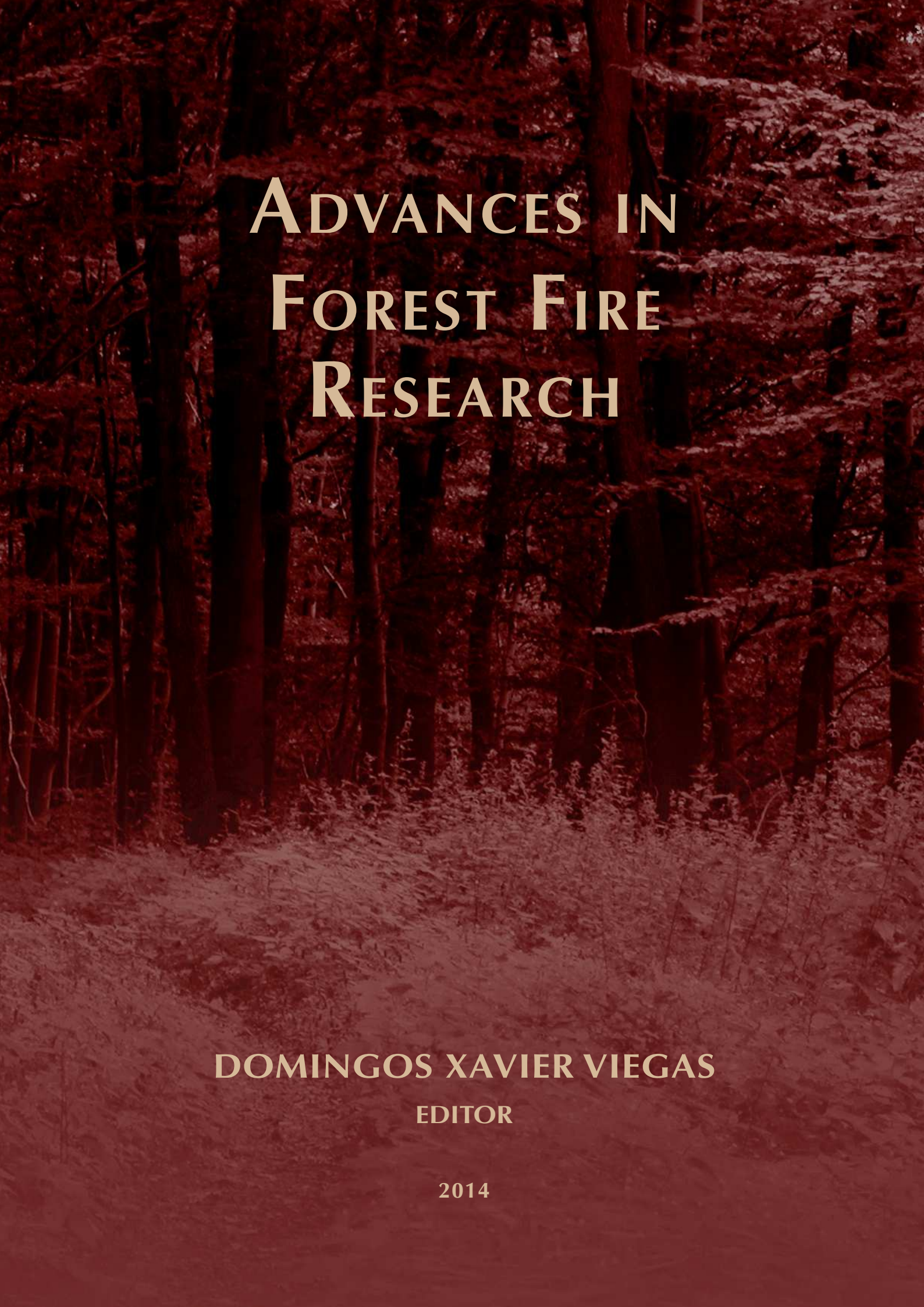

Advances in Forest Fire Research

DOMINGOS XAVIER VIEGAS

EDITOR

2014

EDIÇÃO
Imprensa da Universidade de Coimbra
Email: imprensa@uc.pt
URL: http//www.uc.pt/imprensa_uc
Vendas online: http://livrariadaimprensa.uc.pt

COORDENAÇÃO EDITORIAL
Imprensa da Universidade de Coimbra

COMPOSIÇÃO
Luís Mário Ribeiro

INFOGRAFIA DA CAPA
Mickael Silva

ISBN DIGITAL
978-989-26-0884-6

DOI
http://dx.doi.org/10.14195/978-989-26-0884-6

Advances in Forest Fire Research

DOMINGOS XAVIER VIEGAS
EDITOR

2014

ADAI/CEIF
Associação para o Desenvolvimento da Aerodinâmica Industrial (ADAI)
Centro de Estudos sobre Incêndios Florestais (CEIF)
Rua Pedro Hispano nº12
3030 - 289 Coimbra
Telf: +351 239 708580 | Fax: +351 239 708589

Coimbra 2014

Composition
Luís Mário Ribeiro

Contents

Preface

Forest fires remain a challenge to firefighters, scientists, managers, decision makers, and citizens, in many parts of the World. Conditions brought by a changing climate associated to other trends in land use and fuel management policies along the past years indicate that extreme fire behaviour episodes may occur more frequently than in the past, bringing even more challenges to all.

During the past twenty to thirty years the international fire research community grew in number, quality and diversity of scientific areas involved worldwide. This is reflected in the number of scientific publications and meetings dedicated to forest fires.

The International Conference on Forest Fire Research, that has its seventh edition in 2014 in Coimbra (Portugal), aims to serve its purpose of being a platform to present and discuss the latest results of scientific research on various areas of forest fire management. Almost 300 extended abstracts were submitted for the conference, on the following topics:

- Economic Issues
- Evaluation and management of burned areas
- Fire at the Wildland Urban Interface
- Fire Behaviour
- Fire Detection and Monitoring
- Fire Ecology
- Fire Management
- Fire Safety
- Fire Suppression and New technologies
- Forest Fire Risk assessment and Climate Change
- Forest management and Fire Prevention
- Human and Institutional factors
- Large Fires
- Remote Sensing

Following a process of dedicated evaluation and selection by the Conference Scientific Committee the full papers were put together in this Book.

I hope that this Book may serve the purpose of keeping a record of the recent research in these fields and to illustrate the role that is played by the scientific community in the face of the challenges that these new times bring to fire science. I am sure that it will inspire and provoke more investigation and collaboration.

In the name of the Organizing Committee of the Conference I wish to thank all the authors for their valuable work and for their participation.

I wish to thank Dr. Mike Flannigan for having accepted, once more, the role of Head of the Scientific Committee, who with the help of a group of selected experts revised the submitted abstracts and selected them. Their work was very important to keep the high level of quality that has been the standard of this Conference and I wish to thank the reviewers also.

I would like to express my personal thanks to all the members of the Organizing Committee and in particular to my colleagues of the Local Committee and the Secretariat for all their support, work and dedication during the preparation of the Conference. They carried the largest part of the work load that included the performance of the large and small tasks that are required to put this Conference together and therefore they deserve thanks from all of us.

Coimbra, 1 September 2014

Domingos Xavier Viegas

Chapter 1
Fire Behaviour and Modelling

A Comparative Study of Parameter Estimation and State Estimation Approaches in Data-Driven Wildfire Spread Modeling

M.C. Rochoux[a], C. Emery[a], S. Ricci[a], B. Cuenot[a], A. Trouvé[b]

[a] *CERFACS, SUC-URA1875, CNRS, , 42 Av. G. Coriolis, 31057 Toulouse (France);* melanie.rochoux@graduates.centraliens.net, sophie.ricci@cerfacs.fr, benedicte.cuenot@cerfacs.fr
[b] *Department of Fire Protection Engineering, University of Maryland, College Park, MD 20742 (USA);* atrouve@umd.edu

Abstract
The objective of this work is to demonstrate the ability of the FIREFLY data-driven wildfire simulator to forecast the fire spread behavior over complex terrain topography. The prototype simulator features the following main components: a level-set-based fire propagation solver that adopts a regional-scale viewpoint, treats wildfires as propagating fronts, and uses a description of the local rate of spread (ROS) of the fire as a function of vegetation, topographical and meteorological properties based on Rothermel's model; a series of observations of the fire front location; and a data assimilation algorithm based on an ensemble Kalman filter (EnKF). The data assimilation algorithm also features a choice between a parameter estimation (PE) approach in which the estimation targets are the input parameters of the ROS model, and a state estimation (SE) approach in which the estimation targets are the spatial coordinates of the discretized fire front. This study shows the extension of the FIREFLY data-driven simulator to complex terrain topography. The fire propagation is represented by time-evolving two-dimensional fronts along the horizontal plane in order to remain consistent with the formulation of the PE-/SE-based EnKF algorithms that were initially developed for flat terrain configuration. While evaluated on synthetic cases in this study, the performance of the EnKF algorithm is shown to be preserved in the case of complex terrain. Thus, this study emphasizes the potential of data assimilation to dramatically increase wildfire simulation accuracy in real-world wildfire events.

Keywords: *Data assimilation, Ensemble Kalman Filter, Wildfire, Fire modeling, Terrain topography*

Introduction

The challenges found on the route to developing quantitative fire models are two-fold. First, there is the classical modeling challenge associated with providing accurate mathematical representations of the multi-physics multi-scale processes that involve biomass pyrolysis, combustion, flow dynamics as well as atmospheric dynamics and chemistry (Sullivan 2009a, 2009b). Second, there is the less common data challenge associated with providing accurate estimates of the input parameters required by the models (Viegas 2011). Current regional-scale fire models are limited in scope because of the large uncertainties associated with the accuracy of physics-based models, because also of the large uncertainties associated with many of the environmental conditions that are required as input parameters to the fire problem (Rochoux 2014). A possible approach to overcome the limitations found in numerical simulations of wildfire spread as well as to develop predictive models that are compatible with operational applications is data assimilation (DA). This approach takes advantage of recent progress made in airborne remote sensing that is promising for real-time monitoring of the fire front location (Paugam *et al*. 2013). DA offers a convenient framework for integrating fire sensor observations into a computer model along with the estimated modeling/observation uncertainties with the goal to provide optimal estimates of the control variables and thereby to improve predictions of fire spread behavior. The application of DA and inverse modeling has recently been explored in the area of wildfire research (e.g. Mandel and Beezley 2007; Lautenberger 2013; Rochoux *et al* 2013). The key idea is that, when used alone, neither measurements nor computer models can provide a reliable and complete description of the real state of the physical system.

The present study is an extension of our previous work in Rochoux *et al* (2013, 2014a, 2014b) and Rochoux (2014), in which a prototype data-driven wildfire spread simulator capable of forecasting the wildfire spread behavior was developed. The prototype simulator features the following main components: a level-set-based fire propagation solver (Rehm and McDermott 2009) that treats wildfires as propagating fronts and uses a description of the local rate of fire spread (ROS) as a function of vegetation, topographical and meteorological conditions based on the model due to Rothermel (1972); a series of observations of the fire front location; and a DA algorithm based on the ensemble Kalman filter (EnKF) to account for some of the non-linearities in the mapping between control space and observation space. The DA algorithm also features a choice between a parameter estimation (PE) approach in which the control variables are the input parameters of the ROS model (Rochoux *et al* 2014a) and a state estimation (SE) approach in which the control variables are the spatial coordinates of the fire front (Rochoux *et al* 2014b). This study presents the extension of the FIREFLY-based data-driven wildfire spread simulator to problems with complex terrain topography; the formulation of the PE-/SE-based DA strategies is not affected by the increasing complexity of the wildfire spread model. The paper is organized as follows. The data-driven wildfire spread model (including the fire spread model with complex terrain topography and the DA algorithms) is presented in Section 2; examples for each component of the data-driven simulator are also provided. Its performance is evaluated for synthetic DA experiments in Section 3.

Methodology: Data-driven wildfire spread model

As any current operational fire spread simulator, FIREFLY adopts a regional-scale perspective. This implies that wildfires are assumed to feature a front-like geometry at scales ranging from a few tens of meters up to several kilometers and may be described as a line that propagates normal to itself into unburnt vegetation and over complex topography, at a ROS denoted by Γ_{3D}.

Forward model: Fire spread model

2.1.1. *Geometrical considerations*

A rectangular Cartesian coordinate system (x_0, y_0, z_0) is introduced to geolocalize the propagation of the fire front over complex terrain topography. (x_0, y_0) represents the horizontal plane, with the x_0-axis pointing towards the East direction and the y_0-axis pointing towards the North direction; the z_0-axis is the vertical direction (z_0 = 0 m represents the horizontal plane, where the terrain elevation h is zero). The reference frame is illustrated in Figure 1a.

Based on Sharples (2008) and Lautenberger (2013), the terrain topography is locally characterized in FIREFLY by a pair of angles noted (α_a, α_{sl}), see Figure 1a. α_a [°] is the terrain aspect angle indicating the downslope direction and is defined in a clockwise representation, where 0° indicates the North direction (i.e. the y_0-direction). α_{sl} [°] is the terrain slope angle, taking values between 0° (flat terrain) and 90° (vertical wall). The direction from which the wind blows is noted α_w [°] and is defined in a clockwise representation, where 0° indicates the North direction, see Figure 1b. In this framework, the direction of fire propagation is noted α_{fr} [°].

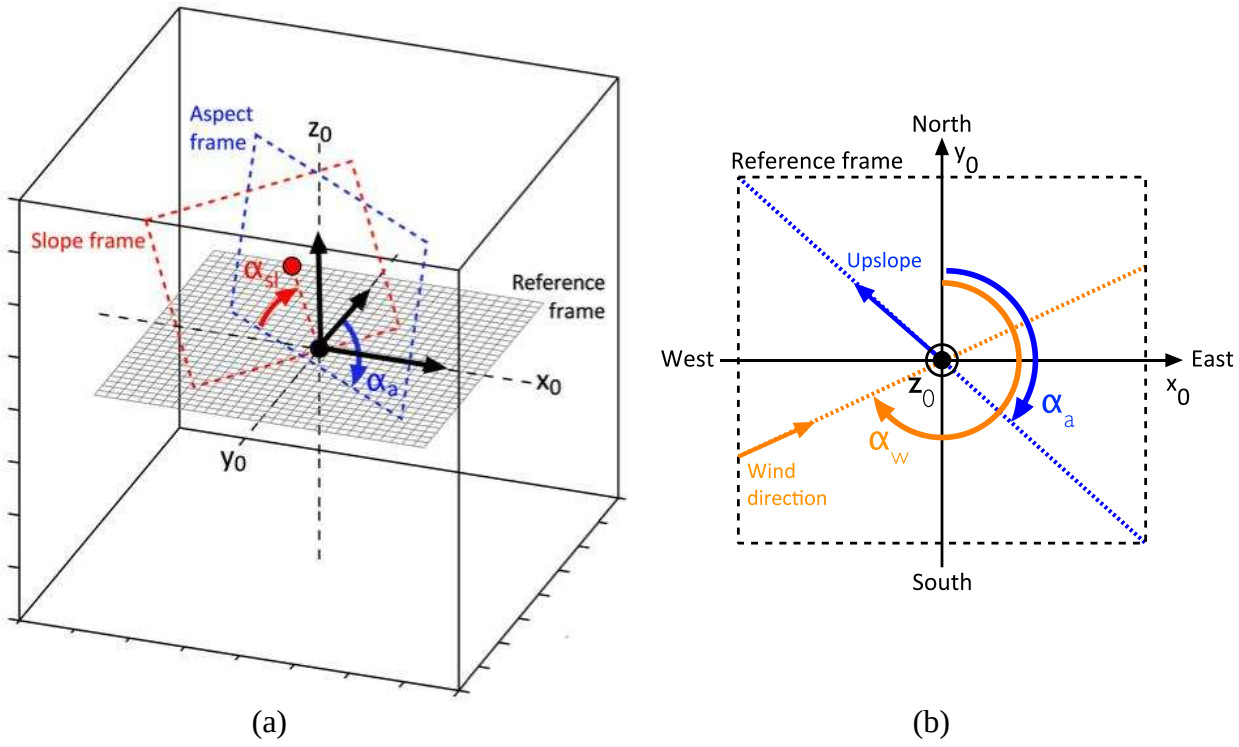

(a) (b)

Figure 1. Formalism to include terrain topography in FIREFLY. (a) Three-dimensional reference frames, where (x0, y0) represents the horizontal plane, where αa represents the aspect angle direction (i.e. the downslope direction) and where αsl represents the terrain slope angle; the blue and red planes are perpendicular. (b) Two-dimensional horizontal plane (x0, y0) with the aspect angle direction αa and the wind direction angle αw.

The pair of local parameters (α_a, α_{sl}) can be retrieved from altimetry elevation data $h \equiv h(x_0, y_0)$ as follows (Vico and Porporato 2009, Emery *et al* 2013):

$$\begin{pmatrix} \sin\alpha_a \\ \cos\alpha_a \end{pmatrix} = -\frac{1}{\tan\alpha_{sl}} \begin{pmatrix} \partial h/\partial x \\ \partial h/\partial y \end{pmatrix}, \quad (1)$$

with:

$$\tan\alpha_{sl} = \sqrt{\left(\partial h/\partial x\right)^2 + \left(\partial h/\partial y\right)^2}. \quad (2)$$

In FIREFLY, the terrain elevation h corresponds to input data that are interpolated at each grid point of the computational domain. The calculation of its gradient is performed through a classical centered finite difference scheme.

2.1.2. *Extension of the Rothermel's model to wind and slope effects*

The original Rothermel's ROS model (noted Γ_{1D}) that was developed for one-dimensional upslope and/or upwind fire propagation is of the following form:

$$G_{1D} = G_0(1 + F_w^* + F_{sl}^*), \quad (3)$$

where Γ_0 [m s^{-1}] is the no-wind no-slope ROS, and where the 1-D coefficients $\Phi_w^* \equiv \Phi_w^*(\mathbf{u}_w)$, $\Phi_{sl}^* \equiv \Phi_{sl}^*(\alpha_{sl})$ represent the wind and slope correction coefficients to account for the additional effects of

wind and slope on the propagating speed of the head fire. Note that the wind correction coefficient depends on the surface wind velocity vector noted $\mathbf{u}_w$ [m s^{-1}], which can be provided for instance by meteorological forecasts.

Following choices made by Lautenberger (2013), a modification of the wind and slope contributions to the Rothermel-based ROS is introduced to account for wildfire spread in other directions than the uphill/upwind direction. The 2-D wind and slope correction coefficients in the modified Rothermel's formulation are noted Φ_w and Φ_{sl}, respectively. The modification of the slope correction coefficient Φ_{sl} relies on the following assumptions: (1) when the fire propagates in the upslope direction (i.e. $\alpha_{fr} = \alpha_a + 180°$), the slope contribution to the ROS is maximum (i.e. $\Phi_{sl} = \Phi_{sl}^*$); (2) if the fire propagation occurs in the normal direction to upslope or downslope (i.e. $\alpha_{fr} = \alpha_a \pm 90°$), the slope does not contribute to the fire front propagation; and (3) if the fire propagates in the downslope direction such that $\alpha_{fr} \in [\alpha_a - 90°, \alpha_a + 90°]$, the ROS is forced to Γ_0, meaning that the fire cannot propagate at a lower ROS than the no-slope no-wind Γ_0. The modification of the wind correction coefficient Φ_w relies on similar arguments. Thus, the Rothermel's formulation of the wind- and slope-aided ROS (noted Γ_{3D}) becomes:

$$\Gamma_{3D} = \Gamma_0 \max(1, 1 + \Phi_w + \Phi_{sl}), \tag{4}$$

with the following expressions for $\alpha_{fr} \notin [\alpha_a - 90°, \alpha_a + 90°]$:

$$\Phi_{sl} = \cos\left(\alpha_{fr} - (\alpha_a + \pi)\right) \Phi_{sl}^*, \tag{5}$$

$$\Phi_w = \cos\left(\alpha_{fr} - (\alpha_w + \pi)\right) \Phi_w^*. \tag{6}$$

Γ_{3D} corresponds here to the evaluation of the ROS in the slope frame (see Figure 1a); this value is projected onto the reference frame (x_0, y_0, z_0) to obtain the ROS Γ_{2D} required by the FIREFLY level-set solver to propagate the fire front on the horizontal plane (x_0, y_0) along its normal direction $\mathbf{n}_{fr}$. Based on geometrical considerations, the projected ROS Γ_{2D} reads:

$$\Gamma_{2D} = \Gamma_{3D} \left(1 + \tan^2(\alpha_{sl}) \cos^2(\alpha_a - \alpha_{fr})\right)^{-\frac{1}{2}}. \tag{7}$$

The derivation of the formulation in Eq. (7) can be found in Emery *et al* (2013). Figure 2 shows the variations of the slope-aided ROS Γ_{2D} evaluated using Eq. (7), with respect to the slope angle α_{sl} (horizontal axis) for different aspect angles α_a (colorbar) varying between 0° (dark-blue-plain line) and 90° (brown-plain line). For $\alpha_a = 0°$, the fire spreads in the upslope direction with a ROS reaching up to 1 m/s for a slope angle α_{sl} above 65°; the effect of the slope is considerable since the ROS Γ_{2D} can be multiplied by a factor up to 25 compared to the no-slope no-wind ROS $\Gamma_0 = 0.048$ m/s. On the contrary, for $\alpha_a = 90°$, the fire propagates in the transverse direction to the slope, implying that the slope does not modify the ROS and $\Gamma_{2D} = \Gamma_0 = 0.048$ m/s.

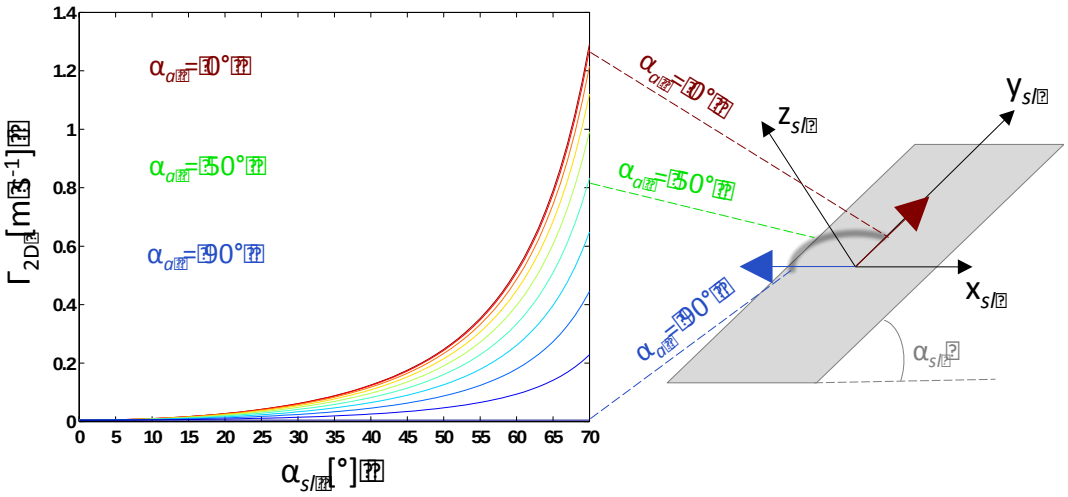

Figure 2. Slope-aided ROS Γ_{2D} with respect to the terrain slope angle α_{sl} (horizontal axis) for different values of the terrain aspect angle α_a (represented by the colorbar) for a no-wind plane configuration and Γ_0 = 0.048 m/s.

2.1.3. *Level-set solver*

FIREFLY tracks the time-evolving fire front location on the horizontal plane (x_0, y_0) using a level-set-based solver, see Figure 3. A progress variable $c \equiv c(x,y,t)$ is introduced as a flame marker: $c = 0$ in unburnt vegetation, $c = 1$ in burnt vegetation, and the contour line $c_{fr} = 0.5$ is identified as the flame front.

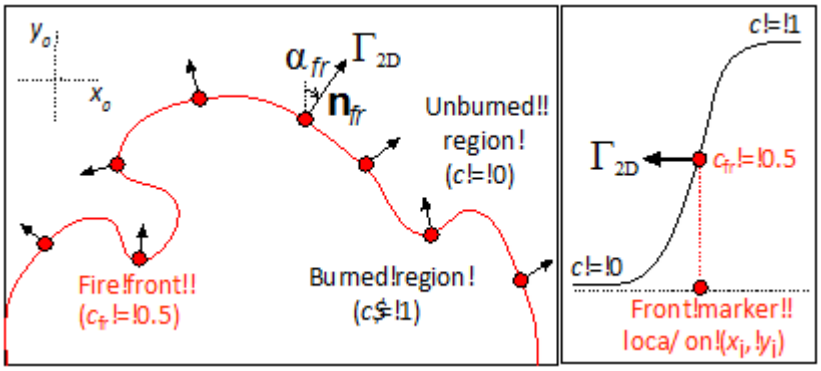

Figure 3. Schematic of FIREFLY. (a) Propagation of the contour line c_{fr} = 0.5 onto the horizontal plane (x_0, y_0), Γ_{2D} measures the local ROS of the fire along the normal direction to the front n_{fr} (defined by the direction angle of fire propagation α_{fr}). (b) Profile of the spatial variations of the progress variable c across the fire front, (x_i, y_i) representing the location of the ith fire front marker.

The progress variable field c is calculated as a solution of the propagation equation:

$$\frac{\partial c}{\partial t} = G_{2D} |\nabla c|, \qquad (8)$$

where $\Gamma_{2D} \equiv \Gamma_{2D}(\mathbf{u}_w, \alpha_{sl}, M_v, \Sigma_v, \beta_v, \delta_{v,\ldots})$ calculated by Eq. (7) is defined along the local normal direction to the fire front $\mathbf{n}_{fr} = -\nabla c/|\nabla c|$ (see Figure 3) and depends on the local environmental conditions such as the biomass fuel moisture content M_v [-], the biomass fuel particle surface-to-volume ratio Σ_v [m^{-1}], the biomass fuel packing ratio β_v [-] and the biomass fuel layer thickness δ_v [m].

Equation (8) is solved by using a second-order Runge-Kutta scheme for time-integration and a second-order total variation diminishing scheme with a Superbee slope limiter for spatial discretization, following choices made by Rehm and McDermott (2009). Convergence of the numerical method was demonstrated in Rochoux (2014).

2.1.4. *Reconstruction of the simulated fire front*

The instantaneous location of the fire front at time t is extracted by geolocalizing the contour line $c_{fr} = 0.5$ and satisfies: $c(x_i, y_i, t) = c_{fr}$ for every marker i of the front, with $i \leq 1 \leq N_{fr}$ (N_{fr} being the total number of simulated markers along the fireline). Two steps are required for this reconstruction of the simulated fire front. First, the algorithm extracts the contour line $c_{fr} = 0.5$ from the two-dimensional progress variable c with respect to the computational grid resolution on the horizontal plane (x_0, y_0) in FIREFLY. Second, this algorithm discretizes the contour line $c_{fr} = 0.5$ with a fixed number (N_{fr}) of equally-spaced markers. Thus, the outputs of FIREFLY are the two-dimensional coordinates of the N_{fr} front markers. Further technical details on the contour line algorithm are provided in Rochoux (2014).

2.1.5. *Examples of fire propagation over terrain topography*

Two synthetic test cases are presented to illustrate the effects of non-uniform terrain topography on the fire front location as simulated by FIREFLY. This terrain topography corresponds to first, an inclined plane and second, a terrain elevation $h(x_0, y_0)$ typical of mountainous regions.

Inclined plane. The fire spread is simulated for a uniform biomass fuel characterized by $\delta_v = 1$ m, $M_v = 15$ % and $\Sigma_v = 11500$ m^{-1}. The terrain is a uniform inclined plane, tilted by $\alpha_{sl} = 15°$ with respect to the horizontal plane, whose aspect angle is $\alpha_a = 225°$ and whose dimensions are 600 m × 600 m (with a mesh step size $\Delta x = \Delta y = 1$ m). The initial condition is described by a circular front centered at ($x_0 = 300$ m, $y_0 = 300$ m) and of radius $r_0 = 5$ m; there is no external flow ($u_w = 0$). FIREFLY is integrated during 1000 s (with a time step $\Delta t = 0.5$ s). Results presented in Figure 4 show that the slope induces a constant propagation in the upslope direction, while the spread at the back of the fire remains very limited. The effective simulated ROS of the head of the fire is equal to 0.264 m s^{-1}, which is consistent with the theoretical value 0.261 m s^{-1} provided by the 0-D Rothermel's model Γ_{1D} (see Eq. 3). The no-slope ROS Γ_0 is equal to 0.068 m s^{-1}; the slope induces a propagation that is 4 times faster than in a no-slope configuration.

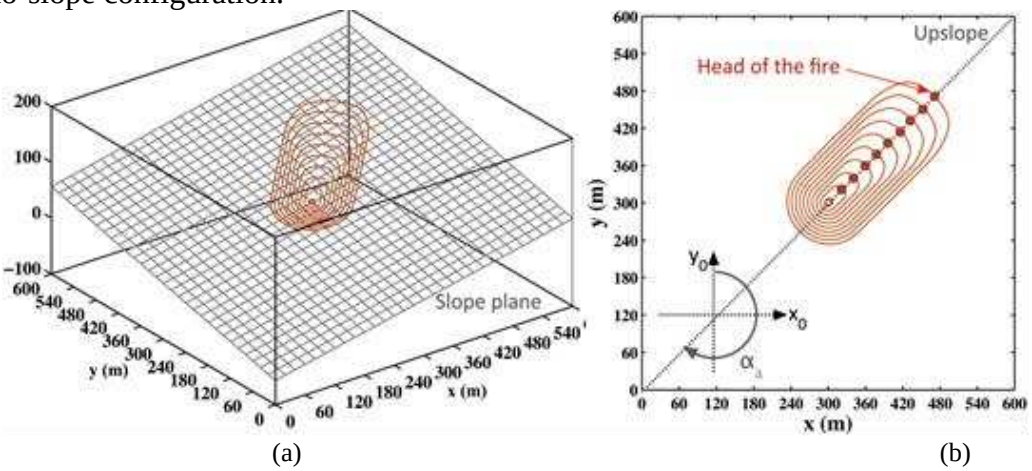

(a) (b)

Figure 4. Time-evolving location of the simulated fire fronts at 100 s intervals on a slope plane with the aspect angle $\alpha_a = 225°$ (a) Three-dimensional representation. (b) Projected representation onto the horizontal plane (x_0, y_0).

Mountainous region. A simulation of wildfire spread induced by complex terrain topography is performed for moderate wind conditions (0.75 m s^{-1}, 315°); the biomass fuel is uniformly-distributed over the 200 m x 200 m field, with $\delta_v = 1$ m, $M_v = 20$ % and $\Sigma_v = 10000$ m^{-1}. The initial condition is

described by a circular front centered at (x_0 = 100 m, y_0 = 100 m) and of radius r_0 = 5 m. FIREFLY is integrated during 1500 s. Figure 5 illustrates the growth of the burnt area over time (at 300 s time intervals). Even though the validation of FIREFLY for the treatment of the wind and slope effects remains to be performed against real-world wildfire events, this simulation is consistent with the main features of wildfire spread: the largest ROS is obtained in the upslope direction (the effect of terrain elevation on the fireline behavior is high compared to the effect of moderate wind, partly due to the high terrain elevation in one corner of the domain).

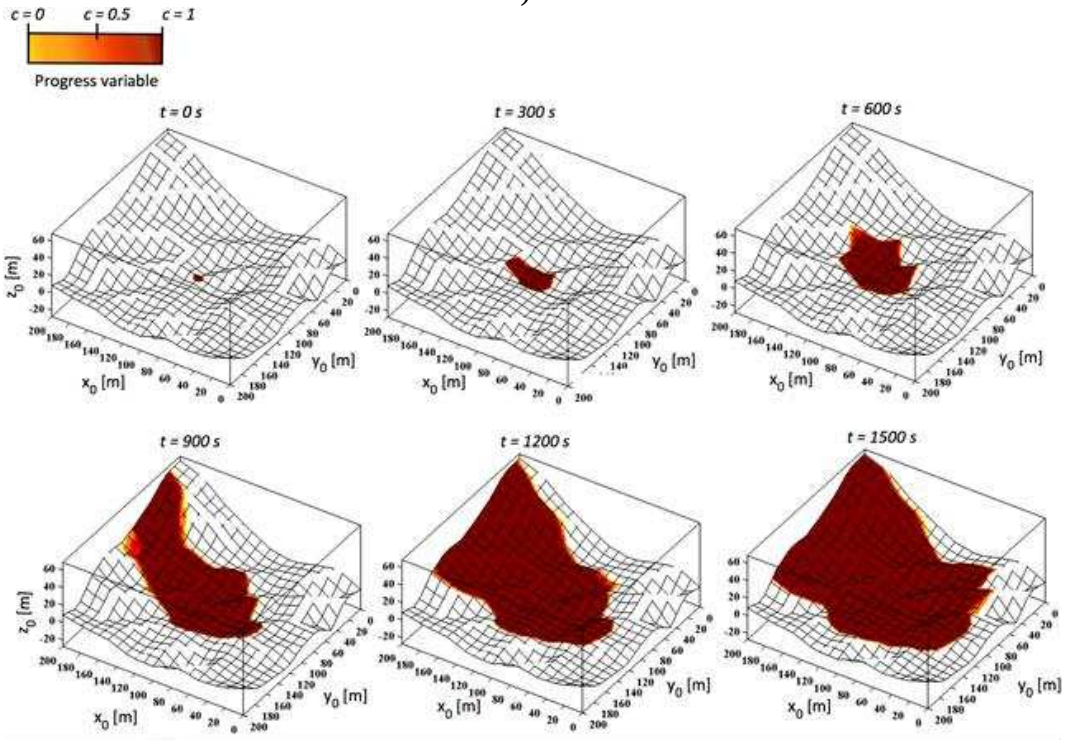

Figure 5. Growth of the burnt area from t = 0 s to t = 1500 s, simulated with FIREFLY over a complex terrain topography; moderate horizontal wind conditions (0.75 m s^{-1}, 315°);

Data assimilation algorithms: parameter estimation versus state estimation

2.2.1. *Model counterparts of the observations*

The correction provided by the DA algorithms relies on a comparison between the (FIREFLY-based) predicted and observed fire front locations at time *t*. The predicted fire front is a high-resolution discretized line described by a set of N_{fr} markers. Since observations of the fire front position are likely to be provided with a much coarser resolution and since they may cover only a fraction of the fire front perimeter, the observed fire front is a discretized line with a set of N_{fr}^o markers, with N_{fr}^o much lower than N_{fr}. In the following, we assume for simplicity that $N_{fr}^o = (N_{fr} / r)$ where *r* is an integer taking values much larger than 1. A selection operator is applied to the simulated fire front in order to pair a subset of N_{fr}^o markers along the simulated fire front with the N_{fr}^o markers along the observation fire front, associating each marker of the observation fire front with its closest neighbor along the simulated fire front.

2.2.2. *Ensemble Kalman filter*

For both parameter estimation (PE) and state estimation (SE) approaches, the EnKF algorithm is sequentially; each assimilation cycle consists of two successive steps (see Figure 6): (1) a prediction step (forecast) in which the system is evolved from time *(t-1)* until time *t* (the next observation time) through an integration of the FIREFLY fire spread model for a large sample N_e of control variables, each realization leading to a new prediction of the fire front location; (2) an update step (analysis) in

which new observations are considered at the analysis time t and the ensemble of forecast realizations is modified consistently with the observations in order to reduce uncertainties in FIREFLY predictions. The new ensemble of N_e realizations is obtained by the application of the classical Kalman filter equation, assuming that the errors on the control variables and on the observations follow Gaussian probability density functions. One advantage of the EnKF algorithm is that the mapping between the control variables and the observation space is estimated stochastically. Thus, the EnKF algorithm is able to handle model non-linearities.

In the PE approach, the control vector includes the n input parameters of the Rothermel-based ROS model that are subject to uncertainties and to which FIREFLY is sensitive (Rochoux *et al*. 2014a). In the SE approach, the control vector is made of the coordinates of the N_{fr} front markers along the simulated fire front such that $n = 2N_{fr}$ (Rochoux *et al*. 2014b). The main difference between PE and SE approaches relies on the definition of the observation operator. In the SE approach, the observation operator is limited to the selection operator introduced in Section 2.2.1. Since in the PE approach the observation operator maps the environmental parameters onto the model counterparts of the observations, it also includes the integration of the FIREFLY fire spread model (this aspect emphasizes the need for a DA approach that accounts for model non-linearities).

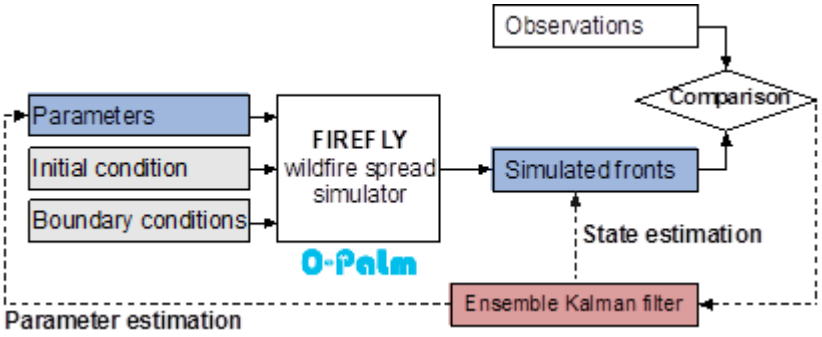

Figure 6. DA flowchart for PE and SE approaches over one assimilation cycle based on the OpenPALM dynamic coupler (www.cerfacs.fr/globc/PALM_WEB/); control variables are colored in blue.

2.2.3. *Validation of the ensemble Kalman filter*

We present results from a validation test in which observations are taken from an experimental database corresponding to a controlled grassland fire (personal communication and unpublished data). This validation test corresponds to a real reduced-scale (4 m x 4 m), flat, open-field grassland lot burning in which the ROS takes values on the order of 1 cm s^{-1} under moderate wind conditions. The properties of the grass are (approximately) known: $\delta_v = 0.08$ m, $M_v = 22$ % and $\Sigma_v = 11500$ m^{-1}. The mean wind conditions are also approximately known: $u_w = 1$ m/s and $\alpha_w = 307$ degrees. The fire spread is recorded during 350 s using a thermal-infrared camera; the fire front (represented by $N_{fr}^o = 40$ markers) is defined at the 600 K iso-temperature contour at 14 s intervals, from $t_0 = 50$ s to $t_4 = 106$ s. In the PE approach, 4 parameters are used as control variables: the fuel moisture content and particle surface-to-volume ratio as well as the wind magnitude and direction angle. These parameters are varied around mean values and with prescribed uncertainties; the EnKF ensemble contains $N_e = 1000$ members. In the SE approach, the control variables are the spatial coordinates of the discretized fire front. An ensemble of $N_e = 100$ members is produced based on assumed uncertainties in the input parameters of the ROS model (i.e., the fuel depth, moisture content and particle surface-to-volume ratio as well as the wind magnitude and direction angle) as well as assumed uncertainties in the initial fire location at t_0.

Figure 7a presents the averaged fire front position at time $t_4 = 106$ s, using the PE and SE ensembles as predicted from a numerical integration of FIREFLY, and with an EnKF update performed at time $t_3 = 92$ s. The numerical integration is performed N_e times for all members of the EnKF ensemble but only the mean predictions are plotted in Figure 7a. It is shown that the mean forecast significantly

underestimates the observed ROS. In contrast, Figure 7b shows that the mean analysis (i.e. a simulation with an EnKF update at current time t_4) successfully reduces the distance between model predictions and observations; this result is achieved by an adjustment of the ROS model parameters in the PE approach or directly of the fire front position in the SE approach.

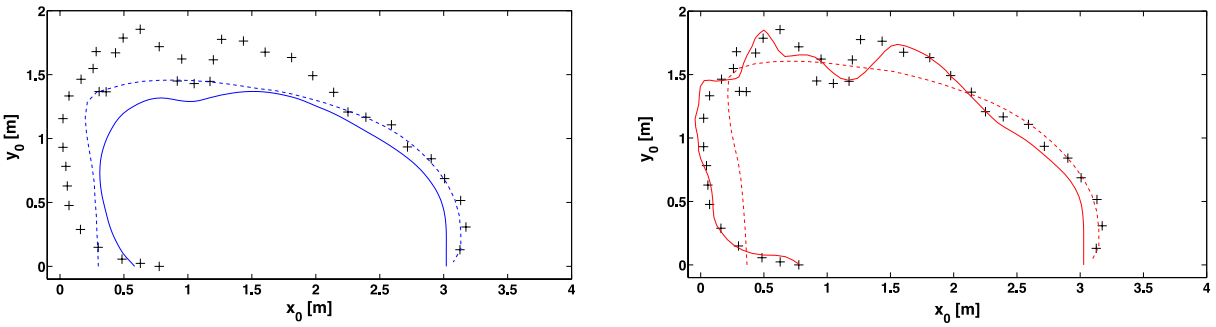

Figure 7. Comparison between simulated (lines) and observed (symbols) front positions at time t_4 = 106 s on the horizontal plane (x_0, y_0). The simulated front position is the mean position calculated as the average of the EnKF ensemble; dashed lines (solid lines) correspond to the PE-based (SE-based) simulations. (a) Forecast (with an EnKF update at t_3 = 92 s). (b) Analysis (with an EnKF update at t_4 = 106 s).

In spite of the quality of the PE-based or SE-based correction, the mean forecast, while still significantly more accurate than the simulations without DA, remains limited. The mean predictions presented in Figure 7a have the benefits of an EnKF update performed at earlier time t_3; however, some of these benefits are lost at time t_4 due to the limited persistence of the initial condition for the SE-based forecast and due to the temporal variability of the errors in the environmental conditions for the PE-based forecast. We find that in this configuration, the PE algorithm provides better forecasts than the SE algorithm but this ranking is problem-dependent. While a DA approach provides excellent forecasting performance at short lead-times, the assimilation frequency (i.e., frequency at which the analysis is renewed by observations) needs to be adjusted to the persistence of the initial condition and/or to the temporal variability of the errors in the environmental conditions.

Evaluation of the performance of the data-driven simulator for complex terrain topography

An anisotropic case of wildfire spread subject to moderate wind conditions is considered for the complex terrain topography illustrated in Figure 5 for a deterministic run. In the present DA test, observations are synthetically generated using a similar deterministic run over the time window [0; 750 s], called *true solution* of the FIREFLY fire spread model, with specified values of the environmental conditions (referred to as the *true parameters* in Table 1); random errors characterized by a 1-m standard deviation (STD) are then added to the true solution to obtain the location of the observation markers ($N_{fr}^{o} = N_{fr} = 100$) at time 750 s (there is a single observation time over [0; 750 s]). Since this observation error STD is low relatively to the size of the fireline perimeter, the objective here is to evaluate the ability of the EnKF algorithm to retrieve the true location of the fire front.
An ensemble of $N_e = 320$ forecasts is produced over the time window [0; 750 s], based on assumed uncertainties in a subset of ROS model parameters, specifically in the fuel layer depth δ_v, the fuel moisture content M_v, the fuel particle surface-to-volume ratio Σ_v and the wind properties (u_w, α_w). Thus, uncertainties are due to variations in 5 parameters, whose mean and STD are presented in Table 1. Note that the perturbed parameters remain spatially-uniform for each ensemble member. Note also that this large ensemble is necessary to accurately describe the spatial variability in the errors in the SE approach as well as to dissociate the effects of each control parameter on the fireline position in the PE approach. Figure 8a presents a comparison between the true and forecast fire front locations at time t = 750 s (the forecast estimates between PE and SE approaches are equivalent). Due to

uncertainties in the ROS model parameters and the presence of heterogeneous terrain topography, the shape of the simulated fire fronts significantly varies between the members (with a burnt area varying between 500 and 10000 m^2).
The EnKF update is performed at time 750 s, either for the PE approach or for the SE approach. While the SE approach leads to a direct adjustment of the fire front location, the PE approach works by an adjustment of the ROS model parameters; the 5 perturbed parameters (δ_v, M_v, Σ_v, u_w, α_w) are used as control variables**.** Figure 8b compares the mean analysis estimate obtained at the same time 750 s using a PE-based EnKF update (red dashed line) and a SE-based EnKF update (red solid line). These analysis estimates are compared to observations (black crosses) and to the mean forecast estimate (blue solid line). For both PE and SE approaches, the analysis estimates feature a much reduced scatter around the true location of the fire front than the ensemble of forecast estimates. At time 750 s, the mean distance between the (PE-/SE-based) mean ensemble estimate and the observations is reduced by a factor of at least 20. Thus, both PE and SE approaches are able to retrieve an accurate estimation of the fire front location, even though the prior information is subject to high levels of uncertainties and the terrain topography is complex. Note that as for the real case presented in Figure 7, the SE approach is more effective at retrieving the topology of the front at the analysis time than the PE approach; the latter provides valuable information on the input parameters to forecast the front at future lead-times (see Rochoux *et al*. 2014a, 2014b for further details).

Table 1. Properties of the ensemble forecast in the control space; anisotropic OSSE test

	True	Forecast (mean/STD)		PE-based analysis (mean/STD)	
δ_v	0.30 m	0.20 m	0.10 m	0.26 m	0.06 m
M_v	10 %	14.0 %	4.0 %	11.7 %	3.6 %
Σ_v	11500 m^{-1}	10000 m^{-1}	4000 m^{-1}	13078 m^{-1}	2436 m^{-1}
u_w	0.75 m s^{-1}	0.65 m s^{-1}	0.20 m s^{-1}	0.83 m s^{-1}	0.15 m s^{-1}
α_w	315°	315°	45°	288°	28°

Conclusions

This study presents a prototype data-driven wildfire simulator capable of correcting inaccurate predictions of the fire front position and of subsqequently providing an optimized forecast of the wildfire behavior over complex terrain topography. The simulator features a regional-scale wildfire spread model FIREFLY coupled with an EnKF-based data assimilation algorithm and a parameter estimation (PE) approach or a state estimation (SE) approach. The study assumes that observations of the fire front location are available at frequent times but possibly provide an inaccurate and incomplete description of the fire front. The results obtained for a controlled grassland fire indicate that the forecasting performance of a PE approach or a SE approach may be limited to short lead-times. Future plans include the development of a dual SE/PE approach that could partly overcome these limitations. The PE approach could be extended to the case of weak spatial variations of the spread-rate model parameters. Assuming that the errors on the parameters vary slowly in time, the PE-based correction can reasonably be used for forecast, thus allowing for mid- to long-term forecast. In addition, the SE correction could be used for short-term forecast in order to locally correct the shape of the fire front. Future plans also include the evaluation of the PE/SE-based estimation strategy for real-world regional-scale wildfire hazards, in order to design the observation requirements (in terms of spatial and temporal resolutions) to obtain reliable forecasts of wildfire spread.

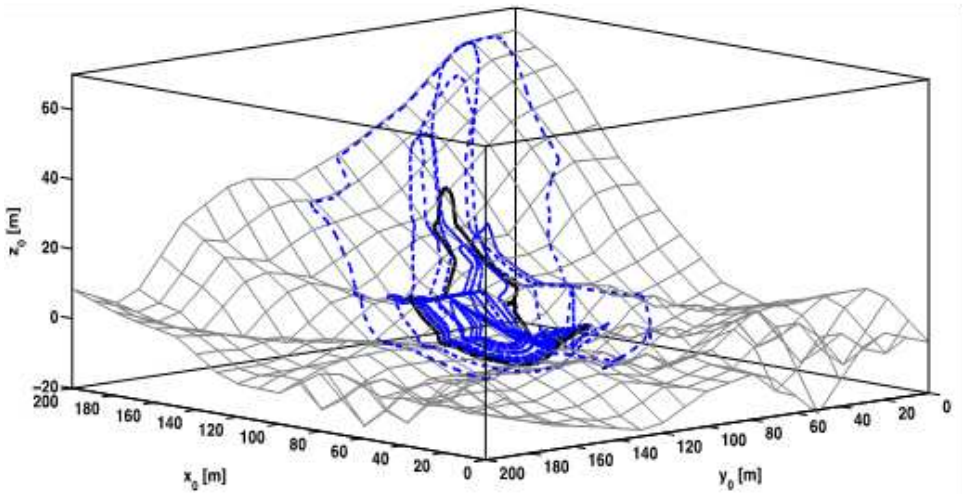

(a) Forecast step at time 750 s

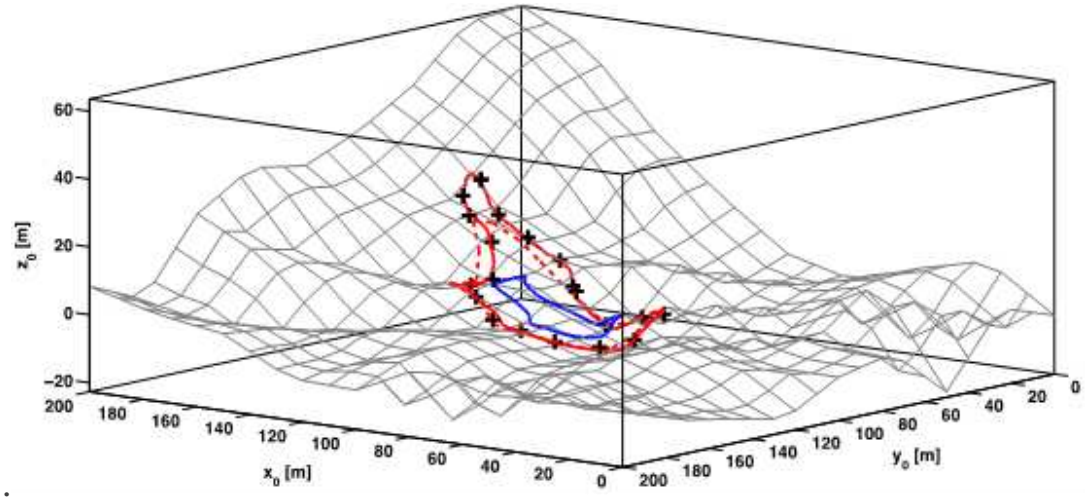

(b) Analysis step at time 750 s.

Figure 8. Comparison between simulated (lines) and observed (symbols) front positions at time 750 s; single assimilation cycle. (a) Forecast step: comparison between the true front location (black solid line) and the ensemble of forecast estimates (blue dashed lines). Only a subset of the ensemble is shown here for clarity purposes (b). Analysis step: comparison between observations (black crosses) and the mean analysis estimate: the dashed line (the solid line) corresponds to the PE-based (SE-based) analysis (with an EnKF update at 750 s and starting from the same initial condition as the forecast at time 0). Only a subset of observation front markers is shown here for clarity purposes.

Acknowledgments

The financial support provided by the Agence Nationale de la Recherche under the IDEA project grant ANR-09-COSI-006 (2010-2013) and by the LEFE-MANU grant (INSU-CNRS program, 2011-2013) was greatly appreciated. The authors also gratefully acknowledge Ronan Paugam and Martin Wooster (King's College London) for sharing the experimental data, Florent Duchaine and Thierry Morel (CERFACS) for support on Open-PALM.

References

Emery C, Rochoux MC, Ricci S, Trouvé A (2013) State estimation using data assimilation for simulation of regional-scale wildfire spread with complex topography. Technical Report TR-CMGC-13-63, CERFACS (France) - University of Maryland (USA).

Lautenberger C (2013) Wildland fire modeling with an Eulerian level-set method and automated calibration, Fire Safety Journal 62, 289–298.

Mandel J, Beezley JD (2007), Morphing Ensemble Kalman filter, Tellus A 60.

Paugam R, Wooster M, Roberts G (2013), Use of handheld thermal imager data for airborne mapping of Fire Radiative Power and Energy and flame front rate of spread, IEEE Transactions on Geoscience and Remote Sensing 51, 3385-3399.

Rehm RG, McDermott RJ (2009) Fire front propagation using the level-set method. NIST, Technical Report 1611.

Rochoux MC, Delmotte B, Cuenot B, Ricci S, Trouvé A (2013) Regional-scale simulations of wildland fire spread informed by real-time flame front observations, Proceedings of the Combustion Institute 34, 2641–2647.

Rochoux MC (2014) Vers une meilleure prévision de la propagation d'incendies de forêt: evaluation de modèles et assimilation de données (PhD Thesis - in English, Ecole Centrale Paris: France)

Rochoux MC, Ricci S, Lucor D, Cuenot B, Trouvé A (2014a) Towards predictive data-driven simulations of wildfire spread – Part I: Reduced-cost ensemble Kalman filter based on poly- nomial chaos surrogate model for parameter estimation, Natural Hazards and Earth System Sciences Discussion 2, 3289–3349.

Rochoux MC, Emery C, Ricci S, Cuenot B, Trouvé A (2014b) Towards predictive data-driven simulations of wildfire spread – Part II: Ensemble Kalman filter for the state estimation of a front-tracking simulator of wildfire spread, Natural Hazards and Earth System Sciences Discussion 2, 3769-3820.

Rothermel RC (1972) A mathematical model for predicting fire spread in wildland fuels. USDA Forest Service, Research Paper INT-115.

Sharples J (2008) Review of formal methodologies for wind-slope correction of wildfire rate of spread. International Journal of Wildland Fire 17, 179–193.

Sullivan AL (2009a) Wildland surface fire spread modeling, 1990-2007. 1: Physical and quasi-physical models, International Journal of Wildland Fire 18, 349-368.

Sullivan AL (2009b) Wildland surface fire spread modeling, 1990-2007. 2: Empirical and quasi-empirical models, International Journal of Wildland Fire 18, 369-386.

Vico G, Porporato A (2009) Probabilistic description of topographic slope and aspect. Journal of Geophysical Research 114, 1–13.

Viegas DX (2011) Overview of forest fire propagation research, in Fire Safety Science - Proceedings of the Tenth International Symposium, International Association for Fire Safety Science 10, 95-108.

A hi-resolution 40-year gridded fire weather/danger climatology for Victoria, Australia

Timothy Brown[a], Graham Mills[b], Sarah Harris[c], Domagoj Podnar[a], Hauss Reinbold[a]

[a] *Desert Research Institute, Reno Nevada USA, tim.brown@dri.edu*
[b] *Monash University, Clayton Victoria Australia, gam4582@gmail.com*
[c] *Monash University, Clayton Victoria Australia, sarah.harris@monash.edu*

Abstract
A homogeneous 40-year (1972-2013) hourly 4-km gridded climate dataset for Victoria, Australia is being generated using a combination of mesoscale modeling, global reanalysis data, surface observations, and historic observed rainfall analyses. The primary purposes of this dataset are optimizing planned burning and land management strategies, and scenario planning for major fire events. Outputs include fire weather and fire danger variables. The output data are created using the Weather Research and Forecast (WRF) model. Error correction techniques are applied to minimize any model biases. Outputs provide an almost limitless opportunity for hitherto unavailable analyses – fields of percentiles of forest fire danger index (FDDI) values, analysis of periods exceeding thresholds at any location, inter-annual and regional variations of fire season characteristics, analysis of prescribed burning windows, of atmospheric dispersion climates, and various atmospheric stability measures that might affect fire behaviour, and to assess climatologies of more esoteric mesoscale weather events, such as mountain waves, that may affect fire behaviour. This presentation describes the generation of the dataset, shows examples of output, and highlights use and relevance for fire management.

Keywords*: Fire weather, fire danger, climatology, dynamical downscaling*

Introduction

There is a need for a detailed understanding of the climatology of fire weather across the Australian landscape if strategic decisions to ameliorate the sometimes-extreme impacts of bushfires on the socio-economic wellbeing of the community are to be based on sound scientific evidence, and if variability and trends in this climatology are to be correctly interpreted. This paper describes the methodology by which a 1972-present high temporal- and spatial-resolution climatology of Victoria's fire weather is being developed. The climatology is intended to combine hourly values of meteorological variables on a regular, high spatial resolution, grid over Victoria, Australia with drought factors based on the Australian Water Availability Project (AWAP) rainfall and temperature analyses (Jones *et al*. 2009) to generate hourly gridded fields of Forest Fire Danger Index (FFDI).
The dataset will provide baseline climatology information for risk management assessments and climate change adaptation planning. The benefits of the dataset to the Victoria Department of Environment and Primary Industries and others include:

- Provides a high-resolution temporally and spatially complete record of temperature, humidity, wind, precipitation, drought and fire danger.
- Allows for analyses at local through regional through state scales.
- Shows interannual and decadal variability for the elements produced, as well as climate trend.
- Quantitatively links climate variability and trend to impacts from fire, heat waves, drought, etc.

- Provides a historical baseline that can be used in comparison studies with downscaled regional or place-based future climate data.
- Serves as input data for decision-support tools to obtain historic baselines.
- Provides quantitative climate values to help test agency strategies and predict ecological outcomes.
- Helps determine if assumptions that go into policy and operations are supported by what is known about the climate record.
- Helps determine the extent that fire management responses have been "driven" by climate versus other forcing factors (e.g., political, economic, public perceptions).

Specific fire management relevance and uses include, but are not limited to:

- Estimating climate related bushfire risk
- Estimating number of days suitable for planned burning
- Input into the allocation of fire management resources - including planned burning
- Bushfire case study analysis, refinement and improvement of burning prescriptions
- Development of climate envelopes for vegetation communities
- Development of weather predictions for "fire use" decision making, and future bushfire climate predictions for strategic planning
- Providing hourly high-resolution weather input for fire spread models

In situ observation networks more typically than not have inhomogeneities in time and space. Thus, there are some considerable barriers to basing a climatology on long-term meteorological observations, as shown by the relatively low number of reliable, long-term observation records available for such analyses (see Lucas *et al*. 2007). This has significant implications for fire weather applications. The bulk of the observations are based near population centres, and so do not necessarily reflect the conditions in the forests where the bulk of major bushfires occur, and which are concentrated in the slopes and valleys of the ranges through central and eastern Victoria. To fulfill bushfire management agency needs, an ideal climatology would be based on a homogeneous high-resolution temporal (i.e., hourly) and spatially gridded fire weather and fire danger dataset. This paper briefly describes the model configuration, running strategy, and quality control/assessment procedures we are using in developing such a dataset for Victoria.

Methods

The mesoscale model used is the Weather Research and Forecasting (WRF) model described by Skamarock *et al*. (2008). It is a well-supported and widely used non-hydrostatic model that includes a wide range of choices of physical parameterization schemes. Three integration domains are used in our configuration (Figure 1) with grid spacings of 36 km (outer mesh), 12 km (middle mesh), and 4 km (inner mesh). Each nest has 33 vertical model levels. Initial state and lateral boundary conditions for the outer mesh are provided by 6- hourly interval global reanalyses. Choices of physical parameterization packages selected are listed in Table 1.

We utilize two global reanalyses for initial state and lateral boundary conditions to start each WRF integration and nudge fields through the 15-day process. The National Centers for Environmental Prediction (NCEP) FNL (Final) Operational Global Analysis (NCEP 2000) data are on 1-degree by 1-degree grids prepared operationally every six hours, and was used for the 2000-2013 period. The ERA-Interim (Dee *et al*. 2011) reanalysis dataset is being used prior to 1999.

There are logistical and data set quality benefits in performing longer (multi-day) rather than shorter (1-2 day) integrations as it is desirable not to have too many discontinuities at the commencement of

each new integration due to the need for the inner mesh to "spin up" from the smooth global reanalysis fields. One would intuitively expect that the model solution would drift somewhat from reality with time, although the use of analysis lateral boundary conditions rather than the forecast conditions used in operational forecast models should reduce this effect somewhat. After considerable testing, we chose to generate the data using 15-day integrations, but with the first day of each integration treated as a spin-up period and thus discarded. Therefore days 2-15 of each integration become Days 1-14 of each two-week data set period.

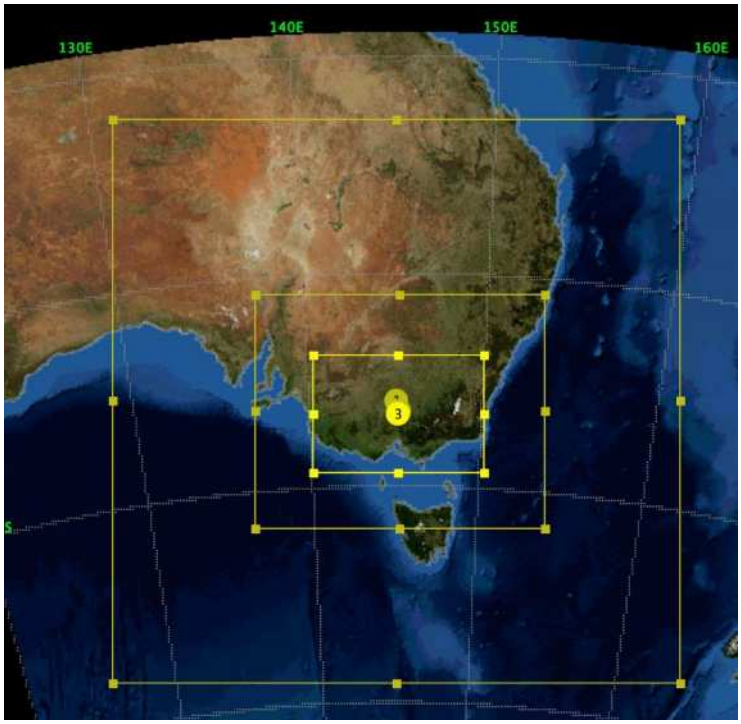

Figure 1. Map showing the three integration grids used in our configuration of the WRF model. Outer grid spacing 36-km, middle 12-km and inner mesh 4-km.

Table 1. List of physical parameterisations used in this WRF configuration.

Microphysics: Thompson *et al.* scheme: A new scheme with ice, snow and graupel processes suitable for high-resolution simulations (8).

*Longwave Radiation***:** RRTM scheme: Rapid Radiative Transfer Model. An accurate scheme using look-up tables for efficiency; it accounts for multiple bands, trace gases, and microphysics species.

*Shortwave Radiation***:** Goddard shortwave: Two-stream multi-band scheme with ozone from climatology and cloud effects.

*Land Surface***:** Noah Land Surface Model: Unified NCEP/NCAR/AFWA scheme with soil temperature and moisture in four layers, fractional snow cover and frozen soil physics.

*Planetary Boundary layer***:** Yonsei University scheme: Non-local-K scheme with explicit entrainment layer and parabolic K profile in unstable mixed layer.

*Cumulus Parameterization***:** Kain-Fritsch scheme: Deep and shallow convection sub-grid scheme using a mass flux approach with downdrafts and CAPE removal time scale.

*Diffusion Option***:** Simple diffusion: Gradients are simply taken along coordinate surfaces.

*K Option***:** 2d Deformation: K for horizontal diffusion is diagnosed from just horizontal deformation. The vertical diffusion is done by the PBL scheme.

The 15-day integrations and model field nudging has produced remarkably small biases. Figure 3 shows cumulative distribution functions (CDFs) for a combined 30 observation dataset and corresponding model grid point for each station for the 10-year period 2004-2013. This includes all hours and days during this period. Further analyses are being undertaken to assess diurnal, seasonal and elevation biases.

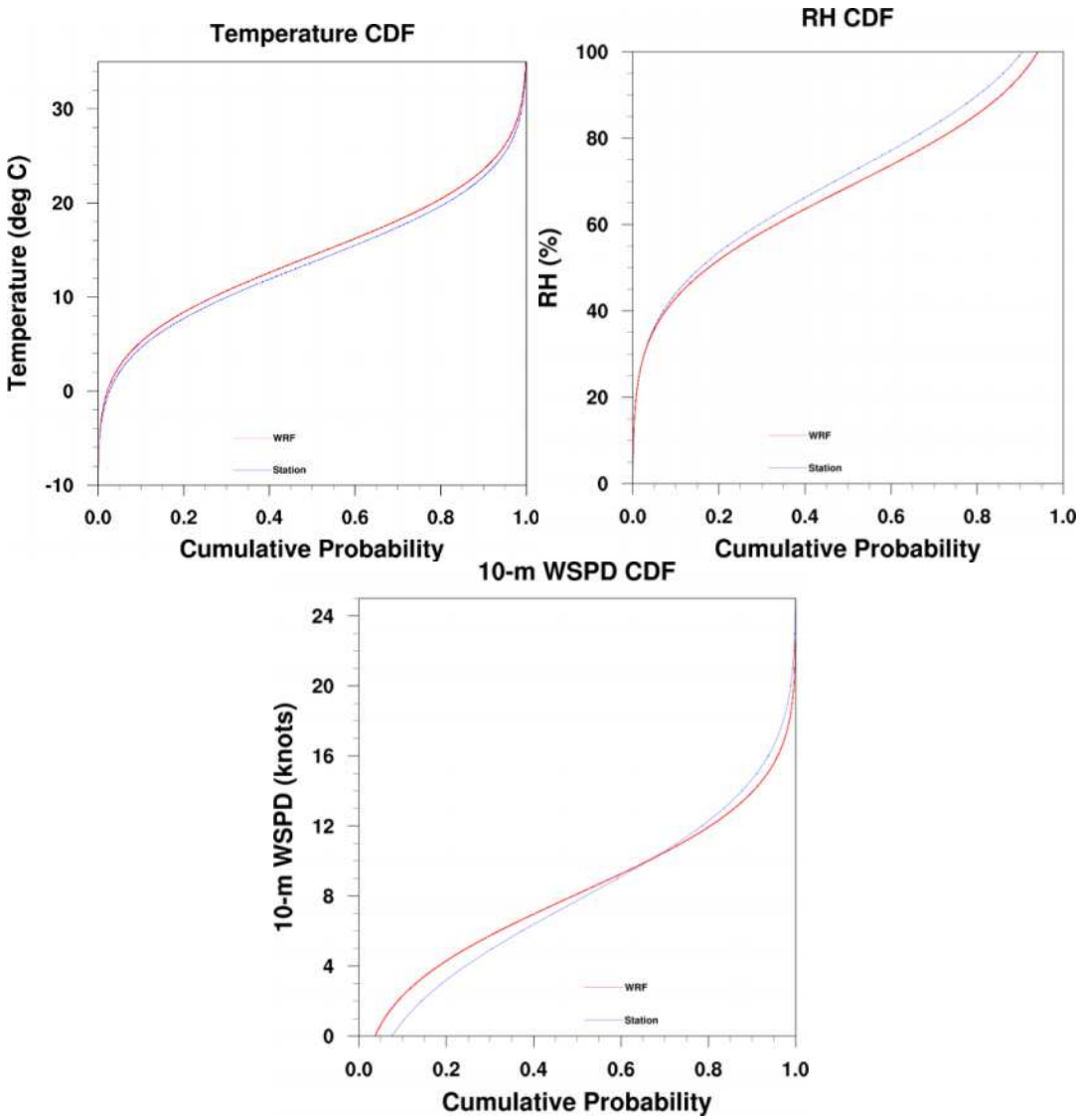

Figure 3. Cumulative distribution functions for 30 stations and corresponding model grid points for all hours and days 2004-2013 for temperature, relative humidity and wind speed.

Results

The surface data from WRF of primary interest include hourly temperature, relative humidity, wind speed, wind direction, Forest Fire Danger Index (FFDI) and precipitation. Daily data of interest include precipitation, Keetch-Byram Drought Index and the Drought Factor. Not surprisingly, a dataset of this size allows for the production of extensive statistics, graphics and analyses. Here we provide a few examples.

Figure 4 shows example maps of 2-m temperature, 2-m relative humidity and 10-m wind speed for 0500 UTC on 22-Jan-2006, a day of extreme fire danger over Victoria. At 0500 UTC a dry cold front has moved onshore in Victoria's west.

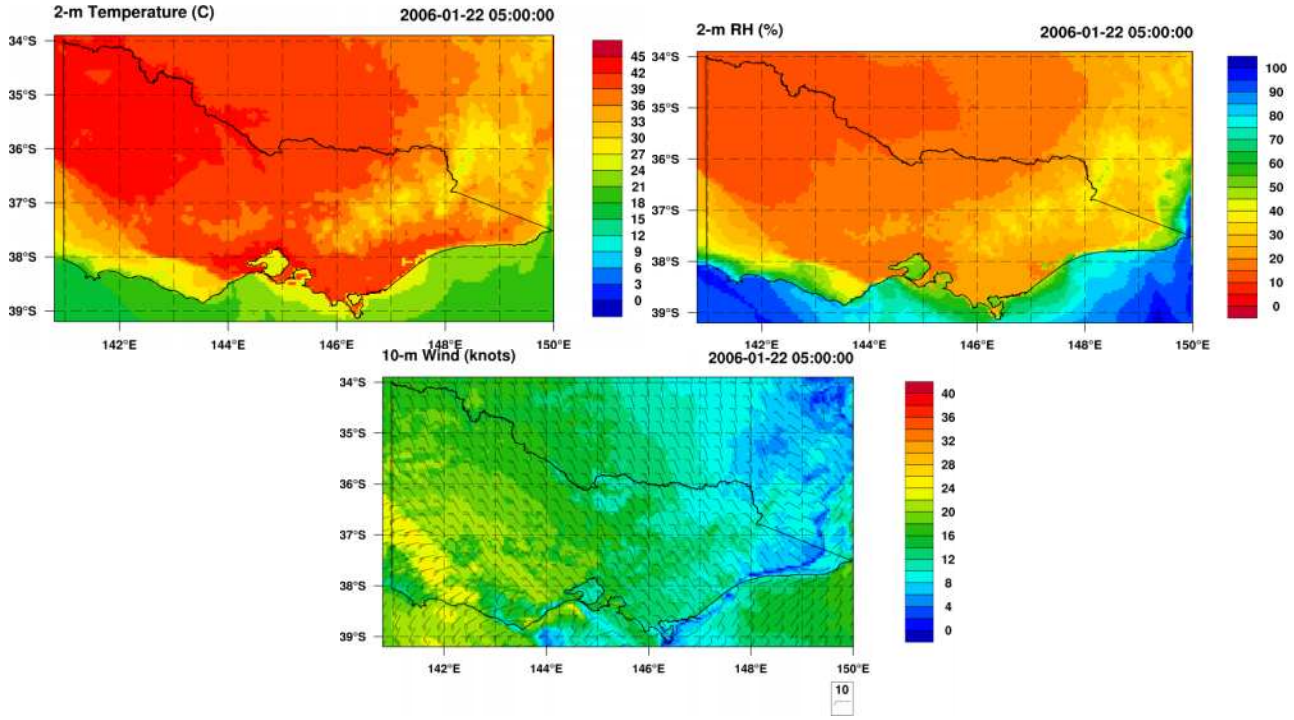

Figure 4. Example maps of 2-m temperature, 2-m relative humidity and 10-m wind speed for 22-Jan-2006.

Figure 5 shows an example of the diurnal cycle of January mean relative humidity by comparing 0500 and 1700 UTC.

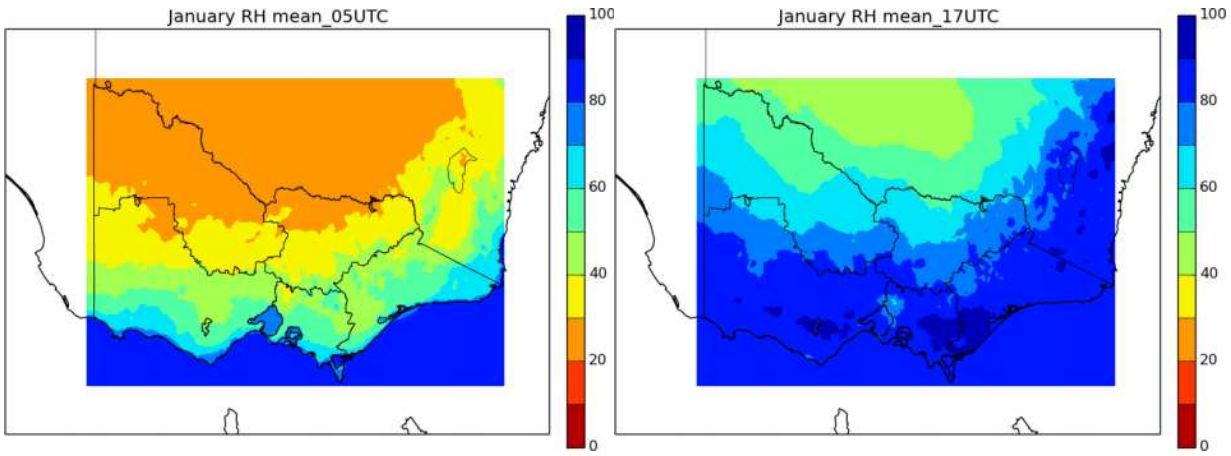

Figure 5. Example maps of January mean relative humidity highlighting the diurnal cycle by contrasting 0500 and 1700 UTC, respectively.

Figure 6 shows the maximum value of the FFDI for the December-February climatological season. The coastal and topographic effects are obvious, and the area of FFDI greater than 125 south of the ranges and west of Melbourne is notable.

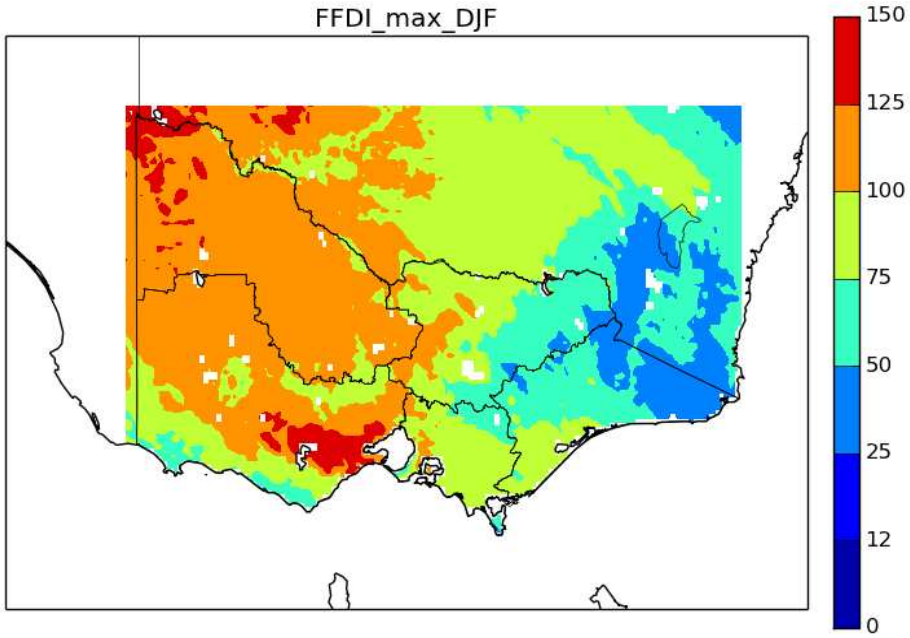

Figure 6. Example map of the climatological maximum FFDI value for the December-February season.

Summary

As of this writing, a 22-year climatology (1992-2013) has been completed. The full dataset is anticipated for completion by the end of 2014. While hourly 4-km surface variables are the primary priority of this project, the fact that the WRF model outputs hourly 3-dimensional fields of all atmospheric variables means that there is the opportunity to assess the climatology of above-surface weather on fire activity that has never been possible at this scale over Victoria before. These studies include the effect of atmospheric stability on fire behavior using indices such as those described by Mills and McCaw (2010), and the potential to perform climatological assessments of foehn/mountain wave events such as those described by Sharples *et al*. (2010) and Badlan *et al*. (2012), or other mesoscale systems that are difficult to analyse climatologically from the observational record.

References

Badlan, R.L., Lane, T.P., Mills, G.A., and Caine, S., 2012. Mesoscale modeling of two "drying events": governing processes and implications for fire danger. *Aust. Meteor. Oceanog. J.*, **62**, 143-156.

Dee, D. P., and 35 co-authors, 2011: The ERA-Interim reanalysis: Configuration and performance of the data assimilation system. *Quart. J. R. Meteorol. Soc.*, **137**, 553-597.

Lucas, C., 2010. On developing a historical fire weather data-set for Australia. *Aust. Meteor. Oceanog. J.*, **60**, 1-14.

Mills, G.A., and L.McCaw 2010. Atmospheric Stability Environments and Fire Weather in Australia – extending the Haines Index. CAWCR Technical Report No20, 158pp.

National Centers for Environmental Prediction/National Weather Service/NOAA/U.S. Department of Commerce, 2000: *NCEP FNL Operational Model Global Tropospheric Analyses, continuing from July 1999*. Research Data Archive at the National Center for Atmospheric Research, Computational

and Information Systems Laboratory, Boulder, CO. [Available online at http://dx.doi.org/10.5065/D6M043C6.]

Sharples, J.J., McRae, R.H.D., Mills, G.A., and Weber, R.O., 2010. Foehn-like winds and elevated fire danger conditions in southeastern Australia. *J. Appl. Met. and Climat.*, **9**, 1067-1095.

Skamarock, W., Klemp, J., Dudhia, J., Gill, D., Barker, D., Duda, M., Wang, W. & Powers, J., 2008. 'A Description of the Advanced Research WRF Version 3', NCAR Technical Note NCAR/TN-475+STR.

A numerical study of crown fires spread using a conjugate formulation

Valeriy Perminov

Tomsk Polytechnic University, Russia 634050, Lenin Avenue, 30, valerperminov@gmail.com

Abstract
The aim of the present paper is to study the behaviour of crown forest fires propagating through crown canopy and to study the mutual influence of crown forest fires and boundary layer of atmosphere using numerical simulation with a physics-based model. It is a coupled atmosphere/crown fire behavior model and is based on conservation of mass, momentum, species and energy. The boundary-value problem is solved numerically using the method of splitting according to physical processes. It allows investigating dynamics of forest fire initiation and spreading under influence of various external conditions: a) meteorology conditions (air temperature, wind velocity etc.), b) type (various kinds of forest combustible materials) and their state (load, moisture etc.).

***Keywords**: forest fire, mathematical modelling, control volume, numerical solution*

Introduction

Fires spreading in crowns are often more intense than fires spreading through surface vegetation. As a result, they are more difficult to suppress, produce higher heat fluxes and more smoke. They can interact with boundary layer of atmosphere that leads to dangerous fire behaviour. The end goal is to develop a range of computationally efficient tools to help land managers and others assess forest fire risk to communities and homes. A suitably validated physics-based approach has the potential to account for realistic variations in the environmental. Considering that, natural investigations of these problems are merely impossible, methods of mathematical modelling are urgent.

Physical and mathematical model

Considering domain consist of two parts: boundary layer of atmosphere and forest. Let us examine a plane problem of radiation-convection heat and mass exchange of forest fuels in all forest strata with gaseous combustion products and radiation from the tongue of flame of the crown forest fire The fire source is modeled as a plane layer of burning forest fuels with known temperature and increasing area of burning**.** It is assumed that the forest during a forest fire can be modeled as a homogeneous two-temperature multiphase non-deformable porous reactive medium [1]. Temperatures of condensed and gaseous phases are separated out. The first includes a dry organic substance, moisture (water in the liquid-drop state), condensed pyrolysis and combustion products (coke, ash) and mineral part of forest fuels. In the gaseous phase it is separated out only the components necessary to describe reactions of combustion (oxygen, combustible products of pyrolysis of forest fuels and the rest inert components). Let the coordinate reference point x_1, $x_2 = 0$ be situated at the centre of the forest fire source at the height of the roughness level, axis $0x_2$ directed upward, axis $0x_1$ directed parallel to the Earth's surface to the right in the direction of the unperturbed wind speed (Fig.1).

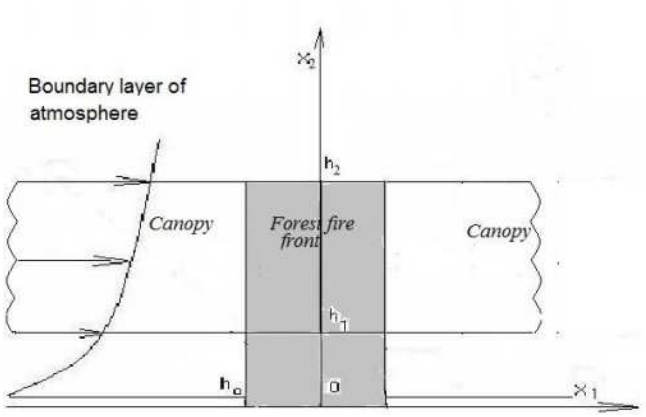

***Figure 1.** Scheme of the domain*

The problem formulated above is reduced to a solution of the system of equations (1)-(6):

$$\frac{\partial \rho}{\partial t} + \frac{\partial}{\partial x_j}(\rho v_j) = \dot{m},\ j = 1,2,\ i = 1,2; \tag{1}$$

$$\rho \frac{dv_i}{dt} = -\frac{\partial P}{\partial x_i} + \frac{\partial}{\partial x_j}(-\rho \overline{v_i' v_j'}) - \rho\, sc_d\, v_i\, |\vec{v}| - \rho g_i - \dot{m} v_i; \tag{2}$$

$$\rho c_p \frac{dT}{dt} = \frac{\partial}{\partial x_j}(-\rho c_p \overline{v_j' T'}) + q_5 R_5 - \alpha_v (T - T_S) + k_g (cU_R - 4\sigma T^4); \tag{3}$$

$$\rho \frac{d\, c_\alpha}{\partial t} = \frac{\partial}{\partial x_j}(-\rho \overline{v_j' c_\alpha'}) + R_{5\alpha} - \dot{m} c_\alpha,\ \alpha = 1,...,5; \tag{4}$$

$$\frac{\partial}{\partial x_j}\left(\frac{c}{3k}\frac{\partial U_R}{\partial x_j}\right) - (k + k_s) c U_R + 4\sigma(k_g T^4 + k_s T_s^4) = 0; \tag{5}$$

$$\sum_{i=1}^{4} \rho_i c_{pi} \varphi_i \frac{\partial T_S}{\partial t} = q_3 R_3 - q_2 R_2 - k_S (cU_R - 4\sigma T_S^4) + \alpha_V (T - T_S); \tag{6}$$

$$\rho_1 \frac{\partial \varphi_1}{\partial t} = -R_1, \rho_2 \frac{\partial \varphi_2}{\partial t} = -R_2,\ \rho_3 \frac{\partial \varphi_3}{\partial t} = \alpha_c R_1 - \frac{M_c}{M_1} R_3, \rho_4 \frac{\partial \varphi_4}{\partial t} = 0; \tag{7}$$

$$\sum_{\alpha=1}^{5} c_\alpha = 1, P_e = \rho R T \sum_{\alpha=1}^{5} \frac{c_\alpha}{M_\alpha}, \vec{v} = (v_1, v_2), \vec{g} = (0, g).$$

The system of equations (1)–(8) must be solved taking into account the following initial and boundary conditions:

$$t = 0: v_1 = 0, v_2 = 0, T = T_e, c_\alpha = c_{\alpha e}, T_s = T_e, \varphi_i = \varphi_{ie}; \tag{8}$$

$$x_1 = -x_{1e}: v_1 = V_e, v_2 = 0,\ T = T_e,\ c_\alpha = c_{\alpha e}, -\frac{c}{3k}\frac{\partial U_R}{\partial x_1} + cU_R/2 = 0; \tag{9}$$

$$x_1 = x_{1e}: \frac{\partial v_1}{\partial x_1} = 0, \frac{\partial v_2}{\partial x_1} = 0,\ \frac{\partial T}{\partial x_1} = 0,\ \frac{\partial c_\alpha}{\partial x_1} = 0, \frac{c}{3k}\frac{\partial U_R}{\partial x_1} + cU_R/2 = 0; \tag{10}$$

$$x_2 = 0: v_1 = 0, (\rho v_2)_0 = h_0 \dot{m}_0,\ T = \begin{cases} T_e + (T_0 - T_e)\exp(-((x_1 - x_{10})/\Delta)^2)t/t_0, t \le t_0 \\ T_e + (T_0 - T_e)\exp(-((x_1 - x_f)/\Delta)^2), \quad t > t_0 \end{cases},$$

$$x_f = \omega(t - t_0),$$

$$-\rho D_t \frac{\partial c_\alpha}{\partial x_2} + \rho v_2 c_\alpha = h_0 \bar{R}_{5\alpha}, -\frac{c}{3k}\frac{\partial U_R}{\partial x_2} = \frac{k_0 h_0}{2}(4\sigma T_S^4 - cU_R); \quad (11)$$

$$x_2 = x_{2e}: \frac{\partial v_1}{\partial x_2} = 0, \frac{\partial v_2}{\partial x_2} = 0, \frac{\partial T}{\partial x_2} = 0, \frac{\partial c_\alpha}{\partial x_2} = 0, \frac{c}{3k}\frac{\partial U_R}{\partial x_2} + cU_R/2 = 0; \quad (12)$$

Here and above $\frac{\mathrm{d}}{\mathrm{d}t}$ is the symbol of the total (substantial) derivative; α_v is the coefficient of gas exchange; t is time; x_i, v_i, (i = 1, 2) are the Cartesian coordinates and the velocity components; x_f is a right boundary coordinate of the surface forest fire source in a wind direction; k_0 is the radiation absorption coefficient in the ground cover, h_0 is the thickness layer in the ground cover; $\Delta = \Delta_0 + 2\omega t$ is the size of the surface fire source, Δ_0 is the initial value of the characteristic size, ω is the normal rate of surface fire spread, t_0 is the time of fire source formation (characteristic time of setting the maximum temperature in the source or the time of ignition), T_0 and T_e are the maximum temperature in the surface fire source and the ambient temperature; index α=1,2,...,5, where 1 corresponds to the density of oxygen, 2 - to carbon monoxide *CO*, 3 - to carbon dioxide and inert components of air, 4 - to particles of black, 5 - to particles of smoke. The thermodynamic, thermophysical and structural characteristics correspond to the forest fuels in the canopy of a pine forest [1].

It should be noted that this system of equations describes processes of transfer within the entire region, which includes boundary layer of atmosphere and forest: crown and the space between the underlying surface and the base of the forest canopy. Because of the characteristic sizes of problem for boundary layer of atmosphere and forest are different; it may be more convenient to divide our domain into two parts. Therefore we can solve this problem using a conjugate formulation. Besides for the second domain the horizontal sizes of forest massif more than height of forest, system of equations of general mathematical model of forest fire was integrated between the limits from height of the roughness level - 0 to top boundary of forest crown. Thus the solution of this problem is reduced to the integration of two systems of differential equations taking into account the correspondence initial and boundary conditions (8)-(12) and condition of conjugation between two domains [1].

Method solution and results

The boundary-value problem is solved numerically using the method of splitting according to physical processes. In the first stage, the hydrodynamic pattern of flow and distribution of scalar functions was calculated. The system of ordinary differential equations of chemical kinetics obtained as a result of splitting was then integrated. A discrete analogue was obtained by means of the control volume method using the SIMPLE like algorithm [2]. Fields of temperature, velocity, component mass fractions, and volume fractions of phases were obtained numerically. At $V_e \neq 0$, the wind field in the forest canopy interacts with the gas-jet obstacle that forms from the forest fire source and from the ignited forest canopy and burn away in the forest canopy. The isotherms of gas phase components moved in the forest canopy by the action of wind. It is concluded that the forest fire begins to spread. The results of the calculation give an opportunity to consider forest fire spread for different wind velocity, canopy bulk densities and moisture forest fuel. Figures 2 a,*b* present the distribution of temperature of gas phase above the crown $\bar{T}(\bar{T} = T/T_e, T_e = 300K)$ (1- 2., 2 – 2.5, 3 – 3, 4 – 4., 5 – 5.) for wind velocity V_e= 5 m/s in different instants of time: I - t=13 sec., II - t=16 sec, III - t=20 sec., IV - t= 23 sec and V - 25

sec. (Fig.2a) and 10 m/s (Fig.2b) (I - t=9 sec., II - t=11 sec, III - t=13.5 sec., IV - t= 15.5 sec.). The distribution of velocity fields is presented also (Fig.3a,b).

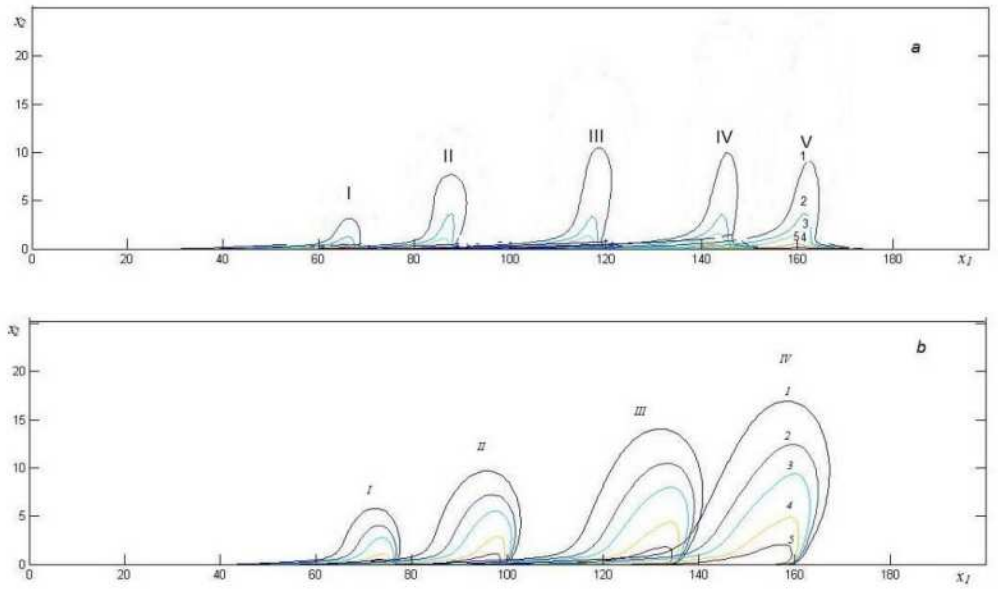

Figure 2. . Field of isotherms of the forest fire spread (gas phase).

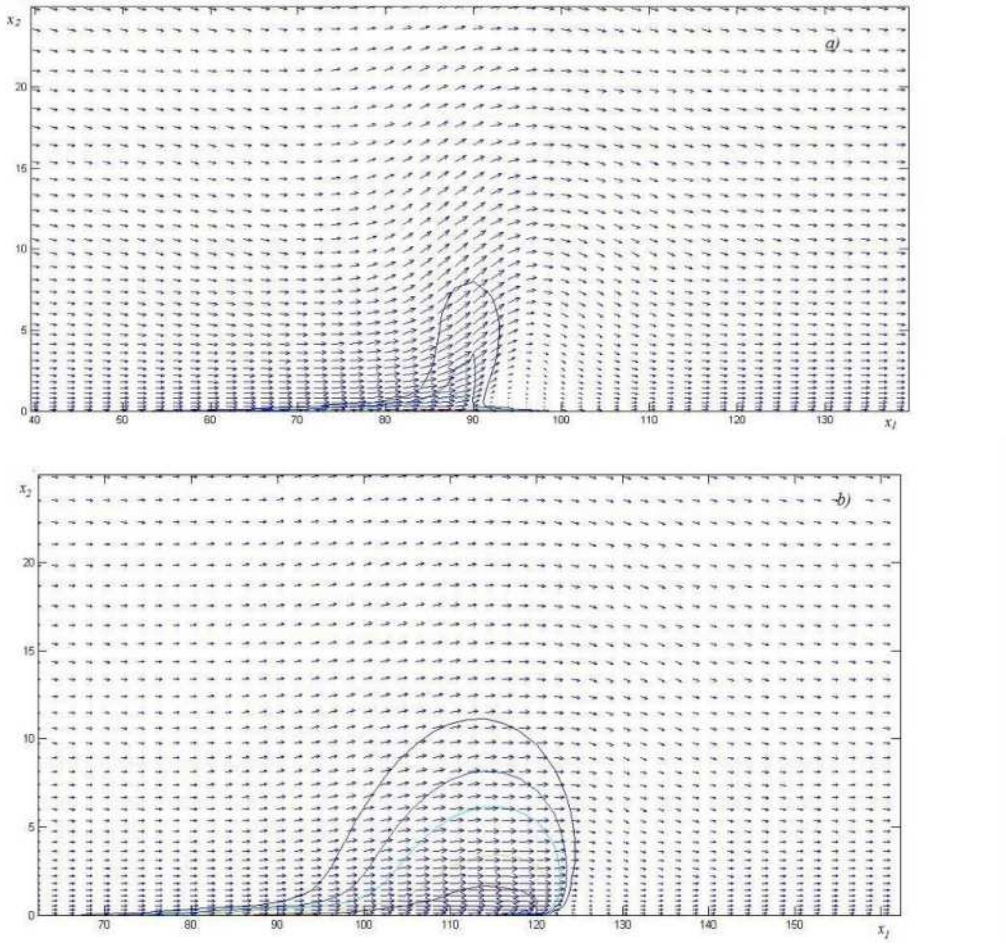

Figure 3- . Fields of velocities for wind: a)V_e=5 m/s(t=16 s)and b) V_e =10m/s (t=10 s).

Figures 3 a and b represent vector fields of velocities and isotherms for different instants of time when a wind velocity V_e= 5 m/s at a height x_2=10 m(Fig.3a) and . It is seen that the effect of the wind results in the tongue of flame defection from the vertical. The wind field above the forest fire front interacts with the gas-jet obstacle that forms from the crown forest fire source. Recirculating flow forms beyond the zone of heat and mass release (Fig.3a), while on the windward side the movement of the air flowing past the ignition region accelerates. But in the second case there is no recirculation flow, because a strong wind destroys it (Fig.3b).

Conclusion

Results of calculation give an opportunity to describe the different conditions of the crown forest fires spread taking account different weather conditions, state of forest combustible materials, which allows applying the given model for prediction and preventing fires. It overestimates the rate of crown forest fire spread that depends on crown properties: bulk density, moisture content of forest fuel, wind velocity and the influence of boundary layer of atmosphere. The model proposed here gives a detailed picture of the change in the temperature and component concentration fields with time, and determine as well as the influence of different conditions on the crown forest fire spreading for the different cases of inhomogeneous of distribution of sources of forest fires initiation. The results of calculation of the rate of crown forest fires are agreed with the laws of physics and experimental data

References

1. Grishin A.M., *Mathematical Modeling Forest Fire and New Methods Fighting Them*, Tomsk: Publishing House of Tomsk University (Russia), 1997.
2. Patankar S.V., *Numerical Heat Transfer and Fluid Flow. New York*, Hemisphere Publishing Corporation, 1981.

An Experimental Approach to the Evaluation of Prescribed Fire Behavior

Eric Mueller[a], Nicholas Skowronski[b], Kenneth Clark[b], Robert Kremens[c], Michael Gallagher[b], Jan Thomas[a], Mohamad El Houssami[a], Alexander Filkov[d], Bret Butler[e], John Hom[a], William Mell[f], and Albert Simeoni[a]

[a] *University of Edinburgh, BRE Centre for Fire Safety Engineering, Edinburgh, UK, e.mueller@ed.ac.uk*
[b] *USDA Forest Service, Northern Research Station, Morgantown, WV, New Lisbon, NJ and Newtown Square, PA, USA*
[c] *Rochester Institute of Technology, Center for Imaging Science, 54 Lomb Memorial Drive, Rochester, NY 14623, USA*
[d] *National Research Tomsk State University, Department of Physical and Computational Mechanics, Russia*
[e] *USDA Forest Service, Rocky Mountain Research Station 5775 W US Highway 10 Missoula MT 59808, USA*
[f] *USDA Forest Service, Pacific Wildland Fire Sciences Laboratory, 400 N 34th St., Suite 201, Seattle, WA 98103, USA*

Abstract
Prescribed fire is a commonly used practice for managing wildland fire spread and intensity. However, due to limits in the current scientific understanding of wildland fire behavior in general, it is difficult to predict the effectiveness and efficiency of a particular regimen of prescribed fire-based fuel treatments in a given environment. As part of a larger project intended to aid in such an assessment, the first in a series of experimental prescribed fires was conducted. Efforts were made to both quantify various aspects of fire behavior and to obtain an accurate measure of pre- and post-fire fuel loadings. This paper focuses on an initial investigation of the fire behavior, as this is necessary for contextualizing the level of fuel treatment achieved. In particular, the range of observed surface fuel consumption and fireline intensities is discussed, the role of ambient wind conditions is considered, and a qualitative assessment of canopy fuel consumption is presented.

Keywords*: Fire behavior, prescribed fire, fuel treatments, fire intensity*

Introduction

Hazardous fuel reduction treatments are important for both the mitigation of wildland fire risk and the support of suppression efforts. In the United States, significant financial resources have been directed to this goal, with an average of $500 million spent by the Federal Government each year from 2002-2012 (Gorte 2011). However, rigorous experimental measurement and proper metrics to measure the success of fuel reduction measures are lacking. As stated by Omi and Martinson (2002), "the lack of empirical assessment of fuel treatment performance has become conspicuous". While the aforementioned report found that fuel treatments were able to modify extreme fuel behavior, questions remain as to the intensity and repetition of treatment needed in a given ecosystem to maintain a desired condition. Further, the success of a certain treatment may not be consistent for different ecosystems or treatment techniques (Gorte 2011). More work is clearly needed to understand and evaluate the effectiveness of these types of treatments.
One technique used to accomplish the reduction of hazardous fuels is prescribed fire, and is the focus of this work. When attempting to develop efficient and effective fire-based fuel treatment strategies, a proper understanding of fire behavior is particularly important. Managers must be able to understand

how a prescribed fire will behave, given a particular set of conditions, as well as predict the subsequent impact on fuel loading. In an effort to improve this understanding, a Joint Fire Science Program (JFSP) funded project is being conducted. This project takes a dual experimental and numerical approach. It aims to use a series of well-instrumented prescribed fires as a source of direct measurements, which can both provide a quantitative analysis of fire behavior and fuel reduction, as well as comparison criteria for use in the development of physical fire behavior models. Such models have the potential to be effective tools for the continued investigation of both general fire behavior and specific topics, such as fuel treatment effectiveness, without requiring extensive experimentation.

The work here pertains specifically to the first of the experimental prescribed fires. The measurement of wildland fire behavior properties is not a novel concept, as can be seen in experiments like those of Santoni *et al*. (2006), Viegas *et al*. (2006), Morandini and Silvani (2010), and Frankman *et al*. (2013). However, the number of such experiments is limited, and each is specific to a particular set of conditions. This work will help to strengthen the scientific understanding of fire behavior by adding to the collection of available measurements. Additionally, due to the focus on fuel reduction, the detail to which pre-fire fuel loading, fire behavior, and post-fire fuel loading are studied and can be correlated is rather unique. This experiment was also designed from the outset so that measurements would be both easily translatable to model inputs and comparable to model outputs.

Though a variety of different measurements were taken, the results analyzed in this paper represent an initial effort to describe the history of the fire spread and its general characteristics. Focus is put on estimates of fireline intensity, the role of ambient wind conditions, and basic characteristics of canopy fuel consumption.

Methods

Study site

The experimental fire was conducted in the Pinelands National Reserve (PNR) of New Jersey, United States. The PNR spans approximately 445,000 ha, and is the site of an active fuel management program by the New Jersey Forest Fire Service (NJFFS) and federal wildland fire managers. Prescribed fires are employed by the NJFFS with the explicit intent of reducing fuel loads and thus mitigating fire risk. These managers, for the most part, rely on professional judgment when planning the intervals and geographic position of these fires. The climate is classified as cool temperate, with mean monthly temperatures of 0.3 in January and 24.3 °C in July, and mean annual precipitation is 1159 mm. The terrain consists of plains, low-angle slopes, and wetlands, with a maximum elevation of 62.5 m. A burn block covering an area of 16.6 acres was used for the experiment, and can be seen outlined in Figure 1. The forest canopy in the block was comprised primarily of Pitch Pine (*Pinus rigida* Mill.), with intermittent oaks (*Quercus* spp.). The understory contained a mixed shrub layer of huckleberry (*Gaylussacia* spp.), blueberry (*Vaccinium* spp.), and scrub oaks (*Quercus* spp.). The perimeter of the block was comprised of access roads, with a narrower track running through the center of the block. These were created to facilitate access for the management of prior prescribed burns.

2.2. Measurement techniques

Point measurements of fire behavior were made using a combination of 4 overstory towers, 12 understory towers, and 3 Fire Behavior Packages (FBP), each supporting various instruments. Each overstory tower provided measurements of turbulence (3D sonic anemometer) at a height of 12.5 meters, and a vertical array of air temperature (8 K-type thermocouples) at even 1.5 m intervals from 0.5 to 11.0 meters. Dataloggers were buried in waterproof boxes and a sampling rate of 10 Hz was used. Each understory tower provided measurements of upward radiative flux (downward facing radiometer) at a height of 6.0 meters, vertical velocity (bi-directional pressure probe) at a height of 6.0

meters, and a vertical array of temperature (5 K-type thermocouples) at even 1.5 m intervals from 0 to 6.0 meters.

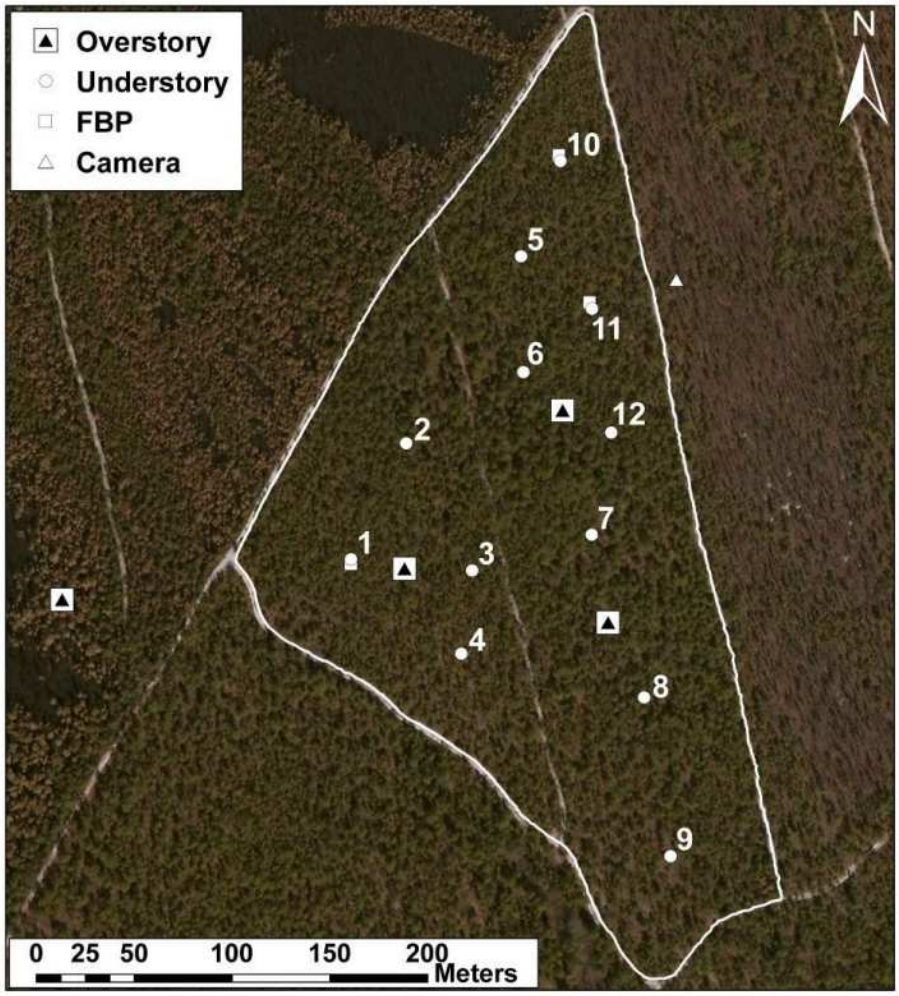

Figure 1. Layout of instrumentation in the study site with understory tower numbers labeled.

Dataloggers were located in protective enclosures at the top of the towers and a sampling rate of 0.5 Hz was used. Each FBP provided measurements of total and radiative incident heat flux (dual radiometer), horizontal and vertical velocity (2 bi-directional pressure probes), and temperature (K-type thermocouple), all at a height of roughly 1 meter (Butler *et al*. 2010). Dataloggers were housed in a protective enclosure and a sampling rate of 10 Hz was used. All instruments were distributed within the area to be burned, excluding one overstory tower, which was situated to the west in order to measure ambient conditions during the time of the fire. Exact instrument locations can be seen in Figure 1. In addition to point measurements, sequential aerial IR images of the fire were recorded from an aircraft using Rochester Institute of Technology's Wildfire Airborne Sensor Program (WASP) (McKeown *et al*. 2011). The WASP records data in short-wave (1.0-1.7 μm), mid-wave (3.0-5.0 μm), and long-wave (8.0-9.2 μm) infrared spectral bands, as well as the visible spectrum (0.4-0.9 μm). Images were time-stamped and georeferenced. Of the above instrumentation, this paper only discusses measurements obtained with the sonic anemometers and the aerial IR camera. As a visual reference, several cameras were placed within and around the burn block. The camera discussed here was placed outside of the site, looking east towards Understory 11 at a distance of about 45 meters.

Field measurements of surface fuel loading were obtained by destructive sampling of the forest floor and shrub layer in 1 m^2 clip plots. 36 of these measurements were made (3 surrounding each understory

tower) both pre- and post-fire, in order to give an indication of surface fuel consumption. Measurements from the litter layer (O_i horizon) were divided into categories of fine fuel, reproductive material (pine cones, acorns, and catkins), 1-hr wood, 10-hr wood, and 100-hr wood, while measurements from the shrub and oak layer fuels were divided into categories of foliage, 1-hr wood and 10-hr wood. It should be noted that a destructive sampling technique inherently excludes colocation of pre- and post-fire measurements. Remote measurements of both pre- and post-fire canopy fuel loading were conducted using an airborne Light Detection and Ranging (LiDAR) technique. This data will allow the generation of a 1 m x 1 m resolution canopy height model, as well as 3D canopy bulk density (CBD) profile at a resolution of 10 m x 10 m x 1 m. CBD will be calibrated to profiles from an upward-sensing LiDAR unit in twelve 20 m x 20 m plots within the burn area. This unit has been previously calibrated to represent profiles of CBD using equations developed through destructive harvest by Clark *et al*. (2013). As this calibration is currently ongoing, only a qualitative discussion of the relative reduction in canopy fuel loading will be given.

2.3. Measurement techniques

In order to characterize the type of fire observed, it is useful to estimate the quantity known as fireline intensity (*I*), which indicates the energy release rate per unit length of fire front (Byram 1959). Fireline instensity is often calculated as $I = H \cdot \Delta m \cdot R$, where R is the rate of spread [$m \cdot s^{-1}$], Δm is the mass of fuel consumed [kg], and H is the heat yield of the fuel. In this study, H is taken as 18700 $kJ \cdot kg^{-1}$ (Alexander 1982). This value of H is the low heat of combustion and is an estimate based on an average value for a number of different fuel species. However, studies have shown that the typical variation between species is only on the order of ±10% (Byram 1959, Van Wagner 1972). Corrections may also be considered to account for completeness of combustion and mass consumption during smouldering combustion, after the fire front passage, but for the purposes of the study this basic value is sufficient. As canopy fuel consumption estimates are not yet available, only the physical measurements of surface fuel consumption were used. Thus, the quantity will be referred to as surface fireline intensity (I_{surf}). Finally, due to the inability to collocate pre- and post-fire physical fuel samples, as mentioned in Section 2.2, consumption estimates for larger fuel elements were considered unreliable, as they were sparsely distributed. For example, 100-hr fuel will likely not be completely consumed, but if no such fuel is located in the post-fire sample plot before the fire, calculation of the difference would suggest that total mass in the pre-fire plot was consumed. Therefore, only fine fuel (primarily needle litter), 1-hr forest floor wood, and 1-hr oak and shrub layer material was used to calculate I_{surf}. Further, thin fuel was considered to be the main contributor to fire intensity. Spread rates were obtained from the aerial IR imagery.

2.4. Burn conditions

The fire was conducted on March 5th, 2013. Ignition was carried out by the NJFFS using a drip torch along the northwest road, moving from northeast to southwest over a roughly 8 minute period, starting at 11:53 (EST). The real-time location of the drip torch on this road was tracked by GPS. Due to safety concerns caused by rapid fire growth, a secondary ignition line was subsequently created along the southwest road. The duration of the fire was determined to be approximately 1 hour, though much of the block was consumed within the first 20 minutes. During this 1 hour period, mean ambient temperature was around 7 °C and mean relative humidity was 39%. Fuel moisture content (FMC) was measured for different classes of vegetation during the burn, details of which can be seen in Table 1. Samples were taken from the stand immediately to the north of the burn block.

Table 1. Measurements of fuel moisture content (FMC ± relative standard deviation) for fuel collected during the time of the fire.

Location	Fuel Type	Sample size	FMC [%]
Canopy (Pitch Pine)	Live needles	7	114.4 ± 2%
	Live stems (1-hr)	7	85.2 ± 8%
Understory	Shrub stems (1-hr)	8	60.9 ± 9%
	Oak stems (1-hr)	5	61.2 ± 12%
Forest Floor	1-hr wood	7	15.3 ± 16%
	10-hr wood	10	30.9 ± 52%
	Needle litter	8	22.5 ± 50%
	Oak leaf litter	7	15.7 ± 45%

Results

3.1. General fire spread

Between the time of 11:56:59 (EST) and 12:38:45 (EST), 16 IR images were captured by the WASP as the plane made passes overhead and allowed the mapping of fire progression (Figure 2). The contours displayed in Figure 2 were obtained by tracing along the sharpest gradient of pixel intensity recorded for each long-wave image. Only 7 of the 16 contours are shown, as these represent the fire behavior of interest for this study. These will be referred to as P2-P8 hereinafter.

The primary fire front, originating from the northwest road, spread as a head fire in a southeasterly direction. It did not completely merge with the secondary (backing) fire front until sometime between fire contour P5 and P6. At certain locations the fire contours sharply dips back to a point which appears to lag behind in the direction of spread (Figure 2). In many places, this feature can be attributed to the narrow track which ran along the center of the block, as can be seen in Figure 1. This track acted functioned as a fuel break, because the only fuel consisted of a thin and intermittent litter layer. However, the resulting discontinuities in the fire front coalesced with continued fire spread, as can be seen when comparing contour P5 to P6 in Figure 2. Other irregular features of the fire contours, such as along the west portion of P3, may be due to fuel heterogeneity, discontinuity in the ignition line, or some combination of the two.

3.2. Local surface fire intensity

Given that each understory tower was surrounded by 3 mass consumption field sample plots, and fire contours were available across the entire burn block, it was possible to calculate local surface fireline intensity to get an indication of the range of fire behavior. A selection of locations are shown in this report, which are, moving from north to south, understory towers 10, 5, 11, and 1. These were chosen as initial sites to investigate as they were situated in a region of headfire which was unaffected by the backfire. Spread rates at each of these locations were determined by measuring distances between fire contours in ArcGIS. Each distance was measured 15 times along a segment of around 60 meters of fire front in order to both minimize measurement uncertainty and to give a general indication of the relative homogeneity of local fire spread. A summary of the calculations for each location, resulting in surface fireline intensity, is presented in Table 2.

At the location of Understory 10, near the northern corner of the plot and the start of the ignition line, the lowest intensities were found (of the locations considered). Estimated values fall between 500-1300 $kW \cdot m^{-1}$. This was a result of both low mass consumption and slow fire spread, as can be seen in Table 2.

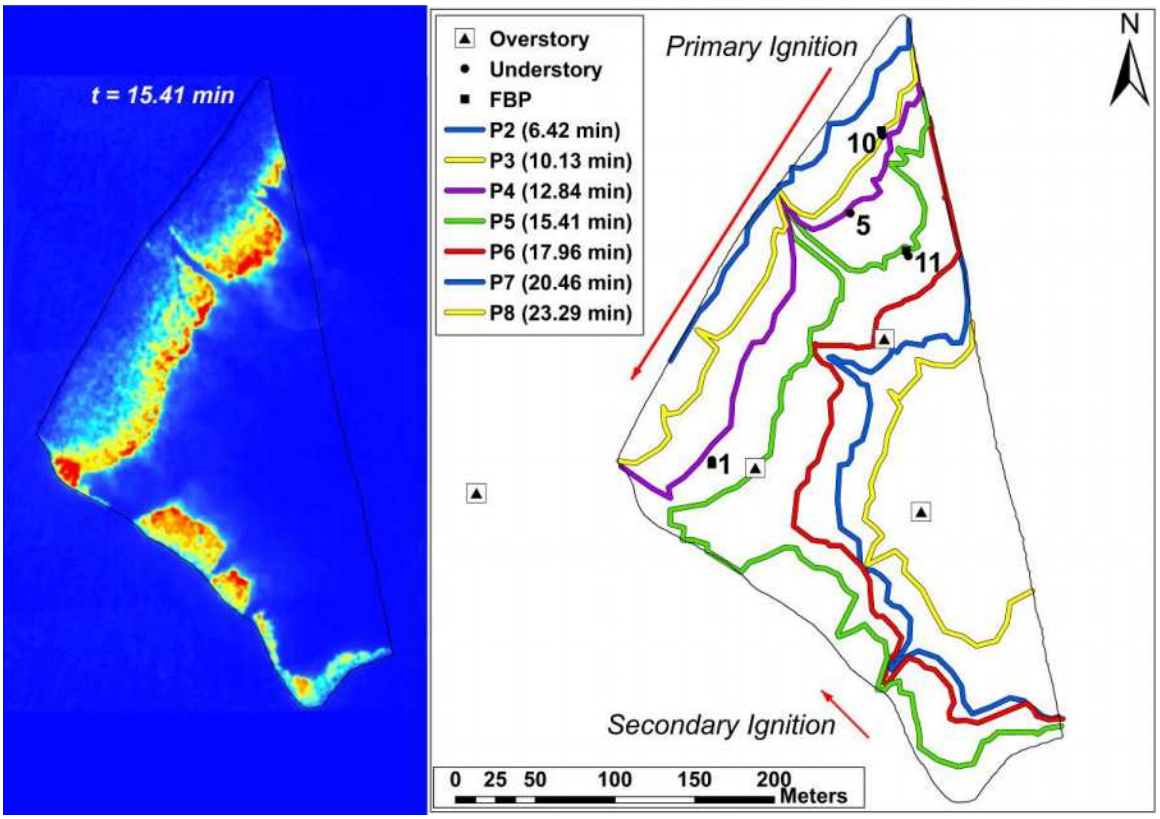

Figure 2. (Left) Example IR image from the WASP (P5). (Right) Progression of the fire front, extracted from IR imagery. The fire progressed from West to East, with consecutive fire contours labeled P2-P8. The time of each contour is given in minutes after the start of ignition.

Table 2. Summary of Δm (± maximum relative difference in the 3 samples), R (± relative standard deviation), and I_{surf}. Values of I_{surf} are rounded to the nearest 100 kW·m^{-1}.

Location	Δm [kg·m^{-2}]	Distance	R [m·s^{-1}]	I_{surf} [kW·m^{-1}]
Understory 10	0.73 ± 41%	P2-P3	0.095 ± 7%	1300 ± 52%
		P2-P4	0.074 ± 10%	1000 ± 51%
		P2-P5	0.073 ± 9%	1000 ± 50%
		P3-P4	0.039 ± 36%	500 ± 77%
		P3-P5	0.055 ± 28%	700 ± 69%
		P4-P5	0.074 ± 49%	1000 ± 90%
Understory 5	0.90 ± 9%	P3-P4	0.088 ± 28%	1500 ± 37%
		P3-P5	0.164 ± 7%	2800 ± 16%
		P4-P5	0.245 ± 9%	4100 ± 18%
Understory 11	1.32 ± 8%	P4-P5	0.245 ± 9%	6000 ± 17%
		P4-P6	0.222 ± 3%	5500 ± 11%
		P5-P6	0.191 ± 7%	4700 ± 15%
Understory 1	1.03 ± 6%	P3-P4	0.166 ± 15%	3200 ± 21%
		P3-P5	0.178 ± 16%	3400 ± 22%
		P4-P5	0.177 ± 10%	3400 ± 16%

Of particular note is a region of slow spread between P3 and P4. There was a deceleration of the fire here, with a 41% reduction in mean spread rate from P2 to P3. The spread increased again from P4 to P5, though increased heterogeneity is observed (± 49% deviation) which is likely due to gaps in fuel loading. The deceleration and acceleration is believed to be partially a result of ambient wind, and will be discussed later.

The Understory 5 and 11 locations are considered together, as they are roughly in line with each other in the direction of fire spread. Surface fireline intensities are considerably higher in this region, ranging from 1500-6000 $kW \cdot m^{-1}$. Here again, a slowing of the fire occurred between P3 and P4. Although the placement of mass consumption measurements does not allow for an accurate measure of intensity from P2 to P3 in this part of the block, the mean spread is between P3 and P4 is a 26% reduction from the P2 to P3 value (0.119 $m \cdot s^{-1}$). There is an increase of fire intensity moving from P3 to P5, with both higher spread rate and higher mass consumption measured at Understory 11. Indeed, of all regions examined in this study, both quantities are at a maximum in this location. Between P5 and P6 there is another slight reduction in spread.

To give a qualitative indication of the type of fire being measured, Figure 3a shows a frame of video footage. The camera was directed towards Understory 11, though it shows fire behaviour closer to the perimeter of the parcel. This region predominantly experienced a surface fire with localized torching into the tree crowns. Fire spread, however, was not supported continuously from crown to crown. Instead, vertical flame spread up the tree trunks resulted in brief periods of crown fuel consumption for individual trees.

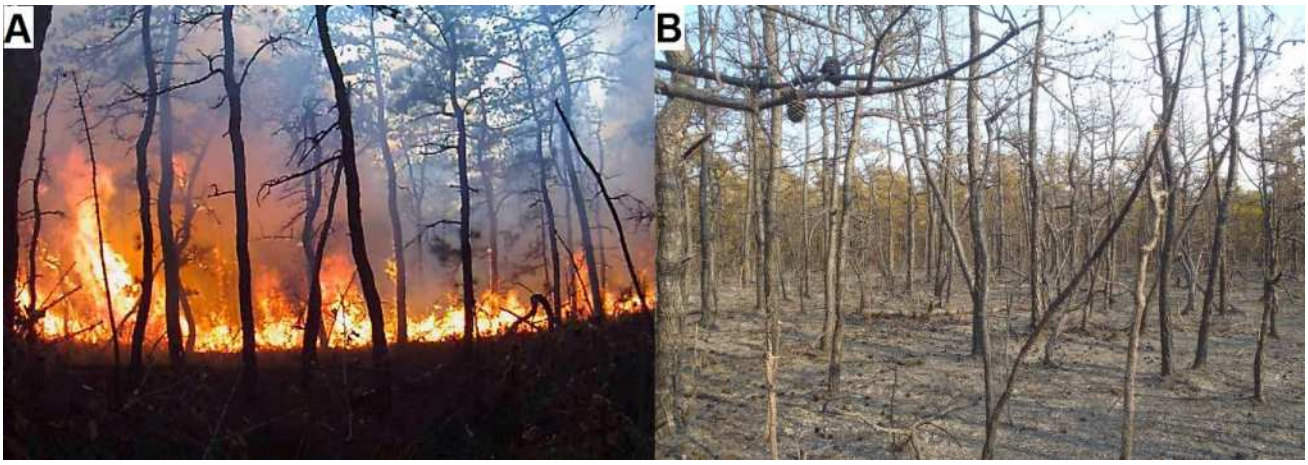

Figure 3. Examples of visual data. (a) Image from camera facing east towards Understory 11 (distortion is due to the wide angle lens used), and (b) image of post-fire fuel consumption in the vicinity of Understory 1.

Understory 1 experienced surface fireline intensities in the range of 3200-3400 $kW \cdot m^{-1}$, which fall between the values at Understory 10 and those at Understory 5 and 11. This region exhibited the most consistent fire behavior, with no obvious accelerations or decelerations. Additionally, observations of significant crown involvement were reported in this area, particularly near P3, close to the ignition line. This is confirmed by post-fire photographs of the region, where very little crown vegetation remains compared to other sections of the burn block (e.g. Figure 3b). However, the location described was to the northwest of Understory 1, beyond the measurements of surface fuel consumption, so the behavior pictured is not well reflected in the values of Table 2.

3.3. Wind

Wind is a critical factor to consider when analyzing the behavior of any wildfire. In the case of this experiment, the focus was first directed to the ambient winds measured by the sonic anemometer on the Overstory Control tower to the west. The magnitude of the horizontal winds at this location is

shown in Figure 4a. The curve was obtained by applying a loess-type moving average filter to the instantaneous values, in order to show the dominant wind gusts more clearly. Over the interval plotted, the average unfiltered horizontal wind is 1.8 $m \cdot s^{-1}$, with a peak magnitude of 6.4 $m \cdot s^{-1}$. Table 3 shows the mean horizontal wind magnitude at the Overstory Control tower for different intervals of fire spread. The instantaneous horizontal wind direction measured at the Overstory Control tower is shown in Figure 4b. Points where horizontal wind magnitude is less than 0.5 $m \cdot s^{-1}$ have been omitted from this figure, as low winds are more susceptible to rapid fluctuations in direction, which do not represent the dominant wind direction and make the data more difficult to interpret.

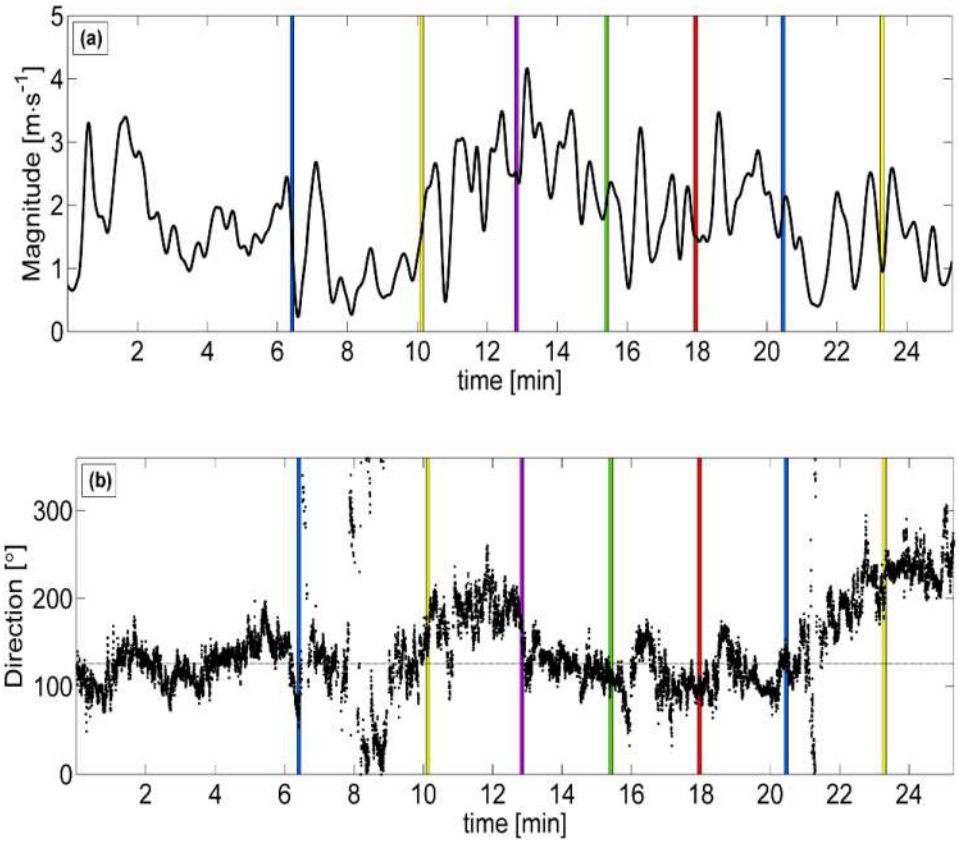

Figure 4. (a) Magnitude and (b) direction of horizontal winds at the sonic anemometer on the Overstory Control tower. Colored lines correspond to the time of fire contours P2-P8 (refer to Figure 2). Time is given in minutes from the start of ignition. Direction is given in compass degrees (clockwise from north). The horizontal line in figure (b) represents the general direction of fire spread.

From this information it can be seen that, as the fire built from ignition, winds were coherent to the direction of initial fire spread (estimated from fire contours as roughly 125°). Between P2 and P3, the wind is reduced somewhat and this corresponds to a shift in direction. From P3 to P4, where a reduction in fire spread was noted at the northeastern section of the burn block, the wind does pick up again, but the direction is oblique to fire spread by about 60°. From P4 to P5, where fire spread was high across the entire block, ambient wind is both relatively strong and consistent with fire spread. It is during this interval that the peak value of 6.4 $m \cdot s^{-1}$ was measured. This wind direction persists until around P7, where a shift is again observed.

Table 3. Mean horizontal magnitude of winds at the sonic anemometers (height of 12.5 m) on the Overstory Control and Overstory West towers.

Interval	Control Magnitude [$m \cdot s^{-1}$]	West Magnitude [$m \cdot s^{-1}$]
Ignition – P2	1.8	1.6
P2 – P3	1.0	2.3
P3 – P4	2.4	2.2
P4 – P5	2.7	3.0
P5 – P6	1.8	3.3
P6 – P7	2.1	2.5
P7 – P8	1.4	2.4

To understand the local influence of the fire on wind conditions within the study site, a comparison is made to the instantaneous horizontal wind direction measured at the Overstory West tower. This data is shown in Figure 5 (with low-velocity data omitted, following the previous convention). Mean horizontal magnitudes are also summarized in Table 3. Deviations from measurements at the Overstory Control tower appear to be fire induced and result from combination of low ambient winds and strong fire behavior. From the ignition to P2, a period of relatively weak ambient wind corresponds with a swing in local wind direction towards the north, where the fire has already established. A similar shift is observed as the fire reaches P3, with even lower ambient winds. From P3 to P4, as the ambient wind shifts to the south, the local wind has more of a westerly direction. This is likely caused by entrainment to the fire plume, which at this point is approaching the Overstory West tower from the northwest. Between P4 and P5, the dominant direction follows the ambient, but the scatter in this data is much greater. This is due to the fact that the anemometer has now started to be impacted by the turbulent plume. Data during this period should be treated with some caution, as the temperature rating of the device only extends to 50 °C. Following the pass of the fire front at P5, the local winds align with the direction of fire spread for the rest of the time shown. The direction is also roughly in line with ambient winds, but the higher magnitude locally suggests there is still an influence of entrainment to the plume.

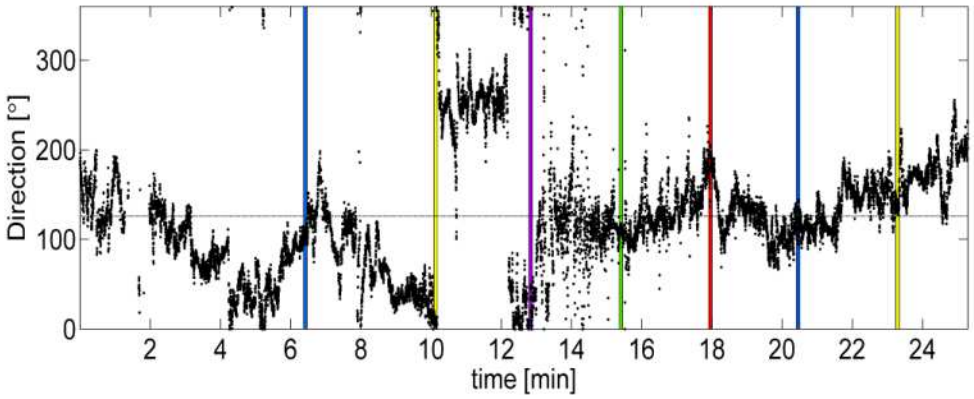

Figure 5. Direction of horizontal winds at the sonic anemometer on the Overstory West tower. Colored lines correspond to the time of fire contours P2-P8 (refer to Figure 2). Time is given in minutes from the start of ignition. Direction is given in compass degrees (clockwise from north). The horizontal line represents the general direction of fire spread.

3.4. **Canopy consumption**

An examination of canopy fuel consumption is also very important to assessing fire behavior. Although the LiDAR data cannot yet be used to obtain direct measures of mass consumption, a

qualitative analysis of the data can still provide valuable information. The percent difference in the pre- and post-fire data was obtained over the 10 m x 10 m x 1 m measurement grid. Transects of this data, which follow the direction of fire spread and pass through grid cells containing understory towers of interest, are shown in Figure 6. Note that because the transects are at an angle to the rectilinear LiDAR grid, the cells shown in Figure 6 have a horizontal extent greater than 10 m.

A comparison of the transects reveals that the Understory 10 and 5 had relatively little canopy fuel consumption, corresponding to the lower surface fireline intensities. In both cases, as the fire reached roughly 40-60 m from the ignition line, a transition to canopy fuel consumption occurred. This type of canopy fuel involvement continued as the fire spread from Understory 5 to Understory 11. The transect for Understory 1 shows somewhat different fire behavior. Canopy fuel is quickly involved in the fire, with this initial region corresponding to the area photographed in Figure 3b. This type of behavior appears to persist along the distance shown, with some small variability, such as a drop in consumption around 40 m.

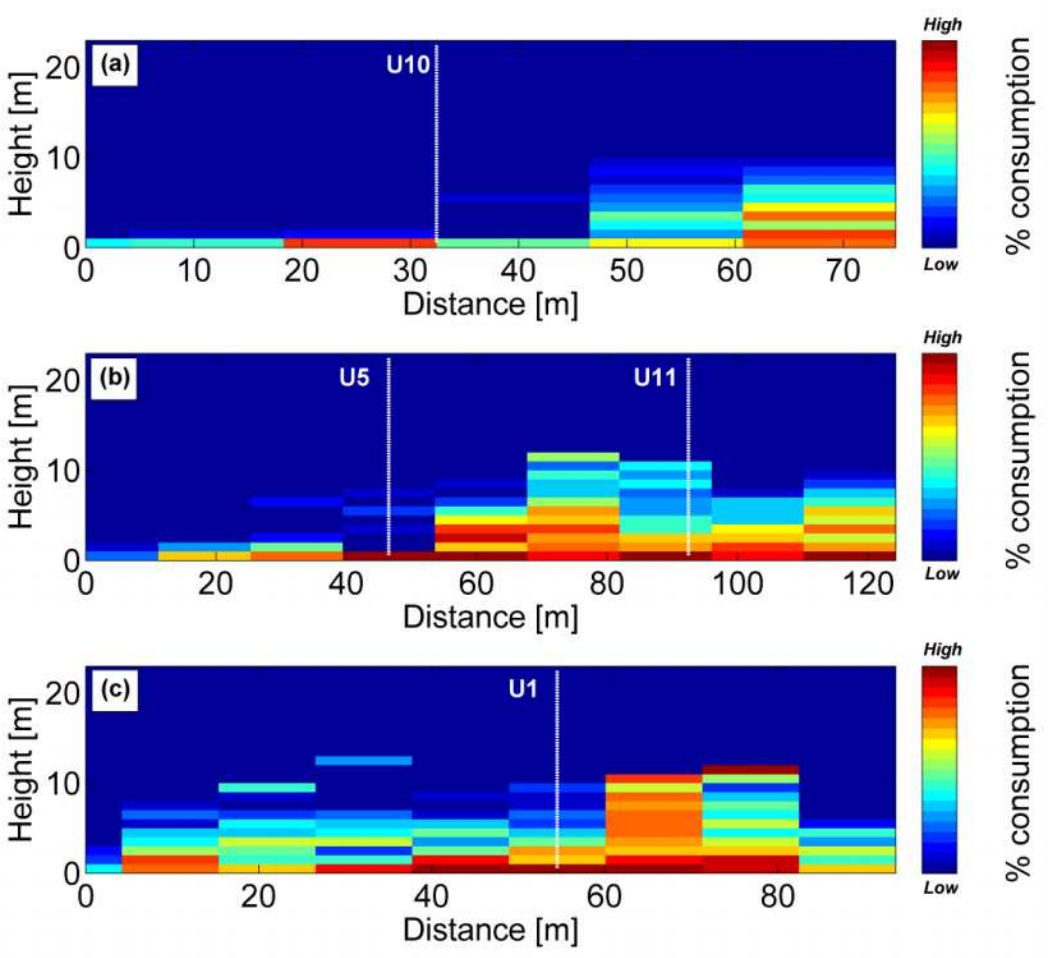

Figure 6. Percent canopy consumption estimated from uncalibrated LiDAR data. Transects are shown in the direction of fire spread for (a) Plot 10, (b) Plot 5 and 11, and (c) Plot 1. Distance is given in meters from the ignition line.

Discussion

The features of fire spread examined in this initial study help quantify the type of fire which was observed. Surface fireline intensities, which range from 500-6000 $kW \cdot m^{-1}$, can be compared to other fires, such as those summarized in Morandini and Silvani (2010). Spread rates reported for several shrubland fires fall within the range of 0.003-0.4 $m \cdot s^{-1}$, which is comparable to those determined here.

However, for the shrubland fire intensities presented by Morandini and Silvani (2010) the upper range was 48000 $kW \cdot m^{-1}$. Wind speed in these studies was within the range of 0-7.9 $m \cdot s^{-1}$, which is again comparable. It should be noted that the measurements discussed from this experiment were made above the canopy, and the drag of the canopy vegetation will cause lower values at the level of the shrubs. The considerably higher intensities can be traced back to the fuel loading. As expected, shrub layers in the open environments of the report tended to be denser than the shrub layer of a forested environment, such as the PNR. Values as high as 25 $kg \cdot m^{-2}$ were found in these previous experiments. Therefore, a prescribed fire which consumes a significant percentage of the shrub layer will be less intense in the environment studied here. However, in the case of this experiment, surface fuels are not the only contributors, and, when considering total fireline intensity, the inclusion of canopy fuel consumption will play a significant role in some areas.

In order to complete this investigation, a full study of canopy fuel structure and consumption will be critical. The different regimes discussed previously in Figure 6 are of particular interest. The transition from surface fire to canopy fuel involvement near Understory 5 is reflected in the fact that surface fireline intensity nearly tripled as the fire passed through this region (see Table 2). However, such a transition is not obvious in the surface fireline intensities near Understory 10. This can be attributed to the fact that the physical fuel samples at this location were taken in the region before the transition. At Understory 1 the more consistent canopy consumption can be seen in the low variation of surface fireline intensity. Examination of the pre-fire canopy arrangement will help provide insight into the presence of transitions. It may be that spatial features of the fuel density played as much or more of a role than wind in causing changes in local fire behavior.

Mean wind speed in this experiment was relatively low compared to what might be considered severe wildland fire conditions. For example, during a famously catastrophic fire in the PNR in 1963, peak wind gusts exceeding 22 $m \cdot s^{-1}$ were measured (Hughes 1987). Despite this, it appears that shifts in wind direction and magnitude may have affected certain observed aspects of fire behavior. One example is the reduction and then increase in fire spread which was observed between P3 and P5, towards the northeast corner of the block. This corresponded with a roughly 60° swing in wind direction. As discussed previously, the fire here did not have significant canopy fuel involvement. Therefore, it is likely that the less intense fire was susceptible to the influence of ambient wind. Conversely, fire spread was quite consistent in the region of Understory 1 during this time. The fire near Understory 1 should be less influenced by ambient winds, however, due to the stronger convective plume where canopy fuels are invloved. The ongoing study of the impact of wind on fire behavior must take into account the fact that measurements shown were taken at 12.5 m, and not within the understory. However, with the largely even topography and fuel loading, shifts above the canopy should correspond to shifts in the lower winds at the level of the shrub layer.

Many other aspects remain to be studied as well. Measurements of upward radiant flux, vertical velocity, and turbulent statistics at understory tower locations will supplement the comparison of variations in fire behavior throughout the burn block. Continued analysis of video footage will also help in interpreting the LiDAR data. The regions in which canopy fuels were involved in fire spread are clearly seen in the Figure 6. However, whether this represents localized torching supported by the surface fire, as shown in Figure 3a, or if true continuous crown fire spread was experienced in some locations, requires further investigation.

Conclusions

This work represents an initial effort to understand the behavior of an experimental fire and the fire spread dynamics. A time series of aerial IR imagery, destructive field sampling of fuel loading and consumption, as well as wind measurements were analyzed, along with a preliminary qualitative discussion of LiDAR data. Several features of fire behavior were identified:

- Observations revealed a predominantly surface fire, with localized torching of tree crowns.
- The involvement of canopy fuels in fire spread was identified with LiDAR measurements, and a clear transition from a pure surface fire was revealed in some locations.
- Ambient winds were relatively low. Wind is believed to have influenced low-intensity surface fire spread, and to have played a role in the aforementioned transition, but had little impact on more intense fire behavior.
- As the fire grew, local winds within the study site appeared to be dominated by fire induced flow, both preceding and following the passage of the fire front.

This analysis will expand, as additional measurements are integrated to provide a more complete description of the behavior. However, the results presented in this investigation give a qualitative baseline and a first understanding of the dynamics of the fire spread. Once coupled with total fuel consumption across the entire burn block, an assessment of the level of fuel reduction, given this type of fire, can be made. In addition, fire contours, spread rates, surface fuel consumption, and wind measurements will all become comparison points for future efforts to model this fire.

Acknowledgements

The authors wish to thank the Joint Fire Science Program (JFSP) for funding this research effort (project #12-1-03-11). Dr. Filkov was supported by the Tomsk State University Competitiveness Improvement Program and the Russian Foundation for Basic Research (project number 14-01-00211-a). The authors would also like to thank the NJFFS for their cooperation in the planning and execution of the experimental fires, as this was critical to the success of the project.

References

Alexander, ME (1982) Calculating and interpreting forest fire intensities. *Canadian Journal of Botany* **60**(4), 349-357.

Butler BW, Jimenez D, Forthofer J, Shannon K, Sopko P (2010) A portable system for characterizing wildland fire behavior. In VI International Conference on Forest Fire Research. D.X. Viegas (Ed.). Coimbra, Portugal, November, 2010.

Byram GM (1959) Combustion of forest fuels. In 'Forest fire: Control and use'. (Ed. KP Davis) pp.61-89, 554-555. (McGraw-Hill: New York)

Clark, KL, Skowronski NS, Gallagher M, Carlo N, Farrell M, Maghirang, MR (2013) Assessment of Canopy Fuel Loading Across a Heterogeneous Landscape Using LiDAR. USDI Joint Fire Science Program, Project #10-01-02-14, Final Report, 47pp.

Frankman David, Webb Brent W., Butler Bret W., Jimenez Daniel, Forthofer Jason M., Sopko Paul, Shannon Kyle S., Hiers J. Kevin, Ottmar Roger D. (2013) Measurements of convective and radiative heating in wildland fires. *International Journal of Wildland Fire* **22**(2), 157–167.

Gorte, RW (2011) Federal funding for wildfire control and management. Congressional Research Service: 7-5700, 29pp.

Hughes, J. (1987) New Jersey, April 1963: can it happen again?. *Fire Management Notes* **48**(1): 3-6.

McKeown D, Faulring J, Krzaczek R, Cavilia S, van Aardt J (2011) Demonstration of delivery of orthoimagery in real time for local emergency response. *SPIE Defense, Security, and Sensing*, International Society for Optics and Photonics.

Morandini F, Silvani X (2010) Experimental investigation of the physical mechanisms governing the spread of wildfires. *International Journal of Wildland Fire* **19**(5): 570-582.

Omi, PN, Martinson, EJ (2002) Effect of fuels treatment on wildfire severity. Final report submitted to the Joint Fire Science Program Governing Board for Project Number 99-1-4-01. Colorado State University, Fort Collins, CO.

Santoni PA, Simeoni A, Rossi JL, Bosseur F, Morandini F, Silvani X, Balbi JH, Cancellieri D , Rossi L (2006) Instrumentation of wildland fire: characterisation of a fire spreading through a Mediterranean shrub. *Fire Safety Journal* **41**(3): 171–184.

Skowronski NS, Clark KL, Duveneck M, Hom J (2011) Three-dimensional canopy fuel loading predicted using upward and downward sensing LiDAR systems. *Remote Sensing of Environment* **115**(2): 703-714.

Van Wagner, CE (1972) Heat of combustion, heat yield, and fire behaviour. Canadian Forest Service, Petawawa Forest Experiment Station, Information Report PS-X-35. (Chalk River, ON)

An update on the WindNinja surface wind modeling tool

Bret Butler, J. Forthofer, N. Wagenbrenner

USDA Forest Service, Rocky Mountain Research Station 5775 W US Highway 10 Missoula MT 59808, USA

Abstract
The WindNinja surface wind modeling tool is being used throughout the world to support wildland fire management. It continues to be updated and improved. Recent improvements include the capability to initialize simulations based on meso-scale weather forecast data or direct observations, an improved tool for accessing elevation data, and access to a momentum solver. This paper describes current status of the tool and planned enhancements.

***Keywords**: Fire behavior, prescribed fire, fire modeling*

Introduction

The temporal and spatial variability in near-surface winds is one of the primary environmental factors influencing wildland fire behavior (Rothermel 1972; Albini 1981; Williams 1982; Linn *et al.* 2007). Historically, fire managers have relied on expert judgment, point measurements, or weather forecasts to estimate local winds (Butler *et al.* 1998; USDA Forest Service and USDI Bureau of Land Management 2002). These methods can lead to large errors in estimated wind speed and direction and subsequently to corresponding uncertainty in fire growth simulations, especially in complex terrain. Others have identified the need for computationally efficient decision support systems for applications involving hazardous chemical or biological releases into the atmosphere and battlefield tactical situations (Davis *et al.* 1984; Homicz 2002; Ling and Shuming 2003; Vaucher and Luces 2011). In order to be useful as a decision support tool for operational fire management, the model must meet several constraints: 1) minimum level of required technical expertise (i.e. not necessarily extensively trained in meteorology); 2) short computational time (i.e. less than 1 hour); 3) minimum computing hardware (i.e. can be run on low cost laptop computers), 4) fine spatial resolution (~ 100 m) of winds at 3 to 10 m above ground level. This paper provides an update on a high resolution surface wind model called WindNinja which meets these constraints (Forthofer *et al.* in press).
WindNinja is a mass-conserving diagnostic model designed for simulating fine-scale, terrain-driven winds. It is widely used in North America to simulate winds in support of wildland fire management. The model seeks to minimize the change from an initial wind field while conserving mass. Details regarding the technical foundation of the model are provided in Forthofer *et al.* (in press). The model can be run via a simple graphical user interface (Figure 1) or a command line interface. Required inputs include a digital elevation model, an initial wind field, and vegetation information. Model outputs are gridded surface or volume wind fields in the following formats: .kmz for viewing in Google Earth, .shp and .asc for viewing in GIS applications, .atm for input to FARSITE and FlamMap fire spread models, and .vtk for viewing in 3-D visualization applications. WindNinja is typically run on domain sizes of up to 50 x 50 km and resolutions on the order of 100 m. Typical simulation times are around 10-30 seconds.
Here we outline the current status of the model with an overview of (1) new features including a diurnal slope flow parameterization, initialization using numerical weather model forecast data, a non-neutral atmospheric stability parameterization, and automated download of terrain data; (2) model validation work with newly collected field observations; and (3) ongoing work including incorporation of an

optional momentum solver, a new GeoPDF output format option, and development of a WindNinja mobile application.

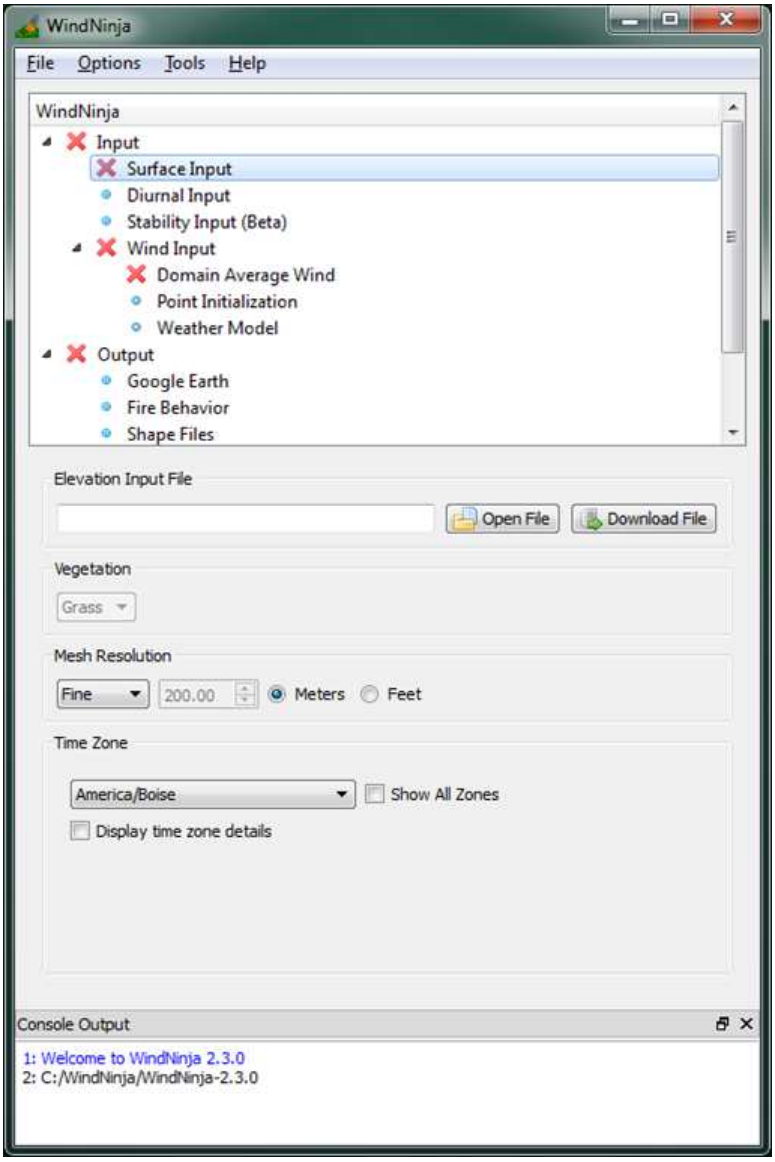

Figure 1. WindNinja graphical user interface.

New features

Diurnal slope flow

An optional diurnal slope flow parameterization has been added to the WindNinja model to simulate local thermally-driven upslope and downslope flows (Forthofer *et al.* 2009). The diurnal slope flow model simulates slope flows induced by local surface heating and cooling. These types of slope flows are most important when gradient wind speeds are low and thermally-induced effects outweigh the mechanically-induced effects on the flow.

The technical foundation of the diurnal slope flow model is described in (Forthofer *et al.* 2009). It includes a micrometeorological model based on (Scire and Robe 1997; Scire *et al.* 2000) which estimates atmospheric stability, surface heat and momentum fluxes, and boundary layer height.

Incident solar radiation is computed within each surface cell using the algorithm from the National Renewable Energy Laboratory (Rymes 2011) and a custom terrain shadow computation. The slope flow model is a one-dimensional model of buoyancy-driven flow along a slope. The magnitude of the slope flow is calculated at each surface grid cell as a function of acceleration distance (distance to ridgetop or valley bottom), percent slope, surface and entrainment drag parameters, and surface sensible heat flux. The direction of slope flow within each cell is exactly upslope or downslope and the depth of the slope flow is assumed to be 5% of the elevation difference to the ridge or valley. Once calculated, the slope flow component in each cell is added to the initial wind field and then the WindNinja solver is run to generate the final mass-conserving flow field.
Since incident solar radiation must be computed, use of the slope flow model requires that the following additional input parameters be specified: date, time, cloud cover, and air temperature. If the simulation is initialized with a weather model forecast, this information is obtained automatically from the weather model data, otherwise it must be supplied. Validation of the diurnal slope flow model with field observations is described below.

Weather model initialization

WindNinja allows initialization with a number of weather model forecasts. Numerical weather models compute gridded predictions of *u*, *v*, *w*, pressure, moisture, and heat on 3-D computational domains. They include sophisticated schemes for boundary-layer dynamics, cloud microphysics, and land-surface interactions. They typically simulate large areas (regional to continental scale), employing computational grids with horizontal resolutions of 4 km or larger. Because of the large computational expense required to simulate detailed physical processes over such large areas, it is not possible to run these types of models at a fine enough resolution to capture local terrain effects on the flow. In contrast, WindNinja is designed to simulate fine-scale winds that are dominated by mechanical terrain modification and local slope flows induced by local surface heating and cooling. Weather model forecasts linked with higher-resolution wind models can produce more accurate surface wind forecasts (Beaucage *et al.* 2014), as synoptic-scale forces and planetary boundary layer processes are resolved by the weather model to generate an initial wind field which is then downscaled by the higher resolution wind model that better resolves individual terrain features. The effect of downscaling weather model surface wind predictions with WindNinja is discussed below.
WindNinja includes built-in support for downloading and initialization with the following forecasts provided by the National Centers for Environmental Prediction: National Digital Forecast Database (NDFD), North American Mesoscale Model (NAM), Rapid Refresh Model (RAP), and Global Forecast System (GFS) (Table 1). Additionally, limited support has been added for the following forecasts via the command line interface: Weather Research and Forecasting (WRF-ARW) (netCDF format), historical NAM (GRIB2 format), and High Resolution Rapid Refresh (HRRR) (GRIB2 format). WindNinja only supports reading and initialization with these additional models, and does not offer download support, so the user must obtain these forecasts from another source.
WindNinja uses the 10-m wind speed and direction, cloud cover, and 2-m temperature from the weather model forecast. Only this subset of variables is downloaded from the full forecast for each output time step so the data transfer is very fast (typically just a few seconds). WindNinja performs an individual WindNinja simulation for every output time step in the weather model forecast. During each WindNinja run, the coarse-scale weather model forecast data is interpolated to the finer-scale WindNinja computational grid. Diurnal winds are added if the diurnal slope flow algorithm is enabled to produce the final initial wind field. Finally, the WindNinja solver is run on this initial wind field to produce a final flow solution that conserves mass.

Table 1. Weather model forecasts available for download in WindNinja

Model Name in WindNinja	Description	Horizontal Resolution	Forecast Duration	Temporal Resolution	Update Frequency
NCEP-NDFD-5km	National Digital Forecast Database	5 km	168 hours (7 days)	Every 6 hours	12 and 18 UTC
NCEP-NAM-12km-SURFACE	North American Mesoscale Model (lower 48 domain)	12 km	84 hours (3.5 days)	Every 3 hours	00, 06, 12, and 18 UTC
NCEP-NAM-Alaska-11km-SURFACE	North American Mesoscale Model (Alaska domain)	11 km	84 hours (3.5 days)	Every 3 hours	00, 06, 12, and 18 UTC
NCEP-RAP-13km-SURFACE	Rapid Refresh Model	13 km	18 hours (0.75 days)	Every 1 hour	hourly
NCEP-GFS-GLOBAL-0_5deg-SURFACE	Global Forecast System	0.5°	168 hours (7 days)	Every 3 hours	00, 06, 12, and 18 UTC

Non-neutral atmospheric stability

Atmospheric stability is a measure of the resistance of the atmosphere to vertical motion due to variations in air density with height above the ground. Under stable atmospheric conditions, vertical motion is inhibited and the flow will tend to flow around, rather than up and over terrain obstacles. Under unstable atmospheric conditions, vertical motion is favored and flow will tend to more easily move up and over terrain obstacles. Atmospheric stability is a dynamic phenomenon and it can vary spatially within a given domain.

The native WindNinja solver assumes a neutral atmosphere (vertical motions are neither suppressed nor favored). An optional atmospheric stability model has been incorporated into WindNinja for simulating non-neutral atmospheric conditions. The model estimates atmospheric stability from the surface heat flux calculated using methods from the diurnal slope flow model. Currently, a single stability value is assigned to the full vertical profile (from the ground surface to the top of the model domain) for each surface grid cell. Future improvements to the stability model will likely use additional information to more fully describe the state of the atmosphere. Because of this, the stability model is considered a beta test version at this time. Use of the stability model requires the following additional input parameters for calculation of the surface heat flux: cloud cover, date, and time. If the simulation is initialized with a weather model forecast, this information is obtained automatically from the weather model data, otherwise it must be supplied.

Elevation file grabber

An option to download a digital elevation model (DEM) has been added to WindNinja. This feature is referred to as the "elevation file grabber." The elevation file grabber uses a Google Maps interface which can be launched either from the graphical user interface or the command line interface (Figure 2). The elevation file grabber allows the user to swoop out an area of interest on the interactive map. After selection of the area, a transparent red box will be drawn on the map indicating the defined area (Figure 2). This box can be enlarged or shrunk by dragging the sides and corners of the box or it can be translocated by dragging the center icon. There are three data sources from which DEM data can be downloaded from: US SRTM, WORLD SRTM, and WORLD GMTED (Table 2). Once the area of interest has been defined and the DEM data source has been selected, the DEM can be downloaded by WindNinja from a United States Geological Survey (USGS) server.

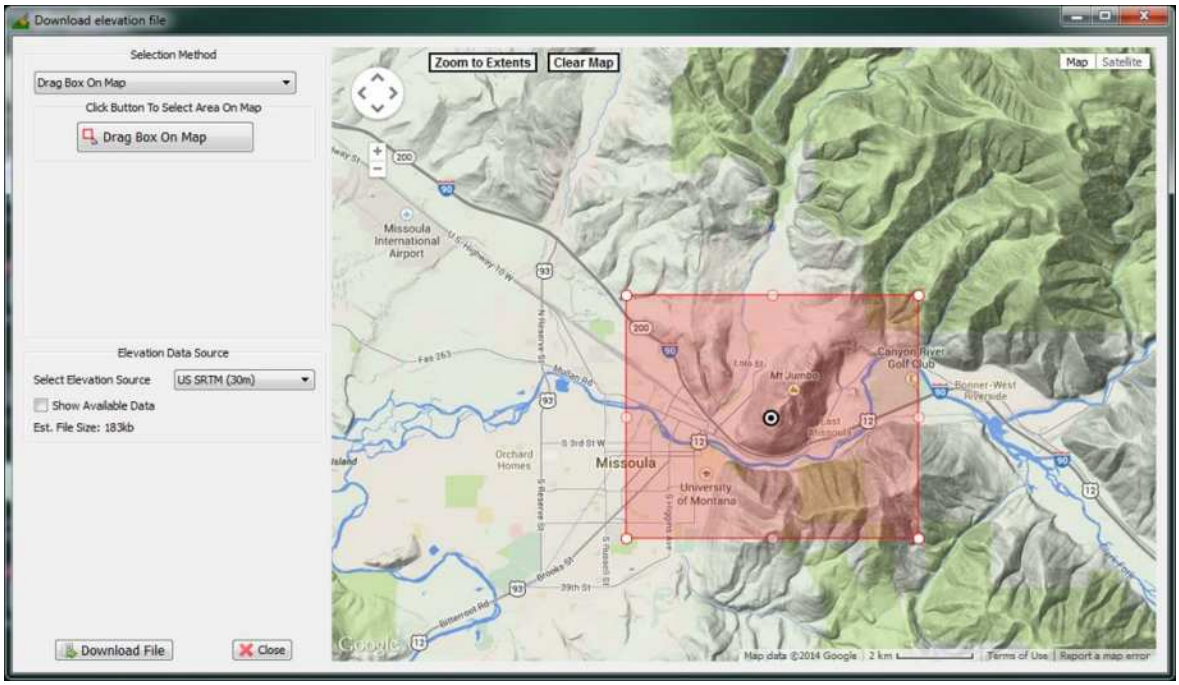

Figure 2. Elevation file grabber.

Table 2. Digital elevation model data sources

Data source	Resolution	Spatial extent	Description
US SRTM	30 m	Contiguous US, Hawaii, Puerto Rico, southern Alaksa	Data from the Shuttle Radar Tomography Mission (SRTM)
WORLD SRTM	90 m	-60° to +60°	Data from the Shuttle Radar Tomography Mission (SRTM)
WORL GMTED	250 m	-60° to +85	Global Multi-resolution Terrain Elevation Data 2010 (GMTED2010)

Model validation

There is little observational data available at appropriate spatial scales for evaluating high resolution wind models like WindNinja. To address this issue and facilitate validation of high-resolution wind models, we conducted a series of intensive field campaigns to collect high-resolution near-surface wind observations from four different field locations in complex terrain. Data from two of these field campaigns has been published (Butler *et al.* 2014) and used to evaluate use of WindNinja for downscaling numerical weather model forecast winds in complex terrain (Wagenbrenner, in preparation). Results from this work demonstrate that WindNinja can improve near-surface wind forecasts in many cases as long as the large-scale flow in the domain is adequately captured by the weather model. The biggest improvements in speed predictions occurred during periods of high winds and the biggest improvements in direction predictions occurred under periods of upslope and downslope flow. The largest errors in WindNinja-predicted wind speed and direction tend to occur on the lee side of terrain obstacles (Forthofer *et al.*, in press; Wagenbrenner *et al.*, in preparation). We found that the diurnal slope flow algorithm helped to correctly orient winds during periods of upslope

and downslope flows, but that the strength of the modeled slope flows tended to be weaker than the observed slope flows (Wagenbrenner *et al*. in preparation). This suggests that additional work could be done to improve parameterizations in the diurnal slope flow algorithm.

Ongoing work

Ongoing work includes incorporation of an optional momentum solver, design of an application for WindNinja simulations on mobile devices, and an additional GeoPDF output format option. Incorporation of the momentum solver should improve wind predictions on the lee side of terrain obstacles, in at least some cases. The new GeoPDF output format will all users to view gridded output surface winds on a map saved locally on their computer or mobile device. This will allow viewing of the output on a dynamic map without an internet connection or cell phone coverage and is expected to be useful to users in remote field locations. The mobile application will allow initiation of a WindNinja simulation from a mobile device. This should improve usability in field settings where use of computers or laptops may not be convenient.

References

Albini, FA (1981) A model for the wind-blown flame from a line fire. *Combusion and Flame* **43**, 155-174.

Beaucage, P, Brower, MC, Tensen, J (2014) Evaluation of four numerical wind flow models for wind resource mapping. *Wind Energy* **17**, 197-208.

Butler, BW, Bartlette, RA, Bradshaw, LS, Cohen, JD, Andrews, PL, Putnam, T, Mangan, RJ, 1998. Fire behavior associated with the 1994 south canyon fire on storm king mountain, Colorado. USDA Forest Service, USA. RMRS-RP-9:

Butler, BW, Wagenbrenner, NS, Forthofer, JM, Lamb, BK, Shannon, KS, Finn, D, Eckman, RM, Clawson, K, Bradshaw, L, Sopko, P, Beard, S, Jimenez, D, Wold, C, Vosburgh, M (2014) High resolution observations of the near-surface wind field over an isolated mountain and in a steep river canyon. *Atmos. Chem. Phys. Discuss.* **14**, 16821-16863.

Davis, CG, Bunker, SS, Mutschlecner, JP (1984) Atmosperic Transport Models for Complex Terrain. *Journal of climate and applied meteorology* **23**, 235-238.

Forthofer, J, Shannon, K, Butler, B (2009) Simulating Diurnally Driven Slope Winds with WindNinja. In 'Eigth Symposium on Fire and Forest Meteorology. Kalispell, MT', October 13-15, 2009. (American Meteorological Society:

Forthofer, JM, Butler, BW, Wagenbrenner, NS (in press) A comparison of three approaches for simulating fine scale surface winds in support of wildland fire management: Part I - wind model formulation and accuracy. *International Journal of Wildland Fire*

Homicz, GF, 2002. Three-dimensional wind field modeling: A review. Albuquerque, N.M. SAND2002-2597

Ling, L, Shuming, D (2003) A computationally efficient particle-puff model for concentration variance from steady releases. *Environmental Modelling & Software* **18**, 25-33.

Linn, RR, Winterkamp, J, Edminster, C, Colman, JJ, Smith, WS (2007) Coupled influences of topography and wind on wildland fire behaviour. *International Journal of Wildland Fire* **16**, 183-195.

Rothermel, RC (1972) A Mathematical model for predicting fire spread in wildland fuels. USDA, Forest Service No. INT-115, Ogden, UT.

Rymes, M, 2011. The SolPos algorithm. National Renewable Energy Laboratory, USA. US Department of Energy, Golden, CO.

Scire, J, Robe, F (1997) Fine-scale application of the CALMET meteorological model to a complex terrain site. In 'Air and Waste Management Association's 90th Annual Meeting and Exhibition. Toronto, ON, Canada'. pp. 1-16.

Scire, JS, Robe, FR, Fernau, ME, Yamartino, RJ (2000) A user's guide for the CALMET meteorological model. Earth Tech, Inc., Concord, MA.

USDA Forest Service and USDI Bureau of Land Management (2002) Price Canyon Fire Entrapment Investigation Report. Missoula, MT. Available at http://www.fire.blm.gov/textdocuments/PriceCONT.pdf.

Vaucher, G, Luces, SA (2011) Urban experiment results characterize building wakes, aiding airborne hazard applications. In '15th Symposium on Integrated Observing and Assimilation Systems for the Atmosphere, Oceans, and Land Surface Seattle, WA'. pp. 9. (American Meteorological Society:

Williams, FA (1982) Urban and wildland fire phenomenology. *Progress in Energy and Combustion Science* **8**, 317-354.

Analysis of firebrand release on the spot fire mechanism

Miguel Almeida[a], Domingos Viegas[a], Jorge Raposo[a]

[a]*Centre for Forest Fire Research ADAI, Rua Pedro Hispano, 12, PT-3030-289 Coimbra, Portugal; miguellmd@yahoo.com, xavier.viegas@dem.uc.pt, jorge.raposo@dem.uc.pt.*

Abstract

Eucalyptus trees are among the most important sources of firebrands with potential to produce spot fires which are one of the most relevant manifestations of extreme fire behaviour. The mechanism of spot fires has several sequential phases starting in the release of a burning ember which is lofted and transported by the airflow, to land in a fuel bed causing a new ignition. In the present study, dedicated to the phase of firebrand release, an analysis of the firebrands released in a process of burning of eucalyptus trees is carried out.

Barks of eucalyptus trees have a great potential to produce firebrands during a forest fire. Sometimes these fuels are lay down on the ground or are attached to the trunk and to large branches of the canopy. In this study, the number and size distribution of firebrands released during the burning of these fuels for different scenarios are analysed. Three tests were made varying the location of the barks (suspended and lay down on a fuel bed) and the orientation of suspended barks (vertical and horizontal). An additional similar test was performed with a fuel bed composed of shrubs.

A particle image velocimetry system available in the Forest Fire Research Laboratory of ADAI was used to analyse the release of firebrands. Additionally, the convective up flow velocity and the temperature 2m above the tree, as well as the weight loss decay were measured. The final results among the several parameters controlled are compared.

Keywords*: forest fire, spot fire, spotting, firebrand, embers, eucalyptus, fire behaviour, extreme fire behaviour.*

Introduction and objectives

The importance of the spotting mechanism in the propagation of forest fires is widely recognized by both the scientific community and the operational elements of civil protection. Its importance is not only due to the effect on increasing the rate of fire spread but also due to the ability to overcome firefighting barriers and fuel breaks, as well as the capacity to surprise and trap people. Additionally, for larger firebrands and particular environment conditions, the long distance spotting mechanism may originate new independent fires which can stress the firefighting system.

For several years ADAI has been studying the spot fires mechanism splitting it in five main stages: (1) release of firebrands, (2) lofting of firebrands in the convection column, (3) downwind transport of the firebrand, (4) landing of the firebrand and possibility of ignition, and (5) interaction between the spot fire and original fire front. This study is focused on the release of firebrands resulting from the burning of eucalyptus trees, specifically the burning of the eucalyptus trees barks. The analysis was made using a particle image velocimetry (PIV) system.

There are several models related to forest fire however the major part is related to the aerodynamic lifting and downwind transport (e.g. Albini, 1979, 1981, 1983a, 1983b; Sardoy *et al.*, 2007) and some are related to the probability of ignition after the firebrand's landing (e.g. Viegas *et al.*, 2012). There are many models (e.g. Ellis, 2000) predicting the spotting mechanism for individual particles, or a set of particles with similar characteristics released in the same location. The major limitation of these models is the understanding of how and where the firebrands are released and what physical properties these firebrands have.

Release of firebrands is actually poorly understood. The use of PIV in this context may be of great useful however it is currently in a very early stage. Several authors have used the PIV technique in the context of fires specifically to determine the flame and the convective flow characteristics (e.g.

Morandini *et al.*, 2012; Horváth *et al.*, 2012) however those application were not in the context of spot fires. Hosseini *et al.* (2010) made a study reporting the characteristics of particle size distributions with focus on chaparral. Manzello *et al.* (2007) made a series of real-scale laboratory fire experiments to determine the size and mass distribution of firebrands generated from 2.6 to 5.2m high Douglas-fir (*Pseudotsuga menziesii*) trees using an array of pans filled with water to collect the firebrands generated from the burning trees.

Eucalyptus trees are among the main sources of firebrands with potential to cause a spot fire (McArthur, 1967). Barks of the eucalyptus trees (*Eucalyptus globulus* Labill.) were assumed in this study as being one of the most important components to produce firebrands. Normally the barks can be found lay down on the ground or may be attached to the trunk or to large branches of the tree. The barks attached to the trunk show an orientation predominantly vertical. The barks attached to the branches show an orientation with a greater horizontal component.

Several burning tests were carried out for three different scenarios: 1) barks lay down on a fuel bed, 2) barks suspended in a tree predominantly with vertical orientation, and 3) barks suspended in a tree mainly in the horizontal position. It is expected a faster and more intense combustion of the suspended barks and specifically the vertical barks (Almeida *et al.*, 2011). Higher intensity leads to a faster and more effective burning of the barks however it increases the up flow convective velocity intensifying the release of firebrands. On the other side, the horizontal orientation of the barks have a larger drag coefficient value (Almeida *et al.*, 2010) facilitating the uplift of the firebrands.

To sustain the combustion and to increase the fire intensity, a fuel bed of shrubs was used. To understand the effect of the shrubs in the release of firebrands, a fourth test with a single fuel bed of shrubs, without barks, was carried out.

The numerical and size distribution of the firebrands released during the burning was determined using a PIV system. In parallel other parameters like weight loss decay, temperature and vertical convective flow at 2m high were measured. A comparative analysis of the results was performed.

Experimental study

All the experiments following described were carried out in the Forest Fires Research Laboratory of ADAI (Association for the Development of Industrial Aerodynamics), in Lousã - Portugal.

Two different types of fuels were used in the experiments, namely eucalyptus barks (*Eucalyptus globulus* Labill.) and a mix of shrubs composed by heather (*Calunna Vulgaris*) and carquesia (*Pterospartium tridentatum*). The barks were detached randomly from the trunk and the large branches of the trees. The shrubs were cut using a brush cutter. All the fuels were collected in typical summer days and were stored inside the laboratory in controlled conditions of $T \approx 25$ºC and $RH \approx 40\%$.

As previously mentioned, four burning tests were carried out using shrubs (*T1*) or shrubs and barks (*T2, T3* and *T4*). Table 1 resumes the experimental conditions of each test. In *T1* the shrubs were lay down on the combustion table (Figure 1a).The fuel bed had the shape of a cone with a base of area of $0.81 m^2$ and 0.4m high. This "basic" fuel bed of shrubs was common to all tests. In *T2* the barks were lay down on the shrubs to cover the upper surface (Figure 1b). In *T3* (Figure 1c) and *T4* (Figure 1d) the barks were suspended in a tree skeleton only with thickest branches. It was assumed that tree skeletons used do not burn to loose significant weight nor to produce firebrands. In *T3* barks were suspended mainly with vertical orientation and in *T4* a predominant horizontal orientation of the barks was forced. The environmental laboratorial conditions (temperature *T* and relative humidity *RH*), the fuels moisture content (*FMC*), the initial fuel weight (m_0), the tree skeleton height (*H*) and diameter ($\varnothing$) and the distance (ΔH) from the surface fuels and the tree canopy were also measured before the burning. The fuels were roughly totally consumed during the test.

Table 1. Main data of the experimental conditions.

REFERENCE	INITIAL CONDITIONS	FUELS CHARACTERISTICS
T1	Fuel: shrubs Temperature (ºC): 29.8 Relative humidity (%): 48	FMC shrubs (% DB): 10.7 m_0 shrubs (kg): 2.7
T2	Fuel: Barks and shrubs lay down on the fuel bed Temperature (ºC): 25.5 Relative humidity (%): 31	FMC barks (% DB): 14.1 FMC shrubs (% DB): 12.8 m_0 barks (kg): 1.94 m_0 shrubs (kg): 2.8
T3	Fuel: Barks suspended with vertical orientation Temperature (ºC): 26.7 Relative humidity (%): 60	FMC barks (% DB): 11.1 FMC shrubs (% DB): 10.7 m_0 barks (kg): 1.99 m_0 shrubs (kg): 2.8 H tree (m): 2.60 ΔH (m):0.95 ∅ (m): 0.5
T4	Fuel: Barks suspended in horizontal orientation Temperature (ºC): 30.1 Relative humidity (%): 47	FMC barks (% DB): 11.1 FMC shrubs (% DB): 10.7 m_0 barks (kg): 1.99 m_0 shrubs (kg): 2.8 H tree (m): 2.10 ΔH (m): 0.95 ∅ (m): 0.6

(a) (b) (c) (d)

Figure 1. Images of the four burning tests carried out: a) T1, b) T2, c) T3 and d) T4.

The ignition was produced using a woollen yarn lying on the perimeter of the shrub fuel bed. The acquisition of weight, temperature and up flow velocity was initiated at the same time of the ignition. The PIV images started being captured when the total weight of the fuel bed was reduced to 88% of the initial value. By total weight of the fuel bed we understand the weight of all the elements over the table which, for example, in *T4* are the shrubs, the barks and the tree skeleton.

The fuel bed was set up on a balance (precision: 0.01kg) allowing the measurement of the weight loss decay during the burning. The temperature and the vertical flow velocity at 2m high in the central axis of the smoke plume were controlled throughout the experiment using a thermocouple and a *Pitot* tube, respectively.

The number and dimensions of the firebrands released were acquired from a PIV system. The PIV system is composed of a camera linked to a computer that store the images. The camera was placed in an elevated position in order to have a horizontal axis of image capture video. Figure 2 shows a representation of the experimental apparatus.

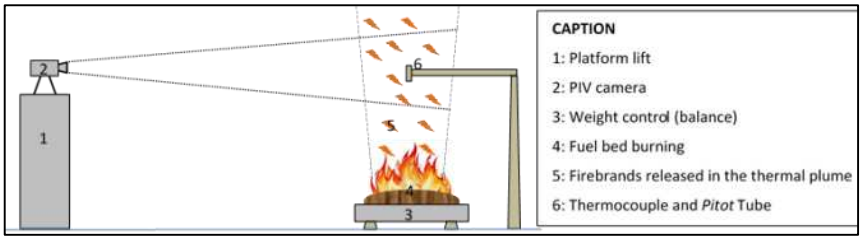

Figure 2. Experimental apparatus.

The images were captured for 25s. As previously mentioned, the image acquisition started when the total weight of the fuels was reduced to 88% of the initial value as it was observed to be the moment when the burning blows up to a higher intensity and more firebrands are released. The area covered by each PIV image is a rectangle of 2320mm width and 1728mm height with the centre 3.5m above the centre of the fuel bed. Particle were identified and characterized using the Dynamic Studio software of Dantec. After the preliminary identification of the particles of interest (Figure 3) only particles with equivalent diameter larger than 1.7mm were considered as interesting for this study. Besides the major part of the firebrands released has an equivalent diameter lower than 1.7mm, we considered that very small particles with lower calorific values do not represent an effective threat to cause a spot fire when lofted in the experimental conditions of burning.

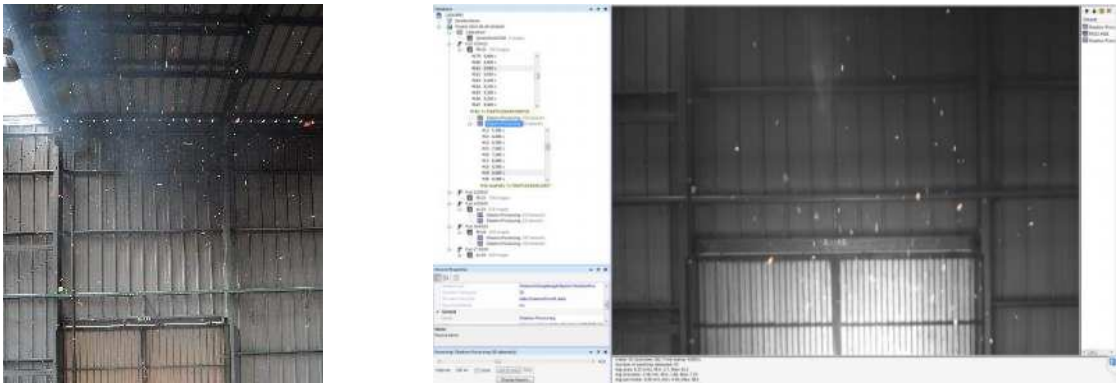

(a) (b)

Figure 3. Images of the firebrand release (test T1): a) photographic image, and b) PIV image after the preliminary identification of the firebrands (red lines involving the particles).

Results and discussion

The weight loss decay was analysed taking into consideration that initial total weight was different among the four tests. Therefore a relative weight loss decay $\dot{m}$ was determined using Equation 1 where m_t is the mass of the fuel bed at any instant t and m_0 is the initial mass of the fuel bed. The weight of the tree skeleton was reduced as this element did not participated in the combustion. In Figure 4 the variation of $\dot{m}$ during the experiments is represented. Following Almeida (2011), the weight loss decay can be fitted with an exponential law as shown in Eqn. 2 where k is the weight loss coefficient represented in **Erro! A origem da referência não foi encontrada.**2. As can be seen the weight loss decay for *T3* and *T4* is quite similar and were the tests with faster decrease of fuel relative weight. On the other side, test *T2* burned slowly essentially due to the coverture of the shrubs fuel bed by the barks that muffled the flames delaying the burning. The values for Test *T1* were below those verified for T3 and T4 because the absence of barks that have a good combustibility rate.

$$\dot{m} = \frac{m_t}{m_0} \qquad \text{[Eqn. 1]}$$

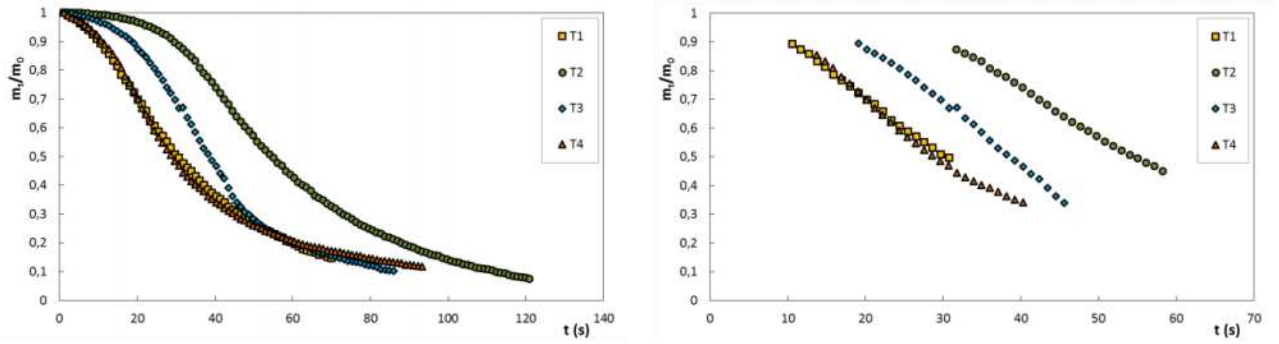

(a) (b)

Figure 4. Relative weight loss decay (Eqn. 1) measured throughout the burning tests: a) all the values of the tests and (b) the values related to the period when the PIV images were captured.

$$m = m_0 \times \exp(-k \times t) \qquad \text{[Eqn. 2]}$$

Table 2. Values of the weight loss decay k.

REFERENCE	T1	T2	T3	T4
k (s^{-1})	0.0299	0.0256	0.0354	0.0360

The combustion rate during the range of time for what the PIV images were captures that is the period of interest for this study was very constant. The fitting of a linear equation of the values represented in Figure 4b drives to correlation coefficients r^2 larger than 0.98. Therefore the determination of average values for the other parameters (temperature, up flow velocity and number and area of firebrands) is reasonable.

The measured temperature *T* and the determined up flow velocity *V* values are represented in Figure 5. In Figure 5a, the values of *T* and *V* during the complete burning in test *T4* is given for exemplification. Figure 5b represents the values of *V* for tests *T1*, *T3* and *T4* during the time of the PIV images acquisition. The respective files of *T2* were corrupted and therefore the results for this test are not presented. Table 3 resumes the average values of T_{av} and V_{av} for each test. It is possible to observe that values of temperature and up flow velocity are lower for *T1* than for *T3* and *T4*, which are very similar. The lower intensity of *T1* verified and described during the analysis of *k* can explain these results. Additionally, the lower distance between the suspended barks and the *Pitot* tube, in *T3* and *T4*, when compared to the larger distance between the shrubs fuel bed and the *Pitot* tube in *T1*, can also explain that discrepancy of T_{av} and V_{av} among the tests.

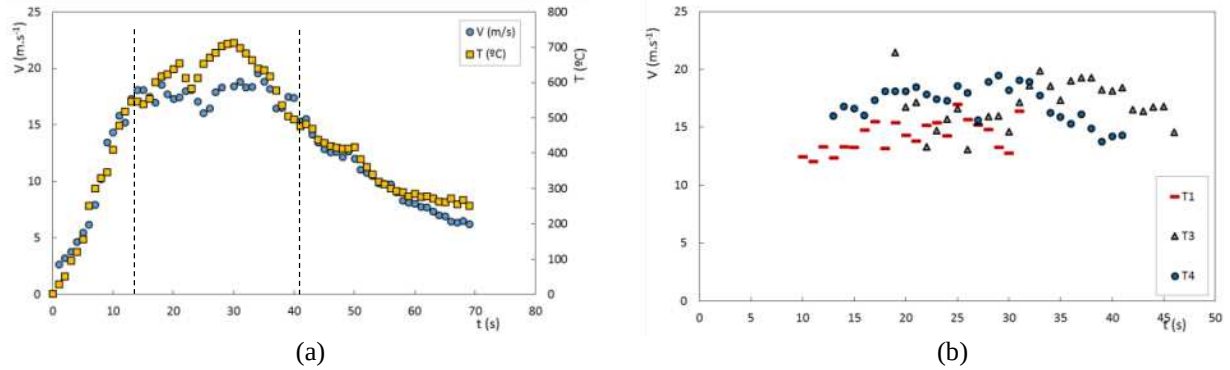

(a) (b)

Figure 5. Example of the values of temperature (T) and convective up flow velocity (V) measured throughout a burning test (T4). Vertical dotted lines correspond to the time period when the PIV images were captured.

Table 3. Values of average temperature T_{av} and average up flow velocity V_{av}.

REFERENCE	T1	T2	T3	T4
T_{av} (ºC)	541.5	N/D	607.7	613.8
V_{av} (m.s^{-1})	14.3	N/D	17.0	17.0

In Figure 6 the total number of particles released and captured by the PIV system for each test is shown. It is possible to see that in general terms the fuel bed composition producing more firebrands was that of test *T1* (shrubs) with an average value of 113 particles per image (Table 4) during the analysed range of time. Test *T2*, with barks and approximately the same load of shrubs than *T1*, produces an average value of 69 particles.image^{-1}. The barks work like a cover of the shrubs do not allowing the lofting of the firebrands. However, when this "cover" is passed through by the firebrands they can be lofted. The number of particles released during *T3* was even lower and N_{av} for *T4* was slightly above of *T2*. We could observe in laboratory that the tree skeleton with the barks suspended work as an obstacle for the lofting of the firebrands released from the shrub fuel bed. As consequence these firebrands were not lofted to the higher level were the PIV camera was pointed. When the barks start burning more intensively the number of firebrands increased assuming being counted 171 particles for *T4*. This was the larger value for all the tests. Surprisingly this increase of intensity was not traduced in an increase of the up flow velocity nor the weight loss decay. The superior number of particles verified in *T4* when compared with *T3* is due the higher drag coefficient of the horizontal barks facilitating the lofting of the particles and the breakage of the burning bark in small particles.

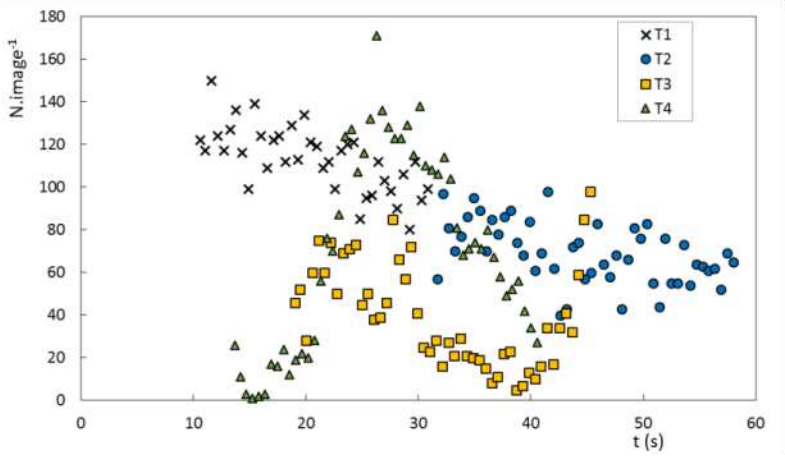

Figure 6. Total number of firebrands released during the burning captured by the PIV camera.

Table 4. Values of average number of particles per PIV image.

REFERENCE	T1	T2	T3	T4
N_{av}	113	69	40	71

In Figure 7the distribution of the released particles by dimensional classes is represented for each test. The area of classes in mm^2 correspond to the projected area of the particles captured by the PIV system. Test *T1* only with shrubs as burning fuel has the larger number of firebrands, as it was mentioned before, however around 77% of the particles have a projected area below 100mm^2. Test *T2* was that one with less particles released however more than 41% of these particles have an area larger than 1000mm^2. The small particles released during the burning of shrubs were not lofted due to the barks cover however the burning of the barks produced firebrands with larger dimensions. Like for *T1* and

T2, particles below 100mm^2 were the most represented in *T3* and *T4*. While *T1* and *T2* roughly did not produced particles in the class [100; 500[mm^2, tests *T3* and *T4* with barks suspended, originate several particles in this range of area. On the other side these two tests produced less firebrands of larger dimensions. The more intensive burning verified in T3 and T4 can explain this achievement.

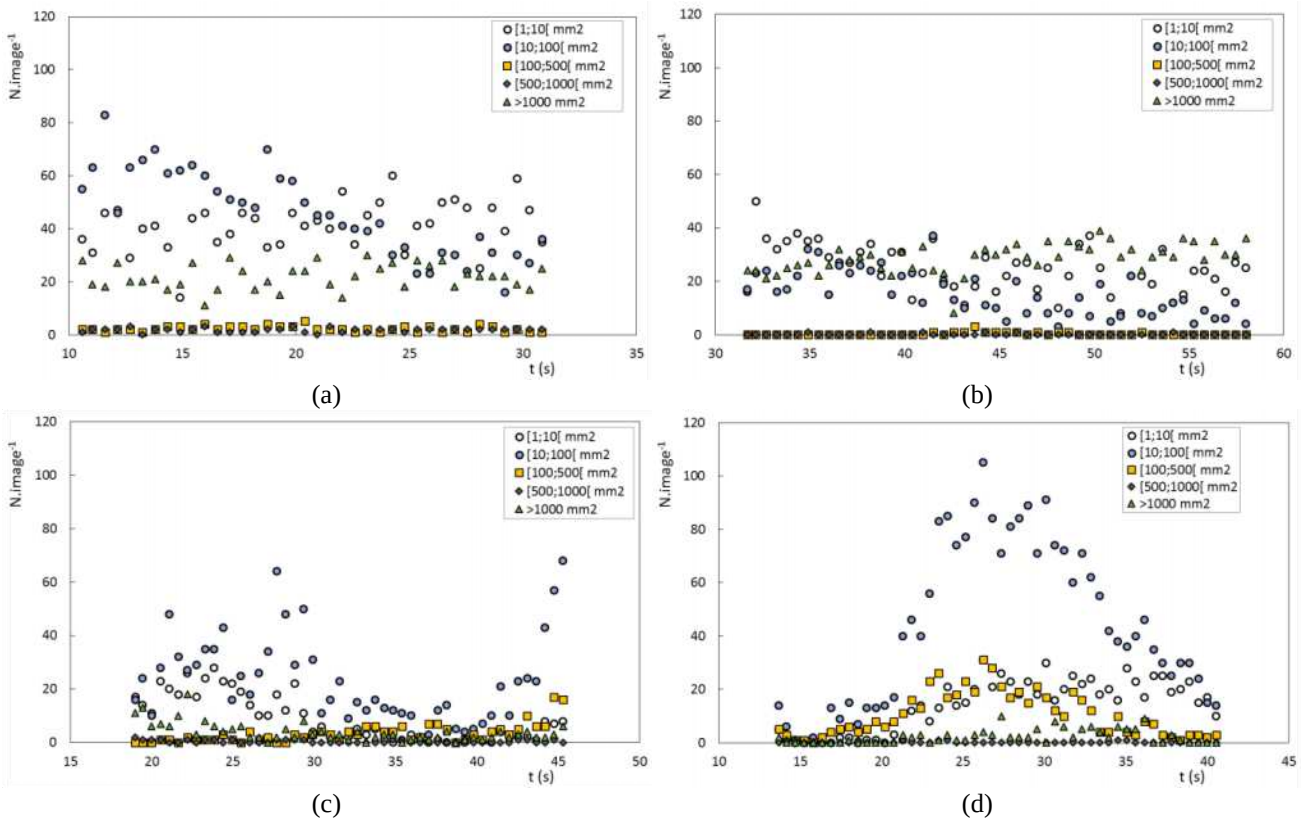

Figure 7. Numeric distribution of firebrands released during the burning captured by the PIV camera for T1 (a), T2 (b), T3 (c), and T4 (d).

The analysis of the projected areas was carried out as well as showed in **Erro! A origem da referência não foi encontrada.** and **Erro! A origem da referência não foi encontrada.**. If we consider that projected areas are proportionally related to the volume of the particles and consequently to the mass, it can be concluded that tests *T1* and *T2* produced a larger mass of firebrands. It can be seen in **Erro! origem da referência não foi encontrada.** that particles larger than 1000mm^2 contribute mainly for this result. The more intense tests *T3* and *T4* produced a lower mass of particles as a great amount of fuel is converted in smoke with particles below 1mm^2. Besides *T4* produced a larger number of particles than *T3*, the total area of the particles per image was similar due to the different distribution per area classes.

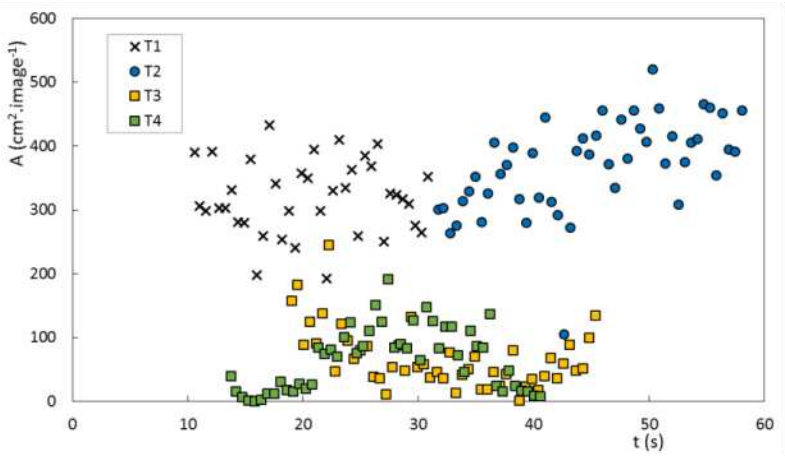

Figure 8. Total projected area of firebrands released during the burning captured by the PIV camera.

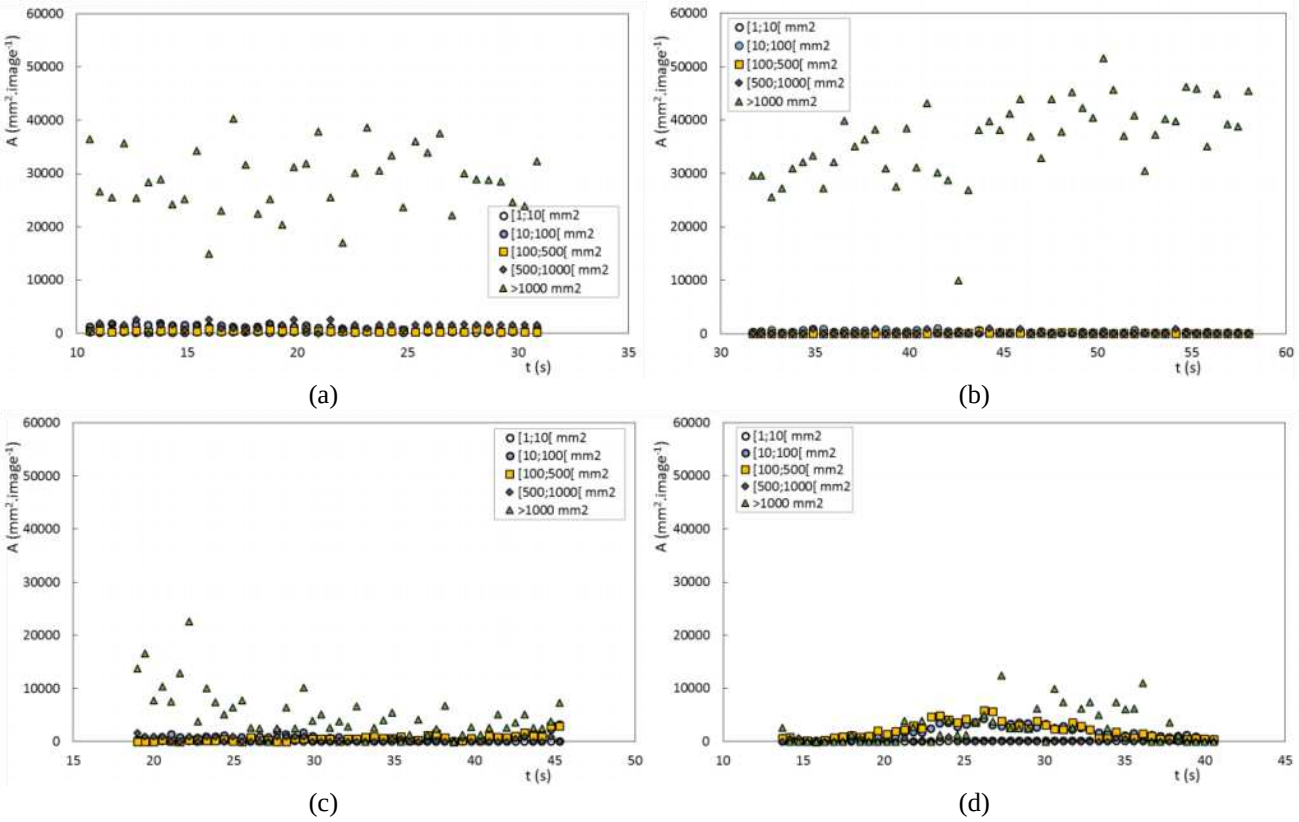

Figure 9. Area distribution of firebrands released during the burning captured by the PIV camera for T1 (a), T2 (b), T3 (c) and T4 (d).

Table 5. Values of average projected area of particles per PIV image.

REFERENCE	T1	T2	T3	T4
A_{av} (cm^2)	320	370	69	65

The four tests carried out are not sufficient to take ending conclusions on the relations among the parameters controlled. In addition the values of temperature and up flow velocity were not determined

for *T2*. Nevertheless in **Erro! A origem da referência não foi encontrada.** the relation among the arameters is presented. As it would be expected, *T*, *V* and *k* vary in the same direction (**Erro! A origem da referência não foi encontrada.**a, **Erro! A origem da referência não foi encontrada.**b and **Erro! A origem da referência não foi encontrada.**c). Parameters *T* and *V* are very related as *V* corresponds to the vertical convective flow that is induced by the heat of combustion. The number of particles released as function of the weight loss decay (**Erro! A origem da referência não foi encontrada.**d) is not well defined however it is possible to see a tendency showing a decrease of A_{av} with rising of *k* (**Erro! A origem da referência não foi encontrada.**h). This is due to the more intense and complete burning of the fuels for larger values of *k*. A negative effect of *T* and *V* to *N* and *A* is also verified in **Erro! A origem da referência não foi encontrada.**e, **Erro! A origem da referência não foi encontrada.**f, **Erro! A origem da referência não foi encontrada.**i and **Erro! A origem da referência não foi encontrada.**j. It would be expected that larger values of *V* would lead to an increase of *N* and *V* however, the larger values of *V* are related to more complete burnings (larger *k* and *T*) producing less particles. If to *V* was added an induced airflow (wind for example) maybe the number and area of the particles would increase in the same direction. The relation N_{av} *vs* A_{av} (**Erro! A origem a referência não foi encontrada.**g) is not well defined for the reasons previously explained.

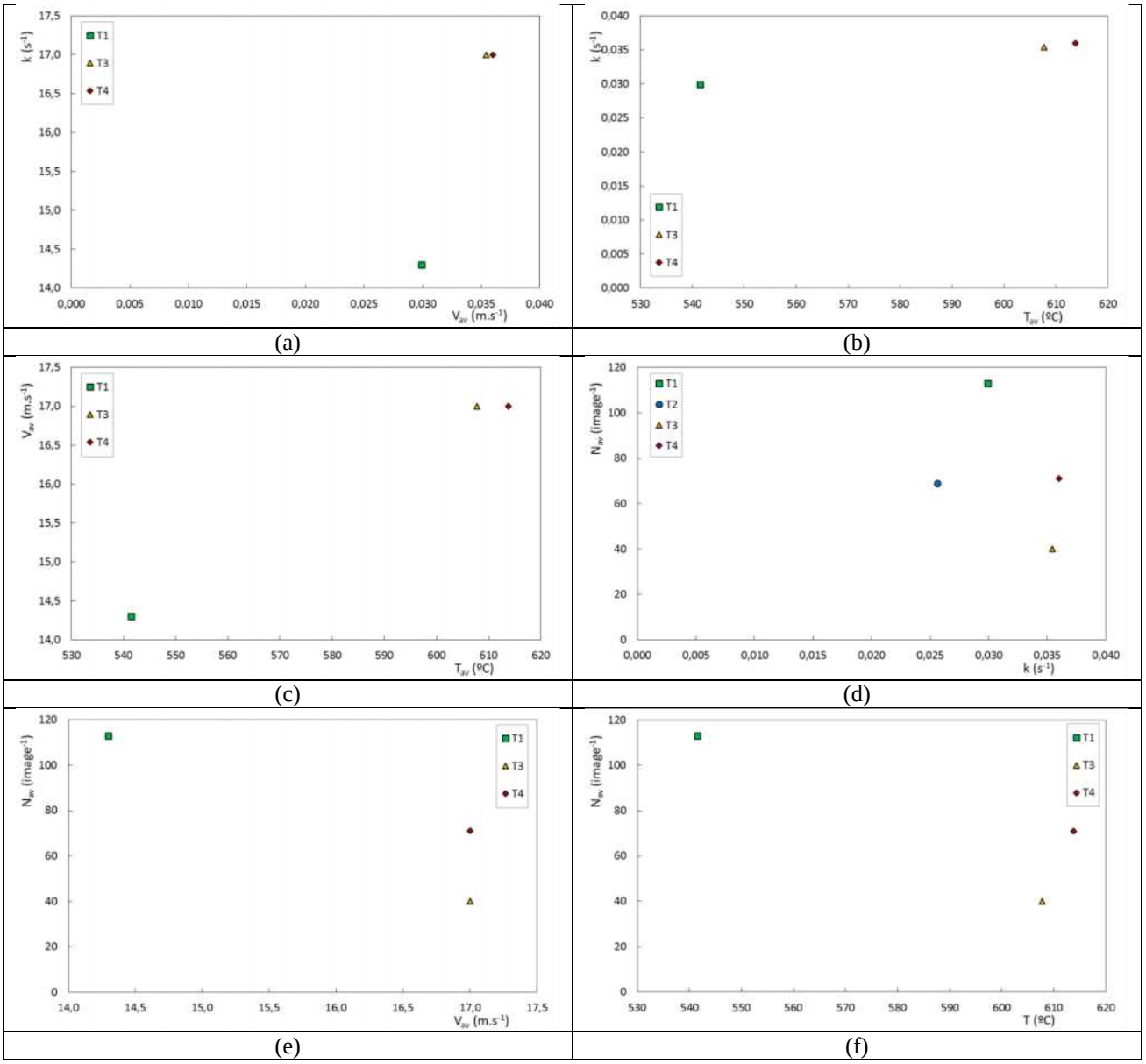

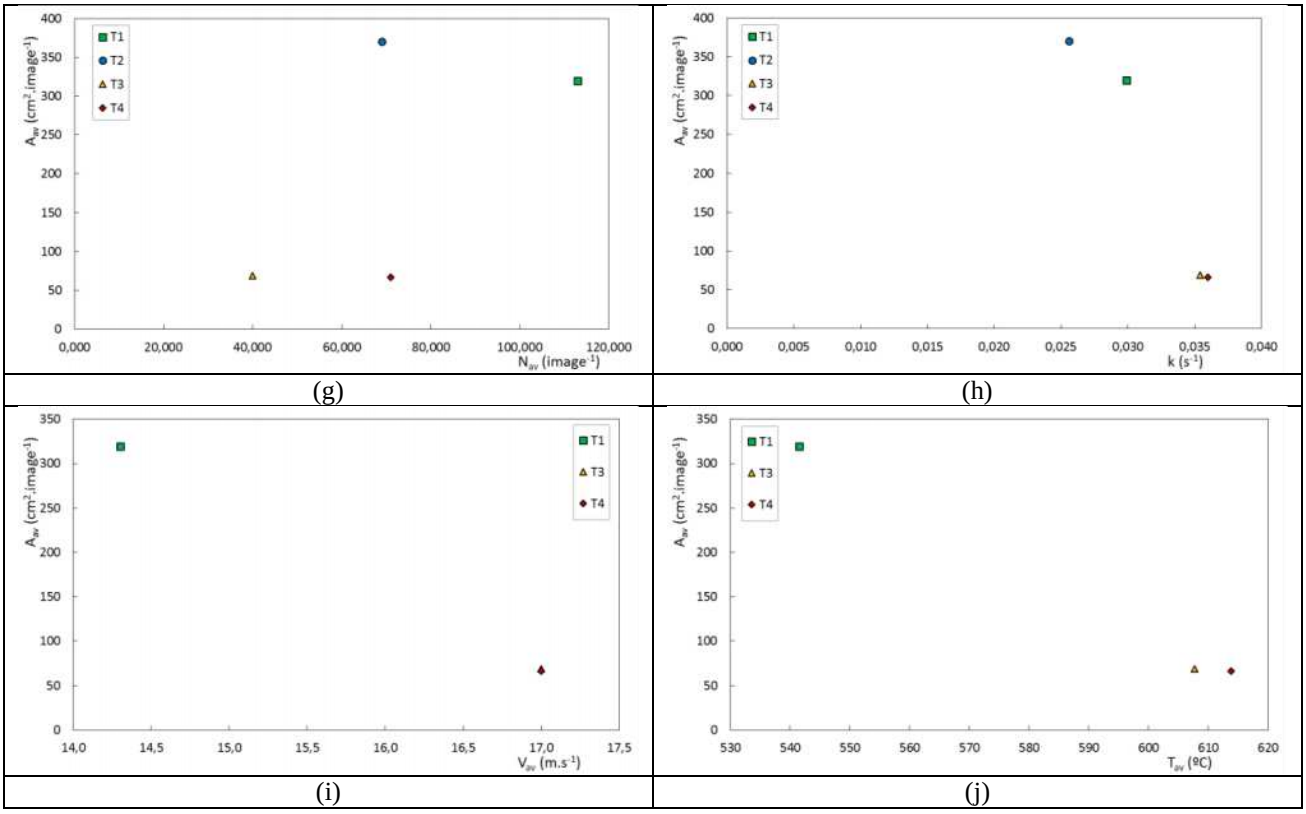

Figure 10. Relation between the parameters determined: (a) k vs V_{av}, b) k vs T_{av}, A_{av} vs k, (c) V_{av} vs T_{av}, (d) N_{av} vs k, (e) N_{av} vs V_{av}, (f) N_{av} vs T_{av}, g) A_{av} vs N_{av}, h) A_{av} vs k, (i) A_{av} vs V_{av}, and (j) A_{av} vs T_{av}.

Conclusions

Four burning tests were carried out in order to analyse the release of firebrands. Three of these tests burned shrubs and eucalyptus barks in different circumstances: 1) lay down of the shrubs fuel bed, 2) suspended in vertical position and 3) suspended in horizontal position. The fourth test consists of the burning of a singles fuel bed of shrubs.

The number and projected area of firebrands released, the weight loss decay, the temperature and the up flow velocity were determined. It was observed that burning shrubs with no barks (*T1*) working as obstacles produce many small particles below 100mm^2 (around 77%) and particles larger than 1000m^2 (around 19%). Test *T2* produced mainly particles larger than 1000m^2 (around 41%) as the less intense burning did not destroy the firebrands. Tests *T3* and *T4* produced mostly particles below 500mm^2 (89% and 97% respectively). Tests *T3* and *T4* were the tests with larger intensity and test *T2* was that with lower value of *k* due to the muffling that the layer of barks produce in the shrubs fuel bed. There was not a clear difference between the results of *T3* and *T4* with different orientation of the barks. The values of *T*, *V* and *k* for both tests were very similar as well as the total project area of the firebrands. The distribution of the particles released was slightly different with *T3* releasing more particles larger than 1000m^2 and *T4* producing more particles in the range [100; 500[mm^2. Maybe the more narrow net of the barks in the horizontal position is a more effective obstacle to the larger particles. However, the larger particle released during the four tests was observed in T4 with 2852mm^2. These particles have potential to produce spot fires at short distance. We believe that induced wind during the burning would lead to the release of larger firebrands with capacity to produce spot fires at superior distances. The number and area of the firebrands released was analysed using one single PIV camera. This limitation may sometimes lead to a number of firebrands released inferior to the real number as some particles may be hidden behind one another. We do not consider this error as very relevant as it is

would not be very frequent and eventual errors would be proportional to all the tests. The use of a second PIV camera capturing images in a perpendicular axis would avoid this fault and additionally would allow the determination of the velocity of firebrands which is much more accurate in a 3D analysis. The determination of the 3D shape of the firebrands would be possible with a second camera as well.

As future work we intend to extend the tests in number and carried out them for other scenarios with other fuels, introducing the induced wind as an additional parameter. The inclusion of a second PIV camera in order to avoid limitations and to analyse the velocity of firebrands is also foreseen.

List of acronyms

A [cm^2 or mm^2]	Projected area of the particles released captured by the PIV system
A_{av} [cm^2 or mm^2]	Average projected area of the particles released captured by the PIV system
ADAI	Associação para o Desenvolvimento da Aerodinâmica Industrial
DB	Dry basis
FMC [%]	Fuel moisture content
H [cm]	Tree height
K [s^{-1}]	weight loss decay coefficient
$\dot{m}$	Relative weight loss decay
m_t [mg]	Mass at the instant *t*
m_0 [mg]	Initial value of mass
N	Number of particles released captured by the PIV system
N_{av}	Number of particles released captured by the PIV system
PIV	Particle image velocimetry
r^2	Correlation coefficient
RH [%]	Relative humidity
t [s]	Elapsed time
T [ºC]	Temperature
T_{av} [ºC]	Average temperature
V [$m.s^{-1}$]	Flow velocity
V_{av} [$m.s^{-1}$]	Average flow velocity
∅ [cm]	Tree canopy diameter
ΔH [cm]	Distance from the surface fuel to the tree canopy base

References

Manzello SL, Maranghides A and Mell WE (2007) Firebrand generation from burning vegetation. International Journal of Wildland Fire, 2007, 16, 458–462.

Morandini F, Silvani X and Susset A (2012) Feasibility of particle image velocimetry in vegetative fire spread experiments. Experiments in Fluids, Volume 53, Issue 1, pp 237-244. DOI: 10.1007/s00348-012-1285-5.

Horváth I, Beeck J and Waterloo C (2012) Large-Scale Particle Image Velocimetry on a Full-Scale Pool Fire. 16th Int Symp on Applications of Laser Techniques to Fluid Mechanics Lisbon, Portugal, 09-12 July, 2012

Hosseini S, Li Q, Cocker D, Weise D, Miller A, Shrivastava M, Miller JW, Mahalingam S, Princevac M and Jung H (2010) Particle size distributions from laboratory-scale biomass fires using fast response instruments. Atmos. Chem. Phys., 10, 8065–8076, 2010 www.atmos-chem-phys.net/10/8065/2010/ doi:10.5194/acp-10-8065-2010

McArthur, A. G. 1967. Fire behaviour in eucalypt forests. Comm. of Australia For. & Timber Bur. Leaflet No. 107

Ellis PF (2000) The aerodynamic and combustion characteristics of eucalypt bark—a firebrand study. Ph.D. Dissertation, Australian National University, Canberra.

Viegas DX, Almeida M, Raposo J, Oliveira R and Viegas CX (2012) Ignition of Mediterranean Fuel Beds by Several Types of Firebrands. Fire Technology. 2012 Springer Science + Business Media, LLC. DOI: 10.1007/s10694-012-0267-8.

Albini FA (1979) Spot fire distance from burning trees—a predictive model. USDA Forest Service, Research Paper INT-56, Intermountain Forest and Range Experiment Station 16.

Albini FA (1981) Spot fire distance from isolated sources—extensions of a predictive model. USDA Forest Service, Research Note INT-309, Intermountain Forest and Range Experiment Station 17.

Albini FA (1983a) Potential spotting distance from wind—driven surface fires. USDA Forest Service, Research Paper INT-309, Intermountain Forest and Range Experiment Station 18.

Albini FA (1983b) Transport of firebrands by line thermals. Combust Science Technology 32:277–288 19.

Sardoy N, Consalvi J, Porterie B, Fernandez-Pello A (2007) Modelling transport and combustion of firebrands from burning trees. Combust Flame 150:151–169.

Almeida M, Viegas DX, Miranda AI, Reva V (2011) Effect of particle orientation and of flow velocity on the combustibility of *Pinus Pinaster* Ait. and *Eucalyptus Globulus* Labill. firebrand material. International Journal of Wildland Fire 20(8):946–962.

Almeida M, Viegas DX, Miranda AI, Viegas C, Leitão N (2010) Aerodynamic Characteristics of Some Potential Embers. In: DX Viegas (ed) 6th international conference on forest fire research, Coimbra, Portugal, (CD-ROM). Associação para o Desenvolvimento da Aerodinâmica Industrial (ADAI), Coimbra, Portugal, 15–18 November 2010.

Analysis of fire spread across a two-dimensional ridge under wind conditions

Jorge Raposo[a]; Salvatore Cabiddu[b]; Domingos X. Viegas[a]; Michele Salis[c,d]; Jason Sharples[e]

[a] *ADAI/CEIF, University of Coimbra, Rua Luís Reis dos Santos, Coimbra 3030-788, Portugal.* *jorge.raposo@dem.uc.pt*
[b] *Sardinia Forest Service (CFVA), Italy;*
[c] *University of Sassari, Department of Science for Nature and Environmental Resources (DIPNET), Italy;*
[d] *Euro-Mediterranean Center on Climate Changes (CMCC), IAFENT Division of Sassari, Italy;*
[e] *University of New South Wales, Australia*

Abstract
Laboratory scale investigation of a fire spreading on the windward face of a triangular section hill of variable shape with wind perpendicular to the ridgeline was performed. The work confirmed previous observations that the fire enlarges its lateral spread after reaching the ridgeline entering the leeward face with a much wider front. Reference fire spread velocities were measured and analyzed putting in evidence the importance of the dynamic effect due to flow velocity and its associated horizontal axis separation vortex strength without great dependence on hill geometry. A similar analysis performed to some real fires confirmed the same trend as was observed in the laboratory scale.

Keywords*: fire channeling; lateral fire spread; horizontal vortices*

Introduction

Predicting fire spread and behavior is one of the main challenges in forest fire research. It is widely recognized that wind, topography and fuels are the dominant factors affecting forest fire spread (Viegas 2004). The joint interactions among environmental factors and fire front influence fire propagation in various ways, particularly in areas with complex topography. In such conditions, many fatal accidents have been reported by a number of studies in different areas of the world. In fact, the interaction between wind, topography and fire front may lead to unusual patterns of fire spread that may surprise fire managers. An example of such a pattern occurs when a fire spreads across a two dimensional hill with wind blowing nearly perpendicular to the ridgeline. Pyrogenic vorticity, which manifests on the lee side of the ridge, produces a lateral enlargement of the fire that will then spread with a much wider front on that face of the hill and from then on (Simpson *et al*. 2013). This problem was first identified by McRae (2004) and it was analyzed by Sharples *et al*. (2011) and Sharples *et al*. (2012). A laboratory scale experimental research on this problem was carried out by the present authors for the case of a fire spreading upslope on the leeward face of the hill (Sharples *et al*. 2011). The interaction of the fire's plume with ambient horizontal vorticity near the top of this slope produced a lateral spread of the fire when it reached the ridgeline. This effect was confirmed in the numerical study presented by Simpson *et al.* (2013). In the above case the fire did not spread on the windward face and therefore this is possibly not the most interesting case to be analyzed.
In this paper the case of a fire spreading on the windward face of a two dimensional hill and its lateral spread at the ridgeline is analyzed. Laboratory scale experiments were performed in the large Combustion Tunnel of the University of Coimbra for various sets of hill configurations and flow velocities. Particular attention was given to the analysis of the lateral spread of the fire, and two models are proposed to estimate the relative growth rate of fire on both sides of the hill as a function of flow velocity and upslope non dimensional rate of spread. Our results put in evidence that the fire lateral growth is mainly due to the vortex flow dynamics, given its direct relationship with the dynamic

pressure of the flow. Moreover, we analyzed three case studies in which lateral fire growth in similar topographic and flow conditions were documented obtaining the same trend on the parameters variation as at laboratory scale.

Methods and Material

Physical problem

We consider a two dimensional hill with a low radius of curvature ridgeline subject to atmospheric flow with a reference velocity U that is assumed to be perpendicular to the ridgeline of the hill. We consider that the fuel bed is homogeneous and has uniform properties in the entire area of interest. In the present analysis we exclude crown fire spread and spot fire occurrence. The windward face (face *A* in Figure 1*a*) has an average inclination angle α_1 and the leeward face (face *B* in Figure 1*b*) has an average inclination angle α_2.

The wind flow will develop along face *A* as a turbulent boundary layer with increasing velocity from the bottom to its top. At the ridge of the hill, depending on the radius of curvature, the Reynolds number of the flow and its turbulence intensity, the flow may separate forming a horizontal axis vortex and reattaching downslope in face *B*. The shape and extension of this separation zone is very much dependent on the incident flow properties and on hill geometry. If the radius of curvature of the ridge is very small, we are in the presence of a sharp ridge like in the case of a bluff body. In this configuration flow separation will certainly occur, because theoretically the flow velocity at the edge of a convex dihedral is equal to infinity, regardless of the Reynolds number. In nature these situations are not uncommon, so we took into consideration this condition in order to avoid dependence on flow Reynolds number and consequently on scale effects.

The complex flow produced around two dimensional hills immersed in a turbulent boundary layer has been studied by Ferreira (1995), among others. Even in the relatively simple cases of sinusoidal or triangular cross sections, the flow topology in the absence of fire is not simple and there is not a uniquely defined reference velocity to characterize this flow. In numerical or experimental studies in which the imposed flow is either uniform or has a well-defined boundary layer profile it is relatively easy to define a characteristic flow or wind velocity, but this is not the case in full scale situations for which other parameters may be required to characterize the flow (cf. Viegas and Neto, 1991).

With reference to Figure 1*a*, we assume that there is a fire starting at a point O_1 in face *A* and spreading upslope along this face, with favorable wind until it reaches the ridgeline. In the limit this fire may have started before, but in that case it is assumed that it reaches this face with a relatively narrow fire front. It is observed that when the fire reaches the ridge and starts to descend face *B* it begins to spread laterally, with a rate that is much larger than the one it had on the windward face. This process has been observed in several real fires and is corroborated by numerical simulations and laboratory experiments like the present ones. Simpson *et al.* (2013) demonstrated that the lateral spread results from the interaction between the fire's plume and the horizontal vorticity due to flow separation near the top of the ridge. This interaction generates vertical vorticity on the fire's flanks, which in turn generates a lateral flow in the immediate lee face of the ridge. For this reason this phenomenon is appropriately designated by Simpson *et al.* (2013) as "Vorticity-driven Lateral Spread (VLS)".

The analysis of the enhanced lateral spread of the fire on both sides of the hill is the main purpose of this study.

Test configuration

In the present study we consider a two dimensional hill of triangular cross section, meaning that both faces *A* and *B* are plane surfaces. The inclination angles are α_1 and α_2 respectively for the windward face *A* and for the leeward face *B* (Figure 1*a*). The two faces intersect as a sharp ridge line. A reference Cartesian system is defined in the following way. The axis *OX* is parallel to the horizontal direction

and has its origin at the edge of the plane surface on which the hill is based; *OZ* axis is vertical and *OY* axis is also horizontal and parallel to the ridgeline of the hill.
Wind with a reference velocity *U* flows perpendicular to the ridgeline and in these conditions a vertical plane containing the *OX* axis is a plane of symmetry of the fire. The oncoming flow velocity may vary with *z* but not with *y*. We assume that a point source fire is ignited at point O_1 at a distance *a=50cm* from the base of the hill in the windward face. We define (cf. Figure 1*b*) the following distances travelled by the fire during its spread:
s_{1A} is the distance from the fire origin to the head of the fire along axis O_{S1} that is a symmetry line on face *A*;
s_{2A} is the distance from the fire origin O_1 to the back fire along the same axis but measured in the downslope direction (it is considered as a positive quantity);
s_{3AR} is the distance measured from the O_{S1} axis to the right flank of the fire on face *A*, measured along O_{S3A} axis that is an horizontal axis placed at a distance *b=20cm* from the ridgeline;
s_{3AL} is a similar distance measured to the left flank of the fire line;
s_{1B} is the distance from the ridgeline to the head of the fire along axis O_{S1A} that is a symmetry line on face *B* (with descending fire);
s_{3BR} is the distance measured from the O_{S1B} axis to the right flank of the fire on face *B*, measured along O_{S3A} axis that is an horizontal axis placed at a distance *c=10cm* from the ridgeline;
s_{3BL} is a similar distance measured to the left flank of the fire line;
We define the average value of the rate of spread along each one of the seven directions that were defined above as the slope of a linear fit of the function $s_i(t)$. This simplification is only acceptable if there are no consistent variations of the rate of spread (ROS) and it implies that the fire is spreading in a quasi-steady state, which may not be valid in all cases (cf. Viegas 2004).
Given the symmetry of the fire, we assume that $s_{3AR} = s_{3AL}$ and $s_{3BR} = s_{3BL}$. Therefore we only need to consider five relevant ROS to characterize the problem. The fire will spread upslope with a ROS R_{1A}, downslope with a ROS R_{2A} and laterally with a ROS R_{3A} (cf. figure 1b)). After reaching the ridgeline, the fire will spread downslope on face *B* with a ROS R_{1B}, and laterally with a ROS R_{3B}.
In order to minimize the effect of small variations of fuel bed properties, namely moisture content, following Viegas and Neto (1991) we use the non-dimensional ROS (NDROS) values given by:

$$R' = \frac{R}{R_o} \qquad [1]$$

In the present analysis we shall use the following five NDROS to characterize the spread of the fire along its main directions.

Upslope NDROS in face A: $$R'_{1A} = \frac{R_{1A}}{R_0} \qquad [2]$$

Downslope NDROS in face A: $$R'_{2A} = \frac{R_{2A}}{R_0} \qquad [3]$$

Lateral NDROS in face A: $$R'_{3A} = \frac{R_{3A}}{R_0} \qquad [4]$$

Downslope NDROS in face B: $$R'_{1B} = \frac{R_{1B}}{R_0} \qquad [5]$$

Lateral NDROS in face B: $$R'_{3B} = \frac{R_{3B}}{R_0} \qquad [6]$$

Given the importance of comparing the relative growth of lateral fire spread in faces *A* and *B* we shall use also the following non-dimensional parameter:

$$k_3 = \frac{R_{3B}}{R_{3A}} \qquad [7]$$

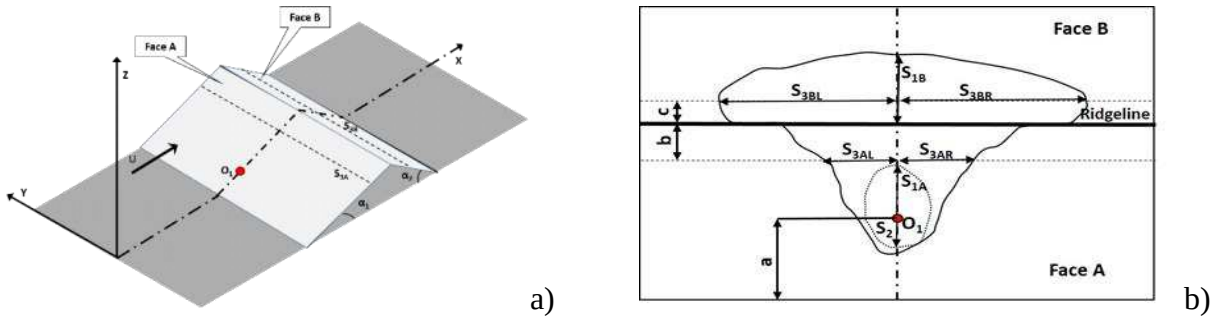

Figure 1. (a) Schematic representation of the fire; (b) Detail of the fire spread analysis.

Experimental Study

The experimental study was performed at the Combustion Tunnel TC 3 of the Fire Research Laboratory of the University of Coimbra in Lousã (Portugal). The Tunnel has a working section of $6\times8m^2$ and a maximum flow velocity of 7m s^{-1} (figure 2). A model of the two dimensional hill composed of two metallic plates hinged at the ridge line was used in the experiments. The width of the model is 4m, and the length of faces *A* and *B* are 1.5m and 1.0m respectively. The fuel bed for the experiments was composed by dry particles of straw with a constant load of 0.6kg m^{-2} (dry basis). Moisture content of the fuel was measured for each test or groups of tests with an A&D ML50 Moisture Analyzer. A reference test to measure the basic ROS R_o in no slope and no wind conditions was made in each test session. The corresponding values are given in Table 1.

The configuration of the model in each series of tests was adjusted fixing the value of α_1 of face *A*. Given the model construction, the slope α_2 of face *B* depended on α_1. Three values of α_1 were used in the present tests: 20º, 25º and 30º. The resulting values of α_2 were respectively close to: 30º, 40º and 50º. For each hill configuration five tests were performed with values of *U* equal to: 0, 1, 2, 3 and 4m s^{-1}. The values of α_1 and α_2 and flow velocity used in each test are reported in Table 1.

Figure 2. General view of the Combustion Wind Tunnel of the Forest Fire Research Laboratory of the University of Coimbra.

A point fire was ignited at point O_1 (Figure 1*a* and 1*b*), 0.5m above the base of face *A* (*a*=0.5m) and then the flow was turned on for the pre-adjusted velocity. Two video cameras, one IR camera and several digital photo cameras were used to record fire spread on each face of the hill. The images obtained were processed using a software developed by the ADAI team to analyze fire evolution and determine ROS values along relevant directions. Though in some cases the fire spread was not steady (cf. Viegas, 2006), we assumed that the ROS was constant along each spread direction (s_i) that was

considered, and therefore the corresponding average value of ROS was estimated as the slope of a straight line fitted to the plot of (s_i, t) using between four and ten data points. Lateral ROS R_{3A} was measured along a horizontal line 0.3m from the ridgeline, and R_{3B} was measured on face *B* along a horizontal line 0.1m from the ridgeline. Although the test configuration was nominally symmetrical, in order to assess this condition the lateral spread was measured separately for both sides (right and left) in each face: R_{3AR} and R_{3AL}, for face *A* and R_{3BR} and R_{3BL} for face *B*. As good symmetry conditions were found in the performed experiments the values of R_{3A} and R_{3B} given in Table 1 and that are used in subsequent analysis are the average of both left and right side estimates.

Table 1. Parameters of Tests performed in the present study

Ref.	α_1 (º)	α_2 (º)	U (m s^{-1})	m_f (%)	R_o (cm s^{-1})	R_{1A} (cm s^{-1})	R_{1B} (cm s^{-1})	R_2 (cm s^{-1})	R_{3A} (cm s^{-1})	R_{3B} (cm s^{-1})
VH 01			2	13.6	0.73	4.75	0.81	0.77	1.12	3.15
VH 02			3	15.5	0.69	4.87	1.09	-	1.49	4.38
VH 03	25	40	4	12.5	1.09	7.88	1.81	0.18	1.04	6.79
VH 04			1	12.5	1.09	5.79	0.81	0.69	3.40	2.27
VH 05			0	13.1	0.84	1.40	0.34	0.63	1.58	0.82
VH 06			2	13.1	0.84	3.74	1.29	0.68	1.52	2.59
VH 07			3	9	0.73	10.35	1.18	0.31	2.36	4.29
VH 08	30	50	0	9	0.73	2.10	0.96	0.59	1.55	1.59
VH 09			1	14.8	1.00	2.11	0.63	0.79	1.07	1.35
VH 10			4	14.8	1.00	7.38	2.84	0.55	1.83	9.63
VH 11			2	14.8	1.00	9.90	1.09	0.33	1.59	3.60
VH 12			3	10.1	0.92	8.18	1.65	0.45	1.59	4.40
VH 13	20	30	1	10.0	0.92	2.66	0.69	0.31	1.62	1.76
VH 14			0	10.0	0.92	1.45	0.76	0.79	1.39	1.55
VH 15			4	10.0	0.92	9.85	3.63	0.53	1.94	8.71

Case Studies

In order to assess the validity of present results obtained at laboratory scale we used data from some real fires in which lateral fire growth most probably due to channeling or horizontal axis formation on the lee side of a ridge have been observed. Some of them were already mentioned and described by Sharples *et al.* (2012).

4.1. Fire of Broken Cart

During the large fires that affected the city of Canberra (Australia) on 18th January 2003, various cases of VLS were observed (McRae 2004). Among these cases we selected the event of the Broken Cart Fire that is described by McRae (2004).

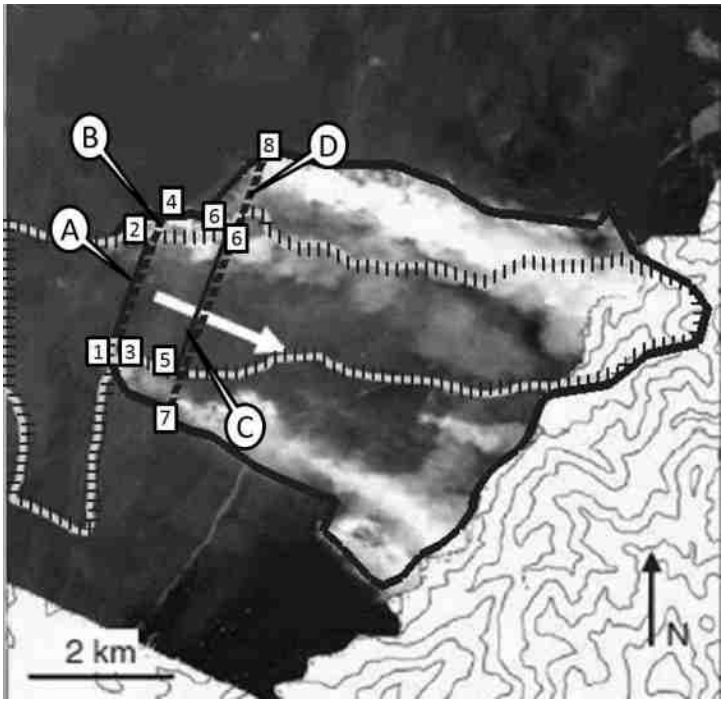

Figure 3. Schematic view of Broken Cart Fire (adapted from Sharples et al. (2012)).

In Figure 3 the white line with black dashes corresponds to 14:00 hours and the black bold line represents the fire at 15:09. The white bold arrow indicates the main spread direction due to the synoptic wind. Line A that is limited by points 1 and 2 represents the width of the main fire front before crossing the ridge at 14:00. Line B located between points 3 and 4, plotted with dashed bold line refers to the width perpendicular to the main spread direction before the ridge crossing at 15:09. The difference between the lengths of segments A and B divided by the time lapse gives the rate of enlargement of the fire front perpendicular to the main spread direction here designated as R_{3A}.
The measurements made after the fire crossed the ridge correspond to line C delimited by points 5 and 6 at 14:00 and line D between points 7 and 8 at 15:09. The rate of enlargement of the fire front after crossing the ridge that results from the analyses of these two lines corresponds to R_{3B}. The coefficient that gives the ratio of enlargement between side A (before the ridgeline) and side B (after crossing the ridgeline) is designated as k_3. The corresponding values are given in Table 2.

Table 2. Parameters of Case Studies analyzed in the present study

Case	R_o ($m\ s^{-1}$)	R_{1A} ($m\ s^{-1}$)	R_{3A} ($m\ s^{-1}$)	R_{3B} ($m\ s^{-1}$)	U ($m\ s^{-1}$)	R'_{1A} -	k_3 -
Broken Cart	0.06	0.69	0.12	0.42	9	11.60	3.59
Sa Costa	0.15	0.43	0.39	0.64	4	2.87	1.64
Golfo Aranci	0.06	0.54	0.18	0.68	10	9.69	5.70

4.2. Fire of Sa Costa

An interesting case study involving the fire spread process that is being analyzed occurred in Sardinia (Italy) on the 5th and 6th August 2010. This fire was reported in Cabiddu *et al.* 2010, and a brief description is presented here.
This fire is designated as Sa Costa and it occurred near the village of Jerzu, in the Province of Ogliastra, Eastern Sardinia.

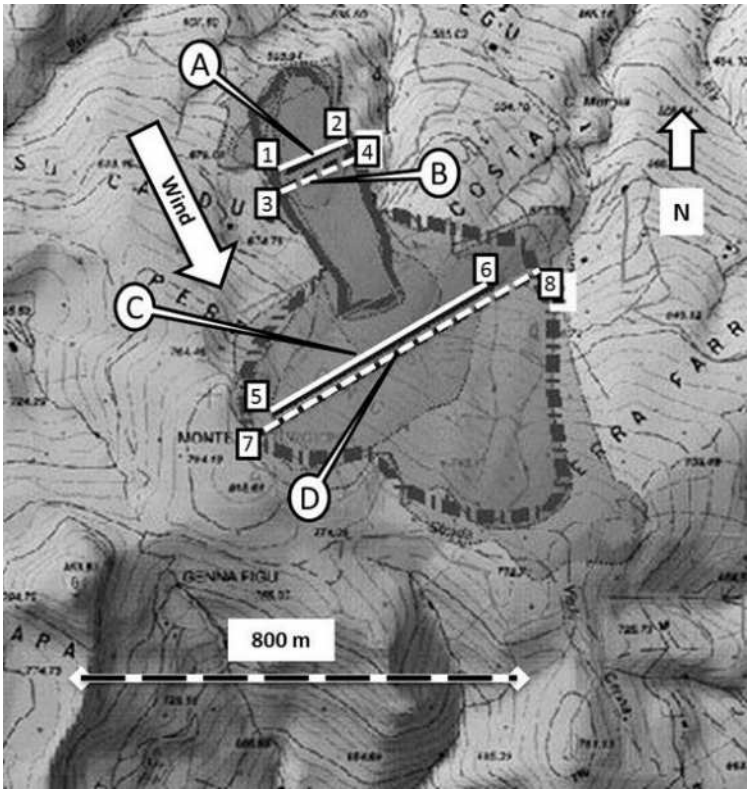

Figure 4. Spread of Sa Costa fire, in Eastern Sardinia, on the 5th of August of 2010.

In Figure 4 the analysis performed with the plots of the fire perimeter at different times are shown. The blue bold line corresponds to 17:05 and the dashed bold line represents the fire perimeter at 17:40. The wind direction was 320-330°.
The line A, plotted in bold white that is limited by points 1 and 2, represents the width of the main fire front before crossing the ridge at 17:05. Line B, located between points 3 and 4, refers to the width perpendicular to the main spread direction before the ridge crossing at 17:40. The difference between the lengths of the segments A and B divided by the lapse of time gives the rate of enlargement of the fire front perpendicular to the main spread direction here designated as R_{3A}.

4.3. Fire of Golfo Aranci

The fire of Golfo Aranci occurred in Northeast Sardinia (Italy) , near the town of Olbia, on the 24th June of 2013. The fire started at 14:43, the wind direction and intensity was practically constant and wind velocity decreased from 40 to 30 km h^{-1} over the duration of the fire.
When the fire reached a ridge with NNW-SSE direction, almost perpendicular to the wind direction, it spread laterally along the lee side of the ridge as it is shown in figure 5. Using the isochrones of fire spread that were provided by the *Sardinia Forest Service*, we estimated the relevant ROS values that are indicated in Table 2.

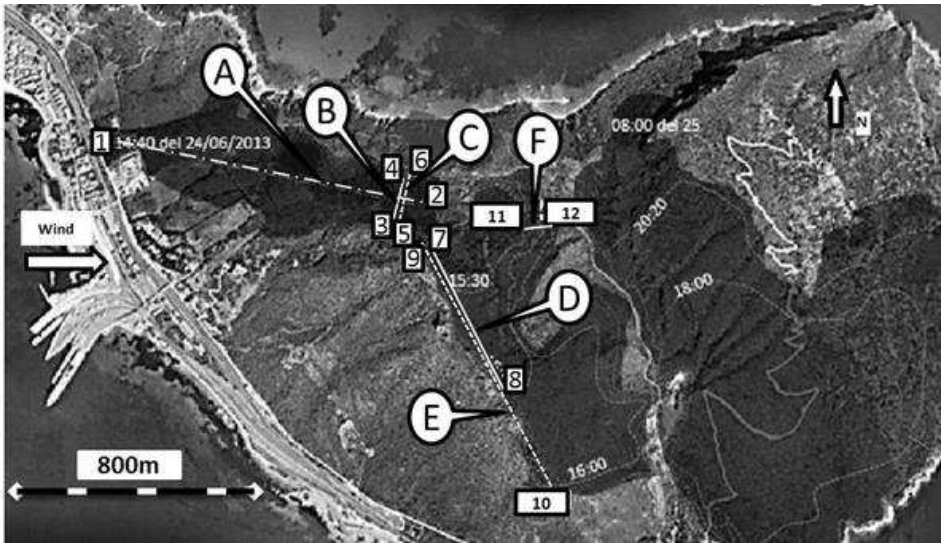

Figure 5. Spread of fire of Golfo Aranci in Sardinia, on the 24th June 2013.

By the analyses of the isochrones represented by the white lines and consequently of the fire perimeters defined at 14:40, 15:30 and 16:00 the rate of spread of the main fire front in side A, that is designated as R_{1A} was estimated. This calculation was based on the measurement of the length of line A located between points 1 and 2. The rate of enlargement of the fire front in side A, R_{3A}, corresponds to the difference of lengths of the segments B and C divided by the lapse of time. Line B is defined between the points 3 and 4, and line C is defined by points 5 and 6.
The rate of enlargement in side B, R_{3B} was estimated by the analysis of the relative growth of line E in relation to line D in the lapse of the time. Line D is limited by the boundary points 7 and 8 and line E is defined by points 9 and 10.
Finally line F, defined by points 11 and 12 and corresponding to a downslope fire spread, was used to estimate the basic rate of spread for this fuel bed in the absence of slope and wind.

Results and Discussion

5.1. Fire Contours

The analysis of the fire contours obtained in each laboratorial test and the respective shapes for the 15 tests performed are presented in figures 6, 7 and 8. In these figures face *A* is below and face *B* is above. The values in the axis correspond to the actual dimensions of the hill model in meter. The ridgeline corresponds to the dotted horizontal line at 1.5m from the bottom. The wind is blowing from the bottom to the up of the figure.

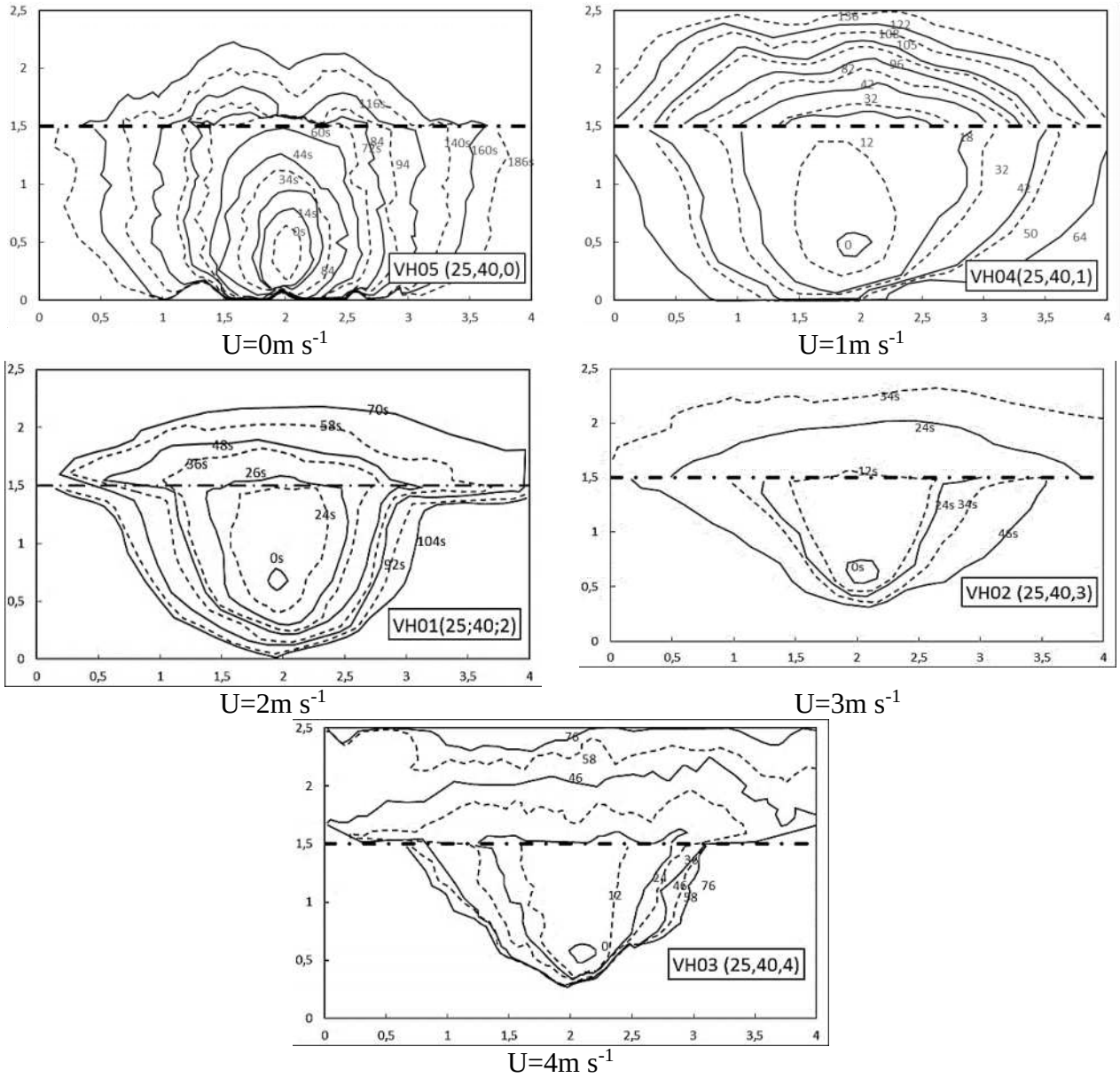

Figure 6. Fire line contours for tests with α_1=25º and α_2=40º for the indicated values of wind velocity.

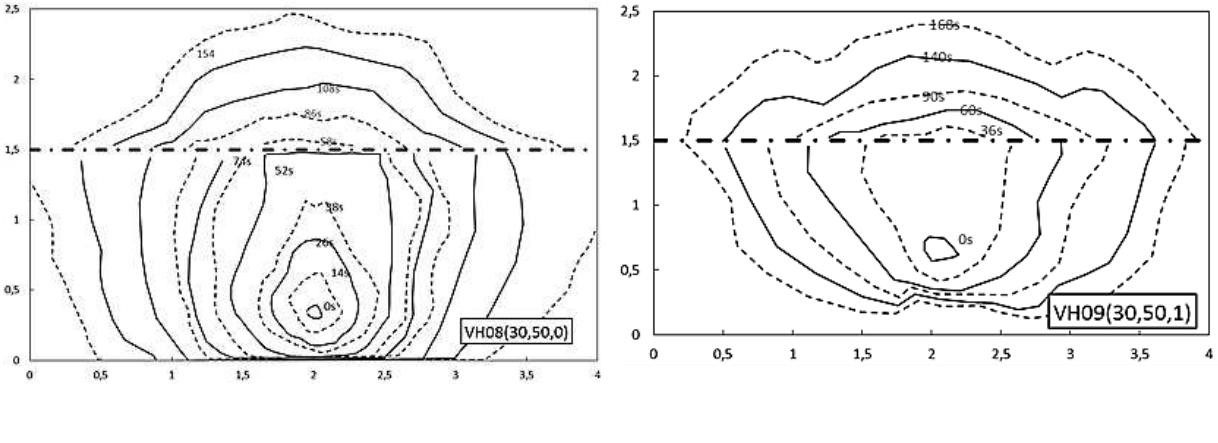

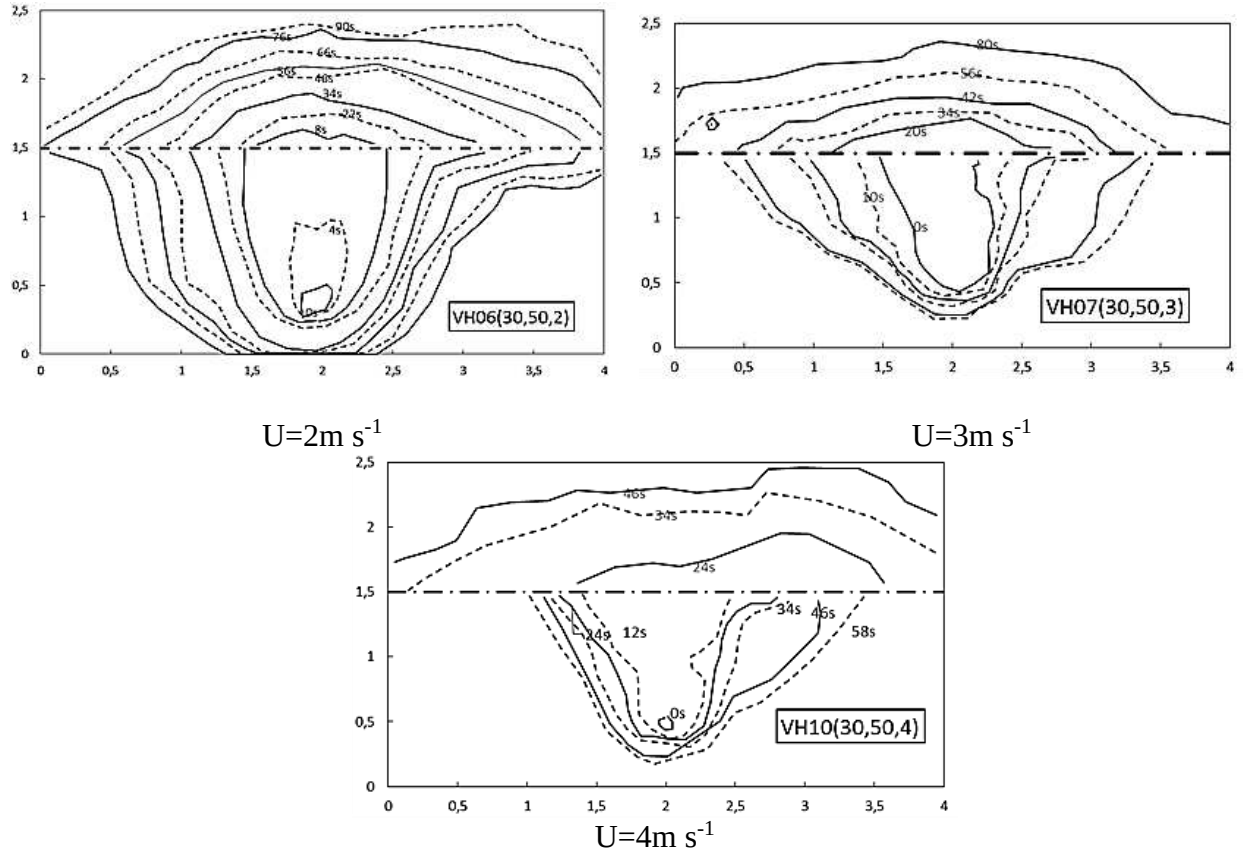

Figure 7. Fire line contour for tests with α_1=30° and α_2=50° for the indicated values of wind velocity

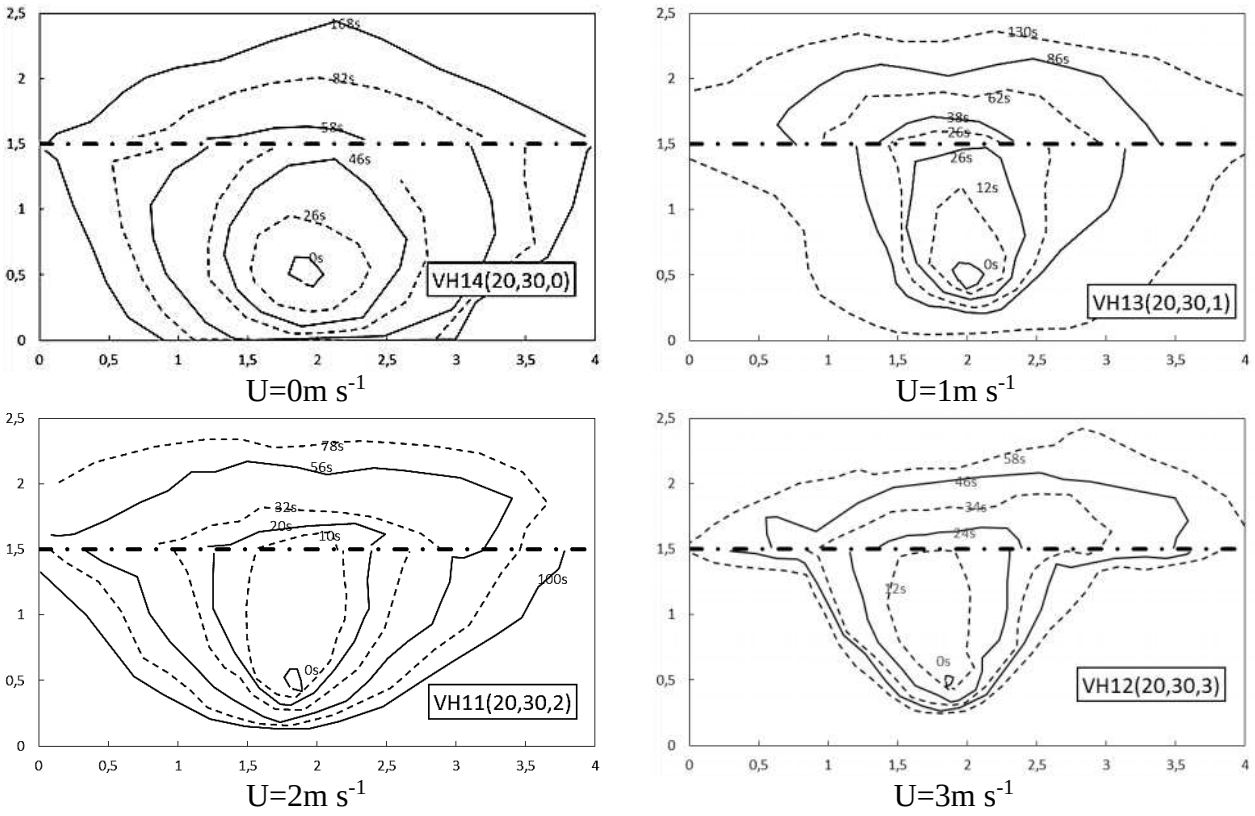

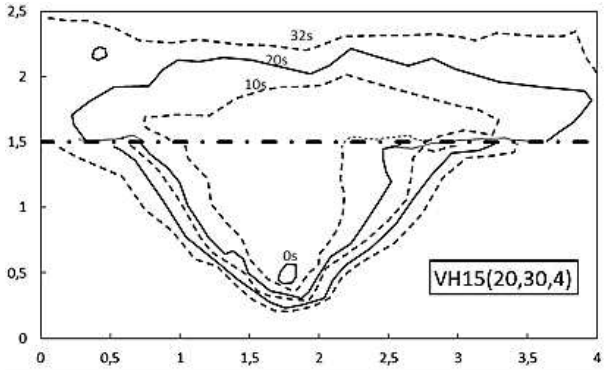

Figure 8. Fire line contour for tests with α_1=20º and α_2=30º for the indicated values of wind velocity

5.2. Rate of spread along wind direction

In Figure 9 the values of R'_{1A} show an increase approximately with the square of the reference flow velocity, but the dependence with slope angle α_1 is not clear. The data points corresponding to the real fires follow the same trend but with a different value of the reference wind velocity.

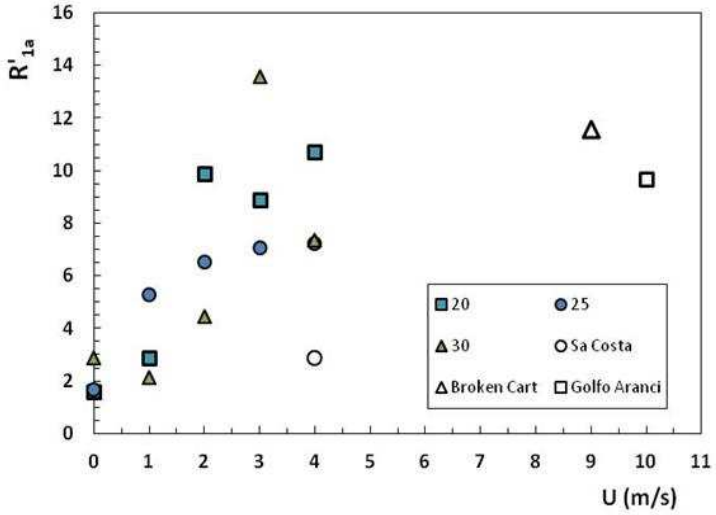

Figure 9. Evolution of **R'**$_{1A}$ *as a function of wind velocity for the three configurations tested and for Sa Costa, Broken Cart and Golfo Aranci Fires.*

As could be expected, the values of R'_2, shown in Figure 10, corresponding to the tail of the fire spreading downslope and with contrary wind, are quite low. These values are usually lower than 1.0 and tend to decrease with increasing wind velocity. In some cases it was observed that the fire would extinguish and fire spread ceased.

The values of R'_{1B}, corresponding to the average NDROS of the fire front descending the slope on face *B* with favorable wind, which are shown in Figure 11, show a practically linear increase with wind velocity with no marked dependence on the hill geometry.

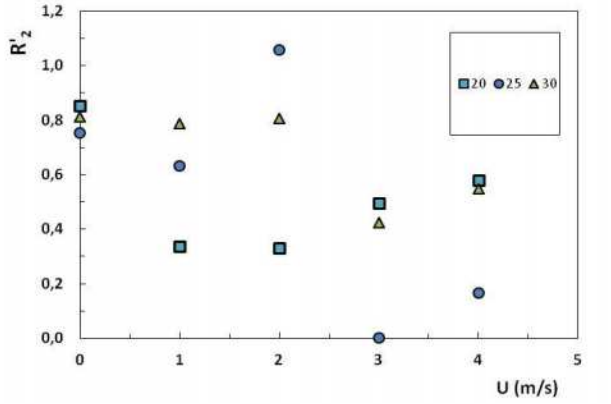

Figure 10. Evolution of **R'**$_2$ *as a function of wind velocity for the three configurations tested*

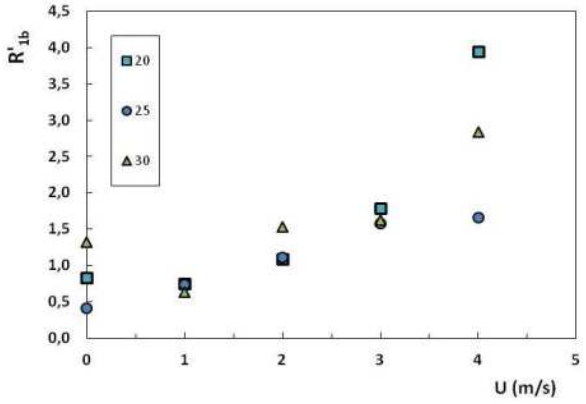

Figure 11. Evolution of **R'**$_{1B}$ *as a function of wind velocity for the three configurations tested*

5.3. Lateral Rate of spread

The analysis of lateral fire spread is of great interest in the context of the present work. In Figure 12 and 13 we show the results obtained for R'_{3A} and R'_{3B} respectively. As can be seen in Figure 10, the average rate of lateral growth of the fire on face *A* is relatively small and does not seem to depend very much either on the slope angle α_1 or on the flow velocity. The corresponding value of 2.6 for the Sa Costa Fire is within the range of our laboratory experiments.

The lateral growth of the fire in face *B* is performed with a NDROS R'_{3B} that is usually larger than R'_{3A} and shows a marked increase with flow velocity, with no clear dependency on hill geometry. The value of 4.26 for Sa Costa fire is slightly above our trend and seems to correspond to a slightly higher value of the reference wind velocity, possibly closer to 2.5ms^{-1}.

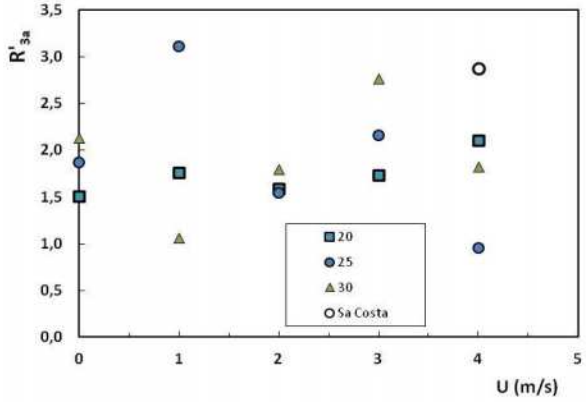

Figure 12. Evolution of **R'**$_{3A}$ *as a function of wind velocity for the three configurations tested. The point corresponding to Sa Costa fire is shown in the figure.*

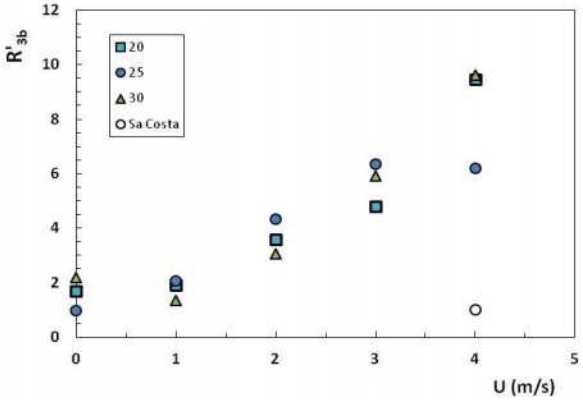

Figure 13. Evolution of **R'**$_{3B}$ *as a function of wind velocity for the three configurations tested. The point corresponding to Sa Costa fire is shown in the figure.*

5.4. Evolution of lateral fire growth ratio k$_3$

Parameter k_3, introduced in equation [7] provides a comparison between the rates of lateral growth of the fire in the windward and leeward faces of the hill (faces *A* and *B* respectively).

The evolution of k_3 as a function of wind velocity is shown in Figure 14. As can be seen, k_3 values increase with the square of *U* and exhibit only a small dependence on the hill geometry in the present set of test conditions. The values of k_3 obtained for the real fires are shown in Figure 14 as well. A good model to estimate k_3 as a function of *U* is obtained with the following equation:

$$k_3 = 1 + a_3.U^2 \qquad [8]$$

The values of coefficient a_3 and of the corresponding r^2 fitness parameter for each configuration and for the entire set of laboratory data, excluding two cases for which $k_3<1$, are given in Table 3. The value of a_3=0.041 obtained for the field cases is much lower than the average value obtained for laboratory experiments (a_3=0.256). This difference can be explained by the already mentioned difficulty in defining a reference velocity for tests in combustion tunnels and for field cases. The ratio between the values of a_3 for laboratory and field cases indicates that the field reference velocity is approximately 2.5 times larger than the combustion tunnel velocity. Assuming that the velocity profile near the ground is logarithmic, this is equivalent to considering that the wind tunnel velocity is measured at the height of 1.5m while the field reference wind velocity is measured at 10m height.

Table 3. Parameters of Model to estimate k_3 as a function of flow velocity

Case	a_3	r^2
α_1=20º; α_2=30º	0.217	0.972
α_1=25º; α_2=40º	0.321	0.850
α_1=30º; α_2=50º	0.230	0.894
All Laboratory Tests	0.256	0.859
Field cases	0.041	0.892

In our opinion, the result expressed by this model is quite relevant as it indicates that the relative rate of growth of lateral fire depends on the dynamic pressure that is proportional to the kinetic energy of the incident flow. This fact puts in evidence that the lateral growth of the fire is a consequence of the flow on the lee side of the ridge which is comprised of horizontal axis vorticity caused by flow separation at the ridge. Without disregarding the effects of the combustion energy added to the flow, this result shows clearly that the lateral growth of the fire is mainly a result of the vortex flow dynamics.

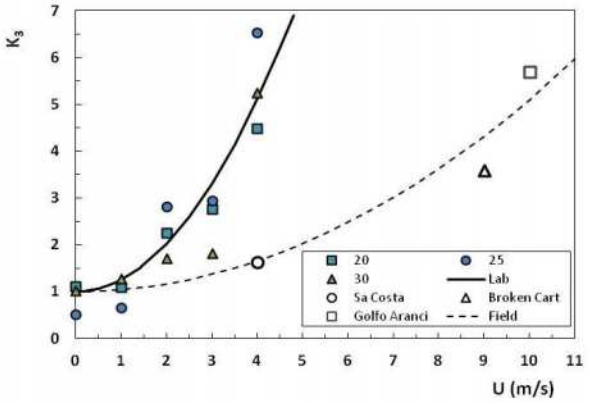

Figure 14. Evolution of k_3 as a function flow velocity for laboratory tests and for the real fires. The two lines correspond to the present model for laboratory and field cases.

Conclusion

The experiments discussed above demonstrate that the interaction of a fire with wind flowing in complex terrain can give rise to dynamic mechanisms that can enlarge a fire front near the top of a crest. In addition, the main direction of fire propagation is different to the expected direction of fire spread.

The authors intend to extend this experimental program considering other hill configurations and the influence of fuelbed composition on the lateral spread parameters. The influence of wind direction in relation to the ridgeline will be analyzed as well.

7. Acknowledgements

The authors wish to thank Portuguese Science Foundation for the support given to project Extreme under contract PTDC/EME-MFE/114343/2009 and for a PhD grant under contract SFRH / BD / 85557 / 2012. The support given by the Portuguese Company *Rede Enérgetica Nacional* to purchase and equip the Combustion Tunnel is also acknowledged. The participation of Dr. Cabiddu was supported by a grant from the Sardinia Region in the context of the Master PIROS program. J.J. Sharples is supported by an Australian Research Council Discovery Indigenous Award (IN130100038). Dr. Salis is supported by the Project "Modeling approach to evaluate fire risk and mitigation planning actions".

8. Symbols

Symbol	Units	Description
α_1	-	Inclination angle of windward face *A* of the two dimensional hill
α_2	-	Inclination angle of leeward face *B* of the two dimensional hill
O	-	Origin of reference Cartesian system
O_1	-	Origin of the fire
OX	-	Horizontal axis is parallel to the horizontal direction and has its origin at the edge of the plane surface on which the hill is based
OY		Horizontal axis parallel to the ridgeline of the hill.
OZ		Vertical axis
U	$m.s^{-1}$	Reference flow velocity
R	$m.\ s^{-1}$	Rate of spread (ROS)
R_o	$cm.s^{-1}$	Basic rate of spread of linear fire in the absence of slope and wind
R_{1A}	$m.\ s^{-1}$	Rate of spread perpendicular to the ridge in the face A driven by the wind
R_{1B}	$m.\ s^{-1}$	Rate of spread perpendicular to the ridge in the face B driven by the wind
R_2	$m.\ s^{-1}$	Rate of spread perpendicular to the ridge in the face A against the wind
R_{3AR}	$m.\ s^{-1}$	Rate of enlargement of the fire front in the face A in the right direction
R_{3AL}	$m.\ s^{-1}$	Rate of enlargement of the fire front in the face A in the left direction
R_{3A}	$m.\ s^{-1}$	Average Rate of enlargement of the fire front in the face A
R_{3BR}	$m.\ s^{-1}$	Rate of enlargement of the fire front in the face B in the right direction
R_{3BL}	$m.\ s^{-1}$	Rate of enlargement of the fire front in the face B in the left direction
R_{3B}	$m.\ s^{-1}$	Average Rate of enlargement of the fire front in the face B
R'	-	Non-dimensional rate of spread (NDROS)
x	m	Distance measured along OX axis
y	m	Distance measured along OY axis
z	m	Distance measured along OZ axis
a	m	Distance from the fire origin to the base of the hill
b	m	Distance from the reference horizontal line on face A to the ridgeline
c	m	Distance from the reference horizontal line on face B to the ridgeline
s_i	m	Distance measured along reference direction i from the fire origin or from the symmetry axis of the fire to its perimeter
k_3	-	Coefficient of relative rate of fire lateral enlargement in faces B and A
a_3	$s^2 \cdot m^{-2}$	Empirical coefficient in equation (8)

9. References

Cabiddu, S., Congiu, F., Lara, G., Usai, L., and Becchia, A. (2010). "Analisi incendio boschivo. Rapporto di analisi e studio dell'incendio di Sa Costa, comune di Jerzu". Archivio CFVA Lanusei (OG), n. prot. 86, Pos. XI 2-5, 24 Settembre 2010...

Ferreira, A.D., Lopes, A.M.G., Viegas, D.X., and Sousa, A.C.M. (1995). "Experimental and numerical simulation of flow around two-dimensional hills." *Journal of Wind Engineering and Industrial Aerodynamics* **54–55**, 173–181.

McRae, R.H.D. (2004). "Breath of the dragon – observations of the January 2003 ACT Bushfires." Conference Bushfire 2004: Earth, Wind and Fire – Fusing the Elements. Adelaide: South Australian Department of Environment and Heritage: Adelaide, SA.

Sharples, J., McRae, R.H.D., and Wilkes, S.R. (2012). "Wind–terrain effects on the propagation of wildfires in rugged terrain: fire channelling." *International Journal of Wildland Fire* **21**, 282–296.

Sharples, J.J., Viegas D.X., McRae R.H.D., Raposo J.R.N., and Farinha H.A.S. (2011). "Lateral bushfire propagation driven by the interaction of wind, terrain and fire." *Proceedings of the 19th International Congress on Modelling and Simulation*, 12–16.

Simpson, C., Sharples, J., Evans, J., and McCabe M. (2013). "Large eddy simulation of atypical wildland fire spread on leeward slopes." *International Journal of Wildland Fire* **22**, 282–296

Viegas, D.X. (2006). "Parametric study of an eruptive fire behavior model." *International Journal of Wildland Fire* **15**, 169-177.

Viegas, D.X. (2004). "On the existence of a steady state regime for slope and wind driven fires." *International Journal of Wildland Fire* **13**, 101–117.

Viegas, D.X., and Neto, L.P. (1991). "Wall Shear-Stress as a Parameter to Correlate the Rate of Spread of a Wind Induced Forest Fire." *International Journal of Wildland Fire* **1**, 177-188.

Analysis of the jump fire produced by the interaction of two oblique fire fronts: Comparison between laboratory and field cases

Jorger Raposo[a]; Domingos X. Viegas[a]; Xiaodong Xie[b]; Miguel Almeida[a]. and Liu Naian [2]

[a]*ADAI/CEIF, University of Coimbra, Rua Luís Reis dos Santos, Coimbra 3030-788, Portugal. Jorge.raposo@dem.uc.pt.*
[b] *State Key Laboratory of Fire Science, University of Science and Technology of China, Hefei, China*

Abstract
The merging of two linear fire fronts intersecting at a small angle creates an accelerating fire that is designated as "jump fire", given the very high value of the rate of spread that it can reach in a relatively short time. In this work an analysis of the jump fire process based on laboratory scale, field scale experiments and large fire scale observation was performed. This confirmed that independently from the scale of analysis the fire in this condition follows the same behaviour pattern that is due to the fire geometry and to the associated heat transfer mechanisms that induce the phenomenon of a quick acceleration followed by a deceleration phase. S type pitot tubes were used to study the flow pattern inside or near the fire front to better understand the mechanisms of fire induced convection given its very important role in these fires.

Keywords*: Forest fire behaviour; Jump fire; Merging fire; Dynamic effect; Extreme Fire*

Introduction
The concept of "jump fire" behaviour associated to the merging of two linear fire fronts that intersect at a point making a small angle between them as was introduced in Viegas *et al.*, (2012, 2013) with a conceptual model of energy release by the fire front, mainly by radiation was proposed to justify the very rapid decrease of a reference rate of spread (ROS) that was observed in laboratory scale tests performed with horizontal fuel beds. In the present study the previous work is extended to consider the effect of slope, various types of fuels, and different fire dimensions. A comparison of the results obtained at laboratory scale with the tests performed at field tests in the Lousã Mountain and also with the case of a very large forest-fire that occurred in Canberra in 2003 was made.

Experimental Study

Physical problem
We consider two linear fire fronts that intersect at point *D* and making an angle θ_o between them spreading on a uniform fuel bed making an angle α with the horizontal. The axis *OX* is assumed to be a symmetry line of the fire (figure 1a)). Particular attention is given in this study to the displacement of the intersection point *D* of the two fire lines that has a velocity or rate of spread *R*. In order to generalize our results we use the reference basic ROS R_o of a linear fire front in the same fuel bed in the absence of slope or wind, to define the non-dimensional ROS $R'=R/R_o$.

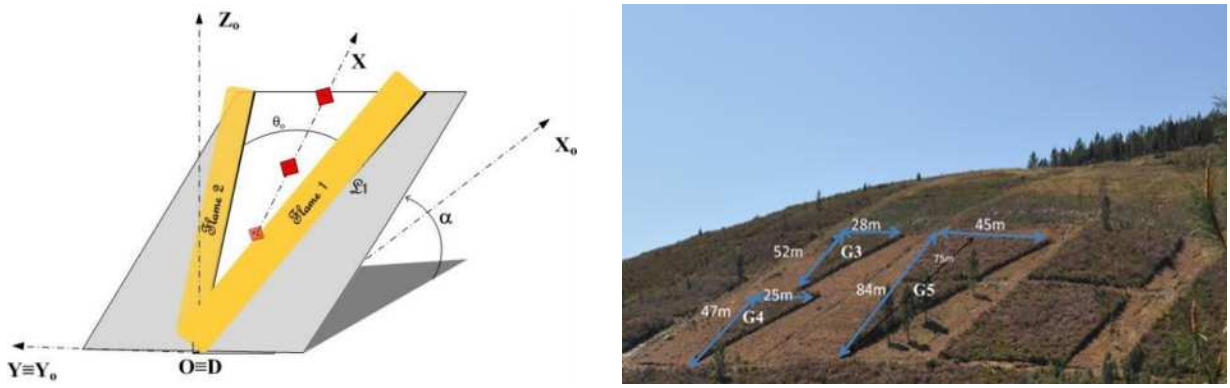

a) *b)*

Figure 1. a) Schematic representation of the problem. b) View of the plots burned at the field tests of jump-fire in Gestosa.

The configuration of the fuelbed is shown in figure 1 schematically for the laboratory and for the field tests respectively. In all tests the fuelbed had a triangular shape with an angle θ_o=30º and the fire front was initiated along the two large sides of the triangle (indicated as Flame 1 and Flame 2 in figure 1a). A large set of tests on the scope of jump fires was performed both at laboratory and at field scale. From these tests some were selected for the present work including a case study of the Canberra 2003 fire. The main parameters of the cases that are considered in this paper are given in Table 1.

Table1: Parameter of jump-fire cases considered in the present study

Designation	Fuel	α	Scale	Series
CF02	PP	40	Lab	S1
CF05	PP	0	Lab	S1
CF07	PP	10	Lab	S1
CF14	PP	20	Lab	s2
CF15	PP	20	Lab	s2
CF17	PP	30	Lab	s2
CF44	PP	20	Lab	s5
CF54	PP	30	Lab	s5
CF55	PP	0	Lab	s5
CF57	SH	30	Field	-
CF59	SH	30	Field	-
CF60	SH	-	Canberra 2003	-

Laboratory Experiments

Laboratory experiments were carried out at the Forest Fire Research Laboratory of the University of Coimbra using the table DE4 that has a useful area of 6x8 m^2 with a slope (α) that can be varied in the range of 0º to 40º.

The methodology used is similar to the one described in Viegas *et al*. (2013) with the addition of flow velocity measurements using S type pitot tubes placed along OX axis at 1, 3 and 6m from point *D* as indicated in figure 1a). The measured properties were temperature, pressure and heat flux. The measurement of the temperature was made with a multi-point system of 25 K type thermocouples, connected to a NI cDAQ-9174 that allows a synchronous data-logging. This 25 thermocouples (TC) were placed in a beam coincident with the OX axis. The position of each thermocouple is known and the gap between thermocouples is constant of 20cm the rate of acquisition was of 1Hz. For a spatial

distribution of the temperature along the fuel-bed infrared images from each experiment were recorded, using an infra-red camera FLIR ThermaCam SC640 The acquisition rate was also 1Hz. In both methods the presence of the fire front was considered for values of temperature above 350ºC that was considered as sign of the existence of flame in the place or time of measurement. Using IR methodology the position of the fire perimeter at given time frames was assessed and from these images the ROS at various positions of the fire perimeter namely at point D were measured. Using the thermocouples and knowing time interval required for the fire to travel from one position to the next the ROS of the fire along OX axis was measured as well. Besides this all the tests were recorded by a Sony high definition video camera and temporized shots were also taken with a Cannon photographic high performance digital camera.

The flow velocity was measured at three different points along OX axis at 1m, 3m and 6m from the origin, with pitot tubes designated respectively P1, P2 and P3. The pitot tubes used were type S specially designed for the purpose as they are indicate to perform measurements inside dirty and high temperature flows. The pitot were placed along the centre line at the high of 15cm from the ground so that the pitot was always above the fuel bed but inside the flame zone. Each pitot was connect by pipes to a differential pressure transducer Gems 5266-50L Very Low Range Differential Pressure Transmitter. These transducers were connect to a multifunctional NI 6009-DAQ that made the data-logging of the signal also with a frequency of 1Hz. With the data collected by this method using the values of synchronous temperature measurements by the application of a calibration it was possible to estimate the flow velocity induced by the fire phenomena.

2.3. Field Experiments

The field tests were performed in Gestosa, Lousã, with *V* shaped plots with dimensions indicated in figure 1 b). The plots were prepared cutting shrub vegetation with height varying between 0.5 and 1.2m using mechanical tools in order to give the plots the desired shape. The average slope of these plots is 30º and the initial angle between the fire fronts was 30º. In order to assure a simultaneous ignition of the two fire lines along their entire length pyrotechnics devices were used. Due to the presence of lateral wind during the experiments full symmetrical conditions were not obtained. During these tests infrared and visible range images were recorded to allow fire spread analysis. Thermocouples were disposed along the central axis of the plots to measure the temperature evolution and consequently the rate of spread in the centre line as in the laboratory experiments. The real case occurred during the merging if two large fires in the vicinity of Canberra in January 2003, that are documented in Doogan (2006), creating a very intense jump-fire phenomenon. In mid-afternoon of the 18th January 2003 the flanks of Bendora and McIntyres large fires merged on undulating ground covered by grass, shrubs and groups of tress under a strong wind of the order of 25m/s. The merging of these fires developed very rapidly towards Canberra and even produced a tornado near one of its flanks. More details on this fire can be found in Sharples *et al.,* (2012).

Results and Discussion

3.1. Effect of fuel bed slope

In Figure 2 the dimensional rate of spread ROS for three different slope angles 0º, 20º, 30º and 40º with fuel bed of dead pine needles of Pinus pinaster is plotted as function of time t. As it is typical for the jump fire phenomena these tests show a pattern of behaviour that involves a sharp acceleration in its initial phase until the peak velocity is reached and afterwards it decreases reaching relatively low values.

The analysis will be mainly focused in speeding up phase of the fires. The deceleration phase was already considered in Viegas *et al*. (2012) but needs to be more investigated. Although some observations and comments on this phase are made here its more detailed analysis will be the scope of future work.

As can be seen in figure 2 for α=0º the acceleration phase lasts less than two seconds and therefore it is not captured with the experimental methodology that was used. Forα=20º this phase lasts about 12 seconds and therefore can be clearly picked up in our laboratory experiments. The same happens for α=30º and 40º for which the acceleration phase takes about 22.5 and 15.1 seconds respectively. The peak ROS value also increases with slope angle. In these tests the following maximum ROS values were observed: 7.7cm/s, 15.4cm/s, 22.5cm/s and 39.4 cm/s for α=0º, 20º, 30º and 40º respectively. It is interesting to notice that on the contrary the deceleration phase duration decreases with slope angle except for the case of α=40º here no deceleration phase was recorded. In these experiments the following values were registered for the duration of the deceleration phase: 300s, 60s and 5s for α=0º, 20º or 30º respectively.

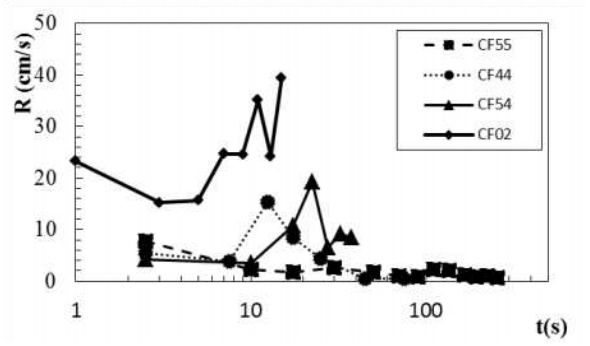

Figure 2. Plot of the Dimensional rate of spread R as function of time t for three different slope angles 0º; 20º 30ºand 40º with fuels

The change of jump fire behaviour from an accelerating ROS to a deceleration indicates that this phenomenon is based on the shifting of the main physic heat transfer processes of convection and radiation. Convective flows generated by the interaction of the fire fronts that are developed during the fire front evolution play a major role in the acceleration phase but there seems to be an opposing effect due both to convection and radiation (associated to the change of flame geometry) that stops the acceleration phase and produces the deceleration phase that seems to be mostly related to this change of flame geometry.

Analysis of the fire acceleration phase

The phase of sharp acceleration can be interpreted at the light of the concept of dynamic fire behaviour due to the feedback between the fire and its surrounding flow proposed in the model to predict eruptive fires presented in Viegas (2006). According to this model the time involved in the acceleration of a pint source fire front in a slope or canyon is associated to a characteristic time of each fuel bed. This time is related to the residence time of the combustion in the fuel bed and therefore it is large for heavier fuels. The special configuration of the jump fire create similar effects due to the heat transfer processes associated to the phenomena particularly to the role of convection in this phase. In spite of this similarity it was realised that contrary to eruptive fires in jump fires the increasing phase has a limit of growth.

In order to better interpret the problem the use non-dimensional parameters based on selected reference parameters is adopted. This method is also required to overcome the problem of scale and allows the application of results of laboratory scale tests to full size experiments or even to real fires with much larger dimensions.

To describe the evolution of ROS in the course of time the non-dimensional parameters *R'* and *t'* were used to present the results of both laboratory and field scale tests in figure 3. The non-dimensional value of $t'=t/t_o$ was evaluated following Viegas (2006) the residence time t_o that was measured in our tests were used. These values are given in Table 2.

Table2: Characteristic Residence time for the different fuels

Fuel	Residence time t_o(s)
Straw	42,81
Pine needles	54,21
Shrubs (lab.)	65,63
Shrubs (field)	286,00

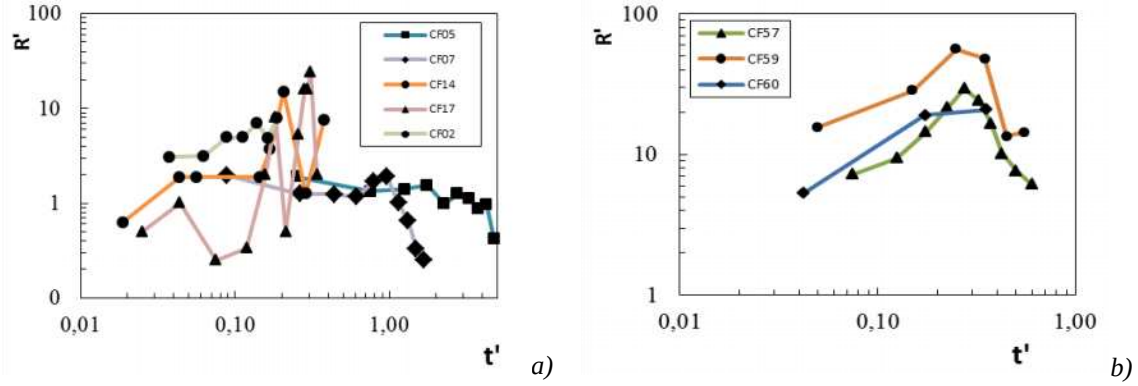

Figure 3. Evolution of non-dimensional rate of spread R' as function of the reference time t', for laboratorial tests a), field tests and the case of Canberra, Australia b).

In figure 3 a) the values of *R*' for a set of laboratory experiments with *Pinus pinaster* needles were plotted as a function of *t'* for slope angle values of 0º, 10º, 20º, 30º and 40º, although this is not the same set of tests of figure 2 they are in agreement with the previous set. The peak values of *R'* are in the range between 3 and 25. The accelerating phase can be clearly observed in these tests for values of t'<0.3. The same trend that was referred above can be observed here: while for the case of α=0º the accelerating phase was not observed in the case of α=40º the deceleration phase is non-existent.
In figure 3 b) the corresponding results for two field tests and for the Canberra fire are shown. The similarity between figures 3 a) and 3b) is quite apparent in spite of the scales of the tests. The similarity can be observed both in the general form of the curves but also in the order of magnitude of the reference parameters like for example the peak values of R' and of the corresponding values of t'.

3.3. Flow analysis

In order to better assess and understand the role of convection induced by the fire during the speeding up process, results of sample flow velocity measurements are presented.
In figure 4 the horizontal flow velocity *U* (m/s) close to the fuel bed measured at each station is plotted as a function of the distance x-x_p of the fire front to the corresponding sensor for three values of slope angle. These figures put in evidence the complexity of the flow associated to fire evolution and of the rapidly changing character of the induced flow near the fire front. We observe periods of negative flow velocity (flow in the negative direction of OX axis), followed by periods of positive velocity. The negative flow velocity acts as a counter flow in relation to flame spread and it may explain the fact that the acceleration phase is limited. The positive or inflow flow velocity is observed mainly after the passage of the fire front and it is an indication of fire acceleration. This is more clearly observed in figure a c) for α=30º. In this case it is interesting to see that at pitot P1 placed 1m above the origin of OX axis the flow is negative after the passage of the fire and then reaches a very high positive peak, corresponding to the acceleration of the fire along the slope while at pitot P2 (x=3m) the flow is positive even before the fire reaches the pitot station.

The peak of the inflow velocity increases with α in correspondence to the increase of the maximum value of ROS.

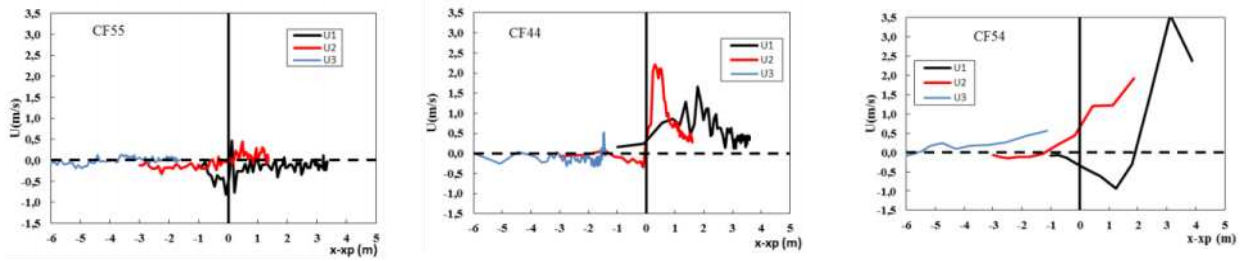

a) b) c)

Figure 4. Flow speed U measured at three differents points along the center line placed at 1m (U1), 3m (U2) and 6m (U3) from point D, for three different slope angles a) 0º; b) 20º and c) 30º .

Conclusion

Analysis of the jump fire process based on laboratory scale, field scale experiments and large fire scale observation shows that in all cases the fire follows the same behaviour pattern that is due to the fire geometry characteristics of two convergent fire lines and to the associated heat transfer mechanisms that induce the phenomenon that is designated as jump-fire.
Taking into account the data presented it is possible to realize that the patterns of behaviour of the jump fires are very much dependent on the convective flows generated by this special way of burn. The complex geometry of jump fires give origin to unstable boundary conditions that will dynamically affect the fire spread both by convective flows and by radiative heat transfer processes that are greatly affected by morphisms in the fire fronts that occur in this phenomena in the course of time.
The S type pitot tubes appeared as important tools to analyse the flow pattern inside or near the fire front contributing to a better understanding of the mechanisms of this phenomenon given the very important role played by induced convection in these fires.
More research is necessary to be able to model the complex heat and mass transfer processes during a jump fire for arbitrary fuel and boundary conditions. The authors will develop an effort towards producing such a model to explain and predict the two phases of jump-fires.

Acknowledgments

The authors wish to thank Portuguese Science Foundation for the support given to project Extreme under contract PTDC/EME-MFE/114343/2009 and for a PhD grant under contract SFRH / BD / 85557 / 2012. The participation of Naian Liu and Xiaodong Xie were supported by the bilateral project of cooperation between Portugal and China founded by the Portuguese Science Foundation.
The authors thank their colleagues who supported the experimental work in laboratory and in the field experiments, namely Ricardo Oliveira, Nuno Luís and Luís Ribeiro.

Symbology

Symbol	Units	Description
α	-	Inclination angle
θ	-	Angle between the fire fronts
O	-	Origin of reference Cartesian system
D	-	Intersection point D of the two fire lines

X	-	Coordinate along reference OX axis
Xo	-	coordinate along reference horizontal axis OXo
Y	-	coordinate along reference OY axis
Yo	-	coordinate along reference horizontal axis OYo
Zo	-	coordinate along reference horizontal axis OZo
$\mathcal{L}_1$	-	Fire line 1
$\mathcal{L}_2$	-	Fire line 2
R	$cm.s^{-1}$	Rate of spread (ROS)
R_o	$cm.s^{-1}$	Basic rate of spread of linear fire in the absence of slope and wind
R'	-	Non-dimensional rate of spread (NDROS)
U_1	$m.s^{-1}$	Flow velocity measured by Pitot 1
U_2	$m.s^{-1}$	Flow velocity measured by Pitot 2
U_3	$m.s^{-1}$	Flow velocity measured by Pitot 3
t_o	s	Residence time
t'	-	Reference time
P1	-	Pitot station 1
P2	-	Pitot station 2
P3	-	Pitot station 3
PP	-	Fuelbed of Pinus pinaster dead needles
SH	-	Fuelbed of dead shrubs
IR	-	Infrared image
TC	-	Thermocouple

References

Doogan M. 2006. Inquests and Inquiry into Four Deaths and Four Fires between 8 and 18 January 2003. (ACT Coroner's Court: Canberra, ACT)

Viegas, D., Raposo, J. and Figueiredo, A. R. 2013. Preliminary analysis of slope and fuel bed effect on jump fire behavior in forest fires. Procedia Engineering. Volume 62, pp. 1032-1039.

Viegas, D., Raposo, J., Davim, D. and Rossa, C. 2012. Study of the Jump Fire Produced by the Interaction of Two Oblique Fire Fronts. Part 2: Analytical Extended Model and Validation with Slope Laboratory Experiments. International Journal of Wildland Fire. 21, 843–856

Viegas, D. 2006. Parametric study of an eruptive fire behavior model. International Journal of Wildland Fire, Volume 15(2), pp. 169-177.

Sharples, J., McRae, R.H.D., and Wilkes, S.R. (2012). "Wind–terrain effects on the propagation of wildfires in rugged terrain: fire channelling." International Journal of Wildland Fire 21, 282–296.

Application of the mean radiant temperature method in the evaluation of radiative heat exchanges between a fire front and a group of firemen

Eusébio Z. E. Conceição, Domingos X. Viegas

FCT – University of Algarve - Campus de Gambelas - 8005-139 Faro, Portugal
FCT – University of Coimbra - Pinhal de Marrocos - Pólo II - 3030 Coimbra, Portugal

Abstract
In this work will be studied the application of the Mean Radiant Temperature method in the evaluation of radiative heat exchanges between a fire front and a group of firemen. The development and the application of the Mean Radiant Temperature method will be presented in this work.
The obtained results are used to analyse the protection made by firemen bodies in the others firemen in front a fire front. The obtained protection can be used in order to reduce the fire front radiative flux value that the firemen are subjected.
In this study will be used a numerical model, that evaluates the human and clothing thermal response, in steady-state and transient conditions. The software calculates not only the temperature field in the human body tissue, arterial and venous blood and clothing, but also the blood and tissue mass field in the human body and the water mass field in body skin surface and clothing.
This model considers the human body divided in 25 cylindrical and spherical elements, being each one sub-divided in 12 layers, which could be protected from the external environment through some clothing layers. The computational model of the human body and clothing thermal system is based on the energy balance integral equations for the human body tissue, blood and clothing as well as mass balance integral equations for the blood and transpired water in the skin surface and in the clothing. A thermoregulatory system model was adapted to control the human body tissue temperature.
The radiative heat exchange numerical model between a fire front and the firemen is based in the Mean Radiant Temperature method. This numerical model considers the view factors determination between the firemen bodies and the surrounding surfaces (fire front and environment) and between the occupants' section. In this calculus the grid generation around the firemen and in the fire front is used to evaluate the view factors.
In the numerical simulation, presented in this study, is considered a fire front, the floor, the environment and a group of firemen. The numerical model calculates the Mean Radiant Temperature, that a group of 9 firemen are subjected.

Keywords*: Fire Behaviour and Modelling, Human and Clothing Thermal Response, Mean Radiant Temperature Method, Numerical Simulation.*

Introduction

This study is a continuation of Conceição (2002), Conceição *et al*. (2006B) and Conceição and Viegas (2010). In the previous work the view factors between a firemen and the fire front was made, while in this work the numerical model considers the view factors determination between the firemen bodies and the surrounding surfaces (fire front, floor and environment) and between the occupants' section.
In Conceição (2002) the numerical model was used to study the fireman thermal sensation nearby a fire front. In the three analyzed situations, the radiant temperature, body skin and clothing temperatures and transpired sweat rate field were calculated. The more uncomfortable situation was verified when the fireman is localized in front to the fire central area and distanced 5 m from the flames, being the allowable exposure time, for a non-acclimatized subject with the warning criteria, of around 4.5 hours. During the fire extinction was suggested that the distance between the fireman and the fire front should be the highest possible. It was also suggested that the fireman should avoid being located in front to the flames central area.

In Conceição *et al*. (2006B) the numerical model, that simulates the human and clothing thermal responses, in steady-state and transient conditions, were used to study the fireman thermal sensation nearby a fire front. This numerical model was used to evaluate the thermal sensation that a fireman, equipped with special protective clothing, is subjected nearby vertical flames, with a height of 2 m and a length of 10 m. In this theoretical study the fireman was placed 5 m distanced from the flames and localized in front to the flames central area. The body and clothing temperatures, the radiant temperature, the heat and mass fluxes field and the comfort levels were calculated. The influence of the clothing thickness and the special protective clothing emissivity coefficient reduces, in the fireman thermal comfort sensation were analyzed. The theory used to evaluate the fireman thermal comfort was based in the extension of the PMV model. This extension, used in warm environments, combines the "static" PMV model and the adaptive model. The idea was to use the traditional PMV model, that considers the human body thermal balance, and the expectations verified in the adaptive model. It was verified that the Predicted Percentage of Dissatisfied people increases lightly when the clothing thickness increases and decreases when the special protective clothing emissivity coefficient reduces. In Conceição and Viegas (2010) the radiative heat exchanges between the fire front and two firemen was evaluated. In the radiative heat exchanges the Mean Radiant Temperature method, with correction, was applied. The Mean Radiant Temperature, the skin and clothing temperature and the Predicted Percentage of Dissatisfied people were evaluated. The fireman located behind was protected to the fire front by the fireman located in front. In accordance with the obtained results the radiant protection, promoted by the fireman located in from, with a Predicted Percentage of Dissatisfied people of 25.0 %, reduced the Predicted Percentage of Dissatisfied people, that the fireman located behind is subjected, for 18.1 %.

Physical Model

In the numerical program the human body is divided in 25 cylindrical or spherical elements: the head, the neck, the trunk divided in three, the arms divided in four, the hands, the legs divided in four and the feet. Each element is sub-divided in 12 cylindrical or spherical layers (1 in the core, 2 in the muscle, 2 in the fat and 7 in the skin) and could be still protected of the external environment through several clothing slices. The main arteries and veins and the capillary blood system is also considered in this work.
In the methodologies used in view factors determination each human body element or surrounding surfaces, with inclinations, dimensions and temperatures equal to the respective body or surrounding section, are divided in infinitesimal areas.
In the radiation by long wave phenomena calculus are also considered the shading effects that the body elements surfaces promote in each element.

3. Mathematical Model

The human body thermal system is based on the energy and mass balance integral equations:

- The energy balance integral equations are developed for each tissue slice and for the arterial and venous blood, of each human body element;
- The mass balance integral equations are developed, in each element, for the blood and for the transpired water in the skin surface.

To simulate the clothing thermal system are also developed energy and mass balance integral equations:

- The energy balance integral equations are developed for each clothing layers, in each element;

- The mass balance integral equations are developed for the clothing layers and for the adsorbed/desorbed water vapour in the clothing fibber layers.

The thermoregulatory system, used in the control of the human body temperature, is constituted by (see Stolwijk, 1970):

- heat transport from internal to external tissue;
- heat loss by evaporation;
- additional heat through shivering.

More details about the numerical model are presented in Conceição (2002), Conceição *et al*. (2006A), Conceição *et al*. (2006B), Conceição and Lúcio (2010) and Conceição *et al*. (2010).

Mean Radiant Temperature

The radiant heat exchanges by long wave phenomena are calculated, in this work, using the Mean Radiant Temperature method (Fanger, 1970), with correction (see Conceição and Lúcio (2010). The Mean Radiant Temperature model, presented in Fanger (1970), considers, only, the heat exchanges by radiation between the human bodies sections and the surrounding surfaces. The Mean Radiant Temperature used the view factors calculated between the human body sections and the surrounding surfaces and the surrounding surfaces temperature.
The Mean Radiant Temperature method, developed in this work, considers:

- the heat exchanges between the human body sections and the surrounding surfaces, namely the fire front, the floor and the environment;
- heat exchanges between the human bodies sections of each occupant;
- heat exchanges between the human bodies sections of different occupants.

The Mean Radiant Temperature method, that also considers the view factors correction, calculates, step by step, the Mean Radiant Temperature, using the human body and surrounding surfaces temperatures, calculated in each iteration, and the pre-calculated view factors.

Results and Discussion

In this work the radiant heat exchanges that 9 firemen are subjected nearby vertical flames, with a height of 4 m and a length of 10 m, is evaluate. In this theoretical study the firemen, placed in front to the fire front, are distanced 4, 5 and 6 m front to the flames central area. In this study the Mean Radiant Temperature, the body and clothing temperature field, that 9 protected fireman are subjected, are evaluated.
The obtained results are used to analyse the protection made by firemen bodies in the others firemen in front a fire front. The obtained protection can be used in order to reduce the fire front radiative value that the firemen are subjected.
In figure 1 the grid generation in the 9 firemen, in the ground, in the environment and in the fire front is presented, while the figure 2 the detailed grid generation in the 9 firemen is presented. The location of the fireman and the flame is also presented in the same figure.
In the grid generation is considered that the surroundings surfaces are divides in 100 elementary surfaces and that each human body sections surface is divided in 68 elementary surfaces. The increase of the elementary surfaces number the computational time increase substantially, while the reduction of the elementary surfaces number the approximation of the view factors is bad.
In the view factors determination, used to evaluate the Mean Radiant Temperature, are considered 9 occupants divided in 25 cylindrical or spherical human bodies sections, namely the head, the neck, the trunk divided in three, the arms divided in four, the hands, the legs divided in four and the feet.

In each human body section are calculated:

- 6 view factor for each surrounding surface (1350 view factor);
- 25 view factors between each human bodies sections of each occupant (5625 view factor);
- 25 view factors between each human bodies sections of different occupant (50625 view factor);

Thus, in general, the total view factors calculated is 57600. However, in each view factors determined between one human body and one plan 6800 calculations is made, while in each view factors determined between two elements 4624 calculations is made.
The Mean Radiant Temperature is presented in figures 3. In the Mean Radiant Temperature evaluation is used the surface temperature field and the view factor between the human body sections and the surrounding surfaces.
The surrounding and firemen temperature is evaluated:

- In the surrounding temperature field the fire front, floor and environment temperature are introduced in the numerical model;
- In the firemen temperature field the human body sections temperature is calculated in the numerical model.

The view factor between the human body sections and the surrounding surfaces is evaluated:

- the view factor between the human body sections and the surrounding surfaces, namely the fire front, the floor and the environment;
- the view factor between the human bodies sections of each occupant;
- the view factor between the human bodies sections of different occupants.

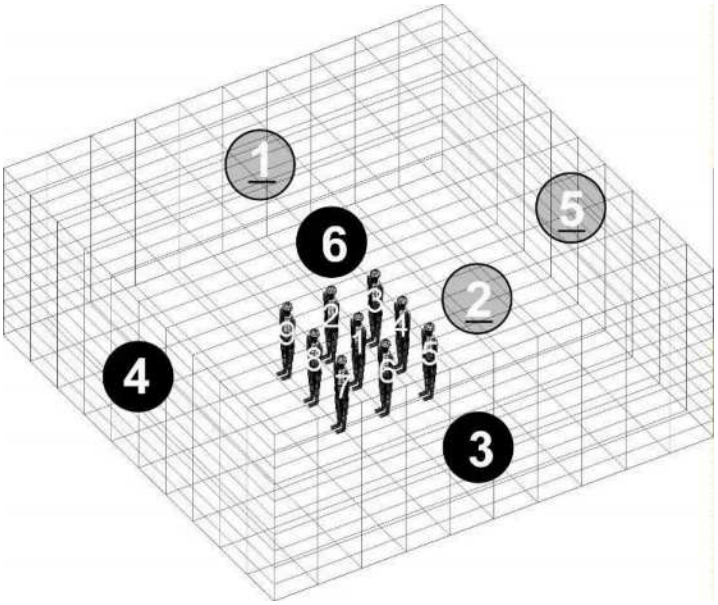

Figure 1. Grid generation in the 9 firemen, in the ground, in the environment in the fire front. Surface 4 are associated with the fire front, surface 2 are associated with the floor and the others surfaces are associated with the environment.

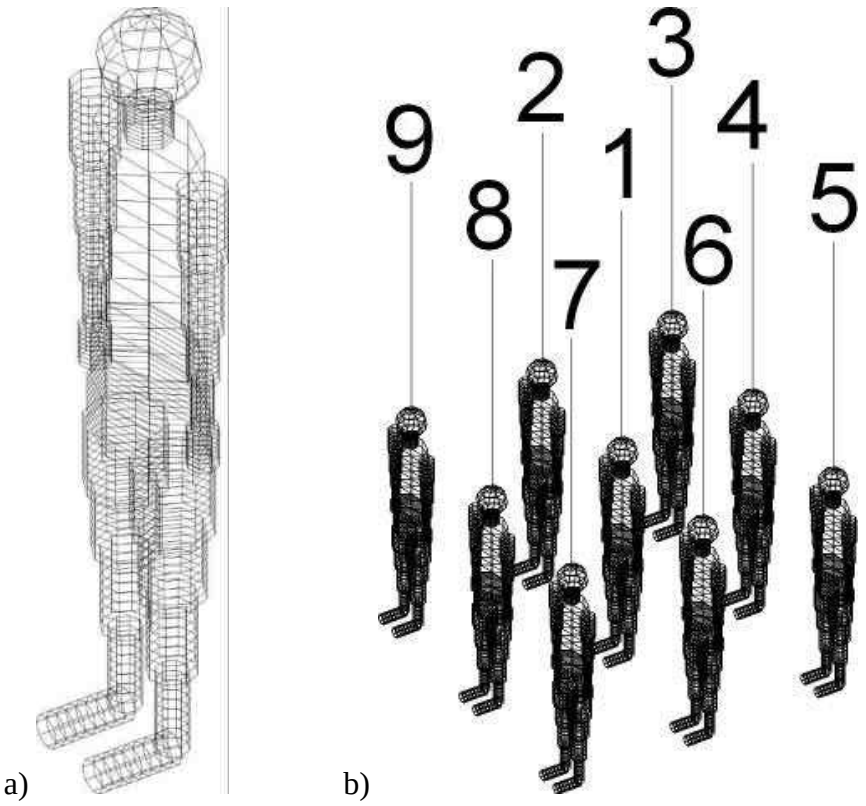

Figure 2. Grid generation around a fireman a) and around a group of firemen b).

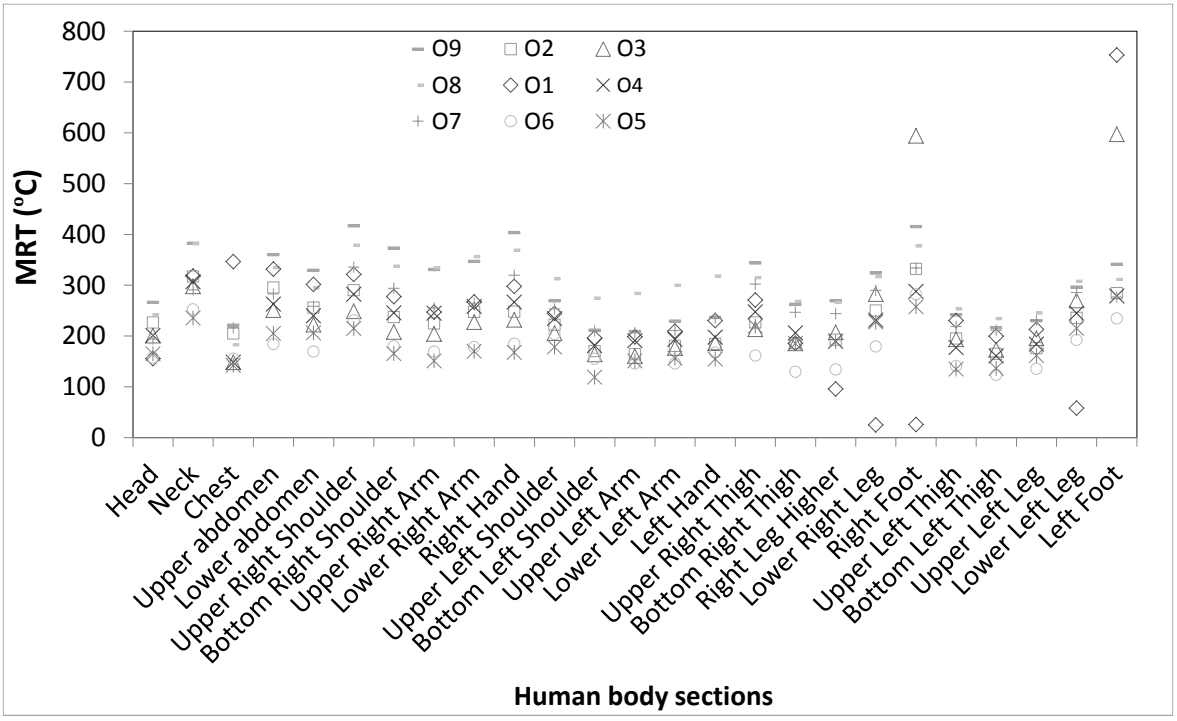

Figure 3. Mean Radiant Temperature.

In accord to the obtained results, is verifying that:

- In general, the highest Mean Radiant Temperature is verified in firemen located in the front of the group and the lowest Mean Radiant Temperature is verified in firemen located in the

behind of the group. This fact is associated with the protection that the fireman located in front promote in the fireman located behind and due the distance between the fire front and the fireman is highest for the fireman located behind;
- However, in some firemen sections, as example in the foot, the previous conclusions are not verified;
- In general, the protection made by the firemen posture, located in front, is higher than 150 ºC (Mean Radiant temperature).

Conclusions

In this work is studied the application of the Mean Radiant Temperature method in the evaluation of radiative heat exchanges between a fire front and a group of 9 firemen placed in front of the fire front. The obtained results are used to analyse the protection made by firemen bodies in the others firemen in front a fire front. The obtained protection can be used in order to reduce the fire front radiative value that the firemen are subjected.

The Mean Radiant Temperature evaluation, used to evaluate radiative heat exchange between the firemen and the surrounding surfaces, is evaluated fiction to the view factors between the firemen body section and the surrounding surfaces and the surrounding surfaces temperature. In accordance with the obtained results, in the view factor determination, the increase of the elementary surfaces number the computational time increase substantially, while the reduction of the elementary surfaces number the approximation of the view factors is bad.

In general, the highest Mean Radiant Temperature is verified in firemen located in the front group and the lowest Mean Radiant Temperature is verified in firemen located in the behind group. In general, the protection made by the firemen posture, located in front of the fire front, is higher than 150 ºC (Mean Radiant Temperature)

References

Conceição E. Z. E. and Lúcio Mª M. J. R. 2010. Evaluation of Thermal Comfort Conditions in a Localized Radiant System Placed in Front and Behind two Students Seated Nearby Warmed Curtains, Building and Environment, Volume 45, Issue 10, October 2010, Pages 2100-2110.

Conceição E. Z. E., Lúcio Mª M. J. R., Capela T. L. and Brito A. I. P. V. 2006A. Evaluation of Thermal Comfort in Slightly Warm Ventilated Spaces in Non-Uniform Environments, International Journal on Heating Air Conditioning and Refrigerating Research, ASHRAE, American Society of Heating, Refrigerating and Air-Conditioning Engineers, Inc., EUA, Vol. 12, Nº 3, July 2006, pp. 451-458.

Conceição E. Z. E., Lúcio Mª M. J. R., Rosa S. P., Custódio A. L. V., Andrade R. L. and Meira Mª J. P. A. 2010. Evaluation of comfort level in desks equipped with two personalized ventilation systems in slightly warm environments, Building and Environment, Vol. 45, Issue 3, March 2010, pp. 601-609.

Conceição, E. Z. E. 2002. Study of Fireman Thermal Sensation Nearby a Fire Front: Evaluation of Human and Clothing Thermal Response, 4th International Conference on Forest Fire Research, Luso, 18 to 21 November 2002.

Conceição, E. Z. E. and Viegas D. X. 2010. Radiative Heat Exchanges Between the Fire Front and the Firemen, Proceedings of the VI International Conference on Forest Fire Research, Coimbra, Portugal, 15 a 18 November 2010.

Conceição, E. Z. E., Lúcio, Mª. M. J. R. and Viegas D. X. 2006B. Numerical Simulation of the Thermal Sensation of a Fireman Equipped with Special Clothing", 5th International Conference On Forest Fire Research, Coimbra, 16 to 20 November 2006.

Fanger , P. O. and Toftum, J., 2002. Extension of the PMV model to non-air-conditioned Buildings in warm Climates. Energy and buildings. Elsevier. N. 34. pp. 533-536.

Fanger P.O. 1970. Thermal Comfort. Copenhagen: Danish Technical Press.

ISO 7730, 2005. Ergonomics of the Thermal Environments – Analytical determination and interpretation of thermal comfort using calculation of the PMV and PPD indices and local thermal comfort criteria. International Standard. Switzerland.

Stolwijk, J. A J. 1970. Mathematical Model of Thermoregulation", In Hardy, J. D., Gagge, A. P. and Stolwijk, J. A. J. "Physiological and Behaviour Thermoregulation", Thomas, Springfield, pp. 703-721.

Calibrating Rothermel's fuel models by genetic algorithms

Ascoli Davide[a], Bovio Giovanni[a], Vacchiano Giorgio[a]

[a] *University of Torino, DISAFA, via Leonardo da Vinci 44, 10095 Grugliasco (TO), Italy*
d.ascoli@unito.it, bovio.giovanni@unito.it, giorgio.vacchiano@unito.it

Abstract
A new method to customize Fire Behaviour Fuel Models was developed by linking Genetic Algorithms (GA) to the Rothermel's equation implemented in the Rothermel package for R. GA randomly generates solutions of fuel model parameters to form an initial population. Each solution is validated against observations of fire rate of spread (ROS) via a goodness-of-fit metric (i.e., RMSE). The population is then selected for its best members, crossed over, and mutated within a range of fuel model parameters space, until fitness is maximized. We tested the performance of GA-optimization against custom fuel models calibrated in two previous studies in grass and shrub fuels. GA was constrained using fuel parameters ranges reported in the selected studies, and was fit against the published ROS measurements. We compared goodness-of-fit (RMSE; R2adj) of fuel models calibrated by GA against that of the original studies. GA improved the fit of Rothermel's model for both studies: RMSE decreased from 5.5 to 4.6 m/min and from 6.9 to 5.4 m/min, respectively for grass and shrub fuel models. R2-adj increased from 0.83 to 0.84, and from 0.73 to 0.83, respectively. We then ran GA-optimization to calibrate a Calluna heaths fuel model against ROS and environmental data measured under experimental conditions. We obtained ranges of fuel model parameters (fuel load; fuel structure) by a field survey in both experimental plots and other Calluna sites of North-West Italy. Ranges of fuel flammability parameters were derived from the literature. We divided fire experiments into a calibration and a validation dataset (20 ROS each) and ran GA-optimization on the calibration dataset to customize the Calluna fuel model. We predicted ROS in the validation dataset by running the Rothermel modelon each of the following fuel models: i) GA-optimized fuel model; ii) the Standard Fuel Model which minimized RMSE against observations; iii) custom fuel models for Calluna heaths, parameterized using modal values from the overall fuel inventory, or inventoried at each experimental plot. Predictions of the Rothermel model reformulation implemented in FCCS, using as input modal values at the vegetation complex or at plot scale, were also evaluated. ROS predictions obtained by GA-optimized fuel model against the calibration dataset had a RMSE of 1.66 m/min and R2-adj of 0.96. When tested against the validation dataset, GA-optimized fuel model produced the lowest prediction error of all the alternative fuel models (RMSE = 1.74 m/min R2-adj = 0.90). FCCS predictions produced RMSE= 3.76 and 2.24 m/min, respectively using modal values from the fuel complex or at the plot scale, and R2-adj= 0.86 in both cases. GA-optimization provided an objective and accurate calibration of custom fuel models. It can be implemented in several fire prediction systems based on the Rothermel model, including the Rothermel package for R. Increasing the range of fuel model parameters beyond the measured values (e.g., +25%, +50%) can further improve GA model performance. However, this raises the question on how far apart from the field truth a fire behaviour fuel model should be stylized.

Keywords*: custom fuel model, optimization, fire rate of spread, prescribed burning, wildfire*

Introduction

Rothermel's model (Rothermel 1972) is the primary surface fire spread model of many fire prediction systems (Sullivan 2009; Finney *et al*. 2011; Andrews 2013). In the Rothermel model the forward rate of spread of a surface fire (ROS) is predicted as a function of topography, fire weather and a "fire behaviour fuel model" (hereafter: fuel model) that consists of a number of fuel parameters for a given fuel complex (Albini 1976; Burgan and Rothermel 1984). Standardized fuel models have been developed to facilitate the prediction of ROS (Anderson 1982; Scott and Burgan 2005). However, using standard fuel models can result in poor predictions and this has prompted the need to develop custom fuel models (Cruz and Alexander 2013). Customizing a fuel model is an iterative process of

comparing predictions to observed fire rate of spread, and subjectively adjusting the fuel model parameters until a satisfactory result is achieved (Burgan 1987). However, due to complex relationships in Rothermel's model, it is not always easy to guess how changes in fuel parameters will affect the fire behaviour prediction (Burgan and Rothermel 1984).
Optimization methods, which explore many possible combinations of fuel model parameters, showed the best solution for calibrating custom fuel models in previous studies (Cruz and Fernandes 2008). However, there are no standard methods or published codes for running an automated optimization of a custom fuel model against observed/expected fire rate of spread.
Genetic Algorithms (GA) (Holland 1975) have been used to calibrate models in several fields (e.g., Wang 1991), including fire science (Finney 2004; Lautenberger *et al*. 2006; Wendt *et al*. 2013). However, an optimization of fuel model parameters using GA has not been attempted yet. GA is a search heuristic which generates numeric solutions to an optimization problem using techniques inspired by natural evolution (e.g., mutation). During GA, many solutions are randomly generated to form an initial population. Each solution is validated against the observations via a user-defined metric of goodness-of-fit. The population is then selected for its best members, crossed over, and randomly mutated within a range of parameter space, until fitness is maximized.
The study objectives are: i) to test a fuel model calibration method based on GA; ii) to implement the GA-optimization method to calibrate a fuel model for *Calluna* heath vegetation.

Methods

GA-optimization testing

To predict the forward rate of spread at the head of a surface fire (ROS), we used Rothermel's equation implemented in the *ros ( )* function of the Rothermel package for R[1] (Vacchiano and Ascoli 2014). To test GA-optimization, we searched for studies with the following characteristics: i) a published dataset of observed ROS, including fuel moisture, wind speed and slope steepness associated to each observation; ii) custom fuel model parameters calibrated using the ROS dataset; iii) inventory and laboratory fuel data from which to infer ranges of fuel model parameters to force the GA-optimization (Table 1, columns A-B); iv) ROS predictions using the same equation implemented in the Rothermel package for R (corrections to original the equation as implemented in BehavePlus). Following these criteria, we found suitable data for both grass (Sneeuwjagt and Frandsen 1977) and shrub fuels (Van Wilgen *et al*. 1985).
GA-optimization was carried out using the *GA* package for R (Scrucca 2014). GA were run with 9999 maximum iterations, a mutation probability of 0.1, and elitism of 0.05 (i.e., the 5 best solutions are retained at each simulation). As a fitness metric, we chose the root mean square error (RMSE) of observed vs. predicted ROS. Then, we compared goodness-of-fit (RMSE; R^2adj) of GA-optimized fuel models against the calibration methods used in selected studies, while keeping constant the fire environment (i.e., fuel moisture; wind speed; slope).

[1] http://cran.r-project.org/web/packages/Rothermel/index.html

Table 1. Fuel model parameters range used to force GA-optimization against observed ROS for both the test analysis (column A-B) and the heath fuel model calibration (column C).

Fuel model	A[2]	B[3]	C
Fuel Type	Grass fuels	Shrub fuels	Calluna heath
Load 1-h (t ha^{-1})	0.5 – 4	1.56 – 6.24	0.24 – 2.625
Load 10-h (t ha^{-1})	–	0.4 – 1.2	–
Load 100-h (t ha^{-1})	–	0.06 – 0.18	–
Load Live Herb (t ha^{-1})	0 – 0.9	1 – 6	0.825 – 7
Load Live Woody (t ha^{-1})	–	0.64 – 6.72	2.175 – 13
SA/V 1-h (m^2 m^{-3})	4600 – 14800	4200 – 8000	6640 – 10036
SA/V 10-h (m^2 m^{-3})	–	358	358
SA/V 100-h (m^2 m^{-3})	–	98	98
SA/V Live Herb (m^2 m^{-3})	4600 – 14800	4200 – 6500	5249 – 6562
SA/V Live Woody (m^2 m^{-3})	–	4200 – 5500	8810 – 10560
Fuel Bed Depth (cm)	9 – 53	100 – 200	19 – 70
Extinction Moisture (%)	12 – 25	20 – 40	27 – 55
Heat content Dead (kJ kg^{-1})	18000 – 19000	18000 – 22000	18719 – 19919
Heat Content Live (kJ kg^{-1})	18000 – 19000	18000 – 22000	20000 – 22504

Heathland fuel model calibration

We implemented the GA-optimization to calibrate a custom fuel model for *Calluna* dry heathlands against ROS and fire weather data recorded under experimental conditions (Ascoli *et al*. 2013; Vacchiano *et al*. 2014). We measured ROS in nine wind-driven field fire experiments using a microplot approach (Simard *et al*. 1984; Fernandes *et al*. 2001). We discarded data recorded during the acceleration, backfire and flank fire phases, retaining a total of 40 ROS observations ranging between 0.9 and 26.3 m/min. Environmental variables (min-max) were as follows: ignition line length = 25-50 m; fire plot size = 1250-4000 m^2; 1h fuels moisture = 10-27%; live woody fuel moisture = 50-70%; wind speed = 0.4-7.9 km/h; slope = 0%.

We obtained ranges of fuel model parameters (Table 1, column C) related to fuel load (1-h, 10-h, 100-h, Live Herb, Live Woody) and structure (Fuel Bed Depth) by a field survey in both fire experiment plots and additional *Calluna* stands in North-West Italy (twelve stands x 6 obs.). Ranges of fuel flammability parameters (SA/V, Moisture of extinction, Heat content) were derived from published datasets and laboratory studies. The fuel model was conceived as Dynamic.

We divided fire experiments into a calibration (four experiments, 20 ROS obs.) and a validation dataset (five experiments, 20 ROS obs.). We ran GA-optimization using the same setting as for the test analysis. Then, we predicted ROS in the validation dataset by using the *ros ( )* function of the Rothermel package for R, and compared goodness-of-fit (RMSE; R^2adj) of predictions obtained by the following fuel models: i) GA-optimized fuel model; ii) the Standard Fuel Model which minimized RMSE against observations, as determined by the *bestFM ( )* function of the Rothermel package (Vacchiano and Ascoli 2014); iii) a custom fuel model for *Calluna* heaths, parameterized with modal values from the overall fuel inventory (72 obs.); iv) a custom fuel model parameterized with modal values from fuels inventoried in each fire experiment plot (6 obs. per plot). Predictions of the Rothermel's model reformulation implemented in the Fuel Characteristics Classification System (FCCS) (Sandberg *et al*. 2007), using modal values at the vegetation complex or at plot scale, were also evaluated.

Results and discussion

GA-optimized fuel models improved the fit of Rothermel's model for both grass and shrub tests, relative to the published fuel models. RMSE decreased from 5.35 to 4.32 m/min and from 7.18 to 5.45 m/min, respectively. R^2-adj increased from 0.83 to 0.84, and from 0.73 to 0.83, respectively.
In heath fire experiments, ROS predictions obtained by GA-optimized fuel model against the calibration dataset had a RMSE of 1.66 m/min and R^2-adj of 0.96. When tested against the validation dataset, GA-optimized fuel model produced the lowest prediction error in comparison to all the alternative fuel models (Figure 1).

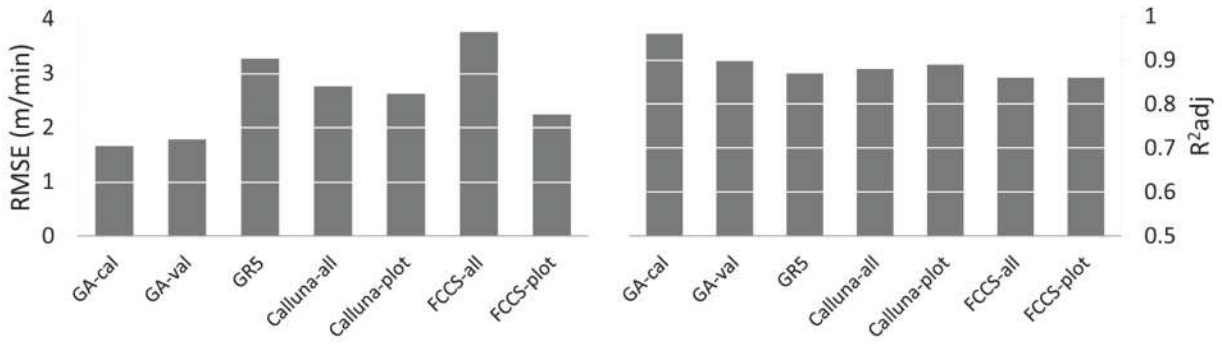

Figure 1. RMSE (left) and R^2adj (right) values for alternative fuel models predictions against the validation dataset

In accordance with previous studies, our results confirms the usefulness of calibrating a custom fuel model to improve Rothermel's model prediction, rather than limit its use to the set of Standard Fuel Models (Cruz and Fernandes 2008). Given the relative homogeneity of fuel conditions in heath vegetation at the study site, our results show that site-specific fuel parameters assessed at the plot scale did not improve predictions of Rothermel's model. However, when using variables measured at the plot scale, FCCS performance was second only to GA. This supports the potential of Rothermel's model reformulation embedded in FCCS, which aims to improve ROS predictions by using modal values of measured plots, bypassing the need to calibrate a stylized custom fuel model (Sandberg *et al*. 2007).
GA-optimization provided an objective and accurate calibration of custom fuel models. It can be implemented in several fire behaviour prediction systems based on Rothermel's model, including the Rothermel package for R. Increasing the range of fuel model parameters beyond the measured values (e.g., +25%, +50%) can further improve GA model performance (analysis not showed). However, this raises the question on how far apart from the field truth a fire behaviour fuel model should be stylized.

References

Albini FA (1976) Computer-based models of wildland fire behavior: a user's manual. USDA Forest Service, Intermountain Forest and Range Experiment Station, Ogden UT.

Anderson HE (1982) Aids to determining fuel models for estimating fire behavior. Gen. Tech. Rep. INT-122. USDA Forest Service, Intermountain Forest and Range Experiment Station, Ogden UT.

Andrews PL (2013) Current status and future needs of the BehavePlus Fire Modeling System. International J. of Wildland Fire 23, 21–33.

Ascoli D, Lonati M, Marzano R, Bovio G, Cavallero A, Lombardi G (2013) Prescribed burning and browsing to control tree encroachment in southern European heathlands. Forest Ecology and Management 289, 69–77.

Burgan RE (1987) Concepts and interpreted examples in advanced fuel modeling. USDA Forest Service, Intermountain Research Station, Ogden UT.

Burgan RE, Rothermel RC (1984) BEHAVE: fire behavior prediction and fuel modeling system – FUEL subsystem. Tech. Rep. PMS 439-1. USDA Forest Service, Intermountain Forest and Range Experiment Station, Ogden UT.

Cruz MG, Fernandes PM (2008) Development of fuel models for fire behaviour prediction in maritime pine (Pinus pinaster Ait.) stands. International J. of Wildland Fire 17(2), 194–204.

Cruz MG, Alexander ME (2013) Uncertainty associated with model predictions of surface and crown fire rates of spread. Environmental Modelling & Software 47, 16–28.

Finney MA (2004) Landscape fire simulation and fuel treatment optimization. In: Hayes JL; Ager AA; Barbour JR, tech. ed. Methods for integrating modeling of landscape change: Interior Northwest Landscape Analysis System. Gen. Tech.Rep.PNW-GTR-610. USDA Forest Service, Pacific Northwest Research Station, Portland, OR: 117–131.

Finney MA, Grenfell IC, McHugh CW, Seli RC, Trethewey D, Stratton RD, Brittain S (2011) A method for ensemble wildland fire simulation. Environmental Modeling & Assessment 16(2), 153–167.

Holland J (1975) Adaptation in artificial and natural systems. Univ. of Michigan Press, Ann Arbor.

Lautenberger C, Rein G, Fernandez-Pello C (2006) The Application of a Genetic Algorithm to Estimate Material Properties for Fire Modeling from Bench-Scale Fire Test Data. Fire Safety J. 41, 204–214.

Ohenoja M, Leiviskä K (2010) Validation of genetic algorithm results in a fuel cell model. International J. of Hydrogen Energy 35(22), 12618–12625.

Rothermel RC (1972) A mathematical model for predicting fire spread in wildland fuels. Tech. Rep. INT-GTR-115. USDA Forest Service, Intermountain Forest and Range Exp. Station, Ogden UT.

Sandberg DV, Riccardi CL, Schaaf MD (2007) Reformulation of Rothermel's wildland fire behaviour model for heterogeneous fuelbeds this article is one of a selection of papers published in the special forum on the fuel characteristic classification system. Canadian J. of Forest Research 37(12), 2438–2455.

Scott JH, Burgan RE (2005) Standard fire behavior fuel models: a comprehensive set for use with Rothermel's surface fire spread model. Tech. Rep.RMRS-GTR-153. USDA Forest Service, Rocky Mountain Research Station, Fort Collins CO.

Scrucca L (2013) GA: a package for genetic algorithms in R. J. of Statistical Software 53(4), 1–37. URL: http://www.jstatsoft.org/v53/i04/.

Simard AJ, Eenigenburg JE, Adams KA, Nissen RL, Deacon AG (1984) A general procedure for sampling and analyzing wildland fire spread. Forest Science 30, 51–64.

Sneeuwjagt RJ, Frandsen WH (1977) Behavior of experimental grass fires vs. predictions based on Rothermel's fire model. Canadian J. of Forest Research 7, 357–367.

Sullivan AL (2009) Wildland surface fire spread modelling, 1990-2007. 2: Empirical and quasi-empirical models. International J. Wildland Fire 18(4), 369–386.

Vacchiano G, Ascoli D (2014) An implementation of the Rothermel fire spread model in the R programming language. Fire Technology. Doi: 10.1007/s10694-014-0405-6

Vacchiano G, Motta R, Bovio G, Ascoli D (2014) Calibrating and Testing the Forest Vegetation Simulator to Simulate Tree Encroachment and Control Measures for Heathland Restoration in Southern Europe. Forest Science 60(2), 241–252.

Van Wilgen BW, Le Maitre DC, Kruger FJ (1985) Fire behaviour in South African fynbos (macchia) vegetation and predictions from Rothermel's fire model. J. of Applied Ecology 22, 207–216.

Wang QJ (1991) The genetic algorithm and its application to calibrating conceptual rainfall-runoff models. Water Resources Research 27, 2467–2471.

Wendt K, Cortes A, Margalef T (2013) Parameter calibration framework for environmental emergency models. Simulation Modelling Practice and Theory 31, 10–21.

Characteristic length of radiative ignition from wildland flames

Yamina Baara[a], K.Khelloufi[a], J.P.Clerc[b], S.Popov[c], B.Porterie[b] and N.Zekri[a,*]

[a] *Université des Sciences et de la Technologie d'Oran Mohamed Boudiaf, Département de Physique Energétique, LEPM, BP 1505 El Mnaouer, Oran, Algeria, nzekri@yahoo.com*
[b] *Aix Marseille Université, EPUM, 5 Rue Enrico Fermi, 13453 Marseille Cedex 13, Jean-Pierre.Clerc@univ-amu.fr, Bernard.Porterie@univ-amu.fr*
[c] *International Char-Network UNESCO Unitwin/ TVET, unesco-tvet-01@yandex.ru*

Abstract
The process of radiative ignition from wild land flames is studied using a simple heat transfer model. For vertical flames (no wind and no slope effects), it is found that the fuel ignition time increases exponentially with distance, which reveals the existence of a characteristic length above which no ignition occurs. The influence of flame size and fuel moisture content on this length is examined. For distances from the flame much smaller than the characteristic length, the ignition time is found to be independent of the moisture content. The existence of such a characteristic length is of major concern for studying percolation-like spread/non spread transition.

Keywords*: Wild land flame radiation, characteristic length, ignition.*

Introduction

Propagation/non-propagation transition threshold is possible only for finite mean free paths [1]. A finite path length is induced by an exponentially decreasing connection probability with the distance between sites. In the frame of propagation of epidemics and forest fires, small world networks seem to be good candidates. They exhibit long-range connections [2] with an exponentially decreasing connectivity distribution. In computer networks (scale free networks), there is no percolation threshold because the connectivity distribution is power-law decreasing (the characteristic length is infinite) [2]. As stated by Albini [3] the dominant mechanism for fire spread is often radiation for the simple reason that the movement of air is toward the burning zone rather than away from it, at least in the near vicinity of the fire edge where rapid heating of unignited fuel is taking place. This situation is obtained even for wind-aided fire spread whenever the flame structure stands erect from the fuel surface rather than being blown through it. Following Billaud *et al*. [4] and Mudan [5], radiation flux is asymptotically power-law decreasing with distance. However, when studying radiative ignition of wildland fuels, a characteristic length can emerge. This is the aim of the present work. The influence of flame properties and fuel moisture content is also examined.

Ignition process

A simple physical model, derived from that of Koo *et al*. [6, 7], is used for steady-state contiguous fire spread in a thermally-thin uniform porous fuel bed (see Fig.1). In this model, the fuel bed is horizontal or inclined with a slope $\boldsymbol{\phi_s}$. It has a length L_{fb} and is assumed to be a thin homogenous, porous fuel layer (its thickness e is small compared to the fuel bed and flame sizes). The fuel medium is preheated to ignition by radiative heat transfer from the flaming zone and losses radiation to the ambient. The solid model of a single flame is used where the visible flame is regarded as a uniformly-radiating solid body with a cylindrical shape, of length L_f and radius r, and with thermal radiation emitted from its surface. Combustion and chemical reactions are thus assumed to be infinitely fast. The reference system is attached to the flame sheet so that the flame is fixed at $y = 0$. The ignition of a fuel bed

control volume located at a constant distance *y* is examined., and the tilt angle of the flame $\boldsymbol{\theta}$ is caused by the wind speed $\boldsymbol{U_w}$ and the gravitational constant $\boldsymbol{g}$. It is approximated as [6]

$$\theta = \tan^{-1}\left[\frac{1.4\ U_W}{\sqrt{g\ L_f}}\right] \quad (1)$$

The heat supplied by the flame radiations leads to the fuel thermal degradation and to rise the temperature until it reaches the ignition temperature $\boldsymbol{T_{ign}}$. The temperature of the combustible layer is thus time and distance dependent ($\boldsymbol{T_y(t)}$). It is at room temperature $\boldsymbol{T_{rt}}$ for $\boldsymbol{y = \infty}$, and at the flame temperature $\boldsymbol{T_f}$ for $\boldsymbol{y = 0}$.

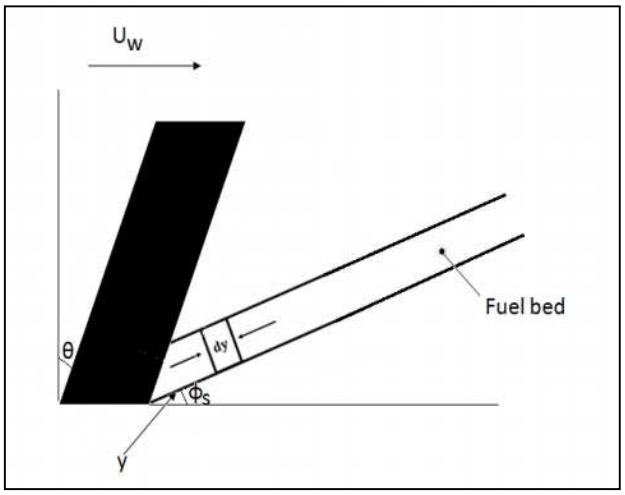

Figure 1. Planar projection of a flame spread schematic.

Consider a volume element $dy \times e \times l$ (l being the width of the fuel bed) of the combustible layer heated by a flame radiation at a distance y. Neglecting the convection flux, the total flux q_T received by this element is

$$q_T = q_{sr} + q_{rl} \quad (2)$$

The radiation flux q_{sr} received from the flame is defined as:

$$q_{sr} = \frac{a_{fb} \times \sigma \times \varepsilon_f \times T_f^4}{e} F \quad (3)$$

Where a_{fb} denotes the absorption coefficient of the combustible element layer, ε_f is the emissivity and σ the Stephan Boltzmann constant. The view factor (F) is determined by Monte-Carlo simulations for a cylindrical flame shape [4, 5]. The Monte-Carlo method used reduces to a stochastic ray-tracing method where discrete energy bundles are sent through the computational domain with the ray direction is sampled.
The radiation loss of the surface element q_{rl} is given by

$$q_{rl} = -\frac{\sigma \times \varepsilon_c \times (T_y^4 - T_{rt}^4)}{e} \quad (4)$$

Where ε_c denotes the emissivity of the combustible element layer. Convective heat transfer is defined as heat transfer between the fuel bed and the ambient air due to bulk fluid motion. The fuel bed may

be heated or cooled by exchanging heat energy with the air by convection both on the surface and in the bulk.
The total heat flux (overhead flame radiation minus radiative losses) increases the temperature of the fuel control volume until it reaches the ignition temperature so that

$$q_T = \begin{cases} \rho_c \times C_p \times \Phi \times \frac{dT}{dt} \,, for\ T \neq 373^0 K \\ -\rho_c \times h_{vap\times} \Phi \times \frac{dW}{dt} \,, for\ T = 373^0 K \end{cases} \quad (5)$$

Here ρ_c is the fuel density, C_p its specific heat, Φ the volume fraction of the solid phase (fine fuel particles), W is the fuel moisture content (FMC), and h_{vap} the latent heat of water evaporation. The boundary conditions associated to Eq. (5) are

$$\begin{aligned} &T(y=0) = T_{ign}, T(y=\infty) = T_\infty \\ &W(y=0) = 0, W(y=\infty) = W_0 \end{aligned} \quad (6)$$

Here W_0 is the initial FMC, T_{ign} and T_∞ are respectively the ignition and ambient temperature. Three different heating processes appear before ignition; wet fuel preheating, drying and pyrolysis. A plateau appears at 373°K due to the phase change as shown in Fig.2.

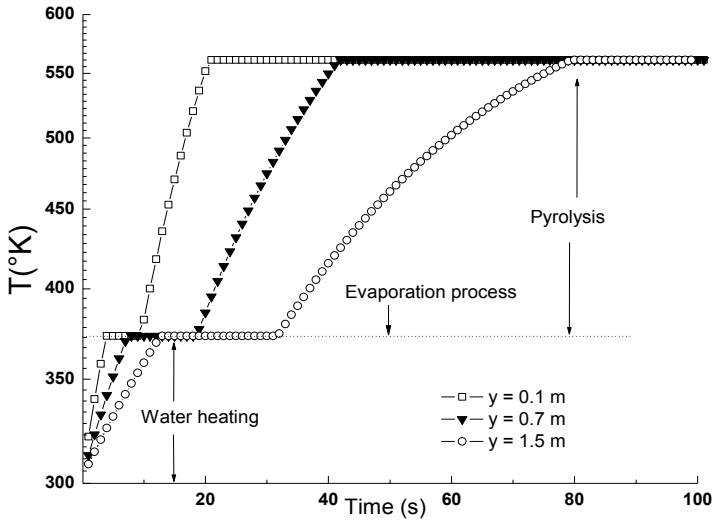

Figure 2. Time evolution of the fuel temperature for various distances y. Ignition temperature is 560°K.The water heating, evaporation and pyrolysis are shown.

Results

In the reference case, the flame is vertical with $L_f = 4\,m$ and $r = 1\,m$, and the FMC is 0.2. The ignition temperature is 560°K and the emissive power of the flame is $120 kW/m^2$. As shown in Fig.3, above $y = 0.5m$, the ignition time exhibits an exponential increase with the distance y from the flame. It behaves as $t_{ign} \propto e^{y/l_c}$ where l_c ($l_c = 2.77 \pm 0.01m$ in Fig.3) is the characteristic ignition length. For $y > l_c$, the ignition time increases faster than the exponential increase.
The existence of a characteristic length of radiative ignition allows reducing the computational time of fire spread simulations, only a small deterministic area of radius l_c (the so-called interaction domain)

being involved in the fire propagation process. This length was empirically introduced in previous studies of forest fire spread and percolation [8].

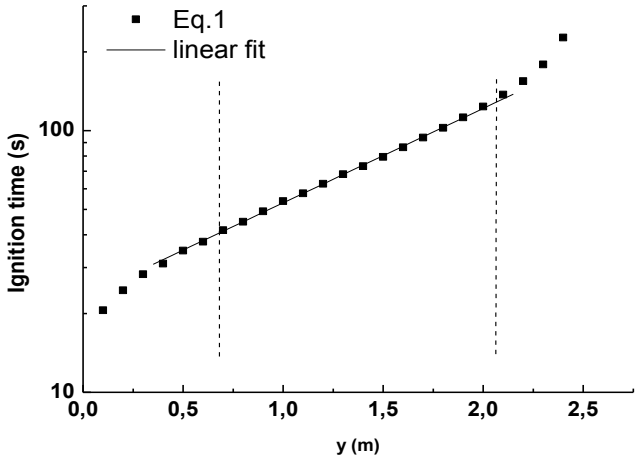

Figure 3. Ignition time vs. y.

The influence of flame height and radius on the ignition characteristic length l_c is shown in Fig.4. The characteristic length l_c increases as a power-law with the flame height. Saturation occurs for L_f around $10m$ (Fig.4a), due to the decreasing contribution of the upper part of the flame. For $L_f = 10m$, the characteristic ignition length increases logarithmically with the flame radius (Fig.4b). This logarithmic behavior indicates a slight dependence on the flame radius.

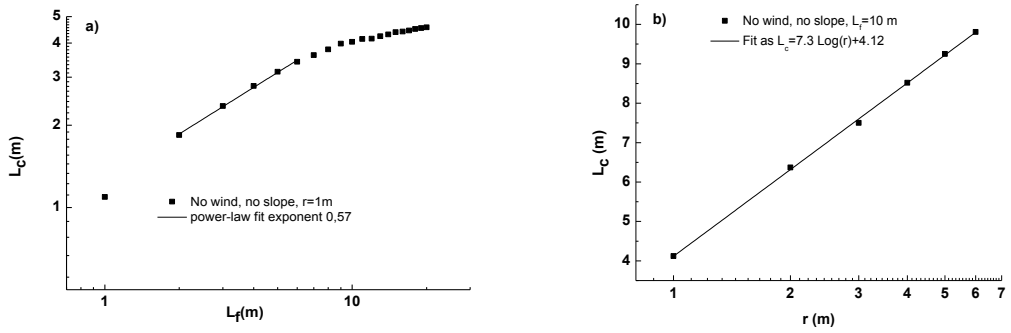

Figure 4. Characteristic length (l_c) vs. a) flame length (logarithmic plot) and b) flame radius (semi-logarithmic plot).

Ignition time increases linearly with FMC, whatever the distance from the flame (Fig.5), according as: $t_{ign} \propto FMC \times e^{y/l_c}$. This indicates that the characteristic length l_c does not depend on FMC, which only delays the ignition time. This result does not agree with the trends obtained experimentally by Trabaud [9], indicating a critical moisture content FMC_{max} above which ignition cannot occur

$$t_{ign} \propto \frac{1}{FMC_{max} - FMC} \quad (7)$$

One of the reasons of this discrepancy is the high flux and small distance y to the flame. Furthermore, flammable gas emission may occur during water heating before evaporation so that, at ignition temperature the remaining gases become insufficient for igniting the fuel. This effect is being included in the present model.

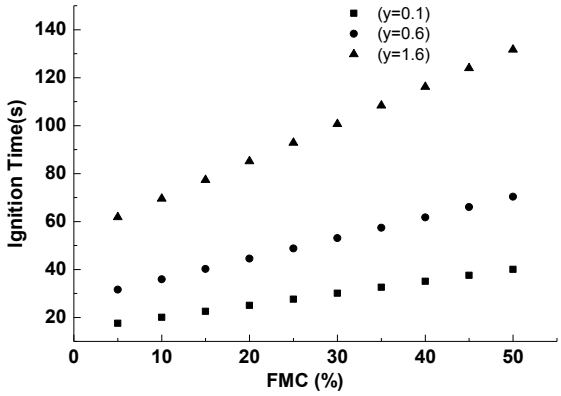

Figure 5. Ignition time dependence on the fuel moisture content for various distances from the flame.

Conclusions

Using a simple thermal model, the existence of a characteristic length of radiative ignition was demonstrated. The dependence of this length on the flame height and radius was investigated. It is also found that this characteristic length was independent of the fuel moisture content. Wind and slope effects on the characteristic length are currently studying.

References

[1] G. Grimmett, Percolation (Springer-Verlag, Heidelberg, 1999); *H.E. Stanley, Introduction to Phase Transitions and Critical Phenomena* (Oxford University Press, London, 1971).
[2] R.Albert and A.-L.Barabasi, Rev.Mod.Phys. **74**, 47 (2002).
[3] F.A.Albini, Shock Waves **32**, 534 (1996).
[4] Y.Billau, A.Kaiss, J.-L.Consalvi and B.Porterie, Int.J.Therm.Science, **50**, 2 (2011).
[5] K. Mudan, Prog. Energy Combust. Sci. **10**, 59 (1984).
[6] E.Koo, P.J.Pagni, J.Woycheese, S.Stephens, D.Weise, and J.Hu, Fire Safety Science–Proceedings of the 8th Intern. Sympos. Intern. Assoc. for Fire Safety Science, London, UK, 2005 pp. 851-862.
[7] Y.Baara, PhD. thesis, USTO, Oran Algeria (2014).
[8] N. Zekri, B. Porterie, J.P. Clerc, and J.C. Loraud, Phys.Rev.E **71**, 046121 (2005).
[9] L.Trabaud, Les feux de forêt. Mécanismes, comportement et environnement (France-sélection, Paris) 1992.

Characterization of custom fuel models for supporting fire modeling-based optimization of prescribed fire planning in relation to wildfire prevention (southern Catalonia, Spain)

Cristina Vega-Garcia[a], Beatriz Duguy[b], Iris Pilar Monfort[c], Sergi Costafreda-Aumedes[d]

[a] *Agriculture and Forest Engineering Department, University of Lleida, Alcalde Rovira Roure 191, 25198, Lleida, Spain, cvega@eagrof.udl.es*
[b]*Departament de Biologia vegetal, Universitat de Barcelona, Diagonal 643, 08028, Barcelona, Spain, bduguy@ub.edu*
[c] *Agriculture and Forest Engineering Department, University of Lleida, Alcalde Rovira Roure 191, 25198, Lleida, Spain, irisenda1818@gmail.com*
[d] *Agriculture and Forest Engineering Department, University of Lleida, Alcalde Rovira Roure 191, 25198, Lleida, Spain, scaumedes@gmail.com*

Abstract
Prescribed fires are an important fuel management tool in Mediterranean fire-prone landscapes, but there is a lack of custom fuel models developed for Mediterranean-type ecosystems and, in particular, for describing ecosystems, which have been treated with a prescribed fire. Such custom fuel models would allow using fire modeling-based approaches for assessing the efficiency of real prescribed fires in relation to fire control at the landscape scale, but also for exploring the efficiency of alternative prescribed fire scenarios under climate change. Pre-burn field-collected vegetation data for shrublands under a *Pinus halepensis* canopy in a semi-arid Mediterranean study area located in southern Catalonia (Northeastern Spain) are presented and compared to values of vegetation parameters published in previous works and commonly used for fuel models characterization. The differences found at the species- and community-levels support the need of developing custom fuel models for improving future fire projections.

Keywords*: prescribed fire, custom fuel models, fire modeling, Mediterranean ecosystems, Aleppo pine*

Introduction

Wildfires are a major cause of environmental degradation in northern Mediterranean countries. The magnitude of the problem will likely be enhanced by climatic change, making necessary the implementation of landscape-level designed fire management strategies (Duguy *et al.* 2013).
Landscape-level fire prevention planning requires a better understanding of how ecosystems, and vegetation in particular, may respond to specific management actions. In recent years, prescribed fires have gained attention as an interesting fuel management alternative to mechanical or chemical tools and livestock grazing, both from economical and ecological points of view (Fernandes 2002, Fernandes and Botelho 2003, Goldammer and Bruce 2004, Rigolot 2005, Cassagne *et al.* 2011). However, while wildfire effects on Mediterranean ecosystems have been comprehensively treated in the literature (Trabaud *et al.* 1985a, 1985b, Pausas *et al.* 1999; Delitti *et al.* 2005; Baeza and Vallejo 2008; Duguy and Vallejo 2008), prescribed fire effects are not so well documented and require further attention before this tool may be extensively applied (Montiel and Kraus 2013).
Short and medium-term effects of prescribed fire are currently being evaluated for shrublands under *Pinus halepensis* canopy within the framework of the ForBurn-Land project funded by the Spanish Ministry of Science and Innovation (AGL2012-40098-C03-02). The focus is on the understory of Aleppo pine stands because almost 367,000 ha of such forests were planted or seeded in Spain between 1940 and 1980, increasing the existing extension of almost 674,000 ha of naturally regenerated *Pinus*

halepensis forests. An additional surface of 786,000 ha, resulting from the secondary succession on abandoned crops, had to be added after 1980.
In general, Aleppo pine forests contribute to the high fire-proneness of Mediterranean landscapes and fire usually plays a major role in the regeneration and dynamics of this pioneer plant community (EEA 2006). The crown structure and the morphology of the pine needles allow ample radiation to reach the soil, so a dense and flammable evergreen sclerophyllous shrub layer (with garrigue to maquis-like physiognomies; EEA 2006), which may cause extreme fire intensities (Martins-Fernandes 2001), is often well developed. Moreover, in the past two decades, the lack of the required preventive silvicultural treatments has resulted in very hazardous stand structures unfavorable for management (Vega-Garcia and Chuvieco 2006). Consequently, we study here the effects of prescribed understory fires under *Pinus halepensis*. Prescribed crown fires are not considered, as they are not allowed in current fuel management planning in Spain (Decreto 312/2006, de 25 de julio in Catalonia and RCARA, de 11 de enero de 2013 in Asturias).
Spatially-explicit fire models, such as FARSITE (Finney 1998), have shown to correctly project fire growth and behavior of hypothetical fires through Mediterranean landscapes (Arca *et al.* 2007, Duguy *et al.* 2007). The reliability of their predictions strongly depends, however, on the accuracy of the fuel-related inputs (Arca *et al.* 2007). Seeking to improve fire simulation options, some scientific precedents in Mediterranean environments have tried to develop new fuel model types (i.e. Prometheus), but few have been based on extensive field measurements; e.g. the UCO40 system developed in Andalucia by Rodriguez y Silva and Molina-Martínez (2012), and most have been limited by scale and budget (Arroyo *et al.* 2008).
The purpose generally stated in previous works is the improvement of fire behavior modeling (Papió and Trabaud 1991; Pereira *et al.* 1995; Bochet *et al.* 2000; Dimitrakopoulos 2001; Viegas *et al.* 2001; Cohen *et al.* 2003; Baeza *et al.* 2006; Pellizzaro *et al.* 2007a; Cassagne *et al.* 2011; Santana *et al.* 2011)., but the evaluation of fuel management alternatives is not explicitly commented.
In that sense, there is still a lack of custom fuel models (CFM, hereafter) developed for Mediterranean ecosystems and, in particular, for describing ecosystems which have been treated with a prescribed fire. Such CFMs would allow using fire modeling-based approaches for assessing the efficiency of real prescribed fires in relation to fire control at the landscape scale, but also for exploring the efficiency of alternative prescribed fire scenarios under climate change.
Consequently, we intend to customize fuel models for pre- and a post-prescribed fire situations in shrublands under a *Pinus halepensis* canopy in a representative study area located in southern Catalonia (Northeastern Spain). The characterization and use of such CFMs are expected to provide more reliable fire modeling projections and, thus, foster the use of fire models as supportive tools for optimizing the landscape-scale planning of prescribed burnings in relation to wildfire prevention. Given that this project is still ongoing, only the pre-fire situation will be presented at this time.

Methods

2.1. Study area

The study area (Figure 1) is located in El Perelló (Southern Catalonia, Spain; UTM Zone 31N; x: 304762, y: 4530927; 250 m a.s.l.). The area is characterized by a semi-arid Mediterranean climate with mild winters and dry and warm summers in which water deficit may reach 300-400 mm. The mean annual precipitation is around 550 mm and mean annual temperature around 17 ºC (POUM Perelló, 2010). Stony Lithic Xerorthents and Lithic Haploxerolls developed over limestones and dolomites (Soil Survey Staff 1999) sustain a forest of *Pinus halepensis Miller* (Vigo *et al.*, 2006) with a canopy cover around 80%. The dominant shrub species in the understory are *Pistacia lentiscus*, *Quercus coccifera*, *Ulex parviflorus*, *Rosmarinus officinalis*, and *Erica multiflora. Rhamnus alaternus*, *Olea europaea* and *Chamaerops humilis* are other common woody species.

The pine stands were planted in 1970 on old crops (cereal, almond and olive groves) that were abandoned in the 1950s. A mechanical treatment was applied in 1998 to reduce the biomass of the understory.

Methods

Three plots (10x10 m) were installed in the study area. The vegetation samplings were carried out in February 2013 and March 2014, before and after, respectively, a prescribed burning for fuel hazard reduction that was conducted over 2.1 ha in May 2013 and that only affected the understory. The three plots were divided in a hundred $1m^2$ quadrats for inventory of specific composition (list of species) and vegetation structure. The minimum and maximum height (of shrub layer and highest individuals among dominant shrubs), the minimum and maximum crown diameters, and the cover percentages (shrub and herbaceous layers) were measured.

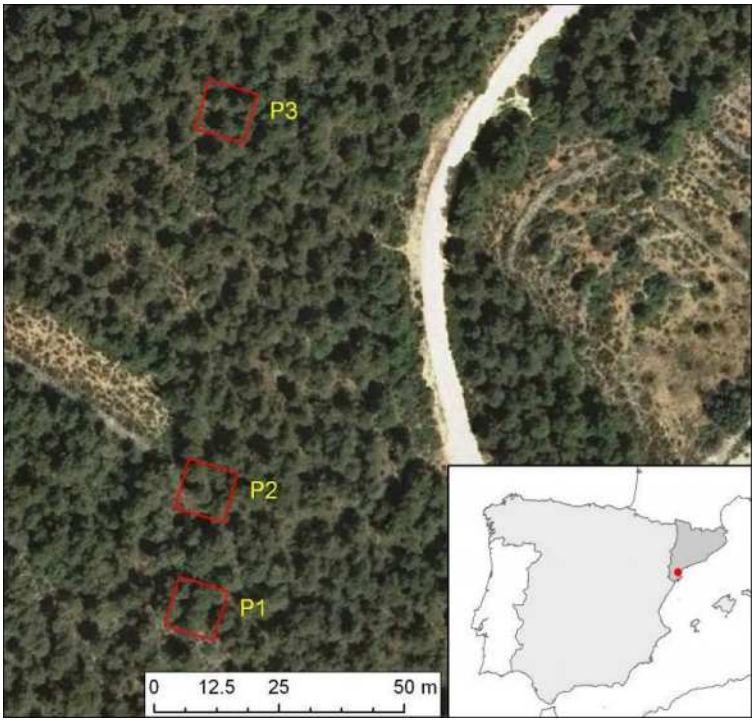

Figure 1. Location of study area and of the three sampling plots. Source: ***PNOA*** *ordered by © Instituto Geográfico Nacional de España*

Outside the plots, 20 individuals of each of the five dominant shrub species (*Rosmarinus officinalis*, *Pistacia lentiscus*, *Quercus coccifera*, *Ulex parviflorus* and *Erica multiflora*) were selected taking into account the dimensional range of each species in the site. Individuals were measured (minimum and maximum crown height and crown diameter), cut, weighted in the field, and reweighted after removing the fine live fraction (diameter < 6 mm) in order to develop allometric relations between the estimated volume and aerial phytomass. The data were processed in order to obtain fuel loads for the description of a CFM. The values of those parameters were then compared to the ranges found in the literature for the same species and similar Mediterranean plant communities. Additionally, those values were also compared to those of analogous fuel model types in the classifications by Scott and Burgan (2005), Anderson (1982) and the UCO40 system by Rodriguez y Silva and Molina-Martínez (2012).
Also, fine live (woody, herbaceous) and dead (fine, coarse) fuel moisture contents were sampled four times along the fire season in 2013 (June, July, August and September). Ten samples were taken by

fuel category and species, sealed, weighted (fresh weight), oven dried (80ºC) during 48h and reweighted afterwards (dry weight). Moisture content was estimated as a dry weight percentage.

Results

The values collected in the field for a set of fuel-related relevant characteristics and for the five sampled shrub species are presented in Table 1 along with the values found in the literature. Under the label "Proxy fuel load variables", the variables used for establishing allometric relationships are presented in the first six rows for our target species. They are followed by four woody fuel load fractions estimated based on those allometries. Below, available direct measurements of fuel load fractions obtained by destructive field sampling are recorded (Live Woody Fuel Load only), followed by total values (added fractions) obtained by any of these procedures (Aerial Phytomass).
Under the label "Custom fuel model input set" are listed some variables that are usually considered for fire modeling under semi-physical models based on Rothermel's (1972) equations, such as FARSITE (Finney 1998). Finally, moisture content data are presented, and the references are provided. In order to facilitate comparisons with fuels described in other studies, data compiled in the table are not restricted only to fuel loads.

Table 1. Fuel-related variables at the species level. The data presented in brackets correspond to FORBURN field data and the rest is bibliographic data. RO: Rosmarinus officinalis; PL: Pistacia lentiscus; QC: Quercus coccifera; UP: Ulex parviflorus; EM: Erica multiflora; (-): not available; H: height; D: diameter.

SPECIES TABLE		NAME	RO	PL	QC	UP	EM
		BIOLOGIC FORM	Nanophanerophyte	Nanophanerophyte	Nanophanerophyte	Nanophanerophyte	Nanophanerophyte
PROXY FUEL LOAD VARIABLES	ALLOMETRIC VARIABLES	Hmax crown (cm)	50-117 (10-110)	106-120 (10-150)	60-75 (10-80)	(10-85)	(15-120)
		Hmin crown (cm)	(0-70)	(0-130)	(0-40)	(0-40)	(0-70)
		Dmax crown (cm)	33.70-165 (5-150)	47.50-146.50 (5-144)	(5-100)	(10-80)	(5-120)
		Dmin crown (cm)	50-124 (3-110)	(5-110)	(5-100)	(5-50)	(5-100)
		Standing necromass length (cm)	-	-	-	-	-
		Basal diameter (cm)	9-112	-	-	-	-
	WOODY FUEL LOAD	Live Woody Fine Fuel Load (t ha-1)	-	-	-	3.89-4.9	-
		Live Woody Coarse Fuel Load (t ha-1)	-	-	-	0.27-17.6	-
		Standing Dead Woody Fine Fuel Load (t ha-1)	-	-	-	0.26-15.8	-
		Standing Dead Woody Coarse Fuel Load (t ha-1)	-	-	-	0-1.46	-
	LOAD FROM DESTRUCTIVE SAMPLING ON THE FIELD	Live Woody Fuel Load (t.ha-1)	0.33-1.30	-	-	1.94-6.36	-

	AERIAL PHYTOMASS	Total Aerial Weight (t.ha-1)	0.76-2.66 (1.69)	(10.72)	(0.90)	5.15-43.08 (0.07)	(1.78)
	ESTIMATED PHYTOVOLUME	PhytoVol_Conic (dm3)	30.80-416 (0.13-280.77)	237.80-3447.60 (0.07-287.90)	(0.07-83.77)	(0.13-62.83)	(0.03-172.79)
		PhytoVol_Cilin (dm3)	(0.39-843.3)	(0.20-864)	(0.20-251.33)	(0.39-188.5)	(0.10-518.36)
	FUEL PARTICLE DENSITY	Density_Vol_Conic (kg m-3)	410-693	530	820-930	614	-
CUSTOM FUEL MODEL INPUT SET	FUEL LOAD BY CATEGORY AND PARTICLE SIZE CLASS	Live Woody Fuel Load (t ha-1)	15-50	2.90-4.5	-	-	-
	SURFACE AREA TO VOLUME RATIO	Live Woody SAV (cm-1)	11.10-55	10.13-70.3	1.30-62.22	40.30-50	-
	EMC	Dead Fuel Moisture of Extinction (%)	-	80-85	>80	-	-
	FUEL PARTICLE PROPERTIES	Live Fuel Heat Content (kJ kg-1)	20.40-24.8	18.90-20.30	18.20-21.1	20-21	-
		Dead Fuel Heat Content (kJ kg-1)	-	-	-	-	-
MOISTURE CONTENT	MEAN DAILY WEATHER CONDITIONS (SAMPLING DAY AND THE 7 PREVIOUS DAYS)	Tmax (ºC)	(24.07-30.3)	(24.07-30.3)	(24.07-30.3)	(24.70-30.3)	-
		Precipitation (mm)	(0-1.84)	(0-1.84)	(0-1.84)	(0-1.84)	-
		Relative Humidity (%)	42-57.3 (64.5-68)	(64.50-68)	(64.50-68)	10-93 (64.50-68)	-
	MOISTURE CONTENT	Standing necromass	(6.36-58.73)	(6.36-58.73)	(6.36-58.73)	(6.36-58.73)	-
		Live Fine fuel	4.40-219 (52.42-194.27)	9.10-119 (81.45-150.48)	65-145 (52.5-85.09)	17.96-85 (52.77-124.86)	-
SOURCE			Bochet *et al.* 2000; Santana *et al.* 2011; Viegas *et al.* 2001; Cohen *et al.* 2003; Baeza *et al.* 2006; Pellizzaro *et al.* 2007a; Pellizzaro *et al.* 2007b; Cassagne *et al.* 2011; Curt 2014 (Unpublished data)	Papió and Trabaud 1991; Dimitrakopoulos 2001; Dimitrakopoulos and Panov 2001; Dimitrakopoulos and Papaioannou 2001; Cohen *et al.* 2003; Pellizzaro *et al.* 2007a; Pellizzaro *et al.* 2007b; GENCAT 2014	Dimitrakopoulos 2001; Dimitrakopoulos and Panov 2001; Dimitrakopoulos and Papaioannou 2001; Viegas *et al.* 2001; Cohen *et al.* 2003; Cassagne *et al.* 2011; GENCAT 2014	Pereira *et al.* 1995; Baeza *et al.* 2002; Cohen *et al.* 2003; Baeza *et al.* 2006; Santana *et al.* 2011; GENCAT 2014	-

For most variables, values are not available for all the species dominating the plant communities of our study area (Table 1). Those species are among the most common species that can be found in shrubland ecosystems of Western Mediterranean basin, though. This lack of data highlights the fact that many fuel-related parameters have not been sufficiently studied in previous work and shows the need of further field-based research on those variables.

The values of fuel-related relevant characteristics for some Mediterranean plant communities similar to the shrublands that have been sampled in the study area are presented in Table 2, as well as the data obtained in our site.

First rows describe the composition and cover variables of the plant communities, followed by fuel fractions estimated through destructive sampling in the field. Total values (added fractions) obtained by any of these procedures are below (Total Shrub Load).

Variables usually considered for fire modeling under semi-physical models based on Rothermel's (1972) equations are listed afterwards and shadowed in grey. Last rows provide fuel moisture data and bibliographic sources of values. Again, in order to facilitate comparisons with communities in other studies, data compiled in the table are not restricted only to fuel loads, but other variables are included.

Table 2. Fuel-related variables at the plant community level. AA: Arbutus andrachne; AU: Arbutus unedo; BR: Brachypodium retusum; BS: Buxus sempervirens; CA: Cistus albidus; CC: Cistus creticus; CH: Chamaerops humilis; CM: Crataegus monogyna; CS: Ceratonia siliqua; EA: Erica arborea; EM: Erica multiflora; FE: Festuca sp.; JC: Juniperus communis; JO: Juniperus oxycedrus; OE: Olea europaea; PA: Phillyrea latifolia; PB: Pinus brutia; PF: Phlomis fruticosa; PH: Pinus halepensis; PL: Pistacia lentiscus; PM: Phyllyrea media; PP: Pinus pinea; QC: Quercus coccifera; QI: Quercus ilex; RA: Rhamnus alaternus; RO: Rosmarinus officinalis; SS: Sarcopoterium spinoum; ST: Stipa sp.; UP: Ulex parviflorus; TV: Thymus vulgaris; (-): not available

PLANT COMMUNITY	SPECIES COMPOSITION	UP, RO, PL, EM, QC	RO, UP, CA	RO, UP, CA	PL, AA, QC, PL, CC, CS, CM, RA	QC, SS, AA, PL	UP, RO, QC, BR	UP, BR, CA, RO	QC, QI, PL, AU, EA	PB, PL, QC, AU, PM
	Species OVER 60% in cover	PL	RO	RO	PL	QC	UP	UP	QC	PB
	OTHER SPECIES	UP, RO, EM, QC	UP, CA	UP, CA	AA, QC, PL, CC, CS, CM, RA	SS, AA, PL	RO, QC, BR	CA, RO	QI, PL, AU, EA	PL, QC, AU, PM
COVER	Dead 1-hr (%)	-	37.80	46.3-90.1	-	-	-	-	-	-
	Live Herbaceous (%)	54	1.30	13.2-31.3	-	-	-	-	-	-
	Specfic Cover (%)	UP 3.8%, RO 18%, QC 16.34%, PL 50.38, EM 10 %	-	-	-	-		UP (>50), CA (1.5)	-	-
	Shrub_Cover (%)	46.7	10.40	59.5-76	-	-	-	-	-	-
	Total Cover(%)	100	-	-		65 - 90	-	-	-	-
LOAD FROM DESTRUCTIVE SAMPLING ON THE FIELD	Live Woody Fine Fuel Load (tn.ha-1)	-	-	-	11.80-21.70	9.50 – 14.50	-	-	-	-
	Live Woody Coarse Fuel Load (tn.ha-1)	-	-	-	-	2.30 – 19.20	-	-	-	-
	Standing Dead Fuel Load Woody (tn.ha-1)	-	-	-	-	4.60 – 8.20	-	-	-	-
SHRUB_LOAD	Total Shrub_Load (tn.ha-1)	(15.24)	-	-	24.70-51.30	19.30 – 36.80	5.00-35.00	-	-	-
FUEL LOAD BY CATEGORY AND PARTICLE SIZE CLASS	Dead Fine Fuel Load 1h (t ha-1)	-	-	-	-	-	-	9.24-18.96	7.39	8.48
	Dead Fuel Load 10h (t ha-1)	-	-	-	-	-	-	-	6.80	3.58
	Dead Fuel Load 100h (t ha-1)	-	-	-	-	-	-	-	3.58	1.80
	Live Fuel Load Herbaceous (t ha-1)	-	-	-	-	-	-	1.87-4.15	-	0.10
	Live Fuel Load Woody (t ha-1)	-	-	-	-	-	-	10.57-20.08	7.68	3.26
SURFACE AREA TO VOLUME RATIO	1hSAV (cm-1)	-	-	-	-	-	-	105.20	24.60	49.21
	10hSAV (cm-1)	-	-	-	-	-	-	-	59.06	59.06
	100hSAV (cm-1)	-	-	-	-	-	-	-	52.49	24.61
	Live Herbaceous SAV (cm-1)	-	-	-	-	-	-	82.02	-	-

	Live Woody SAV (cm-1)	(0.24)	-	-	-	-	-	49.21	-	-
FD	Fuelbed Depth (cm)	-	-	-	-	-	-	-	111.86	24.99
EMC	Dead Fuel Moisture of Extinction (%)	-	-	-	-	-	-	-	14.00	25.00
FUEL PARTICLE PROPERTIES	Dead Fuel Heat Content (kJ kg-1)	-	-	-	-	-	-	21050	-	-
	Live Fuel Heat Content (kJ kg-1)	-	-	-	-	-	-	19500	-	-
MEAN DAILY WEATHER CONDITIONS	Tmax (ºC)	(13.7)	-	-	-	22.50-29.30	-	-	-	-
	Relative Humidity (%)	(49.87)	-	-	-	50-77	-	67-93	-	-
MOISTURE CONTENT	Dead Fuel 1h	-	-	-	13.30-67.60	-	-	52-60	-	-
	Dead Fuel 10h	-	-	-	-	-	-	-	-	-
	Dead Fuel 100h	-	-	-	-	-	-	-	-	-
	Live Fine Fuel	-	-	-	60.30-164	28.20-50.70	-	85-174	-	-
	Live Herbaceous	-	-	-	-	-	-	103-133	-	-
SOURCE		FORBURN	Santana *et al.* 2012	Santana *et al.* 2012	Saglam *et al.* 2008	Bilgili and Saglam 2003	Duguy *et al.* 2007	De Luis *et al.* 2004; Baeza and Vallejo 2008	Kalabokidis *et al.* 2013	Kalabokidis *et al.* 2013

Once more, the compilation of available data presented in the table shows the need of further research for implementing better structural descriptions of some very common Mediterranean plant communities. This lack of reliable data for most fuel-related relevant vegetation parameters makes very difficult an appropriate structural characterization of the corresponding plant communities and, thus, a good description of the derived custom fuel models.

As for our FORBURN data, we found that before the prescribed burning, the total herbaceous cover in the three sampled plots was 50, 61 and 51%, respectively, while the total shrub cover was 58, 41 and 40%, respectively. Among shrubs, *Pistacia lentiscus* was the species with the largest covers (36.6 - 69%) and estimated phytovolumes (in % of total phytovolume of shrub understorey in the community, 33.3 - 73.5%), followed by *Rosmarinus officinalis* (6.5 – 35%, for cover, and 6.1 - 41.7% respectively), *Quercus coccifera* (4.9 - 37.1% cover and 2.3 - 26%), *Erica multiflora* (2.3 - 17.3% cover and 1.5 - 17.8%) and *Ulex parviflorus* (2.2 - 6.4% cover and 1.7 - 4.3% total phytovolume of shrub understorey).

Other species present (*Rhamnus lycioides, Rhamnus alaternus, Chamaerops humilis, Thymus vulgaris* and *Genista sp.*) had very low cover values (always less than 1.8%) and were not considered for our fuel model description purposes. Given the generally rather low percentage covers reached by *Ulex parviflorus* in the studied shrubland, the standing dead woody fuel loads of that species were not considered either.

Over the three plots, shrubs height did not exceed 150 cm. Species averaged heights were weighted by cover (Martins-Fernandes 2001) to provide an integrated site value of 0.68 m. The mean total shrub biomass in the pre-burn situation reached on average 15.25 tn.ha-1. This aerial weight of shrubs or live woody fuel load (LWFL) was lower than those found in Saglam *et al*. (2008) and Bilgili and Saglam (2003), within the range in Duguy *et al*. (2007), De Luis *et al*. (2004) and Baeza and Vallejo (2008), and higher than in Kalabokidis *et al*. (2013). This value is also higher than the total fuel load values provided by Anderson (1982) for shrub-type models 6 and 7 (14.8 and 12.1 t.ha-1, respectively), by Scott and Burgan (2005) for shrub-type model SH2 (12.9 t.ha-1), and by Rodriguez y Silva and Molina-Martínez (2012) for M5, HPM4 and HPM5 models (10.55, 11.13 and 10.74 t.ha-1, respectively). It is smaller than the total fuel load value provided by Anderson (1982) for shrub-type model 4 (32.1 t ha-1), although this fuel load amount includes a large value of dead fuel load (12.4 t ha-1). Our plant community value is also smaller than the fuel load value provided by Scott and Burgan (2005) for shrub-type model SH5 (16.09 t ha-1). This latter fuel model appears, nevertheless, as the

most appropriate standard fuel model that might be attributed to the studied community. SH5 is described as a shrubland with a heavy shrub load, in which the shrub layer height may range from 120 to 180 cm (Scott and Burgan 2005).
Those results are indicative of the wide margin for error that may exist when using for fire modeling fuel models that have not been developed in a customized way, i.e. based on local vegetation structural data collected on the field. They also confirm the need of new CFMs.
An aspect that sometimes makes difficult the appropriate understanding or selection of both standard and custom fuel models, as well as the comparisons between them, is the use of different units by the authors. We have presented all the variables shown in our tables using international system units in order to make those tables more useful for future evaluations and decision processes.

Discussion and management implications.

When considering individual species, Aleppo pine stands in our study site appear to be characterized by a shrub understory with smaller total fuel loads than those found in other Mediterranean ecosystems analyzed in the literature. The dimensional values found for the main shrubs present in our site are similar to those appearing in published works, but their aerial phytomasses and phytovolumes per unit area appear to be smaller. In our site, the understory is dominated in cover, volume and biomass by *Pistacia lentiscus*, although with smaller biomass values (10.72 t.ha-1) than those found by other authors, ranging from 14.19 to 158.20 t.ha-1 (Papió and Trabaud 1991; Dimitrakopoulos 2001; Dimitrakopoulos and Panov 2001; Dimitrakopoulos and Papaioannou 2001; Cohen *et al*. 2003; Pellizzaro *et al*. 2007a; Pellizzaro *et al*. 2007b). The differences may be explained by different conditions in these studies in terms of climatic variables, but also species composition and tree cover. The study by Papió and Trabaud (1991) was placed in a location with a mixed garrigue of *Quercus coccifera* with 919 mm of annual precipitation and no tree cover, while Pellizzaro *et al*. (2007a) and Pellizzaro *et al*. (2007b) worked in maquis and garrigue in a site with about 600 mm and without tree cover. Data in Dimitrakopoulos (2001), Dimitrakopoulos and Panov (2001) and Dimitrakopoulos and Papaioannou (2001) comes from general phrygana and maquis formations, but no climatic data is provided. For Cohen *et al*. (2003) only general locations are referred. Comparability among results is complicated by the lack of descriptions in these cases, but clearly studies in locations with a tree cover are lacking, which justifies our work.
For comparisons at the community level, a lower total shrub biomass in the pre-burn situation was in agreement with the fact that the mean annual rainfall in our study area is lower (300 - 400 mm, with a quite significant water deficit spanning 3-5 months with semiarid conditions, POUM Perello, 2010) than in other studies in which mean annual precipitation ranges between 450 and 700 mm (Lesvos, Greece, Kalabokidis *et al*. 2013), 466 and 700 mm (Valencia Region, Spain, De Luis *et al*. 2004; Duguy *et al*. 2007; Baeza and Vallejo 2008; Santana *et al*. 2012), or even 805 mm and 1200 mm (Turkey, Bilgili and Saglam 2003; Saglam *et al*. 2003). A lower biomass value resulting from more adverse ecological site conditions may be the major causative factor.
However, differences in the procedures followed by different authors for estimating the apparent phytovolumes and other proxy or intermediate variables may certainly have had also an impact on biomass estimations.
Both species and community FORBURN fuel load data estimates highlight the difficulty of carrying out comparative studies considering Mediterranean-type shrublands that may cover a wide range of ecological and land use history situations, and also the crucial need of standardizing the experimental protocols for the characterization of such plant communities in relation to the description of a larger number of custom fuel models. This also applies to other important variables, such as the fuel moisture, which is currently estimated with drying protocols varying from 24 h at 105 ºC (Viegas *et al*. 2001; Saglam *et al*. 2008) to 48 h at 60 ºC (Rodríguez y Silva and Molina-Martinez 2012), for instance.

The fact that in our pine stands the understory is dominated in cover, volume and biomass by *Pistacia lentiscus* raises questions regarding past silvicultural treatments implemented in those stands, but also about future stand treatments. The mechanical fuel reduction treatment applied in 1998 may have favored this species and controlled, on the contrary, the presence of some seeder shrubs (Baeza *et al.* 2003).
Unless excessively tall and thus producing ladder fuels in the pine stands that would increase the risk of crown fires, *Pistacia lentiscus* is a resprouter species, which is usually considered for ecological restoration purposes in Mediterranean fire-prone ecosystems, since its presence gives resilience to those systems (CEAM 2009).
On the contrary, *Ulex parviflorus (gorse)* and *Rosmarinus officinalis* are obligate seeders, which tend to accumulate large amounts of fine dead fuels and need to be controlled (Duguy and Baeza 2009). In gorse communities, in particular, the standing necromass incrases strongly with age, promoting conditions conducive to high intensity fires (Baeza *et al.* 2006). It has been recommended, therefore, to apply a combination of treatments, such as mechanical fuel reduction actions combined with repeated prescribed burnings in order to decrease fuel loads in such communities (Baeza and Duguy 2009).
A single prescribed fire conducted in 2010 in a similar pine stand adjacent to our site seems to have generated this reduction effect over *Ulex parviflorus* cover (M. Castellnou, personal communication, October 2012).
In any case, fuel reduction treatments must be designed taking into account the characteristics and ecological requirements of the species within the target ecosystems (Baeza 2004) and, particularly, the reproductive biology of the key species (Baeza and Duguy 2009). Within a climate change context, treatments strategies should also consider the need of an increased resilience of ecosystems to fire, conservation and promotion of biodiversity, carbon budgets and desertification issues (Hurteau *et al*. 2008).
As this project is still ongoing, post-fire data are not presented at this time, but if those data show that the structural characteristics of the plant community have not been significantly modified by the prescribed fire, the description of a different custom fuel model for the post-fire situation will not be justified. This would, of course, mean that the executed burning has not been an efficient tool in relation to fuel control and, therefore, fire prevention. Prescribed burning may have modified, however, the species composition of the *Pinus halepensis* forest understory. Such changes would require a further analysis, if they happen.
The comparison of total fuel load values (total shrub aerial biomass) of the studied community with those given for existing fuel model types under different classification systems, which are often used in Mediterranean ecosystems, leads to consider that significant errors can be made when using those latter fuel models for fire modeling in our region. It clearly shows the need of describing local custom fuel models for shrublands developed under an Aleppo pine canopy in semi-arid Mediterranean conditions.

Acknowledgements

We gratefully acknowledge funding from the Spanish Ministry of Science and Innovation to the ForBurn-Land project (AGL2012-40098-C03-02), and the field work and literature search tasks by Eduardo Collado, Laura Fuentes López, Jesús Godoy Puertas, Milena Prendin Navarro, Joaquim Garcia Codina and Adrián Cardil.

References

Anderson HE (1982) Aids to determining fuel models for estimating fire behavior. The Bark Beetles, Fuels, and Fire Bibliography.

Arca B, Duce P, Laconi M, Pellizzaro G, Salis M, Spano D (2007) Evaluation of FARSITE simulator in Mediterranean maquis. *International Journal of Wildland Fire* **16**, 563-572.

Arroyo LA, Pascual C, Manzanera JA (2008) Fire models and methods to map fuel types: the role of remote sensing. *Forest Ecology and Management* **256**, 1239–1252.

Baeza MJ (2004) El manejo del matorral en la prevención de incendios forestales. En: Avances en el estudio de la gestión del monte mediterráneo. Vallejo, V.R. y Alloza, J.A., (eds.). Fundación Centro de Estudios Ambientales del Mediterráneo - CEAM. pp. 65-92.

Baeza MJ, De Luis M, Raventós J, Escarré A (2002) Factors influencing fire behaviour in shrublands of different stand ages and the implications for using prescribed burning to reduce wildfire risk. *Journal of Environmental Management* **65**, 199–208.

Baeza J, Duguy B (2009) Prevención de incendios forestales. La gestión del combustible. In: La actividad científica de la Fundación Centro de Estudios Ambientales del Mediterráneo (1991-2008). Investigación Forestal: Los Incendios forestales. Fundación CEAM (ed.). CEAM, Valencia. pp. 155-157.

Baeza MJ, Raventos J, Escarré A, Vallejo VR (2003) The effect of shrub clearing on the control of the fire-prone species *Ulex parviflorus*. *Forest Ecology and Management* **186**, 47-59.

Baeza MJ, Raventós J, Escarré A, Vallejo VR (2006) Fire risk and vegetation structural dynamics in Mediterranean shrubland. *Plant Ecology* **187**, 189–201.

Baeza MJ, Vallejo VR (2008) Vegetation recovery after fuel management in Mediterranean shrublands. *Applied Vegetation Science* **11**, 151–158.

Bilgili E, Saglam B (2003) Fire behavior in maquis fuels in Turkey. *Forest Ecology and Management* **184**, 201–207.

Bochet E, Poesen J, Rubio JL (2000) Mound development as an interaction of individual plants with soil, water erosion and sedimentation processes on slopes. *Earth Surface Processes and Landforms* **25**, 847–867.

Cassagne N, Pimont F, Dupuy J-L, Linn RR, Marell A, Oliveri C, Rigolot E (2011) Using a fire propagation model to assess the efficiency of prescribed burning in reducing the fire hazard. *Ecological Modelling* **222**, 1502–1514.

CEAM. 2009. La actividad científica de la Fundación Centro de Estudios Ambientales del Mediterráneo (1991-2008). Fundación CEAM (ed.). CEAM, Valencia. 201 pp.

Cohen M, Cuiñas P, Diez C, Fernandes P, Guijarro M, Moro C (2003) Wildland fuel particles characterization database content. Contract No. EVG1-CT-2001-00041, Fire Star: A Decision Support System for Fuel Management and Fire Hazard Reduction in Mediterranean Wildland-Urban Interfaces. Deliverable D6-03-A1.

Delitti W, Ferran A, Trabaud L, Vallejo VR (2005) Effects of fire recurrence in Quercus coccifera L. shrublands of the Valencia Region (Spain): I. Plant composition and productivity. *Plant Ecolology* **177**, 57–70.

De Luis M, Baeza MJ, Raventós J, González-Hidalgo JC (2004) Fuel characteristics and fire behaviour in mature Mediterranean gorse shrublands. *International Journal of Wildland Fire* **13**, 79–87.

Dimitrakopoulos AP (2001) A statistical classification of Mediterranean species based on their flammability components. *International Journal of Wildland Fire* **10**, 113–118.

Dimitrakopoulos AP, Panov PI (2001) Pyric properties of some dominant Mediterranean vegetation species. *International Journal of Wildland Fire* **10**, 23–27.

Dimitrakopoulos AP, Papaioannou KK (2001) Flammability assessment of Mediterranean forest fuels. *Fire Technology* **37**, 143–152.

Duguy B, Alloza JA, Röder A, Vallejo R, Pastor F (2007) Modelling the effects of landscape fuel treatments on fire growth and behaviour in a Mediterranean landscape (eastern Spain). *International Journal of Wildland Fire* **16**, 619-632.

Duguy B, Paula S, Pausas JG, Alloza JA, Gimeno T, Vallejo VR (2013) Effects of climate and extreme events on wildfire regime and their ecological impacts. In: Regional Assessment of Climate Change in the Mediterranean, Volume 2: *Agriculture, Forests and Ecosystem Services and People, Advances in Global Change Research* 51 (Eds Navarra A, Tubiana L) pp. 101 - 134. (Springer Science + Business Media. Holanda).

Duguy B, Baeza J (2009) Efecto de la historia de usos en la recuperación de la cubierta vegetal. En: La actividad científica de la Fundación Centro de Estudios Ambientales del Mediterráneo (1991-2008). Investigación Forestal: Los Incendios forestales. Fundación CEAM (ed.). CEAM, Valencia. pp. 167-169.

Duguy B, Vallejo VR (2008) Land-use and fire history effects on post-fire vegetation dynamics in eastern Spain. *Journal of Vegetation Science* **19**, 97-108.

EEA 2006. European forest types. Categories and types for sustainable forest management reporting, European Environmental Agency EEA technical report number 9/2006. (Copenhagen)

España, Consejería de Agroganadería y Recursos Autóctonos. Resolución de 30 de enero de 2012, de la Consejería de Agroganadería y Recursos Autóctonos, por la que se aprueban las normas sobre quemas en el territorio del Principado de Asturias. Boletín oficial del Principado de Asturias, 11 de febrero de 2012, núm. 34, p. 1.

España. Decreto 312/2006, de 25 de julio, por el que se regula la gestión del fuego técnico por parte del personal de los servicios de prevención y extinción de incendios de la Generalitat de Cataluña. *Diario oficial de la Generalitat de Cataluña*, 27 de julio de 2007, núm. 4685, pp. 33769- 33772

Fernandes PM (2002) Prescribed Fire: strategies and management. In: Pardini G, Pintó J (eds). Fire, Landscape and Biodiversity: An Appraisal of the Effects and Effectiveness. Diversitats 29. Universitat de Girona, Institut de Medi Ambient, Girona. pp. 87-200.

Fernandes PM, Botelho HS (2003) A review of prescribed burning effectiveness in fire hazard reduction. *International Journal of Wildland Fire* **12**, 117-128.

Finney MA (1998) FARSITE: Fire Area Simulator–model development and evaluation. USDA Forest Service, Research Paper RMRS-RP-4. Fort Collins, CO, USA.

GENCAT. Generalitat de Cataluña (2014). *Servei Meteorológic de Cataluña*. [online] http://www.meteo.cat/servmet/index.html (Accessed on 23-04-2014)

Goldammer JG, Bruce M (2004) The use of prescribed fire in the land management of Western and Baltic Europe: An Overview. *International Forest Fire News* **30**, 2-13.

Hurteau MD, Koch GW, Hungate BA (2008) Carbon protection and fire risk reduction: toward a full accounting of forest carbon offsets. Front. Ecol. Environ., 6, 493-498.

Kalabokidis K, Palaiologou P, Finney M (2013) Fire Behavior Simulation in Mediterranean Forests Using the Minimum Travel Time Algorithm. In Proceedings of 4th Fire Behavior and Fuels Conference (pp. 468–492). International Association of Wildland Fire.

Martins Fernandes PA (2001) Fire spread prediction in shrub fuels in Portugal. *Forest Ecology and Management* **144**, 67–74.

Montiel C, Kraus D (Eds) (2010) *Best practices of fire use. Prescribed burning and suppression fire programmes in selected case-studies regions in Europe,* European Forest Institut, Joensuu.

Papió C, Trabaud L (1991) Comparative study of the aerial structure of five shrubs of Mediterranean shrublands. *Forest Science* **37**, 146–159.

Pausas JG, Carbó E, Caturla RN, Gil JM, Vallejo R (1999) Post-fire regeneration patterns in the Eastern Iberian Peninsula. *Acta Oecologica* **20**, 499-508.

Pellizzaro G, Cesaraccio C, Duce P, Ventura A, Zara P (2007a) Relationships between seasonal patterns of live fuel moisture and meteorological drought indices for Mediterranean shrubland species. *International Journal of Wildland Fire* **16**, 232–241.

Pellizzaro G, Duce P, Ventura A, Zara P (2007b) Seasonal variations of live moisture content and ignitability in shrubs of the Mediterranean Basin. *International Journal of Wildland Fire* **16**, 633–641.

Pereira JMC, Sequeira NMS, Carreiras JMB (1995) Structural-properties and dimensional relations of some Mediterranean shrub fuels. *International Journal of Wildland Fire* **5**, 35–42.

POUM Perelló (2010) Pla d'Ordenació Urbanística Municipal del Perelló (Urban Development Plan of El Perelló). http://www.elperello.cat/ftp/POUMAPROVINICIAL/1_DOC%201/POUM%20Perello_AI_Doc1.pdf [online]. (Last access: 13/04/2014).

Rigolot E (2005) Bûlage dirigé: Quinze and d'expérimentation. *Espaces Naturales* 12, 16-17.

Rodríguez y Silva F, Molina-Martínez JR (2012) Modeling Mediterranean forest fuels by integrating field data and mapping tools. *European Journal of Forest Research* **131**, 571–582.

Rothermel RC, Forest I (1972) A mathematical model for predicting fire spread in wildland fuels.

Saglam B, Bilgili E, Küçük Ö, Durmaz BD (2008) Fire behavior in Mediterranean shrub species (maquis). *African Journal of Biotechnology* **7**, 4122 - 4129.

Santana VM, Baeza MJ, Vallejo VR (2011) Fuel structural traits modulating soil temperatures in different species patches of Mediterranean Basin shrublands. *International Journal of Wildland Fire* **20**, 668–677.

Santana VM, Baeza MJ, Maestre FT (2012) Seedling establishment along post-fire succession in Mediterranean shrublands dominated by obligate seeders. *Acta Oecologica* **39**, 51–60.

Scott JH, Burgan RE (2005) Standard fire behavior fuel models: a comprehensive set for use with Rothermel"s surface fire spread model. Gen. Tech. Rep. RMRS-GTR-153. Fort Collins, CO: U.S. Department of Agriculture, Forest Service, Rocky Mountain Research Station. 72 p.

Soil Survey Staff (1999) Soil Taxonomy, 2nd edition. NRCS, USDA, Washington.

Trabaud L, Michels C, Grosman J (1985) Recovery of burnt Pinus halepensis mill. forests. II. Pine reconstruction after wildfire. *Forest Ecology and Management* **13**, 167-179.

Trabaud L, Grosman J, Walter T (1985) Recovery of burnt Pinus halepensis Mill. Forests. I. Understorey and litter phytomass development after wildfire. *Forest Ecology and Management* **12**, 269-277.

Vega-Garcia C, Chuvieco E (2006) Applying local measures of spatial heterogeneity to Landsat-TM images for predicting wildfire occurrence in Mediterranean landscapes. *Landscape Ecology* **21**, 595-605.

Viegas DX, Piñol J, Viegas MT, Ogaya R (2001) Estimating live fine fuels moisture content using meteorologically-based indices. *International Journal of Wildland Fire* **10**, 223–240.

Vigo J, Carreras J, Ferré A (Eds) (2006) Cartografia dels hàbitats a Catalunya. Manual d'interpretació. Generalitat de Catalunya, Departament de Medi Ambient i Habitatge.

Data preparation for fire behaviour fuel modelling in the test case of Zlatograd forestry department

Georgi Dobrinkov[a], Nina Dobrinkova[b]

[a] *Institute of Mathematics and Informatics – Bulgarian Academy of Sciences, Acad. Georgi Bonchev str. Bl.8, g.dobrinkov@gmail.com*
[b] *Institute of Infomation and Communication Technologies – Bulgarian Academy of Sciences, Acad. Georgi Bonchev str. Bl.2, nido@math.bas.bg*

Abstract

Since the year 2000 Bulgaria is facing progressive increase of wildland fire occurrence. That is caused mainly because of human mistakes in having fire camps or agricultural land processing after crop harvesting. At the moment Bulgaria has no working mechanism to spot such fires before they become a threat, however the team from Bulgarian Academy of Sciences is working on fire behaviour modelling issues since 2007 and in this work will be presented the first attempts for Bulgarian forestry data classification according to the existing 53 FBFMs, and estimations where custom fuels has to be prepared for better representation of the potential fire spread. Calibrations with FARSITE runs have been performed for the area of Zlatograd Forestry Department (Bulgaria) data set (Dobrinkova et. all 2014). The results are compared with Harmanli (Bulgaria) WRF-Fire/S-Fire simulations (Jordanov et. all 2012) in order to see how the different fire behaviour fuel models estimations reflect in the final simulated burned area. Conclusions for fire behaviour fuel modelling based on both simulation approaches in Zlatograd and Harmanli areas gives future application of the presented work for Bulgarian test cases.

Keywords*: Bulgaria, Forestry data, fire behaviour fuel model data preparation, fuel modelling*

Introduction

FARSITE runs with the standard or custom Fire Behaviour Fuel Models in Bulgaria has never been done until our first attempts for this on the test cases selected randomly for the period 2011-2012 on the territory of Zlatograd Forestry Department. In the previous works on Bulgarian test case nearby the area of Harmanli town has been used CORINE categories (Jordanov et. all 2012; Dobrinkova et. All 2011). The approach in Harmanli test case gives CORINE species division adapted only to the thirteen classes of Anderson (Anderson 1982). However this approach has some weaknesses, because fuel load parameters description with satellite images only is hard to be provided.
The current work present chronologically how the available forestry data from the Zlatograd Forestry department is prepared for the FARSITE runs from turning the list of biological species into FBFMs according to the FARSITE input instructions. Most of the collected data has been provided as paper maps which processing into digital GIS (Geographic Information System's) layers had to meet the requirements of FARSITE. The standard FBFMs (Anderson 1982) and (Scott and Burgan 2005) has been taken into consideration with their parameters for fuel load (1-hr, 10-hr, 100-hr, live herbaceous and live woody), compared to the test cases according to the best collected data.
This work is giving both Harmanli and Zlatograd FBFMs methodologies and how they have been implemented in the WRF-Fire/S-Fire and FARSITE runs. The conclusions give comparison on the achieved results with some plans for future refinements.

Harmanli test case data preparation and FBFMs summary

In the Harmanli test case has been used WRF-Fire/S-Fire computer based tool, which is a combination between the mesoscale atmospheric code WRF-ARW (Skamarock 2008) with a fire spread module, based on the Rothermel model (Rothermel 1972) implemented by the level set method. A simulation

with WRF-Fire/S-Fire requires input data from a variety of sources from meteorological initial and boundary conditions to static surface properties.

For the meteorological inputs the U.S. National Center for Environmental Protection (NCEP) gives a 1 degree resolution grid covering the entire globe with 6 hour reanalysis cycle. The data is freely available and can be downloaded automatically over HTTP by using a simple script. Creating simulation also requires a number of static data fields describing the surface properties of the area. All such data is available as part of a standard global dataset for WRF. The fields in this dataset are available at various resolutions ranging from about 1 km to 10 km, which is sufficient for most mesoscale weather modeling purposes. Each field is stored in a unique format consisting of a series of simple binary files described by a text file. A geogrid utility in the WRF preprocessor (WPS) interpolates the data in these files onto the model grid and produces an intermediate NetCDF file used in further preprocessing steps. While the standard geogrid dataset is sufficient for most weather forecasting applications, it lacks two high resolutions fields. These fields are surface topography and fuel information. Both are essential for modeling fire behavior because they directly affect the rate of spread of the fire front inside the model.

Topography at a resolution of about 90 m for the area of Harmanli is used from the Shuttle Radar Topography Mission (SRTM) at http://eros.usgs.gov. The data received from the server is a GIS raster format (DTED), which is processed and converted to geogrid binary data format.

The final piece of surface data needed for input into geogrid is a categorical field describing the properties of the fuels. In the U.S., this data is readily available from the USGS, however, no such data exists for the Harmanli or any other Bulgarian region region. Instead for this field is used data from the Corine Landcover Project (financed by the European Environment Agency and the member states) see Table 1. This project provides landcover data for Bulgaria with 100 m resolution with a 25 ha minimum mapping unit http://www.eea.europa.eu/data-and-maps/data/corine-land-cover-2006-raster.

Table 1. Fuel categories from satellite imagery and CORINE code (in parentheses)

Category	Description
1	Artificial, non-agricultural vegetated areas (141,142)
2	Sport Complex,Irrigated Cropland and Pasture,Bare Ground Tundra, Arable land (211,212,213), Open spaces with little or no vegetation (331,332,333,334,335)
3	Cemeteries, Dryland Cropland and Pasture, Grassland, Permanent crops(221,222,223), Pastures (231), Heterogeneous agricultural areas(241,242,243,244), Scrub and/or herbaceous vegetation associations (321,322,323,324)
4	Herbaceous Tundra, Parks
5	Wooded Wetland
6	Wooded Tundra, Orchard
7	Mixed Forest
8	Deciduous Needleleaf Forest, Forests (311,312,313)
9-13	N/A
14	Urban fabric (111,112), Industrial, commercial, and transport units (121,122,123,124), Mine, dump and construction sites (131,132,133), Wetlands(411,412,421,422,423), Water bodies (511,512,521,522,523)

The downloaded satellite data along with orthophoto data from the geoportal of the Ministry of Regional Development (MRD) of Bulgaria can be used to estimate the fuel types of the domain like conifer or deciduous woods. All rivers, lakes, villages and forest areas can be vectorized using the orthophoto images combined with CORINE2006 into a GIS vector shape file. The vectorized file provides very high accuracy of representation for non burning areas like rivers and lakes. For the areas

with woods is used Table1, where a description of the fuel categories for the Harmanli simulation corresponds to the Anderson thirteen classes with additional one class for the non burning areas. This fuel level data combined with the vectorized landcover areas gives us a final shape file with attributes for each polygon fuel level. The resulting input files contain all the standard WRF fields along with several additional variables generated from the high resolution topography and fuel categories.
However no fuel load description about 1-hr, 10-hr, 100-hr, live herbaceous and live woody parameters can be estimated with such approach. The problem here is that the satellite images from CORINE project can not provide high resolution with all species information on the land cover. The ortophotoes can provide the canopy cover, but not the fuel load description and in these cases the best solution is to find forestry department plan for any wild land area in Bulgaria. The Bulgarian Forestry department plans contain information which can be used for the fuel load estimations and refinements in the Table 1 categories. Such approach is described in the Zlatograd test case area.

Harmanli test case analysis

The Harmanli test case simulation result is presented on the Figure 1B. The simulated area has significant similarity in the fire spread shape, but it does not fully comply with the real burnt area Figure 1A. The total simulated burnt area also does not correspond with the real one.

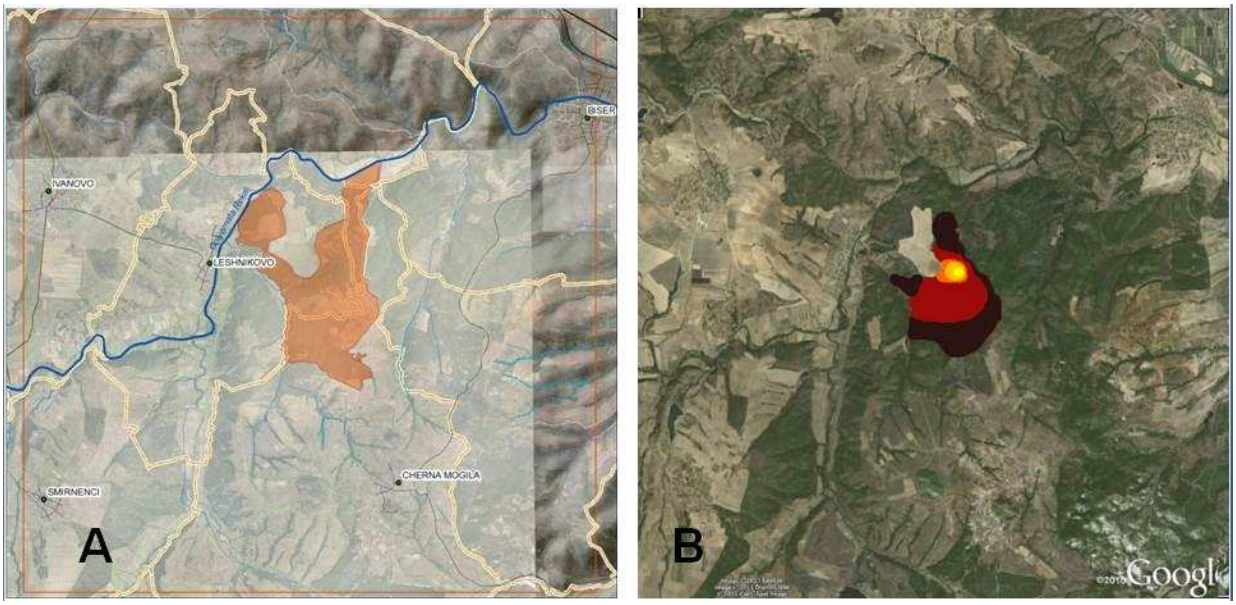

Figure 1. A. Real burned areaof the fire Harmanli(Bulgaria) test case, B. Simulated burned area on the Harmanli(Bulgaria) test case

The difference can be caused mainly from two components the fuel type definitions and weather inputs in the fire zone described in the simulation methodology of Harmanli fire simulation. Further analysis need to be performed and more information on the real fire spread has to be collected in order to be finally defined which components has to be additionally refined. The result however is important, because with this simulation is given the opportunity to operational teams of the responsible authorities in Bulgaria to achieve results on fire spread even with weather inputs and estimations on fuels and topography.

Zlatograd test case data preparation and FBFMs summary

The forestry department of Zlatograd area covers 33,532 ha, of which 31,856 ha are state owned forests. It consist of the municipalities Zlatograd, Madan and Nedelino. In the period 2011-2012 fifteen different size and location wildland fires had occurred in Zlatograd forestsry department (Table 2). These wildfires burned in a variety of vegetation types and were more than likely started by humans to clear agricultural debris or prepare fields, based on the villages nearby. Paper maps from the forestry department identified the ignition location and final fire shape; this data was digitized in a GIS, which allowed each ignition point to be viewed with background orthophotos and the spatial Zlatograd vegetation classification showing pre-fire vegetation (Figure 2).

Table 2. Fire information provided by the Zlatograd Forestry. Department for the period 2011-2012

Fire No.	Vegetation type	Burned area in decares	Date of occurrence	Hour of start	Hour of end
1	Durmast	3.0	25 March 2012	1330	1530
2	Beechwood	5.0	29 March 2012	1400	1800
3	Scotch pine	1.0	16 June 2012	1500	1700
4	Scotch pine	7.0	6Aug. 2012	1640	1950
5	Scotch pine	5.0	6 Aug. 2012	1710	2130
6	European black pine	4.0	27Aug. 2012	1200	1600
7	Scotch pine	3.0	5 Sept. 2012	1400	2030
8	Scotch pine	6.0	6 Sept. 2012	1400	1930
9	Scotch pine	2.0	6 Oct. 2012	1600	2320
10	Scotch pine	1.0	16 March 2011	1310	1400
11	Scotch pine	1.0	5 April 2011	1715	1900
12	Scotch pine	1.0	10 April 2011	1130	1530
13	Grassland	3.0	30 Aug. 2011	1400	1800
14	Scotch pine	4.0	12 Sept. 2011	1230	1900
15	Scotch pine	1.0	15 Sept. 2011	1600	1830

Figure 2a: Digitalized shapes from paper map

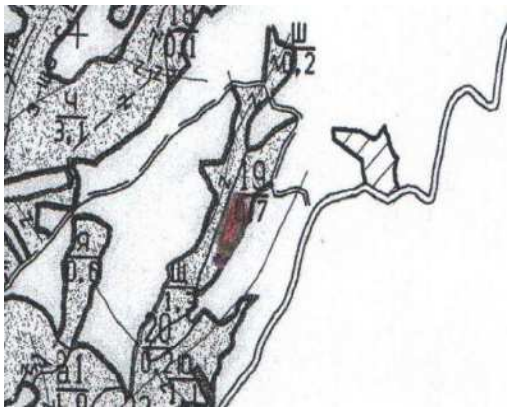

Figure 2b: Paper map sample

Zlatograd test case data preparation and analysis

The first step in preparing data to run spatial fire behaviour analyses was to determine suitable fuel models for fire locations in the Zlatograd test area. This was done by using BehavePlus (Andrews 2007). BehavePlus is a point fire behaviour prediction system that can be used to analyze fire growth and behaviour for homogeneous vegetation with static weather data. Using a number of standard fuel models developed for the United States (Anderson 1982; Scott and Burgan 2005), was evaluated which fuel models were best able to produce estimates of fire behaviour and growth in BehavePlus similar to those observed on each of the fifteen fires.

In addition to fuel model, BehavePlus requires inputs for weather, fuel moisture, slope, and duration of the burning period. Weather data was obtained for each fire from TV Met, a private company in Bulgaria, which provided calculated fine dead fuel moisture values (Rothermel 1983). The weather stations in the area of interest are quite sparse and that let to estimations for some of the zones of fires. Estimations on live herbaceous and live woody fuel moisture values were based on the expected phenological stage for the time of year that the fire occurred. To estimate slope, was used 30 m resolution digital elevation model (DEM) from the National Institute of Geophysics, Geodesy, and Geography in Bulgaria, then subsequently calculated the average slope for each fire using standard geospatial processing in ArcGIS (ESRI 2010). Burn period length for each fire was obtained from the Zlatograd forestry department data (Table 2).

Based on initial BehavePlus results using standard fuel models, custom fuel models were developed for some vegetation types not well represented by the US fuel models. Custom fuel models were developed for native durmast oak and grass as well as one of the Scotch pine sites by modifying fuel loading parameters to better match local vegetation and reflect the lack of woody debris in the understory, as it is collected as firewood by the local population. The custom fuel model developed for grass has a much lower rate of spread and flame length than any of the standard grass fuel models.

Following evaluation of fuel models with BehavePlus, were then performed analyses in FARSITE, a spatial fire growth system that integrates fire spread models with a suite of spatial data and tabular weather, wind and fuel moisture data to project fire growth and behavior across a landscape. It was defined test landscapes using a 500 m buffer zone around each of the fifteen Zlatograd fires (Figure 3); this footprint comprised the extent of the spatial analysis for each individual wildfire.

Input for FARSITE consists of spatial topographic, vegetation, and fuels parameters compiled into a multi-layered "landscape file" format. Topographic data required to run FARSITE include elevation, slope, and aspect. Using the aforementioned 30 m DEM, was calculated an aspect layer, and then clipped elevation, aspect, and slope rasters to the extent of the fifteen test landscapes. Required vegetation data include fuel model and canopy cover. Fuel models within the 500 m buffered analysis area for each individual fire were assigned based on the BehavePlus analyses; fuel model assignments were tied to the dominant vegetation for each polygon based on the Zlatograd forestry department's vegetation data. Canopy cover values were visually estimated from orthophoto images and verified with stand data from the Zlatograd forestry department. Additional canopy variables (canopy base height, canopy bulk density, and canopy height) that may be included in the landscape file were omitted, as these variables are most important for calculating crown fire spread or the potential for a surface fire to transition to a crown fire. None of the fifteen fires analyzed experienced crown fire.

Tabular weather and wind files for FARSITE were compiled using the weather and wind data from TV Met, Bulgarian meteorological company that included hourly records. Tabular fuel moisture files were created using the fine dead fuel moisture values calculated for the BehavePlus analyses for 1-hr timelag fuels. The 10-hr fuel moisture value was estimated by adding 1% to the 1-hr fuel moisture and the 100-hr fuel moisture was generally calculated by adding 3% to the 1-hr fuel moisture. The live fuel moisture values previously estimated for BehavePlus analyses were used to populate live herbaceous and live woody moisture values.

All simulations performed in FARSITE used metric data for inputs and outputs. An adjustment value was not used to alter rate of spread for standard fuel models, rather custom fuel models were created. Crown fire, embers from torching trees, and growth from spot fires were not enabled.

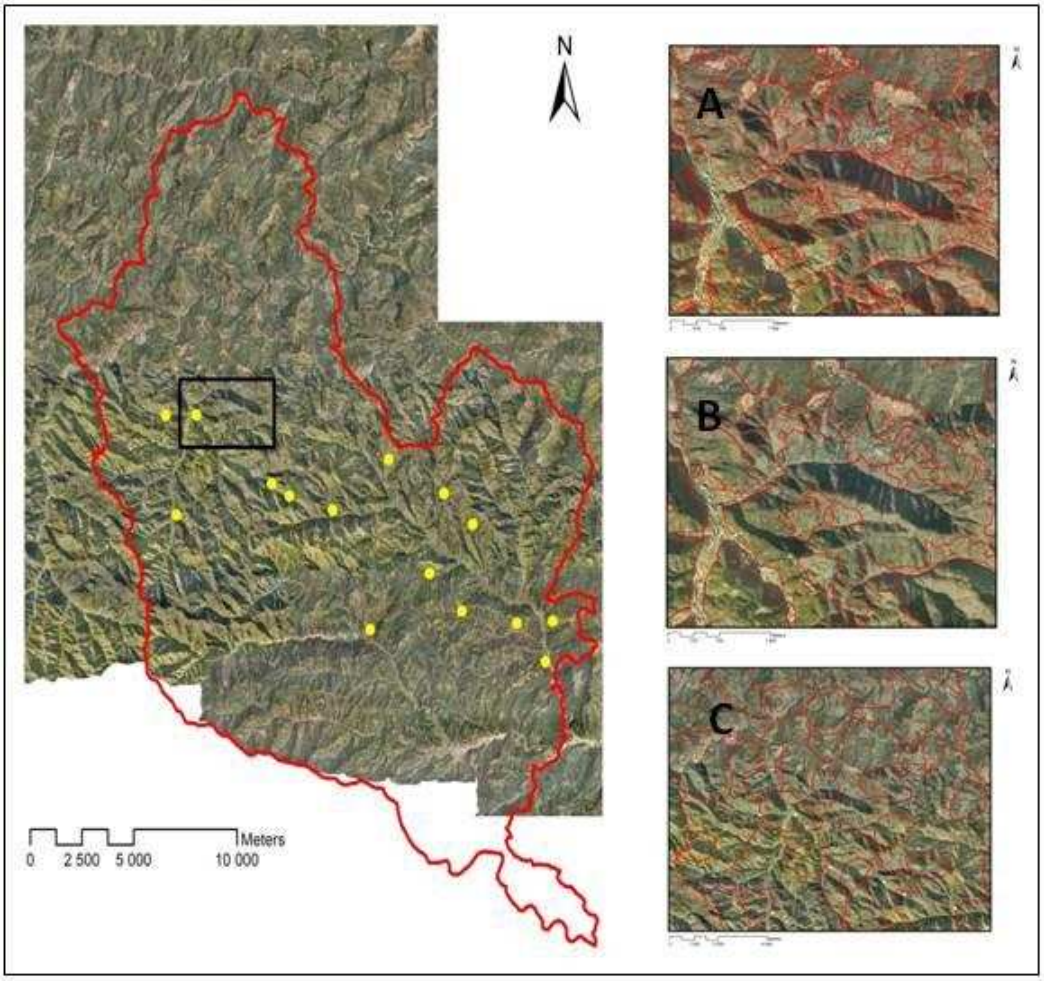

Figure 3. Location of the 15 fires (yellow dots) in the Zlatograd area that occurred in 2011-2012 that were used to develop fire behavior analysis methodology. The outline of the municipality of Zlatograd is shown in red, with the orthophoto imagery used to identify canopy cover underneath. The black box indicates the location of the three inset maps on the right. Inset maps are: A) Zlatograd forestry polygons; B) Corine land cover polygons; and C) Bondev vegetation map polygons.

From the performed analysis and achieved results with the prepared data FARSITE runs gave quite reasonable estimations of burnt areas close to the real burnt one. The results were mainly calculated with custom fuel models and standard ones based on the forty FBFMs (Scott and Burgan 2005).

Conclusions

Based on the work performed with Harmanli and Zlatograd forestry department's test areas summary of the most suitable approximation of classes corresponding to the vegetation types is provided in Table 3.

Table 3. Estimations from 40 standard US Fuel Models to Bulgarian Vegetation/Fuel Models

Vegetation Type	Possible Fuel Models	Logic/Assumptions
Scots pine (Pinus sylvestris)	188 (often used for ponderosa pine) 183 – modified	Ponderosa pine (*Pinus ponderosa*) may be a suitable western US proxy. Otherwise, probably a modified 183 (TL3) to increase rate of spread and flame lengths.
Black pine/Acacia (Pinus nigra/Acacia)	161 183 – probably modified	FBFM 161 works best when the understory is dominated by an herbaceous understory including forbs and grasses (it is dynamic). Creating a custom fuel model starting from FBFM 183 is another solution, to increase the rate of spread and flame lengths. Using FBFM 165 would assume ladder fuels to be present and will probably overpredict rate of spread and flame lengths.
Beechwood (Fagus sylvatica)	182/186 (dormant season fire) 161 (growing season fire)	FBFM 182 or 186 (or a custom FBFM) may be used when a fire is mostly burning through hardwood (round leaf) litter. FBFM 186 tends to have much higher rate of spread and flame lengths than 182. FBFM 161 is dynamic and may be used during the growing season when a fire would be expected to burn through the understory vegetation.
Durmast (Quercus dalechampii)	182/186 (dormant season fire) 161 (growing season fire)	FBFM 182 or 186 (or a custom FBFM) may be used when a fire is mostly burning through hardwood (round leaf) litter. FBFM 186 tends to have much higher rate of spread and flame lengths than 182. FBFM 161 is dynamic and may be used during the growing season when a fire would be expected to burn through the understory vegetation.
Grasslands	101 (may be best for grazed pasture) 102 (ungrazed pasture) Custom FBFM (lower ROS and FL than FBFM 101)	Assumes no irrigation. Rate of spread and flame length drastically change depending on chosen FBFM.

In this table are provided just first estimations on classification which for Bulgarian vegetation types can be further expand and calibrated in further test cases. The fire behaviour fuel modelling work requires future expansion and more tests with different species from all regions of Bulgaria. However the estimated first steps are good basis for development and expansion of what is achieved so far.

Acknowledgement

This work has been partially supported by the European Commission project ACOMIN and by the Bulgarian National Scientific Fund under the grant I01/0006-"Simulation of wild-land re behaviour".

References

Anderson, H.E.: Aids to determining fuel models for estimating fire behavior.USDA Forest Service, Intermountain Forest and Range Experiment Station, Research Report INT-122 (1982)http : //www.fs.fed.us/rm/pubsint/intgtr122.html.

Andrews PL (2007) BehavePlus fire modeling system: past, present, and future. In 'Proceedings of Seventh Symposium on Fire and Forest Meteorology, 23-25 October 2007, Bar Harbor, ME. (American Meteorological Society: Boston, MA)

Dobrinkova N., Hollingsworth L., Heinsch F.A., Dillon G., Dobrinkov G., "Bulgarian fuel models developed for implementation in FARSITE simulations for test cases in Zlatograd area". (E-proceeding) Wade DD & Fox RL (Eds), Robinson ML (Comp) (2014) 'Proceedings of 4th Fire Behavior and Fuels Conference', 18-22 February 2013, Raleigh, NC and 1-4 July 2013, St. Petersburg, Russia. (International Association of Wildland Fire: Missoula, MT), p.513 - p.521.

Dobrinkova N., Jordanov G., Mandel J. „WRF-Fire Applied in Bulgaria", Numerical Methods and Applications 20-24 August, Borovez, Lecture Notes in Computer Science No 6046, Springer, Germany, ISSN 0302-9743, 2011, p.133- p. 140.

Jordanov G., Beezley J.D., Dobrinkova N., Kochansksi A.K., Mandel J., Bedrich Sousedik. "Simulation by WRF-Fire of the 2009 Harmanli Fire (Bulgaria)". 8th International Conference on "Large-Scale Scientific Computations" LSSC'11, Sozopol 6-10 June 2011, Lecture Notes in Computer Science, No 7116, ISSN 0302-9743, 2012, Science, Springer Germany, 2012, p 291 – p. 298.

Rothermel, R. C. (1972) A mathematical model for predicting fire spread in wildland fuels. Research Paper INT-115. Ogden, UT: US Department of Agriculture, Forest Service, Intermountain Forest and Range Experiment Station, pp. 1-40.

Rothermel, RC (1983) 'How to predict the spread and intensity of forest and range fires.' USDA Forest Service, Intermountain Forest and Range Experiment Station General Technical Report INT-GTR-143. (Ogden, UT)

Scott, JH, Burgan, RE (2005) 'Standard fire behavior fuel models: a comprehensive set for use with Rothermel's surface fire spread model.' USDA Forest Service, Rocky Mountain Research Station General Technical Report RMRS-GTR-153. (Fort Collins, CO)

Skamarock,W.C.,Klemp,J.B.,Dudhia,J.,Gill,D.O.,Barker,D.M.,Duda,M.G.,Huang,X.Y.,Wang,W.,Powers,J.G.:AdescriptionoftheAdvancedResearch,WRFversion3.NCARTechnicalNote475(2008) http://www.mmm.ucar.edu/wrf/users/docs/arw_v3.pdf.

Degradation modelling of wildland fuels

Mohamad El Houssami[a], Jan Christian Thomas[a], Aymeric Lamorlette[b], Dominique Morvan[b], Albert Simeoni[a]

[a] *BRE Centre for Fire Safety Engineering, Institute for Infrastructure and Environment, School of Engineering, The king's Buildings, The University of Edinburgh, UK m.elhoussami@ed.ac.uk*
[b] *Laboratoire M2P2, UMR 7340 CNRS, Aix-Marseille Universite, Ecole Centrale de Marseille, France*

Abstract
The combustion of forest fuels at laboratory scale is studied by using a Large Eddy Simulation (LES) fire simulator named ForestFireFOAM (FFF), based on the FireFoam package with the addition of a multiphase formulation adapted for highly porous fuel, such as pine needles. Experiments conducted with the FM-Global Fire Propagation Apparatus (FPA) were reproduced with FFF. Arrhenius-type laws were used to model the evaporation and pyrolysis rates. As these laws are temperature-dependent, the mass loss rate and the temperature distribution inside the fuel sample were selected as comparison criteria to better understand the porous fuel heating process using appropriate convective and radiative models and to better describe the burning dynamics of the fuel.

Keywords*: Pyrolysis, wildland fuel, FireFOAM*

Introduction

This study is dedicated to the modelling of the ignition and burning dynamics of pine needle litters. How these moist and highly porous fuels burn represents a fundamental research gap that leads to bigger gaps when it comes to studying their flammability and wildfire spread. This gap hampers the further development of risk indexes and CFD fire spread models. The main goal of this study is to apply a multiphase approach [1–3] that is often used to describe fire propagation [4–6] to the study of piloted ignition of wildland fuels. The multiphase model is based on the resolution of the set of conservation equations governing the time evolution of the coupled system formed by a porous vegetation and its surrounding gas medium, different sub models such as radiation, convection, turbulence, and combustion are included to close the model (Grishin & Albini, 1997). Some of these sub models are not directly relevant for piloted forest fuel ignition modelling at laboratory scale. Such as in (W Mell, Jenkins, Gould, & Cheney, 2007) where a large scale fire spread is started using an ignition line or in (Margerit & Sero-Guillaume, 2002) where an ignition temperature is used. Indeed, the heat and mass transfer processes involved are the same, but the *in situ* conditions lead to a different modelling of these processes due to the underlying assumptions. These assumptions are valid for propagation modelling but not in ignition modelling, since the flow could be laminar during the ignition phase, particularly under no-wind conditions before changing to a turbulent regime. An attempt to correct these models in order to simulate forest fuel ignition has been realised in (Consalvi, Nmira, Fuentes, Mindykowski, & Porterie, 2011). However, ignition procedure was not described thoroughly: The only given assumption was "the criterion for ignition is the thermal runaway in the gas phase: $\frac{\partial^2 T_{g,max}}{\partial t^2} = 0$, where $T_{g,max}$ is the maximum gas temperature at the vicinity of the pilot flame" (Consalvi *et al*., 2011).

The multiphase formulation was implemented in FireFOAM, a Large Eddy Simulation (LES) solver for fire application, in the C++ object-oriented toolbox of OpenFOAM. The modified solver is called ForestFireFOAM. In addition to presenting the theoretical approach, several strengths and weaknesses

of the current sub-models are identified by comparing simulations to results of fire experiments conducted in the FM-Global Fire Propagation Apparatus (FPA), by burning small samples of dry pine needles exposed to a radiative heat flux. Pine needle beds are used as a reference fuel because they are well characterised in literature and they allow obtaining repeatable fuel bed properties under laboratory settings. Simple modelling of the fuel degradation during the burning of the fuel sample is applied to understand flaming and smouldering. However, in this work the focus is only on heat transfer modelling before and until ignition in order to understand the heating process using appropriate convective and radiative models. It is important to understand this aspect since mass loss rates are highly dependent on the pyrolysis rate, which is usually modelled using an Arrhenius law that is a function of the fuel temperature.

Mathematical formulation

Solid fuel modelling

The solid fuel constituting a forest fuel layer and its interactions with the gas phase are represented by adopting a multiphase formulation [1]. This approach consists in solving the conservation equations (mass, momentum and energy) averaged in a control volume at an adequate scale that contains a gas phase flowing through N solid phases and considering the strong coupling between phases [2]. Here, only one solid phase is considered, and consists of particles of the same geometrical and thermophysical properties, providing the same behaviour. Physico-chemical processes such as pyrolysis, chemical reactions, char oxidation occurring in the solid and gas phases have to be taken into account as well as other phenomena including combustion, radiative and convective heat transfer. The required formulation is made of a set of coupled nonlinear equations, which are presented in (Morvan *et al*., 2009). The fuel bed is considered as a homogeneous distribution of solid particles whose dimensions and physical properties are evaluated from experimental data. Vegetation state must be characterized using the following set of physical variables: Fuel volume fraction (α_s), fuel density (ρ_s), surface area to volume ratio (σ_s), moisture content (Y_{H2O}), fuel temperature (T_s), and fuel composition.

Adjustments were made in order to better estimate the drag force ($\overline{F_i}$) resulting from the interaction between the gas flow and vegetation, in the momentum equation presented in (Morvan *et al*., 2009).

$$\overline{F_i} = \rho C_d \frac{\alpha_s \sigma_s}{2} \left\| \tilde{U} \right\| \tilde{u}_i \qquad (1)$$

The drag force coefficient C_d was averaged and considered constant (C_d =0.15) (Morvan *et al*., 2009). In this study, it is modelled depending on the mesoscopic Reynolds number, defined as:

$$Re_M = \frac{U}{\nu \sigma_s} \qquad (2)$$

where ν represents the air kinematic viscosity. This Reynolds number is compared to a transitional Reynolds number $Re_{M,lim}$ that takes into account the transition from Stokes to inertial flow (Lesieur, 2008). Since an intermediate flow is expected between these two regimes, it is hard to clearly define such a Reynolds number. However, vortices generated by the vortex shedding in the wake of vegetation elements exhibit dislocations responsible for a turbulent break-up (Williamson, 1992). The turbulent flow is then responsible for a constant drag coefficient (Nepf, Sullivan, & Zavitoski, 1997). That is why the Reynolds number accounting for the vortex shedding transition is retained, providing the upper limit for the transition from Darcian to Forchheimer flow. Since the surface area to volume ratio for cylinders of diameter (d) can be define as: $\sigma_s = 4/d$, the transitional Reynolds number for the vortex shedding is evaluated at $Re_{M,lim} \sim 50$ for litters, regarding their typical porosity [10, 11].

For 5% porosity litters:

$$C_d = \begin{cases} \frac{10}{Re_M} \text{ if } Re_M < Re_{M,lim}; \\ C_d = 0.2 \text{ else} \end{cases} \quad (3)$$

For 10% porosity litters:

$$C_d = \begin{cases} \frac{7.5}{Re_M} \text{ if } Re_M < Re_{M,lim}; \\ C_d = 0.15 \text{ else} \end{cases} \quad (4)$$

Turbulence and combustion

The turbulence model is based on the LES approach developed in the solver OpenFOAM ("OpenFOAM User Guide, OpenFOAM The Open Source CFD Toolbox ," 2010). The turbulent sub-grid scale stress is modelled by the eddy viscosity concept through a one-equation model for the turbulent kinetic energy K (Fureby, Tabor, Weller, & Gosman, 1997), with an additional sink term due to dissipation of sub-grid-scale energy in the canopy (Shaw & Patton, 2003):

$$\frac{D\bar{\rho}K}{Dt} = \frac{\partial}{\partial x_j}\left(\mu_t \frac{\partial K}{\partial x_j}\right) - \bar{\rho} C_d \alpha_s \sigma_s |U| K - C_\varepsilon \frac{\bar{\rho} K^{3/2}}{\Delta} - \rho \widetilde{u_i'' u_j''} \frac{\partial \tilde{u}_i}{\partial x_j} + W \quad (5)$$

$$W = -\frac{\mu_t}{Pr_t \bar{\rho}^2} \frac{\partial \bar{\rho}}{\partial x_j} \frac{\partial \tilde{p}_H}{\partial x_j} \quad (6)$$

$\Delta = (\Delta_x \Delta_y \Delta_z)^{1/3}$ represent the sub-grid filter size, Pr_t represents the turbulent Prandtl number and P_H the hydrodynamic pressure. Most combustion models [5, 12] use Eddy Dissipation Concept (EDC) models for the rate of combustion, which was developed for fully developed turbulent flow.

An extension of the EDC model was proposed (Ren, Wang, & Trouvé, 2013) where the characteristic time scale of fuel-air mixing is different under turbulent and laminar flow conditions. The fuel mass reaction is expressed as:

$$\overline{\dot{\omega}_F'''} = \frac{\bar{\rho}}{\min\left(\frac{k_{sgs}}{C_{EDC}\varepsilon_{sgs}}, \frac{\Delta^2}{C_{diff}\alpha}\right)} \min\left(\tilde{Y}_F, \frac{\tilde{Y}_{O_2}}{s}\right) \quad (7)$$

where $\tilde{Y}_F$ and $\tilde{Y}_{O_2}$ are the fuel and oxygen mass fraction, α is the thermal diffusicuity, C_{EDC} = 4 and C_{diff} = 10 [19]. The ratio $\frac{k_{sgs}}{\varepsilon_{sgs}}$ is the turbulent time scale and the ratio $\frac{\Delta^2}{\alpha}$ is the molecular diffusion time scale.

Convective heat transfer

The term representing the contribution due to convective heat transfer Q_{conv} between hot gases, the flame and the unburned solid fuel is written as follows in the energy balance equation (Morvan *et al.*, 2009):

$$Q_{conv} = \chi(T - T_s) \quad (8)$$

With T and T_s the gas and solid phase temperatures, respectively. The heat transfer coefficient χ is estimated for low Reynolds numbers, for which independent particle behaviour is observed (Raupach & Thom, 1981), hence the use Hilpert correlation (Incropera, DeWitt, Bergman, & Lavine, 2007) with the Nusselt number:

$$Nu = \frac{\chi D}{K} = C Re^m Pr^{1/3} \quad (9)$$

Providing the value of χ:

$$\chi = \frac{K}{D} C Re^m Pr^{1/3} \quad (10)$$

K is the air thermal conductivity and D is the effective diameter equivalent to $4/\sigma_s$. Hence, $Re = 4Re_M$. C and m are coefficients (Incropera *et al*., 2007) evaluated for a circular cylinder in cross flow. On the basis of the results on momentum absorption found in (Raupach & Thom, 1981), the same relationship and coefficients at low Reynolds are kept, where interactions between solid particles are negligible. At higher Reynolds, results from (Lamorlette & Collin, 2012) are used to take into account these interactions.

Re < 4	C=0.989	m=0.330
4 < Re < 40	C=0.911	m=0.385
40 < Re < 1560	C=0.683	m=0.466
1560 < Re	C=3.030	m=0.266

2.4. Radiative heat transfer

The term coming from the radiative heat transfer Q_{RAD} can be written as follows:

$$Q_{RAD} = \frac{\alpha_s \sigma_s}{4}[J - 4\sigma T_s^4] \quad (11)$$

$\frac{\alpha_s \sigma_s}{4}$ represents the solid fuel extinction coefficient for spherical particles [17–19]. The total irradiance J is:

$$J = \int_0^{4\pi} I d\Omega \quad (12)$$

Including the contribution of the flames (soot particles) and the embers, the Radiation Transfer Equation (RTE) can be written as follows:

$$\frac{d\alpha_g I}{ds} = \frac{\alpha_s \sigma_s}{4}\left[\frac{\sigma T_s^4}{\pi} - I\right] + \alpha_g \sigma_g \left[\frac{\sigma T^4}{\pi} - I\right] \quad (13)$$

Even if the soot particles in a flame can agglomerate adopting very complex forms, they are assumed spherical (Φ = 1μm). The soot field is calculated solving a transport equation for the soot volume fraction, assuming that the production rate of soot particles in the flaming zone is 5% (in mass) of the solid fuel pyrolysis rate. The contribution of soot oxidation is neglected in the flame. Considering that this soot production rate represents the maximum value reached in the under-oxygenated region of the flame, this source term is multiplied by the ratio $(Y_{O2}^* - Y_{O2})/ Y_{O2}^*$, representing the deviation from the oxygen concentration at atmospheric conditions. Then, the RTE is solved using a finite volume Discrete Ordinate Method (fvDOM), consisting of the decomposition of the radiation intensity I in a finite number of directions. The irradiance J is calculated by integrating this set of discrete contributions with a numerical Gaussian quadrature (Siegel & Howell, 1992).

Simulations, experiments and discussion

3.1. Experimental configuration

Experiments were performed with the FM Global Fire Propagation Apparatus (FPA), which provides controlled and repeatable conditions. Mass loss rate was measured and the exhaust gases were analysed for composition, heat release rate was deduced by calorimetry [21, 22] and vertical temperature was measured in the sample. Experiments were carried for dry *Pinus resinosa* (Red pine) for two different heat fluxes, 20 and 40 kW/m^2 with closed baskets and no flow injected in the FPA chamber where the sample holder is located. More details are provided in (Thomas, Everett, Simeoni, Skowronski, & Torero, 2013). The fuel properties are listed in table 1.

Table 1. Fuel properties

Species	$\alpha_s[-]$	σ_s [m^{-1}]	ρ_s [$kg.m^{-3}$]	$C_p[kJ.kg^{-1}.K^{-1}]$	$Y_{H2O}[-]$
P. resinosa	0.5	7024	776.6	1800	0.7

Numerical conditions

The set of transport equations in the gas phase are solved using a second order implicit Finite Volume (FV) method. Total Variation Diminishing (TVD) schemes have been adopted to avoid introduction of false numerical diffusion. The set of Ordinary Differential Equations governing the evolution of the solid fuel was solved using a second order explicit method. Two-dimensional calculations are performed to simulate ignition of pine needle litters in the FPA. BlockMesh and snappyHexMesh mesh generators supplied with OpenFOAM, generate robust meshes. However, geometrical complexities and rough edges can easily cause instabilities in the calculations. The pine litter is defined as a rectangular zone with the same dimensions as the sample holder. The pilot flame, located 10 mm above the top of the fuel litter, is represented by an area of size 50 mm x 10 mm providing 2 W to the fluid phase. The flow is simply induced by a pressure differential set at top of the FPA. The mesh is made of 0.8 mm by 0.8 mm square cells in the vicinity of the litter and near the lamps. The mesh is stretched vertically above the lamps and to the top, in order to reduce computational time. The domain geometry is presented in figure 1. Lamps were modelled by walls having the same location and orientation as the real lamps to obtain the same view factor. These walls have very high temperatures (see Table 2 in Results section), adapted in order to obtain the heat flux needed on the sample surface.

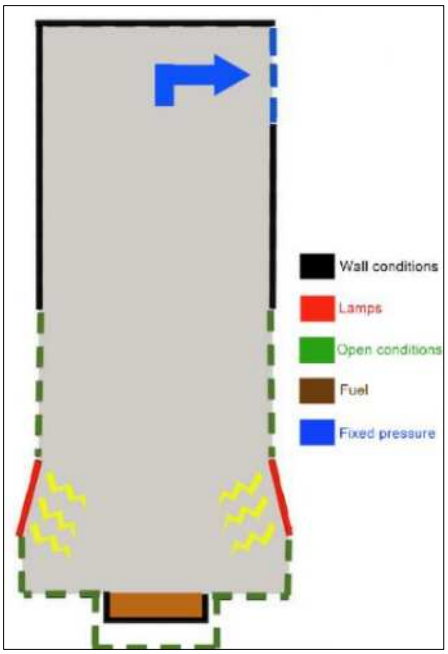

Figure 1. Simulated FPA configuration and boundary conditions

The radiative heat transfer equation is solved for a discrete number of finite solid angles. The accuracy can be increased by using a finer discretisation (Siegel & Howell, 1992):

$$n_{ray} = 4n_{\varphi}n_{\theta} \quad (14)$$

where n_φ and n_θ are the number of discretisation in azimuthal and polar angles, respectively. A sensibility study was carried to determine an adequate amount of discretisation because it is very computationally intensive. $n_\varphi = n_\theta = 8$ was found to be acceptable, providing a uniformly distributed radiative heat flux at the top of the fuel sample, as observed in the FPA.

3.3. Results

The computational time for simulating 10 seconds in parallel on 3 processors was 1h. After conducting a scalability analysis, it was found that the optimal number of cells per processor was 10,000. A snapshot of the temperature field at time t = 5 s after ignition is presented in figure 2.

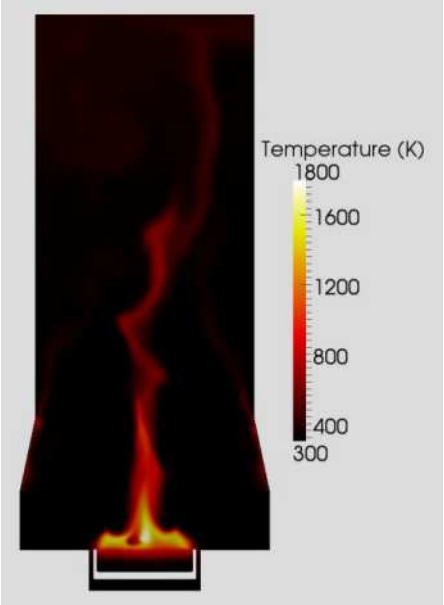

Figure 2. Temperature field 5 seconds after ignition

Preliminary results

In the first attempts to simulate the FPA experiments, the mass loss dropped very quickly. A large number of simulations were conducted to adjust the pyrolysis Arrhenius coefficients in order to have numerical mass loss rates matching the experimental ones. Further simulations were conducted with a maximum pyrolysis rate that could not be exceeded in order to prevent from a rapid mass loss drop. This particular behaviour occurs when the entire fuel is involved in the burning and temperatures become very high, hence the pyrolysis rate increases exponentially. Physically, it represents the fact that pine needles cannot expel all their pyrolysis gases at once. The maximum value of the pyrolysis rate is estimated TGA analysis (Safi, Mishra, & Prasad, 2004) by measuring:

$$\frac{\frac{dm}{dT}}{m} = 0.012\ K^{-1} \qquad (15)$$

with m, the fuel mass and T, the heating temperature. Finally, it was found that the temperature distribution inside the solid fuel was largely over estimated, as presented in figure 3.a and b. Indeed, the simulation for a heat flux of 20 kw/m^2 at the surface of the fuel, temperatures would provide results similar to the experiments done at 40 kw/m^2.

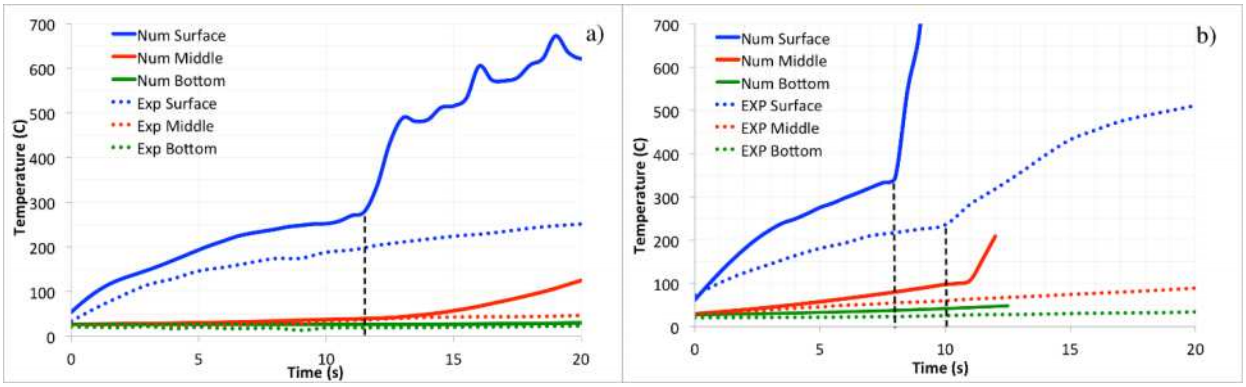

Figure 3. Experimental (dashed) and simulated (solid) temperature distribution in the surface, middle and bottom of the sample with dashed lines representing ignition time a) at 20 kW/m²b) at 40 kW/m².

This was due to the fact that the simulated lamps were assumed to radiate as a black body whereas the FPA heaters operate in very specific spectrum as observed [24, 25] and the fuel emissivity depends on the wavelength number (Monod *et al*., 2009). The halogen lamps of the FPA are very hot and their maximum of emission is shifted towards the lower values of the infrared spectrum, where the absorptivity of the fuels drops dramatically [24]. In consequence, the simulated temperature evolution and ignition times differed from the experiments. Therefore, in order to simulate the experiments performed in the FPA correctly, it was important to estimate the effective absorptivity of the vegetation under the FPA lamps and obtain the correct heat flux absorbed by the fuel.

The absorptivity of vegetation was provided from an experimental study of radiative properties of six vegetal species [18, 26]. Measurements were performed on a large spectrum that covers the spectral radiance spectrum of the FPA infrared heaters, which are very dominant in the near infrared field (0.7-2.5 μm). They can be considered as greybody radiators and the spectral intensity I can be represented by Plank's equation (Marcos Chaos, 2014). The averaged absorptivity is weighted over the normalised spectral radiative intensity at a specific temperature of interest. This temperature is the FPA lamps temperature, corresponding to a specific heat flux (Marcos Chaos, 2014). Simulations were conducted to fit the numerical effective absorptivity to best match the temperature distributions measured in the FPA for 20 kW/m^2 and 40 kW/m^2, as shown in figures 4.a and b, respectively. Experimental and numerical effective absorptivities are presented in Table 2. The main difference comes from the fact that the experimental effective absorptivities are obtained for the available species, whereas the numerical are fitted to match FPA experiments on red pine. Another study (Mcallister *et al*., 2012) using halogen/ quartz bulbs shows that the absorptivity of dry lodgepole pine needles is in the same range (0.576) under 50 kW/m^2 heat flux. The main difference comes from the fact that the experimental effective absorptivities are obtained for the available species, whereas the numerical are fitted to match FPA experiments on red pine.

Table 2. Experimental and numerical effective absorptivities for different heat fluxes

Heat flux (kW/m2)	Lamp Temperatures (K)	Experimental α_{eff}	Numerical α_{eff}
20	820	0.56	0.75
40	900	0.50	0.60

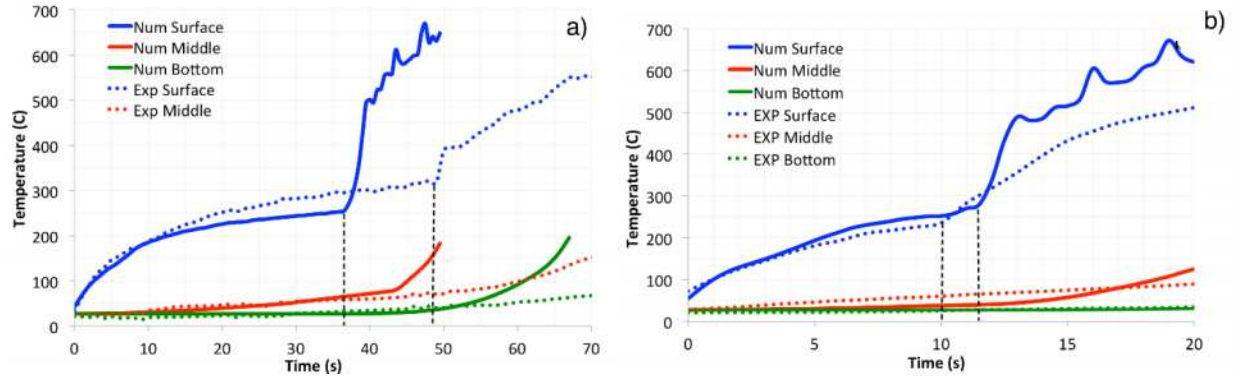

Figure 4. Experimental (dashed) and simulated (solid) temperature distribution in the surface, middle, and bottom of the sample with dashed lines representing ignition time. a) at 20 kW/m²b) at 40 kW/m²

The interesting part of figures 4.a and b covers mainly the temperature variations before ignition, during the heating of the sample only by the lamps of the FPA. In figure 4.a, the temperature evolutions are very similar until the fuel ignites in the simulation 15 seconds before the experiments. The small differences seen in the temperature distribution between experiments and simulations before ignition can be adjusted by modifying the extinction coefficient in equations (11) and (13), as done in (Acem *et al*., 2009). This effect is more pronounced for higher heat fluxes (see figure 4.b). These temperature distributions have large impact on the evaporation and pyrolysis rates, hence on the mass loss rate. The latter are presented for same conditions in figures 5.a and b for 20 kW/m^2 and for 40 kW/m^2, respectively.

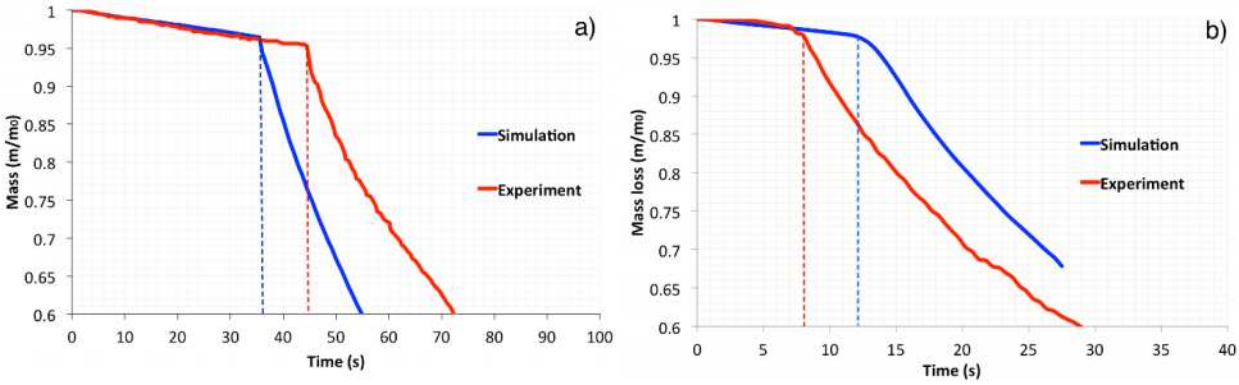

Figure 5. Experimental and simulated mass loss curves for a) 20 kW/m²; b) 40 kW/m². Dashed lines representing ignition time

The experimental ignition times are not exactly the same in figure 4 as in figure 5, since the experiments had to be done separately. Nevertheless, they have very similar tendencies. Mass loss curves are well reproduced until ignition, regardless of the imposed heat flux, but also right after ignition where pyrolysis is still very dominant. Indeed, if the ignition time is quite different, the slope is the same. It should be noticed that it is very difficult to match ignition times as they are happening due to a conjunction of marginal conditions [28, 29].

Conclusion

The use of a multiphase model to study the processes involved in piloted ignition of wildland fuels was found to be promising. However, the experimental conditions of the FPA are not easy to simulate. The fuel sample effective absorptivity has to be taken into account in the near infrared field, which is

quite low for pine needles (~ 0.5). The sub-models for the solid phase were able to describe sufficiently the heating (drying and pyrolysis) and ignition processes, including the mass loss rate prior to ignition for two different heat fluxes. Improvements in the models are currently in progress, such as better estimating the radiation extinction coefficient for pine needle litters, analysing pyrolysis gases with a Fourier Transform Infra Red spectroscopy (FTIR) in order to measure pyrolysis production in different conditions. These measured gases will improve the gas phase combustion modelling. Finally, the contribution of the smouldering phase due to char combustion will be studied, which will allow describing the processes involved at the end of the mass loss.

Acknowledgment

Professor Boulet is gratefully acknowledged for providing the spectral absorptivity of pine needles and the Méso-centre of Aix-Marseille University for providing computational resources.

References

Acem, Z., Lamorlette, A., Collin, A., & Boulet, P. (2009). Analytical determination and numerical computation of extinction coefficients for vegetation with given leaf distribution. International Journal of Thermal Sciences, 48 , 1501–1509.

Alexander, M. E. (2000). Fire behaviour as a factor in forest and rural fire suppression (p. 30). Forest Research; Forest and Rural Fire Scientific and Technical Ser; Rotorua; Wellington. Forest Research Bulletin No. 197; in association with the National Rural Fire Author.

Amorim, J. H. (2011a). Numerical modelling of the aerial drop of firefighting agents by fixed-wing aircraft. Part I: model development. International Journal of Wildland Fire, 20(3), 384–393.

Amorim, J. H. (2011b). Numerical modelling of the aerial drop of firefighting agents by fixed-wing aircraft. Part II: model validation. International Journal of Wildland Fire. doi:10.1071/WF09123

Amorim, J. H., Miranda, A. I., Valente, J., Borrego, C., Viegas, D. X., Pita, L. P., & Ribeiro, L. M. (2010). Effects of chemical retardants on air pollutants emissions: measurements in a combustion chamberNo Title. In D. X. Viegas (Ed.), VI International Conference on Forest Fire Research (ICFFR) (p. 267). Coimbra: University of Coimbra.

Andrews, P. L., Heinsch, F. A., & Schelvan, L. (2011). How to generate and interpret fire characteristics charts for surface and crown fire behavior (p. 48). Gerenal Technical Report RMRS-GTR-253.

Boulet, P. (n.d.). Personal communication 26/02/2014.

Boulet, P., Parent, G., Acem, Z., Collin, A., Försth, M., Bal, N., … Torero, J. (2014). Radiation emission from a heating coil or a halogen lamp on a semitransparent sample. International Journal of Thermal Sciences, 77, 223–232.

Bubb, P. (2004). Cloud forest agenda (p. 36). Cambridge, UK.: UNEP-WCMC.

Carvalho, A., Flannigan, M. D., Logan, K. A., Gowman, L. M., Miranda, A. I., & Borrego, C. (2010). The impact of spatial resolution on area burned and fire occurrence projections in Portugal under climate change. Climatic Change, 98, 177–197. doi:10.1007/s10584-009-9667-2

Carvalho, A., Flannigan, M. D., Logan, K., Miranda, A. I., & Borrego, C. (2008). Fire activity in Portugal and its relationship to weather and the Canadian Fire Weather Index System. International Journal of Wildland Fire. doi:10.1071/WF07014

Carvalho, A., Monteiro, A., Flannigan, M., Solman, S., Miranda, A. I., & Borrego, C. (2011). Forest fires in a changing climate and their impacts on air quality. Atmospheric Environment, 45, 5545–5553. doi:10.1016/j.atmosenv.2011.05.010

Cerda, A., & Robichaud, P. R. (2009). Fire Effects on Soils and Restoration Strategies (p. 605). CRC Press.

Cheney, P., & Sullivan, A. (2008). Grassfires: fuel, weather and fire behaviour. (p. 150). CSIRO Publishing.

Cochrane, M. A. (2003). Fire science for rainforests. Nature, 421(6926), 913–9. doi:10.1038/nature01437

Consalvi, J. L., Nmira, F., Fuentes, A., Mindykowski, P., & Porterie, B. (2011). Numerical study of piloted ignition of forest fuel layer. Proceedings of the Combustion Institute, 33 , 2641–2648.

Cruz, M. G., & Gould, J. S. (2010). Fuel and fire behaviour in semi-arid mallee-heath shrublands. In D. X. Viegas (Ed.), 6th International Forest Fire Research Conference. Coimbra, Portugal: ADAI.

De Mestre, N. J., Catchpole, E. A., Anderson, D. H., & Rothermel, R. C. (1989). Uniform Propagation of a Planar Fire Front without Wind. Combustion Science and Technology, 65(4-6), 231–244.

Frandsen, W. (1997). Ignition probability of organic soils. Canadian Journal of Forest Research, 27(9), 1471–1477. doi:10.1139/x97-106

Frandsen, W. (1998). Heat Flow Measurements From Smoldering Porous Fuel. International Journal of Wildland Fire, 8(3), 137. doi:10.1071/WF9980137

Fureby, C., Tabor, G., Weller, G., & Gosman, D. (1997). A comparative study of subgrid scale models in homogeneous isotropic turbulence. Physics of Fluids, 9(5) , 1416–1429.

Gibbon, A., Silman, M. R., Malhi, Y., Fisher, J. B., Meir, P., Zimmermann, M., … Garcia, K. C. (2010). Ecosystem Carbon Storage Across the Grassland–Forest Transition in the High Andes of Manu National Park, Peru. Ecosystems, 13(7), 1097–1111.

Grishin, A. M., & Albini, F. (1997). A Mathematical Modelling of Forest Fires and New Methods of Fighting Them. Publishing House of the Tomsk University, Tomsk, Russia .

Incropera, F. P., DeWitt, D. P., Bergman, T. L., & Lavine, A. S. (2007). Fundamentals of Heat and Mass Transfer. (F. P. Incropera & F. P. F. O. H. A. M. T. Incropera, Eds.)Water (Vol. 6th, p. 997). John Wiley & Sons. doi:10.1016/j.applthermaleng.2011.03.022

Jain, A. K. (2007). Global estimation of CO emissions using three sets of satellite data for burned area. Atmospheric Environment, 41, 6931–6940. doi:10.1016/j.atmosenv.2006.10.021

Lamorlette, A., & Collin, A. (2012). Analytical quantification of convective heat transfer inside vegetal structures. International Journal of Thermal Sciences, 57 , 78–84.

Larini, M., Giroud, F., Porterie, B., & Loraud, J. C. (1998). A multiphase formulation for fire propagation in heterogeneous combustible media. International Journal of Heat and Mass Transfer, 41(6-7), 881–897.

Lesieur, M. (2008). Turbulence in fluids. (R. MOREAU, Ed.) (fourth.). Springer.

Long, R., Torero, J., Quintiere, J., & Fernandez-Pello, A. (1999). Scale and transport considerations on piloted ignition of PMMA. In Fire Safety Science - Proceedings of the sixth International Symposium (pp. 567–578).

Marcos Chaos. (2014). Spectral Aspects of Bench-Scale Flammability Testing: Application to Hardwood Pyrolysis. In Fire Safety Science-Draft Proceedings of the Eleventh International Symposium.

Margerit, J., & Sero-Guillaume, O. (2002). Modelling forest fires. Part II: Reduction to two-dimensional models and simulation of propagation. International Journal of Heat and Mass Transfer, 45, 1723–1737. doi:10.1016/S0017-9310(01)00249-6

Martins, V., Miranda, A. I., Carvalho, A., Schaap, M., Borrego, C., & Sá, E. (2012). Impact of forest fires on particulate matter and ozone levels during the 2003, 2004 and 2005 fire seasons in portugal. Science of the Total Environment, 414, 53–62. doi:10.1016/j.scitotenv.2011.10.007

Mcallister, S., Grenfell, I., Hadlow, A., Jolly, W. M., Finney, M., & Cohen, J. (2012). Piloted ignition of live forest fuels. Fire Safety Journal, 51, 133–142. doi:10.1016/j.firesaf.2012.04.001

Mell, W., Jenkins, M. A., Gould, J., & Cheney, P. (2007). A physics-based approach to modelling grassland fires. International Journal of Wildland Fire, 16(1), 1–22.

Mell, W., Maranghides, A., McDermott, R., & Manzello, S. L. (2009). Numerical simulation and experiments of burning douglas fir trees. Combustion and Flame, 156 , 2023–2041.

Miranda, A. ., Sá, E., Martins, V., Borrego, C., & Sofiev, M. (2010). The Russian spring 2006 wildland fires effects on air quality over Europe. In D. X. Viegas (Ed.), 6th International Conference on Forest Fire Research (p. 8). Coimbra: University of Coimbra.

Miranda, A. I. (2004). An integrated numerical system to estimate air quality effects of forest fires. International Journal of Wildland Fire, 13, 217–226. doi:10.1071/WF02047

Miranda, A. I., Borrego, C., Martins, H., Martins, V., Jorge, H., Valente, J., & Carvalho, A. (2009). Earth Observation of Wildland Fires in Mediterranean Ecosystems. Earth, 171–187. doi:10.1007/978-3-642-01754-4

Miranda, A. I., Coutinho, M., & Borrego, C. (1994). Forest fire emissions in Portugal: A contribution to global warming? In Environmental Pollution (Vol. 83, pp. 121–123). doi:10.1016/0269-7491(94)90029-9

Miranda, A. I., Marchi, E., Ferretti, M., & Millán, M. (2009). Chapter 9 Forest Fires and Air Quality Issues in Southern Europe. In M. J. A. Andrzej Bytnerowicz Allen R. Riebau and Christian Andersen BT - Developments in Environmental Science (Ed.), Wildland Fires and Air Pollution (Vol. Volume 8, pp. 209–231). Elsevier. doi:http://dx.doi.org/10.1016/S1474-8177(08)00009-0

Miranda, A. I., Martins, V., Cascão, P., Amorim, J. H., Valente, J., Borrego, C., … Ottmar, R. (2012). Wildland smoke exposure values and exhaled breath indicators in firefighters. Journal of Toxicology and Environmental Health. Part A, 75(13-15), 831–43. doi:10.1080/15287394.2012.690686

Miranda, A. I., Martins, V., Cascão, P., Amorim, J. H., Valente, J., Tavares, R., … Pita, L. P. (2010). Monitoring fire-fighters' smoke exposure and related health effects during Gestosa experimental fires (Vol. 137, pp. 83–94). doi:10.2495/FIVA100081

Miranda, AI, Ferreira, J, & Valente. (2005). Smoke measurements during Gestosa-2002 experimental field fires, 14(1), 107–116. doi:10.1071/WF04069

Monod, B., Collin, A., Parent, G., & Boulet, P. (2009). Infrared radiative properties of vegetation involved in forest fires. Fire Safety Journal, 44 , 88–95.

Monteiro, A., Corti, P., San Miguel-Ayanz, J., Miranda, A. I., & Borrego, C. (2014). The EFFIS forest fire atmospheric emission model: Application to a major fire event in Portugal. Atmospheric Environment, 84, 355–362. doi:10.1016/j.atmosenv.2013.11.059

Monteiro, A., Miranda, A. I., Borrego, C., Vautard, R., Ferreira, J., & Perez, A. T. (2007). Long-term assessment of particulate matter using CHIMERE model. Atmospheric Environment, 41, 7726–7738.

Morvan, D., & Dupuy, J. L. (2001). Modelling of fire spread trough a forest fuel bed using a multiphase formulation. Combustion and Flame, 124 , 1981–1994.

Morvan, D., Dupuy, J. L., Rigolot, E., & Valette, J. C. (2006). FIRESTAR: a physically based model to study wildfire behaviour. Forest Ecology and Management, 234S , S114.

Morvan, D., Mèradji, S., & Accary, G. (2009). Physical modelling of fire spread in Grasslands. Fire Safety Journal, 44(1), 50–61.

Myers, N., Mittermeier, R. A., Mittermeier, C. G., da Fonseca, G. A., & Kent, J. (2000). Biodiversity hotspots for conservation priorities. Nature, 403(6772), 853–8. doi:10.1038/35002501

Nepf, H. M., Sullivan, J. A., & Zavitoski, R. A. (1997). A model for diffusion within an emergent plant canopy. Limnology and Oceanography, 42(8) , 85–95.

Ohlemiller, T. J. (2002). Smoldering Combustion. In P. J. DiNenno, D. Drysdale, C. L. Beyler, & W. D. Walton (Eds.), SFPE Handbook of Fire Protection Engineering (3rd ed., pp. 200–210). NFPA.

Oliveras, I., Anderson, L. O., & Malhi, Y. (2014). Application of remote sensing to understanding fire regimes and biomass burning emissions of the tropical Andes. Global Biogeochemical Cycles, 28, 480–496. doi:10.1002/2013GB004664

Oliveras, I., C., D., Cahuana, N., C., E. A., W., H., & Malhi, Y. (n.d.). Andean grasslands are as productive as tropical montane cloud forests. Environmental Research Letters.

OpenFOAM User Guide, OpenFOAM The Open Source CFD Toolbox . (2010).

Ottmar, R. D., Miranda, A. I., & Sandberg, D. V. (2008). Chapter 3 Characterizing Sources of Emissions from Wildland Fires. Developments in Environmental Science. doi:10.1016/S1474-8177(08)00003-X

Ottmar, R. D., Sandberg, D. V, Riccardi, C. L., & Prichard, S. J. (2007). An overview of the Fuel Characteristic Classification System — Quantifying, classifying, and creating fuelbeds for resource planningThis article is one of a selection of papers published in the Special Forum on the Fuel Characteristic Classification Syste. Canadian Journal of Forest Research, 37(12), 2383–2393. doi:10.1139/X07-077

Planas, E., Oliveras, I., Manta, M. I., Urquiaga, E., Quintano, J. A., & Pastor, E. (2013). Soil combustion experiments in the Andean grassland (puna) and tropical montane cloud forests (TMCFs) treeline. In Fourth Fire Behaviour and Fuels Conference (p. 51). Saint Petersburg, Russia.

Raison, R., Woods, P., Jakobsen, B., & Bary, G. (1986). Soil temperatures during and following low-intensity prescribed burning in a Eucalyptus pauciflora forest. Australian Journal of Soil Research, 24(1), 33. doi:10.1071/SR9860033

Raupach, M. R., & Thom, A. S. (1981). Turbulence in and above plant canopies. Annual Review of Fluid Mechanics, 13 , 97–129.

Reh, C. M., Letts, D., & Deitchman, S. (1994). Health hazard evaluation report. California.

Rein, G. (2009). Smouldering Combustion Phenomena in Science and Technology. International Review of Chemical Engineering, 1, 3–18.

Rein, G., Cleaver, N., Ashton, C., & Pironi, P. (2008). The severity of smouldering peat fires and damage to the forest soil. Catena, 74(3), 304–309.

Ren, N., Wang, Y., & Trouvé, A. (2013). Large Eddy Simulation of Vertical Turbulent Wall Fires. Procedia Engineering, 62, 443–452. doi:10.1016/j.proeng.2013.08.086

Román-Cuesta, R. M., Salinas, N., Asbjornsen, H., Oliveras, I., Huaman, V., Gutiérrez, Y., … Malhi, Y. (2011). Implications of fires on carbon budgets in Andean cloud montane forest: The importance of peat soils and tree resprouting. Forest Ecology and Management, 261(11), 1987–1997.

Safi, M. J., Mishra, I. M., & Prasad, B. (2004). Global degradation kinetics of pine needles in air. Thermochimica Acta, 412(1-2), 155–162. doi:10.1016/j.tca.2003.09.017

San-Miguel-Ayanz, J., Schulte, E., Schmuck, G., & Camia, A. (2013). The European Forest Fire Information System in the context of environmental policies of the European Union. Forest Policy and Economics, 29, 19–25. doi:10.1016/j.forpol.2011.08.012

San-Miguel-Ayanz, J. Steinbrecher, R. (2009). EMEP-EEA emissions inventory guidebook (p. 19). Copenhagen.

Sarmiento, F. O., & Frolich, L. M. (2002). Andean Cloud Forest Tree Lines. Naturalness, Agriculture and the Human Dimension. Mountain Research and Development, 22(3), 278–287. doi:10.1659/0276-4741

Schemel, C. F., Simeoni, A., Biteau, H., Rivera, J. D., & Torero, J. L. (2008). A calorimetric study of wildland fuels. Experimental Thermal and Fluid Science, 32(7), 1381–1389.

Séro-Guillaume, O., & Margerit, J. (2002). Modelling forest fires. Part I: a complete set of equations derived by extended irreversible thermodynamics. Int. J.Heat Mass Transfer, 45 , 1705–1722.

Shafizadeh, F. (1978). Combustion, combustibility, and heat release of forest fuels. AIChE Symposium Series, 74:177.

Shaw, R. H., & Patton, E. G. (2003). Canopy element influences on resolved- and sub-grid-scale energy within a large-eddy simulation. Agricultural and Forest Meteorology, 115 , 5–17.

Siegel, R., & Howell, J. R. (1992). Thermal Radiation Heat Transfer (Vol. third ed.). Hemisphere Publishing Corportation .

Simeoni, A., Thomas, J. C., Bartoli, P., Borowieck, P., Reszka, P., Colella, F., … Torero, J. L. (2012). Flammability studies for wildland and wildland–urban interface fires applied to pine needles and solid polymers. Fire Safety Journal, 54(0), 203–217.

Stadmüller, T. (1987). Cloud Forests in the Humid Tropics: A Bibliographic Review. United Nations University Press.

Stroppiana, D., Grégoire, J.-M., & Pereira, J. M. C. (2003). The use of SPOT VEGETATION data in a classification tree approach for burnt area mapping in Australian savanna. International Journal of Remote Sensing, 24(10), 2131–2151. doi:10.1080/01431160210154911

Swezy, D. M., & Agee, J. K. (1991). Prescribed-fire effects on fine-root and tree mortality in old-growth ponderosa pine. Canadian Journal of Forest Research, 21(5), 626–634.

Tamura, H., Kiya, M., & Arie, M. (1980). Vortex shedding from a circular cylinder in moderate-Reynlods-number shear flow. Journal of Fluid Mechanics, 141 , 721–735.

Thomas Simeoni A. Colella F. Torero J.L., J. C. (2011). Piloted Ignition Regimes of Wildland Fuel Beds .

Thomas, J. C., Everett, J. N., Simeoni, A., Skowronski, N., & Torero, J. L. (2013). Flammability Study of Pine Needle Beds. In Proc. of the Seventh International Seminar on Fire & Explosion Hazards (ISFEH7). doi:10.3850/978-981-08-7724-8

Valente, J., Miranda, A. I., Lopes, A. G., Borrego, C., Viegas, D. X., & Lopes, M. (2007). Local-scale modelling system to simulate smoke dispersion. International Journal of Wildland Fire, 16(2), 196. doi:10.1071/WF06085

Van Der Werf, G. R., Randerson, J. T., Giglio, L., Collatz, G. J., Mu, M., Kasibhatla, P. S., … Van Leeuwen, T. T. (2010). Global fire emissions and the contribution of deforestation, savanna, forest, agricultural, and peat fires (1997-2009). Atmospheric Chemistry and Physics, 10, 11707–11735. doi:10.5194/acp-10-11707-2010

Wård, Y. (2007). Tropical Montane Cloud Forest- Fire Disturbance and Water Input after Disturbance (pp. 1–28). Umeå: Swedish University of Agricultural Sciences.

Williamson, C. H. K. (1992). The natural and forced formation of spot-like “vortex dislocations” in the transition of a wake. Journal of Fluid Mechanics, 243 , 393–441.

Zimmermann, M., Meir, P., Silman, M. R., Fedders, A., Gibbon, A., Malhi, Y., … Zamora, F. (2009). No Differences in Soil Carbon Stocks Across the Tree Line in the Peruvian Andes. Ecosystems, 13(1), 62–74. doi:10.1007/s10021-009-9300-2

Effect of layout and below-bed ventilation on burning rate of porous fuel beds

Sara McAllister[a], Mark Finney[b]

[a]*USDA Forest Service, RMRS Missoula Fire Science Laboratory, 5775 W US Highway 10, Missoula, MT 59808, USA, smcallister@fs.fed.us*
[b]*USDA Forest Service, RMRS Missoula Fire Science Laboratory, 5775 W US Highway 10, Missoula, MT 59808, USA, mfinney@fs.fed.us*

Abstract
Wood cribs are often used as ignition sources for room fire tests. A fundamental understanding of the mechanisms that govern the burning rate of a wood crib may also have applications to wildland fires. The burning rate of unconfined cribs has long been identified to occur in two regimes: the densely-packed regime where the burning rate is proportional to the crib porosity and the loosely-packed regime where the burning rate is independent of porosity. Though the cribs used to define these burning regimes were primarily cubic in dimension, there are seemingly endless possible ways to build a crib with a given porosity. This work explores the burning rate of cribs with a wide variety of geometries in the loosely-packed regime to determine whether the porosity-burning rate relation in the literature holds. The porosity was kept approximately constant while the number of sticks per layer, number of layers and the length to thickness ratios (l/b) were varied. For l/b less than 36, the burning rate of all cribs matched the porosity-burning rate relation from the literature. For larger l/b, the burning rate was considerably reduced, implying that the crib porosity is a function of l/b above some critical threshold. A second set of experiments was performed to examine the effect of the spacing distance between the crib and the support platform. The critical spacing distance was shown to be larger than previously thought and a function of the length to thickness ratio. It was quite apparent that as the l/b ratio increases, a significant portion of the required oxidizer comes from the bottom of the crib, even for supposedly loosely-packed cribs. For the cribs with l/b = 48, a larger crib-platform spacing the increased the burning rate of these cribs so that the burning rate was closer to the cribs with smaller l/b. For cribs with l/b = 96, the burning rate was still well below the predicted value, even for large crib-platform spacing. Future work will focus on exploring the burning rate and the effect of the crib-platform spacing for cribs with large l/b.

Keywords*: burning rate, cribs, porosity, residence time*

Introduction

Wood cribs are often used as ignition sources in room fire tests (for example in UL 1715 and ISO 9705 test standards) and for various other tests requiring repeatable heat release rates, such as fire extinguisher performance (ANSI/UL 711). To vary the burning rate of the source fire, cribs can be built with different stick thicknesses and arrangements. Thus predicting the burning behavior of a crib a priori can be particularly useful when designing a new testing procedure. The prediction of the burning rate of a crib may also have applications outside of fire testing. The burning rate of wildland fuels, both in the litter layer on the forest floor and the trees and shrubs themselves is not well understood. Even though wildland fuels do not have the same predictable arrangement as wood cribs, it is possible that a fundamental understanding of what governs the burning rate of a crib will apply to the wildland fire context (Fons *et al*. 1963, Byram *et al*. 1964, and Anderson 1990). All wildland fuels are essentially individual fuel particles with some spacing distance between them. For the needle litter layer, this spacing is small and relatively homogeneous. For trees and shrubs, this spacing will be greater with more variability due to the needles and leaves occurring only along branches. Once the burning rate of wildland fuels is better understood, other aspects of wildland fire behaviour will

become more clear. For example, if the fuel loading and the burning rate of the fuel structure are known, the fireline intensity and flame zone depth can be estimated. These two parameters characterize the fluid dynamics and radiative and convective heat transfer that spread the fire. Thus the fire spread rate can be better predicted with a better understanding of the burning rate. One important complexity of wildland fires that is often overlooked is that most wildland fuels are not homogeneously distributed. Wildland fuels often occur in clumps, such as clumps of native grasses, shrubs, or trees. The residence time of the fire at a particular fuel clump can be determined from the burning rate of that fuel structure. This residence time is itself an important consideration for fire spread – if the residence time for a fuel structure is less than the ignition time for the next structure, the fire won't spread. This is of particular concern when discussing the thresholds for crown fire spread, a currently poorly understood aspect of wildland fire. And finally, this residence time is also important for fire ecologists when evaluating fire effects. An important key to predicting tree mortality is knowing the duration of heating. It is for these reasons that a closer look into the driving mechanisms of crib burning rates is currently being undertaken.

The burning rate of unconfined cribs has long been identified to occur in two regimes: open or loosely-packed and closed or densely-packed. In the loosely-packed regime, the burning rate is more closely approximated by the free burning rate of the individual sticks and is governed by heat and mass transfer processes near the surfaces. In this regime, the burning rate is more of a function of the stick dimensions, and is independent of the "porosity" of the crib. For cribs in the densely-packed regime, the burning rate is limited by availability of oxidizer within the fuel bed. In this regime, the burning rate increases with the inter-stick spacing or the "porosity" of the crib. There are many ways to evaluate the porosity of a crib (see for example Gross (1962), Block (1971), Heskestad (1973), and Anderson (1990)), but perhaps the most commonly used is that of Heskestad (1973). By recorrelating the data of both Gross (1962) and Block (1971), Heskestad suggested that the burning rate is a function of the crib porosity given by

$$\frac{R}{A_s b^{-1/2}} = f\left[\left(\frac{A_v}{A_s}\right) s^{1/2} b^{1/2}\right] \qquad (1)$$

where R is the burning rate (g/s), A_s is the exposed surface area of the sticks (cm^2), b is the stick thickness (cm), A_v is the area of the vertical shafts in the crib (cm^2), and s is the spacing between sticks (cm). This relation predicts the burning rates of the cribs burned in both Gross (1962) and Block (1971) well (±20%).

There are two important aspects that required close consideration when applying knowledge gained from crib theory to the wildland fire context. One is the effect of the crib size and layout. By necessity, wildland fuels will be represented by cribs with a wide range of external dimensions and stick spacing distances. The effect of the ratio of the stick length to the stick thickness will be important when considering different fuel types like needle litter versus slash fuels because this will change the fuel thickness (b) and flame zone depth (l). Another important aspect to consider is the effect of the spacing between the crib and the support platform. Ground fuels, like the needle litter layer, have no way of supplying oxidizer through the bottom surface. These fuels would thus be more like cribs placed directly on the support platform. On the other hand, crown fuels, like trees and shrubs, have ample oxidizer supply from the bottom. These fuels would be more like cribs with a large spacing distance between the crib and the support platform.

Unfortunately, the crib geometries tested by both Gross and Block that were used to generate the relation in Eq. 1 were fairly limited. Gross primarily tested cubic cribs, with ten layers with stick lengths equal to ten times the thickness. Block extended the length to thickness ratio of his cribs to 20. In the wildland context, the fuels clearly are not arranged in such cubic or nearly cubic designs. As one can imagine by looking at Eq. 1, there are seemingly endless possible ways to build a crib with a given porosity. Only a few others have considered a wider range of crib geometries and layouts. Byram

et al. (1964) tested the effect of crib footprint area by keeping the stick spacing (*s*) and crib height constant and increasing the length of the sticks. However, this was an early publication and no attempt was made to correlate the data. O'Dogherty and Young (1964) tested a wide range of crib designs, but were unsuccessful in using applying the Heskestad correlation to their data. Smith and Thomas (1970) and Thomas (1973) had more success in correlating the O'Dogherty and Young data with different relations that included the height of the crib. However, Thomas (1973) excluded cribs with "a large ratio of horizontal to vertical dimensions." In Smith and Thomas (1970), they included the results of Byram *et al*. (1964), but these data were poorly correlated. Clearly, the effect of crib geometry and layout is not well understood.

The only work in the literature found that considered the effect of the distance between the crib and the support platform is that of Block (1970). In this work, Block tested five crib designs with crib-platform spacing distance ranging from 0.159 cm (1/16") to 2.54 cm (1"). The burning rate of all cribs was seen to increase by about 15% as the spacing distance increased from 0.159 cm (1/16") to 1.27 cm (½"). For spacing distances larger than 1.27 cm (½"), no further change in the burning rate was seen. However, only five crib designs were tested and all cribs had a fixed stick length to thickness ratio (*l/b*) of 10, so it is difficult to say that these results are universal to all crib designs.

This work explores the burning rate of cribs with a wide variety of layouts and geometries to determine whether the correlation of Heskestad holds. The effect of the spacing distance between the crib and the support platform is also considered for a selection of crib designs.

Experiment description

The experimental chamber used was very large (12.4m x 12.4m x 19.6m) so that the airflow to the cribs was not restricted. Three load cells spaced equally apart were used to weigh the cribs during each test. As shown in Figure 1, two thin aluminum discs, separated by pins to reduce heat transfer to the load cells, were used as a support platform for the cribs. Multiple sheets of ceramic paper insulation were placed on top of the support platform to further minimize heat transfer to the load cells. A thermocouple was located near the load cells to assure that the temperature remained fairly constant. All cribs were conditioned in an environmental chamber at 35°C and 3% relative humidity for at least three days, resulting in an equilibrium moisture content of approximately 1%.

Simultaneous ignition of the cribs was achieved by quickly dunking the crib in isopropyl alcohol and allowing it to drain. The total mass of fuel used was 10% or less of the crib weight. The liquid fuel was observed to easily burn off before the steady state burning of the crib was achieved. Both mass and temperature were logged at 2 Hz. A sample of the raw data is shown in Figure 2, where four distinct phases of burning can be seen – burning off of the liquid fuel, stick ignition, steady burning, and burnout. Only data from the steady burning portion of the curve was used to calculate the burning rate. The burning rate was found from the slope of the best-fit line through the data.

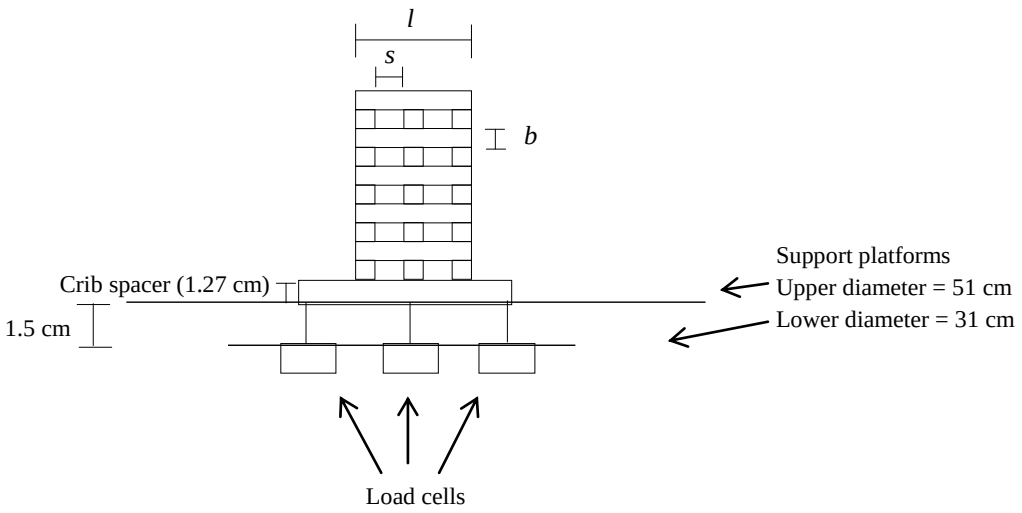

Figure 1. Sketch of apparatus for a crib with 3 sticks per layer (n = 3) and 10 layers (N = 10).

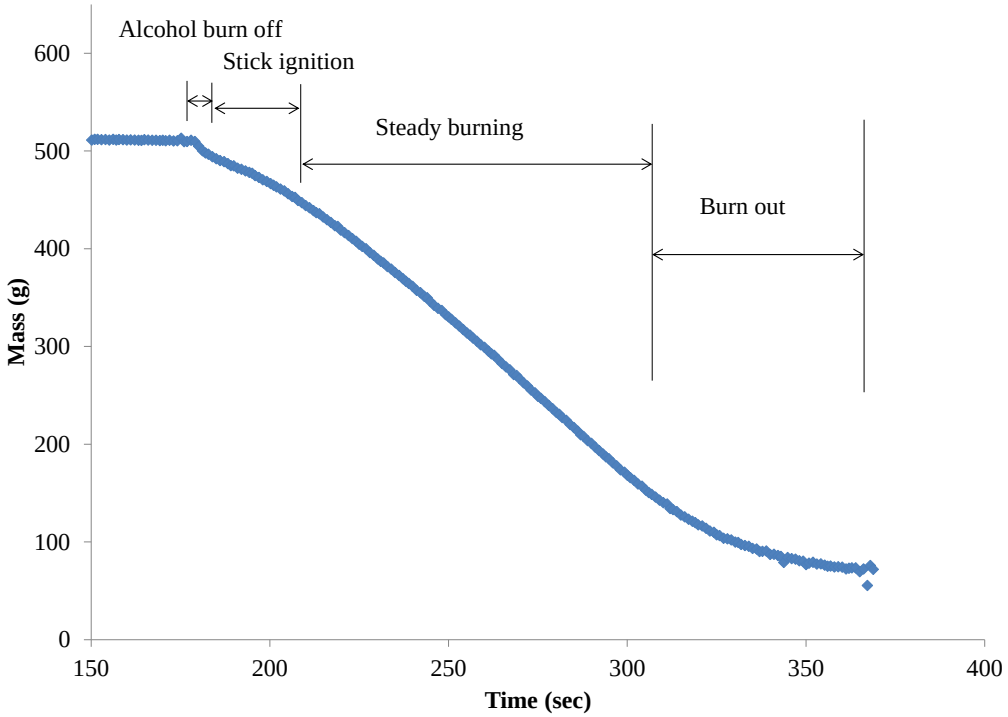

Figure 2. Sample raw data for 1.27-12-3-14 crib.

Wood cribs were built using square ponderosa pine sticks with thicknesses ranging from 0.159 cm (1/16 in) to 1.27 cm (0.5 in). In the first series of tests, a wide variety of crib designs were explored. Table 1 shows the details of all cribs burned. Each crib layout was tested three times and the results averaged. The first phase of experiments was performed to validate the testing apparatus against the known data of Gross (1962). In the second phase of experiments, the effect of crib layout in the loosely-packed regime was explored. The loosely-packed regime was chosen because it was indicated by Fons *et al*. (1963) that all wildland fuels would burn in this regime. For these experiments, the porosity factor of Heskestad (1973) (Eq. 1) was kept approximately constant while the number of sticks per layer, number of layers and the length to thickness ratios (*l*/*b*) were varied. The stick surface area was varied over an order or magnitude and (*l*/*b*) nearly an order of magnitude to really test the range of

validity of the Heskestad correlation. As indicated in Table 1, the number of layers must decrease to keep the porosity constant as more sticks per layer are added. For this set of experiments, the cribs were placed on two steel spacers of 1.27 cm (0.5 in) as this was the critical spacing distance indicated by Block (1970).

A second series of experiments was performed with a subset of the cribs to explore the effect of the spacing distance between the crib and the support platform. Spacing distances of 0 cm, 0.64 cm, 1.27 cm, 2.54 cm, and 7.62 cm were tested. The list of crib designs tested is listed in Table 2. Again, the cribs used here had an approximately constant porosity in the loosely-packed regime while a range of length to thickness ratios (*l/b*) was tested. Each crib layout was tested three times and the results averaged.

Table 1. Crib dimensions for tests with variable crib geometry and layout.

Shorthand (b-l/b-n-N)	Stick thickness (b) [cm]	Stick length (l) [cm]	l/b [ ]	Number of sticks per layer (n) [ ]	Number of layers (N) [ ]	Surface area (A_s) [cm^2]	Porosity (φ) [cm]
0.64-10-3-10	0.64	6.35	10	3	10	442.74	0.0530
0.64-10-5-10	0.64	6.35	10	5	10	665.32	0.0108
0.64-10-7-10	0.64	6.35	10	7	10	829.84	0.00196
1.27-10-3-10	1.27	12.7	10	3	10	1770.96	0.1060
1.27-10-5-10	1.27	12.7	10	5	10	2661.29	0.0215
1.27-10-7-10	1.27	12.7	10	7	10	3319.35	0.00393
0.64-10-2-12	0.64	6.35	10	2	12	370.97	0.1249
1.27-12-3-14	1.27	15.24	12	3	14	3009.67	0.117
0.64-16-2-30	0.64	10.16	16	2	30	1503.22	0.1249
0.64-16-3-12	0.64	10.16	16	3	12	878.22	0.126
0.64-16-4-6	0.64	10.16	16	4	6	574.19	0.1284
0.64-16-5-4	0.64	10.16	16	5	4	471.77	0.1089
0.64-16-6-2	0.64	10.16	16	6	2	290.32	0.1247
0.64-24-3-27	0.64	15.24	24	3	27	3012.09	0.1215
0.64-24-4-14	0.64	15.24	24	4	14	2045.16	0.129
0.64-24-5-9	0.64	15.24	24	5	9	1616.93	0.1246
0.64-24-6-6	0.64	15.24	24	6	6	1277.42	0.123
0.64-36-8-8	0.64	22.86	36	8	8	3406.45	0.118
0.64-48-12-6	0.64	30.48	48	12	6	5051.60	0.119
0.32-48-6-12	0.32	15.24	48	6	12	1328.22	0.123
0.16-96-9-10	0.16	15.24	96	9	10	838.76	0.119

Table 2. Crib dimensions for crib-platform spacing tests.

Shorthand (b-l/b-n-N)	Stick thickness (b) [cm]	Stick length (l) [cm]	l/b [ ]	Number of sticks per layer (n) [ ]	Number of layers (N) [ ]	Porosity (φ) [cm]
1.27-12-3-14	1.27	15.24	12	3	14	0.117
0.64-24-4-14	0.64	15.24	24	4	14	0.129
0.64-48-12-6	0.64	30.48	48	12	6	0.119
0.32-48-6-12	0.32	15.24	48	6	12	0.123
0.16-96-9-10	0.16	15.24	96	9	10	0.119

Results and discussion

Effect of crib geometry and layout

The burning rates of all cribs are listed in Table 3. As mentioned above, three replicates of each crib fire were performed. The average and standard deviation from these replicates are also shown in Table 3. The standard deviation ranged from less than 1% to about 10% of the mean value. The average burning rate for each crib layout is plotted in Figure 3 using the form of Eq. 1. The black line in Figure 3 is the correlation from Heskestad (1973).

Table 3. Burning rate results for cribs with variable geometry and layout.

Shorthand (b-l/b-n-N)	Porosity (φ) [cm]	Burning rate Test 1 [g/s]	Burning rate Test 2 [g/s]	Burning rate Test 3 [g/s]	Mean burning rate [g/s]	Standard deviation [% of mean]
0.64-10-3-10	0.0530	0.4942	0.5510	0.5295	0.5249	5.46
0.64-10-5-10	0.0108	0.3419	0.3517	0.3772	0.3569	5.11
0.64-10-7-10	0.00196	0.1529	0.1516	0.1547	0.1531	1.02
1.27-10-3-10	0.1060	1.7031	1.7632	1.7559	1.7407	1.88
1.27-10-5-10	0.0215	1.9573	1.9474	1.8551	1.9199	2.94
1.27-10-7-10	0.00393	0.7157	0.6913	0.7160	0.7077	2.00
0.64-10-2-12	0.1249	0.5134	0.4991	0.5329	0.4984	8.80
1.27-12-3-14	0.117	3.2160	3.2113	2.8836	3.1036	6.14
0.64-16-2-30	0.1249	2.1110	2.0994	2.2587	2.1564	4.12
0.64-16-3-12	0.126	1.2030	1.1141	1.1540	1.1570	3.85
0.64-16-4-6	0.1284	0.7467	0.7531	0.7396	0.7465	0.90
0.64-16-5-4	0.1089	0.5926	0.5926	0.6198	0.6017	2.61
0.64-16-6-2	0.1247	0.3279	0.3492	0.3655	0.3475	5.43
0.64-24-3-27	0.1215	3.8678	4.3306	4.5316	4.2433	8.02
0.64-24-4-14	0.129	2.8798	2.7776	2.9521	2.8698	3.06
0.64-24-5-9	0.1246	2.1622	2.1000	2.2254	2.1625	2.90
0.64-24-6-6	0.123	1.7096	1.5446	1.7386	1.6643	6.29
0.64-36-8-8	0.118	3.8453	4.3561	4.4014	4.2010	7.35
0.64-48-12-6	0.119	5.6133	5.2003	6.1719	5.6618	8.61
0.32-48-6-12	0.123	1.8529	2.0239	1.6543	1.8437	10.03
0.16-96-9-10	0.119	1.1968	1.2156	1.2585	1.2236	2.58

As mentioned above, the first portion of the experiments were replicates of the experiments of Gross (1962) to validate the experimental procedure. The data from these experiments are marked in Figure 3 as solid diamond-shaped points. Heskestad's correlation fit the data of Gross (1962) and Block (1971) to within ±20% (Heskestad 1973), and the data here comfortably falls in that range. Some variation from the data of Gross is expected due to the differences in wood and moisture content of the cribs, in addition to the difference in spacing between the crib and the support platform. Gross used primarily Douglas-fir wood with average moisture content of approximately 9%, compared to the nearly dry ponderosa pine wood used here. Additionally, it appears that the separation distance used by Gross was equal to the fuel thickness (either 0.64 or 1.27 cm). A constant separation distance of 1.27 cm was used here. As mentioned above, Block noted that the burning rate changes up to 15% as the separation increase from none to a very large distance. These factors help explain the average difference 14% that was observed between the experiments here and those of Gross (1962).

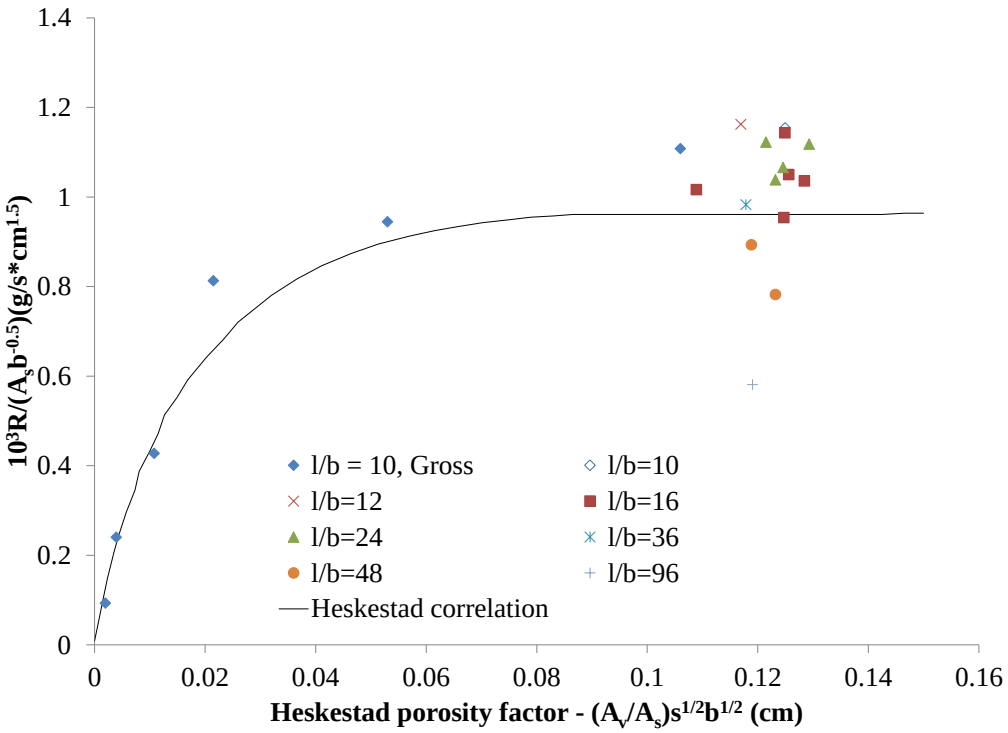

Figure 3. Burning rate results.

Because the layout of the cribs from the second set of experiments varied so widely, the burning rate results in Figure 3 were grouped by their length to thickness ratio (l/b) which ranged from 10 to 96. As listed in Table 1, a fairly wide variety of crib layouts for l/b ranging from 10 to 24 were tested. The burning rates from these cribs are shown in Figure 3 as diamonds for l/b =10, x's for l/b = 12, squares for l/b = 16, and triangles for l/b = 24. Interestingly, it appears that the burning rate of cribs within this range of l/b can be reasonably predicted with the Heskestad correlation, regardless of the crib layout. However, even though the porosity of all the cribs tested was approximately constant (and within the loosely-packed regime), the burning rate appears to decrease as the length to thickness ratio (l/b) further increases. For l/b less than or equal to 36, the burning rate is consistently above the Heskestad correlation. For l/b equal to 48, the burning rate falls below the Heskestad correlation by 7-19%, which is still in the noted range of variability of the correlation. However, for l/b equal to 96, the burning rate falls 40% below that of the correlation. Interestingly, this decrease in burning rate also corresponded to a visual change in burning regime. As this l/b ratio increased to 36 and above, it was observed that the cribs no longer burned simultaneously, but rather burned as propagating region from the outside edges inward as shown in Figure 4. A similar behaviour was noted when burning the densely-packed cribs in the first portion of the experiments. In other words, these loosely-packed cribs behaved like densely-packed cribs of a much lower porosity and the availability of oxidizer is controlling the burning rate as the l/b ratio increases. Thus, it appears that the crib porosity is also a function of the length to thickness ratio above some critical value of l/b.

Fig 4. Crib with l/b = 48 burning from the outside edges inward.

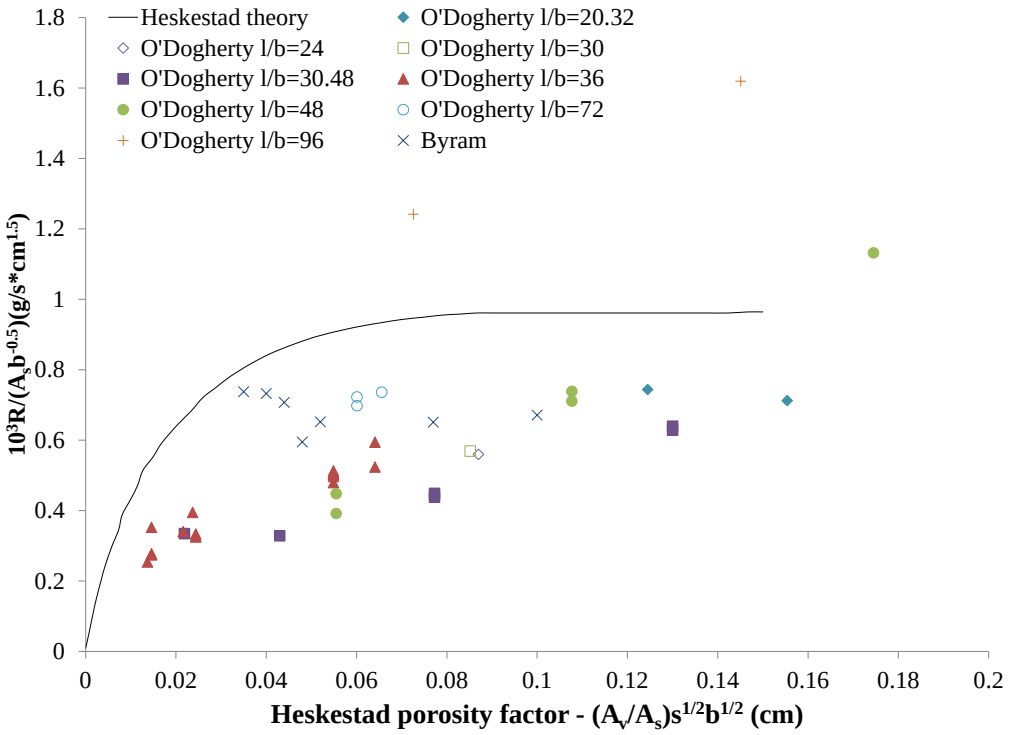

Figure 5. Burning rate data from O'Dogherty and Young (1964) and Byram et al. (1964).

To help clarify whether the porosity is a function of the length to thickness ratio, the results from O'Dogherty and Young (1964) and Byram *et al*. (1964) are considered. These are the only studies found in the literature that consider cribs with *l*/*b* greater than 40. Figure 5 shows the data of both O'Dogherty and Young (1964) and Byram *et al*. (1964) along with the Heskestad correlation. O'Dogherty and Young used white pine of 12% moisture content with *l*/*b* from 20.2 to 96. As mentioned earlier, their data was poorly predicted by the Heskestad correlation and the data is considerably scattered. The burning rate for cribs with (*l*/*b*) = 96 is significantly larger than the others and there is no clear trend in their data with (*l*/*b*). Byram *et al*. tested cribs of white fir with 10% moisture content. No spacing between the crib and support platform appears to have been used. In this study the stick spacing (*s*) and crib height were kept constant as the length of the sticks was increased. Consequently, the porosity of these cribs increased from a densely-packed crib to a loosely-packed crib as *l*/*b* increased from 9.1 to 61.4. As shown in Figure 5, when considered in the form of Heskestad

and Eq. 1, the transformed burning rate was relatively constant for all cribs considered. The densely-packed crib results with lower *l*/*b* ratios are reasonably close to the Heskestad correlation. However, as the *l*/*b* ratio increases above 25 (porosity of 0.048 cm) and the beds become more porous, the burning rates fall considerably below the Heskestad correlation. Interestingly, neither work mentions the spacing distance used between the crib and the support platform. The majority of the data from both studies falls below the Heskestad correlation suggesting that no spacing between the cribs and the platforms was used. Thus it is clear that a more thorough sampling of the burning rates from cribs with *l*/*b* greater than approximately 30 is needed to clarify whether a critical *l*/*b* ratio exists.

Though the studies of O'Dogherty and Young and Byram *et al*. don't help to clarify whether the porosity is a function of the length to thickness ratio, the low burning rates suggest that the spacing between the crib and the support platform could have a greater effect that that listed by Block (1971).

Effect of spacing distance between the crib and support platform

The results of the tests with variable spacing distance between the crib and the support platform are shown in Table 4 and Figure 6. As shown, the burning rate of cribs with *l*/*b* equal to 12 is virtually insensitive to the spacing between the crib and the support platform. In fact, a slight decrease in the burning rate was seen for the largest spacing distance tested (7.62 cm), possibly due to increased convective or radiative heat losses. As the ratio of *l*/*b* increases, however, the effect of that spacing drastically increases. In fact, at *l*/*b* equal to 96, the difference is over 60%. As in the experiments above, this decrease in burning rate is seen visually as well. As shown in Figure 7, cribs with a *l*/*b* ratio equal to or greater than 48 burn as a propagating region from the outside edges inward when the spacing between the crib and the support platform is small (0 to 1.27 cm). As the crib-platform spacing distance increases, the cribs begin to burn simultaneously, in a similar fashion to the cribs with *l*/*b* less than 48. It is quite apparent that as the *l*/*b* ratio increases, a significant portion of the required oxidizer comes from the bottom of the crib, even for supposedly loosely-packed cribs.

Table 4. Burning rate results for crib-platform spacing tests.

Shorthand (b-l/b-n-N)	l/b [ ]	Porosity (φ) [cm]	Mean R (g/s) 0 cm	Mean R (g/s) 0.64 cm	Mean R (g/s) 1.27 cm	Mean R (g/s) 2.54 cm	Mean R (g/s) 7.62 cm
1.27-12-3-14	12	0.117	3.1546	3.1582	3.1036	3.2086	2.9653
0.64-24-4-14	24	0.129	2.2923	2.7081	2.8698	2.8966	2.769
0.64-48-12-6	48	0.119	-	5.0705	5.6618	7.164	7.777
0.32-48-6-12	48	0.123	1.0354	1.5545	1.8437	1.9799	2.3513
0.16-96-9-10	96	0.119	0.4555	0.8644	1.2236	1.3297	1.3425

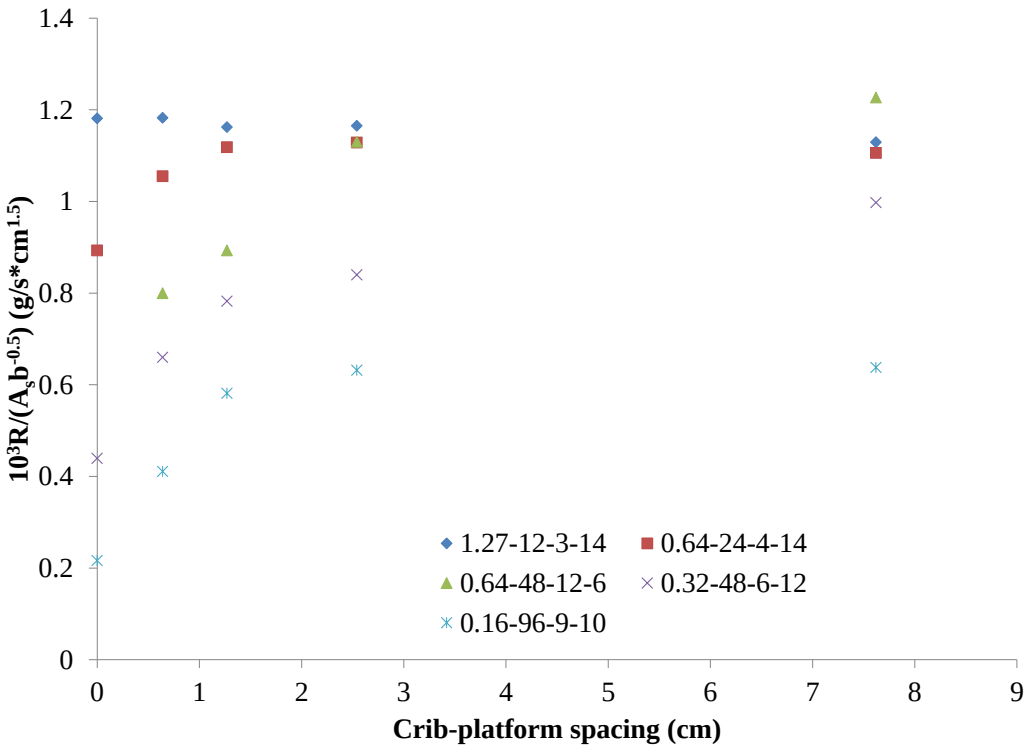

Figure 6. Effect of crib-platform spacing.

Figure 7. Visual change in burning regime for various crib-platform spacings for the 0.64-48-12-6 crib design. Top left: 0 cm spacing; Top right: 1.27 cm spacing; Bottom left: 2.54 cm spacing; Bottom right: 7.62 cm spacing.

Block (1971) noted a critical spacing of about 1.27 cm beyond which the burning rate of his cribs with *l/b* equal to ten did not change. By looking at Figure 6, this critical spacing distance seems reasonable for cribs up to *l/b* up to 24. For larger length to thickness ratios, however, the critical spacing distance is larger. For the cribs tested here with *l/b* of 48, the critical spacing distance appears to be over 2.5 cm. For these cribs, the burning rate increased by 7% for the 0.64-48-12-6 cribs and 15% for the 0.32-48-6-12 cribs as the spacing increases from 2.54 cm to 7.62 cm. Further tests are required at even larger spacing distances to identify the actual critical spacing distance, but it is clear that the change in burning rate is beginning to level off a value much larger than that identified by Block. Interestingly, the change in burning rate for the crib tested with a length to thickness ratio of 96 seems to level off earlier than the cribs with *l/b* of 48. In fact, the critical spacing distance seems to be around 2.54 cm. Because only one crib design with l/b of 96 was tested, it is difficult to know whether the reduction in the critical spacing distance as *l/b* goes from 48 to 96 is real or some artefact of the crib design, in particular the stick thickness. Either way, the critical spacing distance between the crib and the support platform is clearly a function of the length to thickness ratio and can be quite a bit larger than previously thought.

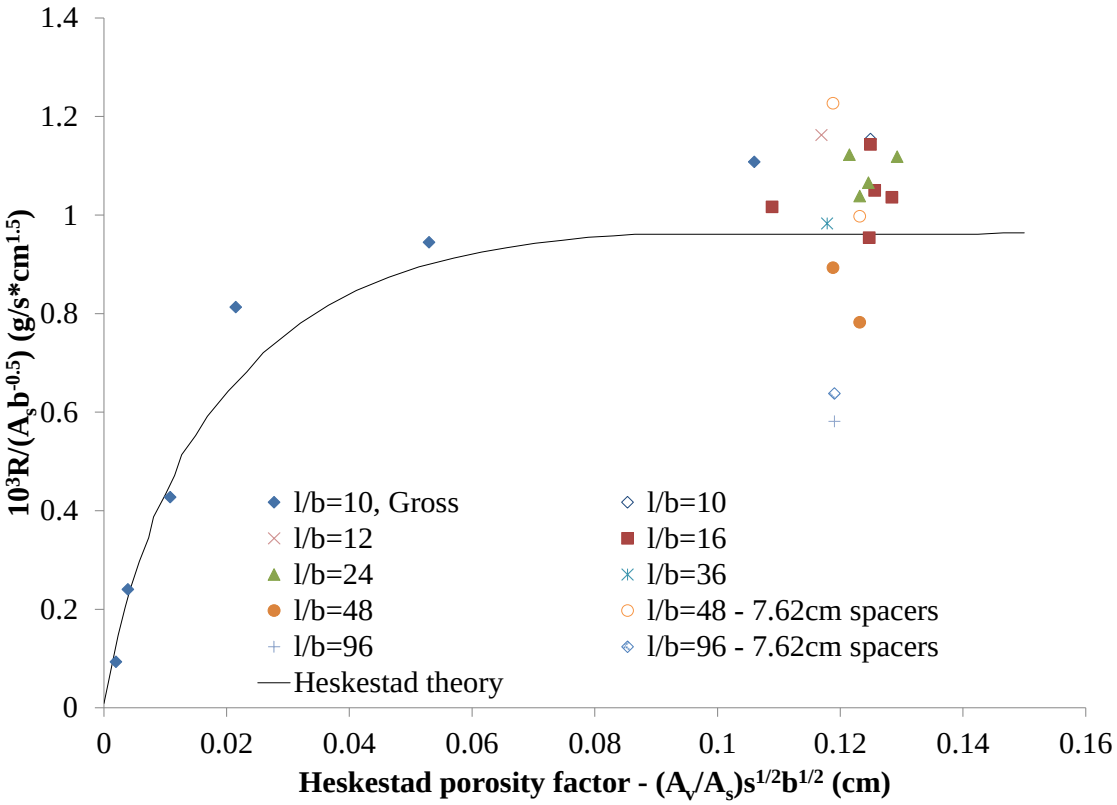

Figure 8. Burning rate including effect of crib-platform spacing.

Because such a large change in the burning rate for cribs with a large *l/b* ratio was seen with the increase in the crib-platform spacing, the Heskestad correlation was reconsidered to determine if the burning rate of these cribs would more closely match the correlation with a larger crib-platform spacing. Figure 8 shows the transformed burning rate as a function of the porosity with both the data from Figure 3 with a crib-platform spacing of 1.27 cm along with the data for cribs with *l/b* of 48 and 96 taken with a crib-platform spacing of 7.64 cm. As shown, the burning rates for the cribs with *l/b* of 48 and crib-platform spacing of 7.64 cm have indeed increased such that they are within the range of burning rate values measured for cribs with smaller *l/b*. However, the critical crib-platform spacing for crib design tested with *l/b* of 96 was much closer to the spacing used in the original series of tests,

so the burning rate for this crib design did not increase much and remains significantly below the Heskestad correlation. It is unknown whether this low burning rate is a real effect of the crib design, due possibly to the extremely thin sticks, or is the result of some effect of the experiment design. Because the sticks are so thin, the steady burning regime is very short (on the order of ten seconds), so it is possible that not all of the liquid fuel is immediately burned off. The measured burning rate would thus be dictated by the liquid fuel and not the sticks themselves and thus not as susceptible to changes in crib design. Additionally, the rate of data logging was fixed at 2 Hz, so fewer data points are available to perform a linear regression on so the error in these measurements may be larger. More crib designs with this stick thickness should be performed, particularly with smaller *l/b* ratios, to determine whether these results are due to the experimental protocol or are a true indication of the behaviour.

Summary and future work

Wood cribs are often used as ignition sources for room fire tests. A fundamental understanding of the mechanisms that govern the burning rate of a wood crib may also have applications to wildland fires. The burning rate of unconfined cribs has long been identified to occur in two regimes: the densely-packed regime where the burning rate is proportional to the crib porosity and the loosely-packed regime where the burning rate is independent of porosity. The cribs used to define these burning regimes were fairly limited in their design – either cubic (Gross 1962) or a fairly limited range of the stick length to thickness ratios (*l/b* = 10-20 in Block 1971). However, there are seemingly endless possible ways to build a crib with a given porosity. The first part of this work explored the burning rate of cribs with a wide variety of geometries to determine whether the porosity-burning rate relation defined by Heskestad (1973) holds. One round of experiments was performed to validate the testing apparatus against the known data of Gross (1962) and good agreement was found. A second round of experiments explored the effect of crib layout in the loosely-packed crib regime. The porosity was kept approximately constant while the number of sticks per layer, number of layers and the length to thickness ratios (*l*/*b*) were varied from 10 to 96. For *l*/*b* less than 36, the burning rate of all cribs matched the porosity-burning rate relation from Heskestad (1973), regardless of layout. For larger *l*/*b*, the burning rate was considerably reduced, indicating that there is an insufficient flow of oxidizer inside the crib even though the defined porosity indicates that it should in the loosely-packed regime. This implies that the crib porosity could be function of *l*/*b* above some critical threshold. The second part of this work explored the effect of the spacing distance between the crib and the support platform. The effect of spacing distance is strongly dependent on *l*/*b*, with no difference seen for *l*/*b* = 10 and over a 60% change for *l*/*b* = 96. From these experiments it was clear that cribs with a large *l/b* ratio require a significant amount of oxidizer to flow through the bottom of the crib. The critical spacing distance was shown to be larger than previously thought and a function of the length to thickness ratio. For the cribs with *l/b* = 48, a larger crib-platform spacing the increased the burning rate of these cribs so that the burning rate was closer to the cribs with smaller *l/b*. For cribs with *l/b* = 96, the burning rate was still well below the predicted value, even for large crib-platform spacing.
Because the number of cribs with *l*/*b* = 36 or larger was limited, future work will explore a wider variety of crib layouts with large *l*/*b* to see if the trends seen here hold and to determine if there is a threshold *l*/*b* where the porosity becomes dependent on *l*/*b*. As wildland fuels tend to be quite thin, more cribs with stick thickness of 0.16 cm should be tested. Understanding the effects explored here will be vital when applying crib theory to wildland fires. For example, the effect of crib spacing above the platform will be important when considering ground fuels versus crown fuels. The effect of (*l/b*) will be important when considering different fuel types (needle litter versus slash fuels will change *b*) and flame zone depths (will change *l*).

Acknowledgements

The authors wish to thank James McGuire for his tireless and careful construction of the cribs and Cyle Wold for setting up the data acquisition system. Funding for this work was provided by the National Fire Decision Support Center.

References

Anderson HE (1990) Relationship of fuel size and spacing to combustion characteristics of laboratory fuel cribs. USDA Forest Service, Intermountain Research Station Research Paper INT-424, 9 pp.

Block JA (1970) A theoretical and experimental study of nonpropagating free-burning fires. Ph.D. Thesis, Harvard University, Cambridge, MA.

Block JA (1971) A theoretical and experimental study of nonpropagating free-burning fires. *Symposium (International) on Combustion* **13**, 971-978.

Byram GM, Clements HB, Elliott ER, George PM (1964) An experimental study of model fires. USDA Forest Service. Southeastern Forest Experiment Station Technical Report No. 3, 36 pp.

Fons WL, Clements HB, George PM (1963) Scale effects on propagation rate of laboratory crib fires. *Symposium (International) on Combustion* **9**(1), 860-866.

Gross D (1962) Experiments on the burning of cross piles of wood. *Journal of Research of the National Bureau of Standards –C. Engineering and Instrumentation* **66c**(2), 99-105.

Heskestad G (1973) Modeling of enclosure fires. *Symposium (International) on Combustion* **14**, 1021-1030.

O'Dogherty MJ, Young RA (1964) Miscellaneous experiments on the burning of wooden cribs. Fire Research Station, Fire Research Note No. 548. (Boreham Wood. Herts.)

Smith PG, Thomas PH (1970) The rate of burning of wood cribs. *Fire Technology* **6**(1), 29-38.

Thomas PH (1973) Behavior of fires in enclosures – some recent progress. *Symposium (International) on Combustion* **14**, 1007-1020.

Environmental thresholds for dynamic fire propagation

Jason J. Sharples[a], Colin C. Simpson[b], Jason P. Evans[c]

[a] *Applied and Industrial Mathematics Research Group, School of Physical, Environmental and Mathematical Sciences, UNSW Canberra, Australia. j.sharples@adfa.edu.au*
[b] *Applied and Industrial Mathematics Research Group, School of Physical, Environmental and Mathematical Sciences, UNSW Canberra, Australia. c.simpson@adfa.edu.au*
[c] *Climate Change Research Centre, Faculty of Science, University of New South Wales, Sydney, Australia. jason.evans@unsw.edu.au*

Abstract
Under conditions of extreme fire weather, bushfires burning in rugged terrain can exhibit highly atypical patterns of propagation, which can have dramatic effects on subsequent fire development. In particular, wildfires have been observed to spread laterally across steep, lee-facing slopes in a process that has been termed vorticity-driven lateral spread (VLS; also known as 'fire channelling'). Coupled fire-atmosphere modelling using large eddy simulation has indicated that the fire channelling phenomenon occurs due to a dynamic interaction between terrain modified winds and the fire's convective plume. This interaction creates pyrogenic vorticity that drives a fire laterally across a leeward slope. In this work we extend previous modelling, using the WRF-Fire coupled fire-atmosphere model, to specifically consider the environmental thresholds that define the likely onset of the VLS phenomenon. In particular we investigate the effects of wind speed and topographic slope on the occurrence of atypical lateral spread.
The simulated behaviour of fires on leeward slopes, and the implied transition in fire propagation that can occur when certain environmental thresholds are breached, highlight the inherent dangers associated with firefighting in rugged terrain. The propensity for dynamic interactions to produce erratic and dangerous fire behaviour in such environments has strong implications for firefighter and community safety. At the very least the research findings provide additional support for careful planning prior to prescribed burning operations and the use of well-briefed observers in firefighting operations undertaken in complex topography.

Keywords*: Dynamic fire propagation; environmental thresholds; wind-terrain-fire interaction; VLS*

Introduction

Dynamic escalation of wildland fires into large conflagrations represents a significant challenge to the management of fires in the landscape. Multi-scale interactions between a fire and the local environment, which includes fuels, weather and topography, can produce highly complex patterns of fire spread that are currently beyond the capabilities of operational fire spread models. Understanding the physical processes that underpin these complex modes of fire propagation is a key step in improving the way extreme bushfires are managed. Recent research into the behaviour of wildfires has identified a number of dynamic modes of fire propagation. These modes of fire spread are referred to as dynamic because they are manifestly at odds with quasi-steady fire propagation, whereby a fire spreads at an approximately constant rate given uniform environmental conditions.
Viegas (2005) and Dold and Zinoviev (2009) examined the ability of a fire to exhibit exponentially increasing rates of spread up steep slopes and canyons, while Viegas *et al.* (2012) discussed the abrupt increases in rate of spread that can occur when two lines of fires intersect at some oblique angle. Another form of dynamic fire propagation was identified by Sharples *et al.* (2012) in connection with the 2003 Canberra bushfires. This phenomenon, which they referred to as *fire channelling*, involved the rapid lateral propagation of a fire across a lee-facing slope in a direction approximately perpendicular to the prevailing wind direction. Sharples *et al.* (2012) conjectured that the lateral spread was due to an interaction between the wind, the terrain and an active fire.

Simpson *et al*. (2013) found support for this conjecture using the WRF-Fire coupled fire-atmosphere model through simulation of the interaction of the terrain modified flow with the fire's convective plume. It was found that this interaction resulted in the intermittent generation of vertical vorticity, which drove the fire laterally across the top of the slope in the immediate lee of the ridge line. As such, Simpson *et al*. (2013) permitted the characterisation of fire channelling as vorticity-driven lateral spread (VLS). Farinha (2011) conducted a number of combustion tunnel experiments to examine the behaviour of fires burning on the leeward slope of a small triangular ridge. He found that in the absence of wind the fires burnt uniformly across the slope at a distinctly quasi-steady rate of spread. In the presence of combustion tunnel winds of 1.5 m s^{-1}or greater Farinha (2011) found that the fire spread rapidly across the top of the leeward slope at a significantly accelerated rate. The rate of lateral spread varied with the speed of the wind, with the greater rates of lateral spread coinciding with the fastest wind speeds.

In the present paper, the study of Simpson *et al*. (2013) is extended to examine the effect of variation in wind speed and topographic slope on the occurrence of VLS across a lee-facing slope. Fires burning on lee-facing slopes under different wind speed and topographic slope regimes were simulated using WRF-Fire. Two sets of simulations were considered. In the first, the winds were taken as coming from the west with the ambient wind speed characterised in terms of a reference wind speed U_0. The topography was taken to be an idealised triangular mountain with a north-south oriented ridge line, such as was considered by Simpson *et al*. (2013). The windward and leeward slopes were taken to be 20° and 35°, respectively. The reference wind speed U_0 was prescribed values of 0, 2.5, 5, 7.5, 10 and 15 m s^{-1}. The aim of this part of the study was to ascertain if there is a wind speed threshold, below which VLS does not occur.

In the second set of simulations, the reference wind speed was fixed at U_0 = 15 m s^{-1}. The topography was again taken to be an idealised triangular mountain with a windward slope of 20°, but with a leeward slope α° that was varied between 10° and 45°. This part of the study was designed to examine the existence of a threshold topographic slope, below which VLS does not occur. Such environmental thresholds are hypothesised to exist based on the role that flow separation in the lee of the ridge plays in driving the VLS phenomenon (Simpson *et al*. 2013). Flow separation is only expected to occur when wind speeds are sufficiently strong and the leeward slope is sufficiently steep (Wood, 1995).

The 'deep flaming' associated with the VLS phenomenon (Sharples *et al*., 2012) can act as a strong source of pyro-convection, and so systematically establishing the environmental thresholds relating to VLS will provide improved guidance for predicting the onset of extreme pyro-convection and blow-up fire behaviour. As such, the present study has direct implications for firefighter and community safety.

Methods

Version 3.5 of the Weather Research and Forecasting (WRF) model (Skamarock *et al*., 2008) is used in a large eddy simulation (LES) configuration (Moeng *et al*., 2007) and coupled to the SFIRE fire spread model (Mandel *et al*., 2011). This coupled atmosphere-fire numerical modelling system, commonly referred to as WRF-Fire, is suited to modelling turbulent atmosphere-fire interactions on length scales of tens of metres to kilometres. The WRF-LES model explicitly resolves grid-scale atmospheric eddies, whereas the effects of subgrid-scale motions are modelled using a subfilter-scale stress model. WRF utilises fully compressible nonhydrostatic equations and has a mass-based terrain-following coordinate system. The WRF-LES model domain has dimensions of 15 km × 5 km × 5 km with open radiative boundaries. The horizontal and vertical grid spacing are both 50 m, although due to the use of mass levels the vertical grid spacing is not constant. A triangular mountain is located within the model domain, as shown in Figure 1, with its ridge line oriented perpendicular to the prevailing wind. The windward and leeward slope angles are 20° and 35°, respectively, and the mountain height is 1 km. The initial and lateral boundary conditions are specified using a 1D sounding

with a vapor mixing ratio of zero, a constant potential temperature of 300 K and a wind profile given by U0, which expressed as a function of the Cartesian coordinates (x,y,z), is

$$\mathbf{U}_0(x, y, z) = U_0 P(z)\mathbf{x} \quad (1)$$

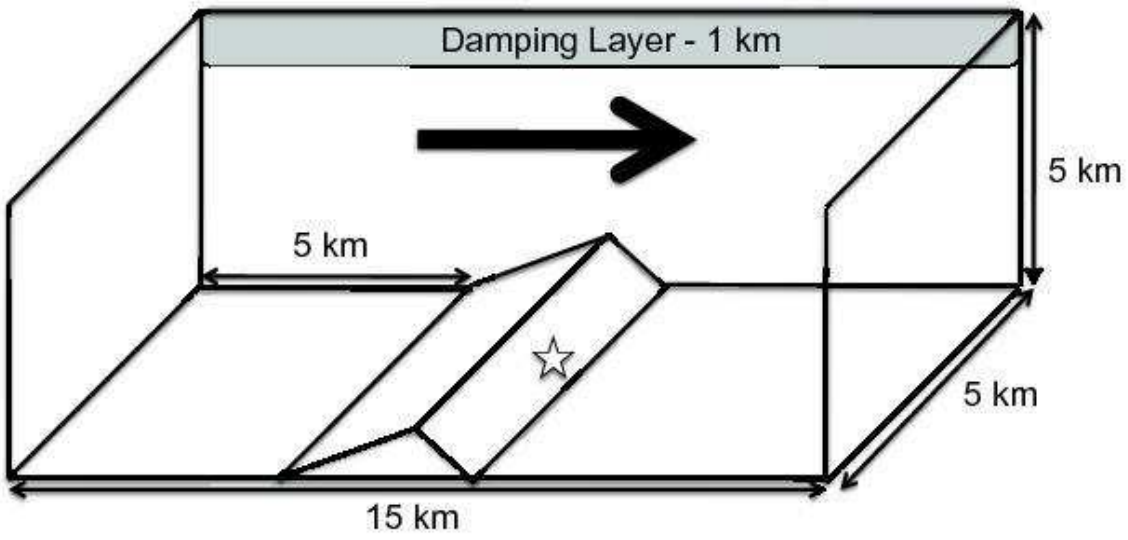

Figure 1. Model domain showing the triangular mountain with its ridge line oriented perpendicular to the input wind field. The windward slope is inclined at 20° and the leeward slope is inclined at an angle of α° (α = 35° in the first set of simulations and is variable in the second set of simulations). The star on the leeward slope indicates the approximate location of the ignition used in the simulations.

Here U0 denotes the reference wind speed – the main variable of interest in this study, and x denotes the unit vector in the x-direction (which coincides with east). The function P(z) in equation (1) prescribes the vertical structure of the initial wind field profile, and is defined as:

$$P(z) = \begin{cases} \left(\frac{z}{200}\right)^2, & z \leq 200, \\ 1, & z > 200. \end{cases} \quad (2)$$

We use a quadratic profile here, rather than the usual logarithmic profile, for the sake of simplicity and, more importantly, so that our results are directly comparable with those of Simpson *et al*. (2013). WRF offers either a physical (not used) or free-slip (used) bottom boundary condition. Since the lowest model level is still above the actual ground level, we don't have a completely zero wind speed on any WRF model level. However, it should be noted that a fuel-dependent roughness length is used in vertically interpolating the wind speeds down to the mid-flame height.

The WRF-LES model is used in an idealised configuration and there is no modelling of the microphysics, radiation physics, cumulus physics and the surface and planetary boundary layers. However, it should be noted that a fuel-dependent roughness length is used in vertically interpolating the wind speeds down to the mid-flame height. Diffusion in physical space is calculated using the velocity stress tensor and the eddy viscosities are calculated using a 3D prognostic 1.5-order turbulence closure scheme. A Rayleigh damping layer in the top 1 km is used to prevent reflection of the pyro-convective plume from the model top. The primary model time integration is performed using a third-order Runge-Kutta scheme and a secondary time step is used to handle acoustic waves. The primary and secondary model time steps are 0.1 s and 0.0125 s, respectively.

A small circular fire is ignited in the SFIRE model near the base of the leeward slope (Figure 1), after a WRF-LES spin-up period of 20 min. The subsequent fire spread is modelled on a 10 m × 10 m

horizontal grid as a temporally evolving fire perimeter using a level set method. The spatially and temporally varying fire spread rate, S, is calculated using the Rothermel equation (Rothermel, 1972):

$$S = R_0(1 + \varphi_W + \varphi_S). \quad (3)$$

The base rate of spread, R_0, is dependent on the parameterised fuel properties. The slope correction factor, φ_S, is calculated using the local terrain in SFIRE. The wind correction factor, φ_W, is calculated from the WRF modelled wind speeds, which are vertically interpolated to an estimated mid-flame height. The "heavy logging slash" Anderson fuel category (Anderson, 1982) is used to initialise the fuel conditions homogeneously across the SFIRE model domain. The parameterised fuel properties include the initial mass loading, fuel depth, surface area to volume ratio, moisture content of extinction and rate of mass loss following ignition.

The two-way atmosphere-fire coupling between SFIRE and WRF-LES is achieved through the release of latent and sensible heat from the modelled fire. For 1 kg of fuel combusted in SFIRE there is 17.43 MJ of sensible heat released into the WRF-LES model, which is about a factor of ten higher than the latent heat released for the fuel type used. These heat fluxes are distributed throughout the WRF-LES vertical levels using an exponential decay function and directly modify the atmospheric conditions surrounding the modelled fire. The two-way coupling in WRF-Fire allows it to directly model atmosphere-terrain-fire interactions down to length scales of tens to hundreds of metres.

Results

Wind speed threshold

Sharples *et al*. (2013) considered the lateral spread characteristics arising for different reference wind speeds. Specifically, they considered reference wind speeds of U_0 = 0.0, 2.5, 5.0, 7.5, 10.0 and 15.0 m s^{-1}. In each case the model output was examined for instances of significant lateral spread (i.e. spread in the north-south direction). Figure 2 summarises the lateral spread rates for each of these cases. For the U_0 = 0.0 m s^{-1} simulation the lateral propagation of the fire occurs at a quasi-steady rate of around 0.2 km h^{-1}. In this case the fire spread predominately towards the west, without any indication of dynamic fire spread. Similarly, Figure 2 shows that the U_0 = 2.5 m s^{-1} case exhibited lateral fire spread consistent with the quasi-steady assumption.

In the U_0 = 5.0 m s^{-1} simulation, the fire spread exhibited a small lateral bulge towards the north (most notably at around 70 minutes after ignition). However, the rate of lateral spread displayed in this case was not significant compared to the other cases for U_0 > 5.0 m s^{-1}. Figure 2 indicates that for all of the cases with U_0 > 5.0 m s^{-1} the fire spread laterally at a significant faster rate. Moreover, this atypical lateral spread occurred immediately after the fire reached the ridge line at about 20-25 minutes after ignition. For the U_0 = 10.0 m s^{-1} and 15.0 m s^{-1} cases the lateral spread rates reach values as a high as 5 km h^{-1}, which is approximately 25 times larger than the quasi-steady lateral spread rates seen in the U_0 = 0.0 m s^{-1} and 2.5 m s^{-1} cases.

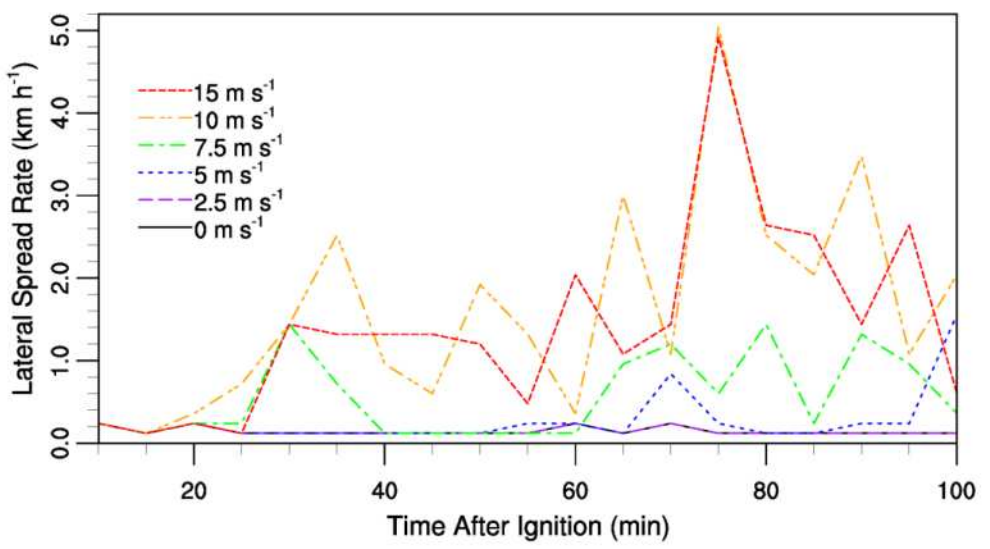

Figure 2. Maximum lateral spread rate for different reference wind speeds.

Topographic slope threshold

The simulations were conducted using a reference wind speed of U_0 = 15.0 m s^{-1}, but assuming different lee slope angles. Specifically, we considered α = 10°, 15°, 20°, 25°, 30°, 35°, 40° and 45°. The resulting patterns of fire spread can be seen in Figure 3, which shows the time of ignition of various points within the domain of interest. Figure 3 shows that for lee slope angles α < 25°, the pattern of fire spread does not exhibit any significant lateral spread beyond what might be expected from a fire spreading under a quasi-steady regime. The simulated fire spread for the α = 25° case indicates some propensity for lateral fire spread, though the pattern of spread is quite different to that observed in the α > 25° simulations. The α = 25° case may therefore be viewed as marginal with regards to the onset of dynamic fire behaviour. For the remaining cases, for which α > 25°, the pattern of fire spread exhibits a clear tendency for significant lateral spread. Moreover, for larger values of α the lateral spread is more confined near the apex of the idealised ridge.

Interestingly, the threshold slope angle of $\alpha \approx 25°$ identified here is in good agreement with the threshold value determined by Sharples *et al*. (2012) in their empirical analysis of VLS events in the 2003 Canberra fires.

Discussion

The propagation of a fire burning on a lee-facing slope was simulated using the WRF-Fire model under a number of different wind speed and topographic slope conditions. In the first set of simulations the fires exhibited two different modes of behaviour. Under the two lowest wind speed regimes the fires did not exhibit any atypical lateral spread, in stark contrast to the two highest wind speed regimes, for which the simulated fires exhibited significantly faster lateral spread. The results suggest the existence of a threshold wind speed, below which the prevailing winds are too weak to drive the vorticity-generating interaction between the wind, the terrain and the fire's plume, so that no atypical lateral spread occurs. The model simulations further suggest that this threshold occurs for wind regimes characterised by $U_0 \approx 5$ m s^{-1} (approx. 20 km h^{-1}).

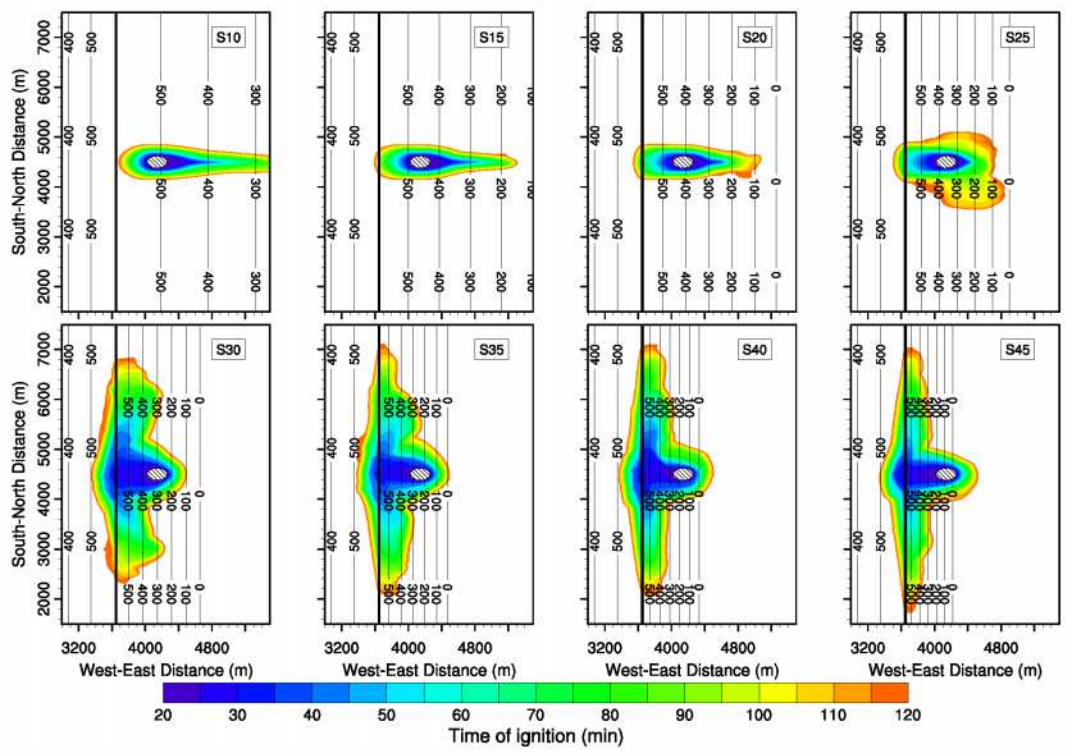

Figure 3. Time of ignition for different lee-facing slope inclinations. The various inclinations are indicated in the top right of each panel; for example, "S15" denotes a lee slope angle of 15°.

In the second set of simulations, in which the wind speed was fixed at U_0 = 15 m s^{-1}, the fires again exhibited two different modes of behaviour. For leeward slope angles less than 25° the fires did not exhibit any significant lateral spread, while for leeward slope angles above 25° the fire spread was dominated by lateral propagation across the leeward slope.

The threshold values determined in this study are in good agreement with the empirically determined values given by Sharples *et al*. (2012). In their study they reported a threshold topographic slope threshold of ~ 26° and a wind speed threshold of 20-25 km h^{-1}. The thresholds determined in the present study are also in general agreement with the values of wind speed and leeward slope angle required for separation of the prevailing winds from the terrain surface (Wood, 1995). As such, the modelling results presented above tend to support the role of flow separation in driving the VLS phenomenon.

Farinha (2011) reported a threshold wind speed of ~ 1.5 m s^{-1} for the occurrence of VLS in their laboratory scale experiments. Although more work is clearly required, comparison of Farinha's value of 1.5 m s^{-1} with the threshold wind speed of ~ 5 m s^{-1} determined above provides preliminary insight into scaling requirements when translating between the laboratory and landscape scales.

The present study has considered the environmental thresholds relating to wind speed and topographic slope. However, this consideration treated the two environmental variables independently, whereas it is quite likely that there is some interdependence of wind speed and topographic slope in defining the threshold to VLS occurrence. For example, for a fixed leeward slope of α = 30°, it is quite possible that the threshold wind speed will be different to that determined for the α = 35° case. These issues will be addressed in ongoing research along with consideration of other environmental variables such as wind direction and topographic aspect.

Conclusions

The existence of environmental thresholds relating to the onset of VLS established here has a number of implications for fire operational and firefighter safety. Indeed, the results obtained here imply that significant changes in fire behaviour can result from relatively small changes in the environmental factors that drive wildfires. For example, with a slight increase in wind speed or a small variation in topographic slope, firefighters working on leeward slopes could very rapidly find themselves in great peril, when only a short time before their safety had not been in doubt.

Acknowledgements

This work is supported by an Australian Research Council (ARC) Discovery Indigenous Award (IN130100038). J.P. Evans is also supported by an ARC Future Fellowship (FT110100576). WRF-Fire model runs were performed using the facilities at the National Computational Infrastructure (NCI) in Canberra.

References

Anderson, H. (1982) Aids to determining fuel models for estimating fire behaviour. *USDA Forest Service, Intermountain Forest and Range Experiment Station INT-122*.

Dold, J. W. and A. Zinoviev (2009) Fire eruption through intensity and spread rate interaction mediated by flow attachment. *Combustion Theory and Modelling* 13, 763–793.

Farinha, H. A. (2011) Formação de vórtices num incêndio florestal - estudo laboratorial de um vórtice de eixo horizontal e de um tornado de fogo. Master's thesis, Universidade de Coimbra, Portugal.

Mandel, J., J. D. Beezley, and A. K. Kochanski (2011) Coupled atmosphere-wildland fire modeling with WRF 3.3 and SFIRE 2011. Geoscientific Model Development 4, 591–610.

Moeng, C., J. Dudhia, J. Klemp, and P. Sullivan (2007) Examining two-way grid nesting for large eddy simulation of the PBL using the WRF model. *Monthly Weather Review* 135 (6), 2295–2311.

Rothermel, R. (1972) A mathematical model for predicting fire spread in wildland fuels , Volume 115. *Intermountain Forest & Range Experiment Station, Forest Service, US Department of Agriculture*.

Sharples, J., R. McRae, and S. Wilkes (2012) Wind-terrain effects on the propagation of large wildfires in rugged terrain: fire channelling. *International Journal of Wildland Fire* 21, 599–614.

Sharples, J., C. Simpson, and J. Evans (2013) Examination of wind speed thresholds for vorticity-driven lateral fire spread. *Proceedings of the 20th International Congress on Modelling and Simulation*, Adelaide, Australia, 1–6 December 2013 (www.mssanz.org.au/modsim2013).

Simpson, C., J. Sharples, J. Evans, and M. McCabe (2013) Large eddy simulation of atypical wildland fire spread on leeward slopes. *International Journal of Wildland Fire* 22, 282–296.

Skamarock, W. C., J. B. Klemp, J. Dudhia, D. O. Gill, D. M. Barker, M. G. Duda, X.-Y. Huang, W. Wang, and J. G. Powers (2008) A Description of the Advanced Research WRF Version 3 (NCAR Technical Note 475 ed.). Available at: http://www.mmm.ucar.edu/wrf/users/docs/.

Viegas, D. (2005) A mathematical model for forest fires blow-up. *Combustion Science and Technology* 177, 27–51.

Viegas, D., J. Raposo, D. Davim, and C. Rossa (2012) Study of the jump fire produced by the interaction of two oblique fire fronts. Part 1: Analytical model and validation with no-slope laboratory experiments. *International Journal of Wildland Fire* 21, 843–856.

Wood, N. (1995) The onset of separation in neutral, turbulent flow over hills. *Boundary-Layer Meteorology* 76, 137-164.

Evaluating crown fire rate of spread from physics based simulations to field data

C.M. Hoffman[a], R.R. Linn[b],W. Mell[c], C.H. Sieg[d], F. Pimont[e], J. Ziegler[a]

[a] *Colorado State University, Fort Collins, CO, USA. c.hoffman@colostate.edu*
[b] *Los Alamos National Laboratory, Los Alamos, NM, USA. rrl@lanl.gov*
[c] *USDA FS Pacific Wildland Fire Sciences Laboratory, Seattle, WA, USA. wemell@fs.fed.us*
[d] *USDA FS Rocky Mountain research Station, Flagstaff, AZ, USA. csieg@fs.fed.us*
[e] *Institut National pour la Recherche Agronomique, Avignon, France. Pimont@avignon.inra.fr*

Abstract
Wildland fire behavior models are commonly used to augment expert opinions, experiments and field observations by both the research and management communities. However, modelling wildfires is challenging in part due to complex set of coupled processes that drive the properties of a spreading wildfire. Further these processes occur over a vast span of spatial and temporal scales that further complicate the development and validation of models. Due to these complications there has been a variety of model types developed for a variety of specific applications. Regardless of the type and purpose of a model, well quantified fire behavior data from wildland fires and field and laboratory experimental fires are necessary for a variety of reasons including the calibration of empirically based models, the evaluation of physically based or theoretical models, and to provide model developers with potential areas to improve model performance by identifying inadequacies in the code. Here we utilize a compiled data set of crown fire rate of spread from Alexander and Cruz (2006) to evaluate published crown fire rate of spread predictions from two physics-based fire behavior models HIGRAD/FIRETEC developed at Los Alamos National Laboratory and the Wildland Urban Interface Fire Dynamics Simulator (WFDS) developed by the National Institute of Standards and Technology and the USDA Forest Service. Our preliminary results suggest that physics based models reasonably predict the crown fire rate of spread given the current data set. In addition we discuss the sensitivity of physics based models to a variety of parameters which likely influence crown fire rate of spread.

***Keywords**: Physics-based model, fire behaviour, model evaluation*

Introduction

Wildland fire behaviour models are commonly used to augment expert opinions, experiments and field observations by both the research and management communities. However, modelling wildfires is challenging in part due to complex set of coupled processes that drive the properties of a spreading wildfire. Further these processes occur over a vast span of spatial and temporal scales that further complicate the development and validation of models. Due to these complications there has been a variety of model types developed for a diversity of specific applications. Along with these developments has also come a wide array of assumptions, simplifications and approximations that are employed in the development of the models to achieve the desired level of detail and calculation time. Regardless of the type and purpose of a model, well quantified fire behaviour data from wildland fires as well as field and laboratory experimental fires are necessary for a variety of reasons including the calibration of empirically based models, the evaluation of physically based or theoretical models, and to provide model developers with potential areas to improve model performance by identifying inadequacies in the code. If model limitations and uncertainties are understood model simulations can provide insights into the interpretation of experimental data, help inform the design of future experiments and be utilized as a cost-effective and safer way to study wildland fire behaviour. However, large field-scale fire experiments or wildland fires can be expensive to conduct, often have limited data about the environmental conditions and fuels complex and rarely if ever have replication;

whereas laboratory-scale experiments, though less expensive and easier to replicate, generally do not provide data that cover the range of spatial and temporal scales typical of free burning wildfires.
The speed at which a fire propagates across a landscape, referred to as the rate of spread, depends upon interactions between a number of processes including the heat transfer rate, moisture evaporation and combustion rates and is one of the most commonly predicted metrics of fire behaviour. Recent studies have compiled empirical data from wildland fires and large-scale experimental fires on the rate of fire spread for surface and crown fires. This data has been utilized to evaluate current empirical surface and crown fire rate of spread models and to suggest potential inadequacies in current empirical fire behaviour modelling systems. However to date there have been no comparisons of simulations performed with physics-based models. Instead these evaluations have primarily involved empirical fire behaviour models.
In this paper we utilize a compiled data set of crown fire rate of spread from Alexander and Cruz (2006) to evaluate published crown fire rate of spread predictions from two physics-based fire behaviour models HIGRAD/FIRETEC developed at Los Alamos National Laboratory and the Wildland Urban Interface Fire Dynamics Simulator (WFDS) developed by the National Institute of Standards and Technology and the USDA Forest Service. In addition to evaluating crown fire rate of spread predictions from physics-based models we also utilize our results to investigate the potential sources of variation in crown fire rate of spread measurements and provide guidance on future research needs.

Description of physics based models

Physics based models such as HIGRAD/FIRETEC and WFDS use a computational fluid dynamics approach and a three-dimensional grid to describe to model the critical physical phenomena and their interactions that control the behaviour of a wildland fire through a set of coupled partial differential equations. This approach allows for the evolution of various quantities such as temperature, velocity of gaseous species and the characteristics of the fuel to be described spatially and temporally in the simulation domain. The vegetation in physics-based models is often described as a porous medium with mean or bulk quantities such as surface area to volume ratio, moisture content and density within the 3-d grid. Such an approach allows for the simulation of fires in areas with complex fuel beds (i.e. varying at small spatial scales) and variable topography.

Methods

Database Compilation

Alexander and Cruz (2006) compiled a total of 57 wildfire observation from North American forests. The data set consisted of 43 fires from Canada primarily occurring in boreal forest fuel types and 14 fires from the United States that occurred in pine dominated fuel types in the interior Rocky Mountains, the Lake States and the south-eastern U.S. During the development of this data set, any case study that lacked adequate data, occurred in areas with a mix of fuel types that do and do not support crown fire or occurred in areas with complex topography (>10% slope, or cross slope fire spread) were removed. For the remaining observations they reported the major fuel type, the temperature (°C), the relative humidity (%), the effective fine fuel moisture (%), the Canopy Bulk Density (kg m^{-3}) and the 10-m open wind speed (km h^{-1}). Although this data set did have a relatively large amount of detailed information regarding the rate of fire spread several calculations were performed by Alexander and Cruz (2006) to ensure a complete data set. Specifically they: 1) adjusted the 6.1 meter open wind speed for the U.S. data by a factor of 15% to approximate the 10-m open wind speed, 2) inferred the canopy bulk density using a variety of methods on a case-by-case basis, and estimated the effective fine fuel moisture content using equations published by Rothermel (1983) and assumed that all fuels were

shaded from solar radiation. Despite the need for additional calculations to complete the data set, this remains the largest data set assembled to date on crown fire rate of spread.

3.2. Crown Fire Rate of Spread Predictions From Physics-Based Models

Because various models require data in different forms and with different levels of details, it was not possible to directly simulate the wildfires contained in the Alexander and Cruz (2006) data set. Rather we identified published crown fire rate of spread values from physics based simulations and developed a data base that included their rate of spread (m s^{-1}), the 10-m open wind speed (m s^{-1}), the maximum canopy bulk density (kg m^{-3}), and the effective fine fuel moisture content (%). We identified a total of 50 simulations from physics based models, 22 of which were conducted using HIGRAD/FIRETEC and 28 of which were conducted using WFDS. These simulations were conducted using primarily fuels data from pine dominated or mixed conifer systems.

3.3. Analysis

Because we were not able to directly simulate the 57 fires contained within the Alexander and Cruz (2006) data set we used linear regression to evaluate the relationship between the 10-m open wind speed and the crown fire rate of spread and predicted non-simultaneous 95% confidence bounds for a new observation. We than compared the simulated crown fire rates of spread from HIGRAD/FIRETEC and WFDS to these bounds.

Results and Discussion

Our results to date show that overall crown fire rate of spread predictions from HIGRAD/FIRETEC and WFDS perform fairly well as compared to the field derived estimates of crown fire rate of spread from Alexander and Cruz (2006). Of the 50 physics-based simulations we compared, 12% (6 total simulations) did not fall within the 95% confidence prediction bounds (figure 1). These 6 points represented 21% of the WFDS simulations and over-predicted the expected rate of spread. There are a variety of reasons that could explain the larger than expected number of points that fall outside the 95% predictive bounds including the sensitivity of the simulated results to wind flow parameters, horizontal and vertical fuel distribution, ignition methods, and fireline shape. Our future work will explore the sensitivity of physics-based models to these parameters. In addition uncertainties in measurements for field experiments such as those compiled by Alexander and Cruz (2006) need to be better documented.

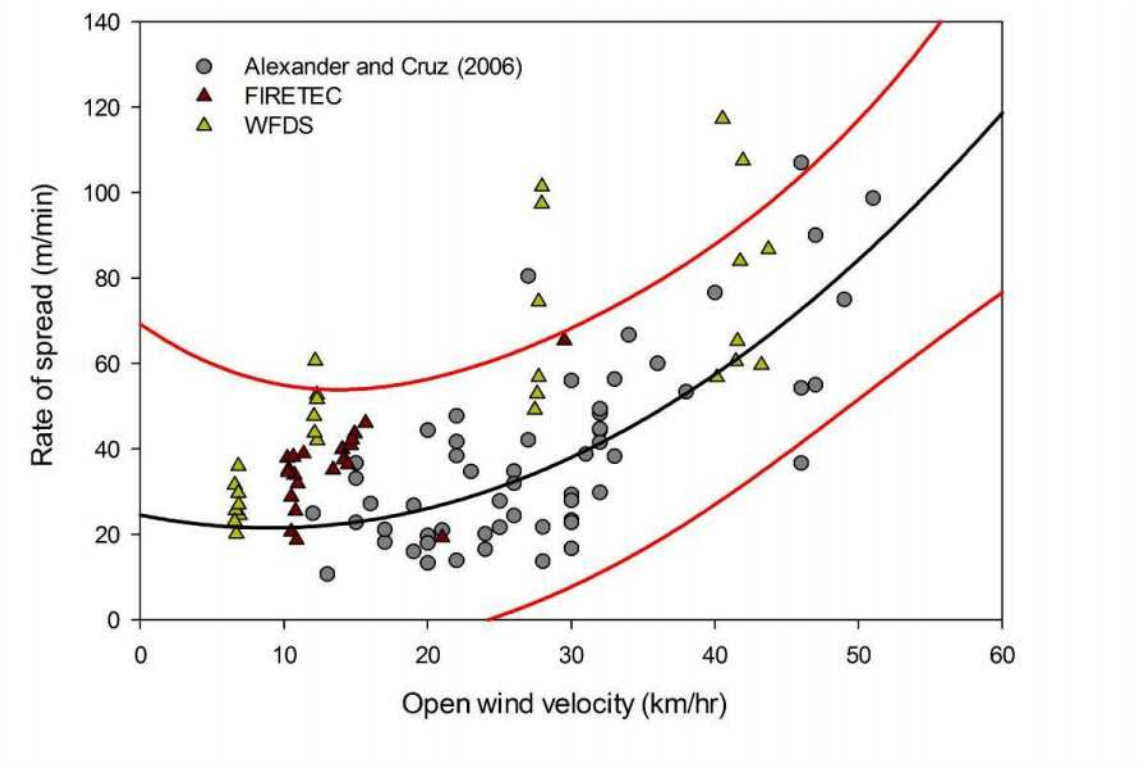

Figure 1. Comparison of crown fire rate of spread predictions from HIGRAD/FIRETEC and WFDS to observed crown fire rates of spread from Alexander and Cruz (2006).

Experimental and numerical study of fire behaviour: effects of the width on the rate of spread

Alexis Marchand, Nicolas Trevisan, Anthony Collin and Pascal Boulet

LEMTA, 2 Avenue de la Forêt de Haye TSA 60604 54518 Vandoeuvre-lès-Nancy cedex,
alexis.marchand@univ-lorraine.fr

Abstract
This study focuses on the influence of the fuel bed width on the rate of spread. An experimental set-up based on visible cameras combined with image processing was used and a direct linear transformation (DLT) algorithm was developed in order to quantify fire propagation features such as the rate of spread, the fire length, ... The present work gathers results aimed at demonstrating the dependence of the rate of spread on the fire front morphology. A new cellular automaton was developed to better understand the heat transfer mechanisms, investigating in particular the role of radiative transfer.

***Keywords**: Fire propagation, cellular automaton model, Fire front width effect, Radiative transfer*

Glossary

HHV	Higher heating value [kW/kg]	Hf	Flame height [m]
LHV	Lower heating value [kW/kg]	RVR	Residual vegetation ratio [kg/kg]
RH	Relative humidity [%]	Cp_{dry}	Heat capacity [kJ/kg/K]
L	Fuel bed width [m]	F	View factor [-]
Lc	Distance from a point to the cylinder centre [m]	V_f	Flame volume [m^3]
		T_f	Flame temperature [K]
Rf	Flame radius	φ	Radiative heat flux [W]
z	Vertical coordinate [m]		

Introduction

Every year, several million hectares of vegetation are burnt by forest fires or bush fires, ravaging both flora and fauna. The knowledge of the fire behaviour is an important issue in order to prevent from disaster or to try to control the fire propagation. In this frame, the accurate estimation of the propagation rate is of major interest for the fire prevention.
It is commonly accepted that the rate of spread depends on the vegetation properties, the topography and the meteorological conditions. Some fire propagation codes, such as Farsite [1] and Behave [2], take these parameters into account when simulating the fire behaviour. However, these models are unable to include the real fire front morphology (fire length, shape ...) in their predictions. The rates of spread are evaluated only for linear fire fronts and can overpredict the fire propagation in many other configurations. Only physical models involving space varying terms in balance equations, namely in radiation or convection models, are really able to reproduce the real fire behaviour.
Fingering (burnt areas with small fire front widths) is an example of a non linear configuration in real fires. In 2001, pictures of real fires taken from satellite were analysed by Caldarelli [3], focusing on the fractal dimension and lacunarities observed in fires. Indeed satellite images show the existence of fingerings. At this scale, the fire propagation is affected by the fire front morphology, as it was already observed experimentally by Anderson in 1968 [4]. It is very important to model efficiently the fire behaviour at small scale (meter scale) in order to predict accurately the fire front evolution against time.

The aim of this contribution is to demonstrate through experimental data or numerical results that the rate of spread depends on the fuel bed width. Moreover this paper gives some issues to explain this phenomenon.
This contribution is divided as follows: Section 1 presents the platform PROMETHEI used to generate surface fires and the experimental data on the fire front. Section 2 details and analyzes the obtained experimental results. Section 3 presents the fire propagation model developed using the concept of cellular automaton. Section 4 proposes some comparisons between experimental and numerical results, giving some issues for a better understanding of the interaction between the fire front morphology and the rate of spread. Section 5 draws some conclusions and perspectives concerning this work.

Experimental set-up

Our experimental fire platform, named PROMETHEI, was used to provide a database on surface fires. This platform was built to better understand the fire behaviour and to calibrate or to validate the fire propagation model.
Experiments were carried out on a combustion table using excelsior as fuel bed (Figure 1). In order to observe different fire front morphologies, the fuel bed width was varied in the range between 25 cm to 3.5 m, the fire being ignited on a line along the whole bed width. In such configurations, the fire fronts are near-parabolic, but the front curvature varies with the line width and the rate of spread is also affected. The vegetation load was set at 0.5 kg/m².

Figure 1. Picture of surface fire front propagation

Image analysis

Pictures of the flame front during the fire propagation were taken with 4 visible cameras, 2 cameras for the back edge and 2 for the leading edge. Typical images are presented in grey-scale in Figure 2(a). The post-processing algorithm which was used, is based on an Otsu algorithm [5]. When this approach is applied, the flame volume is then clearly identified (Cf. Figure 2(b)). The leading edge and the back edge are then localized by two pixel swaps, horizontal and vertical crossing pixel method (Cf. Figure 2(c)). This method was repeated on all the pictures taken during the fire propagation.

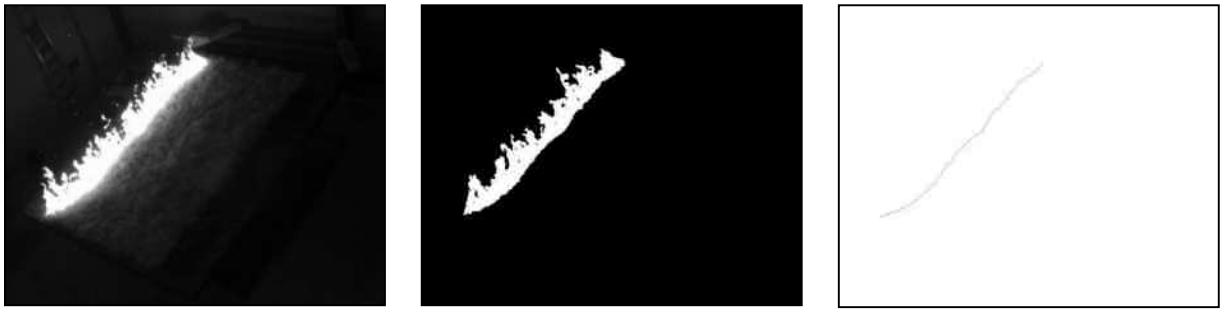

(a) (b) (c)

Figure 2. (a) Image in grey-scale obtained from one camera (b) Binary image after Otsu algorithm application (c) Detected fire front

Front reconstruction

The leading edge and the back edge were first localized on each picture, through pixel coordinates (Cf. Figure 2(c)). A direct linear transformation (DLT), method based on the work by Pastor *et al.* [6] was then applied on each pixel to merge the fire front in a real space in meter. Two examples of fire front detection are given in Figure 3(a) and Figure 3(b) for two different fuel bed widths (*L*).

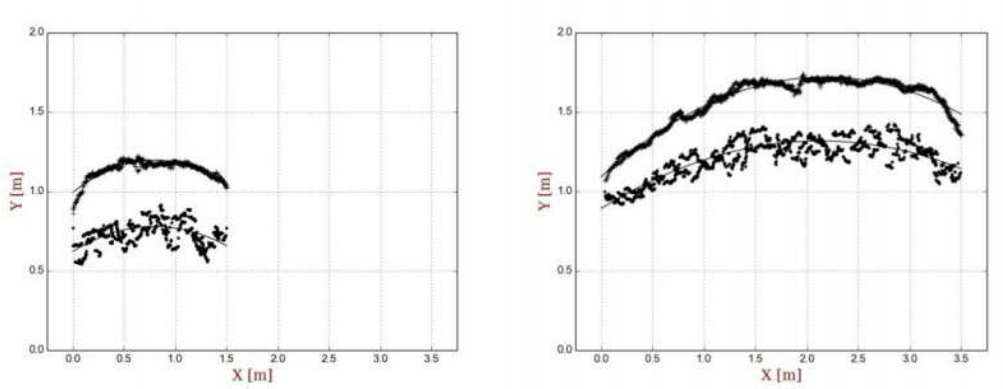

(a) ***(b)***

Figure 3. Fire front (top and back front) reconstructions after DLT algorithm (a) L = 1.5 m at t = 75.1 s after ignition (b) L = 3.5 m at t = 106.3 s after ignition

Repeatability and validation

In order to evaluate the accuracy of the image analysis, the results (in terms of rate of spread) provided by the Otsu-DLT algorithm were compared with the ones obtained using three other methods : (i) evaluation using chronometers (simple measurement of the distance with time of the most advanced point of the fire front) (v_{ch}), (ii) registration based on thermocouples (v_t), (iii) evaluation using dedicated photo-resistors (adapted from the work by Catchpole *et al.* [7]) (v_p). All these techniques were involved on the same experimental conditions, repeated 4 times. For the evaluations based on thermocouples and photo-resistors, the method consists in detecting a peak (of temperature or intensity) at several locations on the combustion table, allowing the estimation of the fire front location and then of the rate of spread. For this test, the experiment involved a fuel bed 2 m wide and 3 m long, with the vegetation load set at 0.5 kg/m². Results are gathered in Table 1.

The results obtained with the Otsu-DLT algorithm (v_{ca}) are first discussed. For the same experiment, the results vary in the range between 1.49 and 1.6 cm/s and the average rate of spread is estimated at 1.55 cm/s. The mean discrepancy is then evaluated at 2.7% which proves the good repeatability of the experimental device. Concerning the comparison with the other experimental methods, the mean

discrepancies are in the range from 1.7 to 4.6%. These small differences demonstrate the good accuracy of the Otsu-DLT algorithm involved in this work.

Table 1. Comparison of the different methods for rate of spread measurements [cm/s]

Experiment number	v_{ca}	v_{ch}	v_p	v_t	Mean discrepancies [%]
#1	1.6	1.51	1.45	1.63	4.6
#2	1.49	-	1.42	1.51	1.7
#3	1.53	1.49	1.45	1.50	3.4
#4	1.59	1.58	1.51	1.59	1.9

2.4. Environmental conditions

The physical properties (Lower Heating Value, Higher Heating Value, Residual Humidity, Residual Vegetation Ratio and Heat Capacity) of E*xcelsior* used in this study were characterized by the LERMAB laboratory, France. All these features are gathered in Table 2.

Table 2. Characteristics of the excelsior combustible

LHV [kW/kg]	HHV [kW/kg]	RH [%]	RVR [kg/kg]	Cp_{dry} [kJ/kg/K]
16180	20180	12.4	0.27	1430

In order to study the change in the rate of spread as a function of the fuel bed width, two series of experiments were carried out in different environmental conditions (see Table 3). For each experiment, relative humidity and temperature were given by a weather station. The environmental conditions were near constant during each experiment as it can be observed in Table 3.

Table 3. Environmental conditions

Width Fire [m]	Relative Humidity [%]	Temperature [°C]
0.25	64	6.1
0.5	66	6.4
0.75	67	6.9
1	67	6.8
1.5	70	6.7
2	69	6.7
2.5	69	7.0
3	68	6.7
3.5	70	6.8

(a) Experiment #1

Width Fire [m]	Relative Humidity [%]	Temperature [°C]
0.25	52	18.0
0.5	51	18.2
0.75	50	18.3
1	50	17.2
1.5	51	17.8
2	50	18.5
2.5	48	18.9
3	47	19.3
3.5	49	18.6

(b) Experiment #2

Results

Rate of spread

Figure 4 gives an example of results provided by the Otsu-DLT algorithm (for experiment #1 with a 3.5 m fuel bed width). The locations of the leading edge and the back edge were estimated as a function of time. The evolution is clearly linear, even at the first instants when the propagation starts. The rate of spread was deduced from the slope of the lines using a least squares method.

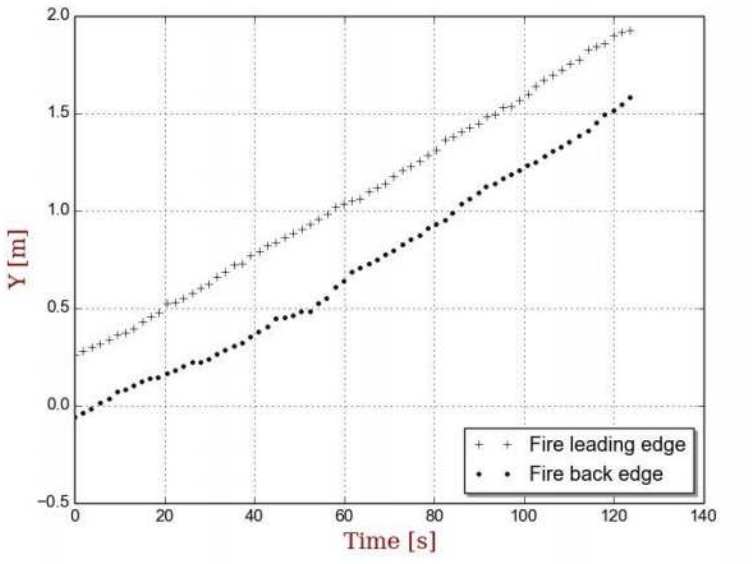

Figure 4. Example of fire front locations as a function of time, fire leading edge and back edge for a bed width L = 3.5 m

The evolution of the rate of spread (ROS) as a function of the fuel bed width is plotted in Figure 5 for Experiments #1 and #2. The ROS quickly increases for small fuel bed widths (between 25 cm to 100 cm) and reaches an asymptotic value above a 100 cm width. The limiting ROS is 1.6 cm/s for Experiment #1 and 1.3 cm/s for Experiment #2. As results tend to follow an exponential law, a fit of the ROS was sought for each experiment with the following relationship

$$ROS(L) = A_1\left(1 - exp\left(-A_2 L\right)\right)$$

The parameters A_1 and A_2 were estimated using a least squares method, yielding the following values:

- Experiment #1: A_1 = 1.28 cm/s and A_2 = 3.04 m^{-1}
- Experiment #2: A_1 = 1.62 cm/s and A_2 = 2.24 m^{-1}

The predictions based on these parameters are in good agreement with the experimental results as presented in Figure 5. A_2 parameter seems to be universal for this kind of experiment (for given vegetation and load) whereas A_1 parameter clearly depends on environmental conditions.

Fire thickness

The fire thickness was measured for the different experiments using the Otsu-DLT algorithm. For a given fire, the two fronts are interpolated with a second order polynomial, such as $Y(X) = aX^2 + bX + c$ (X and Y are the two coordinates associated with the combustion table). Such polynomial interpolations were presented in Fig 3(a) and Fig 3(b). The fronts were represented using

100 points equally spaced along the fire line. The thickness was then defined as the average distance between the two lines for a given *X* coordinate. Figure 6 gives the thickness evolution against the fire width. The fire thickness seems to be independent of the fire width. The average fire thickness is estimated at 33 cm (with average discrepancy of 7%) for Experiment #1 and at 24 cm for Experiment #2 (with average discrepancy of 4%). It can be observed that the ROS of Experiment #1 is slower than the one of Experiment #2, whereas its thickness is larger than the one of Experiment #2.

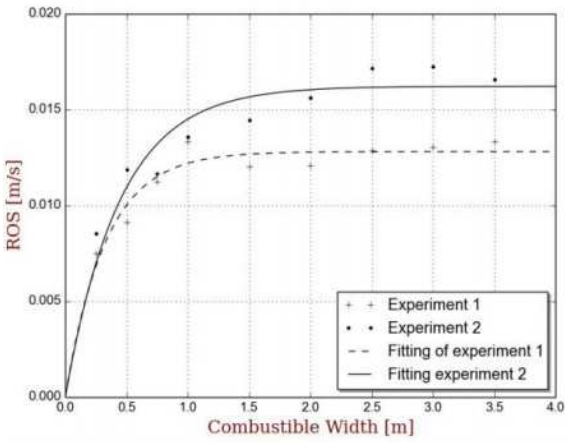

Figure 5. Evolution of the ROS with combustible width

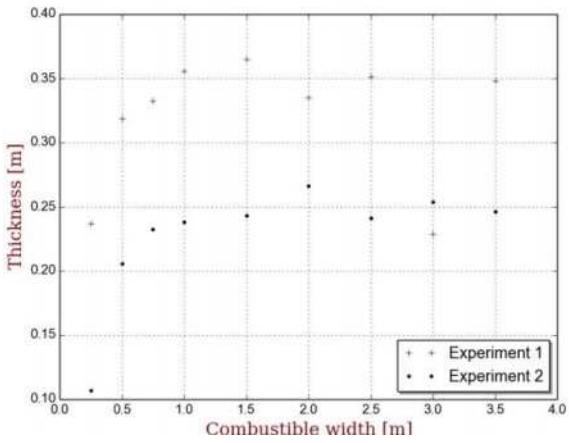

Figure 6. Evolution of the fire thickness with combustible width

3.3. Fire leading edge length

During the fire propagation, for a given time, the fire front is here modelled by a second order polynomial ($Y(X) = aX^2 + bX + c$). The total length of the fire front is then calculated as:

$$Length = \int_{Fire\ Front} ds = \frac{1}{4a}\left(Argsh(2aL+b) - Argsh(b) + (aL+b)\sqrt{(aL+b)^2} - b\sqrt{b^2+1} \right)$$

The evolution of the fire front total length against the fuel bed width is represented in Figure 7. The total length of the fire front is the same for the two experiments. Its evolution is linear with a slope close to 1 (accurate value equal to 1.02). The results demonstrate that the shape (or the length) of the fire front is independent of the environmental conditions.

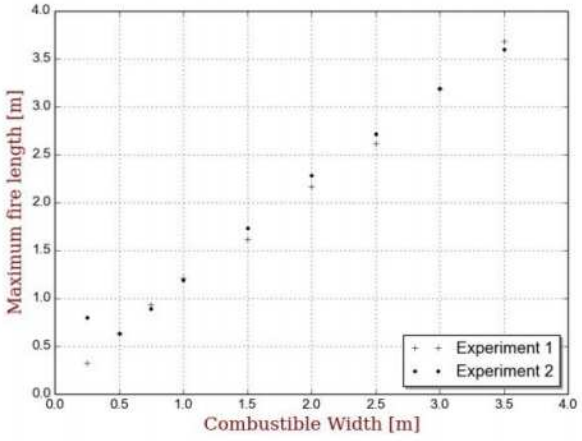

Figure 7. Evolution of the flame front length against the fuel bed width

Automaton model

4.1. Method

This model is based on the work by Porterie *et al.* [8]. The fuel bed is represented by a set of elementary hexagonal cells. The physical properties are assumed to be constant on the numerical domain. Radiation is supposed to be the main heat transfer involved in the fire propagation.

A cellular automaton model consists in associating a given state to each cell. The state of a cell is governed by a dimensionless time, τ. In the present work, the cells are described by one of these states:

(1) raw material ($\tau=0$) **(2)** heating ($0<\tau<\tau_d$)

(3) burning ($\tau_d<\tau<\tau_d+\tau_c$) **(4)** burned vegetation ($\tau_{d+}\tau_c<\tau$)

This kind of models requires a clear definition of the transition law between two states *i* and *j*, and the model parameters τ_d and τ_c. These transition laws can be experimentally defined or they can be extended from a physical model.

When the radiative transfer coming from the flame front is incident on the raw vegetation, the cell state switches from 1 to 2. The cell is heated due to the radiative transfer until a flame appears above the studied cell. At each iteration, an additional $\Delta\tau$ is associated to the characteristic time τ of the considered cell, with $\Delta\tau$ defined as,

$$\Delta\tau = A \sum_{Flame\ cell} \varphi_{Flame\rightarrow vegetation}$$

where *A* is a model parameter and $\sum_{Flame\ cell} \varphi_{Flame\rightarrow vegetation}$ is the total radiative contribution of the fire front toward the studied cell.

$\varphi_{Flame\rightarrow vegetation}$ is the radiative flux from one of the cells located on the fire front toward the "vegetation" cell. The flame is assumed to be represented by an equivalent cylinder with an absorption coefficient κ and a flame temperature T_f. The radiative contribution is evaluated thanks to a view factor calculation and $\varphi_{Flame\rightarrow vegetation}$ is defined by :

$$\varphi_{Flame\rightarrow vegetation} = 4\,F\,\kappa\,\sigma\,{T_f}^4\,V_f S_{cell}$$

V_f is the flame volume, S_{cell} the cell "vegetation" surface and *F* is the view factor evaluated as

$$F = \frac{1}{4\pi V_f}\sum_{\theta i}\left(g\left(Lc,R_f,H_f,\theta i\right) - g\left(Lc,R_f,0,\theta i\right) - g\left(Lc,0,H_f,\theta i\right) + g\left(Lc,0,0,\theta i\right)\right)\Delta\theta$$

where θi is discretized between 0 and 2π using a $\Delta\theta$ step. *Lc* is the distance between the burning cell and the "vegetation" cell. The *g* function is defined by

$$g(l,r,z,\theta) = \sqrt{l^2 - 2rl\cos(\theta) + r^2 + z^2} + l\cos(\theta)\ln\left(r - l\cos(\theta)\right) + \sqrt{l^2 - 2rl\cos(\theta) + r^2 + z^2}$$

The main advantage of this quasi-analytical relationship for *F* is to avoid the use of an accurate but time-consuming numerical method, such as a Monte Carlo Method to model the radiative transfer.

When τ is equal to τ_d (which represents the time of pyrolysis) the cell switches to state (3). It stays in state (3) during a time τ_c which describes the time during which the cell is burning. After burning, the state of cellular changes to (4).

Table 4. Cellular automaton model parameters

Edge of Hexagon [m]	Flame temperature T_f [K]	Absorption coefficient κ [1/m]	Flame height H_f [m]	$\tau_{d/A}$	τ_c
0.025	1733	0.1	0.4	50	13

The parameters used for the numerical study are gathered in Table 4. T_f, κ and H_f are identified using a PSO (Particle Swarm Optimization) algorithm with experimental data on radiative heat flux measured during a fire propagation test.

4.2. Numerical results and comparisons

Numerical simulations were done considering the fuel bed width in the range between 0.25 m and 4.0 m. Figure 8 gives two examples of fire propagations for fuel bed widths equal to 1.5 m and 3.5 m.
At this stage, the present model is able to capture some qualitative trends experimentally observed; in particular the model captures the parabolic shape of the fire fronts. These shapes must be compared with experimental measurements given in Figure 3 (a) and 3(b).

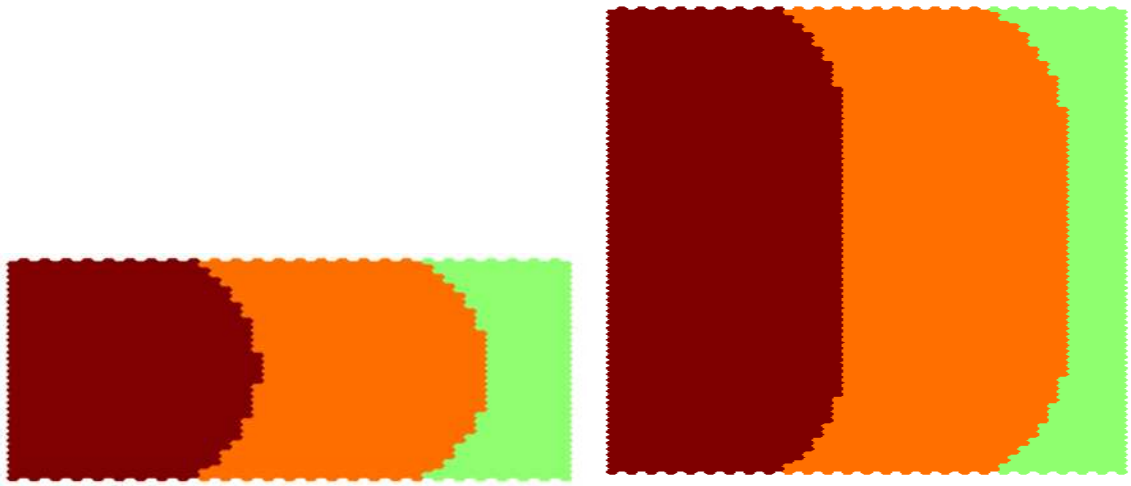

(a) ***1.5 m fuel bed width*** ***(b) 3.5 m fuel bed width***

Figure 8. Fire front spread simulated with the automaton model. Green: cellular in state (2) Orange: cellular in state (3) Brown: cellular in state (4) at 38th iteration.

One aim of the study was to show the ROS dependence on the bed width. As it was previously mentioned, the ROS depends on the environmental conditions, which are not directly involved in the present model. However, as it was observed in Figure 5, the ROS for the two experiments seem to follow the same trend. Hence, in order to compare the results, each rate of spread was divided by its asymptotic value. The corresponding evolution of the normalized ROS with the width is represented in Figure 9 (experimental fits and numerical values). The agreement is quite satisfactory. The evolution of the ROS with the fuel bed width is well described by the cellular automaton model, despite the fact that only the radiative transfer is considered in the heat transfer. Moreover, as the ROS does not vary for a fuel bed width above 1 m, this demonstrates that the radiative transfer coming from the fire front does not affect the vegetation which is located at a distance beyond 1 m. In other words, 1 m is the cut off distance for the radiative transfer in this kind of experiment.

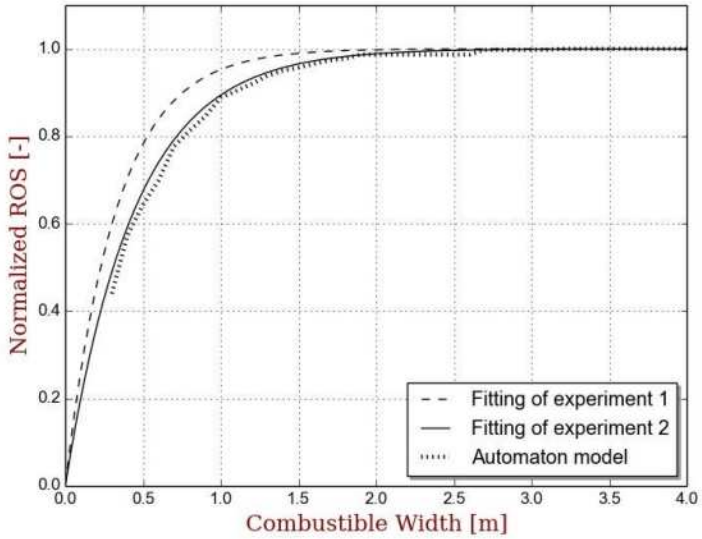

Figure 9. Normalized rate of spread for the two experiments and for the numerical model

Conclusion

A method based on image processing and direct linear transformation was used in order to reconstruct the leading edge and the back edge of a fire spreading in a fuel bed of excelsior. Several experiments were done and the ROS values obtained with the visible cameras were compared with other results obtained using standard methods with a chronometer, thermocouples and photo-resistors. This comparison demonstrated the efficiency of the present method.

The experiments showed a dependence of the ROS with the fuel bed width. Two series of experiments with a fuel bed width varying between 0.25 m and 3.5 m were done in different environmental conditions. These experiments exhibited the same evolution for the rate of spread: an increase with the bed width up to an asymptotic value. The global evolution was well approximated with an exponential law involving two parameters. One parameter was found to be constant for this kind of experiment while the other depends on the environmental conditions (surrounding temperature and humidity).

A simulation was conducted based on a cellular automaton. Only radiative transfer was considered as the heat transfer leading to the fire spread. Radiative transfer between two cells was modeled with view factors between flames represented as cylinders above the burning cells and the surface of a “raw vegetation” cell.

Numerical results showed that the parabolic shape of the fire front is well captured. The evolution of the normalized numerical ROS with the fuel bed width was also found in agreement with the experimental results.

Future work will now extend this fire propagation model in considering the effect of slope or/and wind on the fire propagation in including a convective heat transfer contribution.

References

[1] M.A. Finney. FARSITE: Fire Area Simulator - model development and evaluation. Research Paper RMRS-RP-4. Ogden, UT: USDA Forest Service, Rocky Mountain Research Station. 47 p, 2004.

[2] P.L.Andrews. BehavePlus fire modeling system: Past, present, and future. In ‘Proceedings of 7th Symposium on Fire and Forest Meteorological Society’. 23-25 October 2007, Bar Harbor, Maine.

[3] G. Caldarelli, R. Frondoni, A. Gabrielli, M. Montuori, R. Retzkaff and C. Riccotta. Percolation in real wildfires. Europhys. Lett., Vol. 56 (4), pp. 510-516, 2001.
[4] H.E. Anderson. Fire spread and flame shape. J Fire Technology, Vol. 4, pp. 51-58, 1968.
[5] N. Otsu, A threshold selection method from gray-level histograms, IEEE Trans. Sys, Vol. 9, pp. 62-66, 1979.
[6] E. Pastor, A. Agueda, J. Andrade, M.A. Munoz, Y. Perez and E. Planas. Computing the rate of spread of linear flame fronts by thermal image processing. Fire Safety Journal, Vol. 41, pp. 569-579, 2006.
[7] W. R. Catchpole, E. A Catchpole, B. W. Butler, R. C. Rothermel, G. A. Morris and D. J. Latham, Rate of spread of free-burning fires in woody fuels in a wind tunnel, Combustion Science and Technology, Vol. 131, pp. 1-37, 1998.
[8] B. Porterie, N. Zekri, J.P. Clerc and J.C. Loraud. Influence of firebrands on wildland fire spread. Comptes Rendus de Physique, Vol. 6, pp. 1153-1160, 2005.

Experimental and theoretical study of diameter effect on the ignition of cistus twigs

Virginie Tihay, Paul-Antoine Santoni, Toussaint Barboni, Lara Leonelli

SPE – UMR 6134 CNRS, University of Corsica, Campus Grimaldi,
BP 52, 20250 Corte, France, tihay@univ-corse.fr

Abstract
In this work, the effect of the diameter on the ignition of twigs of *Cistus Monspeliensis* was studied experimentally and theoretically. For this, piloted ignition experiments were carried out in a cone calorimeter. In the first part of the study, the location of ignition, the ignition time and the flame residence time were investigated according to the twig diameter. Different modes of ignition were observed. The ignition could be due to: glowing of embers; flaming near the solid; spark of the pilot. The ignition time and the flame residence time increase strongly with the diameter. For small diameters, ignition time can be considered as proportional to the diameter. For high diameters, the ignition time tends to stabilize around a constant value (about 80 s). The second part of the study was devoted to the modelling of the temperature evolution in a twig. A one-dimensional nonhomogeneous heat-conduction problem was considered in finite medium. An optimization was performed to determine the model parameters (ignition temperature, twig emissivity and total heat transfer coefficient). From the expression of temperature in the twig, the ignition time was calculated for the various diameters. The comparison between these values and the experimental data shows a good agreement. Finally, a sensitivity analysis was carried out highlighting the influence of the ignition temperature and of the total heat transfer coefficient on the results.

Keywords*: ignition time, piloted ignition, ignition modelling*

Introduction

Over the last decades, modelling of wildfires was increasingly used to provide support decision tools for forest management. Among the models of propagation of forest fires, many use the ignition properties of forest fuel such as the ignition temperature (Rothermel 1972, Koo *et al*. 2005, Santoni *et al*. 2011) and the heat required for ignition (Adou 2010). Some also assume that only small fuel particles contribute to the fire dynamics (Morvan *et al*. 2009). Despite the extensive use of ignition properties, misunderstandings persist even if the first works go back into the 19th century (Hill 1887) and have continued until the present time (Simeoni *et al*. 2012). As pointed out by Babrauskas (2001), literature offers a huge quantity of data and it is difficult to extract relevant values for the ignition properties of forest fuels. Among the studies on ignition, there are little works concerning the diameter influence. Studies realized by Mc Arthur (1962) and Peet (1965) suggested that fuels less than 6 mm diameter contribute most to fire behaviour. For them, the rate of spread of the head fire is directly proportional to the load of fine fuel consumed. In 2001, Burrows (2001) studied the flame residence time and the rate of weight loss for different dimensions of Eucalypt twigs. He concluded that round twigs less than 6 mm in diameter and leaves are the most flammable. Given this state of art, it seems necessary to realise new studies to complete the knowledge about ignition. We propose in the present paper to focus on the effect of the diameter on the piloted ignition of twigs of *Cistus Monspeliensis.* This work is composed of two parts. In the experimental study, the location of ignition, the ignition time and the flame residence time are investigated according to the twig diameter. In the numerical study, an ignition model is proposed. An optimization is used to determine the model parameters (ignition temperature, twig emissivity and total heat transfer coefficient) and a sensitivity analysis is

performed to evaluate the influence of these parameters on the numerical results. The aim of this preliminary work is twofold. Firstly, it brings additional data on the ignition of forest fuels. Secondly, it highlights the difficulties encountered during the experiments, leading to new protocols for further study.

Materials and Methods

Piloted ignition experiments were carried out in a cone calorimeter (Figure 1a). Twigs of *Cistus Monspeliensis* oven-dried at 60°C during 24 hours were employed as fuel. Table 1 presents the fuel properties. The twigs of *Cistus* were cut to a length of 10 cm and then sorted according to their diameter (Figure 1b). In this study, only diameters between 2 and 17 mm were investigated. The sample holder was an open basket of 10 cm by 10 cm made on stainless steel. It was maintained over an insulating ceramic by a thin metal support. This device reduces the heating process due to the ceramic and metal while allowing air to circulate under the basket. For each experiment, a mass of 15 g of fuel was placed in the basket with a parallel arrangement. A radiant heat flux of 50 kW/m² was imposed on the top of the fuel sample. To ensure that the radiant flux remained the same for all experiments, the heat flux was calibrated using a fluxmeter prior each experiment. The piloted ignition was obtained by using a spark igniter. The time of ignition was determined visually from the appearance of flaming combustion. A visible camera with a rate of 29 frames per second (Lumix ZS19) was placed in front of the cone calorimeter to observe the ignition location. The flame residence time was also recorded. The ambient temperature was 23°C and relative humidity was 40 %. At least 3 repetitions were performed for all the tests.

Figure 1. a) Experimental device b) Twigs of Cistus Monspeliensis used as fuel

Table 1. Fuel properties

Density ρ (kg/m^3)	Thermal conductivity λ (W/m².K)	Specific heat c_p (J/kg.K)
960	0.42	1834

Experimental Results

3.1. Ignition description

After the shutter opening, the twigs of *Cistus* begin to dehydrate (due to the cone heating) and release white smoke. Once the ignition conditions are met, the ignition occurs. Figure 2 shows the first images recorded by the camera at the time of ignition. According to the pictures, the location of ignition seems to vary. The ignition could be due to: glowing of embers (Figure 2a), flaming near the solid (Figure 2b) or spark of the pilot (Figure 2c). However, these observations should be taken with caution.

Because of the recording speed of the camera, it is possible that the ignition actually occurs between two recorded images. In this case, the picture does not represent the ignition location, since the flame spreads. To refine these results, the use of a high-speed camera seems necessary.

a b c

Figure 2. Location of ignition for different experiment

Ignition time and flame residence time

Figure 3 presents the evolution of the ignition time according to the twig diameter. For diameters under 5 mm, the ignition time increases strongly with the diameter. For a diameter of 2 mm, the mean ignition time corresponds to 25 s whereas for twigs with a diameter of 5 mm, the ignition time reaches 60 s. For these diameters, the evolution of the ignition time can be considered as proportional to the diameter. This is consistent with the ignition theory for thermally thin solids, for which the ignition time t_{ign} is given by the following expression (Quintere 2006):

$$t_{ign} \approx \frac{\rho.c_p.D.(T_{ig} - T_\infty)}{q''} \qquad (1)$$

where ρ is density, c_p is the specific heat, D is the diameter, T_{ig} is the ignition temperature, T_∞ is the ambient temperature and q" represents the incident radiative heat flux.

From a diameter of 9 mm, the ignition time tends to stabilize around a constant value (about 79.5 s). This result is in agreement with the ignition theory of thermally thick solids. In this case, the ignition time is indeed independent of the diameter (Quintiere 2006):

$$t_{ign} \approx \frac{\pi.\lambda.\rho.c_p}{4}\left(\frac{T_{ig} - T_\infty}{q''}\right)^2 \qquad (2)$$

where λ is the thermal conductivity.

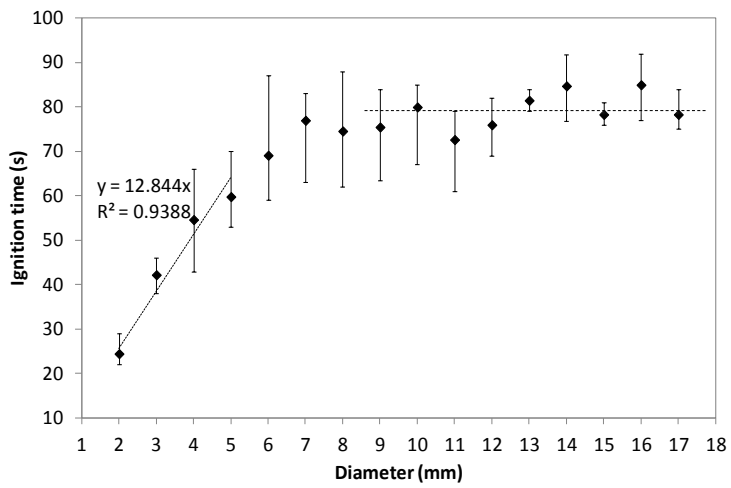

Figure 3. Ignition time according to the twig diameter

Flame residence times for the different diameters are shown on Figure 4. The flame residence time of the twigs increases with the diameter according to the following equation:

$$t_r = 13.2D^{0.96} \quad (3)$$

where t_r is the flame residence time.
This correlation is in agreement with literature (Burrows 2001) even if the increase of the flame residence time with the particle diameter is less significant than that found by Burrows (2001) for eucalypts ($t_r = 0.871D^{1.875}$). This variation is probably due to the fuel but also to the experimental method.

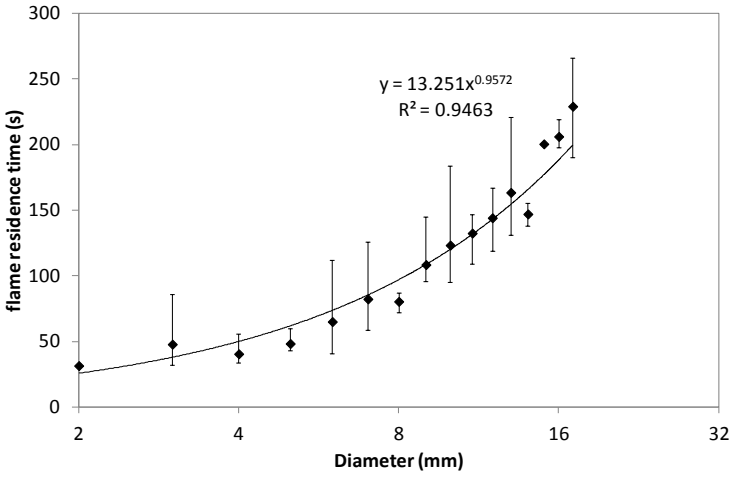

Figure 4. Flame residence time according to a) the twig diameter b) the surface to volume ratio

Given the previous results, it seems that the twigs of C*istus Monspeliensis* can be divided into 3 classes: diameters less than 5 mm, diameters between 5 and 9 mm and diameter above 9 mm. However, these results have to be taken with caution since they depends on our experimental procedure. Indeed, to compare our data with those of Burrows (2001), we kept a same mass for each test. But, this choice has significant consequences. By keeping the same mass, the twig arrangement varies with the twig diameter. For a diameter of 2 mm, the twigs are arranged on three layers on the whole holder surface (Figure 5a). From 4 mm in diameter, twigs are arranged on a single layer (Figure 5b). However, by

increasing the diameter, the number of twigs decreases and they cover no longer the entire surface of the holder (Figure 5c). Above 15 mm, there is only one twig (Figure 5d). Therefore, the energy received by the samples is not the same, since it depends on surface exposure that varies from several small twigs at one side to one big twig at the other side. In addition, for small diameter, the set of twigs can be considered as a porous medium. This is no longer true for larger diameter. These variations of twig arrangement certainly affect the ignition and it is difficult to compare the results between the diameters. For a better understanding of the phenomena, rather than using a same mass, a same area exposed to the radiant heat flux appears to be a better alternative.

a b c d

Figure 5– Twig arrangement for a diameter of a) 2 mm b) 4 mm c) 9 mm d) 15 mm

Ignition model

4.1. Mathematical formulation

The mathematical model for ignition considered in this article is based on the following assumptions:

- Heat flow in the twigs is one-dimensional, i.e. perpendicular to the exposed surface.
- Chemical effects prior to ignition are negligible, i.e., the delay due to kinetics is neglected.
- Delay due to mixing is neglected.
- Ignition occurs when the surface reaches a given temperature
- The twigs are opaque and the Kirchoff's law is valid for the total absorptivity α, emissivity ε and reflectivity r, i.e., $\alpha=\varepsilon=1-r$
- The value of α, ε and r remain constant between the start of exposure and the ignition.
- The heat losses from the surface are partly radiative and partly convective with a constant convection coefficient h_c. The radiative loss term is linearized using an effective coefficient h_{rad} (Quintiere 2006). A total heat transfer coefficient h including the convective and radiant heat transfers is introduced: $h=h_c+h_{rad}$. This coefficient was considered as constant for all experiments.

Under these assumptions, the ignition problem corresponds to a thermal problem with the following mathematical form:

$$\frac{\partial^2 T}{\partial x^2} = \frac{1}{a}\frac{\partial T}{\partial t} \quad \text{for } 0 < x < D,\ t > 0 \qquad (4a)$$

$$-\lambda \frac{\partial T}{\partial x} = \varepsilon . q'' - h(T - T_\infty) \quad \text{for } x = 0,\ t > 0 \qquad (4b)$$

$$-\lambda \frac{\partial T}{\partial x} = h(T - T_\infty) \quad \text{for } x = D,\ t > 0 \qquad (4c)$$

$$T = T_\infty \quad \text{for } x \geq 0,\ t = 0 \qquad (4d)$$

where T is the temperature, T_∞ is the ambient temperature, a is the thermal diffusivity and σ is the Stefan-Boltzmann constant.

To resolve this one-dimensional nonhomogeneous heat-conduction problem in a finite medium, a variable change $\theta = T - T_\infty$ is used. Then, the problem is decomposed into two simpler problems (Ozisik 1993):

- a steady state problem for θ_0(x) given as:

$$\frac{\partial^2 \theta_0}{\partial x^2} = 0 \quad \text{for } 0 < x < D \quad (5a)$$

$$-\lambda \frac{\partial \theta_0}{\partial x} + h\theta_0 = \varepsilon.q'' \quad \text{for } x = 0 \quad (5b)$$

$$\lambda \frac{\partial \theta_0}{\partial x} + h\theta_0 = 0 \quad \text{for } x = D \quad (5c)$$

- a homogeneous problem for θ_1(x,t) given by:

$$\frac{\partial^2 \theta_1}{\partial x^2} = \frac{1}{a}\frac{\partial \theta_1}{\partial t} \quad \text{for } 0 < x < D,\ t > 0 \quad (6a)$$

$$-\lambda \frac{\partial \theta_1}{\partial x} + h\theta_1 = 0 \quad \text{for } x = 0,\quad t > 0 \quad (6b)$$

$$\lambda \frac{\partial \theta_1}{\partial x} + h\theta_1 = 0 \quad \text{for } x = D,\quad t > 0 \quad (6c)$$

$$\theta_1 = -\theta_0(x) \quad \text{for } x \geq 0,\ t = 0 \quad (6d)$$

- Then, the solution of the original problem (5a-d) is determined form:

$$T = T_\infty + \theta_0(x) + \theta_1(x,t) \quad (7)$$

The solution of the steady-state problem (5a-c) is given as:

$$\theta_0(x) = -\frac{\varepsilon.q''}{2.\lambda + h.D}\left(x - \frac{\lambda}{h} - D\right) \quad (8)$$

The solution of the homogeneous problem (6a-d) is obtained as:

$$\theta_1(x,t) = -\frac{2}{D}\sum_{m=0}^{\infty} e^{-a.\beta_m^2 t}\,\frac{1}{N(\beta_m)}\,X(\beta_m,x)\int_0^D X(\beta_m,x').\theta_0(x')dx' \quad (9a)$$

with

$$X(\beta_m,x) = \beta_m.\cos(\beta_m.x) + \frac{h}{\lambda}\sin(\beta_m.x) \quad (9b)$$

$$\frac{1}{N(\beta_m)} = \frac{2}{D\left(\beta_m^2 + \frac{h^2}{\lambda^2}\right) + \frac{2.h}{\lambda}} \quad (9c)$$

$$\tan(\beta_m.D) = \frac{2.\beta_m.h.\lambda}{\beta_m^2.\lambda^2 - h^2} \quad (9d)$$

The temperature T(x,t) of the problem (4a-d) is obtained by performing the integration:

$$T(x,t) = T_\infty - \frac{\varepsilon.q''}{2.\lambda + h.D}\left(x - \frac{\lambda}{h} - D\right) + \frac{2.\varepsilon.q''}{2.\lambda + h.D}\sum_{m=0}^{\infty} \frac{e^{-a.\beta_m^2 t}\left[\beta_m.\cos(\beta_m.x) + \frac{h}{\lambda}\sin(\beta_m.x)\right].\left[\frac{h^2 - \lambda^2.\beta_m^2}{h.\lambda.\beta_m}\sin(\beta_m.D) + 2.\cos(\beta_m.D) - 2 - \frac{h.D}{\lambda}\right]}{\beta_m.\left[D\left(\beta_m^2 + \frac{h^2}{\lambda^2}\right) + \frac{2.h}{\lambda}\right]} \quad (10)$$

At the surface and at the ignition (x=0 and t=t_{ign}), the ignition temperature is given by:

$$T_{ign} = T_\infty + \frac{\varepsilon.q''}{2.\lambda + h.D}\left(\frac{\lambda}{h} + D + \sum_{m=0}^{\infty} \frac{2.e^{-a.\beta_m^2 t_{ign}}.\left[\frac{h^2 - \lambda^2.\beta_m^2}{h.\lambda.\beta_m}\sin(\beta_m.D) + 2.\cos(\beta_m.D) - 2 - \frac{h.D}{\lambda}\right]}{D\left(\beta_m^2 + \frac{h^2}{\lambda^2}\right) + \frac{2.h}{\lambda}}\right) \quad (11)$$

4.2. Numerical results

The calculation of the ignition time with equation 11 is only possible when the three following parameters are known: the ignition temperature T_{ign}, the twig emissivity □ and the total heat transfer coefficient h. To determine the most suitable set of parameters, we decided to realize an optimization based on the gradient descent method. Several values were tested. For each set of values, the experimental ignition times ($t_{ign}^{\exp}$) were compared to the calculated values (t_{ign}^{model}).

The optimized model parameters correspond to the values for which the sum

$$S = \sum_{i=1}^{N}\left(t_{ign,i}^{\exp} - t_{ign,i}^{model}\right)^2 \quad (12)$$

is minimal. Here N is the number of diameters considered.

The set of parameters best describing the experiments is: T_{ign}=491°C, ε=0.982 and h=21.4 W.m².K. For piloted ignition and under radiant heating, the temperature ignition for wood ranges between 296 and 497°C (Babrauskas 2001). This scattering can be explained by the definition used for the ignition, the design of the test apparatus, the specimen conditions and the species of wood. The optimized ignition temperature (T_{ign}=491°C) is therefore in the range of the data found in literature. There is little data concerning the emissivity of forest fuel. Boulet *et al*. (2011) performed experiments using Fourier transform infrared spectrometers to determine the absorption of radiation for different species of forest vegetation. They found values of absorptivity for the vegetation matter between 0.90 and 0.95. The optimized emissivity (ε=0.982) seems therefore to be coherent with these values. In literature, the total heat transfer coefficient is often evaluated by means of the following relationship (Quintiere 2006, Torero and Simeoni 2010):

$$\varepsilon.q''_{ign,crit} = h(T_{ign} - T_\infty) \quad (13)$$

where $q''_{ign,crit}$ is the critical heat flux for ignition

For needles of *Pinus halepensis*, Torero and Simeoni (2010) obtained a value of 22 W/m².K. By using the data given in Quintiere (2006), the total heat transfer coefficient ranges between 34 and 39 W/m².K for wood. As for the other parameters, the value h=21.4 W.m².K is in agreement with literature.

•

Figure 6 presents the ignition times obtained with the experiments and with the optimized set of parameters. The comparison between these data shows a good agreement. Both curves follow the same trend. An increase of the ignition time with the diameter appears for low diameters. Then, the curves

reach an asymptote for larger diameters.The most significant errors appear for diameters of 2 and 3 mm. As described in section 3.2, for these diameters, the twigs are arranged on several layers. Our modeling considering a thickness D is therefore quite away from the experiments and tends to overestimate the time of ignition. Despite these approximations, the two curves are very close. The mean error is indeed less than 8.3%. However, to ensure the validity of this model, an experimental determination of T_{ign}, h and ε is necessary in order to compare the values found with the optimization and with the experiments.

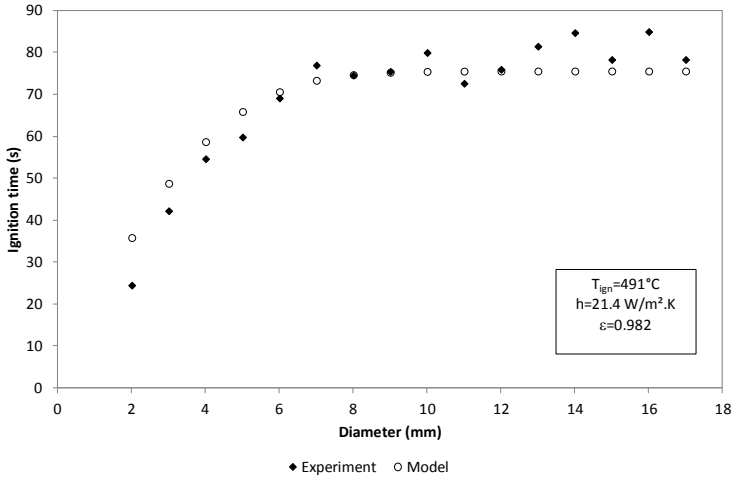

Figure 6– Comparison between the experiment and the numerical simulation

4.3. Sensitivity analysis

To study the effect of the three missing parameters on the ignition time, a sensitivity study was performed. Table 2 shows the three input parameters with their low and high values corresponding to the data found in literature. The interactions between the parameters being unknown, only the interactions between two factors are considered. The factorial design with two levels is therefore built and 2^3 simulations are performed. The software Statgraphics Centurion XVI (StatPoint Technologies) was used to define the numerical design of experiments (Table 3) and to draw the standardized Pareto Chart. The ignition time obtained for high diameters (corresponding to the asymptote of the curve of time ignition according to the diameter) was considered as the output parameter for each case.

Table 2. Variables used for the sensitivity study

Parameter	Low value	High value
T_{ign} (°C)	296	497
ε (-)	0.90	0.95
h (W/m².K)	22	39

Table 3. Numerical design of experiments (DOE)

Test n°	T_{ign} (°C)	ε (-)	h (W/m².K)	Output parameter (Max)
1	497	0.95	22	85.5
2	296	0.95	22	23.7
3	296	0.9	22	26.8

4	497	0.9	22	97.6
5	497	0.9	39	148.8
6	497	0.95	39	126.2
7	296	0.95	39	28.6
8	296	0.9	39	32.7

Figure 7 shows the numerical ignition times according to the diameter for the set of tests. Figure 8 shows the standardized Pareto Chart and the main effects plot. The ignition temperature is therefore the most influent parameter. This is not surprising since this is the parameter which induces the ignition. Increasing the temperature ignition implies an increase of the ignition time. The total heat transfer coefficient affects also the results. By increasing h, the ignition time increases as well. This is due to an increase of the heat losses at the surface. This sensitivity analysis highlights therefore the need to determine accurately the ignition temperature and the total heat transfer coefficient. Specific experiments dedicated to this objective must be considered in the future to obtain these data. This analysis reveals also that the emissivity effect can be neglected in comparison to the effects of ignition temperature and heat transfer coefficient.

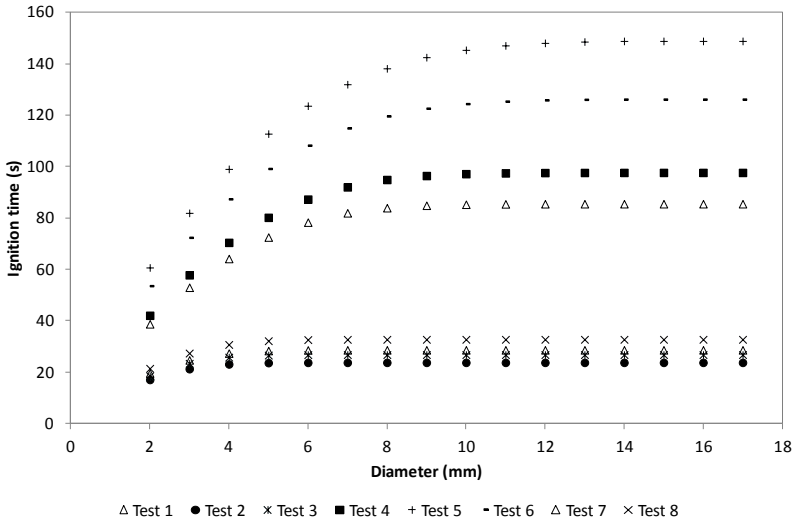

Figure 7– Experimental and numerical time of ignition

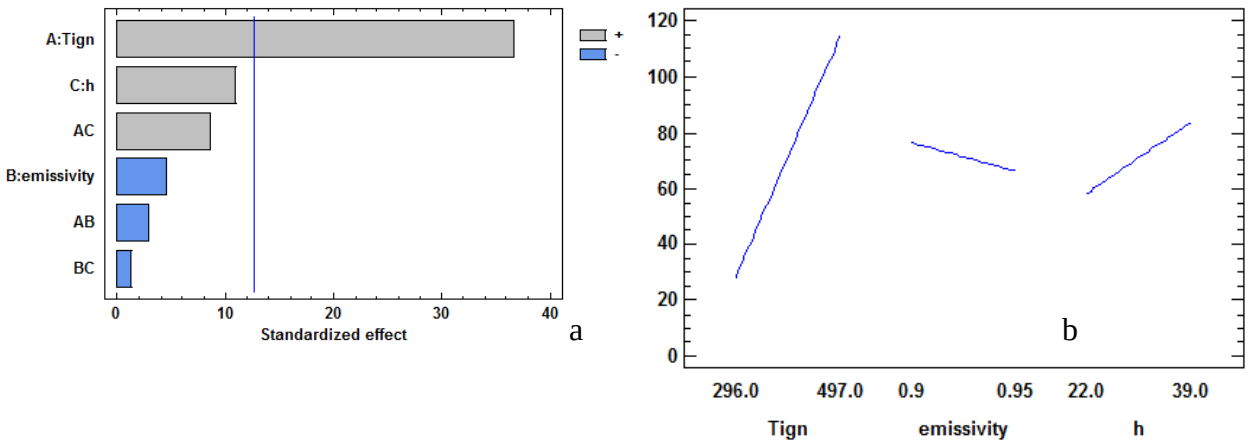

Figure 8– a) Standardized Pareto Chart b) Main effects plot

Conclusion

In this article, the first results of the study of diameter effect on the ignition of *Cistus Monspeliensis* twigs are presented. The location of ignition, the ignition time and the flame residence flame in function to diameter were investigated and a model of ignition was proposed. The main results can be summarized as follows:

- The location of ignition seems to vary. The ignition could be due to: glowing of embers, flaming near the solid or spark of the pilot.
- The ignition time increases strongly with the diameter. For small diameters, the evolution of the ignition time can be considered as proportional to the diameter. For high diameters, the ignition time tends to stabilize around a constant value.
- The flame residence time of the twigs increases with the diameter.
- A model based on one-dimensional nonhomogeneous heat-conduction problem in a finite medium allows modeling the ignition time according to the diameter.

In addition, this study also pointed out the necessity to modify the experimental procedure and to perform specific experiments to better understand the phenomena and to obtain the parameters of the ignition model. Based on these observations, a new study will begin soon, for which:

- A high-speed camera will be used
- A same area exposed to the radiant heat flux will be employed rather than a same mass.
- The ignition temperature will be measured for each experiment
- The model of ignition will be tested with the new set of experimental results.

References

Adou J.K., Billaud Y., Brou D.A., Clerc J.-P., Consalvi J.-L., Fuentes A., Kaiss A., Nmira F., Porterie B., Zekri L., Zekri N. (2010) Simulating wildfire patterns using a small-world network model. *Ecological Modelling* **221**, 1463-1471

Babrauskas V. (2001) Ignition of Wood: A Review of the State of the Art. *Interflam*, 71-88

Koo E., Pagni P., Stephens S., Huff J., Woycheese J., Weise D.R. (2005) A Simple Physical Model for Forest Fire Spread Rate. *Fire Safety Science* **8**, 851-862.

Boulet P., Parent G., Acem Z., Collin A., Séro-Guillaume O. (2011) On the emission of radiation by flames and corresponding absorption by vegetation in forest fires. *Fire Safety Journal* **46**, 21-26

Burrows N.D. (2001) Flame residence times and rates of weight loss of eucalypt forest fuel particles. *International Journal of Wildland Fire* **10**, 137–143

Hill H. B. (1887) On the Behavior of Sound and Decayed Wood at High Temperatures. *Proceedings of the American Academy of Arts and Sciences* **22**, 482-492

McArthur A.G. (1962). Control burning in eucalypt forests. Commonwealth of Australia Forest and Timber Bureau, Leaflet Number 80. Canberra, ACT.

Morvan S., Méradji S., Accary G. (2009) Physical modeling of fire spread in Grasslands. *Fire Safety Journal* **44**, 50-61.

Peet G.B. (1965) A fire danger rating and controlled burning guide for the Northern Jarrah (Euc. Marginata sm) forest of Western Australia (Perth : Forests Dept).

Özisik M.N. (1993) Heat Conduction (Eds John Wiley & Sons, Inc)

Quintiere J.G. (2006) Fundamentals of Fire Phenomena. (Eds John Wiley & Sons Ltd, The Atrium, Southern Gate, Chichester, England)

Rothermel R.C. (1972) A mathematical model for predicting fire spread in wildland fuels, Res. Pap. INT-115. Ogden, UT: U.S. Department of Agriculture, Intermountain Forest and Range Experiment Station.

Santoni P.A., Filippi J.B., Balbi J.H., Bosseur F. (2011) Wildland fire behaviour case studies and fuel models for landscape-scale fire modelling. *Journal of Combustion*, 613424

Simeoni A., Thomas J.C., Bartoli P., Borowieck P., Reszka P., Colella F., Santoni P.A., Torero J.L. (2012) Flammability studies for wildland and wildland–urban interface fires applied to pine needles and solid polymers. *Fire Safety Journal* **54**, 203–217

Torrero J.L., Simeoni A. (2010) Heat and Mass Transfer in Fires: Scaling Laws, Ignition of Solid Fuels and Application to Forest Fires. *The Open Thermodynamics Journal* **4**, 145-155

Experimental evidence of buoyancy controlled flame spread in wildland fires

Mark A. Finney[a], Jack D. Cohen[a], Jason A. Forthofer[a], Sara S. McAllister[a], Brittany A. Adam[b], Nelson K. Akafuah[b], Justin English[b] , Kozo Saito[b], Daniel J. Gorham[c], Michael J. Gollner[c]

[a] *US Forest Service, Missoula Fire Sci. Laboratory, Missoula MT 59808 USA mfinney@fs.fed.us, jcohen@fs.fed.us, jaforthofer@fs.fed.us, smcallister@fs.fed.us*
[b] *Univ. of Kentucky, Lexington, KY 40506, USA, brittany.adam@uky.edu, nelson.akafuah@uky.edu, justin.english@uky.edu, ksaito@uky.edu*
[c] *Dept. Fire Protection Engineering, University of Maryland, 20742, USA, dgorham1@umd.edu, mgollner@umd.edu*

Abstract
Laboratory fires spreading through laser-cut cardboard fuel beds were instrumented and analyzed for physical processes associated with spread. Flames in the span-wise direction appeared as a regular series of peaks-and-troughs that scaled directly with flame length. Flame structure in the stream-wise direction fluctuated with the forward advection of coherent parcels that originated near the rear edge of the flame zone. Thermocouples arranged longitudinally in the fuel beds revealed the frequency of temperature fluctuations decreased with flame length but increased with wind speed. The behaviors are remarkably similar to those of boundary layers, suggesting a dominant role for buoyancy in determining wildland fire spread.

Keywords*: Flame Structure, Buoyancy, Instability, Flame Spread*

Introduction

Despite decades of research on wildland fires, a common understanding has not emerged as to how heat transfer processes are organized to produce fuel particle ignition and flame spread. This has left physical modelling of wildland fires without an experimental basis for the many assumptions, including radiation and convective heat transfer. Strong experimental evidence has now suggested a secondary role for radiation in flame spread in fine fuel beds because 1) the optical attenuation through the fuel bed diminishes irradiance to particles, and 2) cooling by forced or natural convection efficiently prevents fine fuels from reaching ignition. Thus, we focus here on recent laboratory and field experiments designed to determine how convective heating occurs. We found clear evidence that non-steady heating by flame contact produces fuel particle ignition.

Methods

Laboratory fire spread experiments were conducted in uniform fuel beds made of laser-cut cardboard. Cardboard and paper strips have been used previously (Emmons and Shen, 1971) and offer advantages of known homogenous properties such as density and customizable physical dimensions of discrete particles (length, surface area etc.). Fuel beds were burned in the wind tunnel at the Missoula Fire Sciences Laboratory. The wind profiles of the 3m cross-section have been described previously (Rothermel and Anderson 1966, Catchpole *et al*. 1998) and are laminar except along the bottom surface where an upstream trip-fence produces a turbulent boundary layer. Wind speeds were varied from 0.22 m s^{-1} to 2.3 m s^{-1} with relative humidity of approximately 25%.

Figure 1. Picture of laser-cut cardboard laboratory fuel bed. Note that the scale is graduated in inches.

Fuels for the laboratory burns were engineered from cardboard with a commercial CO_2 laser system to produce fuel elements that are connected at regular spacing along a common spine. The cards or "combs" could then be arranged in rows at various spacing to form a fuel bed with vertically standing particles (**Erro! A origem da referência não foi encontrada.**1). The cardboard used was brown "chip board" 1.27mm (0.05 inch) thick with approximately 60% recycled content. Fuel particles were created at different lengths and widths and arranged at different row spacing to achieve specific fuel bed properties. The laser cutter/engraver system was a Universal Laser Systems Inc. ILS12.150D model equipped with two 60W laser cartridges. The beams from both lasers were collimated for cutting. The table accommodates sheets of cardboard 0.61m X 1.22m (2 ft X 4 ft) so that multiple combs can be cut from the same sheet in one operation.

Fuel beds constructed of these cardboard combs were 1.22m to 2.45m in width and 3.05m to 6.1m in length (Figure 1). The combs were supported and arranged on a foundation of cement-board strips (Hardy Board) 0.635cm x 5.08cm (1/4 in. x 2 in) each separated by a steel spacer 0.158cm x 2.54cm (1/16 in x 1.0 in). The steel spacers rested on the floor to preserve a slot at the upper surface which pinched the spine of the fuel combs such that only the vertical tines were exposed (**Erro! A origem da referência não foi encontrada.**). Tine lengths of 2.54cm (1in), 10.1cm (4in), 20.3cm (8in), and 35.6cm (14in) were used in the burns. The longitudinal spacing of the combs could be adjusted every 1.43cm (5/16in). To limit inflow to the combustion zone along the lateral edges during burning, the sides of the beds were lined with paper that was treated with the flame retardant Diammonium Phosphate ($(NH_4)_2HPO_4$). This technique was described by Byram *et al*. (1964), where fire retardant limits independent flaming combustion but allows the paper to burn in conjunction with the advancing fire front. The consumption of the paper sideliners at the trailing edge of the burning zone avoids channelling of air inflow to the rear of the fire which has been shown to affect fire spread on slopes (Smith 1992). Cutouts of the sideliner permitted filming of the ignition process within the fuelbed.

Field-scale fires were assessed to determine potential scaling relationships beyond those possible within the laboratory. At Fort Swift, Texas, grass 1 m deep was burned on separate plots with average winds of 1.7 m s^{-1} and 4.5 m s^{-1} and produced flames of approximately 3m tall. A rectangular wooden crib was also constructed of square ponderosa pine lath 0.025 m thick at 0.12x0.12 m square spacing with overall dimensions of (1.2m wide, 1m tall, and 17m long) and was burned to provide stationary flame source with approximately 6 m flames.

Results

The unprecedented uniformity of the fuel beds from engineered cardboard allowed us to observe flame structure and behaviour isolated from environmental heterogeneity. The first and most obvious characteristic of flame fronts in these flame sources is the peak and trough pattern of the flame edge (Figure 2). This geometry is similar to instabilities in boundary layer flow caused by Taylor-Görtler vortices, oriented in the flow direction, that arise when air inflow to the flame zone is lifted by buoyancy (Floryan 1991). From the literature (*e.g.* Sparrow and Husar 1969), studies of flow over heated plates and of boundary layer transition, pairing of counter-rotating Taylor-Görtler vortices form an alternating series of convergence zones in the transverse direction – with downward force creating the flame trough and up-ward convergence in flame peaks (Figure 2). The significance of these vortices is that they force flame down and forward into the fuel bed and advect secondary instabilities forward through the flame zone. Data from spreading wind tunnel fires, prescribed grassland burns, and stationary crib fires all reveal that the transverse wavelength of these vortices is about ½ the flame length (Figure 2D).

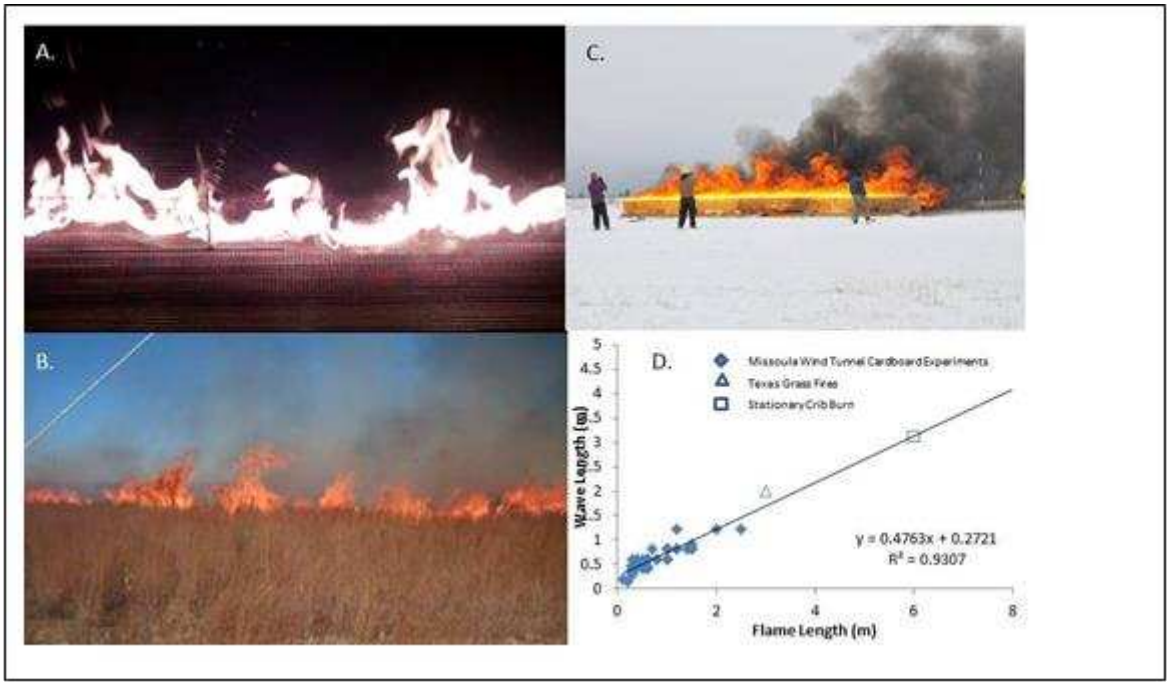

Figure 2. Flame structure in laboratory-scale cardboard fuel beds (2A) reveal the same sawtooth flame structure as grass fires (2B) and stationary crib fires (2C) because of Taylor- Görtler vortices. The transverse wavelength of these flame peaks appears to be about ½ the flame length from all of these fires (2D).

The second dynamic discovered in these experiments is a series of flame parcels (Figure 2a) which are first seen to originate near the back edge of the flame zone. These parcels remain coherent on video and move forward through the flame zone to burst forward and impinge fuel particles for some considerable distance ahead of the combustion interface. Thermocouple temperatures measured in the fuel beds (Figure 3b) fluctuate with predictable average frequencies that showed strong Strouhal-Froude scaling (Figure 3c) similar to the pulsing frequency from pool fires (Malalakasera 2006). This scaling, using the variables of wind speed and flame length, means the bursts frequency increases with wind speed and decreases with flame size. The origin of the bursts appears to be from instabilities arising at the upstream edge of the flame zone similar to Tollmien-Schlichting waves observed in boundary layer instabilities (Floryan 1991). These are visible first as transverse ridges and concave

packets in the upper flame surface (Figure 3A). With downstream movement through the flame zone they are drawn into the circulations from Görtler vorticity and expelled forward past the leading flame edge into the fresh fuels ahead. This bursting frequency was recorded as temperature spikes on thermocouple arrays embedded in the fuel bed (Figure 3B) which demonstrate the coherency of the flame structures as they advect through the flame zone. Remarkably, data from all field sources suggests consistent Str-Fr scaling as laboratory-scale fires (stationary or spreading) (Figure 3C).

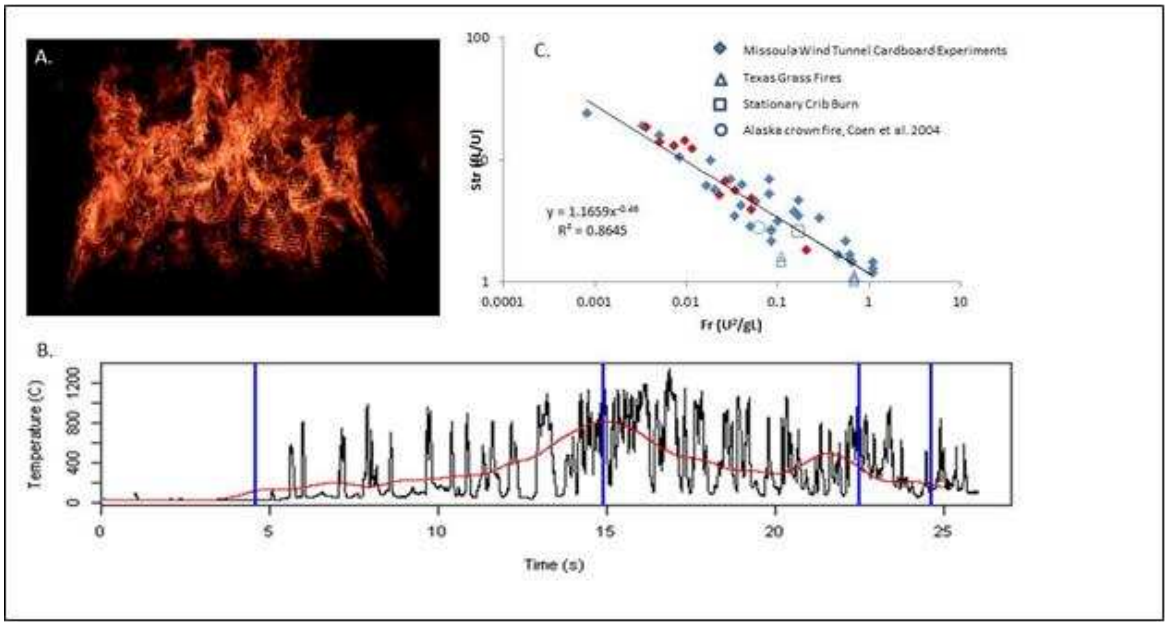

Figure 3. Instabilities in the flame zone are revealed in experimental fires burning in cardboard fuel beds as dish-shaped patterns originating near the rear edge of the flame zone (3A). These produce forward bursts of flame ahead of the combustion interface that result in a pulsing-type temperature signal on thermocouples (3B). Average burst frequencies (f) scale with a Strouhal-Froude correlation (Str-Fr, 3C) using windspeed (U) and flame length (L) of laboratory and field-scale fires (see Figure 2).

Discussion

This research reveals instabilities of the flame that are similar to buoyant dynamics of non-reacting flows (Floryan 1991). These instabilities appear responsible for creating flame intermittency at the leading edge of spreading fires and forcing flames downward into the fuel bed. Similar flame structure and intermittency was recently found using stationary gas flames, with and without forced flow[1]. The use of the Str-Fr scaling of non-steady flame behaviours in both studies suggests broad applicability across a wide range of wildland fire sizes and fuel[2]. The strong dependency of intermittent convective

[1] Gorham, DJ., R. Hakes, A.V. Singh, J. Forthofer, J. Cohen, S. McAllister, M.A. Finney and M.J. Gollner. 2014. Studying wildland fire spread using stationary fires. Paper presented at the 7th International Conference on Forest Fire Research

[2] Adam, B.A., JD. English, NK. Akafuah, K.Saito, M Finney, J Forthofer, J Cohen. 2014. The Strouhal-Froude number scaling for wildland fire spread. Paper presented at the 7th International Conference on Forest Fire Research

heating to thermal behaviour and ignition of individual fuel elements to radiation and convection is revealed in two other studies[1],[2].

Quasi-periodic flame behaviour in spreading fires has been noticed previously for trench fires for pine needle beds, but the role of such non-steady flame impingement in igniting fuel particles and flame spread has not been considered (Atkinson *et al*. 1995, Woodburn and Drysdale 1998, and Dupuy *et al*. 2011). The Strouhal-Froude scaling suggested by our data is consistent with buoyant dynamics of stationary fire phenomena (Malalasekera *et al*. 1996) but new to spreading fires. These findings suggest that the difficulty of identifying an integral length scale for convection related to ignition (Anderson *et al*. 2010) comes from assuming away the time-dependency of particle heating. It also suggests by virtue of the inverse dependency of average pulse frequency on flame dimensions that slower buoyant dynamics of larger flame zones compensate for the increases in energy release and convective heating distance to avoid runaway spread. If buoyant instabilities are responsible for the flame behaviours and particle ignition, then it strongly suggests that laboratory-scale fire spread processes should extend readily to field proportions because flame temperature in diffusion flames (and thus buoyancy) remains approximately the same regardless of fire size. At this time, our limited field-scale experiments and observations seem to be in agreement with this scaling. Much work is yet to be done to understand useful scaling relationships, but the ultimate goal is to someday incorporate these findings into practical tools for wildland fire managers.

Conclusions

These findings may have profound influence on understanding of the flame spread process in wildland fires because they suggest that buoyant dynamics govern the heat transfer processes. Thermocouple measurements on fuel particles show that ignition commences after a series of flame contacts that increase the particle temperature in discrete jumps. This is far from the normally assumed steady processes of particle heating. Even large particles in uniform fuel beds show these temperature jumps from flame contact and do not ignite by radiation because optical attenuation reduces irradiance dramatically.

References

Anderson, W., E. Catchpole and B. Butler 2010. Convective heat transfer in fire spread through fine fuel beds. *Intl. J. Wildl. Fire*, pp. 284-298.

Atkinson, G., D. Drysdale and Y. Wu. 1995. Fire driven flow in an inclined trench. *Fire Safety Journal*, pp. 141-158.

Byram, G., H. Clements, E. Elliott and P. George. 1964. An experimental study of model fires. USDA Forest Service, Southeastern Forest Experiment, Technical Report No. 3. Macon, Georgia.

Catchpole, W., E. Catchpole, B. Butler, R. C. Rothermel, G. A. Morris and D. J. Latham. 1998. Rate of Spread of Free-Burning Fires in Woody Fuels in a Wind Tunnel. *Comb. Sci. Tech.*, pp. 1-37

Coen, J. L., S. Mahalingam, and J. W. Daily, 2004. Infrared imagery of crown-fire dynamics during FROSTFIRE. J. Appl. Meteor. 43:1241-1259

[1] Cohen, J.D. and M.A. Finney. 2014. Fine particle heating during experimental laboratory fires. Paper presented at the 7th International Conference on Forest Fire Research

[2] English, J.D., NK. Akafuah, Brittany A. Adam, M.Finney, J. Forthofer, J.Cohen, S. McAllister and K. Saito. 2014. Ignition behaviour of cardboard fuel particles. Paper presented at the 7th International Conference on Forest Fire Research

Dupuy, JI, J. Marechal, D. Portier and J.-C. Valette. 2011. The effects of slope and fuel bed width on laboratory fire behavior," *Intl. J. Wildl. Fire* , vol. 20, p. 272–288

Emmons, H. and T. Shen. 1971. Fire spread in paper arrays. *Proc. Combust. Institute.,* vol. 13, no. 1, pp. 917-926.

Floryan, J.M. 1991. On the Görtler instability of boundary layers. Prog. Aerospace Sci. 28:235-271.

Malalasekera, W. M. G., H. K. Versteeg and K. Gilchrist. 1996 . A review of research and an experimental study on the pulsation of buoyant diffusion flames and pool fires. *Fire and Materials,* vol. 20, no. 6, p. 261–271.

Rothermel R.C. and H. Anderson. 1966. Fire spread characteristics determined in the laboratory. US For. Serv. , 1966

Smith, D. 1992. Measurements of flame length and flame angle in an inclined trench," *Fire Safety J.,* vol. 18, pp. 231-44.

Sparrow E. and R. Husar. 1969. Longitudinal vortices in natural convection flow on inclined plates. *J. Fluid. Mech.,* vol. 37, pp. 251-255.

Woodburn, P., and D. Drysdale. 1998. Fires in inclined trenches: time-varying features of the attached plume. *Fire Safety Journal,* vol. 31 , pp. 165-172.

Experimental investigation of the influence of geometry on gas accumulation using a V-shape forest model

Bruno Coudour[a,b], Khaled Chetehouna[b], Boris Conan[c], Sandrine Aubrun[c], Jean-Pierre Garo[a]

[a] *Institut P', UPR 3346 CNRS, ENSMA, Univ. Poitiers, Futuroscope Chasseneuil, France.* bruno.coudour@ensma.fr
[b] *INSA-CVL, Univ. Orléans, PRISME EA 4229, Bourges, France.*
[c] *Univ. Orléans, INSA-CVL, PRISME, EA 4229, Orléans, France.*

Abstract
Accumulation of gas inside a valley exposed to a light crosswind is experimented in this paper to evaluate the influence of gas in accelerating forest fire phenomena. Experimentations were done inside a wind tunnel using a 1/400 forest model configured as a valley with two different internal angles. The forest is modelled so that a parallel is possible with a real forest thanks to a similitude law. The emission of gas is ensured by 400 tubes introduced inside the mesh cylinders supplied with ethane. The 400 tubes are divided into four independent parts of 100 tubes to be able to study independently the influence of the different zones before and inside the valley on the accumulation of gases. We focused on the measurements of velocity by Laser-Doppler Velocimetry (LDV) and concentration with a Flame Ionization Detector (FID). Analyzing the velocity, turbulence and concentration results, we observed a stagnation point in the thalweg for the flattest valley and a recirculation zone for the deepest one where gas accumulation reached up to 4 times the concentration measured outside the valley. The study of the influence of the different emission zones showed that gas accumulation mainly comes from the zones inside the valley.

Keywords*: V-shape forest model; gas accumulation; gas emission; Laser-Doppler Velocimetry; concentration*

Introduction

During a forest fire, high concentrations of gases, which may come from fire smoke, pyrolysis products and emissions of vegetation (BVOCs), can be found inside a valley depending mainly on the meteorological conditions and the topography [1,2]. It is noteworthy that some experimented firefighters decide to run away from a forest fire when the surrounding odor is too strong and when the vision becomes hazy. This lets us think that a high concentration of gases is present at that moment. The problem encountered is the observation of Accelerating Forest Fires (AFFs) inside valleys or canyons. Indeed, numerous mortal accidents like those which happened in Mann Gulch (USA, 1949, 13 victims), La Gomera (Spain, 1984, 20 victims) or Kornati Island (Croatia, 2007, 11 victims) are described in the literature [1]. Initially, these AFFs appear to be classic forest fires but change unexpectedly their behavior with impressive rates of spread and heat releases letting behind them large burning areas. One of the possible causes of this phenomenon is the accumulation of gases in narrow areas like thalwegs or canyons with, in one hand, the fire smoke dispersed by complex air flow above and around the forest fire and, on the other hand, BVOCs and pyrolysis products emitted by heated plants because of the fire front radiation. The goal of this project is to have an idea of what happens inside a valley before the arrival of fire regarding the potential of accumulation of both smoke coming from above and BVOCs emitted inside the valley. To address these questions, we reproduced the spatial distribution of gas inside a valley (V-shaped) with a forest model exposed to a light crosswind. Experiments were performed to give information on the location of gas accumulation and whether or not it can be sufficient to form flammable gas pockets to catalyze the fire propagation. Some research studies have been done for street canyons to focus on the dispersion of pollutant [3,4] but, to our knowledge, there is no work on valley configuration with forest models.

Experimental section

Investigations were made in the wind tunnel "Lucien Malavard" of PRISME Laboratory, with a 1/400 forest model configured as a valley with varying angle in order to study the effect of geometry on the global air-flow. The wind tunnel has a 16 m-long rough development plate. Turbulence generators are fixed at the entrance of the test section to develop an atmospheric boundary-layer flow. The forest is modelled using 50 mm-high metallic mesh cylinders which are rolled up to their top to represent the higher leaf density of the tree crown. The cylinder arrangement was chosen to avoid any forced flow direction to the flow going through the canopy [5]. The biogenic emission coming from the forest canopy is represented by a surface source, which is modelled through a series of point sources of a passive tracer. The passive tracer is ethane, chosen for its density close to air. The release height is 40mm (80% of the tree height) and the distance between each point source is 50mm (tree height). Figure 1 illustrates a schematic overview of the wind tunnel and the modelled forest located in the measurement zone. The gas distribution comes from an ethane bottle linked to a first distribution device with which we can chose which of the four emission zones are active (Figure 2). This first distribution device is linked to four other ones built with enough pressure loss to permit an homogeneous surface source when the gas comes out from the tubes (Figure 3). Preliminary testing showed that, right above the canopy, the source was horizontally homogeneous. Consequently, the source is representative of a surface source. The emission zone of 400 tubes, is divided into four independent parts of 100 tubes (Figure 2). This allows us to study the effect of each zone of emission on the accumulation of gases inside the valley.

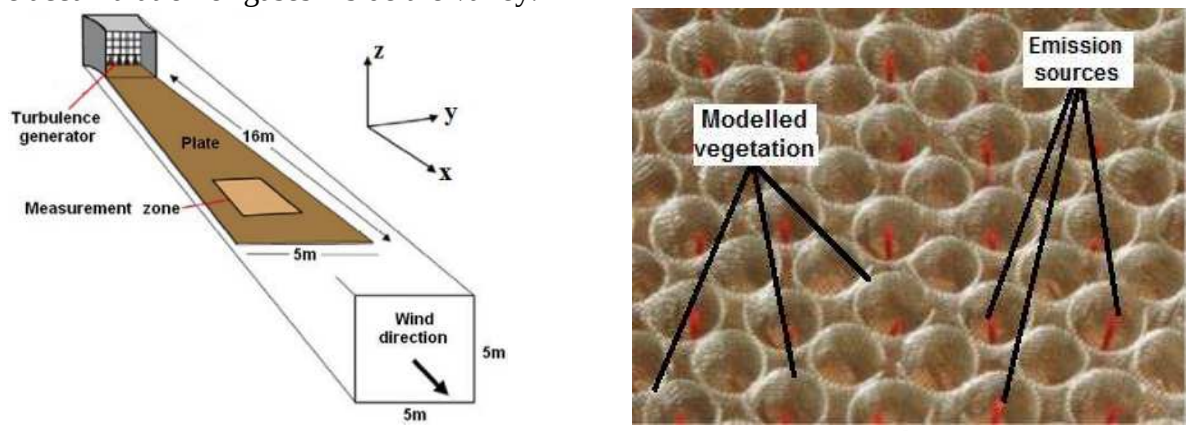

(*a*) (*b*)

Figure 1. Overview of the experimental setup of modelled forest in a wind tunnel: (a) Scheme of the wind tunnel; (b) Metallic mesh cylinders and ethane emission tubes (in red) constituting the model placed in the measurement zone.

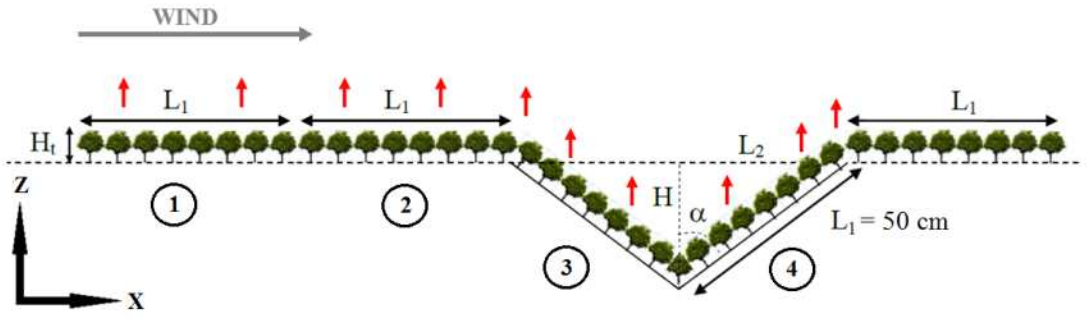

Figure 2. Simplified 2D scheme of the forest model and the four zones of ethane emission, zone 3 is called the lee side and zone 4 the wind side

Figure 3. The two photographs depict the distribution device of ethane placed under the model

Experimentations in the wind tunnel gather two types of measurements above the canopy of the four zones: measurements of velocity with a Laser-Doppler Velocimetry (LDV) and measurements of concentration with Flame Ionization Detector (FID) (Figure 4).

Figure 4. LDV on the left and FID on the right above the V-shaped forest model

For the velocity measurements by LDV, the flow was seeded with olive oil micro-particles upstream of the turbulence generators. By referring to Viegas's work [6], we have chosen two different half internal angles of valley α = 50° and α = 80° (Figure 3). The forest model permits then to make a parallel with a real forest thanks to a similitude law [5]. Indeed, the measured concentrations will be given at reduced scale in a dimensionless form (Eq.1) in order to extrapolate them to full scale situations using real parameters (Eq.2):

$$c^* = \frac{c[m^3/m^3_{mix}] \times U_{ref}[m/s]}{Q_{source}[m^3/s/m^2]} \quad (1)$$

$$c_{full\ scale} = f\left(x, z, c^*, U_{ref}, Q_{source}, \alpha, H_t\right) \quad (2)$$

3. Results

3.1. Velocity

From our different experiments, we measured velocity, turbulence and concentration obtaining grids of values above and inside the valley for the two different angle configurations. To normalize our measurements, we divided them by a reference speed located before the forest at ten times the canopy height. Analyzing the results with the velocity streamlines we observe on the left of Figure 5 below

that there is no recirculation with the flattest valley even if we have a potential of accumulation in the thalweg where the horizontal component of the velocity (U) is almost null. On the right of Figure 5, we observe clearly a clockwise recirculation for the deepest valley. Regarding the turbulence intensity with the Figure 6, we notice that it is located above the canopy for the flat part of the forest and that it increases a lot above the valley with the detachment of the boundary layer. For the 80° angle, the turbulence intensity inside the valley is multiplied by four if we compare it to the flat forest, with a maximum of 1.4%. Turbulence intensity is much stronger for the 50° angle, and reaches up 76% above the valley (Figure 6 and 7) even if there is not so much turbulence near the thalweg. Thus, gas accumulation is possible in this place.

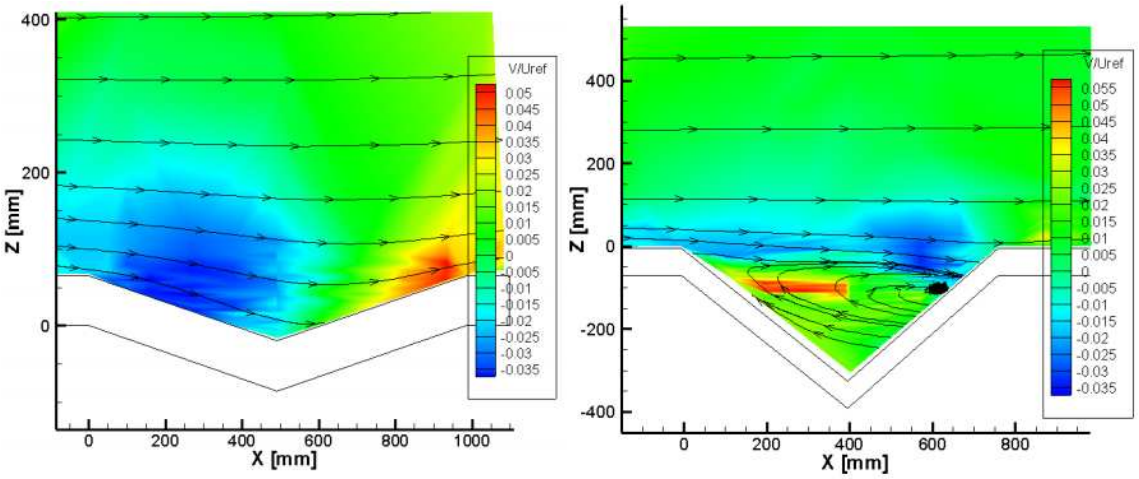

Figure 5. Vertical component of the velocity (V) normalized by Uref with streamlines of the velocity, for α = 80°on the left and α = 50° on the right

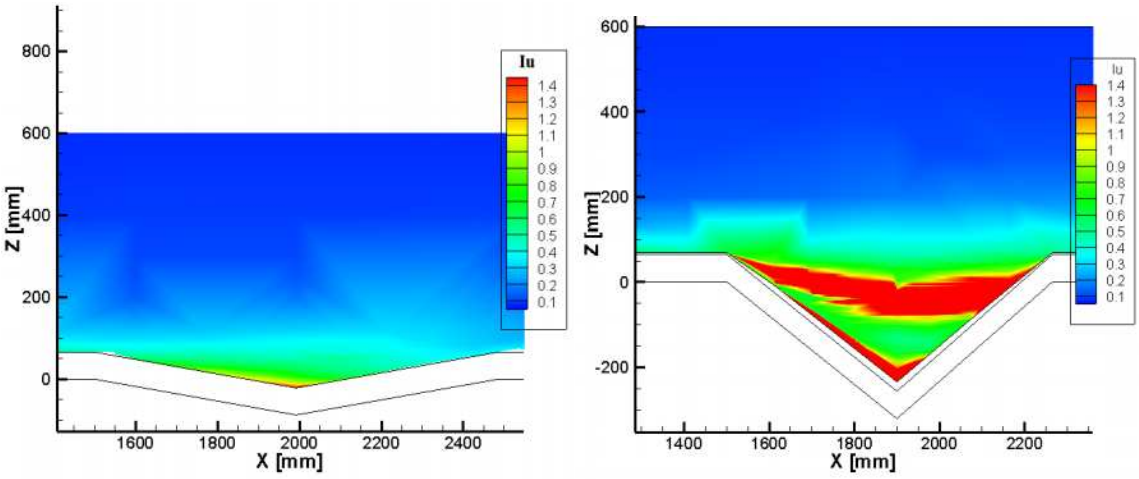

Figure 6. Turbulence intensity on U for α = 80° on the left and α = 50° on the right

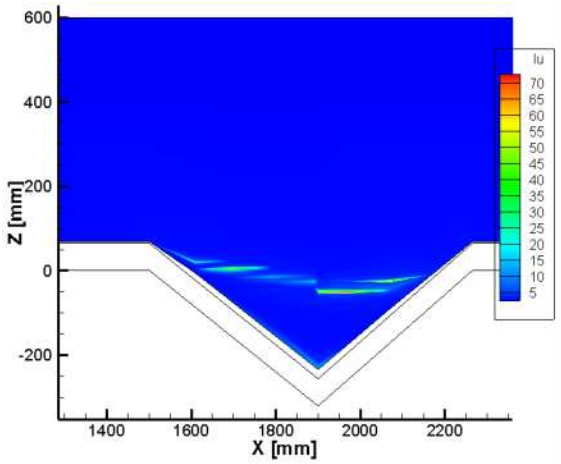

Figure 7. Turbulence intensity on U for α = 50°

3.2. Concentration

If we look now at both concentration and velocity, we obtain the Figure 8 below for 80° and 50°. We notice at 80° that accumulation is located in the thalweg due to the weak velocity in this zone. The maximum concentration is measured at 980 ppm almost twice the concentration measured above a flat forest. At 50°, an accumulation of gas is visible above the lee side due to the recirculation. We reach up a maximum of 1790 ppm increasing the concentration by more than 3.5 times if we still compare to the flat forest.

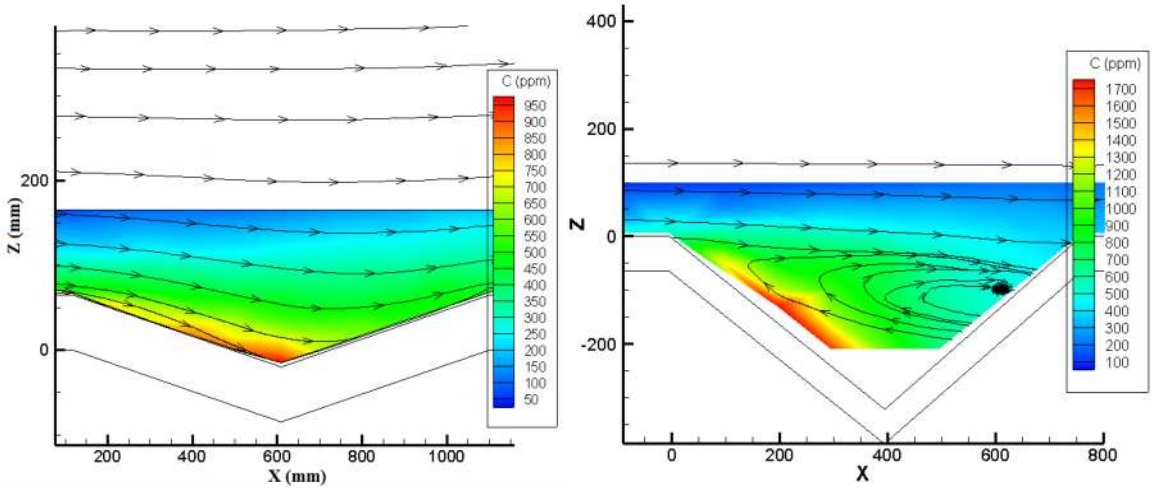

Figure 8. Concentration with velocity streamlines for α = 80° on the right and for α = 50° on the left

3.3. Footprint of the different forest model zones

The following experiments were carried out to know the footprint of the different zones, to know which zones of the forest model are more influent on the gas accumulation. To this end we plugged and unplugged the different emission zones from the distributor. Figure 9 below presents the concentration with all zones emitting on the left graph and only zone 3 on the right. To compare the results we normalized the concentration following the equation 1 page 4. With the 80° angle, we concluded that the inlet part (zone 1 and 2) does not influence the accumulation inside the valley. Focusing on the angle 50° (Figure 9) with the recirculation zone, we observed that it is mainly the lee side (zone 3) which influences the accumulation with a maximum at C* = 152 whereas with all zones emitting we

obtained a maximum of C* = 194. This maximal accumulation is located just above the canopy at the middle of the lee side. Letting now only the wind side emitting (zone 4), we have a maximal accumulation located in the thalweg with a maximal normalized concentration found at 79.

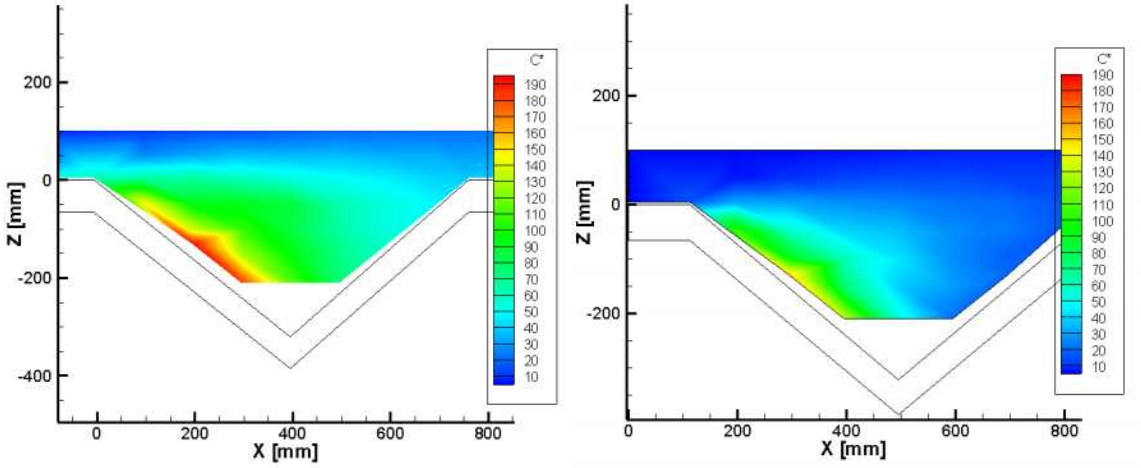

Figure 9. Normalized Concentration all zones emitting on the left and lee side only on the right for 50°

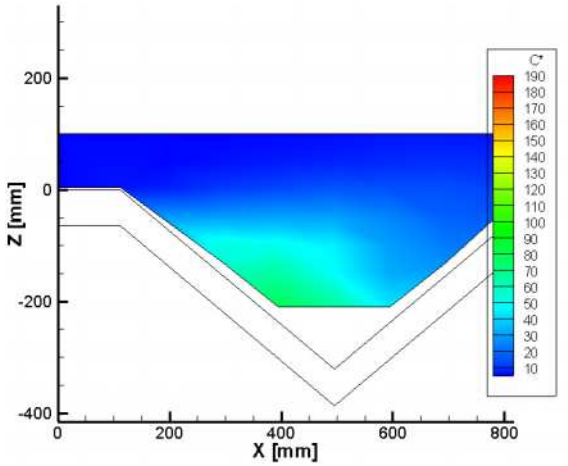

Figure 10. Concentration (ppm) of only wind side emitting for 50°

3.4. Extrapolation to real case

Knowing the influence of each zone, we observe that the risk of accumulation is present if there are emissions from the inside the valley with heated vegetation for example. With the arrival of the fire it is the wind side which will be directly exposed to the radiation and will emit more than the lee side. We could then imagine adding coefficients for each zone to analyze a real case. By plotting the normalized concentration, we see that concentration just above the canopy is multiplied by 3.5 to 4 inside the valley.

Studies of BVOC emissions from real forests evaluate the emission at about 1 g/m².h in favorable regions (dry summers and wooded areas) [7]. Since 50% of emissions are released in July and August, emissions grow to 3 g/m².h during this period. Knowing that *Rosmarinus officinalis*, one of the Mediterranean plant species involved in AFFs, emits eight times more at 175°C than at 50°C [8], we can estimate emissions superior than 24 g/m².h when a forest fire is approaching heating the vegetation with radiation. If we consider now that vegetation is heated during one hour then we have emissions of 24 g/m². If we hypothesize that there are not so much air flow and that emissions are dispersed in 100 m^3. Thus we can evaluate that VOC emissions can reach 0.24 g/m^3 near a forest fire. Then we

know that if these VOCs are emitted near a narrow valley, they can accumulate up to 4 times to get around 1 g/m^3. Studies show that VOCs like α-pinene have a lower flammability limit (LFL) around 1% volumetric [2,9]. According to the density of air and α-pinene we obtain around 0.6% which is rather close to the LFL. Knowing that there are many approximations, the chance of being in presence of a flammable atmosphere inside a narrow valley is still imaginable.

Conclusion

We analyzed velocity, turbulence and concentration results for two different half internal angles of a valley model. Velocity permitted us to observe a potential of accumulation in the thalweg where the velocity is almost null for α = 80°. For α = 50°, we highlighted a recirculation zone inside the valley. Analyses of the turbulence showed that there could be an accumulation of gas in the thalweg of the 50° angle where turbulence is lower than above. By measuring the concentrations, we observed an accumulation in the valley up to twice more than a flat forest for α = 80° and up to four times more for α = 50°. The study of the zone footprint permitted us to say that emissions outside the valley do not have an impact of accumulation inside the valley in our case. Focusing on the 50° angle and studying the emissions of lee side (zone 3) and the wind side (zone 4) independently, we concluded that these are mainly the emissions of the lee side which influence the gas accumulation. Due to the recirculation, gas accumulation is located just above the canopy in the middle of the lee side. Emissions from the wind side accumulate in the thalweg. Numerical study with a Computational Fluid Dynamics code could permit to obtain further results varying the angle (α) with which we could obtain, for example, the threshold of the angle not to overcome to stay in safe concentration, below the LFL of VOCs. The fact that concentration inside the valley is four times the one measured for a flat forest shows that LFL is not so far and that the hypothesis of gas accumulation is still relevant.

References

[1] D.X. Viegas, A. Simeoni, Eruptive behaviour of forest fires, *Fire Technology*, vol. 47, pp. 303-320, 2011.

[2] F. Gerdes and D. Olivari, Analysis of pollutant dispersion in an urban street canyon, *Journal of Wind Engineering and Industrial Aerodynamics*, vol. 82, pp. 105-124, 1999.

[3] M. Pavageau, M. Schatzmann, Wind tunnel measurements of concentration fluctuations in an urban street canyon, *Atmospheric Environment*, vol. 33 pp. 3961-3971, 1999.

[4] K. Chetehouna, L. Courty, J.P. Garo, D.X. Viegas, C. Fernandez-Pello, Flammability limits of biogenic volatile organic compounds emitted by fire-heated vegetation (Rosmarinus officinalis) and their potential link with accelerating forest fires in canyons: A Froude-scaling approach, *Journal of Fire Sciences*, In press, 2014, doi: 10.1177/0734904113514810.

[5] S. Aubrun, B. Leitl, Development of an improved physical modelling of a forest area in a wind tunnel, *Atmospheric Environment*, vol. 38, pp. 2797-2801, 2004.

[6] D. X. Viegas, A mathematical model for forest fires blowup, *Combustion Science and Technology*, vol. 177, pp. 27-51, 2005.

[7] V. Simon, L. Luchetta, L. TorresEstimating the emission of volatile organic compounds (VOC) from the French forest ecosystem, *Atmospheric Environment*, Volume 35, pp. 115-126, 2001.

[8] K. Chetehouna, T. Barboni, I. Zarguili, Leoni A. Simeoni. And A. C. Fernandez-Pello. Investigation On The Emission Of Volatile Organic Compounds From Heated Vegetation And Their Potential To Cause An Accelerating Forest Fire, *Combustion Science and Technology*, Volume 181, Issue 10 (2009)

[9] L. Catoire, V. Naudet, Estimation of temperature-dependent lower flammability limit of pure organic compounds in air at atmospheric pressure, *Process Safety Progress* 24 (2005) 130-137.

Experimental investigations on accelerating forest fires thermochemical hypothesis

Léo Courty[a], Khaled Chetehouna[b], Jean-Pierre Garo[c], Carlos Fernandez-Pello[d]

[a] *Univ. Orléans, PRISME EA 4229, 63 Avenue de Lattre de Tassigny, 18020 Bourges, France.* leo.courty@univ-orleans.fr
[b] *INSA Centre Val de Loire, Univ. Orléans, PRISME EA 4229, 88 Boulevard Lahitolle, 18020 Bourges, France.*
[c] *Institut P', UPR 3346 CNRS, ENSMA, Univ. Poitiers, 1 Avenue Clément Ader, Téléport 2, BP 40109, 86961 Futuroscope Chasseneuil, France.*
[d] *Department of Mechanical Engineering, University of California, Berkeley, CA 94720, USA.*

Abstract
Accelerating forest fire phenomenon is studied in this paper. This phenomenon characterizes fires with a sudden increase of the rate of spread and of the energy released without any changes in the meteorological and topographic conditions. The thermochemical explanation is investigated in this study: acceleration of the rate of spread could be the consequence of the ignition of Biogenic Volatile Organic Compounds emitted by fire heated vegetation. Two experimental setups are used to perform very simple experiments in order to give validation elements to this thermochemical approach. The first experimental setup used permits to show that gases emitted by vegetation (even if they are hot) are diffused mainly in the direction of the ground. The second one shows that the gases emitted by heated *Rosmarinus officinalis* needles can be ignited with a pilot flame. *Rosmarinus officinalis* is a typical vegetal species involved in accelerating forest fires. This work does not prove neither that this hypothesis has been validated nor that this is the only explanation for accelerating forest fire accidents, it only brings arguments for future discussions and for a possible validation of the thermochemical approach.

Keywords: *α-pinene; BVOCs flame; accelerating forest fire.*

Introduction

The main purpose of this work is to give experimental data that would permit to take into account in a better way the combustion process in forest fires models. The aim is of course to better control and prevent wildland fires. A particular care is taken to a special type of accidents, named accelerating forest fires (AFF) and characterized by a sudden increase of the rate of spread and of the energy released. These accidents have been reported and detailed in the literature for several years (Arnold and Buck, 1954; Rothermel, 1993; Dold *et al*. 2009). Different hypothesis have been developed to explain these accidents. During the last ten years, two interesting explanations have been proposed. One suggests that these accidents are the consequence of the feedback effect of the convection induced by the fire (Viegas, 2005). Another explanation suggests that fire acceleration is caused by flow attachment in the direction of the fire propagation (Dold and Zinoviev, 2009). We suggested in previous works (Courty *et al*. 2012; Chetehouna *et al*. 2014) a possible explanation for these accidents, named thermochemical hypothesis to explain accelerating forest fires. This hypothesis is based on the fact that Biogenic Volatile Organic Compounds (BVOCs) emitted by heated vegetation could accumulate near the ground to form with air a flammable mixture. AFF would therefore be the consequence of the ignition of such gas clouds. We identified in previous works the BVOCs emitted by different vegetal species and determined combustion characteristics of these BVOCs by measuring their laminar burning speeds, Markstein lengths and flame thicknesses (Courty *et al*. 2012; Chetehouna *et al*. 2013). We worked with vegetal species typical of the Mediterranean climate, often involved in

forest fires. This work aims at presenting some experimental studies that we performed in order to show that the ignition of BVOCs accumulated in a canyon can be plausible. The thermochemical approach to explain accelerating forest fires is a controversial topic in the wildland fire safety scientific community. This work does not prove neither that this hypothesis has been validated nor that this is the only explanation for AFF, it only brings arguments for future discussions and for a possible validation of the thermochemical approach.

Methods

BVOCs diffusion direction

The main issue we want to solve concerning accelerating forest fires thermochemical approach is to know if BVOCs can accumulate at terrain scale in sufficient concentration to form with air a flammable mixture. One of the necessary conditions to form this flammable mixture is that emitted gases diffuse in the direction of the ground and do not dissipate in the air. Indeed, if BVOCs diffuse in the direction of the ground, it is possible that in canyons the low value of lower flammability limit (1% vol. in air) of BVOCs/air mixtures is reached. We have shown in previous works (Courty, 2012; Courty *et al*. 2012; Chetehouna *et al*. 2014 among others) that the amount of gases emitted is very dependant of temperature and is increasing with the increase of temperature. It is therefore important to prove that the BVOCs diffuse in the direction of the grown, even if they are hot.

To prove it, we used an experimental setup that consisted in a cubic hermetic enclosure made of cellular concrete (Siporex). Its volume is around one cubic meter and it is equipped with a radiant panel simulating an ongoing fire front. It is also equipped with two electrodes providing the ignition energy. The radiant panel is made of sixteen black ceramic plates, each of them providing a maximal thermal power of 1200 W. The maximal power per unit area provided by the panel is around 83000 $W.m^{-2}$. Let us notice that this hermetic enclosure is the same used by Chetehouna *et al*. (2009) to study the gaseous emissions of *Rosmarinus officinalis* vegetal species at plant scale.

Different amounts of different BVOCs (99 % pure from Sigma Aldrich) initially liquid, are placed in a cup inside the enclosure, 50 cm from the radiant panel and at the centre of the enclosure. Different tests are done, the cup being placed above or below the ignition source (i.e. the electrodes). The distance cup-electrodes and the amounts of BVOCs are varied. Figure 1 presents a schematic overview of the experimental setup. Five BVOCs are studied, they correspond to the major component emitted by each of the species studied in Courty (2012): α-pinene, limonene, *p*-cymène, 3-hexen-1-ol and l-fenchone.

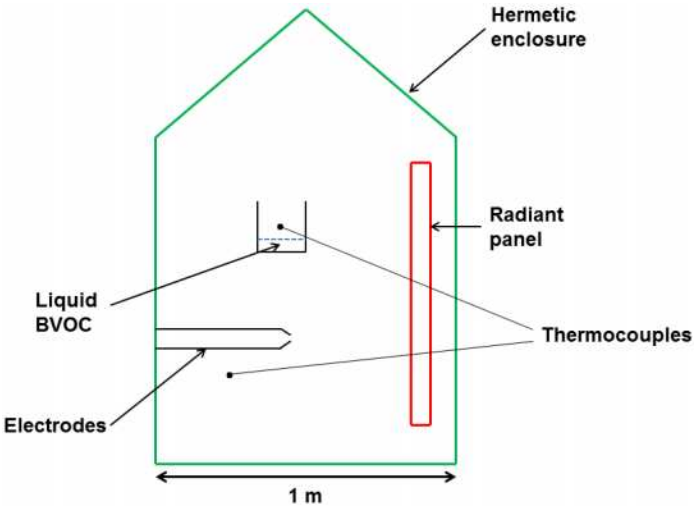

Figure 1. Schematic overview of the experimental setup showing the diffusion direction of BVOC.

BVOCs ignition

This subsection aims at proving with very simple experiments that gas mixtures emitted by vegetal species can ignite. To do so, we just used some heated needles of *Rosmarinus officinalis*. The setup consists in a necked flask of 500 mL heated with a heating mantle. Around 50 g of needles of *Rosmarinus officinalis* vegetal species are placed inside the flask and heated up to a temperature around 443 K. Temperature is measured thanks to a thermocouple placed in the needles bed. Emitted gases are collected in a beaker thanks to a transfer hose connected to the necked flask. Beaker is then placed next to a pilot flame, a candle is used. This setup is illustrated by a schematic overview in Figure 2.

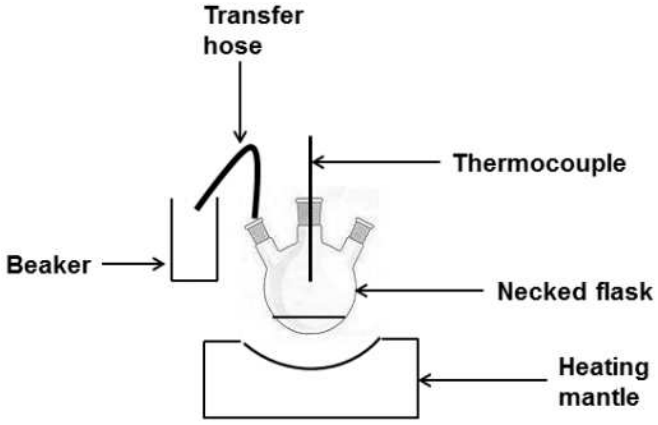

Figure 2. Schematic overview of the experimental setup used to study the ignition of BVOCs.

Results

BVOCs diffusion direction

Two thermocouples, one next to the electrodes and the other in the liquid, are used to study temperature as a function of time. Clearest results are obtained with 7 mL of BVOCs and results will be presented with this amount of BVOCS. Liquid samples are introduced at ambient temperature and spark is ignited at the temperature of maximal emissions. This temperature depends on the BVOCs and is around 443 K (Courty *et al.*, 2014). Ignition is observed or not thanks to the window situated on right side of the enclosure.

We observed that when the spark is situated below the cup, we managed to ignite up to a distance of 40 cm between the electrodes and the cup. On the contrary, when the spark is situated above the cup, no ignition occured for distances electrodes-cup higher than 14.5 cm. This clearly shows that the direction of the VOCs diffusion is downward (even if a small amount is diffusing upward). These results are valid for the 5 studied BVOCs and similar conclusions are obtained with different amounts of BVOCs placed initially in the cup.

A high speed digital camera Photron Fastcam APX RS operating at 2000 images/second has been used to illustrate this phenomenon. Figure 3 illustrates the ignition of α-pinene placed in a cup 3 cm above the electrodes. It is clear reading Figure 3 that the α-pinene vapours are diffusing downward.

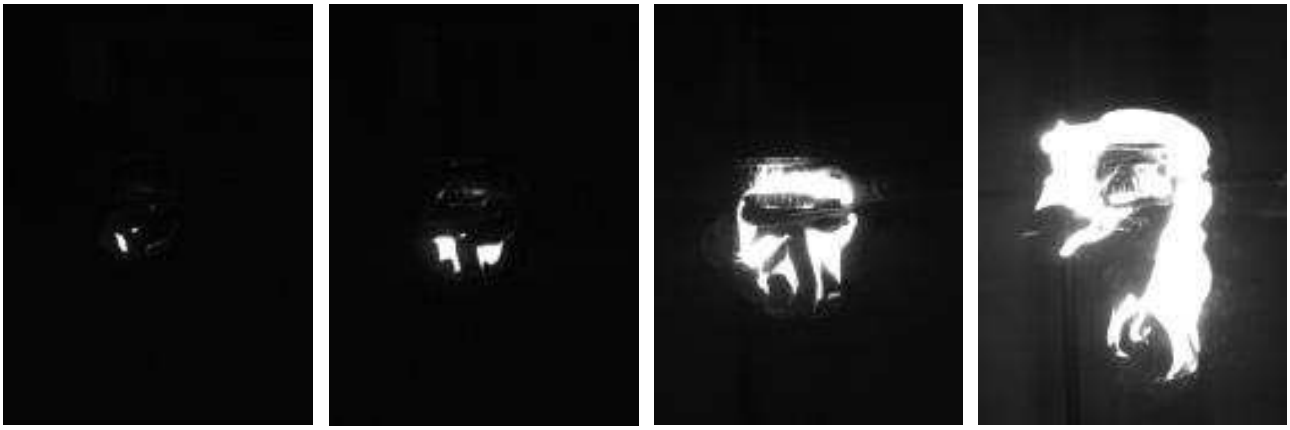

Figure 3. Ignition of α-pinene in the heated hermetic enclosure.

Other experiments have been performed in the same enclosure, with the electrodes placed in a box situated below the cup (filled with α-pinene). In this configuration, emitted gases are concentrated in a box and it is interesting to observe the differences with the previous configuration (without concentrating gases). Electrodes are placed at the center of the box. A color high speed digital camera Phantom V310 operating at 400 images per second is used to follow the flame propagation. Example of flame propagation is presented in Figure 4. This phenomenon was very rapid and not very luminous; this is the reason why we had to use a color high speed camera. Spherical propagation and blue color are characteristics of premixed flames: we actually created a premix α-pinene/air by diffusion of α-pinene in air.

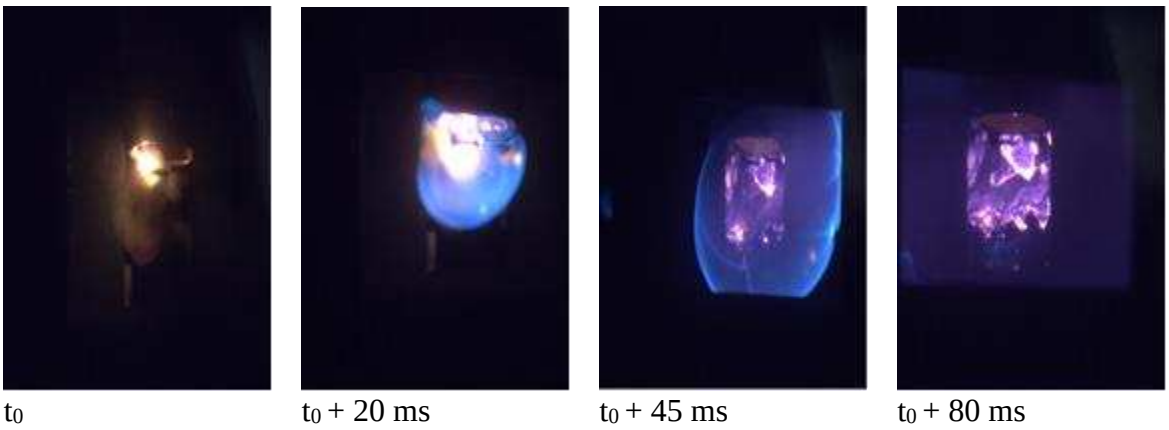

Figure 4. Ignition of α-pinene vapours concentrated in a box.

We have therefore shown that BVOCs are diffusing in the direction of the ground and for this reason they can accumulate at the bottom of a canyon. We have also shown that liquid BVOCs when heated can create with air a flammable mixture. It is now interesting to see if it possible to ignite directly BVOCs mixture emitted by a vegetal species.

3.2. BVOCs ignition

One of the necks of the flask is let open at the beginning of the heating in order to let water vapor going out of the flask. From 393 K, this neck is closed and the gases are transferred in the line that

leads to the beaker. An ignition occurs when the beaker is placed next to a candle. This is illustrated in Figure 5.

Emitted gases are concentrated inside a beaker and of course diffusion effects that can be observed at canyon scale are not taken into account with this very simple experiment. Nevertheless, we can see that heated needles can emit enough BVOCs to create an ignition.

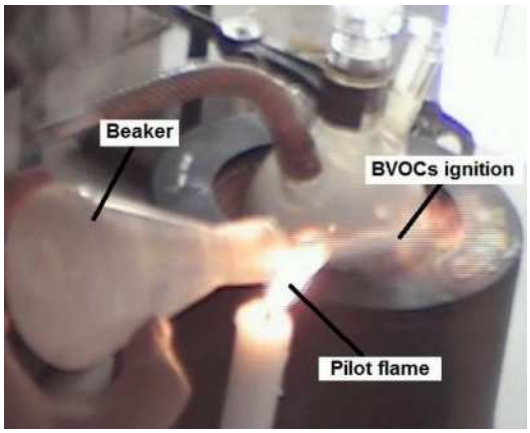

Figure 5. Picture of the ignition of BVOCs emitted by heated Rosmarinus officinalis needles.

Conclusion

Very simple experiments were performed in this study in order to give validation elements to the thermochemical explanation for accelerating forest fires. This hypothesis is based on the fact that almost all vegetal species involved in forest fires emit BVOCs that can form with air a flammable premix. The acceleration of the fire rate of spread could therefore be the consequence of the transition between a diffusion flame characteristic of forest fires and a premixed flame. We have shown in this work that gases emitted by vegetation are diffused mainly in the direction of the ground and that BVOCs mixture emitted by *Rosmarinus officinalis* needles can be ignited with a pilot flame. It will be of course necessary to validate the thermochemical hypothesis for accelerating forest fires to prove that BVOCs are emitted in concentration sufficient to create with air a flammable mixture, this will be investigated in a future work. Up to now, we just proved that this hypothesis can be possible.

References

Arnold K, Buck CC (1954) Blowup fire-silvicultural or weather problems?. *Journal of Forestry* **56**, 408-411.

Chetehouna K, Barboni T, Zarguili I, Leoni E, Simeoni A, Fernandez-Pello C (2009) Investigation on the emission of Volatile Organic Compounds from heated vegetation and their potential to cause an eruptive forest fire. *Combustion Science and Technology* **18**, 1273- 1288.

Chetehouna K, Courty L, Garo JP, Viegas DX, Fernandez-Pello C (2014) Flammability limits of biogenic volatile organic compounds emitted by fire-heated vegetation (Rosmarinus officinalis) and their potential link with accelerating forest fires in canyons: A Froude-scaling approach. *Journal of Fire Sciences* **32**, 316-327.

Chetehouna K, Courty L, Mounaïm-Rousselle C, Halter F, Garo JP (2013) Combustion characteristics of p-cymene possibly involved in accelerating forest fires. *Combustion Science and Technology* **185**, 1295-1305.

Courty L (2012) Etude de l'émission et des propriétés de combustion des composés organiques volatils potentiellement impliqués dans les feux de forêts accélérés, PhD Thesis (in French), Ecole Nationale Supérieure de Mécanique et d'Aérotechnique.

Courty L, Chetehouna K, Halter F, Foucher F, Garo JP, Mounaïm-Rousselle C (2012) Experimental determination of emission and laminar burning speeds of α-pinene. *Combustion and Flame* **159**, 1385-1392.

Courty L, Chetehouna K, Lemée L, Fernandez-Pello C, Garo JP (2014) Biogenic volatile organic compounds emissions at high temperatures of common plants from Mediterranean regions affected by forest fires. *Journal of Fire Sciences*, Accepted (DOI: 10.1177/0734904114536128).

Dold J, Zinoviev A (2009) Fire eruption through intensity and spread rate interaction mediated by flow attachment. *Combustion Theory and Modeling* **13**, 763-793.

Dold J, Simeoni A, Zinoviev A, Weber R (2009) The Palasca fire, September 2000: Eruption or Flashover?. *Recent forest fire accidents in Europe*, Viegas (ed.).

Rothermel RC (1993) Mann Gulch fire: a race that couldn't be won. *General Technical Report INT-299*, U.S. Department of Agriculture, Forest Service, Intermountain Research Station, Ogden, USA.

Viegas DX (2005) A mathematical model for forest fires blowup. *Combustion Science and Technology* **177**, 1-25.

Experimental study on fire behaviour and soil combustion in the high altitude tropical grasslands

Elsa Pastor[a], I. Oliveras[b,c], E. Planas[a], M.I. Manta[d], E. Urquiaga[e], J.A. Quintano[e]

[a] *Department of Chemical Engineering, Centre for Technological Risk Studies, Universitat Politècnica de Catalunya–BarcelonaTech, Diagonal 647, E-08028 Barcelona, Catalonia, Spain. elsa.pastor@upc.edu, eulalia.planas@upc.edu*
[b] *Environmental Change Institute, School of Geography and the Environment, University of Oxford, South Parks Road OX13QY Oxford, UK. imma.oliveras@ouce.ox.ac.uk*
[c] *Nature Conservation and Plant Ecology Group, Wageningen University, Building 100, Droevendaalsesteg 3ª, 6708PB Wageningen, Netherlands.*
[d] *Department of Forest Management, Universidad Nacional Agraria La Molina, Av. de la universidad s/n. Apartado 12-056. Lima 12, Perú. mmanta@lamolina.edu.pe*
[e] *Departamento de Botánica, Universidad de San Antonio Abad del Cusco, Av. Cultura 733, Cusco, Perú. eurquiaga@gmail.com, biojoanqlcp@gmail.com*

Abstract

Tropical mountain cloud forests (TMCFs) are becoming new fire-prone areas in the Neotropics due to ongoing climate change. TMCFs are increasingly suffering from drought episodes during which fires starting at the puna grasslands that occur immediately above the forest, tend to penetrate into the TMCFs causing irreversible damage. Moreover, when the fire reaches the puna-forest treeline it frequently exhibits smouldering propagation consuming the humic soil layer resulting in large carbon emissions.

This paper presents an experimental program set up to study critical conditions that favour fire spread in the puna-TMCFs interface. The objective is twofold: to provide understanding of the threshold environment and fuel conditions allowing sustainable back-fire propagation in puna grasslands when advancing towards the TMCFs and to investigate the onset of smouldering combustion of the humic layers of the puna soil near the TMCFs treeline.

The study area was located at tropical Andean puna grasslands at the Cusco region (Southern Peru, bordering Manu National Park). It involved two different locations, one for the ground fire experiments and the other for the grassfire sustainability and behaviour tests. The first site comprised 20 paired ground plots (0.5 m x 0.5 m) which were ignited by a purpose-standardized ignition procedure and monitored by thermocouples during 48 h. The second site was divided in 12 grassland plots (20 m x 5 m) of two different fuel ages. Each grassfire was recorded with video and infrared cameras and witnessed by ground observers to detect fine scale changes in fire activity due to fuel and wind variability. Environmental conditions were constantly monitored in both type of experiments.

The ground tests provide novel information about smouldering fires in a real environment, going beyond classic laboratory experimentation. Soil temperatures higher than 100ºC were observed to last for around 20 hours with maximum temperatures around 450 ºC. The surface fires experiments revealed dead fuel load and fuel moisture content thresholds (0.2 kg m^{-2} and 20% respectively) that would explain back-fire sustainability, reaching those go-fires pseudo-stationary rates of spread of around 0.4-0.6 m min^{-1}.

These results will allow a more accurate estimation of the magnitude of the fire impact into the TMCFs ecosystems and help envisaging primary fire management policies and recommendations for the correct use of fire by the Andean indigenous communities.

Keywords*: grass fires, smouldering combustion, Peruvian Andes, fire sustainability, infrared imagery.*

Introduction

Fires are one of the largest disturbances in the Neotropics leading to severe environmental impacts in terms of carbon and biodiversity losses. One of the most threatened ecosystems in this ecozone are the tropical mountain cloud forests (TMCF), that albeit they only represent about 2.5% of all tropical forests (Bubb, 2004) they harbour the highest levels of biodiversity of the world (Myers, Mittermeier, Mittermeier, da Fonseca, & Kent, 2000).

TMCFs are mountain forests frequently covered by clouds or mist, and are usually found at altitudes between 1,500 m and 3,300 m a.s.l. (Stadmüller, 1987). Immediately above the forest, high altitude "puna" grasses are found. These grasslands have been populated for millennia by indigenous communities among which the use of fire has been a common practice for agricultural and grazing purposes as well as for supporting cultural and religious beliefs (Sarmiento & Frolich, 2002). Despite their high moisture levels, TMCFs are increasingly suffering from drought episodes due to climate change (Román-Cuesta *et al*., 2011) during which anthropogenic fires starting at the puna grasslands tend to penetrate into the TMCFs causing irreversible changes to the forests structure and composition and pushing the forest-puna treeline downslope (Oliveras, Anderson, & Malhi, 2014). Regardless of the erratic behaviour of fire in complex environments in terms of topography, fuel and wind dynamics, when a fire starts and a self-sustained flame front is formed in the puna grasslands, it usually exhibits backwards downslope flame propagation with high ratios of fuel consumption. Furthermore, under certain conditions, it can also involve smouldering propagation within the humic soil layer. Both the TMCFs and the high-altitude grasslands store large quantities of carbon. Recent studies have quantified the storage at the TMCF humic organic soil layer of 100 Mg C·ha^{-1} and 280 Mg C·ha^{-1} in the first 30 cm of the puna soil in the South-Eastern Peruvian Andes (Gibbon *et al*., 2010; Zimmermann *et al*., 2009), becoming then carbon losses through smouldering fires, a potentially substantial CO_2 emission source.

Notwithstanding the importance of fire activity in the tropical Andes, biomass burning dynamics are still poorly understood (Oliveras *et al*., 2014). Firstly, little is known about the onset environmental conditions for a self-sustained flame propagation in the high-altitude grasslands. Backing fire propagation is hardly affected by wind speed but mostly influenced by fuel moisture and fuel continuity (Cheney & Sullivan, 2008). This is particularly noteworthy in puna grasses, which are organized in discrete clumps favouring discontinuous fire behaviour. Likewise, the puna-tree line exhibits complex water dynamics among fuel and soil moisture and air relative humidity due to persistent ground-level clouds, which may result in an increased catchment water yield compared to other types of fuel (Wård, 2007). Secondly, the knowledge of the critical conditions that determine smouldering fire spread in the humic layers of the puna-tree line is very scarce. Moisture content of the carbon-rich humic layer is a key factor in controlling ignition and the subsequent spread of a smouldering front. Research in lowland rainforests has suggested a moisture content of 65% as a critical threshold for fire ignition and spread (Cochrane, 2003) but high elevation humic layers may have very different flammability characteristics, both because of the nature of the fuel and the low ambient atmospheric pressure and absolute oxygen concentration (Planas *et al*., 2013).

This paper presents an experimental burning program set up to advance our understanding of the critical conditions that favour fire spread in the puna-TMCFs interface. The program was performed at the south-eastern Peruvian Andes during July 2012 (mid dry season) and its objective was twofold: *i)* to investigate the threshold environment and fuel conditions allowing sustainable backing fire propagation in puna grasslands when advancing towards the TMCFs; and *ii)* to study the onset of smouldering combustion of the humic layers of the puna soil near the TMCFs treeline. The main highlights of these experiments are presented and preliminary results are summarized and briefly discussed.

Materials and methods

Experimental sites

The study area was located at tropical Andean puna grasslands at the Cusco region (Southern Peru, bordering Manu National Park). It involved two different locations, one for the ground fire experiments (13°10'50.28''S, 71°35'19.95''W) and the other for the grassfire sustainability and behaviour tests (13º9'4.26''S, 71º38'25.19''W) (**Erro! A origem da referência não foi encontrada.**1). This region experiences a tropical rainforest climate. Average annual rainfall ranges from 1,900 to 2,500 mm, with a wet season spanning from October to April. Mean annual temperature is approximately 11°C at 3,600 m a.s.l. (Gibbon *et al*., 2010). Both sites were covered by typical puna vegetation type, dominated mainly by tussock-forming grasses (*Calamagrostis longearistata, Ageratina sternbergiana, Juncus bufonius, and Scirpus rigidus* (Oliveras *et al*., submitted) with soils typically composed of an organic-rich A-layer, stony B/C-layers, and no Oh-layer (Gibbon *et al*., 2010; Zimmermann *et al*., 2009).

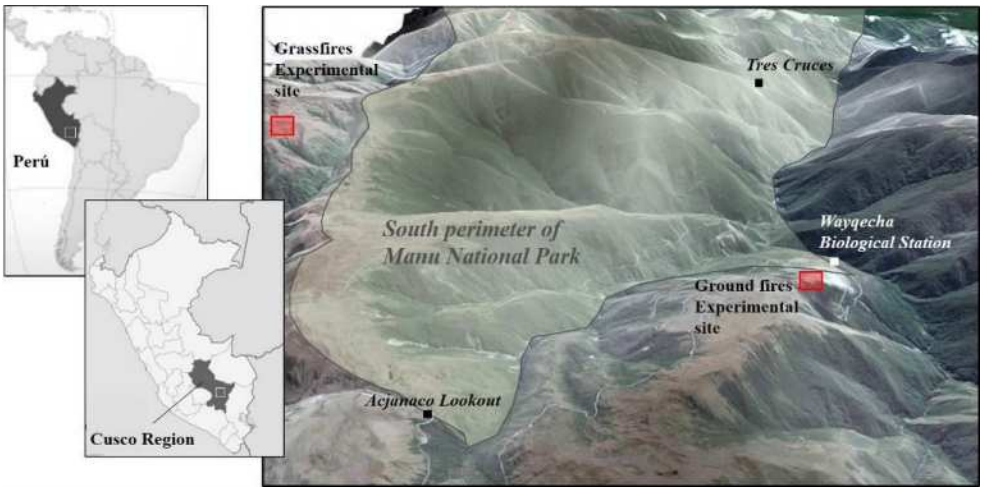

Figure 1. Study area

Ground fire test experimental design

An experimental program of smouldering fires was designed and performed in-situ. To the best of our knowledge, field burns experimentation for studying ground fires is a completely novel approach, far beyond the controlled conditions of laboratories set-ups (e.g. (Frandsen, 1998; Rein, Cleaver, Ashton, & Pironi, 2008)) where the soil usually losses its natural compactness and state. A randomized block of 20 plots (0.5 m x 0.5 m) was designed and replicated once. Five plots in every block were randomly selected as control plots (to be left unburned). Metal plates inserted 0.5 m deep bound all the plots (excepting the control ones), in order to avoid propagation outside the plots. The planning consisted on burning 6 plots at the same time (3 at every block) having then 5 sets available for five burning days. Due to meteorological constraints, only 3 sets were tested (Table 1, **Erro! A origem da referência não foi encontrada.**Figure 2).

Table 1. Random distribution of paired plots burned at each burning day (control plots in brackets)

Date of tests start	Plots in Block W1	Plots in Block W2
Day 1	A1, B2, D1 (CP4)	B1, C1, C2 (CP4)
Day 2	A4, B4, B5 (CP1)	B4, D4, C5 (CP1)
Day 3	B1, D3, D5 (CP2)	A1, A3, A5 (CP2)

An ad-hoc ignition procedure was implemented, which consisted on introducing glowing charcoal in a 30 cm x 10 cm x 20 cm deep dug hole at one of the sides of the plot. An educated guess of the power supply of the ignition source was done according to data available on charcoal heat of combustion and burning rate (Shafizadeh, 1978)(Andreatta, personal communication). 98% of the charcoal energy was assumed to be released within the first 6 hours and a mean heat transfer rate per unit area of 8,4 $kW \cdot m^{-2}$ was found, being only during the first two hours above the minimum necessary for the propagation of a smouldering front, suggested at 10 $kW \cdot m^{-2}$ (Ohlemiller, 2002).Weather data (ambient temperature, relative humidity and wind speed and direction) was measured by a portable weather station placed between the two experimental blocks. Soil moisture content was read at 12 cm and 20 cm deep before ignition at the control plot using a Hydrosense Soil Water Measurement System (Campbell Scientific, Inc.). Grass was clipped at the experimental plots before ignition and some soil samples were extracted from the control plots and sent to the laboratory in order to obtain inorganic content and bulk density. An array of K-type metal-sheathed thermocouples of 0.5-mm diameter, 30-cm length was used to monitor soil temperatures at two deferent depths (5 cm and 15 cm) during the tests, following Figure 3 distribution scheme. This layout was designed in order to both detect ignition (by observing the thermocouple evolution placed 5 cm apart from the ignition source) and pick any possible heat front propagation main direction (by observing the evolution of the rest of the sensors). The plots were left 48h untouched letting the data loggers (HOBO Onset Computer Corp.) connected to the thermocouples register temperatures at a frequency of one datum per minute.

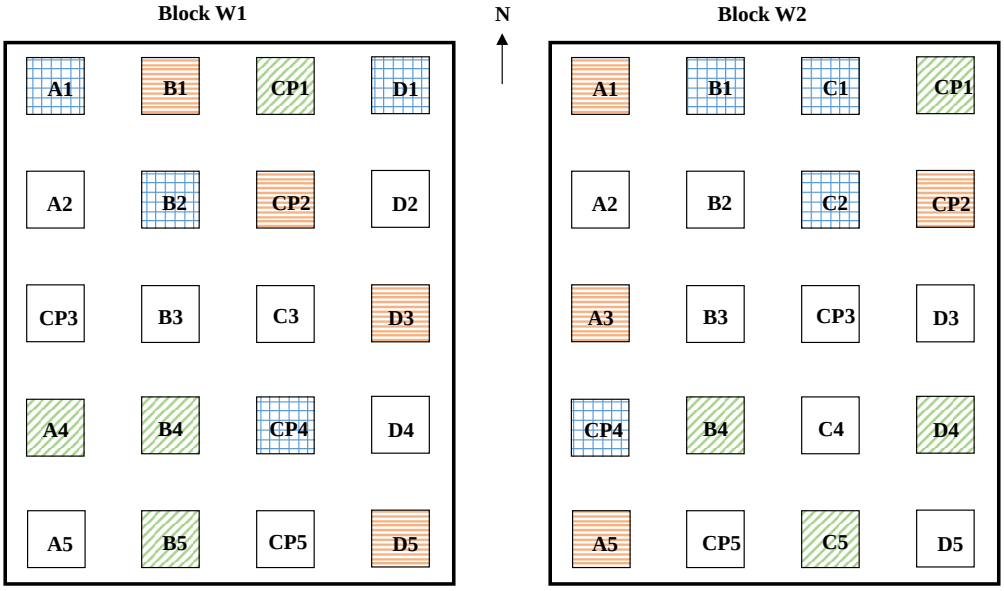

Figure 2. Plots layout at blocks W1 and W2 for ground fire experiments

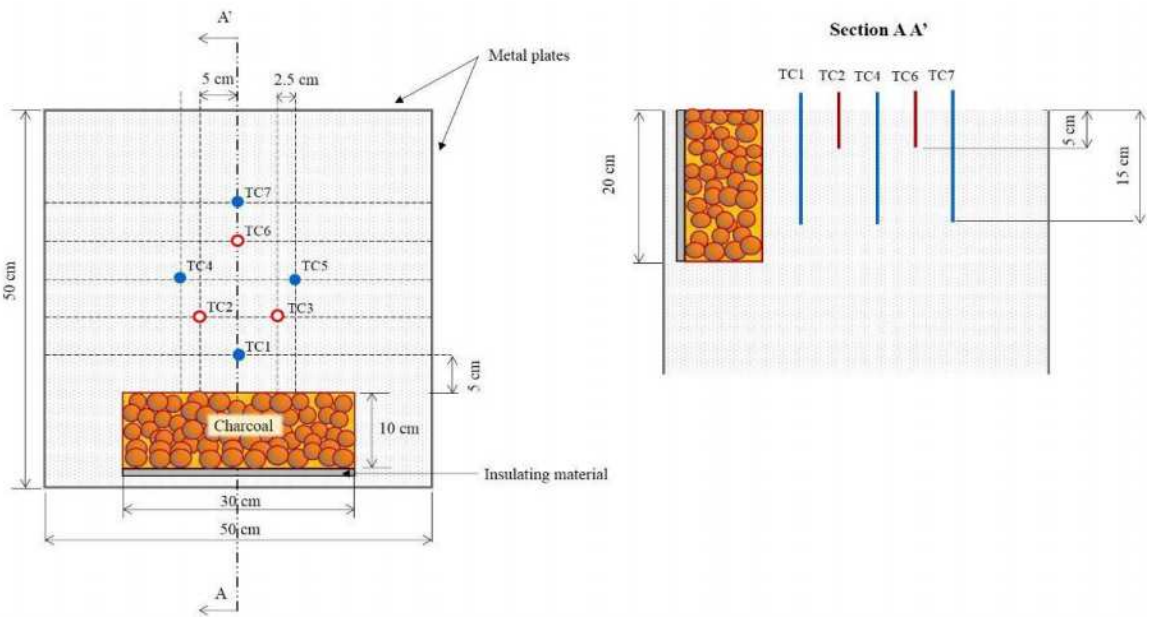

Figure 3. Thermocouples distribution used for monitoring plots temperature

Grassfire sustainability and behaviour tests experimental design

Concerning the experimental grassfires program, it covered thirteen backing fires designed to study the effect of the different weather and fuel variables in grassfire sustainability and behaviour. We stablished two 20 m width by 30 m length plots in a 40º slope spot, one in 3-year old grassland (named P3) and the other in a 7-year old grass (named P7). Six experimental fires were planned in each plot, leaving 5 m for the fire to spread downslope. Every test was ignited with drip-torches along the leeward side of the plot. If the flame front failed to propagate, i.e. exhibited a discontinuous perimeter that tent to self-extinguish, the fire was considered a no-go, and a subsequent ignition was planned for when a significant change of meteorological conditions was observed. If the fire propagated, we would monitor its behaviour until the fire advanced 5 m and proceed to suppress it immediately afterwards using hand firefighting tools.

For planning purposes prior to the experiments, weather records (June-July 2011) from a local station located at 1.5 km from the site (Pumataki weather station) were obtained to analyse rainfall probabilities and to study relative humidity daily variation. Before the experiments, we characterized fuel loads, cover, height and degree of curing, involving a variety of sampling methods (i.e. destructive sampling and point intersect method following a systematic sampling grid within each experimental plot). During burning days, fire weather was monitored every 30 seconds, using a portable weather station located in the vicinity of the experimental plot. Fuel moisture was obtained in-situ before each burn by using an infrared-heated moisture analyser (Sartorius MA-45). Fire direct observation alongside the flame front was performed in order to have fire behaviour information. Two groups of fire observers at each plot would record flame front position, flame length and flame angle at time intervals between 30-60 seconds.

3. Preliminary results and discussion

3.1. Ground fire tests results

Ignitions were performed in eighteen plots in three days (7th, 10th and 11th July 2012) between 10:30h and 14:30h. Ambient conditions followed a similar trend at night time, with stable temperature (around 8ºC), relative humidity (above 90%) and wind speed (below 2 km·h^{-1}) for the whole experimental period. During the day, and particular at noon (from 11h to 14h), weather variables had more

fluctuations. Table 2 shows the experimental range of these environmental parameters coupling the three experimental days, together with soil properties and moisture content values at two different depths.

Table 2. Environmental parameters associated with the ground fire tests

Variable	Measures
Mean midday temperature (ºC)	10.7 – 18.3
Mean midday windspeed ($km \cdot h^{-1}$)	3.4 – 7.8
Mean midday relative humidity (%)	37.7 – 95.9
Soil moisture content at 12 cm (SMC, d.b. %)	90.89 – 130.76
Soil moisture content at 20 cm (SMC, d.b. %)	83.29 – 122.96
Soil inorganic content (IC, %)	18
Soil bulk density (BD, $kg \cdot m^{-3}$)	830

d.b.: dry basis

Ground fire ignition is known to be controlled by soil bulk density, inorganic content and soil moisture content (Frandsen, 1997). The two first parameters were considered constants in all our study area (i.e. no differences per plot) whereas we assumed that soil moisture content could had a variation during burning days responding to meteorological changes at least at the first centimetres of soil depth. Statistical analysis was performed in order to peak possible characteristic soil moisture values per day or plot (data not shown). Significant differences were observed in soil moisture content at the two different depths but this parameter did not show any statistical significant dependence between days or blocks. This result led us to perform an aggregated analysis considering all the tests (18 in total).
For all the experimental plots, we only registered noteworthy temperature response (>60ºC) at some thermocouples named as TC1 (5 cm apart from the ignition source, 15 cm depth) and at some TC2 and TC3 (both 10 cm apart from the ignition source, 5 cm depth). Table 3 summarizes the main findings obtained after processing temperature vs time evolution curves of all the active thermocouples used in our two blocks. In 67% of the cases, at least TC1 showed some significant temperature increase, achieving values above 60ºC, which is roughly the mean value corresponding to protein degradation and at which water loss starts (Cerda & Robichaud, 2009; Swezy & Agee, 1991). The time needed for these thermocouples to reach this threshold oscillated from 8h to 16h after ignition depending on the plot, which is well after the time needed for almost complete (98%) charcoal consumption. Slightly less than half of these thermocouples reached 80 ºC (threshold for many soil microbes death, (Cerda & Robichaud, 2009), with only 3 from 18 sensors peaking values above 100ºC at which water vaporizes and carbon volatizes (Swezy & Agee, 1991). We had only one case from 18 tests, at which typical ground fire front temperatures were registered (Rein *et al*., 2008), with a peak temperature above 400 ºC. Concerning TC2 and TC3 readings, temperatures above 60ºC were achieved in 3 cases and only in one of these, peak temperature reached 80ºC.
These results show that under our experimental conditions, there are only 6% chances for a weak ground fire ignition (i.e. a ground fire that may propagate less than 10 cm from the ignition point tending to self-extinguish). Furthermore, there are 17% chances for the formation of a heat front of around 60ºC which may travel less than 15 cm and finally, 6% chances that the same front may reach the temperature needed for killing most of the microbes present at the soil.

Table 3. Temperature response occurrence of the ground fire experiments.

Peak Temperature	Number of tests	Occurrence
TC1 at T > 60 ºC	12/18	67%
TC1 at T > 80 ºC	5/18	28%
TC1 at T > 100 ºC	3/18	17%
TC1 at T > 400 ºC	1/18	6%
TC2/TC3 at T > 60 ºC	3/18	17%
TC2/TC3 at T > 80 ºC	1/18	6%

Temperature vs time profile of some selected TC1 thermocouples readings are plotted in Figure 4. TC1 of W1B1 plot is the one showing successful ignition. Soil at TC1 vicinity was 5 hours above 400 ºC, it reached a maximum temperature of 463ºC 15 hours after ignition, and it was more than 16 hours at temperatures exceeding 200°C (threshold for N volatilization (Raison, Woods, Jakobsen, & Bary, 1986)). Considering the instant of maximum temperature as the smouldering front characteristic arrival time, we can affirm that the mean spread rate of the ground fire was 3 $mm \cdot h^{-1}$. This value corresponds to a self-extinguishing ground fire front and is below the typical ranges for smouldering fronts of 10-30 $mm \cdot h^{-1}$ (Rein, 2009).
W2A3, W1D1 and W2D4 TC1 profiles show temperature evolution of failed ignition tests. However, it is worth mentioning some interesting patterns of these three sensors: TC1 in W1D1 had a clear drop around 12 hours after ignition which would correspond to the 100% consumption of the ignition source; W2A3 TC1 had one of the longest residence time (14 h) above 60ºC, surpassing in this case any ignition effect. Finally, W2D4 was more than 45 h above this latter threshold, exhibiting plateaus at 80ºC -100ºC corresponding to the evaporation of the moisture in the soil.

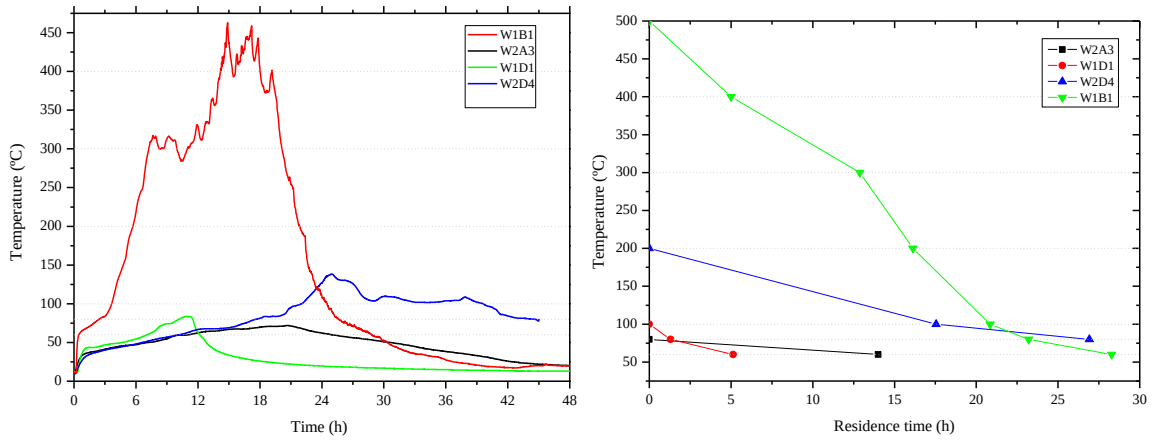

Figure 4. Left) Temperature evolution of four selected TC1 thermocouples; right) thermal severity registered by the same TC1 thermocouples

Grassfires results

The experimental program comprised a set of seven and six experimental fires in the 3-years-old puna and the 7-year-old puna, respectively performed during 4 burning days (July 5th, 6th, 9th and 10th 2012). Figure 5 shows the evolution of the relative humidity (RH) with time for the four days together with the exact time when the experiments were undertaken. Taking into account the expected unfavourable climatology of the area despite being at the dry season (70% of daily raining probabilities were registered during June-July 2011 by the Pumataki weather station), a RH range of around 50 points

could be picked during the four burning days, taking advantage of the daily fluctuation of this variable to perform several tests within the same day.

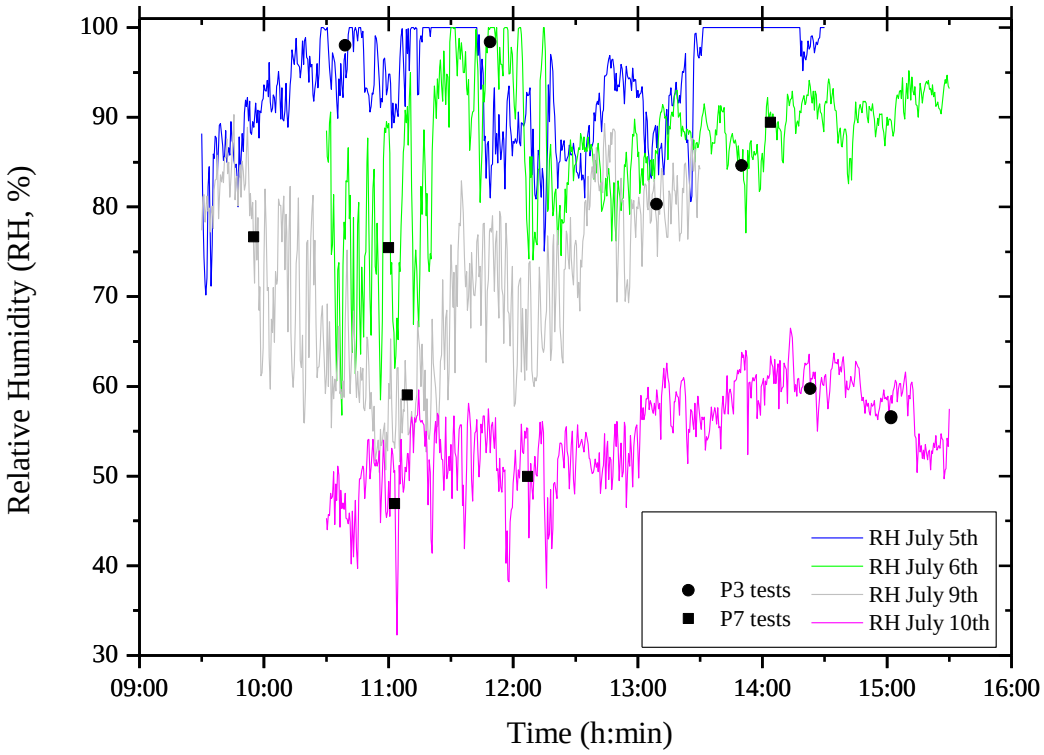

Figure 5. Relative humidity time evolution for the four burning days (5th, 6th, 9th, 10th July 2012)

Environmental parameters (i.e. fuel characteristics and fire weather) changed from one test to another. Table 4 provides the experimental range of these, partitioned by fuel type. Statistical differences between both types of fuels were explored for each variable. 3-year and 7-year old puna differed in terms of dead fuel load, degree of curing and fuel cover, whereas no statistically significant differences were found for FMC, respectively. Air temperature, RH and wind speed varied roughly within the same order of magnitude for both plots, being the latter reasonably well aligned with the slope (leeward side of the plots north/north-westerly oriented).

Table 4. Range in environmental parameters associated with the grassland fires

Group	Variable	3-year puna	7-year puna	Statistical test (p-value)
Fuel	Dead fuel load ($kg \cdot m^{-2}$)	0.2 – 0.5	0.8 – 1.4	Mann-Whitney (p< 0.005)
	Degree of curing (%)	70 – 76	78 – 87	ANOVA (p<0.005)
	Fuel cover (%)	47.5 – 80	75 – 99	ANOVA (p=0.005)
	Dead fuel moisture content, FMC (%)	8.2 – 30.6	7.2 – 23.3	ANOVA (p=0.651)
Fire weather	Air temperature (ºC)	7.8 – 10.6	7.8 – 11.7	ANOVA (p=0.163)
	Relative humidity (%)	57 – 98	47 – 89	ANOVA (p=0.131)
	2-m wind speed ($km \cdot h^{-1}$)	5.4 – 12.9	5.8 – 12.6	ANOVA (p=0.526)
	2-m wind direction (º)	98 – 107	80.8 – 98.1	ANOVA (p<0.005)

We counted 3 go-fires from 7 ignitions in 3-year old puna and 4 go-fires from 6 ignitions in the elder puna. We explored differences between parameters for go and no-go fires (analyzing both P3 and P7

tests together). Figure 6 suggests fire sustainability could be explained by means of dead fuel load and dead fuel moisture content. These results are in agreement with other fire sustainability studies (Cruz & Gould, 2010). Our preliminary results show there could be a FMC threshold between 17-23% which could avoid fire propagation in our experimental set as well as a dead fuel load threshold around 0.2 $kg \cdot m^{-2}$ below which there might be not available fuel for a sustained fire spread. This idea is supported by the fact that FMC differences between go and no-go fires were found to be statistically significant (ANOVA p=0.042). However, we could not find any statistical bases related to DFL, probably because P3 mean dead fuel load is already marginal for sustained fire spread and we do not have any test with DFL significantly lower than this in our dataset.

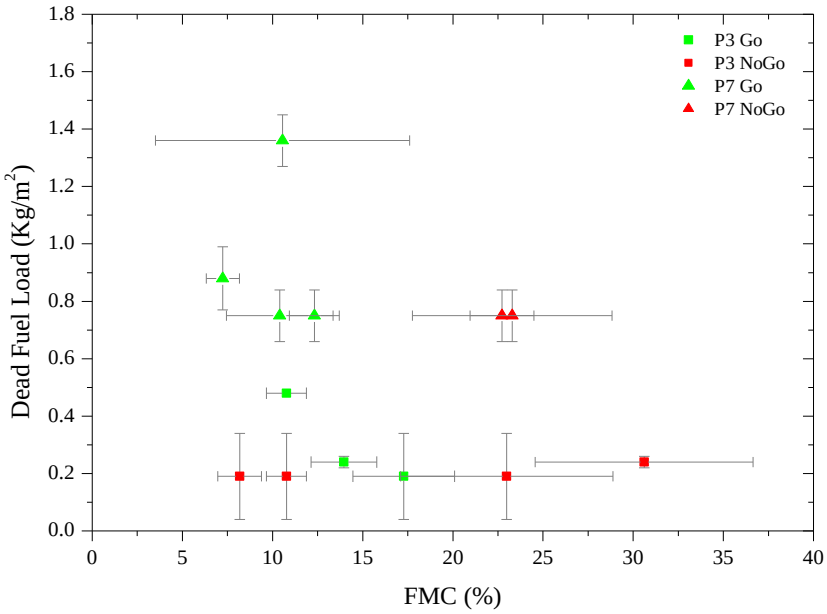

Figure 6. Go/no-Go matrix for P3 and P7 fires

Rate of spread was analysed for P3 and P7 self-sustained fires. There was a convergence to a pseudo-stationary rate of spread for all P3 (a) and all P7 (c) go-fires (Figure 7). Analysing ROS averages at 2-minutes intervals, it can be observed how steady state was achieved after 10 minutes in P3 fires with a mean stationary propagation of 0.37 m/min (s.d. 0.038), and after 8 minutes in P7 fires, at 0.56 m/min (s.d. 0.095). A 2-Sample t-test between all P3 ROS observations and all P7 ones, denoted dissimilarity between groups ($p<0.005$). This difference can be explained in terms of relative humidity (ANOVA p=0.02), curing degree (ANOVA p=0.013) and dead fuel load (ANOVA p=0.02). The latter result highlights the important role of the amount of available fuel on fire behaviour in this type of ecosystem.

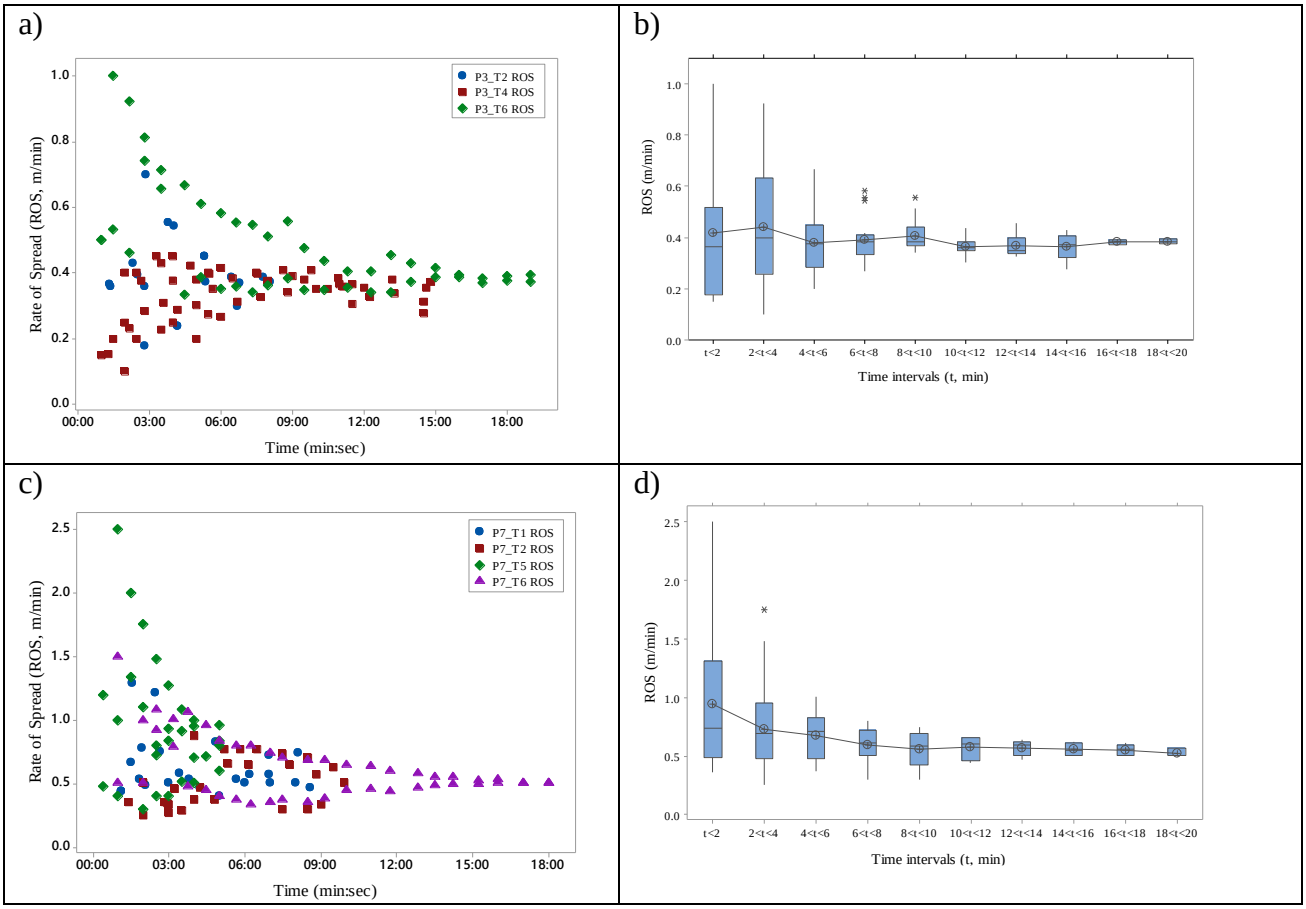

Figure 7. ROS evolution for P3 tests and P7 tests; left) Scatterplots of all fire observations sorted by tests at a) P3 and c) P7; right) evolution of 2-min interval mean ROS value for all b) P3 and d) P7 dataset.

Byram's fireline intensity, flame length of the leading edge and flame angle (defined as the inclination of the leading edge from the vertical) are presented in Table 5. According to these, experimental tests are in agreement with low intensity back-fire regime figures (Andrews, Heinsch, & Schelvan, 2011). The lowest mean fire intensity computed corresponds to test 6 of 3-year puna, and equals to 18.9 $kW \cdot m^{-1}$ (s.d. 4.5) which can be considered the threshold for backfire spread by flaming combustion in the study area. It is to be highlighted that this threshold almost doubles the headfire spread minimum intensity limit set at 10 $kW \cdot m^{-1}$ (Alexander, 2000) which reveals the existing differences between head and backfire propagation mechanisms.

Table 5. Mean values of fireline intensity and flame geometry characteristics

	Fireline Intensity ($kW \cdot m^{-1}$)	Flame angle (º)	Flame length (m)
P3	39.5 (s.d. 27.6)	45.8º (s.d. 12.9)	0.34 (s.d. 0.23)
P7	180.1 (s.d. 82.9)	46.0º (s.d.13.6)	0.94 (s.d. 0.57)

Concluding remarks

A twofold experimental program was performed to study critical conditions that favour fire spread in the puna-TMCFs interface, providing understanding of the threshold environment and fuel conditions allowing sustainable ground smouldering fires and back-propagation grassfires. These results will

allow a more accurate estimation of the magnitude of the fire impact into the TMCFs ecosystems and will help envisaging primary fire management policies.

A novel methodology for in-situ ground fire tests has been developed and found successful, being our experimental dataset the first of these characteristics, far beyond the controlled conditions of laboratories set-ups. Conditions tested have been found marginal for self-sustained propagation (SMC between 91-131%, IC 18% and BD 830 $kg \cdot m^{-3}$). However, in one particular case, a smouldering front has been observed advancing 5 cm in 15 h, with typical temperature ranges above 400ºC. In 67% of the tests, temperatures for biological molecules denaturation have been reached with residence times up to 14h but the water evaporation threshold has been only surpassed in 3 tests, which confirms that given the physical properties of the soil, moisture content has been the factor preventing self-sustained smouldering fires in our dataset. Despite the front propagation has been in all plots weaker than in many of the lab-scale tests reported in the literature, residence times found in our experimentation are substantially larger and not dependent on the ignition source used.

Sustainability of back fires at the puna grasses sitting above the TMCFs is a key aspect when studying fire occurrence and its environmental implications at the forest-puna treeline. A complete understanding of this phenomenon is needed for fire managing purposes, in particular for debriefing indigenous communities about the correct use of fire. Our grassfire behaviour and sustainability experiments have proved that fire sustainability at the Andean puna can be explained by key fuel parameters. Fuel moisture content has a preponderant role and dead fuel load appears to be also important. For dry season, we suggest initial thresholds of 20% and 0.2 $kg \cdot m^{-2}$, respectively, to be used in our study area. However, our dataset would have to be enlarged with more experimental campaigns to precise these figures. Due to the difficulty and cost of this type of experimentation, physical or quasi-physical simulation appears to be the most feasible alternative to burning campaigns. With a complete experimental design, a simulation-based probabilistic model for fire sustainability could be obtained, which should be of great help for management purposes in the zone of influence of our study area and in other Andean emerging fire-prone grasslands, provided the selected fire simulation tool is validated with the already available experimental dataset.

Steady state fire spread at puna of different ages has been achieved in the go-fires of our experimental campaign. Relative humidity, curing degree and dead fuel load are the key parameters that have major influence on the rate of spread in our experimental dataset. The limit for sustained back-fire spread has been found at around 20 $kW \cdot m^{-1}$. This is the minimum power needed for the flame front to overcome grass clumps discontinuities. Rate of spread, fireline intensity and flame dimensions have been accurately quantified for 3-year and 7-year puna grasses. These are the main variables arisen from the heat transfer processes between the fireline and the surrounding environment. This information can be of great help when evaluating different aspects of fire impact and the ecosystem response to it. In particular, this data with such a degree of accuracy shall be useful to improve carbon losses estimations.

Acknowledgements

This research was funded by the Spanish Ministerio de Economia y Competitividad under the project AGL2011-23425. The authors also thank the Autonomous Government of Catalonia for financial support (project No. 2009SGR1118). Support has also been received from Asociación para la Conservación de la Cuenca Amazónica (ACCA) and Parque Nacional del Manu-INRAENA.

References

Acem, Z., Lamorlette, A., Collin, A., & Boulet, P. (2009). Analytical determination and numerical computation of extinction coefficients for vegetation with given leaf distribution. *International Journal of Thermal Sciences, 48* , 1501–1509.

Alexander, M. E. (2000). *Fire behaviour as a factor in forest and rural fire suppression* (p. 30). Forest Research; Forest and Rural Fire Scientific and Technical Ser; Rotorua; Wellington. Forest Research Bulletin No. 197; in association with the National Rural Fire Author.

Amorim, J. H. (2011a). Numerical modelling of the aerial drop of firefighting agents by fixed-wing aircraft. Part I: model development. *International Journal of Wildland Fire*, *20*(3), 384–393.

Amorim, J. H. (2011b). Numerical modelling of the aerial drop of firefighting agents by fixed-wing aircraft. Part II: model validation. *International Journal of Wildland Fire*. doi:10.1071/WF09123

Amorim, J. H., Miranda, A. I., Valente, J., Borrego, C., Viegas, D. X., Pita, L. P., & Ribeiro, L. M. (2010). Effects of chemical retardants on air pollutants emissions: measurements in a combustion chamberNo Title. In D. X. Viegas (Ed.), *VI International Conference on Forest Fire Research (ICFFR)* (p. 267). Coimbra: University of Coimbra.

Andrews, P. L., Heinsch, F. A., & Schelvan, L. (2011). *How to generate and interpret fire characteristics charts for surface and crown fire behavior* (p. 48). Gerenal Technical Report RMRS-GTR-253.

Boulet, P. (n.d.). *Personal communication 26/02/2014*.

Boulet, P., Parent, G., Acem, Z., Collin, A., Försth, M., Bal, N., … Torero, J. (2014). Radiation emission from a heating coil or a halogen lamp on a semitransparent sample. *International Journal of Thermal Sciences*, *77*, 223–232.

Bubb, P. (2004). *Cloud forest agenda* (p. 36). Cambridge, UK.: UNEP-WCMC.

Carvalho, A., Flannigan, M. D., Logan, K. A., Gowman, L. M., Miranda, A. I., & Borrego, C. (2010). The impact of spatial resolution on area burned and fire occurrence projections in Portugal under climate change. *Climatic Change*, *98*, 177–197. doi:10.1007/s10584-009-9667-2

Carvalho, A., Flannigan, M. D., Logan, K., Miranda, A. I., & Borrego, C. (2008). Fire activity in Portugal and its relationship to weather and the Canadian Fire Weather Index System. *International Journal of Wildland Fire*. doi:10.1071/WF07014

Carvalho, A., Monteiro, A., Flannigan, M., Solman, S., Miranda, A. I., & Borrego, C. (2011). Forest fires in a changing climate and their impacts on air quality. *Atmospheric Environment*, *45*, 5545–5553. doi:10.1016/j.atmosenv.2011.05.010

Cerda, A., & Robichaud, P. R. (2009). *Fire Effects on Soils and Restoration Strategies* (p. 605). CRC Press.

Cheney, P., & Sullivan, A. (2008). *Grassfires: fuel, weather and fire behaviour*. (p. 150). CSIRO Publishing.

Cochrane, M. A. (2003). Fire science for rainforests. *Nature*, *421*(6926), 913–9. doi:10.1038/nature01437

Consalvi, J. L., Nmira, F., Fuentes, A., Mindykowski, P., & Porterie, B. (2011). Numerical study of piloted ignition of forest fuel layer. *Proceedings of the Combustion Institute*, *33* , 2641–2648.

Cruz, M. G., & Gould, J. S. (2010). Fuel and fire behaviour in semi-arid mallee-heath shrublands. In D. X. Viegas (Ed.), *6th International Forest Fire Research Conference*. Coimbra, Portugal: ADAI.

De Mestre, N. J., Catchpole, E. A., Anderson, D. H., & Rothermel, R. C. (1989). Uniform Propagation of a Planar Fire Front without Wind. *Combustion Science and Technology*, *65*(4-6), 231–244.

Frandsen, W. (1997). Ignition probability of organic soils. *Canadian Journal of Forest Research*, *27*(9), 1471–1477. doi:10.1139/x97-106

Frandsen, W. (1998). Heat Flow Measurements From Smoldering Porous Fuel. *International Journal of Wildland Fire*, *8*(3), 137. doi:10.1071/WF9980137

Fureby, C., Tabor, G., Weller, G., & Gosman, D. (1997). A comparative study of subgrid scale models in homogeneous isotropic turbulence. *Physics of Fluids*, *9(5)* , 1416–1429.

Gibbon, A., Silman, M. R., Malhi, Y., Fisher, J. B., Meir, P., Zimmermann, M., … Garcia, K. C. (2010). Ecosystem Carbon Storage Across the Grassland–Forest Transition in the High Andes of Manu National Park, Peru. *Ecosystems*, *13*(7), 1097–1111.

Grishin, A. M., & Albini, F. (1997). *A Mathematical Modelling of Forest Fires and New Methods of Fighting Them*. Publishing House of the Tomsk University, Tomsk, Russia .

Incropera, F. P., DeWitt, D. P., Bergman, T. L., & Lavine, A. S. (2007). *Fundamentals of Heat and Mass Transfer*. (F. P. Incropera & F. P. F. O. H. A. M. T. Incropera, Eds.)*Water* (Vol. 6th, p. 997). John Wiley & Sons. doi:10.1016/j.applthermaleng.2011.03.022

Jain, A. K. (2007). Global estimation of CO emissions using three sets of satellite data for burned area. *Atmospheric Environment*, *41*, 6931–6940. doi:10.1016/j.atmosenv.2006.10.021

Lamorlette, A., & Collin, A. (2012). Analytical quantification of convective heat transfer inside vegetal structures. *International Journal of Thermal Sciences*, *57* , 78–84.

Larini, M., Giroud, F., Porterie, B., & Loraud, J. C. (1998). A multiphase formulation for fire propagation in heterogeneous combustible media. *International Journal of Heat and Mass Transfer*, *41*(6-7), 881–897.

Lesieur, M. (2008). *Turbulence in fluids*. (R. MOREAU, Ed.) (fourth.). Springer.

Long, R., Torero, J., Quintiere, J., & Fernandez-Pello, A. (1999). Scale and transport considerations on piloted ignition of PMMA. In *Fire Safety Science - Proceedings of the sixth International Symposium* (pp. 567–578).

Marcos Chaos. (2014). Spectral Aspects of Bench-Scale Flammability Testing: Application to Hardwood Pyrolysis. In *Fire Safety Science-Draft Proceedings of the Eleventh International Symposium*.

Margerit, J., & Sero-Guillaume, O. (2002). Modelling forest fires. Part II: Reduction to two-dimensional models and simulation of propagation. *International Journal of Heat and Mass Transfer*, *45*, 1723–1737. doi:10.1016/S0017-9310(01)00249-6

Martins, V., Miranda, A. I., Carvalho, A., Schaap, M., Borrego, C., & Sá, E. (2012). Impact of forest fires on particulate matter and ozone levels during the 2003, 2004 and 2005 fire seasons in portugal. *Science of the Total Environment*, *414*, 53–62. doi:10.1016/j.scitotenv.2011.10.007

Mcallister, S., Grenfell, I., Hadlow, A., Jolly, W. M., Finney, M., & Cohen, J. (2012). Piloted ignition of live forest fuels. *Fire Safety Journal*, *51*, 133–142. doi:10.1016/j.firesaf.2012.04.001

Mell, W., Jenkins, M. A., Gould, J., & Cheney, P. (2007). A physics-based approach to modelling grassland fires. *International Journal of Wildland Fire*, *16*(1), 1–22.

Mell, W., Maranghides, A., McDermott, R., & Manzello, S. L. (2009). Numerical simulation and experiments of burning douglas fir trees. *Combustion and Flame*, *156* , 2023–2041.

Miranda, A. ., Sá, E., Martins, V., Borrego, C., & Sofiev, M. (2010). The Russian spring 2006 wildland fires effects on air quality over Europe. In D. X. Viegas (Ed.), *6th International Conference on Forest Fire Research* (p. 8). Coimbra: University of Coimbra.

Miranda, A. I. (2004). An integrated numerical system to estimate air quality effects of forest fires. *International Journal of Wildland Fire*, *13*, 217–226. doi:10.1071/WF02047

Miranda, A. I., Borrego, C., Martins, H., Martins, V., Jorge, H., Valente, J., & Carvalho, A. (2009). Earth Observation of Wildland Fires in Mediterranean Ecosystems. *Earth*, 171–187. doi:10.1007/978-3-642-01754-4

Miranda, A. I., Coutinho, M., & Borrego, C. (1994). Forest fire emissions in Portugal: A contribution to global warming? In *Environmental Pollution* (Vol. 83, pp. 121–123). doi:10.1016/0269-7491(94)90029-9

Miranda, A. I., Marchi, E., Ferretti, M., & Millán, M. (2009). Chapter 9 Forest Fires and Air Quality Issues in Southern Europe. In M. J. A. Andrzej Bytnerowicz Allen R. Riebau and Christian Andersen BT - Developments in Environmental Science (Ed.), *Wildland Fires and Air Pollution* (Vol. Volume 8, pp. 209–231). Elsevier. doi:http://dx.doi.org/10.1016/S1474-8177(08)00009-0

Miranda, A. I., Martins, V., Cascão, P., Amorim, J. H., Valente, J., Borrego, C., … Ottmar, R. (2012). Wildland smoke exposure values and exhaled breath indicators in firefighters. *Journal of Toxicology and Environmental Health. Part A*, *75*(13-15), 831–43. doi:10.1080/15287394.2012.690686

Miranda, A. I., Martins, V., Cascão, P., Amorim, J. H., Valente, J., Tavares, R., … Pita, L. P. (2010). Monitoring fire-fighters' smoke exposure and related health effects during Gestosa experimental fires (Vol. 137, pp. 83–94). doi:10.2495/FIVA100081

Miranda, AI, Ferreira, J, & Valente. (2005). Smoke measurements during Gestosa-2002 experimental field fires, *14*(1), 107–116. doi:10.1071/WF04069

Monod, B., Collin, A., Parent, G., & Boulet, P. (2009). Infrared radiative properties of vegetation involved in forest fires. *Fire Safety Journal*, *44* , 88–95.

Monteiro, A., Corti, P., San Miguel-Ayanz, J., Miranda, A. I., & Borrego, C. (2014). The EFFIS forest fire atmospheric emission model: Application to a major fire event in Portugal. *Atmospheric Environment*, *84*, 355–362. doi:10.1016/j.atmosenv.2013.11.059

Monteiro, A., Miranda, A. I., Borrego, C., Vautard, R., Ferreira, J., & Perez, A. T. (2007). Long-term assessment of particulate matter using CHIMERE model. *Atmospheric Environment*, *41*, 7726–7738.

Morvan, D., & Dupuy, J. L. (2001). Modelling of fire spread trough a forest fuel bed using a multiphase formulation. *Combustion and Flame*, *124* , 1981–1994.

Morvan, D., Dupuy, J. L., Rigolot, E., & Valette, J. C. (2006). FIRESTAR: a physically based model to study wildfire behaviour. *Forest Ecology and Management*, *234S* , S114.

Morvan, D., Mèradji, S., & Accary, G. (2009). Physical modelling of fire spread in Grasslands. *Fire Safety Journal*, *44*(1), 50–61.

Myers, N., Mittermeier, R. A., Mittermeier, C. G., da Fonseca, G. A., & Kent, J. (2000). Biodiversity hotspots for conservation priorities. *Nature*, *403*(6772), 853–8. doi:10.1038/35002501

Nepf, H. M., Sullivan, J. A., & Zavitoski, R. A. (1997). A model for diffusion within an emergent plant canopy. *Limnology and Oceanography*, *42(8)* , 85–95.

Ohlemiller, T. J. (2002). Smoldering Combustion. In P. J. DiNenno, D. Drysdale, C. L. Beyler, & W. D. Walton (Eds.), *SFPE Handbook of Fire Protection Engineering* (3rd ed., pp. 200–210). NFPA.

Oliveras, I., Anderson, L. O., & Malhi, Y. (2014). Application of remote sensing to understanding fire regimes and biomass burning emissions of the tropical Andes. *Global Biogeochemical Cycles*, *28*, 480–496. doi:10.1002/2013GB004664

Oliveras, I., C., D., Cahuana, N., C., E. A., W., H., & Malhi, Y. (n.d.). Andean grasslands are as productive as tropical montane cloud forests. *Environmental Research Letters*.

OpenFOAM User Guide, OpenFOAM The Open Source CFD Toolbox . (2010).

Ottmar, R. D., Miranda, A. I., & Sandberg, D. V. (2008). Chapter 3 Characterizing Sources of Emissions from Wildland Fires. *Developments in Environmental Science*. doi:10.1016/S1474-8177(08)00003-X

Ottmar, R. D., Sandberg, D. V, Riccardi, C. L., & Prichard, S. J. (2007). An overview of the Fuel Characteristic Classification System — Quantifying, classifying, and creating fuelbeds for resource planningThis article is one of a selection of papers published in the Special Forum on the Fuel Characteristic Classification Syste. *Canadian Journal of Forest Research*, *37*(12), 2383–2393. doi:10.1139/X07-077

Planas, E., Oliveras, I., Manta, M. I., Urquiaga, E., Quintano, J. A., & Pastor, E. (2013). Soil combustion experiments in the Andean grassland (puna) and tropical montane cloud forests (TMCFs) treeline. In *Fourth Fire Behaviour and Fuels Conference* (p. 51). Saint Petersburg, Russia.

Raison, R., Woods, P., Jakobsen, B., & Bary, G. (1986). Soil temperatures during and following low-intensity prescribed burning in a Eucalyptus pauciflora forest. *Australian Journal of Soil Research*, *24*(1), 33. doi:10.1071/SR9860033

Raupach, M. R., & Thom, A. S. (1981). Turbulence in and above plant canopies. *Annual Review of Fluid Mechanics*, *13* , 97–129.

Reh, C. M., Letts, D., & Deitchman, S. (1994). *Health hazard evaluation report*. California.

Rein, G. (2009). Smouldering Combustion Phenomena in Science and Technology. *International Review of Chemical Engineering*, *1*, 3–18.

Rein, G., Cleaver, N., Ashton, C., & Pironi, P. (2008). The severity of smouldering peat fires and damage to the forest soil. *Catena*, *74*(3), 304–309.

Ren, N., Wang, Y., & Trouvé, A. (2013). Large Eddy Simulation of Vertical Turbulent Wall Fires. *Procedia Engineering*, *62*, 443–452. doi:10.1016/j.proeng.2013.08.086

Román-Cuesta, R. M., Salinas, N., Asbjornsen, H., Oliveras, I., Huaman, V., Gutiérrez, Y., … Malhi, Y. (2011). Implications of fires on carbon budgets in Andean cloud montane forest: The importance of peat soils and tree resprouting. *Forest Ecology and Management*, *261*(11), 1987–1997.

Safi, M. J., Mishra, I. M., & Prasad, B. (2004). Global degradation kinetics of pine needles in air. *Thermochimica Acta*, *412*(1-2), 155–162. doi:10.1016/j.tca.2003.09.017

San-Miguel-Ayanz, J., Schulte, E., Schmuck, G., & Camia, A. (2013). The European Forest Fire Information System in the context of environmental policies of the European Union. *Forest Policy and Economics*, *29*, 19–25. doi:10.1016/j.forpol.2011.08.012

San-Miguel-Ayanz, J. Steinbrecher, R. (2009). *EMEP-EEA emissions inventory guidebook* (p. 19). Copenhagen.

Sarmiento, F. O., & Frolich, L. M. (2002). Andean Cloud Forest Tree Lines. Naturalness, Agriculture and the Human Dimension. *Mountain Research and Development*, *22*(3), 278–287. doi:10.1659/0276-4741

Schemel, C. F., Simeoni, A., Biteau, H., Rivera, J. D., & Torero, J. L. (2008). A calorimetric study of wildland fuels. *Experimental Thermal and Fluid Science*, *32*(7), 1381–1389.

Séro-Guillaume, O., & Margerit, J. (2002). Modelling forest fires. Part I: a complete set of equations derived by extended irreversible thermodynamics. *Int. J.Heat Mass Transfer*, *45* , 1705–1722.

Shafizadeh, F. (1978). Combustion, combustibility, and heat release of forest fuels. *AIChE Symposium Series*, *74:177*.

Shaw, R. H., & Patton, E. G. (2003). Canopy element influences on resolved- and sub-grid-scale energy within a large-eddy simulation. *Agricultural and Forest Meteorology*, *115* , 5–17.

Siegel, R., & Howell, J. R. (1992). *Thermal Radiation Heat Transfer* (Vol. third ed.). Hemisphere Publishing Corportation .

Simeoni, A., Thomas, J. C., Bartoli, P., Borowieck, P., Reszka, P., Colella, F., … Torero, J. L. (2012). Flammability studies for wildland and wildland–urban interface fires applied to pine needles and solid polymers. *Fire Safety Journal*, *54*(0), 203–217.

Stadmüller, T. (1987). *Cloud Forests in the Humid Tropics: A Bibliographic Review*. United Nations University Press.

Stroppiana, D., Grégoire, J.-M., & Pereira, J. M. C. (2003). The use of SPOT VEGETATION data in a classification tree approach for burnt area mapping in Australian savanna. *International Journal of Remote Sensing*, *24*(10), 2131–2151. doi:10.1080/01431160210154911

Swezy, D. M., & Agee, J. K. (1991). Prescribed-fire effects on fine-root and tree mortality in old-growth ponderosa pine. *Canadian Journal of Forest Research*, *21*(5), 626–634.

Tamura, H., Kiya, M., & Arie, M. (1980). Vortex shedding from a circular cylinder in moderate-Reynlods-number shear flow. *Journal of Fluid Mechanics*, *141* , 721–735.

Thomas Simeoni A. Colella F. Torero J.L., J. C. (2011). Piloted Ignition Regimes of Wildland Fuel Beds .

Thomas, J. C., Everett, J. N., Simeoni, A., Skowronski, N., & Torero, J. L. (2013). Flammability Study of Pine Needle Beds. In *Proc. of the Seventh International Seminar on Fire & Explosion Hazards (ISFEH7)*. doi:10.3850/978-981-08-7724-8

Valente, J., Miranda, A. I., Lopes, A. G., Borrego, C., Viegas, D. X., & Lopes, M. (2007). Local-scale modelling system to simulate smoke dispersion. *International Journal of Wildland Fire*, *16*(2), 196. doi:10.1071/WF06085

Van Der Werf, G. R., Randerson, J. T., Giglio, L., Collatz, G. J., Mu, M., Kasibhatla, P. S., … Van Leeuwen, T. T. (2010). Global fire emissions and the contribution of deforestation, savanna, forest, agricultural, and peat fires (1997-2009). *Atmospheric Chemistry and Physics*, *10*, 11707–11735. doi:10.5194/acp-10-11707-2010

Wård, Y. (2007). *Tropical Montane Cloud Forest- Fire Disturbance and Water Input after Disturbance* (pp. 1–28). Umeå: Swedish University of Agricultural Sciences.

Williamson, C. H. K. (1992). The natural and forced formation of spot-like "vortex dislocations" in the transition of a wake. *Journal of Fluid Mechanics*, *243* , 393–441.

Zimmermann, M., Meir, P., Silman, M. R., Fedders, A., Gibbon, A., Malhi, Y., … Zamora, F. (2009). No Differences in Soil Carbon Stocks Across the Tree Line in the Peruvian Andes. *Ecosystems*, *13*(1), 62–74. doi:10.1007/s10021-009-9300-2

Fine fuel particle heating during experimental laboratory fires

Jack D. Cohen, Mark A. Finney

[a] *US Forest Service, Missoula Fire Sciences Laboratory, Missoula, MT 59808 USA*
jcohen@fs.fed.us, mfinney@fs.fed.us

Abstract
Fuel particle temperature measurements were related to measurements of particle irradiance and impinging gas temperatures during seven fire spread experiments at the U.S. Forest Service Fire Sciences Laboratory, Missoula, Montana. Fine particle temperature increases corresponded to pulses of impinging hot gases and thus suggested convection as the primary heat transfer mechanism responsible for particle ignition. An analysis using the flux-time product correlation (FTP) indicated that flame radiation was insufficient to pilot ignite fuels for fire spread. A numerical modeling examination of fine particle heating indicated flame radiation was insufficient for particle ignition and convection heat transfer from flame contact was the primary heating mechanism leading to particle ignition.

Keywords*: Fuel heating, Fire spread, Ignition processes*

Introduction

Since the 1940's wildfire spread has been described as a step-wise process of ignition by heat transfer from the burning zone to adjacent fine fuel particles (Fons 1946). Observations and experiments have identified fine live and dead vegetation (e.g. conifer needles and twigs < 3 mm diameter) as the burning fuels primarily responsible for the intensity of the propagating flame zone and thus wildfire spread (Fons 1946; Rothermel 1972; Pagni and Peterson 1973; Call and Albini 1997; Stocks *et al*. 2004). For example, after fire spreads through shrub and tree canopies the branches larger than 6 mm commonly remain unconsumed after a high intensity wildfire has burned the area. Thus, understanding fire spread requires an understanding of ignition processes at spatial and temporal scales of fine fuels.
Sufficient understanding of wildland fire spread processes does not exist for reliable *ex ante* physical modeling. An indicator of this insufficient understanding is the inconsistency between fire spread models that attempt physical descriptions of radiation and convection (Sullivan 2009). Model developers have largely assumed fuel particle ignition processes without an experimental basis (Finney *et al*. 2013a). For example, radiation heat transfer has been commonly assumed to govern fire spread. However, experimental evidence suggests radiation heat transfer is insufficient for igniting fine fuel particles (Fang and Steward 1969; Baines 1990; Finney *et al*. 2013a). And prior experimental evidence (Rothermel and Anderson 1966; Fang and Steward 1969) and laboratory fire observations (Baines 1990; Fang and Steward 1969) indicated that most fuel particle heating to ignition occurred within the last 0.025 m during fire spread. Given that burning fine fuels are primarily responsible for wildland fire spread, if radiation is insufficient for fine fuel ignition then convection must be the heat transfer mechanism governing fire spread. The convective heating would occur from flame impingement on fuels adjacent to the flaming front, and recent experiments have shown how this occurs (related paper[1]). The following discussion describes measured fuel particle temperatures related to measured incident radiation heat fluxes (irradiance) and gas temperatures during experimental surface fires and how that relates to heat transfer mechanisms governing fire spread.

[1] Finney et al. 2014. Experimental evidence of buoyancy controlled flame spread in wildland fires; VII ICFFR.

Methods

We are experimentally examining wildfire ignition processes to provide a basis for physically modeling fire spread. The following discussion describes fuel particle heating experiments with measurements made at fine fuel particle spatial and temporal scales. The experiments relate measured fine fuel particle temperatures with measured irradiance and impinging gas temperatures during the approach of spreading flame zones. In conjunction with the experiments, heat transfer processes are examined using modeling.

Experiments

Special wood fuel particles were instrumented with thermocouples along with measurements of incident radiation (irradiance) and gas temperatures adjacent to the particles. Machined wood (*Liriodendron tulipiferia*) particles with 1 mm and 12 mm square cross-sections, both 120 mm long were instrumented with fine thermocouples (K Type, 0.05 mm). The 1 mm fuel particles had thermocouples embedded at the center of the front (facing the approaching flames) and back vertical surfaces; the 12 mm particles had thermocouples embedded at the center of each vertical and horizontal surface (front, top, back and bottom) (Figure 1). The fuel particles were horizontally attached to the top of precisely constructed cardboard "comb" fuel beds. The particles were located 130 mm to one side of the center line of the 2.44 m wide fuel bed in the U.S. Forest Service experimental wind tunnel burning facility in Missoula, Montana.

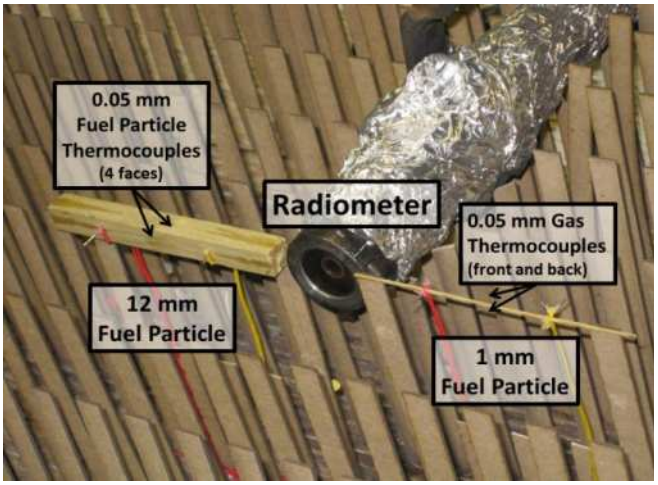

Figure 1 - 1 mm and 12 mm fuel particles were instrumented with 0.05 mm thermocouples. The 1 mm particle had thermocouples embedded in the centers of front and back faces only; the 12 mm particle had thermocouples centered in four faces (ends are neglected). The particles were attached to the top of a "fuel comb" in the cardboard fuel bed. The comb fuel bed shown had tines 152 mm tall and 12.4 mm wide and spaced 46 mm between rows. A water cooled radiometer at fuel particle height estimated particle irradiance and suspended 0.05 mm thermocouples estimated gas temperatures.

Fuel particle irradiance and temperatures of impinging gases were measured as the fire spread to the particles. Fuel particle irradiance was estimated using a water-cooled radiometer placed even with the fuel particles. Temperatures of gases flowing around the fuel particles were estimated using fine thermocouples (K Type, 0.05 mm) suspended approximately 5 mm from the particle's front and back vertical faces (Figure 1). To reliably measure the flame radiation we calibrated the radiometer using a black body cavity having temperatures in the range of a spreading flame front (1000 K – 1400 K). All measurements were taken at a sampling rate of 500 per second (500 Hz). At this rate, the sampling time interval (.002 sec) is less than one-half the time constant (.04 sec) of the fastest responding sensor (thermocouple) and meets Nyquist frequency aliasing criteria (Fritschen and Gay 1979). Measurements began before fuel bed ignition and continued through fine particle ignition and burning.

The "comb" fuel beds were engineered using 1.25 mm thick cardboard (Finney *et al*. 2013b). Each comb was laser cut from a 1.2 m long sheet to specified tine heights and widths (Figure 1). Fuel particles were mounted on combs having tine widths of 2.31 mm, 6.20 and 12.4 mm and comb heights ranging from 102 mm to 203 mm. To change flame zone characteristics fuel beds were constructed with combs at various spacing widths between rows and combinations of combs with different tine

heights and widths. For fuel beds with comb size combinations, fuel particles were mounted on the combs with the highest tines.

Modeling

We used a two-dimensional numerical model of fuel particle heat transfer to further examine particle heating during the fire experiments. The numerical model calculates fuel particle temperatures across the particle mid-section and these temperatures reasonably represent temperatures for most of the particle. This assumes that end effects are negligible and the particle exchanges energy uniformly along its length (120 mm) such that no significant lengthwise temperature gradients occur through most of the particle. The numerical model used a finite difference, explicit method with a grid increment of 2.5×10^{-5} meters between computational nodes and a time increment of 5.0×10^{-4} seconds. We verified that the computational results were stable and independent of spatial and temporal increments. The irradiance and gas temperature measurements from the experiments were used as inputs to the 1 mm particle model.

The initial conditions and boundary conditions were determined by a combination of measured values and assumed values. We assumed the fuel particle initially had uniform temperature corresponding to the measured front face temperature before heating from the flame front. It was assumed the particle was in equilibrium with its surroundings just prior to the first model computation. Radiation boundary conditions were estimated by the measured irradiance for the front face and the designated constant blackbody temperature of the surroundings for the other three faces of the particle. The convection boundary conditions were estimated by a computed convection heat transfer coefficient and the measured gas temperature adjacent to the fuel particle front face. For the lack of a convection coefficient correlation that matched the particle heating context, the Hilpert average correlation for non-circular forms (Incopera and DeWitt 2002) was used. The flow velocities were assumed based on the measured gas temperature. At gas temperatures below 500 C the flow velocity was designated to be the wind tunnel flow speed. For gas temperatures equal to and greater than 500 C, the gas flow velocity was increased to seven times the ambient flow based on observations of higher flow circulations associated with flames. Although the convection coefficient and air properties were determined for the entire particle based on the average film temperature for the front face, the heat transfer was calculated at each computational node. At every time increment, the physical properties of the wood particle were determined by the temperature at each computational node.

The model only accounted for heat exchange and did not include chemical kinetics and mass transfer related to moisture vaporization and pyrolysis. Although particles were not oven-dried prior to the experiments, the 1 mm particles had moisture contents less than six percent and assumed negligible for modeling. Pyrolysis was assumed negligible at particle temperatures below 275 C. The model was considered unreliable at temperatures above 275 C and thus modeling ended prior to particle ignition. The purpose of the modeling was to examine heat transfer processes leading to particle ignition during fire spread. There was no intent to develop a predictive tool with this effort. Thus, model parameters were set without benefit of prior comparisons between model and experimental results and model parameters were not adjusted after comparisons to improve estimates of measured particle temperatures.

Results

Seven fire spread experiments were conducted with instrumented fuel particles. To describe the context of the particle heating experiments related to fire conditions, Table 1 provides the wind speed, fire spread rate, flame length, flame zone depth and particle irradiance for each burn. After ignition the experimental fires spread with a nearly straight flame front across the 2.44 meter wide fuel bed. The flame lengths from Table 1 suggest fire characteristics similar to those burning actual fuel beds composed of short grasses or surface forest litter under dry conditions and low wind speeds. The factors contributing to the variety of spread rates and flame lengths such as fuel bed characteristics are beyond the scope of this discussion and not included in the Table 1.

Table 1. Laboratory Fire Spread Conditions. Wind speed was a constant wind tunnel setting. Rate of spread and flame length were estimated after the influence of the ignition line became negligible. Flaming depth was the estimated distance from the forward edge of the propagating flame front to the rear where coherent flaming ceases due to fuel consumption. The fuel particle irradiance range is from the last four seconds before the 1 mm particle ignition.

Fire Exp.	Wind Speed (m/s)	Rate of Spread (m/s)	Flame Length (m)	Flaming Depth (m)	Irradiance [4 s to ign.] (kW/m^2)
a	0.34	0.028	1.0	0.54	20 - 29
b	0.34	0.024	1.2	0.41	20 - 30
c	0.22	0.016	1.4	0.57	22 - 40
d	0.56	0.032	1.2	0.68	17 - 34
e	0.34	0.031	1.3	0.56	25 - 44
f	0.67	0.034	1.5	0.60	13 - 22
g	0.34	0.031	0.6	0.28	10 - 22

Every experiment produced the same general results regarding the fuel particle thermal response to transient conditions and ignition. The 1 mm particles responded quickly to changing thermal conditions compared to the 12 mm particles (Figure 2). Within the last four seconds of the approaching flame front the 1 mm particle temperatures rapidly increased resulting in sustained ignition while the 12 mm particle had not yet ignited before flame front arrival (Figure 2). Particle ignition was determined by fuel particle and gas temperatures and confirmed with video recordings. In all seven experiments the 1 mm particles ignited before the 12 mm particles.

None of the experiments produced measured fuel particle irradiance capable of piloted ignition. Using a validated irradiance based ignition correlation (Cohen 2004) the flux-time product (FTP) was computed from the measured fuel particle irradiances. The resulting FTP values for all the fuel particle experiments were well below the criteria for ignition. For example, the maximum measured irradiance of the fuel particle experiments was 44 kW/m^2 (Table 1, experiment "e") and the FTP value when the 1 mm particle sustainably ignited was 1313. The minimum value for piloted ignition is 11501, nearly an order of magnitude greater (Figure 3). Thus, radiation heat transfer was insufficient for particle ignition during all the fire spread experiments.

We take a closer examination of fine fuel heating during an approaching flame front. Because the general response characteristics of all fuel particle heating experiments were similar, we use measurements from fire experiment "d" (Table 1) to show the 1 mm particle response related to the irradiance and gas temperatures.

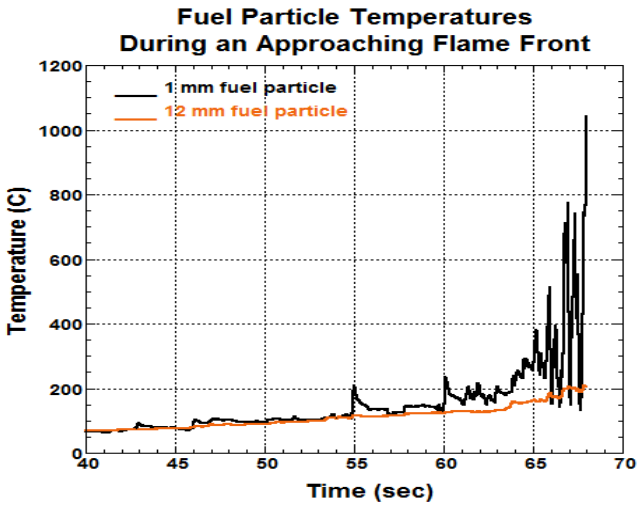

Figure 2 - For the same thermal conditions, the 1 mm particle (black) has a large temperature variation compared to the 12 mm particle (orange). In the last second of data the 1mm particle ignited while the 12 mm particle had not yet reached a temperature corresponding to a pyrolysis rate that could result in piloted ignition (example from

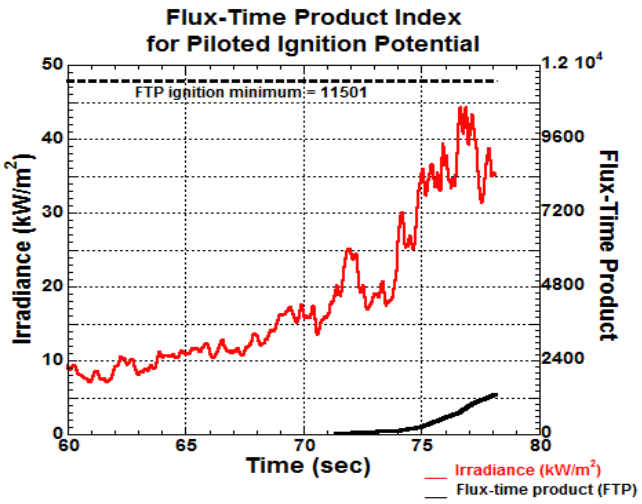

Figure 3 - The FTP (solid black) is calculated based on the measured irradiance (red, from experiment "e"). If the minimum FTP for ignition (broken black) is met and

Examination of the 1 mm particle response uses measurements of the irradiance, gas temperatures adjacent to and in front of the fuel particle and front face surface particle temperature ("front" refers to the side facing the fire). The 1 mm particle temperature graph (Figure 4) starts before significant thermal exposure from the flame front and ends just prior to the 1 mm particle ignition. Gas temperatures (blue) less than the particle temperature (black) indicate convective cooling; gas temperatures higher indicate convective heating. The gas temperature chronology shows intermittent high temperature spikes for approximately 20 seconds prior to ignition whereas radiant flux increases more steadily. Radiation energy absorbed by the particle is indicated by particle temperatures remaining higher than gas temperatures with noticeable particle temperature responses to gas temperature. Pulses of higher gas temperatures result in particle temperature increases. The higher the gas temperature and longer the pulse duration the greater the particle temperature increase. For example, the particle remains at 100 C – 120 C in the 50 – 55 second time interval (Figure 4). Small temperature increases occur only during pulses of gas temperatures above the particle temperature. The significant particle temperature increases occur during impinging pulses of hot gasses such as those that occur at 55, 60 and 64 seconds (Figure 4). In the last 1.5 seconds of the heating sequence the particle temperature increases from below 200 C and approaches 300 C (with subsequent ignition) only after gas temperatures remain above and several hundred degrees Celsius higher than particle temperatures (Figure 4).

Importantly, the pulsing higher gas temperatures result from the spreading flame front; the wind tunnel air flow is temperature controlled. The pulsing occurred in all fire experiments and produced particle heating downwind of the flame front. In Figure 4 pulses greater than 100 C began at about 20 seconds before particle ignition. Using the average rate of spread for experiment "d" from Table 1 (0.032 m/s) and neglecting the pulse advection time, the flame front was about 0.64 meters (0.032 m/s x 20 s) from the fuel particle when this convective particle heating occurred. The high temperature gas pulses at 55 seconds and 60 seconds (graph times; Figure 4) were greater than 600 C and within the range of visible flame temperatures. These pulses could have been observed as lateral extensions of the non-steady flaming front contacting the fuel particle across distances of 0.35 meters and 0.19 meters, respectively.

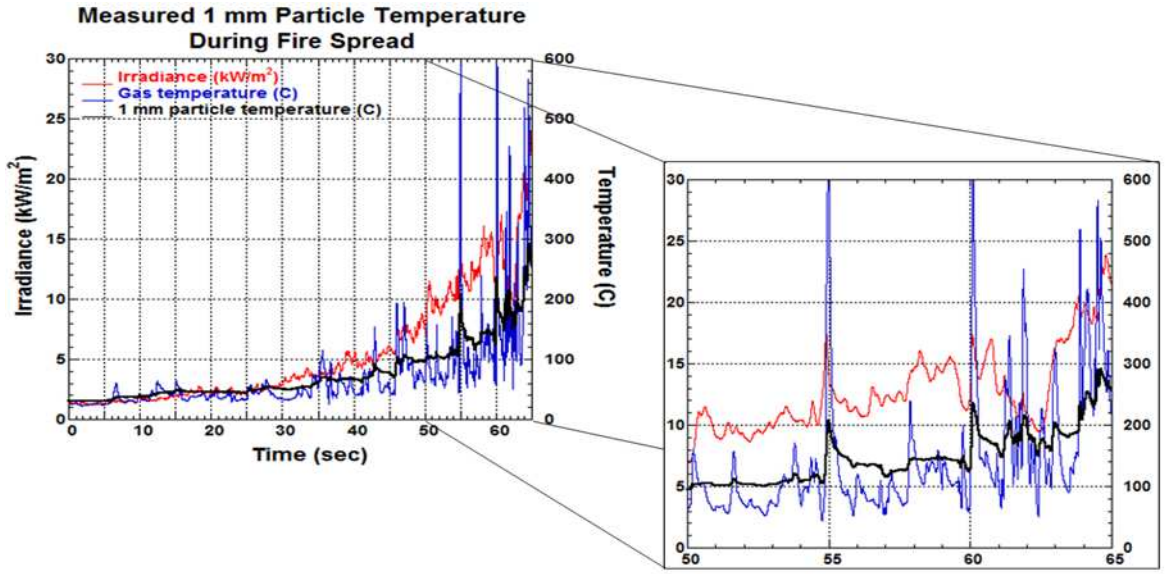

Figure 4. The left graph shows the measured front surface 1 mm fuel particle temperature with the corresponding measured irradiance and front face gas temperature as the fire spread to the particle. The graph ends just prior to particle ignition. The right graph is an enlargement of the last 15 seconds. The right graph shows particle temperatures responding (heating and cooling) to the variations in gas temperature and heating primarily during the pulses of high gas temperatures. (Data from experiment "d" of Table 1.)

The fuel particle heat transfer model computes fuel particle temperatures similar to the measured particle temperatures (Figure 5). Inspection of Figure 5 indicates the model captures the convective heating, both the response time and the magnitude during the high temperature gas pulses at 55 seconds, 60 seconds, and in the last second of the graph. However, the model did not simulate the thermal sensitivity revealed in the measured particle temperatures.

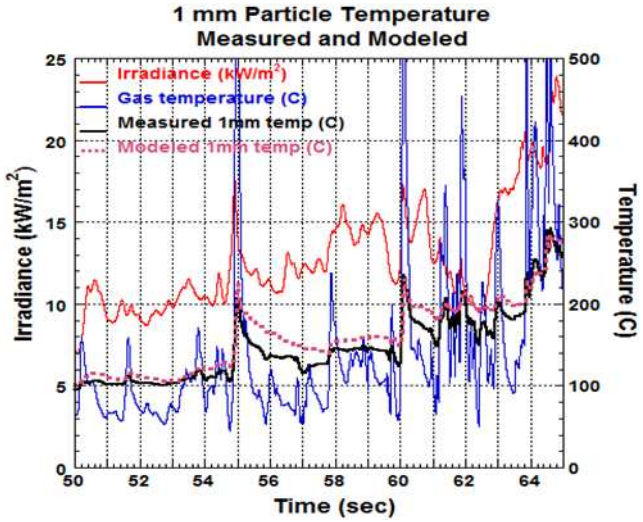

Figure 5. The same measured irradiance and gas temperatures as in Figure 4 are used as inputs for computing the 1 mm particle face temperature (purple). The measured 1 mm face temperature (black) is presented for comparison with the modeled temperature (the last 15 seconds as in the right graph of Figure 4).

In particular, the model does not cool as much as the particle as indicated by the modeled temperature (purple) largely remaining above the particle temperature. It is not clear what factors are causing the

difference but it could be the use of an average particle convection coefficient, higher absorbed radiation than actual and/or measurement errors.

Discussion and Analysis

The fuel particle heat transfer experiments have shown the importance of convection heat transfer. As seen in Figure 2 fine fuel particles convectively exchange heat at a higher rate than coarser particles. Thus, at cooler gas temperatures fine fuel particles will more effectively reduce radiation heating but at high gas temperatures fine particles will more effectively heat to ignition. Initially convective cooling was indicated by the particle temperatures largely staying above the gas temperatures (0 – 35 seconds, Figure 4). As the flame front approached (after 35 seconds), fuel particle temperatures increased primarily in response to convection heat exchange and this was particularly evident in the last 1.5 seconds of the graph (Figure 4). A separate analysis using the flux-time product (FTP) correlation based on the measured irradiance indicated insufficient flame irradiance for piloted ignition and thus the necessity of convective particle heating seen in Figure 4. However, even with fine scale sampling during the particle heating experiments it is difficult to differentiate the radiation and convection heat transfer mechanisms during fire spread. A heuristic examination using computational modeling has the potential to overcome practical limits of experimentation and explore questions such as "What if we stopped the flame radiation without affecting flame convection at the particle and vice versa?".
We used the model to examine the specific contributions of flame radiation and flame convection on fuel particle temperature by eliminating one and then the other.
No flame radiation: The measured irradiance was replaced by the constant irradiance of 300 K (27 C) blackbody surroundings. The measured gas temperatures were used as previously modeled. Inspection of Figure 6 indicates the modeled particle temperature responds to gas temperatures similar to the measured particle.

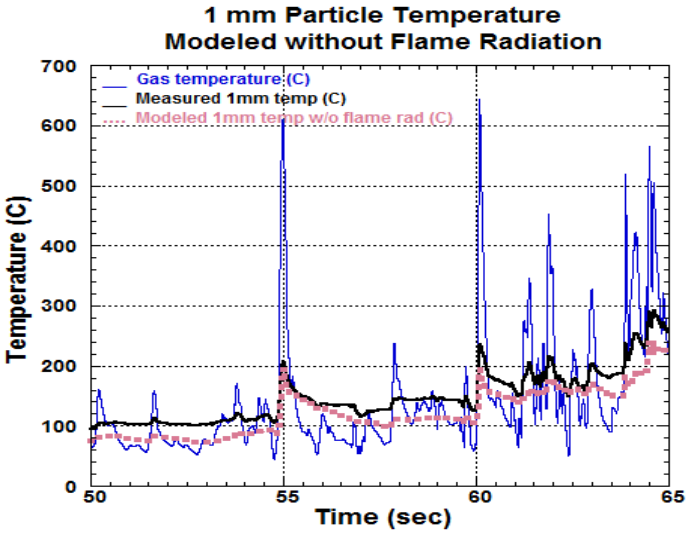

Figure 6. A constant irradiance of 300 K surroundings was substituted for the measured flame irradiance. The measured gas temperatures (blue) were used to compute convection heat transfer as before. The last 15 seconds of the computed particle temperature (purple) was compared to the measured particle temperature (black).

However, without flame radiation the modeled particle temperature remains below the measured temperature and below the modeled temperature in Figure 5. *No flame convection*: The measured gas temperatures were replaced by the constant wind tunnel flow speed of 0.56 meters/second at a constant temperature of 300 K (27 C). The measured irradiance was used as previously modeled. Inspection of

Figure 6 indicates a dramatic change in the modeled particle response characteristics compared to the measured particle.
The rapid increases in measured particle temperatures corresponding to 55 seconds and 60 seconds (Figure 7 graph time) did not occur with the modeled particle. At 63 seconds the modeled particle temperature drops corresponding to the measured irradiance but the measured particle temperature increased.

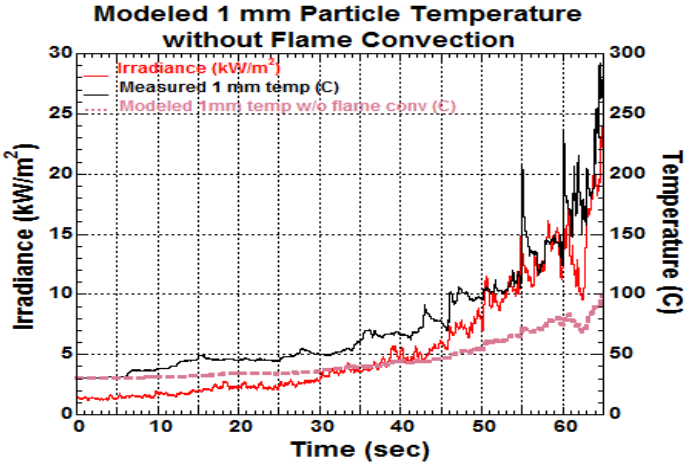

Figure 7. A constant 300 K gas flow was substituted for the flame gases. The measured flame irradiance was used as before. The 65 second sequence shows how the measured particle temperature (black) diverges from the computed temperature (purple) without hot flame gases.

Notably, just prior to ignition the final modeled particle temperature was about 100 C while the measured particle temperature was approaching 300 C. This result is consistent with the FTP analysis indicating that the irradiance was nearly an order of magnitude less than necessary for piloted ignition.

Conclusion

Fuel particle heat exchange experiments and heuristic modeling have demonstrated convection heat transfer as the principal mechanism governing fire spread during experimental laboratory fires. Temperature measurements have shown that fine fuel particles thermally respond at the time scales of significant convective pulses. As the flame front approaches, fine particles primarily heat convectively with increasing gas temperatures and pulse frequencies. In agreement with prior research, our experiments showed that the primary heating to ignition of the fine particles occurred within 0.05 meters of the approaching flame front during our laboratory fires. Measured temperatures along with modeling indicate convection heat transfer from flame contact was the primary mechanism responsible for the rapid particle temperature increases prior to particle ignition.

References

Baines PG (1990) Physical mechanisms for the propagation of surface fires. *Mathematical Computer Modelling* **13**(12), 83-94.

Call PT, Albini FA (1997) Aerial and surface fuel consumption in crown fires. *International Journal of Wildland Fire* **7**(3): 259-264.

Cohen, JD (2004) Relating flame radiation to home ignition using modeling and experimental crown fires. Canadian Journal of Forestry Research **34**(8): 1616-1626.

Fang JB, Steward FR (1969) Flame spread through randomly packed fuel particles. *Combustion and Flame* **13**, 392-398.

Finney MA, Cohen JD, McAllister SS, Jolly WM (2013a) On the need for a theory of wildland fire spread. *International Journal of Wildland Fire* **22**, 25-36.

Finney MA, Forthofer JD, Grenfell IC, Adam BA, Akafuah NK, Saito K (2013b) A study of flame spread in engineered cardboard fuel beds, Part I: Correlations and Observations. August 6-9, 2013, Seventh International Symposium on Scale Modeling, Hirosaki, Japan.

Fons WL (1946) Analysis of fire spread in light forest fuels. *Journal of Agricultural Research* **72**(3):93-121.

Fritschen LJ, Gay LW (1979) 'Environmental Instrumentation.' (Springer-Verlag: New York)

Incopera FP, DeWitt DP (2002) 'Fundamentals of Heat Transfer and Mass Transfer.' 5th Edition (Wiley: New Jersey)

Pagni PJ, Peterson TG (1973) Fire spread through porous fuels. *Fourteenth Symposium (International) on Combustion* **14**(1): 1099-1107.

Rothermel RC, Anderson HE (1966) Fire spread characteristics determined in the laboratory. USDA For. Serv. Res. Pap. INT-30.

Rothermel RC (1972) A mathematical model for predicting fire spread in wildland fuels. USDA For. Serv. Res. Pap. INT-115.

Stocks BJ, Alexander ME, Wotton BM, Stefner CN, Flannigan MD, Taylor SW, Lavoie N, Mason JA, Hartley GR, Maffey ME, Dalrymple GN, Blake TW, Cruz MG, Lanoville RA (2004) Crown fire behavior in a northern jack pine-black spruce forest. *Canadian Journal of Forestry Research* **34**: 1548-1560.

Fire behavior of prescribed burns in grass - woody steppe on Paraná State, Brazil

Celso Darci Seger, Antonio Carlos Batista, Alexandre França Tetto, Ronaldo Viana Soares

Federal University of Paraná - UFPR. Av. Pref. Lothário Mainster, 900, ZIP Code 80210-170, Curitiba, PR, Brazil, celsoseger@terra.com.br; batistaufpr@gmail.br; tetto@ufpr.br; rvsoares@ufpr.br

Abstract

Prescribed burns are widespread in many countries, becoming a management practice in different types of vegetation. In addition to practice pasture renewal and land clearing, prescribed burns also represent a means of preventing forest fires, because through this practice, the fuel load can be reduced significantly. To be used safely and effectively, it is crucial understand the aspects of the fire behavior from the vegetation to be burned. The Grass-Woody Steppe (Natural Fields) consists of the phytogeographic regions of the state of Paraná, covering an area of approximately 20,000 km^2 of east-central region of the state. The vegetation consists mainly of grasses and shrubs, with a large concentration of fine fuels (≤ 0.7 cm), representing a high danger of forest fires. For many years, the region of Grass-Woody of Paraná was used as pasture for the intensive rearing of cattle and sheep, activity that lost momentum in recent years due to the advancement of agriculture and forestry. Many farms, however, still keep areas of fields that are management by the fire. Although the burning of vegetation is still a common practice in the region, there are not however, information about the behavior of fire in this vegetation type. The objective of this research was to characterize the behavior of fire in steppe vegetation of the state of Paraná, through prescribed burns. The results aim to support studies of effects of fire on survival and regeneration of plant species in this environment, considering the hypothesis that controlled burning is a viable and safe activity for pasture management. The survey was conducted in the period preceding the winter in an area with more than eight years without human interference, located in Palmeira county, Paraná state. For the experiment, 10 plots of 3 x 20 m were prepared and burned by backfire and head fire techniques. On the day of burning, the weather conditions were: average wind speed of 2.20 $km.h^{-1}$, average relative humidity of air 60.31% and average temperature of 21.83 °C. The surface fuel load was estimated at 2.53 $kg.m^{-2}$, with an average moisture content of 79.77%. The results obtained in the backfire and headfire burnings were: rate of spread - 0.0536 and 0.0150 $m.s^{-1}$, height of flames - 1.39 and 0.68 m, fire intensity - 119, 11 and 51.96 $kcal.m^{-1}.s^{-1}$ and heat per unit area - 2218.84 and 4259.32 $kcal.m^{-2}$. It concluded with the achievement of the experiment, that the prescribed burns conducted at vegetation of Steppe within the established criteria and burning plans, are feasible and safe from the point of view of fire hazard.

Keywords*: fuel loading; fire intensity; fire danger.*

Introduction

Fire is the result of the rapid combination of oxygen and a combustible substance, releasing large amounts of energy. Although it may cause serious environmental damage, the fire is not only a agent that can cause damage to nature, but can also bring benefits to certain ecosystems, when used in a controlled manner, ie, through burnings that provide management vegetation without compromising the processes of natural regeneration (Soares, 1985).

Prescribed burnings, widespread in many countries, are a practice of manegement of different types of vegetation (Soares, 1995). Basically, consists in using the fire confined to a selected area and in appropriate climatic conditions, so that the rate of spread, the intensity of the fire and the heat released, reach management objectives intended in any vegetation. The use of prescribed burning has, among

other objectives, to reduce the surface fuel load that can generate the most destructive fires in most critical periods, manegement the vegetation of pastures, control of pests and diseases and to promote the clearing of land for agricultural crops and forest (Soares; Batista, 2007).
For conducting prescribed burns properly, it is essential, however, know how fire behaves in relation to vegetation that will be managed. The knowledge of fire behavior allows understanding the factors that have an important role in the onset and spread of fire. This knowledge is thus so important for the management, as being for planning to fight forest fires operations (Souza *et al*., 2003).
Basically, the variables that describe fire behavior are: rate of spread, fire intensity, heat per unit area and residence time (Soares; Batista, 2007). These variables serve to quantify and characterize the behavior of the fire, as well as, to control the difficulty of extinguishing any fire (Vega, 1996). Other variables such as the maximum temperatures reaching in the areas of combustion and the height of the flames, in addition to describing aspects of fire behavior, can establish associations about the effects produced on the various elements of the forest ecosystem (De Ronde *et al*., 1990).
In Brazil, the use of fire in many regions to vegetation management is still a common practice. Although all biomes are subject to burning a greater or lesser extent, the Savanna (Cerrado) and the Steppes (Southern Fields) are handled more frequently by fire (Pivello, 2011). This is the case of natural fields present in the state of Paraná, which are covered by grasses and shrubs and calling of "Estepe Gramineo-Lenhosa". The "Estepe Gramineo-Lenhosa" of Paraná state covers approximately 20,000 km^2, composing a phytogeographic zone with vegetation of grasslands adapted to relatively dry environments (Maack, 1981).
Although the burning of vegetation in the region is still a common management practice, there is, however, information about the behavior of fire in this vegetation type. Therefore, the aim of this research was to characterize the behavior of fire in steppe vegetation of the state of Paraná through prescribed burning in order to generate knowledge related to the effects of fire on the survival and regeneration of vegetation.

Methods

2.1. Study area

The study was conducted in the Private Natural Heritage Reserve "Caminho das Tropas". (Figure 1), coordinates 620334 E and 7196739 S, located in Palmeira county, state of Paraná. Created by decree nº 188/08 of the Environmental Institute of Paraná (Instituto Ambiental do Paraná, 2013), the Reserve with an area of 189.70 hectares, is one of the few private protected areas that conserves "Estepe Gramineo-Lenhosa" vegetation in the region.
The climate of the study area, according to the Köppen classification, is the Cfb, present in the higher portions of Paraná highlands. The summers, are usually fresh, with average temperature of 22 °C, while in the winters the average temperatures are below 18 °C. Severe frosts are frequent, occurring on average of 10 to 25 days annually. Rainfall is evenly distributed throughout the year, however, with higher intensity during the summer. The wind blows constantly, in the prevailing direction northeast (Instituto Agronômico do Paraná, 2013).

***Figure 1. Study area** – Private Natural Heritage Reserve "Caminho das Tropas".*

The experiment

For the realization of the experiment, 10 plots with dimensions of 3 m x 20 m (60 m^2) were bounded with the use of tractor, arranged in the predominant wind direction in the region (Figure 2). The burnings were held in the 5th July (autumn) between 02:00 pm and 6:30 pm, period of the day when weather conditions were more favourable to burn and with less risk of loss of control of the fire. To evaluate the fire behavior, two techniques (treatment) of burning were employed: backfire and headfire.

*Figure 2. **Delimitation of plots to the experiment***

The last rains before of the experiment ocurred on 29 and 30 June with 12.8 and 37.4 mm rainfall respectively (Fundação ABC, 2013). Thus, the burnings occurred 5 days after the last rainfall, covering a period considered relatively safe for burning (within 10 days since the last rain), when the degree of fire danger has not yet reached critical levels (Soares; Batista, 2007).

Fuel characterization

To characterize the fuel, informations about the type, quantity, moisture content and thickness formed by the deposition of material on the ground were obtained (Figure 3). To do so, it were allocated randomly in each plot three samples of 400 cm^2 (20 cm x 20 cm), where fuel was collected and separately in four categories: material with diameter between 0 and 0.7 cm, material with diameters between 0.71 and 2.5 cm and material whith diameter between 2.51 and 7.6 cm. This fuel was oven dried at 75 °C of constant temperature for determination of dry weight.

After drying, it was determined the fuel moisture using the formula U% = [(Mu - Ms) / Ms] .100 (Batista, 1990), where: **U**% is the fuel moisture content (%); **Mu** is the mass of the fuel during the collection (in grams) and **Ms** the mass of fuel after drying (in grams).

Figure 3. Collection and fuel characterization

2.4. Monitoring of weather conditions

During the period in which the burns were done, the weather conditions were monitored. In all plots were recorded the variables: wind speed ($m.s^{-1}$), air temperature (°C) and air relative humidity (%). For the measurement of meteorological variables, an automatic station Kestrel 6000 Station was used, positioned a height of 1.20 meters above the ground.
Data regarding rainfall of days prior the burnings were obtained from de weather station of the locality of Rosario from the city of Ponta Grossa, whose results are available for viewing on the ABC Foundation website (Fundação ABC, 2013).

2.5. Fire behavior variables

While the burning was occurring in each plot, observations about the following fire behavior variables were made, according to standard procedures adopted internationally and recommended by several authors (Ribeiro *et al*., 2006; Garnica *et al*., 2006; Kuçuk *et al*., 2008; McDonald; McPherson, 2011):

- Rate of spread - obtained visually by determining the time required to the fire line cover distances of 2 m, previously demarcated in each plot, along its length (20 m);
- Flame height - visual estimate of the average height reached by the flames in each 2 m at the advancing of line fire, with the aid of comparators (scales) of known dimensions;
- Intensity of the fire - estimated by the equation proposed by Byram (1959):

$I = H. w. r$

Where:
I = intensity of fire in $kcal.m^{-2}.s^{-1}$
H = calorific value in $kcal.kg^{-1}$
w = weight of fuel available in $kg.m^{-2}$
r = rate of spread of fire in $m.s^{-1}$

For the calorific value was used 3875 kcal.kg^{-1}, proposed by Griffin and Friedel (1984) for the grasslands and savannas vegetation.

Figure 4 present the plots before, during and after the prescribed burning.

Figure 4. ***Sequence of operations in the burning plots***

2.6. Processing and analyzing the data

From the collection and processing of data was possible to construct a matrix, composite of environmental (fuel and weather conditions) and fire behavior variables (Table 1). The data, relating to the environment (fuel and weather conditions) and fire behavior, were processed and analyzed with software STATGRAPHICS Centurion XV. The statistical test used for analysis and comparison of data was the "t" test.

Table 1. Environmental and fire behavior variables

Variable	Description	Unit
WCf	Fuel load (average of 3 samples per plot) before burning	kg.m^{-2}
WCc	Residual (average of 3 samples per plot) after burning	kg.m^{-2}
Hch	Flame height during burns (average of 10 observations per plot)	m
T	Air temperature at the beginning of the burning portion	°C
UR	Relative humidity at the beginning of the burning of plot	%
r	Rate of spread (average of 10 observations per plot)	m.s^{-1}
Vv	Wind speed at the beginning of the burning of plot	km.h^{-1}
I	Fire intensity (average of 10 observations per plot)	kcal.m^{-1}.s^{-1}
H_a	Heat per unit area	kcal.m^{-2}

Results

3.1. Weather conditions

The prescribed burnings must be conducted in accordance with established the previous requirements for the weather and fire behavior conditions (Fernandes *et al.*, 2002; Soares; Batista, 2007; Fernandes; Loureiro, 2010). For grasslands, the appropriate recommendations to carry out the burns and achieve the objectives with less risk of fire control losing are shown in table 2.

Table 2. Prescription for burning grassland vegetation

Weather conditions	Optimun	Minimum	Maximum
- Number of days without rain	3 - 7	1	10
- Air temperature (°C)	8 - 20	5	25
- Air Relative humidity (%)	30 - 70	20	85
- Wind speed ($km.h^{-1}$)	5 - 5	1	20
Fire behaviour			
- Rate of spread ($m.s^{-1}$)	0,03 - 0,08	< 0,03	0,13
- Flame height (m)	1 - 4	< 1	5,5

Note: adapted from Fernandes et al. (2002).

Weather conditions recorded at the day of the experiment are presented in table 3

Table 3. Weather conditions

Meteorological variables	Backing fire burning			Head fire burning		
	Mean	Minimum	Maximum	Mean	Minimum	Maximum
Air temperature (°C)	$22,32_a$	20,00	24,00	$21,34_b$	18,50	23,50
Relative humidity (%)	$58,40_a$	54,00	63,00	$62,20_b$	55,50	69,00
Wind speed ($km.h^{-1}$)	$1,36_a$	1,00	1,80	$3,08_b$	2,20	4,00

Note: Results in the same line followed by different letters are statistically different, by "t" test ($p < 0,01$).

It is observed by table 3, as well as verified for the precipitation, that the experiment was accomplished within condition acceptable of weather and fire behaviour for the achievement of the prescribed burn safely, according to the parameters listed in table 2.

The results in table 3 indicate that there were differences in weather conditions for the burnings techniques utilized. These distinct weather conditions demonstrate the difficulties that are often encountered when performing burning experiments outdoors. Despite the variations in the weather, the values of weather variables remained very close to the limits recommended for safely performing burnings as shown in table 2.

3.2. Fuel caracteristics

The fuel, as one of the components of the fire triangle is basic and essential for the occurrence and spread of fire. The amount of fuel in an area and their characteristics define whether there will be ignition and how will be the spread of fire. Therefore, the characterization of the remaining fuel is a decisive factor in plans to prevent and fight fires, especially in prescribed burnings programs (Soares; Batista, 2007).

The characteristics of the fuel in the area of the two burn treatments are shown in table 4.

Table 4. Fuel characteristics

Fuel variables	Backing fire burning			Headfire burning		
	Mean	Minimum	Maximum	Mean	Minimum	Maximum
Fuel load ($kg.m^{-2}$)	$2,72_a$	1,23	4,48	$2,35_a$	1,59	4,18
Fuel moisture (%)	$74,60_a$	52,00	92,19	$86,46_b$	60,61	115,83
Fuel consumed ($kg.m^{-2}$)	$2,09_a$	0,85	3,12	$1,19_b$	0,78	1,81
Fuel consumed (%)	$76,25_a$	69,11	90,98	$56,60_b$	30,12	77,19

Note: Means in the same line followed by different letters are different, by "t" test ($p < 0,01$).

There is not statistical difference in fuel load of the two areas of burns, reflecting the homogeneity of the surface fuels in this type of vegetation.

The fuel moisture was statistically different between the two burning techniques. This variable has great influence on the ignition and the efficiency of combustion, and can vary greatly depending on weather conditions observed on the day or pre-burn period, as well as the season of the year. The fuel moisture found for the 20 plots was approximately 80%, being 74.60% (with a range of 52.00 and 92.19%) in the backfire burning and 86.46% (variations of 60.61 and 115.83%) in headfire burning.The most of the fuel (approximately 70%) was dead and was composed primarily of fine material (≤ 0.7), sorted by Soares (1985) as a hazardous fuel. Although the most of the vegetation was dead, even so, the fuel moisture was high, probably due the amount of rainfall that occurred five days prior to the experiment and due to the overcast sky that prevailed in the following days. However, even with the high fuel moisture, the fire has spread normally, being influenced by the amount of dead fuel, its thickness and also because of the fuel arrangement. Experiments by other authors in grassland vegetation showed that the fuel moisture vary greatly depending on the season and the region. Fidelis *et al*. (2010) reported values between 37.80 and 44.49% for the fine fuels in an experiment conducted with burning of grassland near the Porto Alegre county, south region of Brazil. Miranda *et al*. (1996) found values between 8 and 23% of moisture in fine dead fuel (≤ 0.7 cm) and 113-163% in live fuels in the Savannas near Brasília city. Pivello and Coutinho (1992) reported content of 21-44% moisture of the vegetation of Savannas in the São Paulo State.

Regarding the "burning efficiency" variable that comes to the amount of fuel consumed (in percentage) in relation to fuel load, differences were also recorded. The results of 56.60% for the treatment of headfire burnings and 76.25% for the backfire burnings are significantly different. The burning efficiency of herbaceous vegetation in fields and grasslands may vary from 65 to 95%, according Levine (1996). For savannas of Brazil, Pivello and Coutinho (1992) found values of 63 and 77%, while Miranda *et al*. (1996) determined values between 81 and 94% for the same vegetation. In vegetation of Steppe, Fidelis *et al*. (2010) reported values of 93% in an area with about two years without burning and 95% in an area with six years without fire.

In general, two conditions acting directly for the efficiency of burning: the first related to vegetation type and its characteristics (thickness, arrangement, fuel moisture, etc.), and the second, the meteorological factors during burning (Soares; Batista, 2007).

The differences for the two techniques burning of the experiment can be explained mainly by the physiological state of the fuel load. The moisture checked for fuel from the plots of backfire burnings was greater than moisture of the burned plots of headfire burnings. Other factors, such as, the weather conditions shown in table 3 during the burning may also have influenced the results.

3.3. Fire behavior

It is understood by fire behavior, the result of the interaction between weather, fuel caracteristics, topography, burning technique and form of ignition. The results of the fire behavior variables are represented in table 5.

Table 5. Fire behavior variables of the burning treatments

Fire behavior	Backing fire burning			Headfire burning		
	Average	Minimum	Maximum	Average	Minimum	Maximum
Rate of spread ($m.s^{-1}$)	$0,0150_a$	0,0100	0,0239	$0,0536_b$	0,0391	0,0841
Flame height (m)	$0,68_a$	0,47	0,86	$1,39_b$	1,20	1,75
Fire intensity ($kcal.m^{-1}.s^{-1}$)	$51,96_a$	35,83	73,95	$119,11_b$	65,40	205,08
Heat released ($kcal.m^{-2}$)	$4259,32_a$	1498,85	5754,20	$2218,84_b$	1167,64	2802,29

Note: Means in the same line followed by different letters are different, by "t" test ($p < 0,01$).

The table 5 shows that all variables that characterize the fire behavior are significantly different for the two treatments.

The mean rate of spread of the backing fire burning was 0.0150 $m.s^{-1}$, with a range of 0.0100 and 0.0239 $m.s^{-1}$, classified as slow according to Soares and Batista (2007). At the head fire burning, the rate of fire ranged between 0.0391 and 0.0841 $m.s^{-1}$, with mean of 0.0536 $m.s^{-1}$, classified as medium by the cited authors.

In a research on fire behavior in prescribed burning in grasslands in the Oklahoma State, United States, Bidwell and Engle (1991) obtained values of 0.20 and 0.02 $m.s^{-1}$ for the rate of spread in the headfire and backing fire burnings, respectively.

Fidelis *et al*. (2010) recorded average rate of spread of 0.015 $m.s^{-1}$ in burnings in an area with one year without burning, and 0.013 $m.s^{-1}$ in an area with six years without burning, in the both cases with headfire. Miranda *et al*. (1996) has found values of rate of spread of burnings in brazilian savannas of 0.13 to 0.64 $m.s^{-1}$ (mean of 0.385 $m.s^{-1}$). Brown and Davis (1973) observed in several experiments of burning in the United States of America, a rate of spread of backing fire burnings with variations of 0.009 to 0.018 $m.s^{-1}$, values very similar to those observed in this experiment.

Statistical analysis detected a significant difference between the mean flame height between the two burning techniques, which were of 0.68 and 1.39 m respectively. These values are within the recommended limits to conduce the fire safely (Fernandes *et al*., 2002).

The fire intensity also varied significantly between the two forms of burnings. In the backing fire burnings, the values were lower, mean of 51.96 $kcal.m^{-1}.s^{-1}$, ranging between 35.83 and 73.95 $kcal.m^{-1}.s^{-1}$. In the backing fire burnings performed in prairies by Engle and Bidwell (1991), the mean of intensity observed were 23.18 $kcal.m^{-1}.s^{-1}$, ranging from 7.41 to 34.89 $kcal.m^{-1}.s^{-1}$. In the headfire burnings, the variation was from 65.40 to 205.08 $kcal.m^{-1}.s^{-1}$ (mean of 119.11 $kcal.m^{-1}.s^{-1}$). In the literature very different values of the fire intensity of prescribed burning on grassland vegetation are found. Fidelis *et al*. (2010) determined a mean of 22.35 $kcal.m^{-1}.s^{-1}$for an area with frequent burning and 42.79 $kcal.m^{-1}.s^{-1}$ to an area with more than five years without burning, both headfire burnings. In the study by Miranda *et al*. (1996), values between 299.99 and 3405.95 $kcal.m^{-1}.s^{-1}$ were recorded and an average of 995.33 $kcal.m^{-1}.s^{-1}$. Fidelis *et al.* (2010) cited the following values obtained by various researchers: 6.68 to 4276.53 $kcal.m^{-1}.s^{-1}$ for the African savannah; 36.06 to 2200.72 $kcal.m^{-1}.s^{-1}$ for the Australian savannas; from 23.64 to 273.95 $kcal.m^{-1}.s^{-1}$ for the grasslands of Australia; 7.40 to 2813.12 $kcal.m^{-1}.s^{-1}$ for the prairies of the United States; from 10.27 to 265.59 $kcal.m^{-1}.s^{-1}$ for the heaths (wetlands) of Scotland; from 95.06 to 112.73 $kcal.m^{-1}.s^{-1}$ for the low savannas of Venezuela; from 46.09 to 538.11 $kcal.m^{-1}.s^{-1}$ for the high Venezuelan savannas and 678.80 to 3916.59 $kcal.m^{-1}.s^{-1}$for the Brazilian savannas.

The fire intensity, calculated by the equation of Byram (1959), has proven to be a very useful parameter in the description of fire behavior, and serve as a benchmark to visualize and compare the rates of energy released by different types of burnings or forest fires (Soares; Batista, 2007).

Regarding the heat released per unit area, values of 4259.32 $kcal.m^{-1}.s^{-1}$ at the backing fire burn (ranging from 1498.85 and 5754.20 $kcal.m^{-1}.s^{-1}$), and 2218.84 $kcal.m^{-1}.s^{-1}$ were obtained in the headfire

burnings (range of 1167.64 and 2802.29 kcal.m^{-1}.s^{-1}). Miranda *et al.* (1996) found values from 1999.85 to 3405.94 kcal.m^{-1}.s^{-1} in a experiment with headfire burnings in Brazilian savanna, considered very close to the values determined for the African savannas. This variable of fire behavior is an important parameter to evaluate the effects of fire on soil and on the emission of particles in the atmosphere. Generally, as higher is the rate of spread, the lower the amount of energy directed to the inner layers of the soil. In contrast, as slower is the spread of fire, the greater is the amount of energy concentrated there. The highest values of observed heat per unit area in backing fire burning when compared with the headfire burning, are due to the lower rate of spread in this kind of burning.

Conclusions

Considering that the controlled burns were conducted within the limits of environmental conditions recommended by the guidelines for fire management adopted internationally**,** it can be concluded that**:**

- The prescribed burns in vegetation of Steppe carried out within the criteria set out at burns plans are feasible and safe from the point of view of fire hazard;
- The parameters of fire intensity, the rate of spread, the heat released per unit area and flame height could be quantified easily and accurately, allowing adequate description of fire behavior;
- The values of fire behavior observed in this study are compatible with most results recorded in similar surveys conducted in other regions and are fundamental to evaluate the effects of fire on the dynamics of post-fire period in steppe vegetation of Paraná state.

References

Batista, AC. Incêndios florestais. Recife: Imprensa Universitária da UFRPE, 1990. 115 p.

Bidwell, TG; Engle, DM. Behavior of headfires and backfires on tallgrass prairie. In: International Symposium Fire And Environment: Ecological And Cultural Perpectives, 1990, Knoxville, EUA. Proceedings... Knoxville: USDA Forest Service, 1991. p. 344 - 350.

Brown, AA; Davis, KP. Forest fire: control and use. New York: McGraw-Hill, 2nd. ed., 1973. 686 p.

Byram, GM. Combustion of forest fuels. In: DAVIS, K. P. Forest fire: control and use. New York: Mc Graw Hill, 1959. p. 77 – 84.

De Ronde, C; Goldammer, JG; Wade, DD; Soares, RV. Prescribed fire in industrial plantations. In: Goldammer, J. G. (Ed.) Fire in the tropical biota: ecosystem processes and global challenges. Berlin: Springer-Verlag, 1990. p. 216 - 272 (Ecological Studies, v. 84).

Fernandes, P; Loureiro, C. Handbook to plan and use prescribed burning in Europe. Universidade de Trás-os-Montes e Auto Douro, Vila Real-Portugal, 2010. 37 p. (Project Fire Paradox).

Fernandes, P; Botelho, H; Loureiro, C. Manual de formação para a técnica do fogo controlado. Vila Real: UTAD, 2002. 144 p.

Fidelis, A; Delgado-Cartay, MD; Blanco, CC; Müller, CS; PIlLAR, VD; Pfadenhauer, J. Fire intensity and severety in brazilian campos grassland. Interciencia, Caracas, v. 35, n. 10, p. 739 - 745, Oct., 2010.

Fundação ABC. Sistema de monitoramento agrometeorológico. Available from: <http://sma.fundacaoabc.org.br/monitoramento/grafico/diario>. Accessed on: 15/05/2014.

Garnica, JGF, Gonzalez, Dam; Solorio, JDB. Forest fire behavior in prescribed burns under Different environmental conditions in México. Forest Ecology and Management, Amsterdam, v. 234, n. 1, p. 131, 2006.

Griffin, GF; Friedel, MH. Effects of fire on central Australian rangelands I: fire and fuel characteristics and changes in herbage and nutrients. Australian Journal of Ecology, Carlton, v. 9, n. 4, p. 381 - 393, 1984.

Instituto Ambiental Do Paraná (IAP) Unidades de conservação do Paraná: RPPN Reserva Particular do Patrimônio Natural. Available from: <http://www.uc.pr.gov.br/modules/conteudo/conteudo.php?conteudo=131>. Accessed on: 15/05/2014.

Instituto Agronômico Do Paraná (IAPAR) Mapas climáticos do estado do Paraná. Available from: <http://www.pr.gov.br/iapar/sma/Rosa_dos_ventos.htm>. Accessed on: 15/05/2014.

Kuçuk, O; Bilgili, E; Saglam, B; Baskaya, S; Dinç Durmaz, B. Some parameters affecting fire behavior in anatolian black pine slash. Turk J Agric For, Ankara, v. 32, p. 121 – 129, 2008.

Levine, JS. Biomass burning and global change: biomas burning in South America, Southeast Asia, and temperate and boreal ecosystems, and the oil fires of Kuwait. Massachussts Institute of Technology Press, Cambridge, EUA, v. 2, p. 561 – 568, 1996.

Maack, R. Geografia física do estado do Paraná. Curitiba: BADEP/UFPR/IBPT, 1981. 450 p.

Miranda, HS.; Rocha E Silva, EP.; Miranda, AC. Comportamento do fogo em queimadas de campo sujo. In: Miranda, HS.; Saito, CH.; Dias, BFS. (Org.) Impactos de queimadas em áreas de cerrado e restinga. Brasília: UnB, ECL, 1996. p. 1 - 10.

Pivello, VR. The use of fire in the cerrado and amazonian rainforests of Brazil: past and present. Fire Ecology, v. 7, n. 1, p. 24 - 39, 2011.

Pivello, VR.; Coutinho, LM. Transfer of macro-nutrients to the atmosphere during experimental burnings in an open cerrado (brazilian savanna). Journal of Tropical Ecology, Cambridge, v. 8, n. 4, p. 487 - 497, 1992.

Ribeiro, GA.; Lima, GS.; Oliveira, ALS.; Camargos, VL.; Magalhães, MU. Eficiência de um retardante de longa duração na redução da propagação do fogo. Revista Árvore, Viçosa, v. 30, n. 6, p. 1025 - 1031, 2006.

SOaRES, R. V. Incêndios florestais: controle e uso do fogo. Curitiba: FUPEF, 1985. 213 p.

Soares, RV. Queimadas controladas: prós e contras. In: FÓRUM NACIONAL SOBRE Incêndios Florestais, 1., 1995, Piracicaba. Anais..., Piracicaba: IPEF, 1995. p. 6 - 10.

Soares, RV.; Batista, AC. Incêndios florestais: controle, efeitos e uso do fogo. Curitiba, 2007. 264 p.

Souza, LJB; Soares, RV; Batista, AC. Modelagem do material combustível superficial em povoamentos de *Eucalyptus dunnii*, em Três Barras, SC. Cerne, Lavras, v. 9, p. 231 - 245, 2003.

Vega, JA. Investigacion sobre control de incendios en España. In: Reunião Técnica Conjunta FUPEF/SIF/IPEF, 4., 1996, Curitiba; Curso De Atualização Em Controle De Incêndios Florestais, 2., 1996, Curitiba. Anais…, Curitiba: FUPEF, 1996. p. 40 - 56.

Fire Spread across a Fuel Break in a Ridge

Jorge Raposo[a]; Domingos Viegas[a]; Miguel Almeida[a]; Illenia Crissantu[b]; Michel Salis[b]

[a] *Departamento de Engenharia Mecânica, Pólo II da Universidade de Coimbra, Coimbra, Portugal. jorge.raposo@dem.uc.pt*
[b] *University of Sassari, Department of Science for Nature and Environmental Resources (DIPNET), Italy*

Keywords*: Fire Behaviour; Slope Effect; Fuel Break; Flow velocity.*

Abstract
The size of a fuel break in a top of the ridge with several different configurations of slope is studied on this work.
Laboratorial tests were performed to simulate the same geometric conditions of a fire occurred in centre of Portugal and that was extinguished by itself due to the special configurations of slope and geometric barrier to fire spread that correspond to a fire break. Based on this fire other configurations were tested to measured their impact on the probability of the fire crossing the geometric barrier of a gap.

Introduction

It is observed that in some instances a fire spreading upslope, without wind and in the absence of spotting, stops when it reaches the ridge even with a relatively narrow fire break at the ridge top. Referring to fire fighter safety in Green (1977) it is assumed that a fire spreading along a slope of 35º, in heavy brush fuel, with low humidity, and heavy winds, flames with 15 m long flames a fuel break with 60 m is efficient. But if a sharp ridge marked the centre of a fuel break, protection from radiation would be afforded by crouching in the lee of the ridge top, and somewhat less than 60 m would be needed. Indeed a forest road or a maintained right-of-way such as a power or telephone line often serves as a firebreak (Brown and Davis 1973). In Butler & Cohen (1998) a general rule in wich a safety zone radius must be equal or greater than four times the maximum flame height is proposed. This situation was observed for example at fires in Segade (Coimbra) in 2001 and in Sardinia in 2010. In order to analyse this phenomenon and to assess the effectiveness of fire breaks placed at the ridge tops in general the present research was performed.

Experimental Study

Physical problem

We consider a ridge formed by two planar slopes making an angle α_A in face ***A*** and α_B in face ***B*** and assume that there is a fuel break with a width equal to *c* at the ridge top (Figure 1). A fire spreading upslope on face ***A*** in the absence of wind will reach its top with a ROS R_1, a flame length L_1 and will either spread across the fuel break or not.

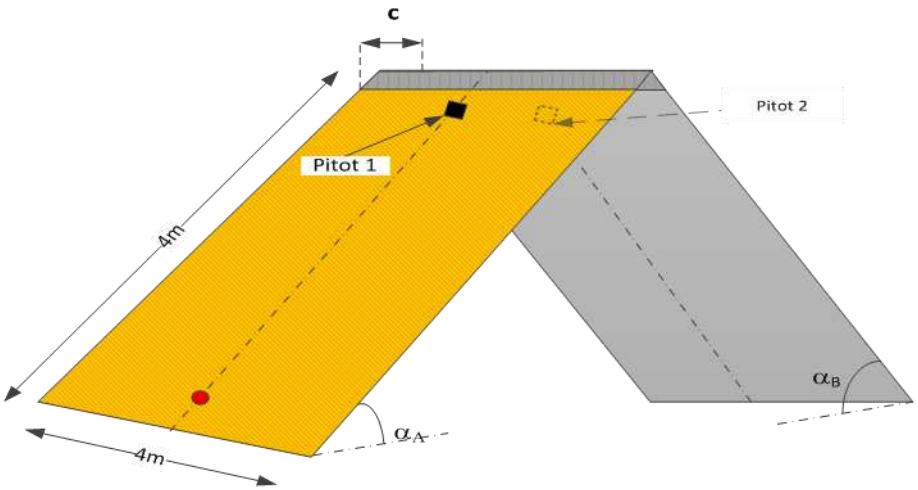

Figure 1. Schematic view of the ridge and the fuel break.

Laboratory Experiments

In the present study an experimental research was carried out at the Forest Fire Research Laboratory of the University of Coimbra on the Dihedral Table that has two faces of 4x4m^2 each that can be inclined independently between -45º and +45º in relation to the horizontal reference (figure 2a).


a)


b)

Figure 2. Picture of the test SE11 with parameters: α_A=40º, α_B= -20º, c=0.30m. a) Front view, b) Side view with detail of the ridge and fuel break.

The fuel bed was made with straw with a fuel load of 0.6 kg/m^2 (dry basis) and the fire was ignited at a point in the centre line of face A 0.25m above its lower edge. The fuel covered the entire face A and only 1.6x4 m^2 on face B. The ROS of the head fire was measured using strings of cotton placed across the fuel bed with a gap of 20cm between them. A pair of S Type pitot tubes equipped with thermocouples was placed near the ridge top to measure flow velocity even inside the flames at the positions indicated in figure 2a). A video camera was used to record and analyse the flame front near the ridge top to capture a side vew of the fire front when it approached the ridge line (figure 2b)). Several tests were performed with various combinations of slope angles αA and αB with fuel break widths in the range of 0 to 0.3m. The main parameters of the tests are given in Table 1.

Table 1. Set of experiments and main parameters.

Ref.	α_1	α_2	C (m)	M_c (kg/m^2)	m_f (%)
SE 1	30	30	0,00	0,6	8,46
SE 2	30	-20	0,00	0,6	8,10
SE 3	30	-30	0,00	0,6	8,10
SE 4	30	-40	0,00	0,6	7,29
SE 5	30	-40	0,00	1	7,64
SE 6	30	-30	0,30	0,6	8,70
SE 7	30	-20	0,30	0,6	8,30
SE 8	30	-10	0,30	0,6	13,89
SE 9	30	0	0,30	0,6	9,89
SE 10	30	10	0,30	0,6	9,76
SE 11	40	-20	0,30	0,6	14,41
SE 12	40	-10	0,30	0,6	9,53
SE 13	40	0	0,30	0,6	9,53
SE 14	40	0	0,15	0,6	8,58
SE 15	40	10	0,15	0,6	9,80
SE 16	30	10	0,15	0,6	9,80
SE 17	30	20	0,15	0,6	13,10
SE 18	30	30	0,15	0,6	13,10
SE 19	30	40	0,15	0,6	11,96
SE 20	30	0	0,15	0,6	11.10
SE 21	30	-10	0,30	0,6	13,00
SE 22	30	20	0,30	0,6	13,00
SE 23	40	10	0,30	0,6	9,00

Results and Discussion

4.1. Probability of fire crossing

In figure 3 a plot of the cases in which the fire went or did not go across the fuel break as a function of c/L_1 is presented. The value one in this graph indicates that the fire passed the fuel break while the value zero indicates the contrary. Only for cases in which the slope angle α_B was positive we had passage of the fire. The terrain configuration in such cases is not really a ridge. As can be seen in this figure a relatively small value of c/L_1 of the order of 0.2 seems to be sufficient to stop the fire which is much smaller than the value of c/L_1 =4 presented in Green, (1977) for the case described above.

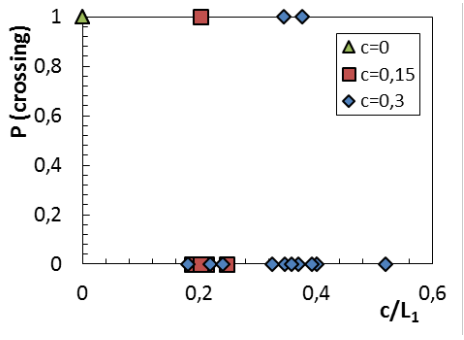

Figure 3. Probability of fire crossing as a function of c/L_1 for all tests.

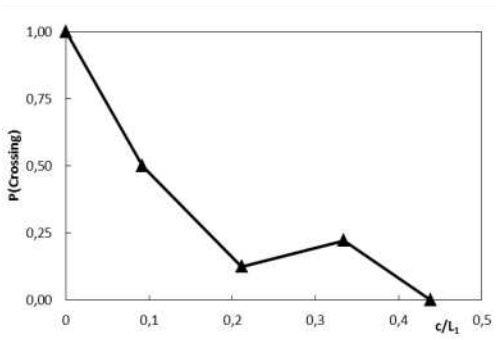

Figure 4. Average probability of fire crossing as a function of c/L_1 for classes with a step of 0.13 between them.

In figure 4 the average probability of crossing for different classes of values of c/L_1 is presented. The range of values were split in groups of values of c/L_1 with a length of 0.13 between them and the correspondent value of the probability for each class of c/L_1 was plotted. In agreement with the previous data a sharp decrease of the probability of the fire crossing with the increase of relation c/L_1 is clear. For c/L_1 >0.2 the probability of crossing becomes constant with a small increase for c/L_1 close to 0.36. Comparing figure 3 with the data of the figure 4 it is possible to relate this small increase with the occurrence of two crossings of the fire to the face B. After this occurrence no more crossings were registered with the increase of c/L_1 making the value of the probability of crossing to decrease to zero for c/L_1=0.4.

Radiation

Using a simple model based on principles of radiation presented in Wong (2003) was estimate the radiation flux from a vertical flame with constant height to an infinitesimal element of area, with an area of 0,05x0,05m^2, placed on face B at the centreline at a distance c from the base of the fire (figure 5) the results were plotted in figure 5 were obtained.

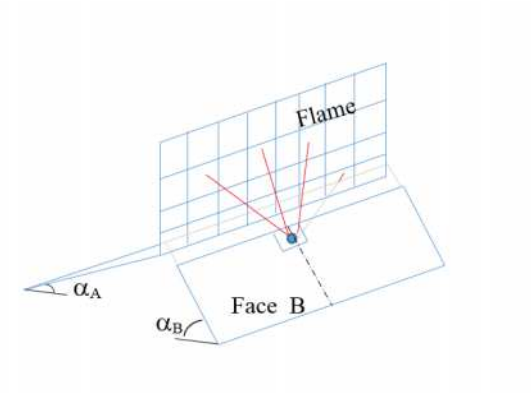

Figure 5. Skecth of the radiation flux from the vertical flame in the side A for the target in face B.

The properties of the flame and the slope of face B were established according to the average values obtained in the tests for the points plotted in figure 4, a table with the values is presented below.

Table 2. Set of data for the computation of the radiant flux.

α_{Bavg}	g/L_1	$q(kW/m^2)$
-40	0,00	94,47
-15	0,09	83,30
-20	0,21	65,12
-15	0,33	52,00
-10	0,44	40,17

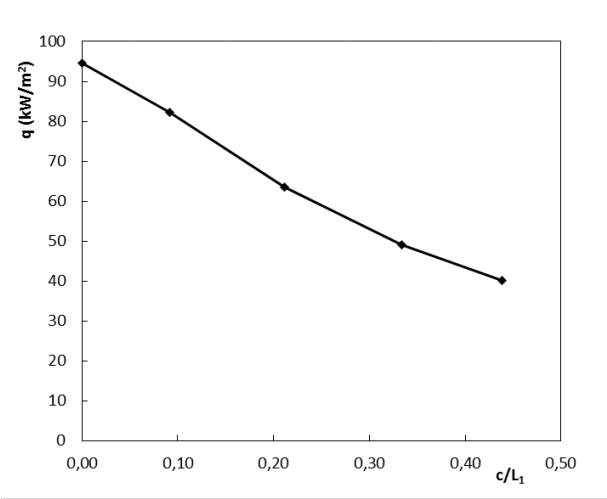

Figure 6. Computation of the net rate at which an infinitesimal element face B gains radiation due to the interaction of the flame in the side a for several values of c/L_1.

By the analysis of the data is possible understand as was expected that the rate of radiation that arrives to the face B is greatly affected by the distance between the two surfaces. It is possible to see that the trend shown in figure 4 for the variation of the average probability of fire crossing as a function of c/L_1 is very similar to the decrease of the radiation flux on the surface element that is shown in figure 5 putting in evidence the role of flame radiation in this process.

4.2. NDROS (R') and Induced Flows

In figures 6 to 8 results from NDROS (R') on face ***A*** and of flow velocity are shown as a function of time. In these tests the fire did not cross the fuel break. The coloured lines indicate the times of the end of spreading of fire for each test. The flow velocity U_1 measured at P1 is shown in figure 7 and the flow velocity U_2 measured at P2 is shown in figure 8.

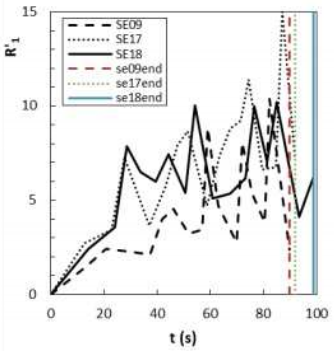

Figure 6 –ROS values as a function of time for tests: SE 09, SE 17and SE 18

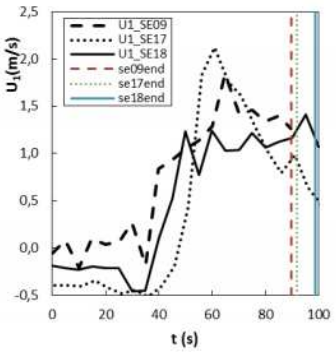

Figure 7. Flow velocity at positions P_1 as a function of time for tests: SE 09, SE 17 and SE 18

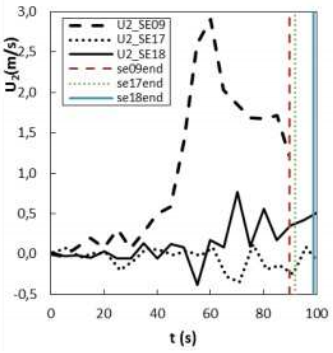

Figure 8. Flow velocity at positions P_2 function of time for tests: SE 09, SE 17 and SE 18

In the case of SE 09, dashed line, with configuration α_B=0º, the increment of the NDROS with a maximum of 10 is visible in figure 5 plotted with dashed line, coincident with this increment is the increment of the flow in both pitot tubes. The presence of a positive flow meaning that the flow is in same direction of the rate of spread was observed. The maximum flow was registered at P_2 (face B), figure 7, with the value of 3m/s. It was noticed at least in U_1 flow (figure 6) some negative periods that could correspond to the indraft of air towards the fire front as the slope of side B is not a barrier to the income of air this type of flow is allowed.

In the case of SE 17 α_B=20º, dotted line, an increment of the NDROS with the course of time until the end of side A, with a peak of 11m/s and then appears the maximum of 15m/s, was also observed.
In figure 6 it is detected that the flow measured at P_1 starts with a decreasing to negative values of -0.5m/s and then have a sharp increase until a maximum of 2.1 m/s. The value of the flow registered at P_2 was mainly negative or close of zero the reason of this behaviour could lie on the fact of the second slope works as a barrier to the feeding air for the fire front and only when the fire front is very close of P_2 it was observed some positive flow.
In the last experiment, plotted with a bold black line, that is the test SE18 with α_B=30º, was registered an increasing of NDROS very sharp and with several fluctuations the maximum value recorded was of 10 the difference in relation with the others is that in all the experiment several times was recorded high values of the NDROS.
The flow velocity U_1 also was high and constant, only at the beginning a negative flow of -0,5 m/s was recorded and then the flow shifted to positive and more or less stable at the values of 8-9 m/s. As in previous case the presence of the second slope of the face B could cause some interference on the free progress of the flow and for that the P_2 in the major part of the test present a negative flow that is against the fire spread direction and only in the very end an increase of the flow velocity to values of less than one 0.5 m/s but favourable to fire spread was registered.

Conclusion

Our results show that with a ridge shape like the one tested by us in the absence of wind the flow induced by the fire does not cause an inclination of the flame front towards the unburned fuel (figure 2b)) and consequently the fire does not spread across the fire break.
The probability of the fire crossing the fuel break decreases with the increase of the parameter c/L_1 and therefore it indicates that radiation is the dominant heat transfer mechanism in this process. The explanation of this lies on the fact that even for small values of the gap between the fire front and the unburned fuel bed on face B the radiation flux is relatively small and consequently the fire does not spread across the fire break.

Acknowledgements

The authors wish to thank Portuguese Science Foundation for the support given to project Extreme under contract PTDC/EME-MFE/114343/2009 and for a PhD grant under contract SFRH / BD / 85557 / 2012. The participation of Illenia Crissantu was supported by a grant from the Sardinia Region in the context of the Master PIROS program. Dr. Salis is supported by the Project “Modeling approach to evaluate fire risk and mitigation planning actions”.

Symbols

Symbol	Units	Description
α_A	-	Inclination angle of face *A*
α_B	-	Inclination angle of face *B*
O	-	Origin of reference Cartesian system
c	*m*	Fuel break dimension
R'	-	Non-dimensional rate of spread (NDROS)
U_1	$m.s^{-1}$	Flow velocity measured by Pitot 1

U_2	$m.s^{-1}$	Flow velocity measured by Pitot 2
P1	-	Pitot station 1
P2	-	Pitot station 2
q	(kW/m^2)	Net rate of radiation

8. References

Brown, A, and Davis, K. 1973. Forest Fire Control and Use. New York: McGraw-Hill Book Company.

Green, Lisle R. 1977. Fuelbreaks and Other Fuel Modification for Wildland Fire Control. U.S. Dep. Agric., Agric. Handb. 499, 79, p., illus.

Butler BW, Cohen JD. 1998. Firefighter Safety Zones: A Theoretical Model Based on Radiative Heating. International Journal of Wildland Fire 8 , 73–77.

Wong, K.F.V. 2003. Intermediate heat transfer. Vol. 155: CRC

FireStar3D: 3D finite volume model for the prediction of wildfires behaviour

G. Accary [a], S. Meradji[b], D. Morvan[c,d], O. Bessonov[d], D. Fougère[e]

[a] *Beirut Arab University, Tripoli, Lebanon, g.accary@bau.edu.lb*
[b] *IMATH, EA 2134, Université de Toulon, Toulon, France, meradji@univ-tln.fr*
[c] *UNIMECA, Aix-Marseille Université, Marseille, France, dominique.morvan@univ-amu.fr*
[d] *M2P2, UMR 7340 CNRS - Aix-Marseille Université, Marseille, France, dominique.fougere@univ-amu.fr*
[e] *Institute for Problems in Mechanics RAS, Moscow, Russia, bess@ipmnet.ru*

Abstract
Most of the operational tools of fire propagation in natural environment are based on statistical or semi-empirical approaches. However, under conditions that deviate from the database used to construct these models, extrapolation may be completely random and, therefore, not very reliable. Subsequently, other models have been developed, taking into account the various interactions occurring between the vegetation and the surrounding fluid medium. This approach is based on a very detailed modeling of the physicochemical phenomena involved in a fire that are quite complex (turbulence, combustion, radiation, interaction between the fluid and vegetation ...). The 3D model developed in this work (referred to as "FireStar3D") is part of the latter class of models, and consists in solving the conservation equations of the coupled system consisting of the vegetation and the surrounding gaseous medium. The model takes into account the phenomena of vegetation degradation (drying, pyrolysis, combustion), the interaction between an atmospheric boundary layer and a canopy (aerodynamic drag, heat transfer by convection and radiation, and mass transfer), and the transport within the fluid phase (convection, turbulence, gas-phase combustion). This paper presents the validation of this 3D model that was conducted for a fire in confined environment, by reproducing experiments of fuelbed fire in a wind tunnel carried out by Catchpole *et al*. in 1998. The comparison between the simulations and the experimental data is mainly based on the rate of spread of fire or ROS (velocity of the fire front). A good agreement is obtained for most of the simulations that were conducted, and a study of the dependence of the rate of spread on the wind speed and on the fuel bed characteristics, particularly the fuel moisture content, is carried out.

Keywords*: Forest fires, turbulent reactive flows, modelling and numerical simulation, high performance computing.*

Introduction

As evidenced by the literature, most of the operational tools of fire propagation in natural environment are based on statistical or semi-empirical approaches [1]. However, under conditions that deviate from the database used to construct these models, extrapolation may be completely random and, therefore, not very reliable. Subsequently, other models have been developed; in these models, the study of the spread of a fire and its behavior are addressed through its physicochemical aspects, taking into account the various interactions occurring between the vegetation and the surrounding fluid medium [2]. This multiphase approach is indeed based on a very detailed modeling of the physicochemical phenomena involved in a fire that are quite complex (turbulence, combustion, radiation, interaction between the fluid and vegetation, ...). To better understand the phenomenon of the spread of fire in natural environment, the model developed in this work is part of the latter class of models, and consists in solving the conservation equations of the coupled system consisting of the vegetation and the surrounding gaseous medium [3]. This model is already operational in a 2D approximation [4] and

consists in solving the multi-physical model in a vertical plane defined by the direction of fire propagation. The 3D extension of the existing model enables to render the 3D effects observed in real fires and to represent the real heterogeneous structure of the vegetation. The objective of this paper is to evaluate the potential of this 3D model (referred to as "FireStar3D") that has been mainly developed within the context of the European integrated project "FireParadox". This leading evaluation was conducted for a fire in confined environment by reproducing experiments of fuelbed fire in a wind tunnel (the so-called Rothermel configuration), carried out by Catchpole *et al*. in 1998 [5].

Modelling and Numerical Method

The present multiphase formulation, detailed in [3, 4, 6, 7], is based on the description of the behaviour of the coupled system formed by the vegetation and the surrounding atmosphere. The model consists of two parts: one part devoted to the calculation of the turbulent-reactive fluid flow resulting from the mixture of the pyrolysis and combustion products and the ambient air, and a second part devoted to the evolution of the state of the solid vegetation subjected to the intense heat flux coming from the flaming zone. Each solid fuel particle is assimilated as a mixture of water, dry foliage (or dry wood), char, and residual ashes. During fire propagation, the degradation of the vegetation is represented using a three steps temperature-dependent mechanism (drying, pyrolysis, and char oxidation), where the constants (activation energy and pre-exponential factor) are evaluated empirically from thermo-gravimetry Analysis (TGA), performed for solid fuel samples [6]. It is assumed that the pyrolysis process can be activated only if the dehydration was completed, and that the surface oxidation can begin only if the pyrolysis was completed. The gas flow around the fire is considered to be fully unsteady and turbulent. To extract a coherent behaviour, the balance equations (mass, momentum, energy, and chemical species) governing the time evolution of the fluid phase are filtered using a weighted average RANS (Favre) formulation [8]. The interaction between the ambient atmosphere and the vegetation is taken into account through additional terms in the equations (gas production due to pyrolysis reaction, drag force, heat transfer by convection and radiation exchange with solid phase, …). The closure of these equations is done using an eddy viscosity concept [9], evaluated from the turbulent kinetic energy and its dissipation rate. An adapted statistical two-equations (k-Epsilon)-RNG version turbulence model in a high Reynolds number formulation is employed [10,11]. The Eddy Dissipation Concept (EDC) combustion model [9,12] is used to evaluate the combustion rate in the gaseous phase, where it is assumed that the reaction is mainly limited by the mixing rate between the pyrolysis and the oxygen of the ambient air. Convection and radiation heat transfers between the hot gazes, the flame, and the unburned solid fuel are taken into account as follows: the convection heat transfer coefficient is modelled using empirical correlations [13] and the radiation heat transfer is obtained by solving the radiation transfer equation (RTE) [14] in which the contribution of the flames (soot particles) and the embers is included [3]. The fluid enthalpy-temperature dependence is treated using the CHEMKIN thermodynamic database [15]. Finally, the soot volume fraction field is obtained by solving a transport equation [16,17] including a thermo-phoretic convective contribution [3] and a soot oxidation term [18].

The fluid flow conservation and transport equations are solved numerically by a fully implicit finite volume method in a segregated formulation [19]. "FireStar3D" predicts turbulent reacting flows in rectangular domains on a structured but non-uniform staggered mesh. The time discretization relies on a third order Euler scheme with variable time step. To ensure the numerical stability, the space discretization is based on second order schemes with flux limiters (Quadratic Upstream Interpolation scheme [20] and ULTRA-SHARP [21]) for convection terms while diffusion terms are approached by central difference approximation with deferred corrections [22] to maintain accuracy. The Radiative Transport Equation (RTE) is solved using a Discrete Ordinate Method (DOM), consisting in the decomposition of the radiation intensity in a finite number of directions. This set of discrete contributions is integrated using a numerical Gaussian quadrature rule (a S8 method is used) for the

calculation of the total irradiance [23]. The set of ordinary differential equations describing the evolution of solid fuel are solved separately using a fourth order Runge-Kutta method. From implementation point of view, the code is parallelized [24] and optimized [25] using the APIs OpenMP and HMPP directives (suitable for shared memory platforms and accelerators) and is operational on a high-performance computing machines consisting of a SMP node using modern processors with INTEL Xeon Phi co-processors and NVIDIA graphic cards. Finally, the hydrodynamic module of the code has been extensively validated on several benchmarks of laminar and turbulent natural convection, forced convection and neutrally stratified flow within and above a sparse forest canopy [26-31].

Rothermel configuration

As mentioned in introduction, in the framework of validating "FireStar3D", several experiments of fuelbed fire carried out by Catchpole *et al*. in a wind tunnel are reproduced numerically. Figure 1 shows a perspective view of the flow computation domain; all the simulations were carried out using the same geometric parameters and the depth of the fuel bed δ was fixed at 20.3 cm. The fuel bed is divided into two zones that have the same characteristics, however only zone (2) is thermally degradable. Zone (1) was added to account for the wire mesh spoiler used in the experiment that was placed on the floor of the wind tunnel from wall to wall, 2 m upwind the fuel trail, and was adjusted to have the same height as the fuel depth; as mentioned by Catchpole *et al*., this wire mesh was placed in order to simulate a longer reach of the fuel and its resulting turbulent boundary layer. Also, vertical strips of metal sheeting (25 cm high) were placed in the experiments along each side of the tray to mimic a wider fire front by preventing indrafts into the combustion zone. These strips were accounted for numerically by placing vertical baffles along each side of the fuelbed (see Figure 1); the velocity component normal to the baffles (y component) is set to zero, while a drag coefficient $C_D = 1.0$ (based on the baffles exposed surface) was introduced in the momentum equations of the velocity components tangential to the baffles (x and z components). The value of the drag coefficient $C_D = 1.0$ resulted in a quasi-uniform fire-front, as observed experimentally.

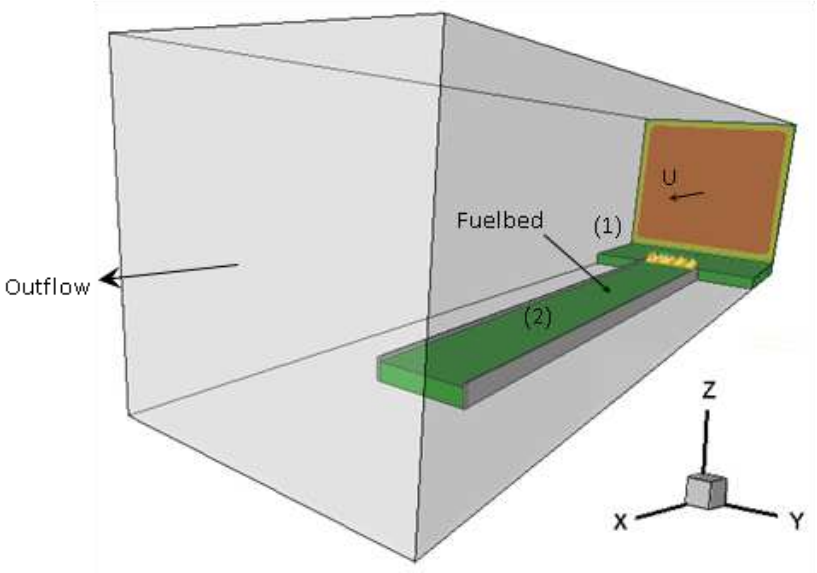

Figure 1. Perspective view of the computation domain corresponding to Catchpole et al. experiment. The flow domain dimensions are $12\times3\times3$ m3 and those of the fuel bed are $10\times1\times\delta$ m3 (δ = 20.3 cm). The fuel bed is divided into two zones, only zone (2) ($2m < x < 10m$) is thermally degradable, vertical baffles (25 cm high) are placed along both sides of zone (2) and fire is set at its entrance.

Before ignition, simulations were run long enough using Neumann conditions at the open boundaries while maintaining a negative pressure gradient in the x-direction that was adjusted in order to reach a turbulent steady state with the desired mean wind speed that was imposed in the experiment; 5 seconds were sufficient for this phase. Then, the turbulent velocity profile, obtained at channel inlet at the end of this phase, is applied (as a Dirichlet condition) at the inlet of the domain during the remaining time

of simulations. At t = 5 s, fire is set at the entrance of zone (2) by injecting carbon dioxide at 1600 K from the bottom of the computation domain for another 5 s. The injection surface lies between x = 2 m and x = 2.16 m, and along the entire width of zone (2). At t = 5 s, the average injection velocity is at its maximum (V_j = 10 cm/s), then it decreases linearly with the burned mass of dry material (m_b) according to the equation (1) in order to avoid destabilizing the fire-front by suddenly ceasing the injection.

$$V_j(cm/s) = 10 \times \left(1 - \frac{m_b}{m_{b0}}\right) \quad (1)$$

where m_{b0} is the initial mass of dry material located above the burner (i.e. the mass of dry material inside the volume $V_{b0} = 0.16 \times 1 \times \delta$ m^3). Eq. (1) is used between t = 5 s and t = 10 s as long as V_j remains positive, injection of carbon dioxide is ceased if V_j reaches zero during this time interval.
Several simulations were conducted for different wind speeds and for different moister contents of the fuelbed. The simulations correspond to experiments EXMC 23, 24, 28, 36, 48, and 69 carried out by Catchpole *et al*., in which regular excelsior is considered; the main physical data of the simulations are shown in Tab. 1. A wall-refined mesh of 300×80×62 grid points was used for the fluid domain, while a uniform mesh was used for the solid domain with a grid size (Δx, Δy, Δz) = (2 cm, 1.25 cm, 1.69 cm). Since a high-Reynolds turbulence model is used in the simulations, the fluid domain mesh was carefully chosen to be fine enough for an accurate description of the solution, while respecting the condition $11.5 < y^+ < 500$ during the entire simulations time. The results were obtained using an adaptive time-step strategy based on a local truncation error approach, with time steps in the range of 0.001 to 0.01 seconds. At each time step, the conservation and transport equations were solved with an accuracy of 10^{-4} in normalized form.

Table 1. Rothermel configuration experiments chosen to show the effect of wind speed and moister content on fire spread dynamics. δ - fuelbed depth, U - wind speed, α - packing ratio, σ - surface area to volume ratio, M - moister content. Regular excelsior (particles density ρ_P = 398 Kg/m^3) is considered in all experiments.

	σ (m^{-1})	α	δ (cm)	U (m/s)	M (%)
EXMC23	7596	0.005	20.3	2.68	5.5
EXMC24	7596	0.005	20.3	0.89	5.2
EXMC28	7596	0.005	20.3	1.79	5.4
EXMC36	7596	0.005	20.3	2.68	10.1
EXMC48	7596	0.005	20.3	2.68	18.0
EXMC69	7596	0.005	20.3	2.68	3.0

Results

Figure 2 shows the temperature field obtained at t = 15 s (i.e. after 10 s of burning) in the simulation corresponding to experiment EXMC23 in Tab. 1 (U = 2.68 m/s and M = 5.5%); figure 2 shows the development of the flame and the expected propagation of fire. Figure 3 shows the corresponding distributions of temperature and dry material fraction at fuelbed-surface; figure 3 shows clearly the quasi-uniform fire-front obtained experimentally as mentioned in the previous section, and we notice also that the fuelbed upstream the ignition line (at x = 2 m) remains intact during the entire simulation time.

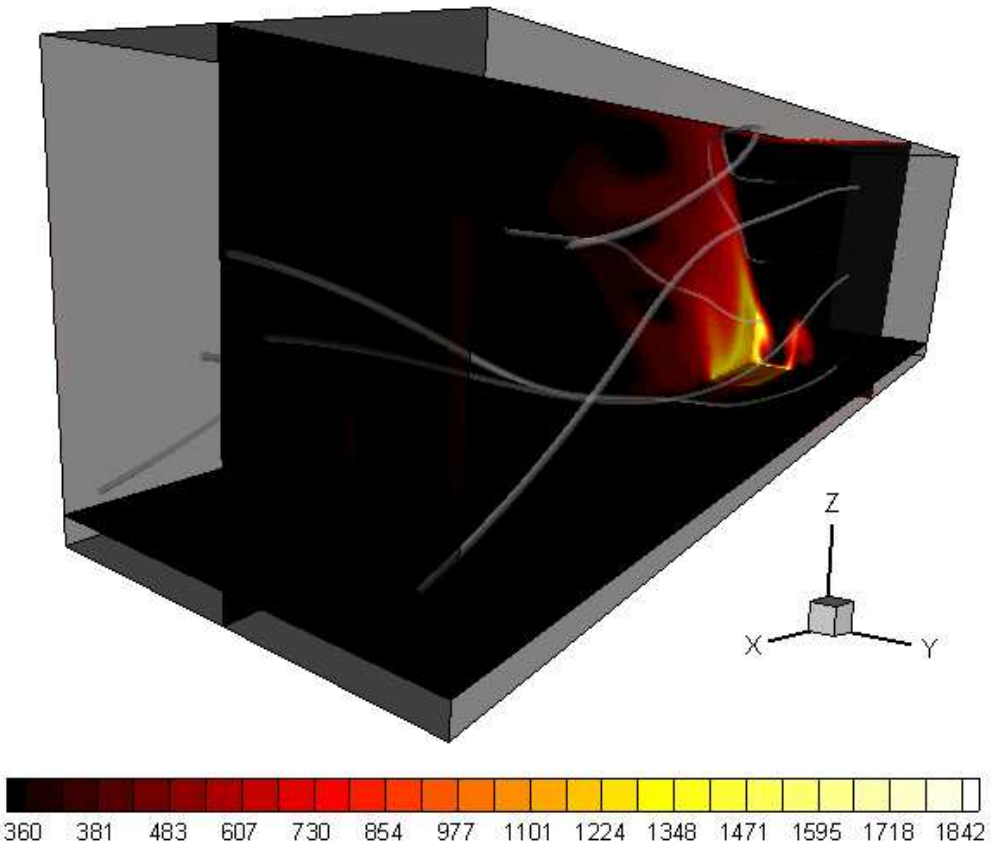

Figure 2. Temperature field and some streamlines obtained at t = 15 s, corresponding to experiment EXMC23 of Catchpole et al. (regular excelsior, wind speed of U = 2.68 m/s, moister content 5.5%, see Tab. 1 for more details).

The comparison between the simulations and the experimental data is based on the rate of spread of fire or ROS (i.e. the average velocity of the fire front). For this purpose, fuelbed characteristics were monitored at several positions along the line (y = 1.5 m, z = 0.203 m) as shown in Figure 4, by analogy to the photocell tubes positioned at 0.5 m intervals in Catchpole *et al*. experiments. Figure 5 shows the time evolution of the fuelbed temperature at duly chosen points of Figure 4; we clearly notice the phases of pyrolysis and char combustion. Indeed, according to the solid-fuel combustion model implemented in "FireStar3D", pyrolysis of dry material takes place between 400 K and 500 K, while char combustion starts once all dry material at a given location has been consumed. The ROS could be easily estimated from Figure 5 by measuring the average time required for the pyrolysis front (isotherm 500 K) to move from a monitoring point to another (covering each time the distance of 0.5 m). However, a simpler and more accurate method for estimating the rate of fire spread consisted in finding at each time step of simulation the average position of the pyrolysis front at the fuelbed surface. This was done by determining the average positions of the furthest points downstream the ignition line where the dry material fraction is equal to zero. In Figure 3(a), we clearly distinguish the pyrolysis front, it corresponds to the white-black interface located at about x = 5 m. Figure 6 shows the time evolution of the fire-front positions for duly chosen simulations; the ROS was obtained by evaluating the average slopes of the curves in Figure 6 after t = 10 s (end of ignition time). We notice, as expected, that increasing the wind speed or decreasing the fuelbed moisture-content increases the rate of fire spread.

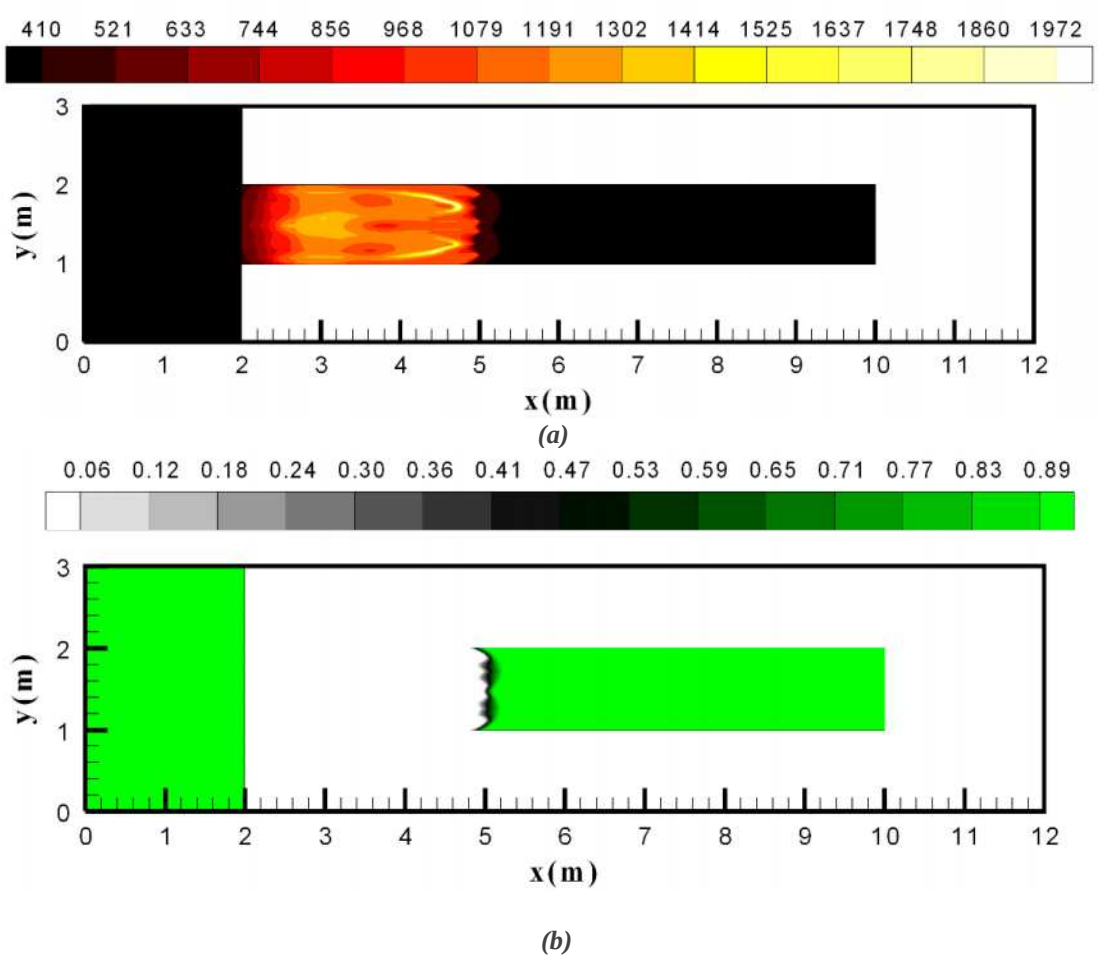

Figure 3. Temperature (a) and dry material fraction (b) distributions at fuelbed-surface (z = 0.203 m) obtained at t = 15 s, corresponding to experiment EXMC23 of Catchpole et al. (regular excelsior, wind speed of U = 2.68 m/s, moister content 5.5%, see Tab. 1 for more details).

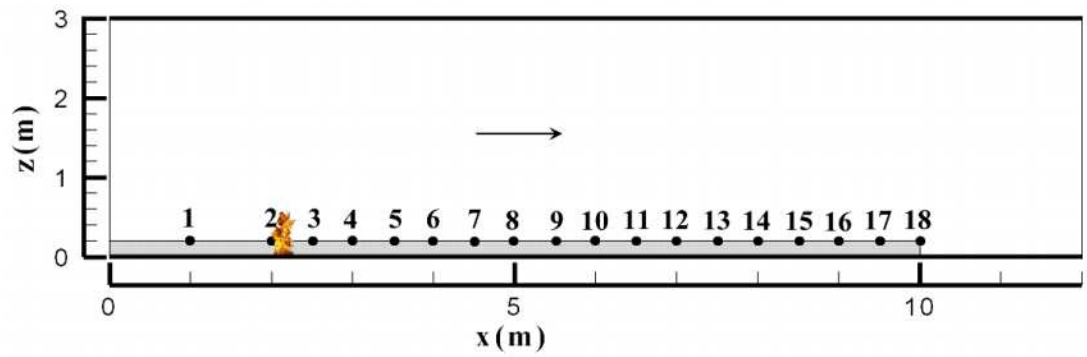

Figure 4. Positions in the vertical median plan of the computation domain (at y = 1.5 m) where fuelbed characteristics are monitored during simulation.

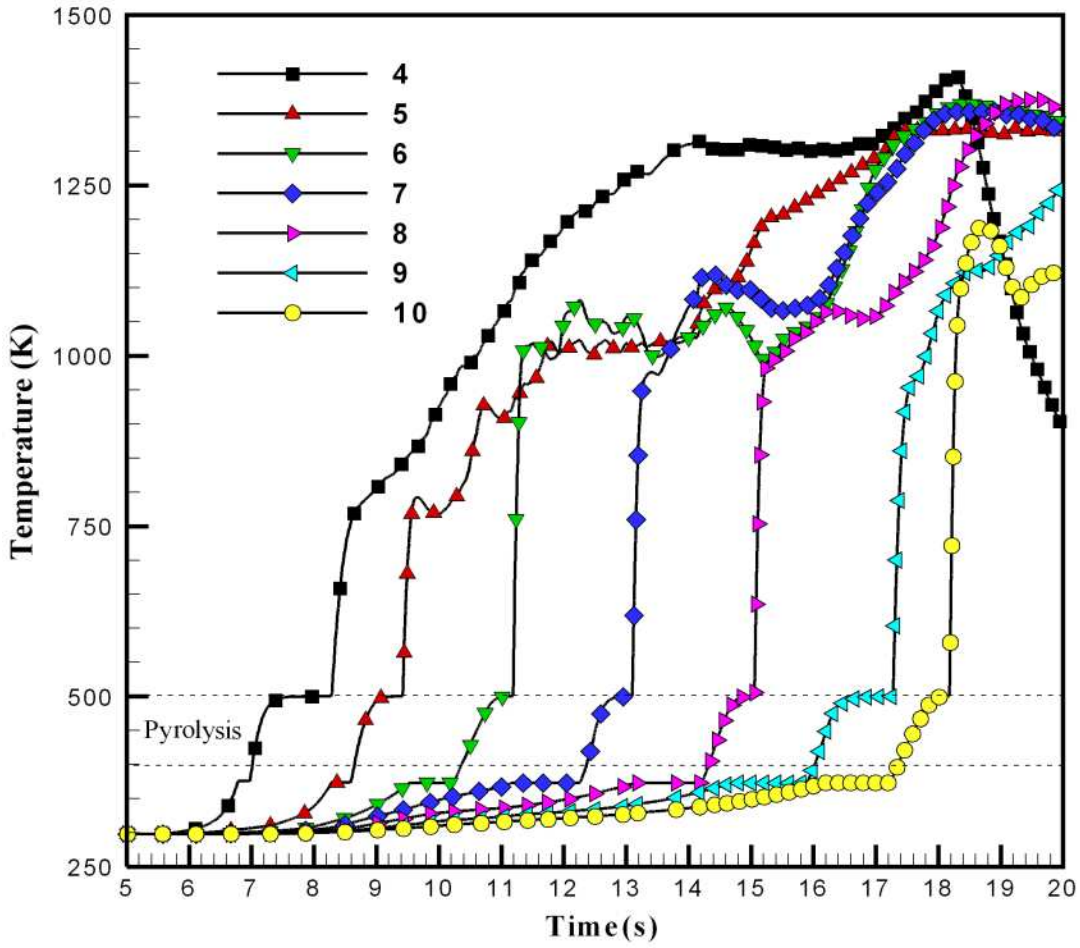

Figure 5. Time-evolution of the fuelbed temperature at positions 4 to 10 of Figure 4, corresponding to experiment EXMC23 of Catchpole et al. (regular excelsior, wind speed of U = 2.68 m/s, moister content of 5.5%, see Tab. 1 for more details).

The rates of fire spread were evaluated for the different simulations that had been conducted and are shown in Tab. 2, compared to those obtained experimentally. Table 2 shows also ROS values obtained using the correlation given by eq. (2) that was established by Catchpole *et al*. for different fuel types and properties using 357 experimental fires.

$$ROS = \frac{\left(I + mU^{n}\right)e^{-347/\sigma}\alpha^{-0.499}e^{-kM}}{\rho_{P}\left(Q_{P} + MQ_{W}\right)} \qquad (2)$$

Where I = 495.5, m = 1934, n = 0.91, and k = – 0.73 are model constants, and Q_P = 711 KJ/Kg and Q_W = 2250 KJ/Kg are the pyrolysis heat and water latent heat respectively.

We notice first that "FireStar3D" predicts the correct order of magnitude of the rate of fire spread (which is not easy to obtain for confined fires) and its correct dependence on the wind speed and on the fuelbed moisture-content. We notice also that, even though FireStrar3D seems to overestimate the rate of fire spread in the case of Rothermel configuration, especially for low wind speeds (EXMC24), the predicted ROS values are comparable to those obtained experimentally or estimated using different analytical models.

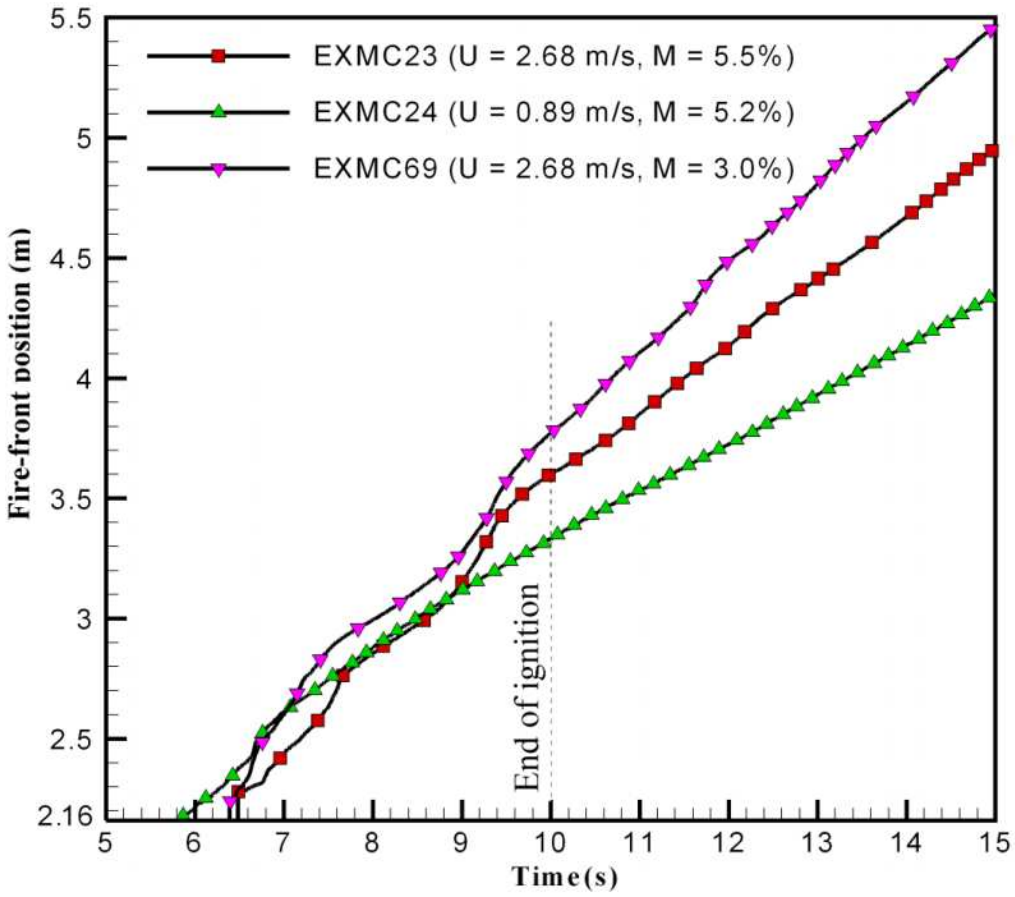

Figure 6. Time-evolution of the average position of the pyrolysis front, corresponding to experiment EXMC23, EXMC24, and EXMC69 of Catchpole et al., showing the effect of wind speed and moisture content on the rate of fire spread. The ROS is the average slope of the curve after t = 10 s (end of ignition time).

Table 2. Comparison of the rates of spread (in m/s) obtained numerically using FireStar3D, experimentally, and using the correlation established in Catchpole et al. (eq. 2) for the different experiments shown in Tab. 1.

	EXMC23	EXMC24	EXMC28	EXMC36	EXMC48	EXMC69
Simulation	0.285	0.201	0.241	0.230	0.199	0.345
Experiment	0.252	0.105	0.129	0.156	0.175	0.242
Correlation	0.221	0.094	0.159	0.203	0.181	0.232

Conclusions

A fully-physical wildfire model was used to simulate a confined fire in a wind tunnel. A preliminary study was carried out in the case of a homogeneous fuel bed to evaluate the potential of the model to predict fire behaviour. The obtained result were analysed in terms of fire front rate of spread (ROS) and shape, for different wind velocities and fuel moisture content values and compared with experimental data from the literature (measurements and empirical correlations). Globally, the obtained results compare well enough to experimental data, despite the relative difficulty of the considered configuration (confinement effects) and a consistent monotonicity is observed numerically

when varying the control parameters (wind speed and moisture content) accordingly to the realistic physical expectations. The next step will be to extend the investigation to other set of parameters (influence of particle size, other fuel types, …) and also to consider heterogeneous fuelbeds in this confined configuration for which correlations also exist. Finally and beyond the scope of this work, prospective numerical simulations for grassland fires were also carried out for different values of wind velocities; the leading results are in good agreement with some previous numerical studies and experimental data from literature.

Acknowledgements

The authors would like to thank the "Méso-Centre de Calcul de Marseille" for granting the access to the computer systems.

References

[1] M.A. Finney and K.C. Ryan. Use of the FARSITE fire growth model for fire prediction in US National Parks. Proc. International Emergency Management and Engineering Conference, Sophia-Antipolis, 1995, p. 186.
[2] A.M. Grishin. Mathematical modeling of forest fires and new methods for fighting them. In: F. Albini (Ed.), Tomsk University, Tomsk, 1997.
[3] D. Morvan and J.L. Dupuy. Modeling of fire spread through a forest fuel bed using a multiphase formulation. Combustion and Flame, 127, 2001, p. 1981-1994.
[4] D. Morvan and J.L. Dupuy. Modeling the propagation of a wildfire through a Mediteranean shrub using a multiphase formulation. Combustion and Flame, 138, 2004, p. 199-210.
[5] W.R. Catchpole, E.A. Catchpole, B.W. Butler, R.C. Rothermel, G.A. Morris and D.J. Latham. Rate of spread of free-burning fires in woody fuels in a wind tunnel. Combustion Science and Technology, 131, 1998, p. 1-37.
[6] D. Morvan, S. Meradji and G. Accary. Wildfire behaviour study in a Mediterranean pine stand using a physically based model. Combustion Science and Technology, 180, 2008, p. 1-19.
[7] D. Morvan, S. Meradji and G. Accary. Physical Modeling of fire spread in Grasslands. Journal of Fire Safety, 44, 2009, p. 50-61.
[8] A. Favre, L.S.G. Kovasnay, R. Dumas, J. Gaviglio and M. Coantic. La turbulence en Mécanique des Fluides. Gauthier-Villars, 1976.
[9] G. Cox. Combustion fundamentals of fire. Academic Press, 1995.
[10] V. Yakhot and M. Smith. The renormalization group, the epsilon-expansion and derivation of turbulence models. J. Scientific Computing, 7(1): 35-61, 1992.
[11] S.A. Orszag. Introduction to renormalization group modeling of turbulence. Oxford University Press, p. 155-183, 1996.
[12] B.F. Magnussen and H. Hjertager. On mathematical modeling of turbulent diffusion flame in cross flow. Combustion Sci. and Tech., 140, p. 93-122, 1998.
[13] F.P. Incropera and D.P. De Witt. Fundamentals of heat and mass transfer. John Wiley and Sons. Chichester, UK (4th edition), 1996.
[14] R. Siegel and J.R. Howell. Thermal Radiation Heat Transfer. Hemisphere Publishing Corporation, Washington D.C., 3rd edition, 1992.
[15] R.J. Kee, F.M. Rupley and J.A. Miller. The CHEMKIN thermodynamic data base. Technical report, Sandia National Laboratories, 1992.
[16] K.J. Syed, C.D. Stewart and J.B. Moss. Modelling soot formation and thermal radiation in buoyant turbulent diffusion flames. In 23rd Symposium (International) on combustion, The Combustion Institute, Pittsburgh, p. 1533, 1990.

[17] J.B. Moss, in G. Cox (Ed.). Turbulent Diffusion Flames. Academic Press, London, UK, p. 221-272, 1990.
[18] J. Nagle and R.F. Strickland-Constable. Oxidation of carbon between 1000-2000°C. In Proceeding 5th Conference on Carbon, vol. 1, p. 154-164, 1962.
[19] S.V. Patankar. Numerical Heat Transfer and Fluid Flow. Hemisphere Publishing, New York, 1980.
[20] Y. Li and M. Rudman. Assessment of higher-order upwind schemes incorporating FCT for convection-dominated problems. Numerical Heat Transfer B, 27, p. 1, 1995.
[21] B.P. Leonard and S. Mokhtari. Beyond first-order upwinding: the ultra-sharp alternative for non-oscillatory steady-state simulation of convection. Int. J. Numerical Methods Engineering, 30, p. 729-766, 1990.
[22] M. Peric. Computational Methods for Fluid Dynamics. Springer-Verlag.
[23] M.F. Modest. Radiative Heat Transfer. Academic Press, 2003.
[24] G. Accary, O. Bessonov, D. Fougère, S. Meradji, D. Morvan. Optimized Parallel Approach for 3D modeling of fire behavior. In V.E. Malyshkin (Ed.), PaCT 2007, LNCS, vol. 4671, p. 96-102, Springer, Heidelberg, 2007.
[25] G. Accary, O. Bessonov, D. Fougère, K. Gavrilov, S. Meradji, D. Morvan. Efficient Parallelization of the Preconditioned Conjugate Gradient Method. In V.E. Malyshkin (Ed.), PaCT 2009, LNCS, vol. 5698, p. 60-72, Springer, Heidelberg, 2009.
[26] G. Accary, S. Meradji, D. Morvan, K. Gavrilov, O. Bessonov and D. Fougère. 3D-Modeling of fire behavior and effects. European Integrated Project "FireParadox", 6th PCRD, Deliverable D2.2-1, 2008.
[27] A. Khalifeh, G. Accary, S. Meradji, G. Scarella, D. Morvan, K. Kahine. Three-dimensional numerical simulation of the interaction between natural convection and radiation in a differentially heated cavity in the low Mach number approximation using the discrete ordinates method. Proc. of the Fourth International Conference on Thermal Engineering: Theory and Applications, Abu Dhabi, UAE, January 12-14, 2009.
[28] G. Accary, S. Meradji, D. Morvan, D. Fougère. Towards a numerical benchmark for 3D mixed-convection low Mach number flows in a rectangular channel heated from below. Journal of Fluid Dynamics and Material Processing, Vol. 141(1), pp. 1-7, 2008.
[29] K. Gavrilov, G. Accary, D. Morvan, D. Lyubimov, S. Meradji, O. Bessonov. Numerical Simulation of Coherent Structures over Plant Canopy. Flow, Turbulence, and Combustion. 86, 2011, p. 89-111.
[30] K. Gavrilov, D. Morvan, G. Accary, D. Lyubimov, S. Meradji. Numerical simulation of coherent turbulent structures in atmospheric boundary layer above a forest canopy. Computer & Fluids, 78, 2013, p. 54-62.
[31] K. Gavrilov. Numerical modeling of atmospheric boundary layer flow over forest canopy. Université d'Aix-Marseille II, Thèse en cotutelle avec l'Université d'Etat de Perm (Russie), 2011.

FIRETEC evaluation against the FireFlux experiment: preliminary results

J-L Dupuy[a], F Pimont[a], RR Linn[b], CB Clements[c]

[a] *INRA, UR 629, Unité d'Ecologie des Forêts Méditerranéennes (URFM), Avignon, France, dupuy@avignon.inra.fr, pimont@avignon.inra.fr*
[b] *LANL, Earth and Environmental Science, Los Alamos NM 87544, USA, rrl@lanl.gov*
[c] *San José State University, Department of Meteorology and Climate Science, San José, CA, USA, craig.clements@sjsu.edu*

Abstract
Local dynamic or thermodynamic variables that are the primary time and space dependent variables predicted by the FIRETEC physics-based model of fire behaviour, including gas velocity and gas temperature, have not been tested against experimental measurements to date. In the present study, we attempt to reproduce the FireFlux experiment with the FIRETEC model and we compare the predicted time evolution of wind velocity components and temperatures above the fire to data measured on a tower up to 43 meters above ground level. Given the complex and somewhat uncertain wind and ignition scenario that cannot be exactly reproduced by the model simulation, FIRETEC captured well the timing and magnitude of downdrafts, updrafts and temperature variations observed during the experiment when the fire plume crossed the measurement tower. The drawbacks of the experimental measurements and the influence of ambient wind fluctuations that cannot all be captured by the model do not allow conclusive comparisons regarding turbulent statistics and fluxes during the fire period.

***Keywords**: grassland, fire plume, temperature, velocity, model testing*

Introduction

FIRETEC is a three-dimensional coupled fire-atmosphere model that allows the simulation of fire spread in natural conditions at a high spatial resolution (one meter) over areas typically 10 to 100 ha. Earlier fire behaviour simulation studies of the physics-based FIRETEC model have provided reasonable results with respect to qualitative and some quantitative observations of global aspects of wildfire behaviour in the field. Previous evaluations considered fire spread in grasslands (Linn and Cunningham 2005), interactions between two fires (Dupuy *et al*. 2011), crown fire behaviour (Linn *et al*. 2012), fuel moisture effect on the rate of spread (Marino *et al*. 2012), or fire shapes as influenced by the combination of wind and terrain slope (Pimont *et al*. 2012). However, local dynamic or thermodynamic variables that are the primary time and space dependent variables predicted by FIRETEC, including gas velocity and gas temperature, have not been tested against experimental data. In fact, only turbulent wind profiles over tree canopies in absence of a fire have specifically been tested to date (Pimont *et al*. 2009).
The FireFlux experiment has already been used to assess the performance of coupled fire-atmosphere models (Fillipi *et al*. 2013, Kochanski *et al*. 2013). The above models are essentially designed to address lower spatial resolution and larger domains than FIRETEC and fire-atmosphere coupling refers to coupling between the atmospheric flow and a fire spread equation, whereas FIRETEC couples the atmosphere with a combustion model. In the present study, we attempt to reproduce the FireFlux experiment (Clements *et al*. 2007, 2008, Clements 2010) with the FIRETEC model. The reader may refer to earlier papers (e.g. Dupuy *et al*. 2011, Pimont *et al*. 2012) for a description of the model.

In the present study, we compare the predicted time evolution of wind velocity components and temperatures above the fire to data measured on a tower up to 43 meters above ground level (AGL). We quickly address the comparison of turbulent statistics and fluxes during the fire period.

The FireFlux experiment

The FireFlux experiment was conducted on 23 February 2006 and is described in detail by Clements *et al*. (2007). The atmosphere was neutral except in the first tens of meter. The experimental burn was conducted in a tall grass over a plot approximately 800 m long in the south direction (x-axis) and 400 m wide in the east direction (y-axis). The plot was surrounded by blocks of forested areas dominated by Chinese tallow trees of a maximum height 12-13 m. The experiment was designed to measure the winds and temperatures over the vertical direction as the plume and the fire passed two instrumented towers. A 43 m height instrumented tower (main tower, MT) and a 10 m height tower (short tower, ST) located 300 m downwind of the MT were equipped with three-dimensional sonic anemometers and thermocouple probes. In the current paper, we will focus on measurements at the MT. ST data have only been used together with MT data for adjustment of the wind scenario. The three-components of velocity were measured by the sonic anemometers at 2, 10, 28 and 43 m above ground level (AGL) at MT and 2 and 10 m AGL at ST. These data were recorded at 20 Hz and post-processed to produce valid data files (1 Hz) in earlier analysis. Temperatures were measured by a set of fine-wire thermocouple probes at 1 Hz from 2 to 43 m AGL, we will use only those probes that are located at 2, 10, 28 and 43 m AGL. The sonic anemometers measure virtual temperature, but they could not measure temperatures above 50°C. Temperature recordings readily show that these sensors underestimated the temperatures measured by thermocouple probes, especially at the lowest levels. On the other hand, thermocouple probes were not at the same position as sonic anemometers except at 2 m AGL level. That prevents their use for computation of turbulent correlation between temperature and velocity components (time shift in signals) at all levels.
Fire was ignited by two teams walking respectively to the west (actually 280°) and to the east (100°) direction from a point located in the central part of the plot, at approximately 120 m north of the MT. The timing of fire ignition was recorded for the eastern branch of the ignition line thanks to a GPS located with the ignition crew member. We used these data to build the simulation scenario of the ignition by FIRETEC. It was assumed that the western part was ignited at the same speed as the eastern branch. The exact MT position was known, the position of the ignition point was known within +/- 10 m. Fire spread and fire line shape were difficult to observe and were not well documented. According to temperature data recorded at lowest levels, fire reached the MT at 12:46:40, and according to photographs ignition started at 12:43:36 (+/-6 s) in the data logger clock time. From videos and photographs, the spread of the fire head was about 1.2 m/s when fire approached the tower.
Wind measured at the MT since 12:00 prior to fire ignition indicate that the mean wind speed was about 6 m/s and the mean wind direction was 11°. Wind data also show that wind speed decreased to 3.5 m/s and wind direction changed to North-East (45°) just before the ignition time. These values were observed for 30-40 s after ignition and then wind speed increased again and wind direction changed to the North roughly after about 1 min from ignition time. Later on, the ambient wind at the MT was modified by the fire and the plume, and thus is basically unknown.

Simulation setup

The simulation domain was 1200 m long (x-axis), 600 m wide (y-axis) and 615 m high. The actual position of the MT in this domain was (x=636 m, y= 330 m). The computational mesh is orthogonal and stretched over the vertical direction. Cell size was 2 x 2 x 1.5 m at ground level. Figure 1 shows a map of the vegetation types that was produced from an aerial image of the area. Tree canopy was represented by a homogeneous layer of 10 m height and a constant plant area density (note that those

deciduous trees were leafed out at the season of the burn). The rest of the area is covered by tall grass (fuel) and some areas of cut grass.

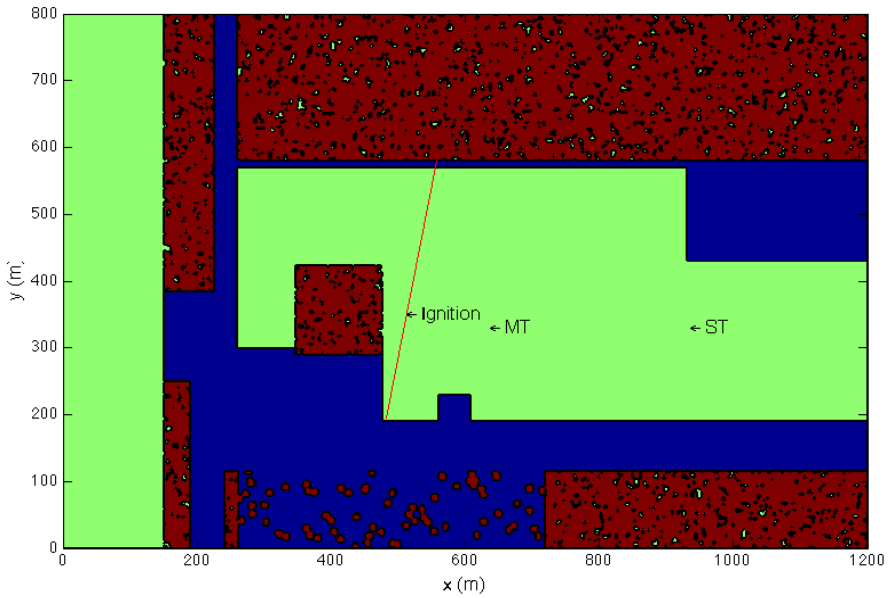

Figure 1. Simulation domain and vegetation map (Red : trees; Green : tall grass; Blue : cut grass)

A turbulent wind field was pre-computed using the same simulation domain dimensions, but the area was covered by a 600 x 600 m strip of tree canopy and two strips of tall grass upwind and downwind of the tree strip. This pre-computation used cyclic boundary conditions and a large-scale pressure gradient force method to allow the development of realistic turbulent structures due to vegetation roughness. In this method, a target wind is specified at some height where drag effects are minor (here 43 m AGL). Then the pre-computed wind field was used to set the initial and the boundary conditions for the computation of fire spread over the map shown in Figure 1. In this simulation, ignition started 300 s after run start to allow the wind field to adjust to the drag effects of the actual map of vegetation. In particular, the block of trees located just upwind of the ignition line influenced the wind field in the area of interest (between ignition line and MT). We adjusted the initial wind of the pre-computation and the (unknown) plant area index (PAI) of the tree blocks to get mean wind speed values closed to the observed ones at 10 m AGL at both the MT and the ST (respectively 4.9 and 5.7 m/s). That led us to use a 7 m/s wind speed and 11° wind direction at 43 AGL in the pre-computation and a PAI of 0.2 for the tree canopy with a drag coefficient set to 0.15. Fuel parameters were set following estimates reported in Clements *et al*. (2007) and ignition reproduced the process described in section 2. Fuel and ignition parameters are reported in Table 1.

Because fuel was removed 5 m around the tower base, we ran two fire simulations, one with no fuel clearing and one with fuel clearing (residual fuel load: 0.05 kg/m^2) in a square of 14 m side centred on the tower location. In fact, fuel clearing in the simulation was not operated at the actual tower location, but at two locations among points that were reached by the head fire within the observed timing. This is explained in the next section.

Table 1. Fuel (tall grass and live shrubs) and ignition parameters of the simulation

Fuel height (m)	1.5	Length of ignition western branch (m)	155
Fuel load (kg/m^2)	1.08	Duration of ignition western branch (s)	138
Dead fuel (% load and cover)	96	Length of ignition eastern branch (m)	237
Dead fuel moisture content (%)	9	Duration of ignition eastern branch (s)	205
Live fuel moisture content (%)	200	x, y position of ignition start (m)	513, 350

Results and discussion

4.1. Ambient wind adjustment

The experimental wind profile at MT, determined from recordings prior to fire ignition, was not perfectly predicted by the model at that location. To get the observed value at 10 m AGL, the mean predicted wind speed was close to 7 m/s at 43 m AGL at MT (the same as in the pre-computation), whereas the observed value was 6 m/s. We suspect that the model overestimates the influence of trees on the mean wind profile downwind of tree canopy since we got a profile close to the measured wind profile some tens of meters downwind of the MT.

4.2. Fire spread

Figure 2 shows the simulated fire front 60 s, 120 s and 190 s after ignition start. According to temperatures predicted at 2 m height, fire reached the x-position of the MT (636 m) within 185 and 195 s after ignition for points located between 340 and 370 m in y-direction, thus exactly the experimental timing. The actual y-position of the MT (330 m) was reached with ~ 10 s delay in the simulation. Owing to the uncertainty on the actual position and timing of the ignition line building, we did not expect a better result. In fact we must consider that within a few tens of seconds, this timing was obtained just by chance. The strong change in wind speed and direction during the initial development of the fire line cannot be rendered by the model simulation and certainly affected the fire line spread and shape and when plume and fire reached the MT just 2-3 minutes later. This change is likely due to large-scale atmospheric structures that cannot be captured with the current technique used to compute the ambient wind.

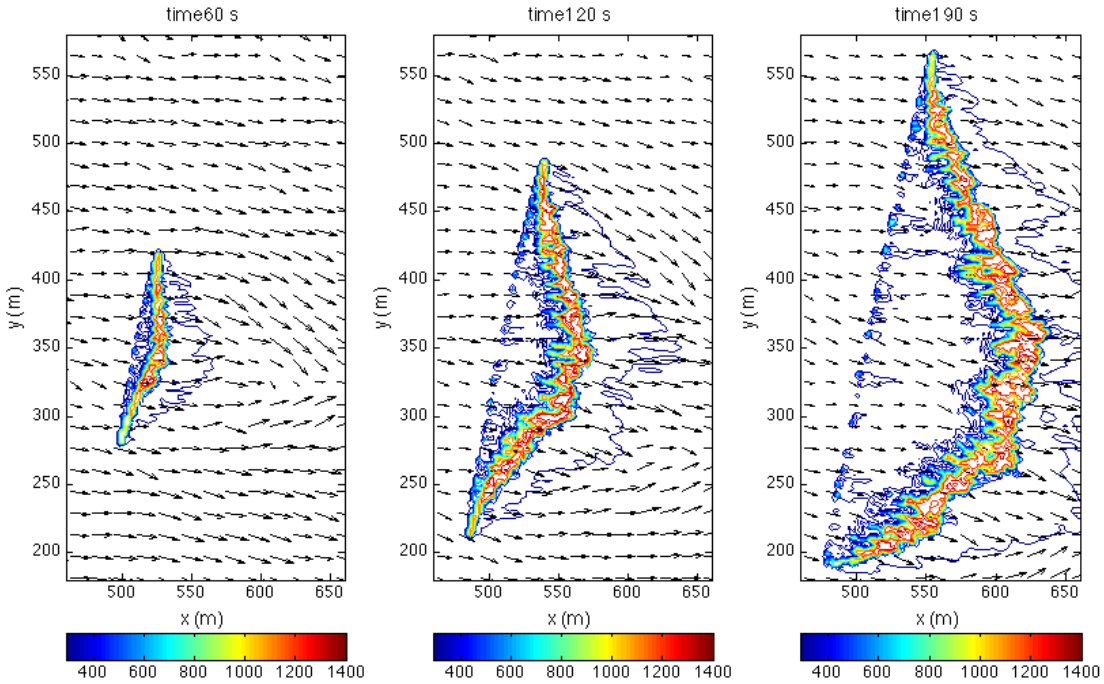

Figure 2. Fields of gas temperature (0.75 m AGL) and horizontal wind (10 m AGL) simulated with FIRETEC, 60 s, 120 s and 190 s (arrival of fire head at x=636 m) after the ignition

In the following, we will focus on those points comprised between y=340 m and y=370 m where fire arrived at x-position of the MT (636 m) in a timing close to the experimental one. In all time series plots of the variables, time zero corresponds to the ignition start time and fire reached the MT at ~ 190 s. Predicted time series are all shown together with the experimental one.

4.3. Horizontal velocity

We will only report results for the u-component of velocity (x-axis), which is the major component of horizontal wind speed (mean angle with North is only 11°) and drives the plume along the x-axis. Figure 3 shows 1 Hz time series of the u-component of velocity at y=340 m and y=370, and at 10, 28 and 43 m AGL. As expected (section 4.1), the mean wind speed is over-predicted at 43 m AGL and to a lesser extent at 28 m AGL, but also at 10 m AGL. In fact, variations in the measured wind are much higher than variations in the computed velocity. This was also observed prior to fire arrival (variance of predicted and measured velocities) and confirms we cannot capture all ambient wind fluctuations. The comparison between predicted and measured horizontal velocities is thus delicate since we cannot separate the largest variations due to the ambient wind flow structures (that cannot be rendered by the model) from the impact of the fire in the experimental data. At least a wind measurement not influenced by the fire should be used to do so. Nevertheless, experimental data exhibit two minimum values at all heights (approaching zero at 10 m AGL), prior to plume arrival, and then an increase of the wind when the plume crosses the MT. The model captures the increase in wind speed as the plume passes, but not the strong wind decay prior to plume arrival.

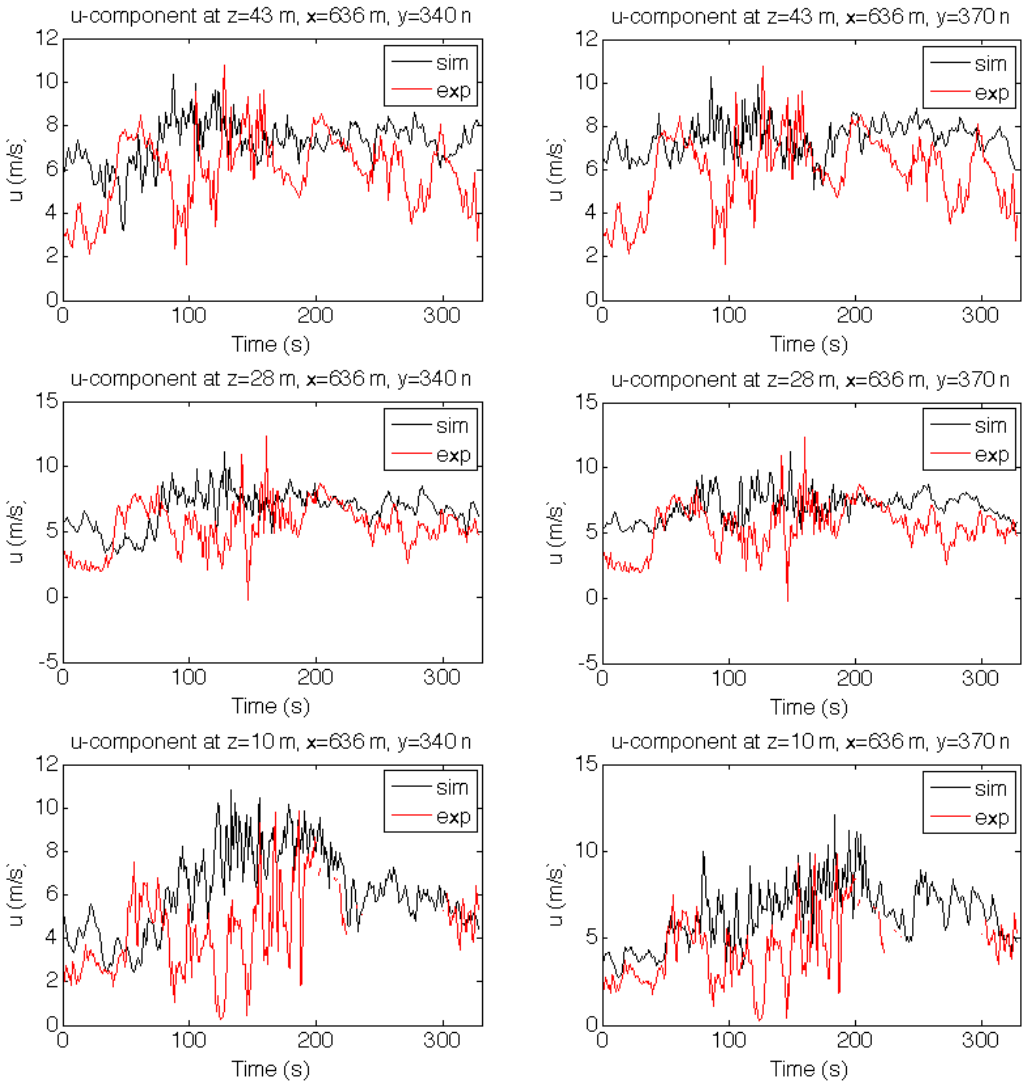

Figure 3. u-component of velocity versus time (1 Hz) at 10, 28, and 43 m AGL, at two points (sim) and at MT position (exp)

4.4. Vertical velocity

Over a flat terrain and in near neutral conditions, the ambient flow should have a small effect on vertical velocity as compared to the fire, which is a high source of buoyancy. In other words, comparisons of the model predictions to measured w-component of velocity should be meaningful for the model assessment. Figure 4 shows 1 Hz time series of the w-component of velocity (vertical velocity) at six points together with the experimental measurement, at 28 m AGL. The predicted and experimental patterns are very similar, in timing and in magnitude. In particular, the model renders the increase in vertical velocity peak values as the plume crosses the points and the downdraft observed just after the plume passed the tower location. Consistency between predicted and measured w-velocity patterns is confirmed at other heights (shown for two points in Figure 5). Figure 6 shows 10 s-averaged data at the six points between 340 and 370 m. It is easier to depict the magnitude of velocity and worth noting that variations among simulated points are important.

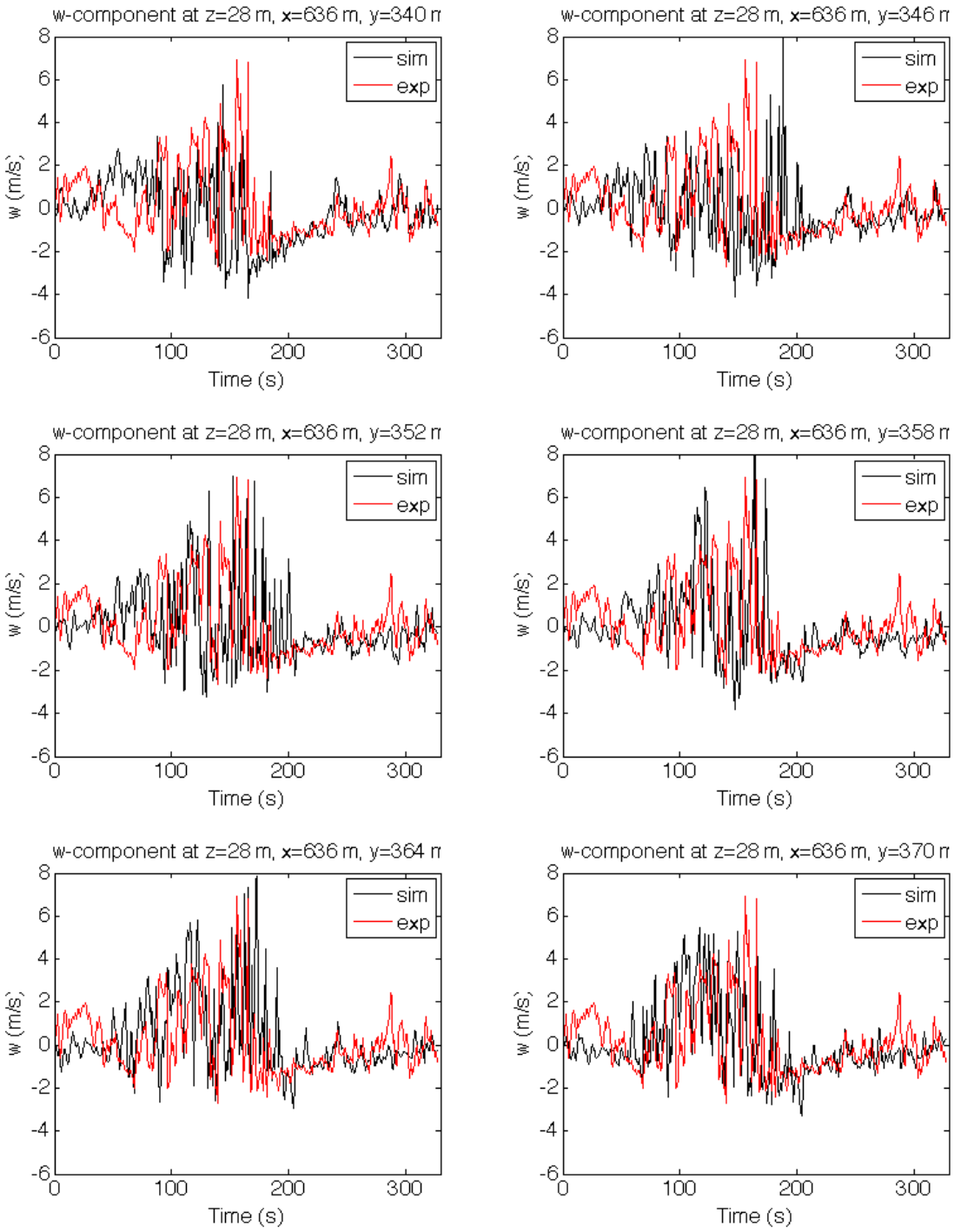

Figure 4. w-component of velocity versus time (1 Hz) at 28 m AGL, at six points (sim) and at MT (exp)

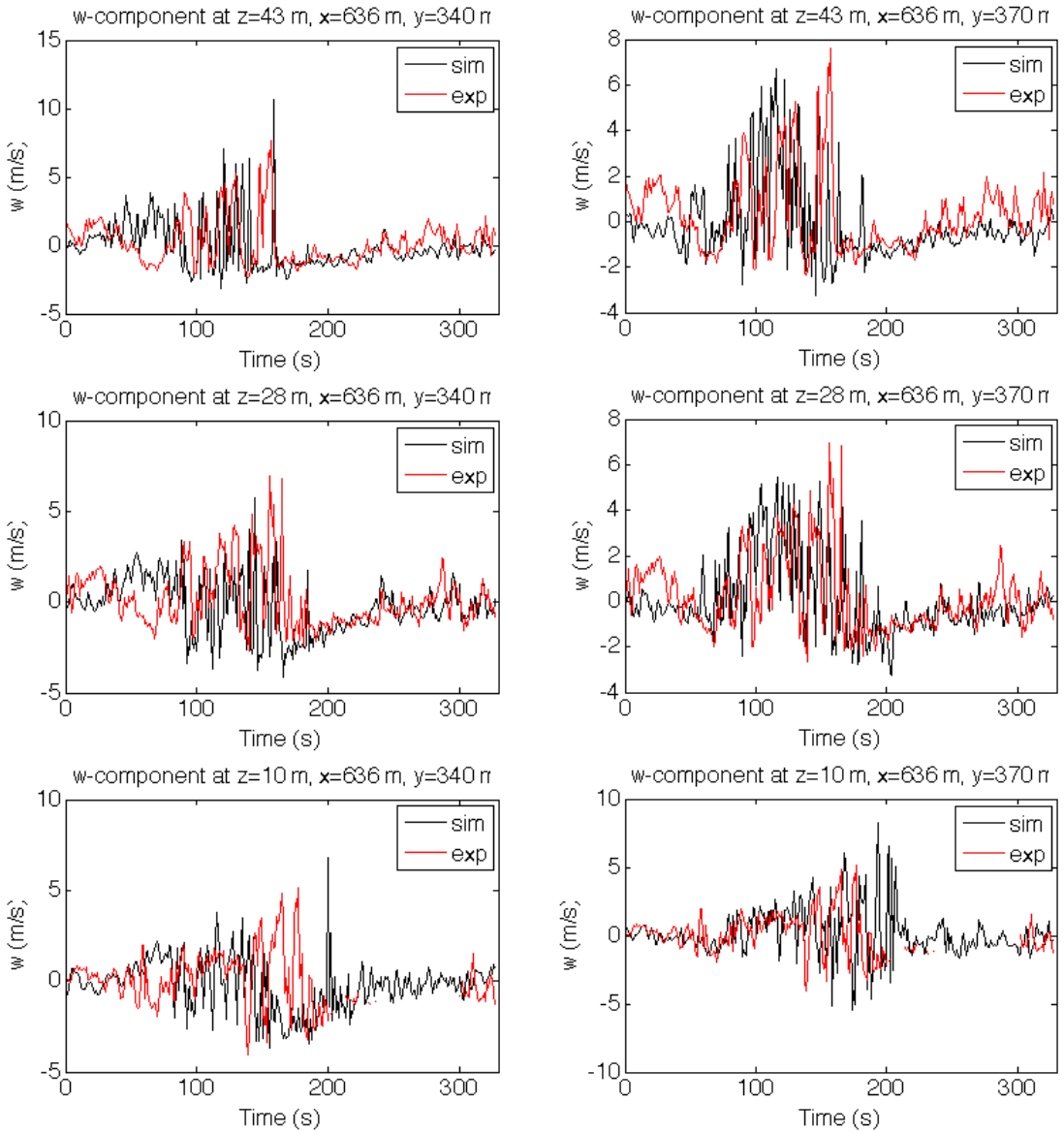

Figure 5. w-component of velocity versus time (1 Hz) at 10, 28, and 43 m AGL, at two points (sim) and at MT position (exp)

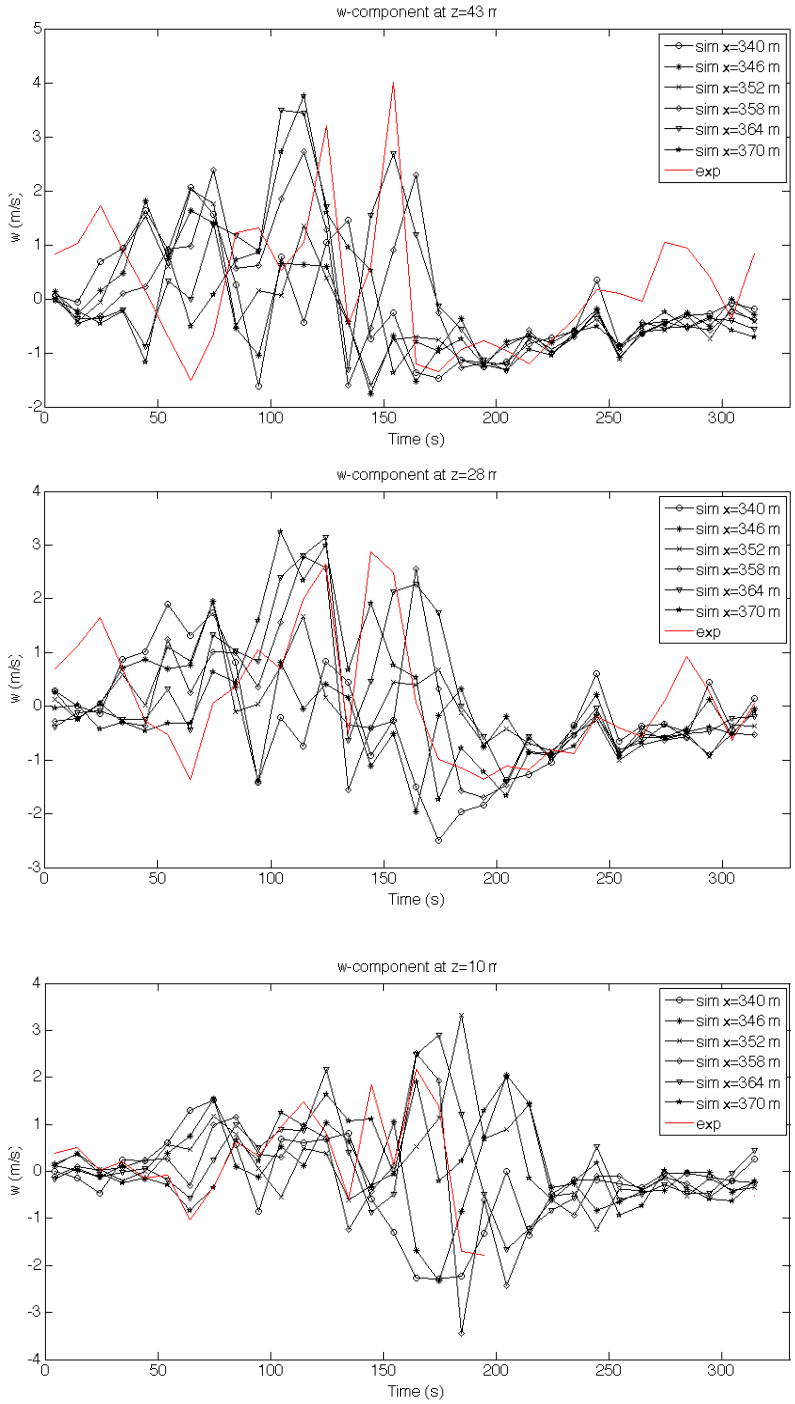

Figure 6. w-component of velocity versus time (10s-averaged data) at 10, 28, and 43 m AGL, at six points (sim) and at MT position (exp)

4.5. Temperatures

Plots of 1 Hz temperature time series at 10, 28 and 43 m AGL all show the same general pattern, but also important variations among points between y=340 and y=370 m (not shown). Figure 7 shows those time series of temperature at two points and three heights AGL (10, 28, 43 m). The plume impinges the upper levels of the tower earlier than in the experiment, typically 40-50 s earlier at 43 m AGL and 20-30 s earlier at 28 m AGL. This results in higher predicted temperatures than observed when the plume starts to cross the tower. That can be easily seen for the six points between 340 and

370 m on 10-s average plots of temperature (Figure 8). We assume that these differences are essentially due to differences in horizontal wind speed described above and to the initial wind change observed in the experiment. Higher wind speeds imply that heat is advected faster. The wind change in both speed and direction in the experiment is likely to have delayed plume impingement on the tower. It is worth noting from Figure 8 that the observed peak value of temperature at the three heights is in the range of predicted values, which however vary a lot among the different points.

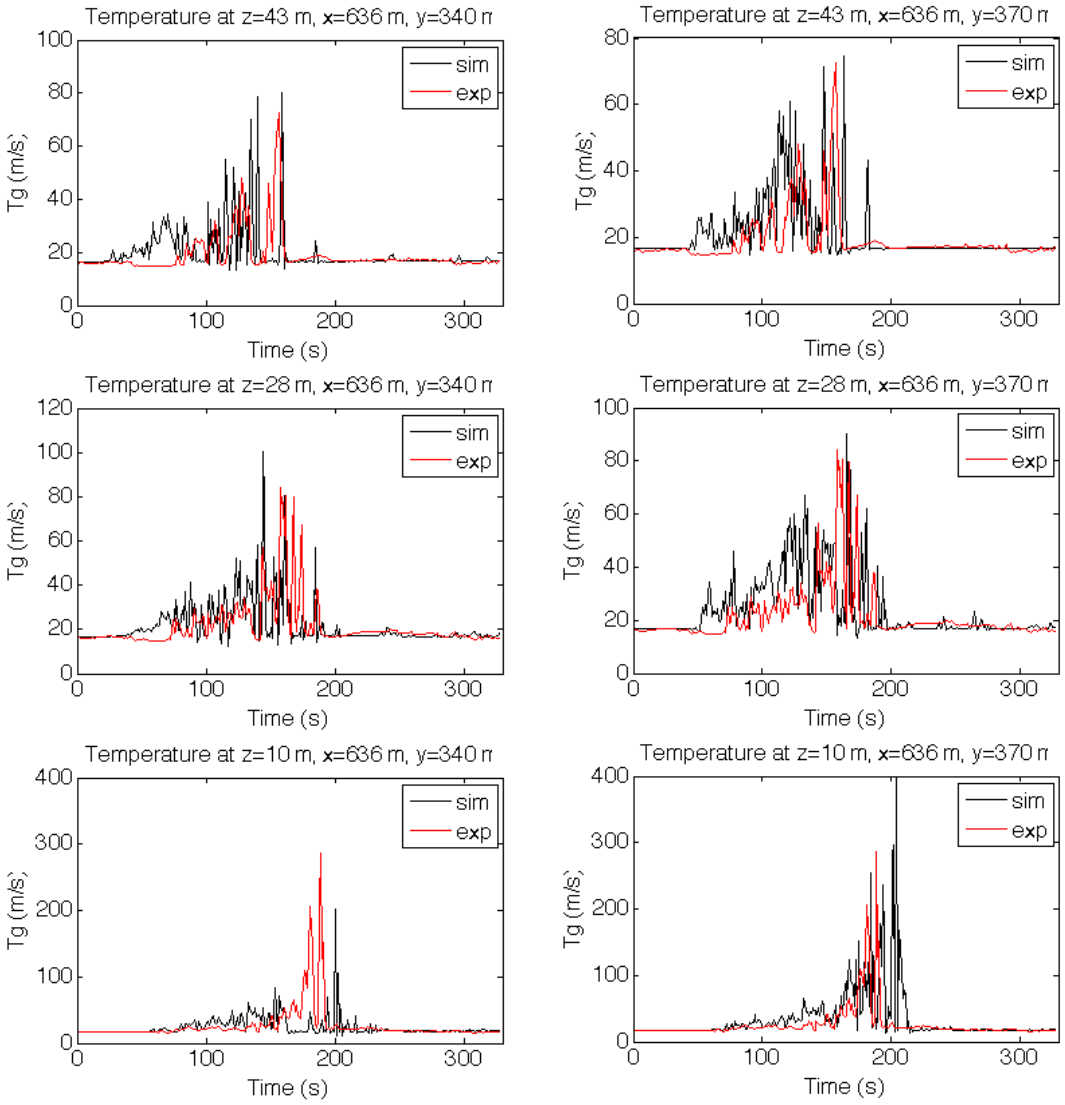

Figure 7. Temperature versus time (1 Hz) at 10, 28, and 43 m AGL, at two points (sim) and at MT position (exp)

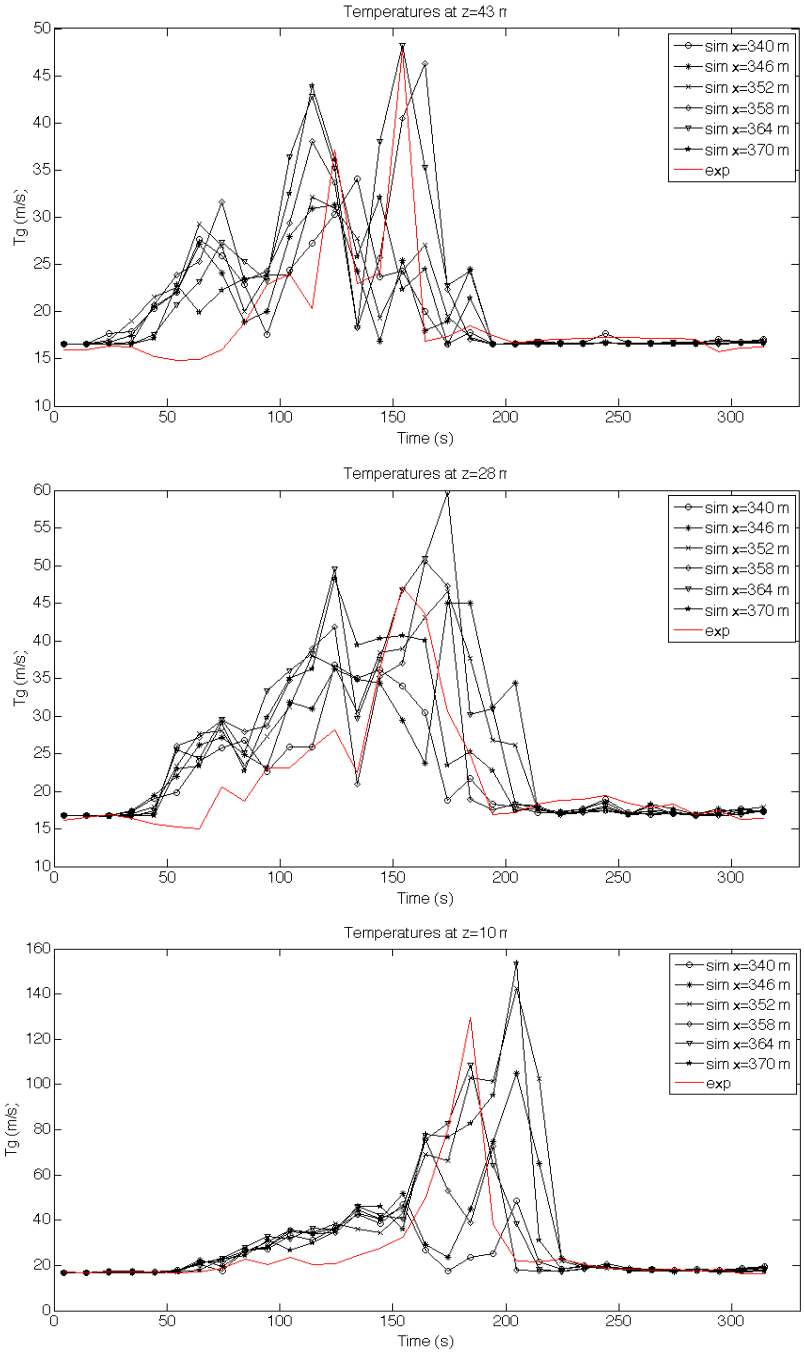

Figure 8. Temperature versus time (10s-averaged data) at 10, 28, and 43 m AGL, at six points (sim) and at MT position (exp)

4.6. **Influence of fuel clearing**

In a second simulation, fuel was cleared at y=340 m and y=370 m. Clearing had little effect on velocity and temperature patterns at the upper levels. We noticed some small changes in the temperature peaks at 10 m (not shown). This was expected since heat is advected faster in the horizontal than in the vertical direction (two times faster in order of magnitude in the simulation). In contrast, changes in temperature were very large at 2 m height. Figure 9 shows that peak temperatures were strongly reduced when clearing was applied and that predicted temperature levels with clearing match the observed values. Clearing also reduced the peak values of vertical velocity reached when the fire crosses the base of the tower (not shown).

4.7. **Turbulent statistics**

Turbulent statistics of atmospheric flows are meaningful when computed over time samples large enough to consider that variables are stationary. During the plume and fire passage, all variables measured at a fixed point are clearly unsteady. In addition, in the present experiment, measurements were taken at a position that was influenced by the initial development of the fire since the duration of ignition and the time to reach the MT were similar. Only point probes "attached" to a steady fire or more realistically 1D or 2D fields of data measurements, would be able to provide such statistics. This is of course a great challenge to perform such measurements.

Statistics may be computed over some reference time period with the purpose of model-experiment comparison only. Unfortunately, both the current technique of ambient flow modelling used by FIRETEC and the drawbacks of the temperature measurements strongly limited the possibility to perform such comparisons. As we mentioned, ambient wind variations are likely to influence the horizontal components of wind in the plume and as such, should influence their variance and co-variance.

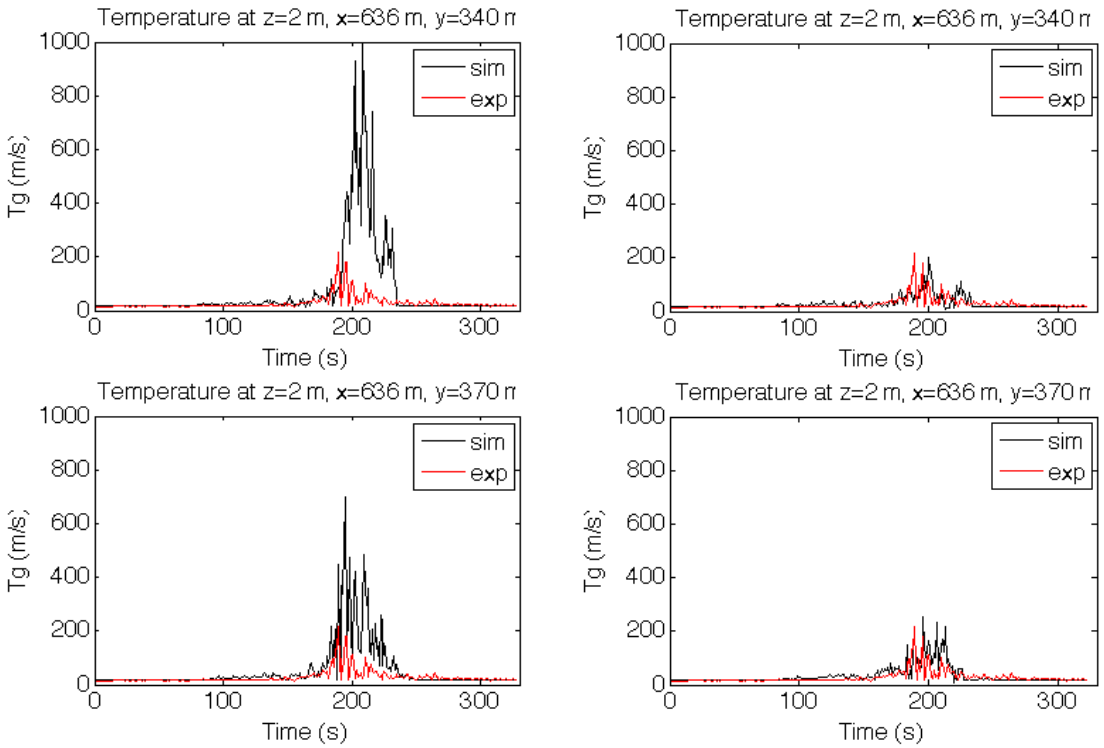

Figure 9. Temperature versus time (1 Hz) at 2 m AGL, at two points (sim) and at MT position (exp). Left : no fuel clearing; right : fuel clearing at point location

We readily found in the pre-fire period that the observed variances of u and v components of velocity were underestimated by the model, because we only capture those variations that are due to the vegetation roughness in the simulated domain we used. Besides, sonic temperatures were underestimated by the sonic anemometers, which compromises the calculation of the vertical sensible heat flux or the vertical buoyancy (e.g. basically the correlation of the vertical velocity and the temperature).

To support the above assertions, we computed one minute moving averages of velocity component variances and co-variances and the covariance of vertical velocity and temperature (w't') on 5 Hz data. We tracked the extrema of these statistics during the fire period (0 to 5 min after ignition). Those statistics were computed for the 16 points of the simulation located between y=340 and 370 m, and for

the experimental data, at 10, 28 and 43 m AGL. As expected, the model underestimated the observed peak variance of horizontal velocity (u'^2, v'^2) and the magnitude of the (negative) peak vertical momentum flux (u'w'). The variance of the vertical velocity (w'^2) from the observations was similar to the model. The experimental w't' correlations (or the sensible heat flux) were clearly below the model predictions and it decreased with decreasing height AGL, whereas it increased in the model predictions.

Conclusion

The current work is the first assessment of temperature and velocity predictions by FIRETEC against data measured in a plume developed from a spreading fire in natural conditions. The updrafts and downdrafts observed in vertical velocity measurements are particularly well captured. Temperature magnitude at different heights is also well captured. This is particularly important because these two variables are mostly determined by the fire and much less by the ambient wind flow. However the model predicts a faster plume impingement on the upper levels of the measurement tower, whereas the arrival of fire at the position of the tower in the simulations is the same as in the experiment. We assumed that it was due to the model not being able to reproduce the actual wind profile at the tower location downwind a block of trees resulting in a 15% overestimation of wind speed at the upper level. The model also cannot incorporate the change in wind speed and direction that was observed during the initial development of the fire in the experiment and was likely to delay this impingement. The current technique used to set up the ambient wind field in the simulations does not allow to take into account such changes in ambient wind speeds that are likely not due to the surrounding vegetation, but to larger atmospheric structures. This is in fact a good illustration of the challenge that represents such model-experiment comparisons. The fact that the ambient wind during the fire was not known (not measured at a point not influenced by the fire) did not help with understanding the differences between predicted and measured horizontal wind speed during the fire passage. It is worth noting also that the model showed a clear effect of clearing the fuel at the tower base on temperature and velocity, which is important for design of future experiments. Finally, the drawbacks of the experimental measurements and the influence of ambient wind fluctuations that cannot all be captured by the model do not allow conclusive comparisons regarding turbulent statistics during the fire period.
These results encourage us to continue the assessment of the model using more recent experiments such as FireFlux II that benefit from progress in fire instrumentation and to simulate a diversity of situations that would help design future experiments by testing the sensitivity to environmental conditions and ignition scenario or the relevance of measurement devices.

References

Clements CB, Zhong S, Goodrick S, Li J, Bian X, Potter BE, Heilman WE, Charney JJ, Perna R, Jang M, Lee D, Patel M, Street S, Aumann G (2007) Observing the dynamics of wildland grass fires: FireFlux – a field validation experiment. *Bulletin of the American Meteorological Society* **88**(9), 1369–1382.

Clements CB, Zhong S, Bian X, Heilman WE (2008) First observations of turbulence generated by grass fires. *Journal of Geophysical Research* **113**, D22102.

Clements C (2010) Thermodynamic structure of a grass fire plume. *International Journal of Wildland Fire* **19**, 895-902.

Dupuy J-L, Linn RR, Konovalov V, Pimont F, Vega JA, Jimenez E (2011) Exploring coupled fire/atmosphere interactions downwind of wind-driven surface fires and their influence on backfiring using the HIGRAD-FIRETEC model. *International Journal of Wildland Fire* **20**,734-750.

Filippi JB, Pialat X, Clements C (2013) Assessment of ForeFire/Meso-NH for wildland fire/atmosphere coupled simulation of the FireFlux experiment. *Proceedings of the Combustion Institute* **34**, 2633-2640.

Kochanski AK, Jenkins MA, Mandel J, Beezley JD, Clements CB, Krueger S (2013) Evaluation of WRF-SFIRE performance with field observations from the FireFlux experiment. *Geoscience Model Development* **6**, 1-18.

Linn RR, Cunningham P (2005) Numerical simulations of grass fires using a coupled atmosphere-fire model: basic fire behavior and dependence on wind speed. *Journal of Geophysical Research* **110**: D13107

Linn RR, Anderson K, Winterkamp J, Brooks A, Wotton M, Dupuy J-L, Pimont F, Edminster C (2012) Incorporating field wind data into FIRETEC simulations of the International Crown Fire Modeling Experiment (ICFME): preliminary lessons learned. *Canadian Journal of Forest Research* **42**,879-898.

Marino E, Dupuy JL, Pimont F, Guijarro M, Hernando C, Linn RR (2012) Fuel bulk density and fuel moisture content effects on fire rate of spread: a comparison between FIRETEC model predictions and experimental results in shrub fuels. *Journal of Fire Science* **30**(4),277-299.

Pimont F, Dupuy J-L, Linn RR, Dupont S (2009) Validation of FIRETEC wind-flows over a canopy and a fuel-break. *International Journal of Wildland Fire* **18**(7),775-790.

Pimont F, Dupuy JL, Linn RR (2012) Coupled slope and wind effects on fire spread with influences of fire size: a numerical study using FIRETEC. *International Journal of Wildland Fire*, **21**(7), 828-842.

ForeFire: open-source code for wildland fire spread models.

Jean-Baptiste Filippi, Frédéric Bosseur, Damien Grandi

SPE – CNRS UMR 6134, Campus Grossetti, BP52, 20250 Corte. filippi@univ-corse.fr

Abstract
Fore fire code has been developed to bridge the gap between research and operational code, it is open source, designed for large scale fire simulation, can be easily extended with any new model formulations and can take typical landscape data as input. The code is composed of a simulation engine that has been numerically tested with numerous bindings for different computer languages to be integrated into other scientific environments ranging from SciPy/Numpy to Fortran parallel coupled numerical weather forecast models. This paper presents the general software architecture and concepts, illustrated by examples and use cases in different context.

Keywords*: software, model, simulation, source code, open source, python, fire front, forecast*

Introduction

Fire front simulation tools have either been targeted with great success for research or for operations (Finney and Andrews 94). If most research oriented codes were designed to handle specific configuration with a complex and possibly time consuming set-up, operational tools are designed to handle almost readily available landscape data in order to provide simulation results relevant for real large scales fire. The ease of use of such software, and their relevance for large scale fire simulation has helped the field of forest fire operational research with application among which fire re-analysis, uncertainty estimation, land use, fuel management. Nevertheless, all these software are monolithic, they are not designed to be modular, extended or used in the context of multiple interactions with other scientific software (model coupling, data analysis, post-processing). An important aspect is also that unlike research purpose code operational software's are mostly closed source, available only as a compiled binary with little opportunity to add or change the numerical scheme or the formulation of the rate of spread of fire intensity.
Fore fire code has been developed to bridge the gap between research and operational code, it is open source, designed for large scale fire simulation, can be easily extended with any new model formulations and can take typical landscape data as input. The code is composed of a simulation engine that has been numerically tested (Filippi *et al*, 2009) with numerous bindings for different computer languages to be integrated into other scientific environments ranging from SciPy/Numpy to Fortran parallel numerical weather forecast models.
This paper will present first the general software architecture, illustrated in a second part by examples and use cases in different context. Finally the conclusion will also review the requirements and future code developments.

Time handling and numerical integration method

The forefire code is based on discrete events simulation, a complete description can be found in (Filippi et.al. 2009). Basically, each action (fire portion moving, wind change …) is performed by a component (fire portion, atmospheric data model) at a specific time. An action, from a component, is scheduled at this specific time by an event, these events are received and time-sorted in a global timetable. Events can be inserted by the user, and each component, when activated, can re-schedule events. Time is

continuous, meaning that there in no time step, and activation times are real numbers, simulation is run by activating the component with the most imminent event, scheduling its output events and moving to the next imminent event.
Discrete events time handling has several advantages, first it does not forbids the use of discrete time stepping methods (with evenly timed events), it is easily integrated in a scripted environment, can easily handle the introduction of heterogeneous components and most of all, can optimize computational time when components have very different characteristic time (such as a between a very slow moving backfire and a strong head-fire).
ForeFire software architecture is not tied to a specific numerical method to simulate fire front propagation, yet, only a Lagrangian front tracking method of markers is implemented.
In the front tracking method, the fire line is decomposed into a set of connected points, or markers. Each marker is a component that has a specific propagation direction and speed, such as shown in figure 1.
The speed at which the marker is traveling along its propagation vector is given by the rate of spread model with many available (isotropic, wind-aided, Balbi (2009), Rothermel (1972), other can be added with a single C++ file. The direction of propagation vector is usually (several methods available) taken as the bisector of the angle formed by the marker, and the location of the immediate left and right markers. Markers are redistributed along the front if separated by more than a resolution distance Δr and removed if separated by less than $\Delta r/4$. A fire line is defined as a full set of interconnected markers. If two points of different fire lines are separated by less than $\Delta r/4$ the two fronts are merging. The integration of a marker advance is performed in a discrete event fashion, with no global time step but specific activation time for markers. Each marker is advancing by the same distance Δq with an event time activation estimated as the time it will take to the parker to move by this distance given its local propagation.

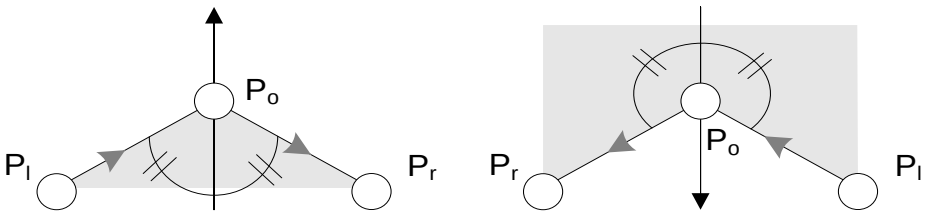

Figure 1. Front tracking and markers. Circles represent markers along the fire line. Arrows show the propagation vector (bisector of the local angle at the marker P0 between the point at left, Pl and point at right, Pr). Grey area represents the burned fuel.

The propagation velocity of the fire front given by the velocity model depends on the flame geometrical properties: tilt angle, curvature and front depth. The two firsts properties are assumed instantaneous in the model and may be observed from the front geometry or computed at a given time. On the contrary the front depth, thickness of the front where the flame is present, depends on front history and fuel properties (for how long and how fuel has been burning). When simulating the effect of a fire this history is also necessary to diagnose the location and intensity of different fire induces phenomenon (mass and heat fluxes for example, requiring user defined fluxed models). In the proposed method a high resolution matrix of arrival time is used to keep track of the fire history top perform instantaneous surface diagnostics. The matrix resolution is a key point and limitation of the method that requires to fix a physical lower limit, making the hypothesis of a minimal propagative front depth (if the front is thinner than this value the fire can't propagate and may go to extinction in non self-sustaining fire conditions). On large domains (tens of square kilometers) this two dimension matrix may contains millions of points at a typical resolution of one meter. Nevertheless, as in large Wildland

fires the active burning area is only a very small fraction of the total domain extension, arrival times is handled as a sparse matrix that may still be handled efficiently.

Software architecture

The general software architecture is presented in Figure 2. Basically, the software compiles in a shared library, that has optional bindings to different programming languages and data formats to use as input/outputs. In addition to these bindings, there is a binary interpreter with a ForeFire specific syntax and scripted commands that is compiled for standalone applications, parameterisation and text format data input/output.

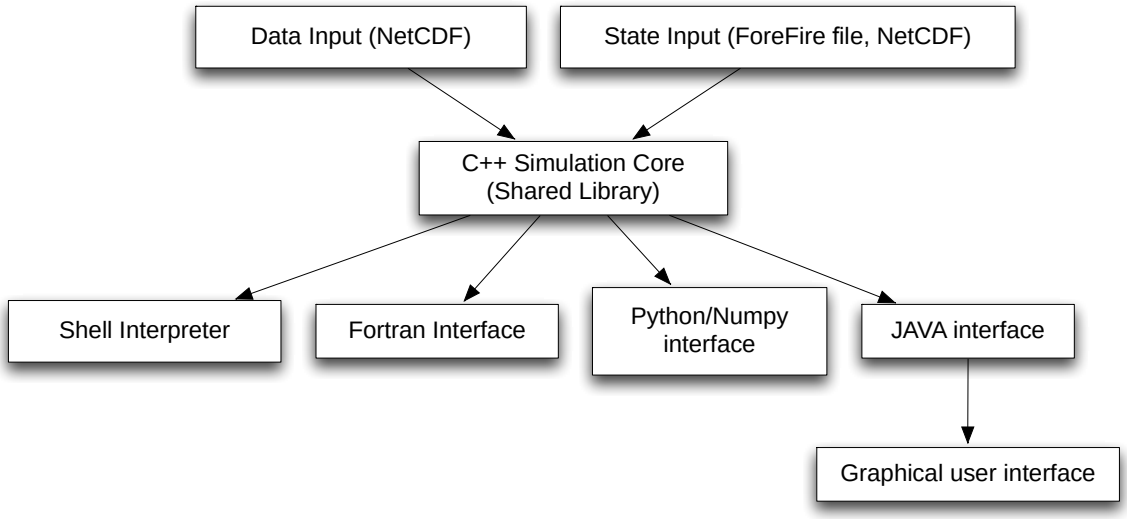

Figure 2. General software architecture and bindings

There are two different kind of input data, with sample format available from the software repository. The first is similar to Farsite's "Landscape" file but in the NetCDF file format, it defines, for a specific data domain a compilation of altitude, wind field, fuel distribution and optional diagnostic (fluxes) model distribution. Fuel state for each fuel classes is defined in a separated file and is highly dependent on the fire velocity model of use. The state input file is composed of the arrival time sparse matrix in NetCDF and ForeFire format for front input.

3.1. Command interaction

Interaction with the simulation is made with so-called commands, these can be either software calls (functions available in Fortran/Python/C++/Java interfaces) or command calls from the interpreter (a binary file launched from the command line). All commands are presented in Figure 3, all interaction with the simulation can be performed with this set of commands, with the exception of accessing the data arrays that cannot be made in text/console mode and can only be stored to files or accessed with programming interfaces.

```
FireDomain[date, location, extension] : creates a fire domain
FireFront[date] : creates a fire front with the following fire nodes
FireNode[location, velocity] : adds a fire node to the given location
step[duration] : advances the simulation for a user-defined amount of time
goTo[date] : advances the simulation till a user-defined time
setParameter[name=value] : sets a given parameter
setParameters[name=value;name=value] : sets a given list of parameters
getParameter[name] : return the parameter from a key
loadData[Netcdf File] : load a landscape file, define a domain
startFire[location, date] : start a triangular fire front
include[command file] : include commands from a file
print[output file(optional)] : prints the state of the simulation
save[NetCDF file] : saves the simulation state in NetCDF format
clear[] : resets the simulation
quit : quit and terminate
```

Figure 3. List of the scripted commands

Launching a simulation

If most of the commands are self-explanatory, some are notable, in particular the FireDomain, FireFront and FireNode commands that actually defines the fire mesh. A Node (marker) is container in a Front (interface) if it is defines just under it, with correct indentation. If it is only possible to define a single domain, it is possible in that way to define as many fronts with inner fronts as necessary. The propagation direction (contraction or dilatation) of the interface is given by the winding order. The Print command outputs the Domain/front/node structure in the same format, so it is directly readable with an Include command, Figure 4 is an example of the most simple isotropic front propagation.

```
1  setParameters[propagationModel=Iso;Iso.speed=1]
2  FireDomain[sw=(-10.,-10.,0.);ne=(10.,10.,0.);t=0.]
3      FireFront[t=0.]
4          FireNode[loc=(-3,-3,0.);vel=(-0.5,-0.3,0.);t=0.]
5          FireNode[loc=(0.,3,0.);vel=(0.2,1.2,0.);t=0.]
6          FireNode[loc=(3,0.,0.);vel=(0.7,0.1,0.);t=0.]
7  step[dt=10s]
8  print[sim1.ff]
9  clear[]
10 include[sim1.ff]
11 step[dt=5.2s]
12 quit[]
```

Figure 4. Simple simulation example

In this simulation, a domain is created between a southwest and a northwest point, and is added a front with three nodes (lines 3 to 7). The simulation is run for 10 seconds (line 8), then the structure is saved to a file, and reloaded (line 11), restarted for 5.2 more seconds then stopped. The “Iso” model is a simple isotropic model, taken as example for the simplicity of parameterisation here. More complex models are already available such as Balbi (Balbi *et al*, 2009) or Rothermel (1972), and the code design is such as it is very easily expandable with a minimum of coding, as one file is necessary (presented in Figure 5).

3.3. Adding new models

Adding a velocity model is simply done by adding a C++ file that define the “getSpeed” function, a name, and a constructor to specify the required parameters.

```
1  namespace libforefire {
2  /* model name */
3  const string ParametricROS::name = "WindSlope";
4  ParametricROS::ParametricROS(const int & mindex, DataBroker* db)
5          : PropagationModel(mindex, db) {
6      /* Locally interpolated values */
7      effectiveSlope = registerProperty("effectiveSlope");
8      normalWind = registerProperty("normalWind");
9      /* Global parameters */
10     windFactor = params->getDouble("WindAided.windFactor");
11     slopeFactor = params->getDouble("WindAided.slopeFactor");
12 }
13
14 /*  Velocity function */
15 double ParametricROS::getSpeed(double* localValue){
16     double speed = windFactor*localValue[normalWind]
17          + slopeFactor*(1.+localValue[effectiveSlope]);
18     if ( speed > 0. ) return speed;
19     return 0;
20 }
21 }
```

Figure 5. C++ fire velocity model

Once this file is added to the source list the model is available, callable by using the provided name (here “WindSlope”, line 3 of Figure 5). An important hidden object in ForeFire is the “DataBroker”, it is responsible to virtualize data access at the node location (here the “effectiveSlope” and the “normalWind”, both layers being a function applied on the elevation field and wind field given the node location). All data (fuel, wind, slope, flux, velocity) is in fact virtualizes as a Layer, that could be either data or a function, a Layer object has a name (eg. “effectiveSlope”) and can interpolate, compute or determine (index, table, vector, function, model) more layer types can be added and the reader is referred to the code for a complete description. The “getSpeed” function works by calling the DataBroker on each node at each activation, that will automatically compile the registered values interpolated at the node location (and with the node properties such as direction) from the different layers, in an array (“localValue”, line 15). Fluxes and diagnostic models can be added in a very similar fashion in the code.

Uses Cases

The originality of the code it its ability to be used in a variety of contexts, so the same developments (on a flux or velocity model, dataset, algorithm..) may be used to be tested in a pure analytic research mode, make its way to operations, and be compared easily with other approaches available from the same code. The open sourced code is essentially the simulation engine and bindings to other environments, there is no graphical user interface because it is intended to a research/developer community. Nevertheless, as a simulation engine, it is embedded in a system that does perform simulation for operational use, marking a clear separation between the simulation code and the user interface code. With this clear separation, any developments made in the research context can make its way to operational use in a very limited time.

Typical contexts of the code use are for research and testing purposes (using here scientific Python), operational use (used here with as a web-service) or even run in parallel embedded in a numerical

atmospheric model (Filippi et.al. 2013). Both scientific and operational use will be briefly presented here.

4.1. Simple simulation in a scientific python environment

The python interface is made with Numpy bindings, yet the interface is functional but minimalistic as it requires inputs from users to gain in usability. A sample script, performing a simulation is presented in Figure 6, only part of the code is shown to concentrate on the simulation aspects, with imports of the numpy and matplotlib libraries hidden.

```
1  ff = forefire.PLibForeFire()
2  ff.setString("propagationModel","Balbi")
3  ff.setString("fuelsTableFile","fuels.ff")
4  # Parameters for the global wind value
5  ff.setDouble("velU",0.)
6  ff.setDouble("velV",12.)
7  # Domain Definition
8  ff.execute("FireDomain[sw=(0.,0.,0.);ne=(300,300,0.);t=0.]")
9  # Adding layers
10 ff.addLayer("data","windU","velU")
11 ff.addLayer("data","windV","velV")
12 # Defining a specific fuel map
13 fuelmap = np.zeros((sizeX,sizeY,1), dtype=np.int32)
14 fuelmap[:,90:110,:] = 1
15 fuelmap[150:,90:110,:] = 3
16 ff.addIndexLayer("table","fuel",0 , 0, 0, sizeX, sizeY, 0, fuelmap)
17 ff.execute("    FireFront[t=0.]")
18 ff.execute("        FireNode[loc=(40,60,0.);vel=(-1.,-1.,0.);t=0.]")
19 ff.execute("        FireNode[loc=(40,65,0.);vel=(-1.,1.,0.);t=0.]")
20 ff.execute("        FireNode[loc=(260,65,0.);vel=(1.,1.,0.);t=0.]")
21 ff.execute("        FireNode[loc=(260,60,0.);vel=(1.,-1.,0.);t=0.]")
22 # Storing 20 fronts
23 for i in range(1,20):
24     ff.execute("goTo[t=%f]"%(i*20))
25     pathes += printToPathe( ff.execute("print[]"))
26 # Plotting the fuel map
27 CS = ax.imshow(ff.getDoubleArray("fuel"))
28 # Plotting the firelines
29 for path in pathes:
30     ax.add_patch(mpatches.PathPatch(path,edgecolor='red'))
31 plt.show()
```

Figure 6. ForeFire simulation in python

In this script a Forefire object is first created (line 1), it contains a simulation context, linked to one domain, parametrisations and data. In line 2 and 3 is defined the model and the comma separated array file that contains the fuel parameters that are relevant to the propagation model used.
The functions “addLayer” adds a parameter layer that will always return the value set in the corresponding parameter. A user defined indexLayer is then added as a numpy array (line 16). This layers contains the indices in the table (defined in the fuel file), so that all parameters linked to this indices may be passed to the velocity model, at the fire location. Finally, the simulation is initiated using the “execute” function, that calls the standards ForeFire commands, and simulation results are stored in an array (line 25).

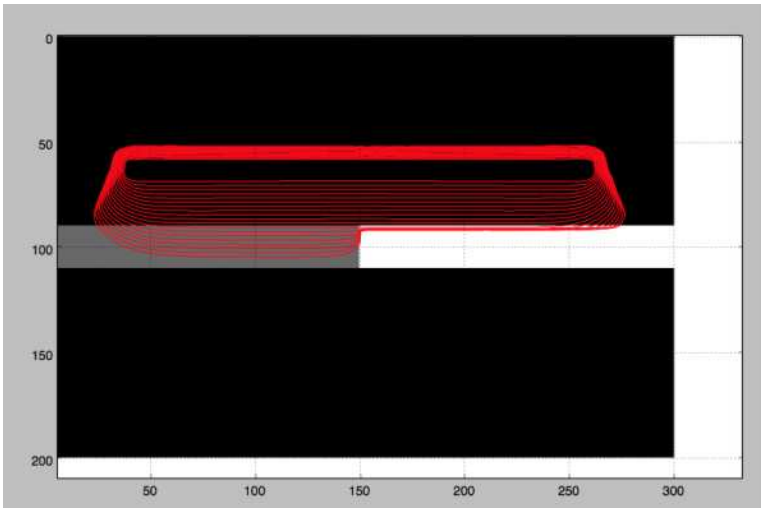

Figure 7. Output from the python script

Figure 7 presents the figure that is outputted from the script. Here MatPlotlib is used to visualize the front and fuel map using the "getLayer" function that return a numpy array.

4.2. Simulation in a operational context

Figure 8 presents a simulation results in a web application that provides a graphical user interface to easily launch simulations (available at http://forefire.univ-corse.fr/sim/dev/). This context is very different, user does not have to take time to prepare data, so everything is already available (a NetCDF file for each small region with all data layers) and the simulation is just run by using the "loadData", then "addFire", and "print" function in a loop on the server and sent back to the web browser.

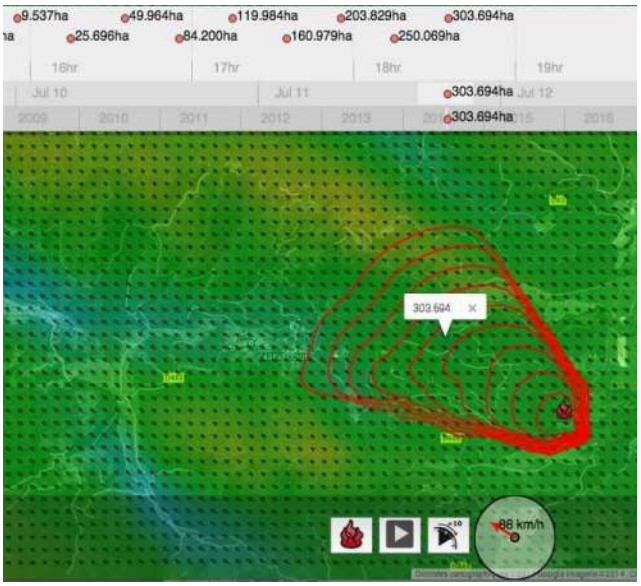

Figure 8. ForeFire in command line, launched on a server trough a web interface

Requirements and conclusion

Forefire library, python, java and command line interpreter is available on GitHub at address https://github.com/forefireAPI/firefront. The minimum requirement is to have NetCDF library

installed with legacy C++ interface. The SWIG (swig, 2014) build platform is used to automate the compilation. Target platform is a Unix compatible system with a C++ compiler available.
This paper presented the philosophy of the software as well as showing its usage in a scripted, command line and a coupled environment [Filippi *et al* 2013]. The same C++ compiled shared library is used here in a graphical user interface, a high performance computing environment and a scripted, scientific oriented environment (Python/Numpy).
The philosophy is typical of both scientific and operational software, with sources available, self compiling and expandable code but also having connections with data formats that allows to simulate real fire on existing data in a very limited time. Further work will be focused to enhance the python interface, optimize the code, add more components and interaction methods.

Acknowledgement

This research was developed within the projects ANR-09-COSI-006-01 IDEA

References

Filippi et.al. 2009. Jean Baptiste Filippi; F. Morandini; Jacques-Henri Balbi; David Hill Discrete event front tracking simulator of a physical fire spread model, hal-00438619, Simulation, 2009, 86 (10), pp. 629-644, DOI : 10.1177/0037549709343117

Balbi et. al. 2009 Jacques Henri Balbi; Frédéric Morandini; Xavier Silvani; Jean Baptiste Filippi; Frédéric Rinieri. A Physical Model for Wildland Fires, hal-00593608, Combustion and Flame, 2009, 156 (12), pp. 2217-2230 . DOI : 10.1016/j.combustflame.2009.07.010

Finney and Andrews, 1994 Finney, M., Andrews, P., 1994. The farsite fire area simulator: Fire management applications and lessons of summer 1994. In: in Proceedings of Interior West Fire Council Meeting and Program. pp. 209–216, coeur Alene, USA.

Filippi et.al. 2013 Assessment of ForeFire/Meso-NH for wildland fire/atmosphere coupled simulation of the FireFlux experiment, J.-B. Filippi, X. Pialat, C.-B. Clements, Proceedings of the Combustion Institute, Volume 34, Issue 2, Pages 2633–2640, 2013.

Swig, 2014. http://www.swig.org

Forest fires effects on the atmosphere: 20 years of research in Portugal

Ana Miranda[a]; Amorim, JH[a]; Valente, J[a]; Monteiro, A[a]; Ferreira, J[a]; Borrego, C[a]

[a] *CESAM & Department of Environment and Planning, University of Aveiro, 3810-193, Aveiro, Portugal, miranda@ua.pt, amorim@ua.pt, joanavalente@ua.pt, alexandra.monteiro@ua.pt, jferreira@ua.pt; borrego@ua.pt*

Abstract
Forest fires are one of the most impressive forces of nature. Large amounts of gases and particles are emitted to the atmosphere, with significant impacts on operational safety, air quality, human health and climate change. In the European context, Portugal, together with other south European countries, has a dark record concerning forest fires, with alarming statistics, concerning occurrences, burnt areas, economic and ecological losses and human casualties.
Due to the frequency, magnitude and effects on the environment, health, economy and security, forest fires have increasingly become a major subject of concern for decision-makers, firefighters, scientists and citizens in general.
The GEMAC (Group of Emissions, Modelling and Climate Change) research team, at the University of Aveiro in Portugal, completed 20 years of experience in dealing with the effects of forest fires on the atmosphere, working on the monitoring and modelling of the impacts on the environment and human health, together with national and international teams, through the participation in numerous national and international projects. This research team has been involved in several experimental fires performed since 1998 in the GESTOSA experiments, at Serra da Lousã, Central Portugal. GEMAC has collected a large quantity of experimental data, used to support the development of new methods and models, aiming to estimate the effects of forest fires on the atmosphere. The work presented summarizes GEMAC's most relevant research in what respects the integrated and multi-scale analysis of the interrelations between forest fires and air quality, human safety and health, suppression and climate change.

Keywords*: fire emissions, air quality, smoke, health effects, visibility impairment, climate change, measurement and modelling*

Introduction

Forest fires are one of the most impressive forces of nature. A forest fire is a large-scale natural combustion process consuming various types of botanical specimen growing outdoors. Among their consequences, is the emission of various gases and solid particulate matter to the atmosphere with significant impacts on operational safety, air quality, human health and climate change.
In the European context, Portugal, together with other south European countries, has a dark record concerning forest fires, with alarming statistics, concerning occurrences, burnt areas, economic and ecological losses and human casualties.
The GEMAC (Group of Emissions, Modelling and Climate Change) research team, at the University of Aveiro in Portugal, completed 20 years of experience in dealing with the effects of forest fires on the atmosphere, working on the monitoring and modelling of the impacts on the environment and human health, together with national and international teams, through the participation in numerous national and international projects. The work here presented summarizes its most relevant research in what respects forest fires atmospheric emissions and its impact on air quality, human exposure and climate change.

Emissions

Smoke from forest fires includes important amounts of carbon dioxide (CO_2), carbon monoxide (CO), methane (CH_4), nitrogen oxides (NOx), ammonia, particulate matter (PM), non-methane hydrocarbon (NMHC) and other chemical compounds. These air pollutants can cause serious consequences to local and regional air quality. Therefore it is essential to understand and establish the relationship between emissions and air quality. The characterization of forest fire emissions is based on two different, but complimentary approaches: direct measurements and estimation of emissions based on emission factors. Miranda *et al.* (2005) measured, among other gases and particulate matter, volatile organic compounds (VOC) emissions in the flaming and smouldering phase of an experimental fire, verifying that despite the small size of the burning plots when compared to wildfires, the measured levels of pollutants were considerable, indicating the effect of these experiments on the local air quality and stressing the serious levels of air pollution that can be expected during wildfires. Moreover, emission measurements have been done in laboratory and during experimental field fires aiming to evaluate the impact of the use of fire retardants, concluding that in that specific case, though the production of smoke is increased by the application of retardants, the extension of the fire (both in area burned and in duration) is reduced, thus contributing to a decrease of the total smoke emissions (Amorim *et al.*, 2010).
Although there is an extensive body of literature on emission factors from forest fires, there are not many works that reflect the specificity of Southern European countries. Miranda (2004) performed and presented a selection of emission factors for South-European forest. This review and summarizing work was further updated and expanded, taking into account more recent works and additional pollutants (Ana I Miranda *et al.*, 2009). The GEMAC team has an extensive work on the estimation of pollutants emissions using emission factors (see e.g. Martins *et al.* 2012, **Erro! A origem da referência não foi encontrada.**1).

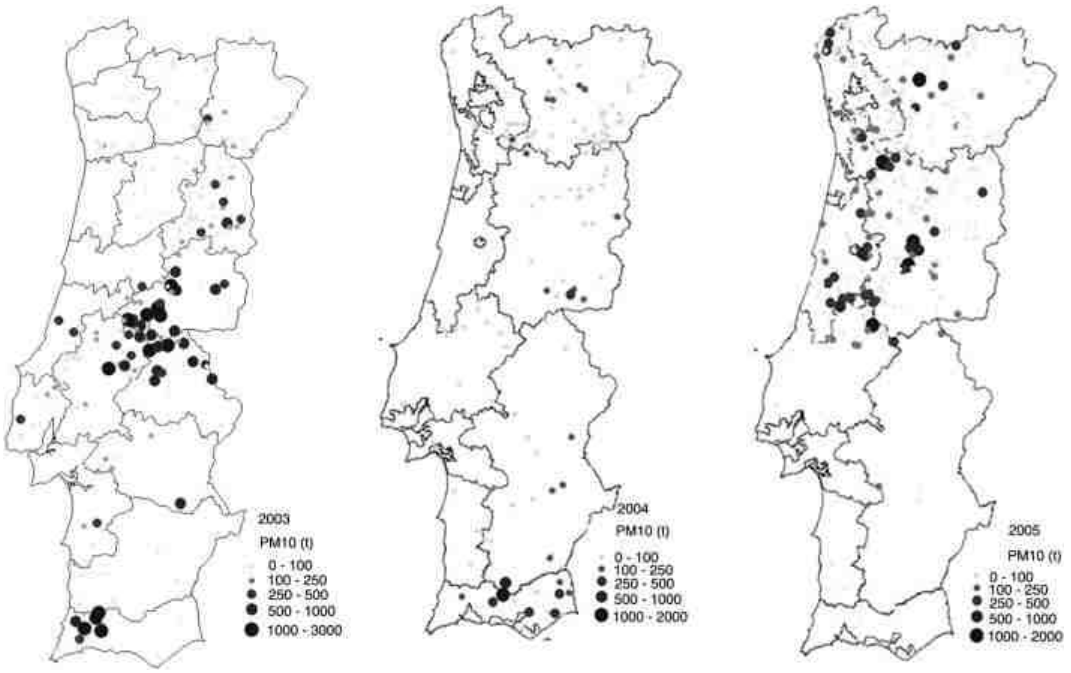

Figure 1. PM10 forest fire emissions spatial distribution for 2003–2005 fire seasons in Portugal (only large forest fires were considered (Martins et al., 2012).

Erro! A origem da referência não foi encontrada.1 shows the spatial distribution of forest fire PM10 emissions for 2003, 2004 and 2005 estimated for air quality modelling purposes. A comparison

between the estimated forest fire emission values and values reported by other available inventories is shown in Table 1, which presents the total forest fire emissions for Portugal (2003–2005) for CO_2, CO, CH_4, NMHC, PM2.5, PM10, total particulate matter (TPM) and NOx, based on three different inventories: the aforementioned Portuguese inventory, the Global Fire Emissions Database (GFED) inventory (Van Der Werf *et al*., 2010), and the European Forest Fire Information System (EFFIS) inventory (San-Miguel-Ayanz, J. Steinbrecher, 2009).

Table 1- Total forest fire emissions (t) in Portugal for 2003, 2004 and 2005 fire seasons based on different methodologies (Martins et al., 2012.).

Source	Forest fire emissions (t)							
Year	CO_2	CO	CH_4	NMHC	PM2.5	PM10	TPM	NO_x
2003								
Portuguese inventory	6,842,000	456,000	26,000	32,000	26,000	53,000	-	21,000
GFED	8,000,000	500,000	70,000	30,000	20,000	-	140,000	14,000
EFFIS	10,510,119	411,945	21,475	17,834	41,406	48,913	68,749	28,745
2004								
Portuguese inventory	2,096,000	137,000	8000	10,000	14,000	16,000	-	7000
GFED	3,000,000	200,000	20,000	10,000	10,000	-	50,000	5000
EFFIS	3,312,543	129,112	6735	5599	13,001	15,361	21,597	9013
2005								
Portuguese inventory	3,470,000	230,000	13,000	16,000	24,000	27,000	-	11,000
GFED	14,000,000	800,000	120,000	50,000	40,000	-	250,000	25,000
EFFIS	7,866,267	325,628	16,843	13,833	32,206	38,034	53,180	22,719

- Not available.

In general, the emission data presents the same order of magnitude, but in some cases it is possible to verify a larger difference, namely: for CH_4 in 2004 and 2005 in the GFED inventory; for NMHC in EFFIS inventory in 2004; for TPM for both GFED and EFFIS inventories. The differences were in some way expected because different methodologies were applied.

The GEAMC team is exploring new methodologies for the estimation of forest fire emissions, based on space borne data and on the fuelbed concept. Currently, large use is made of detailed space borne data to help reduce emissions estimation uncertainties, as shown by a recent comparison exercise at global scale (Jain, 2007; Stroppiana, Grégoire, & Pereira, 2003). In order to reduce these uncertainties, and because real-time information is now increasingly needed for operational use in rapid fire damage assessment, an operational fire emission model has been recently developed at regional/European scale in the European Forest Fire Information System (EFFIS) (San-Miguel-Ayanz, Schulte, Schmuck, & Camia, 2013). This system was applied and tested for a forest fire case study occurred in Portugal on 14th October 2011 (with a total of 4400 ha of burnt area), using detailed fuel maps and sequential mapping of the fire evolution on the basis of satellite imagery (Monteiro *et al*., 2014). In order to evaluate the relevance/importance of these forest fire emissions, they were compared with the anthropogenic emissions estimated for a typical week day over that area (Table 2). The anthropogenic emissions include all Selected Nomenclature for Air Pollution (SNAP) activities like industrial and residential combustion, production processes, solvents use, transports, waste treatment and agriculture, and were compiled using the national emission report developed on an annual basis by the Portuguese Agency for the Environment (Monteiro *et al*., 2007).

Table 2- Anthropogenic emissions (annually) estimated for the study area and the corresponding burnt area calculated by the EFFIS emission model to the study fire event (October 14, 2011) (Monteiro et al., 2014).

Emissions (ton)	CO	VOC	NH_3	NOx	PM10	SO_2
Anthropogenic (annual basis)	660	284	303	373	86	12
Forest fires (EFFIS model)	230000	15000	2000	15000	27000	2500
% anthropogenic/total	0.3	1.9	13.2	2.4	0.3	0.5

As observed from Table 2, the quantity of pollutants emitted by the forest fire event, corresponds to more than 90% of the total annual emissions over the study region. In the case of CO and PM10, forest

fire emissions are three orders of magnitude larger than the total annual emissions by all anthropogenic activities. These high values of forest fires emissions are, in part, explained by the rural characteristics of the study municipality. In this type of rural areas forest fire emissions can be the most important and relevant source of air pollution.
Although air pollutants released from forest fires depend on a number of factors (area burned, fuel loading, fuel consumption, and pollutant-specific emission factors), two factors alone – fuel loading and fuel consumption – account for up to 80% of the error on smoke emissions estimation (Ottmar, Miranda, & Sandberg, 2008). GEMAC is contributing to a higher accuracy of smoke emission estimates for Mediterranean Climate Areas (MCA) by using the Fuel Characteristic Classification System (FCCS) (Ottmar, Sandberg, Riccardi, & Prichard, 2007), to build fuelbeds for Portugal. The FCCS fuelbeds capture the structural complexity, geographic diversity and potential flammability of a fuelbed, encompassing all fuelbed components that have the potential to burn including trees, shrubs, grasses, woody material, litter, and duff. The FCCS evaluates fuelbed hazard by calculating fire potentials, reaction intensity, flame length, and rate of spread. Typical Portuguese fuelbeds were identified and built using the National Forest Inventory, other fuels datasets, published scientific literature, and fuel photo series. The mapping of the defined fuelbeds using vegetation classification and quantitative vegetation data is under development.

Air Quality Monitoring and Modelling

The gases and particles emitted during a forest fire undergo chemical transformations in the atmosphere as they are being dispersed, and its impacts can be found at long distances from the source. Despite current evidence, the connection between forest fires and air quality is still an ongoing topic, that only during the last decade started to be more frequently addressed. For the fire community, the main concern consisted in its direct effects, such as human fatalities and material damage. On the other hand, the air quality community was mainly focused on anthropogenic sources of pollutants, particularly in traditional sectors of industry and road traffic.
To evaluate the effects of forest fires on air quality both measurements and numerical models can be used. The research team has been involved in several experimental fires performed since 1998 in Serra da Lousã, Central Portugal, the GESTOSA experiments, collecting a large quantity of experimental data (e.g. Miranda 2004, Miranda *et al.* 2005; Valente *et al.* 2007), used to support the development of new methods and models. Figure 2 shows some of the equipment used to measure air pollutant concentrations during GESTOSA experimental fires.

Figure 2- Photo of van nr. 2 and its air quality equipment. Photo of passive samplers.

The GEMAC team has developed numerical models, AIRFIRE (A I Miranda, 2004) and DISPERFIRESTATION (Valente *et al.*, 2007), that are able to simulate the effects of fire emissions on air quality, at different scales. DISPERFIRESTATION is a fire behavior system, developed to estimate fire progression, smoke dispersion and visibility impairment, at local scale, while AIRFIRE is a numerical system, developed to estimate the effects of forest fires on air quality, at the mesoscale, integrating several components, namely the meteorological model MEMO, the photochemical model

MARS and the Rothermel fire spread model. These modelling tools have been applied to various case studies in Portugal, showing that concentrations of pollutants attain levels of concern (e.g. Miranda, 2004; and Valente *et al*., 2007). Figure 3 depicts an output of the DISPERFIRESTATION system, a PM10 concentration field resulting from a burning plot in a GESTOSA experiment, and an AIRFIRE output, showing a vertical profile of wind and CO concentrations.

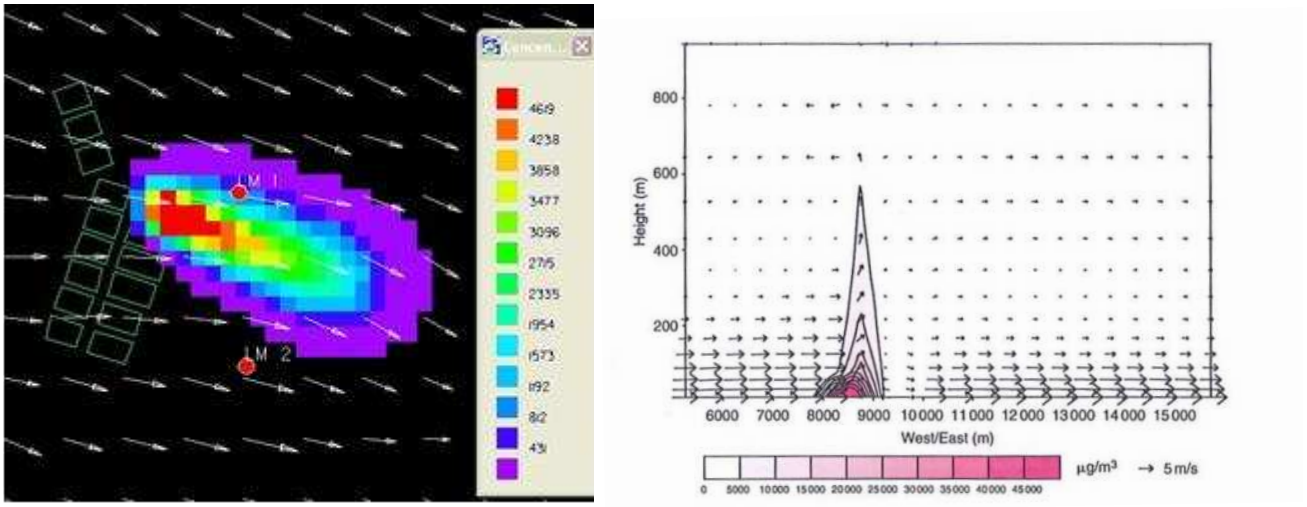

Figure 3. (left) PM10 concentration fields (µg.m^{-3}), at ground level, after the burn of three plots (400m x 330m) at GESTOSA 2004 experiments (Valente et al., 2007). (right) Vertical profile of wind and CO concentration in a forest fire in Arrábida (Portugal)(A I Miranda, 2004) .

At the local scale the effect of fire as a heat source is not considered in DISPERFIRESTATION, but AIRFIRE includes this effect in the simulations.

The GEMAC team also worked on the modelling of wildland urban interface fires. Miranda, Marchi, *et al*. (2009) simulated the temporal evolution of the hourly averaged PM10 concentration fields during September 13, 2003. **Erro! A origem da referência não foi encontrada.**4 shows the surface hourly averaged PM10 concentration patterns for 22.00 LST as estimated by AIRFIRE. There is an obvious contribution by forest fires to the particularly high levels of PM10 measured in the urban area of Lisbon at night.

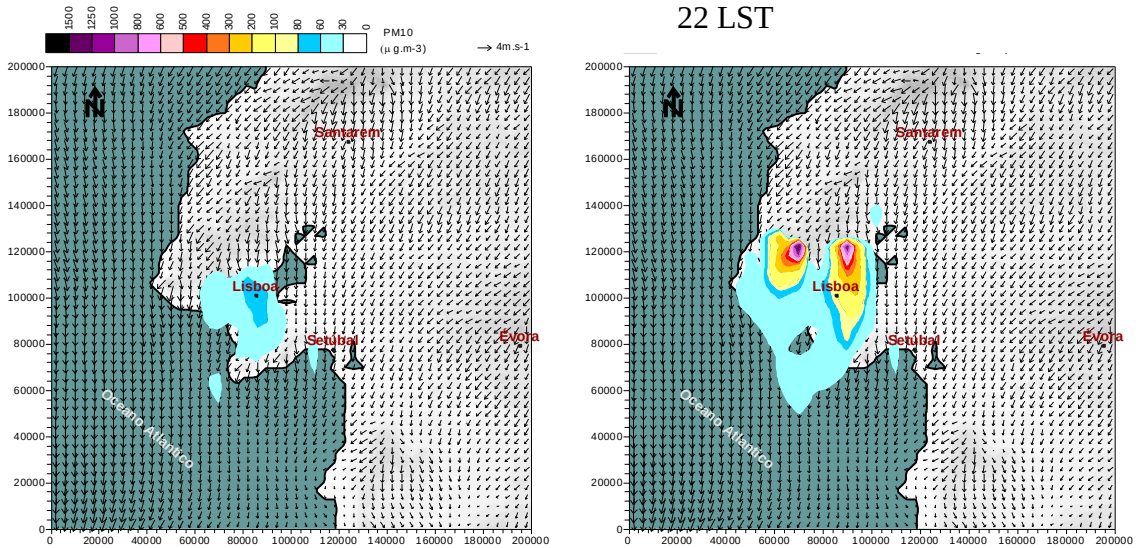

Figure 4. Hourly-averaged surface PM10 concentration (μg m^{-3}) and wind values at 22.00 LST, excluding forest fire emissions(left) and including forest fire emissions (right).

At a larger scale the contribution of 2006 western Russia wildfires, during spring, to the air quality impairment over Europe was evaluated too (A.I Miranda, Sá, Martins, Borrego, & Sofiev, 2010). **Erro! A origem da referência não foi encontrada.**5 presents simulation and measurement results of the PM10 hourly midday spatial distribution for one of the simulation days.

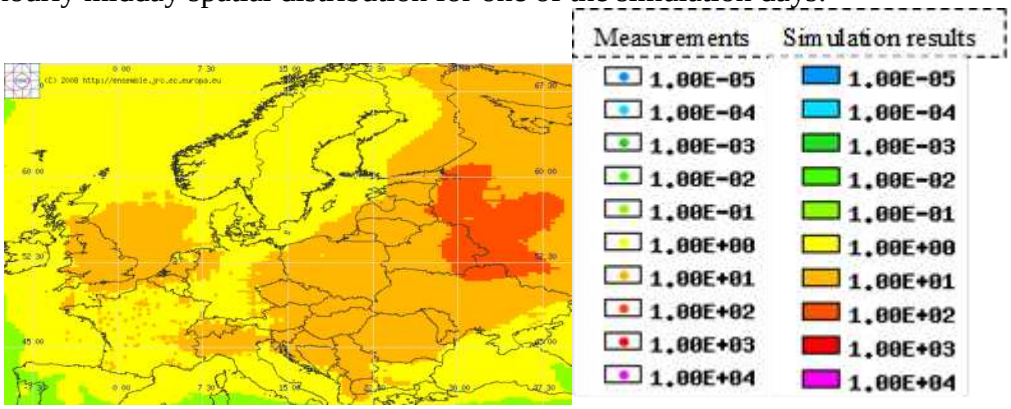

Figure 5. Spatial distribution of PM10 hourly midday concentration values (μg.m^{-3}) May 4 (A.I Miranda et al., 2010).

This simulation of the 2006 spring fires over Europe allowed confirming the transboundary characteristics of wildland fires, clearly showing the impact of fires spreading over Russia in several European countries. The evaluation of the impact of wildfires on the air quality should be included in air quality assessment procedures at the European level, and air quality modelling systems can be important tools to achieve this goal.

Safety

Wildland firefighting implies many hazards to firefighters, including burns, heat stress, tripping and falling hazards, and inhalation exposure to smoke. Personal monitoring is a reliable way of estimating the exposure of an individual to a specific air pollutant. It assesses an individuals' inhalation exposure based on the measurement of a pollutant concentration within a person's breathing zone for a defined time.

Recently, exposure studies were conducted in Portugal to determine firefighter's individual exposure to smoke, using for that purpose personnel sampling devices to monitor CO, VOC, and nitrogen dioxide (NO_2) and a GPS instrument to track their position on site (A. I. Miranda *et al*., 2010; Ana Isabel Miranda *et al*., 2012). The measurement of firefighters individual exposure to smoke was conducted in 2008 and 2009: (i) in Gestosa fire experiments, in Central Portugal, at the end of the spring season; and (ii) during the fire season (May to October) in Central Portugal. Data on individual exposure to CO, PM2.5 and NO_2 were measured for a group of ten firefighters equipped with portable measuring devices.

The selection of monitoring equipment was based on toughness, weight, possibility of continuous data acquisition, and ease of operation. Table 3 presents the main characteristics of the equipment used in the exposure monitoring.

Table 3- Characteristics of the equipment.

Pollutant	Type of data	Equipment	Characteristics	
			Range	Resolution
NO_2	Continuous measurement: 5 seconds interval	GasAlertMicro 5 PID from BW Technologies	0-99.9 ppm	0.1 ppm
CO	Continuous measurement: 5 seconds interval	GasAlertMicroClip from BW Technologies	0-500 ppm	0.1 ppm
		GasAlertextreme from BW Technologies	0-1,000 ppm	1 ppm
PM2.5	Continuous measurement: 1 minute interval	Personal Aerosol Monitor SidePack AM510 from TSI	0-20 $mg.m^{-3}$	0.001 $mg.m^{-3}$

Exposure results were compared to the occupational exposure standards (OES) defined for different air pollutants. According to the American Conference of Governmental Industrial Hygienists (ACGHI), OES are presented as the:

- threshold limit value (TLV) of the time-weighted average (TWA);
- TLV of the short-term exposure limit (STEL); and
- peak limit.

The TWA is calculated over a normal 8-hours working day and a five days working week. The TLV-STEL corresponds to a 15-minutes time-weighted average exposure that should not be exceeded at any time during a workday, even if the 8-hours TWA is under the TLV. The TLV-STEL is the highest concentration to which it is believed that workers can be exposed continuously for a short period of time without suffering effects. **Erro! A origem da referência não foi encontrada.**4 presents the OES values for the different air pollutants analysed under this study.

Table 4. OES limit values for different air pollutants contained in biomass burning smoke. For some VOC these values are not available (n.a.) in National or International regulations.

Air pollutant	TLV-TWA	Reference	TLV-STEL	Reference	Peak Limit	Reference
CO	25 ppm	NP 1796:2007	200 ppm	Australian legislation	400 ppm	Australian legislation
NO_2	3 ppm		5 ppm	NP 1796:2007	20 ppm	NIOSH
Respirable particles without other classification	3 $mg.m^{-3}$	NP 1796:2007	n.a.	n.a.	n.a.	n.a.

Most firefighters use a bandana for respiratory protection, nevertheless, according to (Reh, Letts, & Deitchman, 1994) the pore size of this type of bandanas is approximately 200 μm x 200 μm, roughly

500 to 2000 times larger than the smaller smoke particles (0.100-0.400 μm), and consequently, gases and fine particulate matter can pass through the fabric.
Several exceedances to the OES values for CO were observed (maximum registered was 1000 ppm which is the equipment upper detection limit), meaning that firefighters are exposed to levels higher than the allowed limits of current legislation. NO_2 values are within the OES, except for some peak values exceedances (maximum registered was 33 ppm). Measured PM2.5 is within the OES, however, it should be noted that the OES is much higher than the standard defined by the World Health Organization for air quality.

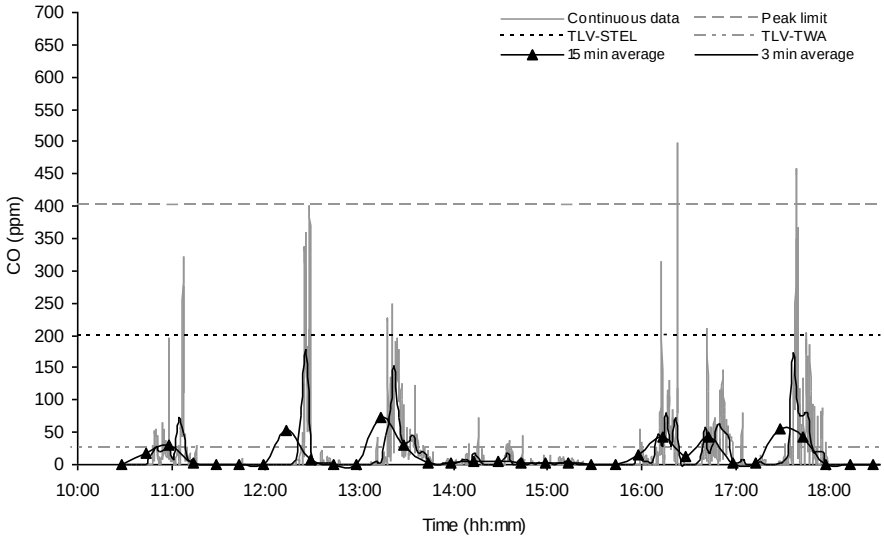

Figure 6. CO concentrations (ppm) measured for one of the firefighters during an experimental fire in GESTOSA.

This data (**Erro! A origem da referência não foi encontrada.**6) shows the magnitude of the exposure peaks that occurred during regular firefighting operations, indicating that the firefighters are exposed to CO concentrations that pose their health and safety at risk and diminish their capability of taking decisions in emergency situations.
Medical tests conducted on the firefighters also indicate a considerable effect on measured medical parameters, with a large increase of CO and a decrease of NO in the exhaled air of majority of the firefighters (Ana Isabel Miranda *et al*., 2012).
Visibility reduction and air quality degradation are a common consequence of biomass burning and a recurring problem in almost every parts of the world. It may lead to a pronounced diminishing of safety conditions during firefighting operations and terrestrial and aerial traffic, even in small scale experimental fires. Valente *et al.* (2007) developed and integrated in a smoke dispersion model, a specific module to calculate the visibility impairment caused by forest fire pollutants emissions, based on its concentrations in the atmosphere.

Suppression

GEMAC's work on fire suppression has been focused on both aerial and ground-based operations. These two lines of research share the objective of optimizing the efficiency of operations while guaranteeing the safety of personnel and civilians in the affected fire zones.
The efficiency of the aerial drop of firefighting agents (water and retardants) using airplanes or helicopters is highly conditioned by local atmospheric conditions (e.g., wind intensity, wind gusts, air turbulence, fire intensity, visibility), together with flight parameters (e.g., altitude, speed, route) and pilot perception. Despite these, and contrarily to commercial aviation, on-board systems for computer-

assisted drops have not yet been used operationally. Aiming to provide an enhanced understanding of the behaviour of aerially delivered firefighting liquids and the factors that influence the overall suppression effectiveness, Amorim (2011a, 2011b) developed the Aerial Drop Model ADM, for water and chemical retardant applications, that can potentially be used in training activities with firefighters; or in testing the effectiveness of new firefighting chemicals or delivery systems, complementing the data obtained from real scale drop tests. This numerical tool allows a near real-time simulation of aerial drops with fixed-wing aircraft, while covering the fundamental stages of the process. It copes with a wide range of product viscosities, from water to highly thickened long-term retardants. **Erro! A origem da referência não foi encontrada.**7 presents a result of a retardant cloud drop as simulated by ADM.

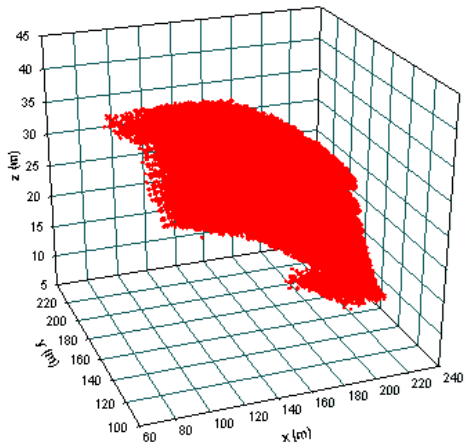

Figure 7. ADM simulation of a 3D retardant cloud, 3s after release initiation.

ADM was validated against experimental data acquired in a large number of real-scale drop tests carried out in Europe and in the United States of America. In general, the model produced a good representation of the spatial distribution of the agent in the ground for various coverage levels and its accuracy was, in fact, within the statistical uncertainty of the experimental sampling method.

On an operational basis too, GEMAC team is currently working on the development of a firefighting Decision Support System, that will combine the monitoring and forecast of smoke exposure, to help decision making in an operational scenario. The goal of this research is to develop an emergency response support system for firefighting ground-based operations during forest fire events. The target of the under-development computational tool is to provide knowledge-based aid to firefighters at critical decision-making situations, helping with the safe and successful management of fire. This DSS will support the following features:

- capture of 'live' sensor data from a set of wearable monitoring equipment that will be based on a previously developed certified medical wearable technology named "VitalJacket®";
- capture of meteorological observations from a mast placed in one of the vehicles;
- enable projections of fire progression, smoke levels and critical exposure in a predefined time-step (up to 30 minutes);
- interpretation of results in an easy and intuitive form to be used by fire managers or firefighters involved in operations.

To achieve this goal hardware technology (e.g. wearable, mobile, communications) was combined with processing/simulation software algorithms and user interactive interfaces. A data assimilation technique will allow near real-time observations from wearable monitoring equipment to be integrated into the exposure forecast modelling system, increasing the accuracy of the estimates.

A first prototype of the DSS, running in off-line mode, will be tested in the terrain during the fire season of 2014. An improved online version of the prototype will be tested in the following autumn in a series of prescribed burns.
In conclusion, this work proposes the development and testing (under real conditions) of a DSS intended to provide optimized firefighting efficiency, enhanced hazard awareness, and knowledge-based response to forest fire events. Advances in the computational modelling of fire and smoke behaviour, in conjunction with personal monitoring data, provide near real-time simulation of local fire conditions and short-term smoke exposure forecasts, with the needed advance in time to permit the safe and efficient positioning of crews in the terrain.

Climate change

Greenhouse gases emissions by forest fires can have an important contribution in climate change (A. I. Miranda, Coutinho, & Borrego, 1994). Forest fire activity and air quality under a changing climate are considered one of the main threats to sustainable development. Carvalho *et al.* (2008a, 2010) investigated the impact of future climate change on fire activity across Portugal, assessing the fire weather and subsequent fire activity under a $2 \times CO_2$ scenario and studying the relationship between the weather, the Fire Weather Index (FWI) System components, and both the area burned and fire occurrence across Portugal. Temperature was predicted to increase and precipitation to decrease, resulting in an increased FWI in all areas studied along with more severe and longer fire seasons. Future fire activity will increase dramatically across the entire country, with area burned and fire occurrence both rising substantially.
Air quality modelling results for Portugal (A. Carvalho *et al*., 2011) pointed out that future forest fire activity will increase the ozone concentration levels by almost 23 $\mu g\ m^{-3}$ by 2100 but a decrease of approximately 6 $\mu g\ m^{-3}$ is expected close to the main forest fire locations. Future forest fire emissions will also impact the PM10 concentrations over Portugal with increases reaching 20 $\mu g\ m^{-3}$ along the Northern coastal region in July. The highest increases are estimated over the north and centre of Portugal where the area burned projections in future climate are higher.

Final Remarks

Due to the frequency of occurrence and the magnitude of forest fires, and also to their effects on the environment, health, economy and security, they have increasingly become a major subject of concern for decision-makers, firefighters, scientists and citizens in general, in many regions of the world, including the southern European countries.
Experimental field fires represent a valuable tool for understanding wildfires in all its extension: behaviour, impacts on environment, security conditions and health, suppression techniques efficiency, among others.
The application of numerical emissions and air quality modelling systems is also an added value when evaluating and assessing air quality levels in areas affected by forest fires. Environmental policies, in particular the south-European ones must integrate both the traditional air pollution-oriented and the forested-land management issues into a unique system. Better forested-land management can help to reduce both the number of air pollution episodes and the risk of unwanted fires.
Wildland firefighting implies many hazards to the population in general, but also for firefighters, including burns, heat stress, tripping and falling hazards, and inhalation exposure to smoke. The development of monitoring solutions and solid science based DSS is of paramount importance both for fire management, but also for the personal safety of operational personnel.
These predicted increases in fire activity in a changing climate will have environmental, social, and economic impacts and would dramatically impact the organizational structures that deal with wildland fire and also society in general.

8. Acknowledgements

This work was supported by European Funds through COMPETE and by National Funds through the Portuguese Science Foundation (FCT) within projects PEst-C/MAR/LA0017/2013 and VitalResponder2 (PTDC/EEI-ELC/2760/2012), and the Post-Doc grants of J.H. Amorim (SFRH/BPD/48121/2008), J. Valente (SFRH/BPD/78933/2011), A. Monteiro (SFRH/BPD/63796/2009) and J. Ferreira (SFRH/BPD/40620/2007).

9. References

Acem, Z., Lamorlette, A., Collin, A., & Boulet, P. (2009). Analytical determination and numerical computation of extinction coefficients for vegetation with given leaf distribution. *International Journal of Thermal Sciences*, *48* , 1501–1509.

Alexander, M. E. (2000). *Fire behaviour as a factor in forest and rural fire suppression* (p. 30). Forest Research; Forest and Rural Fire Scientific and Technical Ser; Rotorua; Wellington. Forest Research Bulletin No. 197; in association with the National Rural Fire Author.

Amorim, J. H. (2011a). Numerical modelling of the aerial drop of firefighting agents by fixed-wing aircraft. Part I: model development. *International Journal of Wildland Fire*, *20*(3), 384–393.

Amorim, J. H. (2011b). Numerical modelling of the aerial drop of firefighting agents by fixed-wing aircraft. Part II: model validation. *International Journal of Wildland Fire*. doi:10.1071/WF09123

Amorim, J. H., Miranda, A. I., Valente, J., Borrego, C., Viegas, D. X., Pita, L. P., & Ribeiro, L. M. (2010). Effects of chemical retardants on air pollutants emissions: measurements in a combustion chamberNo Title. In D. X. Viegas (Ed.), *VI International Conference on Forest Fire Research (ICFFR)* (p. 267). Coimbra: University of Coimbra.

Andrews, P. L., Heinsch, F. A., & Schelvan, L. (2011). *How to generate and interpret fire characteristics charts for surface and crown fire behavior* (p. 48). Gerenal Technical Report RMRS-GTR-253.

Boulet, P. (n.d.). *Personal communication 26/02/2014*.

Boulet, P., Parent, G., Acem, Z., Collin, A., Försth, M., Bal, N., … Torero, J. (2014). Radiation emission from a heating coil or a halogen lamp on a semitransparent sample. *International Journal of Thermal Sciences*, *77*, 223–232.

Bubb, P. (2004). *Cloud forest agenda* (p. 36). Cambridge, UK.: UNEP-WCMC.

Carvalho, A., Flannigan, M. D., Logan, K. A., Gowman, L. M., Miranda, A. I., & Borrego, C. (2010). The impact of spatial resolution on area burned and fire occurrence projections in Portugal under climate change. *Climatic Change*, *98*, 177–197. doi:10.1007/s10584-009-9667-2

Carvalho, A., Flannigan, M. D., Logan, K., Miranda, A. I., & Borrego, C. (2008). Fire activity in Portugal and its relationship to weather and the Canadian Fire Weather Index System. *International Journal of Wildland Fire*. doi:10.1071/WF07014

Carvalho, A., Monteiro, A., Flannigan, M., Solman, S., Miranda, A. I., & Borrego, C. (2011). Forest fires in a changing climate and their impacts on air quality. *Atmospheric Environment*, *45*, 5545–5553. doi:10.1016/j.atmosenv.2011.05.010

Cerda, A., & Robichaud, P. R. (2009). *Fire Effects on Soils and Restoration Strategies* (p. 605). CRC Press.

Cheney, P., & Sullivan, A. (2008). *Grassfires: fuel, weather and fire behaviour.* (p. 150). CSIRO Publishing.

Cochrane, M. A. (2003). Fire science for rainforests. *Nature*, *421*(6926), 913–9. doi:10.1038/nature01437

Consalvi, J. L., Nmira, F., Fuentes, A., Mindykowski, P., & Porterie, B. (2011). Numerical study of piloted ignition of forest fuel layer. *Proceedings of the Combustion Institute*, *33* , 2641–2648.

Cruz, M. G., & Gould, J. S. (2010). Fuel and fire behaviour in semi-arid mallee-heath shrublands. In D. X. Viegas (Ed.), *6th International Forest Fire Research Conference*. Coimbra, Portugal: ADAI.

De Mestre, N. J., Catchpole, E. A., Anderson, D. H., & Rothermel, R. C. (1989). Uniform Propagation of a Planar Fire Front without Wind. *Combustion Science and Technology*, *65*(4-6), 231–244.

Frandsen, W. (1997). Ignition probability of organic soils. *Canadian Journal of Forest Research*, *27*(9), 1471–1477. doi:10.1139/x97-106

Frandsen, W. (1998). Heat Flow Measurements From Smoldering Porous Fuel. *International Journal of Wildland Fire*, *8*(3), 137. doi:10.1071/WF9980137

Fureby, C., Tabor, G., Weller, G., & Gosman, D. (1997). A comparative study of subgrid scale models in homogeneous isotropic turbulence. *Physics of Fluids*, *9(5)* , 1416–1429.

Gibbon, A., Silman, M. R., Malhi, Y., Fisher, J. B., Meir, P., Zimmermann, M., … Garcia, K. C. (2010). Ecosystem Carbon Storage Across the Grassland–Forest Transition in the High Andes of Manu National Park, Peru. *Ecosystems*, *13*(7), 1097–1111.

Grishin, A. M., & Albini, F. (1997). *A Mathematical Modelling of Forest Fires and New Methods of Fighting Them*. Publishing House of the Tomsk University, Tomsk, Russia .

Incropera, F. P., DeWitt, D. P., Bergman, T. L., & Lavine, A. S. (2007). *Fundamentals of Heat and Mass Transfer*. (F. P. Incropera & F. P. F. O. H. A. M. T. Incropera, Eds.)*Water* (Vol. 6th, p. 997). John Wiley & Sons. doi:10.1016/j.applthermaleng.2011.03.022

Jain, A. K. (2007). Global estimation of CO emissions using three sets of satellite data for burned area. *Atmospheric Environment*, *41*, 6931–6940. doi:10.1016/j.atmosenv.2006.10.021

Lamorlette, A., & Collin, A. (2012). Analytical quantification of convective heat transfer inside vegetal structures. *International Journal of Thermal Sciences*, *57* , 78–84.

Larini, M., Giroud, F., Porterie, B., & Loraud, J. C. (1998). A multiphase formulation for fire propagation in heterogeneous combustible media. *International Journal of Heat and Mass Transfer*, *41*(6-7), 881–897.

Lesieur, M. (2008). *Turbulence in fluids*. (R. MOREAU, Ed.) (fourth.). Springer.

Long, R., Torero, J., Quintiere, J., & Fernandez-Pello, A. (1999). Scale and transport considerations on piloted ignition of PMMA. In *Fire Safety Science - Proceedings of the sixth International Symposium* (pp. 567–578).

Marcos Chaos. (2014). Spectral Aspects of Bench-Scale Flammability Testing: Application to Hardwood Pyrolysis. In *Fire Safety Science-Draft Proceedings of the Eleventh International Symposium*.

Margerit, J., & Sero-Guillaume, O. (2002). Modelling forest fires. Part II: Reduction to two-dimensional models and simulation of propagation. *International Journal of Heat and Mass Transfer*, *45*, 1723–1737. doi:10.1016/S0017-9310(01)00249-6

Martins, V., Miranda, A. I., Carvalho, A., Schaap, M., Borrego, C., & Sá, E. (2012). Impact of forest fires on particulate matter and ozone levels during the 2003, 2004 and 2005 fire seasons in portugal. *Science of the Total Environment*, *414*, 53–62. doi:10.1016/j.scitotenv.2011.10.007

Mcallister, S., Grenfell, I., Hadlow, A., Jolly, W. M., Finney, M., & Cohen, J. (2012). Piloted ignition of live forest fuels. *Fire Safety Journal*, *51*, 133–142. doi:10.1016/j.firesaf.2012.04.001

Mell, W., Jenkins, M. A., Gould, J., & Cheney, P. (2007). A physics-based approach to modelling grassland fires. *International Journal of Wildland Fire*, *16*(1), 1–22.

Mell, W., Maranghides, A., McDermott, R., & Manzello, S. L. (2009). Numerical simulation and experiments of burning douglas fir trees. *Combustion and Flame*, *156* , 2023–2041.

Miranda, A. ., Sá, E., Martins, V., Borrego, C., & Sofiev, M. (2010). The Russian spring 2006 wildland fires effects on air quality over Europe. In D. X. Viegas (Ed.), *6th International Conference on Forest Fire Research* (p. 8). Coimbra: University of Coimbra.

Miranda, A. I. (2004). An integrated numerical system to estimate air quality effects of forest fires. *International Journal of Wildland Fire*, *13*, 217–226. doi:10.1071/WF02047

Miranda, A. I., Borrego, C., Martins, H., Martins, V., Jorge, H., Valente, J., & Carvalho, A. (2009). Earth Observation of Wildland Fires in Mediterranean Ecosystems. *Earth*, 171–187. doi:10.1007/978-3-642-01754-4

Miranda, A. I., Coutinho, M., & Borrego, C. (1994). Forest fire emissions in Portugal: A contribution to global warming? In *Environmental Pollution* (Vol. 83, pp. 121–123). doi:10.1016/0269-7491(94)90029-9

Miranda, A. I., Marchi, E., Ferretti, M., & Millán, M. (2009). Chapter 9 Forest Fires and Air Quality Issues in Southern Europe. In M. J. A. Andrzej Bytnerowicz Allen R. Riebau and Christian Andersen BT - Developments in Environmental Science (Ed.), *Wildland Fires and Air Pollution* (Vol. Volume 8, pp. 209–231). Elsevier. doi:http://dx.doi.org/10.1016/S1474-8177(08)00009-0

Miranda, A. I., Martins, V., Cascão, P., Amorim, J. H., Valente, J., Borrego, C., … Ottmar, R. (2012). Wildland smoke exposure values and exhaled breath indicators in firefighters. *Journal of Toxicology and Environmental Health. Part A*, *75*(13-15), 831–43. doi:10.1080/15287394.2012.690686

Miranda, A. I., Martins, V., Cascão, P., Amorim, J. H., Valente, J., Tavares, R., … Pita, L. P. (2010). Monitoring fire-fighters' smoke exposure and related health effects during Gestosa experimental fires (Vol. 137, pp. 83–94). doi:10.2495/FIVA100081

Miranda, AI, Ferreira, J, & Valente. (2005). Smoke measurements during Gestosa-2002 experimental field fires, *14*(1), 107–116. doi:10.1071/WF04069

Monod, B., Collin, A., Parent, G., & Boulet, P. (2009). Infrared radiative properties of vegetation involved in forest fires. *Fire Safety Journal*, *44* , 88–95.

Monteiro, A., Corti, P., San Miguel-Ayanz, J., Miranda, A. I., & Borrego, C. (2014). The EFFIS forest fire atmospheric emission model: Application to a major fire event in Portugal. *Atmospheric Environment*, *84*, 355–362. doi:10.1016/j.atmosenv.2013.11.059

Monteiro, A., Miranda, A. I., Borrego, C., Vautard, R., Ferreira, J., & Perez, A. T. (2007). Long-term assessment of particulate matter using CHIMERE model. *Atmospheric Environment*, *41*, 7726–7738.

Morvan, D., & Dupuy, J. L. (2001). Modelling of fire spread trough a forest fuel bed using a multiphase formulation. *Combustion and Flame*, *124* , 1981–1994.

Morvan, D., Dupuy, J. L., Rigolot, E., & Valette, J. C. (2006). FIRESTAR: a physically based model to study wildfire behaviour. *Forest Ecology and Management*, *234S* , S114.

Morvan, D., Mèradji, S., & Accary, G. (2009). Physical modelling of fire spread in Grasslands. *Fire Safety Journal*, *44*(1), 50–61.

Myers, N., Mittermeier, R. A., Mittermeier, C. G., da Fonseca, G. A., & Kent, J. (2000). Biodiversity hotspots for conservation priorities. *Nature*, *403*(6772), 853–8. doi:10.1038/35002501

Nepf, H. M., Sullivan, J. A., & Zavitoski, R. A. (1997). A model for diffusion within an emergent plant canopy. *Limnology and Oceanography*, *42(8)* , 85–95.

Ohlemiller, T. J. (2002). Smoldering Combustion. In P. J. DiNenno, D. Drysdale, C. L. Beyler, & W. D. Walton (Eds.), *SFPE Handbook of Fire Protection Engineering* (3rd ed., pp. 200–210). NFPA.

Oliveras, I., Anderson, L. O., & Malhi, Y. (2014). Application of remote sensing to understanding fire regimes and biomass burning emissions of the tropical Andes. *Global Biogeochemical Cycles*, *28*, 480–496. doi:10.1002/2013GB004664

Oliveras, I., C., D., Cahuana, N., C., E. A., W., H., & Malhi, Y. (n.d.). Andean grasslands are as productive as tropical montane cloud forests. *Environmental Research Letters*.

OpenFOAM User Guide, OpenFOAM The Open Source CFD Toolbox . (2010).

Ottmar, R. D., Miranda, A. I., & Sandberg, D. V. (2008). Chapter 3 Characterizing Sources of Emissions from Wildland Fires. *Developments in Environmental Science*. doi:10.1016/S1474-8177(08)00003-X

Ottmar, R. D., Sandberg, D. V, Riccardi, C. L., & Prichard, S. J. (2007). An overview of the Fuel Characteristic Classification System — Quantifying, classifying, and creating fuelbeds for resource planningThis article is one of a selection of papers published in the Special Forum on the Fuel Characteristic Classification Syste. *Canadian Journal of Forest Research*, *37*(12), 2383–2393. doi:10.1139/X07-077

Planas, E., Oliveras, I., Manta, M. I., Urquiaga, E., Quintano, J. A., & Pastor, E. (2013). Soil combustion experiments in the Andean grassland (puna) and tropical montane cloud forests (TMCFs) treeline. In *Fourth Fire Behaviour and Fuels Conference* (p. 51). Saint Petersburg, Russia.

Raison, R., Woods, P., Jakobsen, B., & Bary, G. (1986). Soil temperatures during and following low-intensity prescribed burning in a Eucalyptus pauciflora forest. *Australian Journal of Soil Research*, *24*(1), 33. doi:10.1071/SR9860033

Raupach, M. R., & Thom, A. S. (1981). Turbulence in and above plant canopies. *Annual Review of Fluid Mechanics*, *13* , 97–129.

Reh, C. M., Letts, D., & Deitchman, S. (1994). *Health hazard evaluation report*. California.

Rein, G. (2009). Smouldering Combustion Phenomena in Science and Technology. *International Review of Chemical Engineering*, *1*, 3–18.

Rein, G., Cleaver, N., Ashton, C., & Pironi, P. (2008). The severity of smouldering peat fires and damage to the forest soil. *Catena*, *74*(3), 304–309.

Ren, N., Wang, Y., & Trouvé, A. (2013). Large Eddy Simulation of Vertical Turbulent Wall Fires. *Procedia Engineering*, *62*, 443–452. doi:10.1016/j.proeng.2013.08.086

Román-Cuesta, R. M., Salinas, N., Asbjornsen, H., Oliveras, I., Huaman, V., Gutiérrez, Y., … Malhi, Y. (2011). Implications of fires on carbon budgets in Andean cloud montane forest: The importance of peat soils and tree resprouting. *Forest Ecology and Management*, *261*(11), 1987–1997.

Safi, M. J., Mishra, I. M., & Prasad, B. (2004). Global degradation kinetics of pine needles in air. *Thermochimica Acta*, *412*(1-2), 155–162. doi:10.1016/j.tca.2003.09.017

San-Miguel-Ayanz, J., Schulte, E., Schmuck, G., & Camia, A. (2013). The European Forest Fire Information System in the context of environmental policies of the European Union. *Forest Policy and Economics*, *29*, 19–25. doi:10.1016/j.forpol.2011.08.012

San-Miguel-Ayanz, J. Steinbrecher, R. (2009). *EMEP-EEA emissions inventory guidebook* (p. 19). Copenhagen.

Sarmiento, F. O., & Frolich, L. M. (2002). Andean Cloud Forest Tree Lines. Naturalness, Agriculture and the Human Dimension. *Mountain Research and Development*, *22*(3), 278–287. doi:10.1659/0276-4741

Schemel, C. F., Simeoni, A., Biteau, H., Rivera, J. D., & Torero, J. L. (2008). A calorimetric study of wildland fuels. *Experimental Thermal and Fluid Science*, *32*(7), 1381–1389.

Séro-Guillaume, O., & Margerit, J. (2002). Modelling forest fires. Part I: a complete set of equations derived by extended irreversible thermodynamics. *Int. J.Heat Mass Transfer*, *45* , 1705–1722.

Shafizadeh, F. (1978). Combustion, combustibility, and heat release of forest fuels. *AIChE Symposium Series*, *74:177*.

Shaw, R. H., & Patton, E. G. (2003). Canopy element influences on resolved- and sub-grid-scale energy within a large-eddy simulation. *Agricultural and Forest Meteorology*, *115* , 5–17.

Siegel, R., & Howell, J. R. (1992). *Thermal Radiation Heat Transfer* (Vol. third ed.). Hemisphere Publishing Corportation .

Simeoni, A., Thomas, J. C., Bartoli, P., Borowieck, P., Reszka, P., Colella, F., … Torero, J. L. (2012). Flammability studies for wildland and wildland–urban interface fires applied to pine needles and solid polymers. *Fire Safety Journal*, *54*(0), 203–217.

Stadmüller, T. (1987). *Cloud Forests in the Humid Tropics: A Bibliographic Review*. United Nations University Press.

Stroppiana, D., Grégoire, J.-M., & Pereira, J. M. C. (2003). The use of SPOT VEGETATION data in a classification tree approach for burnt area mapping in Australian savanna. *International Journal of Remote Sensing*, *24*(10), 2131–2151. doi:10.1080/01431160210154911

Swezy, D. M., & Agee, J. K. (1991). Prescribed-fire effects on fine-root and tree mortality in old-growth ponderosa pine. *Canadian Journal of Forest Research*, *21*(5), 626–634.

Tamura, H., Kiya, M., & Arie, M. (1980). Vortex shedding from a circular cylinder in moderate-Reynlods-number shear flow. *Journal of Fluid Mechanics*, *141* , 721–735.

Thomas Simeoni A. Colella F. Torero J.L., J. C. (2011). Piloted Ignition Regimes of Wildland Fuel Beds .

Thomas, J. C., Everett, J. N., Simeoni, A., Skowronski, N., & Torero, J. L. (2013). Flammability Study of Pine Needle Beds. In *Proc. of the Seventh International Seminar on Fire & Explosion Hazards (ISFEH7)*. doi:10.3850/978-981-08-7724-8

Valente, J., Miranda, A. I., Lopes, A. G., Borrego, C., Viegas, D. X., & Lopes, M. (2007). Local-scale modelling system to simulate smoke dispersion. *International Journal of Wildland Fire*, *16*(2), 196. doi:10.1071/WF06085

Van Der Werf, G. R., Randerson, J. T., Giglio, L., Collatz, G. J., Mu, M., Kasibhatla, P. S., … Van Leeuwen, T. T. (2010). Global fire emissions and the contribution of deforestation, savanna, forest, agricultural, and peat fires (1997-2009). *Atmospheric Chemistry and Physics*, *10*, 11707–11735. doi:10.5194/acp-10-11707-2010

Wård, Y. (2007). *Tropical Montane Cloud Forest- Fire Disturbance and Water Input after Disturbance* (pp. 1–28). Umeå: Swedish University of Agricultural Sciences.

Williamson, C. H. K. (1992). The natural and forced formation of spot-like "vortex dislocations" in the transition of a wake. *Journal of Fluid Mechanics*, *243* , 393–441.

Zimmermann, M., Meir, P., Silman, M. R., Fedders, A., Gibbon, A., Malhi, Y., … Zamora, F. (2009). No Differences in Soil Carbon Stocks Across the Tree Line in the Peruvian Andes. *Ecosystems*, *13*(1), 62–74. doi:10.1007/s10021-009-9300-2

Fuel and climate controls on peatland fire severity

Grau-Andres, Roger[a]; Davies, G. Matt[b]; Waldron, Susan[c]; Gray, Alan[d]; Bruce, Michael[e].

[a] *School of Interdisciplinary Studies, University of Glasgow, Dumfries DG14ZL, UK,* r.grau-andres.1@resarch.gla.ac.uk
[b] *School of Interdisciplinary Studies, University of Glasgow, Dumfries DG14ZL, UK,* Gwilym.Davies@glasgow.ac.uk
[c] *School of Geographical and Earth Sciences, University of Glasgow, Glasgow G128QQ, UK,* Susan.Waldron@glasgow.ac.uk
[d] *Centre for Ecology and Hydrology, Bush Estate, Penicuik, Midlothian, EH26 0QB,* alangray@ceh.co.uk
[e] *Firebreak Services Ltd., Glen Tanar Estate, Aboyne AB34 5EU, UK,* Michael@glentanar.co.uk

Abstract
A series of experimental fires were conducted to investigate the effect of ground-fuel structure and fuel moisture content in controlling fire severity in a *Calluna vulgaris* dominated environment. Their influence on fire-induced temperature pulses into the soil (peat) was quantified. The effect of fire-related changes in fuel structure on peat microclimate was also examined. We found the moss and litter (M/L) layer to be important in insulating peat from fire-induced temperature pulses, especially at the peat surface. We recorded higher fire-induced peat temperatures and residence times in microplots where a drought had been simulated, with climatic conditions playing a key role. The removal of the heather canopy due to burning and the change in structure of the M/L layer were found to similarly increase both peat daily temperature fluctuation and peat mean temperature.

Keywords*: Calluna vulgaris, drought, fire severity, FMC, litter, moss, peat*

Introduction

Peatlands in high-latitude regions represent a large soil carbon reservoir, and their degradation could have important implications for the climate – ecosystem feedback governed by the carbon cycle (Heimann & Reichstein 2008). As summer droughts in northern regions are projected to intensify due to climate change (IPCC 2013), thus laying the foundations for more severe fires, it is necessary to understand the key mechanisms controlling fire effects on peatlands.
Peat deposits in the U.K. are usually covered by a mixture of mosses and dead shrub foliage a few cm deep. The moisture content of these ground fuel layers respond quickly to weather conditions. The M/L layer is thought to be important in insulating peat from temperature pulses, and possibly ignition, during the passage of a flaming fire-front. The structure of the M/L layer may therefore be a critical factor in keeping fire severity low despite high fire intensity. Drought conditions may lower the moisture content of the M/L layer below its flammability threshold (Davies and Legg 2010), leading to a step change in fire behaviour and fire severity that threatens carbon stores through peat combustion, altered soil respiration or post-fire degradation. We currently have no quantitative evidence demonstrating the extent to which peat is heated or scorched during burning and how the M/L layer mitigates the effects of the fire, both in terms of temperature penetration during burning and post-fire peat microclimate.
We hypothesise that the M/L layer is a key mechanism in controlling fire behaviour and fire severity. To investigate this we conducted a series of experimental fires in Glen Tanar (Aberdeenshire, Scotland, UK), in a heather (*Calluna vulgaris* (L.) Hull) dominated moorland where prescribed burning has traditionally been used to improve habitat for red grouse (*Lagopus lagopus scoticus*), and in Braehead Moss (South Lanarkshire, Scotland), a Special Site of Scientific Interest (SSSI) designated raised bog.

Methods

Ground fuel structure and below-ground temperature penetration

To examine the role of the M/L layer in temperature penetration a series of experimental fires were completed where the M/L layer was manipulated. The M/L layer was either left untouched, removed after the fire, or removed before the fire in 1 x 1 m microplots. Control microplots where set up outside the fire area. This allowed us to separate the relative importance for peat microclimate of the M/L layer, the heather canopy and scorching of the peat surface during the fire. A total of seven experimental fires ignited as head fires were completed in Glen Tanar, with two replicate microplots of each treatment per fire. To study temperature penetration during the fire, two Hobo^{TM} loggers connected to a K-type twisted pair thermocouple were buried at the peat surface and two cm below in each microplot. The loggers were retrieved after 35 min of the start of the fire. As for changes in peat microclimate, long-term peat temperature were recorded two cm below the top of the peat in one microplot per treatment in each fire using an iButton^{TM} temperature logger (0.5°C accuracy, 2h logging interval). Peat microclimate was recorded from April 2013 to April 2014.

The effect of drought on ground fuel moisture content, flammability and fire severity

To investigate the extent to which M/L layer moisture content and flammability controls variation in fire severity, summer drought was simulated in 2 m x 2 m microplots using rain-out shelters (Figure 1). Ten experimental fires were completed in Glen Tanar and another ten in Braehead Moss between September 2013 and September 2014. Each fire comprised two drought-treated microplots and two untreated microplots. Measurements included: fuel load and structure assessment following the FuelRule method (Davies *et al*. 2008), pre-fire peat, M/L layer, live heather and dead heather fuel moisture content (FMC), moss depth above the thermocouple, fire-induced below-ground temperature pulses, weather conditions and moss consumption.

Figure 1. Rain-out shelter (left) and post-fire ground fuel smouldering limited to treated microplots (right)

Results

Ground fuel structure and below-ground temperature penetration

A substantial increase in peat temperature residence (in °C s) was observed at the peat surface in microplots where the M/L layer had been removed: microplots where the M/L layer hadn't been removed presented an average 7800 °C s (SD = 7000, n = 28) while microplots where the M/L layer had been removed had an average temperature residence of 19000 °C s (SD = 11100, n = 14). Effects

2 cm below the top of the peat were less evident although still substantial (Figure 2). Average temperature residence values were 1900 °C s (SD = 2300, n = 26) in microplots where the M/L layer were present at the time of the fire, and 3900 (SD = 3900, n = 12) in microplots where the M/L layer had been removed.

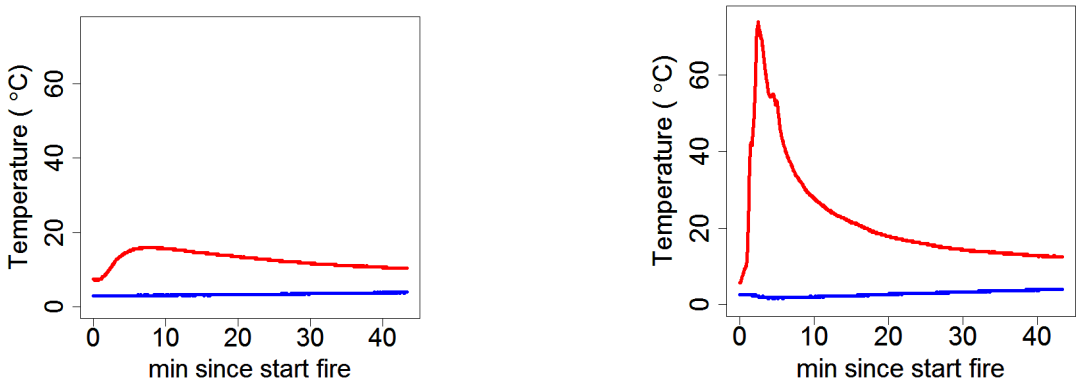

Figure 2. Temperature-time curves during a fire from a microplot with (left) and without (right) the moss and litter layer. Red and blue lines indicate temperatures measured at the top of the peat and 2cm below, respectively.

The peat microclimate data showed that burnt microplots presented higher below-ground daily temperature fluctuations than control microplots. Diurnal fluctuations were further increased in microplots where the M/L layer had been removed (Figure 3). A provisional seasonal linear model was fitted to the data and it was found that mean daily temperature was higher in burnt and burnt and M/L layer removed microplots in spring and summer but the opposite was true in autumn and winter (Figure 4).

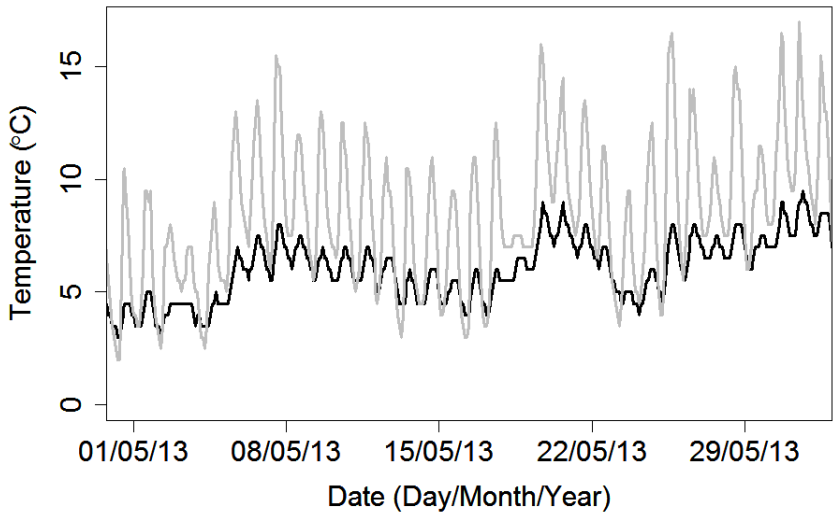

Figure 3. Post-fire peat micro-climate at 2cm depth in a control microplot (black line) and in a burnt microplot where the M/L had been removed (grey line).

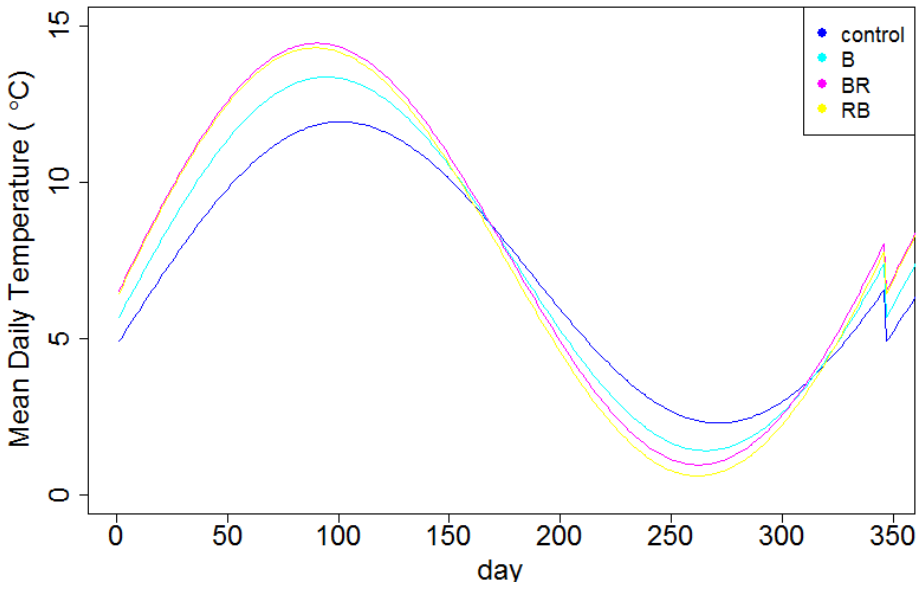

Figure 4. Predicted mean peat temperature values of the seasonal model for the four different treatments. Sampling started in April 2013 and finished in April 2014. "control", unburnt microplots; "B", burnt microplots; "BR", burnt microplots where the M/L layer was removed after the fire; "RB", burnt microplots where the M/L layer was removed before the fire.

The effect of drought on ground fuel moisture content, flammability and fire severity

Rain-out shelters reduced the FMC of the M/L layer in dry heath from an average of 304% in dry base (SD = 186, n = 16) to 124% (SD = 75%, n = 16). Average M/L layer consumption was 0.7 cm (SD = 1.6, n = 16) in control microplots and 2.4 (SD = 2.4, n = 16) in drought microplots. Microplots burnt under simulated summer drought conditions showed higher temperature residence times than untreated microplots at both the peat surface and at a depth of 2 cm (Figure 5).

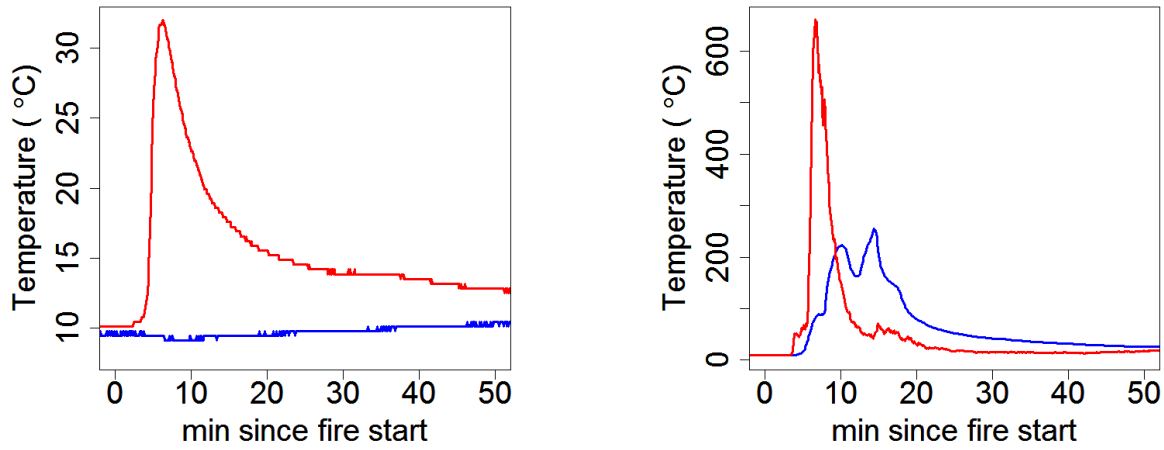

Figure 5. Temperature-time curves during a fire from a control microplot (left) and a drought microplot (right). Red and blue lines indicate temperatures measured at the top of the peat and 2cm below, respectively.

Conclusions

Our results show that the M/L layer has a critical ecosystem function by preventing peat from being exposed to significant temperature pulses during burning. The change in fire severity associated with

a decrease in the moisture content of the M/L layer under drought conditions could have important implications for peat carbon dynamics and post-fire vegetation regeneration. Variation in fire severity can also drive changes in belowground micro-climate with potentially important implications for soil ecosystem function. On-going work is examining how this variation in fire severity and post-fire microclimate affects carbon fluxes following burning.

References

Davies GM, Hamilton A, Smith A, Legg C (2008) Using visual obstruction to estimate heathland fuel load and structure. *International Journal of Wildland Fire* **17**, 380-389.

Davies GM, Legg CJ (2010) Fuel moisture thresholds in the flammability of Calluna vulgaris. *Fire Technology* **47**, 421-436.

Heimann M, Reichstein M (2008) Terrestrial ecosystem carbon dynamics and climate feedbacks. *Nature* **451**, 289-292.

Stocker TF, Qin D, Plattner GK, Tignor M, Allen SK, Boschung J, Nauels A, Xia Y, Bex V, Midgley PM (Eds) (2013) 'IPCC, 2013: Climate Change 2013: The Physical Science Basis. Contribution of Working Group I to the Fifth Assessment Report of the Intergovernmental Panel on Climate Change.' (Cambridge University Press, Cambridge, United Kingdom and New York, NY, USA)

High resolution spatial and temporal variability of fine dead fuel moisture content in complex terrain

Gary Sheridan [a], Petter Nyman[a], Daniel Metzen[a], Patrick Lane[a]

[a]*The Department of Forest and Ecosystem Science, The University of Melbourne, Parkville 3010, Melbourne, Australia, sheridan@unimelb.edu.au*

Abstract

The moisture content of fine dead fuel plays an important role in forest fire behaviour, affecting the probability of ignition at the fire front, the probability of night-time extinguishment, and the availability of the depth of fine fuel for burning. A recent review of dead fuel moisture research by Matthews (2014) concluded that one of the key research and modeling needs is the capacity to represent the complexity of vegetation structure and topography and forecast fuel moisture content across the landscape. Fine fuel moisture content varies at a range of spatial scales due to many factors, however in complex, steep and dissected landscapes, topographic aspect can play a significant role in small-scale (ie. scales in the order of 10's ha) variability.

Experimental sites for monitoring microclimate variables and moisture content in litter and in near-surface soils were established at a control site and on four contrasting aspects (north, south, east and west) in southeast Australia. At each of the four microclimate sites sensors are arranged to measure the soil moisture (2 replicates), fine dead surface fuel moisture at 2.5cm depth (12 replicates), precipitation throughfall (3 replicates), radiation (3 replicates), and screen level relative humidity, air temperature, leaf wetness, and wind speed (1 replicate of each). Temperature and relative humidity are also measured within the dead fine surface fuel using Ibutton's (4 replicates).

All measurements are logged continuously at 15 min intervals. The moisture content of the fine dead surface fuel is estimated using high-replication of low-cost continuous soil moisture sensors placed at the centre of a 5cm deep sample of fine dead surface fuel, referred to here as "dead fine fuel packs" . The dead fine fuel packs were constructed from fuels collected from the area surrounding the microclimate site. The initial results show the moisture regime on the forest floor was highly sensitive to the incoming shortwave radiation, which was up to 6 times higher in the north-facing (equatorial) slopes due to slope orientation and the sparse vegetation compared to vegetation on the south-facing (polar facing) slopes. Differences in shortwave radiation resulted in peak temperatures within the litter that were up to 2 times higher on the equatorial-facing site than those on the polar-facing site. For instance, on a day in November 2013 with maximum open air temperature of 35o C, the temperatures within the litter layer at the north-facing and south-facing sites were 54o C and 32o C, respectively, despite air temperature at the two sites differing by less than 2o C. The minimum gravimetric water content in the litter layer on the same day was 21% on the equatorial-facing slope and 85% on the polar-facing slope. The experimental data is being used to calibrate and test models of fuel moisture spatial variability against an independently collected gravimetric fuel moisture dataset.

Keywords*: aspect, litter, wildfire,*

Introduction

The moisture content of fine dead fuel plays an important role in forest fire behaviour, affecting the probability of ignition at the fire front, the probability of night-time extinguishment, and the availability of the depth of fine fuel for burning. A recent review of dead fuel moisture research by Matthews (2014) concluded that one of the key research and modeling needs is the capacity to represent the complexity of vegetation structure and topography and forecast FMC across the landscape.

Fine fuel moisture content varies at a range of spatial scales due to many factors, however in complex, steep and dissected landscapes, slope orientation (aspect and slope) can play a significant role in small-

scale (ie. in the order of 10's ha) variability. This is because ddifferent topographic positions are often associated with different soils, soil moisture conditions, and forest structure. Forest canopies create distinct understory micro-climates (Geiger 1995, Lee 1978, Oke 1987, Mc- Caughey *et al*. 1997, Grimmond *et al*. 2000). Below the forest canopy, solar radiation and day-time temperature and wind speed is reduced, while humidity is increased. All these factors affect the dead fine fuel moisture content and therefore spatial patterns of fuel moisture (Sharples 2009).
The relationship between slope orientation, soil, vegetation structure, micro-climate and fine fuel moisture dynamics is poorly understood and has not been sufficiently represented or parameterised in models. This project aims to improve the prediction of short- range variability in dead fine fuel moisture using field measurement of aspect related differences in soil, vegetation and microclimate.

Methods

Topographic micro-climate experimental sites

Experimental sites for monitoring microclimate variables and moisture content in dead fine fuels and in near-surface soils were established in March 2013 on the upper slopes of four contrasting aspects (north, south, east and west) within a 0.5km radius in the Upper Yarra Catchment in Victoria, southeast Australia. Rainfall, ambient air temperature, geology, and drainage position, are similar across the four sites, so measured differences between the experimental sites at the ground level are assumed to be due to aspect-related microclimatic-variability. An additional weather station was established in a nearby open, ridgetop position to quantify precipitation, temperature, relative humidity, windspeed and direction for the area. Measurement from these five sites is ongoing.

Microclimate instrumentation

At each of the four microclimate sites sensors are arranged to measure the soil moisture (2 replicates), fine dead surface fuel moisture at 2.5cm depth (12 replicates), precipitation throughfall (3 replicates), radiation (3 replicates), and screen level relative humidity, air temperature, leaf wetness, and wind speed (1 replicate of each). Temperature and relative humidity are also measured within the dead fine surface fuel using ibuttons (Hydrochron, DS1923) (4 replicates). All measurements are logged continuously at 15 min intervals. The layout of the sensors at each microclimate site is illustrated in **Erro! A origem da referência não foi encontrada.**Figure 1.

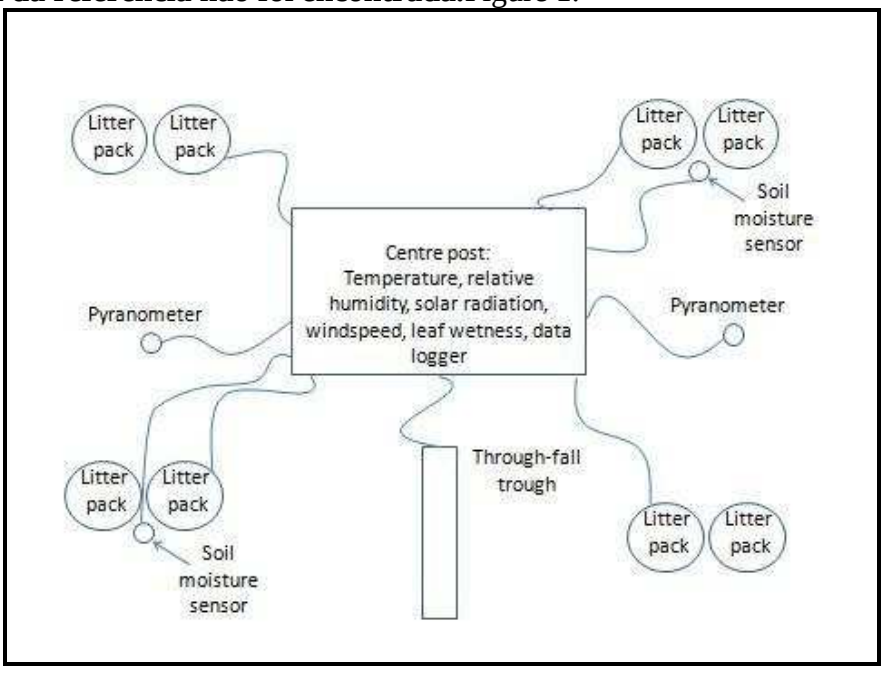

Figure 1 –An illustration of the layout of the instrumentation and sensors at one of the four instrumented microclimate sites.

There have been few attempts to continuously measure fine fuel moisture under field conditions. Here, the moisture content of the fine dead surface fuel is estimated using high replication of low-cost continuous soil moisture sensors (VH400, Vegetronix, Inc., Riverton, USA) (see Figure 2) placed at the centre of a 5cm deep sample of fine dead surface fuel, referred to here as "litter packs".

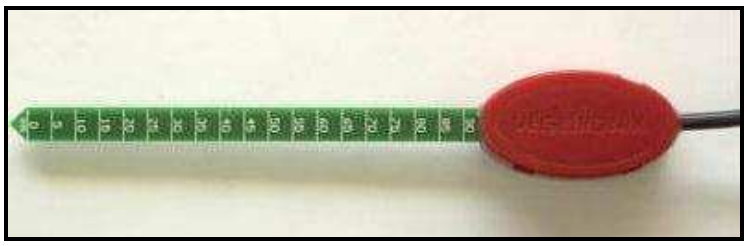

Figure 2. A vegetronix VH400 soil water content probe, used in this study to continuously estimate the gravimetric water content of fine dead surface fuels. (Source: www.vegetronix.com) .

The litter packs were constructed from fuels collected from the area surrounding the microclimate site. Each of the pairs of fuel packs (4 pairs, a total of 8 litter packs at each micro climate site) includes one continuously monitored pack (logged every 10 mins) that contains 3 Vegetronix soil moisture sensors, and one pack that is used to measure fuel moisture content gravimetrically during field visits. The gravimetric litter pack was used to build an empirical relationship between the measured gravimetric fuel moisture content, and the Vegetronix voltage output, under field conditions. This relationship was used to produce a continuous estimate of the fuel moisture content of the dead fine fuel layer. An example of the dead fine fuel packs installed at one of the microclimate sites is shown in Figure 3.

Figure 3. Two of the dead fine surface fuel sample packs used in this study to monitor fuel moisture. The left hand pack is fitted with three Vegetronix VH400 soil water content sensors, recording every 15 minutes. The right hand pack is used for manual gravimetric measurements during field site service visits. (Source: www.vegetronix.com).

The continuous fuel moisture monitoring methods described above were supported by four seasonal field campaigns to quantify dead fine fuel moisture content from 3 additional replicated locations for each aspect, and to measure variability in fine fuel depth, density and spatial arrangement as a function of aspect.

Results & Discussion

The first year of data from the microclimate sites is currently being analysed and the sensors calibrated using recently collected summer field campaign data. As a consequence, no detailed results are available at the time of writing this abstract. However, some interesting observations can be noted. The moisture regime on the forest floor was highly sensitive to the incoming shortwave radiation, which was up to 6 times higher in the north-facing (equatorial) slopes due to slope orientation and the sparse vegetation compared to vegetation on the south-facing (polar facing) slopes. Differences in shortwave radiation resulted in peak temperatures within the litter that were up to 2 times higher on the equatorial-facing site than those on the polar-facing site. For instance, on November 2013 with maximum open air temperature of 35^{o} C, the temperatures within the litter layer at the north-facing and south-facing sites were 54^{o} C and 32^{o} C, respectively, despite air temperature at the two sites differing by less than 2^{o} C. The minimum gravimetric water content in the litter layer on the same day was 21% on the equatorial-facing slope and 85% on the polar-facing slope. A full analysis and summary of the experimental data will be available for the conference presentation. The implications for modelling spatial variability in fuel moisture will be discussed.

Acknowledgements

The authors would like to acknowledge the financial support of the Victorian Department of Environment and Primary Industries, and the Natural Disaster Resilience Grants Scheme.

References

Matthews, S. (2014) Dead fuel moisture research: 1991–2012. International Journal of Wildland Fire **23**, 78–92.

Geiger R, Aron RH, Todhunter P (1995) 'The Climate Near the Ground.' 5th edn. (Friedr.Vieweg and SohnVerlagsgesellschaft mbH: Braunschweig/Wiesbaden)

Lee R (1978) Forest micrometeorology. Columbia University Press, New York

Oke TR (1987) Boundary layer climates. Methuen, London

McCaughey JH, Amiro BD, Robertson AW, Spittlehouse DL (1997) Forest environments. In: Bailey WG, Oke TR, Rouse WR (eds) The surface climates of Canada. McGill Queen's University Press, Montreal, p 247–276

Grimmond, C.S.B., S. M. Robeson, J. T. Schoof (2000) Spatial variability of micro-climatic conditions within a mid-latitude deciduous forest Climate Research 15, 137-149

Sharples J (2009) An overview of mountain meteorological effects relevant to fire behaviour and bushfire risk. International Journal of Wildland Fire 18, 737-754.

Ignition behavior of cardboard fuel particles

Justin D. English[a], Nelson K. Akafuah[a], Brittany A. Adam[a], Mark Finney[b], Jason Forthofer[b], Jack Cohen[b], Sarah McAllister[b] and Kozo Saito[a]

[a] *Univ. of Kentucky, Lexington, KY 40506, justin.english@uky.edu, nelson.akafuah@uky.edu, brittany.adam@uky.edu, ksaito@uky.edu*
[b] *USDA Fire Science Laboratory, Missoula, MT 59808, mfinney@fs.fed.us, jaforthofer@fs.fed.us, jcohen@fs.fed.us, smcallister@fs.fed.us*

Abstract
This paper reports infrared thermal-image-based temperature changes on cardboard fuel surfaces during ignition. Two sets of experiments were designed to separately test the effect of convective heating and radiative heating on ignition of cardboard fuel samples. An air torch was used to provide the convective heating, and a crib fire was used for the radiative heating. An infrared thermography technique developed in our laboratory was used to obtain thermal profiles/signature of the heated cardboard sample surface under two different heating rates, from which the surface temperature change was obtained as a function of heating time. We found that radiation effects increased with an increase in the cardboard sample surface area exposed to radiation while the effects from convection dominated the smaller surface area samples. This finding qualitatively explains the United States Department of Agriculture's (USDA) original findings that millimeter diameter pine needles cannot be ignited by radiation only, even under a long duration fire generated radiant heat flux of an average 10.3 kW/m^2. Our experimental results also justify the use of the cardboard fuelbeds to simulate fire behavior of large scale forest fires.

Keywords*: Ignition, Fuelbed, Fuel Particle, Heat Transfer*

Introduction

Wildland fires are unpredictable and destructive events that use enormous amounts of resources to fight and contain, particularly in the wildland-urban interface where numerous amounts of resources are utilized to protect homes and other structures.

Scientific advances in the form of spread rate models have paved the way in providing more effective means for firefighting and containment for large fires. Such fire behavior models form the core for decision support system (Noonan-Wright, et al., 2011).

Given the limitations and empirical nature of current fire behavior models, the question remains of how to enhance physical understanding and someday enhance operational fire spread modeling (Gollner, 2012). As surmised by Finney *et al*. (2012), correct application of the heat transfer mechanisms contributing to ignition have yet to be reliably applied to fire spread models. Therefore, a more thorough understanding of the underlying physics and theory behind ignition on forest fuels (including live fuels) is needed to develop a coherent theory on the heat transfer mechanisms affecting it. The flame is the source to provide sufficient heat to pyrolyze (solid) forest fuel, and the pyrolyzed gas phase products will then mix with air. When this fuel-air mixture satisfies flammability limit under the ignition temperature, ignition occurs creating flammable combustion. This repeating pattern is the mechanism which allows the flame front to spread, where heat transfer from the front to the unburned fuel particles and gas phase kinetics play an important role (Fernandez-Pello & Hirano, 1983).

Radiation has been thought as the primary mechanism in wildland fire spread, similar to upward flame spread along vertical walls under natural convection (Brehob & Kulkarni, 1998; Brehob, Kim, & Kulkarni, 2001) and flame spread across a continuous horizontal fuel bed under a very high horizontal wind velocity (Steward, 1971). These laboratory experiments use PMMA and wood samples under well controlled laboratory boundary conditions, while flame spread over forest fuel beds involves

many other additional parameters. These parameters include complex mixtures of different types of live and dead fuels, non-uniform porous fuel structure, different terrain, and changing wind speed among others. Emori and Iguchi *et al*. (1988) mimicked forest fuel with excelsior and vertically oriented paper strips coated with candle wax, whose geometry is similar to the cardboard fuelbeds, and showed that flame spread over inclined fuel beds for the paper strip fuels and horizontal and inclined excelsior fuel beds is controlled by convection (Emori, *et al*., 1988). Adam *et al* (2013) further studied scaling laws on flame spread by bringing a Strouhal-Froude number flow instability to convection heat transfer, predicting that flame spread through forest fuelbeds would satisfy these convection-controlled scaling law conditions.

Experimental Methods

To ensure homogenous properties and physical attributes among the fuel samples being used, we engineered cardboard particles 1.27 mm thick with approximately 60% recycled content using a laser engraver. We measured the transient temperature history of the fuel particles when subjected to various heat sources using a FLIR SC4000™ infrared camera (spectral range of 3-5 μm, fitted with a broadband flame filter with spectral range of 3.7 - 4.2 μm, with spatial resolution of 320 x 256 pixels). To reduce the amount of noise and saturation captured in each video image, we employed a super-framing algorithm which takes a set of four images (subframes) of the scene at progressively shorter exposure times, in rapid succession, and then repeats this cycle. The sub-frames from each cycle are then merged into a single super-frame to combine the best features of the four sub-frames. This process, called collapsing, can provide thermal images both high in contrast and wide in temperature range.
The following section provides results from two sets of experiments: convective dominated heating from an air torch and radiative dominated heating from a crib fire.

Convection Dominated Heating: Air Torch Experiment

The cardboard fuel elements were heated from ambient temperature by a convective heater to achieve ignition (recognized by the establishment of a visible flame). Figure 1 depicts a schematic of convection heating experiment. A vertically oriented convection heater provided forced convective heat flow parallel to the cardboard elements suspended approximately 0.5 cm above the exit of the air torch, where two different temperature settings (500 °C and 750 °C) were used. The mass flow rate of air is controlled and held constant, so the airflow velocity at the exit of the torch varied from 1.3 to 1.5 m/s for the two temperatures tested.

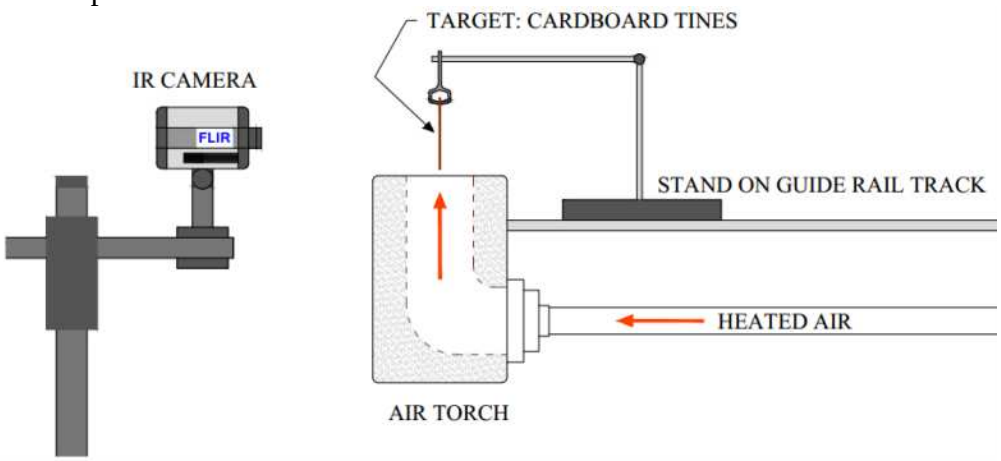

Figure 1. Experimental setup: Air torch - Side view

Three common tine geometries, shown in Figure 2, were used and each experiment was repeated ten times per geometry. Every effort was made to ensure all experimental conditions remained the same and the results were repeatable, since the temperature distribution at the circular exit of the torch was not symmetric which could lead to an uneven temperature distribution across the hot exiting air stream. The cardboard tine samples were suspended in a downward facing manner, as shown in Figure 3, throughout the duration of the experiment to mimic the condition of heated vertical plates subjected to forced convection from an imposed parallel flow.

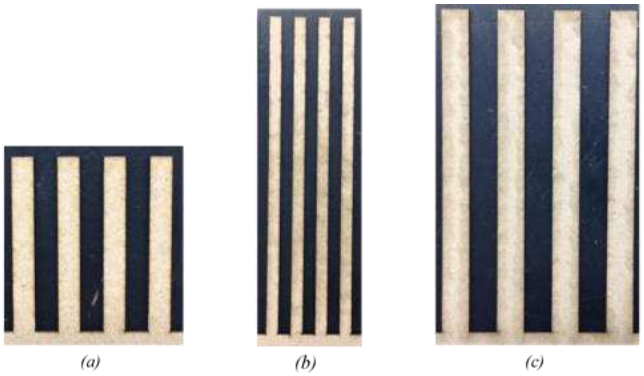

Figure 2 - Tine geometries (a) 0.635 cm wide x 5.08 cm high (b) 0.635 cm wide x 15.24 cm high (c) 1.27 cm wide x 15.24 cm high

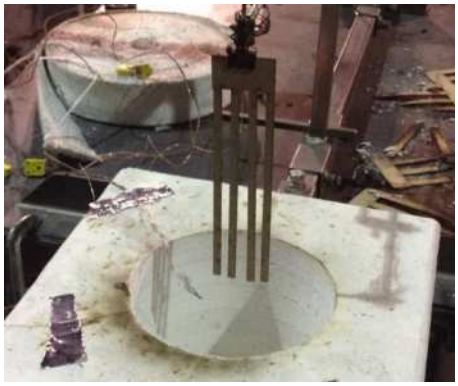

Figure 3 – Tine orientation

Radiation Dominated Heating: Crib Fire

A wood crib (91.44 cm wide x 76.2 cm tall x 91.44 cm long) constructed of Ponderosa pine (*Pinus ponderosa*) sticks was used to provide radiative heating to the cardboard samples under circumstances as close to wildland fires conditions as possible. A schematic of the experimental set up is shown in Figure 4. The crib was constructed with 2.54 cm square sticks with six sticks per layer and 30 layers, such that it burned in the loosely-packed regime. The crib was placed on cinder blocks providing 19.5 cm of space between the crib and the support platform. The crib was housed within a large (12.4 m x 12.4 m x 19.6 m) sealed burn chamber with no imposed flow. This allowed minimal incoming and outgoing drafts, thus limiting convective heating and cooling effects and maximizing the radiative heating effects. Equation (1) can describe the above heat balance

$$\frac{dq''}{dt} = E(T_s^4 - T_{sur}^4) + h(T_s - T_\infty) \quad (1)$$

where E represents the product of the Stefan-Boltzmann constant (5.67 x 10^{-8} W/m^2-K^4), the integrated emissivity of the cardboard elements, and a geometrical view factor and the $h(T_s - T_\infty)$ term is used to define the convective cooling effects.

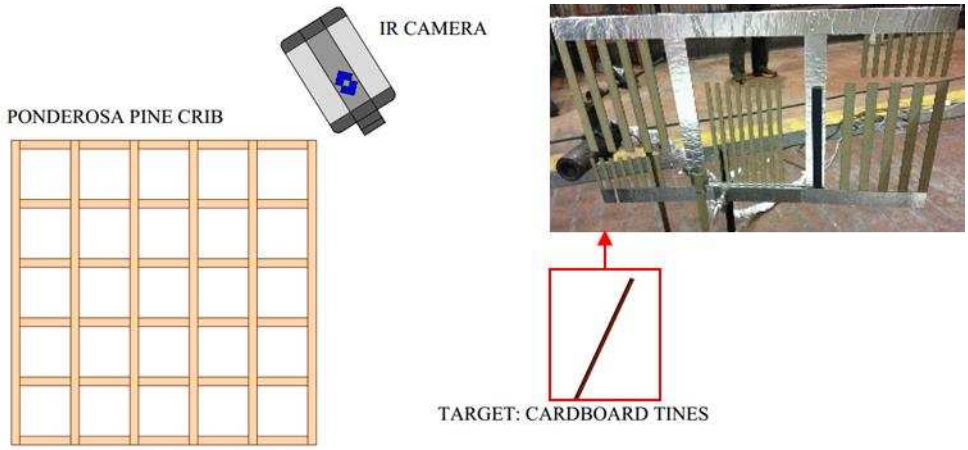

Figure 4 - Crib schematic: Plan view

Three cardboard tine geometries were used for this experiment: 0.635 cm wide x 5.08 cm high, 0.635 cm wide x 15.24 cm high, and 1.27 cm wide x 15.24 cm high. The tines were originally constructed into two foot sections, but cut into smaller segments and taped together using reflective aluminum adhesive tape. To achieve the best viewing angle as possible between the IR camera and the fuel, the tines were positioned at an angle of 25° with respect to the crib with the closest end measuring 91.44 cm away from the edge of the crib and the furthest measuring 109.22 cm away.
A separate cardboard tine was coated with high carbon content black paint ($\varepsilon = 0.95$) to serve as a black body for the IR camera. Additionally, a 1 mm K-type thermocouple was taped to the bottom of the cardboard sample to measure the surrounding air temperature during the heating experiment.

3. Results

3.1. Convection Dominated Heating: Air Torch

The recorded infrared video images provided a rich database for all 30 fuel samples, but this paper only reports the results for the 0.635 cm wide x 5.08 cm high cardboard elements due to space limitations. It should be noted that the results presented are not representative of a single test but rather depict the average of all ten trials for the 0.635 cm wide x 5.08 cm high fuel element.
The software ExaminIR™ (FLIR Systems, Inc., 2014) was used to evaluate the IR video image data. Specific regions of interests (ROI's) located at the tip of each tine were used to determine a temperature history of the cardboard fuel elements. These ROI's were labelled from left to right as Cursor one through four. In the grayscale image, white is representative of hotter temperatures, while dark is indicative of colder temperatures. The results for the air torch outlet temperature of 500 °C show a steady progression in temperature up to the point of flame visibility at approximately 315 °C where temperature rises sharply (Figure 5).

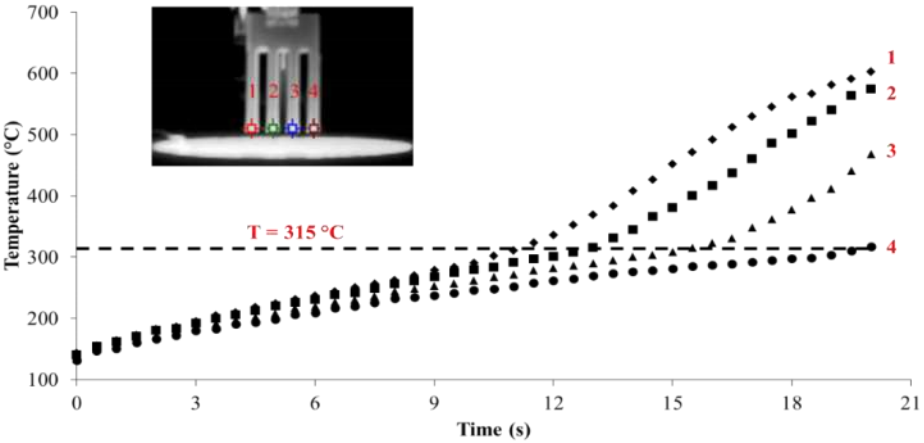

Figure 5. Temperature history for the 0.635 cm wide x 5.08 cm high fuel element subjected to an outlet temperature of 500 °C

Once a stable flame was established, the tines were pulled away from the outlet of the torch to prevent burning fuel elements from falling into the air torch and possibly damaging the equipment. In evaluating each cursor, fluctuations due to flame movements and CO_2 interference, which are visible in the spectral range of the filter, are represented by a larger standard deviation. These fluctuations are shown for Cursor one and Cursor four in Figure 6.

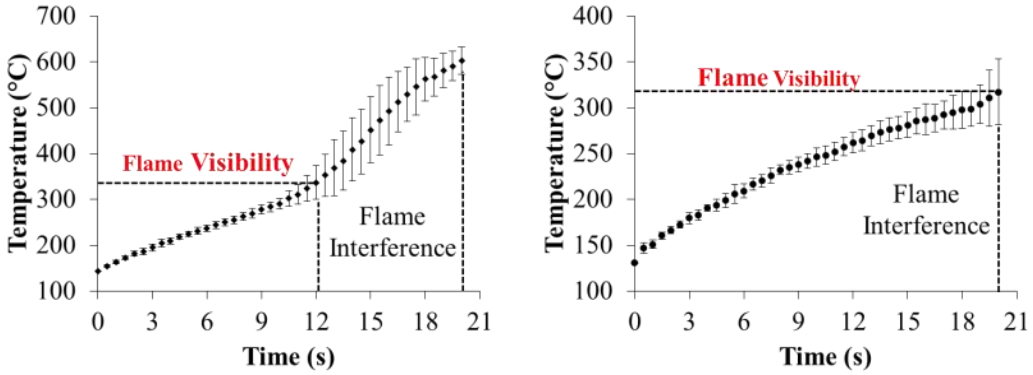

Figure 6. Temperature history showing standard deviations as a result of flame movement and CO2 interference for an outlet temperature of 500 °C for Cursor 1 and Cursor 4

For the case of an outlet temperature of 750 °C (Figure 7), the results show a decrease in flame visibility temperature (307 °C) with an increase in heat flux, as expected (Atreya & Abu-Zaid, 1991). Additionally, more fluctuations in the temperature progression are present as a result of increased turbulence in the airflow (Figure 8). Note that for an outlet temperature of 500°C, it took approximately 12 seconds to reach ignition, while for an outlet temperature of 750 °C it took roughly 1.5 seconds, indicating that an increase in the heat flux increases convective heat transfer rate to the unburned fuel element and consequently increasing the rate of flame spread.

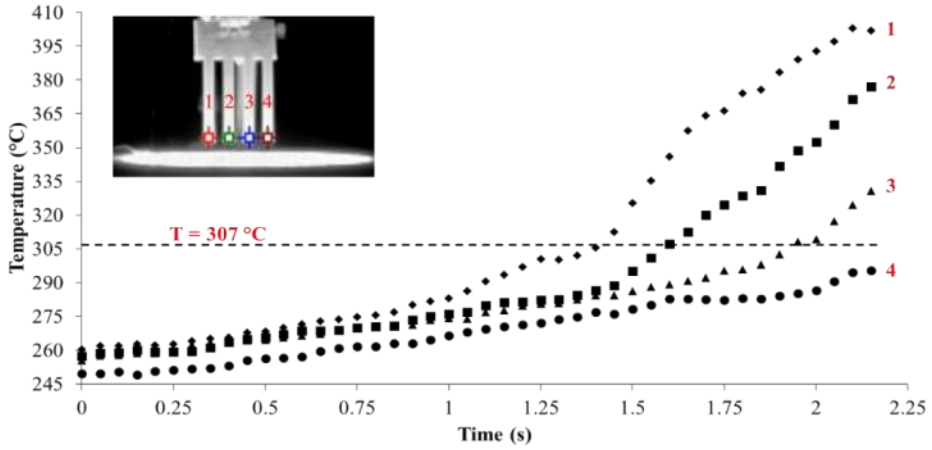

Figure 7. Temperature history for the 0.635 cm wide x 5.08 cm high fuel element subjected to an outlet temperature of 750 °C

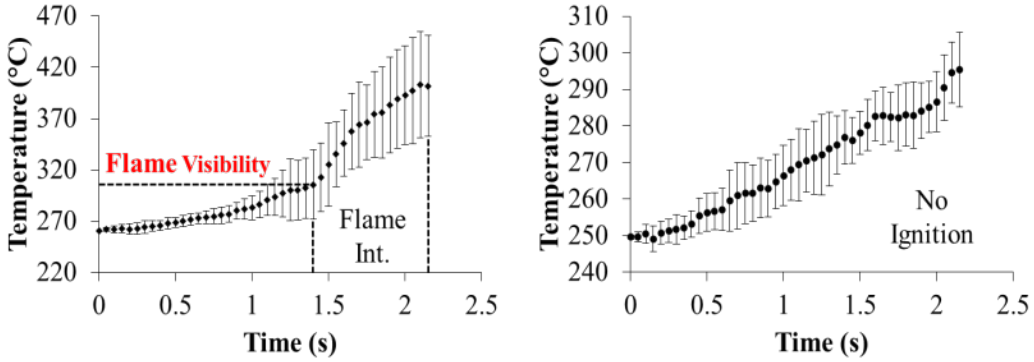

Figure 8. Temperature history showing standard deviations as a result of flame movement and CO2 interference for an outlet temperature of 750 °C for Cursor 1 and Cursor 4

Radiation Dominated Heating: Crib Fire

A similar procedure was used to determine the temperature history of the cardboard fuel elements when subjected to primarily radiative heating. The average radiative heat flux of the crib fire was approximately 10.3 kW/m^2. Within ExaminIR, specific areas of interest were placed at the tip, middle, and bottom of the cardboard fuel elements closest to the burning crib, as these tines were exposed to the largest amount of radiative heat. These fuel particles included the 0.635 cm wide x 5.08 cm high tines and the 1.27 cm wide x 15.24 cm high cardboard elements shown in Figure 9(c).

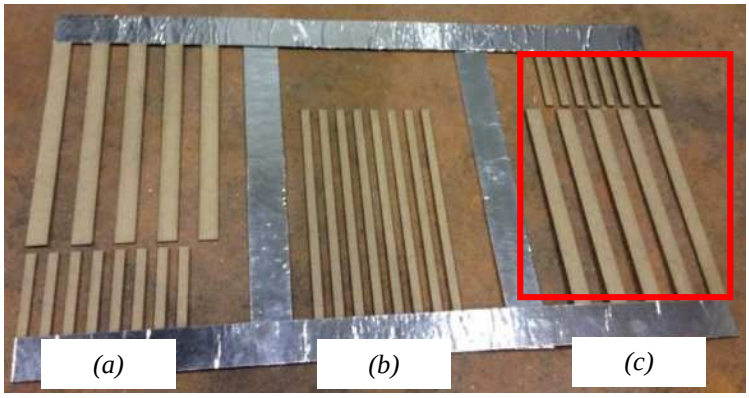

Figure 9 – Tine geometries: (a) 0.635 cm wide x 5.08 cm high (b) 0.635 cm wide x 15.24 cm high (c) 1.27 cm wide x 15.24 cm high

During radiative heating, a natural convection thermal boundary layer will be developed over the heated fuel surface bringing two different benefits for ignition: reducing the heat loss from its heated surface to the surrounding air and promoting a fuel-air mixture layer within the boundary layer. Both are favourable for ignition.

Examining the ratio of exposed heating area to total fuel surface area, we realized that the potential for receiving radiant heat as opposed to losing energy to the surroundings from natural convective cooling was greater for the larger fuel particles. This explains the results of Figure 10 where the larger tines (1.27 cm wide x 15.24 cm high) were able to ignite at the tip.

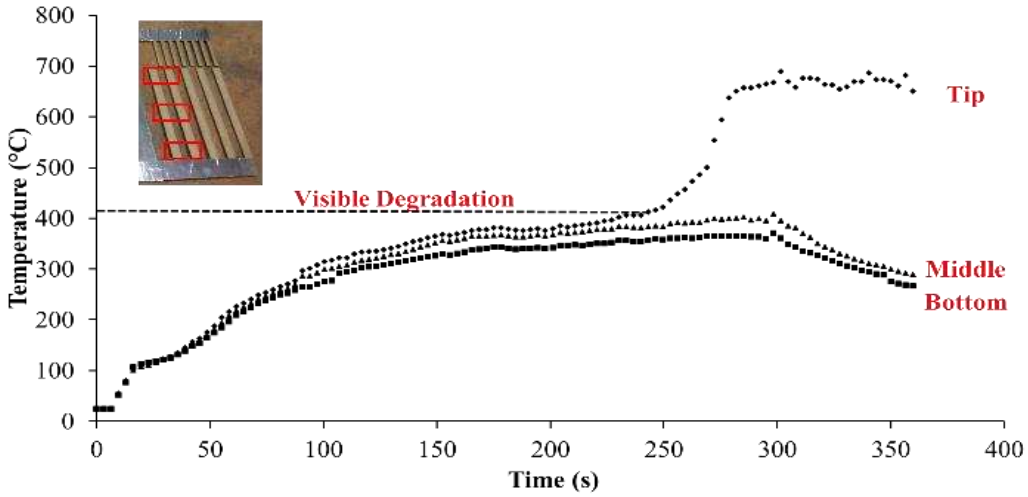

Figure 10 - Temperature history of the 1.27 cm wide x 15.24 cm high fuel element subjected to predominately radiative heating

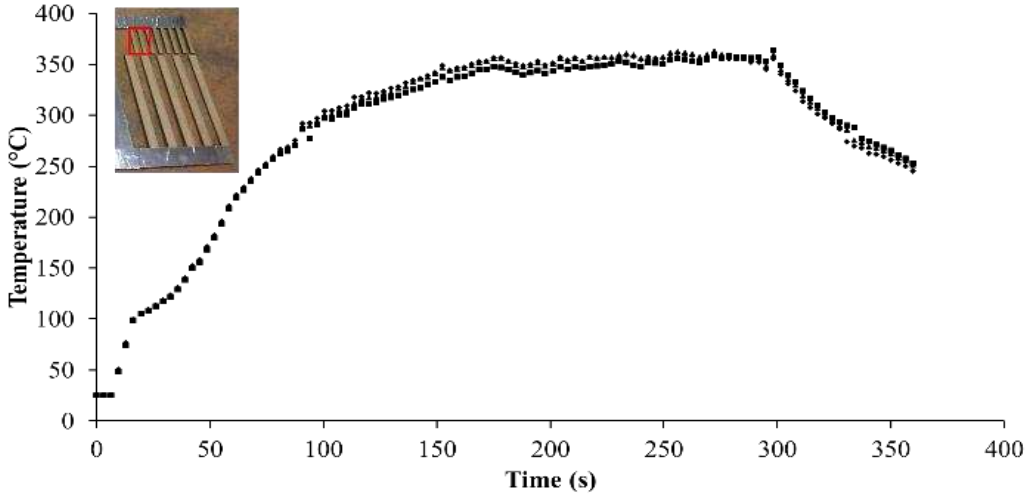

Figure 11 - Temperature history of the 0.635 cm wide x 5.08 cm high fuel element subjected to predominately radiative heating

It should be noted that the ratio of the exposed heating area to the total fuel surface area is an important indicator to assess the effect of radiation on ignition not only for cardboard fuel samples but possibly for actual dead forest fuels, since the underlining governing physics can be also applied. But a more thorough scaling study, perhaps based on previous studies by Adam *et al*. (2013), Emori and Saito (1983), and Emori and Iguchi *et al* (1988), is required to justify whether or not this ratio can be an important scaling factor. As for live forest fuels, however, the above finding may not be directly applicable due to its complex fuel structure (McAllister & Finney, 2014) and therefore, a fundamental study to reveal ignition behaviour of live fuels is certainly needed.

Summary

This paper reports IR thermal image-based temperature history and ignition behavior of engineered cardboard fuel elements subjected to convective and radiative heating. Our results support the USDA's original findings that millimeter diameter pine needles cannot be ignited by radiation only even under a long duration fire generated radiant heat flux of an average 10.3 kW/m^2.
The objective of the air torch experiment was to examine convective heating of fuel particles. The tines above the torch represented the unburned fuel particles that are receiving flame contact near a spreading fire. This layout, however, does not exactly represent forest fire conditions, where fuel particles receive heat from a cross-flow as opposed to a parallel flow. We are planning to perform an additional experiment using a heat gun to simulate forced convection due to an imposed flow along and around cardboard fuel elements in cross-flow.

Acknowledgements

This study was supported by the USDA Forest Service under Collaboration Forest service agreement: 12-CS-11221637-133.

References

Adam, B., Akafuah, N., Saito, K., Finney, M., Forthofer, J., & Grenfell, I. (2013). A Study of Flame Spread in Engineered Cardboard Fuelbeds, Part II: Scaling law approach. Seventh International Symposium on Scale Modeling (ISSM-7). Hirosaki, Japan.

Atreya, A., & Abu-Zaid, M. (1991). Effect of Environmental Variabes on Piloted Ignition. Fire Safety Science 3, 177-186.

Brehob, E. G., & Kulkarni, A. K. (1998). Experimental meaurements of upward flame spread on a vertical wall with external radiation. Fire Safety Journal, 31(3), 181-200.

Brehob, E. G., Kim, C. I., & Kulkarni, A. K. (2001). Numerical model of upward flame spread on practical wall materias . Fire Safety Journal, 36(3), 225-240.

Emori, R. I., & Saito, K. (1983). A study of scaling laws in pool and crib fires. Combustion Science and Technology, 31, 217-230.

Emori, R. I., Iguchi, Y., Saito, K., & Wichman, I. S. (1988). Simplified scale modeling of turbulent flame spread with implication to wildland fires. Fire Safety Science - Proceddings of the Seocnd International Symposium (pp. 263-273). Hemisphere Publishing Corporation.

Fernandez-Pello, A. C., & Hirano, T. (1983). Controlling mechanisms of flame spread. Combustion Science and Technology, 32(1-4), 1-31.

Finney, M. A., Cohen, J. D., McAllister, S. S., & Jolly, W. M. (2012). On the need for a theory of wildland fire spread. International Journal of Wildland Fire.

Gollner, M. J., Williams, F. A., & Rangwala, A. S. (2011). Upward flame spread over corrugated cardboard. Combustion and Flame, 158(7), 1404-1412.

IR camera control and analysis software. (2014). Retrieved from FLIR System, Inc.: http://www.flir.com/thermography/apac/en/view/?id=50079

McAllister, S., & Finney, M. (2014). Convection Ignition of Live Forest Fuels. Fire Safety Science - Draft Proceedings of the Eleventh International Symposium. International Association of Fire Safety Science.

Noonan-Wright, E. K., Opperman, T. S., Finney, M. A., Zimmerman, G. T., Seli, R. C., Elenz, L. M., & Calkin, D. E. (2011). Developing the U.S. Fire Decision Support System (WFDSS). Journal of Combustion.

Saito, K., Quintere, J. G., & Williams, F. A. (1986). Upward turbulent flame spread. Fire Safety Science - Proceedings of the First International Symposium (pp. 75-89). Hemisphere Publishing.

Saito, K., Williams, F. A., Wichman, I. S., & Quintiere, J. G. (1989). Upward turbulent flame spread on wood under external radiation. Journal of Heat Transfer, 111, 438-445.

Stein, S. M., Menakis, J., Carr, M. A., Comas, S. J., Stewart, S. I., & Cleveland, H. (2013). Wildfire, Wildlands, and People: Understanding and Preparing for Wildfire in the Wildland-Urban Interface. Rocky Mountain Research Station: United States Department of Agriculture Forest Service.

Steward, F. R. (1971). A Mechanistic Fire Spread Model. Combustion Science and Technology, 4(1), 177-186.

Influence of the radiative heat exchanges between the fire front and vehicle passengers in a road

Eusébio Z. E. Conceição[a], Manuel C. Gameiro Silva[b], Domingos X. Viegas[b]

[a] *FCT – University of Algarve - Campus de Gambelas - 8005-139 Faro, Portugal*
[b] *FCT – University of Coimbra - Pinhal de Marrocos - Pólo II - 3030 Coimbra, Portugal*

Abstract
The influence of the radiative heat exchanges between the fire front and vehicle passengers' in a road is made in this study. Numerical software, that simulates the vehicle thermal behaviour with complex topology and the human thermal response, in transient conditions, is developed and used.
The numerical model that simulates the vehicle thermal behaviour and the passenger thermal response is based in energy and mass balance integral equations and works in transient conditions. These equations, solved by the Runge-Kutta-Felberg method with error control, are based in conduction, convection and radiation phenomena. All coefficients used in these equations are evaluated by a sub-model that calculates the internal and external view factors, radiative heat exchanges, glass radiative properties, occupation cycle, ventilation strategy, human thermo-physiology and heat and mass transfer coefficients by convection using empirical expressions.
In the numerical simulation a bus, that runs in a road nearby a fire front, occupied with 52 passengers is used. The radiative heat exchanges numerical model between the fire front and the vehicle and between the vehicle and the passengers, based in Mean Radiant Temperature method, is used.
The work is divided in three parts: the bus geometry, the passenger geometry and the fire front geometry (1), the view factor inside the and outside the bus passenger compartment (2) and the Mean Radiant Temperature that each bus bodies and human body section are subject (3).

Keywords*: Vehicle Thermal Behaviour, Human and Clothing Thermal Response, Mean Radiant Temperature, Numerical Simulation, view factors.*

Introduction

The vehicles and the passengers placed near a fire front are subjected to high radiative heat exchange. The passenger is subjected to thermal discomfort and the vehicles are, inclusively, subjected to ignition phenomena. Thus, it is an important and interesting topic to be analysed in detail.
In this preliminary study a numerical simulation of a bus, that runs in a road nearby a fire front, occupied with 52 passengers is used. The radiative heat exchanges numerical model between the fire front and the vehicle and between the vehicle and the passengers, based in Mean Radiant Temperature method, is developed and applied.
This study is a continuation of Conceição *et al*. (1997), Conceição *et al*. (1997), Conceição *et al*. (1997), Conceição *et al*. (2000), Conceição *et al*. (2000) and Conceição (2001). In the previous work only vehicle thermal behaviour and the internal airflow are analysed, while in this and in the following works the vehicle, the passengers and the fire front are considered.
In the vehicle thermal behaviour numerical models, analysed by several authors, have been given special attention to the passenger compartment, namely, the vehicle body (main and interior bodies and windows) and thermal phenomena (radiation, convection, human generation, glass radiative properties, air renovation and others).
The numerical model that simulates the vehicles thermal behaviour, presented in this work, considers all spaces and all vehicle bodies spatially defined. It calculates not only the solar radiation incident in the internal and external surfaces, but also the radiative heat exchange between internal, in each space, and external surfaces, between vehicle and surrounding bodies. In the radiative calculus are considered, in the internal and external calculus, the shading effect.

Finally, to evaluate the passengers thermal comfort level is used a human multi-node comfort model (see, as example, Conceição, 2000, Conceição *et al*., 2006 and Conceição and Lúcio, 2010). More details of the multi-node comfort model, based in Stolwijk (1970), can be see Conceição *et al*. (2014).

Physical Model

In the physical model, the numerical program defines the vehicle, passengers and fire front geometry. The vehicle, in general, is divides in several compartments (passengers, luggage and motor), main bodies (panels, doors, ceiling and floor), interior bodies (benches and motors) and glasses.
The passengers are divided in 25 cylindrical or spherical elements and each element is sub-divided in 12 cylindrical or spherical layers and could be still protected of the external environment through several clothing slices.
The fire front is identifying using one, or more, geometric surfaces.
Using the geometry inputs the programs built the energy and mass balance equations system.

Vehicle Mathematical Model

The vehicles thermal behaviour model is based not only in energy balance integral equations for the air inside each spaces, different slices of vehicle main bodies, several windows glasses and interiors bodies, but also in mass balance integral equations for the several air contaminants inside the spaces. It considers the convective (natural, forced and mixed), conductive (in the main bodies divided in several slices), radiative (shortwave and long wave radiation outside and inside the vehicle) and mass transfer (inside the compartments) phenomena.

In the radiative calculus each surface is sub-divided in several small areas. In the vehicle external surfaces are considered:

- the absorbed solar radiation by the main bodies and windows glasses surfaces;
- the long wave radiative heat exchange between the vehicle external surfaces and the nocturnal sky, during the night, and the surrounding surfaces, during the day.

In the internal surfaces are considered:

- the solar radiation transmitted through the glasses and received by the main and interior bodies surfaces;
- the long wave radiative heat exchange between the internal surfaces (glasses and main and interior bodies), of each space. The diffuse radiations between grey surfaces, in each enclosure, are determined by radiosity equations system and view factors.

It is considered the shading effect caused by the surrounding surfaces (buildings or other vehicles), when the car is parked, and the internal surfaces (main and interior bodies in each compartment).
In the mass transfer inside each space are considered the human respiration and transpiration, outdoor infiltration and mass exchange between different compartments. Using the water vapour concentration and the air temperature value the model calculates the air relative humidity.

Heat exchanges by radiation

The radiant heat exchanges by long wave phenomena are calculated, in this work, using the Mean Radiant Temperature method (Fanger, 1970). The Mean Radiant Temperature, used to evaluate the heat exchanges that each human body section is subjected, considers the view factors calculated between the human body sections and the surrounding surfaces and the surrounding surfaces temperature. In the methodologies used in view factors determination each human body element, vehicle surfaces and external surfaces, with inclinations and dimensions equal to the respective body,

are divided in infinitesimal areas. In the radiation by long wave phenomena calculus are also considered the shading effects that the body elements surfaces promote in each element.

The Mean Radiant Temperature method, with correction, is divided in two parts:
- Heat exchange in the human body;
- Heat exchange in the vehicle.

The human body consider:
- heat exchanges between the human body sections and the surrounding surfaces (main and interiors bodies and glass);
- heat exchanges between the human bodies sections of each passenger and between the human bodies sections of different passengers;

The vehicle body consider:
- heat exchanges between the vehicle surfaces (main and interiors bodies and glass) itself;
- heat exchanges between the vehicle surfaces (main and interiors bodies and glass) and the passengers;
- heat exchanges between the vehicle surfaces (main and interiors bodies and glass) and the external surfaces (floor, environment and fire front).

The Mean Radiant Temperature method, with correction, calculates, step by step, the Mean Radiant Temperature, using the human body and vehicles bodies, calculated in each iteration, and the pre-calculated view factors.

Results and Discussion

This preliminary work is divided in three parts:
- the bus geometry, the passenger geometry and the fire front geometry;
- the view factor inside the and outside the bus passenger compartment;
- the Mean Radiant Temperature that each bus bodies and human body section are subject.

In the bus studied, divided in 6 compartments (frontal ventilation ducts, luggage, motor, passengers and two ventilation ducts over the seats), are considered 99 main bodies, 18 window glasses and 105 interior bodies (see figure 1). The same figure, as example, show also a small fire front, placed in the vehicle left side.
Each of these surfaces, in order to evaluate the view factors, is divided in several infinitesimal areas. In general, in accordance with previously numerical simulation obtained in the view factors determination, all surfaces are subdivided in both directions in a grid spaced in a maximum of 0.2 m and divided in a minimum of 100 elementary areas.
Figure 2 show the grid generation in the vehicle passenger's compartment surfaces and the 52 passengers used in the view factor determination. The passengers considered has 1.7 m of height, 70 kg of weight and 1 met of activity and 0.8 Clo of clothing level.
In figure 2 the vehicles surfaces are subdivided in elementary surfaces, defined previously, while in the passengers the spherical head is divided in 64 elementary areas (a grid in the azimuthal angle direction of 8 divisions and a grid in the polar angle direction of 8 divisions), while the others passenger bodies cylindrical elements are also divided in 64 elements (a grid in the longitudinal direction of 8 divisions and a grid in the radial direction of 8 divisions).
In the geometry definition all vehicles surfaces (main bodies and transparent bodies) are in contact. However, in the interior bodies only the seats, defined by a vertical and an inclined surface, are defined. In the passengers all elements are disposed in similar way to the human body posture. The neck, the arms divided in four and the legs divided in four are connected to the trunk with dimensions and angles

similar to the human body sections. The head is connected to the neck, the hands are connected to the arms and the feet are connected to the legs. In the neck, shoulders, elbows, hips, knees and ankles are placed rotation elements. The dimensions and inclination of each element are obtained using a numerical model based in the human body weight and height.
All passengers are not in contact between them and all passengers are not in contact with the seat and with all vehicle surfaces.

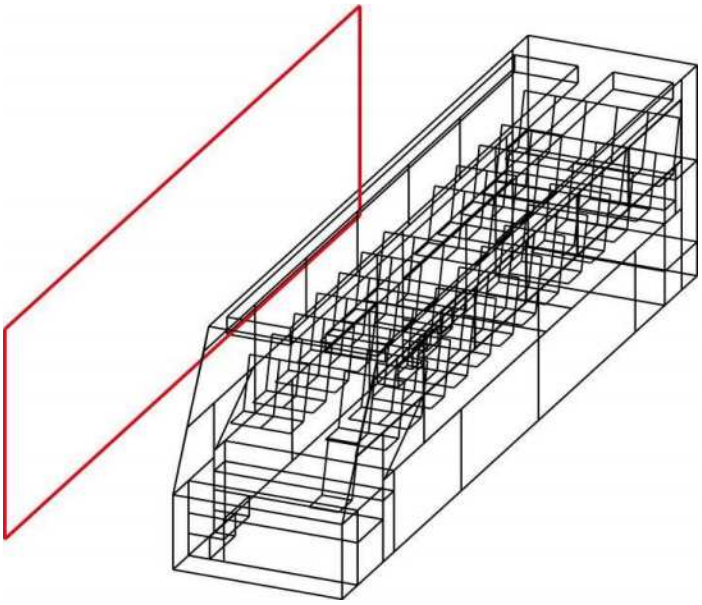

Figure 1. Scheme of a bus with 6 spaces, 99 main bodies, 105 interior bodies, 18 windows and 1 fire front.

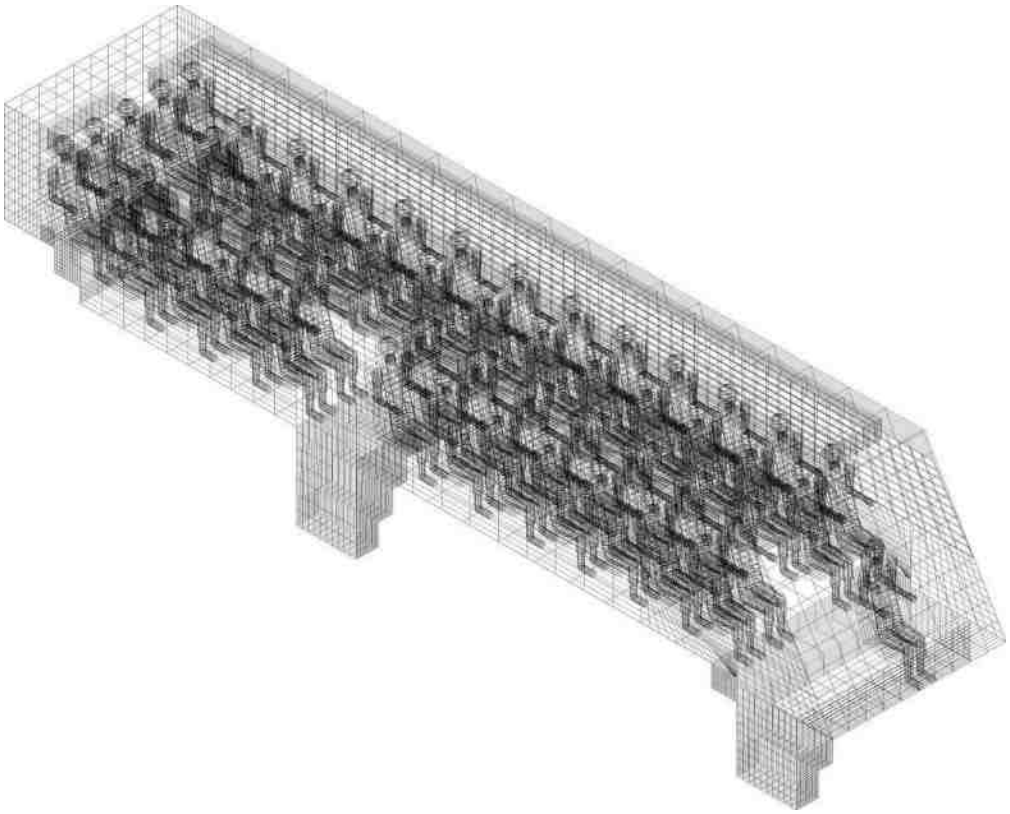

Figure 2. Grid generation in the vehicle passenger's compartment surfaces and in the 52 passengers used in the view factor determination.

In figure 3, as example, the Mean Radiant Temperature that each human body sections are subjected is presented. In these calculus the air temperature and relative humidity, evaluated in the external environment are, respectively, 18 ºC and 50 %, while the external floor is 18 ºC.

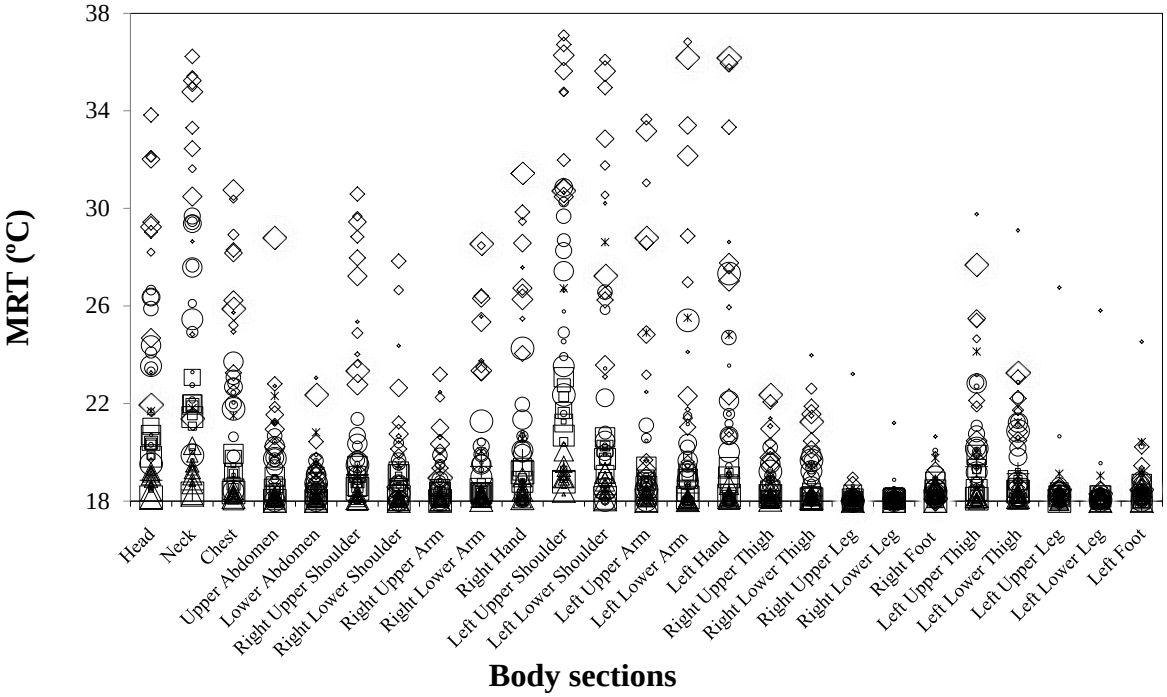

Figure 3. Distribution of the Mean Radiant Temperature that each human body section of the 52 passengers are subjected.

In accordance with the obtained results, in this preliminary study, is possible to verify that:

- The Mean Radiant Temperature is highest for passenger located near the left side vehicle;
- The Mean Radiant Temperature is higher for the left side passenger sections than right side passenger sections;
- The Mean Radiant Temperature is higher in upper passenger sections than in lower passenger sections.

Conclusions

In this work the influence of the radiative heat exchanges between the fire front and vehicle passengers' in a road is made. In the study a numerical software that integrate the vehicle thermal behavior with complex topology and the human thermal response, in transient conditions, is developed and used.
In this preliminary study, divided in three parts, are defined the bus geometry, the passenger geometry and the fire front geometry (1), are calculated the view factor inside the and outside the bus passenger compartment (2) and are evaluated the Mean Radiant Temperature that each bus bodies and human body section are subject (3).
In accordance the obtained preliminary results the grid generation in the vehicle geometry, in the passenger geometry and in the fire front geometry, in general, promote a good compromise between the view factors obtained and the computational time used. The increase of the grid generation increase substantially the computational time used, while the reduction cannot obtained good view factors values.
The preliminary obtained values show a slight asymmetry in the Mean Radiant Temperature values. The Mean Radiant Temperature is highest for passenger located near the left side vehicle, the Mean Radiant Temperature is higher for the left side passenger sections than right side passenger sections

and the Mean Radiant Temperature is higher in upper passenger sections than in lower passenger sections.
In the future the obtained information will be used in the evaluation of the vehicle temperature distribution and the human body temperature distribution. The vehicle temperature distribution will be used to evaluate the ignition risk that a vehicle is subjected near a fire front, while the human body temperature distribution will be used to evaluate the human thermal comfort and local discomfort levels.

References

Conceição E. Z. E. and Lúcio Mª M. J. R. 2010. Evaluation of Thermal Comfort Conditions in a Localized Radiant System Placed in Front and Behind two Students Seated Nearby Warmed Curtains, Building and Environment, Volume 45, Issue 10, October 2010, Pages 2100-2110.

Conceição E. Z. E., Lúcio Mª M. J. R., Capela T. L. and Brito A. I. P. V. 2006. Evaluation of Thermal Comfort in Slightly Warm Ventilated Spaces in Non-Uniform Environments, International Journal on Heating Air Conditioning and Refrigerating Research, ASHRAE, American Society of Heating, Refrigerating and Air-Conditioning Engineers, Inc., EUA, Vol. 12, Nº 3, July 2006, pp. 451-458.

Conceição, E. Z. E., Evaluation of Thermal Comfort and Local Discomfort Conditions Using the Numerical Modeling of the Human and Clothing Thermal System, RoomVent 2000 - 7th Int. Conference, University of Reading, U. K., 9 to12 of June 2000.

Conceição, E. Z. E., Multinodal Models of Vehicles Thermal Behavior and Passenger Thermal Response, 7th Int. Conference, Florence ATA 2001, Florence, Italy, 23 to 25 of May 2001.

Conceição, E. Z. E., Silva M. C. G. and Viegas D. X. Air Quality Inside the Passenger Compartment of a Bus", Journal of Exposure Analysis and Environmental Epidemiology, International Society of Exposure Analysis, EUA, Vol. 7, No. 4, 1997, pág. 521-534.

Conceição, E. Z. E., Silva M. C. G. and Viegas D. X. Airflow Around a Passenger Seated in a Bus, International Journal on Heating Air Conditioning and Refrigerating Research, ASHRAE, American Society of Heating, Refrigerating and Air-Conditioning Engineers, EUA, Vol 3, Nº 4, Outubro de 1997, pág. 311-323.

Conceição, E. Z. E., Silva M. C. G. and Viegas D. X. Application of the Mean Radiant Temperature Method in the Evaluation of Radiative Heat Exchanges Between a Fire Front and a Group of Firemen, VI International Conference on Forest Fire Research, 1014.

Conceição, E. Z. E., Silva M. C. G., André J. C. S and Viegas D. X. Application of the Runge-Kutta Method in the Numerical Modelation of the Thermal Behavior of a Vehicle", Textos de Matemática, Departamento de Matemática da Faculdade de Ciências e Tecnologia da Universidade de Coimbra, Série B, Nº 11, 1997, pág. 19-27.

Conceição, E. Z. E., Silva M. C. G., André J. C. S and Viegas D. X. A Computational Model to Simulate the Thermal Behaviour of the Passengers Compartment of Vehicles", SAE 1999 Transactions - Journal of Passenger Cars, September 2000.

Conceição, E. Z. E., Silva M. C. G., André J. C. S and Viegas D. X. Thermal behavior simulation of the passenger compartment of vehicles", International Journal of Vehicle Design, Volume 24, No. 4, 2000, pág. 372-387.

Fanger P.O. 1970. Thermal Comfort. Copenhagen: Danish Technical Press.

Stolwijk, J. A J. 1970. Mathematical Model of Thermoregulation", In Hardy, J. D., Gagge, A. P. and Stolwijk, J. A. J. "Physiological and Behaviour Thermoregulation", Thomas, Springfield, pp. 703-721.

Investigation of vegetation fire plumes using paragliders tracks and micro-scale meteorological model.

Jean-Baptiste Filippi[a], Miguel Cruz[b], Frédéric Bosseur[a], Antoine Girard[c]

[a] *SPE – CNRS UMR 6134, Campus Grossetti, BP52, 20250 Corte. filippi@univ-corse.fr*
[b] *CSIRO Ecosystem Sciences and CSIRO Climate Adaptation Flagship. Black Mountain, Australia*
[c] *Université Stendhal, Grenoble 3, Valence, France*

Abstract
This work presents an interesting and unique analysis of an open air fire plume extrapolated from a large amount of paragliders tracks flying over a sugarcane fire during a world cup super final event in february 2013 Columbia. Vertical speeds of over 20 m/s were observed into a narrow core just over the fire. Simulation of the same event shown the relatively good ability of micro-scale meteorological models to represent quantitatively the velocity fields and behavior.

Keywords*: fire meteorology, fire weather, plume, convection, simulation, modelling, paragliding*

Introduction

An understanding of the interaction between a free spreading fire and the surrounding weather system requires knowledge on the dynamics of the buoyant fire plume. Insight into this dynamics, namely how the energy released by the fire sustains this plume can be studied experimentally [clements 2007, Church and snow 1985] and numerically. Nevertheless instrumenting a fire plumes is quite a complex task, particularly due to the nature of the energy source and the height to which instruments would need to be located. Remote sensing has also been used to capture the plume dynamics in large fires, although because the signals can be severely blinded by the amount of large particles in the air it is not clear how certain the remotely sensed data reflects the inside of the plume. In situ measurements may be done using Unmanned Aerial Vehicles (UAV) [clements 2007] but as well are limited by extreme flight conditions caused by flying embers and strong convection
A recent paragliding competition (the 2012 World Cup Super Final held in Roldanillo ,Colombia) offered an unique opportunity to characterize the structure of a buoyant plume above a fire. In this event a large number of paragliding pilots flew into a fire plume developing above a controlled burn in a sugarcane field. Mandatory GPS and variometer instruments carried out by the pilots recorded their detailed movement as they navigated the plume. The pilots can be considered synchronized passive tracers that allow us to reconstruct the plume dynamics and namely inform us on the intensity of the convection within the plume and up to a high altitude.
In our unique study we quantify the energy source of the sugarcane fire, present the 3D dynamics of the plume as characterized by the dataset and compare it with a simulation from coupled fire/atmosphere micro meteorological model in order to (1) verify the relevance of such models for such plumes and (2) see if it may be used to generalise the result.
The first part of the study present the dataset, providing specific insight on sugarcane fuels, and how the flight logs were analysed and convection fields extrapolated. Results are presented in the second part, with first guess analyses of simulation results compared to post-processed tracks.

2. Method

Fuel source

The fuel complex is a sugar cane plantation prior to harvesting. At this stage the standing crop is

approximately 3 m tall and carrying an overall biomass varying between 7.5 and 10 kg/m2. Standing biomass will largely depend on the watering and fertilized regime provided to the standing crop. About 20% of the biomass is dead suspended leaves along the stalk and litter forming a well-aerated fuel layer in the lower 1 – 1.5 m of the stand. This dead biomass is the fuel that will be consumed in pre-harvest burning. It is well accepted that these burns will consume between 1.5 and 2 kg/m2 (Cheney, Sullivan 2008)

The high intensity burning in Fig 1 is indicative of productive sites and varieties, so we can confidently assume a fuel consumption in the high end of the range, i.e., 2 kg/m2. Cheney and Just (1974) suggest flame heights of about 9-11 m (from the ground) in 3 m tall crops with good fuel accumulation. These flame heights are consistent with the ones recorded photographically by several pilots (as per Fig 1). Tabled values for sugarcane heat content vary between 18500 kJ/kg (higher) and 17700 kJ/kg (lower). Considering a fuel load of 2 kg/m2 and an heat content of 18000 kJ/kg it will be appropriate to consider a heat per unit area of 36 MJ/m2. The size of the sugarcane field was 5 ha, corresponding to a total energy released of 1.8 GJ.

The photos taken by several of the paraglider pilots as they approached the plume suggest an ignition pattern characteristic of sugarcane burning. The ignition method consist of two igniters walking along the longer sides of the field with one of them slightly ahead of the other. If we assume that (1) the igniters are moving at a rate of 1.4 m/s (walking pace) as they light the long edge of the sugar field; (2) as they move along the plot the two fire fronts merge and move along the igniters direction of travel at 1.4 m/s (Fig 1); then we can assume that the fire front is spreading at 1.4 m/s spread rate.

Given the approximately 500 m length of the sugarcane field, the lighters took about 6 minutes (357 s to be more exact) to burn the full 50000 m2 of the sugarcane block. A raw analysis from pilots pictures during the event are in relative agreement with this estimate (between 6 and 8 minutes as fire front position is difficult to locate precisely). Overall the full burn duration is considered to be about 9 minutes, 6 minutes of lightning procedure and 3 more minutes for the full burn out.

From this and the assumption that the fire is spreading at a steady state determined by the igniters pace, it is possible to estimate the energy release rate from the combustion of those fine dead fuels. Considering a burning duration of 40 seconds, and that 50% of the combustion energy is converted to convective heat fluxes, the surface instantaneous heat fluxes for the numerical model is parameterized as 450Kw.m2 for these 40 second. The propagation pattern is force to mimics the actual fire as seen from the photographs, with fires spreading towards the center of the field.

Tracklogs

The study attempts to leverage the opportunity offered by task 3 of the 2012 paragliding world cup super final that occurred in Roldanillo (near Cali), Columbia the 19th of January 2013, that happened to be at the same time that large sugarcane fields were set to burn before harvest.

More than 120 of the world best competitors were free-flying in this large valley with equatorial climate, all searching for the quickest way to gain altitude in order to reach the finish line first. to be a very effective way to gain altitude, a flock of 80 pilots entered this fire thermal and exited within 10 minutes gaining about 1600 meters in average. This fire thermal was intense enough that some had to deploy their reserve parachute, risking to fall into flames with 20kg of nylon wing and it is since that day forbidden to fly over a fire in the PWC championship rules.

As the format of the competitions requires that tracks must be logged with relatively high frequencies for verification, the resulting dataset may be regarded as a set of relatively well spread and synchronized passive tracers that may inform on the intensity of the convection within the plume and up to a high altitude. The frequency of the tracklogs is in between 5 and 10 seconds, depending on the pilots equipment, all these track points were first compiled into a timed dataset with the computation of the instantaneous vertical velocity for each glider at each point. This vertical velocity was taken as the altitude difference between a point and its next point in time, divided by the duration between those

2 points (5 to 10 seconds). We then subtracted a typical competition glider sink rate (0.7 m/s) to the value.
The second operation required to reconstruct a volume from this dataset in order to interpolate vertical paragliders velocities inside the plume, for that all points within a 120 seconds window were extracted and used to perform a Delaunay triangulation of a volume. Within this volume vertical velocity can then be interpolated as the bilinear interpolate between grid points.
To reconstruct the timely evolution of the plume, the 120 seconds window is moved 10 seconds at a time during the overall burn duration, with a triangulation performed with each window dataset. An animation of this plume rise taken from these tracklogs may be found here: youtube.com/watch?v=Ogsq2yINV6o.

Figure 1 - View of the plume from the sugarcane burn

2.3. Model Set-Up

The coupled simulations were run on a 2.5km×2.5km×3km domain discretized on a 80×80×60 mesh for the atmospheric model simulation ($\Delta x = \Delta y$, 40m, vertical grid up to 5000m, vertical resolution increasing from 20M (ground) to 200m (top)).
Atmospheric conditions were initialized with radio soundings extracted from global model analyses. Simulations were run on a parallel 8 cores computer, with a speedup ration of 0.9 (0.9 seconds of computation for 1 seconds of real time). Mesonh/ForeFire [Filippi *et al* 2010, Filippi *et al* 2013] code was used to perform the computation.

3. Results

Figure 2 presents the reconstructed wind field when the fire was approximately towards the end of the burn and much gliders present, we can see areas in excess of 20 m.s vertical speed. Obviously vertical velocity may be extrapolated only where data is present, but with 80 tracers, this field is composed of about 4800 real points. It is possible to observe a relatively narrow convection core (about 200 meters) rising with some negative velocities area its outer edges of this core.

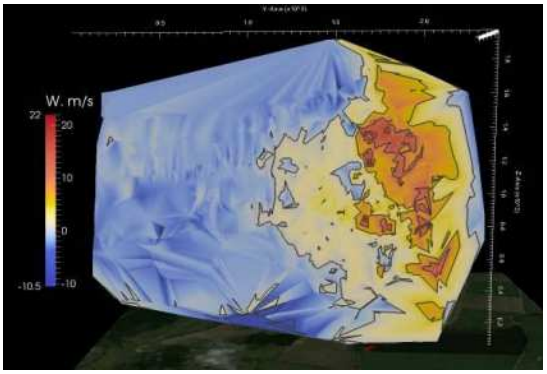

Figure 2 - View of reconstructed plume

The very basic idealized simulations that were performed are presented in figure 3. It might be observed that overall a similar (although obviously much more smooth) vertical velocity pattern is formed. These results shows in particular a nice accordance between the maximum vertical rate, and as well a 200m wide convective core and a plume that rises at about the same height (although no glider went higher than +2000m, so higher than that, no data is there for comparison). The vertical downdrafts is less intense in the simulation, but still present and at the outer edge of the main core.

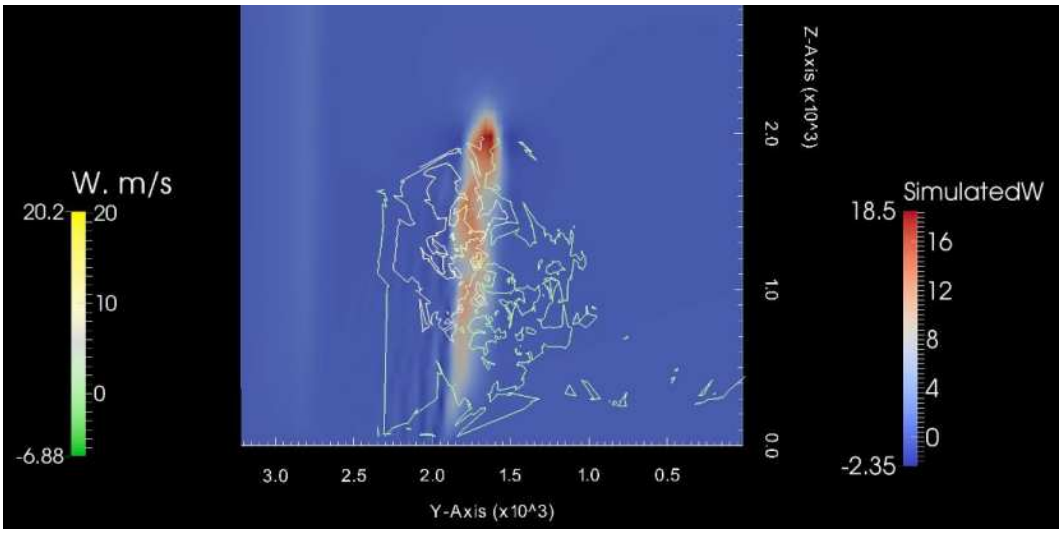

Figure 3. Simulated plume (red/blue vertical wind velocity) and approximately synchronized isolines of the estimated vertical paragliders velocities (-5,0,5,10,15,20 m/s). Time = Ignition + 340s.

Conclusion

This work presented an interesting and unique analysis of an open air fire plume extrapolated from a large amount of paragliders tracks. Vertical speeds of over 20 m/s were observed into a narrow core just over the fire. Simulation of the same event shown the relatively good ability of microscale meteorological models to represent quantitatively the velocity fields and behaviour even with very crude parameterisation consequence of the lack of field data.

Acknownlegements

Authors wishes to thanks competitor Charles Cazaux for its insights, data and contacts with other competitors, Team Russia and S. Gattini for the pictures and the MesoNH team for teir support.

References

CHURCH C. R. ; Snow. T. ; Observations of vortices produced by the météotron. Programme COCAGNE. Séminaire(1984) 1985, vol. 19, no4, pp. 455-467

Clements, C. B., S. Zhong, S. Goodrick, J. Li, X. Bian, B.E. Potter, W. E. Heilman, J.J. Charney, R. Perna, M. Jang, D. Lee, M.Patel,S. Street and G. Aumann, 2007: Observing the Dynamics of Wildland Grass Fires: FireFlux- A Field Validation Experiment. Bulletin of the American Meteorological Society ,88(9),1369-1382.

Filippi, J.B., Morandini, F., Balbi, J.H., Hill, D.R.C. (2010) Discrete event front tracking simulator of a physical fire spread model, Simulation, transactions of the SCS. 2010, vol. 86, no10, pp. 629-644 doi: 10.1177/0037549709343117

J.-B. Filippi, X. Pialat, C.-B. Clements Assessment of ForeFire/Meso-NH for wildland fire/atmosphere coupled simulation of the FireFlux experiment, , Proceedings of the Combustion Institute, Volume 34, Issue 2, Pages 2633–2640, 2013.

Cheney, Sullivan 2008 : Grassfires: Fuel, Weather and Fire Behaviour, CSIRO PUBLISHING. isbn: 9780643099012

Live fuel moisture and wildland fire behaviour

Philip Zylstra[a]

[a] *Centre for Environmental Risk Management of Bushfires, University of Wollongong, Northfields Ave, Wollongong NSW 2522, pzylstra@uow.edu.au*

Abstract

Live fuel moisture content (LFMC) is a parameter that affects the flammability of plants, and the capacity to measure it remotely makes it an accessible variable for use in fire behaviour models. Although the effect of LFMC on the flammability of fuel particles has clear theoretical support however, the way in which this relates to fire behaviour is complex and difficult to quantify so that empirical studies of heath and forest fires at times yield weak or ambiguous results.

This study examines the way in which moisture affects fire behaviour by using a process-based conceptual framework (Zylstra 2011) to identify feedbacks and complexities that may confound empirical analysis.

Z11 links empirically-derived sub-models of flammability characteristics within a dynamic physical framework where heat is transferred convectively across spaces between leaves, branches, plants and plant strata. The ignitability, combustibility and sustainability of flame from burning leaves interacts with the geometry of the fuel array to determine whether flame will spread across horizontal spaces affecting rates of spread, and vertical spaces affecting flame heights.

Factors are identified that should be considered explicitly in experimental design if LFMC is a consideration, and physical arguments presented to show that where such a range of conditions is not present in the experimental design, the results are inadequate to draw conclusions. In some cases, practical considerations will prevent the lighting of experimental fires under the full range of necessary conditions so that the best understanding will be derived from modelling results. In such cases, misleading conclusions will be drawn unless the model can adequately reflect the complexity presented here.

There exists a strong physical argument for the effect of LFMC on fire behaviour, however this effect is not straightforward and will drive threshold changes and feedbacks. Such changes may represent sudden and dangerous escalations in fire behaviour, so understanding and quantifying these is important. Z11 is a model that can calculate such thresholds and can be used to both inform experimental design and risk-based decision making.

Keywords*: Fire behaviour, live fuel moisture, flammability, Forest Flammability Model, complex systems*

Introduction

Live fuel moisture content (LFMC) is a readily accessible metric that can be measured to varying levels of precision via remote sensing (Yebra *et al.* 2013). Physical arguments suggest that it has an influence on fire behaviour as the presence of moisture affects the flammability or ignitability, combustibility and sustainability (Anderson 1970) of leaves; however debate exists as to the extent and nature of the influence in field conditions and it is therefore rarely or inadequately considered as a component of fire behaviour modelling.

Ignitability has two components – the minimum temperature of ignition (Philpot 1970) and the time to ignition (Gill and Zylstra 2005). While the minimum temperature or endotherm appears to be a chemical property, time to ignition is the time taken for a leaf to be heated to ignition and relates to both the surface area to volume ratio and the thermal inertia of the leaf. Various studies (e.g. Xanthopoulos and Wakimoto 1993; Weise *et al.* 2005; Madrigal *et al.* 2011) have identified moisture content as a major influence in this, although more recent studies at higher temperatures (Engstrom *et al.* 2004; Fletcher *et al.* 2007) have failed to find a relationship.

While the effect of moisture on particle ignition is widely accepted under most conditions, the

influence of LFMC on fire behaviour as a whole is more complex. It has been strongly implicated in the incidence and scale of fires across several landscape studies (e.g. Schoenberg *et al.* 2003; Chuvieco *et al.* 2009; Dennison and Moritz 2009; Caccamo *et al.* 2012) and identified as a key determinant in the behaviour of fires burning through simple complexes such as heath and shrub lands (Weise, Zhou, *et al.* 2005; Davies *et al.* 2009; Plucinski *et al.* 2010). The interaction however is harder to detect in more complex arrangements. Alexander and Cruz (2013) have summarised the results of a series of laboratory and field experiments looking at LFMC effects on behaviour, noting that the correlation is either ambiguous or non-existent when all studies of heath and crown fires are considered; although its role in facilitating crown fire commencement was not examined.
This paper addresses the conflicts by providing a theoretical analysis of the mechanisms by which moisture affects fire behaviour, describing trends, feedbacks and complexities which may mask correlations in studies that do not specifically account for them.

Methods

The role of moisture is described and quantified mathematically through a process-driven model that addresses the limitations identified for laboratory studies. The model is then described conceptually as a basis for explaining anomalous observations, and to provide some guidelines for effective analysis of the relationship.

Issues to be addressed

Two main concerns have been raised over attempts to model the effect of moisture and other particle flammability properties; these are:

1. *Exaggerated effects of LFMC due to inadequate experimental technique*. Empirical models of time to ignition are frequently constructed using small radiant heat fluxes (Fernandes and Cruz 2012; Alexander and Cruz 2013) when analyses at higher convective fluxes have reported little to no relationship (Engstrom *et al.* 2004; Fletcher *et al.* 2007). In addition, it is at times erroneously assumed that all moisture is evaporated before a leaf ignites (Pickett *et al.* 2010), so that models of time to ignition may over-estimate the effect of LFMC at high temperatures typical of field conditions.
2. *Flawed assumptions*. The flammability of plant parts does not automatically scale to the flammability of the whole plant (Pérez-Harguindeguy *et al.* 2013) or stand (Fernandes and Cruz 2012).

Model description

The fire behaviour model (Zylstra 2011) hereafter referred to as Z11 currently utilises empirical models of leaf flammability that were developed alongside the main model. The equations for combustibility and sustainability were developed from experiments that utilised candle flames, where the point of heating for the leaves used a measured heat flux of 145kW/m^2 (Hamins *et al.* 2005). This exceeds the values of 61kW/m^2 measured in the field by Silvani and Morandini (2009) and approaches the maximum value of 150kW/m^2 measured by Butler (2010). Both models found a significant influence of leaf moisture, and predicted flame length and duration values for leaves across 10 sclerophyllous species and a wide range of moisture values with R^2 values of 0.87 and 0.74 respectively.
The main concern expressed in the literature however relates to models for time to ignition. Equation 1 used in Z11 was developed across six sclerophyllous species with moisture contents ranging from oven dried to 200% with combined convective and radiative heating to temperatures from 220^{o}C to 700^{o}C, explaining 90% of the variability for the species and conditions studied. Surface area to volume ratio had the effect of regulating the conductance of heat into the leaf so that leaf thickness T and the

number of sides *s* to the leaf combined with moisture content *m* to form the ignitability coefficient *IC* (equation 2). The effect of leaf thickness is thereby negated when moisture is zero. The units for these equations are percent, mm and ^{o}C, and leaves have either two sides when flat or four when terete. Time to ignition is ψ and temperature is *t*.

$$\varphi = IC97805.26t^{-2.10} + 6452280.04t^{-2.40} \quad \text{Equation 1}$$

$$IC = \frac{mT}{s} \quad \text{Equation 2}$$

Although the temperatures in the muffle furnace used were not as high as those of the Chaparral studies (Engstrom *et al.* 2004; Fletcher *et al.* 2007) and the heat fluxes were not measured; figure 1 demonstrates that when reported moisture and leaf thickness values are used to predict the times to ignition that were measured in these studies, the model of Z11 was well within the target range and moisture content did not artificially slow expected ignition times.

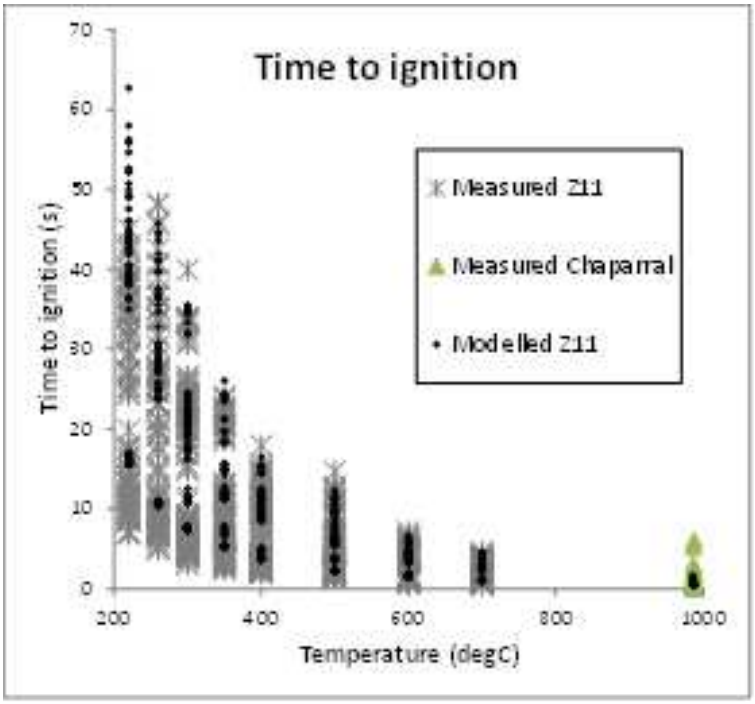

Figure 1. Equation 1 extended to predict the values measured by Engstrom et al. (2004) and Fletcher et al. (2007)

In regard to the second concern, Z11 makes no assumptions about the scaling between leaf flammability and plant or stand flammability, rather this relationship emerges dynamically from a series of interactions calculated in 1s time-steps. Fire propagates in a process analogous to crown fire initiation models such as Xanthopoulos (1990) and Cruz *et al.* (2006), where fuels are ignited by a heat flux that decays across a distance defined by the geometry of the array. Each leaf flammability property explicitly influences propagation as described in Table 1. In this way, the dimensions, position and angle of the flame are adjusted each second according to the capacity for flames to ignite new fuels across spaces between leaves, branches, plants and plant strata, and the time for which these fuels stay ignited.

Table 1. The role of leaf flammability properties in Z11

Flammability component	Influence
Combustibility	The length of flame produced by burning leaves modified by the physics of flame interactions for the number of leaves burning in close proximity defines the flame length for a time-step. Together with the temperature at which these leaves burn, this in turn produces the input to a temperature field. The decay in convective temperature is defined with distance from the base of the flame, and the direction of convective transfer is defined by the angle of the flame as influenced by its length, the wind speed at that point in the forest profile and any blocking effects of the slope.
Sustainability	A cohort of leaves is ignited in each time-step, and these burn for a period of time defined by their sustainability before they extinguish, redefining the flame origin and the total quantity of leaves burning.
Ignitability	Leaves along the vector defined by the flame are exposed to a given temperature defined by their distance from the burning fuels. If this temperature both exceeds the endotherm of the leaves and the time to ignition calculated by equation 1 for that temperature and the ignitability of the leaves is less than the calculation time-step, then the leaves ignite, increasing the quantity of leaves burning. If both conditions are not met, the time-step is considered pre-heating and a proportion of the time to ignition is removed according to the heating received. The leaves are again tested in the next time step.

The way in which the ignitability of a leaf affects flame propagation is shown in figure 2. As the distance increases from the flame base along the *x*-axis, temperature decays along the lower part of the *y*-axis, in this case using the functions given by Weber *et al.* (1995). The time to ignition is modelled against this temperature using equation 1 for a leaf with low ignitability (high moisture content and/or thickness) as shown by the lighter broken line, and for a leaf with high ignitability (low moisture content and/or thickness) by the heavier broken line. At the left of the graph where temperature is highest (such as observed in the chaparral studies), the time to ignition is very short. As temperatures decrease with distance from the flame base, time to ignition increases until it meets the solid horizontal line which marks the time-step used for calculation. The intersection of these lines shows the maximum distance that may be ignited during that time-step. That is, all leaves in a plant crown that lie within this distance will be ignited in that step. As time to ignition is defined by temperature which is in turn defined by distance from the flame base, ignitability can therefore be understood not only as time to ignition, but also as distance to ignition or minimum temperature required to ignite within a given time step.

Equation 1 demonstrates that very high temperatures will indeed overwhelm any small effect of leaf moisture, however high temperatures are not limited to field conditions. Even a candle can produce a temperature of 1400^{o}C (Gaydon and Wolfhard 1979) and thereby exceed the maximum value recorded by Butler (2010) for a crown fire; but in each case this only corresponds to the hottest part of the flame. As time to ignition equates to distance to ignition or minimum temperature required for ignition within a given time, the effect of moisture is to regulate the distance to which leaves can be ignited. Larger gaps can be crossed and more leaves lit simultaneously when they are drier.

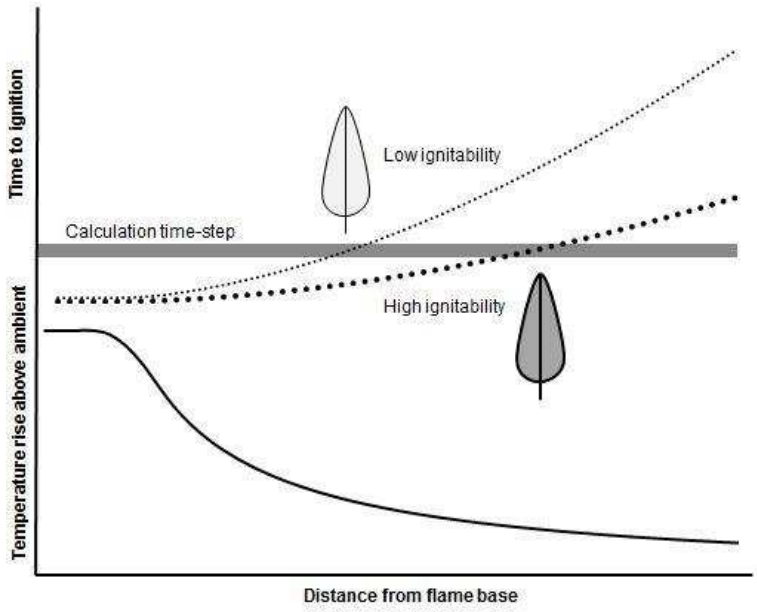

Figure 2. Translating time to ignition into distance to ignition. The curved solid line represents flame temperature, the straight line marks a time-step on the y-axis and the two broken lines mark the time to ignition for two different plant species as calculated using equation 1.

To picture the process, consider a simplified situation where the combustibility and sustainability of leaves are kept constant and can be characterised such that flames are 1.5 times the depth of ignited leaves, the hottest part of any flame is 1300ºC and all leaves burn for 2s. Three different LFMC values will be considered (Table 2) for two-sided leaves in a 0.7m tall shrub with a base extending from the ground, and with leaves separated by 4cm. Pre-heating will be ignored for simplicity and no wind will be considered so that flames are vertical. The value 'minimum temp' in Table 2 is the temperature required to ignite the leaves in 1s or less, found by solving Equation 1 for *t*.

Table 2. Ignitability of leaves in the examples

	Moisture 1	**Moisture 2**	**Moisture 3**
Moisture (%ODW)	70%	220%	250%
Thickness (mm)	0.2	0.2	0.2
IC (Eq. 2)	7.0	22.0	25.5
Minimum temp (ºC)	850	1200	1260

If all three plants are exposed to an identical heat flux from a pilot flame of 0.3m such as might be achieved from a fire burning surface litter, the distances to minimum temperature found using Weber *et al.* (1995) will be 0.28m, 0.12m and 0.08m respectively. That is, in the span of 1s the bottom 28cm of leaves will be ignited in the driest plant producing a plant flame that extends 1.5 times the depth ignited (42cm) beyond the ignited leaves. In the wettest plant however, only 8cm of the lowest leaves will be ignited, producing a flame extending 12cm. The altered heat fields produced by the new flames will allow flame to propagate in the two drier plants, but in the wettest plant the distance to 1260ºC will be less than the separation between leaves and flame will not propagate. As more leaves are ignited in the next second these are added to the total depth of ignited leaves, but because the leaves only burn for 2s the lower cohorts will extinguish in sequence after this time even as new leaves are ignited. The three scenarios are shown in figures 3 to 5.

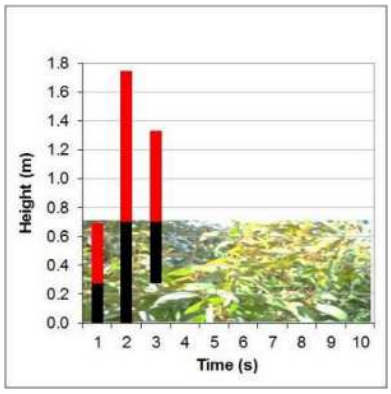

Figure 3. Fire propagation in Moisture 1. Maximum flame height reached is 1.75m, the plant is consumed and flame duration is 3s.

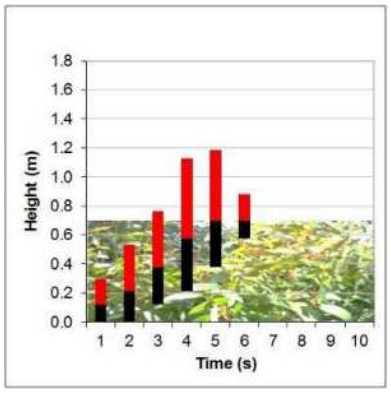

Figure 4. Fire propagation in Moisture 2. Maximum flame height reached is 1.18m, the plant is consumed and flame duration is 6s.

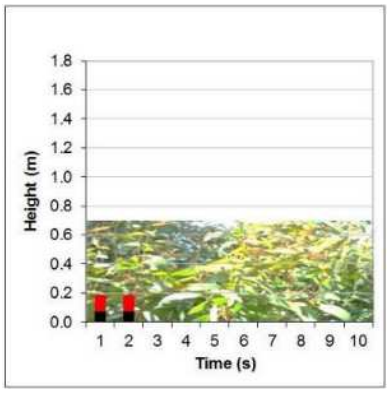

Figure 5. Fire propagation in Moisture 3. Maximum flame height reached is 0.19m, the plant is only partially consumed and flame duration is 2s.

Although these scenarios describe simplified situations and the influence of moisture will be affected to some extent by pre-heating and its effect on combustibility and sustainability of leaves, the basic process by which leaf flammability translates to fire propagation can be understood. Notably, the flammability properties of the leaves did not scale directly to the plant. While only the ignitability of leaves was altered, the sustainability of flame in the plant varied from 2s to 6s and the combustibility varied such that flame heights ranged from 0.19m and 1.75m. In this way, the flammability of plants and stands emerges from numerous factors and should not be assumed from the parts.

Model application

The lack of correlation between LFMC and fire behaviour reported for many field experiments requires explanation, however full treatment is impossible without replication of the exact conditions. In the absence of this information, the principles of fire propagation that have been shown will be used to describe a series of behaviours that can confound the observation of trends.

Much work on fire behaviour has focused on propagation through continuous fuel beds such as dead leaf litter; however such observations can be misleading if applied to discontinuous fuels. Plant communities are characterised by gaps between leaves, branches, plants and plant strata, and the bridging of these gaps can result in threshold changes that are not well captured with statistical methods that do not explicitly account for them.

As convective heat transfer occurs along a vector rather than being radiated in all directions, heat can be directed upward across vertical spaces between strata, or horizontally across gaps between plants. The angle of the trajectory is influenced by the size of the flame providing buoyant uplift, the velocity of the wind acting on the flame and the effect of slope in blocking air intake from one side. In both this way and by the tilting of the fuel array in relation to the flame, the effect of slope may not follow expectations established from fires in continuous surface fuels, but may produce threshold changes in the same way as winds do.

The emergent nature of fire behaviour can introduce feedbacks that obscure trends or even produce opposite trends to those of the larger picture. Consider for example the difference in the height of flames produced in figures 3-5. Larger flames are more buoyant and therefore stand more upright against lateral air movement than do smaller flames, so that if wind was added to those scenarios, the differences in flame height may have been even greater due to tilting of the smaller flames.

Tilting of flames however has the effect of directing the convective stream forward rather than upward, and the propagation of flame between plants in the same stratum requires this forward direction of heat. It can be the case then that when plants produce smaller flames due to higher moisture contents,

the greater tilting of these flames by the wind facilitates forward propagation with resulting faster rates of spread and larger flames as the amount of fuel burning increases. The lowest wind speeds allowing this spread produce a transitional period where temporarily larger flames pulse - in turn standing upright and still due to their size before partially dying out then leaning forward again to spread in a pulsing pattern. Under stronger wind conditions however, the flame of the drier shrub will also propagate forward in the same way, but as it produces a greater convective burst it will also lead to a faster spreading fire.

This phenomenon which may be called *flame angle feedback* is illustrated in figure 6 for a hypothetical heathland modelled with Z11 under two different moisture treatments where LFMC is equal to 80% in one, and doubled to 160% in the other. Rates of spread (ROS) are initially faster in the moist plants than the dry ones, but as wind speeds increase, fire spreads faster in the dry heath.

This is an important aspect that must be factored into experimental design, as the failure to conduct experiments under conditions that will accommodate this feedback can result in weak or erroneous conclusions. Figure 7 illustrates this by examining the correlation between LFMC and ROS for the two scenarios. If experiments in this heath were conducted with winds that did not exceed about 20km/h, it may be concluded that fires spread faster in more moist heaths. It may in fact require experimental burns in wind speeds significantly greater than this threshold speed before any robust correlation can be found. As operational issues frequently preclude burning under such conditions it may be impossible to provide an empirical answer for this situation, however it should be noted that this threshold is specific only to this scenario and others will apply under different slopes, with different species, plant sizes and spacing.

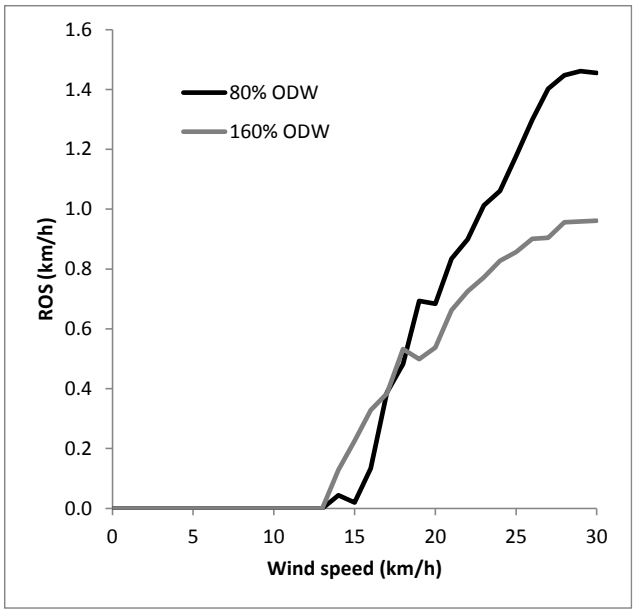

Figure 6. Fire Rate of Spread in two hypothetical heathlands modelled using Z11. Lateral spread initiates under lower wind conditions for the more moist plants, but once initiated, fire spreads faster in the drier plants.

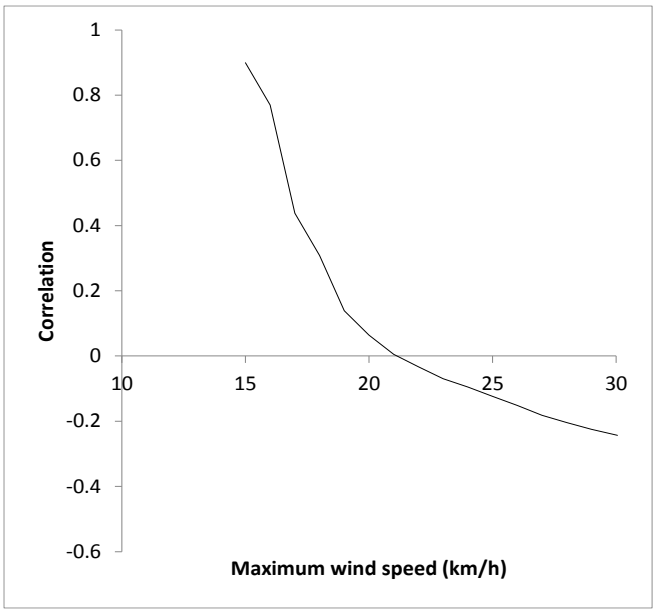

Figure 7. Correlation of ROS with LFMC for the two scenarios in Figure 6. The x-axis indicates the maximum wind speed considered for analysis so that if only fires burning under wind speeds of 20km/h or less are considered, the correlation is positive (i.e. fire spreads faster in more moist fuels). Consideration of higher wind speeds however produces a negative correlation.

Table 3. Summary data from Table 1 in Alexander and Cruz (2013)

Wind speed (km/h)	LFMC (% ODW	ROS (m/min)	Flame height (m)
23	135	16.8	19.8
15	100	10.8	14.8
19	95	27.4	30.5

This relationship is evident in one of the examples reported in Alexander and Cruz (2013), where the results from published fires are summarised in Table 3. As the LFMC is reduced from 135% to 100% the ROS declines along with the flame height, but when the wind speed is increased for a second dry scenario, the ROS and flame height increase to well beyond the value in moist fuels, even though the wind speed remains lower than in this example. Assuming that all other factors are constant, this is exactly the pattern that may be expected if the wind speeds lie across a threshold.

Flame angle feedback becomes more complex when more plant strata are considered, as more vertical gaps between fuels are introduced in the process. High wind speeds may have the effect of tilting the flame so far that crown fire does not initiate (e.g. Luke and McArthur 1978; Buckley 1990) and the fire slows down, or if tilting further forward in a dense shrub layer the greater flame length produced may initiate a crown fire. The response will vary depending again on the flammability, size and density of plants, on the degree of protection from wind provided by the higher strata, and on the vertical gap sizes.

As the length of flame from burning plants relates to the depth of foliage and therefore the number of leaves or quantity of fuels burning, the shape of plant crowns can have an important effect on flame dimensions. In general, the largest flames are produced when the angle of the flame intersects the plant crown at its longest axis, igniting the most leaves. Tall narrow plants will therefore produce the largest flames when the flame angle is close to vertical, so if the leaves are moist and the flame is more easily tilted by wind, the effects of moisture in reducing flame length will be accentuated. Conversely, if the plant is wider than it is tall, smaller initial flames from moist leaves may ultimately ignite more of the plant if directed forward. These effects may however be obscured if plants are in close enough proximity to allow forward spread, as the shape of individual plants will become irrelevant.

Discussion

A fundamental tenet of complex systems theory is that such systems are self-organised (Bak *et al.* 1988); that is, behaviours emerge from many interactions and cannot be predicted from initial trends. While broad trends may be identified, specific predictions cannot be made from these alone and the interactions of the various agents must be modelled. Increasing greenhouse gas concentrations warm the planet for example, but the mean temperature of an upcoming season will not be well predicted without knowledge of factors such as the circulation of heat within the system via the Southern Oscillation Index. The interactions of multiple agents can confound individual predictions, so that even though CO_2 levels increase, global temperatures fall for a short period and even though leaves in a forest become drier, fires under some conditions burn with smaller flames and spread more slowly. The presence of feedbacks and threshold changes (also known as criticality or tipping-points) are part of such systems and do not negate the importance of individual factors.

Modelling of fire behaviour as a complex system suggests that the quantity of moisture in plant leaves is an important influence on the behaviour of wildland fires. The scale and direction of its influence will vary markedly with the conditions, the species and the structure of the fuels burning, but the overall effect is that drier plants produce larger, faster fires.

The apparent influence of LFMC on fire behaviour becomes less discernable as fuel arrays increase in complexity - as expected if the system is self-organised. While Zylstra (2011) showed that the evaporation of water explained 90% of the variability in time to ignition for individual leaves and the

effect of LFMC was discernable in lab experiments with model shrubs etc; field experiments involving more complex fuel arrays have found little correlation. The larger heat fluxes and temperatures involved fail to explain this; however the feedbacks and threshold changes that can be expected from bottom-up simulation of the processes can provide viable answers for these apparent anomalies.
Attempts to quantify the effect of LFMC empirically therefore must be designed around the location of thresholds and account for the influence of feedbacks; although this will not always be possible due to operational constraints. The most vital component of this is that fires are examined across a broad coverage of wind speeds, with less wind required when burning up steeper slopes.
Where adequate studies cannot be carried out for certain fuel arrays, Alexander and Cruz (2013) propose that appropriate physics-based models can be employed to resolve issues. It will be critical that such models are capable of capturing the complexity described here. The Z11 or Forest Flammability Model used in this study is currently undergoing software development and validation through the Centre for Environmental Risk Management of Bushfires at the University of Wollongong.

References

Alexander ME, Cruz MG (2013) Assessing the effect of foliar moisture on the spread rate of crown fires. *Int J Wildl Fire* **22**, 415–427.

Anderson HE (1970) Forest fuel ignitability. *Fire Technol* **6**, 312–322.

Bak P, Tang C, Wiesenfeld K (1988) Self organised criticality. *Phys Rev A* **38**(1), 364–374.

Buckley A (1990) Fire behaviour and fuel reduction burning - Bemm River wildfire, October 1988. Research Report No. 28.

Butler BW (2010) Characterization of convective heating in full scale wildland fires. InViegas DX (ed) "VI Int. Conf. For. Fire Res.," P CD–ROM

Caccamo G, Chisholm LA, Bradstock RA, Puotinen MLA (2012) Using remotely-sensed fuel connectivity patterns as a tool for fire danger monitoring. *Geophys Res Lett* **39**(1), . doi:10.1029/2011GL050125.

Chuvieco E, González I, Verdú F, Aguado IA, Yebra M (2009) Prediction of fire occurrence from live fuel moisture content measurements in a Mediterranean ecosystem. *Int J Wildl Fire* **18**, 430–441.

Cruz MG, Butler BW, Alexander ME, Forthofer JM, Wakimoto RH (2006) Predicting the ignition of crown fuels above a spreading surface fire. Part I: model idealization. *Int J Wildl Fire* **15**(1), 47–60. doi:10.1071/WF04061.

Davies GM, Legg CJ, Smith AA, MacDonald AJ (2009) Rate of spread of fires in Calluna vulgaris - dominated moorlands. *J Appl Ecol* **46**(5), 1054–1063. doi:10.1111/j.1365-2664.2009.01681.x.

Dennison PE, Moritz MA (2009) Critical live fuel moisture in chaparral ecosystems: a threshold for fire activity and its relationship to antecedent precipitation. *Int J Wildl Fire* **18**(8), 1021–1027. doi:10.1071/WF08055.

Engstrom JD, Butler JK, Smith SG, Baxter LL, Fletcher TH (2004) Ignition behavior of live california chaparral leaves. *Combust Sci Technol* **176**, 1577–1591.

Fernandes PM, Cruz MG (2012) Plant flammability experiments offer limited insight into vegetation – fire dynamics interactions. *New Phytol* **194**(3), 606–609. doi:10.1111/j.1469-8137.2012.04065.x.

Fletcher TH, Pickett BM, Smith SG, Spittle GS, Woodhouse M, Haake E, Weise DR (2007) Effects of moisture on ignition behaviour of moist california Chaparral and Utah leaves. *Combust Sci Technol* **179**, 1183–1203. doi:10.1080/00102200601015574.

Gaydon AG, Wolfhard HG (1979) "Flames: their structure, radiation and temperature." (John Wiley and Sons: New York)

Gill AM, Zylstra P (2005) Flammability of Australian forests. *Aust For* **68**(2), 87–93.

Hamins A, Bundy M, Dillon SE (2005) Characterization of candle flames. *Fire Prot Eng* **15**, 265–285. doi:10.1177/1042391505053163.

Luke RH, McArthur AG (1978) "Bushfires in Australia." (Australian Government Publishing Service: Canberra, ACT)

Madrigal J, Marino E, Guijarro M, Hernando C, Díez C (2011) Evaluation of the flammability of gorse (Ulex europaeus L.) managed by prescribed burning. *Ann For Sci* **69**(3), 387–397. doi:10.1007/s13595-011-0165-0.

Pérez-Harguindeguy N, Díaz S, Garnier E, Lavorel S, Poorter H, Jaureguiberry P, Cornwell WK, Craine JM, Gurvich DE, Urcelay C, Veneklaas EJ, Reich PB, Poorter L, Wright IJ, Ray P, Enrico L, Pausas JGH, Vos AC De, Buchmann N, Funes G, Hodgson JG, Thompson K, Morgan HD, Steege H, Heijden MGA Van Der, Sack L, Blonder B, Poschlod P, Vaieretti M V, Conti G, Staver AC, Aquino S, Cornelissen JHC (2013) New handbook for standardised measurement of plant functional traits worldwide. *Aust J Bot* **61**, 167–234.

Philpot CW (1970) Influence of mineral content on the pyrolysis of plant materials. *For Sci* **16**(4), 461–471.

Pickett BM, Isackson C, Wunder R, Fletcher TH, Butler BW, Weise DR (2010) Experimental measurements during combustion of moist individual foliage samples. *Int J Wildl Fire* **19**, 153–162.

Plucinski MP, Anderson WR, Bradstock RA, Gill AM (2010) The initiation of fire spread in shrubland fuels recreated in the laboratory. *Int J Wildl Fire* **19**(4), 512–520. doi:10.1071/WF09038.

Schoenberg FP, Peng R, Huang Z, Rundel P (2003) Detection of non-linearities in the dependence of burn area on fuel age and climatic variables. *Int J Wildl Fire* **12**(1), 1–6. doi:10.1071/WF02053.

Silvani X, Morandini F (2009) Fire spread experiments in the field: Temperature and heat fluxes measurements. *Fire Saf J* **44**(2), 279–285. doi:10.1016/j.firesaf.2008.06.004.

Weber RO, Gill AM, Lyons PRA, Moore PHR, Bradstock RA, Mercer GN (1995) Modelling wildland fire temperatures. *CALMScience Suppl* **4**, 23–26.

Weise DR, White RH, Beall FC, Etlinger M (2005) Use of the cone calorimeter to detect seasonal differences in selected combustion characteristics of ornamental vegetation. *Int J Wildl Fire* **14**, 321–338.

Weise DR, Zhou X, Sun L, Mahalingam S (2005) Fire spread in chaparral —" go or no-go ?" *Int J Wildl Fire* **14**, 99–106.

Xanthopoulos G (1990) Development of a wildland crown fire initiation model. University of Montana, Missoula.

Xanthopoulos G, Wakimoto RH (1993) Time to ignition - temperature - moisture relationship for branches of three western conifers. *Can J For Res* **23**(2), 253–258.

Yebra M, Dennison PE, Chuvieco E, Riaño D, Zylstra P, Hunt ER, Danson FM, Qi Y, Jurdao S (2013) A global review of remote sensing of live fuel moisture content for fire danger assessment: Moving towards operational products. *Remote Sens Environ* **136**, 455–468. doi:10.1016/j.rse.2013.05.029.

Zylstra P (2011) Forest Flammability: Modelling and Managing a Complex System. PhD Thesis, University of NSW, Australian Defence Force Academy. http://handle.unsw.edu.au/1959.4/51656.

Map partitioning to accelerate wind field calculation for forest fire propagation prediction

Gemma Sanjuan, Carlos Brun, Tomàs Margalef, Ana Cortés

Escola d'Enginyeria, Universitat Autònoma de Barcelona, 08193 Cerdanyola, Spain
gemma.sanjuan@uab.es, carlos.brun@uab.es, tomas.margalef@uab.es, ana.cortes@uab.es

Abstract
Forest fire is significantly affected by wind. However, meteorological wind is modified by terrain topography in such a way that a different value of wind speed and direction is given on every point. To estimate forest fire propagation on such conditions it is necessary to couple a wind field model to the forest fire propagation model. These models are time consuming from the computational point of view and may be parallelised to make them feasible in an operational scenario. So, a map partitioning has been applied to accelerate wind field calculation. The results show that the wind field and the forest fire propagation prediction are not significantly affected by map partitioning and the time to reach the forest fire prediction is significantly reduced.

***Keywords**: Wind field, map partitioning, data parallelism, forest fire propagation prediction*

Introduction

Forest fire propagation prediction is a difficult task due to the amount of variables that take part in the process, the complexity to develop a computational model that faithfully describe the real phenomenon and the lack of accuracy in certain environmental measurements or terrain features. Therefore, despite there exists several fire spread simulators [1][2][3], the results are still far from real behaviour. To overcome such difficulty a Two-Stage prediction strategy [4][5] was developed to improve the quality of input parameters. In the first stage a Genetic Algorithm (GA) is used to determine the values of the parameters that best reproduce the fire propagation during an observation interval. GAs work in an iterative way where at each iteration a set of individuals (representing fire scenarios) are executed, the provided results are compared to the actual fire propagation to rank them and the genetic operators are applied to determine the next generation. At the end of the iterative process, the best individual is used in the second stage to predict the fire propagation in the next time interval. In this work FARSITE [2] is used as forest fire propagation simulator.
However, certain parameters, such as wind, present a spatial distribution or variation along the terrain due to topographic effects. The wind provided by a global weather forecast model or measured at a meteorological station in some particular point is modified by the topography of the terrain and has a different value at each point of the terrain. Therefore, a single value does not represent the wind in each point of the terrain. To estimate the wind speed and direction at each point of the terrain it is necessary to apply a wind field model that determines those values at each point depending on the terrain topography [6].
When coupling wind field and forest fire propagation models, each individual consists of executing two computing demanding simulations in a pipeline way. First, a wind field model must be executed to provide a high resolution wind field adapted to the underlying topography. The output provided by this wind field model will be fitted into a forest fire spread simulator to generate the fire front evolution Figure 1).

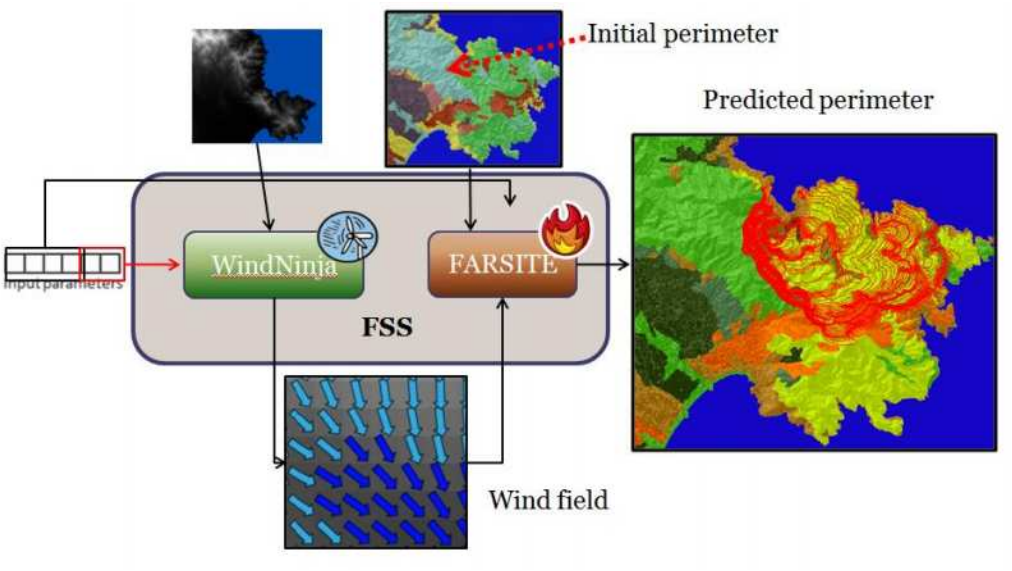

Figure 1 –Coupling Model

WindNinja and map partitioning

WindNinja [7] is a wind field simulator that calculates the effect of topography on wind flow and provides the wind speed and direction at each point of the terrain given a meteorological wind value (Figure 2). The main problem is that, when the map has a considerable size (30x30 Km) and the resolution is high (30x30m), it requires an unaffordable execution time and a huge amount of memory that may not be available on a single computational node. Such limitations make impractical the effective prediction of fire spread with accurate wind field. Moreover, the amount of memory required to solve the wind field increases linearly with the number of cells of the map making unaffordable to be solved a map with a large number of cells in a single node. It means that calculating the wind field of a 1500x1500 cells map on a single node with 4GB of main memory fails and no output is delivered. Therefore, it is necessary to apply some parallelization technique to reduce execution time and memory requirements.

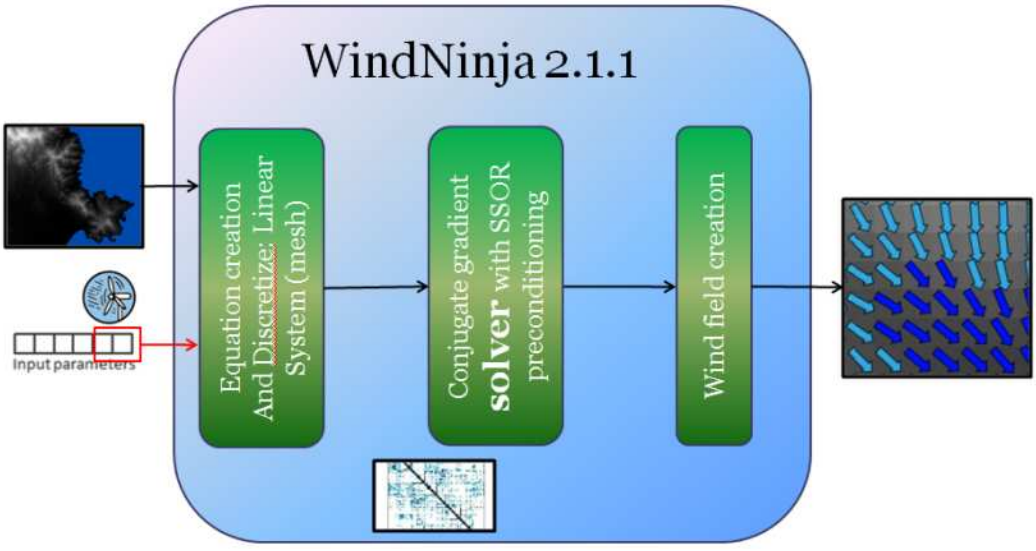

Figure 2 –WindNinja

To reduce the computation time of the wind field calculation a map partitioning method (Figure 3) has been applied to benefit from the parallel architectures. In this case the wind field is calculated in parallel on each part of the map and then the wind fields of the different parts are joined to form the global wind field. Furthermore, by partitioning the terrain map, the data structures necessary to calculate the wind field in each part are reduced significantly and can be stored in the memory of a single node in a current parallel system. Therefore, the existing nodes can perform computation in parallel with data that fit the capacity of the memory on each node.
However, wind field calculation is a complex problem that has certain boundary effects. So, the wind speed and direction in the points close to the boundary of each part may have some variability and differ from those they would have obtained if they were far from the boundary, for example if the wind field is calculated over a single complete map. To solve this problem, it is necessary to include a certain amount of overlapping among the map parts. So, there is a margin from the beginning of each part and the part cells itself. The overall wind field aggregation is obtained by discarding the calculated margin fields overlap of each part. The inclusion of an overlapping to each part increases the execution time, but the variation in the wind field is reduced significantly [8]. This map partitioning approach can easily be implemented in a Master/Worker MPI application where the Master creates the map parts and distributes them to the workers, the workers calculate the wind field for each part and return the results to the Master that aggregates the wind fields in a complete wind field. Once the map partitioning scheme has been applied, the resulting wind field map has the same dimensions as the original one.

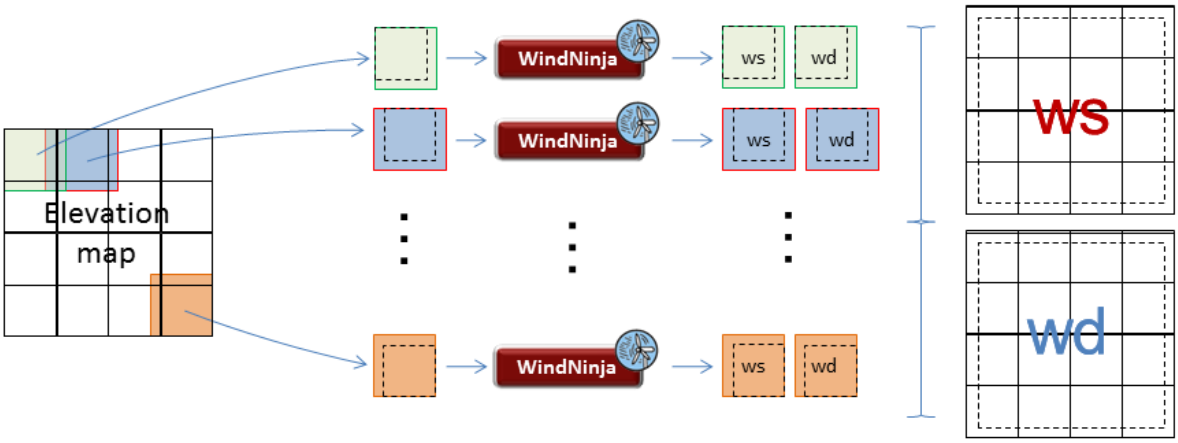

Figure 3. Map partitioning

The methodology has been tested with several terrain maps, and it was found that parts of 400x400 cells with an overlap of 50 cells (table 1) per side provides a reasonable execution time (120 sec) with virtually no variation with respect to the wind field obtained with a global map. With this type of partitioning, each process solves an effective part of a map of 300x300 cells. The inclusion of a wind field should improve the accuracy of forest fire propagation prediction, but it is necessary to test the effect of map partitioning on forest fire propagation prediction.

Table 1- Similarity indexes for different partitioning

Speed (mph)	Partitioning	RSMESp (mph)	Speed >1 (mph)	MaxSp (mph)	RSMEAng (^{0})
5	6x6	0.191	8183	3.76	1.703
5	5x5	0.187	7818	3.76	1.571
5	4x4	0.188	7531	3.76	1.701
10	6x6	0.383	60920	7.50	1.703
10	5x5	0.373	49565	7.50	1.571
10	4x4	0.375	49182	7.50	1.701
15	6x6	0.574	156479	11.3	1.703
15	5x5	0.559	140826	11.3	1.571
15	4x4	0.563	140196	11.3	1.701

Effect of map partitioning on forest fire spread prediction

As it has been stated in previous section map partitioning does not generate extreme differences in wind fields, but it necessary to analyse the influence of such differences in forest fire spread prediction. To carry out such analysis it is necessary to execute a lot of propagation simulations considering maps with different topography terrains, different wind conditions, different vegetation types, different canopy covert and different fire positions. So, different terrain maps corresponding different areas of Spain has been selected. The raster maps used are composed by 1500 rows and 1500 columns with 30m resolution per cell. That means that the map has a dimension of 45km x 45km.
Tables 2 show the difference on burned areas for different types of vegetation (brush, grass, conifer and rough) and different map partitioning considering a meteorological wind of 15mph and a direction of 45º. This meteorological wind has been considered because it is the winds that generate larger differences in wind field. For each configuration, the evolution had shown in the time 24h. In particular, fire rows shows the results considering fire ignition points over terrain zones with a wind speed difference larger than 1mph, shows the results considering fire ignition points near the terrain point with differences larger than 1mph (it means that at some point of the propagation the fire front crosses that zones) and third rows shows the results considering fire ignition points far from those different wind speed zones (it means that the fire front does not cross those zones).

Table 2- Difference for ignition point from different wind zones.

	5x5				15x15			
	Brush	**Conifer**	**Grass**	**Rough**	**Brush**	**Conifer**	**Grass**	**Rough**
Over	0.080	0.213	0.103	0.240	0.114	0.353	0.128	0.420
Near	0.063	0.035	0.072	0.051	0.073	0.047	0.096	0.069
Far	0.037	0.028	0.025	0.013	0.038	0.030	0.040	0.014

From the experiments carried out it can be observed that as the number of parts is increased, the error increases proportionally to that number of parts. This is due to the fact that the wind field generated when the parts are very small has a larger difference from the global map wind field and this larger differences provoke larger differences in fire spread predicted area.
On the other hand, it can be observed, as it was expected, that the position of the fire is very significant. If the fire does not cross points with significant wind speed difference the spread area difference is negligible. When the fire ignition point is on large wind speed difference zones the difference in burned area is larger, but not extremely different. These results are also presented in figures 4 that present an example of each one of the ignition point situation. In these figures the blue dots represent the zones with large wind speed difference, the yellow perimeter represents the Global Map Wind Field fire propagation, the red one represents the partitioning 5x5 map wind field fire propagation and the green

one the partition 15x15 map wind field fire propagation. In figure 4c it can be observed that there is no appreciable difference among the three perimeters. However, figures 4a and 4b show a small difference that is increased when the partitioning divides the map in more parts.
It must be considered that the show results were obtained considering that the fire only cross a large difference zone, but if there are several of such large difference zones on the fire area, differences in fire propagation prediction will be larger since the effects are accumulative.

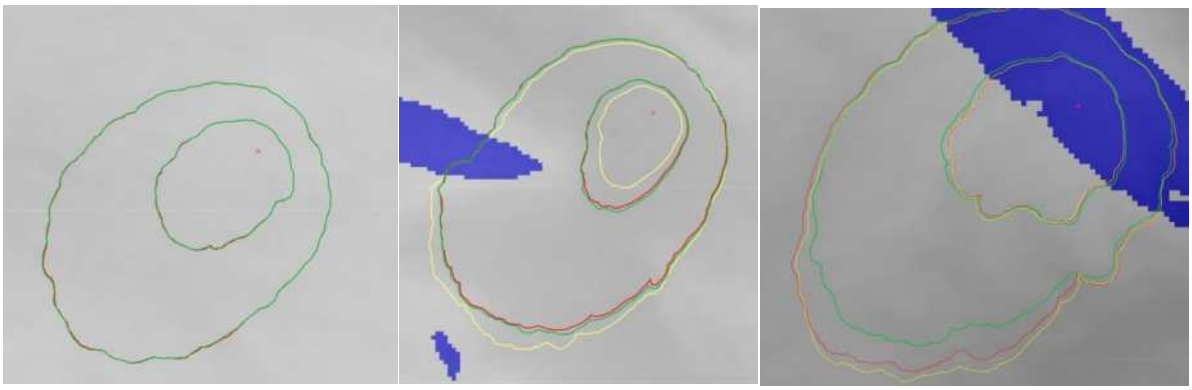

Figure 4 –Propagation Fire

Study case: La jonquera 2012

This analysis was carried out using as study case the fire that occurred in La Jonquera (Catalonia, Spain) in July 2012. In this case, the two-stage methodology has been applied considering 25 individuals per population and iterated for 10 generations. Since the Genetic Algorithm has a stochastic component the experiments have been repeated 3 times using different starting populations. For each case 4 fire fronts are compared:

- The real fire propagation.
- The predicted fire front obtained by considering a homogenous wind value along the whole terrain.
- The predicted fire front obtained by introducing a wind field calculated considering a complete map (1500x1500 cells).
- The predicted fire front obtained by introducing a wind field calculated by map partitioning (5x5 parts of 300x300 cells with 50 cells of overlap on each direction).

The results considered to determine the correctness of the approach are the following ones:

- The RMSE (Root Mean Square Error) estimates the difference among the wind speed (and direction) on each point of the terrain. The Root-Mean-Square Error (RMSE) is shown in equation 1. More precisely, for each map cell (N), the value of wind speed in that particular cell i obtained when no partition is applied to the input DEM map (NP_{ws_i}) is compared to the speed obtained in the same cell when applying the map partitioning strategy with a given partition scheme (SC_{AXBws_i}). The same procedure is also applied to wind direction just changing the corresponding terms of equation 1 to wd.

$$RMSE_{AxB}(ws) = \sqrt{\frac{\sum_{i=0}^{N}(NP_{(ws)_i} - SC_{AxB(ws)_i})^2}{N}} \quad (1)$$

- The Symmetric difference among the real fire perimeter and the fire front obtained by taking into account the three wind field schemes (homogeneous, complete map wind field and map partitioned field). This equation calculates the difference in the number of cells burnt between the predicted area by 2 different WindNinja configurations. In this case, the area predicted using a global map wind field (GMWF) is used as reference propagation. Formally, this equation corresponds to the symmetric difference between the global map wind field area (GMWF) and the partitioned map divided by the GMWF area, so as to express a proportion. ∪(GMCell,PCell) is the union of the number of cells burned in the GMWF and the cells burned in the partitioned map, ∩(GMCell,PCell) is the intersection between the number of cells burned in the GMWF propagation and in the partitioned map wind field, and GMCell is the number of cells burned using Global map wind field.

$$D = \frac{\cup\,(GMCell, PCell) - \cap\,(GMCell, PCell)}{GMCell} \quad (2)$$

- The execution time considering the complete 2 stage process.

4.1. Experimental results

Table 3 summarizes the results. It shows the wind speed RMSE and the prediction error and prediction times for each wind field scheme (homogenous wind, complete map wind field and partition map wind field) considering three initial population. It can be observed that the differences between the wind fields (RMSE) are very small and, on the other hand, the introduction of a wind field improves the quality of the prediction significantly. Comparing the homogenous wind propagation against the complete map wind field propagation the error is reduced between 20% and 35%. When comparing the homogeneous wind propagation against the partition map wind field propagation the error is reduced between 16% and 33%. This means that the map partitioning does not modify the fire propagation prediction significantly. However, the execution time of the two-stage process shows that the execution time to reach a prediction is significantly reduced when applying a map partitioning strategy. The time reduction varies between 47% and 70% which means a significant time saving.

	RSMSE (mph)	**Homogeneous Wind**		**Complete map Wind Field**		**Partition map Wind Field**	
		Pred. Error	**Exec. Time (s)**	**Pred. Error**	**Exec. Time (s)**	**Pred. Error**	**Exec. Time (s)**
Pop. 1	0.14	0.74	255	0.59	967	0.62	295
Pop. 2	0.12	0.53	700	0.42	1407	0.35	739
Pop. 3	0.16	0.42	491	0.28	1195	0.33	530

Table 3.- Comparison of wind field schemes

The four fire perimeters for population 1 are shown in figure 2. The green perimeter represents the real fire propagation, the yellow one represents the homogenous wind fire propagation prediction, the red one represents the complete map wind field fire propagation prediction and the blue one the partition map wind field fire propagation.

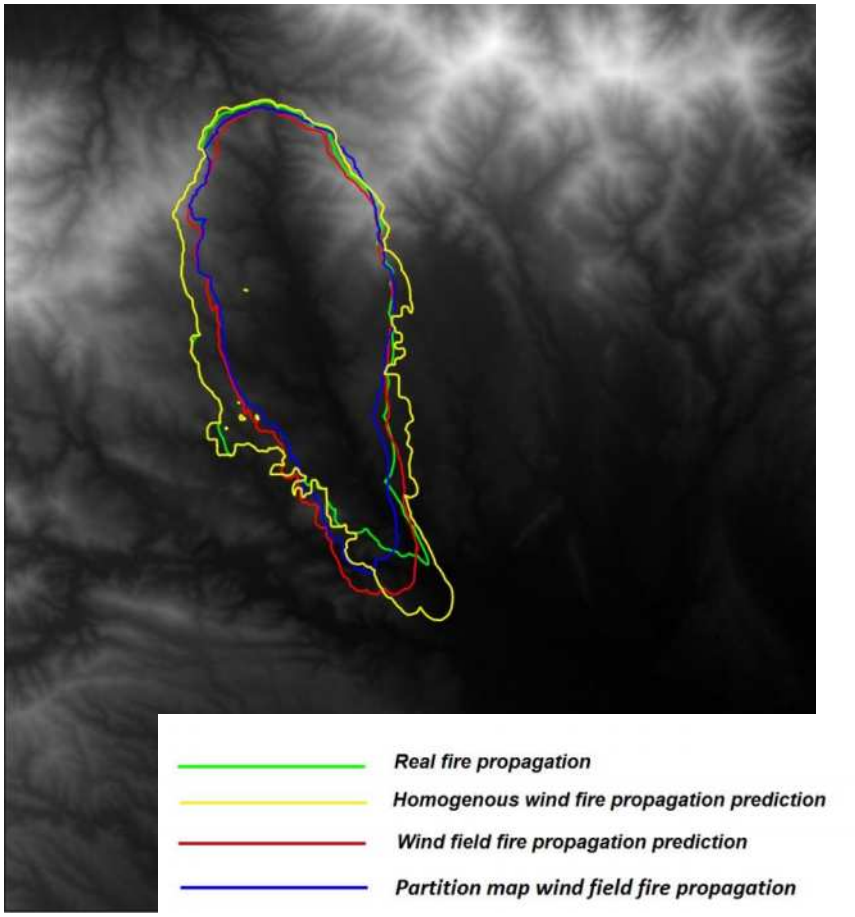

Figure 5. Real and predicted fire perimeters

Conclusions

Coupling wind field and forest fire propagation models is a promising approach to improve forest fire propagation prediction. However, such coupling demands high computing capabilities and takes long execution time. To overcome such difficulties a map partitioning approach has been defined to parallelise wind field calculation and reduce execution time. The results on synthetic and real fires show that the wind field and forest fire propagation prediction are not significantly affected by map partitioning and the parallelisation is effective.

Acknowledgement

This work has been supported by Ministerio de Ciencia e Innovacion under contract TIN-2011-28689-C02-01

References

[1] Hansen-Tansen, Ernst, and Tore Baunan. "Fire Risk Assessment by Stimulation—Firesim." Fire Safety Journal 5.3 (1983): 205-212.

[2] Finney, Mark Arnold. FARSITE, Fire Area Simulator--model development and evaluation. US Department of Agriculture, Forest Service, Rocky Mountain Research Station, 2004.

[3] Lopes, A. M. G., M. G. Cruz, and D. X. Viegas. "< i> FireStation</i>—an integrated software system for the numerical simulation of fire spread on complex topography." Environmental Modelling & Software 17.3 (2002): 269-285.
[4] Abdalhaq, Baker, et al. "Enhancing wildland fire prediction on cluster systems applying evolutionary optimization techniques." Future Generation Computer Systems 21.1 (2005): 61-67.
[5] Cencerrado, Andrés, Ana Cortés, and Tomàs Margalef. "Applying Probability Theory for the Quality Assessment of a Wildfire Spread Prediction Framework Based on Genetic Algorithms." The Scientific World Journal 2013 (2013).
[6] Brun, Carlos, Tomàs Margalef, and Ana Cortés. "Coupling Diagnostic and Prognostic Models to a Dynamic Data Driven Forest Fire Spread Prediction System." Procedia Computer Science 18 (2013): 1851-1860.
[7] Forthofer, Jason, Kyle Shannon, and Bret Butler. "4.4 Simulating Diurnally Driven Slope Winds with WindNinja." (2009).
[8] Sanjuan, G., Brun, C., Margalef, T., Cortés, A. “Wind field uncertainty in forest fire propagation prediction”,Procedia Computer Science29 (2014): 1535-1545.

Model reduction approach for wildfire multi-scenario analysis

Elisa Guelpa[a], Adriano Sciacovelli[b], Vittorio Verda[c], Davide Ascoli[d]

[a] *Energy Department, Politecnico di Torino, C.so Duca degli Abruzzi 24, 10129 Torino, Italy, elisa.guelpa@polito.it*
[b] *Energy Department, Politecnico di Torino, C.so Duca degli Abruzzi 24, 10129 Torino, Italy, adriano.sciacovelli@polito.it*
[b] *Energy Department, Politecnico di Torino, C.so Duca degli Abruzzi 24, 10129 Torino, Italy, vittorio.verda@polito.it*
[d] *Dipartimento di Scienze Agrarie, Forestali e Alimentari, Università degli Studi di Torino, Via da Vinci 44, 10095 Grugliasco (TO), Italy, d.ascoli@unito.it*

Abstract
Wildfire models have been widely applied to the prediction of fire front evolution, in order to obtain useful information for evacuation plans and fire management. A major difficulty in treating wildland fires is related to the complexity of the phenomena that are involved. In addition, it is difficult to obtain accurate input data for the models, especially in the case of on-going fire events. In fact, wind and weather data, available from meteorological stations, fuel characteristics and orographic characteristics data are often inaccurate. Furthermore, some of these data may change during the fire event, so a prediction is necessary. Results obtained from models are therefore affected by errors. Probabilistic approaches are useful in order to overcome some of these problems, but this requires the use of suitable models in order to perform large number of simulations. Over the last decades, empirical and physical based models have been proposed. Physical based models provide detailed results but requires higher computational cost than empirical models. In order to use physical based models for risk analysis and multi-scenario analysis it is necessary to reduce their computational time, which can be achieved through model reduction techniques.
In this paper, Proper Orthogonal Decomposition technique (POD) is applied to the reduction of a physical model. A simple one-dimensional physical model has been selected in order to test the approach. This model is based on conservation equations and it is built by setting some of the parameters through empirical data collected during field fire experiments. In this first work, slope and wind contribution are not considered. POD permits to extract the spatial basis of the problem and capture the main features of the system with reduced requirement of computational resources. A comparison shows that the results of the reduced model are close to that of the full model, but the computational time for solving the energy equation is reduced to about 10% of that required by the full model.

Keywords*: wildfire, reduced model, Proper Orthogonal Decomposition, fast physical model*

Introduction

Wildfires are complex natural phenomena that threaten both human lives and infrastructures and that have caused various disasters in the last years. Wildfire are particularly destructive and difficult to manage if proper and effective fire fighting actions are not taken in time. For this reason the prediction of wildfire evolution and propagation plays a key role and can greatly help in increasing the efficiency of fire-fighting operations. In the last decades several mathematical models have been developed to study the behavior of wildfires. The models available in the literature can be divided in three groups: theoretical, empirical and semi-empirical (Pastor *et al.* 2003). Theoretical model are also called physics-based model (Mell *et al.* 2007). In the literature various software based on physical models exist, including FIRESTAR, FIRETEC, FIRELES, WFDS (Morvan 2011). Physical models of wildfires are based on the conservation equations that describe mass momentum and energy conservation, radiative heat transfer, reaction and diffusion. Such an approach leads to complex

mathematical models involving a system of coupled, non-linear partial differential equations. As a consequence, the prediction of wildfire propagation through physical models require large computational times and relevant hardware resources (Sullivan 2009). Furthermore, wildfire modeling involves large computational domains and a wide range of time scales which makes physical models not suitable as operational tools for real-time calculations. Empirical models are developed correlating experimental data while semi-empirical model are based on energy conservation but do not distinguish the different modes of heat transfer (Mell *et al.* 2007). Typical examples of empirical models are those one proposed by Rothermel (1972) and McArthur (1965) which have been largely employed because of their simple mathematical structure and the capability of predicting key quantities such as the rate of spread (ROS). Empirical models are typically algebraic and very cheap from a computational point of view. For these reasons they represent a valuable operational tool (Mandela *et al.* 2012). However, empirical models treats the interaction between the physical phenomena in a oversimplified manner. This is the case, for example, of wind-wildfire interaction which is often predetermined and does not account of buoyancy and turbulence fluctuations. Furthermore, empirical models cannot predict key local quantities in a wildfire, such as temperature and heat flux. Empirical models are widely used in order to predict the fire spread because they give predictions with a computational cost that is lower and lower than the event evolution. On the other hand these models in some condition are not able to give accurate results.
In this framework, with the aim to reduce the computational cost of physical models, in this paper an approach of modeling based on proper orthogonal decomposition (POD) has been proposed. It is the first time that POD is applied to a wildfire prediction model. Here a one dimensional model for the investigation of fire propagation over a flat ground is proposed. The model is calibrated using a set of experimental measurements gathered during field fire experiments. Then, POD technique is introduced to derive a reduced order model that allows to investigate the fire phenomenon with a reduced computational effort. Finally, the capabilities of the POD model are assessed and a parametric analysis is carried out. To summarize this paper constitute the first work on the use of model order reduction technique for wildfire analysis.

Experiments and Models description

2.1. Collection of experimental data

Fire behaviour was assessed in four field fire experiments (Figure 1) in North-West Italy (Ascoli *et al.* 2013) carried out on a flat terrain in grassland fuels dominated by *Moliniaarundinacea* Shrank. Fire experiments were conducted under moderate weather at one burnday in 2009 during the winter dry season when grass fuel is fully cured.
Fuel characteristics were measured in all fire experiment sites before burning. At each site, fuels were harvested in six 1 m^2 quadrates and dried in the laboratory to determine the fuel load. Fuels were entirely constituted by dead (fully cured grasses) fine fuels (< 6 mm in diameter). Fuel bed depth and cover were measured every 0.5 m along six linear transects (length =10 m) at each fire site. Flammability parameters (surface area to volume ratio, moisture of extinction, heat content) were derived from published values for similar grass fuels (FCCS Inferred variables)[1].Fuel cover was 100% at all sites while mean fuel bed depth was 14 cm. Fuel load and bulk density ranged between 4.29to 5.50 t ha^{-1}, and 2.2 to 7.1 kg/m^3, respectively. Dead fine fuel moisture was assessed at the time of each fire experiment by collecting five samples of grass leaves (50 g of fresh weight each). Fresh samples were weighed in the field using a portable scale, and then dried in laboratory. Fuel moisture (dry weight basis) ranged between 11-19%. In order to let the fire front reach a pseudo-steady state, each fire

[1]http://www.fs.fed.us/pnw/fera/fccs/inferred_variables/table2_metric/table2_metric.htm

experiment was ignited upwind by line ignitions of 25 m in length, and the fire was allowed to spread for 50 m before being suppressed along a fuel break. During each experiment, fire behaviour was assessed at a microplot scale (Fernandes *et al.* 2001; Vacchiano *et al*. 2014) by measuring the arrival time of the fire front at the vertices of a triangle and computing the rate of spread according to the trigonometric method of Simard *et al*. (1984). At each fire experiment site, 8 equilateral triangles (10 m side) were visualized using 2 m rods placed at each triangle vertex. The time of arrival of the fire front was measured using K-Type thermocouples (0.4 mm in diameter) positioned at each triangle vertex within the grass fuel few centimeters above the soil (< 10 cm) and connected to a data-logger buried one meter apart. This allowed to measure flame temperature every second during all combustion phases. Flame height was assessed by four observers which used as a reference scale the increment markers painted on each rod (0.5 m).
Air temperature and moisture, and wind speed and direction were assessed every 30 seconds by two weather stations positioned at a height of 2 m upwind to the experimental plot, so as to couple weather data to fire behaviour observations. In a few cases, marked changes in wind direction occurred during the burn. However, the microplot approach allowed to identify backfire, flank fire and head fire phases. Time since last rain was 19 days, air temperature and moisture, and wind speed ranged between20 to 27%, 19 to 25°C, and 2.8 to 7.1 km h^{-1}, respectively.

Figure 1. Field fire experiment

In total, 32 rate of spread observations and 32 time-temperature profiles were collected, each associated with fuel characteristics (load; bulk density; moisture), environmental conditions (slope; wind speed) fire behaviour (rate of spread; back, flank or head fire phase) and effects (fuel consumption). Rate of spread ranged between 0.8 to 14.2 m min^{-1}. Only observations corresponding with negligible wind velocity and in flat ground have been considered for the model development. Fuel consumption was assessed soon after the fire by collecting remaining charred fuels in six 1 m^2 quadrats and ranged between 75 and 90% of the pre-fire mean fuel load. Maximum flame temperature ranged between 244°C and 733°C. Average residence time above 60°C and 300°C were 183 and 21 seconds, respectively.

Model description

In this paper a one-dimensional model was developed in order to investigate the fire propagation in a grass-shrub flat and the corresponding temperature time evolution. The computational domain considered is the one described in the previous section. The fire front evolves in the domain where four thermocouples (T1, T2, T3, T4) are located, after 10 m, 20 m, 30 m, 40 m from the ignition point. The four zones between the thermocouples will be later on called section A,B,C,D.

In order to show a better description of the domain, a schematic is reported in Figure 2.

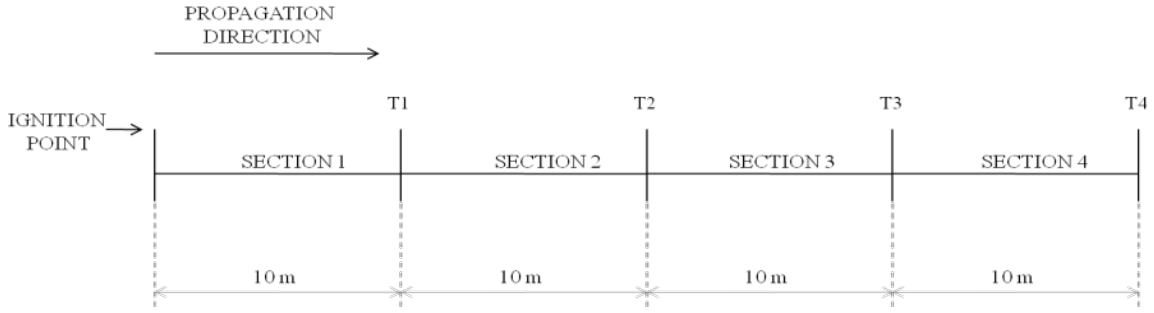

Figure 2. Experimental and model domain

The model is based on energy equation for the fuel array.

$$\rho c \frac{\partial T}{\partial t} = k \frac{\partial^2 T}{\partial x^2} - h(T - T_e) - \frac{H}{s}\frac{dM}{dt} + \Phi_{RAD} \quad (1)$$

The mass rate variation, according to Balbi *et al.* (1999) was described using a constant rate of change after reaching the ignition temperature:

$$\frac{dM}{dt} = -\alpha M \quad (2)$$

The terms of the right-hand side of Eq. (1) account for heat transfer due to thermal diffusion, convection ad radiation. A further term appears and accounts for the heat of reaction due to fuel combustion. Fuel properties are different in the four sections of the domain highlighted in Figure 2. In fact both fuel depth and fuel array density are not the same in all the experimental field. In order to obtain results that describes the overall fire behavior the fuel properties used in the model are the averaged ones. Density and specific heat are evaluated considering the fuel array as a porous medium. The convective losses are considered as proportional to the difference between the fuel array temperature and the environmental temperature. The convective losses coefficient was evaluated using experimental data.

Temperature time evolution measured during the experiment was used to evaluate the unknown coefficient in the energy equation. Experimental temperature profile (Figure 3) was investigated and its portion dominated by convective losses (zone 1) was considered for the evaluation of the convective heat transfer coefficient The linearized reaction rate α was estimated considering the portion of temperature evolution (zone 2) mainly affected by the heat release due to combustion The radiative term was estimated using Stefan-Boltzman law (Incropera, Dewitt 1996). The emissivity has been evaluated as described in Pastor *et al*. (2002) ,while the height of the flame is also experimentally determined. The considered radiative term is:

$$\Phi_{RAD} = r F_{ij} \varepsilon \sigma T^4 \quad (3)$$

where r is evaluated using the same curve used for evaluating convective losses coefficient and mass losses coefficient. In this case the zone C of Figure 3 has been considered, when the arriving flame front exchange radiative thermal flux to thermocouple.

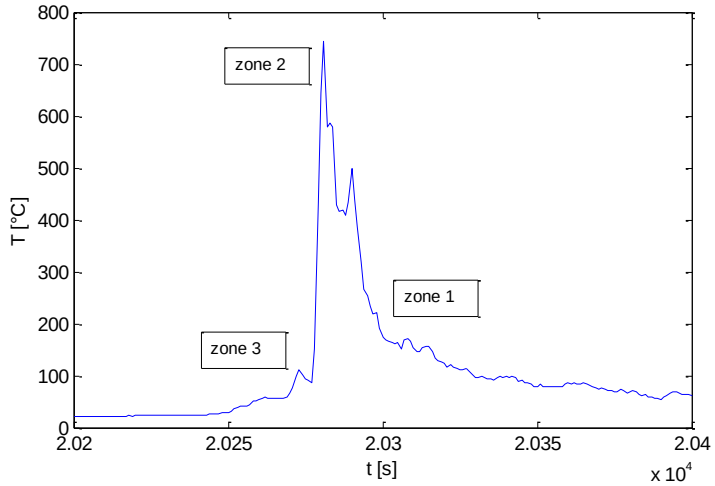

Figure 3. Temperature evolution collected to a thermocouple

Equation (1) is discretized using an implicit finite difference scheme (Ferziger, Peric 2002) and the resulting system of ordinary differential equation is:

$$\boldsymbol{C\dot{T} = AT + DT^4 + f} \tag{4}$$

This is the full-model that is solved in order to obtain the temperature distribution. Time integration is performed using the implicit backward Euler method while non-linearity due to radiative heat transfer are treated through the Newton-Raphson algorithm. Dirichlet boundary conditions were imposed at the left and right boundaries. As initial condition in the first 0.4 m of the domain a sinusoidal temperature distribution with a maximum of 700 K was imposed, in order to represent the fuel ignition. The initial mass per unit area is 0.39 kg/m^2 everywhere.

2.3. POD reduced model

POD is a technique able to capture the main characteristics of a system behavior with a dimensionally reduced model (Sirovich 1987). The reduction is carried out using a collection of sampled values of the considered field called snapshots. The snapshots at M different time are collected in the so-called *snapshot matrix S*, a N x M matrix. Snapshots can be obtained from experiments or simulations. The snapshots matrix can be expressed as:

$$\boldsymbol{S \cong Ba} \tag{5}$$

where $a \in \mathbb{R}^{KxM}$ is the coefficients matrix and $B \in \mathbb{R}^{NxK}$ is the matrix of the truncated basis. N and K are respectively the orders of full model and reduced model.
In order to find the K best "modes" to describes the system an eigenvalue problem is solved. For details refer Bialeki *et al*. (2005). Using this procedure, the system is solved for the temporal contribution of the temperature field α because the space contribution is included yet in the matrix B.

$$\boldsymbol{T = B\alpha} \tag{6}$$

Using (6) and multiplying by B^T equation (4) becomes:

$$\boldsymbol{\tilde{C}\dot{\alpha} = \tilde{A}\alpha + B^T D(B\alpha)^4 + B^T f} \tag{7}$$

where

$$\widetilde{\boldsymbol{C}} = \boldsymbol{B}^{\boldsymbol{T}}\boldsymbol{C}\boldsymbol{B} \text{ and } \widetilde{\boldsymbol{A}} = \boldsymbol{B}^{\boldsymbol{T}}\boldsymbol{A}\boldsymbol{B} \quad (8)$$

The full model dimension is 4000. The POD basis chosen for the analyzed problem are 160, therefore the dimension is reduce to the 5% of the initial one.

Results

Temperature distribution at different instants of time obtained with the full model is detailed in Figure 4. It shows that fire rapidly reaches a shape that does not change anymore in time; this condition will be later on called pseudo steady state. The temperature profile in the combustion region varies only in the first 500 s then pure propagation occurs. As a result, the rate of spread is constant.

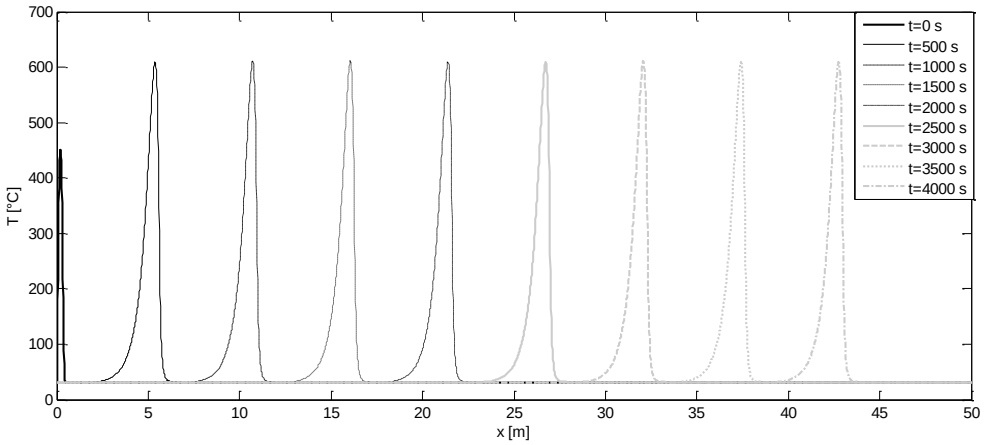

Figure 4. Temperature distribution at different time -Full model

In order to better compare the results obtained with the full model and the experimental ones the average rate of spread in the sections B, C, D of the experiment of the experimental fire front is reported in Figure 5. Figure 5 indicates that a good agreement between experimental ROS and the rate of spread calculated with the proposed model is achieved.

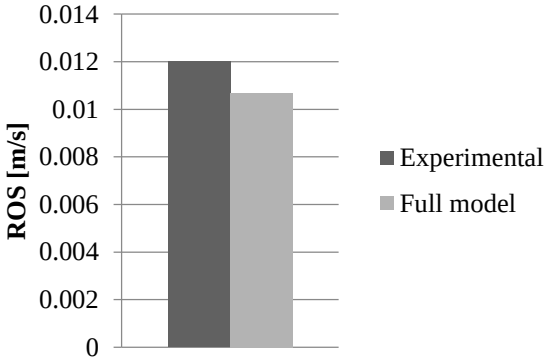

Figure 5. ROS mean value comparison

In Figure 6 the experimental temperature time evolution recorded by thermocouples T1, T2, T3, T4, is reported, which provides information on experimental fire propagation. The evolution of the experimental fire is not constant during time. In fact the front reaches the first thermocouple (section A) after 1000 s, the second after 2000 s, the third after 2800 and the fourth after 3700 s. Therefore , since the thermocouples are equidistant it is clear that the ROS in the sections of the domain are very

different. In Figure 6 the temperature time evolution predicted using the full model is also reported. The results indicate that a good agreement between experimental data and numerical simulation is achieve, although the model slightly under-predicts the fire front velocity in the first half of the domain. Numerical predictions obtained using the POD model are also compared with experimental data and numerical results of the full model. POD model and the full one are in good agreement and also the maximum temperature predicted is very similar. The marginal differences that can be observed in Figure 6 are due to the fact that only 160 autofunctions are used in order to reduce the computational cost. In the case of the described experiment, the computational time required to solve the energy equation using the POD model with a refined grid is about 10% of the full model.

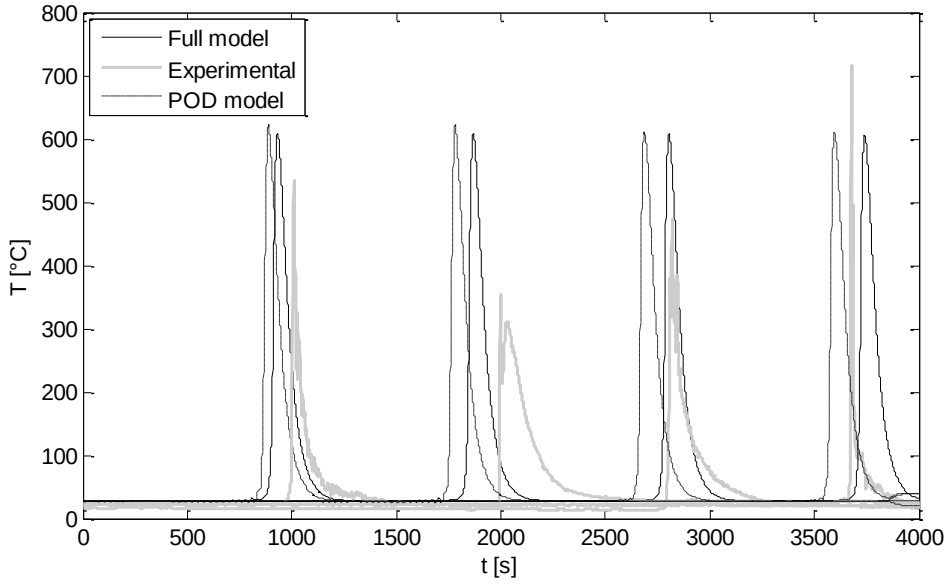

Figure 6. Temperature evolution in the four thermocouple, full model, experimental and POD model

An interesting application of the POD model is the possibility of performing sensitivity or parametric analysis using a reduced model built from a single reference scenario. In particular, it is possible to assess the influence of boundary conditions or model parameters at the expense of small computational costs. In fact the main strength of this approach is the ability to reproduce the behavior of the system with some different characteristics, using snapshots provided to an experiment or simulation executed in other conditions. In this paper the effect of uncertainties in the evaluation of the linearized reaction rate are investigate using the POD model. In particular, a +/- 30% variation of α (Eq. 2) was considered. The resulting variation of ROS are illustrated in Figure 7. The rate of spread evaluated with the full and POD model are very similar; the maximum error obtained is less than 6%. Furthermore the considered case is characterized by a low propagation velocity, therefore the error has a very low value. Figure 7 shows that an higher value of α correspond to a slower propagation, while ROS decrease with smaller value of α.

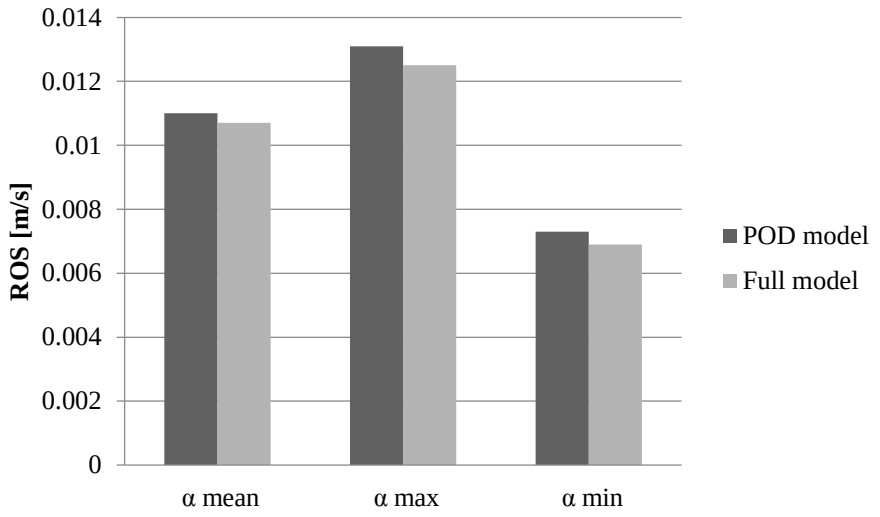

Figure 7. ROS with different mass loss rate coefficient

Conclusions

The present paper reports the use of POD in order to reduce the computational time of wildfire models. POD has been applied to a simple 1D problem based on energy conservation equation. Diffusion, convection, radiation, and heat release associated with the mass rate has been considered. Coefficients are determined experimentally. Time integration is evaluated with the implicit backward Euler method and the resulting nonlinear system of equations is solved using a Newton-Raphson algorithm. This is the first paper in literature that deal with the POD reduction applied to forest fire model.
The full model is able to reproduce the pseudo steady-state behavior of the experimental fire. In fact the ROS of the two model are similar. We found that POD model is able to provide appreciative results using only 160 basis. Therefore the dimension of the solved model is 160 while the dimension of the full one is 4000. The computational time to solve the energy equation is reduced to 10% of the full model. This is a good result but in future in order to increase efficiency of non-linear problems solved using POD techniques as the DEIM decomposition can be used.
The snapshots provided to the full model are used in order to simulate fire evolution with two different value of mass loss rate coefficient. Results show that POD model is able to estimate the ROS with good accuracy, even when the equation parameters differ from that used to obtain the snapshots. Errors are below 6% in each the computed cases. Future work will be focused on increasing of performances of this technique and application to more complex and multi dimensional models.

Nomenclature

c	specific heat of the fuel array	[kJ/kgK]
F_{ij}	view factor	[-]
h	convective coefficient	[W/m^{3}K]
H	heat content of fuel	[kJ/kg]
k	equivalent conductivity coefficient	[W/mK]
M	mass of fuel per unit of surface	[kg/ m^2]
s	fuel array depth	[m]
r	radiation coefficient	[m^{-1}]

T	temperature of the fuel array	[K]
T_e	temperature of environment	[K]
α	mass loss rate parameter	[s^{-1}]
ρ	density of the fuel array	[kg/m^3]
σ	Stefan-Boltzman constant	[$Wm^{-2}K^{-4}$]
Φ_{RAD}	radiative heat flux	[W/ m^3]

References

Ascoli D, Lonati M, Marzano R, Bovio G, Cavallero A, Lombardi G (2013). Prescribed burning and browsing to control tree encroachment in southern European heathlands. *Forest Ecology and Management* 289, 69–77.

Balbi J, Santoni P, Dupuy J (1999). Dynamic modelling of fire spread across a fuel bed. *International Journal of Wildland Fire* 9(4), 275–284.

Białecki RA., Kassab AJ, Fic A. (2005). Proper orthogonal decomposition and modal analysis for acceleration of transient FEM thermal analysis. *International journal for numerical methods in engineering* 62,774–797

Fernandes PM, Catchpole WR, Rego FC (2001). Shrubland fire behaviour modelling with microplot data. *Canadian Journal Forest Research* 30, 889–899.

Ferziger JH, Peric M. (2002) Computational Methods for Fluid Dynamics (Springer)

Incropera FP, Dewitt DP (1996) Fundamentals of Heat and Mass Transfer. (JohnWiley& Sons: NewYork)

Mandela J, Beezleya J D, Kochanskib A K., Volodymyr Y. Kondratenkoa, Kima M., (2012). Assimilation of Perimeter Data and Coupling with Fuel Moisture in a Wildland Fire – Atmosphere DDDAS. *International Conference on Computational Science*, ICCS 2012 Procedia Computer Science 9 1100 – 1109

McArthur AG (1965). Weather and grassland fire behaviour. Country Fire Authority and Victorian Rural Fire Brigades Association Group Officers Study Period, 13–15 August 1965. (Geelong, VIC)

Mell W, Jenkins MA, Gould J, Cheney P, (2007). A physics based approach to modeling grassland fires. *International Journal of Wildland Fire* 16(1),1–22.

Morvan D. (2011) Physical Phenomena and Length Scales Governing the Behaviour of Wildfires: A Case for Physical Modelling. *Fire Technology* 47, 437–460

Pastor E, Rigueiro A, Zárate L, Giménez A, Arnaldos J, Planas E. (2002) Experimental methodology for characterizing flame emissivity of small scale forest fires using infrared thermography techniques. *Forest Fire Research & Wildland Fire Safety*, Viegas (ed.)

Pastor E, Zarate L, Planas E, Arnaldos J (2003). Mathematical models and calculations systems for the study of wildland fire behavior. *Progress in Energy and Combustion Science* 29, 139–153.

Rothermel RC, (1972). A mathematical model for predicting fire spread in wildland fuels. USDA Forest Service, Intermountain Forest and Range Experiment Station General Technical Report INT-11. (Ogden, UT)

Simard AJ, Eenigenburg JE, Adams KA, Nissen RL, Deacon AG (1984). A general procedure for sampling and analyzing wildland fire spread. *Forest Science* 30, 51–64.

Sirovich L, Turbulence and the dynamics of coherent structures (1987). *Quarterly of Applied Mathematics* 45 561-590.

Sullivan A L (2009) Wildland surface fire spread modelling, 1990–2007.1 Physical and quasi-physical models. *International Journal of Wildland Fire* 18(4) 349–368

Vacchiano G, Motta R, Bovio G, Ascoli D (2014). Calibrating and Testing the Forest Vegetation Simulator to Simulate Tree Encroachment and Control Measures for Heathland Restoration in Southern Europe. *Forest Science* 60(2), 241–252.

Modelling fine fuel moisture content and the likelihood of fire spread in blue gum (Eucalyptus globulus) litter

Anita Pinto[a], Juncal Espinosa-Prieto[a], Carlos Rossa[a], Stuart Matthews[b], Carlos Loureiro[c], Paulo M. Fernandes[a*]

[a] *Centro de Investigação e de Tecnologias Agro-Ambientais e Biológicas, UTAD, Quinta de Prados, Apartado 1013, 5000-801 Vila Real, Portugal.* [*] *pfern@utad.pt*
[b] *CSIRO Ecosystem Sciences and CSIRO Climate Adaptation Flagship, GPO Box 1700, Canberra, ACT 2601, Australia*
[c] *GIFF S.A.; Rua D. João Ribeiro Gaio, 9B-1ºE, 4480-811 Vila do Conde, Portugal.*

Abstract
The capabilities of accurately estimating dead fuel moisture content and predicting the likelihood of self-sustained fire spread are crucial to plan prescribed fire operations and achieve the treatment goals, among other fire management objectives. After analysis to determine whether some existing models could be adopted or adapted, we developed user-friendly equations to predict the moisture content of dead fine fuels in blue gum (*Eucalyptus globulus*) litter and examined their prediction ability. Models with vapour pressure deficit, the FFMC code of the Canadian FWI System (or the no. of days since last precipitation in alternative) and noon 10-m open wind speed from the nearest weather station as independent variables fitted the data suitably, as well as a physics based model. The probability of sustained fire propagation in experimental burns carried out in reconstructed blue-gum litter in the laboratory was described through fuel moisture content, litter depth and fire-spread direction (backward or forward). Both types of equations will be further tested in blue gum stands.

Keywords*: Fuel moisture, Eucalyptus globulus, fire behaviour, fire danger, prescribed burning*

Introduction

Blue gum eucalypt (*Eucalyptus globulus* Labill.) stands in Portugal are an important economic resource as well as inherently flammable, hence contributing to the extent of the fire problem. Treatment of fuels in highly flammable forest plantations is an essential component of their sustainable management to minimize burn probability, be able to suppress fire under unfavourable weather conditions, decrease its ecological impact and increase the value of salvaged wood. The advantages of prescribed burning as a fuel management technique warrant investigation of its feasibility in industrial eucalypt plantations. The FIREglobulus project seeks to establish the scientific basis for the technological development of prescribed burning in blue gum plantations. This project studies the behaviour and severity of experimental outdoors fires carried out from autumn to spring, supplemented by laboratory trials data. Data analysis relates fire characteristics with fuel complex descriptors and other environmental factors, examines the performance of currently available fire-behaviour prediction models, and develops predictive relationships for the chain fire environment - fire behaviour - fire effects in blue gum stands.
The moisture content of dead and live fuels plays an important role in fire behaviour and fuel consumption. Usually referred to as 'fuel moisture content' FMC (Viney 1991) it significantly influences fuel flammability and ignition, fuel consumption and overall fire behaviour (Matthews 2006; Pyne *et al.* 1996). Over the past decades several authors have developed research in this area using different approaches. Viney (1991) and more recently Matthews (2014) reviewed the state-of-the art on modelling the moisture of dead fine fuels. The focus of our work is on user-friendly operational models for use in the field, falling inside the group of empirical models based on weather

conditions so that FMC can be expressed through functional relationships like those developed by Pook and Gill (1993), Marsden-Smedley and Catchpole (2001), Ferguson *et al*. (2002), Lin (2004), Sharples *et al*. (2009), Ray *et al*. (2005, 2010) or Sharples and McRea (2011).
Fuel moisture content has been shown to be the main variable determining the likelihood of sustained fire spread in distinct fuel types, but other environmental variables (wind speed, fuel accumulation and continuity, fire direction) further exert an effect (e.g. Fernandes *et al*. 2008; Leonard 2009; Anderson and Anderson 2010; Cruz *et al*. 2013). Prescribed burning is often carried out under marginal conditions, i.e. at the high-end of the fuel moisture range that allows a spreading fire, and so the operational abilities to assess dead fine fuel moisture content and the likelihood of sustained fire spread are critical to plan and carry out prescribed fire operations.
In this study we present modelling results for blue-gum litter concerning (i) estimation of the moisture content of fine litter from environmental variables, and (ii) fire spread sustainability.

Methods

Fuel moisture content

The fuel moisture content of fine surface litter was measured by destructive sampling. The samples were collected daily (n=127) in a forest stand in the UTAD campus (Vila Real, northern Portugal) at 15:00 hours, between August 2012 and December 2013, and were oven-dried for 24 hours at a temperature of 100ºC. The temperature and relative humidity at the time of litter collection were measured at a 1.8-m height and used to calculate vapour pressure deficit (VPD, kPa), which measures the drying power of the air as the difference between the amount of moisture in the air and how much moisture the air can hold when saturated.
Noon weather data from the nearest meteorological station (4 km) and the corresponding indices of the Canadian FWI System (Van Wagner 1987) were also recorded.

Sustainability of fire spread

The sustainability of fire spread was evaluated in indoor burn trials (n=134) for backing (Figure 1) and heading fires under a wide range of litter moisture and structure (load, depth, bulk density) and wind speed.
For each trial we have reconstructed a litter layer (1.5m x 2m) in the combustion table. We tried to cover the natural variation in litter thickness and loading, based in the national forest inventory (2005-2006) data. Fuel loading was estimated by oven drying the material within a randomly-located 0.073 m^2 square. Fuel depth was determined from nails (n=8) inserted in the litter and flushed with its top. Fuel sampling for moisture content assessment proceeded immediately before ignition. Ambient temperature and relative humidity were monitored with a Davis weather station.
The fires were line-ignited (fire front width = 1.5 m) and allowed to propagate downslope with the slope fixed at 30%. The trials were either classified as sustained or non-sustained in case of self-extinction. If the fire failed to spread downslope the trial was repeated upslope with successive laminar-flow wind speeds of 0, 5, 10 and 15 km h^{-1} until attaining sustained fire spread.

Figure 1. A fire-spread sustainability trial in the combustion table.

2.3. Data analysis

We examined the prediction ability of eucalypt litter moisture content models (Gould *et al*. 2007; Sharples *et al*. 2009; Sharples and McRea 2011). FMC was empirically modelled from local weather (and related variables, e.g. vapour pressure deficit) and Canadian FWI moisture codes. FMC was log-transformed and regressed on both the untransformed and log-transformed independent candidate variables; the elected equations were back-transformed and corrected for bias. FMC was also derived through the physically-based model of Matthews (2006), for which hourly weather was estimated using the methods of Matthews *et al*. (2007). Model assessment was based on deviation statistics.

To predict the go/no-go status of fire spread we used two supplementary approaches, respectively CART (Classification and Regression Trees) and logistic regression, which estimates the continuous and non-linear probability *P* of an event (successful fire spread in this case, coded as 1). The logistic equation has the form (Hosmer and Lemeshow 2000):

$$P = 1 / [1 + \exp (- (b_0 + b_1 x_1 + \ldots + b_i x_i))] \quad (1)$$

where x_1 to x_i are the independent variables and b_0 to b_i are the regression coefficients.

Besides FMC we considered fuel structure (litter depth, load, and bulk density) and fire-spread direction as potential independent variables; the number of upslope trials with varying wind speed did not warrant assessment of its effect. The direction of fire spread was coded 0 for backward spread (the downslope back fire) and 1 for forward spread (the upslope head fire). To evaluate model predictions we used concordance analysis and the area under the ROC (receiver operating characteristic) curve, which is independent of an arbitrary decision.

Results and discussion

Fine fuel moisture content

Weather data at the moment of fuel sampling varied in the ranges of 7.0 - 35.8 ºC for ambient temperature, 16.5 - 100% for relative humidity and 0 - 25 km h^{-1} for wind speed. In general, the existing models for eucalypt litter FMC produced underestimates (Table 1), essentially because they were developed to predict the moisture content of fuels unaffected by precipitation. However, multiplying Gould *et al*. (2007) predictions by a factor of 1.5 succeeded in explaining 77% of the observed variation when FMC <35%. The physical model generally produced better predictions because it included precipitation effects. The best-fitting empirical model (Table 2) explained 92% of the observed variation and included the VPD, noon 10-m open wind speed and the FFMC of the Canadian FWI as independent variables (equation A). An alternative, more user-friendly equation (B) that included the number of days since precipitation instead of the FFMC had a poorer fit to data. The performance of both models was comparable to the more complex physical model.

Table 1. Evaluation of the models for estimating the moisture content (%) of fine surface litter.

Model	*n*	FMC range	RMSE	MAE	MAPE
Gould *et al*. (2007)	60	6.1 - 29.2	5.4	4.4	31.5
Sharples *et al*. (2009)	127	6.1 - 193.0	25.1	10.1	24.6
Sharples and McRae (2011)	127	6.1 - 193.0	33.6	15.3	45.3
Matthews (2006)	127	6.1 - 193.0	20.8	8.8	25.1
Matthews (2006)*	107	6.1 - 35.0	4.3	3.1	18.7

RMSE - Root mean square error; MAE - Mean absolute error; MAPE - Mean absolute percent error.
*Subset of results with modelled and observed moisture content below 35%

Table 2. Equations for estimating the moisture content (%) of fine surface litter. Standard errors of regression coefficients appear below the equations by the same order. All independent variables are significant at p<0.001.

Model	Equation	R2	MAE	MAPE
A	77.707 VPD-0,385 exp(-0.018 FFMC) exp(-0.012 U) (8.493; 0.001; 0.004; 0.029)	0.92	4.5	16.9
B	28.701 VPD-0,571 NDWR-0,157 exp(-0.021 U) (1.919; 0.032; 0.034, 0.005)	0.85	6.8	21.8

VPD – Vapour pressure deficit (kPa); FFMC- Fine Fuel Moisture Code; U – 10-m wind speed in the open (km h^{-1}); NDWR - Number of days since precipitation. R^2- Coefficient of determination; MAE - Mean absolute error; MAPE - Mean absolute percent error.

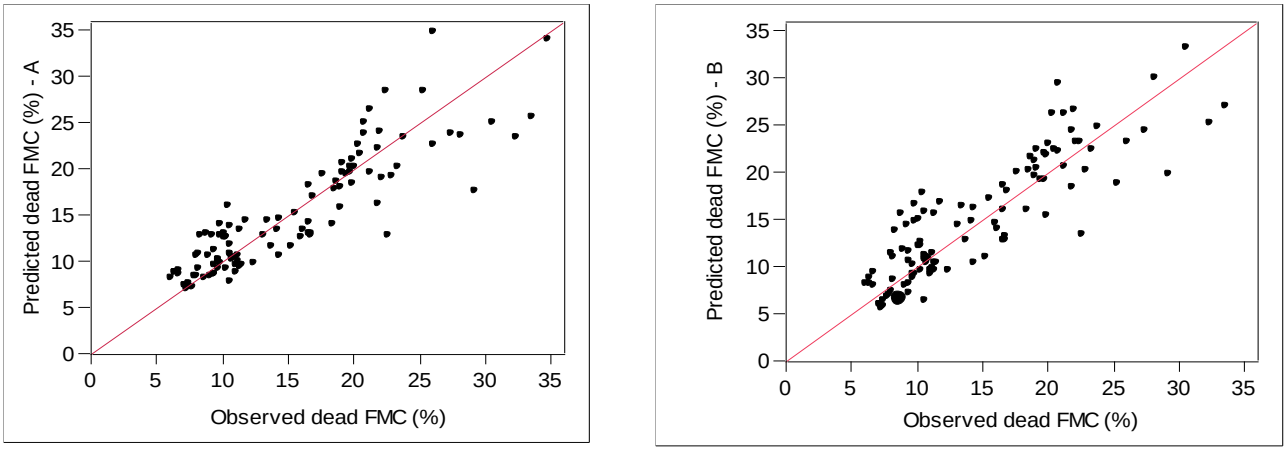

Figure 2. Observed versus predicted blue-gum litter moisture content using models A and B. The line of perfect agreement is overlaid.

Fire spread sustainability

FMC during the burn trials varied from 10.4 to 68%. The CART analysis indicates litter moisture content, its depth (which exerted the major effect) and fire-spread direction (forward or backward in relation to wind and slope) as the variables influent in the sustainability of fire spread (Table 3). When FMC is lower than 32.4% and litter depth is greater than or equal to 3.7 cm, sustained fire spread is virtually certain. In contrast, fire spread is highly unlikely for FMC above 32%, independently of other variables.

The model developed to predict the likelihood of sustained fire spread (Table 4 and Figure 3) has an area under the ROC curve of 0.925, which Hosmer and Lemeshow (2000) consider outstanding. Nevertheless, a comparison between Table 3 and Figure 3 indicates the logistic regression tends to be conservative, i.e. underestimates the fire-spread potential. In fact model predictions are quite sensitive to litter depth, e.g. the likelihood of fire spread increases substantially when LD changes from 3.0 (the data set average) to 3.5 cm. Litter depth probably expresses the effect of fuel continuity in addition to the effect of fuel loading, as the former tends to be partial at shallow depths due to the morphology of blue gum leaves. The fire-spread outcome was correctly predicted by the model in 85% of the experimental trials; out of the failed predictions 10% were underestimates and 5% were overestimates.

Table 3. CART analysis of the likelihood of sustained fire spread in blue gum litter.

<table>
<tr><th colspan="5">Variables and thresholds</th><th>Fire spread probability</th></tr>
<tr><td rowspan="5">FMC <32.4 %</td><td colspan="4">Litter depth ≥ 3.7 cm</td><td>1</td></tr>
<tr><td rowspan="4">Litter depth < 3.7 cm</td><td colspan="3">Forward spread</td><td>0.82</td></tr>
<tr><td rowspan="3">Backward spread</td><td rowspan="2">Litter depth ≥ 2.9 cm</td><td>FMC <28.2 %</td><td>1</td></tr>
<tr><td>FMC ≥28.2 %</td><td>0.20</td></tr>
<tr><td colspan="2">Litter depth < 2.9 cm</td><td>0.07</td></tr>
<tr><td colspan="5">FMC ≥32.4%</td><td>0.16</td></tr>
</table>

Table 4. Coefficients (standard errors) of the model for estimating the probability of sustained fire spread.

Intercept	FMC	LD	FD
3.0182 (0.9490)	0.1852 (0.0342)	-2.3181 (0.4799)	-2.7597 (0.6287)
p=0.0015	p<0.0001	p<0.0001	p<0.0001

FMC – Fuel moisture content (%); LD – litter depth (cm); FD – Fire-spread direction

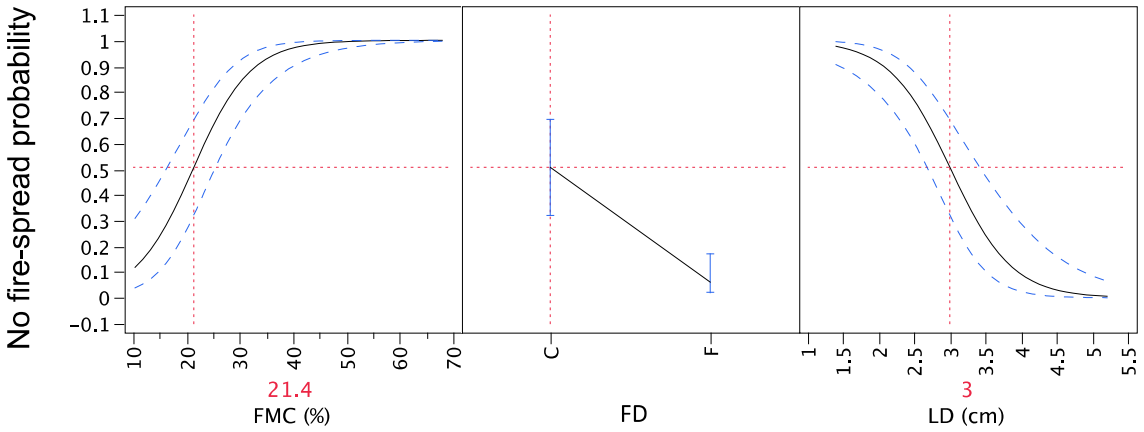

Figure 3. Fire-spread probability with confidence intervals as per the logistic model in Table 4. FMC = 21.4% is the threshold between go / no-go for a back fire and the mean observed litter depth.

Conclusions

Expedite and reasonably accurate estimation of the moisture content of fine surface litter for operational purposes is possible by using an empirical model based on temperature and relative humidity (in the form of the VPD), supplemented by other less relevant variables that account for the drying effects of time since last rainfall and wind speed. The physical model performs similarly, but its use by fire managers is not practical.

Fire-spread sustainability was highly influenced by fuel structure, which contrary to expectations (and because of the experimental design) exceeded the importance of FMC. The performance of the laboratory-base model for fire spread sustainability needs to be assessed during outdoors experimental fires. In case the results indicate good predictive ability, scaling problems will then be ruled out and it will be reasonable to extrapolate the lab-based results to the field and to management-ignited fires. The results will be part of the prescribed burning guide for blue gum plantations.

Acknowledgments

This study wass supported by FIREglobulus, I&DT co-promotion project no. 21555 in the frame of *Quadro de Referência Estratégico Nacional* (QREN), co-funded by the European Regional Development Fund (ERDF) through *Programa Operacional Regional de Norte*.

References

Anderson SAJ, Anderson WR (2010) Ignition and fire spread thresholds in gorse (*Ulex europaeus*). *International Journal of Wildland Fire* **19**, 589–598.

Cruz MG, McCaw WL, Anderson WR, Gould JS (2013) Fire behaviour modelling in semi-arid mallee-heath shrublands of southern *Australia.Environmental Modelling and Software* **40**, 21–34.

Ferguson SA, Ruthford JE, McKay SJ, Wright D, Wright C, Ottmar R (2002) Measuring moisture dynamics to predict fire severity in longleaf pine forests. *International Journal of Wildland Fire* **11**, 267–279.

Fernandes PM, Botelho HS, Rego FC, Loureiro C (2008) Using fuel and weather variables to predict the sustainability of surface fire spread in maritime pine stands. *Canadian Journal of Forest Research* **38**, 190–201.

Gould JS, McCaw WL, Cheney NP, Ellis PF, Matthews S (2007) Field Guide - Fuel Assessment and Fire behaviour Prediction in Dry Eucalypt Forest. Ensis-CSIRO, Canberra, ACT and Department of Environment and Conservation. (Perth, WA)

Hosmer DW, Lemeshow S (2000) Applied logistic regression. 2nd ed. John Wiley & Sons Inc. (New York)

Leonard S (2009) Predicting sustained fire spread in Tasmanian native grasslands. *Environmental Management* **44**, 430-440.

Lin CC (2004) Modeling fine dead fuel moisture in Taiwan red pine forests. *Taiwan Journal of Forest Science* **19**, 27–32.

Marsden-Smedley JB, Catchpole WR (2001) Fire modelling in Tasmanian buttongrass moorlands. III - Dead fuel moisture. *International Journal of Wildland Fire* **10**, 241–253.

Matthews S (2006) A process-based model of fine fuel moisture. *International Journal of Wildland Fire* **15**, 155–168.

Matthews S, McCaw WL, Neal JE, Smith RH (2007) Testing a process-based fine fuel moisture model in two forest types. *Canadian Journal of Forest Research* **37**, 23–35

Matthews S (2014) Dead fuel moisture research: 1991-2012. *International Journal of Wildland Fire* **23**, 78–92.

Pyne SJ, Andrews PL, Laven RD (1996) Introduction to Wildland Fire. John Wiley & Sons, Inc. (New York).

Pook EW, Gill AM (1993) Variation of live and dead fine fuel moisture in *Pinus radiata* plantations of the Australian Capital Territory. *International Journal of Wildland Fire* **3**, 155–168.

Ray D, Nepstad D, Moutinho P (2005) Micrometeorological and canopy controls of fire susceptibility in a forested Amazon landscape. *Ecological Applications* **15**, 1664–1678.

Ray D, Nepstad D, Brando P (2010) Predicting moisture dynamics of fine understory fuels in a moist tropical rainforest system: results of a pilot study undertaken to identify proxy variables useful for rating fire danger. *New Phytologist* **187**, 720–732.

Sharples J, McRae R, Weber R, Gill M (2009) Simple index for assessing fuel moisture content. *Environmental Modelling and Software* **24**, 637–646.

Sharples J, McRae R (2011) Evaluation of a very simple model for predicting the moisture content of eucalypt litter. *International Journal of Wildland Fire* **20**, 1000–1005.

Van Wagner CE (1987) Development and Structure of the Canadian Forest Fire Weather Index System. Canadian Forest Service, Information Report 35. (Ottawa, ON).

Viney NR (1991) A review of fine fuel moisture modelling. *International Journal of Wildland Fire* **1**, 215–234.

Multi-scale kinetic model for forest fuel degradation

Dominique Cancellieri, Valérie Leroy-Cancellieri, Eric Leoni

SPE - UMR CNRS 6134, University of Corsica, Corte, France. vcancellieri@univ-corse.fr

Abstract
In modelling wildfire behaviour, a good knowledge of mechanisms and kinetic parameters controlling the thermal decomposition of forest fuel is of great importance. Generally, the pyrolysis models are determined from experiments carried out in thermal device (i.e. TGA and DSC). This kind of tools ensures an accurate determination of kinetic parameters in perfectly controlled conditions. But the gap of a larger scale, for their uses in forest fire conditions, is still far. To corroborate the kinetic models in realistic forest fire conditions, a mass loss device specially designed for field scale has been developed. The system includes three load cells with a max load at 400 g and 2.7 Hertz for the frequency acquisition. Each load cell is sit on top of a stainless tube in which the sample is hold. The position and height of the sample in the tube could be adjusted to optimize the interaction with the height of the flame and the sample. To obtain the temperature impacting the sample, a thermocouple K is placed at the end of each tube set to the same frequency acquisition as load cells. The device is integrated in a welded ceramic box that was lined with a 15 mm thick refractory lining. The acquisition system is included into an armored thermal box. For this first campaign of measures, we have selected species which have been previously studied for the kinetic modeling and presenting different typologies: Rockrose, Heather and Pine. One of the main advantages of this prototype is that 3 different species can be submitted, in line, to the same external heating conditions and are simultaneous analyzed. The heating source is a fire spread of wood wool bed. This fuel have been selected for a good repeatability of heating conditions Before each test, a fuel bed with various loads (0.5, 1 and 2 kg/m2) has been uniformly distributed and the prototype has been placed around the end of the bed to ensure the steady state. In these experimental conditions the samples, of intact branches and leaves, are closest to their natural state. Experimental field-scale results have been compared to numerical simulations based on Arrhenius law.
The simulations have been performed considering a two-steps mechanism previously obtained by the authors using TGA data. In a general point of view, the simulations have a good agreement with the experimental mass loss rate even if some differences appear (as attempt). For the rockrose, the model do not match accurately in the range of $0.7 < m/m0 < 0.9$ probably because the mechanisms of initiation and preheating are more complex than a simple Arrhenius equation of order n. Concerning the heather, experiments exhibit an accelerate degradation process which can be explain by the very fine structure of this specie. Conversely, Pine has a different structure which is constituted by a single branch with a diameter of 6 mm. This thickness of sample involves an incomplete degradation. Considering the very important gap between laboratory and field scale, the kinetic scheme gives satisfactory modeling.

***Keywords**: field-scale, mass loss prototype, kinetic analysis*

Introduction

In studying forest fire propagation, kinetic modeling of thermal degradation mechanisms is one of the main prerequisites for the determination of source terms, allowing the development of realistic models. Numerous Computational Fluid Dynamics (CFD) codes have been developed for predicting fire spread and providing operational tools for land managers. Those codes include various sub-models describing the different phenomenon involved in case of fire such as the pyrolysis model (Morvan and Dupuy 2004) which describes the thermal decomposition of the solid.
In order to describe the evolution of the solid phase, the mass loss rate of the solid is one of the most important parameters. Indeed it is directly linked with the pyrolysis gas flow rate and represents the initial factor of the combustion process.

In modelling fire behaviour the knowledge of the mechanisms and kinetic parameters controlling the thermal decomposition of forest fuel it is of great important. Indeed, adequate kinetic mechanisms should be coupled with the description of transport phenomena (heat, mass and momentum transfer) in order to provide detailed process simulation.
The thermoanalytical technique commonly used in solid-phase thermal degradation studies is the ThermoGravimetric Analysis (TGA) (Ninan 1989; White *et al.* 2011) which has gained widespread currency in thermal studies of biomass pyrolysis (Di Blasi 2008). TGA measures the decrease in substrate mass caused by the release of volatiles, or devolatilization, during thermal decomposition. In TGA, the mass of a sample being heated at a specific rate is monitored as a function of temperature or time. The TGA requires sample sizes sufficiently small such that the diffusion effects become negligible and the pyrolysis is kinetically controlled (Miller and Bellan 1997). The experimental data gathered in the perfectly controlled conditions of the TGA ensures an accurate determination of kinetic mechanism. Unfortunately, these experimental conditions are not realistic with those encountered in real forest fire. Sometimes, experiments were performed in calorimetry (with cone or FPA)(Schemel *et al*. 2008), but the gap of a larger scale is still far.
Based on these observations, the aim of this study is to propose a kinetic model for Mediterranean fuels adapted to realistic forest fire conditions. In this purpose, a mass loss device specially designed for field scale has been developed. This device can record in real time and simultaneously the mass loss and the temperature of 3 samples when they are submitted to a heat flux. Always with the aim of bringing it closer to a forest fire, the heat flux is a flame front created by the spread of a bed of straw. The experimental values conducted at field-scale have been compared to kinetic laws established in TGA.

Materials and Methods

Biomass fuels

Plant materials have been collected in Corsica from a natural Mediterranean ecosystem situated far away from urban areas in order to prevent any pollution on the samples. Heather, Rockrose and Pine are the representative species of different strata of vegetation concerned by wildland fires. The properties of the species are shown in Table 1. All the fuels are expressed in their chemical equivalent formula, which is a function of their major elements (C, H and O) obtained from the ultimate analysis on a dry basis. The heating values (high and low) were measured using a bomb calorimeter and the calorific capacities were determined using a Differential Scanning Calorimeter (DSC). The surface-to-volume ratio and density were measured following the methodology proposed by Moro (Moro 2006).

Table 1. Physico-chemical parameters of fuels

Properties	Parameters	Rockrose	Heather	Pine
Chemical	Formula	C4,24 H6,49 O 2,66	C4,58 H7,32 O 2,35	C4,26 H6,83 O 2,62
Thermal	High Heating Value (kJ kg-1)	20905	20988	21566
	Low Heating Value (kJ kg-1)	19745	19703	20239
	Calorific capacity (kJ kg-1 °C-1)	1912	1939	2050
Physiologic	Surface to volume ratio (m-1)	2217	3801	3057
	Fuel density (kg m-3)	912	614	511

2.2. Laboratory experiments

For kinetic characterization of thermal degradation mechanisms the mass loss is one of the main prerequisites. This parameter has been chosen as the major driving parameter for the characterization of source terms. Moreover, the mass loss provides qualitative and quantitative information regarding the different reactions taking place in the heated solid (Kissinger H.E. 1957). Thermogravimetric experiments were carried out in a thermogravimetric analyzer (PerkinElmer Pyris 1 TGA). The precision of the temperature measurement was ±2 K. For each sample, 5 mg of dried and ground biomass was heated from 350 K up to 900 K under dynamic conditions at heating rates of 20 K min^{-1}. During the experiments the furnace of the TGA is flushed with 20 mL min^{-1} air to maintain an oxidative atmosphere for thermal degradation of particles. Each experiment was repeated at least three times.

2.3. Field experiments

To cross the gap of real fire, we transpose the principle of the TGA at the field scale. In this purpose, we have created a device in which samples are exposed to a heating source (a fire front) and the weight loss and temperature are simultaneously recorded. The next sections are dedicated to the description of this mass loss prototype and its use.

2.3.1. *Differential mass loss prototype set up*

The prototype consists of two parts: one dedicated to measurement and the other dedicated to data acquisition. The characteristics of each are detailed below.

The instrumental part:

The size of the device has been calculated to be 1/5 of the width of the plot to burn. In this way, the system will completely encompass during the propagation.
The device includes 3 load cells which are integrated in a welded ceramic box (1260 mm × 170 mm × 100 mm) that was lined with a 50 mm thick refractory lining (Thermal Ceramics Kaowool 1600).
Given that the meteorological and fire conditions are difficult to perfectly reproduce, we make the choice of install 3 load cells on apparatus to follow the behaviour for 3 species submitted to the same fire propagation. With three species on the prototype, a differential analysis between samples becomes possible free from the external conditions.
The 3 load cells (Futek®) have a maximum lift of 450 g for 6.8 mm width, 19 mm height and 17.5 mm length. A stainless tube is sit on top of each load cell in order to insert the sample inside. The height and the diameter of this tube (190 mm x 20 mm) have been reckoned to avoid any lift effect. Moreover, the position and height of the sample in the tube could be adjusted to optimize the interaction with the height of the flame and the sample.
The distance between each supporting tube (500 mm) has been chosen so that the decomposition of a branch does not affect the neighbouring branch. Thus, the plant will only be affected by the fire front of the beforehand device.
To obtain the temperature impacting the sample and the punctual heating rate of the fire propagation, thermocouples are placed at the end of each tube. Thermocouples K have been selected according to their temperature ranging to 1300 ± 0.5 °C (Omega® HKMTSS-010G-8) diameter: 25 µm.

The acquisition part:

The acquisition system is integrated into a thermal Multi-Layer Aluminization (Z-Flex®) shield box. A deported wireless acquisition system is actually impossible to use because of disturbances caused by the thermal shield. The temperature inside the thermal box is controlled using a thermocouple and adjusted if necessary by a fan if the temperature of the thermal box is rising. Inside the box, a laptop

is included in which the data are simultaneously transmitted through a USB interface and using custom software.

The mass loss data are recorded using Sensit the Futek's software with a frequency of 2.5 Hz.
The temperature data are synchronized with mass losses data acquisition recorded with the same frequency thanks to acquisition unit Omega® TC-08. This system can accommodate up to 8 thermocouples with an acquisition frequency of 10 Hz. The figure 1 presents the whole mass loss prototype.

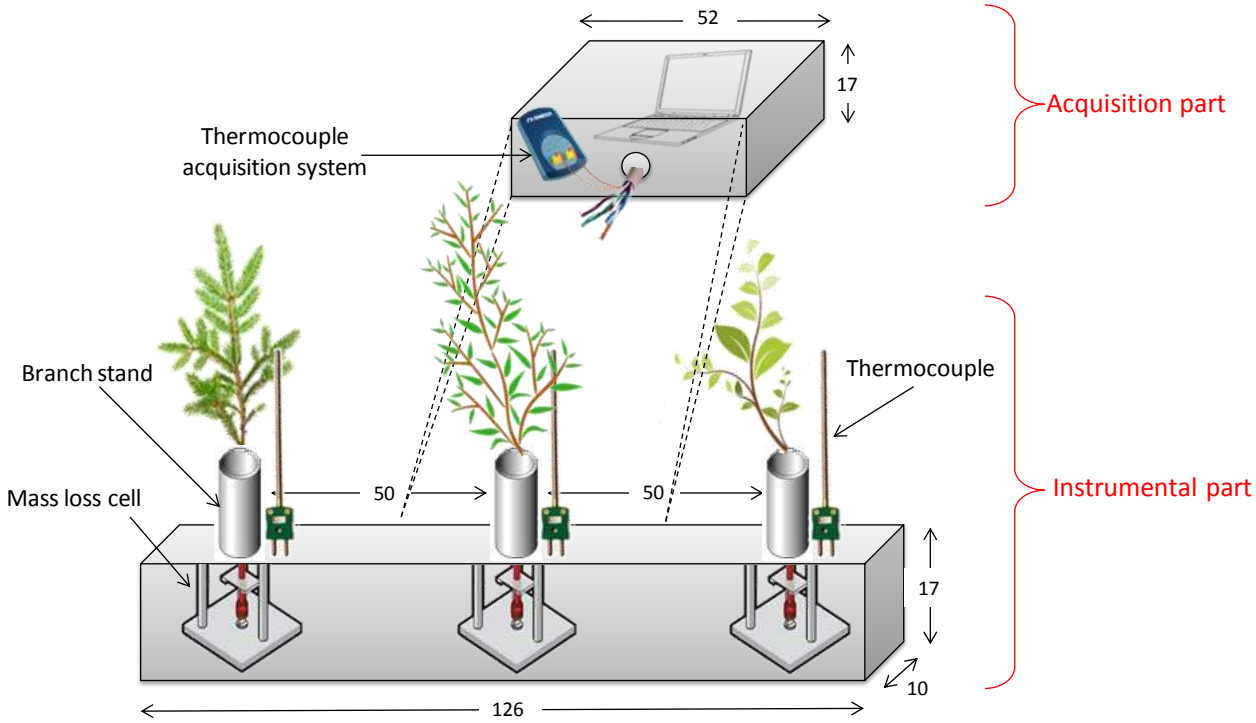

Figure 1. The differential mass loss prototype

One of the main advantages of this prototype is that 3 different species can be submitted, in line, to the same external heating conditions and are simultaneous analyzed in the same field conditions.

2.3.2. *Experimental conditions*

All experiments have been carried out on 3 species presenting different typologies: Rockrose, Heather and Pine. In these experimental conditions the samples of intact branches and leaves, are closest to their natural state. This initial mass of the sample (around 50g) represent a factor 10000 compared to experiments performed at laboratory scale with crushed samples.
The 3 species are submitted to the same heating source which is a fire spread of wood wool bed. This fuel has been selected for a good repeatability of heating conditions.
Before each test, a fuel bed of 6 m wide and 10 m long has been uniformly distributed with a fuel load of 2 kg m^{-2}. The prototype is placed around the end of the bed to ensure the steady state of propagation. The experiments have been performed in an area with no wind and no slope and were replicated three times.

Figure 2. Differential mass loss prototype in field conditions

2.4. Kinetic Analysis

The thermogravimetric data have been used to find the best set of kinetic parameters for three species. Using TGA experiments, in case of non-isothermal conditions, the rate of heterogeneous solid-state reactions can be described by:

$$\frac{d\alpha}{dt} = \frac{1}{\beta} A\, e^{-\frac{E_a}{RT}} f(\alpha) \qquad \text{(Eq. 1)}$$

where f(α) is the conversion function (reaction model) with $\alpha = m_0 - m/m_0 - m_\infty$, A is the pre-exponential factor, Ea is the activation energy, R is the gas constant and β is the heating rate.

The estimation of the kinetic parameters (*A*, E_a, *f(α)*) from TGA experimental data can be done with a variety of techniques (Vyazovkin and Wight 1998; Vyazovkin *et al.* 2011). In order to obtain a reliable kinetic description of the investigated processes, we used an approach that combines the accuracy of isoconversional methods with model-fitting methods (Pratap *et al.* 2007; Chrissafis 2009). This approach, called Hybrid Kinetic Method (HKM), has been developed in a earlier work (Cancellieri *et al.* 2005). It is based on two steps; the first uses isoconversional methods to provide $E_a(\alpha)$ and the reaction model. The second step requires these initiation data to be injected in a model fitting method to obtain the pre-exponential factor and n^{th}-order. This allows selection of models that might otherwise be indistinguishable based on the quality of the regression fit alone. From your point of view, such an approach gives the highest probability of selecting the most accurate kinetic triplet (*A*, E_a, and the model).

3. Results

3.1. TGA experiments

During thermal degradation in air, weight loss occurs continuously until the weight becomes almost constant. Figure 3 presents the experimental results of fuels thermal degradation from 350 to 900 K, under air sweeping.

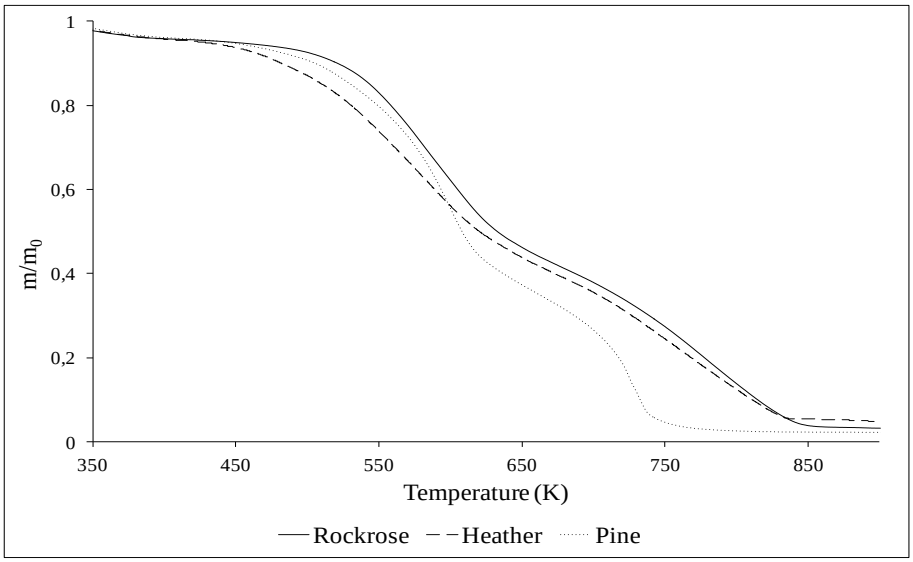

Figure 3: TGA curves of samples obtained with a linear heating rate of 20 K min^{-1} under air atmosphere.

Despite of the complex composition and chemical process, experimental observations suggest that a 2-steps of global reactions can capture the most important behaviour of the thermal and oxidative degradation of plants. Figure 3 highlights that for the heating rate considered in this work, Heather has the lower onset temperature, followed by Pine and in fine, Rockrose. This criterion is very helpful as it can be used as an ignition criterion since onset temperature measures the starting of oxidation reactions. The fuels with low onset temperature are the most ignitable and they burn easily. These results will be confronted to field scale experiments.

Taking the first derivative of such thermogravimetric curves (i.e., −dm/dt) curves, known as derivative thermogravimetry (DTG), provides the maximum reaction rate. The nature of a TGA curve in combination with the corresponding DTG peaks gives a clear indication of the number of stages of the thermal degradation.

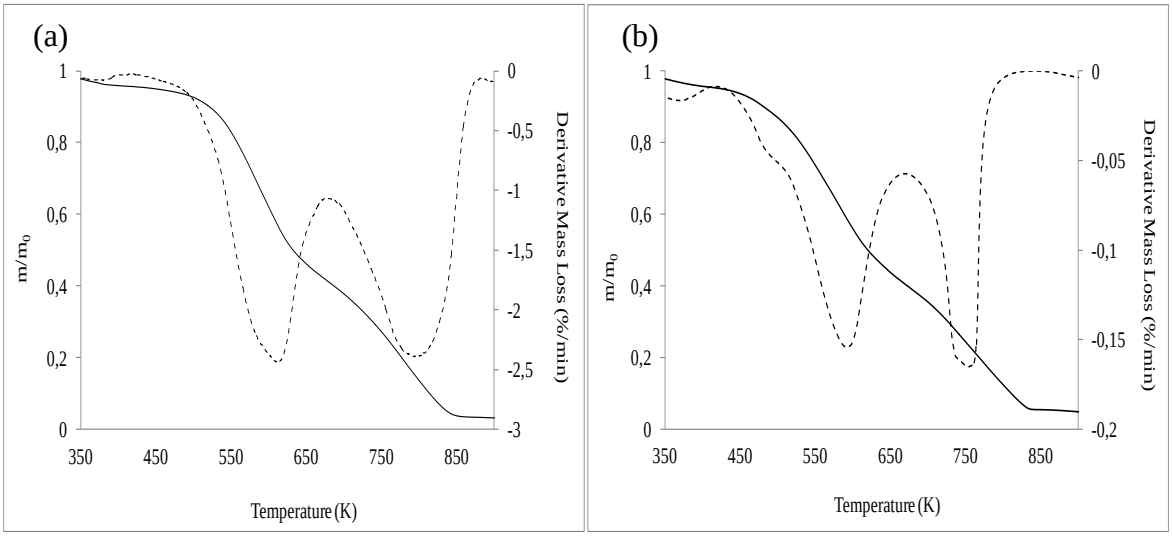

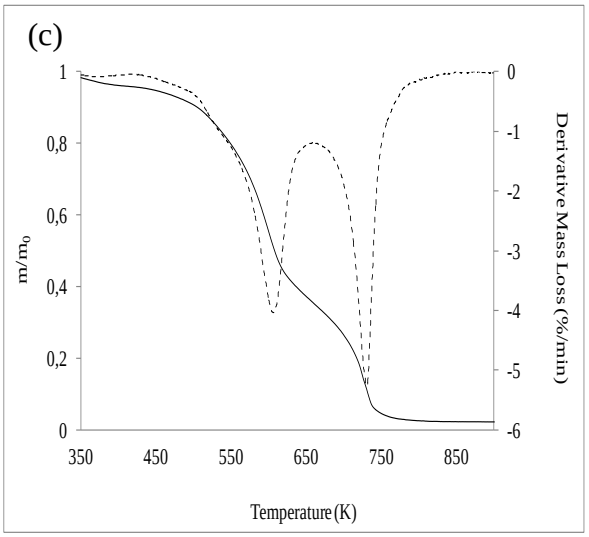

Figure 4: TGA (lines) and DTG (dotted) of oven dried of Rockrose (a), Heather (b), Pine (c) samples obtained with a linear heating rate of 20 K.min^{-1} under air atmosphere (Cancellieri et al. 2013)

TGA curves show two steps of weight loss confirmed in DTG by 2 peaks. The oxidative process is claimed to have two steps: the first step is volatilization of the main biomass constituents and production of char residue at low temperature; the second step includes the decomposition of lignin and the combustion of the charcoal generated in the early stage (Fang *et al.* 2006). The same phenomena are observed and recorded by other authors (Branca and Di Blasi 2004; Safi *et al.* 2004; Shen *et al.* 2009).

Kinetic parameters

According to laboratory experiments, it would seem wise to consider a 2-steps mechanism. This scheme seems to be suitable for the 3 species. The first process is modeled as:

$Virgin_{(s)} \rightarrow Char_{(s)} + Gas_{(g)}$ (1)

The second reaction concerns the oxidation of chars formed during the first process: $Char_{(s)} \rightarrow Residue_{(s)} + Gas'_{(g)}$ (2)

The two reactions (1) and (2) can be traduced in the two following differential equations (Eq. 2) and (Eq. 3), considering a n-th order model.

$$\frac{d\alpha_1}{dt} = \frac{1}{\beta} k_{01}\, e^{-\frac{E_{a1}}{RT}}\, (1-\alpha_1)^{n_1} \quad \text{(Eq. 2)}$$

$$\frac{d\alpha_2}{dt} = \frac{1}{\beta} k_{02}\, e^{-\frac{E_{a2}}{RT}}\, (\alpha_1-\alpha_2)^{n_2} \quad \text{(Eq. 3)}$$

Applying the HKM has allowed to obtain the kinetics parameters presented in the table 2.

Table 2 : Summary of kinetics parameters (Cancellieri et al. 2013).

	$Virgin_{(s)} \rightarrow Char_{(s)} + Gas_{(g)}$			$Char_{(s)} \rightarrow residue_{(s)} + Gas_{(g)}$		
	n_1	Ea_1 (kJ.mol^{-1})	ln k_{01}	n_2	Ea_2 (kJ.mol^{-1})	ln k_{02}
Heather	2.63	80	12.90	0.52	114	12.50
Pine	3.97	118	23.20	0.43	128	14.20
Rockrose	3.74	120	22.10	0.52	128	14.50

3.3. Field Experiements

The experimental campaign took place on 21 June 2012 in Corsica, in the South of France. The plot is located in an area with no slope. The figure 5 presents the temperature versus time data recorded during the burn of a plot.

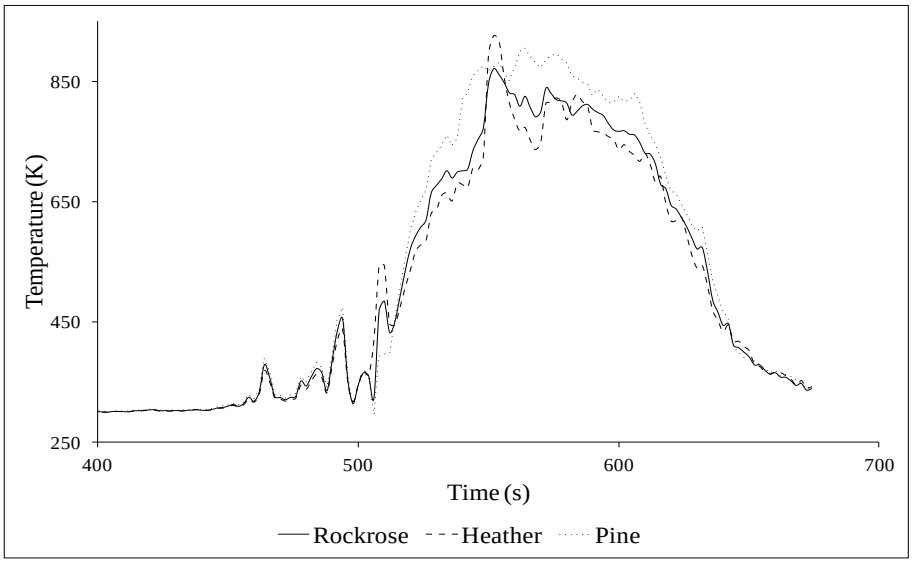

Figure 5: Temperature vs. Time obtained during a field experiment.

The temperature profiles were sensibly the same for the 3 species with a maximum at 926 K. The behavior of the temperature indicates that the fire front can be considered as a straight line impacting the prototype. It is important to note that the temperature behavior is the similar for the 2 other repetitions made during the campaign. Using the evolution of the temperature during the experiment, the heating rate is deduced for each plant. The maximum heating rates obtained are 13.2 for Pine, 12.1 for Heather and 11.1 K s^{-1} for Rockrose. The figure 6 exhibits the mass loss synchronized to the temperature and time data displayed above.

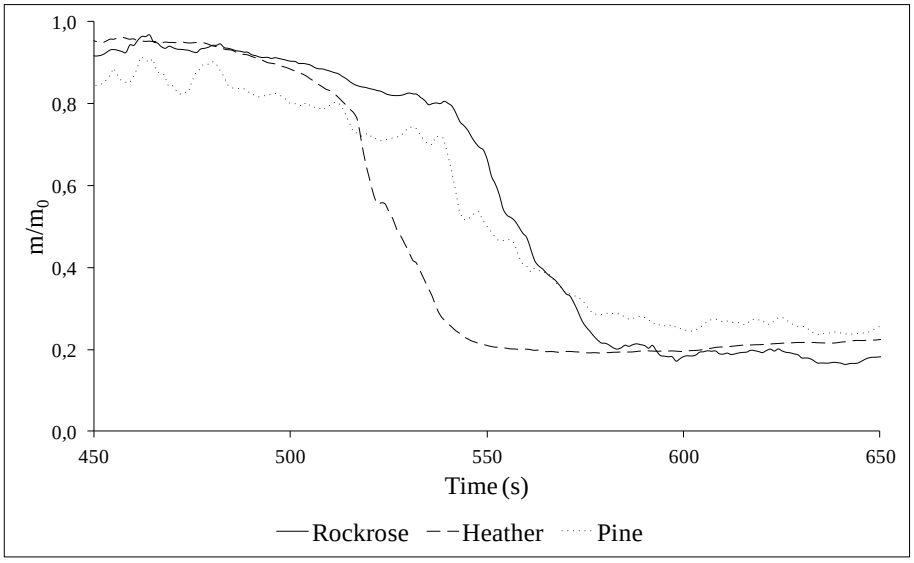

Figure 6. Experimental mass losses obtained at field scale.

The mass loss of Heather starts quickly compared to Rockrose and Pine. This observation is in agreed with the laboratory experiments. Indeed, the Heather presents a low onset which indicates that it is the specie which will ignite firstly compared to the 2 others. The behavior exhibit in TGA is corroborated at field scale. For Heather and Rockrose the degradation is fast while for Pine is slower.

3.4. Comparisons

Experimental field-scale results have been compared to numerical simulations based on Arrhenius law with kinetic parameters obtained for laboratory scale. According to the figure 5 the heating rates deducted are used for the simulations. The simulations have been performed considering the 2-steps mechanism and the kinetic parameters presented in the table 2. The figure 5 compares for each species the mass loss obtained experimentally and the data modelled according to the Eq. 2 and Eq. 3.

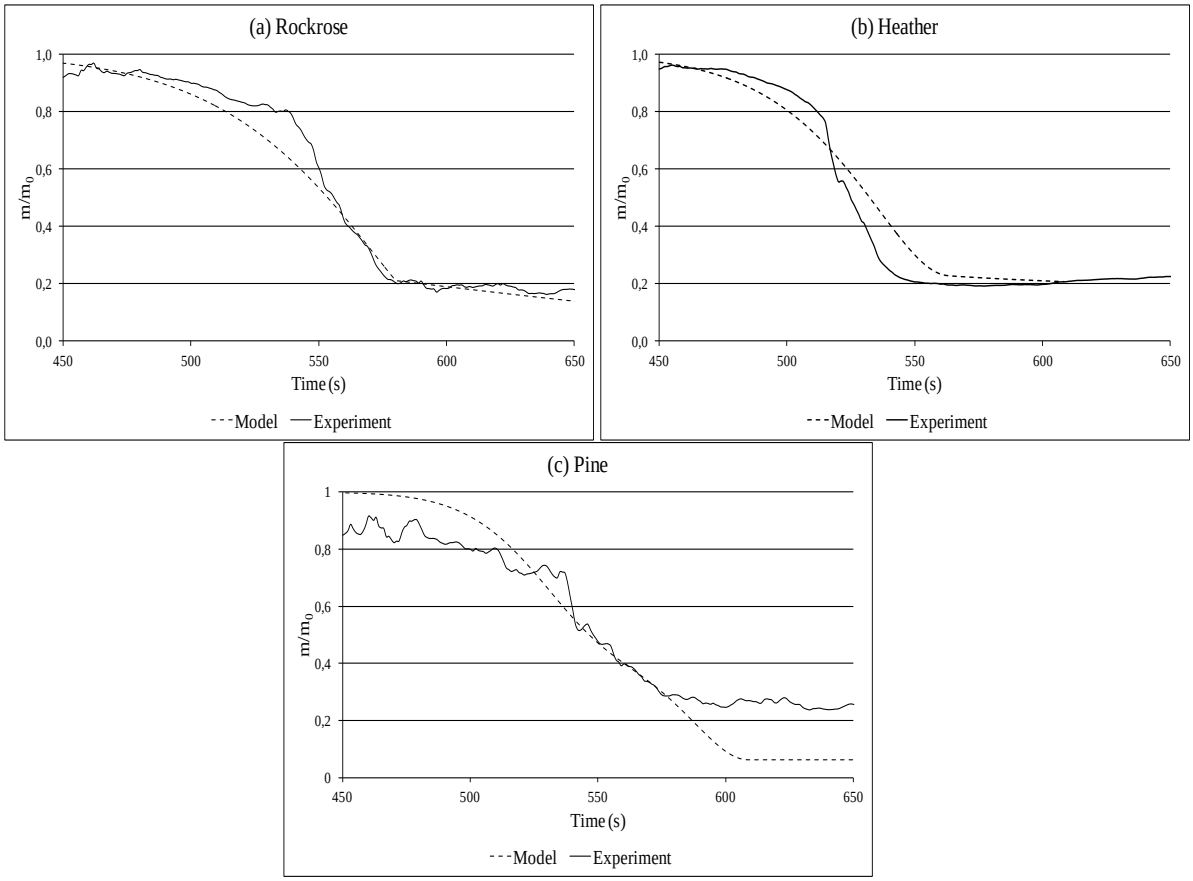

Figure 7. Experimental (solid line) and modeled (dashed line) mass loss for (a) Rockrose, (b) Heather and (c) Pine.

In a general point of view, the simulations have a good agreement with the experimental mass loss rate even if some differences appear (as attempt). For the Rockrose, the model do not match accurately in the range of $0.85 > m/m_0 > 0.60$ probably because the mechanisms of initiation and preheating are more complex than a simple Arrhenius equation of order n. Concerning the Heather, experiments exhibit an accelerate degradation process which can be explain by the very fine structure of this specie with branches of 2 mm. Conversely, Pine has a structure which is constituted by a single branch with a diameter of 6 mm. This thickness of sample involves an incomplete degradation.

Conclusion

A differential mass loss prototype has been designed with the aim to validate kinetic models adapted to field scale. This is the first time that the kinetics of decomposition of solid fuels is validated in real wildland fire condition, thus helping to a reliable characterization of a source term.
The prototype has been tested with 3 species in different conditions of fuel bed loads. Kinetic model previously tested on TGA data seems to well fit the experimental results obtained at field-scale.
The kinetic validity of the schemes is then exported outside the TGA. It is also found that the kinetic scheme with 2-steps gives a good agreement but flawed predictions are occasioned by the natural physiology of the samples (thickness, size of leaves and branches). In fact the initiation step of preheating is strongly related to the physiology. Future works will focus on the integration of the thickness in the model as an inhibitor parameter.

References

Di Blasi C (2008) Modeling chemical and physical processes of wood and biomass pyrolysis. *Prog Energy Combust Sci* **34**(1), 47–90. doi:10.1016/j.pecs.2006.12.001.

Branca C, Di Blasi C (2004) Global interinsic kinetics of wood oxidation. *Fuel* **83**(1), 81–87. doi:10.1016/S0016-2361(03)00220-5.

Cancellieri D, Innocenti E, Leroy-Cancellieri V (2013) WinGPYRO: A software platform for kinetic study of forest fuels. *Fire Saf J* **58**, 103–111. doi:10.1016/j.firesaf.2013.01.005.

Cancellieri D, Leoni E, Rossi JL (2005) Kinetics of the thermal degradation of Erica arborea by DSC: Hybrid kinetic method. *Thermochim Acta* **438**(1-2), 41–50. doi:10.1016/j.tca.2005.07.013.

Chrissafis K (2009) Kinetics of thermal degradation of polymers. *J Therm Anal Calorim* **95**(1), 273–283. doi:10.1007/s10973-008-9041-z.

Colomba DB (2008) Modeling chemical and physical processes of wood and biomass pyrolysis. *Prog Energy Combust Sci* **34**(1), 47–90. doi:10.1016/j.pecs.2006.12.001.

Fang MX, Shen DK, Li YX, Yu CJ, Luo ZY, Cen KF (2006) Kinetic study on pyrolysis and combustion of wood under different oxygen concentrations by using TG-FTIR analysis. *J Anal Appl Pyrolysis* **77**(1), 22–27. doi:10.1016/j.jaap.2005.12.010.

Kissinger H.E. (1957) Reaction kinetics in differential thermal analysis. *Anal Chem* **29**, 1702–1706.

Miller RS, Bellan J (1997) A Generalized Biomass Pyrolysis Model Based on Superimposed Cellulose, Hemicelluloseand Liqnin Kinetics. *Combust Sci Technol* **126**(1-6), 97–137. doi:10.1080/00102209708935670.

Moro C (2006) Détermination des caractéristiques physiques de particules de quelques espèces forestières méditerrannéenes.

Morvan D, Dupuy JL (2004) Modeling the propagation of a wildfire through a Mediterranean shrub using a multiphase formulation. *Combust Flame* **138**(3), 199–210. doi:10.1016/j.combustflame.2004.05.001.

Ninan KN (1989) Kinetics of solid state thermal decomposition reactions. *J Therm Anal* **35**(4), 1267–1278. doi:10.1007/BF01913047.

Pratap A, Lilly Shanker Rao T, Lad K, Dhurandhar H (2007) Isoconversional vs. Model fitting methods. *J Therm Anal Calorim* **89**(2), 399–405. doi:10.1007/s10973-006-8160-7.

Safi MJ, Mishra IM, Prasad B (2004) Global degradation kinetics of pine needles in air. *Thermochim Acta* **412**(1-2), 155–162. doi:10.1016/j.tca.2003.09.017.

Schemel CF, Simeoni A, Biteau H, Rivera JD, Torero JL (2008) A calorimetric study of wildland fuels. *Exp Therm Fluid Sci* **32**(7), 1381–1389. doi:10.1016/j.expthermflusci.2007.11.011.

Shen DK, Gu S, Luo KH, Bridgwater AV, Fang MX (2009) Kinetic study on thermal decomposition of woods in oxidative environment. *Fuel* **88**(6), 1024–1030. doi:10.1016/j.fuel.2008.10.034.

Vyazovkin S, Burnham AK, Criado JM, Pérez-Maqueda LA, Popescu C, Sbirrazzuoli N (2011) ICTAC Kinetics Committee recommendations for performing kinetic computations on thermal analysis data. *Thermochim Acta* **520**(1–2), 1–19. doi:10.1016/j.tca.2011.03.034.

Vyazovkin S, Wight CA (1998) Isothermal and non-isothermal kinetics of thermally stimulated reactions of solids. *Int Rev Phys Chem* **17**(3), 407–433. doi:10.1080/014423598230108.

White JE, Catallo WJ, Legendre BL (2011) Biomass pyrolysis kinetics: A comparative critical review with relevant agricultural residue case studies. *J Anal Appl Pyrolysis* **91**(1), 1–33. doi:10.1016/j.jaap.2011.01.004.

Numerical investigations of 3D aspects of fire/atmosphere interactions

R.R. Linn[a], J.M. Canfield[a], J. Sauer[a], M. Finney[b], J. Frothofer[b], J.L. Winterkamp[a], C.H. Sieg[g], F. Pimont[c], JL Dupuy[c]

[a] *Los Alamos National Laboratory, Los Alamos, NM, USA. rrl@lanl.gov, jessec@lanl.gov, jsauer@lanl.gov, judyw@lanl.gov*
[b] *USDA FS Rocky Mountain research Station, Missoula, MT, USA. mfinney@fs.fed.us, jaforthofer@fs.fed.us, csieg@fs.fed.us*
[c] Institut National pour la Recherche Agronomique, Avignon, France. *pimont@avignon.inra.fr, dupuy@avignon.inra.fr*

Abstract
Idealized FIRETEC grassfire simulations were used to study some of the roles that three-dimensional aspects of coupled atmosphere/fire interactions play on fire behavior. Domains of various widths that were periodic in the cross-stream direction, simulating an infinite-length fireline, were used to isolate local fireline-scale three-dimensional effects. Two-dimensional vertical plane (zero width) simulations were performed for comparison. Idealized finite-length fire simulations were used to study the larger fire-scale three-dimensional effects.
In the infinitely long simulations the fireline remains fairly straight on a macroscale while significant heterogeneities develop along the fireline at fireline-scales. These simulations suggest that the nature of atmosphere–fire coupling and these heterogeneities are influenced by wind speed. At low wind speed, the spread rate is not significantly affected by the width of the domain (for domains greater than 10 m wide). For higher wind speeds, the flank of the simulated firelines is fingered and the front of the fireline exhibits lobes. The average spread rates vary by approximately 20% for the different domain widths.
In the finite-length fireline simulations, the fireline shape was fairly parabolic and the headfire rate of spread (ROS) increased with wind speed and length of ignition line. The curvature of the fire was also influenced by the length of the ignition line. The indrafts of the headfire and flanking fire lines compete for upstream wind. For wider fires, the separation between the flanking fire lines is larger and more of the upstream wind is able to reach the headfire. These finite-length simulations also suggest that there might be an overall negative pressure gradient from upwind of the fireline to downwind of the fireline near the ground. This pressure gradient is believed to be tied to the penetration of wind through the fireline and the convective heating of unburned fuel.
Streamwise-vorticity pairs contribute to the heterogeneous appearance of the fire front by feeding upward momentum in the location where towers are seen on the fireline and thrusting hot gases through the fireline and down to the unburned fuel in the troughs between the firelines. These streamwise vorticies have also been recognized in the periodic infinite length and finite-length simulated firelines as well as laboratory tests.
In the two-dimensional simulations with wind speeds above 3 m/s, one major effect of the two-dimensional restrictions is to preclude the nominally streamwise-vorticity structures from forming upstream of the fireline. This thus diminishes the ability of the wind to mix through the heated plume and entrain hot gases down into the fuels ahead of the fire.
These simulations suggest that caution should be used when attempting to use one or two-dimensional models to simulate wildland fires. These simulations also suggest the significant value of experiments in which details of both flow and fire dynamics can be studied at scales ranging from fireline scale to overall fire geometry scales in order to better understand fire behavior. The hypothesis generated here can help provide insight in support of experimental design and analysis.

Keywords*: coupled fire/atmosphere, FIRETEC, grassfire, wildfire behaviour, vorticity, vortex*

Introduction

A variety of wildfire models have been developed in recent years to predict wildfire behavior, assess wildfire risk or simply gain insight into cause and effect relationships and the sensitivity of wildfires

to their environment. Some of the models are empirical-based, while others are process-model based so they can be used to explicitly simulate some of the processes that control wildfire behavior. In order to reduce complexity or save computational cost, some researchers have tried to develop wildfire behavior models using one- or two-dimensional formulations. In the case of empirical models, local fire-line scale three-dimensional effects can be inherently represented through extensive data collection in ensembles of experiments. However, without a good understanding of the phenomenology driving multi-scale fire dynamics, it is very difficult for these types of models to capture the larger fire-scale three-dimensional effects caused by fireline shape or end effects due to the complexity and number of experiments and/or field observations required to parameterize these effects over the possible size and shape of fires in various weather and topographic conditions. Some researchers have attempted to use computational fluid dynamics techniques to explore fire behavior using a two-dimensional x–z plane, where x is the direction of the wind and spread and z is the vertical direction. Unfortunately, these approaches inherently neglect three-dimensional features of wildfire behavior due to the combination of the two-dimensional formulation and process-based approach.

While the potential benefits of physics-based modeling includes the ability to look at the interplay between processes and explore various cause and effect relationships in fire, this approach has the downside of omitting those processes that are not resolved or explicitly modeled as unresolved processes. In two-dimensional approaches, fluctuations in the third direction are omitted unless explicitly modeled by sub-grid parameterizations. However, such parameterizations have not yet been adequately developed for wildfire behavior. Better understanding of three-dimensional aspects of coupled fire/atmosphere interactions could suggest new ways to represent the effects of three-dimensionality without explicitly resolving them by providing insight into the relative sensitivity of fire behavior to key variables, suggesting functional forms and reducing the number of parameters that must be obtained from experiments. Canfield *et al*. (2014) considered this three-dimensionality in two size-based categories: local fireline-scale aspects such as fireline undulations, which were the main focus of Linn *et al*. (2012), and larger fire-scale aspects such as fire shape.

In order to understand the implications of omitting these aspects of fire behavior, a three-dimensional physics-based simulation tool was used to explore the significance of local fireline-scale heterogeneities (Linn *et al*. 2012) as well as larger fire-scale three-dimensionality (Canfield *et al*. 2014) of coupled fire/atmosphere fireline dynamics. These explorations are intended to compliment experiments by feeding the development of new hypotheses and additional mechanistic perspectives that are very difficult to isolate in experiments.

2. Methods

Idealized simulations with a physics-based fire/atmosphere model, FIRETEC, were used to explore the impacts of the local three-dimensionality of coupled fire/atmosphere interactions on fire behavior (Linn *et al*. 2012). FIRETEC (Linn, 1997; Linn, 2002, Linn and Cunningham, 2005) was developed as an attempt to represent multi-phase chemistry and physics in a bulk sense by resolving quantities at approximately meter-scale. FIRETEC is coupled to a fully compressible, non-hydrostatic, atmospheric-dynamics model, HIGRAD (Reisner *et al*., 2000), that was specifically designed to operate at higher resolution as compared to traditional mesoscale models.

In all of the simulations described in this paper, the grid spacing in both of the horizontal directions is uniform and equal to 2 m. The grid spacing in the vertical direction is nonuniform, with a value of approximately 1.5 m near the ground increasing to about 30 m at the top of the domain (z = 615 m). The fuel bed load is specified to be similar to tall grass of height 0.7 m, with a load of 0.7 kg m^{-2}, contained within the first grid cell above the ground. Within the fuel bed, the surface area per unit volume is specified as 4000 m^{-1}.

In order to isolate local fireline-scale three-dimensionality from larger three-dimensionality such as fireline curvature and end effects, a series of simulations were performed using periodic boundary

conditions in the cross-stream direction (Figure 1) (Linn *et al*, 2012). Fires were uniformly ignited over the cross-stream width of several domain sizes: 10, 20, 40, 80, and 160 m. Since the domains were periodic in the cross-stream direction, these fires could be considered infinite in length with some periodic restrictions on them. In order to further isolate the effects of fire/atmosphere coupling from ambient upstream turbulence or the effects of eterogeneous vegetation, these idealized scenarios included homogeneous grass fuels with no cross-stream or time-dependent ambient wind variations at the domain boundary 100 m upwind of the fire. Two-dimensional, vertical plane (zero crossstream width) simulations were performed with the same model for comparison. Simulations with six different ambient wind speeds - 1 m s^{-1}, 3 m s^{-1}, 6 m s^{-1}, 9 m s^{-1}, 12 m s^{-1}, and 15 m s^{-1} - were performed for each of the two-dimensional and three-dimensional periodic scenarios.

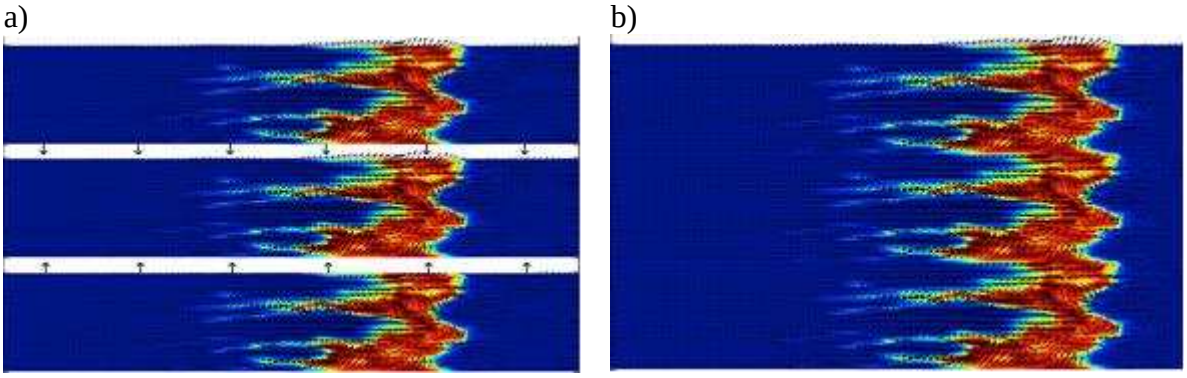

Figure 1. Top down view of 6 m s-1 wind 40 m wide fire simulation a) (in red dotted box) and the use of periodic boundary conditions to conceptually approximate an infinite-length fireline a) and b). In these images the colors indicate gas temperatures (Dark Blue is 300 K and red is greater than 1100K.) These images show the fingering behind the fireline and lobes in front of the fireline. This structure was ftypical for the infinite fireline simulations with 6 m s-1 and stronger winds.

Idealized FIRETEC simulations were also used to study the interactions between fireline shape and rate of spread (Canfield *et al*., 2014). Idealizations/simplifications similar to the infinite fireline approach described above were used except that these fires were finite in length and not periodic in the span-wise direction. These simulations, which were performed with ambient wind speeds of 3 m s^{-1} and 6 m s^{-1}, included finite-length ignition lines ranging from 20 to 400 m in length. In these simulations, the lateral boundary conditions were at least 100 m away from the ends of the ignition line. The winds at the boundaries were relaxed to the upstream flow velocity profile.

Results

All of the infinite-length simulations that were periodic in the stream-wise direction (Linn *et al*., 2012) showed some heterogeneity in the crossstream direction, even though the upstream winds, fuel, and ignition were uniform in this direction. This series of simulations suggest that the nature of atmosphere/fire coupling and the variability along the length of the fireline are influenced by wind speed. At low wind speed, variation along the length of the fireline exists but the fireline remains fairly straight and the spread rate is not significantly affected by the width of the domain (for domains greater than 10 m wide) for the duration of the simulations. For higher wind speeds, the upwind side of the simulated firelines are fingered and the downstream edge of the firelines exhibit lobes. The average spread rates vary by approximately 20% for the different domain widths (Table 1). This may indicate that the variety of sizes of atmosphere–fire structures influence spread rates and become affected by periodic domain constraints as the domain gets smaller. At higher ambient wind speeds, the structure of the wind and temperature fields also show evidence of streamwise vorticity.

Table 1. Rates of spread for periodic infinite-length fireline simulations of various widths and various wind speeds (measured 10 m above ground) (Linn et al., 2012).

Wind Speed U_{10} (m s^{-1})	2D	10 m	20 m	40 m	80 m	160 m
1	.57	.25	.23	.22	.22	.22
3	1.10	1.33	1.35	1.25	1.18	1.14
6	1.24	2.15	2.27	2.14	1.91	1.92
9	.77	2.23	2.81	2.41	2.49	2.28
12	.76	2.67	3.14	2.96	2.94	3.01
15	1.63	3.17	3.31	3.56	3.47	3.44

In the periodic infinite-length simulations, rate of spread increases with wind speed as seen in previous investigations with this model (Linn and Cunningham, 2005) as well as other numerical works and observations. The magnitudes of the spread rates for the periodic simulations were in general larger than those seen in the Linn and Cunningham (2005) finite-length fireline simulations. This result suggests a reduction of rate of spread due to fire-scale three-dimensional features such as end effects and fireline curvature that were present in the Linn and Cunningham (2005) simulations.
In the finite-length fireline simulations (Canfield *et al*., 2014) the fires did not stay relatively straight as they did in the periodic simulations (Figure 2). Instead, they took on a shape that was parabolic-like. In these simulations, rate of spread increased with wind speed and length of ignition line (Table 2) as expected and shown by observations (Cheney *et al*., 1993) and previous numerical studies (Linn and Cunningham, 2005; Mell *et al*., 2007). Flanking fire behavior was also influenced by ignition line length. As a result, fireline shape was affected by ignition line length.

Table 2. Rates of spread for finite-length fireline simulations of various widths and 3 m s^{-1} and 6 m s^{-1} wind speeds (measured 10 m above ground) (Canfield et al., 2012).

Wind Speed U_{10} (m s^{-1})	20 m Ignition line	100 m Ignition line	200 m Ignition line	400 m Ignition line
3	.20	0.68	1.10	1.15
6	.27	1.19	1.45	1.75

Three-dimensional effects at fireline scales

A predominant feature of both the relatively straight periodic infinite-length and the curved finite-length firelines is the presence of stream-wise vorticies that originate well behind the fireline and extend into the fireline itself. Such structures have also been identified in laboratory experiments at the USDA Missoula Fire Lab and are believed to be very important to the spread of fires. These stream-wise vorticies form alternating pairs and occasionally combine into larger vorticies. The development and strengthening of these vorticies is linked to the buoyancy of the sustained burning, which itself is heterogeneous in the crosswind direction. These pairs contribute to the heterogeneous appearance of the heading-fire front by feeding upward momentum in the location where flaming towers are seen on the fireline. The helical nature of the vortices thrust hot gases through the fireline and down to the unburned fuel in the troughs between the towers (Figure 3).

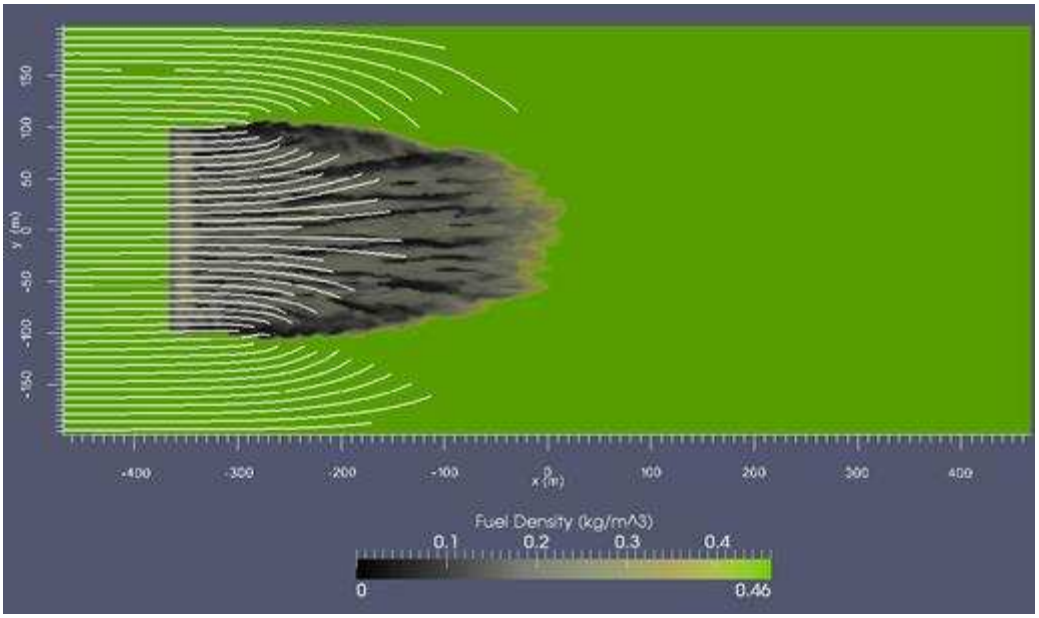

Figure 2. Top down view of 6 m s^{-1} wind 200 m-ignition fire. This image illustrates the parabolic shape of the progressing fire and the white streamlines illustrate the interaction between the upstream air flow and the competing indrafts of the flanking and heading firelines

In the two-dimensional simulations there were no cross-stream variations. These scenarios are more representative of a fire burning between two very-close plates of glass with wind blowing between them than they are of a two-dimensional slice through an infinitely long fireline. With ambient wind speeds of 1 m s^{-1}, the general structure of the plume appeared similar to those seen in the 1 m s^{-1} three-dimensional periodic simulation, but the spread rate was more than twice as fast as in the three-dimensional simulations. For wind speeds above 3 m s^{-1}, a significant effect of the two-dimensional restrictions was to preclude stream-wise and vertically oriented vortex structures. These structures occurred and proved to be important in the three-dimensional calculations, but are prevented in two-dimensional calculations because they require heterogeneity in the cross-stream direction. The elimination of the three-dimensional vorticity under two-dimensional constraints diminishes the ability of the wind to mix through the heated plume and entrain hot gases down into the fuels ahead of the fire. This causes a much slower spread rate in the two-dimensional simulations compared to the periodic three-dimensional simulations for ambient winds of 6 m s^{-1} and higher.

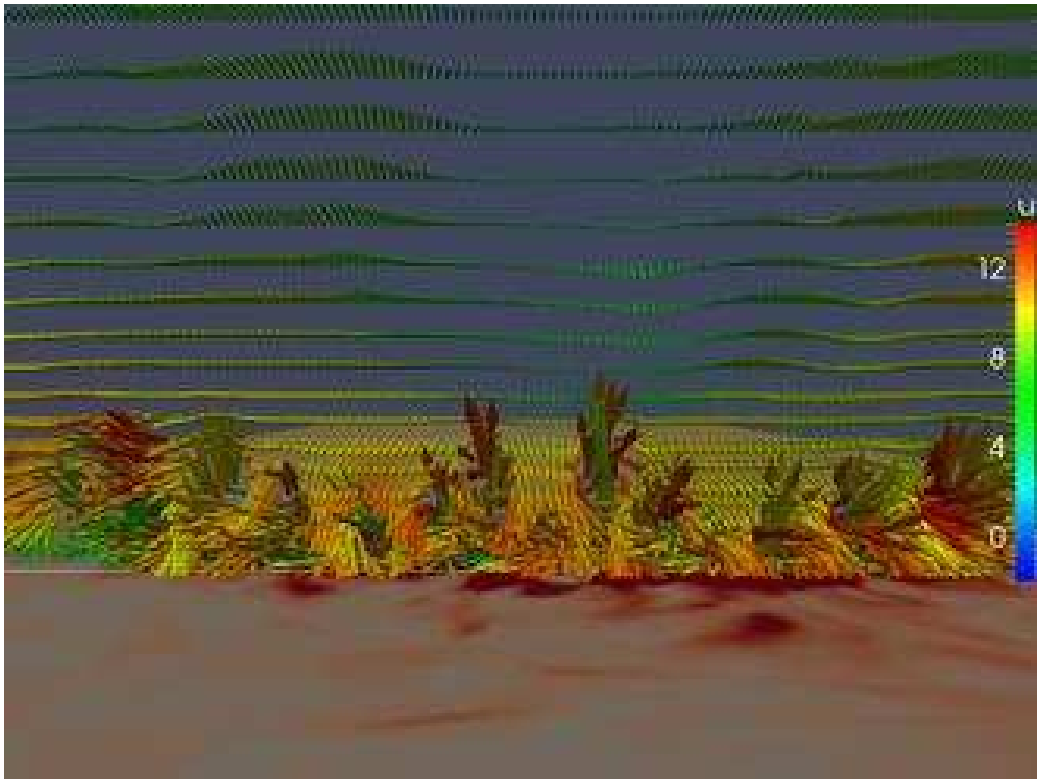

Figure 3 – Head on FIRETEC simulation of finite-length fireline (looking from in front of the fire as it approaches). This image illustrates the significance of the heterogeneity along the fireline in the cross-stream direction (left and right in the image). The fuel surface is colored by convective heating of the fuel where red is heating and blue is cooling. The vectors are in a y-z plane extending vertically above the white line and the vectors are colored by stream-wise velocity and scaled by total velocity

1.2. Three-dimensional effects at fire scales

In the finite-length fireline simulations, the curvature of the fireline and ability for winds to move around the fire lead to different fire behaviour than seen in the infinite-length fire scenarios. These differences are exacerbated by a couple of three-dimensional fire-scale interactions between the fire and the atmosphere. The head and flanking sections of the fire influence each other through their fire-induced indrafts. Indrafts from the flanking portions of the fireline compete with each other for the supply of upstream wind. For example, flanking portions of the fire draw from the airflow upstream, leaving a reduced amount of stream-wise wind to push the head fire forward and thus slowing down the forward spread rate. For wider fires, the separation between the flanking fires is large enough that competition between flanking fires is a non-issue. In scenarios where the flanking portions of the fire are relatively short compared to the length of the head fire, the wind can more effectively reach the headfire and transport hot gases to the unburned fuel in front of the fire. Similarly, as the competition between flanking fire and headfire sections of the fireline decreases, the wind arriving at the inside of the flanking fire sections can increase, enabling more effective heat transfer to the unburned fuel on the flanks as well. The competition between the indrafts of flanking and head fire and the net impacts on spread rate should be investigated experimentally in the future, as it has the potential to tie observable fireline geometry characteristics to corrections for rate of spread calculations.

The idealized finite-length grass fire simulations also suggest that there might be an overall negative pressure gradient from upwind of the fireline to downwind of the fireline. This pressure gradient may affect the penetration of wind through the fireline and the convective heating of unburned fuel. The magnitude of the effective pressure gradient across the fireline is influenced by the upstream in-draft competition between flanking and headfires. These firelines did not extend across the entire domain

and air was free to move around them, unlike in the periodic infinite-length simulations described above where air cannot move around the firelines. The wind flow around the fires in the finite-fire simulations alters the upstream to downstream pressure gradient and therefore can contribute to the differences in spread rate between the infinite firelines and the finite length firelines. This effect contributes to the difference between the finite-length firelines and infinite-length fires where the firelines become much deeper (in the streamwise direction) firelines and have larger rates of spread. In the periodic infinite-fireline scenarios, the larger pressure gradient across the firelines and inability of the winds to move around the fireline increase the flow through the fireline and the heat transfer to the unburned fuel in front of the fire.

Conclusions

This work suggests ways that the three-dimensionality of coupled fire/atmosphere behavior at a variety of scales affect fireline dynamics. The three-dimensional phenomena outlined here (described in detail in Canfield *et al*., 2014 and Linn *et al*., 2012) provide the basis for hypotheses that need to be tested in laboratory and field experiments. The three-dimensionality of the fire/atmosphere interaction also has significant implications for measurement strategies in such experiments. The analysis of any point measurements should include both knowledge of the position of the measurement with respect to the shape of the fireline as well as the context of the measurement with respect to the towers and troughs of the fireline itself.

These simulations suggest that caution be taken when attempting to use a two-dimensional assumption for wildland fire spread modelling. This is especially important when attempting to interpret results in the context of a process-based model such as that of Linn (1997), where the two-dimensional nature of the calculations are believed to have significant impacts on the simulated fire behavior. Care should be taken to account for the combined impacts of the variations in the flow field and plume structure in the third dimension. It is possible that the effects of local three-dimensionality could be represented in a manner similar to how turbulence kinetic energy is modelled without actually resolving the velocity fluctuations; however, this is not a trivial task and has not been accomplished to date. Such advances will likely come from a combination of modelling, laboratory experiments and field observations.

References

Canfield JM., Linn RR., Sauer J., Finney M., Forthofer J., 2014. A numerical investigation of the interplay between fireline length, geometry, and rate of spread. *Agricultural and Forest Meteorology*.

Cheney, N.P., Gould, J.S., Catchpole, W.R., 1993. The influence of fuel, weather and fireshape variables on fire-spread in grasslands. *International Journal of Wildland Fire* 3, 31–44.

Linn, R.R. 1997. A transport model for prediction of wildfire behavior. Los Alamos National Laboratory Report LA-13334-T.

Linn, R.R., Reisner, J. Colman J., Winterkamp J., 2002. "Studying wildfire behavior using FIRETEC." International Journal of Wildland Fire **11**(3-4): 233-246.

Linn, R.R., Cunningham, P., 2005. Numerical simulations of grass fires using a coupled atmosphere–fire model: basic fire behavior and dependence on wind speed. *Journal of Geophysical Research* 110, D13107, doi:10.1029/2004JD005597.

Linn, R.R., Canfield, J.M., Cunningham, P., Edminster, C., Dupuy, J.-L., Pimont, F., 2012. Using periodic line fires to gain a new perspective on multi-dimensional aspects of forward fire spread. *Agriculture and Forest Meteorology* 157, 60–76.

Mell, W., Jenkins, M.A., Gould, J., Cheney, P., 2007. A physics-based approach to modeling grassland fires. *International Journal of Wildland Fire* 16, 1–22.

Reisner, J., Wynne, S., Margolin, L., and Linn, R., 2000. Coupled atmospheric-fire modeling employing the method of averages. Mon. Weather Rev. 128(10): 3683–3691. doi:10.1175/1520-0493 (2001)129<3683:CAFMET>2.0.CO;2.

Numerical simulations of spreading fires in a large-scale calorimeter: the influence of the experimental configuration

Y. Pérez-Ramirez[a], P.A. Santoni[a], J.B. Tramoni[a], W.E. Mell[b]

[a] *CNRS UMR 6134, Campus Grimaldi, BP 52, 20250 Corte, France, perez-ramirez@univ-corse.fr*
[b] *US Forest Service Pacific Northwest Research Station, Pacific Wildland Fire Science Laboratory, 400N, 34th Street, Suite 201 Seattle, WA98103, wemell@fs.fed.us*

Abstract
The validation of physical models of fire spread requires comparing simulated results and experimental observation. Fire tests conducted at laboratory scale are appropriate to measure the finest physical mechanisms that cannot be recorded at field scale. However, particular attention must be paid concerning the influence of the experimental configuration on the fire and the way to take them into account for the simulation. Indeed, one must be sure that the main effects due to the experimental device and design are well reproduced by the models before to investigate the validation of such model by comparison with thermodynamics quantities measured. In this paper a methodology is proposed to be able to test a physical model against experiments conducted in a Large Scale Heat Release calorimeter. The hood effects as well as the ignition are investigated with WFDS, a physical model of wildland fire.

Keywords*: Calorimetry measurements, 3D numerical simulation, WFDS, fire behaviour*

Introduction

The use of physically-based wildland fire models for research purposes has increased in this last decade both due to their potential to capture the basic physical processes regardless of the scale (Porterie *et al*., 2005, Mell *et al*. 2007), and due to the growing improvements offered by computational resources. These models have been assessed at different scales but their validation is still ongoing. Laboratory-scale experiments can provide an important source of data for validating physically-based models at this particular scale. However, laboratory fires are relatively low intensity fires and their behaviour is related to the experimental configuration (e.g. experimental methodologies and design, characteristics of the experimental device, etc.). So, when using laboratory experimental data to validate physically-based models, this aspect should be carefully taken into account in order to avoid misleading conclusions.
Figure 1 depicts the different aspects that must be considered to ideally compare the simulation results provided by a given model with experimental observations done at laboratory scale. Depending on the experimental configuration, the design and device parameters might be different. With regard to the experimental design parameters, we can consider that fuel load and slope are common parameters frequently used by many investigators (Dupuy 1995, Viegas 2004, Tihay 2012). Although the range of variation for these parameters might be different from one author to the other, they can be easily (and implicitly) taken into account by physical models. Another important parameter concerning the experimental design is the ignition pattern. Different ignition types (linear or point) and methods can be found in literature. For linear ignition, Viegas *et al*. (2004) use one or more threads of wool soaked in a mixture of petrol and fuel oil. The threads are located at the edge of the fuel bed and ignited with matches. A linear flame is obtained along the thread in 5s. Santoni *et al*. (2010) spread a line of alcohol (4 to 6 ml) linearly on the fuel with a pipette and use a flame torch to ensure quasi-instantaneous ignition along one edge of the fuel. Although for such ignition patterns the fire will spread similarly under no slope condition, conversely ignition condition might affect the spreading for canyon

configuration for instance. Hence providing a numerical ignition close to the experimental one is of interest for the test of physical models. Some parameters that can also affect the spreading of fire are related to experimental device used. For instance the physical properties of the bench substrate are not thermally negligible (Dupuy, 1995). The thermal conductivity of a metallic bench (Viegas, 2004) for instance is different from an air-entrained concrete plate (Santoni *et al*, 2010). Thus heat transfer between the fuel bed and the bench must be taken into account. Another parameter that can affect fire spreading is the use of an exhaust system. Santoni *et al*. (2010) used such type of system to investigate the heat release rate (HRR) of spreading fires by collecting the smoke released during fire spread. By measuring the consumption of oxygen it is possible to derive the HRR. In previous works we investigated the HRR, the radiant and convective fraction of energy release by fire under slope and no slope conditions (Tihay *et al*., 2012). Those results can be used to validate physical models of fire spread. However the exhaust system has to be taken into account in the numerical study since the air entrainment near the fire can slightly be modified by the extraction system for low intensity fires. Finally, besides experimental design and experimental device parameters that must be accounted for, the numerical computational parameters (grid size sensitivity, parallelisation,) are of primarily importance. The size of the mesh must be fine enough to couple with both combustion of gases and heat transfer within the fuel bed.

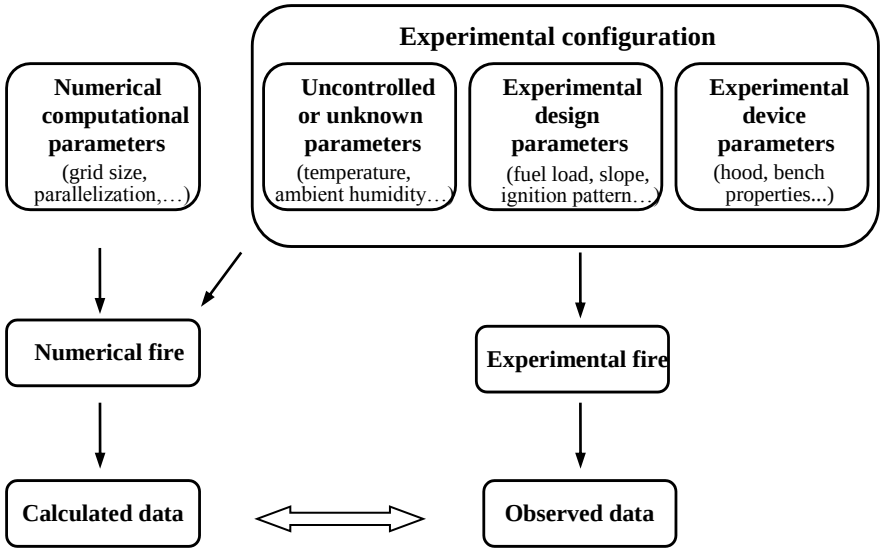

Figure 1. Diagram of the influence of the experimental conditions on numerical and experimental fires

In this paper the use of a physically-based model to simulate spreading fires in a large-scale heat release calorimeter is addressed, paying special attention to the influence of the experimental configuration. The study has been focused on two parameters which could have a major role in the behaviour of numerical fires; this is the hood extraction system and the ignition method. The experimental configuration is first depicted. Then some experimental results are provided to detail the quantities of interest to be modeled. The numerical model is presented in the fourth section. It is the *Wildland urban interface Fire Dynamics Simulator* – WFDS (Mell *et al*., 2007; Mell *et al*., 2009) developed by the National Institute of Standards and Technology (NIST) and the US Forest Service. The air flow in the hood is then studied as well as the numerical ignition. A grid sensitivity analysis is performed for the flow to reach a compromise between precision and simulation time.

Experimental configuration

The fire spread experiments were conducted by using a 1 MW Large Scale Heat Release rate apparatus (LSHR). Fire tests were performed on a 2 m long and 2 m wide combustion table located under a 3 m × 3 m hood with a 1 m^3/s extraction system (Figure 2). Two thermocouples (48 cm spaced) recorded the temperature of the combustion gases in the exhaust smoke duct. The bench was located on a load cell (sampling rate 1 Hz and 1 g accuracy) in order to record the mass loss over time during the fire spread across a fuel bed. Needles of *Pinus pinaster* were distributed uniformly on the table in order to obtain homogenous fuel beds of 1 m width and 2m long that occupy only the central part of the table. Particular attention was paid to the preparation of the fuel bed. Different fuel loads were tested: 0.6, 0.9 and 1.2 kg/m^2 that correspond respectively to fuel beds height of 4 cm and 6 cm for the highest loads. At least four repetitions were carried out for each fuel load.

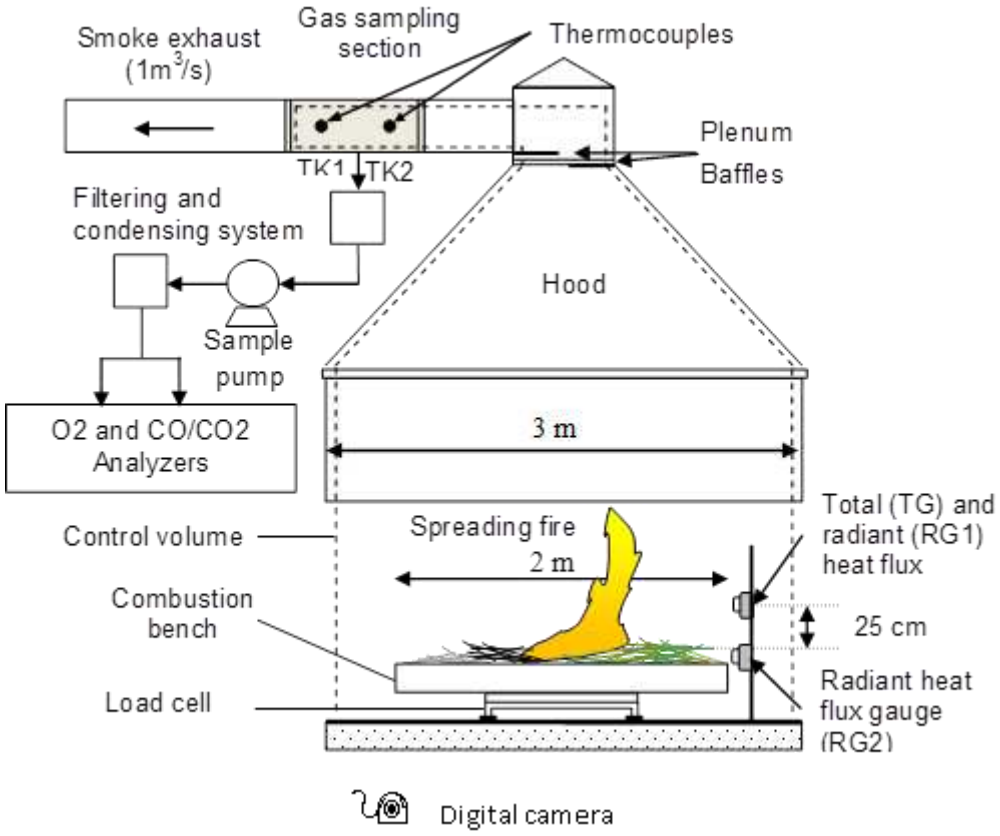

Figure 2. Large Scale Heat Release apparatus used for the fire tests

The net heat of combustion, the surface to volume ratio and density of the particles were $\Delta H_{c,needles}$ = 20313 kJ/kg, σ = 3057 /m and ρ = 511 kg/m^3 respectively. The net heat of combustion was derived from the gross heat of combustion measured in an oxygen bomb calorimeter following the standard AFNOR NF EN 14918. The needles were oven dried at 60°C for 24 hours. The resulting moisture content was between 3-5%. To ensure fast and linear ignition, a small amount of alcohol and a flame torch were used. The fire tests were conducted without wind under slope angles of 0° and 20°. The rate of spread was deduced from the position of the fire over time every 0.25 m. Three heat flux gauges (Medtherm Corporation) were placed at the end of the experimental bench, in the centre of the bed (see Figure 2 for no slope fire). The total heat flux gauge (TG) and a radiant heat flux gauge (RG1) were oriented towards the flame and located 0.20 m above the bed. The second radiant heat flux gauge (RG2) was located at the end of the combustion bench, at mid height of the fuel layer in order to measure radiation from the bed (Figure 2).

HRR measurement and main experimental results

The experiment performed allowed us measuring an important quantity of data: fire front geometry (flame height, flame angle), rate of spread, heat release rate (HRR), burning rate, convective and radiant fraction, radiant heat flux. However for the purpose of this study we solely consider the HRR as it is among the most important parameter for understanding combustion process and fire characteristics (Babrauskas and Peacock, 1992). The measurement of exhaust flow velocity and gas volume fractions were used to determine the heat release rate (HRR) based on the formulation derived by Parker (1992). The heat release rate is given by the oxygen molar flow rate:

$$HRR = E\left(\dot{n}_{O_2}^{\circ} - \dot{n}_{O_2}\right)W_{O_2} \tag{1}$$

where $\dot{n}_{O_2}^{\circ}$ and $\dot{n}_{O_2}$ represent respectively the molar flow rates of O_2 in incoming air and in the exhaust duct and W_{O_2} is the molecular weight of oxygen. The volume flow rate of incoming air, referred to standard conditions is:

$$\dot{V}_a = \frac{\dot{n}_{O_2}^{\circ}}{X_{O_2}^{\circ}}\frac{W_{air}}{\rho_0} \tag{2}$$

where $X_{O_2}^{\circ}$ is the molar fraction of O_2 in incoming air and W_{air} is the molecular weight of dry air at 25 °C and 1 atm. The oxygen depletion factor is introduced for convenience. It is given by:

$$\phi = \frac{\dot{n}_{O_2}^{\circ} - \dot{n}_{O_2}}{\dot{n}_{O_2}^{\circ}} \tag{3}$$

Combining Eq. (1) - (3), one obtains the HRR, $\dot{q}$:

$$\dot{q} = \frac{E\rho_0 W_{O_2}}{W_{air}} X_{O_2}^{\circ}\phi\dot{V}_a \tag{4}$$

Gases are measured on a dry basis since the analyzers cannot handle wet mixtures. Thus, the mole fraction of gases in air is derived from the analyzers' measurement and from air humidity. For instance, the mole fraction of oxygen in air is given by:

$$X_{O_2} = \left(1 - X_{H_2O}\right)X_{O_2}^{a} \tag{5}$$

where superscript *a* denotes the mole fraction in the analyzers. Unfortunately, in an open system, not the incoming air flow rate $\dot{V}_a$ but the flow rate in the exhaust duct $\dot{V}_s$ is measured. A relationship between $\dot{V}_a$ and $\dot{V}_s$ is obtained and after some development (Parker, 1992), the HRR is given by the three following relations:

$$\dot{q} = \frac{E\rho_0 W_{O_2}}{W_{air}}\left(1 - X_{H_2O}^{\circ}\right)X_{O_2}^{a\circ}\dot{V}_{s,298}\left[\frac{\phi}{(1-\phi)+\alpha.\phi}\right] \tag{6}$$

$$\dot{V}_{s,298} = 22.4A\frac{k_t}{k_p}\sqrt{\frac{\Delta P}{T_S}} \tag{7}$$

$$\phi = \frac{X_{O_2}^{a^\circ}\left(1 - X_{CO_2}^{a}\right) - X_{O_2}^{a}\left(1 - X_{CO_2}^{a^\circ}\right)}{X_{O_2}^{a^\circ}\left(1 - X_{CO_2}^{a} - X_{O_2}^{a}\right)} \quad (8)$$

X denotes the molar fraction and ρ_0 is the density of dry air at 298K and 1 atm. $\dot{V}_{s,298}$ is the standard flow rate in the exhaust duct. α is the expansion factor for the fraction of the air that was depleted of its oxygen. The superscript ° is for the incoming air. A is the cross sectional area of the duct, k_t is a constant determined via a propane burner calibration, k_p=1.108 for a bi-directional probe, ΔP is the pressure drop across the bi-directional probe and T_s is the gas temperature in the duct.
Instantaneous heat release rates (HRR) measured during the fire tests are displayed in Figure 3 for fuel loads of 0.6, 0.9 and 1.2 kg/m² and no slope. For experiments performed without slope, a quasi-steady state was reached for all fuel loads. The flameout occurred earlier for higher fuel load due to the increase in the rate of spread. The average HRR were computed during the quasi-steady state. The average heat release rates were 41, 87 and 130 kW for the 0.6 to 0.9 and 1.2 kg/m² fuel load, respectively. The greater the fuel load, the greater the heat release rate. The mean values increased by a factor of 2.1 and 3.2 with increasing the fuel load by a factor of 1.5 and 2. The total heat released (THR) was obtained by integration of the HRR curves during the whole experiment. The average total heat released were 22, 33 and 44 MJ for the 0.6, 0.9 and 1.2 kg/m² fuel load, respectively. The total heat released depends also linearly on the load.

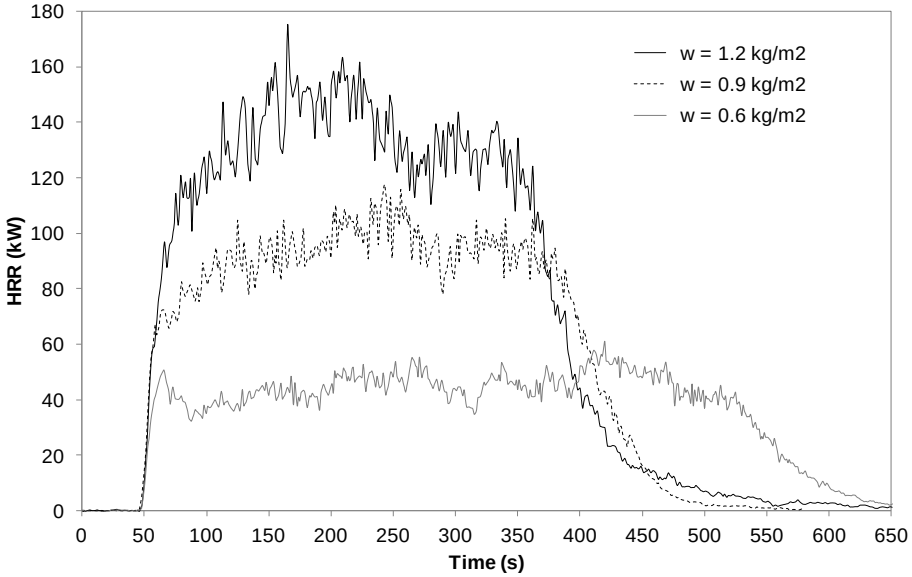

Figure 3 –Heat release rate versus time for fuel load of 0.6, 0.9 and 1.2 kg/m²

Numerical model

The numerical approach, called WFDS for WUI Fire Dynamics Simulator, is an extension of the capabilities of the FDS (Fire Dynamics Simulator) to outdoor fire spread and smoke transport problems that include vegetative and structural fuels and complex terrain. FDS is a fire behaviour model developed by NIST in cooperation with VTT Technical Research Center of Finland, industry, and academics (Mc Grattan *et al*., 2013a). The methods of computational fluid dynamics (CFD) are used to solve the three-dimensional time-dependent equations governing fluid motion, combustion, and heat transfer. The numerical model is based on the large-eddy simulation (LES) approach and provides a time-dependent, coarse-grained numerical solution to the governing transport equations for mass,

momentum, and energy. There are currently two ways of representing vegetative fuel in WFDS. One is restricted to surface fuels (Mell *et al*., 2007). It is called the boundary fuel model. The other, called the fuel element model can be used for raised or surface fuels but requires more spatial resolution (Mell *et al*., 2009). The interested reader is referred to Mell *et al*. (2009) for an extended presentation of WFDS and its capabilities. In the present work, we use the fuel element model to represent the vegetation. We assume that the litter is composed of thermally thin fuel elements. The needles of *Pinus Pinaster* are sufficiently small in size (e.g., branches <1.85 mm in diameter) that the heat transfer is not resolved within the core of each needle on the computational grids used here (2 cm). This is similar to other modelling approaches (Porterie *et al*., 2005). Both convective and radiative heat transfer between the gas phase and the vegetation is accounted for, as is the drag of the vegetation on the airflow. In the modelling approach used here, the temperature equation for the fuel bed is solved assuming a two stage endothermic decomposition process of water evaporation followed by solid fuel pyrolysis. The grid size (2 cm) inside the vegetation litter was evaluated as a fraction of a length scale representative of the radiative heat transfer $\delta_R = 4/(\beta\sigma)$ which constitutes one of the most important modes of heat transfer contributing in many situations to the propagation of the fire. β represents the compactness of the litter. Its value was 0.029 for the fuel loads of 0.6 and 0.9 kg/m^2 and 0.039 for the fuel load of 1.2 kg/m^2. The values of δ_R are respectively 4.4 cm for the fuel loads of 0.6 and 0.9 kg/m^2 and 3.3 cm for the fuel load of 1.2 kg/m^2. Simulations were run with an Intel Xeon cluster whose nodes consists of two 8-core Intel Xeon E5-2650 CPUs running at 2.0 GHz with 32 GB of main memory.

Sensitivity analysis and ignition method

5.1. Sensitivity analysis of the flow in the hood

As detailed previously, calorimetric calculations are based on the measurement of oxygen consumption. A hood extraction system collects the gases released from the combustion, hence this system induces an air flow. Validating a physical model of vegetation requires thus being capable to capture the flow within the hood that could influence the spreading of the fire. In other words, before to test the model against experimental results one must verify previously that it is able to represent the flow without fire, since the flow field could have an influence for fire tests with the smallest fuel load. Indeed, for the load value as 0.6 kg/m^2, the fire front is not regular and it seems formed of an ensemble of individual flamelet. It is not the case for the highest fuel load (0.9 kg/m^2 and 1.2 kg/m^2) for which the fire front is like a wall of flame spreading towards the unburned fuel. To study the flow we have first considered the whole laboratory of experimentation with the LSHR inside as well as the different vents. Figure 3 depicts the laboratory simulated with WFDS.

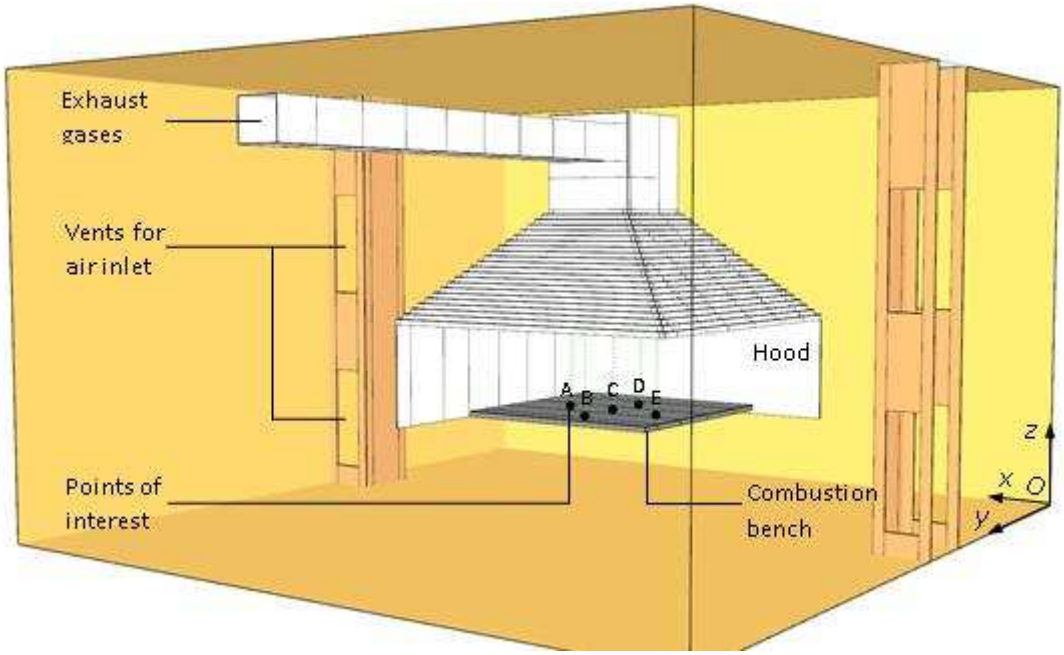

Figure 4. Laboratory with LSHR and vents.

We can see that the domain of calculation is much larger than the LSHR hood where the fire tests were performed. However, before to reduce the size of the calculation domain (to the size of the control volume of the hood as shown in figure 1 for instance) it is important as a first step to conduct a sensitivity analysis with the actual dimension of the experimental laboratory whose dimensions are 6.6 m long, 6.4 m large and 4.4 m high.

Sensitivity analysis

A sensitivity analysis has been performed to find out the more appropriate grid resolution to capture the flow dynamics behavior within the hood. Although the mesh size inside the vegetation is governed by the radiant heat transfer through the fuel bed, conversely a measure of how well the flow field is resolved in the gas phase above the fuel (for simulations involving buoyant plumes) is usually given by the non-dimensional expression $z_c / \delta x$ (Mc Grattan *et al*., 2013b)

$$z_c = \left(\frac{\dot{q}}{\rho_\infty c_p T_\infty \sqrt{g}} \right)^{2/5} \tag{9}$$

where z_c is a characteristic fire scale, δx is the nominal size of a mesh cell and $\rho_\infty = 1.2$ kg/m^3 , $c_p = 1000$ J/(kg.K) and $T_\infty = 293$ K are respectively the density, specific heat and temperature of ambient air. The $z_c / \delta x$ values have to range from 4 to 16 (Mc Grattan *et al*., 2013b). In our case, since the fire is spreading as a line, the characteristic length scale $z_{c,line}$ for a line plume is given by:

$$z_{c,line} = \left(\frac{\dot{q}'}{\rho_\infty c_p T_\infty \sqrt{g}} \right)^{2/3} \tag{10}$$

where $\dot{q}'$ represents the fire line intensity, i.e. the energy release rate per unit length of the fire (Quintiere, 2006). Since the fire front remains quasi-linear during the fire tests, the fire line intensity is equivalent to the HRR: 41, 87 and 130 kW respectively for fuel loads of 0.6, 0.9 and 1.2 kg/m². We obtain $z_{c,line}$ values of 0.11, 0.18 and 0.24 m respectively for the 0.6 to 0.9 and 1.2 kg/m² fuel loads. For these fuel loads, the mesh size δx must respectively be lower than 2.8, 4.6 and 6 cm.

As a first stage, our sensitivity analysis is based on the study of the flow in the hood without the fire. The following mesh sizes were used: 2.5 cm, 5 cm and 10 cm called respectively grid 1, grid 2 and grid 3 in the following. The reason is that away from the fire, the mesh size can be coarse and having mesh size greater than the sizes mentioned previously can provide computational time saving without altering the resolution of the fire region for which the grid has to be finer (less than 2.8, 4.6 and 6 cm for the 0.6 to 0.9 and 1.2 kg/m² fuel loads). For the sensitivity analysis, we will consider 5 positions of interest on the bench on combustion (Figure 4): point C is at the center of the table and points A, B, D and E are positioned 0.5 m aside. The global velocity and the velocity components of the flow will be considered as a function of height above these 5 positions. The interval (Fig 4) between each point along height depends on the mesh size. The total velocity (and deviation) with height are displayed in figure 5 above positions A and C as example. The results presented are representative of simulations obtained at location B, E and F. The better agreement between grid 1 and 2 was obtained at position A while position C is representative of the worst agreement between simulations results obtained with both grids. Figure 5 shows that the values of the total velocity obtained with grid 2 are near to the simulation of reference performed with grid 1. We observe also that grid 3 fails to reproduce the tendency of the variation of the velocity with height observed for grid 1 and 2. The small differences observed between the results obtained with grid 1 and grids 2 suggest that a mesh size of 2.5 cm is sufficient to get convergence in the case of a non reacting flow. Another point that deserves mention is the comparison of inflow at the vent of the domain. The mass balance was checked for the three grids, but we observe that the inflow is very different for grid 3. In that case, a greater amount of air comes into the domain and then flow out at the vent denoting an important recirculation that was very low for grid 1 and grid 2. All these results show that a mesh size of 10 cm is not capable to accurately represent the flow in the hood and in the laboratory.

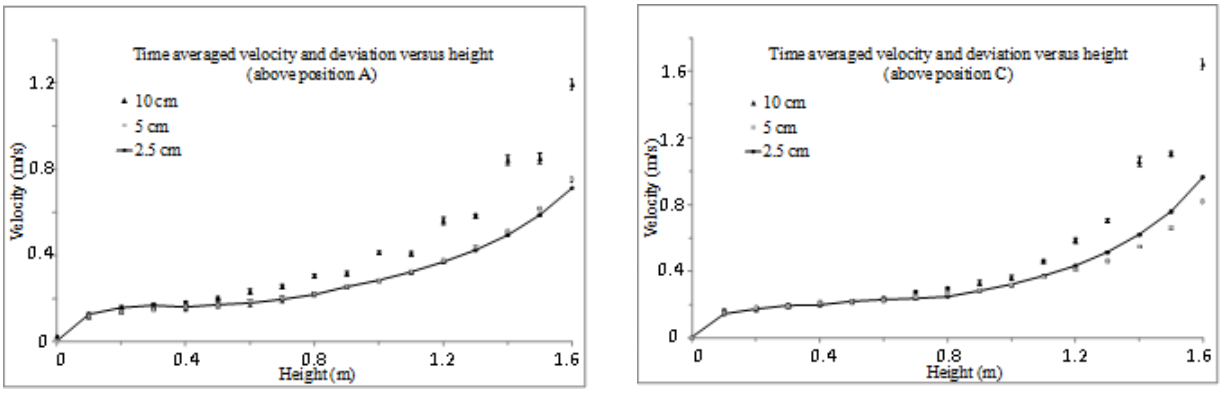

Figure 5. Time averaged velocity and standard deviation versus height in the hood for the large calculation domain (laboratory) above position A and C for the different grids

The quality of a particular simulation is most directly tied to the grid resolution. In order to measure this quality, the fraction of unresolved kinetic energy called the measure of turbulence resolution (MTR) was examined (Mc Grattan *et al*., 2013b). The MTR is similar to the Pope (2004) criterion. The MTR was calculated at each point above the positions of interests as depicted in figure 4. Then the time average of MTR was calculated at each point along height. And finally the mean of these values was calculated versus height above the five positions of interest. Figure 6 displays the results of the mean time averaged MTR along height for the different grid tested. According to Mc Grattan *et al*. (2013b), maintaining mean values of MTR near 0.2 provides satisfactory results (simulation results within experimental error bounds) for mean velocities and species concentrations in non reacting, buoyant plumes. Hence figure 6 shows that grid 1 and grid 2 are convenient for this criterion while grid 3 is not suitable.

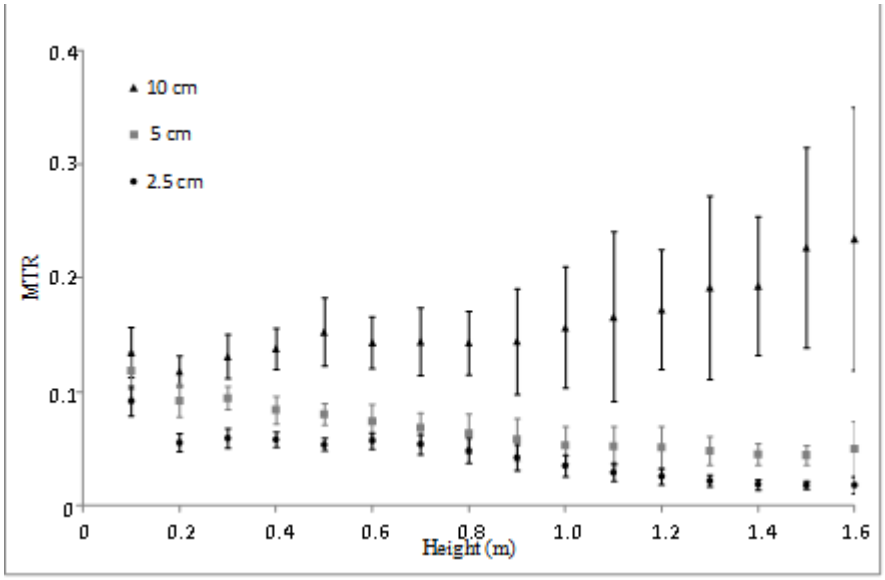

Figure 6. Measure of mean turbulence resolution with standard deviation for the different grids.

Size of the calculation domain and time saving

The size of the calculation domain is an important factor that affect greatly the calculation time. The greater the domain is the larger the time of simulation is. As an example, the simulation time performed per day for the flow is given in table 1 for the mesh sizes of 2.5, 5 and 10 cm (grids 1, 2 and 3). Different domains of calculation have been studied and the simulated results have been compared as previously, attempting to reach a compromise between the precision of the results and the simulation time. Two domains are discussed hereafter. The first one is a little bit larger than the hood (50 cm larger in all direction). It is called 'LSHR and vicinity'. The second one is limited to the size of the hood (see control volume in figure 1). It is called LSHR.

Table 1. Calculation time for the different grids

	Grid 1	Grid 2	Grid 3	Grid 4
Domain	Laboratory	Laboratory	Laboratory	LSHR
Mesh size (cm)	2.5	5	10	2 and 4
Number of mesh	11 489 280	1 436 160	179 520	2 707 200
Number of processor	14	1	1	14
Calculation time (sec/day)	13	29	883	72

In order to optimize the different requirements of the grid (in the litter and in the flame), the mesh size was fixed to 2 cm in the litter, above it and below it (under the bench). A coarse mesh size of 4 cm was used elsewhere in the calculation domain since as seen previously grid 2 (5 cm size) was enough convenient for the flow. We have chosen 4 cm since it is not allowed with FDS to align meshes with size of 2 cm and 5 cm (Mc Grattan *et al*., 2013a). The simulation of the flow done with these domains was compared to a simulation of reference performed with the large domain (see Figure 2) for which a mesh size of 2 cm was used in the hood and 4 cm elsewhere in the domain to be coherent with the mesh of the small domains.

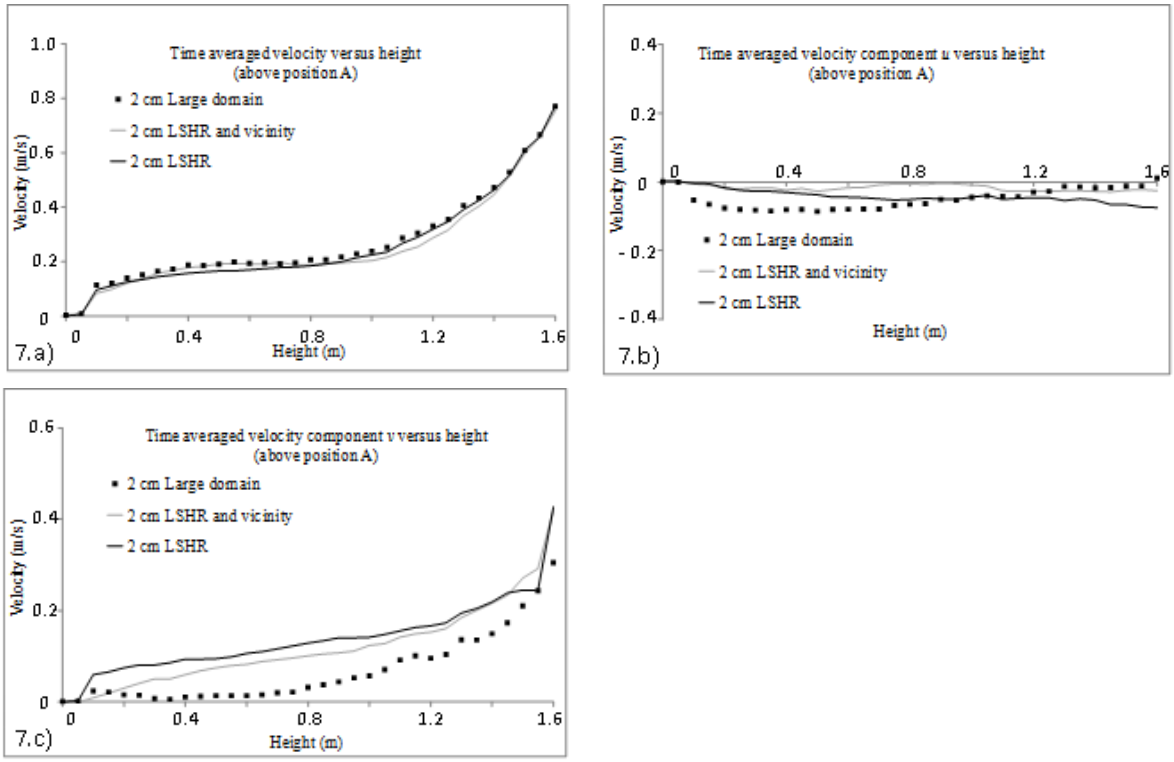

Figure 7. Simulation of the velocity in the hood of the LSHR: comparison between the large calculation domain and the domains limited to the hood and to the hood vicinity: a) global velocity, b) component u, c) component v, d) component w.

Figure 7 shows the time averaged velocity versus height above position A and the time averaged of the three components of the velocity *u*, *v* and *w* along respectively the axis *Ox*, *Oy* and *Oz* as depicted in Fig 2, for the three calculation domain. We observe that for the different positions along the height the three calculation domain provide similar results for the three components of velocity. The LSHR domain is however in better agreement with the large domain than the 'LSHR with vicinity' domain for component *w*. We can note that the values of components *u* is almost zero along the height and simulation results obtained with both domains can be considered in agreement for *u*. The main difference between the small domains and the large one is visible for component *v* which is overestimated with the small domains. However, we can observe that the tendency of components *v* which increases with height is rendered by the simulation performed with the small domains. Here also, the difference between the results of both small domains is negligible. Similar results were obtained along height for points located above the positions B, C, D and E. We can conclude that both small domains are equivalent to simulate the flow by comparison with the simulations performed with the large domain.

5.2. **Ignition method**

Concerning the ignition method, experimental fires were ignited by using a small amount of ethanol and a flame torch to ensure a fast and linear ignition of the fuel beds. The fires were ignited along the entire width of the fuel bed by using between 4 and 6 ml of alcohol. Figure 8 displays a zoom of figure 3 to focus on the HRR just at the ignition. 4 ml were used to ignite the fire tests with fuel load of 0.6 kg/m² while 6 ml were used to ignite fire tests with higher fuel load.

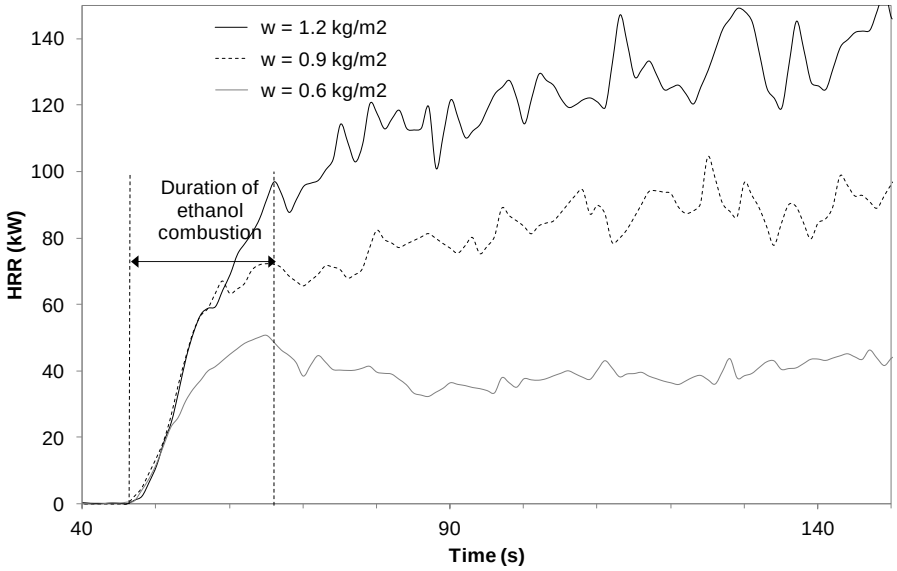

Figure 8 –Heat release rate at the ignition for fuel load of 0.6, 0.9 and 1.2 kg/m²

A study has been performed to investigate the duration time of ethanol burning when it is spread on the combustion bench without the vegetation. We measured this time (see Figure 8) in order to determine the mass of needles burned with ethanol during the ignition, $m_{needles}$:

$$m_{needles} = \frac{\int_0^{t_{ig}} \dot{q}\, dt - V_{ethanol} \times \Delta H_{c,ethanol}}{\Delta H_{c,needles}}$$

where t_{ig} represents the duration of ignition, $V_{ethanol}$ is the volume of ethanol used to ignite the vegetation and $\Delta H_{c,ethanol} = 21300$ kJ/L is the net heat of combustion of ethanol. The mass of needles involved in the ignition has been estimated to 20 g, 32 g and 35 g respectively for the fuel load of 0.6, 0.9 and 1.2 kg/m². The mass of needles used for 0.9 and 1.2 kg/m² are very close because the same quantity of ethanol was used for both fuel loads.

WFDS offers different options to simulate an ignition source that have been tested to reproduce the experimental ignition. Two different numerical methods to ignite the fuel bed have been compared in order to assess their ability to reproduce our experimental ignition in terms of heat release rate. The first method considers a linear strip of a given width located at the edge of the combustion bench for which the HRR per unit area is fixed during a time interval corresponding to the duration of the ignition. With this method and given the mass of fuel involved in ignition a strip of one meter long and 4 cm wide was considered. Although the calculated width was slightly lower than 4 cm, this dimension was chosen to be in agreement with the mesh size (2 cm) within the fuel bed. The HRR per unit area was set to 1100 kW/m^2 for the fuel load of 0.9 kg/m². The strip of ignition was applied during 18 s. It should be noted that the fuel bed length was shorten of 4 cm in order to avoid superimposing the needles and the strip that can be viewed as a burner located in front of the fuel bed. The second method consists of fixing the temperature of an ignitor at 1000°C. The ignitor is 4 cm wide and one meter long. Its height is equal to the fuel bed height. The ignitor is like a set of particle with porosity equal to the porosity of the fuel bed. It is located in front of the fuel bed. The simulated results of HRR for both methods of ignition were very similar. A point that deserves mention is the necessary time required "before to ignite the numerical fire". Even though the time for the flow to reach a quasi-stationary regime is not a problem for experimental fires since the hood is turned on a long time before ignition, it is the case for numerical fires. Indeed, the numerical ignition has to take place once a "quasi-

stationary flow regime" is established. This time is about 60 s for the LSHR domain of calculation and for a fuel load of 0.9 kg/m². Ignition before this time (that is to say during the transient flow regime) might result in a perturbation of the fire line that subsequently affects the spreading of the fire front over time (see Figs. 9a and 9b). In that case, the perturbation of the ignition is due to the flow that is not stabilized and introduces some dissymmetry before a given time that depends on the configuration (height of the fuel bed,…).

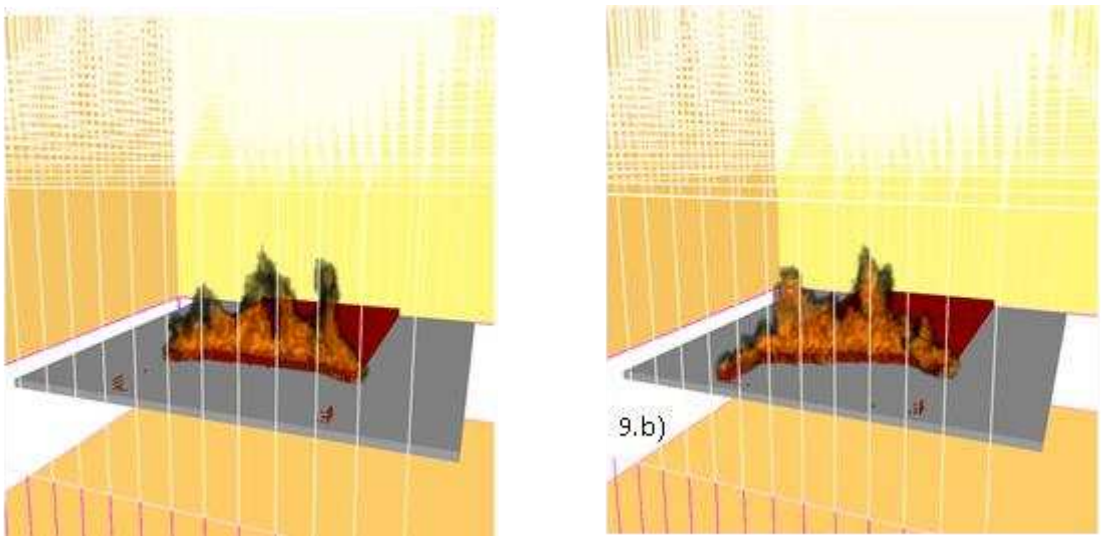

Figure 9. Influence of ignition time on the fire front shape for a fuel load of 0.9 kg/m²: a) numerical ignitions performed after stabilisation of the flow, b) numerical ignition performed before stabilisation of the flow

Conclusion and prospects

Physical model of fire spread are very promising to represent the behavior of wildland fires at a scale useful for risk assessment and fire safety concerns. The aim of our ongoing study is twofold. We propose a set of experimental data that can be used to validate physical model based on thermodynamics quantity of interest. Secondly we propose a methodology to validate such models paying attention to the influence of the experimental conditions that can affect the comparison between numerical and experimental fires. We focused on two parameters which could have a major role in the behaviour of numerical fires: the hood extraction system and the ignition method. This paper represents the first step of our work. Further studies will be devoted to the following activity: measurements of flow velocity within the hood will be done to assess the accuracy of WFDS to represent the flow with no fire. Secondly a full study will be performed to test WFDS against the set of data obtained from experiments conducted with the calorimeter for fire spreading under both slope and no slope condition for the different fuel loads: HRR, mass burning rate, radiant heat flux and exhaust gas composition. The role of the char during the process of spreading will be particularly investigated.

Acknowledgements

Part of this work was carried out in the scope of project PROTERINA-Due supported by the EU under the Axis 3 (Natural and Cultural Ressources) of the Operational Program Italia/France Maritime 2007-2013, contract: G25I08000120007.

8. References

Babrauskas, V., Peacock, R.D. (1992) HRR. The single most important variable in fire hazard. *Fire Safety Journal* **18**, 255-292.

Dupuy J.L. (1995) Slope and fuel load effects on fire behavior: laboratory experiments in pine needles fuel beds, *International Journal of Wildland Fire*, **5(3)** 153-164

McGrattan K., Hostikka S., McDermott R., Floyd J., Weinschenk C., Overholt K. (2013a) Fire Dynamics Simulator Technical Reference Guide, volume 1 : Mathematical Model. Technical Report. NIST Special Publication, 1018-6, National Institute of Standards and Technology, Gaithersburg, Maryland, <http://fire.nist.gov/fds>.

McGrattan K., Hostikka S., McDermott R., Floyd J., Weinschenk C., Overholt K. (2013b) Fire Dynamics Simulator User's Guide. Technical Report NIST Special Publication, 1019-6, National Institute of Standards and Technology, Gaithersburg, Maryland, <http://fire.nist.gov/fds>.

Mell W.E., Jenkins M.A., Gould J., Cheney P. (2007) A physics-based approach to modelling grassland fires. *International Journal of Wildland Fire* **16**, 1-22.

Mell W.E., Maranghides A., McDermott R., Manzello S. (2009) Numerical simulation and experiments of burning Douglas fir trees. *Combustion and Flame* **156**, 2023-2041.

Parker W.J. (1982) Calculations of the heat release rate by oxygen consumption for various applications, NBSIR 81–2427–1.

Pope S.B. (2004) Ten questions concerning the large-eddy simulation of turbulent flows. New Journal of Physics, 6, 1–24.

Porterie B., Consalvi J.L., Kaiss A., Loraud J.C. (2005) Predicting wildland fire behaviour and emissions using a fine-scale physical model. *Numerical Heat Transfer*, Part A **47**, 571–591.

Quintiere J.G. (2006) Fundamentals of Fire Phenomena. (Eds John Wiley & Sons Ltd, The Atrium, Southern Gate, Chichester, England)

Santoni P.A., Morandini F., Barboni T. (2011) Determination of fireline intensity by oxygen consumption calorimetry. *Journal of Thermal Analysis and Calorimetry*, **104**(3), 1005-1015,

Tihay V., Morandini F., Santoni P.A., Pere-Ramirez Y., Barboni T. (2012) Study of the influence of fuel load and slope on a fire spreading across a bed of pine needles by using oxygen consumption calorimetry. **Journal of Physics: Conference Series**, ***395, 012075***

Viegas D.X. (2004) On the existence of a steady state regime for slope and wind driven fires. *International Journal of Wildland Fire*, **13**, 101-117

Overview of the 2013 FireFlux-II Grass Fire Field Experiment

CB Clements[a], B Davis[a], D Seto[a], J Contezac[a], A Kochanski[b], J-B Fillipi[c], N Lareau[a], B Barboni[c], B Butler[d], S Krueger[b], R Ottmar[e], R Vihnanek[e], W E Heilman[f], J Flynn[g], M A Jenkins[b], J Mandel[h], C Teske[i], D Jimenez[d], J O'Brien[j], and B. Lefer[g]

[a] *Fire Weather Research Laboratory, Department of Meteorology and Climate Science, San José State University, San José, CA, USA.* craig.clements@sjsu.edu
[b] *Department of Atmospheric Sciences, University of Utah, UT, USA*
[c] *University of Corsica, Corsica, France*
[d] *Fire Sciences Laboratory, Missoula, MT, USA*
[e] *Pacific Northwest Wildland Fire Sciences Laboratory, WA, USA*
[f] *USFS, Northern Research Station, Lansing, MI, USA*
[g] *University of Houston, Houston, TX USA*
[h] *University of Colorado, CO, USA*
[I] *University of Montana, MT, USA*
[j] *USFS Southern Research Station, GA USA*

Abstract

In order to better understand the dynamics of fire-atmosphere interactions and the role of micrometeorology on fire behaviour the FireFlux campaign was conducted in 2006 on a coastal tall-grass prairie in southeast Texas, USA. The FireFlux campaign dataset has become the international standard for evaluating coupled fire-atmosphere model systems. While FireFlux is one of the most comprehensive field campaigns to date, the dataset does have some major limitations especially the lack of sufficient measurements of fire spread and fire behaviour properties. In order to overcome this, a new, more comprehensive field experiment, called FireFlux II, was conducted on 30 January 2013. This paper will address the experimental design and preliminary results. The experiment was designed to allow an intense head fire to burn directly through an extensive instrumentation array including fixed 42-m and three 10-m micrometeorological towers (Figure 2). The fuels consist of a mixture of native grasses.Each tower was equipped with a variety of sensors, including 3D sonic anemometers, pressure sensors, heat flux radiometers, and an array of fine-wire thermocouples to measure plume temperatures. The experiment was carried out under red flag warning conditions with strong winds of 8 m s-1 and relative humidity of approximately 24%. Instrumentation also included a scanning Doppler wind lidar, microwave temperature profiler, radiosonde balloons for upper-air soundings, a full suite of air quality instrumentation located downwind, and multiple ground and tower mounted infrared and visible video cameras. In addition, the fire spread was monitored from the air using helicopter mounted infrared and visible video cameras. Because the experiment was designed to be conducted under a north wind, the timing of the experimental period only allowed for a northwest wind. This required the instrumentation array to be moved in order to document the fire spread and was a limitation to the experiment. Preliminary results showed that the fire spread rate was ~1.5-2.5 m s-1 for the head fire while the flanks spread at 0.7 m s-1. The surface pressure field indicated that a low-pressure region formed downwind of the advancing fire front. The observations from the 42-m tower show that the strongest fire-induced winds occur a the surface in the cross-wind direction.

Keywords*: Grass fire, field experiment, fire-atmosphere interactions, micrometeorology, fire-induced winds*

Introduction

Studies on the fine-scale structure of fire-atmosphere interactions and fire behaviour have been based mostly on numerical simulations using coupled fire-atmosphere models (Clark *et al*. 1996; Mell *et al*. 2009; Linn and Cunningham 2005; Kochanski *et al*. 2013; Fillipi *et al*. 2013) and few field campaigns (Cheney *et al*. 1999; Clements *et al*. 2007). To better understand the dynamics of fire-atmosphere

interactions and the role of micrometeorology on fire behaviour, the FireFlux campaign was conducted in 2006 on a coastal tall-grass prairie in southeast Texas, USA (Clements *et al*. 2007, 2008). The FireFlux campaign dataset has become an international standard for evaluating coupled fire-atmosphere model systems. While FireFlux is one of the most comprehensive field campaigns to date, the dataset does have major limitations, especially the lack of sufficient measurements of fire spread and fire behaviour properties. In order to overcome these limitations, a new and more comprehensive field experiment, called FireFlux II, was conducted on 30 January 2013. This paper will address the experimental design and preliminary results.

Experimental Design and Instruments

The FireFlux II (FF2) field campaign was conducted at same plot as FireFlux at the University of Houston Coastal Center in Texas, USA, on 30 January 2013. The experiment was designed to allow for an intense head fire to burn directly through an extensive instrumentation array that included four meteorological towers, one fixed 42-m tower and three 10-m towers (Figure 1). The towers were equipped with a variety of sensors (Table 1), including three-dimensional sonic anemometers, pressure sensors, heat flux radiometers, and an array of fine-wire thermocouples to measure plume temperatures. Also located within the prairie were two interspersed grids of 28 surface thermocouples, buried underground, 18 pressure sensors positioned ~3.0 m above the burn plot, and 8 fire behaviour sensor packages that measured flame temperature, heat fluxes and gas velocities ~1 m AGL.
A key platform and instrumentation suite deployed during FF2 was the California State University-Mobile Atmospheric Profiling System (CSU-MAPS) (Clements and Oliphant 2014). The CSU-MAPS includes a truck mounted scanning Doppler wind lidar and a microwave profiling radiometer used to continuously measure background and plume thermodynamic and kinematic properties throughout the experimental period. The Doppler lidar provided high-resolution measurements of smoke plume aerosol backscatter intensity and radial wind velocities across the plot and around the fire front. The lidar has a range gate resolution of 18 m and the temperature profiler has a vertical resolution that scales with height, with a finer resolution of 50 m within the boundary layer. The CSU-MAPS also includes a mobile, trailer-mounted 32 m meteorological tower that is equipped with 5 levels of 2-d sonic anemometers and thermistor/hygristor sensors. In addition, a radiosonde system was used for an in-situ upper-air sounding taken just before ignition. Emissions and air chemistry were measured with a full suite of gas and particle samplers located downwind of the experimental plot (Figure 1). Multiple ground and tower mounted infrared and visible video cameras were used for measuring fire behaviour properties. In addition, the fire spread was monitored from the air using helicopter mounted infrared and visible video cameras. Table 1 provides a detailed description of meteorological instruments used during the experiment.

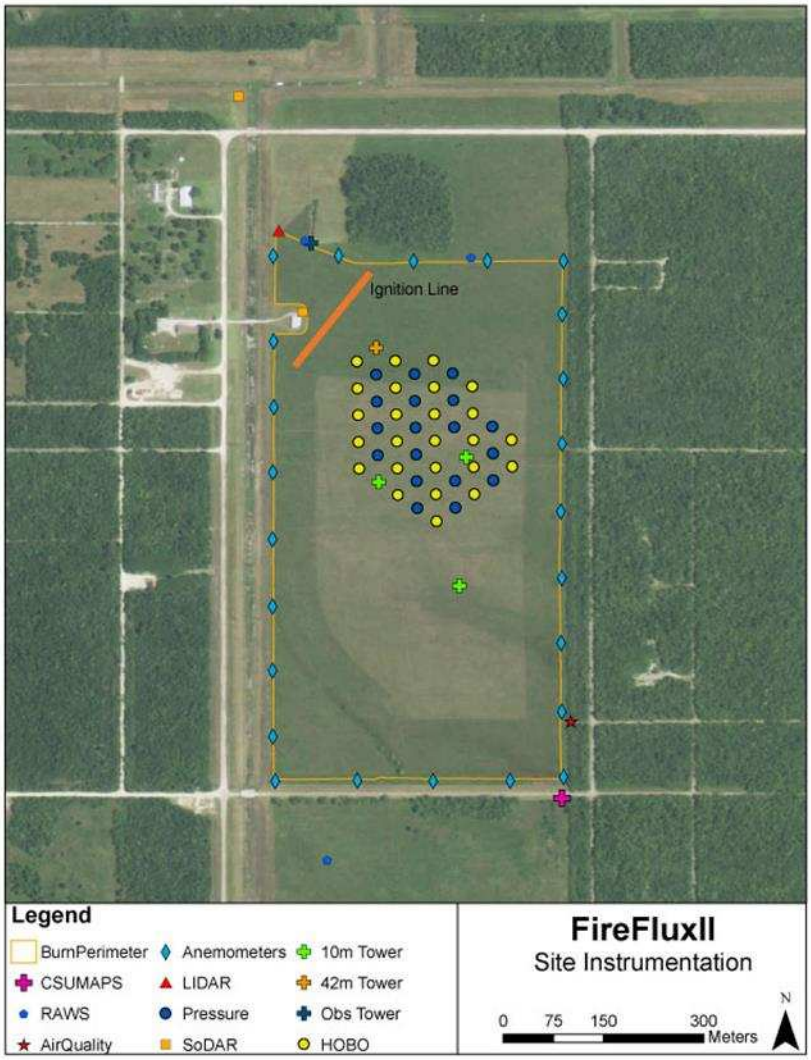

Figure 1. A map of the experimental setup during FireFlux II conducted on 30 Jan 2013.

Site description

The experimental plot was a natural tall-grass, of 155 acres (0.63 km^2) in size. The fuels consisted of a mixture of native grasses, including big bluestem (*Andropogon gerardi*), little bluestem (*Schizachyrium scoparium*), and long spike tridens (*Tridens strictus*). Fuel loading calculations were made from 20 destructive sampling plots. The average fuel loading for the experimental unit was 2.88 tons $acre^{-1}$.

The experiment was to be conducted under a north wind. However, synoptic conditions, as well as the timing of the experimental period, only allowed for a northwest wind as the best scenario. The decision was made to take advantage of the lesser than ideal conditions. WRF-SFire simulations (Mandel *et al*. 2012, Kochanski *et al*. 2013) were conducted to confirm the idealized fire spread under a northwest wind and based on these simulations, the instrumentation array was reconfigured just 24 hours prior to ignition. The reconfiguration was aimed to provide the most efficient experimental configuration for capturing the expected fire spread and maximize the number of instruments in the path of the fire.

Fuel moistures

Fuel moisture calculations were made from 20 different sampling plots. Three different sample types were collected 30 minutes prior to ignition: upper level grass (UL), lower level grass (LL), and forb (a herbaceous flowering plant). The boundary between the two grass layers was assessed based on the visual center of the mass height of the grass. Table 2 describes the moisture content percentages in detail.

Preliminary Results

Synoptic environment

The ignition occurred at 15:04 (CST) local time on 30 January 2013 and was associated with a post-frontal environment. The month of January was associated with above average precipitation and weak frontal systems, limiting ideal experimental conditions that required strong post-frontal northerly winds. Due to the excessive rain, soil conditions were wet with some regions of standing water within the experimental plot. A cold frontal passage the previous night created a strong northwesterly surface flow in excess of 8 m s-1, with gusts up to 12 m s-1, as well as a relative humidity of approximately 24% at the time of ignition (Figure 2). These conditions led to a red flag warning to be issued by the National Weather Service for the day of the experiment. A radiosonde launched 40 minutes prior to the ignition shows that the daytime boundary layer associated with a shallow superadiabatic surface layer and nearly adiabatic to slightly stable above the surface layer up to a capping inversion at nearly 2000 m aloft. The upper-level winds transition to strong westerly flow from the more northwesterly at the surface (Figure 3).

Preliminary spread analysis

The fire quickly spread from its ignition to the southeast side of the plot in 4 min while the flank continued to spread to the south end of the experimental plot. Using the ground based temperature loggers (Fig 4) to determine the fire front position, the fire spread rate was calculated to be ~1.5-2.5 m s^{-1} for the head fire while the flanks spread at 0.7 m s^{-1}.

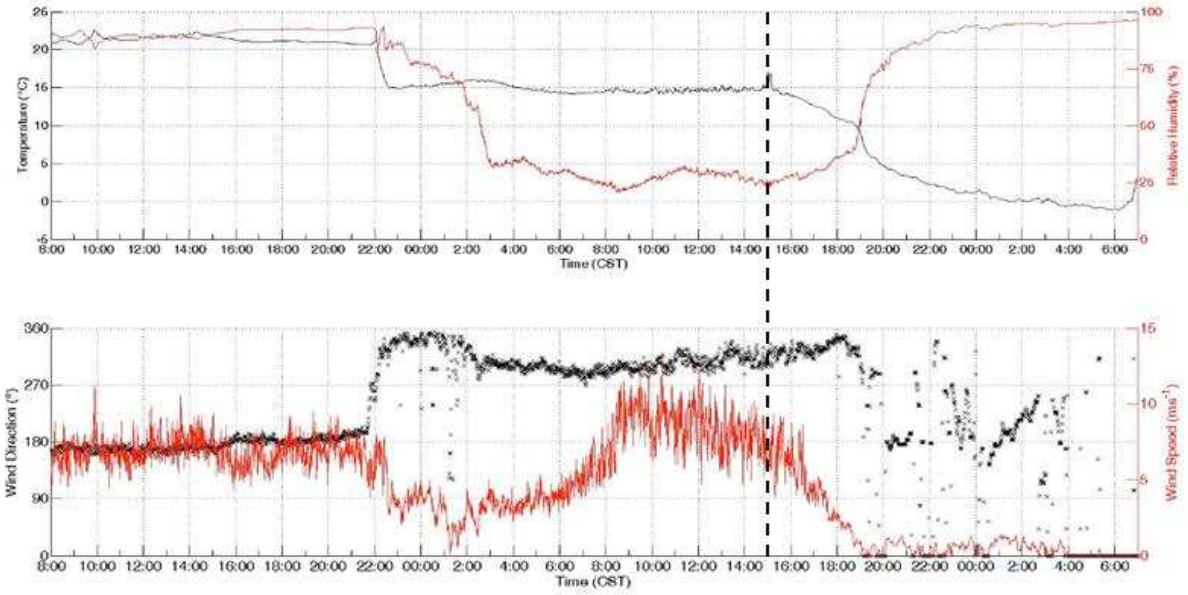

Figure 2. Surface conditions before, during, and after the burn, January 29-30, 2013. Ignition time is marked by the vertical dashed line.

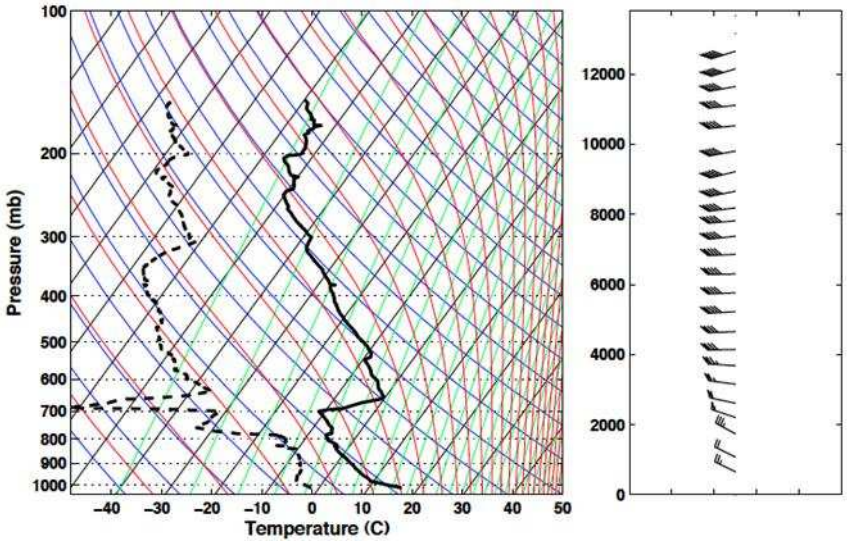

Figure 3. Skew-T diagram of radiosonde sounding taken just prior to the burn experiment.

Table 1. Key meteorological instruments deployed during experiment.

Platform/Instrument	**Sensor Type/ Model**	**Variables**	**Measurement Height (m AGL)**	**Sampling Frequency**
Meteorological tower (10 and 42 m)	3-D sonic anemometers (ATI, SAT-Sx; *RM Young 81000)	*u*, *v*, *w*, T_S	10 m and 6.0, 10.0, 20.0 & *42.0 for the 42 m tower	10 Hz
	Type-E, Fine-wire thermocouples	*T*	0 to top	1 Hz
	Total heat flux	kW m^{-2}	2.8	5 Hz
	Radiative heat flux	kW m^{-2}	2.7 (42 for 42 m tower)	5 Hz
CSU-MAPS 32 m portable tower	Thermistor/hygristors (Vaisala HMP45C)	*T*, *RH*	7.0-31.0	1 min
	3-D sonic anemometers (RM Young 81000)	*u*, *v*, *w*, T_S	7.0 & 31.0	10 Hz
Doppler mini SoDAR	Atmospheric Research & Technology, VT-1	*u*, *v*, *w*	15.0-200	10 min
Doppler SoDAR	Scintec MFAS-64	*u*,*v*,*w*	20-500	10 min
Doppler Lidar	Halo Photonics, Ltd., model Streamline 75	*u*, *v*, *backscatter*	0-1200	1 Hz
Microwave profiler	Radiometrics, Corp., MP-3000A	*T*, *RH*	0-10000	1 Hz
Weather balloon sounding system	GRAW Radiosondes, Gmb, GS-E	*T*,*RH*,*P*, *WS*,*WD*	0-15 km	1 Hz
Cup and Vane Anemometers	S-WCA-M003, Onset Computer Corporation	*WS/WD*	3.3	3 s
Temperature loggers	Onset, Inc, Hobo loggers,	*T*	0.0	1 Hz
Pressure Sensors	SJSU Custom	*T*, *p*	3.0	1 Hz

Table 2. Fuel moisture values (in percent) per sample type taken at the FireFlux II prairie.

Sample Type	Sample Size (n)	Mean (in %)	Median (in %)	Confidence Level (95%)	Standard Error	Standard Deviation
UL Grass	5	8.49	9.05	1.01	0.52	1.15
LL Grass	10	18.14	17.17	2.00	1.02	3.22
Forb	5	16.07	9.56	12.77	6.51	14.57

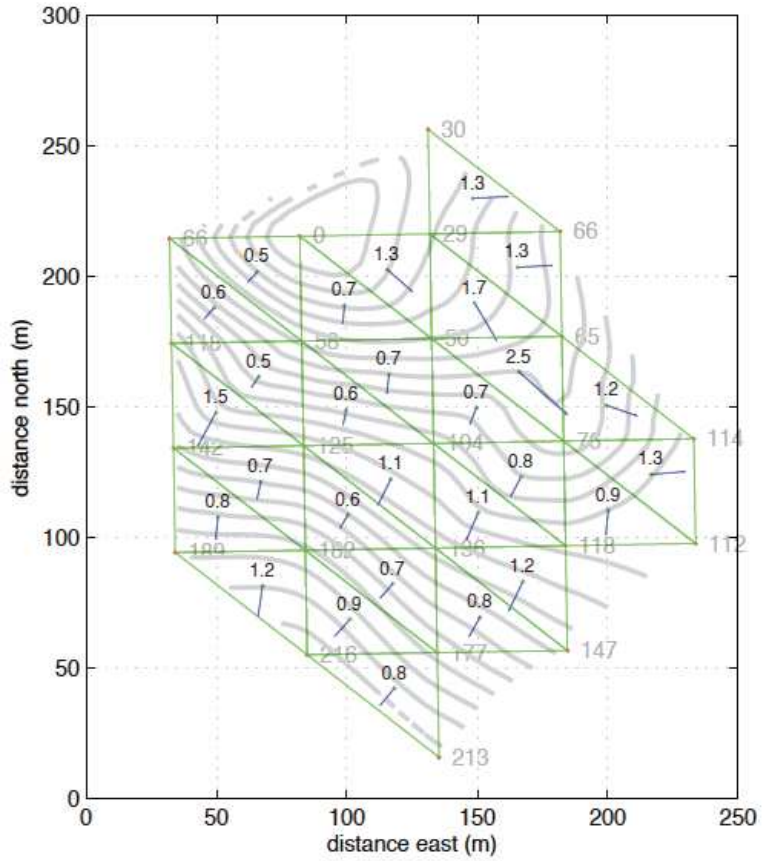

Figure 4. Rate of Spread vector calculation made from 28 ground thermocouples. Arrival times (s) at each HOBO, isochrones at 10-s intervals, ROS vectors, and ROS speed. (m/s).

3.3. In situ tower observations

Wind and temperature observations made from the 42 m tower are shown in Figure 5 for each measurement level. The time series shows little variability in the u-component wind, which is the streamwise component velocity, except for a slight decrease in velocity at the 20 m height just before the fire passes the tower. However, in the crosswind, v-component, the winds change from 2 m s-1 to nearly 6 m s-1 at 6 m AGL. Similar structure was observed at 10 m AGL, but not as large in magnitude (Figure 5). These observations indicate that the strongest fire-induced circulations occur at the surface near the fire front while above the fire, the ambient winds have a more pronounced effect on the plume, as indicated by the 20 m wind speed not changing from ambient. This fire-induced shear layer, where the surface winds accelerate and shift in direction at the fire front, can potentially increase turbulence generation near the surface potentially impacting fire behaviour.

The fire front passage is indicated by the sharp increase in temperature in Figure 5 (lowest panel) where maximum temperatures reached ~150 °C. At this same period, maxima in vertical velocities occurred at each level of the tower associated with the updraft of the plume. The maximum-recorded velocity was 8 m s^{-1} at the 20 m AGL level while at 10 m AGL the maximum updraft velocity was approximately 4 m s^{-1}.

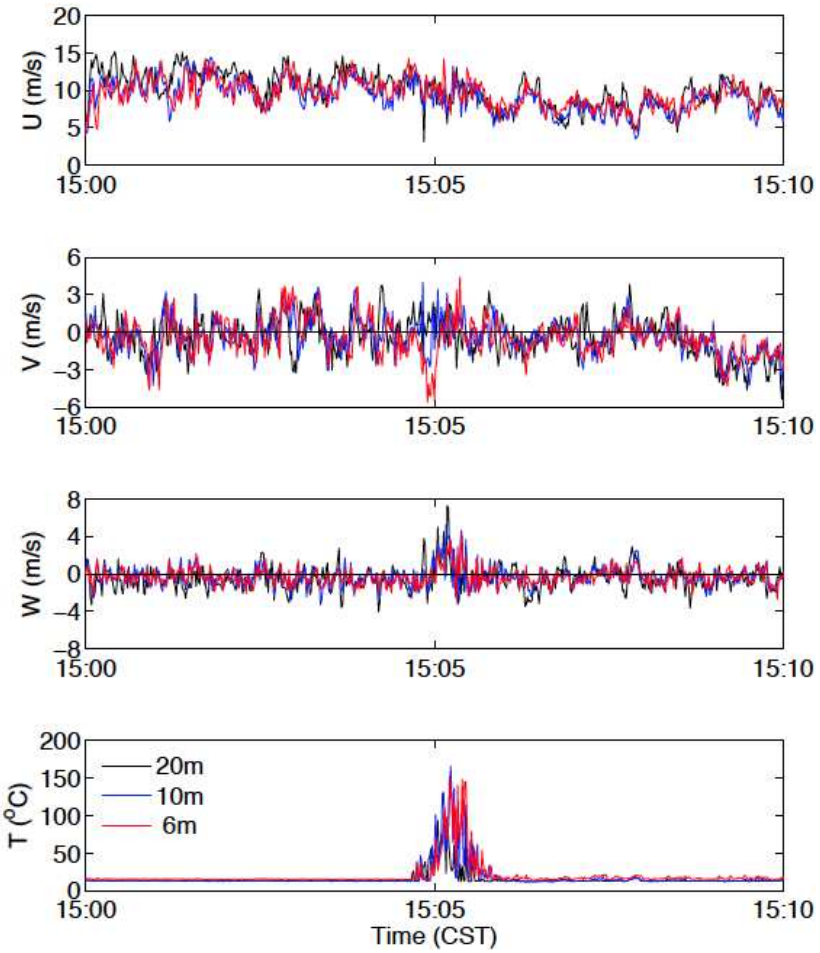

Figure 5. Time series of winds (u,v,w) and plume temperatures (T) during fire front passage (1505 CST) at the 42 m tower. Top panel is the u-component of velocity rotated into mean wind, v-componet is the cross-wise wind, w velocity is vertical component. Temperatures are taken from Sonic anemometers.

3.4. Photogrammetric analysis

For FireFlux II, photogrammetric analysis techniques were implemented in order to identify the fire spread rates for the head and flank fires. The technique, previously applied to fire front passage studies in controlled environments (Pastor et. al 2006), uses georectified high-definition and infrared imagery from a helicopter, correlated with georeferenced Plan Position Indicator (PPI) Doppler lidar scans, tower data, and perimeter anemometer plots, to create a comprehensive view of the wind field of the burn plot. In addition, georectifiying the helicopter high definition and infrared imagery to the prairie also allows for fire front tracing, providing an alternative method to calculating fire spread rates.
Preliminary photogrammetric analysis shows the progression of the fire as it burned across the prairie (Figure 6). Figure 6a, at ignition time, shows strong winds in excess of 10 m s-1 from 300 degrees, consistent with data from the perimeter anemometers, SoDARs, and tower data. Figure 6b, at approximately 86s after ignition, shows the development of the smoke plume moving with the wind

as the fire passes through the main tower, as seen by the black backscatter intensity contours. The smoke created by the backing fire along the edge of ignition also appears. Lidar data immediately downwind of the smoke plume contains errors, likely due to the lidar beam's inability to penetrate past the smoke. Figures 6c and 6d show the continued progress of the smoke plume over the prairie as the fire develops. Fire spread rate calculations using the georeferenced helicopter imagery shows a head fire spread rate of ~1.3-1.5 m s^{-1} and flank fire spread rate of ~0.5-0.7 m s^{-1}, which correlates well with the rate of spread calculations taken from the in ground temperature sensors (Figure 4). However, the error in this technique increased approximately 160 seconds into the burn, due to the change in the helicopter's altitude and angle in relation to the surface, skewing the error.

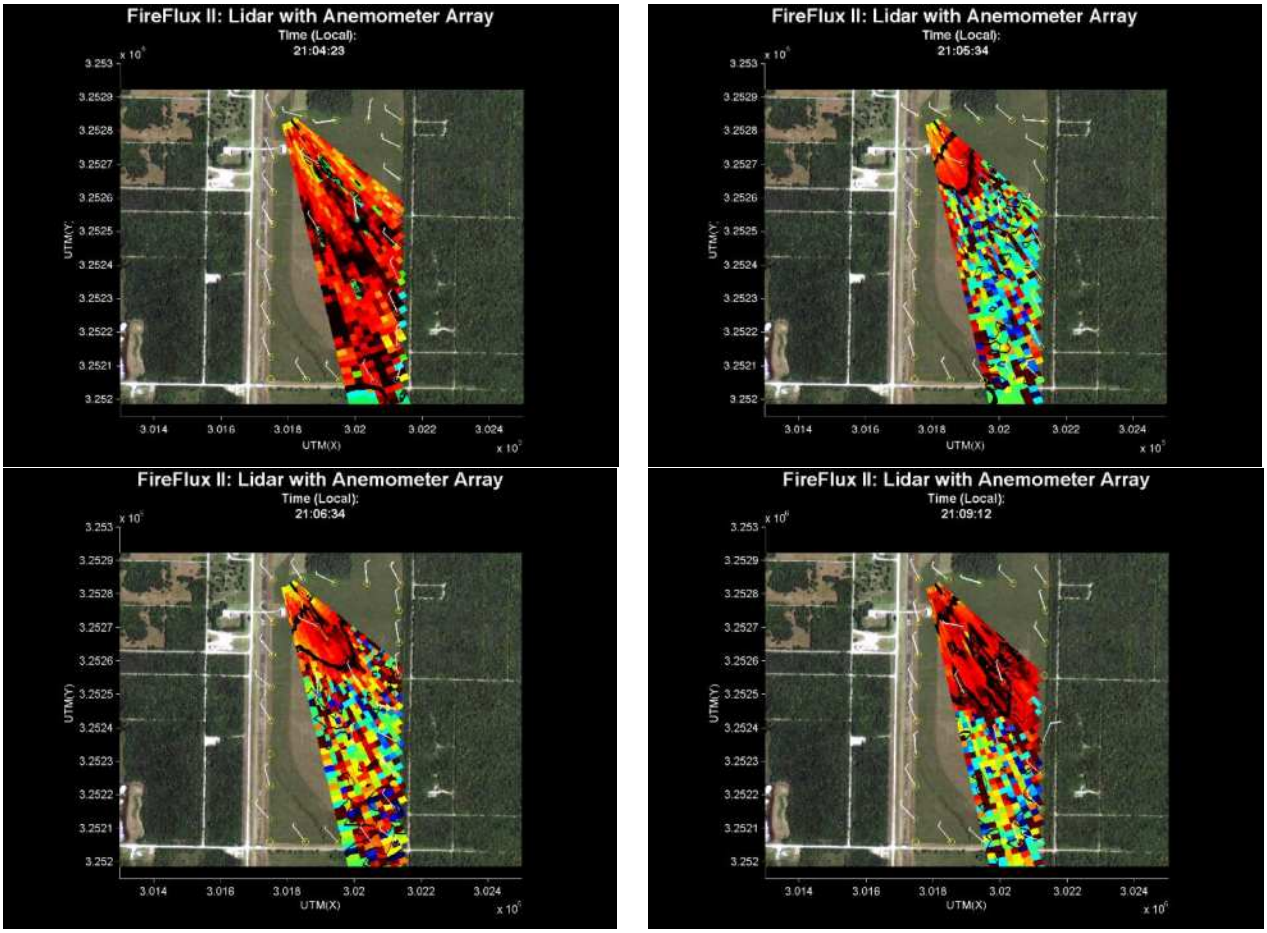

Figure 6. Time series of georectified images from FireFlux II, with Doppler lidar imagery superimposed over perimeter anemometer wind barbs. Black lines within the lidar scan designate the location of the smoke plume.

Conclusions

Analysis on the FireFlux II dataset is ongoing, and the work presented is a preliminary assessment of the potential for the data. The goal of improving upon the limitations of the original FireFlux field campaign is attained, as FireFlux II provides several methods for measuring fire spread rate and fire behaviour properties. Preliminary photogrammetric analysis gives a reliable method for calculating spread rate, coinciding well with values attained from ground thermocouple vector calculations. Future work in this area involves using the photogrammetric analysis method in the vertical, by correlating range height indicator (RHI) Doppler lidar scans to photography of the smoke plume, in order to further study the spread rate of the fire, as well as smoke plume dynamics. Data collected from pressure

sensors located within the experimental plot also shows promise in uncovering more information on pressure perturbations at the fire front.

Additionally, the FireFlux II dataset reinforces information gained in the original FireFlux campaign, providing more vertical wind and temperature measurements within the prairie with more in situ tower measurements. With these supporting datasets, we hope to build a more robust data library for model validation and more in depth fire-atmosphere interaction study.

Acknowledgements

This experiment would not have been possible without help and management from the following individuals and agencies. The Texas A & M Forest Service is thanked for conducting the burn operations. We want to thank the Rich Gray and his team for managing the burn operations, Dave Popoff from Galveston County Emergency Management for helping organizing county operations and personnel, Capt. Todd Weidman from La Margue Fire Dept for logistics and providing his staff of fire fighters, Prof. Steve Pennings and Tim Becker of the University of Houston Coastal Center for the research permit and help with all the logistics at the site, Paul Sopko (USFS), Ben Hornsby (USFS), Joe Restaino (USFS), and Dianne Hall (SJSU) for help with field sampling and setup, and Kent Prochazka (NWS Houston) for the fire weather forecasts. This research was funded by grants from the National Science Foundation (AGS-1151930) and Joint Fire Science Program (#11-2-1-11).

References

Cheney NP, Gould JS, Catchpole WR, 1998: Prediction of fire spread in grasslands. Int J Wildland Fire 8:1-13

Clark, T. L., Jenkins, M. A., Coen, J., Packham, D., 1996: A coupled atmosphere-fire model: Convective feedback on fire-line dynamics. J. Appl. Meteorol. 35, 875-901.

Clements C B et al., 2007: Observing the dynamics of wildland grass fires: FireFlux – a field validation experiment. B Am Meteorol Soc 88:1369–1382

Clements C B et al., 2008: First observations of turbulence generated by grass fires, J. Geophys. Res., 113, D22102, doi:10.1029/2008JD010014.

Filippi J B, Pialat X, Clements C B, 2013: Assessment of FOREFIRE/MESONH for wildland fire/atmosphere coupled simulation of the FireFlux experiment. P Combust Ins: 2633- 2640

Kochanski A K, Jenkins M A, Mandel J, Beezley J D, Clements C B and Krueger S, 2013: Evaluation of WRF-SFIRE performance with field observations from the FireFlux experiment. Geo Model Devel 6:1109-1126

Linn, R. R., and P. Cunningham, 2005: Numerical simulations of grass fires using a coupled atmosphere-fire model: Basic fire behavior and dependence on wind speed. J. Geophys. Res., 110, D13107, doi:10.1029/ 2004JD005597

Mandel J, Beezley, J D, and Kochanski, A K: Coupled atmosphere-wildland fire modeling with WRF 3.3 and SFIRE, Geosci. Model Dev., 4, 591–610, doi:10.5194/gmd-4-591-2011.

Mell, W, Jenkins M, Gould J, Cheney P, 2007: A physics-based approach to modelling grassland fires. Int J Wildland Fire 16:1–22

Pastor, E., et al., 2006: Computing the rate of spread of linear flame fronts by thermal image processing, Fire Safety Journal, Volume 41, Issue 8, Pages 569-579, ISSN 0379-7112.

Physiological drivers of the live foliar moisture content 'spring dip' in Pinus resinosa and Pinus banksiana and their relationship to foliar flammability

W. Matt Jolly[a], John Hintz[b], Rachael C. Kropp[a] and Elliot T. Conrad[a]

[a] *US Forest Service, RMRS, Fire Sciences Labortory, 5775 Hwy 10 W, Missoula, MT, USA, 59808, mjolly@fs.fed.us, rachaelckropp@fs.fed.us, eliotttconrad@fs.fed.us*
[b] *Wisconsin Dept of Natural Resources, 473 Griffith Ave, Wisconsin Rapids, WI, USA, 54494-7859, John.Hintz@wisconsin.gov*

Abstract
A phenomenon known as the 'Spring Dip' in conifer live foliar moisture content (LFMC) has been documented and monitored for decades. This period also corresponds with intense crownfire activity in areas dominated by *Pinus resinosa* (Red pine) or *Pinus banksiana* (Jack pine). Despite a long-standing tradition of measuring LFMC during the dip period, the drivers of these variations have been the source of much speculation but little investigation and the actual causes of foliar flammability change have received even less attention. Here we assess the seasonal drivers of LFMC variations and their impact on foliar flammability. Foliar samples were collected for an entire year from both Red pine and Jack pine at a site in Central Wisconsin. New and previous year's foliage were sampled separately when both were present. From these samples, we determined LFMC, foliar chemistry and foliar density. We also ignited samples in an open flame burner to assess seasonal changes in their flammability. We verified that there is indeed a drop in the foliar moisture content during the spring. However, foliar density changes explained 96.7% of the variation in LFMC across both species and both needle age categories. These density changes were driven by an accumulation of starch and sugar in the previous year's foliage, most likely as a result of the onset of photosynthesis in the spring. Foliar starch, sugar and crude fat content explained 86.4% of the variation in foliar density. Foliar flammability followed the same trend as LFMC, reaching its period of highest flammability during the time of the lowest LFMC. However, these changes were strongly related to changes in foliar density, where density explained 51% and 77.4% of the variations in foliar flammability. Our results challenge the assumption that live conifer foliage flammability is limited by its water content and this study has led to a new theory of the factors that dominate live fuel flammability.

Keywords: Live Foliar Moisture Content, Spring Dip, Foliar Density, Flammability

Introduction

Jack pine (*Pinus banksiana*) and Red pine (*Pinus resinosa*) are distributed throughout much of the high latitude and temperate North American forests and collectively they cover parts of eleven states and eight Canadian provinces. Wildfires are an integral component of their ecology (Ahlgren and Ahlgren 1960). Fires that occur in these areas can vary from low intensity surface fire to high intensity crown fires. Fire severity significantly affects the ecological succession and subsequent distribution of these trees throughout the boreal region (Arseneault 2001). It is therefore important to develop a complete understanding of the factors that drive fire severity in these forests.
Fire behavior in these forests is a crucial component of the development of management strategies for these species (Johnson and Miyanishi 1995). Successful prediction of fire behavior in these stands has been the source of much investigation (Quintilio *et al*. 1977, Stocks 1987, 1989, Stocks *et al*. 2004). Both weather and fuel conditions can significantly influence fire behavior in these stands. Strong winds and dry conditions lead to intense fires that spread rapidly. Fuel factors such as the crown base height, canopy bulk density and foliar moisture content are important determinants of their fire behavior (Van

Wagner 1977, 1993). Variations in crown base height and canopy bulk density happen slowly as stands develop over time, while foliar moisture content can vary significantly throughout the season. As such, foliar moisture content has the largest potential to alter the potential fire behavior of Jack pine and Red pine stands throughout the year.

A phenomenon known as the 'spring dip' in foliar moisture content has been extensively documented (Van Wagner 1967, 1974, Chrosciewicz 1986). It describes a seasonal decline in the foliar moisture before new needle flushing and a subsequent increase in moisture content thereafter. This period of low foliar moisture content corresponds with an increase in crown fire likelihood. While the phenomenon itself has been adequately described, the causes of the dip, and subsequently their potential impact on fire behavior, have not been adequately explored. One difficulty with evaluating seasonal changes in foliar moisture content is that they are driven by a combination of both changes in leaf water content and dry mass. Little (1970) suggests that a similar observed dip in foliar moisture of balsam fir (Abies balsamea), was attributed at least in part to a change in foliar carbohydrates. A complete examination of the seasonal dynamics of foliar moisture content and their influence on crown flammability must then examine changes in foliar dry matter composition as well as changes in foliar water content.

Here we present a study aimed at characterizing the seasonal changes in foliar chemistry during a period the 'spring dip'. We sample current and past year's foliage from mature Red pine and Jack pine trees at varying intervals for an entire year. We measure foliar moisture content, foliar density, chemical composition and each sample is also combusted on an open flame burner to measure their seasonal changes in flammability. We use this extensive dataset to explore the inter-relationships between measured foliar moisture content, foliar water content, foliar dry matter variations and their influence on ignitability.

Methods

Jack pine and Red pine sampling sites were located ~ 0.6 km apart in northern Adams County in central Wisconsin, USA, approximately 10 miles south of the city of Wisconsin Rapids. The red pine collection site is at N44° 14' 33", W89° 49' 44". The jack pine site is at N44° 14' 4", W89° 48' 54". Elevation at both locations is 873 feet. Topography at both sites is level to gently rolling on well-drained Plainfield Sand soils of glacial outwash origin. The area is part of a broad sand plain bisected by the Wisconsin River as it crosses the central part of the state.

The soils and topography of the area have made it prime landscape for growth of vast commercial plantations of red pine (*Pinus resinosa*), interspersed with natural forest cover of jack pine (*P. banksiana*) and "scrub" oak (*Quercus ellipsoidalis, Q. palustris, Q. alba, Q. velutina*). The lands are also ideal for residential, agricultural and recreational development, with numerous homes and cabins dotting the landscape and the major community of Rome (over 3500 homes) located within three miles to the south and southeast of the sampling site.

The landscape has experienced frequent fires of both natural and human origin throughout its history, including the pre-settlement period. It has also seen some of the largest and most destructive fires in Wisconsin during the post WWII era, the most recent being the 3400-acre Cottonville Fire of 2005. The red pine sample site itself is a plantation re-established after a forest fire that occurred in 1995, while the jack pine samples were taken from volunteers found in a separate, younger red pine plantation established after a commercial harvest of an oak/jack pine stand in 2000.

Needles were collected in both "new" (current year growth) and "old" (previous two growth seasons combined) age classes for both red and jack pine. Jack pine samples were collected in metal sampling tins, while larger plastic containers were used for the longer red pine needles. Containers were kept sealed during transport to a lab at the Wisconsin Department of Natural Resources (WDNR) office in Wisconsin Rapids. In the lab, the samples from each species/age class were divided into three subsets. Two subsets were designated for chemical and flammability analysis and were packaged for overnight

shipping to AgriAnalysis for chemical testing and to the US Forest Service Fire Lab in Missoula, Montana. From the third subset, five fascicles of varying size were selected for determination of needle density while the rest of the subset was used for bulk measurement of live foliar moisture content (LFMC). Fresh weights were measured to the nearest milligram for both the fascicles and bulk samples were obtained and the volume of the fascicles was determined using an Ohaus density apparatus. Fascicle and bulk samples were then dried overnight in at 85°C and measured to obtain dry weights, after which all weight measurements were brought together for final calculations of needle density and LFMC. LFMC was converted from a dry weight basis to a wet weight basis to standardize the scales between the foliar chemistry and moisture content measure using the following equation:

$$M_{wb} = (LFMC * 100 / (100 + LFMC)) \quad \textbf{Equation 1}$$

Samples were ignited using an open-flame burner. The apparatus was built specifically for the rapid heating and ignition of live fuel samples and is composed of a pre-mixed propane, a sample holder and timer (**Erro! A origem da referência não foi encontrada.**). Flow rates were set at 0.48 mol/min for fuel and 6.47 mol/min for air. This yields a rich flame that is partially pre-mixed and partially diffuse, yet creates a flame that is very similar to wildland flames and a convective heating environment that is conducive to very rapid heating. Samples were introduced to the flame by the sample holder where they were immersed in flame and their time-to-ignition was recorded as the point where flames were visibly attached to the surface of the sample.

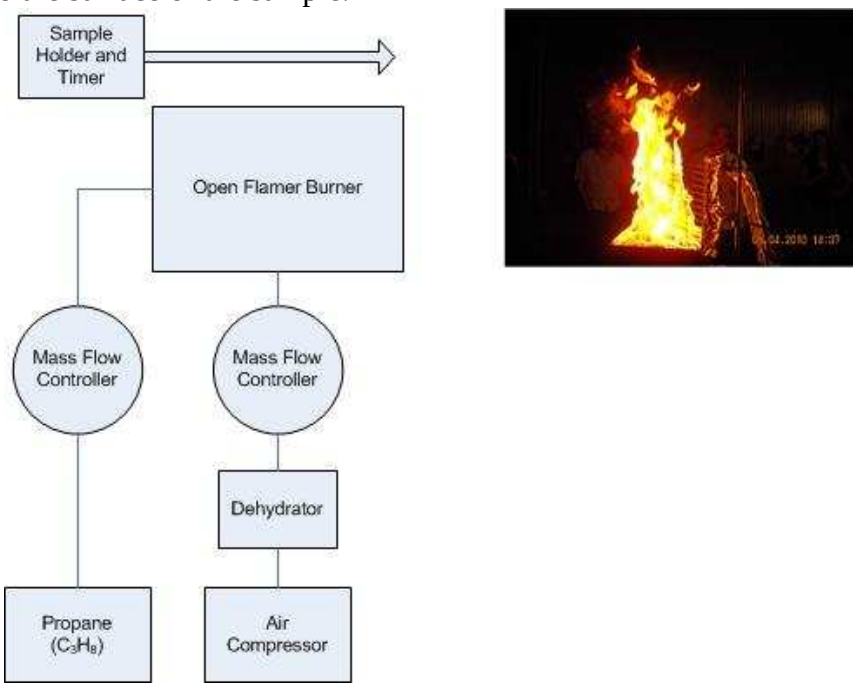

Figure 1. Flow diagram of the open-flame igniter apparatus.

Results

Live foliar moisture content (LFMC) seasonal trends followed patterns similar to those reported by Van Wagner (Van Wagner 1967) (Figure 2). Dormant foliar moisture contents for previous year's needles of red pine (*Pinus resinosa*) and jack pine (*Pinus banksiana*) were high for both species. Red pine needle moisture was 114.3% on March 29th, 2013 and 120.6% for jack pine but both dropped precipitously starting in about April and recovered completely by August (Figure 2). The lowest recorded LFMC recorded for red pine (82.0%) occurred on June 3rd, 2013 and the lowest LFMC for jack pine (91.5%) occurred on May 13th, 2013, representing a 29% and 26% reduction in LFMC during the 'Spring Dip' for Red pine and Jack pine respectively. LFMC recovery coincided with new needle

emergence in mid-June (Figure2). New needle LFMC was >250% for both species and declined rapidly during needle development (Figure 2).

Foliar chemistry varied substantially between needle age classes but was similar between species (**Erro! A origem da referência não foi encontrada.**). The strongest variations were observed in starch concentrations of old needles in both species, while crude fat and sugar content of new needles continued to rise after emergence signally foliar chemical changes due to needle hardening. Starch concentrations of old needles rose from zero to 14.4% and 11.8% of dry weight for Red pine and Jack pine respectively. Both crude fat and sugar content of new needles more than doubled over the study period.

Foliar density tracked seasonal changes in foliar chemistry. Density of old needles increased during the 'spring dip' period reaching a seasonal maximum value of 0.52 g/cm^3 and 0.497 g/cm^3 for Red pine and Jack pine respectively (**Erro! A origem da referência não foi encontrada.**). Density of old needles for both species increased by more than 20% during the dip period. Starch, sugar and crude fat content of needles explained 86.2% of the variations in foliar density across both species and needle ages (**Erro! A origem da referência não foi encontrada.**). Foliar density exhibited a linear relationship with foliar moisture content and it explained 96.7% of the variation, when foliar moisture content was translated from a dry weight to a wet weight basis (Equation 1).

Foliar density also explained much of the variation in time to ignition of both species. Density was most related to Jack pine flammability where it explained 77.4% of the variation in time to ignition, while density explained 51% of the variation in time to ignition for Red pine across both needle ages.

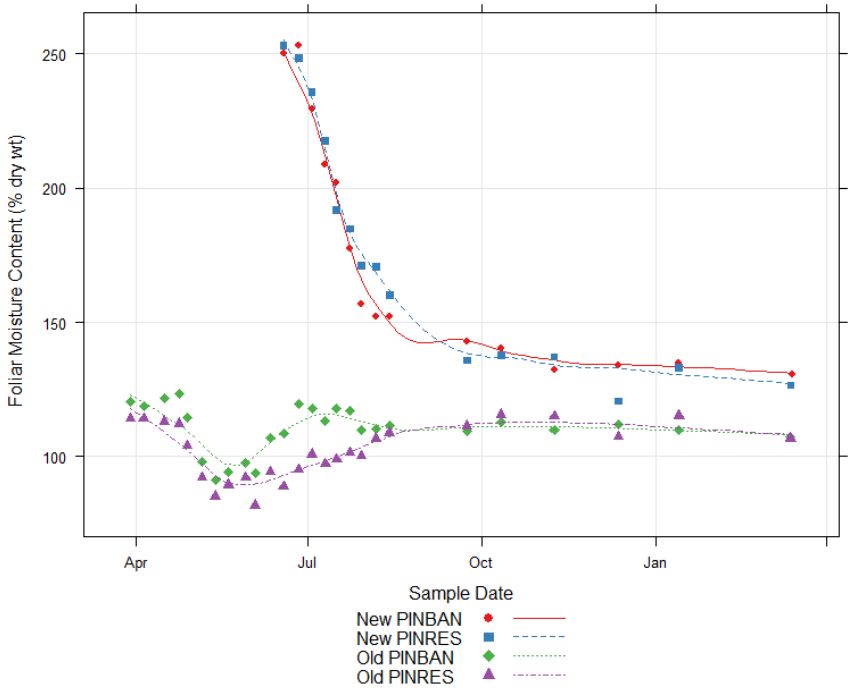

Figure 2. Seasonal variations in live foliar moisture content for Red pine and Jack pine from April 2013 - April 2014. Seasonal low LFMC values were observed in old needs of both species during the 'spring dip' period and the highest recorded values were observed in new needles. By the end of the study period, old and new needles had similar foliar moisture contents but new needle moisture contents were consistently higher for both species.

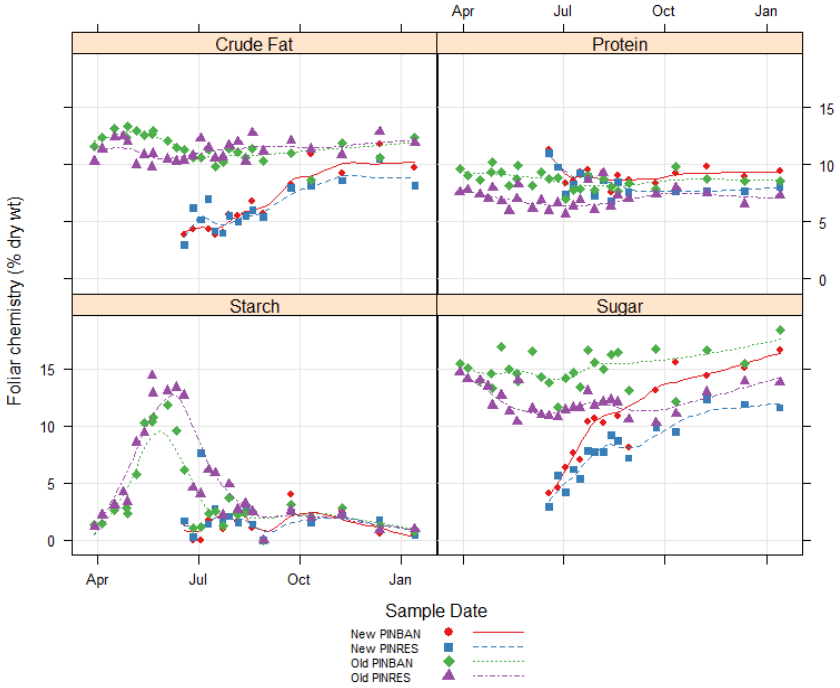

Figure 3. Seasonal variations in live foliar chemistry for Red pine and Jack pine from April 2013 - April 2014. Crude fat was lowest in new needles of both species and increased during needle development. Needle starch content showed over a ten-fold increase during the spring, increasing from 0% during dormancy to 14.4% and 11.8% for Red pine and Jack pine respectively just prior to new needle emergence. Additionally, sugar content of new needles increased during needle development but protein was similar between needle ages and species.

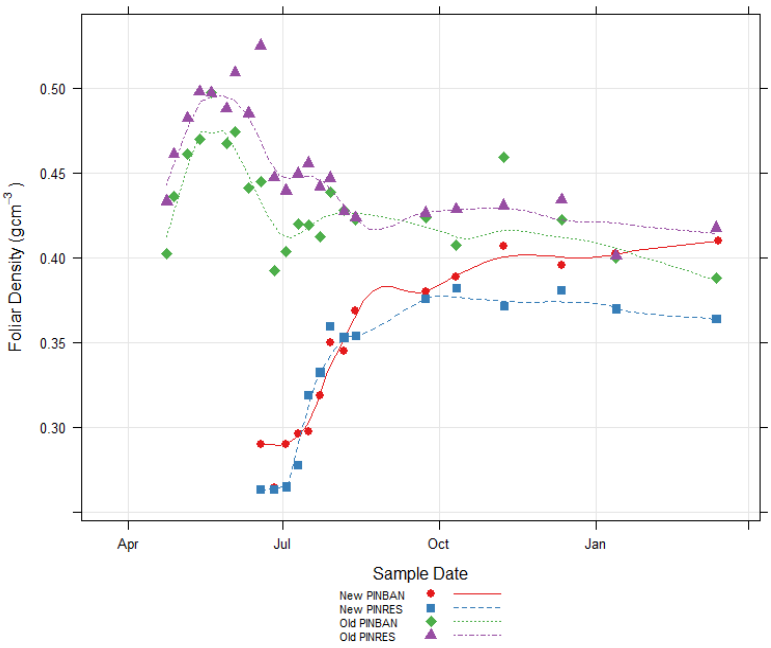

Figure 4. Seasonal changes in the foliar density of old and new Jack pine and Red pine needles from April 2013 to April 2014. Highest needle densities for old needles of both species occurred during the spring while lowest densities observed for both species occurred just after bud break as new needles emerged. New needle density increased as needles matured, while old needle density decreased over that period.

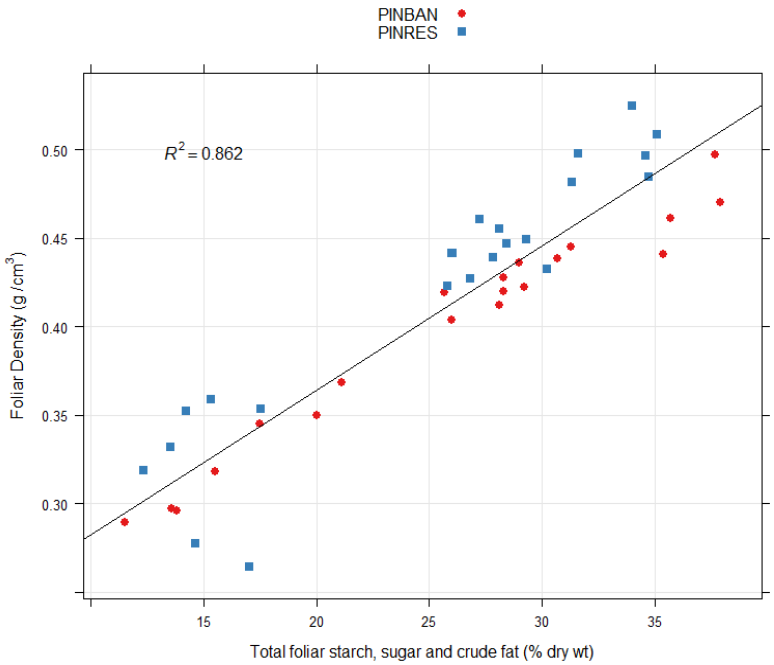

Figure 5. Relationship between total foliar starch, sugar and crude fat concentrations (as a percentage of total dry matter) and foliar density. These variables explained 86.2% of the variation in foliar density across both species and both age classes suggesting that seasonal variations in foliar density are primarily dependent on carbon dynamics (starch and sugar) and needle development (crude fat).

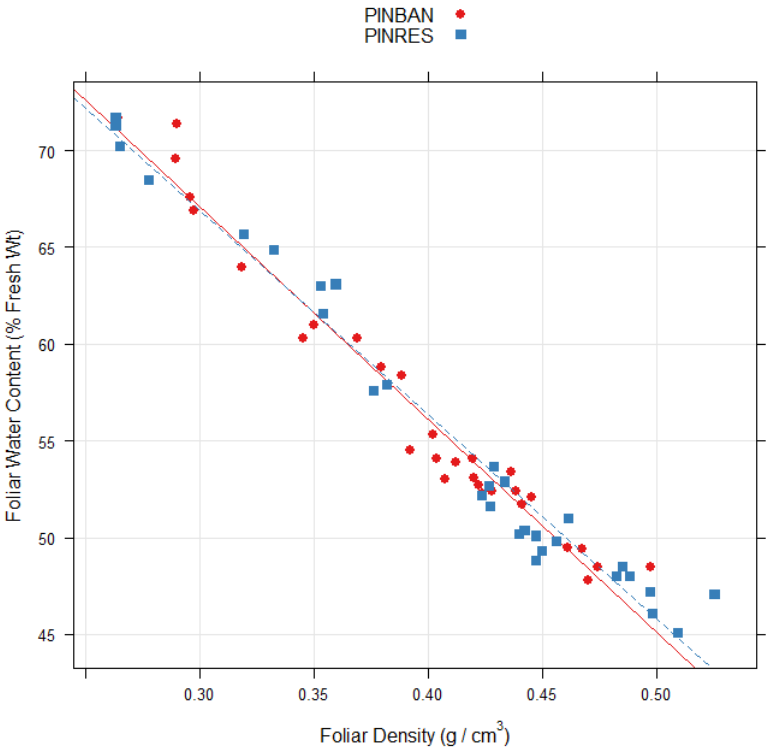

Figure 6. Relationship between total foliar density and foliar water content (% fresh wt). Foliar density explained 96% of the variation in foliar water content across both species and needle ages.

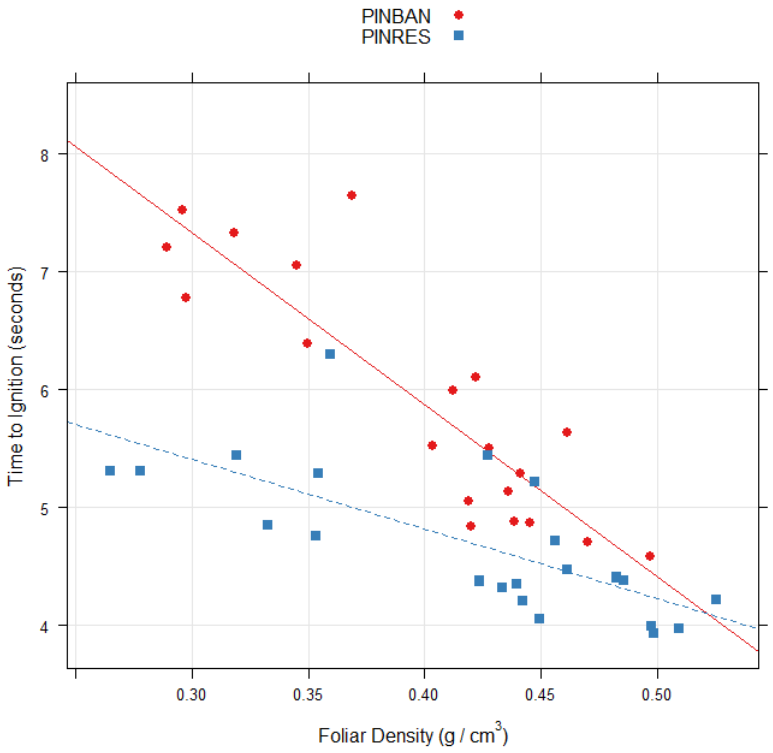

Figure 7. Relationship between foliar density and time to ignition for Red pine (PINRES) and Jack pine (PINBAN). Foliar density explained 51% of the variations in time to ignition for Red pine and 77.4% of the variation in time to ignition for Jack pine.

Discussion

Foliar moisture content has long been assumed to relate to red pine and jack pine flammability but little work has explained the interactive drivers that influence their seasonal changes. Our study has shown that foliar moisture content variations are a direct result of seasonal changes in foliar chemistry, not moisture content variations, which is consistent with previous findings (Little 1970). These chemical changes are reflected in seasonal changes in foliar density and subsequent changes in seasonal foliar flammability.

Foliar moisture content variations coincided with the onset of photosynthesis and the accumulation of carbon compounds prior to the flushing of new needles. During the early season, once trees have broken dormancy, we observed large increases in stored starch prior to the immergence of new foliage (**Erro! A origem da referência não foi encontrada.**). Once new needles emerged, that stored starch was depleted because during needle development, carbon is translocated from old needles to new needles (Gordon and Larson 1968). New needles also have a high demand for carbohydrates during their early development and they only export carbon to other parts of plant several weeks after they are fully developed (Ericsson 1978). Ultimately, photosynthesis is the main driver of the spring dip and the plant-level carbon cycle determines the apparent moisture content of the foliage but these changes could be affecting foliar flammability in ways that have not been previously considered.

It is conceivable that while the apparent moisture content of foliage varies substantially throughout the season, the absolute water content of the foliage could stay relatively constant. If this were the case, it would imply that the true seasonal drivers in foliar flammability lie not in changes in the water content of the foliage but in the chemical changes that compose the foliage. These chemical compounds might alter how rapidly needles can ignite. We noted strong seasonal changes in starch content of old foliage

during the dip. Starch and sugar compose over 28% of the dry weight of foliage yet they have never been considered as driving components of wildland fires. Generally, time-to-ignition is positively related to density (Incropera and DeWitt 2002). However, we found that these two quantities were negatively related, suggested that the drivers of the density increase, were more easily volatilized and thus lead to faster ignition, despite their contribution to particle density. Sugar, starch and crude fat should be studied further to determine whether or not they appreciably alter foliage ignitability.
This is the first study to combine moisture content, chemistry, density and ignition testing during the "Spring Dip" period. We have revealed some previously undiscovered linkages that could change how we assess live fuel flammability in the future. This new knowledge may lead to better tools to help fire managers assess crown fire potential in these dynamic forests.

References

Ahlgren, I. F. and C. E. Ahlgren. 1960. Ecological effects of forest fires. The Botanical Review 26:483-533.

Arseneault, D. 2001. Impact of fire behavior on postfire forest development in a homogeneous boreal landscape. Canadian Journal of Forest Research 31:1367-1374.

Chrosciewicz, Z. 1986. Foliar moisture content variations in four coniferous tree species of central Alberta. Canadian Journal of Forest Research 16:157-162.

Ericsson, A. 1978. Seasonal Changes in Translocation of 14C from Different Age-Classes of Needles on 20-Year-Old Scots Pine Trees (Pinus silvestris). Physiologia Plantarum 43:351-358.

Gordon, J. C. and P. R. Larson. 1968. Seasonal course of photosynthesis, respiration, and distribution of C14 in young Pinus resinosa trees as related to wood formation. Plant Physiology 43:1617-1624.

Incropera, F. P. and D. P. DeWitt. 2002. Introduction to Heat Transfer. 4th edition edition. John Wiley and Sons, New York.

Johnson, E. A. and K. Miyanishi. 1995. The Need for Consideration of Fire Behavior and Effects in Prescribed Burning. Restoration Ecology 3:271-278.

Little, C. H. A. 1970. Seasonal changes in carbohydrate and moisture content in needles of balsam fire (Abies balsamea). Canadian Journal of Botany 48:2021-2028.

Quintilio, D., G. R. Fahnestock, and D. E. Dubé. 1977. Fire behavior in upland jack pine: the Darwin Lake Project. NOR-X-174, Edmonton, Alberta.

Stocks, B. J. 1987. Fire behavior in immature jack pine. Canadian Journal of Forest Research 17:80-86.

Stocks, B. J. 1989. Fire behavior in mature jack pine. Canadian Journal of Forest Research 19:783-790.

Stocks, B. J., M. E. Alexander, B. M. Wotton, C. N. Stefner, M. D. Flannigan, S. W. Taylor, N. Lavoie, J. A. Mason, G. R. Hartley, and M. E. Maffey. 2004. Crown fire behaviour in a northern jack pine black spruce forest. Canadian Journal of Forest Research 34:1548-1560.

Van Wagner, C. E. 1967. Seasonal variation in moisture content of eastern Canadian tree foliage and the possible effect on crown fires.

Van Wagner, C. E. 1974. A spread index for crown fires in spring. Information Report PS-X-55, Petawaw Forest Experiment Station, Chalk River, Ontario.

Van Wagner, C. E. 1977. Conditions for the start and spread of crown fire. Canadian Journal of Forest Research 7:23-34.

Van Wagner, C. E. 1993. Prediction of crown fire behavior in two stands of jack pine. Canadian Journal of Forest Research 23:442-449.

Relationship between the slope and some variables of fire behavior

Guido Assunção Ribeiro,Tiago Guilherme de Araújo, Carlos Miguel Simões da Silva, Mateus Alves de Magalhães

Departamento de Engenharia Florestal, Universidade Federal de Viçosa, 36571-000, Viçosa, MG, Brazil – gribeiro@ufv.br, tiagoguilherme23@gmail.com

Abstract

The topographic features influences fire regime and fire behavior jointly with the remaining environmental variables. The fire regime characteristics can vary due to fine scale topography and variation in stand history according to topographic features. The fire often influences severity with smaller areas of high severity on lower mesic slopes and larger areas on upper xeric slopes. Several researches confirm the severity of wildland fire. Topographic variables were relatively more important predictors of severe fire than either climate or weather variables. Predictability of severe fire was consistently lower during years with widespread fires, suggesting that local control exerted by topography may be overwhelmed by regional climatic controls when fires burn in dry conditions. This was an indoor study conducted at Forest Fire Laboratory, of Departamento de Engenharia Florestal, Universidade Federal de Viçosa (DEF/UFV), Minas Gerais State, Brazil. It was used a combustion table apparatus with a dispositive to simulate six slopes (0º, 5º, 15º, 25º, 35º and 45º). It was measured the flame length to correlate with the fire line intensity. Five replications were used for each slope, both in uphill as the downhill. The fuel bed was formed by a grass Melinis minutiflora Beauv. common in Brazilian grassland. The average values of dry fuel load for each slope were 0.561 kg, uniformly distributed on a platform area of 1.0 x 1.0 meter. The fire line intensity was calculated according to Byram (1969). The relative humidity mean in the downhill and uphill burn day was 48.8% and 57.8% respectively. The result showed that there was increases in the fire line intensity when compared downhill with the uphill slope from range 5 to 45 degrees. The increase was 2.7 times higher in the 45-degree slope compared with the lowest slope. This study will establish a factor for increasing the height of the flames and the fire intensity increased as the surface slope. In all replicates of downhill burning was observed a shorter length of the flames at the beginning and the end portion of plot while on uphill the flame length was shorter only on last plot portion. The flame length was a crescent relationship from 0 until 45 slope degree, represented by Y=1.1136+0.0675X-0.0012X2, with a R2 of 0.9362 for uphill and a polynomial representation of Y=1.0923X + 0.101X – 0.0046X2 - 5E-05X3 with a R2 of 0.8304 for downhill.

Keywords*: slope effect; flame length; fire spread; fire behavior*

Introduction

The great wildfires are occurring on all parts of the world, according to their regional climatic conditions. The relationships between mankind activities and the environment are heavily documented due to the influence of the climatic variations on the human welfare overtime. On the last years we are observing a great demand for food given the population growth requiring the expansion of agricultural areas and a necessary and periodical management of the soil which the fire has been an important tool (JUSTINO *et al*., 2011). Although the fire has been used by man since the remote times, is now growing concern over its use due to the change in the structure of farms, climate and greenhouse gas emissions. These conditions are producing great changes on the landscape and resulting in large accumulations of fuel. In fact, in different parts of the world and by different reasons the amount of fuel has risen considerably and there has been a consequent increase in the number of fires and land burnt each year as reported by Miller *et al*. (2012), Pausas (2012), Pausas (2004), Soares and Batista (2007), Beautling (2009). Miller *et al*. (2012) further state that recent research has indicated an increasing in worldwide fire size, large fires are becoming more frequent, and in at least some locations

percentage of high-severity fire is also increasing. These changes in the contemporary fire regime are largely attributed to changing climate, land management practices, including suppression of fires and abandonment of rural areas.

The topographic features besides others parameters environmental influences the fire regime and fire behavior jointly with the remaining variables that characterize the environment. According Miler *et al*. (2011), the fire regime concept was developed to provide a framework for investigating differences in the way fire influences ecosystems. The fire regime characteristics can vary due to fine scale topography and variation in stand history. These researchers conclude that topographic features however, often influence severity with smaller areas of high severity on lower, mesic slopes and larger areas on upper, xeric slopes.

The environmental complexity leads to different situations and makes not all fire is equal; fire-caused change or fire severity can vary considerably and decisively influences the effects resulting like evolved species largely with low to moderate-severity fire, and those post-fire landscapes are characterized by survival of fire-tolerant and large-diameter individuals. Severe fires kill and consume large amounts of above and belowground biomass and affect soils, resulting in long-lasting consequences for vegetation, aquatic ecosystem productivity and diversity, and other ecosystem properties (DILLON *et al*., 2011). However, in many respects, Dillon *et al*. (2011) confirm it is the severity of wildland fire, rather than whether or not a location burned that has greatest effect on ecological processes. Topographic variables were relatively more important predictors of severe fire occurrence than either climate or weather variables. Predictability of severe fire was consistently lower during years with widespread fires, suggesting that local control exerted by topography may be overwhelmed by regional climatic controls when fires burn in dry conditions.

Fire behavior probabilities are different from each other because they depend on spatial and temporal factors controlling fire growth. That is, the likelihood of fire burning a specific area is dependent on ignitions occurring off-site and the fuels, topography, weather, and relative fire direction allowing each fire to reach that location. The results shown by Mistry and Berardi (2005) indicated that there is a higher probability of fire entry from particular border regions as a result of the fuel characteristics.Wind speed greatly increased the spread and extent of fire. According to Miller *et al*. (2011), species compositions vary widely, influenced by precipitation, topography, and substrate, producing different severity degree.

Moreover, studies have shown that fire is part of several ecosystems on the world. It can be used as a tool land management like a prescribed or controlled burning (RIBEIRO, 2009) and can be used safely to achieve different objectives of land management. Biswell (1989) make several recommendations to describe an area to be burn and the mainly one are the topographic features. The combustion process and fire behavior are complex as well as being compounded by variations caused during the burning that are difficult to predict.

The fuel used in this work was the Millinis minutiflora Beauv. an 1 hr time lag fuel.

The aim of this study was to assess the influence of slope steepness in fire line intensity and flame length in an indoor condition using the Melinis minutiflora Beauv. as a fire bed with no wind flow, and known conditions of fuel moisture and fuel load.

2. Materials and methods

This was an indoor study conducted at Forest Fire Laboratory, of Department of Forest Engineering, Federal University of Viçosa (DEF/UFV), Minas Gerais State, Brazil. It was used an apparatus named combustion table (Figure 1) with a dispositive to simulate the slope steepness in the desired angles and the flame length.

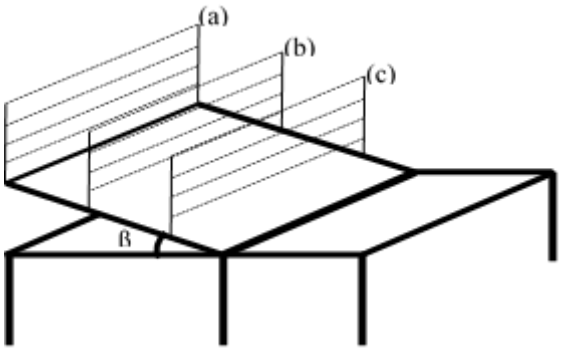

Figure 1. Schematic drawing of the combustion table

The angles ß tested were 0º, 5º, 15º, 25º, 35º and 45º and the flame length was measured from three devices (a,b,c) through the cotton yarns vertically distant every 0.25 m. Five replications were used for each angle, both in uphill as the downhill which were burned on different days.
The fuel bed was formed by a grass Mellinis minutiflora Beauv. Its power heat was determined in the Panels and Wood Energy Laboratory, Department of Forestry Engineering, DEF/UFV finding 4,186 kcal. The relative humidity of the testing room and the fuel humidity throughout the day 1 (uphill) and the day 2 (downhill) are shown in Tabel 1.

Table 1. Relative humidity and fuel humidity on day 1 (uphill) and day 2 (downhill) of burn.

Uphill			Downhill		
Day time (h)	Relative humidity (%)	Fuel humidity (%)	Day time (h)	Relative humidity (%)	Fuel humidity (%)
9:00	43	10,20	9:00	76	20,28
11:00	52	9,20	11:00	75	16,47
13:00	51	10,34	13:00	52	18,58
15:00	52	6,05	15:00	43	19,69
17:00	43	7,65	17:00	42	18,64

The average values of dry fuel load for each angle tested are shown in Table 2. Before each burning the fuel load was uniformly distributed on an platform area of 1.0 x 1.0 meter (Figure 1).

Table 2. Dry fuel load (kg) for each slope.

Uphill		Downhill	
Slope (degree)	Fuel load (kg)	Slope (degree)	Fuel load (kg)
0º	0.545	0º	0.545
5º	0.557	5º	0.508
15º	0.554	15º	0.525
25º	0.577	25º	0.498
35º	0.567	35º	0.511
45º	0.569	45º	0.513

The fire line intensity was calculated by Byram (1969) equation:

$$I = H.w.r$$

where,

I = fire line intensity (kcal/m/s);
H = heat power (kcal);
w = fuel load (kg);
r = fire spread (m/s).

It was measured after each burning the flames length, the burning time, the rate of fire spread and burning intensity by Byram (1969). The analyzes were carried out with the StatGraphic statistical package to determine the correlation between the flames length and burn intensity, the gradient increase in intensity with slop increasing and to establish a propagation factor in accordance with the slope for the fuel type studied.

Results and discussions

The media and standard deviations values of fire line intensity (Figure 2 and 3) recorded small burning values for both slopes. This was expected because the burning was conducted indoor or without the influence of wind besides the controlled conditions of humidity and fuel load. However, they show a significant difference between the two types of burn. The uphill burning recorded higher and increasingly values between the flat condition (0°) and the largest slope (45º). The highest intensity of burning was recorded for the 45° uphill and was about three times higher than the intensity recorded for the 45°downhill. This confirms the expected scattering flames towards the uphill or the effect of topography behavior.

It is clear that the fire behavior has a strong influence of the fire speed in the absence of others variables. In this study both the heat value as fuel load did not vary. The highest fire speed attained was for the 45º uphill and it was 4.5 times higher than the highest speed reported for the downhill.

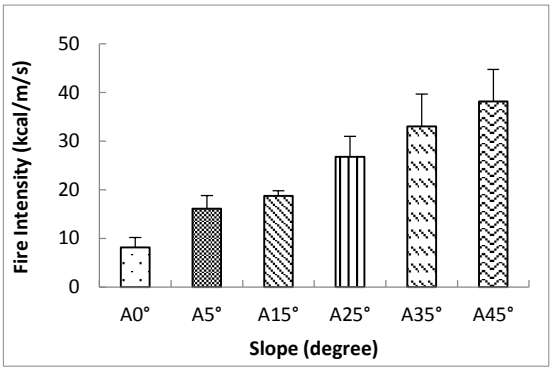

Figure 2. Uphill burning

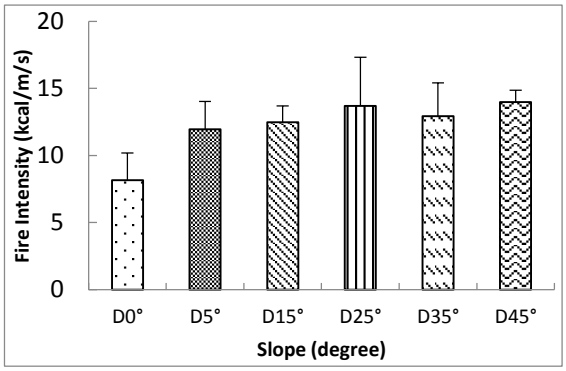

Figure 3. Downhill burning

The relationship between the different levels of slope and the fire line intensity (Figure 4 and 5) showed a better fit of the mathematical model for the firing in the uphill. This relationship was almost direct to which a rectilinear model was fitted.

This profile of fire behavior in uphill is well within the expected. However, in the downhill burning the fire behavior was not the same. The mathematical model fitted was a second degree polynomial equation. In addition, the adjusted model showed a lesser coefficient than the uphill model.

The Figure 5 shows a trend of reduced intensity as the line of fire approaches the lower portion of the burning area. This can be explained by the fact that the fuel load is practically in the end and a less heat flow is produced.

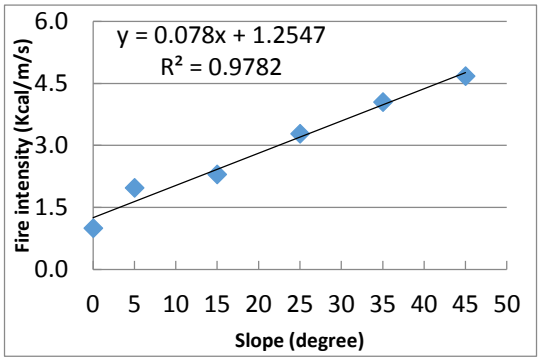

Figure 4. Uphill burning

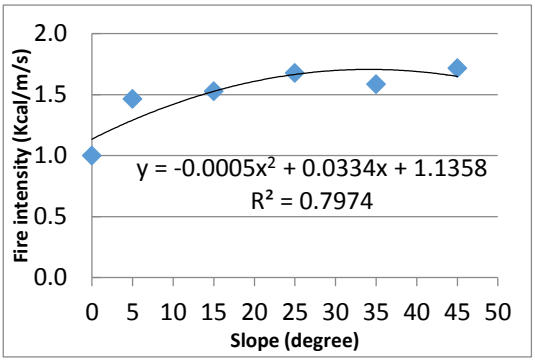

Figure 5. Downhill burning

As noted in other studies, there is a direct relationship between The fire line intensity and the flame length. However, this behavior varies according to other environmental variables and the direction of fire. Burning in the uphill (Figure 6) tends to have a direct relationship with exponential trend. The flames tend to have greater length in relation to the downhill fire and increase in length with increasing slope. However, when reaching the top portion of the flame length decreases by the fact reduce the fuel to be burned and the headwind on the opposite side of the burning surface.
Burning in the uphill shows a different behavior in relation to downhill. Upon reaching the end of the burning surface, the smaller slope, the flames become smaller, probably no more upward flow of warm air and there is no more fuel to be burned.

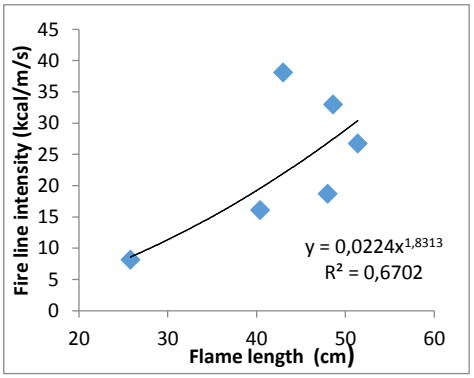

Figure 6. Uphill burning

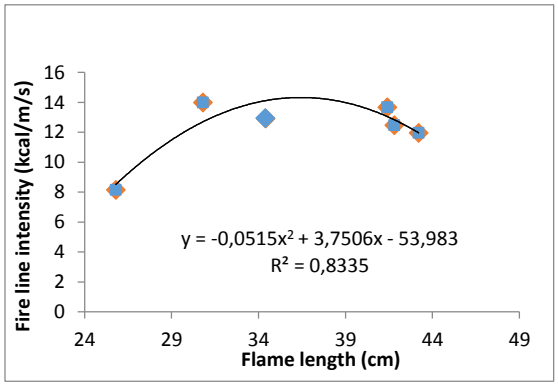

Figure 7. Downhill burning

3. Conclusion

It can be concluded that in the absence of any other variables such as fuel moisture, prevailing winds, different loads and fuel type the slope of the relief has a strong influence on fire behavior. In natural conditions this variables can have an exponential influence that is very difficult to predict because the reaction of combustion promotes local modifications in the combustion area that match the variables in humidity and air flow and are difficult to measure.

References

Beutling, A. (2009). Combustíveis florestais. In: Soares, R.V.; Batista, A.C. e Nunes, J.R.S. (Eds.). Incêndios florestais no Brasil: estado da arte. Curitiba, Brasil, pp. 21-34.

Biswell, Harold Hubert. Prescribed Burning in wildland vegetations management. Berkeley, University of California Press, 1989. 255 p.

Dillon, Gregory K., Zachary A. Holden, Penelope Morgan, Michael A. Crimmins, Emily K. Heyerdahl, and Charles H. Luce. 2011. Both topography and climate affected forest and woodland burn severity in two regions of the western US, 1984 to 2006. Ecosphere 2: art130.

Justino, F; Melo, A.S. de; Setzer, A.; Sismanoglu, R.; Sediyama, G.C.; Ribeiro, G.A.; Machado, J.P.. Sterl, A. (2011). Greenhouse gas induced changes in the fire risk in Brazil in ECHAM5/MPI-OM coupled climate model. Climate Change, 106:285-302. (DOI 10.1007/s10584-010-9902-x).

Miller, Jay D., Collins, Brandon M., Lutz, James A., Stephens, Scott L., Van Wagtendonk, Jan W. and Yasuda, Donald A. (2012). Differences in wildfires among ecoregions and land management agencies in the Sierra Nevada region, California, USA. Ecosphere, vol. 3(9). (Article 80).

Mistry, Jayalaxshmi ; Berardi, Andrea (2005). Assessing fire potential in a Brazilian savanna nature reserve 1. Biotropica, vol. 37(3), pp.439-451.

Pausas, J.G. (2004). Changes in fire and climate in the eastern Iberian Peninsula (Mediterranean basin). Climatic Change. 63, 337-350.

Pausas, J.G. (2012). Incendios Forestales – Una visión desde la ecología. Madri, Catarata, CSIC. 119 p.

Ribeiro, G.A. A queima controlada no manejo da terra. In: Soares, R.V.; Batista, A.C. e NUNES, J.R.S. (Eds.). Incêndios florestais no Brasil: estado da arte. pp. 181-214. 2009. Curitiba, 2009.

Soares, R.V. ; Batista, A.C . Incêndios Florestais: controle, efeitos e uso do fogo. 1. ed. Curitiba: Ronaldo Viana Soares e Antonio Carlos Batista, 2007. v. 1. 264 p.

Soil temperatures and fuel consumption in different species during three experimental fires as a fire severity measure

Baeza MJ[a,b], Pérez EL[b], Santana VM[b], Ayache F[a]

[a] *Departamento Ecología, Universidad de Alicante. Ap. 99. 03080 Alicante, Spain, jaime.baeza@ua.es*
[b] *Fundación de la Generalitat Valenciana CEAM. Centro de Estudios Ambientales del Mediterráneo. C/ Charles Darwin 14, 46980 Paterna (Valencia), Spain, jaime.baeza@ua.es*

Abstract
Forest fires are a recurrent disturbance in Mediterranean ecosystems, and the effect on the structure and dynamics of vegetation may depend largely on fire severity. Our knowledge of how fuel consumption in different species can be an indicator of fire severity is limited, and very few studies have covered this aspect. Our initial work hypothesis is based on the existence of different ecological severities according to each species' structural characteristics. The work aims to determine degree of severity by assessing biomass of different species consumed during a fire. Three experimental fires in Ayora (eastern Iberian Peninsula) were conducted, and subplots dominated by Rosmarinus officinalis, Quercus coccifera, Erica multiflora and Juniperus oxycedrus were selected. The soil temperature during fire was measured using thermocouples in each subplot. Average fuel consumption per species was determined by measuring the minimum diameter of the branches burned in each subplot. Our results indicate fire severity variability between species. The fuel consumption values within the subplots differed significantly between species. The largest were found for E. multiflora and R. officinalis if compared to Q. coccifera and J. oxycedrus. The temperature residence time above 40°C was very important for all species, but the longest occurred in E. multiflora and J. oxycedrus. Soil temperature and its duration were related to fuel type. The results show that fuel accumulation and its spatial distribution in the plant architecture, associated with reproductive strategy, are one of the most important traits in determining fuel consumption and soil temperature and can, therefore, play a key role in fire severity terms. These results indicate the importance of considering fuel structure and flammability of species as potential drivers of new fire regimes.

Keywords*: consumed biomass, fire ecology, fuel type, flammability, Mediterranean shrubland, severity degree*

Introduction

Fire is a recurrent natural disturbance in Mediterranean ecosystems which drives the dynamics of many plant communities (Naveh, 1975; Trabaud, 1980; Gill *et al*., 1981; Pyne, 1995; Baeza *et al*., 2006; Santana *et al*., 2011). However, the level of severity affecting an area depends on the parameters defining the fire regime, such as: extent, frequency, recurrence period, seasonality and intensity of fires. These parameters have been discussed in several papers, but very few have attempted to relate the effects of fire on vegetation by taking into account fire severity (Pérez and Moreno, 1998; Key and Benson, 2005; Lentile *et al.*, 2006; Keely, 2009).
The effects of fire variability on the ecosystem may depend on canopy's dominant species; in particular, the structural characteristics of fuels can modulate the effects on the ecosystem. Availability of fire-prone fuel is determined by its flammability; this property varies from one species to another, and is determined by the interaction of different structural attributes (Cornelissen *et al*., 2003; Alessio *et al*., 2008). Differences in dead twigs retention (Zedler, 1995; Schwilk, 2003; de Luis *et al.*, 2004; Bond and Keeley, 2005), a property that changes with time (Baeza *et al.*, 2011), and structural differences in the arrangement of leaves and stems (van Wilgen *et al*., 1990), affect the temperatures reached during the fire and the heat they emit.
Some research has suggested that differences in fuel structural attributes between different species

induce variability in soil temperature and fuel consumption (Pérez and Moreno, 1998; Molina and Llinares, 2001; Santana *et al*., 2011). Other studies have shown relationships between post-fire regeneration strategies (seeders or resprouters) and flammability traits (Zedler *et al*., 1983; Lloret *et al*., 2003; Bond and Keeley, 2005; Saura-Mas *et al*., 2010). Therefore, further studies are required to clarify the effects of the fuel characteristics of different functional groups in relation to fire severity.
This study focused on fire severity, and specifically on the relationships between two related proxies: fuel consumption and soil temperatures. These relationships were assessed in species with different functional attributes (seeders or resprouters). Our aim was to know how fuel consumption in different species can act as a fire severity indicator.

Methods

This work was conducted in Ayora, eastern Iberian Peninsula (39 º 05'-40 º 15 'N, 0 ° 51'-1 ° 59' W). In April 2009, three plots of 33x33 m were burned. The areas were previously delimited by a 4-metre-wide fire break in which vegetation was eliminated through mechanical brushing. Experimental burnings were carried out under strict safety conditions and were monitored by forest services.
Vegetation was a shrubland dominated by seeders such as *Rosmarinus officinalis* and *Ulex parviflorus*. The resprouting species, these being *Erica multiflora, Quercus coccifera* and *Juniperus oxycedrus*, appeared between the seeder species distributed in a mosaic. This vegetation came from the regeneration of the pine forests burned in the 1979 Ayora fire, which means a vegetation age of 30.
Thirty-six subplots of 50x50 cm were randomly selected prior to the fire. A thermocouple connected to a datalogger was placed in the centre of each subplot on the soil surface, which recorded the temperature every 10 seconds. After the fires, the diameter of burned twig tips were measured for the different species in each subplot following the methodology of Moreno and Oechel (1989).
Furthermore, the average fuel consumption for each species was determined using allometric equations, which were applied to the diameters of the burned twig tips. The differences between the amounts of consumed biomass among the various species were analysed by one-way ANOVA. The residence time of temperature above 40°C was related using regressions with the terminal burned twigs diameter and consumed biomass.

Results

Biomass consumption differed among the three fires. Fire 3, with a maximum temperature of 710°C was the severest, followed by Fire 2 and Fire 1 with 676°C and 670°C, respectively.
The variability in fire severity among the different species was also observed. The highest consumptions were observed for *E. multiflora* and *R. officinalis* rather than for *Q. coccifera* and *J. oxycedrus* (Figure 1).

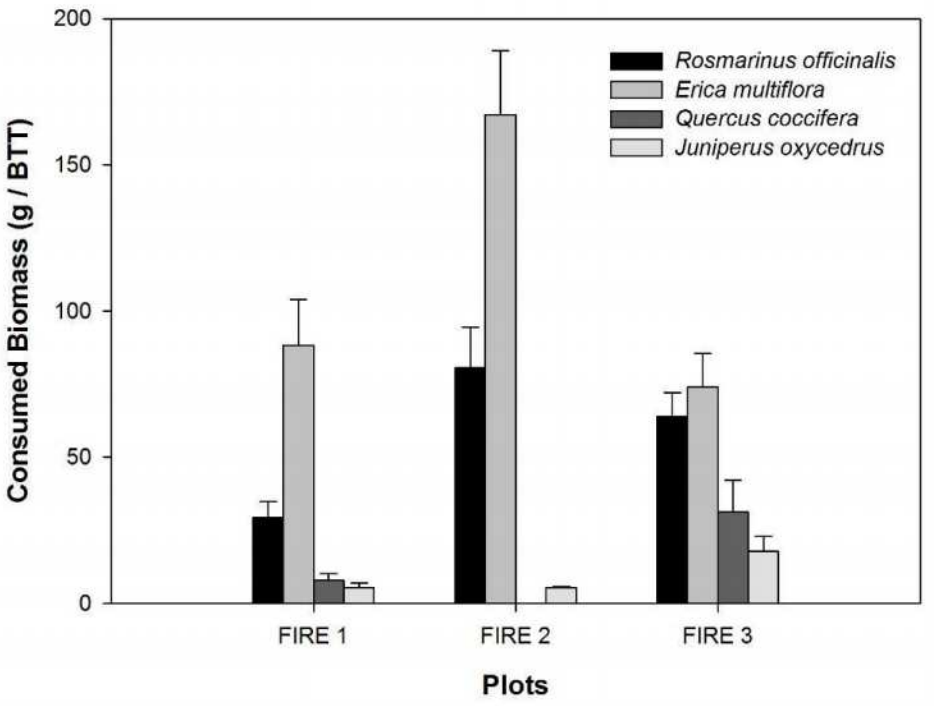

Figure 1. Consumed biomass (mean ± standard error) for the different species during each fire. (BTT: Burned Twig Tips)

The residence time of temperature above 40°C was high for all the species, and ranged between 74 and 92 minutes, but longer durations were recorded for *E. multiflora* and *J. oxycedrus* (Figure 2). Temperatures above 60°C and 80°C were of intermediate duration, and residence time was longer for *Q. coccifera*. For temperatures above 400°C, duration was relatively low (under 5 minutes) for all the species.

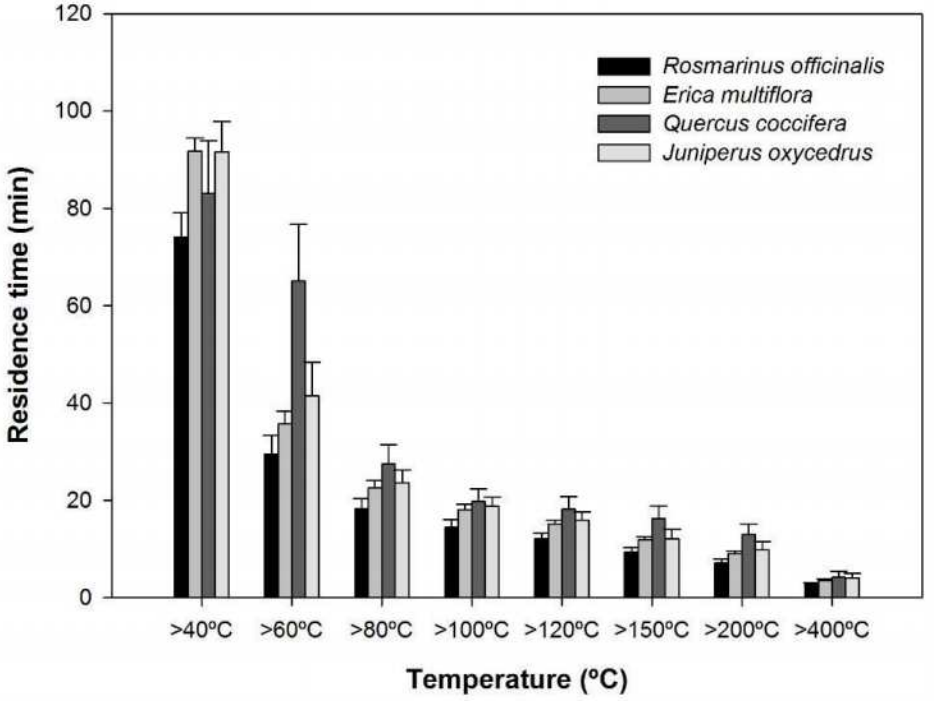

Figure 2. Residence time of temperatures at ground level (0 cm) for the different species (mean ± standard error)

The diameters of the burned twig tips and consumed biomass correlated positively with residence times of above 40°C for *R. officinalis* and *J. oxycedrus* (P <0.01; Table 1). Furthermore, the consumed biomass of *R. officinalis* correlated significantly with the residence times above 100°C and 120°C, while this effect was not observed for the consumed biomass and the diameters of terminal tips of *Q. coccifera* and *E. multiflora*.

Table 1. Correlation between the temperature residence time and the diameters of burned twig tips and biomass consumption (* P<0.05, ** P<0.01); (CB: Consumed biomass, DTT: Diameters of twig tips)

	Rosmarinus		***Quercus***		***Erica***		***Juniperus***	
Temperature residence time (min)	CB (g)	DTT (mm)	CB (g)	DTT (mm)	CB (g)	DTT (mm)	CB (g)	DTT (mm)
>40°C	**0.2146****	**0.2084****	0.1751	0.1363	0.0000939	0.1309	**0.509****	**0.5175****
>60°C	0.0929	0.0821	0.2917	0.2437	0.0126	0.0988	0.1102	0.2437
>80°C	0.1275	0.083	0.2339	0.1857	0.011	0.083	0.0689	0.0422
>100°C	**0.1364***	0.0806	0.3515	0.271	0.005	0.0043	0.129	0.0857
>120°C	**0.1306***	0.1144	0.3575	0.2719	0.0019	0.0031	0.1686	0.1064
>150°C	0.109	0.103	0.4373	0.3351	0.000021	0.0009	0.1273	0.0746
>200°C	0.1035	0.0983	0.4905	0.3792	0	0.0002	0.1491	0.1015
>400°C	0.1071	0.1221	0.2625	0.2041	0.0079	0.0202	0.1864	0.1707

Discussion

The present study reveals the existence of variability in fire severity between our experimental fires, even though they took place at the same time, in similar communities and under similar climatic conditions. This fact has been pointed out in other communities (Baeza, 2001). It has also been suggested that variation in vegetation moisture might be responsible for these differences (Johnson and Miyanishi, 1995). Fuel moisture content is the main factor to control the fire spread rate in controlled burnings applied to young and mature Mediterranean gorse (dominated by *Ulex parviflorus*; Baeza *et al*., 2002b). This variability is also due to the fuel characteristics of the component species and may, thus, depend on the assembly of different compositions in each plot. In fact, specific vegetation composition seems to play a decisive role in the temperatures recorded during a controlled burning in Mediterranean shrublands (De Luis *et al*., 2004).

Our study reveals that seeder species *R. officinalis* was the most flammable species in contrast to resprouter species. One exception was *E. multiflora*, which also showed high flammability. In line with this, some previous studies have correlated flammability characteristics with post-fire regeneration strategies in plants (Bond and Keeley 2005; Ojeda *et al*., 2010; Saura-Mas *et al*., 2010). Mediterranean Basin seeders grow much faster and allocate more biomass on leafs than resprouters. Seeders are mainly non-sclerophyllous and are associated with early succession stages, whereas resprouters are mainly sclerophyllous and are associated with late succession stages (Keeley, 1998; Pausas, 1999; Verdú, 2000). In fact seeders need lower temperatures to produce flame and exhibit fast combustion (Saura-Mas *et al*., 2010, Santana *et al*., 2011). However, the higher temperatures required by resprouters to initiate combustion, together their large fuel loads, can make fires not easily to extinguish (Andrews and Bevins, 2003). These preliminary results suggest that the ecosystems dominated by seeders are more prone to fire and burn more severely than those dominated by resprouting species.

Moreover, fire behaviour and its impact potential are related to the amount of accumulated fuel which, in turn, depends on the time elapsed since the last fire (Baeza *et al*., 2011). In fact, the differences observed between each species' consumed biomass are attributable to not only the structural

differences between species, but also to the retention of dead branches (Schwilk, 2003; Bond and Keeley, 2005). Our results indicate that shrub species such as *E. multiflora* and *R. officinalis* obtain much higher consumed biomass values if compared to tree or semi-tree species such as *Q. coccifera* and *J. oxycedrus*. Baeza *et al*. (2011) suggested that in advanced succession stages, shrub species like *E. multiflora* obtain higher percentages of dead fuel and dead thin twigs than other tree species such as *Q. coccifera* and *J. oxycedrus*. This suggests that the plant communities dominated by these shrub species are more likely to burn.

The fuel structure differences between species are significant in soil temperatures modulation and temperature residence times. In our study, *R. officinalis* displayed shorter temperature residence times despite its greater fuel consumption. This can be explained by its fast combustion due to a more dispersed fuel load in its structure. In contrast, the residence time was longer for resprouters with thicker fuels and larger amounts of fuel. These species require higher temperatures and longer times for the combustion of their biomass.

Indeed as has been widely documented in other fire-prone shrublands with similar fuel loads, the maximum soil temperatures and the longest residence times are significantly higher and longer, respectively, for fuels of lower height and higher bulk density (Molina and Llinares, 2001; Wright and Clarke, 2008). These results agree with other studies in conducted Mediterranean shrublands (Bradstock *et al*., 1992, 1993; Savadogo *et al*., 2006; Baeza *et al*., 2002a; Santana *et al*., 2011).

Our results show that differences in fuel accumulation among species with a different reproductive strategy, as well as their spatial distribution in the plant architecture, represent one of the most important structure features that determine fuel consumption and soil temperature. Consequently, it may play a key role in fire severity determination.

Acknowledgements

This work has been possible thanks to the “CAtastrophic Shifts in drylands: how CAn we prevent ecosystem DEgradation?" CASCADE project (FP7. ENV.2011. 283068) and the RESILIEN project (CGL 2011-30515-C02-02). It has also been possible through a grant from the Spanish Agency for International Development Cooperation, issued to Mrs. F. Ayache.

References

Alessio GA, Peñuelas J, de Lillis M., Llusià J (2008) Implications of foliar terpene content and hydration on leaf flammability of *Quercus ilex* and *Pinus halepensis*. *Plant Biology* **10**, 123-128.

Andrews PL, Bevins CD (2003) BehavePlus fire modeling system, version 2.0: overview. In ´Proceedings of the Second International Wildland Fire Ecology and Fire Management Congress and Fifth Symposium on Fire and Forest Meteorology´, pp. 5-11. (Orlando, FL)

Baeza MJ (2001) Aspectos ecológicos y técnicas de control de combustible (roza y quema controlada) en matorrales con alto riesgo de incendio dominados por *Ulex parviflorus* (Pourr.). Ph.D thesis, Departamento de Ecología. Universidad de Alicante.

Baeza MJ, Raventós J, Escarré A (2002a) *Ulex parviflorus* germination after experimental burning: effects of temperature and soil depth. In ´Fire and Biological Processes´. (Eds Trabaud L, Prodon R) pp. 83-91. (Backhuys Publisher, Leiden, The Netherlands)

Baeza MJ, de Luis M, Raventós J, Escarré A (2002b) Factors influencing fire behaviour in shrublands of different stand ages and the implications for using prescribed burning to reduce wildfire risk. *Journal of Environmental Management* **65**: 199-208.

Baeza MJ, Raventós J, Escarré A, Vallejo VR (2006) Fire risk and vegetation structural dynamics in Mediterranean shrubland. *Plant Ecology* **187**: 189-201.

Baeza MJ, Santana VM, Pausas JG, Vallejo VR (2011) Succesional trends in standing dead biomass in Mediterranean basin species. *Journal of Vegetation Science* **22**: 467-474.

Bond WJ, Keeley JE (2005) Fire as a global 'herbivore': the ecology and evolution of Flammable ecosystems. *Trends in Ecology and Evolution* **20**: 387-394.

Bradstock RA, Auld TD, Ellis ME, Cohn JS (1992) Soil temperatures during bushfires in semi-arid, mallee shrublands. *Australian Journal of Ecology* **17**: 433-440.

Bradstock RA, Gill AM (1993) Fire in semi-arid, Mallee shrublands: size of flames from discrete fuel arrays and their role in the spread of fire. *International Journal of Wildland Fire* **3**: 3-12.

Cornelissen JH, Lavorel S, Garnier E, Díaz S, Buchmann N, Gurvich DE, Reich PB, ter Steege H, Morgan HD, van der Heijden MGA, Pausas JG, Poorter H (2003) A handbook of protocols for standardised and easy measurement of plant functional traits worldwide. *Australian Journal of Botany* **51**: 335-380.

de Luis M, Baeza MJ, Raventós J, González-Hidalgo JC (2004) Fuel characteristics and fire behaviour in mature Mediterranean gorse shrublands. *International Journal of Wildland Fire* **13**: 79-87.

Gill AM, Groves RH, Noble IR (Eds) (1981) Fire and the Australian biota. (Australian Academy of Science, Canberra)

Johnson EA, Miyanishi K (1995) The need for consideration of fire behavior and effects in prescribed burning. *Restoration Ecology* **3**: 271-278.

Keeley JE (1998) Post fire ecosystem recovery and management: the October 1993 large fire episode in California. In ´Large forest fires´. (Eds Moreno JM) pp. 69–90. (Backhuys Publishers, Leiden)

Keeley JE (2009) Fire intensity, fire severity and burn severity: a brief review and suggested usage. *International Journal of Wildland fire* **18**: 116-126.

Key CH, Benson NC (2005) Landscape Assessment: Ground measure of severity, the Composite Burn Index; and remote sensing of severity, the Normalized Burn Ratio. In ´FIREMON: Fire effects monitoring and inventory system´. (Eds Lutes DC, Keane RE, Caratti JF, Key CH, Benson NC, Gangi LJ) pp. 1-51.

Lentile LB, Holden ZA, Smith AM, Falkowski MJ, Hudak AT, Morgan P, Lewis SA, Gessler PE, Benson NC (2006) Remote sensing techniques to assess active fire characteristics and post-fire effects. *International Journal of Wildland Fire* **15**: 319-345.

Molina MJ, Llinares JV (2001) Temperature-time curves at the soil surface in maquis summer fires. *International Journal of Wildland Fire* **10**: 45-52.

Moreno JM, Oechel W (1989) A simple method for estimating fire intensity after a burn in California chaparral. *Acta Ecologica/Ecologia Plantarum* **10**: 57-68.

Naveh Z (1975) The evolutionary significance of fire in the Mediterranean region. *Vegetatio* **29**: 199-208.

Lloret F, Pausas J, Vilà M (2003) Responses of Mediterranean plant species to different fire frequencies in Garraf Natural Park (Catalonia, Spain): field observations and modelling predictions. *Plant Ecology* **167**: 223-235.

Ojeda F, Marañón T, Arroyo J (1996) Post-fire regeneration of a Mediterranean heathland in Southern Spain. *International Journal of Wildland Fire* **6**: 191-198.

Pausas JG (1999) The response of plant functional types to changes in the fire regime in Mediterranean ecosystems. A simulation approach. *Journal of Vegetation Science* **10**: 717-722.

Pérez B, Moreno JM (1998) Methods for quantifying fire severity in shrubland-fires. *Plant Ecology* **139**: 91-101.

Pyne SJ (1995) World Fire: The Culture of Fire on Earth, 384 pp. (University of Washington Press)

Savadogo P, Zida D, Sawadogo L, Tiveau D, Tigabu M, Odén PC (2006) Fuel and fire characteristics in savanna-woodland of West Africa in relation to grazing and dominant grass type. *International Journal of Wildland Fire* **16**: 531-539.

Santana VM, Baeza MJ, Vallejo VR (2011) Fuel structural traits modulating soil temperatures in different species-patches of Mediterranean Basin shrublands. *International Journal of Wildland Fire* **20**: 668-677.

Saura-Mas S, Paula S, Pausas JG, Lloret F (2010) Fuel loading and flammability in the Mediterranean Basin woody species with different post-fire regenerative strategies. *International Journal of Wildland Fire* **19**: 783-794.

Schwilk DD (2003) Flammability is a niche construction trait: canopy architecture affects fire intensity. *American Naturalist* **162**: 725-733.

Trabaud L (1980) Impact biologique et écologique des feux de végétation sur l'organisation, la structure et l'évolution de la végétation des zones de garriques du bas-Lanquedoc. Ph. D. Thesis, University of Montpellier, Monpellier.

van Wilgen BW, Higgins K, Bellstedt D (1990) The role of vegetation structure and fuel chemistry in excluding fire from forest patches in the fire-prone fynbos shrublands of South Africa. *Journal of Ecology* **78**: 210-222.

Verdú M (2000) Ecological and evolutionary differences between Mediterranean seeders and resprouters. *Journal of Vegetation Science* **11**: 265-268.

Wright BR, Clarke PJ (2008) Relationships between soil temperatures and properties of fire in feathertop spinifex (*Triodia schinzii* (Henard) Lazarides) sandridge desert in central Australia. *The Rangeland Journal* **30**: 317-325.

Zedler PH, Gautier CR, McMaster GS (1983) Vegetation change in response to extreme events: the effect of a short interval between fires in California chaparral and coastal scrub. *Ecology* **64** (4): 809-818.

Zedler PH (1995) Are some plants born to burn? *Trends in Ecology and Evolution* **10** (10): 393-395.

Studying wildland fire spread using stationary fires

D.J. Gorham[a], R. Hakes[a], A.V. Singh[a], J. Forthofer[b], J. Cohen[b], S. McAllister[b], M.A. Finney[b] and M.J. Gollner[a]

[a] *Department of Fire Protection Engineering, University of Maryland, College Park, MD 20742, USA. dgorham1@umd.edu, mgollner@umd.edu*
[b] *US Forest Service, Missoula Fire Sciences Lab, Missoula, MT 59808, USA. jaforthofer@fs.fed.us, mfinney@fs.fed.us*

Abstract
Experiments were performed using stationary gas burners and liquid fuel-soaked wicks to study fundamental wildland fire behaviour, including unsteady flame heating. These experiments were motivated by observations of instabilities in spreading fire experiments that suggest they play a critical role in fire spread. Stationary fire experiments in forced flow and on inclined surfaces exhibited instabilities similar to those observed in spreading fires but allowed for more detailed analysis of the mechanisms responsible. Large scale inclined experiments were performed using an ethylene gas-fed burner at angles from 10 to 60 degrees. Forced flow experiments were performed on liquid-soaked wicks and small scale gas burners at wind speeds from 0.2 to 3 $\mathbf{ms^{-1}}$. Results presented include observations of the general flame structure, including streamwise streak spacing and flame fluctuation frequencies which relate to instabilities observed in large spreading experiments. A description and correlations of flame geometry, useful for predictions of wildland fire spread are also presented.

Keywords*: wildland fire, inclined flame spread, diffusion flame, flame pulsation*

Introduction

Predicting the rate of spread (ROS) of large wildland fires is of critical importance for operational firefighting, prescribed burning, and calculating future wildfire potential. Currently, most of these models are based upon correlations derived from experiments performed in the 1970's by Rothermel, Anderson and others (Finney *et al*. 2013a). While these correlations provided a "leap forward" in the prediction of a steady ROS, they failed to capture essential physics and therefore break down under extreme wind, topographic, and other conditions (Finney *et al*. 2013b). A considerable amount of effort is therefore being invested towards better understanding this fire behaviour, especially the mechanisms of heating to fuel particles. While it has proven difficult to study these phenomena in some large-scale spreading fires, a series of stationary, scaled experiments have been designed to determine the underlying physics that occur during fire spread.

Recent experiments of flame spread in discrete fuel beds have revealed the presence of buoyant instabilities which may lead to increased convective heating of fuel particles (Finney *et al*. 2013a). Unfortunately, detailed fluid dynamics and convective heating measurements in spreading fires remain difficult to capture because of the moving burning region of the fire. This is compounded by changes in the flame front and fuel burnout with time, causing non-steady burning rates and dynamic fire behaviour that require dozens of expensive, large scale fire experiments to investigate. Stationary burners have long been used to study fires in the built environment (de Ris and Orloff 1975), therefore they offer an ideal configuration to study non-steady fire effects in a thorough, statistical manner, in essence capturing a snapshot of a moving fire front. Experiments here show these stationary burning regions contain two buoyant instabilities which are similar to spreading fires, appropriately scaling with macro-features of large spreading fires, however they provide enhanced measurement capabilities (Finney *et al*. 2013a).

Motivation

Recent studies of spreading fires in the 3×3 m wind tunnel at the Missoula Fire Science Laboratory have shown coherent structures that form in the streamwise direction of the flow as well as spanwise fluctuations that propagate to the downstream edge of the flame zone contributing to fuel heating. The highly spatially-uniform fuel beds used in these experiments allowed for the observation of these structures with more repeatable results than previous efforts (Finney *et al*. 2013a). The results suggest that flame spread in fine fuel beds is driven by non-steady convective heating and intermittent flame contact on fuel particles. These heating characteristics were measured using micro thermocouple arrays and high speed video. The travelling flaming region, however, made it difficult to carefully study these properties, such as a statistical analysis of these features which appear stochastically in the flow. A technique was therefore needed that could study these new instabilities and other general structures of propagating wildfires in a small-scale configuration that can be utilized over long times.

Figure 1. Photos demonstrating the scales over which coherent streaks and flame towers have been observed. (a) Inclined gas burner, $L_f \approx 0.2$ m, (b) Comb burn experiments in 3×3 m wind tunnel, $L_f \approx 2$ m, and (c) Canadian Crown fire experiments, $L_f \approx 30$ m (Clark et al. 1999).

A stationary, non-spreading fire was chosen as it allows for a thorough statistical analysis of the flame structure. Long-duration experiments allow for a large sample size and more control over variations in experimental parameters, such as decoupling the heat-release rate of the fire from flow conditions, unachievable in spreading fires. The flame zone depth in the direction of fire spread can also be carefully adjusted via the size of the burner. High speed video and micro thermocouples are useful on these fires to reveal and track buoyant instabilities in the fire flow which resemble those appearing in spatially-uniform fuel beds. The same intermittent heating observed in the fuel bed experiments were observed in the stationary burner, but with the ability to collect a larger data set. Other modifications to the flow field, such as the incoming boundary layer thickness is also adaptable in these small scale experiments.

3. Methods

3.1. Experimental Setup

Forced-flow experiments were performed at both the USDA Forest Service's Missoula Fire Science Laboratory and a specially-designed 30 centimeter cross section wind tunnel at the University of Maryland's Fire Phenomenon Laboratory (UMD). In Missoula, a propane burner was constructed in the laboratory, using sintered metal as the porous burner surface which measured approximately 30 by 25 cm. A volumetric flow meter was used to measure the flow rate of propane gas into the burner, and experiments were conducted at fire sizes of 7.5, 10.9, and 15.1 kW. Ceramic insulation board was placed around the burner so as to make a continuous flat, inert surface to limit side-air entrainment. The apparatus was tested in a low-speed tunnel, 3×3 m cross section, at free-stream velocities of 0.22, 0.44, 0.67, 0.89, 1.11, and 1.34 ms^{-1}. Side view video was captured with a Phantom brand high-speed camera at 120 frames per second.

At UMD, a laminar wind blower was designed and built for uniform forced flow combustion experiments. The wind blower was designed to pressurize a 0.75 cubic-meter plenum box with a centrifugal fan. The flow then travels through a converging section into a 30×30 cm rectangular duct into a mesh screen and honeycomb flow straightener. The flow travels another 1.35 m in the duct resulting in a fully-developed laminar boundary layer before it is exhausted at the outlet. The velocity profile of the boundary layer was measured along the centerline of the blower above the burner surface using a hot-wire anemometer. Measurements confirmed the blower is capable of repeatedly producing precise forced flow velocities between 0.6 and 4.8 ms^{-1} with turbulence intensities less than 3% at maximum velocities.

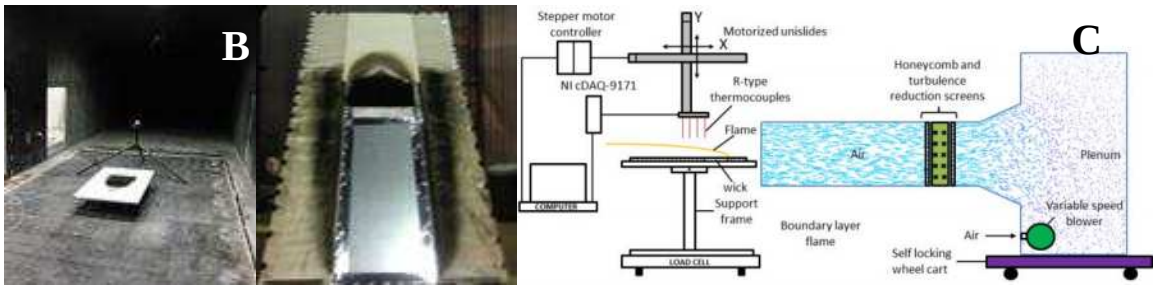

Figure 2: (A) Forced-flow gas burner in the Missoula 3×3 m wind tunnel, (B) Inclined gas burner at Missoula and (C) Forced flow configuration at UMD.

Large-scale inclined experiments were performed in Missoula on a gas burner flame wall repurposed from a vertical configuration (Jimenez *et al*. 2010). The retrofitted burner is rotatable so that experiments could be performed at inclination angles between 0 and 90 degrees relative to the ground. The width of the burner was 0.595 meters and the total burner surface height was 1.83 meters. To produce a line fire, sections of the burner were sealed so that gas flowed out of a ceramic plenum only above the exposed burner surface. The width of the line fire was fixed, based on the flame wall, but the depth of the burning region was changed between experiments by extending the amount of burner surface covered. Non-combustible surfaces were also attached to the top and sides of the flame wall in order to extend its length and width, minimizing side-air entrainment. Sidewalls were also considered for use, however it was found that at this scale such walls would induce the trench effect, drastically increasing flame lengths and flame attachment somewhat different than the open-fire behaviour trying to be studied here (Atkinson *et al*. 1995). A flush transition from the burner to the attachment section was ensured. Similar to vertical flame wall experiments (Finney *et al*. 2010), the burner was first purged with nitrogen and ethylene fuel was then introduced at a rate specified by the mass flow controller. Once the flame was fully developed across the exposed burner area, the flow of nitrogen was cut off.

3.2. Instrumentation

High-speed videography was used to capture digital images of the flame in all configurations from both the side and top view (Figure 1and 2). The side view camera was a Phantom, recording at 120 frames per second and a 1920×1080 pixel resolution, mounted on a tripod and tilted to give a parallel view of the flame relative to the attachment surface. The top-view camera was a high-speed Casio EFX-1, recording at 120 frames per second at a 640×480 pixel resolution, mounted on a tripod mounted to the bottom of the flame wall. This allowed for observation of the flame from the upstream edge at approximately a 45 degree angle. Micro-thermocouple arrays, similar to those used in spreading fire experiments (Finney *et al*. 2013a), were also placed downstream along the centerline of

the burner, raised 1 centimetre above the inert "unburnt fuel" surface with a spacing of 2 cm between thermocouples. Temperature measurements were sampled at a frequency of 120 Hertz.

Results

4.1. Mechanisms of Instability

In both spreading, forced flow (wind-driven) fires and stationary forced flow and inclined (sloped) experiments two dominant instabilities were observed. The first consisted of streamwise streaks, appearing as flame peaks and troughs when observed parallel to the direction of external flow (Figure 3). These structures resemble counter-rotating vortex pairs (Taylor-Görtler vortices) which form over concave surfaces (Saric 1994). The significance of these structures is that they splay flames downward into the fuel-bed, adding heating to the fuel surface that increases rates of flame spread. Similar structures have been observed in experiments on inclined heated surfaces with correspondingly increased rates of heat transfer noted (Jeschke and Beer 2001)**.** In stationary burner experiments, flame attachment was seen to occur downstream of the burner in both forced flow and inclined experiments, facilitating heating of "unburnt" fuel and thus simulating flame spread. Within this attachment region the flame front was also observed to pulse or burst further downstream, extending the direct flame contact zone with the unburnt fuel surface far beyond the mean flame front. The frequency of these observed pulsations were then extracted from oscillations of the flame location within this attachment region. This behavior is important as it could be similar to heating of fuel particles by direct flame contact which may be responsible for flame spread, as observed in larger scale experiments (Finney *et al*. 2013a).

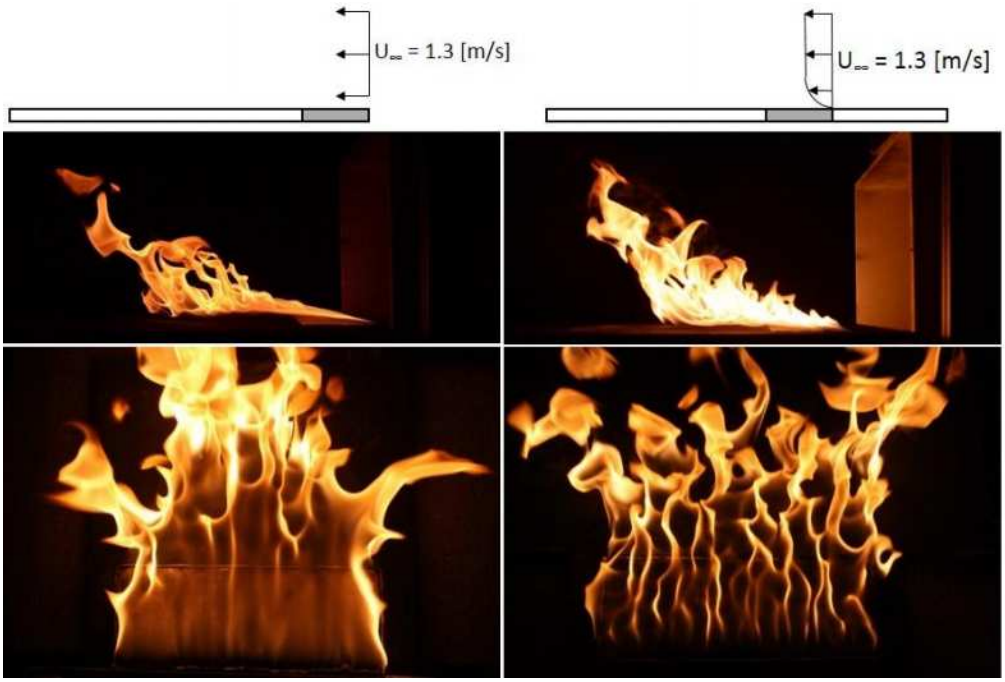

Figure 3. Boundary layer effects on a stationary wind-blown fire. (Left) No boundary layer development surface, i.e. placed directly in the free-stream flow. (Right) 25 cm boundary layer development surface (boundary layer thickness ≈ 2 cm). The fuel source was a heptane-soaked wick and an inert surface was placed downstream for all experiments to observe attachment of the flame.

In order to investigate the mechanisms responsible for these instabilities, experiments were conducted on UMD's forced flow burner apparatus to see what flow configurations were necessary for the formation of streamwise streaks. After a series of experiments, it was found that the length of the flat, inert surface leading into the flame significantly modified observed structures in the flow. A 30 cm wide, 12 cm deep porous ceramic wick was soaked with heptane and ignited in a 1.3 ms^{-1} flow with

two different leading edge conditions. First, the wick was placed directly in the free stream flow, allowing for negligible boundary layer development. Second, the wick was placed parallel to the surface of the wind tunnel, providing an 8 cm boundary layer development length. Figure 3illustrates this effect with two different configurations. The difference in the flames is striking, the uniform flow generated flame with no boundary layer development has almost no observable streaks, with a flatter, more laminar appearance (left-hand side of Figure 3). The flame with the boundary layer, however, forms strikingly coherent streaks which periodically force the flames closer to the fuel surface (troughs) or further into the air (peaks) along the width of the burner. Analysis of the two configurations utilizing methods described in the proceeding sections also showed that the boundary-layer configuration results in higher burning rates (0.8 g/s vs. 0.3 g/s), measured by a load cell and higher flame fluctuation frequencies than the uniform-flow configuration (7.3 Hz vs. 3.5 Hz). Therefore, the formation of streaks appears to be important in understanding downstream heating and thus fire spread.

4.2. Streamwise Streak Analysis

Streamwise streaks were observed to originate at the base of flames where any boundary layer development was present, whether that development occurred due to external forced flows or entrainment into the flame on inclined experiments. Streaks are observable due to up wash regions (peaks) where flames illuminate the structure. In order to further understand the instability which modifies the spacing between these streaks, measurements of the streak spacing were taken under a wide variety of flow configurations. High speed video taken from the top of the experiments was used to determine this average streak spacing 1 cm from the base of the flame.

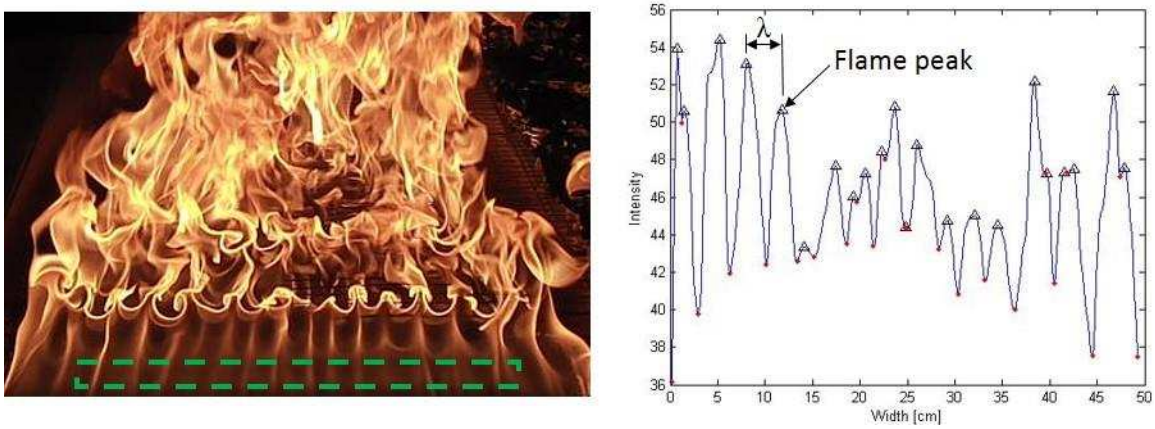

Figure 4. Streak analysis method for stationary gas burners. (Left) Top-view image from the Missoula inclined experiment, with a crop box region identified by dashed green lines. (Right) Smoothed intensity plot across the width of the burner, with local maximums marked as black triangles, representing the flame upwash peak.

The video was loaded into MATLAB and decomposed into individual frames. The region-of-interest started at the base of the flame across the width of the burner. For image analysis, the region was cropped one centimeter from the base of the burner in the flow direction. The intensity for each pixel column in the region-of-interest is averaged and the intensity across the width of the burner smoothed. The local maximums in intensity were determined to be a streak in the flow, and the spacing between the streaks determined for each image (Figure 4). Streak spacings for each experiment were then plotted on a histogram, fit to a log-normal distribution and the peak was used to scale the spacing between streaks for experiments (Figure 5).

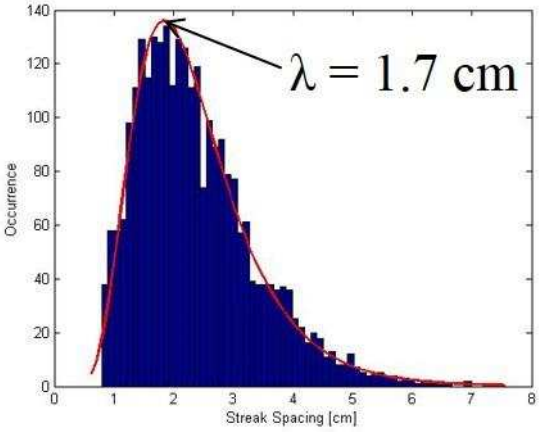

Figure 5. Probability distribution function (PDF) of streak spacing for a single experiment. The vertical axis represents the frequency of occurrence and the horizontal access the streak spacing observed. The red line indicates a log-normal distribution fit to the observed PDF.

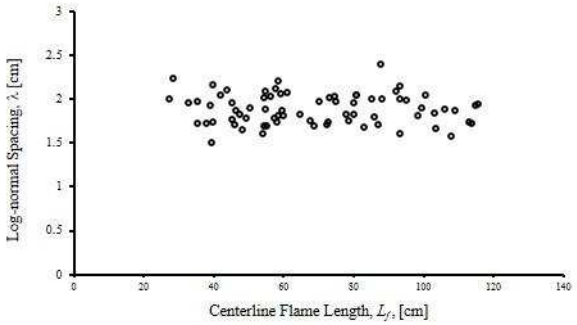

Figure 6. Maximum log-normal streak spacing, λ, remains relatively constant for small scale stationary burner experiments.

Similar to large scale experiments (Finney *et al*. 2013a), a relationship between the streak spacing and flame length were found, shown in Figure 6. This relationship appears nearly linear here over the limited test conditions, however if plotted against large-scale data (Finney *et al*. 2014) a relationship between flame length and streak spacing of the form, $\boldsymbol{\lambda = 0.39 L_f + 0.34}$ is observed. While the streaks meander from side to side during tests, the uniformity of the log-normal distributions observed show that they are coherent in formation for the unique conditions of every test. Their formation requires incoming vorticity of both the boundary layer and flame to interact, forming a centrifugal instability similar to Taylor-Görtler vortex streaks. Other instabilities are also observed, especially in inclined experiments, namely span wise waves that appear on the base of the inclined burner. These are most likely Tollmien-Schlicting waves that form at the base of a boundary layer from small perturbations that slowly grow in size and play a critical role in a laminar flow's transition to turbulence (Goldstein and Hultgren 1989). In these observed boundary layers, these waves cause flames to break off into flamelets so that they are easily observable. Similar structures are also seen in larger spreading fire experiments in the 3×3 m Missoula wind tunnel (Finney *et al*. 2014). They may play a role in the formation of pulsations or bursts of flames discussed in the next section. Further research using stationary burners will explore more effective scaling techniques and ways of predicting their formation and effects.

4.3. Flame Pulsation Analysis

Pulsations, or bursts of the flame beyond the mean flame front location were observed in spreading fire experiments as well as in stationary burners (Figure 7). The flame location in stationary experiments was determined using side-view high-speed video and an array of thermocouples ahead of the burner. A region starting at the downstream edge of the burner and extending fully downstream, 1 cm above the surface was determined as a region of interest where extension of the flame would relate to flame attachment and fuel particle heating. The flame location was then determined in this region-of-interest by tracking the furthest-most downstream tip of the flame. This location fluctuated in time and it was observed that the flame would pulse downstream, "bursting" into what would be the unburned fuel region in a spreading fire experiment.

Experimental videos were loaded into a MATLAB script for analysis. The previously described region of interest was defined from the downstream edge of the burner surface to the end of the image in the downstream direction, with a height above the surface of 1 cm (see the dashed purple rectangle in Figure 7). Each image in the video was cropped to this same region-of-interest and then converted to a black and white image using the same average threshold value from the streak analysis. The attached flame location (xa) was determined as the furthest downstream pixel in the region-of-interest that satisfied the flame threshold level (Figure 7).

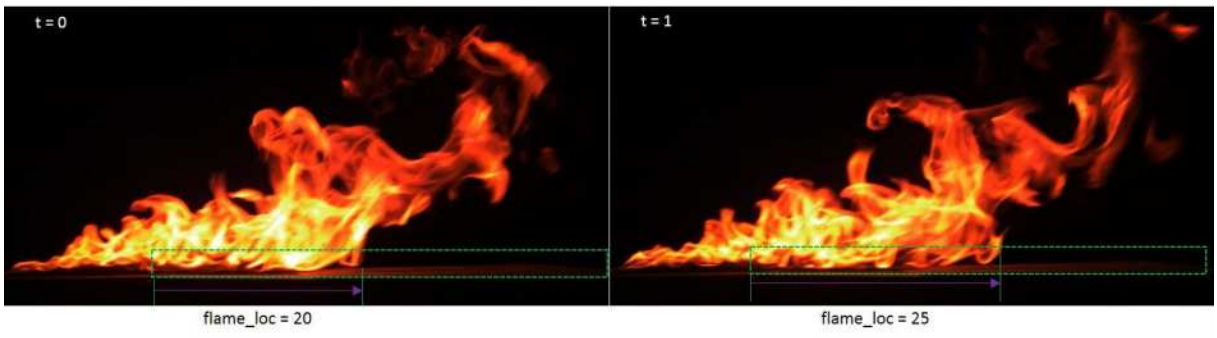

Figure 7: Flame location between two time steps in a forced flow experiment. The flame attachment location (x_a) is measured from the downstream edge of the burner to edge of the flame within the attachment region.

The flame extension downstream within the attachment region fluctuated in time, causing intermittent flame contact (Figure 8). The frequency of the flame pulsations was determined at locations on the downstream end of the burner using a variable interval time average (VITA) method (Blackwelder and Haritonidis 2006). The levels were determined at a range of locations downstream of the burner, starting at the burner edge and increasing in 1 cm increments (Figure 9). The flame position in time was compared to each of these locations and the number of occurrences was tallied. A level-crossing in the VITA technique was only considered for one direction; therefore only when the flame was previously not at a location and then at it in the next time step was it considered a crossing. The frequency for each location was then determined by dividing the number of crossings by the total number of frames analyzed, and multiplying by the frame rate of the video.

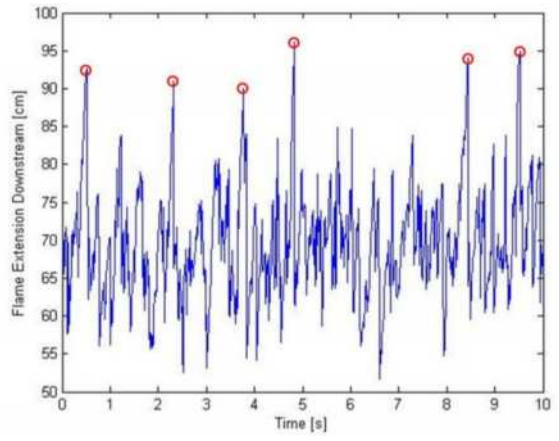

Figure 8. Flame location over time determined with high-speed videography. Flame location fluctuates around maximum frequency pulsation distance, but occasionally "bursts" further downstream (noted by red circles).

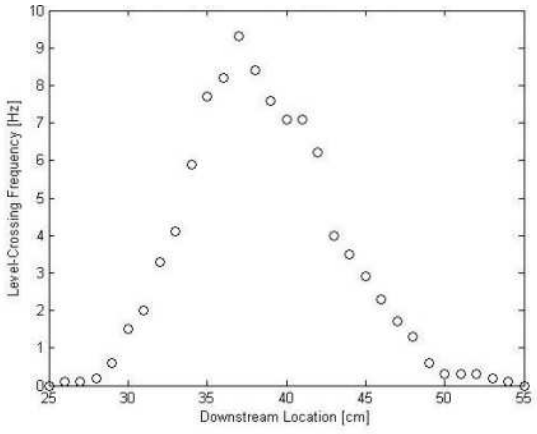

Figure 9. VITA frequency at advancing downstream locations.

In analysis of the trend of the frequency with different configurations, an analogy with pulsating pool fires was applied in the form of a Strouhal-Froude relationship. The Strouhal number, $\boldsymbol{St = fL/U}$, where *f* is the VITA frequency, *L* is a characteristic length scale and *U* is the free-stream velocity, was used to non-dimensionally relate oscillating flow mechanics to a balance of momentum and buoyancy forces. For this, the Froude number was used, $\boldsymbol{Fr = U/(gL)^2}$, where *g* is the acceleration due to gravity. Following the analysis of spreading fires (Finney *et al*. 2014), the flame length L_f was chosen as a characteristic length scale for the system, which represents the magnitude of the buoyant force. Figure 10 shows this scaling, $St = 2Fr^{-0.3}$ which is resolved from forced-flow gas burner experiments. The value of this exponent is below the value of -0.43 found in scaling for larger-scale fire spread experiments (Finney *et al*. 2014) and the -0.5 for diameter scaling of puffing in circular pool fires (Cetgen and Ahmed 1993 and Malalasekera *et al*. 1996). While the flame length may not be the most fundamental quantity for scaling analysis because of its coupling to experimental conditions, it is useful as most wildland fire spread analyses are correlated to this quantity (Byram 1959).

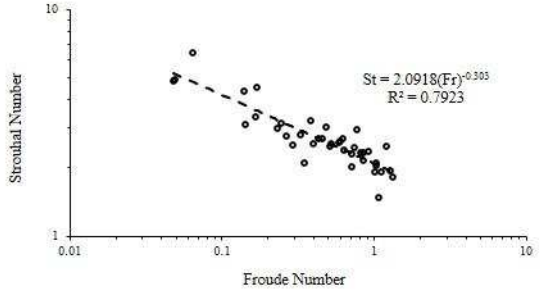

Figure 10. Strouhal-Froude scaling for stationary burners in forced-flow environment.

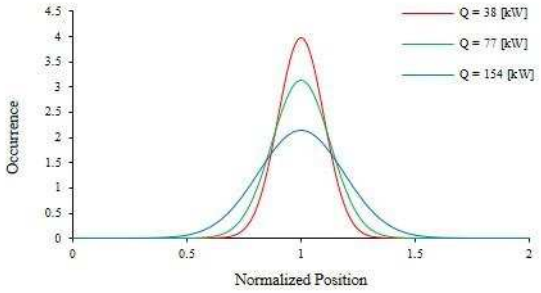

Figure 11. Probability-density function distribution of flame attachment along the free surface for three different heat-release rates (Q).

Statistical analysis of the flame position over time was also performed by producing a probability density function of the normalized flame attachment length (x_a) for different fire and flow configurations on an inclined and forced-flow gas burner. A histogram of the flame attachment length consistently shows a normal distribution of the downstream flame extension along the surface for each experiment. To compare the distribution for experiments, the attachment length was normalized with the average of the flame attachment distance in the attachment region (nominally an average flame extension along the free surface). The mean and standard deviation of the normalized flame location was then used to produce normal probability density functions, one of which is shown in Figure 11.
The representative tests shown in Figure 11 indicate increasing heat-release rates (Q = 38.6, 77.1 and 154.3 kW/m^2) of ethylene on the inclined Missoula flame wall. As the heat-release rate of the fire is increased, it is clear that the peak downstream extension of the flame resides further away from its mean position and extends further downstream more often. While other variables were compared, such as the incoming wind velocity and slope angle of inclined burners, once normalized with the flame length they were found to have little effect on the relationship shown in Figure 11. The implications of this finding are that, despite varying flow conditions and relative fire sizes (L_f), it is the overall heat-release rate of the fire that represents increasing extension of flames beyond the mean flame length into unburnt fuels. This perhaps suggests a means for correlation or future study.
Finally, an analysis was performed to investigate how far downstream of a burner a maximum VITA frequency would occur. Again, the relative fire size in terms of heat-release rates were found to best represent the variation in frequencies observed. Figure 12 shows this relationship, with the distance at which the maximum VITA frequency for a fire is observed downstream of a gas burner for various

inclined and forced-flow conditions versus a dimensionless fire size, $\boldsymbol{Q^* = Q/\left(\rho c_p T g^{1/2} L_f^{5/2}\right)}$, where $\boldsymbol{Q}$ is the heat-release rate of the fire, $\boldsymbol{\rho c_p T}$ representative gas density, specific heat and temperature, respectively, g acceleration due to gravity and $\boldsymbol{L_f}$ the flame length.

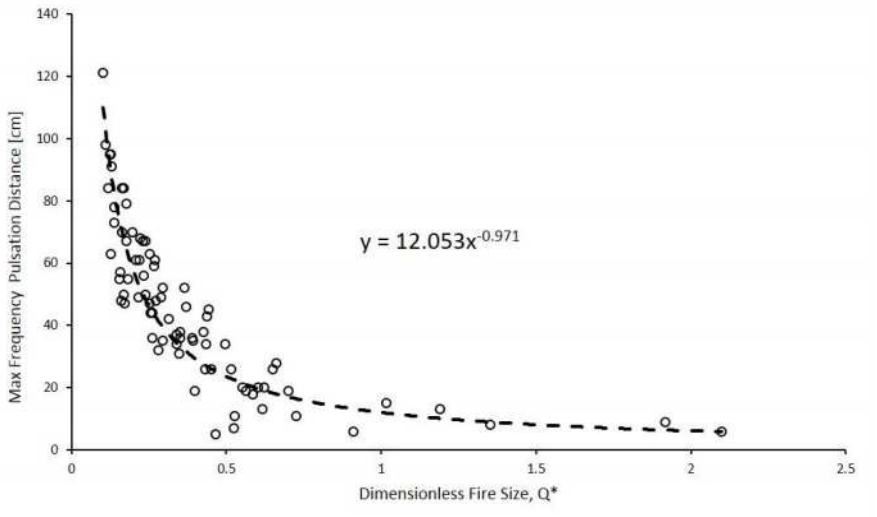

Figure 12. Max-frequency pulsation distance downstream into "unburnt fuel-bed" is considerably far for fires with low dimensionless fire size, Q*, and decreases exponentially with increasing dimensionless fire size.

4.4. Flame Geometry

Knowledge of the mean flame geometry, such as flame length, tilt angle, etc. are useful for assessing fire properties and can be easily obtained from stationary fire experiments. Measurements of the two-dimensional flame geometry were taken from side view images of the each experiment. Videos were processed into gray-scale images in MATLAB for the analysis. To determine the average flame geometry, the image was converted to RGB and all pixels with values between 0.48 and 0.52 were converted to red (Figure 13). To distinguish between flame and non-flame in the images, a thresholding tool was used on five randomly selected frames, from which a threshold was selected for the luminosity of the flame and background (non-flame). An average threshold value was then used for converting all frames in the video. Thresholding converted the gray-scale images to binary, black-and-white images, with 1 indicating flame and 0 indicating no flame. All images were then averaged.

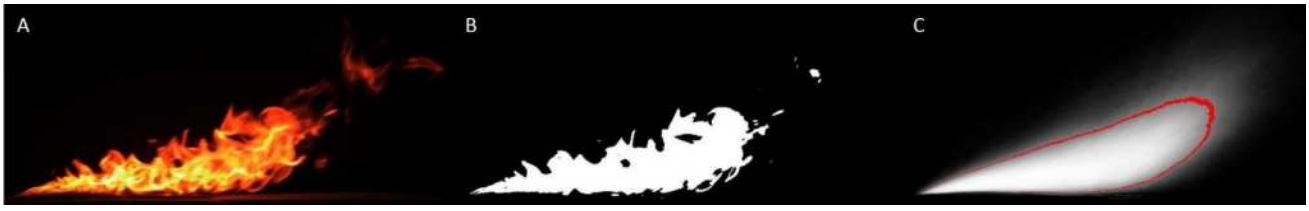

Figure 13. Image averaging technique used to determine flame geometry. (A) Still image from side-view camera (B) Black and white converted image using flame intensity threshold. (C) All black and white images averaged with pixel values between 0 and 1. A threshold line following pixels with value 0.48-0.52 are shown in red, identifying the average flame geometry.

Several flame geometry measurements were made using the average image (Figure 13 and 14). The flame tip was considered to be the highest point, furthest downstream from the burner. Flame length (L_f) was then measured from the midpoint of the burner (d/2) to the flame tip, along the centerline of the flame. The flame height (H_f) and flame extension (x_f) lengths were measured from the top of the

surface and the downstream edge of the burner to the flame tip, respectively. The attachment length (x_a) was defined as the average distance the flame extends downstream within the attachment region (denoted as a dashed box 1 cm above the attachment surface). The boundary-layer thickness incoming to the base of the burner (δ) was determined based on hot-wire anemometer measurements as 99% of the incoming free-stream fluid velocity, which compare favorably to estimates of δ using the Blasius solution (White 2011).

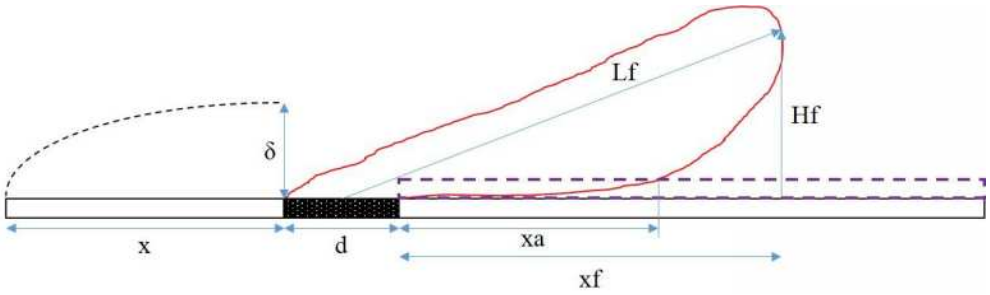

Figure 14. Physical length scales of the experiment. Independent parameters shown include the depth of the burner, d, leading edge, x, and boundary-layer thickness, δ. Dependent variables include the flame length L_f, flame height, H_f, flame length along the surface, x_f, and flame attachment length x_a.

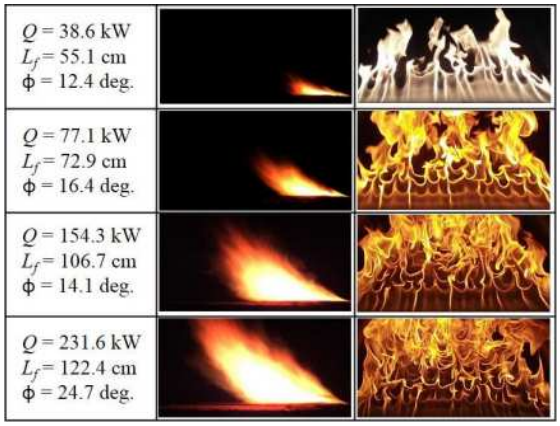

Figure 15. Variation of flame tilt angle based on heat release rate per unit length of the burner width (59.5 cm) at slope angle of 30 degrees. Burner depth = 12.7 [cm]

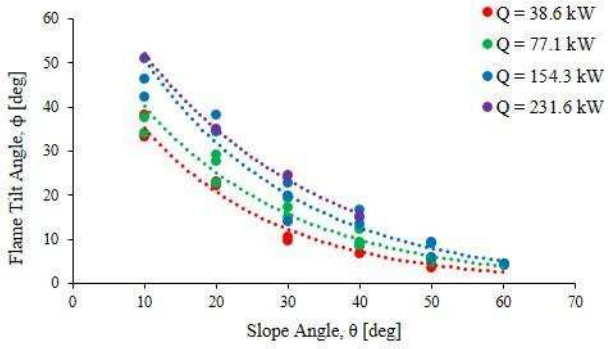

Figure 16. Flame tilt angle for several different heat-release rates (Q) on an inclined gas burner.

Figure 15 shows four representative conditions for tests on an inclined ethylene gas burner. Variations in the heat-release rate per unit length ($\dot{\boldsymbol{Q}}$), the flame length, $\boldsymbol{L_f}$ and the angle of inclination, $\boldsymbol{\phi}$ on the flame geometry are shown in both side-view and front-view images. From the side view, it can be seen that as both the angle of inclination and heat-release rate are increased, the flame length increases, however the attachment region does not experience a linear increase with flame length. The slope angle, which is representative of the attachment of the flame to the surface is shown in Figure 16. As the slope angle of the burner is increased, the flame tilt angle decreases, thereby signifying the flames becoming more and more attached to the surface of the burner. With increasing heat-release rates, it takes a greater angle of inclination for the flames to attach closer to the surface. This is expected as additional buoyant forces propel the flame upwards, compared to incoming entrained air.

A dimensionless length scale, $\boldsymbol{D^* = [\dot{Q}/(\rho c_p T g^{1/2})]^{2/5}}$ has been used in the fire research community to describe the source strength of a buoyant fire source (Quintiere 1989). This non-dimensional length

scale is given by the ratio of the fire heat release-rate $\dot{\boldsymbol{Q}}$ to the ambient air conditions $\boldsymbol{\rho c_p T}$ (density, specific heat, and temperature) and the square root of the acceleration due to gravity, all raised to the 2/5 power. The gravity term contributes to the buoyant force of the fire, and should act parallel to the line of action of the flame. To incorporate the slope angle of inclined fires, a rotated gravity vector term parallel to the inclined surface is used, given by the acceleration due to gravity time the sine of the slope angle. Flame lengths of pool fires, for instance, can be scaled with the dimensionless fire length, $\boldsymbol{D^*}$, and so with an adjusted gravity vector they should be able to as well. In Figure 17, preliminary scaling of the flame length with an adjusted gravity vector is shown to scale linearly with the centerline flame length. This suggests that the flame length for fires over sloped surfaces may be universally correlated if the correct ratios between buoyant forces and the gravity vector are taken into account.

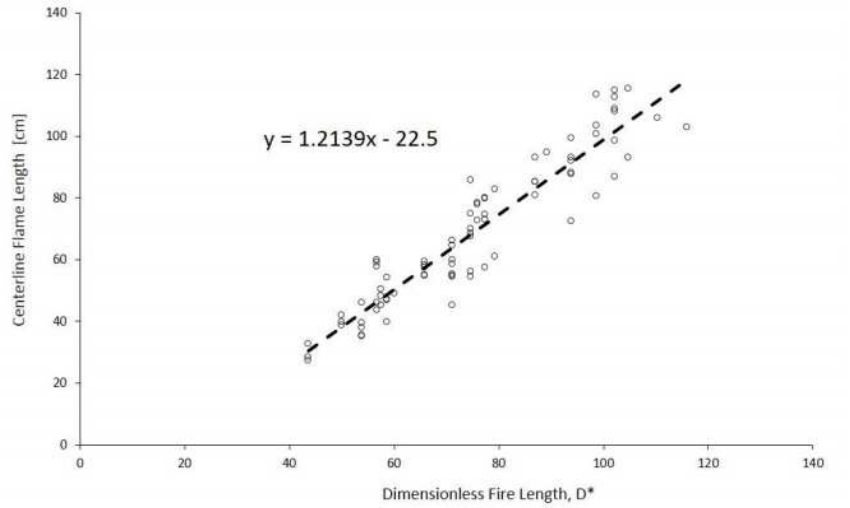

Figure 17. Relationship between centerline flame length and dimensionless fire length parameter D*, shows that for larger fires in steep slope the flame length is increases linearly.

Conclusions

This study has presented a framework for the use of stationary gas burners to study spreading wildland fire behavior, enabling measurements and analysis of key parameters related to instabilities and flame geometry that play a role in flame spread. Numerous techniques used to accomplish this are shown, as well as preliminary scaling analysis. Recently-discovered instabilities and flow structures are shown to be re-created in steady gas burners, allowing for more detailed studies, including statistical analysis made possible by the long time scales stationary flames can be created. Correlations for the mean flame geometry, such as the flame tilt angle and flame length can also be obtained by these studies with appropriate nondimensional scaling.

References

Atkinson, G., Drysdale, D. & Wu, Y., 1995. Fire driven flow in an inclined trench. *Fire safety journal*, 25.

Blackwelder, R. F., & Kaplan, R. E. (2006). On the wall structure of the turbulent boundary layer. *Journal of Fluid Mechanics*, *76*(01), 89.

G.M. Byram, Combustion of forest fuels. In: Davis, K.P., ed. Forest fire: control and use., New York McGraw Hill. (1959) 61–89.

Cetegen B. and T. Ahmed, Experiments on the periodic instability of buoyant plumes and pool fires, *Comb. Flame,* pp. 157-184, 1993

Clark, T.L., L. Radke, J. Coen, and D. Middleton. 1999. Analysis of Small-Scale Convective

Dynamics in a Crown Fire Using Infrared Video Camera Imagery. J. Appl. Meteorology. 38:1401-1420.

Finney, M.A., Forthofer, J. and Grenfell, I., 2013a. A study of flame spread in engineered cardboard fuelbeds; part I: Correlations and observations. *Seventh International Symposium on Scale Modeling (ISSM-7) Hirosaki, Japan, August 6-9, 2013.*

Finney, M.A. *et al*., 2013b. On the need for a theory of wildland fire spread. *International Journal of Wildland Fire*, 22(1), p.25.

Finney, M.A. *et al*., 2010. Structure of Diffusion Flames from a Vertical Burner. *IV International Conference on Forest Fire Research D.X. Viegas (Ed.), 2010.*

Finney, M.A. Cohen, J., Forthofer, J., McAllister, S. Adam, B. Akafuah, N., English, J., Saito, K., Gollner, M.J. and Gorham, D., Experimental Evidence of Buoyancy Controlled Flame Spread in Wildland Fires. VII International Conference on Forest Fire Research, Coimbra, Portugal, 14 to 20 Nov, 2014.

Goldstein, M. E., and Lennart S. Hultgren. "Boundary-layer receptivity to long-wave free-stream disturbances." *Annual Review of Fluid Mechanics* 21.1 (1989): 137-166.

Jeschke, P. & Beer, H., 2001. Longitudinal vortices in a laminar natural convection boundary layer flow on an inclined flat plate and their influence on heat transfer. *Journal of Fluid Mechanics*, 432, pp.313–339.

Jimenez, D., Finney, M.A. & Cohen, J., 2010. Design and Construction of Gas-Fed Burners for Laboratory Studies of Flame Structure. *IV International Conference on Forest Fire Research D.X. Viegas (Ed.), 2010.*

Malalasekera, W.M.G., H.K. Versteeg and K. Gilchrist. 1996. A review of research and an experimental study on the pulsation of buoyant diffision flames and pool fires, *Fire and Materials*, vol. 20, no. 6, p. 261-271

Oka, Y. *et al*., 2000. Modelling Of Unconfined Flame Tilt In Cross-Winds. *Fire Safety Science*, 6, pp.1101–1112.

de Ris, J. and Orloff, L., 1975. The role of buoyancy direction and radiation in turbulent diffusion flames on surfaces. *Symposium (International) on Combustion*, 15(1), pp.175–182.

Saric, W.S., 1994. Gortler vorticies. *Annual Review of Fluid Mechanics*, (2), pp.379–409.

White, F.M., 2011. *Fluid Mechanics* 7th ed., New York, NY: McGraw Hill.

The analysis and simulation of forest fire on Pohang-Si and Uljoo-Kun in Korea

Si-Young Lee[a], HoungSek Park[b], Chun-geun Kwon[a], Chan-ho Yeom[a]

[a] *Professional Graduate School of Disaster Prevention, Kangwon National University, Samcheok, Gangwon-Do, South Korea, lsy925@kangwon.ac.kr*
[b] *Dongguk University, Chung-Ku, Seoul, South Korea, parkhs08@nate.com*

Abstract
The forest fire in Korea was occurred by human activities. Recently, forest fires intended to damage not only forest and related regions but also urban facilities like houses, buildings and citizens. In this study, we simulated the fires which occurred on wildland–urban interface in Pohang-Si and Ulju–Gun in spring, 2013. And we compared real damages of facilities in wildland interface with simulated damaged for applying in Korea forest environment. These results would be good reference data for the prediction about danger zone in wildland-urban interface.

Keywords*: Wildland-urban interface, forest fire simulation, FARSite , Forest fire danger zone, fire intensity*

Introduction

The forest fires in wildland-urban interface especially damaged in human and their properties. Therefore, many researchers have studied about environments in which were more danger (forest floor, topography, weather, the location of houses and etc.). And they classified with danger zone and safety zone in wildland–urban interface from forest fire. Moreover they have developed the treatment for reducing forest fire damages (the fuel treatment, the removal of flammable matter, the change of building material and etc.). In these studies, we investigated the forest fire which occurred in Pohang-Si and Ulju-gun in Korea in 2013. These fires occurred in wildland–urban interface and forest fire in Pohang-SI ignited in mainly urban area and spread in forested area. So, many houses-even 15 floors apartment-were damaged by these forest fires. Because these fire destroyed 30 buildings and facilities, we could analyzed relationships with forest fire intensity and the condition of destroy from forest fire.

Methods

We investigated damaged area for measuring and surveyed an area burned, officers and residents for estimating forest fire damages, forest fire velocities and damaged area. After field surveys, we simulated the forest fires by FARSite for obtaining a detailed forest fire damage data.…

2.1. Field survey

Field surveys were carried out from May to June on Pohang-Si and Ulju-Gun in 2013. We surveyed total burned area and damaged facilities and houses. And we investigated the topographical conditions (a degree, an aspect and an elevation) and forest floors (a density and main species) around damaged building. And we surveyed official records about these fire for getting damage data and forest fire velocities detailed. …

Forest fire Simulation

For analysis relationships with forest fire intensity and conditions around damaged buildings, we used simulation, FARSite which was developed by USDA. FARSite simulated a detailed data about forest fire intensity, burned area, forest fire velocity from topography, weather and forest species. Topographical data were acquired from D.E.M. Weather data were input by an editor contained in FARSite. Forest floor data were getting from digital forest floor map made by K.F.R.I.. These data were processed by ARCGIS 9.3 and inputted in FARSite. FARSite made many data simulated. A fireline intensity, a flame length, a time for arrival, heat per rate from forest fire and burned area were acquired

Results

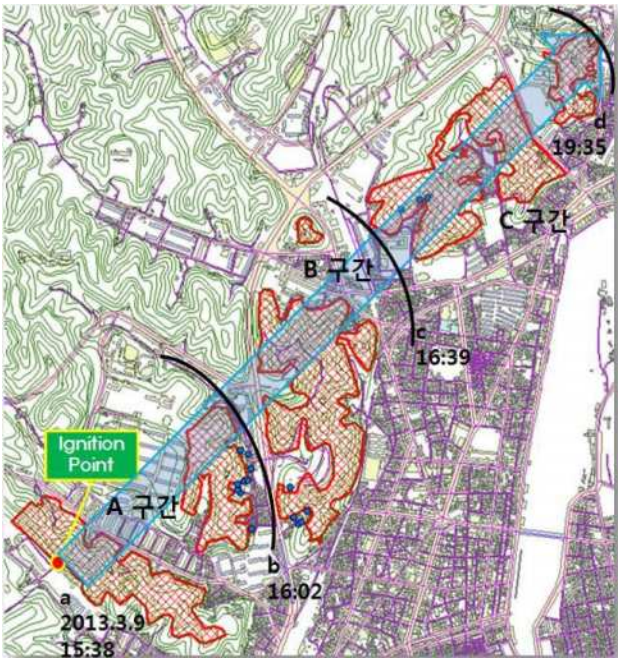

Figure 1. The result of field survey in Pohang-Si

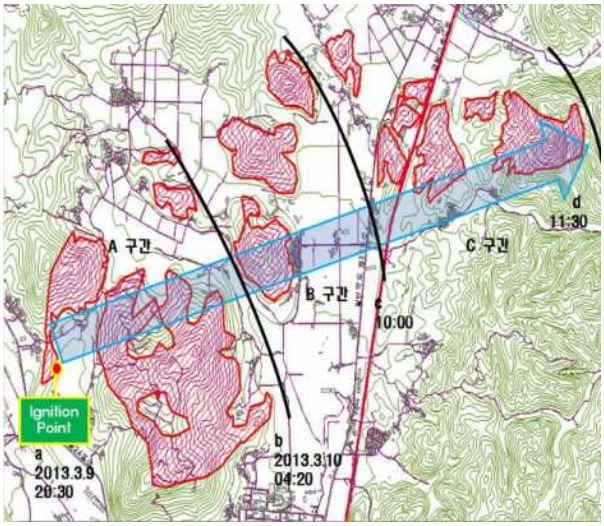

Figure 2. The result of field survey in Ulju-kun

The Pohang forest fire directly moved 3km from 20:30 P.M. 2 March and burned for 237 minutes. 79ha forested area and 110 buildings were damaged. 10 houses and one garage were destroyed wholly. The average velocity was 0.8km/hr. The Ulju forest fire directly moved 5.4km from 20:30 P.M. 9 March and burned for 900 minutes. 280ha forested area and 57 building was damaged. 15 houses and 3 buildings were destroyed wholly. The average velocity was 0.4km/hr.
The burned area from simulation was 184% larger than real burned area and the reason of this difference may be caused by forest fire attack. The average speed of spread was 0.12km/hr in simulation and 0.4km/hr in real fire. The results was similar to former simulation for Samcheok forest fire. The real fire was 3 times faster than real fire because of fuel condition maybe. The average fireline intensity from simulation of Ulju forest fire was 1,255kw/m and the average fireline intensity around destroyed building was 331.85kw/m. The average flame length from simulation of Ulju forest fire was 3.5m and the average flame length around destroyed building was 1.5m. As the results of fireline intensity and flame length were compared with U.S. Wildland-urban interface forest fire assessment guide made by N.W.C.G., this result indicate that Ulju fire was very serious state. Using these results, we analyzed and classified degree and the location of mountainous contour which divided 10class by elevation. The danger zone was classified in over 15 degree and over 3/10 location by elevation

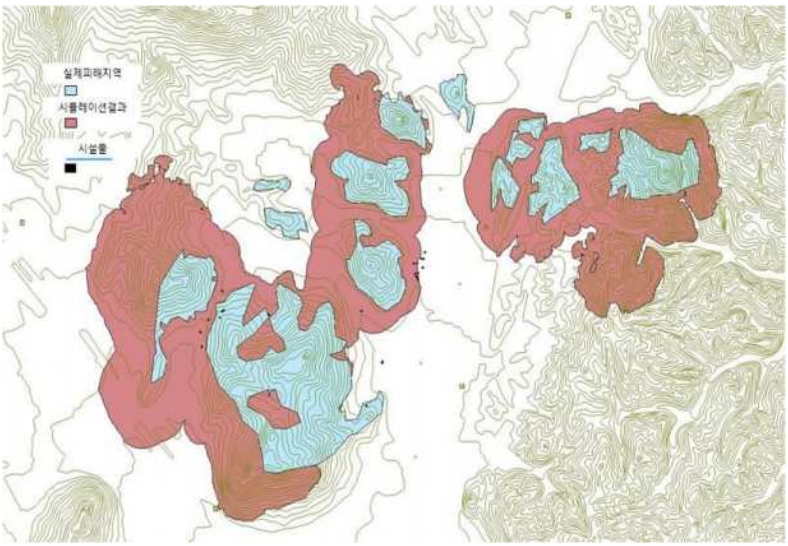

Figure 3. The comparison with simulated burned area , real burned area and locations of destroyed building

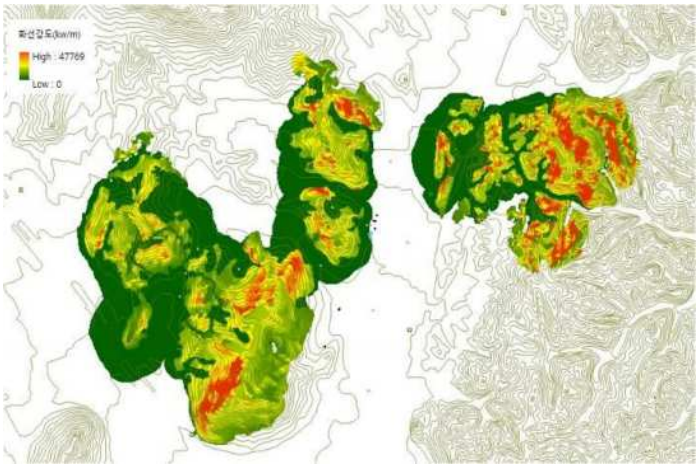

Figure 4– The result of simulation in fireline intensity

References

B. W. Butler, J.M. Forthofer, R.D. Stratton, M.A. Finney, and L.S. Bradshaw (2005) Fire growth simulations of the Price Canyon, Thirtymile, and Storm King mountain fire using high resolution wind simulation tools and FARSITE. Sixth Symposium on Fire and Forest Meteorology, 25-27

Jason M. Forthofer , B. W. Butler, K. S. Shannon, M. A. Finney, L.S. Bradshaw, R. Stratton (2003) Predicting surface winds in complex terrain for use in fire spread models. Proceedings of the Fifth Symposium on Fire and Forest Meteorology and Second Wildland Fire Ecology and Fire Management Congress, 16-20

Geoff Wehmeyer (2012) Simulations and Analysis of a 2012 Kansas Wildland Fire Using FARSITE. The University of Texas at Austin

John Ainsworth, Iain Buchan (2009) Preserving consent-for-consent with feasibility-assessment and recruitment in clinical studies: FARSITE architecture. *Studies in Health Technology and Informatics* **147**, 137-148

Kristen A. Sanders (2001) 'Validation and calibration of the FARSITE fire area simulator for Yellowstone National Park' (The University of Montana)

Mark A. Finney (1998) *FARSITE*: Fire area simulator model development and evaluation. USDA Forest Service, Rocky Mountain Research Station Research Paper RMRS-RP-4 Revised. (Oregon, UT)

Mark A. Finney, Isaac C. Grenfell, Charles W. McHugh, Robert C. Seli, Diane Trethewey, Richard D. Stratton, Stuart Brittain (2011) A Method for Ensemble Wildland Fire Simulation. *Environ Model Assess* **16**, 153-167

Mark A. Finney, Robert C. Seli, and Patricia L. Andrews (2003) Modeling post-frontal combustion in the FARSITE fire area simulator. 2nd International Wildland Fire Ecology and Fire Management Congress

Michele Salis (2008) 'Fire behaviour simulation in Mediterranean maquis using FARSITE (fire area simulator)' (Universita' degli studi di Sassari)

Richard D. Stratton (2004) Assessing the Effectiveness of Landscape Fuel Treatments on Fire Growth and Behavior. *Journal of Forestry* **October/November,** 32-40

Robert E. Keane, Kevin C. Ryan, Steven W. Running (1996) Simulating effects of fire on northern Rocky Mountain landscapes with the ecological process model FIRE-BGC. Tree Physiology **16**, 319-331

Ross J. Phillips, Thomas A. Waldrop, Dean M. Simon (2006) Assessment of the FARSITE model for predicting fire behavior in the Southern Appalachian Mountains. *Proceedings of the 13th biennial Southern Silvicultural Research Conference*, 521-525

Soung-Ryoul Ryu, Jiquan Chen, Daolan Zheng, Jacob J. Lacroix (2007) Relating surface fire spread to landscape structure: An application of FARSITE in a managed forest landscape. *Landscape and Urban Planning* **83**, 275–283

Tonja Opperman, Jim Gould, Mark Finney, and Cordy Tymstra (2006) Applying Fire Spread Simulators in New Zealand and Australia: Results from an International Seminar. *USDA Forest Service Proceedings RMRS-P-41*, 201- 212

The effect of grass curing level on the propagation of grassland fires – an experimental study

David Nichols[a], Rachel Bessell[a], Miguel G. Cruz[b], Jim Gould[b], Richard Hurley[b], Susan Kidnie[a], Vijay Koul[a], Alen Slijepcevic[a]

[a] *CFA, Fire and Emergency Management, PO Box 701, Mt Waverley, Victoria, Australia.*
[b] *CSIRO Ecosystem Sciences, GPO Box 1700, Canberra, ACT 2601, Australia.*

Abstract
Key to understanding fire propagation in grassland fuels is to know their annual growing cycle and the availability of biomass to be consumed by a fire. Curing is the progressive senescence and drying out of grass after flowering (annuals) or in response to drought (perennials) and is the key process transferring biomass from the live to the dead fuel component. Despite the relevance of fires in grasslands and savannah ecosystems in Australia and throughout the world, our understanding of (1) grass senescence effect on overall fuel moisture content and fuel availability, and (2) the degree of grass curing in fire behaviour, is still lacking. To investigate the effect of the curing process on grassland fire behaviour an experimental field study was conducted at two distinct locations in Victoria. Experimental burn plots size were 32 x 32 m. Simultaneous burns were conducted with one plot being fully cured (100%; control) and another being partially cured (treatment). Detailed measurements of fuel bed structure, weather variables (3D wind speed, air temperature, relative humidity and solar radiation) and fire behaviour (rate of spread, flame length, residence time and time-temperature profiles) were recorded on 52 experimental fires. The range of curing in the partially cured plots varied between approximately 35% and 90%. The range of other fire environment parameters were: 2-m wind speed: 5.4 - 20.5 km/h; ambient air temperature: 16-33 C; relative humidity: 14-40 %; Fire spread rates varied between 3.6 and 72 m/min. Preliminary analysis highlights include the observation of sustained fire spread with curing levels between 30-40% and the importance of the dead fuel component from the previous year growth to sustain propagation at these marginal conditions. The data collected is being used to reanalyze functional relationships currently used to express the effect of curing and live fuel moisture on the spread of grassland fires

Keywords*: Grass curing, grass fire behaviour, fire danger ratings*

Introduction

Key to understanding fire propagation in grassland fuels is to know their annual growing cycle and the availability of biomass to be consumed by a fire. Grassland curing is the progressive senescence and drying out of grass after flowering (annuals) or in response to drought (perennials) and is the key process transferring biomass from the live to the dead fuel component within the fuel complex. As senescing progresses, the fuel moisture content gradually decreases and the amount of dead material in the grassland increases. These changes have an important impact on fire behavior in grasslands. In Australia, where grasslands cover approximately 75% of the country, the degree of curing is used as an input into the calculation of grassfire spread and grassland fire danger ratings.

Despite the relevance of fires in grasslands and savannah ecosystems in Australia, and throughout the world, our understanding of (1) grass senescence effect on overall fuel moisture content and fuel availability, and (2) the degree of grass curing in fire behaviour, is still lacking. The ability to accurately assess the degree of curing is therefore important for fire agencies who predict fire danger throughout the fire season.

Grassland curing is a complex and dynamic process. The study examines the dynamics of grass curing levels through the grass life cycle and the relation to grassfire behaviour through the fire season. The

objective is to provide better estimates of grass curing that could be used to predict rate of spread of grassfires.

Methods

Two distinct Victoria, Australia experimental field sites, located at Wangaratta South and Wendouree, with continuous grass cover were selected for studying grass curing dynamics and grassland fire behaviour during the 2013-14 fire season (October to February). The distinct predominant grass species present at each site resulted in distinctive fuel structures. One site consisted of coarser grass and higher fuel loads than the other site which was characterized by finer grass and lower fuel loads. The differences in each site had a significant effect on fire behaviour.

Experimental burn plots size were 32 x 32 m. Simultaneous burns were conducted with one plot being fully cured (100%; control) and another being partially cured (treatment). Detailed measurements of fuel bed structure, weather variables (3D wind speed, air temperature, relative humidity and solar radiation) and fire behaviour (rate of spread, flame length, residence time and time-temperature profiles) were recorded on 52 experimental fires. The range of curing in the partially cured plots varied between approximately 35% and 90%. The range of other fire environment parameters were: 2-m wind speed: 5.4 - 20.5 km/h; ambient air temperature: 16-33 C; relative humidity: 14-40 %; Fire spread rates varied between 3.6 and 72 m/min.

Results

Preliminary analysis highlights include the observation of sustained fire spread with curing levels between 30-40% and the importance of the dead fuel component from the previous year growth to sustain propagation at these marginal conditions. The results indicate that the fire rates of spread of 40 to 60% cured can be as rapid as spread rates previously achieved by cured grasses of 60% and higher. The data collected is being used to reanalyze functional relationships currently used to express the effect of curing and live fuel moisture on the spread of grassland fires.
The results will feed into future grassland fire danger indices which contribute to the overall fire danger rating system. Accurate fire danger ratings allow fire agencies to plan for fire restrictions, resource allocation, total fire bans, fire behaviour modeling and community warnings during the fire season.

The Strouhal-Froude number scaling for wildland fire spread

Brittany A. Adam[a], Justin D. English[a], Nelson K. Akafuahb[a], Kozo Saito[a]
Mark Finney[b], Jason Forthofer[b], Jack Cohen[b]

Univ. of Kentucky, Lexington, KY 40506, brittany.adam@uky.edu
justin.english@uky.edu; nelson.akafuah@uky.edu; ksaito@uky.edu
[b]USDA Fire Science Laboratory, Missoula, MT 59808, mfinney@fs.fed.us;
jaforthofer@fs.fed.us; jcohen@fs.fed.us

Abstract
A study of wildland fires leading to a correct understanding of flame spread in wildland fire would find its foundation firmly situated on an understanding of the governing mechanisms, processes, and threshold of ignition. It is, therefore, very important for effective firefighting efforts and safety reasons to identify the roles of radiative and convective heating. Over the years, the United States Department of Agriculture (USDA) Missoula Fire Sciences Laboratory has conducted a series of experiments in their unique wind tunnel fire experimental facility. This rich database provides years of numerical data and video from burns conducted under a wide range of well-specified conditions. After identifying the need to explore the roles of both convective heat transfer and radiative heat transfer in the ignition process, the USDA's well documented line fire data provided an opportunity to observe ignition and, subsequently fire spread phenomenon, through a uniform fuel bed of laser-cut cardboard combs under controlled conditions. The goal of our study is to identify features distinguishing radiative heat transfer from convective heat transfer. The team worked to explain scaling laws, determine key parameters to support the development of scaling laws, and begin a comparison of the scaling law predictions with USDA data. When the above scaling laws are validated, it would be reasonable to design medium scale prescription fire experiments, which fall between the USDA experiments and the full scale wildland fires. Our step-by-step approach using different size scale model experiments eventually allow us to understand the governing physics that control the mechanism of flame spread through and ignition on the wildland fuel bed.

Keywords*: Scale Modelling, Scaling Laws, Fire Spread, Fuel beds, Forest Fire, Wildland Fire, Fire Behaviour*

Introduction

A correct understanding of flame spread in wildland fire would be based on governing mechanisms, processes, and thresholds of ignition. Critically, the roles of radiative and convective heating must still be discerned (Finney, Cohen, et al. 2013). Over the years, the United States Department of Agriculture (USDA) Missoula Fire Sciences Laboratory has conducted a series of experiments in their unique wind tunnel fire experimental facility. This rich database provides years of numerical data and video from burns conducted under a wide range of well-specified conditions. After identifying the need to explore the roles of both convective heat transfer and radiative heat transfer in the ignition process, the USDA's well documented line fire data provided an opportunity to observe ignition and, subsequently fire spread phenomenon, through a uniform fuel bed of laser-cut cardboard combs under controlled conditions.

The USDA Missoula Fire Sciences Laboratory and University of Kentucky Institute of Research for Technology Development (IR4TD) teams conducted two explorations to further understand ignition on a wildland fuel bed. The team first began by identifying and exploring flame behaviours in the lab environment that were previously only observed in large scale wildland fires (Finney, Forthofer, et al. 2013) (Adam, et al. 2013). The goal of our study is to identify features distinguishing radiative heat transfer from convective heat transfer. The team worked to explain scaling laws, determine key

parameters to support the development of scaling laws, and begin a comparison of the scaling law predictions with USDA data. When the above scaling laws are validated, it would be reasonable to design medium scale prescription fire experiments, which fall in size between the USDA experiments and full scale wildland fires. The USDA – University of Kentucky collaboration already produced two recent articles (Finney, Forthofer, et al. 2013) (Adam, et al. 2013), and we made further progress on the above study. In this paper we report recent field burn tests, organized by USDA Forest Service and conducted in Texas. Our step-by-step approach using different size scale model experiments will eventually allow us to understand the governing physics that control the mechanism of flame spread through and ignition on the wildland fuel bed.

Scale Modelling and Scaling Laws

University of Kentucky and USDA Forest Service in Missoula Science Laboratory have developed mutually beneficial research program to understand the mechanism of fire spread through forest fuelbeds. This paper reports one of our current progresses in this effort, namely focusing on scaling laws and scaling aspects forest fire. We begin with an excellent book: The Use of Models in Fire Research (Bert 1961). This book is the collection of sixteen different papers presented at five different sessions of the International Symposium of the same title as the book held in 1959, and commentaries are provided at the end of each session. This is a book written more than a half century ago when no computer simulation was available, but researchers' wisdom and unique insights in fire phenomena with their attempts to extract the governing physical laws which can help develop simple practical models are still valuable in the age of high speed computation, and therefore serve as an excellent reference for our forest fire research efforts.

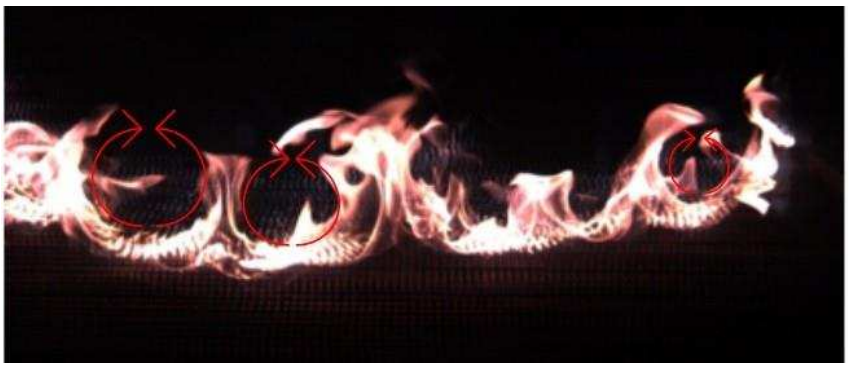

Figure 1. A high speed color photographic image of spreading flame over artificially made cardboard fuelbeds (Finney, Forthofer et al. 2013).

To continue the above book's philosophy, the USDA's Forest Service Fire Science Lab (Finney, Cohen, et al. 2013) (Finney, Forthofer, et al. 2013) made a series of unique observations on forest fires by high speed video photography and thermocouple temperature measurement techniques. These techniques are rather ordinary but their observation results are rather extra-ordinary. The following are except from Finney's observations (Finney, Cohen, et al. 2013). "A series of preliminary burns of the cardboard fuelbeds in the wind tunnel were used to refine the instrumentation. The fires were filmed with digital video cameras from the top, sides, front, back, and various oblique angles. This footage revealed two principal dynamic features of the flame zone. First the flame zone became divided in the transverse or span-wise direction into convective peaks and troughs at fairly regular spacing. The ignition interface (at the leading edge of the combustion zone) was convoluted in association with this flame structure, with a concave segment located directly beneath these peaks (Figure 1) and convex segments in the troughs. Second, the flame zone exhibited clear instabilities, which when viewed at an angle from behind and above the bed, appeared as patches originating near the rear of the burning

zone…… After reaching the ignition interface at the leading edge of the burning zone, they impinged new fuels ahead. When the flame zone was viewed normal to the stream-wise direction, eddies appeared on the upper and lower flame edges which rotated in the opposite direction. Regardless of the local geometry of the fire edge, it progressed at the same rate across the fire front." (Finney, Forthofer, et al. 2013)

Almost 30 years prior to Finney's observations, F.A. Albini (Albini 1984) made a comprehensive review on wildland fires addressing Rothermel's steady-spread model (Rothermel 1972) to predict the rate of spread of surface fire as a successful example, while describing wildland fires as poorly understood phenomena. As of today, many of the unknowns pointed out by Albini (who believed radiation as the key heat transfer mechanism for flame spread) in 1984 still remain to be unknown (for example, the role of live fuels in fire spread and the effect of wind on fire spreading behaviour). As to the wind effect, some progress has been made on fire whirl studies (Emori and Saito 1982; Chuah *et al*. 2011), while an important progress was made recently on the mechanism of fire spread (Finney, Cohen, et al. 2013) (Finney, Forthofer, et al. 2013) based on a serious of unique observations mentioned. This paper mainly focuses on the latter development (Finney, Cohen *et al*. 2013; Finney, Forthofer *et al*. 2013; Finney *et al*. 2014) which establishes a high correlation between Strouhal (St) – Froude (Fr) number based on a series of careful observations over a variety of fuel types and a wide range of size including full scale crown fires, grassland control burn experiments, large scale wood crib fires, and wind tunnel laboratory-scale fire experiments using artificial cardboard fuelbeds. In the following, we provide governing physical laws responsible for the above St-Fr correlation and possible scaling laws on fire spread.

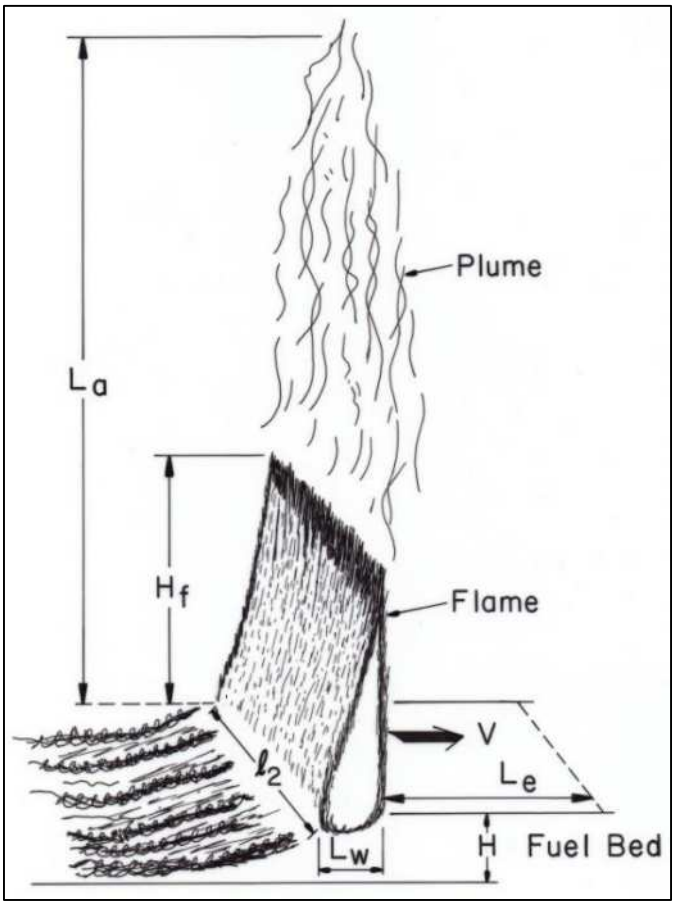

Figure 2. Schematic of one-D flame spread over fuel bed and dimensions of flame height, plume height, and fuel bed (Emori, Iguchi et al. 1988)

Here we use the law approach whose details are provided in refs (Emori and Saito 1985; Emori, Saito and Sekimoto 2000) to obtain seven independent pi-numbers from the above three different forces and five different heats. The scaling criteria demand: $\pi_i = \pi_i'$ for similarity, where $i = 1$ to 7, the left hand π_i represents a full scale scenario, and the right hand π_i' represents a corresponding scale model. Note

that the ratio of the inertial force causing vortex shedding behind a flame, $F_{i,down}$, to the inertial force of the wind, $F_{i,up}$, is unique to the current wildland fire problem, where a flame acts like a vertical solid cylinder to generate a wake in the downstream against an upcoming horizontal flow (Kuwana, et al. 2007), and pi-number constituting between heat and work done by fluid motion can be ignored. Finney *et al*. (Finney, Cohen, et al. 2013) obtained a reasonably strong St-Fr correlation, which is equivalent with the (π_2 - π_1) correlation, over wide range of experimental data including the wind tunnel fire spread experiments on cardboard fuelbeds, a full scale crown fire data, and outdoor large scale wood crib fire experiments. Using the same fuels both for the full scale and the model and assuming the same temperature at the corresponding points, the law approach can produce the following, Equation (1):

$$\phi\left[\frac{u^2}{L_w}, \frac{L_e\omega}{u}, \frac{El_2}{I}, \frac{L_aR}{I}, \frac{L_au^3}{I}\right] = 0 \qquad (1)$$

Previously Emori and Saito (1983) showed liquid pool fires to be radiation-driven and wood crib fires to be convection-driven, each governed by a different set of scaling laws. Later Emori and Iguchi *et al*. (1988) conducted flame spread experiments using two different types of fuel bed: vertically oriented allay of paraffin-coated paper strips and packed excelsior mats. They found that the above two different scaling laws also can be applied to flame spread identifying two different types of spreading mode, radiation-driven and convection-driven. Recently Finney's group in Missoula and the University of Kentucky's group are collaborating to develop scaling laws for flame spread through actual full scale forest fuelbeds (Adam, et al. 2013), which are significantly complex in nature consisting of live and dead fuels of different fuel types and geometry. This work is still in progress. The following provides summary of the above scaling studies (Emori and Saito 1983; Emori, Iguchi *et al*. 1988) and one of recent findings on St-Fr correlations (Finney, Forthofer *et al*. 2013; Finney *et al*. 2014).

Radiation-driven Fire Type: There is little effect of the fluid dynamics on the overall heat balance, and radiation is the main source of the solid fuel evaporation and ignition leading to the flame to spread. For this type of fire, Equation (1) can yield the specific scaling relationships seen in Equation (2).

$$\frac{u}{u'} = \sqrt{\frac{L_w}{L'_w}} \qquad \frac{R}{R'} = \frac{E}{E'} \qquad t = t' \qquad (2)$$

(2) Convection-driven Fire Type: Contrary to the radiation-driven type, fluid dynamics influences the heart transfer mechanism as the form of heat convection, creating a coupling between the force and heat balances, and leading to the following Equation 3.

$$\boldsymbol{\frac{u}{u'} = \frac{R}{R'} = \frac{E}{E'} = \frac{t}{t'} = \sqrt{\frac{L_w}{L'_w}}} \qquad (3)$$

The St – Fr Number Correlation

Figure 3 shows St-Fr correlation over the wide range of scale of fires. Data consist of a full scale crown fire (10m; 100m-1,000m), controlled grassland fires (3 m; 10m-100m), large scale wood crib fires (2m; 3m-10m), and wind tunnel laboratory-scale fire experiments (0.5m; 2m – 5m). The first number in parenthesis indicates a typical flame height, and the second number indicates a typical fuel bed dimension, width x length. There are two important practical implications of the St-Fr correlation that have not been previously known. First, time-varying convective heating derives from buoyant instabilities, explaining the origin of the frequency scaling from laboratory to field-scale wildfires. Second, with frequency related inversely to flame size, it suggests a negative feedback on wildfire spread rate. In other words, as fires move faster (with increasing wind for example) and release more energy, flame size increases but convective frequency decreases (according to St-Fr) and slows the convective heat transfer.

The Figure 3 correlation can provide an approximate correlation: $St \sim Fr^{-0.5}$, which indicates $F_\omega/F_i \sim (F_g/F_i)^{0.5}$, i.e., $F_\omega/(F_iF_g)^{0.5} \sim$ const. Using characteristic parameters, this relationship can yield: $(L^{1.5}\omega^2)/Ug^{0.5} \sim$ const.

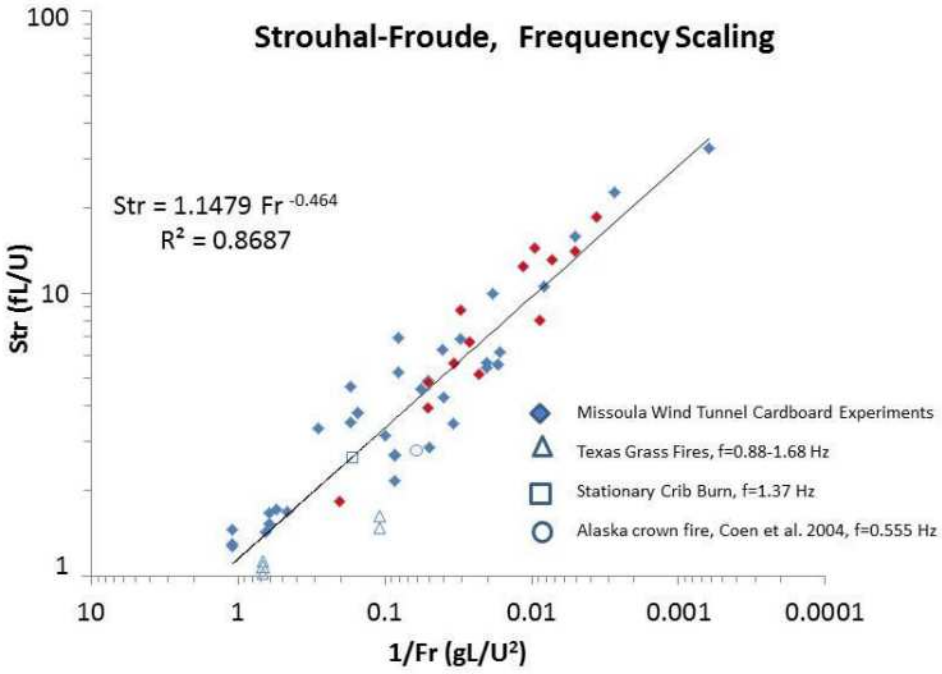

Figure 3. Strouhal (St) – Froude (Fr) number correlation for various size and type of fires including a full scale crown fire (10m; 100m-1,000m), controlled grassland fires (3 m; 10m-100m), large scale wood crib fires (2m; 3m-10m), and wind tunnel laboratory-scale fire experiments (0.5m; 2m – 5m). The first number in parenthesis indicates a typical flame height, and the second number indicates a typical fuel bed dimension (width x length) [32].

3. Summary

We provided background for the need to study spreading mechanism of actual forest fuelbeds. This study is one of our collaborative studies between USDA Forest service and University of Kentucky to achieve that goal with the scale modeling approach. We used the law approach to provide the major governing physical laws on the St-Fr correlation which have been established over a wide range of scale of fires and different types of fuels. The results indicate that previously developed scaling laws on stationary (pool and wood crib) fires and flame spreading can be extended to the current problem with possible some modifications which will be studied in the future.

References:

Adam, B.A., N.K. Akafuah, K. Saito, M.A. Finney, J. Forthofer, and I.C. Grenfell. 2013. "A Study of Flame Spread in Engineered Cardboard Fuelbeds, Part II: Scaling law approach." Proc. the Seventh International Symposium on Scale Modeling (ISSM7) Hirosaki, Japan 2013, and to appear in Progress in Scale Modeling volume 2, Springer 2014.

Albini, F. A. 1984. "Wildland Fires: Predicting the behavior of wildland fires—among nature's most potent forces—can save lives, money, and natural resources." American Scientist 590-597.

Bert, W.G., 1961. International Symposium on The Use of Models in Fire Research, National Academy of Science - National research Council, Washington, D.C.

Chuah, K. H., K. Kuwana, K. Saito, and F.A. Williams. 2011. "Inclined fire whirls." Proc. The Combustion Institute 33 (2): 2417-2424.

Emori, R. I., and K. Saito. 1983. "A study of scaling laws in pool and crib fires." Combustion Science and Technology 31: 217-230.

Emori, R. I., and K. Saito. 1985. "A unified view of scaling laws in fires (First report): Scaling laws in stationary fires." Transactions of JSME, Series B 29: 1892-1898.

Emori, R. I., and K. Saito. 1982. "Model experiment of hazardous forest fire whirl." Fire Technology 18: 319-327.

Emori, R.I., K. Saito, and K. Sekimoto. 2000. Scale Models in Engineering (Mokei Jikken no Riron to Ohyou). Third Edition, Gihodo Publishing Co. Tokyo, Japan, in Japanese.

Emori, R.I., Y. Iguchi, K. Saito, and I.S. Wichman. 1988. "Simplified scale modeling of turbulent flame spread with implication to wildland fires." Fire Safety Science – Proc. the Second International Symposium 263-273.

Finney, M.A., J. Forthofer, B.A. Adam, N.K. Akafuah, and K. Saito. 2013. "A Study of Flame Spread in Engineered Cardboard Fuelbeds, Part I: Correlations and Observations." Proc. the Seventh International Symposium on Scale Modeling (ISSM7) Hirosaki, Japan 2013, and to appear in Progress in Scale Modeling volume 2, Springer 2014.

Finney, M.A., J.D. Cohen, S.S. McAllister, and W.M. Jolly. 2013. "On the need for a theory of wildland fire spread." Intl. J. Wildl. Fire. 25-36.

Finney, M.A., *et al*. 2014, this conference.

Kuwana, K., K. Sekimoto, K. Saito, F.A. Williams, Y. Hayashi, and H. Masuda. 2007. "Can we predict the occurrence of extreme fire whirls?" AIAA Journal 45 (1): 16-19.

Rothermel, R.C. 1972. "A mathematical model for predicting fire spread in wildland fuels." USDA Forest Service Research Paper, INT-115.

The ring of fire: the relative importance of fuel packing versus intrinsic leaf flammability

Saskia Grootemaat[a], Ian J. Wright[a] and Johannes H. C. Cornelissen[b]

[a] *Department of Biological Sciences, Macquarie University, Sydney, NSW 2109, Australia; saskia.grootemaat@mq.edu.au, ian.wright@mq.edu.au*
[b] *System Ecology, Faculty of Earth and Life Sciences, VU University, 1081 HV Amsterdam, The Netherlands; j.h.c.cornelissen@vu.nl*

Abstract
Two different experimental set-ups were used to disentangle the relative importance of intrinsic leaf traits versus fuel packing for the flammability in fuel beds. Dried leaves from 25 Australian perennial species were burnt in fuel bed rings under controlled conditions. The flammability parameters were compared with the results of a previous study where individual leaves from the same species were burnt in a muffle furnace at 400°C. Fuel density (g fuel per volume) was the dominant driver for the combustibility and sustainability of the fire in the fuel bed rings; e.g., loosely packed fuel beds showed higher rates of spread. Specific leaf area (SLA, ratio of leaf area to dry mass) was not only the strongest predictor of "time-to-ignition" in the furnace set-up (higher-SLA species having shorter ignition times), but also played a major role in the build-up of the fuel bed, and thus the flammability in fuel beds.

Keywords*: combustibility, fire behaviour, fuel bed density, leaf traits, specific leaf area*

Introduction

During high intensity wildfires any organic matter will likely burn. However, at lower intensities the intrinsic properties of fuel, like fuel moisture content or leaf dimensions, can strongly influence fire behaviour (Scarff and Westoby 2006; Plucinski and Anderson 2008). In a previous study we showed that intrinsic chemical and morphological properties of leaves had strong and differential effects on the ignitibility and sustainability of fire (Grootemaat *et al*., in review). Species with higher specific leaf area (SLA) and lower moisture content showed shorter ignition times. Leaf nitrogen (N), phosphorus (P) and tannin concentrations favoured the combustion process towards charring rather than tarring, thereby shortening the flame duration and prolonging the smouldering phase (Grootemaat *et al*., in review).
In fuel beds however, fuel bed density (g fuel per volume) and packing ratio (cm^3 fuel per volume) are strong drivers of fire spread (Scarff and Westoby 2006; Engber and Varner 2012; de Magalhães and Schwilk 2012; Van Altena *et al*. 2012). Based on principles of air-flow, more densely packed fuel beds are restricted in their oxygen supply and will therefore face difficulties with their combustion (Byram 1959; Drysdale 2011).
In this study we quantified the relative importance of leaf traits and packing on the sustainability, combustibility and consumability of fire burning through fuel beds. We examined if the same drivers were important for the "flammability" of a) individual leaves and b) fuel beds. Does the ranking in species' flammability differ between the two types of experimental set-ups? We expected that the physical configuration of the leaves would dominate over the "intrinsic' effects of leaf chemistry and morphology. We also expected that leaf size and "curliness" would be the main drivers of fuel bed density, with larger and curlier leaves forming more aerated fuel beds and therefore leading to a higher combustibility (i.e. higher rate of spread, or shorter flame residence time).

Methods

Experimental burns were performed on monospecific fuel beds consisting of dried green leaves from 25 perennial Australian species, a subset of those used in the previous experiments (Table S1). These species were sampled from four vegetation types in New South Wales, eastern Australia (details in Wright *et al*. 2001). The burning experiments were run at the FLARE Lab (Fire Laboratory of Amsterdam for Research in Ecology; VU University, The Netherlands). Fuel beds were burnt following standard procedures (Van Altena *et al*. 2012). In short, air-dried leaves were placed loosely in a steel mesh ring (25 cm in diameter, 3 cm high). The leaves were equally distributed over the ring until the ring was full, resulting in an equal volume of fuel for all replicates. Six thermocouples were positioned approximately 1 cm above the fuel bed. Samples were ignited by lighting a cotton disk injected with 1ml of ethanol (96%), which was placed in the middle of the ring. Different flammability parameters were measured (Table 1) and compared to the results from our previous study. Furthermore, the role of leaf traits (Table S2) for species' flammability was analysed.

Table 1. Overview of the measured flammability variables during the experimental burns (species' means). The first six variables were measured in the fuel bed rings; the last four (shaded) variables came from our previous work on flammability of individual leaves in a muffle furnace at 400°C

Variable	Description	Flammability component	Unit	Range
Ignition frequency	Percentage of replicates that truly ignited (with flames rather than smouldering)	Ignitibility	%	33.3-100
Maximum temperature	Mean maximum temperature for 5 sensors	Combustibility	°C	480-753
Total heat released	Area under the temperature*time curve	Combustibility	°C*min	200-2620
Rate of spread	Distance from the ignition point to the edge of the ring, divided by time to edge	Combustibility	cm/s	0.05-0.64
Burning time	Fire duration; time from ignition at a sensor until the fire dies out at that sensor (mean of 5 sensors, threshold used is 50°C)	Sustainability	s	61-1407
Fuel consumption	Percentage weight lost	Consumability	%	67-98
Time to ignition	Time from the insertion of a leaf into a muffle furnace (400°C) until the first visible flame	Ignitibility	s	1.1-7.0
Flame duration	Time from the first visible flame until no more flames could be seen	Sustainability	s	0.8-10.6
Smouldering duration	Time from the end of the last visible flame until the glowing phase died out	Sustainability	s	2.4-46.0
Total burning time	Sum of flame- and smouldering duration for individual leaves in a muffle furnace	Sustainability	s	3.2-56.7

Preliminary results

3.1. Which leaf traits are important for the flammability in fuel beds?

Fuel bed density (g/cm^3) was by far the most important driver for rate of spread ($R^2 = 0.81$, $p < 0.001$; Figure 1a). Fuel beds which were more densely packed (more mass per ring-volume), showed a slower spread of the fire. This can be understood as a simple "mass-effect", i.e. higher fuel loads require more time for combustion. On the other hand, the combustion process itself could have been limited by oxygen supply. When fuel beds were more densely packed there was less physical space for airflow, leading to partly incomplete combustion. Indeed we found that the mass of unburnt material was higher when the fuel bed density was higher ($R^2 = 0.29$, $p = 0.006$). Interspecific variation in fuel bed density itself was mostly driven by specific leaf area ($R^2 = 0.72$, $p < 0.001$) and leaf curliness ($R^2 = 0.61$, $p < 0.001$), and only to a lesser extent by leaf size (expressed as one side surface area, $R^2 = 0.19$, $p = 0.036$).

Specific leaf area (SLA) and leaf curliness also showed direct effects on the rate of spread (Figure 1b and c). Species with curlier leaves, and species with higher SLA, showed a higher rate of fire spread through the fuel bed. Most likely this is a side effect of the packing: curled leaves or species with higher SLA decreased the density of the fuel beds and therefore increased the rate of fire spread.

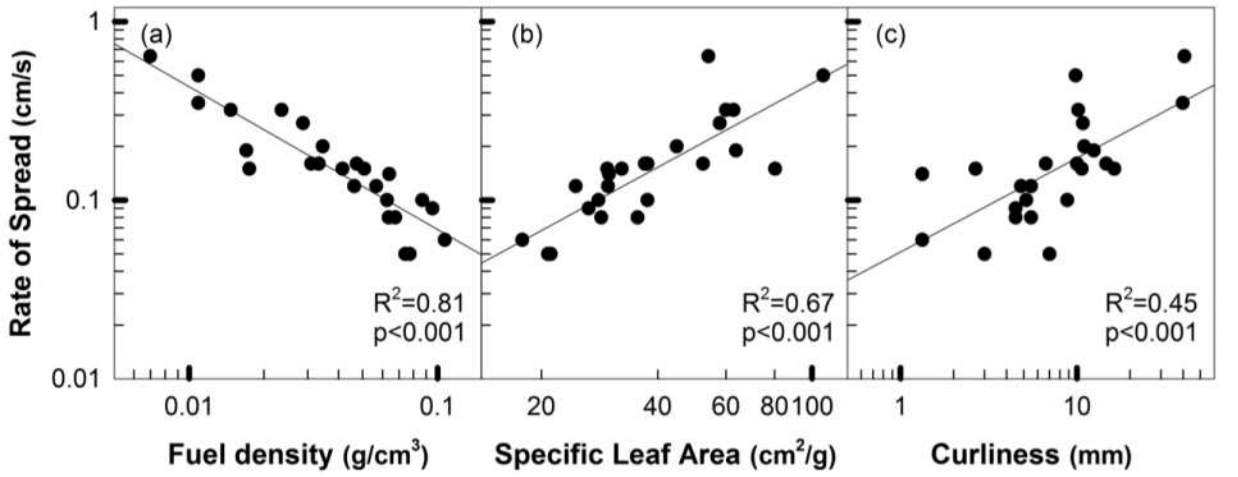

Figure 1. Bivariate relationships between "Rate of Spread" and (a) fuel bed density, (b) Specific Leaf Area and (c) leaf curliness. Each dot represents a species-mean. R^2- and p-values for the regression lines are given in the figure.

3.2. Does the ranking in species' flammability hold in two different experimental set-ups?

In contrast to our expectations we did not find a relationship between the fire-duration (total burning time) in individual leaves and the burning time in fuel beds. However, individual-leaf "time-to-ignition" showed clear relationships with four of the fuel bed fire parameters (Table 2). Most notably, the shorter the time-to-ignition of individually burnt leaves, the higher the rate of spread through the same species arranged in fuel beds ($R^2 = 0.59$, $p < 0.001$). Rate of spread can thus be seen as an accumulation of "ignition-steps".

In our previous study on individual leaves, interspecific variation in ignition times was strongly driven by specific leaf area ($R^2 = 0.70$, $p < 0.001$). Our results here suggest that SLA is the main driver of fuel density and consequently has a major influence of the combustibility in fuel beds. Leaf size and surface area per volume (SA:V) appeared to be less important than SLA.

Table 2. Intrinsic leaf flammability versus flammability in fuel beds. Only leaf intrinsic "time-to-ignition" showed significant relationships with (four out of five) fuel bed flammability parameters. The direction of the relation is expressed by "+" for positive relationships, and "-" for negative relationships; ns = not significant.

	Maximum Temperature (°C)	**Total Heat Released (°C*min)**	**Rate of Spread (cm/s)**	**Burning time (s)**	**Fuel consumption (%)**
Time To Ignition (s)	R^2 = 0.37 (+) p = 0.002	R^2 = 0.67 (+) p < 0.001	R^2 = 0.59 (-) p < 0.001	R^2 = 0.66 (+) p < 0.001	ns
Flame Duration (s)	ns	ns	ns	ns	ns
Smoulder Duration (s)	ns	ns	ns	ns	ns
Total Burning Time (s)	ns	ns	ns	ns	ns

Acknowledgements

Thanks to Richard van Logtestijn for his help with the experimental set up. Veronica Shaw and Vincent Maire helped with the collection of leaf material in Round Hill nature reserve. This project was funded by a scholarship from Macquarie University to S.G. and additional funding by VU University.

References

Byram GM (1959) Combustion of forest fuels. 'Forest Fire: Control and Use' (ed. K.P. Davis), pp. 155-182. McGraw-Hill, New York.

de Magalhães RMQ, Schwilk DW (2012) Leaf traits and litter flammability: evidence for non-additive mixture effects in a temperate forest. *Journal of Ecology* **100**(5), 1153-1163.

Drysdale D (2011) 'An Introduction to Fire Dynamics.'3rd edn. (John Wiley & Sons), West Sussex, UK.

Engber EA, Varner JM III (2012) Patterns of flammability of the California oaks: the role of leaf traits. *Canadian Journal of Forest Research* **42**, 1965-1975.

Plucinski MP, Anderson WR (2008) Laboratory determination of factors influencing successful point ignition in the litter layer of shrubland vegetation. *International Journal of Wildland Fire* **17**(5), 628-637.

Scarff FR, Westoby M (2006) Leaf litter flammability in some semi-arid Australian woodlands. *Functional Ecology* **20**(5), 745-752.

Van Altena C, van Logtestijn R, Cornwell W, Cornelissen H (2012) Species composition and fire: non-additive mixture effects on ground fuel flammability. *Frontiers in Plant Science* **3**, 1-10.

Wright IJ, Reich PB, Westoby M (2001) Strategy shifts in leaf physiology, structure and nutrient content between species of high- and low-rainfall and high- and low-nutrient habitats. *Functional Ecology* **15**(4), 423-434.

Supplementary Information

Table S1- Species list

Genus	**Species**	**Family**	**Rainfall** [a]	**Soil P** [b]	**No. of replicates**
Acacia	doratoxylon	Fabaceae	low	high	5
Acacia	havilandiorum	Fabaceae	low	low	1
Allocasuarina	sp.	Casuarinaceae	high	high	5
Astrotricha	floccosa	Araliaceae	high	high	5
Brachychiton	populneus	Malvaceae	low	low	6

Corymbia	gummifera	Myrtaceae	high	low	6
Dodonaea	viscosa spathulata	Sapindaceae	low	high	1
Eremophila	longifolia	Myoporaceae	low	high	5
Eucalyptus	dumosa	Myrtaceae	low	low	3
Eucalyptus	haemastoma	Myrtaceae	high	low	6
Eucalyptus	intertexta	Myrtaceae	low	high	6
Eucalyptus	socialis	Myrtaceae	low	low	4
Geijera	parviflora	Rutaceae	low	high	6
Hakea	dactyloides	Proteaceae	high	low	4
Hakea	tephrosperma	Proteaceae	low	high	2
Hakea	teretifolia	Proteaceae	high	low	1
Lambertia	formosa	Proteaceae	high	low	1
Lasiopetalum	ferrugineum	Malvaceae	high	high	6
Lomatia	silaifolia	Proteaceae	high	high	6
Macrozamia	communis	Zamiaceae	high	high	5
Persoonia	levis	Proteaceae	high	low	3
Santalum	acuminatum	Santalaceae	low	low	3
Syncarpia	glomulifera	Myrtaceae	high	high	4
Synoum	glandulosum	Meliaceae	high	high	6
Triodia	scariosa	Poaceae	low	low	5

[a] *Low rainfall sites receive approximately 383 mm rainfall per year, high rainfall sites 1233 mm.*
[b] *Low soil phosphorus levels are below 132 µg/g; high soil phosphorus levels are above 250 µg/g (Wright et al. 2001).*

Table S2 - Trait overview

Traits	**Description**	**Units**	**Range**
Fuel bed density	Mass of sample per fuel bed volume	g/cm^3	0.00697-0.10707
Fuel bed packing ratio	Particle volume per fuel bed volume	dimensionless (cm^3/cm^3)	0.000024-0.001129
Leaf curliness	Height above the flat leaf surface, including petiole (perpendicular to leaf length)	mm	1.33-40.67
Leaf size	One sided surface area	cm^2	0.82-32.61
Leaf dry mass	Oven dry weight	g	0.01-1.03
Leaf SA/V	One sided leaf surface area per volume	cm^{-1}	11.42-31.06
SLA	One sided leaf area per dry mass	cm^2/g	17.86-106.89
Leaf N	Nitrogen concentration	% mass	0.61-2.19
Leaf P	Phosphorus concentration	% mass	0.02-0.11
Leaf lignin	Difference between the sum of non-polar, water soluble, and acid soluble fractions from the total sample	% mass	8.72-37.50
Leaf tannin	Soluble polyphenols	% mass	1.79-18.50
Leaf thickness		mm	0.33-1.28
Leaf length		mm	43-128
Leaf width		mm	3-43

The velocity and structure flame front at spread of fire across the pine needle bed. Experiment

Oleg P. Korobeinichev[a] , Alexander G. Tereshchenko[a] , Alexander A. Paletsky [a], Andrey G. Shmakov[a,b], Munko B. Gonchikzhapov[a,b], Dmitrii Bezmaternykh[a,b],
Lilia Yu. Kataeva [c], Dmitriy.A. Maslennikov[c], Naian Liu[d]

[a] *Institute of Chemical Kinetics and Combustion, Novosibirsk 630090, Russia, korobein@kinetics.nsc.ru*
[b]*Novosibirsk State University, Novosibirsk 630090, Russia*
[c] *Nizhny Novgorod State Technical University, Russia*
[d] *State Key Laboratory of Fire Science, University of Science and Technology of China, Hefei 230026, P. R. China, liunai@ustc.edu.cn*

Abstract
The paper addresses an experimental study of the flame speed and of spatial temperature distribution at various depths of the bed of pine needles of Siberian boreal forests, a study of the composition of gaseous species and distribution of their concentrations across the bed during fire spread and the study of the impact of the wind velocity on these characteristics. It has been found that, as the wind velocity rises in the range of 0.12 - 0.2 m/s, the burning regime changes dramatically, as well as the temperature and concentration profiles of gaseous species inside the bed. At low wind velocities, flame penetrates the bed, while at high ones it does not. At wind velocities 0.15 m/s and higher, as the wind velocity grows, together with the dramatic growth of the flame velocity the maximum temperature in the flame front in the middle of the bed decreases from 1200 °C to 600 °C , the width of the combustion zone increases, in accordance with the temperature and O_2 и CO_2 concentration measurements. The flame front in the middle of the bed is biased relative to the flame front on the bed surface The data obtained in the study may be used in developing a ground fire spread model.

Keywords*: pine needles;; fire spread across fuel bed; flame structure; forest fire*

Introduction

Propagation of a ground fire across a fuel forest (FF) bed is a frequently used model of a forest fire. Consideration of this model is also of practical importance, as it describes the general features of the mechanism of ground forest and steppe fires. There are many papers devoted to computer simulation of forest fire spread across a FF bed (Balbi 2007, Grishin 1997, Konev 1977, Lyons 1993, Morandini 2005, Morvan 2001, Porterie 2007, Simeoni 2003, Weber 1990). At the same time, there are unfairly few experimental studies of the process, measuring such parameters as the spread velocity, temperature and FF temperature profiles in a FF bed and outside it (Marcelli 2004, Morandini 2005, Santoni 2002, Simeoni 2003, Sukhinin 1975). The compositions of the pyrolysis and combustion products, their concentration and their profiles both in a FF bed and outside it have never been measured elsewhere. All these data, though, are required for verification of the assumptions made in certain models, by comparing the experimental data and the modeling data. Especially noteworthy are the studies of fire spread across a pine needles bed. In (Morandini 2005) temperature distribution was measured both in the gas phase and inside the bed of pine needles in still air and exposed to wind, the minimum velocity of which was 1 m/s. In (Sukhinin 1975) the same measurements were made in still air, while in (Marcelli 2004) temperature distribution was measured only over a bed of pine needles in still air. In (Morandini 2005) it was found that the minimum temperature approximately in the middle of the bed 2.3. cm thick reaches the value of 1,000 – 1,100 ° C. It is interesting that the maximum temperature

measured with a thermocouple placed over the FF bed surface at the distance of 4 cm from it was about the same. We can suppose diffusion combustion of each needle in the bed to take place. Similar results under similar conditions were obtained in (Sukhinin 1975). In this study, the temperature profile was measured for a pine needle located on the bed surface with a thermocouple embedded inside a needle. The maximum temperature of a needle reached 800 °C. The flame spread velocity across the needles bed was approximately equal to 3 mm/s. It is to be noted that in the above studies temperature profiles of the needles at different distances from the bed surface inside it were mot measured. We did not find the papers in literature which would be devoted to the composition of gaseous products and their concentration distribution in the FF bed. Therefore one of the objectives of the study was to measure under laboratory conditions the temperature profiles inside of the bed of needles of the Siberian boreal forests (SBF), to study the composition of the gaseous products and distribution of their concentrations inside the bed during flame spread across the bed and to investigate the impact of the wind velocity on these characteristics.

Methods

Materials

The materials were the pine needles from SBF. The pine needles litter was sampled from under trees in a pine forest, then leaves and twigs were removed from it, with only litter needles left. The needles thus obtained were dried at the temperature of 60 °C during 24 hours in a drying cabinet. Weight loss after drying was 7.8-9.4 %. The average length of a pine needle was 5 mm, it was 1 mm wide and 0.6 mm thick. Specific surface area was determined using the BET method. It was 0.18 m^2/g.

Measuring the flame spread velocity across the pine needles bed depending on the wind velocity

The experiments were conducted in a chamber (Fig.1.) with the dimension of 70 cm/15 cm/30 cm. A photo of setup is presented in Fig.2. Placed inside the chamber a tray with a bed of pine needles 8 cm wide and 34 cm long. A photo of a tray with a bed of pine needles is presented in Fig.3. The amount of the pine needles was 0.07 g/cm^2. The needles were placed on an asbestos board plate 10 mm thick into a space restricted by fire-clay plates, 17 mm high. The layer porosity was 0.928.

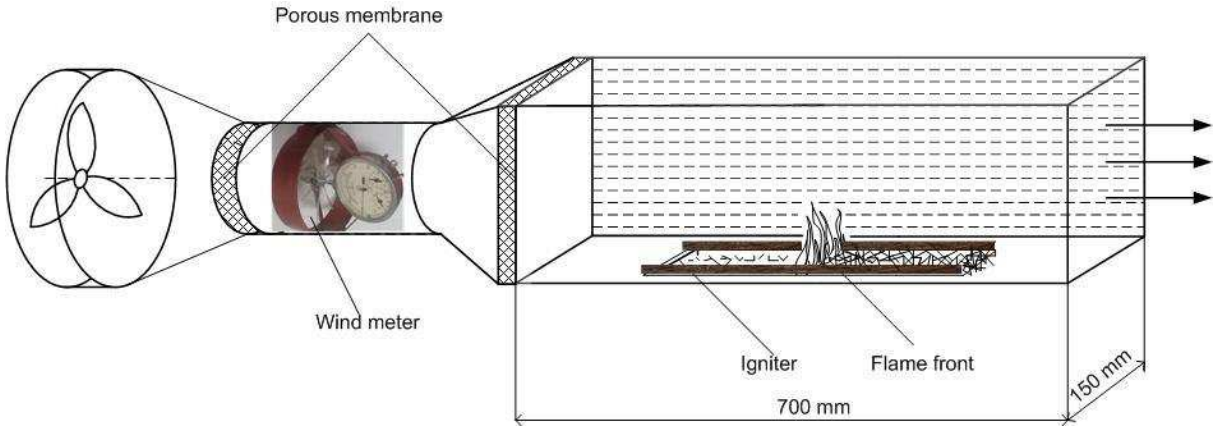

Figure 1- Experimental chamber for measuring the flame spread velocity across pine needles bed

Air was blown into the chamber from an air blower the capacity of 0.11 m^3/s. The wind velocity varied from 0 to 0.5 m/s. The air penetrated a porous filter to generate uniform flow. The air flow velocity was measured with a calibrated anemometer. The error in determining the average wind velocity was ±5%. The pine needles were ignited by a nichrome wire heated by electric current and a nearby glass

wool bundle, impregnated with 1 ml ethanol. To avoid wire sagging during heating, it was mounted with a spring. The flame spread velocity was determined by signals from three thermocouples placed along the pine needles bed near its surface and from a video recording of the burning process. Variance in measuring the velocity of flame spread across a pine needles bed is ± 15%.

Figure 2. Experimental setup for measuring the flame spread velocity across pine needles bed

Figure 3. A photo of a tray with a bed of pine needles

2.3. Measuring the temperature profiles and the composition of the gaseous products on the bed surface and inside the bed exposed to flame spread

The temperature profiles and the composition of the gaseous products on the bed surface and inside the bed were measured with two Π-shaped Pt-Pt 10% Rh thermocouples 50μm in diameter. The junction of one thermocouple (T1) was in the middle of the bed at the 13.2 cm distance from the igniter,

the junction of the other one (T2) was on the bed surface at the 12 cm distance from the igniter. The photo of the thermocouples location is shown in Figure 4.

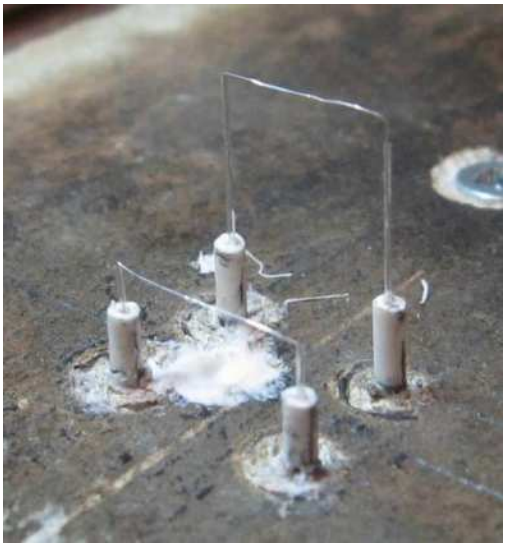

Figure 4. A photo of thermocouples location

To measure the temperature, a multichannel AD converter E14-140-M ("L-Card") was used. The measurement error of thermal EMF was ±0.5%. The temperature measurements were conducted at the frequency of 1 kHz. The thermocouples' signals were shown on the computer.
The composition of the pine needles pyrolysis products was measured by the probe mass spectrometry method. As a sampling probe, a pyrex tube was used with an internal diameter of 1.5 mm, embedded in the middle of the bed at a 18.8 cm distance from the igniter. The sample taken from the flame was cleaned from fine aerosol particles and tar and was delivered to the molecular beam system of the Hiden HPR-60 mass spectrometer. The response time of the sampling system was 2-2.5 sec, which is comparable with the time of recording one mass spectrum. Concentrations of O_2, CO_2, N_2, C_2H_5OH (ethanol), C_3H_6O (acetone), C_4H_4O (furan) in the sample studied were determined by the mass peak intensities with m/e 32, 44, 28, 31, 15 and 43, 68, accordingly. Sensitivity of the mass-spectrometer was determined by the calibration mixtures of the known composition. The ignition time and the starting time of the mass spectrometric measurements were synchronized. The dependences of mass peak intensities were measured, corresponding to the compounds chosen, as a function of time. Considering the measured average flame spread velocity across the pine needles bed, the dependences of temperature and species concentrations on time were recalculated into the respective dependences of temperature and species concentrations on the horizontal coordinate relative to the flame front.

3. Results

3.1. Dependence of the flame spread velocity across the bed of pine needles on the wind velocity

It can be seen from Figure 5, showing the results of measuring the dependence of the flame spread velocity on the wind velocity, that, as the wind velocity grows from 0 to 0.12 m/s, the flame spread velocity varies little, while with the change in the wind velocity from 0.12 m/s to 0.2 m/s, it almost triples. With the wind velocity of 0.15 - 0.2 m/s and higher, the regime of flame spread changes critically. As the wind velocity increases from 0.15 to 0.2 m/s the flame speed dramatically increases to 6 mm/s. Simultaneously, as seen from Fig.5, the temperature in the middle of the bed dramatically drops from 1200 до 600ºC. With the wind velocity higher than 0.2 m/s, probably comparable with the velocity of the pyrolysis products rise, the angle of flame slope to the horizon dramatically decreases

(with the wind velocity of 0.1 m/s, it would be close to 90 degrees), the flame seems to lie down on the pine needles layer (Figure 6).

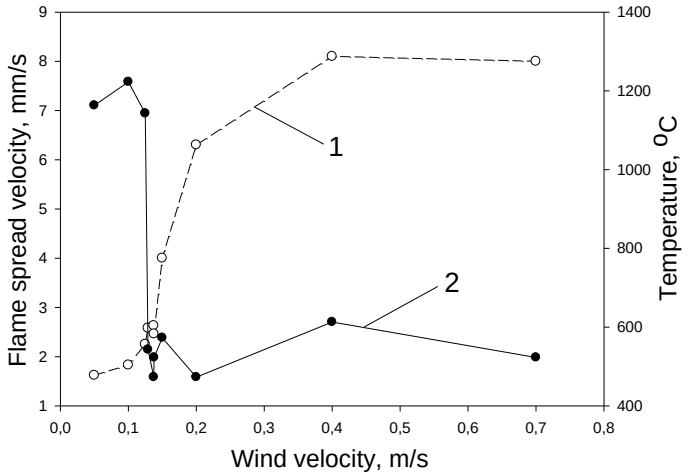

Figure 5. Dependences of the velocity of flame spread across the pine needles bed (1) and temperature in the middle of the bed (2) on the wind velocity

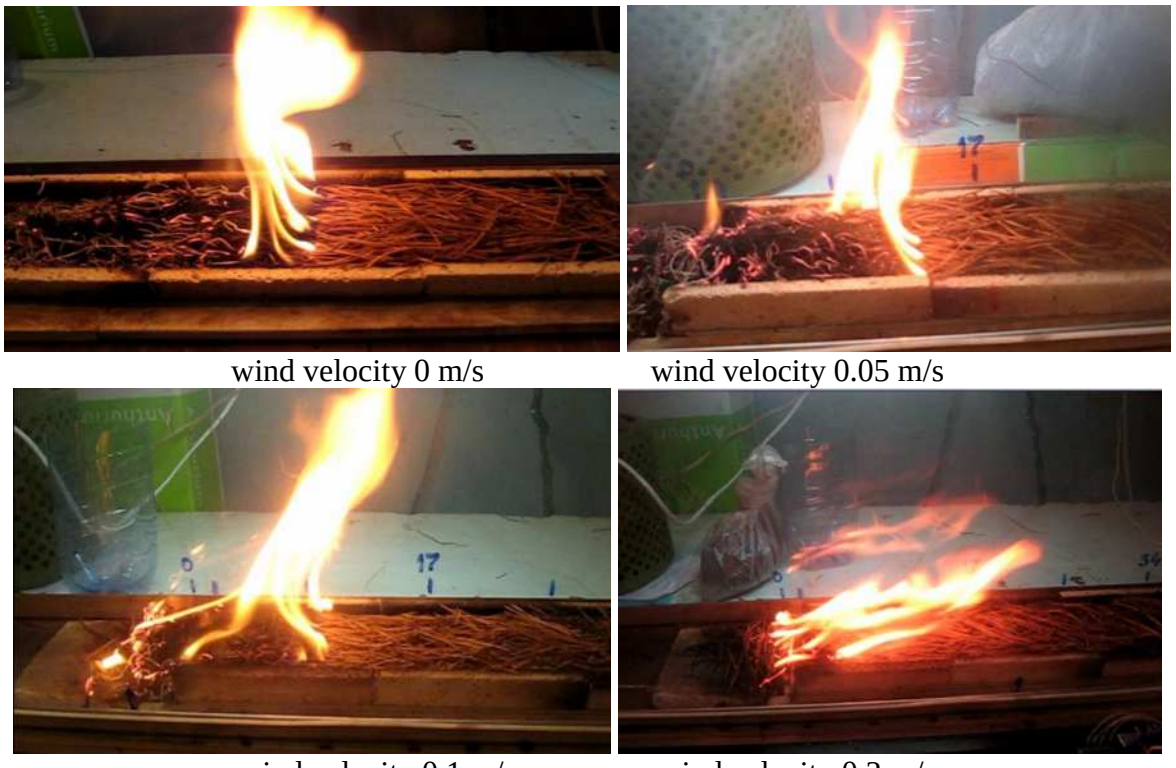

Figure 6. The photos of flame spread across a bed of pine needles depending on the wind velocity in the range from 0 to 0.2 m/s.

3.2. Temperature profiles and concentration profiles of O_2, CO_2 and volatile pyrolysis products in flame spread across a pine needles bed

Shown in the Figure 7 are the temperature profiles in the middle of the bed (T1) and on the surface (T2), considering the fact that the distance between the thermocouples was 11.8 mm, and the concentration profiles of CO_2, O_2 and ethanol inside the bed with the wind velocity of 0.1 m/s. The flame spread velocity is 2.05 mm/s. Analysis of the temperature profiles allows the following conclusions to be made:

1. Flame penetrates into the pine needles bed. The maximum temperature in the middle of the bed is 1300 °C. These data are in good agreement with the data of (Morandini 2005, Sukhinin 1975), obtained for conditions close to those of this study.
2. The flame front in the middle of the bed is 1.2 cm shifted relative to the flame front on the bed surface.
3. The width of the flame zone determined by the T2 profile is 7 cm. The width of the glowing (high temperature) zone is 1.2 cm on the bed surface (which agrees with the video recording data) and 0.9 cm in the middle of the bed.
4. Although combustion behind the flame front on the bed surface finishes at the 7 cm distance from the flame front, the temperature in this place in the middle of the bed is higher than on the bed surface, indicating continuing reactions inside the bed.

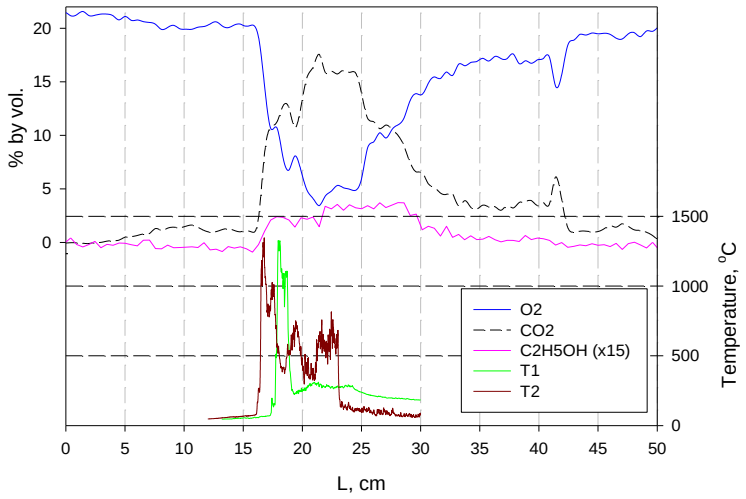

Figure 7. Temperature profiles in the middle of the pine needles bed (T1) and on the surface (T2), as well as CO_2, O2 and ethanol concentrations inside the bed, with the wind velocity of 0.1 m/s.

Thus, it follows from the results of mass spectrometric studies that:

1. As the flame front advances, O_2 concentration in the middle of the pine needles bed decreases to 4-5 %, while the maximum CO_2 concentration is reached at the distances from 6 to 9 cm from the flame front and is equal to 15-17 %. The width of the flame front determined from the O_2 и CO_2 concentration profiles is equal to 6 cm, which is close to the value of 7 cm, obtained from the data of the temperature profiles (T2). Thus, O_2 concentration in the middle of the bed does not decrease to zero. Oxygen may penetrate the bed due to diffusion and gas transfer along the bed. At the distances from the flame front greater than 9 cm, CO_2 concentration gradually decreases, while O_2 concentration goes up.
2. Maximum concentrations of two major volatile products of pine needles pyrolysis ethanol and acetone in the middle of the bed are 0.2 and 0.4-0.9 %, respectively. The width of the yield zone of the main volatile pyrolysis products is 12-13 cm. When the distances from the flame front are greater than this value, char smolders in the middle of the bed.

Similar facts are observed for the wind velocity of 0.05 m/s and in the absence of wind. However, with the wind velocity of 0.2 m/s and higher, the regime of flame spread changes critically. With the wind velocity higher than 0.2 m/s, probably comparable with the velocity of the pyrolysis products rise, the angle of flame slope to the horizon dramatically decreases. Due to this, the width of the heated zone

before the flame front expands and the front zone expands, too, which is confirmed by the temperature profiles and species concentrations in the pine needles bed at the wind velocity of 0.2 m/s shown in Figure 8.

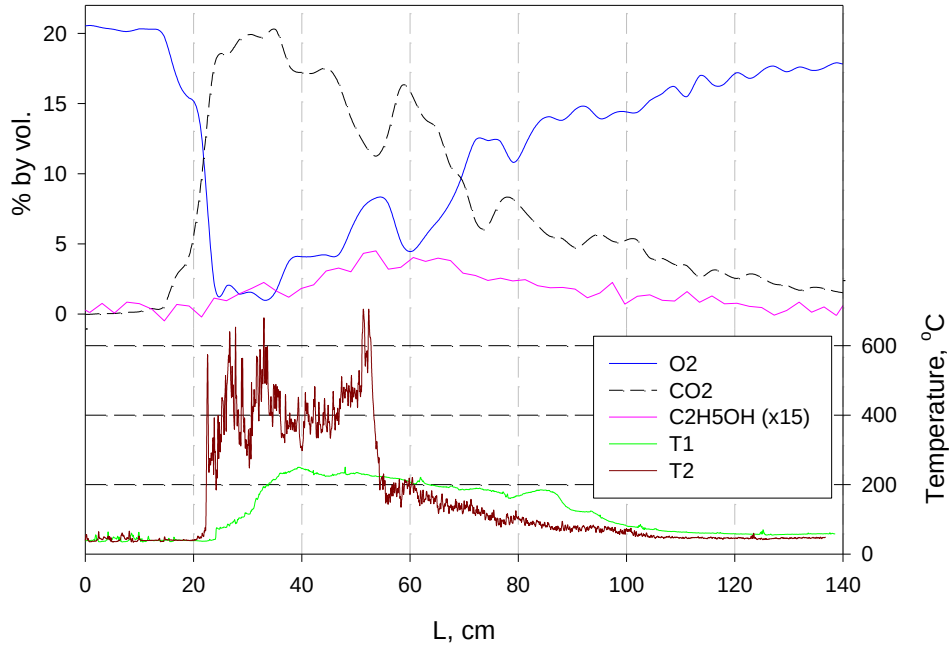

Figure 8. Temperature profiles in the middle of the pine needles bed (T1) and on the surface (T2), as well as CO_2, O_2 and ethanol concentrations inside the bed, with the wind velocity of 0.2 m/s.

It can be seen that the maximum temperature near the bed surface drops to 700 °C, evidently among other factors due to dilution of the combustion and pyrolysis products with air, while in the middle of the bed it drops to 230°C. The flame front width near the bed surface with the temperature 600-700°C increases several times due to the drop of temperature and therefore of the pyrolysis rates to become about 30 cm.

Conclusion

1. First changing the regime of flame spread across a bed of pine needles was found for changing wind velocity. It has been observed that in flame spread across a bed of pine needles there emerges a complex spatial distribution of temperatures and species concentrations, which depends on the wind velocity. The character of combustion essentially changes as the wind velocity changes from one range (0-0.12 m/s) to the other one (0.12 - 0.2 m/s). In the first range of wind velocities, the flame spread velocity is only slightly dependent on the wind velocity, while in the second range the dependence significantly increases. At low wind velocities flame penetrates the bed of pine needles, while at high wind velocities this does not occur. At wind velocities 0.12 m/s and higher, at the wind velocity grows, together with the growth of the flame velocity the maximum temperature in the flame front decreases from 1200 °C and 700 °C , the width of the flame zone, in accordance with the temperature and O_2 и CO_2 concentration measurements. The flame front in the middle of the bed is shifted relative to the flame front on the bed surface.
2. The experimental data on the dependence of the flame spread velocity across the bed of pine needles on the wind velocity obtained in the study and on the flame front structure (distribution of temperature and concentrations of gaseous species inside the bed) may be used in developing a model of ground fire spread.

Acknowledgment

This work was supported by the RFBR under grant #13-03-91164 and by the NNSF of China under Grant 51120165001 and 51176179.

References

Balbi J-H, Rossi J-L, Marcelli T and Santoni P-A (2007) A 3D physical real-time model of surface fires across fuel beds. *Combustion Science and Technology* **179**:12, 2511-2537

Grishin A.M., in: Albini F.A. (Ed.) (1997) "Mathematical Modeling of Forest Fires and New Methods of Fighting Them" (Pub. House of the Tomsk University, Tomsk).

Konev E.V., Sukhinin A.I. (1977) The Analysis of Flame Spread Through Forest Fuel. *Combustion and Flame* **28**, 217-223.

Lyons P.R.A., Weber R.O. (1993) Geometrical Effects on Flame Spread Rate for Wildland Fine Fuels. *Combustion Sciences and Technology* **89** (1), 153-165.

Marcelli T., Santoni P.A., Simeoni A., Leoni E. and Porterie B (2004) Fire spread across pine needle fuel beds: characterization of temperature and velocity distributions within the fire plum. *International Journal of Wildland Fire* **13** (1), 37–48.

Morandini F., Simeoni A., Santoni P.A., and Balbi J.H. (2005) A model for the spread of fire across a fuel bed incorporating the effects of wind and slope. *Combustion Sciences and Technology* **177** (7), 1381-1418.

Morvan D., Depuy J.L. (2001) Modeling of Fire Spread Throught a Forest Fuel Bed Using a Multiphase Formulation. *Combustion and Flame* 127, 1981-1994.

Porterie B., Consalvi J.-L., Loraud J.-C., Giroud F., Picard C. (2007) Dynamics of wildland fires and their impact on structures. *Combustion and Flame* **149**, 314–328.

Porterie B., Morvan D., Loraud J.C., and Larini M. (2000) Physics of fluids, 12(7), 1762–1782.

Santoni P.-A., Marcelli T., Leoni E. (2002) Measurements of Fluctuating Temperature in a Continuous Flame Spreading Across a Fuel Bed Using a Double Thermocouple Probe. *Combustion and Flame* **131**, 47-58.

Simeoni A., Santoni P.-A., Larini M., Balbi J.-H. (2003) Reduction of a multiphase formulation to include a simplified flow in a semi-physical model of fire spread across a fuel bed. *International Journal of Thermal Sciences* **42**, 95-105.

Sukhinin A.I. (1975) Temperature distribution in a burning layer of pine needles. *Comb. Expl. Shock Waves* 11 (5) 726-730.

Weber R.O. (1990) Modelling fire spread through fuel beds. *Prog. Energy Combust. Sci.*, 17, 67–82.

Turbulence structures observed during experimental fires in forest and grassland environments

Daisuke Seto[a], Craig B. Clements[a] and Warren E. Heilman[b]

[a]*Fire Weather Research Laboratory, Department of Meteorology and climate Science, San José State University. San José, CA 95192 USA*
daisuke.seto@sjsu.edu; craig.clements@sjsu.edu
[a]*USDA Forest Service, Northern Research Station . Lansing, MI. wheilman@fs.fed.us*

Abstract
Fire-atmosphere interactions can occur at spatial scales on the order of tens of meters at the fire front and to kilometers in plumes during large fires. However, few studies have focused on the observed turbulence structure in the immediate environment of propagating fires to further understand the relative importance of ambient and fire-induced turbulence on fire front propagation. In this study, turbulence structures during the passage of fire fronts were investigated using the data obtained from two field experiments. One fire was conducted over grass fuel under strong ambient mean winds and the other conducted in a forest sub-canopy environment under light ambient winds. The main objective of this research is to investigate scale-averaged variances over different fuels before, during, and after the fire front passage in relation to different fire intensities and atmospheric conditions. Time series data from in-situ sonic anemometer arrays are analyzed using wavelet signal processing to treat non-stationary process of the fire front passage. Only a small increase in u variance over the 2-4 s band was found during the fire front passage in the grass fire environment under the strong mean winds. The variance associated with low intensity sub-canopy fire was found to increase over 2-4 s and 8-16 s bands, due to intermittent convective smoke plume pulses of the low intensity sub-canopy fire.

Keywords*: Fire-induced wind, Fire-atmosphere interaction, Grass fire, Sub-canopy fire*

Introduction

Turbulent kinetic energy (TKE) is produced in the energy containing range and transported from large to small scales without the energy production or dissipation in the inertial subrange, and it is eventually converted to internal energy in the dissipation range. Turbulent eddy motion in these three regions is well recognized in the atmospheric boundary layer. However, because dynamical coupling of the wildfire and atmosphere (Clark *et al*. 1996) may occur over a very wide range of length and time scales depending upon fire intensity and the atmospheric conditions, it is questionable whether the traditional turbulence theory holds in wildfire environments where the atmosphere becomes highly unstable given extremely high flame temperatures and large sensible heat flux, particularly near the surface.
Sun *et al*. (2009) showed that a strong downdraft caused by an interaction between the fire-induced plume circulation and a strong eddy circulation in the ABL can bring down higher momentum from aloft to the surface and increase the rate of fire spread, especially for a large fire. Downdrafts have been observed during fast spreading grassfires (Clements *et al*. 2007). Seto *et al*. (2014) showed that despite lower plume temperatures low-intensity sub-canopy fires may potentially be able to generate nearly as strong fire-induced winds as wind-driven grass fires under favorable fuel conditions due to strong coupling between fire and atmosphere.
Initial analyses of turbulence spectra during fire front passage revealed that fire can influence the energy of the flow and turbulence over a wide frequency range (Seto *et al*. 2013). Although four datasets that were representative of various fuels and terrain were analyzed in the study, more experimental datasets are now available with better horizontal and vertical coverage of turbulence

measurements. Additionally, the study only addressed qualitative aspect of the spectral energy in the spectral regions, and further investigation of TKE generation and dissipation processes during fire events are essential to corroborate the previous findings.
This paper examines the turbulence structures in fire environments during grass fire and sub-canopy fire experiments.

Experimental designs

FireFlux II, a comprehensive grassfire experiment, was conducted on 30 January 2013 at the University of Houston Coastal Center in Texas, USA and was designed with a head fire being allowed to burn directly underneath a 42-m and three 10-m micrometeorological towers (Figure 2). The fuels consist of a mixture of native grasses, including big bluestem (Andropogon gerardi), little bluestem (Schizachyrium scoparium), and long spike tridens (Tridens strictus). Each tower was equipped with multiple 3D sonic anemometers (20 m, 10 m, and 6 m AGL. The experiment was carried out with a head fire ignition under red flag warning conditions (Clements *et al*. this issue).
Three low-intensity prescribed burns were conducted during the late winter and early spring (February and March) of 2010 and 2011 at The Nature Conservancy's (TNC) Calloway Forest/Sandhills Preserve in North Carolina, USA (Figure 1). A majority of the surface fuels were in the 1-hr (defined as ¼ of an inch or less in diameter) size classification and consisted of long leaf pine litter, both cured and live wiregrass (*Aristida stricta*), American turkey oak (*Quercus laevis*), and regeneration long leaf pine. The mean tree height (h_c) was 20 m. The soil was sandy with little to no organic matter beyond the surface duff layer. In this study, turbulence data collected at a 20-m in-situ tower in 2011 was used for the analysis. The tower was equipped with multiple 3D sonic anemometers at 20 m, 10 m, and 3 m AGL. Backing and strip fire ignitions were employed during the experiment although blackline and strip head fire were also ignited around the tower. Fire propagation was limited to ground fuels. Hereafter, the two experiments discussed above are mentioned as FF2 and NC.

3. Data Processing

Streamwise and vertical velocity wavelet power spectra were computed using a continuous wavelet transform (complex Morlet) following Torrence and Compo (1998). Wavelet transforms are mathematical techniques based on group theory and square integrable representation and they use an analysing function called wavelets, which are localized in space, to decompose signals into space and scale (see Farge, 1992 for details). To examine fluctuations in local power over a range of scales, time series of scale-averaged wavelet power is presented in this study. Three wavelet scales were selected: 2-4 s, 8-16 s, and 32-64 s periods. The velocity data were averaged over 1 s before calculating the wavelet power.

Data Analysis and Discussion

4.1. Time series of averaged variances observed during FF2

Observed streamwise velocities *u* at three measurement heights in Figure 1a showed similar magnitudes to those observed before the fire front passage under a strong ambient wind of 9 m s^{-1} observed prior to the ignition (14:30-15:00 CST). Measured 1 Hz peak vertical velocities of 6 m s^{-1} at 6 m AGL and 9 m s^{-1} at 20 m AGL accompanied with a maximum plume temperature of 200°C observed at 6 m AGL compare well with the observations made at the same site under lighter ambient winds (Clements *et al*. 2007). However, a period of downdraft that was observed in Clements *et al*. did not occur during the FF2 due to the strong horizontal winds that are unfavourable for fire-induced circulations (Jenkins *et al*. 2001).

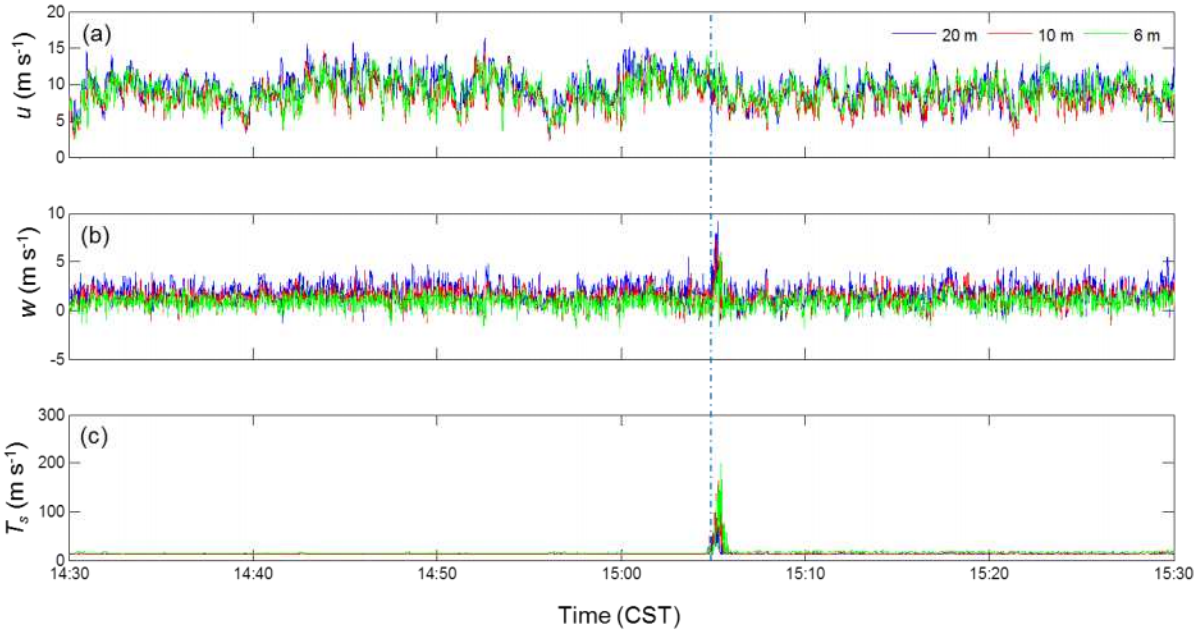

Figure 1. (a) streamwise velocity u, (b) vertical velocity w, and (c) sonic temperature T_s observed at the tower during FF2 experiment. Ignition was made at 15:04:08 CST, and fire front reached the tower around 15:05 CST as indicated by the sonic temperature spikes. Blue dashed line indicates the timing of the fire front arrival at the tower.

Figure 2 shows the *u* wavelet power averaged over three different scales/frequency bands, which give a measure of the scale-averaged variance in a certain band. Increased wavelet power over 2-4 s at 20 m, 10 m, and 6 m AGL at the time of the fire front passage suggests fire generated small-scale turbulence (2-4 s band) within the plume, where the strong updrafts were present. For larger scales than the 2-4 s band, the wavelet power remained below the ambient level over the fire, which suggest no major influence of the fire on the turbulence field for the scales (frequency) larger than 8 s (below 0.1 Hz). The strong mean winds were responsible for the large turbulent energy generation over the 8-16 s and 32-64 s scales on the background turbulence. The results indicate that fire-induced turbulence at larger scales may be supressed in the mean wind direction when the ambient winds are stronger than the fire's convection, and only smaller eddies, perhaps related to the entraining motions of the smoke plume, were enhanced by the fire.

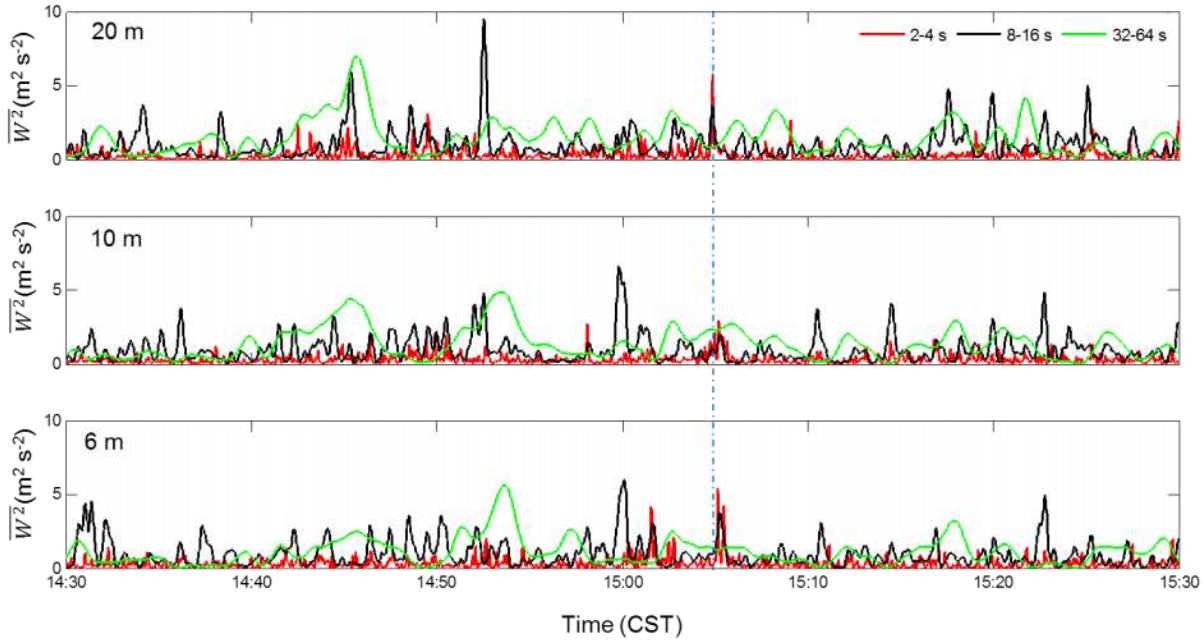

Figure 2. Scale-averaged wavelet power W^2 over the 2-4 s (red line), 8-16 s (black), and 32-64 s (green) bands for the u velocities measured at the main tower during the FF2. Blue dashed line indicates the timing of the fire front arrival at the tower.

The vertical velocity wavelet power shown in Figure 3 is well characterized by the large increases in 2-4 s scale variances at all three measurement heights. The magnitudes of their power were much larger than the variances at larger scales. The fire's strong buoyancy generates turbulence in the vertical direction that is much smaller in scale than the atmospheric turbulence generated within the boundary layer.

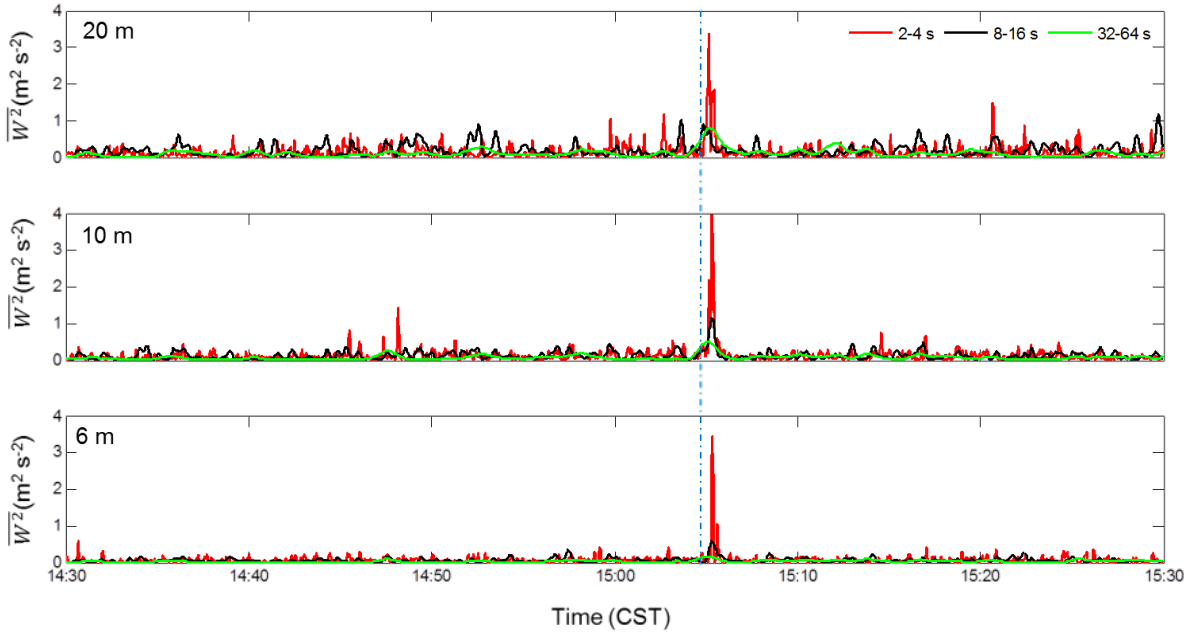

Figure 3. Scale-averaged wavelet power W^2 over the 2-4 s (red line), 8-16 s (black), and 32-64 s (green) bands for the w velocities measured at the main tower during the FF2. Blue dashed line indicates the timing of the fire front arrival at the tower.

4.2. Time series of averaged variances observed during NC

The steamwise velocity *u* at the canopy top (20 m AGL) shows larger fluctuations than those within the canopy (10 m and 3 m AGL) before and after the fire front passage, as indicated by high sonic temperatures near 100°C (Figure 4), due to the momentum absorption by the canopy layer. A head fire at 16:16 EST resulted in increased *u* velocities within the canopy and increased vertical motions at all three heights.

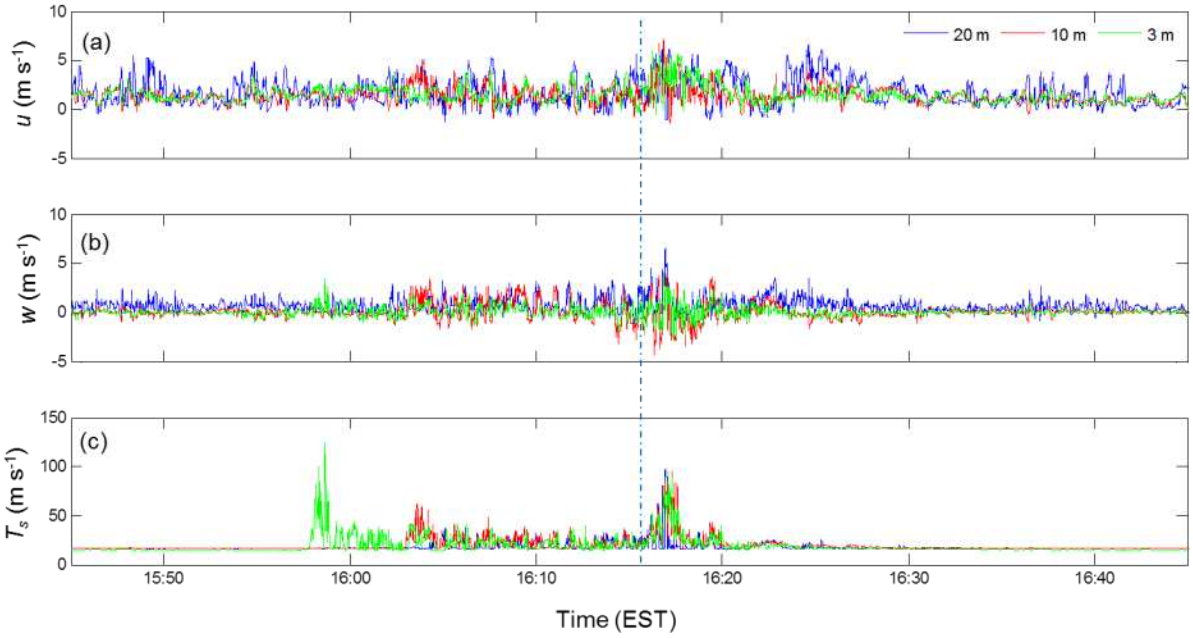

Figure 4. (a) streamwise velocity u, (b) vertical velocity w, and (c) sonic temperature T_s observed during NC experiment. Ignition was made at 11:04:08 EST. Blue dashed line indicates the timing of the fire front arrival at the tower.

The head fire at 16:16 EST was associated with increased *u* variances over the 2-4 s and 8-16 s bands both within and at the top of the canopy as compared to those observed prior to the head fire. It indicates that the turbulence structure within the plume was similar with height up to 20 m AGL. A coherent structure in the 32-64 s band variance may suggest turbulent mixing during the fire although the magnitudes of the variances observed within the canopy were still smaller than the ambient variance above the canopy. The increased wavelet variances within the canopy due to the fire were still smaller than the turbulence observed above the canopy, which indicates relatively weak turbulence generation from the low-intensity fire in the *u* direction.

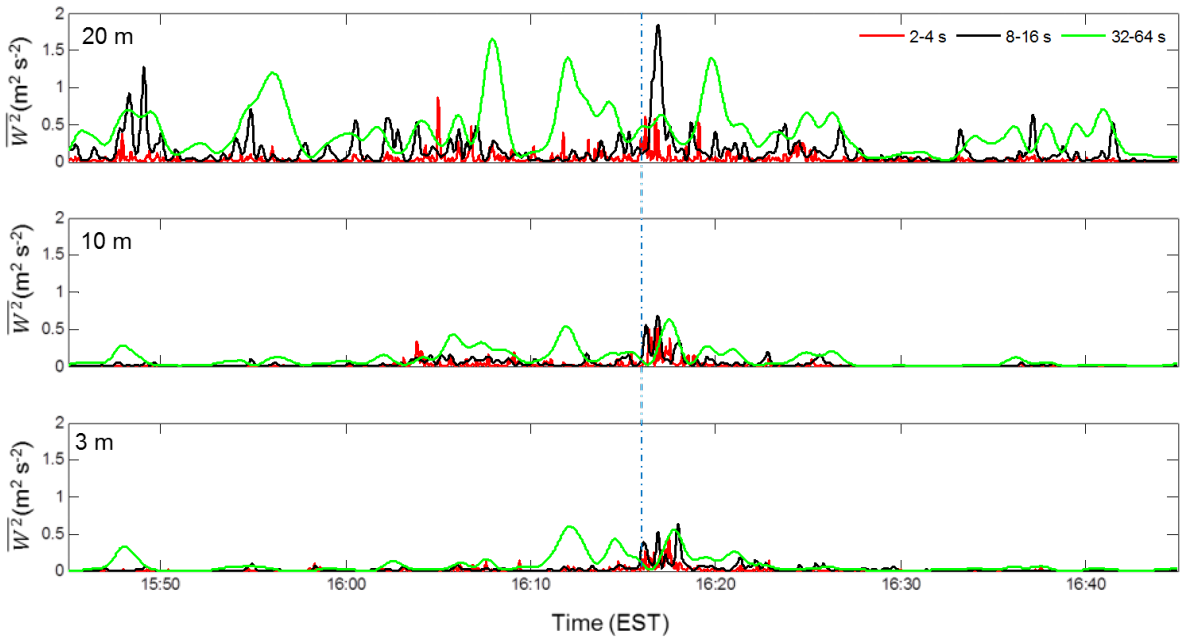

Figure 5. Scale-averaged wavelet power W^2 over the 2-4 s (red line), 8-16 s (black), and 32-64 s (green) bands for the u velocities measured at the main tower during the NC. Blue dashed line indicates the timing of the fire front arrival at the tower.

The vertical velocity variance at the canopy top was dominated by the 8-16 s band with a decreasing trend towards the ground. The *w* wavelet power over the 8-16 s band also shows a large spike similar to the *u* velocity component.

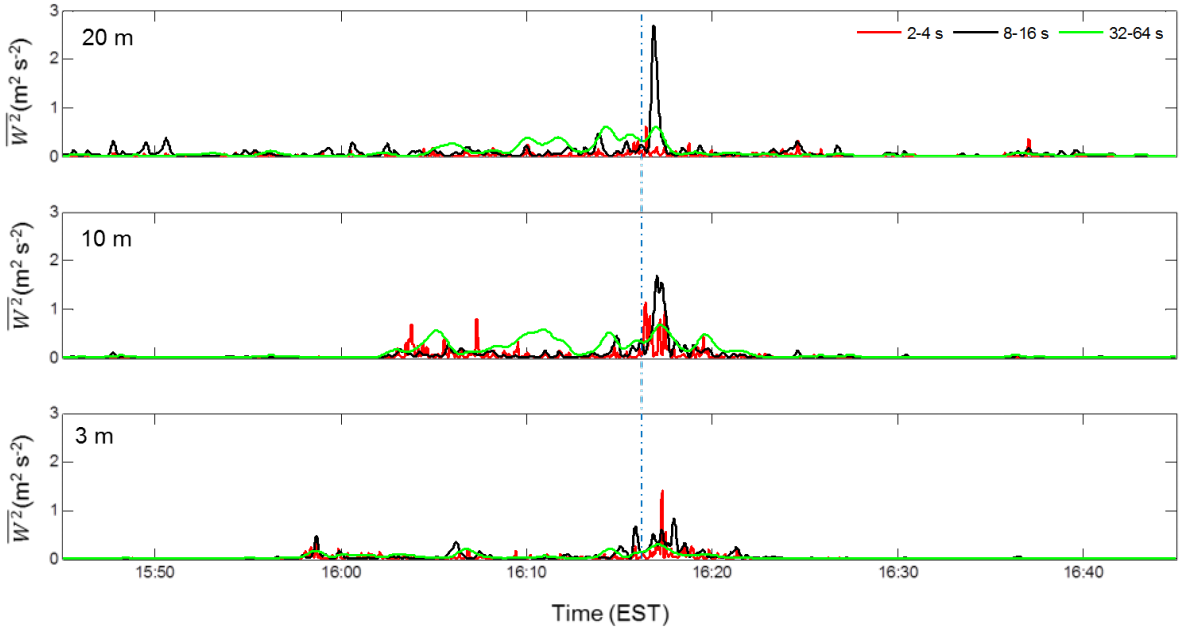

Figure 6. Scale-averaged wavelet power W^2 over the 2-4 s (red line), 8-16 s (black), and 32-64 s (green) bands for the w velocities measured at the main tower during the NC. Blue dashed line indicates the timing of the fire front arrival at the tower.

4.3. Comparisons between the two fires

The turbulence generated by the grass fire showed an increase limited primarily to the smaller (2-4 s) scale turbulence, whereas the sub-canopy fire contained slightly larger scale (8-16 s) turbulence structures. This may be associated intermittent convective smoke plume pulses of the low intensity sub-canopy fire. The magnitudes of the 2-4 s variances induced by the grass fire were 3 to 5 times larger in magnitude than those generated by the low intensity sub-canopy fire. The turbulence structure before and after the fire front passage did not show changes in the velocity spectral behaviour for the two fires under the observed conditions.

Conclusions

Turbulence structures in two experimental fires were examined using a continuous wavelet signal processing for a grass fire under strong ambient winds and a forest sub-canopy fire under light ambient winds. Only a small increase in u variance over the 2-4 s band was found during the fire front passage in the grass fire environment under the strong mean winds. The variance associated with low intensity sub-canopy fire was found to increase over 2-4 s and 8-16 s bands, due to the lower frequency smoke plume pulses. The turbulence structure before and after the fire front passage did not show changes in the velocity spectral behaviour for the two fires for the given conditions. Further analyses will include temperature variances and its relationship with the observed velocity variance signals.

Acknowledgements

The FireFlux II experiment was funded by grants from the National Science Foundation (AGS-1151930) and Joint Fire Science Program (#11-2-1-11). The sub-canopy experiment was funded by the Joint Fire Science Program (Award# 09-1-04-2).

References

Clements, C. B., Zhong, S., Goodrick, S., Li, J., Bian, X., Potter, B. E., Heilman, W. E.,
Charney, J. J., Perna, R., Jang, M., Lee, D., Patel, M., Street, S., Aumann, G., 2007: Observing the Dynamics of Wildland Grass Fires: FireFlux- A Field Validation Experiment. Bull. Am. Meteorol. Soc. 88(9), 1369-1382.

Clements C.B., and Coauthors (2014) Overview of the 2013 FireFlux-II Grass Fire Field Experiment**,** *VII International Conference on Forest Fire Research*, D. X. Viegas (Ed.), 2014

Clark, T. L., Jenkins, M. A., Coen, J., Packham, D., 1996: A coupled atmosphere-fire model: Convective feedback on fire-line dynamics. J. Appl. Meteorol. 35, 875-901.

Jenkins, M.A., Clark, T., Coen, J., 2001: Coupling atmospheric and fire models, in: Johnson, E.A., Miyanishi, K. (Eds.), Forest fire: Behavior and ecological effects. Academic Press, pp. 257-302.

Seto, D., Clements, C. B., Heilman, W. E., 2013: Turbulence spectra measured during fire front passage. Agric. For. Meteorol. 169, 195-210.

Seto, D., Clements, C. B., Strand, T., Thistle, H., Mickler, R., 2014: Turbulence and plume thermodynamic structures during low-intensity subcanopy fires. Agric. For. Meteorol. *In review*.

Sun, R., Krueger, S.K., Jenkins, M.A., Zulauf, M.A., Charney, J.J., 2009. The importance of fire-atmosphere coupling and boundary-layer turbulence to wildfire spread. International Journal of Wildland Fire 18, 50-60.

Uncertainty in model predictions of wildland fire rate of spread

Miguel G. Cruz[a], Martin E. Alexander[b]

[a] *Bushfire Dynamics and Applications, CSIRO Land and Water, GPO Box 1700, Canberra, ACT 2601, Australia, Miguel.cruz@csiro.au*
[b] *Department of Renewable Resources and Alberta School of Forest Science and Management, University of Alberta, Edmonton, Alberta, Canada T6G 2H1, mea2@telus.net*

Abstract
This paper highlights the results obtained from a comprehensive survey recently published by the authors on the error statistics associated with studies that have used independent data derived from field observations of wildfires, prescribed fires and experimental fires to evaluate the performance of 13 models used operationally to predict head fire rate of spread. Answers to the following kinds of questions were sought:

- How accurately can one expect to predict the spread rate of wildland fires with currently available models?
- Can models based on experimental fire data be used to predict wildfire behaviour?
- Are wildfires inherently more difficult to predict the spread rates of than prescribed fires or crown fires compared to surface fires?
- How realistic is it to expect an exact prediction of rate of fire spread?
- What is an acceptable error for rate of fire spread models?

A total of 49 studies, comprising 1278 paired observations vs. model predictions of fire spread rates for four forest fuel types (hardwood, mixedwood, conifer, eucalypt) and three non-canopied fuel types (grassland, shrubland, logging slash) from four continents (North America, Australia, Europe, Africa) were assembled. The answers to the five questions asked above are as follows:

- Mean absolute percent error varied between 20 and 310% and was homogeneous across fuel type groups. Slightly more than half of the evaluation datasets had mean absolute percent errors between 51 and 75 percent. Under-prediction bias was prevalent in 75 percent of the case 49 datasets analysed.
- Empirical-based fire spread rate models founded on solid field observations and well accepted functional forms, can adequately predict rates of fire spread well outside of the bounds of the data used in their development.
- There was no evidence to be found that predicting the rates of spread of wildfires was any more difficult than that of prescribed fires. Spread rates of crown fires were no more difficult to predict that surface fires.
- Only three percent (i.e. 35 out of 1278) of model predictions were considered to be exact (i.e. ±2.5 percent of the observed rate of fire spread).
- A ±35 percent error interval constitutes a reasonable standard for model adequacy.

Keywords*: fire spread models; fire behaviour; error; surface fires; crown fires; wildfires; prescribed fires.*

Introduction

There are a variety of aspects associated with the subject of wildland fire behaviour (Scott *et al.* 2014) and reasons to increase our knowledge on the subject through continuing research and improvements in operational practice (Cruz *et al.* 2014a,b). However, if one could boil down the whole science of wildland fire behaviour to its most practical essence, it might very well be to provide fire operations personnel with a decent estimate of just how fast a free-burning fire (Figure 1), either of planned or of unplanned origin, would likely spread based on the prevailing fire environment conditions (Van Wagner 1985).

This paper highlights the study undertaken by Cruz and Alexander (2013) that addressed the following kinds of questions:

- How accurately can one expect to predict the spread rate of wildland fires with currently available models?
- Can models based on experimental fire data be used to predict wildfire behaviour?
- Are wildfires inherently more difficult to predict than prescribed fires or crown fires compared to surface fires?
- How realistic is it to expect an exact prediction of rate of fire spread?
- What is an acceptable error for fire spread models?

It is fully recognized that the degree of accuracy in model predictions of rate of spread in wildland fires is dependent on the model's applicability to a given situation, the validity of the model's relationships, and the reliability of the model input data (Alexander and Cruz 2013b).

Figure 1. Photo of the Millers Reach #2 Fire near Anchorage, Alaska, during its major run on June 3, 1996 that involved extensive crowning in black spruce forests. Photo by: Anne Raup, Anchorage Daily News. For further information on this wildfire, see Hufford et al. (1998).

Methods

2.1. Compilation of datasets

In order to address the questions poised in the Introduction, a comprehensive effort was made to locate as many evaluation studies of rate of fire spread rate model performance in the literature as possible. The sources included:

- Scientific peer-reviewed journal articles
- Conference and workshop papers
- Technical reports from government agencies
- Post-graduate university theses

The principal requirements for inclusion in the analyses were that the evaluation data be (i) collected on outdoor experimental fires, operational prescribed fires and (or) wildfires, involving a "line fire" pattern similar to that observed on the head of a free-burning wildfire (Figure 1), as opposed to strip-head fires or point-source fire(s) (e.g. Sapsis and Kauffman 1991; Jupen *et al.* 2013) and (ii) that the dataset could not have been used in the model development (i.e. completely independent observational data) as Albini and Stocks (1986) did in their analysis. For example, Cruz *et al.* (2005) used the datasets of Alexander *et al.* 1991, Stocks *et al.* (2004) and Alexander *et al.* (2006) to test their crown fire rate of spread model.

Experimental fires carried out in fuelbeds or with head-fire widths judged too narrow to yield realistic pseudo-steady state rates of spread were excluded (e.g. Neuenschwander 1980; Schimmel and Granström 1997). This also included laboratory studies (e.g. Weise and Biging 1997; Menage *et al.* 2012). To ensure that each study included in the analysis had sufficient data to discern model adequacy for the particular fuel type and burning conditions, we restricted the analysis to studies that had at least five paired observations. Thus, studies like Brown (1982), Pickford *et al.* (1992) and Fogarty *et al.* (1997), for example, were excluded from the analysis. Finally, studies where model outputs were not fully independent, as a result of investigators fine tuning model predictions in relation to the observed rates of fire spread (e.g. Woodall 1998; Beavers 2001), were also not selected for analysis.

It was readily acknowledged that the data quality between studies would vary, especially between data obtained from experimental burning programs versus wildfire monitoring. Experimental fire studies are characterized by detailed sampling of fuel structure, weather and fire behaviour (e.g. Everson *et al.* 1985; Alexander *et al.* 1991; Stocks *et al.* 2004) whereas observations associated with wildfires tend to rely on broad assumptions regarding fuels and representativeness of weather data (e.g. Fogarty *et al.* 1997; Alexander *et al.* 2013).

Calculation of statistics

Error statistics on the rate of fire spread observations versus predictions were calculated for each of the model performance studies that qualified for inclusion. These included the root mean square error (RMSE), the mean absolute error (MAE), the mean absolute percent error (MAPE), and the mean bias error (MBE) as described by Willmott (1982). In most cases, these error statistics were not reported in the studies that we examined so it became necessary to compute them from the data contained in the associated publication or by contacting the study investigators directly for the data pairs.

The percentages of exact, under- and over-predictions were also calculated. To our knowledge, a definition for what constitutes an exact model prediction does not exist. Thus, for the purposes of this study, we elected to consider an exact model prediction as one where the error was less then ±2.5 percent of the observed rate of fire spread.

Results

Assembled database

Our extensive search for evaluation studies of rate of fire spread model performance resulted in the compilation of 49 suitable cases. At least two studies were overlooked, one consisting of eight low-intensity experimental fires (with spread rates less than 1.5 m/min) in an Australian eucalypt forest (Davis 1976) and a second one involving 28 observations (with spread rates of 1.0 to 89 m/min) garnered from a single wildfire in southern California chaparral (Weise and Fujioka 1998). The number (n) of studies by geographic distribution were as follows:

- Africa (n = 3)
- Australia (n = 14)
- Europe (n = 3)
- North America (i.e. Canada and US; n = 29)

The combined database ended up amounting to a total of 1278 individual observed rate of fire spread observation – model prediction pairs. This included three types of data (Figure 2):

- Experimental fires (*n* = 891)
- Operational prescribed fires (*n* = 182)
- Wildfires (*n* = 204)

The data encompassed a wide range in fire behaviour and fire propagation regime types, including low- to high-intensity surface fires in both canopied and non-canopied fuel complexes as well as passive and active crown fires (Van Wagner 1977) in several forest and other vegetation types that are prone to crowning (Table 1 and Figure 3). Seven broad fuel type groups could be identified in the 49 studies (Figures 4 and 5):

- Grasslands (*n* = 6)
- Shrublands (*n* = 9)
- Logging slash (*n* = 3)
- Conifer forest (*n* = 17)
- Hardwood forest (*n* = 3)
- Mixedwood forest (*n* = 2)
- Eucalypt forest (*n* = 9)

All of the studies involved either empirical (*n* = 11) or semi-empirical rate of fire spread models (*n* = 2). The lack of any physics-based models involvement simply reflects the fact that any performance evaluation studies carried out to date with these type of models has involved four or less paired cases of observation and model prediction (Alexander and Cruz 2013a).

Table 1. Sample size, range in rate of fire spread (ROS), and summary of error statistics by type of fire involved in the 1278 pairs garnered from the 49 comparison studies as compiled by Cruz and Alexander (2013)

Type of fire	No. of fires	ROS range (m/min)	Exact predictions	Under-predictions			Over-predictions		
				No. of fires	Mean MAPE (%)	Standard deviation	No. of fires	Mean MAPE (%)	Standard deviation
Surface fires	994	0.1 – 150.9	32	631	48%	25%	346	99%	137%
Crown fires	266	3.4 – 175	3	180	51%	22%	86	61%	63%

Mean absolute percent errors

The mean absolute percent error (MAPE) is a very popular measure of the accuracy of a predictive model or system. It represents the summed differences between the individual predicted versus observed values divided by the observed value; multiplying it by 100 makes it a percentage error. MAPE values were found to vary between 20 and 310 percent and were homogeneous across the seven fuel type groups. The distribution of model comparisons by MAPE classes were as follows:

- 30 percent or less (*n* = 7)
- 31 to 50 percent (*n* = 9)
- 51 to 75 percent (*n* = 26)
- 76 percent and greater (*n* = 7)

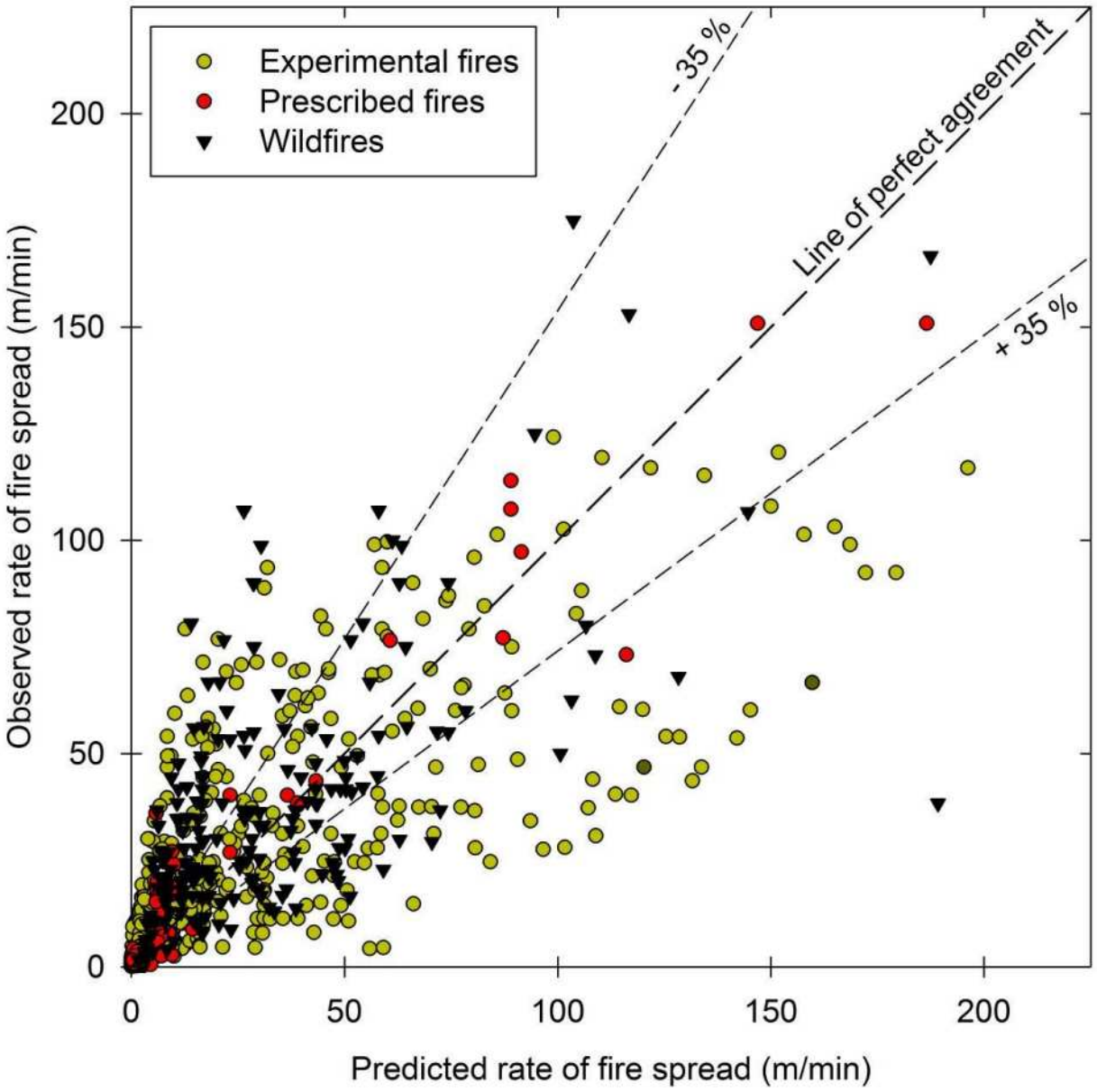

***Figure 2.** Observed rates of fire spread versus model predictions by type of data involved in the 1278 pairs garnered from the 49 comparison studies as compiled by Cruz and Alexander (2013). The two dashed lines around the line of perfect agreement indicate the ±35 percent error interval.*

The lowest errors (i.e., from 20 to 30 percent) were associated with seven studies involving experimental fires and prescribed fires where fuel and weather inputs would have been measured onsite. For comparisons dealing exclusively with wildfires, errors varied from 33 to 59 percent.

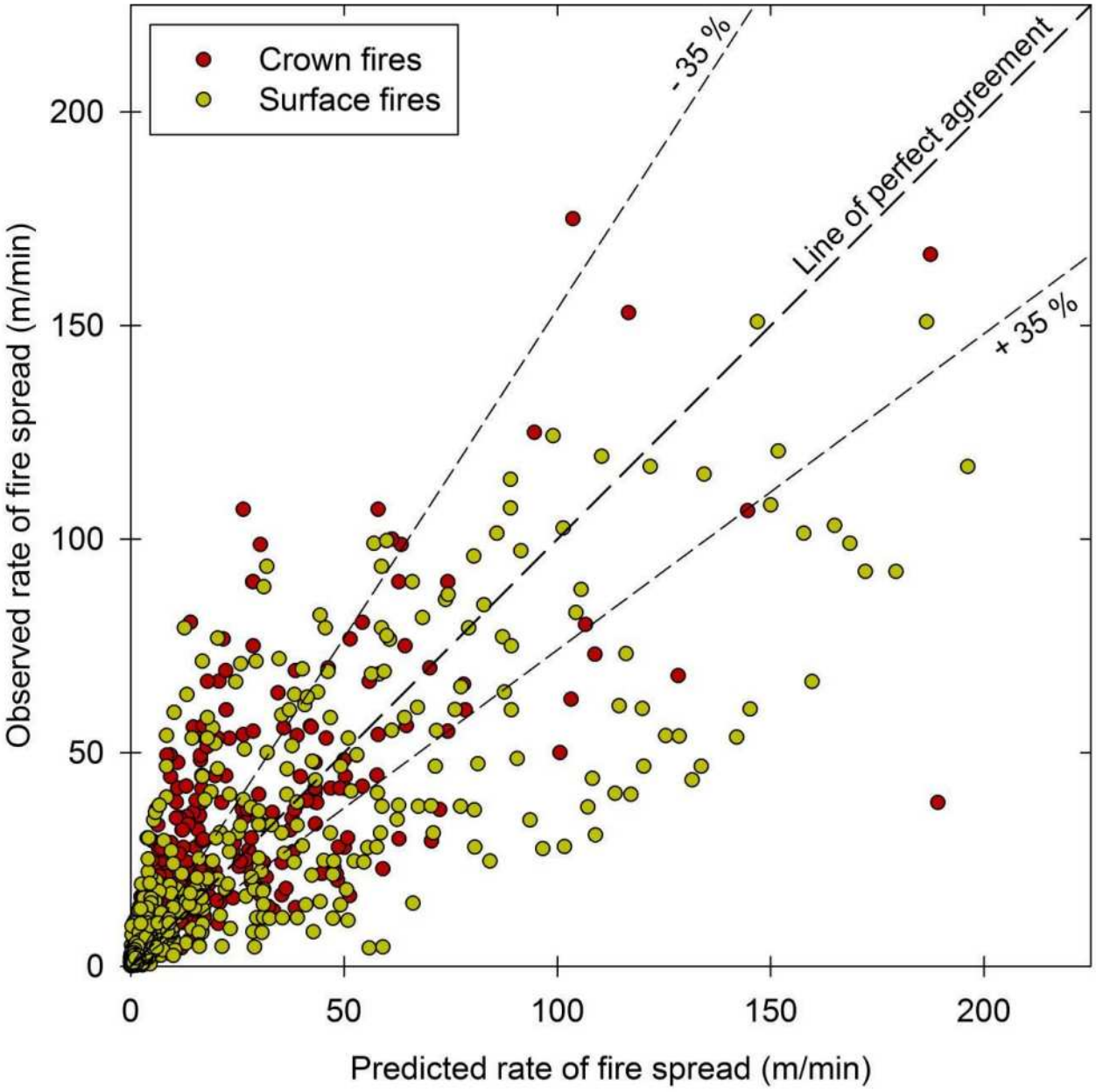

Figure 3. Observed rates of fire spread versus model predictions by type of fire involved in the 1278 pairs garnered from the 49 comparison studies as compiled by Cruz and Alexander (2013). The two dashed lines around the line of perfect agreement indicate the ±35 percent error interval.

Discussion

4.1. How accurately can one expect to predict the spread rate of wildland fires with currently available models?

No significant differences were found for under- and over-prediction errors by the type of data source (Figure 2). However, it was found that the rate of fire spread models examined under-prediction occurred in 818 of the 1278 model comparisons (i.e. 64 percent).

Although the range in rate of fire spread in the independent wildfire datasets was much higher than in the datasets used in model development, the model structure allowed for consistent predictions over the full range of observed fire behaviour. In most cases, under-prediction bias was small. There were,

however, combinations of model and fuel type that resulted in a predominant, if not total, under-prediction bias. This included, for example, Rothermel's (1972) surface fire rate of spread model in conifer forests and in logging slash, and both the Rothermel (1991) and Schaaf *et al.* (2007) crown fire rate of spread models.

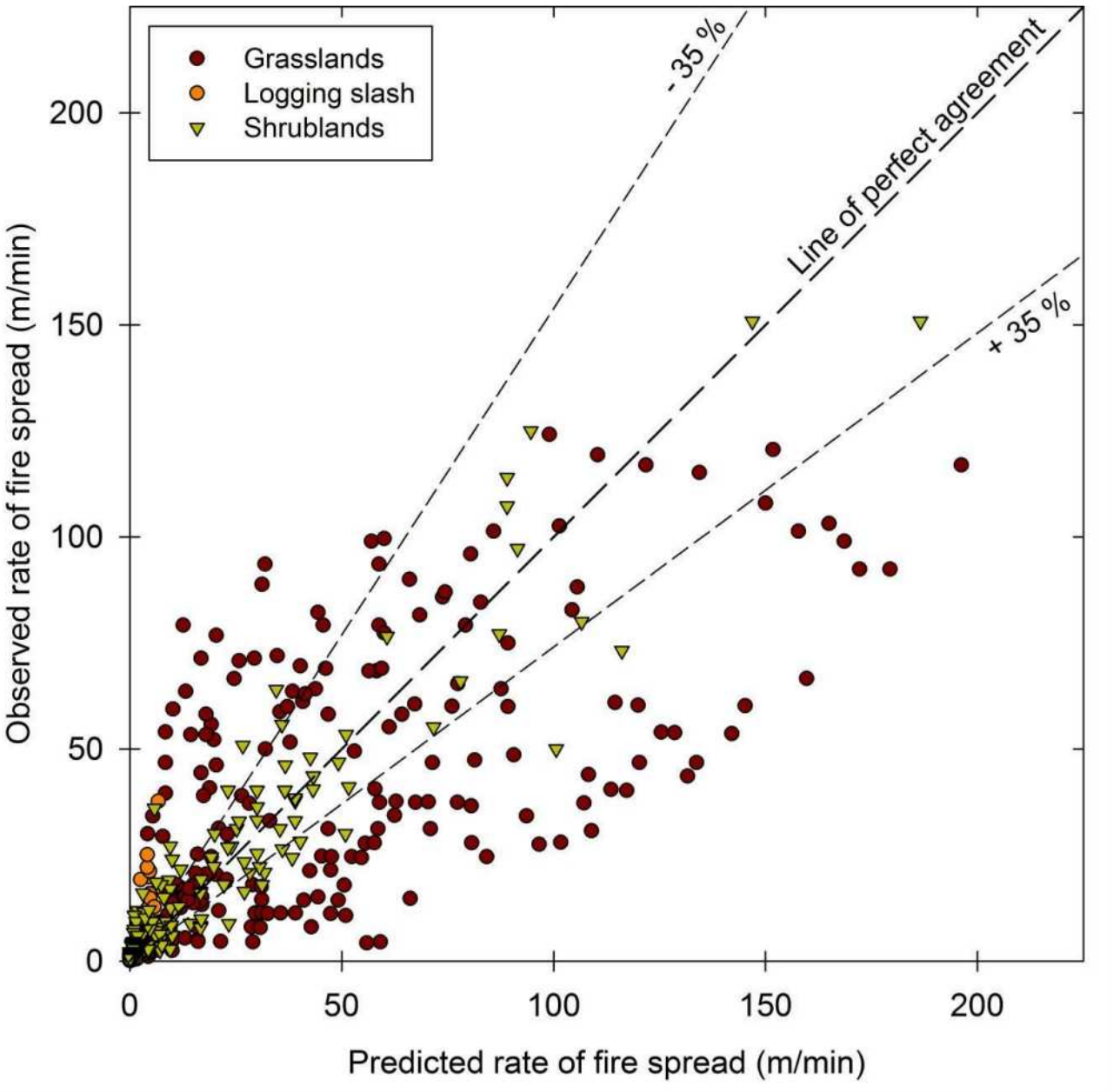

Figure 4. Observed rates of fire spread versus model predictions for non-canopied fuel types (grassland, shrubland and logging slash) involved in the 441 pairs garnered from the 17 comparison studies as compiled by Cruz and Alexander (2013). The two dashed lines around the line of perfect agreement indicate the ±35 percent error interval.

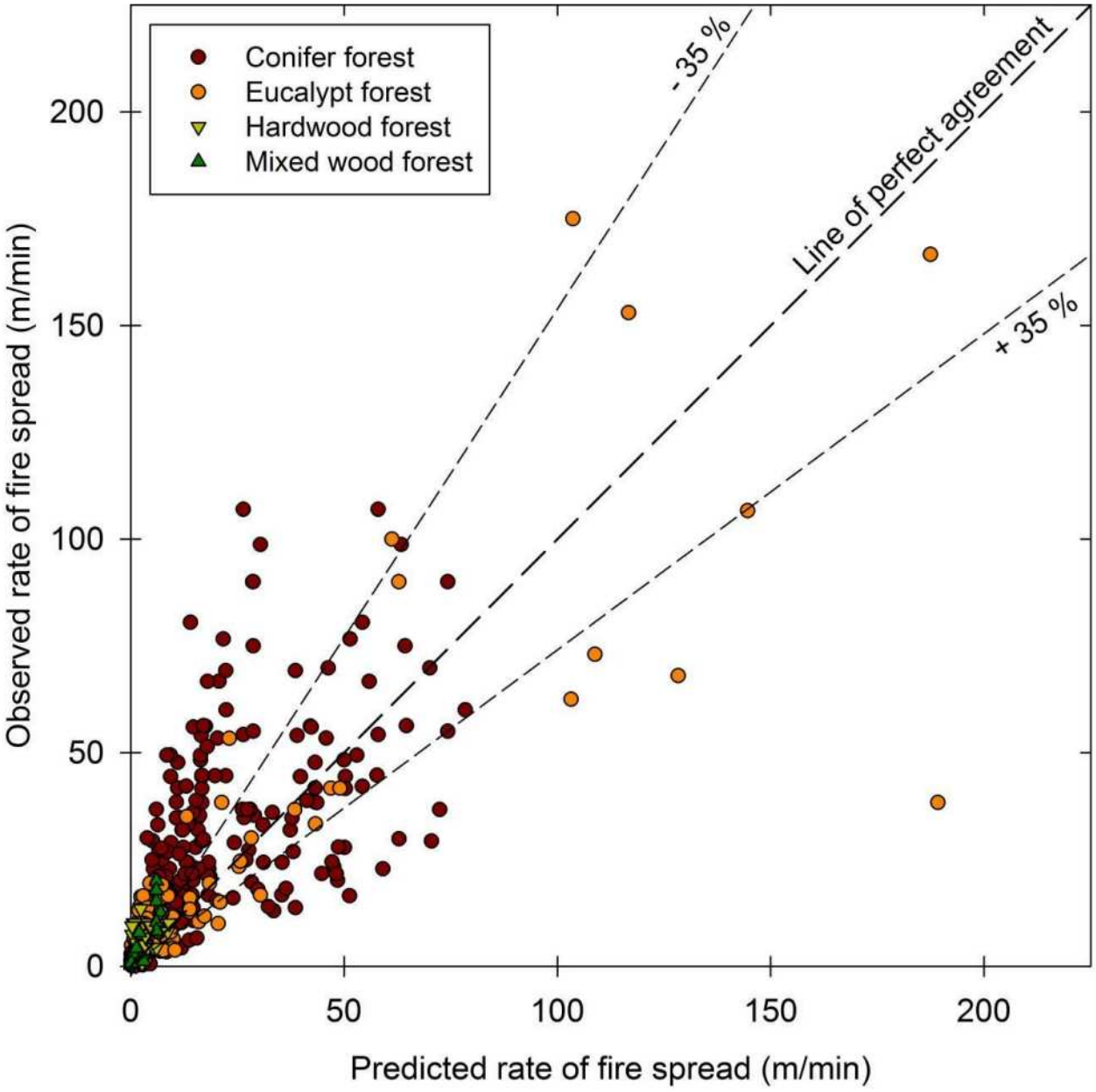

Figure 5. Observed rates of fire spread versus model predictions for forest canopied fuel types (hardwood forest, mixedwood forest, conifer forest and eucalypt forest) involved in the 837 pairs garnered from the 32 comparison studies as compiled by Cruz and Alexander (2013). The two dashed lines around the line of perfect agreement indicate the ±35 percent error interval.

4.2. Can models based on experimental fire data be used to predict wildfire behaviour?

Only two of the 13 rate of fire spread models considered in the study were separately evaluated against both experimental fire and wildfire datasets. This included the models developed by Cruz *et al.* (2005) and Cheney *et al.* (2012) where the MAPE values for the experimental fires where 26 and 35 percent, respectively. In turn, the Cruz *et al.* (2005) model yielded MAPE values of 46 and 52 percent for two separate wildfire datasets, while for the Cheney *et al.* (2012) model, the MAPE was 54 percent.

The increase in MAPE is expected given the uncertain nature of the exact environmental conditions associated with the wildfires. In these evaluations against wildfire data, both the Cruz *et al.* (2005) model, which is the basis for the *Crown Fire Initiation and Spread* (*CFIS*) system (Alexander *et al.*

2006), and the Cheney *et al.* (2012) model were extended well beyond the bounds of dead fuel moisture content, wind speed, and rate of fire spread used in their development. This implies that the underlying functional relationships in these models are valid for far drier and windier wildfire conditions than those involved in the model development, a conclusion that Fernandes (2014) has also recently shown to be valid.

4.3. Are wildfires inherently more difficult to predict the spread rates of than prescribed fires or crown fires compared to surface fires?

Examination of error statistics revealed no discernible difference in the ability to predict wildfire rates of spread from those associated with prescribed fires.

Some fire researchers have contended on the basis of the dynamic nature of crown fires that their behaviour is more unpredictable than that of surface fires (e.g. Cohen *et al.* 2006). However, according to the error statistics computed for surface and crown fires, there appears to be no differences, at least with respect to predicting rate of fire spread (Table 1). In fact, the highest MAPE values were obtained for surface fires rather than for crown fires.

4.4. How realistic is it to expect an exact prediction of rate of fire spread?

On the basis of the 49 studies and 1278 paired observations versus model predictions complied and analyzed, we found that the concept of an exact prediction of rate of fire spread to be an elusive one. Only three percent of the predictions (i.e. 35 out of 1278) were considered to be exact. It thus appears that the only certainty about rate of fire spread predictions is that it is extremely unlikely that a prediction will exactly match the observed fire spread rate.

4.5. What is an acceptable error for fire spread models?

McArthur (1977) considered that the fire danger meters he had developed for Australian grasslands and eucalypt forests could predict rate of fire spread and other fire behaviour characteristics to within ±20 percent of the actual observed value. Kilinc *et al.* (2013) have recently shown this assertion to have been quite optimistic.

From a statistical standpoint one might think that a ±1.0 standard deviation as a reasonable measure for an acceptable error. Assuming a normal distribution, such a quantity corresponds to a 34.1 percent departure from the mean. Richard C. Rothermel (USDA Forest Service retired, personal communication, 2012) was to remark to the authors that "I do like your suggestion of one standard deviation being used as a criteria for evaluating what can be expected in model prediction". This error threshold is also consistent with the average errors associated with several experimental field studies of fire behaviour.

According to the present study only two out of the 49 model performance studies (i.e. 4 percent) had a MAPE of 20 percent and no study had any less of a value. Eight of the 49 model comparisons (i.e. 17 percent) had a MAPE equal to or less than 35 percent suggesting that this could constitute a realistic benchmark by which to judge good model performance when accurate input data is available. On the basis of this outcome and the aforementioned considerations, it would appear that a ±35 percent error would constitute a reasonable and conservative standard for fire spread rate model performance.

Of course a ±35 percent error benchmark is only deemed applicable to research studies. In operational practice, given the uncertainty in the estimation of the input data, often times involving large spatial (e.g. >1000 ha) and temporal (i.e. from one to several hours) scales, would understandably, result in wider error intervals.

Conclusions

A comprehensive survey of the error statistics associated with evaluation studies of rate of fire spread models was undertaken by Cruz and Alexander (2013) in order to gauge the general predictive ability

of such models. This has led to new insights into some of the uncertainties associated with model predictions of free-burning wildland fire behaviour. This survey has also accordingly highlighted the importance of model evaluation (Cruz *et al.* 2003) based on independent datasets and encouraged others to do so (e.g. Anderson *et al.* 2014 in review).

It is worth noting that our evaluation study focused on models of forward or head fire rate of spread (i.e. in one dimension). More recent studies evaluating spatially explicit fire propagation models have relied on a distinct number of metrics to quantify the error associated with wildland fire growth simulations (e.g. Filippi *et al*. 2014a,b). These were not considered in our analysis as the spatial outputs are only partially dependent on the fire spread rate.

Acknowledgment

This paper is a contribution of Joint Fire Science Program Project JFSP 09-S-03-1.

References

Ablini FA, Stocks BJ (1986) Predicted and observed rates of spread of crown fires in immature jack pine. *Combustion Science and Technology* **48**, 65-76.

Alexander ME, Cruz MG (2006) Evaluating a model for predicting active crown fire rate of spread using wildfire observations. *Canadian Journal of Forest Research* **36**, 3015-3028.

Alexander ME, Cruz, MG (2013a) Are the applications of wildland fire behaviour models getting ahead of their evaluation again? *Environmental Modelling & Software* **41**, 65-71.

Alexander ME, Cruz MG (2013b) Limitations on the accuracy of model predictions of wildland fire behaviour: a state-of-the-knowledge overview. *Forestry Chronicle* **89**, 370-381.

Alexander ME, Cruz MG, Lopes AMG (2006) *CFIS*: a software tool for simulating crown fire initiation and spread. In 'Proceedings of 5th International Conference on Forest Fire Research', 27–30 November 2006, Figueira da Foz, Portugal. (Ed. DX Viegas) (CD-ROM) (Elsevier BV: Amsterdam, the Netherlands)

Alexander ME, Heathcott MJ, Schwanke RL (2013) 'Fire behaviour case study of two early winter grass fires in southern Alberta, 27 November 2011.' (Partners in Protection Association: Edmonton, AB)

Alexander ME, Stocks BJ, Lawson BD (1991) Fire behavior in black spruce-lichen woodland: the Porter Lake Project. Forestry Canada, Northern Forestry Centre, Information Report NOR-X-310. (Edmonton, AB)

Anderson WR, Cruz MG, Fernandes PM, McCaw L, Vega JA, Bradstock RA, Fogarty L, Gould J, McCarthy G, Marsden-Smedley JB, Matthews S, Mattingley G, Pearce G, van Wilgen BW (2014) A model for predicting fire spread in shrublands. In review.

Beavers AM (2001) Creation and validation of a custom fuel model representing mature *Panicum maximum* (Guinea grass). Colorado State University, The Center for Environmental Management of Military Lands, CEMMIL TPS 01-12. (Fort Collins, CO)

Brown JK (1982) Fuel and fire behavior in big sagebrush. USDA Forest Service, Intermountain Forest and Range Experiment Station General Technical Report INT-290. (Ogden, UT)

Cheney NP, Gould JS, McCaw WL, Anderson WR (2012) Predicting fire behaviour in dry eucalypt forest in southern Australia. *Forest Ecology and Management* **280**, 120-131.

Cohen JD, Finney MA, Yedinak KM (2006) Active spreading crown fire characteristics: implications for modeling. In 'Proceedings of 5th International Conference on Forest Fire Research', 27–30 November 2006, Figueira da Foz, Portugal. (Ed. DX Viegas) (CD-ROM) (Elsevier BV: Amsterdam, the Netherlands)

Cruz MG, Alexander ME (2013) Uncertainty associated with model predictions of surface and crown fire rates of spread. *Environmental Modelling & Software* **47**, 16-28.

Cruz MG, Alexander ME, Wakimoto RH (2003) Definition of a fire behavior model evaluation protocol: a case study application to crown fire behavior models. In 'Fire, Fuel Treatments and Ecological Restoration: Conference Proceedings', 16-18 April 2002, Fort Collins, CO. (Tech Eds PN Omi, JA Joyce) USDA Forest Service, Rocky Mountain Research Station, Proceedings RMRS-P-29, pp 49-67. (Fort Collins, CO)

Cruz MG, Alexander ME, Wakimoto RH (2005) Development and testing of models for predicting crown fire rate of spread in conifer forest stands. *Canadian Journal of Forest Research* **35**, 1626-1639.

Cruz MG, Sullivan AL, Alexander ME (2014a) Fire behaviour knowledge in Australia: Knowledge gaps and Fire Behaviour Analyst (FBAN) training revision plan. CSIRO Ecosystems Sciences and CSIRO Digital Productivity and Services Flagship, Client Report No. EP145697. (Canberra, ACT)

Cruz MG, Sullivan AL, Leonard R, Malkin S, Matthews S, Gould JS, McCaw WL, Alexander ME (2014b) Fire behaviour knowledge in Australia: a synthesis of disciplinary and stakeholder knowledge on fire spread prediction capability and application. CSIRO Ecosystems Sciences and CSIRO Digital Productivity and Services Flagship, Client Report No. EP145189. (Canberra, ACT)

Davis KM (1976) Behaviour and effects of fire during mild weather. CSIRO Division of Forest Research, Internal Report No. 3. (Canberra, ACT)

Everson TM, Smith FR, Everson CS (1985) Characteristics of fire behaviour in the montane grasslands of Natal. *Journal of the Grassland Society of Southern Africa* **2**(3), 13-21.

Fernandes PM (2014) Upscaling the estimation of surface-fire rate of spread in maritime pine (*Pinus pinaster* Ait.) forest. iForest **7**, 123-125.

Filippi J-B, Mallet V, Nader B (2014a) Representation and evaluation of wildfire propagation simulations. *International Journal of Wildland Fire* **23**, 46-57.

Filippi J-B, Mallet V, Nader B (2014b) Evaluation of forest fire models on a large observation database. *Natural Hazards and Earth System Sciences Discussion* **2**, 3219–3249.

Fogarty LG, Jackson AF, Lindsay WT (1997) Fie behaviour, suppression and lessons from the Berwick Forest Fire of 26 November 1995. New Zealand Forest Research Institute, FRI Bulletin No. 197, Forest and Rural Scientific and Technical Series Report No. 3. (Rotorua, New Zealand)

Hufford GL, Kelley HL, Sparkman W (1998) Use of real-time multisatellite and radar data to support forest fire management. *Weather Forecasting* **13**, 592-605.

Junpen A, Garivaita S, Bonneta S, Pongpullponsakc A (2013) Fire spread prediction for deciduous forest fires in northern Thailand. *ScienceAsia* **39**, 535–545

Kilinc M, Anderson W, Price B, McCaw L (2013) Testing the performance of Australian grassland and forest fire spread models. Research poster presented at 10th Annual Bushfire Cooperative Research Centre Conference, Melbourne, Victoria, 2 September 2013. Available at: http://www.bushfirecrc.com/sites/default/files/managed/resource/72_depi_musa_kilinc.pdf

McArthur AG (1977) Fire danger rating systems. Food and Agriculture Organization of United Nations, FAO Document FO: FFM/77/3-01. (Rome, Italy)

Menage D, Chetehouna K, Mell WE (2012) Numerical simulations of fire spread in a *Pinus pinaster* needles fuel bed. In '6th European Thermal Sciences Conference', 4–7 September 2012, Poitiers, France. (Eds D Petit, NC Le) (Société française de thermique: Paris)

Neuenschwander LF (1980) Broadcast burning of sagebrush in the winter. *Journal of Range Management* **33**, 233-236.

Pickford S, Suharti M, Wibowo A (1992) A note on fuelbeds and fire behavior in Alang-alang (*Imperata clylindrica*). *International Journal of Wildland Fire* **2**, 41-46.

Rothermel RC (1972) A mathematical model for predicting fire spread in wildland fuels. USDA Forest Service, Intermountain Forest and Range Experiment Station, Research Paper INT-115. (Ogden, UT)

Rothermel RC (1991) Predicting behavior and size of crown fires in the Northern Rocky Mountains. USDA Forest Service, Intermountain Research Station, Research Paper INT-438. (Ogden, UT)

Sapsis DB, Kauffman JB (1991) Fuel consumption and fire behaviour associated with prescribed fire in sagebrush ecosystems. *Northwest Science* **65**, 173-179.

Schaaf MD, Sandberg DV, Schreuder MD, Riccardi CL (2007) A conceptual framework for ranking crown fire potential in wildland fuelbeds. *Canadian Journal of Forest Research* **37**, 2464-2478.

Schimmel J, Granström A (1997) Fuel succession and fire behaviour in the Swedish boreal forest. *Canadian Journal of Forest Research* **27**, 1207-1216.

Scott AC, Bowman DMJS, Bond WJ, Pyne SJ, Alexander ME (2014) 'Fire on Earth: An Introduction'. (Wiley-Blackwell: Chichester)

Stocks BJ, Alexander ME, Wotton BM, Stefner CN, Flannigan MD, Taylor SW, Lavoie N, Mason JA, Hartley GR, Maffey ME, Dalrymple GN, Blake TW, Cruz MG, Lanoville RA (2004) Crown fire behaviour in a northern jack pine – black spruce forest. *Canadian Journal of Forest Research* **34**, 1548-1560.

Van Wagner CE (1977) Conditions for the start and spread of crown fire. *Canadian Journal of Forest* Research **7**, 23-34.

Van Wagner CE (1985) Fire behavior modelling – how to blend art and science. In 'Proceedings of the Eighth Conference on Fire and Forest Meteorology', 29 April-2 May 1985, Detroit, MI. (Eds LR Donoghue, RE Martin) Society of American Foresters, SAF Publication 85-04, pp. 3-5. (Bethesda, MD)

Weise DR, Biging GS (1997) A qualitative comparison of fire spread models incorporating wind and slope effects. *Forest Science* **43**, 170-180.

Weise DR, Fujioka FM (1998) Comparison of fire spread estimates using weather station observations versus nested spectral model gridded weather. In 'Preprint Volume of the Second Symposium on Fire and Forest Meteorology', 11-16 January 1998, Phoenix, AZ. pp. 75-79. (American Meteorological Society: Boston, MA)

Willmott CJ (1982) Some comments on the evaluation of model performance. *Bulletin of American Meteorological Society* **63**, 1309-1313.

Woodall CA (1998) Prescribed fire behavior and custom fuel modeling in the pitch pine-scrub oak barrens and pine-oak forests of New England. University of Massachusetts, Department of Forestry and Wildlife Management, Course FOREST 698 Report. (Amherst, MA) Available at: http://www.umass.edu/nebarrensfuels/publications/pdfs/claiborne_woodall.pdf

Unsteady phenomena affecting the propagation of surface fires

Dominique Morvan

Laboratoire de Mécanique, Modélisation et Procédés Propres (M2P2)
UMR 7340 CNRS, Aix-Marseille Université, Ecole Centrale de Marseille
UNIMECA 60 rue Joliot Curie, Technopôle de Château Gombert
13453 Marseille cedex 13 France dominique.morvan@univ-amu.fr

Abstract
The unsteadiness coming from thermo-convective and shear instabilities or from the time variations of the external conditions affecting the fire (wind gusts for example), affecting the propagation of a surface fire, has been studied numerically using a multiphase approach. Two regimes of propagation (plume dominated and plume driven) have been identified, governed by two forces: the buoyancy resulting from the density gradient inside and outside the plume and the inertia of the wind. The degree of non-linearity associated with these two physical mechanisms, can explain the magnitude of unsteadiness of the fire behaviour. It participates also of the impact (sometimes linear and sometimes strongly non-linear) of the impact of wind conditions upon the fire spread. For weak wind conditions (exhibiting potentially a more non linear behaviour), a sinusoidal time variation of the wind speed has been tested with five frequencies (0.25, 0.5, 1, 2 and 3 Hz) nearly equal to the frequency (1.4 Hz) characterizing the thermo-convective instability (in assimilating the fire front as a pool fire) and to the shear instability (0.26 Hz).

Keywords*: surface fire, multiphase model, wind/fire interaction*

Introduction

With ambient temperature and relative air humidity, the wind is certainly one of the most important weather parameter affecting the conditions of ignition and propagation of wildland fires. Various experimental studies carried out at small scale in a wind tunnel and at large scale on the field, have highlighted a power law relationship ($ROS \sim U_W^B$) between the rate of spread (ROS) of a surface fire and the wind velocity (U_W) [1, 2, 3, 4, 5]. The fact that the wind's exponent B varies from 0.4 [3] to 2 [5], shows that this relationship is not fully understood. Direct observations of fires in grassland [6], have highlighted that the curve representing the relation ROS versus U_W can be decomposed in three zones: a linear zone (wind's exponent B nearly equal to one), bounded by two non-linear zones for weak (B>1) and strong (B<1) wind conditions. Because experimental fires must be conducted in safe conditions, the range of variations of wind conditions cannot be extended sufficiently, to observe in all cases, these changes of fire behaviour. Numerical simulations performed in shrubland, which are not submitted to the same constraints, have been able to reproduce this kind of behaviour [7]. Analysis of experimental results obtained in a fire wind-tunnel [8], seem indicating that sudden changes of slope in the curve ROS vs U_W can be attributed to a change in the main mode of heat transfer (by convection and radiation) between the flame and the solid fuel layer. It is well known that the relative importance between these two mechanisms of heat transfer, is strongly affected by the view angle between the flame and the unburned fuel and consequently by the trajectory of the flame (more or less vertical). This trajectory is affected by two forces along two directions: vertically the buoyancy and horizontally the inertial force of the wind. The relative importance of these two forces can be evaluated from a non dimensional parameter, the Byram's convective number [9]:

$$N_C = \frac{2gI_B}{\rho C_P T_0 \left(U_W - ROS\right)^3} \quad \text{(Eq.1)}$$

where g is the acceleration of gravitation, I_B is the fireline intensity, ρ , C_P , and T_0 are the density, the specific heat and the temperature of the ambient air.
From the value taken by this similitude parameter, two great regimes of fire propagation have been identified:

- For $N_C >> 1$, the plume dominated fires, characterized by a flame trajectory more or less vertical, a general trend of the air flow (near the fire) to be symmetrically aspirated by the fire front,
- For $N_C << 1$, the wind driven fires, characterized by a flame horizontally sheared by the wind flow, pushing hot gases toward the vegetation layer located ahead of the fire front,

The propagation of surface fires can be affected by unsteady phenomena coming from the fire itself (internal fluctuations of the fire intensity) and from variations of external parameters such as time variations of the wind velocity (gusts). Depending of the fire propagation regime (plume dominated or wind driven) the consequences for the forecasting of fire behaviour are more or less significant. Previous experimental observations have shown that the relationship between the fire rate of spread and the wind velocity was not as straightforward (as a monotonous curve) in all wind conditions [10, 11].
It is in this general context, that the present study has been conducted, in focussing our attention on the effects of these two sources of unsteadiness upon the behaviour of a surface fire in propagation through a homogeneous fuel layer representative of grassland.

The study was based on numerical simulations, in using a multiphase formulation, details of the physical and numerical models can be found in previously published articles [7, 9, 12, 13].

In the first part of the paper, unsteady signals of fireline intensity have been analyzed for various quasi steady wind conditions (U_W) ranged between 1 and 25 m/s (10m open wind velocity). With these values, the simulations covered a large range of conditions of propagation from plume dominated to wind driven fires (N_C ranged nearly between 0.1 and 1000). Then the effects of a sinusoidal time variation of the wind flow (representing wind gusts) have been explored for relatively moderated wind conditions (U_W=2 m/s , ΔU_W= +/- 1 m/s). In this case, four frequencies were tested 0.25, 0.5, 1, 2 and 3 Hz.

Physical multiphase model

The numerical simulation of the behaviour of wildland fires is very challenging and can be qualified as a complex multi-scale and multi-physics problem. The main difficulty results from the wide spectral band of length scales, associated to physical mechanisms governing the fire behaviour (atmospheric turbulence, combustion, pyrolysis, radiation heat transfer …) which are for most of them non-linear. Even if we limit the description of the problem to the immediate neighbourhood of the fire front, a large range of spatial scales are concerned: the turbulent integral length scale of the boundary layer flow above the canopy (more or less equal to the height of the canopy, 0.7 m here), the corresponding Kolmogorov micro-scale (< 1 mm), the length of extinction characterizing the vegetation layer (0.5 m here), the flame thickness (~ 500 □m for a hydrocarbon flame) [9]. Of course, it is impossible to explicitly take into account all these length scales, the effects of the smallest ones (Kolmogorov micro-scale and flame thickness) must be reproduced using physical models [15]. In the same order of idea, it is impossible to reproduce with all details, the structure of the vegetation layer. In place of representing in details all the elements constituting the vegetation (foliage, twigs, trunk), an averaging procedure has been introduced which consists in representing the vegetation as an equivalent sparse porous media. This approach can be assimilated as a sort of homogenization step, is often referenced in the literature as a multiphase formulation of forest fire modelling [7, 12, 14]. The main advantage of this formulation is the possibility of taking into account all the terms of interaction between the gas

phase and the vegetation, without the necessity of representing in detail the very complex interface (fractal) between these two phases. The numerical simulations (2D) have been carried out in a computational domain, 170 m long and 35 m high, inside which a 150 m long and 0.7 m high homogeneous vegetation layer has been positioned (see Figure 1). The inlet wind flow has been reproduced with a logarithmic velocity profile (Eq. 2) at the left end side of the domain (the constant A was adjusted to ensure a known value of the wind velocity 10 m above the ground level), z0 = 0.01 m corresponding to a nude soil. A 20 m long nude zone (without any vegetation) has been built near the entrance, to ensure the establishment of the boundary layer flow (see Figure 1).

$$U_X(z) = A \times U_{10} \times Ln\left(\frac{z + z_0}{z_0}\right) \qquad \text{(Eq.2)}$$

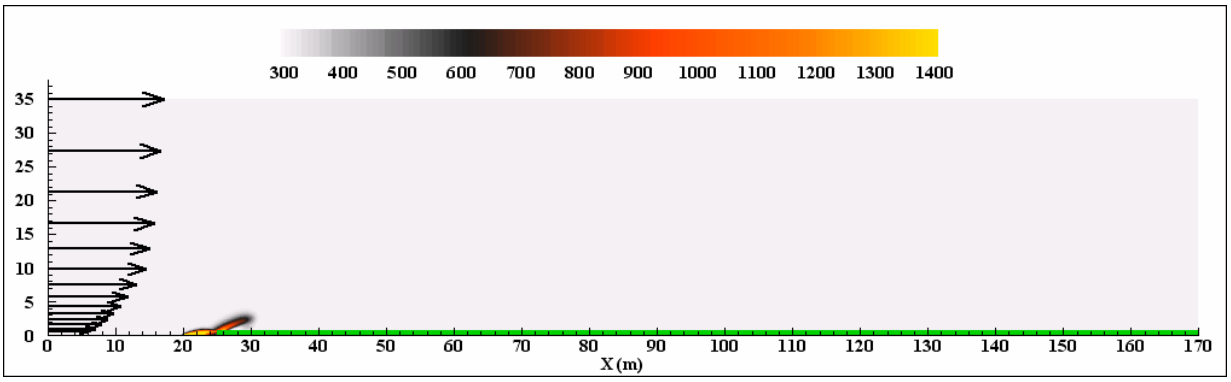

Figure 1. Computational domain and boundary conditions.

The vegetation layer (here a homogeneous grass) has been represented using the set of physical properties from data collected on the field [16]. To guarantee an optimal accuracy, the simulations have been performed using a dynamic adaptive mesh attached to the fire front (positioned from the first pick of temperature inside the vegetation). The size of the grid mesh in the vicinity of the fire front, has been adjusted to guarantee that the radiation heat transfer and the turbulent flow inside the vegetation were correctly reproduced [9, 17].

Table 1. Solid fuel physical properties and external conditions imposed in the present numerical simulations (Anderson 1982).

Solid fuel density (kg/m^3)	500
Volume fraction x 10^3	2
Fuel moisture content (FMC) (%)	10
Fuel depth (m)	0.7
Fuel load (t/ha)	7
Surface area to volume ratio (m^{-1})	4000
Length of extinction (m)	0.5
Leaf Area Index (LAI)	2.8
10m open wind velocity (m/s)	1-25

Plume dominated fires are supposed to be mainly governed by the buoyancy force resulting from the difference of density between the external atmosphere and the hot gases inside the thermal plume. For this reason, the behaviour of this kind of fire must present some similarities with pool fire. It is well known that the dynamic of pool fires is governed by thermal-convective instabilities, marked by vertical oscillations of the flame height and of the heat release rate, with a frequency f_B related to the acceleration of gravity (g) and the diameter (D_{Fire}) of the pool fire as following:

$$f_B = (0.5 \pm 0.04)\left(\frac{g}{D_{Fire}}\right)^{1/2} \qquad \text{(Eq.3)}$$

Wind driven fires are more affected by the inertia force of the wind, a consequence of that is that the dynamics of the fire can potentially be affected by the shear layer instability (Kelvin-Helmholtz) resulting from the rapid deceleration of the external flow due to the presence of the vegetation. For this reason, we have also introduced in our analysis the characteristics frequency f_{KH} associated with this instability along the steamwise direction:

$$f_{KH} = \frac{0.15 \times U_H}{H} \qquad \text{(Eq.4)}$$

where U_H is the wind velocity at the top (Z = H) of the canopy.
Because the behaviour of surface fires can be affected by these two forces (the buoyancy and the inertia of the wind), we have compared the frequencies extracted from the fast Fourier transform (FFT) analysis of the fire intensity signals with these two characteristics frequencies.

Results and discussion

A first set of numerical simulations has been performed for a large range of wind velocity (from 1 to 25 m/s) in order to cover both, plume dominated and wind driven fires. The results shown in Figure 2 is a good illustration of the difference of interaction between the fire front and the surrounding atmosphere, for weak (UW = 1 m/s) and strong (UW = 20 m/s) wind conditions. For weak wind conditions, the trajectory of the flame was nearly vertical, promoting the development of a vertical thermal plume forming an obstacle for the incoming wind which was not able to cross the fire front (the same tendency has also been observed in 3D for the same wind conditions [21]). The burning zone was fed in fresh air symmetrically on both side of the fire front (see Figure 2 on top).

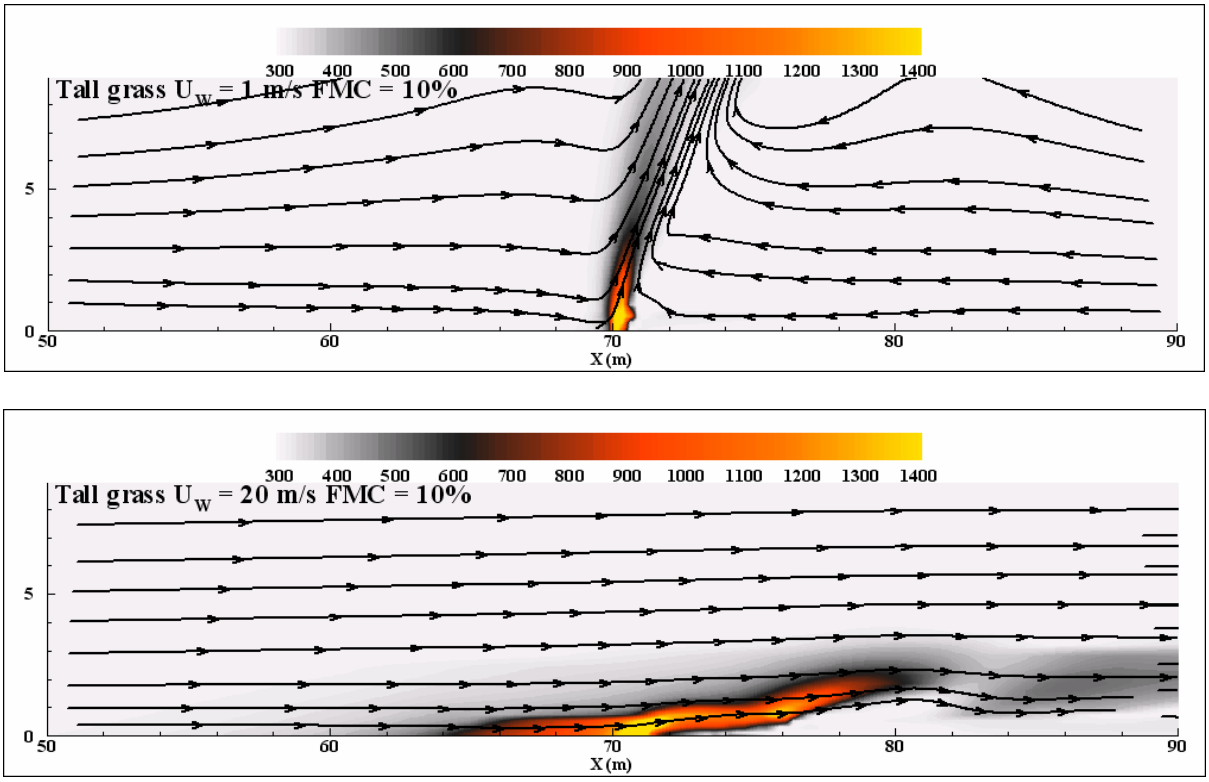

Figure 2. Snapshot of the temperature field and gas flow (streamlines) calculated for two values of the wind velocity: UW = 1 and 20 m/s.

We must underline that 2D simulations contribute to enforce this behaviour (in 3D the formation of peaks and troughs along the fire front [8], allowed to reduce the role of barrier played by the fire front). For strong wind conditions, the trajectory of the flame was significantly deviated by the wind flow (see Figure 2 on bottom) and the incoming wind flow was able to cross the fire front, contributing to transport hot gases from the burning zone toward the vegetation layer. As shown in Table 2, the action of the wind flow upon the fire behaviour (in terms of rate of spread and fire intensity) cannot be reduced to a monotonic curve, confirming the existence of multiple regimes of propagation. This kind of non linear interaction between wind and fire has already be observed experimentally and reported in the literature [10, 11, 12]. The signals of fire intensity obtained for the same wind conditions (UW = 1 m/s and 20 m/s) are shown in Figure 3 (see also Table 2).
Between 1 and 20 m/s, the rate of spread and the fire intensity, has increased by a factor 2.8 and 2.6 respectively. An other interesting information extracted from these fire intensity signals, is the ratio between the standard deviation and the average value, which decreased from 0.28 to 0.18 (as the wind speed increases from 1 to 20 m/s). This trend was confirmed for the whole range of variation of the wind speed (see Figure 4), indicating that the relative level of unsteadiness of the fire behaviour was more pronounced for plume dominated fires than for wind driven fires. The same kind non-linear effect has already been observed experimentally [6] and numerically [7] for the relationship linked the rate of spread and the wind velocity. It is already known that the behaviour of plume dominated fires is more difficult to predict compared to fires piloted by a strong wind.

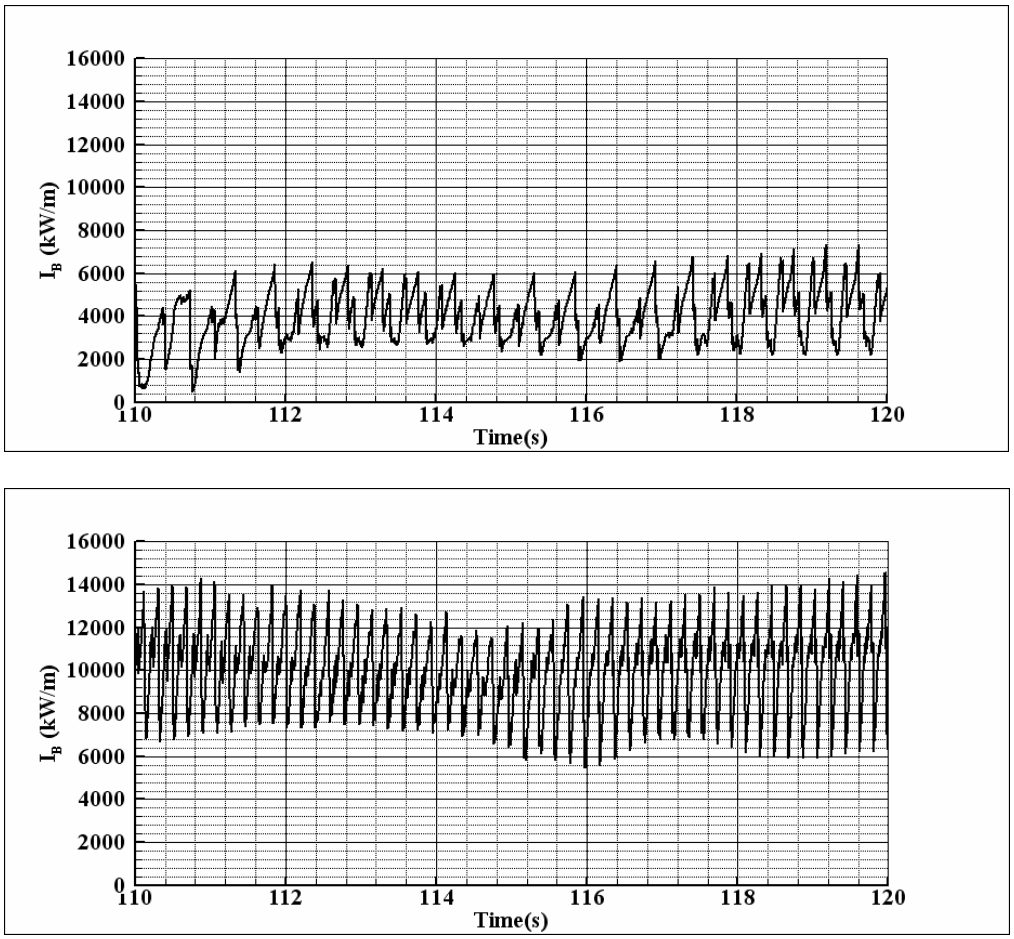

Figure 3. Time history of fireline intensity for two values of wind velocity: UW = 1 (top) and 20 m/s (bottom).

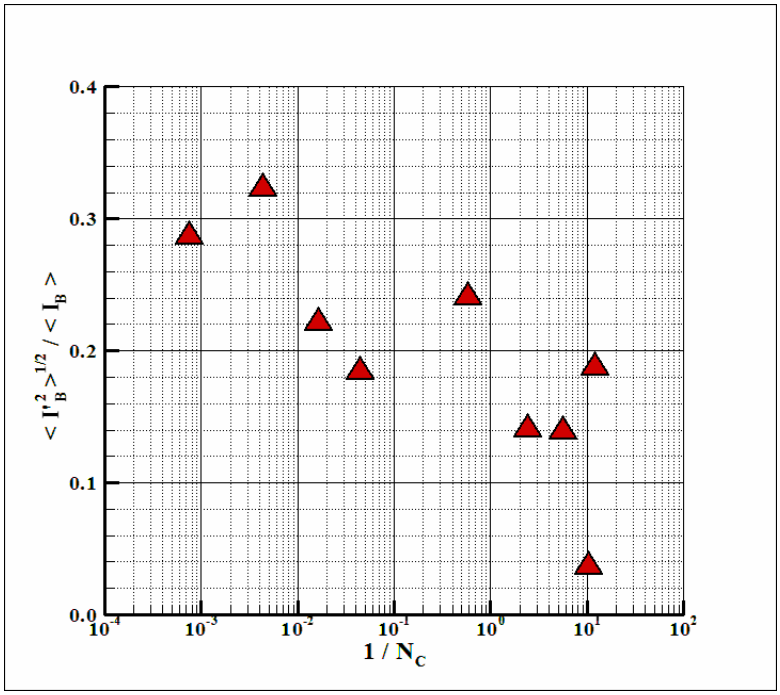

Figure 4. Ratio standard deviation / mean value of the fireline intensity as a function of the convective Byram number.

This difference of behaviour versus the wind velocity, results mainly from the dominant mechanism of heat transfer between the flame and the vegetation. If the radiation heat transfer plays a major role in the propagation of the fire, because this physical mechanism is intrinsically more non-linear compared to convection heat transfer (because of the σT4 of the Stefan-Boltzmann law), it is not surprising that this kind of surface fire can exhibited less predictable sudden changes [12].

Fast Fourier transform (FFT) of the fire intensity signal (see an example in Figure 5) has allowed identifying the energy distribution on a frequency domain. As shown in Figure 5, for UW = 1 m/s, the major contribution (maximum level of energy) was associated to a σto the frequency characterizing the buoyancy instability (1.6 Hz) compared to the Kelvin-Helmholtz instability (0.1 Hz).

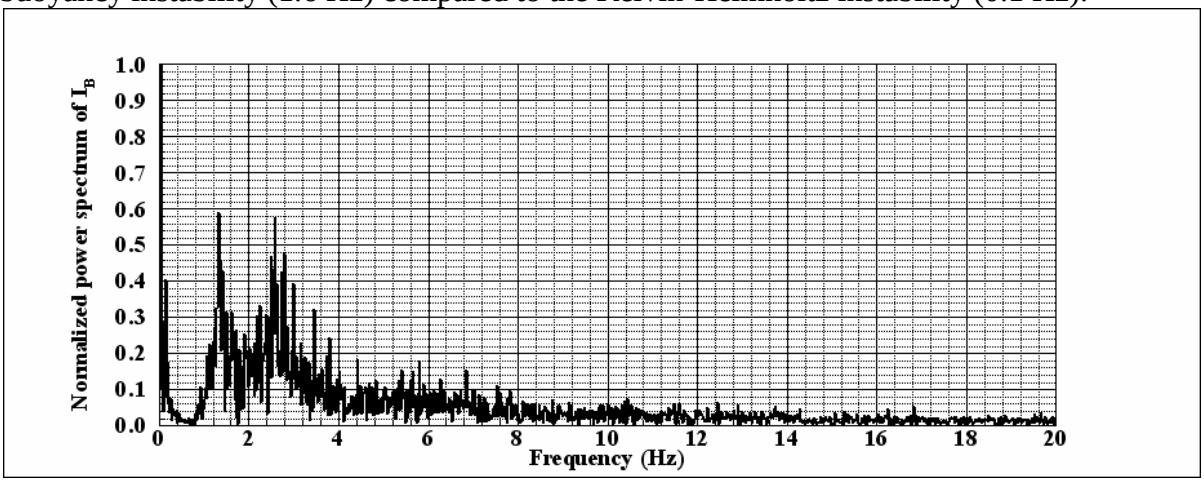

Figure 5. FFT analysis of fireline intensity signal obtained for U_W = 1 m/s.

In analysing the data in Table 2 and considering that the wind velocity promoted an increase of the depth of the fire front (see Figure 2), consequently its effect upon the two frequencies associated to the two forces (buoyancy and inertia) were symmetrically opposed: it decreased for the first one, and it increased for the second one. Considering that the situation observed during the propagation of a

surface fire differed from the two simplified models used for the analysis in frequencies (steady pool fire and boundary layer canopy interaction), we can still conclude that, as the behaviour of the fire moved from plume dominated fire to wind driven fire, the instability governing the fire intensity signal, changed from a thermal-convective type instability to a shear type instability.
In order to study the response of a surface fire in propagation, we have performed a second set of simulations, in adding a sinusoidal variation, in order to reproduce schematically wind gusts.

$$U_X(z) = A \times U_W \times Ln\left(\frac{z + z_0}{z_0}\right) + \Delta U_W \sin(2\pi \times F \times t)$$

where ΔU_W and F are respectively the amplitude and the frequency of wind variations. The present study has been limited to one wind conditions U_W = 2 m/s and ΔU_W = 1 m/s (the wind speed varied between 1 and 3 m/s), the frequency F varied between 0.25 and 3 Hz. This wind condition (U_W = 2 m/s) has been chosen because it represented a situation for which we have found (in quasi steady wind conditions) a relatively high value of the variation of the rate of spread (*ROS*) versus U_W (see Table 2).

Table 2. Wind speed, Rate of spread, Fire intensity (average value, standard deviation, frequency), Thermal-convective and Kelvin-Helmholtz frequencies.

UW (m/s)	1	2	3	4	8	12	15	20	25
ROS (m/s)	0.46	0.84	1.06	1.18	1.24	1.23	1.10	1.28	2.51
IB (kW/m)	3798	6468	8179	9155	9604	9331	8602	9913	20098
<I'B2>1/2 (kW/m)	1088	2090	1806	1683	2313	1311	1191	1856	738
f (Hz)	2.3	3.4	4.2	4.8	5.0	5.0	5.5	5.5	5.5
fB (Hz)	1.6	1.4	1.2	1.1	0.9	0.8	0.7	0.6	0.5
fKH (Hz)	0.1	0.2	0.4	0.5	3.2	1.1	1.6	2.0	2.6

The curve shown in Figure 6 is the time evolution of the fire intensity obtained with a sinusoidal variation at a frequency of 0.25 Hz, in comparison we have also added the result obtained in quasi-steady wind conditions.

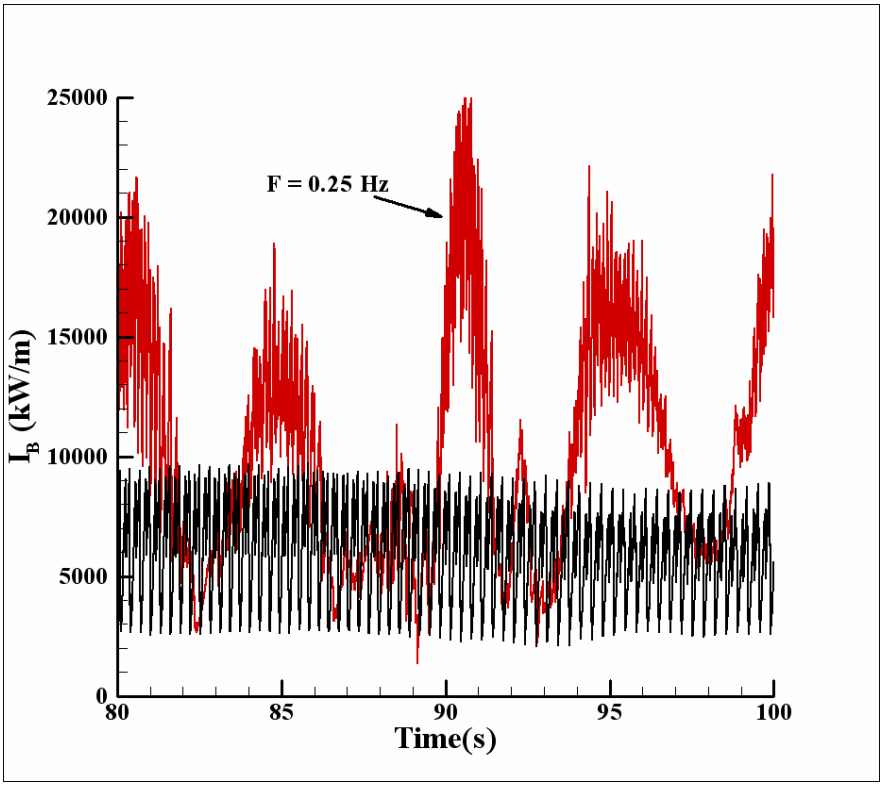

Figure 6 –Time evolution of the fireline intensity obtained for U_W = 2 m/s with and without a sinusoidal variation (F = 0.25 Hz).

This is for this frequency (0.25 Hz), nearly equal to the frequency characterizing the Kelvin-Helmholtz instability (see Table 2) that we have obtained the maximum effect. We can notice that this relatively small change in wind conditions, has promoted a huge modification of the behaviour of the fire. While the maximum value observed in quasi-steady state varied from 7000 to 12000 kW/m, for a wind velocity ranging between 1 and 3 m/s, the same value has increased up to 20000-25000 kW/m (the fire intensity signal was modulated with a sinusoid at frequency of 0.21 Hz) in simply adding an unsteady variation. We have also noticed that this sort of resonance mechanism decreased rapidly as the excitation frequency exceeded this critical value, the maximum fire intensity observed with a frequency F = 0.5 Hz reached 18000 kW/m and decreased to 10000 kW/m for F = 1 Hz (quasi identical than the value observed in quasi steady wind conditions for U_W = 2 m/s).
The normalized spectra of the fire intensity signals shown in Figure 7, has confirmed this coupling mechanism between the frequency at which the wind velocity was excited and the characteristic frequency of the Kelvin-Helmhotz instability. The evolution of the fire intensity (average value and standard deviation) as a function of the wind gusts frequency F is represented in Figure 8.

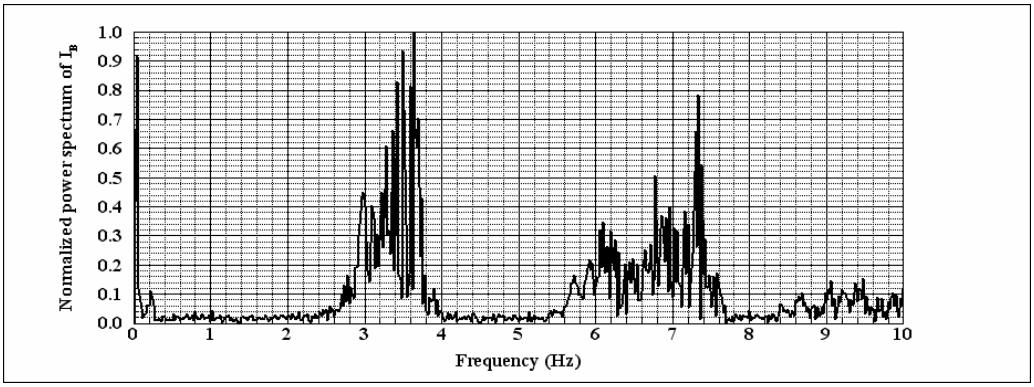

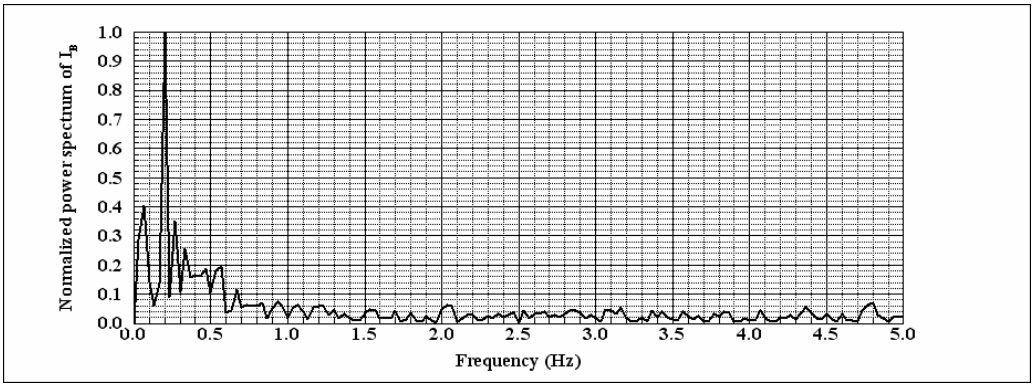

Figure 7. FFT analysis of fireline intensity signal obtained for U_W = 2 m/s without (top) and with (bottom) a sinusoidal time variation (amplitude 2 m/s, frequency 0.25 Hz).

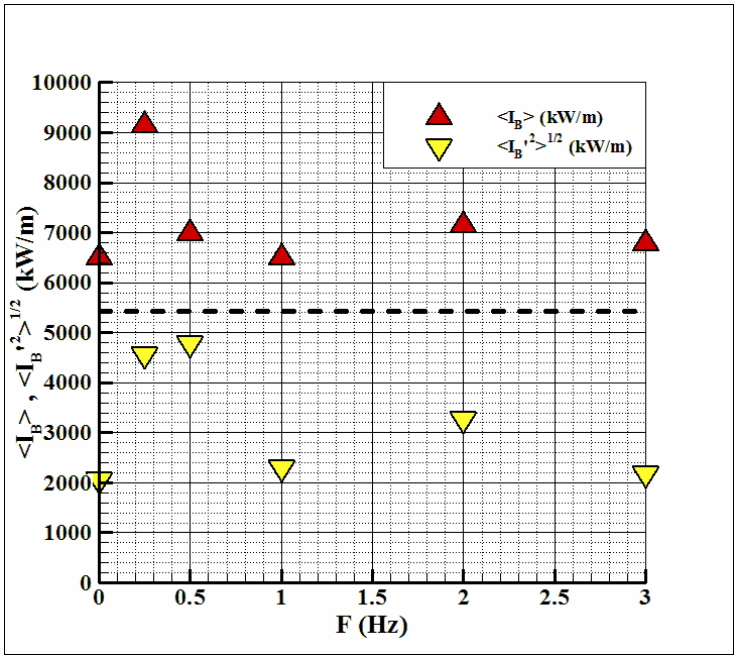

Figure 8. Fireline intensity and standard deviation obtained for UW = 2 m/s and a sinusoidal time variation (frequency ranged between 0.25 Hz and 3 Hz).

These numerical data show that two frequencies seemed increasing the unsteady effects, a first one (with the larger effect) for F = 0.25 Hz (near the Kelvin-Helmoltz frequency for these conditions of wind and vegetation) and a second one for F = 2 Hz (not far from the plume instability).

Conclusion

Numerical simulations of surface fires propagating through homogeneous vegetation layer on a flat terrain have been carried out for a large range of wind conditions, covering the two regimes of propagation (plume dominated and wind driven) referenced in the literature. The FFT analysis of the time variation of the fireline intensity signals, has allowed identifying that the unsteady motions of the flame front were governed by two instabilities (by shear and by density gradient). Then a second set of numerical simulations, reproducing the wind gusts, has allowed to highlight a coupling mechanism between forced and internal instability modes, which was able to modify significantly the fire behaviour.

References

[1] Rothermel R.C., Anderson H.E. Fire spread characteristics determined in the laboratory USDA Forest Service RP INT-30, 1966.
[2] Catchpole W.R., Catchpole E.A., Butlet B.W., Rothermel R.C., Morris G.A., Latham D.J. Rate of spread of free-burning fires in woody fuels in a wind tunnel, *Combustion Science and Technology*, Vol.131, pp.1-37, 1998.
[3] Trabaud L. Etude du comportement du feu dans la garrigue de chêne kermès à partir des températures et des vitesses de propagation, *Annals of Forest Science*, Vol.36(1), pp.13-38, 1979.
[4] Fernandes P.A.M. Fire spread prediction in shrub fuels in Portugal, *Forest Ecology and Management*, Vol.144, pp.67-74, 2001.
[5] McArthur A.G. Weather and grassland fire behaviour, Forest Research Institute, Forestry and Timber Bureau, ACT, Australia, 1966.
[6] Fogarty L.G., Alexander M.E. A field guide for predicting grassland fire potential, *Fire Technology Transfer Note*, Vol.20, 10p., 1999.
[7] Morvan D., Dupuy J.L. Modeling the propagation of a wildfire through a Mediterranean shrub using a multiphase formulation, *Combustion and Flame*, Vol.138, pp.199-210, 2004.
[8] Beer T. The interaction of wind and fire, *Boundary-Layer Meteorology*, Vol.54, pp.287-308, 1991.
[9] Morvan D. Physical phenomena and length scales governing the behaviour of wildfires: a case for physical modelling, *Fire Technology*, Vol.47, pp.437-460, 2011.
[10] McArthur A.G. The Tasmanian bushfire of 7th February 1967, and associated fire behaviour characteristics. Technical Co-operation Programme, Mass Fire Symposium (Canberra, Australia 1969), Maribyrnong, Victoria, Defence Standards Laboratories, Vol.1, 23p, 1969.
[11] Rothermel R.C. A mathematical model for predicting fire spread in wildland fuels, USDA Forest Service RP INT-115, 43p., 1972.
[12] Morvan D., Meradji S., Accary G. Physical modelling of fire spread in grasslands, *Fire Safety Journal*, Vol.44, pp.50-61, 2009.
[13] Morvan D. Wind effects, unsteady behaviour and regimes of propagation of surface fires in open field. *Combustion Science and Technology, (in press), 2014.*
[14] Grishin A.M. Mathematical modelling of forest fires and new methods of fighting them. Albini F. (Ed.) Tomsk State University, 367p., 1997.
[15] Libby P.A., Williams F.A. Turbulent reacting flows. Academic Press, 1994.
[16] Anderson, H.E. Aids to determining fuel models for estimating fire behaviour, Gen. Tech. Rep. INT-122, Ogden UT, USDA-FS, Intermountain Research Station, 22p., 1982.
[17] Morvan D., Larini M. Modeling of one dimensional fire spread in pine needles with opposing air flow, *Combustion Science and Technology*, Vol.164, pp.37-64, 2001.
[18] Cox G. Combustion fundamentals of fire. Academic Press, London, 1995.
[19] Hamins A., Kashiwagi T., Burch R.R. Characteristics of pool fire burning. ASTM STP 1284, 1996.
[20] Kaimal J.C., Finnigan J.J. Atmospheric boundary layer flows, Oxford University Press, 1994.
[21] Morvan D., Méradji S., Mell W. Interaction between head fire and backfire in grasslands, *Fire Safety Journal*, Vol.58, pp.195-203, 2013.

Wildfires in Mediterranean shrubs and grasslands, in Greece: In situ fire behaviour observations versus predictions

Miltiadis Athanasiou[a], Gavriil Xanthopoulos[b]

[a] *"Environmental Impact Assessment Studies". 8 Thoma Paleologou st., 13673 Acharnes, Attica, Greece. info@m-athanasiou.gr*
[b] *Hellenic Agricultural Organization "Demeter". Institute of Mediterranean Forest Ecosystems and Forest Products Technology. Terma Alkmanos, Ilisia, 11528, Athens, Greece. gxnrtc@fria.gr*

Abstract
This paper presents a testing of surface wildfire rate of spread (ROS) field observations ($ROS_{observed(surface)}$) versus rate of spread predictions ($ROS_{predicted(surface)}$) from BehavePlus (Andrews *et al*., 2005) for tall and short Mediterranean shrublands, Sarcopoterium spinosum (small xeric shrub, up to 0.5 m height) and grass. In order to evaluate the degree of their agreement and analyse the results of their correlations, surface or passive crown fire behaviour data as well as meteorological, topography and forest fuels data had to be prepared according to specific criteria in order to ensure their quality and compatibility.
Ninety five fire behaviour data records were created from field observations and measurements made during the evolution of specific wildfires in Greece, in the last seven fire seasons (2007-2013). The data were classified depending on the fuel model that describes the fuel types they had spread in and, thus, four data subsets were generated that correspond to the following four fuel models for Greece which had been developed in 2001 (Dimitrakopoulos *et al* 2001, Dimitrakopoulos 2002): a) "Evergreen-schlerophyllous shrublands (1.5 - 3 m)" for tall maquis (38 cases), b) "Evergreen schlerophyllous shrublands (up to 1.5 m)" for short maquis (13 cases), c) "Phrygana II (Sarcopoterium spinosum)" for phryganic areas where the dominant species was Sarcopoterium spinosum (26 cases) and d) "Mediterranean grasslands" for grass (18 cases). After creating the database, the BehavePlus system was used to produce rate of spread predictions for each of the ninety five cases and flame length (FL) predictions ($FL_{predicted}$ values) for the twenty six cases of *Sarcopoterium spinosum* dominated phrygana fields.
The main finding is that for the four Greek fuel models tested, BehavePlus can be a useful tool for predictions of fire behaviour. However, there is a relatively consistent over-prediction of ROS for the models "Evergreen-schlerophyllous shrublands (1.5 - 3 m)" for tall maquis, "Evergreen schlerophyllous shrublands (up to 1.5 m)" for short maquis (13 cases), and "Phrygana II (Sarcopoterium spinosum)", while there a significant under-prediction for the "Mediterranean grasslands" fuel model.
Four linear regression equations describing mathematically the relation of the predicted to the observed ROS were developed. They are statistically significant and can be used for adjusting BehavePlus predictions to match "real world" fire behaviour.
A further finding was that flame length is seriously under-predicted when using BehavePlus with the Phrygana II fuel model to predict fire behaviour in *Sarcopoterium spinosum* dominated phrygana fields. This is an important result that can be very useful for the safety of firefighters.

Keywords*: Mediterranean shrubs, maquis, phrygana, fuel model, wildfire behaviour prediction, BehavePlus, wildfire field observations, Greece*

Introduction

Modern wildfire management requires use of reliable fire behaviour prediction and fire spread simulation systems. However, broad operational adoption of such systems can be achieved and benefits can be maximized only if their strengths and generalizations, weaknesses or limitations are well known. Continuous and extensive testing of fire behaviour prediction systems in the laboratory, in experimental field burns as well as in actual wildfires, is necessary since it detects their "limits",

documents their proper use and increases, eventually, their contribution to fire fighting safety and efficiency. Globally, fire managers and scientists often utilise data sets that come from documented wildfires and test the predictions of fire behaviour modelling systems, such as the popular system BehavePlus (Andrews *et al*., 2005), versus field observations, aiming to evaluate the degree of their agreement. Measurements of weather conditions and topography as well as information about the forest fuels (fuel models), are necessary as inputs for using the BehavePlus system. Until now, many studies have shown minor or significant disagreements between fire behaviour observations and predictions which have often been attributed to the inadequacy of stylized fuel models to represent the existing forest fuel conditions.

In Greece, some testing of BehavePlus took place after the fires of 2007 which had mostly spread under extreme weather conditions and had caused huge damages (Athanasiou and Xanthopoulos, 2010). That testing had shown a very good agreement between fire behaviour observations and predictions for tall Mediterranean shrublands that were described by the "Evergreen-schlerophyllous shrublands (1.5 - 3 m)" fuel model for tall maquis, which had been developed and published earlier (Dimitrakopoulos *et al* 2001, Dimitrakopoulos 2002). The collection of fire behaviour data continued in the field during the following fire seasons, enriching the database and allowing a "stress test" of the initial and preliminary conclusions for the above model, in a wider range of conditions.

Moreover, additional fire behaviour data were recorded presenting an opportunity for testing BehavePlus surface fire behaviour predictions for three more fuel types: a) short maquis, b) small xeric shrubs, up to 0.5 m height (called phrygana in Greece) and c) grass. These types can be described by three previously developed fuel models for Greece by the same authors: a) "Evergreen schlerophyllous shrublands (up to 1.5 m)", b) "Phrygana II (*Sarcopoterium spinosum*)" and c) "Mediterranean grasslands".

The current paper is part of the Ph.D. thesis of the first author. A data subset of documented wildfires of the last seven fire seasons (2007 – 2013) in Greece were utilised, aiming to evaluate the degree of agreement of BehavePlus predictions with observed fire behaviour for four out of the seven fuel models that have been developed for Greece, to introduce adjustments if needed, and ultimately to contribute towards wider adoption of prediction systems into fire management.

2. Methods

A database including meteorological, topography, forest fuels and fire behaviour data was initially created in 2007 and is continuously enlarged with field measured observations made during specific fires. It now consists of detailed data collected during 32 low, medium or high intensity wildfires which took place under a variety of meteorological conditions, topography and fuels. More than one data records (fire behaviour cases) resulted from each of these fires as most of them run their course for many hours. The database now includes 185 records. Its fields contain detailed information about the observed fire rate of spread and flame length and reliable data about the fire type, crowning initiation and propagation, crown fire type, spreading in canyon, spotting (Athanasiou and Xanthopoulos, 2013), wind direction versus slope, wind adjustment factor and midflame wind speed (Rothermel, 1983), downslope or upslope fire spread, fire spread direction in relation to wind (head fire, backward, or sideward moving) and, where relevant, such observations as strong wind turbulence occurrence, convection column generation, etc.

Fieldwork and data processing

The fire behaviour observations were matched with the related meteorological, topography and forest fuels information following specific procedures (Athanasiou and Xanthopoulos, 2010). The forest fuel types, in which the fires spread, were identified through visual assessment and were described by the suitable fuel models for Greece when such a description was possible. Slope, aspect and altitude were

measured using a Garmin etrex Summit GPS device in the field, and later using the ArcGIS 9.3 Geographic Information System (GIS) software by ESRI Corporation in the office. Air temperature in degrees Celsius (^{o}C), relative humidity in (%) and wind speed and gusts in kilometers per hour (km/h), were measured using an electronic weather instrument (type: Thermometer – Anemometer - Hygrometer Model N^{o} AM4205). Additionally, wind direction azimuth was determined using a compass.

Fire rate of spread ($ROS_{observed}$), in (km/h), was calculated by knowing the exact time for every fire head, finger, tail or flank location (Alexander and Thomas, 2003) and applying simple geometry (Clements *et al*., 1983) or using the GIS software, through the following steps:

a) recording the geographic coordinates of observer's positions with the GPS device and measuring the observations' horizontal azimuth with a compass,
b) taking plenty of sequential digital photographs (in JPG format and known time) using a Canon Powershot S3is digital camera [which has a lens with a focal length ranging from 36 mm (wide Angle) to 432 mm (telephoto)],
c) pinpointing the sequential locations of the fire on the photograph (figures 1, 2, 3 and 4) or on the map.

Flame length ($FL_{observed}$) in (m), was calculated also by applying simple geometry (Clements *et al*., 1983) for the cases that this was possible.

Defining the fire behavior data samples

The first step of the analysis was the preparation of the data according to specific criteria in order to ensure data quality and compatibility. Active crown fires and cases of surface fire behaviour affected by spotting, a strong convection column or other factors that resulted in extreme fire behaviour (e.g. box canyon or turbulence) were excluded. The excluded cases fall in two main categories of: a) fires that were dominated by factors that cannot be explained by the ordinary fire spread physical laws, therefore these cases are not comparable with BehavePlus predictions or b) fires which spread in fuel situations and complexes that consist of several mixed fuel types that cannot yet be described by the existing seven fuel models, for Greece. The remaining 95 cases of surface or passive crown fire behaviour ($ROS_{observed(surface)}$) were then classified depending on the fuel model that describes the fuel types they had spread in. Four data subsets were generated that correspond to the following four fuel models for Greece:

a) "Evergreen-schlerophyllous shrublands (1.5 - 3 m)" for tall maquis (38 cases),
b) "Evergreen schlerophyllous shrublands (up to 1.5 m)" for short maquis (13 cases),
c) "Phrygana II (*Sarcopoterium spinosum*)" for phryganic areas where the dominant species was *Sarcopoterium spinosum* (26 cases) and
d) "Mediterranean grasslands" for grass (18 cases).

1(a): Photo captured at 18:22:36

1(b): Photo captured at 18:57:38

Figure 1(a) & (b) - Fire spread of 55 meters in tall maquis (yellow arrow), downslope, within a period of 35 minutes and 2 seconds. $ROS_{observed}$ = 0.09 km/h

2(a): Photo captured at 14:34:36

2(b): Photo captured at 14:35:36

Figure 2(a) & (b) - Fire spread of 12.5 meters in low maquis (yellow arrow), upslope, within a period of 1 minute. $ROS_{observed}$ = 0.75 km/h

Figure 3. Fire spread of 80 meters in phrygana (yellow arrow), downslope, within a period 3 minutes and 54 seconds. $ROS_{observed}$ =1.23 km/h

4(a): Photo captured at 15:44:00

4(b): Photo captured at 15:44:15

Figure 4(a) & (b) - Fire spread of 36 meters in grass (yellow arrow), on flat terrain, within a period of 15 seconds. $ROS_{observed}$ = 8.64 km/h

Analysis

On-site meteorological measurements, measured slope values and the four fuel models for tall maquis, short maquis, *Sarcopoterium spinosum* dominated phryganic areas and grass, were used as inputs for predicting surface fire rate of spread values ($ROS_{predicted\ (surface)}$) with BehavePlus. The values of the four fuel models parameters are summarized and reported in table 1 and typical photos are shown in Figure 5 in an effort to facilitate further testing by researchers and use by fire managers in Mediterranean countries with fuel situations that can be described by these fuel models.
The NEWMDL module of the original BEHAVE system (Burgan and Rotrhermel 1984) was used to calculate the overall fuel load in the dead fine fuels (1hr) category of the fuel models, adding the load of litter to that of the rest of 1 hr fuels and then to calculate a weighted fuel bed depth. Furthermore, NEWMDL produced an estimate for the "dead fuel moisture of extinction" for each model. Such values had not been reported previously.
Fine (1-h) dead Fuel Moisture Content (FMC %) value was calculated using Rothermel's methodology (1983) using: a) air temperature and relative humidity measurements, b) month and time of day of the observation, c) elevation difference between the location where the meteorological measurements were made and the fire spread location, d) slope and aspect of the fire spread location and e) surface fuels shading percentage.

Table 1. The values of the parameters of the four fuel models that were used as inputs for predicting surface fire rate of spread ($ROS_{predicted(surface)}$) with BehavePlus.

FUEL MODEL / **PARAMETER**	**Evergreen schlerophyllous shrublands (1.5 – 3.0 m)**	**Evergreen schlerophyllous shrublands (up to 1.5 m)**	**Phrygana II (*Sarcopoterium spinosum*)**	**Mediterranean grasslands**
1 HR (MTON/HA)	17.88	9.91	3.50	4.82
10 HR (MTON/HA)	13.30	6.80	1.02	0.49
100 HR (MTON/HA)	8.5	3.60	0.28	0
LIVE HERB (MTON/HA)	0	0	0	0
LIVE WOODY (MTON/HA)	10.60	7.70	0.85	0
1 HR S/V (1/CM)	55	55	65	78

LIVE HERB S/V (1/CM)	-	-	-	-
LIVE WOODY S/V (1/CM)	55	55	65	-
FUEL BED DEPTH (CM)	203.58	102.19	40.00	27.53
EXT MOISTURE (%)	34	34	20	14
HEAT CONTENT (J/G)	20000	20000	19054	18600

The 10-h dead FMC value was assumed equal to the 1-h dead FMC also (Andrews *et al*., 2005) (which is a commonly applied and acceptable approach) while the necessary 100-h dead FMC% and live woody FMC% values were assigned according to values of unpublished measurements in Attica for that time period and year.

Figure 5(a). Tall maquis fuel model

Figure 5(b). Short maquis fuel model

Figure 5(c). Phrygana II fuel model

Figure 5(d). Grass fuel model

The 26 surface fire behaviour observations in phryganic areas included 26 $FL_{observed}$ values that consist a complete subset which could be compared with predictions ($FL_{predicted}$ values) that were obtained using the fuel model "Phrygana II (*Sarcopoterium spinosum*)".

Results

The maximum, minimum, mean and standard deviation of $ROS_{observed(surface)}$ values for the subsets of 38, 13, 26 and 18 observations, referring to surface fire behaviour during pure surface fires or passive crown fires, are reported in table 2.

Table 2. Descriptive statistics summary of surface $ROS_{observed(surface)}$ values for the four fuel types (N:number of observations / cases)

ROS values (km/h)	**Tall maquis N = 38**	**Short maquis N = 13**	**Phrygana II (dominant species: *Sarcopoterium spinosum*) N = 26**	**Grass N = 18**
max	3.31	1.65	2.71	11.03
min	0.09	0.05	0.02	0.04
mean	0.90	0.45	0.54	1.95
std. deviation	0.80	0.45	0.59	3.28

The pairs of rate of spread observed values ($ROS_{observed(surface)}$) and BehavePlus predicted values ($ROS_{predicted(surface)}$), were correlated via linear regression, for every fuel model subset, resulting in the four following equations. The plots of these equations are shown in figure 6.

$$\mathbf{ROS_{observed} = 0.165 + 0.886 * ROS_{predicted}},\ \text{adjusted } \mathbf{R^2 = 0.806}, \text{ (tall maquis)} \quad (1)$$

$$\mathbf{ROS_{observed} = 0.127 + 0.709 * ROS_{predicted}},\ \text{adjusted } \mathbf{R^2 = 0.873}, \text{ (short maquis)} \quad (2)$$

$$\mathbf{ROS_{observed} = 0.101 + 0.783 * ROS_{predicted}},\ \text{adjusted } \mathbf{R^2 = 0.681}, \text{ (*Sarcopoterium spinosum*)} \quad (3)$$

$$\mathbf{ROS_{observed} = -0.023 + 1.562 * ROS_{predicted}},\ \text{adjusted } \mathbf{R^2 = 0.847}, \text{ (grass)} \quad (4)$$

The four equations are statistically significant ($p<0.001$) and the p-values of their slope coefficients are statistically significant ($p<0.001$). The p-values of the constants of equations (1), (3) and (4) are not statistically significant ($p\text{-value}_1=0.052$, $p\text{-value}_3=0.266$ and $p\text{-value}_4=0.950$, respectively) while the p-value of the constant of equation (2) is statistically significant ($p\text{-value}_2=0.046$).
The adjusted R^2 values of the regression equations (1), (2) and (4) indicate that their unexplained errors are low while the adjusted R^2 value of equation (3) shows that the unexplained error is relatively higher. This is probably the result of using this fuel model to describe fuel situations and complexes of significant heterogeneity (figure 6c).
The ROS data subsets analysis was followed by a preliminary investigation that concerned the FL of surface fires in phryganic areas (figure 7). Plotting the observed and predicted FL values for the 26 cases in this subset it became clear that in only two cases $FL_{observed}$ was lower than $FL_{predicted}$. The ratio between $FL_{observed}$ and $FL_{predicted}$ varied between 0.3 and 5.0 with an average value of 2.3 and a standard deviation of 1.2. In general, $FL_{observed}$ values were more than twice the values of $FL_{predicted}$ for the fuel model Phrygana II.

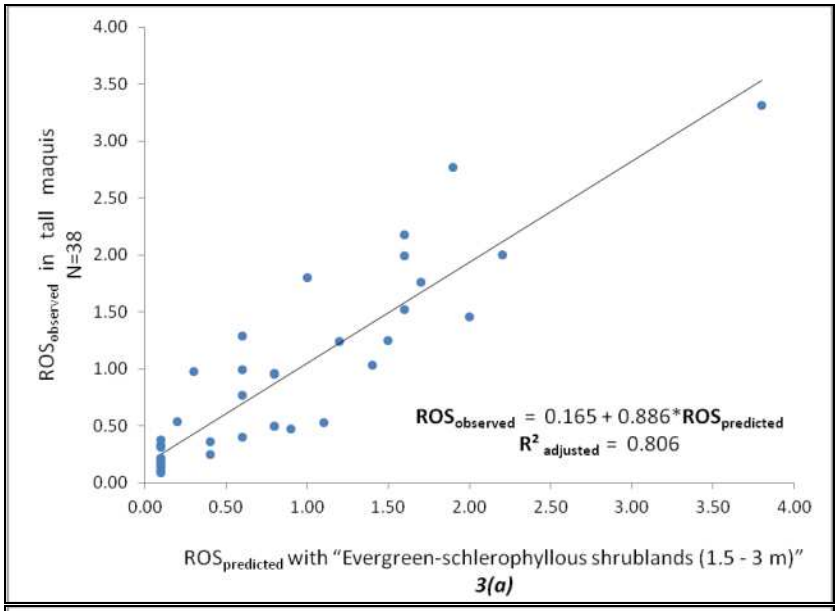

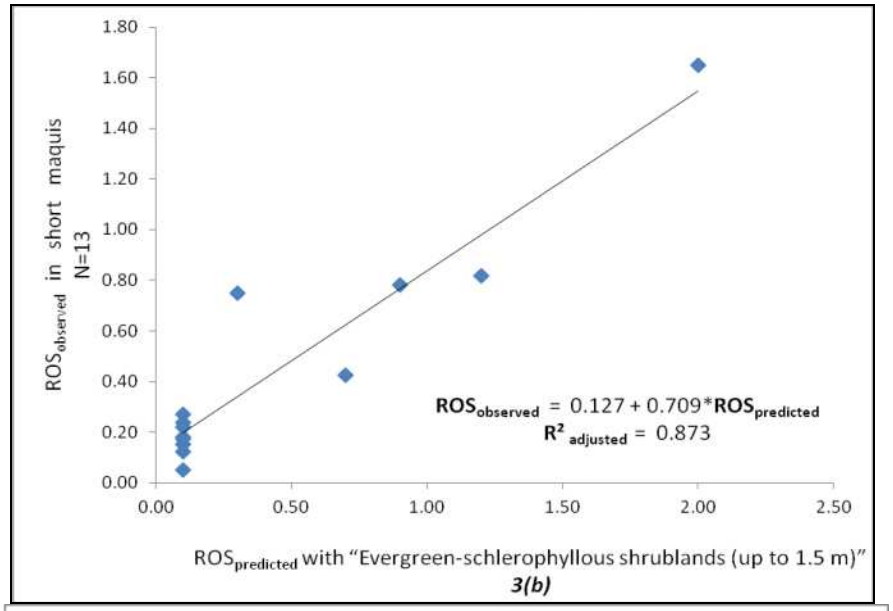

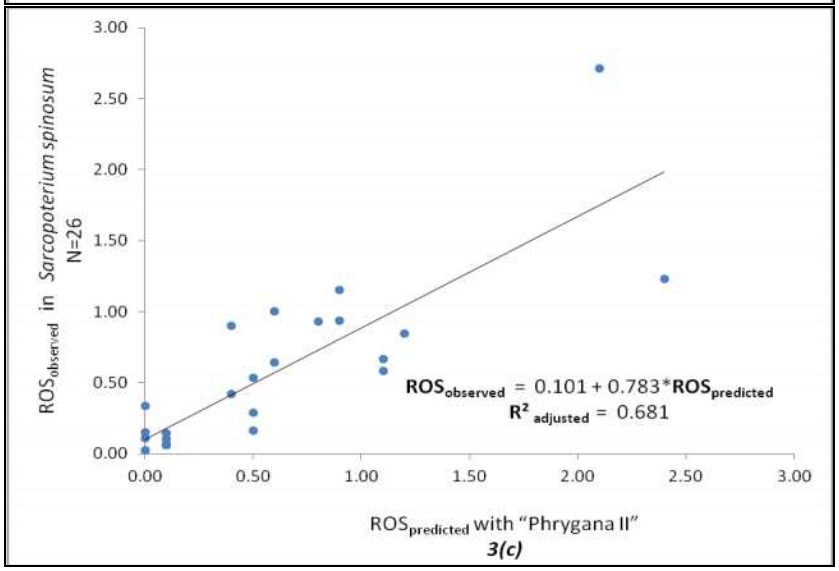

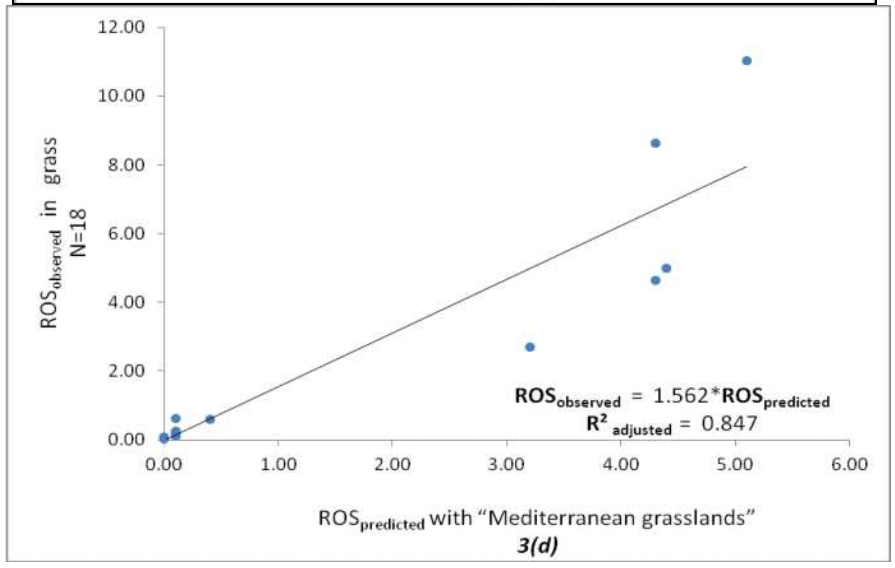

Figure 6 (a), (b), (c) & (d): – Correlations of surface $ROS_{observed}$ and $ROS_{predicted}$ values (in km/h) for the four data subsets

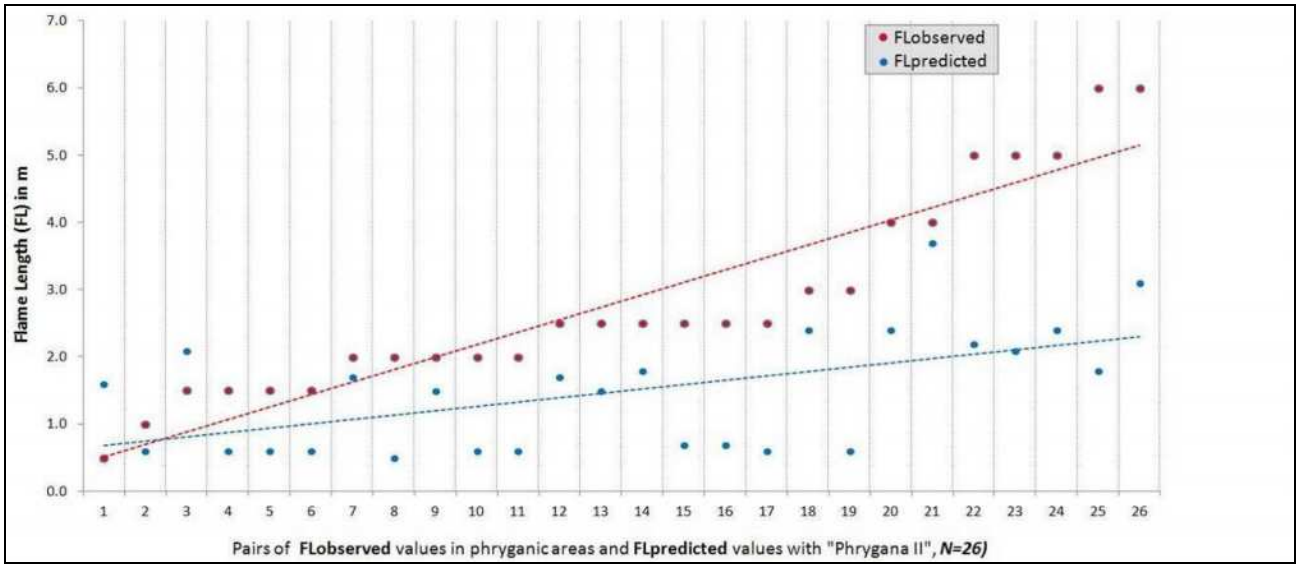

Figure 7. Plot of observed and predicted flame length for Sarcopoterium spinosum dominated phrygana fields. The pairs of values are sorted in ascending order of $FL_{observed}$.

Discussion

The pairs of $ROS_{observed(surface)}$ values and BehavePlus $ROS_{predicted(surface)}$ values, were correlated via linear regression for each of the data subsets, resulting in four statistically significant ($p<0.001$) equations with good adjusted R^2 values. The p-values of their slope coefficients were also statistically significant ($p<0.001$). This was not true for the constants of the equations for tall maquis, *Sarcopoterium spinosum* and grass, whereas the constant of the equation for short maquis was statistically significant. The non-significance of the constants of the three equations means that this term is not significantly different from 0.

The unexplained error of the equations was low for the short and tall maquis as well as for grass but was higher for the quite flammable xeric shrub *Sarcopoterium spinosum*. This higher unexplained error may be attributed to the fact that the fuel model "Phrygana II (*Sarcopoterium spinosum*)" was used to describe relatively heterogeneous fuel situations, including for example a variable percentage of other phryganic species such as *Cistus creticus*, *Cistus salvifolius*, etc.

Table 3 shows the calculated $ROS_{observed(surface)}$ values from solving the four equations for a range of plausible $ROS_{predicted(surface)}$ values, providing an insight on the degree of agreement of predictions vs observations for the level of accuracy that is required in operational applications. From this table it becomes clear that the agreement for the fuel model "Evergreen-schlerophyllous shrublands (1.5 - 3 m)" is very good, confirming the conclusions of Athanasiou and Xanthopoulos (2010). Due to this good agreement it seems unnecessary to adjust BehavePlus ROS predictions to the somewhat lower "real world" values that would result from corrections based on equation (1).

The agreement for the "Evergreen schlerophyllous shrublands (up to 1.5 m)" and for the "Phrygana II" models is also relatively good although it is clear that BehavePlus predictions are quite higher than the ROS observations. Because of this over-prediction it is advisable, when obtaining ROS estimates for fires in these two fuel models, to adjust these estimates using equations (2) and (3) respectively. It should be mentioned here that equation (2), in spite of its good adjusted R^2 value and the fact that its constant and slope coefficient are statistically significant, should be considered as preliminary. The number of observations that were analysed was small (N=13) so the result does not inspire confidence for broad operational use. Further work is needed for this fuel type.

Table 3. Solution of equations (1)-(4) for a range of values of $ROS_{predicted(surface)}$ (km/h).

	ROSobserved(surface)			
ROSpredicted(surface)	Tall maquis	Short maquis	Phygana II	Grass
0	0.165	0.127	0.101	-0.023
1	1.051	0.836	0.884	1.539
2	1.937	1.545	1.667	3.101
3	2.823	2.254	2.450	4.663
4	3.709	2.963	3.233	6.225
5	4.595	3.672	4.016	7.787
6	5.481	4.381	4.799	9.349
7	6.367	5.09	5.582	10.911
8	7.253	5.799	6.365	12.473
9	8.139	6.508	7.148	14.035
10	9.025	7.217	7.931	15.597

In the case of grasslands, table 3 shows that BehavePlus strongly underpredicts ROS. As equation (4) is statistically significant and its adjusted R^2 value is high ($R^2_{adjusted}$ = 0.847), this under-prediction should be taken into consideration when using BehavePlus for ROS prediction in grasslands with the Greek grass fuel model. Equation (4) should be used for obtaining adjusted $ROS_{observed(surface}$ i.e. "real world" ROS estimates.

The analysis of flame length in phryganic areas showed that on average $FL_{observed}$ was 2.3 times greater than the $FL_{predicted}$ values obtained through BehavePlus using the Phrygana II fuel model. The FL predictions tended to underestimate notably the actual FL that was measured in the field. There were only two exceptions, out of the twenty six cases, in which $FL_{predicted}$ was greater than the $FL_{observed}$ value (figure 7).

Underestimating the expected FL in phrygana is a serious problem for another reason as well: as shown in figure 7 the underestimation takes place in a narrow band of FL values that includes the FL threshold value of 1.2 m which is considered as the limit for direct attack on the flames with hand tools (Deeming *et al*., 1977, Hirsch and Martell, 1996). For ten out of the twenty six cases the prediction value was lower than the hand tools threshold value while the actually observed flame length was greater than that.

Phrygana have been the cause of many firefighting accidents in Greece as they are flashy fuels and respond very quickly to changes of the environmental conditions (wind, topography, relative humidity) (Xanthopoulos, 2007). The reliability of FL predictions for a wide range of meteorological conditions, topography and fuel situations is crucial and mandatory since flame length affects the personnel extinguishment capacity and FL predictions inaccuracy could jeopardize the safety of the firefighters in these fine, quite flammable and flashy fuels.

Conclusions

The main finding of the work presented here is that for the four Greek fuel models tested, BehavePlus can be a useful tool for predictions of fire behaviour. However, there is a relatively consistent over-prediction of ROS for the models "Evergreen-schlerophyllous shrublands (1.5 - 3 m)" for tall maquis, "Evergreen schlerophyllous shrublands (up to 1.5 m)" for short maquis (13 cases), and "Phrygana II (*Sarcopoterium spinosum*)", while there is a significant under-prediction for the "Mediterranean grasslands" fuel model.

The four linear regression equations that were developed are statistically significant and can be used for adjusting BehavePlus predictions to match "real world" fire behaviour, at least as documented in

the present study. Such an adjustment could also be incorporated in fire spread simulation systems used in Greece.
The finding that flame length is seriously under-predicted when using BehavePlus with the Phrygana II fuel model to predict fire behaviour in Sarcopoterium spinosum dominated phrygana fields is an important result that can be very useful for the safety of firefighters. It should be seriously taken into consideration in operational firefighting in the country.
Future work, as data continue being collected and the data base is expanded, are expected to shed additional light in the issues discussed in this paper, ultimately improving fire behaviour prediction and firefighter safety in Greece.

7. Aknowledgements

The research reported here is part of the Ph.D. thesis of the first author and was sponsored, in part, by the International Association of Wildland Fire (IAWF) through the Doctoral Student Scholarship Award for 2014. Participation of the second author was supported by a research project of the Institute of Mediterranean Forest Ecosystems and Forest Products Technology (IMFE&FPT) titled "Forest fuels standardization and management methodology in Attica"; The project was co-funded by the European Regional Development Fund (ERDF) through the Greek General Secretariat for Research and Technology (Project code: ATT-63), and also by a research project of IMFE&FPT titled "Investigation of the relation between the water potential of forest plants and forest fires".

8. References

Alexander, M.E., Thomas D.A., 2003. Wildland Fire Behavior Case Studies and Analyses: Other Examples, Methods, Reporting Standards, and Some Practical Advice. Fire Management Today, 63 (4): 4-12.

Andrews, P.L., Bevins, C.D., Seli, R.C., 2005. BehavePlus fire modeling system, Version 3.0: User's Guide. General Technical Report RMRS-GTR-106WWW revised. Ogden, UT: U.S. Department of Agriculture, Forest Service, Intermountain Forest and Range Experiment Station. 132 p.

Athanasiou, M. and G. Xanthopoulos 2010. Fire behaviour of the large fires of 2007 in Greece. In proceedings of the 6th International Conference on Forest Fire Research, 15-18 November 2010, Coimbra, Portugal. D.G. Viegas, Editor. ADAI/CEIF, University of Coimbra, Portugal. Abstract p. 336, full text on CD.

Athanasiou M. and G. Xanthopoulos 2013. *Observations of the spotting phenomenon, in wildfires in Greece*. 30-40 p. In proceedings of the 16th National Forestry Conference, October 6-9, 2013, Thessaloniki, Greece. Hellenic Forestry Society. 1144 p. (in Greek).

Burgan, R.E., Rothermel, R.C. 1984. BEHAVE: fire behavior prediction and fuel modelling system—FUEL subsystem. Gen. Tech. Rep. INT-167. Ogden, UT: U.S. Department of Agriculture, Forest Service, Intermountain Forest and Range Experiment Station. 126 p.

Clements, H., D. Ward, and C. Adkins. 1983. Measuring fire behaviour with photography. Photogrammetric Engineering and Remote Sensing: Series II, vol. 49: 213-217.

Deeming, J.E.; Burgan, R.E.; Cohen, J.D. 1977. The National Fire-Danger Rating System -1978. United States Department of Agriculture, Forest Service, General Technical Report INT -39, Intermountain Forest and Range Experiment Station, Ogden Utah.

Dimitrakopoulos, A.P., V. Mateeva, and G. Xanthopoulos. 2001. Fuel models for Mediterranean vegetation types in Greece. Geotechnical Scientific Issues (Geotechnical Chamber of Greece): Series VI, vol. 12(3): 192-206 (in Greek).

Dimitakopoulos, A. P. 2002. Mediterranean fuel models and potential fire behavious in Greece. International Journal of Wildland Fire, 11:127-130.

Hirsch KG, Martell DL (1996) A Review of Initial Attack Fire Crew Productivity and Effectiveness. International Journal of Wildland Fire 6, 199–215.

Rothermel, R.C. 1983. How to predict the spread and intensity of forest and range fires. Gen. Tech. Rep. INT-143. Ogden, UT: U.S. Department of Agriculture, Forest Service, Intermountain Forest and Range Experiment Station. 161 p.

Xanthopoulos, G. 2007. Forest fire related deaths in Greece: confirming what we already know. p. 339. In book of abstracts of the "IV International Wildland Fire Conference", May 13-17, 2004, Seville, Spain. Full paper on the CD accompanying the book of abstracts.

Wind flow characterization associated with fire behaviour measurements

Dan Jimenez[a], Bret W. Butler[a], Casey Teske[b] , Joseph O'Brien[c], Louise Loudermilk[c], Ben Hornsby[c], Craig Clements[d]

[a] *USDA Forest Service, Rocky Mountain Research Station 5775 W US Highway 10 Missoula MT 59808, USA*
[b] *National Center for Landscape Fire Analysis, University of Montana, Missoula, MT 59812, USA*
[c] *USDA Forest Service, Southern Research Station, 200 W.T.Weaver Blvd. Asheville, NC 28804, USA*
[d] *Fire Weather Research Laboratory, Department of Meteorology and Climate Science, San Jose State University San Jose, CA USA*

Abstract

The relationship between fire behaviour and ambient wind flow is often presumed, but seldom measured. General understanding of observed fire behaviour suggests an increase in fire intensity associated with increased wind speed (Van Wagner 1987, Rothermel 1991, Finny *et al*. 2006, Forthofer 2007). Fire behaviour characteristics (such as temperature, radiant and total heat flux, 2- and 3-dimensional velocities, and air flow) are extremely difficult to measure in-situ (Jimenez *et al*. 2007). Studies base on these phenomena often correlate empirical data either from observed wildland fire or laboratory experiments, but few data sets exist that capture ambient wind flow simultaneously with corresponding in-situ fire behaviour measurements.

This paper reports on the corresponding fire behaviour and wind field relationship on six field study plots that were instrumented with several fire behaviour packages (Butler el al. 2004), and a network of wind anemometer towers deployed around the perimeter of each plot. The study plots were part of the Prescribed Fire Combustion and Atmospheric Dynamics Research Experiment (RxCADRE) 2012 field campaign, with the objectives aimed at developing synergies between fuels, fuel consumption, fire behaviour, smoke management, and fire effects measurements for fire model development and evaluation.

Keywords*: Fire behaviour, prescribed fire, surface wind flow, anemometer, thermograghy*

Introduction

Fire-atmosphere interactions (FAI) are defined as the interactions between presently burning fuels and the atmosphere, in addition to interactions between fuels that will eventually burn in a given fire and the atmosphere (Potter 2012). Currently, much of the meteorological sampling for fire behaviour applications and science is performed at a very coarse resolution (i.e., hundreds of meters to kilometers), such as the standard Remote Automated Weather Stations (RAWS) networks in existence throughout the United States (Horel and Dong 2010). Additionally, these data are often captured or averaged at a coarse time resolution (i.e., hourly to daily), although surface flows are constantly fluctuating.

Wildland fire researchers have recognized the benefit of in-situ measurements of fire intensity and behaviour as a critical component in the effort to develop improved fire management decision support models. Past measurements consisted primarily of observations of rate of spread, gas temperatures, and fuel consumption, and have been both field based (Barrows 1951; Cheney *et al*. 1993; Fons 1946) and laboratory based (Catchpole *et al*. 1998; Fons 1946; Rothermel 1972). New mathematical models include additional physics which has led to the need for additional measurements, particularly of the basic heat and chemical processes occurring in fire in addition to the local surface wind flow.

Recent studies have focused on understanding the role of both radiative and convective energy transport to wildland fire ignition and spread (Morandini and Silvani 2010).

When considering relationships between energy transport in wildland flames and particle ignition it is unclear how small particles respond to temporal fluctuations in the heating source. Thus the temporal characteristics of the heating regime are relevant to increased understanding of wildland fire behaviour (Frankman *et al*. 2012)

There is an increasing need to measure fire-atmosphere interactions at finer scales in order to better understand the role of near-surface wind and thermodynamic structures of fire behaviour (Clements *et al*. 2007). While useful at a landscape scale and possibly for the largest fires, both spatial and temporal scales of near-surface wind and thermodynamic structures presently are highly generalized. Interpolation between these sparsely dispersed points does not consider the spatial heterogeneity or micro-scale influences that impact the smaller fires on the landscape, nor do they capture the fluctuations at a fine temporal scale.

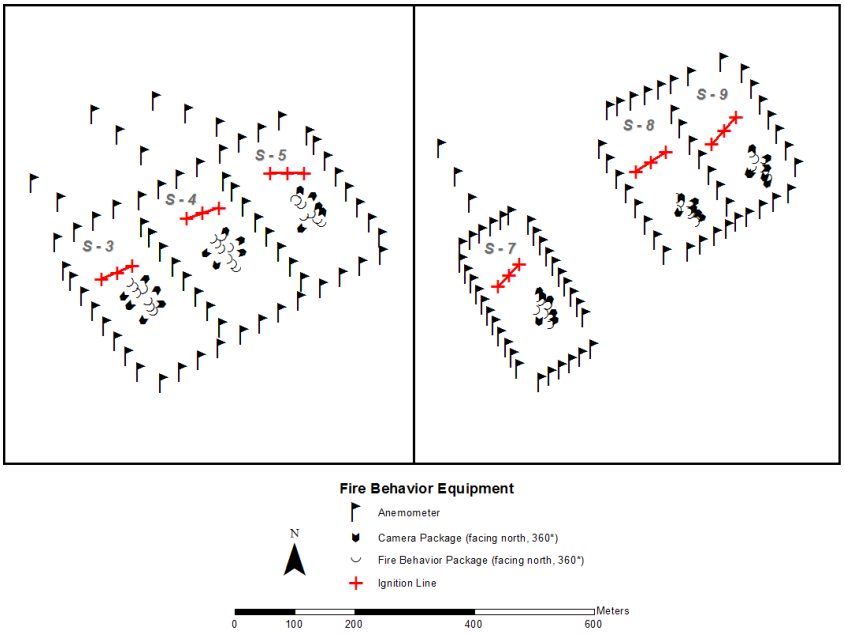

Figure 1. Equipment layout for the six 100mx200m plots.

For this study, six plots (S3, S4, S5, S7, S8, S9) measuring roughly 100m x 200m, and oriented in a northwest/southeast (long-axis) alignment, were highly instrumented in order to capture time-resolved surface wind flow and corresponding in-situ fire behaviour (Figure 1). The plots were chosen and aligned based on generally homogenous fuels and predicted general wind direction. Plots S3, 4, and 5 were in a predominantly grass fuel type, while plots S7, 8, and 9 were in a predominantly grass/shrub fuel type. Multiple cup-and-vane anemometers were set up with 20m spacing around each plot, with adjacent plot edges sharing anemometers. Additionally, five to seven in-situ fire behaviour packages (FBPs) recording heat flux, air temperature, and 2-D mass flow at 10Hz were deployed within each of the plots in order to characterize the fire behaviour throughout plot ignition. Finally, visible and infrared 1Hz-averaged imagery were collected from an elevated 26m platform located at the upwind edge of each plot. All instruments were synchronized to Greenwich Mean Time (GMT).

Methods – Surface Wind Field Measurements

The six replicate burn blocks were burned during two separate burning periods. Three of the replicates (S3, S4, S5) were individually burned on November 1, 2012; the other three replicates (S7, S8, S9) were individually burned on November 7, 2012. In order to provide a continuous flaming front, two

lighters with drip torches uniformly and rapidly ignited the burn blocks, starting at the middle point of the ignition line and simultaneously working in opposite directions toward both ends; these points are marked in Figure 1. Detailed fuels, fuel consumption, fire behaviour, heat flux, and fire effects data were collected on the plots before and during the burns. Table 1 provides instrumentation and ignition specifics for each replicate burn block.

Surface wind and surface fire behaviour measurements were collected on all burn units. Multiple cup-and-vane anemometers (S-WCA-M003, Onset Computer Corporation) were set up with approximately 20m spacing around each small plot, with adjacent plot edges sharing anemometers (Figure 1; Table 1). These instruments measure wind speed and direction at 3.3m above ground level (AGL); the data are used to characterize surface flow patterns before and during the burns. Cup revolutions and unit vector components are accumulated every three seconds for the duration of the logging interval. Wind speed is the average speed for the entire logging interval (0-44 m/s ± 0-4%). Gust speed is the highest three-second wind recorded during the logging interval. Average direction is calculated from the average of the vector components (0-358 º ± 5º).

Table 1. Burn plot instrumentation and ignition information.

Burn Unit	Burn Date	Burn Start Time (Zulu)	Data Collection End Time (Zulu)	Plot Instrumentation
S3	11/1/2012	21:20	22:30	Anemometer: 24 adjacent to plot; 2 NW of plot FBPs: 7; Cameras: 6
S4	11/1/2012	19:35	21:15	Anemometer: 24 adjacent to plot; 3 NW of plot FBPs: 8; Cameras: 5
S5	11/1/2012	18:10	19:30	Anemometer: 24 adjacent to plot; 3 NW of plot FBPs: 7; Cameras: 5
S7	11/7/2012	17:25	18:50	Anemometer: 33 adjacent to plot; 3 NW of plot FBPs: 7; Cameras: 6
S8	11/7/2012	20:16	21:30	Anemometer: 25 adjacent to plot FBPs: 6; Cameras: 6
S9	11/7/2012	18:54	20:10	Anemometer: 23 adjacent to plot FBPs: 7; Cameras: 7

Methods – In-Situ Energy Measurements

In-situ fire behaviour was measured using portable fire behaviour packages (FBPs) developed at the US Forest Service, RMRS Fire Science Lab. The FBPs measure air temperature during fire passage, radiant and convective heat flux emitted from the flames and horizontal and vertical air flow. The sensor package measures 27 cm by 15 cm by 18 cm and in its current configuration weighs approximately 5.3 kg. Various enclosure materials consist of 0.37mm thick aluminium welded at the seams. A 12 volt 4.5 Ah sealed lithium polymer battery provides power to the sensor array and data logger. The data loggers used are Campbell Scientific® model CR1000 and are capable of logging over one million samples, providing 3.5 hours of continuous data logging at 10 Hz. This logger is user-programmable and accepts a wide range of analog and digital inputs and outputs. All of the FBPs incorporate a Medtherm® Dual Sensor Heat Flux sensor (Model 64-20T) that provide incident total and radiant energy flux, a type K fine wire thermocouple (nominally 0.05 mm diameter wire) for measuring gas temperature, a custom designed narrow angle radiometer (Butler 1993) to characterize flame emissive power, and two pressure based flow sensors (McCaffrey and Heskestad 1976) to characterize air flow. Table 2 provides details about individual sensors and their engineering specifications.

Table 2. In-situ Fire Behaviour Package (FBP) Specifications

Narrow Angle	
Sensor	20-40 element thermopile
Spectral Band of Sensor	0.15 – 7.0 μm with sapphire window
Field of View	~4.5º controlled by aperture in sensor housing
Transient Response	Time constant of sensor nominally 30msec
Units of Measurement	Calibrated to provide emissive power of volume in FOV in kW/m^2
Total Energy Sensor	Medtherm Corp® Model 64-20T Dual total Heat Flux Sensor/Radiometer
Sensor	Schmidt-Boelter Thermopile
Spectral Band of Sensor	All incident thermal energy
Field of View	~130º controlled by aperture in sensor housing
Transient Response	< 290msec
Units of Measurement	Total heat flux incident on sensor face in kW/m^2
Hemispherical Radiometer	Medtherm Corp® Model 64-20T Dual total Heat Flux Sensor/Radiometer
Sensor	Schmidt-Boelter Thermopile (Medtherm Inc)
Spectral Band of Sensor	0.15 – 7.0 μm with sapphire window
Field of View	~130º controlled by window aperture
Transient Response	< 290msec
Units of Measurement	Radiant energy incident on sensor face in kW/m^2
Air Temperature	
Sensor	Type K bare wire butt welded thermocouple, new, shiny, connected to 27ga lead wire
Wire Diameter	0.05mm
Bead Diameter	~0.08-0.13mm
Units of Measurement	Degrees Celsius
Air Mass Flow	
Sensor	SDXL005D4 temperature compensated differential pressure sensor
Pressure Range	0-5 in H_2O
Sensor Design	Pressure sensor is coupled to custom designed bidirectional probe with ±60º directional sensitivity.
Units of Measurement	Calibrated to convert dynamic pressure to velocity in m-s-1 assuming incompressible flow
Sensor Housing	150× 180 × 270 (mm)
Housing Weight	7.7 kg
Insulation Material	Cotronics Corp® 2.5cm thick ceramic blanket
Tripod Mount	½ inch female NCT fitting permantly mounted to base of enclosure.
Power Requirements	12V DC
Power Supply	Rechargeable Internal Battery
Data Logging	Campbell Scientific Model CR1000
Sampling Frequency	Variable but generally set at 10 Hz

The sensors were calibrated prior to deployment as described elsewhere (Butler and Jimenez 2009). Integration of the heat flux time histories can provide a measure of fire total, radiative and convective energy per unit area as a function of heating time. In all cases the FBPs were positioned to sense fire from the expected spread direction (e.g., facing the oncoming fire front) based on wind direction, terrain, and lighting procedures. All FBPs were located nominally 1.0 m above the mineral soil.
Incident radiant and total heat flux at the surface of the FBPs were evaluated to determine convective heating at the sensor face (Frankman *et al.* 2010). The fine wire thermocouple has a response time of approximately 0.01 s and was used to sense flame presence and flame residence time. Flame arrival at the FBP was indicated by a nearly vertical increase (~3000-5000°C/s) in temperature to several hundreds of degrees above ambient. This temperature increase was almost always associated with a nearly instantaneous increase in heat flux at the sensor (4 to 25 $kW/m^2/s$). The completion of the flame event was indicated by a rapid decay in air temperature. In some cases the thermocouple failed, in which case the radiometer data alone was used to gauge the arrival and completion of flaming combustion. Flame radiative and convective energy were calculated by integrating the respective signals over the period of flaming combustion.

Methods – Infrared Thermography Measurements

Visible and near infrared (IR) imagery were captured using cameras situated on a 26 m boom lift. To lessen the likelihood of unburned fuels obscuring the IR signal from the fire, the lift was located 10-25 m from the control lines demarcating the small units; it was positioned at the centre of and perpendicular to the ignition line upwind of the units in all cases except S9. Prior to ignition of each plot, an image of the plot indicating the ambient temperature range (0-300 C) was collected. The oblique IR imagery was collected using a FLIR Inc SC660. The SC660 has a focal plane array resolution of 640 x 480 pixels, a sensitivity of 0.03°C, spatial resolution of 1.3 mrad and a thermal accuracy of ± 2%. The field of view of the oblique imagery covered the majority of the area of the small burn blocks and captured the entire fire perimeter from ignition until the fire passed the central instrument cluster and/or reached the downwind control line. Emissivity was set at 0.98 and the air temperature and relative humidity were noted for post processing. The temperature range for all cameras during the fires was set to 300-1500°C for collecting active fire IR data. High definition digital visual imagery was collected before and during the fire from video cameras located adjacent to the IR cameras. Post-processing resolution of this imagery is 1m x 1m.
Twelve ground control points for each small burn block were identified using surveyed positions of hot targets, instruments, and ignition points. The pre-fire IR image was critical for identifying ground control points.
For all IR imagery, the native file format was converted to an ASCII array of temperatures in K with rows and three columns where x,y,z = pixel row, pixel column, and temperature. Temperatures were then converted into W m^{-2} using the Stefan-Boltzmann equation for a gray body emitter. Mean residence time was calculated as the average amount of time a pixel was measured to be >525°C (Draper point) and maximum residence time was the maximum number of times a single pixel was measured to be >525°C.
For the oblique platform, images were processed using Python 2.7 programming language and rectified using GDAL (Geospatial Data Abstraction Library, 1.10.1, www.gdal.org). Once rectified, each image was converted back to radiometric temperature values, by back calculating using the previous equations, and estimates of fire radiative power (FRP) by pixel were calculated using the Stefan-Boltzmann Law for a grey body emitter.
Fire pixel values were summed across units at each time step to give total fire radiative energy (FRE) for the whole fire. Total fire radiative energy density (FRED) was calculated across oblique IR images (Figure 2). The total FRED images visually illustrate the area recorded by the oblique IR camera, as well as the distortion caused by the oblique angle.

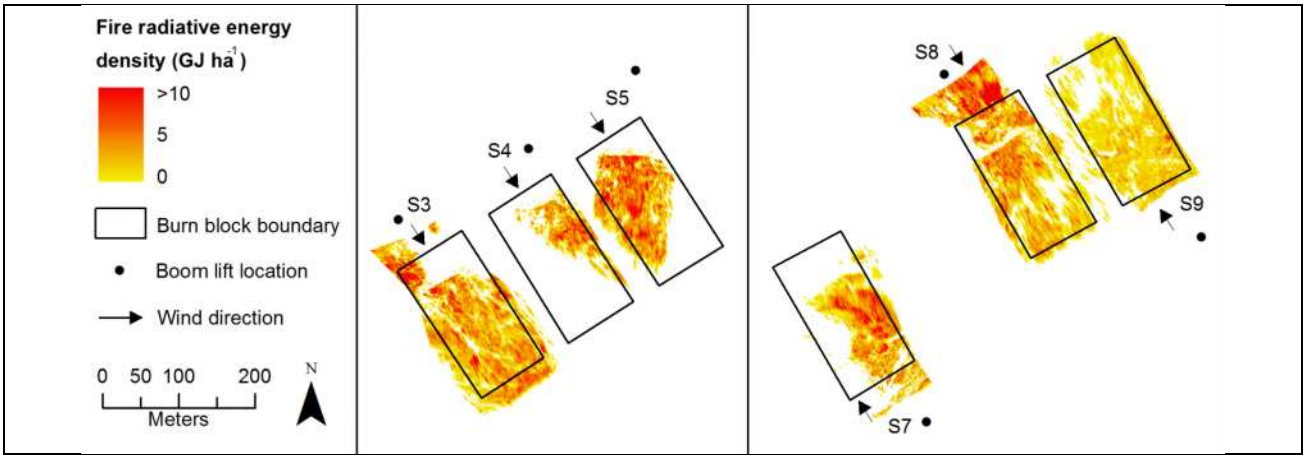

Figure 2. *Total FRED (GJ ha^{-1}) across oblique IR imagery.*

Results and Discussion

The aim of the RxCADRE campaign effort was to simultaneously acquire fine- to coarse-scale fuels, weather, and fire behaviour information during a suite of low-intensity prescribed fire experiments. This paper outlines a dense instrumentation network designed to measure the fine-scale meteorology within and around each burn block and couple that with fire behaviour and effects.

Preliminary results suggest that multiple fire behaviour and fire weather platforms can successfully capture small scale fire and terrain induced fluctuations, which may influence local fire-atmosphere interactions at the fire front. Initial analyses of the cup-and-vane anemometer data suggest that the relatively low fire intensity may not have been powerful enough to influence local weather conditions, as wind speed and direction differences related to the passage of the fire front were not detectable within the gridded surface level anemometer array. Table 3 outlines the overall average wind direction and speed, as well as the minimum and maximum wind speed, measured during each burning period for each of the six plots.

Table 3. Overall measurements for the cup-and-vane anemometer

Plot	Average Wind Direction, ø	Average Wind Speed, mph	Minimum Wind Speed, mph	Maximum Wind Speed, mph
S3	275.66	5.29	0.00	14.94
S4	275.06	7.65	0.00	18.03
S5	251.12	6.51	0.00	16.20
S7	274.69	8.08	0.00	19.15
S8	292.35	9.01	0.00	21.97
S9	270.30	9.03	0.00	21.59

For this study fire intensity was measured both in-situ by FBPs and remotely from IR cameras on an elevated oblique angle platform. The fire behaviour per unit (e.g., each of the six plots) is further interpreted using visual observations of flame properties; derived rate of spread values (based on observations of visual video footage, calculations based on infrared images, and fire time of arrival at fire behaviour packages); air temperature measurements; total and radiant energy measured incident on the in-situ FBPs; and derived values for fire radiative energy and fire convective energy.

Table 4 presents measurements derived from the FBP data for each of the six replicate burn blocks. These measurements include average radiative heat flux over the flaming period (Q_R), average convective flux over the flaming period (Q_C), average total heat flux at sensor for the flaming period

(Q_T), averaged flame emissive power from the narrow angle sensor (E_F), averaged kinetic air temperature (T_{air}) and averaged flame residence time from heat flux data (t_{flame}) for each of the burn plots. In general, the shrub/grass plots (S7,8,9) showed higher radiant, convective, and total heat flux, as well as higher emissive power than the grass plots (S3,4,5).
Table 5 outlines measurements derived from the oblique IR imagery for each of the six plots. Measurements include the active flaming duration, mean active flaming area, total area burned, total FRE, Mean FRP, Max FRP, and mean FRED. Total area burned is the mean number of $1m^2$ pixels burned at 1Hz (across IR images), and excludes unburned areas (pixels) within burn blocks.

Table 4. Averaged in-situ fire behaviour package data for each plot.

Plot	Average Radiant Heat Flux (kW/m^2)	Average Convective Heat Flux (kW/m^2)	Average Total Heat Flux (kW/m^2)	Average Flame Emissive Power (kW/m^2)	Average Kinetic Air Temperature (C)	Average Flame Residence Time (sec)
S3	7.5	5.9	12.1	23.0	821.6	103
S4	3.6	1.2	4.5	15.1	463	211
S5	3.7	5.5	8.6	14.5	682	12.3
S7	10.5	10.2	19.9	44.1	707	204
S8	12.9	12.5	23.7	42.8	922	122
S9	11.7	8.9	19.4	30.3	780.6	93

Table 5: Oblique IR imagery data for each plot.

Plot	Active flaming duration (min)	Mean (SD) active flaming area (m^2)	Total area burned (ha)	Total FRE (GJ)	Mean (SD) FRP (MW)	Max FRP (MW)	Mean (SD) FRED ($GJ\ ha^{-1}$)
S3	26	324 (286)	2.16	5.7	4.2 (3.8)	15.4	3.0 (2.5)
S4	20	88 (86)	0.50	1.3	1.2 (1.4)	5.5	3.0 (2.5)
S5	29	289 (203)	1.14	5.9	3.9 (3.0)	14.0	3.9 (2.9)
S7	29	150 (217)	1.14	3.1	2.1(3.3)	18.8	3.0 (2.6)
S8	23	353 (356)	2.31	6.3	5.1 (6.7)	41.4	3.0 (3.1)
S9	17	177 (173)	1.82	1.9	2.0 (2.0)	7.8	1.2 (1.0)

Comparisons between the in-situ fire behaviour measurements and oblique IR are not complete and therefore are not presented in this paper. However; the in-situ point source data show slightly greater heat flux measurements in plots S7-S9 which is in alignment with the grass/shrub fuel complex versus the dominant grass fuel component in plots S3-S5. A similar trend is not as apparent in the oblique IR data.
The calculations and analysis used between point source measurements (FBPs) and landscape scale measurements (IR) show promising similarities and it is our belief that the two techniques provide in depth detail pertaining to the micro scale fire environment. In these six low intensity grass fires, the interactions between fire behaviour and ambient wind flow are non-existent or difficult to detect. However, similar replicated measurements in a high intensity shrub or forest fire might elucidate some relationship between fire behaviour and micrometeorology. From this study we hope to determine that precise measurements at multiple scales in space and time are important for capturing and understanding the variability associated with both large and small scale fires in terms of wind flow and fire behaviour.

References

Barrows JS (1951) 'Fire behaviour in northern Rocky Mountain forests. USDA Forest Service, Station Paper No. 29. (Missoula, MT)

Butler, BW (1993) Experimental measurements of radiant heat fluxes from simulated wildfire flames. In '12th International Conference of Fire and Forest Meteorology, Oct. 26-28, 1993. Jekyll Island, Georgia', Oct. 26-28, 1993. (Eds JM Saveland, J Cohen) Volume 1 pp. 104-111. (Society of American Foresters, Bethesda, MD:

Butler, BW, Jimenez, D (2009) In situ measurements of fire behavior. In '4th International Fire Ecology & Management Congress: Fire as a Global Process. Savannah, GA', 30 November - 4 December, 2009. (Ed. S Rideout-Hanzak) (The Association for Fire Ecology:

Butler, BW, Cohen, J, Latham, DJ, Schuette, RD, Sopko, P, Shannon, KS, Jimenez, D, Bradshaw, LS (2004) Measurements of radiant emissive power and temperatures in crown fires. Canadian Journal of Forest Research 34, 1577- 1587.

Catchpole WR, Catchpole EA, Butler BW, Rothermel RC, Morris GA, Latham DJ (1998) Rate of spread of free-burning fires in woody fuels in a wind tunnel. Combustion Science Technology 131, 1-37.

Cheney NP, Gould JS, Catchpole WR (1993) The influence of fuel, weather and fire shape variables on fire-spread in grasslands. International Journal of Wildland Fire 3, 31-44.

Clements, C. B., S. Zhong, S. Goodrick, J. Li, X. Bian, B.E. Potter, W. E. Heilman, J.J. Charney, R. Perna, M. Jang, D. Lee, M.Patel,S. Street and G. Aumann 2007: Observing the Dynamics of Wildland Grass Fires: FireFlux- A Field Validation Experiment. Bull. Amer. Meteor. Soc., 88(9), 1369-1382.

Finney, M.A., R.C. Seli, C.W. McHugh, A.A. Ager, B. Bahro, J.K. Agee. 2006. Simulation of long-term landscape-level fuel treatment effects on large wildfires. USDA Forest Service Proceedings RMRS-P-41.

Fons WL (1946) Analysis of fire spread in light forest fuels. Journal of Agricultural Engineering Research 72, 93-121.

Forthofer, J. M. 2007. Modeling wind in complex terrain for use in fire spread prediction. Fort Collins, CO: Colorado State University, Thesis. (528 KB, 123 pages).

Frankman, D, Webb, BW, Butler, BW, Jimenez, D, Forthofer, JM, Sopko, P, Shannon, KS, Hiers, JK, Ottmar, RD (2012) Measurements of convective and radiative heating in wildland fires. International Journal of Wildland Fire 22, 157-167.

Horel, John D., and X. Dong 2010: An evaluation of the distribution of Remote Automated Weather Stations (RAWS). Journal of Appl. Meteor. and Clim., 49, 1563-1578.

Jimenez, D, Forthofer, JM, Reardon, JJ, Butler, BW (2007) Fire Behavior sensor package remote trigger design. In 'The Fire Environment-innovations, management, and policy. Destin, FL', 26-30 March, 2007. (Eds BW Butler, W Cook) Volume RMRS-P-46CD pp. 662. (US Dept. of Agriculture, Forest Service, Rocky Mountain Research Station

McCaffrey, BJ, Heskestad, G (1976) A robust bidirectional low-velocity probe for flame and fire application. COMBUSTION AND FLAME 26, 125-127.

Morandini, F, Silvani, X (2010) Experimental investigation of the physical mechanisms governing the spread of wildfires. International Journal of Wildland Fire 19, 570-582.

Potter BE (2012) Atmospheric interactions with wildland fire behaviour – I. Basic surface interactions, vertical profiles and synoptic structures. International Journal of Wildland Fire 21(7) 779-801 http://dx.doi.org/10.1071/WF11128

Rothermel RC (1972) 'A Mathematical model for predicting fire spread in wildland fuels.' USDA Forest Service, Intermountain Forest and Range Experiment Station Research Paper INT-115 (Ogden, UT)

Rothermel, R. C. 1991. Predicting behaviour and size of crown fires in the Northern Rocky Mountains. Research Paper INT-438. Ogden, UT: U. S. Department of Agriculture, Forest Service, Intermountain Research Station. (23,585 KB; 46 pages).

Van Wagner, C.E. Development and structure of the Canadian Forest Fire Weather Index System. 1987. Van Wagner, C.E. Canadian Forestry Service, Headquarters, Ottawa. Forestry Technical Report 35. 35 p.

Chapter 2
Fire Ecology

Bibliometric study of fires in tropical rain forests

Sonia Juárez-Orozco [a], Siebe-Grabach C [b], Fernández y Fernández D and Michán L[c]

[a, b] *Instituto de Geología, Universidad Nacional Autónoma de México, Mexico City, E-mail: soni@ciencias.unam.mx, siebe@unam.mx*
[c] *Laboratorio de Cienciometría, Información e Informática Biológica (CIIB), Departamento de Biología Comparada, Facultad de Ciencias, UNAM, laylamichan@ciencias.unam.mx, danielafyf@gmail.com*

Abstract
Bibliometrics allows to analyze on behalf of literature searches the existing knowledge around a specific topic and identify tendencies in its development. Tropical forests are characterized naturally by a low regime of fires. However human activities have dramatically changed this phenomenon. Since tropical rain forests are a hot spot of world's diversity, we conducted a bibliometric study of occurrence and effects of fires in tropical rain-forests. The aim of this work is to identify the main tendencies in biological literature about this subject, diagnose knowledge areas with a poor development and to define the geographic location of the performed studies and their methodological approach. This analysis will allow to identify the main gaps in the research of fires in tropical rain forests and contribute to direction the following research projects. We retrieved more than 2000 documents of indexed journals from the following bibliographic databases: Web of Science, Scopus, Science Direct, Biosis and Zoological abstracts. We selected the papers of words related with forest fires and tropical rain forests by an advanced search using logic and boolean operators. We considered for this study the fields: the document title, authors, adscription institution, publication year, journal name,
Keywords and descriptors, country, knowledge area and abstract. With this information we designed and normalized the database. Then, we considered all the papers focused on the study of fires in tropical forests and we classified other works that not specifically worked on fires but mention it as an important element of their studies. We did this by looking for the words "fire" and "tropical forest" in the
Keywords and abstracts. Then we analysed the documents by their geographic location and by the field of knowledge. We found an increasing interest in this topic in the scientific community since early 1950 to the present. The journals with more works in the theme were Forest ecology and management and Biotropica. We consider that this bibliometric review will help to the decisions making.

Keywords*: publication temporality, authors, indexed journals, knowledge fields, study site locations, bibliometrical studies*

Introduction

The generation of new information has impacted scientific work since the appearance of computers and the development of software. This technology allows to analyze on behalf of literature searches the existing knowledge on a specific topic and to identify tendencies in its development (Michán-Aguirre and Muñóz-Velasco 2013). It known as bibliometrics, which is a set of methods to quantitatively analyze academic literature (Wilson 1999; Hull *et al*. 2008).
Forest fires are related with global warming, decrease of forested area, loss of biodiversity and an increase of erosion. There are a lot of ecological parameters that change after a forest fire like vegetation cover, density, structure, composition, diversity and productivity. Therefore, forest fires are recognized as an interesting topic among foresters. Tropical forests are characterized naturally by a low fire regime (Bowman *et al*. 2011). However, in the last decades forest fires have become increasing events in these fragile ecosystems (Cochrane 2001). This relationship has been widely explored in temperate and mediterranean forests where plants have adapted to fire.

Agricultural and ranching activities are highly associated with forest fires. It is known that swidden cultivation is still an important agricultural practice, especially in areas where intensive agriculture is not possible (Van Vliet *et al*. 2012). However, fire plays also an important role in many parts of the world where it induces land uses change to for example cattle production or the cultivation of biofuel plants.
Bibliometric studies have been used for example to understand the direction of several ecologic phenomena such as changes in diversity and impact of conservation strategies (Song and Zhao 2013), by studying the information process and its change over time (Young and Wolf 2006; Stork and Astrin 2014).

According to FAO (1993) tropical forests are located in tropical areas within different biogeographic origins. They have a high plant and animal richness and show a wide range in composition, structure, functionality and productivity. The evergreen tropical rain forests are located in regions where the total annual rainfall is greater than 2500 mm and the dry season is either short or inexistent.
Since tropical rain forests are a hot spot of world's diversity and lately have been increasingly affected by fire to induce land use change, the objective of this study is to know the state of the art of tropical rain forest fire research. In particular, we wanted to determine which countries that possess tropical rain forest have reported fires and how this subject is addressed by the scientific community. It is important to detect the causes of unusual fire regime in tropical forest and which are the expected changes. The aim of this work is to identify the main tendencies in biological literature about this subject, detect the knowledge gaps and to define the geographic location of the performed studies and their methodological approaches.

Methods

We retrieved articles of indexed journals published until April 2013 from the following bibliographic databases: Web of Science, Scopus, Science Direct, Biosis and Zoological abstracts. We selected the papers by an advanced search (filtered) using the logic and boolean operators AND, OR, NOT, ?, * and "" that included words related with forest fires and tropical rain forests (Figure 1). We considered for this study the following fields: (1) the document's title, (2) authors, (3) adscription institution, (4) publication year, (5) journal name, (6) keywords and descriptors, (7) country, (8) discipline and (9) abstract. With this information we constructed a database and normalized records eliminating all the papers that were within the scope of our objectives and completed and annotated all the nine fields. Pre-processing included duplicate deletion and pertinence selection. In addition, we selected the documents that mention in their title the word soil, as it is an important compartment that changes after a forest fire and we re-classified the soil types according to the WRB soil classification (IUSS, 2007). Then, we considered all the papers focused on the study of fires in tropical forests and we classified other works that not specifically worked on fires but mention it as an important element in their studies. We did this by looking for the words "fire" and "tropical forest" in the keywords and abstracts and all of their synonyms and homonyms which were defined utilizing the Cab Abstracts thesaurus. The results of the search were restricted to only articles from environmental disciplines. The whole process of the method is resumed in Figure 2.

TITLE-ABS-KEY ("Tropical rain forest" OR "Tropical timber*" OR "Tropics" OR "Tropical countr*" OR "Tropical climat*" OR "Tropical America" OR "tropical crop*" OR "Tropical burn weed*" OR "Tropical forest*" OR "Tropical dry forest*" OR "Tropical seasonal forest*" OR "Semi-evergreen seasonal forest*" OR "Deciduous seasonal forests" OR "Equatorial forest*" OR "Rain forest*" OR "Tropical rain forest*" OR "Tropical timber*" OR "Tropics" OR "Tropical countr*" OR "Tropical climat*" OR "Tropical America") AND TITLE-ABS-KEY ("Fire regime*" OR" Managed wild land fire*" OR "Prescribed natural fire*" OR "Prescribed fire*" OR "Natural fire*" OR "Wild fire*" OR "Wildfire*" OR "Let burn" OR "Manager-ignited fire*" OR "Wild land fire*" OR "Burn*" OR "Ignition*" OR "Shifting agriculture*" OR "Shifting cultivation*" OR "Hot spot*" OR "Indian fire*" OR "Slash-and-burn*" OR "Fire*" OR "Slash and burn*" OR "Ash*" OR "Fuel*" OR "Fire trend*" OR "Fire *adapted" OR "fire-*" OR "Fire regime*" OR "Managed wild land fire*" OR "Prescribed natural fire*" OR "Prescribed fire*" OR "Natural fire*" OR "Wild fire*" OR "Wildfire*"OR "fire history" OR "fire trend*")*

Figure 1. Terms and algorithms used in the advanced search

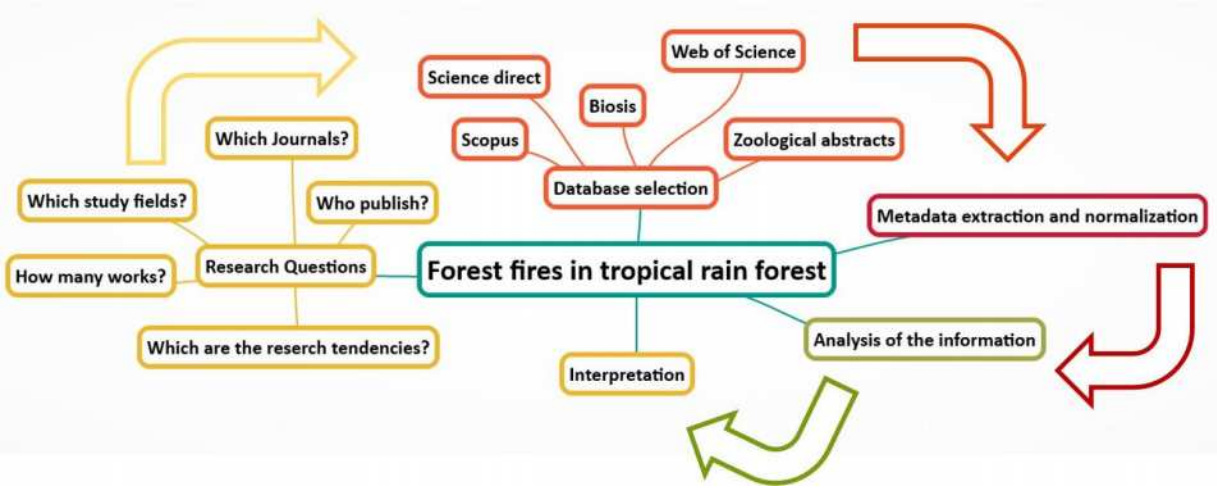

Figure 2. Stages of the documental research

Statistical analysis

Absolute and relative frequencies of the above fields were obtained. We analysed the documents by their geographic location and by field of knowledge. We also calculated the frequency of words appearing in the title and keywords of the documents to see which are the main fields addressed by the scientific community. We conducted a keyword analysis, by calculating the probability to find one word by inserting another one.

3. Results

In total we recorded 2000 publications. The following results belong to the analysis of these records. Reports on fires in tropical rain forests started in 1960. From the beginning of the 1980's articles on fire in tropical rain forests have been growing steadily. This growth pattern is shown for papers that either just report a forest fire in a tropical forest (N = 1982) or focus specifically on this phenomenon (N = 498) (Figure 3).

Research about tropical rainforest fires was conducted in 42 countries. Most of these studies have been done in the American continent (49.34 %), followed by Asia (26.54 %), Australia (15.79 %) and Africa (8.33 %). The most productive countries of each region were Brazil (141), Venezuela (18) and México (16) for America; Indonesia (55), India (25) and Malaysia (23) for Asia; Australia (63) for Australia

and Cameroon (10) and Madagascar (7) for Africa. However, the distribution in the number of these studies does not reveal which countries have more forest fires in their corresponding tropical rainforests. Tropical rain forest are decreasing their area due to deforestation and in many cases fire is a tool that facilitates the advance of agriculture. Figure 4 shows the remains of tropical forests distributed around the world. The Amazon, for example is the greatest area covered with rainforest in the world, and also one of the regions in which forest fires are most studied. Although, this is not related with the real number of forest fires in this area, but rather is related with the number of investigations conducted in these areas. These data show that rather few studies exist on fire studies in these forests, in which plants have not adapted to cope and to recover after a fire and in consequence allows exotic plants to disseminate.

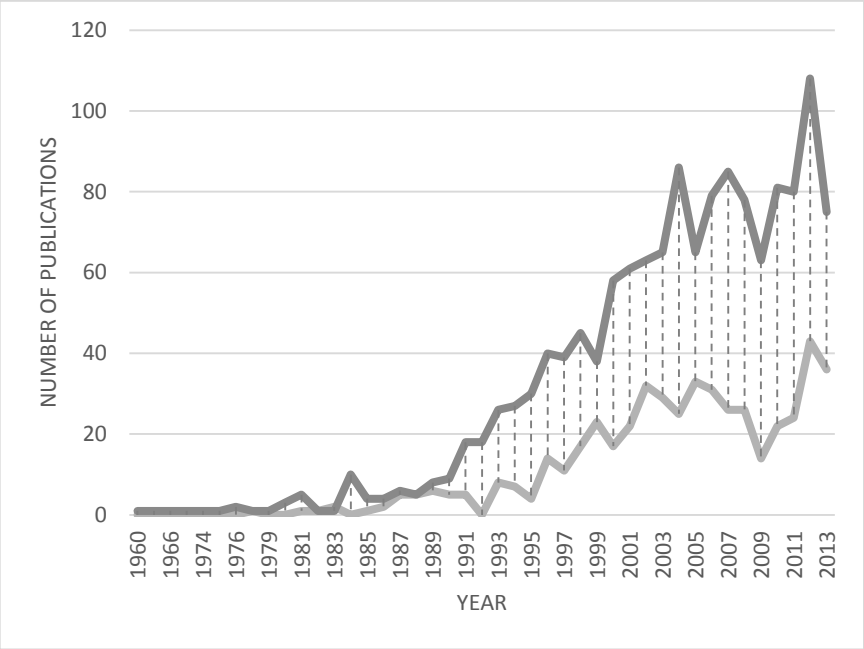

Figure 3. Temporal variation in the number of publications. Lines in dark grey denote studies in which forest fires are mentioned (N = 1982), and lines in light grey represent publications focused on tropical rainforest fires until April 2013 (N = 498).

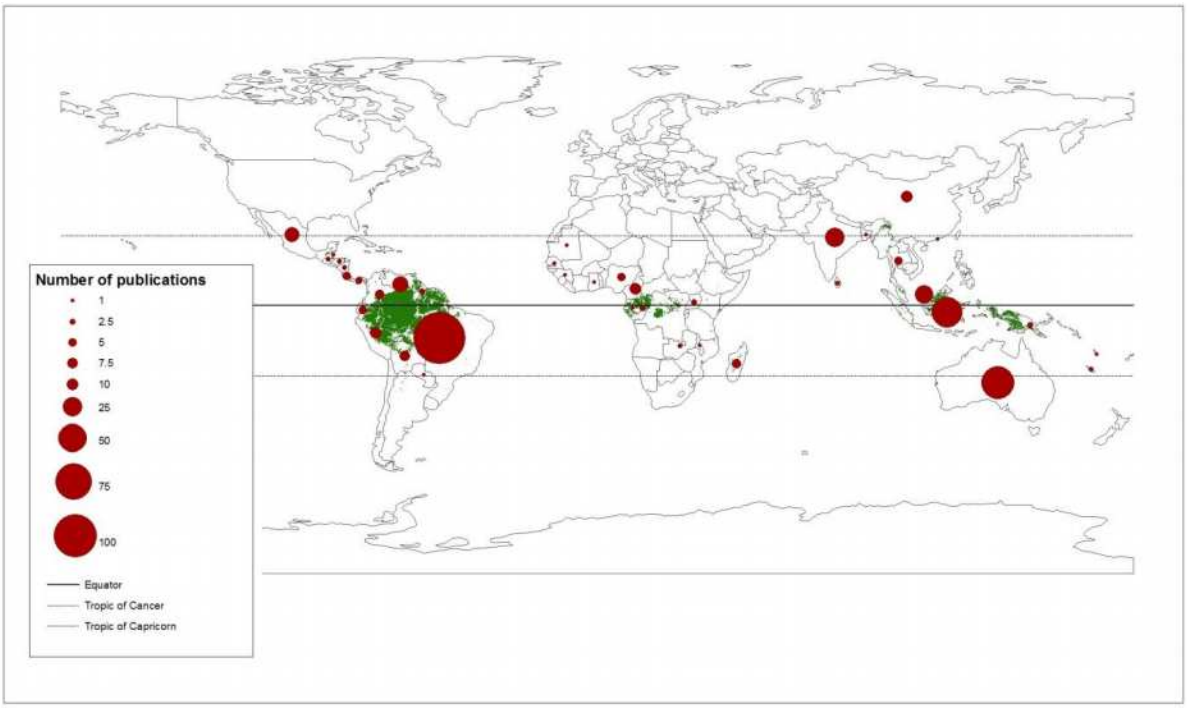

Figure 4. Spatial distribution of publications at global scale focused on fires in tropical rainforests. Green areas represent the principal remains of tropical rainforests (Wildlife Conservation Society). Red dots represent the number of publications.

The journals with most studies dealing with the topic were Forest Ecology and Management, Biotropica and the International Journal of Remote Sensing with 24, 20, 18 and 17 publications, respectively. Terms like slash and burn agriculture are frequent. The papers were published in 192 international journals. We identified ten journals that form together 31.53% of the published scientific articles related with fires in tropical forests. The contribution of each journal was: Forest Ecology and Management (4.82 %), Biotropica (4.02 %), International Journal of Remote Sensing (3.61 %), Journal of Tropical Ecology (3.61 %), Remote Sensing of Environment (3.21 %), Biodiversity and Conservation (2.81 %), Agriculture, Ecosystems and Environment (2.61 %), Ecological Applications (2.41 %), Journal of Biogeography (2.41 %) and Austral Ecology (2.21 %) (Figure 5).

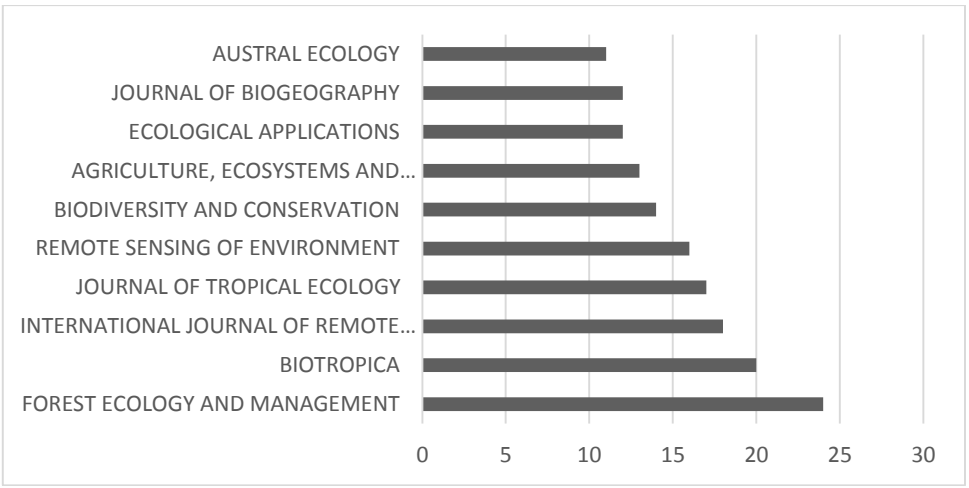

Figure 5. Main journals and the number of publications related with fires in tropical rain forests. N = 498 articles.

There were 5195 terms in our keyword analysis. These terms provide information on the main interests in the scientific community related with fires in tropical rainforests. As expected, fire, forest, tropic, burn and shifting are the words that appear most in the literacy, since these were the terms selected in the advanced search. Other terms are *cultivation*, *effect*, *use*, *Amazon* and *change*, which were the five most repeated terms among the key words in the published documents. The key words *cultivation* and *use* are related with human activities such as agricultural practices in which fire is used for several purposes. On the other hand, the term *effect* shows that the effect of fire is one of the main research topics. Apparently, rainforest are unnaturally burned with more frequency than expected in nature. It is of particular interest that *Amazon* is one of the most frequent words since it is the largest area covered with tropical forests and also the area where more scientific articles are produced. Table 1 shows the most used terms among which regions or countries can be identified, in which the causes of fire are being studied around the world. The majority of documents are associated with ecological disciplines followed by soil science, agronomy and remote sensing (Figure 7).

Table 2. Stemmed key word frequency (N = 498)

Global	freq.	Global %	Global	freq.	Global %	Global	freq.	Global %
Fire	308	5.929	brazilian	29	0.558	northern	18	0.346
Forest	244	4.697	speci	29	0.558	recover	18	0.346
Tropic	127	2.445	amazonian	28	0.539	savanna	18	0.346
Burn	99	1.906	australia	27	0.52	spatial	18	0.346
Cultiv	69	1.328	system	27	0.52	borneo	17	0.327
Shift	67	1.29	rainforest	26	0.5	composit	17	0.327
Effect	56	1.078	area	25	0.481	landscap	17	0.327
Use	55	1.059	divers	25	0.481	regim	17	0.327
Amazon	47	0.905	eastern	23	0.443	studi	17	0.327
Slash	45	0.866	amazonia	22	0.423	swidden	17	0.327
Chang	40	0.77	data	22	0.423	brazil	16	0.308
Rain	40	0.77	respons	22	0.423	central	16	0.308
Biomass	39	0.751	log	21	0.404	fallow	16	0.308
tree	38	0.731	communiti	20	0.385	nutrient	16	0.308
veget	34	0.654	southern	20	0.385	region	16	0.308
agricultur	33	0.635	year	20	0.385	wildfir	16	0.308
dynam	32	0.616	deforest	19	0.366	east	15	0.289
impact	32	0.616	indonesia	19	0.366	global	15	0.289
soil	32	0.616	manag	19	0.366	analysi	14	0.269
land	31	0.597	structur	19	0.366	bird	14	0.269

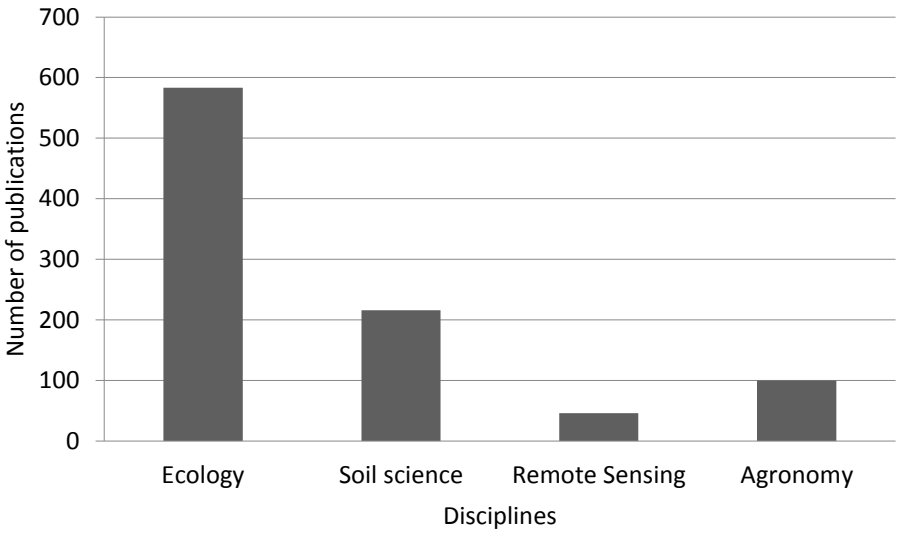

Figure 7. Disciplines that study forest fires in tropical rainforests

Only 32 of the reviewed articles were focused on the changes occurring in soil after a fire in tropical rainforests. From these studies, 15 did not report the kind of soil present in the study area. The principal topics taken into account were physicochemical changes in the soils after a fire, but also the effects of fires on macro and microbiota. In soil the most commonly reported changes are the soil pH, organic matter content and exchangeable cations like potassium and calcium, as well as changes in nitrate and phosphorus contents. These properties are important for farmers to assure a good harvest. Their loss over time leads to soil degradation.

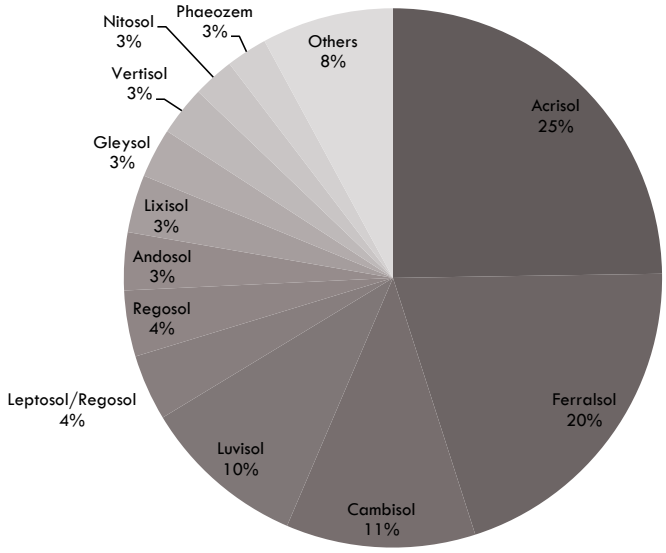

Figure 7. Main soil reference groups in which studies on fires in tropical rainforests have been done.

Discussion

Forest fires represent a threat for the relicts of tropical forests around the world. Natural fires in these ecosystems are rarely reported. Instead, publications on forest fires are increasing. Fires on tropical rainforests appear to be more frequent, intense and extended over the time (Pyne 1995; Cochrane 2002). Mouillot and Field (2005) estimate that in the 1990's alone 54 Mha yr^{-1} of tropical rainforests were affected by fire. Some consequences on the environment are gas emissions, which between 1997 and 1998 represented approximately 40% of the emissions produced by burning of fossil fuel (Cochrane 2003). It is necessary to know the real numbers of fires occurring in the tropical rain forest over the world and which is the extent of these events. These studies ought to reveal the causes, which can be a high rate of land conversion to agriculture or pasture, proximity to roads and rural roads, population density or climatological causes which include long periods of dryness related to the climatic global changes. Taking in account a mesoscale approach (mesoscales γ and β, 2-20, 20-200 km, respectively; Stull 1988), relatively few remote sensing studies were focused in detection, burned area calculation and land use change.

Spatially, forest fires are reported worldwide. According with information of the World Bank (2014) most of the countries in the tropics have a high rural population and low GDP per capita, excepting Australia. Conversely, continents like Africa show less reports of fires in their forest than more developed regions as Australia. In the case of America, there is a vast production of articles in the Amazon region, such as Brazil, Venezuela and others. Nevertheless, there is a smaller productivity of articles in Central America. In Asia the largest number of articles have been published in Indonesia, India and Malaysia.

The discipline of most research studies was ecology. Among the most studied ecological factors were: *diversity*, *structure*, *recovery* and *composition*. These variables reflect that most of the ecological studies are focused on the community level, but also some investigations deal with landscape and ecosystem scale. Biomass, for example is one of the most important elements in ecology, but also in management and prevention of fires. In the case of remote sensing the principal interests were focused in detection of forest, the calculation of the burned area and on land use change. Therefore biomass should be included in the remote sensing studies to make models with an ecosystem approach that explain a huge part of the fire dynamic and improve the fire management and prevention programs.

Agriculture activities usually are the origin of fire and soil properties change are a consequence of these activities which also are related with crop productivity. A deep bibliometric study can help us to understand how and which changes in soil properties, after fires and over time, are generalizable. We need to synthetize and make deep bibliometric studies to relate all the ecosystem properties studied until now to bigger scales. This initial bibliometric study is a first step in a research topic to understand how bibliometric studies in different fields, as in other cases have shown to understand different phenomena and how they have helped on making decisions about different topics like conservation of biodiversity (Stork and Astrin 2014) or which are the ecological consequences of land use change (Hasanagas *et al*. 2010). Bibliometric studies in different fields have allowed to understand complex phenomena and in some cases they can help to take decisions (Hasanagas *et al*. 2010). Finally, we consider that this bibliometric review will help to the decisions making helping us to understand the relevance of the different scale approaches and the gaps in fire ecology to evaluate both the effects of climatic change, the real relevance of shifting cultivation and other anthropogenic activities on fire dynamics, its consequences, management and prevention.

References

Bowman DM, Balch J, Artaxo P, Bond WJ, Cochrane MA, D'Antonio CM, DeFries R, Johnston FH, Keeley JE, Krawchuk MA, others (2011) The human dimension of fire regimes on Earth. Journal of biogeography 38(12), 2223–2236.

Cochrane MA (2001) In the line of Fire Understanding the Impacts of Tropical Forest Fires. Environment: Science and Policy for Sustainable Development 43(8), 28–38.

Cochrane MA (2002) Spreading like wildfire: tropical forest fires in Latin America and the Caribbean: prevention, assessment and early warming.

Cochrane MA (2003) Fire science for rainforests. Nature 421(6926), 913–919.

FAO. 1993. The Challenge of Sustainable Forest Management. Chapter 2: The world's forests. Rome. http://www.fao.org/docrep/t0829e/T0829E04.htm#Tropical forests

Hasanagas ND, Styliadis AD, Papadopoulou E (2010) Environmental Policy \& Science Management: Using a scientometric-specific GIS for e-learning purposes. International Journal of Computers, Communications and Control 5(2), .

Hull D, Pettifer SR, Kell DB (2008) Defrosting the digital library: bibliographic tools for the next generation web. PLoS computational biology 4(10), e1000204.

Michán-Aguirre L, Muñóz-Velasco I (2013) Cienciometr'\ia para Ciencias Médicas: Definiciones, aplicaciones y perspectivas.

Mouillot F, Field CB (2005) Fire history and the global carbon budget: a 1$\times$ 1 fire history reconstruction for the 20th century. Global Change Biology 11(3), 398–420.

Pyne SJ (1995) "World fire: the culture of fire on earth." (Holt)

Song Y, Zhao T (2013) A bibliometric analysis of global forest ecology research during 2002-2011. SpringerPlus 2(1), 1–9.

Stork H, Astrin JJ (2014) Trends in Biodiversity Research—A Bibliometric Assessment. Open Journal of Ecology 4(07), 354.

Stull, R. 1988, An Introduction to Boundary Layer Meteorology, Kluwer Academic Press, Dordretch.

The World Bank Group. 2014. http://data.worldbank.org/. Accessed 10/06/2014

Van Vliet N, Mertz O, Heinimann A, Langanke T, Pascual U, Schmook B, Adams C, Schmidt-Vogt D, Messerli P, Leisz S, others (2012) Trends, drivers and impacts of changes in swidden cultivation in tropical forest-agriculture frontiers: a global assessment. Global Environmental Change 22(2), 418–429.

Wildlife Conservation Society - WCS, and Center for International Earth Science Information Network - CIESIN - Columbia University. 2005. Last of the Wild Project, Version 2, 2005 (LWP-2): Last of the Wild Dataset (Geographic). Palisades, NY: NASA Socioeconomic Data and Applications Center (SEDAC). http://dx.doi.org/10.7927/H4348H83. Accessed 10/06/2014.

Wilson CS (1999) Informetrics. Annual Review of Information Science and Technology (ARIST) 34, 107–247.

Young R, Wolf S (2006) Goal attainment in urban ecology research: A bibliometric review 1975-2004. Urban Ecosystems 9(3), 179–193.

Changing fire regimes: The response of litter-dwelling invertebrates to altered seasonality and frequency of fire

Alan York

University of Melbourne, 4 Water Street Creswick VIC 3363 Australia, alan.york@unimelb.edu.au

Abstract
Mediterranean climate regions are experiencing changes that are projected to have significant impacts on patterns of temperature and rainfall, thereby affecting key ecosystem drivers such as fire regimes. In the sclerophyll-dominated vegetation communities of southern Australia, land managers are responding to increased wildfire probabilities through the use of more frequent low intensity (prescribed) fire. With burning occurring more often throughout the year, plant and animal communities are experiencing altered fire regimes; with changes to both frequency and season of burn. Here I report on the results of a long-term, replicated study, investigating the effects of fire frequency (high vs low) and seasonality (autumn vs spring) on a biodiverse and functionally important component of the fauna (litter-dwelling invertebrates). At the ordinal level, three broad patterns of response were detected: (i) no effect of fire treatment on abundance, (ii) a burning treatment effect, suggesting that fire in any season and at any frequency lowers abundance, and (iii) a significant negative effect of fire frequency on abundance. No season of fire effects were apparent for any group. The mechanisms underpinning these responses warrant further investigation, particularly in light of proposed increases in the amount of prescribed fire to be applied to these forest systems in coming years.

Keywords: climate change, fire regime, invertebrates, prescribed fire

Introduction

The application of prescribed fire in many regions is becoming more common amid forecasted increases in the frequency and severity of wildfire under climate change (Stephens *et al.* 2012; Cary *et al.* 2012; Flannigan *et al.* 2013). For example, in the state of Victoria in south-eastern Australia, a long term program of prescribed burning on an annual rolling target of 5% of public land (equating to a minimum of 385,000 ha per year) was introduced following severe wildfires in 2009 (Attiwill and Adams 2013). Historically, primarily for safety reasons, prescribed burning in these temperate ecosystems has been undertaken during autumn (Luke and McArthur 1978), however to meet new burn targets managers are now applying fire whenever weather conditions allow. As a consequence prescribed fires are occurring across a broader range of seasons and, potentially, with increased frequency (i.e. reduced intervals between successive burns). Understanding the implications of such changes in the fire regime for biodiversity is therefore critical (Bradstock *et al.* 2010; Penman *et al.* 2011).

As a group, invertebrates are numerous, diverse, and play important functional roles in ecosystems (Beattie 1995; Raven and Yeates 2007). Through their role in the breakdown and decomposition of organic matter and the release of materials to the soil environment, invertebrates have a positive influence on the availability of nutrients for plant growth and on soil physical properties. In Australia there have been a number of studies on the effects of low-intensity prescribed fire on invertebrates, particularly in regard to the interval between such fires (fire frequency); with fewer examining the season of burn. Following two short rotation (three-year interval) low-intensity fires in spring in Victoria, Collett *et al.* (2003) found that arthropod diversity had increased following the second fire, caused by greater evenness of individuals among taxa rather than any change in taxon richness. Three fires over an eight-year period had no cumulative impact on springtails and earthworms (Collett 1999)

or on richness or composition of beetle communities (Collett and Neumann 1995), but the effects of individual fires were quite variable. In contrast, two autumn fires over a five-year period produced a significant decrease in springtails, mites and earwigs and an increase in ant activity (Collett 1998). From studies based in Western Australian, Majer (1980, 1985) concluded that spring burning may be more detrimental to the soil-surface fauna than autumn burning. Some impacts however may be cumulative and take many years to manifest themselves. Examining the effects of seven fires over a 20 year period in sclerophyll forest in New South Wales, York (1999a) showed significantly lower ordinal diversity of surface-active and litter-inhabiting invertebrates in frequently burnt sites compared to unburnt sites.

With changing management practices involving the use of fire, concern has been recently expressed about the potential impacts of altered fire regimes on invertebrate diversity in both Mediterranean woodlands (Quartau 2009) and Australian temperate forests (New *et al.* 2010; York 2012). This paper utilises a long-term fire experiment to build on existing research; evaluating both the independent and combined effects of changed frequency and season of planned fire on litter-dwelling terrestrial invertebrates.

Methods

The study incorporates five areas (known locally as the 'Fire Effects Study Areas', FESA) within a 25 km radius in the Wombat State Forest, about 100 km north-west of Melbourne, Victoria, south-eastern Australia. The areas have an underlying geology of Ordovician sedimentary rock, and are at elevations ranging from 590 to 760 m above sea level. Topography varies from mostly flat (slopes 0-4°) to hills of low to moderate relief (slopes up to 21°). The climate is temperate, with annual rainfall in the range 814-901 mm, with the majority falling in winter and spring (Tolhurst and Flinn 1992). Native vegetation of the study areas is open to tall-open forest (tree heights 10 to >30 m, projective foliage cover 30-70%; Specht 1981). Dominant trees are Messmate Stringybark *Eucalyptus obliqua*, Narrow-leaf Peppermint *E. radiata* and Candlebark *E. rubida*. The understorey is characterised by a sparse shrub layer up to four metres in height (e.g. *Acacia* spp.), and ground layer of Austral Bracken (*Pteridium esculentum*) and native perennial grasses, forbs and rushes. Open to tall-open forests such as these are likely to be burnt more frequently under ongoing commitments to extensive use of prescribed fire on Victoria's public land (DSE 2012).

The study was established in 1985, and used a randomised block design involving a long-unburnt control (reference state) and four prescribed fire treatments randomly allocated within each of the five study areas (total of 25 treatment areas). The four fire treatments involved a factorial combination of two fire seasons (autumn or spring), and two fire frequencies (nominally every 3 or 10 years); that is, Autumn High-frequency (AH), Autumn Low-frequency (AL), Spring High-frequency (SH), and Spring Low-frequency (SL). Nominal prescribed fire intervals of three and ten years were chosen to represent, respectively, the shortest interval for sufficient recovery of surface fuels to carry a fire in these forests, and the likely return interval of prescribed fire based on local fire management practice. Prescribed fires in all treatments in this study were considered to be of low intensity (Tolhurst & Flinn 1992). Mean inter-fire intervals ranged from 2.7–5.7 years in the High-frequency treatments, and 8.5-16 years in Low-frequency treatments (see Bennett *et al.* 2013 for further detail).

To sample topographic variability, three plots (ridge, slope and gully) were established in each of the five burn treatments in each of the five areas; giving 75 plots overall. In 2012, twenty 2000 cm^3 samples of surface litter were systematically collected along 2 x 18 m orthogonal transects at each plot. Samples were bulked and sieved on site using a litter sifter (Upton & Mantle 2010); with a single sample for each plot returned to the laboratory. Invertebrates were extracted over four days using Tullgren funnels at the University of Melbourne. Samples were stored in 70% alcohol and identified to Order or equivalent using a binocular dissecting microscope and appropriate taxonomic keys.

Effects of prescribed fire treatments on invertebrate abundance were tested using Analysis of Variance (ANOVA) in Genstat 16th Edition. A factorial plus added control model with area as a random factor, treatment as a fixed factor, and plot nested within treatment by area, was used to examine the overall effects of prescribed fire (Control versus Fire treatments), as well as the effects of prescribed fire season (Autumn versus Spring) and frequency (High versus Low), and their interactions.

Results

In total 276,314 individuals from 23 broad taxonomic groups were collected. A number of groups were poorly represented and/or unlikely to be effectively sampled using litter extraction, with data for 15 groups sufficient to undertake analyses (Table 1). Overall, there was a significant effect of fire frequency on total invertebrate abundance (P = 0.009) with both Autumn High-frequency (AH) and Spring High-frequency (SH) treatments resulting in a substantial decline in mean invertebrate abundance (Table 1).

Table 1. Summary statistics of invertebrate abundance and ANOVA results for comparisons of five burning treatments (AL: Autumn Low-, AH: Autumn High-frequency; C: Unburnt; SL: Spring Low-, SH: Spring High-frequency). B: significant burn treatment effect, F: significant burn frequency effect (P<0.05), ns: not significant. – indicates groups poorly represented and/or unlikely to be effectively sampled using litter extraction (not tested).

Taxon	Treatment (Abundance MEAN±S.E.)					ANOVA
	AL	AH	C	SL	SH	
Mites	2542.7±424.5	1901.9±264.4	2220.7±279.8	2770.7±373.3	1797.5±259.1	F
Amphipods	28.7±11.7	4.1±0.9	27.7± 5.8	26.3±7.6	9.1±3.5	F
Spiders	66.9±11.4	49.0±12.1	77.7±7.2	58.8±9.5	48.1±8.0	B,F
Cockroaches	9.1±1.5	7.5±1.1	7.0±1.1	0.7±0.7	6.8±0.8	ns
Centipedes	8.1±2.7	8.7±1.9	7.0±1.6	9.8±1.8	7.2±2.4	ns
Beetles	131.7±19.0	97.5±11.7	119.9±15.1	133.7±13.9	89.2±10.8	F
Springtails	701.5±149.2	340.2±50.1	1507.3±358.6	917.5±272.2	566.3±122.4	B
Earwigs	1.4±0.6	1.9±0.5	0.3±0.2	1.5±0.5	1.1±0.4	-
Diplopods	25.4 15.4	5.5±2.1	21.7±9.1	10.6±2.9	5.0±2.0	ns
Bristletails	0.0 0.0	0.1±0.1	0.1±0.1	0.0±0.0	0.0±0.0	-
Flies	0.4±0.2	0.6±0.2	1.2±0.3	1.1±0.3	0.3±0.1	-
Webspinners	0.0±0.0	0.0±0.0	0.4±0.3	0.0±0.0	0.0±0.0	-
Bugs	18.1±2.3	10.4±1.6	17.8±2.9	12.5±2.6	12.7±1.9	ns
Ants	43.9±7.2	41.7±7.9	46.3±14.7	48.3±6.2	59.2±12.4	ns
Wasps	7.3±1.1	8.4±1.1	10.6±3.5	8.9±1.5	5.6±0.9	ns
Woodlice	13.9±3.1	9.7±2.7	23.7±4.0	15.3±2.9	7.9±3.4	B
Larvae	251.9±33.9	182.0±23.9	243.4±35.4	267.3±31.9	206.0±22.8	F
Velvet worms	0.1±0.1	0.0±0.0	0.0±0.0	0.1±0.1	0.0±0.0	-
Grasshoppers	0.1±0.1	0.1±0.1	0.1±0.1	0.1±0.1	0.1±0.1	-
Pseudoscorpions	2.7±0.7	3.2±0.9	5.7±1.7	6.0±2.1	1.2±0.4	ns
Barklice	1.9±0.6	0.1±0.3	1.1±0.4	1.9±0.5	1.2±0.3	-
Scorpions	0.2±0.1	0.3±0.2	0.1±0.1	0.2±0.1	0.0±0.0	-
Thrips	73.9±19.4	66.9±11.5	100.6±26.2	94.1±17.9	98.5±19.9	ns
Total	3931.0±555.1	2741.3±282.2	4442.2±576.0	4393.7±566.5	2924.1±317.1	F

When individual groups were considered, there were 3 basic patterns of response (Figure 1). Firstly, for seven groups (cockroaches, centipedes, diplopods, bugs, ants, wasps and barklice) there was no effect of fire treatments on their abundance at plots, suggesting that numbers of these groups were not

impacted by fire in any season or at any frequency. Secondly, for three groups (spiders, springtails and woodlice) there was an effect of the burning treatment, suggesting fire (in any season and at any frequency) lowers their abundance. Thirdly, for five groups (mites, amphipods, spiders, beetles and larvae), there was a significant effect of fire frequency on their abundance. No season of fire effects were apparent for any group.

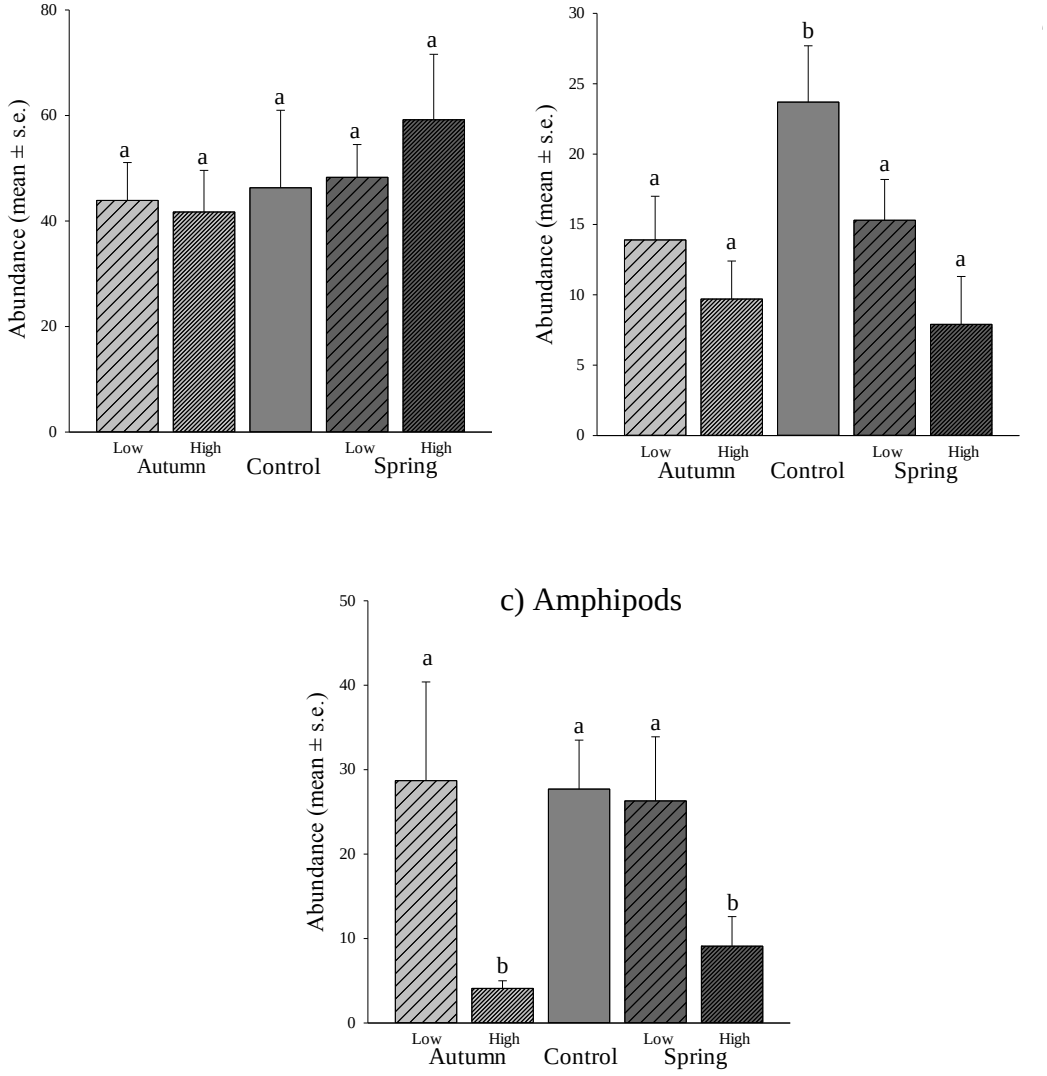

Figure 1. Examples of the three basic patterns of response. a) No effect of fire treatments on abundance e.g. ants. b) Significant effect of the burning treatment, irrespective of season and frequency e.g. woodlice. c) Significant effect of fire frequency e.g. amphipods. Columns with the same letters do not differ significantly, while those with different letters are significantly different in mean abundance (SNK post-hoc test). No season of fire effects were apparent for any group.

Discussion

Recent catastrophic wildfire events in Mediterranean-type ecosystems, including in Australia (Cameron *et al.* 2009), California (Keeley *et al.* 2009) and Greece (Pyne 2008), have led to increasing pressure on governments to mitigate fire risk (Teeter 2008; Teague *et al.* 2010). Fire prescriptions often target surface fuel loads in an attempt to reduce the intensity and spread of future wildfires (e.g.

McArthur 1967; Gould *et al.* 2007). In Australian dry forest systems however, leaf litter can accumulate quickly, often reaching pre-fire levels within 3 years (Penman and York 2010). Maintaining low fuel levels in strategic locations, and/or increasing annual area burnt by prescribed fire, will inevitably lead to increases in the frequency of fire and changed season of burning, as land managers seek to maximise burning opportunities. While sclerophyll forests, woodlands and heaths are dominated by plant species with adaptive responses than enable them to survive periodic burning (Gill 1981; Noble and Slatyer 1981), the impact of fires on terrestrial invertebrates is poorly understood. Because low-intensity fires are often patchy in nature and invertebrates can seek shelter within the soil and in unburnt habitat refuges, it has been suggested (Majer 1980; Campbell and Tanton 1981; Abbott 1984) that periodic fires used for fuel management purposes have few long-term effects on most soil and litter invertebrates. Little is known, however, about the effects of the repeated use of fire over long time scales; particularly as frequent fires can reduce spatial and structural heterogeneity and could have long-term consequences for the survival of invertebrate populations (Collett *et al.* 1993).

This study investigated the impact of 30 years of low-intensity fire on a functionally important component of the forest biodiversity, litter-dwelling invertebrates. Soil- and litter-dwelling invertebrates play an important role in the breakdown of litter and soil organic matter; facilitating the decomposition process and contributing to nutrient availability (York *et al.* 2012). Results from this long-term fire study indicated three broad response patterns. Firstly, for seven groups (cockroaches, centipedes, diplopods, bugs, ants, wasps and barklice) there was no effect of fire treatments on their abundance at plots, suggesting that numbers of these groups were not impacted by fire in any season or at any frequency. York (1999a) found negative effects of frequent fire on cockroaches, centipedes and bugs, although the low numbers caught in that study warrant cautious interpretation. Secondly, for three groups (spiders, springtails and woodlice) there was an effect of the burning treatment, suggesting fire (in any season and at any frequency) lowers their abundance. Collett (1998) found that two autumn fires over a five-year period produced a significant decrease in springtail abundance, while York (1999a) reported reductions in the numbers of spiders, springtails and woodlice with frequent autumn fire. The third broad response identified concerned five groups (mites, amphipods, spiders, beetles and larvae), where there was a significant negative effect of fire frequency on their abundance. High fire frequency has previously been shown to reduce the numbers of these groups (York 1999a).

It is of potential concern that high frequency fire (every ~3 years) significantly reduces the number of mites, amphipods, beetles and insect larvae. Amphipods (landhoppers) and larvae play major roles in litter fragmentation (Schowalter 2000) while many litter-dwelling beetles are associated with decomposer fungi (Lawrence and Slipinski 2013). This suggests a reduction in rates of decomposition and nutrient cycling with more frequent fire; which has implications for both rates of post-fire litter accumulation and forest health (see Brennan *et al.* 2009). The mechanisms underpinning these responses warrant further investigation, particularly in light of proposed increases in the amount of prescribed fire to be applied to these forest systems in coming years. It is most likely that frequent fire influences litter biomass and associated moisture levels (York 1999b; Penman and York 2010), and simplifies habitat structure. Several studies have reported the importance of litter depth and structure as a control of litter invertebrate composition (e.g. Uetz 1979; Michaels and McQuillan 1995). Because of this, litter fauna may take longer to recover after fire than the soil fauna (Majer 1984) and unburnt plants, logs and patches of litter become important refuges for fauna in burnt areas (Majer 1980; Whelan *et al.* 1980; Andrew *et al.* 2000). An interesting finding concerned the lack of a season of fire effect for any group. In earlier studies at this site Collett (1993, 1998, 1999) and Collett and Neumann (1995) observed that effects of individual fires were quite variable, with outcomes for most groups more dependent on the severity of individual fires rather the season of burn. Koch and Majer (1980) have previously emphasised that an understanding of the phenology (seasonality) of invertebrate abundance and activity is needed to fully assess the potential impacts of burning. Future work on this

project will target focal groups with an emphasis on understanding responses at the feeding guild or functional group level.

References

Abbott I (1984) Changes in the abundance and activity of certain soil and litter fauna in the jarrah forest of Western Australia after a moderate intensity wildfire. Australian Journal of Soil Research 22, 463-469.

Andrew N, Rodgerson L, York A (2000) Frequent fuel-reduction burning: the role of logs and associated leaf litter in the conservation of ant biodiversity. Austral Ecology 25, 99-107.

Attiwill PM, Adams MA (2013) Mega-fires, inquiries and politics in the eucalypt forests of Victoria, south-eastern Australia. Forest Ecology and Management. 294, 45-53.

Beattie AJ (1995) (Ed) 'Australia's Biodiversity. Living Wealth.' (Reed Books Australia)

Bennett LT, Aponte C, Tolhurst KG, Löw M, Baker TG (2013) Decreases in standing tree-based carbon stocks associated with repeated prescribed fires in a temperate mixed species eucalypt forest. Forest Ecology and Management 306, 243-255.

Bradstock RA, Hammill KA, Collins L, Price O (2010) Effects of weather, fuel and terrain on fire severity in topographically diverse landscapes of south-eastern Australia. Landscape Ecology 25, 607-619.

Brennan KEC, Christie FJ, York A (2009) Global climate change and litter decomposition: more frequent fire slows decomposition and increases the functional importance of invertebrate decomposers. Global Change Biology 15, 2958–2971.

Cameron PA, Mitra B, Fitzgerald M, Scheinkestel CD, Stripp A, Batey C, Niggemeyer L, Truesdale M, Holman P, Mehra R, Wasiak J, Cleland H (2009) Black Saturday: the immediate impact of the February 2009 bushfires in Victoria, Australia. The Medical Journal of Australia 191, 11–16.

Campbell AJ, Tanton MT (1981) Effect of fire on the invertebrate fauna of soil and litter of a eucalypt forest. In 'Fire and the Australian biota' (Eds AM Gill, RH Groves, IR Noble) pp. 215-242. (Australian Academy of Science, Canberra, Australia)

Cary GJ, Bradstock RA, Gill AM, Williams RJ (2012) Global change and fire regimes in Australia. In 'Flammable Australia. Fire regimes, biodiversity and ecosystems in a changing world' (Eds RA Bradstock, AM Gill, RJ Williams) pp.149-169 (CSIRO Publishing Australia)

Collett NG (1998) Effects of two short-rotation prescribed fires in autumn on surface-active arthropods in dry sclerophyll eucalypt forest of west-central Victoria. Forest Ecology and Management 107, 253-273.

Collett NG (1999) Effects of three short rotation prescribed fires in autumn on surface-active arthropods in dry sclerophyll eucalypt forest of west-central Victoria. Australian Forestry 62, 295-306.

Collett NG (2003) Short and long-term effects of prescribed fires in autumn and spring on surface active arthropods in dry sclerophyll eucalypt forest of west-central Victoria. Forest Ecology and Management 182, 117-138.

Collett NG, Neumann FG (1995) Effects of two spring prescribed fires on epigeal Coleoptera in dry sclerophyll forest in Victoria, Australia. Forest Ecology and Management 6, 69–85.

Collett NG, Neumann FG, Tolhurst KG (1993) Effects of two short rotation prescribed fires in spring on surface-active arthropods and earthworms in dry sclerophyll eucalypt forest of west-central Victoria. Australian Forestry 56, 49–60.

DSE (2012) 'Code of Practice for Bushfire Management on Public Land'. Department of Sustainability and Environment (East Melbourne, Victoria, Australia)

Flannigan M, Cantin AS, de Groot WJ, Wotton M, Newbery A, Gowman LM (2013) Global wildland fire season severity in the 21st century. Forest Ecology and Management 294,54-61.

Gill AM (1981) Adaptive responses of Australian vascular plant species to fires. In 'Fire and the Australian biota'. (Eds AM Gill, RH Groves, IR Noble) pp. 243-272. (Australian Academy of Science, Canberra)

Gould JS, McCaw WL, Cheney NP, Ellis PF, Matthews S (2007) Field Guide – Fuel Assessment and Fire Behaviour Prediction in Dry Eucalypt Forest. (Ensis–CSIRO: Canberra, ACT; and WA Department of Environment and Conservation: Perth, WA)

Keeley JE, Safford H, Fotheringham CJ, Franklin J, Moritz M (2009) The 2007 Southern California wildfires: lessons in complexity. Journal of Forestry 107, 287–296.

Koch LE and Majer JD (1980) A phenological investigation of various invertebrates in forest and woodland areas in the south-west of Western Australia. Journal of the Royal Society of Western Australia 63, 21-28.

Lawrence JF, Slipinski A (2013) 'Australia Beetles. Morphology, Classification and Keys. Volume 1'. (CSIRO Publishing, Australia)

Luke RH, McArthur AG (1978) 'Bushfires in Australia'. (Commonwealth of Australia)

Majer JD (1980) Report on a study of invertebrates in relation to the Kojonup Nature Reserve fire management plan. Bulletin Department of Biology Western Australian Institute of Technology 2, 1–22.

Majer JD (1984) Ant return in rehabilitation mines – an indication of ecosystem resilience. In 'Medicos IV: Proceedings of the 4th International Conference on Mediterranean Ecosystems' (Ed B Dell) pp. 105–106. (Botany Department, University of Western Australia, Nedlands, Australia)

Majer JD (1985) Fire effects on invertebrate fauna of forest and woodland. In 'Symposium on Fire Ecology and Management in Western Australian Ecosystems'. (Ed JR Ford) pp. 103-106. (WAIT Environmental Studies Group Report No. 14. Western Australia)

McArthur AG (1967) Fire behaviour in eucalypt forests. Forestry and Timber Bureau, Department of National Development. (Canberra, ACT)

Michaels KF, McQuillan PB (1995) Impact of commercial forest management on geophilous carabid beetles (Coleoptera, Carabidae) in tall, wet Eucalyptus obliqua forest in southern Tasmania. Australian Journal of Ecology 20, 316–323.

New TR, Yen AL, Sands DPA, Greenslade P, Neville PJ, York A, Collett NJ (2010) Planned fires and invertebrate conservation in south east Australia. Journal of Insect Conservation 14, 567-574.

Noble IR and Slatyer RO (1981) Concepts and Models of Succession in Vascular Plant Communities Subject to Recurrent Fire. In 'Fire and the Australian Biota'. (Eds AM Gill, RH Groves, IR Noble) pp. 312-335. (Australian Academy of Science, Canberra)

Penman TD, Christie FJ, Andersen AN, Bradstock RA, Cary CJ, Henderson MK, Price O, Tran C, Wardle GM, Williams RJ, York A (2011) Prescribed burning: how can it work to conserve the things we value? International Journal of Wildland Fire 20, 721-733.

Penman TD, York A (2010) Climate and recent fire history affect fuel loads in Eucalyptus forests: Implications for fire management in a changing climate. Forest Ecology and Management 260, 1791-1797.

Pyne SJ (2008) Passing the torch: why the eons-old truce between humans and fire has burst into an age of megafires, and what can be done about it. The American Scholar 77, 22–32.

Quartau JA (2009) Preventative fire procedures in Mediterranean woods are destroying their insect biodiversity: a plea to the EU Governments. Journal of Insect Conservation 13, 267-270.

Raven PH, Yeates DK (2007) Australian biodiversity: threats for the present, opportunities for the future. Australian Journal of Entomology 46, 177-187.

Schowalter TD (2000) 'Insect Ecology. An Ecosystem Approach'. (Academic Press, New York)

Specht RL (1981) Foliage projective cover and standing biomass. In 'Vegetation Classification in Australia'. (Eds AN Gillson, DJ Anderson). Pp. 10-21. (CSIRO. Canberra, Australia)

Stephens SL, McIver JD, Boerner REJ, Fettig CJ, Fontaine JB, Hartsough BR, Kennedy PL, Schwilk DW (2012) The Effects of Forest Fuel-Reduction Treatments in the United States. Bioscience, 62, 549-560.

Teague B, McLeod R, Pascoe S (2010) 'The 2009 Victorian Bushfires Final Report'. Parliament of Victoria. (Melbourne)

Teeter L (2008) Wildfire mitigation. Forest Policy and Economics 10, 341–343.

Tolhurst KG, Flinn D (1992) Ecological impacts of fuel reduction burning in dry sclerophyll forest: first progress report. Forest Research Section, Department of Conservation and Environment. (Kew, Victoria, Australia)

Uetz GW (1979) The influence of variation in litter habitats on spider communities. Oecologia 22, 373-385.

Upton MS, Mantle BL (2010) 'Methods for Collecting, Preserving and Studying Insects. 5th Edition'. Australian Entomological Society (Miscellaneous Publication No. 3, (Indooroopilly, Queensland)

Whelan RJ, Langedyk W, Pashby AS (1980) The effects of wildfire on arthropod populations in Jarrah-Banksia woodland. Western Australian Naturalist 14, 214-220.

York A (1999a) Long-term effects of frequent low-intensity burning on the abundance of litter-dwelling invertebrates in coastal blackbutt forests of southeastern Australia. Journal of Insect Conservation 3,191-199.

York A (1999b) Long-term effects of repeated prescribed burning on forest invertebrates: management implications for the conservation of biodiversity. In 'Australia's Biodiversity – Responses to Fire'. Biodiversity Technical Series No. 1, pp. 181–266. (Environment Australia, Canberra)

York A (2012) Invertebrates and fire – Challenges and opportunities for conserving biodiversity. Proceedings of the Royal Society of Victoria 124, 47-55 (Melbourne, Australia)

York A, Bell TL, Weston C (2012) Fire regimes and soil-based ecological processes: implications for biodiversity. In 'Flammable Australia: Fire Regime, Biodiversity and Ecosystems in a Changing World'. (Eds RA Bradstock, RJ Williams, AM Gill) pp. 127-148 (CSIRO Publishing, Collingwood, Victoria)

Effect of prescribed burning on chlorophyll fluorescence and sap flow of *Pinus laricio*, a preliminary study

Lapa Gauthier, Lecomte Léa, Morandini Frédéric, Cancellieri Valérie, Cancellieri Dominique, Ferrat Lila

UMR CNRS SPE 6134, Université de Corse, 20250 Corte, France, lapa@univ-corse.fr, lecomtelea10@gmail.com, morandin@univ-corse.fr, vcancellieri@univ-corse.fr, cancelie@univ-corse.fr, ferrat@univ-corse.fr

Abstract
Forest fires constitute important perturbations in Mediterranean ecosystems, and preventing methods are used (e.g. prescribed burning) to avoid large scale fires during dry periods. This preliminary study aims to investigate the effects of prescribed burning on Corsican pine (*Pinus nigra* ssp. *laricio* (Poir.) Maire var. *corsicana* (Loud.) Hyl.) in field conditions. Two complementary approaches were tested: chlorophyll fluorescence and sap flow measurements. Chlorophyll fluorescence parameters allowed showing short term effects of prescribed burning, with a decrease of photochemical process on burned pines. However, at medium term, no significant difference was visible between burned and reference trees. Sap flow monitoring provided information about daily and seasonal cycles, it was greatly correlated with vapour pressure deficit, but no effect of prescribed burning was observed.

Keywords*: Prescribed burning, Pinus laricio, chlorophyll fluorescence, sap flow*

Introduction

Forest fires constitute one of the major perturbations for Mediterranean ecosystems, with real human, economic and ecological hazard. Mediterranean pines are well known for their flammability and their vulnerability to natural fires, and in Corsica (France), in order to prevent large scale fires and protect forests, prescribed burning are conducted under Corsican pine forests (*Pinus nigra* ssp. *laricio* (Poir.) Maire var. *corsicana* (Loud.) Hyl.). Today, a scientific framework is asked by forest managers to help guide this practice.
Previous studies (Ferrat *et al.* 2009; Cannac *et al.* 2009, 2011) brought beginnings of answers with laboratory experiments on needles and experimental fires in nursery, and it is now necessary to go on with tools that can be used on the field. The aim of this preliminary study is to test the potentialities of some vitality/stress indicators in quantifying impacts of a prescribed burning in a natural pine stand: chlorophyll fluorescence and sap flow measurements.
Chlorophyll fluorescence is widely used in plant physiological studies due to the ease of the field measurements and the quality of information provided. Indeed, changes of chlorophyll fluorescence are correlated with changes of CO_2 assimilation and therefore with changes of photosynthetic rate (Baker 2008), it is also a good indicator of stress (Peñuelas *et al.* 1998). Three parameters are usually monitored, the quantum yield photosystem II (ΦPSII), the maximum quantum yield of PSII (F_v/F_m) and the non-photochemical quenching (NPQ). The first are indicators of photochemical process: ΦPSII corresponds to the proportion of absorbed light used in photochemistry, and F_v/F_m is an indicator of photosynthetic performance, with optimal value around 0.83, lower value indicating a photoinhibition. NPQ is correlated to energy dissipated as heat and is studied as a mechanism of protection (Maxwell and Johnson 2000; Calatayud *et al.* 2006; Baker 2008).
These parameters are influenced by soil mineral content (Laing *et al.* 2000; Shangguan *et al.* 2000; Gough *et al.* 2004) and by drought (Shangguan *et al.* 2000; Pukacki and Kamińska-Rożek 2005;

Boureima *et al.* 2012), as demonstrated on coniferous and crop plants. They also undergo important seasonal variations (Vogg *et al.* (1998); Gielen *et al.* (2000) on coniferous; and Damesin (2003) on deciduous trees).
Sap flow is widely used to measure whole tree water use, due to its high degree of reliability and accuracy (Lu *et al.* 2004). Many studies have investigated effects of abiotic parameters on sap flow, mainly drought, with disparate results depending on the species considered (Anfodillo *et al.* 1998 for pinaceae). It is greatly influenced by climatic conditions (radiation, rain, VPD…) on different coniferous (Köstner *et al.* 1996; Simpson 2000; Iijima *et al.* 2004) and deciduous trees (Zalesny Jr *et al.* 2006; Nasr and Mechlia 2007). Ducrey *et al.* (1996), highlighted an alteration of sap flow after an important experimental heating of young *Pinus halepensis* trunk.
To our knowledge, literature regarding the effect of prescribed burning with chlorophyll fluorescence and sap flow on a natural pines stands is quite poor (Ducrey *et al.* 1996; Ferrat *et al.* 2009; Pasqualini *et al.* 2009) and generally realized experimentally and for short periods.

Methods

Study site

The study site was a mountain (900 m a.s.l.) natural pure Corsican pine stand situated in the Venaco Forest, Corsica, France (42°11'51.3"N 9°06'53.5"E). Trees were 20-25 years old, 11-17 m tall, with 13.5-18.5 cm DBH in average. Prescribed burning was performed March 29, 2012 on an usual fuel load surface (pine needles bed) of about 1500 $g.m^{-2}$, leading to a fire intensity between 50 and 100 $kW.m^{-1}$ (Trabaud 1979; Ferrat *et al.* 2011).
Measurements of chlorophyll fluorescence and sap flow were realised daily, then monthly, on burned and reference (unburned) trees.

Chlorophyll fluorescence

Measurements of chlorophyll fluorescence were realised in situ on attached needles of the previous year with a Portable Chlorophyll Fluorometer (PAM-21000, Walz, Germany), needles were dark-adapted during 30 minutes before measurement to open the reaction centres of the PSII. All of these measurements were realised at the sunrise, before the burning and daily then monthly after the burning, from March 27 to July 13, 2012. When light energy is absorbed by chlorophyll, the light not used in photosynthesis is dissipated as heat or is re-emitted as light fluorescence. Chlorophyll fluorescence is measured by exposing a leaf to light and measuring light re-emitted, different intensity/flash of light is used to measuring different parameters (figure 1). Measurement light (MB) allows measurement of the zero fluorescence level (F_o), the maximum fluorescence level (F^o_m) is measured after a saturating flash (SP), a second saturating flash is applied under an actinic light (AL) to measuring the maximum fluorescence in the light (F'_m) and the fluorescence level under actinic light, before the second flash (F_t), the zero level fluorescence (F'_o) is measured under far-red light (Maxwell and Johnson 2000).

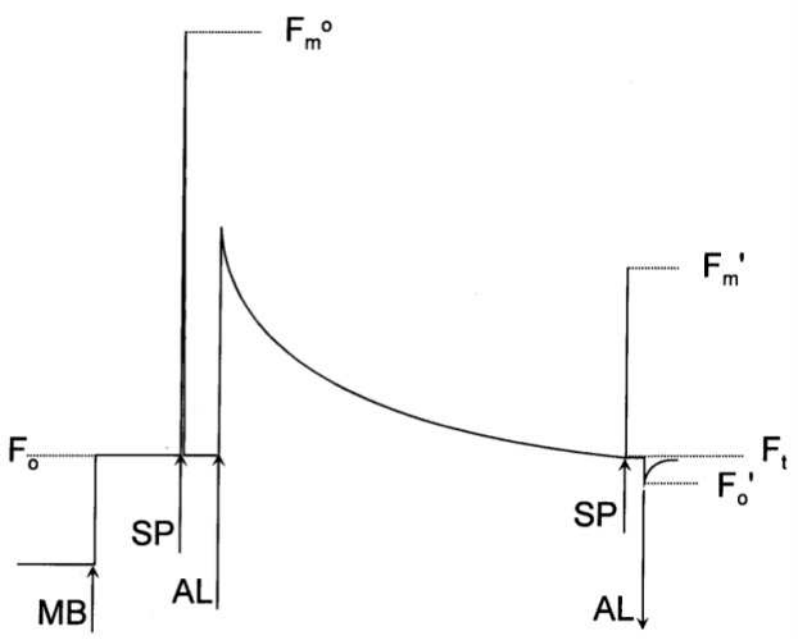

Figure 1. Sequence of a typical fluorescence trace (from Maxwell and Johnson 2000).

Three parameters were monitored: the quantum yield of photosystem II (ΦPSII), the maximum (or intrinsic) quantum yield of photosystem II (F_v/F_m) and the non-photochemical quenching. These parameters were calculated according to Maxwell and Johnson (2000), i.e.:

$$\Phi\text{PSII} = \frac{(F'_m - F_t)}{F'_m}$$

$$F_v/F_m = \frac{(F^o{}_m - F_o)}{F^o{}_m}$$

$$NPQ = \frac{(F^o{}_m - F'_m)}{F'_m}$$

with F'_m is the maximum fluorescence in the light, Ft is the level of fluorescence before the second saturating flash, F^o_m is the maximum fluorescence from dark-adapted leaves.

2.3. Sap flow

Sap flow measurements were realised with thermal dissipation probes (TDP, Dynamax, USA) according to the method developed by Granier (Granier 1985; Granier and Gross 1987). This method is based on temperature differences between two probes inserted radially into the trunk. The upper probe is continuously heated, both probes have a thermocouple. When sap flow is null, the difference between the two probes is maximal, when sap flow is high it dissipates heat produced by the upper probe by convection, and the difference of temperature between the two probes will depend on the speed of sap (Granier 1985; Granier and Gross 1987).

Depending on the thickness of sapwood, two length of probes were used (30 for DBH between 13.5 and 14.5 cm and 50 mm for DBH between 15.5 to 18.5cm) to improve the measurement (Lu *et al.* 2004). All probes were installed at East to avoid the influence of azimuth (Do and Rocheteau 2002). These measurements were recorded continuously before and after the burning from March 28 to October 30, 2012. Data were recorded in a CR3000 Micrologger (Campbell Scientific, USA) supplied by a battery charged by a solar panel. Together relative humidity and temperature were monitored, these allow computation of vapour deficit pressure (VPD, in kPa):

$$\boldsymbol{VPD = e_s - e_a}$$

$$\boldsymbol{e_s = 0.6108 \times e^{\left(\frac{17.27 \times T}{T+273.3}\right)}}$$

$$\boldsymbol{e_a = e_s \times \frac{RH}{100}}$$

with e_s is the saturation vapour pressure (kPa), e_a is the actual vapour pressure (kPa), T is the temperature (°C) and RH is the relative humidity (%).
Sap flow were calculated according to Granier and Gross (1987):

$$\boldsymbol{k = \frac{\Delta TM - \Delta T}{\Delta T}}$$

$$\boldsymbol{V = 0.0119 \times k^{1.231}}$$

with k is a dimensionless number, ΔTM is the maximal temperature difference between the two probes (°C), ΔT is the temperature difference between the two probes (°C) and V is the sap velocity ($cm.s^{-1}$).

Results - Discussion

The prescribed burning influenced all chlorophyll fluorescence measurements at short term, the maximum quantum yield of burned pines decreased strongly immediately after the burning, from 0.84 to 0.76. It increased few days later but remained always under the reference values (resp. 0.82 vs. 0.84 during summer). F_v/F_m of the reference pines remained constant during the entire measurement period (approx. 0.84, figure 2).
Quantum yield increased the day after the burning, from 0.22 to 0.37 (68% up), but there was no difference between burned and reference pines few days later. Furthermore, this parameter underwent seasonal variations with a peak (0.44) at the end of May (figure 3).
Non-photochemical quenching decreased 2 and 3 days after the burning, from 2.3 to 1.2 (48% down) then increased to the initial value the 4th day. Later, it was under the reference (65% of the reference value, May, 5), except for the last record (figure 4).

The decrease of F_v/F_m immediately after the burning could reveal an alteration of photosynthetic performances due to a thermal stress. Previous study (Pasqualini *et al.* 2009) showed a decrease of this parameter after a burning on *Pinus laricio* needles, but this decrease did not have any effect on the survival of populations. It was shown that F_v/F_m was not long term affected if the value was kept upper than 60% of reference value (Ferrat *et al.* 2009), it is in accordance with our results, as Fv/Fm was about 98% of the reference value at the end of the experiment while it was about 90% of the reference value 2 days after the burning. NPQ corresponds to energy dissipated at heat, its increase would be a protection mechanism to dissipate energy excess and photo damage of PSII (Calatayud *et al.* 2006), this mechanism has not been implemented here. In the medium term, none of these three parameters seemed significantly affected by the burning.

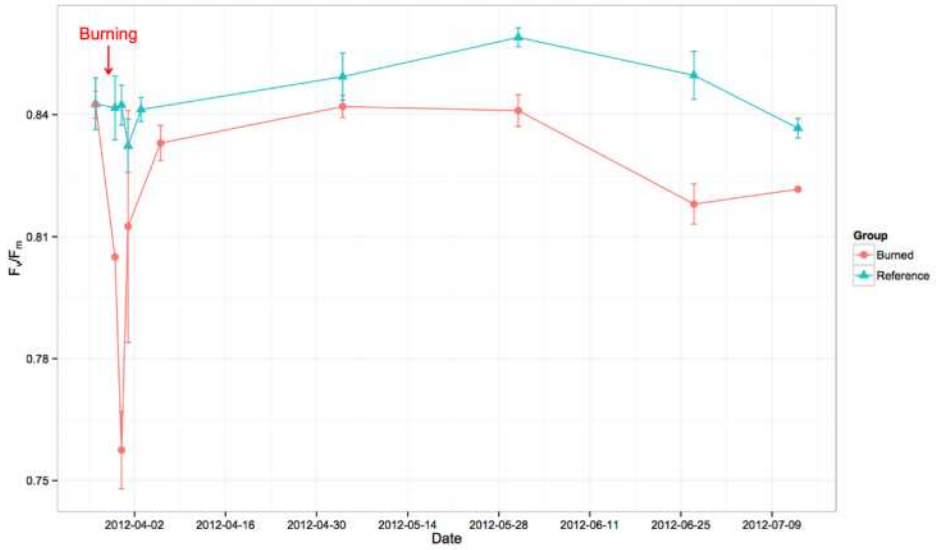

Figure 2. F_v/F_m for burned and reference pines. Means ± standard error.

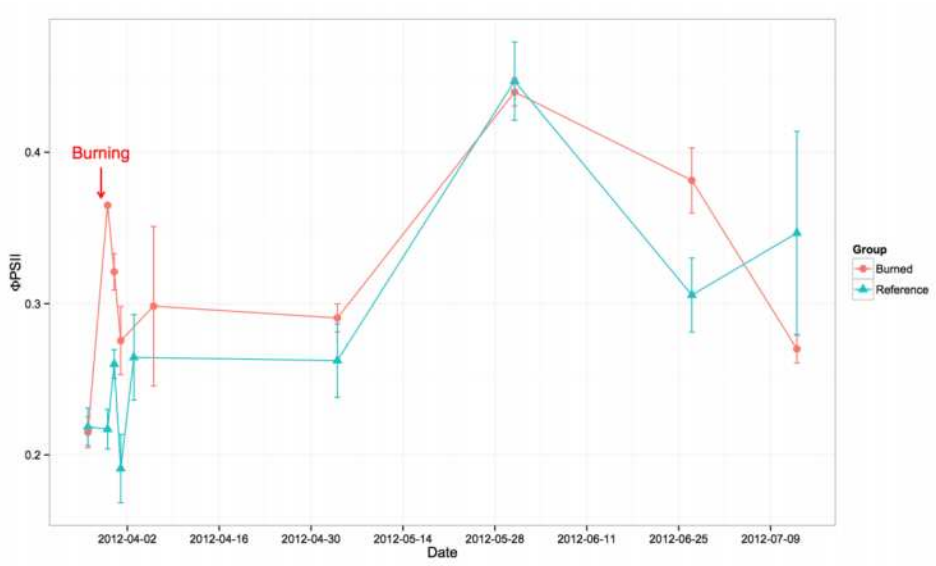

Figure 3. ΦPSII for burned and reference pines. Means ± standard error.

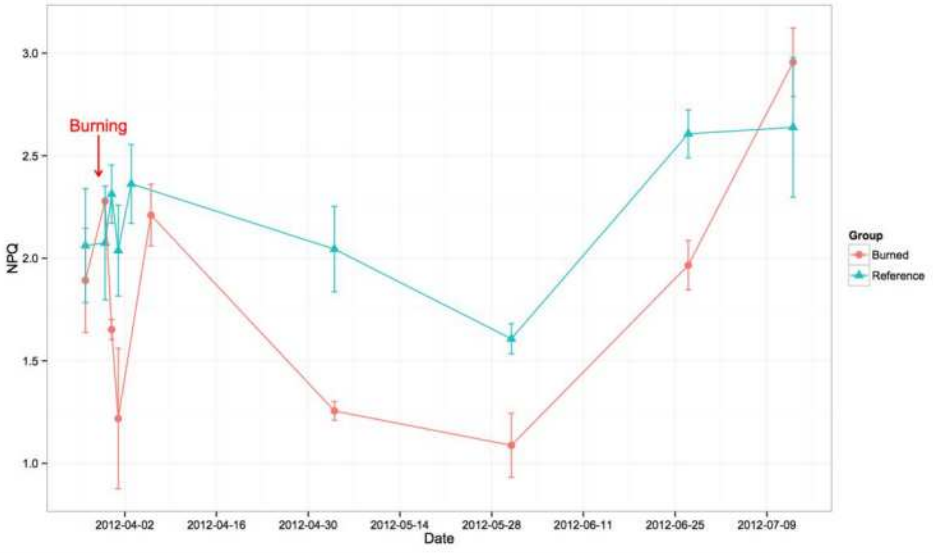

Figure 4. NPQ for burned and reference pines. Means ± standard error.

Figure 5 shows the sap velocity for two representative trees (a burned and a reference) and the VPD. Sap flow of reference tree was lightly under the sap flow of burned tree during spring (mean: 7.8 10^{-4} $cm.s^{-1}$, max: 4.39 10^{-3} $cm.s^{-1}$ for reference; mean: 1 10^{-3} $cm.s^{-1}$, max: 6.3 10^{-3} $cm.s^{-1}$ for burned) and summer (mean: 6.5 10^{-4} $cm.s^{-1}$, max: 4.5 10^{-3} $cm.s^{-1}$ for reference, mean: 8.5 10^{-4} $cm.s^{-1}$, max: 4.8 10^{-3} $cm.s^{-1}$ for burned). During autumn they were close (mean: 4.7 10^{-4} $cm.s^{-1}$, max: 2.2 10^{-3} $cm.s^{-1}$ for reference, mean: 4 10^{-4} $cm.s^{-1}$, max: 2.9 10^{-3} $cm.s^{-1}$ for burned). The global sap flow difference between reference and burned tree can be explained by difference of DBH (resp. 14 cm vs. 15 cm) and mainly by difference of probe length (resp. 30 mm vs. 50 mm). It will be important in further studies to homogenize probes for a better discrimination of sap flow trends.
Nevertheless, it can be noticed that sap flow of reference and burned trees had similar variation from the start to the end of the monitoring, the prescribed burning did not seem to affect sap flow.

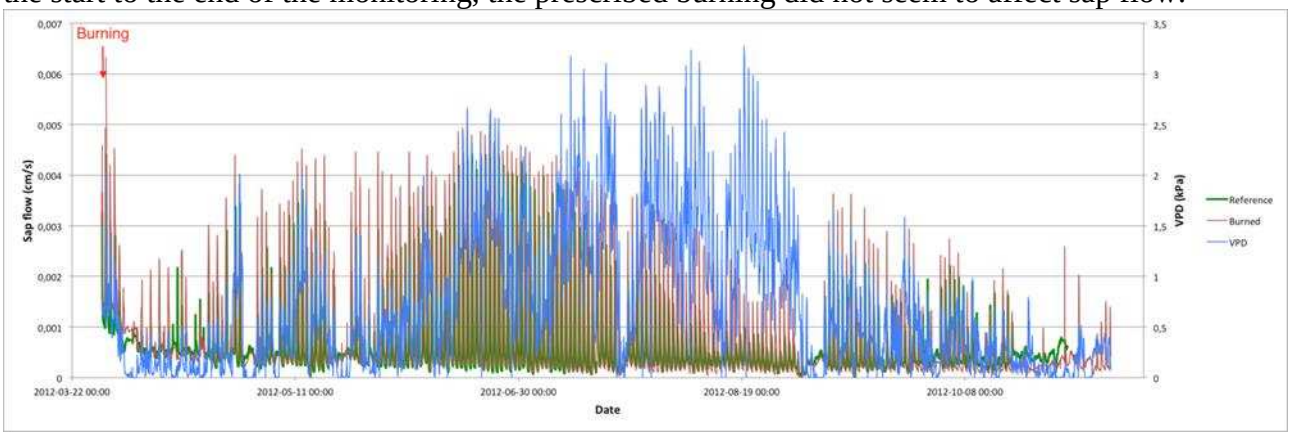

Figure 5. Sap flow velocity for burned and reference pines, and VPD.

The VPD varied daily and seasonally, it was low during spring (mean: 0.47 kPa, max: 2.66 kPa) and greater during summer (mean: 1.19, max: 3.27 kPa) and decreased during autumn (mean: 0.26 kPa, max: 1.58 kPa). Daily and seasonally variation of VPD can be explained by the great influence of relative humidity (RH) on the calculation, indeed during night and rain period RH is very high and thus VPD is very low. Temperature influences also VPD, more the temperature is important, more the saturation pressure is important and more the VPD may be important (Allen *et al.* 1998).

These data show that sap flow was greatly correlated, daily and seasonally, with vapour pressure deficit (VPD). An exception was measured during July and August, with a decrease of sap flow (from 0.004 to 0.002 $cm.s^{-1}$) while VPD was very high (over 3 kPa), this drop could be explained by low water availability during drought period (Anfodillo *et al.* 1998), and would reveal a water saving behaviour (Anfodillo *et al.* 1998; Badalotti *et al.* 2000). It will be interesting to survey this behaviour in case of severe drought.

This preliminary study has provided the beginnings of a reply regarding the effect of prescribed burning on photosynthetic and hydric parameters, and also provided information on daily and/or seasonal variation of these parameters. Chlorophyll fluorescence and sap flow measurements are promising tools to evaluate the impact of thermal stress on field, at short, medium and long term. A longer study with more replicate and complementary tools is in progress to provide more accurate answers.

References

Allen RG, Pereira LS, Raes D, Smith M, others (1998) 'Crop evapotranspiration-Guidelines for computing crop water requirements-FAO Irrigation and drainage paper 56.' (Rome, Italy)

Anfodillo T, Rento S, Carraro V, Furlanetto L, Urbinati C, Carrer M (1998) Tree water relations and climatic variations at the alpine timberline: seasonal changes of sap flux and xylem water potential in Larix decidua Miller, Picea abies (L.) Karst. and Pinus cembra L. Annales des Sciences Forestières 55(1-2), 159–172. doi:10.1051/forest:19980110.

Badalotti A, Anfodillo T, Grace J (2000) Evidence of osmoregulation in Larix decidua at Alpine treeline and comparative responses to water availability of two co-occurring evergreen species. Annals of forest science 57(7), 623–633. doi:10.1051/forest:2000146.

Baker NR (2008) Chlorophyll Fluorescence: A Probe of Photosynthesis In Vivo. Annual Review of Plant Biology 59(1), 89–113. doi:10.1146/annurev.arplant.59.032607.092759.

Boureima S, Oukarroum A, Diouf M, Cisse N, Van Damme P (2012) Screening for drought tolerance in mutant germplasm of sesame (Sesamum indicum) probing by chlorophyll a fluorescence. Environmental and Experimental Botany 81, 37–43. doi:10.1016/j.envexpbot.2012.02.015.

Calatayud A, Roca D, Martínez PF (2006) Spatial-temporal variations in rose leaves under water stress conditions studied by chlorophyll fluorescence imaging. Plant Physiology and Biochemistry 44(10), 564–573. doi:10.1016/j.plaphy.2006.09.015.

Cannac M, Ferrat L, Barboni T, Chiaramonti N, Morandini F, Pasqualini V (2011) Identification of flavonoids in Pinus Laricio needles and changes occurring after prescribed burning. Chemoecology 21(1), 9–17. doi:10.1007/s00049-010-0060-4.

Cannac M, Pasqualini V, Barboni T, Morandini F, Ferrat L (2009) Phenolic compounds of Pinus laricio needles: A bioindicator of the effects of prescribed burning in function of season. Science of The Total Environment 407(15), 4542–4548. doi:10.1016/j.scitotenv.2009.04.035.

Damesin C (2003) Respiration and photosynthesis characteristics of current-year stems of Fagus sylvatica: from the seasonal pattern to an annual balance. New Phytologist 158(3), 465–475. doi:10.1046/j.1469-8137.2003.00756.x.

Do F, Rocheteau A (2002) Influence of natural temperature gradients on measurements of xylem sap flow with thermal dissipation probes. 1. Field observations and possible remedies. Tree Physiology 22(9), 641–648. doi:10.1093/treephys/22.9.641.

Ducrey M, Duhoux F, Huc R, Rigolot E (1996) The ecophysiological and growth responses of Aleppo pine (Pinus halepensis) to controlled heating applied to the base of the trunk. Canadian Journal of Forest Research 26(8), 1366–1374.

Ferrat L, Morandini F, Baconnais I, Silvani X, Berti L, Pasqualini V (2009) Impact of thermal stress on Pinus laricio: determining tolerance levels to prescribed burning through field experimentation.

In ‘Proceedings of the 24th Tall Timbers Fire Ecology Conference: The Future of Prescribed Fire: Public Awareness, Health, and Safety.’, Tall Timbers Research Station, Tallahassee, Florida, USA. Pp 127–134. (K.M. Robertson, K.E.M. Galley, and R.E. Masters: Tall Timbers Research Station, Tallahassee, Florida, USA)

Ferrat L, Morandini F, Mascarenhas F, Elineau A, Cochard H, Poggi I (2011) Effects of prescribed burning on photosynthesis and water status of Pinus laricio. In ‘Medpine 4: 4th International Conference on Mediterranean Pines.’, Avignon, France.(Avignon, France)

Gielen B, Jach ME, Ceulemans R (2000) Effects of season, needle age, and elevated atmospheric CO2 on chlorophyll fluorescence parameters and needle nitrogen concentration in Scots pine (Pinus sylvestris). Photosynthetica 38(1), 13–21. doi:10.1023/A:1026727404895.

Gough CM, Seiler JR, Maier CA (2004) Short-term effects of fertilization on loblolly pine (Pinus taeda L.) physiology. Plant, Cell & Environment 27(7), 876–886. doi:10.1111/j.1365-3040.2004.01193.x.

Granier A (1985) Une nouvelle méthode pour la mesure du flux de sève brute dans le tronc des arbres. Annales des Sciences Forestières 42(2), 193–200. doi:10.1051/forest:19850204.

Granier A, Gross P (1987) Mesure du flux de sève brute dans le tronc du Douglas par une nouvelle méthode thermique. Annales des Sciences Forestières 44(1), 1–14. doi:10.1051/forest:19870101.

Iijima Y, Ishikawa M, Suzuki K, Battogtokh D, Sharkhuu N, Kadota T, Ohata T (2004) Preliminary report of environmental regulation of xylem sapflow at the northern faced forest slope. In ‘The third International Workshop proceedings on Terrestrial Change in Mongolia’, Tsukuba, Japan. Pp 78–81. (Tsukuba, Japan)

Köstner B, Biron P, Siegwolf R, Granier A (1996) Estimates of water vapor flux and canopy conductance of Scots pine at the tree level utilizing different xylem sap flow methods. Theoretical and Applied Climatology 53(1-3), 105–113. doi:10.1007/BF00866415.

Laing W, Greer D, Sun O, Beets P, Lowe A, Payn T (2000) Physiological impacts of Mg deficiency in Pinus radiata: growth and photosynthesis. New Phytologist 146(1), 47–57. doi:10.1046/j.1469-8137.2000.00616.x.

Lu P, Urban L, Zhao P (2004) Granier’s thermal dissipation probe (TDP) method for measuring sap flow in trees: theory and practice. Acta Botanica Sinica 46(6), 631–646.

Maxwell K, Johnson GN (2000) Chlorophyll fluorescence—a practical guide. Journal of Experimental Botany 51(345), 659–668. doi:10.1093/jexbot/51.345.659.

Nasr Z, Mechlia NB (2007) Measurements of sap flow for apple trees in relation to climatic and watering conditions. In ‘Water saving in Mediterranean agriculture and future research needs’, Valenzano, Italy. Pp 91–98. (Valenzano, Italy)

Pasqualini V, Fernandez C, Giroud F, Bousquet-Mélou A, Cannac M, Ferrat L, Gauquelin T, Greff S, Guilmard M, Lavoir AV, Mevy JP, Picard C, Vila B (2009) Conséquence des brûlages dirigés sur le métabolisme primaire et secondaire de deux pins méditerranéens et relation avec les potentialités d’inflammation. Convention n°E 11.07.

Peñuelas J, Filella I, Llusia J, Siscart D, Piñol J (1998) Comparative field study of spring and summer leaf gas exchange and photobiology of the Mediterranean trees Quercus ilex and Phillyrea latifolia. Journal of Experimental Botany 49(319), 229–238. doi:10.1093/jxb/49.319.229.

Pukacki PM, Kamińska-Rożek E (2005) Effect of drought stress on chlorophyll a fluorescence and electrical admittance of shoots in Norway spruce seedlings. Trees 19(5), 539–544. doi:10.1007/s00468-005-0412-9.

Shangguan Z, Shao M, Dyckmans J (2000) Effects of Nitrogen Nutrition and Water Deficit on Net Photosynthetic Rate and Chlorophyll Fluorescence in Winter Wheat. Journal of Plant Physiology 156(1), 46–51. doi:10.1016/S0176-1617(00)80271-0.

Simpson DG (2000) Water use of interior Douglas-fir. Canadian Journal of Forest Research 30(4), 534–547. doi:10.1139/x99-233.

Trabaud L (1979) Etude du comportement du feu dans la garrigue de chêne kermes à partir des températures et des vitesses de propagation. Annales des sciences forestières 36, 13–38. doi:10.1051/forest/19790102.

Vogg G, Heim R, Hansen J, Schäfer C, Beck E (1998) Frost hardening and photosynthetic performance of Scots pine (Pinus sylvestris L.) needles. I. Seasonal changes in the photosynthetic apparatus and its function. Planta 204(2), 193–200. doi:10.1007/s004250050246.

Zalesny Jr RS, Wiese AH, Bauer EO, Riemenschneider DE (2006) Sapflow of hybrid poplar (Populus nigra L.×P. maximowiczii A. Henry 'NM6') during phytoremediation of landfill leachate. Biomass and Bioenergy 30(8–9), 784–793. doi:10.1016/j.biombioe.2005.08.006.

Experimental prescribed burning in Turkey oak forest of Cilento and Vallo di Diano National Park (Southern Italy): effects on vegetation and soil

Assunta Esposito[a], Ascoli D.[b], Croce A.[a], Giordano D.[c], Catalanotti A.E.[a], Mazzoleni S.[c], Bovio G.[b], Salgueiro A[d], Palheiro P.[d], Loureiro C.[d], Rutigliano F.A.[a]

[a] *Second University of Naples, Dip.DiSTABiF, Via Vivaldi 43, 81100 Caserta, Italy, Tel.: +39 0823274544. assunta.esposito@unina2.it*
[b]*University of Torino, Dip. DISAFA, Largo Paolo Braccini 2, 10095 Grugliasco, Italy*
[c]*University of Naples Federico II,Dip. Agraria, Via Università 100, 80055-Portici, Italy*
[d] *GIFF, Gestão Integrada de Fogos Florestais SA. Rua D. João Ribeiro Gaio, 9B 1º Esq. 4480-811,Vila do Conde, Portugal.*

Abstract
An experimental prescribed burn was conducted in February 2011 in a Quercus cerris forest in the Cilento e Vallo di Diano National Park (Southern Italy) to analyze fire effects on vegetation and soil.
Fuel fire behavior characteristics and were assessed to define the burning conditions that allowed a rate of fire spread between 0.10 and 0.22 m min-1, fireline intensity never below 50 kW m-1 and maximum flame temperatures in the litter of 600°C but the average residence time above 60°C and 300°C were 198 and 12 seconds, respectively. Litter fuel consumption ranged between 80% and 90%.
The effect of fire on vegetation was evaluated in terms of floristic composition and structure by means of phytosociological and dendrometric samplings randomly located in burned and unburned plots two years after fire. The effect of fire on soil was evaluated by determining soil chemical (pH, water content, total and extractable organic C content, total and mineral N) and microbial properties (microbial biomass, soil potential respiration) in the 0-5 cm soil at different time since fire (3 hours, 30, 94, 209 and 394 days). Moreover, water holding capacity and bulk density were measured in burned and unburned plots at first sampling.
Results on vegetation evidenced no significant differences in species richness and diversity, in both burned and unburned plots. No changes have been found in frequency and cover values of endemic species (Digitalis micrantha, Echinops ritro subsp. siculus, Lathyrus jordanii, Teucrium siculum). Woody species showed a great resilience with very low tree mortality. Sapling persistence by high sprouting rootstocks evidenced no significant difference in the abundance of some species (Quercus cerris, Acer campestre, Carpinus betulus, Crataegus monogyna) or an increase for few species (Ruscus aculeatus, Ilex aquifolium, Erica arborea, Fraxinus ornus, Sorbus torminalis, Carpinus orientalis) in burned plots.
Results on soil showed that prescribed burning did not affect soil chemical and microbial properties, so indirect effects on plants deriving on effect of fire on soil may be excluded. Our findings highlight the sustainability of prescribed burning in Quercus cerris forests and support its future use as a management tool of fire risk reduction without significant impact on vegetation and soil.

Keywords*: Quercus cerris forest, prescribed burning, biodiversity, resilience*

Introduction

Fire has played an important role in shaping the distribution and composition of many biomes worldwide (Keeley *et al*. 2011), including temperate forests of the Northern Hemisphere (Abrams 1992; Bradshaw *et al*. 1997). In particular, natural and anthropogenic fire regimes have been one of the main drivers in determining life traits of oak species and the structure of oak forests in both North America (e.g., Cutter & Guyette 1994; Shumway *et al*. 2001) and Europe (Clark *et al*. 1989; Mason 2000; Robin & Nelle 2014).

Oaks have several fire related traits which enable them to survive on frequent fire. Mature oaks have thicker bark than most other hardwood species (Nicolai 1986). They are capable of living for decades after bole injury. Litter displays a relatively marked flammability (Kane *et al*. 2008). Regeneration from root and stump sprouts can be enhanced by fire (Hutchinson 2008). A synergistic interaction of fire and masting may result in burned sites having high oak seedling density following a mast year (Brose *et al*. 2006; Abrams & Johnson 2013). Fires may also kill acorn predators, which may result in increased acorn viability and germination (Johnson *et al*. 2002). Acorns germinate well below the soil surface where they are protected from the heat of a surface fire. The reduced shading and competition, and prepared seedbed that result from litter removal combine to provide favourable oak regeneration conditions (Wang *et al*. 2005).

For the above mentioned reasons, prescribed burning is broadly used to manage oak forests of North Eastern America with the objective to promote oak natural regeneration, reduce invasive species, restore biological diversity, and decrease hazardous fuel build-up (Peterson & Reich 2001; Burton *et al*. 2011; Cavender-Bares & Reich 2012; Brose *et al*. 2013). Such management goals are often achieved integrating prescribed burning with other sylvicultural treatments such as thinning and shelterwood cutting (Albrect & McCarthy 2006; Brose *et al*. 2006).

Several oak species of Northern America managed by prescribed burning (i.e. *Quercus alba, Q. ellipsoidalis, Q. macrocarpa, Q. marilandica, Q. rubra, Q. shumardii, Q. stellata*), are vicariant of main European oak species, e.g., *Q. alba* vs. *Q. petraea*, *Q. macrocarpa* vs. *Q. robur*, *Q. stellata* vs. *Q. cerris* (Box & Manthei 2005), with which share similar ecological traits and regeneration strategies. However, the use of prescribed burning for forest management goals has been relatively recent in Europe in comparison to North America (Fernandes *et al*. 2013).In particular, very little knowledge exists regarding prescribed fire behaviour and its ecological effects in deciduous oak forests of Europe. In order to assess the ecological sustainability of this management practice, investigations are needed to reduce undesirable fire effects on the ecosystem components, such as tree seedlings mortality, soil degradation and floristic impoverishment (Franklin *et al*. 2003; Hutchinson *et al*. 2005; Neary *et al*. 2010; Williams *et al*. 2012).

With these aims, an experimental prescribed burning was carried out in 2011 in a *Quercus cerris* forest of the Cilento e Vallo di Diano National Park, Southern Italy (Ascoli *et al*. 2012). Since this forest is located in a Site of Community Importance (IT8050002 included in Annex I of the Directive 92/43/EEC), ecological monitoring was particularly important in order to evaluate the effects on biodiversity and to exclude possible negative impact to holly (*Ilex aquifolium*) and ruscus (*Ruscus aculeatus*), being both species protected by a regional law.

In particular the specific objectives of the present study are: i) to characterize fuels and fire behaviour observed during the experimental prescribed burning; ii) to assess short term effects of fire on understory plant species diversity, oak regeneration andprotected plant species ; iii) to analyse fire effects on soil chemical and microbial properties.

Methods

Study area

The study site (40°17’10’’N; 15°16’51’’E) is located in the National Park of Cilento, Vallo di Diano and Alburni, Sothern Italy (Figure 1), about 20 km apart from the sea in a hilly area. The site is 455 m a.s.l., with a SW aspect and an average of 40% slope. The climate is mesotemperate humid with mean annual temperature of 14.7°C (ranging from 6.3°C in January to 23.6°C in August) and annual precipitation of 825 mm with a dry period in summer with less than 100 mm. (Gioi meteorological station, 684 m a.s.l., 22 km apart from the study site).

Soil is Calcari-Vertic Cambisols and geologic substrate is Marls and Calcarenites of the Stream Trenico of the Chattian (FAO 1998; di Gennaro, 2002).

Vegetation is characterized by *Quercus cerris wood* 14-16 m high with an average cover of 80% and a low scattered presence of *Sorbus domestica*, *Ostrya carpinifolia* e *Fraxinus ornus*. The woody understorey is dominated by *Carpinus orientalis, Crataegus monogyna, Ilex aquifolium, Ruscus aculeatus* and *Erica arborea,* whereas the main representative herbs are *Festuca exaltata, Echinops ritro subsp. siculus, Digitalis micrantha.*

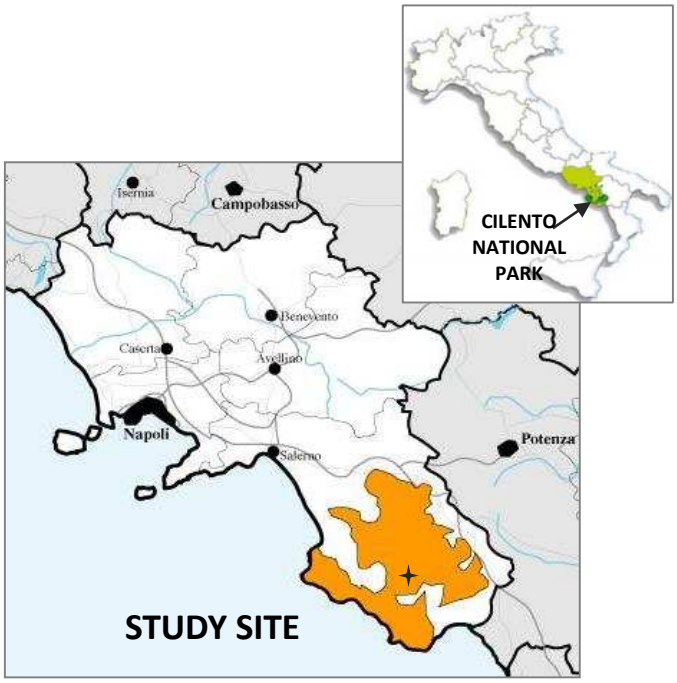

Figure 1. Study site location

Fuel and prescribed fire characterization

The prescribed burn was conducted in winter 2011 on an area of 0.7 ha. Fuel characteristics were assessed few days before burning. Dead fine (< 6 mm) surface fuels were constituted by *Q. cerris* litter, cured grasses and dead woody material. Live grasses and forbs, and elevated live woody fuels such as *Erica arborea*, were sparse. Dead surface fuels were harvested in six 1 m^2 quadrats and dried in the laboratory to determine the fuel load. Fuel bed depth and cover of dead fuels were also measured every 0.5 m along six linear transects (10 m).Dead fine fuel moisture was assessed at the time of the burn by collecting 5 litter samples. Fresh samples (50 g each) were weighed in the field by a portable scale, and then dried in laboratory.

Fire behaviour was assessed at a microplot scale (Fernandes *et al*. 2001) by measuring the arrival time of the fire front at the vertices of a triangle and computing the rate of spread according to the trigonometric method of Simard *et al*. (1984). Five equilateral triangles (2 m side) were visualized using 2 m rods placed at each triangle vertex. The time of arrival of the fire front was measured using K-Type thermocouples (0.4 mm) positioned at each triangle vertex within the litter fuel (5 cm from the soil surface), and connected to a data-logger buried one meter apart. Flame temperature was measured every second during all combustion phases. Flame height was assessed by two observers which used as a reference scale the increment markers(0.5 m)painted on each rod. Fireline intensity was calculated using the Byram (1959) formula applying a high heat content of 20000 kJ kg^{-1}. Air temperature and moisture, and wind speed and direction were assessed every time fire was spreading through a triangle using a portable weather stations positioned at midflame height at a distance of 5 m upwind the triangle. In total, 5 rate of spread observations and 15 time-temperature profiles were collected. Fuel consumption was assessed soon after the fire by harvesting remaining charred fuels in a 1 m^2 quadrat within the triangle.

2.3. Vegetation sampling

The effects of prescribed burning were assessed in summer 2013 to analyze the following parameters: floristic and structural composition, plant community sintaxonomy, species richness, species density, demography and regeneration of structural species. Plant community was sampled by the phytosociological method (Braun-Blanquet, 1964) on sampling area of 100 m^2 for sintaxonomical characterization. Moreover the phytosociological method was applied on 1 m^2 sampling plots along randomly located transects to analyze the effects of burning application on plant biodiversity. In total, 40 plots were surveyed in both burned and control sites. Thesurvey was carried outin accordance with theBraun-Blanquet scale and then converted in Van der Maarel (1979) scale in the data matrix.

The data matrix (60 species x 80 relevés) was analyzed by Principal Component Analysis (PCA) with algorithm Euclidean distance contained in SYN-TAX package (Podani, 2001) to test the degree of floristical similarity between burned and control plots. The software EstimateS (Colwell, 2013) was used to calculate rarefaction curve of richness estimators and biodiversity for sample based data (40 burned plots and 40 control plots). The nomenclature of species follows Pignatti (1982), Med Check list (Greuter *et al*., 1989), and Conti *et al*. (2005, 2007).

Stand structure (tree species density, basal area, height, and status: alive, dead, fallen, fire scar) was also assessed. Trees with a diameter at breast height >5 cmwere measured in a circular plot of 20 m in diameter. Tree regeneration with a diameter <5 cm and a height >30 cm was assessed in a circular plot of 8 m in diameter. Regeneration with a height <30 cm was assessed in the same plot used for phytosociological relevés. Regeneration was characterized by stem density, height and status (live/dead; seedling, sapling, post-fire sprout). For each plot, environmental data such as slope, litter cover and depth, bare soil, rocks, herb and shrub cover and height) were also recorded to evaluate their potential effects. A total of 40 plots were surveyed in both burn and control sites. Statistical analysis was performed to evaluate significant differences of individual number (test Chi^2) and average height (test U-Mann-Whitney) between burned and control plots.

2.4. Soil collection and analysis

To evaluate the effect of prescribed burning on soil properties that could affect oak, soil samples were collected at 0-5 cm depth in 6 randomly selected sub-plots (40 x 40 cm) of burned and unburned plots at different times since burn (3 hours, 30, 94, 209 and 394 days).

In the first sampling, in both control and burned plots, soil water holding capacity and bulk density were determined by gravimetric method (USDA, 2004). At each sampling time sieved soil samples (2-mm mesh) were analysed for chemical (water content, pH, total organic C, extractable organic C, total N, ammoniacal N and nitric N) and microbial properties (microbial C and soil potential respiration).

Water content was measured by gravimetric method (Allen, 1989). Soil pH was determined by potentiometric method on air dried soil:water suspension with a 1:2.5 ratio using a calibrated electrode (Hanna Instruments mod. HI1230). Total organic carbon content was measured on air dried soil by humid oxidation method (Springer and Klee, 1954). Extractable and microbial C were determined on fresh soil by chloroform-fumigation extraction method (Vance *et al*., 1987). Total N was determined with NCS Elemental Analyser (ThermoFlash EA 1112). The ammonium and nitrate contents were determined by potentiometric method (Beck, 1993) on fresh soil stored at 4 °C until measurement, by using specific potentiometric electrode for ammonia (ORION, Mod. 9512BNWP) and one specific for nitrate (ORION, Mod. 290A) after Castaldi and Aragosa (2002). Soil potential respiration, indicating microbial activity, was determined measuring, by gas chromatography, CO_2 evolved from samples incubated in standard conditions (25 °C, 55 % of water holding capacity, in the dark) for one hour (Kieft *et al*., 1998).

Results

Fuel characteristics and prescribed fire behaviour

Pre-fire fuel cover was 100%.Mean fuel bed depth was 8 cm. Dead fine fuel load ranged between 3.4 and 5.7 t ha^{-1}. During the burn, mean fine dead fuel moisture content (dry weight basis) was 38% (Table 1).Weather conditions are reported in Table 1.

Table 1– Mean weather, fuels and fire behavior characteristics observed during an experimental prescribed burning in Quercus cerris litter fuels. Photos shows prescribed fire behavior and fuel consumption.

Weather	
Air temperature (°C)	16
Air moisture (%)	43
Wind speed (km h^{-1})	6
Days since rain (days)	5
Fuel load	
Litter fuels(t ha^{-1})	4,24 ± 0,34
Cured grasses + fine dead woody(t ha^{-1})	2,44 ± 0,46
Fuel moisture	
Litter (%)	38 ± 5
Duff (%)	132 ± 19
Fire behaviour	
Ignition pattern	Backfire
Rate of spread (m min^{-1})	0,17 ± 0,04
Flame height (m)	0.1-0.3
Fireline intensity (kW m^{-1})	25 ± 5,7

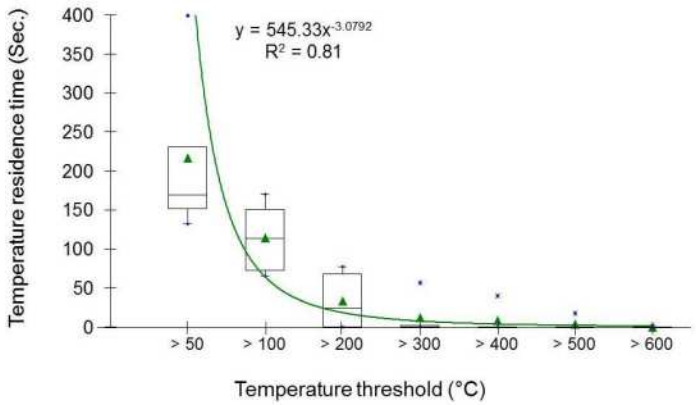

Figure 2. Flame temperature residence time above threshold temperatures measured at the soil surface during a prescribed burning in Q. cerris litter fuels.Boxes show the first and third quartiles; the black line is the median.Green triangles are the mean.Negative exponential function, its equation and R2 are also displayed.

Fire rate of spread varied between 0.10 and 0.22 m min^{-1}. Fuel consumption ranged between 80 and 90% of the pre-fire mean fuel load (see figure in Table 1). Maximum flame temperature ranged between 159°C and 601°C. Average residence time above 60°C and 300°C were 198 and 12 seconds, respectively. Figure 2 shows the flame temperature residence time above threshold temperatures measured at the soil surface. The temperature decay displayed a negative exponential function.

Vegetation

On the basis of phytosociological relevés the studied forest formations can be classified as part of mesotemperate *Quercus cerris* wood, referring to the association *Lathyro digitati quercetum cerridis* Bonin and Gamisans 1976 and subassociation *festucetosum exaltata* (Rosati *et al*.2005). These forestsare distributed in the clay-marl and sandstone areas of hilly and mountain between 400 and 850 m a.s.l. and are referred to suballiance *Ptilostemo-Quercenion cerridis* (*Teucrio siculi-Quercion cerridis*). Burned and control area show a great homogeneity in the floristic composition especially

highlighted by the high number of species frequency V (at least 80% of the relevès). In the phytosociological relevés all the species characteristic of association (*Lathyrus jordanii*, *Carpinus orientalis*, *Ptilostemon strictus* and *Melittis melissophyllum*), were found while between the characteristics of sub-association *Erica arborea* and *Drymochloa drymeja* are very common.

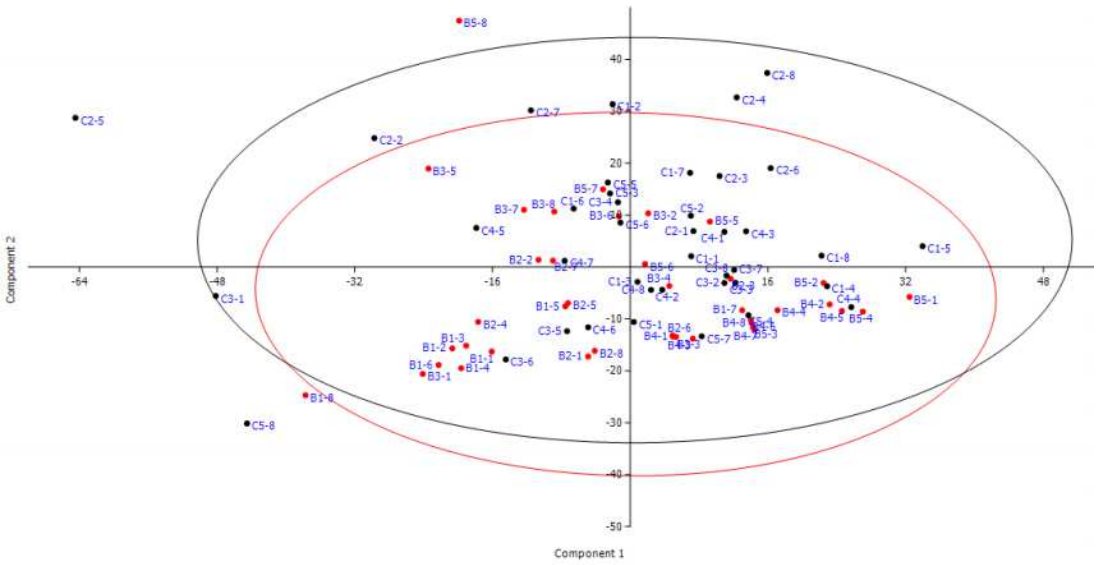

Figure 3. Principal Component Analysis of sampled 80 plots in burned (red) and control (black)area.

The prescribed burning did not affect the understory floristic composition as showed in the Figure 3. The PCA obtained by the analysis of a data matrix (60 species x 80 relevès) does not show a clear separation of burned and control plots along the axis 1 and 2 (explaining35%of the total variability). The ellipses enclose 95% of the variability and are strongly overlapping.

Prescribed burning did not affect the understory plant biodiversity. The rarefaction curve of richness estimators and biodiversity for sample based data (40 burned plots and 40 control plots) showed a similar pattern of variation with a not significant distance. In fact, considering the 95% confidence limits, the curves are superimposed (Figure 4A). No changes were found also in species density as reported in Figure 4B that evidence the same values in the average species number in both treatments.

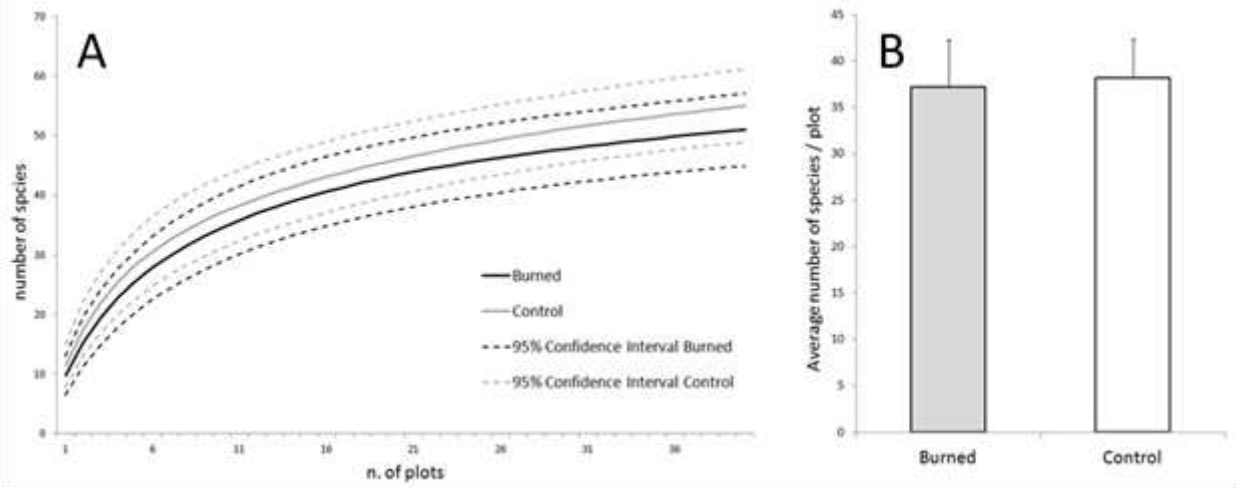

Figure 4. Rarefaction curve of species richness (A) and Average number of species/plot in burned and control area (B).

The analysis of the regeneration was carried out on all tree species present in both seedling and the sapling state. As showed in Table 2 the burning treatment produced a different effect in relation to life trait of species. In particular, *Erica arborea*, *Fraxinus ornus*, *Ilex aquifolium*, and *Sorbus torminalis* evidenced a significant increase of individual number in burned area while *S. domestica* show a decrease.

Table 3. Total number of individuals and average height of woody species in burned and control area. ***For each species significant differences between burned and unburned are reported (n.s.= not significant; *= p<0,05; **= p<0,01; ***= p<0,001).***

	Number of individuals			Average height (±STD)		
Species	**Burned**	**Control**	**test X^2**	**Burned**	**Control**	**U test**
Acer campestre	17	13	n.s.	0.39 (±0.09)	0.65 (±0.34)	n.s.
Carpinus betulus	20	32	n.s.	0.99 (±0.29)	0.81 (±0.32)	n.s.
Carpinus orientalis	37	49	n.s.	0.51 (±0.23)	0.85 (±0.39)	***
Crataegus monogyna	25	27	n.s.	0.63 (±0.33)	0.56 (±0.23)	n.s.
Erica arborea	194	45	n.s.	0.62 (±0.22)	0.90 (±0.34)	***
Fraxinus ornus	304	169	***	0.46 (±0.16)	0.63 (±0.30)	***
Ilex aquifolium	65	20	***	0.58 (±0.26)	0.58 (±0.31)	n.s.
Quercus cerris	177	202	n.s.	0.43 (±0.24)	0.40 (±0.10)	**
Sorbus domestica	6	15	*	0.50 (±0.00)	0.47 (±0.12)	n.s.
Sorbus torminalis	27	7	***	0.51 (±0.16)	0.55 (±0.17)	n.s.

The ability to survive burning treatment with vegetative regrowth was found particularly interesting both in the structural species *Quercus cerris* but especially in some species of conservation interest as *Ruscus aculeatus* and *Ilex aquifolium*. These species responded to burning by resprouting from both the stem and the rhizome (Figure 5).

Figure 5. Regrowth after prescribed burning in Quercus cerris seedlings (right) and Ilex aquifolium (left).

3.3. Effects on soil

Results show that soil samples collected in control and burned plots did not affect soil water holding capacity or bulk density (Table 4).

Soil chemical and microbial properties determined at different times in burned and unburned plots showed that sampling time is the main factor affecting properties of soil compared to fire (Table 5, Figure 6). In fact, all parameters were significantly ($P<0.05$; two-way ANOVA) affected by sampling time, except for soil pH and total N, probably because of temporal variation of climatic conditions. By

contrast, only nitric N appeared significantly (P<0.05; two-way ANOVA) affected by fire. It has to be underlined that accidental changes of some parameters (pH, water content and nitric N), observed only much time after prescribed fire (Table 5), did not appear due to fire treatment. It is not surprising that no effect on soil was found because litter surface temperature was higher than 100°C only for 114 seconds. Similarly, Tecimen and Sevgi (2011) found no effect on C or N fractions if soil from *Quercus* forests (*Q. petrea*, *Q. robur*, *Q. frainetto* and *Q. cerris*) was heated until to 100 °Cfor 1-4 h, whereas a loss of C content and an increase in ammoniacal N were observed at higher temperature.

Table 4. Mean values (±standard deviations) of water holding capacity and bulk density of soil determined in the first sampling (February 2011) in burned and unburned plots of Q. cerris stand.

Treatment	Water holding Capacity(%)	Bulk density (kg m^{-3})
Control	41.5 (±11.0)	0.94 (±0.2)
Burned	45.7 (±16.0)	0.95 (±0.2)

Table 5. Mean values (± standard deviations) of soil pH, water content, total N (N_{tot}), ammoniacal N (NH_4^+-N) and nitric N (NO_3^--N) in burned and unburned plots of Q. cerris stand at different sampling times. For each sampling date significant differences (one-way ANOVA) between burned and unburned are reported (* P<0.05: ** P<0.01).

Sampling date (times after fire) Treatment	pH	Water content (% d.w.)	N_{tot} (μg g^{-1})	NH_4^+-N (μg g^{-1})	NO_3^--N (μg g^{-1})
8/2/2011 (3 h)					
Control	5.5 (±0.5)	63.0 (±19.1)	6.1 (±1.8)	74.1 (±35.6)	2.1 (±1.2)
Burned	5.6 (±1.0)	63.5 (±9.4)	7.0 (±2.2)	68.1 (±30.8)	7.7 (±8.3)
10/3/2011 (30 d)					
Control	5.4 (±0.5)	73.5 (±18.8)	7.7 (±2.0)	52.0 (±34.8)	1.9 (±0.6)
Burned	5.6 (±0.6)	62.1 (±13.9)	5.7 (±1.7)	45.3 (±9.4)	2.6 (±1.4)
13/5/2011 (94 d)					
Control	5.7 (±0.5)	50.4 (±4.8)	5.7 (±1.0)	44.8 (±17.2)	1.8 (±1.9)
Burned	6.5 (±0.4)*	42.7 (±2.7)**	6.6 (±0.6)	45.1 (±13.0)	7.8 (±5.2)*
16/9/2011 (209 d)					
Control	6.1 (±0.9)	25.2 (±3.1)	6.7(±1.5)	8.1 (± 2.3)	0.2 (±0.2)
Burned	5.4 (±0.6)	27.3 (±8.0)	6.1 (±0.9)	9.0 (±3.5)	0.1 (±0.1)
8/03/2012 (394 d)					
Control	5.0 (±0.4)	59.1 (±9.1)	6.3 (±1.3)	21.1 (±8.5)	0
Burned	4.7 (±0.6)	44.9 (±11.0)**	4.7 (±1.4)	13.6 (±7.0)	0

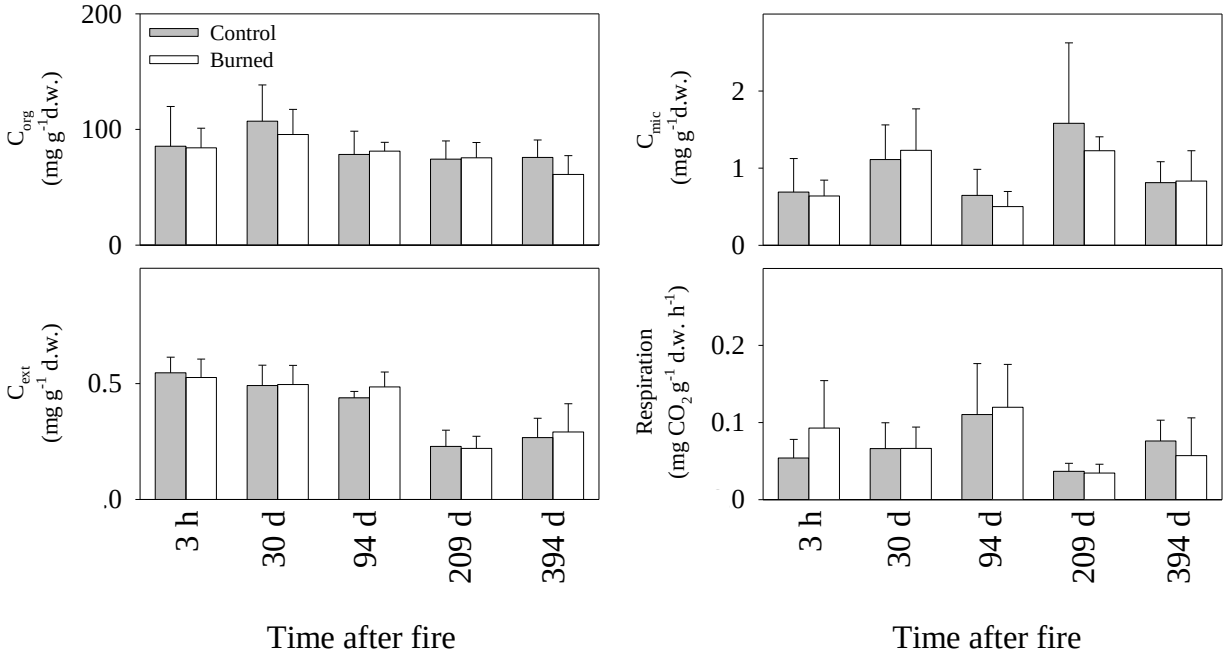

Figure 6. Mean values (+ standard deviations) of soil total organic C (C_{org}), extractable organic C (C_{ext}), microbial C (C_{mic}) and respirationin burned and unburned (control) plots.

Conclusion

In the studied Quercus cerris forest (*Lathyro digitati quercetum cerridis-subassociation festucetosum exaltata*) the prescribed burning application did not affect vegetation and soil during the two year after treatment. No significant changes occurred in floristic composition, species richness and density. The structural species Quercus cerris and some interesting protected taxa (*Ruscus aculeatus and Ilex aquifolium*) evidenced a high regeneration ability by regrowth of killed stem through resprouting new young shoot.

Moreover changes in soil chemical and microbial parameters due to fire were generally not significant and smaller than those occurring during the year, suggesting that fire-induced changes do not overcome the natural temporal variability of these parameters.

Our first results highlight the sustainability of prescribed burning in *Quercus cerris* forests as a management tool both in fire risk reduction and quercus cerris regeneration. Further monitoring activities should be continued to know the impact on all ecosystem components in the medium and long term and to evaluate the most appropriate burning prescriptions and time of frequency application.

References

Abrams M.D., 1992. Fire and the development of oak forests. Bioscience 42(5): 346-353.

Abrams M.D., Johnson S.E., 2013. The Impacts of Mast Year and Prescribed Fires on Tree Regeneration in Oak Forests at the Mohonk Preserve, Southeastern New York. Natural Areas Journal 33(4): 427-434.

Albrecht M.A, Brian C. McCarthy B.C., 2006. Effects of prescribed fire and thinning on tree recruitment patterns in central hardwood forests. Forest Ecology and Management 226: 88-103.

Allen S.E., 1989. Chemical analysis of ecological materials. Blackwell Scientific Publications, Oxford.

Ascoli D., Catalanotti A., Valese E., Cabiddu S., Delogu G., Driussi M., Esposito A., Leone V., Lovreglio R., Marchi E., Mazzoleni S., Rutigliano F.A., Strumia S., Bovio G., 2012. Esperienze di fuoco prescritto in Italia: un approccio integrato per la prevenzione degli incendi. Forest@ 9: 20-38.

Beck T., 1993. Die N-Mineralisation von Boden im Laborbrutversuch Z. Plflanzenernaehr Bodenkd. Vol. 146, pp. 243-252.

Bradshaw R.H.W., Tolonen K., Tolonen M., 1997. Holocene records of fire from the boreal and temperate zones of Europe. Sediment Records Biomass Burning and Global Change. NATO ASI Series 51: 347-365.

Braun Blanquet 1964. Pflanzensociologie: Grundzuge der Vegetationskunde. 3te aufl. Springer-Verlag, Wein. 865 pp.

Brose P.H., Shuler T.M., Ward J.S., 2006. Responses of Oak and Other Hardwood Regeneration to Prescribed Fire: What We Know as of 2005. GTR-NRS-P-1, 123-135.

Brose P.H., Dey D.C., Phillips R.J., Waldrop T.A., 2013. A Meta-Analysis of the Fire-Oak Hypothesis: Does Prescribed Burning Promote Oak Reproduction in Eastern North America? Forest Science 59(3): 322-334.

Box E.O., Manthey M., 2005. Oak and other deciduous forest types of Eastern North America and Europe. Botanika Chronika 18(1): 51-62.

Burton J.A., Hallgren S.W., Fuhlendorf S.D., Leslie D.M., 2011. Understory response to varying fire frequencies after 20 years of prescribed burning in an upland oak forest. Plant Ecology 212: 1513-1525.

Byram G.M., 1959. Combustion of forest fuels. In 'Forest Fire: Control and Use'. (Eds AA Brown, KP Davis) pp. 61–89. (McGraw-Hill Book Company: NewYork)

Castaldi S., Aragosa D., 2002. Factors influencing nitrification and denitrification variability in a natural and fire-disturbed Mediterranean shrubland. Biology and Fertility of Soils 36: 418–425.

Cavender-Bares J., Reich P.B., 2012. Shocks to the system: community assembly of the oak savannain a 40-year fire frequency experiment. Ecology 93(8): S52-S69.

Cutter B.E., Guyette R.P., 1994. Fire Frequency on an Oak-Hickory Ridgetop in the Missouri Ozarks American Midland Naturalist 132(2): 393-398.

Clark J., Merkt J., Muller H., 1989. Post-glacial fire, vegetation and human history on the northern Alpine forelands, south-western Germany. Journal Ecology 77: 897-925.

Colwell R.K., 2013. EstimateS: Statistical estimation of species richness and shared species from samples.Version 9 and earlier. User's Guide and application. http:/viceroy.eeb.uconn.edu/EstimateS

Conti F., Abbate G., Alessandrini A., Blasi C. (eds.), 2005. An annotated check-list of the italian vascularflora.Palombi ed., Roma.

Conti F., Alessandrini A., Bacchetta G., Banfi E., Barberis G., Bartolucci F., Bernardo L., Bonacquisti S., Bouvet D. ,Bovio M., Brusa G., Del Guacchio E., Foggi B., Frattini S., Galasso G., Gallo L., Gangale C., Gottlisch G., Grunanger P., Gubellini L., Iriti G., Lucarini D., Marchetti D., Moraldo B., Peruzzi L., Poldini L., Prosser F., Raffaelli M., Santangelo A., Scassellati E., Scortegagna S., Selvi F., Soldano A., Tinti D., Ubaldi D., Uzunov D., Vidali M., 2007. Integrazioni alla Checklist della flora vascolare italiana. Natura Vicentina, 10: 5-74. (2006).

di Gennaro A., 2002. I sistemi di terre della Campania. Edizioni S.EL.CA., Firenze.

FAO, 1998. World Reference Base for Soil Resources, World Soil Resources, Report No.84, FAO, Rome.

Fernandes P.M., Catchpole W.R., Rego F.C., 2001. Shrubland fire behaviour modelling with microplot data. Canadian Journal Forest Research 30: 889-899.

Fernandes P.M., Davies M.D., Ascoli D., *et al*. 2013. Prescribed burning in southern Europe: developing fire management in a dynamic landscape. Frontiers in Ecology and the Environment 11: e4-e14.

Franklin S.B., Robertson P.A., Fralish J.S., 2003. Prescribed burning effects on upland Quercus foreststructure and function. Forest Ecology and Management 184: 315-335.

Greuter W., Burdet H. M. & Long G. (eds) (1984–1989): Med-Checklist. Vols 1, 3, 4. – Conservatoire et Jardin Botaniques de la Ville de Genève, GenèveKane J.M., Varner J.M., Hiers J.K., 2008. The burning characteristics of southeastern oaks: Discriminating fire facilitators from fire impeders. Forest Ecology and Management 256: 2039-2045.

Keeley J.E., Pausas J.G., Rundel P.W., Bond W.J., Bradstock R.A. 2011. Fire as an evolutionary pressure shaping plant traits. Trends Plant Science 16(8): 406-411.

Kieft T.L., White C.S., Loftin S.R., Aguilar R., Craig J.A., Skaar D.A., 1998. Temporal dynamics in soil carbon and nitrogen resources at a grassland-shrubland ecotone. Ecology 79: 671-683.

Hutchinson T.F., 2008. Proceedings of the 3rd Fire in Eastern Oak Forests Conference. 20-22 May 2008, Illinois. General Technical Report NRS-P-46, Northern Research Station, p. 161.

Hutchinson T.F., Sutherland E.K., Yaussy D.A., 2005. Effects of repeated prescribed fires on the structure,composition, and regeneration of mixed-oak forests in Ohio. Forest Ecology Management 218: 210-228.

Maarel Van der, E., 1979. Transformation of cover-abundance values in phytosociology and its effects oncommunity similarity. Vegetatio 39: 97-114.

Mason S.L.R., 2000. Fire and Mesolithic subsistence - managing oaks for acorns in northwest Europe? Palaeogeography Palaeoclimatology Palaeoecology 164: 139-150.

Neary D.G., Gottfried G.J., Koestner K.A., Folliott P.F., Morale R.A., 2010.Burning temperatures and fire severity in cool and warm season prescribed fires and wildfire in an oak savanna of the southwestern USA. VI International Conference on Forest Fire Research, Coimbra (PT), D. X. Viegas (Ed.): 1-14.

Nicolai V., 1986. The Bark of Trees: Thermal Properties, Microclimate and Fauna Oecologia 69(1): 148-160.

Peterson D.W., Reich P.B., 2001. Prescribed fire in oak savanna: fire frequency effects on stand structure and dynamics. Ecological Applications 11(3): 914-927.

Pignatti S., 1982 - Flora d'Italia. 1-3. Edagricole, Bologna

Podani J. (2001): SYN-TAX 2000. Computer programs for data analysis in ecology and systematics. User'smanual. Scientia Publ., Budapest

Robin V., Nelle O., 2014. Contribution to the reconstruction of central European fire history, based on the soil charcoal analysis of study sites in northern and central Germany. Vegetation History and Archaeobotany.doi:10.1007/s00334-014-0438-2.

Shumway D.L., Abrams M.D., Ruffner C.M., 2001. A 400-year history of fire and oak recruitment in an old-growth oak forest in western Maryland, USA. Canadian Journal of Forest Research 31: 1437-1443.

Simard A.J., Eenigenburg J.E., Adams K.A., Nissen R.L., Deacon A.G., 1984. A general procedure for sampling and analyzing wildland fire spread. Forest Science 30: 51-64.

Springer U., Klee J., 1954. Prüfung der Leistungsfähigkeit von einigen wichtigeren Verfahren zur Bestimmung des Kohlemstoffs mittels Chromschwefelsäure sowie Vorschlag einer neuen Schnellmethode. Z. Pflanzenernähr. Dang. Bodenk 64: 1.

Tecimen H.B, Sevgi O., 2011. Heating induced changes in mineral nitrogen and organic carbon in relation with temperature and time. Journal of Environmental Biology 32: 295-300.

Vance E.D., Brookes P.C., Jenkinson D.S., 1987. An extraction method for measuring soil microbial biomass C. Soil Biology & Biochemistry 19: 703-707.

USDA Natural Resources Conservation Service, 2004. In: Burc, R. (Ed.), Soil Survey Laboratory Methods Manual. Soil Survey Investigations Report No. 42, Version 4. 0. National Soil Survey Center, Lincoln, NE.

Wang G.G., Van Lear D.H., Bauerle W.L., 2005. Effects of prescribed fires on first-year establishment of white oak (Quercus alba L.) seedlings in the Upper Piedmont of South Carolina, USA. Forest Ecology and Management 213: 328-337.

Williams R.J., Hallgreen S.W., Wilson G.W.T., 2012. Frequency of prescribed burning in an upland oak forest determines soil and litter properties and alters the soil microbial community. Forest Ecology and Management 265: 241-247.

Fire as a tool to manage pollination services

Julian Brown[a], Fiona Christie[a], Alan York[a]

[a] *University of Melbourne, Department of Forest and Ecosystem Science, Creswick Campus, 4 Water Street, Creswick, VIC, 3363, j.brown3@student.unimelb.edu.au*

Abstract
As a tool of land management and conservation there are a number of applications for which fire is poorly developed. One of those applications is the management of ecosystem services such as pollination and pest control that are provided by mobile organisms. Pollination in particular is an ecosystem service that requires improved management, in response to global declines in pollinators that present a threat to the plants that are dependent on them for reproduction. Much recent attention has been given to the effects of land use and land management generally on pollination, but little to fire as a particular form of land management. Here we develop a conceptual model describing hypothesised causal chains linking fire to pollination, and then report the initial findings of a study investigating fire effects on pollination as informed by this model for an orchid species native to Australia.

Keywords*: pollination, Caladenia tentaculata, fire, succession.*

Introduction

Fire is a tool with a wide variety of applications in land management and conservation. One potential application that has received little attention is as a means to manage ecosystem services provided by mobile organisms, such as pollination and pest control. Fire can influence the population and community dynamics of mobile organisms (Whelan *et al.* 2002), so it might be used to manage the services they provide. There is an urgent need to improve management of pollination services as recent declines in pollinators across the globe (including fire-prone regions) raises concerns over the loss of pollination services to crops and wild plant populations (Potts *et al.* 2010; Vanbergen and IPI 2013). Pollinators and consequently pollination services are affected by habitat conditions at the landscape-scale (Kremen *et al.* 2007) and fire is a relatively inexpensive tool for managing habitat at this scale. Recent research has indeed demonstrated the role of fire in structuring pollinator communities through habitat alteration (e.g. Potts *et al.* 2003a, b, 2005, 2006). However, pollination rate can be determined by factors other than pollinator population and community dynamics (Kremen *et al.* 2007); so it is important to consider whether fire might influence pollination through additional pathways to avoid unintended consequences of management. No single study has considered all the possible pathways through which fire might influence pollination.

A conceptual model describing hypothesised causal chains linking fire to pollination is developed here to guide research into the effects of fire on pollination. A general model of the effects of land use and land management on pollination has recently been developed (Kremen *et al.* 2007) and underpinned a recent quantitative model of pollination services across landscapes that performed well when evaluated against independent data (Lonsdorf *et al.* 2009). Within this tested framework the conceptual model of interactions between fire (as a particular component of land management) and pollination services is developed by combining the body of research in pollination ecology underlying Kremen *et al.*'s model with the relevant body of research in fire ecology. Kremen *et al.* propose that land use/management influences pollination by affecting the target plant to which pollination services are of interest (at the individual, patch, and population level), the plant community (with which the target plant interacts in competition or facilitation through shared pollinators), the pollinator community, and the biotic and abiotic factors that influence these groups. The model developed here (Figure 1)

describes the mechanisms (Blue boxes) linking fire (Orange box) to groups (Green boxes) to pollination (Yellow box). The mechanisms linking fire to groups can be direct (e.g. direct mortality) or indirect (e.g. alteration of nesting sites) effects that are immediate and/or occur along a time-since-last-fire trajectory (Dafni *et al.* 2012).

Kremen *et al.* (2007) highlight the importance of both local-scale changes in groups and their aggregation into landscape structure in influencing pollination. That is, there are multiple spatial scales at which changes in groups can influence pollination, which might be of particular relevance to fire management of pollination services. For example, flower visitation by bumblebees is related to the abundance of co-flowering plants within an area of 100-500 m^2, but not at larger or smaller scales (Thomson 1981; Johnson *et al.* 2003). Flower visitation by bumblebees is related to bumblebee habitat conditions within an area several orders of magnitude larger, corresponding to the bumblebees' home range (Westphal *et al.* 2006). The implication is that the size of a fire might determine its impact on pollination by determining the degree to which different pathways influencing pollination are affected; a fire that is 500 m^2 might alter competition or facilitation for pollination with little effect on pollinator populations, whereas a larger fire might impact both.

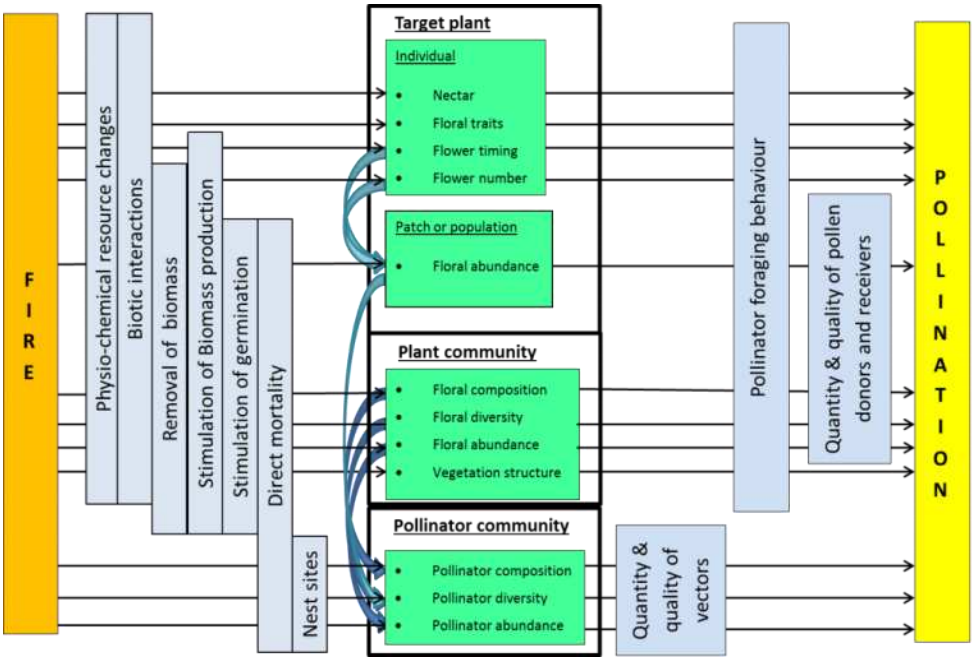

Figure 1. Conceptual model outlining hypothesised pathways of the relationships between fire and pollination. Fire may influence groups (Green boxes) through a range of mechanisms (Blue boxes). Groups may influence pollination directly (black arrows) or indirectly via a number of biotic interactions (blue arrows) through a second set of mechanisms (Blue boxes).

This model has been used to guide a PhD research project (J. Brown) into the effects of fire on pollination in a species of the Orchidaceae family (*Caladenia tentaculata*). There is a need to learn about fire effects on pollination in orchids because many inhabit fire-prone environments across the globe (Naveh *et al.* 1994; Swarts and Dixon 2009; Lamont and Downes 2011) and fecundity is generally limited by pollen (Trembley *et al.* 2005). A group of particular concern in Australia is the sexually-deceptive orchids that achieve pollination through mimicry of the sex pheromones of female insects. They occur in some of the most flammable ecosystems in the country (e.g. heathy woodlands) and are one of the most pollen-limited orchid groups (Tremblay *et al.* 2005; Phillips *et al.* 2009). The critically threatened status of a number of sexually-deceptive orchids has been attributed to the highly specialised, and so sensitive to ecological change, pollination system characteristic of this group (Swarts and Dixon 2009). Many sexually-deceptive along with other groups of terrestrial orchids are

stimulated to flower by fire (Jones 2006; Coates and Duncan 2009; Duncan 2012), and the promotion of flowering and emergence through regular burning is a common management recommendation for these plants (Cropper *et al.* 1989; Lunt 1994; Coates *et al.* 2006; Coates and Duncan 2009). However, the effects of fire on pollination through any of the possible pathways is unknown, so there is no way of predicting the effect of regular burning on pollination and determining to what extent this will depend on fire size. Reported here are the findings from the pilot study of a PhD project (J. Brown) investigating the effects of fire on pollination in the sexually-deceptive orchid *C. tentaculata*.

Methods

Study System

The study landscape was an area of approximately 15,000 km^2 in south-west Victoria, Australia (Figure 2). The area encompassed the Grampians National Park and numerous forests on public land between the National Park and the South Australian border. The native vegetation consists of sclerophyllous heaths, shrub lands, and woodlands interspersed with open grasslands (Gibbons and Downes 1964; Dodson 2001). The area has a Mediterranean-type climate (hot dry summers and mild wet winters), and has experienced recurring fires throughout the Holocene (reviewed in Dodson 2001). Prescribed fire is currently applied to vegetation on public land in an attempt to protect lives and property and achieve ecological objectives (DEPI 2013a, b). The area was chosen because the orchid and its pollinator have been detected at a number of localities in this area (Bower 2009), there is a broad range of fire histories, and minimal topographic variation between sample locations. In order to cover a wide range of post-fire successional stages this research was based on a chronosequence of 52 heathy woodland sites ranging from several months since last fire to several decades since last fire.

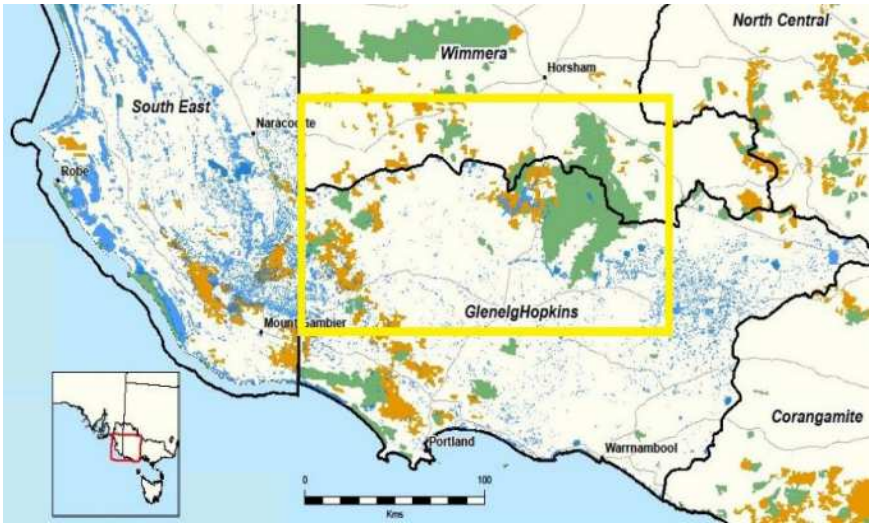

Figure 2. Area (yellow rectangle) of south-west Victoria within which all samples were collected. Green and brown areas are native vegetation (National Park and State Forest respectively), blue areas water bodies, and white rural and residential.

The native orchid *C. tentaculata* has been chosen for this study for a number of reasons. It is stimulated to flower by fire (Jones 2006; Duncan 2012). It is also known to be pollinated by a single species of parasitoid wasp from the thynnine subfamily – *Thynnoides pugionatus* – by sexual deceit (Peakall and Beattie 1996; Jones 2006). Both plant and pollinator are widespread and common in south-east Australia (Jones 2006; Bower 2009), allowing for relatively large sample sizes.

Data collection

The main response variable of interest was the visitation rate of *T. pugionatus* to *C. tentaculata* flowers. The pollinators of *C. tentaculata* respond rapidly to the presentation of its flowers (Peakall and Beattie 1996), so at each of the 52 sites four *C. tentaculata* flowers (growing in pots) were placed at a single location for 10 minutes and the number of times pollinators made contact with (visited) the flowers was observed (sexually-deceptive orchids typically exhibit one-to-one relationships with their pollinators and the pseudo-copulatory flower visiting behaviour is distinct [Gaskett 2011], such that pollinators could be identified by observing visitation). This was done multiple times at each site to allow for the development of a model that accounts for the probability of detecting the pollinator (i.e. number of visits being greater than zero) given its presence. Also obtained at each location was the time-since-last-fire (TSLF) at the site (sites 55 years or greater were classified as 55 years old which corresponds roughly to senescence for heathy woodlands [Cheal 2010] and the limits of accurate fire records for this region) from GIS layers provided by the Department of Environment and Primary Industries, temperature (since this is known to influence wasp activity) at the time of pollinator sampling, and for the recently burnt sites (less than three years before the time of sampling) the distance to the nearest edge of the burnt site (i.e. distance to nearest unburnt vegetation).

2.3. Data analysis

Only observations made above the critical temperature threshold for wasp activity of 17°C (determined using repeat observations at sites to model the probability of detecting the pollinator given its presence as a function of temperature, which is not presented here) were used for the analysis presented here. Zero visits were observed at a large proportion of the sites, so logistic regression was first used to model pollinator presence/absence (i.e. greater than zero visits/zero visits respectively) as a function of TSLF, and simple linear regression was used to model the maximum number of visits observed at each site where pollinators were present (that is, excluding sites where no pollinators were observed) as a function of TSLF. For the logistic regression, R^2 was calculated using the method developed in Nakagawa and Schielzeth 2013). For the subset of the data corresponding to recently burnt sites, simple linear regression was used to model the maximum number of visits observed at each site as a function of distance to the nearest edge of the burnt site. All analyses were performed in the R statistical environment (R Development Core Team 2011).

3. Results

The model of pollinator presence/absence as a function of TSLF was a poor fit to the data ($R^2 = 0.00$). When the maximum number of *T. pugionatus* visits to *C. tentaculata* observed at each site was modelled as a linear function of TSLF, the model explained a negligible amount of the variation ($R^2 = 0.02$). The relationship between the maximum number of visits and TSLF is shown in Figure 3 below, and it can be seen that unusually high visitation values were observed in two very recently burnt sites and one long unburnt site, but that lower values were observed across all sites (thus explaining the poor model fit).

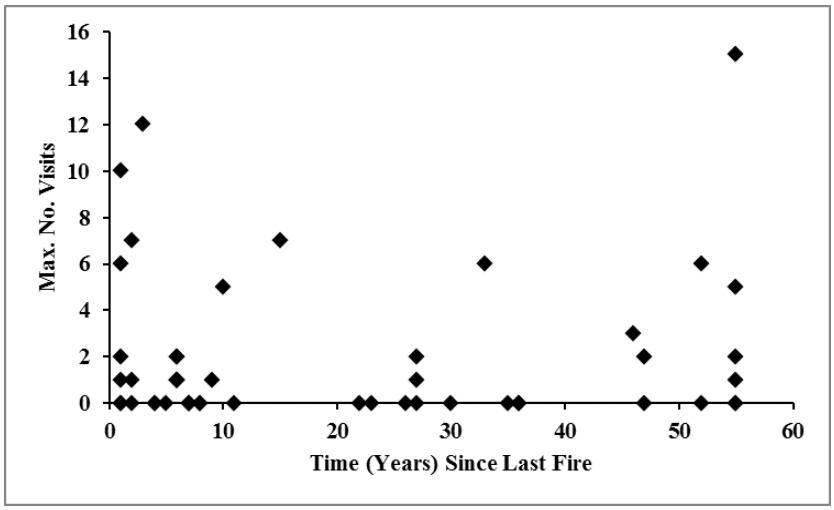

Figure 3. Show the maximum number of visits to C. tentaculata flowers by thynnine wasps at each site as a function of the number of years since the last fire at each site.

The model of the maximum number of visits to flowers at recently burnt sites as a linear function of distance from the nearest edge of the burn site was also a poor fit to the data ($R^2 = 0.00$). Figure 4(a) shows that this can be attributed to an extreme outlier. With this outlier removed (Figure 4(b)), model fit improved substantially ($R^2 = 0.45$). Inspection of Figure 4(b) suggests that inclusion of polynomial terms would further enhance model fit, though there were not enough observations to allow the addition of further parameters.

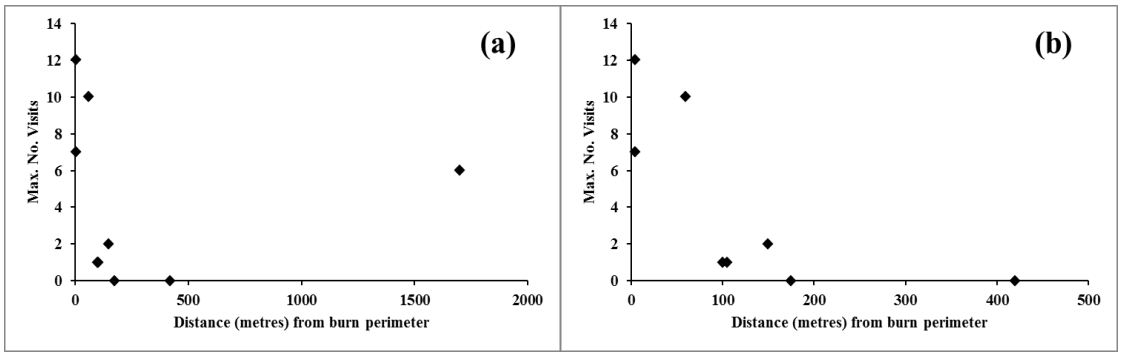

Figure 4. Shows the maximum number of visits to C. tentaculata flowers by thynnine wasps at (a) each recently burnt site and (b) each recently burnt site except for the outlier site, as a function of the distance of the flowers from the nearest edge of the burn site

Discussion

Statistical models developed here were generally poor fits to the data. Pollinator presence or visitation rate showed no clear relationship with TSLF, and visitation rate in recently burnt sites only showed a relationship to distance from the nearest edge of the burn site when an outlier was removed. The value of this pilot study lies in the potential explanations for the failure of fitted models to explain observed variation.

The outlier in the data pertaining to the recently burnt subset of sites is interesting. It lay approximately 1,700 m from the burn perimeter, which is well beyond the distance from the perimeter where the model without the outlier predicts zero visitation. It has been suggested that some thynnine wasps (the subfamily to which *T. pugionatus* belongs) might be capable of travelling up to 1,600 m, but most are

thought to be restricted to distances of 800 m (Ridsdill-Smith 1970) and the greatest distance *T. pugionatus* has been observed to travel between *C. tentaculata* flowers was 58 m (Peakall and Beattie 1996). Thus, either the observed outlier extends the known foraging range of thynnine wasps, or the wasps were resident in the recently burnt site. The TSLF GIS layer used in this analysis does not include information about variation in fire severity within fire perimeters, which may provide faunal refugia that allows fire-sensitive animals to be present immediately after fire (Whelan *et al.* 2002; Penman *et al.* 2007). Alternatively, the wasps are capable of rapidly recolonizing from surrounding unburnt vegetation or surviving the passage of fire of any severity.

Although models were generally poor fits to the data, the patterns observed are interesting in the context of the conceptual model developed in the introduction. From the patterns shown in Figure 3 and Figure 4(b) it would appear as though when *C. tentaculata* flowers in the early post-fire environment (as it tends to do) it is capable of attracting more visits from its pollinators compared to other post-fire seral stages (except perhaps for very long unburnt sites), provided it is not too far from unburnt vegetation. In other words, small fires centred on the orchid may enhance pollination, but as fire size increases the pollination benefits may eventually disappear such that visitation is equal to or less than what is experienced in later seral stages. Thus, the size of a fire may be important in determining its impact on *C. tentaculata* pollination. However, this requires more formal testing as the data presented here are suggestive at best.

Although this tentative model is yet to be tested, it is interesting to consider the underlying mechanisms. Petit and Dickson (2005) found that the pollination rate of a sexually-deceptive orchid decreased as the amount of vegetation within close proximity increased, which they attributed to increased difficulty for pollinators in locating orchid flowers. In the heathy woodland system studied in the present paper, vegetation structure is low in the early post-fire environment, gradually increasing to a maximum in mid successional stages, and then declining again late in succession (Cheal 2010; Brown 2013). Thus, the highest potential (depending on other factors such as perhaps distance from burn edge) pollination rates would be expected in recently burnt sites, and then again much later in succession, which is what was observed in the present study. A decrease in visitation in recently burnt sites with increasing distance from unburnt vegetation might occur if pollinators are incapable of inhabiting or otherwise avoid recently burnt sites, entering only when enticed by a signal (in this case indicating the possibility of a mating opportunity, since the orchids are sexual mimics) that presumably decreases in strength with greater distance from the source (the ability of an insect to detect a sex pheromone decreases as a logarithmic function of distance from the odour source [Andersson *et al.* 2012]). Further work is required to investigate these possible mechanisms in the study system.

The next stage of the PhD project is to explore some of the possible interpretations of the data presented here. The main focus will be on determining the relationship between visitation and distance from the edge of the burn site. Observations will be made of visitation to *C. tentaculata* flowers placed at a number of fixed distances from the fire perimeters of a number of recently burnt sites, and attempts will be made to control for burn severity. Processes operating at different spatial scales will also be explored. In particular, relationships between *C. tentaculata* pollination and vegetation structure (and co-flowering heterospecifics) measured within close proximity to the orchid, and between pollinator activity and seral stage composition at the landscape scale. Together the findings from this research will contribute to the knowledge base required to effectively use fire to manage *C. tentaculata* and other sexually-deceptive orchids with fire-stimulated flowering, which are among the most threatened in Australia (Victoria Flora and Fauna Guarantee Act 1988).

Acknowledgements

We would like to thank the Department of Environment and Primary Industry and the University of Melbourne for financial and technical support, Colin Bower and Garry French for training in the use

of orchids to detect their pollinators, and Julio Najera, John Loschiavo, and Rowena Booth for assistance with data collection.

References

Andersson P, Löfstedt C and Hambäck PA (2012) How insects sense olfactory patches – the spatial scaling of olfactory information. Oikos 122, 1009–1016.

Brown T (2013) The effects of fire on invertebrate pollinator communities. Honours Thesis, University of Melbourne, Victoria, Australia.

Bower CC (2009) Pollinators of sexually deceptive spider orchids (Caladenia) in Victoria. Report to the Australian Orchid Foundation, Melbourne.

Cheal D (2010) Growth stages and tolerable fire intervals for Victoria's native vegetation data sets. Fire and Adaptive Management Report No. 84. Department of Sustainability and Environment, East Melbourne, Victoria, Australia.

Coates F and Duncan M (2009) Demographic variation between populations of Caladenia orientalis – a fire-managed threatened orchid. Australian Journal of Botany 57, 326–339.

Coates F, Lunt I and Tremblay R (2006) Effects of disturbance on population dynamics of the threatened orchid Prasophyllum correctum D.L.Jones and implications for grassland management in south-eastern Australia. Biological Conservation 129, 59–69.

Cropper SC, Calder DM and Tonkinson D (1989) Thelymitra epipactoides F. Muell. (Orchidaceae): the morphology, biology and conservation of an endangered species. Proceedings of the Royal Society of Victoria 101, 89–101.

Dafni A, Izhaki I, and Ne'eman G (2012) The Effect of Fire on Biotic Interactions in Mediterranean Basin Ecosystems: Pollination and Seed Dispersal. Israel Journal of Ecology and Evolution 58(2-3), 235-250.

Department of Environment and Primary Industry (DEPI) (2013a) Fire Operations Plan 2013/14-2015/16 Barwon South West Region. Department of Environment and Primary Industries, Victoria, Australia, Melbourne.

Department of Environment and Primary Industry (DEPI) (2013b) Fire Operations Plan 2013/14-2015/16 Wimmera Region. Department of Environment and Primary Industries, Victoria, Australia, Melbourne.

Dodson JR (2001) Holocene vegetation change in the mediterranean-type climate regions of Australia. Holocene 11, 673-80.

Duncan M (2012) Response of Orchids to Bushfire: Black Saturday Victoria 2009 – Natural values fire recovery program. Department of Sustainability and Environment, Heidelberg, Victoria.

Gaskett AC (2011) Orchid pollination by sexual deception: pollinator perspectives. Biological Review 86, 33–75.

Gibbons F R and Downes RG (1964) A Study of the Land in South Western Victoria. Soil Conservation Authority, Victoria, Melbourne.

Johnson SD, Peter CI, Nilsson LA and Agren J (2003) Pollination success in a deceptive orchid is enhanced by co-occurring rewarding magnet plants. Ecology 84, 2919–2927.

Jones DL (2006) A complete guide to native orchids of Australia including the island territories. Reed New Holland, Sydney.

Kremen C, Williams NM, Aizen MA, Gemmill-Herren B, LeBuhn G, Minckley R, Packer L, Potts SG, Roulston T, Steffan-Dewenter I, Vázquez DP, Winfree R, Adams L, Crone EE, Greenleaf SS, Keitt TH, Klein AM, Regetz J and Ricketts TH (2007) Pollination and other ecosystem services produced by mobile organisms: a conceptual framework for the effects of land-use change. Ecology Letters 10(4), 299-314.

Lamont BB and Downes KS (2011) Fire-stimulated flowering among resprouters and geophytes in Australia and South Africa. Plant Ecology 212, 2111–2125.

Lonsdorf E, Kremen C, Ricketts T, Winfree R, Williams N and Greenleaf S (2009). Modelling pollination services across agricultural landscapes. Annals of Botany 103, 1589–1600

Lunt ID (1994) Variation in flower production of nine grassland species with time since fire, and implications for grassland management and restoration. Pacific Conservation Biology 1, 359–366.

Nakagawa S and Schielzeth H (2013) A general and simple method for obtaining R2 from generalized linear mixed-effects models. Methods in Ecology and Evolution 4(2), 133-142.

Peakall R and Beattie AJ (1996) Ecological and genetic consequences of pollination by sexual deception in the orchid Caladenia tentaculata. Evolution 50, 2207–2220.

Penman TD, Kavanagh RP, Binns DL and Melick DR (2007) Patchiness of prescribed burns in dry sclerophyll eucalypt forests in south-eastern Australia. Forest Ecology and Management 252(1), 24-32.

Petit S and Dickson CR (2005) Grass-tree (Xanthorrhoea semiplana, Liliaceae) facilitation of the endangered pink-lipped spider orchid (Caladenia syn. Arachnorchis behrii, Orchidaceae) varies in South Australia. Australian Journal of Botany 53(5), 455-464.

Phillips R, Faast R, Bower C, Brown G and Peakall R (2009) Implications of pollination by food and sexual deception for pollinator specificity, fruit set, population genetics and conservation of Caladenia (Orchidaceae). Australian Journal of Botany 57, 287–306.

Potts SG, Vulliamy B, Dafni A, Ne'eman G, O'Toole C, Roberts S and Willmer P (2003a) Response of plant pollinator communities to fire: changes in diversity, abundance and floral reward structure. Oikos 101, 103–112.

Potts SG, Vulliamy B, Dafni A, Ne'eman G and Willmer P (2003b) Linking bees and flowers: how do floral communities structure pollinator communities? Ecology 84, 2628–2642.

Potts SG, Vulliamy B, Roberts S, O'Toole C, Dafni A, Ne'eman G and Willmer P (2005) Role of nesting resources in organising diverse bee communities in a Mediterranean landscape. Ecology Entomology 30, 78–85.

Potts SG, Petanidou T, Roberts S, O'Toole C, Hulbert A and Willmer P (2006) Plant-pollinator biodiversity and pollination services in a complex Mediterranean landscape. Biology Conservation 129, 519–529.

Potts SG, Biesmeijer JC, Kremen C, Neumann P, Schweiger O and Kunin WE (2010) Global pollinator declines: trends, impacts and drivers. Trends in Ecology and Evolution 25, 345 – 353.

R Development Core Team (2011) R: A Language and Environment for Statistical Computing. R Foundation for Statistical Computing.

Ridsdill-Smith TJ (1970) The behaviour of Hemithynnus hyalinatus (Hymenoptera: Tiphiidae), with notes on some other Thynninae. Journal of the Australian Entomological Society 9, 196–208.

Swarts ND and Dixon KW (2009) Terrestrial orchid conservation in the age of extinction. Annals of Botany 104, 543–556.

Thomson JD (1981) Spatial and temporal components of resource assessment by flower-feeding insects. Journal of Animal Ecology 50, 49–59.

Tremblay RL, Ackerman JD, Zimmerman KK and Calvo RN (2005) Variation in sexual reproduction in orchids and its evolutionary consequences: a spasmodic journey to diversification. Biological Journal of the Linnaean Society 84, 1–54.

Vanbergen AJ and the Insect Pollinators Initiative (IPI) (2013) Threats to an ecosystem service: pressures on pollinators. Frontiers in Ecology and the Environment, 11(5), 251–259.

Westphal C, Steffan-Dewenter I, and Tscharntke T (2006) Bumblebees experience landscapes at different spatial scales: possible implications for coexistence. Oecologia 149(2), 289-300.

Whelan RJ, Rodgerson L, Dickman CR and Sutherland EF (2002) Critical life cycles of plants and animals: developing a process based understanding of population changes in fire-prone landscapes. In 'Flammable Australia: The fire regimes and biodiversity of a continent' (Eds RA Bradstock, JE Williams, AM Gill) pp. 94-124. (Cambridge University Press: Cambridge).

Is remote sensing a good method to define forest fire resilience? A particular case in the South-eastern of the Iberian Peninsula

Javier Hedo[a], Eva Rubio[b], Tarek Dadi[c], Francisco Ramón López-Serrano[c], Raquel Alfaro-Sánchez[a], Daniel Moya[a], Jorge de las Heras[a]

[a] *Department of Plant Production and Agricultural Technology. School of Agricultural Engineering of Albacete. University of Castilla-La Mancha. Campus University s/n 02071, Albacete. Javier.Hedo@gmail.com; R.Alfarosanchez@gmail.com; Daniel.Moya@uclm.es; Jorge.Heras@uclm.es*
[b] *Department of Applied Physics, School of Industrial Engineering of Albacete. University of Castilla-La Mancha. Campus University s/n 02071, Albacete. EvaMaria.Rubio@uclm.es*
[c] *Department of Genetics and Agroforestry Science and Technology, School of Agricultural Engineering of Albacete. University of Castilla-La Mancha. Campus University s/n 02071, Albacete. Fco.Lopez@uclm.es; Tarek.Dadi@uclm.es*

Abstract

Fire is one of the most drastic disturbances in forest ecosystems, particularly in Mediterranean ecosystems. Global change, including climate change and land use changes, is strengthening the rising of frequency and intensity of them. The knowledge of the resilience of the main Mediterranean ecosystems would allow defining policies and actions to protect the most vulnerable species.

One of the problems that the concept of resilience presents it is to be a concept associated to the dynamic of the ecosystem and there is no definition to quantify in a normalized and standardized way. This work propose an original methodology that involves the definition of type curves of recovery based on a time series of NDVI data, from Landsat satellite images, and the analysis of the potential changes in the taxonomic composition of the ecosystem after fire. We present the analysis of two areas affected by forest fires in the southeast of the Iberian Peninsula. It involves representative plant communities in this region, specifically esparto-grassland, esparto and rosemary shrubbery, and Aleppo pine forest.

Keywords*: resilience, site quality, landscape ecology, forest dynamics.*

Introduction

Fire is one of the main drastic disturbances in forest ecosystems, mainly in Mediterranean ecosystems, and plants have developed traits to cope with fire. Resilience has been defined as the capacity of an ecosystem to respond to a disturbance by resisting damage and recovering in a relatively short period of time in plant communities. The resilience is a function of the composite resiliences of the assemblage of species populations (Keeley 1986).

Global change, climate change and changes in land use or land cover, modified fire regime in South-eastern Spain in the last three decades (Pausas 2004). The changes promoted an increase in the number and recurrence of wildfires, its intensity and severity, burned surface and the period of fire risk. Those changes in fire regime could induce changes in the climax stage of plant community and/or ecosystems, relegated to secondary stages in the succession or, even, to paraclimax stages (San Miguel Ayanz *et al*., 2012). It implies a decrease in productivity and a reduction in plant diversity, in addition to variations in spatial distribution and vegetation structure. Forest management based on natural disturbances could maintain and restore ecological resilience (Drever *et al*., 2006) which should be taken into account in planning and policies to protect the less resilient species and improve it.

Tools helping decision makers should include analysis of resilience and adaptive resource management based in scientific knowledge. The concept of resilience is associated with ecosystem dynamics and different approaches have been developed for concrete cases of study, however, there is still a lack

regarding to obtain a normalized and standardized method to quantify relative resilience. The main objective of the current framework was to develop a tool for landscape-scale monitoring and prediction of vegetation resilience, related to management objectives.

Methods

Study area

This work was carried out in two areas burnt in 1994 in the municipality of Hellin (province of Albacete). Before fire, mature and natural Aleppo pine forests (*Pinus halepensis* Mill) and esparto-grasslands (*Macrochloa tenacissima* (L.) Kunth) covered the study area. The study area was characterized as a semiarid type and the potential natural vegetation was a shrubland of *Quercus coccifera* L. (*Rhamno lycioidis - Quercetum cocciferae* sigmetum) (Rivas-Martinez 1987). After fire, the vegetation was mainly composed of Aleppo pine, esparto grass and rosemary (*Rosmarinus officinalis* L.). Physical and climatic characterization of the study areas is shown in Table 1.

Table 1. Physical and climatic characterization corresponding to the analysed areas. Rainfall and temperature were calculated for the last 30 years

Site	"Sierra de los Donceles"	"Peñalavada"
Date	04/01/1994	07/19/1994
Slope(º)	18-35	ene-40
Aspect	All	All
Altitude (m)	618 – 770	427 - 825
Soil type (IGME, 2013)	Aridisols	Entisols
Rainfall (mm)	275	285
Temperature (ºC)	15.6	16.1

Experimental design

Resilience concept includes multiple aspects, such as taxonomic composition and pre-fire community structure changes, changes in ecosystem functions and impacts of processes rates (Holling, 1973). In this work it is formulated a methodological approximation to the resilience concept, centered on the study of plant community composition changes (successional stages) and on structure changes (recovery dynamics). In addition, those changes are analyzed in terms of plant community external factors, as fire severity and site quality. Here, the site quality concept is approximated by the amount of vegetation before the fire.

In particular, the study of changes in the taxonomic composition of communities after fire has been carried out based on pre-and post-fire cartography and forest inventories (Table 2). Structural changes in vegetation have been determined from the estimation of the recovery dynamics based on the amount and greenness of the vegetation. For that end, it has been proposed the assessment of the temporal evolution curves of the *Normalized Difference Vegetation Index* (NDVI) in the burnt areas. We use seventeen Landsat images, all of them distributed in the period 1992-2011. The acquisition dates of all Landsat images used were in spring, to avoid potential seasonal changes in NDVI due to phenological variations. Landsat images were also used to determine fire severity in terms of the *differenced Normalized Burn Ratio* (dNBR) (Key and Benson, 2006). For each pixel in the image of the study areas a record with all the fields from the databases showed in Table 2 was assigned. This information was used to analyse the changes in the taxonomic composition of communities, to define site quality and resilience.

Table 2. List of databases, cartography and satellite imagery used in this work.

Database	Source
Spanish Forest Map 1:200,000 (MFE200)	MMA
Spanish Forest Inventory 2 (IFN2)	MMA
Forest Inventory Spanish 3 (IFN3)	MMA
Spanish Forest Map 1:50,000 (MFE50)	MMA
Climatological DB (1980-2012)	AEMET
Digital Terrain Model (DTM)	IDE-CLM
Map 1:1,000,000 lithologies of Spain	IGME
Soil Map of Spain 1:1,000,000	IG ME
Series vegetation Rivas-Martínez	MMA
Landsat 5/7 and derivatives (NDVI, DNBR)	USGS, National Remote Sensing Plan

Results

The vegetation present in the area was classified into five general plant formations and two plant sub-types in order to analyse their different post-fire behaviours (Table 3).

Table 3. Plant formations in the study area

		Plant formation	Name	Description
90%	68%	Formation 1	Esparto grassland	Mainly esparto grassland
		Formation 2	Grass-shrub	Land associated with scrub grassland. Scrub surface does not exceed 20%.
		Formation 3	Shrub	Predominance of shrubs and suffrutescent plants.
	32%	Formation 4	Aleppo pine open forest	Aleppo pine high pole wood forest (canopy cover fraction 10 %)
10%		Formation 5	Aleppo pine dense forest	5.1. Aleppo pine high pole wood forest (canopy cover fraction 30 %)
				5.2. Aleppo pine high pole wood forest (canopy cover fraction 60 %)

Taxonomic composition changes

Changes in land cover were analysed. Table 4 shows the changes in the percentage of soil coverage by each plant formation before (PRE) and after fire (POST). These results have been analyzed based on fire severity, site quality, and physiographic factors as slope and aspect. Table 5 summarizes these external factors. Site quality has been assimilated to the amount of vegetation before the fire and discretized into five levels, with the AAA category the highest quality, and the BB the category of lowest quality. Likewise, we have established four levels of severity: high, moderate-high, moderate and low.

Table 4. Vegetation before and after fire, percentages of land cover changes according to the taxonomic composition (Table 3)

POST / PRE	Esparto grassland	Grass-shrub	Shrub	Aleppo pine open forest	Aleppo pine dense forest	**% Before fire**
Esparto grassland		93		7		**5**
Grass-shrub	17	35	2	42	4	**29**
Shrub	16		80	4		**34**
Aleppo pine open forest		75		15	10	**23**
Aleppo pine dense forest	8	2	20	18	52	**9**
% Post-fire	**10**	**43**	**10**	**25**	**11**	

Recovery dynamics post-fire vegetation

From NDVI time series, until eight different patterns or curve types of the dynamics of regeneration of the vegetation structure were identified and defined. The eight characteristic patterns are regarded as 'recovery curves' Figures 1-2 grouped the individual behaviours of all analyzed pixels. In particular, Figure 1 shows for the less mature plant formations (i.e. Esparto grassland, Grass-Shrub and Shrub) these recovery curves in relation to post-fire vegetation, site quality conditions and fire severity, factors which modulate the recovery dynamics.

Table 5. Pre and post fire vegetation, site quality, fire severity, altitude and dNBR.

Pre-fire vegetation	**Post-fire vegetation**	**Site quality**	**Altitude (m)**	**Severity**	**dNBR**
Esparto grassland	Grass-shrub	BB	530 ± 30	Low	160 ± 30
	Aleppo pine opened forest	BB	461 ± 15	Low	197 ± 10
Grass-shrub	Esparto grassland	B	630 ± 90	Low	220 ± 70
	Grass-shrub	B	530 ± 80	Low	240 ± 70
	Shrub	A	690 ± 60	Mod-Low	330 ± 60
	Aleppo pine opened forest	B	530 ± 40	Mod-Low	280 ± 80
	Aleppo pine dense forest 30%	AAA	780 ± 30	Mod-Low	370 ± 80
Shrub	Esparto grassland	B	530 ± 50	Low	200 ± 50
	Shrub	B	530 ± 50	Low	220 ± 70
	Aleppo pine opened forest	AA	585 ± 15	Mod-Low	354 ± 7
Aleppo pine opened forest	Grass-shrub	B	550 ± 70	Low	200 ± 60
	Aleppo pine open forest	B	570 ± 70	Low	260 ± 80
	Aleppo pine dense forest 30%	B	580 ± 50	Low	220 ± 50
Aleppo pine dense forest 30%	Shrub	BB	510 ± 15	Low	144 ± 24
	Aleppo pine dense forest 30%	A	514 ± 7	Mod-Low	283 ± 4
Aleppo pine dense forest 60%	Esparto grassland	B	640 ± 110	Baja	260 ± 130
	Grass-shrub	BB	470 ± 20	Low	202 ± 8
	Aleppo pine opened forest	AA	500 ± 50	Mod-Low	360 ± 170

	Aleppo pine opened forest	AA	730 ± 30	Mod-Low	380 ± 90
	Aleppo pine dense forest 30%	B	770 ± 18	Mod-Low	280 ± 9
	Aleppo pine dense forest 30%	AAA	680 ± 60	Mod-High	400 ± 100
	Aleppo pine dense forest 60%	AA	696 ± 24	Mod-Low	350 ± 60

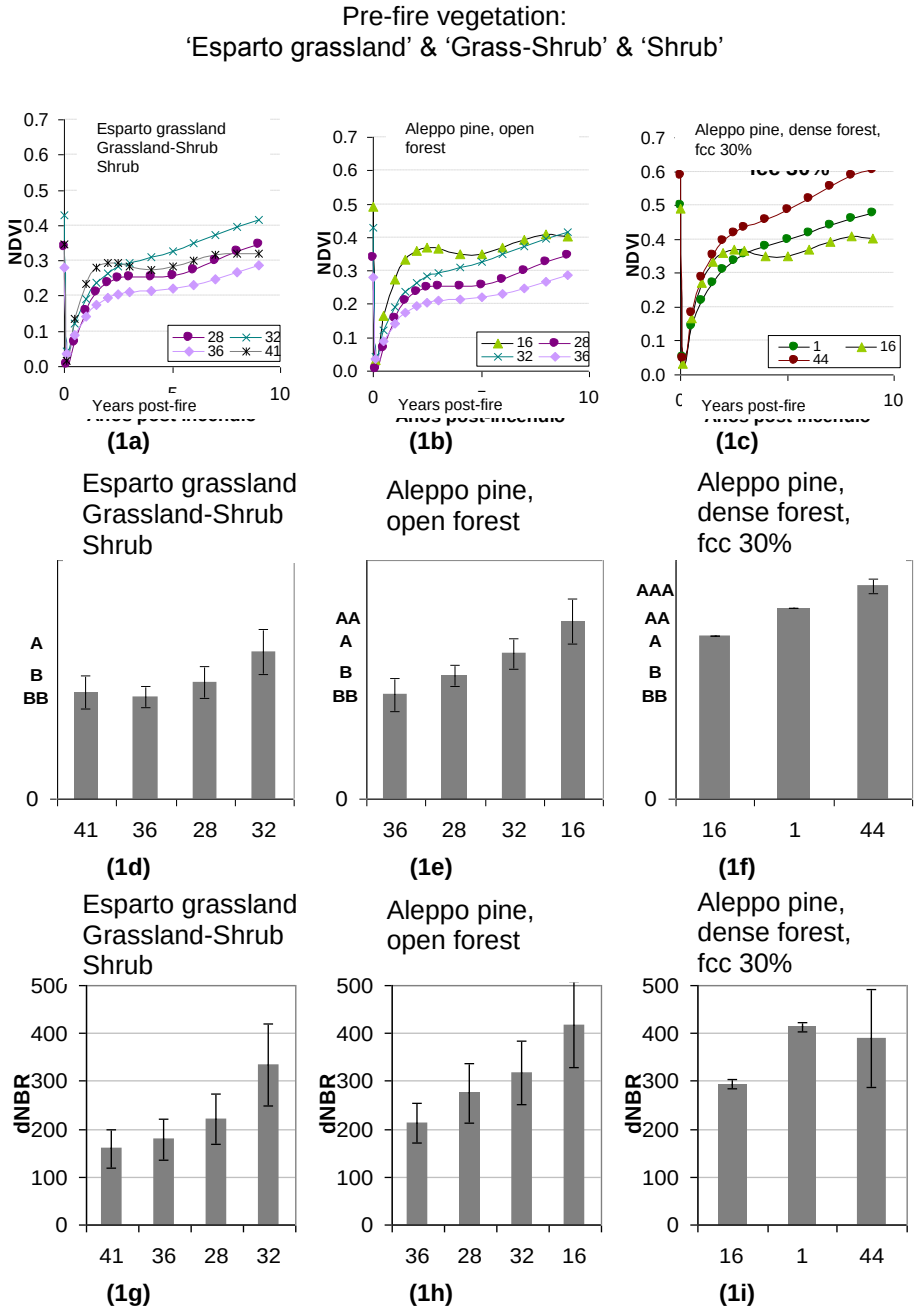

Figures 1a-1c: Recovery curves of the original vegetation formations: Esparto grassland, Grassland-Shrub and Shrub after fire: (1a) Esparto grassland, Grassland-Shrub and Shrub; (1b) Aleppo pine open forest; y (1c) Aleppo pine dense forest with canopy cover fraction of 30 %. Figures 1d-1f: Quality site. Figures 1g-1i: Average and standard deviation of fire severity (dNBR).

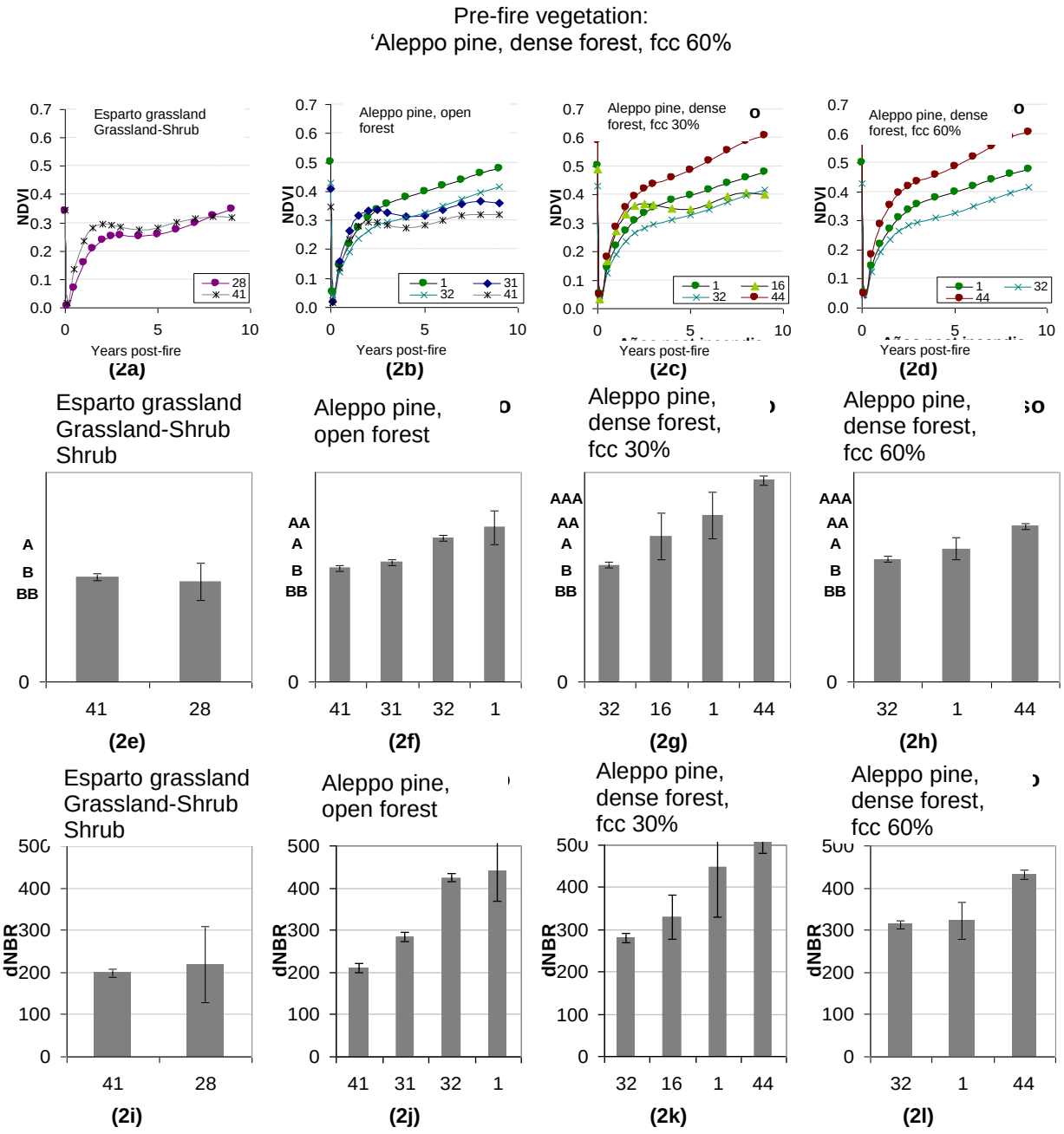

Figures 2a-2d: Recovery curves of the original vegetation formations: Esparto grassland, Grassland-Shrub and Shrub after fire: (2a) Esparto grassland, Grassland-Shrub and Shrub; (2b) Aleppo pine opened forest; (2c) Aleppo pine dense forest with canopy cover fraction of 30 % and (2d) Aleppo pine dense forest with canopy cover fraction of 60 %. Figures 2e-2h: Quality site. Figures 2i-2l: Average and standard deviation of fire severity (dNBR).

Discussion

Immature formations mainly predominate in the study area, which is coherent in a semiarid climate. Indeed, there is no climacic vegetation (*Rhamno lycioidis-Quercetum cocciferae* sigmetum) in the area, regressive climax only. About 33% of the pre-fire vegetation changed to regressive stages of autosuccession, one third of vegetation remained in the same successional stage after disturbance and other 33% developed in a more mature successional stage. Surface of Esparto grassland increased based in changes of its spatial distribution. In most of Esparto grasslands before fire, we recorded regeneration of Aleppo pine after fire. However, shrublands and open marginally in Aleppo pine forest before fire regenerated as Esparto grass. In a similar way, surface of shrubland increased after fire. We

found similar surface of Aleppo pine forest pre and post-fire. The low site quality in semiarid Mediterranean stands promoted an unstable equilibrium. In this case, fire severity is a key variable influencing recovery after fire.
Related to the dynamics of the structure recovery, patterns are related to the post-fire vegetation. Aleppo pine dense forest with a canopy cover fraction of 60% showed three different patterns being the resulting post-fire vegetation the same. For the same vegetation formation and canopy cover fraction, curve 44 in comparison with curves 1 and 32, would correspond to vegetation with higher greenness. Moreover, low quality site areas showed the 1998 and 1999 drought effect, as can be seen in the 16, 31, 28 and 41 curves.

Conclusions

The methodology is suitable for the evaluation of the evolution of regeneration of forests after fire. The first results of this study allow us to distinguish areas with different "characteristic curves". This kind of study is interesting for decision making, aimed to optimize resources and improve the management of burned areas. Forest external factors, such as fire severity, site quality or physiography are determinants to post-fire resilience. This contribution is a first step to develop a methodology based on both, fire and recovery sensitive to contextualize short and medium-term change with respect to any potential or desired pre-wildfire stand condition.

Acknowledgements

This work has been possible thanks to funding by the Ministry of Education and Science of Castilla-La Mancha (Ref. PBCC08-0109); the Ministry of Science and Technology under the National R + D + I, Ingenio 2010 (Ref. CSD2008-00040); and the Ministry of Science and Innovation (MICINN) co-financed by ERDF (Ref. AGL2011-27747).

References

Broncano MJ, Retana J, Rodrigo A (2005) Predicting recovery of Pinus halepensis forests after a large wildfire in the northeastern Spain. Plant Ecol 180: 47–56.

De Las Heras, J, Moya, D, Vega, JA, Daskalakou, E, Ramón Vallejo, V, Grigoriadis, N, Tsitsoni, T, Baeza, J, Valdecantos, J, Fernández, C, Espelta, J and Fernandes, P. 2012. Post-Fire Management of Serotinous Pine Forests. En Post-Fire Management and Restoration of Southern European Forests. Moreira, F.; Arianoutsou, M.; Corona, P.; De las Heras, J. (Eds.). Series: Managing Forest Ecosystems, Vol. 24

Díaz-Delgado, R., Lloret, F., Pons, X. Y Terradas, J. (2002). Satellite evidence of decreasing resilience in Mediterranean plant communities after recurrent wildfires. Ecology 83 (8): 2293-2303.

Fox, B.J. Y Fox, M.D. 1986. Resilience of animal and plant communities to human disturbance. In"Resi1ience in Mediterranean-type ecosystems". (Ed. B.Dell, A.J.M. Hopkins and B.B. Lamont). (Junk, Dordrecht). pp. 39-64.

Holling, C.S. 1973. Resilience and stability of ecological Systems. Annu. Rev. Ecol. Syst. 4 (1): 1-23. doi:10.1146/annurev.es.04.110173.000245.

IFN2. Segundo Inventario Forestal Nacional. Servicio de Inventario Forestal. Dirección General de Medio Natural y Política Forestal. Ministerio de Medio Ambiente, y Medio Rural y Marino.

IFN3. Tercer Inventario Forestal Nacional. Servicio de Inventario Forestal. Dirección General de Medio Natural y Política Forestal. Ministerio de Medio Ambiente, y Medio Rural y Marino.

IGME, 2013, Mapa de litologías de España 1/1.000.000.

Keeley J.E. 1986. Resilience of Mediterranean shrub communities to fire. In: Dell B, AJM Hopkins & BB Lamont (eds.). Resilience in Mediterranean-type ecosystems: 95-112. Dr. W. Junk, Dordrect, The Netherlands.

Key CH, Benson NC. 2006. Landscape Assessment (LA). In 'FIREMON: Fire Effects Monitoring and Inventory System'. (Eds DC Lutes, RE Keane, JF Carati, CH Key, NC Benson, LJ Gangi) USDA Forest Service, Rocky Mountains Research Station General Technical Report RMRS-GTR-164-CD. p. LA-1–55. (Fort Collins, CO).

Lloret, F.; 1998. Fire, canopy cover and seedling dynamics in Mediterranean shrubland of northeastern Spain. Journal of Vegetation Science 9:417-430.

Moya, D., Espelta, J. M., López-Serrano, F. R., Eugenio, M. And De Las Heras, J. (2008a). Natural post-fire dynamics and serotiny in 10-year-old Pinus halepensis Mill stands along a geographic gradient. International Journal Wildland Fire, 17(2):287-292.

Pausas, J.G. (2004). La recurrencia de incendios en el monte mediterráneo. En Avances en el estudio de la gestión del monte mediterráneo (Vallejo, V.R. y Alloza, J.A. Eds.). CEAM, Valencia, 47-64.

Pimm, S.L. 1984. The complexity and stability of ecosystems. Nature 307:321–6.

Quijada-RoSAS, M. 1992. Glosario de Términos de Genética, Fitogenética y Afines. Universidad de los Andes. Mérida. Venezuela. 436 pp.

Ruiz De La Torre, J. Mapa Forestal De España. Escala 1:200.000. Dirección General de Medio Natural y Política Forestal. Ministerio de Medio Ambiente, y Medio Rural y Marino. Memoria General. ISBN: 84-85496-63-9.

Trabaud, L. 1993. From the cell to the atmosphere: an introduction to interactions between fire and vegetation In: L. Trabaud & R. Prodon (eds.), Fire in mediterranean Ecosystems: 13:12. CEC-DG XII/D-1. Brussels.

Valladares, F. 2004. Capítulo 4. Lloret, F. Ecología del bosque mediterráneo en un mundo cambiante. Páginas 101-126. Ministerio de Medio Ambiente, EGRAF, S. A., Madrid. ISBN: 84-8014-552-8.

Westman, W. E., And J. F. O'leary. 1986. Measures of resilience: the response of coastal sage scrub to fire.Vegetatio 65(3): 179-189.

Monitoring post-fire forest regeneration of *Pinus brutia* in North Lebanon

Amira El Halabi[a], George Mitri[ab], Mireille Jazi[b]

[a] *Department of Environmental Sciences, Faculty of Sciences, University of Balamand, Lebanon.*
[b] *Institute of the Environment, University of Balamand, Lebanon. george.mitri@balamand.edu.lb*

Abstract
Forest fires represent a major threat to Lebanon's forests. More precisely, *Pinus brutia* forests, which occupy relatively large areas in Lebanon, are affected by frequent fire events. Lebanon's National Strategy for forest fire management highlighted the need to facilitate natural forest regeneration and undertake reforestation activities in areas where regeneration is not possible. Accordingly, this study aimed at assessing post-fire regeneration of *Pinus brutia* in the Mediterranean region of North Lebanon. A total of 540 samples of 1x1m² were collected on 18 different sites affected by fires throughout the past 20 years. The density of seedling regeneration was calculated for each plot. The highest regeneration density (10.33 seedlings/m²) was observed on plots that were sampled one year after fire. The regeneration density decreased by 68% on plots sampled four years after fire when compared to plots sampled one year after fire. Also, the plots that were sampled five years after fire showed a 93.8% decrease in regeneration density. This continuous could be attributed to a high mortality rate due to prevailing severe weather conditions and human disturbances. The results highlighted the need to implement efficient post-fire management measures within the first four years after a fire event to decrease the mortality rate of young pine seedlings and to assist in the successful recovery of fire affected sites.

Keywords*: forest fires, post-fire natural regeneration, Pinus brutia*

Introduction

Lebanon's forest cover is a unique feature in the semi-arid environment of the Mediterranean. Lebanon's forests play an important role in supporting high biodiversity and providing a variety of environmental goods and services. Nevertheless, several biophysical and anthropogenic factors have shaped biodiversity in Lebanon (MOE/UNDP, ECODIT 2011).
Increasingly, fire occurrence risk was observed in association with high maximum temperatures and long dry seasons (Salloum and Mitri, 2014). Forest fires represent a major and continuous threat to Lebanon's forests (Mitri *et al*., 2014). In this context, monitoring post-fire regeneration of *Pinus brutia* is expected to support National efforts in restoring healthy ecological conditions of burned forest lands by providing useful and insightful information about the status of natural regeneration after fire (Mitri and Fiorucci, 2012).
Lebanon's National Strategy for forest fire management clearly indicated the need to facilitate natural forest regeneration and undertake reforestation activities in areas where regeneration is not possible (MOE/AFDC, 2009). Until present, Lebanon lacks comprehensive studies for assessing trends in post-fire forest regeneration. Accordingly, the aim of this study was to assess post-fire regeneration of *Pinus brutia* in North Lebanon.

2. Study area and dataset description

Lebanon is situated on the eastern shores of the Mediterranean. The country is characterized by its Mediterranean climate with warm and dry summer and cool and wet winters. Forests in Lebanon cover around 139,376 ha which accounts for 13.3 % of the Lebanese territory. Coniferous forests occupy 31

% of the total forest cover (MOE/UNDP/ECODIT, 2011). More specifically, pine forests including *Pinus pinea*, *Pinus brutia*, and *Pinus halepensis* are mostly found on the western slopes of the Mount Lebanon chain and they are constantly affected by fire events.
During the year of 2013, sampling of *Pinus brutia* fire affected forests was conducted on 8 different fire sites located between 500 m and 1000 m above sea level in North Lebanon (Table 1). A total of 540 samples of 1x1m² were collected and the number and height of seedlings was recorded for each sample. Historical weather data showed that around 95% of the annual precipitation fall between October and April. The average rainfall in this region has an average 1210 mm per year (MOE/UNDP/ECODIT, 2011).

Table 1. Characteristics of fire affected sites

Year of fire	Slope percent	Elevation (m)	Aspect
1993	30	703	North East
2004	5	710	West
2006	45	722	South
2007	30	794	North west
2007	10	416	South west
2008	15	642	North East
2009	30	670	South east
2012	45	1139	North east

Methods

3.1. Field sampling

The field sampling comprised surveying 20x20m plots. Each plot comprised three different locations of sampling across the slope (namely, top, middle, and bottom). A total of 30 samples of 1m² were collected within each plot using the belt transect sampling method. The length of the belt transect was 20 meters and the sampling interval was 5 meters. A quadrat of 1 m x 1 m was placed on each side of the line at the interval level. Accordingly, the number and height of individual seedlings were collected.

3.2. Statistical analysis of field data

The calculation of the regeneration density was developed based on the number of seedlings per square meter (Equation 1), an approach that was also used by Titsoni (1997).

$$\frac{\Sigma \text{ number of seedlings}}{\text{Total number of plots}} \qquad \text{Equation 1}$$

Consequently, the variation in the post-fire regeneration density of *Pinus brutia* based on descriptive statistics, and the average regeneration density was calculated for each year. ANOVA-stepwise analysis was applied to investigate significant changes in regeneration density and height of seedlings throughout the years.

Results and discussion

The highest regeneration density (average of 10.33 seedlings/m²) was recorded on plots that were surveyed one year after fire. This could be attributed to seed availability on site and lack of long-term natural stresses and human disturbances (Figure 1).

Sites surveyed three years after fire showed a decreased density by 68% (7.11 seedlings/m²) when compared to the results of sites surveyed one year after fire. Following the same comparison approach, sites sampled five years after fire showed an abrupt decrease in the regeneration rate (0.44 seedlings/m²), while sites sampled six years after fire showed only 0.22 seedlings/m². These gradual decreases in regeneration density could be attributed to both environmental and anthropogenic conditions including severe climatic conditions, human disturbances, and the effect of local environmental characteristics of the sites. Other factors such as fire characteristics (fire severity), could also affect regeneration density of *Pinus brutia* (Pausas *et al*., 2008).
Finally, the results from plots sampled twenty years after fire showed a regeneration density of 1 seedling/m². This could be attributed either to insignificant variation in regeneration density or to a continuous enrichment of young seedlings from the surrounding forested areas (Tsitsoni, 1997).

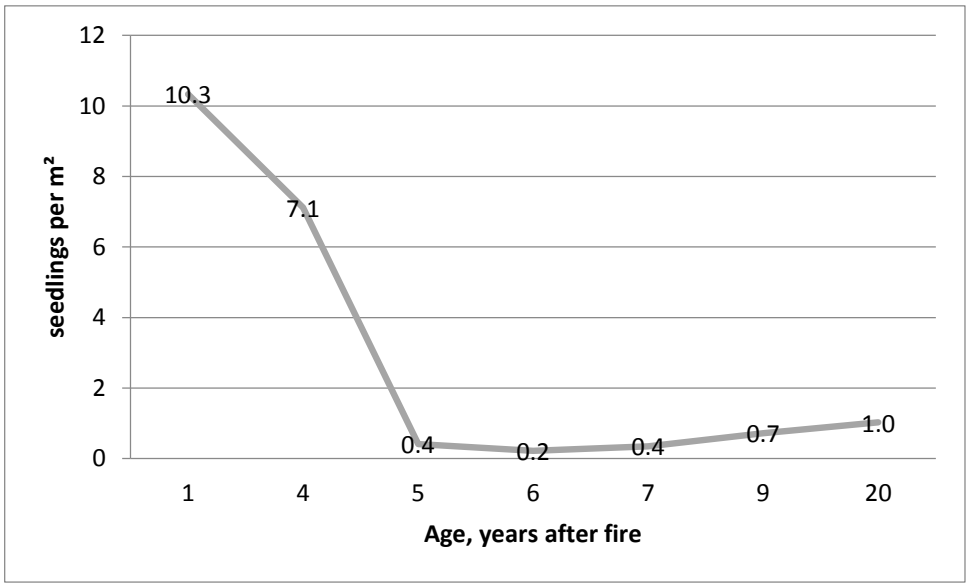

Figure 1. Multi-temporal rate of regeneration density of Pinus brutia

The regression analysis showed post-fire average height increment of 9.26 cm (Figure 2), while other studies in the Mediterranean showed an average growth of 5-20 cm per year (Neyisci, 1989; Thanos *et al*., 1989; Spanos, 1994; Spanos el al., 2000).

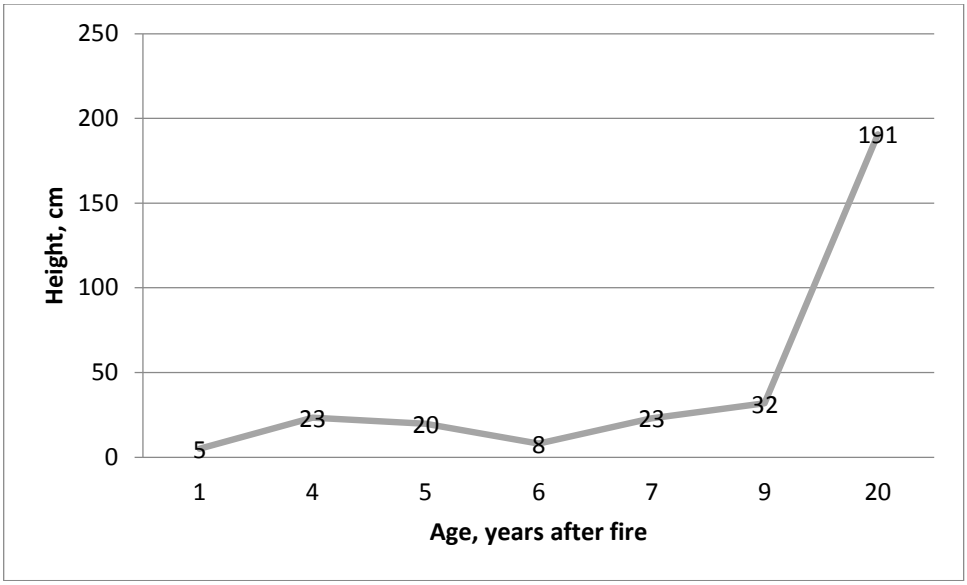

Figure 2 Post-fire variation of average seedling height

Conclusions

The highest regeneration density (10.33 seedlings/m²) was observed on plots that were sampled one year after fire. When compared to plots sampled five years after fire, the regeneration density abruptly decreased to 0.44 seedlings/m².

In the light of these findings, it is essentially important to invest more post-fire restoration efforts in assisting natural regeneration in order to promote natural recovery of pine burned forests. The implementation of certain protection measures during the first two years after a fire event is expected to facilitate a higher survival rate of established seedlings. This is expected to be a cost saving initiative in comparison to costly reforestation campaigns.

Future work will involve conducting further studies to understand the different factors that affect the natural regeneration of pine forests in Lebanon as an attempt to come out with improved post-fire management initiatives.

Acknowledgments

The authors would like to thank the Lebanon Reforestation Initiative (LRI) (a project funded by the United States Agency for International Development (USAID) and implemented by the US Forest Service (USFS) for their financial support to the conducted work. The contents do not necessarily reflect the views of USAID or the United States Government.

References

Mitri, G. and Fiorucci, P. (2012). Towards monitoring post-fire vegetation cover dynamics in the Mediterranean with the use of object-based image analysis of Landsat images. In. 1st Workshop on Temporal Analysis of Satellite Images (Ban, Y., Ed.), (pp. 2 -25). Mykonos Island, Greece: European Association of Remote Sensing Laboratories.

Mitri, G., Jazi, M., and McWethy, D. (2014). Investigating temporal and spatial variability of wildfire potential with the use of object-based image analysis of downscaled global climate models. *South-Eastern European Journal of Earth Observation and Geomatics, 3*(2S), 251-254.

MOE/AFDC. (2009). *Lebanon's National Strategy for Forest Fire Management*. (Mitri, G. Ed.). Beirut, Lebanon: Association for Forests, Development and Conservation.

MOE/UNDP/ECODIT. (2011). *State and trends of the Lebanese environment*. Beirut, Lebanon: ECODIT.

Neyisci, O. (1989). Effects of prescribed burning on soil chemical properties and subsequent seedling growth in Pinus brutia Ten. ecosystems (in Turkish). *Turkish Forest Research institute: Technical Bulletin, 225*, 1-56.

Pausas, J. G., Llovet,J., Rodrigo, A. and Vallejo, R. (2008). Are wildfires a disaster in the Mediterranean basin? A Review. *International Journal of Wildland Fire, 17*, 713-723.

Salloum, L. and Mitri, G. (2014). Assessing the temporal pattern of fire activity and weather variability in Lebanon. *International Journal of Wildland Fire*, *23*(4), 503-509.

Spanos, E. A. (1994) Natural Regeneration of Pinus brutia in north-west areas of Thanos Island, burned in 1989 (in Greek). *Geotechnika Epistimonika Themata*, *4*, 33-39.

Spanos , I., Daskalakou, E., and Thanos, C. (2000). Postfire, natural regeneration of Pinus brutia forests in Thasos Island, Greece. *Actaoecologica, 21*(1), 13-20.

Thanos, C.A., Marcou, A., Christoduoulakis, D., and Yannitsaros, A. (1989). Early post-fire regeneration in *Pinus brutia* forest ecosystems of Samos Island (Greece), *ActaOecological, 10*, 79–94.

Tsitsoni, T. (1997). Conditions determining natural regeneration after wildfires inI the *Pinus halepensis* (Miller, 1768) forest of Kassandra Peninsula (North Greece). *Forest Ecology and Management, 92*, 199-208.

Natural and anthropogenic fire regimes in boreal landscapes of Northwest Russia

Andrei Gromtsev , Nikolai Petrov

Forest Research Institute, Karelian Research Centre, Russian Academy of Sciences,
11 Pushkinskaya St., Petrozavodsk, Russia, gromtsev@krc.karelia.ru, nvpetrov@krc.karelia.ru

Abstract
Patterns in the natural fire regime in different types of geographical landscape and its present-day transformations are considered. Surveys were carried out in the north-west of the Russian boreal zone at the junction of two North-European physiographic domains – Fennoscandian Shield (Fennoscandia) and East-European (Russian) Plain. The resultant data disclose the history of fires and their landscape-related characteristics over the past millennium. The frequency and intensity of wildlife fires may differ drastically among landscapes – from 1-2 in a century to 1-2 in a millennium. Multiple intermediate variants fill the range between these two poles. It is demonstrated that conservation of pristine forests with their spontaneous dynamics in protected areas is possible only under a natural fire regime. The total and average size of fires has been gradually decreasing. In the study area, e.g. the indices have over the past half a century ranged within 100-10 000 ha, and 5-20 ha a year, respectively. Humans have significantly increased the frequency of forest fires. The patterns identified can be quite confidently extrapolated to the whole boreal zone of European Russia. The characteristics of geographical landscapes (the range, ratio and spatial arrangement of their types) and land use history must however be taken into account.

Keywords*: boreal landscapes, natural fire regimes, current situation*

Introduction

Various aspects of the natural development of European boreal forests as related to fires are discussed in a great number of publications, including the authors' own (Gromtsev 1996, 2002, 2008, etc.). It is obvious the topic is of high interest to researchers. Fires (lightning-ignited) used to be the weightiest ecological factor shaping the structure and dynamics of pristine forests. Man-induced fires are now an equally important factor.
In an overwhelming majority of cases systematized data on natural fire regimes in Russia were obtained either by dating fire scars on trees or from archives. In the first case retrospective analysis is limited to 250-350 years (maximum age of the oldest tree generation). In the second case only very strong fires were recorded, but were not referenced to specific locations and ecotopes. Furthermore, averaged data for a region or habitat with no connection to the landscape features of boreal areas are usually given. They however also focus on individual sites without linking the situation to specific characteristics of boreal landscapes. Let us analyze the successions of spontaneous boreal forests in different types of geographical landscape in the second half of the Holocene and follow the major trends in them.

Study area, methodological background, and methods

Surveys were carried out in the north-west of the Russian boreal zone in the drainage basins of Lakes Ladoga and Onega, and west of the White Sea. Administratively, the central position in this region is occupied by the Republic of Karelia (total area ca. 15 mln ha excluding the water area of the named waterbodies). The area lies at the junction of two North-European physiographic domains – Fennoscandian Shield (Fennoscandia) and East-European (Russian) Plain (Fig.1). Hence, the study

area features a high diversity of geographical landscapes, even in terms of the relief (from flat marine plains to crystalline uplands rising higher than 1000 m above sea level).
Different types of geographical landscape were surveyed using the classification and map prepared in advance (Tab.1). The landscapes were distinguished by genetic types of relief, degree of paludification, and prevalent forest vegetation (prior to human impact on the forest cover). The classification was based on the zonal and the typological principles. The former differentiated the territory into the northern, middle and southern taiga subzones. The latter implied that contours similar in all landscape-forming traits but spatially discontinuous were combined into one 'type'. An average area of a landscape contour was ca. 100,000-150,000 ha. Over 30 landscape types have been identified and comprehensively studied (forests, wetlands, flora and fauna, land use history, etc.). Both the natural and the human-induced change of the landscape biotic components was studied. As applied to fires the main methods were: 1) stratigraphic analysis of peat deposits with dating of fire layers according to the peat deposition rate (ca. 1000 cores were treated); 2) recording of charcoal underneath the forest floor and the remains of burnt tree trunks with simultaneous analysis of the forest cover composition and age structure (ca. 5 000 pits); 3) dating of fire scars on trees (several hundreds records); 4) analysis of various archival materials (since mid-19th century) and modern fire statistics (covering the past 60 years).

Table 1. Classification of landscapes (example of the Republic of Karelia)

Predominant habitats	Degree of paludification		
	heavy >50%	moderate 20-50%	low <20%
I. Lacustrine, glacio-lacustrine and marine (m) plains			
Spruce	1/1,5[A]	2/4,0	-
Pine	3/8,5	4/2,0	5/+[B]
II. Glacial (g) and fluvioglacial (fl) hilly-ridge plains			
Spruce	-	6/4	-
Pine	7/5,0	8/4,5	9/1,0
III. Glacial accumulation plains with rugged topography			
Spruce	-	10/2,5	-
Pine	-	11/2,0	-
IV. Tectonic denudation hilly-ridge plains with a complex of glacial deposits (g) and low mountain topography (lm)			
Spruce	-	2/12,5	-
Pine	13/8,0	14/37,5	-
V. Tectonic denudation ridge (selga)			
Spruce	-	15/+	16/1,0
Pine	-	17/2,5	18/1,5
VI. Rock			
Pine	-	19/1,0	20/0,5

[A] - number of the landscape type/percent of the region's area;
[B] - less than 0,5%

Results

The resultant data disclose the history of fires and their landscape-related characteristics over the past millennium. Distinct fire layers (FL) were detected in deposits at different depths. The deepest-lying FL was at 2.85 m, and a charred organic-mineral layer – at 3.7 m. The layers are roughly dated to 5.5-7.5 Ka B.P. Searching for older FL involves sampling from deeper peat deposits (down to 10 m), few of which have been found in our landscape profiles. Thus, fires were a common ecological factor influencing the forest cover in the Holocene. Note here that only the fires reaching into peatland habitats are considered. Their traces can be clearly identified in the field. Fires confined to dry areas were identified separately by fire scars on trees and stags, or by charcoal underneath the forest floor.

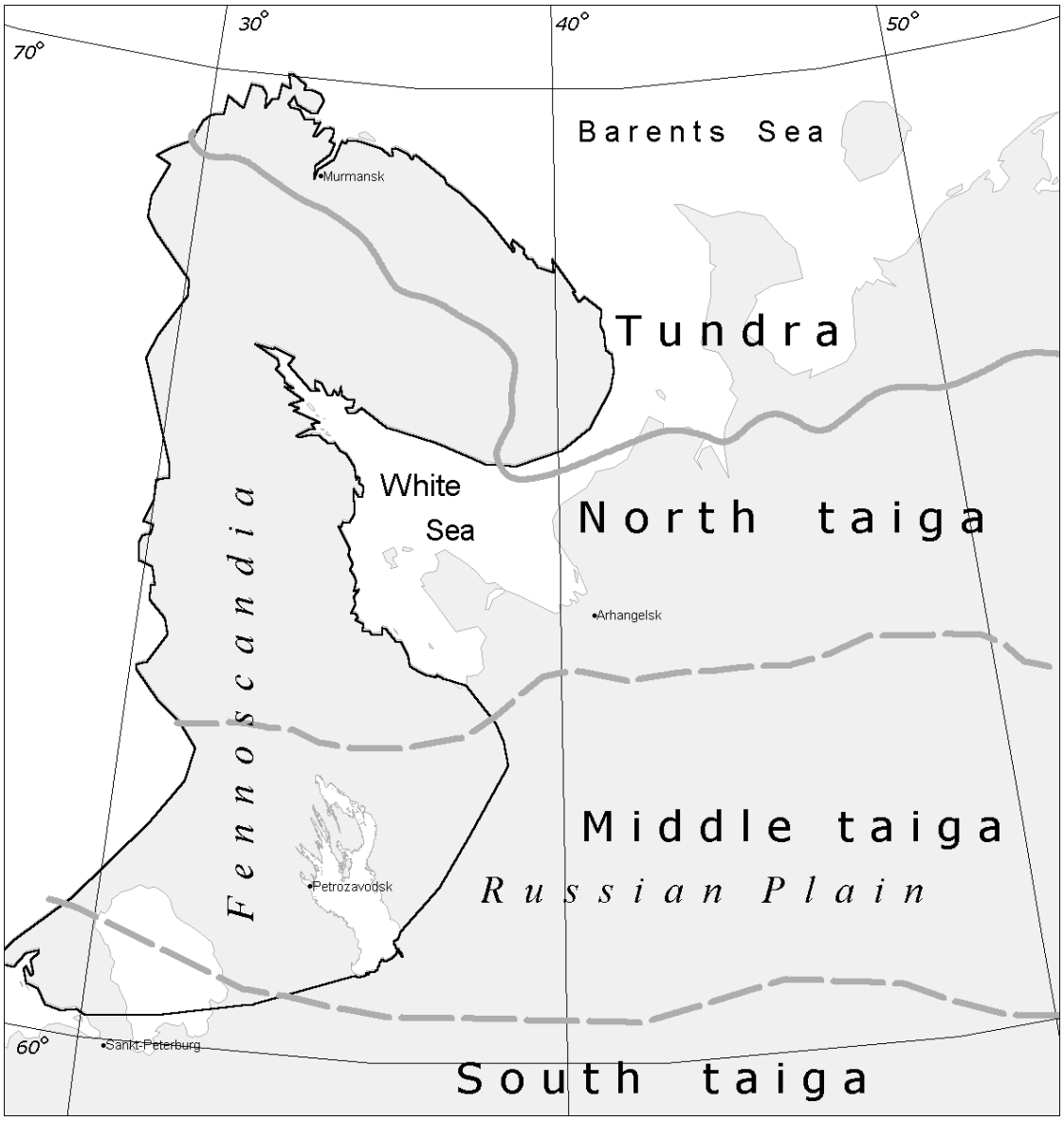

Figure 1. Taiga zone of the Western European Russia

Landscape-related patterns of the fire regime are quite vivid. The fire regime is more or less specific to each landscape type. The overall situation is however quite predictable – the number of FL was the lowest in landscapes of different genesis and paludification clearly dominated by spruce forests. Landscapes of different genesis and paludification dominated by pine forests were the most susceptible to fires (Tab.2).

Table 2. Frequency of forest fires in different types of geographical landscapes (data from the stratigraphic analysis of peat deposits, only the most illustrative types of landscapes are included)

Max number of fires (according to data for an individual drill hole, years ago)	Fire frequencies in different types of geographical landscape (the names of landscape types are abridged)					
	North taiga subzone			Middle taiga subsone		
	Low mountain spruce	Rocky pine	Fluvioglacial hilly-ridge pine	Tectonic denudation hilly ridge spruce	Tectonic denudation hilly ridge pine	Fluvioglacial hilly-ridge pine
<300	0	0	0	0	1	1
300-750	0	2	0	0	4	7
751-1500	0	3	4	2	5	11
1501-2200	0	-[A]	4	0	0	-
Total	0	5	8	2	10	19

[A] - the age of the peat deposit with the max number of layers is below 1500 years

Thus, some 'spruce' landscapes were affected by fires approximately once or twice in a thousand years. They were apparently catastrophic events induced by abnormal weather (droughts). Such stand-replacing fires destroyed nearly totally large spruce forests on mineral land. The only refugia were wet sites with flowing water, swamps, etc., from where the surviving spruce dispersed to the surrounding areas. These landscapes are a kind of a model of top fire resistance. The conditions there are least favorable for fire emergence and spread. The landscape biotic components have been affected by fires only sporadically, but with all-embracing effect.

Some 'pine' landscapes experienced stand-replacing fires (when even part of wetland habitats burnt down) 1-3 times every 300 years. Running understory fires in pine forests on dry sandy soils were even more frequent (sometimes twice a century). These habitats are a showcase of fire vulnerability. The conditions there are the most favorable for fire emergence and spread. The biotic components of these landscapes have grown adapted to frequent fire impact. Their structure and spontaneous dynamics have been controlled by fires for millennia.

Multiple intermediate variants filled the range between these two poles of the natural fire regime.

Fires as an ecological factor. Primary taiga forests in the Russian taiga zone represent, with very few exceptions, different stages and patterns of pyrogenic succession series. Prior to the commencement of human activities boreal forests had represented different stages of secondary successions – from pioneer vegetation groupings on naturally emerging burnt areas or areas of wind-fallen forest to climax forest communities. A whole spectrum of phytocenoses at different stages of the secondary succession lay between these two extreme variants. The boreal territory in general was however dominated by coniferous communities approaching their climax. The situation changed abruptly only after stand-replacing fires, which were real natural catastrophes. Leaving alone the modifications in the forest cover induced by the global climate change in the late Holocene one can claim that changes in primary boreal ecosystems were of a cyclic nature. They followed the pattern: pre-climax – catastrophe (fire or windstorm) – series of regeneration stages – pre-climax.

The pyrogenic factor has for millennia controlled the forest formation process. Fires destroyed dead organic matter, affected the forest vegetation properties of habitats, enhanced the formation of specific faunistic complexes, etc. In the absence of fires the structure of primary taiga forests underwent transformation in which the forest-forming tree species ratio changed towards shade-tolerant species. Coarse non-decayed litter deteriorating the soil suitability for forest vegetation was accumulated. The productivity of forest areas decreased, and their structure was simplified, including the less mosaic pattern of the landscape forest cover, etc. Corresponding modifications occurred in the biota in general.

Fires are a powerful natural factor that has ensured renewal and homeostasis in spontaneous forest ecosystems for at least several millennia. Preservation of primary boreal forests in protected areas in their primeval state can only be achieved if a certain fire regime that has established in the boreal landscape in the post-glacial period is maintained.

Human-induced modification of natural fire regimes. Natural fire regimes have been profoundly modified by humans. In the boreal zone of Europe this process commenced at different times and in different scope. Formally, human impact on natural fire regimes in the European part of Russia's boreal zone began some 5-10 Ka B.P., as people colonized the territory after glacial retreat. Obviously, with the arrival of ancient hunters and fishermen lightning was no longer the only cause of ignition. The number of fire outbreaks grew sharply over the past centuries due to the wide use of slash-and-burn agriculture and widespread selective forest felling. Thus, 19th century sources already state that at least 90 of 100 fires were caused by slash-and-burn (fire spreading beyond the sites). Generally speaking, humans significantly increased the frequency of forest fires. Until the last century they had spread spontaneously, restrained only by natural firebreaks (hydrographic network), or stopped due to weather (rainfall).

The total and average size of fires has lately been gradually decreasing. E.g., in the Republic of Karelia (area almost 15 mln. ha of area in total) the indices have over the past half a century ranged within 100-100 000 ha (Fig.2), and 50-2500 fires per year (Fig.3). Some large fires affected an area of several thousands hectares (one ignition is 2013 burnt over 6,000 ha). These cases are however exceptional. An average fire in the past decades rarely exceeds 10 ha due to timely detection and quick localization by modern technology.

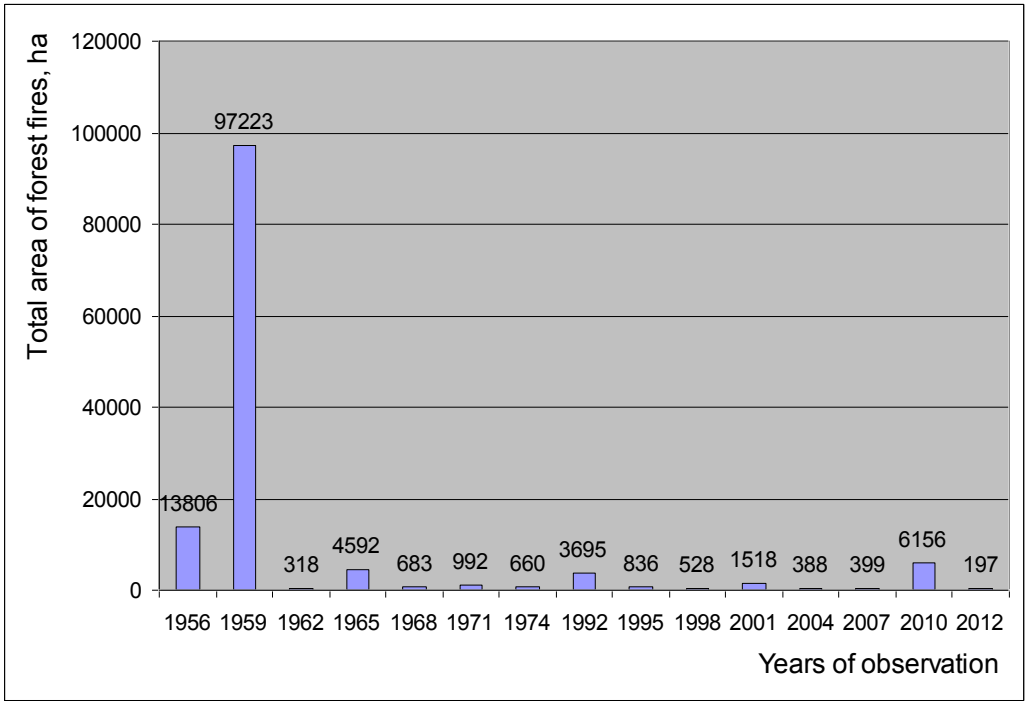

Figure 2. Total area affected by fires in the Republic of Karelia (selected data are presented)

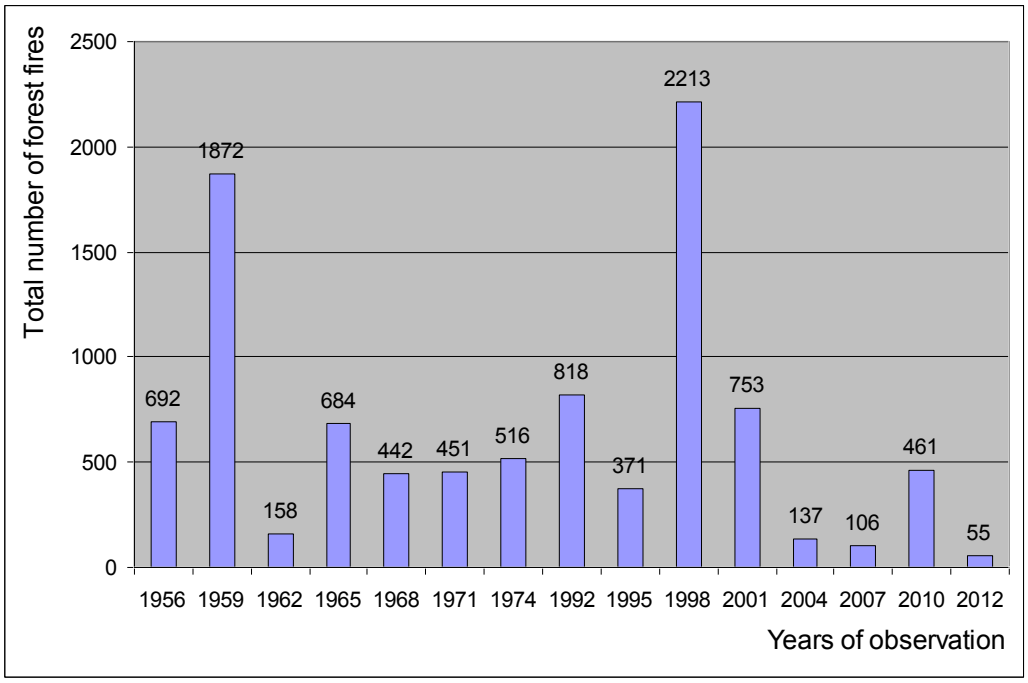

Figure 3. Total number of fires in the Republic of Karelia (selected data are presented)

Variation of the total area, number and average size of fires is due to the summer weather alone. Fires are expressly taken under control and eliminated by specialized agencies, using aircraft where needed. Thus, natural fire regimes have been fundamentally changed, mainly through a reduction in the size of a fire – from tens and hundreds of thousands hectares in primeval landscapes to some tens of hectares now. Human impact has dramatically increased the frequency of outbreaks. As mentioned above, it ranged from 1-2 in a century to 1-2 in a millennium depending on the landscape. The number has now grown to a total of several thousands a year. Yet, all the indices still correlate quite clearly with the landscape characteristics, and can vary by a factor of tens of times. Conservation of pristine forests with their spontaneous dynamics in protected areas is possible only under a natural fire regime.

Conclusions

The patterns identified can be quite confidently extrapolated to the whole European part of boreal forests in Russia. The characteristics of geographical landscapes (the range, ratio and spatial arrangement of their types) and land use history must however be taken into account.

References

Gromtsev AN (1996) Retrospective analysis of natural fire regimes in landscapes of eastern Fennoscandia and problems of their antropogenic transformation. In 'Fire in ecosystems of boreal Eurasia'. (Eds JG Goldammer, VV Furyaev) pp. 45-54. (Kluwer Academic Publishing: Dordrecht)

Gromtsev AN (2002) Natural disturbance dynamics in the boreal forests of European Russia: a review. *Silva fennica* **36 (1)**, 41-55

Gromtsev AN (Eds) (2008) 'Fundamentals of the landscape ecology of the European taiga forests of Russia' (Karelian Research Centre, Russian Academy of Sciences Publishing: Petrozavodsk) (in Russian)

Past and present fire regimes in temperate forest zone of lowland Central Europe

Ewa Zin[a,b], Mats Niklasson[b], Ryszard Szczygieł[c]

[a] *Forest Research Institute (IBL), Department of Natural Forests, ul. Park Dyrekcyjny 6, 17-230 Białowieża, Poland, Ewa.Zin@slu.se, ezin@las.ibl.bialowieza.pl*
[b] *Swedish University of Agricultural Sciences (SLU), Department of Southern Swedish Forest Research Centre, P.O. Box 49, SE-230 53 Alnarp, Sweden, Mats.Niklasson@slu.se*
[c] *Forest Research Institute (IBL), Department of Forest Fire Protection, ul. Braci Leśnej 3, Sękocin Stary, 05-090 Raszyn, Poland, R.Szczygiel@ibles.waw.pl*

Abstract
Fires in Central European lowland forests are nowadays numerous but efficiently suppressed and hence usually very small. Poland is one of the countries with highest annual number of forest fires in the region, with as many as 9–10 000 individual fire events per year (with record of 17 000 fires in 2003), however of relatively limited size, with 0.5–0.95 ha being mean values of area burned in a single forest fire. Main fire season in Poland lasts from March to September and is driven largely by weather conditions and litter humidity, with people being the dominant source of ignition. Active forest fire prevention and suppression is carried both by the regular fire services and State Forest Administration – the main forest manager in Poland due to the ownership structure of forest land in the country (>80% state-owned). In Białowieża Forest, one of the best preserved lowland forest ecosystems in temperate Europe fires happen at present rather incidental, alike in the rest of the country are effectively controlled and thereby affect very small areas (0.5 ha). However numerous stands with fire scarred trees, stumps and snags, especially in the conifer dominated areas, can be found; indicating substantial fire presence in the past. The first tree ring fire history records from that area evidenced frequent fires in Pinus sylvestris-dominated forests during the 17th up to early 19th centuries, with dramatic decrease in fire presence over the last 150+ years, most likely linked to changes in human fire use and forest management. We conclude that there is a large need for fire history and fire ecology studies in Central Europe due to high population density and strong dominance of flammable conifers in forests of that region. Extended knowledge about past disturbance dynamics and reference conditions may be essential for future sustainable forest management and nature conservation throughout this part of European continent.

Keywords*: annually burned area, Białowieża Forest, dendroecology, fire ecology, fire history, fire protection, fire scars, fire suppression, forest fires, forest fire statistics, mean annual number of fires, Pinus sylvestris, Poland, tree rings*

Introduction

Fires in Central European lowland forests are nowadays numerous but efficiently suppressed and hence usually very small (Szczygieł *et al.* 2009*a*; Schmuck *et al.* 2011). However, that region has evidenced a significant rise in the number of forest fires in the recent decades (Szczygieł *et al.* 2008, 2009*a*,*b*), alike the whole European continent (Schelhaas *et al.* 2003).
Although fire has been proven to be one of the key elements of European lowland forest ecosystems during the Holocene (e.g. Hannon *et al.* 2000; Rösch 2000), the knowledge on fire ecology in that region is limited (Bradshaw *et al.* 1997; Hille 2006; Niklasson *et al.* 2010). Forest fires in that part of Europe are still associated with threat and large economic losses (Ubysz and Szczygieł 2002; Ubysz *et al.* 2006; Szczygieł *et al.* 2009*a*), which may impede the acceptance of fire as one of the important natural factors shaping forest structure and dynamics throughout the region (*cf.* Faliński 2001).
Given the significant share of fire-prone coniferous forests and the observed increase in fire activity throughout Central Europe, projected climate change and its possible influence on forest fire risk in

the near future (Badeck *et al.* 2003; Schelhaas *et al.* 2003, 2010; Szczygieł *et al.* 2008, 2009*a*; San-Miguel-Ayanz *et al.* 2011), extended knowledge on the ecological role of fire in forest ecosystems of that region is valuable.

Poland is one of the largest countries in Central-Eastern Europe (Szczygieł *et al.* 2009*a*), with the total country area of approx. 312.7 th. km^2 and total population of approx. 38.5 mill people, reflecting high population density of 123 people/km^2 (GUS 2014). Over 9 mill ha, accounting for ca. one third of the country area is covered by forests (San-Miguel-Ayanz *et al.* 2011; Zajączkowski *et al.* 2014), which locates Poland among the countries with substantial forest cover in the region (San-Miguel-Ayanz *et al.* 2011). Polish forests are largely dominated by coniferous forest habitats on sandy soils (51%) and coniferous stands (approx. 70% of the forest area), with *Pinus sylvestris* L. (Scots pine) being the dominant tree species (approx. 60%). Stands younger than 80 years cover approx. 70% of the forest area, with age class 41–60 yrs accounting for as much as 26.0%. Over 80% of forests in Poland is owned by the state (Zajączkowski *et al.* 2014).

Active forest fire prevention and suppression in Poland is carried both by the regular fire services and State Forest Administration (LP = Lasy Państwowe, State Forests National Forest Holding) – the main forest manager in the country, administrating 77.3% of the forest area (Zajączkowski *et al.* 2014), obliged to conduct forest fire prevention by the Forestry Act (1991).

In Białowieża Forest, one of the best preserved lowland forest ecosystems in temperate Europe (Faliński 1986; Peterken 1996) fires happen at present rather incidental, alike in the rest of Poland are effectively controlled and thereby affect very small areas (ca. 0.5 ha) (E. Zin and M. Niklasson, unpubl.). However numerous stands with fire scarred trees, stumps and snags, especially in the conifer dominated areas, can be found (e.g. Faliński 1986); indicating substantial fire presence in the past. This has been also confirmed by the first tree ring fire history reconstruction in that area (Niklasson *et al.* 2010).

To conclude on past and present fire regimes in temperate forest zone of lowland Central Europe we used Poland as a case study and applied both: (1) literature review (including actual fire inventory reports throughout the last decades) on current data concerning present fire activity in the country and (2) tree ring fire history record from two locations in Białowieża Forest, obtained by dendroecological analyses of tree ring samples from *Pinus sylvestris*, spanning over the period 1650–2010.

Methods

To achieve data on the present forest fire activity in Poland we did literature review. Additionally, selected actual fire inventory reports throughout the last decades were reviewed in the National Information System on Forest Fires database (available online at https:// bazapozarow.ibles.pl/ ibl_ppoz/faces/index.jsp). To summarize data on the annual number of forest fires, burnt area in forest fires and mean area burned in a single forest fire in Poland in 1990–2013, we used the following publications: Szczygieł and Piwnicki (2011); Piwnicki and Szczygieł (2011, 2012); Zajączkowski *et al.* (2014). The first one may be found in Schmuck *et al.* (2011). The three latter ones are available online at http://www.gios.gov.pl/monlas/raporty.html (Annual Reports: 2011, 2012) and at http://www.lasy.gov.pl/informacje/publikacje/ informacje-statystyczne-i-raporty/raport-o-stanie-lasow/raport-o-stanie-lasow-2013/view (Annual Report: 2013), respectively.

Tree ring fire history data from two locations in Białowieża Forest were obtained by dendroecological analyses of wood samples from *Pinus sylvestris*, spanning over the period 1650–2010. Exact fire dates were identified by cross dating of fire scars according to the standard dendrochronological techniques. Details on field and laboratory procedures are given in Niklasson *et al.* (2010).

Results and discussion

Present-day forest fire activity in Poland

Poland is one of the countries with the highest annual number of forest fires in Central-Eastern Europe (Szczygieł *et al.* 2009*a*), with as many as 9–10 000 individual fire events per year, however of relatively limited size, with 0.5–0.95 ha being mean values of area burned in a single forest fire in the recent decades (Tab. 1).

Although most of the burnt area occurs nowadays in the Mediterranean part of the European continent (Schmuck *et al.* 2011), Poland still has accounted for as much as 60% of all forest fires in Central-Eastern European countries in 1999–2001, with as many as approx. 240.5 th. fires which burned approx. 465 th. ha. In that period larger burnt area has been noted only once, in 1996, when the highest value has been recorded in the Ukraine (Szczygieł *et al.* 2009*a*). In the recent past (1990–2013) the highest number of forest fires in Poland occurred in 2003, with the record value of 17 088 fires. The largest area (43 755) burned in Polish forest fires in 1992 (Tab. 1). This has been a year with a disastrous fire situation (Szczygieł *et al.* 2008, 2009*a*), when the two largest, catastrophic forest fires in Poland in the recent history have occurred. In the Potrzebowice Forest District in north-western Poland more than 5 000 ha have burnt, whereas the Rudy Raciborskie fire in Upper Silesia (south-western Poland), being the largest forest fire in the country since 1948, has damaged over 9 000 ha in Forest Districts: Rudy Raciborskie, Rudziniec and Kędzierzyn (Hawryś *et al.* 1998, 2004; Dobrowolska 2008; Szczygieł *et al.* 2008).

As weather conditions and litter humidity are the main drivers of the fire risk in Poland (Ubysz *et al.* 2006; Szczygieł *et al.* 2009*b*) the anticipated changes in temperature and precipitation patterns may considerably increase the burning hazard in the near future (Schelhaas *et al.* 2010). In fact, a significant rise in the forest fire activity in Poland has been already observed over the last decades due to the increasing trend in temperature and decreasing precipitation (Ubysz *et al.* 2006; Szczygieł *et al.* 2008). Furthermore, mild winters and shortening of the snow cover period have prolonged fire season (Szczygieł *et al.* 2008), that nowadays lasts from March–April to September (Ubysz *et al.* 2006; Piwnicki and Szczygieł 2011, 2012; Szczygieł and Piwnicki 2011; Zajączkowski *et al.* 2014). In 2011–2012 the highest forest fire risk has been recorded in April, May and June (Piwnicki and Szczygieł 2011, 2012), whereas in the last year in April and July (Zajączkowski *et al.* 2014). Nevertheless the effective fire suppression system in Poland may successfully prevent the increase in annually burnt forest area (Szczygieł *et al.* 2008). Mean area of a single forest fire in 1990–2013 was 0.93 ha (Tab. 1) – a value considerably lower than the average for earlier periods, given by Szczygieł *et al.* (2008): 3.25 ha in 1948–1950, 2.35 ha in 1951–1960, 1.78 ha in 1961–1970, 1.43 ha in 1971–1980 and 1.41 ha in 1981–1990. However, extreme weather conditions in certain years (like e.g. 2003) may still significantly increase the forest fire activity and hence the mean forest fire size (Tab. 1).

The main cause of fires in Poland are people as natural, lightning-ignited fires account for about 1% only. It has been also observed, that the number of forest fire outbreaks has been larger on holidays than on workdays (Ubysz and Szczygieł 2006). Arson cases have represented as much as approx. 40% of forest fire causes throughout the recent past (Szczygieł *et al.* 2009*a*; Piwnicki and Szczygieł 2011, 2012; Szczygieł and Piwnicki 2011; Zajączkowski *et al.* 2014). Fire spreading from nonforest areas due to the burning of grasslands has been another important cause of forest fires in Poland (Rydzak and Trebecki 2009; Szczygieł *et al.* 2009*a*). This practice, although illegal according to Polish legislation (Nature Conservation Act 2004), has been traditionally aiming at improving grazing conditions by removal of old plant remains and post-fire fertilizing effect (Rydzak and Trebecki 2009; Szczygieł *et al.* 2009*a*). The decrease in number of fires caused by setting grasslands ablaze has been observed in the most recent years only (Rydzak and Trebecki 2009; Szczygieł and Piwnicki 2011; Zajączkowski *et al.* 2014), likely as an effect of educational campaigns by the State Forest

Administration (Rydzak and Trebecki 2009; Szczygieł and Piwnicki 2011) and/or of people's concern for EU-subsidies, that could have been eventually withdrawn (Szczygieł *et al.* 2009*a*).

Table 1. Data on forest fires in Poland in 1990–2013 (Sources: Piwnicki and Szczygieł 2011, 2012; Szczygieł and Piwnicki 2011; Zajączkowski et al. 2014).

Year	No of forest fires	Burnt area (ha)	Mean fire area (ha)
1990	5 756	7 341	1.28
1991	3 528	2 567	0.73
1992	11 858	43 755	3.69
1993	8 821	8 290	0.94
1994	10 710	9 171	0.86
1995	7 681	5 306	0.69
1996	7 924	14 120	1.78
1997	6 818	6 598	0.97
1998	6 166	4 019	0.65
1999	9 820	8 307	0.85
2000	12 428	7 013	0.56
2001	4 480	3 429	0.77
2002	10 101	5 593	0.55
2003	17 088	28 554	1.67
2004	7 219	4 338	0.60
2005	12 803	7 387	0.58
2006	11 828	5 912	0.50
2007	8 302	2 841	0.34
2008	9 090	3 027	0.33
2009	9 161	4 400	0.48
2010	4 680	2 126	0.45
2011	9 220	2 850	0.31
2012	9 265	7 235	0.78
2013	4 883	1 289	0.26
Mean values for the periods			
1990–2013	**8 735**	**8 145**	**0.93**
1990–1999	7 908	10 947	1.38
2000–2013	9 325	6 142	0.66
1999–2003	10 783	10 579	0.98
2004–2008	9 848	4 701	0.48
2009–2013	7 442	3 580	0.48

Fire prevention together with creating and maintaining fire protection infrastructure are obligatory tasks of the Polish State Forest Administration (LP = Lasy Państwowe, State Forests National Forest Holding), as defined by the Forestry Act (1991). Current fire prevention and suppression measures applied by the State Forest Administration, besides education activities for the public, include construction of fuel- and fire breaks, silvicultural operations, fire observation system, communication

and alarm network, water supply points and professional fire suppression equipment (Szczygieł and Piwnicki 2011). All that has amounted to the total fire protection cost (incurred by the State Forest Administration) of 294 mill PLN (approx. 71 mill EUR) in 2003–2004 (Szczygieł *et al.* 2007) and of 63 mill PLN (approx. 15.2 mill EUR) in 2010 only (Szczygieł and Piwnicki 2011). According to the Polish law State Forest Administration is not obliged to conduct active fire suppression. Nevertheless it belongs to its important activities. In 2003–2004 fire suppression carried out by the State Forest Administration has accounted for 17.2% of the total fire protection cost incurred, corresponding to the cost of approx. 8–10 mill PLN (approx. 1.9–2.4 mill EUR) annually. As many as 9% of all forest fires in that period have been supressed by the employees of the State Forest Administration alone, with no fire brigades involved (Szczygieł *et al.* 2007).
At present there is no prescribed burning practice in Polish forests as it is legally restricted (e.g. Forestry Act 1991; Nature Conservation Act 2004). In the other neighbouring countries in the temperate Europe fire use is still practiced at the experimental level only, for nature conservation and landscape management purposes (Goldammer and Bruce 2004).

Historical forest fire record from Białowieża

The first tree ring fire history records from two locations in Białowieża Forest evidenced frequent fires in *Pinus sylvestris*-dominated stands during the 17th up to early 19th centuries, with dramatic decrease in fire presence over the last 150+ years, most likely linked to changes in human fire use and forest management (Niklasson *et al.* 2010; Zin *et al.*, unpubl.).
Despite the considerable fire occurence in Central-Eastern Europe nowadays (e.g. Szczygieł *et al.* 2009*a*; Schmuck *et al.* 2011), there are hardly any annually resolved data on fire activity in temperate European forests spanning over time periods longer than the 20th and the 21st centuries (*cf.* Niklasson *et al.* 2010). As main reasons for the lack of such research in that region Niklasson *et al.* (2010) gave both the traditional perspective on fire as less important disturbance agent in the vegetation dynamics of this biome (e.g. Ellenberg 1988; Vera 2000; Timbal *et al.* 2005) and the paucity of old-growth woodlands enabling dendrochronological analyses spanning over several centuries, mainly linked to the long history of forest use and management throughout this part of the European continent (e.g. Pyne 1997; Farrell *et al.* 2000).
Białowieża Forest however, a large woodland in the borderland between north-eastern Poland and western Belarus, offers an extraordinary value for dendroecological studies. Thanks to its status as a royal hunting area since the early 1400s (Samojlik 2007) it withstood deforestation and commercial timber exploitation that made thousands of hectares of old-growth woodlands all over the continent disappear and survived until today as one of the best preserved temperate lowland deciduous and mixed forests in Europe (Faliński 1986; Peterken 1996). Considering dendrochronological recunstructions, Białowieża Forest is most likely unique among other European lowland forests. Old-growth forest stands with deadwood continuity and numerous ancient, large-size trees that are still present in that area (Faliński 1986; Sokołowski 2004) deliver annually resolved tree ring record of past stand and forest dynamics.
The first tree ring fire history record from a site located in the Polish part of Białowieża Forest (Niklasson *et al.* 2010), being to our knowledge also the first dendrochronological fire history reconstruction from the temperate forests of lowland Central Europe, has evidenced fire as a factor of major importance for the past forest dynamics. It has been proven that historical fires were recurring at very short intervals (approx. 10 years on average) over the last 350+ years (1650–2007), which favoured *Pinus sylvestris*-dominated forest. However, significant temporal changes in the past fire frequencies have been recorded at the end of the 18th century, when fire intervals have significantly increased. The complete cessation of fire occurrence has been documented since 1920s. This change in historical fire regime has resulted in a remarkable shift in tree establishment patterns, towards the dominance of fire-sensitive, shade-tolerant Norway spruce (*Picea abies* (L.) Karst.) (Niklasson *et al.*

2010) – a phenomenon described also in boreal Europe (e.g. Linder 1998; Wallenius *et al.* 2004). Furthermore, substantial human impact on the reconstructed fire regime has been suggested (Niklasson *et al.* 2010), alike in other studies from Northern European locations (e.g. Niklasson and Granström 2000; Groven & Niklasson 2005; Storaunet *et al.* 2013).
Interestingly, the second tree ring fire history record from Białowieża Forest, coming from a study site located in the Belarusian section of that area (Zin *et al.*, unpubl.), brought similar information on the historical forest fire activity over the analogous period. That site, although separated in space, evidenced comparably high fire frequency between 1650s and the first decades of the 1800s, when the onset of fire decline appeared. Similarly to the Polish location, no fires were recorded since the first decades of the 20th century (Zin *et al.*, unpubl.).

Conclusions

We conclude that there is a large need for fire history and fire ecology studies in Central Europe due to high population density and strong dominance of flammable conifers in forests of that region. Extended knowledge about past disturbance dynamics and reference conditions may be essential for future sustainable forest management and nature conservation throughout this part of European continent.

References

Badeck F-W, Lasch P, Hauf Y, Rock J , Suckow F, Thonicke K (2003) Steigendes klimatisches Waldbrandrisiko. *Allgemeine Forst Zeitschrift für Wald und Forstwirtschaft* **59**, 90–92.

Bradshaw RHW, Tolonen K, Tolonen M (1997) Holocene records of fire from the boreal and temperate zones of Europe. In 'Sediment Records of Biomass Burning and Global Change'. (Eds JS Clark, H Cachier, JG Goldammer, B Stocks) pp. 347–365. (Springer Verlag: Berlin–Heidelberg).

Dobrowolska D (2008) Odnowienie naturalne na powierzchniach uszkodzonych przez pożar w Nadleśnictwie Rudy Raciborskie. *Leśne Prace Badawcze* **69(3)**, 255–264.

Ellenberg H (1988) 'Vegetation Ecology of Central Europe'. (Cambridge University Press: Cambridge)

Faliński JB (2001) Fires in the long-term dynamics of pine subcontinental forests. In 'Coniferous forest vegetation – differentiation, dynamics and transformations', Seria Biologia Nr 69. (Eds A Brzeg, M Wojterska) pp. 131–170. (Wydawnictwo Naukowe UAM: Poznań)

Faliński JB (1986) 'Vegetation Dynamics in Temperate Lowland Primeval Forest. Ecological Studies in Białowieża Forest'. (Dr W. Junk Publishers: Dordrecht)

Farrell EP, Führer E, Ryan D, Andersson F, Hüttl R, Piussi P (2000) European forest ecosystems: building the future on the legacy of the past. *Forest Ecology and Management* **132**, 5–20.

Forestry Act (1991) Ustawa z dnia 28 września 1991 r. o lasach (Dz.U. 1991 Nr 101 poz. 444, ze zm.). Kancelaria Sejmu (Warszawa)

Goldammer JG, Bruce M (2004) The use of prescribed fire in the land management of Western and Baltic Europe: An overview. *International Forest Fire News* **30**, 2–13.

Groven R, Niklasson M (2005) Anthropogenic impact on past and present fire regimes in a boreal forest landscape of southeastern Norway. *Canadian Journal of Forest Research* **35**, 2719–2726.

GUS 2014. Polska w liczbach. Główny Urząd Statystyczny, Zakład Wydawnictw Statystycznych. (Warszawa) Available at http://www.stat.gov.pl [Verified 13 July 2014]

Hannon GE, Bradshaw R, Emborg J (2000) 6000 years of forest dynamics in Suserup Skov, a seminatural Danish woodland. *Global Ecology and Biogeography* **9**, 101–114.

Hawryś Z, Zwoliński J, Kwapis Z, Wałecka M (2004) Rozwój sosny zwyczajnej na terenie pożarzysk leśnych z 1992 roku w Nadleśnictwach Rudy Raciborskie i Potrzebowice. *Leśne Prace Badawcze* **2**, 7–20.

Hawryś Z, Zwoliński J, Matuszczyk I, Olszewska G, Zwolińska B, Batko B (1998) Zmiany i odbudowa ekosystemów leśnych zniszczonych przez pożar na przykładzie wielkoobszarowego pożarzyska w lasach Rudzko-Rudziniecko-Kętrzyńskich. *Postępy Techniki Leśnej* **67**, 33–40.

Hille M (2006) Fire Ecology of Scots Pine in Northwest Europe. Wageningen University, Ph.D. thesis. (Wageningen)

Linder P (1998) Structural changes in two virgin Boreal forest stands in central Sweden over 72 years. *Scandinavian Journal of Forest Research* **13**, 451–461.

Nature Conservation Act (2004) Ustawa z dnia 16 kwietnia 2004 r. o ochronie przyrody (Dz.U. 2004 nr 92 poz. 880). Kancelaria Sejmu (Warszawa)

Niklasson M, Granström A (2000) Numbers and sizes of fires: long-term spatially explicit fire history in a Swedish boreal landscape. *Ecology* **81**, 1484–1499.

Niklasson M, Zin E, Zielonka T, Feijen M, Korczyk AF, Churski M, Samojlik T, Jędrzejewska B, Gutowski JM, Brzeziecki B (2010) A 350-year tree-ring fire record from Białowieża Primeval Forest, Poland: implications for Central European lowland fire history. *Journal of Ecology* **98**, 1319–1329.

Peterken GF (1996) 'Natural Woodland: Ecology and Conservation in Northern Temperate Regions'. (Cambridge University Press: Cambridge)

Piwnicki J, Szczygieł R (2011) Pożary lasów. In Raport 2011. Stan zdrowotny lasów Polski w roku 2011. Monitoring lasów w Polsce. Państwowy Monitoring Środowiska, Instytut Badawczy Leśnictwa – Główny Inspektorat Ochrony Środowiska, Annual Report 2011, pp. 39–41. Available at http://www.gios.gov.pl/monlas/raporty/raport_2011/01.html [Verified 13 July 2014]

Piwnicki J, Szczygieł R (2012) Pożary lasów. In Raport 2012. Stan zdrowotny lasów Polski w roku 2012. Monitoring lasów w Polsce. Państwowy Monitoring Środowiska, Instytut Badawczy Leśnictwa – Główny Inspektorat Ochrony Środowiska, Annual Report 2012, pp. 38–39. Available at http://www.gios.gov.pl/monlas/raporty/raport_2012/12.html [Verified 13 July 2014]

Pyne SJ (1997) 'Vestal Fire. An Environmental History, Told through Fire, of Europe and Europe's Encounter with the World'. (University of Washington Press: Seattle)

Rösch M (2000) Long-term human impact as registered in an upland pollen profile from the southern Black Forest, southwestern Germany. *Vegetation History and Archaeobotany* **9**, 205–218.

Rydzak W, Trebecki J (2009) Modes of Wildland Fire Fighting through Educational Campaign in Transition Countries in Europe: Case Study of Poland. *Journal of Forestry* **107(8)**, 419–424.

Samojlik T (2007) Antropogenne przemiany środowiska Puszczy Białowieskiej do końca XVIII wieku. Mammal Research Institute, Polish Academy of Sciences – Jagiellonian University, Ph.D. thesis. (Białowieża – Kraków)

San-Miguel-Ayanz J, Ståhl G, Vidal C, Bonhomme C, Cienciala E, Korhonen K, Lanz A, Schadauer K (2011) Criterion 1: Maintenance and Appropriate Enhancement of Forest Resources and their Contribution to Global Carbon Cycles. In 'FOREST EUROPE, UNECE and FAO 2011: State of Europe's Forests 2011. Status and Trends in Sustainable Forest Management in Europe' pp. 17–27. (Ministerial Conference on the Protection of Forests in Europe: Oslo)

Schelhaas MJ, Hengeveld G, Moriondo M, Reinds GJ, Kundzewicz ZW, ter Maat H, Bindi, M (2010) Assessing risk and adaptation options to fires and windstorms in European forestry. *Mitigation and Adaptation Strategies for Global Change* **15(7)**, 681–701.

Schelhaas MJ, Nabuurs GJ, Schuck A (2003) Natural disturbances in the European forests in the 19th and 20th centuries. *Global Change Biology* **9**, 1620–1633.

Schmuck G, San-Miguel-Ayanz J, Camia A, Durrant T, Santos de Oliveira S, Boca R, Whitmore C, Giovando C, Libertá G, Corti P, Schulte E (2011) Forest Fires in Europe 2010. European Commission, Joint Research Centre – Institute for Environment and Sustainability, JRC Scientific and Technical Reports, Report No 11. (Luxembourg, Publications Office of the European Union)

Sokołowski AW (2004) 'Lasy Puszczy Białowieskiej'. (Centrum Informacyjne Lasów Państwowych: Warszawa).

Storaunet KO, Rolstad J, Toeneiet M, Blanck Y (2013) Strong anthropogenic signals in historic forest fire regime: a detailed spatiotemporal case study from south-central Norway. *Canadian Journal of Forest Research* **43**, 836–845.

Szczygieł R, Piwnicki J (2011) Country Report: Poland. In Forest Fires in Europe 2010 (Eds. G Schmuck, J San-Miguel-Ayanz, A Camia, T Durrant, S Santos de Oliveira, R Boca, C Whitmore, C Giovando, G Libertá, P Corti, E Schulte) pp. 44–48. European Commission, Joint Research Centre – Institute for Environment and Sustainability, JRC Scientific and Technical Reports, Report No 11. (Luxembourg: Publications Office of the European Union)

Szczygieł R, Piwnicki J, Ubysz B (2007) Analiza ekonomiczna funkcjonowania ochrony przeciwpożarowej lasu w Lasach Państwowych. *Leśne Prace Badawcze* **1**, 27–50.

Szczygieł R, Ubysz B, Piwnicki J (2008) Wpływ zmian klimatycznych na kształtowanie się zagrożenia pożarowego lasów w Polsce. Leśne Prace Badawcze **69(1)**, 67–72.

Szczygieł R, Ubysz B, Zawiła-Niedźwiecki T (2009*a*) Spatial and temporal trends in distribution of forest fires in Central and Eastern Europe. In 'Wildland Fires and Air Pollution' (Eds A Bytnerowicz, M Arbaugh, A Riebau, C Andersen) pp. 233–245. (Elsevier: Amsterdam – Oxford)

Szczygieł R, Ubysz B, Kwiatkowski M, Piwnicki J (2009*b*) Klasyfikacja zagrożenia pożarowego lasów Polski. *Leśne Prace Badawcze* **70(2)**, 131–141.

Timbal J, Bonneau M, Landmann G, Trouvilliez J, Bouhot-Delduc L (2005) European non-boreal conifer forests. In 'Ecosystems of the World. Coniferous Forests' (Ed F Andersson) pp. 131–162. (Elsevier: Amsterdam – San Diego – Oxford – London)

Ubysz B, Szczygiel R (2002) Fire Situation in Poland. *International Forest Fire News* **27**, 38–64.

Ubysz B, Szczygieł R (2006) A study on the natural and social causes of forest fires in Poland. *Forest Ecology and Management* **234S**, S13.

Ubysz B, Szczygieł R, Piwnicki J (2006) Analysis of the trends in the forest fire risk for recent years in Poland against the background of long-term trends. *Forest Ecology and Management* **234S**, S248.

Vera F (2000) 'Grazing Ecology and Forest History'. (CABI Publishing: Wallingford)

Wallenius TH, Kuuluvainen T, Vanha-Majamaa I (2004) Fire history in relation to site type and vegetation in Vienansalo wilderness in eastern Fennoscandia, Russia. *Canadian Journal of Forest Research* **34**, 1400–1409.

Zajączkowski G, Jabłoński M, Jabłoński T, Małecka M, Kowalska A, Małachowska J, Piwnicki J (2014) Raport o stanie lasów w Polsce 2013. Państwowe Gospodarstwo Leśne Lasy Państwowe, Dyrekcja Generalna Lasów Państwowych, Centrum Informacyjne Lasów Państwowych, Annual Report 2013. (Warszawa) Available at http://www.lasy.gov.pl/informacje/ publikacje/informacje-statystyczne-i-raporty/raport-o-stanie-lasow/raport-o-stanie-lasow-2013/view [Verified 14 July 2014]

Utilizing random forests imputation of forest plot data for landscape-level wildfire analyses

Karin L. Riley[a], Isaac C. Grenfell[b], Mark A. Finney[c], and Nicholas L. Crookston[c]

[a] *College of Forestry and Conservation, University of Montana, 32 Campus Drive, Missoula, Montana, USA, 59812, karin.riley@umontana.edu*
[b] *RTL Networks, US Highway 10 W, Missoula, Montana, USA, 59808, igrenfell@gmail.com*
[c] *Missoula Fire Sciences Laboratory, Rocky Mountain Research Station, U.S. Forest Service,5775 US Highway 10 W, Missoula, Montana, USA, 59808, mfinney@fs.fed.us* [d]*Moscow Forestry Sciences Laboratory, Rocky Mountain Research Station, U.S. Forest Service, 1221 South Main Street, Moscow, Idaho, USA, 83843, nrcrookston@fs.fed.us*

Abstract
Maps of the number, size, and species of trees in forests across the United States are desirable for a number of applications. For landscape-level fire and forest simulations that use the Forest Vegetation Simulator (FVS), a spatial tree-level dataset, or "tree list", is a necessity. FVS is widely used at the stand level for simulating fire effects on tree mortality, carbon, and biomass, but uses at the landscape level are limited by lack of availability of forest inventory data for large contiguous areas. Detailed mapping of trees across large areas is not feasible with current technologies, but statistical methods for matching forest plot data with biophysical characteristics of the landscape offer a practical means to populate landscapes with a limited set of forest plot inventory data. We used a modified random forests approach, with Landfire vegetation and biophysical predictors at 30m grid resolution. In essence, the random forests method creates a "forest" of decision trees in order to choose the forest plot with the best statistical match for each grid cell in the landscape. Landfire data was used in this project because is publicly available, offers seamless coverage of variables needed for fire models, and is consistent with other datasets, including burn probabilities and flame length probabilities generated for the continental US by Fire Program Analysis (FPA). We used the imputed forest plot data to generate a map of forest cover and height as well as existing vegetation group for a study area in eastern Oregon, and examined correlations with Landfire data. The results showed good correspondence between the two data sets (84-97% within-class agreement, depending on the variable). In future research, the new imputed grid of inventory data will be used for landscape simulation studies to determine risk to terrestrial carbon resources from wildfire as well as to investigate the effect of fuel treatments on burn probability and fire sizes.

Keywords*: imputation; forest plot data; Landfire; random forests*

Introduction

For many research applications ranging from estimation of terrestrial carbon resources to the impact of fuel treatment projects on wildfire propagation, to name a few, it is desirable to know the location, size, and species of each tree on the landscape. However, such a mapping effort is not feasible with current technologies. LiDAR and similar technologies may make such a tree-level map a reality in coming years, but in the interim, various statistical efforts can produce spatial models, known as "tree lists", suitable for a wide range of research applications.
To this end, a number of statistical methods have been evaluated in the literature, ranging from gradient nearest neighbour imputation (GNN), linear models (LM), classification and regression trees (CART), kriging, universal kriging (UK) and most similar neighbour (MSN) (Moeur and Stage 1995; Pierce *et al.* 2009). Among these, Pierce *et al.* (2009) found GNN performed best for forest structure variables in Oregon, while LMs and UK demonstrated stronger performance for both forest structure and canopy variables in Washington and California. Drury and Herynk (2011) produced a national tree list by stratifying plot data by existing vegetation type, biophysical setting, succession class, and canopy bulk

density. Because this method generally left several potential matches for each grid cell on the landscape, and because the purpose of the tree list was to model tree mortality from fire, they then identified the median bark thickness for each plot, and chose the plot with the median of the median bark thickness to assign.

This project had several specific requirements that precluded use of most of these methods. For this project, we required our tree list to be consistent with two already existing datasets. The Landfire project provides over 20 national geo-spatial layers, including topographic, fuel, and vegetation layers, on 30m grids (www.landfire.gov). These layers, in turn, are used as inputs to Fire Program Analysis (FPA), which runs national-level wildfire simulations to output burn probability and flame length probabilities on a 270m grid, accompanied by a set of modelled fire perimeters. Therefore, we leveraged the Landfire dataset as inputs to our tree list, to ensure consistency with that dataset as well as the FPA outputs. In order to model forest type, introduction of a categorical variable, existing vegetation group, into our model along with numeric variables was necessary. That limited the set of possible methodologies to classification trees. We chose random forests as our methodology, since it leverages a "forest" of classification trees in order to produce high accuracies and model complex interactions among predictor variables, two notable strengths of this methodology over other statistical classifiers (Cutler *et al.* 2007). The random forests method as used here in essence evaluates a set of forest plots, and identifies the best-matching plot for each grid cell on the landscape. Our methodology is distinct from that of Pierce *et al.* (2009) in that it has the capacity to use categorical variables and is consistent with Landfire and FPA data. Several important differences exist between our methodology and that of Drury and Herynk (2011) as well: 1) we limited our data to a single set of nationally consistent plot data, whereas they obtained a variety of fixed- and variable-plot designs from multiple agencies, 2) since tree mortality was not the primary variable of interest, we did not use it as a predictor, and 3) we wanted to identify a single best matching plot for each point on the landscape rather than utilizing the median plot in a class, retaining more variability on the landscape.

Here, we demonstrate high model accuracies for a random forests imputation run on an approximately 40,000 km^2 area of forest in the western U.S., indicating the output would be suitable for a wide range of research applications.

2. Methods

In order to test and refine our methodology, we chose a Landfire zone, Zone 9, which lies mainly in eastern Oregon, as our study area (Figure 1). The zone contains large forested areas, amounting to about 25% of the total area of the zone, or approximately 40,000 km^2.

In this random forests imputation, a set of reference observations was imputed to a set of target points (Crookston and Finley 2008). The reference observations consisted of a set of forest plot data acquired from the US Forest Service's Forest Inventory Analysis (FIA) program. Beginning in 1999, FIA has been using a standardized plot design to conduct forest surveys across the US (O'Connell *et al.* 2014). Among the variables collected at these plots that we utilized in the imputation are: elevation, slope, aspect, latitude, and longitude. The Landfire program calculates additional variables needed for the imputation and stores them in their Landfire Reference Database (LFRDB), including forest height, forest cover, and existing vegetation group (EVG) computed from a classification method devised by NatureServe (2009) for Landfire. We derived additional biophysical variables via overlays of plot locations with gridded data from the Landfire project for photosynthetically active radiation, precipitation, relative humidity, maximum temperature, minimum temperature, and vapour pressure deficit. The target points in this study consist of a grid of 30m pixels that comprise the Landfire dataset. So, in essence, we use random forests to find the best matching FIA plot for each 30m pixel, imputing an FIA plot number to each pixel.

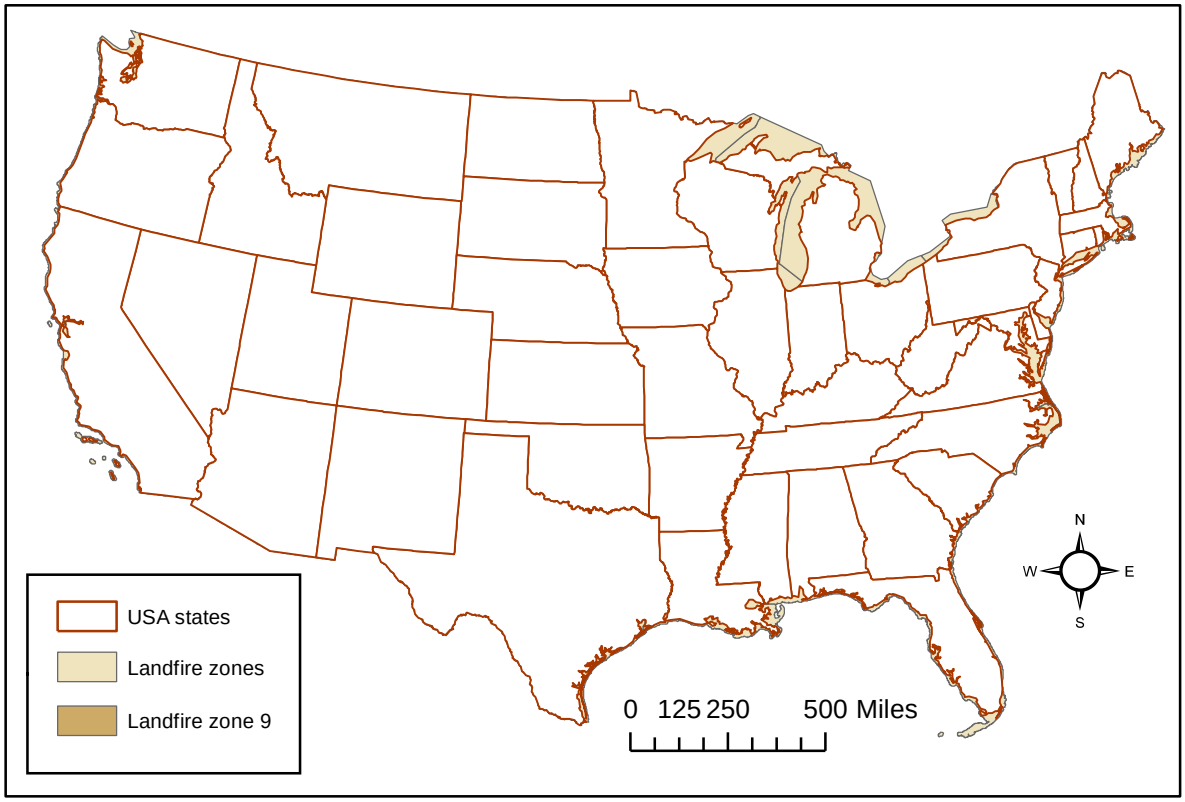

Figure 1. Location of the study area, Landfire Zone 9, in the western United States.

For this project, we retained only FIA plots that utilized the national design, were single condition (meaning they did not cross ownership boundaries or major vegetation types), and appeared in the LFRDB. Thus, we began with 15,333 plots in the western half of the continental United States, and then created a subset consisting only of the plots with EVGs appearing in Zone 9. Then, we formed the random forest model using the yaImpute package in the statistical program R. To do this, we used 250 total decision trees to predict tree height, tree cover, and EVG for each plot. To predict these, we used the following predictors: latitude, longitude, tree cover, tree height, elevation, slope, EVG, PAR (photosynthetically active radiation), precipitation, relative humidity, maximum temperature, minimum temperature, VPD (vapour pressure deficit), cosine of aspect (northing), and sine of aspect (easting). Notice that the variables we wish to predict also appear as predictors. This may appear odd, but the reason we do this is that the objective with random forest imputation is to build a model that assigns a set of predictor values to a plot associated with the response variables. Accuracy in the response variables can be heightened by also including them as predictors. The random forest method involves building many classification trees (in this case, 83 for each response variable, adding to the total 249). Each tree is formed using a subset of the plots, and the remainder (referred to as the out-of-bag observations) are set aside to assess accuracy. As Cutler *et al.* (2007) eloquently describes it, "Observations in the original data set that do not occur in a bootstrap sample are called out-of-bag observations. A classification tree is fit to each bootstrap sample, but at each node, only a small number of randomly selected variables (e.g., the square root of the number of variables) are available for binary partitioning." Binary partitioning continues until the variance in each bucket cannot be reduced significantly, or until further divisions cannot be made without reducing the number of observations in a bucket to less than 5. Each "fully grown" decision tree is used to predict the out-of-bag observations. "The predicted class of an observation is calculated by the majority vote of the out-of-bag-predictions for that observation, with ties split randomly" (Cutler *et al.* 2007).

We can obtain an overall accuracy of the model by taking the out-of-bag misclassification for each tree and considering them in aggregate to assess the overall quality of the forest model. In this case,

the out-of-bag error rates for Zone 9 were 6.99%, 1.79%, and 0.897% for forest cover, forest height, and EVG respectively, an indication of high model accuracy.
Once the forest of decision trees is in hand, we can impute new target observations to determine which reference plots are most closely associated with the targets (pixels, in this case). Our dataset consisted of 44,138,635 forested pixels. The imputation is done by evaluating the target predictor variables for each pixel through each of the 3 sets of trees associated with each response variable. Then, the plot most frequently imputed amongst all 500 trees is considered the winner. Once we obtain this list of reference plots, we can build imagery of the variables of interest associated with each imputed plot. In this case, we output raster images of forest cover, forest height, existing vegetation group, and plot number. The plot number can be used to reference the number, size, and species of trees in each plot via a lookup table.
Validation consisted of assessing within-class accuracy for the three response variables (forest cover, forest height, and existing vegetation group) using confusion matrices and the kappa statistic. Barplots were used to assess the proportion of pixels in each class in the target data versus the imputed data.

Results and Discussion

Accuracies for imputed forest height were high. Landfire maps forest height in four classes: 0-5 m, 5-10 m, 10-25 m, and greater than 25 m. The Landfire organization also computes the height of FIA forest plots in its LFRDB to tenths of a meter. We compared the height of each imputed plot to the height class mapped by Landfire for the corresponding pixel (Table 1). The resulting confusion matrix represents a type of accuracy assessment of the outputs. We do not assess the accuracy of the Landfire data itself, which has its own error rates, but we compute the accuracy of our imputation compared to the gridded target data. Within-class accuracy for forest height was 97% in Zone 9. The number of pixels in each height class compared quite favourably across the imputed plot data and the Landfire gridded target data (Figure 2).

Table 1. Confusion matrix of forest height in meters in gridded Landfire data and imputed forest plot data.

		Imputed plot				
		0-5m	**5-10m**	**10-25m**	**>25m**	**Accuracy**
Gridded Landfire	**0-5m**	1,059,777	98,042	820	13	**0.91**
	5-10m	47,313	7,842,084	6,227	63	**0.99**
	10-25m	852	66,957	23,609,236	107,949	**0.99**
	>25m	316	2,734	1,100,876	10,195,377	**0.90**
	Accuracy	**0.96**	**0.98**	**0.96**	**0.99**	**0.97**

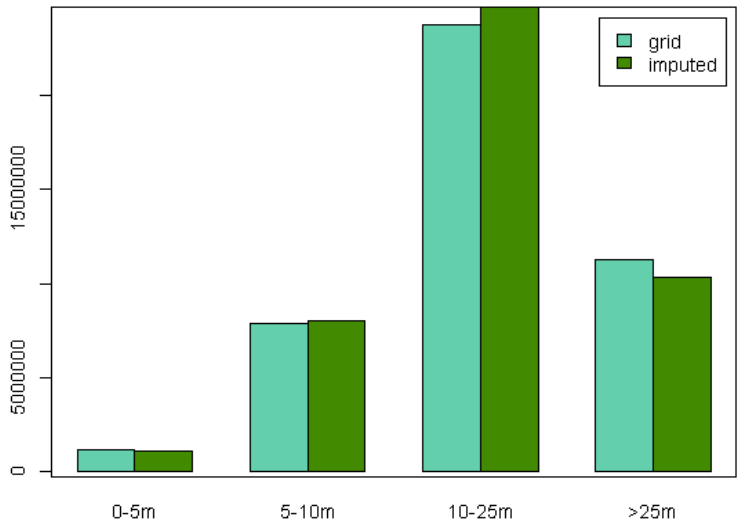

Figure 2. Barplots comparing height class of imputed forest plot data and gridded Landfire reference data. Units of the y axis are numbers of pixels.

The accuracy of the imputation was also high for forest cover. Forest cover is mapped in nine classes in Landfire (Table 2), with areas of tree cover less than 10% not considered forested. For FIA plots, forest cover is estimated to the nearest percent in the LFRDB. Overall accuracy for the zone was 86%, with within-class accuracy ranging from less than 1% in the two densest forest cover classes (80-89% and 90-100%) to 98% in a moderate cover class (30-39%). The proportion of cover classes compared favourably across the imputed forest plots and gridded target Landfire data (Figure 3). The largest discrepancies were in the sparsest cover class (10-19%), which was underestimated by the imputed plot data, and the 20-29% cover class, which was conversely overestimated by the imputed plot data. Forest cover greater than 60% was rare in the Landfire reference data.

Table 2. Confusion matrix of forest cover in percent in gridded Landfire data and imputed forest plot data.

Imputed plot

Gridded Landfire	10-19%	20-29%	30-39%	40-49%	50-59%	60-69%	70-79%	80-89%	90-100%	Accuracy
10-19%	9,052,029	3,321,677	345,886	42,645	26,675	1,066	3,105	3	0	**0.71**
20-29%	171,230	7,960,416	62,318	4,945	10,694	42	45	2	0	**0.97**
30-39%	76,663	79,301	7,984,875	34,055	6,778	3	734	0	0	**0.98**
40-49%	13,698	38,271	289,665	9,001,039	109,372	25,566	1,255	0	0	**0.95**
50-59%	23,696	22,807	151,700	464,473	3,859,002	362,658	64,946	1,741	2,154	**0.78**
60-69%	123	1,071	12,445	39,498	64,997	306,547	60,585	9,197	2,100	**0.62**
70-79%	32	34	1,087	1,472	2,456	4,044	5,367	1,860	83	**0.33**
80-89%	2	35	2,066	2,182	308	3,220	154	38	396	**0.00**
90-100%	0	1	4	0	2	0	0	0	0	**0.00**
Accuracy	**0.97**	**0.70**	**0.90**	**0.94**	**0.95**	**0.44**	**0.04**	**0.00**	**0.00**	**0.86**

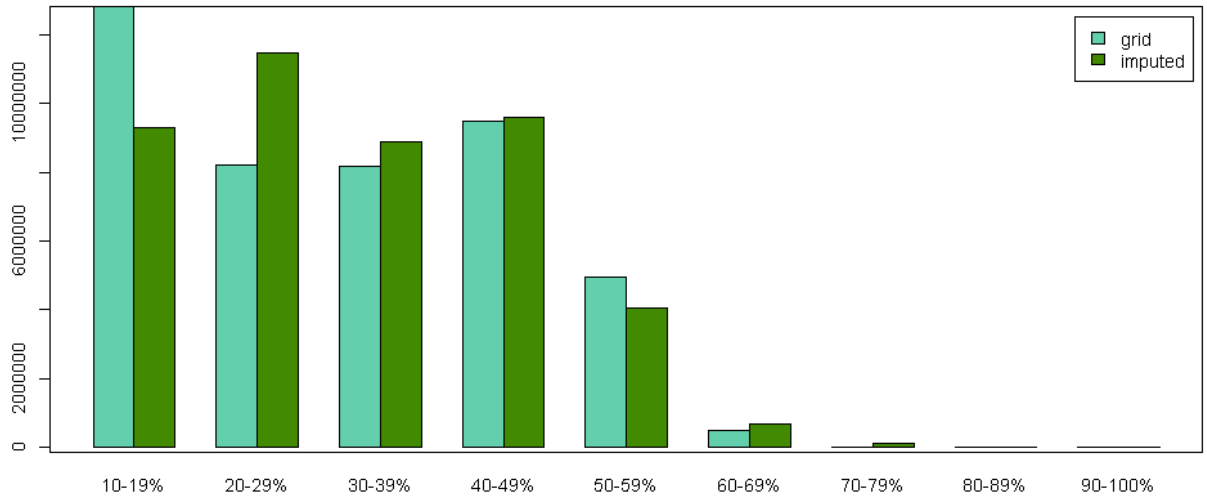

Figure 3. Barplots comparing forest cover class of imputed forest plot data and gridded Landfire target data. Units of the y axis are numbers of pixels.

The third response variable in our study was existing vegetation group (EVG). There were 14 EVGs in Zone 9 (Table 3). EVG is mapped to the gridded target data by Landfire, and also assigned to FIA forest plots in the LFRDB. Within-class accuracy of EVG was 84% for the study area as a whole. Class proportions compared favourably across the gridded Landfire data and the imputed plot data, but the most common EVG classes tended to be somewhat over-represented in the imputed plot data (Figure 4).

Table 3. Landfire Existing Vegetation Groups (EVGs) in zone 9, by numeric code and text description

EVG Code	EVG Description
602	Aspen Forest, Woodland, and Parkland
603	Aspen-Mixed Conifer Forest and Woodland
614	Douglas-fir Forest and Woodland
620	Juniper Woodland and Savanna
621	Limber Pine Woodland
622	Lodgepole Pine Forest and Woodland
625	Douglas-Fir-Ponderosa Pine-Lodgepole Pine Forest and Woodland
628	Mountain Mahogany Woodland and Shrubland
630	Pinyon-Juniper Woodland
631	Ponderosa Pine Forest and Woodland and Savanna
635	Western Riparian Woodland and Shrubland
639	Spruce-Fir Forest and Woodland
640	Subalpine Woodland and Parkland
643	Douglas-fir-Grand Fir-White Fir Forest and Woodland

Table 4. Confusion matrix of Existing Vegetation Group (EVG) in gridded Landfire data and imputed forest plot data.

Imputed plot

Gridded Landfire	602	603	614	620	621	622	625	628	630	631	635	639	640	643	Accuracy
602	314,840	249,598	95,978	1,385,619	7,993	59,758	334,829	107,570	64,309	535,962	1,714	19,841	7,251	586,985	**0.08**
603	4,550	154,112	23,785	25,385	609	13,355	213,861	743	135	50,873	222	8,258	823	96,633	**0.26**
614	38	349	2,571,261	16,626	1,162	860	47,797	42	3,563	10,060	294	86	894	2,609	**0.97**
620	730	118	16,363	5,807,709	751	5,691	27,071	15,083	89,344	60,399	2,000	816	21,819	3,970	**0.96**
621	0	0	2	0	2,439	186	0	0	4	52	0	266	1,076	461	**0.54**
622	3	3,139	919	2,883	659	402,396	10,222	7	1	70,926	249	31,867	826	9,664	**0.75**
625	540	359	3,831	6,904	375	171,844	15,500,221	107	253	36,256	1,593	25,714	141	5,903	**0.98**
628	602	9,372	19,380	62,687	901	3,432	70,707	304,824	9,576	112,518	187	7,306	3,469	41,835	**0.47**
630	0	159	100	13,145	0	376	1,120	700	205,741	7,978	0	2,451	102	21,165	**0.81**
631	0	2,605	2,590	89,693	702	6,818	119,542	163	69,293	7,527,132	51	7,345	7,183	225	**0.96**
635	209	62,056	59,712	493,731	39	102,195	141,945	4,645	2,221	383,109	646,482	21,820	2,907	70,895	**0.32**
639	101	2,506	1,108	1,892	11	1,911	2,818	120	11	7,804	395	1,023,592	0	338	**0.98**
640	1	0	31	0	0	843	28	16	0	461	0	298	347,194	10	**1.00**
643	1,126	4,455	139,042	1,802	3	13,250	214,882	161	8	7,863	658	57,759	3,668	2,211,945	**0.83**
Accuracy	**0.98**	**0.32**	**0.88**	**0.73**	**0.16**	**0.51**	**0.93**	**0.70**	**0.46**	**0.85**	**0.99**	**0.85**	**0.87**	**0.72**	**0.84**

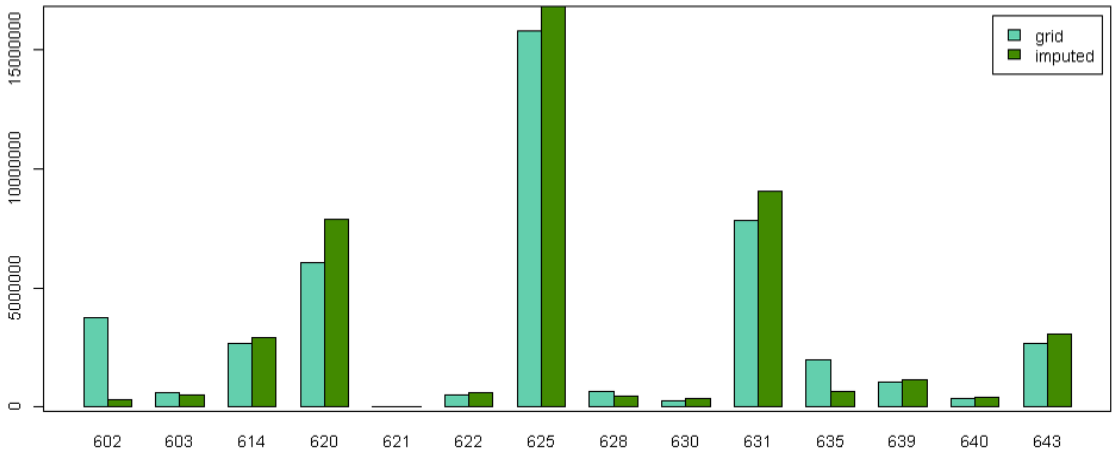

Figure 4.
Barplots comparing Existing Vegetation Group (EVG) of imputed forest plot data and gridded Landfire reference data. Units of the y axis are numbers of pixels.

In general, within-class accuracies were lower in rarer classes. This result makes sense, since it is unlikely in rare types that random forests can match all three of the response variables (forest cover, height, and existing vegetation group) when choosing from a limited pool of candidate forest plots, and must in essence choose which of these response variables is most important to match. If increased accuracy was desired in future implementations of this methodology, increasing the sample size of rare types would likely be the most effective way to boost accuracies.

Conclusions

Here, we have demonstrated that a modified random forests approach is a feasible method for imputing forest plots to a set of target landscape grids. This method produces a seamless grid of tree data at the landscape level. The modified random forests method produced high correlations between the target gridded data and the imputed plot data for the response variables of forest cover, forest height, and existing vegetation group (86%, 97%, and 84% respectively), an indication of high model accuracy. Very high classification accuracy is one of the strengths of the random forest method, along with its ability to utilize categorical as well as numerical variables (Cutler *et al.* 2007). Due to the high accuracy, the output imputed forest plot data should perform well in a number of applications, including estimation of risk from wildfire to terrestrial carbon resources, and analysis of the effect of fuel treatments on fire sizes and landscape-level burn probability.

References

Crookston, NL, Finley, AO (2008) yaImpute: an R package for kNN imputation. Journal of Statistical Software 23, 1-15.

Cutler, DR, Edwards, TC, Beard, KH, Cutler, A, Hess, KT, Gibson, J, Lawler, JJ (2007) Random forests for classification in ecology. Ecology 88, 2783-2792.

Drury, S, Herynk, J, 2011. The national tree-list layer: a seamless spatially-explicit tree-list layer for the continental United States.

Moeur, M, Stage, AR (1995) Most similar neighbor: an improved sampling inference procedure for natural resource planning. Forest Science 41, 337-359.

NatureServe (2009) 'International ecological classification standard: terrestrial ecological classifications.' NatureServe Central Databases. Arlington, VA, U.S.A. Data current as of 06 February 2009.).

O'Connell, BM, LaPoint, EB, Turner, JA, Ridley, T, Pugh, SA, Wilson, AM, Waddell, KL, Conkling, BL (2014). The Forest Inventory and Analysis Database: Database Description and User Guide Version 6.0 for Phase 2. Available at http://www.fia.fs.fed.us/library/database-documentation/current/ver6.0/FIADB_user%20guide_6-0_p2_5-6-2014.pdf [Accessed 16 July 2014].

Pierce, KB, Ohmann, JL, Wimberly, MC, Gregory, MJ, Fried, JS (2009) Mapping wildland fuels and forest structure for land management: a comparison of nearest neighbor imputation and other methods. Canadian Journal of Forest Research 39, 1901-1916.

Variation in peatland wildfire severity – implications for ecosystem carbon dynamics

G. Matt Davies[a], Alan Gray[b], Ruth Domenech Jardi[c], and Paul Johnson[d]

[a] *Solway Centre for Environment and Culture, University of Glasgow, Dumfries, DG1 4ZL, UK, gwilym.davies@glasgow.ac.uk*
[b] *Centre for Ecology and Hydrology, Bush Estate, Penicuik, Midlothian, EH26 0QB, UK, alangray@ceh.ac.uk*
[c] *Solway Centre for Environment and Culture, University of Glasgow, Dumfries DG1 4ZL, UK, rdomenja@yahoo.es*
[d] *Institute of Biodiversity, Animal Health and Comparative Medicine, University of Glasgow, Glasgow, G12 8QQ, paul.johnson@glasgow.ac.uk*

Abstract

Globally peatlands contain ca. 550 GT of ancient carbon and there is the potential for a positive feedback between peatland degradation and global climate change. Peatlands cover a substantial area of the British Uplands and the effects of wildfire and traditional managed burning on their ecological integrity are issues of growing debate. Land-managers and conservationists continue to argue over the effects of managed and wild fire on peatland carbon dynamics. Clear differences do exist in the severity of moorland fires and wildfires, though often intense, are not necessarily severe. The aim of our project was to document variation in the severity and ecological effects of a spate of peatland wildfires that burnt during the springs of 2011 and 2012. We identified a number of fire locations that included coverage of variation in major north-south and east-west bioclimatic conditions and peatland types. Fire severity was described using a modified form of the semi-quantitative Composite Burn Index. Fuel consumption was assessed using destructive harvesting of burnt- and unburnt fuel loads. Carbon dioxide and methane fluxes were assessed using samples taken from gas flux chambers. Fire severity varied substantially both within and between individual fires. Average severity varied up to two-fold between fires but as much as three-fold within some fires. Total carbon loss varied substantially between and within wildfires. Average fire-level consumption was 0.64± 0.12 kg C m^{-2} but this estimate should be treated with caution. Consumption was best described by a mixed effects model than included random intercepts for different fires and plots within fires and random slopes for different plots. The evidence for differences in consumption between fires was weak due to the small sampling size and the substantial within plot and fire variation in fuel load. There was a linear relationship between pre-fire fuel surface load and surface fuel consumption but no obvious difference between the prescribed and wild fires in how the proportion of fuel consumed changed with increasing fuel load. Soil methane fluxes were consistently lower on burnt sites whilst carbon dioxide fluxes were generally higher. Day-night temperature fluctuations in burnt plots were frequently more than twice that seen in unburnt plots. Our results demonstrate substantial variation in fire severity both within and between individual wildfire events. Assessment of the effects of wildfires requires intensive sampling efforts and drawing robust conclusions about the implications of wildfire on ecosystem C dynamics is thus fraught with difficulties.

Keywords*: carbon dioxide, Composite Burn Index, fuel consumption, methane, soil gas flux, soil microclimate*

Introduction

Globally peatlands contain ca. 550 GT of ancient carbon (Mitra *et al.* 2005) but there is considerable concern about the potential for a positive feedback between peatland degradation and global climate change (Turetsky *et al.* 2002, Dorrepaal *et al.* 2009). Many temperate and boreal peatlands experience wildfires and when these fires ignite peat deposits substantial amounts of carbon can be released (e.g. Davies *et al.* 2013). Ecosystem recovery following such severe burns can be extremely slow due to

the destruction of below-ground plant propagules (Granström and Schimmel 1993). More pernicious fire effects, such as scorching of the peat surface or removal of ground fuel layers overlying peat deposits, are also possible but the ecosystem implications of such impacts are relatively poorly-studied. The results of Maltby *et al.* (1990) however suggest that ecosystem recovery in such cases can take decades or longer. Little quantitative evidence exists of the extent to which peatland wildfire severity varies, the fuel and fire weather drivers of variation in severity or the ecological impacts of such variation.

Peatlands cover a substantial area of the British Uplands and the effects of wildfire and traditional managed burning on their ecological integrity are issues of growing debate (Davies *et al.* 2008a). Fire is an integral part of the traditional management of heaths and moorlands and is used to create a diversity of heather (*Calluna vulgaris*, hereafter *Calluna*) dominated habitat structures that support large surplus populations of red grouse (*Lagopus lagopus scoticus*) for hunting (Tharme *et al.* 2001). Traditional burning also provides fresh growth of heather for sheep and deer grazing (Smith and Thomas 1956), creates habitats for rare wildlife (Tharme *et al.* 2001) and may help to manage fuel loads reducing the potential for large or severe wildfires (Davies *et al.* 2008a). Nevertheless, land-managers and conservationists continue to argue over the effects of fire on peatland habitat structure, biodiversity and soil carbon dynamics. With regards to the latter there remains rather little scientific information to inform best-practice fire management (Blodau 2002).

Relatively few studies have directly examined the effects of fire on soil carbon fluxes or hydrology in U.K. peatlands. For the studies that do exist, most come from a single long-term experiment at Moor House in northern England. Here Ward *et al.* (2007) recorded increased net ecosystem respiration and reduced methane emissions as a result of burning. Additionally, Worrall *et al.* (2007) observed higher water tables in plots subject to more frequent managed burns. A larger number of studies have examined the effect of fire on the production of dissolved organic carbon though the results remain difficult to interpret and somewhat controversial. Holden *et al.* (2012) point to discrepancies between plot and catchment scale experiments and suggest that the results of catchment scale studies showing increased DOC production (e.g. Clutterbuck and Yallop 2010) should be treated with some caution.

Clear differences do exist in the severity of moorland fires and we can distinguish between high severity burns, that consume surface and ground fuels, whilst igniting or scorching underlying peat (e.g. Maltby *et al.* 1990) and lower severity prescribed burns that have more limited ecosystem effects (Davies *et al.* 2010). However, wildfires, though often intense, are not necessarily severe (Bullock and Webb 1995). There is thus a clear need to describe the extent to which fire severity varies in peatland ecosystems and to understand what processes drive this variation. During the springs of 2011 and 2012 a large number of intense and severe wildfires burnt across heaths and moorlands throughout the UK. The extent of these fires, associated environmental degradation and the costs of restoration have added to increasing concern about potential feedbacks between climate, fire frequency, fire severity and carbon fluxes from moorlands (e.g. Davies *et al.* 2008a). Research on the impacts of such fires on UK peatlands is urgently needed to inform the development of fire danger rating systems (e.g. Kitchen *et al.* 2006) and to fill fundamental knowledge gaps regarding fire, peatland and global change.

The aim of our project was to document variation in the severity and ecological effects of a spate of peatland wildfires that burnt during the springs of 2011 and 2012. Here we report the results of preliminary analyses of variation in i) peatland fire severity; ii) carbon lost from direct combustion of above-ground biomass and iii) changes in methane and carbon dioxide fluxes following burning.

Methods

Study sites

Though regional Fire and Rescue Services collect some data on the occurrence of wildfire there is currently no national system in place for reporting wildfire outbreaks. We therefore worked in collaboration with land management agencies, land owners and other stakeholder groups to identify a

number of fire locations that included coverage of variation in major north-south and east-west bioclimatic conditions and peatland types (Figure 1).

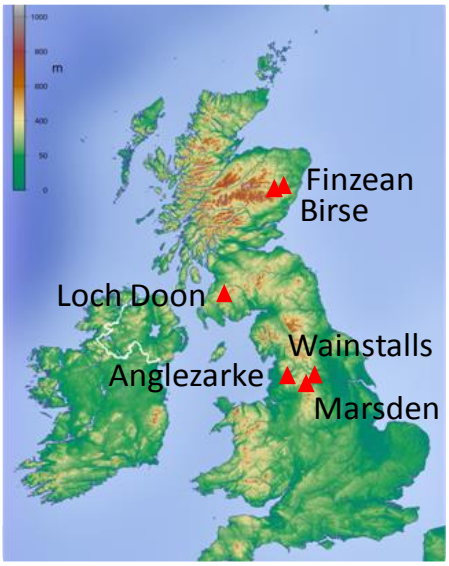

Figure 1. Location of wildfire study sites across the U.K. Sites covered a range of bioclimatic conditions and included fires in dry heath communities on shallow, stony organic soils (Finzean, Birse), active blanket bogs dominated by* Molinia caerulea *and* Sphagnum *spp. (Loch Doon) as well as wet and dry* Calluna*- and grass/sedge dominated moorland on peat soils (Angelzarke, Wainstalls, Marsden).

Each wildfire was assessed using a walk-over survey with the relevant land-owner. We created or obtained maps of the fire perimeter and carefully noted qualitative evidence of variation in fire severity. In each fire we selected three to six locations for further monitoring that best represented the range of severities we observed.

Monitoring fire severity

Fire severity was described using a modified form of the semi-quantitative Composite Burn Index (CBI; Key and Benson 2006). This method was adapted for use on treeless moorlands and bogs similarly to Schepers *et al.* (2014). The CBI uses qualitative descriptions of fire effects on a number of vegetation strata and ecosystem properties each scored on a rating of zero to three. These scores are then averaged within strata and the averages summed across strata to produce an overall severity index. Our method included assessment of fire effects on surface and ground fuel layers. We thus examined: litter/ light fuel consumption, duff/peat consumption, exposure of mineral soil, damage or loss of *Sphagnum* capitula, moss scorching and consumption, recovery of *Sphagnum*/moss species, percentage of shrubs top-killed, fine/crown fuel consumption, frequency of burnt shrubs or grass/sedge tussocks resprouting, evidence of new colonizers and the potential for changes in species composition.

CBI plots were circular, 20 m in diameter and established both as stand-alone plots in the fire interior and as paired burnt/unburnt plots close to the fire perimeter (Figure 2). For paired plots, we avoided edge-effects by ensuring the burnt plot centre was always located < 30 m from the edge of the fire. No part of any plot was < 5 m from the fire perimeter or, for unburnt plots, in obviously scorched vegetation. We were careful to ensure that burnt and unburnt plots had similar pre-fire fuel structures by locating them in the same pre-fire *Calluna* stand through careful observation of stem density and basal diameters either side of the fireline. Due to the large size of the wildfires, the substantial spatial separation of the plots and variation in pre-fire fuel structure we considered each CBI plot or paired-plot to be an independent observation in a manner similar to the "microplot" approach of Fernandes *et al.* (2000).

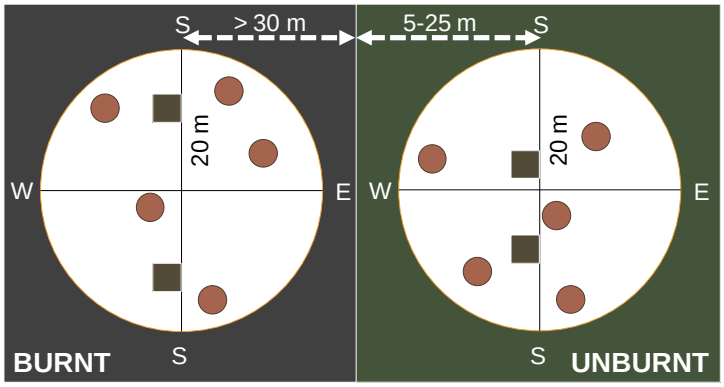

Figure 2. Layout of CBI monitoring plots showing the two fuel quadrats (squares), located at random distances along the N-S axis, and five soil gas flux chambers (circles) located at random co-ordinates in each plot

2.3. Variation in above ground carbon loss

Fuel consumption was assessed using destructive harvesting of fuel loads in two 50 x 50 cm quadrats located at random co-ordinates within the paired burnt/unburnt plots (two paired plots per fire). All above ground biomass was harvested down to the top of the peat. We harvested surface fuels (shrubs, grasses, etc.) separately from ground fuels (*Sphagnum* spp., other mosses + plant litter, grass/sedge tussock bases and duff). Fuel was also harvested in a similar manner from five gas flux chambers (diameter = 38 cm; see below) located at random locations throughout each plot. Samples were processed in the lab and dried at 80°C for 48 hours before being weighed. Fuel consumption was defined as average unburnt plot biomass minus average burnt plot biomass. Combustion completeness was defined as the proportion of fuel consumed and above-ground carbon loss was estimated by assuming all fuel components had a C proportion of 0.48 (Legg *et al.* 2010). We compared consumption and combustion completeness of our wildfires with data from 26 prescribed fires described by Davies *et al.* (2009). This comparison was however limited to changes in surface fuels (herbaceous and shrub species) as data on consumption of ground fuels were limited for the prescribed burns.

Total fuel consumption (i.e. all fuel components pooled) was analysed by making a square root transformation of the data and using a General Linear Mixed Model in the "lme4" package (Bates *et al.* 2013) of R 2.15.0 (R Development Core Team 2012). Plot and fire were defined as random effects whilst status (burnt/unburnt) and sample (chamber/quadrat ID) were defined as fixed effects. We initiated analysis using the full model (random slopes, according to status, and intercepts) and simplified the model by reference to AIC. Parametric bootstrapping was used to fit 95% confidence intervals around mean fire-level fuel consumption that accounted for uncertainty due to sampling variation in quadrats/chambers and plots.

2.4. Assessing soil carbon fluxes

Carbon dioxide and methane fluxes were assessed using samples taken from five gas flux chambers permanently located at random co-ordinates within each side of our burnt/unburnt plot pairs (Figure 2). The chambers were made of black plastic, had a diameter of ca. 38 cm and a volume of ca. 30 l. Chamber bases were buried 3-5 cm below the top of the peat. We made five measurements of the distance from the chamber top to the internal ground level in order to determine the installed chamber volume. As we were interested in variation in fire effects on the soil ecosystem we chose to contrast carbon fluxes in our burnt plots with a "zero severity burn" in the unburnt plot and in the absence of plant photosynthesis and respiration. This was achieved by removing all vegetation (surface and ground fuels) in the chambers down to the top of the peat. Any variation in flux was thus solely a result of varying fire effects on the soil. We acknowledge that the removal of vegetation can cause changes

in the production of root exudates which might alter the structure and activity of soil microbial communities. However, since the above ground components of plants were removed in both burnt and unburnt plots, we suggest any difference should be attributable to temperature pulses from the fire, scorching or heat induced alteration of peat structure. Chambers were sealed using metal lids and gas samples extracted using a syringe. The sample was then used to fill an airtight vial. Samples were extracted immediately following closure and at ten minute intervals thereafter to produce a total of five samples per chamber. Methane and carbon dioxide concentrations were analysed using a gas chromatograph and fluxes estimated by standard regression-based methods.

Due to the importance of soil temperature in determining peatland soil carbon fluxes (e.g. Updegraff *et al.* 2001) we buried iButton™ temperature loggers 2 cm below the top of the peat (and thus below overlying layers of moss, litter and duff in unburnt plots) in a random subsample of our paired plots. Two loggers were buried in each plot – one each in the burnt and unburnt subplot. Loggers recorded soil temperature hourly and were left in place for up to a month and half during August and September.

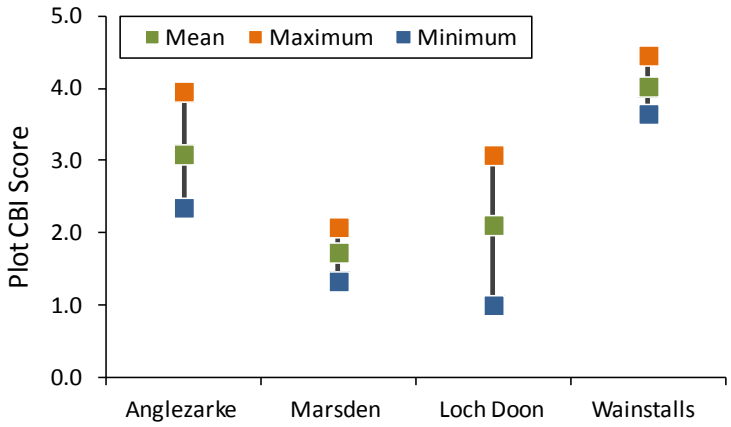

Figure 3. Variation in fire severity between and within four wildfires (data for Finzean to be analysed). Symbols show fire mean (green), minimum (blue) and maximum (orange) Composite Burn Index score.

Results

3.1. Variation in fire severity

Fire severity varied substantially both within and between individual fires. Interestingly average severity varied up to two-fold between fires but as much as three-fold within some fires (Figure 1).

3.2. Variation in above ground carbon loss

Total carbon loss varied substantially between and within wildfires (Figure 4) but average fire-level consumption was 0.64± 0.12 kg C m^{-2} across the five wildfires we studied. Average fire-level losses were relatively consistent with the exception of Finzean. Here mean carbon losses were both notably higher than other fires and the amount of variation between plots rather small.

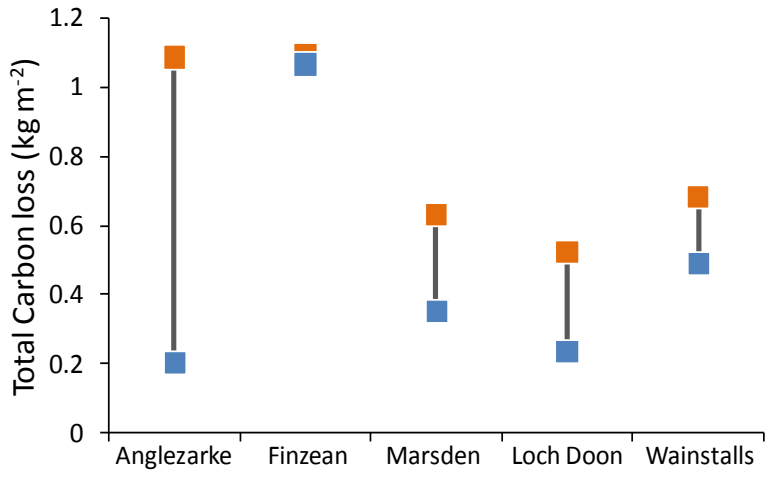

Figure 4. Variation in total (ground and surface fuels) carbon loss due to combustion across five wildfires. Blue and orange points are the minimum and maximum losses recorded respectively.

Fuel consumption was best described by a model than included the fixed effects of plot status (burnt/unburnt), quadrat ID and random intercepts for different fires and plots within fires and random slopes for different plots. The evidence for differences between fires was weak but was retained in the model as the relatively small sample size meant such differences couldn't be categorically discounted. Consumption thus varied substantially between plots within fires but there was limited evidence of a difference in average consumption between fires (Figure 2). Parametric bootstrapping was used to fit 95% confidence intervals and revealed substantial uncertainty in the prediction of mean fire fuel consumption due to sampling variation in quadrats/chambers and plots (Figure 2).

There was a linear relationship between pre-fire surface fuel load and surface fuel consumption but no obvious difference between the two types of fire in how the proportion of fuel consumed changed with increasing fuel load (Figure 6). Surface fuel consumption increased linearly with increasing fuel load up to a load of ca. 1.25 kg m^{-2}, thereafter fuel consumption appeared to reach an asymptote. This was reinforced by the apparent decline in combustion completeness with increasing fuel load. It was noticeable that the surface fuel load of the prescribed fires was, on average, higher than that found on the wildfire sites we monitored.

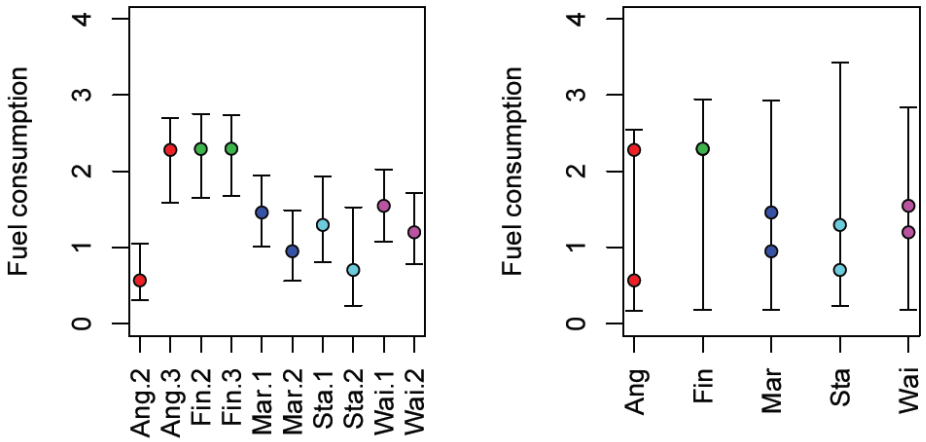

Figure 5. variation in total fuel consumption (kg/m2) between and within five different wildfires (left). Bootstrapped 95% Confidence Intervals showing uncertainty in fire mean fuel consumption due to within plot and within fire variation in fuel load (right).

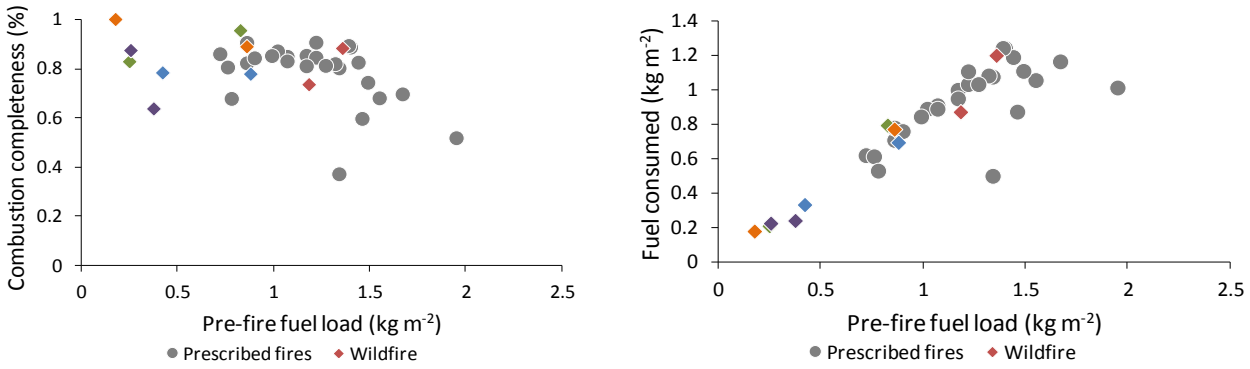

Figure 6. The relationship between pre-fire surface (herbaceous and shrub) fuel load and combustion completeness (left), and fuel consumption (right) for five wildfires (diamonds) and the 26 prescribed burns (grey circles) described by Davies et al. (2009). For wildfires each point is a CBI paired plot rather than a fire per se. Colours define each wildfire – Angelzarke (green), Finzean (red), Loch Doon (purple), Marsden (orange) and Wainstalls (blue). Note that for clarity errors are not shown here but they are likely to be large (see Figure 5)

3.3. Variation in soil gas fluxes

Both CO_2 and CH_4 fluxes were noticeably different between burnt and unburnt plots but substantial differences also existed between different fires. Methane fluxes were consistently lower on burnt sites whilst carbon dioxide fluxes were generally higher (Figure 7).

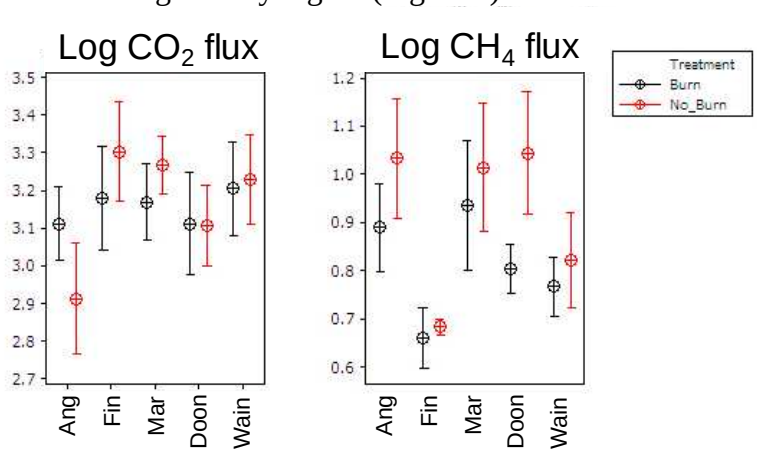

Figure 7. Variation in mean carbon dioxide (left) and methane (right) fluxes recorded in paired burnt/unburnt CBI plots across five different wildfire sites.

Substantial differences were recorded in both mean soil temperature and diurnal temperature trends between brunt and unburnt plots. Day-night temperature fluctuations in burnt plots were frequently more than twice that seen in unburnt plots (Figure 8).

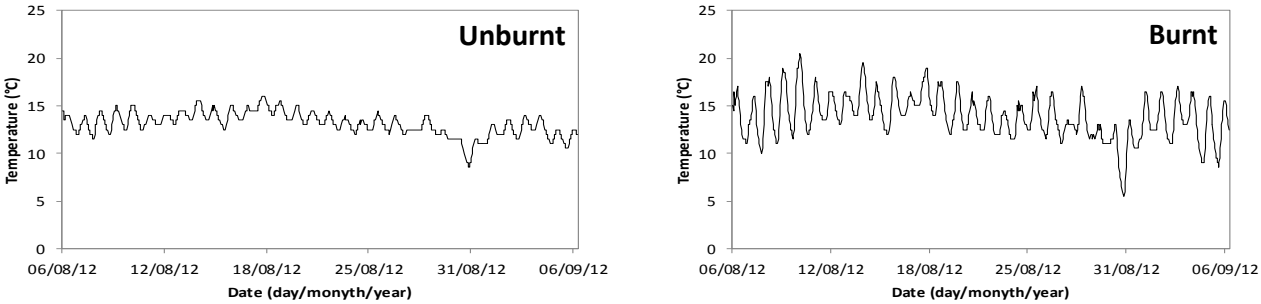

Figure 8. Example of typical patterns of diurnal soil temperature variation in unburnt and burnt plots

Discussion

Our results demonstrate substantial variation in fire severity both within and between individual wildfire events (Figure 4). Given the potential for substantial variation in fuel structure (Davies *et al.* 2008b) and fire weather (Legg *et al.* 2007) in the British uplands this is perhaps not surprising. A key finding of our work is therefore that robust assessment of the effects of wildfires requires substantial sampling effort. Variation in CBI and our estimates of fuel consumption were greater within a number of fires than that recorded, on average, between different burns. Managers needing to understand the effects of wildfires on landscapes, or researchers and policy makers wanting to quantify the effects of burning on landscape C storage, must therefore ensure that their monitoring is representative of this variation. Despite investing substantial monitoring effort in assessing fuel structure in burnt and unburnt stands the variation in fuel load encountered at both the sub-plot and fire levels mean we were unable to draw any robust conclusions about differences in consumption between fires (Figure 5). It is also clear that the estimate of mean carbon released by combustion we present should be treated with caution.

Though our monitoring captured a range of fuel structures it was clear from comparison with data from prescribed burns that this did not adequately reflect the range of fuel loads found on British peatlands (Figure 6). Broad differences in fuel consumption between and within wildfires could generally be related to pre-fire fuel composition. High levels of combustion completeness were recorded across all sites but this tended to be lower on wetter sites like Loch Doon. In such bog communities strong vertical gradients in the moisture content of standing *Molinia* litter may limit fuel consumption (Hamilton 2000). Prescribed fires in *Calluna*-dominated fuels generally consume all fine fuels < ca. 2 mm in diameter leaving behind larger, live woody stems (Davies 2006). This relationship is apparent in Figure 6 where the asymptote in fuel consumption as a function of fuel load is a consequence of the higher proportion of coarse, woody fuels in these older stands. In very severe burns this woody material may also be consumed but, the relationship we observed between pre-fire fuel load and fuel consumption (Figure 6) suggests that carbon release from the direct combustion of surface fuels only can be predicted from pre-fire fuel load for all but the most severe fires. Further analysis is needed to allow for comparison of consumption of ground fuels during prescribed burns and wildfires, and on fuel consumption during higher severity wildfires. This will allow us to determine whether, or under what burning conditions, differences in combustion processes operate and lead to altered rates of C emission.

For fires that do not lead to consumption or scorching of ground fuel layers and peat the carbon lost from combustion should, in theory, be of comparatively little concern. *Calluna* and other moorland plants such as *Molinia* and *Erica* spp. are able to regenerate rapidly both from seed and vegetatively (e.g. Hobbs and Gimingham 1984, Davies *et al.* 2010). Regeneration may, however, be delayed, lacking or follow alternative successional trajectories in older stands (Hobbs and Gimingham 1984, Davies *et al.* 2010), where fire severities are high (Legg *et al.* 1992) or where there are compounded

disturbances such as grazing and trampling by livestock (e.g. Legg *et al.* 1992). Understanding the consequences of wildfire for landscape carbon storage thus requires robust monitoring of post-fire vegetation regeneration. Assuming regeneration progresses communities back towards their pre-fire state, there are nevertheless substantial consequences of fire for carbon dynamics. Authors have provided contrasting data on dissolved organic carbon production and CO_2 and CH_4 fluxes and most of this information comes from low severity prescribed burns. Severe moorland wildfires have the potential to deliver large temperature pulses belowground, to remove insulating ground and surface fuel layers all of which may alter soil temperature (Figure 8), moisture, water table and microbial community dynamics. Previous authors (e.g. Worrall *et al.* 2007) have observed a raised water table in more frequently burnt sites and others were surprised to see reduced CH_4 fluxes following burning (Ward *et al.* 2007) at the same site. Our results mirror those recorded by for methane by Ward *et al.* (2007), albeit for wild rather prescribed fires and for a wider range of sites. There is this increasing evidence for a decline in CH_4 production in at least the first year following burning. Data on longer-term trends is now needed. Contrary to Ward *et al.* (2007), burning generally reduced CO_2 fluxes for our sites. Differences between burnt and unburnt plots were, however, very small for two of our fires and CO_2 production increased at Angelzarke. Our results suggest fire-related disturbance of microbial communities but identifying the underlying processes, and understanding site-to-site differences in response, will require further research. We also recorded substantial changes in diurnal soil temperature fluxes (Figure 8). Given that soil temperature is closely related to soil C flux (Updegraff *et al.* 2001) additional fine-temporal scale assessment of variation in C fluxes would be worthwhile.

In conclusion our data show that drawing robust conclusions about the implications of wildfire on ecosystem C dynamics is fraught with difficulties. Characterising the effects of fuel consumption is made difficult by substantial variation in fuel structure between and within individual fires and the need to understand the nature of post-fire regeneration. Wildfires appeared to have substantial effects on soil ecological processes generally leading to reduced CH_4 and CO_2 fluxes. At this point it is difficult to determine whether this is due to the direct impacts of the fires themselves or associated changes in vegetation and soil microclimate. Key objectives of our on-going research include:

- Quantifying the relationship between carbon fluxes and fire (CBI) severity
- Modelling variation in carbon fluxes to differences in fire weather
- Describing how vegetation recovery varies as a function of fire severity
- Defining the mechanisms by which fuel structure and fire weather control fire severity (see Grau *et al.* this volume).

Acknowledgements

Thanks are due to Emily Taylor, Sophie Philbrick and Roger Grau for field and lab assistance. Julia McMorrow and the England & Wales Wildfire Forum helped us obtain records of wildfires and our thanks go to all those who contributed data/information. We are particularly grateful to the owners and managers of the sites we used: Yorkshire Water, United Utilities, National Trust, Forestry Commission Scotland, Finzean Estate, Birse Community Trust, Bo Scholefield, Carl Prenton, Ian Harper, Kate Snow, Gemma Wren, Judith Patrick, Rob Soutar, Andrew Jarrott, Andrew Farquharson and Paul Chapman. This research was funded by the Natural Environment Research Council.

References

Bates D, Maechler M, Bolker B, Walker S (2013) lme4: Linear mixed-effects models using Eigen and S4. R package version 1.0-4. Available from: http://CRAN.R-project.org/package=lme4 [last accessed 15 Jul 2014].

Blodau C (2002) Carbon cycling in peatlands: a review of processes and controls. *Environmental Reviews,* 10 111-134.

Bullock JM, Webb NR (1995) Responses to severe fires in heathland mosaics in Southern England. Biological Conservation, 73, 207-214.

Clutterbuck B, Yallop AR (2010) Land management as a factor controlling dissolved organic carbon release from upland peat soils 2: changes in DOC productivity over four decades. *Science of the Total Environment*, 408, 6179-6191.

Davies GM (2006) Fire behaviour and impact on heather moorlands. PhD Thesis, The University of Edinburgh. Available from: https://www.era.lib.ed.ac.uk/handle/1842/2609 [last accessed 15 Jul 2014].

Davies GM, Gray A, Hamilton A, Legg CJ (2008a) The future of fire management in the British uplands. *International Journal of Biodiversity Science and Management*, 4, 127-147.

Davies GM, Legg CJ, Hamilton A, Smith AA (2008b) Using visual obstruction to estimate heathland fuel load and structure. *International Journal of Wildland Fire*, 17, 380-389.

Davies GM, Legg CJ, Smith AA, McDonald AJ (2009) Rate of spread of fires in *Calluna vulgaris*-dominated moorlands. *Journal of Applied Ecology*, 46, 1054-1063.

Davies GM, Smith AA, McDonald AJ, Bakker JD, Legg CJ (2010) Fire intensity, fire severity and ecosystem response in heathlands: factors affecting the regeneration of *Calluna vulgaris*. *Journal of Applied Ecology*, 47, 356-365.

Davies GM, Gray A, Rein G, Legg CJ (2013). Peat consumption and carbon loss due to smouldering wildfire in a temperate peatland. *Forest Ecology and Management*, 308, 136-144.

Dorrepaal E, Toet S, van Logtestijn RSP, Swart E, van de Weg MJ, Callaghan TV, Aerts R (2009) Carbon respiration from subsurface peat accelerated by climate warming in the subarctic. *Nature*, 460, 616-619.

Fernandes PM, Catchpole WR, Rego FC (2000) Shrubland fire behaviour modelling with microplot data. *Canadian Journal of Forest Research*, 30, 889-899.

Granström A, Schimmel J (1993) Heat effects on seeds and rhizomes of a selection of boreal forest plants and potential reaction to fire. *Oecologia*, 94, 307-313.

Hamilton A (2000) The characteristics and effects of management fire on blanket-bog vegetation in north-west Scotland. PhD Thesis, The University of Edinburgh.

Hobbs RJ, Gimingham CH (1984) Studies on fire in Scottish heathland communities II. Post-fire vegetation development. *Journal of Ecology*, 72, 585-610.

Holden J, Chapman PJ,Palmer SM, Kay P, Grayson R (2012) The impacts of prescribed moorland burning on water colour and dissolved organic carbon: a critical synthesis. *Journal of Environmental Management*, 101, 92-103.

Key CH, Benson NC (2006) Landscape Assessment (LA): Sampling and Analysis Methods. USDA Forest Service General Technical Report RMRS-GTR-164-CD. (Fort Collins, CO)

Kitchen K, Marno P, Legg C, Bruce M, Davies GM (2006) Developing a fire danger rating system for the UK. *Forest Ecology and Management*, 234, Supplement 1, S21.

Legg CJ, Maltby E, Proctor MCF (1992) The ecology of severe moorland fire on the North York Moors: seed distribution and seedling establishment of *Calluna vulgaris*. *Journal of Ecology*, 80, 737-752.

Legg CJ, Davies GM, Kitchen K, Marno P (2007) Developing a Fire Danger Rating System for the UK: FireBeaters Phase I final report. Report to the Scottish Wildfire Forum. Available from: https://www.era.lib.ed.ac.uk/handle/1842/3011 [last accessed 15 Jul 2014].

Legg CJ, Davies GM, Gray A (2010) Comment on "Burning management and carbon sequestration of upland heather moorland in the UK". *Australian Journal of Soil Research*, 48, 100-103.

Maltby E, Legg CJ, Proctor MCF (1990) The ecology of severe moorland fire on the North York Moors: effects of the 1976 fires, and subsequent surface and vegetation development. *Journal of Ecology*, 78, 490-518.

Mitra S, Wassmann R, Vlek PLG (2005) An appraisal of global wetland area and its organic carbon stock. *Current Science*, 88, 25-35.

R Development Core Team (2012). R: A language and environment for statistical computing. (R Foundation for Statistical Computing, Vienna, Austria)

Schepers L, Haest B, Veraverbeke S, Spanhove T, Vanden Borre J, Goossens R (2014) Burned area detection and burn severity assessment of a heathland fire in Belgium using airborne imaging spectroscopy (APEX). *Remote Sensing*, 6, 1803-1826.

Smith AN, Thomas B (1956) The nutritive value of *Calluna vulgaris* IV. Digestibility at three, seven and fourteen years after burning. *The Journal of Agricultural Science*, 47, 468-475.

Tharme AP, Green RE, Baines D, Bainbridge IP, O'Brien M (2001) The effect of management for red grouse shooting on the population density of breeding birds on heather-dominated moorland. *Journal of Applied Ecology*, 38, 439-457.

Turetsky MT, Wieder K, Halsey L, Vitt D (2002) Current disturbance and the diminishing peatland carbon sink. *Geophysical Research Letters*, 29, 21-1-21-4.

Updegraff K, Bridgham SD, Pastor J, Weishampel P, Harth C (2001) Response of CO_2 and CH_4 emissions from peatlands to warming and water table manipulation. *Ecological Applications*, 11, 311-326.

Ward SE, Bardgett RD, McNamara NP, Adamson JK, Ostle NJ (2007) Long-term consequences of grazing and burning on northern peatland carbon dynamics. *Ecosystems*, 10, 1069-1083.

Worrall F, Armstrong A, Adamson JK (2007) The effects of burning and sheep-grazing on water table depth and soil water quality in a upland peat. *Journal of Hydrology*, 339, 1-14.

Chapter 3
Fire Management

A focused analysis on lean fire management systems

Jeremiah S. Fugate[a], M. Abbot Maginnis[b], Nelson K. Akafuah[c], Kozo Saito[d], Mark A. Finney[e], Jason Forthofer[f]

[a] *Univ. of Kentucky, Lexington, KY 40506, jeremiah.fugate@uky.edu*
[b] *Univ. of Kentucky, Lexington, KY 40506, amaginnis@uky.edu*
[c] *Univ. of Kentucky, Lexington, KY 40506, nelson.akafuah@uky.edu*
[d] *Univ. of Kentucky, Lexington, KY 40506, ksaito@uky.edu*
[e] *USDA Fire Sciences Laboratory, Missoula, MT 59808, mfinney@fs.fed.us*
[f] *USDA Fire Sciences Laboratory, Missoula, MT 59808, jaforthofer@fs.fed.us*

Abstract
A primary role of the Incident Command System (ICS) is to learn from past incidents, particularly in the case of wildland fires. As such, a successful ICS application is critically dependent on its capability to function as a learning organization in order to continuously improve emergency response effectiveness. The objective of this study is to evaluate the potential to apply fundamental principles of the Toyota Production System (Lean manufacturing) to improve the learning effectiveness within the ICS. An in-depth review of literature and training documents regarding both systems reveals common goals and functional similarities, including the importance of continuous improvement. These similarities point to the validity of applying Lean principles to the ICS. Subsequently, a focus on systematic problem solving and the learning function of the ICS culminated in the discovery of gaps between the two systems. Finally, recommendations are made that the application of systematic problem solving including rigorous root cause analysis and effective standardization of successful problem solving countermeasures could be adapted from Lean principles in order to benefit the system.

Keywords*: Toyota Production Systems, Lean Manufacturing, Fire Management, Wildland Fire Management, Incident command System.*

Introduction

The objective of this study is to evaluate the potential to apply fundamental principles of Lean Manufacturing (LM) to facilitate continuous improvement of the Incident Command System (ICS). The ICS drives management of all major incidents including human and lightning caused wildfires in forests, grasslands, and preserved or monitored areas of the United States. The term "Lean" indicates that operational methods based on Toyota Production System (TPS) principles are in place within some model area of, or throughout the entirety of, an organization.

1.1. Wildland Fire in the United States

The inevitability of wildland fire occurrence has prompted dedicated annual seasons where precautions are taken and emphasized publically in hopes of reducing the frequency and severity of incidents. Since 2005, annual costs for wildland fire suppression have ranged from approximately one to two billion U.S. dollars for private, state, and federal land combined (National Interagency Fire Coordination Center, 2014). *Figure 1* illustrates the variation of wildland fire suppression costs form 2005 to 2013. According to the figure, suppression costs in 2013 reached $1.74B, a reduction from $1.9B in the previous year (National Interagency Fire Coordination Center, 2013). However, the National Oceanic and Atmospheric Administration (NOAA, 2012) classified 2012 as a warmer and drier year than average, which likely increased the risk of wildfires.

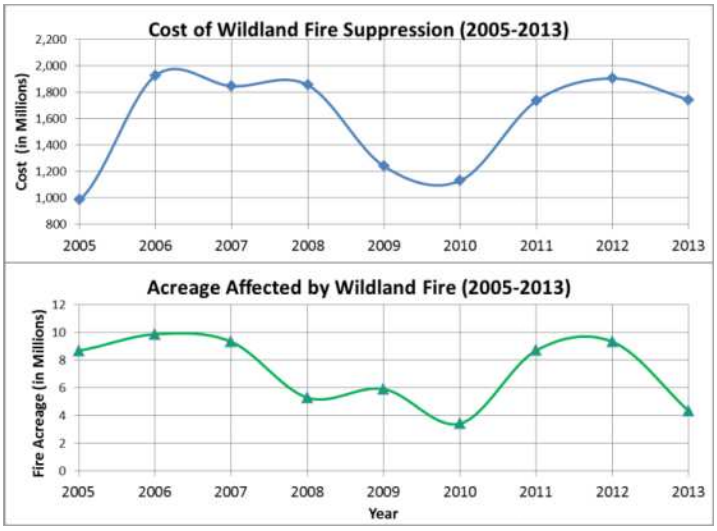

Figure 1. Wildland Fire Statistics (2005-2013) (National Interagency Fire Coordination Center, 2013).

ICS plays a key role in effectively managing hazardous incidents and preventing loss of valuable lives. To do this, ICS streamlines the overall decision making process to effectively cope with all aspects of urgency associated with wildland fire, ranging from strict monitoring of an incident to full extinguishment depending on geographic and fuel management considerations, proximity to wildland-urban interfaces (WUI), weather conditions, and available resources. .

Management Systems

Using available key references, the ICS is compared with a successful LM management system to identify similarities and differences. As main facilitators of the ICS use throughout the country, the Federal Emergency Management Agency (FEMA) and the National Incident Management System (NIMS) provide training documents, while the University of Kentucky's Lean Systems Program (UK-LSP) provides a variety of courses on LM principles and practices created through 20 years of close collaboration with Toyota. Over those 20 years, UK-LSP has served more than 20,000 people from different types of organizations including manufacturing, food service industry, healthcare and public services, as well as education.

The Incident Command System

ICS is an expert system developed in response to lessons learned during past experiences. In the fall of 1970, southern California suffered significant fires that burned over 500,000 acres, more than 700 structures, and caused 16 fatalities (Countryman, 1974). In response, the FIRESCOPE program was developed as "the first practical application of systems design to a major, complex wildland fire management operational problem." The FIRESCOPE team discovered that inefficient interagency communications and unclear organizational structures within the fire management system were regularly at fault during out of control incidents (Chase, 1980). As part of the FIRESCOPE program, the ICS evolved throughout the 1970s and was implemented as a stand-alone management response system in southern California in the 1980s (Chase, 1980). Over time, the ICS proved its effectiveness in meeting the demands of each fire based incident by uniquely scaling an organizational structure and facilitating coordination of resources (Buck *et al*, 2006). In the early 2000s, the ICS was extended nationwide through the National Response Framework (NRF) to create a uniform management system for all incidents (not just fire related) under a National Incident Management System (NIMS). Today, the ICS emphasizes the importance of systematic problem solving and a standardized planning process

to meet its objectives. These activities are supported by a dynamic organizational structure based on clear roles and standardized terminology (Deal *et al*, 2010; Emergency Management Institute, 2014).

Lean Manufacturing

The Toyota Production System was developed in response to lessons learned during past experiences, and thus, shares similar background with the ICS. The tough economic climate of post-World War II Japan led Japanese manufacturing companies to fight for their very survival. In 1950, American scientist and statistician W. Edwards Deming travelled to Japan to assist post-war recovery efforts. Deming introduced Japanese officials to the concept of statistical quality control (Deming and Orsini, 2013) and the idea that focusing on "built-in" quality rather than inspection could increase the quality of products or services without increasing costs (Deming, 1986). Deming also introduced the Japanese to the Plan-Do-Check-Act (PDCA) learning cycle, as well as his "14 Principles of Management" (Deming, 1986), both of which serve as the foundation for managing the ability to achieve and sustain built-in quality. Eventually these ideas were embraced and successfully implemented into many Japanese companie, including Toyota, who continue to apply them, eventually developing the Toyota Production System (TPS or Lean Manufacturing).

As it stands today, TPS places a great deal of importance on "providing products and services with craftsmanship, pride, zeal, history, spirit, joy, and more" (Saito *et al*, 2012) as well, the company strives to promote lifelong learning in its employees to produce well-rounded professionals who possess not only well-developed specialized technical skills but also overall knowledge and keen interest in continuously improving their work (Saito and Finney, 2014). Fujio Cho, the most respected world leader in TPS states: *a company must provide service to society, and the way a company must go about that is to produce good products honestly and consistently without compromise* (Saito *et al*, 2012), *offering service-oriented concepts to create a highly effective and efficient modern system consisting of people, information, machine and material* (Cho 1995).

The UK-LSP teaches a standard definition of what Lean should mean to an organization. The definition of "True Lean" is meticulously crafted as illustrated in the following 5 points: 1) The group by themselves, 2) use systematic problem solving, 3) to improve the work they do, 4) towards achievement of the company's targets and goals, 5) when and only when the company culture is the reason the improvement occurs (Lean Systems Program, 2013). Each point of this definition holds a certain principle of TPS. The first point focuses on the workers and places them first in the definition of "True Lean," signifying their importance in the system. The second point states that there exists a systematic method of problem solving. The third point stresses the focus on continuous improvement but only within the work that one is responsible for, not in other sections outside of their control. The fourth and fifth points outline that the company's culture is what drives the system towards achieving the measurable targets and goals set by the company. The foundation of a Lean system is standardization and revision of those standards through diligent problem solving to resolve abnormalities, to reduce/eliminate waste, and to continuously improve the system's ability to provide products or services (Lean Systems Program, 2013, Saito and Finney, 2014).

3. Discussions

The dynamic nature of the ICS mission is met using a best practices approach, which relies heavily on its ability to learn from previous incidents indicating that learning occurs not only on an individual basis, but also at an organizational level (Fiol and Lyles, 1985). The application of Lean principles and practices have been shown to greatly increase individual learning, and by extension, organizational learning (Maginnis, 2013). Because of this, Toyota has been called "the gold standard" of learning organizations (Liker and Hoseus, 2008). The PDCA learning cycle encourages the continuous improvement typical of learning systems because of its reliance on timely operational information feedback (Argyris, 1982, Spears and Bowman, 1999, Hall, 2006). The need to develop an ever-

increasingly effective learning organization provides a common goal for both LM and ICS, and indicates that the ICS could benefit in its efforts for continuous improvement by adopting Lean principles. To support this claim, we need to look closely at the ICS: their key functions and components.

Figure 2 provides a diagram of organizational structures and direction of communication flow for LM and ICS, where two-way communication and workforce education play a key role in success.

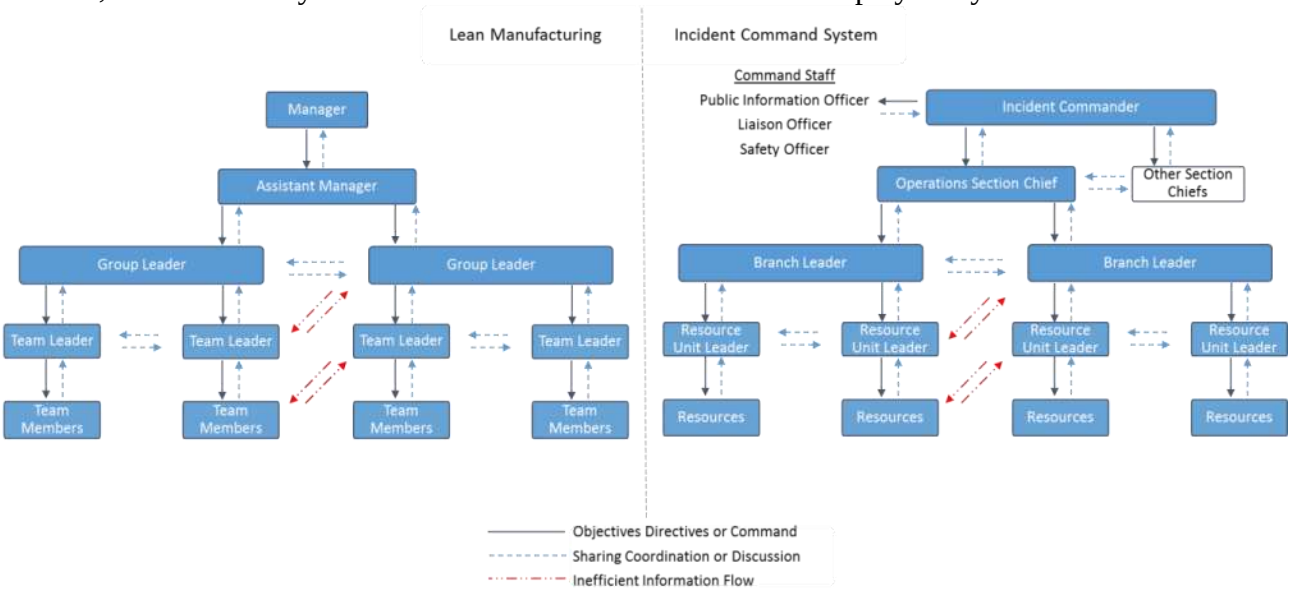

Figure 2. Comparison of structure, roles, and information flow for Lean and ICS.

Groupings within the ICS are comprised of 3 to 7 individuals per supervisor to improve management (Emergency Management Institute, 2014). Similarly, Lean systems employ the same type of control span for supervisors to have around 4 to 6 members reporting to them. Each system also has standards in place to inform workers of their role and corresponding responsibilities. In Lean systems, standardized work is developed and maintained to promote stability and recognition of abnormalities. Similarly, the ICS employs Standard Operating Procedures (SOPs) that promote the best known practices based on previous responses for the same purpose.

Figure 3 shows that the ICS problem solving method shares the same foundation of PDCA as LM problem solving, but that it differs from LM in one key aspect, the focus on problem recurrence.

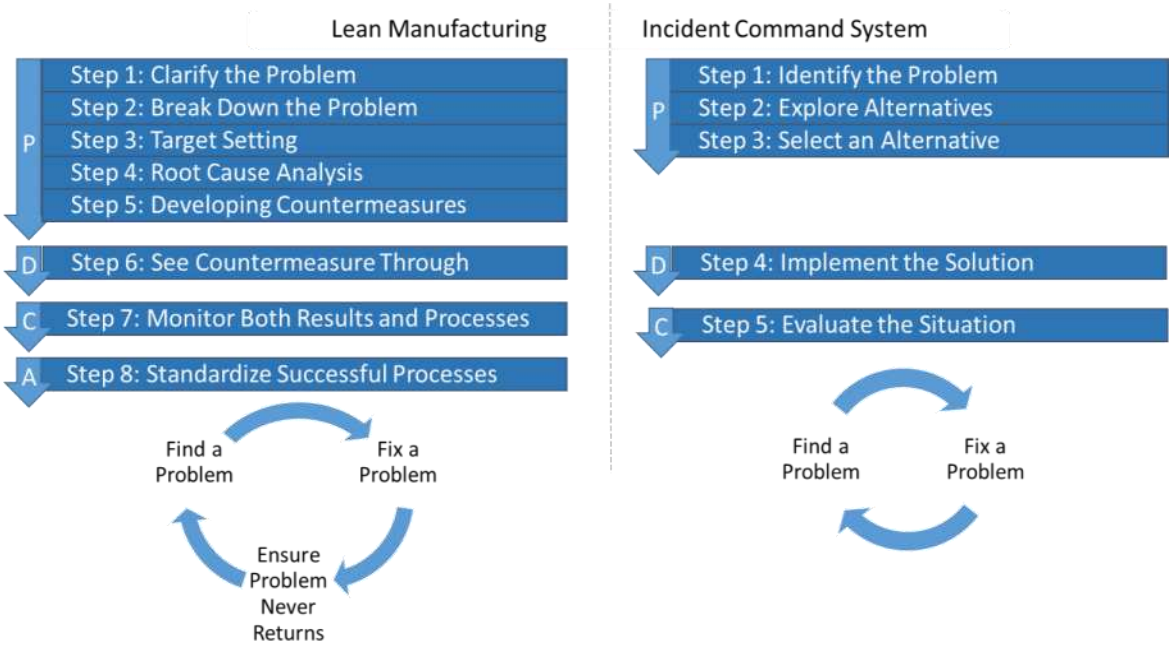

Figure 3. Comparison of Problem Solving Methods used in Lean and the ICS.

A high emphasis is placed on planning in both methods during the initial stage to better understand a problem and develop effective solutions. The ICS method has supportive materials to guide the user towards clarifying, breaking down, and setting goals for problems in the first step of its method (Emergency Management Institute, 2014). LM emphasizes root cause analysis and standardization of successful results following the PDCA to promote the cycle (finding/fixing a problem and tracing back to a root cause to prevent recurrence) (Lean Systems Program, 2013). Unsuccessful applications of LM typically result from an over-emphasis on immediate improvement which often ignores the importance of thorough problem solving and well maintained standardization (Angelis *et al*, 2011). The ICS training documents do not explicitly state standardization and incorporation as part of the current best method, but they are clearly required for continuous improvement, since resolving issues without finding the root cause will risk in recurrence of problems. The ICS process shown in *Figure 3* encourages finding and fixing problems, but will not prevent recurrence unless problems are traced to the root cause, and the results are incorporated into the standard procedures of the ICS.

Donahue and Tuohy (2006) recognized recurrence of problems in their analysis of learning capabilities within the ICS. After careful review of post incident reports, they concluded the need for the drive and ability to solve problems permanently rather than suffer them repeatedly (Donahue and Tuohy, 2006). Moynihan (2009) further explored the concepts of organizational learning in the ICS with regards to learning that takes place during the management of an incident (intra-crisis learning) and learning that takes place as reflection outside of an incident (inter-crisis learning). Moynihan also noted that the development and revision process taking place during inter-crisis learning would effectively minimize the amount of intra-crisis learning required (Moynihan, 2008).

Figure 4 demonstrates the ICS cycle of continuously evaluating how effectively it responds through each iteration of addressing incidents (Fires 1,2,3,…,n). The ICS then uses this data from each incident to improve the efficiency of response and goes on to repeat the process.

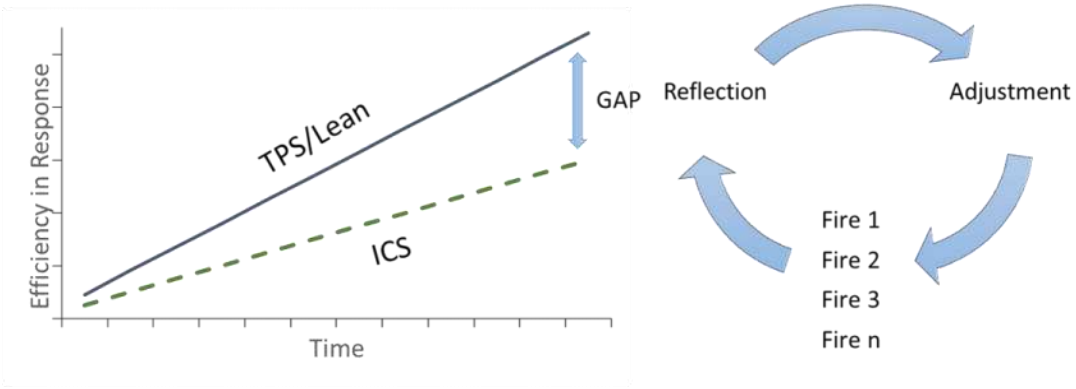

Figure 4. Anticipated Incremental Improvement of TPS/Lean organizations versus the ICS (based on Maginnis, 2013).

The figure also illustrates the anticipated gap that would occur between systems applying TPS/Lean methods and the ICS without root cause analysis and strict adherence to standardizing successful results (Maginnis, 2013).

Conclusions

The robust learning cycle present within the Lean method of PDCA facilitates continuous improvement when followed rigorously. This is due to a deeper level of learning achieved from investigations of root cause to eliminate problems (Tucker and Spears, 2002). In addition, Lean systems retain and spread information regarding improvements throughout the system by continual revision of standards and effective communication in response to problem solving successes. This also serves to drive the system towards future efforts for continuous improvement as goals have been effectively raised and set. The Incident Command System attempts to follow the PDCA cycle, but if the system struggles with problem recurrence as suggested by the literature, application of root cause analysis may be able to significantly contribute to the effectiveness of future emergency responses. Furthermore, ICS training documents regarding problem solving do not guide the user to post-problem solving efforts intended to retain and spread knowledge throughout the system. This highlights an area where loss of valuable incident based knowledge would occur, which could be remedied through more diligent revision of standards.

Many factors are understood to impact the use and effectiveness of the ICS regardless of system design itself. Moynihan (2009) stated that barriers to intra-crisis learning may result from limited time, political consequence, and weak working relationships between responders. As well, a recent comprehensive literature review published by Jensen and Waugh (2014) noted various factors regarding the application of ICS procedures within various emergency response areas. In order to improve the system overall, it is important to maintain continuous improvement efforts within areas that do use the ICS regularly, such as the firefighting community. These efforts would result in a model area of the system that demonstrates efficiency and effectiveness to lead by example and encourage further integration as a unified response community.

Acknowledgements

The first author, JSF has been supported by the Institute of Research For Technology Development (IR4TD) “Lean Systems Graduate Fellowship” for the duration of his MS studies at the University of Kentucky.

References

Argyris, C. (1982). Reasoning, Learning and Action: Individual and Organizational. San Francisco, CA, Jossey-Bass.

Angelis, J., Conti, R., Cooper, C., & Gill, C. (2011). Building a High-Commitment Lean Culture. *Journal of Manufacturing Technology Management, **22***(5), 569-586.

Buck, D. A., Trainor, J. E., & Aguirre, B. E. (2006). A Critical Evaluation of the Incident Command System and NIMS. *Journal of Homeland Security and Emergency Management, **3***(3), n. pages.

Chase, R. A. (1980). FIRESCOPE: A New Concept in Multiagency Fire Suppression Coordination. Berkeley, California: U.S. Department of Agriculture, Forest Service, Pacific Southwest Forest and Range Experiment Station, General Technical Report PSW-040, 17 p.

Cho, F. (1995). *Toyota Production System, Principles of Continuous Learning Systems.* (K. Saito, Ed.) McGraw-Hill.

Countryman, C. M. (1974). Can Southern California Wildland Conflagrations be Stopped? Berkeley, California: U.S. Department of Agriculture, Forest Service, Pacific Southwest Forest and Range Experiment Station, General Technical Report PSW-007, 11 p.

Deal, T., Bettencourt, M. d., Huyck, V., Merrick, G., & Mills, C. (2010). *Beyond Initial Response: Using the National Incident Management System's Incident Command System.* Authorhouse.

Deming, W. E. (1986). *Out of the Crisis.* Cambridge, Massachusetts: Massachusetts Institute of Technology. Center for Advanced Engineering Study.

Deming, W. E., & Orsini, J. N. (2013). *The Essential Deming: Leadership Principles from the Father of Quality Management.* New York: McGraw-Hill.

Donahue, A. K., & Tuohy, R. V. (2006). Lessons We Don't Learn: A Study of the Lessons of Disasters, Why We Repeat Them, and How We Can Learn Them. *Homeland Security Affairs*. Retrieved from http://hdl.handle.net/10945/25094

Emergency Management Institute. (2014). ICS Training Courses: IS-100.b, IS-200.b, IS-241.b. [Department of Homeland Security, Federal Emergency Management Agency]. Retrieved April 2014, from Emergency Management Institute: https://training.fema.gov/EMI/

Fiol, C. M., & Lyles, M. A. (1985). Organizational Learning. *Academy of Management Review, **10***(4), 803-813.

Hall, A. (2006). Introduction to Sustainable Quality Systems Design: An Integrated Approach from the Viewpoints of Dynamic Scientific Inquiry Learning and Toyota's Lean System Principles and Practices. Lexington Kentucky.

Jensen, J., & Waugh, W. L. (2014). The United States' Experience with the Incident Command System: What We Think We Know and What We Need to Know More About. *Journal of Contingencies and Crisis Management, **22***(1), 5-17.

Lean Systems Program. (2013). Lean Three Week Public Certification Series: Class Notes and Handouts. Lexington, Kentucky: [University of Kentucky College of Engineering, Institute of Research for Technology Development].

Liker, J. K. & Hoseus, M, (2008). Toyota Cultur; the Heart and Soul of the Toyota Way, New York, NY. McGraw-Hill

Maginnis, M. A. (2013). The Impact of Standardization and Systematic Problem Solving on Team Member Learning and its Implications for Developing Sustainable Continuous Improvement Capabilities. *Journal of Enterprise Transformation*, **3**, 187-210.

Moynihan, D. P. (2008). Learning Under Uncertainty: Networks in Crisis Management. *Public Administration Review, **68***(2), 350-365.

Moynihan, D. P. (2009). From Intercrisis to Intracrisis Learning. *Journal of Contingencies and Crisis Management, **17***(3), 189-198.

National Interagency Fire Coordination Center. (2013). *Federal Firefighting Costs (Suppression Only).* Retrieved from http://www.nifc.gov/fireinfo/fireInfo_documents/SuppCosts.pdf

National Oceanic and Atmospheric Administration. (2012, December). *State of the Climate: Drought for Annual 2012.* Retrieved January 2014, from National Climatic Data Center: http://www.ncdc.noaa

Saito, A. and Saito, K., Edt. (2012). *Seeds of Collaboration: Seeking the Essence of the Toyota Production System,* Monterey, Kentucky: Larkspur.

Saito, K., & Finney, M. A. (2014). Scale Modeling in Combustion and Fire Research. *Journal of the Combustion Society of Japan, **56**, to appear*.

Spear, S., & Bowen, H. K. (1999). Decoding the DNA of the Toyota Production System. *Harvard Business Review, **77***(5), 97-106.

Tucker, A., Edmondson, A. C. & Spear, S. (2002). When Problem Solving Prevents Organizational Learning. *Journal of Organizational Change Management,* **15**(2), 122-137.

A tool for mapping rural-urban interfaces on different scales

Christophe Bouillon [a], Fernandez Ramiro MM[b], Sirca C[cd], Fierro Garcia B[b], Casula F[c], Vila B[b], Long Fournel M[a], Pellizzaro G[e], Arca B[e], Tedim F[f], Trebini F[c], Derudas A[c],Cane S[c]

[a] *Irstea, Ecosystemes méditerranéens et risques , Aix-en-Provence, France, christophe.bouillon@irstea.fr*
[b] *Tragsatec, Madrid, Spain, mfra@tragsa.es*
[c] *Dipartimento di Scienze della Natura e del Territorio , University of Sassari, Italy,cosirca@uniss.it*
[d] *CMCC, Euro-Mediterranean centre for Climate Change, IAFENT Division, Sassari, Italy*
[e] *Institute of Biometeorology (CNR-IBIMET), Sassari, Italy, g.pellizzaro@ibimet.cnr.it*
[f] *Faculdade de Letras, Universidade do Porto, Portugal, ftedim@letras.up.pt*

Abstract
The aim of this paper is to present the methodologies, a software and results developed in the European FUME program to map the rural-urban interfaces (RUI).
Three methodologies were set up for RUI mapping: two on the local scale (the community scale) and one on the global scale (the European scale).
The first local scale method was developed in a French context by IRSTEA. In this case the RUI is defined by a radius of 100 metres around each house located at a distance inferior to 200 metres from forests or scrublands. The building density was used to create four classes of housing configuration. Then the structure of vegetation was characterized and mapped to emphasize its horizontal continuity with landscape ecology metrics. The RUI map was created by a combination of housing configuration and vegetation characterisation.
The second local scale method developed by TRAGSATEC is based on three phases. First a settlement map creation with the union of a land use cover and a vegetation cover defines the housing and the landscape that surrounds them. Then a buffer is created around settlements which are located at a distance inferior to 400 m from the forest; its size depends on the difficulty in protecting the houses against fire. In the final phase the different types of RUI are defined from the type of settlement and vegetation-settlement connection around houses.
The global scale method developed by IRSTEA makes possible the comparison of the situations and the importance of RUI in the different European countries.
On the global scale, the rural urban interfaces are defined by a radius of 400 metres around houses located at less than 200 metres from forests or shrubland. The global rural urban interface map results from the combination of criteria from the Corine Land Cover database and from the soil sealing database.
A major step of the work was the development of a software named RUImap with the three different methods above.
The use of the tool could be very advantageous for fire risk analysis on RUI scale, and for local quantification of fuel charge and continuity. This information linked with the direct knowledge of the general context is very important for the local fire risk assessment.

Keywords*: forest fire, wildland urban interface, rural urban interface, software, geographic information system, fire prevention, mapping.*

Introduction

Each summer wildfires burn 500 000 ha of forests in the European Mediterranean regions (source EFFIS). 90% of forest fires are of human origin and most of them start in the wildland-urban interfaces. A better understanding of these spaces was obtained through numerous studies in the USA and Canada. The description and characterization of these interfaces have been developed at Irstea (Lampin C., 2009). To make operation easy and fast, an ArcGis extension was developed to create maps on a large area. A first prototype of the software was developed with funding from the FIREPARADOX Program (FP6) .The first operational version

of this tool and user's guide (Lampin –Maillet *et al*, 2010) were created in 2010 with the support from the Ministry of Ecology and published and distributed to regional services.
The framework of the European FUME (Forest fires under climate, social and economic changes in Europe, the Mediterranean and other fire-affected areas of the world) program has defined the creation of a common tool to map rural urban interfaces (RUI). It is a WUI concept for all types of interconnections between the urban area and forest areas around, or wildlands with agricultural areas and with various types of vegetation. Within RUI, buildings and human infrastructures are closely mixed with fuel vegetation and create high wildfire risk. The dynamics can be controlled by land management and planning measures.

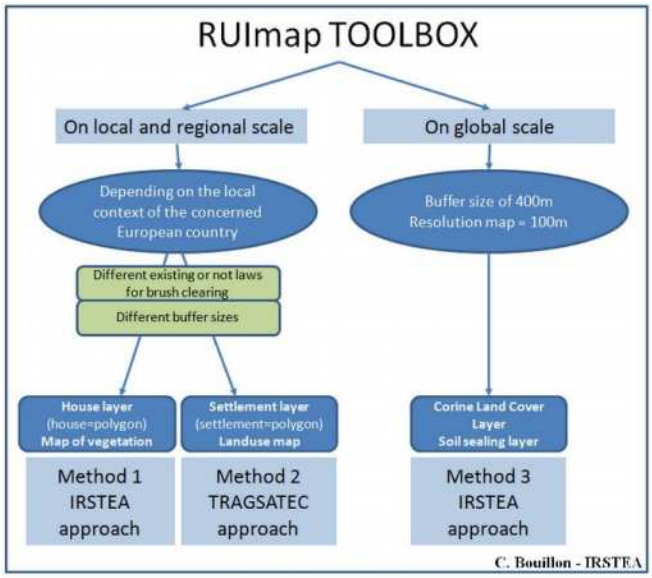

Figure 1. Schema of the tool

Three partners are involved in the creation and testing of this tool: Tragsatec, Spain; Irstea , France and the University of Sassari , Italy. Tragsatec developed a method for mapping interfaces on the local (municipal) level. Irstea developed two methods , a local method by improving the method already set (Lampin&Bouillon, 2011) and a global method, the European scale. The University of Sassari is responsible for testing and validating the results with data from three sites located in Spain, the Alicante region , in France , the Bouches-du-Rhône and in Sardinia, Italy. All developments were made with the ESRI ™ ArcGIS ™ platform and were integrated by Tragsatec in a common software called RUImap (Figure 1). Some recent uses of the methods and maps presented in this paper show a direct operational use of the results to improve the knowledge of the territory under the RUI approach and mapping.

Methods

Local scale Irstea

In the methodology developed in France (C. Lampin -Maillet , 2009), RUI is defined according to the July 9th, 2002 French Forest Orientation Law which makes brush clearing obligatory within a maximum radius of 100 metres around each house located at a distance inferior to 200 metres from forests (Figure 2).

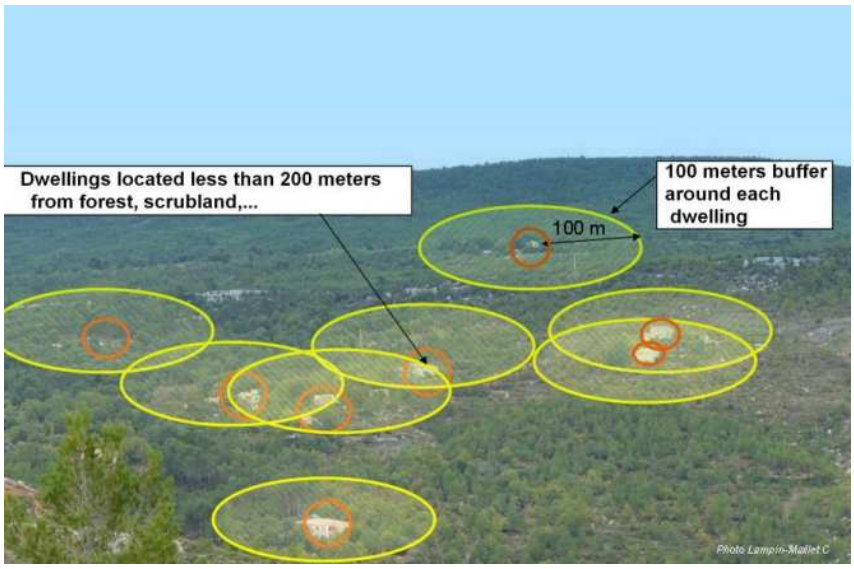

Figure 2. RUI definition

The 12 types of RUI (Figure 3) are created by integrating the density of buildings with a vegetation structure, more or less continuous. The process includes a combination of four housing configurations based on building density (isolated: from 1 to 3 buildings, scattered: from 3 to 50 buildings, dense: more than 50 buildings and very dense: more than 50 buildings at a distance of less than 15m between buildings) and three vegetation connectivity types (null, low, high) based on a landscape metrics : Aggregation Index (AI) (Turner, 1990), which can be mapped using FRAGSTATS3.3© software (McGarigal & Marks, 1994).

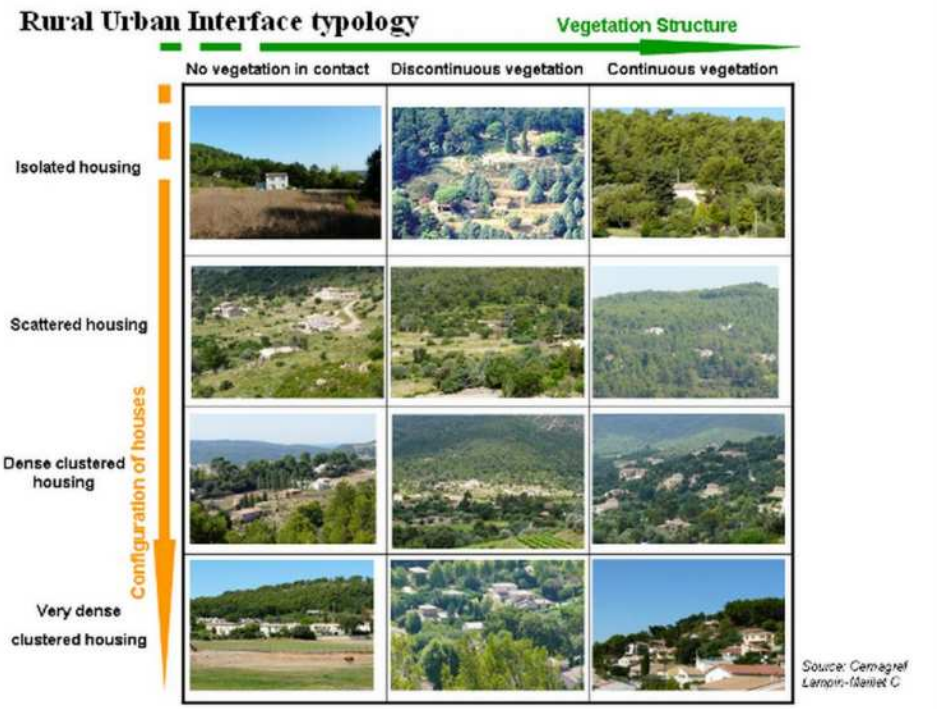

Figure 3. The 12 types of RUI

The map was created by the tool and set up with a colour code for an easy interpretation. (Figure 4)

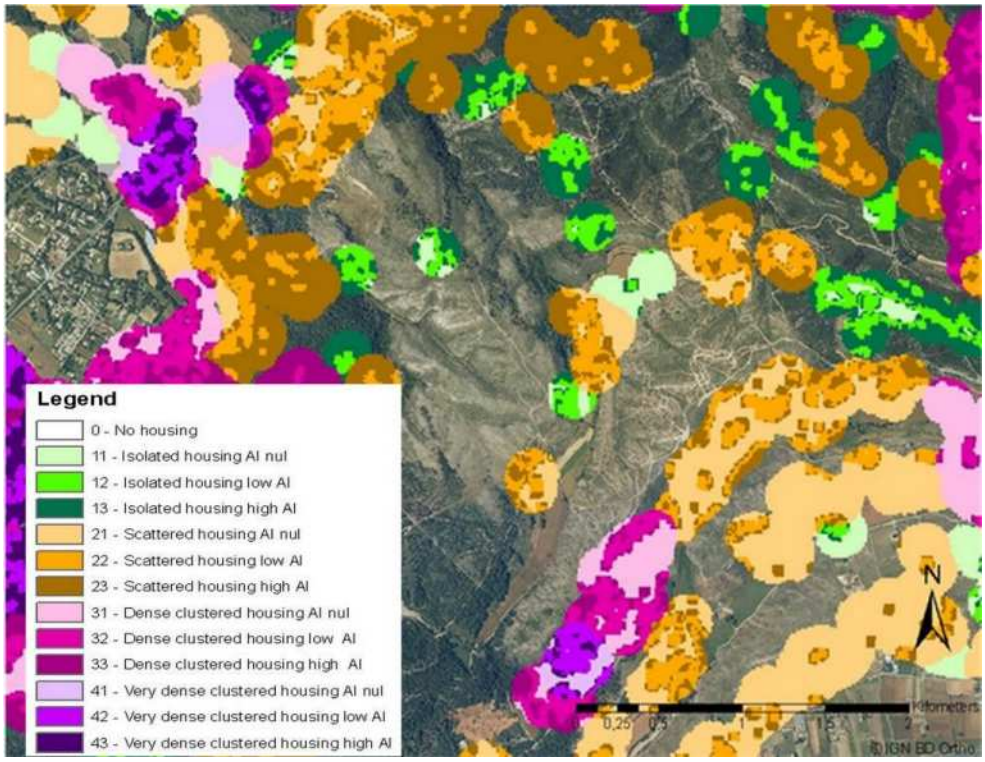

Figure 4 Local scale RUI map

Methods Local scale Tragsatec

The second local scale method was developed by TRAGSATEC. The method is based on three phases. First a settlement map creation with two layers : a land use cover (in Spain : SIGPAC) and a vegetation cover (the National Forest Map of Spain). The result of the union of the layers is a territory which is distributed in plots depending on the housing (Figure 5) - urban cores, spread buildings, isolated houses, etc... - and the different uses of land - forestry or agricultural -, taking as a basic aspect how the dispersion of the buildings is on the land and the landscape that surrounds them with the rules defined below:

- Urban area (plot > 50 ha)
- Habitat in agricultural areas (1 ha < plot <50 ha, forest < 30%)
- Habitat in forest areas (1ha < plot <50 ha, forest >= 30 %)
- Habitat dispersed in agricultural area (plot < 1 ha , forest < 30% , 3 > buildings > 5)
- Habitat dispersed in forest areas (plot <1 ha , forest >= 30% , 3 > buildings > 5)
- Habitat isolated agricultural area (plot < 1 ha , forest < 30% , buildings < 3)
- Habitat isolated forest area (plot < 1 ha , forest >= 30% , buildings < 3).

The second phase is a buffer creation. The Rural-urban interfaces only are considered in settlements which are located at a distance inferior to 400 m from the forest (according to the Regional Spanish laws). A buffer is created around the established settlements from the first phase and its size depends on the difficulty in protecting the houses against fire. In the final phase the different types of RUI are defined from the type of settlement and vegetation-settlement connection around houses, the buffer for each type of settlement is the area called the rural-urban interface.

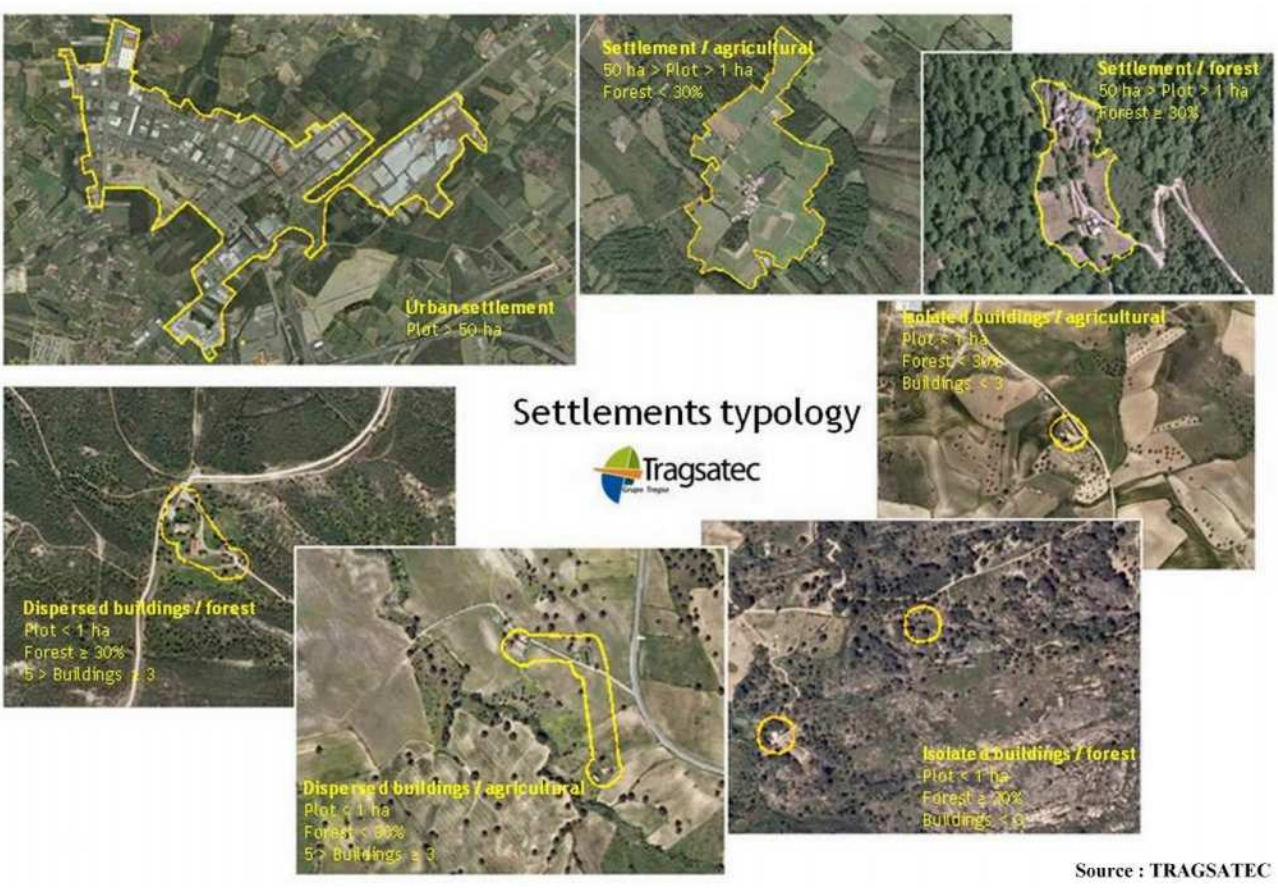

Figure 5. Tragsatec settlement typology-

The Rural-urban interfaces are considered in settlements which are located at a distance inferior to 400 m from the forest. This distance can be modified in the tool according to the laws of each country. Then the RUI map is created (Figure 6) by applying differentiated buffers, varying from 100m up to 400m, according to the type of habitat and risk.(Table 1)

Table 1- Buffer sizes

Settlement Type	Buffer size
Urban settlement	400
Settlement in forested area	300
Settlement in agricultural area	200
Dispersed buildings in forested area	300
Dispersed buildings in agricultural area	100
Isolated buildings in forested area	200
Isolated buildings in agricultural area	100

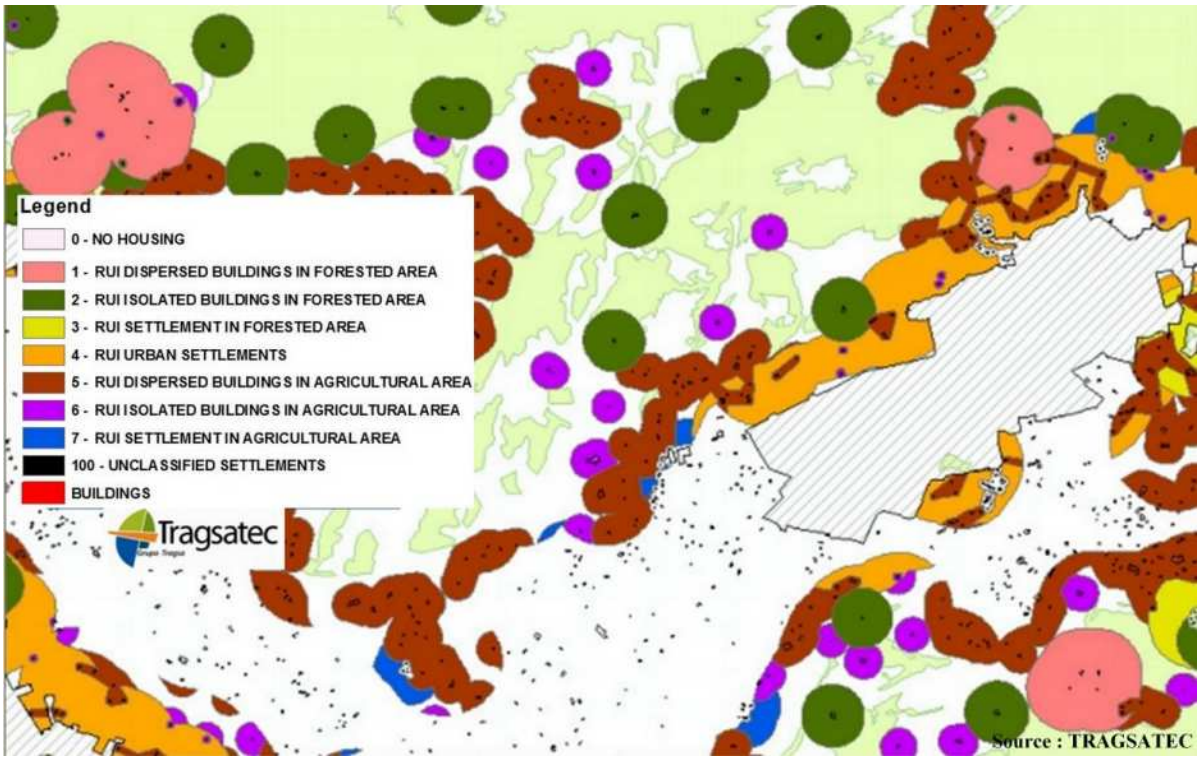

Figure 6. Map of RUI local scale - Tragsatec

2.3. Global scale Irstea

The global scale has been considered as the European level. This level of work has been taken into account in order to compare the situations and the importance of RUI in the different European countries.

The main database used is the 2006 CORINE Landcover with a pixel resolution of 100 metres. In order to characterize RUI, two main landcover types were used : vegetation and urbanization.

On the global scale, the rural urban interfaces are defined by a radius of 400 metres around houses located at less than 200 metres from forests or shrubland. The distance of 400 metres takes into account the perimeter where fuel reduction operations can be imposed on homeowners by different laws or regulations but also the possible burning of houses by spot fires.

The global rural urban interface map results from the combination of 2 criteria:

- the general land cover characterization (mineral, agricultural, sparse vegetated or forested area) resulting from the simplification of the Corine Land Cover database;
- the housing configuration (isolated, scattered, dense cluster housing) resulting from the combination of urban fabric classes of the Corine Land Cover database and from the soil sealing database.

A nine class typology was created during the process with a repartition of housing in three classes : isolated, scattered and dense, combined with different contexts : mineral, agriculture or sparse vegetation and forest. (Figure 7)

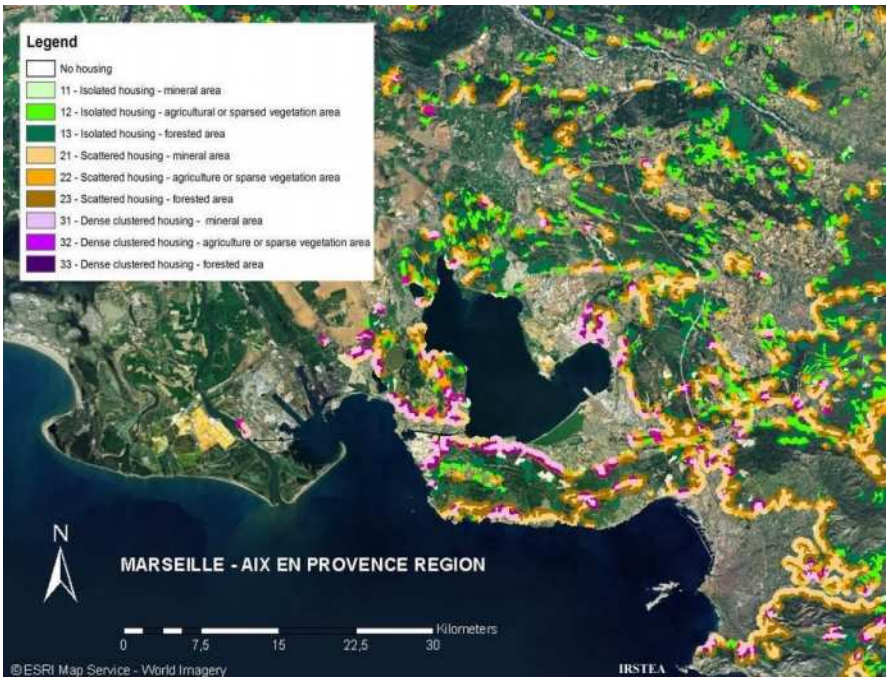

Figure 7. Global RUI map

Results

The RUImap software

This tool called RUImap (Figure 8) is an extension for ESRI™ ArcGis™. It was designed to run the three methodologies detailed above automatically and to gain in time and easiness. Each partner developed some parts of the tool. The Irstea local and global scale modules were developed with the Python programming language using ArgGis™ functions. The TRAGSATEC local scale was written in VBA language. The design and integration of the module in the final version was made by Tragsatec.

Figure 8. The RUImap software

3.2. Application of RUImap methodologies in different contexts

The methodology was used in different programs and researches in Europe. Town managers (in charge of planning, risks and expenditure) could directly apply the methods developed and use the software designed for an easy-and-direct use. The tool could quickly create easily-readable maps, show the location and categories of Rural urban interfaces. The several outputs produced by the tool were compared and a significant coherence was noticed between the different methodologies. The knowledge of the territory and some comparisons of the outputs with the real situation show a good correlation between the software results and the real RUI distribution on the territory.
The two approaches, global and local, are both useful to know, describe and map the territory on different scales and with different definitions. The general map produced by the global tool can be used to have a general view of the territorial characteristics. Then, it is possible to use the local and regional scale to focus the areas and update the analysis.
The IRSTEA and TRAGSATEC methodologies can be considered as complementary. The first method developed by Irstea analyses the residential buildings and the presence and continuity of vegetation. The Tragsatec method works on the dwellings too but it takes into account the environment in which they are located (forested, urban, agricultural). When running the local tool with both methods, more information can be collected and a more complete description of single RUI contexts can be obtained.
The use of the tool could be very useful for fire risk analysis on RUI scale and for local quantification of fuel load and continuity. The information with the direct knowledge of the general context is very important for the local fire risk assessment.

Municipality of Arcos de Valdevez, Portugal

The Portuguese National Fire Plan (2006) promoted fire prevention, population sensitization using passive means such as improvement of surveillance, detection and alert. It focused the need to protect the WUI/RUI through the establishment of defensible space of at least a hundred metres around the buildings and settlements. In this way, "WUImapping" has been used in different research projects.
The local scale methodology was used in the European project MOVE (Methods for the Improvement of Vulnerability Assessment in Europe) to define the vulnerability of the territories in order to find a more cost-effective risk management (funded by European Commission (7th Framework Programme). (Figure 9)

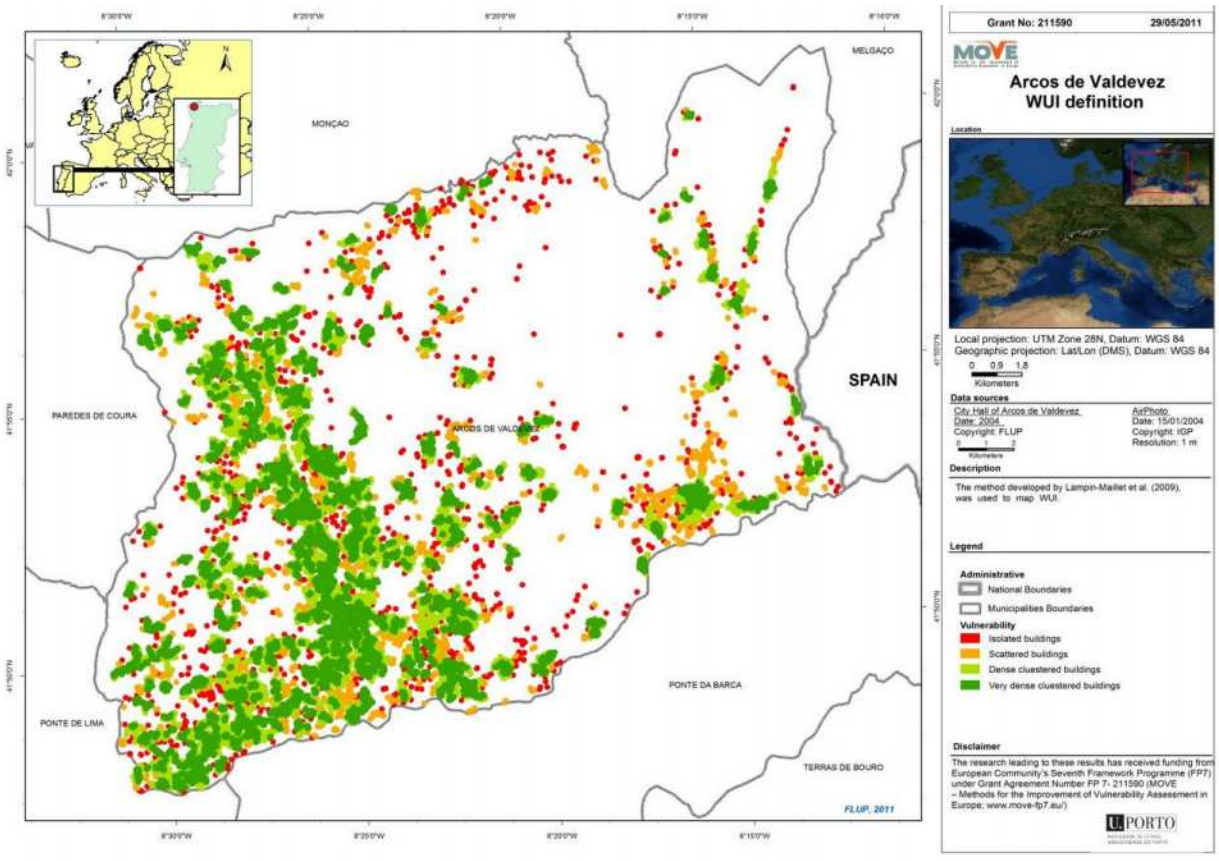

Figure 9. WUI mapping – Program MOVE

A project dealing with the implementation of a Forest Fire Risk Communication Program, will start in 2014 and will use the WUI/RUI methods in collaboration with several municipalities and stakeholders such as the Institute for Nature Conservation and Forests which is responsible for the coordination of all actions. The WUI/RUI typology will make possible a classification of the different forest fire prevention problems and will address them in a coherent way, both providing the capacity of transferability and capitalization.

Golfo Aranci area , Sardinia, Italy

Throughout most Mediterranean coastal areas, potential fire risk is really high for villages, tourist resorts, and people particularly in the summer. With a more important human presence and with extreme weather conditions, vegetation is highly flammable.
Therefore, developing planning policies is essential to find out strategies to prevent and reduce wildfire risk in WUI/RUI areas. Recently, several authors stressed the importance of estimating trends in expansion of WUI/RUI areas.
Tracking past and recent expansion trends allows to minimize their impact, to determine likely extent, location and pattern of WUI/RUI in the future, and to provide information for long-term land use planning and natural resource management. The study focuses on analysing and evaluating the temporal evolution of WUI/RUI areas in North Sardinia coastal regions in the 1954-2008 period with a great tourism development. (Figure 10)
Several simulations by Farsite(fire spread and behaviour simulator) were also performed in order to evaluate the accuracy of this approach in providing useful information for mitigating fire danger and risk in WUI/RUI areas.

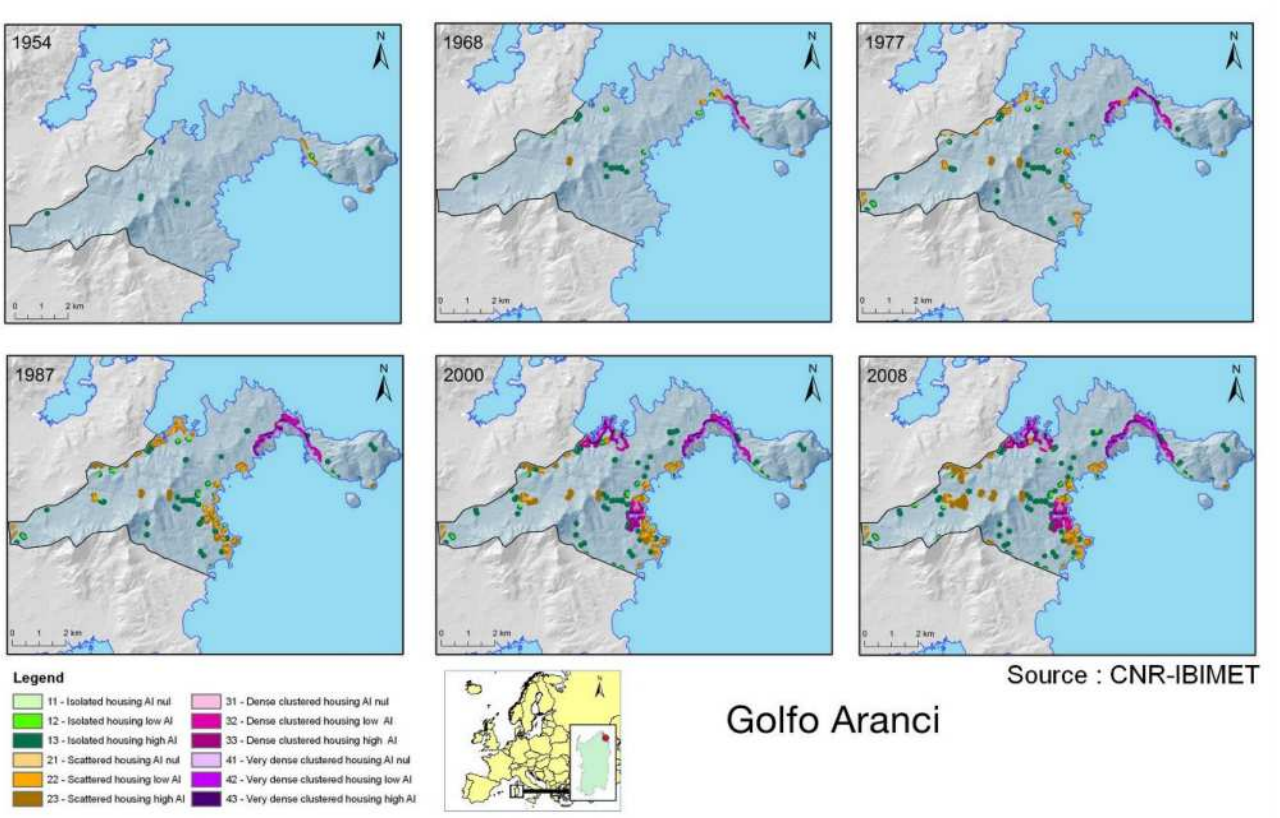

Figure 10. Evolution of the WUI/RUI 1954 – 2008 – Gofo Aranci, Italy

Oristano region, Sardinia, Italy

In the province of Oristano (central-western Sardinia), the mapping and characterization of the interface areas and the adaptation of the methodology to the Iocal context were tested in 22 municipalities, 21 are in the forestry district of Arci-Grighine, using the RUImap tool and the local scale as a methodological basis.(Lampin-Maillet *et al*.2010a and 2010b) .
An adaptation of the RUI mapping procedure was performed, as the French procedure is closely linked to their definition of the RUI and to the brush clearing law (Law Art L.322.3). This adaptation permits the application of the methodology to the Italian territory where a precise definition of the interface is still lacking and were immediate identification of areas that may be more sensitive to the problem of forest fire does not correspond to Italy. The alternative use of this input data allowed us to divide the territory into a forest area and rural area rather than in an area with a requirement / non-requirement trimming.
In the derivation of the vegetation map, the use of aerial orthophotography and of the filter (ICS Index Soil color) has revealed the fragmentation of forest vegetation with satisfying results, highlighting areas of bare soil present in some portions of the territory. BCZ (Brush clearing zone) was not used in this procedure as it is different in Italy. The change in the size of the floating window has made it mandatory to change the thresholds that define classes. AI low e high have been fixed respectively to 0-88% and> 88%.
The piedmont forest district of Arci-Grighine is an area with a high priority level in terms of land management and fire prevention actions.

Among the different RUI types Isolated and Scattered housing and AI low and high are those that require the highest security costs as they have a large surface area exposed to the fire and are difficult to reach. The map of RUI (figure 11) shows high-risk areas with very low population density and in the mountain ranges of Grighine (red) and the Monte Arci (blue). The last area was burned on July 4th, 2014 from a forest to a more dense housing RUI, causing huge damage to farms and dwellings.

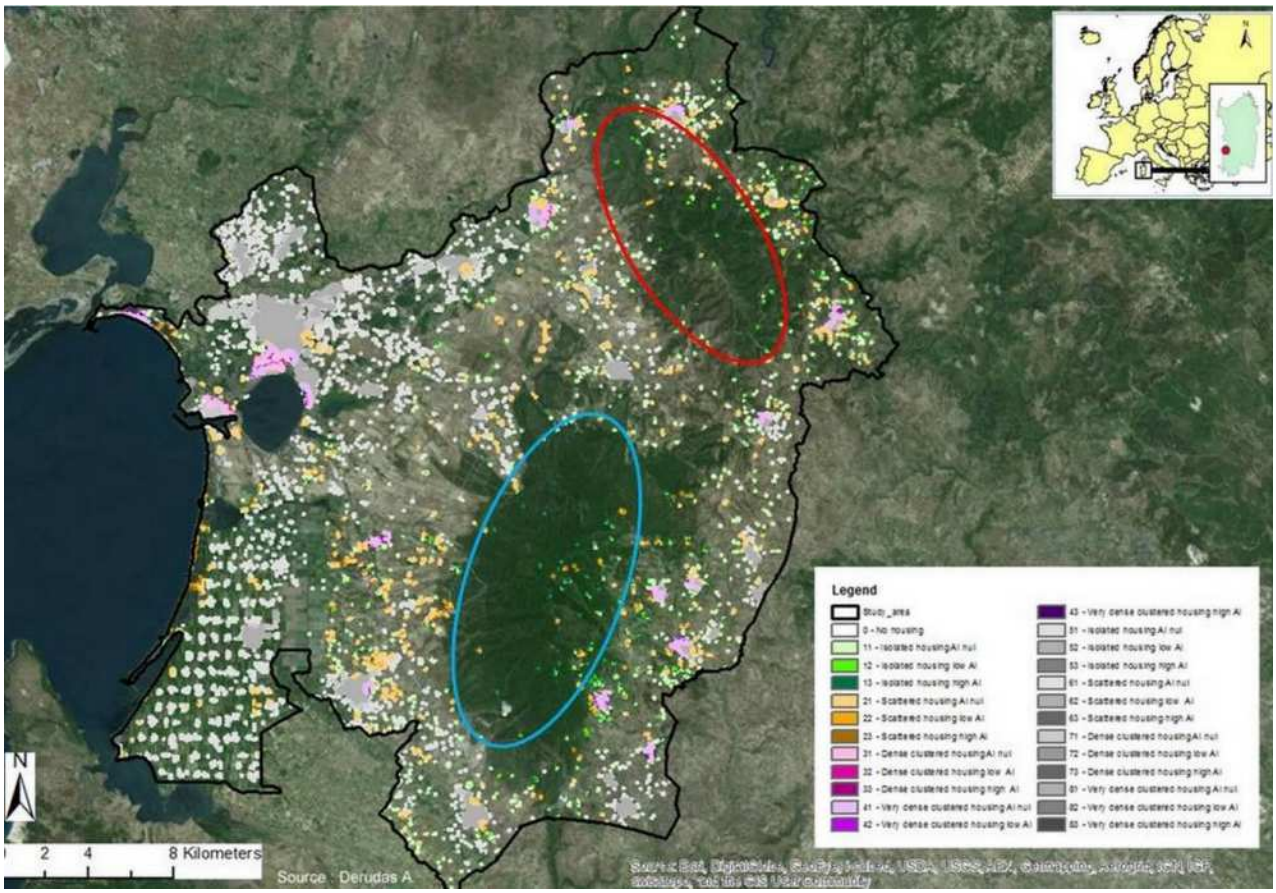

Figure 11– Priority zones to monitor, isolated houses, high vegetation aggregation

Molentargius regional park, Cagliari, Italy

The Molentargius regional park is an area of 1600 ha in the vicinity of Cagliari. The park stretches on wetland, lagoon areas (Ramsar convention) and abandoned salt flats frequented by numerous bird species.
The park area is also made of different terrestrial ecosystems with a patchwork of various vegetation: reed beds, meadows, groves and degraded scrublands interconnected with an a man-made system of some dwellings next to urbanization.
A plan was made to mitigate and lower the fire risk to human high value belongings like commercial buildings on the edge of the park.
The use of the RUImap software allowed to add information to the general knowledge of the park area, as a large part is included in an Rural Urban interface area. An analysis of the territory of the Molentargius regional park was performed (Figure 12) with the results obtained with the application of the RUImap software and the burned areas from 2005 to 2012. We can observe that most of the fires occurred in the areas where dwellings are surrounded by more or less dense vegetation.

Figure 12. RUI map and burnt area

Mimose village, Sinnai community, Sardinia, Italy

In this chapter the study uses the RUImap local methodology for mapping interface areas. This method is different from the method indicated in the guidelines issued by the Department of National Civil Protection Plan. France and Sardinia have different fire protection requirements . RUImap tool was used to point out the differences between the two countries.
The main interesting points of these RUI cartography are :
• a better knowledge of the interface areas and understanding of the dynamics;
• the identification of the most immediate at risk areas for fire operators.
• In the design phase of fire prevention :
- the identification and estimation of the areas to be cleaned;
- the assessment of the scope of the areas at risk and the consequent dividing up fire fighting teams and equipment;
- the design of the escape routes for the population as well as firebreaks or areas of cleaning required in the vicinity of the towns;
- the evaluation of suitable location basins or points for fire water supply.

The mapping urban-forest interfaces is one of the key elements for assessing the risk of fire. It is indeed a method to identify the critical present in an area and the sensitive points such as residences to be protected in case of fire, the presence of people and their assets. It is thus a valuable aid in the fight against fires through the knowledge of the spatial organization of housing in addition to being a tool to identify the people who live in urban-forest interfaces and so it is important to provide information focused on the risk of fire for preventive purposes.

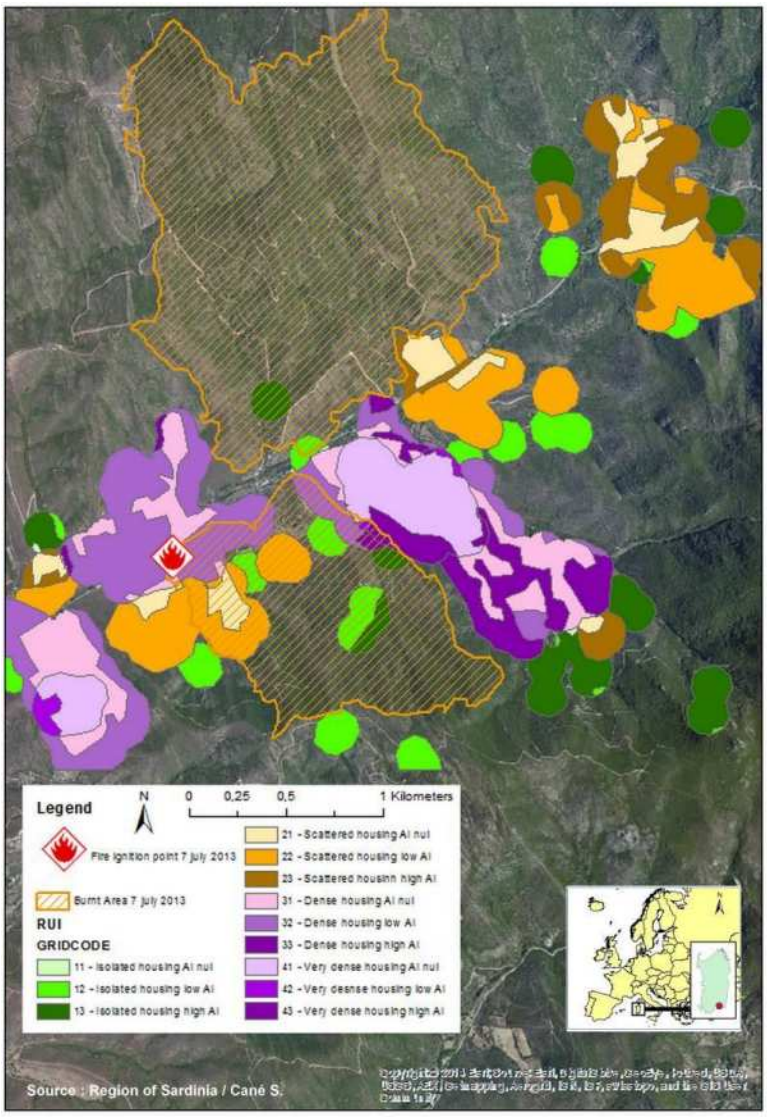

Figure 13. Mimose village -RUI map and burnt area

Bouches-du-Rhône, France

Irstea did a study for the regional ministry of the environment office. The aim was to get an overview of the RUI in the Bouches-du-Rhône department including the metropolitan area of Aix Marseille. The RUI of all the area was performed with two sets of data with a lapse of ten years. The results show an increase of 11% of the WUI area. The data were used later in the FUME program and related to fire historic data. The result shows a high number of ignition points located within the RUI zone with a higher density. The results are useful for stakeholders to make prevention action in this areas
In the study area of the Bouches-du-Rhône the evolution of the RUI between 1999 and 2009 shows changes in the composition and areas of RUI. The first results concerning housing configuration show a global intensification of urbanization in the area with several trends. The densification of the already built RUI zones evolve towards higher density classes. The densification concerns also isolated housing with an increase despite planning policy recommendation over soil sealing of the territory.
The main cause of this fact is an increase of the urban territory on the outskirts of the metropolitan area of Aix-Marseille. The attractiveness of southern France for its climate and lifestyle is part of the increase of built areas even in the remote towns with cheaper building prices.

According to figures it is possible to give some conclusion. The area of the RUI is increasing globally by 10%. The main increase in RUI types occurs principally in dense areas.

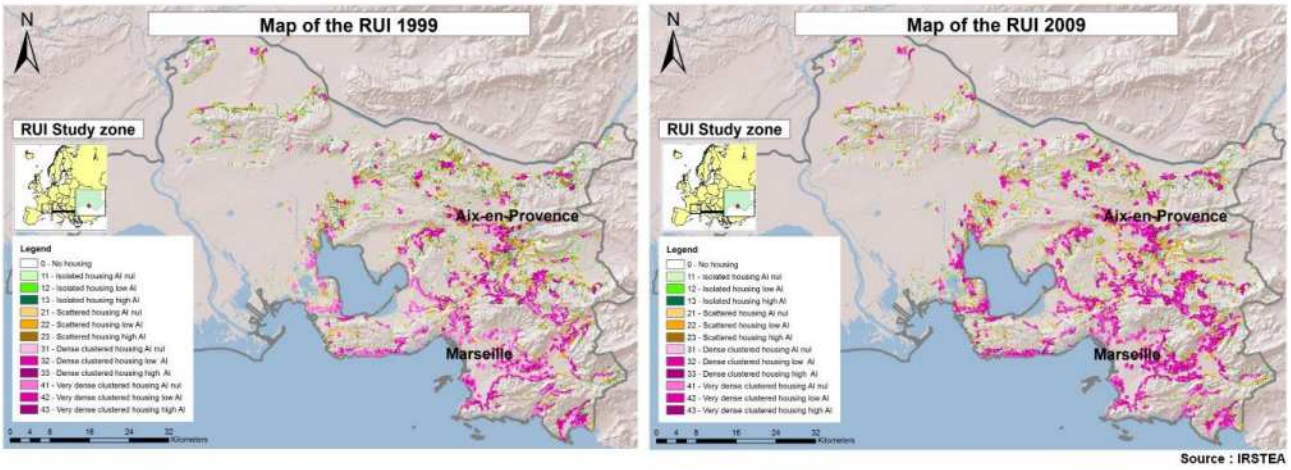

Figure 14. Bouches-du-Rhône, France :RUI evolution 1999-2009

Conclusion

The several outputs produced by the tool were compared and a genuine consistency between the obtained maps was noticed. The direct knowledge and some surveys in the territory are useful to compare the outputs with the real situation. A clear agreement between the software results and the RUI distribution on the territory was checked.

The two approaches, global and local, are both useful to know, describe and map the territory on different scales and definition. The general map that the global tool produces can be used to have a general view of the territorial characteristics on the regional scale and to focus the areas where the use of the local tool would complete the analysis.

In a general interpretation of the local tool application, the IRSTEA and TRAGSATEC methodologies could be considered as complementary. The first method developed by Irstea analyses the residential buildings and the presence/continuity of vegetation; the Tragsatec one also works on the dwellings but it considers the environment (forested, urban, agricultural) in which they are located. Running the local tool with both methods, more information can be collected and a more complete description of single RUI contexts can be obtained.

The use of the tool could be very advantageous for fire risk analysis on RUI scale, and for local quantification of fuels charge and continuity. The information, associated with the direct knowledge of the general context is very important for the local fire risk assessment.

The growing of RUI zone in all the Mediterranean study sites is a challenge for community leaders. This zone is at high risk due to numerous fire ignition density in a zone of human density and high valuable goods. The RUI expansion is a problem for prevention, organisation and fire-fighting. It increases the costs of protection as in these areas great losses are observed when a fire occurs. (human lives, houses).

RUI mapping can participate to prevent devastating loss for homeowners through assessment of information, to protect homes and lives in a better way in the interface where "lives community at risk".

Acknowledgements

The research leading to these results has received funding from the European Union Seventh Framework Programme (FP7/2007-2013) FUME program (Forest Fires under Climate, Social and Economic changes in Europe, the Mediterranean and other fire-affected areas of the world) under grant agreement n°243888 and Sixth Framework Programme. (FP6/2002-2006) FIRE PARADOX program under contract no. FP6-018505.
Produced with the support of the Ministère de l'Ecologie, de l'Energie, du Développement Durable et de l'Aménagement du Territoire – France.

Technical details

RUImap is an extension for ESRI™ ArcGis™ v9.3.1, Spatial Analyst™ and ArcInfo™ licences required. Available for free on request: contact christophe.bouillon@irstea.fr

References

Casula, F (2013) Wildland Urban Interface: Mapping and Wildfire Risk Assessment, PhD thesis, (University of Sassari, Sassari, Italy)

Farina A.(2001) Ecologia del paesaggio, principi, metodi e applicazioni, UTET, Torino, Italy

Lampin-Maillet C (2009). Caractérisation de la relation entre organisation spatiale d'un territoire et risque d'incendie : Le cas des interfaces habitat-forêt du sud de la France. Thèse de doctorat, (université Aix-Marseille, Géographie- Structures et dynamiques spatiales, Aix-en-Provence, France)

Lampin-Maillet C, Jappiot M *et al* (2009) Characterization and mapping of dwelling types for forest fire prevention. Computers, Environment and urban systems 33,224-232.

Lampin-Maillet C, Bouillon C *et al* (2010).' Guide de cartographie et caractérisation des interfaces habitat-forêt'. Convention n°2008 11 9 071. (Ministère de l'Écologie,de l'Énergie, du Développement durable et de la Mer. 68 p.)

Lampin-Maillet C, Jappiot M *et al* (2010). Mapping wildland-urban interfaces at large scales integrating housing density and vegetation aggregation for fire prevention in the South of France. Journal of Environmental Management 91(3), 732-741.

Lampin-Maillet C, Bouillon C (2011) WUImap : A software for mapping Wildland-urban interfaces in the mediterranean european context. Journal of Environmental Science and Engineering, 5, 631-642.

Madrigal Olmo J, Ruiz J.A *et al* (2013) Characterization of wildland-urban interfaces for fire prevention in the province of Valencia (Spain). Forest Systems 2013 22 (2), Short communication, pp. 249-254.

McGarigal K. (2002), Landscape Pattern Metrics Chapter of Encyclopedia of Environmentrics, Vol. 2, John Wiley & Sons, Sussex, England, , pp. 1135-1142.

McGarigal K, Marks, B. (1994) Spatial patterns analysis program for quantifying landscape structure. FRAGSTATS version 2.0. Forest Science Dept, Oregon State Univ., (Corvallis, OR, USA)

Plano Nacional de Defesa da Floresta Contra Incêndios (PNDFCI). Resolução do Conselho de Ministros n.º 65/2006, N°102 DIÁRIO DA REPÚBLICA — I SÉRIE-B, 3511 ,(Lisboa, Portugal)

Piano Regionale di previsione, prevenzione et lotta attiva contro gli incidi boschivi 2014-2016, Regione autonoma della sardegna. Deliberazione, N. 14/41 del 18.4.2014, (Cagliari, Italy)

Website FUME program (Forest Fires under Climate, Social and Economic changes in Europe, the Mediterranean and other fire-affected areas of the world). http://fumeproject.uclm.es/

Turner, M.G. (1990). Landscape changes in nine rural counties of Georgia. *Photogrammetry Engineering and Remote sensing*. **56**, 379-386

An integrated approach to fire emission forecasting

Adam Kochanski[a], Jonathan Beezley[b], Mary Ann Jenkins[c], Martin Vejmelka[d], Jan Mandel[e]

[a] *Atmospheric Sciences Department, University of Utah , Salt Lake City, Utah, USA*
adam.kochanski@utah.edu
[b] *Kitware, Inc., Clifton Park, New York, USA*
jon.beezley@gmail.com
[c] *Department of Earth and Space Science and Engineering, York University, Toronto, Canada*
maj@yorku.ca
[d] *Department of Mathematical and Statistical Sciences, University of Colorado, Denver, USA*
Martin.Vejmelka@ucdenver.edu
[e] *Department of Mathematical and Statistical Sciences, University of Colorado, Denver, USA*
jan.mandel@ucdenver.edu

Abstract
In this study, we describe how WRF-SFIRE is coupled with WRF-Chem to construct an integrated forecast system for wildfire and smoke prediction. The integrated forecast system has the advantage of not requiring a separate plume-rise model and assumptions about the size and heat release from the fire in order to determine fire emissions into the atmosphere. With WRF-SFIRE, wildfire spread, plume and plume-top heights are predicted directly, at every WRF time-step, providing comprehensive meteorology and fire emissions to the chemical transport model WRF-Chem. Evaluation of the system was based on comparisons between available observations to the simulations of the 2007 Santa Ana fires. The study found overall good agreement between forecasted and observed fire spread and smoke transport for the Witch-Guejito fire. Also the simulated PM2.5 (fine particulate matter) peak concentrations matched the observations. However, the NO and ozone levels were underestimated in the simulations and the peak concentrations were mistimed. Determining the terminal or plume-top height is one of the most important aspects of simulating wildfire plume transport, and the study found overall good agreement between simulated and observed plume-top heights.

Keywords*: fire modeling, smoldering, smouldering, smoke, air quality, emissions, dispersion, plume rise*

Introduction

A wide suite of tools exists that can be used to help assess smoke dispersion. They range from simple Gaussian smoke models that aim to assess the area affected by smoke based on fuel type, fire area and wind conditions, to complex multi-model systems predicting the emissions, dispersion and air quality effects associated with wildland fires. The latter ones generally use a set of specialized sub-models, designed to perform specific tasks associated with the fire emission forecasting. The multi-model systems typically consist of a fuel consumption model, providing an estimate of the amount of burnt fuel, an emission model, computing fluxes of chemical species, a plume rise model, assessing the injection height, and a chemical and transport model, computing how the species react and disperse in the atmosphere. The fire emissions and plume dispersion may be linked to meteorological conditions, by feeding these models with weather data provided by a separate numerical weather prediction model. There are two major limitations of this approach. First, this modular approach generally does not capture the two-way interactions between the system components. For instance, even if fire spread and fuel consumption are computed based on the simulated weather forecast, the fire's convection is not coupled to, and represented in, the weather model. The weather prediction used for fire progression will not therefore include local, fire-affected weather conditions. As a consequence, the inaccuracies in the prediction of the local weather conditions may adversely affect estimates of the plume height and dispersion, both which depend heavily on the weather input.

The second drawback is the limited fidelity of such a system in terms of realistic representation of the fire progression, fire emissions, plume rise, and plume dispersion. For example, a typical plume-rise model is based on classical plume theory, and assumes a single idealized Gaussian-shaped plume (in most cases, rising vertically; i.e., not bent-over) placed over a point-source fire. In reality, both the surface fire emissions and fire plume behaviour are much more complex. The majority of the flaming emissions take place at the fire perimeter, while the smoldering may be a source of emissions within it. Regions of high fire activity can induce more than one strong updraft core, ingesting fire emissions at much higher rates than is estimated by the typical plume rise model, while strong winds may limit the plume rise to much lower elevations than those predicted by an idealized plume rise model.
In this paper we present a new integrated approach to the problem of the simulation of the fire emissions. We show an integrated modelling framework that predicts fire progression, taking into account the fire-weather and fuel-weather feedbacks, and explicitly resolves fire-induced convective plumes, as well as simulates the chemical reactions, transport, and dispersion of the fire-emitted species in the atmosphere.

Model description

The core of the system is the WRF-SFIRE model (Mandel *et al*., 2011), which is a two-way coupled fire atmosphere model based on Weather Research and Forecasting model (WRF – Skamarock *et al*., 2005) and Rothermel (1972) fire spread model implemented by a level set method. WRF-SFIRE has evolved from the CAWFE code (Clark *et al*., 1996, 2004), which was built on the Clark-Hall code. The switch to WRF allowed faster than real time parallel execution on fine meshes and a natural coupling with WRF-Chem. WRF-SFIRE predicts fire spread based on local meteorological conditions, taking into account the feedback between the fire and atmosphere.
To capture the effects of local weather on fuel characteristics, WRF-SFIRE is also coupled with a fuel moisture model, which assesses the fuel moisture based on local meteorology (air humidity, temperature, and precipitation). The fire-emitted heat (computed by the fire model) is fed into the atmospheric component of the model, so WRF-SFIRE dynamically simulates and resolves the fire convection and plume rise. The mass of the burnt fuel in the WRF-SFIRE simulation is used to estimate the fire emissions associated with flaming and smoldering in every time step. The linked WRF-Chem (Grell *et al*., 2005) predicts the transport, dispersion, and chemical conversion in the atmosphere of the fire-emitted chemical species as the plume evolves. The impact of fire emitted heat on the plume characteristics accounts for different plume injection heights. Emissions from regions of high intensity fires are carried higher by stronger updrafts and greater plume rise, than from lower intensity fires generating weaker updrafts.

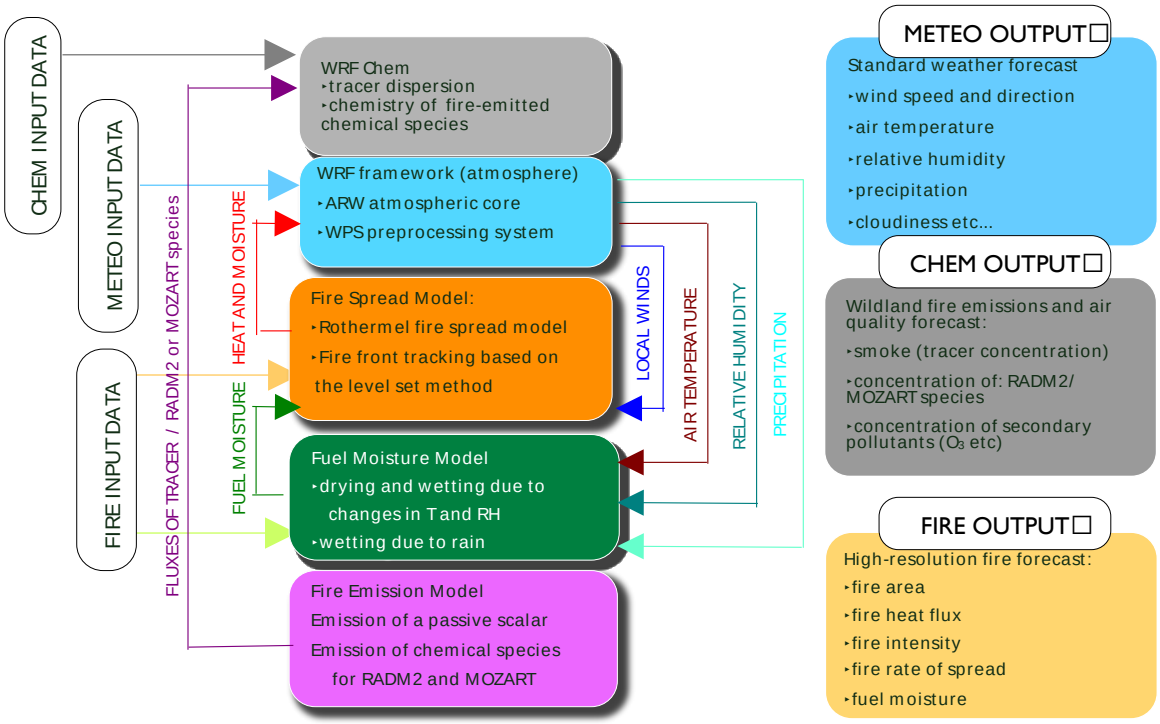

9

Figure 1. Diagram of the integrated fire emission system based on WRF-SFIRE coupled with moisture model and WRF-Chem

In this model framework, the model resolves the fire plumes instead of parameterizing them, and instantaneous fire activity at any given place is linked with the fire-driven emissions, fluxes, buoyancy, and local winds. Assumptions about the vertical distribution of the fire emission as part of a sub-grid scale parameterization based on classical plume theory are therefore avoided, as the vertical dispersion of the fire emissions are simulated by the model explicitly. The diagram showing the WRF-SFIRE model components is presented in Figure 1.

The fire emissions are estimated based on the combustion rates computed for each fire-grid point as the mass of fuel consumed within one WRF time step. Once the fuel consumption is known, emission fluxes are computed as the products of the fuel-combustion rates and the fuel-specific emission factors. Currently the global fire emission factors from FINN (Fire INventory from NCAR, Wiedinmeyer *et al*., 2011) are used, however; the model also accepts user-defined emission factors provided in one of the model configuration files. The fire emissions are represented as a sum of the fluxes of the chemical species compatible with two chemical mechanisms supported by WRF-Chem – MOZART (Emmons *et al*. 2010), and RADM2 (Stockwell *et al*. 1990) as presented in Figure 2. The emission fluxes are then ingested into the first model layer of WRF-Chem, which handles dispersion and chemical transformation of the fire emissions.

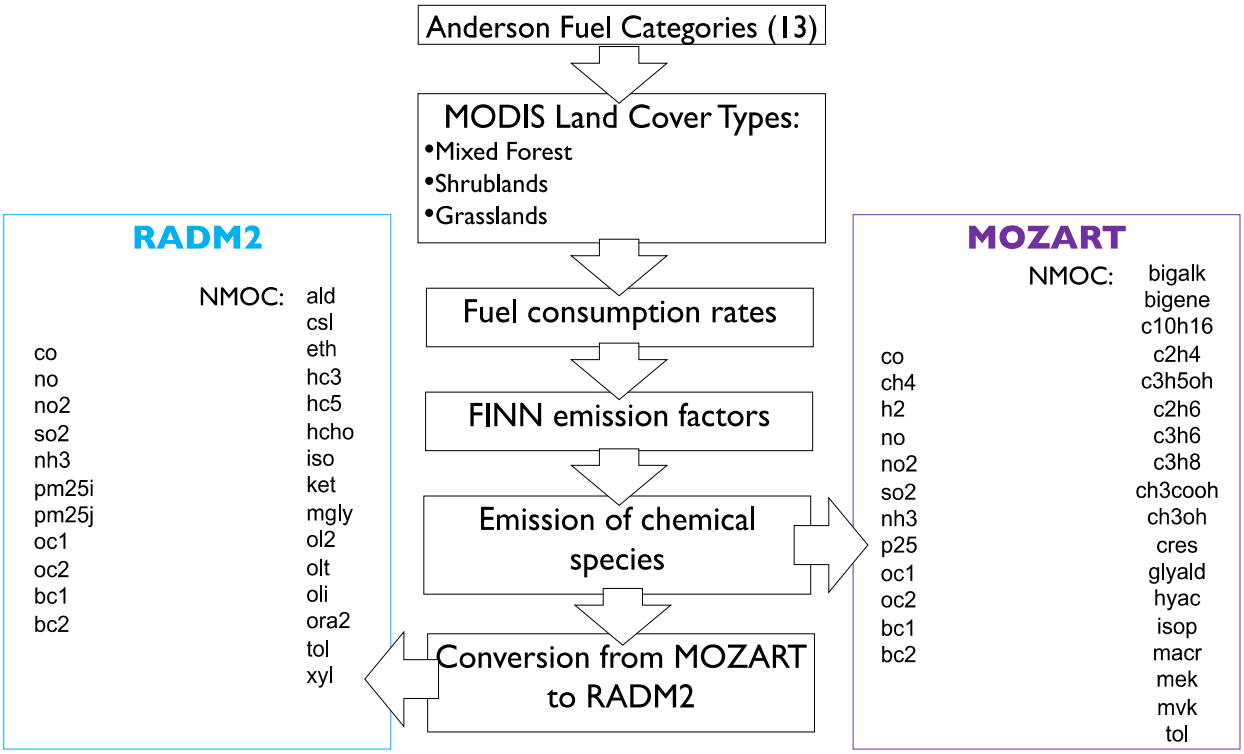

Figure 2. Computation of fire emissions in the WRF-based integrated system for fire and air quality simulations.

Model setup

We tested the system on the 2007 Witch and Guejito Santa Ana fires. In order to model evolution of the Santa Ana event, together with the local circulation dictated by the complex topography of southern California, WRF was configured with four nested domains: D01, D02, D03, and D04, of horizontal-grid sizes 32km, 8km, 2km, and 500m, respectively, as shown in Figure 3. The model's vertically-stretch grid extended up to 15.4 km, with a surface layer roughly 20 m thick and the top-most vertical layer roughly 2000 m thick. The surface fire mesh located in domain D04 had a refinement ratio of 25, making the horizontal fire-grid cell size 20 m. Output from the fire simulation was saved every 10 minutes. The fire model, SFIRE, used 30m-resolution elevation and fuel data, while the atmospheric model, WRF, used approximately 1.5km-resolution MODIS land-use representation. Further details of this setup can be found in Kochanski *et al*. (2013).

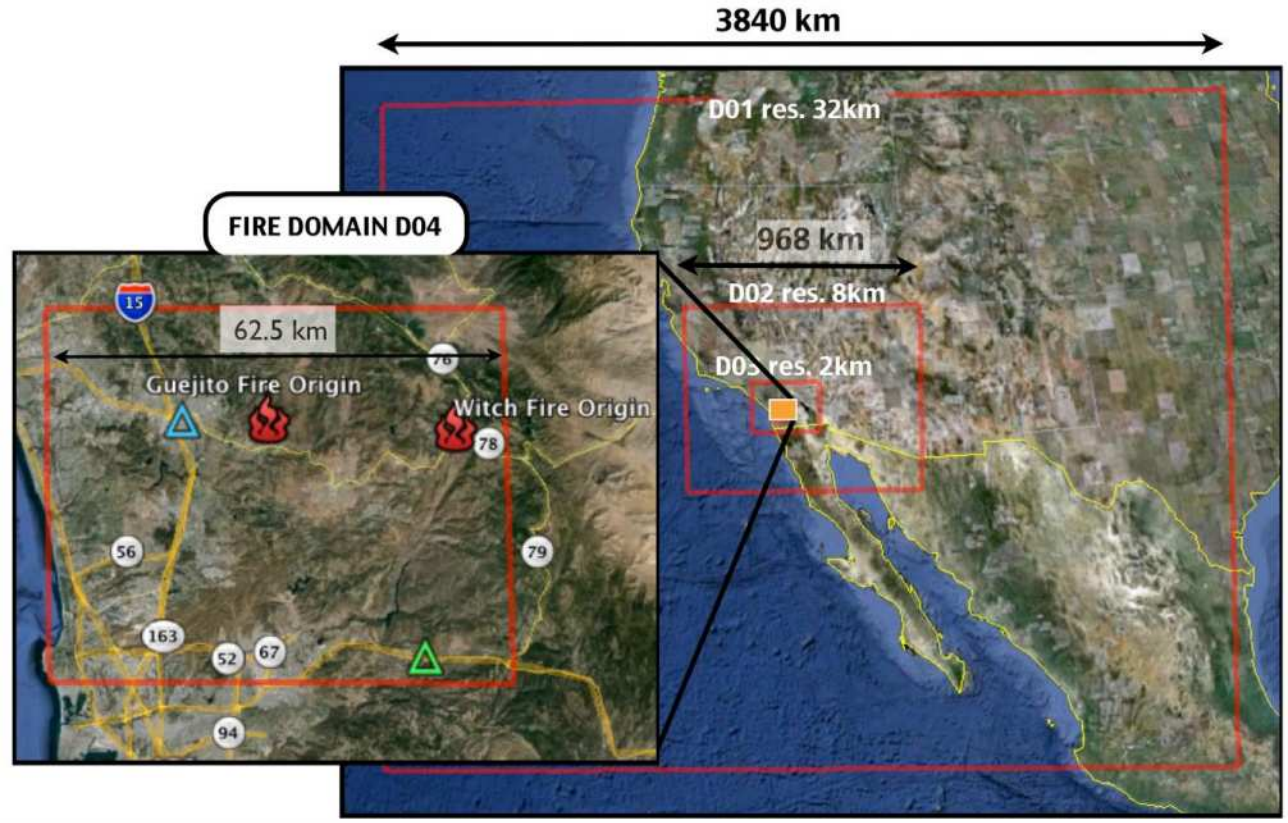

Figure 3. The multi-scale WRF setup in this study, including locations of the Witch and Guejito fire origins and the air quality stations used for model validation (Escondido - blue triangle; Alpine - green triangle). Horizontal domain resolutions vary from 32km (D01) to 500m (D04).

Results and discussion

The model's ability to accurately resolve the plume height was evaluated using available satellite data. There was no MISR (Multi-angle Imaging SpectroRadiometer) data collected for this particular fire, but there were two other nearby fires actively burning at approximately the same time (see Table 1).

Table 1. MISR plume retrieval data for wildfires in the vicinity of Witch-Guejito fire on date 200710-21 and time 18:39:52 UTC. SDev = Standard Derivation

Longitude	Latitude	Plume Perimeter Length	Plume Area [km²]	Median Plume Height [m AGL]	Top Plume Height [m AGL]	SDev
-117.441	33.244	70	259	943	1260	269
-116.562	32.623	269	2168	684	1017	314

The maximum simulated plume top height for the Witch and Guejito fires computed from the PM2.5 field using 1 μg/m^3 threshold was 1574m. This is slightly higher than suggested by the MISR data for the two nearby fires, but it has to be noted that they were also smaller than the Witch and Guejito fires. The two-way coupling between the WRF domains enables pollution transport across the domains, so the smoke emitted from the fire simulated within the inner most domain is also present in the outer domain D03, which may resolve larger-scale smoke transport. An example of the smoke dispersion simulated in the D03 and the visible satellite picture are presented Figure 4.

Figure 4. Smoke dispersion within domain D03 (2km resolution) simulated by WRFSC (left panel) and MODIS satellite image (right panel). The red color fill in left panel represents the fire area projected from the nested fire domain D04 (500m resolution). Red contours in right panel represent remotely detected hot spots.

The transport and dispersion of the fire-emitted pollutants as well as the chemical processes simulated by the model were tested based on the surface measurements of the PM25 and NO. An example of the time series of the PM2.5 and NO concentrations simulated by the model and observed by Escondido air quality station (green triangle in Figure 3) are presented in Figures 5 and 6.

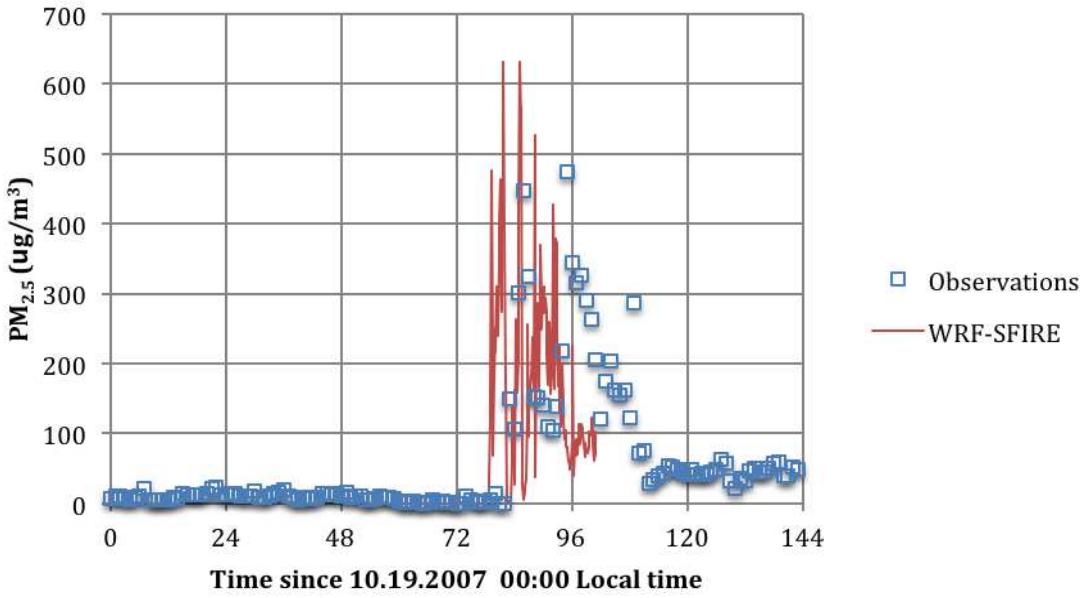

Figure 5. Time series of the simulated (red line) and observed (blue squares) PM25 concentrations at Escondido air quality station.

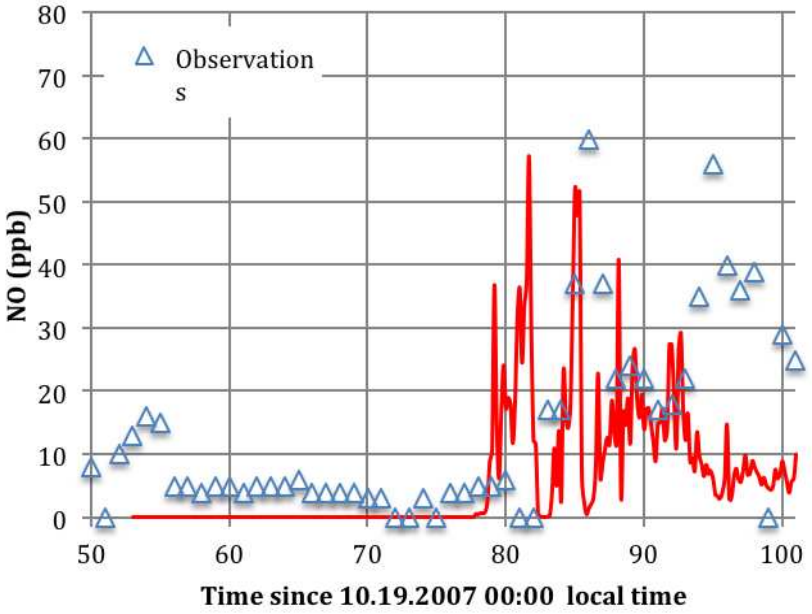

Figure 6. Time series of simulated (red line) and observed (blue triangles) NO concentration at Escondido air quality station.

In terms of the PM2.5 the modelled instantaneous values were slightly higher than the observed ones. The model estimated peaks at 632 μg/m^3 while the observations show maximum hourly values at 475 μg/m^3. It has to be noted that the WRF-predicted values peaked a couple of hours earlier than observed ones. The time shift between observed and simulated peaks can possibly be attributed to an overestimation in the north-west fire progression toward Escondido. Kochanski *et al*. (2013a) determined that the simulated fire progressed approximately 10km further in the north-west direction than the actual fire.

In terms of the NO concentrations, the model slightly underestimated the concentration, predicting peak values of 57.3 ppb, while the observed NO peaked at 60 ppb. Similarly like in the case of PM2.5, the timing of the simulated NO peaks appear earlier than in observations.

In a complex modelling system like WRF-SFIRE coupled with WRF-Chem, it is very difficult to determine directly reasons for the discrepancies between the simulated and observed pollutants levels. One reason may be that the three MODIS Land Cover Types used for emission computations (i.e., mixed forest, shrublands, and grasslands) are not detailed enough to represent the chemical smoke composition from fires spreading across 13 different fuel-bed categories (Anderson 1982). Another reason may be that global NO emission factors for grass and shrubs may be slightly lower than the actual NO emission factors for the fuel types in the Witch-Guejito region of Southern California. Finally the simulated local meteorology and smoke dispersion, as well as the fire progression are not perfect. Nonetheless, these differences between PM2.5 and NO simulated and observed are relatively low, and show promise for integrated fire-emissions forecasts.

Summary

In this paper, we presented an integrated system for simulating fire progression and fire impacts on air quality. The system utilizes the WRF-SFIRE as a component resolving the fire spread forecast and plume rise, and the WRF-Chem handling the chemical transport of fire-emitted pollutants. This pilot study is designed to demonstrate the potential of WRF-Sire and WRF-Chem as an integrated system for use by researchers and resource managers. What the study does establish is the increased level of detail provided by the system, such as locations of high reaction intensity, smoke emissions, and plume

injection heights that can provide a more comprehensive understanding of the wildfire environment, wildfire behaviour, and downwind ramifications of wildland fire emissions on air quality. Future quantitative research is warranted to prove the validity WRFSC, and evaluation of the model by comparison to new and different data sets is necessary. Observations that provide information for all components of the system - local micrometeorology, fire spread, fire emissions, plume rise, and dispersion and chemistry - are needed. Coordinated field measurements of fire spread data, fire heat release, and in-situ meteorological conditions are required to evaluate the fire spread component of the system. Radiosonde data are needed to provide information on the vertical structure of wind, moisture and temperature. Airborne measurements in the smoke plume of the updraft velocities, temperature, and chemical composition, combined with estimates of local emission factors, are needed to analyse fire-plume dynamics, dispersion, and chemistry. A comprehensive dataset providing information on all these aspects is essential to fully understand how the integrated system performs and what components need to be improved.

Acknowledgements

This research was partially supported by the National Science Foundation (NSF) grant DMS-1216481, and National Aeronautics and Space Administration (NASA) grants NNX12AQ85G and NNX13AH9G. This work partially utilized the Janus supercomputer, supported by the NSF grant CNS-0821794, the University of Colorado Boulder, the University of Colorado Denver, and the National Center for Atmospheric Research.

References

Anderson H (1982) Aids to determining fuel models for estimating fire behavior. Technical Report INT-122, USDA Forest Service, Intermountain Forest and Range Experiment Station, Ogden, UT, USA, 22 pp.

Clark TL, Jenkins MA, Coen J, Packham D (1996) A coupled atmospheric-fire model: Convective feedback on fire line dynamics. J. Appl. Meteor, 35, 875–901, doi:10.1175/1520-0450(1996)035<0875:ACAMCF>2.0.CO;2.

Clark TL, Coen J, Latham D (2004) Description of a coupled atmosphere-fire model. International Journal of Wildland Fire, 13, 49–64, doi:10.1071/WF03043.

Emmons L, Walters S, Hess P, Lamarque J, Pfister G, Fillmore D, Granier C, Guenther A, Kinnison D, Laepple T, Orlando J, Tie X, Tyndall G, Wiedinmeyer C, Baughcum S, Kloster S (2010) Description and evaluation of the model for ozone and related chemical tracers, version 4 (MOZART-4). Geoscientific Model Development 3, 43-67, doi:10.5194/gmd-3-43-2010.

Grell G, Peckham S, Schmitz R, McKeen S, Frost G, Skamarock W, and Eder B (2005) Fully coupled "online" chemistry within the WRF model. Atmospheric Environment 39, 6957-6975, doi:10.1016/j.atmosenv.2005.04.027.

Kochanski AK., Jenkins MA, Krueger S, Mandel J, Beezley JD (2013a) Real time simulation of 2007 Santa Ana fires. Forest Ecology and Management, 15, 136-149, doi:10.1016/j.foreco.2012.12.04

Kochanski A., Jenkins, MA, Mandel J, Beezley JD, Clements CB, Krueger S (2013b): Evaluation of WRF-SFIRE performance with field observations from the FireFlux experiment. Geoscientific Model Development, 6, 1109–1126, doi:10.5194/gmd-6-1109-2013

Mandel J, Beezley JD, Kochanski AK (2011) Coupled atmosphere-wildland fire modeling with WRF 3.3 and SFIRE 2011. Geoscientific Model Development, 4, 591-610, doi:10.5194/gmd-4-1-2011.

Rothermel R (1972) A mathematical model for predicting ire spread in wildland fuels. Technical Report Research Paper INT 115. (Ogden, UT), USDA Forest Service, Intermountain Forest and

Range Experiment Station, 46pp.
Stockwell WR, Middleton P, Chang JS, Tang X (1990) The second generation regional acid deposition model chemical mechanism for regional air quality modeling, J. Geophys. Res., 95(D10), 16343–16367, doi:10.1029/JD095iD10p16343.
Wiedinmeyer C, Akagi S, Yokelson R, Emmons L, Al-Saadi J, Orlando J, Soja A (2011)
The Fire INventory from NCAR (FINN): a high resolution global model to estimate the emissions from open burning. Geoscientific Model Development 4, 625–641, doi:10.5194/gmd-4-625-2011.

Analysis of fire hazard in camping park areas

Miguel Almeida[a], José Raul Azinheira[b], Jorge Barata[c], Kouamana Bousson[c], Rita Ervilha[e], Marta Martins[d], Alexandra Moutinho[b], José Carlos Pereira[e], João Caldas Pinto[b], Luís Mário Ribeiro[a], Jorge Silva[c], Domingos Xavier Viegas[a]

[a] *Centre for Forest Fire Research ADAI – LAETA, Rua Pedro Hispano, 12, PT-3030-289 Coimbra, Portugal, miguellmd@yahoo.com, luis.mario@adai.pt, Xavier.viegas@dem.uc.pt*
[b] *IDMEC/CSI – LAETA, Instituto Superior Técnico, Universidade de Lisboa, Av. Rovisco Pais 1, PT-1049-001 Lisboa, Portugal, jraz@dem.ist.utl.pt, alexandra.moutinho@tecnico.ulisboa.pt, jcpinto@dem.ist.utl.pt*
[c] *AEROG – LAETA, Departamento de Ciências Aeroespaciais, Faculdade de Engenharia, Universidade da Beira Interior, Calçada Fonte do Lameiro, PT-6201-001 Covilhã, Portugal; jbarata@ubi.pt, bousson@ubi.pt*
[d] *INEGI – LAETA, Instituto de Engenharia Mecânica e Gestão Industrial, Campus da FEUP. Rua Dr. Roberto Frias 400, PT-4200-465 Porto, Portugal; mmartins@inegi.up.pt*
[e] *IDMEC/LASEF – LAETA, Instituto Superior Técnico, Universidade de Lisboa, Av. Rovisco Pais 1, PT-1049-001 Lisboa, Portugal, rita.ervilha@tecnico.ulisboa.pt, jcfpereira@tecnico.ulisboa.pt*

Abstract
The common location of camping parks in forested or wooded areas, the normal use of combustible material by the campers and the frequent use of campfires to cook turn camping parks into areas with a high propensity for the occurrence of fires. Moreover, fires occurring close to parks induce to evacuations that disturb their normal activities. Despite the occurrence of several of such events, the associated risk is not yet well studied.
Project FireCamp is being developed in Portugal to analyse the propensity of fires in camping parks. This project has as main objectives: (1) analysis of past occurrences; (2) analysis of the combustibility of typical materials used in camping parks such as tents, sleeping bags or camping mattresses; (3) characterization of the camping park fuel cover and its surrounding by image analysis taken by UAV; (4) modelling of fire spread in camping parks; and (5) security measures for fire prevention and mitigation. A pilot study is being carried out in the Camping Park of Coja, in Arganil - Coimbra, which in September of 2012 was threatened by a forest fire that arrived to the perimeter of the camping park. A survey of this occurrence was done.
Several laboratory tests have been carried out in order to analyse the properties of the camping materials. Real tents with and without typical material inside (e.g., sleeping beds) were burnt in controlled environment in order to determine the mass loss decay, the increase of temperature and the convective winds produced. In parallel, each type of typical camping materials were analysed to determine the calorific power value.
Considering that external fires frequently threat camping parks, the survey of the neighbourhood of camping parks is also of great interest. In FireCamp Project, the aerial photographic survey of the camping park of Coja was carried out in order to produce a fuel map of this area. Based on this fuel map, a stochastic model to predict the fire spread in the covered area was set up.
The results obtained in the pilot study of the project applied to the Camping Park of Coja are also presented.

***Keywords**: forest fire, camping parks, wildland urban interface, WUI, modelling, mapping, fuel characterization, tents, camping materials*

Introduction

The occurrence of fires in Camping Parks (CP) are relatively frequent and in several cases they drive to wounded people or even to dead fatalities. The most serious fire incident occurred in camping parks took place in the CP Los Alfaques, in Terragona-Spain in 1978, where cascading explosions of fuel storages led to 217 deaths and more than 300 wounded people. Several other fire incidents have been reported by, for example, Fraser *et al*. (2003) or Klein *et al*. (2005).

Fires affecting camping parks may have origin inside the park or may come from the outside since parks are typically located in forested areas. The main ignition sources of fires starting inside the park are: electric equipment, use of fire for cooking or other practices, or neglect use of some common potentially igniter camping accessories like gas lighting, candles and others. Fires coming from outside the camping area may request the evacuation of the CP, endangering people and goods.

Fires in camping parks also assume great relevance given the many common ignitable camping accessories used such as tents, caravans, sleeping beds, mattresses, etc, which can sustain the fire and, when supported by other forest fuels, increase the fire spread through the camping park by conductivity and radiation mechanisms or by spotting. Besides all these risks, the knowledge of fire ignition, spreading and suppression in camping parks is still poor and requires a methodical analysis.

In Portugal there is a set of regulations about this matter like the regimes applicable to the installation and operation of public and private camping parks to simplify and standardize the respective licensing procedures, or the measures to prevent and control any actions that may cause damage to natural resources and facilities including (naturally) fire hazards:

- outside the CP and during the highest fire hazard season it is prohibited to burn anything within a certain distance of any woodland or brushland during the most part of the day; the law is intended to prevent forest fires by allowing outdoor burning only when the weather conditions are in general less favourable to spread an eventual wildfire;
- there are peripheral circulation paths with a reasonable width along the CP not only to prevent the spread of any fire to its interior but also to facilitate the passage of emergency and fire fighting vehicles;
- inside the CP only campfires and charcoal BBQs are allowed, and in specified fixed places; even so it is prohibited leaving a fire without completely extinguishing it, or failing to maintain it under control.

Albeit in a more or less insipid way and yet revealing the positive trend of the authorities in this matter, among the legislation set out one can list: the impacts of the legislation on CP in specific emergency plans of some Portuguese municipalities; the framework of CP in broader plans for local and regional spatial planning and management; and the existence of specific emergency plans for temporary CP.

The work presented in this paper is integrated in the FireCamp Project that is an internal project of the Associated Laboratory for Energy, Transports and Aeronautics (LAETA). The main objective of FireCamp is to understand and model the fire spread in camping parks as well as present alternatives to reduce the fire risk in CP. A pilot case study to apply the methodologies established in FireCamp was developed in the Camping Park of Coja. Several laboratorial experiments were carried out in order to determine the most important characteristics for modelling the fire spread. Burning tests with real tents and other camping accessories were performed as well. A survey of the area where the CP of Coja is located using Unmanned Aerial Vehicles (UAV) was carried out. A stochastic model to predict the fire spread in CP was produced. The methodologies used and the main results of the work developed are described in the following chapters. Some simulations of the fire spread in the CP of Coja are presented.

Methodology

In order to develop a tool for simulate the fire spread in a camping park, two set of inputs related to the combustible materials are necessary. The first set of inputs consists of the properties of typical camping accessories that can influence the fire spread. Several laboratorial tests were carried out with several different materials under different conditions to obtain these data. The second set of results is related to the characterization of the fuel cover of the area where the CP is located. As it was previously

mentioned, the survey methodology was applied to the Camping Park of Coja that was the pilot case of the project. The methodologies used to achieve the required inputs to modelling are described below.

Analysis of the combustibility of typical accessories used in camping parks

There are many combustible accessories used in camping activities and, for a question of simplicity, tests were restricted to the accessories that were considered to be more relevant, namely: tents, sleeping beds and camping mattresses. On the other side, accessories have different shapes and sizes, and these accessories may be composed by several different materials depending on the brand manufacturer, quality, etc. For example, the walls of some tents only have one layer of fabric while other tents have an additional interior layer of cotton. Therefore, a limited but representative number of the existing types of materials and accessories were analysed. Table 1 and Table 2 resume the accessories and materials tested.

Table 1. Resume of the materials analysed.

Code Sample	R1	E1	B1	W1	I1	P1	SB1	CP1
Picture								
Description	Tent roof	Tent entrance door	Tent base	Tent wall	Tent interior	Tent entrance mosquito protective net	Sleeping bag	Camping mattress
Material	Polyester or polyamide coated with a PU or silicone	Rip stop nylon	Woven PE Sheeting "Poly Tarp"	coated polyester and vinyl	cotton with polyester	Oxford cloth and mesh	100% polyester	PE foam

Since the amount of materials to be tested was limited, it was decided that focus should be given on the determination of the Higher Calorific Value (HCV) of sample materials mainly used in camping tents. These tests were performed in the calorimetric bomb according to standard EN ISO 1716. The bomb calorimeter is the most common device for measuring the heat of combustion or calorific value of a material. A small test specimen with a specified weight is combusted completely during constant volume and oxygen atmosphere inside a high-pressure calorimetric bomb. The calorimeter measures the temperature rise of the surrounding water and calculates the gross heat of combustion. Before testing, samples were conditioned at a temperature of 23 ± 2 ºC and relative humidity of 50 ± 5 %.

Besides the analysis of HCV, other tests of burning tents were also performed in order to understand the mechanism and the main factors affecting the burning. Table 3 resumes the burning tests carried out varying the initial conditions.

Table 2. Resume of the accessories tested.

Ref.	Weight (kg)			Fabric composition (m^2)	Number of layers of fabric	Dimensions (cm)	Photo
	total	structure	fabric				
Can01	0.92	0.64	0.28	B1: 2.28 W1: 3.71 E1: 0.92 P1: 0.46	1	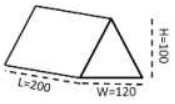	
Igl01	6.44	1.86	4.58	B1:6.67 W1: 9.42 P:0.38 I1: 6.14	2	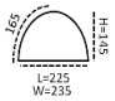	
Igl02	3.67	1.30	2.37	B1: 4.19 W1: 9.51 P1: 0.95 I1: 5.73	2	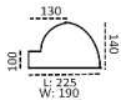	
Igl03	1.15	0.47	0.68	B1:3.36 W:4.64 P:0.20	1	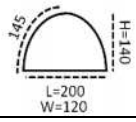	
SB01	0.86	--	--	SB:0.9	--	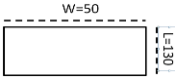	
CM01	0.16	--	--	CM:0.9	--	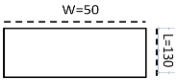	

Table 3. Resume of the burning tests.

Reference	Type of tent	Filling	Induced wind	Type of ignition
110516_TC01	Igl01	1 blanket 4 duvets	no	Fb+St
130125_TC02	Can01	empty	no	Fb*
130616_TC03	Igl02	empty	no	Fb
140127_TC04	Igl03	1 sleeping bag 1 camping mattress	no	St**
140127_TC05	Igl03	1 sleeping bag 1 camping mattress	1.1 m.s-1	St

* Fb – Ignition by firebrands falling over the tent.
**St – Propagation of the fire to the tent by a linear fire front spreading on a straw fuel bed.

Tent ignition was achieved using a firebrand generator as can be seen in Figure 1. The firebrands were provided from the burning of cylindrical pellets with less than 10mm high and with a diameter lower than 4mm. In some cases, the firebrands were directly projected to the tent (Fb). In other experimental tests, a linear fire front spreading on a straw fuel bed propagates the fire to the tent. In one particularly case, the firebrands were simultaneously projected to the tent and to the straw fuel bed adjacent to the tent (Fb+St), resulting in several ignition points in both tent and straw fuel bed. The fuel load of the straw fuel bed was always 0.6 $kg.m^{-2}$.

Figure 1. Experimental apparatus of the burning tests.

The total mass decay (tent, filling and fuel bed) and the convective velocity were the parameters considered for control. The burning tests were carried out in the Forest Fire Research Laboratory (LEIF) using the platform of combustion that is a combustion table fitted on a weight balance that automatically registers for every second the total weight during the experiment. Up flow velocity was automatically measured using Pitot tubes installed on the top of the tent. The experimental installation and equipments can be seen in Figure 1.

Characterization of the camping park fuel cover and its surrounding by image analysis taken by UAV

The determination of the risk of fire in a CP area requires the characterization of factors such as vegetation type, fuel load, distribution of occupied spaces, neighbour water sources and available access routes. In order to facilitate the characterization procedure, either by doing it remotely or even automatically, a high-resolution digital mosaic may be obtained from aerial images acquired by UAVs flying over the camping park area.

With this purpose, some flight tests were made in June 2013 over the CP of Coja, near of Coimbra – Portugal, using the UX-401 quadcopter from UAVision. The quadcopter was equipped with a GoPro HD Hero camera, set for 5MP still image acquisition every 2 seconds. In each of these flights a set of pre-determined waypoints was defined as reference for the quadcopter autonomous navigation. One of these flights is represented in the left image of Figure 2. The right image shows one of the photos taken during the flight.

Figure 2. Left: Trajectory described by the quadcopter while on autonomous navigation over the area of the CP of Coja (seen on Google Earth). Right: One of the pictures taken during the flight with a GoPro camera.

In order to be used as an input variable in fire spread modelling systems, the fuel cover of the camping site and surrounding must be spatially characterized. The processed followed was based on photointerpretation of the produced high-resolution digital mosaic. The photo mosaic was loaded into ArcGIS and the different fuels were identified and vectorized. The fuel models used to characterize the vegetation were the ones produced by M. Cruz (2005) and represent the typical vegetation found in Portugal. A fuel model is by definition a complete set of fuel inputs needed for a mathematical fire spread model (e.g., Rothermel, 1972). It represents a homogeneous vegetation formation in which fire behaviour is expected to be constant and predictable. For each continuous vegetation group identified in the photos a polygon was designed and the corresponding fuel model was assigned in the attributes table. The same was done to non-fuels such as roads, urban areas or water bodies. In the end of the process a continuous fuel map of the entire region was produced.

2.3. Modelling of fire spread in camping parks

Based on the laboratorial experiments results and on the characterization of the camping park fuel cover and its surrounding by image analysis taken by UAV a simulation of a fire front propagation was made. Given the non-deterministic nature of some available data, the fire propagation model was also developed to investigate the quantification of the complex fire propagation uncertainty using stochastic equations and a parametric study (number of variables, stochastic dimension of space) to determine the various parametric influences on the numerical solution of the asymptotic state.
Faster than real time stochastic fire spread predictions were obtained using a Non-Intrusive Spectral Projection (NISP) method in which the solution is expanded in a series using Polynomial Chaos. The unknown coefficients of the expansion terms were calculated from deterministic solutions using a conventional fire growth model. In the present case, the fireLib functions were used for the calculation of the rate of spread together with raster surface fire growth algorithms. The fire growth model of the raster type was ported to the Graphical Processor Units (GPUs) architecture using the Compute Unified Device Architecture (CUDA) programming language.
For the present case three input parameters were considered uncertain, namely the wind speed, the wind direction and the fuel moisture. These three variables were characterized by a Gaussian Distribution with a coefficient of variation of 20%. The stochastic simulations with input parametric uncertainty as random variables were simulated under the complex realistic terrain of the camping park of Coja.

3. Results and discussion

The methodologies previously described were applied in order to obtain the results detailed and discussed in this section. The division into different themes follows the same approach of the previous chapter.

3.1. Analysis of the combustibility of typical materials used in camping parks

The tests performed with the typical camping materials previously described resulted in the values of HCV shown inTable 4.

Table 4. Values of HCV for the different materials tested.

Code Sample	R1	E1	B1	W1	I1	P1	SB1	CP1
HCV (MJ/Kg)	23.13	29.27	45.51	22.58*	22.09	22.86	22.45	41.45

*this sample requires specific accessories for measurements as it contains halogenated components

According to the Portuguese legislation, the tested materials fall within the use-type IX "Leisure and Sports Venues" whose characterization is described in paragraph 1i) of Article 8 of Decree-Law no. 220/2008. This decree-law is regulated by Decree no. 1532/2008 of 29 December, which in point a) of Article 282 stipulates that "in camping parks, coverings used in camping tents, caravans or motorhomes are allowed only when they are constructed with materials with fire reaction classification of at least grade C-S2-d0". This kind of classification is obtained by performing SBI (Single Burning Item test) or the small flame test. However, for SBI tests a very large amount of material is requested by test (1.5x1.5m^2) restraining this to be used mainly for certification of construction and building materials.
Classifications A-B-C-D are dependent of materials fire reaction properties. According to standard NP EN 13501-1, these classes can be related with HCV according to Table 5. In this table, class C does not have a correspondence with HCV.

Table 5. Relation between material classes and HCV according to NP EN 13501-1.

Class	Classification Criteria*
A1	HCV ≤ 1.4MJ/Kg HCV ≤ 3.0MJ/Kg
A2	HCV ≤ 3.0MJ/Kg HCV ≤ 4.0MJ/Kg

*depending on the application

The analysed materials have high calorific values (about 7 to 13 times) above the criteria stipulated for A1 or A2 classes. Based on these high values, it is predicted that they cannot be categorized as class C, suitable for use-type IX "Leisure and Sports Venues" in Portuguese legislation.
The parameters initially considered for control show some problems of measurement due to the convective flow effects, as can be seen in Figure 3. When a tent starts burning, the temperature inside the tent increases creating an uplift which drives to a fake reduction of weight. Occasionally, during the burning some holes in the top of the tent are created and thus the hot air inside the tent can be dissipated. Consequently, the total weight increases suddenly and the up flow velocity abruptly increases to higher values. As the hole enlarges, the exhaust air velocity decreases, even if the tent is burning more intensively. Therefore, these measurements were considered invalid and a qualitative evaluation was made as it is presented in Table 6.

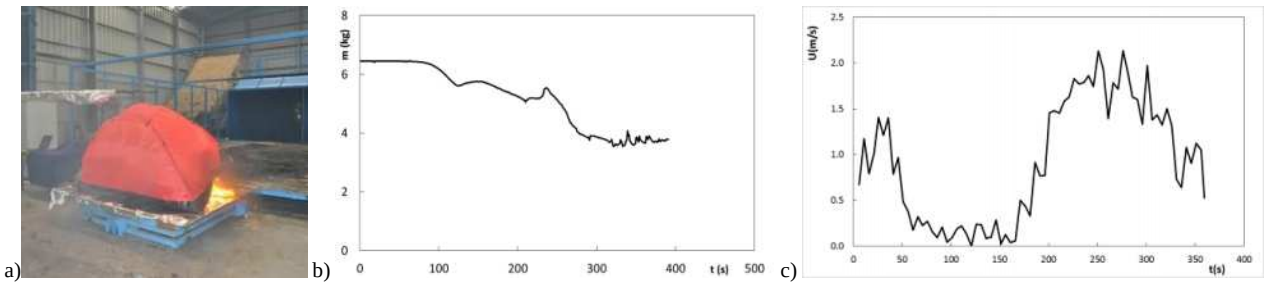

Figure 3. (a) Evidence of the up lift effect caused by the convective flow (140127_TC04); (b) mass loss decay (110516_TC01); (c) up flow variation (140127_TC04).

It was observed the shape of the tent is an important parameter to have ignition. The Canadian tent burned completely because the firebrands felled in the wrinkles accumulating heat. In igloos tents with the fabric well taut, the firebrands did not have that heat accumulation and firebrands just made a hole in the fabric not leading to a sustainable combustion.

The existence of flammable materials inside the tent, a common situation in camping parks, leads to a complete burning of the tent, even if the tent has a specific fabric with favourable combustion behaviour.

Table 6. Qualitative results of the burning tests.

Reference	Characteristics	Results
110516_TC01	Igloo with 2 layers and filling inside; ignition by firebrands and fire line	Complete burn. Ignition in parallel by the straw and by the firebrands. Some firebrands fell on the tent making some holes with no sustainable combustion. Some firebrands passed the fabric of the tent and fell in the blanket and in the duvets that started burning intensively.
130125_TC02	Canadian with 1 layer and no filling inside; ignition by firebrands	Complete burn. Some firebrands fell in the wrinkles of the fabric igniting the tent.
130616_TC03	Igloo with 2 layers and no filling inside; ignition by firebrands	Not burned. Some firebrands fell on the tent making some holes with no sustainable combustion. Some firebrands passed to the floor creating holes which rapidly self-extinguished.
140127_TC04	Igloo with 1 layer and filling inside; ignition by fire line.	Complete burn. The sleeping bed and the camping mattress started burning very intensively, however, when the fire reached these accessories the tent was already burning sustainably.
140127_TC05	Igloo with 1 layer and filling inside; ignition by fire line; induced wind of 1.1m.s^{-1}.	Partially burned. The tent started burning very intensively and the filling was completely burned. At a certain time the tent was inflated by the wind and turned over stopping the experience.

In the presence of wind, if a tent starts burning it can be inflated and dragged by the wind and, consequently, behaving itself as a firebrand spreading the fire to other tents or wounding people. This is a very dangerous situation that shall be taken into account.

3.2. Characterization of the camping park fuel cover and its surrounding by image analysis taken by UAV

The images acquired during the flights in Coja allowed to automatically construct a high-resolution mosaic of the camping site (Coito, 2013), (Costa, 2013). This mosaic is represented in the left image of Figure 4, as an over layer in Google Earth, while the right image represents a zoom of the area indicated by the red rectangle in the left image.

Figure 4. Left: High-resolution mosaic, constructed from aerial images acquired by a quadcopter over the camping site of Côja, overlaying Google Earth. Right: Zoom of the area indicated in red in the image on the left.

Observing the zoom image, one confirms the higher resolution of the resulting mosaic when compared with the available aerial images provided by Google Earth, allowing a clearer identification of the area. Another advantage of the UAV based imagery is that it may be acquired when conveniently, allowing, for example, the characterization of the camping site in different seasons (e.g., summer and winter) corresponding to a quite different distribution of occupied spaces as well as vegetation type and fuel load.

During the photointerpretation phase four fuels were identified: herbaceous (HER-01), low shrubs (MAT-01), pine stand with understory (PPIN-04), and deciduous broadleaves (FOLC-01). The physical parameters of these fuels can be found in Table 7.

Table 7 –Fuel models parameters (from Cruz, 2005)

	Fuel load (kg.m^{-2})				S/V ratio (cm^2.cm^{-3})		Depth (m)	Heat content (kJ.kg^{-1})	Moisture of extinction (%)
	Dead fuels			Live woody					
Model	1 hr	10 hr	100 hr	(Ø<6mm)	1 hr	Live woody			
HER-01	0.3	0	0	0	80	-	0.35	18000	30
MAT-01	0.2	0	0	0.7	60	60	0.4	22500	40
PPIN-04	0.7	0.3	0.2	0.6	60	60	0.7	22000	50
FOLC-01	0.3	0.3	0.2	0	79	-	0.06	18500	21

The area covered by the quadcopter was limited to the Coja camping site but in order to simulate the approach of a wildfire, the surroundings were mapped as well. To do so, Google Earth imagery were used. The final fuel map for the area is shown in Figure 5. The red polygon shows the area covered by the photo mosaic. The surroundings were mapped based on Google Earth.

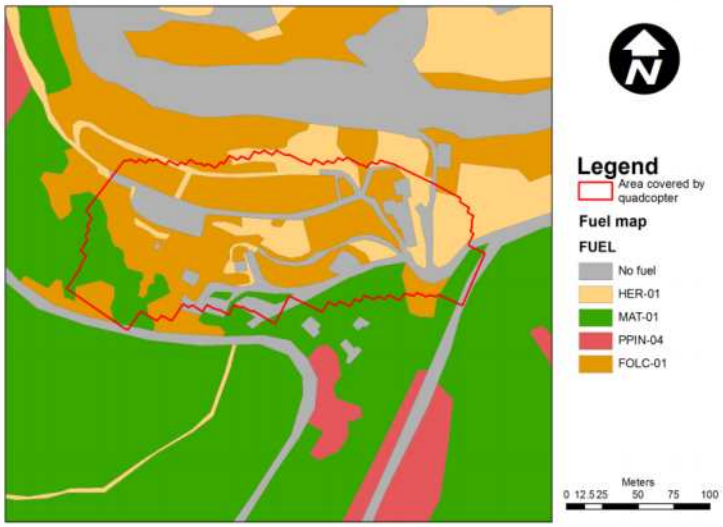

Figure 5. Fuel map of the Coja Camping Site

The fuel map was produced at a resolution of 1 m. The detail obtained with the photographs of the quadcopter is undoubtedly better than the one on Google Earth, thus, the precision of the fuel map inside the camping site is greater than outside. Besides the use of the quadcopter, a fixed-wing UAV (a Twinstar II) is planned to be used for imaging the surroundings of the camping park area. Preliminary imaging will be conducted with a remotely controlled flight of the vehicle and then autonomous flight tests will be performed for the same task. While the quadcopter dealt with the imaging of the camping park and its immediate surroundings, the fixed-wing UAV will focus on taking images of the outer surrounding area.

3.3. Modelling of fire spread in camping parks

Stochastic simulations allow predicting the effect of parametric input uncertainty through the model and, consequently, on the simulation results such as: burned area; fire front velocity and fire front propagation direction. Figure 6 shows the forecast of the fire front (stochastic mean) and its error bar area, based on a 95% confidence interval, at 4 hours of fire propagation.

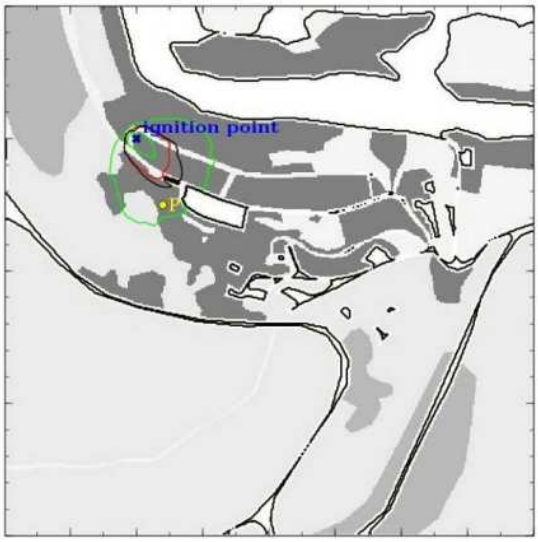

Figure 6. Forecast of the fire front in the CP of Coja after4 hours of ignition: deterministic mean (black); stochastic mean (red); error area with 95% CI (between green lines).

The statistical output of the predicted fields allows to know the probability of fire occurrence at a selected point (any location, as a function of time) and to decide accordingly about actions to have in real wildfires. This becomes particularly interesting when specific locations are of utmost importance and require priority protection. Figure 7 presents the temporal normalized Probability Density Function (PDF) at a selected point (see Figure 6, yellow point) that quantify the uncertainty on the fire spread.

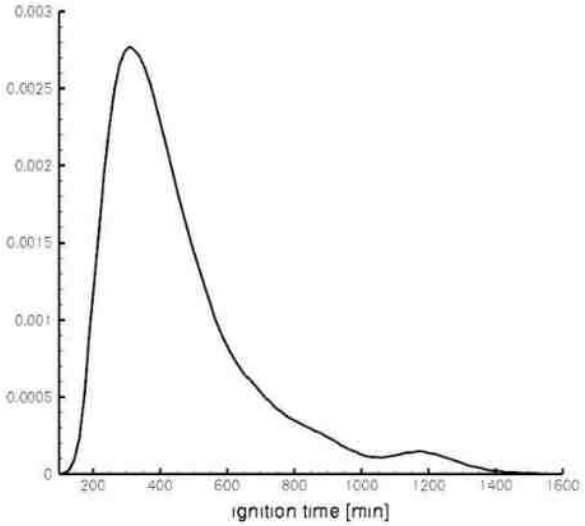

Figure 7. Normalized Probability Density Function (PDF) of ignition time at P location (see Figure 6, yellow point P)

The novel algorithm targeted for GPU architectures achieved a speedup of 176x against serial Central Processing Unit (CPU) execution. The GPU have allowed to obtained two orders of magnitude faster

stochastic fire spread predictions than the real time fire propagation. These results may prove useful toward firefighting methodologies.
The proposed methodology can be used for any camping park scenario. The output provides the time evolution of the ensemble mean fire front location and burned area error bars for a certain confidence interval and the PDF at each point as a function of time. In addition, the hierarchy of input parametric uncertainties based on the stochastic coefficients in the fire spread simulation was quantified. These estimators may add relevant information because wildland fire growth is an intrinsic stochastic process.
Figure 8 shows the stochastic mean (first bar) and the first (second to fourth bars) and second order (last six bars) stochastic coefficients at point P (see Figure 6), where v1, v2 and v3 represent wind speed, wind direction and fuel moisture, respectively. For instance, v1.v2 is the second order cross stochastic coefficient between wind speed and wind direction parameters. The stochastic coefficients characterize the respective parameter variability weight into the final solution. These results permit a sensitivity analysis about the influence of each parameter variability on the fire propagation.

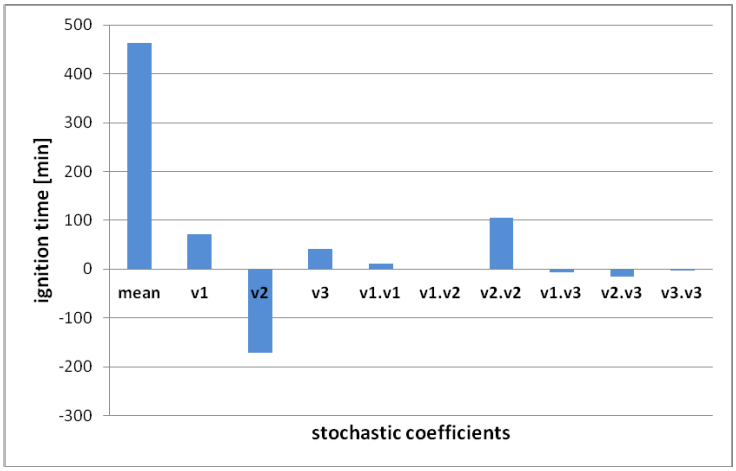

Figure 8. Stochastic coefficients at point P, being the uncertain input parameters: v1 – wind speed; v2 – wind direction; and v3 – fuel moisture.

Conclusion

Several conclusions can be vased on the work performed previously described.
The burning tests of tents resulted in some interesting conclusions. The ignition of the tent by a fire front is very effective, showing the importance of having the area adjacent to the tent free of fuels like straw, needles, garbage, etc. The ignition of tents by firebrands is very alike, and tents not well stretched have a greater probability to ignite as the firebrands accumulate in the wrinkles. The material inside the tent has a great relevance on the probability of the tent burning. Tents should be made of non-flammable fabrics (class C), being observed that when the fabric was taut, firebrands only caused some holes in the tent not leading to a sustained combustion. However, when firebrands crossed the fabric, falling in the other fuel accessories (for example, sleeping beds), they ignited and the tents were completely burned, even if the fabric material was of class C. Since the common situation is tents with accessories inside, it is extremely important to reflect about the need of the actual existing mandatory rules demanding the use of fabric class C in tents or if other camping materials, namely accessories, should have the same compulsory.
This set of tests also highlighted the fact that on windy days a burning tent may become very dangerous. The holes in the tent created by the fire allow the entrance of air, causing the inflation of the tent that is easily pulled from the ground. In this situation, the tent may be dragged over the CP

causing spot fires or even wounding people. As the material of tents is synthetic, the flaming drops released by this kind of materials may cause deep burns.
Regarding to the characterization of the camping park fuel cover and its surrounding, it is clear the advantage of using imagery acquired by an UAV as opposed to Google Earth images. UAV-based imagery results in a high resolution mosaic from which a more detailed fuel map may be obtained. Moreover, with UAVs it is possible to determine when the images are acquired, and thus have fuel maps for different times of the year, corresponding to different camping park occupancies or vegetation degrees of curing.
An accurate and reliable characterization of input variables is necessary because they strongly affect forest fire simulations. Despite the successfully effort in characterizing some fire spread dependencies, such as the fuel cover well featured during this work, there are some parameters that are not easily defined because their values are not constant neither in time nor in space. The non-deterministic behaviour of such parameters leads to stochastic simulations of fire propagation with methods that consider the input variability in the model used. The results obtained provide, admitting a certain confidence interval, error bars of the ignition time in space, as well as sensitivity analysis studies about the influence of each input parameter variability into the final solution. Moreover, the results obtained were faster than real time fire propagation which is mandatory when model predictions are applied to real-time fires.

List of abbreviations

BBQ – Barbeque
CP – Camping Park
CPU – Central Processing Unit
CUDA – Compute Unified Device Architecture
GHC – Gross Heat of Combustion
GPU – Graphical Processor Units
HCV – Higher Calorific Value
LAETA – Associated Laboratory for Energy, Transports and Aeronautics
LEIF – Forest Fire Research Laboratory
NISP – Non-Intrusive Spectral Projection
PDF – Probability Density Function
PE – Polyethilen
PU – Polyurethan
SBI – Single Burning Item test
UAV – Unmanned Aerial Vehicle
WUI – Wildland Urban Interface

Acknowlegments

The authors would like to acknowledge the contributions provided by Domingos Viegas, Valeria Reva, Jorge Raposo and Jorge Neves. The financial support given by LAETA was critical to the development of FireCamp Project which is the base of this paper. To FCMP (Portuguese Camping and Mountaineering Federation) our thanks for the possibility to use the CP of Coja.

References

Fraser JF, Choo KL, Sutch D, Kimble RM (2003). The morning after the night before: campfires revisited. Med J Aust 2003.

Cruz, MG (2005). Guia fotográfico para identificação de combustíveis florestais – Região Centro de Portugal. Centro de Estudos sobre Incêndios Florestais - ADAI, Coimbra. 38 p

Coito T, Caldas Pinto JR, Azinheira JR (2013). Building and Evaluation of a Mosaic of Images using Aerial Photographs. Proceedings of International Conference on Image Analysis and Recognition, Póvoa de Varzim, Portugal, June 2013.

Costa J, Coito T, Caldas Pinto JR, Azinheira JR (2013). Building and Evaluation of a Mosaic of Images using Aerial Photographs", Proceedings of 19th Portuguese Conference on Pattern Recognition, Lisbon, Portugal, November 2013.

Klein MB, Heimbach DM, Honari S, Engrav LH, Gibran NS (2005). Adult campfire burns: two avenues for prevention. J Burn Care Rehabil.

Rothermel RC (1972). A mathematical model for predicting fire spread in wildland fuels. Research Paper INT-115. Ogden, UT: U.S. Department of Agriculture, Forest Service, Intermountain Forest and Range Experiment Station. 40 p.

Assessing the fire risk in the wildland-urban interfaces of SE France: focus on the environment of the housing

Anne Ganteaume, Marielle Jappiot

Irstea, UR EMAX, 3275 route de Cézanne- 13183 Aix-en-Provence cedex 5- France.
anne.ganteaume@irstea.fr, marielle.jappiot@irstea.fr

Abstract
In order to assess the fire risk in Wildland-Urban Interfaces (WUIs) of SE France according to the environment of the housing, several descriptive parameters (ornamental species, types of vegetation adjoining the environment of the housing, types of fence, structure of the hedges and implementation of the regulation on brush-clearing) assumed to either increase or decrease the fire propagation, thus the fire risk, were surveyed according to the types of WUI (isolated, scattered, dense and very dense clustered), in two different locations (coastal and inland) of the study area (département Bouches du Rhône). The flammability of the most frequent ornamental species was assessed at the levels of live and dead surface fuels.
Results showed that the two areas differed according to the main WUI type, the main ornamental species, the main type of fence, the main type of vegetation adjoining the environment of the housing. There was also a variation of these parameters between the different types of WUI, especially according to the ornamental species. The fire risk, assessed through the parameters surveyed and through the flammability of the main ornamental species, increased from the very dense and dense clustered WUIs to the isolated and scattered WUIs and from the coastal area to the inland area.
The improvement of the knowledge on WUI environment at the small scale will allow an increase in the efficiency of the wildfire prevention targeting the areas most at risk.

***Keywords**: Wildland-Urban Interfaces, wildland fire, fire risk, flammability of ornamental vegetation*

Introduction

In the South of France, urbanization, along with the phenomenon of forest extension is generating new spatial configurations called wildland urban interfaces (WUI). In the context of high urban pressure and the accumulation of wildland biomass, WUIs represent serious issues in terms of fire risk management (Davis 1990; Vélez 1997; Cohen 2000). The WUI is becoming a priority region for fire prevention and suppression (Stephens, 2005) and assessing the risk of forest fire in WUI is essential for wildfire prevention and land management. Indeed, wildfires in these areas are a serious threat to communities in many countries worldwide as they can be extremely destructive, killing people and destroying homes and other structures (Mell *et al*. 2010; Haynes *et al*. 2010), thus having ecological, social, and economic consequences. Research using modelling, experiments, and WUI case studies indicates that home ignitability during wildland fires depends on the characteristics of the home and its immediate surroundings, area called the "home ignition zone" (Cohen 2000). A home's ignition potential during extreme wildfires is determined by the characteristics of its exterior materials and design and their response to burning objects, within one hundred feet (30-40 metres), and firebrands (burning embers). Actual case examinations found that most destroyed homes ignite from smaller flames and directly from firebrands and unconsumed vegetation surrounding most destroyed homes (Cohen 2008). Thus, addressing conditions within the home ignition zone can significantly reduce the home ignition potential.
In the present paper, and according to previous works (Stewart *et al*. 2007; Lampin-Maillet *et al*. 2009, 2011), we use the term WUI to refer to the conjunction of housing as well as vegetation characteristics and human presence can be measured by the density of houses and other infrastructures (Lampin *et al*. 2006a, 2006b; Caballero 2004; Camia *et al*. 2003). A WUI typology has been built regarding the spatial

organization of residential houses (Lampin-Maillet *et al.* 2010) and four types of WUI were identified accordingly: (i) isolated (I), (ii) scattered (S) and clustered dwellings divided into (iii) dense clustered (D) and (iv) very dense clustered (VD). The authors of this work hypothesized that the fire behaviour in WUIs was influenced by the pattern of urban areas within a natural landscape and taking into account three variables of fire risk (ignition density, wildfire density and burned area ratio), they showed that isolated and scattered WUI were the most at risk. Hence, it was interesting to explain these results working at a smaller scale, regarding the environment around the housing. At this scale, a first approach assessing the flammability of some ornamental species in SE France was made by Ganteaume *et al*. (2013a, 2013b).

In the present work, we wanted to assess the fire risk at this small scale, taking into account the area surrounding the housing (Cohen's home ignition zone) which corresponds to the ornamental garden commonly found in WUI of SE France. Within this zone, we recorded several indicators which can enhance (vector of the fire propagation) or mitigate the fire risk such as the main ornamental species whose flammability was assessed in laboratory conditions, the structure of the ornamental hedges, the fence type, the vegetation adjoining the environment of the housing and the implementation of the regulation on brush-clearing. The aims of this work were, first, to describe the environment of the housing in each type of WUI in different locations of the study area, and then to assess the fire risk in these WUIs determining which type was the most at risk according to the environment of the housing.

Methods

Study area

The study area is located in the département Bouches du Rhône (Northwestern coordinates: 43.655°N, 5.495°E; Southeastern coordinates: 43.832°N, 5.672°E; total area: 508 700 ha), one of 15 administrative districts composing Southeastern France (Fig 1) which is among the areas most affected by wildfires (54 fires/year and 1247.3 hectares burned per year in the 2000-2010 period according to the regional forest fire database Prométhée). The main natural fuel types of the study area, located mostly on limestone-derived soils, are *Pinus halepensis* forests (Quézel 2000) and mixed pine-oak (*Quercus ilex* and *Q. pubescens*) forests, often the pre-forest vegetation type before oak forests (Quézel and Barbéro 1992). Shrublands, called "garrigue" on limestone-derived soils, are another dominant fuel that corresponds to the predominant successional stage after woodland degradation (Barbéro *et al*., 1998). Wildfires occur frequently in the whole area and overall, the study area is a mosaic of all the previously mentioned types of vegetation and agricultural areas. Because of the difference in climatic conditions between the coastal fringe and the inland part, the study area was divided into two sub-areas (coastal and inland) for sampling, as the variables recorded in the WUI (especially the ornamental vegetation) may differ depending on their location. Thus, 117 housings were surveyed in four coastal locations and 110 housings in five inland locations.

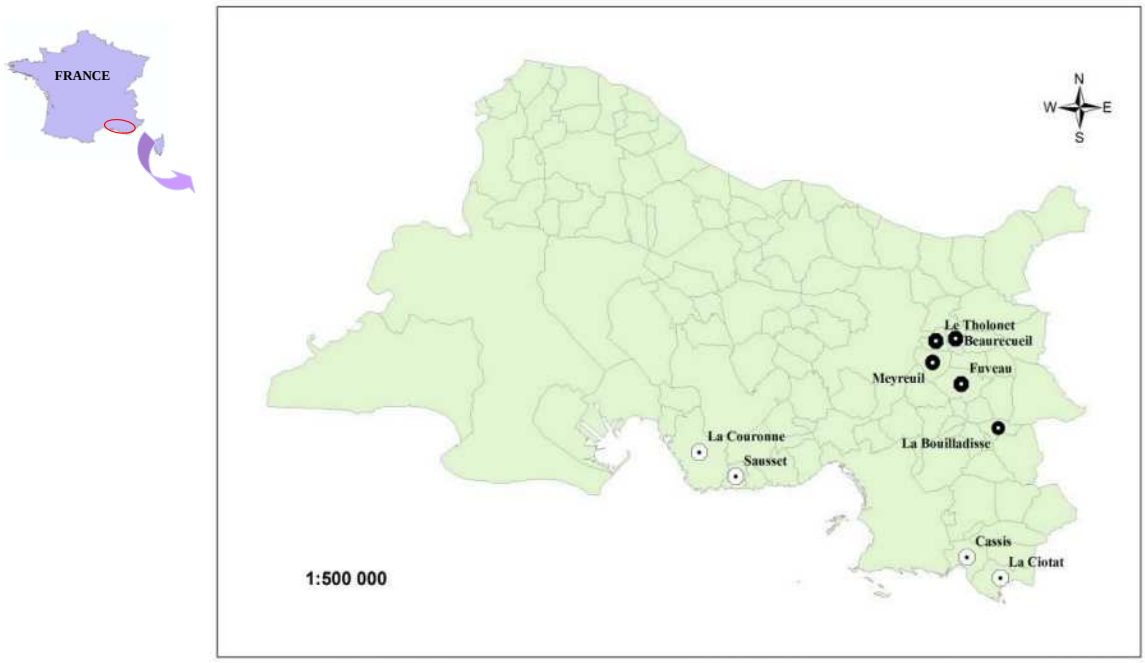

Figure 1. Map of the study area (Département des Bouches du Rhône) in Southeastern France showing where the hedges were surveyed (BD Carto). White spots: coastal area, black spots: inland area

Parameters surveyed for the characterization of the area surrounding the housing

The surveys were also carried out according to the four types of WUI defined by Lampin-Maillet *et al*. (2010): isolated, scattered, dense and very dense clustered. The ornamental species present in each hedge, the structure of the hedge (continuous, discontinuous), the fence type (wall, low wall, low wall and wire, wire, none) surrounding the housing, the vegetation adjoining the ignition zone area (forest, shrubland, crops, another ornamental garden) and if the regulation on brush-clearing was implemented or not, were recorded in each survey. Multiple correspondence analysis (MCA) was carried out in order to highlight the relationships between the parameters recorded in the field and the different types of WUI. This multivariate analysis was performed with R software (R 2.11-1, ADE-4 1.5-1 package).

2.3. Assessing the fire risk according to the flammability of the ornamental species

The flammability of the most frequent ornamental species was assessed during burning experiments of both live and dead fuel samples which were performed at the Irstea Aix-en-Provence facility. Litters (dead fuels), which are the targeted fuel bed in case of spot fires, were burned on a fire bench (experimental conditions described in Ganteaume *et al*. 2013a) and the ignitability, sustainability and combustibility variables were recorded during these experiments. Following the definitions of Anderson (1970), these variables were: (i) the ignition frequency (IF in %) which was computed as the number of successful ignitions relative to the number of trials for a same species; (ii) the time-to-ignition (TTI in s) which corresponded to the time necessary for the appearance of a flame after the firebrand had been placed on the sample; (iii) the flaming duration (FD in s) and (iv) the number of opposite directions of the sample reached by flames (0 to 4) assessing the initial flame propagation.
Live leaves, which are the targeted fuels during the fire propagation from plant to plant, were burned on an epiradiator (experimental conditions described in Ganteaume *et al*. 2013b) and their ignitability and sustainability variables were recorded.
Hierarchical cluster analysis was performed on the flammability variables recorded during the burning experiments of live and dead fuel samples to rank the most frequent species from the least flammable to the most flammable. This analysis was performed with R software (R 2.11-1, ADE-4 1.5-1 package).

2.4. Assessing the variation of the fire risk in the study area

The fire risk was assessed according to the descriptive parameters recorded in the environment of the housing. Multiple correspondence analysis allowed the determination of the types of WUI and the area that were the most at risk and the characterization of the different level of fire risk.

Results and discussion

3.1. Results of the surveys in the study area

Regarding the 227 housings surveyed in the study area, the main types of WUI identified were "very dense clustered" (37%) and "scattered" (31.3%) and a total of 20 ornamental species were recorded. The cypress (all species taken into account) was the most common plant regardless of the WUI type (up to 45% of the ornamental vegetation in the "isolated" WUI type), especially *Cupressus arizonica* (except in the "dense clustered" type). The other most frequent species were *Prunus laurocerasus* and *Thuya plicata* (in scattered WUI), *Eleagnus ebbingei* and *Viburnum tinus* (in dense clustered WUI) as well as *Nerium oleander* and *Pittosporum tobira* (in very dense clustered WUI). The distribution of the ornamental species varied according to the WUI types (Figure 2). Species characterizing the "dense" and "very dense" clustered types clearly differed and differed also from those characterizing the "isolated" and "scattered" types; these two last types did not form two separated clusters of species.

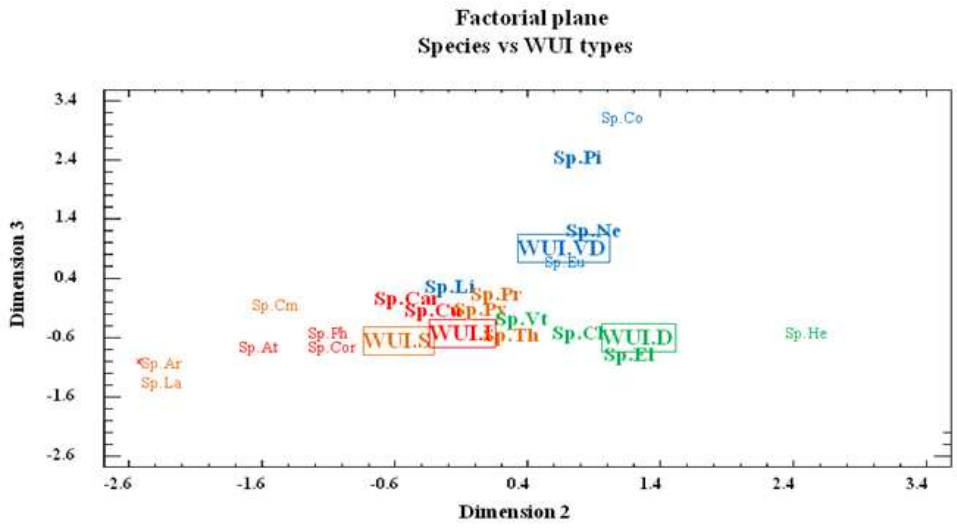

Figure 2. Factorial plane of the MCA showing the characterization of the different WUI types (I: isolated, S: scattered, D: dense clustered, VD: very dense clustered) by the ornamental species (in bold: most frequent species; Ar: Arundo donax, La: Laurus nobilis, At: Atriplex maritimus, Cor: Coronilla sp., Ph: Phyllostachys sp., Cu: Cupressus sempervirens, Cm: Cupressus macrocarpa, Car: Cupressus arizonica, Li: Ligustrum japonicum, Pr: Prunus laurocerasus, Py: Pyracantha coccinea, Vt: Viburnum tinus, Cl: Cupressus leylandii, Th: Thuja occidentalis, El: Eleagnus ebbingei, Eu: Euonymus japonicus, Ne: Nerium oleander, Pi: Pittosporum tobira, Co: Cotoneaster sp., He: Hedera helix).

Among the descriptive parameters recorded in the environment of the housing, we found that the hedges composed of ornamental vegetation were mostly continuous (87%) and the main types of fence were "low wall + wire" (39%, mostly in dense and very dense WUI types) and "wire" (35%, mostly in scattered and isolated WUI types). On the contrary, the "wall" was the less frequent type of fence (16%). The main vegetation types adjoining the buffer around the housing were another ornamental garden (43% especially in dense and very dense WUI types) and forest (31%, especially in scattered

and isolated WUI types). In total, 49% of the houses surveyed were directly adjoining wildland vegetation and the mandatory brush-clearing was implemented at 96%.

3.2. Results of the spatial variation within the study area

The very dense clustered WUI was the most frequent type in the coastal area (47%) whereas the scattered WUI was the most frequent type in the inland area (36%).
The main ornamental species also differed spatially. *Prunus laurocerasus* and *Pyracantha* (in mostly in scattered and very dense types), *Eleagnus ebbingei* and *Cupressus leylandi* (mostly in dense type) as well as *C. sempervirens* and *C. arizonica* (mostly in isolated type) were the most frequent species in the inland area whereas *Nerium oleander* (mostly in scattered, dense and very dense types), *Pittosporum tobira* (mostlin very dense and isolated types), *Thuya plicata* (mostly in dense type) and the cypress (all species regardless of the WUI type) were the most frequent in the coastal area.
There was no spatial difference in the type of hedge (mostly continuous) and the main types of fence were "low wall + wire" in the coastal area (49%) and "wire" in the inland area (53%).
The main vegetation types adjoining the environment of the housing were another ornamental garden (58% especially in dense and very dense types) in the coastal area and forest (42%, especially in scattered and dense types) inland. In total, 30% of the houses surveyed were directly adjoining wildland vegetation in the coastal area against 70% in the inland area and the mandatory brush-clearing was implemented at more than 90% in both areas.

3.3. Flammability experiments

Among the 20 species recorded during the surveys, which were hypothesized to be representative of the species planted in the whole study area, eight species were chosen for the study of their flammability, either because of their frequency in the study area, e.g. *Prunus laurocerasus* (Pr), *Pyracantha coccinea* (Py), *Cupressus sempervirens* (Cu) assumed to have the same flammability characteristics as the other species of *Cupressus* and as *Thuya plicata* (because of the same foliar structure), *Nerium oleander* (Ne), *Eleagnus ebbingei* (El), *Ligustrum japonicum* (Li) and *Pittosporum tobira* (Pi), or because of their uniqueness, e.g. *Phyllostachys sp.* (Ph), the only monocotyledon recorded, which may have particular flammability characteristics.
Results of the flammability experiments are presented in table 1. At the litter level, *Cupressus sempervirens* and *Pyracantha coccinea* litters ignited very frequently (IF $\geq$ 90%) in contrast of *Pittosporum tobira* litters (20%). Litters sampled in the hedges of *Ligustrum japonicum* and *Nerium oleander* were the quickest to ignite (47 and 49 s) in contrast of these of *Prunus laurocerasus* and *Pyracantha coccinea* (153 s and 188 s). The longest flaming duration were recorded in *Eleagnus ebbingei*, *Cupressus sempervirens* and *Pyracantha coccinea* litters (between145 and 148 s) and the shortest in *Pittosporum tobira* litter (55 s). Initial flame propagation was the best in *Ligustrum japonicum* litter (on average 3.7 sides of the sample were reached by the flames) in contrast of *Cupressus sempervirens* litter (on average, 2.4 sides of the sample were reached by the flames). At the live leaf level, *Cupressus sempervirens*, *Eleagnus ebbingei*, *Phyllostachys sp.* and *Pyracantha coccinea* litters ignited very frequently (IF $\geq$ 90%) in contrast of *Ligustrum japonicum* and *Pittosporum tobira* litters (42 and 46%). Litters sampled in the hedges of *Phyllostachys sp.* were the quickest to ignite (11 s) in contrast of these of *Cupressus sempervirens* and *Pittosporum tobira* (36 s and 30 s). *Eleagnus ebbingei* litters burned the longest (12 s) in contrast of these of *Prunus laurocerasus* (5 s).

Table 1. Flammability variables of the litter and live leaf recorded on each species studied (mean and standard deviation; IF: ignition frequency, TTI: time-to-ignition, FD: flaming duration, Ph: Phyllostachys sp., Cu: Cupressus sempervirens, Ne: Nerium oleander, Li: Ligustrum japonicum, El: Eleagnus ebbingei, Pi: Pittosporum tobira, Pr: Prunus laurocerasus and Py: Pyracantha coccinea)

	IF_litter(%)	TTI_litter(s)	FD_litter(s)	FS_litter(#)	IF_live(%)	TTI_live(s)	FD_live(s)
El	57	70.71 (37.88)	145.12(83.57)	3.47(1.01)	98	16.39(5.4)	11.88(3.75)
Li	60	46.72 (50.77)	86(54.51)	3.72(0.75)	42	21.38(8.26)	7.71(4.26)
Ph	70	56.24(33.27)	66.10(33.28)	3.43(0.51)	96	10.71(4.15)	8.4(3.56)
Pi	20	116.85(113.50)	55(45.96)	2.54(1.71)	46	29.57(11.73)	8.96(6.8)
Ne	57	49.26(36.42)	66.89(22.86)	3.11(1.24)	86	23.67(6.81)	8.14(4.2)
Pr	83	153.39(109.32)	75.33(36.89)	3.5(0.74)	98	17.43(4.27)	4.92(2.04)
Py	93	188.32(132.14)	145.32(81.79)	2.58(1.03)	88	15.86(5.7)	7.11(4.99)
Cu	90	92.12(79.61)	147.91(107.25)	2.36(1.29)	94	35.55(6.61)	6.51(2.72)

The combination of the flammability variables recorded on live fuel and dead fuel (litter) using hierarchical cluster analysis highlighted three groups of species with different flammability (Figure 3): the most flammable species (*Phyllostachys sp. , Eleagnus ebbingei , Ligustrum japonicum* and *Nerium oleander*), the least flammable species (*Pittosporum tobira*) and the group of species having intermediate flammability (*Cupressus sempervirens, Prunus laurocerasus* and *Pyracantha coccinea*). According to the type of fuel (live or dead), some species showed the same type of flammability like *Pittosporum* (always poorly flammable), *Cupressus* and *Pyracantha* (always moderately flammable) or *Eleagnus* (always highly/extremely flammable) in contrast of other species (*Phyllostachys sp., Prunus laurocerasus , Ligustrum japonicum* and *Nerium oleander)* which were less flammable at the live leaf than at the litter level.

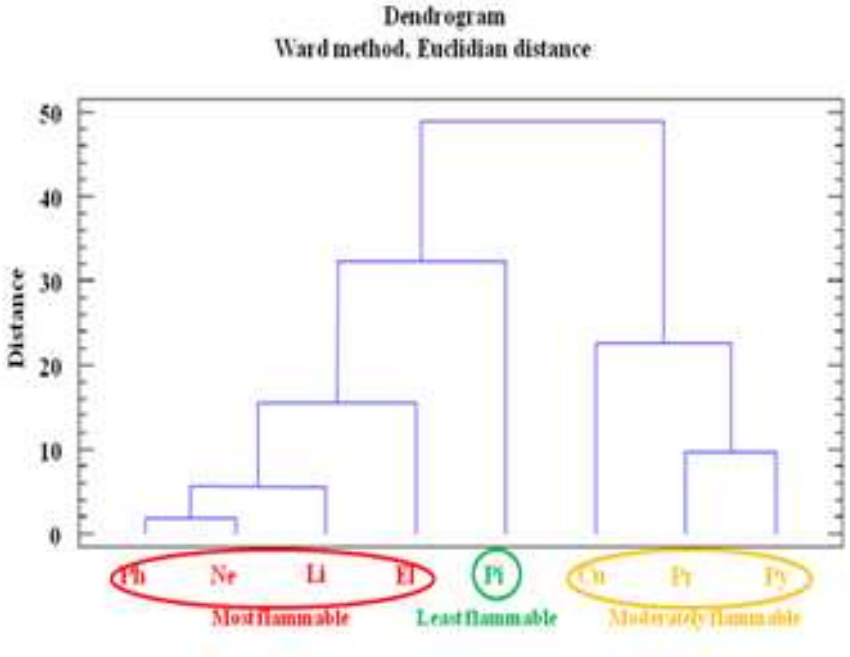

Figure 3 : Dendrogram of hierarchical cluster analysis based on the flammability variables recorded on live leaves (time-to-ignition, flaming duration, ignition frequency) and litters (time-to-ignition, flaming duration, ignition frequency, initial propagation) sampled in the different species studied (Ph: Phyllostachys sp., Cu: Cupressus sempervirens, Ne: Nerium oleander, Li: Ligustrum japonicum, El: Eleagnus ebbingei, Pi: Pittosporum tobira, Pr: Prunus laurocerasus and Py: Pyracantha coccinea)

3.4. Assessment of the fire risk

The fire risk was assessed taking into account the flammability of the main ornamental species, the type of vegetation adjoining environment of the housing, the type of fence, the structure of the hedges and the implementation of the regulation on brush-clearing.

Among these descriptive parameters, some can mitigate the fire propagation toward the housing, thus mitigate the fire risk, such as crops and another garden as vegetation types adjoining the environment of the housing, discontinuous hedges or high wall surrounding the housing. Poorly flammable species (like *Pittosporum*) as well as the implementation of the regulation on brush-clearing around the housing also contribute to mitigate the fire risk. On the contrary, other parameters can enhance the fire risk, such as shrubland and forest adjoining the environment of the housing, the absence of fence or fence made of wire that cannot mitigate the radiant heat or the firebrands emitted by the flaming vegetation. Continuous hedges, particularly composed of very flammable species as well as the non-implementation of the regulation on brush-clearing can also enhance fire propagation toward the housing.

The multivariate analysis showed that the fire risk increases from the dense and very dense clustered WUIs to the isolated and scattered WUIs on axis 1 with a gradient of fire risk from low fire risk (other garden, high wall, discontinuous hedges) to high fire risk (shrublands which means a vegetation burned at least one time, no fence or wire-made, continuous hedges). The presence of, at least, seven species characterized by intermediate or high flammability and no poorly flammable species in the isolated and scattered WUI types also indicates higher fire risk in these areas whereas the presence of at least one poorly flammable species and five species characterized by intermediate or high flammability in the dense and very dense clustered WUI types contribute to decrease the fire risk. The same trend as on axis 1 was also highlighted from the coastal area to the inland area on axis 2. Implementation of the regulation on brush-clearing was not a significant parameter in the analysis (Figure 4).

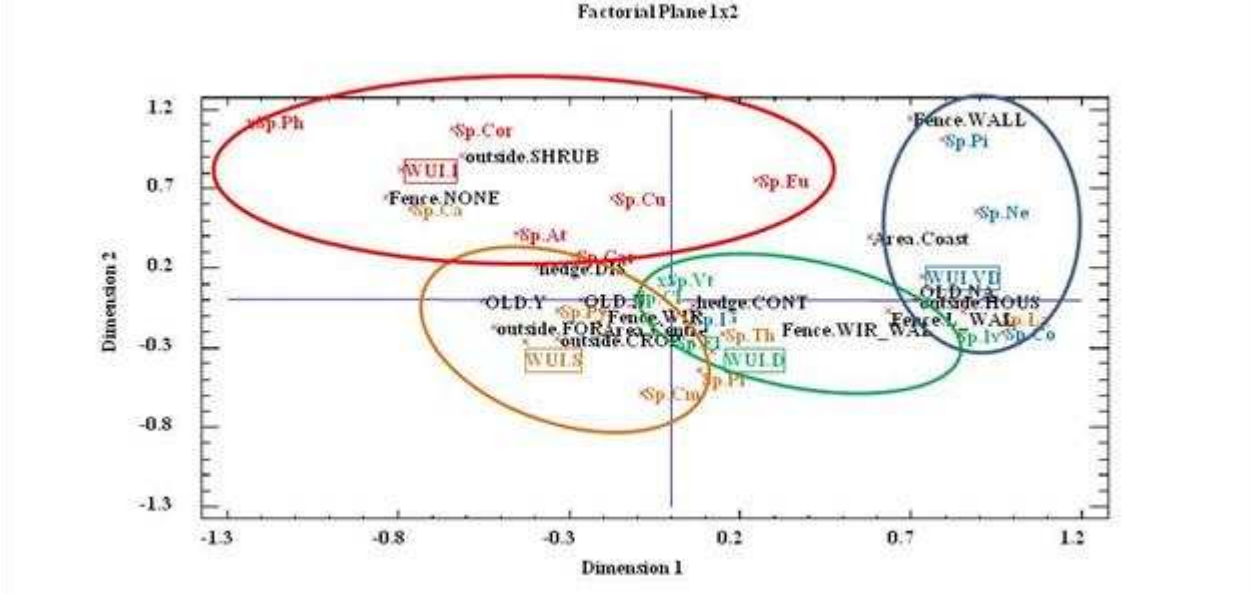

Figure 4. Factorial plane of the MCA showing the variation of the fire risk (red: high, orange: medium, green: low, blue: very low) between the different WUI types (I: isolated, S: scattered, D: dense clustered, VD: very dense clustered) and the location in the study area (coastal vs inland) according to the parameters recorded in the area surrounding the housing. (Sp: Ar: Arundo donax, La: Laurus nobilis, At: Atriplex maritimus, Cor: Coronilla sp., Ph: Phyllostachys sp., Cu: Cupressus sempervirens, Cm: Cupressus macrocarpa, Car: Cupressus arizonica, Li: Ligustrum japonicum, Pr: Prunus laurocerasus, Py: Pyracantha coccinea, Vt: Viburnum tinus, Cl: Cupressus leylandii, Th: Thuja occidentalis, El: Eleagnus ebbingei, Eu: Euonymus japonicus, Ne: Nerium oleander, Pi: Pittosporum tobira, Co: Cotoneaster sp., He: Hedera helix;Outside: HOUS: house, FOR: forest, SHRUB: shrubland; Type of fence: WAL: high wall, L_WAL: low wall, WIR_WAL: wall and wire, WIR: wire; type of hedge: CONT: continuous, DIS: discontinuous; implementation of mandatory brush-clearing: OLD_Y: yes, OLD_N: No, OLD_NA: no data)

Conclusion

The improvement of the knowledge on WUI environment at small scale will allow an increasing efficiency of the wildfire prevention targeting the areas most at risk. Assuming that the parameters recorded in the environment of the housing correspond to important aspects of fire risk, we showed that isolated and scattered WUI, especially in the inland area, are in fact at high risk of wildfire. This result agrees with the work of Lampin-Maillet *et al*. (2010) who also highlighted a higher fire risk in isolated and scattered WUI types than in the clustered types taking into account different fire metrics.

Acknowledgements

The authors wish to thank the Irstea's technical staff for their contribution in the field and in the burning experiements.

References

Anderson HE (1970) Forest fuel ignitability. *Fire Technology* **6**, 312-319

Barbéro M, Loisel R, Quézel P, Richardson DM, Romane F (1998) Pines of the Mediterranean Basin. Ecology and Biogeography of *Pinus*. Cambridge University Press, Cambridge.

Caballero D (2004) Conclusions of the Third WARM Workshop on Forest Fires in the Wildland-urban Interface in Europe. Madrid, Spain, 26–27th of May.WARM Project Final Report. European Commission.

Camia A, Valera V, Marzano R, Etchifidis G (2003) Spatial Analysis in European Wildland-urban Interface Environment Using GIS. WARM project, http://www.fria.gr/chapters/warmCh21Camia.pdf.

Cohen JD (2000) Preventing Disaster- Home Ignitability in the Wildland-Urban Interface. *Journal of Forestry* **98**(3),15-21.

Cohen JD (2008). The wildland urban interface fire problem: a consequence of the fire exclusion paradigm. *Forest History Today*, 20-26.

Davis JB (1990) The wildland-urban interface: paradise or battleground? *Journal of Forestry* **88** (1), 26–31.

Ganteaume A, Jappiot M, Lampin C (2013a) Assessing the flammability of surface fuels beneath ornamental vegetation in wildland–urban interfaces, in Provence (south-eastern France). *International Journal of Wildland Fire* **22**(3), 333-342.

Ganteaume A, Jappiot M, Lampin C, Guijarro M, Hernando C (2013b) Flammability of some ornamental species in wildland-urban interfaces in Southeastern France: laboratory assessment at particle level. *Environmental Management*, **52**, 467-480.

Haynes K, Handmer J, McAneney J, Tibbits A, Coates L (2010) Australian bush- fire fatalities 1990–2008: exploring trends in relation to the "Prepare, stay and defend or leave early" policy. *Environmental Science Policy* **13**, 185–194.

Lampin C, Jappiot M, Long M, Mansuy N, Borgniet L (2006a) WUI and road networks/vegetation interfaces characterizing and mapping for forest fire risk assessment. *Forest Ecology and Management* **234** (Suppl. 1), S137–S140.

Lampin C, Jappiot M, Borgniet L, Long M (2006b) Cartographie des interfaces habitat-foreˆt: une approche spatiale pour estimer le risque d'incendie de forêt. *Revue internationale de géomatique. European. Journal of GIS and Spatial analysis* **16** (3–4), 321–340.

Lampin-Maillet, C., Jappiot, M., Long, M., Morge, D., Ferrier, J.P., 2009. Characterization and mapping of dwelling types for forest fire prevention. *Computers, Environment and Urban Systems* **33**, 224–232. doi:10.1016/j.compenvurbsys.2008.07.003.

Lampin-Maillet C, Jappiot M, Long M, Bouillon C, Morge D, Ferrier JP (2010) Mapping wildland-urban interfaces at large scales integrating housing density and vegetation aggregation for fire prevention in the South of France. *Journal of Environmental Management* **91**, 732–74.

Mell WE, Manzello SL, Maranghides A, Butry D, Rehm RG (2010) The wildland–urban interface fire problem—current approaches and research needs. *International Journal of Wildland Fire* **19**, 238–251.

Quézel P (2000) **Taxonomy and biogeography of Mediterranean pines (*Pinus halepensis* and *P. brutia*)**. In: Néeman G and Trabaud L (eds.) *Ecology, Biogeography and Management of Pinus halepensis and Pinus brutia Forest Ecosystems in the Mediterranean Basin*, Backhuys, Leiden, NL, pp 1-12.

Quézel P, Barbero M (1992) Le pin d'Alep et les espèces voisines : répartition et caractères écologiques généraux, sa dynamique récente en France méditerranéenne. *Forêt méditerranéenne* **XIII**, 158-170.

Stephens SL (2005) Forest fire causes and extent on United State Forest Service lands. *International Journal of Wildland Fire* **14**, 213-222.

Stewart, S.I., Radeloff, V.C., Hammer, R.B., Hawbaker, T.J., 2007. Defining the wildland–urban interface. *Journal of Forestry*, 201–207.

Vélez R (1997) Recent history of forest fires in Mediterranean area. In: Balabanis P, Eftichidis G, Fantechi R (Eds.), Forest Fire Risk and Management. Proceedings of the European School of Climatology and Natural Hazards, Greece, 27 May–4 June 1992. European Commission, Brussels, pp. 15–26.

Assessment of fire risk in relation to land cover in WUI areas

María Calviño-Cancela[a], María L. Chas-Amil[b], Julia Touza[c]

[a] *Dept. Ecology and Animal Biology, University of Vigo, Experimental Sciences Building, University Campus, 36310 Vigo, Spain, maria@uvigo.es*
[b] *Dept. of Quantitative Economics, University of Santiago de Compostela, Baixada Burgo das Nacións s/n, 15782 Santiago de Compostela, Spain, marisa.chas@usc.es*
[c] *Environment Dept., University of York, Heslington Road, YO10 4AD, York, UK, julia.touza@uvigo.es*

Abstract
Areas where urban and wildland intermingle, known as wildland-urban interface (WUI), are increasing worldwide over the last decades (Theobald and Romme 2007; Montiel and Herrero 2010). These WUI areas are of particular concern in forest fire risk management because the presence of housing developments in contact with forestlands increases the likelihood of a fire starting as a consequence of human activities. In Spain, for example, there is increasing evidence that the wildland-urban interface constitutes a highly risk prone area (Herrero *et al*. 2012; Chas-Amil *et al*. 2013). Given the recognised role of land cover distribution in fire risk (Bajocco and Ricotta 2008; Oliveira *et al*. 2013), this paper evaluates recent fire activity across different land cover categories, and the causes and motivations, comparing WUI and non-WUI areas. Fire data were collected in Galicia, Spain, where fires are mostly due to deliberately-caused ignitions. We show that arsonist are more likely to ignited a fire in WUI areas than in non-WUI; and the same seems to be true for fires ignited by agricultural activities. Moreover, land cover types only have a significant impact on the patterns of fire occurrence in WUI areas.

Keywords*: fire hazard, land-use cover, wildland-urban interface, intentional-caused fires, Galicia, Spain.*

Introduction

Fire is a natural process in many ecosystems, with an important role in shaping species adaptations and landscapes (Bond and Keeley 2005). However, human activities have altered fire regimes in areas such as southern Europe, increasing fire frequency, especially of large fires (Moreno *et al*.1998). In Spain, for instance, more than 90% of wildfires are caused by human activities, according to official statistics (MAGRAMA, 2010). Therefore, areas where wildland and human developments intermingles, known as wildland-urban interface (WUI), are especially vulnerable to the risk of fire ignitions (Chas-Amil *et al* 2013; Lampin-Maillet et. al. 2010; Syphard *et al*. 2007). In addition, the presence of population living close to forestlands increases the likelihood of severe consequences in properties and land-use activities and may also pose serious threats to lives.
The fire risk (or ignition risk) is the chance of a fire starting as determined by the incidence of causative agents (FAO 1986; NWCG 2006). A good understanding of the patterns and causes of fire ignition is essential for effective fire prevention (Finney 2005). Land use and land cover (LULC) have been recognized as a major determining factor of fire risk (Bajocco and Ricotta 2008; Moreira *et al*. 2009; Carmo *et al*. 2011; Xystrakis and Koutsias, 2013) and, in contrast with other factors such as weather and topography, it can be subject to active policy management, which makes the analysis of fire risks associated with LULC types especially interesting for fire prevention policies. In addition, it can provide useful information for local residents, as these are often not aware of the fire risk associated with their behaviour. The type of LULC determines fuel load and characteristics (e.g. flammability and moisture content; Saura-Mas *et al*. 2010; Ganteaume *et al*. 2009) and is associated with human activities with contrasting levels of fire risk (e.g. use of fire as a management tool for agricultural waste disposal in farmlands or for pasture renewal in rangelands; Vélez 2002; Ganteaume *et al*. 2013).

Moreover, socio-economic factors may lead to land-use conflicts that can trigger intentionally-caused fires (e.g. urbanization pressure or unemployment; Prestemon *et al*. 2012; Romero-Calcerrada *et al*. 2010).
In this paper, we analyse the level of fire risk at different land covers and the causes and motivations of fires, comparing WUI and non-WUI areas. We analyze whether different land cover types are equally fire-prone, i.e. fires occur in direct proportion to the availability of those land cover types in the landscape, or otherwise some land cover types burn more or less frequently than expected given their abundance. We contribute to the previous literature on fire ignition selectivity towards different land cover types by comparing WUI and non-WUI areas, in order to determine whether the contrasting socio-economic contexts in these types of areas have a significant impact on the patterns of fire occurrence and its causes.

Materials and methods

Study area

The study was carried out in Galicia (NW of Iberian Peninsula). Its ancient mountains, with an average altitude of 508 meters, characterize the territory. Climate is rather humid and because of Galicia's meridional latitude, it can be quite warm in some areas. Galicia is the most important forestry region in Spain (Manuel and Gil 2002), with c. 70% of the land being forested. More than half of the forested area is covered by tree plantations of *Pinus pinaster* and *Eucalyptus globulus*, in pure and mixed stands. Depopulation and farming abandonment has led to an increase of forested land, as in many other rural areas in Europe, particularly the expansion of eucalypt plantations, resulting in important changes in the regional landscape, mainly in rural lowland areas (Marey-Pérez *et al*., 2006; Cramer and Hobbs, 2007). Native forests dominated by *Quercus robur*, which occupied large areas in the past, have now been reduced to small, isolated patches (Ramil-Rego *et al*., 1998; Teixido *et al*., 2010). Based on Chas-Amil *et al*. (2013), the interface between urban and forested areas (WUI) totals 2,442 km^2 in Galicia, which represents 8.3% of the region, with many WUI areas located along the Atlantic coast and in the southwest of Galicia. A significant proportion (79%) of the WUI areas are classified as non-forested areas, while the forested land in WUI is mainly characterized by a high level of fragmentation. On the other hand, forestlands dominate non-WUI areas, covering nearly three-quarters of these areas. Compact forestlands with little fragmentation cover more than half of the territory outside the interface (56%), while highly fragmented forestland covers 14%.
With an annual average of more than 4,000 forest fires and 30,000 ha burned between 2006 and 2009, Galicia is the region of Spain with the highest frequency of fires; more than 30% of forest fires in Spain each year are located in this region, even though it represents only 6% of the Spanish territory. In addition, most fires are human-caused (99%), mainly associated with intentional behaviour (80%) (Chas-Amil *et al*. 2010).

Fire and land cover data and analyses

We defined wildland-urban interface (WUI) as the intersection of the forest area and/or forest influence areas (up to 400 m from forestland) with the buffer of 50 m around buildings, where bush clearing is compulsory by law (Law 3/2007 of April 9, 2007, addressing the issues of wildfire prevention and suppression, as modified by Law 7/2012 of June 28, 2012). The identification and mapping of WUI en Galicia was obtained from Chas-Amil *et al*. (2013).
A database of the daily forest fire ignition points for the period from January 1, 2006 to December 31, 2011 was employed for this study. These fire ignition data were obtained from the Rural Affairs Department of the Regional Government (Xunta de Galicia), and the Spanish Ministry of Agriculture, Food and Environment (MAGRAMA). Forest fire reports list general information on burned areas, date and estimated time of ignition, the geographic coordinates of the ignition point, causes and motivations, and the fire-fighting measures applied. A fire is included in the official database only if

it fully or partially affects forest and other woodland areas. The coordinates of the ignition points for all fires in the database were evaluated and corrected if errors were detected. We refined the coordinates by using maps of administrative boundaries (parishes, municipalities, population entities) at a scale of 1:25000, a raster topographic map 1:25000, and Landsat TM images. All computations were performed with ArcGIS® 9.3.1 by ESRI and Geomedia Professional 6.0 by Intergraph.
We then combined the WUI layer and the geographic coordinates of the ignition points to randomly select a total of 600 wildfires (100 per year), 300 in WUI areas and 300 in non-WUI areas, together with all their characteristics included in the wildfire database. Fire causes were grouped in 4 classes: deliberate, negligence, unknown, others (natural causes and accidents that are not considered negligence). For deliberated fires, the motivation behind the fires is also included in fire reports, and was grouped in the following categories: farmers (fires caused by farmers for clearing shrubland areas), rangers (burning of shrublands for pasture renewal), arsonists, vandals, chasing wildlife away (e.g. wolfs or wild boars), others or unknown motivations. Note that causes are, in most cases, presumed by the technical staff in the field, and only in c. 10% are confirmed caused.
The land cover type of all these locations was identified, using information from the Fourth National Forest Inventory (IFN4), which was developed in Galicia in 2008-2009. The IFN4 has been based on the cartography of the Forest Map of Spain at 1:25.000 (MFE25) carried out on aerial orthophotos of the PNOA of the National Geographic Institute that are divided in homogeneous polygons of 0.5 to 2 ha in size (depending on the cover type) and are classified according to a hierarchic classification with a total of 63. We re-grouped these categories according to our research interest into the following categories: broadleaved forests (broadleaved natural forest, as differing from tree plantations, dominated by native broadleaved trees, mostly *Quercus robur* and *Quercus pyrenaica*; plantations of broadleaved trees such as *Castanea sativa* or *Betula pendula* has been included also in this category), tree plantations (pure or mixed stands dominated by *Eucalyptus globulus*, *Pinus pinaster*, *Pinus radiata* and *Pinus sylvestris*), shrublands (dominated by shrubs, with no tree cover), farmland (used for crops and pastures for livestock), and artificial (areas devoted to urban or industrial developments and infrastructures).
In order to determine fire selectivity for different land cover, the frequency of different land covers between ignition points and a random null model, was investigated using Maximum Likelihood Ratio tests (G test, Sokal and Rohlf 1995). For this, we selected a total of 200 random points (100 in WUI and 100 in non-WUI areas) and determined their cover type. Significant differences indicate that fires would not occur randomly in the landscape, with different proportion of ignition points and available land-cover types. We also estimated the selection ratio (w_i) for a given cover class, an index estimated as $w_i = U_i/A_i$, where U_i is the proportion of the ignition points belonging to cover class i and A_i is the proportion of available area belonging to that cover class i (Manly *et al*. 1993). A cover type with a percentage of ignition points proportionate to its availability has a value $w_i = 1$, a class with a percentage of ignition points exceeding that expected by chance (i.e. selected positively by fire, thus more fire-prone than expected by random) had a value $w_i > 1$, whereas a cover type with a less than expected proportion ignition points (i.e. avoided by a fire, less fire-prone than expected by random), has a value $w_i < 1$ (e.g. Moreira *et al*. 2001; Nunes *et al*. 2005).

3. Results

3.1. Wildfire causes

Most wildfires in Galicia were considered deliberate for the period 2006-2011. Differences between WUI and non-WUI in regard to causes of wildfires were marginally significant ($G=13.5$, 3 d.f., $p<0.05$), with a higher number of fires due to negligence in WUI areas (1.9 times more than in non-WUI areas) (Figure 1).

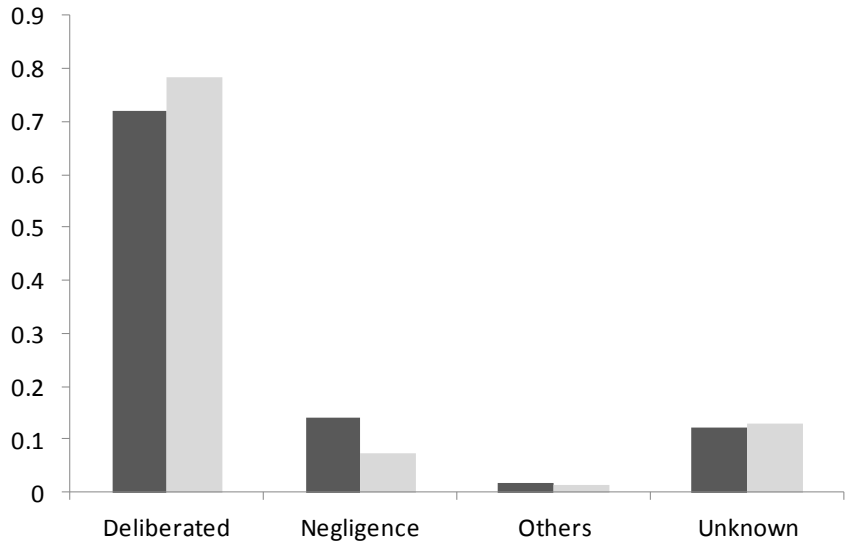

Figure 1. Relative frequencies of wildfire causes in WUI (dark gray) and non-WUI areas (light gray).

Motivations behind deliberate fires differed markedly between WUI and non-WUI areas (G=58.0, 5 d.f., $p < 0.05$), especially in regard to fires caused to chase wildlife away, which were more than 15 times more frequent in non-WUI than in WUI areas (Figure 2). Fires caused by ranchers were also somewhat more frequent in non-WUI than in WUI areas (1.6 and 1.3 times more), whereas those caused by arsonist and farmers showed the opposite pattern (1.6 and 1.2 times more frequent in WUI than in non-WUI areas).

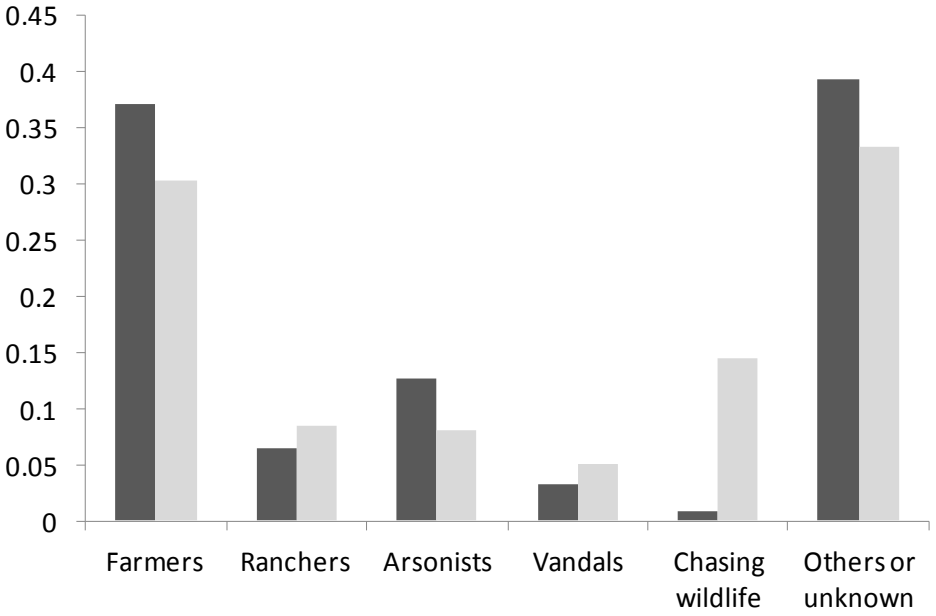

Figure 2. Relative frequencies of motivations behind deliberated wildfire in WUI (dark gray) and non-WUI areas (light gray).

In non-WUI areas, causes of wildfires had similar frequencies among land cover types. However, in WUI areas, the frequency of fire causes in farmlands and plantations differed from the general pattern (pooling together all cover types). In farmlands, deliberated fires and those caused by negligence were the most frequent (87%), but fires caused by negligence were 1.8 times more frequent than expected

by the general pattern, whereas deliberated fires were 13% less frequent than expected. In plantations, deliberated fires were the most frequent (72%), similarly as for all cover types pooled, whereas fires caused by negligence were 25% less frequent than expected.

3.2. Patterns of cover types and wildfire distribution

The coverage of land uses differed between WUI and non-WUI areas, with more land devoted to farms in WUI than in non-WUI (77% vs. 22%) and less to shrublands (3% vs. 26%), plantations (13% vs. 37%), and broadleaves forests (7% vs. 10%).

Table 1. Estimated selection ratio index in WUI and non-WUI in the study area.

Land cover types	Area (%) with respect to total	Ignition points (%) of those randomly selected	w_i
WUI			
Artificial	6	12.8	2.14
Farmland	70	51.0	0.73
Shrublands	3	3.7	1.24
Tree plantations	13	25.3	1.95
Broadleaved forests	7	5.4	0.77
Others	1	1.7	1.7
			G = 21.63*
Non-WUI			
Artificial	5	1.3	0.27
Farmland	22	27.4	1.25
Shrublands	26	29.1	1.12
Tree plantations	37	29.1	0.79
Broadleaved forests	10	12.0	1.20
Others	0	1.0	-
			$G = 5.60^{ns}$

* Significance at 5%.

The proportion of fire ignitions in land cover types differs between WUI and non-WUI areas (G = 108.2, 5 d.f., $p<0.001$), with more frequent fires at shrublands and broadleaved forests in non-WUI areas compared to WUI areas (with fires being 7.8, 2.2 times more frequent in non-WUI than in WUI areas, respectively). However, ignitions are less frequent in artificial areas and farmlands in non-WUI compared with WUI areas (with fires being 9.8 and 1.9 times more frequent in WUI than non-WUI areas). The proportion of fires ignited at tree plantations is similar in WUI and non-WUI areas (25.3% vs. 29.1% respectively).

In WUI areas, the location of wildfire starting points in relation to land cover types differ from that expected by random (Table 1), with artificial areas and tree plantations being positively selected (2.14 and 1.95 more wildfires than expected according to a random distribution), as well as shrublands, in a lesser degree (1.24 times more fires than expected). On the other hand, farmlands and broadleaved forests had fewer fires than expected by random (27% and 23% less wildfires than expected by random; Table 1). In non-WUI areas, the distribution of wildfires did not differ significantly from a random distribution among land cover types (Table 1).

Discussion and conclusions

The great majority of fires are linked to deliberate-caused fires, both in WUI and non-WUI areas, as expected. Looking at the apparent motivations behind deliberated fires, most of them seem to be caused by activities that use fire as a managing tool. Those caused by arsonists or vandals are however less frequent. Farmers and rangers seem to cause most deliberated fires, farmers using fire mostly for clearing and rangers for pasture renewal. In addition, fires related to chasing animals away to avoid damage to crops and livestock may be also cause by farmers or rangers. It is interesting to note the different incidence of negligence and deliberate fires between WUI and non-WUI areas. Outside WUI areas, where the danger of fires due to negligence related to human-activities is lower, there was a higher incidence of deliberate fires, an especially of those related to extensive farming practices. Thus, fires caused to chase animals away or for pastures renewal for livestock were more frequent here than in WUI areas. The higher incidence of negligence in WUI areas might be related to a higher intensity of human activities, for instance related to crop cultivation. Interestingly, in farmlands in WUI areas the incidence of negligence was much higher than in other cover types, this negligence being mostly related to agricultural waste disposal.

Selectivity patterns of fire for particular cover classes were only apparent in WUI areas. Here, the high fire-proneness of artificial areas might be related to a higher human activity concentrated in these areas, which favors human-related fires, either deliberated or due to negligence or accidents. Regarding plantations, the other cover class positively selected by fire, their higher fire-proneness contrasts with the negative selection showed for broadleaved forests (see also Moreira *et al*. 2009, Moreno *et al*. 2011). This might be related to a higher flammability of plantations, which increases the chances for a fire to actually start after a deliberate attempt or a negligent conduct. *Eucalyptus globulus* and *Pinus pinaster* litter is highly flammable (Ganteaume *et al*. 2009), and they can grow more biomass of understory vegetation, which also is dominated by highly flammable species such as Ulex spp. and grasses (Ganteaume *et al*. 2009, Calviño-Cancela *et al*. 2012). This is especially true in the case of *Eucalyptus globulus* plantations with very low-management, which are very common in Galicia due to rural depopulation and land abandonment (Marey-Pérez *et al*., 2006, Robak, 2008; Díaz-Balteiro *et al*., 2009). Broadleaved forests, on the contrary, are more humid and less biomass in the understory (although with higher diversity; Calviño-Cancela *et al*. 2012). The expansion of plantations in many parts of Galicia, especially those of *Eucalyptus globulus* (MAGRAMA 2011), at the expense of broadleaved forests (Marey-Pérez *et al*., 2006) may have contributed to increased fire hazard in this region.

Acknowledgments

This research was funded in part by Ministerio de Economía y Competitividad (Project ECO2012-39098-C06-05). The Spanish Ministry of Agriculture, Food and Environment (MAGRAMA), and the Rural Affairs Department (Xunta de Galicia) provided the wildfire database.

References

Bond, W.J., Keeley, J.E. (2005). Fire as a global 'herbivore': the ecology and evolution of flammable ecosystems. Trends in Ecology & Evolution. 20(7): 387-94.

Bajocco, S., Ricotta, C. (2008). Evidence of selective burning in Sardinia (Italy): which land-cover classes do wildfires prefer? Landscape Ecology 23 (2), 241-248.

Calviño-Cancela, M., Rubido-Bara, M., van Etten, E.J.B., (2012). Do eucalypt plantations provide habitat for native forest biodiversity? Forest Ecology and Management 270, 153-162.

Carmo, M., Moreira, F., Casimiro, P., Vaz, P. (2011). Land use and topography influences on wildfire occurrence in northern Portugal. Landscape and Urban Planning 100, 169–176.

Chas-Amil M.L., Touza J. and Prestemon J.P. (2010). Spatial distribution of human-caused forest fires in Galicia (NW Spain). In G. Perona and C. A. Brebbia (eds.). Modelling, Monitoring and Management of Forest Fires. WIT Press. pp. 247-258.

Chas-Amil M.L., Touza J., García-Martínez E. (2013). Forest fires in the wildland-urban interface: a spatial analysis of forest fragmentation and human impacts. Applied Geography, 43: 127-137.

Cramer, V.A. and Hobbs, R.J. (editors) (2007) Old fields: Dynamics and Restoration of Abandoned Farmland. Island Press, Washington D.C. ISBN: 978-1-5972-6074-9.

Díaz-Balteiro, L., Bertomeu, M., Bertomeu, M., (2009). Optimal harvest scheduling in Eucalyptus plantations. A case study in Galicia (Spain). Forest Policy and Economics. 11, 548–554.

FAO, 1986, Wildland Fire Management Terminology. FAO Forestry Paper 70 (Rome: Food and Agriculture Organization of the United Nations).

Finney, M.A., 2005, The challenge of quantitative risk analysis for wildland fire. Forest Ecology and Management, 211, pp. 97–108.

Ganteaume, A., Lampin-Maillet, C., Guijarro, M., Hernando, C., Jappiot, M., Fonturbel, T., Perez-Gorostiaga, P., Vega, J.A. (2009). Spot fires: fuel bed flammability and capability of firebrands to ignite fuel beds. International Journal of Wildland Fire 18, 951-969.

Ganteaume A., Jappiot M., Lampin C., Guijarro M., Hernando C. (2013). Flammability of some ornamental species in wildland-urban interfaces in Southeastern France: laboratory assessment at particle level. Environmental Management 52, 467-480.

Herrero-Corral, G., Jappiot, M., Bouillon, C., & Long-Fournel, M. (2012). Application of a geographical assessment method for the characterization of wildlandurban interfaces in the context of wildfire prevention: a case study in western Madrid. Applied Geography, 35, 60-70.

Lampin-Maillet, C., Jappiot, M., Long-Fournel, M., Bouillon, C., Morge, D., Ferrier, J.P. 2010. Mapping wildland-urban interfaces at large scales integrating housing density and vegetation aggregation for fire prevention in the South of France. Journal of Environmental Management 91, 732-741.

MAGRAMA (2011): Cuarto Inventario Forestal Nacional. Galicia. [DVD]. Ministerio de Agricultura, Alimentación y Medio Ambiente.

Manly, B., McDonald, L.L., Thomas, D.L., (1993). Resource Selection by Animals: Statistical Design and Analysis for Field Studies. Chapman and Hall, London, UK.

Manuel, C., Gil, L., (2002). La transformacio´n histo´ rica del paisaje forestal en Galicia. Tercer Inventario Forestal Nacional. Ministerio de Medio Ambiente, Madrid, Spain.

Marey-Pérez, M.F., Rodríguez-Vicente, V., Crecente-Maseda, R. (2006). Using GIS to measure changes in the temporal and spatial dynamics of forestland, experiences from North-West Spain. Forestry 79, 409–423.

MAGRAMA. (2010). Los incendios forestales en España. Decenio 2001–2010 (Madrid: Ministerio de MedioAmbiente. Centro de Coordinación de la InformaciónNacional sobre Incendios Forestales).

Montiel, C., Herrero, G. (2010). Overview of policies and practices related to fire ignitions. In J. Sande (Ed.), Towards integrated fire management-outcomes of the European project fire paradox (pp. 35e46). European Forest Institute.

Moreira F, Rego FC, Ferriera PG. (2001). Temporal (1958–1995) pattern of change in a cultural landscape of northwestern Portugal: implications for fire occurrence. Landscape Ecology 16:557–567.

Moreira, F., Vaz, P., Catry, F., Silva, J.S., (2009). Regional variations in wildfire susceptibility of land-cover types in Portugal: implications for landscape management to minimize fire hazard. International Journal of Wildland Fire 18, 563-574.

Moreno, J.M., Vázquez, A. and Vélez, R. (1998). Recent history of forest fires in Spain. In: J.M. Moreno (ed.), Large forest fires, p. 159-185. Backhuys Pub., Leiden, The Netherlands.

Moreno, J.M., Viedma, O., Zavala, G., Luna, B., (2011). Landscape variables influencing forest fires in central Spain. International Journal of Wildland Fire 20, 678-689.

Nunes MCS, Vasconcelos MJ, Pereira JMC, Dasgupta N, Alldredge RJ, Rego FC 2005 Land-cover type and fire in Portugal: do fires burn land cover selectively? Landscape Ecology 20:661–673.

NWCG, 2006, Glossary of Wildland Fire Terminology (Boise, ID: National Wildfire Coordinating Group, PMS 205).

Oliveira, S., Moreira, F., Boca, R., San-Miguel-Ayanz, J., Pereira, J.M.C. (2013). Assessment of fire selectivity in relation to land cover and topography: a comparison between Southern European countries. International Journal of Wildland Fire (in press).

Prestemon, J. P., Chas-Amil, M. L., Touza, J., Goodrick, S. J. (2012). Forecasting intentional wildfires using temporal and spatio-temporal autocorrelations. International Journal of Wildland Fire, 21(6), 743-754.

Ramil-Rego, P., Muñóz-Sobrino, C., Rodríguez-Guitián, M., Gómez-Orellana, L., (1998). Differences in the vegetation of the north Iberian Peninsula during the last 16,000 years. Plant Ecology 138, 41–62.

Robak, E.W., (2008). Sustainable forest management for Galicia. Forestry Chronicle. 84, 530–533.

Romero-Calcerrada, R., Barrio-Parra, F., Millington, J.D.A., Novillo, C.J. (2010). Spatial modelling of socioeconomic data to understand patterns of human-caused wildfire ignition risk in the SW of Madrid (central Spain). Ecological Modelling 221: 34–45.

Saura-Mas S., Paula J., Pausas J.G. and Lloret F. (2010). Fuel loading and flammability in the Mediterranean Basin woody species with different post-fire regenerative strategies. International Journal of Wildland Fire 19, 783-794.

Syphard, A. D., Radeloff, V. C., Keeley, J. E., Hawbaker, T. J., Clayton, M. K., Stewart, S. I. (2007). Human influence on California fire regimes. Ecological Applications, 17(5), 1388-1402.

Sokal, R. R., and F. J. Rohlf. (1995). Biometry, 3rd edn. Freeman, New York, New York, USA.

Assessment of the effectiveness of the forest fire fighting ground forces in Greece

Michail Simos[a], Gavriil Xanthopoulos[b]

[a]*Leoforos Rodopoleos 5, Rodpoli, 14574, Athens, Greece . slok@windowslive.com*
[b]*Hellenic Agricultural Organization "Demeter". Institute of Mediterranean Forest Ecosystems and Forest Products Technology. Terma Alkmanos, Ilisia, 11528, Athens, Greece. gxnrtc@fria.gr*

Abstract
Efficient dispatching of firefighting forces to a forest fire and effective management of those requires good knowledge of their capabilities and limitations. The study presented here tries to develop knowledge and equations for evaluating the performance and limitations of the ground forces attacking fires in Greece taking into consideration the firefighting methods used in the country. It is based on a questionnaire with photos of fires that was answered by 67 individuals with varying firefighting experience and involvement in firefighting. Among the results reported here are equations for selecting "direct attack on all points" of a fire as a function of flame length and of rate of spread and equations for estimating the probability that a fire will be considered as being beyond the capacity of any of a series of suggested firefighting resources combinations. Also, equations were developed for estimating the length of fire front and of fire flank that can be extinguished by a light fire truck with a water capacity of 600 liters and a fire truck with a capacity of 2500 liters, as a function of flame length. The results of the study provide useful input for understanding and modelling forest fire suppression in Greece and can probably be useful for other Mediterranean countries as well.

Keywords*: Forest fire fighting, fire suppression effectiveness, fire truck, fire extinction rate, direct attack*

Introduction

Efficient dispatching of firefighting forces to a forest fire and effective management of those forces in the field of operations requires good knowledge of their capabilities and limitations. Numerous studies in international fire literature have been devoted to assessment of the effectiveness of ground and aerial resources and to modelling of firefighting operations. However, such knowledge and models are not universal as performance is affected by various local factors such as firefighting methods, tools and equipment, firefighter training, professionalism and motivation, weather conditions, vegetation characteristics, topography, road network density, etc. (Hirsch and Martell 1996). Consequently, although published work on the subject is certainly valuable, some local knowledge of firefighting effectiveness is definitely required. In Greece, so far, there have been no published studies on firefighting effectiveness. When such knowledge was required for the development of a decision support system for dispatching of ground and aerial resources the required information was obtained from interviews with a small number of experienced foresters (Xanthopoulos 1994). Since then, a lot has changed in the way firefighting is carried out in the country. For example, firefighting responsibility has been transferred from the Forest Service to the Fire Brigades in 1998, the number of volunteer firefighters increased sharply, firefighting techniques and priorities as well as training changed, and the types of resources improved. On the other hand, the lack of formal knowledge on the effectiveness of the firefighting forces did not change.
The study presented here is an effort to fill this knowledge gap. It focuses specifically on the performance and limitations of the ground forces attacking a fire and takes into consideration the firefighting methods used in Greece. Its findings are certainly of value for Greece but they may be relevant in other Mediterranean countries as well.

Methods

Aiming to develop a first overall picture of the effectiveness of the ground forces, it was decided to employ specifically designed questionnaires for collecting the necessary data. The choice of the method took into consideration difficulties encountered in other studies for collecting valid productivity information using traditional data collection methods that has sometimes led to discrepancies and made, for example, Fried and Gilles (1989) to embark on a major expert opinion study on fireline construction rates.

Estimated

Rate of spread
ROS=120 m/h

Flame length
FLAME=1 m

Attack method (Choose **only one**)
1)☐ 2)☐ 3)☐ 4)☐

Firefighting resources (Choose **all** that can be used)
1) ☐ 2)☐ 3)☐ 4)☐ 5)☐ 6)☐ 7)☐ 8)☐ 9)☐

Minimum Resource Required (Choose **only one**)
1) ☐ 2) ☐ 3) ☐ 4) ☐ 5) ☐ 6) ☐ 7)☐ 8)☐ 9)☐ 10) ☐

Estimated

Rate of spread
ROS=700 m/h

Flame length
FLAME=18 m

Attack method (Choose **only one**)
1)☐ 2)☐ 3)☐ 4)☐

Firefighting resources (Choose **all** that can be used)
1) ☐ 2)☐ 3)☐ 4)☐ 5)☐ 6)☐ 7)☐ 8)☐ 9)☐

Minimum Resource Required (Choose **only one**)
1) ☐ 2) ☐ 3) ☐ 4) ☐ 5) ☐ 6) ☐ 7)☐ 8)☐ 9)☐ 10) ☐

The four options in regard to attack method:
1. Direct attack at all points (front, flanks, heel)
2. Indirect attack at the front, direct at the flanks
3. Indirect attack along all the perimeter (from firebreaks, roads, natural vegetation breaks, etc.)
4. Attack impossible until conditions change

Figure 1. Two of the twelve photos of the first question of the questionnaire and the four options in regard to the method of attack for the type of fire shown in each photo.

2.1. The questionnaire

The questionnaire consisted of two parts. The first part aimed at collecting information about the respondent including age, sex, employment, education level, general training, training about forest fires, years of involvement in fire management, years and way of participating in firefighting operations. Providing the name and contact data of the respondent was optional.

The second part of the questionnaire consisted of three main questions, each presenting a number of cases illustrated by photos. The first question presented 12 photos of fires and provided an estimated flame length and rate of spread (ROS) for each of those fires. These flame length estimates ranged between 0.2 and 50 m, while ROS ranged between 80 and 2500 m/h. The respondent was asked to choose from four options about the type of attack appropriate for the depicted part of the fire (including a "no-attack possible" option), nine options in regard to the required type of resources, and ten options in regard to combinations of resources that would be required at a minimum to control a 100 m wide fire front of the portrayed type of fire from a 6 m wide road (Figure 1).

The second question presented 9 photos of fires with an estimate of the depicted flame length. Assuming scenarios of fighting such flames at the front or at the flanks (2 cases) by a) One driver and two firefighters with a light fire truck having a 600 liter tank and using 25mm diameter hoses, or by b) the same people with a heavier fire truck (2500 liter tank) using 45 mm diameter hoses, the respondent was asked to provide estimates (in meters) of the length of the perimeter (front or flank) that can be extinguished using the water in the tank of the truck. An option was provided to mark X if direct attack on the flames with the particular resource was considered as impossible. Flame length estimates for the fire fronts ranged between 0.5 and 60 m and for the flanks between 0.3 and 30 m.
The third question presented 6 photos of typical vegetation in Greece. The respondent was asked to provide an estimate of the length of a 2 m wide fireline that an 8 person crew could build within an hour for combinations of slope (flat, medium) and time of day (early morning, midday, night).

Analysis and Results

Sixty seven (67) people of varying experience and involvement in firefighting responded to the questionnaire. Forty nine (49) of them work for the Greek Fire Service either as permanent personnel or as volunteers, while fifteen (15) of them belong to the unpaid volunteer groups of the General Secretariat for Civil Protection. Sixteen (16) of the 67 respondents stated that they have high or very high experience in firefighting while 30 more replied that they have average (medium) experience. The data formed a database that was analyzed with the R and SPSS statistical software. Selected results are reported below.
The responses to the first question were examined first in regard to frequencies of selection of certain options (e.g. selection of initial attack). This allowed to investigate trends in the responses versus fire characteristics and to identify certain thresholds. A focal point of the analysis was the assessment made by the respondents about the limits of direct attack. This was done through development of models for the probability of selecting direct attack on the flames on all parts of a fire ($PROB_{direct}$) as a function of flame length (FLAME in m) and of rate of spread (ROS in m/h).
The replies selecting direct attack for the fire depicted in each of the twelve (12) photos of the first question, allowed an estimate of probability of such selection for each flame length. The same was done for ROS. For example, for the upper photo of figure 1, with flame length of 1 m, 88% of the respondents selected the first of the four options "Direct attack at all points (front, flanks, heel)"; no-one selected the fourth option "Attack impossible until conditions change". For the lower photo with flame length of 18 m, only 7% of the respondents selected direct attack; the majority (45%) chose the third option "Indirect attack along all the perimeter" while 21% of the respondents considered this fire as impossible to attack (fourth option).
The probability of selecting "direct attack on all points" of a fire ($PROB_{direct}$) as a function of flame length and of rate of spread was analyzed using the data set of twelve records (N=12), i.e. one record for each of the photos of the first question. Two regression equations were developed with $PROB_{direct}$ as the dependent variable and the natural logarithm of FLAME and ROS. The equations are as follows:

a) $PROB_{direct} = 64.609 - 19.051 * \ln(FLAME)$ with Adj. $R^2 = 0.857$ (1)

b) $PROB_{direct} = 210.999 - 28.389 * \ln(ROS)$ with Adj. $R^2 = 0.814$ (2)

Both equations are statistically significant ($p<0,005$). Plotting of the first equation revealed that the probability of direct attack all around the fire perimeter drops to 40% when the flame length is 3.5 m (Figure 2). Plotting of the second equation showed that $PROB_{direct}$ approaches zero when ROS exceeds 1600 m/h (Figure 3). Actually, the equation produces negative $PROB_{direct}$ values for ROS>1689 m/h.

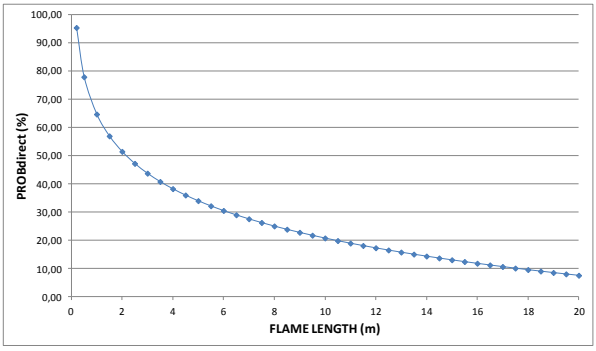

Figure 2. Plotting of the probability to engage in direct attack on all parts of a fire which is exhibiting a particular flame length, according to equation 1.

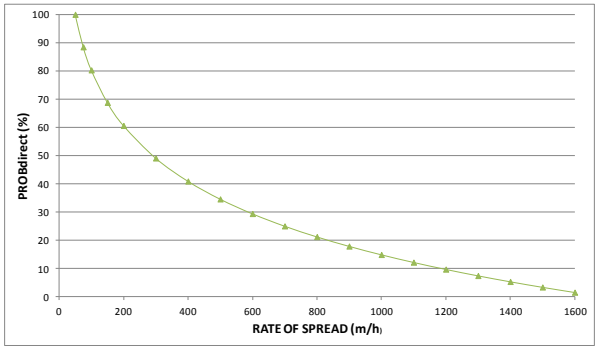

Figure 3. Plotting of the probability to engage in direct attack on all parts of a fire spreading with a particular rate of spread, according to equation 2.

Another important finding, based again on the responses regarding the twelve photos of the first question (N=12), has to do with the probability that a fire will be considered as being beyond the capacity of any of the firefighting resources combinations that were suggested to the respondents (PROB_NO), as a function of FLAME and of ROS. The strongest suggested combination was 4 fire trucks plus aerial resources for fighting a 100 m wide fire front from a 6 m wide road. Again, two regression equations were developed with PROB_NO as the dependent variable and FLAME and ROS as the independent variables respectively. The equations are as follows:

c) PROB_NO = 1.814 + 1.407 * FLAME with Adj. R^2= 0.951 (3)

d) PROB_NO = 6.001 + 0.028 * ROS with Adj. R^2= 0.862 (4)

Both equations are statistically significant (p<0,005).

The second question which focused on the length of extinction of the front and of the flanks of a particular fire, shown in photograph and associated with estimates of frontal and flank flame length. The requested length estimates (m) were for two different firefighting resources as explained earlier. Many respondents omitted providing estimates for some of the photos. Also, many replies were marked X indicating that direct attack on the flames with the particular resource was considered as impossible. The data were analyzed with regression aiming to establish models for estimating extinction lengths of fire front or flank for each resource with flame length as the independent variable. Furthermore, logistic regression analysis provided models for estimating the probability that direct attack is possible. The results are as follows:

Case 1:

Resource: One driver and two firefighters with a light fire truck having a 600 liter tank, using 25mm diameter hoses.

Operation type: Attack to the fire front.

Results: The maximum number of replies from the 67 respondents for the 9 photos was 603. The number of length estimates were 233 while 287 responses were marked with X (direct attack impossible with this resource) and were given a value of 0 for the logistic regression. The number of "no replies" was 83. The equation is:

$EXT_{600L\_Front} = 1.969 + 37.038 / FL_{front}$ (5)

Where the extinction length EXT_{600L_Front} and the frontal flame length FL_{front} are expressed in meters, Adj. R^2 = 0.294, the p-value for the equation is p<0.001, the constant's p=0.282 and of 1/ FL_{front} p <0.001.

The logistic regression equation is:

$$P(EXT_{600L\_Front}) = \exp(1.537-0.,184*(FL_{front}))/(1+ \text{Exp}(1.537-0.184*(FL_{front}))) \quad (6)$$

Case 2:

Resource: One driver and two firefighters with a light fire truck having a 600 liter tank, using 25mm diameter hoses.
Operation type: Attack to the flank of the fire.
Results: The number of extinction length estimates was 333 while 190 responses were marked with X (direct attack impossible with this resource) and were given a value of 0 for the logistic regression. The number of "no replies" was 80. The equation is:

$$EXT_{600L\_Flank} = 6.321 + 27.711 / FL_{flank} \quad (7)$$

Where the extinction length EXT_{600L_Flank} and the flank flame length FL_{flank} are expressed in meters, Adj. R^2 = 0.269, the p-value for the equation is p<0.001, the constant's p=0.019 and of 1/ FL_{flank} p <0.001.

The logistic regression equation is:

$$P(EXT_{600L\_Flank}) = \exp(1.692-0.152 *(FL_{flank}))/(1+ \text{Exp}(1.692-0.152*(FL_{flank}))) \quad (8)$$

Case 3:

Resource: One driver and two firefighters with a fire truck having a 2500 liter tank using 45 mm diameter hoses.
Operation type: Attack to the fire front.
Results: The number of extinction length estimates were 329 while 192 responses were marked with X (direct attack impossible with this resource) and were given a value of 0 for the logistic regression. The number of "no replies" was 82. The equation is:

$$EXT_{2500L\_Front} = 9.354+77.453 / FL_{front} \quad (9)$$

Where the extinction length EXT_{2500L_Front} and the frontal flame length FL_{front} are expressed in meters, Adj. R^2 = 0.292, the p-value for the equation is p<0.001, the constant's p=0.014 and of 1/ FL_{front} p <0.001.

The logistic regression equation is:

$$P(EXT_{2500L\_Front}) = \exp(1,828-0,1 *(FL_{front}))/(1 + \text{Exp}(1.828-0.1*(FL_{front}))) \quad (10)$$

Case 4:

Resource: One driver and two firefighters with a fire truck having a 2500 liter tank using 45 mm diameter hoses.
Operation type: Attack to the flank of the fire.
Results: The number of extinction length estimates were 405 while 120 responses were marked with X (direct attack impossible with this resource) and were given a value of 0 for the logistic regression. The number of "no replies" was 78. The equation is:

$$EXT_{2500L\_Flank} = 20.756 + 57.493 / FL_{flank} \quad (11)$$

Where the extinction length EXT_{2500L_Flank} and the flank flame length FL_{flank} are expressed in meters, Adj. $R^2 = 0.236$, the p-value for the equation is $p<0.001$, the constant's $p=0.001$ and of $1/ FL_{flank}$ $p <0.001$.

The logistic regression equation is:

$$P(EXT_{2500L\_Flank})= \exp(2.444-0.163 *(FL_{flank}))/(1+ Exp(2.444-0.163*(FL_{flank}))) \quad (12)$$

Figure 4 is a plot of equations 5, 7, 9 and 11 showing the quick drop in extinction effectiveness with increasing flame length.

Discussion and conclusions

The results of the study provide useful input for understanding and modelling forest fire suppression in Greece. For example, the result of equation (1) that there is a 40% chance of direct attack on fires with 3.5 m flame length and a 24% chance at 8.5 m flame length, can be evaluated versus the limits of successful attack at the fire front suggested and discussed by Deeming *et al*. (1978), Andrews and Rothermel (1982), Rothermel (1983), Alexander and DeGroot (1988), Alexander and Lanoville (1989), and Hirch and Martell (1996). In interpreting equation (1) it should be taken into consideration that following firefighting practice in Greece the respondents have use of water from fire trucks as the default method of attacking a fire. In general the results of equation 1 appear to be in agreement with the other studies, taking of course into consideration that the photos in the present questionnaire represented various fuel types whereas some of those studies focused on specific fuels types.

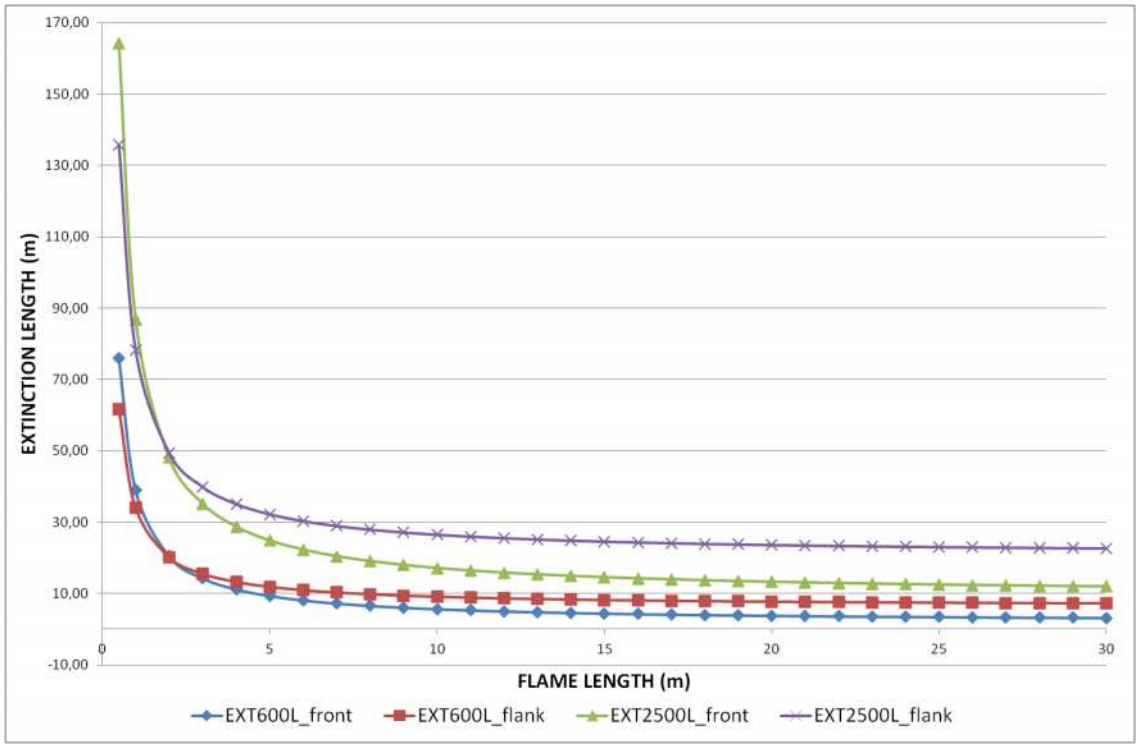

Figure 4.Plotting of the predicted extinction length for a range of flame lengths according to equations 5, 7, 9 and 11.

Equation 2 is also interesting as it provides an estimated ROS limit (1690 m/h) beyond which direct attack is not possible, not taking a particular fuel type into consideration. Such information is less commonly available in the international literature. The results of this equation can be challenged since fast running grass fires can be chased along the flanks by fire trucks equipped with appropriate water spraying capability, aiming to achieve an extinguishing rate faster than the ROS of the fire and ultimately catch and extinguish the head of the fire. Topography, which is generally steep, might make use of such a technique an exception rather than the rule for grass fires in Greece.

Equations 5-12 have generally low Adj. R^2 statistics. This is not surprising as there was a lot of variation in regard to the estimates of extinction length provided by the respondents. Part of this variability is due to the variety of fuel types depicted in the photos. It is well known that the water required to extinguish a grass fire is much less than that needed for a heavier fuel type even if the flame length is the same. The varying background and experience of the respondents is also an important source of variability. Nevertheless, the behaviour of the equations is rational and can provide a good baseline for calculations that will be useful for dispatching of fire trucks for initial attack and for planning extended attack in the future in Greece.

Bibliography

Alexander ME, De Groot WJ (1988) Fire Behavior in Jack Pine Stands as Related to the Canadian Forest Fire Weather Index (FWI) System. Forestry Canada, Northern Forestry Centre. Poster (with text).

Alexander ME, Lanoville RA (1989) Predicting fire behavior in the black spruce-lichen woodland fuel type of western and northern Canada. Forestry Canada, Northern Forestry Centre. Poster (with text) (http://cfs.nrcan.gc.ca/publications/download-pdf/23093)

Andrews PL, Rothermel RC (1982) Charts for interpreting wildland fire behavior characteristics. USDA Forest Service, Intermountain Forest and Range Experiment Station Gen. Tech. Rep. INT-131. (Ogden, UT)

Deeming, J. E., Burgan, R. E., & Cohen, J. D. (1977). The National Fire-Danger Rating System–1978. USDA Forest Service, Intermountain Forest and Range Experiment Station. General Technical Report INT-39. (Ogden, UT)

Hirsch KG, Martell DL (1996) A review of initial attack fire crew productivity and effectiveness. International Journal of Wildland Fire 6(4), 199-215.

Fried JS, Gilles JK (1989) Expert opinion estimation of fireline production rates. Forest Science 35(3), 870-877.

Xanthopoulos G (1994) Development of a decision support system for water bomber dispatching in Greece. In proceedings of the 2nd International Conference on Forest Fire Research, November 21-24, 1994, Coimbra, Portugal. (Ed. D.X. Viegas) pp. 139-149. (Univ. of Coimbra, Coimbra, Portugal).

Building vulnerabilities to fires at the wildland urban interface

João Laranjeira[a], Helena Cruz[b]

[a] *Coimbra, Portugal, joaopslaranjeira@gmail.com*
[b] *Laboratório Nacional de Engenharia Civil (LNEC), Av. do Brasil 101, 1700-066, Lisboa, Portugal, helenacruz@lnec.pt*

Abstract
Fires on the Wildland Urban Interface (WUI) have caused significant loss of life and colossal property and natural environment damages in numerous countries around the world. The solutions to mitigate this fire problem are complex, as it results from the fuel source changes from vegetation to structural materials in a fire-prone environment and it involves the interaction of several factors that act synergistically to increase the frequency of fires with severe potential destruction. In order to understand how and why buildings are damaged and destroyed under wildland fire attack, several surveys following historical large scale fire events, which resulted in significant building damages and/or losses, have been conducted worldwide. This paper aims to review and analyse the main characteristics of buildings and other structures that contributed to their vulnerability during fires at the WUI, based on the analysis of several post fire studies developed in Australia, United States of America and Mediterranean Europe (particularly Portugal, Spain, Greece). The different building traditions between the selected countries are discussed, as long as they affect building vulnerability to fires.

Keywords*: wildland urban interface, fire, building vulnerability, structure vulnerability*

Introduction

Fires on the Wildland Urban Interface (WUI) have caused significant loss of life and colossal property and natural environment damages in numerous countries around the world. Table 1 shows some of the worst wildland fire events that, recently, reached WUI areas in Australia, United States of America (U.S.A.) and Mediterranean Europe (particularly Portugal, Spain, Greece).

Table 1. Some recent wildland urban interface fires and side effects in Australia, United States of America (U.S.A.), Spain, Greece and Portugal (adapted from Xanthopoulos et al., 2003; Cohen, 2008; CAL FIRE, 2009; Viegas et al., 2009; Galiana-Martín, 2011; Viegas et al., 2011; Tedim et al., 2012; Trindade et al., 2012; Infoplease, 2014)

Year	*Country*	*Localization*	*Mortal victims*	*Burned houses*	*Burned area (ha)*
2001	*Australia*	*New South Wales*	*without data*	*121*	*3 000 000*
	Greece	*Northern Attica*	*without data*	*without data*	*3 397*
2002	*U.S.A.*	*Lake George, Colorado*	*without data*	*132*	*without data*
		Heber-Overgaard, Arizona	*without data*	*426*	*468 638*
2003	*Australia*	*Australian Capital Territory (ACT)*	*4*	*519*	*1 300 000*
	Portugal	*Monchique Sierra and Silves*	*1*	*28*	*32 700*
		Mação	*17*	*12*	*21 869*
		Mafra	*without data*	*without data*	*2 891*
	Spain	*Catalonia*	*5*	*without data*	*6 287*
	U.S.A.	*Summerhaven, Arizona*	*without data*	*340*	*without data*
		Southern California	*22*	*3 400*	*320 000*
2005	*Greece*	*Attica*	*without data*	*150*	*1 000*
	Portugal	*Coimbra*	*18*	*without data*	*9 000*
	Spain	*Guadalajara*	*without data*	*without data*	*12 000*

2006	*Portugal*	*Famalicão da Serra*	*6*	*without data*	*without data*
	Spain	*Galicia*	*4*	*without data*	*80 000*
	U.S.A.	*Texas and Oklahoma*	*11*	*723*	*238 000*
2007	*Greece*	*Artemida*	*78*	*3 000*	*270 000*
	Spain	*Canary Islands*	*without data*	*without data*	*37 285*
	U.S.A.	*Southern California*	*17*	*3 069*	*210 000*
2009	*Australia*	*Victoria*	*173*	*3 500*	*450 000*
	U.S.A.	*Southern California*	*2*	*209*	*64 983*
2010	*U.S.A.*	*Fourmile Canyon, Colorado*	*without data*	*161*	*6 181*
2011	*U.S.A.*	*Texas*	*2*	*1 709*	*32 000*
2012	*U.S.A.*	*Colorado*	*6*	*946*	*262 947*
2013	*U.S.A.*	*Toulumne, California*	*without data*	*112*	*257 314*

The solutions to mitigate this fire problem are complex (Kyle *et al.*, 2008), as it results from the fuel source changes from vegetation to structural materials in a fire-prone environment, since the fire travels from a wildland area to a rural, peri-urban and/or urban area which borders the wildland area. Moreover, the fire spread in a WUI area involves the interaction of several factors (such as topography, weather conditions, human behaviour, besides vegetation and building fuels), that act synergistically to increase the frequency of fires with severe fire behaviour and potential destruction (Cohen, 2008; Maranghides and Mell, 2009).

In geographical locations with potential fire risk (e.g. rugged topography), the combination of prolonged drought conditions and particular strong winds, as a result of climate change, leave vegetation particularly vulnerable. Combination of these facts with an increasing number and extent of WUI areas, often leads to fuel accumulation that create conditions that are beyond the fire suppression capacity of any firefighting mechanism (Xanthopoulos *et al.*, 2011).

The most effective ways to improve fire safety are preventive actions (White and Dietenberger, 2010). The knowledge of the critical aspects that make buildings and other structures vulnerable to fires in WUI areas is crucial to reduce or eliminate the risks of ignition, leading to the reduction of their potential losses during fire events (Manzello, 2014).

In order to understand how and why buildings are damaged and destroyed under wildland fire attack, several surveys following historical large scale fire events, which resulted in significant building damages and/or losses, have been conducted worldwide. However, despite these efforts, more should be done to understand the structure ignition potential during fires at the WUI since this problem is getting increasingly worse (Maranghides and Mell, 2009; Manzello, 2014).

This paper aims to review and analyse the main characteristics of buildings and other structures that contributed to their vulnerability during fires at the WUI, based on the analysis of several post-fire studies. In order to carry out this study, some of the post-fire studies developed in Australia, U.S.A. and Mediterranean Europe (particularly Portugal, Spain, Greece) were analysed since these countries have extensive WUI areas with severe fire-prone environments (Xanthopoulos *et al.*, 2011), which resulted in some of the worst fire events in the WUI (Table 1). Moreover, Australia and the U.S.A. have large experience and knowledge in the analysis of fire occurrences (Viegas *et al.*, 2012) and learning from the examples in other parts of the world is of great value.

Building vulnerabilities

2.1. Fire attack mechanisms

During a fire in the Wildland Urban Interface (WUI), buildings may be a fuel source to initial ignition and to the potential for flame-spread. Moreover, some of the components of the building envelope may allow fire penetration into it, and consequently, the ignition of materials inside it.

The main characteristics of a building (and other structures) in the WUI that can significantly contribute to its vulnerability under wildland fire attack are its material characteristics (i.e.

combustible, non-combustible, fire resistant), design features and details of its different parts and the openings or weak points in the building envelope. Furthermore, the susceptibility to ignition of the elements in the building's immediate surrounding may also influence the risk of exposure that a building experience during a fire event.

Post-fire studies have shown that several fire spread mechanisms may be responsible for ignition and propagation of wildland fires into the WUI, as buildings and their immediate surroundings may be exposed to firebrands, radiant heat, and/or flame contact, resulting in building damage or destruction. Firebrands (or embers, or burning debris) may be produced by vegetation of the type that supports fire front spread and/or by the fuel load of other sources from the rural, peri-urban or urban setting. As firebrands can be carried by winds and by convective air rising off the fire front (Fairbanks and Ingalsbee, 2006), they can be transported ahead of the main fire, creating spot fires in the building surrounding close to the building envelope, and even inside the building by entering into it through openings or weak points. As an example, during the 2005 Coimbra fire (Portugal), firebrands (from the main fire front) crossed Mondego river and caused several spot fires inside the urban area (Viegas *et al.*, 2011).

The risk from firebrands attack is complex, as it depends on the vulnerability of the building , as well as from several other factors, such as firebrands quality (i.e. configuration, size), amount and type (source), distance from source, and the duration of the attack (Leonard and Bowditch, 2003; Victorian Bushfires Royal Commission (VBRC), 2009). Furthermore, weather conditions play a relevant role in firebrands propagation (Foote *et al.*, 2011), particularly wind conditions, as it affects firebrands generation, transport, and landing (Koo *et al.*, 2010). Despite the complexity of this fire spread mechanism, it is well understood that firebrands is the most predominant cause of ignition and loss of buildings during fire events at the WUI (Maranghides and Mell, 2009; VBRC, 2009), mainly as this type of attack may occur before, during and after a fire front has passed (Blanchi and Leonard, 2005).

While firebrands offer a discontinuous fire spread mechanism, radiant heat exposure and flame contact are continuous ones, originated from the fire front spread and/or from any combustible elements in building surrounding (VBRC, 2009; Potter and Leonard, 2010). As a result, the external building elements may be ignited or radiant heat and/or flame contact may act on the building envelope until a weak point of it opens up, allowing firebrands' entry into the building and the ignition of building contents (Potter and Leonard, 2010). Radiant heat and flames present a risk based on the level of radiant heat exposure, the time over which this exposure occurs, as well as on the building vulnerability under attack (Leonard *et al.*, 2009).

In the following sections, the main characteristics of buildings (and other structures) and the elements in their immediate surroundings, that contributed significantly to their vulnerability during past fire events, are reviewed and analysed. The different building traditions between the selected countries are discussed, as long as they affect building vulnerability to fires.

Building construction materials

The material characteristics (i.e. combustible, non-combustible, fire resistant) used in buildings construction (and in other structures) influence the ignition of their external and internal components, depending on the material ability to support localised flame development (i.e. material reaction to fire), which may be initiated by firebrands attack, radiant heat exposure and/or flame contact.

In the U.S.A. most buildings are traditionally made with timber (a combustible material). Particularly, for exterior wall cladding, wood or wood based products (such as plywood or oriented strand board) are commonly used, as well as vinyl or other plastics (also combustible materials) (Quarles *et al.*, 2010).

In Australia, building construction traditions changed over years. Early in the 20th Century, with the population growth in coastal areas, traditional buildings (particularly in Queensland) were constructed of timber with a corrugated iron roofing, large verandas all around, and were elevated on stumps above the ground (Xanthopoulos *et al.*, 2011). From the 1930's, in Australian cities (Melbourne, Sydney,

Brisbane), particularly where termites existed, instead of timber (as it is a biological termite-prone material) buildings were constructed of brick or corrugated iron, and cladded with plaster lined fibrocement or brick veneer (Xanthopoulos *et al.*, 2011).
Post-fire studies have indicated that there is a clear relationship between timber buildings destruction and the severity of fire weather conditions, which is a characteristic of fires in the Wildland Urban Interface (WUI), since hot, dry, windy weather dries out timber (hygroscopic material) in the same way that it dries out vegetation (VBRC, 2009). Moreover, during the fire event, radiation heat exposure from surrounding burning fuels also modifies timber temperature and moisture content (Potter and Leonard, 2010). Therefore, in these conditions, timber is more easily ignited. Examination of several fire disasters in the WUI revealed that buildings clad with timber or even fibrocement or cellulose cement sheet, as well as building walls constructed with mud brick (Leonard *et al.*, 2009), have responded significantly worse to wildland fire attack than building walls constructed with bricks (Bell, 1985; Ramsay *et al.*, 1996; Leonard *et al.*, 2009).
In regard to roof covering materials, several researches indicated that untreated timber roofing material (i.e. without impregnated fire retardant treatments), particularly wooden shake and shingle roofs, were a major contributor to buildings destruction in past fire events at the WUI (Foote *et al.*, 1991b; Mitchell and Patashnik, 2007; Quarles *et al.*, 2013). It has been reported that firebrands were the dominating fire spread mechanism on timber roof combustion (Foote *et al.*, 2011). Furthermore, particularly during the 1983 Ash Wednesday fires (in Victoria) and the 1994 New South Wales fires, both in Australia, buildings with masonry tiles or steel deck roofs survived more often than those with corrugated iron or fibrocement roofs (Ramsay *et al.*, 1996).
Taking into account material characteristics, particularly of combustible ones that may be used in building construction in the U.S.A. and Australia, the ignition of the building envelope (cladding and/or roof covering) is a major concern during a fire at the WUI (Xanthopoulos, 2004), as the buildings themselves can easily become fuel. As an example, Figure 1a shows a building envelope damaged that resulted from the 2007 Grass Valley Fire (Southern California, U.S.A.). On one hand, it is visible the burned vinyl cladding and underlayment, as well as the burned timber cladding, which according to Cohen and Stratton (2008) resulted from the thermal exposure from the nearby buildingand the burned surrounding vegetation. On the other hand, it is visible that the burned blackened asphalt shingles in the roof valley resulted from the accumulation of pine needles that ignited due to the flames spread up along the building wall (Cohen and Stratton, 2008).

a **b** **c**

Figure 1. Influence of the construction materials characteristics on building vulnerabilities to wildland fire threats: a) building envelope damage due to the combustible construction materials (U.S.A.) (Cohen and Stratton, 2008); b) buildings destruction due to house-to-house fire spread (U.S.A.) (Cohen and Stratton, 2008); and c) building destruction due to its combustible contents (Greece) (Xanthopoulos et al., 2011).

Therefore, the proximity of more buildings means concentration of fuel loads (Xanthopoulos *et al.*, 2011), thus increasing fire risk propagation. Actually, several field investigations in the U.S.A. (Mitchell and Patashnik, 2007; Cohen and Stratton, 2008; Texas A&M Forest Service, 2012; Colorado

Springs Fire Department, 2013; Quarles *et al.*, 2013) and Australia (Blanchi and Leonard, 2005; Leonard *et al.*, 2009), have evidenced house-to-house fire propagation. This fire spread mechanism acts in the following way: during the fire event, some buildings on fire (due to the main fire front or firebrands attack) provide radiant heat exposure and flame contact to adjacent buildings and/or on their surrounding elements, which in turn ignite adjacent buildings, leading to their destruction (Figure 1b) (Leonard *et al.*, 2009). Moreover, the building itself can become a significant firebrands source (Blanchi and Leonard, 2005; Texas A&M Forest Service, 2012). Besides material characteristics and surrounding elements, the close proximity of buildings and the slope of the terrain also influence this fire transfer mechanism (Quarles *et al.*, 2013). In the 2012 Waldo Canyon Fire (Colorado, U.S.A.), where buildings in peri-urban or urban neighbourhoods were within 10 meters to each other, fire propagated through house-to-house (Mitchell and Patashnik, 2007).

In Mediterranean Europe (particularly Portugal, Spain, Greece), buildings are mostly built with fire resistant materials (Xanthopoulos *et al.*, 2011), such as reinforced concrete frame, bricks, stones, tiled roofs. However, timber may be found in specific building elements, such as in roof structures, window frames, doors, and others (Xanthopoulos *et al.*, 2003).

When compared with the reality in the U.S.A. and Australia, a high density of buildings in Mediterranean Europe generally entails a reduction of the available fuel loads (Xanthopoulos *et al.*, 2011) to fire propagation, due to the construction material characteristics used in the building envelope components. Notwithstanding this, buildings in Mediterranean Europe have also been damaged or destroyed during fires in the WUI, but in most cases, it is a consequence of the ignition of the materials inside it, as the fire managed to enter the buildings through openings or breakthrough weak points (Figure 1c) (Caballero, 2004; Xanthopoulos *et al.*, 2011).

Other difference between the analysed countries arise from post-fire studies in the WUI, as while in the U.S.A. and Australia, a large number of buildings were destroyed and just a few were damaged (VBRC, 2009; Quarles *et al.*, 2013), in Mediterranean Europe, building destruction happens in a minimum fraction of the number of buildings threatened by fire (Caballero, 2004).

2.3. Building design features and openings or weak points

Building design features and details of its different parts play an important role in the survivability of a structure during a fire at the Wildland Urban Interface (WUI), since any part of a building envelope where firebrands can penetrate and/or accumulate is susceptible to ignition and spread, particularly if these building parts are combustible. Some building details are also susceptible to dead vegetation accumulation (e.g. pine needles or other vegetation), increasing the available fuel loads and leading to firebrands spread, thus threatening nearby combustible building elements. Furthermore, openings or weak points in the building envelope entail the ignition of building contents due to the opportunity that they may present to firebrands penetration into the building.

- **Exterior subfloor systems elevated on stumps above the ground**

Subfloor systems of buildings that are elevated on stumps above the ground, revealed to be a vulnerable part of the building during past fire events in the WUI, particularly to firebrands penetration or even accumulation on gaps or crannies (Bell, 1985), as buildings on stumps were more likely to be destroyed than buildings constructed on slab on ground (Ramsay *et al.*, 1996; Leonard *et al.*, 2009). Ramsay *et al.* (1996) reported that, along with combustible material characteristics of stumps (i.e. timber unlike fire resistant concrete slabs on ground), the use of timber gap-boards to enclose the underfloor space of timber and the fibrocement clad buildings appeared to contribute to buildings vulnerability.

- **Windows and external doors**

Windows (either open or closed ones) may be a weak point of the building envelope during a fire at the WUI, depending on their components, such as framing material (Fairbanks and Ingalsbee, 2006) and their conservation conditions (Blanchi and Leonard, 2005), window sills material (Bell, 1985;

Ramsay *et al.*, 1996), shutters material and their conservation conditions (Xanthopoulos *et al.*, 2011), and the use of metal fly wire screens (Bell, 1985). Moreover, glass type (Blanchi and Leonard, 2005), windows dimension (Ramsay *et al.*, 1996), and/or the number of glass panes (Caballero, 2004; Xanthopoulos *et al.*, 2011) may also influence their vulnerability.

Open windows are reported as to be one of the most common entrance point of firebrands in Mediterranean Europe (Xanthopoulos, 2003), which usually ignite nylon curtains, rugs, upholstery, polyurethane and/or timber furnishings, all quite common inside Mediterranean homes (Xanthopoulos, 2004). Besides firebrands attack, nylon curtains may also be exposed to radiant heat from the burning surrounding elements (Xanthopoulos, 2003). Vinyl and old timber shutters are examples of radiant heat sources, as they have shown to be easily destroyed when threatened by fire (Xanthopoulos *et al.*, 2011).

In turn, closed windows are weak points when threatened by flame contact (Blanchi and Leonard, 2005) or by radiant heat exposure (Bell, 1985; Ramsay *et al.*, 1996) from flame front or burning surrounding elements, leading to glass to break, which create an entry point to firebrands into the building (Texas A&M Forest Service, 2012). As an example, a survey after the 2003 Canberra fires evidenced that some windows were broken or cracked from radiant heat, allowing that curtains were heat affected and firebrands entered causing burn marks on carpets (Blanchi and Leonard, 2005). However, there were situations where fire resistant windows shutters (e.g. aluminium, steel) that were closed (either hinged or roll-down), provided optimum protection to glass, timber frames and sills (shutters usually cover window sills). Furthermore, the use of metal fly wire screens on windows seems to have protected them during the 1983 Ash Wednesday fires, as windows unprotected were found apparently cracked and broken by radiation heat exposure (Bell, 1985).

Combustible window frames may also contribute to (closed) windows vulnerability, either due to timber ignition from firebrands accumulation in the re-entrant corner of the window sill, which potentiate glass to break by providing radiant heat exposure and/or flame contact (Blanchi and Leonard, 2005), or due to vinyl melt, causing the glass to fall out (Fairbanks and Ingalsbee, 2006), allowing firebrands to enter into the building. Combustible window sills may also ignite, contributing to window vulnerability (Ramsay *et al.*, 1996). Moreover, gaps around window frames are reported to be common firebrands' accumulation points, as well as around windows and external doors (Blanchi *et al.*, 2006).

In the same way, combustible external doors, frames and even their assemblies increase the risk of ignition and fire spread, as frequently it was observed in re-entrant corners of timber doors, frames, and assemblies, due to firebrands accumulation (Blanchi *et al.*, 2006). Door gaps also present an opportunity for firebrand's entry (Blanchi *et al.*, 2006). Several post-fire field observations evidenced that by screening the external door with non-combustible screen door or using low or non-combustible materials in door assembly, it is possible to reduce the vulnerability of this building component (Blanchi *et al.*, 2006).

Window dimensions may also affect their vulnerability (Quarles *et al.*, 2010). After the 1983 Ash Wednesday fires (in Victoria) and the 1994 New South Wales fires, field observations reported that building destruction increased with the increasing glass area of buildings envelope (Ramsay *et al.*, 1996).

Finally, there are examples where single pane windows revealed to be more vulnerable to cracking and breaking, than dual pane windows (Caballero, 2004; Xanthopoulos *et al.*, 2011; Colorado Springs Fire Department, 2013), such as during the 2011 Texas wildland fire season, where dual pane windows helped to stop fire spread, as the first pane was compromised, but the inner pane withstood facture (Texas A&M Forest Service, 2012).

- **Vents**

Vents revealed to be particularly vulnerable to firebrands penetration into buildings (Quarles and TenWolde, 2004; Texas A&M Forest Service, 2012), specially unscreened ones (Bell, 1985; Blanchi

et al., 2006). Actually, they were one of the most common entrance points to firebrands in past fires in Mediterranean Europe (Xanthopoulos, 2003).
Field observations revealed that vents are also vulnerable to flames penetration (i.e. flames from burning surrounding elements), both vents located in attics or cathedral ceilings, and in crawl spaces under buildings (Quarles and TenWolde, 2004; Quarles *et al.*, 2010).
As an example, the post-fire survey conducted after the 2003 Southern California Fire (U.S.A.) evidenced that several buildings were destroyed due to firebrands and flame penetration through vents located under wide roof overhangs (Quarles and TenWolde, 2004). The combustible items that may be stored in attics or cathedral ceilings, as well as timber trusses, which are easily ignited, due to the lower moisture content (attics or cathedral ceilings tend to be dry spaces) (Quarles *et al.*, 2010), increase the available fuel load to fire propagation, leading to building destruction.

- **Roof systems**

A complex roof design, e.g. with intersections between roof and walls (e.g. a dormer) (Quarles *et al.*, 2013) or geometric features such as valleys or gullies (Blanchi *et al.*, 2006), increases roof vulnerability to fire as it provides the accumulation of firebrands or even dead vegetation (e.g. from overhanging trees), which may be ignited by firebrands. Actually, roofs with multiple ridges (which dictate roof valleys) and gullies appeared to perform fare worse than flat roofs, when threatened by firebrands (Blanchi *et al.*, 2006). Furthermore, roof systems contain several components that proved to be vulnerable to fire penetration into the building (such as roof covering, edge, overhang, gutters, chimneys), depending of their material characteristics, as well as other design features and details of its different parts.
Studies from past fire events at the WUI, particularly in Mediterranean Europe, where tiled roofs are quite common, evidenced that while tiled roofs in good shape and clean from dead vegetation protected buildings from firebrands penetration, along with their fire resistance characteristics, tiled roofs with gaps, dislocated or even broken tiles, that presented a fuel continuity to the building interior (Xanthopoulos *et al.*, 2011) (e.g. dead vegetation accumulation), allowed firebrands penetration into the building (Xanthopoulos *et al.*, 2003), leading to their destruction. It has been reported that the layer of bituminous membrane placed between timber trusses and ceramic tiles (to prevent water leaks), ignited quite easily from firebrands attack, setting the roof on fire (Xanthopoulos *et al.*, 2011). Moreover, poorly maintained timber trusses revealed to increase ignition easiness (Xanthopoulos *et al.*, 2003).
Ceramic roof tiles are commonly supported by timber trusses in southern Europe but concrete roofs covered with ceramic roof tiles may also be found, and past fire events evidenced that the last ones performed better to exterior fire threats, than ceramic tiled roofs supported by timber trusses (Xanthopoulos *et al.*, 2011).
Spanish tiles (or curved or Mediterranean style) roofs contributed to building destruction through firebrands penetration in the 2003 Southern California Fire, as a result of poor construction, missing tiles (which created gaps in the roof covering) and/or dislocated "birdstops" (i.e. cement filler that blocks the eave openings under concave tiles limiting firebrands entry (Foote *et al.*, 1991a)) (Mitchell and Patashnik, 2007). Moreover, they behaved significantly worse than flat-tile/concrete roofs, as well as stone-covered steel roofs (Mitchell and Patashnik, 2007).
Therefore, tiled roofs can be a weak point to the building envelope, during fires in the WUI, particularly when they contain many gaps, typically where the tiles overlap (as tiles rarely fit together tightly enough to maintain a less than 2 mm gap (Blanchi and Leonard, 2005)), and at the roof edge between the roof covering and the roof sheathing (Quarles *et al.*, 2010). Moreover, gaps can also exist at the roof ridge (Quarles *et al.*, 2010), where tiles are dislocated or even broken, creating more gaps.
Roof overhangs may be another weak point of the roof system during fires at the WUI (with or without vents (Quarles *et al.*, 2010)), as combustible soffits can either melt or ignite, leading to firebrands penetration into attic spaces (as it appears that has occurred during the 2011 Texas wildland fire season

(U.S.A.)) (Texas A&M Forest Service, 2012), or eaves area can accumulate firebrands, or even concentrate flames from ignited cladding or burning surrounding vegetation (particularly for open eave construction) (Quarles and TenWolde, 2004), leading to eaves ignition. Actually, during the 2009 Black Saturday Bushfire (Victoria, Australia), eaves were reported to be the part of the building that most commonly caught fire in the first place (VBRC, 2009).
Roof gutters evidenced to be a weak point in the roof system, particularly when filled with dead vegetation (Xanthopoulos, 2003; Quarles *et al.*, 2010), as after firebrands ignition (Blanchi *et al.*, 2006), the flames that may result would provide flame contact to the edge of the roof, particularly to fascia boards (Bell, 1985), which after destruction, may lead to flames entry into the attic space (Quarles *et al.*, 2010).
Chimneys are also pointed out as a weak point, as firebrands proved to be able to enter through them, particularly in the absence of a protective wire mesh (Xanthopoulos, 2003). Actually, they evidenced to be one of the most common firebrands entrance points in past fire events in the WUI of Mediterranean Europe.

2.4. Building immediate surrounding

After past fire events in the Wildland Urban Interface (WUI), field observations reported that, either the elements in the immediate building surrounding played a role of radiant heat barrier to the building, reducing the risk of building destruction (Blanchi *et al.*, 2006), or once ignited, they contributed to fire spread to other elements or even to other buildings, leading to their ignition and consequent loss (Blanchi *et al.*, 2006; Leonard *et al.*, 2009; Texas A&M Forest Service, 2012).
Several post-fire surveys highlighted that buildings were more likely to be destroyed as the vegetation in the immediate surrounding increases in terms of amount or density (Ramsay *et al.*, 1996; Cohen, 2000; Leonard and Bowditch, 2003; Mitchell and Patashnik, 2007). This applies to vegetation in direct contact with buildings (Texas A&M Forest Service, 2012), overhanging (e.g. trees) and immediately adjacent to them (e.g. forest, trees, ground cover such as shrub, mulch bed, dry grass) (Blanchi *et al.*, 2006; Leonard *et al.*, 2009). Thus the distance between vegetation and buildings plays an important role (Blanchi *et al.*, 2006; Leonard *et al.*, 2009). Furthermore, both the type of vegetation (Ramsay *et al.*, 1996) and weather conditions (especially long periods of hot dry conditions) (Potter and Leonard, 2010) influence the fuel loading, fuel moisture content, and heat content (Foote *et al.*, 1991a). Radiant heat and flame exposure play an important role in building ignition from burning surrounding vegetation (Ramsay *et al.*, 1996; Leonard and Bowditch, 2003; Mitchell and Patashnik, 2007).
Poor maintenance of the surrounding vegetation has also shown to affect building vulnerability during fires in the WUI, as it leads to dead vegetation accumulation, alike the accumulation of dead fuel as a result of their cut (Caballero, 2004). Field observations after the 2000 Cerro Grande Fire in Los Alamos (U.S.A.) (Cohen, 2000) revealed that in many areas of buildings destruction, ignition of timber cladding appeared to be triggered by pine needles fuel beds around buildings, while in some cases, whereas pine needles were removed, particularly from the base of timber walls, they did not ignited.
However, well located and selected plants that are properly maintained can reduce the risk of exposure that a building experience during a fire event (Blanchi *et al.*, 2006), e.g., pruning and thinning of ladder fuels in Gambel oak (*Quercus gambelii*) clumps, appeared to be effective in keeping fire on the ground and reducing crown fire potential (i.e. fire spread from treetop to treetop) during the 2012 Waldo Canyon Fire (Quarles *et al.*, 2013).
Generally, timber decks or verandas (either solid or composite products) are attached to buildings. After firebrands attack (common ignition source), decks ignition (particularly of decks untreated with fire retardant products) and even their timber steps (Ramsay *et al.*, 1996), skirting or railings ignition, conducted flames right up to the external parts of the building envelope, leading to building destruction (Texas A&M Forest Service, 2012). However, while in the U.S.A. and Australia, combustible decks are common, in Mediterranean Europe, they do not pose a risk to building destruction, since decks are

mostly built with fire resistant materials (Xanthopoulos, 2004) or they are close to non-combustible walls.
Field observations revealed that decks ignition (through flame contact) may also result from the burning material stored under it (e.g. firewood piles) or on the top of the deck (e.g. combustible garden furniture), or even from burning adjacent vegetation (e.g. trees, bushes) (Colorado Springs Fire Department, 2013).
Timber fencing systems that are adjacent to the buildings, after ignited have the potential to break windows, ignite combustible features of the building itself, and/or even spread fire to neighbourhood buildings, as it happened in the 2003 Canberra fires (Blanchi *et al.*, 2006). Moreover, timber fences with adjacent vegetation are particularly susceptible to ignition (Potter and Leonard, 2010). On the other hand, non-combustible fences demonstrated to provide radiation barriers, as well as timber fences that were regularly wetted (Potter and Leonard, 2010), either to the main fire front or to the burning of an adjacent structure, reducing the potential for fire attack (Blanchi *et al.*, 2006).
Garages and sheds showed to be more readily lost compared with the main structure, since generally they have more gaps and openings, being more susceptible to firebrands' ignition (Blanchi *et al.*, 2006). After ignited, they became localised flame, radiation and firebrands' sources, threatening the main structure, as a function on their proximity, garage or shed design, size, and materials stored inside it (Blanchi *et al.*, 2006). Actually, during the 2011 Texas wildland fire season, garages or sheds after ignited, revealed to generate a tremendous amount of heat, as well as combustible garden furniture, vehicles, and firewood piles (Texas A&M Forest Service, 2012).
Non-combustible retaining walls (e.g. brick retaining walls (Texas A&M Forest Service, 2012)), paths and gravel borders appeared to be effective in stopping fire spread during past fire events at the WUI, particularly in lighter fuel types (Quarles *et al.*, 2013), while combustible retaining walls (e.g. railway sleepers) demonstrated to be easily ignited and burned intensely for long durations (Texas A&M Forest Service, 2012).

Conclusions

The main characteristics of buildings (and other structures) in the Wildland Urban Interface (WUI) that contributed significantly to their fire vulnerability during past fire events are:

- Building material characteristics (i.e. combustible, non-combustible, fire resistant) used in their external and internal parts;
- Design features and details of their different parts and the openings or weak points in buildings envelope, such as gaps or crannies on exterior subfloor systems elevated on stumps above the ground, windows frame, glass and sill (particularly in re-entrant corners), door frames and assemblies (also in re-entrant corners), gaps around window frames and doors, vents, complex roof design with dormers, valleys or gullies, gaps on roof covering and edges, and roof overhang, gutters (particularly filled with dead vegetation), and chimneys.

The building vulnerabilities to fire threats may act by themselves or synergistically with each other and lead to building damage or destruction, depending on several factors, such as topography, weather conditions, human behaviour, and/or fuel loads of the elements in the immediate building surrounding. The elements on, attached to and around buildings most susceptible to ignition and fire spread are live or dead vegetation, untreated combustible decks or verandas and their steps, skirting and railings, firewood piles, timber fences, garages, sheds, awnings, combustible garden furniture, vehicles, and combustible retaining walls.
Despite the colossal property losses that resulted from past fire events at the WUI, several buildings survived. The use of non-combustible or fire resistant materials on buildings envelope appeared to decrease building susceptibility to fire threats, leading to building survivability. Some of the building openings or weak points also appeared to be less susceptible when in good conditions and protected

with particular elements, such as fire resistant windows shutters (that were closed during fire event), metal fly wire screens on windows, fire resistant screens on vents and doors, wire mesh on chimneys, concave tiles filled with cement on eave openings, as well as the use of low or non-combustible materials in door assemblies. Furthermore, an adequate maintenance of live and dead vegetation in buildings' immediate surrounding, non-combustible fences, timber fences regularly wetted, and non-combustible retaining walls, paths and gravel borders appeared to be effective in preventing fire spread.

The materials used in buildings construction (and in other structures) is the main difference observed between the analysed countries (i.e. U.S.A., Australia, Portugal, Spain, Greece), that affected directly building vulnerability to fires. In the U.S.A. and Australia, the use of combustible construction materials, particularly on buildings external parts (i.e. cladding, roof covering and/or decks) clearly increased buildings susceptibility to fire, which most probably led to building destruction, either way through building ignition from the exterior or from inside. Untreated timber elements (i.e. without impregnated fire retardant treatments) were particularly vulnerable to fire, especially as their hygroscopicity allowed it to be easily ignited during severe fire weather conditions (i.e. characteristic of fires in the WUI). In that context, fire ignition of a building may easily lead to fire propagation to adjacent buildings, which was evident in several post-fire surveys. It should be stressed however that the ignition of a building is highly influenced by other variables, besides building materials combustibility, as above discussed.

On the contrary, the building envelope components in Mediterranean Europe are generally fire resistant, leading to a substantial reduction of the available fuel loads to initial ignition and flame-spread to other building components. Actually, from the analysed studies, building destruction in Mediterranean Europe generally happened as a result of fire penetration into the building through openings or weak points (such as open windows, vents, chimneys without a protective wire mesh, tiled roofs with gaps, dislocated or even broken tiles, with dead vegetation accumulation), leading to building ignition from inside.

References

Bell, A. 1985. How bushfires set houses alight lessons from Ash Wednesday. Ecos 43:3-7, Autumn 1985.

Blanchi, R. and Leonard, J. 2005. *Investigation of bushfire attack mechanisms resulting in house loss in the ACT bushfire 2003*. Bushfire Cooperative Research Centre (CRC) Report. Australia.

Blanchi, R., Leonard, J. E., and Leiceste, R. H. 2006. Lessons learnt from post bushfire surveys at the urban interface in Australia. Forest Ecology And Management 234. DOI:10.1016/j.foreco.2006.08.184.

Caballero, D. 2004. III Workshop on Forest Fires in the Wildland-Urban Interface and Rural Areas in Europe Fires of 2003: lessons learnt and how can we use them - conclusions. (http://www.docstoc.com/docs/27147545/III-Workshop-on-Forest-Fires-in-the-Wildland-Urban-Interface-and). Retrieved 2014-06-04.

CAL FIRE. 2009. Top 20 largest California wildland fires. (http://www.fire.ca.gov/communications/downloads/fact_sheets/20LACRES.pdf). Retrieved 2014-06-04.

Cohen, J. D. 2000. Examination of the home destruction in Los Alamos associated with the Cerro Grande Fire July 10, 2000. United States Department of Agriculture (USDA) Forest Service. (http://ebookbrowsee.net/cohen-cerro-grande-fire-examination-of-home-destruction-in-los-alamos-2000-pdf-d577803467). Retrieved 2014-06-03.

Cohen, J. D. 2008. The wildland-urban interface fire problem: a consequence of the fire exclusion paradigm. Forest History Today, Fall 2008: 20-26.

Cohen, J. D., and Stratton, R. D. 2008. *Home destruction examination - Grass Valley Fire*. USDA Forest Service Report R5-TP-026b.

Colorado Springs Fire Department. 2013. *Ignition Resistant Construction Design Manual - A guide to smart construction and wildfire mitigation in the wildland/urban interface*. Colorado: City of Colorado Springs Fire Department - Division of the Fire Marshal.

Fairbanks, R. and Ingalsbee, T. 2006. A homeowner's guide to fire-resistant home construction. Firefighters United for Safety, Ethics, and Ecology. (drupalweb.forestry.oregonstate.edu/forest-owner/sites/default/files/fireresistance.pdf). Retrieved 2014-06-03.

Foote, E. I. D., Liu, J., and Manzello, S. L. 2011. Characterizing firebrand exposure during wildland-urban interface fires. *In proceedings of the 12th International Conference on Fire and Materials*, 1-12. San Francisco, United States of America (U.S.A.).

Foote, E. I. D., Martin, R., and Gilless, J. K. 1991a. The defensible space factor study: a survey instrument for pos-fire structure loss. *In Proceedings of the 11th Conference on Fire and Forest Meteorology*, 91-04: 66-73. Montana, U.S.A..

Foote, E. I. D., Martin, R. E., and Gilless, J. K. 1991b. The Santa Barbara Paint Fire: data collection for urban-wildland interface structure loss analysis. (http://www.bushfirecrc.com/managed/resource/foote-martin-gilless-1991-santa-barbara-paint-fire.pdf). Retrieved 2014-06-12.

Galiana-Martín, L. 2011. The wildland-urban interface: a risk prone area in Spain. (https://www.ucm.es/data/cont/docs/530-2013-10-15-Luis%20Galiana-Martin.pdf). Retrieved 2014-06-12.

Infoplease. 2014. Worst U.S. Forest Fires. (http://www.infoplease.com/ipa/A0778688.html). Retrieved 2014-06-04.

Koo, E., Pagni P. J., Weise, D. R., and Woycheese, J. P. 2010. Firebrands and spotting ignition in large-scale fires. Internation Journal of Wildland Fire, 19: 818-843.

Kyle, G. T., Theodori, G. L., Absher, J. D., and Jun, J. 2008. The influence of home and community attachment on Firewise behavior. Society and Natural Resources, 23: 1–18.

Leonard, J. E. and Bowditch, P. A. 2003. *Findings of studies of houses damaged by bushfire in Australia*. Commonwealth Scientific and Industrial Research Organisation (CSIRO), Manufacturing & Infrastructure Technology. Melbourne, Australia.

Leonard, J., Blanchi, R., Lipkin, F., Newnham, G., Siggins, A., Opie, K., Culvenor, D., Cechet, B., Corby, N., Thomas, C., Habili, N., Jakab, M., Coghlan, R., Lorenzin, G., Campbell, D., and Barwick, M. 2009. Building and land-use planning research after the 7th February 2009 Victorian bushfires - Preliminary findings. CSIRO Sustainable Ecosystems, Bushfire CRC and Geoscience Australia. Final Report. Australia.

Manzello, S. L. 2014. Special issue on wildland–urban interface (WUI) fires. Springer Science+Business Media, Fire Technology, 50: 7–8. DOI: 10.1007/s10694-012-0319-0.

Maranghides, A. and Mell, W. 2009. *A case study of a community affected by the Witch and Guejito fires*. National Institute of Standards and Technology (NIST) Technical Note 1635.

Mitchell, J. W. and Patashnik, O. 2007. Firebrand protection as the key design element for structural survival during catastrophic wildfire fires. (http://www.mbartek.com/FM07_FirebrandsWildfires_1.1F.pdf). Retrieved 2014-06-04.

Potter, M. and Leonard, J. 2010. *Spray system design for ember attack - Research findings and discussion paper*. Bushfire CRC. Australia.

Quarles, S. L. and TenWolde, A. 2004. Attic and crawlspace ventilation: implications for homes located in the urban-wildland interface. *In Proceedings of the Woodframe Housing Durability and Disaster Issues*, 227-232. Las Vegas, U.S.A..

Quarles, S., Leschak, P., Cowger, C. R., Worley, k., Brown, R., and Iskowitz, C. 2013. *Lessons Learned from Waldo Canyon*. Fire Adapted Communities Mitigation Assessment Team Findings. Insurance Institute for Business & Home Safety.

Quarles, S. L., Valachovic, Y., Nakamura, G. M., Nader, G. A., and Lasaux, M. J. 2010. Home survival in wildfire-prone areas: building materials and design considerations. University of California, Agriculture and Natural Resources, May 2010: 83-93.

Ramsay, G. C., McArthur, N. A. and Dowling, V. P. 1996. Building in a fire-prone environment: research on building survival in two major bushfires. *In Proceedings of the Linnean Society of New South Wales*, 116: 133-140.

Tedim, F., Remelgado, F., Borges, C., Carvalho, S., and Martins, J. 2012. Exploring the occurrence of mega-fires in Portugal. Forest Ecology and Management Journal. dx.doi.org/10.1016/j.foreco.2012.07.031.

Texas A&M Forest Service. 2012. 2011 Texas wildfires - Common denominators of home destruction. Texas A&M Forest Service. (http://tfsweb.tamu.edu/uploadedFiles/FRP/New_-_Mitigation/Safety_Tips/2011%20Texas%20Wildfires.pdf). Retrieved 2014-06-06.

Trindade, C. J. B., Ribeiro, P., and Figueiredo, A. 2012. Land use survey in the municipality of Mafra - a contribution of GIS to the municipality sustainability (in portuguese, *Levantamento da ocupação do solo do concelho de Mafra - um contributo dos SIG para a sustentabilidade do concelho*). XIX Ordem dos Engenheiros Congress (in portuguese, *Congresso*). Society, Territory and Environment (in portuguese, *Sociedade, Território e Ambiente*). The Engineer Intervention (in portuguese, *A Intervenção do Engenheiro*). Lisbon.

Victorian Bushfires Royal Commission (VBRC). 2009. *Building in bushfire prone areas*. VBRC. February 2009. Australia.

Viegas, D. X., Figueiredo, A. R., Almeida, M. A., Reva, V., Ribeiro, L. M., Viegas, M. T., Oliveira, R., and Raposo, J. R. 2012. *Wildland fire report of Tavira/São Brás de Alportel* (in portuguese, *Relatório do incêndio florestal de Tavira/São Brás de Alportel*). Centro de Estudos sobre Incêndios Florestais, ADAI/LAETA. Coimbra University. Coimbra.

Viegas, D. X., Rossa, C., and Ribeiro, L. M. 2011. *Wildland fires* (in portuguese, *Incêndios florestais*). Lisbon: Verlag Dashofer.

Viegas, D. X., Simeoni, A., Xanthopoulos, G., Rossa, C., Ribeiro, L. M., Pita, L. P., Stipanicev, D., Zinoviev, A., Weber, R., Dold, J., Caballero, D., and San Miguel, J. 2009. *Recent forest fire related accidents in Europe*. EUR 24121 EN. Joint Research Center (JRC). Institute for Environment and Sustainability (IES). Scientific and Technical Research series. ISSN 1018-5593. Luxembourg.

White, R. H. and Dietenberger, M. A. 2010. *Wood handbook, Chapter 18: Fire safety of wood construction*. General Technical Report FPL-GTR-190. Madison, WI: U.S. Department of Agriculture, Forest Service, Forest Products Laboratory.

Xanthopoulos, G. 2003. Forest fires in the wildland-urban interface and rural areas in Europe: an integral planning and management challenge - conclusions of the workshop. *In Proceedings of the II International Workshop on Forest Fires in the Wildland-Urban Interface and Rural Areas in Europe: an integral planning and management challenge*, 229-231. Athens. Greece.

Xanthopoulos, G. 2004. Factors affecting the vulnerability of houses to wildland fire in the Mediterranean region. *In Proceedings of the II International Workshop on Forest Fires in the Wildland-Urban Interface and Rural Areas in Europe: an integral planning and management challenge*, 85-92. Athens, Greece.

Xanthopoulos, G., Bushey, C., Arnol, C., and Caballero, D. 2011. Characteristics of wildland-urban interface areas in Mediterranean Europe, North America and Australia and differences between them. *In Proceedings of the 1st International Conference in Safety and Crisis Management in the Construction, Tourism and SME Sectors*, 702-734. Nicosia, Cyprus.

Xanthopoulos, G., Labris, C., and Golfinos, C. 2003. The June 4, 2001 fire in the wildland-urban interface areas of Northern Attica: evolution, firefighting problems and damages. *In Proceedings of the International Workshop on Forest Fires in the Wildland-Urban Interface and Rural Areas in Europe: an integral planning and management challenge*, 19-28. Athens, Greece.

Bushfire fatalities and house loss in Australia: Exploring the spatial, temporal and localised context

Raphaele Blanchi[a,b], Justin Leonard[a,b], Katharine Haynes[b,c], Kimberley Opie[a], Melissa James[a], Felipe Dimer de Oliveira[c]

[a] *CSIRO Land and Water, PO Box 56, Highett, Victoria 3190, Australia.*
Raphaele.Blanchi@csiro.au
[b] *Bushfire Cooperative Research Centre, Australia*
[c] *Risk Frontiers Macquarie University*

Abstract:
This paper examined the spatial, temporal and localised context of bushfire fatalities and house loss in Australia. The analysis focused principally on understanding the strength of correlations between location where fatal exposure occurred, fire weather conditions (using the McArthur Forest Fire Danger Index (FFDI) and its individual components), proximity to fuel, proximity to other objects (houses and/or vehicles) and fatality activity and decision making leading up to the death.
The analysis is based on a dataset containing bushfire related life loss and house loss in Australia over the past 110 years (1901-2011). Over this time period 260 bushfires have been associated with a total of 825 known civilian (733) and firefighter fatalities (92), and 8778 houses destroyed. The analysis included spatial, temporal and localised context in which the fatalities have occurred.
The analysis demonstrated that:

- The losses are dominated by major events that have occurred under very severe weather conditions
- The location of fatal exposure provides a useful context to better understand the specific level of shelter a person had when they died with 58% occurring out in the open, 28% occurring inside structures and 8% in vehicles.
- Male and female civilian fatalities within structures were evenly represented, while male fatalities out in the open were approximately 3 times greater than female fatalities out in the open (mainly in earlier years)
- 41% of fatalities within structure occurred in rooms with reduced visibility to the outside
- Fatalities within structures represent over 75% of all fatalities under very severe conditions (weather conditions exceeding an FFDI value of 100). These are associated with people dying while attempting to shelter mainly in their place of residence. Conversely lower values of FFDI are associated with people who are caught outside while defending their property.
- Over 60% of fatalities occurred within 100m of a residence
- 80% of all fatalities and 60% of the house loss occurred within 30 m of the forest.

Keywords*: Wildland fire, Fatalities, WUI, House loss, Risk*

Introduction

In Australia the studies of community safety at the urban interface were mainly based on post bushfire surveys and subsequent analysis to better understand the mechanisms of bushfire attack at the urban interface. The important points of consideration in those studies were on the building design, the immediate landscape, the type of urban interface and human activity and how they significantly influence the risk of loss (e.g. Barrow, 1945; Raphaele Blanchi & Leonard, 2008; Leonard & McArthur, 1999; Ramsay *et al*., 1987).
Some studies have been performed on the behaviour of civilian fatalities during bushfires (e.g. Handmer & Haynes, 2008; Haynes *et al*., 2010; O'Neill & Handmer, 2012; Tibbits, Blanchi, & Gill, 2006). While these studies on civilian fatalities have mainly focused on the behaviour of the victims

and are mainly conducted within the context of the 'Stay or Go' policy[1], they have not included the spatial and environmental circumstances of their death.
Other studies have investigated the circumstances of firefighter fatalities involving entrapment and burnovers (Butler & Cohen, 1998; Cheney *et al*., 2001; Viegas *et al*., 2008). Meanwhile some studies have focused on the influence of environmental circumstances on house loss for individual events or multiple events in Australia (e.g. Ahern & Chladil, 1999; Blanchi *et al*., 2010; Butler & Cohen, 1998; Gibbons *et al*., 2012; Harris *et al*., 2012; Newnham *et al*., 2012) and the US (e.g. Cohen, 2000; Menakis *et al*., 2003; Syphard *et al*., 2012).
This study examined the environmental circumstances of bushfire fatalities and house loss in Australia over the last 110 years, using a specific data set that included spatial, temporal and localised context (Life Loss database). The results presented in this paper are related to the relationship between fatal exposure location, house loss, weather conditions, and proximity to fuel and additional analysis components are presented in Blanchi *et al*. (2014).

Methods and data

The database (Life Loss database) developed for the analysis is a spatial dataset of bushfire related fatalities and related losses (such as house loss) and circumstances, in Australia over the past 110 years (1901-2011). It also captures the circumstances leading up to the fatal exposure such as weather context using the McArthur Forest Fire Danger Index (FFDI) (McArthur, A.G., 1978; McArthur, 1967), fire severity, distance to forest, fatality activity and decision making (Blanchi *et al*., 2014; Blanchi *et al*., 2012).
A number of different data sources were accessed in order to assemble the Life Loss database. This includes coronial inquest records, royal commission reports, journal papers, books, post bushfire study reports, fire agency review documents of major fires, newspaper articles and collated datasets on past bushfire fatalities (Blanchi *et al*., 2012; Haynes *et al*., 2010).
Different types of data have been compiled in the dataset: quantitative variables (e.g. weather information), and categorisation variables (e.g. location of fatality). Some information was categorised to facilitate spatial and statistical analysis. The detail of the data collection is presented in Blanchi *et al*. (2012, 2014).
The Life Loss database contains 825 fatalities, 733 are civilian and 92 are listed as firefighters. Of the fatalities contained in the database 741 were directly related to the fire itself (674 civilians and 67 firefighters). Fifty fatalities were indirectly related to a fire event and the specific cause of death for 34 persons was unknown or unclear.
The data was grouped into three time periods: for the entire time period of data, pre 1965, and post 1965. This segregation of data also happens to be useful in distinguishing some patterns over the years, and provided an opportunity to compare demographic context relating to social behaviour and prevalence of technologies such as automobiles.

The analysis examined the:
- demographics
- distribution of fatalities and house loss in time

[1] Referred to as the 'Stay or Go' policy, the policy recommended that either actively defending a well-prepared home or evacuating/relocating well in advance of a fire threat are the best survival options during a bushfire. formed the basis of the Bushfire and Community Safety Position developed by the Australasian Fire and Emergency Service Authorities Council (AFAC) before the 2009 Victorian fires AFAC (2005) Position Paper on Bushfires and Community Safety. AFAC Limited, Victoria, Australia. This position was translated into the prepare, stay and defend or leave early policy in most jurisdictions.

- location of fatal exposure
- importance of weather conditions on loss
- influence of distance to forest on loss

Results and discussion

3.1. Demographics

The gender and age distribution of all fatalities (civilians and firefighters) was studied to help inform specific trends relating to assumed behaviours or activities. Data was grouped into three time periods; for the entire time period of data, pre 1965, and post 1965. The gender role could also demonstrate an evolution of behaviour in the different roles of men and women over the century.
In summary, in earlier fires a higher proportion of the lives claimed were of young children, whereas more recent fires have claimed the lives of a higher proportion of older people. The distinction between civilians (further broken into gender) and firefighters is shown in Figure 1 for the two periods considered and for all known genders (29 unknown). This figure highlights the significant increase of female civilian fatalities in recent fires.

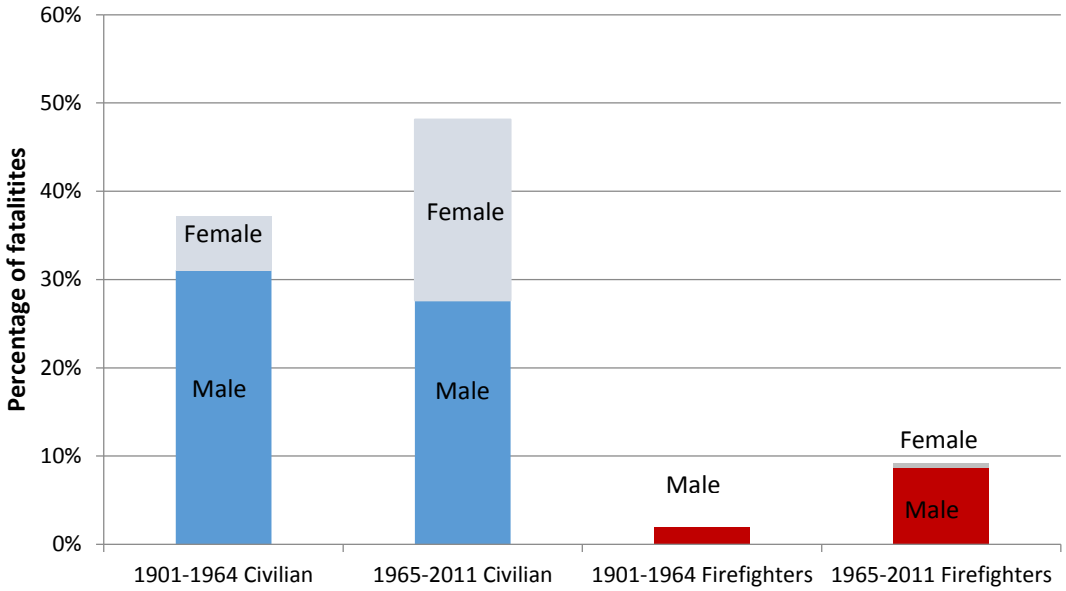

Figure 1. Number of fatalities by gender between the period 1901-1964 and the period 1965-2011 (distinction between civilian and firefighters)

3.2. Distribution of fatalities and house loss in time

The number of fatalities and house loss is dominated by a few major events resulting in large number of the fatalities and house destruction (Figure 2 and Figure 3). This is in accordance with the finding of Haynes *et al*. (2010) and Blanchi *et al*. (2010) which has shown that the losses per event and spatial distribution of loss are strongly influenced by fire weather severity.

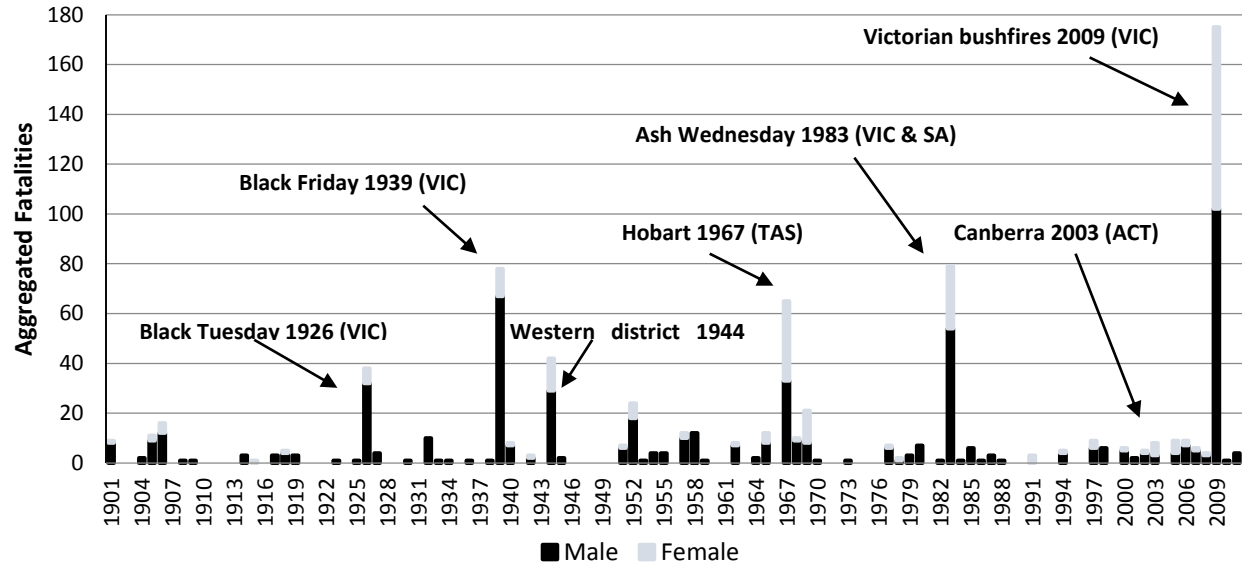

Figure 2. Distribution of number of fatalities over the time period (1901-2011) including civilian and firefighters in Australia

While the graph shows no consistent trend there is an increase in the loss per year rate when comparing the two time period categories (1901-1964 and 1965-2011). For the period 1901-1964, 5.1 civilian fatalities occurred per year and for 1965-2011, 8.6 fatalities occurred per year.
The number of houses lost for the period 1901-2011 shows a similar pattern (see Figure 3) and is dominated by the same iconic events (Blanchi *et al* 2010). There is a more noticeable bias toward losses in more recent years. This is in part due to the lack of house loss data in the 1901-1926 time period and also due to better record of house losses in recent years and an increase of population and houses in fire prone area. Keeping this in mind the 1901-1964 house loss average is 44 per year and the 1965-2011 average is 168 per year.

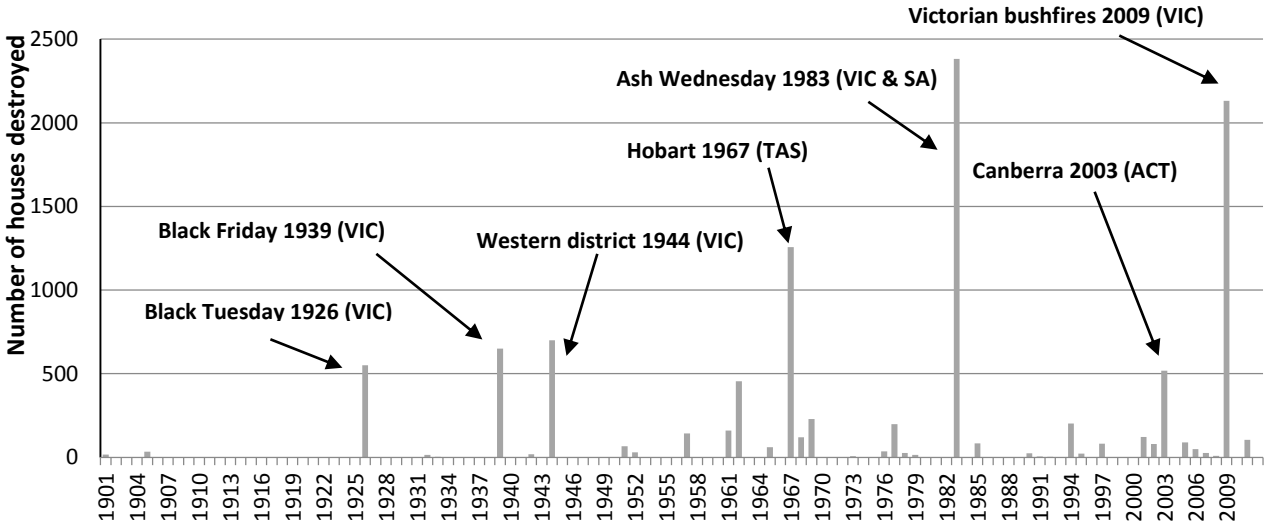

Figure 3. Distribution of number of house burnt (destroyed) over the time period (1901-2011) in Australia

Figure 4 profiles the time of fatal exposure (when known) for both firefighters (44) and civilians (397). This figure shows a clustering of civilian fatalities from 10am through to 11pm with one peak at 10am.

This peak is mainly due to a single loss event, where 17 motorists lost their lives on the Princes Highway between 10am and 11am in the Victorian Lara fire in 1969. Without this anomaly, the civilian fatalities exhibit a normal distribution around 6pm. Firefighter fatalities have a similar fatality time distribution to civilians, with a peak at 3pm and 9pm (which correspond to the Ash Wednesday fire where 12 firefighters died during a burnover).

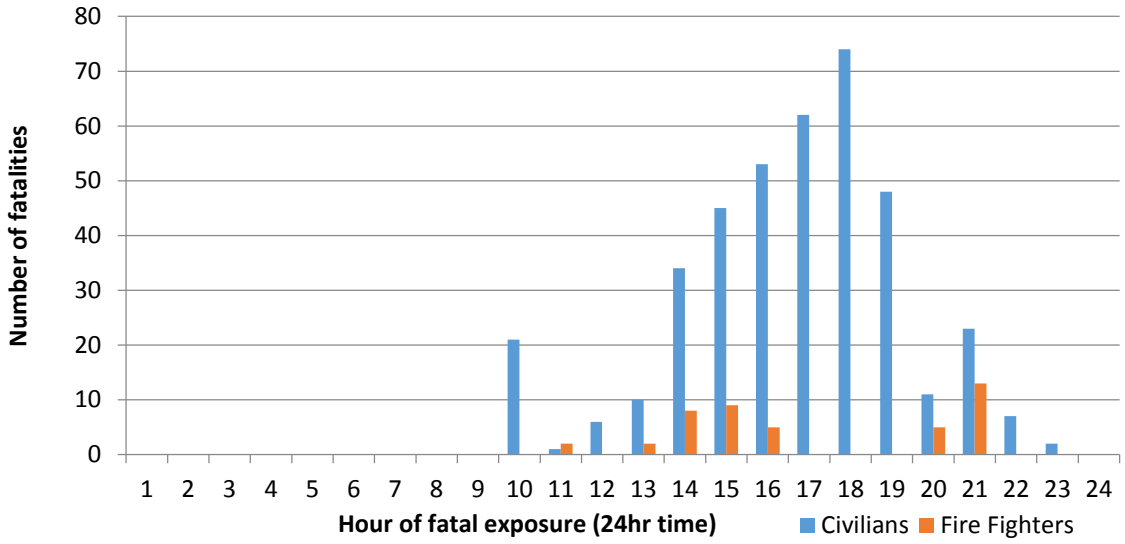

Figure 4. Hour of civilian and firefighter fatal exposure for all directly related deaths

3.3. Location of fatal exposure

The location of fatalities was categorised into 'In structure', 'In vehicle' & 'Open air' to better understand the specific level of shelter a person had when they died. Table 1 summarises the location categories of fatal exposure for the three time periods (1901-2011; 1901-1964; and 1965-2011) with 58% occurring out in the open, 28% occurring inside structures and 8% in vehicles.

A significantly greater proportion of fatalities occurred inside structures or inside vehicles in recent fires, compared to earlier fires. The higher proportion of fatalities inside vehicles in the time period 1965-2011 is explained by higher prevalence of cars and their use during this period. This summary also highlights that in earlier fires a significantly greater proportion of fatalities occurred in the open air, compared to more recent fires.

Male and female civilian fatalities within structures were evenly represented, while male fatalities out in the open were approximately 3 times greater, particularly earlier in the century. This is possibly related to job profiles that involve remote location work such as timber felling where shelter is not easily found or farmers attempting to save livestock (Blanchi *et al*., 2012).

Firefighter fatalities occurred in open air, in fire fighting vehicle burn-over incidents or from falling trees. Sheltering within a structure is a relatively rare and often unavailable strategy for firefighters.

Table 1. Fatal exposure location categories over the three time periods (civilian)

	1901-1964	**1965-2011**	**1901-2011 (total)**
Inside structure	21 (7.1%)	167 (44.4%)	188 (27.9%)
Inside vehicle	11 (3.7%)	45 (12.0%)	56 (8.3%)
Open air	232 (77.8%)	158 (42.0%)	390 (57.8%)
Unknown	34 (11.4%)	6 (1.6%)	40 (5.9%)
Total	298 (100 %)	376 (100%)	674 (100%)

The distance of a fatality to their residence can help qualify the prevalence of behaviours in relation to last minute evacuation or alternative shelter and defence strategies. A sample set of 116 fatalities from the Life Loss database for which residential address and fatal exposure locations were both accurately known was analysed. This sample set included 79 fatalities that occurred in open air, 18 that occurred inside a vehicle and 19 inside a structure (other than their residence, e.g. a neighbouring house, bunker etc). These cases have been plotted as cumulative graph in Figure 5.

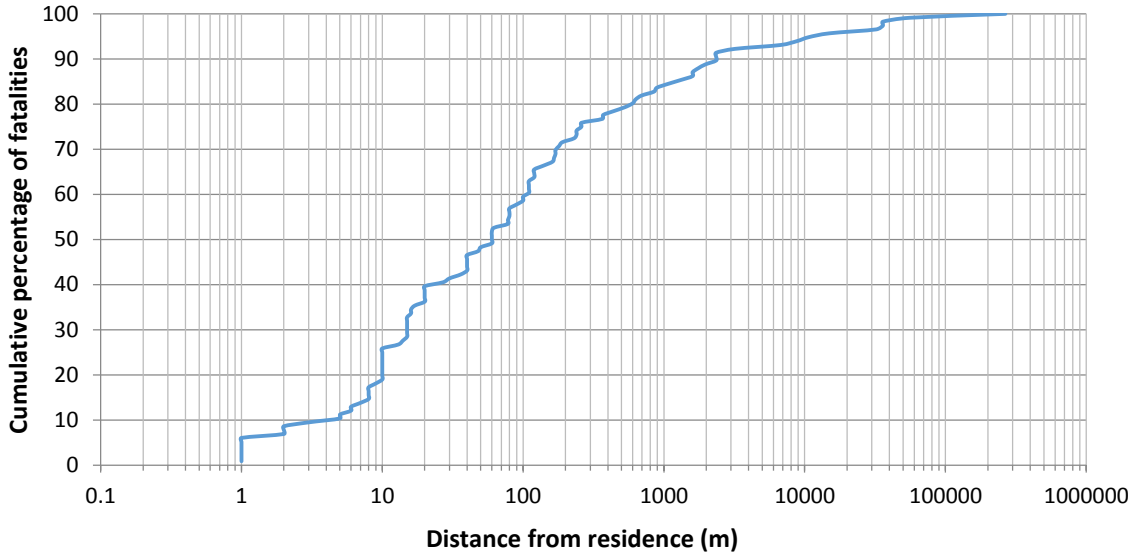

Figure 5. Distance between residential address and fatal exposure location (civilian)

Table 2 shows a close association with the place of residence, with 61% of fatalities occurring within 100m of their location of residence and 84% occurring within 1km. Analysis of the locations of residence of the deceased showed that 10 houses were not damaged and were not used as a shelter, 89 houses were completely destroyed and of these 20 houses were used as a place of refuge during the event. The main activity of the fatalities considered in the analyses was late evacuation (48.3%), followed by saving livestock, livelihood or defending wider property outside (20.7%), and people sheltering as a group (11.2%).

For the fatalities that occurred inside structures it is useful to understand the location within the structure in which the fatal exposure occurred, as this will help to understand the behaviour adopted and the modes in which the house may have lost its tenability. Table 2 shows the location of fatality inside residential structures.

Table 2. Known fatality locations inside residential structures

Location inside structure	Number of fatalities	Percentage of known
Bathroom	36	33%
Kitchen	25	23%
Bedroom	17	16%
Study	10	9%
Enclosure under house	9	8%
Entrance	5	5%
Lounge	4	4%
Laundry	3	3%
Total	**109**	**100%**

Of these cases 33% of the fatalities occurred in bathrooms which typically have no clear visual cues to outside conditions. All other cases either involved an opportunity to monitor outside conditions or be adjacent to an exit to facilitate egress when the house approaches untenable conditions. Eight percent of cases were in either the entrance or laundry: both typically are adjacent to an exit door providing an option to egress if conditions allowed.
Fifty-eight percent involved fatalities in the bathroom, bedroom or study which all typically have only one point of exit to the rest of the house. Twenty-seven percent of cases involved kitchens and lounge areas which usually have opportunities for viewing outside conditions and multiple options to progress through the house towards an exit if it is recognised that the house is losing tenability.
In summary, for 59% of the fatalities there was the opportunity to effectively monitor both the internal and external conditions and make decision to move towards an exit as the house lost tenability. So either people were not aware of this strategy (or the need to leave) or the houses lost tenability at a rate in which safe passage from these locations to an exit door was not possible. This raises several questions in relation to egress, sheltering and the rate of loss of tenability of houses. Also to consider are the air toxic emitted and exposure concentrations inhaled by residents both indoors and outdoors (Reisen, Blanchi, & Tibbits, 2006).

3.4. Weather conditions and loss

The influence of meteorological conditions on loss has been shown in previous studies (Raphaele Blanchi *et al*., 2010; Bradstock, Gill, Kenny, & Scott, 1998). The weather conditions (using forest fire danger index) and aggregated fatalities and house loss by fire event is studied.
The FFDI is categorised according to the existing national danger rating scheme[1]:

- 0-11: low - moderate
- 12-24: high
- 25-49: very high
- 50-74: severe
- 75-100: extreme
- >100: catastrophic (Code Red in Victoria)

The cumulative percentile of both house loss and fatalities is related to the 3pm FFDI on the day of the loss (see Figure 6). Less than 3% of house losses and fatalities occurred when the FFDI was less than 49 (moderate to very high), roughly 7% occurred when the FFDI was between 25 and 50, and 25% of either house or life loss occurred when the FFDI was below 74. Over 60% of all fatalities and 75% of all house loss in Australia has occurred on days where the 3pm FFDI exceed 100.
Three large events dominate the results in the over FFDI 100 category: the Black Tuesday fires (7 February 1967) in Hobart, the Ash Wednesday fires (16 February 1983) in Victoria and South Australia, and the Victorian bushfires (7 February 2009).

[1] http://www.cfa.vic.gov.au/warnings-restrictions/about-fire-danger-ratings/ (accessed 15/06/2014)

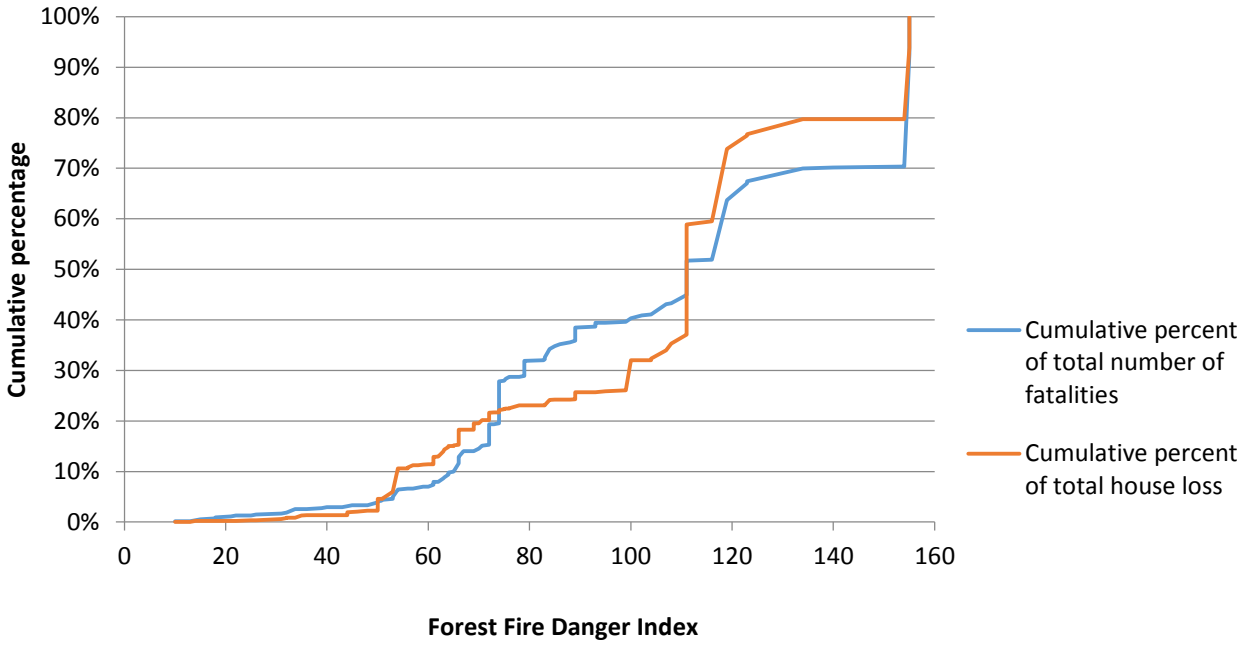

Figure 6. Cumulative percent of total number of fatalities and house loss versus FFDI

The location category of fatal exposure was compared to FFDI classes in Figure 7. There is an expected link with the location of fatal exposure and fire weather severity owing to the different vulnerabilities of each location context. The most noticeable result is the high prevalence of deaths inside structure for an FFDI of 100 plus category (fire danger rating 'catastrophic'). This may be due to a tendency to seek shelter from both the severe weather and the fire under such intense conditions. It also indicates that houses are likely to lose tenability more rapidly under these conditions and cause entrapment. At lower levels of FFDI (0-74) civilians are caught outside as the predominant loss location category.

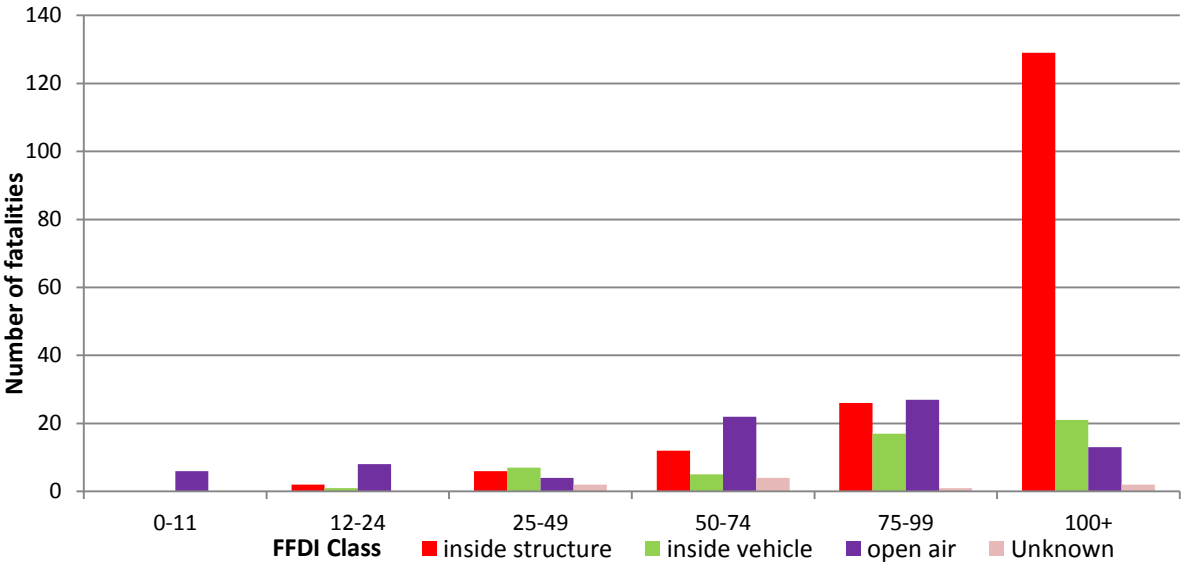

Figure 7. FFDI at 3pm and location of fatality (Blanchi et al. 2014)

3.5. Distance to forest

The separation between bushfire fuels and the fatality is an important risk assessment metric to classify likely exposure levels on the person, vehicle or structure. For the spatial analysis, the forest layer of the closest preceding year to the fire was used to determine the distance to forest. It is assumed that the layer which coincides with the year of the fire has a high likelihood of the fire scar affecting extent of forest for that year.

Of particular interest is the observation that over 50% of all fatalities occurred less than 10m from the forest, 78% in less than 30m and 85% in less than 100m. This provides a strong qualification of the possible influence of forest proximity as a factor in defining exposure resulting in fatal outcomes (Blanchi *et al*. 2014).

Comparing these percentages with the broader dataset of house loss as a function of distance to forest demonstrates that house loss involving fatal exposure are far more dominant in the 0-30m from forest regions. Compared to house losses not involving fatalities, less than 60% of all house losses occurred less than 30m from the forest (Newnham *et al*., 2012). It is to be noted that 30m is a distinctive threshold for direct radiant heat ignition of structures identified by Cohen (Cohen, 2008).

Conclusion

The database developed integrate information on losses including details of fire weather severity (using the McArthur Forest Fire Danger Index (FFDI) and its individual components), fire behaviour, proximity to forest, incident circumstances, fatality details, activities and the location of objects and structures related to the fatality. This paper focused on a subset of the analysis developed in the study, more information is available in Blanchi *et al*. (2012, 2014).

The study provided a better understanding of the circumstances of losses in particular the importance of fire weather conditions and proximity to fuel hazard in setting the context for loss. The findings of the study can be directly integrated in policies and community education initiatives for bushfire related life risk reduction.

Acknowledgement

This research was funded by the Australian Attorney General's Department (via Bushfire CRC). We gratefully acknowledge all the people who contributed to this research from various governmental and research organisations: The Australasian Fire and Emergency Service Authorities Council, Department of Environment and Conservation, Department of Fire and Emergency Services formerly the Fire and Emergency Services Authority of WA, New South Wales Rural Fire Service, Country Fire Authority Victoria, Tasmanian Fire Service, Department of Sustainable Ecosystem, ACT Emergency Services, Queensland fire and rescue service; Coroners Court of Victoria, New South Wales, and South Australia, Public record from Victoria, New South Wales and South Australia; Department of Climate Change and Energy Efficiency, Lucinda Coates and Robin Van den Honert (Risk Frontiers), Chris Lucas (BOM), Joshua Whittaker and John Handmer (RMIT).

We would like to thank Fabienne Reisen, Glenn Newnham and the anonymous reviewer for their helpful reviews, suggestions and comments.

References

Ahern, A., & Chladil, M. (1999). How far do bushfires penetrate urban areas? Proc. Australian Disaster Conf. 1999, Disaster Prevention for the 21st Century. Canberra: Emergency Management Australia.

Barrow, G. J. (1945). survey of houses affected in the Beaumaris fire, January 14, 1944. Journal of the Council for Scientific and Industrial Research, 18(1).

Blanchi, R., & Leonard, J. (2008). Property safety: judging structural safety. In J. Handmer & K. Haynes (Eds.), Community Bushfire Safety (pp. 77–85).

Blanchi, R., Leonard, J., Haynes, K., Opie, K., James, M., Kilinc, M., … Van den Hornet, R. (2012). Life and house loss database description and analysis - Final report (p. 92p). Melbourne: CSIRO, Bushfire CRC report to the Attorney-General's Department. CSIRO EP-129645.

Blanchi, R., Leonard, J., Haynes, K., Opie, K., James, M., & Oliveira, F. (2014). Environmental circumstances surrounding bushfire fatalities in Australia 1901-2011. Environmental Science and Policy, 37, 192–203.

Blanchi, R., Lucas, C., Leonard, J., & Finkele, K. (2010). Meteorological conditions and wildfire-related houseloss in Australia. International Journal of Wildland Fire, 19(7), 914–926.

Bradstock, R. A., Gill, A. M., Kenny, B. J., & Scott, J. (1998). Bushfire risk at the urban interface estimated from historical weather records: consequences for the use of prescribed fire in the Sydney region of south-eastern Australia. Journal of Environmental Management, 52(3), 259–271. Retrieved from <Go to ISI>://000074067700005

Butler, B., & Cohen, J. (1998). Firefighter safety zones: a theoretical model based on radiative heating. International Journal of Wildland Fire, 8(2), 73–77.

Cheney, P., Gould, J., & McCaw, L. (2001). The dead-man zone - a neglected area of firefighter safety. Australian Forestry, 64(1), 45–50. Retrieved from <Go to ISI>://CABI:20013072244

Cohen, J. D. (2000). Preventing disaster. Journal of Forestry., 98(3), 15. Retrieved from http://proquest.umi.com/pqdweb?did=55322153&sid=1&Fmt=1&clientId=82754&RQT=309&VName=PQD

Cohen, J. D. (2008). The wildland-urban interface fire problem. A consequence of the fire exclusion paradigm. Forest History Today, (Fall 2008, 20–26.

Gibbons, P., van Bommel, L., Gill, A. M., Cary, G. J., Driscoll, D. A., Bradstock, R. A., … Lindenmayer, D. B. (2012). Land Management Practices Associated with House Loss in Wildfires. PLoS ONE, 7(1), e29212. Retrieved from http://dx.doi.org/10.1371/journal.pone.0029212

Handmer, J. W., & Haynes, K. (2008). Community bushfire safety (p. xv, 205 p.). Collingwood, Vic.: CSIRO Publishing. Retrieved from http://csiro.aquabrowser.com/?itemid=|library/m/CSIRO-voyager|380524

Harris, S., Anderson, W., Kilinc, M., & Fogarty, L. (2012). The relationship between fire behaviour measures and community loss: an exploratory analysis for developing a bushfire severity scale. Natural Hazards, 63(2), 391–415. doi:DOI 10.1007/s11069-012-0156-y

Haynes, K., Handmer, J., McAneney, J., Tibbits, A., & Coates, L. (2010). Australian bushfire fatalities 1900-2008: exploring trends in relation to the "Prepare, stay and defend or leave early" policy. Environmental Science & Policy, 13(3), 185–194. Retrieved from http://www.sciencedirect.com/science/article/B6VP6-4YNT93S-2/2/1345112f4c3c3a1815fffac6277a739e

Leonard, J., & McArthur, N. A. (1999). A history of research into building performance in Australian bushfires. Proc. Bushfire 99: Australian Bushfire Conference. Albury, 7–9 July 1999.

Luke McArthur, A.G., R. H. (1978). Bushfires in Australia. Reprinted with corrections 1986. Canberra Publishing and Printing Co.

McArthur, A. G. (1967). Fire behaviour in eucalypt forests. Leaflet No. 107. Comm. of Australia For. & Timber Bur.

Menakis, J. P., Cohen, J. D., & Bradshaw, L. S. (2003). Mapping wildland fire risk to flammable structures for the conterminous United States. (K. E. M. Galley, R. C. Klinger, & N. G. Sugihara, Eds.)Fire Conference 2000: The First National Congress on Fire Ecology, Prevention and Mangement. Tallahassee, FL: Timber Research station.

Newnham, G. J., Siggins, A. S., Blanchi, R. M., Culvenor, D. S., Leonard, J. E., & Mashford, J. S. (2012). Exploiting three dimensional vegetation structure to map wildland extent. Remote Sensing of Environment, 123, 155–162. doi:10.1016/j.rse.2012.02.026

O'Neill, S. J., & Handmer, J. (2012). Responding to bushfire risk: the need for transformative adaptation. Environmental Research Letters, 7(1). doi:Artn 014018 Doi 10.1088/1748-9326/7/1/014018

Ramsay McArthur, N.A. Dowling, V.P., G. C. (1987). Preliminary results from an examination of house survival in the 16 February 1983 bushfires in Australia. Fire and Materials, 11, 49–51.

Reisen, F., Blanchi, R., & Tibbits, A. (2006). Potential health impacts to residents from smoke exposure during bushfires. (D. X. Viegas, Ed.)V International Conference on Forest Fire Research, 27-30 November 2006. Figueira da Foz, Portugal.

Syphard, A. D., Keeley, J. E., Massada, A. B., Brennan, T. J., & Radeloff, V. C. (2012). Housing arrangement and location determine the likelihood of housing loss due to wildfire. PLoS ONE, 7(3). Retrieved from http://www.scopus.com/inward/record.url?eid=2-s2.0-84859025192&partnerID=40&md5=9e97acec962c6cd7e196d8e133948af9

Tibbits, A., Blanchi, R., & Gill, A. M. (2006). A Resident's experiences of the 2003 Canberra bushfire. Australasian Bushfire Conference. Brisbane.

Viegas, D. X., Stipanicev, D., Ribeiro, L., Pita, L. P., & Rossa, C. (2008). The Kornati fire accident - eruptive fire in relatively low fuel load herbaceous fuel conditions. Modelling, Monitoring and Management of Forest Fires, 119, 365–375. Retrieved from <Go to ISI>://000260498200036

Classification of large wildfires in South-Eastern France to adapt suppression strategies

Lahaye S. [abc], Curt T. [b], Paradis L. [c], Hély C. [c]

[a] *Service Départemental d'Incendie et de Secours des Bouches-du-Rhône, 1 av de Boisbaudran 13326 Marseille France, slahaye@sdis13.fr*
[b] *Irstea EMAX Mediterranean Ecosystems and Risks, route Cézanne, 13182 Aix-en-Provence cedex 5 France, thomas.curt@irstea.fr*
[c] *Centre de Bio-Archéologie et d'Ecologie, UMR 5059 (CNRS/Univ. Montpellier 2/EPHE), Institut de Botanique, 163 rue A. Broussonet, 34090 Montpellier France, christelle.hely-alleaume@univ-montp2.fr*

Abstract
Large wildfires keep on developing in the French Mediterranean region, regularly threatening responders. We tested if these large fires could be classified into types, and if these types were representative of different environmental drivers. To proceed, we established a database comprising 153 of the largest fires from the last 25 years. For each fire we collected three datasets to describe the environment, the fire behavior and the control operations. We performed a hierarchical clustering analysis followed by a predictive analysis with *Bootstrap Regression Trees*. Fires were classified in 8 types that could a posteriori be reduced to 5 types. The *One-way* type was featured by moderate environmental parameters, the *Multi-way* type was featured by slope, the *Winding* and *Rapid* types were featured by wind, while the *Very large* type was featured by the drought code. Moreover, the probability of having vehicles trapped in a large fire was primarily correlated with the number of vehicles assigned for suppression. This study provides the basis for upcoming trainings of Fire Analyst in France. It paves the way for further research on predictive wildfire danger mapping.

Keywords*: Forest fires, Firefighters, Hierarchical classification, Danger, Wind direction, Propagation rate.*

Introduction

South-Eastern Mediterranean France is the major fire hotspot region in this country since each year it records about two-thirds of the 4,000 fire ignitions, and the mean annual burned area is 20,000 ha (Promethee 2014). Wildfires in this region constitute a major threat to human life and infrastructures thus generating high damages and costs like in other worldwide Mediterranean regions (San-Miguel-Ayanz *et al.* 2013). Fires are also a major landscape driver and the main disturbance for many ecosystems (Keeley *et al.* 2012). Most fires occur during the summer drought period and are crown stand-replacing fires. Wildfires are a major challenge for policy makers due to their costly suppression (San-Miguel-Ayanz *et al.* 2013).
Wildfires are especially active in South-Eastern France because this region encompasses many fire conducive features: the Mediterranean climate characterized by long summer droughts and frequent strong winds (mistral) (Curt *et al.* 2011), a high population density inducing numerous fire ignitions in the road and house vicinities (Curt and Delcros 2010), and large connected stands of flammable forests and wildland fuels due to natural afforestation and a positive fire-fuel feedback in shrublands (Curt *et al.* 2013). The increasing population density and the extension of rural-urban interfaces favor fire ignitions and enhance human vulnerability (Lampin-Maillet *et al.* 2008). Models for the next decades predict the same trends in land cover and land use changes than along the past decades ; therefore inducing an enlarged expected proportion of vulnerable areas (Moreira *et al.* 2011).

Based on the climate part of the global change, increase in mean temperature associated with more frequent heat waves should also extend fire seasons and should in turn generate higher pressure on fire suppression forces (Moriondo *et al.* 2006).

Wildfire size distribution is typically asymmetric with many small fires and few large fires. However, as in many regions around the Mediterranean basin, these large fires are those which threaten the most people and ecosystems (San-Miguel-Ayanz *et al.* 2013). Definitions for large fires vary according to the context: in France fires larger than 100 ha are generally considered as large. They are 741 among the 442,000 recorded from 1989 to 2013 and archived in Promethee database. They are often characterized by spotting and high rate of spread, these characteristics making them difficult to control, and reducing the range of suppression options (Moreira *et al.* 2011).
In 1992 a new policy and strategy for French fire prevention and suppression has been established after a number of large and destructive fires along the previous decades (Battesti 1992). First, it is based on improved prediction of daily fire danger, increased communication on fire risk, and banning of human frequentation in forests during the days at risk. Secondly, it relies on a hard-hitting, initial attack of all fires, concentrating all the fire suppression means available (Direction de la Sécurité Civile 1994). This strategy has been proved effective for small-to-medium fires since the mean annual burned area has decreased since 1992, while ignitions have remained rather constant and population and infrastructures have increased (Promethee 2014). However, large and destructive fires still occur every year escaping initial attack and burning hundreds or thousands of hectares.
We hypothesize that large fires will remain frequent in the South of France for two main reasons. First, the improved fire suppression leads to a negative selection to the benefit of the largest ones. This process paradoxically favored by an efficient fire policy has been referred to as the 'fire paradox' (Sande Silva *et al.* 2010): if fire suppression is effective and reduces the area burned, then wildland fuels accumulate and fuel connectivity increases across the landscape, thus increasing in turn the likelihood of large fires when fire suppression forces cannot control them at the initial stage. Secondly, fire suppression forces will face new challenges: climate change will likely favor more intense and more frequent fires and the extension of the area at fire risk while fire suppression crew and equipment may remain constant due to stagnation of financial resources allocated. The firefighters will have to operate on larger territories, including abroad.
All these arguments pledge for better understanding of the large fires and their drivers. We proposed to build a classification of main large fire types and to explore conditions for their propagation. Such classification has already been established for Catalonia (Spain) (Costa *et al.* 2011). While climate and fuel are similar in both regions, this classification has not been applied for France mainly due to differences in suppression strategies, as well as to coarse database information preventing such analysis. However such knowledge would allow fire brigades to base their intervention on a scientific, fast and robust methodology for forecasting fire risk and fire behavior. This approach is typically that of 'Fire Analysts' whose expertise is to predict the likely behavior and danger of a fire in relation to weather, topography and fuels (Castellnou *et al.* 2010). A high technical level based on scientific analysis has to be promoted to offset the empiric knowledge of local conditions that tends to decrease in Fire Services due to the decline of training over small fires.
In this study we investigated French Mediterranean fires larger than 200 ha that have occurred along the 25 last years in order to answer the two following questions: are there different types of large fires characterized by a typical behavior and typical level of danger for responders? What are the specific environmental drivers (vegetation, topography, fire weather) for these fire types?

Materials & methods

Fire database

293 wildfires larger than 200 ha are reported on the Promethee database for the 1989-2012 period. To proceed, we collected *fire behavior data* describing the fire scenario, *environmental data* describing the fire environment (weather, fuel and topography), and *fire suppression data* in relation with human response to fire. This data collection required to get sufficiently detailed reports on each fire or to interview fire managers and commanders in 15 different fire agencies throughout the South of France. 38 Fire Officers and Forest Officers in charge of key positions during the fires were questioned and 81 paper or computer reports were investigated. We compiled detailed information for a subset of 153 among the 293 fires. The covered area extends from the Alps to the Pyrenean Mountains including Provence and Languedoc limestone plateaus as well as Corsica Island.

Each fire perimeter has been georeferenced on a dataset stored by the French Forest Department (Office National des Forêts). The accuracy of this database has been previously tested (less than 0.05% difference) by comparing ground collected fire perimeters with remote sensing inferred perimeters (Curt *et al.* 2013).

All spatial analyses were performed using the open source Geographical Information System *QuantumGIS 2-2 Valmiera* (http://www.qgis.org).

Fire behavior data

We investigated three variables of fire behavior. The first one was the final area (SURF, in hectares) representative of the total area burned georeferenced. It can be slightly different from the one registered on the Promethee database which is given by responders sometimes with less accuracy, especially for the oldest fires. We interpreted SURF as an indirect and synthetic indicator which differentiates the large fires (hundreds of hectares) from the very large ones (thousands of hectares).

The second variable was the mean rate of propagation (HaH, in hectares per hour), featuring the overall fire increase and not only its axial rate of spread. It was extrapolated from both officer interviews and post-fire reports. The method consisted in rebuilding the isochrones of fire propagation. Assuming that the precise time of ignition and the final time of extinction were difficult to know, we focused only on the 10 to 90% extension of final area burned of each fire. Rapid fires were interpreted as dangerous since they spread more rapidly than the fighting resources can move.

The third variable was the angle change of the main propagation direction (DIRCHG). It was investigated assuming that changes result from specific combination of environmental data. When the main axis of the fire trajectory opened to an angle lower than 60°, it was considered as a non-significant change of direction (coded as 0). When the direction angle change was higher than 60° but less than 90° with constant wind, it was assumed to be a 'winding' fire (coded as 1). In all other cases with angle change higher than 90°, it was coded as 2. These fire direction changes are challenging for responders since they modify the position of active fire lines.

2.3. Environmental data

Weather during a fire event is crucial for explaining its size, its shape, and its danger (Pyne *et al.* 1996). Fire weather is often assessed using the Fire Weather Index (FWI), which is an integrative and unitless index that was designed originally to forecast fire risk in Canada on the basis of daily past and current weather conditions (Van Wagner 1987). The FWI consists of six components accounting for air temperature, relative humidity, surface wind speed, and the last 24-hour rainfall (Groot *et al.* 2007). The FWI and its sub-indices provides a uniform, numeric method of fire danger rating throughout an area and have been extensively used in the Mediterranean basin regions (Giannakopoulos *et al.* 2012). In this study we computed the FWI and its sub-indices for each fire using a daily integrative model on a 2 * 2 km grid. As some fires were very large, each of them was assigned the mean value of the index

within the fire perimeter. We especially focused on: (i) the duff moisture code (DMC), representative of the average moisture content of loosely compacted organic layers of moderate depth, it gives an indication of fuel consumption in medium-size woody material such as shrubs; (ii) the drought code (DC), representative of the average moisture content of deep, compact, organic layers, it indicates the seasonal drought effects on forest fuels. By selecting these two indexes, we integrated together rainfall, temperature and relative humidity. We chose to directly use the wind speed variable (WINDSP in meters per hours) without going through the fine fuel moisture code of the FWI because this last sub-index has been recognized to be nearly saturated during the entire summer season in Mediterranean region. WINDSP values were collected from the closest weather station to the fire (Meteo France 2014).
Vegetation composition within the area burned was characterized using the 1986 and 2006 French Forest Institute maps (Institut Forestier National, BDForêtV1; http://inventaire-forestier.ign.fr). These maps being updated from inventories performed every 10 years, the last statement before fire was considered. The vegetation type of every 2.25Ha forest or natural unit is given from photo interpretation of aerial images in infrared color. Depending on the inventory date, there were up to 75 different fuel classes that we aggregated in only four classes for the purpose of this study: broadleaved forests, pine forests, shrublands and other – this last class covering all agricultural, grassland and urban spaces. The considered data were the percentage of each vegetation class within the area burned.
The average slope for each fire was obtained by crossing the Digital Elevation Model from the National Geographical Institute (Institut Geographique National, BDAlti25; http://www.ign.fr) with the layer of fire final area.

2.4. Fire suppression

We collected the number of vehicles considered as terrestrial resources (RESS) and indicative of the means for suppression. The chosen value represents the maximum number of fire appliances simultaneously committed, excluding logistic support and command vehicles.
Any reported accident injuring a responder or destroying an appliance was finally pointed as a trap (TRAP). The cases of little diseases, very common on such large fires and often linked to warmth and efforts in smoky conditions were not considered. Neither were traffic accidents of responders outside the fire perimeter.

2.5. Data analysis

All statistical tests and modeling were performed using the statistics program R (R Core Team 2013). The final area (SURF) and mean rate of propagation (HaH) variables were both divided into three classes each using the Jenks natural optimization method which minimizes each class average deviation from the class mean, while maximizing each class deviation from the means of the other groups (Jenks 1967).
A first fire classification was performed on fire behavior data, using the R Cluster package (Maechler *et al.* 2013). The Partitioning Around Medoids (PAM) method was used with Euclidean distances and standardized data (Reynolds *et al.* 1992). Results were plotted on a map to identify homogeneous areas in term of fire types.
To assess the influence of the environmental data on each fire class, we used the *Bootstrap Regression Trees* (BRT). This statistical method is particularly suitable to explore ecological drivers and to optimize the predictive performances (De'Ath 2007). Furthermore, it is flexible and easy to read (Elith *et al.* 2008) and it considers any collinearity among variables. We proceeded with the *dismo* and *gbm* packages (Hijmans *et al.* 2013; Ridgeway and others 2013) using a Bernoulli type error. Several regression trees were calculated on calibration data using a "boosting" process. Half the dataset was used to build the model and the other half to test the class accuracy. The number of trees in each BRT was automatically set at 20 with a 0.5 fraction and a 0.005 learning rate. We assessed model prediction

accuracies using the area below the receiving operator curve (AUC) (Pearce and Ferrier 2000). The performance was considered as excellent when AUC>0.9 and weak when AUC<0.6.

In order to assess if the types isolated with BRT correspond to different level of danger for responders, we calculated for each of them the rate of fire where resources were trapped and the Student confidence interval (Eq.1) where this rate would have been statistically supposed to be:

$$CI_{\alpha} = [f - z_{\alpha/2}\sqrt{(f(1-f)/(n-1))} \; ; \; f + z_{\alpha/2}\sqrt{(f(1-f)/(n-1))}] \qquad (Eq.1)$$

with CI_{α} the interval with α probability, f the rate of trap in the database, $z_{\alpha/2}$ Student coefficient, and n number of fires in the type.

Assuming that the probability to have resources trapped (TRAP) is closely linked to the quantity of resources assigned (RESS), the correlation between these two parameters was tested separately with a parametric test of average comparison (Eq.2):

$$H_0: \mu 1 = \mu 2, \text{ with } CI_{(\mu_1 - \mu_2)} = [(\bar{a}_1 - \bar{a}_2) - z_{\alpha/2} * s\sqrt{(1/n_1 + 1/n_2)} \; ; \; (\bar{a}_1 - \bar{a}_2) + z_{\alpha/2} * s\sqrt{(1/n_1 + 1/n_2)}] \qquad (Eq.2)$$

where, for each of both distributions 1 (number of vehicles on fires with trap) and 2 (number of vehicles on fires without trap), μ is the population mean, $\bar{a}$ the observed mean, n number of fires in the distribution and s the weighted variance of both distributions.

Results

Collected datasets

The 153 fire dataset distribution was compared with the 293 fires recorded in the Promethee database (Figure 1). The very large fires, which are generally the best documented, are better represented in the present study: 74% of the > 1000 Ha events *versus* 42% of the 200-500 Ha fires. If geographical distribution of data partly results from the ability to access different regional agency records, the underrepresentation of Haute Corse, where the number of large fire was the most important, is likely explained by the fact that in this territory written reports were few, thus we investigated only through interview and therefore we focused on the post-1995 fires. Moreover, the oldest are the fires, the less information is available, arguing why the 153 dataset includes 37% of 1989-1999 incidents versus 72% of 2000-2012 incidents. Finally, the seasonal variability is clearly represented with 93% of large fire occurrences recorded from June and September.

Dealing with the fire behavior and environmental datasets (Tabl. 1), the windspeed values spread nearly totally on the Beaufort scale, varying from “calm” to “storm” with a mean being “fresh breeze”. The averaged drought index values can be considered as exceptionally high compared to original North-American classification values (Van Wagner 1987). Thus the fires studied here have spread with variable windspeeds but often with important or very important fuel dryness. Shrubland is the most represented vegetation type in areas burned. Most forest stands are dominated by pine, while pines can also be mixed with broadleaved species, generally oak trees.

Data on fire direction change and suppression showed that among the 153 fires, winding was present on 16% of the fires (DIRCHG=1) and a shift on 22% (DIRCHG=2), while 16% of the fires recorded an accident (25 TRAP records).

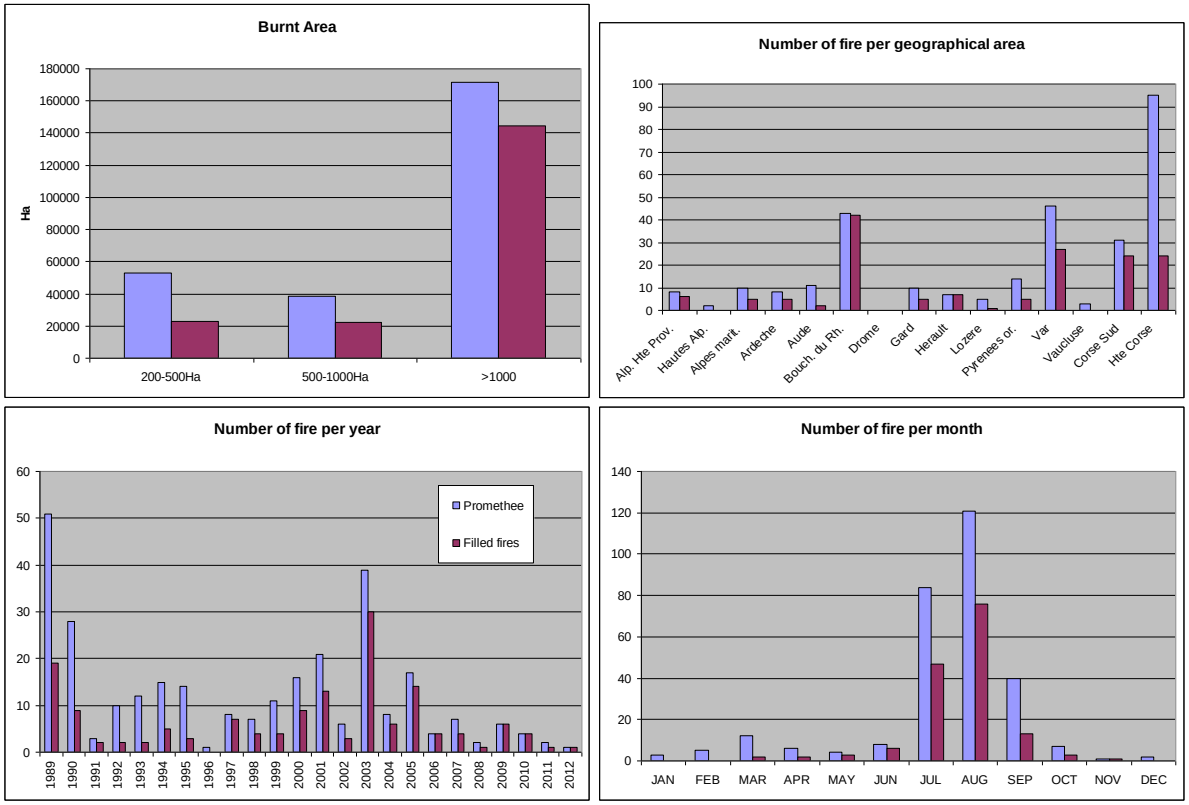

Figure 1 – Comparison of the 153 fires dataset (red bars) with the data recorded on Promethee base (blue bars).

Table 1. Recorded data: windspeed (WINDSP) ; Drought Code (DC), Duff Moisture Code (DMC) ; average slope (SLOPE) ; shrubland (SHRUB), pine (PINE), broadleaved (BRDLV), other fuel (OTHER) ; number of vehicles (RESS) ; prpagation rate (HaH) ; area burned (SURF).

	WINDSP	DC	DMC	SLOPE	SHRUB	PINE	BRDLV	OTHER	RESS	HaH	SURF
Unit	*(km.h^{-1})*	*(--)*	*(--)*	*(degre)*	*(ratio)*	*(ratio)*	*(ratio)*	*(ratio)*	*(engine)*	*(ha.h^{-1})*	*(Ha)*
Mean	32	650	146	15	0.61	0.19	0.08	0.11	95	163	1239
Stand.dev.	17	193	81	7	0.30	0.25	0.13	0.16	83	208	1738
Min.	0	24	18	3	0.00	0.00	0.00	0.00	9	1	208
Max.	90	1067	376	35	1.00	1.00	0.57	0.93	400	1359	14020

3.2. Fire classification

According to Jenks method results, the final area burnt was splitted in three classes: the 200-1990 Ha class including 84% of the fire, the 2000-7000 Ha class including 15% and the > 7000 Ha class representative of the remaining 1%. In the same way, the three classes for the propagation rate were 1-219 Ha/H for 78%, 220-800 Ha/H for 19% and > 800 for 3% of the fires.

The PAM clustering was optimal with seven groups based on a strong structuration with an average proximity of data of 87% and six of the seven groups with an average proximity > 50%. We gave a describing name to each group based on the three investigated variables (Tabl.2).

In the first three groups, fires have not reached very important area burnt neither very important propagation rate. Among them, the *One-way* represents fires with linear direction, the *Winding* fires with angled propagation axis and the *Multi-way* includes fires that totally changed their propagation axis. The fourth group is named *Vast* because fires have reached an important area with a moderate rate of spread. Finally, the last three groups represent fires that developed the most rapidly, even

extremely quickly concerning the *Mega*. Among these three groups only fires in the *Rapid* did not reach the final area burnt of 2000Ha.
When visually analysed, the spatial distribution of fire groups displays five areas (Figure 2): Western coast (Pyrénées-Orientales, Aude, Hérault and southern Gard), Provence (Bouches-du-Rhône and western Var), Maures/Esterel (Eastern Var and west of Alpes-Maritimes), Mountain (North and east of Alpes-Maritimes, Alpes-de-Haute-Provence, Gard cévenol, Ardèche and Lozère) and finally Corsica (Corse). Three of these areas (Provence, Maures/Esterel and Corsica) seem to be particularly affected by the largest fires but more information would be required to go further in the spatial interpretation, which is out of the present study scope.

Table 2. Fire group based on the PAM clustering and fire number in each group. Each group is assumed to be homogeneous when the average proximity is > 0.5. The group specifications are given for each variable used in the clustering : SURF, HaH, DIRCHG. The final name outlines these specifications.

Gr.	Fire number	Average proximity	SURF *(ha)*	HaH *($ha.h^{-1}$)*	DIRCHG	Name
1	26	0.78	<2000	<800	2	**Multi-way**
2	70	1.00	<2000	<220	0	**One-way**
3	16	1.00	<2000	<220	1	**Winding**
4	10	0.50	>2000	<220	0,1,2	**Vast**
5	16	0.88	<2000	220à800	0,1	**Rapid**
6	11	0.41	>2000	220à800	0,1,2	**Rapide&vast**
7	4	0.79	2000-7000	>800	0,1	**Mega**

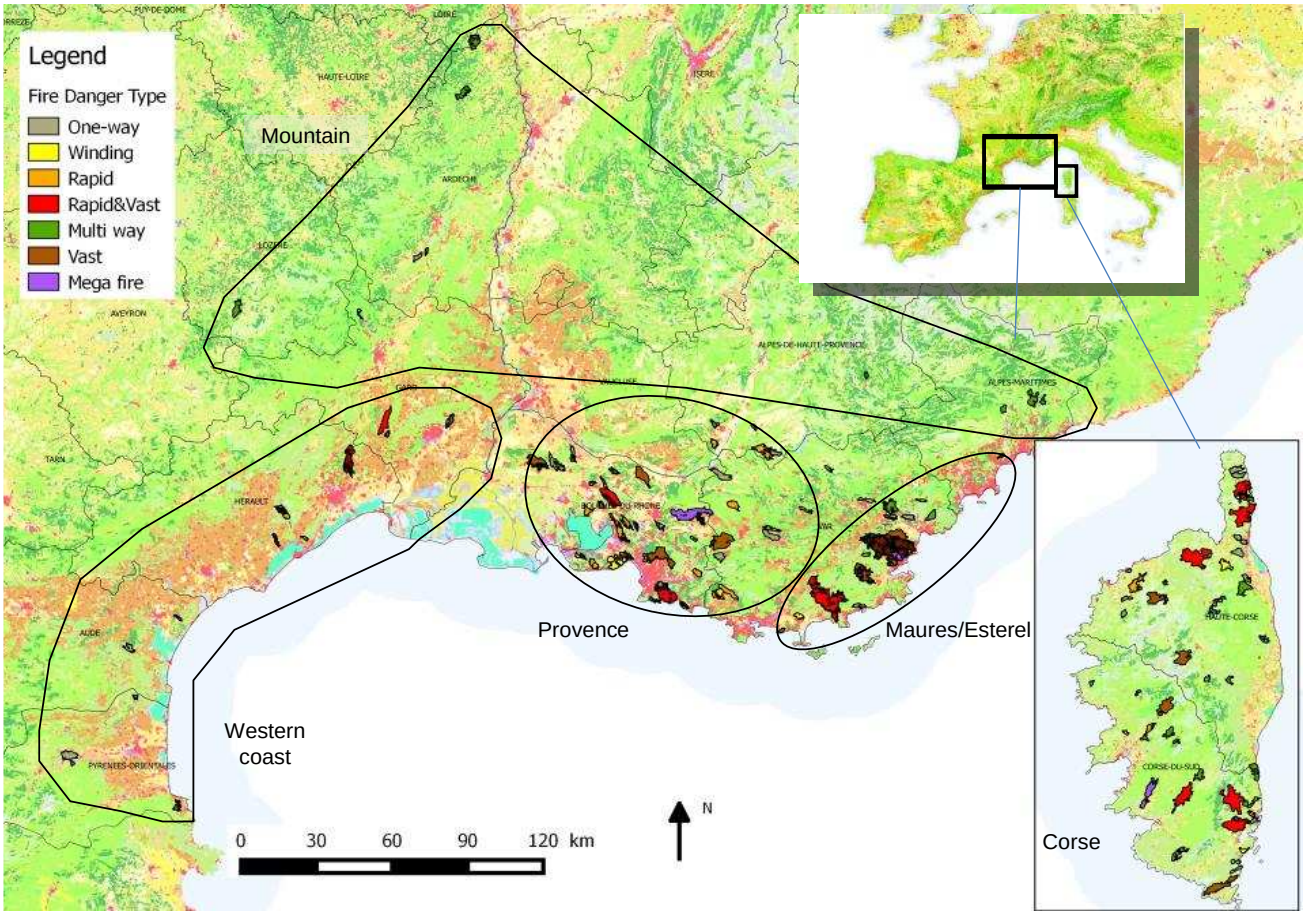

Figure 2. Spatial distribution of fires regarding their group.

3.3. BRT

The number of fires in groups 4 (*Vast)* and 7 (*Mega)* being insufficient to get convincing results with the BRT method, we gathered all the fires over 2000Ha, ie *Vast*, *Rapid&vast* and *Mega*, in a unique group thereafter called *Very large*.

Positive values of fitted function for each variable determine the data scale linked to the given group (Fig.3). Thus, fires in the *One-way* group are substantially linked to low slope (<12°) with large parts of shrublands (>85%, ie the upper quartile of the distribution), moderate wind (<40 km/h) and low DC (<600 ie the lower third). The *Multi-way* fires are in relation with strong slopes (>17° ie the upper third), >50% of pine and <40% of shrublands. The *Winding* fires occur with >75% of shrublands, DC>750 (extreme value, upper quartile) and significant wind (>30km/h). The *Rapid* fires firstly happen with strong wind (>40 km/h ie the upper third), moderate DC (<500) and slope under 12°. Finally, the *Very large* fires are linked with important DC (>600), between 50 and 90% of shrublands in the landscape and low slope (<13°),.

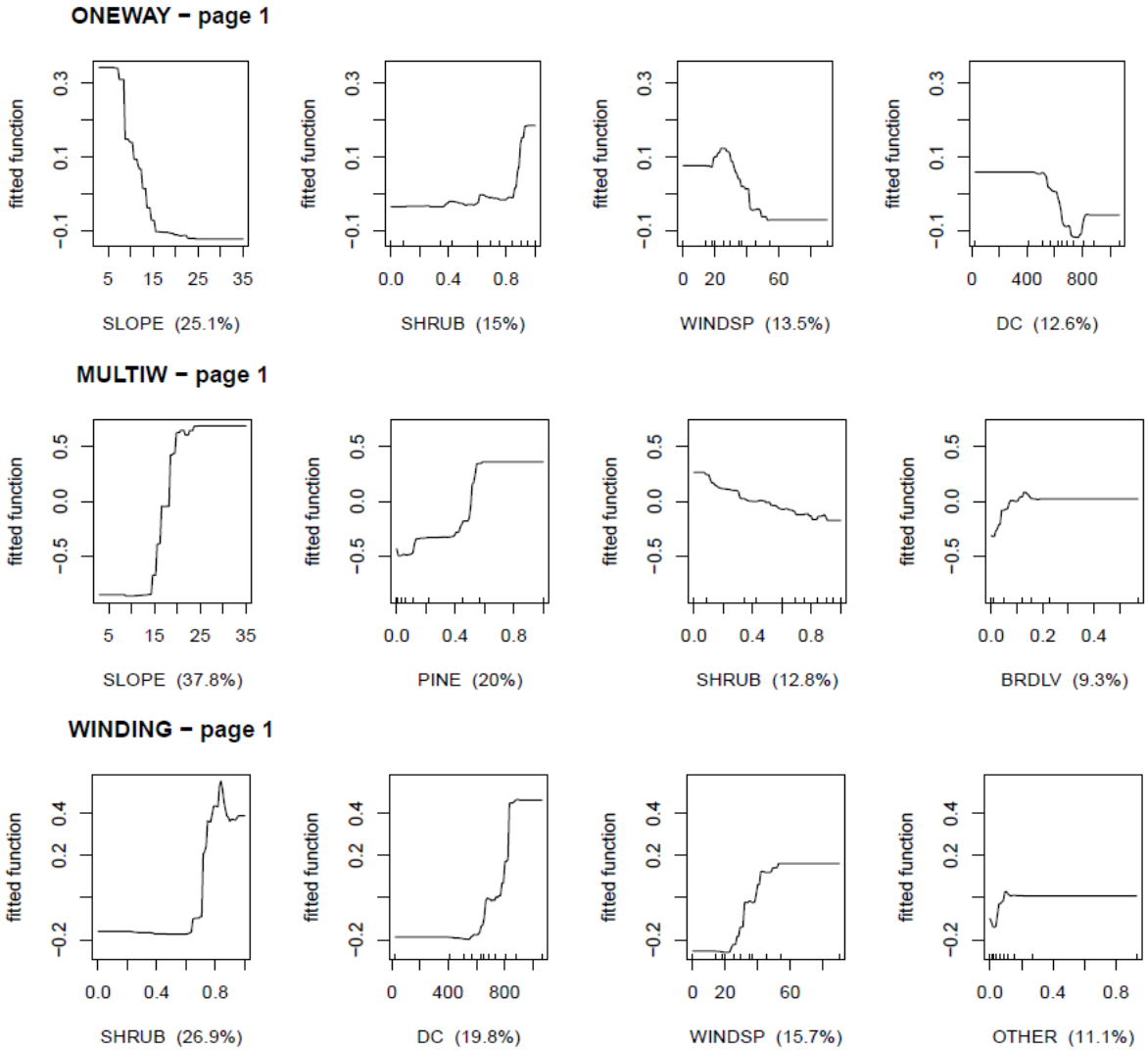

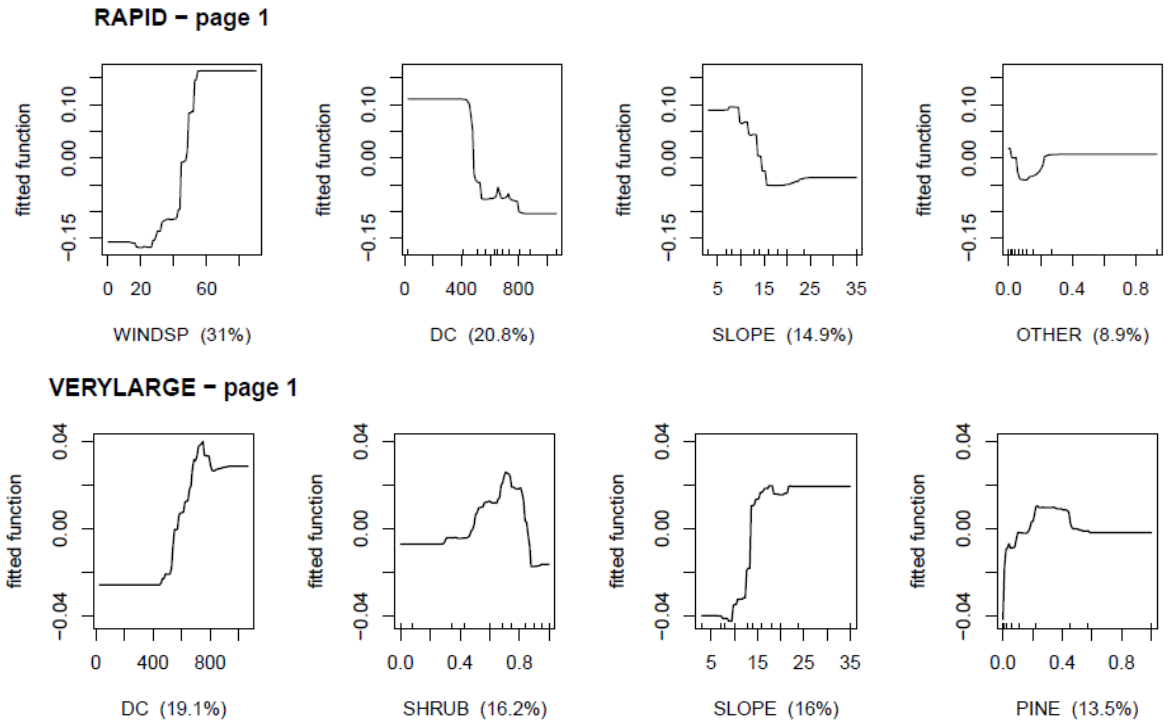

Figure 3. Variance of the 4 most significant variables for each group (horizontal panel including 4 subpanels): One-way, Multi-way, Winding, Rapid and Very large.

We propose in Fig.4 a logical dichotomous synthetizing key to deduce the most likely large fire subtype from environmental data highlighted in the different fire groups. Low DC and low slope will give *One-way* or *Rapid* fire subtypes depending on the wind. High DC values will generate the *Winding* subtype with strong wind and the *Very large* subtype with strong slope. Strong slope will mainly lead in *Multi-way* subtype.

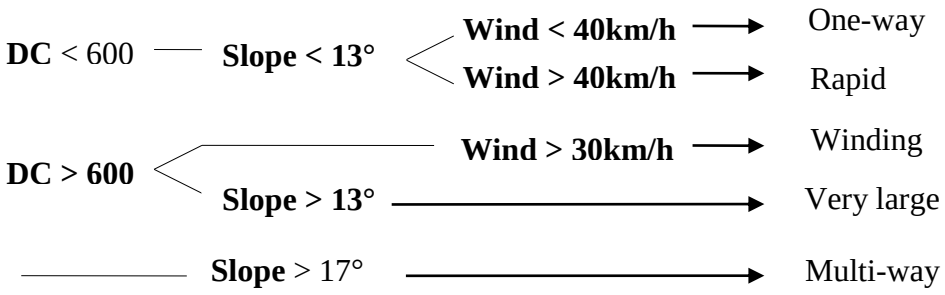

Figure 4. Synthesis of expected fire subtypes according to environmental data.

3.4. **Vehicle traps**

There is no significant difference in any fire group ratio with the overall mean value of 0.16 calculated from the entire studied database, even with a 90% confidence interval (Tabl.3). Nevertheless, based on the regional distribution, we found a significant higher risk in Provence and lower risk in Corsica than elsewhere in average.

Table 3. Accident ratio (TRAP) and 90% confidence interval for each group and area.

	Name	Fire nb.	TRAP ratio	90% C.I.
Group	Multi-way	26	0.11	0.03 – 0.28
	One-way	70	0.17	0.09 – 0.23
	Winding	16	0	0 – 0.32
	Rapid	16	0.31	0 – 0.32
	Very large	25	0.20	0.03 – 0.29
Area	**Corsica**	48	**0.06**	**0.07** – 0.24
	Maures/Esterel	18	0.11	0 – 0.31
	Provence	52	**0.27**	0.07 – **0.24**
	Western coast	18	0.22	0 – 0.31
	Montain	17	0.12	0 – 0.32

Finally, the homogeneity test of mean values of resources assigned with a 99% confidence interval ($CI_{(\mu_1-\mu_2)}$ = [31 ; 119]) showed that there are significantly more accidents in fires with numerous assigned resources.

Discussion

4.1. A suitable classification for France

One of the aims of this study was to check if large fires in South of France could be classified into subtypes. We have found that 46% of them are *One-way* and 10% are *Winding*. That means that 56% of the fires are mainly driven by a constant wind, which may locally take a different direction due to terrain. A small part of fires (17%) belongs to the *Multi-way* subtype. The change of wind direction can either result from a reverse of topographic breeze or from a wind shear, which is frequent in the Maures/Esterel area. Whatever the cause, the fire behavior can be anticipated for this subtype thanks to an adequate knowledge of the local meteorology. Finally, the two last subtypes, *Rapid* (10%) and *Very large* (16%), regroup the fires for which the fighting operations are the most difficult, the less effective and the most dangerous for suppression crews. These fires burned the largest area or reached the fastest propagation rate, sometimes both together.

To our knowledge, there are only similar studies for the Mediterranean region in Catalonia (Spain), conducted by Castellnou *et al*. (Castellnou *et al.* 2010). While we similarly investigated historical fires, we however used a slightly different methodology. Indeed, while the Catalan team considered the synoptic regional weather for each analysed fire, we focused on FWI index parameters in the vicinity of each fire. Moreover, we did not consider the three types of fires commonly accepted (i.e.topographic, wind driven and plume dominated), but we rather observed how our fires were naturally distributed in our study area considering their direction changes and their rate of propagation. Our results are convincing, introducing new subtypes of fires, and call for further research, especially on explosive or convective issues.

4.2. Environmental data as driver of fire types

Our large fire types were driven by environmental data, especially Drought Code, Windspeed and Slope. On The fact that the Duff Moisture Code has not been identified as a driver of any type of large fire could suggest that it may rather characterize smaller fires than 200Ha but this would need more investigations.

We have not kept the fuel composition as a determining factor because the shrubland cover raised as an explaining variable in almost every type. Indeed its fitted functions were all providing information in the same way, with shrub cover being positively correlated to the fire types. *Multi-way* fires are the

exception with shrub cover being negatively correlated to the type and pine and broadleaved cover being positively correlated (the broadleaved signal was nearly flat, so difficult to read). In conclusion, we haven't found relevant to consider forest cover as a driver of *Multi-way* fires since it is an evidence that mountainous areas are the most propitious to this type of fire and together the most forested. The drivers of this fire type are thought to be more likely mountainous environment with wind breezes.

4.3. Link between number of resources assigned and trap probability

No fire type was significantly more propitious to endanger responders. Nevertheless, the trap likelihood was positively correlated to the number of vehicles assigned for suppressing fire. That is likely why accidents are prevalent in Provence area where there is a need to deploy many trucks to protect all the houses threatened by any fire. Conversely, accidents are less frequent in Corsica where the number of engines is much smaller.

4.4. Possible bias in the data

The large fire types we found are based on data coming from reports and interviews that may be partly subjective. Indeed, we called for data records up to 25 years after fires occured in order to rebuild fireline isochrones. Nevertheless, the accuracy of this oral information has been generally tested with crossing the interviews or comparing them to factual archived data.
Moreover, the type of fuel could likely be the less accurate of environmental variables since the vegetation cover was based on geodatabases up to 10 years old. Within this time interval, some land use changes can have occurred such as afforestation of agricultural parcels. That is another reason why fuel data has been interpreted with caution.

Conclusion: implications for fire suppression

In this study we have provided the first classification of large fires dedicated to help fire suppression in South-Eastern France. We have stated several large fire types characterized by their typical fire behavior and environmental drivers. These fire types range along a gradient of difficulty for fire suppression. Some types are predictable using their typical environmental drivers, which suggest that improvements in fire suppression safety and efficiency are possible using this approach.
The basis for classification being established, it is now challenging to have further research on certain types of fire. In particular, we have to investigate 'explosive' fires and convective behaviors to link them to responder traps. Further studies should also focus on the geographical distribution of different groups of fire.
In the workplace, first Fire Analyst trainings are in process in Europe for responders. This study will contribute to set the foundations for training program by proposing a typology related to environmental drivers for Mediterranean France.

Acknowledgements

This study has been funded by the Service Departemental d'Incendie et de Secours (SDIS) 13 through S. LAHAYE's lifelong learning. It would not have been possible without the valuable debriefings of firefighters and foresters from Alpes-de-Hautes-Provence, Alpes-Maritimes, Ardèche, Aude, Bouches-du-Rhône, Corse, Var, Gard, Herault, Pyrennées-Orientales and Var. We thank Marine PASTUREL for her help in data processing.

7. References

Battesti JP (1992) Projet feux de forets; rapport d'étape. Ministère de l'intérieur; Direction de la sécurité civile (Paris)

Castellnou M, Larranaga A, Miralles M, Vilalta O, Molina D (2010) Wildfire Scenarios: Learning from Experience. European Forest Institute (Joensuu)

Costa P, Castellnou M, Larranaga A, Miralles M, Kraus D (2011) Prevention of large wildfires using the fire types concept. Fire Paradox European Project (Generalitat de Catalunya)

Curt T, Borgniet L, Bouillon C (2013) Widfire frequency varies with the size and shape of fuel types in southeastern France: Implications for environmental management. *Journal of Environmental Management* **117**.

Curt T, Delcros P (2010) Managing road corridors to limit fire hazard: a simulation approach in southern France. *Ecological Engineering* **4**, 1-12.

Curt T, *et al*. (2011) Litter flammability in oak woodlands and shrublands of southeastern France. *Forest Ecology and Management* **261**, 2214-2222.

De'Ath G (2007) Boosted trees for ecological modeling and prediction. *Ecology* **88**, 243-251.

Direction de la Sécurité Civile (1994) Guide de stratégie générale pour la protection de la forêt contre l'incendie. Ministère de l'intérieur (Paris)

Elith J, Leathwick JR, Hastie T (2008) A working guide to boosted regression trees. *Journal of Animal Ecology* **77**, 802-813.

Giannakopoulos C, *et al*. (2012) Comparison of fire danger indices in the Mediterranean for present day conditions. *iforest-Biogeosciences and Forestry* **5**, 197-203.

Groot WJd, Field RD, Brady MA, Roswintiarti O, Mohamad M (2007) Development of the Indonesian and Malaysian Fire Danger Rating Systems. *Mitigation and Adaptation Strategies for Global Change* **12**, 165-180.

Hijmans RJ, Phillips S, Leathwick J, Elith J (2013) dismo: Species distribution modeling. R package version 0.9-3.

Jenks GF (1967) The Data Model Concept in Statistical Mapping. *International Yearbook of Cartography* **7**, 186-190.

Keeley J, Bond W, Bradstock R, Pausas J, Rundel P (2012) Fire in Mediterranean Ecosystems. Ecology, Evolution and Management. *Cambridge University Press* 450 pp.

Lampin-Maillet C, Long M, Jappiot M (2008) A Method for Characterising and Mapping Habitat/Forest Interfaces - a Means for Preventing Forest Fires. *Revue Forestiere Francaise (Nancy)* **60**, 363-380.

Maechler M, Rousseeuw P, Struyf A, Hubert M, Hornik K (2013) cluster: Cluster Analysis Basics and Extensions.

Meteo France (2014) http://www.meteofrance.com

Moreira F, *et al*. (2011) Landscape - wildfire interactions in southern Europe: Implications for landscape management. *Journal of Environmental Management* **92**, 2389-2402.

Moriondo M, Good P, Durao R, Bindi M, Giannakopoulos C, Corte-Real J (2006) Potential impact of climate change on fire risk in the Mediterranean area. *Climate Research* **31**, 85-95.

Pearce J, Ferrier S (2000) Evaluating the predictive performance of habitat models developed using logistic regression. *Ecological Modelling* **133**, 225-245.

Promethee (2014) Base de données sur les incendies de forêt en région méditerranéenne en France depuis 1973. https://www.promethee.com/.

Pyne SJ, Andrews PL, Laven RD (Eds) (1996) 'Introduction to wildland fire.' (John Wiley and Sons Publishing)

R Core Team (2013) R: A Language and Environment for Statistical Computing. (R Foundation for Statistical Computing Publishing: Vienna, Austria)

Reynolds A, Richards G, De la Iglesia B, Rayward-Smith V (1992) Clustering rules: A comparison of partitioning and hierarchical clustering algorithms. *Journal of Mathematical Modelling and Algorithms* **5**, 475–504

Ridgeway G, others wcf (2013) gbm: Generalized Boosted Regression Models.

San-Miguel-Ayanz J, Manuel Moreno J, Camia A (2013) Analysis of large fires in European Mediterranean landscapes: Lessons learned and perspectives. *Forest Ecology and Management* **294**, 11-22.

Sande Silva J, Rego F, Fernandes P, Rigolot E (2010) Towards Integrated Fire Management - Outcomes of the European Project Fire Paradox. (Joensuu)

Van Wagner C (1987) Development and structure of the Canadian Forest Fire Weather Index System. Canadian Forestry Service (Ottawa)

Coupling a meshless front-tracking method with a hybrid model of wildfire spread across heterogeneous landscapes

Y. Billaud[a], M. De Gennaro[a,b], A. Kaiss[a], Y. Pizzo[a], N. Zekri[c], B. Porterie[a]

[a] *Aix-Marseille Université, CNRS, IUSTI UMR 7343, 13453 Marseille, France,* Bernard.Porterie@univ-amu.fr
[b] *NOVELTIS, 153 rue du Lac, 31670 Labège, France*
[c] *Université des Sciences et de la technologie d'Oran Mohamed Boudiaf, LEPM, BP 1505 El Mnaouer, Oran, Algérie*

Abstract
The objective of the study is to present a method for improving the capability of a semi-physical network model to predict large fire patterns in heterogeneous landscapes. The method, which can be viewed as an Autonomous System, consists in generating an amorphous network by sowing vegetation cells on-the-fly. All the information on fire behavior is contained in the very few digital elevation map pixels close to the fire front, in which fuel items are heated or burning. The method is applied to two distinct scenarios: a no-wind and no-slope academic case and a historical Mediterranean fire that occurred in the South-East of France in 2005. Both cases are discussed in terms of CPU time and memory allocation gains.

Keywords*: front-tracking method, meshless method, network model, large fire, autonomous system, amorphous network*

Introduction

As underlined by (Strauss et al., 1989), it is an all too familiar fact that a relatively small number of large fires are responsible for a very high proportion of the total damage. Therefore, simulating the spread of large wildfires, with size up to several tens of kilometers, is a major environmental issue and an active area of research. However this requires the storage and handle of a vast amount of data. As an example, a 10km × 10km landscape, with 60 percent covered by vegetation sites of 2m in diameter, contains approximately 1.5×10^7 sites. Assuming an average number of connections per site of 100, the total number of connections to handle is 1.5×10^9. In order to reduce computational resources, a front-tracking method is here propose.
Another important issue concerns the use of regular lattices (triangular or square lattices) to represent vegetation patterns. However, regular lattices only consider single-class vegetation cover, so they cannot mimic the complexity of natural ecosystems (*e.g.* fuel distribution, polydispersity, mosaic of vegetation types). To overcome this issue, we recommend using an amorphous network.
The combination of the front-tracking method and amorphous network may be viewed as a meshless front-tracking method, hereafter called MFT method.

2. Model overview

Vegetation is here modeled as an amorphous network of cylindrical items where the combustible sites are randomly distributed. A digital elevation model (DEM) represents topography. A weighting procedure on combustible sites is considered in order to account for the effects of ignition and flaming duration (Billaud et al., 2012). The physical model, largely inspired from that of (Koo et al., 2007), is based on the energy balance equation for a control volume of thickness δ located at the top of the cell. δ corresponds to the mean free path of radiation $\delta = 4/\alpha_k\sigma_k$, where α_k is the solid-phase volume fraction, σ_k the surface-to-volume ratio of fine fuel elements. The energy-transfer mechanisms of

preheating considered are the radiation coming from the flame $q^{+}_{rad,fl}(i)$ and the embers $q^{+}_{rad,e}(i)$, and $q^{+}_{conv}(i)$ is the wind-driven convection to the top surface of the receptive cell j

$$\sum_{i=1}^{N_{bc}} \begin{bmatrix} q^{+}_{rad,f}(i) + \\ q^{+}_{rad,e}(i) + q^{+}_{conv}(i) \end{bmatrix} = q^{-}_{rad}(j) + \begin{cases} \rho_{WFF}\ c_{p_{WFF}}\ \alpha_k \dfrac{dT(j)}{dt} & T(j) < 373K \\ -\rho_{DFF}\ L_{vap} \alpha_k \dfrac{dFMC(j)}{dt} & T(j) = 373K \\ \rho_{DFF}\ c_{p_{DFF}} \alpha_k \dfrac{dT(j)}{dt} & 373K < T(j) < T_{ign} \end{cases}$$

$q^{-}_{rad}(j)$ is the radiative heat loss to the ambient, T the fuel temperature, ρ and c_p the density and the specific heat of the solid phase. The subscripts DFF or WFF refer to variables evaluated on a dry or wet basis. L_{vap} is the heat of water vaporization and FMC is the fuel moisture content. The ignition delay is the time required for a site under the influence of N_{bc} burning sites to reach a critical temperature T_{ign}. The dynamic of the system clearly depends on the ignition and flame residence times, t_{ign} and t_c. Details can be found in (Billaud et al., 2012).

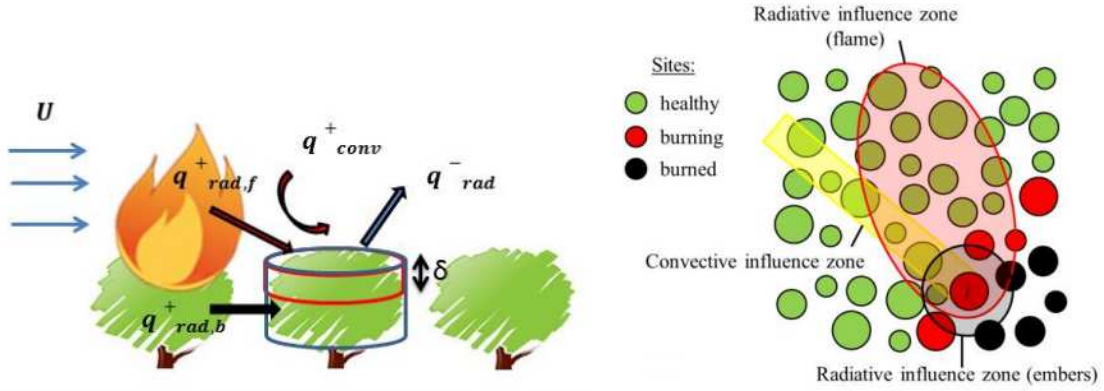

Figure 1. a) Physical problem and b) radiative and convective interaction domains associated to a burning site.

3. Numerical method

The method principle is based on the concept of double indexing: the first is a local indexing of the sites (Holme, 2007), the second is a global indexing of DEM pixels. The main task consists in finding the neighbors of any active site that belongs to a DEM pixel. This can be split into two stages: first, the eight neighboring DEM pixels are identified; second, the sites that belong to these pixels are specifically numbered and stored (Pasquale et al., 2014). If a DEM pixel contains at least one new burning site, the network is updated in order to ensure the continuity of the propagation process. When all the sites of a DEM pixel are burned or too far away from the fire front, the DEM pixel is deallocated.

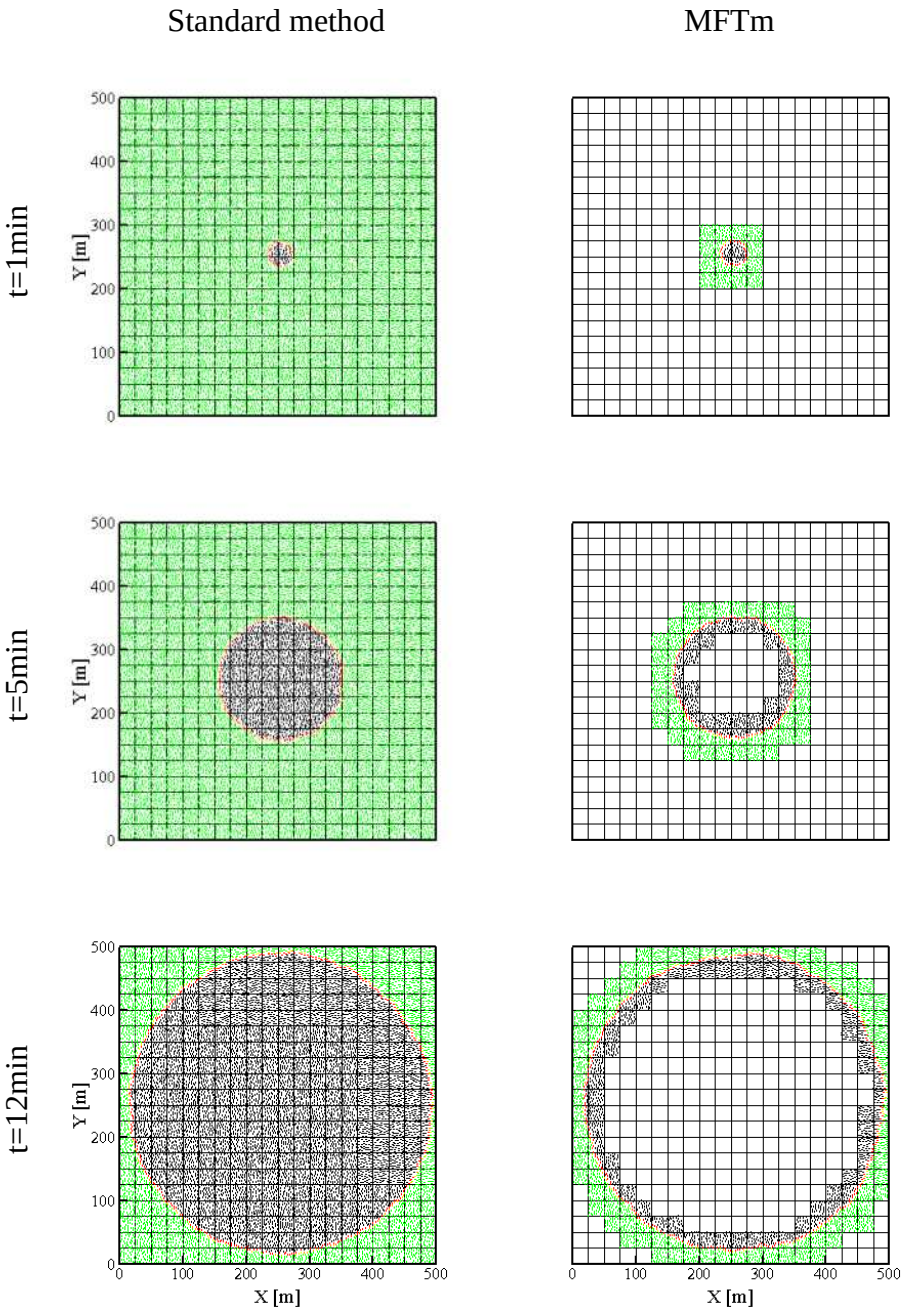

Figure 2. Fire patterns at different instants. Comparison between fire patterns obtained from standard and MFT methods.

Method validation

In order to demonstrate how such a methodology might work in practice, we consider a 500m×500m monodisperse amorphous network of kermes oak shrubs with a diameter of 2m (Figure 2). The terrain is flat and there is no wind. Ignition occurs in the center of the domain. The vegetation coverage is 0.5. Calculation using the MFT method takes 13s on the Intel Xeon CPU E5-3643 (3.30 GHz, 64 bits), whereas it takes 21s using the standard method, leading to a 38% gain in CPU time. As shown in Figure 2, in the early stages of fire spread (*e.g.* t=1min), only 4% of the network is involved using the MFT method. As time progresses, the memory allocation increases due to an increase of active DEM pixels but remains significantly lower than that of the standard method due to the withdrawing of

burned pixels. There are some small discrepancies between the two methods that are due to the stochastic nature of the amorphous network construction.

Small world effects

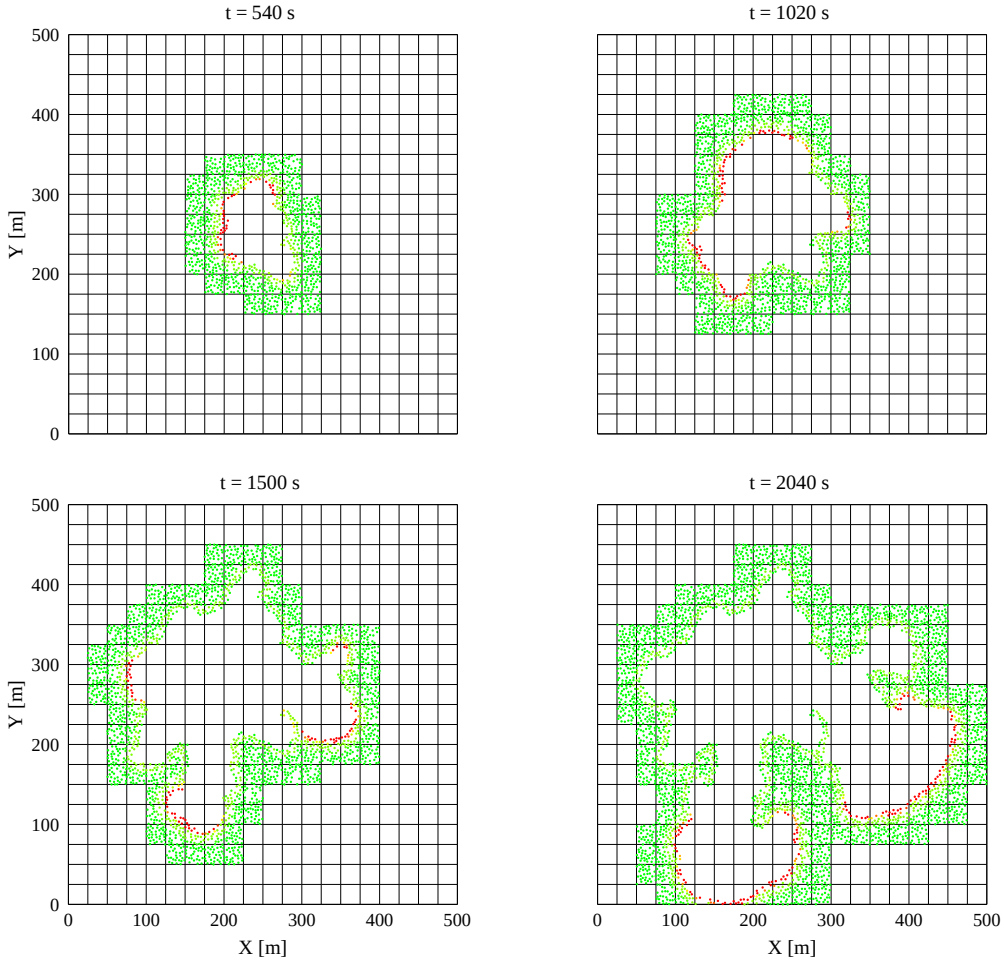

Figure 3. Fire patterns after a) t=540s, b) t=1020s, c) t=1500s and d) 2040s of simulation. The active areas represent about 10%, 17%, 26% and 37% of the total network, respectively.

Here we consider fire spread under the same conditions, except that the vegetation coverage is 0.4. This value is so close to the percolation threshold that small-world effects (clustering, lacunarity, and digitation) occur, as can be observed inFigure 3. Although not shown, similar results are obtained using the standard and MFT methods, with a significant reduction in CPU time and memory allocation.

Large scale simulation

The MFT method is now evaluated by simulating an arson fire that occurred at Lançon de Provence, in France, in July 2005. This fire has been extensively studied and documented by the authors (Adou et al., 2010). Geographical data include a digital elevation model and vegetation map at a resolution of 50 m. The dominant species was kermes oak shrub (*Quercus coccifera*). The weather conditions at the time of fire were: an average wind speed of 46km/h at 10 m above the ground level, an average direction of 330° (NNW), and a dry bulb temperature of 30°C. The CFD program Flowstar© was used to calculate local wind direction and speed from the average wind speed, taking into account the effects of topography and surface roughness of the land site. Two ignition points were reported whose geographic coordinates are 5°11’39’’E; 43°36’6’’N and 5°12’21’’E; 43°35’53’’N.

We consider a 10km×7km monodisperse amorphous network of kermes oak shrubs with a diameter of 3m. The vegetation coverage is 0.5.

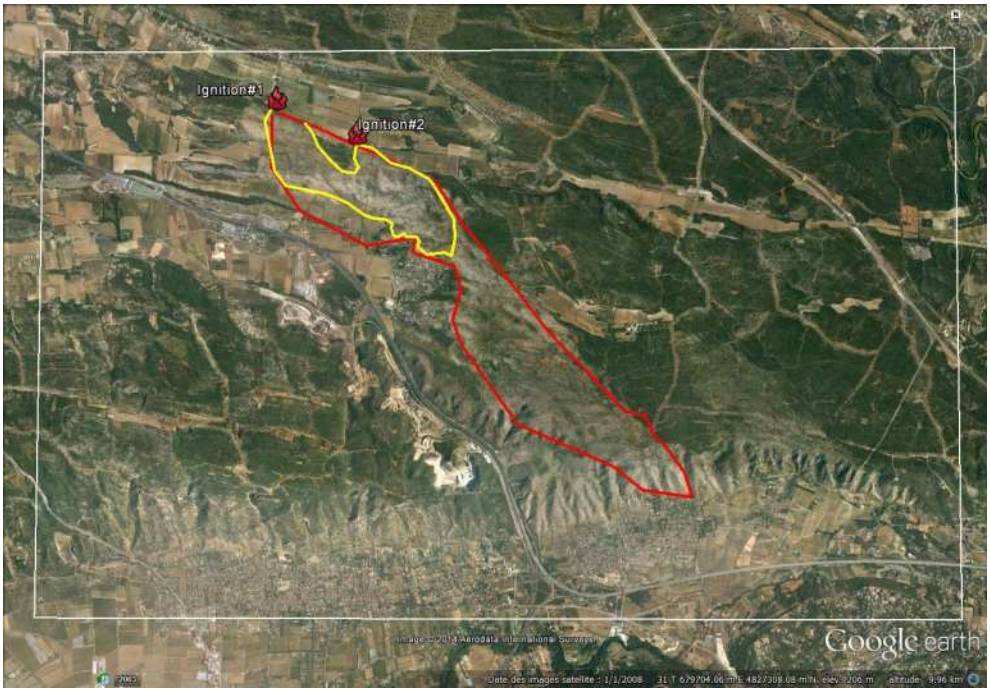

Figure 4. Domain of the study and real fire patterns after t=140min (yellow) and t=300min (red) of propagation.

Contours predicted by the model are compared with field measurements after 140min (Figure 5b) and 300min (Figure 5d) of fire. At t=140min, the average rate of spread is slightly overestimated which leads to a more advanced position of the head fire front. This may be due to time variations in wind properties which are averaged in the model. Integration of time-dependent meteorological conditions is possible but such information is unavailable for the present case. At t=300min, the agreement remains effective. Discrepancies between predicted and real contours, in particular in the lateral extension of the fire, are mainly due to the fire crew intervention which was not introduced into the model because of lack of information on the location and nature of the fire-fighting task force deployed. It may be noted that the model can easily take into account the action of fire fighters by rendering soaked vegetation inactive.

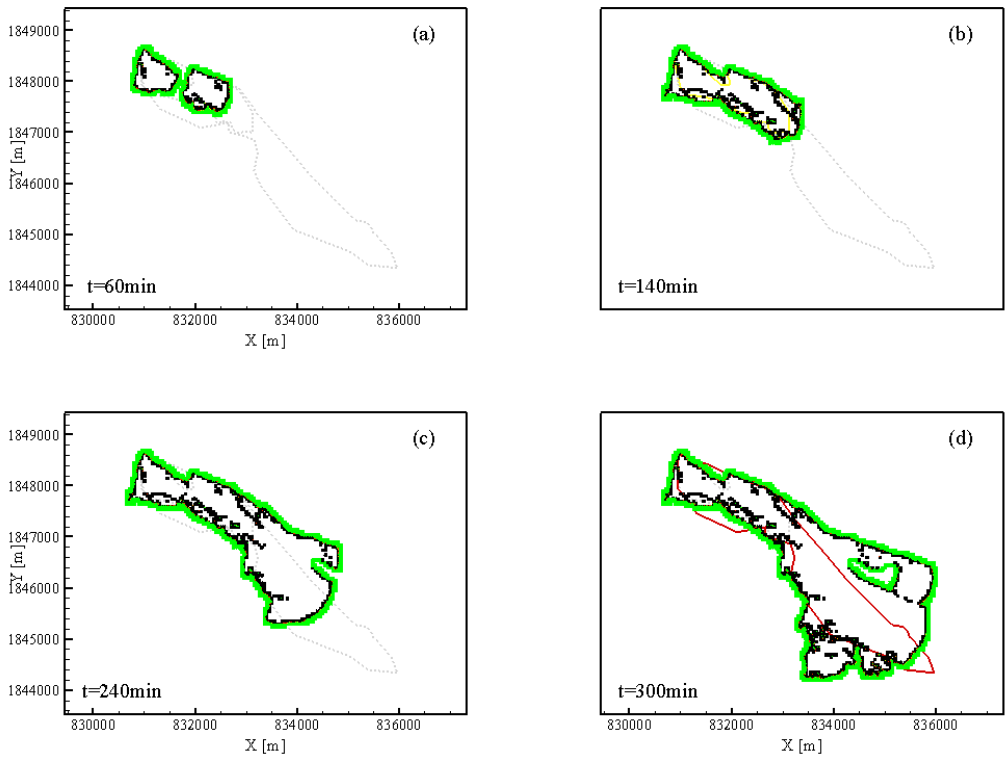

Figure 5. Fire patterns after a) t=60min, b) t=140min, c) t=240min and d) t=300min of simulation. a) and c) are compared with real fire pattern.

As mentioned before, two ignition points were reported for this fire. At t=60min (Figure 5a), the two independent fire fronts interact and merge into a single one. This shows the capability of the method to handle phenomena frequently observed in wildland fire propagation in complex terrains, such as splitting and coalescence of fire fronts. The model can thus be used to evaluate the efficiency of counterfire.

The overall CPU time gains are substantial when using the MFT method as it gives, in the present case, a 450% overall performance gain compared to the standard method. This gain is mainly due to the memory allocation/deallocation strategy, reducing memory allocation and the search space of connections between sites.

Conclusion

A method for improving the capability of a semi-physical network model is used to simulate large fire patterns in heterogeneous landscapes. The basic concepts of the model are recalled and the last improvements, including the use of an amorphous network and the front-tracking method, are presented. The strengths of the meshless front-tracking method are illustrated through an academic case. Method validation is achieved to an acceptable degree through comparison of results with data from a well-documented historical Mediterranean fire. The performance of the method is evaluated in terms of computational resources.

Acknowledgments

MDG gratefully acknowledges the financial support from NOVELTIS and ANRT (CIFRE/ANRT contract n°566/2013).

References

Adou, J. *et al*., 2010. Simulating wildfire patterns using a small-world network model. Ecological Modelling, 221, pp.1463–71.

Billaud, Y. *et al*., 2012. A hybrid small-world network/semi-physical model for predicting wildfire spread in heterogeneous landscapes. J. Phys. Conf. Series, 395.

Holme, P., 2007. Efficiency of Navigation in Indexed Networks. Dynamics on and of networks, pp.189-98.

Koo, E.P.P. *et al*., 2007. A Simple Physical Model for Forest Fire Spread Rate. In Proceeding of the Tenth International Symposium of Fire and Materials. Interscience Communications, San Francisco, CA, 2007.

Pasquale, D.M., Emilio, F., Giacomo, F. & Alessandro, P., 2014. Mixing local and global information for community detection in large networks. Journal of Computer and System Sciences, 80(1), pp.72-87.

Strauss, D., Bednar, L. & Mees, R., 1989. Do One Percent of the Forest Fires Cause Ninety-Nine Percent of the Damage? Forest Science, 35(2), pp.319-28.

Data assimilation of satellite fire detection in coupled atmosphere-fire simulation by wrf-sfire

Jan Mandel[a], Adam Kochanski[b], Martin Vejmelka[c], and Jonathan D. Beezley[d]

[a] *University of Colorado Denver, Denver, CO, USA, jan.mandel@gmail.com*
[b] *University of Utah, Salt Lake City, UT, USA, adam.kochanski@utah.edu*
[c] *University of Colorado Denver, Denver, CO, USA, and Institute of Computer Science, Academy of Sciences of the Czech Republic, Prague, Czech Republic, vejmelkam@gmail.com*
[d] *Kitware, Inc., Clifton Park, NY, USA, jon.beezley@gmail.com*

Abstract
Currently available satellite active fire detection products from the VIIRS and MODIS instruments on polar-orbiting satellites produce detection squares in arbitrary locations. There is no global fire/no fire map, no detection under cloud cover, false negatives are common, and the detection squares are much coarser than the resolution of a fire behavior model. Consequently, current active fire satellite detection products should be used to improve fire modeling in a statistical sense only, rather than as a direct input. We describe a new data assimilation method for active fire detection, based on a modification of the fire arrival time to simultaneously minimize the difference from the forecast fire arrival time and maximize the likelihood of the fire detection data. This method is inspired by contour detection methods used in computer vision, and it can be cast as a Bayesian inverse problem technique, or a generalized Tikhonov regularization. After the new fire arrival time on the whole simulation domain is found, the model can be re-run from a time in the past using the new fire arrival time to generate the heat fluxes and to spin up the atmospheric model until the satellite overpass time, when the coupled simulation continues from the modified state.

Keywords*: VIIRS, MODIS, WRF, WRF-SFIRE, Data assimilation, Fire spread, Fire detection likelihood, Fire arrival time, Least squares, Maximum-a-Posteriori estimate, Tikhonov regularization, Bayesian*

Introduction

Active fire detection products using the VIIRS and MODIS instruments provide planet-wide monitoring of fire activity several times daily as detection squares or polygons at a resolution of 375 m to 1 km. Because the data products are continuously available online, they present an attractive data source for automated fire behavior simulations and forecasts. Unfortunately, fire detection errors are frequent (Csiszar *et al*., 2012; Hawbaker *et al*., 2008; Sei, 2011) , and geolocation errors can be significant, up to 1.5 km (Sei, 2011). An improved data product at 375 m resolution and with better error rates exists (Schroeder *et al*., 2014), but it is not available for general use yet. In any case, satellite active fire detection data have significant error rates, and they have much coarser resolution than the resolution of fire behavior models, which is typically few meters to tens of meters.
Fire detection data consist of squares of polygons (from now on, squares) with associated satellite overpass times. A fire detection square means that a fire of sufficient intensity and size was detected somewhere in the square; it does not mean that the whole square is burning. The fire detection squares are in arbitrary locations; a global fire-detection map where every pixel is marked as either fire or no fire is "neither required or desired" by VIIRS Active Fires specifications (Sei, 2011). In addition, an existing fire is often not detected (a false negative). For example, MODIS has a 50% probability of detecting a 100m^2 flaming fire (Giglio *et al*., 2003). The improved 375m VIIRS product has 50% probability of detecting about a 2 m^2 flaming fire at night, and about 40 m^2 flaming fire during the day of (Schroeder *et al*., 2014). False positives are possible, particularly in areas of high contrast (the data products' algorithms are contextual), but less frequent. Finally, if a location is under cloud cover, the

fire detection is turned off completely. Unfortunately, the cloud mask used was not provided in the data products we found, so we could not distinguish between missing data and negative fire detection. Consequently, current satellite fire detection products do not determine the fire area and the fire perimeter to a degree that could be relied upon. Although the use of satellite fire detection to initialize a fire simulation directly was an important advance (Coen and Schroeder, 2013), satellite fire detection is better suited to improve a fire behavior simulation in a statistical sense only, that is, by data assimilation. Data assimilation fuses the forecast obtained from a model with the data by balancing their uncertainties, and it can also take advantage of more reliable fire detection in future by putting more weight on the data and less weight on the model.

Data assimilation modifies the state of the simulation in analysis cycles. Each cycle consists of advancing the model in time and an analysis step, which takes account of the new information. The analysis cycles steer the simulation periodically and help to avoid an accumulation of modeling errors. Analysis steps at every satellite overpass also help to account for uncertainties caused by incorrect fuel information and by fire-fighting efforts. We propose a new data assimilation method for satellite fire detection, inspired by techniques used for contour detection in computer vision, such as in the Microsoft Kinect (Blake, 2014). The method takes advantage of encoding the state of the fire propagation as the fire arrival time (Finney, 2002), which can be modified by an additive correction. We employ a Bayesian approach and obtain a Maximum-a-Posteriori (MAP) estimate as a solution of a generalized nonlinear least squares problem, similarly as in Stuart (2010), to simultaneously maximize the log likelihood of the fire detection (or lack od detection) and minimize the change in the fire arrival time. The method is implemented efficiently using Fast Fourier Transform (FFT), and its computational cost is negligible compared to the coupled atmosphere-fire simulation itself.

Another challenge of data assimilation in coupled fire-atmosphere models is how to change the state of the atmospheric model when the state of the fire model changes in response to data. Atmospheric circulation evolves in response to the heat flux from the fire over time, and when the state of the fire model changes, the consistence between the state of fire and the state of the atmosphere is lost. Encoding the fire model state as the fire arrival time allows to go back in time, blend the new fire arrival time with the original one, and spin up the atmospheric model with heat fluxes generated by replaying the modified fire arrival time instead of running the fire propagation model itself (Mandel *et al*., 2012). Then, at the fire detection time (the satellite overpass time), the fire spread model takes over, and the simulation continues.

Methods

Fire detection data likelihood

We assimilate the fire detection data in the form of a likelihood of the detection data at a location (x, y). The data likelihood is proportional to $e^{f(t,x,y)}$, where t is the number of hours the fire has arrived at the location (x, y) before the satellite overpass time. The function $f(t, x, y)$ is called log likelihood. For locations (x, y) within the fire detection squares, the data likelihood should be high for when the fire has arrived recently, and low otherwise. For locations outside of the fire detection squares, the data likelihood should be high if the fire has not arrived yet, or has arrived long ago, and low if the fire has arrived at the location recently. Of course, this is a very simplified view; more accurately, the fire detection data likelihood depends on the fire behavior (some fires burn longer and can be detected longer after the fire arrival, and some only for a shorter time), the atmospheric state between the fire location and the satellite, and the properties of the sensor and processing algorithms. Some active fire detection products also provide a level of confidence, e.g. Schroeder *et al*. (2014), which should be a part of the calculation of the data likelihood. In this paper, however, we consider only a simple data likelihood functions modelled as in Figure 1.

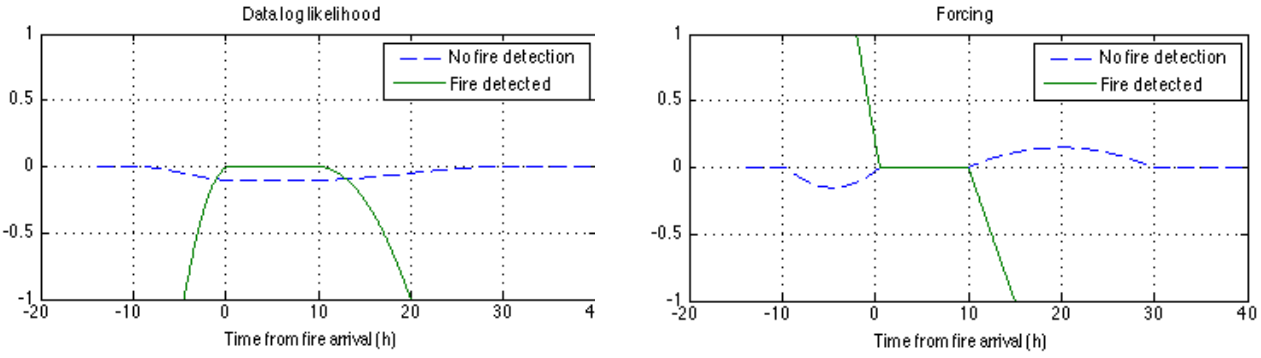

Figure 1. The log likelihood function $f(t)$ (left) and its derivative $f'(t)$ (right) as a function of time t elapsed since fire arrival (hours), in locations inside and outside of fire detection squares.

The model log likelihood f shown in Figure 1 is a function with continuous first derivative in the time t since fire arrival, and it is specified by parameters $T_{\min}$, $T_{\max}$, T_{pos}, T_{neg}, $\gamma > 0$. Within the fire detection squares, we choose $f(t) = 0$ for $T_{\min} \le t \le T_{\max}$, the function f is a quadratic polynomial for $t < T_{\min}$ with $f(T_{\min} - T_{\text{neg}}) = -1$, and a quadratic polynomial for $t > T_{\max}$ with $f(T_{\max} + T_{\text{pos}}) = -1$. Outside of the fire detection squares, $f(t) = -\gamma$ has a constant negative value for $T_{\min} \le t \le T_{\max}$, $f(t) = 0$ for $t < T_{\min} - 2T_{\text{neg}}$ or $t > T_{\max} + 2T_{\text{pos}}$, and f is blended by cubic polynomials in between. However, if the location is under a cloud cover, we would use $f(t) = 0$ for any t.

For the sake of simplicity, the data likelihoods at different locations are assumed to be independent. Then, the overall data likelihood of all detection squares at the satellite overpass time T^S over the whole simulation domain, given fire arrival time $T = T(x, y)$, is proportional to the product of the data likelihoods at all grid nodes (x, y). We also weigh each log likehood by the cell area $\Delta x \Delta y$, which gives

$$p(\text{detection squares} \mid T) \propto \prod_{(x,y)} e^{f(T^S - T, x, y)\Delta x \Delta y} = e^{\sum_{(x,y)} f(T^S - T, x, y)\Delta x \Delta y} \approx e^{\int f(T^S - T, x, y)\, dx\, dy}, \qquad (1)$$

with the understanding that the integral is computed numerically over the fire simulation domain.

Analysis step

In the analysis step, the data likelihood (1) is combined with the forecast fire arrival time $T^f = T^f(x, y)$ to obtain the analysis fire arrival time T^a. For this purpose, we need the probability density of the forecast fire arrival time. We assume that the difference of the fire arrival time from the mean fire arrival time T^f is a smooth random function, and we model the probability density of the fire arrival time as Gaussian, with mean T^f and covariance A^{-1} such that the associated norm

$$\|u\|_A = \langle u, Au \rangle^{1/2}$$

is small for spatially smooth functions u, defined on the model grid, and large for oscillatory u. For this purpose, we choose the covariance A^{-1} as a negative power of a discretization of the Laplace operator

$$\Delta u = \frac{\partial^2 u}{\partial x^2} + \frac{\partial^2 u}{\partial y^2}$$

on the model grid, multiplied by a penalty parameter. Thus, the forecast probability density of the fire arrival time T is

$$p^{\mathrm{f}}(T) \propto e^{-\frac{\alpha}{2}\left\|T-T^{\mathrm{f}}\right\|_A^2}, \quad A=(-\Delta)^p, \quad \alpha, p>0.$$

We also requite that the ignition time of the fire does not change, so $p^{\mathrm{f}}(T)>0$ only if $T=T^{\mathrm{f}}$ at the ignition point. The analysis probability density is obtained from the Bayes theorem as

$$p^{\mathrm{a}}(T) \mu\ p(\text{detection squares}\,|\,T)\,p^{\mathrm{f}}(T) \mu\ e^{\int f(T^{\mathrm{S}}-T,x,y)\,dx\,dy}\, e^{-\frac{\alpha}{2}\left\|T-T^{\mathrm{f}}\right\|_A^2} = e^{\int f(T^{\mathrm{S}}-T,x,y)\,dx\,dy-\frac{\alpha}{2}\left\|T-T^{\mathrm{f}}\right\|_A^2}.$$

The analysis distribution is non-Gaussian due to the presence of the data likelihood. To obtain a single analysis value, we use the standard Maximum-a-Posteriori estimator, which is the maximizer T^{a} of the analysis probability density $p^{\mathrm{a}}(T)$. Maximization of the analysis density is equivalent to the minimization of the exponent, which is the generalized least squares problem

$$J(T)=\frac{\varepsilon}{2}\left\|T-T^{\mathrm{f}}\right\|_A^2-\int f(T^{\mathrm{S}}-T,x,y)\,dx\,dy \to \min_{T:\,T=T^{\mathrm{f}} \text{ at the ignition point}}. \tag{2}$$

Note that the optimization problem (2) can be also understood as the maximization of the log likelihood with a Tikhonov regularization by the added quadratic term. In this context, the matrix A is chosen to penalize non-smooth increments $T-T^{\mathrm{f}}$. To find a descent direction, consider the difference

$$\begin{aligned} J(T+h)-J(T) &= \frac{\alpha}{2}\left\langle A(T-T^{\mathrm{f}}+h),T-T^{\mathrm{f}}+h\right\rangle-\int f(T^{\mathrm{S}}-T-h,x,y)\,dx\,dy \\ &\quad -\left(\frac{\alpha}{2}\left\langle A(T-T^{\mathrm{f}}),T-T^{\mathrm{f}}\right\rangle-\int f(T^{\mathrm{S}}-T,x,y)\,dx\,dy\right) \\ &= \alpha\left\langle A(T-T^{\mathrm{f}}),h\right\rangle+\int\left\langle\frac{\partial}{\partial t}f(T^{\mathrm{S}}-T,x,y)\,dx\,dy,h\right\rangle+O\left(\|h\|^2\right) \\ &= \left\langle\nabla J(T),h\right\rangle+O\left(\|h\|^2\right), \end{aligned}$$

which gives the gradient of J as

$$\nabla J(T)=\varepsilon A(T-T^{\mathrm{f}})-F(T), \quad \text{where } F(T)=\int\frac{\partial}{\partial t}f(T^{\mathrm{S}}-T,x,y)\,dx\,dy$$

is from now on called the forcing function. This gradient direction, however, is not suitable for our purposes, because it is not very spatially smooth, and, consequently, gradient descent iterations converge to the smoother solution of (2) only very slowly and, in addition, they are liable to get caught in local minima. A better gradient direction is obtained by considering the gradient $\nabla^A J(T)$ with respect to the inner product $\langle u,v\rangle_A=\langle Au,v\rangle$:

$$\left\langle\nabla^A J(T),h\right\rangle_A=\left\langle A\nabla^A J(T),h\right\rangle=\left\langle\nabla J(T),h\right\rangle$$

$$\nabla^A J(T)=\alpha(T-T^{\mathrm{f}})-A^{-1}F(T).$$

Now we add the constraint that the increment h is zero at the ignition point and introduce Lagrange multiplier λ, which leads to the saddle point problem

$$\begin{aligned} \varepsilon A h+C\lambda &= \alpha A(T^{\mathrm{f}}-T)+F(T) \\ C^{\mathrm{T}}h &= 0, \end{aligned} \tag{3}$$

for a descent direction h, where C is a zero-one vector such that $C^{\mathrm{T}}h=0$ expresses the condition that h is zero at the ignition point. The saddle point problem (3) is easily solved with access to multiplication by A^{-1} only: Calculating h from the first equation in (3) gives the descent direction

$$h=T^{\mathrm{f}}-T+\alpha^{-1}A^{-1}F(T)-\alpha^{-1}A^{-1}C\lambda=-\alpha^{-1}\left(\nabla^A J(T)+A^{-1}C\lambda\right),$$

where the Lagrange multiplier is determined by substituting in the second equation, which gives

$$\lambda = \left(C^{\mathrm{T}} A^{-1} C\right)^{-1} C^{\mathrm{T}} \left(\alpha(T^{\mathrm{f}} - T) + A^{-1} F(T)\right) = \left(C^{\mathrm{T}} A^{-1} C\right)^{-1} C^{\mathrm{T}} \nabla^{A} J(T).$$

Note that the descent direction h is obtained by a spatial smoothing of the forcing $F(T)$, or, equivalently, from the gradient in the inner product defined by the inverse covariance A, plus an adjustment for the constraint that the fire arrival time at the ignition location should not change. In each step of the descent method, the cost function J is then minimized by a line search over $T + ht$, t real. The first iteration starts from $T = T^{\mathrm{f}}$. Note that the penalty parameter α does not have any effect on the first search direction.

Results

The method is illustrated on two real fires simulated by WRF-SFIRE, with the assimilation of MODIS and VIIRS Active Fire detection data. WRF-SFIRE (Mandel *et al*., 2009, 2011) builds on CAWFE (Clark *et al*., 2004), and it is available from openwfm.org. A limited version from 2010 is currently distributed in WRF release as WRF-Fire (Coen *et al*., 2013).
In both examples below, we have used the parameters

$$\alpha = 1000,\ T_{\min} = 0.5,\ T_{\max} = 10,\ T_{\mathrm{pos}} = 10,\ T_{\mathrm{neg}} = 5,\ \gamma = 0.5,\ \rho = 1.02.$$

2012 Wood Hollow fire

The present data assimilation method was applied to adjust the fire arrival time obtained from a fire simulation up to 24th Jan 2014 23:45 UTC, from 151 MODIS fire detections, which occurred on the same day approximately at 20:00 UTC (Figure 2). The practical implementation of the method implements a line search strategy, in which a maximal step is set (here, 1.0) and the objective function is sampled 6 times in regular intervals. The step with the lowest objective function value and its two neighbors are selected as the new limits and the line search is repeated to determine the best step size with more precision.
In this instance, only the first iteration resulted in an improvement of the objective function, a line search along the second direction did not yield any more improvements, even for smaller step sizes. However, the single iteration has already found a satisfactory modification of the fire arrival time. The seemingly large value of the penalty parameter α was needed to stop the method from adjusting the fire arrival time in later iterations near the fire detection squares only.

2012 Barker Canyon fire

The data assimilation method was applied to a simulation of the 2012 Barker Canyon Fire, 1.71 days from ignition. Figs. 3-6 show how the analysis fire arrival time is obtained from the forecast by adding a correction in the direction of a smooth search direction, which is in turn obtained by the spatial smoothing of the forcing function. Again, a single iteration was sufficient to find a satisfactory solution.

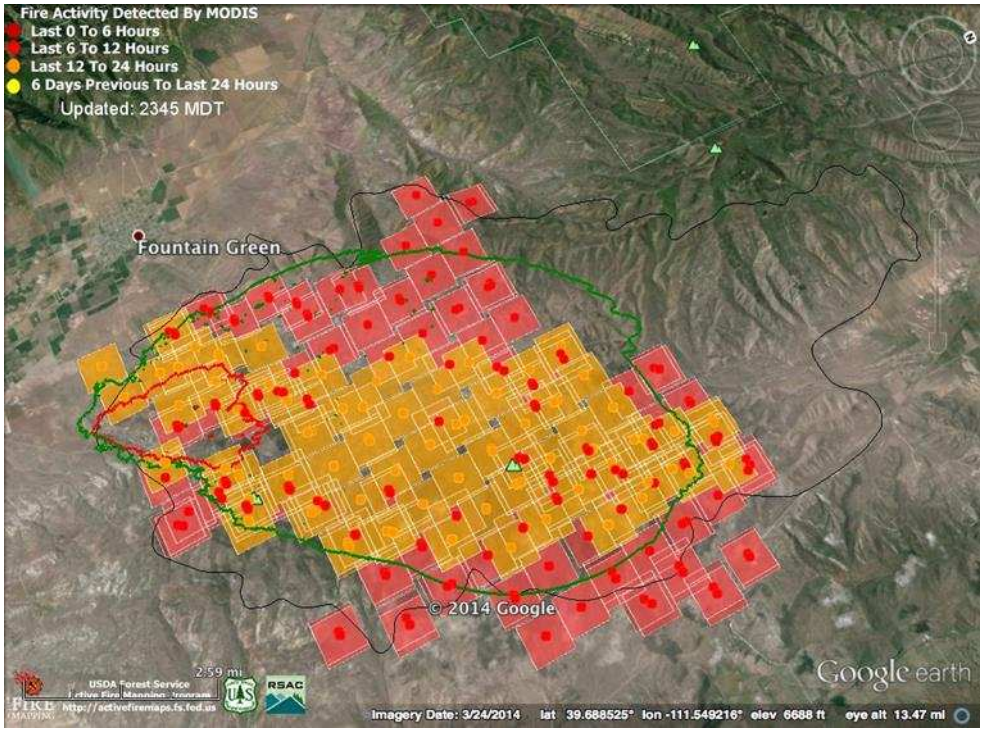

Figure 2. Data assimilation for the 2012 Woods Hollow fire, simulated by WRF-SFIRE, with MODIS Active Fire detection squares. The black contour is the actual fire perimeter on 25th Jun 2012, the red line is the forecast fire perimeter and the green line is the fire perimeter after assimilation, or the analysis. The analysis adjusts the shape of the fire for the fire detection data by a smooth correction, which automatically fills the fire arrival time between the detection squares.

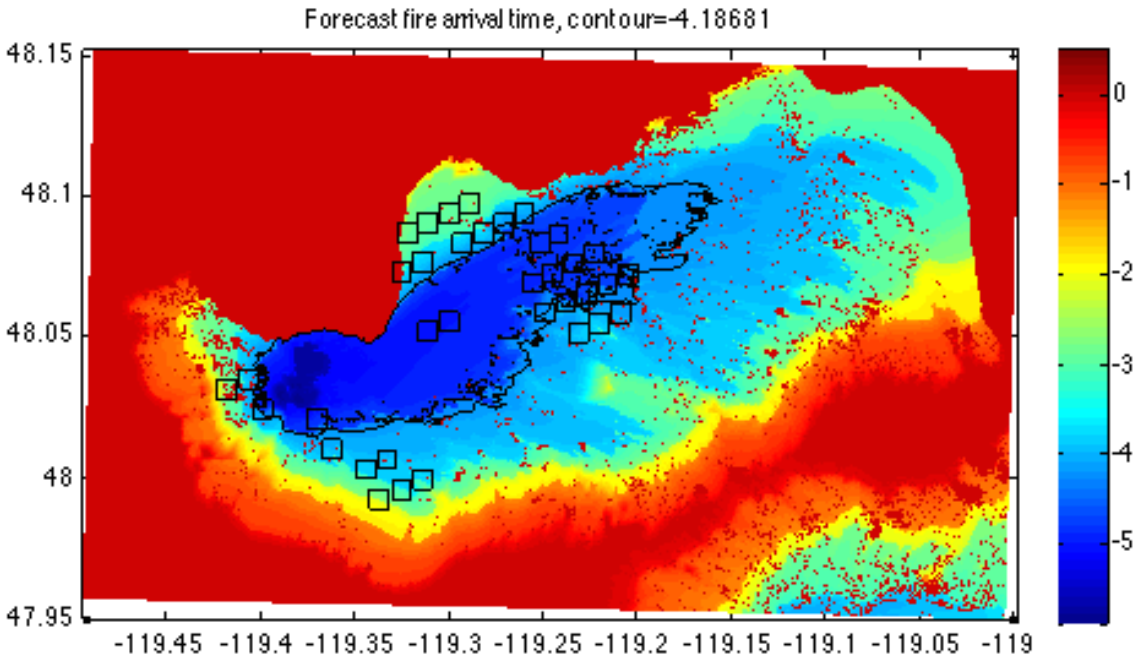

Figure 3. Forecast fire arrival time for the 2012 Barker fire, simulated by WRF-SFIRE, and VIIRS Active Fire detection squares. The black contour is the simulated fire perimeter at the satellite overpass time. The color bar shows fire arrival time in days before the end of the simulation. The axes are longitude and latitude.

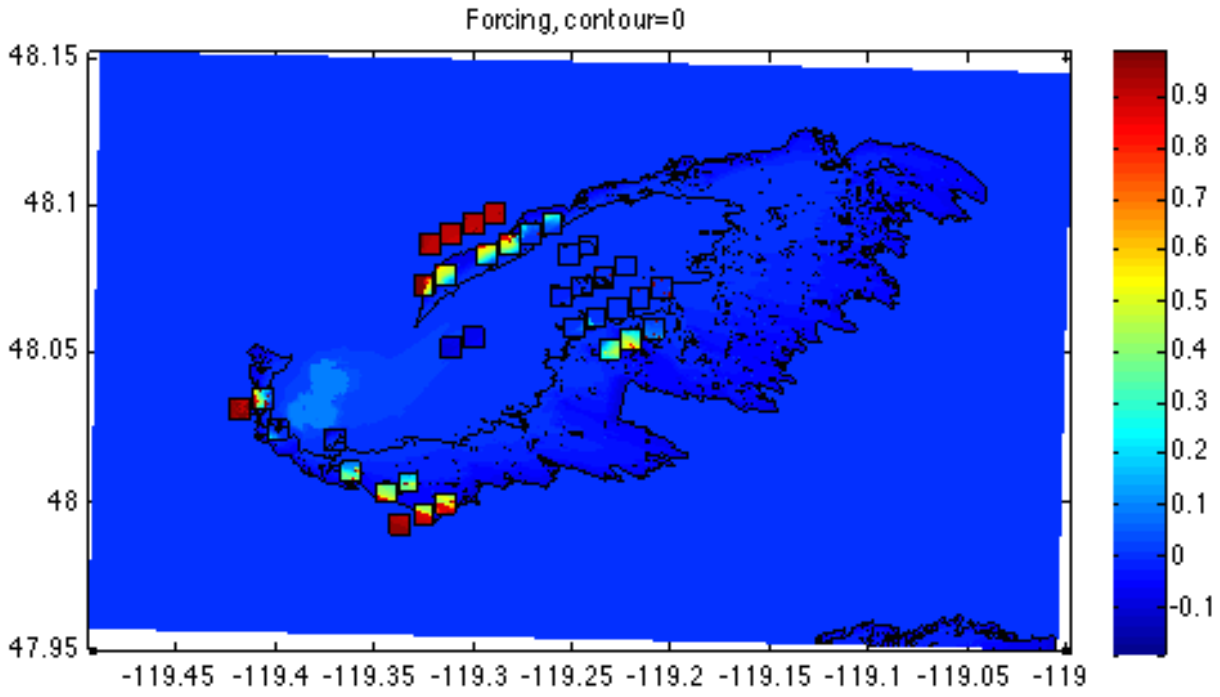

Figure 4. Forcing function F for the forecast in Figure 3. Positive values mean that the fire arrival time at the location should be adjusted down, while negative value mean that the fire arrival time should be adjusted up. The black contour marks the locations where the forcing is zero. Note that the forcing has jumps at the boundaries of the detection squares.

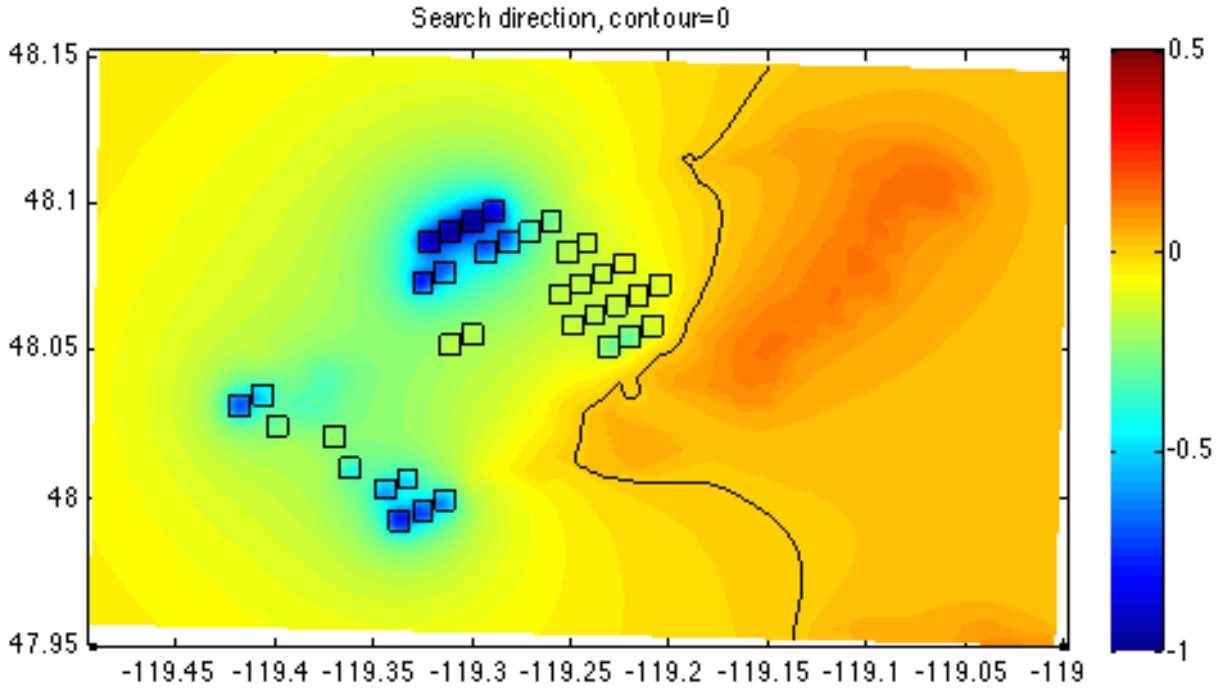

Figure 5. Search direction for the forecast in Figure 3. The forecast fire arrival time will be adjusted by a positive multiple of the search direction. In particular, the fire arrival time at the location of the detection squares colored in blue may be decreased, so the fire will be there at the satellite overpass time. The black line marks the locations where the search direction is zero.

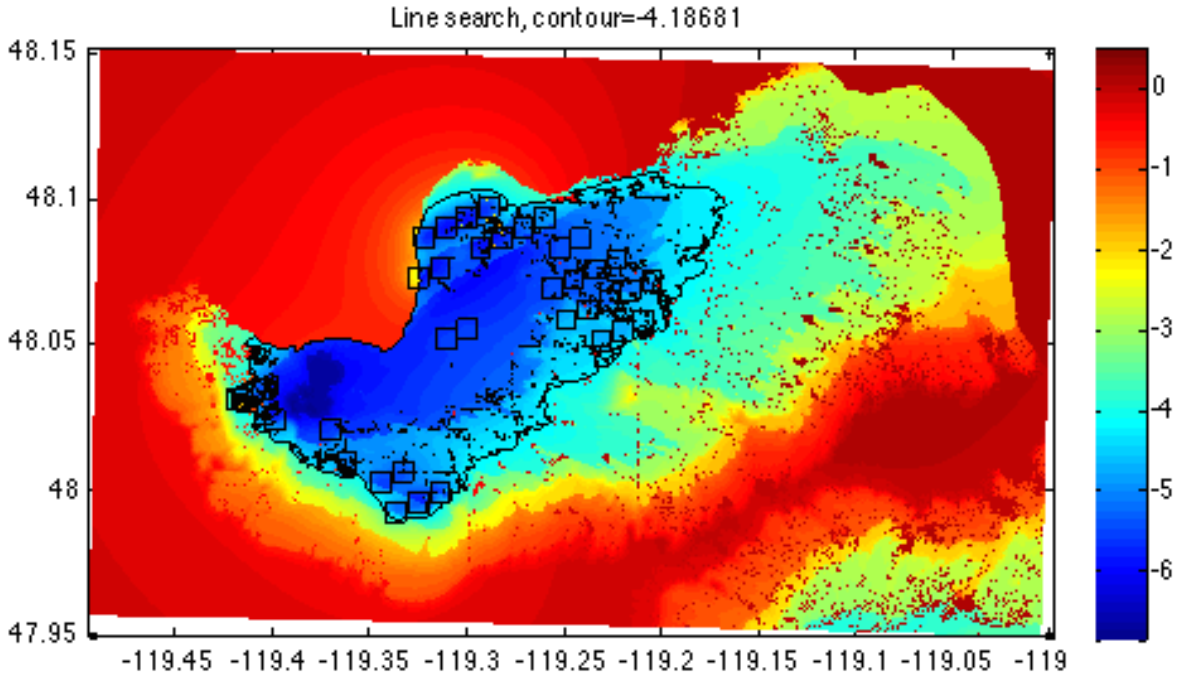

Figure 6. Analysis for the forecast in Figure 3. The method has filled in the fire arrival time based on the forecast from the model and incomplete information from the fire detection squares. The black contour is the resulting analysis fire perimeter.

Conclusion

We have described a new methodology to assimilate satellite active fire detection data into the state of a fire spread model, which is encoded as the fire arrival time. The methodology relies on standard Bayesian framework of data assimilation, which leads to a nonlinear least squares problem to simultaneously minimize the change of the fire arrival time from the forecast in a suitable norm (which penalizes spatially smooth changes less) and maximize the integral of the log likelihood of the fire detection (or non-detection) over the fire simulation domain. An efficient method to solve such problems was presented, which generates smooth increments and it found good approximate solutions in a single gradient descent iteration.

There are many uncertainties affecting fire spread simulations. They are associated with limitations of the fire spread and atmospheric models as well as limited accuracy in the estimate of the initial state of the fuel and atmosphere. As the length of the atmospheric simulation grows, its accuracy deteriorates, and as a consequence, the errors in the fire spread prediction also grow. The presented method allows for objective corrections of the simulated fire progression based on the assimilation of the satellite fire detection data. As the simulation period extends, also more satellite data showing the fire progression becomes available, so the simulated fire may be cyclically nudged to the observations. The method was illustrated on two examples, in which just a single arrival time adjustment to the coupled atmosphere-fire simulations by WRF-SFIRE was made. The same method, however, can be also used for cyclic corrections of the simulated fire progression, where the model continues its fire progression from the adjusted fire state till the new observations become available. A spin-up of the atmospheric state is then needed to restart the coupled model from the modified fire arrival time. An illustration of the cyclic application of this method will be presented elsewhere.

Acknowledgements

This research was partially supported by the National Science Foundation (NSF) grants DMS-1216481, National Aeronautics and Space Administration (NASA) grants NNX12AQ85G and NNX13AH9G, and the Grant Agency of the Czech Republic grant 13-34856S. The authors would like to thank the Center for Computational Mathematics University of Colorado Denver for the use of the Colibri cluster, which was supported by NSF award CNS-0958354. This work partially utilized the Janus supercomputer, supported by the NSF grant CNS-0821794, the University of Colorado Boulder, University of Colorado Denver, and National Center for Atmospheric Research.

References

Blake A (2014) *Machines that see, powered by probability*. Gibbs lecture at the Joint Mathematics Meeting, Baltimore, January 2014.

Clark TL, Coen J, Latham D (2004) Description of a coupled atmosphere-fire model, *International Journal of Wildland Fire* **13**, 49–64. doi:10.1071/WF03043

Coen JL, Cameron M, Michalakes J, Patton EG, Riggan PJ, Yedinak K (2013) WRF-Fire: Coupled weather-wildland fire modeling with the Weather Research and Forecasting model. *J. Appl. Meteor. Climatology* **52**, 16–38. doi:10.1175/JAMC-D-12-023.1

Coen JL, Schroeder W (2013) Use of spatially refined satellite remote sensing fire detection data to initialize and evaluate coupled weather-wildfire growth model simulations, *Geophysical Research Letters* **40**,1–6. doi:10.1002/2013GL057868

Csiszar I, Schroeder W, Giglio L, Justice CO, Ellicott E (2012) Establishing active fire data continuity between Aqua MODIS and Suomi NPP VIIRS, *92nd AMS Annual Meeting, New Orleans.*

Finney MA (2002), Fire growth using minimum travel time methods, *Canadian Journal of Forest Research* **32**, 1420–1424. doi:10.1139/x02-068

Giglio L, Descloitres J, Justice CO, and Kaufman YJ (2003) An enhanced contextual fire detection algorithm for MODIS. *Remote Sensing of Environment* **87**, 273–282. doi:10.1016/S0034-4257(03)00184-6

Hawbaker TJ, Radeloff VC, Syphard AD, Zhu Z, Stewart SI (2008) Detection rates of the MODIS active fire product in the United States, *Remote Sensing of Environment* **112**, 2656–2664. doi:10.1016/j.rse.2007.12.008

Mandel J, Beezley JD, Coen JL, Kim M (2009), Data assimilation for wildland fires: Ensemble Kalman filters in coupled atmosphere-surface models, *IEEE Control Systems Magazine* **29**, 47–65. doi:10.1109/MCS.2009.932224

Mandel J, Beezley JD, Kochanski AK (2011) Coupled atmosphere-wildland fire modeling with WRF 3.3 and SFIRE 2011, *Geoscientific Model Development* **4**, 591–610. doi:10.5194/gmd-4-591-2011

Mandel J, Beezley JD, Kochanski AK, Kondratenko VY, Kim M (2012) Assimilation of perimeter data and coupling with fuel moisture in a wildland fire – atmosphere DDDAS, *Procedia Computer Science* **9**, 1100–1109. doi:10.1016/j.procs.2012.04.119

Schroeder W, Oliva P, Giglio L, Csiszar IA (2014) The New VIIRS 375 m active fire detection data product: Algorithm description and initial assessment. *Remote Sensing of Environment*, **143** 85–96. doi:10.1016/j.rse.2013.12.008

Sei A (2011) *VIIRS active fires: Fire mask algorithm theoretical basis document*. Joint Polar Satellite System (JPSS) document 474-00030, NASA Goddard Space Flight Center. Available at http://npp.gsfc.nasa.gov/sciencedocuments/ATBD_122011/474-00030_Rev-Baseline.pdf, retrieved November 2013.

Stuart AM (2010) Inverse problems: a Bayesian perspective, *Acta Numerica* **19**, 451–559. doi:10.1017/S0962492910000061

Estimating daily fire risk in the mesoscale by means of a Bayesian network model and a coupled GIS

Panagiota Papakosta, Anke Scherb, Kilian Zwirglmaier, Daniel Straub

Engineering Risk Analysis Group, Technische Universität München, Munich, Germany
panagiota.papakosta@tum.de

Abstract
A probabilistic spatio-temporal model for fire risk prediction based on Bayesian networks is presented. It predicts daily fire risk on houses and vegetated areas in the mesoscale (1 km² spatial resolution). The BN model consists of three parts. (1) The fire occurrence model, which involves as predictive variables the weather conditions (expressed by the Fire Weather Index - FWI), land cover types, population and road density. It predicts the probability of a fire occurring daily in each 1km². (2) The fire behavior model, triggered by the occurrence model, which includes the influence of actual and past weather conditions, fire behavior indices and topography. (3) The damage model, which predicts the expected losses relevant to houses and vegetated areas conditional on a fire hazard. Vulnerability (resistance capacity) and exposure (values at risk) indicators are used to quantify the damage, which also depends on the fire suppression efficiency. The final output of the model are the expected house damage costs (the risk to houses) and the restoration costs for the vegetation (the risk to vegetated areas). The BN model is exemplarily established for Cyprus. The conditional probability distributions of the BN variables are populated with data from the time period 2006-2009, regression model results and expert knowledge. Data from 2010 for Cyprus are used as verification dataset. The results are shown in daily maps with 1 km² spatial resolution.

Keywords*: wildfire risk, Bayesian networks, GIS*

Introduction

Fire risk prediction can support the planning of measures for fire prevention (e.g. thinning, prescribed burning) and risk mitigation (e.g. allocation of suppression resources, raising preparedness). In order to quantify fire risk, the predictive model must include models for fire occurrence, fire behavior and fire consequences. Due to the randomness inherent in the wildfire process and because the modeling is subject to uncertainty in all three stages (occurrence, behavior, damages), fire risk prediction is ideally carried out in a probabilistic format. Fire occurrence is influenced by weather conditions, human presence and vegetation types. Fire behavior is influenced mainly by local weather conditions (e.g. wind speed), topography and fuels (Forestry Canada 1992). Fire damages depend to a large extent on fire severity and the vulnerability of assets (Cohen 2000).
In this study, we focus on the Mediterranean area, where most fires occur due to human intervention as a result of arson or negligence, favored by long dry summer periods (Keeley *et al*. 2012).We propose a probabilistic spatio-temporal model based on Bayesian networks, which predicts daily fire risk on houses and vegetated areas in the mesoscale (1 km² spatial resolution). Bayesian Networks (BN) are graphical probabilistic models that can effectively represent complex processes with multiple random variables, their interdependencies and the associated uncertainties.

2. Methods

The predictive BN model consists of three parts: (1) The fire occurrence model, which includes as predictive variables weather conditions (expressed by the Fire Weather Index - FWI of the Canadian Forest Fire Weather Index System - CFFWIS), land cover types, population and road density, and

which predicts the probability of a fire occurring in each spatial-temporal unit, i.e. daily and per 1km². (2) The fire behavior model, triggered by the occurrence model, which is a function of the actual and past weather conditions, the fire behavior indices of the CFFWIS and the topography. (3) The damage model, which predicts the expected losses relevant to houses and vegetated areas conditional on fire hazard. Vulnerability (resistance capacity) and exposure (values at risk) indicators are used to quantify the damage, which also depends on the fire suppression efficiency. The final results of the combined model are the risk to houses (expected house damage costs [€]) and the risk to vegetation (vegetated area damage costs [€]). After a short introduction to BN in section 2.1, the three parts of the model are presented in sections 2.2 – 2.4, and the combined model is provided in 2.5.

Bayesian networks

Bayesian Networks (BN) are directed acyclic graphs and consist of nodes, arcs and conditional probability distributions attached to the nodes (Jensen and Nielsen 2007). In a discrete BN, which is used in this study, each node represents a discrete random variable, whose sample space consists of a finite set of mutually exclusive states. The arcs qualitatively describe the dependence structure among the random variables.

A conditional probability table (CPT) is attached to each of the nodes, defining the probability distribution of the variable conditional on its parents. If we consider a BN with discrete random variables $\mathbf{X} = [X_1, \dots, X_\mathrm{n}]$, then the full (joint) probabilistic model of these variables is the joint Probability Mass Function (PMF), $p(\boldsymbol{x}) = p(x_1, \dots, x_\mathrm{n})$, which can be specified with the help of the chain rule:

$$p(\mathbf{x}) = p(x_n|x_{n-1}, \dots, x_1)p(x_{n-1}|x_{n-2}, \dots, x_1) \dots p(x_2|x_1)p(x_1) \tag{1}$$

By making use of the independence assumptions encoded in the graphical structure of the BN, this chain rule reduces to

$$p(\mathbf{x}) = \prod_{i=1}^{n} p(x_i|pa(x_i)) \tag{2}$$

wherein $pa(x_\mathrm{i})$, are realizations of the parents of X_i (i.e. the variables with a link pointing to X_i). In words, the joint probability mass function (PMF) of all random variables in the BN is the product of the conditional PMFs of all random variables given their parents. Therefore, the graphical structure of the BN, together with the conditional PMFs $p(x_i|pa(x_i))$, are sufficient for specifying the full (joint) probabilistic model of $\mathbf{X} = [X_1, \dots, X_\mathrm{n}]$.

Inference in the BN model is performed through updating. When one or several variables are observed, this information (evidence e) is propagated through the network and the joint prior probability of all nodes is updated to its posterior. The posterior joint probability of a set of variables $\mathbf{Y} \in \mathbf{X}$ in the network given the evidence $\mathbf{e}$ is:

$$p(\mathbf{y}|\mathbf{e}) = \frac{p(\mathbf{y}, \mathbf{e})}{p(\mathbf{e})} \tag{3}$$

The joint probabilities $p(\mathbf{y}, \mathbf{e})$ and $p(\mathbf{e})$ are computed following Eq. 2. Efficient algorithms for performing these computations in rather complex networks exist, which are implemented in software such as GeNIe (Decision Systems Laboratory 2013) or Hugin (HUGIN EXPERT 2012).

In the context of the proposed model for wildfire risk assessment, the main advantage of the BN is not its computational effectiveness but that it facilitates the combination of information from various sources in a single model.

Fire occurrence model

The fire occurrence model, which is described in detail in (Papakosta and Straub 2014), is based on the assumption that fire occurrences are independent of each other for a given fire rate. Hence the number of fires in an area of size α during one day, N, has the Poisson distribution, with PMF:

$$p(n|\,\lambda) = \frac{(\lambda\alpha)^n}{n!}\exp(-\lambda\alpha)\,, n = 0,1,2,\ldots \tag{4}$$

wherein $\lambda\ \left[\frac{\text{Nr.Fires}}{\text{day}\cdot\text{km}^2}\right]$ is the mean occurrence rate and α = 1km² is the area of the cell.
λ is calculated by a regression model with explanatory variables *FWI*, *population density*, *road density* and *land cover types*. The predictive model based on the regression results of (Papakosta and Straub 2014) is

$$\log(\lambda) = -10.90 + 0.0329 \cdot FWI + 0.3217 \cdot Road\ density - 0.0234 \cdot (Road\ density)^2 - 0.0010 \cdot Population\ density \tag{5}$$

The resulting BN for fire occurrence is shown in Figure 1.The node *fire occurrence rate* λ is a parent of the node *Fires N*, whose CPT is defined by the Poisson PMF, Eq. (4). The fire occurrence rate is a child of the nodes *FWI*, *population density*, *road density* and *land cover types*, following the deterministic relation of Eq. (5). The CPTs of the explanatory variables are learnt from data of the test bed area.

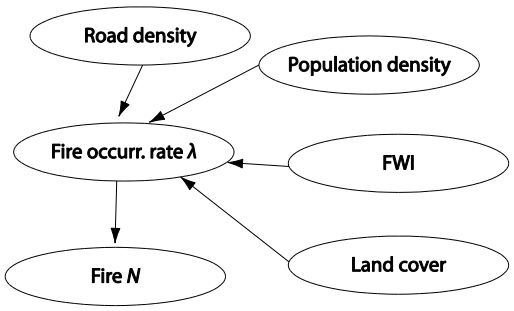

***Figure 1.** Bayesian network for Fire occurrence. The fire occurrence rate $\left[\frac{Nr.Fires}{day\cdot km^2}\right]$ is a function of road density, population density, Fire Weather Index (FWI) and land cover types.*

Fire behavior model

The fire behavior model presented in Figure 2 is adapted from (Zwirglmaier *et al*. 2013). The variables are chosen from a wider range of potential variables to represent the processes influencing the resulting burnt area of a fire. In the fire behavior model, the target/predicted node is *Burnt area*. *Burnt area* is influenced by *fire occurrence*, *land cover types*, *topography*, *recent weather conditions*, and *fire behavior indices*. The latter three are hidden variables, meaning that they cannot be observed. They are included to reduce the number of parents of the node *Burnt area*. *Topography* combines the influence of the variables *Wind Speed* [km/h], *Slope* [°] and *Aspect Minus Wind Direction* [same, opposite, perpendicular]. *Recent weather conditions* summarizes the effect of *Relative humidity* (*RH*) [%], *mean RH over the last 3 days* [%], *mean RH over the last 21 days* [%], *accumulated precipitation over the last 21 days* [mm], *mean temperature of the last day* [°C] and *mean temperature over the last*

7 days [°C]. *Initial fire behavior* influences the three Indices of the CFFWIS, namely *Fine Fuel Moisture Code* (*FFMC*), *Initial Spread Index* (*ISI*) and *Build-up index* (*BUI*).
The BN for fire occurrence (Figure 1) is included in the BN for fire behavior. The variable land cover, which is used for predicting the fire occurrence rate, is also influencing the burnt area directly. However, the node *LC grouped* is introduced to group the land cover types grouped in fewer classes. This reduces the number of free parameters of the variable burnt area and facilitates the parameter learning with hidden variables.

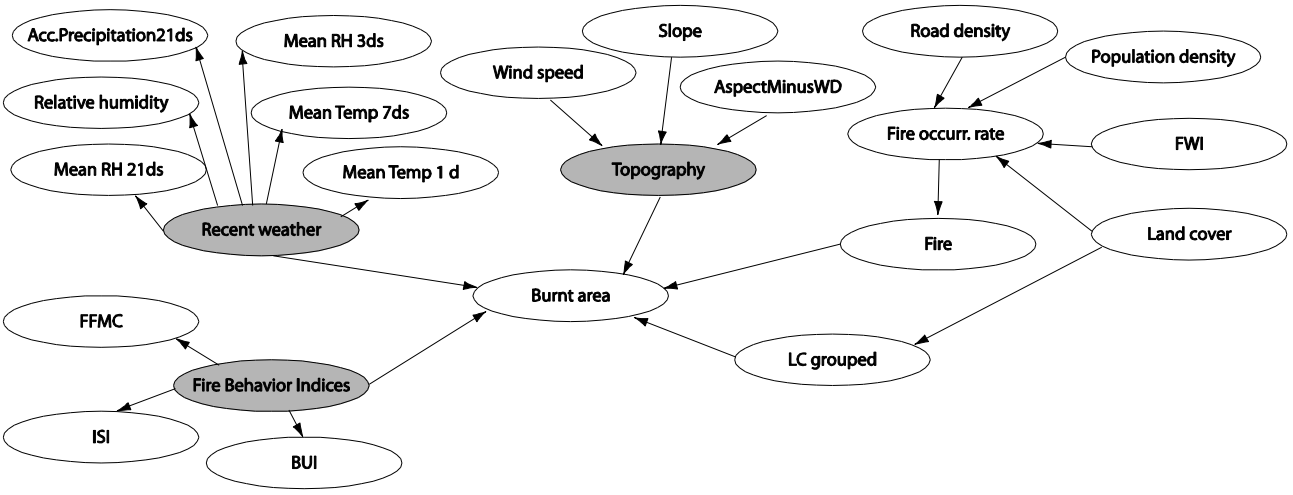

Figure 2. Bayesian network for the prediction of Burnt area. Hidden variables are shown in grey. Indices of the CFFWIS - FWI: Fire Weather Index, FFMC: Fine Fuel Moisture Code, ISI: Initial Spread Index, BUI: Built-Up Index.

2.4. Fire consequences model

The fire consequences model estimates the house damage cost and the restoration cost for vegetated areas. The cost is a function of the hazard characteristics, and the consequences that might occur. Wildfire consequences are a function of vulnerability and exposure of the affected biotic and abiotic systems (e.g. human properties, infrastructure, soil and air quality). Vulnerability describes the degree of expected damage as a function of hazard intensity (UNDRO 1991, Thywissen 2006). Exposure refers to the items at risk, such as house density.
Risk is the expected consequences of wildfires and can be formulated as a function of the hazard H, the resulting damages D and the consequences C as,

$$R = \mathrm{E}_{H,D}[C] = \int_H p(H) \int_D p(D|H) C(D,H) dD\, dH \qquad (6)$$

$\mathrm{E}_{H,D}$ denotes the expected value with respect to H and D. $p(D|H)$ is the probability distribution of damage D conditional on the hazard H, i.e. it describes the vulnerability, and $\mathrm{C}(D,H)$ is the cost as a function of damage and hazard. The inner integral in Eq. (6) describes the expected consequences for a given hazard:

$$\mathrm{E}_D[C \mid H] = \int_D p(D|H)\, C(D,H) dD \qquad (7)$$

In the consequence model, the expected costs conditional on hazard characteristics $E_D[C \mid H]$ are estimated.

We introduce a model to estimate wildfire consequences on house damage and vegetated area damage (Figure 3). The model is based on the assumption that consequences are influenced by the exposure of the items to fire, the flammability of the items and the suppression effectiveness. As with the fire occurrence and behavior models, the modeling is conducted at the mesoscale.

The variables that describe the hazard H, and which are outputs of the fire occurrence and behavior models, are *Burnt area detailed*, *Fire type and FWI*. *Fire type* can be a surface fire with flame length <3.5m, surface fire with flame length >3.5m and crown fire. Burnt area is here expressing wildfire severity.

Vulnerability is expressed by the suppression effectiveness and the damage on houses and vegetated areas (nodes *House damage*, *Area damage* and *Construction type*). The node *Fire Containment in 24 hrs* and its parents represent the probability of a fire being contained by the firefighting crews within 24 hrs. *Fire containment in 24 hrs* is influenced by *FWI*, *Time for ground attack, Air suppression* and *Vegetation type*. The nodes influencing the vulnerability variable *Fire containment in 24 hrs* are based on (Plucinski *et al*. 2012, Plucinski 2012), where fire containment is the dependent variable and the parameters are defined as a result of logistic regression analysis (Table 1). The probability P of fire containment in 24hrs is defined as,

$$\ln\left(\frac{P}{1-P}\right) = b_0 + b_1 FFDI + b_2 groundtime + b_3 airtime \quad (9)$$

wherein *FFDI* is the McArthur Forest Fire Danger Index, $groundtime$ is the time needed for ground suppression crews to reach a fire spot and $airtime$ is the corresponding time for air suppression crews.

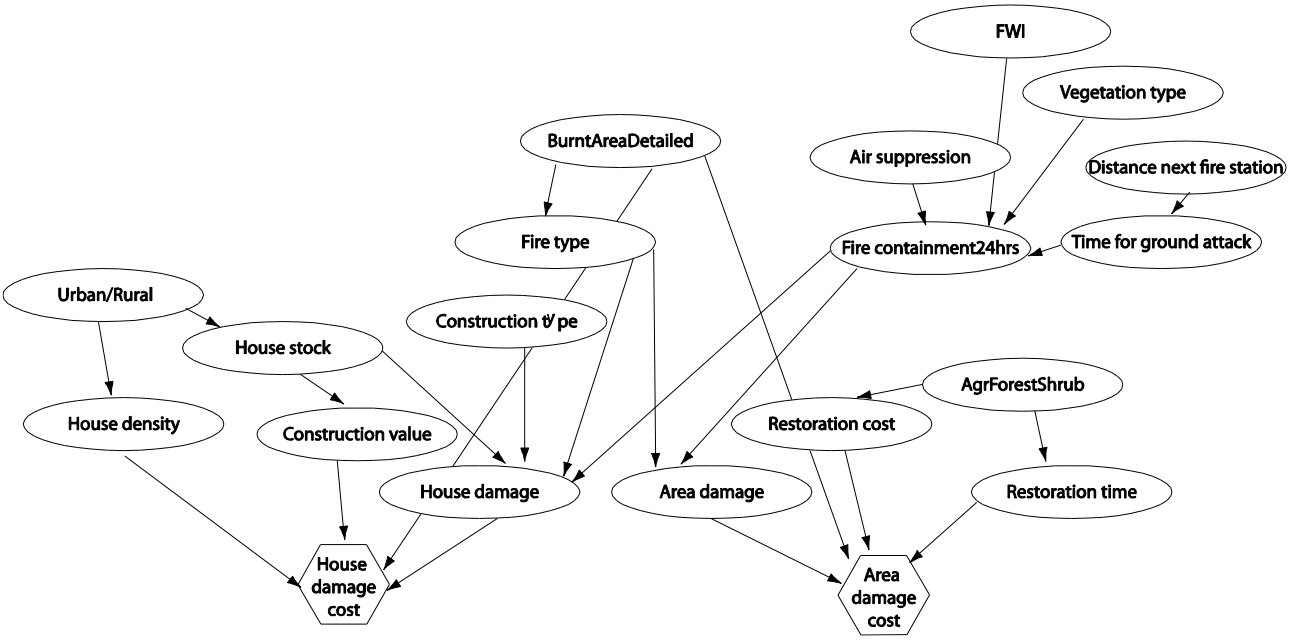

Figure 3. Bayesian network for fire consequences

The vulnerability node *House damage* represents the degree of damage, i.e. the susceptibility of the house portfolio in the cell. The vulnerability is influenced by *Fire type*, *Fire containment in 24 hrs*, *Construction type* and *House stock*. It is expressed as percentage of houses totally damaged in 1 km².

The node *Area damage* is the corresponding vulnerability node for the vegetated area damage. It represents the degree of damage in 1 km². It is expressed as a percentage of the total area (1km²).
Urban/Rural, *House Stock*, *Construction Value*, *House Density*, *Land Cover types*, *AgricultureForestShrub*, *Restoration cost*, *Restoration time* are considered as exposure indicators. *Urban/Rural* discriminates urban from rural areas, which influences the house density [house/km²] and the house stock. *House stock* accounts for the house type portfolio in the mesoscale. It describes the combination of house types in 1km², which include single houses, semi-detached/row houses, and apartments. The node House damage cost is calculated as

$$\begin{aligned} &House\ damage\ cost \\ &= Burnt\ area \cdot House\ damage \cdot Construction\ value \cdot House\ density \end{aligned} \tag{10}$$

The node *Land Cover types*, represents the land cover types as classified in the nomenclature of the Corine Land cover types. The node *AgricultureForestShrub* classifies the land cover types based on the vegetation type. *Restoration cost* [€] is the cost for restoring previous land cover based on premiums paid country wise by the EU Rural Development Programs. *Restoration time* [yrs] is the time needed for restoring previous land cover type (Oehler *et al*. 2012). The node *Area damage cost* is calculated based on results in (Oehler, Oliveira *et al*. 2012) as

$$\begin{aligned} &Area\ damage\ cost = \\ &Burnt\ Area \cdot Area\ damaged \cdot Restoration\ cost \cdot (1+r)^{Restoration\ time} \end{aligned} \tag{11}$$

where $r = 3\%$ is the discount rate.

Table 1. Fire Containment in 24hrs: regression parameters (Eq.9) (Plucinski et al. 2012), (Plucinski 2012)

Vegetation Type	Suppression	b_0 intercept	b_1 F/G FDI	b_2 ground time	b_3 air time
grass	ground	2.41124	−0.02454	−0.51708	
forest	ground	1.168703	−0.024632	−0.20104	
shrub	ground	1.664122	−0.019558	−0.282204	
grass	ground&air	4.80436	−0.042789	−0.66977	−0.3253
forest	ground&air	3.83561	−0.05031	−0.29845	−0.34783
shrub	ground&air	3.75257	−0.03704	−0.3184	−0.08101

2.5. Fire risk model

The Fire risk model of Figure 4 is obtained as the combination of the fire occurrence model, the fire behavior model and the fire consequences model. This model predicts the risk to Houses and vegetated areas.

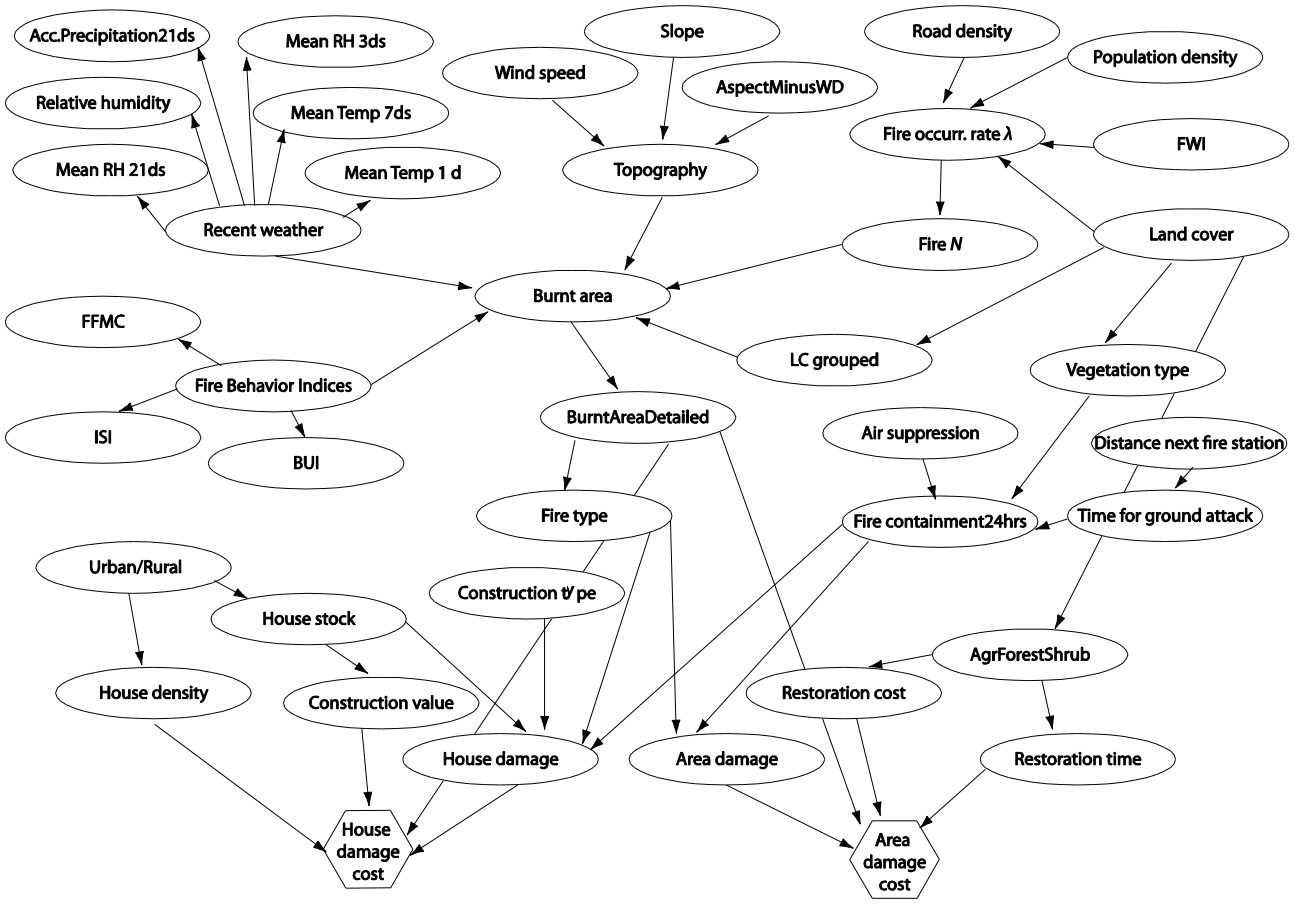

Figure 4. Combined Bayesian network for fire risk.

The BN is coupled with a GIS. Spatial feature groups, such as points, lines and polygons, are processed, stored and managed in a GIS database. Georeferenced spatial features are projected onto a grid with 1 km² cell size, which serves as the spatial resolution of the model. The geospatial features are associated with variables in the BN. In each cell, an instance of the BN models the wildfire risk. With the specific geospatial features associated with a cell, the wildfire risk associated to that cell can be calculated from the BN model. Spatial dependence is represented through the dependence of the observed indicator variables, but not through the BN itself. ArcGIS 10.1 is used for geospatial analysis and mapping (ESRI 2012).
The parameters of the exposure indicators are learned with the attribute data of the geospatial features. Evidence (information on the observed variables) is given on the hazard characteristics and exposure indicators and is propagated in the network and the posterior marginal distributions for each variable are estimated.

Testbed implementation

The BN model is established for Cyprus. The conditional probability distributions of the BN variables are populated with data from the time period 2006-2009, regression model results and expert knowledge. Data from 2010 for Cyprus are used as verification dataset. The results are shown in daily maps with 1 km² spatial resolution.
Figure 5 and Figure 6 exemplarily show the estimated expected damage cost (risk) for the two days of 2010 that had the maximum number of registered fires. The figures differentiate between house risk,

vegetated area risk and the accumulated risk. The calculated FWI with 1km² spatial resolution for each day is displayed as well. The risk in each spatial-temporal unit is low due to the low probability of fire occurrence (in the order of 10^{-5}). In both examples, the highest values of risk occur in wildland-urban interface areas.
The effect of different influencing variables on the probability of fire occurrence is shown inTable 2. For fire behaviour, Table 3 summarizes the effect of the direct influencing variables on the probability of a burnt area > 0.1 km².

Table2. Effect of influencing variables on fire occurrence probability

Variable	States	Pr(Fire) Prior: 9.45e-5	Change in Probability [%]
FWI	0-10	4.50e-5	-52
	10-30	7.22e-5	-24
	30-60	1.60e-4	+70
	60-120	2.82e-4	+199
LandCoverTypes	1 : Urban/Wetland/Pastures	2.17e-5	-77
	2: Arable land	2.72e-5	-71
	3: Permanent crops	1.33e-4	+40
	4: Heterogeneous agriculture	8.31e-5	-12
	5: Forests	1.80e-4	+91
	6: Shrubs/Herb. vegetation	9.34e-5	-1
	7: Open spaces	2.21e-4	+133
Population density	0-20	7.81e-5	-17
	20-300	7.78e-5	-18
	300-4000	3.21e-4	+240
Road density	0-0.5	9.36e-5	-1
	0.5-2	7.35e-5	-22
	2-26	1.16e-4	+23

Table3. Effect of influencing variables on burnt area

Variable	States	Pr(BurntArea>0.1) Prior=1.70e-5	Change in Probability [%]
LCgrouped	1,4,6	1.65e-5	-3
	2,3,5	1.56e-5	-8
	7	6.54e-5	+284
Topography	1:middle	1.97e-5	+16
	2:gradual	8.59e-6	-50
	3:steep	2.88e-5	+69
Recent weather	1: dry	2.49e-5	+46
	2: moderate dry	1.82e-5	+7
	3: moderate humid	1.28e-5	-25
	4: humid	1.12e-5	-34
Fire behavior indices	1: moderate	1.78e-5	+4
	2: low	1.35e-5	-21

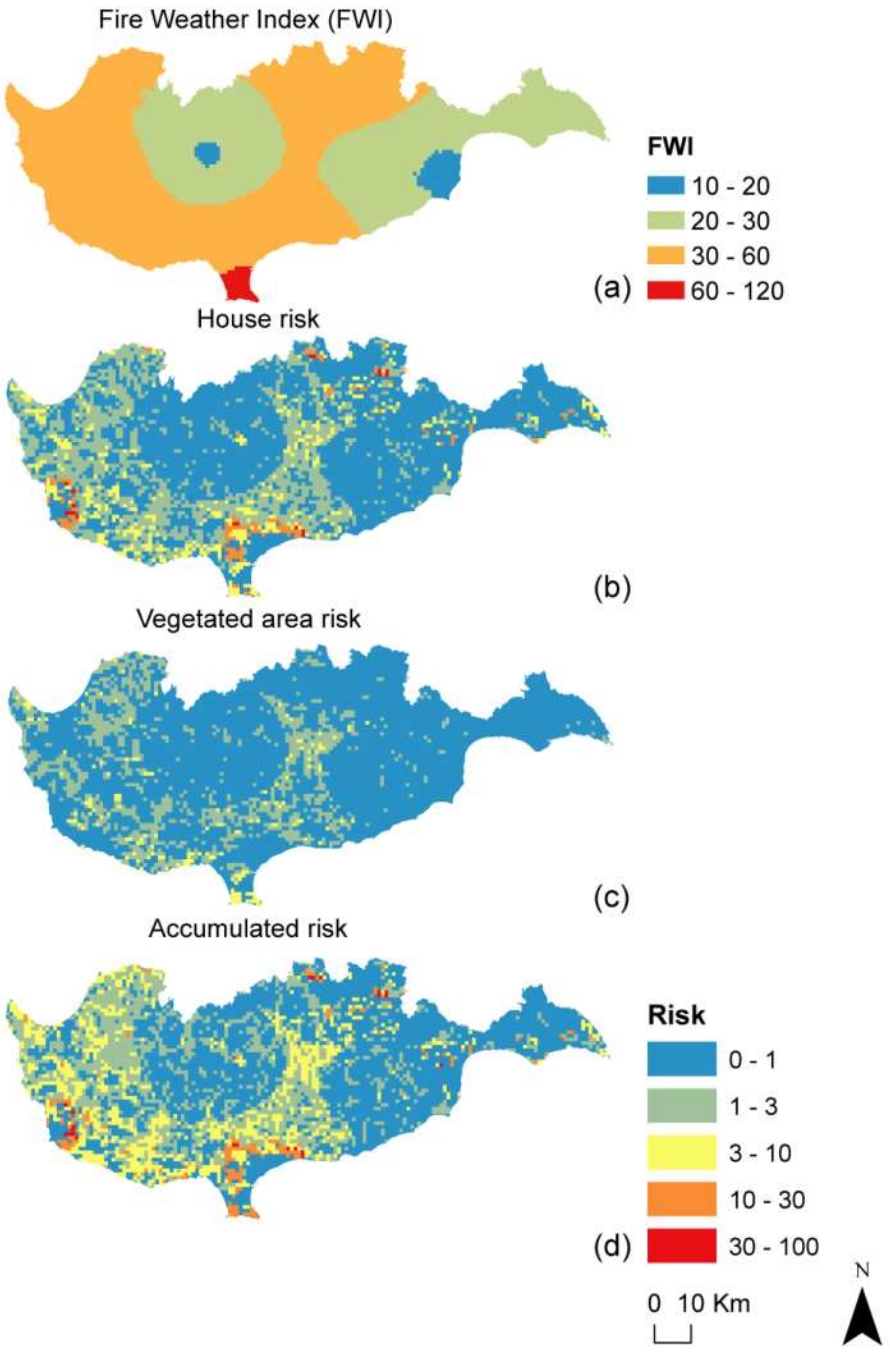

Figure 5. (a) Fire Weather Index (FWI), (b) House risk, (c) Vegetated area risk, (d) Accumulated risk on 08.10.2010

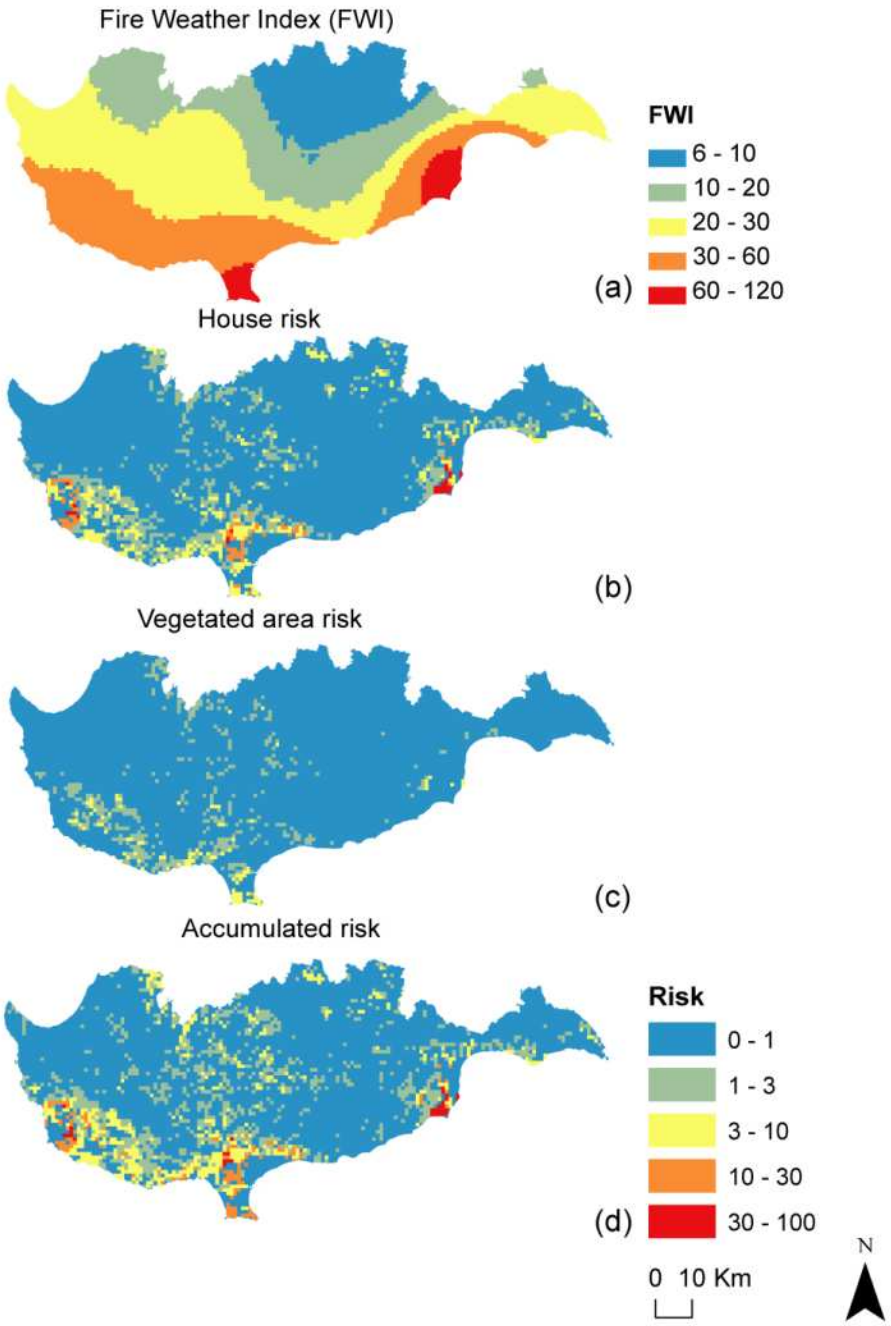

Figure 6. (a) Fire Weather Inx (FWI), (b) House risk, (c) Vegetated area risk, (d) Accumulated risk on 26.06.2010

Concluding remarks

While the understanding and prediction of wildfire occurrence has made significant progress in recent years, research on wildfire risk estimation based on exposure and vulnerability quantification is still evolving (Tutsch *et al*. 2010). Wildfire risk estimation may be facilitated by Bayesian Networks, which, as demonstrated in this paper, can be employed to model the wildfire risk in the mesoscale. The mesoscale requires that the indicators included in the model are representative for a 1 km² spatial

unit. This has strong implications on the modelling; as an example, it is necessary to identify representative building stocks and construction types not of individual buildings, but of portfolios of buildings. A main advantage of the BN is that different models from different sources can easily be combined. Of the BN for wildfire risk proposed in this paper, some parts are learned from data, some parts are derived from models published in the literature and other parts are based on expert knowledge. The graphical nature of the BN facilitates to consistently combine these model parts probabilistically and, not least, also facilitates the communication of the final model.

References

Cohen, J. D. (2000). "Preventing disaster: Home ignitability in the wildland-urban interface." Journal of Forestry 98(3): 15–21.

ESRI (2012). ArcGIS 10.1. ESRI (Environmental Systems Resource Institute), Redlands, California, US.

Forestry Canada, F. D. G. (1992). Development and Structure of the Canadian Forest Fire Behavior Prediction System. Information Report ST-X-3. S. a. S. D. D. Forestry Canada. Ottawa, Canada: 63.

Keeley, J. E., W. J. Bond, R. A. Bradstock, J. G. Pausas and P. W. Rundel (2012). Fire in Mediterranean ecosystems: Ecology, evolution and management. Cambridge, Cambridge Univ. Press.

Oehler, F., S. Oliveira, J. I. Barredo, A. Camia, J. SanMiguel-Ayanz, D. Pettenella and R. Mavsar (2012). Assessing European wildfire vulnerability. European Geoscience Union General Assembly 2012. Vienna, Austria.

Papakosta, P. and D. Straub (2014). "Probabilistic prediction of daily fire occurrence in the Mediterranean based on weather and anthropogenic factors." submitted.

Plucinski, M., G. McCarthy, J. Hollis and J. Gould (2012). "The effect of aerial suppression on the containment time of Australian wildfires estimated by fire management personnel." International Journal of Wildland Fire 21(3): 219-229.

Plucinski, M. P. (2012). "Factors affecting containment area and time of Australian forest fires featuring aerial suppression." Forest Science 58(4): 390-398.

Thywissen, K. (2006). Core terminology of disaster reduction: A comparative glossary. Measuring vulnerability to natural hazards. J. Birkmann. Tokyo, Japan, United Nations University Press: 448–496.

Tutsch, m., W. Haider, B. Beardmore, K. Lertzman, A. B. Cooper and R. C. Walker (2010). "Estimating the consequences of wildfire for wildfire risk assessment, a case study in the southern Gulf Islands, British Columbia, Canada." Canadian Journal of Forest Research(40): 2104–2114.

UNDRO (1991). Mitigating natural disasters: phenomena, effects and options.: A manual for policy makers and planners. Geneva, (UNDRO, Office of the United Nations Disaster Relief Co-Ordinator).

Zwirglmaier, K., P. Papakosta and D. Straub (2013). Learning a Bayesian network model for predicting wildfire behavior. Proceedings of the 11th International Conference on Structural Safety & Reliability.

Exploring the capability to forecast wildfires: spatial modelling of the Tavira/São Brás de Alportel 2012 wildfire

Renata Machado dos Santos Pinto[a], Ana Sá[a], Akli Benali[a], José Miguel Cardoso Pereira[a], Paulo M. Fernandes[b]

[a] *Centro de Estudos Florestais, Tapada da Ajuda, Instituto Superior de Agronomia, 1349-017 Lisboa, Portugal, renatamspinto@sapo.pt*
[b] *Centro de Investigação e de Tecnologias Agro-Ambientais e Biológicas, Universidade de Trás-os-Montes e Alto Douro (UTAD), Apartado 1013, 5001-801 Vila Real, Portugal*

Abstract
We explore the forecasting capability of two spatially-explicit fire spread models, HFire and FARSITE, and the potential of combining fire spread models and satellite data. A well-documented wildfire that occurred in southern Portugal in July 2012 (approx. 24800ha) is investigated. Accuracy of the fire spread models is evaluated by comparing simulated fire spread perimeters with the reported spatio-temporal distribution of the wildfire event, at three different time steps. Results show good agreement between the simulated and observed burned area perimeters (Sørensen metric). Some differences are found in specific fire propagation time intervals. When simulations are initialized using the reported ignition point, FARSITE progressively shows an underestimation of the fire's time of arrival, whereas HFire shows an overestimation for some time steps. Initializing fire-spread simulations with active-fires ignition points improves time of arrival predictions for some time steps. FARSITE is able to predict abrupt changes in rate of spread and fire line intensity, consistent with the reported information for the wildfire event. Both models show good capability to forecast fire spread. The use of fire spread models with satellite data has great potential since the combination of both improves fire growth and behavior predictions, providing valuable supplementary information to fire management and decision support during large wildfire events.

Keywords*: HFire, FARSITE, fire spread modelling, satellite active-fires, fire suppression, MODIS, fire behaviour*

Introduction

Portugal has one of the highest fire incidences in southern Europe with extreme landscape susceptibility to fire, aggravated during the last four decades due to rural abandonment (Pereira *et al*. 2005). In recent years, catastrophic fires that occurred under extreme weather conditions have challenged the country's fire suppression capabilities.
In Portugal, burnt area extent is mainly controlled by two factors: long dry periods without precipitation in late spring and early summer (climate anomaly), and the occurrence of very intense hot and dry spells in days of extreme synoptic conditions (weather anomaly) and in fact, 80% of the burnt area is due to fire events occurring in 10% of summer days (Pereira *et al*. 2005). During the 2003 fire season, extremely anomalous weather conditions were observed, with a devastating sequence of large wildfires resulting in a total of 450.000ha of burned area, approximately twice the previous highest record (220.000ha in 1998) and four times the 1980-2004 average (Trigo *et al*. 2006). Future climatic scenarios show an increase in fire risk in the Mediterranean basin (Mouillot *et al*. 2002; Moriondo *et al*. 2006; Flannigan *et al*. 2009). In particular, Portugal is expected to experience a temperature increase in spring and summer and an increase in the frequency of heat waves (Ramos *et al*., 2011), likely leading to longer and more severe fire seasons with greater incidence of large uncontrolled wildfires.
Predicting fire spread and behaviour during large wildfire events can greatly improve the efficiency of fire suppression, providing valuable information during firefighting activities enabling more efficient resource allocation and implementation of control lines. One of the most effective tools to study how

the main drivers of wildfire spread and behaviour interact - meteorological conditions, topography and vegetation - is fire spread modelling (Keane *et al*. 2004).
Recently, some authors have also explored the potential of satellite data to monitor large wildfire events (Smith *et al*. 2005; Loboda *et al*. 2007). For example, the MODerate Resolution Imaging Spectroradiometer sensor (MODIS) has been integrated in operational systems to assist fire managers detecting active-fires that are burning at the time of overpass (Lee *et al*., 2002), providing inter- and intra-daily spatio-temporal distributions of individual wildfire events propagation, which is usually done by post-fire collection of field data and interviews. Coen & Schroeder (2013) have used spatially remote sensing data to initialize and evaluate coupled weather-wildfire growth model simulations, with improved results from this approach arising from initialization with more current weather analyses and updated maps of fire location.
In this paper, we explore the capability of two spatially-explicit landscape fire spread models - HFire (Petersen *et al*. 2009) and FARSITE (Finney 1998) - to forecast fire spread and behavior during a large fire event, and the advantage of combining fire-spread modelling with satellite data. Inaccuracies in input data (e.g. maps of surface fuels developed without field validation; inaccurate estimates of canopy cover and crown characteristics) produce errors that propagate during simulations. Combining simulations with satellite-derived active-fires from consecutive MODIS passages can help overcome some of these errors, since simulations are updated in space and time at each passage. The feasibility of these approaches is examined based on the analysis of a well-documented wildfire that occurred in Tavira, southern Portugal in July 2012 (Tavira wildfire hereafter). The performance of both fire spread models is evaluated by comparing the observed fire perimeter with the simulated fire perimeters and the temporal distribution of the Tavira wildfire, derived from the information reported for the event. A performance assessment from the combined use of both tools is also performed.

Methods

Fire spread models

HFire (Highly Optimized Tolerance Fire Spread Model) (Morais 2001) is a computationally efficient raster-based fire growth model capable of simulating surface fire spread (Rothermel 1972) through shrubland fuels. HFire uses an adaptive time step allowing for the fire to spread into a cell from all neighbouring cells over multiple time steps (contact-based approach). It has been developed to support simulations of single fire events and long-term fire regimes (Petersen at al. 2009; Petersen *et al*. 2011).
FARSITE (Fire Area Simulator) is a two-dimensional deterministic fire growth and behaviour model, developed by the USDA Forest Service, and widely used to simulate wildfire spread (e.g. Keane *et al*. 2001; Stratton 2004; Loureiro *et al*. 2006; Arca *et al*. 2007). FARSITE incorporates a surface fire spread model (Rothermel 1972), and additional crown fire spread, spotting, post-frontal combustion and fire acceleration models. The spatial growth of fire perimeters is based on Huygens' Principle of wave propagation (Finney 1998).

Model inputs and parameters

The variables required for modelling an individual fire event are similar in both fire spread models (Table 1).

Table 1. List of input variables and outputs for FARSITE and HFire landscape fire spread models.

Inputs types	HFire	FARSITE	
Landscape (GIS layers)	Elevation (m) Slope (º) Aspect (º) Fuel (categories)	Latitude (º) Elevation (m) Slope (º) Aspect (º) Fuel (categories)	Canopy cover (%) Canopy height (m) Canopy base height (m) Canopy bulk density (kg m^{-3})
Fuel	Fuel model Fuel moisture (10-hr, live herbaceous, live woody) (%)	Fuel model, Fuel rate of spread adjustment Fuel moisture (1-hr, 10-hr, 100-hr, live herbaceous, live woody) (%)	
Weather		Precipitation (mm) Relative humidity (%) Temperature (ºC) Cloud cover (%)	
Winds	Wind speed (km h^{-1}) Wind direction (º)	Wind speed (km h^{-1}) Wind direction (º)	
Ignition	Ignition point	Ignition point	
Outputs	Burned area Time of arrival (hours)	Fire perimeters Fire behavior parameters: Time of arrival (hr); Fire line intensity (kW m^{-1}); Flame length (m); Rate of spread (m min^{-1}); Heat per unit area (kJ m^{-2}); Reaction intensity (kW m^{-2}) Crown-noCrown (cat.); Spread direction (cat.)	

Aspect, elevation and slope maps were derived from the Digital Elevation Model provided by the Shuttle Radar Topography Mission (90m resolution). Canopy cover was derived from the MODIS tree cover dataset (250m resolution) (DiMiceli *et al*. 2011).
Fuel maps consisting of the 13 fire behavior fuel models (Anderson 1982) were produced by the Tavira and São Brás de Alportel municipalities, for the Municipal Forest Defense Plan Against Fires.
In order to have the most representative wind data at the time of the fire, wind speed and direction were obtained from the ENEOP2-MJ250 (Exploração de Parques Eólicos SA) station (Viegas *et al*. 2012). WindNinja (Forthofer *et al*. 2009) was used to model the prevailing hourly wind inputs, simulating the spatially varying wind fields given the effect of topography. The meteorological data used in this study was collected from the Faz Fato weather station (http://www.wunderground.com/). Temperature, relative humidity and precipitation were summarized on a daily basis, using the time of maximum and minimum temperature. Cloud cover was assumed to be zero for the entire simulation period.
Reference values for live fuel moisture in the dry season for chaparral fuels (Morais 2001) were used for live herbaceous and woody fuels, 50% and 70 % respectively, in both models. The 10-hr dead fuel moisture, required by HFire in an hourly basis, was estimated using an algorithm based on Nelson's dead fuel moisture model (Nelson, 2000), which determines moisture content of dead and down woody fuels. For FARSITE, initial fuel moistures were set at 5, 8 and 10% for 1-hr, 10-hr and 100-hr dead fuels respectively. These values were empirically derived from the previous estimates for HFire.

2.3. Case Study – background and description

All the descriptive information referred in this section, related with the case study, was obtained from three reports (ANPC 2012; ICNF 2012; Viegas *et al*. 2012). These reports thoroughly describe the development and behavior of the Tavira wildfire event, providing the qualitative and quantitative information necessary to assess the performance of the fire spread models.

The Tavira wildfire occurred between the 18th and 21st of July 2012, in the Tavira and São Brás de Alportel municipalities (Figure 1). It burned approximately 24.800ha, mainly through shrubland (61% of the affected area), and was one of the largest fires recorded in the last years.

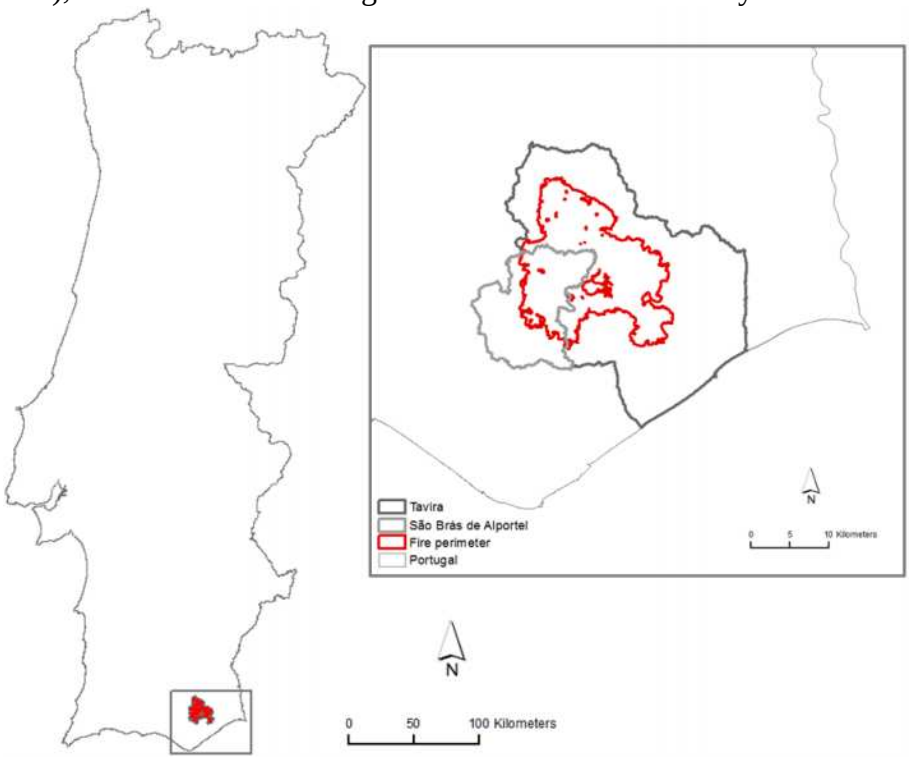

Figure 1. Location of the Tavira Wildfire occurred in July 2012 (Portugal)

The area affected by the fire is orographically heterogeneous, with steep slopes (>20%) covering most of the area and higher elevation in the north part of the Tavira municipality. Less steep terrain (between 0 and 20%) and lower elevation are found at the southeast area of Tavira and southwest area of the São Brás de Alportel municipality, reaching zero meters at several locations (Figure 2). Maximum temperature presents annual mean values between 10°C and 22°C, ranging from 25°C to more than 30°C in August, with maximum absolute temperatures around 39°C. In the summer, relative humidity registers mean values below 65%.

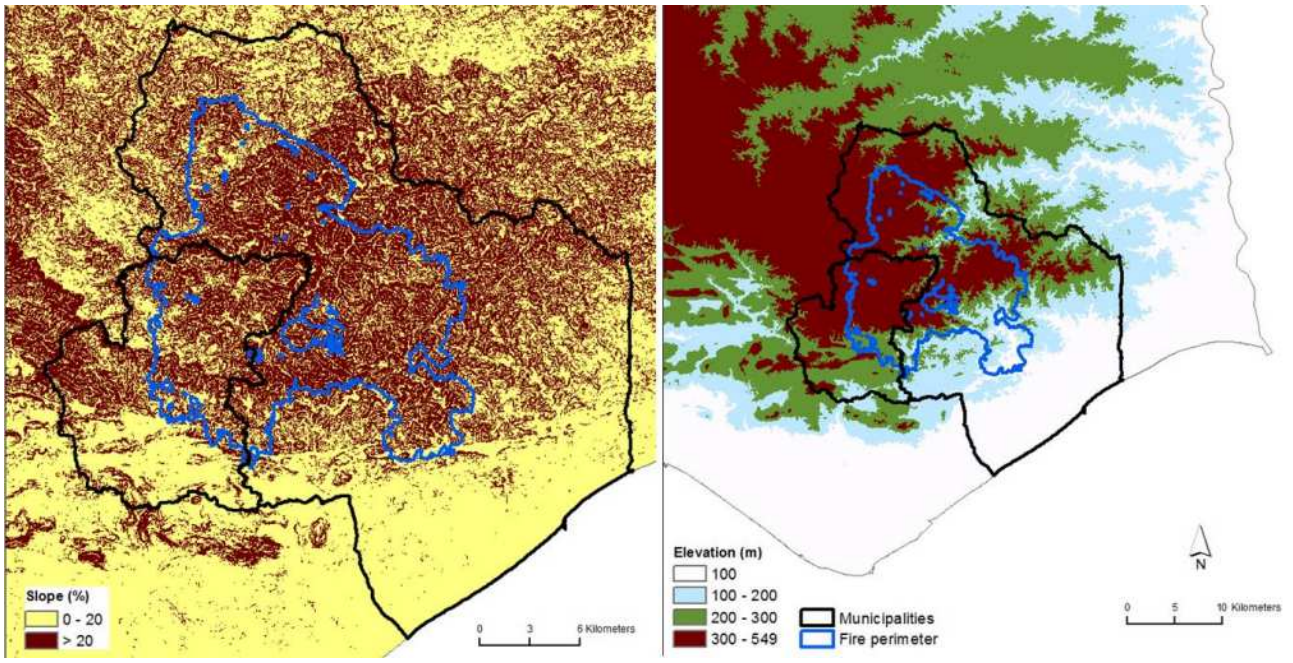

Figure 2. Slope and elevation maps of the study area

In 2012, the precipitation was 45% below the normal record and all the study area was in extreme drought condition, with a soil water content value below 10% at the time of the fire. The vegetation moisture content was estimated to be less than 80% for woody fuels, from 5 to 7% for fine fuels, and no higher than 7% for herbaceous fuels. In addition, the years of 2010 and 2011 experienced above average precipitation favoring vegetation growth and fuel build up. Fire danger as per the Canadian Fire Weather Index (FWI) System was *Extreme* with FWI=56.7 as the average for the most active period of the fire.

The Tavira wildfire was first reported at 14h10 July 18th, contained at 17h46 on July 21st and considered completely extinguished on July 27th. Two important stages for our analysis are identified and will be briefly described.

First stage – Initial development, from 14h10 July 18th to 18h00 July 19th (approx. 28 hours)

The fire burned approximately 5000ha (approx. 20% of total burned area) under favorable conditions for fire spread: fuel moisture was very low, allowing for embers (projected up to hundreds of meters) to ignite and result in multiple spot fires; weak wind but highly variable in direction, causing the fire to spread in every direction and making the initial attack difficult. Fire suppression was hampered by the unfavorable steep, rugged terrain. The unfavorable steep, rugged terrain hampered fire suppression. The fire started spreading through steep slopes along the Ribeira de Odeleite basin (Figura 3).

Second stage – conflagration with very fast spread towards south, from 18h00 July 19th to 1h00 July 20 (approx.7 hours)

The fire reached the Ribeira de Odeleite basin and turned into a major conflagration, turning fire suppression extremely difficult. Several factors led to this loss of control. Reaching Ribeira de Odeleite, the fire increased its intensity by aligning with canyons and steep slopes, spreading alongside the basin. An increase in wind speed led to fast and intense fire growth towards south with a 10km fire front with two advanced fronts heading west and east to the São Brás de Alportel and the Tavira municipalities respectively. Spotting occurred up to two kilometers from the fire front. Fire spread between this stage and the final southern limit in approximately 7 hours.

2.4. Simulation framework

The spatial resolution of the gridded data was set to 100 meters and the temporal resolution was set to 1 hour time step for both models. Fire suppression activities were not simulated in either model. In

FARSITE, fire acceleration and No-Wind No-Slope rate of spread for the spread rate of backing fires, were enabled during simulations. Rate of spread adjustment was set to 1.0 (no adjustment). Three different time steps (Table 2), i.e. burning periods are simulated, based on the documented Tavira wildfire development and behavior (Figure 3).

Table 2. Time steps used to evaluate FARSITE and HFire performances.

Time step	Time of arrival	Milestones
1	2012-7-19 18h00	The fire reached Ribeira de Odeleite
2	2012-7-19 21h00	Blow-up fire behavior, until the fire front reached the area burned in 2009
3	2012-7-20 1h00	The fire reached its south limit

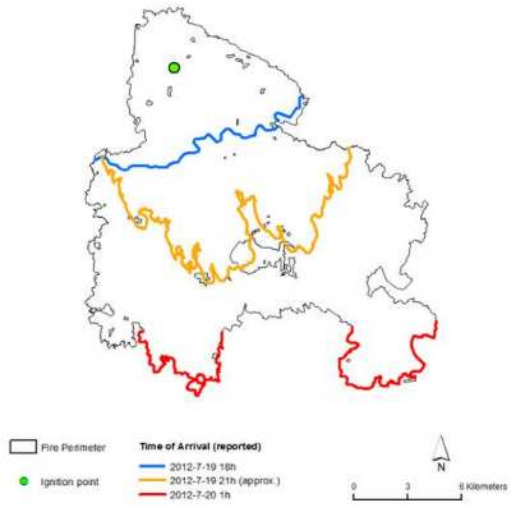

Figure 3. Spatial representation of the fire's time of arrival, for the three defined time steps (Time step 1 corresponds to Ribeira de Odeleite)

Three simulations were performed for both fire-spread models: simulation 1 - initialized at the reported ignition point (start: 2012-7-18 14h); simulation 2 and 3 – initialized with satellite-derived active-fires ignition points from MODIS passages (start: 2012-7-18 22h and 2012-7-19 14h, respectively).

2.5. Simulations performance assessment

The performance of the fire simulations was assessed both spatially and temporally, using the observed burned scar fire perimeter (ICNF 2012) as reference. We used the Sørensen coefficient (Legendre and Legendre, 1998) which indicates the exclusive association between the simulated and the reference burned areas (Eq. 1):

$$SC = \frac{2a}{(2a + b + c)} \quad \text{(Eq. 1)}$$

where *a* is the intersection of the burned area in the two models, *b* is the area burned exclusively by the model, and *c* the area exclusively burned in the actual event. A value of 1.0 indicates perfect agreement.

Other descriptors used to evaluate fire spread simulations performances were the time of arrival (TOA), rate of spread (ROS) and fire line intensity (FLI). FLI is commonly used as a measure of fire suppression capacity (Andrews and Rothermel 1982).

Results and discussion

The Tavira wildfire spread mainly towards southeast, with winds from northeast, which is clearly observed in the simulations performed with FARSITE (Figure 4) and HFire (Figure 5). However, both models underestimated the burned area in the west part. The wind forecast predicted winds from east, which was not reflected in the wind data used to simulate the event and can explain the lack of burn in the west flank of the fire.

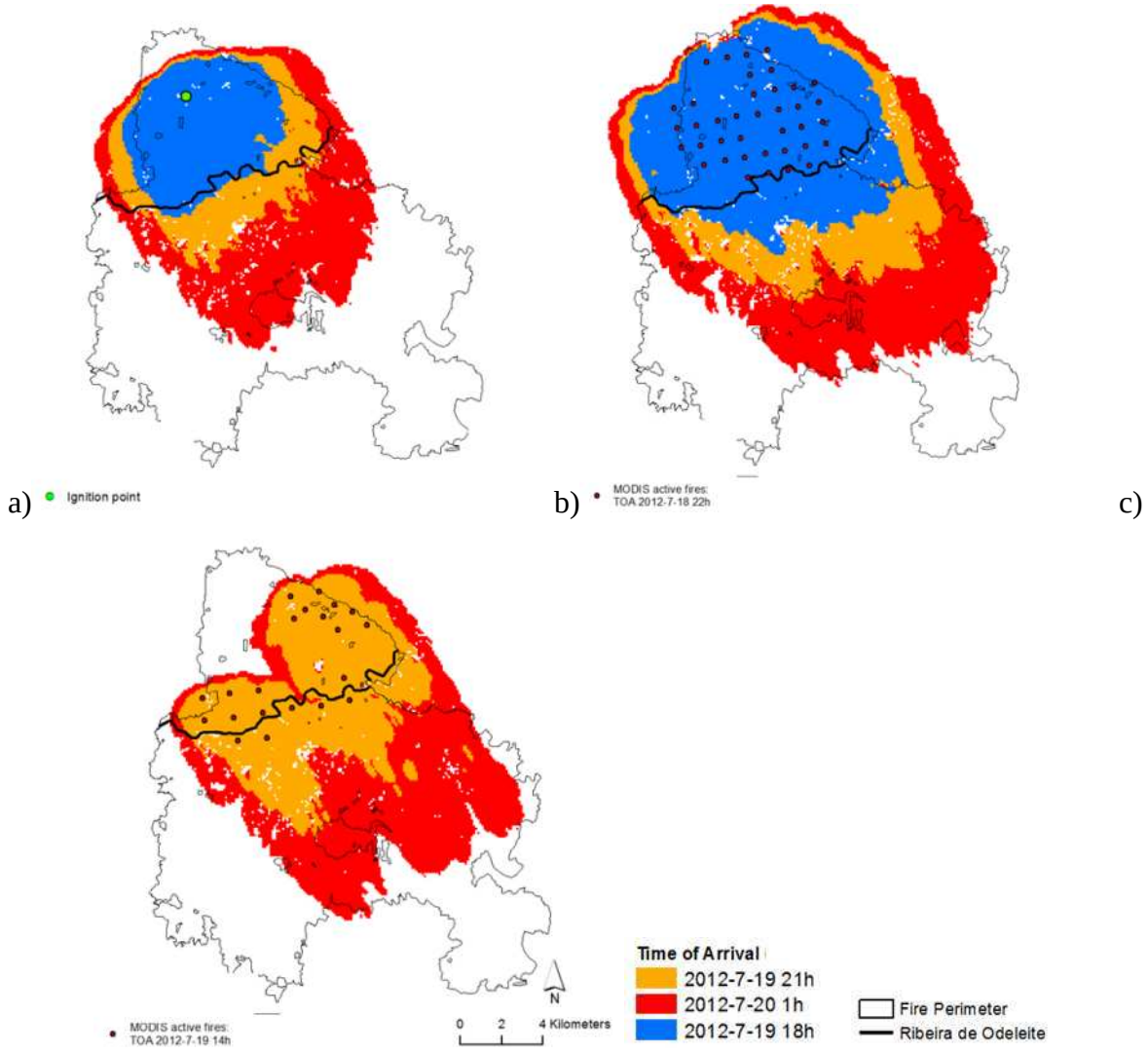

Figure 4. Spatial representation of the simulated time of arrival at the different time steps, using FARSITE. a) Simulation 1 - initialized at the reported ignition point (start: 2012-7-18 14h); b) Simulation 2 - initialized with satellite-derived active-fires ignition points (start: 2012-7-18 22h); c) Simulation 3 - initialized with satellite-derived active-fires ignition points (start: 2012-7-19 14h).

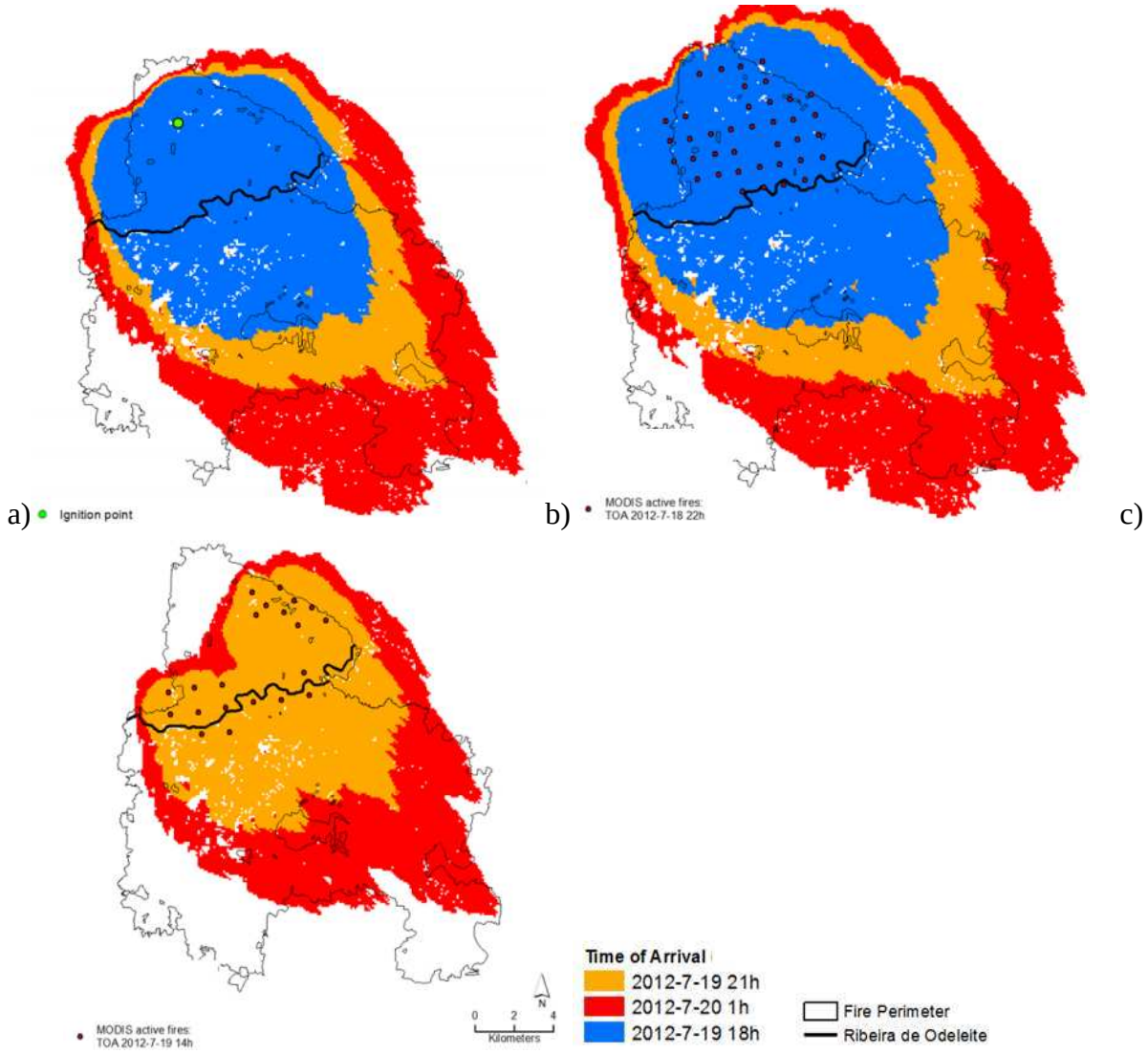

Figure 5. Spatial representation of the simulated time of arrival at the different time steps, using HFire. a) Simulation 1 - initialized at the reported ignition point (start: 2012-7-18 14h); b) Simulation 2 - initialized with satellite-derived active-fires ignition points (start: 2012-7-18 22h); c) Simulation 3 - initialized with satellite-derived active-fires ignition points (start: 2012-7-19 14h).

To evaluate FARSITE and HFire performances, the spatial and temporal agreement between the three time steps of the Tavira wildfire (Table 2, Figure 3) are compared with the three time steps obtained for each simulation with both models.

FARSITE's simulations of burned area and TOA are shown in Figure 4. FARSITE's simulation 1 shows good agreement between the simulated and observed TOA for time step 1, but both estimated TOA for time steps 2 and 3 were underestimated. As expected, starting simulation 2 with active-fires ignition points from the MODIS passage at 22h00 July 18th, improved the estimated TOA of time step 2, now equivalent to the observed TOA for the Tavira wildfire, but continued to underestimate time step 3. Starting simulation 3 with active-fires ignition points from the MODIS passage at 14h00 July19th, underestimated both the estimated TOA for time steps 2 and 3. These differences are probably due to different fuel models available at the start of each simulation, given that in simulation 2 the fire started spreading mainly through grass (fuel models 1 and 2), and in simulation 3 it began to spread mainly through shrub (fuel model 6). Duguy (2007) and Arca (2005) refer the need to increase the ROS adjustment factor for fuel model 6, in order to tune fire spread growth during simulations. Since

this fuel model covers approximately 46% of the area affected by the fire, it can be one of the reasons why all simulations underestimated time step 3, and simulation 3 in particular underestimated time steps 2 and 3.

TOA of time steps 1 and 2 were overestimated for HFire's simulations 1 and 2 (Figure 4). Starting simulation 2 with active fires ignition points from the MODIS passage at 22h00 July 18th, did not change the fire´s time of arrival. Setting the ignition points with active fires from the MODIS passage, at 14h00 July 19th, improved the estimated TOA of time step 2, now equivalent to the observed TOA for the Tavira wildfire, but underestimated time step 3. Again, this underestimation may be related to the fuel type at the ignition location.

The SC values were calculated for each FARSITE and HFire simulations, at the defined times steps (Table 3). Results show good agreement between observed and modeled perimeters for time step 3, for both fire spread models.

Table 3. Values of the Sørensen coefficient for time steps 1, 2 and 3, for the 3 simulations performed with FARSITE and HFire.

		Simulation 1	**Simulation 2**	**Simulation 3**
FARSITE	Time step 1	0.29	0.43	-
	Time step 2	0.41	0.55	0.40
	Time step 3	0.60	0.71	0.68
HFire	Time step 1	0.60	0.61	-
	Time step 2	0.72	0.72	0.53
	Time step 3	0.73	0.68	0.74

Overall results show the best TOA estimates for FARSITE and better SC values for HFire, which was also able to burn into areas that did not burn in FARSITE. When Petersen (2009) compared both models performances, concluded that HFire was better at using narrow corridors to reach additional areas of fuel. While vector-based fire growth models (like FARSITE) produce more realistic fire shapes, raster-based models like HFire can cope better with heterogeneity in fuels and weather (French *et al*. 1990).

For the period between time step 2 and 3, the reported ROS ranged from 20m/min to 25m/min. Figure 6 shows the spatio-temporal variation of the ROS simulated by FARSITE. The simulations predict lower spread rates in the same period. The mean values of ROS for the referred time step, for simulations 1, 2 and 3, were 9 ± 6 m/min, 12 ± 10 m/min, 10 ± 8 m/min respectively. These values are an underestimation of the observed ROS. Nevertheless, simulation 2 presented higher ROS values when compared to simulation 1 and 3. Arca (2005) developed a custom fuel model for shrubland vegetation (maquis) that provided more realistic values of ROS when compared to the values obtained using the standard fuel models. Custom fuel models have also been developed for Portugal (Fernandes *et al*. 2009), and will be considered in future work to produce more realistic ROS estimates.

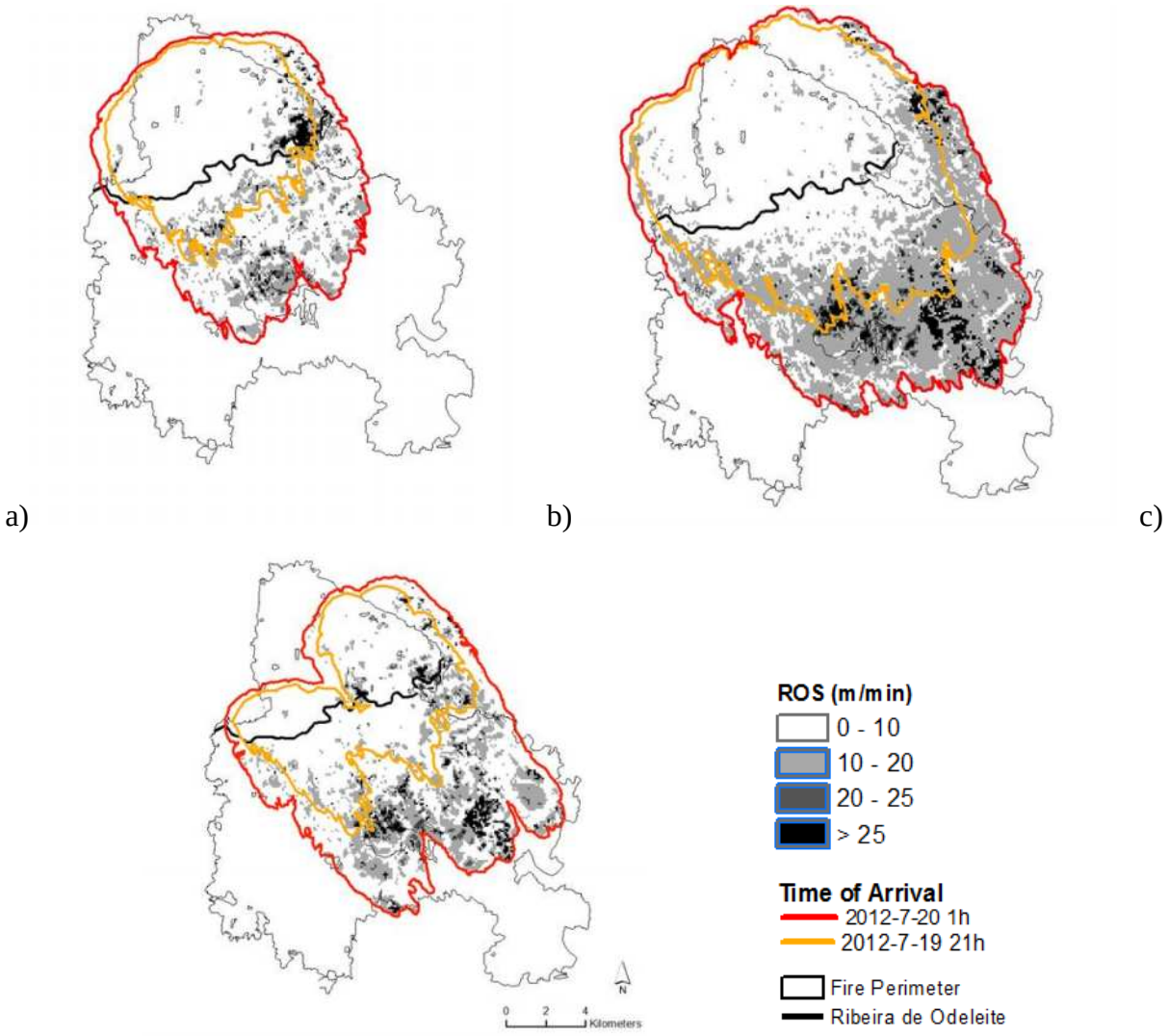

Figure 6. Spatial variation of rate of spread simulated using FARSITE. a) Simulation 1 - initialized at the reported ignition point (start: 2012-7-18 14h); b) Simulation 2 - initialized with satellite-derived active-fires ignition points (start: 2012-7-18 22h); c) Simulation 3 - initialized with satellite-derived active-fires ignition points (start: 2012-7-19 14h).

The Tavira wildfire blow-up behavior, once the fire passed Ribeira de Odeleite is apparent in all simulations, with FLI values simulated by FARSITE generally ranging from 350 to 1750 kW m^{-1} (Figure 7), meaning fires are too intense for direct attack on the head by persons using hand tools and equipment such as dozers, pumpers, and retardant aircraft can be effective.

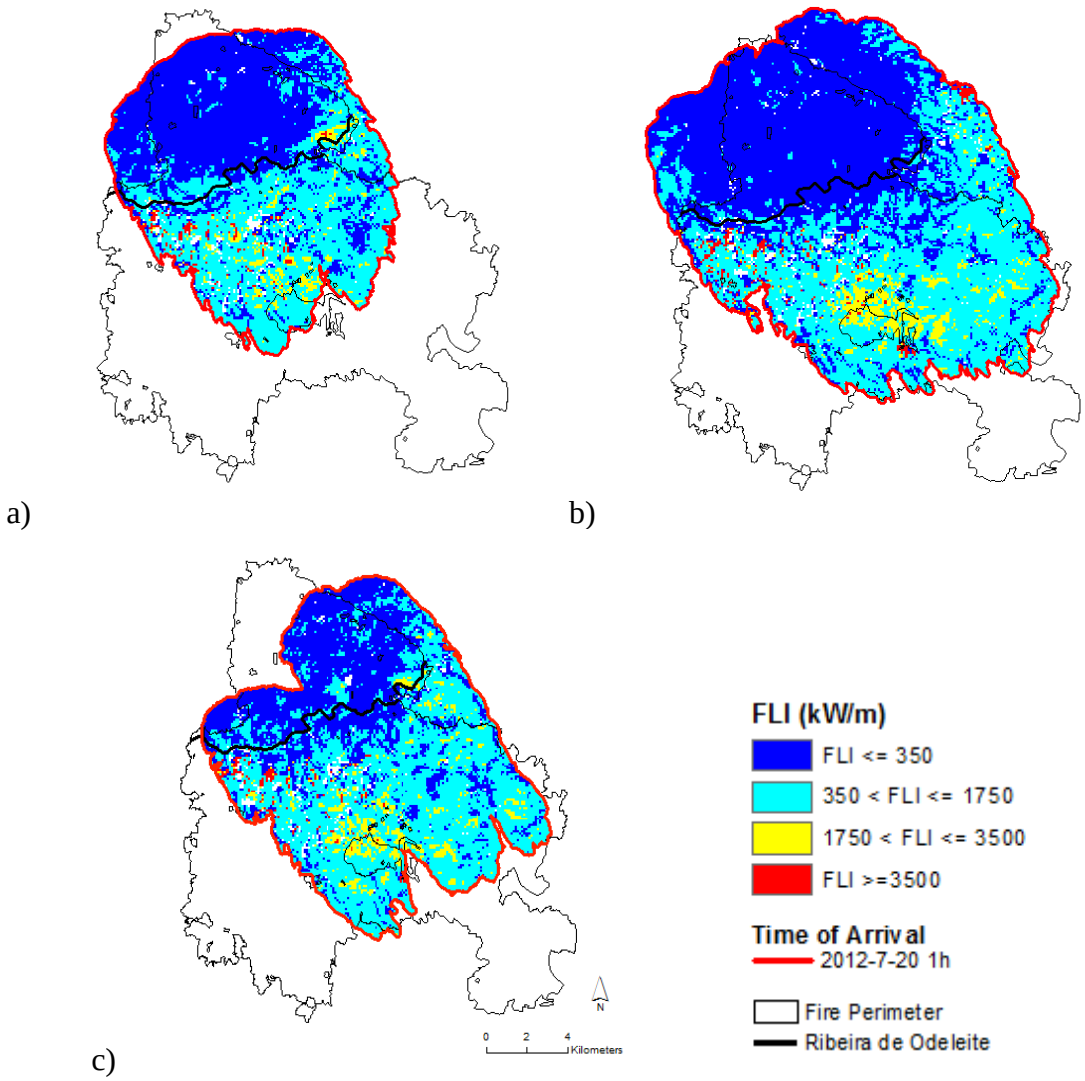

Figure 7. Spatial variation of fire line intensity simulated using FARSITE. a) Simulation 1 - initialized at the reported ignition point (start: 2012-7-18 14h); b) Simulation 2 - initialized with satellite-derived active-fires ignition points (start: 2012-7-18 22h; c) Simulation 3 - initialized with satellite-derived active-fires ignition points (start: 2012-7-19 14h).

Conclusions

In this paper we evaluated the capability of two landscape fire spread models, FARSITE and HFire, to forecast the development of the Tavira wildfire event. A first assessment of the combination of fire spread modelling and MODIS satellite derived active-fires was also performed.

Both fire spread models showed similar estimates regarding fire spread direction and shape. FARSITE produced better time of arrival estimates, i.e. for a given time step, the spatial distribution of the fire front (observed vs. simulated) were similar. HFire presented better Sørensen coefficient values and was also better able to cope with heterogeneity in fuels, reaching additional areas of fuel not burned during FARSITE simulations. However, FARSITE incorporates several other modules other than surface fire spread, taking into account phenomena (crowning and spotting) that play an important role in fire growth during extreme wildfire conditions. It also outputs important fire behavior descriptors

other than time of arrival and burned area. FARSITE was capable of anticipating abrupt changes in rate of spread and fire-line intensity, useful to identify opportunity windows for fire control.
Combining fire spread simulations with satellite-derived active-fires allows splitting a single simulation for the entire duration of the event, into as many simulations as the number of satellite passages, attenuating the errors that propagate throughout a single simulation, since simulations are updated in time and space at each satellite passage. We conclude that this combination improved time of arrival estimates and Sørensen coefficient values for some time steps, presenting great potential for use in near-real time fire spread forecasts.
FARSITE and HFire show good capability to forecast fire spread. The combination of fire spread models with satellite data improves fire growth and behavior predictions, providing valuable supplementary information that can be used in fire management and decision support during large wildfire events.

References

Anderson HE (1982). Aids to determining fuel models for estimating fire behaviour. USDA Forest Service General Technical Report INT-122. Ogden, UT.

Andrews PL, Rothermel RC (1982). Charts for interpreting wildland fire behavior characteristics. Gen. Tech. Rep. INT-131. Ogden, UT: U.S. Department of Agriculture, Forest Serivce, Intermountain Forest and Range Experiment Station. 21 p

Arca B, Laconi M, Maccioni A, Pellizzaro G, Salis M (2005). Validation of FARSITE models in Mediterranean area. In proceeding of: Fire and forest meteorology 6th Symposium, Fire and forest meteorology.

Arca B, Duce P, Laconi M, Pellizzaro G, Salis M, Spano D (2007). Evaluation of FARSITE simulator in Mediterranean maquis. International Journal of Wildland Fire, 16: 563-572.

ANPC (2012). Relatório de Ocorrência 2012080021067 Tavira/Cachopo/Catraia. 10 de Agosto de 2012.

DiMiceli, C.M., M.L. Carroll, R.A. Sohlberg, C. Huang, M.C. Hansen, and J.R.G. Townshend (2011), Annual Global Automated MODIS Vegetation Continuous Fields (MOD44B) at 250 m Spatial Resolution for Data Years Beginning Day 65, 2000 - 2010, Collection 5 Percent Tree Cover, University of Maryland, College Park, MD, USA.

Duguy B, Alloza JA, Roder A, Vallejo R, Pastor F (2007). Modelling the effects of landscape fuel treatments on fire growth and behaviour in an Mediterranean landscape (eastern Spain). International Journal of Wildland Fire, 16: 619-632.

Fernandes P, Gonçalves H, Loureiro C, Fernandes M, Costa T, Cruz MG, Botelho H (2009). Modelos de Combustível Florestal para Portugal. In proceeding of: 6º Congresso Florestal Nacional.

Finney MA (1998). FARSITE: Fire Area Simulator - Model Development and Evaluation. Research Paper RMRS-RP-4, Ogden, UT: U.S. Department of Agriculture, Forest Service, Rocky Mountain Research Station. 47p

Flannigan MD, Krawchuk MA, de Groot WJ, Wotton BM, Gowman LM (2009). Implications of changing climate for global wildland fire. International Journal of Wildland Fire, 18: 483-507.

Forthofer J, Shannon K, Butler B (2009). 4.4 simulating diurnally driven slope winds with windninja. USDA Forest Service, Rocky Mountain Research Station, Missoula, MT.

French IA, Anderson DH, Catchpole EA (1990) Graphical simulation of bushfire spread. Mathematical Computing and Modelling, 13: 67-71.

ICNF (2012). Recuperação da Área Ardida do Incêndio de Catraia (Julho de 2012). Relatório Técnico. Versão de 12 de Setembro. Documento em fase de elaboração.

Keane RE, Burgan R, van Wagtendonk J (2001). Mapping wildland fuels for fire management across multiple scales: integrating remote sensing, GIS, and biophysical modeling. International Journal of Wildland Fire, 10: 301-319.

Keane RE, Cary GJ, Davies ID, Flannigan MD, Gardner RH, Lavorel S, Lenihan JM, Li C, Rupp TS (2004). A classification of landscape fire succession models: spatial simulations of fire and vegetation dynamics. Ecological Modelling, 179: 3-27.

Legendre P, Legendre L (1998). Numerical Ecology. Elsevier: Amsterdam.

Loureiro C, Fernandes P, Botelho H, Mateus P (2006). A simulation-based test of a landscape fuel management project in the Marão range of northern Portugal. Forest Ecology and Management, 234(S1).

Morais M (2001). Comparing Spatially Explicit Models of Fire Spread through Chaparral Fuels: A New Model Based Upon the Rothermel Fire Spread Equation. MA Thesis. University of California, Santa Barbara.

Moriondo M, Good P, Durao R, Bindi M, Giannakopoulos C, Corte-Real J (2006). Potential impact of climate change on fire risk in the Mediterranean area. Climate Research, 31: 85-95.

Mouillot F, Rambal S, Joffre R (2002). Simulating climate change impacts on fire frequency and vegetation dynamics in a Mediterranean-type ecosystem. Global Change Biology, 8: 423-437.

Nelson RM (2000). Prediction of diurnal change in 10-h fuel stick moisture content. Canadian Journal of Forest Research 30: 1071-1087.

Lee B, Alexander M, Hawkes B, Lynham T, Stocks B, Englefield P (2002). Information systems in support of wildland fire management decision making in Canada.

Loboda T, Csiszar I (2007). Reconstruction of fire spread within wildland fire events in Northern Eurasia from the MODIS active fire product. Global and Planetary Change, 56 (3): 258-273.

Pereira MG, Trigo RM, daCamara CC, Pereira JMC, Leite SM (2005). Synoptic patterns associated with large summer forest fires in Portugal. Agricultural and Forest Meteorology, 129: 11-25.

Petersen SH, Morais ME, Carlson JM, Dennison PE, Roberts DA, Moritz MA, Weise DR (2009). Using HFire for spatial modelling of fire in shrublands. Research Paper PSW-RP-259. Albany, CA: U.S. Department of Agriculture, Forest Service, Pacific Southwest Research Station. 44p

Petersen SH, Moritz MA, Morais ME, Dennison PE, Carlson JM. (2011) Modelling long-term fire regimes of southern California shrublands. International Journal of Wildland Fire, 20: 1-16.

Ramos A, Trigo RM, Santo FE (2011). Evolution of extreme temperatures in Portugal: reporting on recent changes and future scenarios. Climate Research, 48: 177-192.

Rothermel, RC (1972). A mathematical model for predicting fire spread in wildland fuels. Research Paper INT1143-115, USDA Forest Service, Intermountain Forest and Range Experiment Station. Ogden, UT.

Smith AM, Wooster MJ (2005). Remote classification of head and backfire types from MODIS fire radiative power and smoke plume observations. International Journal of Wildland Fire, 14 (3): 249-254.

Stratton R (2004). Assessing the effectiveness of landscape fuel treatments on fire growth and behaviour. Journal of Forestry, 102: 32-40.

Trigo RM, Pereira JMC, Pereira MG, Mota B, Calado TJ, daCamara CC, Santo FE (2006). Atmospheric conditions associated with the exceptional fire season of 2003 in Portugal. International Journal of Climatology, 26: 1741-1757.

Viegas DX, Figueiredo AR, Ribeiro LM, Almeida M, Viegas MT, Oliveira R, Raposo JR (2012). Relatório do Incêndio Florestal de Tavira/São Brás de Alportel, 18 a 22 de Julho de 2012.

Fire effects on the physical environment in the WUI using FIRETEC

F. Pimont[a], J-L. Dupuy[a], R.R. Linn[b]

[a] *INRA, UR 629, Site Agroparc F-84914 AVIGNON Cedex 9, pimont@avignon.inra.fr*
[b] *LANL, EES, Los Alamos NM 87544, rrl@lanl.gov*

Abstract
In France, the clearing distance between buildings and forest edge is 50 m, to allow fire fighters to protect those buildings. Current building recommendations in the wildland-urban interface derive from fire-safety tests on building materials using heat exposures (duration and magnitude) that are expected to be different from those produced by wildfires. Beyond a few experimental data released after the International Crown Fire Modelling Experiment, there is a lack of characterisation of the physical environment of a building or human target within a cleared area, that receives hot gases and radiant fluxes from a crown fire. In the present study, we evaluate FIRETEC's ability to simulate heat fluxes based on some available experimental data and subsequently use it to characterize the radiant fluxes, gas temperatures and velocities around a human or building target.
Simulations have been performed in a mature Aleppo pine forest within a 600 by 400 m domain. The conditions of the fire spread were severe (30°C, wind up to 50 km/h, slope until 30%). Radiant fluxes and gas temperatures were computed for several distances between the forest tailing edge and a target that represents either a building or a fire fighter.
Peak radiant heat flux magnitudes decreased by about 80% when the target was at 50 m compared to a target at 10 m. This is between 90 and 95% reduction o0f radiant flux reduction observed at 50 m compared to the forest edge. For the purpose of comparison with reference acceptable thresholds for both materials and fire fighters, the peak values of the average over one minute of the instantaneous radiant fluxes and gas temperatures were computed. These values support the notion that a clearing distance of 50 m is appropriate in the tested conditions for both thermal radiation and gas temperature, even if radiant fluxes remain high is the sloped case.
This study shows a new type of application for physics-based models such as FIRETEC. Simulations demonstrate the interest of clearing around buildings and can help provide recommendations about the appropriate clearing distance. It can also be used for building material specifications.

Keywords: WUI, clearing, radiant flux, gas temperature, building, FIRETEC

Introduction

In France, the clearing distance between buildings and forest edge is 50 m. The aim of this recommendation is to limit fire effects on building, but also to offer safe conditions for fire fighters protecting the building. Current building recommendations in the wildland-urban interface have been derived from fire safety tests on building materials using heat exposures (duration and magnitude) that are of different ranges from those produced by wildfires. Beyond the experimental data released after the International Crown Fire Experiment (Cohen 2004), there is a lack of characterisation of the thermal exposure of a building within a cleared area receiving hot gases and radiant fluxes from a crown fire. Modeling radiatives fluxes is challenging because of its extreme sensitivity to, among other parameters, gas temperature due to the fourth-power dependence of temperature of the emissive power. An error of 20 % on temperature induces an error of 100% on radiative flux. Most of the modelling approaches used up to now assume a value for gas temperature and a shape for the source (Ellis 2000, Billaud *et al*. 2011). In physics-based models such as FIRETEC (Linn & Cunningham, 2005), the local values of gas and solid temperatures and absorption coefficients are computed in 3D by the model itself. These types of models resolve gas transport and combustion equations, coupling heat transfer, transport and combustion. Because of the physical basis of such a model, a satisfactory evaluation over some specific experimental data can give some confidence in the prediction within a slightly broader context. For instance, Linn *et al*. (2012) show some first results demonstrating a reasonable agreement

between the model and the crown fire experiment, even if large uncertainties in wind conditions were complicating the validation process.
In the present study, we evaluate FIRETEC's ability to simulate radiant heat flux using data collected during the International Crown Fire Experiment (Cohen *et al*. 2004). We thus used the model to characterize the radiant fluxes, gas temperatures and velocities to a human or building target. For an evaluation of FIRETEC's predictions of gas temperature and velocities in front and above a fire, the interested reader can refer to Dupuy *et al*. (2014).

Methods

Model evaluation: ability to simulate a radiant heat flux on a vertical target

Following the work of Linn *et al*. (2012), fire behaviour was simulated on four different plots of the International Crown Fire Experiments. Plot 1, 4, 6 and 9 were selected because of the relatively uniform fire behaviour observed during the experiment (Taylor *et al*. 2004, see figure 4). Cohen *et al*. (2004) provided information concerning radiant heat fluxes to a target at 10, 20 and 30 m from the trailing edge: figure 6 shows the temporal variation in incident heat flux for Plot 4 and 9 and table 2 the peak total incident heat ($kW.m^{-2}$) for plot 1, 4, 6 and 9 (except at 10 m for plot 1 and 20 m for plot 6).
The experimental fuels were simulated using the Fuel Manager (Rigolot *et al*. 2010), that provides an explicit representation of each individual tree, based on ICFME data inventory (Alexander *et al*. 2004). Canopy load maps are plotted on Figure 1.

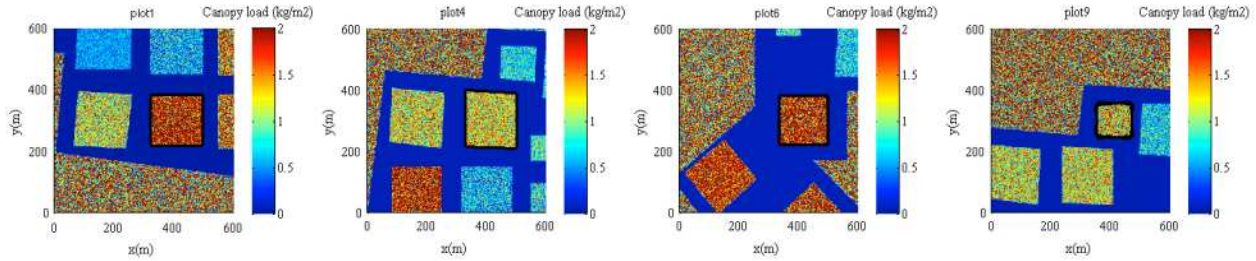

Figure 1. Canopy load maps for the four plots of the ICFME used for the model evaluation. The reference plot is circled in black. On these plots, the wind comes from the left side.

The ambient wind were precomputed using the large scale pressure gradient forcing described in Pimont *et al*. (2014) over homogeneous canopies and were used as boundary conditions for each fire run in order to match the order of magnitude of the reference value in the open (respectively 2.8 m/s, 4.1 m/s, 4.8 m/s, 6.9 m/s at 10 m for plot 1, 4, 6 and 9). Fire was ignited using a "terratorch" procedure, similar to the one used by Linn *et al*. (2012) to reproduce the progressive linear ignition used during those experiments.
FIRETEC uses a Monte-Carlo approach to compute the radiative transfer from any computational voxel of gas and fuel to another one. More details can be found in Dupuy *et al*. (2011). To compute radiative flux toward a vertical target, the number of photons that crosses the vertical cell faces corresponding to target positions were counted. Another specificity of this application is that it required a good accuracy of radiant heat fluxes "far from the flame", whereas what really matters for fire propagation is a good accuracy of radiant heat fluxes "close to the flame". To reach a better accuracy on targets at up to 30 m from the flame, we increased the number of photons thrown by the Monte-Carlo code.
The simulated fires had spread rates of respectively 0.7, 0.65, 0.8 and 1.06 m/s for plot 1, 4, 6 and 9. The experimental spread rates were 0.6, 0.74, 0.6, 1.16 m/s for the same plots. It should be noticed that these experimental fires were performed in a wide range of wind conditions, temperature and fuel

characteristics. Considering the uncertainties associated to wind field description in the experiment and the sensitivity of the model to wind fields (Linn *et al*. 2012), the agreement between experimental and modelled spread rates was found satisfactory.

Using data provided by Cohen *et al*. (2004), FIRETEC's radiant fluxes to targets were plotted against experimental data on Figure 2 for plot 4 and 9. For each distance to the trailing edge (10, 20 and 30 m), data was collected from FIRETEC simulations were at three different lateral positions (centered, 10 m right and 10 m left from the central axis parallel to wind direction) in order to illustrate the spatial variability of the simulated data. For plot 4, the agreement with the experiment was found to be satisfactory: the abrupt rise was very well captured by the model, as well as satisfactory values of peak. The decline occurs quicker in the model than in observations, which can be attributed to the fact that fuels thicker than 6 mm are not accounted for in the model and might play a significant role after the fire front has passed. Radiant heat flux peaks were underestimated on plot 9 by about 30 %. However, it should be noticed that the model rendered the fact that the peak was significantly higher in plot 9 than in plot 1, 4 and 6. Among the reasons that could help to understand the discrepancy, we noted that the modelled spread rate was underestimated (1.06 instead of 1.16 m/s) and Figure 3 illustrates that the modelled fire was more tilted and not as straight as the experimental fire. This might explain why the radiant heat flux was underestimated in this context.

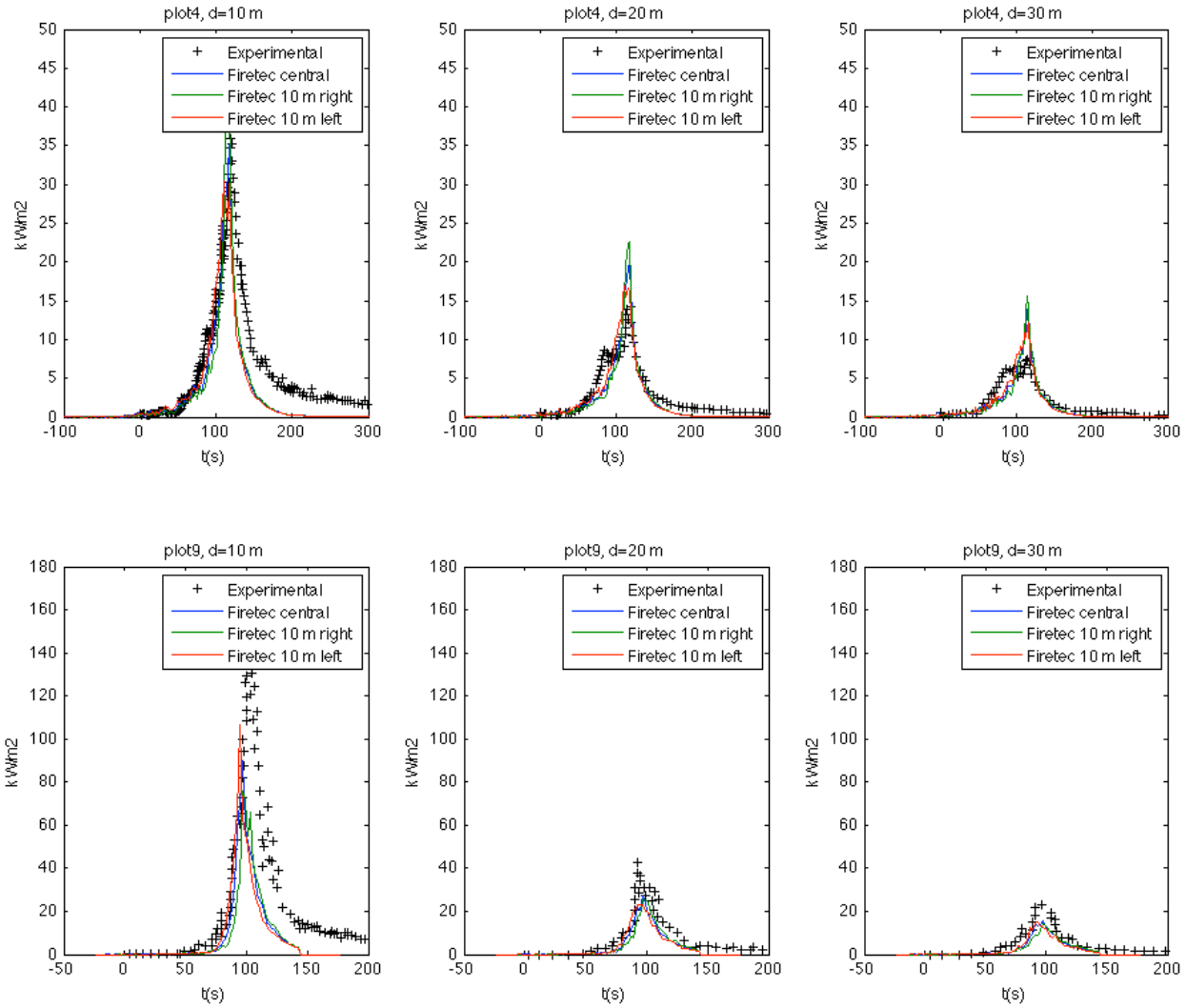

Figure 2. Simulated radiant heat flux at a target at d=10, 20 and 30 m downwind of the trailing edge of plot 4 and 9. Experimental data were taken from Cohen et al. (2004)

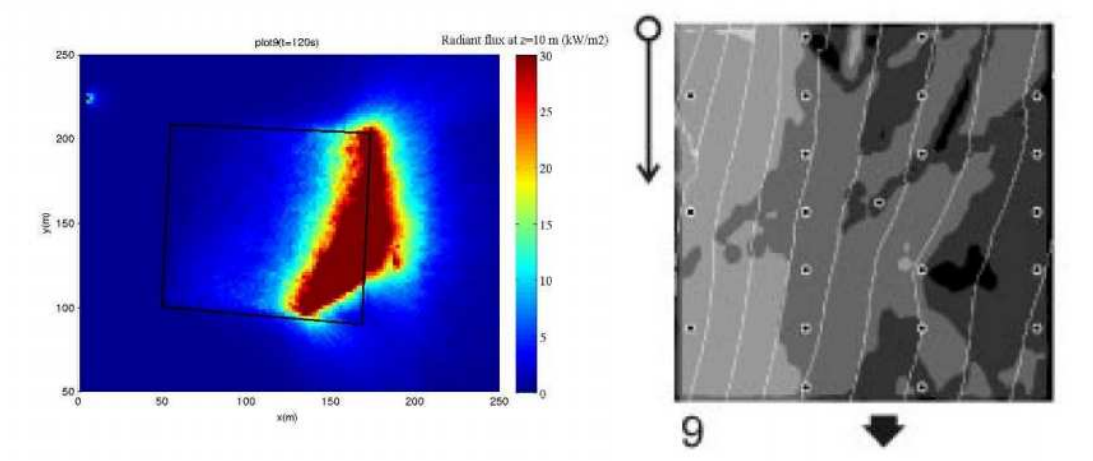

a) Radiant heat flux at z=10 m b) Experimental isochrons for plot 9, taken in Taylor et al. (2004)

Figure 3. Simulated peak radiant heat flux at a target at d=10, 20 and 30 m downwind for plot 1, 4, 6 and 9

Cohen *et al*. (2004) also provided radiant heat flux peak values for plot 1, 4, 6 and 9. **Figure 4** represents the simulated peak values against the experimental ones (FIRETEC's center value was chosen here). A log scale was chosen because of the wide range of radiant fluxes among cases and distances. Again, the agreement was satisfactory.

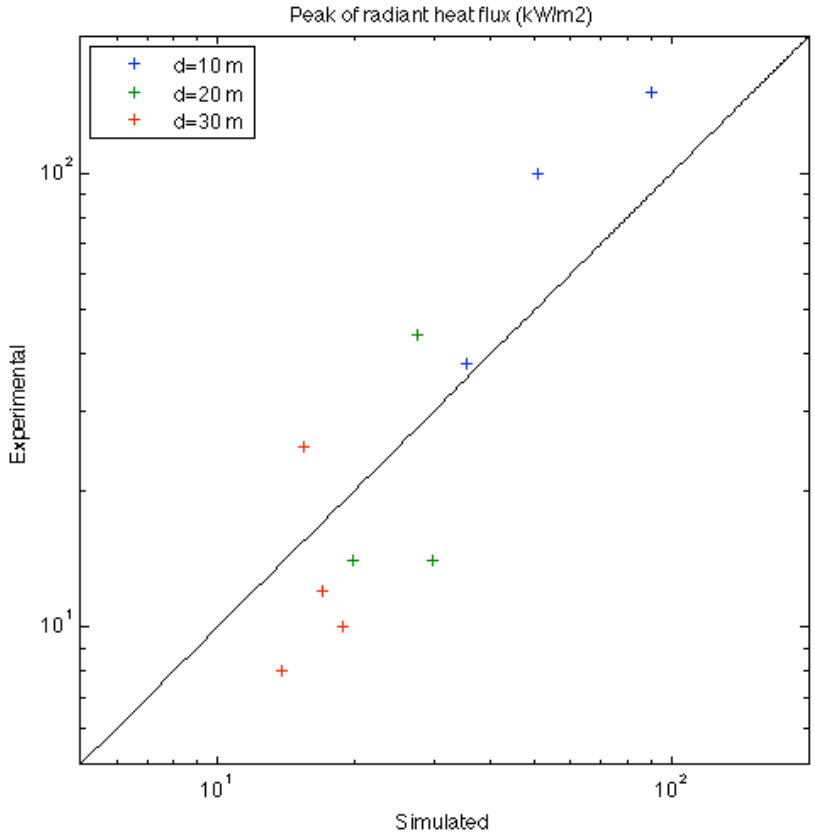

Figure 4. Simulated peak radiant heat flux at a target at d=10, 20 and 30 m downwind for plot 1, 4, 6 and 9.
NB: d=10 m is missing for plot 1 and d=20 m is missing for plot 6

Radiant fluxes in Aleppo pine stand

Four simulations were carried in a mature Aleppo pine forest over a 600 by 400 m domain (Table 1, Figure 5). The forested area is a 40 year old Aleppo pine stand of medium fertility class (corresponding to a dominant height at 50 year old of 12 m) with 1100 stems per ha. The understory is a mixed oak shrubland of 40 year old and has a cover fraction of 80 %. The fuel scene was simulated with the Fuel Manager (Rigolot *et al*. 2010) and can be seen on Figure 5. The simulated fuel scene has a pine/oak cover fraction of 88 % and a fuel load of 1.35 kg/m2, whereas the oak understorey has fuel load of 0.72 kg/m2.

Two different options were tested in the cleared area (see Table 1). Run1 and run2 have some remaining Aleppo pines on the first 20 m of the cleared area, but those pines were thinned so that distances between tree crowns are everywhere greater than 3 m. In the second scenario (run 3 and run4), all the pine trees and oaks were removed. We assumed that there was no ground fuel in the cleared area. Even if this assumption might be found restrictive in such a study, the mesh size of FIRETEC (2 m) is not really appropriate to deal with propagation of a fire in heterogeneous resprouts or patchy fuel at a scale much smaller than grid size. For that reason, this study focuses on the fire effects of the main fire front, spreading from the untreated region (and through thinned trees in the first 20 m of the cleared area when pine trees were only thinned at 3 m between crowns). The reader must be aware that the effect of the fuel recovery in the cleared area is not accounted for. The consequences of this assumption will be discussed in section 4.

The conditions of the fire spread were severe: the air temperature was 30 °C, with a wind speed of 50 km/h (at 10 m in the open that is upwind to the forest), the slope can reach 30 % and the fuel moistures were dry (100 % for Aleppo pine needles, 70 % for live understorey fuel and dead fuel moisture of 10 %). In addition, the cleared area is reached frontally by a crown fire with a wide firefront (about 100 m, when if reaches the cleared area).

Table 1. Description of the four Aleppo pine simulations

	Wind at 10 m in the open	Slope (%)	Presence of trees in the first 20 m of the cleared area
Run1	50 km/h	0 %	Yes
Run2	50 km/h	30 %	Yes
Run3	50 km/h	0 %	No
Run4	50 km/h	30 %	No

The fluxes and gas temperatures were computed at several distances (d=10, 30 and 50 m) downwind of the full-forest trailing edge including a 10 m height target that represents a building (Figure 5). To account for spatial variability, ten different virtual targets were used at each of the three reference distances. As in the evaluation procedure described in section 2.1, the number of photons used in the MonteCarlo scheme was increased to increase long distance accuracy. It should be noticed that the target is virtual here, so that no computation of the flow motion around the building or fire fighter is done, which might affect the gas temperatures, but not the radiant fluxes.

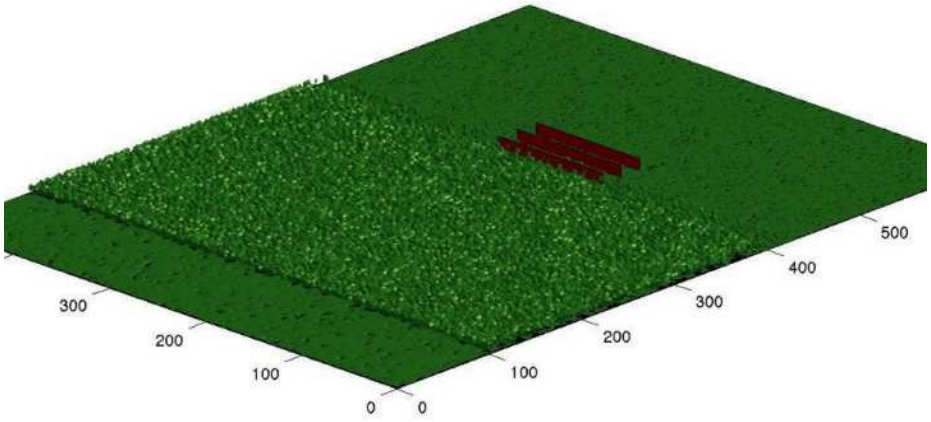

Figure 5. Schematic view of the numerical experiment in the no-slope scenario with tree thinning on the first 20 m of the cleaned area. The three red planes represent target location at respectively 10, 30 and 50 m from the forest edge.

In addition to the instantaneous radiant fluxes and temperatures similar to Figure 2, the peaks of 1 min-averaged radiant fluxes and temperatures where computed at 30 different locations in order to compare them to some known thresholds. The 30 different locations (10 for each distance *d*=10, 30 and 50 m) were then used to compute a maximum and mean value of peak time-averaged quantities over space.

Results

Fire behaviour

The fire behaviour computed by FIRETEC in the scenario described above was always an active crown fire (Figure 6), with computed spread rates of 1.05 m/s for the no slope scenarios (run1 and run3) and of 1.30 m/s for the 30 % slope scenarios (run2 and run4). For the no slope scenarios, the fire intensities reached 27000 kW/m at the head of the fire with a residence time of about 70 s. For the 30 % slope scenarios, the head-fire intensity reached 36500 kW/m with a residence time of about 100 s. Even if the fuel types are different, those values can be compared to the most documented crown fire experiments to date (ICFME, see above, Taylor *et al*. 2004), in which spread rates of more than 1.1 m/s were experimented with wind of less than 25 km/h on similar fire fronts without slope. Residence times between 63 and 94 s were reported at the ground and close to 30 s in the canopy.

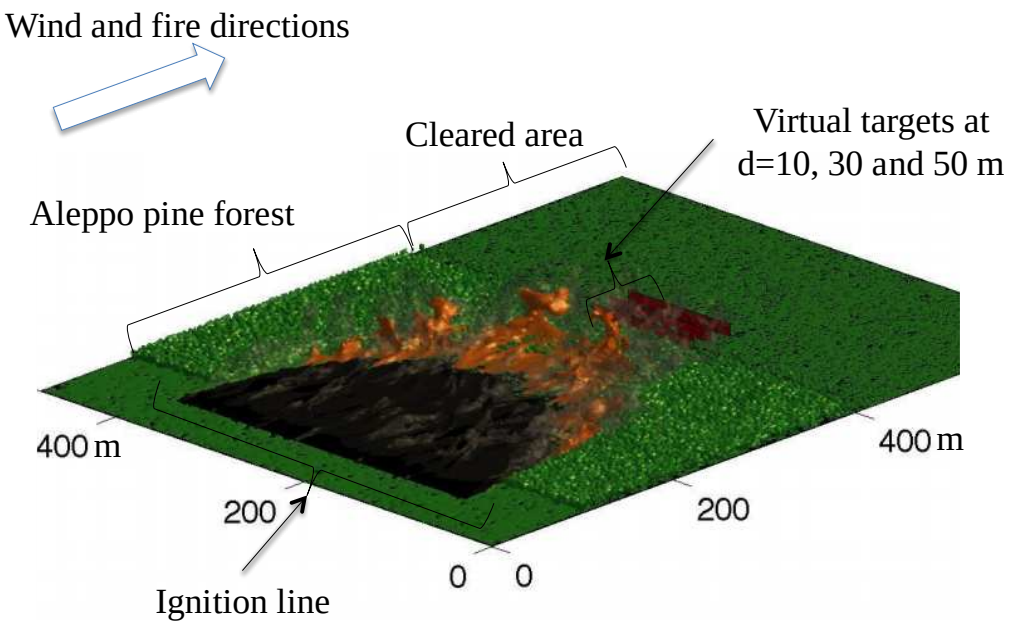

Figure 6. Fire propagation on the forest zone in the no-slope case

Instantaneous and time-averaged radiant heat fluxes

Figure 7 shows how the radiant heat flux decreased of approximately 80 % when the target was 50 m from the forest compared to a target at 10 m. This is up to 90 to 95 % of radiant flux reduction at 50 m compared to the values at the forest edge, that reach 200 kW/m^2. In Table 2, the mean and maximum (in brackets) value corresponds to spatial mean and max among virtual targets of the peak values of time-averaged fluxes. Mean peak average fluxes at 50 m were about 5 kW/m for the no slope cases and of 8 kW/m for the 30 % slope cases. The decrease associated with distance from forest edge was slightly lower for time-averaged quantities than for instantaneous quantities, with a reduction about of about 75% between 10 and 50 m data. The presence of thinned trees in the first 20 m of the cleared area (with distance between crowns of 3 m in run1 and run3) generally induced a small decrease of radiant heat fluxes for distances higher than 10 m (about 4 %), suggesting that those trees are not strong shelter for the targets. However, at 10 m the ignition of those trees can result in a 10 % increase of heat flux.

The standard deviation of the peak of 1 min-averaged fluxes among the targets at various crosswind positions was limited (not shown), suggesting that spatial variability was limited with a wide and homogeneous fire front. The maximum of the peak averaged flux was about 10 % higher than the mean value. It should be noticed that the maximum value for run4 at 10 m was 20 % higher than the mean value, illustrating that variability could be higher close to the forest edge with slope.

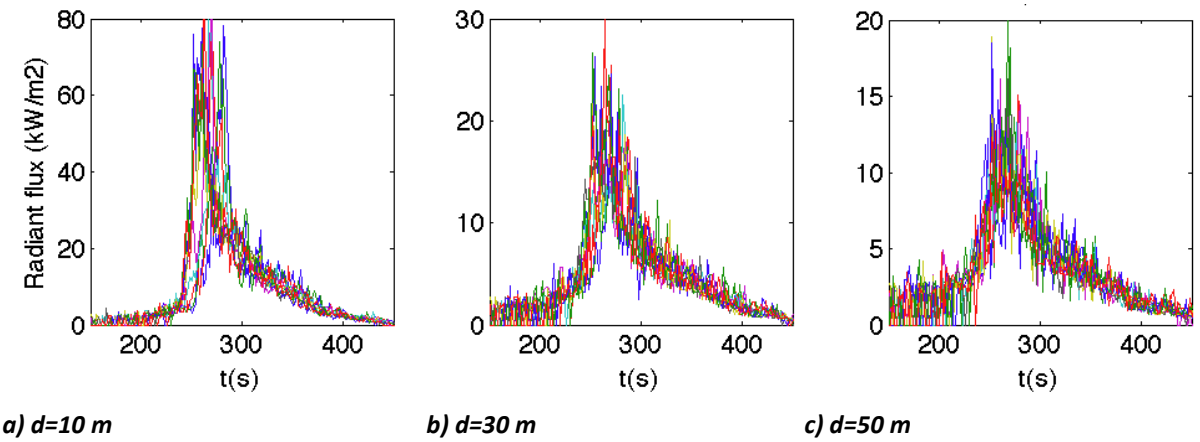

Figure 7. Radiant fluxes to targets at 10, 30 and 50 m from the forest edge in the 30% slope case

Table 2. Spatial mean (max) as a function of distance d of the peak of 1 min-averaged radiant heat flux (kW/m2)

	d=10 m	d=30 m	d=50 m
Run1 (no slope, trees)	24.6 (27.8)	8.6 (9.2)	5.5 (5.9)
Run2 (30 % slope, trees)	31.1 (34.6)	12.2 (13.2)	8.4 (9.1)
Run3 (no slope, no trees)	22.0 (25.8)	8.3 (8.8)	5.4 (5.9)
Run4 (30 % slope, trees)	30.0 (38.8)	11.8 (13.1)	8.0 (8.9)

3.3. Instantaneous and time-averaged temperatures

Figure 8 illustrates how the distance to the edge affects gas temperatures on the 10 m height target. The instantaneous values were much smaller than inside the forest, where they could reach 1000-1100 °C. Peak duration was always shorter than 2 minutes. Due to the large fluctuations associated with instantaneous data in the plume (Dupuy *et al*. 2014), the peak values of the 1 min-average were computed for each of the 30 targets, so that mean and max peak average temperature were computed in Table 3. The peak 1 min-averaged temperature decreased significantly with clearing distance to reach values significantly lower than 90°C, with can be considered as a reasonable threshold for fire fighters. One interesting result is that peak 1 min-averaged temperatures could be 10 % lower in the slope cases, than in the flat cases at 50 m, whereas there were very significantly higher at 10 m (+15-25 %). The stronger plume associated with the more intense fire in the sloped cases could result in their plumes being less tilted from vertical, with lower temperatures at long distances (50 m), whereas they are higher at short distances (10 m) close to the more intense plume and due to the slope effect. Lower gas temperatures in front of higher intensity fires have already been observed by Pimont *et al*. (2011), in the context of fuel treatment.

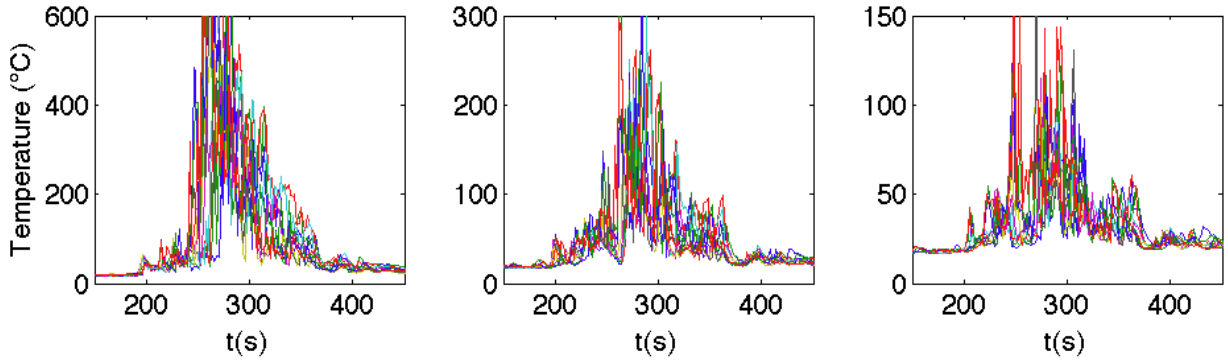

a) d=10 m *b) d=30 m* *c) d=50 m*

Figure 8. Gas temperature fluxes around targets at 10, 30 and 50 m from the forest edge in the 30% slope case

Table 3. Spatial mean (max) as a function of distance d of the peak of 1 min-averaged temperature (°C)

	d=10 m	d=30 m	d=50 m
Run1 (no slope, trees)	287 (323)	105 (111)	71 (78)
Run2 (30 % slope, trees)	329 (404)	110 (130)	59 (70)
Run3 (no slope, no trees)	280 (336)	108 (120)	68 (75)
Run4 (30 % slope, trees)	345 (422)	113 (143)	63 (70)

Discussion and conclusion

The evaluation of the fire behaviour and radiant flux predictions against the ICFME, as well as the results presented by Dupuy *et al*. (2014) suggest that FIRETEC is able to reproduce the main trends associated with physical variables with the right orders of magnitude. This evaluation is limited for the moment, but we can expect to evaluate the model in a wider range of conditions in the future, thanks to new field experiment campaigns. However, no model deficiency was identified in these first comparisons, so that the model can be used with some degree of confidence to contribute to the evaluation of the effects of various clearing distance or to investigate how wind, slope and fuel treatment can affect radiant heat fluxes and gas temperatures. Certainly such modelling results should be used in a complementary fashion with additional more detailed experiments.

The results of the present study confirm that a significant clearing distance around houses can have a huge impact to enable the intervention of fire fighters. For instance, the clearing distance of 50 m induced a decrease of 90 to 95 % of the peak radiant flux, as well as a reduction of 80 % of the peak 1 min-averaged heat flux. The peak 1 min-averaged temperatures below 90°C. It should be noticed that with the 30 % slope and severe conditions, a clearing distance of 30 m was not sufficient to allow defensibility, mainly because of the radiant fluxes.

Concerning building protection, the heat fluxes show that a clearing distance of 10 m is clearly insufficient to avoid direct ignition of woody materials, whereas a clearing distance of 50 m would be enough to limit the risk of direct ignition. In the present study, the cleared area was assumed to contain no burnable fuel, with the exception of low cover of pines trees in the first 20 m of the cleared area in run1 and run2. It should be noticed that even when the cleared area has been cleared very recently, some fuels and remaining litter can spread the fire to the building. And because the treatment are not done every year, the law allows the owner to have a phytovolume that can reach 5000 m3/ha, which can represent a fuel load 0.3 to 0.5 kg/m^2. FIRETEC is not the most appropriate model to deal with fire spread in area that has been cleared very recently, with sparse fuel or duff that will carry low intensity fire. The presence of fire fighters or house inhabitants is in general sufficient to avoid house ignition due to these low intensity fires associated with sparse fuels. However, the scenario of a

significant accumulation of phytovolume (5000 m^3/ha) would worth to be simulating: the model is appropriate to do it, if the fuel is relatively homogeneous, as in a low garrigue and the presence of those fuel is likely to significantly modify the heat fluxes and temperatures. Such simulations will be done in the future and could be used to advise prescriptions concerning the fuel accumulation allowed on cleared area around houses.

This study shows a new type of application for physics-based models such as FIRETEC. Simulations demonstrate the value of clearing around house and can help provide recommendations about the appropriate clearing distance. It can also be used for building material specifications such as those released by the French Scientific and Technical Building Center (CSTB).

References

Alexander ME, Stefner CN, Mason JA, Stocks BJ, Hartley GR, Maffey ME, Wotton BM, Taylor SW, Lavoie N, Dalrymple GN. 2004. Characterizing the Jack Pine – Black spruce Fuel Complex of the International Crown Fire Modelling Experiment (ICFME). Information Report NOR-X-393. Canadian Forest Service Northern Forestry Centre. 49 pp.

Billaud Y, Kaiss A, Consalvi JL, Porterie B. 2011. Monte Carlo estimation of thermal radiation from wildfire. International Journal of Thermal Sciences 50, 2-11.

Cohen JD. 2004. Relating flame radiation to home ignition using modeling and experimental crown fires. Canadian Journal of Forest Research 34, 1616–1626. doi:10.1139/X04-049

Dupuy JL, Pimont F, Linn RR, Clements CB. 2014. FIRETEC evaluation against the FireFlux experiment: preliminary results. VII International Conference on Forest Fire Research D.X. Viegas (Ed.)

Dupuy J-L, Linn RR, Konovalov V, Pimont F, Vega JA, Jimenez E. 2011. Exploring coupled fire/atmosphere interactions downwind of wind-driven surface fires and their influence on backfiring using the HIGRAD-FIRETEC model. International Journal of Wildland Fire, 20, 734-750.

Ellis PF. 2000. Review of current methodology of assessment of bushfire hazard and the prescription of appropriate separation distances and building standards. CSIRO Forestry and Forest Products Client Report 901. (Canberra, ACT)

Linn RR, Cunningham P. 2005. Numerical simulations of grass fires using a coupled atmosphere-fire model: basic fire behavior and dependence on wind speed. Journal of Geophysical Research, 110, D13107.

Linn RR, Anderson K, Winterkamp J, Brooks A, Wotton M, Dupuy J-L, Pimont F, Edminster C. 2012. Incorporating field wind data into FIRETEC simulations of the International Crown Fire Modeling Experiment (ICFME): preliminary lessons learned. Canadian Journal of Forest Research 42(5), 879-898.

Pimont F, Dupuy J-L, Linn RR, Dupont S. 2011. Impact of tree canopy structure on wind-flows and fire propagation simulated with FIRETEC. Annals of Forest Sciences, 68(3), 523-530.

Pimont F, Dupuy JL, Linn RR. 2014. A specific large-scale pressure gradient forcing for computation of realistic 3D wind fields over a canopy at stand scale. Submitted.

Rigolot E, de Coligny F, Dreyfus L, Leconte I, Pezzatti B, Vigy O, Pimont F. 2010. FUEL MANAGER: a vegetation assessment and manipulation software for wildfire modeling. Proceedings of the VI International Conference on Forest Fire Research. D. X. Viegas (Ed.).

Taylor SW, Wotton BM, Alexander ME, Dalrymple GN. 2004. Variation in wind and crown fire behaviour in a northern jack pine – black spruce forest. Canadian Journal of Forest Research 34, 1561–1576.

Firebrand generator system applied to wildland-urban interface research

Ricardo Oliveira[a], Clara Quesada[b], Domingos X. Viegas[a,c], E. Freitas[a], J. Raposo[a]

[a] *Forest Fire Research Centre (CEIF / ADAI); Rua Pedro Hispano n12, 3030 - 289 Coimbra, Portugal. ricardo@adai.pt , Jorge.raposo@dem.uc.pt*
[b] *University of Cordoba, Spain. claraquesada@gmail.com*
[c] *Dep. Mechanical Engineering, Univ. of Coimbra, Portugal. xavier.viegas@dem.uc.pt*

Abstract
The problem of forest fires in the Wildland Urban Interface (WUI) areas is increasing in all countries that have problems with forest fires. This phenomenon is well known and studied in USA, Canada or Australia.
In European countries the problem is identified and studied. In the last 50 years Portugal experienced an unprecedented rural exodus in all its history. Rural areas faced the decreasing of population every year on the one hand emigration, on the other hand young people moved to urban areas. This led to difficulties of management and increased problems related with combat of wildland fires.
The problem of WUI is growing so fast in Portugal in last decade, mainly as a result of the events occurred in 2003, 2005, recently 2012 and 2013. This problems of WUI were identified as a priority, immediately afterwards to personal safety.
Given the importance of spot fires in the context of WUI fires the Centre of Forest Fire Studies (CEIF) developed several studies to increase the knowledge on this problem.
A study of the probability of penetration of firebrands in typical Portuguese house roofs was carried out. Studies on ember aerodynamic transport and on new ignitions inside houses caused by embers. In particularly this second work about ignitions inside houses is being developed with test that involves the generation of embers in a special device designed to create embers, similar to the ones generated in a real forest fire that can transpose structural gaps of the models tested and start a new fire inside of the structure.
In order to carry out this study program a firebrand generator similar to the Baby Dragon developed at NIST by Suzuki and Manzello in 2011 was built. The original device was used in 2013 by Manzello for a similar study.

Keywords*: wildland-urban interface, spot fire, firebrand generator, firebrand particles, burning particles.*

Introduction

The problems of forest fires in the Wildland Urban Interface (WUI) areas are increasing in all the countries that have problems with forest fires (Ribeiro *et al*, 2010). This phenomenon is well known and study in USA (Cohen, 2010), Canada (Cohen *et al*, 2004, 2008) or Australia (Harrap, 2004). In European countries the problem has been identified and studied (Caballero *et al*, 2007).
In the last 50 years Portugal experienced as well other Mediterranean territories an unprecedented rural exodus in all its history (Freire, 2006). Rural areas faced the decreasing of population every year on the one hand emigration, on the other hand young people moved to urban areas. This led to difficulties of management and increased problems related with combat of wildland fires. The problem of WUI is growing so fast in Portugal in last decade, mainly as a result of the events occurred in 2003 and 2005 (Ribeiro *et al*, 2010) and recently in 2012 in the south region of Portugal in Algarve (Viegas *et al*, 2012), and 2013 in Alfândega-da-Fé, Bragança district in the northeast region of Portugal (Viegas *et al*, 2013), as consequence the WUI problem was identified as a priority, immediately afterwards to personal safety (Viegas, 2008).
The situation in Portugal and Mediterranean areas and countries is quite different from the point of view of structures that could be burned. Structures are made of bricks that are not combustible and so in terms of fire the houses of this type of construction are much more resistant although they could be affected if they were not well maintained or have some weakness of constructions as gaps in windows,

doors, roofs and ventilation systems.. In the other hand many places such as USA, Canada have different types of constructions based on wood that are greatly affected by the occurrence of forest fires, despite of this they have some particularities that made is construction attractive as the low price of construction and quick time of construction or reconstruction after a fire.
It is also remarkable that despite of less construction on wood structures is not a synonym of lees problems in an occurrence of a fire many new fuels could appear in a forest fire context as the wastes drooped in the forests.
Given the importance of spot fires in the context of WUI fires the Center of Forest Fire Studies (CEIF) developed several studies to increase the knowledge on this problem. A study of the probability of penetration of firebrands in typical Portuguese house roofs was carried out (Viegas *et al*, 2008). It is not correct believe that wildfires ignite homes by the direct contact of flames on flammable surfaces, Mediterranean structures are not. It is very unusual to have a home ignition this way because of the non flammable nature of the materials.
Studies on ember aerodynamic transport and on new ignitions inside houses caused by embers transposing gaps are being developed. In order to carry out this study program a firebrand generator similar to the *Dragon* developed at NIST by (Suzuki and Manzello, 2011) was built at CEIF by Freitas (Fig.1). The original device was used in Manzello *et al.* (2013) for a similar study.

Figure 1. Firebrand Generator Device

Methodology and Results

An extensive experimental program to calibrate the equipment and to develop a methodology of test was established by Freitas (2013) for the study we have mentioned before.
The fuel particles used to generate the burning embers were pellets. Pellets were chosen because of their known characteristics of calorific value (not important in these tests), dimensions of weight and volume and their facility to burn and generate large amount of particles. Using this type of initial fuel is the best way to reach a repeatable experiment.
The device was manually fed with given amounts of fuel with initial mass (m_i). The tested quantity was considered at 300g of pellets. Greater amounts of pellets were not reflected in more number of generated particles by the device.

Other test control parameters are the gas burner pressure (p), the flow velocity that is linearly related to the radial fan velocity or frequency (Hz) and different opening gaps. Calibration tests to determine the flow of burning particles mass flow rate dm/dt for various sets of control parameters were performed.

A variation on the opening sizes sample results of the mass flow rate for different values of m_i performed with gas pressure equal to 0.3 bar and fan frequency of 50 hz are shown in figure 2.

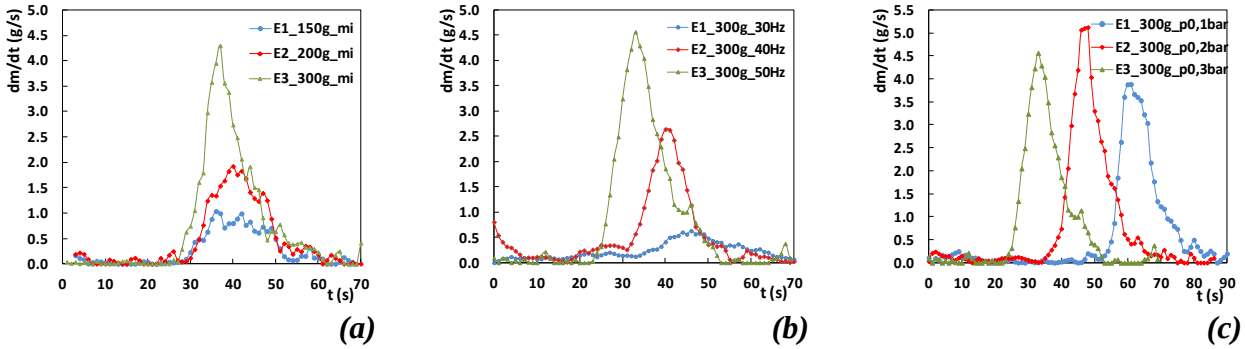

Figure 2. Plot of the rate of ember production dm/dt (g/s) as a function of time t(s). a) varying initial mass; b) varying flow velocity; c) varying gas pressure.

According to figure 2a) the duration of the shower of embers does not depend on the value of $\boldsymbol{m_i}$ but the peak value of *dm/dt* increases with $\boldsymbol{m_i}$. Figure 2b) shows that the maximum value of *dm/dt* increases with flow velocity and occurs earlier in the test. Figure 2c) show that the peak value of *dm/dt* is larger for gas pressure equal to 0.2bar and it decreases for larger or smaller values of ***p***.

In order to analyze the flow of embers through the gap created by a partially closed window or door simulating an opening in a house or building, a special structure that is shown in figure 1 was built specially for this experiment. The results of mass collected in five series of tests with vertical gap values set manually between 0 and 5 cm are shown in figure 3. The reason of choosing 5 cm is the consideration of a small but sufficient size opening to permit a burning particles cross inside the structure. The points corresponding to ***h***=80 cm Standard dimensions of a completely opened window are not shown in the figure but they are very similar to those obtained for h=5 cm A small side opening but wide enough, to the pass of particles. We consider 5 cm as a maximum threshold.

In these tests the following control parameters were kept fixed: *p*=0.3bar, $\boldsymbol{m_i}$ =100g and Frequency=50Hz. During the test the particle generator was placed always in the same position in relation to basis of the gap (from 5 to 80 cm openings). During the ember shower the particles that passed in the gap were collected in a wet surface that would quench immediately the burning particles in order to conserve their mass. After the test these particles were carefully collected and weighted. After that remaining water was eliminated by an oven process drying. The complete evaporating process of water particles took a 24 hours period. The results obtained of completely dried particles in a series of tests in which the gap height ***h*** was varied between 0.5 (almost closed) and 80 cm (completely opened) are shown in figure 3. These results show that the mass of particles collected inside the gap increases sharply for relatively small values of ***h***. For 0<***h***<3 cm the collected mass increases in average from 0 to 7g while for 3<***h***<80 cm it increases in average only to 8g.

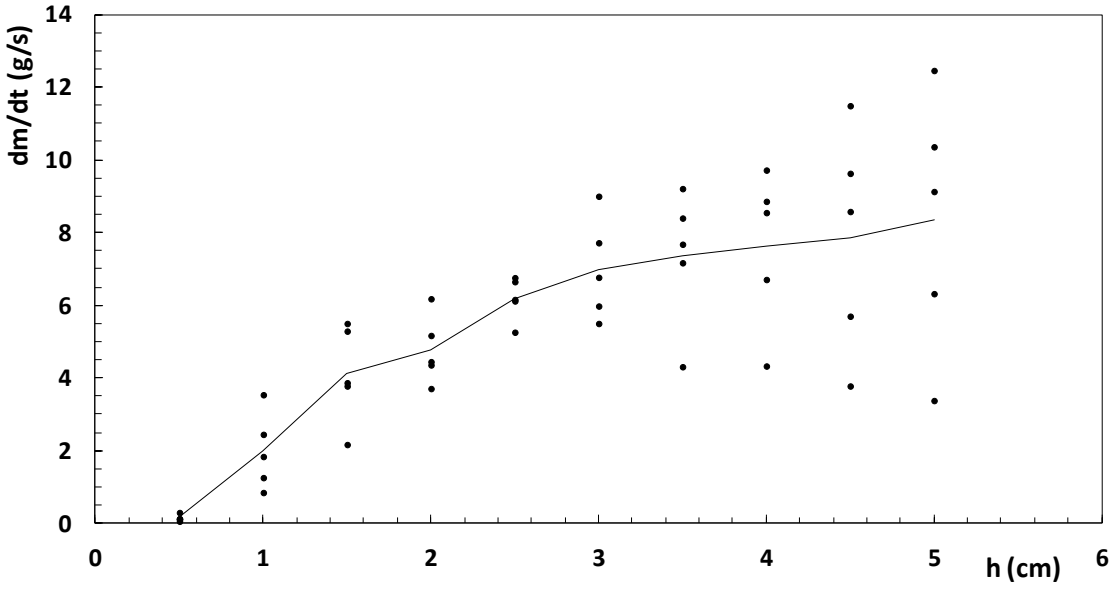

Figure 3. Mass of embers that transposed the gap as function of gap height h (cm). The continuous line is the average of five tests.

Further work

It is expected to extend the analysis for other particle sizes different of the ones represented in figure 4.

Figure 4. An example of firebrand dimensions obtained in the tests are showed in a 3 mm x 3 mm grid

To characterize the generated embers as a function of the feed particles properties could be used a new technique applied to the forest fires called PIV that are being used in CEIF laboratory to the study of firebrands generated by the burning of trees as showed in figure 5

Figure 5. An example of firebrand generated by the burning of trees

Particles position inside the structure can be studied as a limit parameter of an Inside Home Ignition Zone (IHIZ), the inside home fuels (curtains, armchairs, carpets) that an ember could find next to an opening like a window or a door and burn them.
We intend also to continue the experiments submitting different real structures to the tests with showers of firebrands like doors, windows and other structural weaknesses or openings that present in a real structure (figure 6).

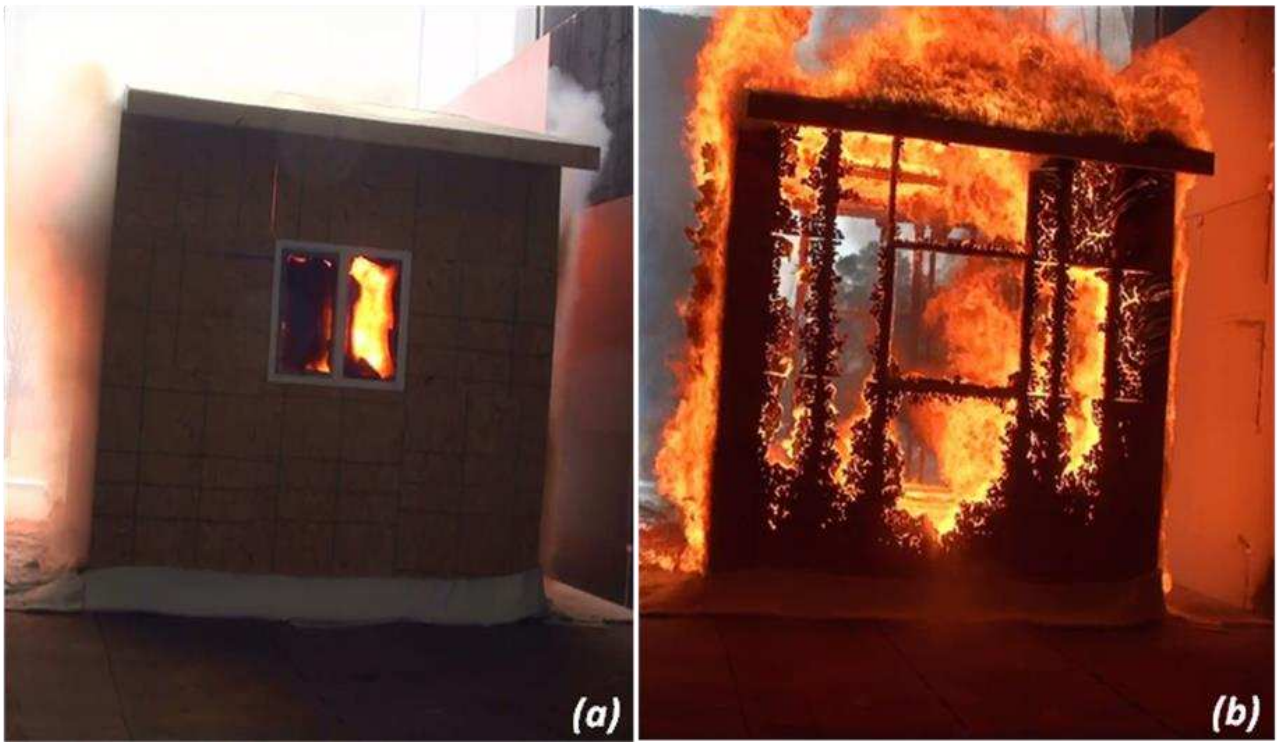

Figure 6. An example of real structures tested used in similar studies (a) after 4 minutes (b) the same structure after 10 minutes (source NIST, 2013)

Conclusions

This paper aims to contribute to a better understanding about the houses ignition by firebrands. Recent studies conducted in several countries that have serious problems of house ignition by firebrands allowed us to understanding the risks of houses ignitions in WUI areas.
The embers generator device installed at the CEIF laboratory allows us to lead several projects to propose mitigation measures to decrease the risk of home ignition in Mediterranean areas. This device working together with the PIV system could be a powerful tool to get reliable data about this problem such as the characterization of the generated embers as a function of the burned fuels and consequently the probability of the ignition as function of the type of the s released particle.
More studies should be effected whit the generator device to have more consistent results as gaps in doors or windows and whit real structures to testing different construction materiaisl to mitigate the problems in WUI areas.

Acknowledgements

The authors wish to thank Portuguese Science Foundation for the support given to project Extreme under contract PTDC/EME-MFE/114343/2009.
The authors acknowledged Doctor Samuel Manzello from NIST to is contribution to construction of the firebrand generator device.
The authors thank their colleagues who supported the experimental work in the Fire Research Laboratory.

References

Cohen J.D. 2004. Relating flame radiation to home ignition using modeling and experimental crown fires. Canadian Journal of Forest Research 34: 1616-1626.

Cohen J.D., and R.D. Stratton. 2008. Home destruction examination: Grass Valley Fire. Technical Paper, R5-TP-026b. USDA Forest Service, Region 5, Vallejo, CA.

Cohen, J. 2010. "The wildland urban interface fire problem". Fremontia, volume 3 8 : 2 / 3 8 : 3 , April 2010/July 2010.

Caballero, D., Beltrán, I., Velasco, A. (2007). Forest fires and wildland-urban interface in Spain: types and risk distribution. *In proc. of the IV International Wildfire Conference*, Seville, Spain, 13-17 May 2007.

Freire, D. (2006). Entre a Propriedade e o Salário. Memórias dos Trabalhos Agrícolas em Alpiarça (anos 50/80). Publicado en *AIBR. Revista de Antropología Iberoamericana, Ed. Electrónica* Vol 1. Num. 3. Agosto-Dezembro 2006. Madrid: Antropólogos Iberoamericanos en Red. ISSN: 1578-9705

Freitas, E. C. (2013). Construção e Calibração de um Gerador de Partículas Incandescentes - Dissertação apresentada para obtenção do grau de Mestre em Engenharia Mecânica na Especialidade de Energia e Ambiente. Faculdade de Ciências e Tecnologia da Universidade de Coimbra. 64p

Harrap, K. (2004). Protecting the Wildland/Urban Interface Community: The Australian Perspective.

Manzello, S.L., Suzuki S., and Hayashi Y. (2013) *Enabling the Study of Structure Vulnerabilities to Ignition from Wind Driven Firebrand Showers: A Summary of Experimental Results*, Fire *Safety Journal*, 54:181-196 (FY).

Ribeiro, L. M., Viegas, D. X., Caballero, D. (2010). Wildland Urban Interface – a diagnostic analysis for Portugal VI International Conference on Forest Fire Research, November 18-23, 2010. Coimbra Portugal. DX Viegas Ed.

Suzuki, S., and Manzello, S. L. (2011). *On the Development and Characterization of a Reduced Scale Continuous Feed Firebrand Generator*. USA: International Association of Fire Safety Science.

Viegas, D. X. (2008). Estudo Laboratorial sobre os Principais Fatores de Ignição nas Habitações – Resistência do Telhado das Habitações aos Incêndios Florestais. ADAI. Coimbra.

Viegas D.X, Gabbert W., Figueiredo A.R., Almeida M.A., Reva V., Ribeiro L.M., Viegas M.T., Oliveira R., Raposo J.R., 2012. Relatório do Incêndio Florestal de Tavira/São Brás de Alportel, 18 a 22 de Julho de 2012. Centro de Estudos sobre Incêndios Florestais, ADAI/LAETA, Universidade de Coimbra, Coimbra, Setembro 2012.

Viegas D.X, Figueiredo A.R., Almeida M.A., Reva V., Ribeiro L.M., Viegas M.T., Oliveira R., Raposo J.R., 2013. Os Grandes Incêndios Florestais e os Acidentes Mortais Ocorridos em 2013 - Parte 1 – Centro de Estudos sobre Incêndios Florestais, ADAI/LAETA, Universidade de Coimbra, Coimbra, Dezembro 2013.

Gaining benefits from adversity: the need for systems and frameworks to maximise the data obtained from wildfires

Thomas J. Duff[a], Derek M. Chong[a], Brett A. Cirulis[a], Sean F. Walsh[a], Trent D. Penman[b], Kevin G. Tolhust[b]

[a] *University of Melbourne, Burnley, Victoria Australia 3121, tjduff@unimelb.edu.au, derekmoc@unimelb.edu.au, sean.walsh@unimelb.edu.au*
[b] *University of Melbourne, Creswick, Victoria Australia 3363, trent.penman@unimelb.edu.au, kgt@unimelb.edu.au*

Abstract
The organisations that manage wildfires are expected to deliver scientifically defensible decisions. However, the limited availability of high quality data restricts the rate at which research can advance. The nature of wildfires contributes to this; they are infrequent, complex events and occur rapidly. While some information about wildfires is usually collected, it is often not of an appropriate standard for research. Valuable information may be discarded or not collected as it is not seen as operationally useful. The harmonisation of fire data management worldwide could increase the availability and quality of information for research. We propose a three tiered approach where agreements are created to standardise data quality, define the scope of information to be collected and establish access protocols for sharing. Standardisation of data collection would facilitate the aggregation of data throughout the world, providing leverage on data collected and reduce unnecessary duplication. If the scope of collection can be expanded, there are a wide range of research fields that stand to benefit. Appropriate data sharing between agencies would increase the value of the data and enable robust conclusions to be reached. It is imperative that the losses caused by severe fires are not in vain; losses should be offset by efforts to maximise the information obtained, helping to prevent a repeat of such events in the future.

Keywords*: bushfire, data, enquiry, experimental design, framework, investigation, observations*

Introduction

In the last decade there has been a high number of catastrophic wildfires throughout the world. In Australia alone, fires burning under extreme weather conditions have resulted in mass house loss in the state Victoria in 2009 (Cruz *et al.* 2012), Western Australia in 2011 and New South Wales and Tasmania in 2013 (Kepert *et al.* 2013). These fires have resulted in substantial social, economic and environmental impacts and recovery activities may take many years. In response to the increasing threat of fire, land managers in vulnerable jurisdictions have made substantial investments in mitigation, preparedness, response and recovery capabilities (McLoughlin 1985; Gebert and Black 2012). Due to the complexity of managing fires, it is not always clear how best to make investments to reduce fire impacts. As a consequence, there has recently been a rapid development of tools to aid decision support for landscape managers in fire prone environments. These include the development of systems that can evaluate complex information to optimise investment levels (Prestemon *et al.* 2008), resource placement (Chow and Regan 2011) or provide information on fire behaviour to aid suppression planning (Sullivan 2009). The development of systems that can support decisions for complex landscape scale events requires research that can differentiate the contributions of numerous interacting factors to an outcome. The analysis of such 'noisy' events requires large amounts of data in order for models to have adequate predictive power. However, the nature of wildfires means that obtaining such data is challenging.

Wildfires typically occur with limited notice, burning in heterogeneous natural landscapes driven by complex weather patterns (Cary *et al.* 2009). The behaviour of fires and their subsequent impacts are consequently the product of multiple interacting parameters and as a result, it can be difficult to quantify relationships and predict outcomes. While some research into wildfires has attempted to address this problem through the use of controlled experiments (Cheney *et al.* 2012), the need to safely manage trials has meant that it is prohibitive to use such experiments to evaluate emergent fire behaviour under extreme conditions. However these events are where losses are typically highest and are consequently of greatest interest to managers (Strauss *et al.* 1989). In addition, many elements of fire management need to be in a realistic landscape context to be relevant; activities such as evacuation or fire suppression are difficult to emulate experimentally.

As research into fields relating to extreme fire behaviour cannot be done experimentally, alternative sources of information are required to allow systematic management planning. The sole remaining way to source observations of fire dynamics is to collect information from fires as they occur. While up to date information is recognised as a critical need for managing 'going' fires, to date there has been a limited focus on collecting information during fires for post-fire analysis. Typically, post-fire investigations are driven by coronial or governmental requirements; it is rare for there to be a systematic process for collecting information during and after severe fires specifically for research purposes. Without such information, fire research and the development of subsequent decision support systems will stall. Case-study fires are commonly used in research; however there is currently no formal process for ensuring the data collected during and post-fire is appropriate for meeting research requirements.

While up to date information is recognised as a critical need for managing 'going' fires, to date there has been a limited focus on collecting information during fires for post-fire analysis. We contend that the collaborative development of a fire data management framework across multiple jurisdictions will have broad benefits for all involved. It has the potential to enhance cross border collaboration, increase the power of datasets and make research findings more internationally relevant.

1.1. The current state of data management

In jurisdictions where fires occur, it is typical that some information about wildfires is collected. This may be details of ignitions (Penman *et al.* 2013), severity (Harris *et al.* 2012) or economic impact (Donovan and Noordijk 2005). However there is currently no unified set of standards or methodologies that define a) what information needs to be collected and b) when collected, what data standards are appropriate. Furthermore there is no standardised system for sharing information that has been collected. As a result, the information that is generated during a fire may not be of an appropriate standard for research, it may be discarded if it is not seen as operationally useful or it may not be seen as important and it may not be collected at all (Figure 1).

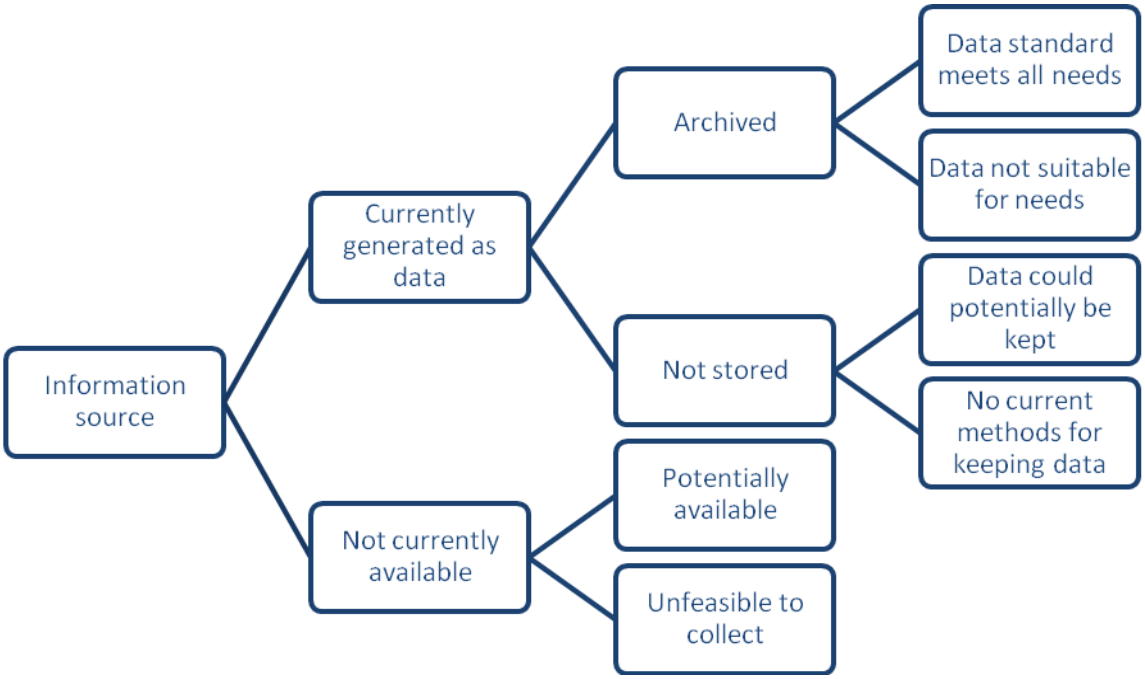

Figure 1. Data hierarchy for information generated at a fire incident

Proposed methods

Determining the breadth of information requirements

Experimental emulation of the most extreme fire conditions is not possible, particularly as many elements of fire management need to be in a real landscape context to be relevant; activities such as evacuation or fire suppression are difficult to emulate experimentally. At the moment, any agency managing a fire incident has specific information requirements to meet its daily operational and planning needs. While meeting these needs has been the priority for managers, there are potentially other needs that are not being met. These may be the needs of external groups (such as university researchers), other intra-governmental agencies (such as the police), inter-governmental agencies (such as the fire management agencies of other jurisdictions or states) or future needs within departments. In addition, at small scales (such as in relation to a single fire) some forms of information may not seem informative. However, when pooled, sample size and consequent model power is increased and the information may then be much more valuable. Without consistent data collection and management protocols, fire information may be useful only within the jurisdiction in which it is collected. Consequently to get the maximum value from information, discussions should be held at the highest level possible – the ultimate benefit would result if data could be effectively pooled across international borders, regions and continents. To do this agreement must be reached on three broad areas; ***scope***- what to collect, ***standards*** – how to collect, and ***access*** – how to share.

Scope: It would be necessary to obtain agreement on the scope of data to be collected. While there is typically a focus on fire behaviour and fuel, information regarding suppression strategies, logistics and command structures are often overlooked. Such information is invaluable for operational research. To optimise the scope of data collected, fire management agencies would need to look more broadly than within their organisations. Other interested parties include other emergency services, utilities, administration bodies and universities.

Standards: Data will need to be standardised, with quality controls on types, units, resolutions, formats and metadata. Standardised methodologies would greatly enhance cross jurisdiction collaboration and allow for broader, more widely applicable studies.
Access: In addition to data collection protocols, for value to be extracted it is important to ensure that contributing agencies are able to access the information provided by others. This is likely to require licensing agreements and the establishment of repositories. There is the potential for privacy issues to manifest, so limitation of access for some datasets may be a consideration.

The degree of difference in fire data collection protocols within a single country can be demonstrated with a search of the Australian public geospatial data directories using the term 'fire'. Table 1 indicates that there are orders of magnitude in difference between the numbers of records available for each state. Wildfires occur within all states of Australia.

Table 1. Number of spatial records discoverable using the term 'fire' on the 5/2/2014 in Australian state based spatial data directories

State	Records available
Australian Capital Territory	48
New South Wales	42
Northern Territory	2
Queensland	65
South Australia	4
Tasmania	11
Victoria	169
Western Australia	149

The three areas of fire information that need to be unified are described briefly below.

Data standards

Of the information typically stored by land managers in relation to fire, a large proportion of the data relates to infrastructure and other relatively invariant landscape attributes. There are a number of datasets that are in common between various states (for example fire history and ignition location), however metadata indicates that there is potentially substantial variation in the collection standards both within and between agencies (Walsh *et al.* 2007). While there are some barriers to the complete standardisation of data collection due to scale, access and technological issues, the degree of difference between the state data collection methodologies means there are likely to be interpretation issues when attempting inter-state investigations. In addition, while many agencies collect information on fire perimeters, for it to be of practical use to science, accessory data such as fuel details, topography, local weather observations, assets at risk and infrastructure must also be made available. Inconsistencies between jurisdictions in accessory data can further compound errors due to inconsistent fire data. For example, while approaches to evaluating fuel have been converging, there is still no system that is consistently applied or is suitable for all jurisdictions and vegetation types in Australia (Gould and Cruz 2012).
Inconsistencies in data can result in severe issues with regards to its access. Differing scales, units and margins of error can make it difficult to determine equivalence between datasets and can confound analysis. As there is much in common in the vegetation, weather and fire behaviour between states in Australia, it would be expected that many of the findings in one jurisdiction would also be appropriate in another. However with differing information, cross-border collaboration and model application is constrained. A common issue with fire science is that due to the complexity, rapidity and infrequent

nature of wildfire incidents it is difficult to collect enough observational data to provide suitable replication for statistical analysis. Standardisation of data collection will facilitate the aggregation of data throughout not only Australia, but the world, providing leverage on data collected, reduce unnecessary duplication and allow robust conclusions to be reached sooner and with less expense.

2.3. Scope of data

Considering Australia as a case study, there are a small number of data sets that are consistently collected by the majority of states despite the fact that wildfires are an issue to varying degrees in them all (Walsh *et al.* 2007). We believe that of the data available, only a small portion of data relevant to fire research is currently being archived as 'fire data' and made available for future needs. While it is common to collect information on impacts such as final perimeters and the locations of house losses, other information pertaining to fire spread predictions, firefighter accomodation and suppression deployments is not available. Table 2 provides an indication of potential information that may be generated; however this list is not exhaustive. Very few of the information sources listed are routinely collected.

Table 2. Information sources potentially available for typical fire incidents. Information is grouped by research group and incident management system category (AIIMS ICS 2013)

Research Potential	Information source	AIIMS ICS category	Routinely available?
Management / Social Science	Incident type	Incident Control	
	Escalation / de-escalation	Incident Control	
	Emergency declarations	Incident Control	
	Control structures	Incident Control	
	Ignition point / points	Investigation	Y
	Ambulance callouts	Investigation	
	Hospitalisation by cause	Investigation	
	Insurance claims	Investigation	
	Fencing / stock losses	Investigation	
	Urban infrastructure	Investigation	
Management Science	Vehicle types	Logistics	
	Supplies	Logistics	
	Catering	Logistics	
	Accommodation	Logistics	
	Medical	Logistics	
	Communications	Logistics	
	Facilities	Logistics	
	Finances	Logistics	
	Resourcing	Logistics/Planning	
	Emergency calls	Investigation	
Operational Research	Weather radar	Intelligence	
	Satellite images	Intelligence	
	Weather Forecasts	Intelligence	
	Aircraft GPS tracks	Operations	
	Vehicle GPS tracks	Operations	
	Response structures	Operations	
	Deployments	Planning	
	Situation reports	Operations/IC control	
Fire Behaviour	Progression isochrones	Intelligence	
	Ground/air observations	Intelligence	
	Line scans	Intelligence	
	Suppression strategies	Operations/Planning	
	Final perimeters	Planning	Y
	Fire behaviour predictions	Intelligence	

	Weather observations	Intelligence	
	Fuel /fire history	Planning	Y
	Objectives	Planning	
	Media strategy	Public information	
All	Recovery	All	
	Post fire impacts	All	

A secondary issue relating to data scope relates to the type of fires that are evaluated in detail. Due to the coronial and reactive nature of large fire investigations, there is a greater likelihood of data being available for extreme events. Data that is consistently collected at these fires includes maps of the final fire perimeter, headfire rates of spread, post-fire aerial imagery, weather conditions, fuel properties and the locations of house losses and deaths. However for more minor fires, the quality of information is generally much poorer. While it may be argued that larger fires are more important to study due their disproportionate impact, a strong counter argument is that some of the smaller fires may have had the potential to be catastrophic but effective preparedness or response measures prevented that from eventuating. Correspondingly it could be argued that smaller fires that occur under severe weather conditions deserve greater attention rather than less.

As it stands currently, a bias of data collection towards particular fire types has the potential to confound research and lead to incorrect conclusions. For example, evidence suggests that the predominant mechanism of house loss under the most extreme fire conditions differs to that under less severe but more common conditions. In addition, fire suppression and fuel reduction are less likely to be seen to be effective under extreme conditions; however they have clear value in preventing incidents from escalating under less severe conditions.

An additional issue is information decay. While information from some sources is robust, providing for simple post-fire collation, other forms are more transient. Highly temporally specific data is common in fires –it is important to be able to track and understand fast moving fire fronts. However if detailed information is not recorded at the time of the fire, information is easily lost and there may be limited opportunity to reconstruct occurrences post fire. This means that management agencies need to develop pro-active data policies. There need to be processes in place to actively target and record information while it is available and before its quality decays. While there is likely to be some overhead cost to this information gathering, such data can lead to improved decision support tools which reduce the overall overheads of fire management. Examples of information that can be transient include the location and rate of spread of fire fronts, the location, number and activity of suppression resources, and the behaviour and activity of civilians in the fire zone. After a fire event, there is greater luxury to collect data from some sources at a slower rate, however it remains important to actively target and record information before it is lost.

The scope of information being collected during and after fires is currently very limited. If information collection can be expanded, there are a wide range of research fields that stand to benefit. While the nature of Australian Eucalyptus forests mean that embers can play a disproportionate role in fire spread than in other forest types throughout the world (Cruz *et al.* 2012), fire remains a physical process. As such, standardisation of the scope and quality of data would be of greater benefit if it could be on an international scale, enabling research projects to be more expansive and enabling conclusions to be more broadly applicable.

2.4. Availability of data

Even if data is of high quality and correctly scoped, fire research may still be hindered by lack of access. This results from two primary issues. The first is that can be difficult for anyone (both internal and external to management agencies) to determine what data is being stored and is available. While spatial data directories have made substantial progress towards transparency of fire information in some jurisdictions, not all information that is collected is formally stored in a manner that is discoverable through such systems (e.g. Table 2). Much of the information gathered during a fire by a

managing agency would be stored in some manner, however only a small proportion is centralised and can be accessed using a query focused on a particular fire. The discovery of such information can require substantial resources; coronial reconstructions of fires take significant time and money to reconstruct particular events, even though much of the necessary information would be generated and available at the time of the event. Currently, the data recorded during fires shows limited consideration to the likely post-fire reconstruction information needs.

A second issue relates to data infrastructure. States, and within states; agencies, currently independently manage their own information. Obtaining data for a large geographic area is likely to mean that access must be negotiated from a number of different bodies. Once data is available, variability in formats and resolutions mean that further processing is typically required to ensure information from various sources is compatible and equivalent. Both obtaining data access and data processing can pose a significant time burden on users. The development of tools to access shared information is a necessary step towards effective cooperation and collaboration on informational needs. One issue that would need to be overcome in relation to information sharing is what limits would need to be applied. Many countries and states now have legislated privacy laws. Some of the information collected during fires may full under the jurisdiction of such laws – undeniably information relating to fatalities and events at particular residences is going to be sensitive and require some limitations on sharing under specific circumstances.

More broadly, the development of systems to recognise, tag, store and share fire related information could greatly reduce data discoverability issues. Furthermore, appropriate data sharing between agencies would create economies of scale, and more comprehensive data would enable more robust conclusions to be reached. If methods, scope and storage of fire data were standardised, substantial benefits may be realised, including greater success in preventing impacts from major fires in the future.

Proposed process

The development of a fire information system is expected to be a complex process as it would require the commitment and collaboration of a large number of emergency service agencies in disparate jurisdictions. It would be necessary to develop any new framework as a multi-stage project.

- Phase one would be to audit the ‘status quo’ and determine in detail how information is being managed within agencies.
- Phase two would be to undertake a needs analysis, evaluating informational requirements of both agencies and scientists. This would need to be carefully planned to ensure that findings are broadly applicable and not merely convenient for a single country.
- Phase three would be to analyse information sources and end-user needs to address data ‘gaps’, making recommendations on data standards, scope and storage mechanisms. This must also include the potential for the recognition of new needs and the inclusion of novel information sources. As technology is continually improving, the future improvement of information collection standards and the inclusion of new sources must remain an option even when a data framework is operating.
- Phase four would focus on the establishing compatible systems between agencies with an overarching aim to develop a centralised system for discovering and accessing data. This would require some reciprocal understanding in relation to data access, licensing, privacy and public availability.

To be effective, this process should be cooperative. While a considered analysis of informational needs will have immediate tangible benefits for a single agency, the greatest benefit overall would be the potential for cross border cooperation and increased research leverage.

We suggest that initial steps towards establishing an effective fire information system should be:

- The allocation of a unique code to each reported fire ignition. Any information pertaining to a particular ignition should be associated with this code. To avoid the risk of duplicates, a composite code could be used such as *country/state/year/fire_number*. Such a code would assist in the development of databases for the archiving of data.
- The existing fire command and control system should be used as a template for structuring and storing fire information. This will ensure that all relevant aspects of a fire are considered. Each function group (i.e Planning, Intelligence etc.) should be responsible for ensuring that information is collected at a suitable standard (Australasian Fire and Emergency Service Authorities Council 2013).

Following this it will be necessary for substantial communication between agencies. This would need to be a forum style process, where views and perspectives can be shared to ensure the proposed procedures and policies best meet the needs of all involved.

The development of any new standards and processes requires careful consideration. Poorly designed standards can 'lock in' unsatisfactory methods or result in competing standards where the interested parties have not come to full agreement (Monroe 2011).

Summary

A common issue with fire science is that due to the complexity, rapidity and rarity of fire incidents it is difficult to collect enough observational data to provide suitable replication for statistical analysis. Standardisation of data collection will facilitate the aggregation of data throughout the world, providing leverage on data collected, reduce unnecessary duplication and allow robust conclusions to be reached sooner and with less expense.
Land and emergency response organisations are increasingly being expected to deliver scientifically defendable decisions and to demonstrate continuous improvement in management and resource use. The limited availability of high quality data restricts the rate at which research can advance and predictive capacity can improve. It is imperative that the losses caused by severe fires are not in vain; losses should be offset by efforts to maximise the information obtained, helping to prevent a repeat of such events in the future.

References

Australasian Fire and Emergency Service Authorities Council (2013) 'Australasian Inter-service Incident Management System (AIIMS) 4th Edition.' (Australasian Fire and Emergency Service Authorities Council: Melbourne, Australia)

Cary, GJ, Flannigan, MD, Keane, RE, Bradstock, RA, Davies, ID, Lenihan, JM, Li, C, Logan, KA, Parsons, RA (2009) Relative importance of fuel management, ignition management and weather for area burned: evidence from five landscape fire succession models. International Journal of Wildland Fire 18, 147-156.

Cheney, NP, Gould, JS, McCaw, WL, Anderson, WR (2012) Predicting fire behaviour in dry eucalypt forest in southern Australia. Forest Ecology and Management 280, 120-131.

Chow, JYJ, Regan, AC (2011) Resource location and relocation models with rolling horizon forecasting for wildland fire planning. INFOR 49, 31-43.

Cruz, MG, Sullivan, AL, Gould, JS, Sims, NC, Bannister, AJ, Hollis, JJ, Hurley, RJ (2012) Anatomy of a catastrophic wildfire: The Black Saturday Kilmore East fire in Victoria, Australia. Forest Ecology and Management

Donovan, GH, Noordijk, P (2005) Assessing the accuracy of wildland fire situation analysis (WFSA) fire size and suppression cost estimates. Journal of Forestry 103, 10-13.

Gebert, KM, Black, AE (2012) Effect of suppression strategies on federal wildland fire expenditures. Journal of Forestry 110, 65-9.

Gould, J, Cruz, MG (2012) Australian Fuel Classification: Stage II.(Ed. G Featherstone.) (Australasian Fire and Emergency Services Council (AFAC) and the Commowealth Science and Industrial Research Organisation (CSIRO): East Melbourne, Australia). [Accessed

Harris, S, Anderson, W, Kilinc, M, Fogarty, L (2012) The relationship between fire behaviour measures and community loss: an exploratory analysis for developing a bushfire severity scale. Natural Hazards 63, 391-415.

Kepert, JD, Fawcett, RJB, Tory, KJT, W. (2013) Applications of very high resolution atmospheric modelling for Bushfires. In 'AFAC13 Shaping Tomorrow Together. Melbourne, Australia'. (Ed. RP Thornton) (Bushfire Cooperative Research Centre)

McLoughlin, D (1985) A framework for intergrated emergency management. Public Administration Review 45, 165-172.

Monroe, RP, 2011. Standards. XKCD. http://xkcd.com/927/,

Penman, TD, Bradstock, RA, Price, O (2013) Modelling the determinants of ignition in the Sydney Basin, Australia: implications for future management. International Journal of Wildland Fire 22, 469-478.

Prestemon, JP, Abt, K, Gebert, K (2008) Suppression cost forecasts in advance of wildfire seasons. Forest Science 54, 381-396.

Strauss, D, Bednar, L, Mees, R (1989) Do one percent of forest fires cause ninety-nine percent of the damage? Forest Science 35, 319-328.

Sullivan, AL (2009) Wildland surface fire spread modelling, 1990–2007. 1: Physical and quasi-physical models. International Journal of Wildland Fire 18, 349-368.

Walsh, DJ, Rumba, KE, Hoare, J, Parsons, M, Thackway, R (2007) Reporting fire in Australia's forests and vegetation. Bureau of Rural Sciences, Canberra, Australia.

Global burned area maps from MERIS

Itziar Alonso-Canas, Emilio Chuvieco

Environmental Remote Sensing Research Group, Universidad de Alcalá, Colegios 2, Alcalá de Henares, Spain; e-mail: itziar.alonsoc@uah.es, emilio.chuvieco@uah.es

Abstract
Biomass burning is a global scale phenomenon that affects annually around 3.5 million Km2. This phenomenon has a very critical relevance for vegetation dynamics, atmospheric emissions and carbon budgets, increasingly affecting human lives and property, particularly in catastrophic conditions (heat waves, drought, strong winds). Properly characterizing burned areas on a global scale has become a relevant factor when studying these processes. The Fire CCI project, in the framework of the ESA's Climate Change Initiative, aims at providing consistent time series of burned areas (BA) globally, over the period 1995 to 2009. Global BA products are obtained by merging information from three sensors: the ATSR series, VEGETATION and MERIS. In this case, the algorithm developed to obtain burned areas from the MERIS sensor will be presented. The MERIS BA algorithm is based on MERIS reflectance bands, spectral indices and both post-fire and multi-temporal analysis controlled by HS locations. BA detection is performed in a two phase process: the first one aims to detect seed pixels while the second one will develop contextual criteria around these seed pixels. Global BA maps have been obtained with the MERIS algorithm for years 2006 to 2008.

***Keywords**: Burned Area, Climate Change, MERIS*

Introduction

Fire is a key component of the carbon cycle affecting greenhouse gases and aerosols emissions to the atmosphere (Andreae and Merlet 2001; van der Werf, Randerson *et al.* 2010), as well as global vegetation dynamics (Kloster, Mahowald *et al.* 2012; Thonicke, Spessa *et al.* 2010). Therefore, it becomes highly critical to monitor fires on a global scale and to estimate their impacts through global climate model simulations, biogeochemical models and dynamic global vegetation models.
Monitoring areas affected by biomass burning has been performed over the last decades using a wide variety of sensors, including very high-spatial resolution such as Ikonos for fine scales (Kachmar and Sanchez-Azofeifa 2006), high spatial resolution sensors such as Landsat-TM/ETM+ or SPOT-HRV for regional areas (Bastarrika, Chuvieco *et al.* 2011b; Pu and Gong 2004) and medium resolution sensors for continental to global studies (Chang and Song 2009; Chuvieco, Opazo *et al.* 2008; Giglio, Randerson *et al.* 2010; Roy, Boschetti *et al.* 2008; Tansey, Grégoire *et al.* 2008).
In the context of the fire_cci project, the goal of this work is to present a global BA algorithm specifically designed for the ENVISAT MERIS sensor. MERIS was mainly designed for ocean colour applications, as it provides high spectral resolution in the range of the blue to the near infrared regions (Gower and Borstad 2004). The application of MERIS data to fire applications is scarce: identification of smoke plumes (Huang and Siegert 2004), discrimination of burn severity (De Santis and Chuvieco 2007; Roldan-Zamarron, Merino-De-Miguel *et al.* 2006). Mapping BA with MERIS has only been performed at regional level (Oliva, Martin *et al.* 2011) using different vegetation indices while (González-Alonso 2009) combined fire hotspots from MODIS and NIR reflectance values from MODIS and MERIS imagery.
The potentials of MERIS for improving current information of BA rely on its greater spatial resolution, complementing other existing global BA products, particularly in areas where under or overestimations have been shown (Chang and Song 2009), thus reducing the uncertainty of current collections. Furthermore, this sensor has a follow up version on the OLCI (Ocean and Land Colour

Instrument) on board Sentinel 3, scheduled for launch in 2015 as part of the EC Copernicus programme.

Methods

The design of a global BA algorithm requires considering the great diversity of biomass burning conditions worldwide. The most extended approaches for mapping BA can be classified in two groups: those that use the thermal contrast of active fires (hot spots, HS) from the surrounding background (Giglio, van der Werf *et al.* 2005), and those based on reflectance changes caused by burning effects (changing of leaf and soil colour, leaf losses, char, etc) (Bastarrika, Chuvieco *et al.* 2011a; Roy, Jin *et al.* 2005). The former approach is more reliable because thermal radiance increases exponentially with temperature, while reflectance changes are more subtle. However, thermal signal lasts very shortly (minutes to hours), while the fires are active, where as post-fire reflectance changes are more lastly (days to years). In addition, BA mapping based on active fires only implies a sample of the total area burned (what is burning when the satellite observes the area), while reflectance changes cover the whole area affected by the fire.

Considering the pros and cons of each approach, several authors have proposed hybrid algorithms, where HS information is used to guide somehow the analysis of reflectance changes in the discrimination of BA, particularly to avoid commission errors (i.e. reflectance changes caused by non-fire causes, such as crop harvest, seasonal flooding, or topographic shade). After analyzing the spectral and temporal characteristics of MERIS, it was decided to follow a similar approach for developing the global BA algorithm, using a synergetic use of HS information derived from MODIS thermal data and temporal trends of MERIS reflectance bands. The hypothesis is that (Kaufman and Justice 1998) the combination of spectral reflectance information with active fires to identify BA should provide a more reliable discrimination of BA. In order to consider a proper balance between omission and commission errors, the algorithm includes two different phases (Chuvieco, Englefield *et al.* 2008): seed identification, which aims to minimize commission errors by selecting only those pixels more clearly burned, and contextual analysis, which applies region growing analysis to improve the delimitation of burned patches.

The algorithm was developed and tested in 10 different study sites, which were selected to take into account the diversity of burning conditions worldwide, including different biomes and fire regimes (Figure 1). (Olson, E. Dinerstein *et al.* 2001)

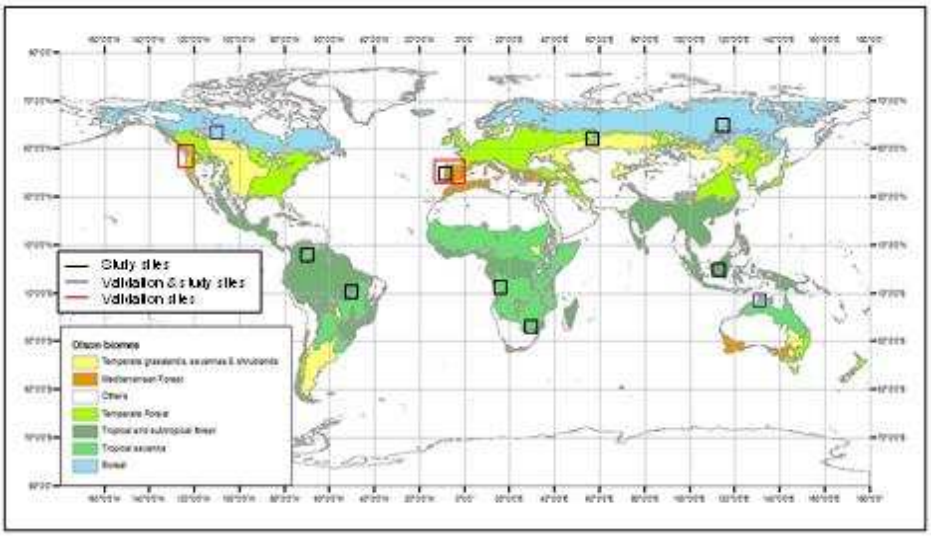

Figure 1. Study sites selection

Generation of corrected reflectances and spectral indices

Corrected MERIS reflectances were received from Brockman Consult. The pre-processing chain was based on the one developed for the Land CCI project with modifications to obtain daily reflectances instead of weekly composites as was required by this project. Geometric correction is obtained through the AMORGOS (Accurate MERIS Ortho Rectified Geo-location Operational Software), improving MERIS FR geolocation better than 70 RMS. Calibration and smile correction are also performed, as well as land water delineation, cloud screening and atmospheric correction. More details of these processes can be found in the ATBD from the Land CCI project (http://www.esa-landcover-cci.org/). The surface directional reflectances are floats between 0 and 1.0. As an output from the pre-processing, additional information layers are included with the MERIS images. Standard error associated to each band is provided. The angles are taken from the respective MERIS L1B input, sun and zenith viewing angles and sun and azimuth angles are provided in degrees. Also, a status layer is provided, with values 1 (clear land), 3 (snow/ice), or 0 (i.e. water, cloud, no observation).

In order to improve performance of the algorithm, the corrected reflectances were gridded into 10x10 degrees tiles (3600x3600 pixels at MERIS spatial resolution). These tiles were the input files for all processes of the BA algorithm.

The NIR region was selected as main input for the MERIS algorithm, since this spectral band has been shown to be highly sensitive to recent burns, especially when pre-fire fuel loadings are high and combustion produces large amounts of charcoal that are deposited on the ground (Pereira, Sa *et al.* 1999). Both green and dry vegetation have substantially higher reflectance than recent burns in the NIR. The suitability of this band to detect burned areas has been shown in previous studies (Chuvieco, Martín *et al.* 2002; Koutsias and Karteris 2000; Trigg and Flasse 2001).

In addition to the NIR band, we computed the Global Environmental Monitoring Index (GEMI) (Pinty and Verstraete 1992), which was proven the best performing to detect burned areas among the spectral indices based on the red-NIR space (Barbosa, Stroppiana *et al.* 1999; Chuvieco 2002; Chuvieco, Englefield *et al.* 2008; Martín, Gómez *et al.* 2005; Pereira, Sa *et al.* 1999). GEMI was computed as follows:

$$GEMI = \frac{\eta(1-0.25\eta)-(\rho_R-0.125)}{(1-\rho_R)}$$

$$\eta = \frac{2(\rho_{NIR}{}^2-\rho_R{}^2)+1.5\rho_{NIR}+0.5\rho_R}{(\rho_R+\rho_{NIR}+0.5)},$$

where ρ_{NIR} is the reflectance in the NIR (MERIS Band 10) and ρ_R is the reflectance in the Red (MERIS Band 8).

The selection of MERIS Bands 8 (673.75 nm to 688.75 nm), and 10 (746.25 nm to 761.25 nm), was based on the results from (Oliva, Martin *et al.* 2011), which showed a better sensitivity of the short NIR bands (bands 9 to 12) over the long NIR bands (bands 13 to 15) to discriminate BA areas. Following their conclusions, band 10 was used for the NIR region and bands 8 and 10 for computing the GEMI index.

Generation of composites

Temporal resolution of input data is quite relevant to build a global BA algorithm, since the analysis of post-fire reflectance may be easily contaminated by clouds or be affected by quick vegetation recovery. Therefore, the number of observations is a limiting factor for detecting fires in areas where images are not available for long periods of time. In order to improve spatial coherence of areas with low temporal continuity, monthly composites of near infrared reflectance (NIR) were generated. These composites were the basis for the two phases of BA detection. Composites were built for each month by selecting NIR information from a bi-monthly time space. This helps ensuring continuity in fire detection and is particularly relevant when a fire occurs in the final dates of a month.

The criteria for generating the monthly NIR-GEMI composites were chosen as to emphasize the sensitivity of the outputs to the burned signal. Two criteria were used: maximize the contiguity to fire dates and minimize the NIR signal. Since HS provide a very accurate estimation of burning dates (Boschetti, Roy *et al.* 2010), we first generated the composites selecting for each location the closest date to the closest HS. For doing so, a Thiessen matrix was created for each period, computing for each pixel the closest HS coordinates and labelling it with the date of that HS. For the Thiessen matrix we also considered HS located within a buffer of 0.5 degrees around the edges of each tile. This option mitigated potential continuity problems between tiles, when for instance a fire was in the edge between tiles.
The second compositing criteria selected minimum NIR reflectance values of the temporal series. However, since low NIR can be caused also for other reasons (cloud or topographic shadows, for instance), instead of selecting the minimum NIR of the 60 day period, we chose the first minimum after the date stored in the Thiessen HS matrix , as this would select a more immediate value to the post-fire burn reflectance. If no minima exist after that date, then the second minimum was chosen.
In addition to the monthly post-fire composites, an annual reference composite was created to help the contextual phase of the algorithm. This annual composite was obtained as the per pixel difference between the annual maximum GEMI value per year and the monthly GEMI composite. The former was created to obtain an estimation of the maximum annual greenness of each pixel time series. The expected change between that maximum value and the post-fire value (the GEMI monthly composite) should be the highest, which should emphasize post-fire spectral changes.

2.3. Seed selection

The first part of the seed selection focused on generating statistics of burned and unburned areas for each tile, based on the composite NIR values and HS distribution. Since burned conditions may be very diverse worldwide, we tried to obtain regional-oriented NIR thresholds, which could be tailored to different post-fire reflectance conditions. Cumulative distribution functions (CDF) were created to establish discrimination thresholds of NIR values that would be better adapted regionally to separate between burned and unburned categories.
The burned pixels to obtain the CDF of BA were obtained from the information provided by the MODIS HS to select the minimum NIR values. Since HS have an original resolution of 1000x1000 m, instead of assuming that all MERIS pixels covered by the HS are active fires, we assumed that the potential active fire (PAF) was more likely located where the MERIS NIR value was lowest in the 3x3 window around the HS. To avoid commission errors, we introduced an additional temporal change constrain, and accepted only those PAF where NIR values were lower than in the previous period. Otherwise, the minimum NIR values were not considered PAF to build the CDF of the burned category. The CDF of the unburned category was generated from the values of those pixels that did not have any HS in a 64x64 pixel matrix and were not detected by the BA algorithm in the previous months.
Specific discrimination thresholds were established for each tile and month. In order to compute them, the NIR threshold value of the burned category (TB) was defined as the decile of the burned pixels CDF that intersected the first decile of the CDF of unburned pixels (NIR values of burned pixels were expected to be lower than those of unburned ones) (fig 2). The more separated the CDFs between burned and unburned categories are, the higher the decile to define the burned category, as there are less chances of confusion with unburned category. On the opposite, the closer the CDFs the more pixel values are shared by the burned and unburned distributions, and therefore a more restrictive condition was chosen. It was considered a good discrimination between burned and unburned CDF when the threshold was established at 7 or more decile value, and bad discrimination otherwise. This classification was later used for phase 2 of the algorithm.

Seed pixels of burned category were selected based on three criteria:

a) The NIR value was lower than the TB for each tile and period.

b) At least one PAF should be found in a neighbour 9x9 matrix;

c) NIR value for month n should be lower than NIR of month n-1.

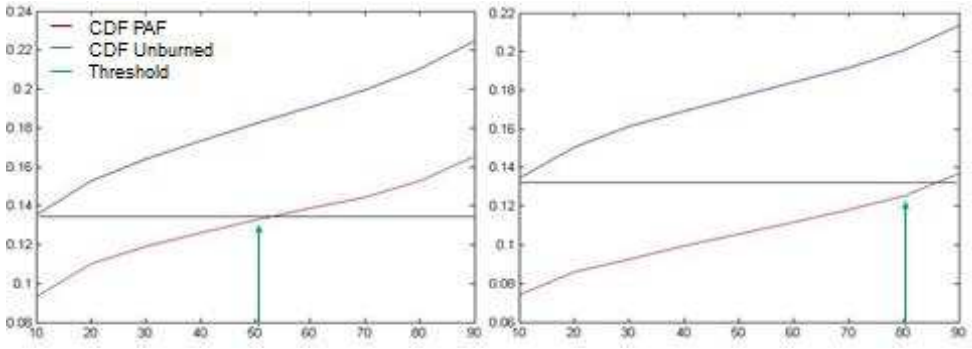

Figure 2. Threshold based on decile 10 of the unburned for a case with worse (left) and better (right) separation between classes for the Australian study site, correspondent to July & October 2005 respectively

2.4. Region growing

Contextual algorithms have been previously used for BA mapping (Bastarrika, Chuvieco *et al.* 2011b; Pu, Li *et al.* 2007). The goal of these algorithms is to reduce omission errors from the seed phase, while avoiding increasing commission errors. One of the critical issues to obtain a good performance of these algorithms for BA mapping relies on obtaining a sound method to stop the region growing process (Zhang, Pavlic *et al.* 2005).

Once the seeds were obtained, a region growing mechanism was applied to refine the characterization of burned patches. Only pixels surrounding the BA seeds were analyzed. This second phase of the BA algorithm included three conditions. These three conditions tried to account for a proper balance between extending the burned patches and avoiding commission errors. They were analyzed recursively around each seed pixel until their neighbour pixels did not meet them, which implied the end of the region growing process. If the criteria were met, the pixel will be included as seed and also its surrounding pixels will be studied. These criteria were:

a) The NIR threshold values were reviewed for this phase. If the TB was based on decile 6 or lower, it was assumed that the discrimination between categories is not good enough to increase the threshold. In this case the value was kept as it was for the seed phase. Otherwise, we assumed a better discrimination of burned and unburned categories and therefore, the NIR thresholds were increased for the region growing process up to the TB found at decile 9.

b) The decrease in NIR in burned pixels should be more negative than the threshold NIR decrease of unburned pixels. To define this new threshold we only considered those pixels more clearly unburned. We selected the first decile of the unburned CDF that has a higher value than decile 9 of the burned curve. For all pixels that satisfy this condition the difference with the composite from the previous month was computed. A new curve is built with these values. The minimum drop is defined as the percentile 90 of this curve.

c) Finally, the third condition was based on detecting the vegetation loss as a result of fire, based on the differences in GEMI values between the target monthly composite and the annual GEMI composites. This criterion was defined as 0.9 times the difference found in the GEMI value between the target pixel and those labelled as burned (either seeds or neighbour detected burns).

Results and validation

Three years of MERIS data (2006 to 2008) were processed with the described algorithm. Global BA obtained for years 2006, 2007 and 2008 was 3650268, 3772086 and 362327 km2 respectively. Figure 3 shows the BA obtained for year 2008.

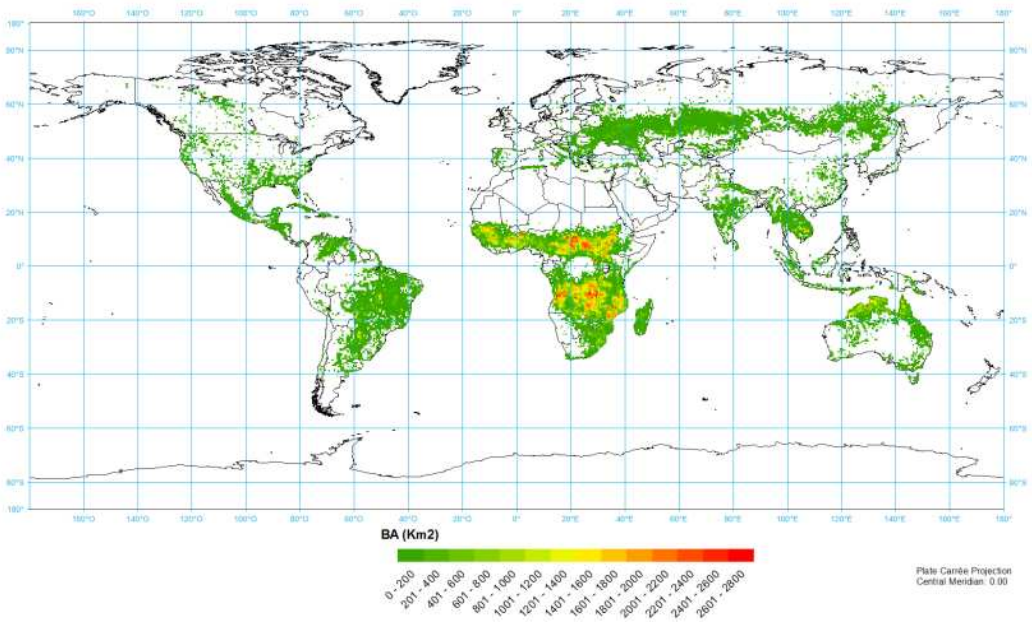

Figure 3. Global BA from MERIS in 2008

A complete global and temporal validation strategy has been developed within the Fire-CCI project. In this framework, a validation of the MERIS BA product performed with a LANDSAT validation dataset was performed. Results can be found in Padilla *et al*, 2014 (in preparation). The validation presented here is based on the use of perimeters obtained from different agencies and aims at validating the product in larger areas. The validation was performed for the 3 years where MERIS BA product is currently available (2006 to 2008).

Four areas were chosen:

- Canada: perimeters were downloaded from the Canadian Wildland Fire information System (cwfis.cfs.nrcan.gc.ca/ha/nfdb/). The Canadian National Fire Databse (CNFDB) is a collection of forest fire data from various sources, provided by Canadian fire management agencies (provinces, territories, and Parks Canada). The area designed to perform the validation is the Canadian study site (Figure 1). MERIS BA product and perimeters from the fire information system were reprojected to UTM.
- Australia: the Australian perimeters were downloaded from the North Australian Fire Information database (www.firenorth.org.au/nafi2/). Also the study site area was chosen to perform the validation (Figure 1). Both MERIS and perimeter databases were projected to UTM. Fire scars are sourced from the Darwin Centre for bushfires research at Charles Darwin University (for NT and northern WA fire scars) and Cape York Peninsula sustainable futures (for Queensland). They are obtained from 250 m MODIS imagery. Two images are used to map the affected areas, by using segmentation and visual interpretation (http://www.firenorth.org.au/nafi2/about/faq.pdf).

- The Californian perimeters were downloaded from the Fire and Resource Assessment program (FRAP) webpage (frap.fire.ca.gov). Fire perimeters information is obtained by several agencies. The validation site chosen covers an area of 572000km2 (Figure 1). MERIS data were reprojected to the perimeters database projection (alberts_conic_equal_area).
- Iberian Peninsula Perimeters were obtained from the European Forest Fire Information System (EFFIS). EFFIS makes use of satellite imagery acquired with MODIS. The area was selected to include the Iberian Peninsula, as shown in Figure 1. MERIS data were reprojected to the perimeters projection, standard European spatial reference system ETRS-LAEA, ETRS89, Lambert azimuthal equal area.

Validation results are shown in Table 1 for the 4 areas under study. Through the years same tendencies and range of commission and omission errors are identified. Overall there is a tendency towards omission for the 3 years. Australia shows higher omission errors. The Californian validation site shows a higher balance between omission and commission except for year 2008. The Canadian area has higher omission values, where as in the Iberian Peninsula the MERIS BA algorithm tends to overestimate the BA leading to higher commission errors.

Table 1. Validation for 4 areas, years 2006 to 2008.

	2006			2007			2008		
	CE	OE	OA	CE	OE	OA	CE	OE	OA
Australia	0.0854	0.4251	0.7887	0.1105	0.4291	0.8075	0.1416	0.4488	0.8498
California	0.3256	0.3409	0.9971	0.3538	0.3333	0.9955	0.1706	0.4568	0.9953
Canada	0.3062	0.4669	0.9809	0.0322	0.5597	0.9924	0.1412	0.7126	0.9807
SP & PT	0.4400	0.2363	0.9984	0.6545	0.3954	0.9994	0.8300	0.6327	0.9997

Figure 4 shows cumulative distribution curves that relate the number of fires detected per fire size for both the validation dataset (dotted line) and the MERIS one (black line) for year 2008. In the case of the validation datasets, perimeters are already identified by a number that differs for each perimeter. In the case of MERIS, perimeters were obtained by assuming that the pixels burned are part of the same perimeter when the dates between neighbour pixels do not differ in more than 15 days. In the Australian site, both NAFI and MERIS show the same tendency. Omission errors found in the validation exercise are shown by the fact that the MERIS line follows under the NAFI one for all fire sizes. For the other 3 validation sites the number of fires detected by MERIS is higher for small fire sizes where as it becomes lower for bigger size patches. This trend is especially clear for the Canadian site. Similar results and behaviour were obtained for years 2007 and 2006.

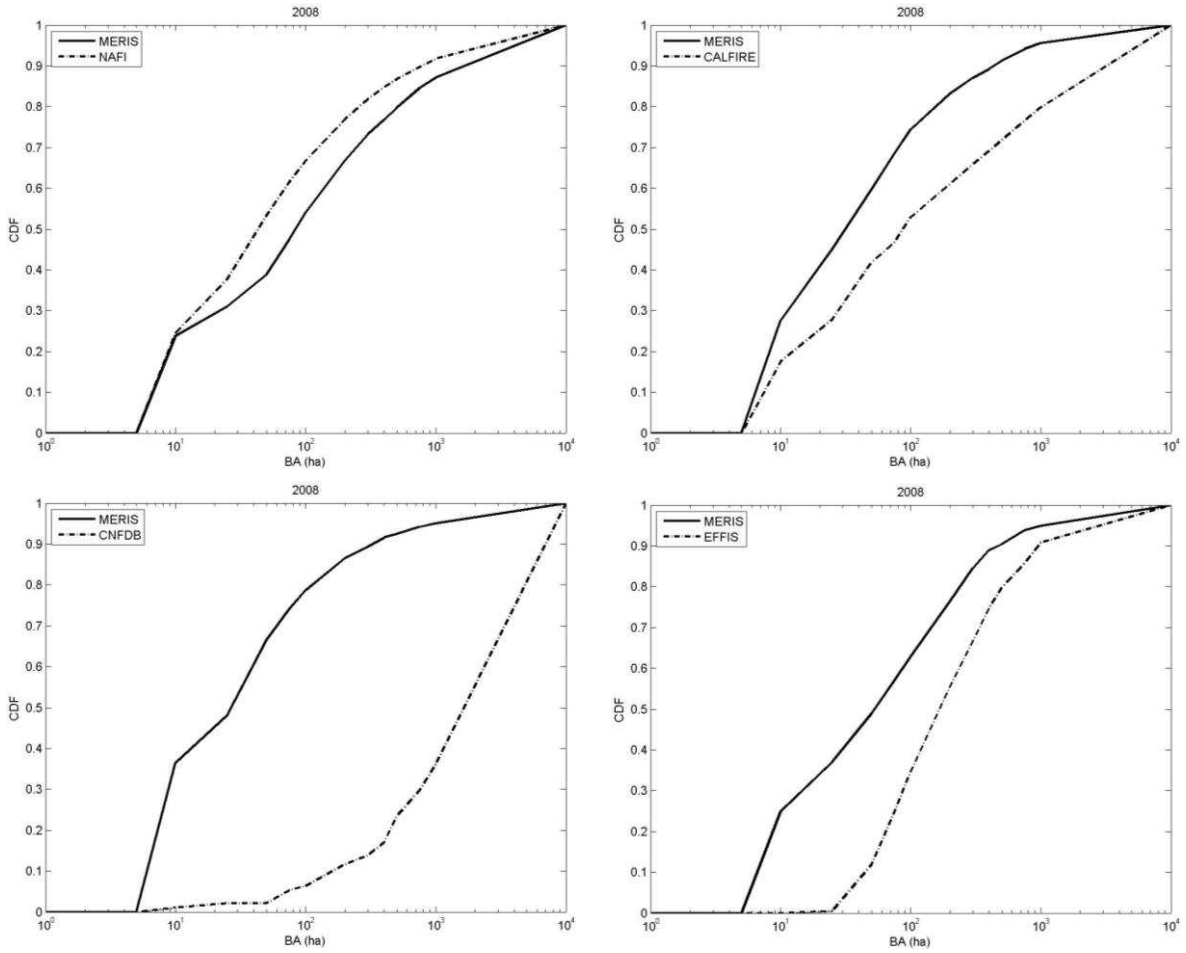

Figure 4. Fire size classification for 2008

We separated the BA by ecosystem, following the classification defined in (Giglio, Loboda *et al.* 2009). Results are shown in Table 2. The areas with higher fire activity are AUS, BOAS, CEAS, NHAF, SHAF, SHSA showing similar tendencies for the 3 years. When comparing the product globally to the MDC 64 (Table 2) results show that MERIS estimates more BA than MCD64 for the 3 years where the comparison has been performed, having the largest difference in 2008. Results are consistent in the order of magnitude for all regions. For 9 regions (CEAM, CEAS, EURO, NHAF, NHSA, SEAS, SHAF, SHSA, TENA) MERIS estimates are higher or in the same order as the GFED ones. In these cases, the trend is consistent between years, i.e. if a BA value increases from one year to the next in the MERIS case, the same behaviour occurs in the GFED. In another 3 regions (AUS, BONA and MIDE) BA MERIS estimates are lower or in the same order than GFED. There are only 2 regions where results are less consistent between the two products (BOAS and EQAS). In BOAS, 2006 has an order of magnitude higher in MERIS estimates, where as 2007 is higher than GFED but in the same range and 2006 is lower than GFED but in the same order. In EQAS 2006 has lower estimates than GFED, where as 2007 and 2008 have higher values.

Table 2. MERIS and GFED values for years 2006 to 2008 separated by ecoregion.

	2008		2007		2006	
ECO REGION	GFED	MERIS	GFED	MERIS	GFED	MERIS
AUST	266319	223018	487099	374883	530913	339800
BOAS	120490	106510	32399	43208	43288	113926
BONA	14465	6350	15458	9656	19117	13133
CEAM	11648	16153	10611	16085	12571	17256
CEAS	139938	171311	124669	151462	175395	172419
EQAS	4239	6068	4776	6370	26826	15085
EURO	5367	12624	9655	14450	4771	9891
MIDE	6036	6945	11770	8481	9015	8637
NHAF	1176668	1275054	1234422	1236476	1151535	1227041
NHSA	17754	24726	25153	27424	14925	15591
SEAS	69744	99912	98740	113824	59303	87737
SHAF	1315416	1473301	1242137	1396252	1221849	1395718
SHSA	133827	188187	338357	338256	124969	204359
TENA	14524	13118	26641	35257	24214	29676
GLOBAL	3296434	3623277	3661888	3772086	3418690	3650268

Discussion and conclusion

MERIS BA estimates are higher than the ones obtained by other collections such as GFED for the 3 years that have been processed, but remain in the same range. In 2 of these areas (AUS, BONA) validation was performed and results showed a tendency towards omission for the 3 years tested. More detailed identification of omission and commission errors will be available soon in Padilla *et al*, 2014. but from this preliminary study there seems to be an underestimation of BA in certain regions. There are 2 possible reasons for this:

- Omission inherent to the HS: as shown in (Hantson, Padilla *et al.* 2013), commission errors in the MOD14 product tend to be small, but omission errors can be significant, especially for some areas (South Africa, Colombia, Australia).
- Conditions too restrictive in both seed and growing phases. In the seed phase the algorithm does not consider all HS as seeds, pixels that do not satisfy the conditions detailed in the previous sections will not be classified as seeds. Filtering out some of the HS should not be a significant problem for large fires, since pixels around the detected PAFs will also be studied. Nevertheless, excessive filtering can become relevant for smaller fires, or in areas where there are less HS, as all HS could be filtered out in the seed phase, leading to non detection of the fire. In the growing phase conditions could be too restrictive particularly for some regions. In this case, larger fires will be considered smaller, and if there are several seeds for the fire this will probably lead to fragmentation of fires. This will lead to an over estimation of smaller number of perimeters in cases where the same fire is fragmented. This could explain the results shown in Figure 4, where smaller fires were more abundant that in the database due to the fact that the fire might be fragmented, and it was considered as more than one perimeter. Although when designing the algorithm the aim was to make it tailored for each region, the growing conditions might not be optimal for all types of land cover and ecosystems.

An algorithm to estimate burned areas on a global scale for the MERIS sensor has been presented. It is an hybrid algorithm that makes use of thermal and spectral information to detect fire scars. It is based on a two steps process: seed and growing phases. Results have been obtained for 3 years of data, and show consistency with other BA collections such as GFED. According to preliminary validation

results, there is a tendency towards omission. Future versions of the algorithm will consider these findings to refine the BA estimates.

References

Barbosa PM, Stroppiana D, Gregoire JM, Pereira JMC (1999) An assessment of vegetation fire in Africa (1981-1991): Burned areas, burned biomass, and atmospheric emissions. Global Biogeochemical Cycles 13, 933-950.

Bastarrika A, Chuvieco E, Martin MP (2011a) Automatic Burned Land Mapping From MODIS Time Series Images: Assessment in Mediterranean Ecosystems. IEEE Transactions on Geoscience and Remote Sensing 49, 3401-3413.

Bastarrika A, Chuvieco E, Martín MP (2011b) Mapping burned areas from Landsat TM/ETM+ data with a two-phase algorithm: balancing omission and commission errors. Remote Sensing of Environment 115, 1003-1012.

Boschetti L, Roy DP, Justice CO, Giglio L (2010) Global assessment of the temporal reporting accuracy and precision of the MODIS burned area product. International Journal of Wildland Fire 19, 705-709.

Chang D, Song Y (2009) Comparison of L3JRC and MODIS global burned area products from 2000 to 2007. Journal of Geophysical Research 114, 10.1029/2008JD11361.

Chuvieco E (2002) 'Teledetección Ambiental: La observación de la Tierra desde el Espacio.' (Ariel Ciencia: Barcelona)

Chuvieco E, Englefield P, Trishchenko AP, Luo Y (2008) Generation of long time series of burn area maps of the boreal forest from NOAA–AVHRR composite data. Remote Sensing of Environment vol. 112, 2381-2396.

Chuvieco E, Martín MP, Palacios A (2002) Assessment of different spectral indices in the red-near-infrared spectral domain for burned land discrimination. International Journal of Remote Sensing 23, 5103-5110.

Chuvieco E, Opazo S, *et al*. (2008) Global Burned Land Estimation in Latin America using MODIS Composite Data. Ecological Applications 18, 64-79.

De Santis A, Chuvieco E (2007) Burn severity estimation from remotely sensed data: performance of simulation versus empirical models. Remote Sensing of Environment 108, 422-435.

Giglio L, Loboda T, Roy DP, Quayle B, Justice CO (2009) An active-fire based burned area mapping algorithm for the MODIS sensor. Remote Sensing of Environment 113, 408-420.

Giglio L, Randerson JT, van der Werf GR, Kasibhatla PS, Collatz GJ, Morton DC, DeFries RS (2010) Assessing variability and long-term trends in burned area by merging multiple satellite fire products. Biogeosciences Discuss. 7, 1171-1186, doi:10.5194/bg-7-1171-2010,.

Giglio L, van der Werf GR, Randerson JT, Collatz GJ, Kasibhatla P (2005) Global estimation of burned area using MODIS active fire observations. Atmospheric Chemistry and Physics 5, 11091-11141.

González-Alonso F, Salgado, V., Calle, V., Casanova, J.L., Sanz, J., de la Fuente, D., Goldammer, J.G., Li, Z., Qin, X., Zhang, X., Deng, G., Liu, Q., Li, G., Cai, H. and Huang, Z. (2009) Forest burn in China by means of MERIS and MODIS images. Dragon 2 Symposium, June 2009, Barcelona.

Gower JFR, Borstad GA (2004) On the potential of MODIS and MERIS for imaging chlorophyll fluorescence from space. International Journal of Remote Sensing 25, 1459-1464.

Hantson S, Padilla M, Corti D, Chuvieco E (2013) Strengths and weaknesses of MODIS hotspots to characterize global fire occurrence. Remote Sensing of Environment 131, 152-159.

Huang S, Siegert F (2004) ENVISAT multisensor data for fire monitoring and impact assessment. International Journal of Remote Sensing 25, 4411-4416.

Kachmar M, Sanchez-Azofeifa GA (2006) Detection of post-fire residuals using high- and medium-resolution satellite imagery. Forestry Chronicle 82, 177-186.

Kaufman YJ, Justice CO (1998) 'MODIS Fire products.' NASA, EOS ID# 2741.

Kloster S, Mahowald N, Randerson J, Lawrence P (2012) The impacts of climate, land use, and demography on fires during the 21st century simulated by CLM-CN. Biogeosciences 9, 509-525.

Koutsias N, Karteris M (2000) Burned area mapping using logistic regression modeling of a single post-fire Landsat-5 Thematic Mapper image. International Journal of Remote Sensing 21, 673-687.

Martín MP, Gómez I, Chuvieco E (2005) Performance of a burned-area index (BAIM) for mapping Mediterranean burned scars from MODIS data. In 'Proceedings of the 5th International Workshop on Remote Sensing and GIS applications to Forest Fire Management: Fire Effects Assessment'. (Eds J Riva, F Pérez-Cabello and E Chuvieco) pp. 193-198. (Universidad de Zaragoza, GOFC-GOLD, EARSeL: Paris)

Oliva P, Martin P, Chuvieco E (2011) Burned area mapping with MERIS post-fire image. International Journal of Remote Sensing 32, 4175-4201.

Olson DM, E. Dinerstein, *et al*. (2001) Terrestrial Ecoregions of the World: A New Map of Life on Earth. BioScience 51, 933-938.

Pereira JMC, Sa ACL, Sousa AMO, Silva JMN, Santos TN, Carreiras JMB (1999) Spectral characterisation and discrimination of burnt areas. In 'Remote Sensing of Large Wildfires in the European Mediterranean Basin'. (Ed. E Chuvieco) pp. 123-138. (Springer-Verlag: Berlin)

Pinty B, Verstraete MM (1992) GEMI: a non-linear index to monitor global vegetation from satellites. Vegetatio 101, 15-20.

Pu R, Gong P (2004) Determination of Burnt Scars Using Logistic Regression and Neural Network Techniques from a Single Post-Fire Landsat-7 ETM+ Image. Photogrammetric Engineering and Remote Sensing 70, 841-850.

Pu RL, Li ZQ, Gong P, Csiszar I, Fraser R, Hao W-M, Kondragunta S, Weng F (2007) Development and analysis of a 12-year daily 1-km forest fire North America from NOAA/AVHRR data. Remote Sensing of Environment 108, 198-208.

Roldan-Zamarron A, Merino-De-Miguel S, Gonzalez-Alonso F, Garcia-Gigorro S, Cuevas JM (2006) Minas de Riotinto (south Spain) forest fire: Burned area assessment and fire severity mapping using Landsat 5-TM, Envisat-MERIS, and Terra-MODIS postfire images. Journal of Geophysical Research-Biogeosciences 111.

Roy D, Jin Y, Lewis P, Justice C (2005) Prototyping a global algorithm for systematic fire-affected area mapping using MODIS time series data. Remote Sensing of Environment 97, 137-162.

Roy DP, Boschetti L, Justice CO (2008) The collection 5 MODIS burned area product — Global evaluation by comparison with the MODIS active fire product. Remote Sensing of Environment 112, 3690-3707.

Tansey K, Grégoire JM, Defourny P, Leigh R, Peckel JF, Bogaert EV, Bartholome JE (2008) A new, global, multi-annual (2000–2007) burnt area product at 1 km resolution. Geophysical Research Letters 35, L01401, doi:10.1029/2007GL03156.

Thonicke K, Spessa A, Prentice IC, Harrison SP, Dong L, Carmona-Moreno C (2010) The influence of vegetation, fire spread and fire behaviour on biomass burning and trace gas emissions: results from a process-based model. Biogeosciences 7, 1991–2011.

Trigg S, Flasse S (2001) An evaluation of different bi-spectral spaces for discriminating burned shrub-savannah. International Journal of Remote Sensing 22, 2641–2647.

van der Werf GR, Randerson JT, *et al*. (2010) Global fire emissions and the contribution of deforestation, savanna, forest, agricultural, and peat fires (1997-2009). Atmospheric Chemistry and Physics 10, 11707–11735.

Zhang QF, Pavlic G, Chen WJ, Fraser R, Leblanc S, Cihlar J (2005) A semi-automatic segmentation procedure for feature extraction in remotely sensed imagery. Computers & Geosciences 31, 289-296.

Global mapping of burned areas from European satellites: the fire_cci project

Emilio Chuvieco, Itziar Alonso-Canas, Marc Padilla and Ruben Ramo

Environmental Remote Sensing Research Group, Universidad de Alcalá, Colegios 2, Alcalá de Henares, Spain; emilio.chuvieco@uah.es

Abstract
This paper presents the results of phase 1 of the fire_cci project. This project is part of the Climate Change Initiative of the European Space Agency, and aims to generate global, long-term burned area maps from European sensors (VEGETATION and MERIS). This information is intended to help modelling efforts of climate and atmospheric and carbon scientists, by adjusting to their needs in terms of product specifications. The project has done an extensive effort of validation and error characterization of the results. Intercomparison with other existing datasets has also been carried out.

***Keywords**: Burned area, Remote Sensing, Climate Change Initiative, GCOS, Earth Observation*

Introduction

The European Space Agency (ESA) Climate Change Initiative (CCI) is part of the European contribution to the Global Climate Observing System (GCOS) program. The CCI aims to produce consistent and accurate time series of Essential Climate Variables (ECV), which may be used by climate, atmospheric and ecosystem scientists for their modelling efforts Plummer 2009. The CCI stresses the importance of improving scientific impact of data acquired by ESA sensors, while maintain close links with key science bodies and other agencies currently generating ECV data. The first call of the CCI program has included 13 ECVs covering atmospheric products (ozone, greenhouse gasses, aerosols andclouds), oceanic variables (ocean colour, sea ice, ocean height and temperature), and terrestrial (fire, glaciers, ice sheets, soil moisture and land cover): http://www.esa-cci.org/.
Biomass burning is widely recognized as one of the critical factors affecting vegetation succession and carbon budgets worldwide (Chuvieco 2008; Thonicke *et al.* 2010). At regional and local scale, fires have also important socio-economic implications, both affecting lives and structures (Chuvieco *et al.* 2010). At a global scale, the effects of fire on the atmospheric chemistry, both in terms of CO2 and aerosols emissions are very relevant (Bowman *et al.* 2009; van der Werf *et al.* 2010). The most recent studies estimate that an average area of 3.5 million km2 is burned every year (Giglio *et al.* 2010; Tansey *et al.* 2008), mostly in the Tropical savannahs, temperate grasslands and boreal forests. Other impacts of fire on the global climate are still poorly understood, such as the direct and indirect role of aerosols, their impact on land use change and surface albedo, the relation with tropospheric ozone and the deposition of black carbon on soils (Bowman *et al.* 2009).
The fire_cci project aims to improve mapping of burned areas (BA), including proper validation and error characterization, as well as the use of BA information in global vegetation and atmospheric models. The fire-cci project has been developed by a consortium of ten teams from five different European countries: University of Alcalá, CIFOR-INIA and GMV (Spain); GAF, DLR and Julich (Germany), IRD and LSCE-CEA (France), ISA (Portugal), and University of Leicester (UK). These groups cover the different specialities required for the project: Earth Observation scientists, Climate-atmospheric-vegetation modellers and System engineers.

Methods

Figure 1 includes the general flowchart of the fire_cci project. The project started with the definition of user requirements, which guided the generation of product specifications. The Burned Area (BA) product was initially based on the analysis of ERS and ENVISAT-ATSR, SPOT VEGETATION (VGT) and ENVISAT MERIS sensors, although finally the ATSR datasets were discarded as they did not provide significant improvement over VGT data. The project included geometric and radiometric corrections, masks, BA and merging algorithms (to fuse BA results from VGT and MERIS sensors), as well as validation and intercomparison analysis.

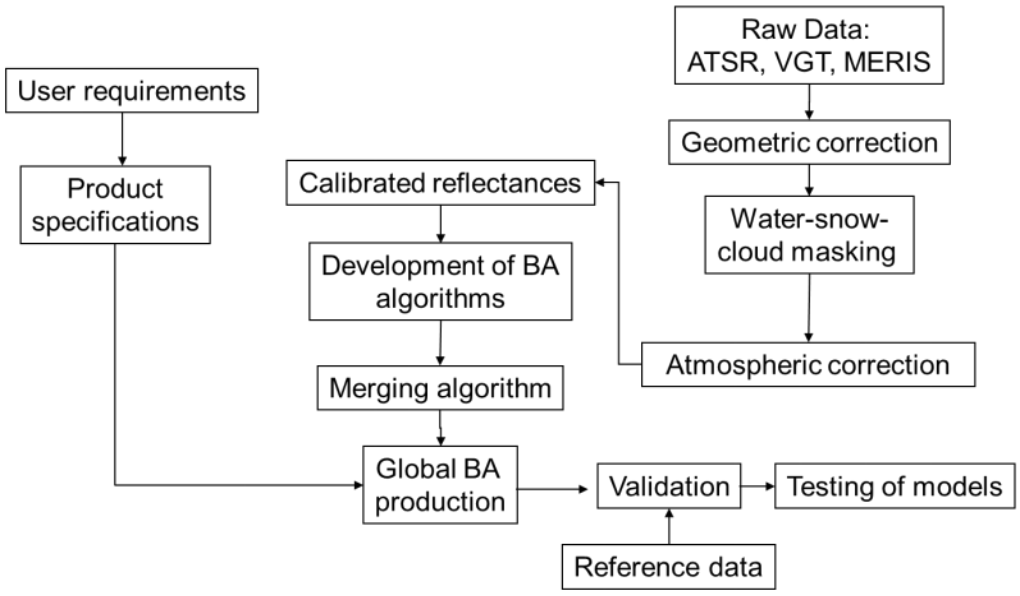

Figure 1. Fire_cci project flowchart

User requirements and product specifications

A proper understanding of user requirements of any product is a critical step to assure that the product will benefit the target community. In the case of the CCI program, the definition of user requirements was part of the program strategy. For the fire_cci project, a detailed questionnaire was addressed to potential users. Forty seven scientists from different fire-related communities (modellers, remote sensing experts, natural hazards, forestry sector...) provided their answers. They were complemented by an extensive literature review on past and present uses of available burned area (BA) products (Mouillot *et al.* 2014).

From this analysis, the product specifications (PSD) were generated. The fire_cci project includes two BA products, one at pixel level at 300 m resolution, and the other one at grid level at 0.5 degree resolution, following the most standard climate grid modelling (CGM) size). The pixel product includes four variables: day of burned detection, confidence level, sensor detecting the burn, and burned land cover. It will be distributed in monthly Geotiff format files, dividing the world in six tiles to make files more manageable (Figure 2). These tiles were agreed with the landcover_cci project to facilitate across-product consistency. The grid product includes 22 layers: sum of BA for each cell, standard error, fraction of observed area in the period, number of burn patches and burned area of each land cover (derived from globcover2005:Arino *et al.* 2007). These grid BA files are produced for 15-day periods in NetCDF format. Both pixel and grid products use the Plate Carré projection and geographical coordinates.

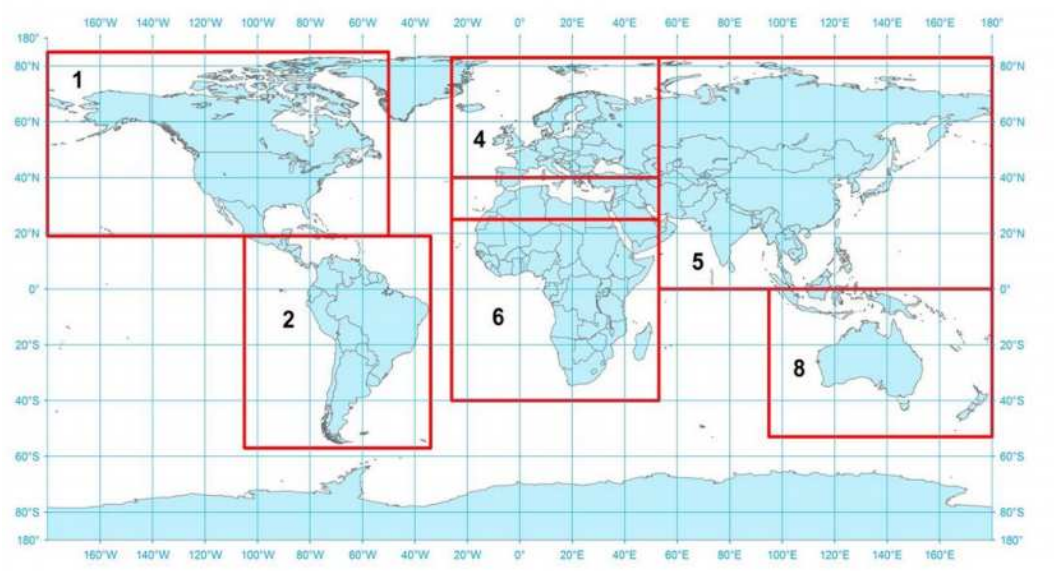

Figure 2. Tiles for the fire_cci pixel project

Pre-processing

The pre-processing, the BA products of the fire_cci project was based on level-1B and level-2 calibrated radiances from VEGETATION and MERIS. To derive corrected level 2 products, advanced image geometrical matching was applied to all sensors. Atmospheric correction was initially based on the ATCOR algorithm (Brazile *et al.* 2008) for ATSR and MERIS, by adapting the wide field of view of both sensors for this project. However, the final version of the processing chain was based on simpler atmospheric correction to improve process performance. Water, cloud snow and cloud shadow masks were developed to reduce the potential confusions in the BA algorithms, since these covers may present similar spectral characteristics to BA. Particularly challenging was the water mask, since water bodies may be seasonal (flooded areas), and the low radiances of water may be easily mixed up with post-fire char.

2.3. BA algorithms

Burned area algorithms were developed based on ten study sites selected from the main ecosystems affected by fire. These algorithms were adapted to VGT and MERIS sensors. Global BA algorithms are particularly challenging, as fire detection is affected by a wide range of factors: pre-fire conditions, burn severity, burn size and regeneration capacity of affected ecosystems (Bastarrika *et al.* 2011a; Giglio *et al.* 2009). The VGT algorithm was developed by the Instituto Superior de Agronomía (Pereira *et al.* 2014) and it is based on multitemporal trend analysis of near infrared reflectance. The process applies robust temporal filters to reduce the impact of instability of the time series, and provides scores of automatically detected changes to select those most likely connected to actual burnings. Initially the algorithm was also tested with ATSR data, but since the temporal resolution of this sensor is lower than VGT, the quality of outputs was considerably lower, and therefore it was decided to focus the global processing on VGT datasets.

The MERIS algorithm was developed from a hybrid two-phase approach, and took into account temporal changes of near infrared reflectance, as well as active fire detections from MODIS thermal channels. The algorithm is regionally adapted, as it estimates threshold values from cumulative distribution functions for both the seed and the region-growing phase (Alonso-Canas and Chuvieco 2014).

The final step was the merging of VGT and MERIS results into a single BA product. This merging was based on confidence levels derived from each sensor results, using a sample of the reference datasets.
A Round-Robin exercise was conducted between October, 2011 and January 2012, in which all available BA algorithms for VGT and MERIS images were tested. The results were compared using a set of statistical metrics. The goal of this exercise was to select the best performing algorithm for global production of burned area maps. The exercise was open to public participation. Once the final algorithms were selected, they were implemented in the global processing chain. For the current phase 1 of the fire_cci project, three global years have been processed (2006 to 2008).

2.4. Validation

Validation of the BA product was carried out by comparing BA outputs with reference fire perimeters generated from Landsat-TM/ETM+ multitemporal images. A standard protocol based on the CEOS LPV recommendations (http://lpvs.gsfc.nasa.gov). was generated and agreed between the internal validation teams to extract fire perimeters from Landsat data, based on a semi-automatic algorithm (Bastarrika *et al.* 2011b). Two samples of reference sites were obtained, one to measure the spatial variation of accuracy using 100 Landsat pairs acquired in 2008 (global validation), and the other one aiming to measure the temporal stability using a temporal series of Landsat scenes (one each year, whenever available in the Landsat archive) for ten representative study sites (temporal validation) (Figure 3). A total of 242 Landsat pairs were processed, including more than 147.000 burn patches and more than 126.000 km^2 of burned area.

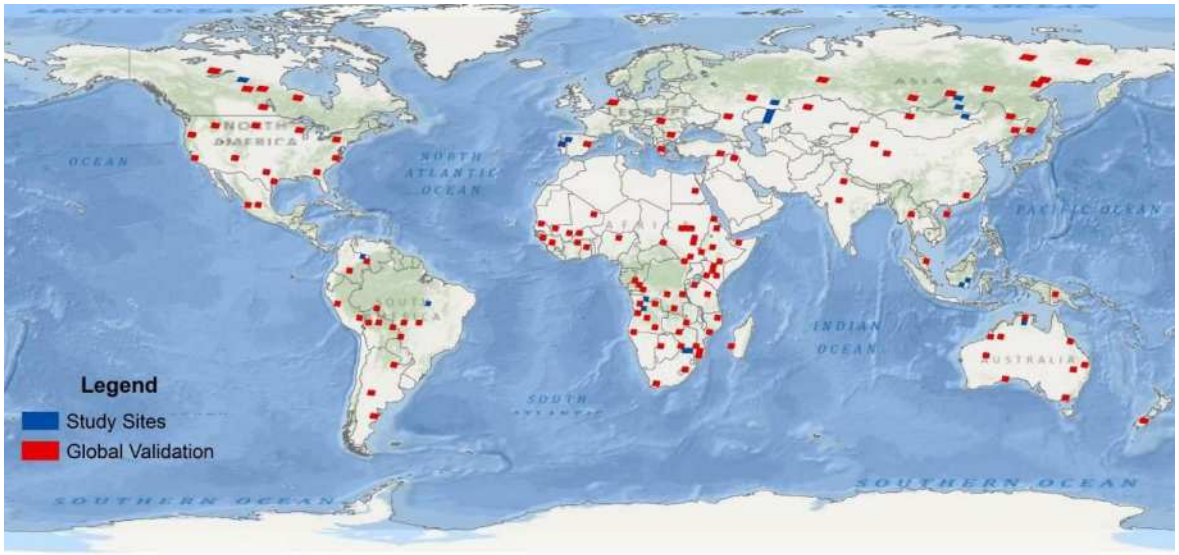

Figure 3. Location of validation sites for the fire_cci project

Validation was based on a fuzzy error matrix and covered three aspects: global accuracy (closeness to the true burned area), error balance (equilibrium between omission and commission errors) and temporal stability (temporal consistency of accuracy). Specific methods to tackle these three aspects were developed (Padilla *et al.* 2014a; Padilla *et al.* 2014b).

2.5. Intercomparison

The intercomparison analysis was based on comparing the total burned area for the fire_cci products and existing global BA products (Geoland, Globcarbon, GFED3 and MCD45) for each of the three years processed. Correlation analysis was also calculated between our results and existing products considering different ecoregions (those used by the GFED database: Giglio *et al.* 2010).

Results

Global datasets from 2006 to 2008 have been generated and are currently being assessed by climate modellers. In terms of sensors outputs, VGT identified less BA area than MERIS, particularly in tropical regions, as we can notice in Figure 4, and higher values in temperate regions, mainly in agricultural areas.
From preliminary validation, MERIS provides much higher accuracy than VGT, both when comparing with our validation sample and with existing BA products. The merged product showed an intermediate estimation of BA, higher than VGT but still lower than MERIS and other existing BA products (table 1).

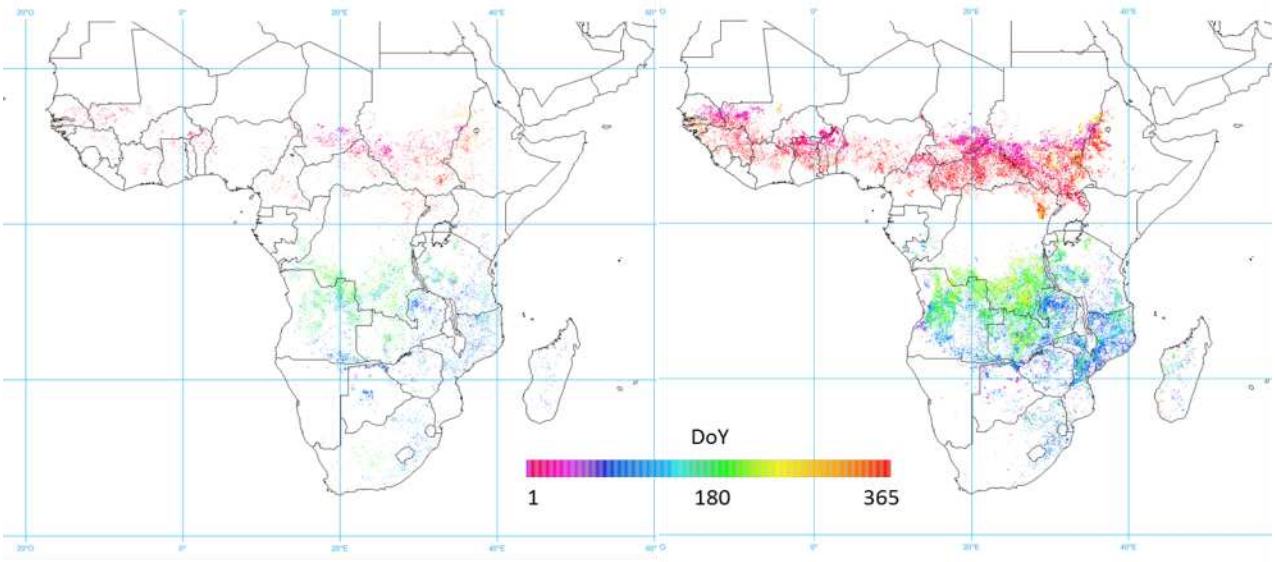

Figure 4. Date of Year (DoY) of Burned Detection from VGT (left) and MERIS (right) over the African continent (2008)

Table 1. Total Burned Area estimated by different global products (sq km)

	GFED	VGT	MERIS	MERGED	MCD45
2006	3418690	2374032	3650268	2853270	3372924
2007	3661888	2239012	3772086	2817410	3522453
2008	3296434	2228610	3623277	2687650	3307390

In terms of spatial variability, Figure 5 shows the estimated burned area from MERIS BA algorithm. The most extensive burnings occur in the Tropical regions, particularly in the African continent and, with less severity, in the Northern regions of Australia, Central Brazil, Venezuelan and Colombian Llanos, and SE Asia. A second belt of burned regions is noticeable in the temperate grasslands and croplands of central Asia, and SE USA. The boreal forest of Russia and Canada have also a substantial role in global biomass burnings.

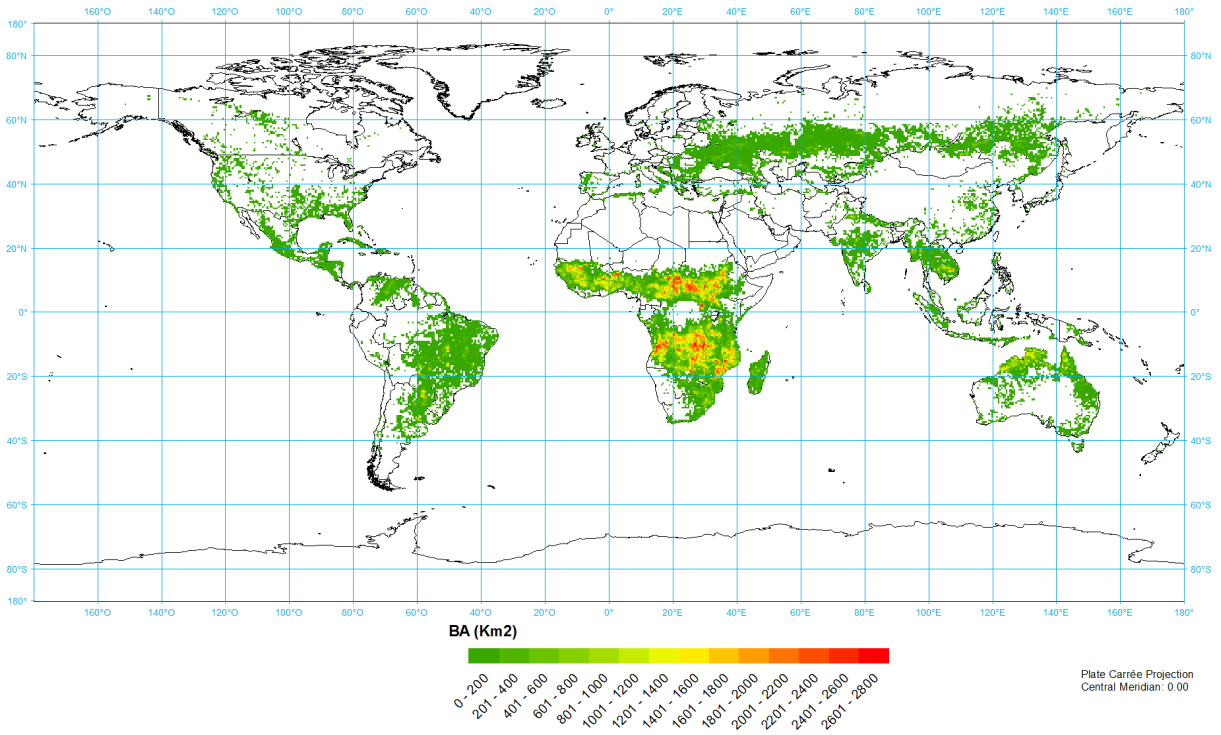

Figure 5. Burned Area estimated from MERIS (2008)

Finally, in terms of estimations produced by our product and other existing global BA products, Figure 6 includes scattergraphs that show the estimated BA in different ecoregions and products. The geographical units were defined by the Global Fire Emissions Database (GFED: Giglio *et al.* 2010), which is a widely-used information source for burned area information, based on MODIS data. Our MERIS product has very high correlations with GFED, with a tendency of around 10% to overestimation. Comparing with the standard MODIS BA product (MCD45), the results are similar in terms of trends, although in this case the tendency is towards underestimation.

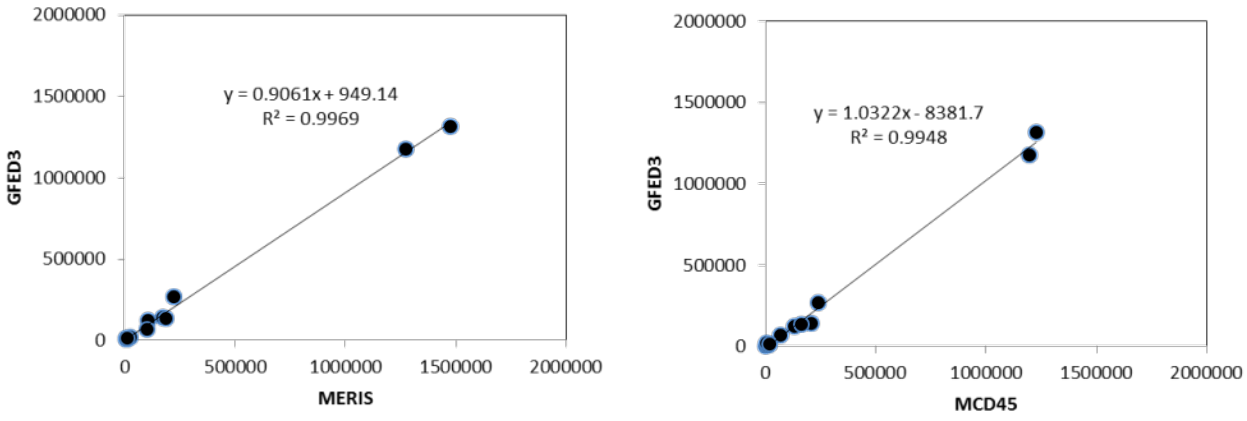

Figure 6. Correlations of BA estimations between MERIS, MCD45 and the GFED in different ecoregions (2008)

Conclusions

This paper has presented the first results of the fire_cci project, which aims to map global burned areas from European sensors. Results are currently in the validation stage, but preliminary assessments show good correspondence between our estimations and existing BA products. A climate assessment report to measure the performance of our product as input to existing carbon and atmospheric models is also under development.

Acknowledgements

This work has been performed within the ESA CCI program (http://www.esa-cci.org/), under the Fire Disturbance project contract.

References

Alonso-Canas I, Chuvieco E (2014) Global Burned Area Mapping from ENVISAT-MERIS data Remote Sensing of Environment (submitted).

Arino O, Gross D, Ranera F, Bourg L, Leroy M, Bicheron P, Latham J, Di Gregorio A, Brockman C, Witt R (2007) GlobCover: ESA service for global land cover from MERIS. 'IGARSS Symposium' pp. 23-28: Barcelona.

Bastarrika A, Chuvieco E, Martin MP (2011a) Automatic Burned Land Mapping From MODIS Time Series Images: Assessment in Mediterranean Ecosystems. IEEE Transactions on Geoscience and Remote Sensing 49, 3401-3413.

Bastarrika A, Chuvieco E, Martín MP (2011b) Mapping burned areas from Landsat TM/ETM+ data with a two-phase algorithm: balancing omission and commission errors. Remote Sensing of Environment 115, 1003-1012.

Bowman DMJS, Balch JK, Artaxo P, Bond WJ, Carlson JM, Cochrane MA, D'Antonio CM, DeFries RS, Doyle JC, Harrison SP, Johnston FH, Keeley JE, Krawchuk MA, Kull CA, Marston JB, Moritz MA, Prentice IC, Roos C, Scott A, Swetnam T, Van der Werf G, Pyne SJ (2009) Fire in the Earth system. Science 324, 481-484.

Brazile J, Richter R, Schlapfer D, Schaepman ME, Itten KI (2008) Cluster versus grid for operational MODTRAN-based look generation of ATCOR's up tables. Parallel Computing 34, 32-46.

Chuvieco E (2008) Satellite observation of biomass burning: implications in global change research. In 'Earth Observation and Global Change'. (Ed. E Chuvieco) pp. 109-142. (Springer: New York)

Chuvieco E, Aguado I, Yebra M, Nieto H, Salas J, Martín P, Vilar L, Martínez J, Martín S, Ibarra P, de la Riva J, Baeza J, Rodríguez F, Molina JR, Herrera MA, Zamora R (2010) Development of a framework for fire risk assessment using remote sensing and geographic information system technologies. Ecological Modelling 221, 46-58.

Giglio L, Loboda T, Roy DP, Quayle B, Justice CO (2009) An active-fire based burned area mapping algorithm for the MODIS sensor. Remote Sensing of Environment 113, 408-420.

Giglio L, Randerson JT, van der Werf GR, Kasibhatla PS, Collatz GJ, Morton DC, DeFries RS (2010) Assessing variability and long-term trends in burned area by merging multiple satellite fire products. Biogeosciences Discuss. 7, 1171-1186, doi:10.5194/bg-7-1171-2010,.

Mouillot F, Schultz MG, Yue C, Cadule P, Tansey K, Ciais P, Chuvieco E (2014) Ten years of global burned area products from spaceborne remote sensing—A review: Analysis of user needs and recommendations for future developments. International Journal of Applied Earth Observation and Geoinformation 26, 64-79.

Padilla M, Stehman SV, Chuvieco E (2014a) Validation of the 2008 MODIS-MCD45 global burned area product using stratified random sampling. Remote Sensing of Environment 144, 187-196.

Padilla M, Stehman SV, Litago J, Chuvieco E (2014b) Assessing the Temporal Stability of the Accuracy of a Time Series of Burned Area Products. Remote Sensing 6, 2050-2068.

Pereira JM, Mota B, Calado T, Alonso IJ, Oliva P, González-Alonso F (2014) 'ESA CCI ECV Fire Disturbance - Algorithm Theoretical Basis Document - Volume II - BA Algorithm Development.' ESA Fire-CCI project.

Plummer S (2009) 'The ESA Climate Change Initiative. Description.' (ESA-ESRIN: Frascati)

Tansey K, Grégoire JM, Defourny P, Leigh R, Peckel JF, Bogaert EV, Bartholome JE (2008) A new, global, multi-annual (2000–2007) burnt area product at 1 km resolution. Geophysical Research Letters 35, L01401, doi:10.1029/2007GL03156.

Thonicke K, Spessa A, Prentice IC, Harrison SP, Dong L, Carmona-Moreno C (2010) The influence of vegetation, fire spread and fire behaviour on biomass burning and trace gas emissions: results from a process-based model. Biogeosciences 7, 1991–2011.

van der Werf GR, Randerson JT, Giglio L, Collatz G, Mu M, Kasibhatla PS, Morton DC, DeFries RS, Jin Y, van Leeuwen TT (2010) Global fire emissions and the contribution of deforestation, savanna, forest, agricultural, and peat fires (1997-2009). Atmospheric Chemistry and Physics 10, 11707–11735.

Hardening structures to resist wildland-urban (WUI) fire exposures

Samuel L. Manzello

Fire Research Division, National Institute of Standards and Technology (NIST)
Gaithersburg, MD USA, samuelm@nist.gov

Abstract
Wildfires that spread into communities, referred to as Wildland-Urban Interface (WUI) fires, have destroyed communities throughout the world. In the USA, over 46 million homes in 70,000 communities are at risk of WUI fires [1]. Historically, fire safety science research has spent a great deal of effort to understand fire dynamics within buildings. Research into how to potentially mitigate the loss of structures in WUI fires is far behind other areas of fire safety science research. This is due to the fact that fire spread in the WUI is incredibly complex, involving the interaction of topography, weather, vegetation, and structures. Since the best way forward to address the WUI problem is the hardening of structures [2], the technical basis for improved test standards and fire and building codes are being developed. This paper provides a brief description of the NIST Dragon technology, recent application of the technology to various building assemblies and mulch, and closes with a series of research gaps that must be addressed to be able to design building components to resist firebrand ignition from WUI fire exposures.

***Keywords**: Wildland-Urban Interface (WUI), firebrands, ignition*

Introduction

Wildland-Urban Interface (WUI) fires continue to burn in the USA, and are rapidly getting worse, with attendant increased economic costs [1]. Some recent examples include the Bastrop Complex Fire in Texas in 2011, the Waldo Canyon Fire in Colorado in 2012, and fires in Arizona, Colorado, and California, in 2013. Firebrands are generated as vegetation and structures burn in these fires. While firebrand showers are responsible for a majority of structure ignitions in WUI fires (see any number of post-fire investigation reports over the past 60 years; for example Foote [3]), there exist no scientifically-based standard laboratory test methods to evaluate individual building component's resistance to ignition from wind-driven firebrand showers. Without standard laboratory test methods, it is impossible to evaluate and compare the performance of building elements ability to resist firebrand ignition. It cannot be overstated that current understanding of building component type to WUI exposure is still mainly predicated on *anecdotal* evidence. As a result, the limited WUI fire and building codes and standards in practice lack scientific rigor and, when implemented, it is not clear if these provide any benefit to structures in the path of hazardous WUI fires.

Before test standards are developed, full-scale experiments that systematically evaluate individual building component vulnerabilities to ignition to firebrand showers are required. It is critical to understand the full-scale assembly performance when exposed to wind-driven firebrand showers since weak points in a given assembly can be investigated. In turn, this will lead to determining the necessary scale of building component mock-ups that can be used in standard laboratory test methods. As wind is a critical component required to transport firebrand showers observed in actual WUI fires, and wind plays a major role in whether ignition is observed, full-scale experiments must be able to consider the influence of an applied wind field to understand such ignition vulnerabilities.

The Fire Research Division at NIST has embarked on research to begin to determine the vulnerabilities of structures to firebrand showers using the NIST Dragon coupled to a full-scale wind tunnel at the Building Research Institute (BRI). The BRI facility (Japan) has been used since it is the only facility

in the world to examine or study the behaviour of building component under wind-driven firebrand showers. Most recently, the NIST Dragon technology was improved to allow for the generation of continuous firebrand showers, as opposed to the original batch-feed Dragon (as described below). With this technology, it is now possible to systematically ascertain building component vulnerability to wind-driven firebrand showers of any duration [4-6]. The Dragon technology directly feeds into the NIST developed WUI Hazard Scale [7]. While beyond the scope of this paper, the WUI Hazard Scale attempts to provide a framework to quantify expected WUI fire exposure, and assign severity scales, for a given parcel and community. The vision is to establish a basis for the levels of hardening (ignition resistance) needed for buildings and communities to protect against exposure from WUI fires. As a result, with the Dragon technology, it will be possible to expose any type of building assembly to different levels of (radiative and convective) heat transfer and firebrand flux, thus enabling design of structures by tailoring fire resistance to the fire exposure and the hazard.

This paper provides an overview of the NIST Dragon technology, recent application of the technology to various building assemblies and mulch, and identifies a series of applied and fundamental research gaps that must be addressed to be able to begin to design building components to resist firebrand ignition from WUI fire exposures.

NIST Dragon Technology

The NIST full-scale Continuous Feed Firebrand Generator (NIST Dragon) consists of two parts: the main body and continuous feed component (**see Figure 1**). A brief overview is provided of the device; the interested reader is referred to recent review articles [5-6]. The feed system is connected to the main body and is equipped with two gates to prevent fire spread from ignition chamber back to the wood supply reservoir. A blower is connected to the main body and the purpose of the blower, described in more detail below, is to vary the combustion state of the generated firebrands from either glowing combustion or flaming combustion. The feed system consists of a pneumatic cylinder coupled to a cylindrical container where wood pieces, that will be ignited to produce firebrands, are stored. The pneumatic cylinder is contained inside a metal sleeve. Inside the metal sleeve, the sliding rod of the pneumatic cylinder is connected to a plate that allows the volume of wood contained within the sleeve to be varied. This volume can be set precisely to allow a specific mass of wood to fall into this volume. When the air pressure was applied, the sliding rod of the pneumatic cylinder moves forward, forcing the wood pieces that have fallen by gravity within the volume of the metal sleeve to the first gate, where they are then dropped into second gate that leads to the Dragon where they are ignited (see **Figure 1**). Douglas-fir wood pieces machined to dimensions of 7.9 mm (H) by 7.9 mm (W) by 12.7 mm (L) are used to produce firebrands. Firebrands generated from combustion of these wood pieces in the NIST Dragon have been shown to be consistent with sizes measured from full-scale burning trees, as well as size distributions obtained from actual WUI fires [6]. The number flux and mass flux of generated firebrands may be adjusted by varying the feeding rate of wood pieces into the device.

An operational parameter that is also varied is the blower speed. When the blower is set to provide an average velocity below 3.0 m/s measured at the exit of the Dragon when no wood pieces were loaded, insufficient air is supplied for combustion, and this results in a great deal of smoke being generated in addition to firebrands. At blower velocities above 3.0 m/s, smoke production is mitigated, and many of the firebrands are in a state of flaming combustion rather than glowing combustion. When firebrands contact ignitable fuel beds, they are typically in a state of glowing combustion, not open flaming. It is possible for firebrands to remain in a flaming state under an air flow, and it is reasonable to assume that some firebrands may still be in a state of flaming combustion upon impact. The purpose of this device is to simulate firebrand showers observed in long-range spotting and therefore firebrands in a

state of glowing combustion are desired. Yet, the NIST Dragon is also capable to generate showers of flaming firebrands as well.

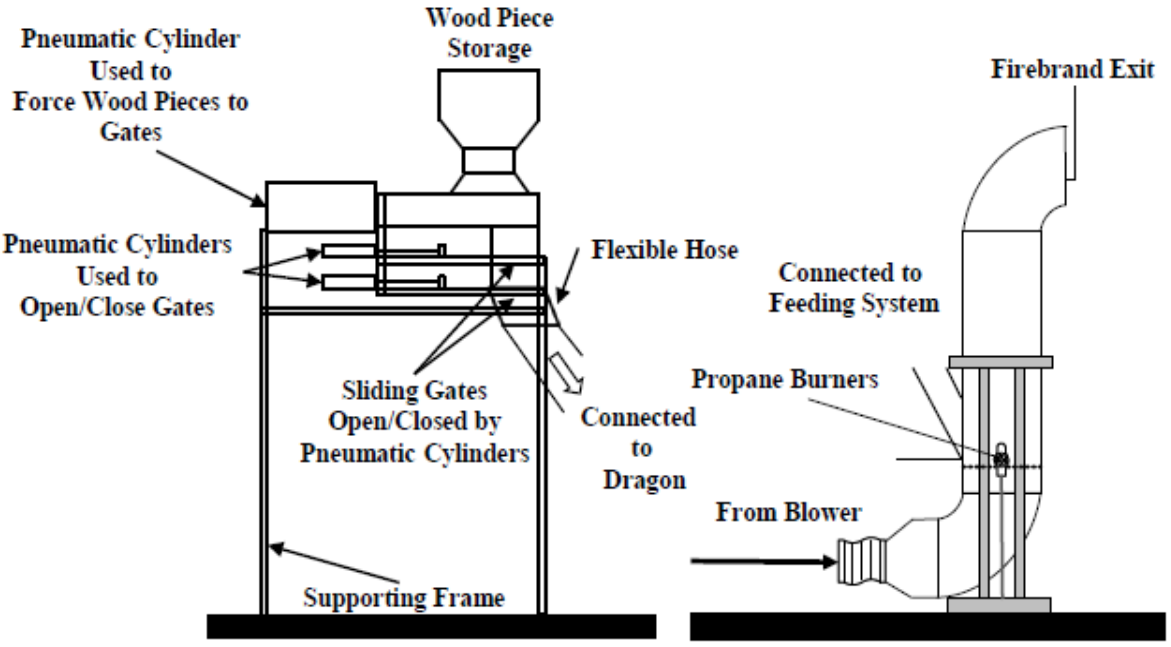

Figure 1Schematic of Full-Scale Continuous Feed Firebrand Generator

3. Current Knowledge Gaps – Applied Research Gaps

3.1. Decking Assemblies

In WUI fires, wood decking assemblies have been observed to be an ignition vulnerability based on post-fire damage surveys conducted by NIST and elsewhere. The California Office of the State Fire Marshal (OFSM) adopted the test method known as State Fire Marshal (SFM) STANDARD 12-7A-4 [8]. The SFM test method is intended to determine the response of decks to firebrand exposure and is very similar to the ASTM E108 [9] roofing test Namely, a firebrand is simulated by placing a burning wood crib (either Class A, B, or C firebrand) on top of a section of a deck assembly under an air flow. Class A is intended to represent the most severe firebrand exposure as it represents the largest crib size (30.48 cm x 30.48 cm x 5.715 cm). The dynamic process of multiple firebrands bombarding decking materials as a function of time is not taken into account in this standard test method. In addition to not simulating a dynamic firebrand attack, no attempt is made to relate the size and mass of the firebrand used in this standard to actual firebrands produced from burning vegetation and structures. There is no evidence to suggest that this test is a 'worst-case' firebrand exposure for decking assemblies.

Recent experiments using the NIST Dragon have demonstrated the dangers of the dynamic process of continual, wind-driven firebrand showers landing onto decking assemblies for the first time [9]. For each wood decking assembly type tested (cedar, Douglas-fir, and redwood), the accumulation of glowing firebrands resulted in flaming ignition of the deck boards. It was also observed that ignition of the deck boards produced smoldering ignition in the support members under the decking assembly (**see Figure 2-3**). Additional experiments must consider more wood types as well as composite (wood/plastic) decking assemblies to determine its performance when exposed to continuous wind-driven firebrand showers. These experiments should be compared to experiments using protocols outlined in SFM STANDARD 12-7A-4 [8]. Finally, it is important to determine whether decking

assemblies, once ignited, can result in a fire spreading to adjacent building components. Therefore, future full-scale experiments are required to address the questions:

- Is the current decking test method that uses Class A firebrand exposure adequate?
- If decking assemblies are ignited, are they capable to ignite adjacent building components?

Figure 2. Picture of the underside of the decking assembly (cedar); overall view [10].

Figure 3. Detail of the underside of the decking assembly (cedar). The ignition process was observed to spread to the wood supporting members [10].

Roofing Assemblies

As indicated above, the ASTM E108 [8] roofing test is used to evaluate ignition of roofs to firebrands by placing a burning wood crib on top of a section of a roof assembly under an air flow, yet, similar to decking assemblies, the dynamic process of multiple firebrands landing under ceramic tiles/gaps as a function of time is not taken into account [6]. Post-fire studies have identified a building ignition mechanism where small firebrands penetrate under non-combustible tile roof coverings [6]. Experiments conducted using the NIST Batch-Feed Dragon has provided experimental confirmation of this ignition mechanism for ceramic tile roofing assemblies (see **Figure 4** and [11] for more details).

Figure 4. ***Images of experiments conducted using oriented strand board/ceramic tile (OSB/CT) without bird stops installed [11]. Intense smoldering ignition (SI) was observed within the OSB base layer and eventually flaming ignition (FI) was observed. The wind tunnel speed was 7 m/s and the Firebrand Generator was located 2.0 m from the CT roofing assembly. The dimensions of the roof assembly were 122 cm by 122 cm.***

In addition, concrete tile roofing assemblies (flat and profiled tile; **see Figure 5**) as well as terracotta tile roofing assemblies (flat and profiled tile) commonly used in the USA, Australia, and elsewhere were exposed to wind-driven firebrand showers [12]. The purpose of these *scoping* experiments was to determine if firebrands were able to penetrate the roofing tile assemblies and melt the underlying sarking material. No sheathing layer was included in the roof support structure as these experiments were intended to replicate Australian construction details [12]. The results, however, are relevant to US construction since the same concrete (flat and profiled) and terracotta (flat and profiled) tiles are used in both countries. Underlayment or sarking, in the form of a layer of aluminium foil laminate bonded with a fire retardant adhesive to a polymer fabric, was placed under the tile battens. The results showed that firebrands penetrated the tile gaps and subsequently melted the sarking material for both types of concrete tile roofing assemblies (flat and profiled tile) and the profiled tile terracotta roofing assembly when exposed to wind-driven firebrand showers (**see Figure 6**). The flat tile terracotta roofing assembly appeared to perform better due to its interlocking design. For these tiles, the firebrands were observed to become trapped within the interlocking sections of the tiles and as a result, the firebrands were not able to penetrate past the tiles toward the sarking material. Based on the findings of these experiments, a potential cost-effective mitigation strategy might be to use a continuous underlayment of firebrand-resistant sarking [12].

Figure 5. Concrete Tile Roofing Assembly (profiled tile) Exposed to Wind-Driven Firebrand Showers. The dimensions of each tile were 420 mm long by 320 mm wide. The Height, from the Wind Tunnel Floor to the Base of the Gutter of Roof Deck was 1250 mm [12].

Figure 6. Images of Sarking Placed Under Concrete Tiles (profiled tile) Taken Immediately after the Experiment was Completed. The Tiles have been removed [12].

To further address the issue of wind-driven firebrands, the State of California in the USA mandated the use of a non-combustible mineral surfaced cap sheet under roof tiles [13]. These requirements have never been tested to wind-driven firebrand exposure. A series of open questions remain:

- All roofing assembly experiments conducted by NIST (described above) have made use of the batch feed NIST Dragon. What happens to roofing assembly performance when experiments are revisited with the improved continuous feed Dragon capable of longer firebrand exposures?
- Is the current requirement mandated in California [12] on the use of a non-combustible cap sheet under roof tiles adequate?
- Should the legacy ASTM E108 [9] roofing test be modified to consider continuous wind-driven firebrand exposure to roofing assemblies?

3.3. Mulch Located Adjacent to Structures

Buildings are often surrounded by vegetation that, when ignited, can produce intense, localized firebrand showers, and provide direct flame contact onto building elements, leading to ignition of buildings. The creation of defensible space around structures is a common mitigation strategy, yet in many areas the requirement for the creation of defensible space is either not popular due to resistance to modify the natural environment and landscaping around structures, or not practical due to limited lot/land parcel size. Of particular concern are wood landscape mulches located adjacent to buildings. While there have been some studies of mulch ignition in the literature, none of these studies have investigated the ignition of mulch installed in realistic building configurations exposed to wind-driven firebrand showers; conditions seen in real WUI fires.

Figure 7 displays a typical experiment to expose shredded hardwood mulch beds to continuous wind-driven firebrand showers. In this image, the wind tunnel speed was 6 m/s and the mulch bed moisture content (MC) was 11 % (dry basis). While full details of these results are beyond the scope of this paper (see [14] for full details, it is rather clear that continuous-wind driven firebrand showers are capable of rapidly igniting mulch beds (**see Fig.7**).

Figure 7. Image of 1.2 m by 1.2 m by 51 mm (depth) shredded hardwood mulch bed at 11 % MC exposed to continuous wind-driven firebrand showers. The re-entrant corner, with dimensions of 1.2 m by 1.2 m by 2.44 m high, was lined with gypsum board to investigate the ignition of the mulch bed itself; the ability of the mulch bed to ignite the wall assembly was not considered [14].

- Are wind-driven firebrand showers capable of igniting common wood mulches found in WUI communities?
    - Shredded hardwood mulch was observed to ignite. How about other common mulch types such as pine bark, pine bark nuggets, and pine straw?
- Once ignited, is the wood mulch bed capable of producing ignition of the structure itself?

3.4. Wood/Vinyl Fencing Assemblies

Post-fire studies conducted by NIST on the Waldo Canyon Fire in Colorado (2012) suggested that wood fencing assemblies are vulnerable to ignition from firebrand showers in WUI fires, but again there has never been any experimental verification of this ignition mechanism. Fencing assembly ignition has also been observed in Australia [15]. Presently, there is lack of understanding on fence assembly ignition vulnerabilities under wind-driven firebrand exposure. **Figure 8** displays results obtained when exposing redwood fencing to continuous firebrand showers. Redwood fencing assemblies were observed to produce their own firebrands.

- Do fence assemblies, if ignited by wind-driven firebrand showers, transfer or link the fire to the structure?
- Are certain fencing assembly types more amenable to firebrand generation?

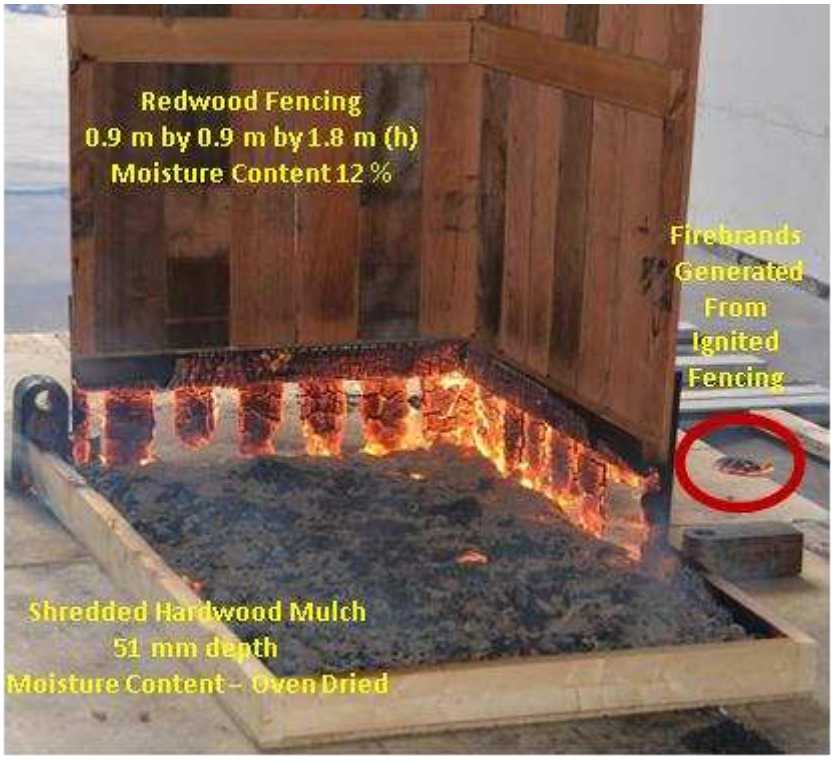

Figure 8 Redwood fencing (inside corner section), exposed to wind-driven firebrand showers at 8 m/s from the NIST Dragon. The firebrands produced smoldering ignition in the shredded hardwood mulch bed (foreground; depth 51mm), this transitioned to flaming ignition in the mulch, and the redwood fencing was subsequently ignited by the mulch. Shredded hardwood mulch was intended to represent various fuels that are adjacent to fencing in the Wildland-Urban (WUI). As the redwood fence continued to burn, firebrands were generated with large projected area and low mass, and were blown downstream (far right).

3.5. Different Wall Siding Types

Complete lack of understanding on wall ignition vulnerabilities under wind-driven firebrand exposure.

- Are test standards [16] that exist for direct flame impingement adequate?
- Once ignited, are certain combustible siding types more likely to generate firebrands?

Translating Full-Scale Experimental Results to Laboratory Test Standards

As needed physical understanding is being collected from the full-scale experiments, work is required to develop reduced-scale test methods that will be able to reproduce results of the full-scale experiments above. The specific exposure ranges (*e.g.* duration of firebrand flux) will be determined as further understanding of WUI fire exposure develops. It is important to understand that is a significant challenge.

As mentioned, a very important characteristic of the NIST Dragon is that the firebrand size and mass produced using the device can be tailored to those measured from full-scale tree burns [17-18], and actual WUI fires [19], which are in stark contrast with the size of firebrands referenced in existing test standards and wildfire protection building construction recommendations. In collaboration with the California Department of Forestry and Fire Protection (CALFIRE), NIST quantified firebrand distributions from a real WUI fire (2007 Angora Fire) [19]. Specifically, digital image analyses of burn patterns from materials exposed to the Angora Fire were conducted to determine firebrand size distributions. The firebrand size distributions reported were compared to firebrand size distributions from experimental firebrand generation using the NIST Dragon, as well as historical firebrand field studies. The most salient result reported in [19] was the documentation of the consistently small size of firebrands (<0.5 cm^2) and the close correlation of these results with the sizes of experimentally generated firebrands from the NIST Dragon. The Texas Forest Service has used this methodology to collect firebrand size distributions from the recent Texas Bastrop Complex fires in 2011, as well, and reported similar findings to the 2007 Angora fire; significant numbers of very small firebrands were produced [20].

- More information of this type is clearly needed from actual WUI fires - this is an important challenge for future WUI fire research.
- Other than the Angora Fire and Bastrop Fire data sets, which are limited, no other information on firebrand distributions from actual WUI fires is available.

Rapidly deployable instrumentation packages that can be placed in the path of WUI fires to collect information on firebrand fluxes generated in *actual* WUI fires are needed. The authors have developed such a system to quantity heat flux from WUI fires and the concept was vetted in prescribed fires, but this methodology must be extended to collect needed firebrand flux [21] from actual WUI fires. It is difficult to simulate the range of WUI fuels (*e.g.* structures) and wind speeds in prescribed fires, and as a result, using only firebrand data from prescribed fires will not give meaningful data from actual WUI events. Prescribed fires are, however, a useful place to test a conceptual firebrand flux instrument package.

Fundamental Research Needs

As indicated above, much applied research is needed to be able to begin to consider designing structures to resist firebrand ignition in WUI fires. Yet, it is important not to overlook fundamental research needs that are an integral part of this problem as well. Important fundamental needs also link WUI research to materials science research, as better fundamental ignition data will lead to enhanced, firebrand resistant materials. Specifically, these needs are:

- Fundamental understanding of ignition of building elements by firebrands, answering questions such as:
  - What is the mechanism of ignition of building elements by firebrands?
  - How does firebrand accumulation influence the heat flux applied to adjacent ignitable materials?
  - How does wind influence accumulation as well as the burning and heat transfer from accumulated firebrands to an ignitable material?
- Forensic analysis of firebrands collected from WUI fires, answering questions such as:
  - What are firebrands comprised of?
  - Is it possible to determine the source of firebrands from burned samples?
    What types of firebrand materials have a greater potential of igniting materials (vegetative and building elements)?

Summary

Research into WUI fires, and how to potentially mitigate the loss of structures in such fires, is far behind other areas of fire safety science research. This is due to the fact that fire spread in the WUI is incredibly complex, involving the interaction of structures with topography, weather, and vegetation, and other structures [6]. While WUI research is challenging, this paper attempts to delineate a series of current research gaps in order to be able to begin to harden structures to firebrand showers, an important aspect of WUI fire exposure.

References

[1]"U.S. Communities Dealing with WUI Fire Fact Sheet (ICC) 1.1.2011," Headwaters Economics, www.headwaterseconomics.org.

[2]J. Pellegrino, J., N.P. Bryner, and E.L. Johnsson, Wildland-Urban Interface (WUI) Fire Research Needs - Workshop Summary Report, NIST SP 1150 (2013).

[3]E.I.D. Foote, Structure survival on the 1990 Santa Barbara "Paint" fire: A retrospective study of urban-wildland interface fire hazard mitigation factors, MS thesis, University of California at Berkeley, p. 129; 1994.

[4]S.L. Manzello, S. Suzuki, S., and Y. Hayashi, Enabling the Study of Structure Vulnerabilities to Ignition from Wind Driven Firebrand Showers: A Summary of Experimental Results, *Fire Safety Journal*, 54:181-196 (2012).

[5] S.L. Manzello, and S. Suzuki, Experimentally Simulating Wind Driven Firebrand Showers in Wildland-Urban Interface (WUI) Fires: Overview of the NIST Firebrand Generator (NIST Dragon) Technology, *Procedia Engineering*, 62:91-102 (2013).

[6]S.L. Manzello, Enabling the Investigation of Structure Vulnerabilities to Wind-Driven Firebrand Showers, *Fire Safety Science* 11, in press, (2014). Presentation available on YouTube: http://www.iafss.org.

[7]A. Maranghides, W. Mell., Framework for Addressing the National Wildland Urban Interface Fire Problem—Determining Fire and Ember Exposure Zones using a WUI Hazard Scale , NIST Technical Note 1748 (2012).

[8]Office of the State Fire Marshal (SFM), Decking, STANDARD 12-7A-4.

[9]ASTM E108 (2003) Fire Standards and Flammability Standards, ASTM International, West Conshohocken, PA.

[10] S.L. Manzello, S. Suzuki, Exposing Wood Decking Assemblies to Continuous Wind-Driven Firebrand Showers, *Fire Safety Science* - in press (2014).

[11] S.L.Manzello, Y. Hayashi, Y. Yoneki, Y. Yamamoto, Quantifying the Vulnerabilities of Ceramic Tile Roofing Assemblies to Ignition During a Firebrand Attack, *Fire Safety Journal* 45:35-43, (2010).
[12] S.L. Manzello, The Performance of Concrete Tile and Terracotta Tile Roofing Assemblies Exposed to Wind-Driven Firebrand Showers, NIST Technical Note 1794, 2013.
[13] California Building Standards Code, Title 24, California Code of Regulations, Volume 1, Chapter 7A, 2013.
[14] S. Suzuki, S.L. Manzello, K. Kagiya, J. Suzuki, and Y. Hayashi, Ignition of Mulch Beds Exposed to Continuous Wind-Driven Firebrand Showers, *Fire Technology*, in review, 2014**.**
[15] S. Suzuki, E. Johnsson. A Maranghides, and S.L. Manzello, Ignition of Wood Fencing Assemblies Exposed to Continuous Wind-Driven Firebrand Showers, *Int'l J. Widland Fire*, in review, (2014).
[16] Office of the State Fire Marshal (SFM), Exterior Wall Siding and Sheathing, STANDARD 12-7A-1.
[17] S.L. Manzello, A. Maranghides, and W. Mell, W. Firebrand Generation from BurningVegetation*, Int'l J. Wildland Fire*, 16: 458-462 (2007).
[18] S.L. Manzello, *et al*., (2009) Mass and Size Distribution of Firebrands Generated from Burning Korean Pine (Pinus koraiensis) Trees, *Fire and Materials* 33:21–31 (2009).
[19] S.L. Manzello, S.L., and E.I.D. Foote, Characterizing Firebrand Exposure from WildlandUrban Interface (WUI) Fires: Results from the 2007 Angora Fire, *Fire Technology* 50:105-124 (2014).
[20] S.Rissel, S., and K. Ridenour, Ember Production During the Bastrop Complex Fire, Fire Management Today, 72: 7-13 (2013).
[21] S.L. Manzello, S.H. Park, J.R. Shields, and T.G Cleary, Development of Rapidly Deployable Instrumentation Packages for Data Acquisition in Wildland–Urban Interface (WUI) Fires, *Fire Safety Journal*, 45: 327-336 (2010).

Ignition of wood subjected to the dynamic radiant energy flux

Alexander Filkov, Kuznetsov V.T., Guk V.O

National Research Tomsk State University, 36 Lenin Ave., Tomsk, Russia, aifilkov@gmail.com

Abstract
In this paper we analyzed the ignition of the wood samples subjected to the dynamic heat flux. The experimental setup was created on the base of the optical wave "Uran-1" with a radiation source. The intensity of the heat flux was changed during the experiment by moving the test sample along the optical axis of the elliptic reflector in the setup. Pine wood was used as the test samples. We received the delay times for ignition of pine wood during heating under conditions of the decreasing and increasing heat flux. The received data were compared with the data for a static heat flux.

***Keywords**: wood, dynamic radiant energy flux, wood, ignition time*

Introduction

In [1] it is reported that the ignition process is essentially dependent on the type of heat flux, whether it is static or dynamic (when the ignition of fuels is initiated by time-dependent heat flux). At the same time, the ignition of fuels under dynamic conditions has been insufficiently studied. There are only some experimental work [2, 3], where the ignition of fuels was carried out under dynamic conditions of heat supply. Taking into consideration that the dynamic type of the heat flux dominates in the real conditions, the urgency of this problem is obvious.

Methods

In [1] the first results were received, in particular, it was developed an experimental technique. The radiant energy source was an Uran-1 optical wave with a DKsR-10000 (Figure 1).

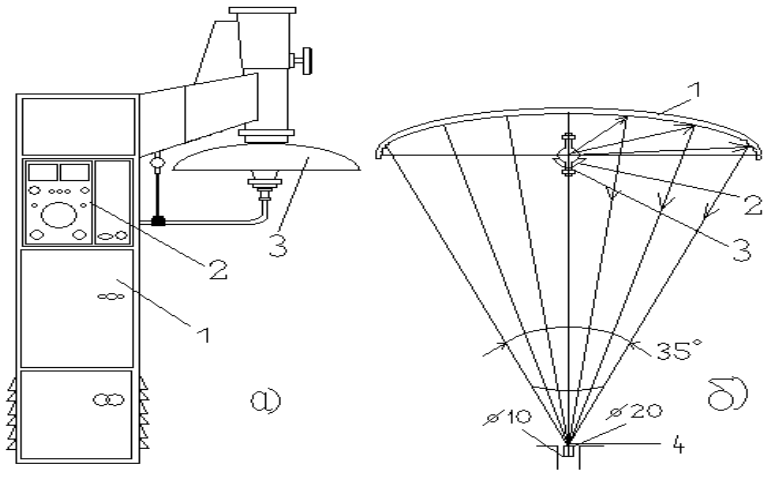

Figure 1. The scheme of experimental installation: a) optical furnace URAN-1: 1- power supply, 2 - control panel, 3 - radiator; b) optical radiator: 1 - reflector; 2 – counter reflector; 3 - lamp; 4 – action spot

Of the 10-kW power generated by the lamp, optical radiation accounted for only 5.5 kW. The radiation spectrum distribution was as follows: 0.5 kW (9%) was in the ultraviolet region, 2 kW (36%) in the visible region, and 3 kW (55%) in the infrared region. The setup provided not less than 95% stability of the radiation in time and not less than 87% uniformity of the radiant energy flux distribution in a

spot of diameter $2 \cdot 10^{-2}$ m. With a deviation of $2 \cdot 10^{-3}$ m from the focal plane along the optical axis, the change in the radiant flux density did not exceed 5%. The diameter of the focused flux was about $2 \cdot 10^{-2}$ m.

The recording unit provided measurements of the radiant flux density, exposure time, the onset of flame and controlled experimental conditions. It included a radiant flux density sensor, diodes, relays and N-117 light-beam oscillograph.

The density of a radiant energy flux in a focal spot was controlled by using radiation attenuators and a smooth change of electric power applied to the xenon lamp. The attenuators of the radiant energy flux were a metal grid that was placed perpendicularly to the optical axis at a distance of 0.3-0.4 m from the focal plane. The system of gates protects the test sample against heating by the radiant flux and dosed supply of energy radiation.

The dynamic flow was modeled by the movement of the sample along the optical axis. For the movement of the sample it was used the following installation (by the example of the decreasing flux of radiant energy, Figure 2).

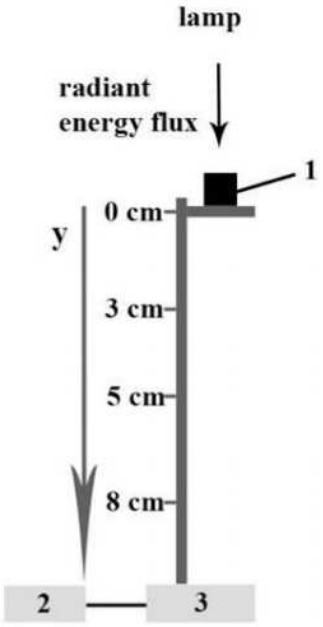

Figure 2. Installation for the movement of the sample: 1 is the sample, 2 is the remote control of motion platform with a sample; 3 is the mechanism that move the sample, y = 0 cm is the focal plane; 3, 5, 8 cm are the distances from the focal plane

Simultaneously with the opening of the gate, the transporter was turn on and the sample started moving with a constant speed of 0.117 m/s. The opening (closing) time of the gate was $4\ 10^{-2} \cdot$ sec.

The test procedure was as follows. The intensity of the radiant flux was measured by a calorimeter fixed to the holder at the upper and lower points of the optical axis. Then the test sample was located on the place of the calorimeter and tested. The registration unit recorded the opening time of the gate and the appearance of flame. Ignition of the condensed substance was determined by the appearance of flame on the sample surface.

The calorimeter was a copper disk 10^{-2} m in diameter and $3 \cdot 10^{-3}$ m thick with a thermocouple calked in the center of the disk to a depth of $1.7 \cdot 10^{-3}$ m. The thermocouple was obtained by contact welding of copper and constantan wires with a diameter of 100 microns.The receiving surface of the calorimeter was coated with lampblack. In the radiation spectrum of 0.36–1.1 μm, the reflection coefficient of the

blackened surface of the calorimeter was 1.5–2.0%. The measurement error of the radiation intensity did not exceed 10%. The heat flux density was measured in the range q = 20–110 W/cm^2.
To determine the density of radiant flux, we experimentally measured the heating rate of the copper disc subjected to radiation coming to the blackened surface. The radiant flux density was calculated by the formula:

$$q = \frac{mc}{(1-b)S} \cdot \frac{\Delta T}{\Delta t} \tag{1}$$

where m is the mass of the disk; c is the specific heat; S is the area of the blackened surface of the disc; b is the reflection coefficient; $\frac{\Delta T}{\Delta t}$ is the rate of heating.
The delay time of ignition was determined by a photoelectric method. The ignition time was taken as the time interval from the beginning of exposure to the radiant energy flux to the occurrence of flame over the surface of the sample. Radiation of flame was registered using photodiodes. The H-117/1 oscilloscope was used for recording electrical signals. In measurements of the ignition time from the occurrence of flame, the error is not more than 4% and is determined mainly by the physicochemical properties of the material studied.
Pine wood (Pinus Silvestris) was used as the test samples (Figure 3). The samples were cylinders $1.9 \cdot 10^{-2}$m in diameter and $1.5 \cdot 10^{-2}$m in height. The surface of the samples, absorbing radiation, was covered by lampblack.

Figure 3. Wood sample before (left) and after experiment (right)

The light radiation was incident on the sample perpendicularly to the wood fibers. The investigations were carried out in air at atmospheric pressure. The initial temperature of the samples corresponded to room temperature — 297 K. The moisture content of the samples was W≈1.8%. The absolutely dry state of wood was achieved by predrying in a drying box at 376 K for 48 hours. Unchangeable moisture content of the samples was provided by a desiccator filled with silica gel. The moisture content of the samples was determined with an accuracy of 0.01% using a A&D MX-50 moisture content analyzer.

3. Results and discussion

To compare the delay time of ignition under static and dynamic conditions, the heat flux was averaged under dynamic conditions. For this purpose, the following method was used. The intensity of the radiant energy flux was measured with a microcalorimeter at fixed distances from the focal plane of the reflector. Knowing the velocity of the sample along the optical axis of the elliptical reflector we

can turn from fixed values of the distance to the time. In this case, the dependence of the heat flux on time is well enough (correlation $R^2 = 0.997$) approximated by the function (Figure 4):

$$q = ae^{\pm 0.7t} - 2, \quad (2)$$

where q is the heat flux, W/cm^2; t is the time, s; a is the nondimensional coefficient, "+" – increasing heat flux; "-" – decreasing heat flux.

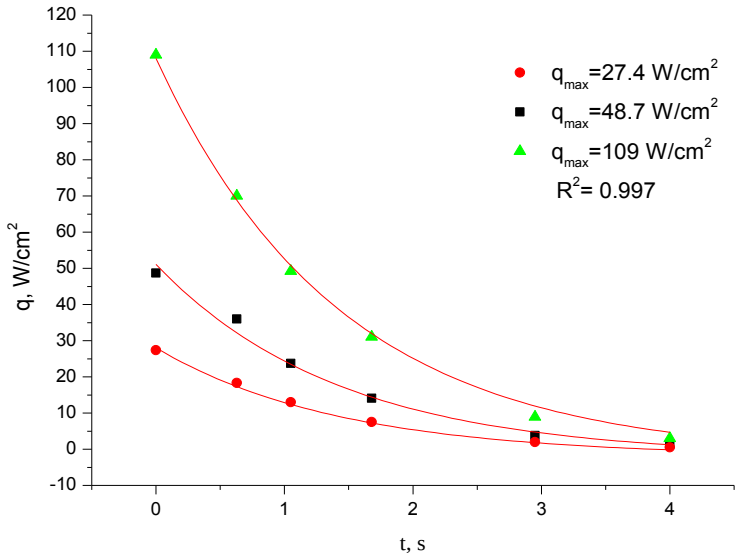

Figure 4. Heat flux versus time when the sample is moved from the focal plane

Thus, depending on the value of heat flux in the focal plane (t=0) we can determine a coefficient *a* and dynamic changes of the heat flux at the surface of the moving sample. The delay time of ignition was measured using a photodiode. Knowing the ignition delay time of the sample we can find a heat flux in the ignition point using a distribution curve q(t). Since the sample of pine ignites within one second in the tested range of the heat flux, then from Figure 4 it can be seen that the curve is quasilinear in this range. In this connection, the average heat flux was determined as the arithmetic mean value for dynamic conditions.

Figure 5 shows the ignition delay times of the pine samples under decreasing (q=f(t)) and static (q=const) heat flux.

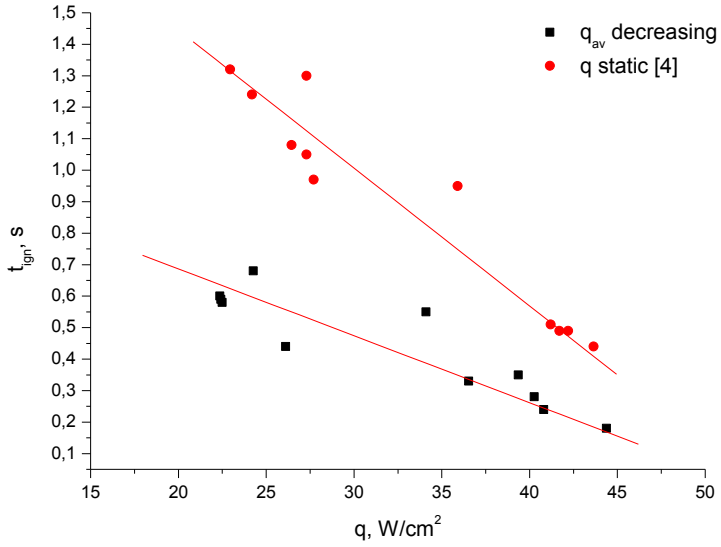

Figure 5. Ignition delay times of the pine samples versus heat flux for dynamic (decreasing heat flux) and static conditions

When the radiation flux decreases, the delay time for ignition of the pine samples is 2-2.5 times less than that for the constant radiation flux. At the same time, Figure 5 shows that the decrease in value of heat flux leads to the fact that the delay time of ignition increases faster under static conditions than under dynamic ones. These results do not contradict the paper [3], where it was experimentally shown that in the case when the heat flux increases, the delay time for ignition of nitrocellulose is greater than that for the constant heat flux.

In a similar way, according to the formula (2) the flux of radiant energy was determined at the moment of ignition for increasing flux. The average heat flux was determined using the method for determination of the average value for interval dynamic rows [5]. Figure 6 shows the delay time to ignite the pine samples for the increasing (q=f(t)) and static (q=const) radiant energy flux.

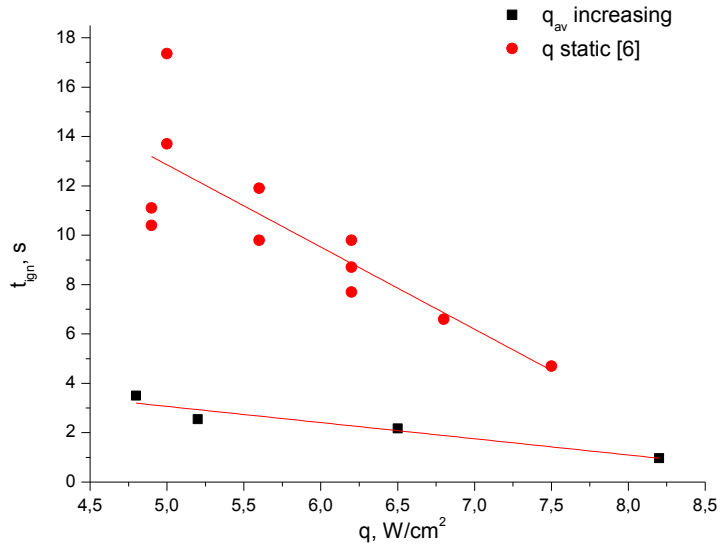

Figure 6. Ignition delay times of the pine samples versus heat flux for dynamic (increasing heat flux) and static conditions

The analysis of the curves in Figure 6 shows that the ignition delay time for the increasing flux of radiant energy is smaller than for a constant flux. The difference in time is from 2 to 3 times. For the decreasing flux (Figure 5), a similar pattern is observed. However, the ignition delay time for the increasing flux of radiant energy decreases slower than for the decreasing flux with the increase in time. The data obtained are in qualitative agreement with the results of mathematical modeling of dynamic conditions for heating of wood in [7].

At a result we have received the delay times for ignition of pine wood during heating under conditions of the decreasing and increasing heat flux. The received data were compared with the data for a static heat flux [4, 6].

The results obtained can be used to improve the prediction of dangerous zones for ignition of wood in wildland and anthropogenic fires.

Acknowledgements

This work was supported by the Tomsk State University Competitiveness Improvement Program, the Government Assignment in the Field of Scientific Activity (number 1624), the Russian Foundation for Basic Research (project number 14-01-00211-a and 14-33-50115-mol-nr) and a Scholarship from the President of the Russian Federation (number SP-3968.2013.1).

References

1. Filkov A.I., Kuznetsov V.T., Guk V.O., Telyakov E.Sh., Enalejev R.Sh. Ignition of Wood Under Dynamic Conditions of Supply of Radiant Energy Flow // Proceedings of the 4th Fire Behavior and Fuels Conference (Saint-Petersburg, Russia, July 1-4, 2013). – USA, IAWF. 2013. Pp. 57.
2. Rosenband R.Sh., Barzykin V.V., Merzhanov A.G. Ignition of Condensed Substances by the Convective Flux of Average Intensity under Dynamic Conditions. Combustion, Explosion and Shock Waves, 1968. V.4. No. 2. Pp. 171-175. (in Russian)
3. Enaleev R.Sh., Mateosov V.A., Sinaev K.N., Dinavetsky V.D., Gainutdinov R.Sh. Experimental Research into Ignition of Condensed Substances under Dynamic Conditions for Supply of Radiant Energy. In the book: Physics of Combustion and Methods of Research, Cheboksary: Chuvash Univ. 1973. Pp. 80-86. (in Russian)
4. Kuznetsov V.T., Fil'kov A.I. Ignition of Various Wood Species by Radiant Energy // Combustion, Explosion, and Shock Waves. 2011, Vol. 47, No. 1. Pp. 65-69.
5. Baliiova V.S. Statistics of Questions and Answers. Textbook. M.: T.K. Welby, 2004. 344 p. (in Russian)
6. Boonmee N., Quintiere J. G. Glowing and flaming autoignition of wood // Proceedings of the Combustion Institute. Vol. 29. 2002. Pp. 289–296.
7. Enaleev R.Sh., Krasin I.V., Gasilov V.S., Chistov Yu.S., Tuchkova O.A. Ignition of Wood // Herald of Kazan Technological University, 2013. V. 16. No. 10. Pp. 99-106.

Improving wildfire spread simulations using MODIS active fires: the FIRE-MODSAT project

Ana Sá[a], Akli Benali[a], Renata Pinto[a], Paulo Fernandes[b], Ana Russo[c], Fábio Santos[c], Ricardo Trigo[c], José Pereira[a], Sónia Jerez[d], Carlos da-Camara[c]

[a] *Centro de Estudos Florestais, Instituto Superior de Agronomia da Universidade de Lisboa, Tapada da Ajuda, 1349-017 Lisboa, Portugal, anasa30@gmail.com*
[b] *Centro de Investigação e de Tecnologias Agro-Ambientais e Biológicas, Universidade de Trás-os-Montes e Alto Douro, Quinta de Prados, Apartado 1013, 5001-801 Vila Real, Portugal*
[c] *Instituto Dom Luís, Faculdade de Ciências da Universidade de Lisboa, Campo Grande. Edifício C8, Piso 3, 1749-016 Lisboa, Portugal*
[d] *University of Murcia, Department of Physics-Physics of the Earth. Edificio CIOyN, Campus de Espinardo, 30100 Murcia, Spain*

Abstract

Wildfires are an important ecological disturbance in Mediterranean forests and have dramatic social, economic and environmental impacts. Portugal is already experiencing an increase in the number and extent of wildfires, with records of burnt extent exceeding 400,000ha and 300,000ha in 2003 and 2005, respectively. With the projected future increase in the frequency of large wildfires, those negative impacts and fire suppression difficulties will also likely increase.

Spatially explicit wildfire spread models (e.g. FARSITE) are one of the most effective tools to understand complex interactions among topography, vegetation fuel and weather conditions. These models can be used not only to study past fire events but also for forecasting fire spread and behavior. MODIS active fires have a large potential to provide relevant information regarding the spatio-temporal distribution of large wildfire events. When combined with fire spread models, they may provide crucial information to overcome the error propagation that arise when simulating large and long duration wildfire events, which is crucial for monitoring and forecasting fires in an operational fire-fighting context.

We investigated nine large wildfires (>=10,000ha) that occurred in Portugal between 2001 and 2012 in order to evaluate if combining fire growth simulations with active fire data improves the accuracy of fire spread predictions. To achieve this goal we propose to: 1) simulate fire growth using FARSITE model in combination with the time and spatial information of the MODIS active fires during the fire event propagation; and 2) assess the performance of fire spread simulations comparing them with the spatio-temporal distribution of the active fires. Additionally we performed a sensitivity analysis to evaluate the impact of key model parameters and variables on fire growth simulations, to understand the main sources of error and identify future work needed to improve the use of combined model-satellite approach in an operational context.

Results show that fire growth simulations are improved when satellite-derived active fires were used to reinitialize the simulation while the fires are occurring. Sørensen coefficients obtained for these simulations assisted by MODIS active fires were all above 0.5, showing a significant improvement over full fire growth event simulations. This innovative approach of combining satellite active fires data with fire spread simulations reduces the propagated errors of the large and long duration fire events and improves the forecasting ability of fire spread models.

Keywords*: Fire growth simulations, satellite active-fires, FARSITE, FIRE-MODSAT.*

Introduction

Large wildfires while infrequent are responsible for severe environmental, ecological and socio-economic impacts. In Portugal, wildfires have consumed an average of 140,000ha/year during the last decade (Sá and Pereira 2011). Portugal has been experiencing significant increments of both maximum and minimum temperature at annual and seasonal scales (Ramos *et al*. 2011) and all regional climate

models indicate an increased likelihood of future increases in the frequency and amplitude of summer heat waves (Barriopedro *et al*. 2011). Therefore, most climate change studies point to an increase in the number and extent of forest fires (Flannigan *et al*. 2013), thus the negative impacts of wildfires and fire suppression difficulties will also likely increase. Portugal is already experiencing this reality, with records of burnt extent exceeding 400,000ha and 350,000ha in 2003 and 2005, respectively (Oliveira *et al*. 2012), and several very large and catastrophic wildfires in the South and Centre of Portugal (Trigo *et al*. 2006).

The scientific community is becoming increasingly aware of the significance of large wildfires impacts, being essential to understand the complex interactions among the main drivers of wildfire spread and behaviour, such as topography, fuel and meteorology. Spatially explicit wildfire spread models are one of the most effective tools to understand such complex interactions and have been commonly used to simulate wildfire growth and behaviour (e.g. Arca *et al*. 2007). They can provide relevant descriptors directly related with fire suppression, such as the rate of spread and fireline intensity of the fire front (Finney 2004). However, fire spread models have been seldom used to monitor real wildfire events, particularly large wildfires (Arca *et al*. 2007, Kochanski *et al*. 2013).

Since large wildfires have extensive burn scars and are in general active for several days, some authors have recently explored the potential of using satellite data to monitor such events events in a quasi-continuous mode (Smith and Wooster 2005, Loboda and Csiszar 2007, Benali and Pereira 2013, Coen and Schroeder 2013). The MODerate Resolution Imaging Spectroradiometer (MODIS) detects active fires that are burning at the time of overpass up to four times per day (Giglio *et al*. 2003) and has been integrated in operational systems assisting fire managers to define strategic decisions regarding fire suppression resource allocation (e.g. Lee *et al*. 2002, USDA 2014).

Modelling and monitoring large wildfires is limited by the accuracy and availability of information about the spatio-temporal distribution of fire spread which is usually taken from subjective eye-witness interviews and limits the accuracy of model calibration and validation. The skill of forecasts in simulating future fire states is basically dependent on accurate weather forecasts, and therefore, both decrease significantly with time (Coen and Schroeder 2013, Lilly 1990). In this context, satellite active-fire data can provide detailed and objective information regarding the dynamics of those events improving the implementation of fire spread models. Both satellite data and fire spread models provide different types of information about the spatial and temporal distribution of large wildfires. However, they have not been combined in a manner that fully exploits their potential and minimizes their limitations. Remote sensing and modelling have been successfully combined to provide useful and accurate predictions in other earth sciences contexts, for instance in hydrological applications (Moradkhani 2008) but very few studies have explored this combination for wildfire applications (Lee *et al*. 2002). Combining active fires satellite data with fire-spread simulations may reduce error propagation during simulations of large, long duration wildfire events. To the best of our knowledge a single recent study moved towards this direction exploring the use of satellite active fires data to initialize and evaluate coupled weather-wildfire growth model simulations in a long lasting fire event (Coen and Schroeder 2013).

FIRE-MODSAT (Supporting FIRE-suppression strategies combining fire spread MODelling and SATellite data in an operational context in Portugal) is an one-year funded project by the Portuguese Foundation for the Science and Technology (FCT) that aims at providing crucial information to understand how large wildfire impacts can be minimized in the future, by combining fire spread simulations and satellite data to support fire management decisions in an operational context improving the efficiency of the fire suppression system.

The study presented here shows some preliminary results of the former project. We selected extreme wildfires (above 10,000ha) that occurred in Portugal between 2001 and 2012 to evaluate the potential of combining fire growth simulations with active fire data, and improve the accuracy of fire spread predictions. We propose to: 1) simulate fire growth using FARSITE (Fire Area Simulator, Finney 2004) model in combination with the temporal and spatial information of the MODIS active fires

during the fire event; 2) assess the performance of fire spread simulations comparing them with the spatio-temporal distribution of the active fires. Additionally we carry out a sensitivity analysis to evaluate the impact of key model parameters and variables on fire growth simulations, to understand the main sources of error. This will contribute to identify future work needed to improve this new approach, producing valuable information to be integrated in a fire-fighting operational context.

Data and Methods

Data

2.1.1. *Case studies*

Nine unusually large wildfires (larger than 10,000ha) which took place in the centre and south of mainland of Portugal between 2001 and 2012 were selected for analysis (Figure 1). Corresponding burnt area perimeters were extracted from the annual 35-years fire atlas of Portugal (1975-2009) (Sá and Pereira 2011) and were used as reference data.

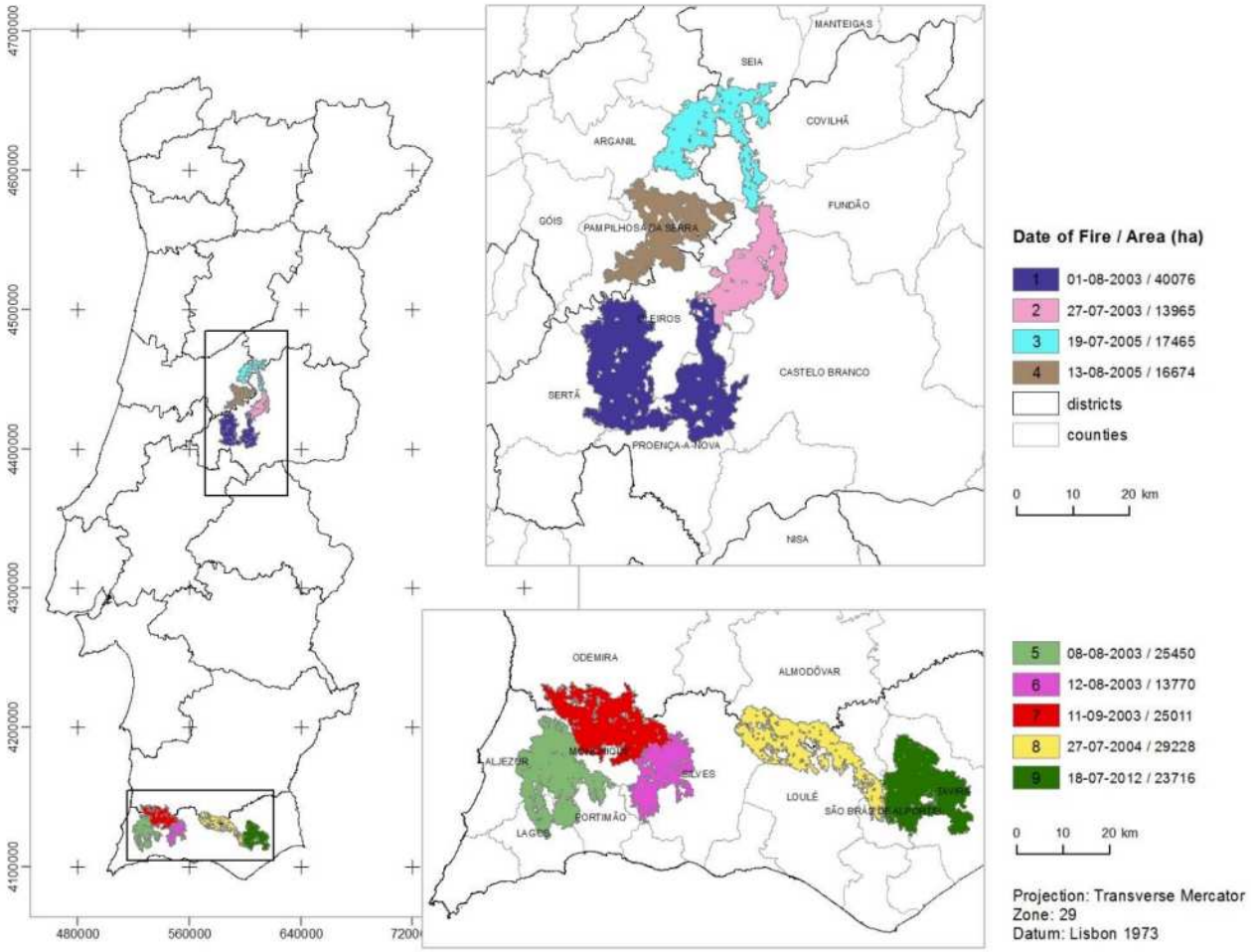

Figure 1. Case studies: nine very large fire events (larger than 10,000ha) that occurred in the mainland of Portugal between 2001 and 2012. Fire events are named as: (1) CasteloBranco1 (Cb1 2003); (2) CasteloBranco2 (Cb2 2003); (3) Covilhã1 (Cov1 2005); (4) Covilhã2 (Cov2 2005); (5) Monchique1 (Mcq1 2003); (6) Monchique2 (Mcq2 2003); (7) Monchique3 (Mcq3 2003); (8) Loulé (Lou 2004); and (9) Tavira (Tav 2012). In the legend we can see each fire date of ignition and the corresponding burnt area extent.

2.1.2. *Landscape and weather data*

Fire spread simulation requires spatial information of the landscapes, and on the weather conditions prevailing during the entire simulation period. Spatial data comprise fuels, weather, and topography. In the simulations, weather variables are input as streams of data, whereas fuels and topography are provided as GIS raster themes. Based on the input variables spatial resolution, and on the time-consuming resources of each simulation, the landscape cell-size spatial resolution was set equal to 100m, which provides an acceptable level of detail for heterogeneous landscapes.

Elevation was obtained from the Shuttle Radar Topography Mission (Farr *et al*. 2007). This dataset was also used to derive the slope and aspect variables.

Fuel maps as per the Northern Forest Fire Laboratory (NFFL) 13 fuel models (Anderson 1982) were provided by the Portuguese municipalities affected by the selected fire events. Some municipal fuels maps were not available for this study, so those maps were derived using a Classification Tree algorithm (Breiman *et al*. 1984) setting as predictor variable the Corine Land Cover (CLC, Caetano *et al*. 2009) class and the fuel class model as the response variable. Burnt areas up to two years before the date of the land cover map were updated to shrublands. The fires that occurred in the same fire season as the fire events were classified as non-burnable.

Tree cover was derived from the MODIS Vegetation Continuous Fields (MOD44B) at 250 m spatial resolution (DiMiceli *et al*. 2011). Stand and tree-based variables were set constant for the entire simulated landscapes (canopy height = 5m; crown base height = 2m and crown bulk density = 0.1 kg $/m^{-3}$).

FARSITE requires daily weather observations of minimum and maximum temperatures, humidity and precipitation at a specified elevation, and hourly observations of wind speed and direction. These data characterize the daily weather pattern and are used to calculate the dead fuel moisture contents. Spatially variable wind fields were modelled wind the WindNinja software to account for the effect of complex topography (Forthofer *et al*. 2009).

Weather (temperature, precipitation, insolation, relative humidity and wind speed and direction) hourly simulated data were derived from the 10km regional climate model (MM5), which is able to reproduce the main regional circulation patterns as well as the temporal variability of the wind series (Jerez *et al*. 2013a). This model was already applied to various applications that require reliable fine-scale meteorological fields (Jerez *et al*. 2013b, Jerez *et al*. 2010).

2.1.3. *MODIS active fires satellite data*

Satellite data has large potential to provide relevant and innovative information about the spread dynamics of large wildfire events, such as the direction and rate of fire spread (Benali and Pereira 2013). The MODIS active fire product detects fires in 1km pixels that are burning at the time of overpass under relatively cloud-free conditions up to four times per day (Giglio *et al*. 2003). MODIS active fires satellite data were aggregated in day and night time overpasses and, within each overpass, we identified the early and late active fires. Each overpass has a different viewing geometry and thus a different pixel size (Wolfe *et al*. 1998). The active fire *footprint* was defined based on the viewing zenith angle and on the azimuth of each MODIS overpass (Ichoku and Kaufman 2005).

MODIS active fires satellite data were coupled with fire growth models in four stages: 1) to initialize simulations from ignition points; 2) to define the start and end date of each wildfire event; 3) to restart fire spread simulations at each satellite overpass; and 4) to evaluate the accuracy of the simulated fire growth. Only the early overpass active fires were used to reinitialize the simulations to ensure a significant simulation time and capture the relevant fire spread periods. However, to evaluate model's performances both the late active fires of the previous overpass and the early active fires of the next overpass were used.

Wildfire simulation

We used FARSITE 4.0 (Fire Area Simulator, Finney 2004) fire growth model simulator, which incorporates existing models of surface fire spread, crown fire spread, spotting and fuel moisture. Fuel moisture (live and dead) has to be provided for each fuel model. Live fuel moistures (woody and herbaceous) were assumed constant during the simulations. Dead fuel moisture varies over time as a function of fuel particle size, weather conditions, and exposure to wind and sun (Finney 1998). Thus, FARSITE uses an initial fuel moisture condition and throughout the simulation it re-calculates dead fuel moisture contents for each time. Considering the weather conditions that usually prevail during the Portuguese fire season, fuel moisture contents were set based on the low scenarios (Table 1) of Scott and Burgan (2005).

Table 1. Dead (1-hr, 10-hr and 100-hr time-lag classes) and life (herbaceous and woody) fuel moisture contents (Scott and Burgan 2005).

Dead fuel moisture content (%)			Live fuel moisture content (%)	
1-hr	10-hr	100-hr	herbaceous	woody
6	7	8	60	90

The rate of spread adjustment factor is a fuel model specific parameter that adjusts the simulated rate of spread to match observed fire patterns. Thus, its value is dependent on the user expertise of fire behaviour in the local fuel complex. Changes in this parameter are based on limitations of the temporal/spatial scales of the simulations, or to adjust errors in fuel classification, inaccurate fuel moistures or improperly represented local winds (Finney 1998). We kept this parameter equal to 1 to keep the original fire spread rate.

Crown fires were simulated using the previously defined constant stand and tree-based variable values. Fire suppression activities were not considered during simulations. Fire growth simulations were performed for i) the full length of the wildfire event using as ignition points the first active fires detected within the reference burnt area perimeter (hereafter *Full simulation*) and, ii) the fire growth simulations were reinitialized at each MODIS overpass during the lifetime of each fire event (hereafter *Satellite simulation*). Thus, the satellite-assisted simulations used all the active fires derived from each satellite passage as ignition points to restart fire growth simulations until the next satellite passage.

2.3. Performance of the fire simulations

In order to assess the performance of fire growth simulations with and without combining actives fires detected from each satellite passage, we compared the simulated final burnt area perimeters with the respective reference burnt area perimeter extent. For this analysis of performance we used the Sørensen coefficient (SC, Sorensen 1948), which is widely used in ecology to compare the similarity of two samples (Eq. 1):

$$SC = \frac{2a}{(2a+b+c)} \quad \text{(Eq. 1)}$$

where, *a* is the intersection of the simulated burnt area extent values (from the full or the satellite combined simulations) with the reference burnt area extent, *b* is the area burned exclusively by the simulation, and *c* the area exclusively burned in the reference data. It ranges from 0 to 1, with the former value corresponding to a completely failed simulation and the latter indicating a perfect agreement between the fire growth simulations and the reference burnt area perimeter.

Additionally, for both the *full* and *satellite* simulations for each MODIS overpass we calculated the distance between the active fire footprint and the position of the nearest correspondent simulated burnt area pixel. This provided a measure of the spatial displacement error between simulations and the position of the fire front observed by the MODIS satellites during the length of each fire event.

2.4. Sensitivity analysis

Sensitivity analysis was performed to evaluate the impact that small changes of selected variables/parameters had on the simulated final burned area extent. Given the model complexity, a large number of variables and parameters affect simulated fire growth and behaviour. Therefore we limited the sensitivity analysis to the variables wind speed and direction, the rate of spread adjustment factor and the position of the ignition point. In order to restrict this analysis to a common fire lifetime period, we set a common simulation period of three days for all case studies.

Wind speed has a strong influence on fire spread and can be one of the most important factors shaping fires (Beer 1993). Changes in wind direction are also considered important because of its interaction with the topography, and also because this information may be used to define fire-fighting strategies. The rate of spread adjustment factor is usually defined empirically based on user's expertise and impacts on the simulated burnt area extent. Additionally, we also evaluated the impact of the uncertainty in the position of active fires within their footprint. The MODIS active fire product can identify a fire as small as 10% of the pixel's footprint, however the correct position of the actual fire within the latter is unknown. Thus, we varied the position of the ignition point in each quadrant of its footprint and varied its distance to the centroid in intervals of 20, 40, 60, 80 and 100% of the maximum distance between the centroid and the footprint's boundaries.

Table 2 shows the sensitivity analysis for the range of values of the selected variables/parameters. For each variable we performed 21 simulations, which resulted in a total of 672 simulations comprising the nine case study fire events. Within the simulations for each variable there is one that is the reference. In the case of the wind speed and direction reference values were those observed during the three-day simulation period. For the rate of spread adjustment factor the reference value is 1, meaning no adjustment. Active fires centroids were used as the ignition reference points.

Table 2. Variables used in sensitivity analysis, with respective interval unit change, with a total number of simulations of 21 each. Dmax is the maximum distance between a centroid of an active fire and its footprint borderline.

Variable	Interval range / (step)
Wind speed (km/h)	(-10; +10) / (1 km/h)
Wind direction (º)	(-50; +50) / (5º)
Rate of spread adjustment factor (adim.)	(0.25; 1.75) / (0.075)
Active fire position (% dmax, m)	(0; dmax) / (0.2)

Results and Discussion

3.1. Model performance

For each case study the fire event simulations performance was assessed using the Sørensen coefficient (Figure 2). Based on the coefficient values there is clear evidence that fire simulations are improved when they are coupled with active fires to reinitialize the simulations at each satellite aggregated overpass (with only one exception). These simulations had Sørensen coefficients above 0.5 (often higher than 0.6) indicating an accuracy improvement when compared with a full event simulation.

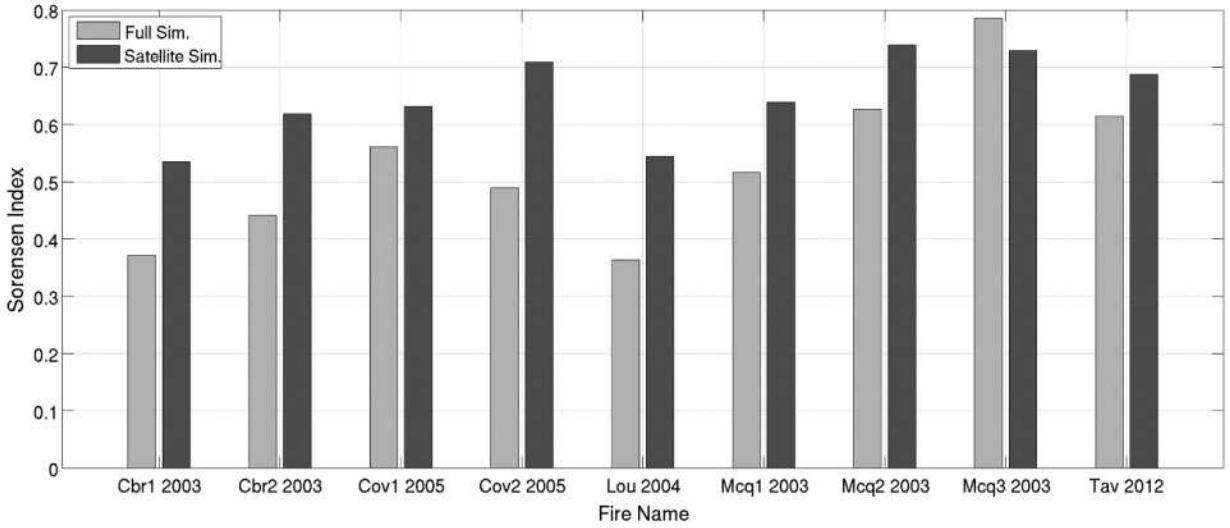

Figure 2. Assessment of the performance of the fire growth simulations using the Sørensen coefficient for: a) a full event lifetime simulation where the ignition points are derived from the first detected active fires satellite passage after the beginning of the event (grey bars); b) simulation of the fire event supported by the MODIS active fires satellite passages during the lifetime of the fire event (black bars).

Figure 3 shows the distribution of simulation accuracies along the duration of the fire events. Full simulations show that the error is almost always higher than the one derived from the satellite simulations and, propagates over time, with a maximum which is more than three times higher at 65% of the time of a fire event completed. The complex interactions between weather, fuels and topography are often difficult to reproduce with fire models producing inaccuracies on the fire spread that increase for long periods of simulations. Additionally, these errors have larger variance than the ones observed for the satellite simulations. Reinitializing simulations with the actual positions of the active fires reduces the propagation of these errors as well as its variability. For most of the time steps, the satellite-assisted simulations have a significantly lower error (around 1 km) than the full simulations.

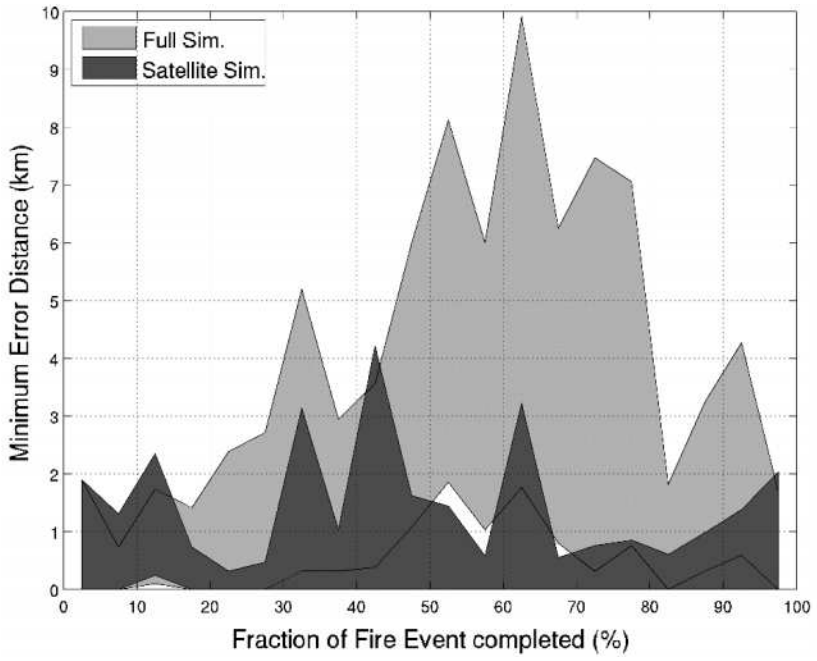

Figure 3. Interquartile range of the minimum error distance for the full and satellite simulations as a function of the fraction of the fire event completed.

Sensitivity analysis

Figure 4 shows the impact that wind speed and direction, rate of spread adjustment factor and the position of the ignition point have on the simulated burnt area (Figure 4, bottom left panel). As expected, wind speed has a large impact on the simulated burnt area extent. Positive wind speed increments produce more variation in the simulated burnt area extent than the negative increments. Two fire events cases are contributing to this wide variation: Lou 2004 and Mcq1 2003. The Loulé fire was more resilient to wind speed increments showing a simulated burnt area extent variation less than ~25% when compared with the simulation using the reference data. The reason for this may be the fact that prevailing wind speed during the simulation period was already quite high so additional increments did not have a significant impact on the new simulated burnt area extent (Figure 5). The length-to-breadth ratio of a fire increases with wind speed, implying that increasingly higher wind speeds will increase fire size at an increasingly lower rate (Alexander 1995). On the other hand, any small increase in wind speed in the Monchique1 fire event (which overall has a low length-to-breadth ratio) produced a large change on the burnt area extent because the reference wind speed values for this fire were low. Other reasons might be involved in the differences between fires, as fire spread rate as a non-linear function of wind speed varies with fuel characteristics (Rothermel 1972).

Changing the wind direction produces a lower extent of burnt area variations than introducing small changes on the wind speed (Figure 4, top right panel). The effect of wind direction increments over the variation of burnt area is more pronounced also on the Loulé fire event, but with an opposite response in terms of burnt area extent. This fire propagated under strong wind conditions with a prevailing direction (from North), thus any change from north to northeast direction will reduce the simulated burnt area extent. Negative increments (from north to northwest) have a smaller and positive effect on burnt area.

As expected, the impact of changing the rate of spread adjustment factor is also very high, with large positive values producing an increase in burnt area extent that can be four-fold larger than the no-adjustment reference value value (Figure 4, bottom left panel). Again, the Loulé fire showed more resilience in terms of burned area variation while CasteloBranco2 showed an opposite response. One explanation for this impact may be that ~40% of the fuels in this fire event are litter (NFFL fuel model 9) and they are concentrated around the area where the fire started. Fire propagation on this type of fuel bed is high and, increases in both wind speed and spread of rate, largely promote the increase in the simulated burnt area extent.

Another source of variation on fire growth simulations evaluated here is the location of the ignition point inside the footprint of MODIS active fire. Sensitivity analysis on this variable (Figure 4, bottom right panel) shows that increasing the distance of the ignition point from the centroid increases the variability on the output simulated burnt area extent. Several factors affect this measure namely the vegetation fuel map where the ignition point is located.

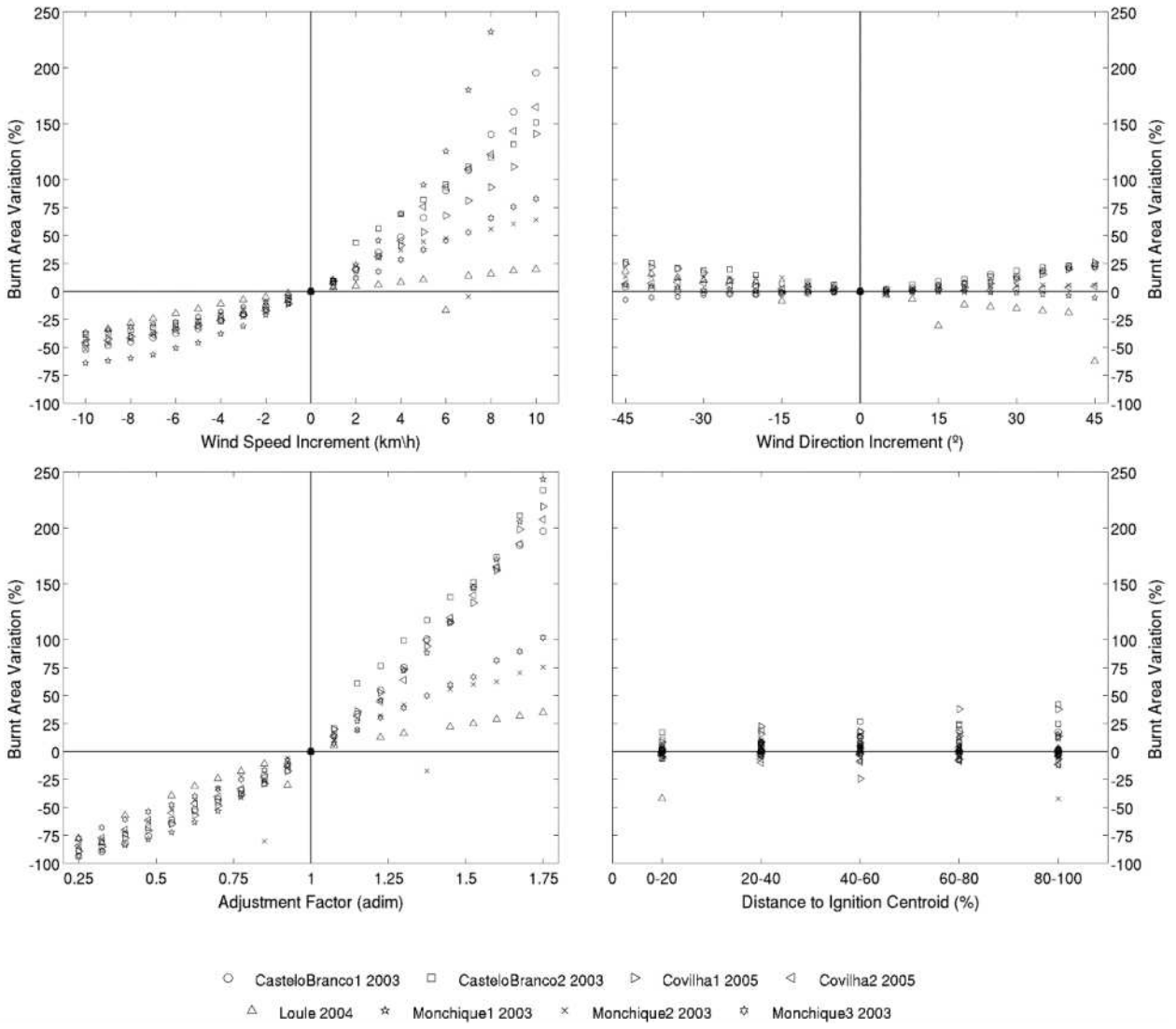

Figure 4. Sensitivity analysis for the wind speed and direction, rate of spread adjustment factor and distance to the ignition centroid variables. Analysis was based on the variation of the burnt area extent derived from introducing small increments of each variable and comparing it with the simulation derived using the corresponding variable reference values.

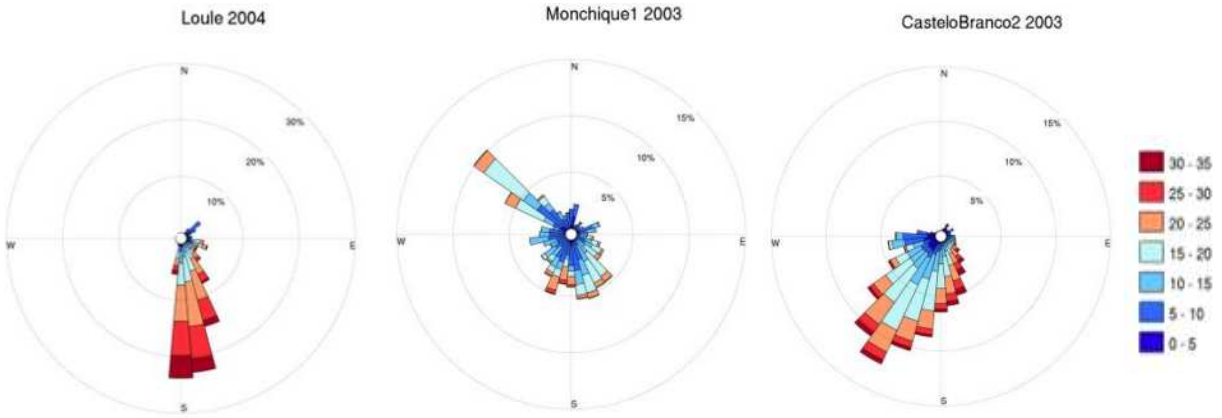

Figure 5. Wind speed (km/h) and direction (º)for the Loulé2004, Monchique1 and CasteloBranco2 fire events for the entire 3-day fire simulation period.

Conclusions

Fire-spread simulations can be improved using MODIS active fires satellite data for monitoring large and long duration wildfires. Estimated burnt area extent derived from fire growth simulations reinitialized with MODIS active fires detected at each overpass showed an improvement when compared with the single ignition point simulation for the entire fire duration.
We evaluated the impact of wind speed and direction, rate of spread adjustment factor and ignition point position, given the potential effect these variables have on fire propagation. As expected, small changes on the wind speed and on the rate of spread adjustment factor had a large impact on the simulated burnt area extent. This response enhances the importance of having accurate information on the wind variable when using fire spread models either for studying past fire events or for fire spread modelling in an operational context.
This innovative approach of combining satellite active fires data with fire spread simulations minimized the observed propagation error through the single fire event simulation. This improvement arises from reinitializing fire-spread simulations for each satellite aggregated overpass with updated maps of fire location for the next simulation.
Attempts to integrate fuel and weather data inaccuracies on the simulations may also improve the fire spread and behaviour simulations.
Future work will encompass uncertainties in fire spread and behaviour simulations using custom fuel models derived from other fuel classification systems (e.g.,Fernandes *et al*. 2009, Scott and Burgan 2005), changing some of its most influential parameters, namely live fuel moisture contents, weather-dependent variables, and stand level variables derived from the Portuguese National Forest Inventory. This information will be integrated in this innovative combination of fire spread and behaviour simulations assisted by MODIS active fires, in order to have a tool that will support decisions in a fire-fighting operational context.

References

Alexander M.E. (1985). Estimating the length-to-breadth ratio of elliptical forest fire patterns. In: Donoghue L.R. and Martin R.E. (Eds.), Proceedings of the 8th Conference on Fire and Forest Meteorology, April 29-May 2, Detroit, Michigan. SAF Publication 85-04. Society of American Foresters, Bethesda, Marylan.

Anderson H.E. 1982. Aids to determining fuel models for estimating fire behavior. General Technical Report INT-122, USDA Forest Service.

Arca B., Duce P., Laconi M., Pellizzaro G., Salis M. and Spano D. (2007). Evaluation of FARSITE simulator in Mediterranean maquis. International Journal of Wildland Fire, 16 (5), 563-572.

Barriopedro D., Fischer E.M., Luterbacher J.R., Trigo R.M. and Garcia-Herrera R. (2011). The hot summer of 2010: redrawing the temperature record map of Europe. Science, 332 (6026), 220-224.

Beer, T. (1993). The speed of a fire front and its dependence on wind speed. International Journal of Wildland Fire, 3, 193-202.

Benali A.A. and Pereira J.M.C. (2013) Monitoring and extracting relevant parameters of wild fire spread using remote sensing data. Anais XVI Simpósio Brasileiro de Sensoriamento Remoto - SBSR, Foz do Iguaçu, PR, Brasil, 13-18 April, INPE.

Breiman L., Friedman J.H., Olshen R.A. and Stone C.J. (1984). Classification and Regression Trees. Wadsworth and Brooks, Monterey, CA.

Caetano M., Nunes V. and Nunes A. (2009). CORINE Land Cover 2006 for Continental Portugal. Technical report, Instituto Geográfico Português.

Coen J. and Schroeder W. (2013). Use of spatially refined satellite remote sensing fire detection data to initialize and evaluate coupled weather-wildfire growth model simulations. Geophysical Research Letters, 40, 5536-5541, doi 10.1002/2013GL057868

DiMiceli C.M., Carroll M.L., Sohlberg R.A., Huang C., Hansen M.C. and Townshend J.R.G. (2011). Annual Global Automated MODIS Vegetation Continuous Fields (MOD44B) at 250 m Spatial Resolution for Data Years Beginning Day 65, 2000 - 2010, Collection 5 Percent Tree Cover, University of Maryland, College Park, MD, USA.

Farr T.G., Rosen P.A., Caro E., Crippen R., Duren R. et al. (2007). The Shuttle Radar Topography Mission, Reviews of Geophysics, 45, RG2004, doi:10.1029/2005RG000183.

Fernandes P., Gonçalves H., Loureiro C., Fernandes M., Costa T., Cruz M.G. and Botelho H. (2009). Modelos de Combustível Florestal para Portugal. In: Actas do VI Congresso Florestal Nacional, 348-354.

Finney M.A. (1998). FARSITE: Fire Area Simulator—model development and evaluation. Res. Pap. RMRS-RP-4. Fort Collins, CO. U.S. Department of Agriculture, Forest Service, Rocky Mountain Research Station. 47p.

Finney M.A. (2004). FARSITE, Fire Area Simulator--model development and evaluation. US Department of Agriculture, Forest Service, Rocky Mountain Research Station.

Flannigan M., Cantin A.S., de Groot W.J., Wotton M., Newbery A. and Gowman, L.M. (2013). Global wildland fire season severity in the 21 st century. Forest Ecology and Management, 294, 54-61.

Forthofer J., Shannon K. and Butler B. (2009) Simulating diurnally driven slope winds with WindNinja. In: Proceedings of 8th Symposium on Fire and Forest Meteorological Society; 2009 October 13-15; Kalispell, MT (2,037 KB; 13 pages).

Giglio L., Descloitres J., Justice C.O. and Kaufman Y.J. (2003). An enhanced contextual fire detection algorithm for MODIS. Remote Sensing of Environment, 87 (2), 273-282.

Ichoku C. and Kaufman Y.J. 2005. A method to derive smoke emission rates from MODIS fire radiative energy measurements. IEEE Transactions on Geoscience and Remote Sensing, 43, 2636-2649.

Jerez S., Montávez J.P., Gómez-Navarro J.J., Jiménez-Guerrero P., Jiménez P. and González-Rouco J.F. (2010). Temperature sensitivity to the land-surface model in MM5 climate simulations over the Iberian Peninsula. Meteorologische Zeitschrift, 19 (4), 363–374, doi:10.1127/0941-2948/2010/0473.

Jerez S., Trigo R.M., Vicente-Serrano S.M., Pozo-Vázquez D., Lorente-Plazas R., Lorenzo-Lacruz J., Santos-Alamillos F. and Montávez J.P. (2013a) The impact of the north atlantic oscillation on renewable energy resources in southwestern europe. Journal of Applied Meteorology and Climatology, 52(4), 2204–2225, doi: http://dx.doi.org/10.1175/JAMC-D-12-0257.1

Jerez S., Montávez J.P., Jiménez-Guerrero P., Gómez-Navarro J.J., Lorente-Plazas R. and E. Zorita (2013b). A multi-physics ensemble of present-day climate regional simulations over the Iberian Peninsula. Climate Dynamics, 40 (11-12), 3023–3046, doi:10.1007/s00382-012-1539-1.

Kochanski A.K., Jenkins M.A., Mandel J., Beezley J. and Krueger S. (2013). Real time simulation of 2007 Santa Ana fires. Forest Ecology and Management, 294, 136-149.

Lee B., Alexander, M., Hawkes B., Lynham T., Stocks B. and Englefield P. (2002). Information systems in support of wildland fire management decision making in Canada. Computers and Electronics in Agriculture, 37 (1-3), 185-198.

Lilly D.K. (1990). Numerical predictions of thunderstorms – Has its time come? Quarterly Journal of the Royal Meteorological Society, 116, 779-798.

Loboda T. and Csiszar I. (2007). Reconstruction of fire spread within wildland fire events in Northern Eurasia from the MODIS active fire product. Global and Planetary Change, 56 (3), 258-273.

Moradkhani H. (2008). Hydrologic remote sensing and land surface data assimilation. Sensors, 8 (5), 2986-3004.

Oliveira S.L., Pereira J.M. and Carreiras J.M. (2012). Fire frequency analysis in Portugal (1975-2005), using Landsat-based burnt area maps. International Journal of Wildland Fire, 21 (1), 48-60.

Ramos A.M., Trigo R.M. and Santo F.E. (2011). Evolution of extreme temperatures over Portugal: recent changes and future scenarios. Climate Research, 48 (2), 177.

Rothermel, R.C. (1972). A mathematical model for predicting fire spread in wildland fuels. USDA For. Serv. Res. Pap. INT-115, Intermt. For. and Range Exp. Stn., Ogden.

Sá A.C.L. and Pereira J.M.C. (2011). Cartografia de Áreas Queimadas em 2009 em Portugal Continental. Final Report. Protocol between the Portuguese Forestry Service and the Forest School of Agriculture. Lisbon.

Scott J.H. and Burgan R.E. (2005). Standard fire behavior fuel models: a comprehensive set for use with Rothermel's surface fire spread model. General Technical Report RMRS-GTR-153. USDA Forest Service, Rocky Mountain Research Station, Fort Collins, CO. 80 p.

Smith A.M. and Wooster M.J. (2005). Remote classification of head and backfire types from MODIS fire radiative power and smoke plume observations. International Journal of Wildland Fire, 14 (3), 249-254.

Sørensen, T. (1948). A method of establishing groups of equal amplitude in plant sociology based on similarity of species and its application to analyses of the vegetation on Danish commons. Biologiske Skrifter /Kongelige Danske Videnskabernes Selskab, 5 (4), 1-34.

Trigo R.M., Pereira J.M.C, Pereira M.G., Mota B., Calado T.J., Dacamara C.C. and Santo F.E. (2006). Atmospheric conditions associated with the exceptional fire season of 2003 in Portugal. International Journal of Climatology, 26 (13), 1741-1757.

USDA Forest Service, Active Fire Mapping Program. URL: http://activefiremaps.fs.fed.us/ (last visited: 2014, 16 June).

Wolfe R.E., Roy D.P. Vermote E. (1998). MODIS Land Data Storage, Gridding, and Compositing Methodology: Level 2 Grid. IEEE Transactions on Geoscience and Remote Sensing, 36(4), 1324-1338.

Influence of relief on the vegetation fires occurrences in the urban area of Juiz de Fora, MG, Brazil

Fillipe Tamiozzo Pereira Torres, Guido Assunção Ribeiro, Sebastião Venâncio Martins, Gumercindo Souza Lima

Universidade Federal de Viçosa, DEF, campus universitário 36570-000, torresftp@yahoo.com.br, gribeiro@ufv.br, venancio@ufv.br, gslima@ufv.br

Abstract
Wildfires cause irreversible damage to the environment, whether in the flora, fauna, people and large economic losses. Knowing the profile of forest fires, traced through different variables, it is essential to have guidelines to establish polices for protection planning. The statistics of occurrences are the main tools to know the profile of fires to planning the prevention and to control more efficiently, reducing costs, time and fight risk. This study used the coordinates of each of the 3,754 occurrences in the city of Juiz de Fora, MG, Brazil, for the period 01/01/2002 to 12/31/2011. The land aspect, the shape and the slope land of each event was determined in order to analyze the influence of the relief on the number of fire occurrence. According to the results, the relief influences directly the occurrence and fire spread. The northern aspect with greater slope and forms that facilitate the flow of water had a higher number of cases. The influence of relief is also confirmed by the relationship between wind direction and occurrences. Land exposures that directly receive the daily prevailing winds have a higher probability of occurrence of fire.

Keywords*: Relief, Fire, Susceptibility*

Introduction

The fires in vegetation are directly responsible, not only for environmental damage, but also economic and social losses whose dimensions often reach invaluable levels (Vosgerau *et al*., 2006).
There are two types of factors that determine the degree of fire danger: the constant factors, represented by the fuel type, which involves different types of vegetation and topography; and variable factors, represented by atmospheric conditions (Torres *et al*., 2011). Besides the listed factors it includes the land use and occupation.
The topography, according to Batista (2000), influences the climate and determines the type of fuel. Considering that fire behaviour is largely the result of the climate and fuel available, it can be said that the topography indirectly influence on the behaviour of the fire and the flames directly by the greater proximity the higher slope. So, we conclude that the relief is fundamental in establishing prevention and control plans.
To preserve the environment from the harmful effects of fires, it is essential that protectionist policies be appropriate to the characteristics of each region. It is necessary to know when and why the events occur. The statistics of occurrence are the main tools to trace its profile. With these data, the control can be planned more efficiently. The lack of this information can underestimate or overestimate the expenses relating to the protection of the environment, endangering the survival of forests and fighters (Santos, Soares and Batista, 2006). According to Vosgerau *et al*. (2006) in Brazil, there is a lack of effective plans for prevention and control. These plans can only be organized and put into practice by evaluating information to report precisely the characteristics of the occurrences of fires
To prioritize areas of greatest risk with intensive programs of protection and structure services of fire fight, in economically feasible limits, it is important to know the locations and the cause of occurrences and the factors of spread. Knowing the factors that contribute to the higher incidence of fire, it may

concentrate efforts and resources to fight it, because these systems are relatively expensive and would be impossible to keep them continuously in all locations.
The aim of this study was to analyse the influence of relief, such as the Sun aspect, The shape of the slopes, the inclination and its position in relation to the prevailing winds, on the occurrence of vegetation fires in the city of Juiz de Fora, Minas Gerais State, Brazil in order to trace the events, giving to the government tools to improve the prevention and fight policies.

Methods

The municipality of Juiz de Fora, with a population of 516,247 inhabitants (IBGE, 2010) and coordinates 21° 41' 20"S and 43° 20' 40"W, is located in the southeastern state of Minas Gerais, (Figure 1).,

Figure 1. Location of the study area

The area is extremely mountainous, reaching 1,000 meters of altitude at the highest point and 670-750 m in the valley bottom. The urban area falls entirely on the middle reaches of the Paraibuna River belonging to the Paraíba do Sul river basin (PJF, 1996).
The relief patterns show a strong tendency to a structural orientation. Their lithologies are characterized by having coverages of thick soils and rock exposures, mainly in the areas of occurrence of charnockitic rocks, to south of the city. In general geomorphological features tend to a convexity of slopes from the top, together with the formation of large number of amphitheatres and plains. The central core of the city, taking advantage of this natural condition, lodged in the enlarged section of the Paraibuna river valley, strangled by a sturdy bar, downstream (PJF, 1996).
The data of fires occurrences in vegetation were obtained in the 4th Battalion of Military Firefighters (4th BBM). We use 3,754 fire occurrences taking the nature, date, time and address for the period 01/01/2002 to 31/12/2011, within the urban area.
All places of occurrences were geocoded and tabulated. The exposures were grouped into strands North (315° to 45°), East (45° to 135°), South (135° to 225°) and West (225° to 315°), by using a compass. The shapes were got by visual interpretation, classified in concave and convex rectilinear. The slopes classes was determined with the Abney clinometer and grouped into classes from 0° to 10°, 10° to 20°, 20° to 30°, 30° to 40° and > 40°.

The preferred directions of the winds were recorded in Principal Climatological Station, located at the Federal University of Juiz de Fora (UFJF). Data were collected at 9:00, 15:00 and 21:00 UTC. From the readings of the three times, the preferred direction for each day of the series divided into North, Northeast, Northwest, West, East, South, Southeast and Southwest was determined.

Results and Discussion

Figure 2 shows that there was a significant influence of exposure of the slopes on events where most of the fires occurred in North aspect (N) followed by the West aspect (W), East aspect (E) and the lowest on the South aspect (S).

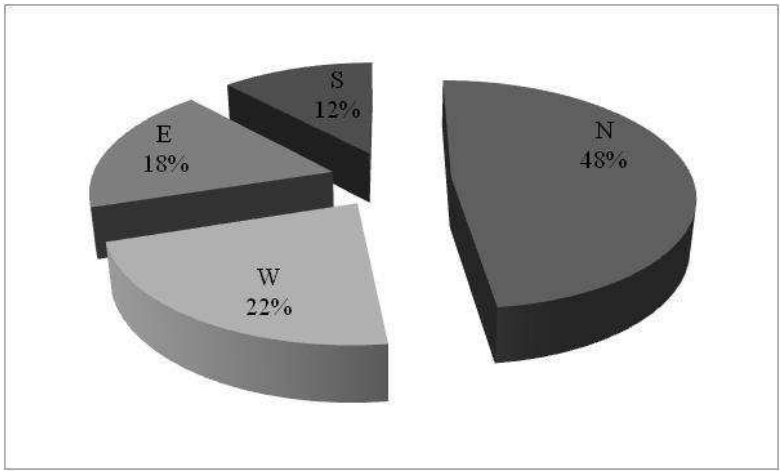

Figure 2. Occurrences of fires in agreement with the exhibition of the slope

This distribution is due to the fact that surfaces with different orientations and inclinations receive different amounts of solar radiation compared to a flat surface, in the same location and time of year (Torres & Machado, 2011). The Sun culminates at zenith (representing greater energy gain) in places whose latitude is equal to the tilt of Earth's axis. Thus, the equinoxes (March 21 and September 23) the Sun culminates at zenith over the equator, with these dates, in all places on Earth , days and nights of equal length. At the Summer Solstice in the South and Winter Solstice in the Northern Hemisphere (December 22), the Sun culminates at zenith for latitude 23° 27' (South), because this is the greatest declination reached the southern hemisphere, this latitude is called the Tropic of Capricorn. On June 21 the Sun culminates at the zenith to 23° 27' (North) latitude that defines the position of the Tropic of Cancer, has thus the Summer Solstice in the Northern Hemisphere and Winter Solstice in the Southern Hemisphere for the higher latitudes 23° 27' the sun does not culminate on zenith on any day of the year.

We observe, therefore, that the sun for much of the year culminates in Zenith north of the city of Juiz de Fora, located at latitude 21° 41' 20" S. This factor tends to raise the temperature in the areas of North orientation directly influencing the physical characteristics of fuel and fire occurrences.

The difference between the West and te East aspect can be explained by the hour of greatest concentration of occurrences (between 15 and 16 hours), during this time the slope the West aspect is getting greater amount of solar energy relative than East aspect, increasing the percentage of occurrences. Another factor is the West aspect receives more energy in the afternoon when the earth's surface and the air are already heated and usually there is no fog. Beside these, the East aspect get humid winds from the Atlantic Ocean, distant, straight, about 150 km from the city.

Hugget (1995) points out that in the southern hemisphere, oriented north slopes receive more insolation than facing the South, which, in turn, receive higher rainfall due to moisture-laden winds from the sea (SW, S and SE). Oliveira *et al*. (1995) found significant differences in the two approaches

with respect to parameters such as temperature, precipitation and humidity. According to these authors, the South aspect has leaf litter on average 41.9% more humid than those toward the North. The authors also claim that the loss of this moisture also occurs much faster on North aspect, because the South one retains moisture 1.6 times more. Consequently soil moisture behaves the same way, only varying according to the type of associated vegetation.

This moisture variation is reflected primarily due to different rates of temperature of these two types of aspects, since the North are significantly warmer due to higher incidence of heat that turned to the South, with 98% occurrence of maximum temperatures on those aspects. The minimum temperature also occurred mostly in the northern aspect (86 %), which should be attributed to higher relative humidity in the South, over the longer period of deposition of dew that acts as a "buffer" effect reducing extreme temperatures (Oliveira *et al*., 1995).

At low relative humidity, the probability of occurrence and spread of fire is greater in view of the direct correlation with the drying of the fuel. The thinnest material, represented by one of time lag of an hour, according the Brown (1982) classification is present in greater quantities and in most environments. In critical weather situations, this material comes to lose up to 66 % humidity in the range of an hour, leading the fuel moisture below the extinction moisture.

According to Nunes (2005) this is due to atmospheric humidity have a direct effect on the flammability of fuels, with a constant moisture exchange between the atmosphere and plant dead. The dry material in a humid atmosphere absorbs water and releases water when the air is dry. The amount of moisture that dead material can absorb or release depends on the relative humidity. During extremely dry periods, moisture may even affect the moisture content of dead or live material.

Furthermore, there are internal variations within geomorphological character that individualize the slopes more or less favorable to the fire occurrence. These are geometric segments which are presented in three main forms: concave, convex and straight. The concave shapes are characterized as areas of convergence of flow and consequently a higher concentration of moisture, while the convex and straight (on slopes) influence the formation of zones of divergence of water and low moisture content and thus more susceptible to the fire occurrence (Coura, Souza & Fernandes, 2009).

This influence is confirmed by the results of the study (Figure 3), showing the largest number of occurrences and the convex rectilinear strands in relation to concave.

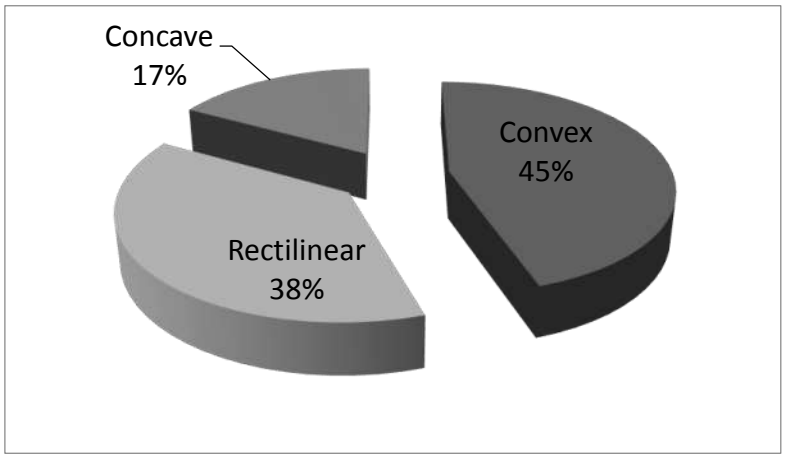

Figure 3. Fire according to the shape of the slope

Regarding the slope, the data point to the following results (Figure 4), confirming that greater when the slope the greater the percentage of occurrences.

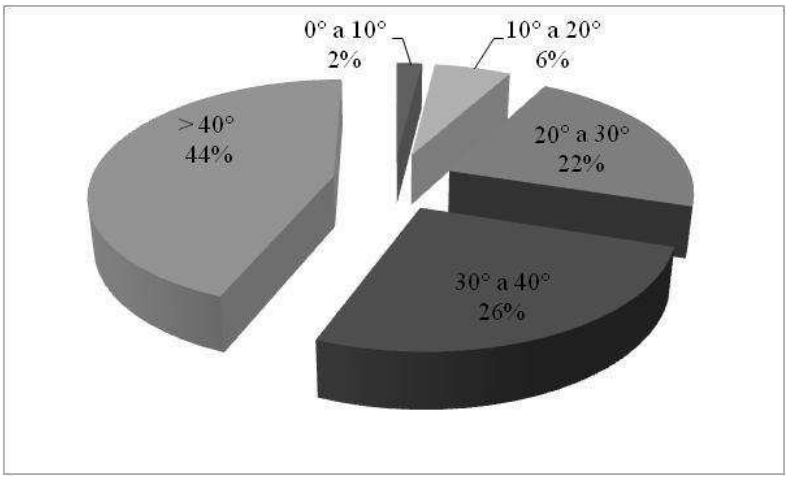

Figure 4. Fires according to the slope

The influence of slope can be explained due to the humidity, according Valeriano (2008), on steeper slopes, it can realize easily that rainwater flows very quickly, seeping in smaller quantities, making it the driest place.

Besides the interference of inclination in water flow, Viegas (2004) explains that the spread of fire in places with some slope is distinct from behavior that occurs in areas without slope, due the effect of additional factors such as convection and radiation. If there are minimum declivity, the rate of spread tends to grow and will be greater the larger the microclimatic changes in the combustion zone. This fact is also confirmed by Ribeiro *et al*. (2008) when they argue that the intensity of the fire in the areas of acclivity is greater due to overheating of fuel above the front of the fire line, the flames closer when compared to flat terrain. On the other hand, the wind tends to help as much on the drying of the fuel material as the spread of fire.

The wind is a major factor in the combustion rate and spread of the fire like described by Torres *et al*. (2011) in addition to affecting the rate of oxygen supply during the burning. The drying of the fuel is accelerated by the removal of the air layer in contact with the surface and induce the tilt of the flames, approaching those of the material not yet burnt and hastening the preheating stage.

The data (Table 1) show the relation between the wind direction and the occurrences of fires. Slopes to windward of the preferred daily winds have higher numbers of occurrences of fires. When the preferred wind direction is north, there is a predominance of fires in windswept strand with the same direction 71 % of the occurrences. When the wind direction is north-west, 87 % of the occurrences are located on slopes facing N and W; when the direction is north-east there is a greater number of occurrences in the areas N and E with 81 % of fires in these respects; with the wind direction West, 77 % of cases occur in the present toward the W; the preferred direction of the wind when it favours eastern occurrences hillsides N and E. This influence can be best observed when the winds are predominant directed in the southern quarter (SW, S , SE), where there is a superiority of occurrences in the southern side, countering the dominance of events that occurs in slopes with further guidance. When the situation is calm (C) without occurrence of winds, the situation normalizes in relation to the order observed in Figure 2 with higher occurrences in the present N, then the slopes neatly Exposure W, E and S.

Table 1. Percentage of occurrences according to the location of the fire and the wind direction

Slope occurrence	Wind direction								
	N	**NW**	**NE**	**W**	**E**	**SW**	**SE**	**S**	**C**
North (N)	71%	44%	54%	23%	40%	22%	28%	33%	65%
West (W)	15%	43%	15%	77%	25%	41%	12%	23%	26%
East (E)	10%	8%	27%	0%	29%	9%	29%	8%	6%
South (S)	4%	5%	4%	0%	6%	28%	31%	36%	3%
% of days with prevailing wind	20%	11%	19%	1%	11%	5%	15%	14%	4%

In summary, when the wind direction is the same as the orientation of the slope, there is the named "wind up the hill" in this situation the wind accelerates the spread of fire, whereas it tends to raise the flames of bottoms for higher still unburned.

Conclusion

The results of this study allow us to conclude that:

- the land aspect has a direct correlation on the fires occurrences;
- the North aspect have a higher percentage of occurrences for receiving greater amount of solar energy during the year;
- the west aspect were in second place with more fire occurrences, which can be explained by the time in which they receive higher solar radiation that coincides with the time of lower humidity;
- the slopes to windward of the preferred daily winds are more susceptible to the occurrence;
- those aspects that favour the spread of water tend to have higher number of occurrences;
- the higher the slope the greater the number of events;
- the strategies to prevent fires must take into account the influences of topography and the prevailing winds through preventative in areas more conducive to the event work. Also the fight actions must take into account such information, reducing the costs and risks of operations.

References

Batista, A. C. (2000). Mapas de risco: uma alternativa para o planejamento de controle de incêndios florestais. *Floresta*, Curitiba, v.30, n.1/2, p.45-54.

Brown, J. K. *et al*. (1982). *Handbook for inventorying surface fuel and biomass in the Interior West*. Ogden: Intermountain Forest and Range Experiment Station.

Coura, P. H. F.; Sousa, G. M. E Fernandes, M. C. (2009). Mapeamento geoecológico da susceptibilidade à ocorrência de incêndios no Maciço da Pedra Branca, município do Rio de Janeiro. *Anuário do Instituto de Geociências - UFRJ*, Rio de Janeiro, v.32, n.2, p.14-25.

Hugget, R. J. (1995). *Geoecology: an evaluation approach*. Londres: Editora London.

IBGE. (2010). *Censo Demográfico 2010*. Rio de Janeiro: Instituto Brasileiro de Geografia e Estatística.

Nunes, J. R. S. (2005) *FMA+ - Um novo índice de perigo de incêndios florestais para o Estado do Paraná – Brasil*. Tese (Doutorado em Engenharia Florestal) – Setor de Ciências Agrárias, Universidade Federal do Paraná, Curitiba.

Oliveira, R. R. *et al*. (1995). Significado ecológico da orientação de encostas no Maciço da Tijuca. *Oecologia Brasiliensis*, Rio de Janeiro, v. 1, p.523-541.

PJF. (1996). *Plano Diretor de Juiz de Fora*. Juiz de Fora: Concorde, 1996.

Ribeiro, L. *et al*. (2008). Zoneamento de riscos de incêndios florestais para a fazenda experimental do Canguiri, Pinhais (PR). *Floresta*, Curitiba, v.38, n.3, p.561-572.

Santos, J. F.; Soares, R. V. E Batista, A.C. (2006). Evolução do perfil dos incêndios florestais em áreas protegidas no Brasil, de 1993 a 2002. *Floresta*, Curitiba, v.36, nº1, p.93-100.

Torres, F. T. P. *et al*. (2001). Correlações entre os elementos meteorológicos e as ocorrências de incêndios florestais na área urbana de Juiz de Fora, MG. *Revista Árvore*, Viçosa, v.35, n.1, p.143-150, 2011.

Torres, F. T. P. E Machado, P. J. de O. (2011). *Introdução à Climatologia*. São Paulo: Cengage Learning.

Valeriano, M. M. (2008). Dados topográficos. In: FLORENZANO, T. G *Geomorfologia: conceitos e tecnologias atuais*. São Paulo: Oficina de textos.

Viegas, D. X. (2004). *Cercados pelo fogo*. Coimbra: Editorial Minerva.

Vosgerau, J. L. *et al*. (2006). Avaliação dos registros de incêndios florestais no Estado do Paraná no período de 1991 a 2001. *Floresta*, Curitiba**,** v.36, n.1, p.23-32.

Integrated and integral forest fire management – Operation Roraima 2013, Brazil

Morais, J. C. M.[a], Barreto, R. V., Alves, R[c], Lima, J. P. P.[d], Silva, M. M.[e], Felix, H. C.[f], Barcelos, M. A.[g], Cunha, A. M. C.[h], Balderramas, A. J. P.[i], Pinho. M. C.[j], Olivato, C. M. O.[l], Rocha, M. C.[m], Macedo, C. F.[n],

[a] *Brazilian Institute of Environment and Natural Renewable Resources, jose.morais@ibama.gov.br*
[b] *Fire Brigade of the Federal District, vianna1975@gmail.com*
[c] *State Committee for the Prevention and Fight against forest fires. Government of the State of Roraima, ramonwalves@yahoo.com.br*
[d] *Brazilian Institute of Environment and Natural Renewable Resources, terroada@yahoo.com.b*
[e] *1st Jungle Infantry Brigade Brazilian Army, marcelomarcant@hotmail.com*
[f] *Chico Mendes Institute for Biodiversity, hudson.felix@icmbio.gov.br*
[g] *Fire Brigade of the Federal District, barcelos.cbmdf@gmail.com*
[h] *Brazilian Institute of Environment and Natural Renewable Resources, anacanut@yahoo.com.br*
[i] *Brazilian Institute of Environment and Natural Renewable Resources, ncbalderramas@oi.com.br*
[j] *Brazilian Institute of Environment and Natural Renewable Resources, marlenecpinho@hotmail.com*
[l] *Brazilian Institute of Environment and Natural Renewable Resources, creusaolivato@gmail.com*
[m] *Brazilian Institute of Environment and Natural Renewable Resources, mrocha41@gmail.com*
[n] *Brazilian Institute of Environment and Natural Renewable Resources, clemilton.macedo@ibama.gov.br*

Abstract

In 1998, the indiscriminate use of fire to manage agricultural and forest areas in favourable weather conditions in the state of Roraima resulted in one of the largest forest fires in the modern era, which was immensely aggravated by the lack of preparation of public institutions that are responsible for fire prevention and protection.

This event, however, left important lessons and prompted the establishment of new forest fire fighting and prevention policies across Brazil. Fifteen years later, Operation Roraima Green 2013 adopted a new fire prevention and fighting model based on concepts, methods and routines of "Integrated and integral forest fire management". Joint coordination was established to constitute the Integrated Multi-Agency Operational Coordination Centre (*Centro Integrado Multi Agências de Coordenação Operacional*) - CIMAN Federal - with a situation room to monitor high fire-risk forest areas, namely protected federal, state and municipal zones, public forests and forest areas of national interest. Greater emphasis was placed on the detection of hotspots by means of remote sensing, warning and quick initial attack on behalf of response bodies, in accordance with priorities established by all the involved entities and institutions.

A Unified Command Unit was constituted to establish priorities for forest fire fighting and prevention activities based on the doctrine of the Incidents Command System - SCI.

Key challenges of integral management were:

1 – Forecasting risk situations;
2 – Fire prevention actions and control of intentional forest burning;
3 – Fire fighting preparation;
4 – Forest fire fighting;
5 – Civil and criminal accountability of offenders;
6- Recovery and reconstitution of affected areas.

The Centre also promoted intense flow of information on implemented actions, which allowed perfect integration between the involved institutions.

Keywords*: Integrated management, Comprehensive management, Prevention, Combat, Accountability*

Introduction

The Climate Report Data, prepared by the Amazon Protection System - Sipam for the period of September, October and November/2012, indicated that during the quarter the coastline of eastern Amazonia was under the influence of a subsidence branch, with short rains in region increasing temperatures. The fallout would be below the climatological patterns, particularly the south-central Amapá, Pará northeast, northwest of Maranhão, Tocantins and Amazonas northern, and **Roraima** south.

These data also indicated a probable **occurrence of *El Niño,*** where its effects enhance normal climate, i.e., change the dry period of the state of Roraima which tends to have a more severe and prolonged summer (drought), with rising temperatures, gusty winds and consequently low relative humidity, favoring the spread of flame in case of wildfires.

At the request of the Environmental Protection Director -Dipro/IBAMA a **Special Report** was drafted by the Operating Technical Center of Manaus / Meteorology Division DivMet-CTO/MN/Sipam for **Roraima** where the study indicated the following prognosis: ***"Precipitation below the climatological patterns, especially at the beginning of the quarter, however the maximum and minimum temperatures may be slightly (about 1-2 ° C) above their climatological values."***

Later the Prevention and Environmental Monitoring Division of Femarh located in Roraima, based on the Climate Report of the Amazon under No. 97, Year 9, prepared by the Amazon-Sipam Protection System with forecasts for December 2012, January and February 2013, noted that the state of Roraima would present precipitation from normal to below the climatological pattern, the temperatures being normal and above the climatological pattern.

Based on climatological information, the Director of Environmental Protection - Dipro / IBAMA decided to conduct an operation targeting preventive actions to protect federal and / or public interest areas in the state of Roraima.

With the assigned mission, the operation was based on the applicable legislation: Article 18 of Decree No. 2.661, of July 8th, 1998, Complementary Law No. of December 8th, 2011, Law No. 12.651, of May 25th, 2012, Law No. 12.727, of October 17th, 2012, MMA Ordinance No. 94 of March 19th , 2012, and we found that with the current legal basis we had to establish a relationship among the federal institutions.

On November 26th the shared planning proposal was submitted following the model of multi-agency Integrated Centers of Operational Coordination - CIMAN's deployed statewide in 2009, 2010 and nationally in 2010.

The proposal was to establish a Joint Coordination, the multi-agency Federal Integrated Operational Coordination Center - **CIMAN RR / Federal,** where a situation room was established. Such structure was conditional on the formation of a unified command that uses the doctrine of the Incident Command System - ICS.

The operating period from December 1st, 2012 to March 31st, 2013 was set, therefore the data used for comparisons of hotspots, combat, visits, burning and supervision observe this period of work.

2. Integrated Multi-Agency Center - CIMAN RR / Federal

The purpose of CIMAN RR / Federal within the 2013 Green Roraima Operation was to enhance the actions of the federal institutions involved, optimize the human and material resources looking for integrated and comprehensive management in preventing and fighting wildfires where the challenge was to predict risk situations, propose and implement preventive actions, prepare institutions for firefighting, hold offenders accountable and finally reconstruct areas affected by the fires.

CIMAN also installed a unique situation room and therein shared information about ongoing operations as well as search for joint solutions among participating entities. The results of actions undertaken were evaluated, seeking to optimize the strategies adopted. In every meeting an Integrated

Action Plan – PAI was prepared, which contains, among other directives, the specific objectives for the operational period, pointing to each institution involved the requested activities, as well as actions already implemented.
Throughout the period 17 meetings of CIMAN RR / Federal were held, 02 Non-Face-To-Face and 15 Face-To-Face meetings; with the presence of 14 federal agencies, plus the participation of a member of the State Committee for Prevention and Control of Wildfires, and the support of the Fire Brigade of the Federal District (CBMDF), constituting the integrated management of wildfires in Roraima (table 1).

Table 1. Agencies composing CIMAN RR / Federal. 2013 Green Roraima Operation. Source: CIMAN RR / Federal.

N	Logo:	Institution	Agency	No.	Logo:	Institution	Agency
1		1st Jungle Infantry Brigade of the Brazilian Army - **1st BIS**	**Ministry of Defense**	09	Eletrobras Eletronorte	Regional Management / RR, Brazilian energy company **Eletrobras / Eletronorte**	**Ministry of Mines and Energy**
02		Boa Vista Air Base of the Brazilian Air Force - **BABV**	**Ministry of Defense**	10	INFRAERO	Supervisory Office / RR Brazilian Airport Infrastructure Company - **INFRAERO**	**Ministry of Defense**
03	IBAMA MMA	State Supervisory Office of the Brazilian Institute of Environment and Renewable Natural Resources - **IBAMA**	**Ministry of Environment**	11	INCRA	Supervisory Office / RR National Institute of Colonization and Agrarian Reform - **INCRA**	**Ministry of Agrarian Development**
04	ICMBio MMA	Regional Coordination - CR-2 Chico Mendes Institute for Biodiversity - **ICMBio**	**Ministry of Environment**	12		Supervisory Office / RR Brazilian Agency of Intelligence - ABIN	**Institutional Security Office**
05	FUNAI	Regional Coordination / RR National Indian Foundation - **FUNAI**	**Ministry of Justice**	13	MRE	Vice Consul of Brazil in Santa Elena of Uairén - Venezuela - **ITAMARATY**	**Ministry of Foreign Affairs**
06		5th Regional District / RR Federal Highway Police - **DPRF**	**Prosecutors Office**	14	Embrapa	Agro Forestry Research Center / Brazilian Agricultural Research Corporation - **EMBRAPA**	**Ministry of Agriculture**
07	MANAGER	State Committee for the Prevention and Combat of Wildfires. Government of the State of Roraima	**Government of the State of Roraima**	15	INPE	National Institute for Space Research - **INPE**	**Ministry of Science and Technology**
08		Manaus Regional Center Amazon Protection System - **SIPAM**	**Ministry of Defense**	16	**CBMDF** **SUPPORT**	Fire Brigade Federal District - **CBMDF**	**Government of the Federal District**

The Integrated Center meetings were held every Wednesdays, always at 10am maintaining a routine with the opening followed by a brief introduction of the participants, the agenda exposed forecasts prepared by SIPAM, after which an analysis was made of hotspots of the operational period and the previous day. When we did not have a GIS specialist present at the meeting we made the analysis directly on the official monitoring of federal areas, an INPE website especially developed for the Green Roraima Operation, and at the end we updated and signed the PAI.
In the second half of January we had additional support with the arrival of technicians from the Brazilian Environmental Protection Agency (IBAMA) and the Fire Brigade of the Federal District - CBMDF in the operation to assist in the logistics and implementation of the Incident Command System- ICS. Thus the logistics establishing physical structure plus the ICS, which assigns concepts of command and control, with the GIS support, established a Situation Room idealized since December 2012 as follows in the chart below (Figure 1).

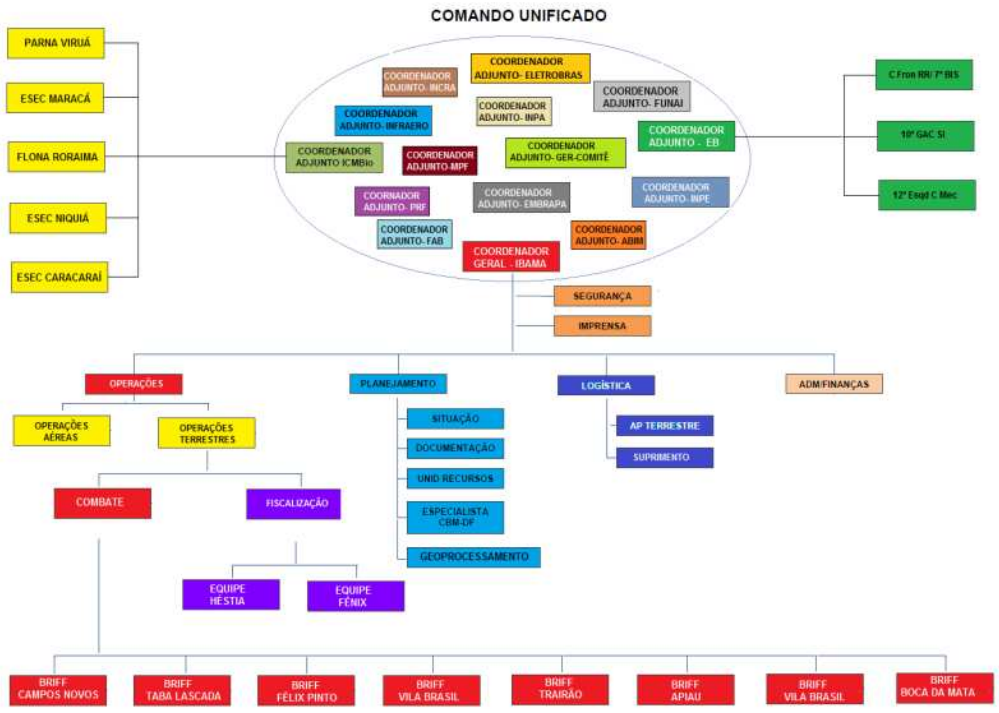

Figure 1. Chart of CIMAN RR / 2013 Federal. Green Roraima Operation. Source: CIMAN RR / Federal.

Remember that the participation of the institutions in this plan was voluntary and did not involve any transfer of funds, where each institution had contributions of capital already budgeted for the implementation of its final activities.

A logo was also created referring to the operation, inspired in similar events, keeping the brand already registered in other Brazilian states (Figure 2).

Figure 2. Logo of CIMAN RR / Federal. Source: CIMAN RR / Federal.

In the situation room the risk areas susceptible to deforestation when associated with burning and wildfires, the federal protected areas, forests and other public areas of security, economic and social interest were monitored, such as federal highways, GURI transmission lines and airfields. Emphasis was given on detection of hotspots, warning to quick initial attack by the response agencies, according to the priorities established by the agencies, institutions and organizations involved. For illustrative

purposes, find below pictures of the situation room assembled in the Supervisory Board of IBAMA in Roraima. The pictures were captured from the four corners of the room, with an emphasis on the meeting table (Figure 3).

Figure 3. Situation Room CIMAN RR / Federal - SUPES / IBAMA / RR. 2013 Green Roraima Operation. Source: CIMAN RR / Federal.

CIMAN RR also had a mission to find mechanisms to predict risk situations and provide information to participating agencies and maintain the situation room provided with information.
CIMAN RR initiated the monitoring of hotspots in the conventional manner, i.e., used a GIS Specialist who intersected the hotspots overlapped in the features of protected areas, indigenous lands, right of way, easement strips, military areas, rural settlements, border areas and aerodromes (Table 2).

Table 2. Areas monitored by CIMAN RR / Federal on the INPE website. 2013 Green Roraima Operation. Source: CIMAN RR / Federal.

Monitored Features	Responsible Agency	Monitored Areas
Overview	IBAMA	Throughout the State of Roraima
Federal protected areas	ICMBio	1,615,971 ha
State protected areas	Femarh	Not available
Indigenous lands	FUNAI	10,331,521.34149 ha
Federal highways	DPRF	1404 km
Aerodromes (Boa Vista, Caracaraí and Pacaraima)	Brazilian Airport Authority (INFRAERO)	Radius of 6 km from the center point of the aerodrome
GURI Transmission line	Eletronorte	190 km
Federal Settlements	INCRA	1,371,856 ha
Military areas	Army	279 421 hectares
Border area	Vice Consul of Brazil in Venezuela	954 km border

The daily monitoring has been replaced by the Special Report for Roraima developed by INPE. The report for the monitoring of outbreaks of fires in Green Roraima Operation presents all outbreaks detected by all satellites (blank) used in the monitoring of fires by **INPE,** in a radius of up to 400 kilometers (per 100 km) around the airport Boa Vista - Roraima. The figure also showed the Points of Attention representing significant persistent fires over the last 24 hours (yellow dots); 48 hours (orange dots) and 72 hours (red dots). Moreover, the red areas are the indigenous territories, the green areas are the state protected areas and the dark green areas are the federal protected areas (figure 4).

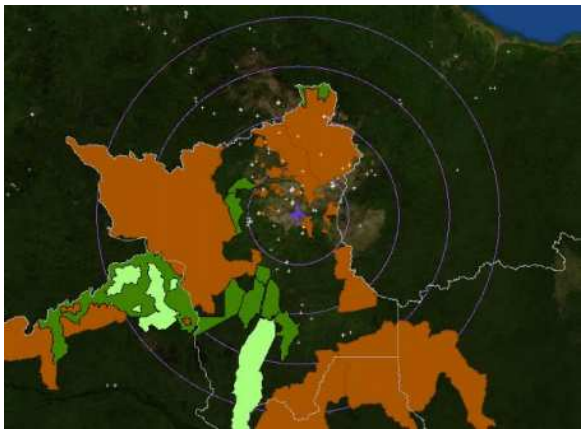

Figure 4. Active fire outbreaks detected by the monitoring satellites - Overview. Source: INPE.
http://peassaba.cptec.inpe.br/queimadas/boletim_roraima/

The monitoring exposes a list of fires presented according to an index that combines the duration and extent of events detected by the nine satellites currently used by the INPE monitoring system.
All the features of interest were also monitored individually and automatically, and when some hotspot is registered in these areas the information was passed along by email to the Situation Room and the agency responsible for the area.
In the figure below, from the top left to the bottom right corner, pictures of the monitoring of federal protected areas administered by ICMBio, Indigenous Lands managed by FUNAI, the easement of Guri line maintained by ELETRONORTE settlements promoted by INCRA , federal highways policed by DPRF, border areas where the Brazilian Consulate in Helena and Venezuela was reported (Figure 5).

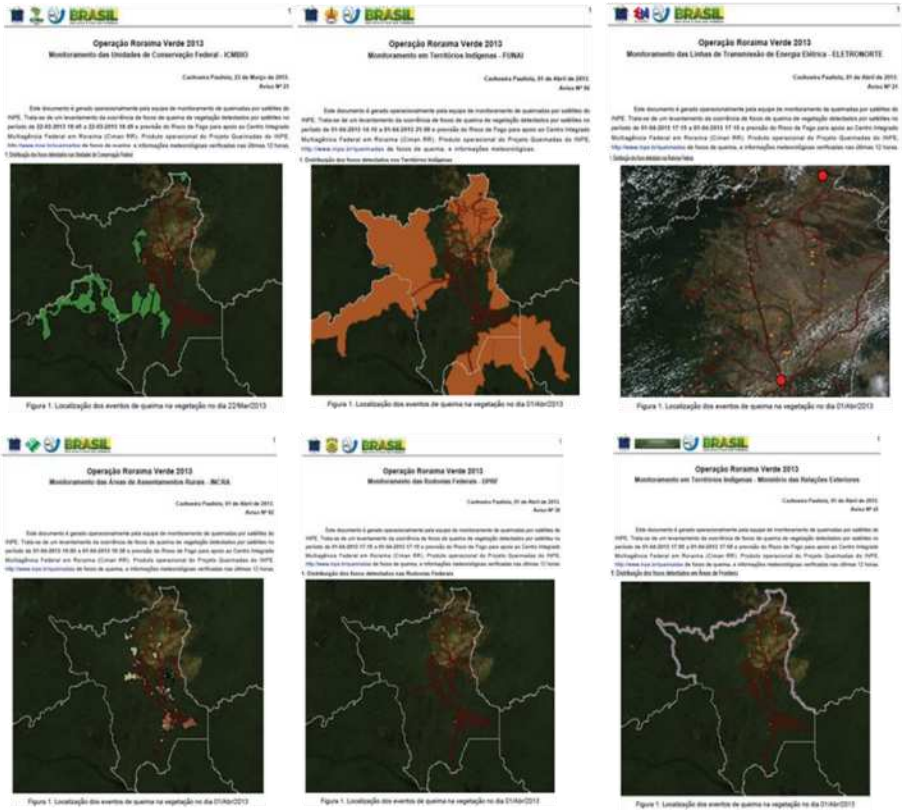

Figure 5. Features monitored by satellites. Source: INPE

The documents were generated operationally by the team of fire monitoring by satellites of INPE. The survey of outbreaks of wildfire outbreaks detected by satellites in the period and the prediction of fire risk for support to CIMAN RR.

Climatology, Forecasting risk situations

Climatological Report is a product based on data from INPE (National Institute for Space Research), INMET (National Institute of Meteorology) and SIPAM (Amazon Protection System), which presents the systematization of meteorological information related to spatial and temporal coverage of Roraima in the quarter January-February-March 2013 and it has strong application in the planning and operation of public services, among others. The information contained herein represents the assessment, treatment and secure dissemination of data, usefully contributing to the expansion of knowledge and the direction of public policy.

The average behavior of the oceans during the month of January is shown in Figure 6. The Pacific Basin was marked by the predominance of colder water (negative anomalies) of sea surface temperature (SST), especially in the equatorial zone comprising the *Niño* region. On the west coast of South America, there was expansion of surface waters with negative anomalies (colder than average) extending from the *Niño* 1 +2 region towards the region of *Niño* 3.

In the Tropical Atlantic Ocean there was a decrease in the area with warm anomalies in the northern tropical basin, while isolated areas of south tropical basin had a water colder than average. In the South Atlantic region there is a predominance of Negative SST anomalies, which created favorable conditions for the cold front in the southeastern of Brazil, resulting in precipitation.

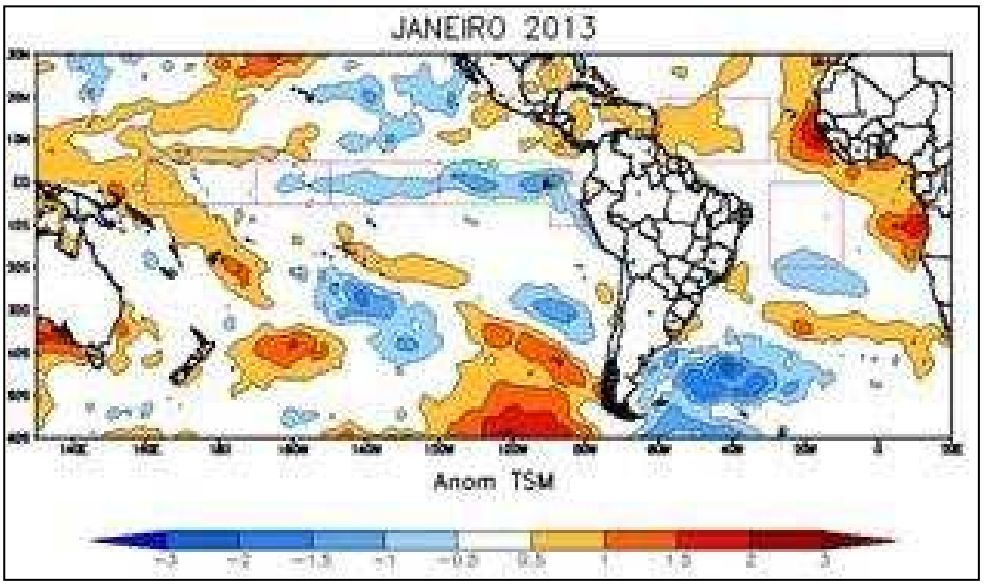

Figure 6. SST anomalies (° C) in January 2013.Rectangles in the Pacific represent areas of Niño 1 +2 (red), Niño 3 (green), 3.4 (dashed red) and Niño 4 (blue). Source: Data from CPC/NCEP processed by SIPAM.

During the month of January 2013, the Convergence Zone of the South Atlantic (SACZ) operated in the region resulting in very irregular spatial distribution of precipitation in the rest of the country, but in Roraima this system does not contribute to accumulated rain, particularly in the northeast sector of the State. ZCAS is a weather system characterized by a region of moisture convergence oriented from northwest to southeast, forming a deep band of cloudiness able to generate abundant precipitation. So in January, low precipitation was recorded across the state of Roraima as in figure 7.

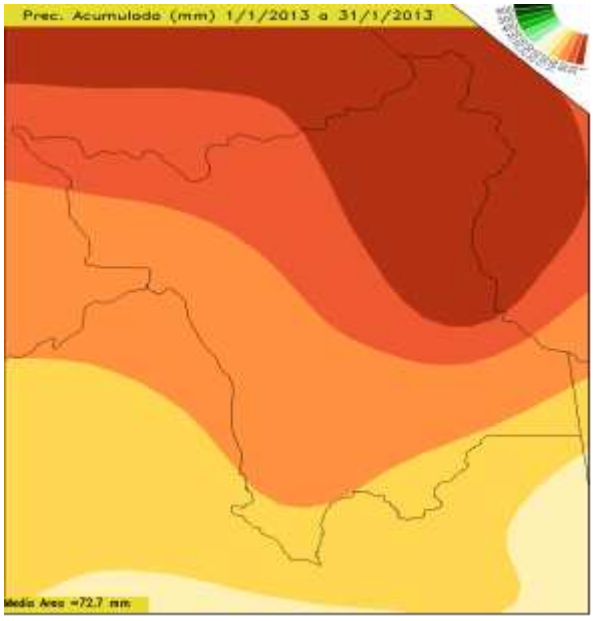

Figure 7. Precipitation recorded in January 2013 in the State of Roraima. Source: INPE.

Such low accumulated precipitation in January, or absence thereof, in some cases, contributed significantly to the increase in fire outbreaks in Roraima, as per the histogram below (Table 3).

Table 3. Histogram of fire outbreaks in the state of Roraima. Listing only of the states municipalities with occurrence of outbreaks in January 2013. Source: INPE.

- HISTOGRAM OF FIRE OUTBREAKS -
2013-01-01 00:00 p.m.: 00 to 01/31/2013 11:59 p.m.: 59
(AQUA Tarde)

Distribuição dos 191 focos de 2013-01-01 a 2013-01-31 em RR	
Municípios	
(1) Rorainópolis / RR	*(31)*
(2) Bonfim / RR	*(22)*
(3) Amajari / RR	*(19)*
(4) Caracaraí / RR	*(18)*
(5) Boa Vista / RR	*(17)*
(6) Normandia / RR	*(15)*
(7) Cantá / RR	*(14)*
(8) Pacaraima / RR	*(14)*
(9) São João da Baliza / RR	*(10)*
(10) Iracema / RR	*(8)*
(11) Alto Alegre / RR	*(8)*
(12) Caro Ebe / RR	*(6)*
(13) Uiramutã / RR	*(5)*
(14) São Luiz / RR	*(3)*
(15) Mucajaí / RR	*(1)*

In February 2013, the average behavior of the ocean is shown in Figure 08. The Pacific Basin was marked by the predominance of colder water (negative anomalies) of sea surface temperature (SST), especially in equatorial regions comprising *Niño*. On the west coast of South America, there was

expansion of surface waters with positive anomalies (warmer than average) in the entire length of the Chilean coast.

In the Tropical Atlantic Ocean there was a decrease in the area with warm anomalies in the northern tropical basin. While in the southern tropical basin there was predominantly standard of neutrality, except on the African coast where surface waters were warmer than average. In the South Atlantic region negative SST anomalies remained predominantly. The performance of the Alta da Bolívia together with the cooling in the Pacific Ocean intensified convection in western Amazonia and the ITCZ activity (Figure 8).

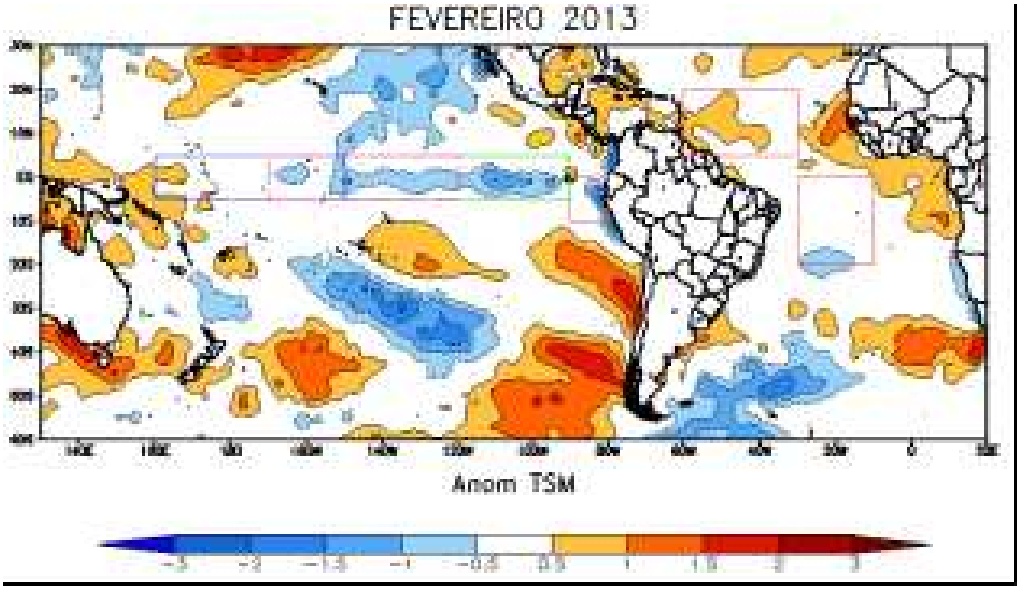

Figure 8. SST anomalies (° C) in February 2013. Rectangles in the Pacific Ocean represent areas of Niño 1 +2 (red), Niño 3 (green), 3.4 (dashed red) and Niño 4 (blue). Source: Data from CPC / NCEP processed by SIPAM.

Figure 09 shows the Accumulated Precipitation during the month of February 2013. The performance of the Intertropical Convergence Zone (ITCZ) in the region caused great irregularity in the spatial distribution of precipitation. The ITCZ is a weather system formed by clusters of clouds of great vertical development with the potential to cause large volumes of rain. The most northerly position of the ITCZ and warming in the tropical north Atlantic basin, which contributed to an increase in the transport of moisture from the ocean toward the continent, were primarily responsible for the emergence of positive anomalies over the state of Roraima.

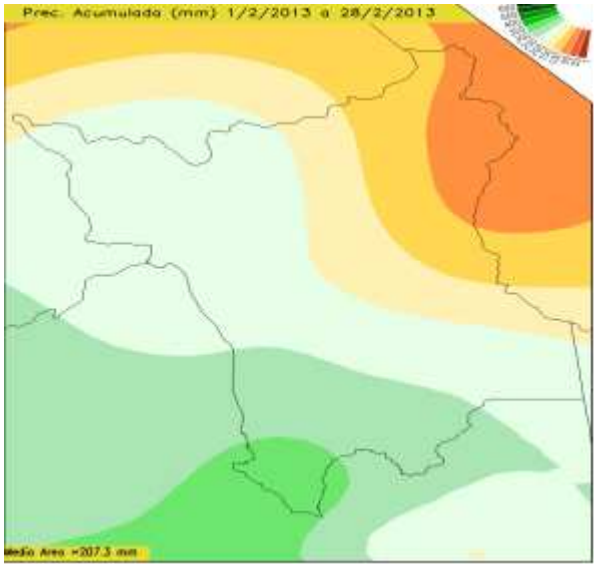

Figure 9. Accumulated Precipitation in February 2013 in State of Roraima. Source: INPE.

Such increased precipitation in the previous month led to a reduction of hotspots in the State of Roraima, as per the histogram below (Table 4).

Table 4. Histogram of fire outbreaks in the state of Roraima. Listing only of states municipalities with occurrence of outbreaks in February 2013. Source: INPE.

- HISTOGRAM OF FIRE OUTBREAKS -
01/02/2013 00:00: 00 TO 28/02/2013 23:59: 59
(AQUA Tarde)

Distribuição dos 10 focos de 2013-02-01 a 2013-02-28 em RR	
Municípios	(1) São Luiz / RR *(4)*
	(2) Cantá / RR *(2)*
	(3) Boa Vista / RR *(2)*
	(4) Caracaraí / RR *(1)*
	(5) Normandia / RR *(1)*

In March 2013, Figure 10 shows the weekly oceanic pattern observed until the 24th day. The monitored areas in the Equatorial Pacific show large spatial and temporal variability of SST anomalies, predominantly colder water than average in the first two weeks of March. In the period from 17 to 24 March there was a significant increase in positive SST anomalies in the equatorial Pacific region, with warmer water than average.

In the Atlantic Basin Tropical there was no significant change over the past three weeks, keeping two extensive areas with positive SST anomalies in the northern portion. In the Subtropical South Atlantic, near Brazil's east coast, there was a slight reduction in the negative SST anomalies, with an almost neutral standard.

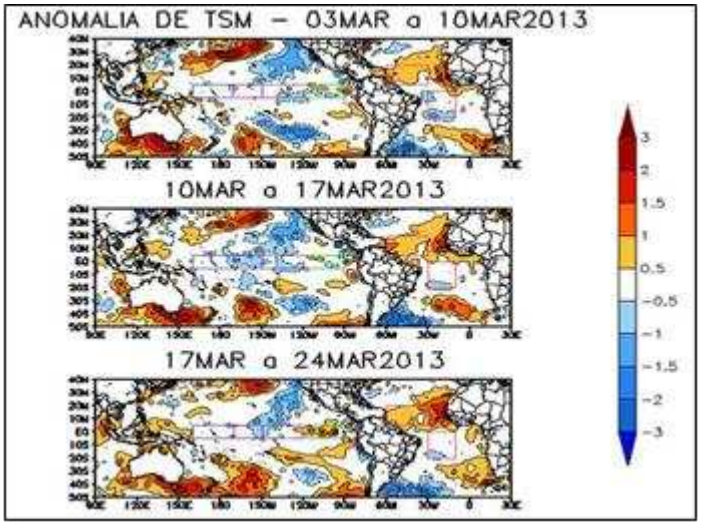

Figure 10. Weekly SST Anomaly (° C) for month of March 2013 over the range between 40 ° N and 50 ° S. Source: Data from NWS / CPC processed by SIPAM.

The performance of the Intertropical Convergence Zone (ITCZ) to the north of its climatological position contributed to the below average precipitation in Roraima during the month of March 2013. The anomalous position of the ITCZ is occurring in response to warming of surface waters in the tropical North Atlantic.

Another reason that explained the lack of rain in much of the state was the anomalous westward displacement of the flow at high levels between the past months of January and February. Over the past few months, signs of intraseasonal variability have interfered in oceanic and atmospheric patterns in tropical areas around the globe.

As a result, these same patterns sometimes contribute to the occurrence of precipitation, sometimes to the inhibition of the rains. As a result Figure 11 shows that the accumulated precipitation was below normal in March 2013.

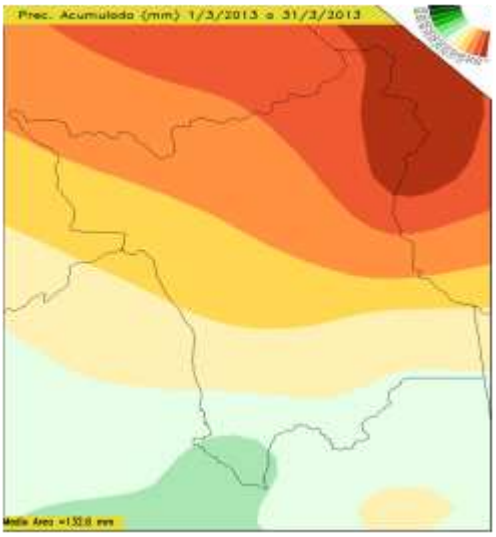

Figure 11. Accumulated Precipitation in March 2013 in the State of Roraima. Source: INPE.

Making a general summary, the data from INMET show that in the quarter January-February-March there was low precipitation as per Figure 12.

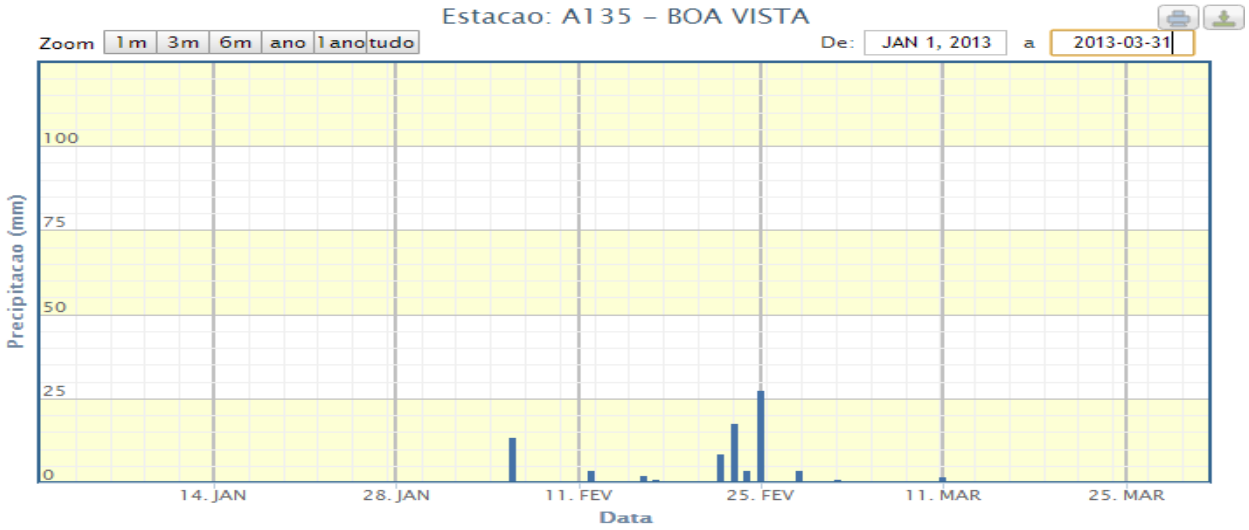

Figure 12. Monthly accumulated precipitation of Boa Vista-RR in the months of January, February and March. Source:INMET. **http://www.inmet.gov.br/portal/index.php?r=home/page&page=rede_estacoes_auto_graf**

That is, in January no precipitation was recorded in Boa Vista. Back in February there were 10 days with rains, registering a cumulative 81.4 mm in the capital. In March the record was 14.5 mm in 5 days of rain. These values indicate a low precipitation for the whole northeast sector of Roraima, where the major cities at risk of fire and wildfires are located. As per the histogram below (Table 05) 267 outbreaks were recorded in this critical quarter of low precipitation, thus showing that this joint operation of CIMAM RR achieved the expected success.

Table 05 - Histogram of fire outbreaks in the state of Roraima. Listing only of states municipalities with occurrence of outbreaks in the period presented. Source: INPE.

- HISTOGRAM OF FIRE OUTBREAKS -
01/01/2013 00:00p.m.: 00 to 30/03/2013 11:59 p.m.: 59
(AQUA Tarde)

Distribuição dos 267 focos de 2013-01-01 a 2013-03-30 em RR	
Municípios	(1) Bonfim / RR *(34)*
	(2) Rorainópolis / RR *(33)*
	(3) Boa Vista / RR *(33)*
	(4) Caracaraí / RR *(25)*
	(5) Amajari / RR *(20)*
	(6) Pacaraima / RR *(20)*
	(7) Cantá / RR *(19)*
	(8) Normandia / RR *(19)*
	(9) São João da Baliza / RR *(13)*
	(10) Iracema / RR *(13)*
	(11) Alto Alegre / RR *(11)*
	(12) Uiramutã / RR *(10)*
	(13) São Luiz / RR *(7)*
	(14) Caro Ebe / RR *(7)*
	(15) Mucajaí / RR *(3)*

Statistics of hotspots

4.1. Quantitative Analysis

Hotspot is the heat record captured in the ground surface by a satellite sensor, the sensor captures and records any temperature above 47 ° C and interprets it as "hotspot" The data are generated and made available by the National Institute for Space Research - INPE, on http://www.dpi.inpe.br/proarco/bdqueimadas .

When comparing with other years (2007/2008 and 2012/2013), the detection of hotspots of the years 2012/2013 is below the expected average for the period (Table 6 and Figure 13).

Table 6. Comparison of the number of hotspots for the period described.

Ano	Número acumulado de focos entre 01/12/2013 a 31/03/2013 de cada ano utilizando o satélite referência	Percentual dos focos de 2012/2013 em relação aos anos anteriores
2007/2008	813	-13,55
2008/2009	379	47,07
2009/2010	1528	-113,41
2010/2011	501	30,03
2011/2012	695	2,93
2012/2013	**716**	

Tabela de análise quantitativa de focos de calor entre o período de 01/12 a 31/03 do ano de 2007/2008 ao período de 01/12 a 31/03 do ano de 2011/2012 com relação ao período de 01/12 a 31/03 do ano de 2012/2013.
Fonte dos dados: INPE.

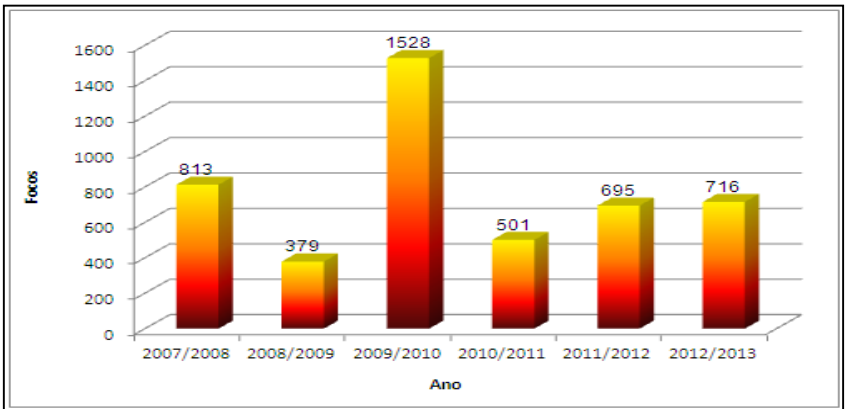

Gráfico de análise quantitativa de focos de calor entre o período de 01/12 a 31/03 do ano 2007/2008 ao período de 01/12 a 31/03 do 2011/2012 com relação ao período de 01/12 a 31/03 do ano de 2012/2013.
Fonte dos dados: INPE.

Figure 13. Graph comparing the number of hotspots for the period described.

According to historical concentration of hotspots (reference sensor) grouped by month for the period 2007-2013, the most critical period of the occurrence of fire in Roraima is between November and March, with the peak detection in months from January to March (Figures 14 and 15).

This year the hotspots showed the same trend, but there was considerably greater number of hotspots detected in January (analysis through the reference satellite in the period from 12/01/2012 to 03/31/2013), and this number has decreased considerably in the following month (Figure 16).
The distribution of hotspots (reference satellite) was also analyzed for the same period, between the municipalities of Roraima where hotspots occurred and the result is shown in Figure 17.
We emphasize that the most critical region in this period (12/01/2013 to 03/31/2013) was the Northwest region, an area with predominant savannah vegetation, for this analysis all hotspot monitoring sensors were used in the period described for the case of monitoring of hotspots (Figure 18).

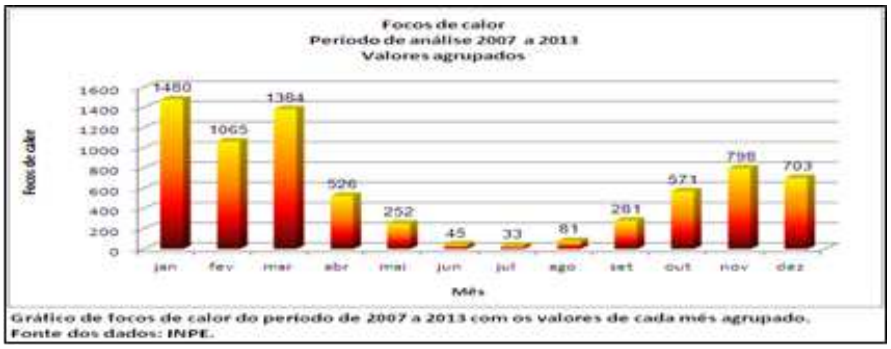

Figure 14. Graph comparing the number of hotspots for the period described.

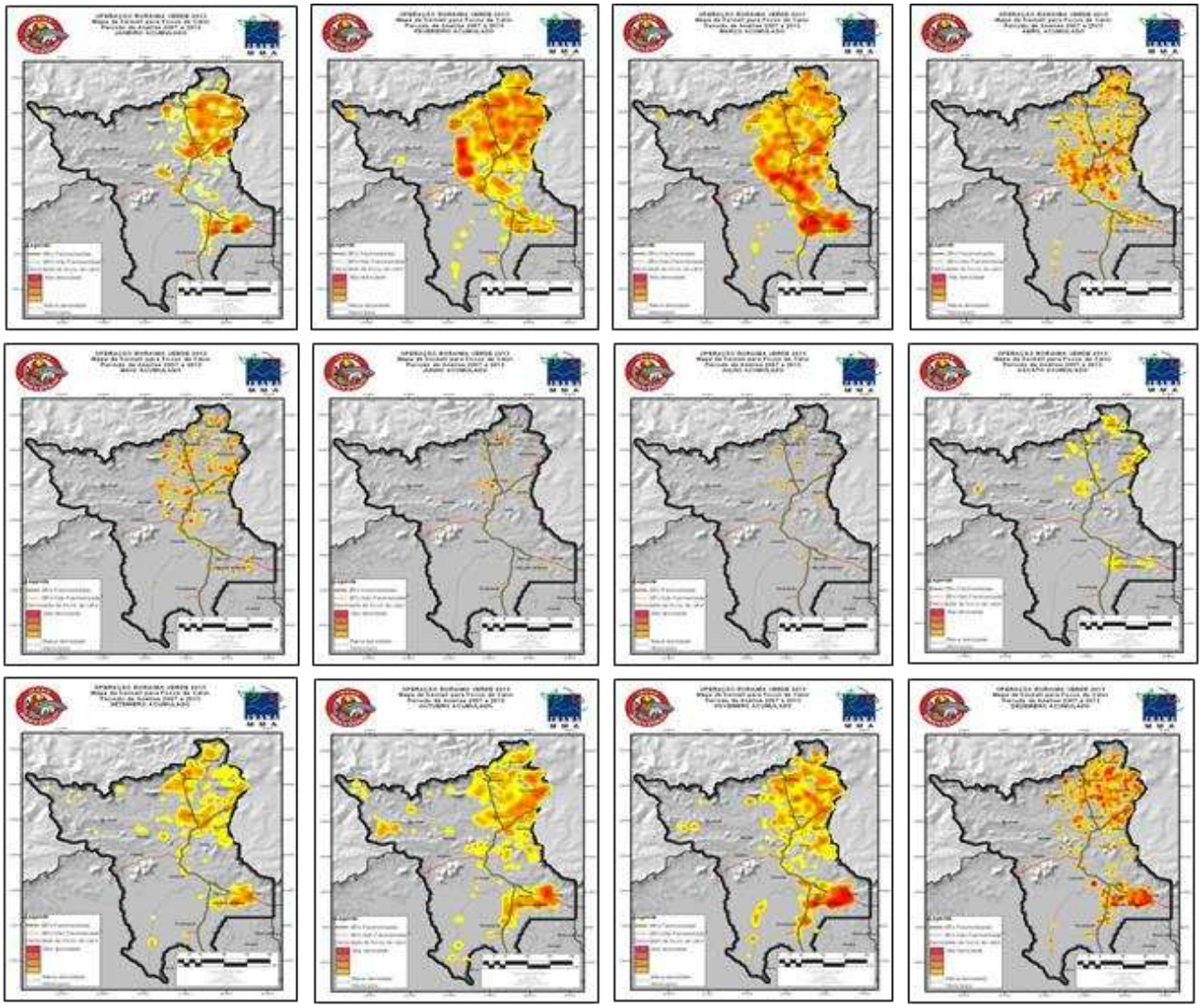

Figure 15. Comparison of the number of hotspots by month, grouped for the period 2007-2013. Source: INPE data processed by CIMAN RR / Federal. 2013 Green Roraima Operation.

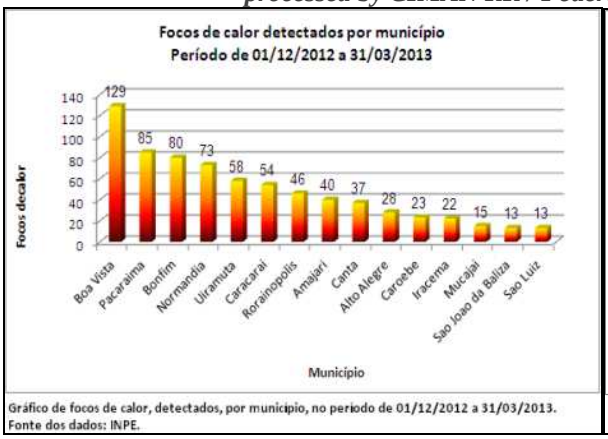

Gráfico de focos de calor, detectados, por municipio, no periodo de 01/12/2012 a 31/03/2013.
Fonte dos dados: INPE.

Figure 16. Graph comparing the number of hotspots for the period described.

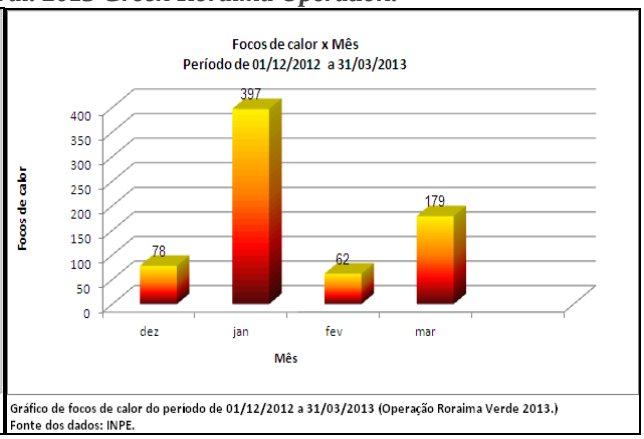

Gráfico de focos de calor do periodo de 01/12/2012 a 31/03/2013 (Operação Roraima Verde 2013.)
Fonte dos dados: INPE.

Figure 17. Graph comparing the number of hotspots per municipality in the state of Roraima for the period described.

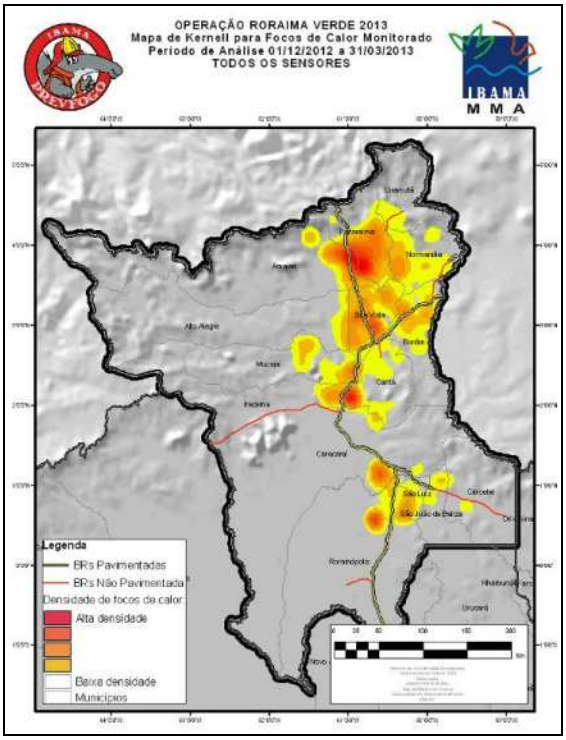

Figure 18. Density map for hotspots for the period described. Source: CIMAN RR / Federal.

4.2. Spatial Analysis

To better understand the dynamics of fires during the operational period of 2012/2013 (2013 Green Roraima Operation), an analysis of the evolution of hotspots was made from 12/01/2012 to 03/31/2013 within federal areas: military areas, border area, federal highways, settlement projects, indigenous lands, federal protected areas and other areas (Figure 19). The maps for hotspots were generated using parameters for kernel[1] map (Figures 15, 18, 20, 21, 22, 23, 24 and 25) the result enables better visualization of the region where the hotspots occur during the year.

[1] Statistical method for estimating concentration density of events and highlighting critical points

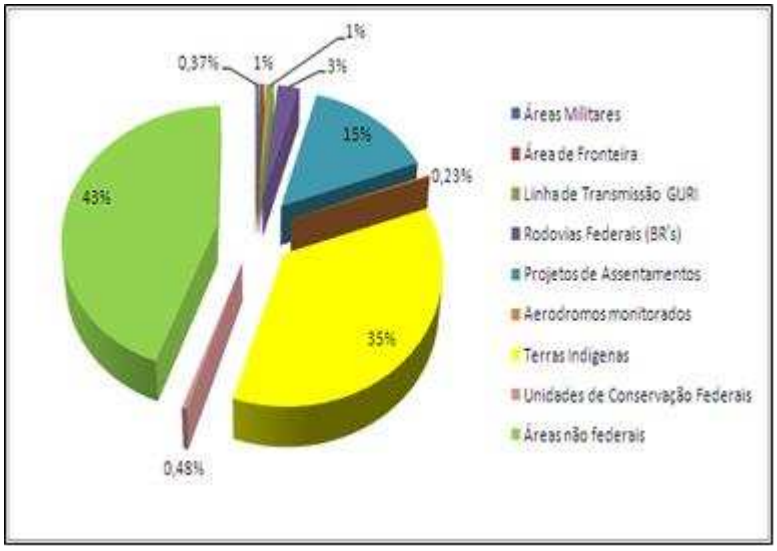

Figure 19. Distribution of hotspots (all sensors, for the case of monitoring) for the period from 12/01/2012 to 03/31/2013 in the areas monitored by CIMAN RR / Federal. 2013 Green Roraima Operation. Source: CIMAN RR / Federal.

Military areas:

Concerning military Areas of the State of Roraima only plots used by the Brazilian Army were considered for monitoring, specifically the 1st Jungle Brigade with a forest area of 279,421.00 ha.

Among the military areas monitored by CIMAN RR / Federal, the plot Serra do Tucano, located in the municipality of Bonfim - RR, was the one with the highest concentration of hotspots (Figure 20). The monitored Military Areas represent 0.37% of the hotspots for the operational period.

Military areas were used for military exercises, being totally bounded with signs indicating the property and warning the use, in some places there are physical barriers that prevented the passage of people in risk areas. This care to warn the military use of the space, in addition to enclosure thereof, prevented the passage of pedestrians in the military unit.

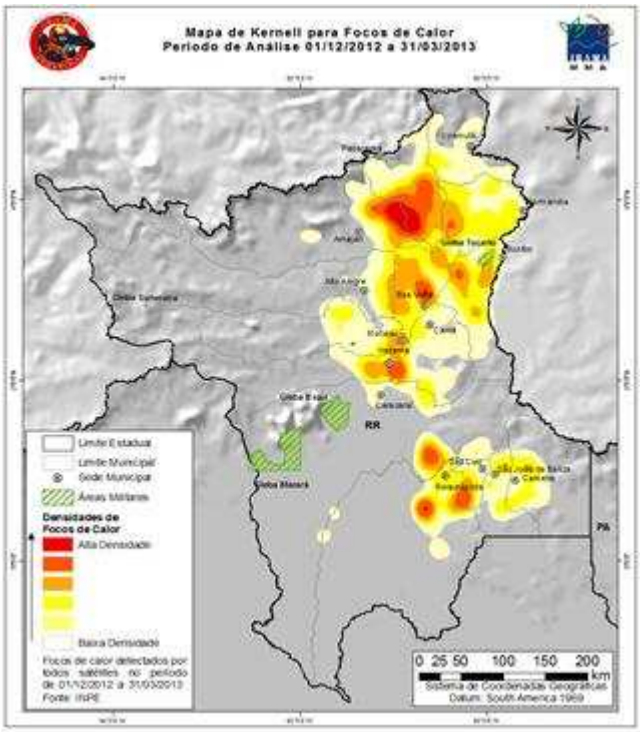

Figure 20. Concentration of hotspots x Military Areas. Source: CIMAN RR / Federal

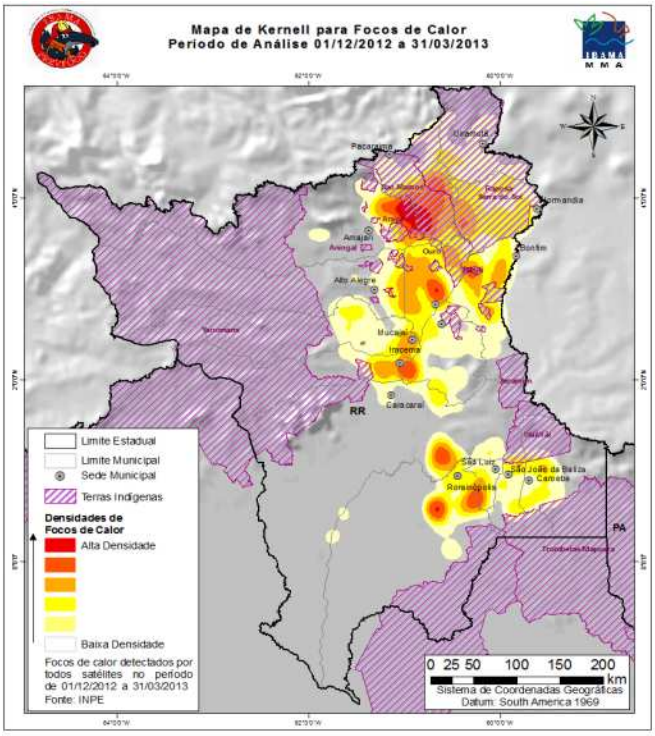

Figure 21. Concentration of hotspots x Indigenous Lands. Source: CIMAN RR / Federal.

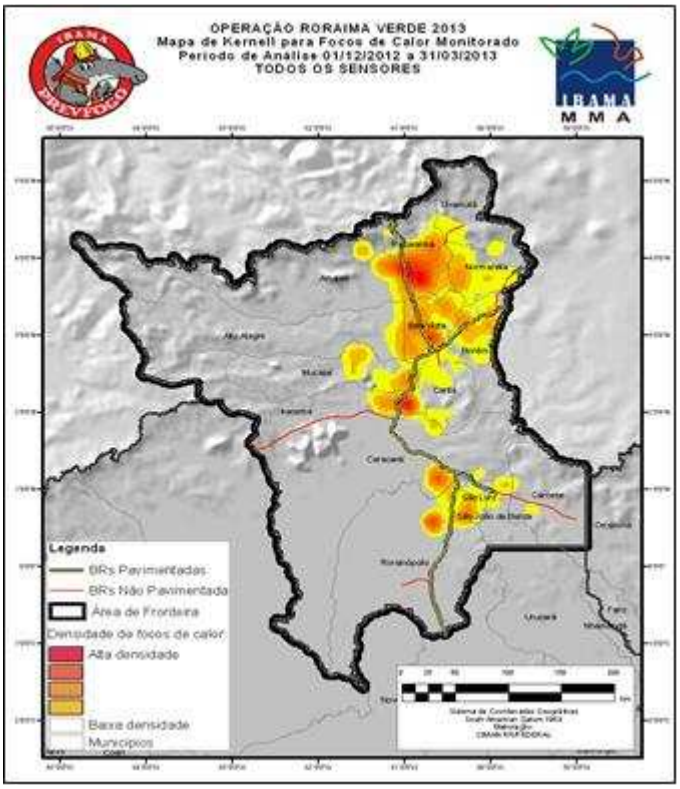

Figure 22. Concentration of hotspots x Border Area. Source: CIMAN RR / Federal.

Indigenous lands:

CIMAN RR / Federal monitored Indigenous Lands in the period from 12/01/2012 to 03/31/2013, i.e., throughout the 2013 Green Roraima Operation, and the Indigenous Lands had the highest number of outbreaks (35% of total outbreaks recorded for the period), compared with the areas monitored by the Multi-Agency Integrated Centers. Indigenous lands with more numbers of hotspots were Raposa Serra do Sol and São Marcos, which together represent approximately 55% of the hotspots detected on indigenous lands (Figure 24).

A part of the natives has also given good contribution to the increase of fires in Roraima, because they usually set fires to process food, get rid of undesirable insects or just put fire in the forest without any purpose.

Border Area:

The boundaries that border with the State of Roraima were monitored by CIMAN RR/ Federal, Venezuela (954 km from the border) and Guyana (964 km from the border), and the hotspots for the period from 12/01/2013 to 03/31/2013, 2013 Green Roraima Operation, concentrated on the border with Guyana and the municipalities of Bonfim and Normandia and of the state of Roraima (Figure 21). The Border Area monitored represents 1% of the hotspots for the operational period.

Through the Sub Consulate of Brazil a contact was made with the institutions of neighboring countries to exchange information related to the prevention and fighting of wildfires in the border area.

In the event of an accident there would be no physical intervention unless we were contacted through diplomatic channels. But the exchange of information related to fire behavior in potential accidents was planned..

INCRA Settlement Projects:

In Settlement Projects, 15% of hotspots monitored for the period were detected, as shown in Figure 23.
The highest incidence of wildfires is undoubtedly due to lack of care when causing burning, whether for pasture renewal, elimination of rest of cultivation or for pest control. These typically agricultural activities without due care to contain the advancing flames have generated the largest wildfires in Roraima.

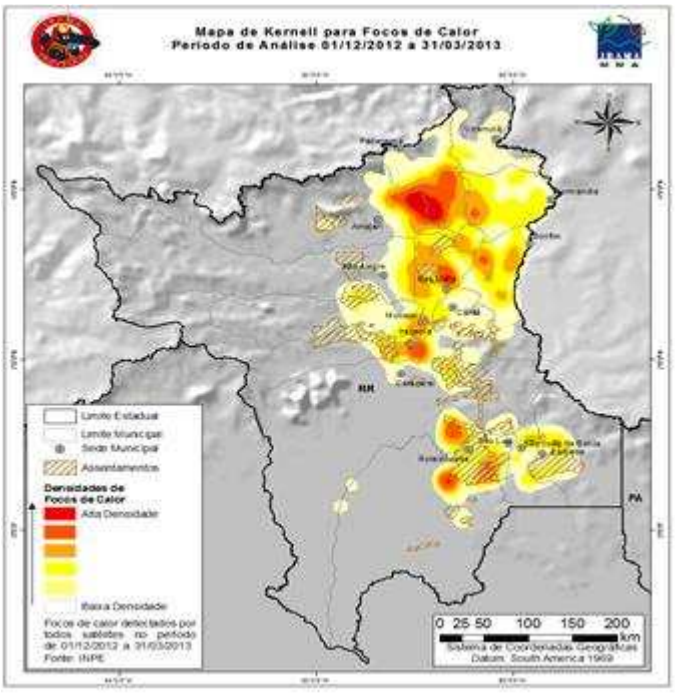

Figure 23. Concentration of hotspots x INCRA Settlement Projects. Source: CIMAN RR / Federal.

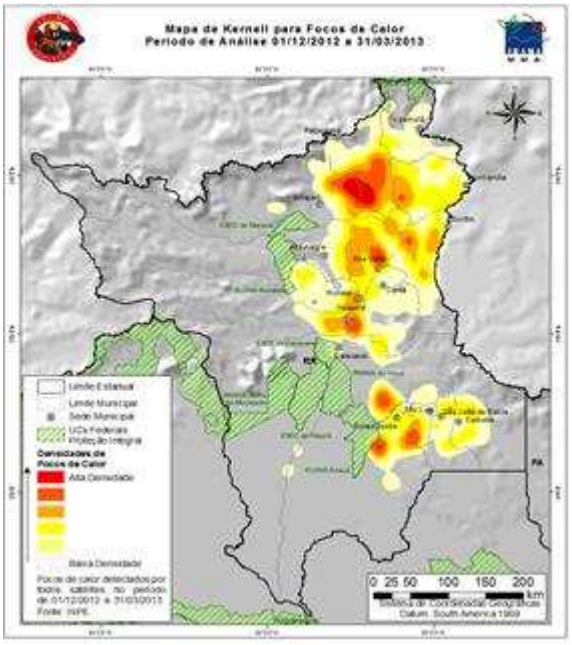

Figure 24. Concentration of hotspots x Federal Protected areas Source: CIMAN RR / Federal. Source: CIMAN RR / Federal.

Protected areas:

The analysis was made for Federal Protected areas of full protection and sustainable use. 0.48% of hotspots were detected during the analysis period. From this number, only one spot is on protected areas for sustainable use: FLONA of Roraima. The rest is on Full Protected areas: ESEC Caracaraí and PARNA and Monte Roraima (Figure 25).
Protected areas of Roraima, though protected by equipped brigades, are of difficult access, which prevents the presence of the main causal agent of fire, man.

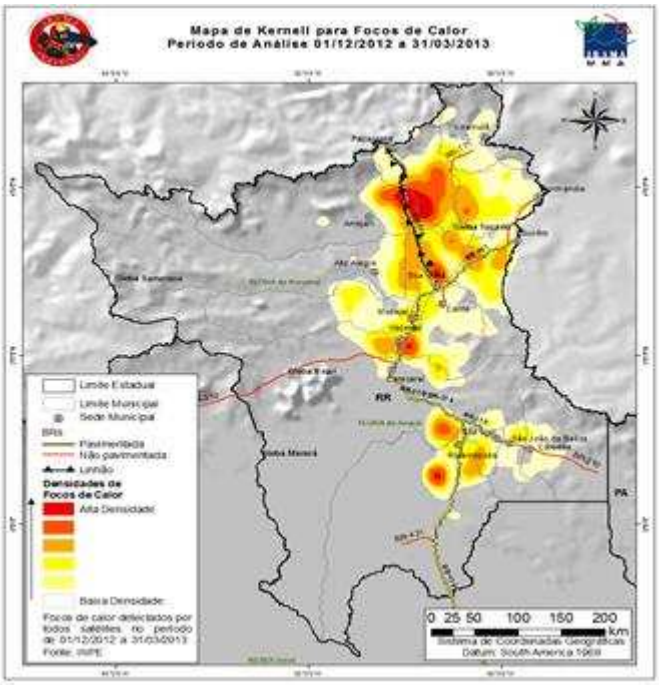

Figure 25. Concentration of hotspots x Federal Highways, GURI line and monitored Airstrip. Source: CIMAN RR / Federal.

Federal Highways, GURI Transmission Line and Monitored Airstrip:

1404 km of Federal Highways were also monitored (3% of hotspots for the period), 190 km of Transmission Line (1% of hotspots for the period) and a radius of 6 km from the center point of aerodromes in the municipalities of Boa Vista, Caracaraí and Pacaraima (0.23% of total hotspots for the period), as shown in Figure 22.

Wildfires in federal, state and municipal roads and highways occur due to lack of maintenance of the right of way, combined with the traffic of vehicles with low compression engines. These engines tend to accumulate carbon particles in the cylinders and the exhaust system when used for long periods and overheat causes softening and loosening of the accumulation of deposited carbon, whose deposited particles can be expelled by the exhaust, usually when the vehicle shifts gears.

The high-voltage lines in forests and lack of maintenance of the easements in transmission networks can cause serious problems, because the contact of wires with vegetation can cause sparks that will cause the fire. And also with the occurrence of fire in these lines wires can heat up, causing network outages resulting in disconnection of power supply.

The accumulation of particles in suspension near the aerodromes, particularly in the headwaters of the strips, can hinder or impede landing and takeoff procedures. As in previous years, it can even close the aerodromes for takeoffs and landings.

Preventive Actions

With preventive actions implemented when the brigades were not acting in firefighting, the main activity was visiting indigenous communities, settlements or farms aiming to educate the local population about the consequences of the problems arising from fires and burning in the region and disseminate controlled burning techniques seeking to establish a safety belt between the edges of the settlements and the rest of the forest, as per Table 07 and Figures 26 and 27.

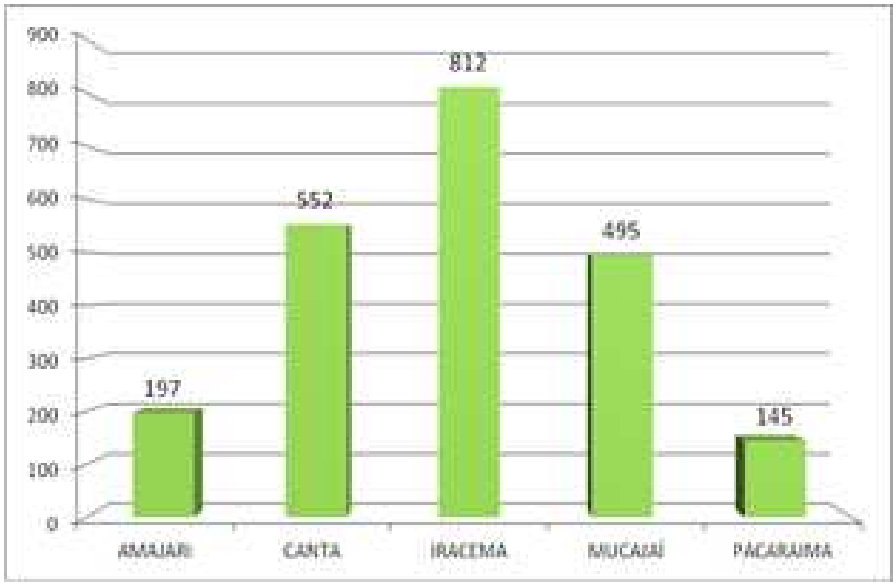

Figure 266 Graph of the distribution of preventive visits in municipalities having Brigades. Source: CIMAN RR / Federal.

Table 7. Distribution of preventive visits in municipalitie having Brigades Source: CIMAN RR / Federal

PREVENTIVE VISIT	
LOCATION	**GRAND TOTAL**
AMAJARI	197
CANTA	552
IRACEMA	812
MUCAJAÍ	495
PACARAIMA	145
GRAND TOTAL	**2201**
Updated on 03/31/2013	

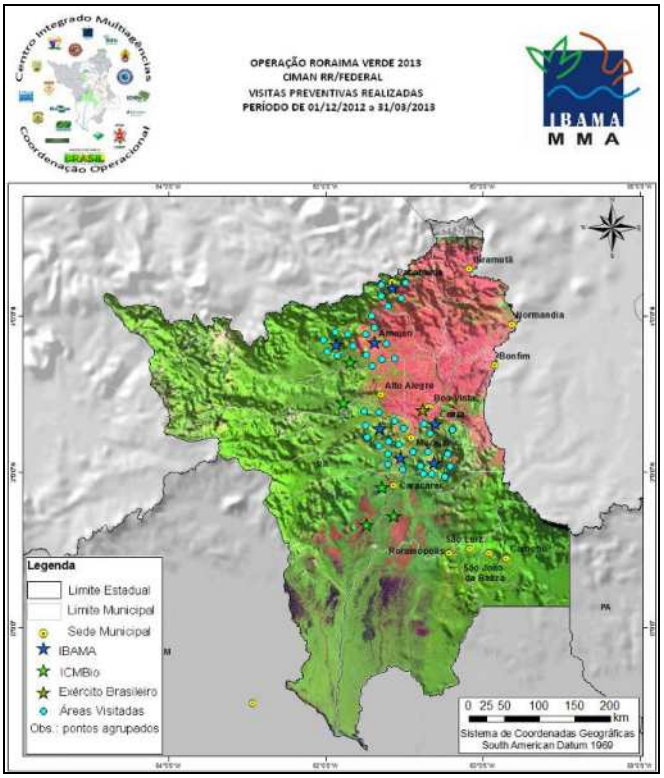

Figure 27. Distribution of the areas visited by the Brigades, grouped points. Period from 12/01/2012 to 03/31/2013. Source: Source: CIMAN RR / Federal.

In a joint effort between the State Foundation for the Environment and Water Resources - FEMARH, IBAMA-RR and RR CIMAN / Federal for the dissemination and issuing of controlled burning. The permits were issued on the basis of the Federal Wildfire Brigades / BRIFF 'S of Prevfogo / IBAMA, as shown in Table 08 and Figure 28.

Table 8. Commitments of controlled burning. Source: Source: CIMAN RR / Federal

AUTORIZAÇÕES DE QUEIMA		
LOCALIDADE	PERIODO	QUANTIDADE
AMAJARI	18/02 a 20/02	16
CANTA	14/02 a 16/06	25
CARACARAI	24/02 a 26/02	2
CAROEBE	03/03 a 05/03	70
IRACEMA	09/02 a 10/02	4
MUCAJAI	11/02 a 12/02	36
SÃO JOÃO DA BALIZA	03/03 a 05/03	0
SÃO LUIS DO ANAUÁ	22/02 a 23/02	6
TOTAL		159
1- Calendario estabelecido pelo Comitê Gestor de combate as queimadas em Roraima , no dia 06/02/2013		
2- Os municipios desta tabela são os que o CIMAN RR atua.		
Fonte FEMARH-RR (Informativo : DPMA/DMCA)		

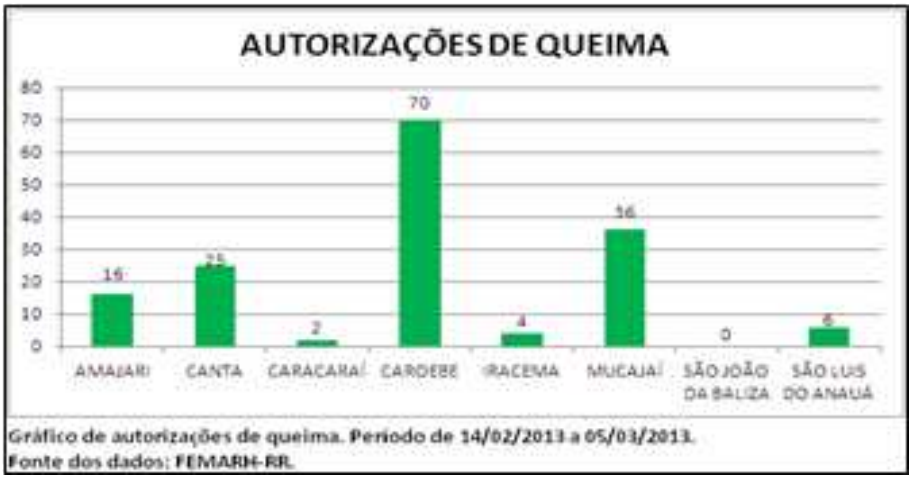

Figure 28. Comparison of controlled burns released by municipalities of Roraima. Source: Source: CIMAN RR / Federal

Preventively a helicopter became available for operation aiding in preventing and fighting wildfires, as well as in enforcement actions. We conducted a flight next to conservation areas and settlement projects, at the time instructions and guidelines were given to the Brigades on procedures for boarding and unboarding. There were two monitoring flights, one in the mosaic of military areas and another to the northeast of the state, such location covering Indigenous Lands and Military Areas (Table 09 and Figure 29).

Figure 29. Graph of distribution of flight hours. Source: Source: CIMAN RR / Federal.

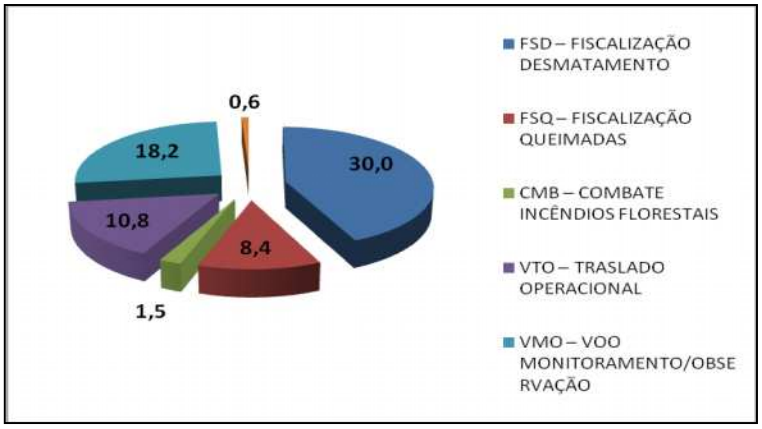

Table 9. Distribution of flight hours. Source: Source: CIMAN RR / Federal.

Purpose of flight	HOURS
FSD – DEFORESTATION SUPERVISION	30.0
FSQ – PURPOSE OF FLIGHT	8.4
CMB – WILDFIRE FIGHTING	1.5
VTO – OPERATING TRANSFER	10.8
VMO – FLIGHT MONITORING/OBSERVATION	18.2
VOU – OTHER	0.6
TOTAL FLIGHT HOURS	69.5

As actions of interaction with Civil Society, 25 dampers were donated to the Club of jeeps the State of Roraima for purposes of fighting small wildfires, Fire Brigade training for handling GPS-Global Positioning System and motor-pumps, lectures on labor unions and rural workers, indigenous communities and monitoring of environmental education project of Eletronorte.
The Brazilian Army, the Brazilian Air Force and employees of the company FIT Manejo Florestal Ltda., were trained on techniques for preventing and fighting wildfires in a course taught by experts of Prevfogo, 72 (seventy-two) students completed the course.
A mission of the National Institute for Space Research-INPE was conducted for monitoring and validation of hotspots detected during 2013 Green Roraima Operation. This validation consisted of analyzing the hotspots detected by the passage of satellites used by INPE, in relation to omission and commission, taking into account hotspots with the indications of burning on images of medium spatial resolution sensors. The missions were conducted by land and air (aircraft assigned by FUNAI) to collect data on photographs, geographic coordinates and local information.
Aiming at the preparation of a Letter of Intent on rebuilding of affected areas, three meetings were held at IBAMA / SUPES RR-03 in the scope of the Green Roraima Operation, where the following entities were present: IBAMA, the Brazilian Agricultural Research Corporation- Embrapa, the National Indian Foundation - FUNAI, Eletronorte and Department of Agriculture and Food Supply and Production of Roraima and the company FIT Manejo Florestal Ltda., which assume the commitments listed below:.
A Climate Meeting was held with the participation of the Head of the Meteorology Division of the Amazon Protection System-Sipam, who discussed in his presentation the mission of Sipam, diagnosis, analysis and prognosis for the weather in Roraima.
At the meeting, where ABIN, UFRR, IBAMA, ICMBio, FUNAI, FEMARH, EB, CBMDF, CBMRR, Civil Defense and SIPAM were present, the importance of creating a representation of SIPAM in the State of Roraima was highlighted, as well as the need to identify weather stations available, assess conditions and provide access by establishing a minimum network of shared information.
Find below a summary of preventive actions during the Green Roraima Operation (table 10).

Table 10. Summary of preventive activities. Source: Source: CIMAN RR / Federal.

Activity	Performers / Participants	Dec	Jan	Feb	Mar
Preventive orientation visits in PA's and TIs.	IBAMA.				
Disclosure and issuance of controlled burning permits.	FEMARH and IBAMA.				
Helicopter available in the operation.					
Check easement of the GURI transmission line under indigenous lands and settlements by INCRA.	IBAMA, FUNAI, DPRF and ELETRONORTE.				
Check possible risks in the Brazil / Venezuela border area.	IBAMA, Consul and THE ARMY.				
Assessment of risk areas in BR 174 and Indigenous Lands. Suggested setting: IBAMA, FUNAI, DPRF.	IBAMA, DPRF, FUNAI.				
Instructions and guidelines for the Brigade on boarding and unboarding procedures.	IBAMA.				
Monitoring flights conducted at UC's mosaic of Baixo Rio Branco and the army areas.	IBAMA, ABIN and ICMBio.				
Flight on the northeastern region of the state covering Military Areas and Indigenous Lands.	IBAMA, ABIN and THE ARMY.				
Donation of dampers for jeeps.	IBAMA and the Club of jeeps.				

Training in techniques for preventing and fighting wildfires (Brigade Training).	IBAMA AND THE ARMY.		■		
Training in techniques for preventing and fighting wildfires (Brigade Training).	IBAMA, Air Force, Fit Manejo Florestal.			■	
GPS Training to the Brigade.	IBAMA.	■	■		
Training on motor-pumps to the Brigade.	IBAMA.	■	■		
Monitoring and validation of hotspots detected by INPE in the state of Roraima.	INPE, IBAMA and FUNAI.		■	■	■
Meetings for the preparation of the letter of intent concerning the Rebuilding of Affected Areas affected by Fire.	IBAMA, EMBRAPA, FUNAI, ELETRONORTE SEAPA/RR and FIT.				■
Climate Meeting – diagnostic, analysis and prognosis for the climate in Roraima.	SIPAM, IBAMA, ABIN, UFRR, ICMBio, FUNAI, FEMARH, THE ARMY, CBMDF, Civil Defense of Roraima and CBMRR.				■
Lectures on unions and indigenous communities.	IBAMA.	■	■	■	■
Environmental Education Project of ELETRONORTE.	ELETRONORTE and IBAMA.	■	■	■	

As part of the preparation for the fight five (05) Brigades of IBAMA were hired, with 143 (one hundred and forty-three) Brigades installed inside or near Settlement Projects and Indigenous Lands. ICMBio also hired its Brigades to prevent and fight wildfires with a total of 77 (seventy seven) Brigades distributed in the units that offer greater risks, added to 52 (fifty two) soldiers of the Armed Forces, who were trained and equipped by IBAMA, CIMAN RR / Federal had 272 (two hundred seventy-two) Brigades directly for preventing and fighting wildfires in Roraima during the 2013 Green Roraima Operation (table 11).

Table 11. Human and material resources. 2013 Green Roraima Operation. Source: Source: CIMAN RR / Federal.

LOCAL	INSTITUIÇAO	RECURSOS HUMANOS UTILIZADOS							RECURSOS MATERIAIS						
		BRG IBAMA	Coord. de fogo	BRG ICMBIO	Coord. ICMBIO	EB	FAB	TOTAL	RODOFOG	VIATURA	HEL. IBAMA	HEL. ICMBIO	AV. CISTERNA	AV. MONITOR	AV. FAB
BOA VISTA	IBAMA		11					**10**		4	1				
BRIFF TRAIRÃO	IBAMA	14	1					**15**		2					
BRIFF VILA BRASIL	IBAMA	15	1					**16**		2					
BRIFF FÉLIX PINTO	IBAMA	14	1					**15**		2					
BRIFF TABA LASCADA	IBAMA	13	1					**14**		2					
BRIFF IRACEMA	IBAMA	29						**29**		2					
BRIFF APIAU	IBAMA	29						**29**		2					
BRIFF BOCA DA MATA	IBAMA	29						**29**		2					
ESEC MARACÁ	ICMBIO			14	1			**15**		1					
FLONA RORAIMA	ICMBIO			14	1			**15**		1					
PARNA VIRUÁ	ICMBIO			28	1			**29**		1					
ESEC CARACARAÍ	ICMBIO			14	1			**15**		1					
ESEC NIQUIÁ	ICMBIO			7	1			**8**		1					
10º GAC SI	EB					15		**15**		2					
12º ESQD. C. Mec.	EB					15		**15**		1					
C front. RR/7 BIS	EB					15		**15**		1					
BABV	FAB						7	**7**		1					
TOTAL		**143**	**15**	**77**	**5**	**45**	**7**	**291**		**28**	**1**				

Federal brigades for the Prevention and Fighting of Wildfires of IBAMA-BRIFs / IBAMA

Since 2001, the National Center for Prevention and Control of Wildfires - Prevfogo seeks to establish control over wildfires through the hiring of prevention and fighting brigades. Primarily restricted to the federal protected areas, such brigades have achieved important goals for the conservation of local

biodiversity by creating prevention routines, providing first response to frequent occurrences and composing field teams in large-scale fighting.
In 2009, hiring UC's brigades became the responsibility of the Chico Mendes Institute for Biodiversity Conservation - ICMBio. In 2008, Prevfogo began developing the "Wildfire Brigades of Prevfogo in Critical Municipalities" program, which aims to promote the prevention and fighting of fire incidents in locations especially threatened by wildfires.
The selection of municipalities for the implementation of the brigades observed the technical and objective criteria for detection of hotspots in remnants of native areas and coverage of protected areas (indigenous lands, and federal and state conservation), forest remnants and settlement projects.
In 2013 Prevfogo hired 143 (one hundred and forty-three) Brigades in five municipalities of Roraima: Cantá, Mucajaí, Iracema, Pacaraima and Amajari, which were located in forward bases, prioritizing the contact areas of savannah with temperate rainforest (Figure 30). The period of hiring Brigades in 2013 in the state is December to April, except Cantá whose hiring was during December extending until April.
When Prevfogo Brigades were not acting in firefighting, the main activity was visiting indigenous communities, settlements or farms aiming to educate the local population about the consequences of the problems arising from fires and burning in the region and promote controlled burning techniques. Altogether 2201 (two thousand two hundred and one) preventive visits (see Figure 27) were done. When possible, the brigade supported the authorized controlled burning.

7. Brigades for the Prevention and fighting of Wildfires of ICMBIO

The Chico Mendes Institute for Biodiversity Conservation has, among its duties, the responsibility for the protection of Federal Protected areas. Among the activities for the protection, Firefighting and prevention is one of the most important.
The existing fire brigades in federal protected areas has as their main goal to work under the command of the head of the unit and the manager of fire in all actions to prevent and fight wildfires within the protected areas and their surroundings provided in the Management Plans (Figure 30).
In 2012 ICMBio hired 77 (seventy-seven) Brigades to act in five protected areas in the state of Roraima. Their distribution was as follows: Parna do Viruá with 28 (twenty eight) Brigades; ESEC Caracaraí with 14 (fourteen) Brigades; ESEC Niquiá with 07 (seven) Brigades; ESEC Maracá with 14 (fourteen) Brigades and Flona Roraima with 14 (fourteen) Brigades. The hiring period of the brigades in the state starts in November and goes until April.
When the risk of fire within the UC's is zero, the brigades of ICMBio usually work on prevention of incidents along the nearby communities, conducting lectures, educational visits and supporting authorized controlled burning. In fact, firefighting in Federal Protected areas is the last resort of the unit, after completion of all the efforts in prevention and public awareness, causing Brigades of ICMBio, after all, to act as social actors in their communities.

8. Brigades for the Prevention and Fighting of Wildfires of the Army

During the month of November 2012, meetings between IBAMA servants and a representative of the 1st Jungle Infantry Brigade were held, where it was agreed that the Army would indicate a representative to participate in the situation room that would be installed and that IBAMA would promote prevention and fighting courses for one hundred (100) Soldiers.
At the beginning of December 2012, the Commander of the 1st Jungle Infantry Brigade signed Service Order No. 27, regulating the activities to be performed to support CIMAN in case of fighting wildfires in Roraima and determining the initial composition of fifty (50) Soldiers for the "Fire Brigade" of the Army in Roraima, after training with the staff of IBAMA - Prevfogo (Figure 30).

Thus, in the period from January 21st to 25th, 2013, the Course for the Prevention and Fighting of Wildfires was conducted, promoted by CIMAN, through IBAMA and the 1st Jungle Infantry Brigade. 46 (forty six) Soldiers successfully completed the course: 26 (twenty six) from C Fron RR / 7th BIS; 10 (ten) from the 12th Esqd C Mec and 10 (ten) from the 10th GAC S1.
Finally, the Brigade is interested in training more fifty (50) Brigades, with the goal of assigning them to the Special Border Platoons (with road access) in the future.

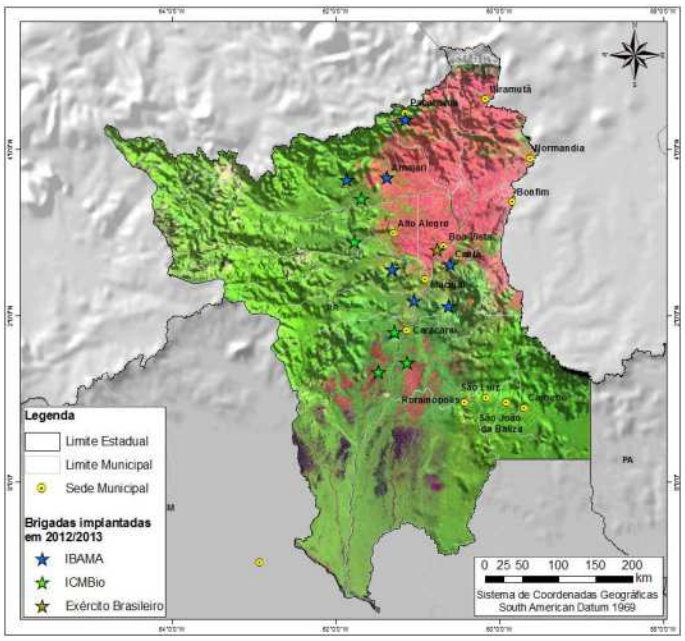

Figure 30. Distribution of brigades deployed in 2012/2013. Source: Source: CIMAN RR / Federal.

9. Fire Record – ROI

The records of occurrences of wildfires and the statistical analysis thereof are essential tools for defining strategies for prevention and firefighting, indispensable for countries that seek to manage the issue of fire in an efficient and organized manner.
The ROI's are filled by field teams and entered into the National Fire Information System - SisFogo. It is a system of IBAMA in which it is possible to enter and search ROI's with information on the agency itself, ICMBio and Fire Stations. It integrates information and allows the use of data safely and autonomously by users and is available on the following website: http://siscom.ibama.gov.br/sisfogo/.
Also according to the ROI's of the 2013 Green Roraima Operation, Canta is the municipality that has the highest number of records, followed by Pacaraima and Amajari. It is worth-mentioning that these data do not fully reflect the reality of the occurrences of wildfires, since there are a lot of gaps in the records, as well as records without dates and coordinates.
425 (four hundred twenty-five) firefighting actions were recorded by CIMAN RR / Federal during the 2013 Green Roraima Operation, distributed by the deployed Brigades (Table 12 and Figure 31).

Table 12. Firefighting actions. Source: CIMAN RR / Federal

BRIGADA/LOCAL	TOTAL
10º GAC Sl	0
12º Esqd C Mec	0
BRIFF APIAU	61
BRIFF BOCA DA MATA	71
BRIFF CAMPOS NOVOS	52
BRIFF FÉLIX PINTO	61
BRIFF TABALASCADA	87
BRIFF TRAIRÃO	37
BRIFF VILA BRASIL	31
BRIFF VILA NOVA	0
C Fron RR/ 7º BIS	1
ESEC CARACARAÍ	4
ESEC MARACÁ	5
ESEC NIQUIÁ	0
FLONA RORAIMA	0
PARNA VIRUÁ	15
TOTAL	425

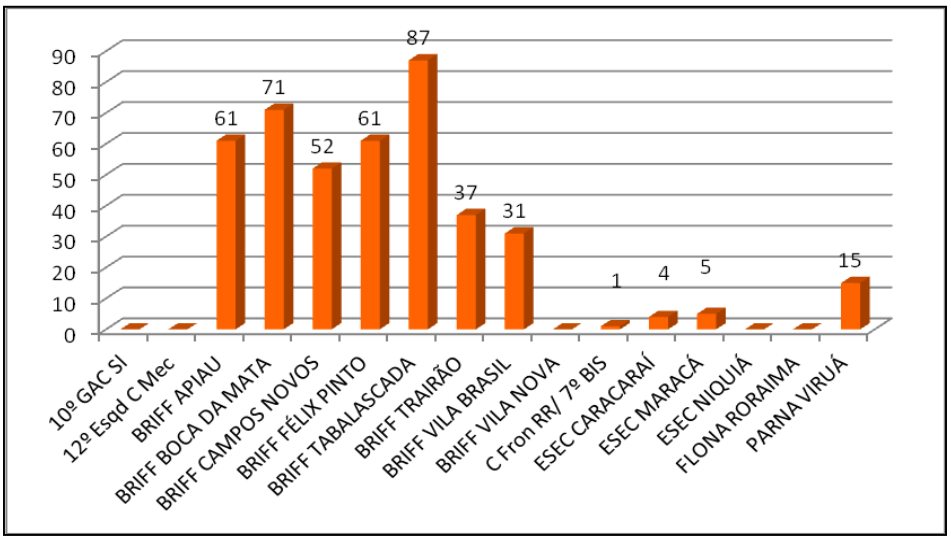

Figure 31. Graph of the firefighting actions distributed among deployed Brigades. Source: CIMAN RR / Federal.

10. Accountability for Environmental Crimes

In order to be successful, wildfire fighting actions were accompanied by actions of enforcement activities. The inspection teams conducted educational and repressive actions in the critical regions of fires, illegal deforestation, illegal logging and other illegalities. The intensive supervision contributed to the inhibition of infringing actions and reduction of environmental crimes, in particular those related to wildfires, fires and deforestation.

Table 13. Work done by NUCOF. Source: CIMAN RR / Federal

Ações de Fiscalização	Número
Autos	14
Embargo	8
Apreensão	8
Notificações	9
Visitas	29
Total	**68**

Tabela dos trabalhos realizados pelo Núcleo de Fiscalização da SUPES/IBAMA-RR. Período de 01/12/2012 a 31/03/2013. Fonte dos dados: NUCOF/DITEC/IBAMA-RR.

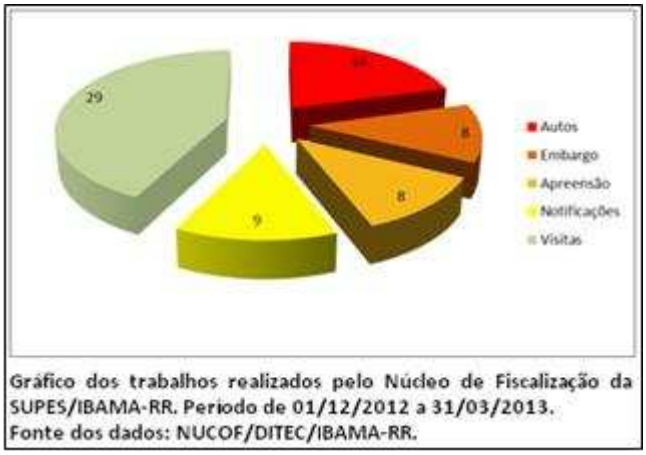

Gráfico dos trabalhos realizados pelo Núcleo de Fiscalização da SUPES/IBAMA-RR. Período de 01/12/2012 a 31/03/2013. Fonte dos dados: NUCOF/DITEC/IBAMA-RR.

Figure 32. Graph of the work done by NUCOF. Source: CIMAN RR / Federal.

The years 2012/2013 prioritized the fight against deforestation, especially in the Amazon. Most of the inspection teams of IBAMA were focused on these activities, but by no means the supervisory activities of misuse of fire was impaired. 14 notices of violation were issued for illegal burning during 2013 Green Roraima Operation; such number is insignificant when compared to 2010, when 347 notices of violation (Table 13, Figures 32 and 33) were issued.

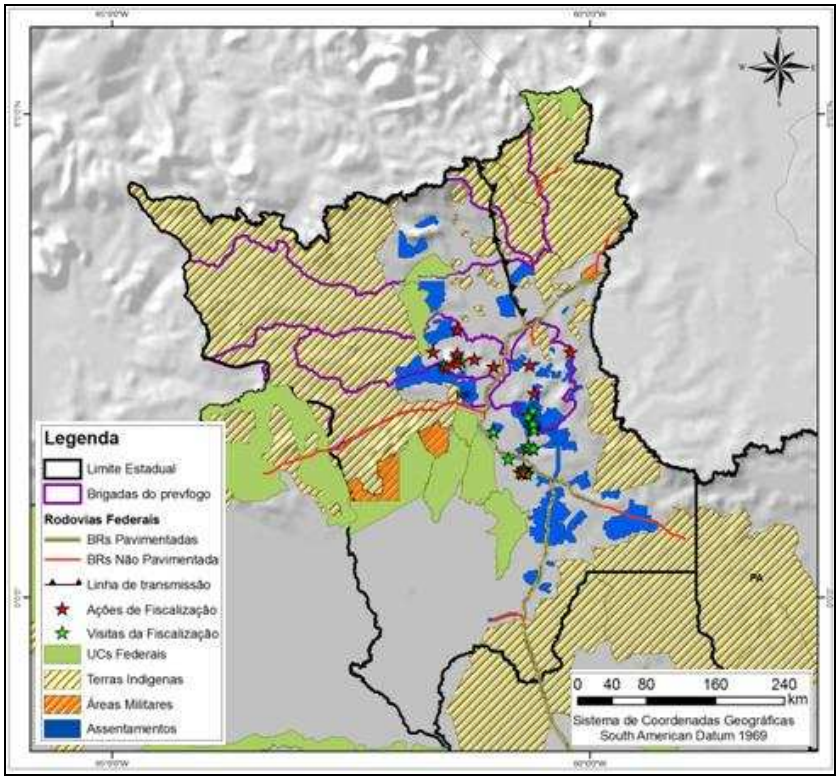

Figure 33. Work done by NUCOF. Source: CIMAN RR / Federal

11. Difficulties

Notably the lack of a specific and compatible structure of the agencies can be considered as the main obstacle to satisfactory response of CIMAN/RR Federal. The deficiencies are: insufficient system of communication, means of transport and capacity below what is needed.

11.1. Equipment

Regarding communication, the lack of adequate means results in difficulty of calling some Brigades located in the most isolated municipalities, loss of agility in firefighting activities and huge delay in informing the situation to the central coordination, which is critical for efficient management of available resources.

The personal and vehicle tracking devices, currently nonexistent, are an important and complementary part of a communication system, and increase situational awareness of national coordination and security of the Brigade members.

The transport was also deficient during the whole operation, making it difficult to mobilize teams for firefighting and prevention. Vehicles available for operation are rented, the maintenance and supply being the responsibility of the lessee. Even so, the maintenance issue was demonstrably very poor and there is a huge delay in service authorization and release of substitute vehicles. The supply is made only in Boa Vista, which complicates the operationalization of the brigades.

Brigades of Prevfogo were strongly damaged by the delay of delivery of PPE or the absence of some items.

11.2. Deficit of skilled personnel

While servants from other states have been made available to integrate the operation, some areas were not covered during the operation.

The lack of know-how on the Incident Command System-ICS, by some members of Ciman / RR caused the tool to be underused, jeopardizing the establishment of standardization activities.
Another activity that was jeopardized was geoprocessing, where there were difficulties in providing technicians to work with the tool.

12. **Final Remarks**

The Green Roraima operation is a milestone in the implementation of the national policy for preventing and fighting wildfires with integrated and comprehensive management giving a new direction to actions of firefighting, prevention and control.
Again, the need for expansion and consolidation of the Integrated Centers - CIMAN was clear in all regions of Brazil where recurrent wildfires occur.

Participants of the Green Roraima Operation:

Alexandre Ramos	ABIN	Fabiano Morelli	INPE	Marcos da Conceição Rocha	IBAMA/SEDE
Alcides Galvão dos Santos	EMBRAPA	Flávio Rosas de Oliveira Júnior	IBAMA	Marlene da Costa Pinho	IBAMA/RR
Ahmed C. Sobrinho	INFRAERO	Flávio Marcelo de Souza	IBAMA/RR	Moisés Alves Barcelos	CBMDF
Aline Souza	FEMARH	Francisco Wilson de Oliveira Pequeno	IBAMA/RR	Nilton Barth Filho	ICMBIO
Adailton Paulino Vieira	IBAMA	Gildenio de Jesus Sousa	IBAMA/PI	Ozelio Izidorio Messias Junior	EMBRAPA
Antonio Francisco Beserra Marques	INCRA	Guilherme Silva Rodrigues	FEMARH	Oziel Furquim Pinto	FEMARH
Anderson F. Jose da Silva	EXERCITO	Guilherme Jose F. Colares	PRF	Operácio Alves Lobato	IBAMA/SEDE
Ana Maria Canut Cunha	IBAMA/SEDE	Heliezer R. Ferreira	ELETROBRAS	Paulo Baltazar Diniz	IBAMA/RO
André Lopes dos Santos	ABIN	Hugo Américo Rubert Schaedler	IBAMA/PA	Paulo Roberto Lopes Soares	IBAMA/RR
Anderson Peixoto Amparo	IBAMA/AC	Hudson C. Felix	ICMBIO	Pedro Rogerio Rodrigues Coelho	FEMARH
Antonio Jorge Passos Balderramas	IBAMA/PA	Inayê Wiana Perz	FUNAI	Pedro Augusto Lagden de Souza	INPE
Antônio Carlos de Lima	IBAMA/SEDE	Italo Chaves de A. Barbosa	PRF	Raimundo Neto Alves Lopes	IBAMA/RR
Arivelto Mendes Borbas	FEMARH	Jaider da Silva Esbell	ELETROBRAS	Raimundo Nonato de C. Bezerra	IBAMA/RR
Augusto Avelino de Araújo	IBAMA/GO	Janneson Nilo Monteiro Sobral	CIPA	Rafael B. Mendes	BA BV
Azemar Marques	IBAMA/RR	Jeferson dos Prazeres Silva	CIPA	Ramón Alves	FEMARH
Cap. Marcelo Marcant da Silva	EXERCITO	Jerffeson Sérgio Souza Soares	CIPA	Renata Bocorny de Azevedo	ICMBIO
Carlos José Dantas	IBAMA/RR	Joaquim Parimé Pereira Lima	IBAMA/RR	Ricardo Vianna Barreto	CBMDF
Celso Luiz Ambrosio	IBAMA/ESREG/SP	José Braz Oliveira Filho	FUNAI	Ricardo Luiz Godinho Dallarosa	CENSIPAM
Clemilton Firmino de Macedo	IBAMA/SEDE	José Carlos Mendes de Morais	IBAMA/SEDE	Rosangela Lima de Oliveira	FEMARH
Creusa Monteiro Olinto Olivato	IBAMA/SEDE	José Neto Francisco de Souza	IBAMA/SEDE	Roberto Fernande Abreu	IBAMA/RO
Diego Milleo Bueno	IBAMA/RR	José Gonçalo de Paula	IBAMA/SEDE	Rodrigo de Moraes Falleiro	IBAMA/SEDE
Dirlan Alves da Costa	CIPA	Josue Claudio da Silva Filho	IBAMA/RR	Sgt Lazaro Bessa	BASE AÉREA
Ediley da Silva Costa	CIPA	Lourival Pereira da Silva	DPRF	Sandra M. Gomes	INFRAERO
Emerson Luiz da Assumpção	ABIN-RR	Laurenço de Souza Cruz	EMBRAPA	Saul Abreu Lavor	FEMARH
Emilton Paixão Caxias	IBAMA	Lon Guaranay C. Lopes	FAB	Sebastião Lima Ferreira Junior	IBAMA/RR
Erwin João de Morais	SEAPA/DATER	Luismar Araujo de Souza	IBAMA/RR	Sebastião Vicente Pereira	IBAMA/RR
Erisvaldo da Silva Pereira	IBAMA	Luiz Emi de Souza Leitão	FEMARH	Silvio Nogueira S. Junior	EB-1 BDA
Estevão Vieira Tanajura	IBAMA/GO	Luiz Carlos Lima Magalhaes	IBAMA/RR	Soraia Maria Peixoto de Caldas	IBAMA/RR
Adalberto Ortale Junior	IBAMA/NOA	Moacy Azevedo Conto	BVA IRF SL	Taise Rachel Sarmento	EMBRAPA
Marcelo José Lourenço	IBAMA/NOA	Maria Soleane Lemos Barbosa	IBAMA	Taylor Nunes	ASSEMBREIA
José Carlos Oliveira Ribeiro	IBAMA/NOA	Marcelo Antônio P. de Oliveira	IBAMA/MT	Ubiraci T. Reis Basto	MRE
Wendell Rodrigues de Brito	IBAMA/NOA	Carlos Alberto Rofimann	IBAMA/NOA	Valdercir José Albino	CIPA
Pedro Ivo Bastos Baldo	IBAMA/NOA	Thiago de Souza	IBAMA/NOA	Valdecir P. da Costa	FEMARH
Ederson Souza da Silva	IBAMA/NOA	Ezequias Aguiar de Assis	IBAMA/NOA	Valdemar Soares dos Santos	IBAMA/SEDE
Everton Pimentel	IBAMA/NOA	Anderson Felipetto	IBAMA/NOA	Wanja Soraia de M. Carneiro	IBAMA/GO

"Be the change you want to see in the world"

Dalai Lama

Large airtanker use in the United States: what do we know?

Matthew P Thompson, Crystal Stonesifer, and David E Calkin

Rocky Mountain Research Station, US Forest Service, Missoula, MT, USA,
mpthompson02@fs.fed.us, csstonesifer@fs.fed.us, decalkin@fs.fed.us

Abstract
In this paper we will review recently uncovered trends in large airtanker (LAT) use in the U.S., explore implications, and discuss opportunities for improving efficiencies. First, we will review results of two studies attempting to characterize LAT use between initial attack (IA) and extended attack and/or large fire support (EA) missions. Collectively these studies identified significant LAT use for EA despite a history of prioritizing LATs for IA, and further identified potentially counterintuitive results where fires receiving LAT support during IA were more likely than not to escape IA efforts. These results suggest potential operational efficiencies in LAT use, and that improving success in IA efforts may be in part premised on reducing the time between ignition and LAT arrival on the fire. Here we examine trade-offs between LAT usage for IA and LAT unavailability for IA operations due to EA use. To do so we use a mathematical optimization model to identify efficient LAT air base location and deployment strategies. The model is designed to minimize the total deployment time of meeting LAT IA demand, with demand quantified as a function of a fire weather index. Results indicate, as expected, that model performance degrades as LATs are increasingly unavailable. Results further indicate substantial sensitivity of LAT air base location strategy to LAT availability, with potentially significant implications for air base staffing and capacity decisions, as well as fleet composition decisions. To conclude we will describe ongoing and future work analysing opportunities for efficiency gains in LAT management, focusing on the role of forecasting and optimization frameworks, as well as ongoing data collection and analysis regarding retardant drop conditions and outcomes.

Keywords*: initial attack, resource use, large fire management, efficiency*

The views expressed here are the authors', and do not necessarily represent the views of the USDA

Introduction

Large airtankers (LATs) are part of a broader suite of aviation assets including scoopers, helicopters, and single-engine airtankers, each with different operational capacities and limitations that can perform a wide variety of mission critical activities. LATs are prized for their large storage capacity and their ability to quickly travel to fire starts to facilitate containment during initial attack operations. Nominally, initial attack has been the primary role for LATs in federal fire suppression in the United States. Subsequently, optimization models supporting LAT fleet composition and location-allocation decisions are premised on the primary use of LATs being for initial attack (Fire Program Solutions 2005; Keating *et al*. 2012). These analyses have great policy relevance, as the U.S. Forest Service is facing decisions about how best to address an aging fleet of contracted aircraft. Questions to consider include whether to contract or purchase aircraft, how many aircraft to contract/purchase, of which type, in what mix, with what equipment, and for what role.
But is initial attack really the primary role for federally contracted LATs in the United States? And do the data exist to support comprehensive analysis of the costs and benefits of alternative fleet composition strategies? In 2013 the U.S. Government Accountability Office (GAO) released the findings of an investigation into federal agency actions regarding their fleet modernization and analysis efforts, which identified a need for improved data collection systems (GAO 2013). Similarly, our past and ongoing research has identified inadequacies and deficiencies in data collection, ranging from a limited ability to track and characterize LAT use at the national level, to an even more limited ability

to characterize the objectives and outcomes of individual drops at the incident level. Fine-scale evaluation of LAT drop effectiveness is the fundamental piece of information for supporting decisions related to choosing efficient combinations of aviation and ground-based firefighting resources and establishing appropriate flight mission objectives at the incident-level, for prepositioning and dispatch decisions across multiple incidents, and ultimately for arriving at efficient aviation resource mixes across fire seasons at the national level. Fortunately, recent work in the U.S. and elsewhere around the globe is providing new data and tools to better characterize the costs and benefits of aerial suppression efforts.

Three recent studies are particularly relevant to analyses of aerial firefighting effectiveness and efficiency. First, Plucinski and Pastor (2013) outlined a set of criteria and methodologies for evaluating the effectiveness of aerial suppression drops, and applied their methods during field fire experiments performed in eastern South Australia. The authors identified information needs for environmental and delivery conditions to support evaluation of drop effectiveness, including characteristics related to the type of aircraft, the drop location, fire behaviour, and ground suppression activities. Questions related to evaluation of drop success include whether a drop objective was clearly defined, whether drop placement and coverage were sufficient, and whether spatiotemporal effects on fire behaviour met drop objectives. In the U.S. the ongoing Aerial Firefighting Use and Effectiveness study will ideally be able to provide much of this information, but in the interim critical knowledge gaps remain.

Second, Thompson *et al*. (2013) examined the availability and sufficiency of U.S. federal agency aviation data to support cost-effectiveness analysis, finding that significant data quality issues and limited interoperability across data management systems precluded an in-depth analysis of the sort recommended by Plucinski and Pastor (2013). Instead, the authors as a first step summarized LAT flights according to mission type (initial attack (IA) versus extended attack and/or large fire support (EA)) across the years 2007-2010, using information on both the flight's job code description, and fire size class at the time of the drop. Depending upon assumptions for how to group job codes, results indicated that somewhere between 6.6% and 48.1% of flights were used for IA operations. Fire size results similarly showed limited usage for IA (10.8%), and further indicated extensive use on very large fires. Nearly 35% of drops occurred on fires larger than 4,047 ha (10,000 ac), and nearly 23% of flights occurred on fires larger than 8,094 ha (20,000 ac).

Third, in a more in-depth study, Calkin *et al*. (2014) linked spatially-explicit drop location data with fire occurrence and firefighting resource ordering records to better identify the period in the fire history when drops occurred as well as the resulting outcomes of fires that received drops during IA. The authors analysed LAT drops across 2010-2011, and results confirmed earlier work indicating extensive use of LATs on EA. In 2010, a relatively quiet fire season, 34.4% of all drops were used in EA; this increased to 50.9% in 2011. The number of drops per incident exhibited high variability, largely a reflection of heavy usage for significant events during EA operations, including multiple incidents with more than 75 drops. Results further indicated that drops during IA tended to be associated with incidents that escaped IA and transitioned into EA. In 2010, 67.5% of IA LAT use incidents eventually escaped, and this increased to 84.8% in 2011.

Results of these two latter studies highlight possible inadequacies in contemporary LAT usage, as well as significant complexities in quantifying cost-effectiveness given limited understanding of the marginal contribution of LAT usage to reduced damage across of the spectrum of LAT drop objectives during EA operations. That the majority of overall drops occurred during EA operations suggests that LATs are "sticky" and that fire managers tend to retain LATs for use outside of what has historically been considered their most suitable role. EA LAT use could still be cost-effective under a range of circumstance, of course, but potentially comes at the cost of diverting resources from IA demands. Additionally, that a large majority of drops occurring during IA are associated with escaped wildfires suggests that fire managers are appropriately calling for LAT support on incidents with high escape potential, but also suggests inefficiencies in the positioning, dispatch, availability, and delivery of

LATs for IA operations. The degree to which LAT use on EA can directly degrade IA operational efficiencies has yet to be rigorously quantified, however.
In this paper, we rely on a formalized optimization framework to better understand trade-offs in LAT usage patterns, with the aim to generate information useful for future cost-effectiveness analyses. Specifically we build upon a resource allocation model tested on a select set of units managed by the California Department of Forestry and Fire Protection (Chow and Regan 2011). We develop a static allocation model where LATs are assigned to the same air base for the entire season, and focus on isolating the influence of systemic LAT unavailability for IA due to use for EA operations. In the following sections we introduce the reformulated optimization model along with a sensitivity analysis, present results, discuss implications, and offer recommendations for future research.

Model Formulation

Our model expands upon a previously developed model by Chow and Regan (2011), and has similarities to facility location problems. The problem is defined as the allocation of LATs to air bases over the course of a fire season to minimize the cost (using travel time as a proxy) of deploying LATs to wildfires. The problem formulation is designed to recognize important features of LAT location and deployment, such as the potential demand for multiple LATs to respond to a wildfire, and the ability to co-locate multiple LATs at a given air base. Demand for LATs is dependent upon location-specific seasonal averages for the National Fire Danger Rating System's Burning Index. Structurally, the problem considers a network of nodes (air bases) and arcs with fixed travel times between air bases. Model outputs include assignments of LAT air base locations as well as LAT deployment rules to cover LAT demand from other air bases. We expand upon this formulation by accounting for the possibility of LATs being unavailable for IA due to EA use, and explore how total deployment time changes with various LAT availability rates.

$$\text{Min} \quad \sum_i \sum_j d_{ij} Z_{ij} \tag{1}$$

$$\text{s.t.} \quad Z_{ij} - \gamma_j X_j \leq 0, \ \forall\, i,j \tag{2}$$

$$\sum_j Z_{ij} \geq k_i \quad \forall\, i \tag{3}$$

$$\sum_j X_j = P \tag{4}$$

$$X_j \geq 0 \ \ \forall\, j, \ UD_i \geq 0 \ \forall\, i, \ Z_{ij} \geq 0, \ \ \forall\, i,j, Z_i, X_j \text{ integers} \tag{5}$$

Where

Z_{ij} integer number of LATs at node *j* covering node *i*
d_{ij} matrix of travel times from *i* to *j*
X_j integer number of LATs based at node *j*
k_i minimum demand threshold for number of LATs covering node *i*
γ_j LAT availability rate at node *j*
P number of LATs

Equation 1 minimizes the travel times of the closest tanker bases delivering LATs to demand nodes. Equation 2 limits the number of LATs that can be assigned to node *i* by the availability-weighted number of LATs at node *j*. Equation 3 forces assignment of the *k* closest available LATs to node *i*. Lastly, Equation 4 limits assignment of LATs to the total number of LATs in the fleet, and Equation 5 ensures non-negativity.
To examine the sensitivity of model performance to LAT availability, we first uniformly vary LAT unavailability rates in 0.05 increments from 0.05 to 1.00. We then consider variable LAT availability rates across air bases. As a simple rule we define air bases as low or high demand nodes (and therefore high or low availability nodes, respectively) based upon whether their demand levels are below or above the median demand across all air bases. We then vary the availability rates according

to three paired sets of (0.70, 0.90), (0.60, 0.80), and (0.50, 0.70), which correspond to average availability rates of 0.80, 0.70, and 0.60, respectively.
Additionally we explore introducing penalties for otherwise infeasible solutions with unmet demand. To account for unmet demand in the model the objective function is updated to include penalty costs (Equation 6) and the constraint to meet LAT demand is updated to include a dummy variable for unmet demand (Equation 7). We explore three weights (1, 10, and 25) for the penalty that in effect act as a scaling parameter to convert unmet LAT demand into the equivalent deployment time. In practice, the ρ parameter could be based on the cumulative travel times of alternative firefighting resources necessary to achieve an equivalent level of firefighting production capacity.

$$\sum_i \sum_j d_{ij} Z_{ij} + \sum_i \rho_i UD_i \quad (6)$$

$$\sum_j Z_{ij} + UD_i \geq k_i \quad \forall i \quad (7)$$

Where
UD_i unmet demand at node *i*
ρ_j unmet demand penalty at node *j*

For parameterization of the model we use the same set of demands and travel times for the test network applied by Chow and Regan (2011). This test case includes 20 LATs and 12 California Department of Forestry and Fire Protection air bases. Table 1 presents summary information on the demand levels and availability classifications we used.

Table 1. Summary information on air bases in test network

Air Base #	Air Attack Base Name	# of LATS	Demand Level	Availability Classification
1	Hollister	2	4.16	High
2	Chico	1	10.4	Low
3	Fresno	1	9.8	Low
4	Rohnerville	1	5.58	Low
5	Sonoma	2	4.8	High
6	Ukiah	2	6.2	Low
7	Ramona	2	9.9	Low
8	Hemet	2	5.12	High
9	Redding	2	5.69	Low
10	Paso Robles	2	5.47	High
11	Columbia	2	5.18	High
12	Porterville	1	4.06	High

Results

Figure 1 displays how total deployment time varies with LAT availability, using the first model presented in Equations 1-5. As expected, total deployment time decreases as LAT availability increases, reaching an overall minimum of 31.46 at full availability. Results are not presented below an availability rate of 0.55 because solutions are infeasible. At the rate of 0.55 total deployment time (63.64) is more than double that of full availability.
Figure 2 instead focuses on LAT air base assignments, summarizing how these assignments can vary with LAT availability. The figure compares the number of LAT assignments per air base under the baseline (full availability) scenario to the mean number of assignments across availability rates ranging from 0.55 – 0.95. Results indicate substantial variation in LAT air base assignments, suggesting a high

degree of sensitivity to LAT availability. Particular prominent differences are observed for air bases 2 and 3 (fewer assignments under baseline scenario) as well as air base 8 (more assignments under baseline scenario). Optimal LAT air base locations also differ significantly from current (as of 2011) actual LAT assignments (see Table 1).

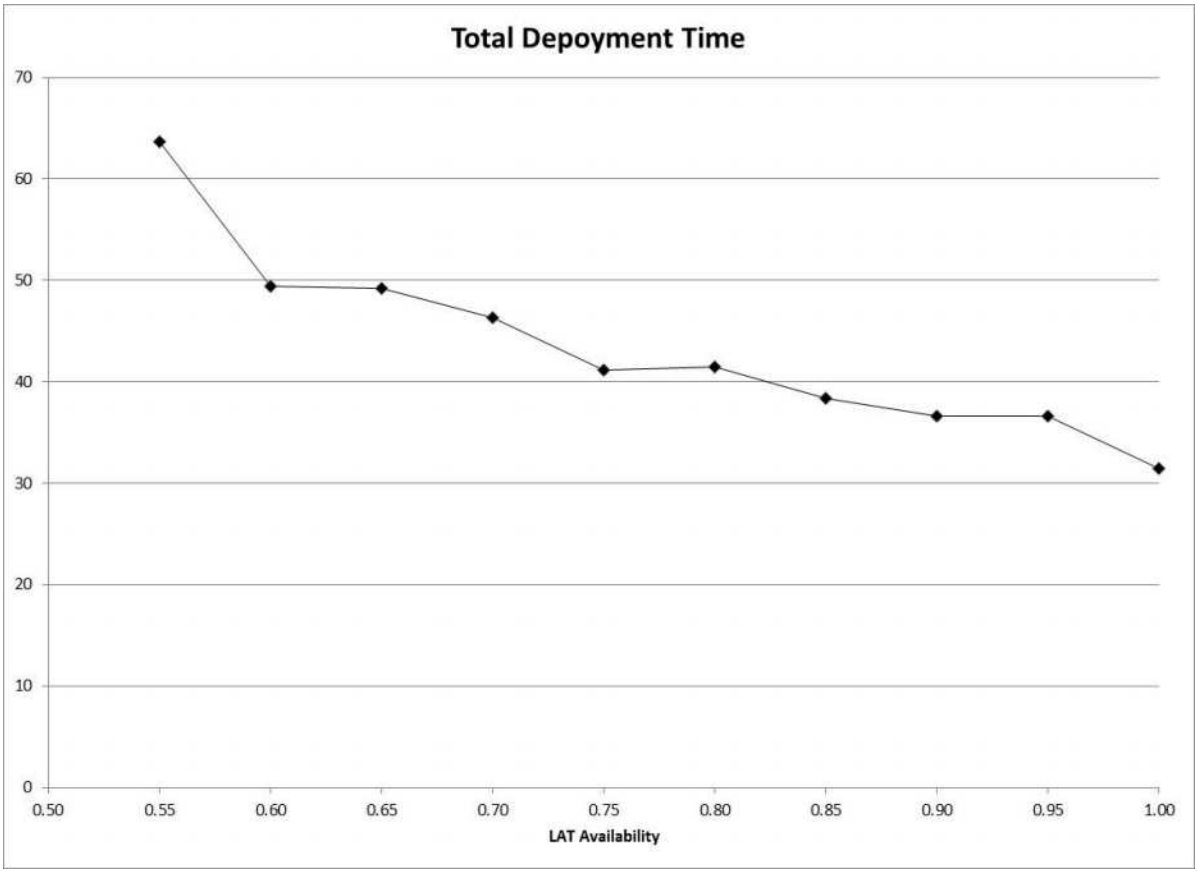

Figure 1. Total deployment time as a function of LAT availability

Table 2 compares total deployment times and LAT air base assignments across six LAT availability scenarios – those for uniform availability rates of 0.80, 0.70, and 0.60, as well as the low/high paired sets. At least over these availability rate combinations, the model performs better with variable availability rates, and in general shows substantial sensitivity to LAT availability. This is because the model preferentially selects air bases with low demand levels and therefore higher availability rates (see Table 1). For instance compare the number of LAT assignments to air bases 2 and 3 under uniform and variable availability rates.

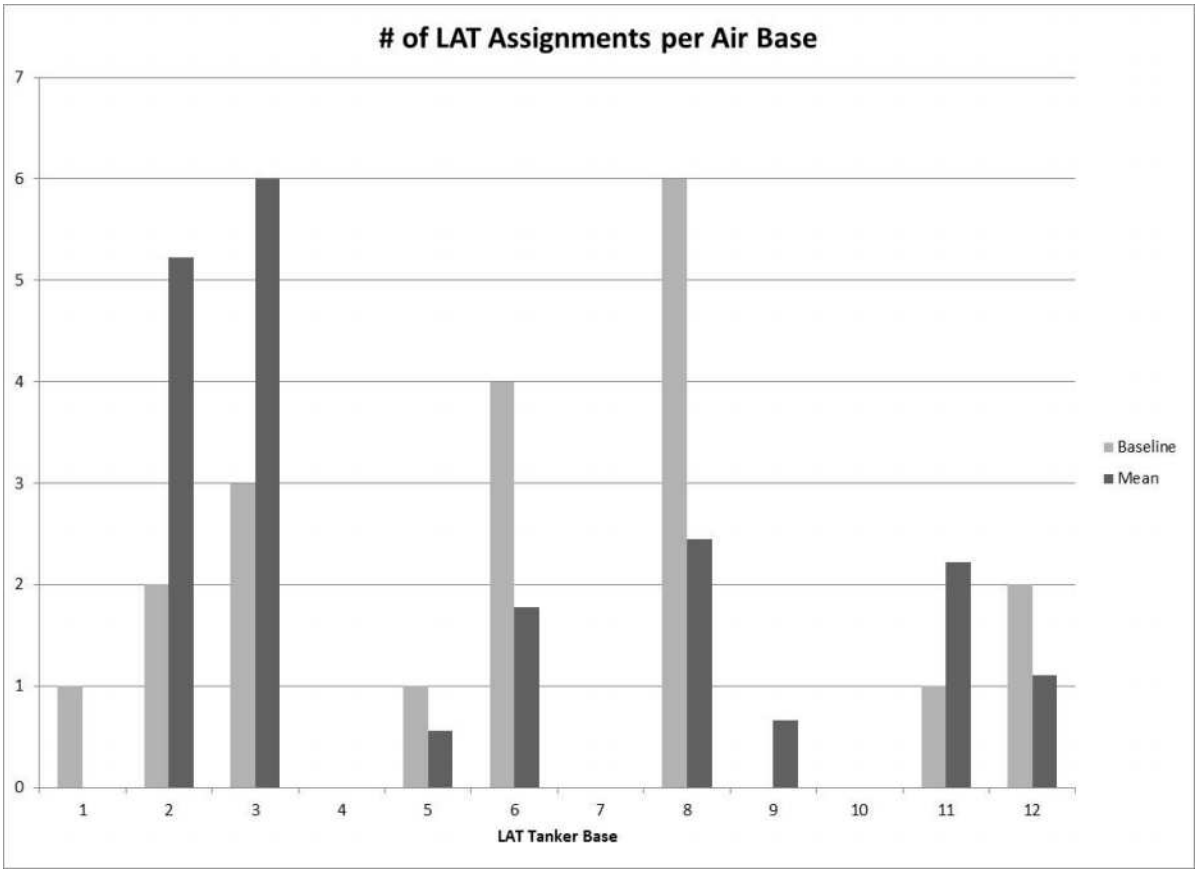

Figure 2. Number of LAT assignments per air base across different LAT availability scenarios

Table 2. Total deployment times and LAT air base assignments under different LAT availability rate scenarios

Air Base #	Uniform LAT Availability Rate Across Air Bases			Variable LAT Availability Rate Across Air Bases		
	0.80	0.70	0.60	0.70, 0.90	0.60, 0.80	0.50, 0.70
	Total Deployment Times					
	41.5	46.27	49.45	39.59	42.68	47.5
	Number of LAT Assignments per Air Base					
1	0	0	0	0	0	0
2	5	10	5	0	0	0
3	5	10	5	0	0	0
4	0	0	0	0	0	0
5	0	0	5	8	5	10
6	3	0	0	0	0	0
7	0	0	0	0	0	0
8	4	0	0	6	5	0
9	0	0	0	0	0	0
10	0	0	0	0	0	0
11	0	0	0	0	5	0
12	3	0	5	6	5	10

Figures 3-5 incorporate unmet demand based on the updated model incorporating Equations 6 and 7. Figure 3 displays total penalty-adjusted deployment times as a function of LAT availability, using a log-scale to better differentiate results at the higher availability rates. At rates below 0.55, where the original model becomes infeasible, objective functions with higher penalty rates begin to climb more steeply. Over the range 0.55 to full availability, results for the penalty weight of 25 are identical to results presented in Figure 1. Where the penalty for unmet demand is only 1, the solutions never fully me*et al*l demand because it is cheaper to incur the penalty than to travel to other air bases. Figure 4 further illustrates this relationship between unmet demand and deployment time where the penalty is 1, showing that unmet demand never drops to zero. Neither does deployment time exhibit a negative slope after availability of 0.55 (see Figure 1), again because the gains in availability are less important relative to the low penalty of not meeting demand. By contrast, Figure 5 shows the same relationships but where the penalty is 10. Travel time rises and unmet demand drops steeply until roughly the point where the problem becomes feasible. From that point forward deployment time continues to drop as availability increases, consistent with Figure 1.

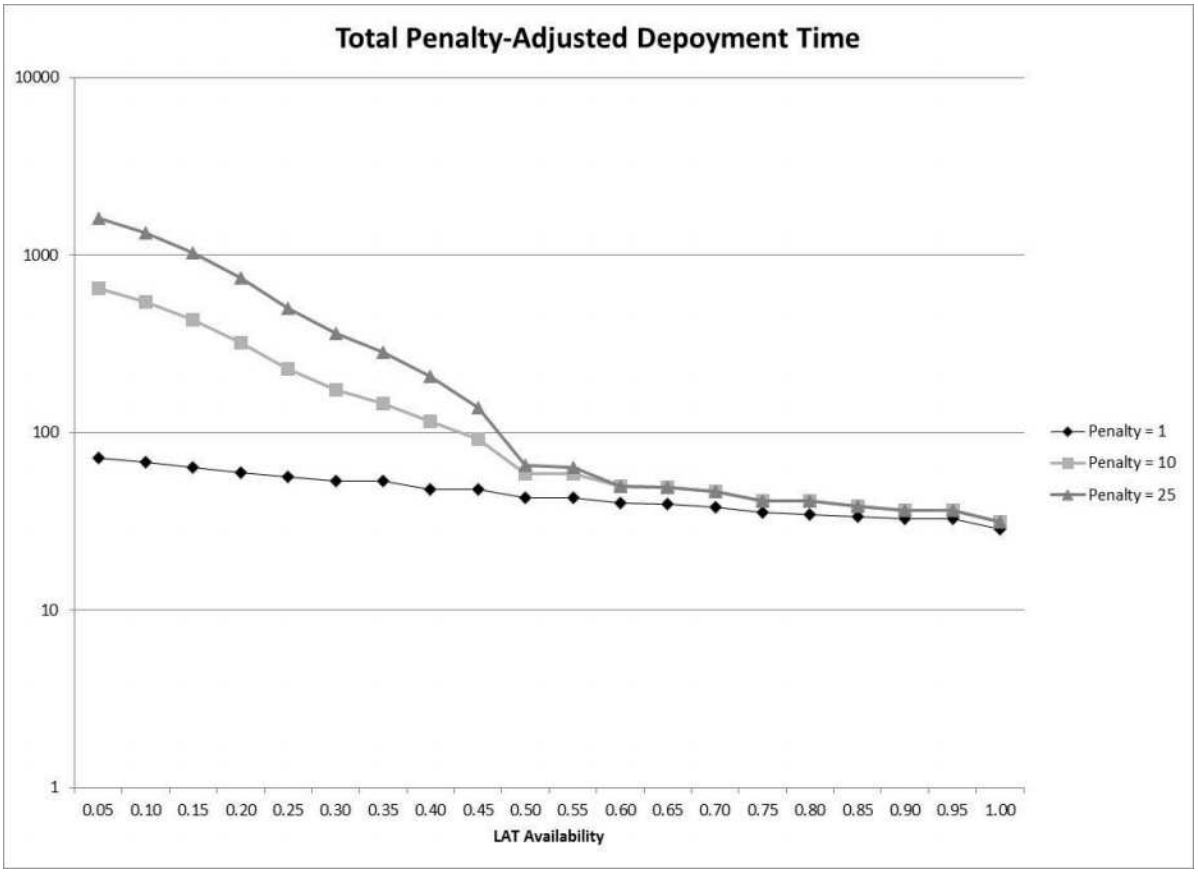

Figure 3. Total penalty-adjusted deployment time as a function of LAT availability

Discussion

We reviewed recent research indicating significantly different LAT usage patterns than has been typically assumed within LAT location and deployment optimization efforts. Specifically these models have assumed near total use for IA, whereas recent evidence suggests EA use can comprise a significant share of overall use. Additionally, recent research indicating low IA success rates on fires that receive LAT support during IA suggest possible inefficiencies in LAT usage. In response we

augmented a mathematical optimization model to explore trade-offs between IA and EA use, and examined model sensitivity to LAT unavailability for IA efforts.

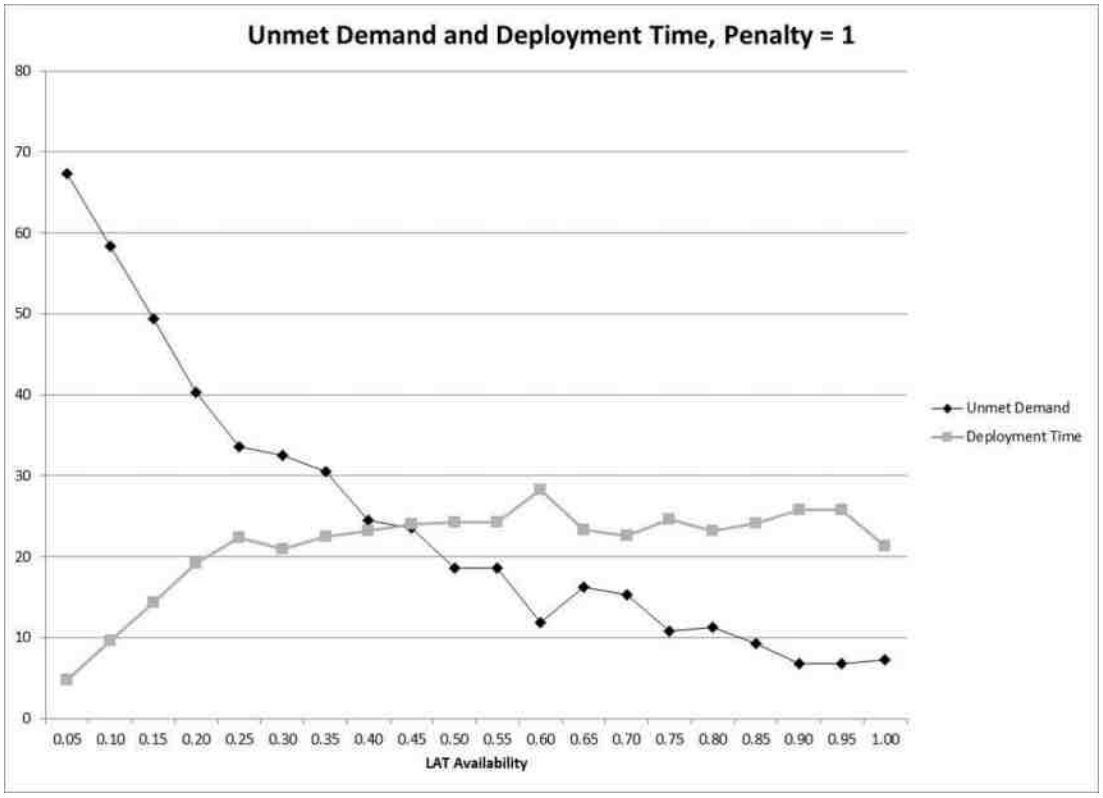

Figure 4. Unmet demand and deployment time as a function of LAT availability, penalty = 1

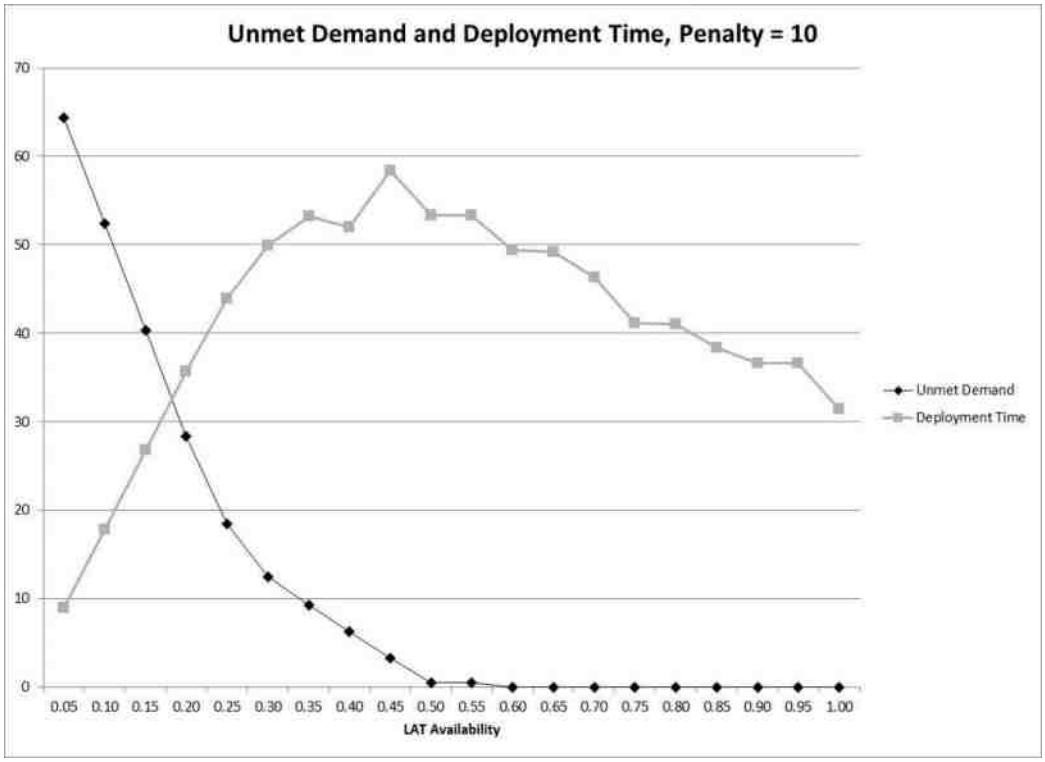

Figure 5. Unmet demand and deployment time as a function of LAT availability, penalty = 10

Our results indicated that model performance degrades as LATs become less available, and that results are highly sensitive to LAT unavailability. This sensitivity is particularly evident when examining optimal LAT air base locations (the same is true for optimal LAT deployment rules, not provided here for economy of presentation). These results could carry significant implications for efficient updating of LAT location and deployment strategies, especially when considering additional real-world factors like staffing needs and air base capacities. Our results also lead to questions of how changes in fleet size could mitigate or exacerbate potential IA/EA trade-offs. A more complete model would ideally seek to better compare with a common metric the costs and benefits of LAT use for IA and EA rather than focus on degraded IA performance, although data gaps still present significant challenges to building such a model.

One immediate extension to our model is to consider a dynamic model that can relocate LATs on a daily basis in response to observed and/or predicted fire activity (Chow and Regan 2011). This extension requires a more complicated framework and increased computational demands, a verifiable ability to forecast future aerial firefighting needs, and an approach to translate relocation costs to the value of improved deployment time considering factors such as avoided damages. Further, incorporating LAT unavailability into the model on a daily basis would require a more complicated model to characterize LAT unavailability due to EA support. However, this approach can better capture the nature of a truly dynamic suppression organization that makes responsive location and relocation decisions. This modelling approach may also better illustrate opportunities for efficiency gains relative to current practice.

Additional future modelling efforts could consider variation in demand in addition to supply, could explore probabilistic efforts to better capture possible pulses of high IA activity, and adopt combined simulation-optimization efforts. Additional research to calibrate and parameterize these models is necessary as well. These efforts could seek to quantify the predictive skill of fire weather forecasts as well as the degree to which these forecasts influence suppression resource prepositioning. Critically, research efforts will need to better characterize the benefits and costs of LAT usage to move beyond the simplistic model based on travel time alone. Thus, beyond modelling efforts, continued empirical analysis of LAT usage, fire outcomes, and particularly drop effectiveness are warranted.

Acknowledgements

The Rocky Mountain Research Station and the National Fire Decision Support Center supported this effort.

References

Calkin, D. E., C. S. Stonesifer, M. P. Thompson, and C. W. McHugh (2014), Large airtanker use and outcomes in suppressing wildland fires in the United States, International Journal of Wildland Fire, 23(2), 259-271.

Chow, J. Y., and A. C. Regan (2011), Resource location and relocation models with rolling horizon forecasting for wildland fire planning, INFOR: Information Systems and Operational Research, 49(1), 31-43.Fire Program Solutions 2005

Fire Program Solutions (2005) Wildland Fire Management Aerial Application Study. Available at http://www.fs.fed.us/fire/publications/aviation/nats3_wfmaas_report_final.pdf [Verified 24 July 2014]

GAO (2013) Improvements Needed in Information, Collaboration, and Planning to Enhance Federal Fire Aviation Program Success. US Government Accountability Office, Report number GAO-13–684. Available at http:// http://www.gao.gov/products/GAO-13-684 [Verified 14 July 2014]

Keating EG, Morral AR, Price CC, Woods D, Norton D, Panis C, Saltzman E, Sanchez R (2012) Air attack against wildfires: understanding US Forest Service requirements for large aircraft. (RAND Corporation) Available at
http://www.rand.org/content/dam/rand/pubs/monographs/2012/RAND_MG1234.pdf [Verified 14 July 2014]

Plucinski, M. P., and E. Pastor (2013), Criteria and methodology for evaluating aerial wildfire suppression, International Journal of Wildland Fire, 22(8), 1144-1154.

Thompson, M. P., D. E. Calkin, J. Herynk, C. W. McHugh, and K. C. Short (2013), Airtankers and wildfire management in the US Forest Service: examining data availability and exploring usage and cost trends, International Journal of Wildland Fire, 22(2), 223-233.

Mapping of forest habitats vulnerable to fires using Corine Land Cover database and digital terrain model

Edyta Woźniak[a], Mirosław Kwiatkowski[b], Bartłomiej Kołakowski[c]

[a] *Space Research Center, Bartycka 18A, 00-716 Warszawa, e-mail: ewozniak@cbk.waw.pl*
[b,c] *Forest Research Institute, Sękocin Stary, Braci Leśnej 3, 05-090 Raszyn, m.kwiatkowski@ibles.waw.pl, b.kolakowski@ibles.waw.pl*

Abstract
An appropriate system of fire detection and proper preparation of the forested areas for emergency and fire extinguishing activities have a significant impact on the magnitude of losses caused by forest fires. The basis of the forest fire protection planning is the forest categorisation in the context of fire risk, which is performed on the basis of the percentage of area covered by the most vulnerable habitats: dry coniferous, fresh coniferous, fresh mixed coniferous, wet coniferous, wet mixed coniferous and riparian forest. Maps of forest habitat are available for the State Forests however for private forests this information does not exist, so the proper categorisation of fire risk in these forests is very difficult and costly. The object of the study is to develop a method for the estimation of the area cover of the above-mentioned forest habitats using open source data Corine Land Cover (CLC) database and SRTM - Digital Terrain Model in order to fill the information gaps for the private forests. Employing GIS environment the analysis of the correlation between CLC land cover classes and specific forest habitat was performed. Then, the terrain characteristics such as curvature and slope were correlated with habitat humidity. Also, the shape analysis of units was carried out. On the basis of these three parameters was estimated the areas covered by fire vulnerable habitats for forest inspectorates in central and north-west Poland where the state forests constitute 98% of the area so the ground verification data was accessible for almost the entire terrain. The overall agreement between obtained and reference maps is 89%, and the error of the estimation of the specific fire vulnerable habitats is lower than 20%. The proposed method is relatively fast and low-cost and may be used for fire risk categorisation of the forested areas where the ground verification information is not available.

Keywords*: fire detection, Corine Land Cover (CLC), forest habitat*

Introduction

The appropriate organisation of the fire detection system and preparation of forest areas to conduct prevention-extinguishing activities has a significant influence on the size of losses caused by forest fire. The basis for planning activities in the extent of forest fire protection is the forest fire risk category (KZPL). It is determined according to the requirements specified in the Ordinance of the Minister of the Environment of the 22nd of March 2006 concerning detailed principles of forest fire protection of forests (Journal of Laws No. 58 entry 405 with subsequent amendments). It concerns forests of a similar level of susceptibility to fire, established on the basis of frequency of fire occurrence, stand and climatic conditions and anthropogenic factors. This category is established on the basis of the sum of points resulting from calculations for four, following parameters:

a) average annual number of forest fires in the period of the last 10 years per thousand hectares of afforested area,
b) sums of percentage participation of stands growing in habitats: dry forest, fresh forest, moist forest, moist mixed forest and riparian forest,
c) average relative air humidity at height of 0.5 m and percentage of days with air humidity less than 15% at the hour of 9.00,
d) average number of inhabitants per hectare of forest area.

The range of forest habitat types (STL) considered in the establishment of KZPL results from analysis of flammability of forests presented in the study "Categorisation of fire risk of Polish forests" (Szczygieł *et al*. 2009, in which to categorise flammability is used the flammability indicator, being the quotient of the share of the number of fires of given stands to the areas of these stands. As flammable habitats, the share of which is influences KZPL, those are recognised, for which this indicator is greater than the units. They are: dry coniferous forest (Bs)-4.39, moist coniferous (Bw)-1.81, fresh coniferous forest (Bśw)-1.66, fresh mixed broadleaved forest (BMśw)-1.30, moist mixed coniferous forest (BMw)-1.18 and riparian forest (Lł)-1.03.
Insofar as for forests managed by State Forests National Forest Holding the decisions of KZPL do not give rise to greater difficulties and are updated each time while drawing up forest management plans, to that extent for remaining forests, principally private, its decisions cause significant difficulties. This is connected primarily with the lack of detailed information, concerning the proportion of surface area covered by particular forest habitat types. In individual provinces these forests consist of from 2.9 to 54.2 per cent of the afforested area. Equally the density of occurrence of fires in particular years in the period 2003-2012, as also the average area of one fire are clearly greater for forests in other forms of ownership, in comparison to forests managed by State Forests (Figure 1).

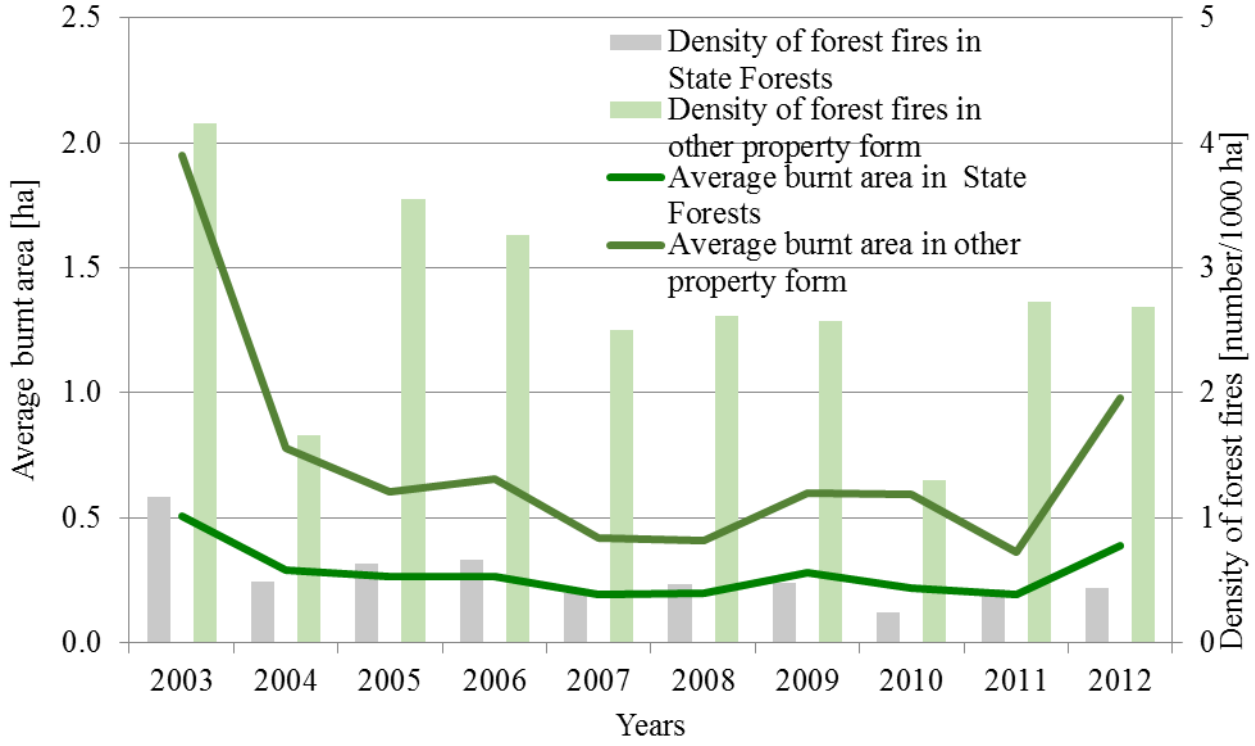

Figure 1. The occurrence of forest fires in the years 2003-2012

Density of occurrence of fires in State Forests is fivefold less in comparison to forests in other forms of ownership, fluctuating in particular years between 3.4 and 6.4. Equally the average area of a single forest fire in forests in other forms of ownership is significantly greater (from 1.9 to 3.8) than in State Forests. In this situation it is essential to seek a method determining the proportion of surface area taken by habitats Bs, Bw, Bśw, BMśw, BMw, Lł, enabling appropriate determination of KZPL for these forests, and in consequence appropriate preparation of forest areas for the conduct of prevention-extinguishing activities. This problem is diligently solved by drawing up a modelling method for proportion of selected forest habitat types on the basis of the Corine Land Cover land-use map and numerical terrain models.

Comparative works to the CORINE maps and models exist in the databases of national forest maps and for defining its suitability in forest cartography on regional scales (Waser, Schwarz, 2006). Because of the great generalisation of information, direct interpolation of data is not possible, especially in mountainous areas typified by great heterogeneity. In such a situation it is essential to use various auxiliary materials in order to increase the spatial resolution of CORINE. Such assumptions were accepted by Pekkarinen *et al*. (2009) in the cartography of afforested areas. It is simultaneously supported by Landsat ETM+ satellite photographs. In the work presented below the increase of CORINE spatial resolution is obtained by use of numerical terrain model.

Area of research

For the purpose of drawing up the habitat designation method two research areas were chosen. The first research area served as a research area, the second as a testing area. For the research area was chosen the territory of the following Forest Districts: Dobieszyn, Kozienice, Marcule, Radom and Zwoleń of a combined area of approximately 500 000 ha, among which almost 63 000 ha is covered by forest, managed by these forest districts. The combined area of forests on the territory of these forest districts according to CORINE amounts to 101 816 ha. The basic characteristic of the stands of these forest districts in comparison to conditions for the area of all Poland is shown in figures 2-4. These forest districts are typified by proportions of high flammability class habitats: dry coniferous forest, fresh coniferous forest, moist coniferous forest, fresh mixed broadleaved forest, moist mixed broadleaved forest and riparian forest that are close to the national average. Equally the distribution of forests in specified age group is similar to the national average. In relation to Polish forests as a whole, in these forest districts there is an approximately 20% greater proportion of pine stands.

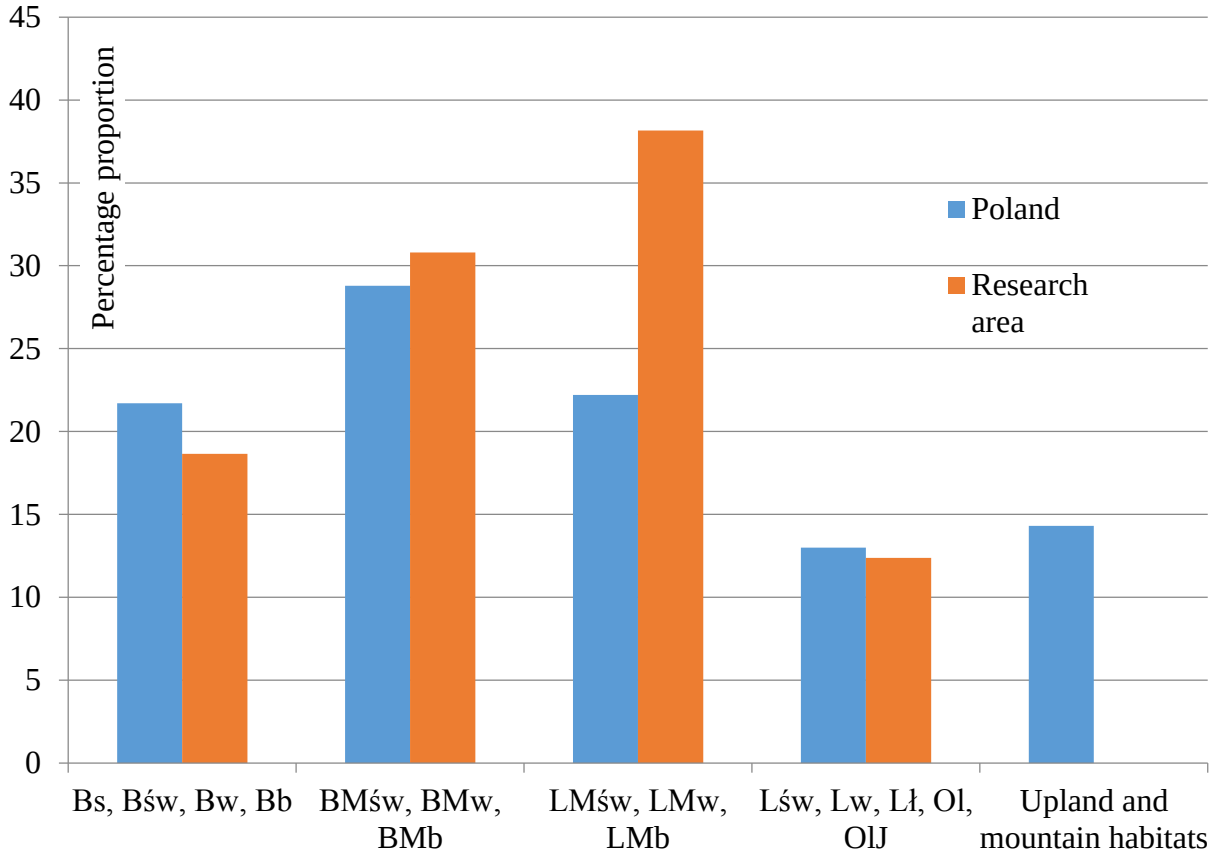

Figure 2. Percentage proportion of stands according to forest habitat types

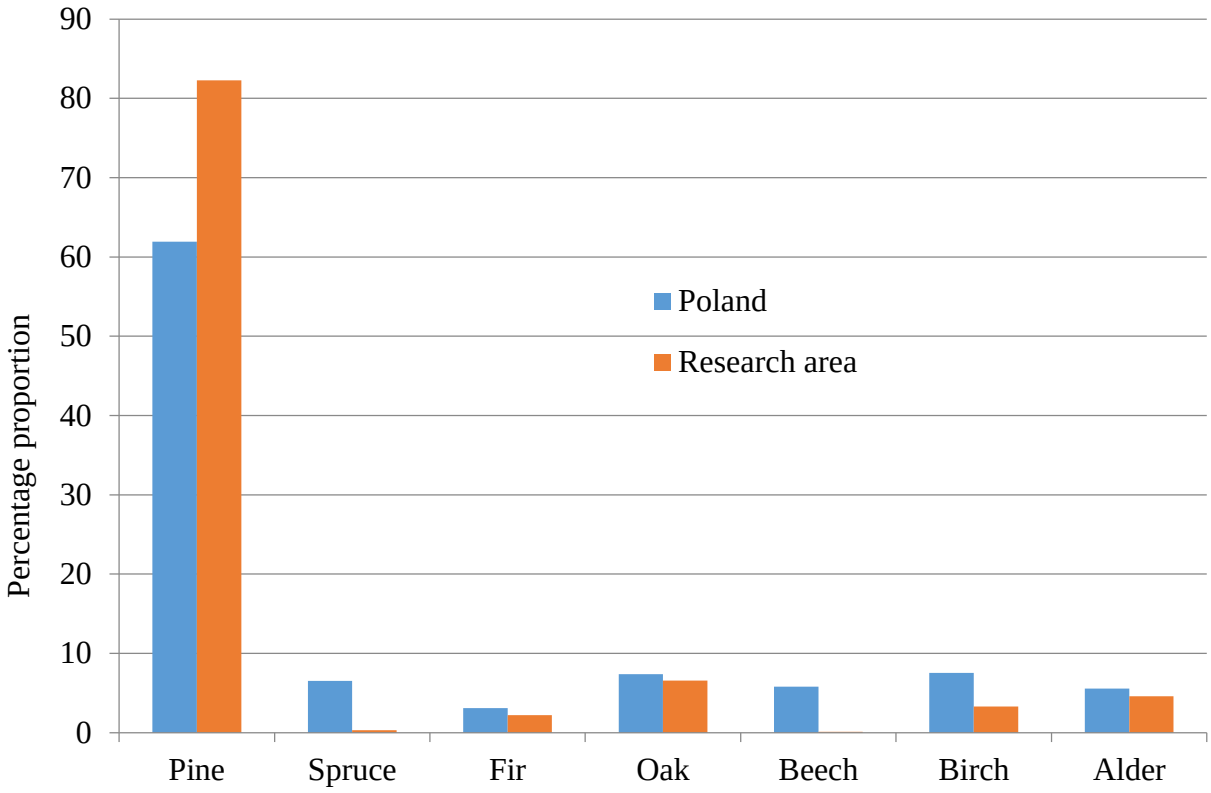

Figure 3. Percentage proportion of stands according to prevailing species

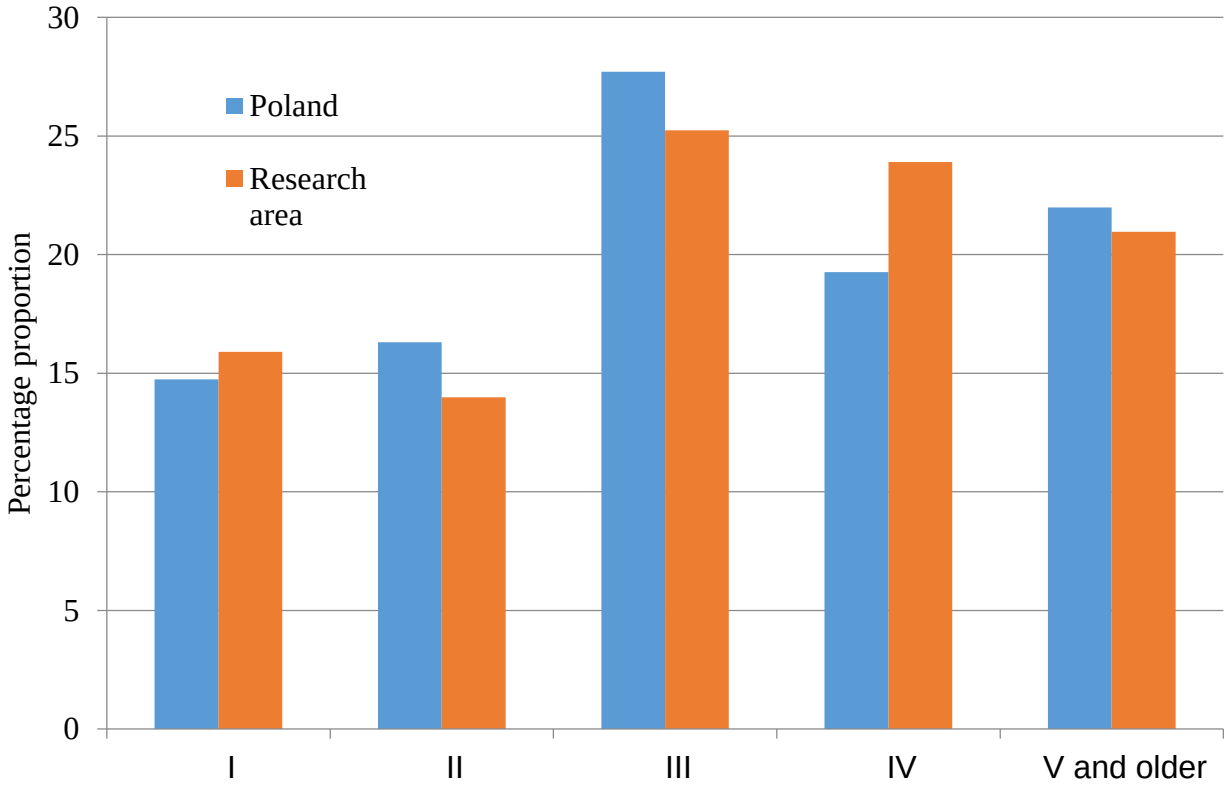

Figure 4. Percentage proportion of stands according to stands age

In the verification of the drawn up method it was applied to the area of forest districts within the whole or part of the province of Western Pomerania (57 forest districts). This area was chosen with regard to the virtually 98% share of state forests in the ownership structure of forests in the given province.

Source data

In the study, data generally available with the aid of Internet services was used. The basis for the performance of the work was the terrain use data CORINE Land Cover – CLC2000 and also data of the numerical terrain model SRTM (Shuttle Radar Topography Mission). For reference material the Forest Numerical Map supplied from the State Forests database was used.

3.1. CORINE Land Cover 2000 Database

The CLC2000 database is constructed in three hierarchical levels. The first level (European) differentiates 5 basic groups of terrain cover, agricultural, forest and semi natural ecosystems, boggy terrains and water. The second level (regional) separates 15 classes and the third (national) distinguishes 44 classes, of which 31 occur within Poland. In the study only three classes are used from the third group - forests and semi natural ecosystems: 3.1.1 deciduous (broadleaved) forests, 3.1.2 coniferous forests, 3.1.3 mixed forests. Their definitions are placed below.

Deciduous forest - code 3.1.1. - This class includes botanical communities consisting primarily of trees, with regard to the undergrowth layer, where deciduous species are dominant. The crowns of the trees should cover over 30% of the surface and deciduous trees should represent over 75% of the stand. The height of trees of this class should exceed 5 m in normal climatic conditions.
Coniferous forest - code 3.1.2. - Flora classified as coniferous forest should consist primarily of trees, with regard to the undergrowth layer, where coniferous species are dominant. Similarly to the deciduous forests the height of the trees in this class should exceed 5 m. Coniferous trees should represent over 75% of the stand.
Mixed forest - code 3.1.3. - General class definition is similar to the preceding cases i.e. flora should consist primarily of trees, with regard to the undergrowth layer and height of trees in this class should exceed 5 m. Nonetheless however percentage participation of deciduous or coniferous may not be dominant.

CORINE Land Cover map sheets covering the study terrain were taken from the website of the European Environment Agency (European Environment Agency) http://www.eea.europa.eu/themes/landuse/interactive/clc-download in .shp. format. Subsequently the reproduction of the maps obtained was changed to UTM zone 34, reference system WSG84.

3.2. Numerical Terrain Model

Numerical Terrain Model (NMT) SRTM was obtained for Polish terrain from the website http://srtm.csi.cgiar.org/SELECTION/inputCoord.asp in format GeoTiff. This model has spatial definition of 80 m. For the needs of the work the terrain definition of the model was increased to 30 m. The sheets taken were joined in one layer and the reproduction was changed to UTM zone 34, reference system WGS84. Then two types of errors occurring in the model were located: height value anomaly, above 2600 m above sea level and lacking pixels and designated as no data. Corrected anomalous pixel values and supplementation of lacking pixels through interpolation with nearest surroundings.

3.3. Numerical forest map

Reference data are obtained from Numerical Forest Map, which contained basic data concerning all designated forest areas lying within the boundaries of the research polygon. These areas are designated

during the drawing up of forest management plans for piece of land constituting a part of uniform forest section with regard to biotope and biotic forest community. For each of these data is available relating to:

- forest habitat type,
- layered vertical zones structure,
- area,
- layer structure,
- species composition,
- age of stand
- height of stand
- density.

Methodology and results of studies

4.1. Analysis of occurrence of CLC terrain cover class and types of forest habitats.

In order to verify the comparability of data of particular habitat types they were pre-classified according to CORINE nomenclature, those in which percentage share of coniferous trees in the stand exceeded 80% were classified as class 3.1.2, those in which percentage share of deciduous trees in the stand exceeded 80% were classified as class 3.1.1 and the remainder as mixed 3.1.3. Percentage proportional quantities of particular CLC classes in succeeding habitat types being the object of interest are shown in table 1. From the table it is seen that with a very high probability it may be stated, that CLC classes of coniferous and mixed forests shall correspond to forest classes on forest map. Riparian forest habitat type completely fulfils the criterion of CLC deciduous forest. Remaining types in an exceptional majority correspond to CLC criterion for deciduous or mixed forest degree.

Table 1. Percentage share of quantity allocation of specific classes of Corine Land Cover in analysed habitat types.

Habitat type	CLC 3.1.1	CLC 3.1.2	CLC 3.1.3
Dry coniferous forest	2%	89%	9%
Moist coniferous forest	4%	74%	22%
Fresh coniferous forest	4%	67%	29%
Fresh mixed coniferous forest	4%	52%	44%
Moist mixed broadleaved forest	10%	36%	54%
Riparian forest	98%	0%	2%
Other forests	65%	15%	20%

4.2. Study of profile indicators on the basis of numerical terrain model to achieve a more detailed localisation of habitats

Each habitat is associated with a specific genetic soil type, which in turn is associated with the sediment deposit type, from which it is created. Depending on the origin and mechanical composition of deposit subjected to various types of geomorphologic processes and differing intensities, it is reflected in the shape of the terrain. The predominant part of Poland is covered with Quarternary formations of glacial, water, river, lake and aeolian origin. Various types of loose sands, clay sands, clays, dusts or silts dominate. Bearing in mind equally: origin, manner of settlement, resistance to processes occurring on the surface, as also age of deposit it may with considerable generalisation be stated, that terrains constructed of older substrates are flatter, and those in areas with a sandy substrate have a less varied terrain topography. Together with increase of the values of silts in surface formations, reaching the level of heavy clay, the morphological sculpting is ever more varied. Areas formed from silts are typified by a large quantity of deep cut ravines. Areas formed from silts are normally flat. This is the result of sedimentation processes, which lead to the creation of geological formations.

On the basis of the numerical terrain model the degree of terrain topography variation may be defined through definition of two parameters: terrain inclination and its curvature (Zeverbergen, Thorne, 1987, Moore *et al*. 1991). Variable terrain inclination is generally known and does not require further comment, if however it concerns curvature of terrain this defines three basic situations: flat terrains, concave terrains and convex terrains.
In table 2 are shown an average dimensions of standard deviation values, and also span of extent of terrain curvature and inclination of slopes for particular types of forests, with the exception of dry coniferous forest, the rare appearance of which in the studied terrain prevented taking the appropriate samples. From the table it is shown that terrain curvature enables separation of fresh and moist habitats. Fresh habitats are typified by an average terrain curvature exceeding 0, corresponding to areas with "curvature" dominance, moist habitats though are typified by values less than 0.006, corresponding to "concave". Mixed forest habitats are characterised by greater deviation of standard terrain inclination.

Table 2. Values of terrain shaping indicators for forest habitats

	Incline of slopes			**Curvature**		
STL forest types	Variation extent	Average	Standard deviation	Variation extent	Average	Standard deviation
Fresh coniferous	5.5874	1.2071	**0.8887**	0.6719	**0.0071**	0.0644
Fresh mixed forest	7.2093	1.1821	**0.9588**	0.6563	**0.0070**	0.0600
Moist mixed forest	6.0675	1.2246	**0.9511**	0.4688	**-0.0022**	0.0581
Moist coniferous	3.4723	1.0994	**0.8445**	0.3438	**-0.0048**	0.0590

4.3. Study of terrain shape indicators to achieve very detailed habitat localisation.

Shaping indicators may provide information on circularity, extension and degree of complication of polygons. In the case of definition of types of forest habitats, shape parameters have great significance in the emergence of riparian forests among all deciduous forests. The PARA shape indicator being the relationship of the polygon circumference to its surface area describes the degree of elongation of polygons or their shape complication. Poligony, for which the PARA indicator is less than 0.007, does not correspond to riparian forest shape criteria. Polygons described in PARA with greater value than given threshold value may be riparian forests, but additional criteria are necessary in order to separate them from other forests with an elongated shape.

4.4. Developing method of habitats designation on the basis of CLC and previously enumerated indicators.

With regard to excessive numbers of polygons for showing on CLC maps (minimal area 25 ha) additional terrain division was made. Utilising the numerical terrain model, areas were designated every 30 m of height, and then CLC polygons were "fragmented" with the use of the designated areas. Thus was segmentation achieved of terrain surface polygons, which enabled the obtaining of more precise statistics for smaller polygons. For particular habitats of high flammability groups a procedure was drawn up leading to the imaging of the given habitat on map. Dry coniferous forest constitutes an exception, because of the very small statistical size of the classification. Basic layers used to designate these habitats are: CORINE Land Cover (CLC) map and also those received from numerical terrain model of declines and curvatures. In some instances other variables were also used, which were described together with the necessitating case.

Moist coniferous forest was designated on the basis of the following routine:

1. polygons coded as coniferous forest were selected from the CLC map (3.1.2),
2. average terrain curvature and standard deviation from terrain inclination values were calculated for the selected polygons,
3. polygons of curvature less than 0.006 and standard deviation of terrain inclination less than 0.9 were reclassified as moist coniferous forest. Fresh coniferous forest was designated on the basis of the following routine:
4. polygons coded as coniferous forest were selected from the CLC map (3.1.2),
5. average values of terrain curvature and standard deviation of terrain inclination were calculated for the selected polygons,
6. polygons of curvature greater than 0.006 and standard deviation of terrain inclination less than 0.9 were reclassified as fresh coniferous forest. Fresh mixed coniferous forest was designated on the basis of the following routine:
7. polygons coded as coniferous forests were selected from the CLC map (3.1.2),
8. average values of terrain curvature and standard deviation of terrain inclination were calculated for the selected polygons,
9. polygons of curvature greater than 0.006 and less than 0.02 and standard deviation of terrain inclination greater than 0.9 were reclassified as fresh coniferous forest,
10. polygons coded as mixed coniferous forest were selected from the CLC map (3.1.3),
11. polygons of curvature less than 0.007. Moist mixed forest was designated on the basis of the following routine:
12. polygons coded as coniferous forest (3.1.2), were selected from the CLC map
13. average values of terrain curvature and standard deviation of terrain inclination were calculated for the selected polygons,
14. polygons of curvature less than 0.006 and standard deviation of terrain inclination greater than 0.9 were reclassified as fresh coniferous forest. Riparian forest was designated on the basis is the following routine:
15. polygons coded as deciduous forest (3.1.1) were selected from the CLC map
16. PARA indicator values were calculated for selected polygons,
17. selected polygons of PARA indicator greater than 0.007,
18. water flows system was generated from the numerical terrain model,
19. only those deciduous forests were classified as riparian forests, which fulfilled the condition of elongated shape and at least partially covered with water flows and having a surface area less than 500 ha.

4.5. **Method validation**

Habitat maps received with the aid of described procedures were compared with the Digital Forest Map. Analysis was conducted of the percentage surface share taken by particular habitats (figure 5). A large conformity of results is visible, though an increased share of riparian forest habitats should be noted. Perhaps is a result of fact that they are mainly outside the area of State Forests.

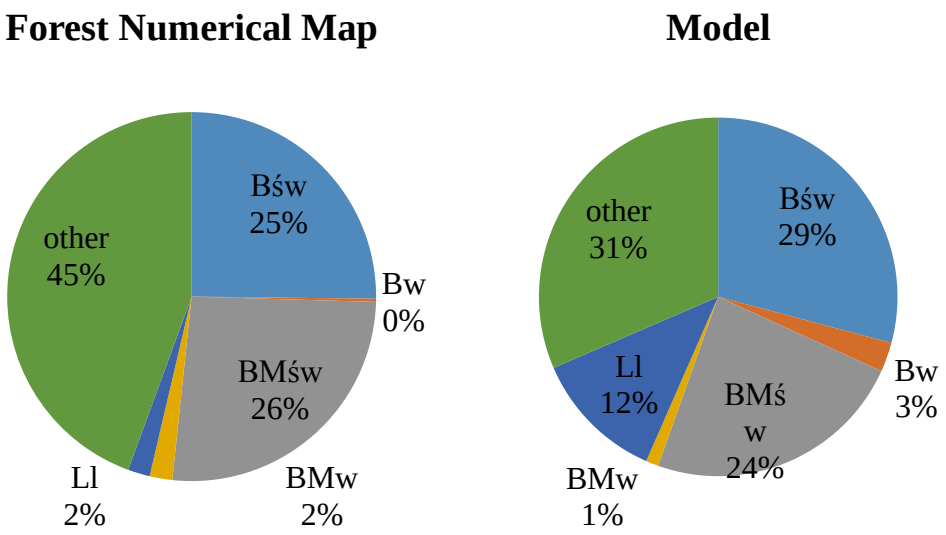

Figure 5. Percentage share of habitats according to numerical forest map and model

Application of method for the Western Pomerania province

On the terrain of forest districts being at least partially within the Western Pomerania province there are 1 130 918 ha of forest according to Corine CLC and 1 006 647 according to forest reports. As a whole the difference of forest areas between the two sources of information amounts to 124 270 ha, which constitutes 12% of the total area.
Habitat modelling results are shown in figure 6. The greatest percentage participation of habitats with a high flammability indicator is found in forest districts located in the southern and eastern parts of the province. The least percentage of these habitats may be noted in the central part of the province.

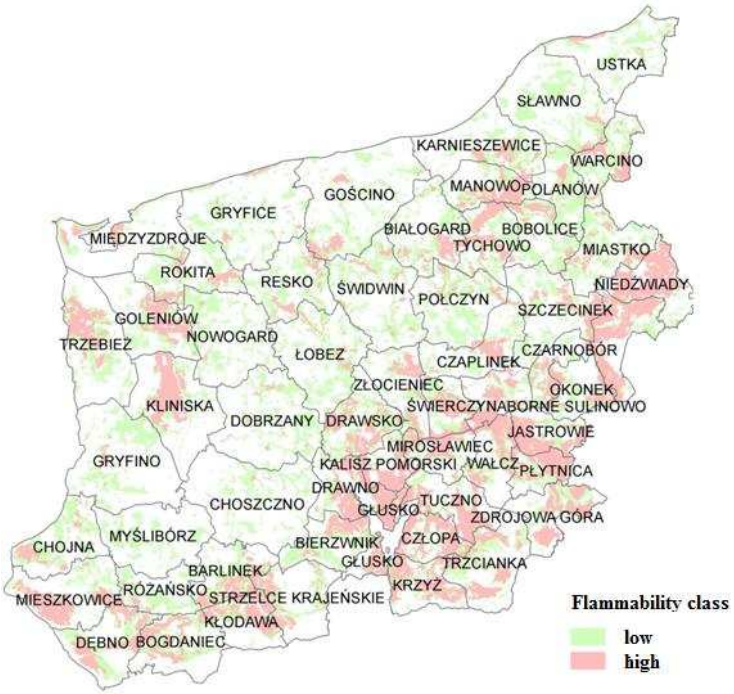

Figure 6. Habitat map according to flammability class indicator in forest districts of Western Pomerania province

At the provincial level 89% conformity was received, relating to surface area of groups of habitats of high flammability. In 39 out of 57 cases the error of designation of percentage of habitats of high flammability class did not exceed 20%. In 4 cases, where this error was greater than 20% it might equally be noted that the total forest surface difference according to Numerical Forest Maps and Corine Land Cover is greater than 21%. One may therefore accept that the difference in percentage participation of flammable habitats may arise from differences of types of habitats of forests contained in the digital forest map and those charted in the CORINE database. From this it results that 76% of forest districts estimated percentage participation of flammable habitats with an error not exceeding 20%. In 44 cases follows the estimation that may equally result from a greater forest area charted in comparison with the CORINE database. Considerable non-estimation, exceeding 30%, was noted only in two forest districts: Barlinek and Kłodawa. Perhaps this results from generalisation of the CORINE database, where small single patches of forest other of mixed and coniferous forest interlaced with each became jointly classified as mixed.

Summary

The method presented above enables the definition of percentage participation of habitats of a high flammability in forests on the basis of generally available low resolution data.
The difference of proportion of flammable habitats in the study area is established according to Forest Numerical Map and the study model is connected with the significant difference in forest area of forests being managed by forest districts being part of this area and areas of forests charted on the basis of Corine data.
Differences in the precision of methods for the study area (Forestry Districts: Dobieszyn, Kozienice, Marcule, Radom and Zwoleń) and the control check area (forestry districts being at least partially in the Western Pomerania province) may suggest that it requires local calibration of thresholds accepted in the method. This may be associated with a different geological substrate and type of terrain shape in both areas, which have an influence on values of indications.

Abbreviation:

BMśw – *fresh mixed coniferous forest*
Bs – *dry coniferous forest*
Bśw – *fresh coniferous forest*
Bw – *moist coniferous forest*
BMw – *moist mixed coniferous forest*
Bb – *bog coniferous forest*
BMb – *bog mixed coniferous forest*
Ł – *riparian forest*
Ol – *alder forest*
OlJ – *alder-ash forest*
Lw – *moist broadleaved forest*
LMśw – *fresh mixed broadleaved forest*
LMw – *moist mixed broadleaved forest*
LMb – *bog mixed broadleaved forest*
Lśw – *fresh broadleaved forest*

References

Moore, I.D., Grayson, R.B., Landson, A.R. Digital. 1991. Terrain Modelling: A Review of Hydrological, Geomorphological, and Biological Applications. Hydrological Processes 5: 3–30.

Pekkarinen, A., Reithmaier, L., Strobl, P. 2009. Pan-European forest/non-forest mapping with LandsatETM+ and CORINE Land Cover 2000 data. ISPRS Journal of Photogrammetry and Remote Sensing 64, 171-183

Szczygieł, R., Ubysz, B., Kwiatkowski, M., Piwnicki, J. 2009. Klasyfikacja zagrożenia pożarowego lasów Polski. Leśne Prace Badawcze 70 (2): 131-141.

Waser, L.T, Schwarz, M. 2006. Comparison of large-area land cover products with national forest inventories and CORINE land cover in the European Alps. International Journal of Applied Earth Observation and Geoinformation 8 (3), 196-207

Zeverbergen, L. W., R. Thorne. 1987. Quantitative Analysis of Land Surface Topography. Earth Surface Processes and Landforms 12: 47–56.

Minimum travel time algorithm for fire behavior and burn probability in a parallel computing environment

Kostas Kalabokidis[a], Nikolaos Athanasis[a], Palaiologos Palaiologou[a], Christos Vasilakos[a], Mark Finney[b], Alan Ager[c]

[a] *Department of Geography, University of the Aegean, GR-81100 Mytilene, GREECE. kalabokidis@aegean.gr*
[b] *USDA Forest Service, Rocky Mountain Research Station, Fire Sciences Laboratory, 5775 Hwy 10 West, Missoula, MT 59808, USA, mfinney@fs.fed.us*
[c] *USDA Forest Service, Pacific Northwest Research Station, Western Wildlands Environmental Threat Assessment Center, 3160 NE 3rd Street, Prineville, OR 97754, USA, aager@fs.fed.us*

Abstract
Fire management systems materialize the integration of fire science models and decision support planning modules. Their operational usage often requires the concurrent execution of a large number of fire growth simulations by multiple users. Intensive computations such as the creation of burn probability maps demand not only high expertise but also high computing power and data storage capacity.
The purpose of this paper is to present some of the initial results of the AEGIS platform, which is a Web-GIS wildfire prevention and management information system currently under development. More specifically, the paper focuses on the utilization of the Minimum Travel Time (MTT) algorithm as a powerful fire behavior prediction system. MTT in AEGIS will be applied in a transparent way through its graphical user interface. Several end users will be able to conduct on-demand fire behavior simulations. To achieve this, end users must provide a minimum amount of inputs, such as fire duration, ignition point and weather information. Weather inputs can be either inserted directly or derived from selected remote automatic weather stations or forecasted weather data maps based on the SKIRON system (Eta/NCEP model).
Seasonal burn probability maps will be also prepared and provided to the end users. Socioeconomic data, weather predictions, topographic and vegetation data will be combined with artificial neural networks to produce an ignition probability map. Based on the ignition probability map, thousands of potential ignition points located in areas of anticipated high risk will be generated. These ignitions will be further used as inputs on MTT simulations, running FConstMTT as a command line-based executable. FConstMTT calculations will be conducted on a parallel mode in Microsoft Azure infrastructure using a different subset of ignition points in each simulation.
The current deployment of the AEGIS platform consists of a number of machines resided on premises and a scalable Cloud Computing environment based on the Microsoft Azure infrastructure. This parallel computing environment ensures high processing power availability and high data storage capacity. During a fire emergency, the scalability of the Cloud can also provide extra processing power and storage, if needed. It is anticipated that by integrating MTT into the AEGIS platform, the firefighting and civil protection agencies will gain great assistance to organize better and more reliable plans for fire confrontation.

Keywords*: Minimum Travel Time (MTT); Ignition Risk; Wildfire Behavior; Burn Probabilities; FConstMTT; Cloud Computing; Web-GIS*

Introduction

Large wildfires break out on an annual basis causing problems for societies and firefighting agencies across several fire prone areas of the world. Information technology provides the means for the utilization of sophisticated solutions on pre-fire management and planning, post-fire effects mitigation and potential wildfire behavior evaluation.

Towards the development of effective fire management operational systems, the integration and utilization of fire behavior and risk models and decision support planning modules plays an important role. Today's firefighting needs demand systems that are able to conduct on a timely manner and without devastating delays multiple concurrent fire behavior predictions for several different users of fire suppression and civil protection agencies involved. However, this kind of operation requires trained and skilled operators with expertise in fire propagation simulation and behavior modeling. In advance, substantial computing resources are required to conduct these intense spatiotemporal calculations; nevertheless, local civil protection agencies often do not own these resources due to limited financial means (Kalabokidis *et al*. 2014).

To deal with the aforementioned issues, the Web-GIS wildfire prevention and management information system AEGIS is currently under development. AEGIS will be a cost effective, easy to use forest fire management system that will utilize the Minimum Travel Time (MTT) algorithm (Finney 2002) as a powerful and sophisticated cell-based tool for fire behavior predictions, fuel treatments and fire risk estimation. The MTT algorithm is applied in strategic and tactical fire management planning throughout the United States (Andrews 2009) integrated into the Wildland Fire Decision Support System (WFDSS) (Pence and Zimmerman 2011). It actually typifies wildfires in the Mediterranean region, which are relatively short in duration with respect to those in the western USA. AEGIS is applied on seven study areas of Greece with different environmental and socioeconomic characteristics.

The scope of this paper is to present some of the initial results of MTT incorporation into the AEGIS platform. MTT in AEGIS is applied in a transparent way through a Web-GIS platform for a single fire simulation. Several end users are able to conduct concurrently on-demand fire behavior simulations by providing a minimum amount of inputs, such as fire duration, ignition point and weather data. Beside the predefined weather data by the user, the simulation can be also based either on real weather data retrieved from Remote Automatic Weather Station (RAWS) of the study area or can be based on predicted weather conditions retrieved from a weather prediction model that supports the platform.

Seasonal burn probability and flame length maps are automatically generated periodically (when the weather pattern is suspected to change), by simulating thousands of possible wildfire ignitions across each study area. Simulations are conducted by applying parallel computer processing techniques of High Performance Computing (HPC) that resides on premises and/or Cloud Computing of Microsoft Azure. ArcGIS Server is utilized for storing the outputs in geo-databases and creating the visualization services that enables end-users to see the results in the Web-GIS platform over high resolution satellite Bing Maps[1].

The Minimum Travel Time algorithm

The MTT algorithm can either compute the potential fire behavior characteristics (spread rate, fireline intensity, time of arrival, flow paths, etc.) for a single fire or burn probabilities/ flame length for the entire landscape from thousands of simulated fires based on landscape data, weather and fuel moisture information. The fire perimeters created by MTT are similar to wave-front expansion (Richards 1990; Finney 2002), but they are mathematically and computationally more efficient. Holding all environmental conditions constant, the MTT algorithm searches for the fastest path of fire spread along straight-line transects connected by nodes (cell corners) (Finney 2006) and it exposes the effects of topography and arrangement of fuels on fire growth (Ager and Finney 2009).

The MTT algorithm replicates fire growth by the Huygens' Principle, where the fire edge growth (and behavior) is a vector or wave front (Richards 1990; Finney 2002). While holding environmental

[1] http://www.bing.com/maps

conditions constant, fire growth calculation exposes the effects of topography and arrangement of fuels on fire growth (Ager and Finney 2009). Extensive testing over the years has demonstrated that the Huygens' Principle, originally incorporated into FARSITE (Finney 1998) and later approximated in the more efficient MTT algorithm, can accurately predict fire spread and replicate large fire boundaries on heterogeneous landscapes (Ager *et al*. 2010; Arca *et al*. 2007; Carmel *et al*. 2009).
In addition to fire spread that is predicted when a new fire spot is provided, MTT has the advantage of producing the burn probability of the entire study area by simulating thousands of potential fires that could burn throughout the area. It permits Monte Carlo simulations of many fires (>100,000), to evaluate burn probability and fire intensity for very large (>2 million ha) landscapes (Ager and Finney 2009). Burn probability is an estimate of the likelihood of a pixel burning given a single random ignition under burn conditions in the simulation. The likelihood measures are required for quantitative risk assessments. Burn probability modeling represents a major advancement in wildfire behavior modeling compared to previous methods, such as those where fire likelihood was quantified with relatively few (<10) predetermined ignition locations. As a result, the product of this process is the burn probability map that reveals which areas are more susceptible to encounter a fire event and which are less.

Methodology

The system architecture is structured by combining different on-premises and Cloud resources. On demand single fire simulations are conducted inside an on-premise Datacenter, while seasonal burn probability outputs are initially calculated in four Virtual Machines (VMs) in the Cloud infrastructure of Microsoft Azure (8x cores machines, 14 GB RAM, 1.6 GHz) and then finalized in an on-premise HPC cluster environment (24x cores machines, 8 GB RAM, 2.9 GHz) that contains 4 VMs. All fire behavior outputs are handled and visualized by using an ArcGIS Server deployment, installed on premises.
For the creation of the burn probability maps, cloud resources are utilized on specific time frames, when the weather pattern is suspected to change. During such a time frame, the VMs in the Cloud are allocated and command line-based executables of MTT (called FConstMTT) are running simultaneously on each VM. On the other hand, on demand fire simulations are better suited to run on premises than in the Cloud. This is because of the significant amount of time overhead (approximately 15 min) required to allocate new VMs in Microsoft Azure. On demand fire behavior simulations need to be conducted instantly and thus, time overheads should be minimized to achieve a timely and effective response when a wildfire breaks out.
After the execution in the Cloud's and/or on-premises VMs, output results are handled by the ArcGIS Server on premises which enables the visualization of the results from the graphical interface of AEGIS (Figure 1).

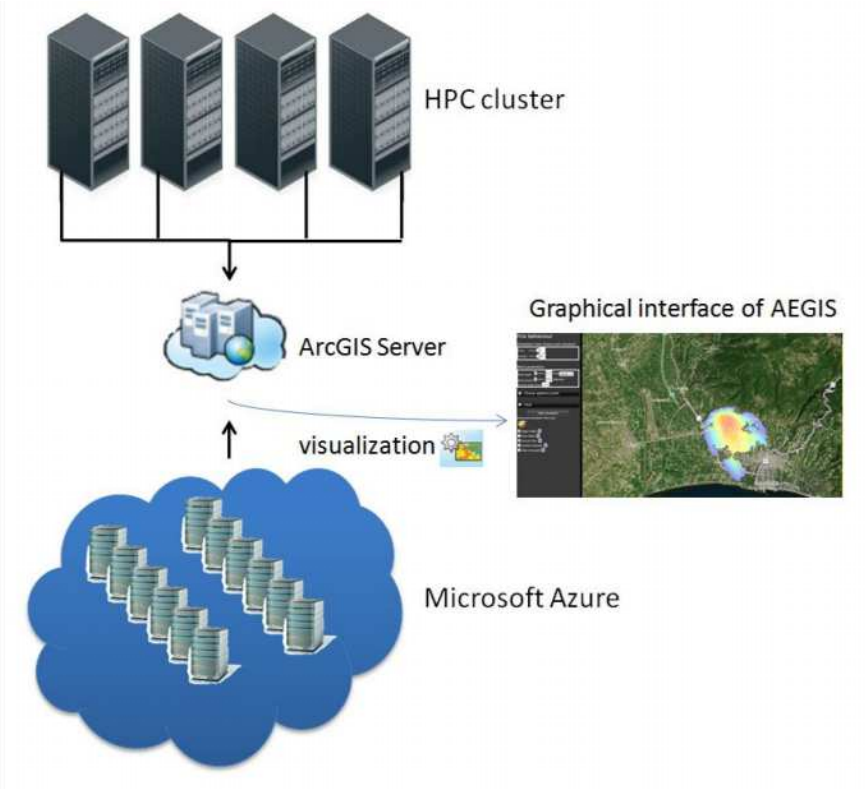

Figure 1. Combining Cloud resources and HPC for simulating fire behavior and burn probability in AEGIS

Running on demand fire simulations

When a new fire simulation is triggered, a command line execution of MTT is starting. If multiple users begin their fire simulations simultaneously, each simulation will be assigned to one of the available VMs and execution takes place in parallel. Before the execution starts, a configuration file is generated on the fly that stores all the necessary input parameters of the simulation (duration, wind speed and direction). Similar to FARSITE simulations, conditional fuel moisture is calculated by providing the corresponding weather and wind files. These files are automatically created if a conditioning period is defined, calculated from RAWS data of the past five days. If the user does not define a preferable RAWS, then the system automatically finds the closest to the fire ignition. Users have also the ability to use forecasted wind data from the closest gridded prediction point provided by the weather forecast prediction model called SKIRON, based on Eta/NCEP model (Kallos *et al*. 1997). Upon the completion of execution, several output files are generated either in ascii format (arrival time, fireline intensity, ignition point and rate of spread) or vector files with information for regular and major flow paths. After the creation of the output files, several ArcGIS Server geoprocessing services are running to transform ascii files to vector and to store them in corresponding ArcSDE geo-database feature classes. Data from different users are separated by providing the user name and execution date and time. Finally, ArcGIS Server mapping services retrieve the appropriate information from the geo-database feature classes, by performing filtering that request's the corresponding simulation outputs and then, visualize them over the AEGIS platform.
In Figure 2, the architecture behind the on demand MTT execution is explained. End users trigger a new simulation (step 1) and then, the first available machine retrieves the input parameters and starts a new process of MTT execution (step 2). Outputs are stored in a shared repository (step 3) from where a geo-processing service retrieves them (step 4), performs the necessary data transformations, adds descriptive information, stores them in a geo-database (step 5) and, finally, notifies the users that the

execution is finished. Visualization of the results is achieved by mapping services directly over the AEGIS graphical interface (step 6).

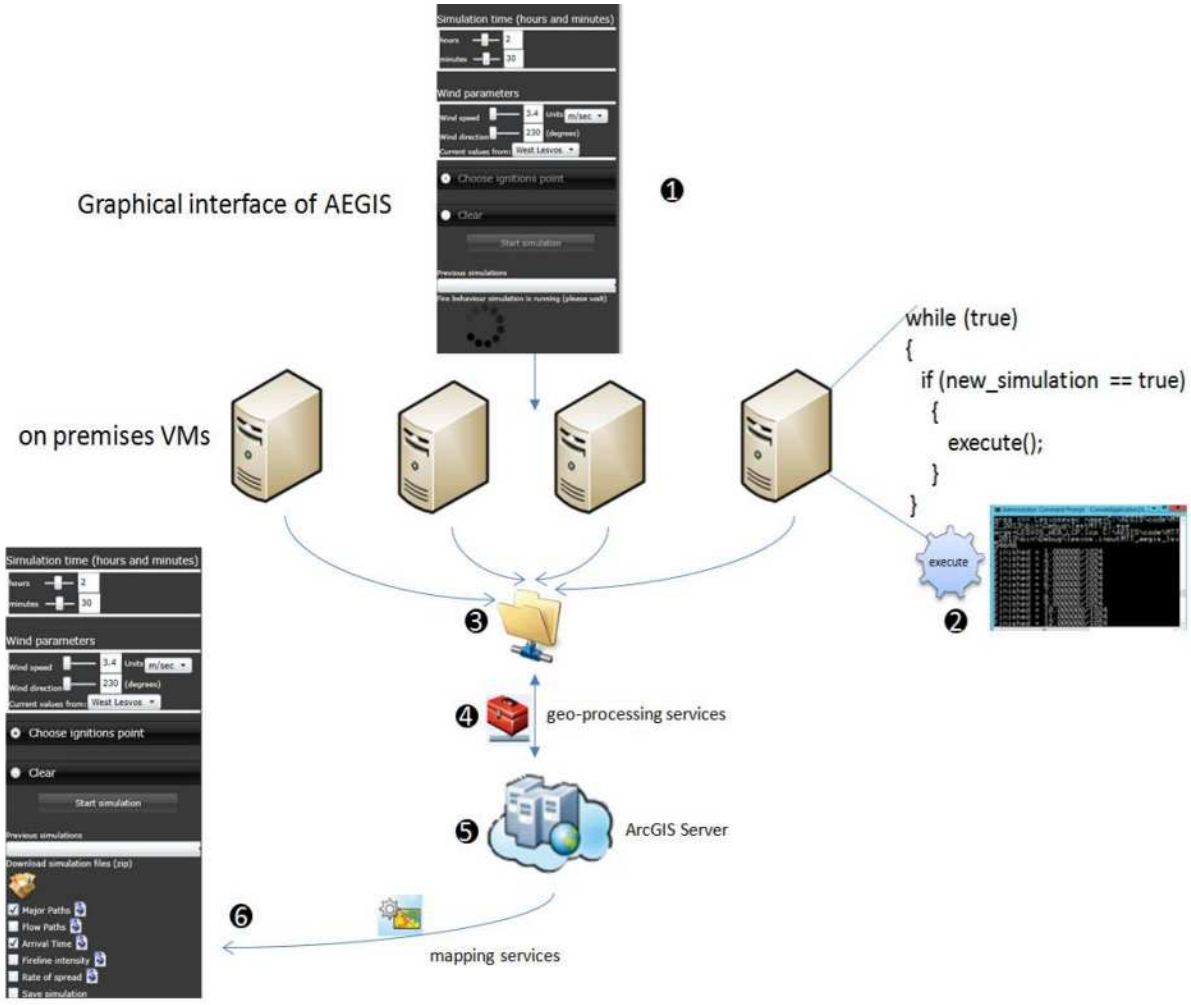

Figure 2. Information flow for on demand MTT simulations

Running MTT for fire burn probabilities

Conducting an on-premise FConstMTT simulation for a single study area takes approximately 24 hrs to be completed (3,000 km^2, 30 m cell size, 100,000 fires). This extraordinary execution time reveals the need for a parallel processing approach, to make the results available on a timely manner for each of the seven study areas. The phases for conducting a parallel processing FConstMTT simulation on Microsoft Azure cloud infrastructure are the following:

1. **Initialization.** A deployment is uploaded in the Microsoft Azure cloud infrastructure. The deployment encapsulates the FConstMTT command line-based executable.
2. **Execution.** Parallel execution of the FConstMTT executable is conducted, by dividing the overall number of ignition points (i.e. 100,000) equally among the available VMs. This partitioning of the ignitions significantly reduces the execution time.
3. **Merging.** The output results are combined into a new ascii text file to calculate the burn probabilities and the flame length categories (i.e. 20 categories) for the entire number of ignitions.

4. **Extraction.** The burn probability and every flame length category are extracted from the merged output.
5. **Visualization.** The extracted outputs are loaded in a geo-database to be visualized through the AEGIS platform. Furthermore, outputs are available for download from the end-users to perform meta-analysis on them (e.g. with ArcFuels).

At the initialization phase, a .NET deployment is uploaded in the Microsoft Azure cloud. The deployment encapsulates the FConstMTT binary executable. Once the deployment has been uploaded, execution of the executable is starting concurrently in four VMs in the Cloud. Each of the VMs starts a new process that initializes the executable. With a total number of 100,000 ignition points, each of the VMs is running FConstMTT with 25,000 of them. Every FConstMTT calculation produces a flame length probability file that contains for each calculation point the corresponding burn probability and flame length probabilities for each of 20 flame length classes. Currently, the ignition points are generated randomly across each study area. However, it is planned to locate the ignition points based on an ignition probability map in areas of anticipated high risk. Socioeconomic data, weather predictions, topographic and vegetation data will be combined with artificial neural networks (Vasilakos *et al.* 2007; 2009) to produce a daily fire ignition probability map.
After the parallel execution of the executables, the intermediate results are combined together and merged. For this merging, the calculated burn probability is transformed to total numbers of burnings on each pixel, a methodology described in Kalabokidis *et al*. (2014). If t1, t2, t3 and t4 are the total numbers a pixel is burned from each FConstMTT calculation, the mean burn probability (BP) for each pixel is calculated as:

$$BP = \frac{(t1 + t2 + \cdots + tN)}{(f1 + f2 + \cdots fN)} = \frac{\Sigma_{i=1}^{N} t_i}{\Sigma_{i=1}^{N} fi} \qquad (1)$$

where:

- N is the number of the available machines in the Cloud (in the current deployment N = 4)
- fi is the fraction of the total fire ignition points (in the current deployment f = 25,000)
- t_i is the partial number of burnings, calculated at the i^{th} VM.

In a similar way, the mean flame length probability (FLP) for each flame length category is calculated as:

$$FLP = \frac{\Sigma_{i=1}^{N} ti}{BP} \qquad (2)$$

Given the FLP, the conditional flame length (CFL) is calculated as:

$$CFL = 0.25 \times FIL1 + 0.75 \times FIL2 + 1.25 \times FIL3 + \cdots + 9.75 * FIL20 \qquad (3)$$

After the calculation of the (1), (2) and (3) for each pixel of the study area, the values are stored in a file with the following structure:

XPOS,	YPOS,	BP	FLP1,	FLP 2,	…	FLP 20,	CFL
X_{ij},	Y_{ij},	BP_{ij},	FLP 1_{ij},	FLP 2_{ij},	…	FLP 20_{ij},	CFL_{ij}

From this merged file, 22 separated ascii output files are generated (one output file for the burn probability, 20 output files for the flame length probabilities and one CFL output file). This extraction takes place in parallel on the HPC cluster environment. Each machine reads the merged file, extracts and transforms one of the categories in a corresponding file. Every file contains three columns: the latitude and longitude of the ignition point and the value of the corresponding category. After the extraction, the GDAL/OGR utility is used to convert each file to raster format. Geo-processing services

retrieve the raster files and store them in a corresponding geo-database to visualize them over the AEGIS graphical interface through corresponding mapping services. In Figure 3, the information flow for the creation of a seasonal burn probability map in AEGIS is presented. At a specific time, the deployment is uploaded from one of the on-premises machines to the Cloud (step 1). Execution starts concurrently at available VMs (step 2). Partial output results are created and a merged file is generated that stores all values for all output categories (step 3). From the merged file, all output categories are extracted in separated output files (step 4), converted to raster files (step 5) and stored in a geo-database (step 6) for visualization purposes (step 7).

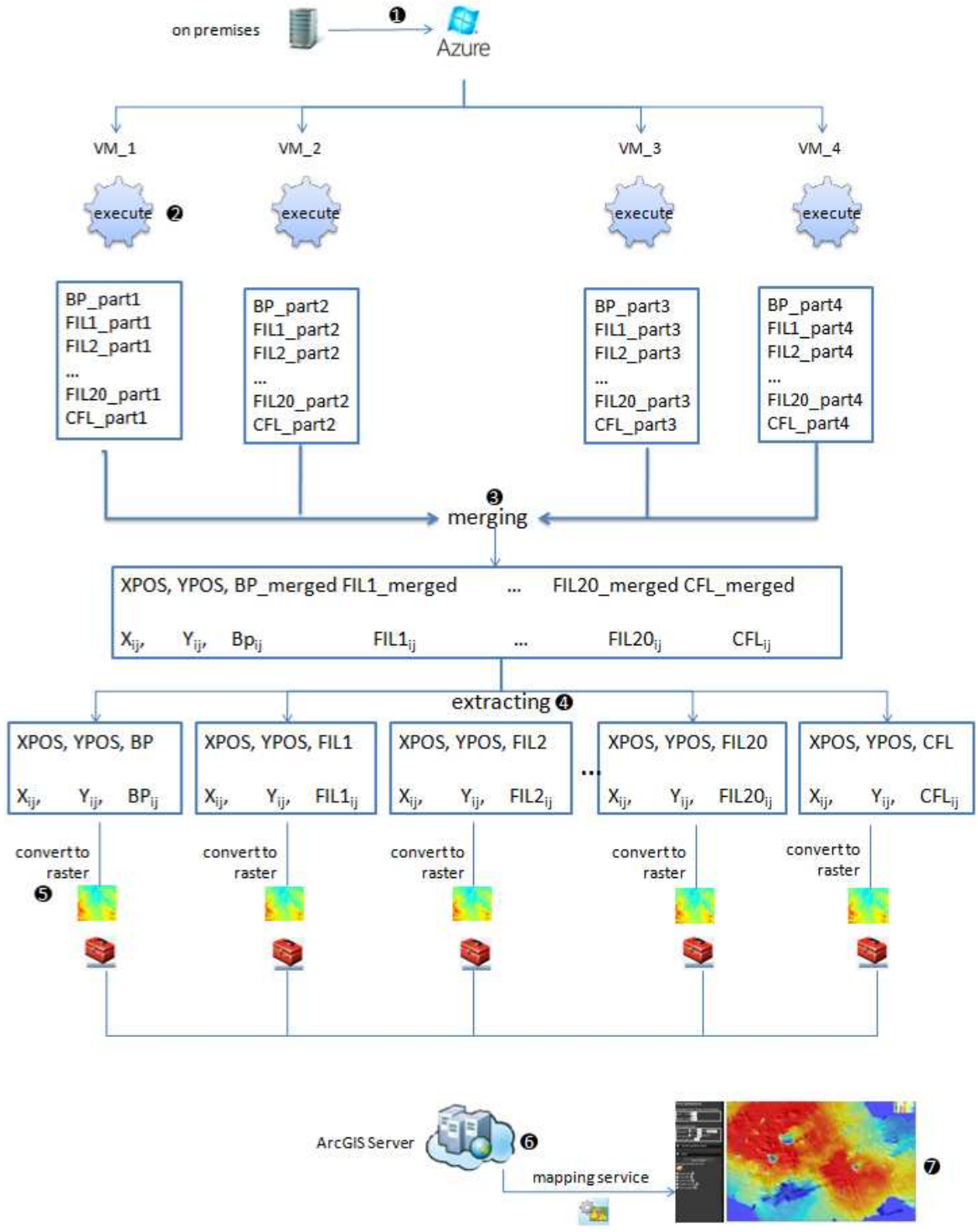

Figure 3. Information flow for the conduction of burn probabilities maps

Visualization of MTT results in AEGIS

Authorized users of AEGIS are able to conduct new MTT simulations or view older stored simulations. If the user decides to conduct a new simulation, the ignition point and the duration time (hrs and min) of the simulation must be specified. The duration time cannot exceed six hrs, since MTT provides better simulations for short term time periods. Real-time wind parameters (speed and direction) are retrieved from RAWS of the study area or can be user-specified to conduct "what if" scenarios simulations. After providing the required inputs, users can trigger the "Start Simulation" button. The platform steadily provides information about the status of the simulation for as long as the execution is in progress. At the end of the simulation, all outputs can be directly visualized over the AEGIS platform by enabling a checkbox next to each mapped attribute. Individual output files can also be downloaded as kml layers or alternatively, can be downloaded in their raw format as a zip file (flow paths, major flow paths, fireline intensity, rate of spread, time of arrival and ignition point). In Figure 4, a visualization of MTT fire simulation from the AEGIS GUI is portrayed (arrival time and major flow paths). Simulation time was set to three hrs, while wind data were retrieved from a nearby RAWS. The check box "store the simulation" is used to store the simulation in the simulations archive.

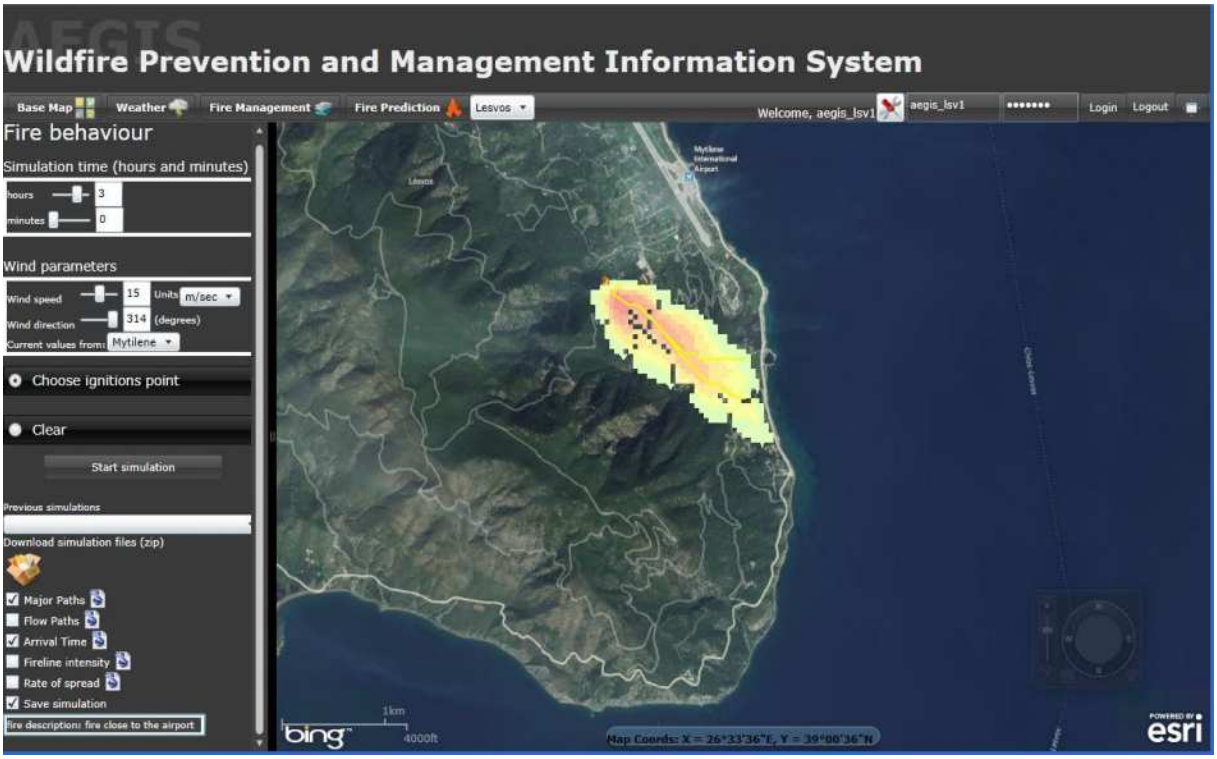

Figure 4. Visualization of on demand MTT results in AEGIS

Seasonal FConstMTT outputs can be visualized by selecting the desired attribute (mean burn probability, conditional flame length and each flame length class probabilities) from a drop down menu (Figure 5).

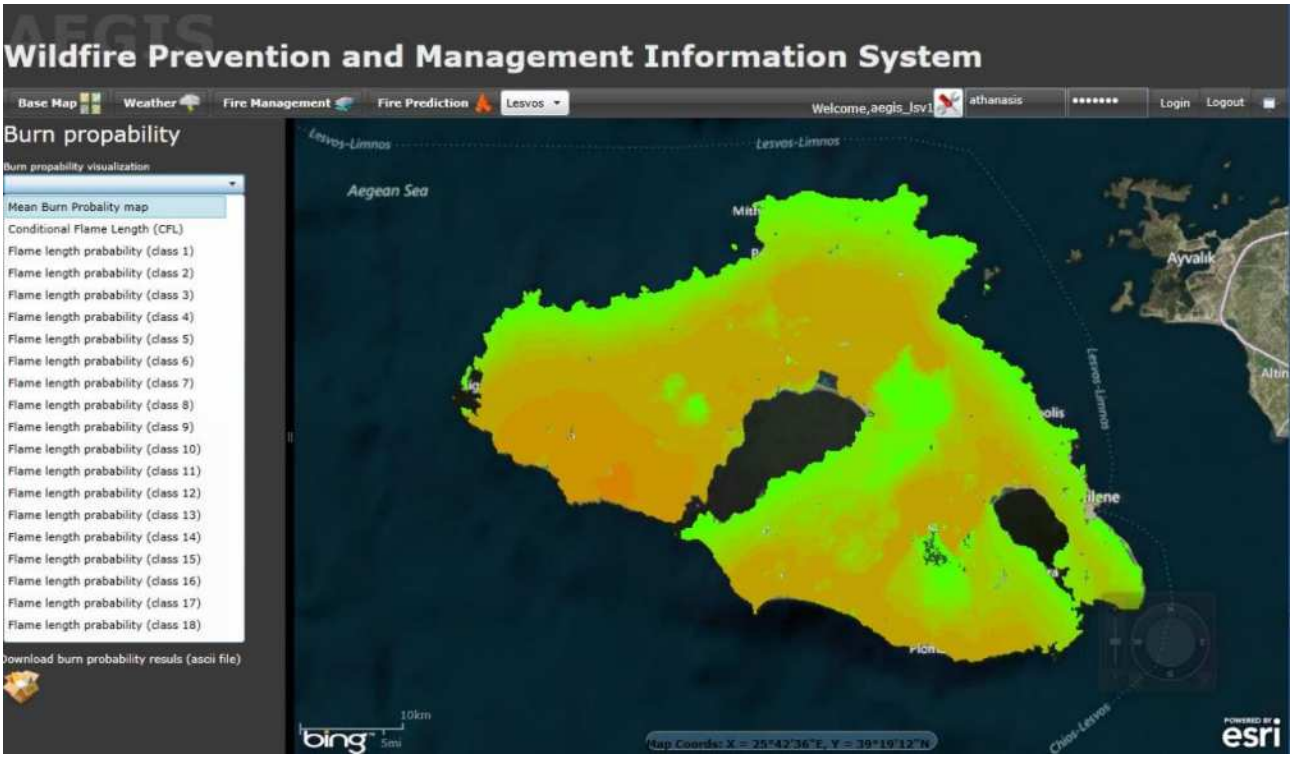

Figure 5. Visualization of burn probabilities in AEGIS

Conclusions

This paper describes the utilization of the fire behavior prediction algorithm of Minimum Travel Time (MTT) algorithm in the AEGIS platform. Calculations are conducted in a parallel computing environment, combining Cloud and HPC resources. More specifically, on demand fire simulations are conducted on premises, while seasonal burn probability maps are first conducted in the Cloud infrastructure of Microsoft Azure and then finalized in the HPC cluster environment. This combination of cloud and HPC resources provides the means to produce useful fire prediction maps without devastating delays.

On an operational basis, the system's functionalities may assist local authorities of wildfire management to extract useful information towards the design of an effective operational wildfire prevention and management plan. Fire behavior predictions are visualized through the web-based front end of AEGIS, eliminating the need to install special desktop software. Users have the ability, without the requirement of knowing the handling of complicated fire management systems, to integrate fire science models and decision support planning modules and to utilize the capabilities of the system.

The visualization of burn probability maps can reveal which areas are more susceptible to encounter a wildfire event. Furthermore, multiple on demand simulations can be conducted simultaneously by changing the weather parameters and simulate different "what if" scenarios. During a fire emergency, the fire behavior can be easily simulated by integrating real time weather measurements. The computation architecture follows the software design principles of parallel processing of high performance computing and cloud computing. All software modules are developed in the .NET language. Execution requires also third-party software of the MTT binary executables. By integrating MTT into the AEGIS platform for all seven study areas of AEGIS, firefighting and civil protection agencies may gain a great assistance to organize better and more reliable plans for fire confrontation.

8. Acknowledgments

The research project “AEGIS: Wildfire Prevention and Management Information System” {Code Number 1862}, is implemented within the framework of the Action ARISTEIA of the Operational Program "Education and Lifelong Learning" (Action’s Beneficiary: General Secretariat for Research and Technology), and is co-financed by the European Social Fund (ESF) and the Greek State. Final results and outcomes of the project are expected by September 2015.

9. References

Ager, A.A. and Finney, M.A., 2009. Application of wildfire simulation models for risk analysis. *Geophysical Research Abstracts*, **11**, (2009) (EGU2009-5489, 2009; EGU General Assembly 2009).

Ager, A.A., Vaillant, N.M., Finney, M.A., 2010. A comparison of landscape fuel treatment strategies to mitigate wildland fire risk in the urban interface and preserve old forest structure. *Forest Ecology and Management*, **259**, 1556-1570.

Andrews, P.L., 2009. BehavePlus fire modeling system, version 5.0: Variables. USDA Forest Service, Rocky Mountain Research Station, General Technical Report RMRS-GTR-213.

Arca, B., Duce, P., Laconi, M., Pellizzaro, G., Salis, M., Spano, D., 2007. Evaluation of FARSITE simulator in Mediterranean maquis. *International Journal of Wildland Fire*, **16**, 563-572.

Carmel, Y., Paz, S., Jahashan, F., Shoshany, M., 2009. Assessing fire risk using Monte Carlo simulations of fire spread. *Forest Ecology and Management*, **257**, 370-377.

Finney, M.A., 2002. Fire growth using minimum travel time methods. Canadian Journal of Forest Research **32**, 1420-1424.

Finney, M.A., 1998. FARSITE: fire area simulation model development and evaluation. USDA Forest Service, Rocky Mountain Research Station, Research Paper RMRS-4.

Finney, M.A., 2006. An overview of FlamMap fire modeling capabilities. In: Proceedings of Fuels Management-How to Measure Success, Portland Oregon, USA, 28–30 March, pp. 213-220.

Kalabokidis K., Athanasis N., Vasilakos C. and Palaiologou P., 2014. Cloud Computing in Geospatial Analysis of Wildfire Danger and Fire Growth. In Wade DD & Fox RL (Eds), Robinson ML (Comp): Proceedings of 4th Fire Behavior and Fuels Conference, 18-22 February 2013, Raleigh, NC, USA and 1-4 July 2013, St. Petersburg, Russia. Published by the International Association of Wildland Fire: Missoula, MT, USA. pp. 457-467.

Kalabokidis, K., N. Athanasis, C. Vasilakos, P. Palaiologou. 2014. Porting of a wildfire risk and fire spread application into a cloud computing environment. International Journal of Geographical Information Science, **28(3)**, 541-552.

Kallos, G., Nickovic, S., Papadopoulos, A., Jovic, D., Kakaliagou, O., Misirlis, N., Boukas, L., Mimikou, N., Sakellaridis, G., Papageorgiou, J., Anadranistakis, E. Manousakis, M., 1997. The regional weather forecasting system SKIRON: An overview. In Proceedings of the International Symposium on Regional Weather Prediction on Parallel Computer Environments, Athens, Greece, pp. 109-122.

Pence, M., Zimmerman, T., 2011. The wildland fire decision support system: Integrating science, technology, and fire management. Fire Management Today **71**, 18-22.

Richards, G.D., 1990. An elliptical growth model of forest fire fronts and its numerical solution. *International Journal for Numerical Methods in Engineering*, **30**, 1163-1179.

Vasilakos, C., Kalabokidis, K., Hatzopoulos, J., Kallos, G. and Matsinos, Y., 2007. Integrating new methods and tools in fire danger rating. *International Journal of Wildland Fire*, **16(3)**, 306-316.

Vasilakos, C., Kalabokidis, K., Hatzopoulos, J. and Matsinos, Y., 2009. Identifying wildland fire ignition factors through sensitivity analysis of a neural network. *Natural Hazards*, **50(1)**, 125-143.

Modelling of fire managers' decision making method

Agoston Restas

National University of Public Service, Budapest, Hungary, Restas.Agoston@uni-nke.hu

Abstract
During fighting against forest fires the situation can change quickly, thus, managers must also be ready to change the strategy and tactic. Firefighting managers have a typical profession, during which – depending on the time – making both analytical and naturalistic decision. Trainings usually focus on traditional – analytical based – decision making, which takes time, however, in many cases there is not enough time to do that. Therefore managers make many times recognition-primed decisions as a symbol of naturalistic decision-making. The first part of this article gives a thorough review of the topic. The second shows a simple and a complex model, created by the author. Method: the author used different tools and methods to achieve his goals; one of them was the study of the relevant literature, the other one was his own experience as a firefighting manager. Other results come from two surveys that are referred to; one of them was an essay analysis, the second one was a word association test, specially created for this research. Results and discussion: the author created a simple and a complex model for firefighting managers making decisions, taking into account time pressure, the limited capability of processing information and also a mechanism complementing the recognition-primed decision.

Keywords*: decision making, fire managers, recognition primed decision, model for making decisions in emergencies*

Introduction

The background of recognition of a special decision-making mechanism in the focus of this paper was given that, in some cases, no sufficient time is available, necessary for classic decision-making. Therefore, strategists sought to design and plan the details of military operations in advance, just as today, however, their proper implementation, the application of different decision support instruments in live situations, designed for optimal decisions, failed many times in spite of these. Decisions made in reality, e.g. fighting against forest fire are often not harmonized, could not be harmonized, considering the circumstances, with the pre-formulated strategies, mostly because there was not enough time needed to achieve them.
In the paper, author illustrates the limits of the possibilities of analytical decision-making, presents the general operating mechanism of recognition-primed decision-making, elaborates on its special model relevant to firefighting managers, as well as explores and systemizes the factors that facilitate (catalyze) the processes.

Characteristic circumstances of emergency interventions

An important element of the activities of emergency responders is that they cannot or only to a very limited extent can modify the terms of the task, improve them as desired. Despite the differences of environment, indications of the *complexity* of the situation, the possibility of the *radical change* in the given situation, *uncertainty* and *ambiguity* of the information available can be recognized and well identified. During fighting against forest fire the weather condition can change radically – for this, a typical example is the change of wind direction –, the accessible resources, because of the intensive plum convection can be new hot spots also behind the existing fire fronts, firefighters can be injured seriously or can fallen in trap requiring help immediately.

The peculiarities of each specialized branch can be illustrated through the examples of several authors: Klein dealt with the analysis of the decision circumstances of the military also using the examples of firefighters (Klein, 1989), Killion took examples from the navy (Killion, 2000), Bruce shows his own medical case (Bruce, 2011), Johansen simplifies difficult circumstances (Johansen, 2007).
Most of above factors are present; occasionally all of them may be present at a certain level of emergency decisions: including the strategic, operational and tactical levels, but certainly with a different focus or at different times. On strategic and operational level, in general, not only more time is available, but also human and technical resources are at hand more broadly, and decision support instruments as well to reduce uncertainties occurring.
The extinction of fire in a smaller grass land requires the implementation of a completely different, simpler scope of tasks than to control forest fire in an extra dry weather period and high articulated area. The different scopes of tasks exist in different environments and structures, so the solution of similar basic problem also exists in other dimensions. Based on author's own experience, the more extensive case we are dealing with in time, space and from the aspect of involvement in the incident, the more the above factors cumulatively prevail, but because of the protracted implementation, it is, however, easier to solve them.
The most limiting factor from the above is *time*, proven also in author's own studies. This provides a framework impossible to burst and a forced drift, a *pressurized channel* for the decision-maker, entangled in which one can no longer break free.

3. General model of recognition-primed decisions

The above proves that, in certain situations, the multi-criteria, analyzing, evaluating decision-making simply cannot be used or in a limited manner. However, it can be seen that managers, directors or commanders are many times in situations that they simply *cannot elude from their decisions*; they should make them in a short time. The functional background of decisions made in a short time, their mechanism different from the conventional was first studied in depth by Klein, who gave the name *recognition-primed decision* to this special decision procedure (Klein, 1989).
Author refers, at the general model of recognition-primed decisions, mostly to Klein's work (Klein, 1989; Klein, 1999), which is analyzed by Cohen with others from the direction of critical thinking (Cohen *et al*., 1996). Killion supplements and combines with his multi-aspect decision-making model, (Killion, 2000). Based on Klein's work, the essence of recognition-primed decisions is that the decision-maker, through his previous experience, has several different solution schemes in his mind, which he is capable of recalling in a new situation from memory. The decision-maker immediately applies the first pattern that matches the typical features of the given problem of, that is to say, makes decisions fast as a result of previous experience.
Supplementing the general model with the assessment of action versions, we receive the model of *analysis of possibilities* (Killion, 2000). In this case, if the action version is not satisfactory, a new action version will be modified or assessed. If the decision-maker has a significantly longer time to assess his concepts, naturally within the framework offered by a recognition-primed decision, there is the possibility to assess on the level of critical analysis (Cohen *et al*. 1996), or according to options characterizing analogical thinking (Killion, 2000).
Recognition-primed decisions do not exclude the possibility to amalgamate conventional, analyzing decision-making (Killion, 2000; Radnóti & Faragó, 2005). At complex tasks, where a given situation is examined from several aspects – and choose from the options with analogical thinking – recognition-primed decision-making can be automatically applied by experienced decision-makers while solving some partial tasks to reduce the time of the decision process.
The above issues harmonize with the observation that decision-makers simplify complex problems, i.e. create partial problems, until the elements broken down become manageable and resolvable (Simon, 1960; Paprika-Zoltay, 2002). By enlarging its interpretation range, of course, we can reach

the point where the decision-maker may say the problem does not exist until he sees its solution (Duggan, 2002), or the problem does not exist at all if it does not have a solution (Ribárszki, 1999). Many times we can see that forest fire managers come face to face with fire and without any time of thinking they are able to give instructions immediately. We say, routine works but it means they use schemes rather than making ad-hoc decision.
It springs forth from the above that the relative position of multi-aspect decision-making and recognition-primed decision-making is not constant. Recognition-primed decision can be the partial process and decision unit of analogical thinking. In this case, the main decision-making mechanism is analogical thinking; recognition-primed decision is the additional element.

Decision-making mechanism of a firefighting manager

Limited time frame allows the elaboration and management of limited amount of information. We know from Miller's researches that the *short-term memory* of the vast majority of people can only process simultaneously 7±2 units of information (Miller, 1956). This information, of course, can be quite different, e.g. a characteristics of fire, the capacity of the response unit, a number, or even the absence of information searched. Our memory handles the combinations, "operations" between the information units as information units (Ribárszki, 1999), from which clearly springs forth that the capacity of the short-term memory of a firefighting manager is exhausted very quickly.
Author has proven by essay analysis how complex the tasks of emergency responders are (Restas, 2013); this shows that in several cases, simultaneously, there is or would be a need to process many more units of information than the capacity of our short-term memory would allow. *The maintenance of our decision-making capability, i.e. our short-term memory, based on the above, clearly requires that we should omit analyzing and evaluating decision-making processes protracted and use the recognition-primed decision-making procedure, based on previous experience.*
Author wishes to create a model element to demonstrate the decision-making mechanism of firefighting managers, which takes into account the limits of the simultaneous processing of information, that is, it also illustrates *Miller's decision-making capacity*. Since the information units may be qualitatively independent of each other, author choses the simplest *graphical representation of the unit-based discrete difference* to separate them from each other. A model element must be such, which can graphically demonstrate the schemes based on earlier experience, the characteristics of different fires, and the interlocking of the former as the application of the scheme, which represents the technically correct solution of the task, i.e. effective decision. The model refers, at the general model of recognition-primed decisions, mostly to Klein's work (Klein, 1989; Klein, 1999).

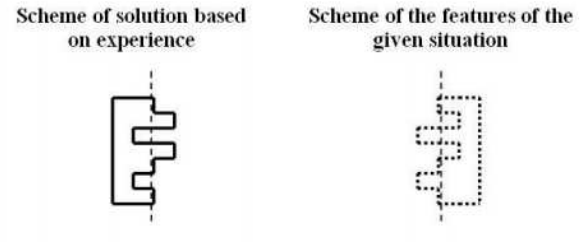

Figure 1. Graphic representation of the empiric scheme of recognition-primed decisions matching a given situation

The schemes in figure 1 represent 7 graphical discrete values each, which are marked by positive or negative protrusions and their "center line"; these values indicate the amount of simultaneous decision-making capacity. Thus, the "negatives" of the schemes can be matched as a given situation and the solution necessary therefor. As an integration of above processes, decision mechanism functions as

follows: an experienced firefighter has performed the elimination of a large number of and forest fires. Despite the fact that as far as the parameters each forest fire is different from another, some characterizing features can be well conceived (figure 2).

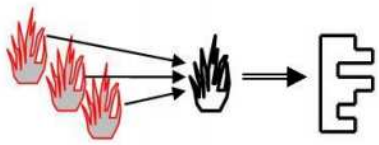

Figure 2. Evolvement of the scheme on forest fire

The characterizing features of identical types of fires are crystallized by experience, and are fixed in our *long-term memory*. Similarly, to the characteristics of a forest fire, the characteristics of successful extinguishing, the facilitating decisions are also fixed (figure 3); just as the mistakes desired to be avoided and the unsuccessful procedures and failures. Experience gained through many years, based on the features of forest fires, formulate the system of schemes, behind which we can find actions (decisions) efficiently applicable to eliminate them.

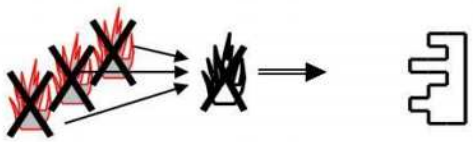

Figure 3. Evolvement of the scheme on the lessons learnt from extinguishing a forest fire

If another incident has almost the same circumstances as one already many times successfully eliminated by a firefighting manager previously (model of positive confirmation), he will attempt to use the same ones in the procedures. Therefore, another fire, quasi bearing the typified properties of previous similar fires, a decision-maker involuntarily immediately recalls the typified decisions in his conscience. The properties of a fire and of previous successful extinguishing operations, based on the above, are closely interlinked; they are each other's "reflections" (figure 4). Author proved with the results of association studies that the above, i.e. the characteristics of a fire and the thoughts directed towards its extinguishing, the schemes of response, in the case of firefighters, are very closely connected in a complex way (Restas, 2013).

When a firefighting manager identifies a fire, he imagines what would happen if he applies the usual tactics to fight it. If the scheme of solution matches, he accepts it, if not, he rejects it and thinks of the next most typical action. Thus, it is a recognition-primed, model-matching process, which can be followed by a quick and almost automatic decision. The above process is naturally not limited only to forest fire managers; it can be used more broadly to firefighting managers.

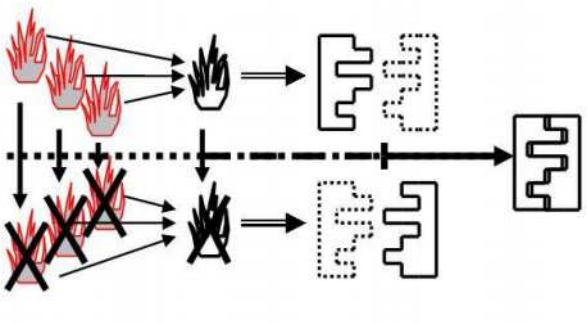

Figure 4. Aggregated scheme on fire and the evolvement of the lessons learnt from extinguishing it

The amalgamation of previous schemes into a given incident is shown in figure 5. The long-term memory of a firefighting manager, through practical experience, has the schemes of both different fires and their extinguishing characteristics. During another alert, information available and collected on a fire automatically generates the recollection of the scheme necessary to solve it, based on which a firefighting manager defines the firefighting tactics necessary. However, the results of association studies clearly point in the direction that at a given fire (problem) managers do not focus on the fire as a problem but rather on its immediate solution (Restas, 2014). From this, author makes the conclusion that a decision-maker will not follow the change of the characteristics of a fire, but the validity of solution scheme, that is, the dynamics of the implementation of the extinguishing process. This does not mean a contradiction with the previous, but rather a difference in views, the shift of emphasis of the focus of attention.

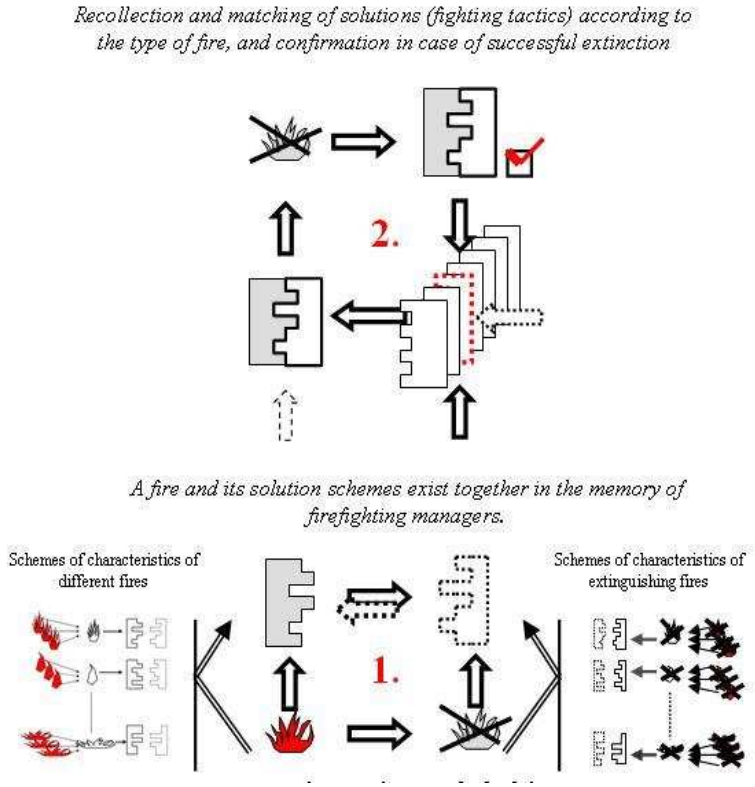

Figure 5. Decision-making mechanism of a firefighting manager

The difference in views, that is, the shift of emphasis means that a firefighting manager does not focus on the change of characteristics of a fire, but rather on the expected evolvement and dynamics of the scheme selected, i.e. extinguishing tactics. Based on the previous, these are, of course, inseparable from each other; however, author finds the dominance of the interventions trend in the results of association studies in the case of firefighters so strong that, based on it, author judges his above conclusion to be justified.

The above do not contradict Klein's model, they rather complement it. Klein, in his model, evaluates (imagines what will happen) the results of matching schemes by the decision-maker prior to performing action version, which, based on author's own experience, is so without doubt, however the aftermath of the decision, in author's opinion, is much more significant in case of firefighting managers. Since the problem immediately and automatically generates both the direction of the solution and start of the action version, rather the process itself is important in terms of efficiency, which is caused by the decision. The schemes based on experience certainly contain the information on the dynamics of the process of fire, so if it meets the expectations, we do not have to modify the original firefighting tactics. However, if the dynamics of the process does not suit the expected, the

change is inevitable in the performance of efficiency. Based on the above, the recognition-primed decision is not just an individual act before extinguishing the fire, but it is also the continuous accompaniment as needed. By doing this, author shares the view that the experienced decision-maker perceives the problem together with its solution, furthermore, author extends the continuous co-existence of the problem and of the whole process of solution of an emergency (firefighting and technical rescue).

Mechanisms complementing a recognition-primed decision

5.1. Triggers

Different triggers, internal resources ensure the operation of recognition-primed decisions. Klein, in his work, assumes 5 markedly distinct abilities, these are *intuition*, *imagination*, *perception of the invisible*, the *ability to formulate, metaphors* and *analogies* (Klein, 1999). In the joint work of Cohen, Freeman and Thomson (Cohen *et al*., 1996), draws the attention to the importance and benefits of critical thinking as criticism of actions planned by ourselves.

Despite the fact that one could assume, based on the previous issues, that recognition-primed decision-making enjoys exclusivity on a tactical level, it is absolutely not true. We can compare it with several fires or incidents, still, one of the essential features is that it protracts in time. It allows the decision-maker to think through the situation, collect information, develop action versions and consider. Not just forest fires but peat fires, or in many cases, fires of storage facilities or other hall-type buildings, burning for several hours or days and covering a large area are categorized specifically into the above types. During protracted decision-making, the recognition-primed processes, based on author's experience, proved to be irreplaceable assistance rather in solving partial tasks.

5.2. Analytical thinking

Killion sees the combination of recognition-primed decision-making with the analyzing and evaluating procedure in two ways (Killion, 2000). In both cases, the conditions are that adequate time should be available for analyzing the options. In the first case, prior to recognition-primed decisions, focusing on the given circumstances, we set up options and analyze them. In the second case, a more detailed analysis of the action version of our recognition-primed decision may take place. In the latter case, the spectrum of the task is obviously significantly narrower than in the first case. The two mechanisms, depending on the situation, can be harmonized or one of them may become predominant.

The observation of the elemental parts of multi-aspect decision-making shows that decision-makers divide complex problems to smaller and smaller partial problems until they become such a basic level problem that a decision-maker is able to solve even with little effort (Simon, 1960). This latter process can also be a recognition-primed decision-making, but logically we can find Duggan's view (2002), previously referred, at the end of thought list, according to which successful decision-makers not perceive a problem until they can solve it.

5.3. Critical thinking on tactical level

Cohen, Freeman and Wolf studied the possible decision support role of critical thinking on a tactical decision-making level (Cohen et. al., 1996). In their work, active naval officers and case reports were studied based on which they state that experienced emergency decision-makers, in new situations, using their previous experience, make decisions with help of recognition-primed mechanisms.

Cohen's model explains in detail the critical analytical strategies that contribute to the operation of recognition-primed thinking. Systematic situation models often based on informal narratives as schemes organize our information in cause and effect relationship in individual cases and underpin the development of recognition-primed thinking.

One of the most important elements of Cohen's model is the quick test. A quick test is a higher-level control mechanism for critical analysis and its accuracy. Its recognition strategies are formed, similarly

to other decision-making processes, by the success or failure experience of past events. The complex recognition mechanism comes to the fore when the demand on time and resources for critical analysis is overweighed. It is possible in three well-definable cases (Cohen *et al*., 1996). *A quick test considers the conditions in the light of the above factors, and if they appropriate, prevents recognition-primed decision, and focuses on critical thinking. When circumstances are not adequate, a quick test will allow for an instant reply.* (Cohen, 1996).

5.4. Satisfactory procedure mechanism

We have seen previously that a firefighting manager's time, just as the time of other decision-makers in an emergency to make a decision is limited. Since this time limit precludes the possibility to carry out the necessary analyses of the classic model, objectively the choice of an optimum option is not achievable for a decision-maker[1]. In response to the difficulties of the collection of information and the reduction of the costs in relation, a decision-maker does not strive for optimum results, but, depending on the circumstances, settles for satisfactory solutions.

The above process, unlike analytical thinking, is enforced by several factors. Some of these factors are the impossibility of obtaining all information necessary to select the best solution, or the shortage of time; the latter induces a compulsion of decision-making. The limited nature of the processing information available is also of significant influence. Filtering of information and by this the selection of response to the tasks is necessary because the capacity of our short-term memory is quite limited. According to Miller's studies, it allows the parallel processing of only 7 ± 2 bits of information at one time (Miller, 1956). If a firefighting manager made all the basic decisions, his decision-making capacity would be immediately exhausted at a complex firefighting task.

Despite the small capacity, thanks to recognition-primed mechanisms, correct decision is made in most cases (acceptable, given the effectiveness of firefighting). A firefighting manager, using his experience, in situations not requiring decisions different from the previous solutions, implement automatic measures, protocol procedures, thus continuously maintains his decision-making capacity. In this case, using his own experience, a firefighting manager is not interested in by which series of best elementary decisions he can eliminate fires, but only in satisfying the conditions of professional firefighting through the decisions made as a whole.

5.5. Decisions by exceptions

The aim of the application of the method is that the leadership responsibilities of managers should be drastically reducible; its essence is that we should only intervene into processes having permanent characteristics in majority, if they cross the pre-specified lower and upper limits. The method developed later (management by sensitive exception), so derived from the dynamics of the processes, the necessary interventions are now possible even before crossing the borders (Hoványi, 2002). The method of management (decision) by exceptions, based on author’s experience, is the greatest help for a firefighting manager to continuously maintain his decision capacity. It can appear in different ways, like protocol procedures, individual way of speaking, silence approval, peripheral vision, information-processing in zones.

The experience and competence of the persons performing a given activity allows that every firefighter make his basic decisions in his own field of work. This shows the arrangement in zones of information processing (figure 6). Of course, not every incident or moment requires response. This zone does not require action that is practically ignored by a firefighter, because it is a natural consequence of extinguishing. A significant part of problems outside the zone, as a result of a firefighter's decision in

[1] Except the single case when the random choice exactly coincides with the decision made with the method of analysis. Its magnitude can be identified through statistical methods.

that location, is solved by intervention (firefighting), this information now reaches the firefighting manager, but he usually does not require a decision yet. A firefighting manager manages the problems outside this zone that exceed the decision-making competence of subordinate firefighters. This originates in the fact that, on the one hand, based on the information from reconnaissance and radio traffic, he can create a comprehensive and dynamic picture of the entire process, the evolvement of fire or the efficiency of extinguishing, on the other hand, legislation entitles firefighting managers to take actions.

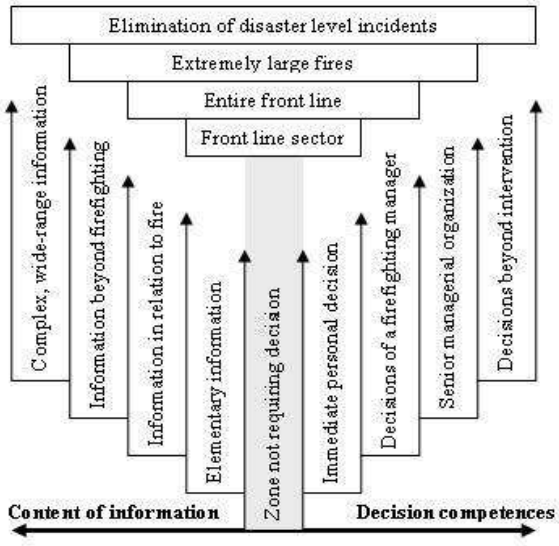

Figure 6. Decisions based on exceptions

5.6. **Creativity**

Creativity has many definitions. Munteanu, in one of his works, presents 35, which approach creativity in different ways, however, there is no single definition generally accepted or used, either (Munteanu, 1994). Analyses researching creativity show that there are three general directions of study (Csíkszentmihályi, 1996; Paprika-Zoltay, 2002). The first concerns the *nature* of creative thinking, the second one the *development* of creativity and the third one the *characterizing properties* of creative people. Amongst the properties, there is practically none, which would not be advantageous for efficient work in a VUCA environment describing the working conditions of a firefighting manager. Based on the above, author made the conclusion that the creative capabilities of a firefighting manager can be explicitly beneficial for facilitating the technically correct decisions relating to firefighting and technical rescue tasks.

Creativity can significantly increase professional efficiency of decisions made by firefighting managers in unexpected situations. This can be seen when firefighters are able to turn local conditions, in a moment, exploitable advantages. However, author found that a significant part of properties characterizing innovativeness do not prefer everyday work, free of interventions, in structured organizations, in respect of firefighting managers. This is confirmed by research findings as well, according to which it is explicitly problematic to follow strict rules for people producing creative results (The Reader's Digest Association Ltd., 1992). Maybe this is why it is a typical example that chief fire officers can safely trust the professional firmness of subordinates at incidents, in everyday life, even though the working relationships of managers and subordinates are burdened with tension.

5.7. **Heuristics**

Heuristics means that certain distortions are not incidental and unarranged errors, but the results of simplifying mechanisms, with which decision-makers make the complicated tasks manageable for

themselves, which cut the Gordian knot (Paprika-Zoltay, 2002). Based on researches related to the names Tversky and Kahneman, we distinguish 5 basic groups of heuristics (Tversky & Kahneman, 1974). These are representativeness, availability, fixing (imprint) and adjustment heuristics, retrospective distortion, as well as overconfidence and calibration. Studying the activities of firefighting managers, there are many examples of practical heuristics.
Overconfidence, based on author's judgment, is one of the greatest risk factors to the efficiency of decisions of a firefighting manager. A firefighting manager, quite often, stops searching for the necessary information earlier than sufficient, based on his experience, he trusts his own judgment, many times, assuming unnecessary risks. The extent of rational risk assumed during interventions should be always chosen proportionate to the given task; a risk assumable at a fire in a grain storage facility is incomparable with a fight for the life of a human being.
Researches show (Lichtenstein & Fischhoff, 1977) that overconfidence means that the division between actual and putative knowledge is around 50%. We are best able to judge the certainty of our decisions around 80% of knowledge, over this value, we underestimate our abilities. The above have shown that our actual knowledge does not grow parallel with certainty, the increase of our knowledge does not automatically mean the growth of self-assurance (Paprika-Zoltay, 2002). During firefighting (technical rescue), the characteristic VUCA environment exactly expresses that the actual knowledge of a decision-maker can only be partial, he can only be sure temporarily of the reliability of his knowledge. Aggregating the above, we can see that the risk of overconfidence continuously prevails in the decisions of a firefighting manager.

The complex model of decision-making of firefighting managers

In this article, author made efforts to examine and show the mechanisms promoting the more efficient decision-making of firefighting managers. Author demonstrated the linking opportunities of recognition-primed decision procedure and analogical thinking, pointing out the fact that the two do not exclude each other. If an intervention is protracted or longer time is available for the decision, many times, firefighting managers may achieve more efficient firefighting by using the latter.
If not enough time is available for analyzing and evaluating decision-making, recognition-primed procedures receive a greater role. Critical thinking uses recognition procedures, during which the decision-making process can be accelerated or analyzed with the help of a quick test and depending on the time available. The quick test, considering the circumstances, hinders recognition-primed decision and prefers critical thinking. However, when the circumstances are inappropriate for critical analyzing thinking, the quick test allows immediate reply.
Despite the limited decision capacity, thanks to recognition-primed mechanisms, in most of the occasions, correct decision is made by firefighting managers. Time limit precludes the possibility for the firefighting manager to carry out analyses necessary for the classic model, therefore, the selection of the optimal possibility is objectively not attainable by the decision-maker. The decision-maker is not striving to achieve ideal results, as a response to the difficulties of collecting information and reducing costs in relation, but depending on the circumstances, he is satisfied with the its satisfactory solution.
By reducing the time available for decision-making and for maintaining decision-making capacity, a firefighting manager applies the management (decision-making) method based on exceptions in numerous situations. Its essence is that several moments of interventions proceed protocol-like, thus, they need not be controlled all the time; on the other hand, not all the phases of the processes require direct management decision.
During the study of creativity, author has concluded that there is no such a feature characteristic of the working circumstances of firefighting managers that would not be advantageous to perform efficient work in a VUCA environment. Therefore, it is sure that the creative capabilities of firefighting managers can be explicitly advantageous to facilitate the professionally correct decisions on

firefighting and rescue tasks even if a significant part of the characteristics of innovativity does not favor the performance of an everyday work free of interventions with respect to firefighting managers. Heuristics are not random-like errors or specific distortions facilitating our everyday activities. These are the results of simplifying mechanisms, through which decision-makers can make difficult tasks manageable for themselves. Besides the benefits of heuristics, the greatest challenge for a firefighting manager can mean the inherent erroneous distortions, which surely often help, but their uncritical acceptance, in certain cases, can end up in fatal dangers.
The declared objective and sense of the decisions of firefighting managers is the efficient implementation of emergency interventions. It is symbolized by the principles of firefighting with structured division, on the top of which we clearly find the saving of human lives.

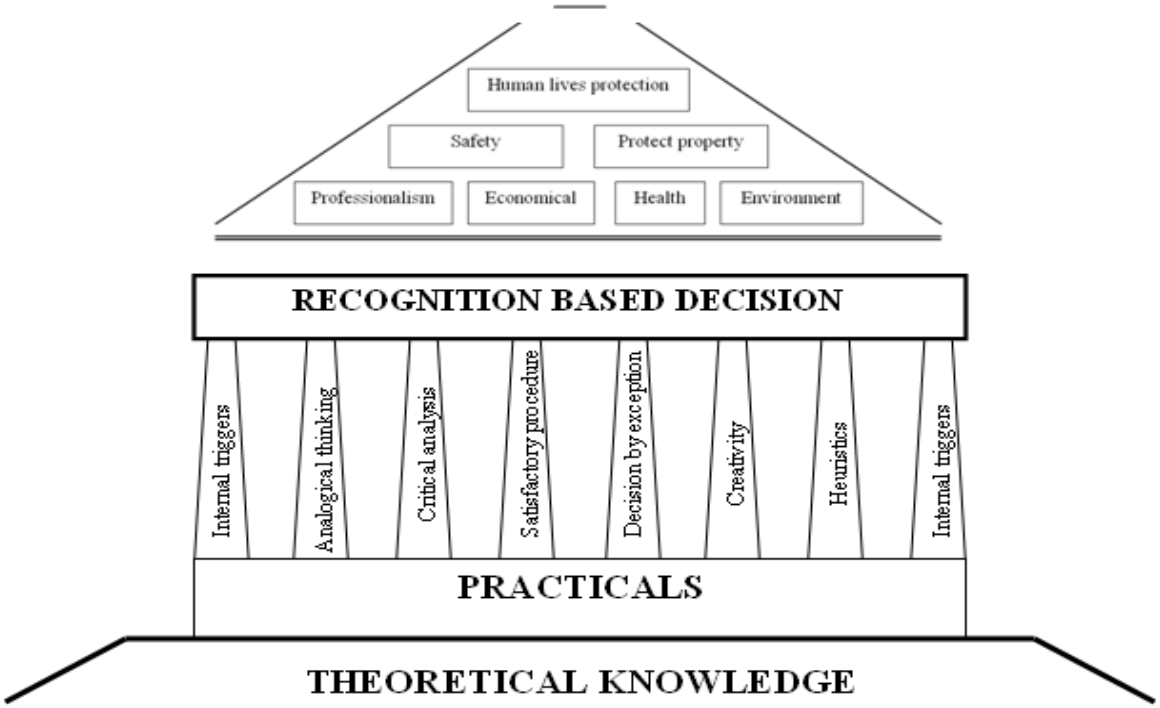

Figure 7. Complex model of decision-making of firefighting managers in emergencies

Firefighting managers certainly have less time to make their decisions compared to the time interval of classic decisions, so, their decision mechanism is strongly based on recognition procedures due to the peculiar environment (VUCA), and the limited process possibility of simultaneous pieces of information. The competence of firefighters is based on the unity of theoretical knowledge and practical experience. Building on practical experience, the different mechanisms like analogical thinking, critical analysis, satisfactory procedure, decisions based on exceptions, creativity and heuristics, together with the internal triggers, hold as pillars and make recognition-primed decision procedure of firefighting managers operational. Author illustrates the above as a complex system of emergency decision-making of firefighting managers in figure 7.

References

Bruce, E. [2011] A Picture is Worth a Thousand Words – at Least; Pentington Media Inc. USA, 2011.
Cohen, S. M., Freeman, J.T., Thompson, B.B. [1996] Integrated Critical Thinking Training and Decision Support for Tactical Anti-Air Warfare; Report, Cognitive Technologies, Inc., Naval Air Warfare Center Training System Division, Contract No. N61339-96-R-0046.

Csíkszentmihályi,M. [2008] Kreativitás – A flow és a felfedezés, avagy a találékonyság pszichológiája; Akadémiai Kiadó, 2008

Duggan, W. [2002] Napoleon's Glance: The Secret of Strategy (New York: Nation/Avalon, 2002), p.17.

Hoványi, G. [2002] A menedzsment új horizontjai; Közgazdasági Szemle, XLIX. évf., 2002. 03., pp 251-264.

Johansen, B. [2007] Get There Early: Sensing the Future to Compete in the Present. San Francisco, CA: Berrett-Koehler Publishers, Inc.. pp. 51–53. ISBN 9781576754405.

Killion,T.H. [2000] Decision Making and the Levels of War; Military Review, United States Army Combined Arms Center, Fort Leavenworth, Kansas, 2000 novemer-december,

Klein, G. A. [1989]: Strategies of decision making , Military Rewiev, No.5.

Klein, G. A.: [1999]: Sources of Power: How People Make Decisions Cambridge, MA: MIT Press 1999 ISBN 0262611465

Klein,G.A. [2004] The Power of Intuition: How to Use Your Gut Feelings to Make Better Decisions at Work Currency, 2004 ISBN 0385502893

Lichtenstein, S. & Fischhoff, B. [1977] Do those who know more also know more about how much they know? Organizational Behaviour and Human Performance, Vol. 20. 159-183.

Miller, G. A. [1956] The Magic Number 7 Plus or Minus 2; Some Limits on our Capacity for Processing Information, Psychology Review, Vol. 63

Munteanu, A. [1994] Incursiune în creatologie. Timişoara, Editura Augusta.

Radnóti, I., Faragó, K. [2005] A kockázatpercepció és kockázatvállalás vizsgálata egy fegyveres testületnél; Magyar Pszichológiai Szemle, Akadémiai Kiadó, Volume 60, 2005. április, ISSN 0025-0279, pp. 29-50.

Restas, A.: Principles of Decision-Making of Firefighting Managers, Based on Essay Analysis; 11th NDM International conference on Naturalistic Decision Making, Marseilles, France, 2013

Restas, A.: Special Decision Making Method of Internal Security Managers at Tactical Level; NISPAcee conference, Budapest, Hungary, 2014

Ribárszki, I. [1999] Döntéspszichológia, Zrínyi Miklós Nemzetvédelmi Egyetem, Jegyzet, Budapest

Simon, H. A. [1960] The new science of management decisios; Harper & Brother, New York

Twersky,A. & Kahneman,D. [1974] Judgment under uncertainity: heuristics and biases,; Science, vol. 185, pp. 1124-1131

Zoltayné Paprika, Z. [2002] Döntéselmélet; Alinea Kiadó, Budapest ISBN 9638630612

PREFER FP7 project for the management of the pre- and post-fire phases: presentation of the products.

G. Laneve[a], Roberto De Bonis[a], Lorenzo Fusilli[a], Fabrizio Ferrucci[b], Ana Sebastian Lopez[c], Sandra Oliveira[d], Stephen Clandillon[e], Lucia Tampellini[f], Barbara Hirn[g], Dimitris Diagourtas[h] and George Leventakis[i]

[a] *University of Rome 'La Sapienza', Dipartimento di Ingegneria Astronautica, Elettrica e Energetica, Roma, Italy; laneve@psm.uniroma1.it; robertodebonis@yahoo.it*
[b] *University of Calabria, Rende, Italy; f.ferrucci@gmail.com*
[c] *GMV, Madrid, Spain; asebastian@gmv.com*
[d] *University of Coimbra, Coimbra, Portugal; sisoliveira@gmail.com*
[e] *SERTIT, Strasbourg, France; stephen@sertit1.u-strasbg.fr*
[f] *CGS, Milano, Italy; ltampellini@cgspace.it*
[g] *IESConsulting, Roma, Italy; b.hirn@iesconsulting.net*
[h] *SATWAYS, Athens, Greece; d.diagourtas@satways.net*
[I] *KEMEA, Athens, Greece; george.leventakis@gmail.com*

Keywords*: severity, remote sensing, risk, burned, erosion*

Introduction

The PREFER FP7 project aims at responding to major fire prevention needs in Southern Europe. The Mediterranean area is systematically affected by uncontrolled forest fires with large impact on ecosystems, soil erosion, slope instability, desertification trends, and local economies as a whole, with a negative mid-to-long term prospect because of Climate Change. In this scenario, the need to improve the information and the intelligence support to forest fire prevention is widely recognized to be relevant. Fire prevention is still the most cost-effective strategy when compared to firefighting and extinguishing that are costly, local, and triggered only in response to already ongoing crises. The PREFER project intends to contribute to responding to such a pragmatic need of Southern Europe's forests by: 1) providing timely multi-scale and multi-payload information products based on exploitation of all available spaceborne sensors; 2) offering a portfolio of EO products focused both on Pre-crisis and Post-crisis forest fire emergency cycle in the EU Mediterranean area; 3) preparing the exploitation of new spaceborne sensors available by 2020 (e.g.: Sentinels) and 4) contributing to the definition of User requirements for the new EO missions.
The paper is devoted to illustrate the results of the R&D activity and the results of the preliminary validation of the project products.

Methods

The main objective of the PREFER project is to set up a space-based end-to-end information services to support prevention/preparedness and recovery phases of the Forest Fires emergency cycle in the EU Mediterranean Region (Figure 1). The satellite data The PREFER Service portfolio consists of two main services (see Table 1):

1. Information Support to Preparedness/Prevention Phase" (ISP) Service, and
2. Information Support to Recovery/Reconstruction Phase" (ISR) Service

Hereafter the peculiarities of such information services are listed:

- They will be based on an harmonized set of user requirements, defined by the different users from Portugal, Spain, Italy, France and Greece, also taking into account the different legal frameworks existing in such countries.
- They will be as general as to be usable in the different countries of the Mediterranean Region.
- They will be demonstrated by an interoperable service provision infrastructure (based on OGC / INSPIRE), that will allow easy access to the information.
- They will be complementary to the products provided by the GMES Land and Emergency services of the GMES Initial Operations.
- They will be complementary to the products provided by the EC JRC EFFIS (European Forest Fires Information System) System.
- They will be based on the exploitation of the data from the GMES space infrastructure.
- They will optimise integration of different data: EO, Digital Terrain Models, socio-economic data, in-situ data, meteorological data.

The PREFER consortium has the ambitious objective to start up the formation of a cluster of research institutes, industries and SMEs focused on the provision of space-based information services and products in support to Forest fires emergency management in the Mediterranean Area.

Figure 1. In gray the countries where the PREFER project partners are located and in red the project test areas.

Table 1. List of products to be developed in the framework of the PREFER project.

Service: Information Support to Preparedness/Prevention Phase	**Service: Information Support to Recovery/Reconstruction Phase**
Seasonal Fuel Map	Post-fire Vegetation Recovery Map
Seasonal Fire Hazard Map	Burn Scar map HR Optical and SAR
Seasonal Exposure (Vulnerability & Economical Value) Map	Burn Scar Map VHR
Seasonal Risk Map	Biomass Burning Aerosol Map
Daily Fire Hazard	3D Fire Damage Assessment Map
Prescribed Fires Map	Damage Severity Map

Results

This paragraph is devoted to describe more in detail the PREFER products providing, for those that are at a most advanced stage of development (namely: burn scar map, damage severity map and daily fire hazard), a description of results of the preliminary validation procedure. Figure 2 provides an example of one of the products which has been developed in the project. In particular, it shows the accuracy in the estimate of the burned areas reachable by using a suitable automatic algorithm applied on a high spatial resolution satellite images compared with the results routinely provided by JRC's EFFIS (European Forest Fire Information System) system.

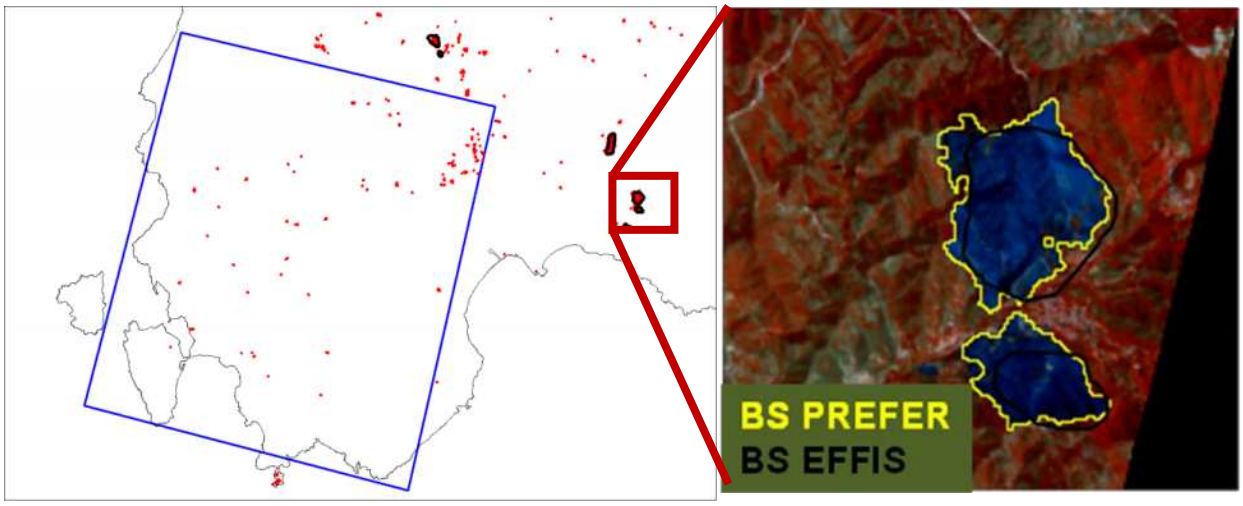

Figure 2. An example of the PREFER product burn scar. The PREFER product based on Landsat is compared with the same product provided by the EFFIS system of JRC.

Figure 3 provides an example of the damage severity map computed for a case study regarding a fire occurred last summer (2013) in Sardinia. The area of interest, Golfo Aranci, has been selected because of its relevance as SCI (Site of Community Interest). A couple of Landsat 8 images (pre and post fire) of the area were used for the computation of the damage severity index. Presently, three indices have been selected for the estimate of the fire severity, namely:

1. the well known dNBR (differential Normalized Burn Ratio) defined as follows (Key and Benson 1999, 2002):

$$dNBR = NBR_{pre} - NBR_{post}$$

where NBR_{pre} and NBR_{post} are the NBR indices computed on the pre and post-event images, according to the López García and Caselles relationship:

$$NBR = \frac{NIR - MIR}{NIR + MIR}$$

The dNBR provided a continuous scale of difference that could be related to a magnitude of ecological change, which in turn offered a conceptual model for burn severity: the greater the detected change caused by fire, the higher the severity.

2. a combination of indices called BSI which is composed of the three indices dNDVI, dNBR and dNDII:

$$BSI = (dNDVI + dNDII + dNBR)/3$$

$$NDII = \frac{NIR - SWIR}{NIR + SWIR} \quad NDVI = \frac{NIR - RED}{NIR + RED} \quad dNDII = NDII_{pre} - NDII_{post} \quad dNDVI = NDVI_{pre} - NDVI_{post}$$

This index, according to some tests made on fires occurred in Sardinia seems to be able to improve the fire damage severity estimation.

3. the DSI (Damage Severity Index) defined as:

$$DSI = MNBR_{pre} - MNBR_{post}$$

based on an optimized version of NBR called Modified Normalized Burn Ratio (MNBR) expressed as:

$$MNBR = \frac{NIR - \frac{1}{1.68} MIR}{(0.7 - NIR)^2 + MIR^2}$$

In the previous equation SWIR and MIR refer to the channels at 1.6 and 2.1 μm, respectively. Each one of the indices has presents some advantages and disadvantages summarized in Table 2.

Table 2. Comparison of the advantages and disadvantages of the developed indices.

Index	**Advantages**	**Disadvantages**
dNBR	Classical index; Tested in many cases; Thresholds known;	Saturation; Poor optimality; Sensitivity to external effects (Atmosphere, noise, etc…);
BSI	Composed by classical index; Increase of information considered respect other two;	Poor optimality; Sensitivity to external effects (Atmosphere, noise, etc…); Research of new threshold in calibration phase for damage assessment.
DSI	Optimized for change detection in burned areas; Increased sensitivity in changes due to fire. Using only two bands (less noise) Low sensitivity to external effects	Research of new threshold in calibration phase for damage assessment. Using only two bands (less information)

In figure 3 the damage severity maps computed, in an automatic way, by each one of the previously introduced indices have been compared with the damage level estimate done through the use of field data (MCBI, see below) and very high resolution images (Rapid Eye and Kompsat).
The index that best correlates with ground truth map is the DSI.

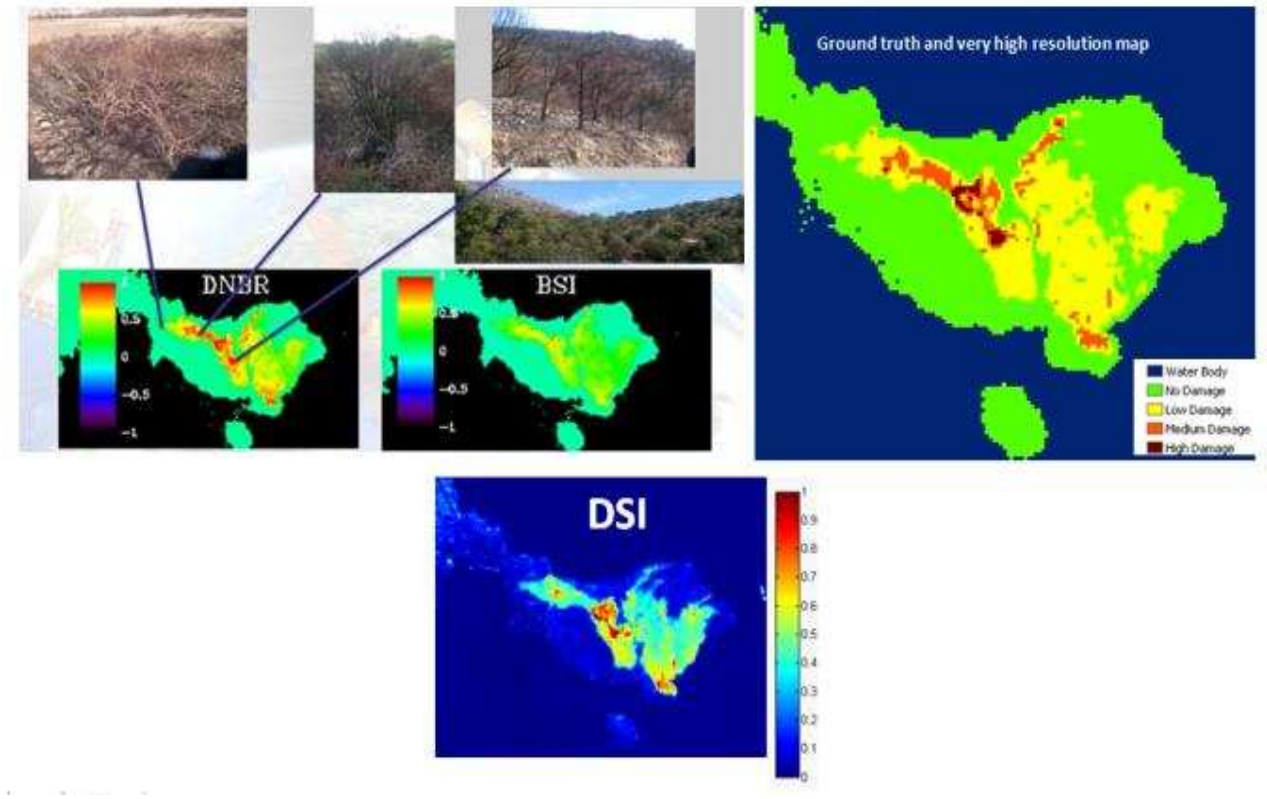

Figure 3. Comparison of the three indices with ground truth data.

The scale of the damage more used in the scientific international field is the CBI (composite burn index), a description of this parameter was given in Key and Benson 2006. In CBI, synthetically, the vegetation is considered made of 5 possible strata: 1) substrates, 2) herbs, low shrubs and trees less than 1 m, 3) tall shrubs and trees from 1 to 5 m high, 4) intermediate trees, 5) big trees.
The CBI was an innovation in the field of damage estimation because it provides an overall view of the damage associated with a number that varies continuously in a established range (0-3), this is a great advantage if we want to connect CBI to satellite observations.
However, we lightly changed the CBI definition for making it more consistent with our definition of damage. In particular, when the plots do not contain all strata, the missing strata have to be considered not damaged if these strata are upper than the existing strata and completely damaged if the missing strata are lower than existing strata."
Another change that we have made to CBI, is the reduction of the strata from 5 to 3: 1) herbs, low shrubs and trees less than 2 m, 2) tall shrubs and trees from 2 to 4 m high, 3) big trees. This new version of CBI is named Modified Composite Burn Index (MCBI).
Figure 4 shows an example of the third product recalled above, the Daily Fire Hazard Map (DFHI). This index is based on the FPI (Fire Potential Index) derived by Burgan (Burgan, 1998) for U.S. and takes into account the JRC experience (Lopez *et al*., 2002). The model requires the NDVI to compute the *Relative Greenness*, meteorological data (air temperature, relative humidity, cloudiness and rainfall) for estimating the Ten Hours Time Lag Fuel Moisture (FM10hr) and a fuel map to estimate the percentage of dead vegetation. The relative greenness (RG) or vegetation stress index represents how much green is a pixel, with reference to the range of historical observation of the NDVI used (Burgan, 1993). This quantity allows the estimate of the percentage of green fuel, as function of the fuel model assigned to each pixel.

The *Ten Hours Time Lag Fuel Moisture* has been selected as the quantity representative of the humidity available in the dead vegetation (Nelson, 2000). Such a quantity can be computed by using the meteorological parameters and the relationship described by Lopez (Lopez, San-Miguel, 2002).
However, the classic definition of FPI does not allow to take into account the effect of solar illumination conditions in determining the moisture content of the dead vegetation, therefore its proneness to burn. Actually, in Lopez *et al*. 2002 is declared that the *emc* values were corrected to take into account the solar heating but the way how this is obtained was not explained. Therefore, in order to introduce such parameter we decided to apply the formulas used for estimating the vegetation evapotranspiration rate, ET_0, and to use the computed values as a sort of weight for obtaining the *FM10hr* term for similar vegetation types characterized by a different solar *aspect angle*.
ET_0 has been computed by using the Penman-Monteith formula (Allen *et al*., 1998), modified according with FAO:

$$ET_0 = \frac{0.408 \cdot \Delta \cdot (R_n - G) + \gamma \cdot \frac{900}{T} \cdot u_2 (e_s - e_a)}{\Delta + \gamma \cdot (1 + 0.34 \cdot u_2)} \quad (5)$$

where ET_o is the reference evapotranspiration [mm day^{-1}], R_n the net radiation available at the vegetation [MJ m^{-2} day^{-1}], G the heat flux [MJ m^{-2} day^{-1}], T the daily mean temperature at 2 m [K], u_2 the wind velocity at 2 m [m s^{-1}], e_s water vapour saturation pressure [kPa], e_a actual vapour pressure [kPa], e_s - e_a the deficit of saturation pressure [kPa], Δ the slope of the vapour pressure curve [kPa $°C^{-1}$], γ psychometric constant [kPa $°C^{-1}$]. Therefore, the needed meteo data are: the mean temperature and humidity, the wind speed, the net solar radiation computed, in our case by using slope and aspect angle retrieved from a DEM of the area of interest. However, the whole process to obtain the quantities needed can be found in (Allen *et al*. 1998). Anyway others relationship, like these of Hargreaves (Hargreaves, 2003) and Thornthwaite (Thornthwaite, 1948), can be used for computing the same quantity.
Since also the presence of water in the alive vegetation can be considered relevant in determining the fire regime, the problem of estimating the vegetation water content, by using satellite images, has been dealt with. This estimate is made through an index called the *Equivalent Water Thickness* (EWT)**.** We adopted the expression given by Ceccato (Ceccato, 2002) which allows to estimate the value of EWT as a function of GVMI (Global Vegetation Moisture Index), although this index has been defined for the sensor SPOT/VEGETATION. Therefore, it was necessary to compute new coefficients allowing to apply the Ceccato EWT relationship to MODIS images. This was made by carrying out an extended series of simulation by using PROSAIL software. The new parameters have been computed by simulating more than 650000 profiles by using PROSAIL.
The results obtained by means of the simulation have been used for adapting the coefficients of the Ceccato model to the MODIS sensor and, above all, to the Mediterranean vegetation.

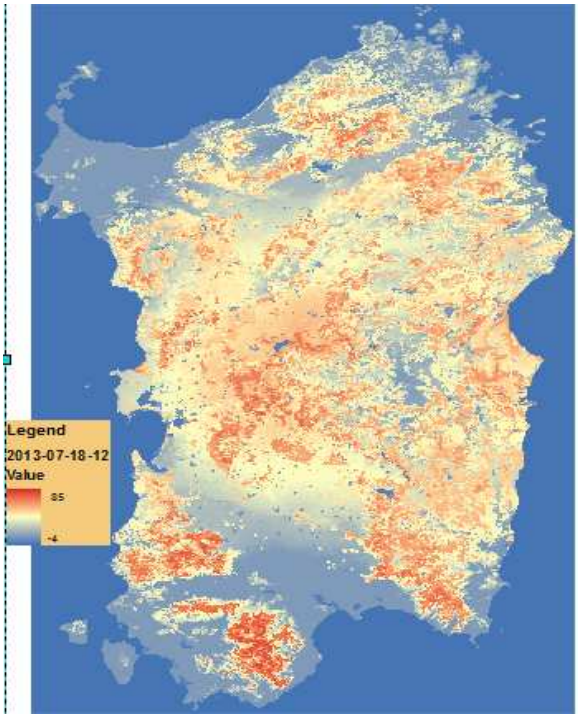

Figure 4. Example of DFHI index computed on the Sardinia region for the day 18 July 2013 at 12:00 UTC.

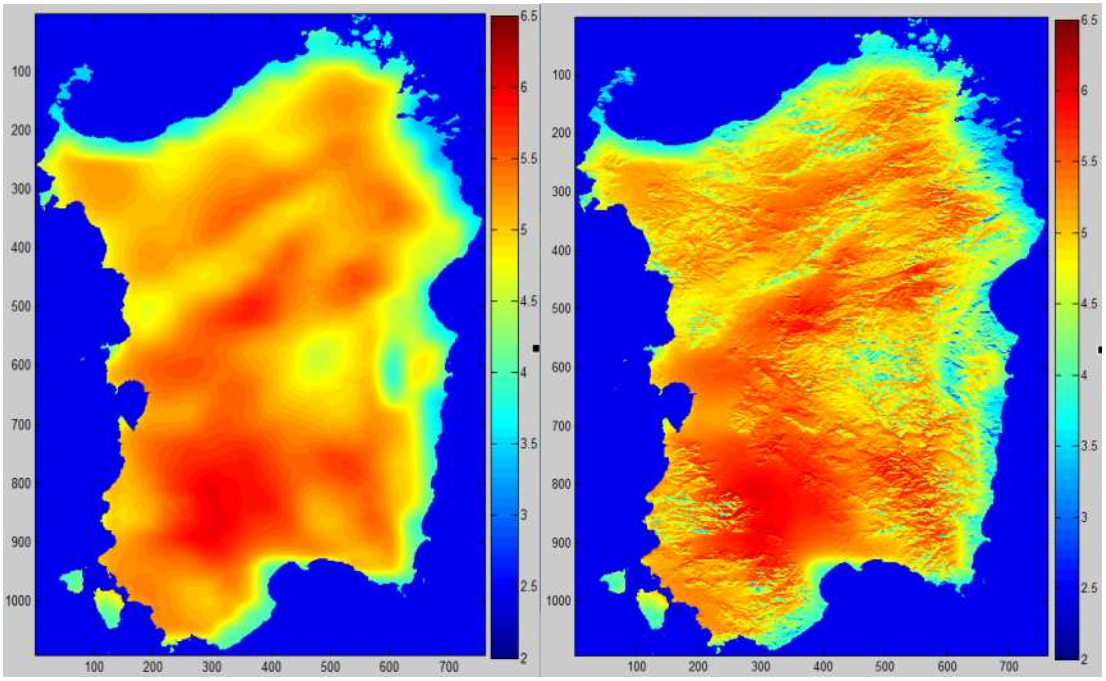

Figure 5. Comparison between the evapotranspiration (ET_0) maps computed by assuming a flat surface (right map) or taking into account the topography (left image) for the Sardinia region.

The solar illumination conditions are taken into account for estimating the DFHI by using ET_0 as a way for correcting the air temperature values used for retrieving the emc parameter. This has been done as follows:

- the Rn term (eq. 5), depending from the local aspect and slope of the surface with respect to the sun, allows us introducing the effect of the illumination conditions. In fact, we can estimate ET_0 assuming a flat surface and using the known meteorological parameters. See Figure 5 (right), as an example for Sardinia. Then, we can estimate the same quantity taking into account

the topographic characteristics of the area of interest (Figure 5, left). From eq. (5), written as function of T, it is possible to estimate the temperature (equivalent temperature) value capable to provide that ET_0 value computed taking into account the topographic effects.

In other words, a LUT has been computed containing 6 parameters: temperature, humidity, latitude, day of the year, available radiation and ET_0. For each pixel, we enter the LUT looking for the row of the table that minimizes the difference between the actual humidity and the one reported in the LUT, between the actual Rn and the one reported in the LUT and the actual ET_0 and the one reported in the LUT. The corresponding temperature represents the temperature that takes into account the illumination conditions present in the pixel as consequence of its slope and aspect.

Conclusions

The FP7 PREFER project objectives originate from the circumstance that, notwithstanding the improvements in the efficiency of the fire fighting, the phenomenon is not showing any tendency to decrease. Therefore, the European Commission has recently adopted a Communication on the prevention of natural and man-made disasters that focuses on the concept that a common approach is more effective than separate national approaches: for example, developing knowledge, linking actors and policies, and efficient targeting of community funds to prevention. In fact, the prevention is still the most cost-effective strategy, when compared to fire fighting and suppression, able to efficiently mitigate this major environment threat. PREFER intends to contribute at responding to such a pragmatic need of southern Europe's forests by: providing timely information products based on the exploitation of all available spacecraft sensors, offering a portfolio of products focused on pre- and post-crisis forest fire emergency, suitable for the users in the different countries of the European Mediterranean area.

Therefore PREFER will set up a regional service, able to process and distribute the information to end users. The service will be ready for operational deployment at the end of the project, as a new powerful tool at the disposal of the authorities in charge of forest fire management in the Mediterranean area.

References

Key, C.H. and N.C. Benson. 2006. Landscape Assessment: Ground measure of severity, theComposite Burn Index, and remote sensing of severity, the Normalized Burn Ratio. In D.C.Lutes, R.E. Keane, J.F. Caratti, C.H. Key, N.C. Benson, S. Sutherland, and L.J. Gangi.2005. FIREMON: Fire Effects Monitoring and Inventory System. USDA Forest Service,Rocky Mountain Research Station, Ogden, UT. Gen. Tech. Rep. RMRS-GTR-164-CD:LA1-51.

Key, C. H. and N. C. and Benson. 1999. Measuring and remote sensing of burn severity. In L.F. Neuenschwander and K. C. Ryan (Eds.), Proceedings Joint Fire Science Conference andWorkshop, Vol. II, Boise, ID, 15-17 June 1999. University of Idaho and InternationalAssociation of Wildland Fire. 284 pp.

Key, C.H. and N.C. Benson. 2002. Post-fire burn assessment by remote sensing on NationalPark Service lands, and Measuring and remote sensing of burn severity. U.S. GeologicalSurvey Wildland Fire Workshop, Los Alamos, NM October 31-November 3, 2000. USGSOpen-File Report 02-11: 55-56.

López-García, M.J. and V. Caselles. 1991. Mapping burns and natural reforestation using Thematic Mapper data. Geocarto International 1: 31-37.

Burgan, R. E., R. W. Klaver and J. M. Klaver, "Fuel models and fire potential from satellite and surface observations," Int. J. Wildland Fire 8 (3), 159-170, 1998.

Lopez Garcia, M.J. & Caselles, V., Mapping burns and natural reforestation using Thematic Mapper data. Geocarto International, 1, 31-37, 2002.

Burgan R. E. and Hartford R. A., Monitoring Vegetation Greenness with Satellite data, General Technical Rep. INT-297, USDA Forest Service, 1993.

Nelson R. M., Prediction of diurnal change in 10-hour fuel moisture content, Canadian Journal of Forest Research 30:1071-1087, 2000.

Lopez A. S., San-Miguel-Ayanz J. and Burgan R. E., Integration of satellite sensor data, fuel type maps and meteorological observations for evaluation of forest fire risk at the pan-European scale, Int. J. Remote Sensing, 23 (13), 2713-2719, 2002.

Allen R. G., Pereira L. S., Raes D. and Smith M., Crop evapotranspiration: guidelines for computing crop requirements. Irrigation and Drainage paper N. 56, FAO, Rome, 1998.

Hargreaves G. H. and Allen, R. G.: "History and Evaluation of Hargreaves Evapotranspiration Equation", *Journal of Irrigation and Drainage Engineering*, 129 (1), 53–63, 2003.

Thornthwaite W., An approach toward a rational classification of climate. Geographical Review 38 (1), pp. 55-94, 1948.

Ceccato, P., Gobron, N., Flasse, F., Pinty, B., & Tarantola, S., Designing a spectral index to estimate vegetation water content from remote sensing data: Part 1 Theoretical approach. Remote Sensing of Environment, 82, 188, 2002.

Reconstructing the spread of landscape-scale fires in semi-arid southwestern Australia

Lachlan McCaw[a], Vicky Reynen[b], Katherine Zdunic[b] and Mika Peace[c]

[a] *Department of Parks and Wildlife, Manjimup Western Australia, lachie.mccaw@dpaw.wa.gov.au*
[b] *Department of Parks and Wildlife, Kensington Western Australia, vicky.reynen@dpaw.wa.gov.au*
[b] *Department of Parks and Wildlife, Kensington Western Australia, katherine.zdunic@dpaw.wa.gov.au*
[c] *Bureau of Meteorology, Adelaide South Australia, m.peace@bom.gov.au*

Abstract
Landscape-scale fires are a regular feature of semi-arid south-western Australia where the dominant vegetation types are shrubland and eucalypt woodland. Fuel discontinuity limits the spread of fire in some eucalypt woodlands under moderate weather conditions, but fires can spread extensively in woodland under severe fire weather conditions. This paper reconstructs the spread of five large fires ignited by lightning that each burnt more than 90 000 ha. Fires remained active for up to 70 days after ignition until they encountered areas of sparse fuel associated with salt lakes and previous burn scars, or were extinguished by rain. Fire perimeters were mapped using daily NOAA AVHRR and MODIS satellite imagery and used to determine periodic growth in fire area. Weather conditions associated with each fire were examined using observations from a limited number of sites. Fire growth was episodic and strongly associated with periods of high temperature, extreme dryness and strong winds. An event of extraordinary fire growth was identified during the 1994 Forrestania fire which increased in area by more than 350 000 ha during a 24 hour period. The influence of weather on fire spread is being examined using re-analysis data from the European Centre for Medium-Range Weather Forecasting (ECMWF) Interim Re-analysis project ERA-1 which provides spatial and temporal data coverage not otherwise available due to the sparse observation network. South-western Australia provides a unique opportunity to examine factors influencing the duration, scale and growth characteristics of fires burning in semi-arid landscapes unimpeded by fire suppression. High intensity fires can cause widespread mortality of mature woodland trees with recovery to a mature structure taking several centuries, and the role of fire in development and persistence of eucalypt woodlands is currently a topic of scientific interest. This study forms part of a broader examination of the extent of active fire management, including prescribed burning and fire suppression, appropriate in these landscapes.

Keywords*: large fires, semi-arid landscapes, lightning ignition, Mediterranean woodlands, satellite imagery*

Introduction

Landscape-scale fires are a regular feature of remote semi-arid areas in south-western Australia where the dominant vegetation types are shrubland and eucalypt woodland. This region of Western Australia is recognised as being of global significance for biodiversity conservation and supports the largest remaining area of intact Mediterranean climate woodland on Earth, known as the Great Western Woodlands (Watson *et al*. 2008, DEC 2010). The semi-arid landscapes of south-western Australia provide a valuable opportunity to understand factors influencing the duration, scale and growth characteristics of fires burning unimpeded by suppression activities. Weather conditions conducive to the ignition and spread of fire occur from October to April in most years, with regular occurrence of severe fire danger resulting from high temperatures, low relative humidity and strong winds associated with the development of pre-frontal troughs during the summer months (McCaw and Hanstrum 2003). Lightning is a common source of ignition during late spring and summer, and fires may be left to burn without intervention for periods of weeks and sometimes months in remote areas where the human population is small and there are few assets threatened by fire. Patterns of fire spread in the landscape

are strongly mediated by vegetation type and fuel structure, time since fire, and by the location of natural barriers to fire spread including rocky outcrops and extensive salt lakes (O'Donnell *et al*. 2011a). The occurrence of very large fires (eg. >100 000 ha) has been linked to climatic patterns that facilitate more extensive spread of fire in eucalypt woodland communities (O'Donnell *et al*. 2011b, O'Donnell *et al*. in press). Large fires appear to be driven by inter-annual variation from extremely wet periods to drought periods that promote increased fuel mass and continuity of ephemeral grasses and small shrubs.

Improved understanding of factors controlling the occurrence and scale of fires in semi-arid woodlands and shrublands would benefit land management programs that seek to conserve biodiversity and cultural heritage values (DEC 2010, Prober *et al*. 2013) and to maintain biomass carbon stocks in long-lived woody vegetation (Berry *et al*. 2009). High intensity fires can cause widespread mortality of mature woodland trees, with recovery to a mature structure taking up to several centuries (Gosper *et al*. 2013a, b). There is also a need to predict the spread of fires that have potential to impact on communities and settlements, infrastructure such as powerlines and pipelines, and on regional transport corridors vital for communication and economic activity.

This paper reconstructs the spread of five large fires ignited by lightning that developed with little or no effect of fire suppression activity. Our study seeks to better understand the dynamics of large fires by documenting patterns of fire spread and examining weather conditions associated with periods of rapid fire growth. We also identify and discuss topics that will be investigated further as the study develops.

Methods

Study area

The five fires examined in this study occurred in or close to the Great Western Woodlands which are bounded on the western and southern sides by the interface with cleared agricultural land, and on the northern and eastern sides by the limits of eucalypt woodland associations and the transition to rangelands held under pastoral lease and subject to extensive grazing by cattle and sheep (Figure 1). Outside of the major regional centre of Kalgoorlie and the towns of Southern Cross and Norseman, the area is sparsely populated by residents of remote pastoral stations, mines and communities of traditional owners. Only a small proportion of the area has been subject to grazing by introduced cattle or sheep, and the vegetation generally retains its natural species composition and structure.

Mean annual rainfall declines across the Great Western Woodlands from 400 mm in the south-west corner to 250 mm at the northern limit (Fig.1). Land surfaces are of great antiquity and derived from Archean granite and gneiss of the Yilgarn craton intersected by formations of greenstone and banded ironstone (Beard 1998). The surface of the Yilgarn plateau is gently undulating at elevations between 200 and 500 m above sea level, with occasional higher points on rocky ranges and granite outcrops. Drainage is occluded with extensive salt lakes indicating the alignment of ancient paleo-drainage systems. Salt lakes are typically bare of vegetation and larger lakes (>1 km wide) are a major barrier to fire spread other than by airborne firebrands.

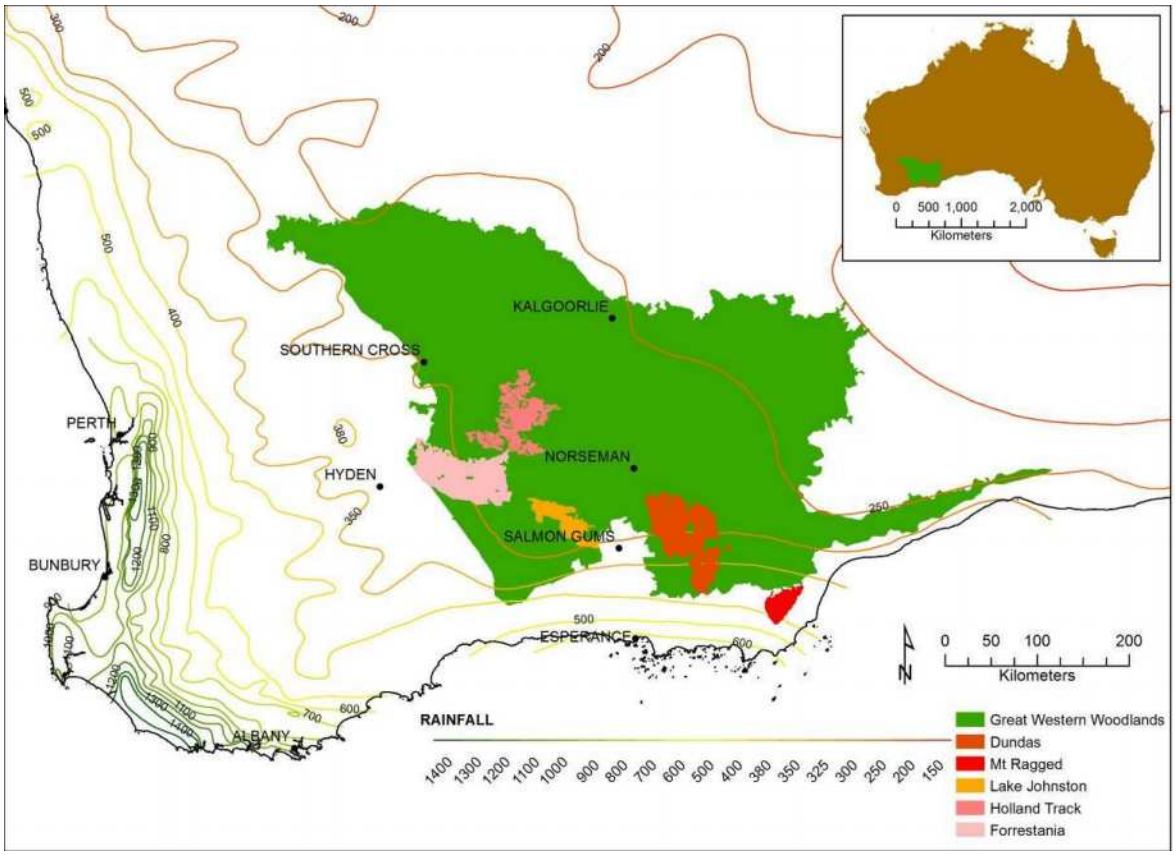

Figure 1. Location of the Great Western Woodlands in south-western Australia

2.1. Re-constructing fire growth from satellite imagery

The date and location of ignition, duration of fire activity and final area burnt for the five fires examined in the study are presented in Table 1. Fire perimeters were mapped from sequential satellite imagery dating to a minimum of every second day during the period of fire activity, subject to image availability and cloud coverage. Images were analysed daily during periods when fires were active and fire perimeters changed significantly from one image to the next. Imagery from the AVHRR sensor on the NOAA-11 and NOAA-12 satellites was used to map the perimeters of the Lake Johnson, Dundas, Mt Ragged and Forrestania fires. The NOAA-11 satellite was operational from 1998 to 2004 and the NOAA-12 satellite from 1991 to 2007. The AVHRR sensor acquired data in five bands (red, near infrared and three thermal bands) with an image resolution of 1.09 km. This satellite imagery data is suitable for detecting active fires (Lentile *et al*. 2006), particularly where fires are large in size and much of the area was burnt at high intensity resulting in significant change in vegetation cover, as was the case for these fires. Fire perimeters were digitised in ERDAS ER Mapper software and subsequently imported into ArcMap for final data manipulation. This analysis utilised archived NOAA imagery held by the CSIRO Earth Observation Centre (http://www.eoc.csiro.au/cats/) and Western Australian Land Information Authority (http://www.rss.dola.wa.gov.au/newsite/noaaql/NOAAsearch.html).

Progression of the 2004/05 Holland Track fire was derived from MODIS constellation imagery. Imagery from both the Terra satellite (launched 1999) and the Aqua satellite (launched 2002) was used, and contains 36 bands at varying resolutions from 250 to 1000 metres. Natural colour displays using bands red, green and blue were created and used to interpret burnt areas. Digitizing of fire perimeters was undertaken in ArcMap. The archive of MODIS data was accessed from the

Western Australian Land Information Authority Firewatch service (http://firewatch.landgate.wa.gov.au/landgate_firewatch_public.asp).

Table 1. Details of large fires reconstructed using satellite imagery

Fire	Ignition date (dd/mm/yyyy)	Ignition location (Lat./long.)	Duration of fire activity (days)	Final fire area (ha x 10^3)
Lake Johnston	19/12/1990	-32.7/120.7	36	151
Dundas	20/12/1990	-32.6/122.3	70	478
Mt Ragged	6/01/1991	-33.3/123.5	53	93
Forrestania	21/01/1994	-32.2/119.3	9	466
Holland Track	5/12/2004	-31.8/120.2	37	311

Weather

The network of weather observation sites representative of the Great Western Woodlands is sparse and restricted to larger settlements mostly located on the margins of the area including Southern Cross, Hyden, Kalgoorlie and Salmon Gums, with Norseman being more centrally located (Figure 1). Automatic weather stations capable of continuous recording began to be installed at these sites from the mid-1990s but did not exist at the time of the Lake Johnson, Dundas, Mt Ragged and Forrestania fires. Balloon sondes launched daily at Kalgoorlie provide atmospheric observations above the surface level. The ignition points of all fires examined for this study were at least 75 km from the closest weather observation site, and in some case much further. In selecting weather observations representative of each fire important considerations are how well the observations reflect the location of the fire relative to pre-frontal troughs and cold fronts advancing from the west, and relative to coastal influences that may moderate extremes of temperature and dryness but be influenced by sea breezes from the Southern Ocean.

Re-analysis data from the European Centre for Medium-Range Weather Forecasting (ECMWF) Interim Re-analysis project ERA-1 provides spatial and temporal coverage of weather data not otherwise available due to the sparse observation network in the study area and is being utilised as an additional source of information for fire reconstructions. Re-analysis data are available 3 hourly on a 75 km grid worldwide and provide basic variables (T, T_d, wind speed and direction) from 1979 onwards. Wain and Kepert (2013) used ERA-1 re-analysis data to develop a comprehensive and nationally consistent climatology of fire weather parameters for the whole of Australia including derived indices for fire danger and atmospheric stability that can provide important insights into factors influencing fire dynamics.

3. Results

The five fires examined in our study spanned the southern half of the Great Western Woodlands, with the 1991 Mt Ragged fire in the Cape Arid National Park at the southern extremity of the woodland region (Fig 1.). Three of the fires occurred during the summer (Dec-Feb) of 1990/91 resulting in a burnt area of 722 000 ha. Individual fires ranged in final size from 93 000 ha for the Mt Ragged fire to 478 000 ha for the Dundas fire. The Lake Johnston and Dundas fires were ignited by lightning from dry thunderstorms on 19 December 1990, and the Mt Ragged fire was ignited by lightning on 6 January 1991.

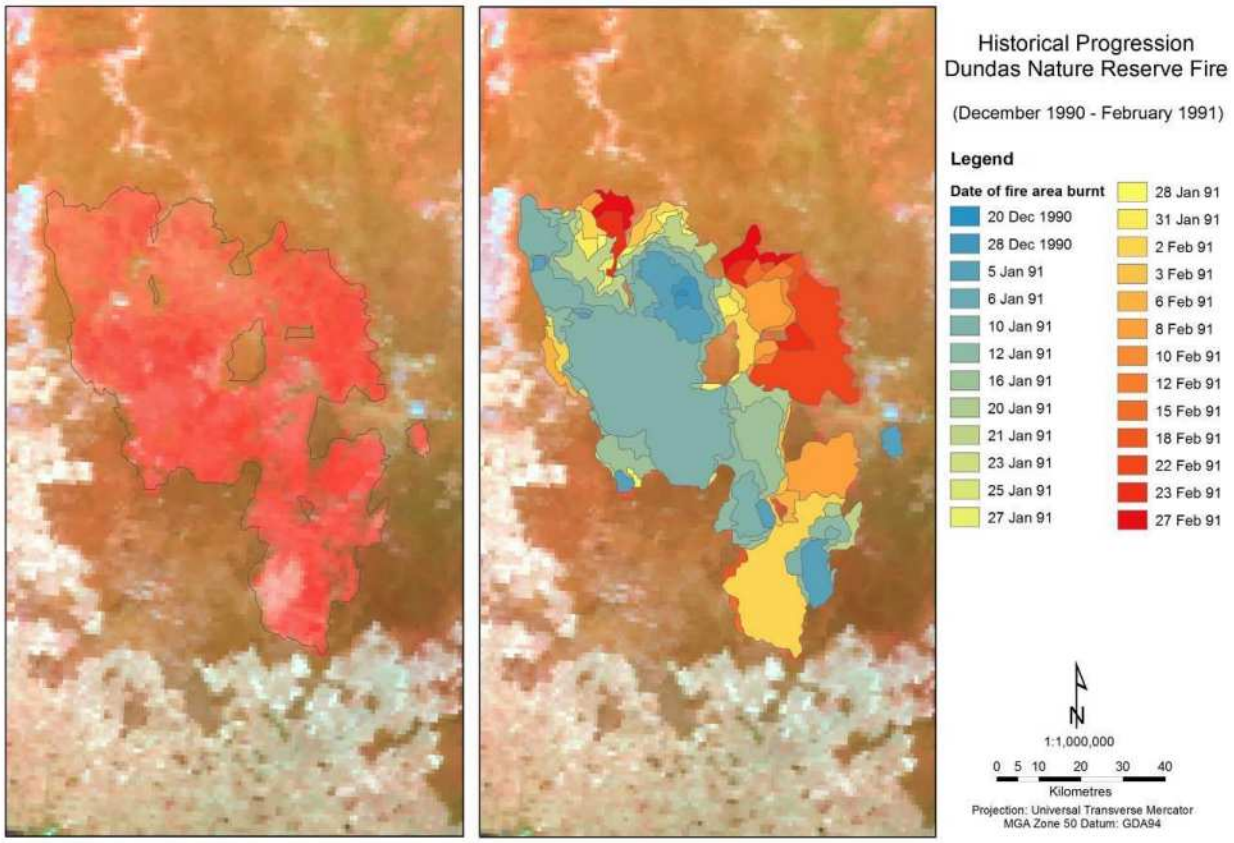

Figure 2. Reconstruction of the Dundas fire from AVHRR satellite imagery between 20 December 1990 and 27 February 1991 showing (a) burnt area and (b) periodic spread

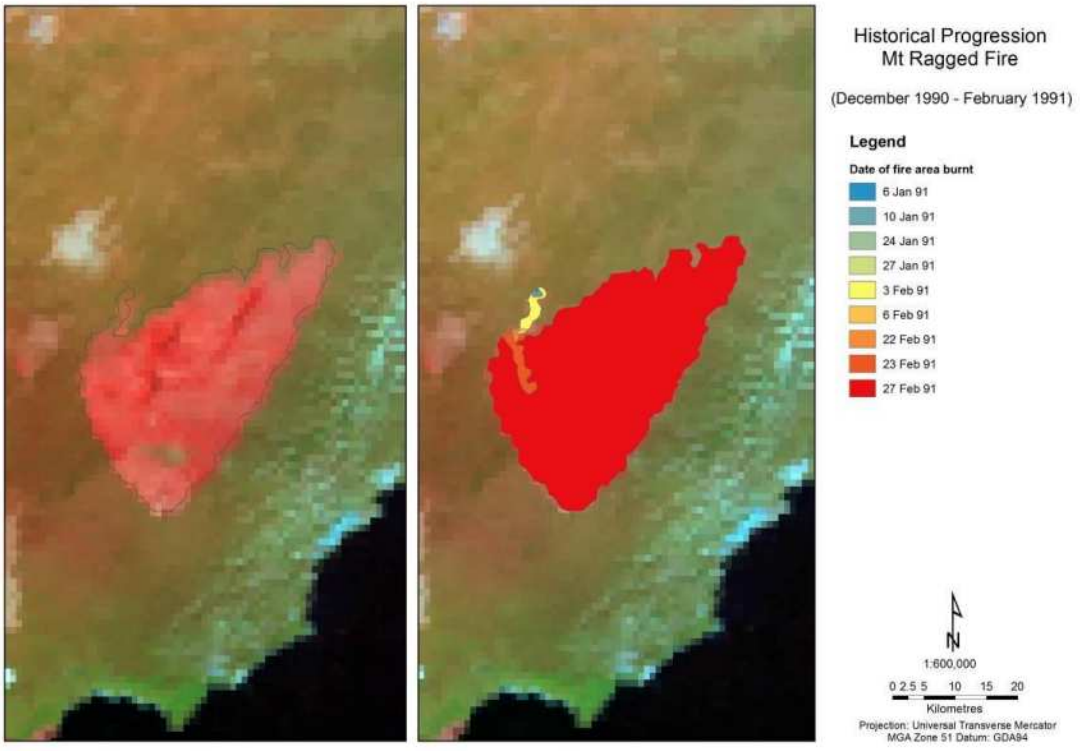

Figure 3. Reconstruction of spread of the Mt Ragged fire from AVHRR satellite imagery between 6 January and 27 February 1991 showing (a) burnt area and (b) periodic spread

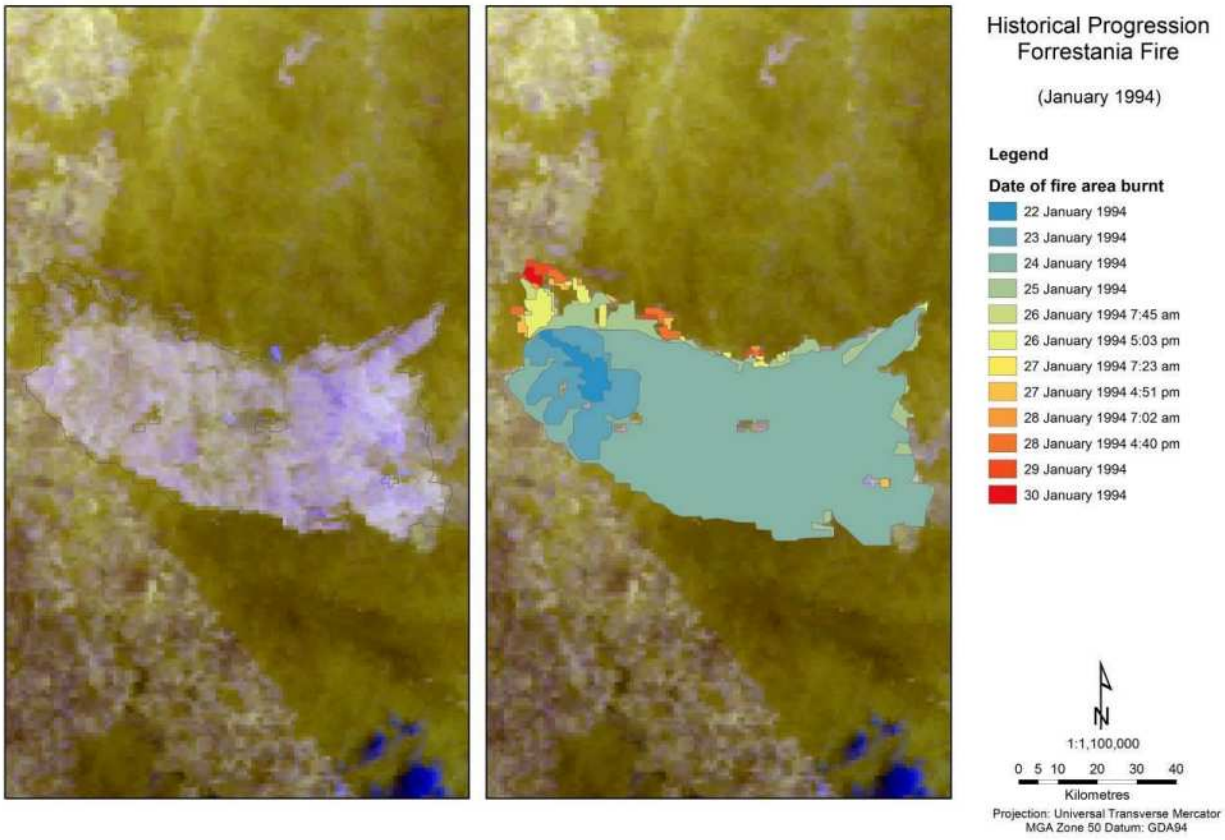

Figure 4– Reconstruction of spread of the Forrestania fire from AVHRR satellite imagery between 22 and 30 January 1994 showing (a) burnt area and (b) periodic spread

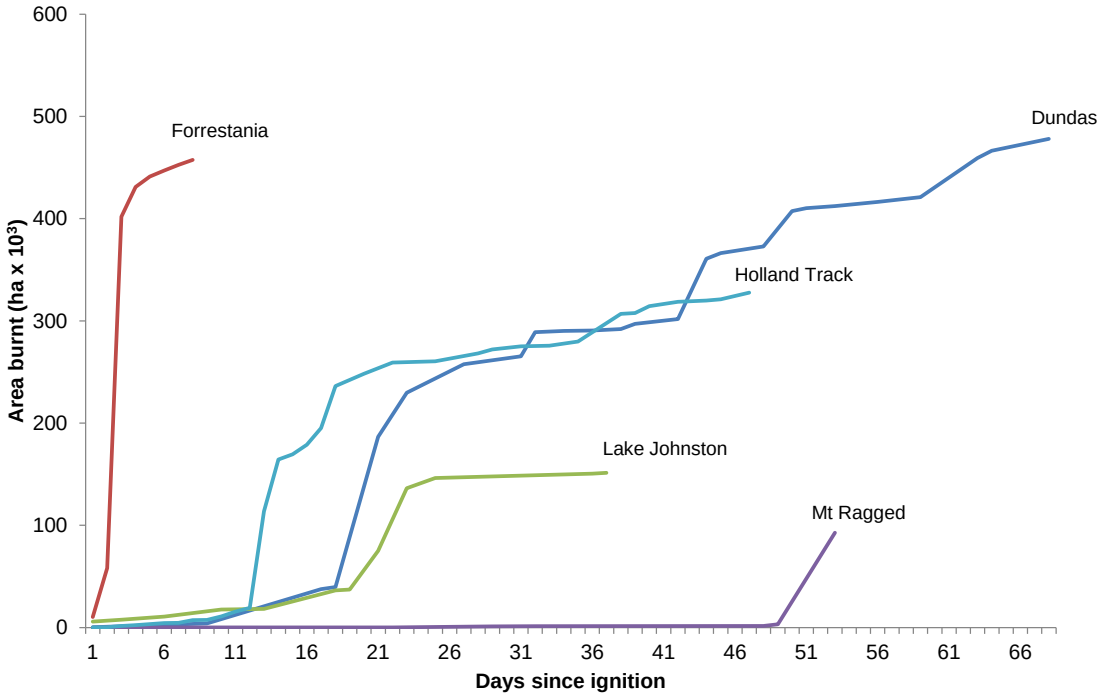

Figure 5. Increase in area burnt following ignition for five large fires

Fire reconstructions from satellite imagery show that the Mt Ragged and Dundas fires continued to grow through until late February 1991, with corresponding active periods of 53 and 70 days (Figs 2 & 3). The 1994 Forrestania fire burnt a very large area (466 000 ha) but was only active between 22 and 30 January, with the major spread event taking place on 24 January (Figure 4). The Holland Track fire was ignited by lightning on 5 December 2004 and remained active for 37 days attaining a final burnt area of 311 000 ha.

Fires exhibited different patterns of growth and development (Figure 5). The Lake Johnston and Dundas fires developed at a similar rate to each burn about 40 000 ha by 6 January 1991. Both fires then exhibited major spread between 7 and 9 January increasing in size by more than 100 000 ha under the influence of dry north-westerly winds and very high temperatures; a maximum temperature of 41°C was recorded at Salmon Gums on 8 January. The Lake Johnson fire travelled a distance of approximately 60 km to Peak Charles where its further spread was constrained by extensive salt lakes. The Dundas fire continued to develop and exhibited further periods of major spread to the south between 28 January and 3 February, and towards the north-east in mid-February. These spread events were also associated with periods of very high temperature (>42°C) and strong northerly to westerly wind. The Mt Ragged fire exhibited a quite different pattern of development following ignition on 6 January 1991. This fire remained small (<200 ha) throughout January and then grew to 1500 ha in early February, under the same weather pattern that drove the expansion of the Dundas fire. A further period of very high temperature and northerly winds increased the fire size to 3250 ha on 23 February. The major fire spread event took place on 27 February, initially under north-westerly winds through an area burnt previously by a lightning caused fire in 1983, and then under the influence of a strong south-westerly flow that extended the northern flank of fire. Fire growth on 27 February was estimated to be approximately 90 000 ha.

The Forrestania fire was ignited by lightning on 22 January 1994 and grew to approximately 10 000 ha within the first day of spread. Back-firing from the interface with the cleared agricultural land on 23 January increased the fire area to approximately 58 000 ha, with the pattern of the back-firing evident from the remote sensing imagery. An event of extraordinary fire growth took place on 24 January during which the fire increased in size by more than 350 000 ha under the influence of north-west and westerly winds. The head of the fire spread up to 80 km and reached the extensive salt lake at Lake Johnston. Upper air observations from Kalgoorlie show a dry adiabatic atmosphere to more than 5 km and wind speeds of 46 knots at the 900 hPa (1000 m) level (Figure 6). Growth of the Forrestania fire on the subsequent five days was relatively small in extent and confined to the northern flank of the fire.

The Holland Track fire was ignited by lightning on 5 December 2004, and underwent an initial period of growth for 10 days similar to that of the 1991 Dundas and Lake Johnston fires (Figure 5). Fire size increased by almost 100 000 ha on 17 December, after which time the rate of growth followed a similar trajectory to that of the Dundas fire. Some limited suppression activity including track construction and back-burning was undertaken on the Holland Track fire and this may have influenced its pattern of development during later stages.

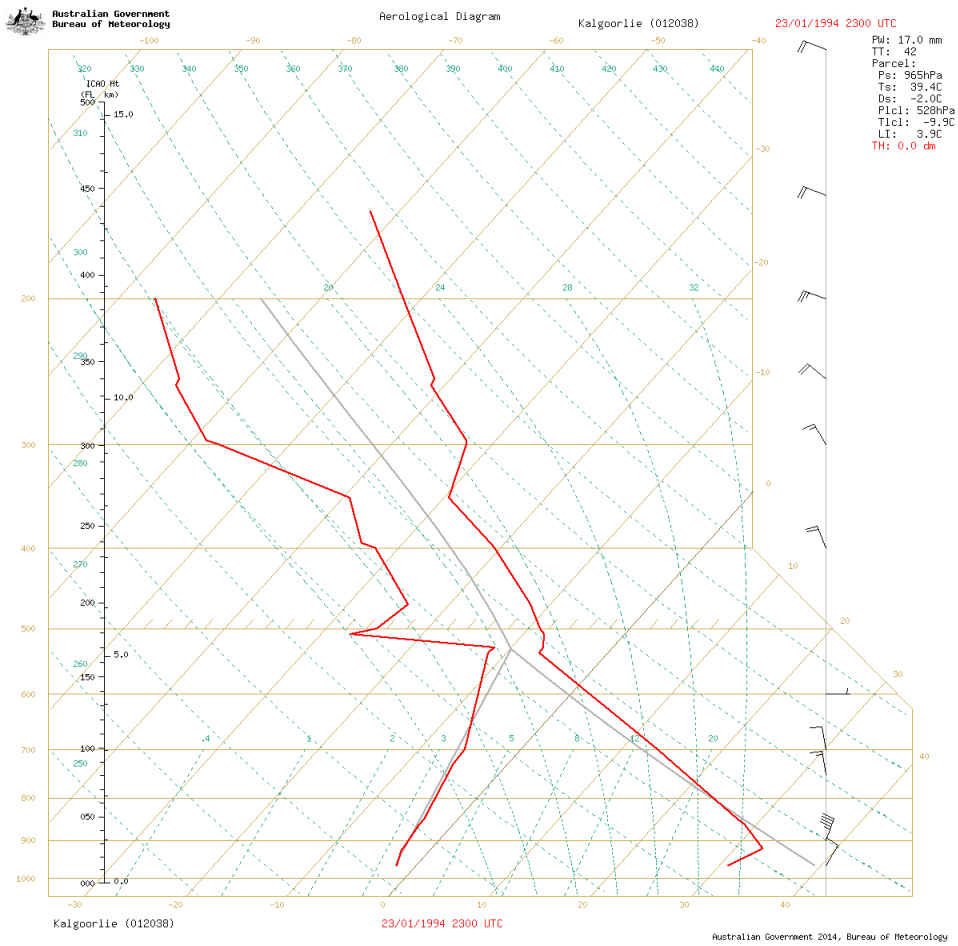

Figure 6. Aerological diagram for Kalgoorlie for 0700 hr Western Standard Time on 24 January 1994

Discussion

The fires examined in this study are of a size significant at the scale of the Australian continent, and potentially at a global scale. Indeed, the rate of growth of the Forrestania fire may represent one of the largest fire spread events documented for a single fire on one day. The scale of area burnt and rates of fire development are comparable with those documented for Black Saturday 7 February 2009 in south-eastern Australia which burned over 450,000 ha and resulted in 173 human fatalities (Cruz *et al*. 2012). The Kilmore East fire was the most significant of these fires, burning 100,000 ha in less than 12 hours and travelling a distance of around 55 km under northerly winds before being forced northwards by the passage of a cold front. Understandably, fires burning in remote areas of Australia that do not pose a direct threat to human life or economic activity attract little attention from the community or from fire researchers. However, these large remote fires warrant detailed study because of their environmental impacts on a range of values including biodiversity, atmospheric emissions and carbon storage in long-lived woody vegetation. They also offer insights into dynamic processes of fire spread that are rarely available in more densely populated landscapes.

Further work will be undertaken for this study to examine in greater detail the weather patterns associated with periods of major fire spread and to investigate the association between fire growth and existing fire danger indices used in Australia. We also intend to examine how fire spread is affected by broadscale patterns of vegetation and time since previous fire.

References

Beard JS (1998) Position and development of the central watershed of the Western Shield, Western Australia. *Journal of the Royal Society of Western Australia* **81**, 157-164.

Berry S, Keith H, Mackey B, Brookhouse M, Jonson J (2009) Biomass carbon stocks in the Great Western Woodlands. Report for the Wilderness Society (ANU Enterprise Pty Ltd: Canberra)

Cruz MG, Sullivan AL, Gould JS, Sims NC, Bannister AJ, Hollis JJ, Hurley RJ (2012) Anatomy of a catastrophic wildfire: The Black Saturday Kilmore East fire in Victoria, Australia. *Forest Ecology and Management* **284**, 269-285.

DEC (2010) A Biodiversity and Cultural Conservation Strategy for the Great Western Woodlands. (Government of Western Australia, Department of Environment and Conservation: Perth)

Gosper CR, Prober SM, Yates CJ (2013a) Multi-century changes in vegetation structure and fuel availability in fire-sensitive eucalypt woodlands. *Forest Ecology and Management* **310**, 102-109.

Gosper CR, Prober SM, Yates CJ (2013b) Floristic diversity in fire-sensitive eucalypt woodlands shows a 'U'-shaped relationship with time since fire. *Journal of Applied Ecology* **50**, 1187-1196.

Lentile LB, Holden ZA, Smith AMS, Falkowski MJ, Hudak AT, Morgan P, Lewis SA, Gessler PE, Benson NC (2006) Remote sensing techniques to assess active fire characteristics and post-fire effects. *International Journal of Wildland Fire* **15**, 319-345.

McCaw WL, Hanstrum B (2003) Fire environment of the Mediterranean south-west of Western Australia. In 'Fire in ecosystems of south-west Western Australia: impacts and management'. (Eds I Abbott, N Burrows) pp. 87-106. (Backhuys Publishers: Leiden, The Netherlands)

O'Donnell AJ, Boer MM, McCaw WL, Grierson PF (2011a) Vegetation and landscape connectivity control wildfire intervals in unmanaged semi-arid shrublands and woodlands in Australia. *Journal of Biogeography* 38, 112-124.

O'Donnell AJ, Boer MM, McCaw WL, Grierson PF (2011b) Climatic anomalies drive wildfire occurrence and extent in semi-arid shrublands and woodlands of southwest Australia. *Ecosphere* **2**, Part 127.

O'Donnell AJ, Boer MM, McCaw WL, Grierson PF (in press) Vegetation type and fuel age control wildfire size in semi-arid southwest Australia. *Ecosphere* accepted 29 May 2014.

Prober SM, Yuen E, O'Connor MH, Schultz L (2013) Ngadju kala: Ngadju fire knowledge and contemporary fire management in the Great Western Woodlands. (CSIRO Ecosystem Sciences: Perth)

Wain A, Kepert JD (2013) A comprehensive, nationally-consistent climatology of fire weather parameters. Report prepared under the National Emergency Management Program, Department of the Attorney General, Canberra.

Watson A, Judd S, Watson J, Lam A, Mackenzie D (2008) The extraordinary nature of the Great Western Woodlands. The Wilderness Society of Western Australia, Perth.

Rekindles or one-σ quality in forest fire fighting: validating the pressure on firefighters and implications for forest fire management in Portugal

Abílio Pereira Pacheco[a], João Claro[a], Tiago Oliveira[b]

[a] *INESC TEC (formerly INESC Porto) and Faculdade de Engenharia, Universidade do Porto, Campus da FEUP, Rua Dr. Roberto Frias, 378, 4200-465 Porto, Portugal, abilio.pacheco@fe.up.pt*
[b] *Forest Protection, grupo PortucelSoporcel, Edifício Mitrena, Apartado 55, 2901-861 Setúbal, Portugal*

Abstract
A long time after many business activities started struggling for six sigma quality in their operations, in Portugal, fire suppression operates at a one sigma quality level with disappointing performance results expressed by too many rekindles – re-work caused by defects in the suppression process. Indeed, they represent a high burden on wildland fire suppression resources, but despite the relevance of this phenomenon in Portugal, related research is still scarce.
Seeking to contribute to address this gap, the purpose of this study was to organize and provide an overview of the problem of rekindles in Portugal, and to verify whether evidence exists that the high proportion of rekindles in Portugal is related to the double duty of Portuguese firefighters to perform initial attack and mop-up operations.
Our study included informal meetings, formal recorded interviews, dispatch centre visits, actual rekindle observation, and an analysis of the National Forest Authority database.
From the study of genealogies of rekindles, we concluded that 17.2% additional forest fires (rekindles in successive generations) had their origin in only 7.4% of primary fires. Through regression analysis, we found that their proportions increase in days with more occurrences, preliminarily supporting the hypothesis of premature abandonment of mop-up operations, as a result from the pressure to immediately attack starting fires by the same crews.
A more detailed analysis of two representative districts highlighted specific organizational and natural challenges to successful mop-up efforts and provided further evidence of the hazardousness of rekindles. Finally, we suggest management practices to mitigate this problem and increase the level of quality of forest fire suppression in Portugal.

Keywords*: wildfire, rekindle, mop-up operations, reburn, initial attack, suppression*

Introduction

A complex and hazardous part of forest fire are rekindles, or reignitions, that reburn an area over which a previous fire has passed, but has left fuel that later ignites due to latent heat, sparks, or embers (NWCG 2011). Throughout the 2010 summer, Portugal had 14,551 primary wildfires, of which 17.2% rekindled into an additional 2,497 fires, leading to a total of 17,048. That summer accounted for 94.7% of the wildland annual burnt area of 132,241 ha. However these figures may be more severe. Several authors suggest that the number of rekindled forest fires is higher than that officially reported (ANIF 2005; Lourenço and Rainha 2006). Expert-judgment elicitation in field interviews performed by the authors points to the double. Even assuming that the available information is correct, the number of rekindles is too high (Beighley and Hyde 2009). This is a concerning situation that has been getting worse over the years (ANIF 2005), and results from ineffective mop-up operations (Murdock *et al.* 1999; ANIF 2005; ISA 2005; Lourenço and Rainha 2006; Lourenço 2007; Beighley and Hyde 2009), despite effective initial attacks (ANIF 2005; Lourenço and Rainha 2006; Lourenço 2007). Although there is a danger of fatalities during the mop-up stage (Alexander *et al.* 2007), this danger is even higher in a rekindle scenario (NWCG 2005). Finally, ineffective mop-ups and lack of surveillance

(Lourenço 2007) result in rekindles that often become large fires (ANIF 2005; Lourenço and Rainha 2006; Lourenço 2007). These are usually bigger than the wrongly judged extinguished primary fire, with larger burnt areas and considerable damage (ANIF 2005), even when the initial perimeter was just tens of meters (Lourenço and Rainha 2006).
After the disastrous fires of 2003 (Fernandes 2008), repeated two years later, the government commissioned a technical strategy (ISA 2005) to address this problem. In 2006, a modified version (shifting the emphasis from prevention to an increase in suppression capability) was approved and published (C.M. 2006) as the national strategy for forest protection against fires (Beighley and Hyde 2009). The plan recognizes the impact of rekindles and establishes mitigation as one of the priorities, with a goal of 1% by 2010 defined as an accepted value for the rekindle rate (Oliveira 2011). However, this goal was never achieved (AFN 2011) and the national figures are still much higher than, for instance, the USA 2004-2008 rekindle annual averages, which vary between 2 and 6% (Ahrens 2010).

Methods

For this study we use data kindly provided by *Autoridade Florestal Nacional* (AFN). This wildfire dataset, although having undergone several changes throughout the years, has been relatively stable in the last 12 years. The current version gathers information regarding the location of the fire, date and time (i.e., alert, ignition and extinction), burnt area, type of event, and causes. The events could be false alerts, fires in agricultural lands, or wildland fires (forests and shrublands). Information about the nature of the fire (single or reignition) is recorded since 1984 (Pereira *et al.* 2011). We focused our attention on 2010 because this is the first year for which more complete data on rekindles is available. For instance, it is now possible to know, for each rekindle, the specific fire whose bad mop-up originated it.
The country mainland is divided in 18 main administrative regions (districts), their corresponding municipalities (278 counties) and 4,050 parishes. There are significant geomorphologic, climatic and demographic differences between the northern and southern parts of Portugal (Pereira *et al.* 2011). Fire policies, suppression and prevention efforts are organized at the district level. They are therefore too heterogeneous, and we chose them as units of analysis.
Rekindles represent a high burden on suppression resources. Our goal (and hypothesis) was to find whether there was evidence that in days with more ignitions, the firefighters are compelled to prematurely abandon fire mop-up operations, thus promoting more rekindles. In other words, we wanted to know if the high number of rekindles was associated with the pressure to immediately combat all the new fires, to prevent them from becoming big fires. To accomplish this, we conducted a linear regression study, considering two variables. We consider as explanatory variable the number of fires that were simultaneously fought in each day (active fires). For the first component of the dependent variable, we counted the number of fires with a bad mop-up in that same day, i.e., the fires erroneously declared extinct, and origin of some later rekindle. However, because it is expected that bad mop-ups increase with adverse climatic conditions and the number of fires in each day, we divided this component by the number of active fires in that day. To count the number of fires with a bad mop-up in a particular day, we performed a detailed treatment of the database to uncover the genealogies of rekindles, identifying for each rekindle the bad mop-up that originated it. We used Microsoft Excel® and MapPoint Europe 2011® for the pivot tables and maps, IBM SPSS Statistics 19® for descriptive statistics, and STATA/IC 12® for regression analysis.

3. Results

Among the districts with a relevant number of rekindles, only one – Viana do Castelo – did not present a statistically significant positive correlation between the proportion of bad mop-ups and the number of active fires. The plot of the relationship between the two variables (**Erro! A origem da referência não**

foi encontrada. 1, left) displays no discernible trend; however it shows very clearly a persistently very high proportion of bad mop-ups. In our contacts with experts, a key explanation that was put forward for this result was the fact that this is the district in the country with the lowest ability to mobilize volunteer firefighting efforts, which leaves mop-up activities permanently understaffed. Another potential cause is the fact that the district has a very large mountain area, where wildfires are more difficult to control, resulting in higher burnt areas and perimeters, and therefore higher probabilities of rekindling.

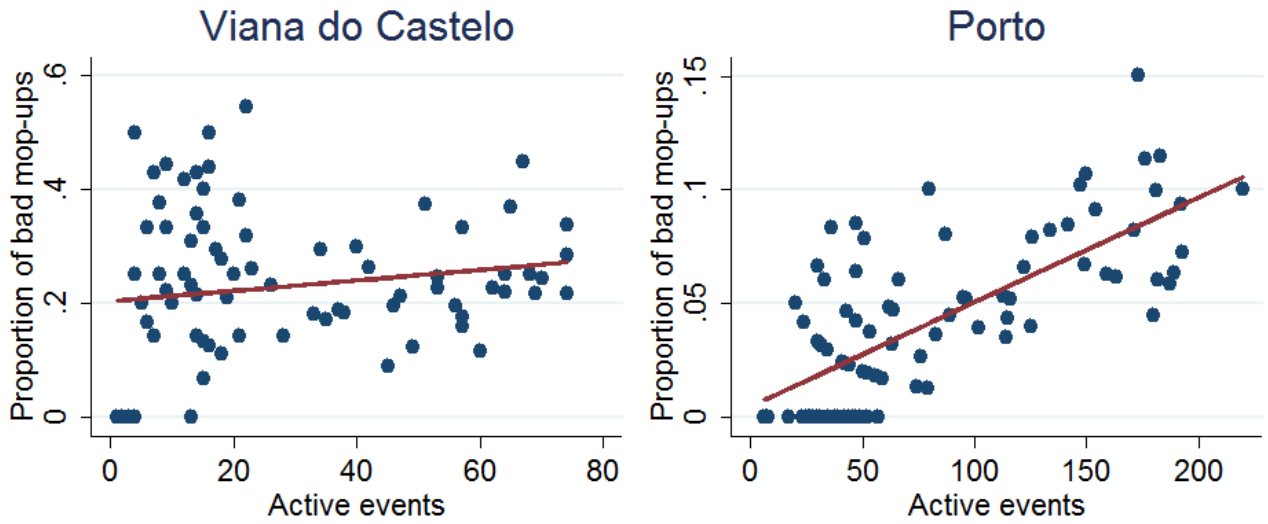

Figure 1. Plots of values and fitted values for Viana do Castelo and Porto.

The district where the effect of suppression pressure on bad mop-ups is clearer is the district of Porto; the correlation is high and the plot (**Erro! A origem da referência não foi encontrada.** 1, right) shows a distinct trend of increase in the proportion of bad mop-ups with the increase in active events. The district of Porto has a historical trend of a very high number of forest fires, which remained through 2010, with a very high proportion of forest fires with a burnt area below 1 ha – 90.6% of the six thousand incidents (Pacheco 2011). This very high number of incidents puts a huge pressure on the suppression system, which not only works at constantly very high levels of capacity utilization, but also is constantly being requested for initial attack of new fires or rekindles.

Starting from a literature review and the results of our fieldwork to identify, organize, and relate the set of physical, natural, technical and organizational factors that influence the occurrence of rekindles, we used data analysis and descriptive statistics to present evidence of the size and impact of the problem of rekindles in Portugal (Pacheco *et al.* 2012). A key contribution of our work resulted from a simple linear regression analysis of the relationship between active events and the proportion of bad mop-ups to active events. A statistically significant positive relationship was found for six of the seven districts with a relevant number of rekindles. Finally, a more detailed view of rekindle dynamics in the districts of Viana do Castelo (the only district with a non-significant regression) and Porto (the district with the higher significant correlation) highlighted specific organizational and natural challenges to a successful mop-up effort and provided further evidence of the hazardousness of rekindles. As future work, we plan to extend this study to new data that is becoming available for more recent fire seasons, and analyse the performance of alternative organizational architectures for suppression efforts, with specialized teams assigned to the different suppression tasks.

Acknowledgements

This work was financed by the European Regional Development Fund (ERDF) through the COMPETE Programme (Operational Programme for Competitiveness), by National Funds through

the Fundação para a Ciência e a Tecnologia (FCT, Portuguese Foundation for Science and Technology) within projects «FCOMP - 01-0124-FEDER-022701» and «FIRE-ENGINE - Flexible Design of Forest Fire Management Systems/MIT/FSE/0064/2009», in the scope of the MIT Portugal Program, and by grupo Portucel Soporcel. FCT has also supported the research performed by Abílio P. Pacheco (Grant SFRH/BD/92602/2013).
The authors are grateful to Manuel Rainha (ICNF), and Paulo Bessa (GTF Penafiel), for their invaluable input and feedback on this research. They would also like to thank Rui Almeida (ICNF), who was key in facilitating access to data, and Cândido Resende, for technical support on SQL issues.

References

AFN, I (2011) Monitorização e Avaliação do Plano Nacional de Defesa da Floresta Contra Incêndios, 2009/2010 - Relatório Final Preliminar. Autoridade Florestal Nacional.

Ahrens, M (2010) Brush, Grass, and Forest Fires. National Fire Protection Association, Fire Analysis and Research Division No. 0877650357.

Alexander, ME, Mutch, RW, Davis, KM (2007) Wildland fires: Dangers and survival. In 'Wilderness Medicine.' (Ed. PS Auerbach.) pp. 286-335. (Elsevier:

ANIF (2005) Relatório Final (Vol I). Autoridade Nacional para os Incêndios Florestais Available at http://www.bombeiros.pt/Arquivo1/Perdidos_e_achados/Relat%F3rio%20Inc%EAndios%202005%20-%201.pdf. Accessed: 2012-03-07. (Archived by WebCite® at http://www.webcitation.org/65zfKdsAT).

Beighley, M, Hyde, AC (2009) Systemic Risk and Portugal's Forest Fire Defense Strategy.

C.M., 2006. Resolução do Conselho de Ministros n.º 65/2006, PNDFCI. Diário da Republica, I SÉRIE-B, nº102 (26 de Maio de 2006).

Fernandes, PM (2008) Forest fires in Galicia (Spain): The outcome of unbalanced fire management. Journal of Forest Economics 14, 155-157.

ISA (2005) Proposta técnica de Plano Nacional de Defesa da Floresta contra Incêndios. In 'Volume I.' Vol. I Available at http://www.isa.utl.pt/pndfci/ [Accessed

Lourenço, L (2007) Incêndios florestais de 2003 e 2005. Tão perto no tempo e já tão longe na memória! Colectâneas Cindínicas-Riscos Ambientais e Formação de Professores 7, 19-91.

Lourenço, L, Rainha, M (2006) As mediáticas 'mãos criminosas dos incendiários'e algumas das 'lições dos fogos florestais de 2005 em álbum fotográfico. Contributo para a desmistificação dos incêndios florestais em Portugal. Territorium 71-82.

Murdock, JI, Borough, MS, Wasilla, A (1999) 'Cross-training Standards for Structural and Forestry Personnel in Urban Interface Wildfires: One Alaskan Solution.' (National Fire Academy:

NWCG (2005) 'Wildfire Origin & Cause Determination Handbook.' (National Wildfire Coordinating Group, Fire Investigation Working Team:

NWCG (2011) 'Glossary of wildland fire terminology.' Available at http://www.nwcg.gov/pms/pubs/glossary/ (Archived by WebCite® at http://www.webcitation.org/65wjoO4i7) [Accessed 5 March].

Oliveira, T, 2011. Relatório da visita ao Chile. grupo Portucel Soporcel,

Pacheco, AP (2011) Simulation Analysis of a Wildland Fire Suppression System. University of Porto.

Pacheco, AP, Claro, J, Oliveira, T (2012) Rekindle dynamics: validating the pressure on wildland fire suppression resources and implications for fire management in Portugal. In 'Modelling, Monitoring and Management of Forest Fires III.' Vol. 3 pp. 258. (Wessex Institute of Technology: Ashurst, Southampton, UK)

Pereira, MG, Malamud, BD, Trigo, RM, Alves, PI (2011) The history and characteristics of the 1980–2005 Portuguese rural fire database. Nat. Hazards Earth Syst. Sci. 11, 3343-3358.

Risk assessment to achieve fire adapted communities in the US

David Calkin[a], Jack Cohen[b], Mark Finney[b], and Matt Thompson[a]

[a] *US Forest Service Rocky Mountain Research Station, Forestry Sciences Laboratory, Missoula, MT, USA, decalkin@fs.fed.us and mpthompson02@fs.fed.us*
[b] *US Forest Service Rocky Mountain Research Station, Fire Sciences Laboratory, Missoula, MT, USA, mfinney@fs.fed.us and jcohen@fs.fed.us*

Keywords: Risk Assessment, Cohesive Strategy, WUI

Extended Abstract

The US Cohesive Strategy on Wildfire Management has established three primary goals: 1) Fire Adapted Communities, 2) Fire Resilient Landscapes, and 3) Safe and Effective Fire Response. Risk assessment has been put forward as an organizing framework to achieve these established goals. However, there is considerable uncertainty in identifying the most effective way to reach the goals and how the goals complement or compete with each other in reducing potential future losses to human development and natural resource values from wildfire while recognizing the critical ecological importance of wildfire within fire adapted ecosystems.

In this presentation we focus on the application of a wildfire risk assessment framework to achieve fire adapted communities. To start we identify the sequence of events and necessary conditions that lead to Wildland Urban Interface (WUI) disasters, and outline a structured framework to examine the risk components that influence expected wildfire losses with particular emphasis on goal 1, Fire Adapted Communities. WUI disasters where numerous structures are destroyed with potential human fatalities typically follow a common sequence of events (see Figure 1). Environmental conditions related to the location of the community relative to potential severe wildfire behaviour, numerous homes susceptible to ignition, and high severity fire weather overwhelm and limit the effectiveness of firefighting resources resulting in WUI fire disasters.

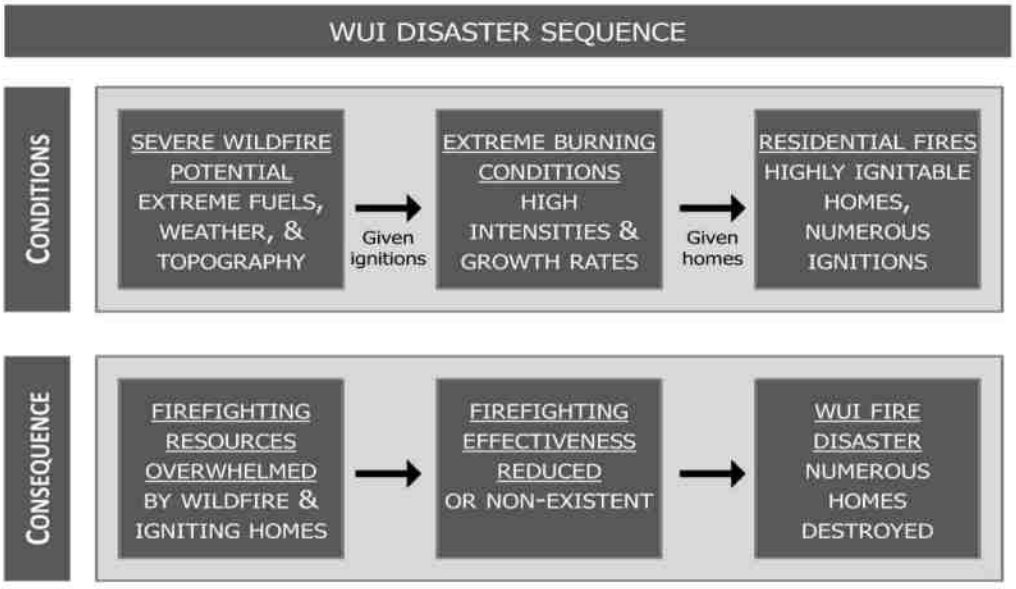

Figure 1. The WUI disaster sequence (taken from Calkin et al. 2014).

Evaluation of risk mitigation options to eliminate WUI fire disasters begins with the questions of what the appropriate wildfire management objectives are, how risk mitigation options realistically vary in terms of cost, the likely effectiveness if those options, and the appropriate identification of who bears the responsibility. Figure 2 presents a conceptual framework of mitigation objectives and methods to achieve those objectives in reducing the risk to life and property within the WUI.

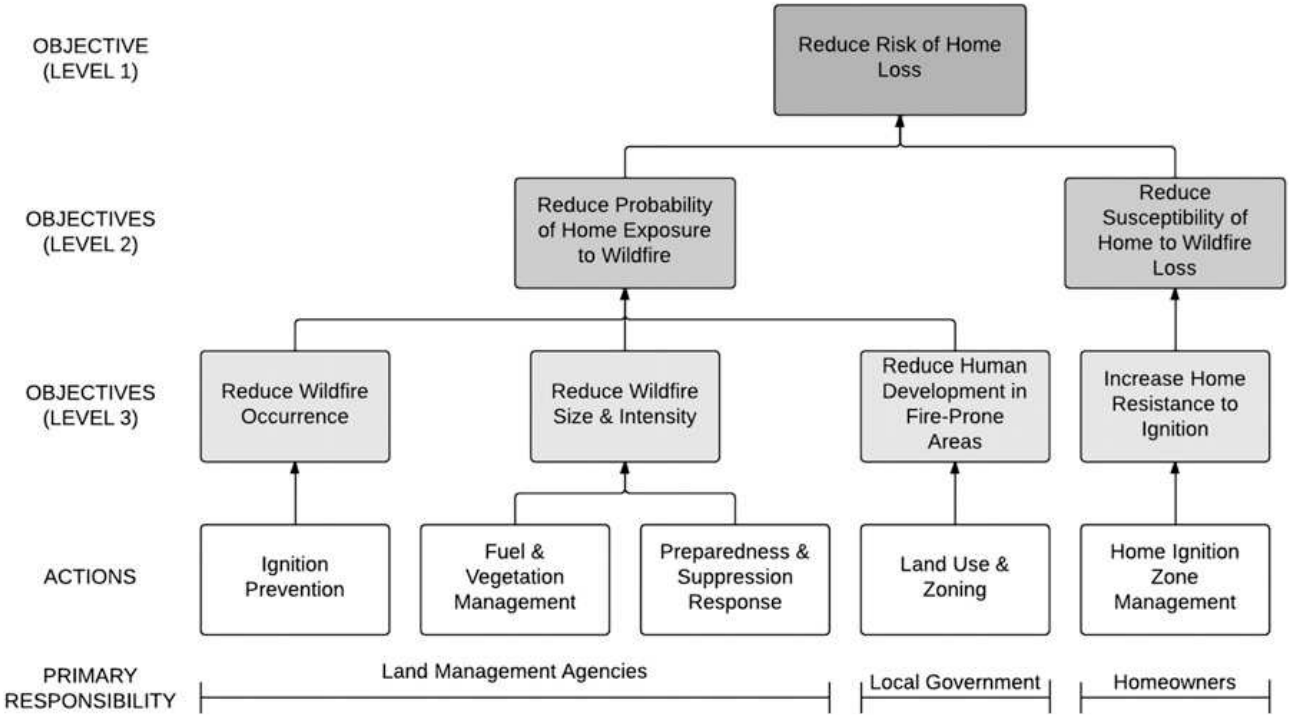

Figure 2. Conceptual framework of risk reduction to reduce risk to life and property.

Public land management agencies with wildfire management responsibilities in the US have focused significant attention on efforts to reduce the size and intensity of wildfire through aggressive suppression efforts and fuel treatment programs that focus effort within and adjacent to the WUI (US Public Law 108-148, 2003). However, extensive research has demonstrated that the destruction of residential structures is defined by the conditions of the structure itself and a 30 m buffer that surrounds the structure (see for example Cohen, 2000, 2010); an area which is typically private land. Public land agencies face several challenges in implementing aggressive fuel treatment programs near populated areas include limited budgets, sensitivity to smoke from prescribed burns, and concern that escaped prescribed fires may increase risk to the community (Calkin *et al*. 2011). Additionally, most WUI fire disasters occur under extreme wildfire conditions when suppression resources fail to contain the fire. Therefore, the ability of traditional fire management response to limit WUI fire disasters is limited.
We suggest the current paradigm that views wildland urban interface disasters as a failure of wildfire control needs to be reframed to recognize the inevitability of wildfire and that these disasters can best be prevented by focusing on the home ignition conditions. This is not to suggest that public land agencies do not have a significant role in achieving fire adapted communities. Significant investments in fuels treatments are necessary to maintain the environmental quality and landscape amenities that draw people to these environments. Application of these concepts will require engagement and risk sharing from all parties involved in fire management within the WUI. However, the described approach presents an opportunity to effectively and efficiently achieve fire adapted communities within the US.

References

Calkin, D.E., J.D. Cohen, M.A. Finney, and M.P. Thompson. 2014. How risk management can prevent future wildfire disasters. Proceedings of the National Academy of Sciences. 111(2): 746-751.

Calkin, D.E., M.A. Finney, A.A. Ager, M.P. Thompson, K.G. Gebert. 2011. Progress towards and barriers to implementation of a risk framework for Federal wildland fire policy and decision making in the United States. Forest Policy and Economics. 13(5): 378-389.

Cohen JD (2000) Preventing disaster, home ignitability in the wildland-urban interface. *J. For.* 98(3):15-21.

Cohen J (2010) The wildland-urban interface fire problem. *FREMONTIA* 38(2,3):16-22.

US Public Law 108-148 (2003) Healthy forests restoration act of 2003. Healthy Forest Restoration Act.

Searching for a reliable remote sensing method to detect burned area scars for the Andean Cusco region in Southern Peru

E. Planas[a], A. Guix[a], E. Pastor[a], I. Oliveras[b,c]

[a] *Department of Chemical Engineering, Centre for Technological Risk Studies, Universitat Politècnica de Catalunya–BarcelonaTech, Diagonal 647, E-08028 Barcelona, Catalonia, Spain. eulalia.planas@upc.edu, alan.guix@upc.edu, elsa.pastor@upc.edu*
[b] *Environmental Change Institute, School of Geography and the Environment, University of Oxford, South Parks Road OX13QY Oxford, UK. imma.oliveras@ouce.ox.ac.uk*
[c] *Nature Conservation and Plant Ecology Group, Wageningen University, Building 100, Droevendaalsesteg 3ª, 6708PB Wageningen, Netherlands.*

Abstract
According to the literature, MODIS burned area product MCD45 has been shown to have low reliability in the tropical Andes, with omission errors around 50%. Instead, Landsat images can provide good results but current processing methodologies are very time consuming. This study presents a new method for the tropical Andes, based on spectral unmixing applied to MODIS and Lansat images, with the aim of improving the methods currently available to estimate burned area in the region. Results show that the technique is not appropriate for MODIS images, which have not enough spatial resolution distinguishing between burned and unburned pixels. However, spectral unmixing applied to Landsat images lead to results with only 20% of omission errors and 9% of commission errors.

Keywords*: tropical mountain cloud forest, linear unmixing, Peruvian Andes, MODIS, Landsat TM5*

Introduction

The Andes are one of the most biologically rich regions on the planet, where the occurrence of fires is believed to be increasing. In the Andean region of Cusco there are, on the one hand, high mountain pastures where the use of fire by local communities for agriculture and livestock as well as for cultural and religious practices is common (Sarmiento & Frolich, 2002). On the other hand, there are the tropical mountain cloud forests, ecosystems of high ecological value but extremely sensitive to fire which, due to climate change, are being increasingly affected by fires (Cochrane, 2003). However, the fire regime and the emissions associated with the combustion of biomass in the region are still relatively poorly understood, mainly due to the lack of systematic national fire monitoring policies but also due to the characteristics of the region with very remote areas of difficult access. Remote sensing can therefore become a very effective tool for the estimation of burned areas in these regions.
There are numerous studies in the literature on the detection of burned area scars from satellite images, but there are really very few studies focused on the Tropical Andean region (Bradley & Millington, 2006; Oliveras, Anderson, & Malhi, 2014; Román-Cuesta *et al*., 2014). Moreover, all of these few studies also agree that the majority of remote sensing products currently used have a high degree of underestimation in the detection of the number and area of fires in this region. Several reasons can be argued to explain this underestimation (Bradley & Millington, 2006), mainly: spatial resolution of imagery, topographic effects causing shadows on the image, climatic seasonality which affects fuel moisture contents and cloud cover, local fire characteristics (most fires in the tropical Andes are small and of short duration) and the spatial and temporal scales of human activity in managing the grasslands. Oliveras *et al*. (Oliveras *et al*., 2014) observed a remarkable underestimation of fire ignitions and burned area from MODIS fire products. Particularly, their data suggested that the MODIS burned area product (MCD45) failed to detect not only small burn scars but also large burn scars, probably due to the limitation of this global algorithm to overcome issues of cloud frequency and shadows caused by

the complex topography of this region. These authors have therefore suggested that a calibration would be needed for the Tropical Andes in order to improve the performance of these products. The use of higher resolution images such as the ones provided by the Landsat thematic mapper could also be a solution, but current processing methodologies are very time consuming, of difficult validation and limited by the temporal resolution of the Landsat imagery.

The basic unit of a satellite image is the pixel that varies in size depending on the image's resolution. Regardless its resolution, a pixel is not usually homogeneous, because the signal measured by the sensor is always a mixture of the electromagnetic radiation of different constituents that are in pixels. Recognizing that pixels are combinations of different components has introduced the need to decompose quantitatively these mixtures. The basic premise of the mixture modelling techniques is that in an image most of the area is dominated by a small number of different materials that have relatively constant spectral properties. These materials (eg water, soil, metal, vegetation, etc.) are called *endmembers* and the fractions appearing in a mixed pixel are called *abundances*. The endmembers are elements considered spectrally pure. The spectral decomposition or spectral unmixing is thus the procedure by which the measured spectrum of a mixed pixel is decomposed into the endmembers and their corresponding abundances. During the last decades, several methods have been proposed to solve the mixture problem (Atkinson & Tatnall, 1997; Brown, Gunn, & Lewis, 1999; Carpenter, Gopal, Macomber, Martens, & Woodcock, 1999; Guilfoyle, Althouse, Chang, & Member, 2001; Nascimento & Dias, 2005; Wang, 1990). Among all methods, the most widely used is the spectral mixture analysis (Adams, Smith, & Johnson, 1986; Keshava & Mustard, 2002) using linear models (LMM) and non linear models (NLMM). The question of whether linear or nonlinear processes dominate spectral signatures is still an unsolved problem (Somers, Asner, Tits, & Coppin, 2011). The linear approach has proven to be a useful technique for the interpretation of remote sensing data variability and a powerful mean of converting spectral information on products which may be related to the abundance of natural materials on the surface (Keshava & Mustard, 2002). Nevertheless, it does not include the possible interactions between the endmembers present in a pixel, which may lead to results with absolute errors of up to 30%. The NLMM, although it considers the possible interactions between endmembers and thus reduces the error, has a much higher computational cost (Adams & Gillespie, 2006). For this reason, the use of LMM is much more extensive in the literature.

The key to achieve good results in spectral mixture analysis is an accurate selection of type and umber of endmembers (Elmore, Mustard, Manning, & Lobell, 2000; Tompkins, Mustard, & Forsyth, 1997). The most common way achieving this is the use of iterative testing with different combinations and sets of endmembers (Franke, Roberts, Halligan, & Menz, 2009; Somers *et al*., 2010). Once the endmembers have been determined and the number of spectral bands available is known, if a LMM is used, an overdetermined system of linear equations have to be solved in order to obtain, for each pixel, the respective abundances of the endmembers. The solving method used must ensure the minimum error of the solution. Generally, the selection of this method is arbitrary, for example (Ball, Kari, & Younan, 2004) use the singular value decomposition, (Adams *et al*., 1995) use the Gramm-Schmidt orthogonalization, (Chen, Jia, Yang, & Matsushita, 2009; Du, 2004) use quadratic programming, (Settle, 2006) uses maximum similarity and (Anderson *et al*., 2005; Barducci & Mecocci, 2005) use the least squares regression analysis.

This study aims to develop a systematic and reliable methodology for obtaining accurate data on burned area scars for the Tropical andes, by using unmixing modelling on remote sensing images from different satellites (MODIS and Landsat).Following the work performed by Anderson *et al*. (Anderson *et al*., 2005), we used three types of endmembers (soil, vegetation and water), performing a specific study to characterize them (Somers *et al*., 2011) for the study area.

Study area

The study area, of about 2.8 million hectares, is located on the eastern slope of the southeastern Peruvian Andes, at altitudes over 2000 meters above sea level (see the red line in Figure 1), and is characterized by very steep gradients both longitudinally and latitudinally. The coordinates used to delimitate the study area were: -12° S, -14°S, -69.5° W, -73.2° W

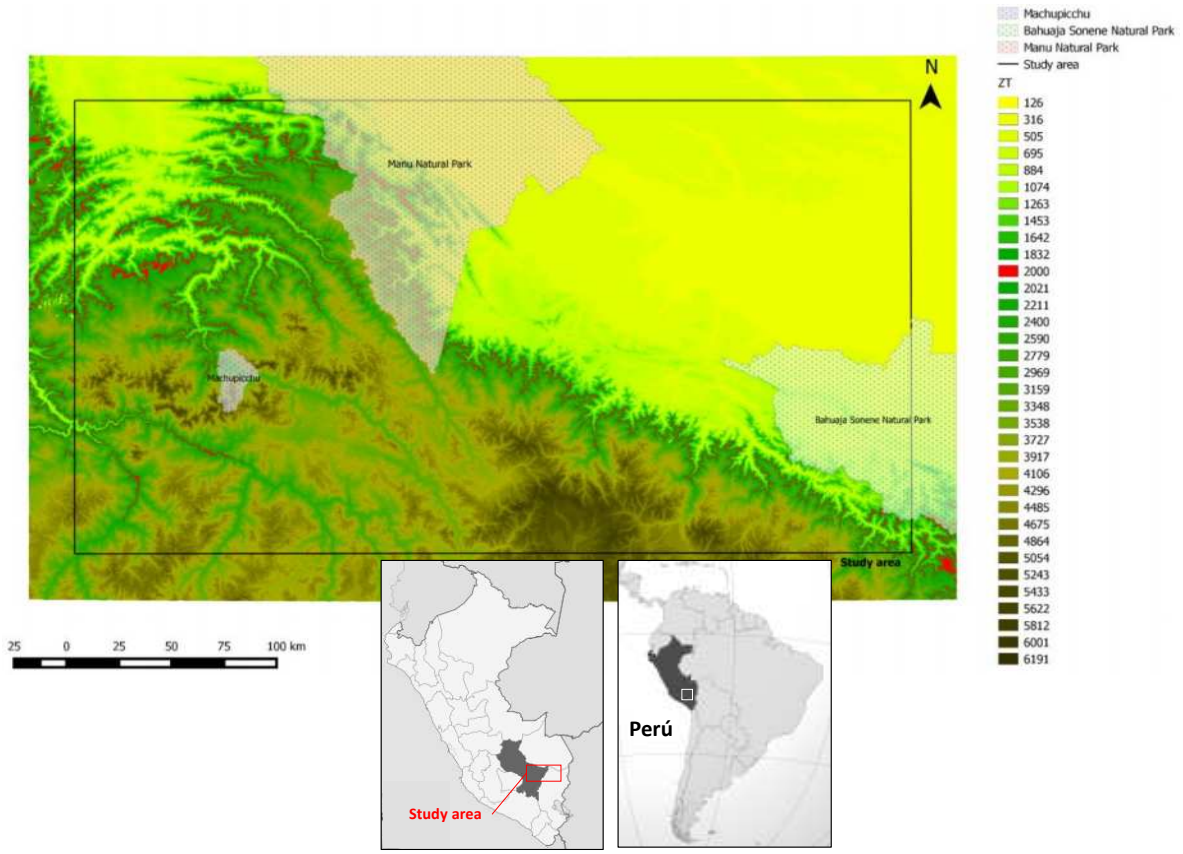

Figure 1. Location of the study area. Colour legend indicates altitude in meters a.s.l.

Methodology

3.1. Data

Three different sets of data were used: MODIS to develop the linear unmixing model, the ASTER Global Digital Elevation Model (GDEM) to develop an elevation mask over 2000 m a.s.l. at the study area and the Landsat TM5 for validation purposes.

MODIS instruments are onboard satellites Terra (EOS AM), launched in late 1999, and Aqua (EOS PM), launched in mid-2002; both following the Earth polar orbit and covering its entire surface every 1 to 2 days. MODIS instruments provide high radiometric sensitivity (12 bit) in 36 spectral bands, ranging from 0.4 to 14.4 microns wavelength, with spatial resolutions ranging from 250 to 1000 m (http://modis.gsfc.nasa.gov/about/design.php). Here, following the previous work of Anderson *et al*. (Anderson *et al*., 2005) we used the MOD09 product (MOD09GQ and MOD09GA) for obtaining the reflectance in the following wavelengths: band 1 (620-670nm), band 2 (841-876nm), band 3 (459-479nm), band 4 (545-565nm), band 5 (1230-1250nm), band 6 (1628-1652nm) and band 7 (2105-2155nm). Bands 1 and 2 correspond to MOD09GQ and have a spatial resolution of 250 m, while the other bands correspond to MOD09GA and have a spatial resolution of 500 m. We also used the product MODIS 250 m land-water mask (MOD44W) to help us making a mask of water bodies. Images from

MODIS were reprojected to WGS84/UTM18 using the Modis Reprojection Tool (MRT) free software (https://lpdaac.usgs.gov/tols/modis_reprojection:tool). MRT was also used to standarize pixel size to 250 m resolution in the three MODIS products (MOD09GQ, MOD09GA and MOD44W). For each MODIS product, we downloaded tiles h10v10 and h11v10 (that cover the study area) for the period January 2000-December 2012.

Aster is an earth observing sensor developed in Japan to be onboard the satellite "Terra". It is in operation since December 1999. Aster GDEM is a product from NASA and the Japan's Ministry of Economy, Trade and Industry, released on June 2009 and giving a complete mapping of 99% of the earth surface with a 30 m theoretical resolution. Previously the most comprehensive map was the NASA's Suttle Radar Topography Mission (SRTM) that covered 80% of the Earth's surface with 90 m resolution. Aster GDEM images can be obtained on the website: http://gdem.ersdac.jspacesystems.or.jp/search.jsp. The ASTER images corresponding to the study zone (S13W074- S14W074- S13W073- S14W073- S13W072- S14W072- S13W071- S14W071- S13W070- S14W070) were used to create an altitude mask to the MOD09GQ and MOD09GA reprojected images. After, another mask has been created by means of the MOD44W images to eliminate all water pixels. MODIS images used in the subsequent analysis had therefore a uniform 250x250 m^2 pixel size, were referred to the WGS84/UTM18 system and only non-water pixels above 2000 m a.s.l. were considered. All the algorithms developed to characterize endmembers, to perform the linear unmixing and to obtain the burned areas were implemented with MATLAB®.

The Landsat TM5 (Landsat 5 Thematic Mapper, Landsat TM5) is a sensor flying aboard the Landsat 4 and 5 satellites, released in 1984 and decommissioned in June 2013. It performed a full observation of the Earth once every 16 days. This sensor provided information on reflectance in seven spectral bands: band 1 (450-520nm), band 2 (520-600nm), band 3 (630-690nm), band 4 (760-900nm), band 5 (1550-1750nm), band 6 (10400-12500nm) and band 7 (2080-2350nm). Band 6 corresponds to the thermal band and has a resolution of 120m, while the other bands have a resolution of 30m. Landsat images corresponding to Path/Row 03/69 and 04/69 (covering the study area) were obtained on the website: http://glovis.usgs.gov/. These images were used to test the applicability of the LMM technique on higher resolution scenes. Data provided by Landsat is not directly the pixel reflectance value but the Digital Number (DN), therefore they have been converted to reflectance following the steps described on: https://earth.esa.int/ers/sysutil/069c.html.

3.2. Endmembers characterization

Three types of endmembers were used in this study: vegetation, soil and water (also referred to as shadow).

Each endmember requires a characteristic reflectance value per spectral band. To test the dependace of this value on the image tile and on time of the year (dry/rainy season), we randomly selected one cloud-free image per month for each MODIS product (MOD09GQ/GA) and tile (h10v10 and h11v10) for the period February 2000 – December 2012 (i.e. 620 images). In each image three areas of 5x5 km^2 were selected, each area corresponding to pure vegetation, soil or water. The reflectance values for each of the three endmembers were statistically analyzed, individually for each spectral band and, as a function of the tile and whether it corresponded to the dry season (May to October) or to the rainy one (November to April). The results showed that no significant differences existed, neither among tiles nor among season. Therefore, mean global values for each endmember and spectral band were used (see Figure 2).

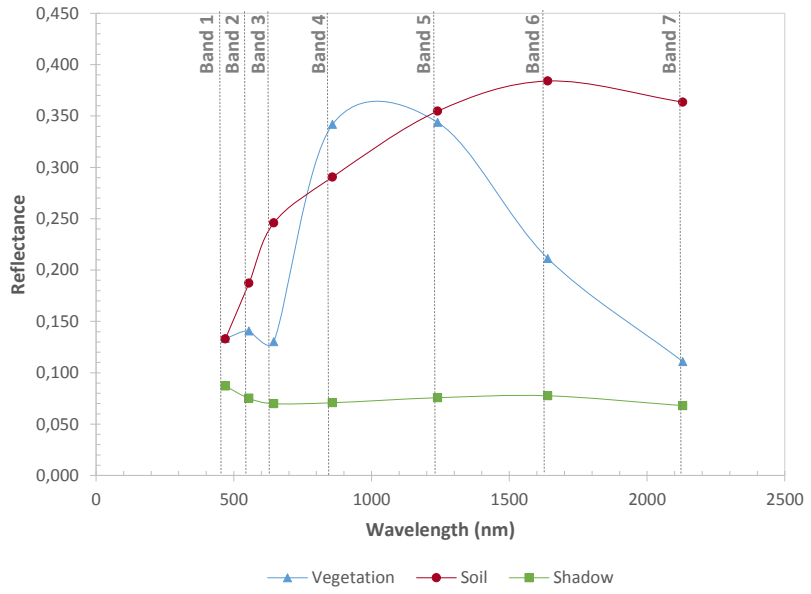

Figure 2. Reflectance values of the three endmembers used in the study as a function of the spectral band (from cloud-free images).

One of the main problems arisen in previous studies, that caused a low detection of the burn scars, was the large presence of clouds in the study area. To avoid that error, the endmembers were also characterized in those pixels identified as being medium cloudy –called "mixed"– and highly cloudy –called "cloudy"– (Figure 3).

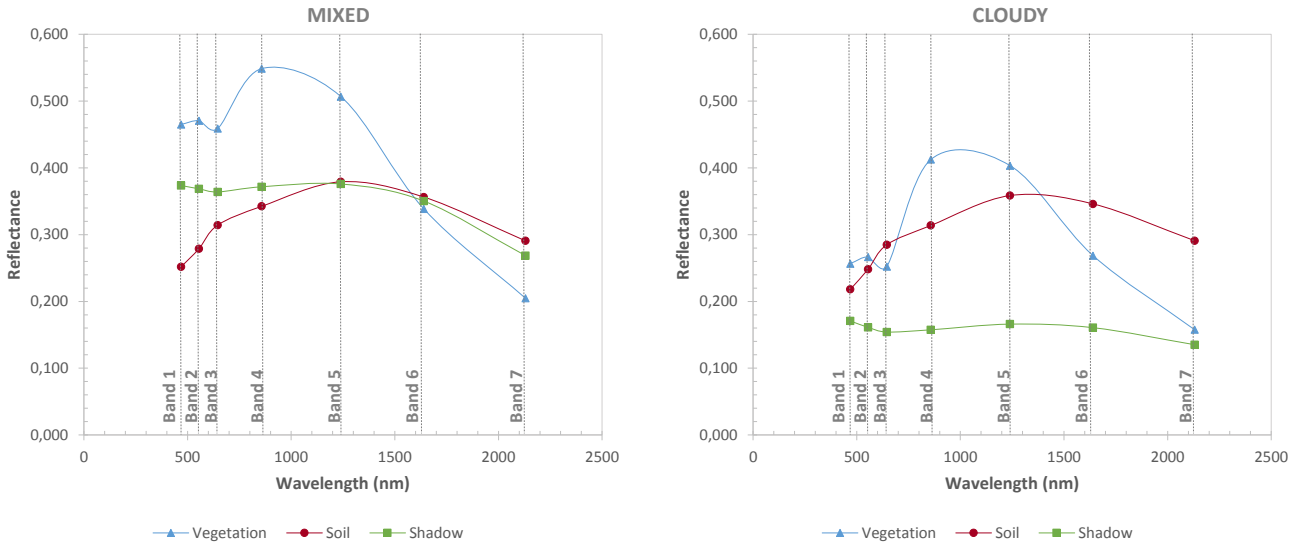

Figure 3. Reflectance values of the three endmembers used in the study as a function of the spectral band for pixels showing some degree of cloudiness. On the left values corresponding to mixed pixels; on the right values corresponding to cloudy pixels.

As it can be observed from the previous figures, there were clear differences between the reflectance of endmembers based on the degree of cloud cover. Being mixed pixels the ones that have the highest values and pixels free of clouds the ones that have lowest values.

3.3. Linear unmixing model

The LMM used in this study can be represented by the following equation:

$$r_i = a \cdot vegetation_i + b \cdot soil_i + c \cdot shadow_i + e_i$$

Where r_i is the reflectance of a pixel in the spectral band i; a, b and c are the proportions of vegetation, soil and shade respectively in this pixel; $vegetation_i$, $soil_i$ and $shadow_i$ are the reflectance values of the three endmembers in the spectral band i; e_i is the error of band i.

For each pixel, depending on whether it is clear, mixed or cloudy, a set of seven linear equations was obtained (one for each spectral band with the corresponding endmembers as a function of the cloudiness) with three unknowns (a, b and c) and two constrains: $(a, b \; and \; c \geq 0)$ and $(a + b + c = 1)$. The least squares regression analysis was used to solve this system of linear equations.

Once the relative abundances of the three endmembers are known for each pixel, the burned areas can theoretically be recognised as made of pixels having large proportions of shade. In section 4 we show the analysis of two known burn scars in the study area (described in section 3.4) in order to identify the thresholds in the shadow abundance that allow defining a pixel as burned.

3.4. Reference burn scars

Two previously known burn scars were used in this analysis. One corresponded to a fire occurred between the 2nd and 4th of July 2012 (named BS2012 from now on) covering around 129 ha and the other corresponds to a larger fire occurred at the end of August 2008 (named BS2008 from now on) with an area of approximately 1410 ha. Figure 4 shows these two burn scars superimposed over a Google Maps image of the zone together with a grid corresponding to the MODIS pixel size and distribution. Location of both fires in the study area is also given in Figure 5, the centre of BS2012 can be found in coordinates -13.23° S, -71.57° W; the centre of BS2008 can be found in coordinates: -13.81° S, -71.58° W.

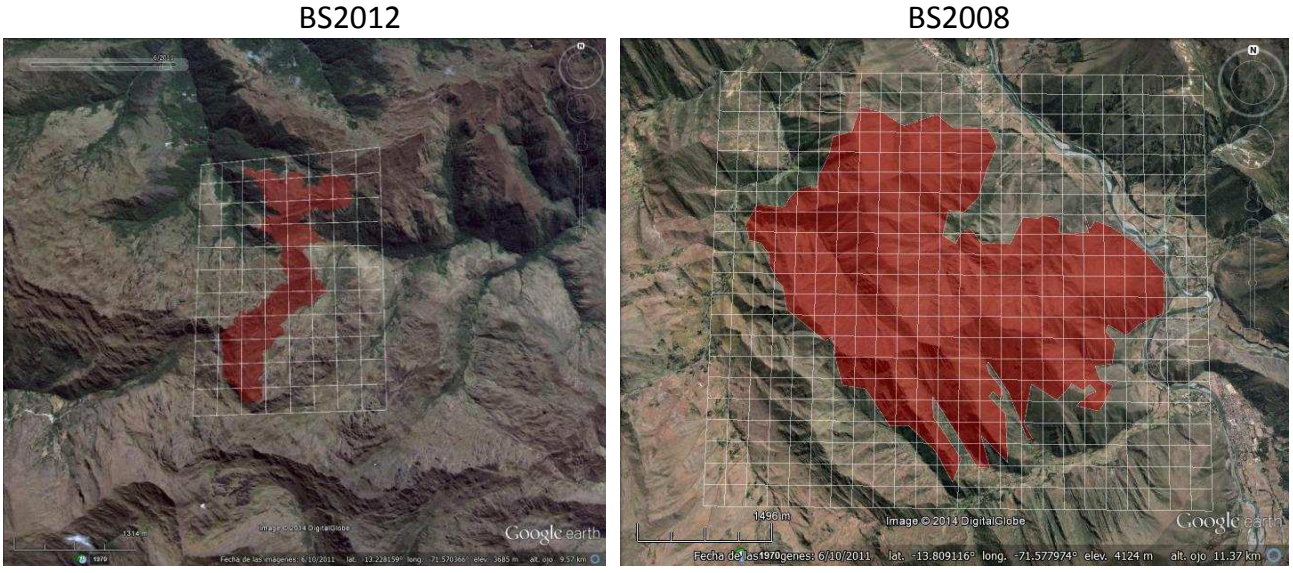

Figure 4. Area covered by the two burn scars used in this study. White line grid representing pixel size and number on the corresponding MODIS images.

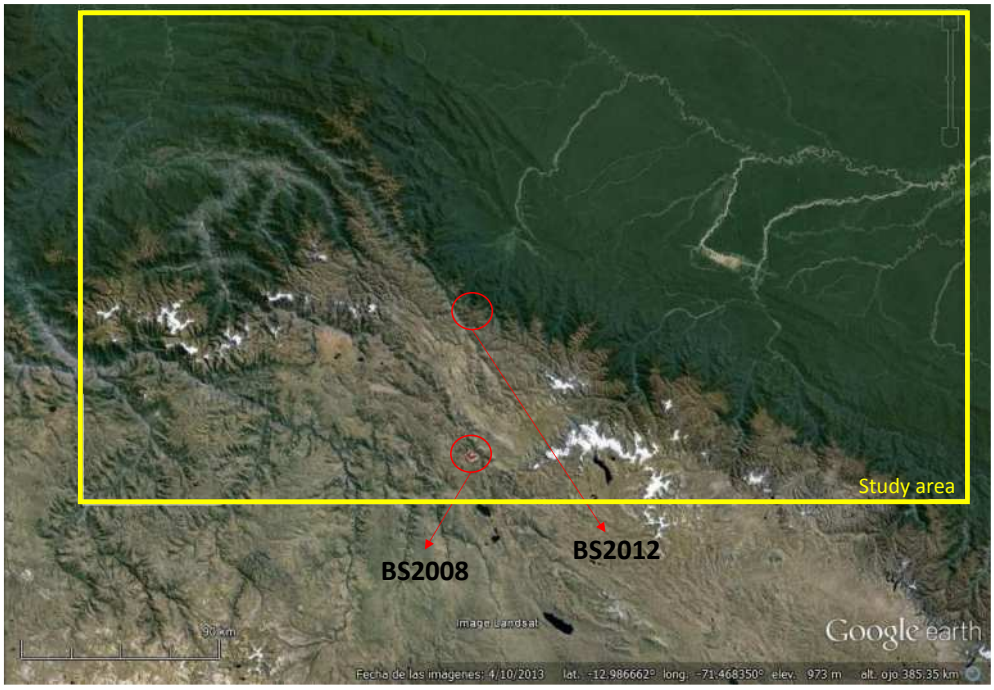

Figure 5. Location within the study area of the two burn scars used in this study.

Taking into account that MODIS pixel size is 250x250 m^2, BS2012 contained around 21 pixels while BS2008 contains around 226 pixels, which was a low number of data for any statistical analysis if only one image is taken. Therefore, 9 images corresponding to days previous to the BS2012 fire and 9 images just after the BS2012 fire were used to analyse the differences between burned and unburned pixels. In the case of BS2008, 5 images prior and 5 after the fire were used to extract the data.

Results and discussion

For each image previous and after the two fires analysed, BS2012 and BS2008, we obtained the abundances of the three endmembers considered: vegetation, soil and shadow. The frequencies of these abundances extracted from the images previous to the fire were plotted against the ones obtained after the fire. Because burned areas tend to have larger proportions of shadow (Anderson *et al.*, 2005), we expected to see differences in the abundances distribution previous and after the fire.

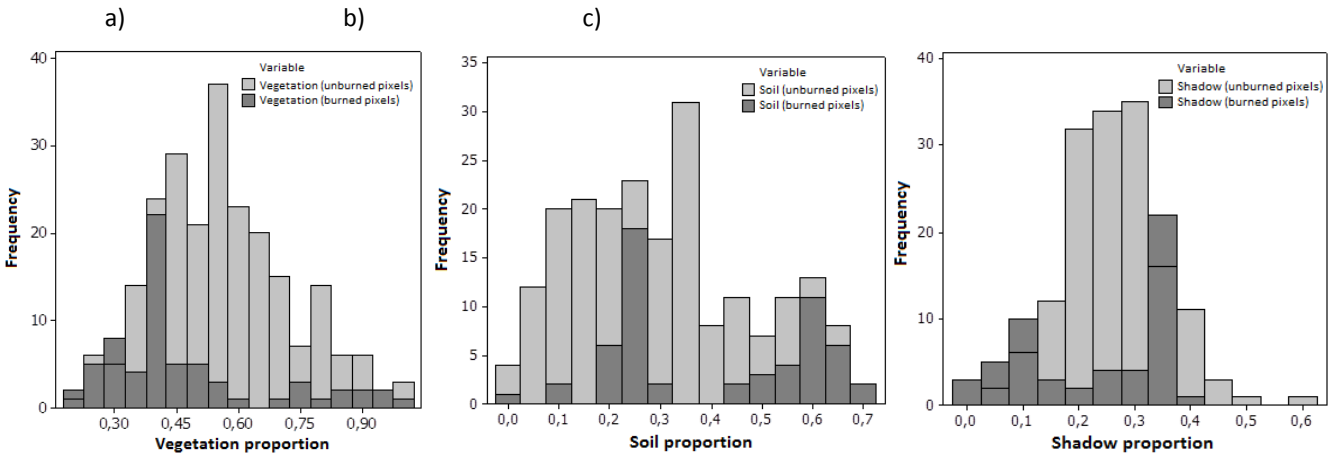

Figure 6. Frequencies distribution of the endmember abundances prior and after the fire BS2012: a) vegetation, b) soil, c) shadow.

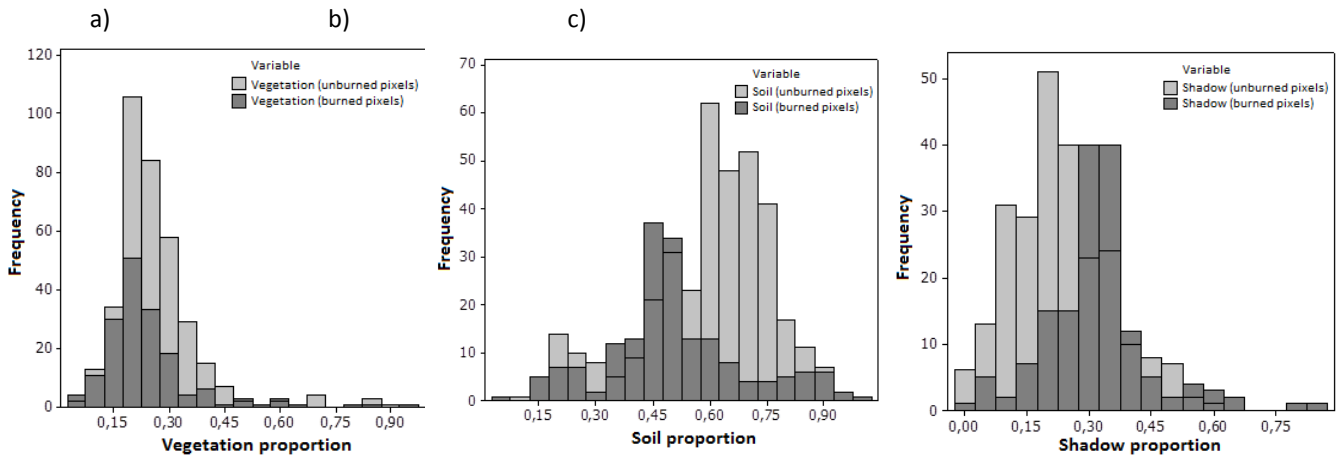

Figure 7. Frequencies distribution of the endmember abundances prior and after the fire BS2008: a) vegetation, b) soil, c) shadow.

Although vegetation abundances tended to diminish after the fire while soil and shadow abundances tended to increase, data dispersion was too large to enable us to distinguish a pixel from being burned or unburned according to its endmember proportion values (Figure 6). The large dispersion could be a result of the small size of the burn scar when compared to the pixel size, as there were many pixels that belonged to the burn scar boundary and were therefore half burned. Nevertheless, the same problem appeared inFigure 7, although in this case fire BS2008 was much larger and thus the boundary effect was smaller. These results show that that, even solving the problem of large presence of clouds in the area, linear unmixing method is unable to capture differences among MODIS reflectance values for burned and unburned pixels and therefore once again MODIS seems to fail to provide good data to obtain burn scar information in the study area. We hypothesized that MODIS spatial resolution was probably too low to capture with enough precision the differences in the reflectance values before and after the fire, taking into account the noise effect caused by the complex topography of the study area on the reflectance values.

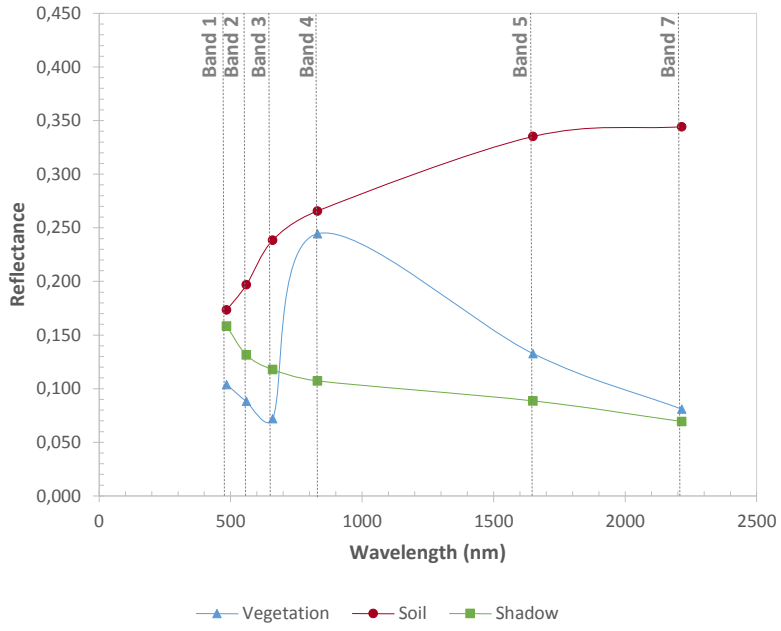

Figure 8. Endmembers characterization obtained from Landsat TM5 images.

To test this hypothesis the same method was applied to images provided by Landsat TM5. A new endmembers characterization was performed following the method described in section 3.2, but using Landsat data on the spectral bands 1 (485 nm), 2 (560 nm), 3 (660 nm), 4 (830 nm), 5 (1650 nm) and 7 (2215 nm), Figure 8 shows the results obtained. In this case, the study of the endmember abundances distribution before and after the fire was performed with BS2008 whereas BS2012 was saved for validation purposes.

Figure 9 shows the endmember proportion before and after the BS2008 fire obtained with Landsat images. Results for soil and shadow abundances, showed large dispersion and a great number of extreme values, therefore not being useful for burned/unburned discrimination purposes. However, vegetation abundances were clearly different depending on whether the pixel was or was not burned. Burned pixels had a vegetation abundance below 40% while unburned pixels have always a vegetation percentage above 40%. Using this criterion to distinguish between burned and unburned pixels, the method was applied to BS2012 in order to see if it was possible to detect the burn scar.

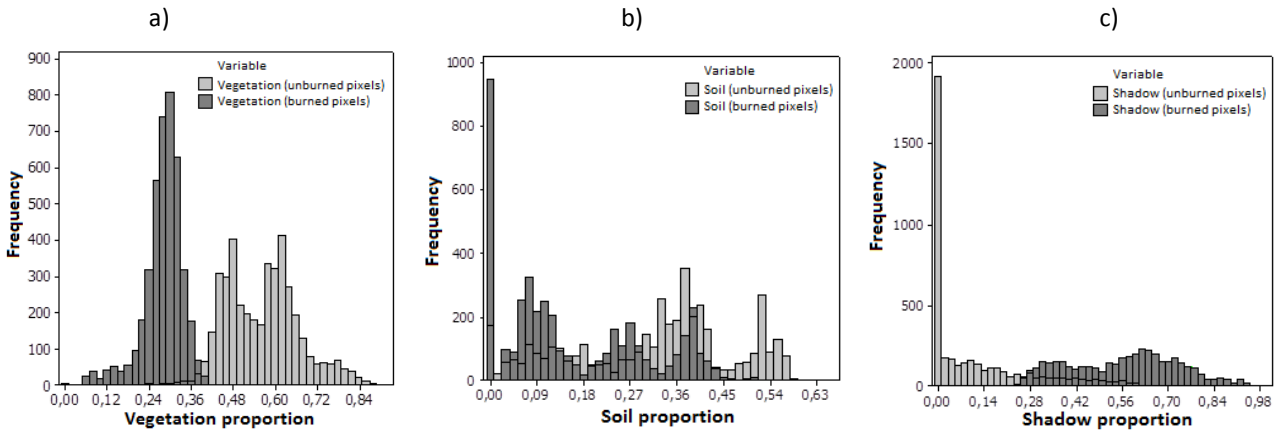

Figure 9. Frequencies distribution of the endmember abundances previous and after fire BS2008 using Landsat TM5 images: a) vegetation, b) soil, c) shadow.

Due to a number of difficulties that Landsat TM5 has been dragging since December 2008, no data was available for this sensor for the year 2012. Therefore, we used the images obtained by Landsat 7 ETM + that, despite the failure of one of their scanners, continues providing images. As it can be seen in Figure 10 (left and centre), Landsat 7 ETM+ images of the area were BS2012 was located show three black bands without data, due to problems with the sensor. This was transformed into three grey bands after applying the spectral unmixing model, corresponding to undefined pixels due to the lack of data. Despite this, the method was able to locate and draw the burn scar quite accurately.

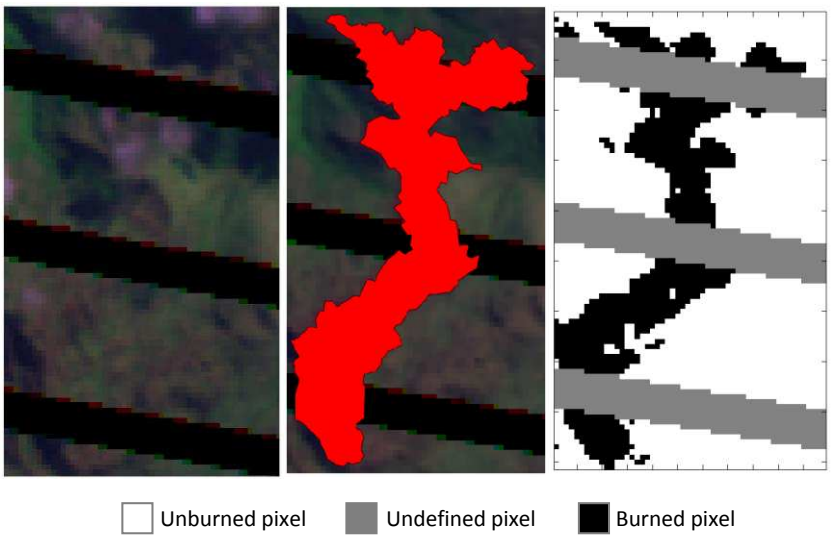

Figure 10. left: Landsat 7 ETM+ image prior to the BS2012 fire (16/06/2012); Centre: Landsat 7 ETM+ image after the BS2012fire (03/08/2012) with burn scar area superimposed; Right: image obtained with the linear unmixing model

An estimated value of 9% of commission error and 20% of omission error was computed for this fire, the only one for which the perimeter has been ground validated. Although omission error was still high, it significantly improved omission errors of 48% for the MODIS MCD45 burned area product in the study area (Oliveras *et al*., 2014).

Conclusions

The literature survey has shown that current methodologies to estimate burned areas in the tropical Andes need to be significantly improved. One of the methods that could provide better results is the spectral unmixing. This technique require the characterization of specific endmembers for the study area. In this paper a specific study to characterize the endmembers for the tropical Andes has been performed. It has shown that, for the study area, reflectance values of the endmembers are independent of the MODIS tile and of the season but change according to the degree of cloudiness.
MODIS images were not valid for the technique studied, probably due to their spatial resolution (250 m). However, Landat images, with 30 m spatial resolution, proved to be relatively accurate in the detection of burned area scars with spectral unmixing modelling. However, the complex topography and meteorology of the study area makes the development of any automatized technique for detecting burned area scars especially challenging, and further efforts are needed to achieve a reliable, standardized method that allows the accurate detection of burned area scars in the tropical Andes.

Acknowledgements

This research was funded by the Spanish Ministerio de Economia y Competitividad under the project AGL2011-23425. The authors also thank the Autonomous Government of Catalonia for financial support (project No. 2009SGR1118). Authors are grateful to Erickson Urquiaga and Toño Quintano for providing the GPS perimeter of BS2012. Support has also been received from Asociación para la Conservación de la Cuenca Amazónica (ACCA) and Parque Nacional del Manu-INRAENA.

7. References

Adams, J. B., & Gillespie, A. R. (2006). Remote Sensing of Landscapes with Spectral Images. A Physical Modeling Approach (1st ed., p. 379). New York: Cambridge University Press.

Adams, J. B., Sabol, D. E., Kapos, V., Filho, R. A., Roberts, D. A., Smith, M. O., & Gillespie, A. R. (1995). Classification of Multispectral Images Based on Fractions of Endmembers : Application to Land-Cover Change in the Brazilian Amazon. Remote Sensing of Environment, 52, 137–154.

Adams, J. B., Smith, M. O., & Johnson, P. E. (1986). Spectral mixture modeling: A new analysis of rock and soil types at the Viking Lander 1 Site. Journal of Geophysical Research, 91(B8), 8098. doi:10.1029/JB091iB08p08098

Anderson, L. O., Aragão, L. E. O. e C. de, Lima, A. De, & Shimabukuro, Y. E. (2005). Detecção de cicatrizes de áreas queimadas baseada no modelo linear de mistura espectral e imagens índice de vegetação utilizando dados multitemporais do sensor MODIS / TERRA no estado do Mato Grosso , Amazônia brasileira. Acta Amazonica, 35(4), 445–456.

Atkinson, P. M., & Tatnall, A. R. L. (1997). Introduction Neural networks in remote sensing. International Journal of Remote Sensing, 18(4), 699–709. doi:10.1080/014311697218700

Ball, J. E., Kari, S., & Younan, N. H. (2004). Hyperspectral Pixel Unmixing using Singular Value Decomposition. In IEEE Transactions on Geoscience and Remote Sensing. IEEE International Geoscience and Remote Sensing Symposium Proceedings (pp. 3253–3256). Anchorage, Alaska, Sept. 20-24, 2004: Institute of Electrical and Electronics Engineers, Inc.

Barducci, A., & Mecocci, A. (2005). Theoretical and experimental assessment of noise effects on least-squares spectral unmixing of hyperspectral images. Optical Engineering, 44(8), 087008. doi:10.1117/1.2010107

Bradley, A. V., & Millington, A. C. (2006). Spatial and temporal scale issues in determining biomass burning regimes in Bolivia and Peru. International Journal of Remote Sensing, 27(11), 2221–2253. doi:10.1080/01431160500396550

Brown, M., Gunn, S. R., & Lewis, H. G. (1999). Support vector machines for optimal classification and spectral unmixing. Ecological Modelling, 120, 167–179. doi:10.1016/S0304-3800(99)00100-3

Carpenter, G. A., Gopal, S., Macomber, S., Martens, S., & Woodcock, C. E. (1999). A Neural Network Method for Mixture Estimation for Vegetation Mapping. Remote Sensing of Environment, 70, 138–152. doi:S0034-4257(99)00027-9

Chen, J., Jia, X., Yang, W., & Matsushita, B. (2009). Generalization of Subpixel Analysis for Hyperspectral Data With Flexibility in Spectral Similarity Measures. IEEE Transactions on Geoscience and Remote Sensing, 47(7), 2165–2171. doi:10.1109/TGRS.2008.2011432

Cochrane, M. a. (2003). Fire science for rainforests. Nature, 421(6926), 913–9. doi:10.1038/nature01437

Du, Q. (2004). Optimal Linear Unmixing for Hyperspectral Image Analysis. In IEEE Transactions on Geoscience and Remote Sensing. IEEE International Geoscience and Remote Sensing Symposium Proceedings (pp. 3219–3221).

Elmore, A. J., Mustard, J. F., Manning, S. J., & Lobell, D. B. (2000). Quantifying Vegetation Change in Semiarid Environments : Precision and Accuracy of Spectral Mixture Analysis and the Normalized Difference Vegetation Index. Remote Sensing of Environment, 73, 87–102. doi:S0034-4257(00)00100-0

Franke, J., Roberts, D. a., Halligan, K., & Menz, G. (2009). Hierarchical Multiple Endmember Spectral Mixture Analysis (MESMA) of hyperspectral imagery for urban environments. Remote Sensing of Environment, 113(8), 1712–1723. doi:10.1016/j.rse.2009.03.018

Guilfoyle, K. J., Althouse, M. L., Chang, C., & Member, S. (2001). A Quantitative and Comparative Analysis of Linear and Nonlinear Spectral Mixture Models Using Radial Basis Function Neural Networks. IEEE Transactions on Geoscience and Remote Sensing, 39(8), 2314–2318.

Keshava, N., & Mustard, J. F. (2002). Spectral Unmixing. IEEE Signal Processing Magazine, (January), 44–57.

Nascimento, J. M. P., & Dias, J. M. B. (2005). Vertex Component Analysis : A Fast Algorithm to Unmix Hyperspectral Data. IEEE Transactions on Geoscience and Remote Sensing, 43(4), 898–910.

Oliveras, I., Anderson, L. O., & Malhi, Y. (2014). Application of remote sensing to understanding fire regimes and biomass burning emissions of the tropical Andes. Global Biogeochemical Cycles, 28, 480–496. doi:10.1002/2013GB004664

Román-Cuesta, R. M., Carmona-Moreno, C., Lizcano, G., New, M., Silman, M., Knoke, T., … Vuille, M. (2014). Synchronous fire activity in the tropical high Andes: an indication of regional climate forcing. Global Change Biology, 20(6), 1929–42. doi:10.1111/gcb.12538

Sarmiento, F. O., & Frolich, L. M. (2002). Andean Cloud Forest Tree Lines. Naturalness, Agriculture and the Human Dimension. Mountain Research and Development, 22(3), 278–287. doi:10.1659/0276-4741(2002)022[0278:ACFTL]2.0.CO;2

Settle, J. (2006). On the effect of variable endmember spectra in the linear mixture model. IEEE Transactions on Geoscience and Remote Sensing, 44(2), 389–396. doi:10.1109/TGRS.2005.860983

Somers, B., Asner, G. P., Tits, L., & Coppin, P. (2011). Endmember variability in Spectral Mixture Analysis: A review. Remote Sensing of Environment, 115(7), 1603–1616. doi:10.1016/j.rse.2011.03.003

Somers, B., Delalieux, S., Verstraeten, W. W., van Aardt, J. a. N., Albrigo, G. L., & Coppin, P. (2010). An automated waveband selection technique for optimized hyperspectral mixture analysis. International Journal of Remote Sensing, 31(20), 5549–5568. doi:10.1080/01431160903311305

Tompkins, S., Mustard, J. F., & Forsyth, D. W. (1997). Optimization of Endmembers for Spectral Mixture Analysis. Remote Sensing of Environment, 59, 472–489. doi:S0034-4257(96)00122-8

Wang, F. (1990). Fuzzy Supervised Classification of Remote Sensing Images. IEEE Transactions on Geoscience and Remote Sensing, 28(2), 194–201.

Severe fire activity and associated atmospheric patterns over Iberia and North Africa

Malik Amraoui[a,b], Mário G. Pereira[c,a], Carlos C. DaCamara[a], Teresa J. Calado[a]

[a] *Instituto Dom Luiz, Universidade de Lisboa, Lisboa, Portugal, malik@utad.pt, cdcamara@fc.ul.pt, mtcalado@fc.ul.pt*
[b] *Universidade de Trás-os-Montes e alto Douro, UTAD, Quinta de Prados, 5000-801 Vila Real, Portugal,*
[c] *Centro de Investigação e de Tecnologias Agro-Ambientais e Biológicas CITAB, Universidade de Trás-os-Montes e alto Douro, UTAD, Quinta de Prados, 5000-801 Vila Real, Portugal, gpereira@utad.pt*

Abstract
Biomass burning is extremely important at the global, regional and local scales and has impressive impacts at the atmospheric, climatic, environmental and socio-economical levels. The temperate biome of the Mediterranean regions is characterised by rainy and mild winters followed by warm and dry summers that make the region especially prone to the occurrence of a large number of summer fire events. In this context, the 10-year (2003 – 2012) MODIS fire data, provided by the MODIS Fire Team (University of Maryland) is used to characterize the spatial and the temporal distribution of fire activity over western region of the Mediterranean basin, paying special attention to large fire episodes. Finally, an assessment of the role of meteorological conditions on large fire events is performed based on the analysis of low and mid atmospheric fields of geopotential, air temperature, relative humidity and wind.

Keywords*: Extreme fire activity; MODIS; Fire pixels; fire weather; atmospheric circulation patterns; Mediterranean*

Introduction

Biomass burning is an extremely important process from local to global scales with significant impacts at the atmospheric, environmental and socio-economical levels. Encompassing the lands around the Mediterranean Basin is associated to Mediterranean type of forests, woodlands, and shrub. This temperate biome is characterised by rainy and mild winters followed by warm and dry summers that make the region especially prone to the occurrence of a large number of fire events and to the onset of extreme episodes that account for the bulk of burned area in the whole fire season (Pereira *et al*., 2005, Trigo *et al*., 2006; Amraoui *et al*., 2010). The Western part of Mediterranean basin, which includes the Iberian Peninsula, Southern France and Sardinia in Europe and Northern coastal areas of Morocco, Algeria and Tunisia in North Africa, has been the most affected by vegetation fires in the last decades (Schmuck *et al*., 2013). In the above mentioned countries, fire ignition is strongly conditioned by human behaviour and socioeconomic activities (Costa *et al*., 2010). Nevertheless, natural factors like the morphology of the landscape, land use, land cover, weather and climate strongly affect wildfire activity (Amraoui *et al*., 2013). In fact, weather and climate have a profound influence on all stages and aspects of biomass burning from ignition, spread and behaviour up to severity and effects (Benson *et al*., 2008).
The vast majority of burned area in Mediterranean regions is due to a reduced number of extreme events that occur during a short period of time, and are associated to several atmospheric processes interacting at different temporal and spatial scales (Pereira *et al*., 2005). These facts motivate focusing attention on the extreme events of fire activity and on the role of weather conditions on fire activity during these cases.

In terms of accuracy and reliability, satellite information appears as a very appealing tool to monitor fire activity over the entire globe and have led to the development of a consistent long-term record of global fires (Justice and Korontzi, 2001) due to: (*i*) its homogeneity in space and time and (*ii*) its several advantages over classical databases of ground-based measurements where the computation of burned area or number of fire occurrences not only depend on the policies of the different countries but are also usually estimated by visual inspection (Pereira *et al*., 2011; Amraoui *et al*., 2013).
In this context, the Moderate Resolution Imaging Spectroradiometer (MODIS) on board the polar orbiting Terra and Aqua satellites of National Aeronautics and Space Administration (NASA) Earth Observing System (launched in 1999 and 2002, respectively) was the first instrument with spectral characteristics designed specifically for active fire detection (Kaufman *et al*., 1998) and, consequently, the MODIS active fire product (Justice *et al*., 2002) is the most consistent database of burned area and active fires at different spatial and temporal scales (Csiszar el al., 2005; Oom and Pereira, 2013).
The main objective of this work is to use the 10-year (2003 – 2012) database of the MODIS active fire product, composed by daily numbers of fire pixels: (*i*) to characterize the extreme fire activity episodes (hereafter EFAE) occurred over the Iberian Peninsula and the Northern Africa, throughout the year (extending the study to the months outside the fire season) and (*ii*) to characterize the associated meteorological conditions of these extreme events based on the analysis of low and mid atmospheric fields such as wind, air temperature, relative humidity, mean sea level pressure and geopotential.

Data and Methods

Active fire data

The fire dataset covers a 10-year period, from January 2003 to December 2012, of the MCD14ML Collection 5 active fire product (Justice *et al*., 2002), obtained from MODIS imagery data with a spatial resolution of 1 km at nadir. Fire detection is performed using a contextual algorithm that exploits the strong emission of mid-infrared radiation from fires and is based on brightness temperatures derived from the 3.9 and 10.5 μm channels (Giglio *et al*., 2003).
During the considered 10-year period, there is a grand total of 126 887 fire pixels detected in the study area. The spatial distribution of these fire pixels suggests the existence of two separated sub-regions with highest fire activity namely, the Northern and Western parts of Iberian Peninsula (hereafter NWIP) and the Northern Africa and South-Eastern Iberia (hereafter NAFR) accounting for about 57% and 40% of the grand total, respectively. This evidence is even consubstantiated by the impressive anti-correlation (- 99%) between relative number of fire activity in these two sub-regions (Figure 1).

Meteorological data

The meteorological conditions associated to extreme fire activity were derived using the horizontal fields of ERA-Interim data (Dee *et al*., 2011) provided by the European Centre for Medium-Range Weather Forecasts (ECMWF). The following meteorological data were extracted over the Western Mediterranean sector (30^0W – 20^0E, 20^0N – 60^0N), at 12 UTC, for the period of 30 years (1983 – 2012), and then projected onto a $0.75^0 \times 0.75^0$ latitude/longitude grid:

- mean sea level pressure (hereafter MSLP);
- air temperature at 2 metres height (hereafter T2m);
- wind speed and direction at 10 metres (hereafter W10m);
- air temperature, geopotential height and relative humidity at 850 hPa which corresponds to approximately 1 500 m of altitude (hereafter T850, Z850 and RH850, respectively); geopotential height at 500 hPa, in the mid atmosphere, at about 5 000 m of altitude (hereafter Z500).

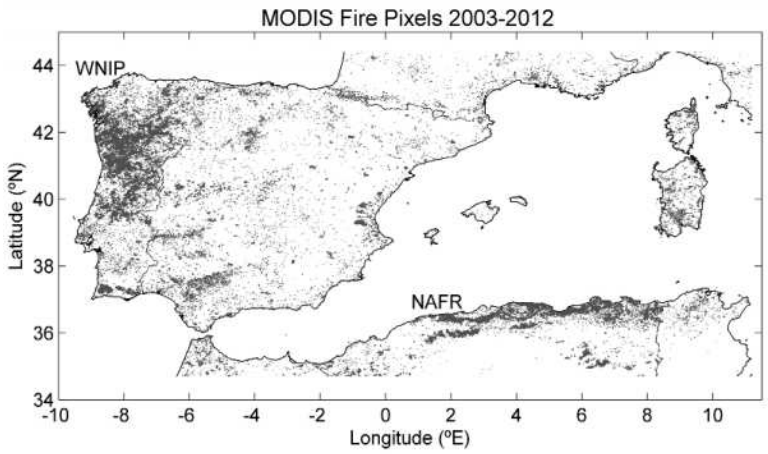

Figure 1. MODIS Fire pixels over Western Mediterranean region from January 2003 to December 2012.

2.3. Methods

The EFAE throughout the study period were identified by the use of two criteria: (*i*) at least 3 consecutive days with number of fire pixels above the 95th percentile; and, (*ii*) a minimum of 10 fire pixels per day in the same sub-region. These criteria led to the identification of a total number of 35 EFAE with the following spatial distribution: 31 of cases in NWIP; 3 events in NAFR; and 1 particular case that cannot be clearly classified in any of the previous clusters. It is worth noting that 18 of EFAE located in NWIP sub-region have occurred during summer period (May to October) and the remaining 13 episodes during winter period (November to April). On the other hand, all the 3 EFAE occurred in the NAFR sub-region were detected in the summer months (June, July and August).

An assessment of the role played by the meteorological conditions during the EFAE may be performed by analysing the associated horizontal patterns of meteorological fields. For this purpose, reference fields of meteorological variables were computed for each day of the year by averaging the respective 12 UTC meteorological fields for the same day over the entire reference period of 1983 – 2012. Daily anomalies were then computed as departures of each daily field from the reference field (for that day). Finally, composites and anomalies of the meteorological fields were derived by averaging the field's daily values and anomalies for the days of each EFAE.

Results

An exhaustive analysis of all meteorological variables listed in section 2.2 was performed for each day of the 34 EFAE. The spatial patterns of the obtained composites and anomalies allow stating that the atmospheric conditions were very similar for all days of EFAE in each sub-region and season which lead to the definition of three clusters of EFAE, namely NWIP-Summer, NWIP-Winter and NAFR-Summer.

The similarity between the meteorological patterns of each day of the EFAE associated to the same cluster, leads to present results of only one case for each cluster that illustrate the typical atmospheric conditions associated to extreme fire activity of the respective cluster. The chosen extreme episodes are: 11 – 18 October 2011, 21 February – 2 March 2012 and 27 – 30 August 2007 corresponding to the NWIP-Summer, the NWIP-Winter and the NAFR-Summer clusters, respectively. For sake of simplicity, only the anomaly composites of meteorological variables obtained for each EFAE will be presented (Figures 2 to 4).

The episode of 11 – 18 October 2011 (NWIP-Summer)

The anomalous synoptic conditions at the surface (Figure 2b) and at 850 hPa (Figure 2c) are characterized by an amplified Azores anticyclone extending from the Atlantic to Central Europe and by a sub-Saharan thermal low centred at South Algeria. The MSLP and W10m dynamical fields over the region are characterised by isobars with SE-NW orientation and geostrophic winds resulting from the convergence of NE winds over Europe and SE winds from the Northern Africa. This circulation pattern leads to strong North-Eastern and South-Eastern advections of continental dry and warm air, resulting in high surface air temperatures over the Western Iberia and in the extreme air temperature anomalies, exceeding 7ºC in both 2 metres height temperature and temperature at 850 hPa.

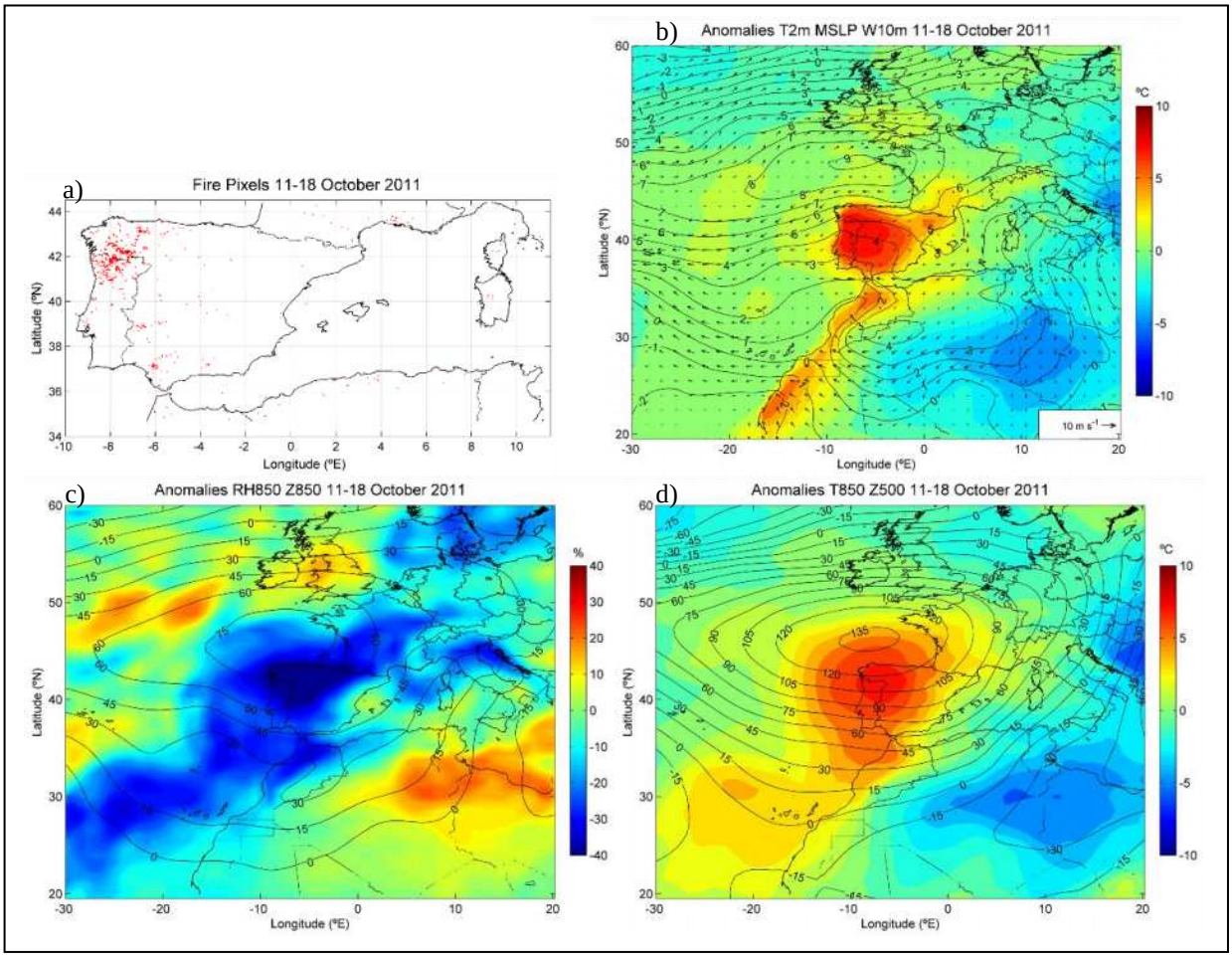

Figure 2. MODIS Fire pixels (red dot) over Western Mediterranean region detected during the EFAE of 11 – 18 October 2011 belonging to the NWIP-Summer cluster (upper left panel). The associated anomalies composites of multiple low and mid atmospheric fields are also shown: (b) air temperature (°C) at 2m height (T2m) mean sea level pressure (MSLP) and wind ($m \cdot s^{-1}$) at 10 m (W10); (c) relative humidity (%) at 850 hPa (RH850) and geopotential height (gpm) at 850 hPa (Z850); (d) air temperature (°C) at 850 hPa (T850) and geopotential height (gpm) at 500 hPa (Z500).

Relative humidity at 850 hPa level reveals the presence of very dry air over the Western and the Northern parts of the Iberian Peninsula reaching the impressive value of 25% with anomalies lower than -35%. Composite of the atmospheric flow at 500 hPa (not shown) reveals synoptic baroclinic activity with a pronounced ridge with axes in the Southwest to Northeast direction over the Atlantic Ocean and at Iberia, forcing warmer and drier air mass into the NWIP sub-region. The patterns of composite anomalies at 500 hPa level (Figure 2d), exhibit positive departures of 135 gpm enhancing

the subsidence of air into the Troposphere and reinforcing the increase of air temperature through adiabatic heating at lower levels.

3.2. The episode of 21 February – 2 March 2012 (NWIP-winter)

The synoptic conditions are characterized by an anticyclonic blocking activity over Eastern Atlantic which evolved in altitude into a predominant omega pattern located West of Europe and constituted by the huge high-pressure ridge and two troughs, the first one positioned over Central Atlantic at West of the Canary Isles, and the second one over Central Europe. It is worth stressing that the above mentioned anomalous circulation patterns at the low and mid-Troposphere levels exhibit positive departures of Z850 and Z500 reaching, respectively, to the impressive values of about 100 and 200 gpm (Figures 3c and 3d) North of the Iberian Peninsula.

The temperature anomalies over the sub-region are lower than the previous episode reaching values of about 3ºC for both the T2m ant T850 temperatures (Figures 3b and 3d). As in the preceding episode, relative humidity at 850 hPa level shows the presence of very dry air over the sub-region decreasing to the impressive value of 30% with anomalies lower than -40%.

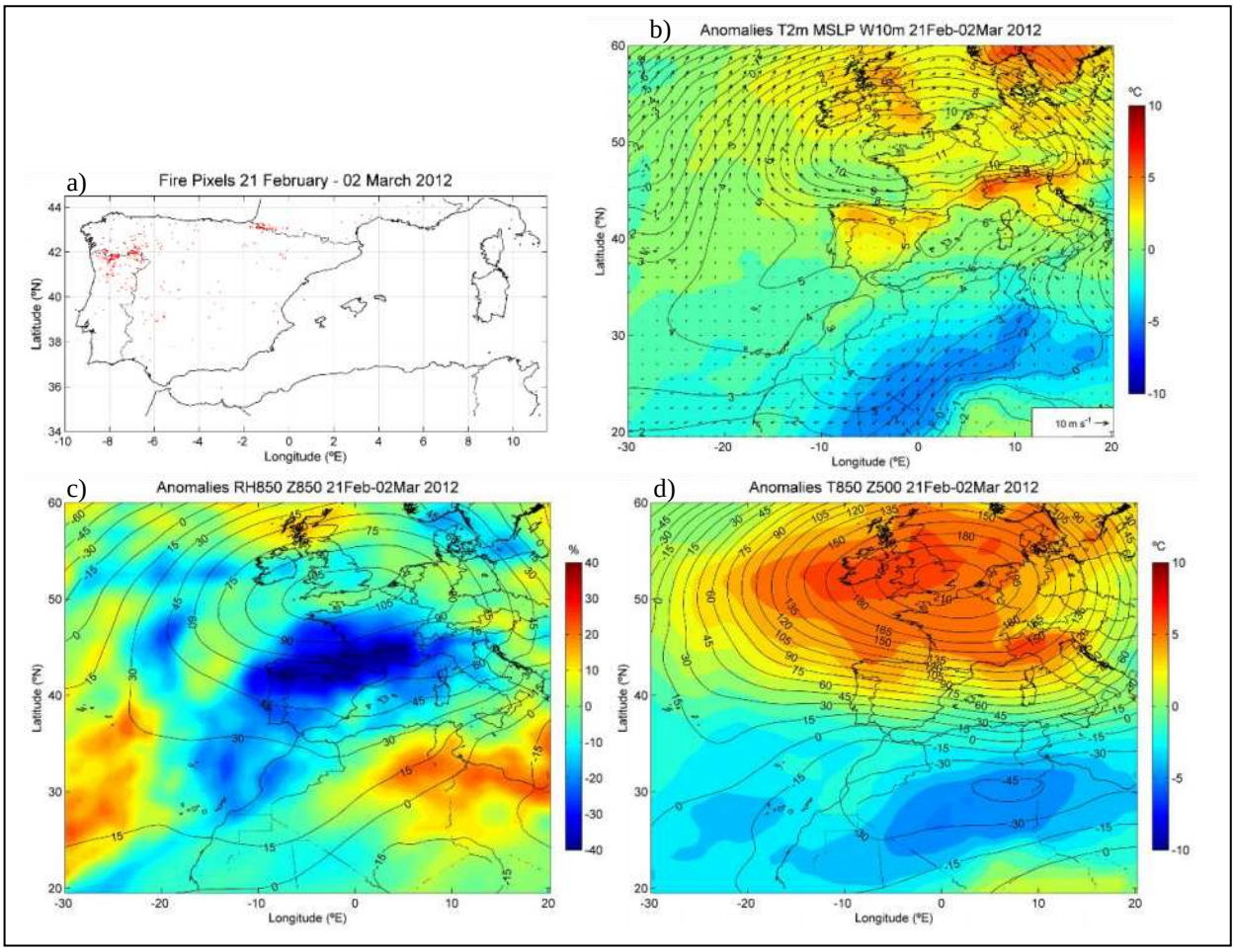

Figure 3. As in Figure 2 but respecting to the EFAE of 21 February – 2 March 2012 belonging to the NWIP-Winter cluster.

3.3. The episode of 27-30 August 2007 (NAFR-Summer)

The atmospheric conditions of the episode occurred during the month of August 2007 in North African sub-region is quite different from those obtained for NWIP during winter or summer periods. At the surface, the circulation is dominated by an intense Southerly/South-Easterly advection of very hot and

very dry Saharan air, brought to the region by the anticyclonic circulation centred over South Italy and the cyclonic flow due to the presence of a Saharan heat low centred over South-Western Algeria and to the Atlas Low located in Central Morocco. The associated high departure values of air temperature (above 7 ºC) obtained in both T2m and T850 (Figures 4b and 4d), and very low departure values of relative humidity at 850 hPa reaching the value of -25% (Figure 4c) are well apparent over this sub-region.

The atmospheric circulation at the 500 hPa level is dominated by a pronounced ridge whose axis is directed from Southwest to Northeast (not shown), affecting the Northern Algeria and Tunisia and bringing warmer and drier air mass to the region. It may be observed that the location of the referred ridge over Western Mediterranean basin is associated to positive departures of Z500 of about 60 gpm (Figure 4d), which delimit a region over Eastern part of Iberia and Northern Algeria and Tunisia, revealing a region characterized by enhancement of the air subsidence into Troposphere, leading to an increase of air temperature through adiabatic heating at lower levels.

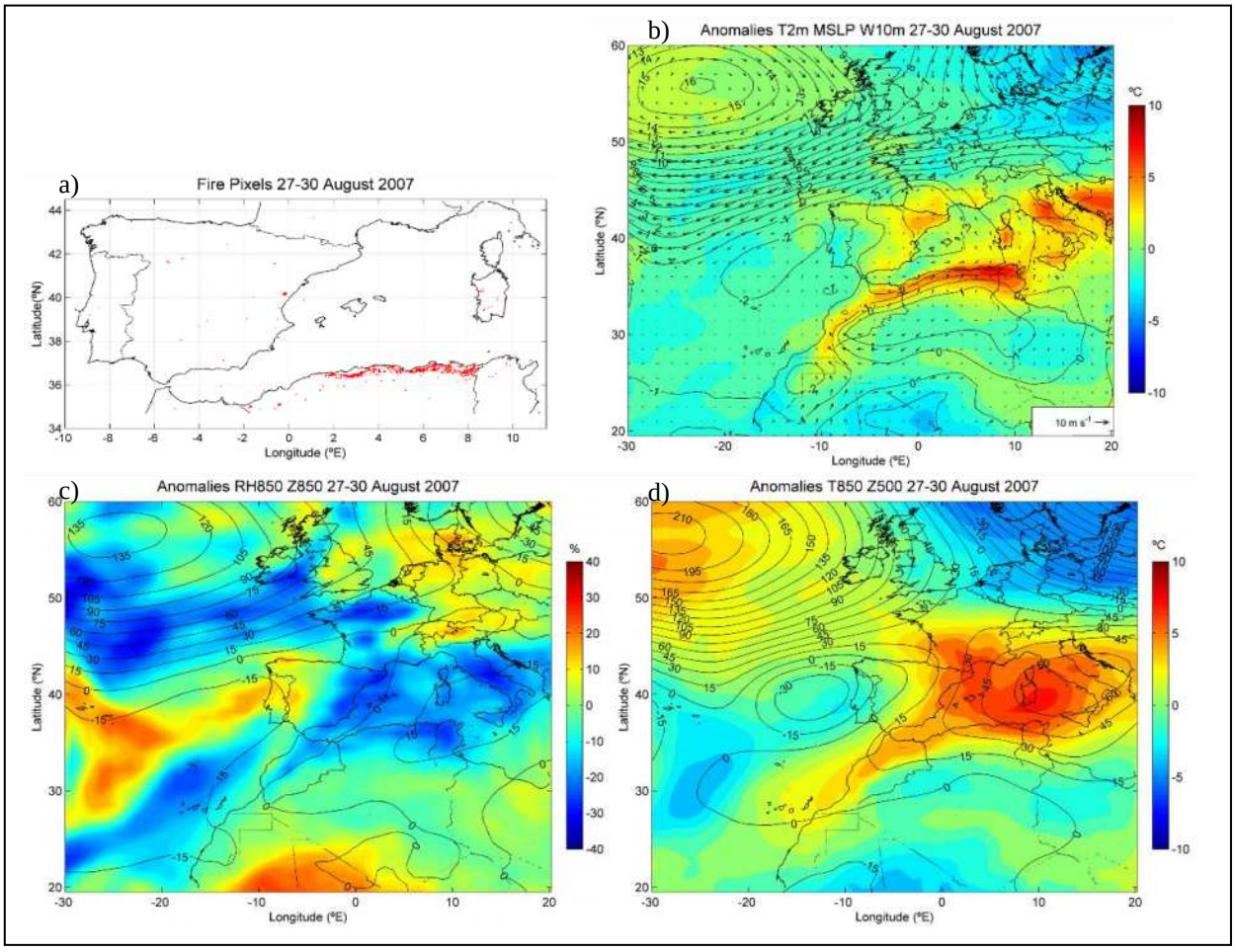

Figure 4. As in Figure 2 but respecting to the EFAE of 27 – 30 August 2007 belonging to the NAFR-Summer cluster.

Conclusions

The main objective of the present study is to identify and characterize the atmospheric conditions associated with extreme fire activity episodes occurred over Iberia and Northern Africa mainly because: (*i*) these regions comprises the European and North African countries most affected by fires

(Pereira *et al*., 2011, Schmuck *et al*., 2013); and, (*ii*) weather and climate proved to be the most important factor to the fire regime in the region (e.g. Rasilla *et al*., 2010; Amraoui *et al*, 2013).
The spatial distribution of fire pixels detected by MODIS over Western Mediterranean region during the 10-year (2003 – 2012) period reveals the existence of two sub-regions particularly affected by this natural hazard (Figure 1): the Western and Northern parts of Iberian Peninsula (NWIP); and South-Eastern Iberia and Northern region of Algeria and Tunisia, in North of Africa (NAFR).
The non-seasonal approach used in this study, based on the two criteria mentioned in section 2.3, allows the identification of the major extreme fire activity episodes over the region and the determination of the associated atmospheric patterns, applying the methodology previously validated for Portugal, Italy and Greece during summer (Pereira *et al*., 2005; Trigo *et al*., 2013; Amraoui *et al*., 2013). Thereby, the EFAE were identified in the two sub-regions: 3 episodes observed in the NAFR sub-region and occurred during summer season (June, July and August) and 31 episodes detected in the NWIP and occurred throughout the year even outside the summer fire season, 13 of them during the winter season (November to May) and the remaining 18 episodes during the summer season (June to October). Accordingly, all EFAE were grouped into 3 clusters depending on the sub-region and on the season of occurrence: NWIP-summer, NWIP-winter and NAFR-summer clusters. The similarity between the meteorological patterns of the EFAE associated to the same cluster, leads to present results of only one case for each cluster that illustrate the typical atmospheric conditions associated to extreme fire activity of the respective cluster.
The most important features of the meteorological anomaly fields associated with the presented 3 EFAE belonging to the 3 different clusters are the positive anomalies of T2m and T850 and the impressive negative anomalies of RH850 over most of the corresponding sub-region. It is worth noting that the temperature parameter (T2m) is not the most critical factor to the occurrence of vegetation fires during the winter season. For instance, the T2m of the EFAE belonging to the NWIP-Winter cluster presented in this study (21 February – 2 March 2012), reached a small value of 13ºC (with an anomaly that does not exceed 3ºC) over the NWIP sub-region corresponding to a typical value for the mentioned sub-region and season.
The atmospheric circulation patterns of the EFAE occurred in NWIP during summer and winter are essentially characterized by Eastern advection of air at surface and higher levels usually associated to the influence of the Azores high pressure system and the occurrence of heat waves episodes during summer and Atlantic anticyclone blocking events during winter which imply clear sky conditions and enhanced of radiative heating/cooling over the sub-region.
Atmospheric patterns responsible for the occurrence of EFAE in NAFR sub-region during summer season are dominated by very hot and dry South-Easterly winds (*Scirocco* winds), due to the anticyclonic circulation centred over South Italy, and by the cyclonic flow resulting from the presence of a Saharan heat low centred over South-Western Algeria and the Atlas Low located in Central Morocco. The atmospheric circulation at the 500 hPa level is dominated by a pronounced ridge affecting the Northern Algeria and Tunisia that brings warmer and drier air mass to the sub-region.
Finally, the identification and characterization of the atmospheric conditions associated with extreme fire activity episodes is of paramount importance for (*i*) the planning and management of fire prevention activities and fire suppression resources, because the time of occurrence and persistence of such conditions may be predicted with current weather forecasting systems for periods of days up to a 1 – 2 weeks and (*ii*) to improve future projections of fire activity based on estimated changes on their frequency, magnitude and duration for different scenarios of climate change (Dury *et al*., 2010; Pereira *et al*., 2013).

References

Amraoui M, Calado T, Pereira M, DaCamara C (2010) High fire activity and associated atmospheric circulation patterns over the Mediterranean basin. *EGU General Assembly 2010* **12**, EGU2010-15533.

Amraoui M, Liberato MLR, Calado TJ, DaCamara CC, Pinto Coelho L, Trigo RM, Gouveia CM (2013) Fire activity over Mediterranean Europe based on information from Meteosat-8. *Forest Ecology and Management* **294**, 62-75.

Benson RP, Roads JO, Wiese DR (2008) Climatic and weather factors affecting fire occurrence and behaviour. In ´Developments in Environment Science´. (Eds A Bytnerowicz, M Arbaugh, A. Riebau, C. Andersen) **8**, pp. 37–59. ISSN: 1474–8177. DOI: 10.1016/S1474-8177(08)00002-8.

Costa L, Thonicke K, Poulter B, Badek FW (2010) Sensitivity of Portuguese forest fires to climatic, human, and landscape variables: subnational differences between fire drivers in extreme fire years and decadal averages. *Regional Environmental Change* **11(3)**, 543–551.

Csiszar I, Denis L, Giglio L, Justice CO, Hewson J (2005) Global fire activity from two years of MODIS data. *International Journal of Wildland Fire* **14**, 117-130.

Dee DP, Uppala SM, Simmons AJ, Berrisford P, Poli P, Kobayashi S, Andrae U, Balmaseda MA, Balsamo G, Bauer P, Bechtold P, Beljaars ACM, van de Berg L, Bidlot J, Bormann N, Delsol C, Dragani R, Fuentes M, Geer AJ, Haimberger L, Healy SB, Hersbach H, Hólm EV, Isaksen L, Kållberg P, Köhler M, Matricardi M, McNally AP, Monge-Sanz BM, Morcrette J-J, Park B-K, Peubey C, de Rosnay P, Tavolato C, Thépaut J-N, Vitart F (2011) The ERA-Interim reanalysis: configuration and performance of the data assimilation system. *Quarterly Journal of the Royal Meteorological Society* **137**, 553–597.

Dury M, Hambuckers A, Warnant P, Henrot A, Favre E, Ouberdous M, François L (2010) Responses of European forest ecosystems to 21st century climate: assessing changes in interannual variability and fire intensity. *iForest Biogeosciences and Forestry* **4**, 82-99.

Giglio L, Descloitres J, Justice CO, Kaufman YJ (2003) An enhanced contextual fire detection algorithm for MODIS. *Remote Sensing of Environment* **87**, 273-282.

Justice CO, Korontzi SA (2001) A review of the status of satellite fire monitoring and the requirements for global environmental change research. In ´Global and regional vegetation fire monitoring from space: planning a coordinated international effort´. (Eds FJ Ahern, JG Goldammer, CO Justice) pp. 1–18. (SPB Academic Publishing: New York, NY, USA).

Justice CO, Giglio L, Korontzi S, Owens J, Morisette JT, Roy D, Descloitres J, Alleaume S, Petitcolin F, Kaufman Y (2002) The MODIS fire products. *Remote Sensing of Environment* **83**, 244-262.

Kaufman YL, Justice CO, Flynn L, Kendall JD, Prins E, Giglio L, Ward DE, Menzel WP, Setzer AW (1998) Potential global fire monitoring from EOS-MODIS. *Journal of Geophysical Research* **103**, 215-238.

Oom D, Pereira JMC (2013) Exploratory spatial data analysis of global MODIS active fire data. *International Journal of Applied Earth Observation and Geoinformation* **21**, 326-340.

Pereira MG, Trigo RM, DaCamara CC, Pereira JMC, Leite SM (2005) Synoptic patterns associated with large summer forest fires in Portugal. *Agricultural and Forest Meteorology* **129**, 11-25.

Pereira MG, Malamud BD, Trigo RM, Alves PI (2011) The history and characteristics of the 1980–2005 Portuguese rural fire database. *Natural Hazards and Earth System Science* **11**, 3343 - 3358.

Pereira MG, Calado TJ, DaCamara CC, Calheiros T (2013) Effects of regional climate change on rural fires in Portugal. *Climate Research* **57**,187-200.

Rasilla DF, García-Cordon JC, Carracedo V, Concepción D (2010) Circulation patterns, wildfire risk and wildfire occurrence at continental Spain. *Physics and Chemistry of the Earth* **35**, 553-560.

Trigo RM, Pereira JM, Pereira MG, Mota B, Calado MT, DaCamara CC, Santo FE (2006) The exceptional fire season of summer 2003 in Portugal. *International Journal of Climatology* **26**, 1741-1757.

Trigo RM, Sousa PM, Pereira MG, Rasilla D, Gouveia CM (2013) Modelling wildfire activity in Iberia with different atmospheric circulation weather types. *International Journal of Climatology*, doi: 10.1002/joc.3749.

Schmuck G, San-Miguel-Ayanz J, Camia A, Durrant T, Boca R, Libertá G, Schulte E (2013): Forest fires in Europe, Middle East and North Africa 2012. Publications Office of the European Union, JRC Technical Reports.

Short term forecasting of large scale wind-driven wildfires using thermal imaging and inverse modelling techniques

Oriol Rios[a], Elsa Pastor[a], Diana Tarragó[a], Guillermo Rein[b], Eulàlia Planas[a]

[a] *Department of Chemical Engineering, Centre for Technological Risk Studies, Universitat Politècnica de Catalunya–BarcelonaTech, Diagonal 647, E-08028 Barcelona, Catalonia, Spain.* *oriol.rios@upc.edu, diana.tarrago@upc.edu, elsa.pastor@upc.edu, eulalia.planas@upc.edu*
[b] *Department of Mechanical Engineering, Imperial College London, SW72AZ, London, UK.* *g.rein@imperial.ac.uk*

Abstract
A key factor in decision-making process during a wildfire incident is counting on the forecast of how the fire is likely to behave in different fuels, weather conditions and terrain. Wildfire models and simulators attempt to assist fire responders in gaining understanding of the fire behaviour. The main hurdle to overcome when applying such technologies at operational level is the lack of a complete model that describes wildfire governing physics and the trade-off between accuracy and computing time. A forecasting prediction must be delivered within a positive lead time and current physical models are far beyond this requirement.
Inverse modelling and data assimilation techniques offer a great potential of operational applicability in wildfires, coupling fire monitoring and fire behaviour forecast at real time. With this approach, a better description of the processes simulated by the fire behaviour models can be achieved when adding real-state information of the system, since discrepancies between simulated fire behaviour variables and observed variables are minimized. The use of this approach accelerates fire simulations without loss of forecast accuracy.
In this paper we explore the adaptation to real fire scenarios of a synthetic-data-based inverse modelling structure for fire behaviour forecast. Improvements are investigated to extrapolate the already existing algorithm to real data assimilation from IR aerial monitoring. The technique explores elliptical Huygens expansion coupled with simple -yet effective- semi-empirical wildfire models. The algorithm assimilates fire fronts positions extracted from airborne thermal imaging and additional available data as wind speed and direction or fuel characteristics. The invariants -set of governing parameters that are mutually independent and constant for a significant amount of time- are resolved by means of forward model and linear tangent minimization.
The technique has been adapted to be employed in large-scale mallee-heath shrubland fires experiments conducted in South Australia in 2008. Fires were filmed with a helicopter transported TIR camera. The IR images were processed to obtain the position of the fire perimeter at a maximum frequency of one isochrone every 10 seconds. The algorithm shows great capability to simulate fire fronts observations and opens the door to keep developing a fully automatic data assimilation algorithm with forecasting capacity.

Keywords*: inverse modelling, data assimilation, infrared imagery, shrubland fire behaviour.*

Introduction

Fire managers need to obtain real-time information as fast as possible in order to make quick potentially impactful decisions. They have to keep track of fire behaviour and suppression activities at all times with the responsibility of safeguarding physical integrity of all the individuals involved in the emergency. In response to this need, numerous activities have been recently under way to take advantage of new opportunities and technology for wildland fire management. Over the past few years several public wildfire agencies have been benefiting from different information technology tools that allow monitoring fire activity and fire brigades. A good example of such advances is the implementation of airborne fire monitoring apparatuses combined with global geo-positioning systems so that both fire and suppression resources can be tracked. With these systems, images of any interesting spot of the fire scenario can be obtained in the infrared (IR) and visible spectrum and

transferred in real-time to the commander work station of the fire incident, so that fire managers can have more readily available information for decision-making. However, the use of this systems is currently less cost-effective than it could, not only because of the specificity of all the compounds and the costs associated to the airborne platform (e.g. surveillance helicopters and aircrafts) but also because the information they provide is not exploited quantitatively, particularly, for forecasting purposes.

A key factor in decision-making process during a wildfire incident is counting on the forecast of how the fire is likely to behave in different fuels, weather conditions and terrain. Wildfire models and simulators attempt to assist fire responders in gaining understanding of the fire behaviour. The main hurdle to overcome when applying such technologies at operational level is the lack of a complete model that describes wildfire governing physics (Finney *et al*., 2013) and the trade-off between accuracy and computing time. A forecasting prediction must be delivered within a positive lead time (time ahead of the predicted event) and current physical models are far beyond this requirement. Inverse modelling and data assimilation techniques offer a great potential for operational applicability in wildfires, coupling fire monitoring and fire behaviour forecast at real time. With this approach, a better description of the processes simulated by the fire behaviour models can be achieved when adding real-state information of the system, since discrepancies between simulated fire behaviour variables and observed variables are minimized. The use of this approach accelerates fire simulations without loss of forecast accuracy (Mandel *et al*., 2008), (Jahn *et al*., 2011), (Rochoux *et al*., 2012).

In this paper we explore the adaptation of a synthetic data assimilation-based forecasting algorithm to deal with large scale real sensed data. The algorithm to be adapted is based on the identification of some invariants (model components that are constant for a given period of time and area, such as fuel depth, moisture content, packing ratio, etc.) that are determined through an optimization process during a given assimilating window. This technique has shown great performance when challenged with synthetic data (Rios, Jahn, & Rein, 2014) but its adaptation to a real case scenarios will require special attention. The real data that will be used are fire fronts isochrones obtained by airborne infrared imaging in mallee-heath shrublands experimental burns conducted in South Australia in 2008 (Cruz, McCaw, Anderson, & Gould, 2013; Pérez, Pastor, Planas, Plucinski, & Gould, 2011).

Data assimilation and inverse modelling

Data assimilation has been historically developed and applied in the weather forecasting discipline to combine observations with the models and improve forecasts with available sensed data (Kalnay, 2003). One of the most common strategies used to merge assimilated data with the model is by means of inverse modelling.

Inverse modelling is particularly appropriate for wildfires modelling due to large amount of unknowns in terms of environmental parameters, such as fuel physical properties (e.g. fuel elements distribution and thermal characteristics), weather inputs (e.g. wind profile, ambient temperature gradient and relative humidity) and terrain features (e.g. slope and aspect variability). There are numerous necessary variables to initialise a physical classical forecasting model and hardly ever can all be measured. By contrast, the inverse approach can use any kind of available data to improve the forecast if the forward model is tweaked accordingly.

Despite its great capacity for coping with complex problems with a large number of variables, still few authors have tried to apply it to the fire field. Among these, Jahn *et al*. (Jahn, Rein, and Torero 2011, Jahn, Rein, and Torero 2012) successfully pioneered this approach to forecast fires in enclosures using both simple and complex models (two zones models and Computer Fluid Dynamics, CFD models).

In the field of wildfires, Mandel *et al*. (Mandel, Beezley, Coen, & Kim, 2009) explored this technique to predict time-temperature curve of a sensor placed in the way of an advancing fire. They examined a reaction-diffusion equation and a semi-empirical fire line propagation model coupled with an

Eulerian level-set-based equation. Additionally, they coupled weather forecast information to the model demonstrating the powerful potential of data assimilation. Despite its potential, their implementation was found to be unstable due to the ill-definition of temperature measurements in a wildfire.
Following this work, Rochoux *et al*. (Rochoux, Delmotte, Cuenot, Ricci, & Trouvé, 2012b), (Rochoux, Emery, Ricci, Cuenot, & Trouvé, 2014) developed a data assimilation algorithm using ensemble Kalman filters and a state estimation approach. The forward model (named "Firefly") was composed of a Rothermel based propagation equation for rate of spread (RoS) and a level set approach to propagate the front. The algorithm was tested with synthetically generated data and with a controlled small scale (4 x 4 m) grassland experiment with spatially-varying fuel depth and temporally-varying wind speed and direction. One of the main drawbacks of the algorithm lies in the fact that the model deals with errors using Kalman Filters which implies the assumption that the errors are normally distributed. However, in fire, errors do not follow a Gaussian distribution (Johns & Mandel, 2008). Nevertheless, the approach reinforces the potential of data assimilation in wildfire forecasting.

Simple synthetic validation

As has been mentioned, the work at hand is the improvement an adaptation to a real data context of a forecasting algorithm developed by Rios *et al*. (Rios *et al*., 2014). The algorithm is based on Huygens light propagation principle applied to wildfires propagation (Richards, 1990), (Richards, 1993) together with Rothermel model (Rothermel, 1972) to compute RoS. The Huygens principle assumes that each node in the front acts as a new elliptical propagation ignition point. Each ellipse –firelet– has the main axis directed towards the wind-slope vector (assumed to be the main propagation direction) and the magnitude of its axis is defined by equations [1-3] (Figure 1). The curve that envelopes all the firelets is then the new fire front (Figure 2).

$$a(s,t) = RoS(s,t) \cdot \frac{1 + \left(LB - \sqrt{LB^2 - 1}\right)^2}{2 \cdot LB} \quad \textbf{[1]}$$

$$b(s,t) = RoS(s,t) \cdot \frac{1 + \left(LB - \sqrt{LB^2 - 1}\right)^2}{2} \quad \textbf{[2]}$$

$$c(s,t) = b(s,t) - \frac{RoS(s,t)}{\left(LB + \sqrt{LB^2 - 1}\right)^2} \quad \textbf{[3]}$$

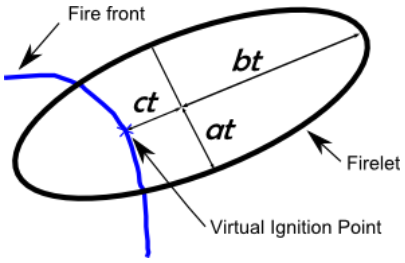

Figure 1:Firelet axis geometry

Where *LB* is the length-to-breadth ratio and is defined by Anderson *et al*. (Anderson, Catchpole, De Mestre, & Parkes, 1982) throughout an experimental correlation with the wind-slope vector and *s* is the front parameterization variable.

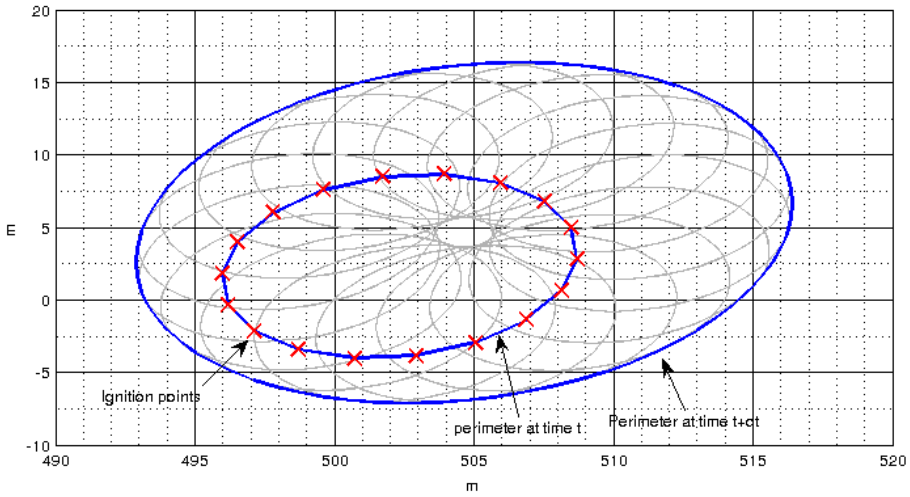

Figure 2. Illustration of the Huygens' Principle applied to fire spread. The fire front at time t is discretized into vertices (red crosses). Each of this vertex become the point source for local elliptical expansions (firelets). The curve that envelopes all the firelets is the new fire perimeter at time t + dt.

The optimization problem to find the invariants that best reproduce the assimilated fire fronts used a Tangent Lineal Model approach and an automatic differentiation of the forward model. To check the performance of the algorithm, different configurations of invariants were checked. In some cases, up to 4 invariants were estimated during the optimization loop and non-homogeneous fuel distribution together with temporally-varying wind direction and speed were used to recreate more real scenarios. The algorithm showed good capacity to identify the correct invariants and reproduce the assimilated fronts even when the first guested invariants value was 150% off the true value (see Figure 3). The computational process was fast and large lead times were achieved.

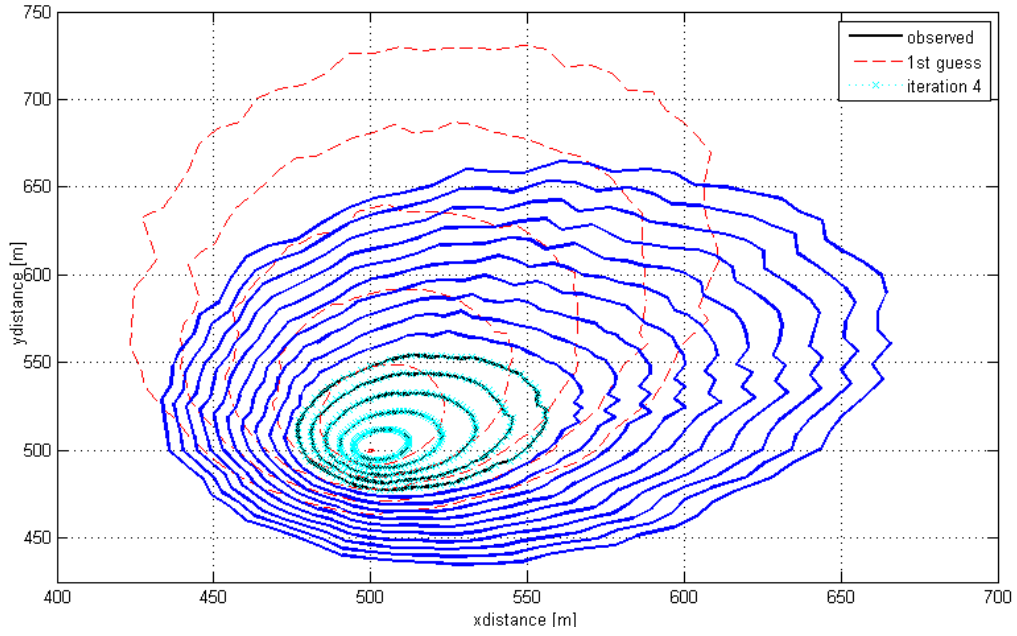

***Figure 3. Fire front convergence(dotted light blue lines) towards observed data (solid black line) after 4 iterations (after* Rios *et al.*, 2014)**

The complete flow diagram of the algorithm is presented inFigure 4. A first invariant's vector guess is needed to create the first forward model run. Together with the available assimilated fronts, the optimization loop identifies the most suitable invariants by means of automatic differentiation. When

a certain convergence is achieved the invariants are assumed to be properly estimated and a forecast can be delivered. This forecast will be valid as long as the invariants remain constant.

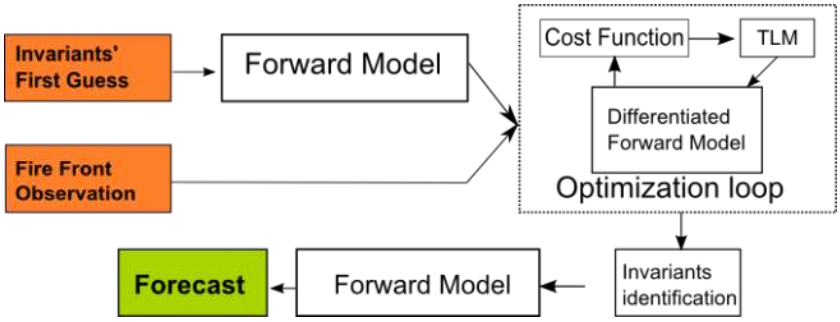

Figure 4: Diagram flow of the data assimilation algorithm. Orange boxes are input data whereas green box is the output of the algorithm.

Real data pitfalls

The use of real data to check the performance of the model rises some mathematical and computing problems that need to be addressed. First of all, a real fire front hardly is a closed curve, which is, however, one of the bases of the already existent algorithm (see Figure 3). There are many circumstances that may disable the fire to expand in all directions, e.g. line vs point ignition, perimeter interception by a firebreak, suppression activities, etc. Thus, the existing forward model has to be adapted to this reality and hence handle open ignition curves. For this reason, a new set of forward model differential equations needs to be implemented and integrated. Moreover, the simulated fire needs to stop on firebreaks (natural or suppression-made) or overtake them if they are inefficient. At this stage of our algorithm, when a simulated fire overtakes little fire breaks or vegetation has a great local change, the front creates sharp areas (see Figure 5) that have to be smoothed, hence improvements in terms of regridding and adding extra nodes on the perimeter have to be done. Due to this overtaking, the current code simulates front fingers that will overlap as fire propagates and recovers a convex shape (Figure 5), and because of that a filtering algorithm that correct this non-physical situations will need to be coupled to the model.

Regarding the assimilated data, in real scenarios data income concerning environmental parameters can be highly variable so the algorithm needs to be prepared to integrate data that are not regularly supplied on time and space.

Beyond the inherent algorithm difficulties, the use of the inverse modelling framework with real data also requires some additional remarks. While the assumption of the existence of some invariants parameters may remain correct for certain scenarios and time periods, it might not be such an invariant magnitude in the model that can reproduce the assimilated data, due to model simplicity. Therefore the forward model needs to be kept flexible enough to allow large adjustments and complex behaviours and front shapes. Similarly, the cost function optimization target value should not be kept too small since perfect convergence (i.e. perfect matching of simulated and observed fronts) might be impossible. Even in the cases where it converges close to zero, the correct invariant's value will not be known, and therefore the individual invariant convergence cannot be analysed as it was done in the synthetic data case.

Real case algorithm adaptation

In order to use our existing inverse modelling data assimilation structure with real sensed data some adaptation algorithms had to be implemented. This included new integration of the Huygen's expansion differential equations, a regridding algorithm, a loop clipping algorithm and a degridding algorithm.

3.1. Forward model equations

The previously implemented forward model equations did not allow the initial fire perimeters to be opened curves. Thus we implemented the integration of the differential equations originally developed by Richards (Richards, 1990) for the firelets enveloping curve defined by x and y coordinates:

$$\frac{\partial x(s,t)}{\partial t} = \frac{a^2 \cos\theta\left(\frac{\partial x}{\partial s}\sin\theta + \frac{\partial y}{\partial s}\cos\theta\right) - b^2 \sin\theta\left(\frac{\partial x}{\partial s}\cos\theta - \frac{\partial y}{\partial s}\sin\theta\right)}{\sqrt{\left(b^2\left(\frac{\partial x}{\partial s}\cos\theta - \frac{\partial y}{\partial s}\sin\theta\right)\right)^2 + \left(a^2\left(\frac{\partial x}{\partial s}\sin\theta + \frac{\partial y}{\partial s}\cos\theta\right)\right)^2}} + c\ \sin\theta \quad \textbf{[4]}$$

$$\frac{\partial y(s,t)}{\partial t} = \frac{-a^2 \sin\theta\left(\frac{\partial x}{\partial s}\sin\theta + \frac{\partial y}{\partial s}\cos\theta\right) - b^2 \cos\theta\left(\frac{\partial x}{\partial s}\cos\theta - \frac{\partial y}{\partial s}\sin\theta\right)}{\sqrt{\left(b^2\left(\frac{\partial x}{\partial s}\cos\theta - \frac{\partial y}{\partial s}\sin\theta\right)\right)^2 + \left(a^2\left(\frac{\partial x}{\partial s}\sin\theta + \frac{\partial y}{\partial s}\cos\theta\right)\right)^2}} + c\ \cos\theta \quad \textbf{[5]}$$

Where a, b and c are the firelet axis calculated with equations [1-3], θ is the wind-slope vector direction and s the curve parameterization parameter. These equations were numerically integrated using a Prediction-Corrector method based on central difference approximation.

3.2. Complementary algorithms

3.2.1. *Regridding algorithm*

As mentioned in section 2.2 a regridding algorithm was needed in order to avoid sharp zones formations due to firebreaks or rapid local fuel changes. The algorithm implemented, successively analyses the angles between three correlative segments. Then, if any of the two adjacent angles is larger than a given threshold a new node is inserted in the corresponding segment and the process is repeated until all the angles meet the condition. The effect of this step can be observed in Figure 5 (before applying the algorithm) and Figure 6 (after using it). In this case, the implemented open curve differential equations are used to propagate the front.

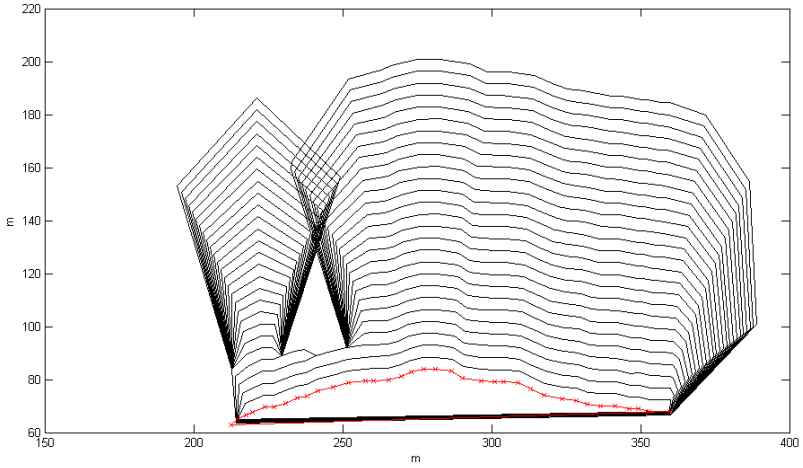

Figure 5. Propagation model showing pitfalls due to the presence of a firebreak (a rectangular 20x10m fire break is placed at coordinates [230, 90]). Line ignition (red crossed line), is taken from real fire data (shrubland experiments in South Australia 2008)

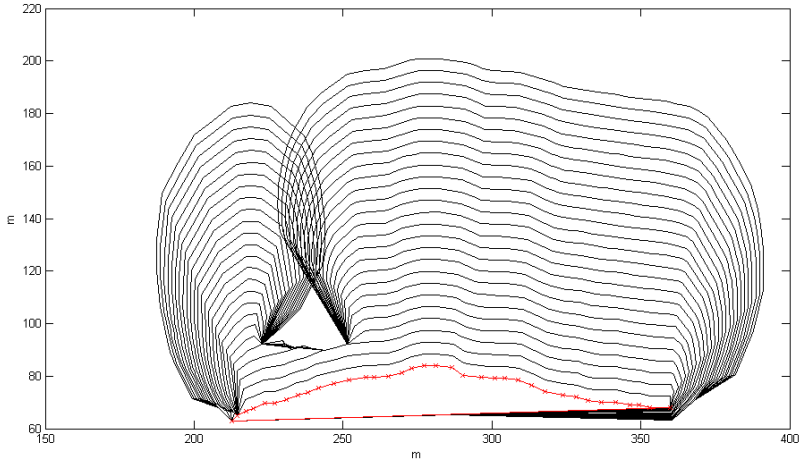

Figure 6. Effect of the regridding algorithm for the same front propagation around a firebreak as figure 5 for a threshold value of π/4 radians.

3.2.2. *Loop-clipping algorithm*

When the front became a convex curve and kept propagating, after overtaking a fire break or due to a local fire spread acceleration, our code created overlapping loops between two front fingers or even self-crossing loops. A loop-clipping algorithm was then implemented to avoid meaningless propagations such as fire propagating inwards in a self-crossing loop. The algorithm checks for intersections at any segment and identifies the section that has to be directly removed from the propagating front. Loop clipping can create sharp curves on the loop's intersection and therefore the regridding algorithm is again called afterwards.

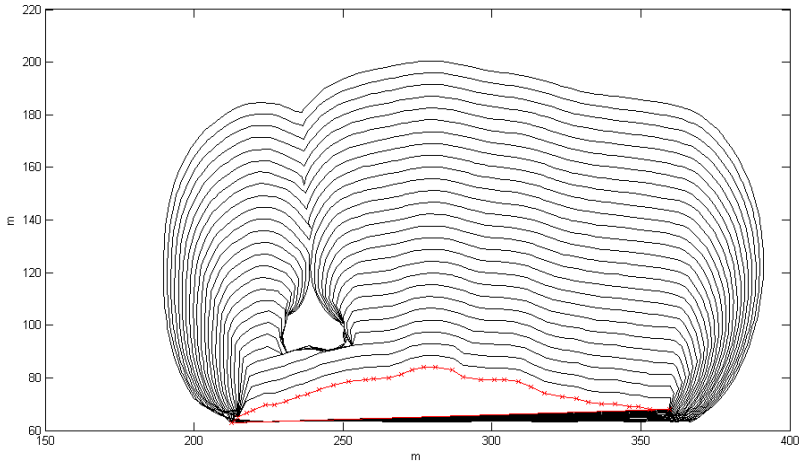

Figure 7. Effect of the loop clipping algorithm when applied to the same propagating case as Figure 6.

3.2.3. *Degridding algorithm*

After applying the mentioned improvements, as the forward model generated fire fronts and the loop clipping and regridding algorithms were run when needed, unnecessary nodes appeared in a non-curved region. To maintain performance and coherence a degridding algorithm had to be implemented. The algorithm looks for segments that are shorter than a given length (taken to be a multiple of the

spatial sensibility) and checks that the adjacent angle is smaller than this of regrinding algorithms. If both conditions are met, the node is removed from the front (Figure 8).

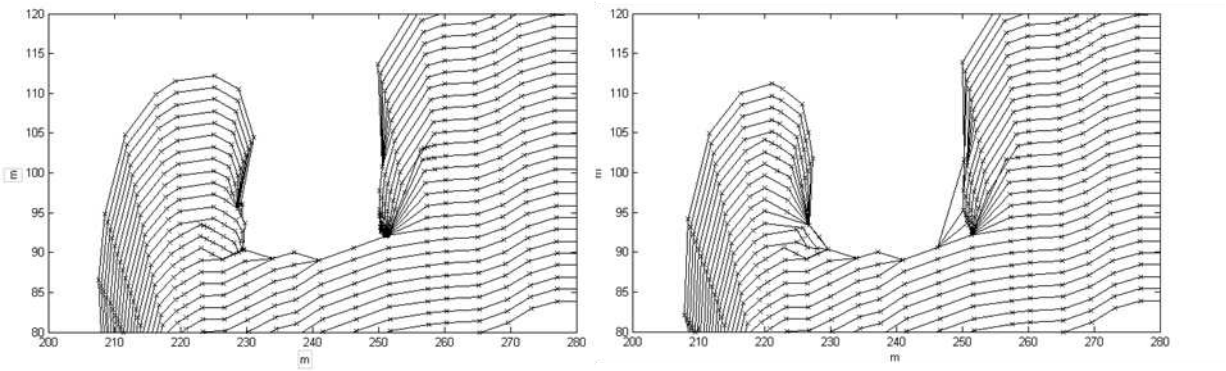

Figure 8. Around fire brake zones, the propagation algorithm creates regions of high and unnecessary node density (left figure). When the degridding algorithm is applied (right figure) those regions are reduced and the forward model can be run faster.

3.3. Inverse modelling

In our inverse modelling-data assimilation structure, a cost function that accounts for the discrepancies between modelled and sensed fire fronts has to be evaluated in each forward model run to determine the invariants. The best set of invariants are calculated by minimising this cost function. The cost function plays a central role in the algorithm. It has to be simple enough so its evaluation is not computationally expensive while it has to be accurate and drive the algorithm towards a meaningful convergence.

3.3.1. *Cost Function*

The cost function implemented in the previous algorithm used an angular discretization scheme to select the points on both, the model and the observed fronts. The summed up distance between each angularly related pair of points was then computed as the cost function value:

$$J(p) = \sum_{t=t_i}^{t_f} \sqrt{[\overline{y_i} - y_i(p)]^T W [\overline{y_i} - y_i(p)]} \qquad \textbf{[6]}$$

Where $\overline{y_i}$ and y_i are the observed and modelled front coordinates respectively, p is a given set of invariants value and W is a weight diagonal matrix that can be used to give more value to certain observations depending on their reliability and accuracy. In each cost function evaluation, all the available fronts are computed and summed up.

In the real data scenario the angular discretization is no longer valid due to the complex shapes. Thus, the cost function was modified by finding the Euclidian norm of a vector that connects each modelled segment mid-point with its correspondent assimilated front following the local propagation direction (perpendicular to the local curve slope). Since this distance is quantified for every assimilated fire front and the number of segments are not kept constant in each front as the perimeter expands, the total distance between each pair of isochrones is divided by the number of vectors. Figure 9 illustrates the Euclidian norm evaluation for four fire fronts assimilation. Note that some intersection vectors diverge due to the local geometry of the modelled front. In this cases, a filter is applied so vectors that are larger than the mean value plus/minus 2 times the standard deviation are removed. As both perimeters converge, the intersection vectors behaviour improves.

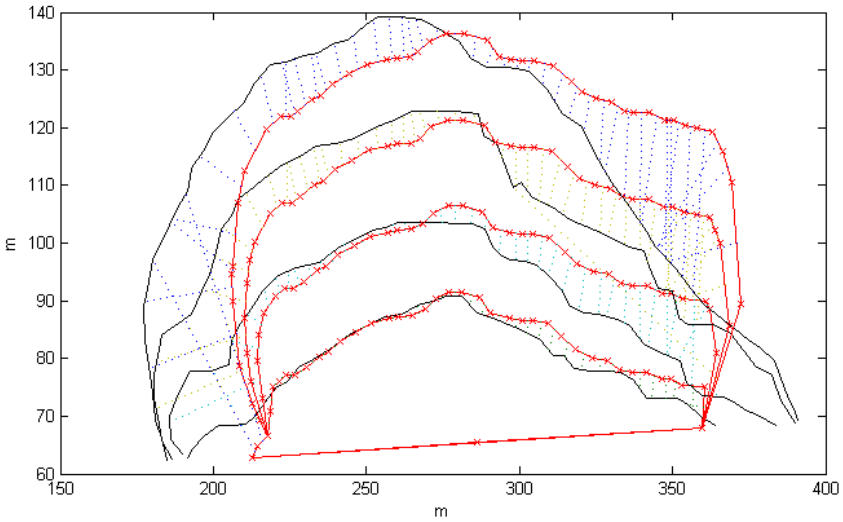

Figure 9. Paired isochrones of assimilated (black solid lines) and modelled (red dotted lines) fire fronts (real fire data from South Australia experiments 2008). The cost function is calculated by averaging the Euclidian norm of the lines perpendicular to the modelled front that intersect the corresponding observed perimeter.

3.3.2. *Tangent Lineal Model*

The optimization loop is the most critical part of the algorithm since it will affect the total computing time (and therefore compromise the lead time). The two main approaches to optimize the cost function are gradient-free and gradient-based algorithms. While the first group sweeps all the available domain and identifies absolute minimums, their algorithms are also more computationally expensive. The gradient-based algorithms assume an initial guess for the estimating parameters and use the gradient to drive the solution towards a minimum. They are particularly suitable for systems where variables are limited within a range of values. Using the later, and using a Tangent Linear Model local approximation for the forward model (based on Taylor's expansion series on the vicinity of the initial guess) the optimization step can be reduced to a linear system of equations that can be easily solved by using a QR factorization with column pivoting (Nocedal & Wright, 1999):

$$\sum_{t=t_i}^{t_f} H_i^T H_i \bar{p} = \sum_{t=t_i}^{t_f} H_i^T (\bar{y} - y_i(p))$$

Where $\bar{p}$ is the difference between an old and an updated invariant's vector, $(\bar{y} - y_i(p))$ is the discrepancy between the observed and the modelled fronts and the term $H_i^T H_i$is the Jacobian of the forward model. The most common numerical algorithm to calculate this term need to evaluate the forward model itself multiple times (a centred difference approach for example) which may dramatically increase the computational time. Alternatively, an automatic differentiation approach can be used to directly evaluate this term. This approach uses the chain-rule for derivatives to systematically derive the scripted code. Once this is done, the Jacobian term can be calculated with one run. If the process is repeated in a loop, the final invariant's vector is obtained when the term that contains the difference between the observations and the model converge. This algorithm is not yet implemented for the real data assimilation case due to the changes in the forward model equations. The automatic differentiation process has to include the correcting algorithms, and therefore is not straightforward. Moreover, since the complexity of the model increases, the adjoint model instead of the forward model is needed.

Model testing with real fire data

The improvements implemented so far in our inverse modelling – data assimilation structure were tested using real fire data coming from experimental fires performed in eastern South Australia in March 2008. Despite being within a framework of a scientific experimental burning program, fires exhibited real behaviour patterns as were performed in extremely severe weather conditions and plots dimensions were all above 6 ha. These experiments were conducted in Ngarkat Conservation Park (35º45'S, 140º51'E) which is constituted by a characteristic dune and swale system comprising large flat areas of mallee-heath shrublands (130 m a.s.l.). Fire behaviour in mallee-heath fuel types is characterized as being discontinuous and highly variable due to the heterogeneous characteristics of the various fuel layers that comprise mallee-heath fuel complexes (Cruz *et al*., 2013). Data used in this paper comes from the experimental burn performed in a 9 ha 8 year-old heath plot in March 4th 2008. This fuel complex was characterized by scattered small-leafed shrubs, organized in clumps, and a discontinuous litter layer partially buried by sand. The main fire carrying fuel layer was the discontinuous shrub canopy (1.5 m depth). Ambient conditions were temperature of 32 ºC and relative humidity of 25%. Wind speed (10-m open) averaged 15 km/h, with gusts up to 30 km/h. Wind direction was from south-south-westerly. Characteristic dead fuel moisture of the fuel complex was 7.7%. The fire was ignited with a 130-150 m long line and two minutes after ignition, flame heights were about 2-2.5 meters, with flashes up to 4 meters. The fire spread vigorously throughout the plot with sustained flames heights of 4-5 meters. Eight minutes after ignition, the main flame front hit the northern border of the plot, concluding a 350 m head fire run (Planas, Pastor, Cubells, Cruz, & Grenfell, 2011) The fire was filmed from an helicopter with a IR camera (AGEMA Thermovision 570-Pro, FSI-FLIR Systems). This camera operated within the 7.5-13 μm range and was equipped with a frame grabber to control and store sequences of IR images (240 x 320 pixel) onto a laptop computer at an approximate rate of 5 frames per second. The helicopter was hovering positioned so that the majority of the plot was in view for the duration of each fire, allowing fire behaviour to be recorded and monitored. Isochrones map (1 every 10 seconds frequency) and RoS map of this fire experiment were subsequently obtained applying a methodology for IR analysis developed with MATLAB® computing software and described elsewhere (Pastor *et al*., 2010).

Using the first observed perimeter as an ignition line, the forward model was run fed with the moisture content, wind speed and direction and fuel load and depth values. Figure 10 shows the comparison between 5 min of real burning fronts, sampled every 10 sec. and the modelled isochrones for the same period of time. While individual isochrones shape do not perfectly match all the observed fronts, the total distance travelled by the head fire is well predicted. Similarly, the left flank of the fire is properly predicted as time passes by. Taking into account that the plot had a high fuel discontinuity not added to the model, and also that the wind variation was neither considered, the simulations are reasonably accurate and support the need for and the suitability of an automatic data assimilation algorithm capable of identifying this factors difficult to obtain with enough accuracy during operational scenarios.

Conclusions

The required steps to adapt a data assimilating system to work with real sensed data have been investigated and implemented in a wind-driven short-term forecasting algorithm. Difficulties such as front concavity, fire breaks and fuel irregularities have been identified and addressed in the forward model. The assimilating capacity of the algorithm can be now explored by casting different invariants configurations and performing the optimization step with an automatic differentiation approach to ensure positive lead time. The preliminary check with airborne thermal images of a large scale experiment showed the capacity of the implemented forward model of reproducing head fire

propagation and overall fire growth with a reasonable accuracy and highlights the potential of an automatic assimilation algorithm implementation.

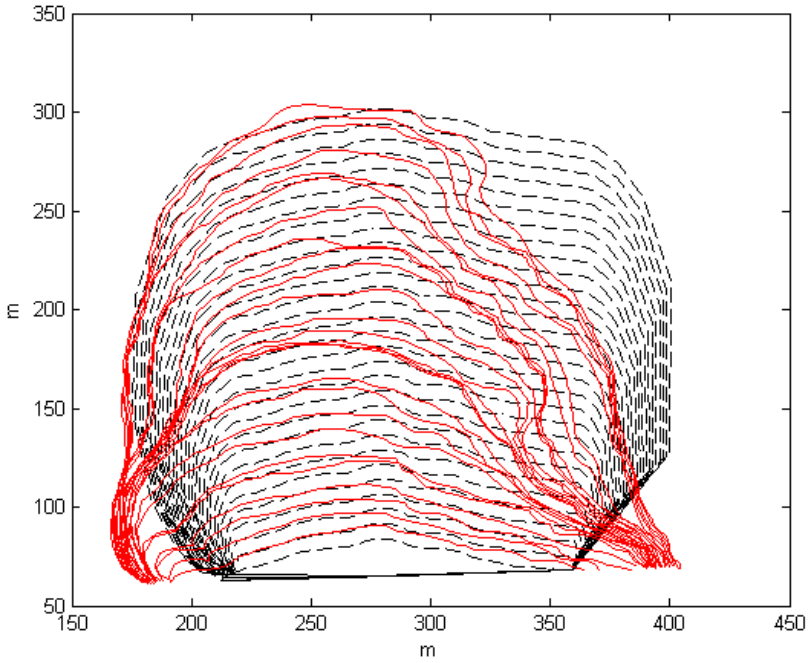

Figure 10. Modelled fronts (dashed lines) versus Ngarkat's plot "A" real perimeters (solid lines). Isochrones are plotted every 10 secons during 5 min. (i.e. 30 isochrons are depicted). The fuel depth is estimated of 1.3m and the wind is set to 3m/s.

Acknowledgements

This work is supported by Agaur (FI-DGR 2014FI-00133). The authors also thank the Autonomous Government of Catalonia for financial support (project No. 2009SGR1118).

References

Anderson, D. H., Catchpole, E. A., De Mestre, N. J., & Parkes, T. (1982). Modelling the spread of grass fires. Journal of the Australian Mathematical Society, 23, 451–466.

Cruz, M. G., McCaw, W. L., Anderson, W. R., & Gould, J. S. (2013). Fire behaviour modelling in semi-arid mallee-heath shrublands of southern Australia. Environmental Modelling & Software, 40, 21–34.

Finney, M., Cohen, J. D., McAllister, S. S., & Jolly, W. M. (2013). On the need for a theory of wildland fire spread. International Journal of Wildland Fire, 22(1), 25. doi:10.1071/WF11117

Jahn, W., Rein, G., & Torero, J. L. (2011). Forecasting fire growth using an inverse zone modelling approach. Fire Safety Journal, 46(3), 81–88.

Jahn, W., Rein, G., & Torero, J. L. (2012). Forecasting fire dynamics using inverse computational fluid dynamics and tangent linearisation. Advances in Engineering Software, 47(1), 114–126.

Johns, C. J., & Mandel, J. (2008). A two-stage ensemble Kalman filter for smooth data assimilation. Environmental and Ecological Statistics, 15(1), 101–110.

Kalnay, E. (2003). Atmospheric modeling, data assimilation and predictability (p. 203). UK: Cambridge University Press.

Mandel, J., Beezley, J. D., Coen, J. L., & Kim, M. (2009). Data assimilation for wildland fires. Control Systems, IEEE, 29(3), 47–65.

Mandel, J., Bennethum, L. S., Beezley, J. D., Coen, J. L., Douglas, C. C., Kim, M., & Vodacek, A. (2008). A wildland fire model with data assimilation. Mathematics and Computers in Simulation, 79(3), 584–606.

Nocedal, J., & Wright, S. J. (1999). Numerical Optimization. (J. Nocedal & S. J. Wright, Eds.). New York: Springer-Verlag. doi:10.1007/b98874

Pastor, E., Pérez, Y., Cubells, M., Planas, E., Plucinski, M., & Gould, J. (2010). Quantifiable assessment of aerial suppression tactics in wildland fires using airborne infrared imagery. In D. X. Viegas (Ed.), VI International Conference on Forest Fire Research (p. 15 pp.). Coimbra, Portugal.

Pérez, Y., Pastor, E., Planas, E., Plucinski, M., & Gould, J. (2011). Computing forest fires aerial suppression effectiveness by IR monitoring. Fire Safety Journal, 46, 2–8. doi:10.1016/j.firesaf.2010.06.004

Planas, E., Pastor, E., Cubells, M., Cruz, M. G., & Grenfell, I. C. (2011). Fire behavior variability in mallee-heath shrubland fires. In 5th International Wildland Fire Conference (p. 10 pp.). 9-13 May, 2011. Sun City, South Africa.

Richards, G. D. (1990). An elliptical growth model of forest fire fronts and its numerical solution. International Journal for Numerical Methods in Engineering, 30(6), 1163–1179.

Richards, G. D. (1993). The properties of elliptical wildfire growth for time dependent fuel and meteorological conditions. Combustion Science and Technology, 95(1-6), 357–383.

Rios, O., Jahn, W., & Rein, G. (2014). Forecasting wind-driven wildfires using an inverse modelling approach. Natural Hazards and Earth System Science, 14(6), 1491–1503. doi:10.5194/nhess-14-1491-2014

Rochoux, M. C., Delmotte, B., Cuenot, B., Ricci, S., & Trouvé, A. (2012a). Regional-scale simulations of wildland fire spread informed by real-time flame front observations. Proceedings of the Combustion Institute.

Rochoux, M. C., Emery, C., Ricci, S., Cuenot, B., & Trouvé, A. (2014). Towards predictive simulation of wildfire spread at regional scale. In Iafss 2014. IAFSS 11th.

Rothermel, R. C. (1972). A mathematical model for predicting fire spread in wildland fuels. Intermountain Forest & Range Experiment Station, Forest Service, US Department of Agriculture.

Susceptibility of forest fire in urban area of Uba, MG, Brazil

Fillipe Tamiozzo Pereira Torres, Guido Assunção Ribeiro, Elias Silva, Sebastião Venâncio Martins

[a] *Universidade Federal de Viçosa, DEF, campus universitário 36570-000, torresftp@yahoo.com.br, gribeiro@ufv.br, eshamir@ufv.br, venancio@ufv.br*

Abstract

The aim of this study was to produce a map of susceptibility to fires in vegetation within the urban perimeter of the city of Uba, MG, Brazil, with the use of information related to topography, land cover and land use and the proximity of access roads and urban areas, using GIS techniques. From the validation of the generated cartogram, it was observed that 80 % of cases were located in areas of high and very high risk, 15 % in medium-risk and 5 % in areas of low and very low risk. Was observed in this study that the largest number of occurrences is concentrated near urban areas. In other studies, these authors found that, besides the favourable physical environment it is necessary a causative agent to fire occur. In area of very high or very low risk, the event will only occur from an initial cause or source of heat. This mapping will serve as a tool for establishing public policies to prevent power, acting in promoting awareness and control measures in the areas of highest risk.

Keywords*: Vegetations fires, susceptibility, map.*

Introduction

Fire is a growing problem in the remaining tropical forests in the world. Despite years of scientific study and all the media attention in relation to forest fires, the effects they cause to the environment have also been ignored (Silva *et al*., 2003).

Fires in vegetation generate various economic, landscape and ecological damage and can occur in protected or conservation areas, farms, roadsides, proximity to urban areas and reforestation areas, besides other places (Fiedler *et al*., (2006). Anyway, fires occur when several factors associated with combustion and fire propagation become favorable to the ignition and spread of flame (Nogueira *et al*., 2002).

There are two types of factors that determine the degree of fire danger. The constant factors that are represented by the type of fuel, which involves different types of vegetation and topography and the variable factors that are represented by atmospheric conditions (Torres *et al*., 2011). The slope, aspect and the use and occupation of land are examples of these variables.

According to Batista (2000), the topography influences the climate and determines the type of fuel. Considering that fire behavior is largely the result of climate and fuel available, it can be said that the topography also has a decisive influence on fire behavior.

Surfaces with different orientations and slope receive different amounts of solar radiation compared to a horizontal surface at the same location and time of year (Torres & Machado, 2011). The studies of Torres *et al*. (2010a) shown that the concentration of largest number of fires on the North (43 %), followed by Western a (27 %), East (18 %) and South aspect (12 %) with fewer occurrences. This is due the sun, during most of the year, culminates in Zenith north of the city, because of latitudinal position. This factor tends to raise the temperature in the North aspect influencing more fuel load and fire occurrences. Regarding the slope Ribeiro *et al*. (2007) shown that the increased of the fire intensity in this areas is due to the approaching flames and fuel compared with smooth areas, heating the fuel quickly.

According to Viegas (2004), the spread of fire in slopes is distinct from that in areas without slope due to the effect of additional factors such as convection and radiation behavior. If there is slope and the presence of wind, the propagation rate tends to increase.
In addition to relief, the fuel is crucial in the fire occurrence. Evaluating coverage torched in the city of Uba (MG), Torres *et al*. (2010a) observed that the most forest vegetation tends to hold moisture better than herbaceous, recording 80 % of the occurrences of fires in fields and pastures and 5 % in forests.
The type of material and their arrangement facilitate the ignition and spread of fire. The thinner material has lower ignition temperature and loses their moisture faster (Nunes, Soares & Batista, 2006), facilitates the start of the fire and accelerates its spread. Also according to these authors, the proximity and uniform distribution of the fuel particles facilitate the spread, also favoring the occurrence of fire on the fields, pastures, and urban vegetation areas.
On the other hand, bushes or trees intercept the radiation, reducing the temperature of the air and the fuel in its interior (Nunes *et al*., 2008). They also act as a barrier, preventing the free passage of air currents, reducing the wind speed inside. This reduces evaporation, making the drying of the fuel. Furthermore, transpiration of forest material provides an increase in relative humidity in the forested area.
However, it is not enough that the factors directly associated with the occurrence of forest fires are favorables, the initial flame is necessary to fire occurrence. Thus, any action to prevent forest fires should seek the elimination of its causes (Nogueira *et al*., 2002).
According to Soares and Cordeiro (1974), Soares and Santos (2002), Bonfim, Ribeiro and Silva (2003), Santos, Soares and Batista (2006), and Torres *et al*. (2010b), the main cause of fires is human activity, such as smoking, burning to clean, incendiary fires and recreation. Thus, next to roads and urban areas tend to be more susceptible to fire occurrences.
Because of the constant character of the listed factors (slope, aspect and land use), they become valuable in establishing susceptibility maps to fires. It is essential to know where the fires occur to determine the areas of high risk or high susceptibility (Soares and Santos, 2002) for these regions by establishing specific programs. The risk zoning or fire risk maps according to Batista (2000) have been used very effectively as a fundamental tool in the rational planning of resources for prevention and pre-suppression of fires on vegetation.
Faria, Silva and Goes (2003) affirm that the use of tools linked to a Geographic Information System (GIS), allows increase knowledge about the relationships between environmental phenomena, estimating risk areas, potential environmental and defining zoning. The cartograms generated provide a layer on the various components of the environment, such as slope, use and cover, soils, geomorphology, and others, besides to allow the overlap of the generated maps.
The aim of this study was to produce a map of susceptibility or risk to fires in vegetation inside the urban area of Uba city (MG), using informations related to relief, use and land cover. This mapping will serve as a tool for establishing public policies for prevention, acting in the public awareness of power as well as control measures in the areas of highest risk.

2. Methods

The Municipality of Uba is located in the physiographic mesoregion denominated Zona da Mata Mineira, Minas Gerais State, Brazil. It lies between latitudes 21°16' to 20°57' south and longitudes 43°07' to 42°57' west. Its length is approximately 40,750 hectares and its population is about the 101,466 inhabitants (IBGE, 2010).
The topography is represented by areas of strong wavy slope, comprising about 16,556 hectares (40.6 %) of its entire territory. However, other 11,354 hectares (27.9%) can be considered flat whereas 8,790 hectares (21.6 %) has an intermediate topography. The remaining area (4,050 hectares, 8.9 %) has a mountainous structure.

The vegetation type is compound by pasture cover an area of 75,51 %, followed by brushwood (capoeira) and woods with 16.2 % and agriculture with 4.9 %.
The susceptibility cartogram of fires was done using ArcGIS 9.3 software to generate the maps of Slope, Aspect and Use and Occupation of the soil. These maps were overlaid, allowing the determination of more susceptible areas to fires.
In this sense, to construct the maps of declivity and exposure of slopes was produced a Digital Elevation Model (DEM) (Figure 1) by interpolating the contours of 10 - 10m, extracted from Aerial Images Orthorectified range of 1:10,000, November 2005.

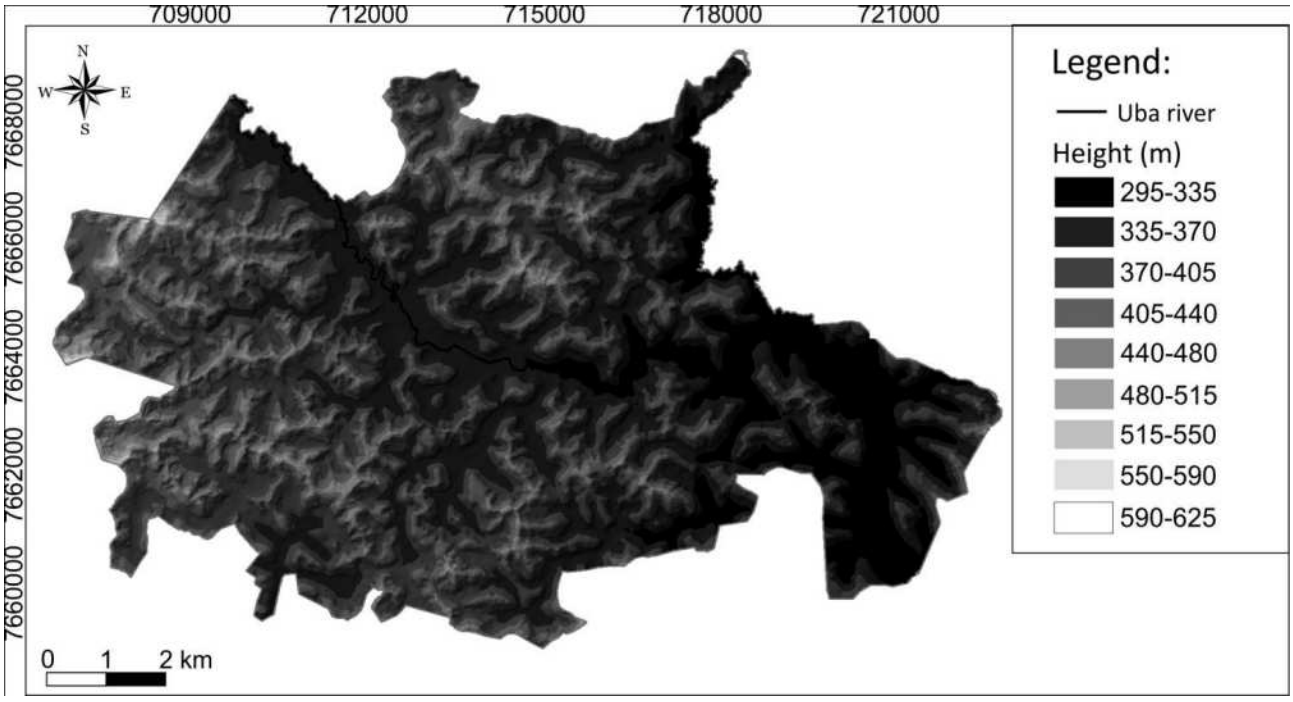

Figure 1. Modelo Digital de Elevação do perímetro urbano de Ubá – MG

The land use map was originated by visual interpretation of orthorectified images. They were vectored the major classes of land use in the urban area of the municipality: forest, brushwood (capoeira), pasture, agriculture, water bodies, exposed soil and constructed area. To check the classification performed in the laboratory, georeferenced points in the field were collected, thus ensuring the reliability of the data.
After generation of cartograms regarding declivity (Figure 2), Aspect (Figure 3) and Use and Occupation of the soil (Figure 4), the classes were analyzed relating to each of these maps. Grades were assigned to each of these classes according to weight of respective class of occurrence (Table 1).

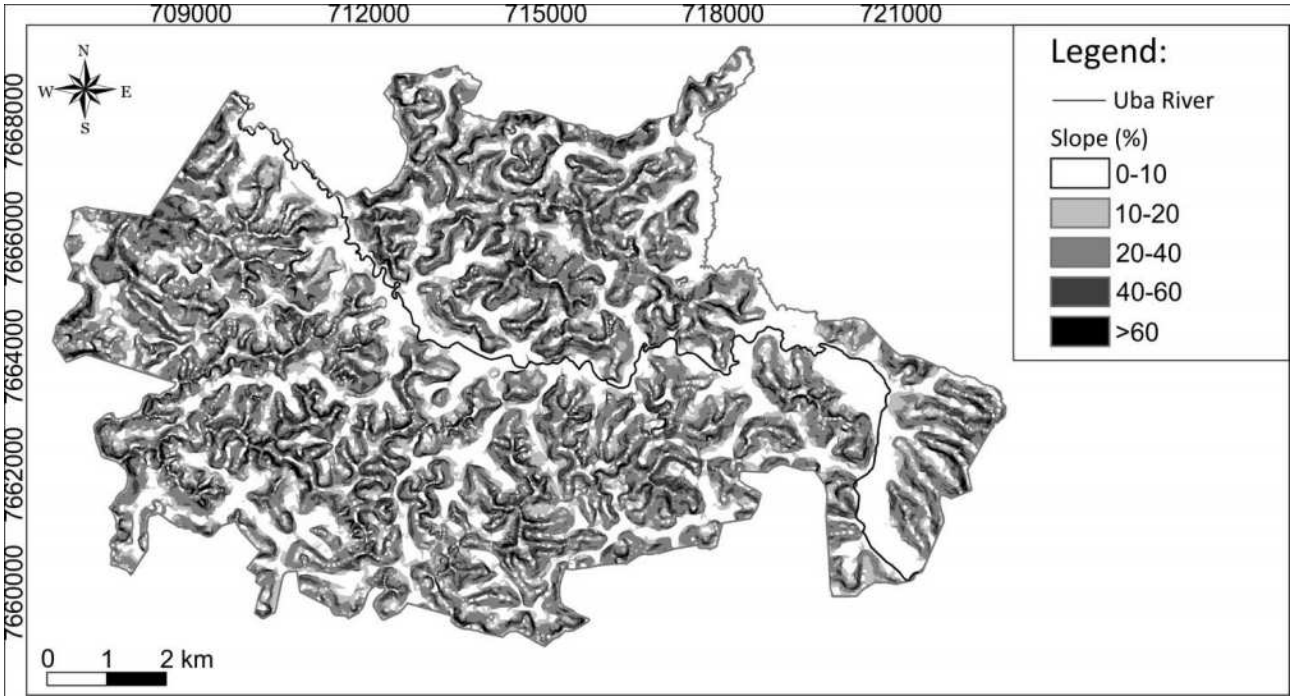

Figure 2. Slope of the urban perimeter Uba - MG

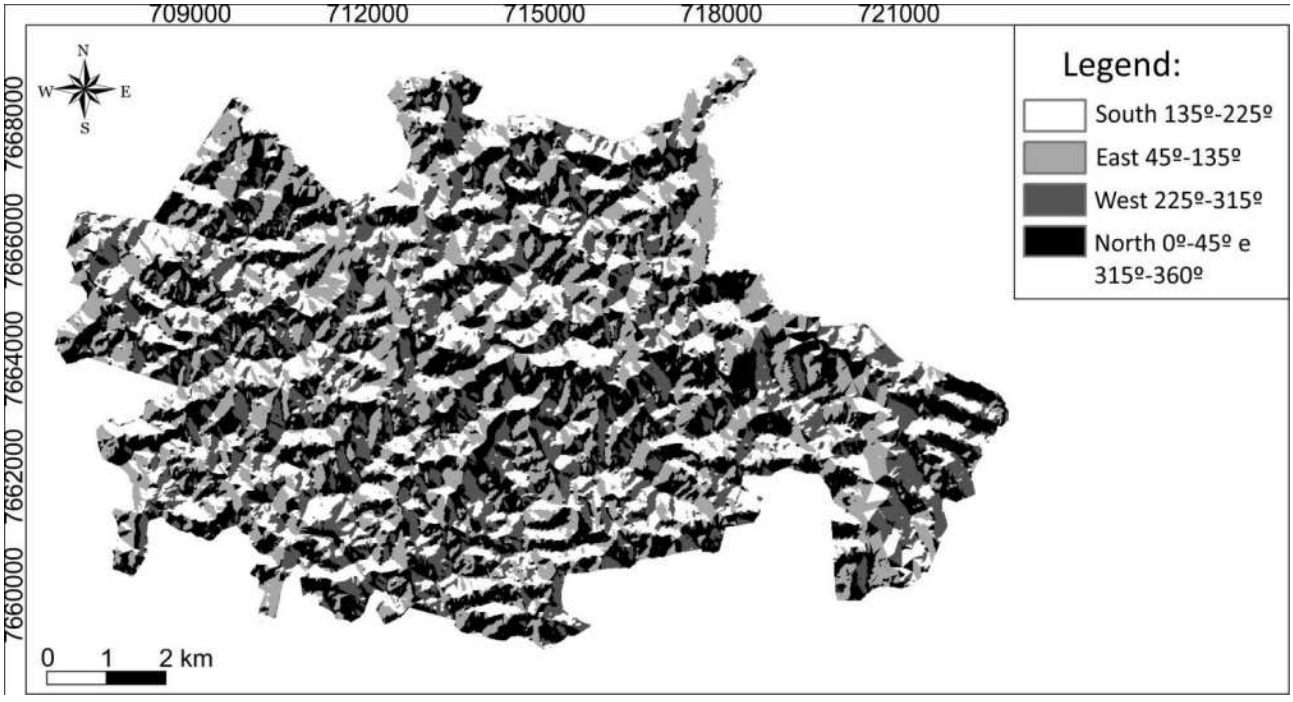

Figure 3. Exposition of the Sun aspects the urban perimeter of Uba - MG

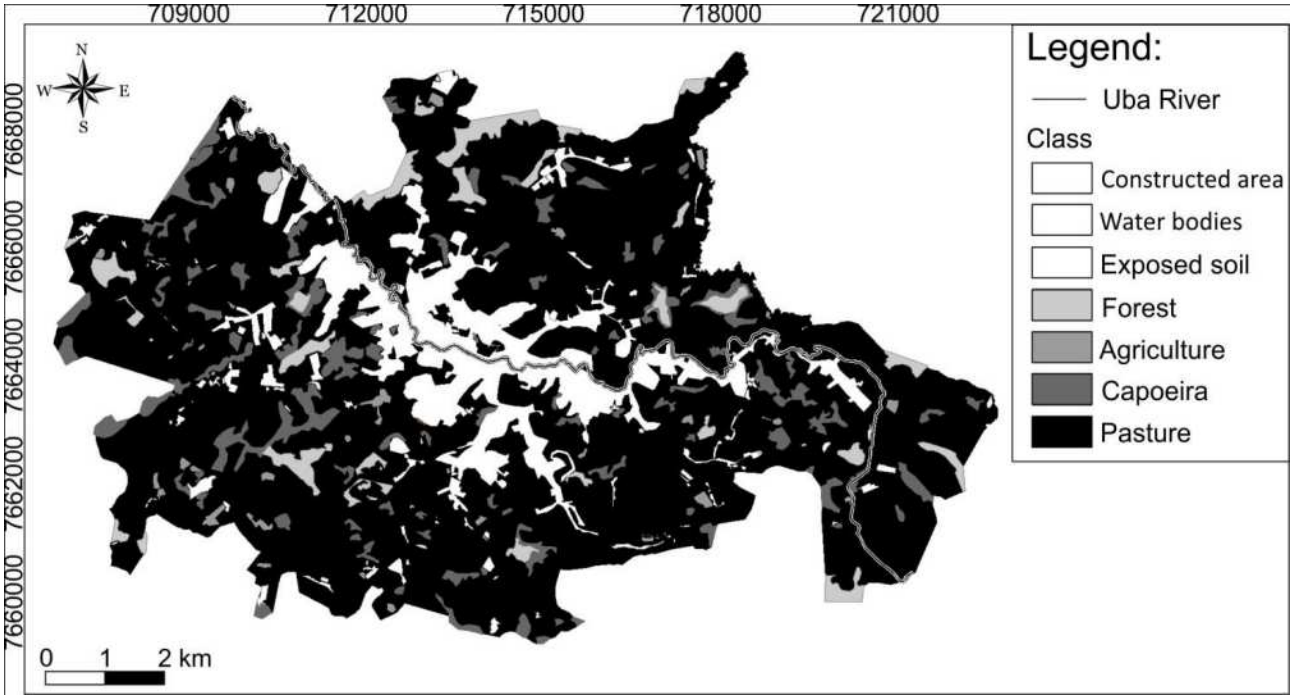

Figure 4. Use and occupation of urban perimeter Uba - MG

Table 1. Table notes the statement of the Fire Risk

Use and occupation		Exposition of the Sun		Slope	
Class	Weight	Class	Weight	Class	Weight
Forest	3	North	10	0º a 10º	2
Capoeira	7	West	8	10º a 20º	4
Agriculture	5	East	6	20º a 30º	6
Constructed area	0	South	4	30º a 40º	8
Exposed soil	0			>40º	10
Water bodies	0				
Pasture	10				

The notations used in Table 1 were based on Torres *et al*. (2008) and Torres *et al*. (2010a) who studied the profile of vegetation fires in the cities of Juiz de Fora and Ubá, both located in the Zona da Mata Mineira, Minas Gerais State, Brazil. The data of reclassified maps were overlaid, according to the tree of Figure 5 decision.

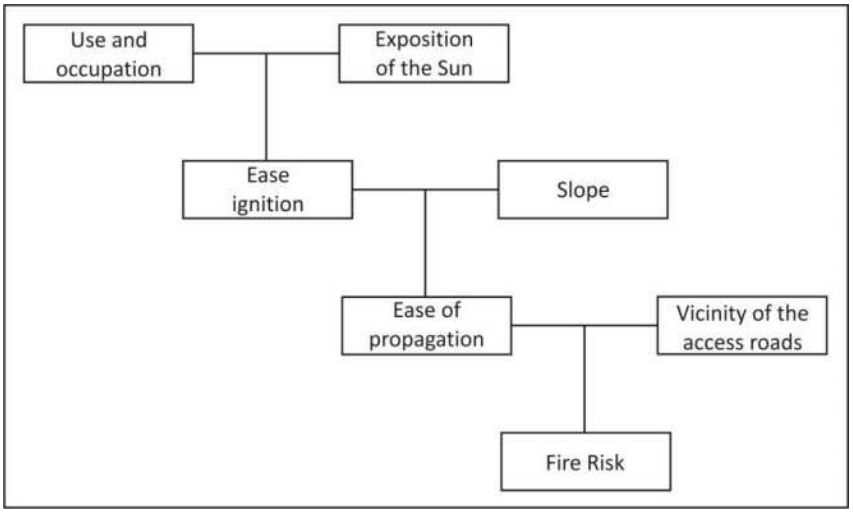

Figure 5. Decision tree for fire risk

The Use and Occupation cartogram was crossed with the Aspect cartogram, both with same weight, generating a Ease Ignition cartogram. Both cartogram has a weight of 66% when crossed with the Slope cartogram (weight 34%), generating the Ease of Propagation cartogram.
This cartogram was overlaid to the proximity of roads and urban areas, creating a 15-meter buffer around them. This was based on Torres *et al*. (2008) that describe the risks of fires in road borders and urban areas peripheries. The final product of these crossings was the cartogram of Susceptibility of Fires in vegetation within the urban area of the municipality of Uba, Minas Gerais Brazil (Figure 6).

Results and Discussion

The cartogram of susceptibility of fires in vegetation in the urban area vegetation of the municipality of Uba - MG (Figure 6) is supported by hazard classes shown in Table 2.

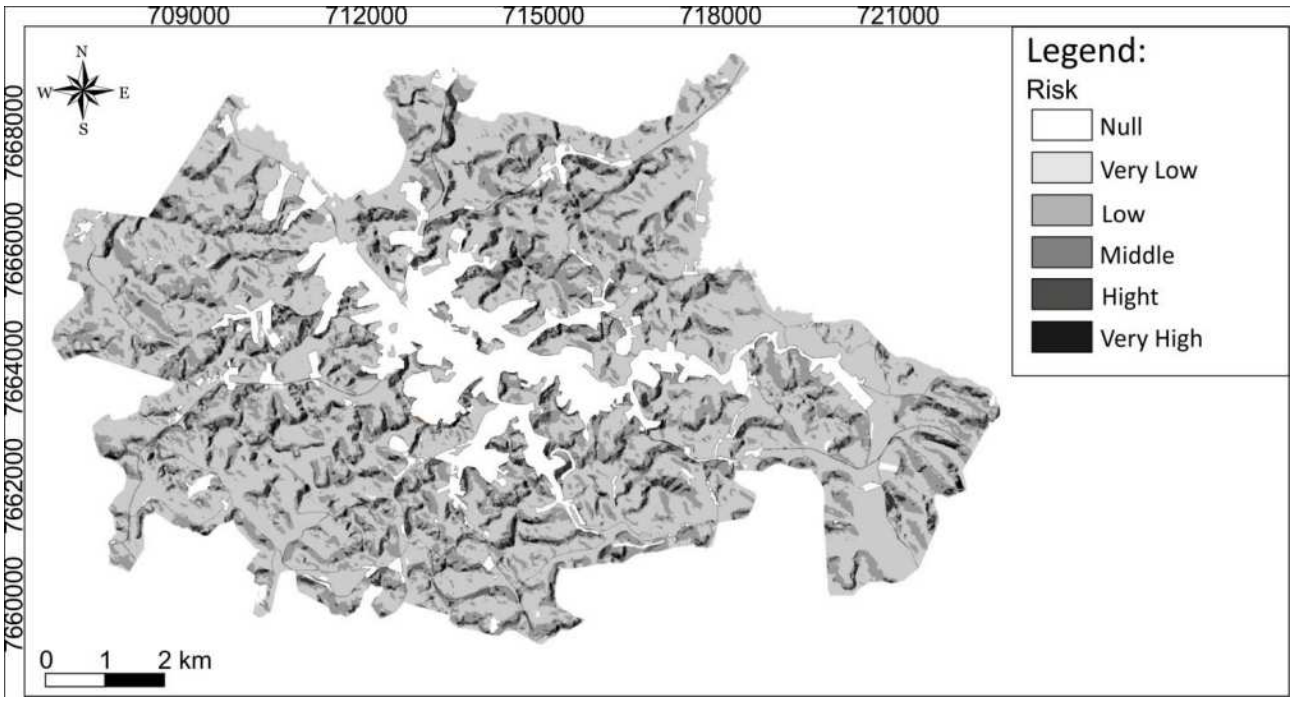

Figure 6. Map of forest fires in the urban perimeter of Uba - MG

Table 2. Areas according to the class of risk

Class	Ha	(%)
Null	1276,1	13.7
Very Low	4636,7	49,8
Low	2480,5	26,5
Middle	289,0	3,1
High	555,8	5,9
Very High	96,0	1,0
Total	**9334,1**	**100%**

It is observed that the risk areas are concentrated near urban areas. This is due to the human presence as the main source of ignition of fires. In studies conducted by Torres *et al*. (2008) and Torres *et al*. (2011), was identified that although the scenario created by the physical environment (slope, aspect, use and occupation of land) without causal agent there is no occurrence of the fire. On other hands, even in an area classified as very high risk area, the fire will occur only if the initial flame, ordinarily, is associated with cleaning burning, smoking and arson. The same occurs in areas classified as very low risk; if there is the ignition, the risk of fire is high in these areas.
To analyze the effectiveness of the cartogram generated, were used the geographical coordinates of all occurrences in the urban area in the period 2006-2012 (Table 3). It was recorded 732 events in the urban perimeter of study area, with 80 % of those located in areas of high and very high risk and 5 % in areas of low and very low risk. These data demonstrate that the generated map portrays well the situation of vegetation fires in the urban area.

Table 3. Percentage of occurrences according to risk class

Risk Class	% of occurrences
Null	0%
Very Low	1%
Low	4%
Middle	15%
High	28%
Very High	52%

The results were similar to those of Coura, Souza and Fernandes (2009) for the city of Rio de Janeiro, Brazil. The authors crossed the maps of geomorphology, aspect and land use and they obtained 79% of occurrences in areas of high risk, 16% on middle and 5% in low susceptibility.

Conclusion

According to the results, it was concluded that:

- The scores and weights used have produced a cartogram that reflects the susceptibility to fires in the urban area of Uba, Minas Gerais, Brazil;
- Areas with Northern aspect, greater slope and near the roads were major points of susceptibilities to occurrences;
- Most of the areas classified as very high risk, as well as incidents recorded by the Fire Department, surrounding the urban area and access roads reflect the high influence of anthropogenic activity;
- the inclusion of changeable factors in the methodology will increase the reliability of the generated cartogram;

- the cartogram generated serves as a tool to aid the development of strategies for fighting fires in the municipality;
- the methodology is simple and shows likely to be used in other areas with the same issue.

References

Batista, A. C. (2000). Mapas de risco: uma alternativa para o planejamento de controle de incêndios florestais. Curitiba: *Floresta*, v.30, n.1, p.45-54.

Bonfim, V. R.; Ribeiro, G. A. E Silva, E. (2003). Diagnóstico do uso do fogo no entorno do Parque Estadual da Serra do Brigadeiro (PESB), MG. Viçosa: *Revista Árvore*, vol.27 n.1, p.87-94.

Coura, P. H. F.; Sousa, G. M. E Fernandes, M. C. (2009). Mapeamento geoecológico da susceptibilidade à ocorrência de incêndios no Maciço da Pedra Branca, município do Rio de Janeiro. Rio de Janeiro: *Anuário do Instituto de Geociências - UFRJ*, v.32, n.2, p.14-25.

Faria, A. L. L De; Silva, J. X. Da E Goes, M. H. de B. (2003). Análise ambiental por geoprocessamento em áreas com susceptibilidade à erosão do solo na bacia hidrográfica do Ribeirão do Espírito Santo, Juiz de Fora (MG). Uberlândia: *Caminhos de Geografia*, v.4, n.9, p.50-65.

Fiedler, N. C. *et al*. (2006). Avaliação das condições de trabalho, treinamento, saúde e segurança de brigadistas de combate a incêndios florestais em unidades de conservação do Distrito Federal: estudo de caso. Viçosa: *Revista Árvore*, vol.30 n.1, p.55-63.

IBGE. (2010). *Censo Demográfico 2010*. Rio de Janeiro: Instituto Brasileiro de Geografia e Estatística.

Nogueira, G. S. *et al*. (2002). Escolha de locais para instalação de torres de detecção de incêndio com auxílio do SIG. Viçosa: *Revista Árvore*, v.26, n.3, p.363-369.

Nunes J. R. S.; Soares, R.V.E., E Batista, A. C. (2006). FMA+ - Um novo índice de perigo de incêndios florestais para o Estado do Paraná, Brasil. Curitiba: *Floresta*, v.36, n.1, p.75-91.

Nunes, J. R. S., *et al.* (2008). Relação entre a qualidade da paisagem e o risco de incêndios florestais. Curitiba: *Floresta*, v.38, n.1, p.145-154.

Santos, J. F.; Soares, R. V. E Batista, A.C. (2006). Evolução do perfil dos incêndios florestais em áreas protegidas no Brasil, de 1993 a 2002. Curitiba: *Floresta*, v.36, nº1, p.93-100.

Silva, J. C. da, *et al*. (2003) Avaliação de brigadas de incêndios florestais em unidades de conservação. Viçosa: *Revista Árvore*, v.27, n.1, p.95-101.

Soares, R. V. E Cordeiro, L. (1974). Análise das causas e épocas de incêndios florestais na região centro-paranaense. Curitiba: *Floresta*, v.5, n.1, p.46-49.

Soares, R. V. E Santos, J. F. (2002). Perfil dos incêndios florestais no Brasil de 1994 a 1997. Curitiba: *Floresta*, v.32, n.2, p.219-232.

Ribeiro, L. *et al*. (2008). Zoneamento de riscos de incêndios florestais para a fazenda experimental do Canguiri, Pinhais (PR). Curitiba: *Floresta*, v.38, n.3, p.561-572.

Torres, F. T. P. *et al*. (2008). *Incêndios em vegetação na área urbana de Juiz de Fora: Minas Gerais.* Ubá: Editora Geographica.

Torres, F. T. P. *et al*. (2010a) Perfil dos Incêndios em Vegetação nos Municípios de Juiz de Fora e Ubá, MG, de 2001 a 2007. Seropédica: *Floresta e Ambiente*, v. 17, n.1, p.83-89.

Torres, F. T. P. *et al*. (2010b). Determinação do período mais propício às ocorrências de incêndios em vegetação na área urbana de Juiz de Fora, MG. Viçosa: *Revista Árvore*, v.34, n.2, p.297-303.

Torres, F. T. P. *et al*. (2011). Correlações entre os elementos meteorológicos e as ocorrências de incêndios florestais na área urbana de Juiz de Fora, MG. Viçosa: *Revista Árvore*, v.35, n.1, p.143-150.

Torres, F. T. P. E Machado, P. J. de O. (2011). *Introdução à Climatologia*. São Paulo: Cengage Learning.

Viegas, D. X. (2004). *Cercados pelo fogo*. Coimbra: Editorial Minerva.

Temporal changes to fire risk in Disparate WUI communities in Southern California, USA

Christopher A. Dicus[a], Nicola C. Leyshon[b], David B. Sapsis[c]

[a] *California Polytechnic State University, Natural Resources Management & Environmental Sciences Department, San Luis Obispo, CA 93402, USA; cdicus@calpoly.edu*
[b] *California Polytechnic State University San Luis Obispo, Natural Resources Management & Environmental Sciences Department, San Luis Obispo, CA 93402, USA; nleyshon@calpoly.edu*
[c] *California Department of Forestry & Fire Protection, PO Box 944246, Sacramento, CA 94244, USA; dave.sapsis@fire.ca.gov*

Abstract
To aid policy development that reduces fire losses in the wildland-urban interface, we are evaluating changes to risk through time in dissimilar communities that are expanding into fire-prone areas of southern California, USA. Conventional wisdom states that escalating losses are caused, in part, by an expansion of residential development into fire-prone areas. However, various mitigation strategies such as defensible space and improved construction standards have recently been mandated for new developments in California so as to reduce the risk of these losses. Subsequently, older high-risk communities may actually become buffered from wildfires as the WUI expands and subsequently lessens their exposure to flames and embers. Thus, expanding WUI may either increase or decrease risk of residential loss dependent upon the extent of altered fire exposure and the application of mandated mitigation strategies.
To help elucidate this seeming dichotomy, we are utilizing various GIS strategies to spatially analyze changes to development and subsequent risk of structural ignitions through time in three expanding, but demographically dissimilar, residential communities in southern California. Here, we quantify temporal changes in the area exposed to fire hazards in each of the communities over a 26-year period. The amount of area exposed to wildfire increased in each of the communities. The degree and location of newly exposed development, however, differed between communities, which may influence fire risk in an impending assessment we will conduct as part of a larger research project of the area.

Keywords*: Wildland Urban Interface, Land Use, Urban Expansion, Wildfire, Risk, Urban Resiliency, San Diego County*

Introduction

Even with increasing proportions of governmental budgets allocated to fire suppression resources, wildfires annually destroy great numbers of homes and critical infrastructure in the wildland-urban interface (WUI). Indeed, since 2002 in the US, the largest fires in the histories of California, Arizona, Colorado, New Mexico, Utah, Oregon, and Texas have occurred in spite of increased fire agency staffing, equipment, and training (National Interagency Fire Center 2014). In California alone, thirteen fires over 40,500 ha in size have burned since 1990, with 7 of the 10 most destructive wildfires having occurred during this period, resulting in the loss of 53 lives and almost 12,000 structures (California Department of Forestry & Fire Protection 2013). To aid policy development that reduces these losses, we are evaluating how risk changes through time in communities that are expanding into fire-prone areas, but which vary in demographics and socioeconomic status.
The cause of increased fire losses in the WUI is related to a myriad of complex and interacting factors, the influence of each which varies by time and by place. Of especial concern, burgeoning population growth into fire-prone areas has resulted in greater exposure of residential development to wildland fire. Further, with increased population growth into the WUI, there are increased ignitions through accident or arson (Syphard *et al.* 2008).

To better facilitate sustainable communities in the WUI, managers need an accurate and detailed assessment of not only the fire hazard in a given area, but also its risk to assets of value. Many methods of WUI risk assessment involve the use of maps or spatial data (Bar Massada *et al*., 2009; Prestemon *et al*. 2002). Mapping and defining the WUI is critical for wildfire risk management because as the WUI expands, it must be monitored in order for planners to make effective policy decisions to mitigate risk (Stewart *et al.* 2007). Such maps provide powerful visual images and are commonly used as tools to direct policy, which has contributed to their increasing use in the US (Radeloff *et al*. 2005; Theobald and Romme 2007). Many studies of WUI fire risk have used Geographic Information Systems (GIS) to examine changes through time (Greenberg *et al.* 1997; Jain *et al.*, 1996; Nourbakhsh *et al.* 2006), which is an effective approach because fire risk analysis commonly employs both spatial and temporal attributes (Chuvieco *et al.* 2010). A GIS-based model is an especially effective approach for areas in which a large part of the land is being encroached upon by development (Jaiswal *et al*. 2002).

Conventional wisdom is that escalating WUI losses are caused, in part, by an expansion of residential development into fire-prone areas. However, if new construction and landscaping adheres to strict mitigation strategies, then expansion of the WUI (with higher-resistant development) may actually buffer the older, high-risk communities from exposure to flames and embers. Thus, expanding WUI may either increase or decrease risk of residential loss dependent upon the extent of adhering to mandated mitigation strategies.

To help elucidate this seeming dichotomy, we are utilizing various GIS and remote sensing strategies to spatially analyze changes to urban expansion and subsequent potential risk of structural ignitions (including differing wildfire exposure via roofing materials, defensible space, and housing density) through time in growing, fire prone communities in southern California. While these communities are geographically nearby, they are demographically dissimilar, which may influence the ability to mitigate risk. The work presented here is the first stage of a larger, multi-phase project that is investigating changes in fire risk in those communities and the overriding causative agents influencing any changes to risk.

Methods

Study Site

Three residential communities in San Diego County, California, USA were assessed including Rancho Santa Fe, Ramona, and Julian (Figure 1). All of the communities have conditions conducive to high fire hazard, including a Mediterranean climate with extended drought, regular occurrence of high-velocity foehn winds (commonly referred to as Santa Ana winds), steep terrain, and flammable vegetation, all of which have led to several high-intensity, high-loss wildfires there in the past 10 years. The three specific communities represent a range of rates of development, demographics, housing density and geographic area deemed WUI.

Figure 1. Location of study sites and map of 12-year fire history around study sites (Top Left)

Specific demographics of each of the three communities are detailed in Table 1. Rancho Santa Fe has a population of 3,100 with an average household income of over $200,000. The community has taken numerous additional measures above county and state regulations to mitigate fire hazard and lower the likelihood of structural ignitions during wildfires. Some of these measures include mandatory installation of residential fire sprinklers, fire-resistant landscaping, setbacks, and widening of roadways (District 2004). Rancho Santa Fe is regularly viewed as a leader in the US in terms of mitigating fire risks.

While geographically near Rancho Santa Fe, Ramona and Julian differ in demographics, including population size and annual household income. A recent wildfire hazard risk assessment (Botts *et al.* 2013) found that Ramona and Julian had the most residential properties at risk in San Diego County. Both communities have significantly lower mean household incomes and subsequent ability to mitigate against wildfire) than Rancho Santa Fe. Ramona is over six times larger than Rancho Santa Fe. Conversely, Julian has half the population of Rancho Santa Fe.

Table 1. Demographics of the three assessed communities.

Study Site	Population	Average Income (USD)	Average House Value (USD)	WUI type
Rancho Santa Fe	3117	$180,612	$1,139,911	Interface
Ramona	20,292	$60,033	$485,597	Interface
Julian	1,502	$65,781	$510,138	Intermix

Data Analysis

In order to determine land use changes from non-urban to urban through time, we utilized publicly available land use data from the San Diego Regional Data Warehouse (SanGIS 2014). Land use data were available for pre-1986, 1990, 1995, 2000, 2004, 2008 and 2012. The data contained many classes of land use; for the purpose of this study, each year of land use data was classified as either urban or

non-urban. Agricultural and landscaping uses (e.g., vineyards and parks) were considered non-urban. All land uses involving clearing of vegetation and/or paving (e.g., telecommunication right-of-way) were considered urban.
The years of land use were then layered chronologically to show development over time (Figure 2). To quantify the changes in land use over time, the area of the polygons were clipped to a defined study area. In order to be inclusive of all structures within the WUI, a 3.2 km buffer was created around each of the US census-designated place (CDP) boundaries of the study sites, the size of which was chosen because embers regularly travel 1.6 km (i.e., half the buffer size) or more during extreme weather conditions. Also, we included any structures that resided within the 3.2 km buffer from the CDP boundary. Given the nature of urban expansion, it is intuitive to include structures on the outskirts of current boundaries, as the developments of the future are likely to be located here. The land-use data was then clipped to each buffer zone, and the area for each polygon was calculated using GIS. Evaluation included percentage change in urban land use.

Results

Figure 2 shows the results of the land use mapping over time. Rancho Santa Fe has clustered recent development in the eastern portion of the community, which was expected because other existing communities on the western portion limit development there. As can be seen in Figure 1, wildfire events have historically approached Rancho Santa Fe from the east, which is due to the general direction of Santa Ana winds. The newer developments (purple and pink polygons) therefore have the potential to act as a buffer for the town if developed with more fire-resistant construction and landscaping is maintained.

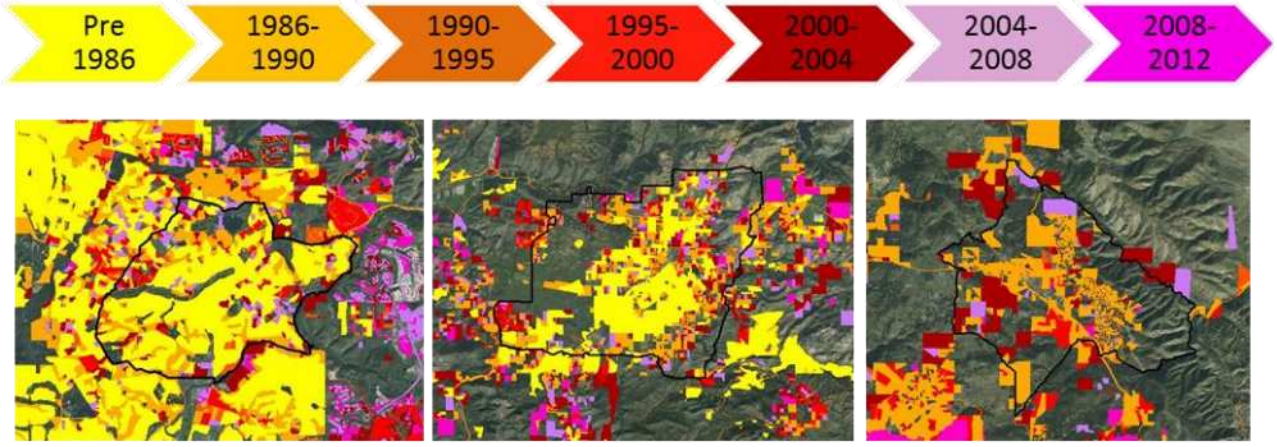

Figure 2. Change in designated land use from "non-urban" to "urban" over time in Rancho Santa Fe (A), Ramona (B), and Julian (C). Data per SanGIS (2014)

Much of the new development in Ramona has taken place on the outskirts of the town to the northeast and southwest, which might be result of the topography of the area limiting new development to those areas. The 2007 Witch Creek burned through the northeast portion of Ramona.

Land use data was not available for Julian pre-1986. The community has experienced little development in the past 8 years. Although the polygons depicting new development in Julian may appear large compared to Rancho Santa Fe and Ramona (Figure 2), many of these polygons only contain 1-3 structures within them. Julian differs from the former two communities that form a classic interface between the built and natural environments. Instead, Julian represents a classic intermix WUI community, where many structures are isolated from each other and have larger areas of vegetative

fuels between them. This is especially the case near the borders of the community. This differs greatly from Rancho Santa Fe, where there is a higher density of structures in both the new and old developments.

Figure 3 illustrates the change in urban land use over time in each of the communities. Each community demonstrated an upward trend over the 26-year period in the percentage of total lands deemed urban development. Results indicate that the majority of urban development in all three of the study sites is taking place as a result of expanding WUI (vs. residential infill into the existing communities). Rancho Santa Fe had the greatest rates of development of the three study sites.

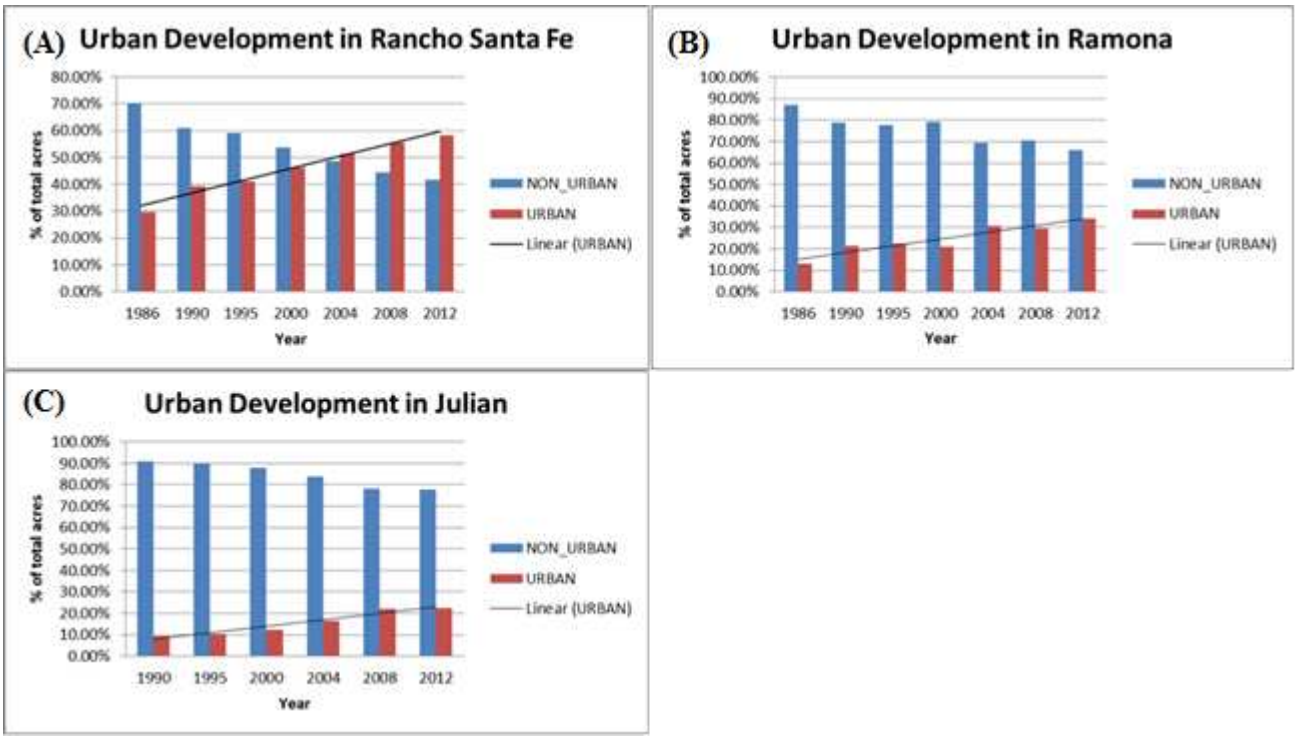

Figure 3. Proportional changes over time of urban and non-urban land uses in Rancho Santa Fe (A), Ramona (B), and Julian (C), including 3.2 km buffer outside of CDP boundaries). (SanGIS 2014)

Discussion

The results confirm that all three communities experienced expansion of the WUI over the past 26 years. Despite major wildfires in San Diego County in 2003 and 2007, which destroyed thousands of buildings, structures continue to be built in fire-prone areas, both to replace existing homes destroyed during wildfires and because of increasing populations in these communities. As previously noted, however, this new development could either exacerbate an already tenuous situation or could provide a means to reduce fire risk to older building interior to the new development, dependent on the nature and degree of fire mitigations that are employed.

Figure 4 illustrates how newer communities could potentially buffer the older communities if appropriate mitigation measures are employed in the new developments. In Rancho Santa (Figure 4A), the parcels east of the yellow line were developed 2004-2010 and could potentially provide a buffer to the structures built 1986, which are west of the yellow line. Likewise, in Julian (Figure 4B), the purple polygon contains a parcel developed in the 2004-2008 time frame (represented by the purple line) could buffer the structure built pre-1990 (the parcel of which is represented by the orange line).

(A) **(B)**

Figure 4. Examples of how new developments (with stricter construction and landscaping standards) could buffer older developments in Rancho Santa Fe (A) and in Julian (B).

Fire managers have multiple mitigation strategies to reduce the risk of fire loss in the WUI at their disposal. One mitigation activity is management of vegetative fuels. There is considerable evidence that fire intensity (and subsequent loss) is reduced when a fire advances through vegetation that has recently been treated by prescribed fire or by mechanical means (Martinson and Omi 2003, Skinner *et al*. 2004, Finney *et al*. 2005). Thus, there has been an escalating call by both land management agencies and the public to significantly modify the amount and arrangement of vegetation in wildlands near the communities so as to mitigate the potential negative impacts of high-severity fires (Dombeck *et al.* 2004; Abrams and Lowe 2005; Ostergren *et al.* 2008). Indeed, the 2001 National Fire Plan, the 2003 Healthy Forest Restoration Act, and the 2014 National Cohesive Wildland Fire Management Strategy all prioritized fuel treatments into national fire policy in the US.

That said, many argue that treating vegetation outside the area immediately surrounding a structure (commonly referred to in the US as the "Home Ignition Zone") is largely futile because of its minimal impact on the factors that impact structural ignition (Cohen 2000). Creation of a defensible space immediately surrounding a building would reduce structural ignitions via direct flame impingement or radiant heat transfer (Cohen and Butler 1998). To that end, the California Public Resources Code Section 4291 has required 9.15 m of defensible space around structures since 1991, which was increased to 30.48 m in 2006.

Even if current regulations are enforced, it must be noted that defensible space would not impact structural ignition from lofted embers, which is a more critical factor in residential losses than flame impingement or radiant heat (Cohen 2000). To mitigate potential residential losses, in 2008 California enacted building standards for new construction in areas in which the state has primary fire protection responsibility. California Code of Regulations Title 24, Part 2, Section 701.A now requires standards for some portions of dwellings that are most prone to ignition, including roofs, siding, attic ventilation, windows, decks, and others. While the new standards will likely reduce fire losses in future development, they obviously cannot impact vulnerability of existing structures.

Additionally, there has been a greater call to limit new construction into areas in which topography, such as steep slopes, naturally facilitates active fire spread (Syphard *et al.* 2008). Indeed, some areas in California now require a minimum setback of structures away from slopes so as to limit their exposure to convective heat transfer from burning vegetation. Of interest, some high-value communities (e.g., Rancho Santa Fe in this study) have taken novel approaches to meet setback regulations such as constructing enormous retaining walls (costing in excess of $400,000 USD) on the

sides of slopes in order to artificially meet the setback standards there (Mike Scott, Rancho Santa Fe Fire District, personal communication).

Unfortunately, W U I residents seem to frequently resist the very regulations that were developed to protect them and their property. For example, residents of one fire-prone area in California did not adhere to defensible space standards because of privacy concerns and a desire to be immersed in "natural" conditions (Delfino and Dicus 2007). Further, fire agencies commonly do not enforce the state-mandated defensible space regulations due to reasons such as lack of budget and personnel or unwillingness to play a perceived adversarial role with the public that they serve. Thus, adherence to sound mitigation standards varies by place and depends in part on the fiscal ability of residents to implement these strategies and the willingness of fire agencies to enforce existing regulations.

The buffer zones identified in this portion of the study, which demonstrate changes to urban expansion through time, will be used for future analysis to assess changing fire risk over time to these communities. In addition to the more traditional parameters of housing density, vegetation, and fire probability, there is a great need to develop a WUI risk assessment that more fully considers aspects of individual structure ignition (Calkin *et al*. 2014; Chuvieco *et al.* 2010; Menakis *et al*. 2003). For example, the inclusion of near-structure vegetation and defensible space in a remote sensing analysis would provide a better means of quantifying fire risk in WUI communities (Calkin *et al*. 2014; Menakis *et al.* 2003). Further, knowledge of a structure's location and arrangement relative to other structures or flammable materials is critical in effective risk analysis (Cohen, 2000; Murnane, 2006). Unfortunately, many risk analysis studies have not considered the fine-scale characteristics of vegetation immediately surrounding a home or have assumed that all structures are equally flammable (Bar Massada *et al.* 2009; Menakis *et al.* 2003; Prestemon *et al.* 2002).

Risk analysis has also traditionally emphasized the ignition and propagation potential of a wildfire, rather than it potential damages (Chuvieco *et al.* 2010). The idea of vulnerability is an important new addition to fire risk assessment models (Calkin *et al.* 2010; Chuvieco *et al.* 2012), which is a result of multiple high-loss wildfire events in the US in recent years (Calkin *et al.* 2014).

Sound risk analysis must therefore include elements of both fire hazard and the susceptibility of assets of value (Calkin *et al.* 2010). Thus, in subsequent phases of this on-going work, we will employ a WUI risk assessment protocol that more fully considers aspects of individual structural ignition as well as surrounding fire hazard and community variables such as housing density and proximity to fuels (Menakis *et al.* 2003; Chuvieco *et al.* 2010; Calkin *et al.* 2014). In order to have an accurate assessment of risk, we will consider roofing materials, vegetation proximity, structure density, eaves, windows, decking and siding materials. We will also measure compliance with defensible space legislation and general homeowner maintenance within the home ignition zone (Figure 5). All of these factors are critical in measuring structural vulnerability as defensible space may not impact structural ignition from lofted embers, which is a more critical factor in residential losses than flame impingement or radiant heat (Cohen 2000; Quarles *et al.* 2010).

Figure 5. Management of the home ignition zone must include implementation of defensible space at multiple scales, the most important of which is the 30 m immediately surrounding a structure.

Conclusions

As new buildings and infrastructure are developed into fire-prone WUI areas, measures must be taken to prevent losses from wildfire. Strategic placement of new developments to buffer vulnerable communities could provide multiple benefits the community. It is significantly more cost-efficient to build a community in a fire resistant manner at the onset than it is to retrofit an existing community. Our on-going research, of which this manuscript details the initial stages, will investigate if and how fire risk is being changed through time in these communities, which while geographically close vary significantly in community demographics and in socioeconomic status. We expect that there will be differences between the three communities in the implementation of mitigation strategies (and subsequent risk of loss) based upon the disparate abilities of residents to pay for modifications and jurisdictional differences in enforcement of the existing regulations.

To sustainably manage the WUI, stakeholders from diverse disciplines and worldviews must collaborate to reduce fire risk in a manner that is environmentally sound (Dicus and Scott 2006). Our ongoing research will provide land managers and policymakers with a means to facilitate that endeavor, creating a process that fosters meaningful dialogue between individuals and groups that sometimes have conflicting objectives. Indeed, while our research is regional in nature, it is hoped that the process that we develop will be able to be utilized by scientists, land managers, and policymakers on an international scale.

Acknowledgements

Funding for this work was provided by the California Department of Forestry & Fire Protection, the California State University Agricultural Research Initiative, and the McIntire-Stennis Cooperative Forestry Research Program. We are grateful to ongoing advice and insight provided by Dan Turner (Cal Fire, retired), Kate Dargan (Intterra), and Steve Quarles (Insurance Institute for Business & Home Safety).

References

Abrams, J., and K. Lowe (2005) Public perceptions of forest restoration in the southwest: A synthesis of selected surveys and literature. Ecological Restoration Institute. Northern Arizona University, Flagstaff, Arizona, USA.

Bar Massada, A., V.C. Radeloff, S.I. Stewart, T.J. Hawbaker (2009) Wildfire risk in the wildland–urban interface: a simulation study in northwestern Wisconsin. Forest Ecology and Management 258:1990-1999.

Botts, H., T. Jeffery, K. Stephen, S. Mcabe, B. Stueck, L. Suhr (2013) Wildfire Hazard Risk Report, Corelogic.

California Department of Forestry & Fire Protection (2013) 20 Largest California Wildland Fires (By Structures Destroyed). Available at http://interwork.sdsu.edu/fire/resources/documents/20LSTRUCTURES.pdf , <2-14-14>.

Calkin, D.E., J.D. Cohen, M.A. Finney, M.P. Thompson (2014) How risk management can prevent future wildfire disasters in the wildland-urban interface. Proceedings of the National Academy of Sciences 111:746-751.

Chuvieco, E., I. Aguado, S. Jurdao, M. Pettinari, M. Yebra, J. Salas, S. Hantson, J. de la Riva, *et al*. (2012) Integrating geospatial information into fire risk assessment. International Journal of Wildland Fire.

Chuvieco, E., I. Aguado, M. Yebra, H. Nieto, J. Salas, M.P. Martín, L. Vilar, J. Martínez, *et al*. (2010) Development of a framework for fire risk assessment using remote sensing and geographic information system technologies. Ecological Modelling 221:46-58.

Cohen, J.D. (2000) Preventing disaster: home ignitability in the wildland-urban interface. Journal of Forestry 98:15-21.

Cohen, J.D., B.W. Butler (1996) Modeling potential structure ignitions from flame radiation exposure with implications for wildland/urban interface fire management, Thirteenth Fire and Forest Meteorology Conference, Lorne, Australia.

Delfino, K., and C.A. Dicus (2007) Kennedy Meadows Community Wildfire Protection Plan. Available at http://www.krvfiresafecouncil.org/KennedyMeadowsCWPP.pdf <01 November 2008>

Dicus, C.A., and M.S. Scott (2006) Reduction of potential fire behavior in wildland-urban interface communities in southern California: a collaborative approach. P. 729-738 in Andrews, Patricia L.; Butler, Bret W., comps. Fuels Management—How to Measure Success: Conference Proceedings. 28-30 March 2006; Portland, OR. Proceedings RMRS-P-41. Fort Collins, CO: U.S. Department of Agriculture, Forest Service, Rocky Mountain Research Station.

District, R.S.F.F.P. (2004) Sheltering in Place During Wildfires: a Modern Approach to Living Safely in a Wildland–Urban Interface Community. Rancho Santa Fe, CA.

Dombeck, M.P., J.E. Williams, and C.A. Wood (2004) Wildfire policy on public lands: integrating scientific understanding with social concerns. Conservation Biology 18(4):893-889.

Greenberg, J.D., G.A. Bradley (1997) Analyzing the urban-wildland interface with GIS: two case studies. Journal of Forestry 95.

Jain, A., S.A. Ravan, R. Singh, K. Das, P. Roy (1996) Forest risk modeling using remote sensing and geographic information systems. Current Science 70:928-933.

Jaiswal, R.K., S. Mukherjee, K.D. Raju, R. Saxena (2002) Forest fire risk zone mapping from satellite imagery and GIS. International Journal of Applied Earth Observation and Geoinformation 4:1-10. DOI: http://dx.doi.org/10.1016/S0303-2434(02)00006-5 .

Menakis, J., J. Cohen, L. Bradshaw (2003) Mapping wildland fire risk to flammable structures for the conterminous United States, Proceedings of Fire Conference. pp. 41-49.

Murnane, R.J. (2006) Catastrophe risk models for wildfires in the wildland–urban interface: What insurers need. Natural Hazards Review 7:150-156.

National Interagency Fire Center (2014) Historically significant wildland fires. Available at http://www.nifc.gov/fireInfo/fireInfo_stats_histSigFires.html <15-July-2014>

Nourbakhsh, I., R. Sargent, A. Wright, K. Cramer, B. McClendon, M. Jones (2006) Mapping disaster zones. Nature 439:787-788.

Ostergren, D.M., J. Abrams, and K. Lowe (2008) Fire in the forest: Public perceptions of ecological restoration in north-central Arizona. Ecological Restoration 26(1): 51–60.

Prestemon, J.P., J.M. Pye, D.T. Butry, T.P. Holmes, D.E. Mercer (2002) Understanding broadscale wildfire risks in a human-dominated landscape. Forest Science 48:685-693.

Quarles, S. L., Y. Valachovic, *et al*. (2010). "Home survival in wildfire-prone areas: building materials and design considerations." ANR Publication 8393.

Radeloff, V.C., R.B. Hammer, S.I. Stewart, J.S. Fried, S.S. Holcomb, J.F. McKeefry (2005) The Wildland Urban Interface in the United States. Ecological Applications 15:799-805. DOI: 10.1890/04-1413.

SanGIS (2014). Regional Data Warehouse, County of San Diego.

Stewart, S.I., V.C. Radeloff, R.B. Hammer, T.J. Hawbaker (2007) Defining the wildland-urban interface. Journal of Forestry 105:201-207.

Syphard. A.D., V.C. Radeloff, N.S. Keuler, R.S. Taylor, T.J. Hawbaker, S.I. Stewart, and M.K. Clayton (2008) Predicting spatial patterns of fire on a southern California landscape. International Journal of Wildland Fire 17:602-613.

Theobald, D.M., AND W.H. Romme (2007) Expansion of the US wildland– urban interface. Landsc. Urb. Plan. 83(4):340 –354.

The development of forest fire danger mapping method for wildland urban interface in Korea

HoungSek Park[a], Si-Young Lee [b], Chun-geun Kwon [b], Chan-ho Yeom [b]

[a] *Dongguk University, Chung-Ku, Seoul, South Korea, parkhs08@nate.com*
[b] *Professional Graduate School of Disaster Prevention, Kangwon National University, Samcheok, Gangwon-Do, South Korea, lsy925@kangwon.ac.kr*

Abstract
Facilities in wildland-urban interface were main causes of forest fire ignition or protection objects from forest fire. In Korea, many facilities-for example, ancient temples and pensions-lied in wildland-urban interface and suffered from forest fire extremely. For preventing forest fire damage to these facilities, Korea national government designated the wildland-urban interface, which was located within 30m from forest.
In this study, we established some manuals which were resulted from analysis of damaged facilities records in Korea and referred other management tool-FIREWISE and FIRESMART for estimation of the forest fire danger rating around these facilities and a protection of the life and the property. The manual was consisted by two parts. One was related by environment factors (forest species, forest density, slope, a distance from forest and etc.) and another by artificial factors (a condition of road, distance from forest fire attack agency, distance from water source and etc). Theme maps were made by this factor which was graded by this manual and analyzed using ARCGis 9.3. The map was made on three districts (Kyeongjoo-Si, Uljin-Gun and Bongwha-Gun) in Keongsangbuk-Do and the resolution was 10m. In mapping and analyzing, we graded these factors and classified according to this grade rule using G.I.S tool.
In results, the forest fire danger rate in Uljin-Gun and Bonghwa-Gun was much higher than Kyungjoo-Si. Because of Coniferous forest, the forest fire danger rate in Uljin-Gun and Bonghwa-Gun was much higher than Kyungjoo-Si. And forest fire danger rates related with artificial condition in Uljin-Gun and Bonghwa-Gun much higher than that in Kyungjoo-Si.

Keywords*: Wildland-urban interface, forest fire danger map, GIS , Forest fire danger zone*

Introduction

In Korea, many facilities-for example, ancient temples and pensions, houses, hospitals, gas stations, powerline, etc. - lied in wildland-urban interface and were exposed by high danger rate from forest fire extremely. The large forest fire in Korea, for example, East region forest fire in 2000, YangYang Forest fire in 2005 and other large forest fire, destroyed many houses and building in wildland-urban interface. Especially, Naksan temple, ancient bell and other Buddhism structure, important cultural properties, were destroyed by Yangyang forest fire in 2005. And many houses in highly urbanized area with urban forest on Pohang-Si were damaged and destroyed in 2012. So , in Korea, central and local government were interested in how to protect structures in wildland-urban interface and to lessen damages from forest fire. Therefore, for preventing possibilities of forest fire damage for these facilities, first of all, Korea national government classified the facilities in forest and wildland-urban interface and designated the wildland-urban interface zone, which was located within 30m from forest.
In U.S.A., Willam E. Mell *et al* (2010) reviewed whole method for reducing structure losses. They focused on fuel treatment, risk assessment strategies and test for fire-resistant designs and metarials. In our country, as packaged measure for forest fire would be needed, we would plan to analyze characters of damaged structures and facilities according to forest factors and others for first steps and would make forest fire danger map for risk assessment in wildland-urban interface for next step.
In many countries, many mapping method for forest fire danger map in wildland-urban interface were developed. In Spain, Roul R. Calcerrada *et al* (2008) focused on socio-economic factors and analyzed

the ignition risk characteristics in Mediterranean regions. In U.S., Robert E. Keans *et al* (2008) made fire hazard and fire risk using FIREHARM. FIRE HARM calculate risks of forest fire from fuel moisture and other fire variables. James K. Lein and Nicole I. Stump (2009) assessed wildfire potentials in wildland-urban interface using GIS based models. The vegetation, a intensity of solar radiation, topographic wetness, population densities and near roadway were using for models from forest fire records

In this study, we analyzed damaged facilities records in wildland-urabn interface in Korea and referred to other management tool for facilities in wildland-urban interface-FIREWISE and FIRESMART. Using these results, we established a manual for estimation of the forest fire danger rating of facilities in wildland-urban interface. This manual must be needed for a protection of the life and the property

Methods

The manual was consisted by two parts. One was related by environment factors (forest species, forest density, slope, a distance from forest and etc.) and another by artificial factors (a condition of road, distance from forest fire attack agency, distance from water source and etc).

The survey of environment and natural and artificial factors

Field surveys from forest fire records about damaged structure were carried out in Korea from 2010 to 2012. The main damaged structures were house and storage. Especially in Korea, many farmers houses were located in mountainous topology and near to forest. So, we focused on which natural and artificial factor make to ignite structure. For proving these questions, we analyzed the relationship with facility damages and road condition, vegetation, topographical condition, factors for forest fire attack and other relation factors. These factors which were surveyed factors for estimating forest danger rating were referred to FIREWISE in U.S. and other country mapping results. After surveying, we analyzed the relationship and selecting the factor having high relationships.

The selection of environment and artificial factor

After analyzing whole data about damaged facilities and their natural and artificial environment, we selected a few factor for damaging facilities from forest fire. These were main facfor - the number, width, degree and condition of road to access, road sign, space for attack engine, main species of forests, tree height of trees, D.B.H. of forests, tree density of forests, a fuel condition of shrub, a condition of ladder fuel, a fuel condition of surface, a condition of crown, a distance from forest, a gradient of neighboring ground, a existence of water in near and the distance from forest fire attack facilities.

After selecting factors, we found a relationship with damage rating of facilities per factor. And we designated a weight between factors which was referred to NIST reports about estimating house danger rating from forest in wildland-urban interface.

Using these factors, we made theme maps from D.E.M. and digital forest floor map from K.F.R.I.. We used ARCGis 9.3 for making theme maps. And we wrapped these theme maps using ARCGis 9.3 for making a forest fire danger rating map for facilities in wildland-urban interface.

Results

In results, the forest fire danger rate in Uljin-Gun and Bonghwa-Gun was much higher than Kyungjoo-Si. Because of Coniferous forest, the forest fire danger rate in Uljin-Gun and Bonghwa-Gun was much higher than Kyungjoo-Si. The forest fire danger rate according to the distance from forest in Uljin-Gun and Bonghwa-Gun was much higher than Kyungjoo-Si. Absolutely safety area (distance was above 300m from forest) was 78.6% in Kyungjoo-Si, 52.5% in Uljin-Gun and 48.6% in Bonghwa-Gun. The danger area according to slope was 15.5% in Kyungjoo-Si, 42.1% in Uljin-Gun and 53.7%

in Bonghwa-Gun. And forest fire danger rates related with artificial condition in Uljin-Gun and Bonghwa-Gun much higher than that in Kyungjoo-Si.

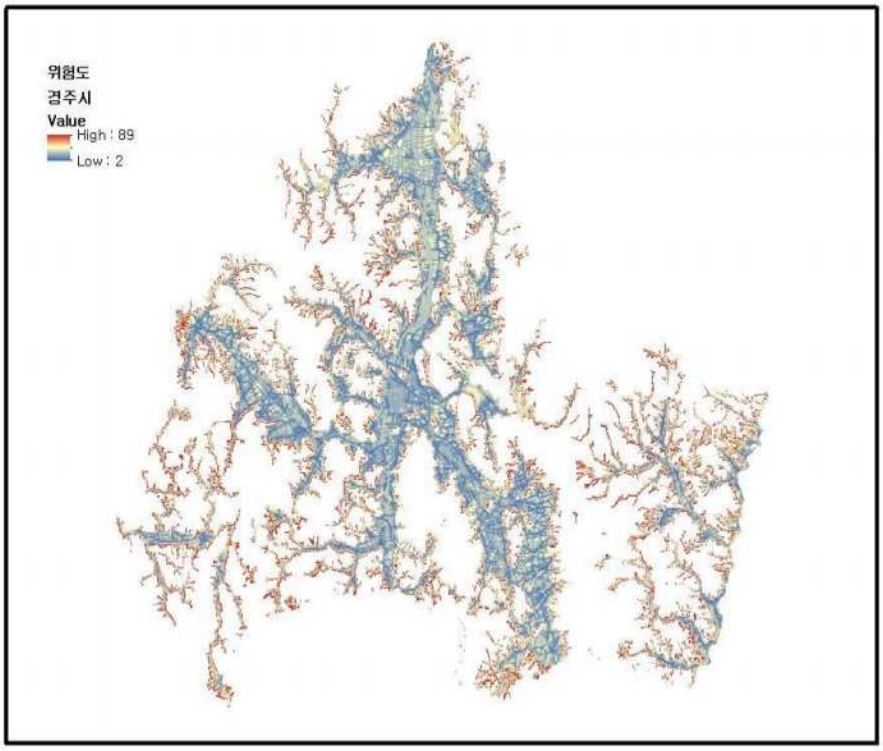

Figure 1. The results of danger rating for forest fire in Wildland-urban interface in Kyeongjoo-SI

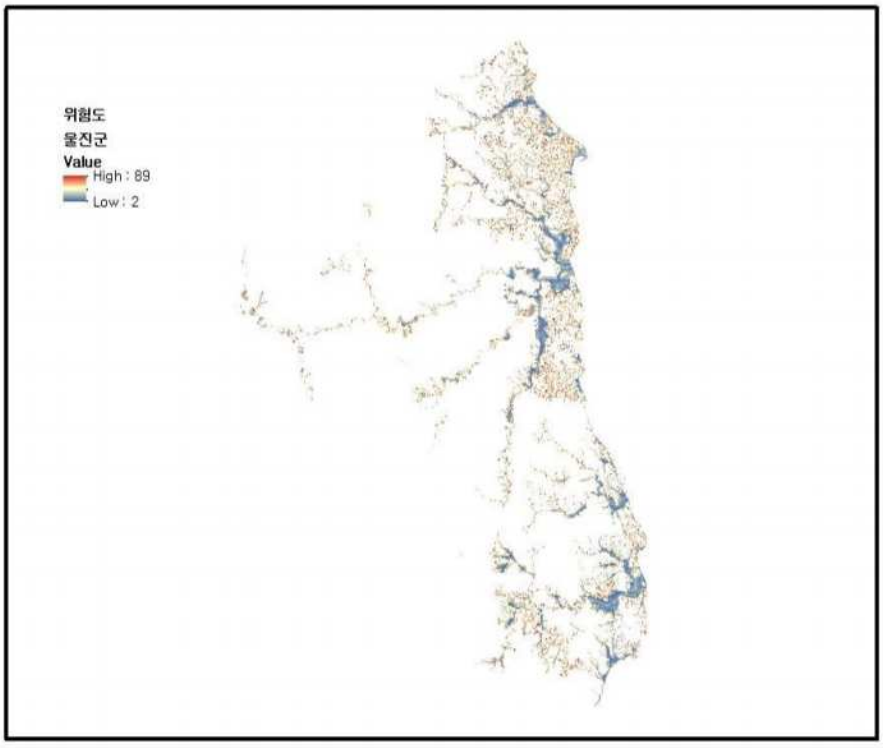

Figure 2. The results of danger rating for forest fire in Wildland-urban interface in Uljin-Kun

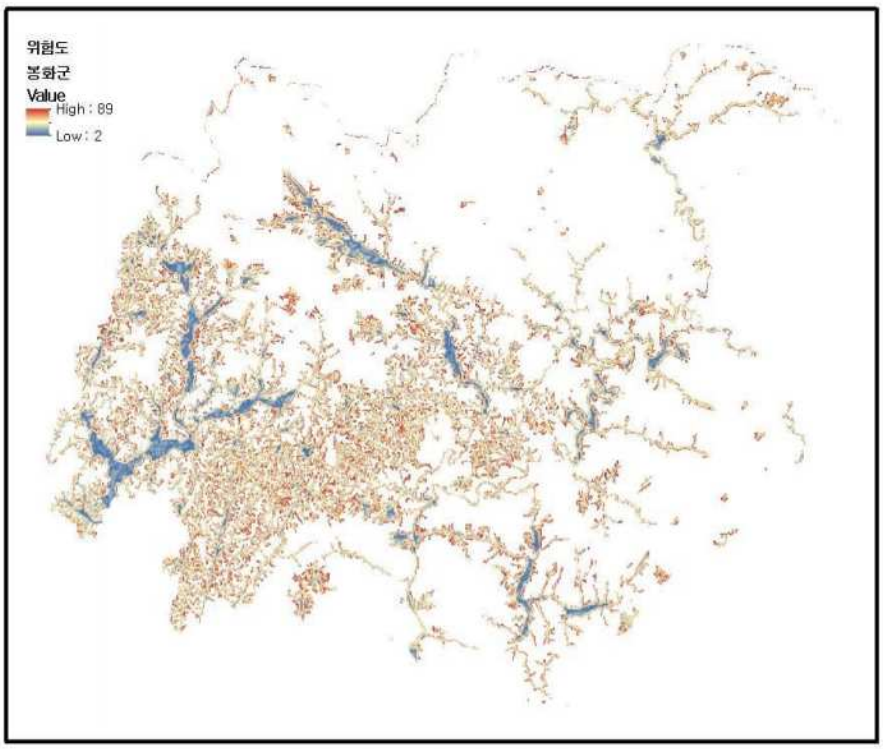

Figure 3. The results of danger rating for forest fire in Wildland-urban interface in Bonghwa-Kun

In results, the proportion of forest danger had a difference between three regions in 5% significant level. For verifying this algorithm, we applied this algorithm to facilities in other region. We tested 11 damaged facilities in wildland-urban interface on Seomi-Ri and Jungmyeong-Ri in Kyeongsangbuk-Do. These facilities damaged from forest fire which occurred in 2011. The mean in a radius of 30m of damaged facilities was 46.98 in 89 scales. the maximum was 70.61. That is over 'danger rate(37/89)' which was referred to home ignition manuals of 'FIREWise'

Using these algorithms, we calculated and estimated the danger rating of main facilities in three regions. In results, Bongwha-Kun was most danger region. An average Danger rating was 44/89. The danger rating according to facilities categories was analyzed. In results, cultural assets were most danger facility category(39.3/89).

The forest management like a fuel management or deploying of forest fire attack resources would be needed for this region and cultural assetsext…

Acknowledgement.

This study was carried out with the support of 'Forest Science & Technology Projects (Project No. S121214L140110)' provided by Korea Forest Service.

References

Alan A. Ager, Nicole M. Vaillant, Mark A. Finney (2010) A comparison of landscape fuel treatment strategies to mitigate wildland fire risk in the urban interface and preserve old forest structure . *Forest Ecology and Management* **259,** 1556–1570

Avi Bar Massada , Volker C. Radeloff , Susan I. Stewart , Todd J. Hawbaker (2009) Wildfire risk in the wildland–urban interface: A simulation study in northwestern Wisconsin. *Forest Ecology and Management* **258,** 1990–1999

Casey Cleve, Maggi Kelly, Faith R. Kearns, Max Moritz (2008) Classification of the wildland–urban interface: A comparison of pixel- and object-based classifications using high-resolution aerial photography. *Computers, Environment and Urban Systems* **32,** 317–326

James K. Lein*, Nicole I. Stump (2009) Assessing wildfire potential within the wildland–urban interface: A southeastern Ohio example. *Applied Geography* **29,** 21-34

John Talberth, Robert P. Berrens, Michael MCkee, and Michael Jines (2006) Averting and insurance decisions in the Wildland-Urban interface: Implications of survey and experimental data for wildfire risk reduction policy. *Contemporary Economic Policy* **24**, 203-223

Paul F. Hessburg, Keith M. Reynolds, Robert E. Keane, Kevin M. James, R. Brion Salter (2007) Evaluating wildland fire danger and prioritizing vegetation and fuels treatments. *Forest Ecology and Management* **247,** 1-17

Raul Romero-Calcerrada, C. J. Novillo, J. D. A. Millington, Gomez-Jimenez (2008) GIS analysis of spatial patterns of human-caused wildfire ignition risk in the SW of Madrid (Central Spain) *Landscape Ecol*

Robert E. Keanea, Stacy A. Drurya, Eva C. Karaua, Paul F. Hessburg, Keith M. Reynolds (2010) A method for mapping fire hazard and risk across multiple scales and its application in fire management. *Ecological Modelling* **221**, 2-18

Robert G. Haight, David T. Cleland, Roger B. Hammer, Volker C. Radeloff, and T. Scott Rupp (2004) Assessing Fire Risk in the Wildland-Urban Interface. *Journal of Forestry* **October/November,** 41-48

Susan I. Stewart, Bo Wilmer, Roger B. Hammer, Gregory H. Aplet, Todd J. Hawbaker, Carol Miller, and Volker C. Radeloff (2009) Wildland–Urban Interface Maps Vary with Purpose and Context. *Journal of Forestry* **March,** 78-83

Vassilis Spyratos, Patrick S. Bourgeron, and Michael Ghil (2007) Development at the wildland–urban interface and the mitigation of forest-fire risk. *PNAS* **104,** 14272-14276

Wendel J. Hann, Diane J. Strohm (2003) Fire Regime Condition Class and Associated Data for Fire and Fuels Planning: Methods and Applications. *USDA Forest Service Proceedings* **RMRS-P-29,** 397-434

William E. Mell, Samuel L. Manzello, Alexander Maranghides, David Butry and Ronald G. Rehm (2010) The wildland–urban interface fire problem – current approaches and research needs. *International Journal of Wildland Fire* **19**, 238–251

The evolution of the Wildland Fire Decision Support System (WFDSS): future direction after five years of implementation

Noonan-Wright, Erin[a], Sexton, Tim[b], Burgard, Mitchell[c]

[a] *U.S. Forest Service, WFM RDA, 5765 West Broadway St., Missoula, Montana 59808 USA, enoonan02@fs.fed.us*
[b] *U.S. Forest Service, WFM RDA, 3833 S. Development Ave., Boise, Idaho 83705 USA , timsexton@fs.fed.us*
[c] *U.S. Forest Service, WFM RDA, 344 6th Avenue East, Kalispell, Montana 59901 USA , mburgard@fs.fed.us*

Abstract
The Wildland Fire Decision Support System (WFDSS) was unveiled to the United States (U.S.) fire community in 2009 to facilitate a flexible, agile and scalable risk-informed decision-making process on complex wildland fires. Composed of a collection of spatial and non-spatial data, economic, fire behaviour, smoke, and weather tools, the WFDSS was designed to guide a decision-maker through a deliberative and thoughtful decision. After five years of operational use on federal wildland fires, user trends suggest greater involvement with the decision-making process and an increase in the number of documented decisions made on wildland fires. Despite these trends, increased wildland fire costs and continued fire-fighter fatalities each year reinforces the need to improve fire management decision-making to achieve better performance. After reviewing the intent, implementation, components and usage statistics of the WFDSS, we discuss the strengths, weaknesses, and further opportunities to support the U.S. fire management community with making risk informed decisions. International audiences who are developing similar wildland fire decision-making systems may find value in evaluating the strengths, opportunities, and lessons learned from a national decision support system like the WFDSS.

Keywords*: fire management, United States, risk, decision-making, Wildland Fire Management Research Development and Application (WFMRDA)*

Introduction

The Wildland Fire Decision Support System (WFDSS - Noonan-Wright et.al 2011) was officially unveiled to the U.S. fire community in 2009 to facilitate continued implementation of the 1995 U.S. federal fire policy which acknowledged fire as a critical process that will be planned for in land and resource management planning documents (USDI-USDA 2001, 2009). The revised implementation of this policy in 2009 specified "a new wildfire analysis and decision process, the Wildland Fire Decision Support System (WFDSS), to improve decision documentation, risk assessment, decision support, and operational implementation" (NWCG 2009). The integration of the best available science and tools in the WFDSS was intended to increase decision makers' ability to acquire and synthesize information in order to more make timely and applicable risk informed decisions on wildland fires (Zimmerman 2011).

Two decision processes had been in place for federal agency administrators and fire managers to use in making decisions on wildfires. One very simple process, the Wildland Fire Situation Analysis (WFSA) was used for fires necessitating an aggressive suppression response. The WFSA was a PC-based desktop application with decision tree analysis using expert opinions. Another more complicated process, the Wildland Fire Implementation Plan (WFIP) was required for fires that were deemed to be beneficial to natural and cultural resources and might be allowed to achieve land management plan objectives. After several severe wildfire years affecting almost all portions of the United States, federal agency administrators and fire managers from U.S. land management agencies [including the United States Department of Agriculture, National Forest System (USDA FS); the United States Department

of Interior Bureau of Land Management (USDOI BLM); National Park Service (USDOI – NPS); Bureau of Indian Affairs (USDOI – BIA); and the Fish and Wildlife Service (USDOI – FWS)], agreed that a single process for all wildland fires would be more effective. It was further agreed that the single process would be a deliberative, risk-based process which would provide decision support and also serve as an archive of decisions for organizational learning. Initial research and development of the conceptual design of the WFDSS began in 2005 and was tested during the 2007 and 2008 fire seasons through a new web based fire behaviour model, Fire Spread Probability (FSPro). A decision framework process was quickly added to assist fire and land managers with rapidly evaluating the emerging fire situation and producing a quality strategic decision. The WFDSS was being utilized by all 5 of the largest federal land management agencies in the U.S. by 2010. The primary users of the WFDSS have been Agency Administrators, who have the ultimate responsibility and approval authority for how wildland fire is managed on their home unit. Though the focus of the WFDSS is on strategic decision-making, over time, it has incorporated more tools and data that additionally assist incident command teams and other firefighting resources with gaining situational awareness and developing short-term tactics from the broader strategic direction. Emerging science and technologies are continually integrated, such as the Near-Term and Short-Term fire behaviour models, to further support risk informed decisions that are integral to the WFDSS (Zimmerman 2011).
Despite increased use of a deliberative, risk-based decision process, even the partial costs for suppressing federal fires often exceeds 1 billion dollars a year (Calkin *et al*. 2005, NIFC 2013). The U.S. Forest Service continues to experience annual wildfire costs of approximately 3 billion dollars a year, when both preparedness and suppression costs are included in the estimate (Lichtenstein, 2014). Costs incurred by other federal, state, and local governments push the total costs of wildland fire in the United States far higher. In addition, there are episodic tragedies of loss of firefighter and civilian lives. Consequently, there is a compelling need to enhance the WFDSS as well as improve user understanding and use of this application.

Risk Assessment Process in the WFDSS

The WFDSS is a system for wildfire decision support and analysis based on a deliberative decision process (Figure 1). A risk informed decision process in the WFDSS begins with gathering, analysing and synthesizing new and existing information. Land managers are, by definition, geographically oriented decision makers; therefore, much of the WFDSS information is displayed as spatial data over a variety of different map base layers. The location of the fire start, its size, and the responsible agency is populated and available to a decision maker. Maps with reference data layers showing highly valued resources and assets are evaluated with hazard and fire potential to develop a preliminary risk assessment. Management Requirements and Strategic Objectives from land management planning documents are automatically displayed for the fire area. Users develop incident specific requirement and objectives tiered to the Strategic Objectives, informed by the Management Requirements and tailored to the specific spatial and temporal attributes of the fire. A course of action defining operational actions to meet incident specific objectives is drafted, reviewed, and validated. Collectively, the Agency Administrator, local staff and fire specialists develop a decision, which the Agency Administrator has the option of approving or rejecting. If it is approved, the Agency Administrators document the decision with the rationale behind it and provide it to the incident management team that has been assigned to the fire. After approval, a periodic assessment allows a decision maker to revisit their decision and evaluate its relevance to the current fire situation. All parts of a decision require iterative steps to re-evaluate when conditions change and new information is provided. All components of a risk-informed are available in the WFDSS.

Figure 1. There are seven linear steps to develop and document a wildland fire decision in the WFDSS.

Five Years of Operational Use

After 5 years of implementation, the need to review how the WFDSS is supporting the field to facilitate and document decisions is necessary. Given the capacity of the WFDSS to store analyses and other components of a risk-informed decision, the ability to query the database has enabled retrospective evaluation of the system, which, in part, is described below.

General User Statistics

User statistics in the WFDSS were summarized to evaluate the over-all use and application of the system. Data were normalized by the total number of federal fires per year and scaled by 1000 in order to compare yearly trends (NWCG 2013).

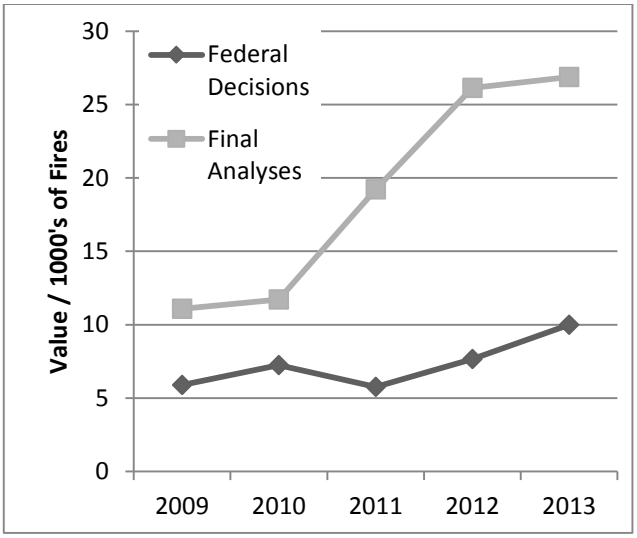

Figure 2. Analyses and Decisions in the WFDSS

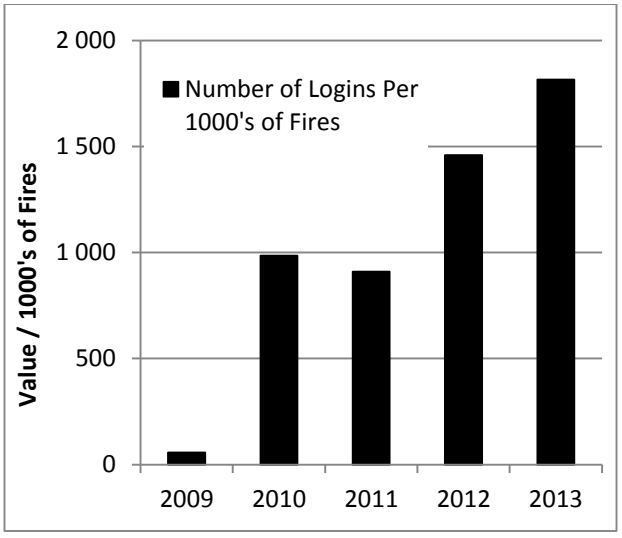

Figure 3. WFDSS Use Since 2009

In Figure 2, it is not surprising that there are more analyses than decisions because multiple analyses would provide part of the information to develop a decision. “Final analyses” are defined as all fire behaviour modelling analyses (Basic, STFB, NTFB, and FSPro) used on wildland fires and formally published in the WFDSS by the fire behaviour specialist. “Federal Decisions” are published documents excluding local, county and state fires that follow a risk assessment process in the WFDSS to document how a wildland fire will be managed. Trends suggest that fire modelling use has been increasing over time with the greatest increase between 2010 and 2012, possibly reflecting the expanded utilization of fire behaviour specialists to support short-term tactics and long-term strategy on wildland fires. There has been a moderate increase in the number of decisions since 2011. The dip in the number of federal decisions in 2011, however, does not correspond with a fewer number of federal fires. In fact, 2011 had more fires than any other year since 2009. Figure 3 shows the number of logins into the WFDSS since 2009 normalized by the total number of federal fires. For example, in 2013, on average, for every thousand federal wildland fires in the U.S. there were 1,800

logins into the WFDSS (or 1.8 logins per fire), which was a slight increase compared to previous years and suggests greater involvement in the decision support tools in the WFDSS.

3.2. Fire Behaviour Analysis to Support Decision-making

Enabling users to gain access to national geo-spatial data layers such as surface and canopy fuels and topography (Rollins 2006) resulted in increased use of fire behaviour modelling systems dependent upon these data sources. The WFDSS contains four primary fire behaviour modelling systems: Basic, Short-term (STFB), Near-term (NTFB) and the Fire Spread Probability (FSPro) Simulator for longer term analyses.

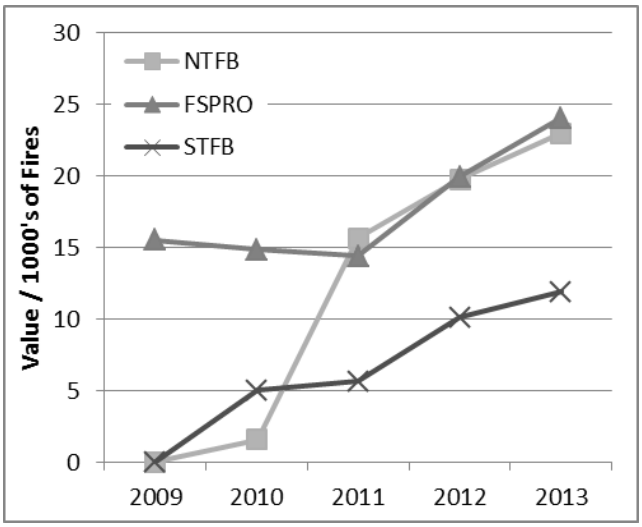

Figure 4. Usage statistics per every thousand federal fires for fire behaviour modeling systems, such as Near-term Fire Behaviour (NTFB), Fire Spread Probability (FSPro) Simulator, and Short-term Fire Behaviour (STFB) in the WFDSS from 2009 to 2013.

The first fire behaviour modelling system in the WFDSS, FSPro, was initially tested in 2007 to support long-term fire behaviour projections. As hardware and software capacity increased, STFB and NTFB modeling systems were added to support short (1-3 days) to mid term (1-7 days) spatial analyses. Usage of FSPro was initially greater than other modeling systems, but an increase in NTFB usage from 2010 to 2011 resulted in almost equal usage to FSPro by 2011. Small fires that were suppressed in the first 24 hours would likely not use fire behaviour modelling systems to gain situational awareness; however, by 2013 for every 1000 fires, there were approximately 11 short-term and over 20 mid to long term fire behaviour analyses simulated for all federal fires. Since 2011, usage for all fire behaviour modelling systems has increased, in addition to the number of federal decisions and logins, suggesting greater usage of the system over time (Figure 4).

Opportunities and Challenges of Risk Informed Decision-making

4.1. Social Science and Fire Management

Developing tools and processes to facilitate smart information sharing, communication, and decision-making was an objective of the WFDSS and continues to be a main challenge for wildland fire management (Zimmerman 2011). Identifying and understanding the institutional practices of the people who will use a process or collection of tools is crucial for implementing a decision support process like the WFDSS. Early adopters within the user community were recruited to assist with training others on the WFDSS and this contributed greatly to its acceptance as a process and a useful tool for fire management. Regional leaders, called Geographic Area Editors, were given authority for managing their user community by assigning user roles and access to the WFDSS based on skill level and need. They were relied upon to provide direction and training on how the WFDSS was

implemented in their region. This collaborative relationship with the user community gave users a sense of ownership and created a feedback loop between them and the developers so that changes and enhancements could be made in a responsive and agile fashion.

The use of the WFDSS to make risk-informed decisions continues to evolve for numerous reasons. The decision makers and their support personnel, including the host unit and incident management team, may vary in their understanding and application of decision science and risk management. This can result in failing to utilize the WFDSS to its full potential by not adequately considering all of the alternatives in developing a course of action or, simply, by using the system to document decisions that were made external to the process

There can be a tendency to reject low probability, large fire growth events when drafting a planning area; a user defined spatial extent that incorporates all of the land the fire may burn during the period that the decision is relevant. Since 2010, 16% of incidents with a decision had two or more planning areas, suggesting that some decision makers draw too small a planning area to manage their fire incident and eventually need to redraw a bigger area as the fire encroaches upon the planning area boundary (Figure 5). When these events occur, decision makers are often forced to rapidly respond to emergency situations and can neglect the careful and deliberative process utilized by the WFDSS. Using a fire behaviour modelling tool such as FSPro could help delineate a planning area that would serve the entire length of the decision. This example illustrates that the process to apply the various tools and information to optimize risk-informed decision-making is still evolving.

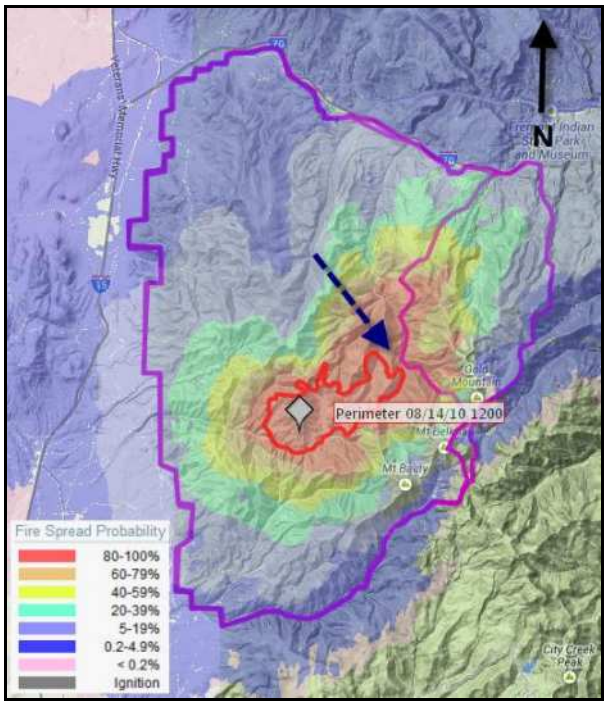

Figure 5. The 8/14 fire perimeter (red line) encroached with 0.2 miles of the first of two planning areas (purple lines) on the east side: the first drawn on 8/14 and the second 8/18 – see black arrow. FSPro is displayed in the background and can be helpful to evaluate fire potential (and the probability) that certain areas will be impacted by the fire over a designated time period, in addition to delineating where the planning area could be located.

4.2. User-friendly, Best Available Science

A current effort amongst land management agencies is to take historically text and paper based fire planning documents (referred to as the land and resource management plans and fire management plans) and convert them into digital and spatially explicit formats. As an alternative to providing lengthy text describing where and how a fire will be managed on the landscape, a location can now be

drawn on a map, and only the pertinent objectives and requirements will be presented for evaluation. Spatial Fire Planning (SFP) is an optional planning process available in the WFDSS that can spatially describe how fire will be managed according to planning documents. The visual depiction of these data allow for greater data control because data managers can upload, manage, and associate spatial polygons, lines or points to represent the planning direction, and make changes as needed throughout the year. The WFDSS initially provided lengthy planning documents in electronic text-based format and made them available to decision makers when they were developing their strategy. While a notable first step, spatial fire planning is the evolution of a process to make information from planning documents more easily consumable during the formulation of wildland fire management strategy and decisions.

Emphasis on pre-fire planning is facilitated by recent advances in quantitative risk assessment (Finney 2005, Calkin *et al*. 2010, Ager *et al*. 2011, Scott *et al*. 2012,) where values on the landscape that are most important are identified and evaluated for their hazard and susceptibility for experiencing harm or benefit from wildland fire. The integration of spatial fire planning and quantitative risk assessment, could result in less exposure to wildland fire fighters, and optimize the strategic wildfire response, i.e. resources are allocated where the probability of containment is highest and values are likely to interact with fire in a negative manner.

4.3. Information Sharing Via the Risk and Complexity Analysis

Gathering and communicating timely information on an emerging wildland fire is challenging for an incident commander. The process to determine wildland fire complexity and what level of an incident management organization is needed on a wildland fire was recently merged into one process called a Risk and Complexity Analysis (NWCG 2013). Historically, a separate risk assessment was done by an incident commander (in the field) and a land manager (in the WFDSS). With this change, intelligence gained in the field can be more readily shared with remotely located Agency Administrators who are ultimately responsible for making wildland fire decisions.

The Risk and Complexity Analysis provides users with the ability to make notes and document mitigations for elements identified as moderate or high complexity on wildland fires. Users evaluate components of risk including values (infrastructure, natural and cultural concerns; the proximity and threat of the fire to values; and social and economic concerns), hazard (fuel conditions and fire behaviour) and probability (the likelihood of a long duration event; barriers to fire spread; and the seasonal severity). The Risk and Complexity Analysis is designed to be completed on paper, and the information easily transferred into the WFDSS. Reinforcing a similar risk assessment process across all vested parties is central to the ideology of the WFDSS.

Conclusion

There are number of decision support systems (DSS) for fire management available internationally (Martell 2011, Mavsar 2013) both for management of fire ignitions and fuels planning. Implemented operationally on a national-scale in 2009, the WFDSS may be considered unique because of its application to a range of different ecosystem types and agencies across the United States. After five years of use, the WFDSS showed a general increase of system application to wildland fires and fire behaviour modelling tools. Challenges remain regarding the optimization of the system to evaluate all facets of ecosystem management, mitigate fire fighter exposure, and utilize fire-fighting resources to manage fire where values are most likely to have a negative impact from wildland fire. As new research methods and products are created, the WFDSS is designed to support and implement new practices to address many of these challenges. Research focused on fire management and decision science (Maguire *et al*. 2005, Thompson *et al*. 2013) is especially relevant. Continued investment in technology transfer to the decision makers and support staff is necessary for continued use and elevated application of the WFDSS as wildland fires become larger (Dennison 2014).

Acknowledgements

Funding for the WFDSS was provided primarily by the USDA Forest Service Fire and Aviation Management, State and Private Forestry, and the Department of Interior Office of Wildland Fire Coordination. Contributing staff and associated work accomplishments by the Department of Interior Bureau of Indian Affairs, National Park Service, and Office of Wildland Fire Coordination also contributed to the implementation of the WFDSS.

References

Ager, A.A., Vaillant, N.M., and M.A. Finney. (2011) Integrating Fire Behaviour Models and Geospatial Analysis for Wildland Fire Risk Assessment and Fuel Management Planning. *Journal of Combustion*. 2011: Article ID 572452: doi: 10.1155/2011/572452 19 p.

Calkin, D. E., Gebert, K. M., Jones, J. G., and Neilson, R. P. (2005) Forest service large fire area burned and suppression expenditure trends, 1970-2002. *Journal of Forestry, 103*(4), 179-183.

Calkin, David E.; Ager, Alan A.; Gilbertson-Day, Julie, eds. (2010) Wildfire risk and hazard: procedures for the first approximation. Gen. Tech. Rep. RMRS-GTR-235. Fort Collins, CO: U.S. Department of Agriculture, Forest Service, Rocky Mountain Research Station. 62 p.

Dennison, P. E., Brewer, S. C., Arnold, J. D., and M. A. Moritz (2014) Large wildfire trends in the western United States, 1984–2011, *Geophys. Res. Lett*.(41): 2928–2933, doi:10.1002/2014GL059576.

Finney, M. A. (2005) The challenge of quantitative risk analysis for wildland fire. *Forest Ecology and Management*. 211(1): 97-108.

Lichtenstein, Mark (2014) Personal communication. US Forest Service, National Headquarters, Fire Budget Branch Chief.

Martell, D. (2011) The Development and Implementation of Forest Fire Management Decision Support Systems in Ontario, Canada: Personal Reflections of Past Practices and Emerging Challenges. *Mathematical and Computational Forestry and Natural Resource Sciences*. 3 (1): 18-26.

Mavsar, R., Gonzalez Caban, A., and E. Varela (2013) The state of development of fire management decision support systems in America and Europe. *Forest Policy and Economics* (29): 45-55.

Maguire, L.A. and E. A. Albright (2005) Can behavioural decision theory explain risk-averse fire management decisions? *Forest Ecology and Management* (211): 47-58.

National Interagency Fire Center (2013) *Federal Firefighting Costs (Suppression Only)*. Available online: http://www.nifc.gov/fireInfo/fireInfo_documents/SuppCosts.pdf [Verified 14 July 2014].

National Interagency Fire Center [NIFC] (2013) Total Wildland Fires and Acres (1960-2013). Available online at https://www.nifc.gov/fireInfo/fireInfo_stats_totalFires.html [Verified 09 July 2014].

National Wildfire Coordinating Group [NWCG] (2009) Update on the modifications to the interagency strategy for the implementation of Federal Wildland Fire Management Policy *(*NWCG #001-2009). Boise: Idaho. Print.

National Wildfire Coordinating Group [NWCG] (2013) Adoption and Release of the Risk and Complexity Assessment (NWCG #015-2013). Memorandum and Attachement. Boise: Idaho, 2013. Print.

Noonan-Wright, E.; Opperman, T. S.; Finney, M. A.; Zimmerman, T. G.; Seli, R. C.; Elenz, L. M; Calkin, D. E.; and J. R. Fiedler (2011) Developing the U.S. Wildland Fire Decision Support System (WFDSS). *Journal of Combustion*. 2011: Article ID 168473: doi: 10.1155/2011/168473. 14 p.

Rollins, M. G. and C. K. Frame, tech. eds. (2006) The LANDFIRE Prototype Project: nationally consistent and locally relevant geospatial data for wildland fire management. Gen. Tech. Rep.

RMRS-GTR-175. Fort Collins: U.S. Department of Agriculture, Forest Service, Rocky Mountain Research Station. 416 p.

Scott, J. H.; M.P. Thompson, and D.E. Calkin (2013) A wildfire risk assessment framework for land and resource management. Gen. Tech. Rep. RMRS-GTR-315. U.S.Department of Agriculture, Forest Service, Rocky Mountain Research Station. 83 p.

Thompson, M.P., Marcot, B.G., Thompson III, F.R., McNulty,S., Fisher, L.A., Runge, M.C., Cleaves, D. and M. Tomosy (2013) The Science of Decisionmaking: Applications for Sustainable Forest and Grassland Management in the National Forest System. General Technical Report WO-88. 54p.

U.S. Department of the Interior, U.S. Department of Agriculture, U.S. Department of Energy (and others) [USDI – USDA] (2001) Review and update of the 1995 Federal Wildland Fire Management Policy. January 2001. Available at: https://www.nifc.gov/PIO_bb/Policy/FederalWildlandFireManagementPolicy_2001.pdf Verified [14 July 2014].

U.S. Department of the Interior, U.S. Department of Agriculture [USDI-USDA] (2009) Guidance for Implementation of Federal Wildland Fire Management Policy. February 2009. Boise, Idaho, USA, Available at: http://www.nifc.gov/policies/policies_documents/GIFWFMP.pdf [Verified 14 July 2014].

Zimmerman, T. (2011) Fire science application and integration in support of decision-making. Wildfire 2001: 5th International Wildland Fire Conference, South Africa. Available online at: http://www.wildfire2011.org/material/papers/Tom_Zimmerman.pdf Verified [14 July 2014].

The flammability of ornamental species with potential for use in highways and wildland urban interface (WUI) in southern Brazil

Daniela Biondi, Antonio Carlos Batista, Angeline Martini

[a] *Universidade Federal do Paraná, Av. Lothário Meisnner, 900 Curitiba-Brasil, dbiondi@ufpr.br, batistaufpr@ufpr.br, martini.angeline@gmail.com*

Abstract

The areas of wildland urban interface (WUI) are sites that have mixed characteristics, from the influence of rural and urban areas. With the increase in urban population in national and global level, the areas are losing this characteristic transition with diversity of functions. One of the most common problems due to this rural/urban proximity are forest fires that cause damage to many homes in urban areas. The highway is a transportation infrastructure located in the area of the wildland urban interface that can serve as a barrier or mitigation of forest fires that threaten urban areas, through its landscaping. For the highway integrate with the local landscape is necessary that this landscaping provide conservation or ecological, cultural and aesthetic function. The objective of this study was to evaluate the flammability of native ornamental species with potential for use in the prevention of forest fires in the vicinity of highways. The selected species are native from southern Brazil due the presence of interesting aesthetic features. They are: *Aspilia montevidensis* (Spreng.) Kuntze - the family Asteraceae species with ornamental potential both by the beauty of the flowers of bright yellow color, like the long flowering period that occurs almost all year round and can be used in landscaping as ground cover, is indicated for public areas by not requiring maintenance and also for treatment of degraded areas; *Peltodon rugosus* Tolm. - herbaceous species of the family Lamiaceae, native to southern Brazil, on "Estepe Gramíneo-lenhosa" presents both its ornamental inflorescence globose form and by its leaves with visible vein, can be used in degraded areas due to its hardiness; and *Verbena rigida* Spreng - the Verbenaceae family, is a little branched herbaceous perennial, rhizomatous, erect, popularly known as "grass-wire", native of the fields of the plateau in southern Brazil, can reach 20-30 cm in height with decorative flowering, stiff and rough leaves, inflorescences with small flowers blue-purple color formed in spring-summer. For each species were performed 50 burnings in epiradiator of 1 g of material freshly harvested. During the experiments burning in the epiradiator, the following variables were collected: Frequency of ignition (FI), time to ignition (TI), duration of combustion (DC), flame height (AC) and combustion index (IC). Statistical analysis was done by SNK test at 95 % probability. The results of the species flammability show that *Aspilia montevidensis* and *Peltodon rugosus* differ statistically of the *Verbena rigida* for FI and TI, indicating to be less flammable, although all species show low flammability. Given the results, it is concluded that the analyzed species exhibit excellent characteristics for landscape composition on highways both due its aesthetic appearance and functional, and can also serve as a barrier against forest fires in areas of wildland urban interface in southern Brazil.

Keywords*: in forest fuels, epiradiator, native ornamental species.*

Introduction

The Wildland Urban Interface areas, otherwise known as WUI, are places that have mixed features, with influence of rural and urban areas (BIONDI, 2013). Are multifunctional spaces where there are fragmented presence of land use and the absence of urban structure, with deep economic, social and physical transformations and that still feature a dynamic closely linked to the presence of a nucleus around (MIRANDA, 2009).

Radeloff *et al*. (2005) complements the concept of WUI stating that this area is a zone of conflict between humans and the environment, where there is destruction of houses by forest fires, fragmentation of natural habitats, introduction of exotic species and the loss of biodiversity.

According to Biondi (2013), with the increase of urban population, these areas are losing that characteristic of transition and acquiring a rural or urban physiognomy, moreover, to be removed shall

become the boundary between urban and rural zone. With that, one of the most common problems that occur are the forest fires that eventually reach the homes of the urban areas. Thus, since the highway is a transportation infrastructure in urban and rural transition area, could serve as a barrier and mitigation or forest fires that threaten urban areas

The assessment of forest fires risk on the landscape planning of roads should be an essential element to reduce the damage caused by the fire in the wildland urban interface areas of Paraná-Brazil (BIONDI *et al*., 2013). According to the same authors, from the characterization of the degree of risk of fire it is possible to perform the selection and planning of less flammable species composition in order to impede the spread of fire.

The knowledge of how the species differ in their flammability characteristics it is necessary to develop more reliable lists of plants recommended for residential landscaping in wildland - urban interface (WHITE and ZIPPERER, 2010).

According Ganteaume *et al*. (2013) currently, there is no research on the evaluation of flammability of ornamental species.

Flammability can be defined as how easy it is for a material to catch fire, both spontaneously and through exposure to certain conditions (ZHANG *et al*., 2011). According to Anderson (1970) flammability initially was defined based on three components: the potential of ignition, which is the time needed for the fuel reaches the ignition after being exposed to a source of heat; sustainability, refers to the ability to maintain combustion after ignition; and combustibility, which is the rate of burn after ignition.

The plant species that provide the fuel for the fires have specific flammabilities (CURT *et al*, 2011), which varies according to the species and with moisture content (VÉLEZ, 2000). In addition, the volatile organic compounds, such as monoterpenes, constitute other possible factors contributing to the increased flammability vegetation (ALESSIO *et al*., 2008).

The aim of this study was to evaluate the flammability of native ornamental species with potential for use in the prevention of forest fires in the surrounding highways.

Methods

The experiment was conducted in the laboratory of forest fires at the Campus III of the "Universidade Federal Paraná" (UFPR), in Curitiba, Brazil. The original vegetation of the city, before the anthropic action, consisted of "Estepe Gramíneo-Lenhosa" (fields), intermingled of arboreal groupings (with the presence of *Araucaria angustifolia*), next the downloaded and streams (RODERJAN *et al*., 2002)

The climate of Curitiba, according to Köppen classification, is Cfb, humid subtropical, humid, without dry season, with cool summers and winters with frequent frosts and occasional snow precipitation. Has average temperatures of 19.7° C in summer and 13.4° C in winter, with average annual precipitation of 1419.9 mm (IPPUC, 2011).

The species selected for the experiment are native from southern Brazil, on the "Estepe Gramíneo-Lenhosa", and present interesting aesthetic characteristics for use in landscaping. They are: *Aspilia montevidensis* (Spreng.) Kuntze, *Peltodon rugosus* Tolm and *Verbena rígida* Spreng.

Aspilia montevidensis is a species of the Asteraceae family that boasts great potential both for ornamental beauty of flowers of bright yellow color, as for the long flowering period that occurs almost the whole year. In landscaping, can be used as lining plant in flower beds to homogeneous full sun, being indicated for public areas and also in degraded areas, not requiring great care in maintenance.

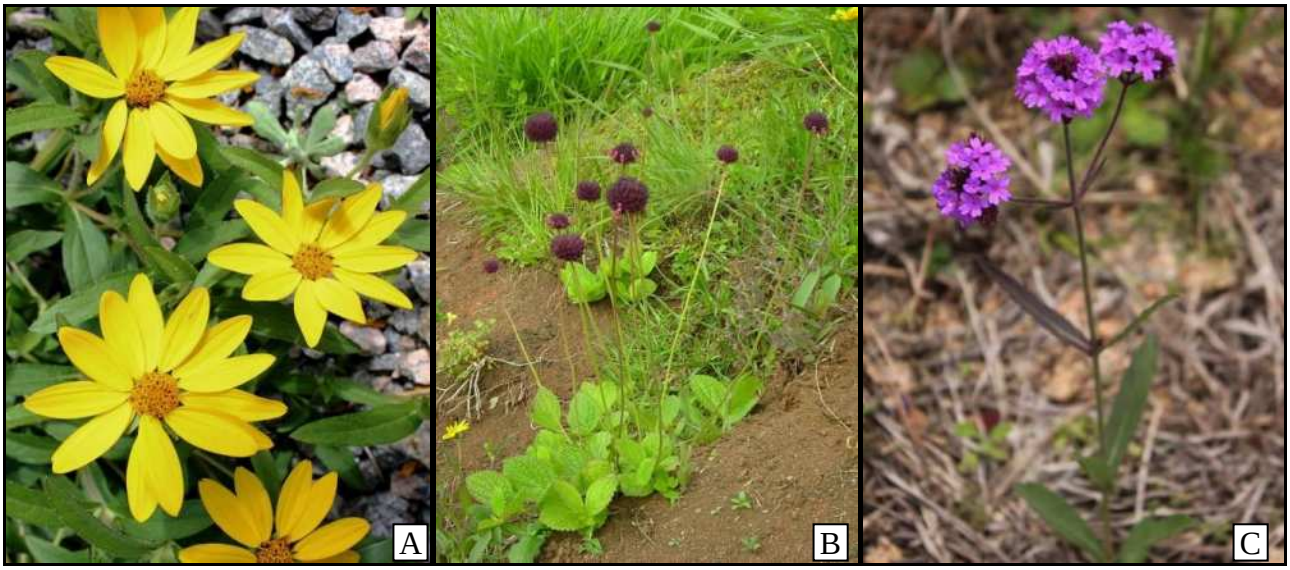

Figure 1. The selected species: A) Aspilia montevidensis; B) Peltodon rugosus, C) Verbena rigida

Peltodon rugosus, of the family Lamiaceae, is a herbaceous plant which features ornamental potential both for its inflorescence shape globe, as by their apparent ribbed leaves. Due to its hardiness can be used in recovery of degraded areas.

Verbena rigida, family Verbenaceae, is a little branched herbaceous perennial, rhizomatous, erect, popularly known as wire weed. Can reach of 20 to 30 cm tall, with decorative flourish, stiff and rough leaves, inflorescences with small flowers-blue color formed in spring-summer.

The concept of flammability can be reduced to distinct aspects of combustion, according to the type of metric used in its assessment (WHITE and ZIPPERER, 2010). Thus, it can be experimentally evaluated by fuel burning in the laboratory, whether in the form of discrete elements (such as a leaf or branch), or as a fuel bed and a heterogeneous set of individual units (FERNANDES and CRUZ, 2012). In this research the flammability was analyzed from the combustion experiments, performed in a chapel (a draught-free location), with an epiradiator of 500 W nominal power constant, kept in a controlled temperature range of 250 °C. The material used in the experiment consists only of leaves of selected species, which were collected in the vicinity of the building of Forestry and Wood of the UFPR, moments before the beginning of the experiment, which was carried out within a maximum of 2 hours after collecting.

Flammability tests were conducted according to the methodology proposed by Petriccione *et al*. (2006) and Petriccione (2006). For each species were performed 50 repetitions, each with 1 g of green fuel material, determined with the aid of a precision balance. The forests fuel was exposed to epiradiator for 60 seconds. In all the steps performed were taken the care required to be no direct contact with the material, so as to avoid interference in their properties.

During the experiment, conducted in the epiradiator, were collected the following variables: ignition frequency (FI), ignition time (TI), duration of combustion (DC) and height of the flame (AC). Flammability values were obtained from the potential of ignition (PI) and the average combustion time (TC) based on table 1 (VALETTE, 1990). This index is calculated based on the values of frequency ignition (FI), which refers to the number of positive ignitions (less than 60 seconds) of a total of 50 repetitions and the combustion time (time that the flame remains visible). Statistical analysis of the data was made by SNK test the 95% probability.

Table 1. Flammability Values (Valette, 1990)

PI TC - s	< 25	25-38	39-48	42-44	45-47	**48-50**
>32,5	0	0	0	1	1	2
27,5 – 32,5	0	0	1	1	2	2
22,5 – 27,5	0	0	1	2	2	2
17,5 – 22,5	1	1	2	2	3	3
12,5 - 17,5	1	1	2	3	3	4
< 12,5	1	2	3	3	4	5

Note:
PI – potential of ignition (positive number of ignitions a total of 50 trials); TC – combustion time in seconds.
0 = very low flammability; 1 = low flammability; 2 = flammable; 3 = moderately flammable; 4 = very flammable; 5 = extremely flammable.

Results

The variables of flammability were analyzed separately, which has shown the difference in behavior between the species studied. The ignition timing in each repetition performed for the species can be observed in Figure 2.

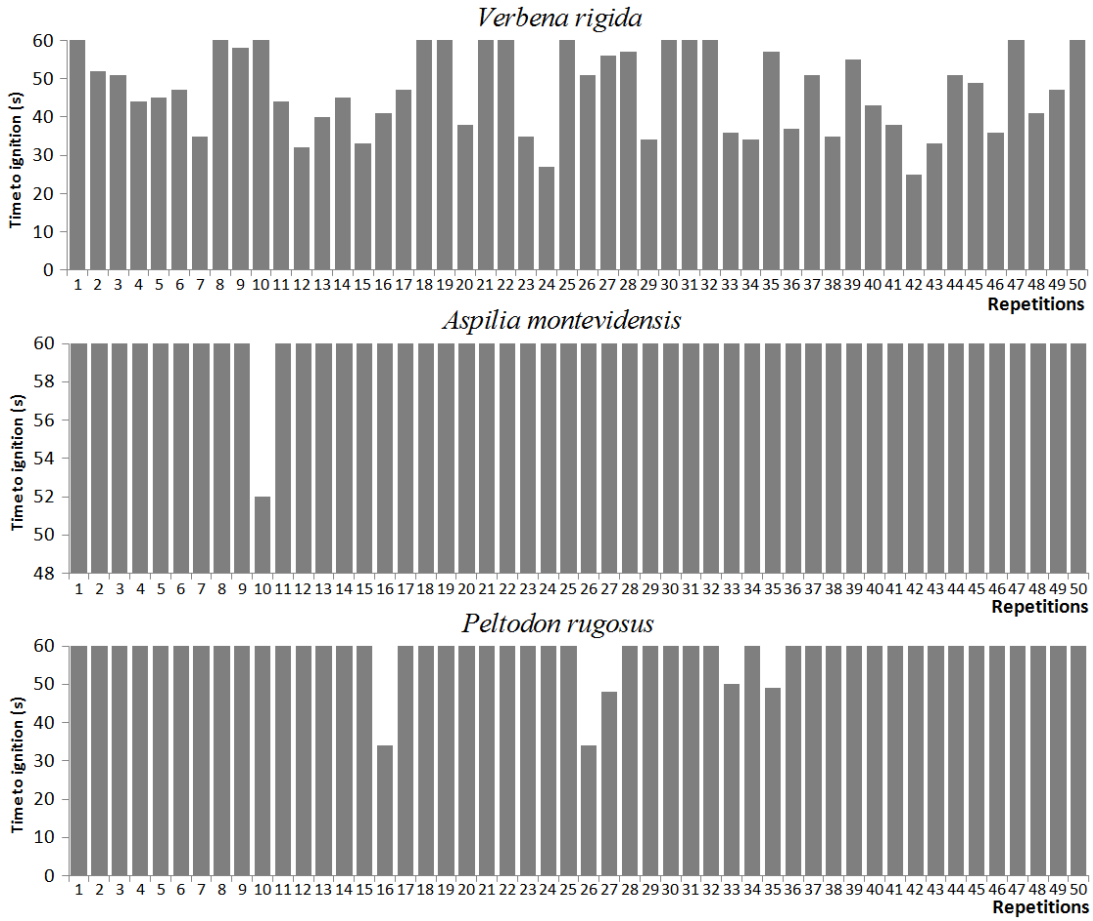

Figure 2. TI of the species in each repetition

It is observed that *Verbena rigida* was the species that presented greater variation in TI, being that most of the repetitions performed less than 60 s, corresponding to positive ignitions.

Aspilia montevidensis presented only one positive ignition, while *Peltodon rugosus* presented five positive ignitions. These results support the use of *Aspilia montevidensis* and *Peltodon rugosus* as barriers to the ignition of the forest fires in the edges of the WUI.
DC and AC variables were only possible to analyze in detail the species *Verbena rigida* (Figure 3 and 4). This is because the other species present in the vast majority of the repetitions, TI greater than 60 seconds, indicating negative ignition, and if "no ignition, no combustion".

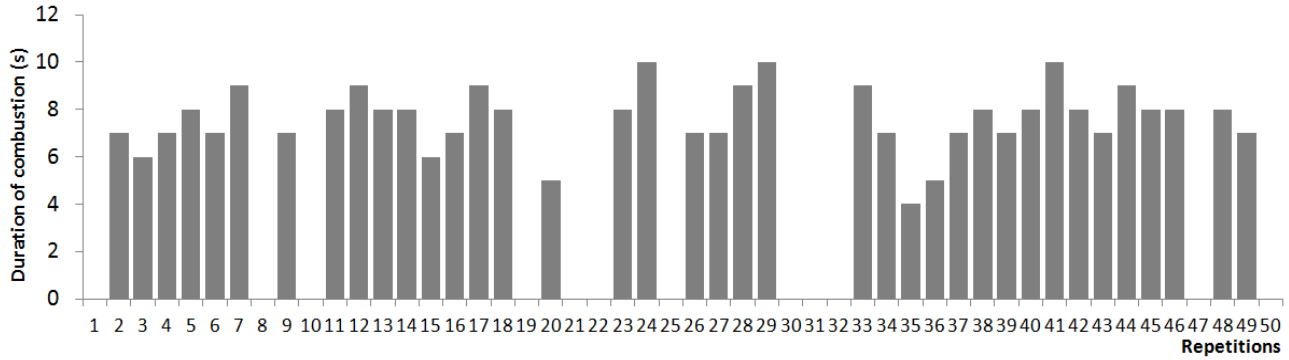

Figure 3. DC of Verbena rigida in each repetition.

It can be observed that there was wide variation in the DC of species in the repetitions performed. The average DC of *Verbena rigida* lasted 7.6 seconds, varying between 4 and 10 seconds.

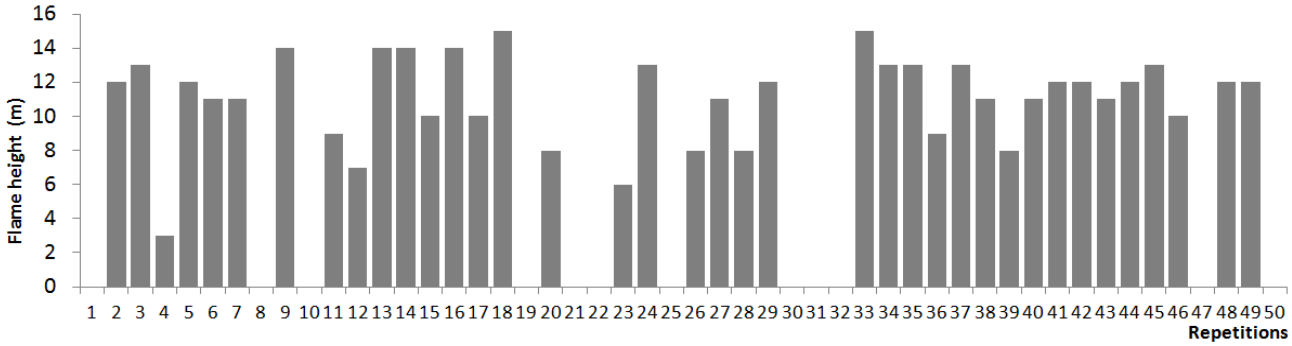

Figure 4. AC of Verbena rigida in each repetition

The flame height of *Verbena rigida* also showed wide variation, with an average of 11.1 cm, ranging from 3.0 to 15.0 cm.
After the analysis of the variables held separately, was assessed the flammability of the species, which allows to obtain a more accurate result regarding its use as a fuelbreak (table 1).

Table 1. Avaliação da inflamabilidade de espécies ornamentais

Species	FI (%)	TI (s)	DC (s)	AC (cm)	Combustion Index (IC)
Aspilia montevidensis	2 (a)	> 60 (a)	13	9	1 - Low flammability
Peltodon rugosus	10 (a)	> 60 (a)	9,2	14	1 - Low flammability
Verbena rigida	76 (b)	43,9 (b)	7,6	11,1	2 - Moderately flammable

Note:
FI -ignition frequency; TI - ignition time; DC duration of combustion; AC - height of the flame.
For FI and TI variables, means followed by the same letter in the column do not differ at 5% significance level by SNK test.

It is observed that *Aspilia montevidensis* and *Peltodon rugosus* differ statistically from *Verbena rigida* for variables FI and TI, indicating they are of low flammability although all species demonstrate weak flammability.

Conclusion

By the results, it is concluded that the analyzed species exhibit excellent characteristic to landscape composition on highways both for its aesthetic aspect as functional, and may also serve as a barrier against forest fires in WUI areas in southern Brazil.
In relative terms of flammability can be concluded that the species analyzed presented the following behavior: *Aspilia montevidensis* < *Peltodon rugosus* < *Verbena rígida.*

References

Alessio GA, Peñuelas J, Llusià J, Ogaya R, Estiarte M, De Lillis M (2008) Influence of water and terpenes on flammability in some dominant Mediterranean species. *International Journal of Wildland Fire* 17, 274-286.

Anderson HE (1970) Forest fuel ignitibility. *Fire Technology* 6, 312-319.

Biondi D (2013) 'Paisagismo Rodoviário: indicação de espécies.' (O Autor: Curitiba)

Biondi D, Batista AC, Martini A (2013) Fire risk in the road landscape patterns of the state of Paraná, Brazil - planning grants for the Wildland-Urban Interface. *Pacific Southwest Research Station - General technical report PSW-GTR-245*, 326 -337.

Curt T, Schaffhauser A, Borgniet L, Dumas C, Estève R, Ganteaume A, Jappiot M, Martin W, N'Diaye A, Poilvet B (2011) Litter flammability in oak woodlands and shrublands of southeastern France. *Forest Ecology and Management* 261, 2214-2222.

Fernandes PM, Cruz MG (2012) Plant flammability experiments offer limited insight into vegetation–fire dynamics interactions. *New Phytologist* 194, 606-609.

Ganteaume A; Jappiot M; Lampion C; Guijarro M; Hernando C (2013) Flammability of Some Ornamental Species in Wildland–Urban Interfaces in Southeastern France: Laboratory Assessment at Particle Level. *Environmental Management* 52,467–480.

Instituto de Pesquisa e Planejamento Urbano de Curitiba - IPPUC (2011) 'Desenvolvimento sustentável: Indicadores de sustentabilidade de Curitiba – 2010.' (IPPUC: Curitiba)

Miranda LIB (2009) Planejamento em áreas de transição rural-urbana: velhas novidades em novos territótios. *Revista Brasileira de Estudos Urbanos e Regionais* 11, 25-40.

Petriccione M (2006) Infiammabilità della lettiera diverse specie vegetali di ambiente Mediterraneo. *Tesi di Dottorato in Biologia Applicata* - Università Degli Studi di Napoli Federico II.

Petriccione M, Moro C, Rutigliano FA (2006) Preliminary studies on litter flammability in Mediterranean Region. In: International Conference on Forest Fire Research 5, Proceedings of… Portugal.

Radeloff VC, Hammer RC, Stewart I, Fried JS, Holcomb SS, Mckeefry JF (2005) The wildland –urban interface in the United States. *Ecological Applications* 15, 799-805.

Roderjan CV, Galvão F, Kuniyoshi YS, Hatschbach GG (2002) As unidades fitogeográficas do Estado do Paraná. *Ciência & Ambiente* 24, 75-92.

Valette, JC (1990) Inflammabilités des espèces forestières méditerranéennes. *Rev. Forest. Fr* 42, 76-92.

Vélez R (2000) 'La defensa contra Incendios Forestales: Fundamentos y experiencias.' (McGraw Hill: Madrid)

White RH, Zipperer WC (2010) Testing and classification of individual plants for fire behaviour: plant selection for the wildland–urban interface. *International Journal of Wildland Fire* 19, 213-227.

Zhang Z, Zhang H, Zhou D (2011) Flammability characterization of grassland species of Songhua Jiang-Nen Jian Plain (China) using thermal analysis. *Fire Safety Journal* 46, 283-288.

The history of a large fire or how a series of events lead to 14000 Hectares burned in 3 days

Luís Mário Ribeiro[a], Ricardo Oliveira[a], Domingos X. Viegas[a,b]

[a] *Forest Fire Research Centre (CEIF / ADAI) of the University of Coimbra; Rua Pedro Hispano n12, 3030 - 289 Coimbra, Portugal.* luis.mario@adai.pt, ricardo@adai.pt
[b] *Dep. Mechanical Engineering, Univ. of Coimbra, Portugal.* xavier.viegas@dem.uc.pt

Abstract
The year 2013 was particularly negative with regard to forest fires in Portugal. Besides of the large burned area (around 141000 ha until October 15th, according to official data), for a small country, 8 firefighters and a Mayor lost their lives while fighting the fires. In this paper we try to describe the series of events that led to the burning of around 14000 ha in the Northern Region of Portugal, in an unusually short period of time, and in what was the largest fire of the civil year. This fire was to be known as the *Picões* fire. The work described here is based on a report ordered by the Portuguese Minister of Internal Administration, and is part of a larger study involving another large fire (in Serra do *Caramulo*, Central Portugal) and the analysis of the accidents that caused the death of the 9 referred persons.
Countryman's fire environment (1972) and the series of events that potentially led to the unusually large burned area for that region are described in this paper. Fire behaviour is also analysed, with the help of fire behaviour simulations produced for specific periods of the fire.

Keywords*: Large fires; extreme fire behaviour; fire behaviour simulation*

1. Introduction

The forest fire that occurred between July 8th and July 12th in the Northeast of Portugal, the *Picões* fire, burned around 2000 ha of forest stands and 12000 Ha of shrubland, making it the largest one that year. The fire spread across 4 Municipalities: *Alfândega da Fé, Mogadouro, Freixo de Espada-à-Cinta* and *Torre de Moncorvo* (Figure 1).
On July 8th 2013, at 14h44, a fire ignited on the right bank of River *Sabor*. The fire was controlled on that evening, at 20h53 with an estimated burned area of 180 hectares. During the night and the next morning two teams of fire-fighters stayed on watch, monitoring the extinguished fire line. Despite of the vigilance, at 14h00 of July 9th, the fire rekindled and spread, sometimes with extreme violence, until it was dominated very early in the morning of July 12th, leaving an area of approximately 14000 ha burned.
During the afternoon of July 9th the violent fire propagation, with episodes of extreme propagation, burned through 18km in little over 5 hours. Approximately ten of the fourteen thousand hectares burned in less than one day, between 14h00 of July 9th and 10h00 of July 10th.
The reconstruction of a large fire is a slow and meticulous process. For this particular fire all of the major actors involved were interviewed: Civil Protection Authorities, Fire Brigade Commanders, representatives from the municipalities, local inhabitants and others. Also, as a work basis, some important documents were used: the official ANPC (National Civil Protection Authority) Incident Reports and a technical report focusing on the restoration of the burned area, produced by the National Forest Service (ICNF, 2013). MODIS satellite data about the fire progression was obtained from the Joint Research Centre (JRC) of the European Union and the "*MODIS Active Fire and Burned Area Products*" from Maryland University (EUA).

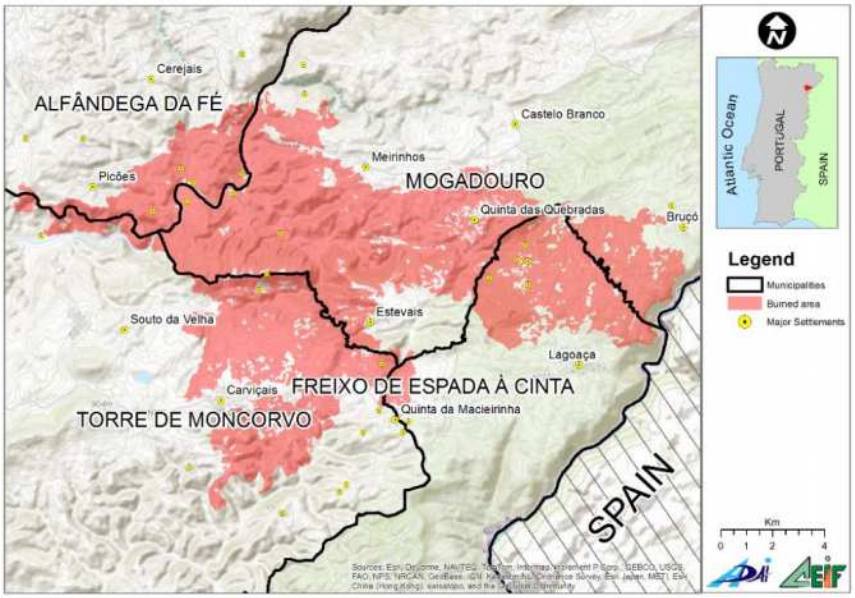

Figure 1. Burned area location, across 4 municipalities of the Northeast of Portugal

It was not possible to visit the area during the fire itself but we did it during October (17^{th}/18^{th}). In this visit we were also able to interview all the above mentioned intervenients.

2. Characterization of affected area

2.1. General characterization

The fire took place in an aged and low populated region, in a mountainous area where most of its inhabitants dedicate their few resources to subsistence agriculture and olive and almond trees. Some *Eucalyptus globulus L*. and *Pinus pinaster Ait*. stands are also present, maintained by the largest Portuguese paper pulp related company.

There are very few settlements in the region, as seen on Figure 1, and of small dimension. Many of them are named "*Quintas*" and consist of only 2 or 3 houses. Considering the fire perimeter and a buffer of 2000 meters outwards we counted 44 small villages and *Quintas.* The largest villages are on the margin of the fire perimeter.

The particularly rainy winter of 2013 had an important impact on the growth of fine fuels all over the country, but particularly in these areas due to 2 important factors. First, the construction of a big dam in the *Sabor* river was being finalized. In order to fill that dam all the vegetation (herbs, shrubs and trees) in the flooding area was being removed in the past months. During 2013 spring, all the basin along these main water tributaries of *Sabor* got covered with rapid growth herbaceous vegetation. Secondly, there is a common practice in the region of superficially ploughing two times the ground of the olive and almond fields, in early spring and in late spring/early summer, basically to remove all herbaceous fuels. The later was not possible, due to the high levels of moisture in the ground. These fields, usually good passive defense areas against fire, ended up with an unusual load of fine fuels. Apart from the described areas, most of the region is covered by shrubs.

2.2. Fire defense related infrastructures

The road network is not very dense, a common pattern found in many mountainous regions of the interior. The main roads (Municipal Roads) usually connect the municipalities' major villages or cities. In the area affected by the fire we found the Forest Road Network to be deficient, not covering most of the area. This aspect is a constraint when managing heavy firefighting vehicles and their positioning, as they have to travel for long distances. With very few exceptions there is one fire brigade per municipality and usually distancing more than 20 km from each other.

The closest brigades from the fire origin were from *Alfândega da Fé* and *Torre de Moncorvo*, approximately 10 km in a straight line.
The first crew to arrive to the fire, composed of 5 men, was transported by helicopter and arrived at the scene 10 minutes after the initial alarm. The ground crews (2 vehicles, 10 men) took 20 minutes.
The water sources or points used by the fighting crews are depicted in Figure 2. There's a main river (4th order) on the East side (*Douro River*) but the orography of the surroundings makes it difficult for the aerial means to use it as a water source. The same for *Rio Sabor* (3rd order), crossing the area from North to West. Besides these two rivers there are only 2 water sources for aerial means identified in the Municipal Defense Plans Against Fires (PMDFCI) obtained from the municipalities. Also, considering a buffer of 2 km from the final perimeter we count 14 terrestrial and 9 mixed water points. We ignore the conservations and usability conditions of these water points.

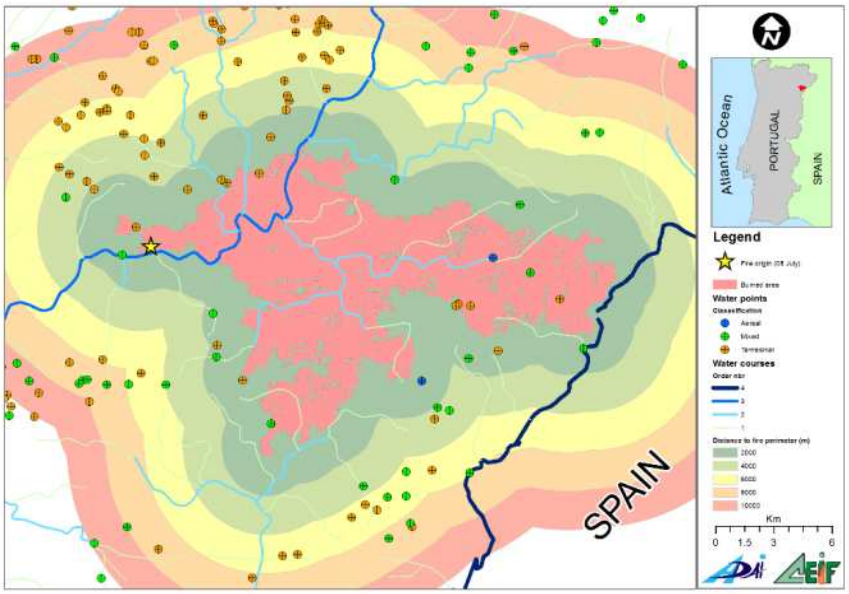

Figure 2. Water points in the area of the fire

Although not inventoried in the Plans, there are also a few dams of different dimensions in the surrounding, which we assume would have good operating conditions for the helicopters.
In such a large fire we consider the water resources to be scarce, even assuming they were all 100% operational. In the fire area itself there are practically no water supplies, and the large concentration of point on the Northwest was progressively being farther away as the fire progressed towards East.

2.3. Fire history

Knowing the fire regime of a particular area is of great importance for forest, fire and land managers.

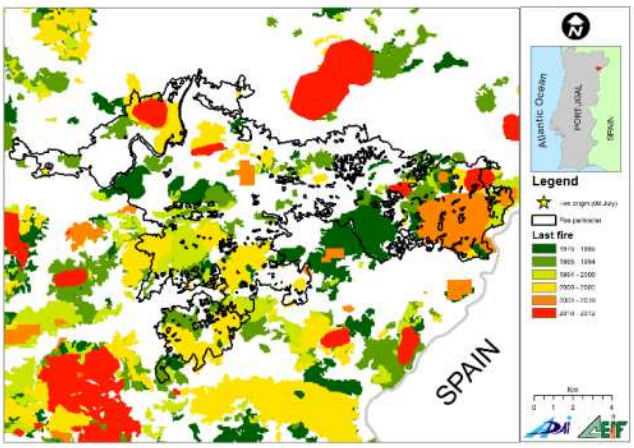

Figure 3. Last recorded fire in the region

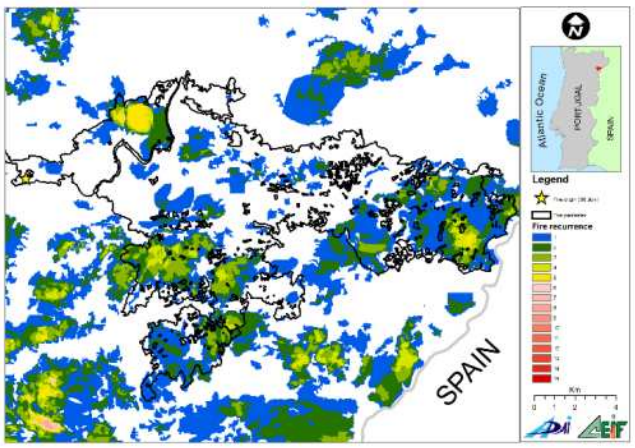

Figure 4. Fire recurrence in the region

In Figures 3 and 4 we can observe that a large portion of the area that burned in this event had not been burned since we have consistent and systematic records of fire perimeters in Portugal (1975).
The Southern part of the 2013 perimeter has burned between 1 and 4 times since 1975 but the last recorded fire was in 2005. The Eastern part has also been frequently affected by fire, some in 2010 and 2011.
The absence of fire in a large part of the region for the last decades, and the progressive abandonment of ancient agricultural practices results in an increasing accumulation of surface fuels, namely herbaceous and shrubs. This is a crucial factor in the increment of the fire potential in the region.

3. Fire environment

The fire environment is a well-known concept (Countryman, 1972) that describes the three main characteristics of the environment that affect the development of a forest fire: topography, fuels and meteorology.

3.1. Topography

The role of topography on fire spread is well known (e.g. Van Wagner, 1977; Pyne *et al*, 1996), namely the slope, by conditioning the rate of spread (ROS), or the orientation, by influencing the solar radiation received by the exposed fuels.
The area affected is mostly a mountainous region, with some open valleys mostly parallel to the wind and fire direction during the most important part of the fire development. The slopes are high in most of the area covered by the fire, in some cases greater than 45%, usually corresponding to the slopes that flank the rivers *Douro* and *Sabor* and their tributaries. A panoramic view of part of the area can be seen on Figure 5.

Figure 5. Panoramic view of part of the burned area

3.2. Fuels

Similarly to most of Portugal interior region, the predominance in this area in terms of land use is agriculture or related activities. However, the area directly affected by fire was mainly composed of shrubs and herbaceous vegetation. The municipal defense plans (PMDFCI) mentioned earlier are obliged to map forest fuels corresponding to a set of fuels derived from the standard American 13 NFFL fuel models (Anderson, 1982). Although there are technical guidelines published by ICNF the identification and mapping of these fuels is still very subjective as it relies on the knowledge and analysis of the different end users (the personnel responsible for the field work and cartography). Figure 7 is a composite of the individual fuel maps obtained from the municipalities. Even visually it is possible to see the lack of uniformity (Figure 6). Not only the resolutions used were different but also there are many cases where the same fuels are mapped with different codes, which denotes different identification criteria.

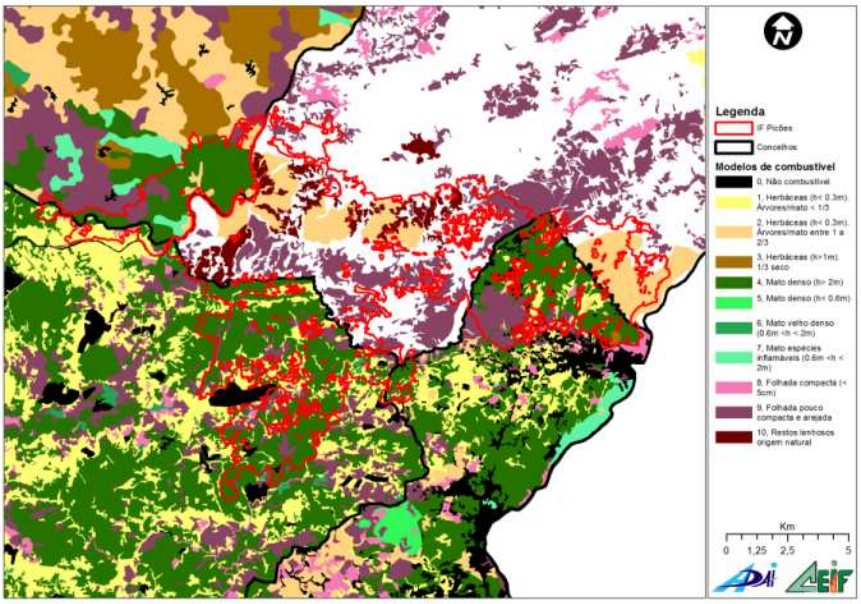

Figure 6. Fuel map of the area affected by the fire

In the surroundings of the ignition zone the prevailing fuels were described as natural herbaceous vegetation and dense shrubland (models 2 and 4). In this type of fuel bed fire spreads very rapidly and the existence of some scattered woody fuels increments its intensity. As the fire progressed to East herbaceous fuels dominate the landscape on the margins of the water courses. Apart from that, the majority of the central region of the fire was dominated by shrubs of different heights and loads (Models 4, 5 and 6). In these models fire propagates rapidly and intensely, even with high moisture contents. There are some forest stands, mainly composed of *Pinus pinaster Ait*. and *Eucalyptus globulus* L..

Very few fuel management activities were identified in all the region affected by the fire and the surroundings. The only management activities carried during the last 3 to 4 years were on the sides of some major roads and along the high and very high tension power lines. It was clearly not enough and not planned in a fire management perspective. Fuel moisture for fine fuels was estimated to be around 7% between 14h00 and 16h00, doubling during the night.

3.3. Meteorology

The year 2013 began with precipitation values above the average (IPMA, 2013a) until the end of May. June and July were below the climatic mean for the period 1971-2000.

According to the Portuguese Institute for the Sea and Atmosphere (Novo *et al.*, 2013; IPMA, 2013b) on July 3rd a heat wave affected Portugal, staying in the Northeast until July 13th. The precipitation on July was half of the mean value in almost all the country, with the exception of the Northwest.

Between 11th and 18th July some atmospheric instability was present in the North of the Iberian Peninsula, originating periodic episodes of light rain and thunderstorms.

To describe the period from July 8th to 11th, during which the fire spread, we used the meteorological stations owned by IPMA that are located very close to the affected area. One example of the constructed meteograms is shown on Figure 7.

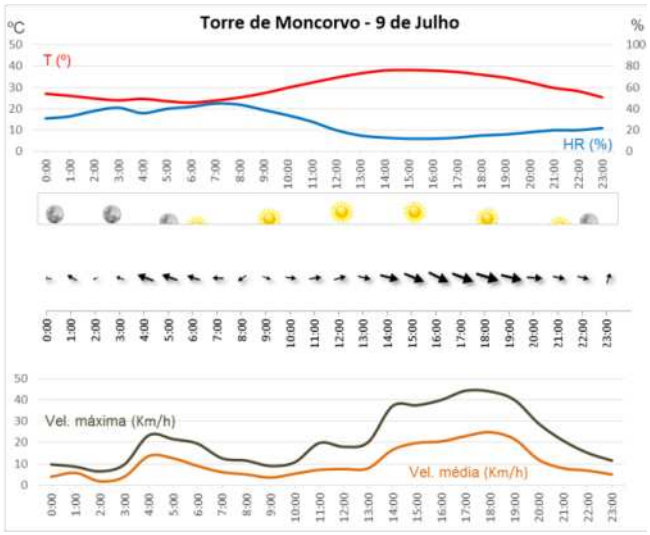

a

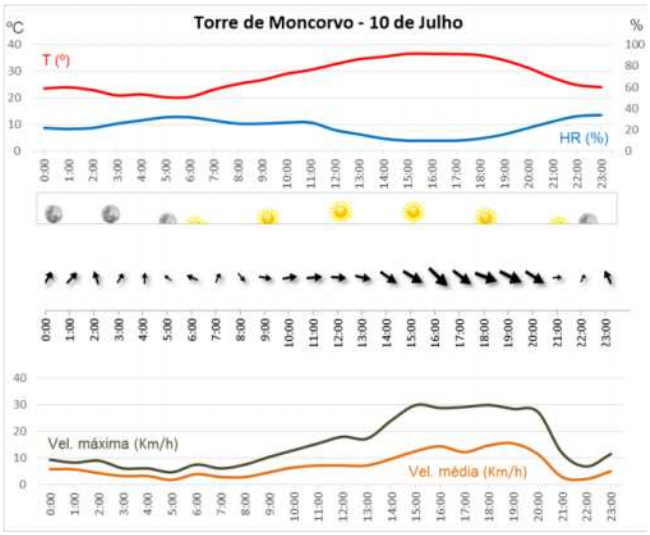

b

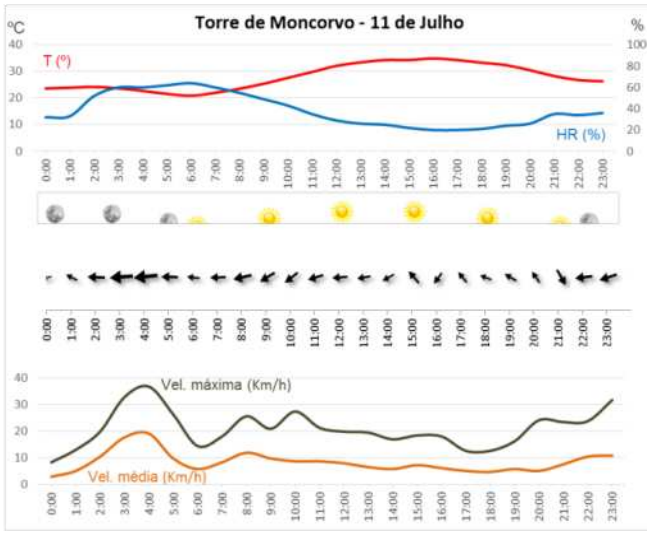

c

Figure 7. Meteorological data recorded for July 9 (a), 10 (b) and 11 (c)

The recorded values are good reference but may not coincide with the ones registered locally on the different fire sections, mainly due to topographic effects and also to the influence of fire itself.
The values show 3 very hot days with maximum temperatures up to 40ºC and minimum above 20ºC. Relative humidity was also extremely low during the afternoons (around 10%).

3.3.1. July 9th

During the night and morning of July 9th, the wind always presented values of low speed, usually of the order of 5 km/h. During the night the wind was from the East shifting to West during the morning. At night high temperatures between 23 and 27 °C were recorded, together with relative humidity often less than or equal to 40 %.
Between noon and two o'clock the weather worsened. At 14h00 temperature was around 38 °C and humidity of 13%. The wind blew from W-NW with an average speed of 17 km/h and gusts of 37km/h. These values provided a rapidly developing fire after its rekindle. Throughout the afternoon wind speed varied from 17 to 25 km/h with gusts up to 44 km/h. The maximum values were recorded between 17h00 and 19h00, when the village of *Quinta das Quebradas* was hit by the fire.
At the beginning of the night the wind rotated to the South and its intensity decreased to around 5 km/h.

3.3.2. July 10th

During the night of July 10th the wind was from the South. Early in the morning started blowing from West and it increased the speed as the day passed.
At around 14h00 the wind shifted to Northwest and throughout the afternoon the wind remained with velocity varying between 10 and 15 km/h. Starting from 20h00, there has been a pronounced decrease in wind speed to values of around 3 km/h.

3.3.3. July 11th

The night from July 10th to July 11th brought increased wind intensity, unlike the previous two nights that had been very calm. Wind came from the East with gusts up to 40km/h. During the morning speed decreased to 10 km/h, maintaining direction, until it shifted to the Southeast at 15h00.
At the end of July 9th and 10th, in particular to the middle of the afternoon, the wind was weak, rarely exceeding 10 km/h. Under these conditions, in a region of complex topography and with the observed intense insolation, the local effects are dominant. Thus, the extrapolation of the wind behaviour from one location to another is subject to a certain degree of uncertainty.

4. Fire Chronology

4.1. The *Cilhade* fire – July 8th

At 14h44 of July 8th a fire started near a small uninhabited Quinta named *Cilhade*, in the municipality of *Torre de Moncorvo* (*Bragança* District). In less than 10 minutes after the initial alert, the initial attack crew was on the ground fighting a fire that was developing in a highly sloped area.
The fire burned about 180 hectares, according to our reconstitution (Figure 8). This fire was dominated in the early evening (20h53) the same day and the consolidation and mop up were initiated shortly after. During all night and the following morning two crews from the fire brigades involved in the extinction operations remained in the area on surveillance.

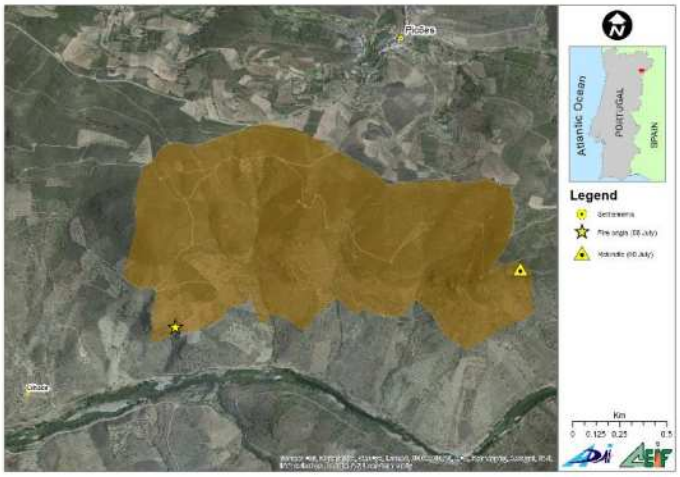

Figure 8. Approximate perimeter of the Cilhade fire on July 8th

4.2. The *Picões* fire – July 9th

Despite the vigilance operations, around 14h00, the *Cilhade* fire rekindled and quickly spread by adjacent sloping areas covered with shrubs. At this time the nearest weather station maintained by IPMA (*Torre de Moncorvo*) recorded temperature values of 38ºC and relative humidity of 13%.
The fire progressed rapidly to the East/Northeast, with the wind blowing from the West at an average speed of about 20 km/h but with gusts reaching 40 km/h. Due to the construction of the *Baixo Sabor* dam almost all the area across the river valley had been cleaned out of vegetation in the last months. The rainy spring of 2013 resulted in the growth, above average, of herbaceous vegetation, especially in these areas, which were relatively clean of trees and shrubs. The orientation of these areas, which would be filled with water when the dam started operating, is a perfect match with the general propagation of the fire in its initial stages.
At approximately 15h30 we estimate that the fire jumped to the left bank of the river *Sabor* (Figure 9).

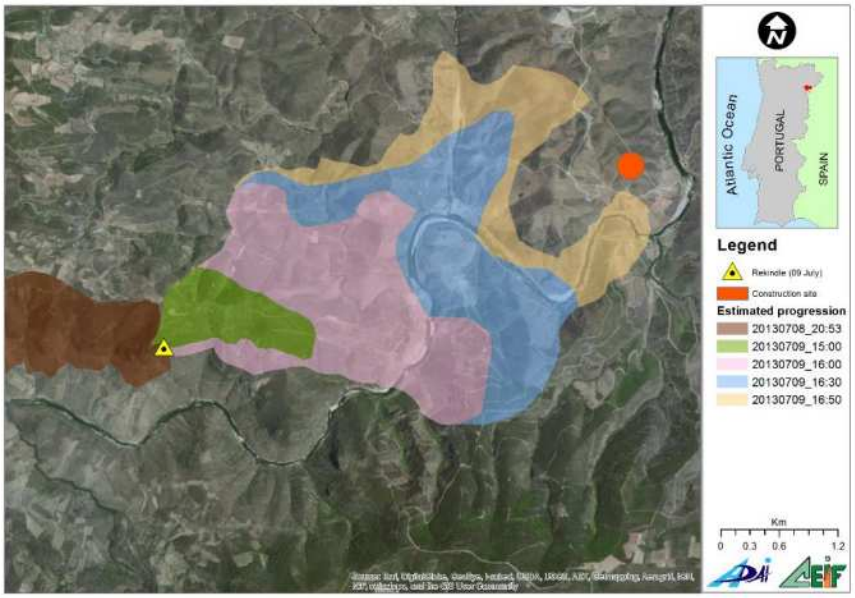

Figure 9. Estimated progression at 16h50 of July 9th

At around 16h50 a request for help was received from the chief of a construction site (marked in orange in Figure 9) who felt was being surrounded by fire, along with 30 workers. This call for help had a direct impact on the firefighting strategy. Although the fire officers had the perfect notion that the construction site was a safe place (that particular mountain had been cleared of vegetation from the middle to its top) they made the decision to displace several crews to evacuate the construction workers.

Between 17h00 and 17h30 the fire entered the long valley of a small water line called *Ribeira do Medal* and spread with a high velocity for about 3.5 km in a Northwest-Southeast orientation. It then split and entered the valleys of 3 other water lines (*Meirinhos*, *Resinal* and *Inferno*), as shown in Figure 10. The orange arrows show the direction of the fire propagation. Eventually the fire also spread North through another smaller water line.

The configuration of the terrain and the waterlines pushed the propagation of the fire towards the existing settlements, mainly *Meirinhos*, *Estevais* and *Quinta das Quebradas*. Also the wind was blowing from the West, which increased the ROS.

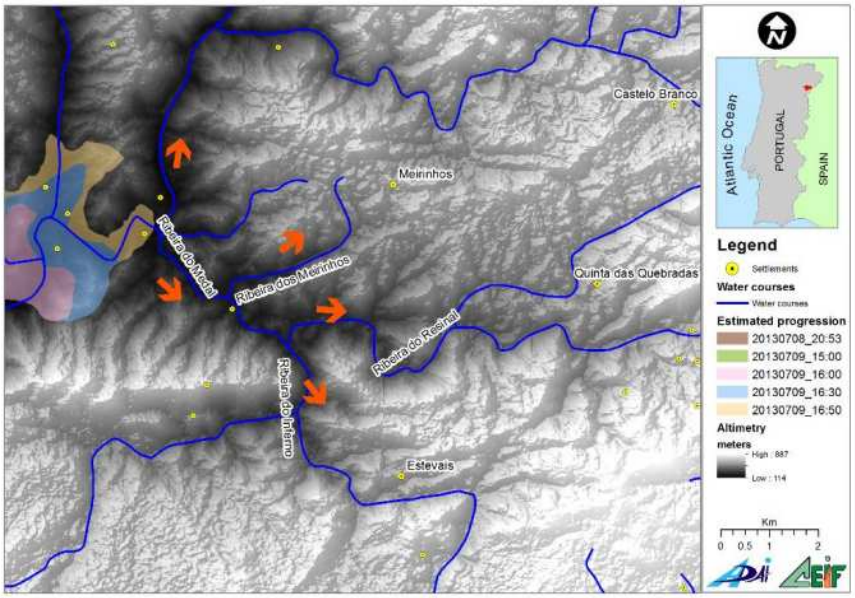

Figure 10. Scheme of the topography, water lines and direction of fire propagation

Around 17h30, with the fire progressing with unusually high rates of spread one of the fire Brigade Commanders identified the small village of *Quinta das Quebradas* as a priority target for defense, as it was located ahead, and on the most likely path, of the fire front. Although the fire front was approximately 6 km away, taking into account the observed ROS and the knowledge about the poor road network, it was decided to allocate some firefighting resources to protect the houses and people still there.
Between 17h00 and 19h00 the wind was blowing with an average of 20 km/h but with gusts up to 40 km/h. The fire was progressing not only by surface but with a considerable amount of flying embers, creating numerous spot fires. One of them was registered flying about 3 km from the main front, originating a spot fire less than 3 km west of *Quinta das Quebradas*. Another one was registered 1 km South/Southwest of the small village around 19h00. Shortly after another one at Southeast. Figure 11 represents the estimated propagation on the afternoon of July 9th. The orange arrows indicate the approximate location of the described spot fires.

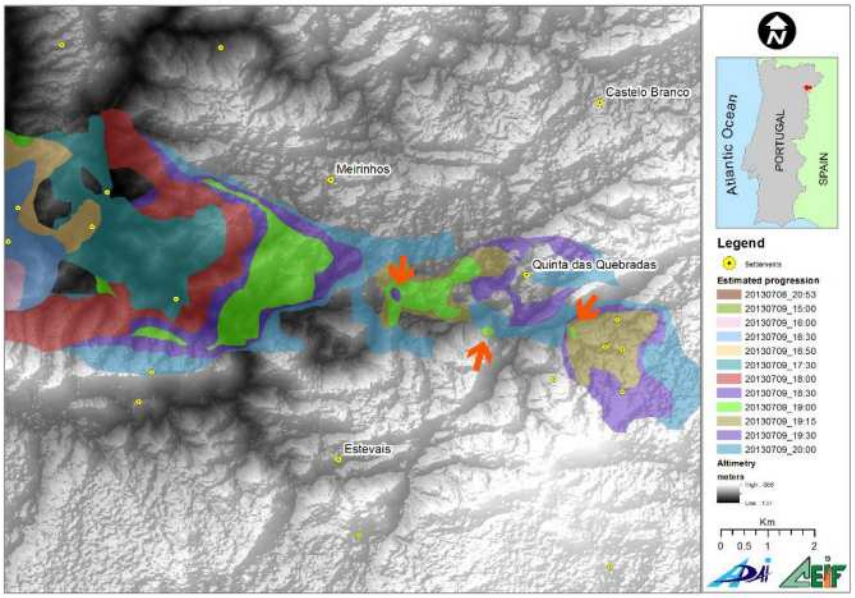

Figure 11. Estimated propagation on the afternoon of July 9th

The protection to *Quinta das Quebradas* was an important milestone of the fire as it coincided to the time of the most violent propagation of the fire, either by the rapid surface propagation and the numerous spot fires. By this time (around 19h00) 30 vehicles and 99 men were protecting the village and the fire was spreading freely. It even spread through the middle of the village.
The time from the decision of going to protect the village and the passing of the fire was of around one and a half hours. The fire spread through 6 km, which represents roughly 4 km/h, quite above the "normal" rate of spread.
The development of the spot fires helped accelerate the spread of the fire at this stage and lengthened it. Shortly after 19h00 traffic was cut on National Road EN221, which connects *Mogadouro* to *Freixo de Espada-à-Cinta*, about 2 km East from *Quinta das Quebradas*. At the end of the day, early evening, the wind calmed. Already in the early morning of the 10th, the front advancing Eastward stopped its progression on extremely steep slopes, often devoid of vegetation, leading down to the *River Douro*. One or two burning embers flew across the river and fell in Spain but were immediately extinguished by the Spanish firefighting crews.

The events that were just described, were the most important on the history of this fire, with a West-East axis of progression, perfectly aligned with the wind direction and most of the valleys and watercourses present in the area.

4.3. The *Picões* fire – July 10th

During the night (July 9th to 10th) the wind swirled South and decreased in intensity, registering speeds varying between 2 and 6 km/h and the fire began to expand laterally, with lower propagation speed.
During the morning of the 10th the fire was progressing very slowly all over the perimeter. The prevailing wind was from the West once again with hourly average below 10 km/h.

Figure 12. View from Google Earth of the fire going downslope into the Ribeira do Inferno

By late morning, a small section of the fire was spotted on the right flank, progressing downslope, and slowly heading to the valley of the *Ribeira do Inferno*. At this time the wind was weak and from the West but the forecast predicted a slight rotation to the Northwest accompanied by a small increase in speed. In low wind conditions and in the presence of a heat source (fire) the local effects induced by the topography in the wind dispersion are more pronounced.
Analysing the topography South of the region where this situation was detected, and knowing that the wind would be aligned with the valley of *Ribeira do Inferno,* it could probably be anticipated an increase in intensity and ROS of the fire as soon it reached the base of the slopes that are seen in Figure 12.
Indeed, around 14h00 on the 10th the wind increased in intensity and suffered a rotation to the Northwest. Virtually the entire left flank (North) and the back of the fire (West) were dominated or in mop up actions. Progression to East was contained in the *Douro* river. This change mainly resulted in the right flank gaining intensity and rapidly propagating South, in the direction of three small villages. By this time a large number firefighting crews and all available aerial means were dislocated to this area to protect the villages and its inhabitants, especially *Carviçais*, South of the fire. Figure 13 shows the estimated area burned at 22h00 of July 10th.

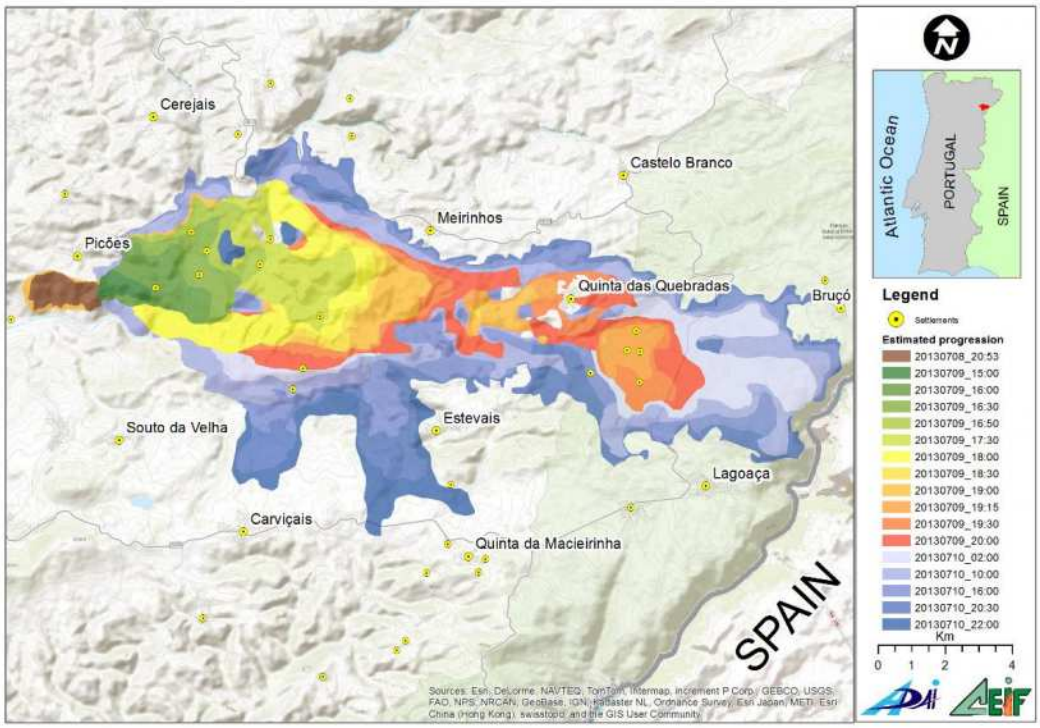

Figure 13. Estimated fire progression at 22h00 of July 10th

4.4. The *Picões* fire – July 11th and 12th

The morning of July 11th was not as favourable in meteorological terms. From 02h00 the wind increased in intensity prevailed from East, favouring the spread of the fire to the West. The average speed became of 15-20 Km/h with gusts of 30 to 40 Km/h.

The North area of *Carviçais* has an intensive and active agricultural occupation, posing as a natural barrier to the fire spread. There is also a major road crossing in an E-W direction, used as a support to the firefighting actions. Still, the fire jumped through in a small area occupied by shrubs. The wind changes that followed brought the fire, more than once, near the mentioned village of *Carviçais*, first in the North and then by South (Figure 14).

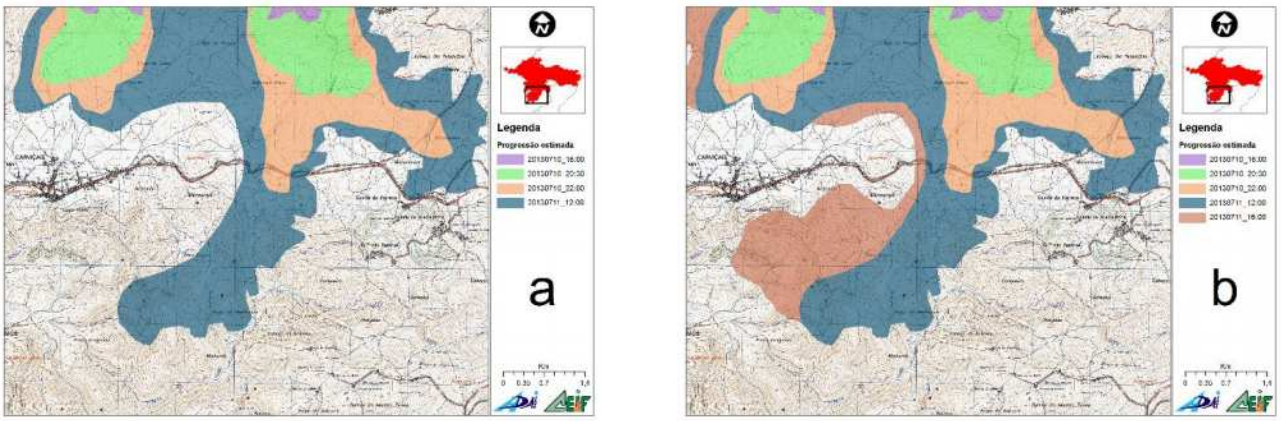

Figure 14. Detail of the estimated fire progression threatening Carviçais: at 12h00 (a) and at 16h00 (b)

During the night of 11th to 12th the prevailing East wind was of the order of 7-8 km/h and the fire did not propagate much more.

According to the Incident Report from ANPC the fire was finally declared extinguished at 09h30 on July 12th. The final burned area by registered ICNF was 13706 hectares, 1983 hectares of forest plantations and 11723 hectares of shrubland. Later on the final perimeter was released showing an area of 14136 hectares burned.

5. Analysis

5.1. Fire behaviour

The described fire evolution and its final burned area, depicted in Figure 16, were strongly affected by 3 major events: i) the rekindle of the original fire, ii) the defense of *Quinta das Quebradas* and iii) the wind shift that turned the right (South) flank into a fire front.

5.1.1. The rekindle of the original fire (beginning of the afternoon, July 9th)

The initial attack on the *Cilhade* fire was quick and effective. Given the location of the fire and the lack of good access road that hinders the arrival of heavy combat trucks, containing the fire in six hours and about 180 hectares can be considered a positive performance. Despite of the vigilance throughout all night and the next morning, at 13h47 the fire rekindled. This was probably the key element on the final outcome of the large *Picões* fire.

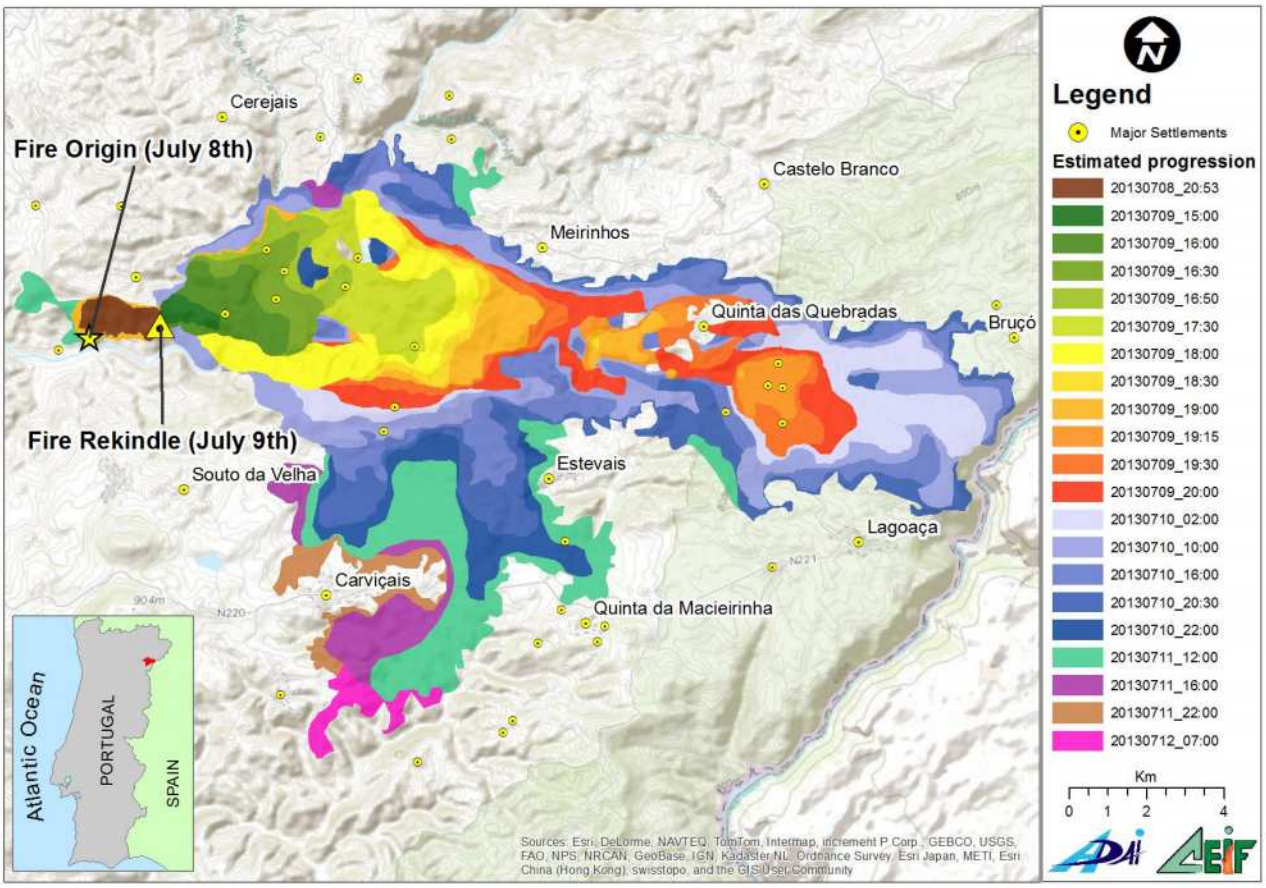

Figure 15. Global estimated fire evolution

Being able to predict changes in the wind field is extremely useful in fire management activities, especially if one is able to predict the influence of topography in its dispersion. IPMA provides atmospheric wind forecasts but using the fire behaviour simulator *Firestation*, developed in ADAI (Lopes *et al* 2002), we can simulate the effect of topography on the distribution of the wind field (Figure 16).

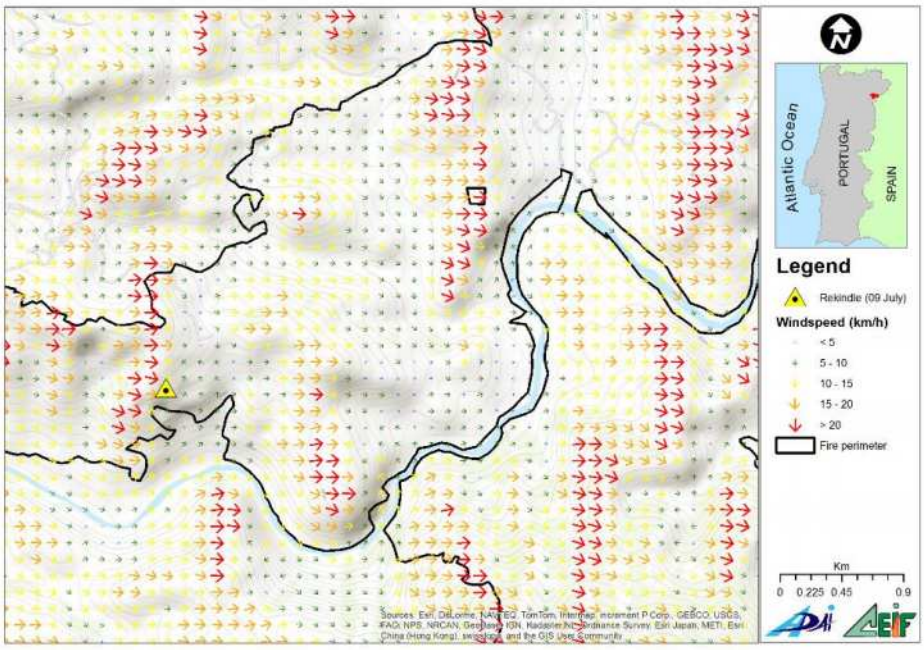

Figure 16. Simulated wind field at the time of the rekindle

At the time of the rekindle the West winds had higher overall speeds when going up the slopes facing West. The lower speed would be registered in the more sheltered valleys, with prevailing downslope East exposure. Jumping over river *Sabor* wouldn't have been hard as the strong winds easily carried burning embers across the valley. As described earlier, the herbaceous fuel load along the banks of the water lines was considerably high, as well as its curing degree. We assume the ROS at this early stage would have been very high. The air temperature was 38ºC and the relative humidity 13%. The surrounding area was still warm and the unburned fuels desiccated from the heat released from the fire of the previous day. When the fire started again it spread very quickly to adjacent fuels.
The alarm was not as swift as it should be and the initial attack on this rekindle was not strong enough to prevent the fire from spreading. In the first 3 hours of propagation the fire ran approximately 5 km in a W-E orientation (in a straight line) which corresponds to a mean rate of spread of 1.67 km/h. Figure 17 shows the vertical profile and the slope variation along the mentioned line of 5 km. Slope has several abrupt changes but sometimes is negative (fire progressing downslope). It is generally between 20 and 40%.

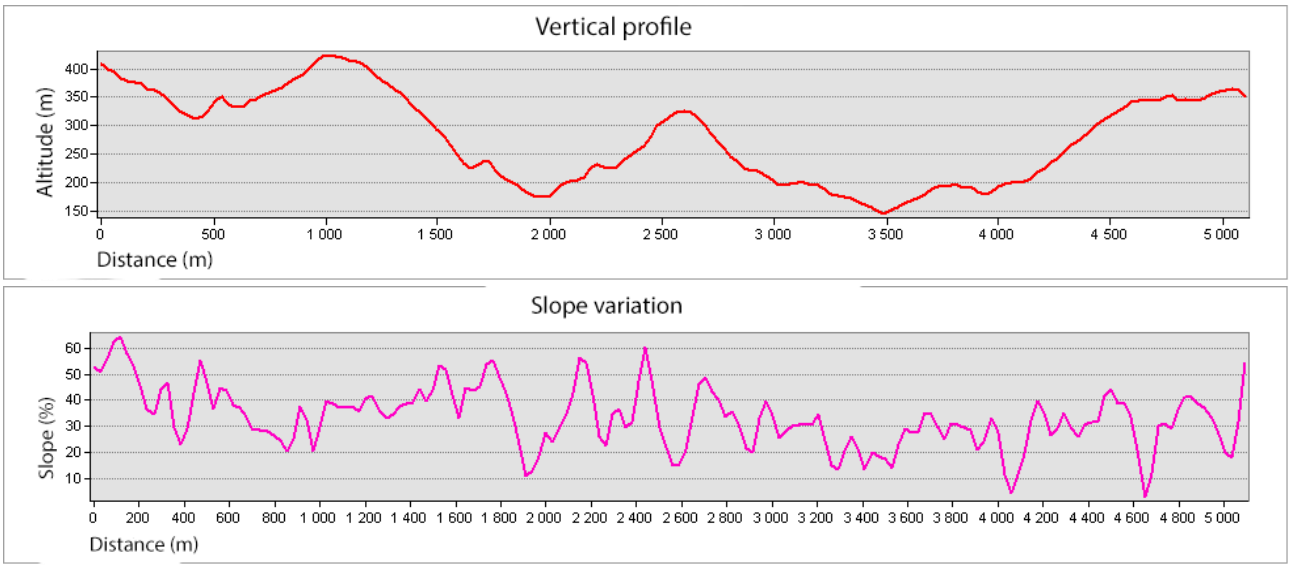

Figure 17. Vertical profile and slope variation in the first 5 km of fire spread (after the rekindle)

Using BehavePlus (Andrews *et al*, 2008) we estimated the fire rate of spread herbs and shrubs, in function of the slope and, assuming the slope is always positive, the predicted ROS was always below the observed (**Erro! A origem da referência não foi encontrada.**1):

Table 1. Predicted ROS according to BehavePlus

Slope	%	20	30	40
Rate of spread (km/h)	Herbaceous	1.25	1.33	1.45
	Shrubs	1.05	1.10	1.19

From the middle of the afternoon the fire progressed with very high speed, not only through the surface but also with numerous spot fires.

5.1.2. The defense of the small Quinta das Quebradas village (late afternoon, July 9th)

During the afternoon of July 9th, and at the time of the most violent fire propagation, this village of around 100 inhabitants was stroke by the main fire front. At this time, in about one and a half hours the fire ran 6 km in a straight line, averaging approximately 4 km/h of ROS. Several spot fires were identified. There were practically no passive defensive structures around the village so, as it usually happens, firefighters stopped fighting the fire and concentrated on defending the structures, livestock

and, most important, the people living there. An important number of means were dislocated to this action: 30 vehicles and 99 men.
As the night progressed the meteorological conditions became more favourable and the fire slowed its W-E progression and eventually stopped on the steep scarps of river *Douro*.
At this stage the fire propagated very slowly on the flanks.

5.1.3. The wind shift that turned the right (South) flank into a fire front (morning, July 10th)

During the morning of July 10th the fire kept burning slowly on the flanks and the National Incident Command Structure in charge of the strategy believed it would soon be controlled. Despite the fact that wind predictions indicated a shift in the wind direction the overall strategy failed to adapt in time to the probable fire behaviour change. At the time the wind changed we estimate that the area burned should be around 8000 ha, far from the final 14000 ha. The fire was being pushed by slow Westerly winds into the East.
In the area identified and described earlier (see Figure 12) the fire was burning slowly and downslope, with the wind blowing sideways, but there weren't any firefighting crews nearby. In any fire, particularly a large fire, constant observation over the entire perimeter is of the utmost importance (either by terrestrial or by aerial means), as is the analysis of weather forecasts and topography and their expected influence on fire behaviour. We believe the reaction to the predictable wind shift was very late. We cannot tell for sure that, had this situation been anticipated, the fire would be contained, but evidence suggests that if the descending fire was attacked during the morning there was a strong possibility that it would be contained at this time.
After the wind has changed to the Northwest the right (South) flank of the fire became an active fire front and propagated to the South endangering some villages, one of them multiple times (*Carviçais* – see Figures 14 and 15).
During July 11th practically all manoeuvres were concentrated near *Carviçais*, where the fire reached from multiple points, as described earlier.

5.2. Fire behaviour simulation

Fire behaviour simulation is nowadays a very important tool in fire management, although a perfect knowledge of its fundaments and limitations is required. ADAI team has been developing a spatial simulation software called *FireStation* (Lopes *et al*, 2002), based on Rothermell's surface fire spread model (1972). The system takes as input static maps of fuels (obtained from the mentioned PMDFCI) and topography (in for of Digital Elevation Map) and point measurements of wind characteristics, that can be updated as needed. *Firestation* uses a wind simulation model called *Canyon* (Lopes *et al*, 1998), which is a model used for complex topography and that takes into account the different thermal and recirculation effects.
We chose 3 instants to simulate, corresponding to the 3 key events described earlier.

5.2.1. Phase 1 – the rekindle

For this first stage we used an ignition on the spot where the rekindle was identified. The area corresponding to the original fire was simulated as already burned, in order to avoid any interaction with the fire and wind simulation. Figure 18 represents the predicted and estimated fire progression for this period. Time since ignition and fire line intensity are shown.

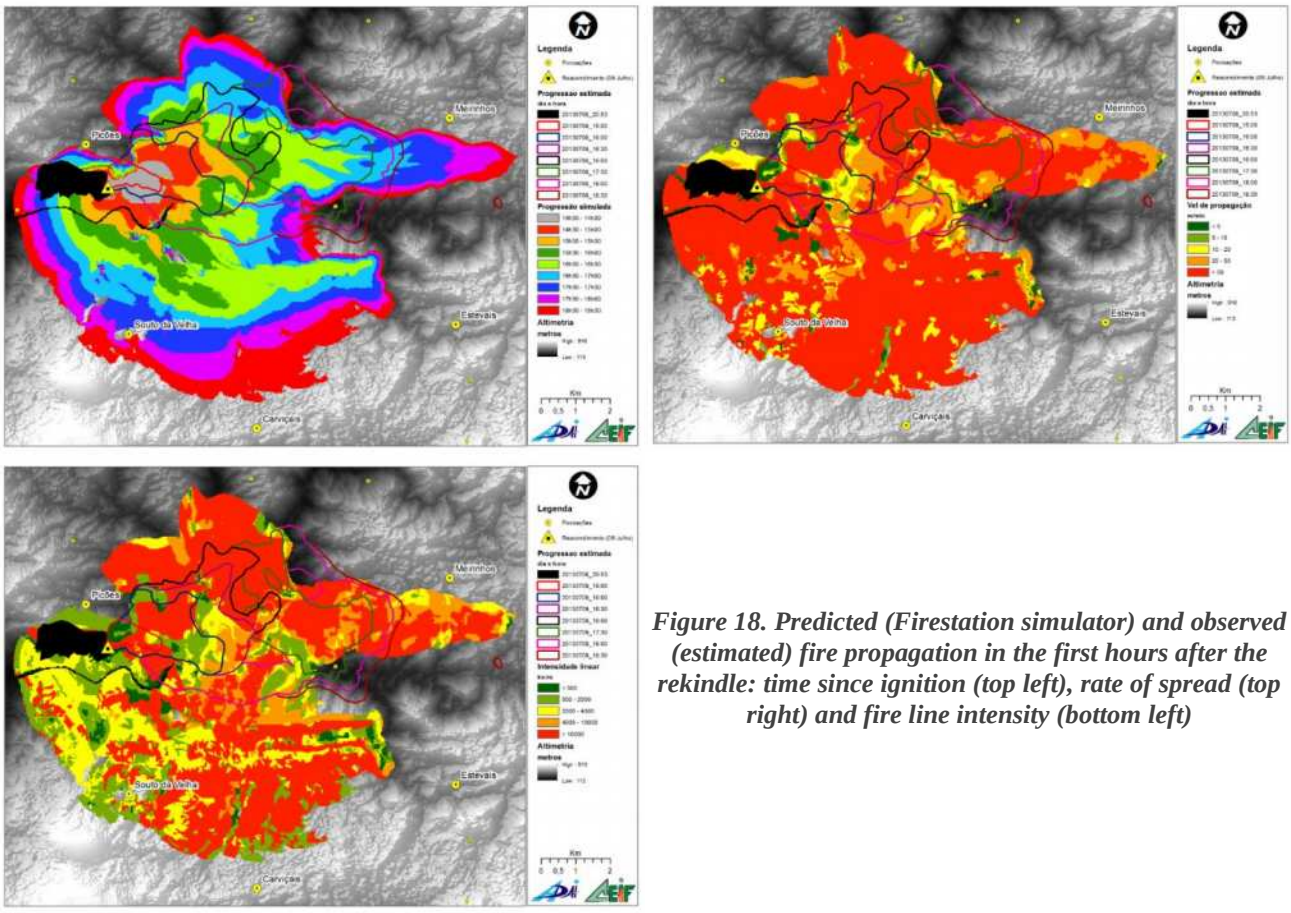

Figure 18. Predicted (Firestation simulator) and observed (estimated) fire propagation in the first hours after the rekindle: time since ignition (top left), rate of spread (top right) and fire line intensity (bottom left)

The coloured areas represent the simulation while the contours represent the observed (estimated) progression.

At a first glance we can see that the final shape of the simulated fire does not correspond to reality. Looking in more detail we observe however important results. The simulated fire has spread extensively to the South because it crossed river *Sabor* immediately after the rekindle and we know that that did not happen. We also know that, on the hill below the rekindle, the fuels were very scarce and the fuel map we used did not reflect that. Also the fuel map doesn't map the river in its whole, making fuels continuous from one bank to the other. This wrongly allows the fire to easily cross the river. If we limit the analysis to the Northern half of the simulation similarities with reality increase.

In the initial zone of fire propagation the simulated ROS exceeds 50 meters per minute (approximately 3 km/h), as seen in Figure 18. Moreover, according to the simulation, and with the exception of the period between the estimated progression of 16h00 and 16h30 (blue and violet lines), the entire area burned with ROS exceeding 50 m/min.

The intensity of a fire at the front can be related to the difficulty of attacking it and the probability of success, as shown in Table 2. Observing again the simulated fire intensity (Figure 19 - bottom left) we see that, during the first moments of the fire, its intensity could have been above 10000 kw/m, were any efforts to contain it would be virtually impossible.

Observing all these data we can assume that, after escaping initial attack, and with the few resources available in the field, the fire spread with a ROS that would make unfruitful any firefighting strategy

Table 2. Difficulty of fire control related to fire line intensity

Danger class	Fire Control	Fire line intensity (kW/m)	Fire suppression interpretations
Low	Relatively easy	I< 500	Direct attack at fire's head or flanks by firefighters with hand tools and back-pack pumps possible. Light aerial means effective.
Moderate	Moderately difficult	500 < I <2000	Firefighting along the flanks and eventually some spots in the fire front. Water is needed to control the fire. Medium to heavy aerial means can be effective
High	Very difficult	2000 < I <4000	Any attempt to contain the fire's head limited to the use of aerial means. Control efforts may fail.
Very High	Extremely difficult	4000 < I <10000	Suppression action restricted to back and flanks of the fire. Direct control of the fire likely to fail. Indirect attack with heavy aerial means. Spot fires expected to appear.
Extreme	Virtually impossible	I > 10000	Extreme fire behavior. Number of spot fires can increase rate of spread. Direct attack ineffective. Ground attack limited to flanks and back. But with low probability of success.

(adapted from Alexander & Lanoville, 1989)

5.2.2. Phase 2 – fire approaching Quinta das Quebradas

The ignition used for the 2nd phase was coincident with the estimated perimeter of the fire at 18h30 of July 9th, including the spot fire. The results are shown in Figure 19.

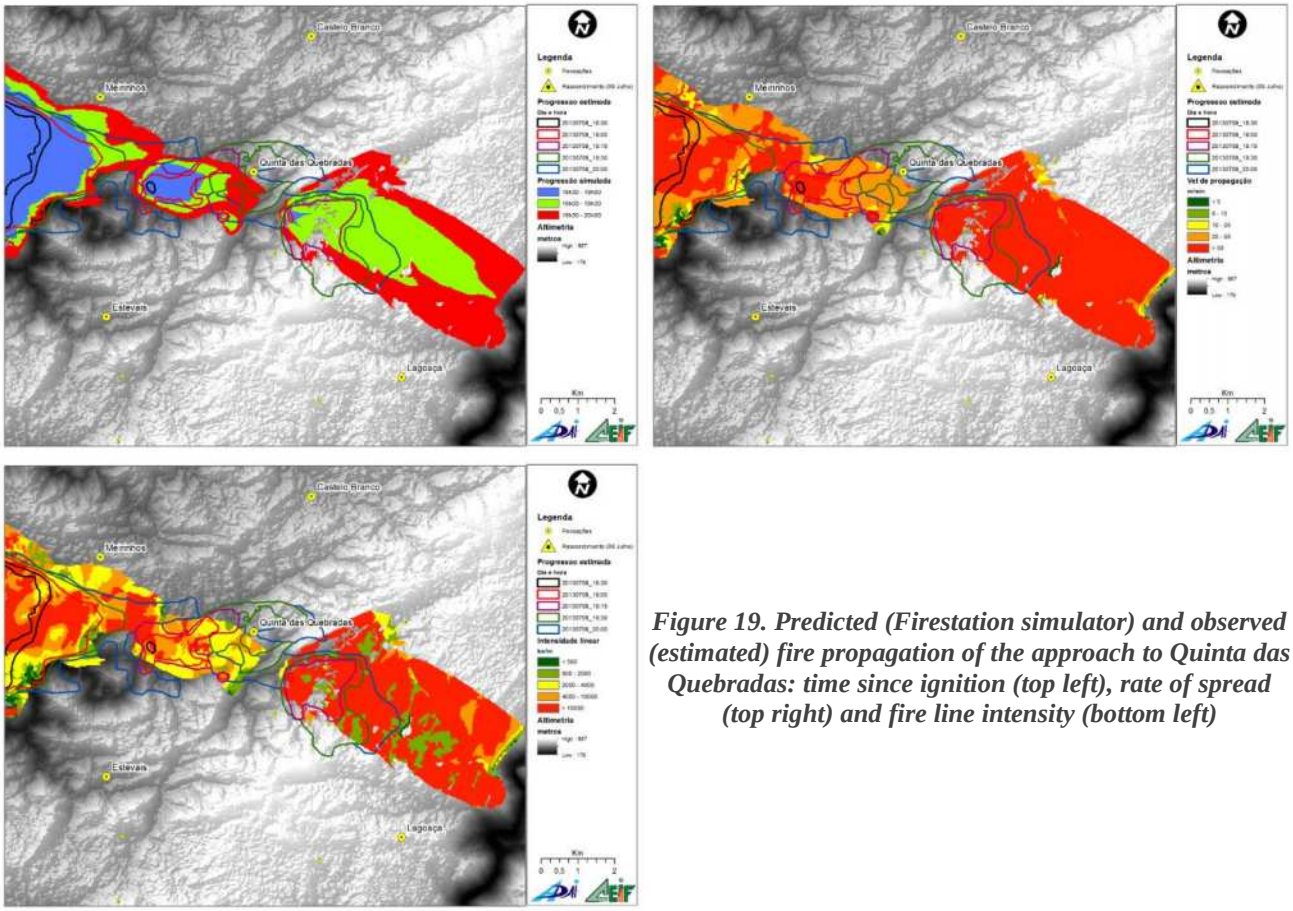

Figure 19. Predicted (Firestation simulator) and observed (estimated) fire propagation of the approach to Quinta das Quebradas: time since ignition (top left), rate of spread (top right) and fire line intensity (bottom left)

Simulation shows a fire intensity between 2000 and 10000 kw/m, with very few possibilities of a direct attack on the fire front. After passing through *Quinta das Quebradas* the fire gained intensity, mainly due to the change in fuels that were then dominated by shrubs.

5.2.3. Phase 3 – fire entering Ribeira do Inferno

The ignition in this phase corresponds to the area identified earlier when fire was progressing downslope (Figure 12) and at the time of the wind change. The simulation doesn't predict two fire "heads" but only one continuous front (Figure 21). Nevertheless the predicted rate of spread is above 20 m/min (1.2 km/h) and in a considerable area above 50 m/min (3 km/h). The higher values of intensity correspond to the fire entering *Ribeira do Inferno* and to the Southwest and Southeast of the simulated burned area.

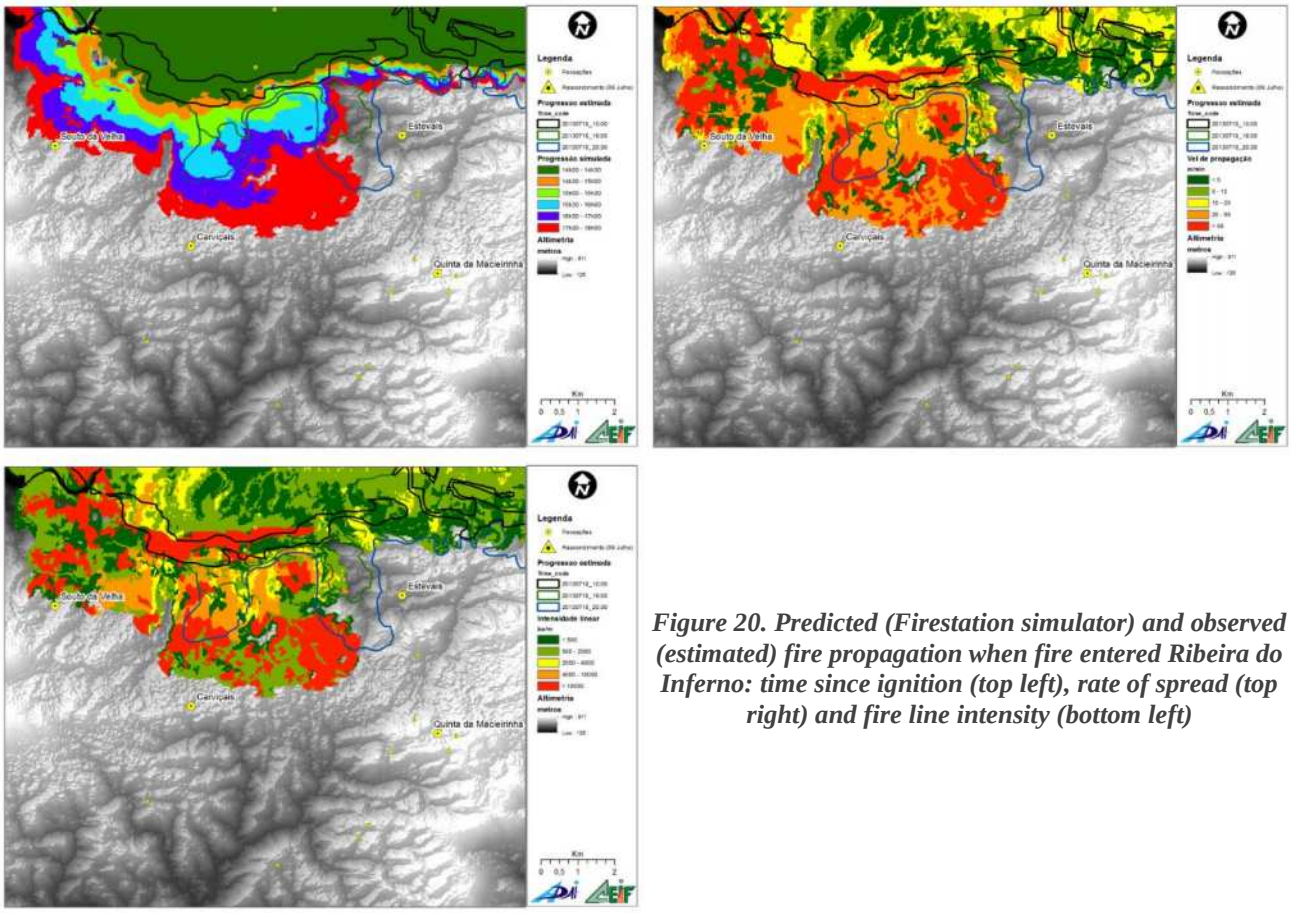

Figure 20. Predicted (Firestation simulator) and observed (estimated) fire propagation when fire entered Ribeira do Inferno: time since ignition (top left), rate of spread (top right) and fire line intensity (bottom left)

6. Conclusions and recommendations

The large fire of *Picões* had some moments in which any efforts from the firefighting crews to control it would not have been enough. There are 3 key moments, 2 of which with direct implications, that can explain the large area burned. The reconstitution we made is the closest possible to the real progress of the fire, although we admit that there may be some discrepancies with the actual progression. However, except for errors of detail, we believe to have recreated all the most important events accurately. The main conclusions we withdrew from this study were:

- The fire that occurred on July 8th in *Cilhade* was dominated and finished with an area of approximately 180 hectares burnt. After the mop up actions, surveillance was assured by teams who had already participated in the firefighting. These teams would perhaps not have the best state of mind and physical conditions to remain overnight and the following morning on surveillance. Vigilance was long because it was understood that, if there were any rekindle this would have to be controlled quickly under the threat of the fire gaining strength again. Probably would be a wiser decision to place new (fresher) crews on the vigilance. Despite of the

vigilance, on July 9th around 13h47 a rekindle of this first fire occurred. This was the first key moment of *Picões* large fire.

- The rekindle took place in a difficult access to ground crews and at a time when weather conditions were particularly adverse. A rekindle usually develops faster than a starting fire even more with these weather conditions. Although we have no data to confirm this, we believe that it was not detected in time. The difficulty in accessing the area allowed the fire to rapidly grow in area and intensity.
- The population of the affected area has a high aging index, on average 2 times higher than the national average but in some regions gets to be 10 times higher. This aging results in some degree of abandonment of agricultural practices and a lower availability to implement self-protection measures near the urban centres. This is particularly noticeable in the small villages, like *Quinta das Quebradas*.
- The villages and *Quintas* are not in large numbers but they are disperse and their access is very difficult. The firefighting crews deployed to protect the buildings had great difficulty, not only in reaching there but also later on in reallocating to actively fight the fire.
- There's an enormous lack of self defense culture among the majority of urban areas, despite of their size, as well as in isolated houses. Not only by managers, or politicians but also by the inhabitants themselves. The major consequence is that in most cases fighting the fire becomes secondary for the crews, as they have to protect houses and people first.
- The construction of the *Baixo Sabor* dam was at a very advanced state of execution, as were the preparatory measures necessary before the filling. Much of the valleys in this region, especially the main water lines had already been cleared of shrubs and trees. A very wet spring of 2013 resulted in a substantial herbaceous production, all over the country but especially in those areas that were devoid of vegetation. The existence of a large amount of dry and cured grass favourably influenced the rapid progression of the fire, especially on day 9th.
- During the afternoon of July 9th the fire reached velocities much higher than what we consider normal fire behaviour. Between 17h30 and 19h00 the fire ran about 6 km towards East, reaching *Quinta das Quebradas* with great violence. The protection of this small village was the second key moment of the fire. A large number of human and material resources were required for the defense of people and their assets, consequently abandoning the combat against the propagating fire.
- Fuels management in the area affected by the fire was incipient. Almost no fuel breaks are present in the area and the ones that exist lack maintenance.
- The water points' network in the area was not adequate, requiring extensive travel for water refuelling.
- Data analysis about terrain and weather forecasting is of great importance in fire behaviour prediction, even without taking into account the fuel. During the morning of July 10th this prediction did not motivate a timely reaction by the Commanding Officers and this was the third key moment of the *Picões* fire.
- Expert fire behaviour prediction is still not being taken into account on normal fire management activities, and we believe this to be a gap in the system that should be filled.

7. References

Alexander, M.E.; Lanoville, R.A. (1989). Predicting fire behavior in the black spruce-lichen woodland fuel type of western and northern Canada. For. Can., North. For. Cent., Edmonton, Alberta, and Gov. Northwest Territ., Dep. Renewable Resour., Territ. For. Fire Cent., Fort Smith, Northwest Territories. Poster (with text).

Andrews, Patricia L.; Bevins, Collin D.; Seli, Robert C. 2008. BehavePlus fire modeling system, version 4.0: User's Guide. Gen. Tech. Rep. RMRS-GTR-106WWW Revised. Ogden, UT: Department of Agriculture, Forest Service, Rocky Mountain Research Station. 116p.

Countryman, C. M. 1972. The fire environment concept. Berkeley, CA: U.S. Department of Agriculture, Forest Service, Pacific Southwest Forest and Range Experiment Station.

Anderson, Hal E. Aids to determining fuel models for estimating fire behavior. Gen. Tech. Rep. INT-122. Ogden, UT: U. S. Department of Agriculture, Forest Service, Intermountain Forest and Range Experiment Station; 1982.20 p.

ICNF 2013. Recuperação da área ardida do incêndio de Picões (julho de 2013). Relatório Técnico. Instituto da Conservação da Natureza e Florestas

IPMA 2013a. Vento nos dias 9 e 10 de julho de 2013 na região de Alfândega da Fé. Relatório técnico. Instituto Português do Mar e da Atmosfera

IPMA 2013b. Boletim Climatológico Mensal de Portugal Continental. Julho 2013. Instituto Português do Mar e da Atmosfera

Lopes, A.M.G.; Cruz, M.G and Viegas, D.X. (1998). FireStation – An Integrated System for the Simulation of Wind Flow and Fire Spread over Complex Terrain. II International Conference on Fire and Forest Meteorology, Vol. I, pp. 741-754, Luso – Coimbra.

Lopes, A.M.G, Cruz, M.G. and Viegas, D. X. (2002), "FireStation - An integrated software system for the numerical simulation of wind field and fire spread on complex topography" Environmental Modelling & Software, Vol.17, N.3, pp. 269-285

Novo, I.; Rio, J.; Silva, P; Ramos, R. e Moreira, N. (2013). Incêndios Florestais no Verão de 2013: Análise Meteorológica e Comportamento do Vento. Novembro de 2013. Divisão de Previsão Meteorológica, Vigilância e Serviços Espaciais. Instituto Português do Mar e da Atmosfera.

Pyne, S.J., Andrews, P.L. & Laven, R.D. (1996) Introduction to Wildland Fire, p.50. Wiley, New York

Rothermel, Richard C. 1972. A mathematical model for predicting fire spread in wildland fuels. Res. Pap. INT-115. Ogden, UT: U.S. Department of Agriculture, Intermountain Forest and Range Experiment Station. 40 p

Van Wagner, C.E. 1977b. Effect of slope on fire spread rate. Canadian Forestry Service Bi-monthly Research Notes. 33: 7–8

The MODIS-based perpendicular moisture index as a tool for mapping fire hazard: indirect validation in three areas of the Mediterranean

Carmine Maffei[a], Laura Bonora[b], Fabio Maselli[c], Adrien Mangiavillano[d], Massimo Menenti[e]

[a] *Delft University of Technology, Stevinweg 1, 2628 CN, Delft, Netherlands, c.maffei@tudelft.nl*
[b] *Institute of Biometeorology of the Italian Research Council, Via Madonna del Piano 10, 50019 Sesto Fiorentino, Italy, l.bonora@ibimet.cnr.it*
[c] *Institute of Biometeorology of the Italian Research Council, Via Madonna del Piano 10, 50019 Sesto Fiorentino, Italy, maselli@ibimet.cnr.it*
[d] *Entente pour la forêt Méditerranéenne - Département Essais et recherche (CEREN), Centre Francis Arrighi, Domaine de Valabre, 13120 Gardanne, France, a.mangiavillano@valabre.com*
[e] *Delft University of Technology, Stevinweg 1, 2628 CN, Delft, Netherlands, m.menenti@tudelft.nl*

Abstract

Several spectral indices based on measurements in the optical domain have been proposed for the estimation of equivalent water thickness (EWT), which is defined as the mass of liquid water per unit of leaf surface. However, fire models rely on the live fuel moisture content (LFMC) as a measure of vegetation moisture. LFMC is defined as the ratio of the mass of the liquid water in a fresh leaf over the mass of oven dry leaf, and traditional vegetation moisture spectral indices are not as effective in capturing LFMC variability. Recently, the perpendicular moisture index (PMI), based on MODIS, was proposed to overcome this limitation and provide a direct measure of LFMC. The aim of this research was to understand the potential and limitations of the PMI in predicting fire hazard. To this purpose, more than 19000 fire records in Provence-Alpes-Côte d'Azur (31400 km^2), France, Toscana (22994 km^2), Italy and Campania (13595 km^2), Italy, over heterogeneous periods between 2000 and 2012 were compared against PMI derived from MODIS reflectance images. Results show that PMI maps capture both year-to-year variability of vegetation condition and its evolution during the advancement of the dry season. The PMI appears to be correlated with mean rate of spread and mean number of fires.

Keywords*: MODIS; Live Fuel Moisture Content; Perpendicular Moisture Index; Fire hazard.*

Introduction

The remote-sensing community has developed a number of spectral indices based on broadband satellite measurements in the optical domain for the assessment of vegetation water content measured as equivalent water thickness (EWT), which is defined as the mass of liquid water per unit of leaf surface (e.g. Hunt and Rock 1989; Gao 1996; Pinty *et al.* 2002). However, fire models rely on the live fuel moisture content (LFMC) as a measure of vegetation moisture (Yebra *et al.* 2013). LFMC is defined as the ratio of the mass of the liquid water in a fresh leaf over the mass of oven dry leaf, and spectral indices proposed so far are not as effective in capturing LFMC variability as with EWT (Danson and Bowyer 2004; Caccamo *et al.* 2012).

In a recent paper (Maffei and Menenti 2014), the perpendicular moisture index (PMI) was introduced to exploit MODIS spectral characteristics and to overcome some of the limitations of the traditional vegetation moisture spectral indices. The PMI is a direct measure of LFMC, but its potential in the evaluation of fire hazard is unexplored.

The objective of this research was to understand the potential and limitations of the PMI in predicting fire hazard, i.e. in providing relevant information on the characteristics of fires that might occur in a certain area. To this purpose, three large study areas were selected, and MODIS-derived maps of PMI

were evaluated against fire occurrence records. The relationship between the PMI, the average fire propagation speed and the mean number of fires was investigated.

Materials and methods

Study areas

The research was performed on three study areas of the Western Mediterranean basin (Figure 1):

- Provence-Alpes-Côte d'Azur (PACA, 31400 km^2), France;
- Toscana (22994 km^2), Italy;
- Campania (13595 km^2), Italy.

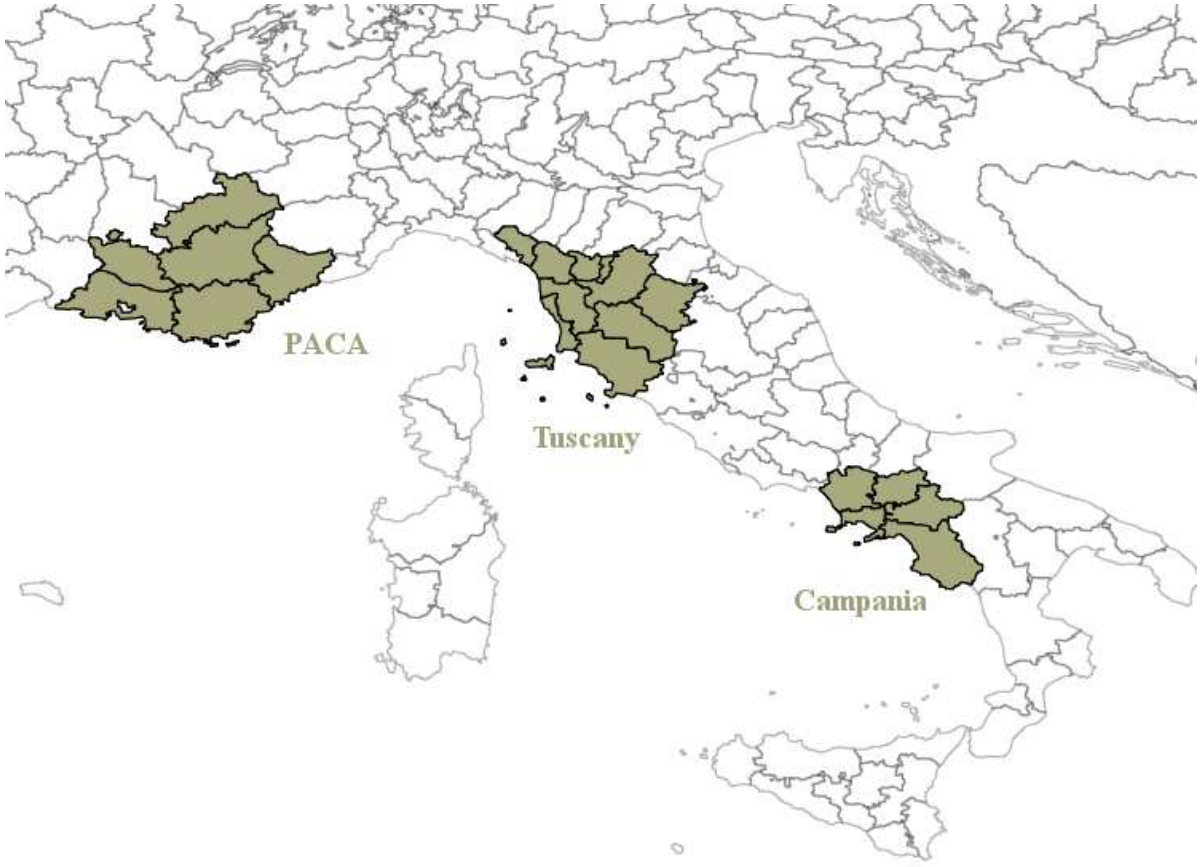

Figure 1. Study areas.

Fire data

Fire records from different sources were used in this research:

- PACA: a collection of more than 9400 fires between 2000 and 2012 extracted from the Prométhée database ("Prométhée: Forest fires database for Mediterranean area in France");
- Toscana: a database of more than 2300 fires records between 2000 and 2007, provided by the Regional Administration of Toscana;
- Campania: a database of more than 7700 fire records covering years between 2000 and 2008, provided by the Italian Forest Corps (*Corpo Forestale dello Stato*, CFS).

2.3. MODIS data

Moderate Resolution Imaging Spectroradiometer (MODIS) sensors mounted on Terra and Aqua satellites from NASA view the entire Earth's surface almost on a daily basis, recording radiance in 36 spectral channels ranging from the optical to the thermal domains. MODIS data are free of charge, and can be downlinked and processed at ground stations for the near-real-time delivery of derived products. For this research, 8-day composites of Terra-MODIS reflectance data (product MOD09A1) were retrieved from the Land Processes Distributed Active Archive Center ("LP DAAC") hosted by the United States Geological Survey (USGS). All composites covering June to September were selected, for the years corresponding to the availability of fire data in each study area.

2.4. The perpendicular moisture index

The perpendicular moisture index (PMI) was developed from the observation that, in the spectral plane spanned by MODIS channels 2 (0.86 μm) and 5 (1.24 μm), points characterised by the same value of LFMC lay on straight parallel lines. This led to the definition of a measure of vegetation moisture as the distance of a reflectance point in this plane from a reference line, according to equation:

$$PMI = -0.73 \cdot (R5 - 0.94 \cdot R2 - 0.028)$$

where R2 and R5 are reflectance measurements in MODIS channels 2 and 5 respectively.

2.5. Indirect validation of the PMI

Maps of PMI were calculated from MODIS data, and masked basing on CORINE Land Cover (CLC) classes. Due to a difference in the way the Italian and French fires databases were constructed, CLC mask for the Italian sites included all forests and natural areas classes, whereas in France it also included agricultural lands.

For each fire in the data sets, the value of the PMI was sampled from the PMI map corresponding to the MODIS 8-day compositing period previous to the date of the event. PMI values at fires' locations were compared to fire rate of spread. This parameter was computed from fire size and duration, and in this sense it does not give any information about the actual rate of spread; however, it provides information on "how fast" the area affected by the fire was burnt.

To understand the relationship between the number of fires and the PMI values, within each intermediate administrative unit (departments in PACA, provinces in Toscana and Campania), the median PMI in an 8-day compositing period was calculated and the fires in the following compositing period counted. This led to the construction of a number of couples of values of PMI and number of fires that were grouped by regular intervals of PMI; in each group, the mean number of fires was calculated and assessed against PMI values.

3. Results

Maps of PMI show clear seasonal trends as well as year-to-year variability. In Figure 2 four maps produced from the MOD09A1 data of the 208th day (composite of days 201-208) of years 2003, 2004, 2005 and 2006 in PACA clearly show how spatial patterns of PMI vary for the same compositing period on a yearly base. Similar considerations can be drawn in Toscana (Figure 3) and Campania (Figure 4).

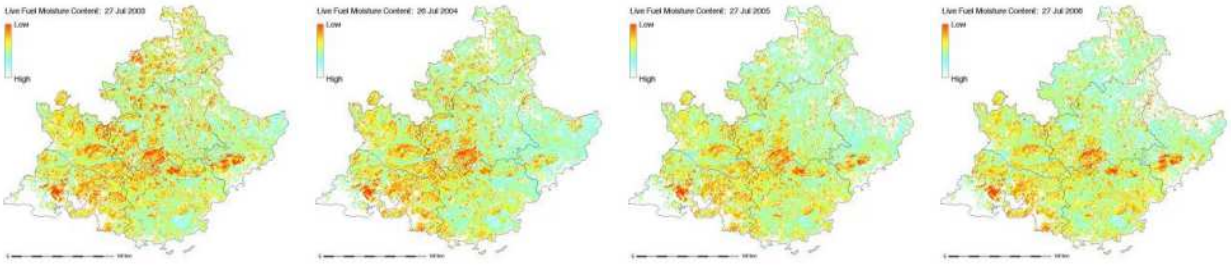

Figure 2. Maps of PMI in the same date of four successive years in the study area of PACA.

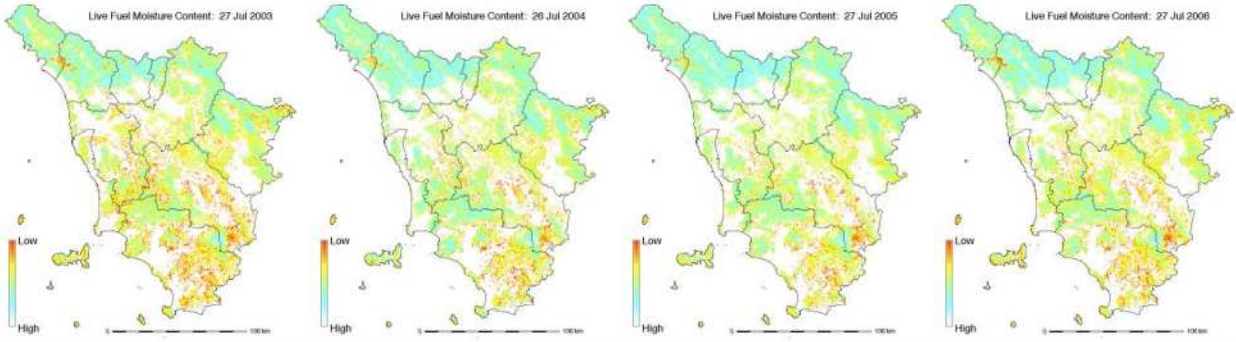

Figure 3. Maps of PMI in the same date of four successive years in the study area of Toscana.

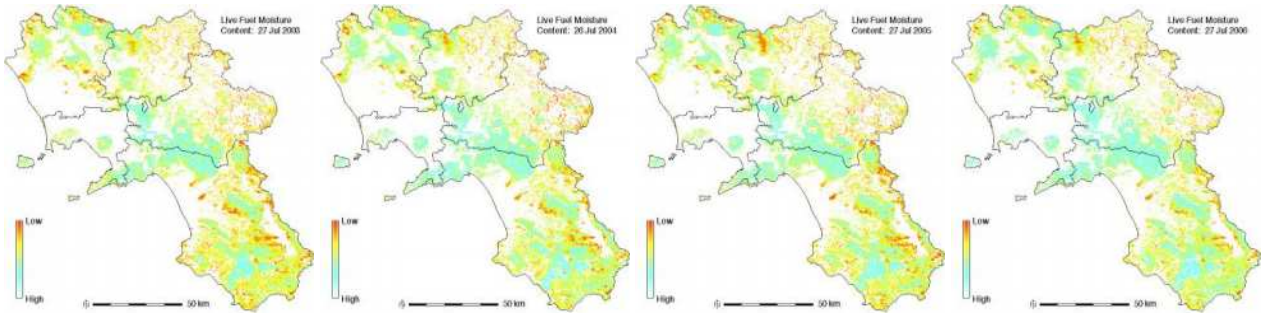

Figure 4. Maps of PMI in the same date of four successive years in the study area of Campania.

Figure 5 shows four successive 8-day maps of PMI of year 2003 in PACA. The PMI appears to capture the evolution of vegetation condition during the summer (dry) season, toward conditions of lower moisture content. Also in this case, similar considerations can be drawn in Toscana (Figure 6) and Campania (Figure 7).

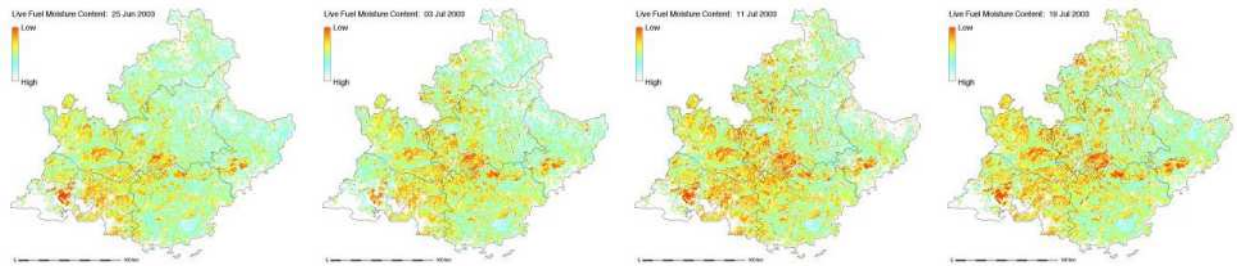

Figure 5. Maps of PMI in four successive compositing periods of the same year in the study area of PACA.

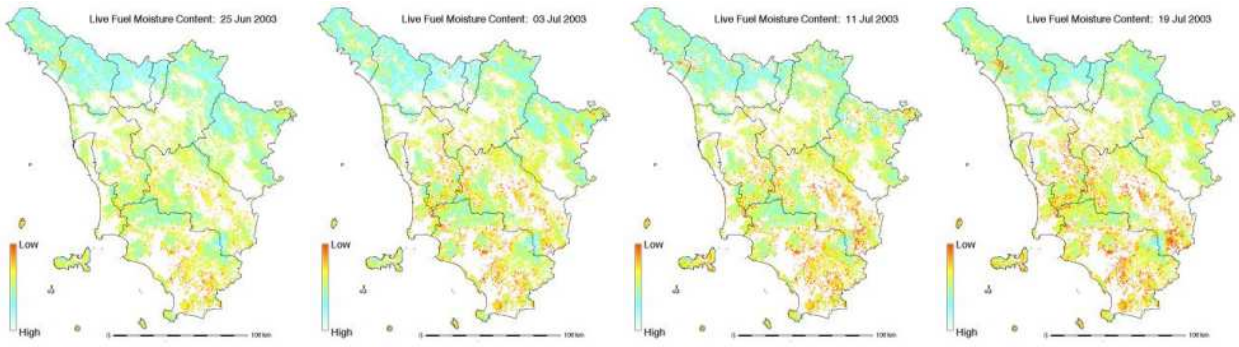

Figure 6. Maps of PMI in four successive compositing periods of the same year in the study area of Toscana.

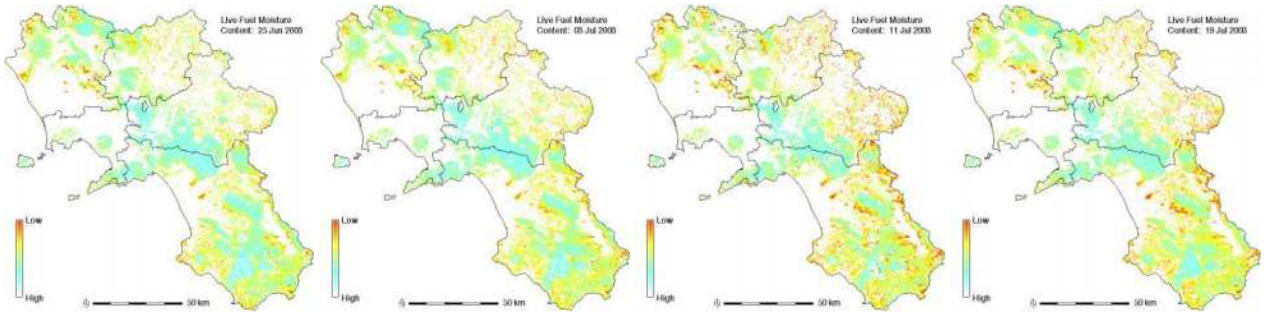

Figure 7. Maps of PMI in four successive compositing periods of the same year in the study area of Campania.

Fire rate of spread is affected by several factors of different nature. To isolate the role of vegetation moisture (as estimated by the PMI) from that of all the other factors, the PMI values associated to all fires in a study area were divided into bins delimited by their 0th, 10th, …, 100th percentiles. Within each bin, the mean value of the rate of spread was associated to the corresponding median value of PMI. This observation was only performed in Toscana and Campania, since the Prométhée database does not contain information on fire duration. Figure 8 shows evidence of the observed relationship between PMI and fire rate of spread. Higher PMI values imply a lower rate of spread, as would be expected in conditions of higher moisture content in leaf tissues. In both study areas the regression is linear; however, the dynamic range of the rate of spread differs.

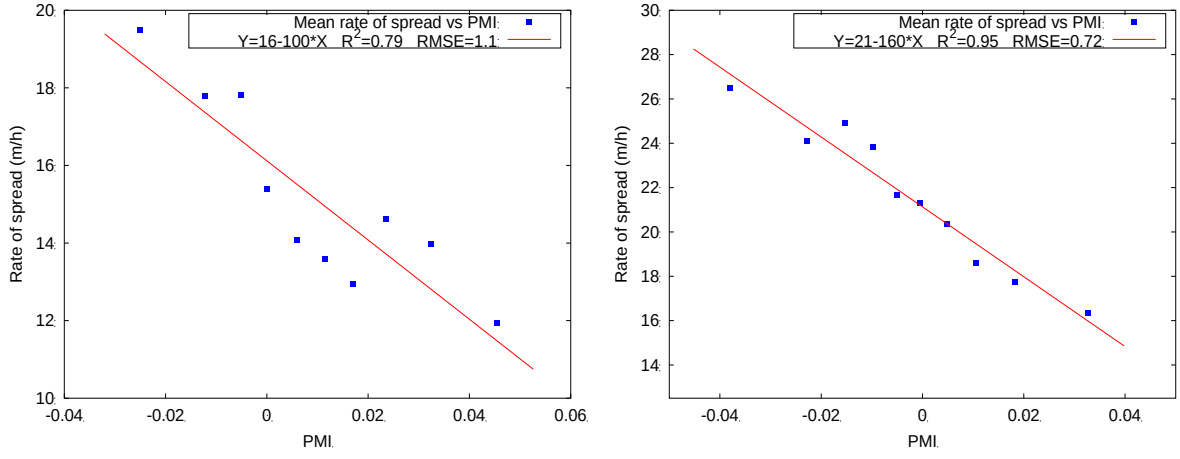

Figure 8. Relationship between PMI and mean rate of spread in Toscana (left) and Campania (right).

The variation of the mean number of fires with the median PMI value recorded in each department of PACA appears to follow a general trend (Table 1): when the vegetation moisture content is higher (the

PMI is higher), a lower number of fires is observed. Similar results were found in Toscana (Table 2) and Campania (Table 3).

Table 1. Relationship between the mean number of fires and the median PMI value in 8-day observation periods, for each department of PACA.

	Mean number of fires				
Department	PMI<-0.02	-0.02<PMI<-0.01	-0.01<PMI<0	0<PMI<0.01	PMI>0.01
Alpes-de-Haute-Provence	2.71	1.45	1.11	0.71	-
Hautes-Alpes	-	0.43	0.26	0.21	-
Alpes-Maritimes	-	4.75	5.53	4.48	4.00
Bouches-du-Rhône	9.86	10.41	7.19	7.25	-
Var	10.14	10.45	8.48	4.58	-
Vaucluse	1.34	1.80	1.47	1.11	-

Table 2. Relationship between the mean number of fires and the median PMI value in 8-day observation periods, for each province of Toscana.

	Mean number of fires					
Province	PMI<-0.01	-0.01<PMI<0	0<PMI<0.1	0.01<PMI<0.02	0.02<PMI<0.03	PMI>0.03
Massa Carrara	-	-	2.37	2.28	1.28	0.69
Lucca	-	-	2.25	2.98	4.13	2.06
Pistoia	-	-	-	1.71	1.68	1.67
Firenze	-	4.73	4.83	3.43	1.75	0.67
Livorno	-	1.06	0.71	0.55	0.33	-
Pisa	-	2.26	2.51	1.70	0.64	-
Arezzo	-	4.18	4.40	1.61	1.71	-
Siena	2.81	1.79	0.93	0.36	-	-
Grosseto	3.68	2.48	1.79	0.64	-	-
Prato	-	-	-	0.70	0.69	0.72

Table 3. Relationship between the mean number of fires and the median PMI value in 8-day observation periods, for each province of Campania.

	Mean number of fires					
Province	PMI<-0.01	-0.01<PMI<0	0<PMI<0.1	0.01<PMI<0.02	0.02<PMI<0.03	PMI>0.03
Caserta	4.25	4.83	4.46	2.42	0.96	0.5
Benevento	6.80	7.56	2.58	1.57	0.14	-
Napoli	-	-	4.14	4.08	1.43	-
Avellino	6.37	9.11	7.45	1.14	1.17	-
Salerno	13.08	20.98	15.48	3.31	0.75	-

Discussion

The recently introduced PMI tries to overcome some of the limitations of the traditional broadband spectral indexes in the quantification of LFMC. Its main limitation is given by its sensitivity to the leaf aria index. It is expected that the PMI underestimates vegetation moisture when vegetation cover is less dense. Its application to fire hazard mapping was here evaluated in three large study areas in France and Italy.

From a qualitative point of view, the PMI appears to capture the seasonal variation of vegetation moisture, exhibiting decreasing values of PMI during the evolution of the dry season (Figures 5, 6, 7). Although not shown here, this pattern was observed in every year under consideration. Similarly, the proposed spectral index shows clear year-to-year variability for any selected compositing period (examples shown in Figures 2, 3, 4).

More quantitative observations lead to the clear identification of a linear relationship between PMI and average fire rate of spread (Figure 8). However, it must be noted that the regression lines are different in Toscana and Campania, suggesting that landscape factors may affect it.
Clear trends are observed between median PMI value calculated at department / province level and the mean number of fires in each 8-day observation period (Tables 1, 2, 3). No assumptions were made on the actual distribution of the number of fires in each observation period, as this is part of further investigations.

Acknowledgements

We are grateful to the Forest Fires office of the Italian Forest Corps (CFS), the Italian Civil Protection and the Regional Administration of Toscana for providing fire data in Toscana and Campania.

References

Caccamo G, Chisholm L a., Bradstock R a., Puotinen ML, Pippen BG (2012) Monitoring live fuel moisture content of heathland, shrubland and sclerophyll forest in south-eastern Australia using MODIS data. Int J Wildl Fire 21(3), 257. doi:10.1071/WF11024.

Danson FM, Bowyer P (2004) Estimating live fuel moisture content from remotely sensed reflectance. Remote Sens Environ 92(3), 309–321. doi:10.1016/j.rse.2004.03.017.

Gao B-C (1996) NDWI—A normalized difference water index for remote sensing of vegetation liquid water from space. Remote Sens Environ 58(3), 257–266. doi:10.1016/S0034-4257(96)00067-3.

Hunt ER, Rock BN (1989) Detection of Changes in Leaf Water Content Using Near- and Middle-Infrared Reflectances. 54, 43–54.

LP DAAC https://lpdaac.usgs.gov/. Accessed 26 June 2014.

Maffei C, Menenti M (2014) A MODIS-based perpendicular moisture index to retrieve leaf moisture content of forest canopies. Int J Remote Sens 35(5), 1829–1845. doi:10.1080/01431161.2013.879348.

Pinty B, Tarantola S, Ceccato P, Gobron N (2002) Designing a spectral index to estimate vegetation water content from remote sensing data : Part 1 Theoretical approach. 82, 188–197.

Prométhée: Forest fires database for Mediterranean area in France http://www.promethee.com/. Accessed 26 June 2014.

Yebra M, Dennison PE, Chuvieco E, Riaño D, Zylstra P, Hunt ER, Danson FM, Qi Y, Jurdao S (2013) Remote Sensing of Environment A global review of remote sensing of live fuel moisture content for fi re danger assessment : Moving towards operational products. 136, 455–468.

Time series of land surface temperature from daily MODIS measurements for the prediction of fire hazard

Carmine Maffei, Silvia Alfieri, Massimo Menenti

[a]*Delft University of Technology, Stevinweg 1, 2628 CN, Delft, Netherlands, c.maffei@tudelft.nl, s.m.alfieri-1@tudelft.nl, m.menenti@tudelft.nl*

Abstract
Prolonged heat and absence of rainfall drive vegetation into water stress conditions that lead to an increase of its temperature. Since stressed vegetation is more prone to fire, it is expected that remote sensing mapping of temperature anomalies might be a viable tool to predict fire hazard. The identification of these anomalies requires the prior definition of a reference temperature against which compare actual recorded temperatures. This can be achieved by using long time series of satellite data and the HANTS (Harmonic ANalysis of Time Series) algorithm. The objective of this research was the characterisation of fire hazard using temporal series of land surface temperature (LST) derived from Terra-MODIS measurements. The investigation was based on a sequence of MODIS LST data from 2000 to 2008 in Campania (13595 km^2), Italy, and on a data set of 7700 fires recorded in the area in the same period. Missing and/or cloudy LST data were reconstructed by means of the HANTS algorithm applied to annual sequences of daily observations. The coefficients of the Fourier analysis were assessed against spatial patterns of fire occurrence. HANTS algorithm was also used to construct daily reference temperature maps against which to evaluate temperature anomalies and cumulated temperature anomalies. Results show that fires tend to occur in areas characterised by specific values of several Fourier coefficients with high significance, and to avoid the other areas. The amplitude of the second harmonic is the only Fourier coefficient dictating mean fire size. The mean fire size and the proportion of large fires correlate with both daily and cumulated thermal anomalies.

Keywords*: Land surface temperature; MODIS; Time series; HANTS; Fire hazard.*

Introduction

Prolonged heat and absence of rainfall drive vegetation into water stress conditions that lead to an increase of its temperature. Since stressed vegetation is more prone to fire, there might be a potential role for Earth observation technologies in mapping fire hazard (Leblon 2005), whereas it is proved that current orbiting instruments are able to detect anomalies in vegetation temperature.
The identification of temperature anomalies requires the prior definition of a reference temperature against which compare actual recorded temperature. By using long time series of satellite data it is possible to identify expected temporal patterns on a pixel-by-pixel basis. The HANTS (Harmonic ANalysis of Time Series) algorithm accomplishes this task by means of a Fourier series (Verhoef *et al.* 1996). HANTS has been reported to successfully provide reference data for both vegetation spectral indexes and land surface temperature (Julien *et al.* 2006).
The objective of this research was to develop and test a methodology for the characterisation of fire hazard from anomalies of daily land surface temperature (LST), as derived from thermal infrared measurements of the Moderate Resolution Imaging Spectrometer (MODIS) on board Terra satellite, evaluated against a reference temperature calculated with HANTS algorithm. Since maps of HANTS coefficients provide a detailed characterisation of the spatial and temporal pattern of surface temperatures, their potential to explain spatial patterns of fire occurrence was also investigated.

Materials and methods

Study area

The research focussed on Campania (13595 km^2), Italy. The Italian Forest Corps (*Corpo Forestale dello Stato*) provided a dataset of more than 7700 fire records covering years between 2000 and 2008. Data included date and time, coordinates, duration and extent of each event.

Figure 1. Study area.

MODIS land surface temperature data

A collection of daily diurnal (approximately 10.30 am local time) Terra-MODIS LST data from 2000 to 2008 was used for this research. These data are publicly available at the Land Processes Distributed Active Archive Center ("LP DAAC") hosted by the United States Geological Survey (USGS).

2.3. Fourier analysis of LST data

Series comprising three harmonics (365, 180 and 120 days) were fit to the data with two different methods, to achieve the diverse purposes of this research:

- HANTS was executed on each yearly sequence of daily LST data separately, to reconstruct missing or cloudy data (Roerink *et al.* 2000). The retrieved yearly images of Fourier coefficients (mean LST, amplitude and phase of the three harmonics) were then compared against spatial patterns of fire occurrence.
- The algorithm was executed on the whole 2000-2008 dataset to construct daily maps of reference temperature (Azzali and Menenti 1999). These served as a basis for the calculation of thermal anomalies.

2.4. Spatial patterns of fire occurrence

Yearly maps of Fourier coefficients were masked on forest and natural areas (as from the CORINE Land Cover 2000 map) and segmented into labelled classes. Masking was performed to ensure

consistency between the characteristics of the database, which includes only fires occurred in forests and other natural areas, and further analyses based on the spatial distribution of fires.
Spatial patterns of fire occurrence were assessed with respect to fire number and mean burnt area in terms of selectivity, i.e. by understanding whether in each class fire incidence is higher (preferred) or lower (avoided) than expected from a random null model (Bajocco and Ricotta 2007).

2.5. Analysis of LST anomalies

Daily maps of thermal anomalies (TA) were computed by subtracting the daily reference temperature from MODIS LST. Forest fires are expected to occur in areas where there has been a prolonged exposure to lack of rainfall and high air temperature. In these circumstances a temperature anomaly is observed over a number of consecutive days. For this reason cumulated anomalies (CTA) were calculated as the sum of all the observed thermal anomalies from the day when the thermal anomaly was first recorded in the pixel up to the current day. Each fire in the database was then associated to the values of TA and CTA observed at fire's location in the day previous to the event.

Results

The mean annual temperature and the amplitudes of the three harmonics used in the analysis have an evident role in determining spatial patterns of fire occurrence (Tables 1 to 4). Among the phase components, fire occurrence shows clear spatial selectivity only against the first (Table 5, other tables not shown). Mean fire size shows unambiguous spatial selectivity solely in the amplitude of the second harmonic (Table 3).
Temperature anomalies and cumulated temperature anomalies were evaluated against fire size by first calculating the conditional mean fire size observed when the TA (CTA) was larger of the considered value, and then plotting the calculated means against the values of anomaly (cumulated anomaly) used in the calculation. In a similar manner, the conditional proportion of large fires (larger than 16 ha, which is the 90th percentile in the study area) was evaluated against anomaly and cumulated anomaly.

Table 1. Selectivity of fires' number and mean size for mean temperature classes. Symbol "+" means class preference, "-" class avoidance. One symbol: selectivity non significant. Two symbols: significant P<0.05. Three symbols: significant P<0.01.

Constant component of Fourier analysis (K)				
Class	Number of fires		Mean fire size	
<288	34	---	15,74	+++
288-289	47	---	7,09	+++
289-290	121	--	5,39	+
290-291	264	+++	7,34	+
291-292	494	+++	4,4	-
292-293	782	+++	4,23	-
293-294	904	+++	4,85	-
294-295	751	+++	3,99	--
295-296	560	-	5,52	+
296-297	279	---	4,81	+
297-298	127	---	9,67	+++
>298	41	---	4,79	+

Table 2. Selectivity of fires' number and mean size for classes of amplitude of the first harmonic. Symbol "+" means class preference, "-" class avoidance. One symbol: selectivity non significant. Two symbols: significant P<0.05. Three symbols: significant P<0.01.

Amplitude of the first harmonic (K)				
Class	Number of fires		Mean fire size	
<8	59	-	7,79	+
8-9	203	+	4,97	+
9-10	453	+++	5,8	+
10-11	984	+++	4,55	-
11-12	1242	+++	4,94	+
12-13	872	---	4,71	-
13-14	411	---	4,39	-
14-15	158	---	6,02	+
>15	22	---	27,05	+++

Table 3. Selectivity of fires' number and mean size for classes of amplitude of the second harmonic. Symbol "+" means class preference, "-" class avoidance. One symbol: selectivity non significant. Two symbols: significant P<0.05. Three symbols: significant P<0.01.

Amplitude of the second harmonic (K)				
Class	Number of fires		Mean fire size	
0-1	2083	+++	3,52	---
1-2	1723	+	6,01	+++
2-3	570	---	7,24	+++
>3	28	---	12,85	+++

Table 4. Selectivity of fires' number and mean size for classes of amplitude of the third harmonic. Symbol "+" means class preference, "-" class avoidance. One symbol: selectivity non significant. Two symbols: significant P<0.05. Three symbols: significant P<0.01.

Amplitude of the third harmonic (K)				
Class	Number of fires		Mean fire size	
0-1	1486	+++	5,06	+
1-2	2450	+++	4,99	-
2-3	447	---	5,2	+
>3	21	---	4,88	+

Table 5. Selectivity of fires' number and mean size for classes of phase of the first harmonic. Symbol "+" means class preference, "-" class avoidance. One symbol: selectivity non significant. Two symbols: significant P<0.05. Three symbols: significant P<0.01.

Phase of the first harmonic (°)				
Class	Number of fires		Mean fire size	
<180	21	---	10,15	++
180-185	126	---	3,12	---
185-190	645	---	3,21	---
190-195	1438	+++	4,29	--
195-200	1329	+++	6,63	+++
200-205	623	++	5,28	+
205-210	193	+++	5,27	+
>210	29	+	6,9	+

Daily thermal anomalies appear to be related to fire size: with increasing values of the thermal anomaly, the expected mean fire size in all areas with thermal anomaly larger of that value increases (Figure 2, left). A similar pattern is observed with the conditional fraction of large fires (Figure 2, right). A wider dynamic range in fire size and fraction of large fires is observed when the same analysis is performed against CTA (Figure 3).

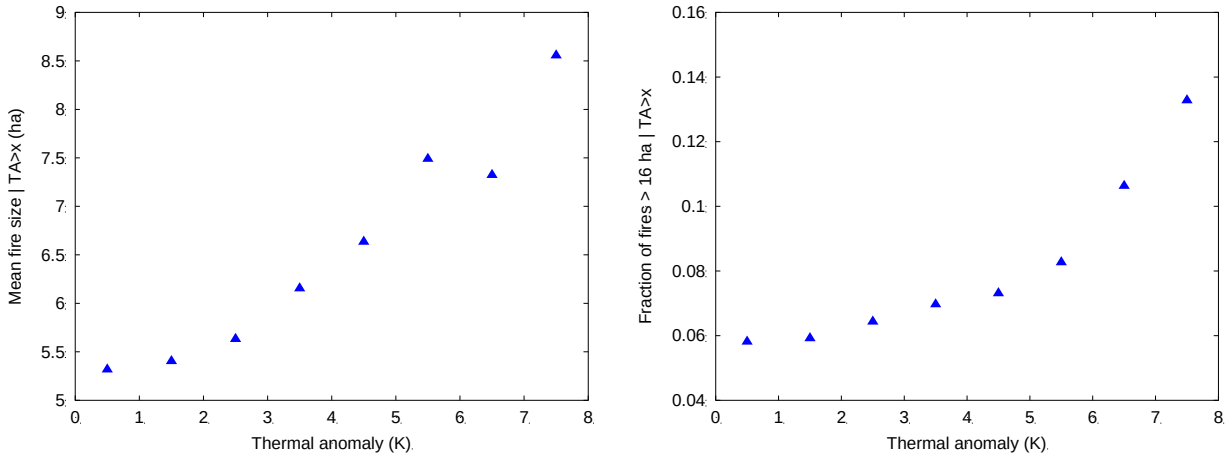

Figure 2. Relationship between conditional mean fire size (left) and conditional fraction of large fires (right) against values of thermal anomaly (TA) observed in the day previous to the event at fires' locations.

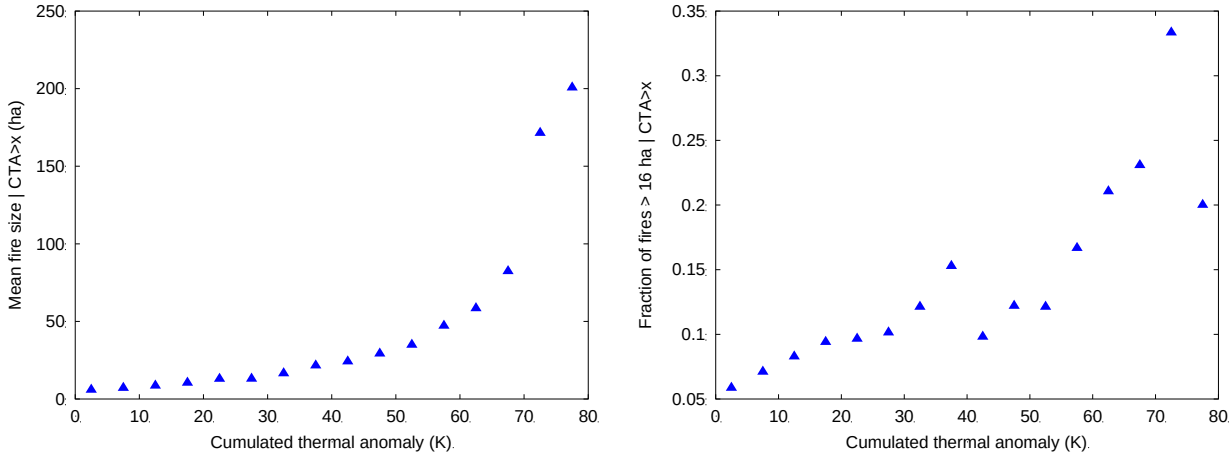

Figure 3. Relationship between conditional mean fire size (left) and conditional fraction of large fires (right) against values of cumulated thermal anomaly (CTA) observed in the day previous to the event at fires' locations.

Discussion

Results show that the HANTS algorithm plays an important role in both characterising spatial patterns of fire occurrence and in predicting mean fire size. Indeed, fires occurrence shows clear selectivity against mean value, amplitude of the three harmonics and phase of the first harmonic of LST computed on a yearly basis. Mean fire size shows selectivity only against the amplitude of the second harmonic. Here, a clear inverse relationship between number of fires and mean fire size is observed, with larger fires significantly preferring areas where the amplitude is larger (Table 3).
The only phase component of the Fourier analysis related to fires incidence is that of the first harmonic; fires significantly prefer areas where this phase is higher. The phase carries information on the timing

of fire events, and indeed a larger number of fires is observed where the phase is higher, i.e. when a prolonged warm season occurs.
A relationship was found between conditional mean fire size and thermal anomalies (Figure 2). With increasing values of the thermal anomaly, the conditional mean fire size increases. A similar trend is observed with the conditional fraction of fires larger than 16 ha. From the point of view of fire size, cumulated thermal anomaly maps carry a stronger informative content. CTA is a measure of heat "accumulated" in a certain area, providing more direct information on the prolonged exposure of vegetation to stress conditions. This is reflected in the prediction of expected mean fire size over two orders of magnitude (Figure 3). Moreover, when the cumulated anomaly is larger that about 60 K, a steep increase in mean fire size is observed, potentially allowing the production of more meaningful fire hazard maps as compared to TA.

Acknowledgements

We are grateful to the Forest Fires office of the Italian Forest Corps (CFS) and the Italian Civil Protection for providing fire data in the study area.

References

Azzali S, Menenti M (1999) Mapping isogrowth zones on continental scale using temporal Fourier analysis of AVHRR-NDVI data. Int J Appl Earth Obs Geoinf 1(1), 9–20. doi:10.1016/S0303-2434(99)85023-5.

Bajocco S, Ricotta C (2007) Evidence of selective burning in Sardinia (Italy): which land-cover classes do wildfires prefer? Landsc Ecol 23(2), 241–248. doi:10.1007/s10980-007-9176-5.

Julien Y, Sobrino JA, Verhoef W (2006) Changes in land surface temperatures and NDVI values over Europe between 1982 and 1999. Remote Sens Environ 103, 43–55. doi:10.1016/j.rse.2006.03.011.

Leblon B (2005) Monitoring Forest Fire Danger with Remote Sensing. Nat Hazards 35(3), 343–359. doi:10.1007/s11069-004-1796-3.

LP DAAC https://lpdaac.usgs.gov/. Accessed 26 June 2014.

Roerink GJ, Menenti M, Verhoef W (2000) Reconstructing cloudfree NDVI composites using Fourier analysis of time series. Int J Remote Sens 21(9), 1911–1917. doi:10.1080/014311600209814.

Verhoef W, Menenti M, Azzali S (1996) A colour composite of NOAA-AVHRR-NDVI based on time series analysis (1981-1992). Int J Remote Sens 17, 231–235. doi:10.1080/01431169608949001.

Waste in non-value-added suppression activities: simulation analysis of the impact of rekindles and false alarms on the forest fire suppression system

Abílio Pereira Pacheco[a], João Claro[a], Tiago Oliveira[b]

[a] *INESC TEC (formerly INESC Porto) and Faculdade de Engenharia, Universidade do Porto, Campus da FEUP, Rua Dr. Roberto Frias, 378, 4200-465 Porto, Portugal, abilio.pacheco@fe.up.pt*
[b] *Forest Protection, grupo PortucelSoporcel, Edifício Mitrena, Apartado 55, 2901-861 Setúbal, Portugal*

Abstract[1]
Rekindles and false alarms are phenomena that have a significant presence in the Portuguese forest fire management system and an important impact on suppression resources in particular and fire management resources in general. As illustration, in 32,357 incidents that the suppression system handled in 2010, 12.3% were false alarms and 13.0% were rekindles, rising to 12.5% and 15% respectively, during the summer, the critical period.
In this work, we propose a discrete-event simulation model of a forest fire suppression system designed to analyze the joint impact of primary fires (ignitions), and non-value-added fire suppression activities such as rekindles (defects, inappropriate processing) and false alarms (motion) on the performance of the system. The work contributes to address a research gap concerning that impact, and features a novel application of simulation to suppression systems, as a screening tool to support more holistic analyses.
The model was implemented in ®ARENA and is applied to a case study of the district of Porto, Portugal, for the critical period of the forest fire season, between July and September 2010.
We study the behavior of the system's point of collapse, comparing the real base scenario with a benchmark scenario built with reference values for rekindles and false alarms, and also as a function of the number of fire incidents, considering historical variations.
The results of the analysis are useful for operational decision-making and provide relevant information on the trade-off between prevention and suppression efforts. In particular, we have found that reducing false alarms and rekindles to benchmark values would significantly reduce pressure on firefighting teams, enabling more effective suppression operations.

Keywords*: wildland fire suppression, rekindles, false alarms, hoax calls, discrete event simulation, wildfire*

Introduction

We propose in this work a discrete-event simulation model of a forest fire suppression system, designed to analyse the joint impact of ignitions and non-value-added fire suppression activities such as rekindles (defects, inappropriate processing) and false alarms (motion) on the performance of the system. The application of the model is illustrated with a case study of the district of Porto, in Portugal, for the critical period of the forest fire season, between July and September 2010. Our motivation for this work comes from the perception that rekindles (RK) and false alarms (FA) – malicious or good intent calls – have unusually high values in the Portuguese forest fire management system, and thus

[1] In this work we extend, with additional cost and optimization analysis, the recently published paper: Pacheco, A. P., J. Claro, and T. Oliveira. 2014. "Simulation analysis of the impact of ignitions, rekindles, and false alarms on forest fire suppression." Canadian Journal of Forest Research no. 44 (1):45-55. doi: 10.1139/cjfr-2013-0257.

represent an also unusually high burden on the suppression resources in particular, and fire management resources in general.
Since fire departments cannot presume that a call is an FA and must respond as they would to a fire (Ahrens 2003), the deployment of crews to non-existing fires, cause them to be unavailable for real fires, deprived of time to rest and recover, or hastily redeployed from other incidents, prematurely abandoning mop-up efforts and possibly creating conditions for fires to rekindle. In the little research available about FA performance measures (Flynn 2009), we have found values for the U.S. - 4.4% of all calls in 2009 and 4.1% in 2010 (Karter 2011); New Zealand - between 4.6% and 5.4% (Tu 2002); and the U.K. - 5.0% in Derbyshire (Yang *et al.* 2003) and 6.2% in South Wales (Corcoran *et al.* 2007), accounting for all emergency calls. These numbers suggest that there is still room for improvements regarding FA in Portugal.
The proportion of RK is also extremely high, still very much above the target defined in the "Technical Proposal for a National Plan of Defence of the Forest against Fires", PTPNDFCI (ISA 2005), or the values of other countries, such as the US, for which, in a report on the factors that contribute to new ignitions, Ahrens (2010) mention rekindles as responsible for 3% to 6% of the local fire department responses, between 2004 and 2008. The figures for FA and RK reveal futile suppression efforts that contribute to an overload of the suppression system.
Fire occurrence rates vary over both time and space (Martell 2001) and an increased response time is considered intrinsically linked to a decreased probability of containment of new fires (Quince 2009) and a larger intensity-weighted burned area (Mercer *et al.* 2008). Hence, it is reasonable to use response time as a performance measure to evaluate an initial attack (IA) and for operational decision-making. Minimizing fire response time is crucial to minimize the number of fires that escape IA (Islam *et al.* 2009). Therefore, the use of response time as a proxy of suppression effort is meaningful because it is related to available suppression resources (Butry 2007) and most strategic fire management planning models use this simple performance measure to reflect suppression cost effectiveness (Martell 2007; Quince 2009). For any fixed quantity of mobile suppression resources, such as IA crews, as the occurrence rate increases, so do response times, and thus, daily IA effectiveness will saturate at some rate, beyond which the proportion of fire escapes will increase (Cumming 2005). This limit where the system starts to fail is what we call "point of collapse", which we define as an average waiting time above ten minutes, based on conducted field interviews.

Materials and Methods

The model that we present was designed based on a literature review, field trips, informal meetings, formal recorded interviews, and data analysis of a database of fire suppression interventions. It was implemented in ®Arena, and used for a case study of the district of Porto in the critical period, between July and September 2010 (Pacheco *et al.* 2012b, 2012a).
There are four key motives for the choice of the district of Porto as a case study: the district is particularly interesting as it has a high number of fire occurrences and available data about deployed resources; the proportion of rekindles and false alarms is slightly below, but still in line with national figures; 84% of the ignitions, corresponding to 96% of the burnt area, occur in the three-month period considered; and 2010 is the first year to have appropriate data on false alarms available. The database was used, jointly with non-parametric statistical analysis, to parameterize and validate the model, which was subsequently used with sensitivity and optimization analyses to understand the impact of ignitions, rekindles and false alarms on the performance of the suppression system, particularly on the "point of collapse", the system dimension below which the mean time between the alarm and the IA starts to grow exponentially (Pacheco *et al.* 2014).

Results

Our data analysis of forest fire incidents in the district of Porto, between July and September 2010, highlights the importance of addressing the phenomena of rekindles and false alarms. Jointly, rekindles and false alarms represent almost 20% of the incidents, with daily peaks that are exactly coincident with the peaks of requests of suppression resources for real new forest fires. Although on average false alarms use resources for a time interval lower than an IA, there is a very high opportunity cost to that time. In the case of rekindles, this is worsened by the fact that rekindle suppression operations are much harder, as made clear from the fact that initial and extended attack durations are higher for rekindles.

The extra pressure that these additional classes of incidents put on the suppression system raises difficult challenges to its management. We believe that deviations from operational standards found in our analysis, such as the number of crews dispatched to an IA, or its duration, are evidence of this pressure. In a fire prone country with an extensive wildland urban interface (WUI), where the average number of fires in the last decade corresponds to over 50% of the whole EU Mediterranean region (San-Miguel-Ayanz *et al.* 2013), increasing suppression effectiveness is particularly important to avoid that small fires become mega-fires in days of critical fire danger (Tedim *et al.* 2013).

Using our simulation analysis, we found that bringing RK and FA down to benchmark levels, would lead to a reduction in the point of collapse of approximately 9.8%. This means that managing FAs, for instance, will lead to a lower number of events in the system, which reduces pressure and releases resources that become available for real fires and to invest more time in mop-up, thus reducing the number of rekindles, contributing again to reduce the number of events, and so on, in a positive feedback loop. This highlights as well the risk of not managing FAs (Pacheco 2011).

Another very important challenge for the suppression system is the huge inter-annual variability of the number of ignitions. We sought to characterize the impact of overall ignitions on the point of collapse and, for the range of values observed between 2001 and 2010, we found a linear relationship between the number of ignitions and the point of collapse, with a decrease of 1.00% in the daily rates of ignitions leading to between 0.85% and 0.96% reduction in the number of required suppression teams, in the range that we studied. Since 98% of ignitions are of human origin (arson, negligence or accidental) this indicator provides a relevant threshold for the investment in prevention: a reduction of 1% in ignitions allows for a reduction of the point of collapse of one firefighting team, inverting the vicious circle more fire, more teams.

A final analysis that we performed aimed at comparing the point of collapse criterion with a cost criterion. Two simulation optimization analyses, with each of the criteria, led to the same result in the minimum number of crews, supporting the relevance of the point of collapse as a useful indicator in capacity decisions for a suppression system. Arriving early increases the probability of containing the fire in its initial stage and, additionally, if the resources are insufficient, the pressure to attack starting fires increases the premature abandonment of mop-up operations of already controlled fires, leading later to more rekindles and thus even more fires.

Acknowledgements

This work was financed by the European Regional Development Fund (ERDF) through the COMPETE Programme (Operational Programme for Competitiveness), by National Funds through the Fundação para a Ciência e a Tecnologia (FCT, Portuguese Foundation for Science and Technology) within projects «FCOMP - 01-0124-FEDER-022701» and «FIRE-ENGINE - Flexible Design of Forest Fire Management Systems/MIT/FSE/0064/2009», in the scope of the MIT Portugal Program, and by grupo Portucel Soporcel. FCT has also supported the research performed by Abílio P. Pacheco (Grant SFRH/BD/92602/2013).

We are deeply grateful to Rui Almeida (ICNF), Coronel Teixeira Leite and Alberto Costa (Porto CDOS), Manuel Rainha (ICNF), Paulo Fernandes (UTAD), and Ross Collins (MIT) for their invaluable input and feedback on this research.
We would also like to thank Tenente-Coronel António Paixão (GIPS), Paulo Bessa (GTF Penafiel), João Bandeirinha (Afocelca), Comandante José Morais (BV Paredes), Tânia Rodrigues Pereira (ICNF), Isidro Alves da Costa (Portucel), and Comandante Elísio Oliveira (Lisboa CDOS) for their enthusiasm and advice.

References

Ahrens, M (2003) The US fire problem overview report: leading causes and other patterns and trends. Fire Analysis and Research Division, National Fire Protection Association, 1 Batterymarch Park, Quincy, MA 02269-7471. Available at www.nfpa.org .

Ahrens, M (2010) Brush, Grass, and Forest Fires. Fire Analysis and Research Division, National Fire Protection Association No. USS89, 1 Batterymarch Park, Quincy, MA 02269-7471. Available at www.nfpa.org/osds .

Butry, DT (2007) Estimating the Efficacy of Wildfire Management Using Propensity Scores. Dissertation thesis, North Carolina State University.

Corcoran, J, Higgs, G, Brunsdon, C, Ware, A, Norman, P (2007) The use of spatial analytical techniques to explore patterns of fire incidence: A South Wales case study. Computers Environment and Urban Systems 31, 623-647.

Cumming, SG (2005) Effective fire suppression in boreal forests. Canadian Journal of Forest Research 35, 772-786.

Flynn, JD (2009) Fire Service Performance Measures. Fire Analysis and Research Division, National Fire Protection Association, 1 Batterymarch Park, Quincy, MA 02269-7471.

ISA (2005) 'Plano Nacional de Defesa da Floresta contra Incêndios: Um Presente para o Futuro.' Available at http://www.isa.utl.pt/pndfci/ (Archived by WebCite® at http://www.webcitation.org/5zjuImZzu) [Accessed 2011-03-07].

Islam, KS, Martell, DL, Posner, MJ (2009) A Time-Dependent Spatial Queueing Model for the Daily Deployment of Airtankers for Forest Fire Control. Infor 47, 319-333.

Karter, MJ (2011) False Alarm Activity in the U.S. 2010. Fire Analysis and Research Division, National Fire Protection Association, 1 Batterymarch Park, Quincy, MA 02269-7471. Available at www.nfpa.org/osds .

Martell, DL (2001) Forest Fire Management. In 'Forest Fires.' (Eds AJ Edward, M Kiyoko.) pp. 527-583. (Academic Press: San Diego)

Martell, DL (2007) Forest Fire Management. In 'Handbook Of Operations Research In Natural Resources.' (Eds A Weintraub, C Romero, T Bjørndal, R Epstein, J Miranda.) Vol. 99 pp. 489-509. (Springer US:

Mercer, DE, Haight, RG, Prestemon, JP (2008) Analyzing trade-offs between fuels management, suppression, and damages from wildfire. In 'The Economics of Forest Disturbances.' pp. 247-272.

Pacheco, AP (2011) Simulation Analysis of a Wildland Fire Suppression System. Thesis thesis, University of Porto.

Pacheco, AP, Claro, J, Oliveira, T A González-Cabán (Ed.) (2012a) 'Análisis de la Simulación de un Sistema de Extinción de Incendios Forestales, IV International Symposium on Fire Economics, Planning, and Policy: Climate Change and Wildfires.' Ciudad de México, México. (USDA Forest Service:

Pacheco, AP, Claro, J, Oliveira, T A González-Cabán (Ed.) (2012b) 'Simulation Analysis of a Wildfire Suppression System, IV International Symposium on Fire Economics, Planning, and Policy: Climate Change and Wildfires.' Ciudad de México, México, November 5-11, 2012. (USDA Forest Service. Available at

http://www.fs.fed.us/psw/publications/documents/other/psw_2012_gonzalescaban_FireSympAbstracts.pdf

Pacheco, AP, Claro, J, Oliveira, T (2014) Simulation analysis of the impact of ignitions, rekindles, and false alarms on forest fire suppression. Canadian Journal of Forest Research 44, 45-55.

Quince, AF (2009) Performance measures for forest fire management organizations: Evaluating and enhancing initial attack operations in the province of Alberta's Boreal Natural Region. Thesis thesis, University of Toronto.

San-Miguel-Ayanz, J, Moreno, JM, Camia, A (2013) Analysis of large fires in European Mediterranean landscapes: Lessons learned and perspectives. Forest Ecology and Management 294, 11-22.

Tedim, F, Remelgado, R, Borges, C, Carvalho, S, Martins, J (2013) Exploring the occurrence of mega-fires in Portugal. Forest Ecology and Management 294, 86-96.

Tu, YF (2002) Assessment of the Current False Alarm Situation from Fire Detection Systems in New Zealand and the Development of an Expert System for Their Identifications. Thesis thesis, University of Canterbury.

Yang, L, Gell, M, Dawson, C, Brown, M (2003) Clustering Hoax Fire Calls Using Evolutionary Computation Technology. In 'Developments in Applied Artificial Intelligence.' (Eds P Chung, C Hinde, M Ali.) Vol. 2718 pp. 644-652. Springer Berlin / Heidelberg)

Wooden buildings in Wildland-Urban Interface areas − flammability of solid woods used in wood-framed construction in Portugal

Valeria Reva[a], João Gomes[b], José J. Costa[b], A. Rui Figueiredo[b]

[a] *Centre for Forest Fire Research, ADAI-LAETA, Rua Pedro Hispano, 12, PT-3030-289 Coimbra, Portugal, valeria.reva@yahoo.com*
[b] *ADAI-LAETA, Department of Mechanical Engineering, University of Coimbra, Portugal. joao_antonio13@hotmail.com; jose.costa@dem.uc.pt; rui.figueiredo@dem.uc.pt*

Abstract
The problem of forest fires in the wildland-urban interface raises the issue of security of wood-framed constructions. The ability of external wooden walls to resist against fire exposure constitutes the framework of the present study. The flammability of the samples of wooden planks from framing lumber of *Pinus sylvestris, Apuleia leiocarpa* and *Pinus pinaster* used in a house construction in Portugal was assessed. The influence of the wood density on time to ignition, position and time of combustion phases (drying, pyrolysis and char combustion), mass loss decay, heat release rate and total heat released was evaluated.

Keywords*: wildland urban interface, flammability, wood-framed construction*

Introduction

In the United States of America, Canada, Australia and some countries in Northern Europe, wood-framed houses with up to two floors are the most common type of residential buildings, particularly in rural areas. According to Gustavsson *et al.* (2006), the market share of wood in construction of single-family houses constitutes 90-94% in North America, and 76-85% in Canada. It varies largely in Europe. In Scandinavian countries and Scotland, the share of timber-framed housing is 60-90% (Tykkae *et al.* 2010), while in Central Europe it ranges between 10 and 50% (Richter, 2012). Lowest values (<5%) were registered for Mediterranean countries (Gustavsson *et al.* 2006, Richter 2012). Regarding multi-family (multi-story) residential houses, the use of wood as the main structural material is much lower, with a market share of 2-10% in European countries and 4% in North America (Tykkae *et al.* 2010, Richter 2012).
Low construction costs, durability, thermal comfort, attractive facade, and limitless architectural possibilities of wooden houses encourage the use of wood in construction. The problem of GHG emissions and efficient ways of carbon storage enhances the usefulness of wooden buildings and the benefits of wood as a sustainable building material within the concept of green buildings (Naturally: wood 2011). Satisfactory performance of wood-framed buildings in earthquakes is another positive factor for use of wood in construction (Rainer and Karacabeyli 2000, Ceccotti 2008).
The efforts of industry, research activities, policies and governmental initiatives create the basis for wood-based construction systems, and statistics confirm the increased use of wood in residential and commercial buildings, especially in European countries. Portugal follows this trend, and the construction of wood-framed houses in rural areas is growing. Since 2006, an increase of the number of small enterprises working in wood-building construction sector was verified (Morgado *et al.*, 2011).
The problem of forest fires in the wildland-urban interface (WUI), which is critical in USA, Canada, Australia, Mediterranean countries and Portugal, raises the issue of security of wood-framed constructions, which constitutes the framework of the present study.
Many different types of soft and hard wood with a wide variety of characteristics are available for building construction. Soft and hardwoods are considerably different in flammability properties and combustion (Janssens 1991, Drysdale 2011, Cholin 1997, White and Dietenberger 1999, Van Loo and

Koppejan 2008). Wood type and species influence the combustion process through physical/chemical characteristics such as chemical composition, volatile content, density and porosity. The chemical composition is related with the gross calorific value, emissions and ash-content. Together with the volatile content, it also influences the thermal behaviour of wood. The density, varying within each tree and also significantly between hardwoods and softwoods, is related with the burning time and the total energy released. The porosity influences the burning rate.
Ignitability and heat release rate are determining parameters in the evaluation of fire hazards and combustibility of a material, and are essential for fire safety engineering towards a building design. The objective of the present work was to study the flammability of *Pinus sylvestris*, *Apuleia leiocarpa* and *Pinus pinaster* woods, used in wood-framed construction in Portugal. The influences of the wood density on the time to ignition, the time and duration of the combustion phases (drying, pyrolysis and char combustion), the mass loss decay, the heat release rate and the total heat released were evaluated.

Materials and methods

Wooden material

The samples of wooden planks from framing lumber used in a house construction were provided by the company Exotic House - Casas de Madeira, Lda (http://www.exotic-house.pt/Index.html). In the house under construction where the samples were collected (Figure 1), *A. leiocarpa* wood, imported from Brazil, was used for external walls, and *P. sylvestris* wood, imported from Northern Europe, for internal walls. The response of these wood species to heat flux exposure was compared with that of *P. pinaster* wood, the native species with a great potential for the construction industry.

Figure 1. Wood-framed house under construction

The density of wood at 12% moisture content for collected wooden planks was 870 kg/m^3 for *A. leiocarpa*, 472 kg/m^3 for *P. sylvestris*, and 582 kg/m^3 for *P. pinaster*.
To protect wood from insect and fungal attack, wooden planks were submitted to chemical treatment. Used for internal walls, low dense *P. sylvestris* wooden planks were treated by substances against insect and fungal attack and impregnation and thixotropic varnishes. Used for external walls, denser *A. leiocarpa* wooden planks were treated only by impregnation and thixotropic varnishes. Flammability of wooden samples with and without chemical treatment was studied.

Samples preparation

Samples of 60×60×35 mm and 60×60×20 mm were cut from wooden planks (Figure 2). To measure the variation of the temperature inside the wood sample, holes were drilled at 5, 15 and 25 mm from sample surface to fix thermocouples (Figure 3).

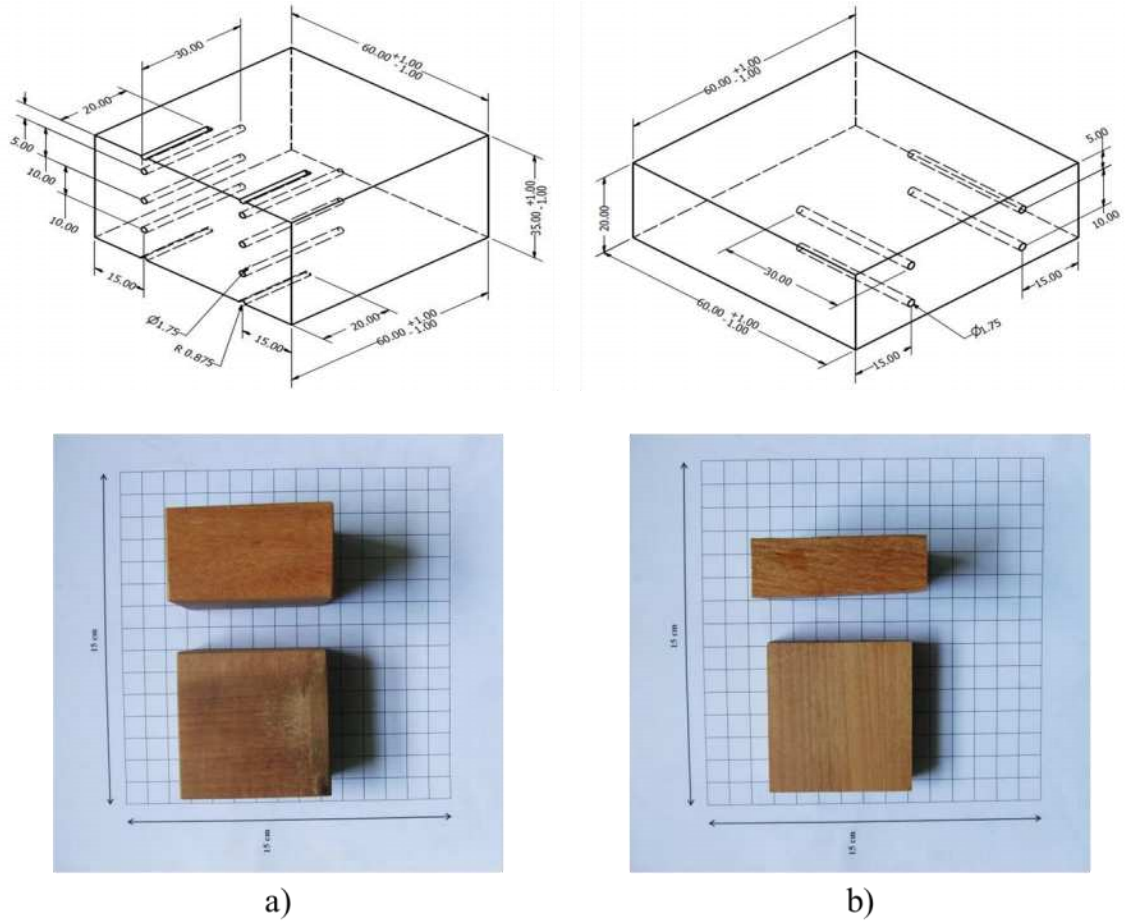

Figure 2. Two types of studied samples: a) 60×60×35 mm; b) 60×60×20 mm. In this figure, samples of Apuleia leiocarpa wood are presented.

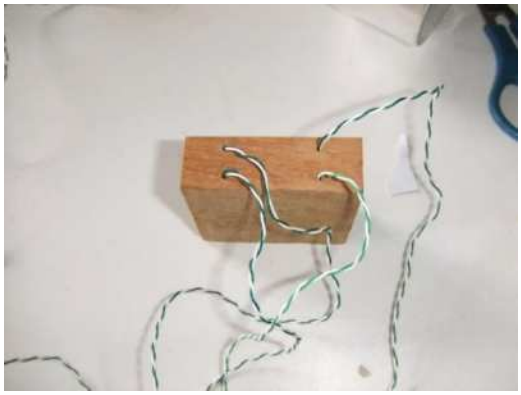

Figure 3. Apuleia leiocarpa wood sample with thermocouples fixed inside

2.3. Flammability test

Flammability tests were performed in a cone calorimeter (Figure 4) at a constant heat flux of 16kW/m^2. At least three replicates of each sample types were made. Samples were laterally wrapped in a single layer of aluminium foil and placed in horizontal orientation on calcium silicate support. A fuel sample was permanently radiated and an ignition source (pilot flame) provided. During the test, the sample mass was continuously measured using an AND FXi3000 electronic balance and the time variation of the temperature inside the wood samples was measured and registered using thermocouples, fixed inside and on the sample surface and connected to a PICO TC-08 data logger. Mean values of the studied parameters are reported.

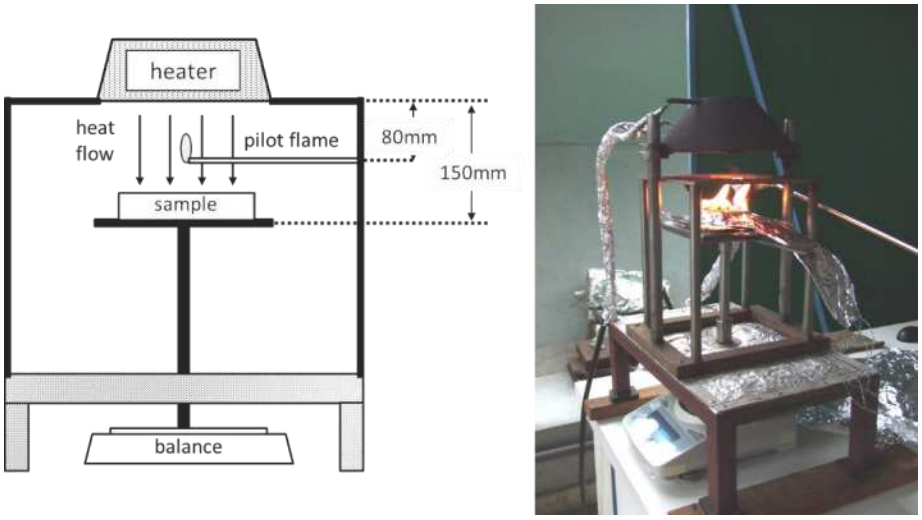

Figure 4. Sketch of cone calorimeter and experimental set-up for the flammability test

The heat release rate (HHR) was evaluated using the equation:

$$HRR = \dot{m} \times NCV$$

where $\dot{m} = -dm/dt$ is the mass loss rate and *NCV* is a net (or low) calorific value. Values of the *NCV* referred by Telmo and Lousada (2011) were assumed. For *P. pinaster*, the *NCV* was of 16.936 MJ/kg. For *P. sylvestris* and *A. leiocarpa*, mean values for softwoods (16.423 MJ/kg) and hardwoods (16.030 MJ/kg) were taken as a reference.

The total energy released was evaluated by:

$$q = \int_0^{t_f} \dot{q}\, dt = (m_i - m_f) \cdot NCV$$

where t_f is the time when the test was complete (flameout); $\dot{q}$ is the heat release rate; and m_i and m_f are the initial and final masses of the sample, respectively.

Results and discussion

3.1. Time to ignition

Figure 5 shows the results of time to ignition (t_i) measurements for *A. leiocarpa*, *P. sylvestris*, and *P. pinaster* wood samples, with and without chemical treatment. Characterized by highest density (870 kg/m^3), *A. leiocarpa* wood has longest time to ignition (t_i = 66 s) as compared with *P. pinaster* (582 kg/m^3, t_i = 28 s) and *P. sylvestris* (472 kg/m^3, t_i = 24 s) woods. Despite the small difference in density,

denser *P. pinaster* wood took a longer time to ignition than less dense *P. sylvestris* wood. Chemical treatment reduced time to ignition by 23% for *P. sylvestris* wood (24 s for non-treated and 18 s for treated wood) and 27% for *A. leiocarpa* (66 s for non-treated and 48 s for treated wood).

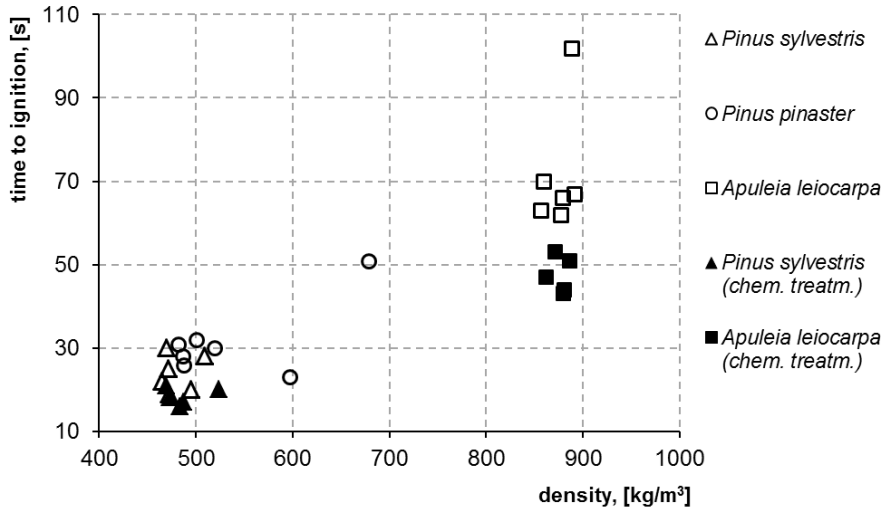

Figure 5 –Influences of density of wood and of chemical treatment on the time to ignition

Temperature variation

Figure 6 shows time-temperature curves for the surface and interior parts of the samples (at 5, 15 and 25 mm from the surface) for *P. sylvestris* and *A. leiocarpa* wood samples. The effect of wood density on the temperature variation, where higher density corresponds to lower temperature for all depth levels, was observed. The difference in the registered temperatures is greater on the sample surface and at a 5 mm depth, which may be explained by time to ignition, which is shorter for less dense *P. sylvestris* wood. Smaller and similar differences of temperature for *P. sylvestris* and *A. leiocarpa* wood were observed at 15 and 25 mm depths.

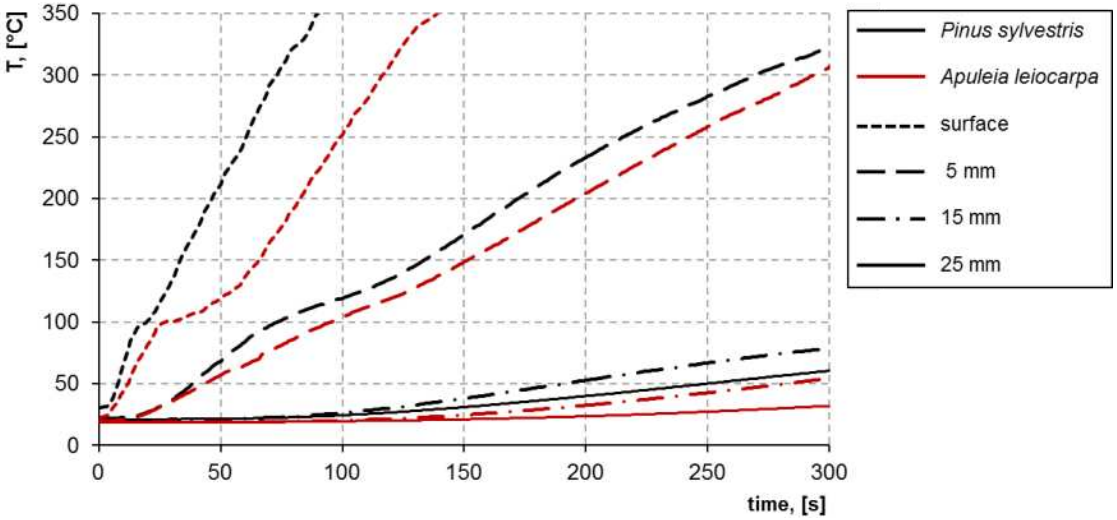

Figure 6. Temperature variation on the surface and inside the sample for Pinus sylvestris and Apuleia leiocarpa woods

The effect of chemical treatment on the temperature variation on the surface of the sample is more notable for *P. sylvestris* wood (Figure 7**)**. The difference between surface time-temperature curves for non-treated and treated *P. sylvestris* wood is higher as compared with *A. leiocarpa* wood, which may be related to the more complex chemical treatment applied to *P. sylvestris* wooden planks.

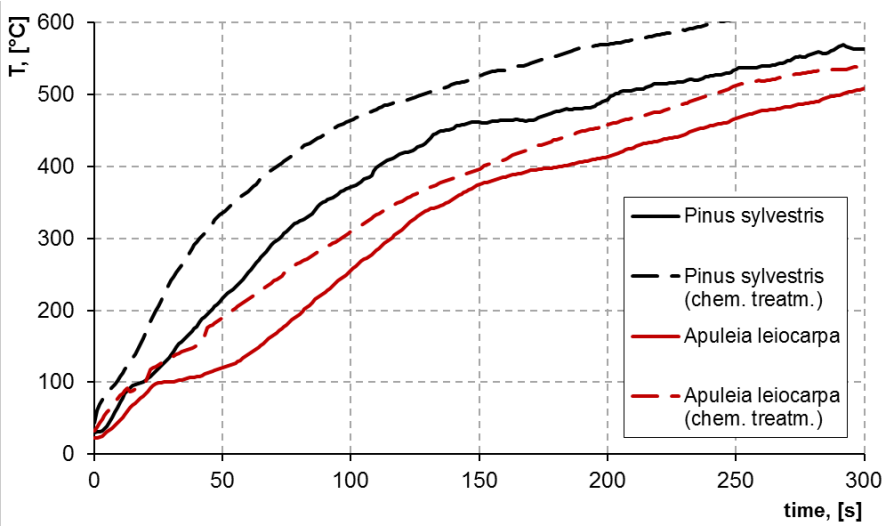

Figure 7. Temperature variation on the surface of the sample for Pinus sylvestris and Apuleia leiocarpa woods, with and without chemical treatment

3.3. Mass loss rate, heat release rate and total energy released

The mass loss ($\Delta m = m_f - m_i$), the heat release rate, HRR, and the total energy released (q) increase with increasing density of the wood. **Erro! A origem da referência não foi encontrada.** shows the mass loss rate and HRR curves for the studied wood species. Due to the greater time to ignition, the mass loss rate for *A. leiocarpa* wood starts growing later than for *P. sylvestris* and *P. pinaster* woods (Figure 8a). The highest maximum value of mass loss rate (0.051 g/s) was obtained for *A. leiocarpa* wood. Similar and lower values were found for *P. sylvestris* and *P. pinaster* wood (0.047 and 0.045 g/s, respectively). As the gross and net calorific values are lower for hardwoods than for softwoods, the difference in positioning of HRR curves as compared mass loss rate curves will decrease. Figure 8b shows that the HRR curve obtained for *A. leiocarpa* wood is less distant from HHR curves for *P. sylvestris* and *P. pinaster* wood. The maximum values of HRR are 214 kW/m^2 for *P. sylvestris*, 213 kW/m^2 for *P. pinaster* and 228 kW/m^2 for *A. leiocarpa* woods. The values of mass loss Δm and of the total energy released are 28.37 g and 10.53 MJ/kg for *P. sylvestris*, 32.28 g and 10.79 MJ/kg for *P. pinaster*, and 54.26 g and 12.12 MJ/kg for *A. leiocarpa*, respectively.

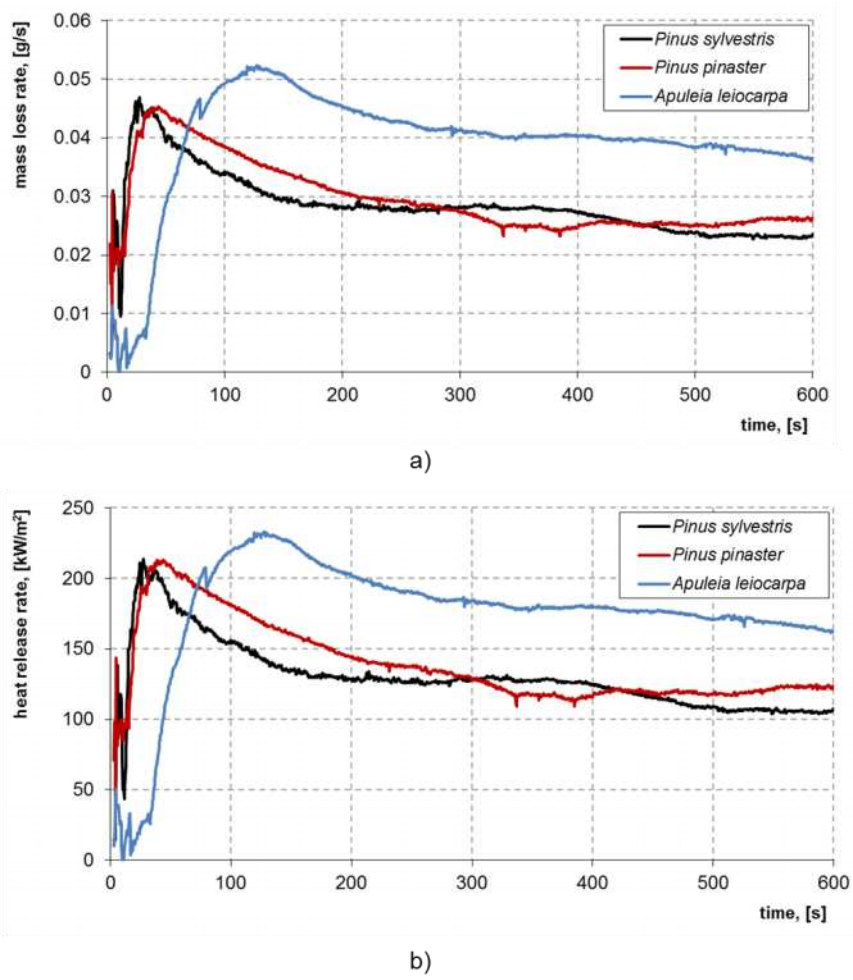

Figure 8. Mass loss rate (a) and heat release rate (b) for Pinus sylvestris, Pinus pinaster and Apuleia leiocarpa woods

Conclusions

Most hardwoods have a higher density than softwoods and, consequently, are more resistant to fire than softwoods. The use of hardwood for external walls in wood-framed buildings increases the resistance of these constructions to fire exposure. Flammability parameters such as time to ignition, mass loss, heat release rate, temperature of ignition and variation of temperature inside the wooden samples of one hardwood (*Apuleia leiocarpa*) and two softwood species (*Pinus sylvestris* and *Pinus pinaster*) used in construction of wood-framed buildings in Portugal were studied. Under a constant heat flux of 16kW/m^2, the time to ignition of *A. leiocarpa* wood (hardwood) was more than twice longer as compared with two softwood species (*P. sylvestris* and *P. pinaster*) and, consequently, a slower temperature rise on the wooden sample surface was verified. However, *A. leiocarpa* wood showed higher peak values of the mass loss and heat release rates, i.e. higher fire intensity, when ignition occurs. Higher mass loss rate also results on higher quantity of toxic gases resulting from combustion. The use of chemical treatments shortens the time to ignition, an effect that was more pronounced in the case of *A. leiocarpa* wood than with *P. sylvestris* wood. On the other hand, resistance of denser hardwood to insect and fungal attack allows moderate chemical treatment usage, which positively leads to lower temperatures on the surface of the wooden samples after ignition. Inside the wood samples, the temperature tends to present similar variations in softwoods and in hardwoods as the depth increases. Thus, for any wood type, the thickness of the wooden planks used in the building envelope construction may be an important parameter to control the temperature rise at the inner

surface of the external walls, in case of intense heat fluxes in the outside, and thus prevent ignition of flammable materials inside the construction.

Acknowledgments

Authors are thankful to Eng. José Neves of the company Exotic House - Casas de Madeira, Lda. for supplying wooden planks from framing lumber, and to Armindo G. Teixeira (UTAD) and António Cardoso (ADAI) for the technical support in preparing the samples.

References

Ceccotti A. New technologies for construction of medium-rise buildings in seismic regions: the XLAM case, Structural Engineering International, 2008, 2: 156–165.

Cholin JM. Wood and wood-based product. In: Fire protection handbook, 18th edition, NFPA-National Fire Protection Association, Quincy, MA, 1997, 3680p.

Drysdale D. An introduction to fire dynamics. John Wiley & Sons, 3rd edition, 2011, 574p.

Naturally:wood. Building green & The benefits of wood, British Columbia Forest Facts, 2011. (www.naturallywood.com)

Gustavsson L, Madlener R, Hoen HF, Jungmeier G, Karjalainen T, KlÖhn S, Mahapatra K, Pohjola J, Solberg B, Spelter H. The role of wood material for greenhouse gas mitigation. In: Mitigation and adaptation strategies for global change, 2006, 11(5): 1097-1127.

Janssens M. A thermal model for piloted ignition of wood including variable thermophysical properties. In: Cox G, Langford B. (eds.) Fire safety science – proceedings of the third international symposium, 1991, pp. 167-176.

Morgado L, Pedro JB, Cruz H, Pontífice P. Projecto e construção de casas de madeira em Portugal. Jonadas LNEC. Engenharia para a sociedade: investigação e inovação. Lisboa, 18-20 junho 2012. http://www.lnec.pt/organizacao/ded/nau/estudos_id/com_casasdemadeira.pdf

Rainer JH, Karavabeyli E. Performance of wood-frame construction in earthquakes. In: Proceedings of 12th World Conference on Earthquake Engineering, Auckland, New Zealand, 30 January - 4 February, 2000.

Richter K. Wood in construction – including multi-storey building. In: Proceedings 2012 IUFRO conference Divison5: Forest products, 2012, p. 31-34.

Van Loo S, Koppejan J. (eds). The handbook of biomass combustion and co-firing. Earthscan, 2008, UK: Earthscan.

White RH, Dietenberger MA. Fire safety. In: Wood handbook – Wood as an engineering material. U.S. Department of Agriculture, Forest Service, Forest Products Laboratory, 1999, 463p.

Chapter 4
Fire Risk Assessment and Climate Change

A new calibration for Fire Weather Index in Spain (AEMET)

Romero, R., Mestre, A., Botey, R.

Agencia Estatal de Meteorología (Aemet), Spain, rromerof@aemet.es, amestreb@aemet.es, mboteyf@aemet.es

Abstract
The Fire Weather Index (FWI) is an index based on meteorology. The system consists of six components and it depends on weather variables taken each day at 12 UTC (or forecasted for 12 UTC): temperature, relative humidity, wind speed and rain during the previous 24 hours. FWI is an accumulative index, that is, subindexes values for a day D are used for the calculation of the final index the following day D+1. The procedures for the calculation for Iberian Peninsula and Balearic Islands were initialized by AEMET in 2008 March, being executed daily without interruption since then. Canarias Islands procedures are being executed since 2013 May. Procedures include analysis for day D and forecasts for day D+1, D+2 and D+3 in a 0.5ºx0.5º horizontal resolution grid cells with data provided by the HIRLAM numerical weather prediction model.
FWI values calculated for a determinate localization have no meaning for themselves. It's necessary to make a correspondence between the danger classes and those FWI values in order to calibrate it. For this, five danger classes split has been calculated only from a climatological point of view. Each class or risk level corresponds with a range of values of FWI between different percentiles. Thus, fire low risk corresponds with FWI values below its percentile 40; moderate risk with FWI values between percentile 40 and 65; high risk between percentile 65 and 85; very high risk between percentile 85 and 95 and extreme fire risk above its percentile 95. In the calculation of the different percentiles, a data period from May 2008 until December 2013 has been used. This period will be updated with most recent values according to the month pass.

***Keywords**: FWI, fire risk, danger classes, calibration, validation*

Introduction

The purpose of the Fire Weather Index (FWI) system, based on the Canadian system, is to account for the effects of weather on forest fuels and forest fires. The system consists of six components: three primary subindexes representing fuel moisture and following daily changes in the moisture contents of three classes of forest fuel with different drying rates, two intermediate subindexes representing rate of spread and fuel consumption, and a final index representing fire intensity as energy output rate per unit length of fire front.
The three primary subindexes are, according to *Van Wagner, C.E., (1987)* :

- Fine Fuel Moisture Code (FFMC), which represents the moisture content of litter and other cured fine fuels in a forest stand, in a layer of dry weight about 0.25 kg/m^2.
- Duff Moisture Code (DMC), which represents the moisture content of loosely compacted, decomposing organic matter weighing about 5 kg/m^2 when dry.
- Drought Code (DC), which represents a deep layer of compact organic matter weighing perhaps 25 kg/m^2 when dry.

Those three primary subindexes plus wind are combined in pair to produce the two intermediate subindexes, ISI and BUI. Final index, FWI, is formed by a combination of the two intermediate subindexes. According to *Van Wagner, C.E., (1987)* :

- Initial Spread Index (ISI), a combination of wind and the FFMC that represents rate of spread alone without the influence of variable quantities of fuel.
- Buildup Index (BUI), a combination of the DMC and the DC that represents the total fuel available to the spreading fire.

- Fire Weather Index (FWI), a combination of the ISI and the BUI that represents the intensity of the spreading fire as energy output rate per unit length of fire front.

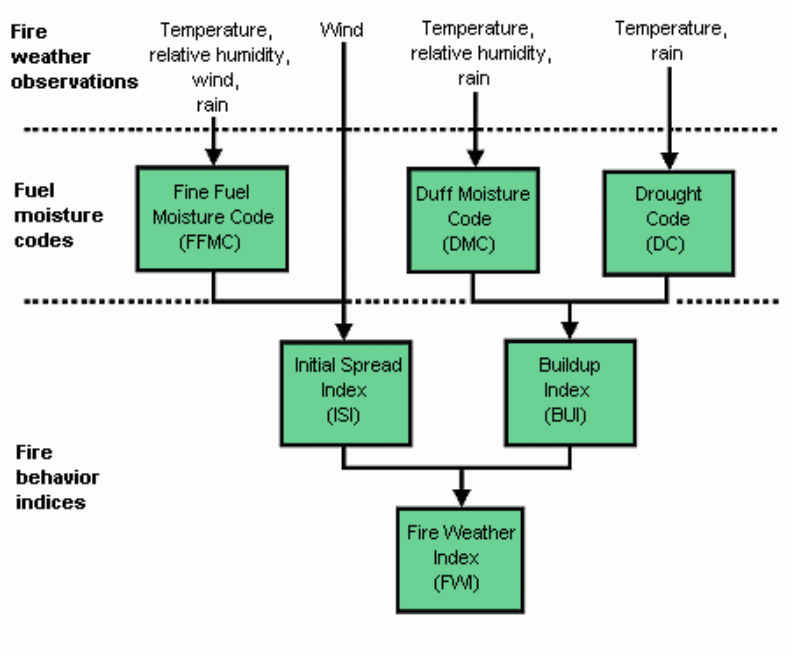

Figure 1. FWI system components.

The system depends on weather variables taken each day at noon Universal Time Coordinated UTC (or forecasted for 12 UTC): temperature, relative humidity, wind speed and 24 hours-precipitation values. FWI is an accumulative index, that is, subindexes values for a day D are used for the calculation of the final index the following day D+1. Moreover, in order to guarantee the estimations stability, calculations must be initialized in a high rain period, when fine fuel moisture content is maximum.
Two different procedures are used in AEMET in order to calculate the FWI system components: *Iberian Peninsula and Balearic Islands* on the one hand and *Canary Islands* on the other hand.
Procedures for the calculation for *Iberian Peninsula and Balearic Islands* were initialized by AEMET in 2008 March, being executed daily without interruption since then. Procedures include analysis for day D and forecasts for day D+1(H+24), D+2(H+48) and D+3(H+72) in a 0.05ºx0.05º horizontal resolution grid cells for D+1 and 0.16ºx0.16º horizontal resolution grid cells for D+2 and D+3. Meteorological data are provided by the HIRLAM numerical weather prediction model. *Canary Islands* procedures are being executed since 2013 May. Procedures include analysis for day D and forecasts for day D(H+12), D+1(H+36) and D+2(H+60) in a 0.05ºx0.05º horizontal resolution grid cells for D and D+1 and 0.16ºx0.16º horizontal resolution grid cells for D+2. Meteorological data are provided by the HIRLAM numerical weather prediction model.

Examples of weather variables provided by HIRLAM:

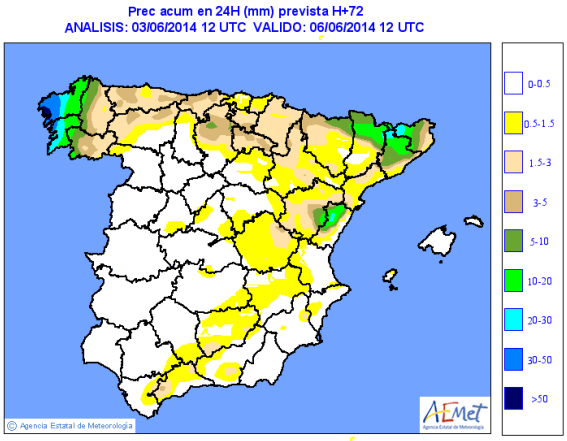

Figure 2. Precipitation during the previous 24 hours

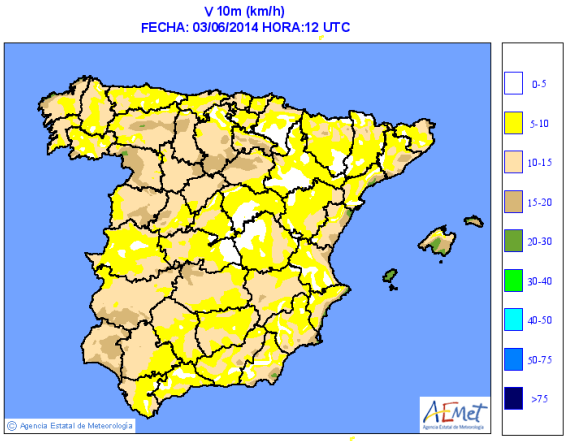

Figure 3. 10 m wind speed

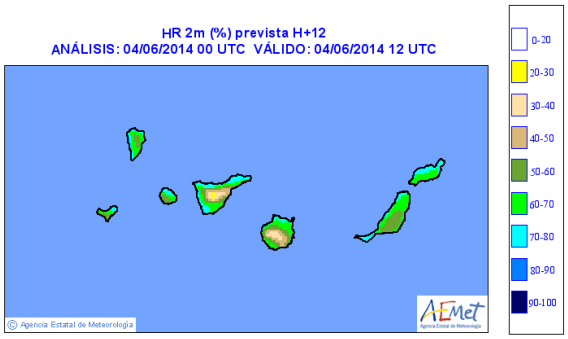

Figure 4 –2m Temperature

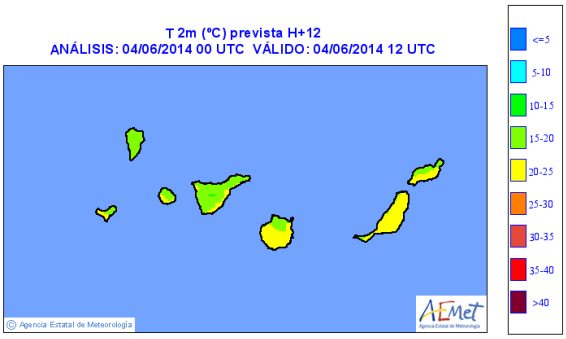

Figure 5. 2m Relative Humidity

Examples of subindexes for Iberian Peninsula/Balearic Islands and Canary Islands:

Figure 6 –Drought Code (DC)

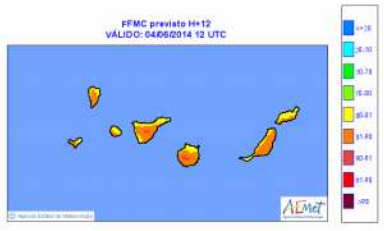

Figure 7 –Fine Fuel Moisture Code(FFMC)

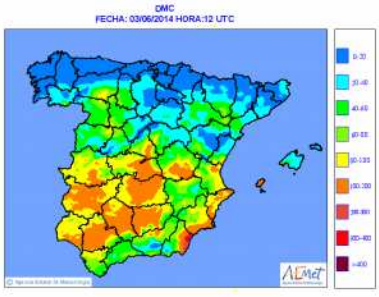

Figure 8 –Duff Moisture Code (DMC)

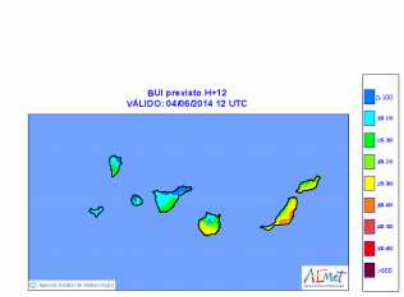

Figure 9 –Buildup Index (BUI)

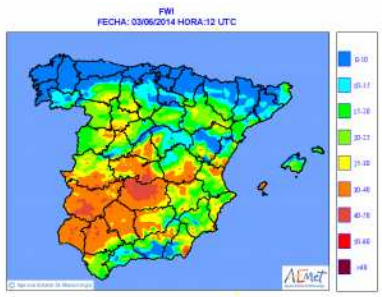

Figure 10–Fire Weather Index(FWI)

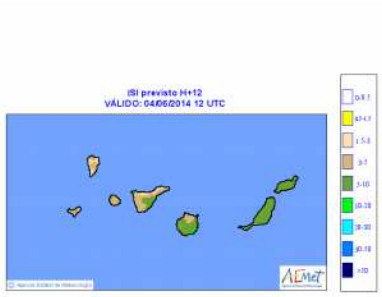

Figure 11 –Initial Spread Index(ISI)

Methods

FWI values calculated for a determinate localization have no meaning for themselves. It's necessary to make a correspondence between the danger classes and those FWI values. Furthermore, non meteorological factors such as type, quantity and fuel distribution must be taken in account when assigning danger classes in the different areas. In order to represent a range of climatological conditions, FWI values are calculated using daily weather data provided by the numerical weather prediction model HIRLAM during several years. Cutoff values for the different danger classes are calculated from the value at different percentiles.

Old calibration Peninsula and Balearic Islands.

Five danger classes have been established in AEMET: low, moderate, high, very high and extreme fire risk level. Until 2013, according to that division, FWI had been calibrated for the location of a set of observatories and automatic meteorological stations by setting four threshold values for delimitating those five danger classes. From those four threshold values, by interpolating, a file with the four threshold values in every grid point was generated. Fire risk level is calculated by comparing, in every grid point, FWI daily value with the corresponding four threshold values for that grid cell. That calibration has been carried out by starting off FWI values at meteorological stations and historical records of burned area of fires surrounding those stations. A 10 years period (1997-2006) only with months between June and October was considered.

New calibration Peninsula and Balearic Islands.

However, as we have considered that the fire risk level provided should only take into account meteorological and climatological factors, it's necessary to try another different calibration according to the above requirements. For this, five danger classes division has been calculated only from a climatological point of view. Each class or risk level corresponds with a range of values of FWI between different percentiles. Thus, fire low risk corresponds with FWI values below its percentile 40; moderate risk with FWI values between percentile 40 and 65; high risk between percentile 65 and 85; very high risk between percentile 85 and 95 and extreme fire risk above its percentile 95. In the calculation of the different percentiles, a daily data period from May 2008 until December 2013 has been used by using weather data provided by the numerical weather prediction model HIRLAM. This period will be updated with most recent values according to the month pass.

FWI values have been separated in two different periods; from May to October, and from November to April. Thresholds obtained for May-October period have been generated from FWI series values ranging from April to November during 2008-2013, thus, 8 months. In the other hand, thresholds generated for November-April period have been calculated from the whole FWI values series(2008-2013).

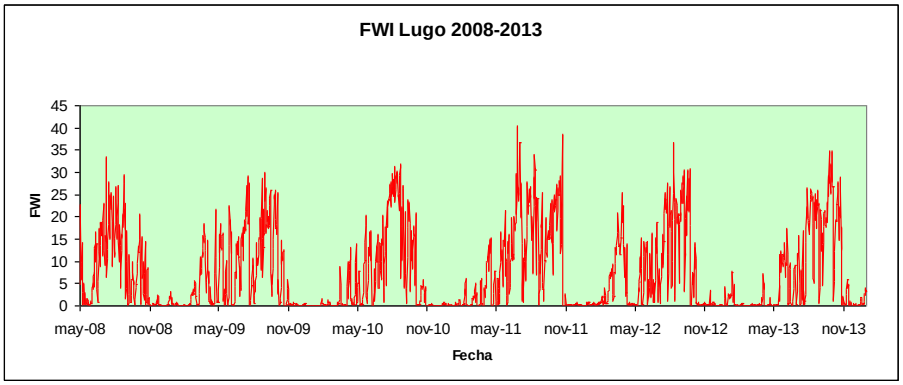

Figure 12. FWI values from January 2009 to December 2013

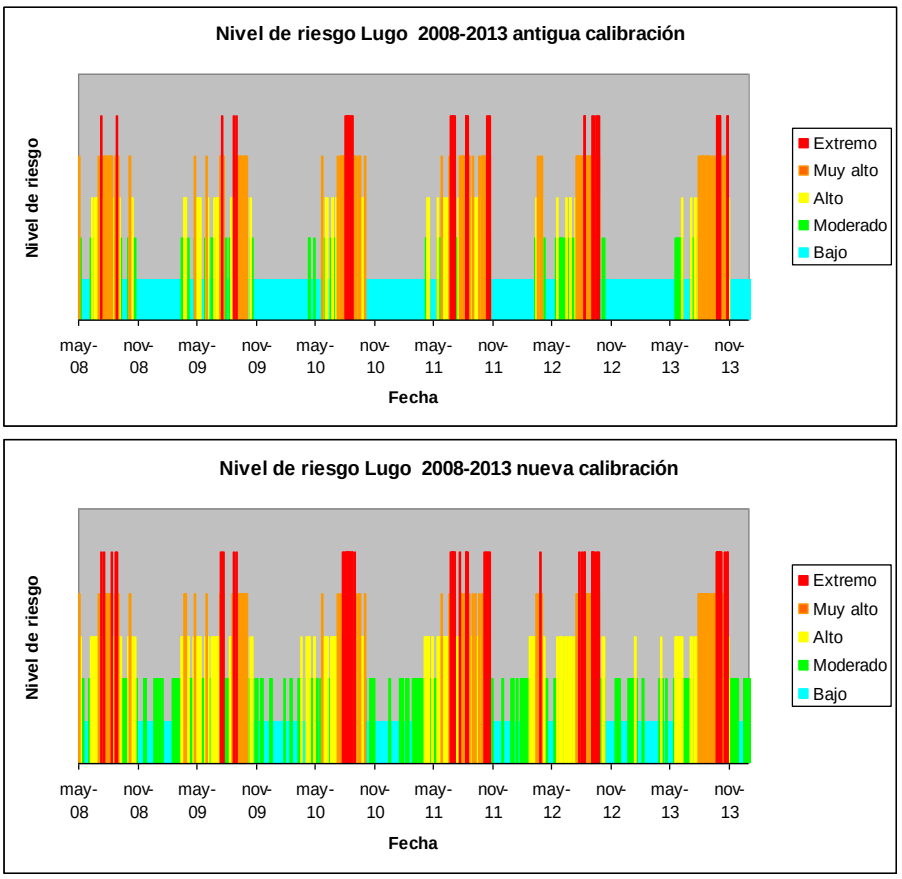

Figure 13. Risk levels January 2009 to December 2013(old calibration-top/new calibration-bottom)

.

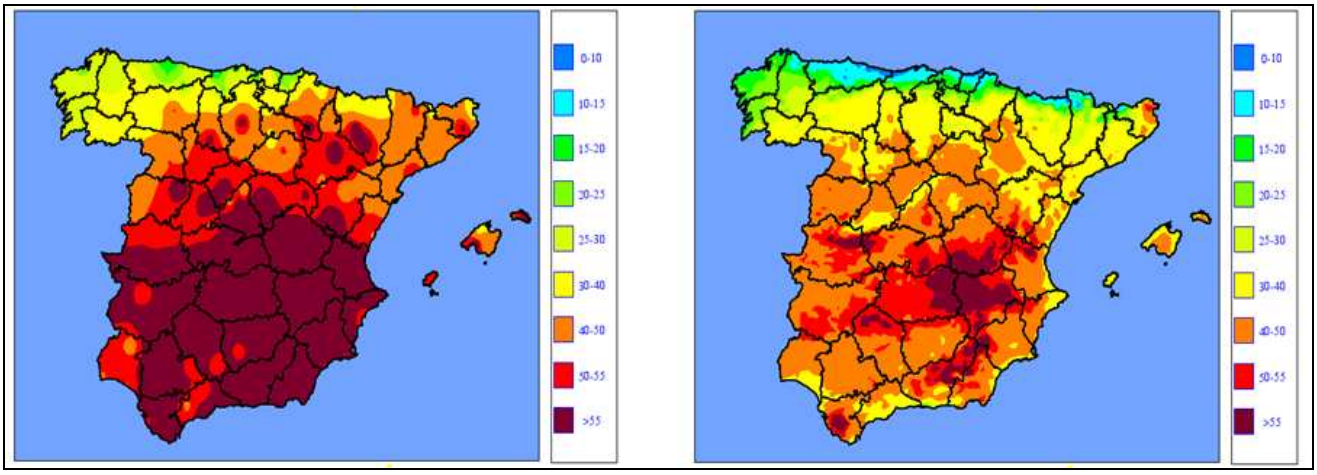

Figure 14. Percentile 95 FWI values. Old Calibration (left / New Calibration(right).

2.3. Old calibration Canary Islands.

Unlike the old calibration previous to 2014 calculate in Peninsula and Balearic Islands, Canary Islands calibration has always been calculated taking into account only meteorological and climatological factors. Again, five danger classes have been established: low, moderate, high, very high and extreme fire risk level. Each class or risk level corresponds with a range of values of FWI between different percentiles. Thus, fire low risk corresponds with FWI values below its percentile 40; moderate risk with FWI values between percentile 40 and 65; high risk between percentile 65 and 85; very high risk between percentile 85 and 95 and extreme fire risk above its percentile 95. In the calculation of the different percentiles, a daily data period from March 2009 until February 2011 has been used by using weather data provided by the numerical weather prediction model HIRLAM.

2.4. New calibration Canary Islands.

The only different with the old calibration is the extension of the period from January 2009 to December 2013. Due to the special characteristic of the Canary Islands climate, FWI values used for percentile calculation and the threshold generation are ranging for the whole year.
This period will be updated with most recent values according to the month pass.

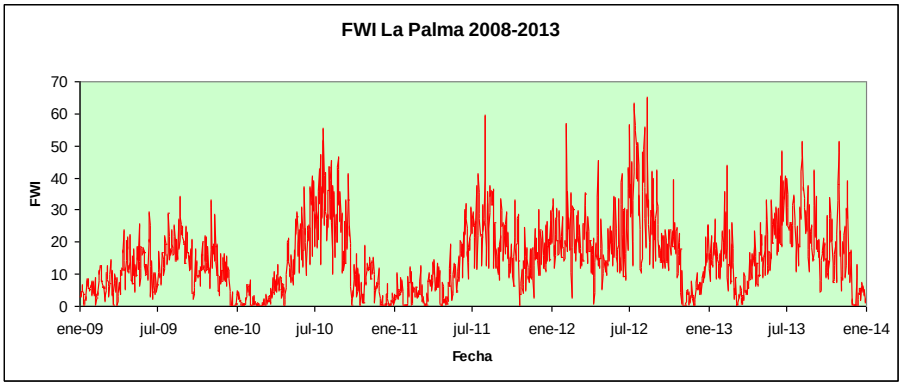

Figure 15– FWI values from January 2009 to December 2013

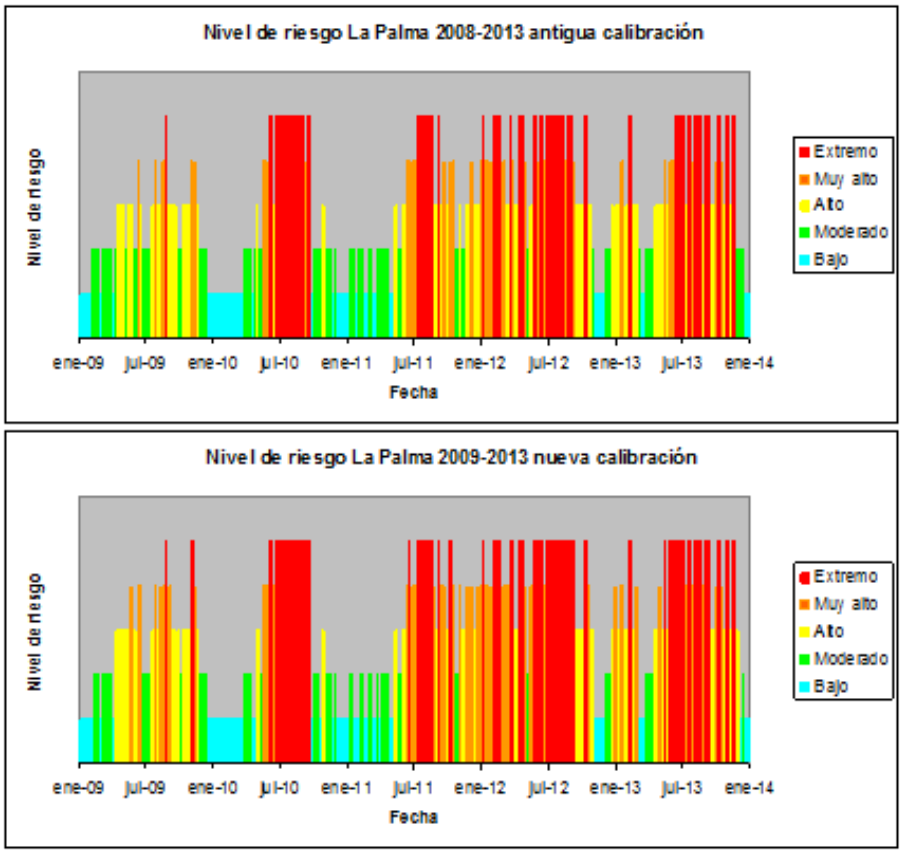

Figure 16. Risk levels January 2009 to December 2013(old calibration-top/new calibration-bottom).

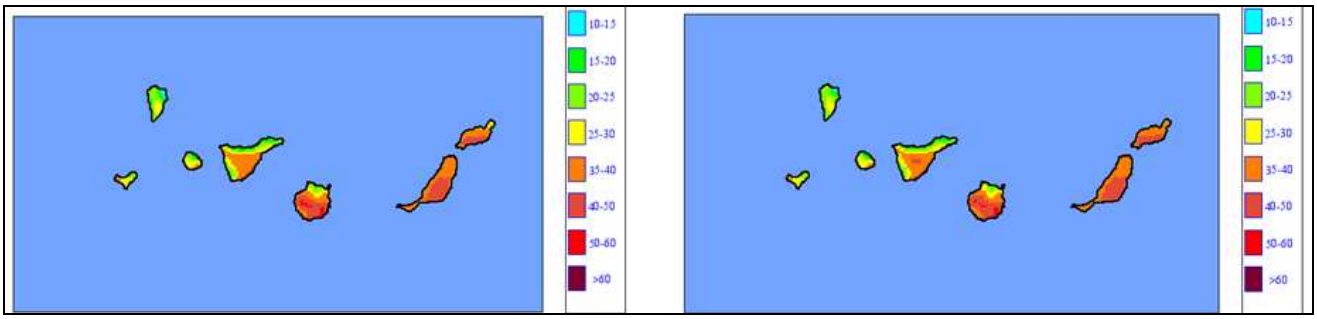

Figure 17- Percentile 95 FWI values. Old Calibration (left)/ New Calibration(right).

3. Results.

3.1. Iberian Peninsula and Balearic Islands.

Fire occurrences during 2010 year have been used in order to validate the new calibration behaviour, taking only into account those ones with burned area greater than 5 hectares, what makes us to have 230 fires spread all over the Iberian Peninsula and Balearic Islands.

For each fire coordinates, FWI value in the nearest grid point has been calculated. Then, two risk levels have been associated to that FWI value, one calculated with the old calibration, and another one calculated with the new calibration. Thresholds obtained for May-October period have been generated from FWI series values ranging from April to November during 2008-2013, thus, 8 months. In the other hand, thresholds generated for November-April period have been calculated from the whole FWI values series (2008-2013). In figures 18 and 19 results are presented by comparing the two different

calibrations for the whole 2010 year. As we can see, the risk level associated to each fire with the new calibration appears, in most of the fires, in a higher danger class.

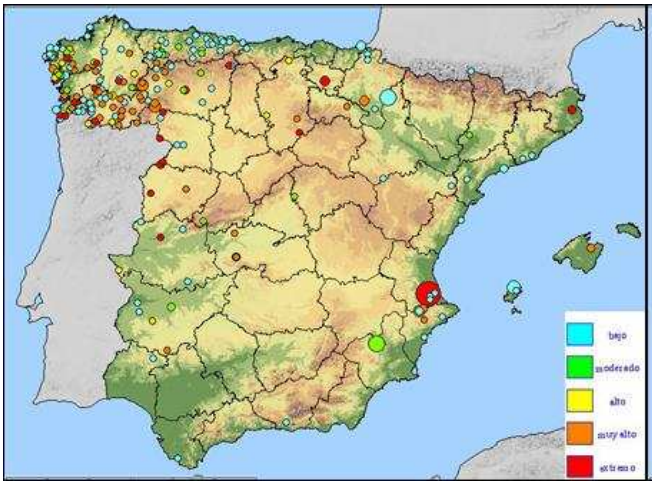

Figure 18. Fire risk level during 2010 old calibration

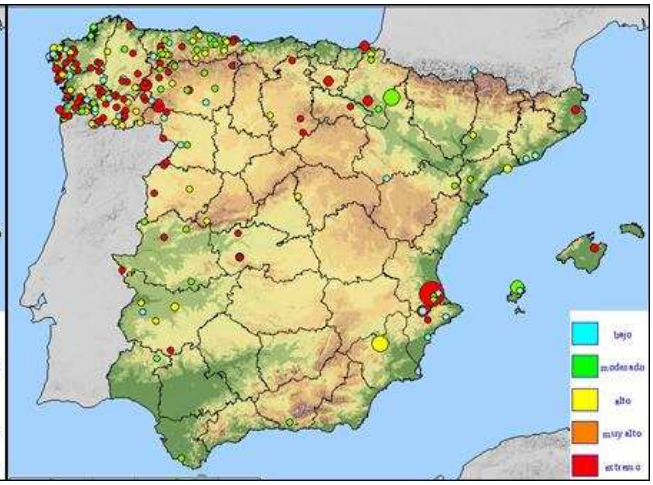

Figure 19. Fire risk level during 2010 new calibration

Later, fire data records were validated by separating two different periods; from May to October, and from November to April. In the next figures we can see the different calibrations for the two different periods as well as the fire risk level associated to each fire.

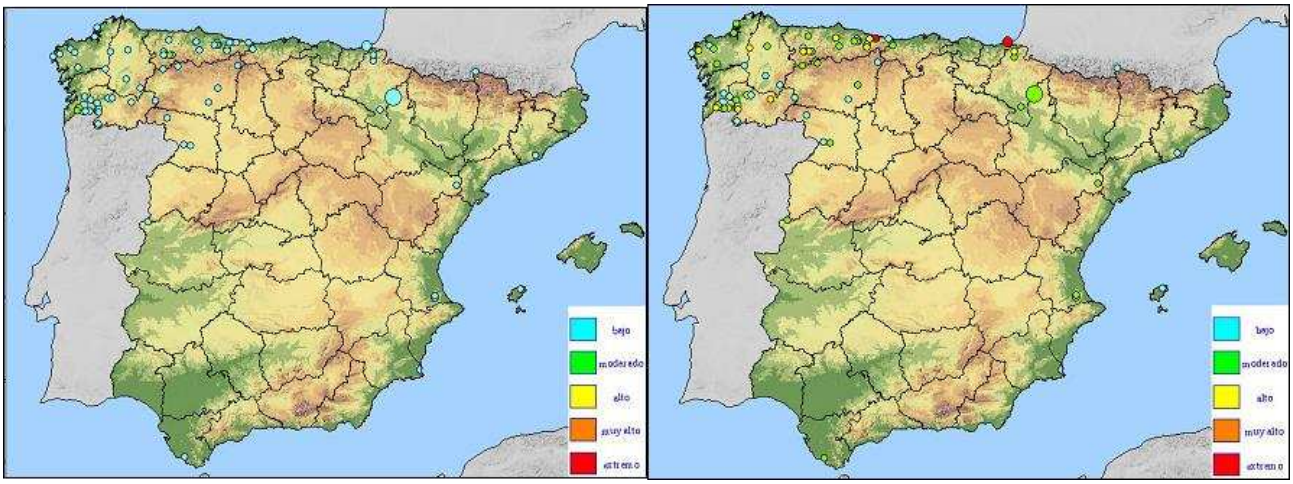

Figure 20. Fire risk level during November-April 2010 period with old (left) and new (right) calibration

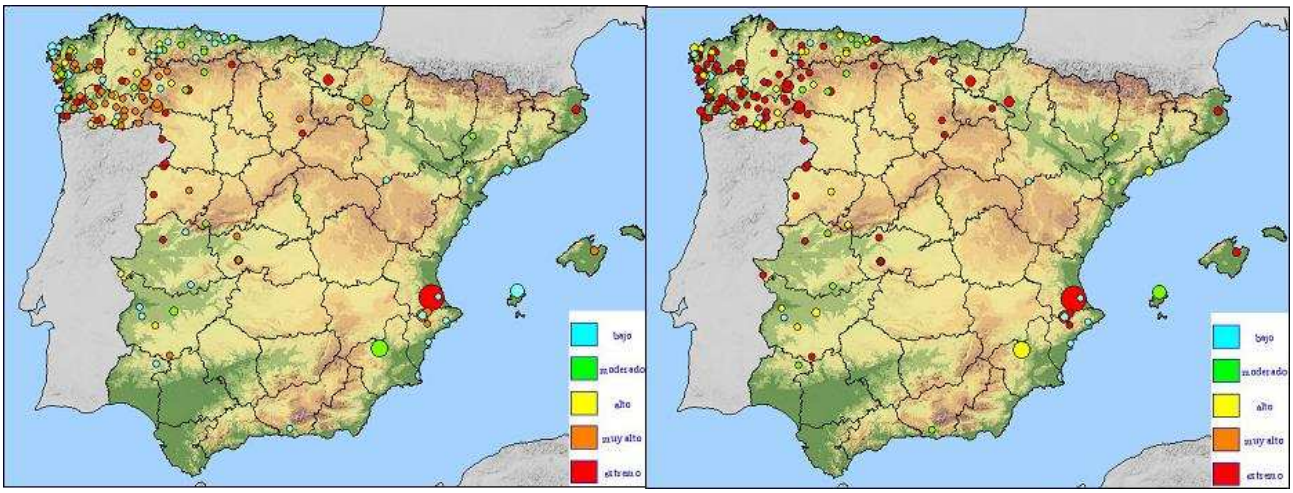

Figure 21. Fire risk level during May-October2010 period with old (left) and new (right) calibration.

Canary Islands.

Same validation procedures have been used for the fire occurrences in the Canary Islands during 2010 year, by comparing the old and the new calibration. Results are presented in the next figures. We can observe similar results to the ones obtained in the Iberian Peninsula and Balearic Islands, where the risk level associated to each fire with the new calibration appears, in most of the fires, in a higher danger class.

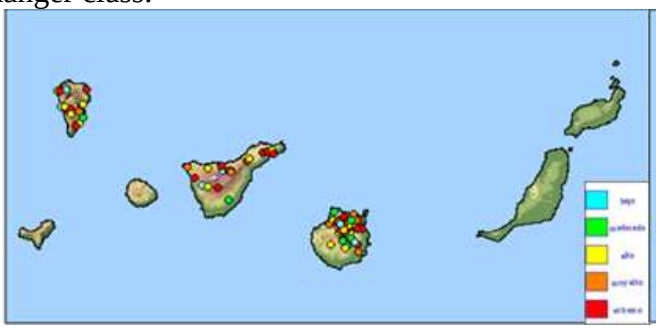

Figure 22. Fire risk level during 2010 old calibration

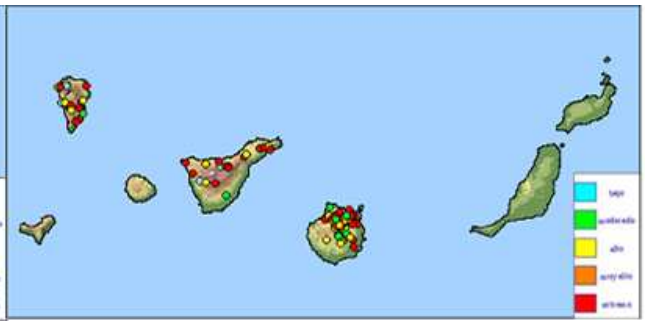

Figure 23. Fire risk level during 2010 new calibration

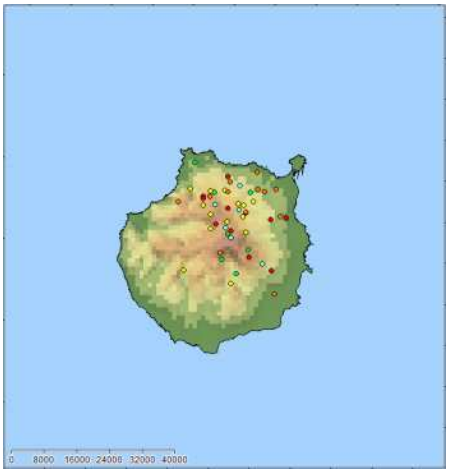

Figure 24. Fire risk level during 2010 old calibration

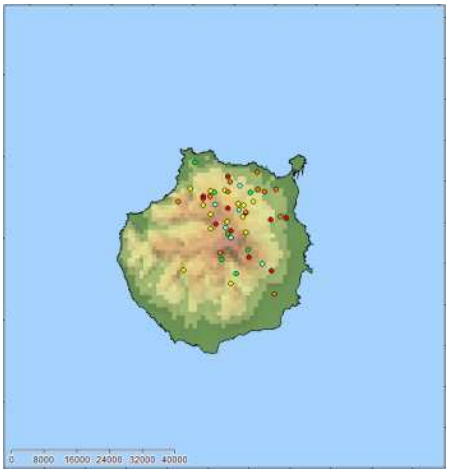

Figure 25. Fire risk level during 2010 new calibration.

References.

Heinsch, F. A. Andrews, P. L., Kurth, L. L. 2009 *"Implications of using percentiles to define fire danger levels,"* in Proceedings of the 8th Symposium on Fire and Forest Meteorology, Kalispell, Mont, USA.

Mestre, A., Allue, M., Peral, C., Santamaría, R., Lazcano, M. 2008. *Operational Fire Danger System in Spain*, International Workshop on Advances in Operational Weather Systems for Fire Danger Rating. GOFC-GOLD/WMO. Edmonton(Canada), 14-16 July 2008.

Van Wagner, C.E., 1987. *Development and structure of the Canadian Forest Fire Weather Index System. 1987.* Canadian Forestry Service, Headquarters, Ottawa. Forestry Technical Report 35, 37 pp.

Van Wagner, C. E., Pickett, T. L. 1987. *Equations and Fortran program for the Canadian Forest Fire Weather Index System*. Canadian Forestry Service, Forestry Technical Report 33, Ottawa.

Assessing the association of drought indicators to impacts. The results for areas burned by wildfires in Portugal

Carlo Bifulco[a], Francisco Rego[a], Susana Dias[a], James H. Stagge[b]

[a] *Universidade de Lisboa, Instituto Superior de Agronomia, Centro de Ecologia Aplicada Prof. Baeta Neves/InBio; Tapada da Ajuda,1349-017 Lisboa, Portugal; ceabn@isa.ulisboa.pt*
[b] *University of Oslo, Department of Geosciences, Oslo, Norway; j.h.stagge@geo.uio.no*

Abstract
In the FP7 European project "DROUGHT-R&SPI - Fostering European Drought Research and Science-Policy Interfacing" CEABN works together with partners from other eight countries on monitoring and prediction tools to manage drought impacts at different scales.
The wildfire extent was one of the impacts studied in relation to recent drought events in Portugal. The identification of specific periods where shortage of water is relevant to the extent of wildfires is of prime importance to counteract drought impacts. Meteorological droughts can be characterized using indices such as SPI (Standardized Precipitation Index). In this study we explored the links between area burned by wildfires and meteorological drought indicators using data series from mainland Portugal. Significant correlations were found between wildfire burned area and drought indices (SPIs 1, 3 and 6), which can be useful to understand and manage the risk of forest fires.

Keywords: Portugal, drought, SPI, forest fires

Introduction

Drought is a recurrent climatic event occurring worldwide and intensively perceived by the Mediterranean countries (Pereira *et al.*, 2009). Projections indicate an increased in the observed trend (Sousa *et al*., 2011) towards drier conditions for this region (Van Lanen *et al.*, 2013) with substantial foreseen impacts that need to be properly addressed (EEA, 2012).
"DROUGHT-R&SPI - Fostering European Drought Research and Science-Policy Interfacing" is a FP7 European project aiming at improving drought preparedness across Europe (http://www.eu-drought.org). In this framework, Portugal, along with eight other countries, works on monitoring and prediction tools to manage drought impacts at different scales (from pan-European to sub-national or river basin level).
Meteorological droughts can be characterized using indices such as SPI, Standardized Precipitation Index (Moreira *et al.*, 2008). They calculate anomalies in precipitation, accumulated over several periods: 1, 2, 3, 6, 9, 12, 24 months, compared with its multiyear average (Zargar *et al.*, 2011). In the last 70 years there were ten major drought events in mainland Portugal: 1944-45 (extreme), 1948-49, 1964-65, 1974-76, 1980-83, 1990-92, 1994-95, 1998-99, 2004-2005 (extreme) and 2012 (extreme). The drought episode of 2004-2005 can be considered the most severe in terms of meteorological data, extent of the area affected, and impacts on different socio-economic and environmental sectors (Comissão para Seca 2005, 2006). The wildfire extent was one of the most important impacts of recent drought events in Portugal (MAMAOT, 2013). In fact, precipitation deficits, by reducing soil and fuel moisture, ease up the ignition and spread of forest fires (Shoennagel *et al.*, 2004; Gouveia *et al.*, 2009; Jurdao *et al.*, 2012). The identification of specific periods where the shortage of water is crucial to maximise wildfire extent is of prime importance for counteract drought impacts. However, although the climate drivers of area burned have been extensively studied, both in Portugal (Viegas & Viegas, 1994; Pereira *et al.* 2005; *Trigo et al.*, 2006) and elsewhere (e.g., Flannigan & Harrington, 1988;

Pausas, 2004; Littel *et al.*, 2009), the links between drought indices and wildfire extent have only recently been modeled (e.g., Stagge *et al*., 2014).
The objective of this study is thus to explore the link between area burned by wildfires and meteorological drought indicators using long-term data series (fire and climate) from Portugal analysed at sub-national level (NUTS2).

Methods

The **Standardized Precipitation Index (SPI) as a** drought indicator

The Standardized Precipitation Index (SPI) (McKee *et al.* 1993) is a probability index that was developed to give a representation of abnormal wetness and dryness, and compares precipitation with its multiyear average. It is essentially a seasonally normalized, backwards-looking moving average of precipitation. SPI overcomes the difficulty of comparing sites with different climate and highly variable precipitation distributions by transforming the precipitation distribution record to a normal distribution (Paulo & Pereira, 2006). The first step in calculating the SPI is to determine a probability density function that describes the long term time series of precipitation observations. The series can be for any time duration (typically for total precipitation of 1, 2, 3, 6, 9, 12, 24 months). Once the probability density function is determined, the cumulative probability of an observed precipitation amount is computed. The inverse normal Gaussian function, with mean zero and variance one, is then applied to the cumulative probability. The result is the SPI (Guttman, 1999).
Positive SPI values indicate a wetter than typical period, i.e. accumulated precipitation greater than the median, while negative SPI values indicate a dryer period with less precipitation than normal. A value of zero corresponds to the median accumulated precipitation. The magnitude of the departure from zero is a probabilistic measure of the severity of a wet or dry event that can be used for risk assessment (Paulo *et al.,* 2012). The time series of the SPI can be used for drought monitoring. Accumulated values of the SPI time series are used to analyze drought severity. Threshold values of the SPI define drought beginning and ending (Moreira *et al*., 2008). If SPI reaches a value of -1 or less a drought is said to have occurred. Different duration of SPI reflected different phenomena (Zargar *et al.*, 2011). One month SPI (SPI1) is related to short-term conditions as short-term soil moisture and vegetation stress during growing season. Three months SPI (SPI3) is related to short/medium-term conditions, roughly approximating seasons, while the six-month SPI (SPI6) shows the precipitation across distinct seasons. When the nine months SPI (SPI9) is less than -1.5 substantial impacts occur in agriculture and other sectors, one year SPI (SPI12) is tied to evolution of streamflows and reservoir and groundwater levels (Paulo & Pereira, 2006).

To explore correlations of drought with the areas burned by forest fires in Portugal we used monthly SPIs of different duration: SPI1, SPI2, SPI3, SPI6, SPI9 and SPI12. These SPI values were calculated on the basis of long-term series of monthly precipitation (1979-2009) based on the WFDEI (Watch Forcing Data ERA-Interim) for each NUTS2 (Nomenclature of Territorial Units for Statistics level 2) area of the Portuguese mainland (Norte, Centro, Lisboa, Alentejo and Algarve).

2.2. **Proportional change to standardize continuous variables as crop or forest fire in long-term data series**

Monthly SPIs were used as candidate explanatory variables to model wildfire extent, defined by area burned. Annual area burned by wildfires in Portugal (1985-2010) is the dependent variable, extracted at the NUTS2 level from the European Fire Database (compiled by the EU JRC) and used after log-transformation to rescale the data.

Data from long-term series as areas burned by wildfires typically do not fluctuate around a constant mean. Therefore, in order to detect the signal of drought in wildfire areas, it is important to remove

these multi-annual trends that are not related to drought. This was accomplished by using moving averages, whose length was determined by the structure of the time series data as detected by autocorrelation analyses. Burned area anomaly was defined as:

$$\text{Log(fire area)}_{\text{anomaly}} = \text{Log(fire area)}_{\text{observed}} - \text{Log(fire area)}_{\text{mov.average}}$$

The standardization was accomplished by a proportional change as:

$$\text{Log(fire area)}_{\text{proportional change}} = \\ = (\text{Log(fire area)}_{\text{observed}} - \text{Log(fire area)}_{\text{mov.average}}) / \text{Log(fire area)}_{\text{mov.average}}$$

Proportional change has a minimum value of -1 (when there is no burned area in that year), zero when the observed burned area is equal to the expected value (the moving average), and greater than 0 when the observed burned area is higher than expected.

Once defined the moving average period, we performed a correlation analysis (Pearson r) to detect the most significant links between monthly SPIs (of the current year and the last 3 months of the previous year) and the proportional change of log-transformed annual burned area. This later variable was in turn modelled using a multiple regression model (stepwise method) with all the SPIs as candidate independent variables (Draper & Smith, 1998). Correlation values and regression coefficients were considered statistically significant for $p<0.05$.

Results and discussion

The analyses of long-term series for burned areas (log transformed) in Portugal indicated that statistically significant partial autocorrelations of these data exist for lags 1 and 2 years. These results suggested that four year moving average (2 previous years and 2 following years) was adequate to smooth these data in order to better detect the annual anomaly and calculate the proportional changes in log-transformed burned areas. Figure 1 represents burned area by wildfires in the five NUTS2 for mainland Portugal (1985 - 2009), whereas its log-transformed and standardized trends are depicted in figure 2.

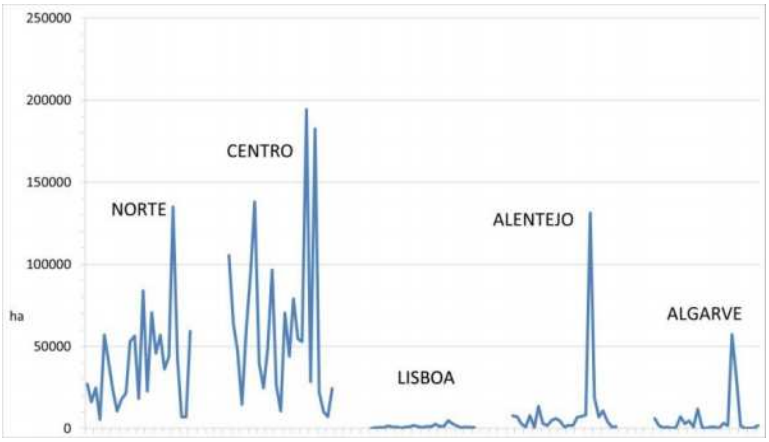

Figure 1. Burned area (ha) by wildfires in mainland Portugal (1985 - 2009) by NUTS2. The x-axis corresponds to the sampling years for each NUTS2.

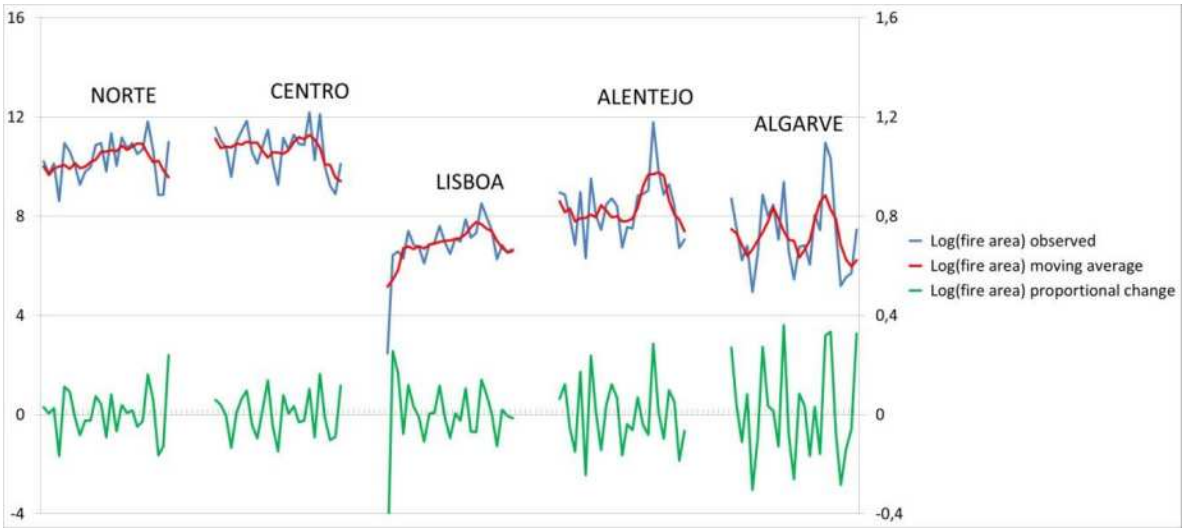

Figure 2. Log(fire area) observed, Log(fire area) moving average and Log(fire area) proportional change, by NUTS2 in mainland Portugal (1985 - 2009). The x-axis corresponds to the sampling years for each NUTS2; the left y-axis correspond to observed and moving average of Log(fire area), the right y-axis to Log(fire area) proportional change.

Investigating the correlations between short-term SPI1 and Proportional Change of log-transformed burned area we found two significant correlations (Figure 3). For short-term meteorological droughts, measured by SPI1, the most significant is the negative correlation occurring in May (R=-0.271). A negative correlation suggests that as meteorological drought severity increases (SPI becomes more negative), the wildfire area burned increases. It can be also speculated that, larger precipitation values in May result in lower areas burned, probably due to higher moisture in soil and vegetation before the summer (Dias *et al.* 2006). While statistically non-significant, all months from Abril to August show negative correlations, with the same interpretation as before.

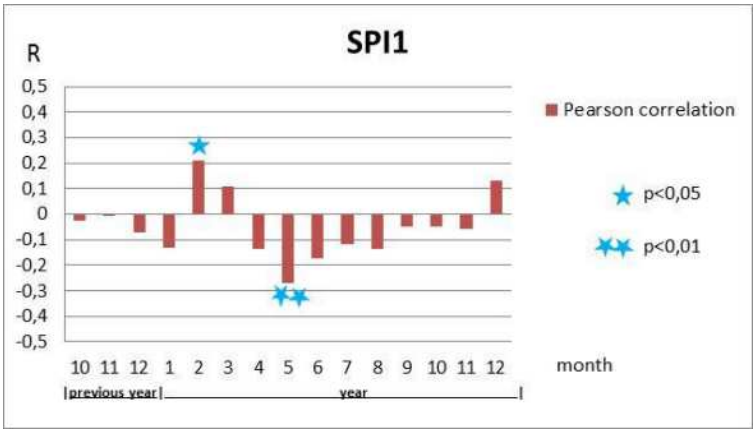

Figure 3. Correlations between Proportional Change of log (fire area) and monthly SPI1

The results also showed a positive (R=0.208) significant correlation, with SPI1 of February, meaning that extensive wildfire burned area is correlated with higher than average precipitation in February. In a Mediterranean country such as Portugal, a water surplus by the end of winter benefits fuel accumulation, namely the biomass of the herbaceous layer, which is easy to burn during the summer (Schoennagel *et al.* 2004; Gouveia *et al.* 2009). A similar explanation, in line with those provided by Viegas & Viegas (1994), can be used for March, even if the correlation is not statistically significant.

SPI3 involves the total rainfall of the current month and of the two previous months. In this case (Figure 4) the significant negative correlations for SPI3 are found between May and August, with

highest values for June (R=-0.348) and July (R=-0.367). Thus according to our results, accumulated deficit of precipitation from May to July is a good candidate for predicting larger annual wildfire area. A significant positive effect of summer drought (especially when evaluated by SPEI) in wildfire extent, was also found by Stagge *et al.* (2014) for several European regions.

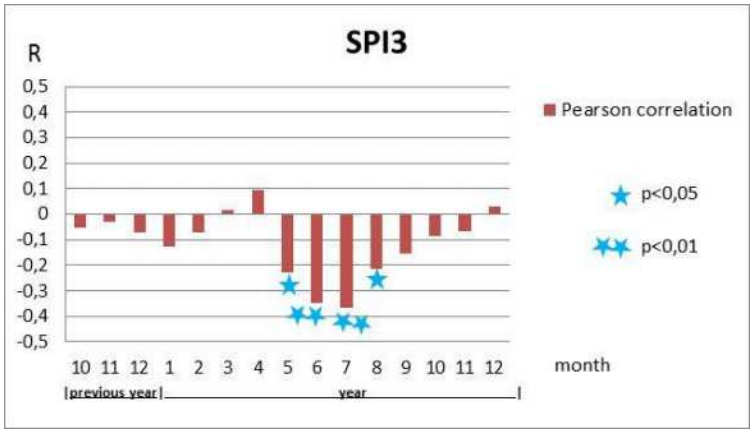

Figure 4. Correlations between Proportional Change of log (fire area) and monthly SPI3

Medium-term SPI6, commonly used to indicate drought impacts in rainfed agriculture, (Zargar, 2011) was also well correlated with burned area. SPI6 involves precipitation of the current month and of the previous five. The highest negative correlations were found from August to October (Figure 5).

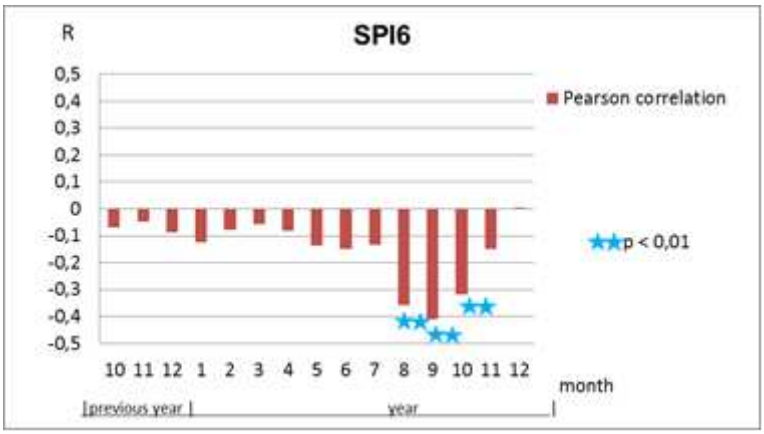

Figure 5. Correlations between Proportional Change of log (fire area) and monthly SP6

The highest negative correlation (R=-0.412) in this study was found for the SPI6 in September. This means that accumulated precipitation deficits from April to September correspond to accumulated dryness of soil, litter and vegetation (Dias *et al.*, 2006; Pellizzaro *et al.*, 2007), therefore triggering larger burned areas (Canyameres *et al.*, 2006; Jurdao *et al.*, 2012).
Though this correlation does not allow for a detailed analysis of the process, it can be useful in making the general association between drought and wildfire extent. In fact, we found that SPI6 of September was the first and only independent variable selected by the multiple regression model where all possible linear combinations of SPI1, SPI2, SPI3, SPI6, and SPI9 were used as explanatory candidates of the proportional change of area burned (log-transformed) in mainland Portugal:

$$Y_{LogFireChange} = -0.047 \times SPI6_{September},\ R = 0.412,\ p<0.001,\ n=125.$$

This indicates that it is possible to establish a solid negative association between cumulative precipitation deficits in late spring and summer months and wildfire extent, and that this association summarizes well the relationship between drought and burned area for mainland Portugal.

Conclusions

Climate scenarios estimate a significant increase in the forest fire danger (Bedia *et al.,* 2014) and in the total burned area (>66%, Amatulli *et al.,* 2013) for the EU-Mediterranean countries by the end of the 21st century. The identified link between meteorological drought and fire impact can be a step towards the improvement of an early-warning system for seasonal wildfire severity for both Portugal and other countries sharing the same climatic conditions.
The medium-term drought index, SPI6, in September provided the best explanation for burned areas in an interpretable way. Accumulated precipitation deficit results in low moisture content in forest fuels and therefore in larger areas burned due to more intense wildfires.
Short-term (SPI1 of May) and short-medium-term indices (SPI3 of May, June, July and August) can be used in real-time, giving some forecast lead time, to evaluate for possible major risk of forest fires and to engage field measures to implement in the forthcoming months.
The assessment of the SPI1 of February can provide important warning information when deciding whether to enact measures, in the four months ahead, to reduce herbaceous biomass, which may increase risk of wildfires.

Acknowledgments

The study was financed by FP7 European project "DROUGHT-R&SPI - Fostering European Drought Research and Science-Policy Interfacing" (contract no. 282769).
We acknowledge the Joint Research Centre (Jesus San-Miguel and Andrea Camia) for providing the data on forest fires in Europe.

References

Amatulli G, Camia A, San-Miguel-Ayanz J (2013) Estimating future burned areas under changing climate in the EU-Mediterranean countries. Science of the Total Environment 450-451C. 209-222.

Bedia J, Herrera S, Camia A, Moreno JM, Gutiérrez JM (2014) Forest fire danger projections in the Mediterranean using ENSEMBLES regional climate change scenarios. *Climatic Change* **122**(1-2). DOI: 10.1007/s10584-013-1005-z.

Canyameres E, Castro FX, Galante M, Rosello G, Marchetti M, Ferrer N, Dias S, Sambucini V, Picard C, Giroud F, Tudela T, Russo F, Barichello R, Sorbi S, Cruz M, Catry FX, Pinho JR, Buhours S, Moyà J (2006). GRINFOMED+MEDIFIRE, a project for the prevention of great forest fires in the Mediterranean (abstract). *Forest Ecology and Management* **234** (supp. 1). 50.

Comissão para a Seca 2005 (2006) Seca em Portugal Continental - 31 de Dezembro 2005 - Relatório de balanço. Conselho de Ministros (RCM 83/2005, Art.º 8)

Dias S, Rego F, Catry F, Guerrero C, Portela C (2010) Fuel moisture content in Mediterranean woody species throughout the year. In 'VI International Conference on Forest Fire Research'. ADAI, Coimbra. pp. 25.

Draper N R, Smith H (1998) *Applied Regression Analysis*, John Wiley & Sons Inc.

EEA (2012) Climate change, impacts and vulnerability in Europe 2012 - An indicator-based report. EEA Report No 12/2012. Copenhagen 2012. Available at:
http://www.eea.europa.eu/publications/climate-impacts-and-vulnerability-2012

Flannigan MD, Harrington JB (1988) A Study of the Relation of Meteorological Variables to Monthly Provincial Area Burned by Wildfire in Canada (1953-80). *Journal of Applied Meteorology* **27**. 441-452.

Gouveia C, Trigo RM, Da Camara CC (2009) Drought and vegetation stress monitoring in Portugal using satellite data. *Nat. Hazards Earth Syst. Sci*. **9**.185-195.

Guttman NB (1999) Accepting the standardized precipitation index: a calculation algorithm. *Journal of the American Water Resources Association* **35** (2). 311-322.

Jurdao S, Chuvieco E, Arevalillo JM (2012) Modelling fire ignition probability from satellite estimates of live fuel moisture content. *Fire Ecology* **8**(1). 77-97.

Littell JS, McKenzie D, Peterson DL, Westerling AL (2009) Climate and wildfire area burned in western US ecoprovinces, 1916–2003. *Ecol Appl* **19.** 1003–1021

MAMAOT (2013) *Seca 2012. Relatório de balanço.* Ministério da Agricultura, do Mar, do Ambiente e do Ordenamento do Território. 132 pp. Available at:
http://www.portugal.gov.pt/media/916024/Relatorio_Balanco_GTSeca2012_v1.pdf

McKee TB, Doeskin NJ, Kieist J (1993) The relationship of drought frequency and duration to time scales. In *'Proc. 8th Conf. on Applied Climatology'.* American Meteorological Society, Boston. pp. 179-184.

Moreira EE, Coelho CA, Paulo AA, Pereira LS, Mexia JT (2008) SPI-based drought category prediction using loglinear models, *J. Hydrol*. **354**. 116–130.

Paulo AA, Pereira LS (2006) Drought concepts and characterization. Comparing drought indices, *Water Int.* **31**. 37–49.

Paulo AA, Rosa RD, Pereira LS (2012) Climate trends and behaviour of drought indices based on precipitation and evapotranspiration in Portugal *Nat. Hazards Earth Syst. Sci*. **12**. 1481–1491.

Pausas JG (2004) Changes in Fire and Climate in the Eastern Iberian Peninsula (Mediterranean Basin). *Climatic Change* **63**. 337-350.

Pellizzaro G, Cesaraccio C, Duce P, Ventura A, Zara P (2007) Relationships between seasonal patterns of live fuel moisture and meteorological drought indices for Mediterranean shrubland species. *International Journal of Wildland Fire* **16**(2). 232-241.

Pereira MG, Trigo RM, Da Câmara CC, Pereira JC, Leite SM (2005) Synoptic patterns associated with large summer forest fires in Portugal, *Agricultural and Forest Meteorology*, **129**. 11–25.

Pereira LS, Cordery I, Iacovides I (2009) *Coping with water scarcity. Adressing the challenges.* Springer, Dordrecht,

Schoennagel T, Veblen TT, Romme WH (2004) The interaction of fire, fuels and climate across Rocky Mountain forests. *BioScience* **54**(7). 661**–**676.

Sousa PM, Trigo RM, Aizpurua P, Nieto R, Gimeno L, Garcia-Herrera, R (2011) Trends and extremes of drought indices throughout the 20th century in the Mediterranean, *Nat. Hazards Earth Syst. Sci*. **11**. 33–51.

Stagge JH, Dias S, Rego F, Tallaksen LM (2014) Modeling the effect of climatological drought on European wildfire extent. *Geophysical Research Abstracts* (**16**). EGU2014-15745.

Trigo, RM, Pereira JC, Pereira MG, Mota B, Calado TJ, Câmara CC, Santo FE (2006) Atmospheric conditions associated with the exceptional fire season of 2003 in Portugal, *International Journal of Climatology*, **26**(13). 1741-1757.

Van Lanen HAJ, Marcel AJ, Alderlieste AA, van der Heijden A, Assimacopoulos D, Dias S, Gudmundsson L, Monteagudo DH, Andreu J, Bifulco C, Rego F, Paredes J**,** Solera A (2013) Likelihood of future drought hazards: selected European case studies. *DROUGHT-R&SPI Technical Report No.11*. Available at: http://www.eu-drought.org/technicalreports.

Viegas DX, Viegas MT (1994) A relationship between rainfall and burned area for Portugal, *International Journal of Wildland Fire*, **4**(1). 11–16.

Zargar A, Sadiq R, Naser B, Khan FI (2011) A review of drought indices. *Environmental Reviews* **19**. 333-349.

Assessing the effect on fire risk modeling of the uncertainty in the location and cause of forest fires

Marcos Rodrigues[ac], Juan de la Riva[bc]

[a] *University of Zaragoza, Pedro Cerbuna 12 50009 Zaragoza (Spain), rmarcos@unizar.es*
[b] *University of Zaragoza, Pedro Cerbuna 12 50009 Zaragoza (Spain), delariva@unizar.es*
[c] *GEOFOREST-IUCA, University of Zaragoza, http://geoforest.unizar.es/*

Abstract
Wildfire risk assessments in Spain usually make little or no reference to the uncertainty of the results due to ignition data quality, or the implications that this potential uncertainty may have on wildfire management decisions. In Spain the autonomous regions have historically been the competent authorities in forest management and environmental protection as a result of the 1978 Constitution and, therefore, responsible on the operational application of the criteria defined for the country for wildfire classification and location. This competency framework has generated significant regional differences in the application of the criteria for wildfire classification among the different autonomous regions, arising potential uncertainty on wildfire assessments and fire risk models based on this historical series of data. This work explores six scenarios based on the classification of fire ignition causes and location data, reported in the General Statistics of Wildfires database (EGIF), to address the potential uncertainty from the point of view of the variability in predicted ignition probability and the changes in its spatial patterns. The analysis is focused on analyzing the effects on human-caused wildfires by using Random Forest algorithms to predict the ignition likelihood and cluster and outlier analysis (hot and cold spot) to detect changes in the spatial pattern of probability. Results suggest that there is significant uncertainty both in predicted human-caused ignition and spatial pattern related to the ignition source and location of fire events compiled in the EGIF database. The accuracy of the predictions ranges from AUC values of 0.90, when considering most of the records of the database, to around 0.76 in scenarios characterized by using only known-caused allocated fire events, probably due to differences in the proportions of unidentified and allocated fires within the mainland Spain.

***Keywords**: Uncertainty, wildfire, point location, ignition cause*

Introduction

During the last decades, the Spanish forest fire authorities have encouraged the investigation of fire causes, which is decisive to better understand patterns of fire occurrence and improve fire prevention measures (Martínez *et al*., 2009). However, the 29% of the fire causes remain unidentified in the period 1988-2007. According to Lovreglio *et al*. (2006), little is known about wildfire causes, which often are more diverse than what is assumed by the traditional classifications employed for statistical purposes. In face of the arising uncertainties, a better knowledge on spatial patterns of fire occurrence and their relationships with its underlying causes becomes a necessity to locate and make prevention efforts more efficient (Martínez *et al*., 2009). From a scientific perspective, improving decision quality in natural resource management begins with uncertainty management (Borchers, 2005). Uncertainty is essentially a lack of information; complete ignorance represents one end of the spectrum and perfect information (i.e., certainty) the other (Thompson and Calkin, 2011). However, viewing uncertainty as 'information about information' may be the first step in transforming a problem into knowledge (Bradshaw and Borchers, 2000).
The aim of this paper is to deal with the potential uncertainty linked to location and ignition cause of wildfires, with special attention to the human-caused fires in the mainland Spain. The analysis of human factors in forest fire is widely recognized as very critical for fire danger estimation (Kalabokidis *et al*., 2002; Martínez *et al*., 2009), especially in human-dominated landscapes where anthropogenic

ignitions widely surpass natural ignitions, like the peninsular Spain (Amatulli *et al*., 2007; Chuvieco *et al*., 2010; Chuvieco *et al*., 2012).

In Spain, fire events are recorded in the General Statistics of Wildfires database (EGIF). The EGIF database is one of the oldest 'complete' wildfire databases in Europe, beginning in 1968 (Vélez, 2001), though its data is not considered as completely reliable until 1988 (Martínez *et al*., 2009). The database is compiled by the Ministry of Environment, Rural and Marine affairs (MARM) using forest fire reports of the autonomous regions (Moreno *et al*., 2011). The autonomous regions have received competition in forest fires from the 1978 Constitution (article 148), and therefore are responsible of the application of the criteria and procedures defined for the entire national territory concerning wildfire classification and location. However, the fact that there is no single administration responsible on this topic has led to differences in the application of the criteria among the autonomous regions. A quick overview on the data collected in the historical database arises some inconsistences in the reported information. For instance, the proportion of unknown causes or the proportion of correctly located fire events (located with coordinates) differs from one region to another, becoming a potential source of uncertainty. This is especially important since research on forest fires in Spain is made from data collected in the EGIF database (Amatulli *et al*., 2007; Chuvieco *et al*., 2010; Chuvieco *et al*., 2012; de la Riva *et al*., 2004; Martinez *et al*., 2009; Padilla and Vega-García, 2011; Rodrigues *et al*., 2014; Rodrigues and de la Riva, 2014). Notwithstanding, the influence of uncertainty in historical fire data is scarcely considered (or at least not specifically addressed) and is mainly focused on location precision rather than ignition cause (Amatulli *et al*., 2006; Amatulli *et al*., 2007). Assessing the effects of uncertainty of Spanish ignition data is particularly interesting since it is a component of the wildfire information compiled European Forest Fires System Database (EFFIS), thus analyzing the effects of uncertainty at the Spanish level could be very helpful to understand wildfire patterns in the European scale, even more since Spain is the more fire-affected country within the European Union (Rodrigues *et al*., 2013).

In this work, we will explore six scenarios based on the classification of ignition causes and location data reported in the EGIF database to assess the potential uncertainty from the point of view of the variability in predicted ignition probability and changes in the spatial pattern of probability.

The occurrence probability will be calculated using Random Forest (RF) algorithms (Breiman, 2001) whereas the changes in the spatial probability patterns will be addresses through local Hot Spot analysis. RF algorithms have proved to be a useful tool for wildfire modeling (Bar Massada *et al*., 2012; Rodrigues and de la Riva, 2014), improving the performance of traditional regression techniques (e.g. logit Generalised Linear Models). The comparison of the proposed occurrence scenarios is conducted from the point of view of the accuracy in the classification based on a k-fold procedure (Fielding and Bell, 1997) and according to the variation in variable importance (Breiman, 2001). On the other hand, Hot Spot methods are one of the most adequate for the analysis of large-scale fire occurrence patterns (Allgöwer *et al*., 2005). The analysis of the changes in the predicted ignition probability patterns in each scenario is carried out by cluster and outlier analysis through the Anselin's Local Moran's I (Anselin, 1995).

2. Materials and methods

Study area and fire data

The study area covered the whole mainland Spain excluding the Balearic and Canary Islands as well as the autonomous cities of Ceuta and Melilla, due to the lack of data in those areas. Thus the total area of the study region was around 498 000 km^2. The fire events considered in this work are those occurred during the period 1988-2007.

An overview to the EGIF database

The EGIF database is compiled by the Ministry of Environment, Rural and Marine affairs (MARM) using the forest fire reports from the autonomous regions. The database classifies each fire event following a hierarchy of criteria which first differences between known (K) and supposed (S) cause and then into the most likely ignition source (natural or human). In turn, the ignition source is classified according to six categories: natural (lightning; L), human (negligence, accident or arson; H), restarted fires (R) and unknown or unidentified fires (U). Ideally, only K fires should be considered when developing any kind of fire analysis as they appear to be the most reliable. However, an insight into the classification of fire events in terms of number of fires in each category (Table 1) reveals that the proportion of fires with a S cause is more than 73 % of the total number of fires in the period 1988-2007. Hence, by excluding S fires the majority of fire events are being discarded (Figure 1).

Table 1. Classification of fire events according to its ignition causes (number of fires).

	Lightning	Human	Unknown	Restarted	All
Known	6775	35443	30952	1957	75127
Supposed	7931	228694	44706	2420	283751
Total	14706	264137	75658	4377	358878

This classification system also influences the proportion of fires according to its ignition source. Attending to K source, L fires represent the 9% of the occurrence whereas H fires are only the 47%. The remaining fires mostly correspond to U sources. This proportion changes drastically when S cause fires are accounted for, decreasing the proportion of L fires to 4% and raising H fires to a 73%. However, this 73 % of H fires is still far from the 90% value usually reported for Mediterranean European Countries (San-Miguel-Ayanz *et al*., 2012; San-Miguel-Ayanz, 2009) and, particularly, for Spain (Martínez *et al*., 2009). This fact suggests that there is great amount of U fires potentially related to H ignition factors and thus, when excluding unknown fires in human-caused wildfire assessments, a significant part of the human occurrence is not taken into account. However, while U fires are quite important attending to national overall values, mapping the spatial distribution of these proportions uncovers the existence of high spatial heterogeneity, increasing the uncertainty on the data (Figure 1). On the other hand, a second source of uncertainty is related to the location of fire events. In the EGIF database wildfires are located following to different procedures: (i) geocoding the location on the basis of a reference 10x10 km ICONA grid (used by the firefighting services for approximate location of fire events) and the municipality origin of the ignition; and (ii) georeferencing fire events using spatial coordinates. Again, the existence of coordinates should imply a precise allocation of the ignition points, however not all the fire events are georeferenced –only the 11% (Table 2)– and, as in the case of the ignition source, the proportion of fire events with coordinates varies from one region to another (Figure 2). This situation usually led to face the spatialization of the fire occurrence using geocoded location information (Amatulli *et al*., 2007; Chuvieco *et al*., 2010; Chuvieco *et al*., 2012; de la Riva *et al*., 2004; Martínez *et al*., 2009). On top of this, sometimes the assigned coordinates are incorrect. For instance, 2267 fires are located outside Spain, 23 are assigned a wrong UTM zone and 757 are located in the exact intersection of the ICONA grid (Table 2). This means that the 7.6% of the forest fires with spatial coordinates are mistakenly allocated.

Table 2. Number of fires with coordinates and wrong located wildfires.

	Located	Outside	Wrong zone	Intersects Grid	Total incorrect
Known	16435	962	18	347	1327
Supposed	23581	1305	5	410	1720
Total	40016	2267	23	757	3047

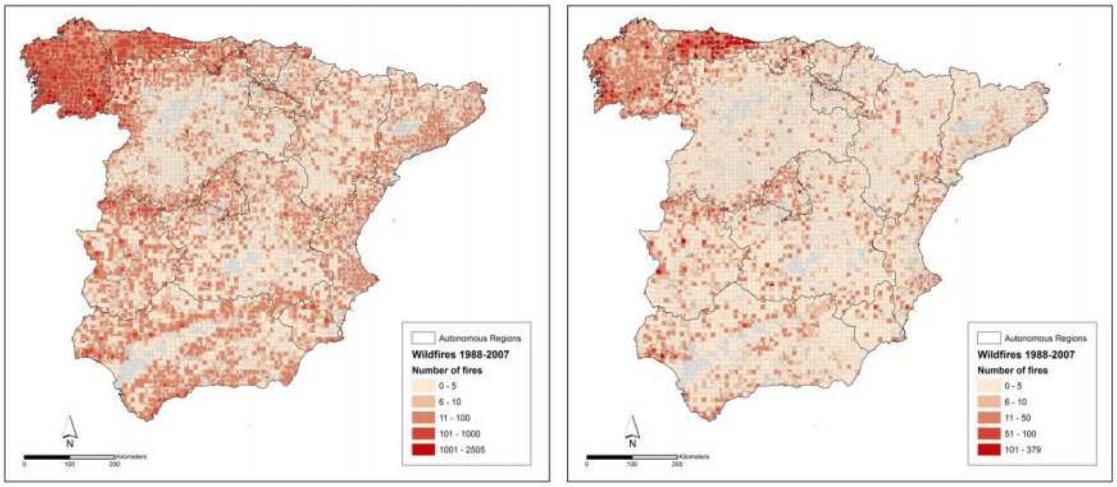

Figure 1. Spatial distribution of wildfires. Left total number of fires, right K fires.

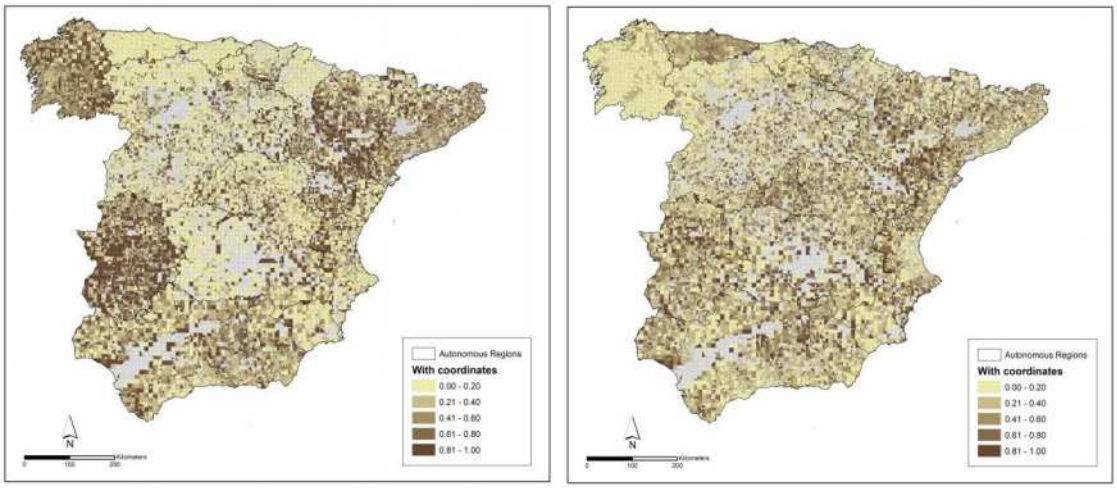

Figure 2. Spatial distribution of the proportion of points with coordinates. Total number of fires (left), fires with known cause (right).

2.3. EGIF scenarios

In this work, we explored six scenarios based on the classification of ignition causes and location data reported in the EGIF database. The proposed scenarios were constructed to simulate the most probable assumptions to select an occurrence sample for wildfire modeling purposes. The criteria followed to design the scenarios were based mainly in three parameters: certainty of the cause (known or supposed), certainty of the source (human or unknown) and presence of coordinates. Thus, the proposed scenarios are:

- Scenario 1: this scenario considers all human-caused fires, including both known and supposed cause, and a proportion of unknown fires according to the observed proportion of human-caused fires in the corresponding autonomous region.
- Scenario 2: this scenario considers all human-caused fire, including both known and supposed cause, excluding those fires with an unknown source.

- Scenario 3: this scenario considers all human-caused fire, but only those with known cause, excluding fires with a supposed cause, but including a proportion of unknown fires according to the observed proportion of human-caused fires in the corresponding autonomous region.
- Scenario 4: this scenario considers all human-caused fire, but only those with known cause, excluding fires with a supposed cause or an unknown source.
- Scenario 5: this scenario considers all human-caused fire, including both known and supposed cause located using coordinates, excluding fires with an unknown source or those which are wrongly located according to Table 2.
- Scenario 6: this scenario considers all human-caused fire, but only those with known cause and located using coordinates, excluding fires with a supposed cause, an unknown source or those which are wrongly located according to Table 2.

2.4. Wildfire modelling

The assessment of human-caused wildfire occurrence was carried out using RF algorithms an ensemble classifier which uses decision trees as base classifiers (Breiman, 2001).

The dependent variable for each scenario was constructed by selecting human-caused fires (e.g. negligence, accident or arson). Then wildfires were spatialized through the assignment of each fire to its respective combination of ICONA grid, municipality and forest perimeter (Amatulli *et al*. 2007; Chuvieco *et al*., 2010,2012; de la Riva *et al*., 2004; Rodrigues *et al*., 2014; Rodrigues and de la Riva, 2014). This allowed the calculation of fire density maps at a spatial resolution of 1 Km^2 by overlaying the random point cloud with the Spanish 1x1 Km UTM grid. The dependent variable was developed for each scenario by classifying the occurrence values into two categories: high occurrence (presence) in locations with two or more fires, and low occurrence (pseudo-absence or background) in locations with only one fire.

The explanatory variables were selected based on the experience of the authors in models at regional and national scales (Amatulli *et al*., 2007; Chuvieco *et al*., 2010, 2012; de la Riva *et al*., 2004; Martínez *et al*., 2009; Rodrigues *et al*., 2014; Rodrigues and de la Riva, 2014). The predictive variables considered were: wildland-agricultural interface (WAI), wildland-urban interface (WUI), density of agricultural machinery (DAM), changes in demographic potential 1991-2006 (CDP; Calvo and Pueyo, 2008), protected areas (PA), forestry area in public utility (FAPU), forestry tracks (TRCK), railroads (RRDS) , power lines (PWR) and land use change 1991-2006 (LUC).

The comparison of the outputs (predicted probability of occurrence) from each proposed scenario was conducted from the point of view of the accuracy in the classification based on a k-fold cross-validation procedure (Fielding and Bell, 1997) and according to the variation in the variable importance (Breiman, 2001). In k-fold cross-validation, the original sample is randomly partitioned into *k* equal size subsamples (*k*=5 in this work). Each time, one of the *k* subsets is used as the test set and the other *k* -1 subsets are putted together to conform the training set. The cross-validation process is then repeated *k* times (the folds), with each of the *k* subsamples used exactly once as the validation data. The *k* results from the folds then can be averaged to produce single error estimation (Bar Massada *et al*., 2012).

Variable importance assessment was carried out by summarizing the influence of the explanatory variables according to the increase in mean square error (*IncMSE*) and the increase in node purity (*IncNP*). *IncSME* is defined as the increase in the mean of the error of a tree in the forest when the observed values of this variable are randomly permuted in the *out-of-bag* samples. *IncNP* is measured using the Gini criterion, from all the splits in the forest based on a particular variable (Breiman, 2001). The variability in variable importance was addressed through the fluctuations in the ranks obtained by ordering the explanatory variables from more to less importance according to *IncSME* and IncNP.

2.5. Spatial variation in the ignition probability patterns

Changes in the spatial probability patterns were addressed through local Hot Spot analysis, one of the most adequate for this purpose (Allgöwer *et al*., 2005). The assessment of changes in the spatial pattern of predicted probability was based on the assumption that one of the key factors in wildfire management was guiding governments or responsible authorities through prioritization across fires and resources at risk. We considered that the identification of areas with high values of occurrence probability (Hot Spot) is linked to the identification of priority intervention areas.

The assessment of the changes in the predicted spatial pattern at each scenario is carried out by cluster and outlier analysis through the Anselin's Local Moran's I (Cluster and Outlier Analysis). This kind of analysis allows identifying and allocating Hot Spot areas as well as characterizes its typology of cluster. Given a set of weighted features, the Cluster and Outlier Analysis tool identifies clusters of features with values similar in magnitude. The tool also identifies spatial outliers. To do this, the tool calculates a Local Moran's I value, a Z score, a p-value, and a code representing the cluster type for each feature. The Distance Band or Threshold established for the cluster detection was 10 km. The results were mapped according to the significant detected cluster typology: Hot Spot (HH), Hot Spot surrounded by Cold Spot (HL), Cold Spot (LL) and Cold Spot surrounded by Hot Spot (LH).

Results

3.1. Predicted probability of occurrence

There is high variability (and therefore uncertainty) in predicted probability values among the six scenarios (Figure 3). In general terms, scenarios characterized by the use of both K and S causes, mainly scenarios 1 and 2, show high performance with AUC values stand above 0.9 (McCune *et al*., 2002). Scenarios 2 and 3, where the occurrence used to construct the dependent variable only consider K causes are less accurate (AUC near 0.83) and values in the high probability interval (0.8 to 1) are almost inexistent. Scenarios where the ignition points are georeferenced using coordinates show the poorest accuracy and probability values are grouped in the first interval (0 to 0.2). In addition, the range of AUC values (difference between minimum and maximum value) shows a similar behavior, with lower values in scenarios 1 and 2, and increasing until scenarios 5 and 6. This means that the models fitted using a dependent variable constructed with both K and S causes are more stable and therefore more reliable. Table 3 summarizes the obtained AUC values. On the other hand, the same comportment is observed when considering the values of Max TPR+TNR. This parameter represents the best threshold to distinguish between presence/absence according to the maximum value of the kappa index i.e. the highest values of true positive rate (TPR) and true negative rate (TNR). In general terms, the higher the threshold the higher the accuracy of the model since it means that the model distinguish more efficiently between presence and background values.

The uncertainty observed in the probability values is also detected in the contribution of the explanatory variables for each scenario. Although the variability is higher in the importance ranks for *IncSME* than in *IncNP* (Table 4) there is a general tendency to promote always the same variables: DAM, CDP, WAI, PA and TRCK (the later only is observed in the *IncNP*). The rest of the variables are swapping ranks among the different scenarios.

Table 3. Summary of k-fold validation with k=5.

	Scenario 1	**Scenario 2**	**Scenario 3**	**Scenario 4**	**Scenario 5**	**Scenario 6**
Max AUC	0.908	0.904	0.838	0.844	0.845	0.784
Min AUC	0.906	0.899	0.827	0.829	0.821	0.746
Max TPR+TNR	0.341	0.324	0.125	0.146	0.123	0.062

Table 4. Importance ranks for the explanatory variables. Top IncSME, bottom IncNP.

	Scenario 1	Scenario 2	Scenario 3	Scenario 4	scenario5	Scenario 6	ranks
DAM	1	1	1	1	1	1	0
CDP	2	2	2	2	2	3	1
WAI	3	3	4	5	6	5	4
PA	4	4	3	3	3	4	3
FAPM	5	5	6	7	4	2	5
WUI	6	6	5	4	5	6	3
RAIL	7	8	7	6	7	9	4
PWL	8	9	9	8	9	8	2
LUC	9	10	10	10	10	10	2
TRCK	10	7	8	9	8	7	4
DAM	1	1	1	1	1	1	0
CDP	2	2	2	2	2	2	0
WAI	3	3	3	3	3	3	0
PA	5	5	5	5	5	5	0
FAPM	6	6	7	7	8	7	3
WUI	10	10	10	10	10	10	3
RAIL	9	9	9	9	7	8	3
PWL	7	7	6	6	6	6	2
LUC	8	8	8	8	9	9	2
TRCK	4	4	4	4	4	4	0

Variation in spatial patterns of probability

Figure 4 shows the spatial distribution of the cluster characterization of the predicted probabilities. In the same way that occurs in the predicted probability of occurrence, there is high heterogeneity in the spatial pattern at each scenario. However, in this case a similar spatial pattern of cluster is observable among the six scenarios, with HH clusters in the northwest of the peninsula and the Mediterranean coast, HL clusters in Pyrenees and the central area of the peninsula and LH in the Cantabrian coast. However, the scenarios using known causes (scenarios 4 and 6) are presenting LL clusters in some regions of the Northwest of the peninsula which is not that would be expectable since this area presents the highest occurrence values (Figure 1).

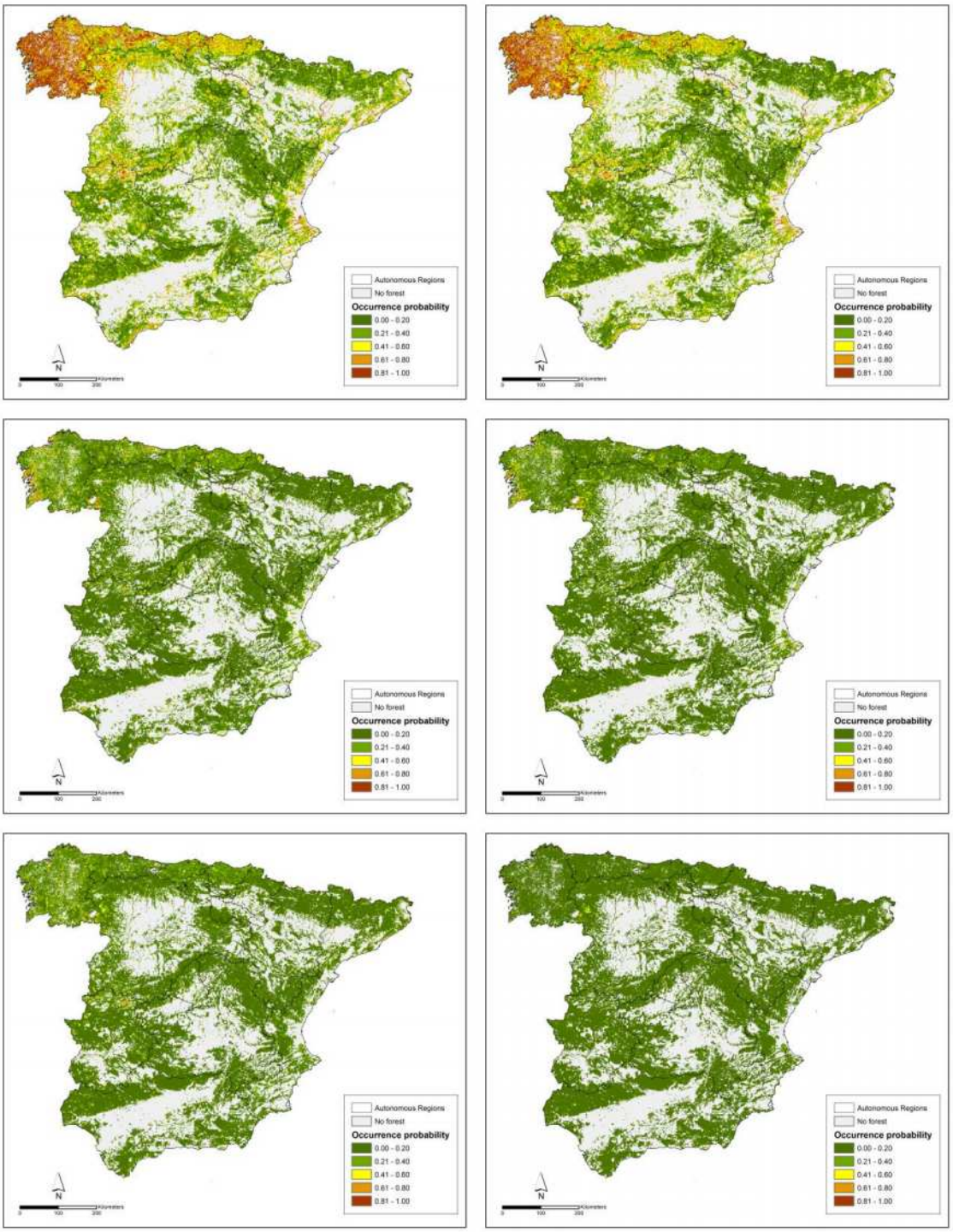

Figure 3. Spatial distribution of the predicted probability values. Scenarios are ordered consecutively left-right-top-bottom.

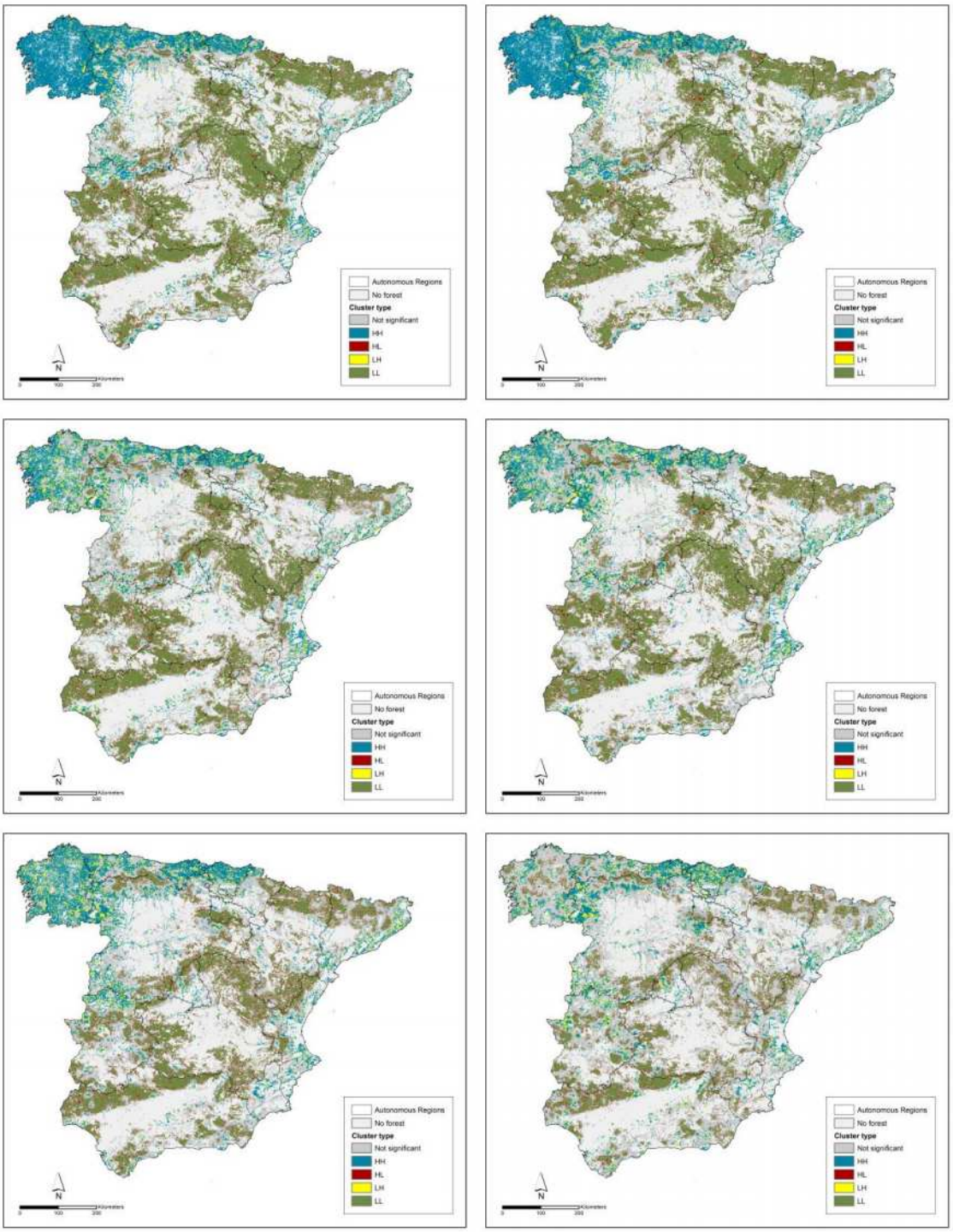

Figure 4. Spatial distribution of the cluster type. Scenarios are ordered consecutively left-right-top-bottom.

Discussion

Multiple sources of uncertainty remain with regard to modelling wildfire occurrence (Thompson and Calkin, 2011). Therefore there is a need to better understand how uncertainty and errors propagate through models (Sullivan, 2009). As little is known about wildfire causes (Lovreglio *et al*., 2006) many authors have chosen to deal globally with human-caused fires, avoiding uncertain specifications of causes, and have been able to derive useful recommendations for management (Stephens, 2005).

Nevertheless, using a coherent framework informs management authorities by facilitating the identification of potential sources of uncertainty and the quantification of their impact.
In Spain, near a 29% of the fire events in the period 1988-2007 have an unidentified cause and the remaining 71% are not fully reliable because the existence of certain degree of uncertainty regarding ignition source and location. This uncertainty is firstly detected while analyzing and mapping fire data; and secondly when occurrence data is used for wildfire modeling. Uncertainty is affecting both to the predicted probability values as well as the spatial pattern of probability.
According to the results may vary greatly depending on to the assumptions made when constructing the dependent variable. Results suggest that the scenarios based on the consideration of all causes (K and S) as well as a proportion of the fires with a U source are more accurate, with AUC values above 0.9. We believe that this is mainly because when considering the whole occurrence, the dependent variable is less 'spatially biased' since there is no partial criterion to leave out a particular set of fire events and, thereby, the spatial pattern should be closer to reality. It is expectable that the scenario with the less uncertainty in its occurrence data, i.e. a scenario with known causes and (scenario 6), would be the most accurate. However, the fact that there are differences in the proportions of unidentified and allocated fires within the Spanish peninsula is harming the quality of the data.
In addition, there is also uncertainty in the contribution/importance of the predictive variables. This might be a big issue in research works aiming to determine the factors that are explaining wildfire occurrence because the assumptions made when constructing the dependent variable are influencing the contribution of the explanatory variables.
Regarding to the predicted probability spatial pattern, although the variability is lower than the detected in the case of the predicted probability, it is still great. As in the case of the probability of occurrence, scenarios based on the consideration of all causes (K and S) including a proportion of the fires with an unidentified source seem to be the most realistic approach.

Conclusions

The lack of uniformity in the application of the criteria among the autonomous regions on forest fire management is a potential source of uncertainty for wildfire risk assessment which is affecting both the predicted probability values as well as the spatial pattern of probability. This is especially significant since research on forest fires in Spain is made from historical data collected in the EGIF database (Amatulli *et al*., 2007; Chuvieco *et al*., 2010, 2012; de la Riva *et al*., 2004; Martínez *et al*., 2009; Padilla and Vega-García, 2011), being more affected the older the data, as technological advances have greatly contributed to improve the quality of the data (such as GPS measurements or database administration capabilities) and, thus, reducing the uncertainty. In any case, some studies have been able to derive useful recommendations for management avoiding uncertain specifications of causes (Stephens, 2005), addressing arising uncertainty in occurrence data can help improve assessments.
The spatial distribution of wildfire ignition greatly varies depending on the assumptions made when considering the ignition cause and source, leading to different predictions. However, it is possible to determine the best scenarios for modeling wildfire occurrence or risk. According with our results the best choice is consider both K and S causes with a proportion of forest fires with unknown source. There is a big amount of unidentified fires potentially related to a human ignition source and thus, when excluding unknown fires in human-caused wildfire assessments, a significant portion of the occurrence is not accounted for. Considering this supposedly human-caused occurrence reduces the spatial biased conducting to more robust and reliable predictions.
Uncertainty is also affecting the contribution of the explanatory variables. Results suggest that DAM, CDP, WAI and PA are the least sensitive variables to variations in the spatial distribution of the occurrence.

Acknowledgements

This work was financed by the National Plan of I+D of the Spanish Ministry of Science and Innovation: FPI grant BES-2009-023728. The research was conducted within the framework of the projects FIREGLOBE: Analysis of fire risk scenarios at the national and global scales (CGL2008-01083/CLI) and PYRORAMA Modeling future scenarios of fire risk and land use changes at national scale (CGL2011-29619-C03-01) subproject 1 of the PYROSKENE project (CGL2011-29619-C03).

References

Allgöwer B, Camia A, Francesetti A, Koutsias N (2005) Fire hot spot areas in Southern Europe. Detection of large-scale wildland fire occurrence patterns by adaptive kernel density interpolation, In 'Proceedings of the 5th International Workshop on Remote Sensing and GIS Applications to Forest Fire Management: Fire Effects Assessment'. (Eds J de la Riva, F Perez-Cabello, E Chuvieco) pp. 47-50 (EARSeL-UZ: Zaragoza).

Amatulli G, Rodrigues MJ, Trombetti M, Lovreglio R (2006) Assessing long-term fire risk at local scale by means of decision tree technique. *Journal of Geophysical Research* **111**, G04S05.

Amatulli G, Peréz-Cabello, F, de la Riva J (2007) Mapping lightning/human-caused wildfires occurrence under ignition point location uncertainty. *Ecological Modelling* **200**, 321-333.

Anselin L (1995) Local Indicators of Spatial Association-LISA. *Geographical Analysis* **27**, 93-115.

Bar Massada A, Syphard AD, Stewart SI, Radeloff VC (2012) Wildfire ignition-distribution modelling: a comparative study in the Huron–Manistee National Forest, Michigan, USA. *International Journal of Wildland Fire* **22**(2), 174-183.

Bradshaw GA, Borchers JG (2000) Uncertainty as information: narrowing the science-policy gap. *Conservation Ecology* **4**, 7.

Breiman L (2001) Random forests. *Machine Learning* **45**, 5-32.

Borchers JG (2005) Accepting uncertainty, assessing risk: Decision quality in managing wildfire, forest resource values, and new technology. *Forest Ecology and Management* **211**, 36-46.

Calvo JL, Pueyo A (2008) Atlas Nacional de España: Demografía (CNIG: Madrid).

Chuvieco E, Aguado I, Yebra M, Nieto H, Salas J, Martín MP, Vilar L, Martínez J, Martín S, Ibarra P, de la Riva J, Baeza J, Rodríguez F, Molina JR, Herrera MA, Zamora R (2010) Development of a framework for fire risk assessment using remote sensing and geographic information system technologies. *Ecological Modelling* **221**, 46-58.

Chuvieco E, Aguado I, Jurdao S, Pettinari ML, Yebra M, Salas J, Hantson S, de la Riva J, Ibarra P, Rodrigues M, Echeverría M, Azqueta D, Román MV, Bastarrika A, Martínez S, Recondo C, Zapico E., Martínez-Vega FJ (2012) Integrating geospatial information into fire risk assessment. *International Journal of Wildland Fire*.

de la Riva J, Pérez-Cabello F, Lana-Renault N, Koutsias N (2004) Mapping wildfire occurrence at regional scale. *Remote Sensing of Environment* **92**,363-369.

Fielding AH, Bell JF (1997) A review of methods for the assessment of prediction errors in conservation presence/absence models. *Environmental Conservation* **24** (1), 38–49.

Kalabokidis KD, Gatzojannis S, Galatsidas S (2002) Introducing wildfire into forest management planning: towards a conceptual approach. *Forest Ecology and Management* **158**, 41-50.

Lovreglio R, Leone V, Giaquinto P, Notarnicola A (2006) New tools for the analysis of fire causes and their motivations: The Delphi technique. *Forest Ecology and Management* **234**, S18.

McCune B, Grace JB, Urban DL (2002) Analysis of ecological communities. MJM Software Design (Glenden Beach).

Martínez J, Vega-García C, Chuvieco E (2009) Human-caused wildfire risk rating for prevention planning in Spain. *Journal of Environmental Management* **90**, 1241-1252.

Moreno MV, Malamud BD, Chuvieco E (2011) Wildfire Frequency-Area Statistics in Spain. *Procedia Environmental Sciences* **7**, 182-187.

Padilla M, Vega-García C (2011) On the comparative importance of fire danger rating indices and their integration with spatial and temporal variables for predicting daily human-caused fire occurrences in Spain. *International Journal of Wildland Fire* **20**, 46-58.

Rodrigues M, San Miguel J, Oliveira S, Moreira F, Camia A (2013). An insight into Spatial-Temporal Trends fo Fire Ignitions and Burned Areas in the European Mediterranean Countries. *Journal of Earth Science and Engineering* **3**, 497-505.

Rodrigues M, de la Riva J, Fotheringham S (2014) Modeling the spatial variation of the explanatory factors of human-caused wildfires in Spain using geographically weighted logistic regression. *Applied Geography* **48**, 52-63.

Rodrigues M, de la Riva (2014) An insight into machine-learning algorithms to model human-caused wildfire occurrence. *Environmental Modelling & Software* In Press.

San-Miguel-Ayanz J (2009) Forest fires at a glance: facts, figures and trends in the EU. In 'Living with wildfires: what science can tell us. A contribution to the Science-Policy dialogue'. (Eds Y Birot) pp. 11-18 (European Forest Institute).

San-Miguel-Ayanz J, Rodrigues M, Oliveira S, Pacheco C, Moreira F, Duguy B, Camia A (2012) Land Cover Change and Fire Regime in the European Mediterranean Region. In 'Post-Fire Management and Restoration of Southern European Forests'. (Eds F Moreira, M Arianoutsou, P Corona, J de las Heras) pp. 21-43 (Springer: Netherlands).

Sullivan AL (2009) Wildland surface fire spread modelling, 1990–2007. 1: Physical and quasi-physical models. *International Journal of Wildland Fire* **18**, 349-368.

Stephens SL (2005) Forest fire causes and extent on United States Forest Service lands. *International Journal of Wildland Fire* **14**, 213-222.

Thompson MP, Calkin DE (2011) Uncertainty and risk in wildland fire management: A review. *Journal of Environmental Management* **92**,1895-1909.

Vélez R (2001) Fire Situation in Spain. In 'Global Forest Fire Assessment 1990-2001'. (Eds JG Goldammer, RW Mutch, P Pugliese). (FAO:Roma).

Assessment and management of cascading effects triggering forest fires

Alexander Garcia-Aristizabal[a], Miguel Almeida[b], Christoph Aubrecht[c], Maria Polese[a], Luís Mário Ribeiro[b], Domingos Viegas[b], Giulio Zuccaro[a].

[a] *Center for the Analysis and Monitoring of Environmental Risk (AMRA), Via Nuova Agnano, 11; IT-80125 Napoli, Italia; alexander.garcia@amracenter.com;mapolese@unina.it zuccaro@unina.it.*
[b] *Centre for Forest Fire Research ADAI, Rua Pedro Hispano, 12, PT-3030-289 Coimbra, Portugal; miguellmd@yahoo.com, luis.mario@adai.pt, xavier.viegas@dem.uc.pt.*
[c]*AIT Austrian Institute of Technology GmbH, Energy Department, Giefinggasse 6, 1210 Vienna, Austria; Christoph.Aubrecht@ait.ac.at.*

Abstract
A crisis situation may be due to the occurrence of a single hazard event with large impacts or due to several hazard events occurring simultaneously. Hazard events occurring at the same time may have independent causes or may result from a sequence of triggering effects. The outcome of a situation for which an adverse event triggers one or more sequential events is generally called "cascading effects".
The perception and understanding of the potential occurrence of cascading effects is of great relevance for planning and response activities since an unexpected scenario in an emergency may worsen the situation endangering people, goods, and may nullify a strategy that was developed accounting for a scenario in which the triggering event was considered as a single occurrence.
This paper presents an analysis of possible scenarios of cascading effects triggered by an earthquake. A detailed quantitative example in which an earthquake causing an electric cable failure that potentially ignites a fire is presented. In particular, a methodology to assess the occurrence probability of the event chain earthquake→cable failure→fire ignition is presented. The final results are presented as conditional probability maps representing each transition, namely: earthquake→cable failure, cable failure→fire ignition, and the assessment of the full path earthquake→cable failure→fire ignition.
This study is a part of a pilot application built to test the integrated crisis management system which is being developed in the FP7 European Integrated Project – CRISMA ("Modelling crisis management for improved action and preparedness").

Keywords*: Forest fire; earthquake, multi risk assessment; multi-hazards, cascading effects, domino effects.*

Introduction

Similarly to other natural and man-made hazard events forest fires can be triggered by some other event or they can themselves trigger one or more hazard events in a situation that is designated by a cascading effect (Marzocchi *et al.*, 2009, 2012). In a cascading process we may have either a series of events occurring in sequence or in parallel at the same time. From the operational and management points of view, the possibility of having cascading effects involving forest fires as triggering or triggered event are of great importance for the following reasons:

- The response forces will have to face two or more simultaneous or sequential events of different nature requiring a distribution of human and material resources;
- The possible diversity of events occurring in a cascading effect scenario claim for a respective versatility of the crisis response system;
- It may be possible that the strategies designed to respond to a single hazard event are not feasible due to the triggering hazard event(s).

For these reasons, it is important to investigate and assess the risk of cascading effects scenarios that may trigger forest fires, in order to improve mitigation procedures and preparation activities, but also to reduce impacts.

In this paper we explore scenarios of cascading event in which forest fires triggered after earthquakes (EQ) are studied and propose a probabilistic framework for their assessment. The presented example is based on the simulation of an EQ occurring in the surroundings of L'Aquila province, in the Italian region of Abruzzo. The spatial domain used for the analyses is shown in Figure 1. This area was affected by a Mw6.3 EQ in 2009 (Pondrelli *et al.*, 2010). This event caused 308 victims, 1,500 injured and the temporary evacuation of more than 65,000 people from their houses in L'Aquila and surrounding municipalities (Alexander and Magni, 2013). Several aftershocks were felt after the main shock compromising the rescue operations. All the available civil protection authorities were allocated in these response efforts. In the proposed scenario the situation is even more stressed assuming the possible occurrence of a forest fire due to damages to the electricity network (cable failure) caused by the EQs. It is assumed that the forest fire spreads in the direction of a village threatening the population, the houses and other assets. An efficient distribution of human resources and equipment is required to face the two interconnected disasters. In addition to earthquake induced risk for people inside houses, also the possibility that people cannot stay outdoors is to be considered because the village can became immersed in smoke. Several options are highlighted and a multi-criteria analysis, based on pre-defined indicators, criteria and costs, is carried out in order to find the most efficient way to deal with the situation.

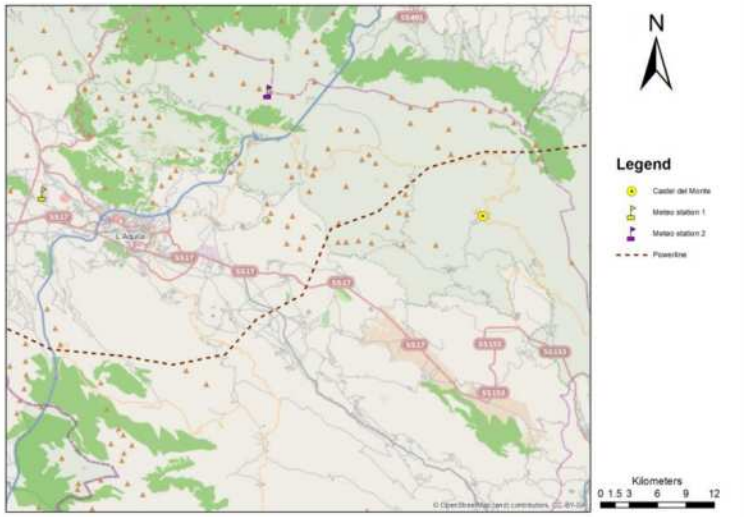

Figure 1. Map showing the area of interest for the study. The location of a hypothetical power line considered for the scenario assessment is also presented.

The analysed scenario refers to a pilot application of the EU-FP7 CRISMA Project. CRISMA focuses on large scale crisis scenarios with immediate and extended human, societal, structural and economic, often irreversible, consequences and impacts. The developed Integrated Crisis Management Simulation System (ICMS) is a simulation-based decision support system for modelling crisis management, improved action and preparedness. In this paper only the part directly related to the cascading effects of the described scenario will be elaborated on.

The methodology herein described for the probabilistic assessment of cascading effects scenarios begins with the selection of the event chain to be assessed. The first step is to identify and to structure the possible event chains and select those of interest for quantitative analyses. The result of this process is illustrated in Figure 2. In this study we focus our attention on the event chain earthquake (EQ)→cable failure (CF)→fire ignition (FI). After selecting an event chain of interest, all the necessary input parameters need to be identified and calculated in order to produce information on the occurrence probability for the scenario(s) of interest. In this case, it is necessary to calculate the following conditional probabilities (hereinafter called "transition probabilities"): EQ→CF: $p(CF|PGA)$, where PGA (peak ground acceleration) is an example of intensity measure used to characterize the EQ hazard,

and CF→FI: $p(FI|CF)$. Using this information is therefore possible to calculate the probability of occurrence of the scenario EQ→CF→FI. The outputs are provided as probability maps in order to facilitate interpretation.
Once the most problematic spots are identified, new simulations may be carried out in order to evaluate the importance of the triggered events. Some indicators may be produced to compare different scenarios and to support the final decisions. These last tasks are a consequence of the cascading effects evaluation and some examples are given in this paper.

Structuring scenarios: the event chains database

After the implementation of a detailed procedure for scenario identification and structuring, a database with various identified possible cascading event chains was created for a set of triggering events, including earthquakes (Figure 2). The sequence of events is often cyclic as a certain event type may occur in the same chain more than once. This repetition may be direct (e.g. EQ→EQ) or indirect (e.g. forest fire →WUI/urban fire →Forest fire). When a potential cycle is verified, the symbol […] was used to indicate the cyclic chain.
The possibility to have certain scenarios strongly depends on the specific case under analysis. For example, the possibility of having an explosion triggered by damages to an industrial facility depends on the type of industrial facility damaged in the area of interest. Under this perspective, the proposed diagrams must be adapted to the characteristics of the hazard event and to the area of interest.
The event chains database is of great importance as it allows the choice of the path of interest and the cascade event analysis that shall be performed. The quantitative example in this paper is centred in the specific scenario of an EQ causing damage to the electricity network (cable failure), leading to fire ignition and triggering a forest fire. In this demonstrative scenario, a Mw5.6 EQ occurring in the NE part of the study area was simulated as the triggering event. In the considered scenario, the EQ may provoke damages to the electricity network, specifically to the cables joints/couplings devices (Figure 3a) near to the pole, which may cause a rupture in the electric cable. As this electric cable is energized, it may ionize the air to the ground and consequently an electric discharge may occur. Figure 3b shows an example of air ionization caused by the proximity of a tree branch and Figure 3c shows a fire ignition caused by an electric discharge. Both examples follow the same principle of the application managed in this paper, however in this scenario we consider the case in which the area reached by the electric arc is covered by surface fine forest fuels where it is possible to trigger an ignition that may develop to a forest fire.

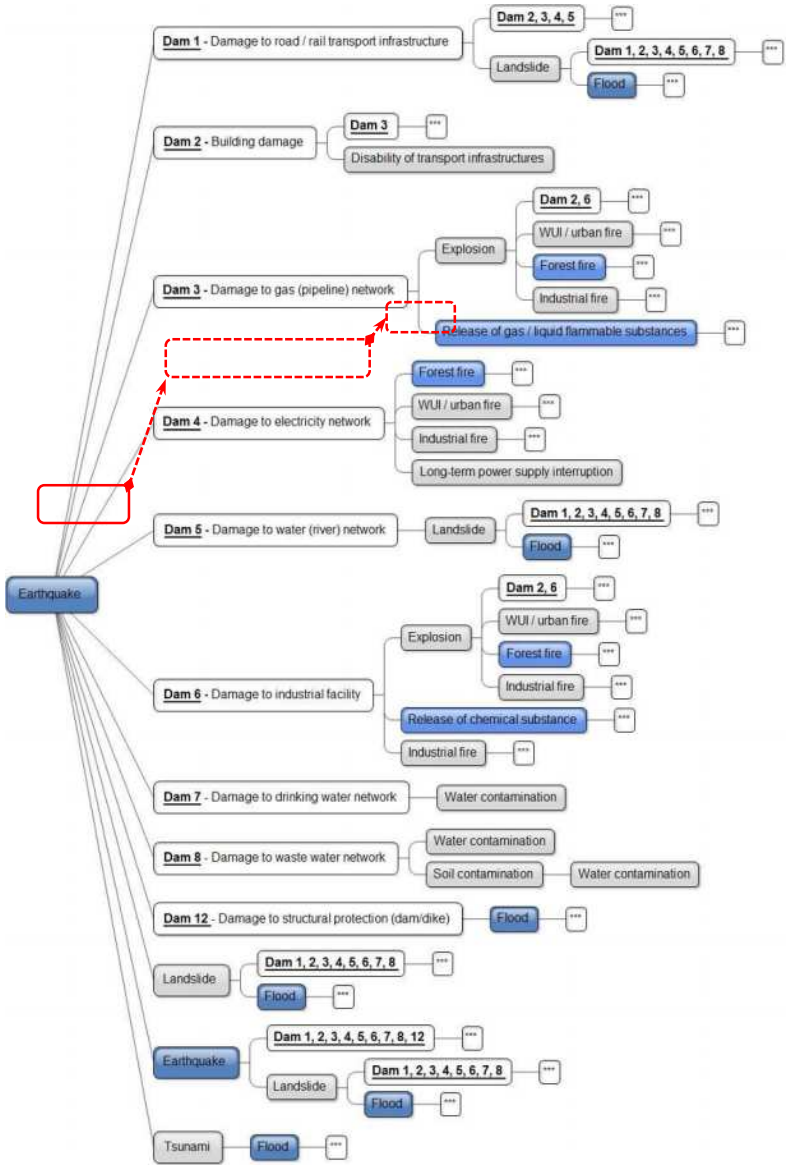

Figure 2. Diagram of the identified cascade event chains for Earthquake

(a) (b) (c)

Figure 3. Images showing an example of electric poles, electric discharge, and fire ignition. (a) Detail of a cable joint/coupling; (b) example of air ionization caused by the proximity of a tree branch; (c) fire ignition caused by an electric discharge.

Quantitative data analysis

In this section we assess the occurrence probability of the selected scenario. To assess the scenario of interest, different input information is required, namely information related to the initial world state and information about the probabilities for the occurrence of transition between events. As "world state", in CRISMA, we understand a particular status of the world, defined in the space of parameters describing the situation in a crisis management simulation that represents a snapshot (situation) along the crisis evolvement (Almeida *et al.*, 2014). The change of world state, that may be triggered by simulation or manipulation activities, corresponds to a change of (part of) its data contents.
After the triggering EQ event, the initial world state changes as a consequence of the impacts resulting from it. Some impacted elements may be vulnerable in a time-dependent manner; therefore, the word state may in fact be considered to be continuously changing after the triggering event. Nevertheless, to assess the possibility of cascading effects, the world state at each moment exactly before a plausible triggering effect must be identified.
The transition probabilities are the conditional probabilities required to determine the likelihood of a transition, and primarily depend on the intensity of the triggering events in the chain.
Figure 4 schematically presents the flow of information necessary for the quantitative assessment of the event chain of interest in this work. Besides the probability functions regarding the fragility curve of the electric system and the probability of ignition after the electric cable failure, other three categories of inputs must be previously available in the world state. These are the location of the electricity network (Figure 1), the intensity distribution (shake map) of the EQ (Figure 5), and the fuel cover in the area of interest (Figure 6).

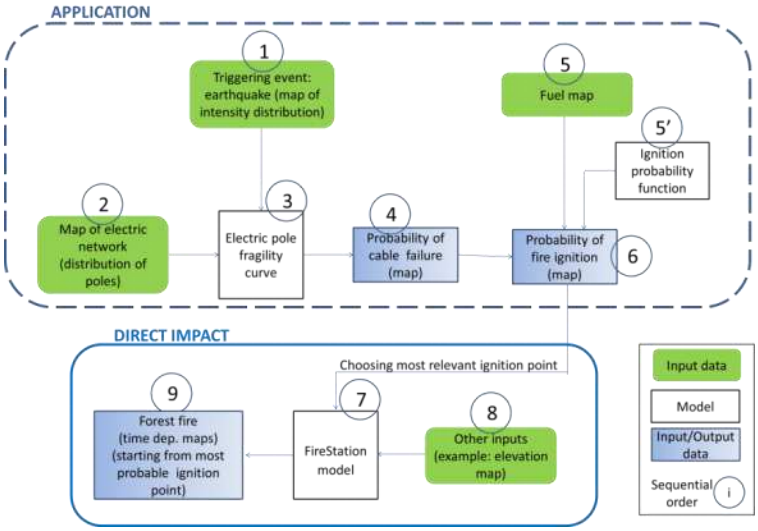

Figure 4. Flow of information necessary for the computation of the selected cascading effects scenario.

The conditional probability of a cable failure in the electric system given the EQ occurrence (and the consequent formation of an electric arc) is estimated considering the intensity distribution of the EQ (shake map) and the fragility function of the electric pole. The intensity of the EQ along the electric network is calculated using regional ground motion prediction equations that provide the intensity measure (in PGA or macro seismic intensity) at each electric pole position. On the other hand, the fragility function relating the intensity of the earthquake to the probability of cable rupture is calculated attaining a limit value of displacement at the pole top varying the intensity of the seismic input. The probability of an ignition started by an electric discharge is estimated considering the fuel classification of the area where the electricity cable failure occurs and the associated ignition model. The fuel classification is part of the world state and is available in form of a fuel map of the area of interest (Figure 6). If the electric discharge occurs in a non-fuel area, as for example a road, the probability of

ignition is zero. However, if the electric discharge occurs in a fuel area, as for example a grass land, the probability of ignition is determined by using the ignition probability model described in Section 3.2.2.

If we address the whole event chain (i.e. EQ-DEN-FI), the probability of a fire ignition due to an EQ is given by the product of the respective conditional probabilities at each node of the sequence, i.e., the probability of fire ignition given an electric cable failure, $p(FI|CF)$, the electric cable failure probability given the intensity of the ground shaking, $p(CF|PGA)$, and the probability of observing the EQ intensity, $p(PGA)$. Note that in this example we do not consider uncertainties in the ground motion prediction equation used and therefore $p(PGA)$ is assumed to be 1.

Input data

Location of the electric network

The location of the hypothetical electric network considered in this study is presented in Figure 1 and was defined at the most opportune location, only taking precautions to not locate a pole in an unlikely place such as in the middle of a river. The separation between two successive poles is 300m.

Map of EQ intensity distribution

The occurrence of a Mw5.6 EQ in the NE part of the study area has been simulated as the triggering event for this scenario. The shake map of this event, represented by the intensity of the ground motion in the area of interest, is shown inFigure 5. Using that shake map, the peak ground acceleration (PGA, in %g) is calculated at the base of each pole of the electric network considered for this study.

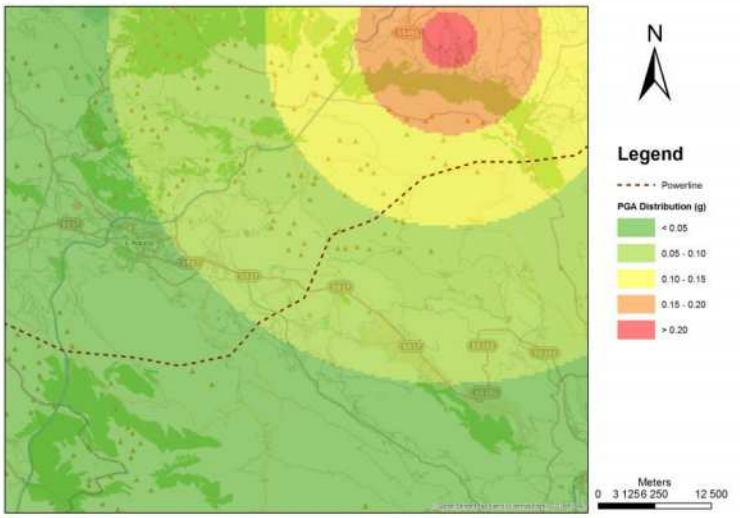

Figure 5. Map of the triggering earthquake intensity distribution with location of the electric power network (distribution lines - smaller poles)

Fuel map

The fuel map is crucial to evaluate the probability of ignition as it includes the information on the class of fuel in the cell(s) where each electricity pole is located. To be harmonized with the fire behaviour prediction model used (FireStation, Lopes *et al.*, 2002), the classes defined in the fuel map are consistent with those used in the FireStation model. As can be seen in Figure 6, in the area of interest there are seven different fuel classes, with grassland being most prominent.

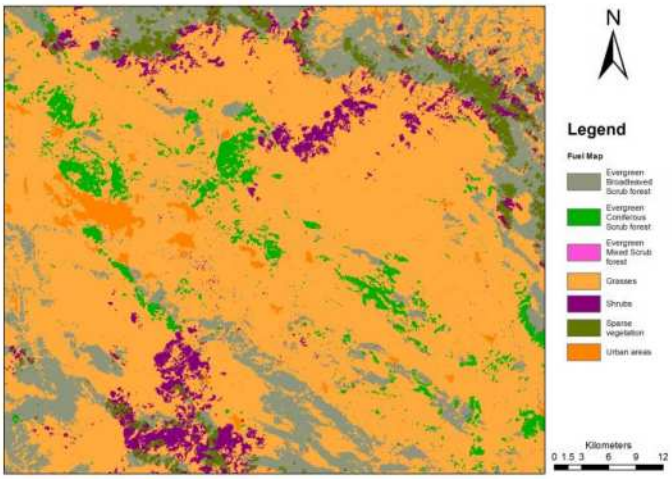

Figure 6. Fuel map for the region of L'Aquila. This fuel map was developed in April 2014 by the ArcFUEL Project Consortium from a cooperation protocol established between CRISMA Project and the European LIFE+ Project ArcFUEL.

Conditional probabilities

Each event transition requires a conditional probability. In the example herein presented, the event "damage to electricity network" is caused by an electric cable disruption (cable failure). However, the same event could also be caused by the fall of a pole. These two different cases require two different probability functions.

3.2.1. *Transition probability function for the cable failure triggered by an earthquake*

The fragility of the electricity poles used in electricity distribution lines is dependent on several factors as their dimensions, material, state of maintenance, etc. The fragility curve represents the probability of cable rupture as a function of the displacement at the pole top varying with the intensity of the seismic input. Such limit value is represented as a fraction of a displacement X_{MAX} (three hypotheses are considered: 0.5 X_{MAX}, X_{MAX} and 1.25 X_{MAX}), where X_{MAX} is defined as the displacement corresponding to the static application of a transversal force. The shaking of a pole may lead to tensions in the cables which may consequently disrupt. Cable disruption normally occurs in the connections which are the most fragile parts of the network.

In Figure 7, the fragility curve of a pole (type: 12B14) as function of the peak ground acceleration (PGA) is shown. In order to simplify the use case, all the electricity poles in the study area will follow the fragility curve X_{MAX}.

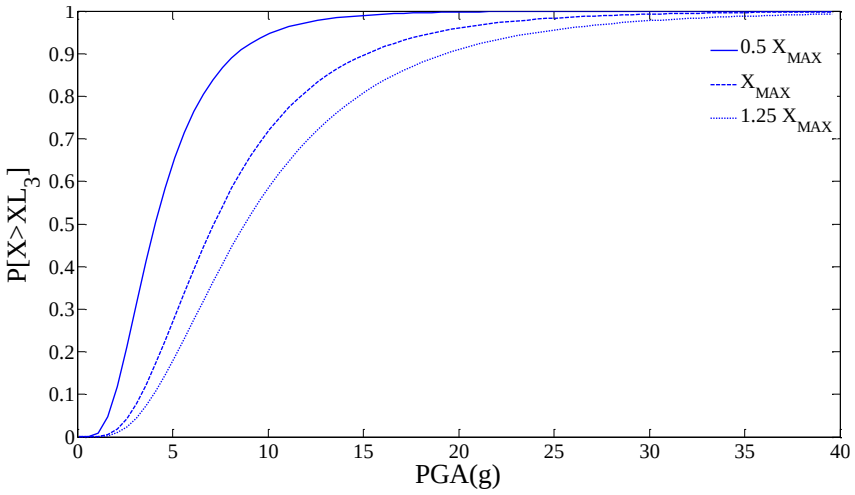

Figure 7. Fragility curves of electric poles to a transversal force T1.

3.2.2. *Transition probability function for fire ignition triggered by cable failure*

The transition from the electric cable failure to a fire ignition has two evolutionary steps: 1) the production of the electric arc from the electricity cable to the fuel bed, and 2) the ignition of the fuel bed by the electric arc.

It is assumed that the failure of an electric cable imperatively causes an electric arc. Due to the existing protection systems, the electric charge is normally interrupted in case of failure and after that, for brief instants, the residual electric charge continues flowing. After the cable breakage, the cable takes some time to land or to reach a sufficient distance to establish the electric arc. The time to ignition by electric arc with high voltage is very short (tenths of seconds) and therefore in this sense it is reasonable to consider the production of an electric arc for a short period as inevitable. On the other hand, the time to ionize the air path from the cable failure to the fuel bed and the consequent production of the electric arc is strongly dependent on the distance and on the resistance of this path. This dependency is a function of many additional factors such as topography, cable height, air humidity, and pressure. For simplification reasons we will not take those aspects into consideration in this paper, but rather assume that the cable failure will always drive to an electric arc that reaches the fuel bed.

In a laboratory environment, several tests were carried out in order to determine the total amount of energy required to ignite a certain amount of fuel. These tests were performed for straw and pine needles (*Pinus pinaster*) for a range of fuel moisture content (FMC) between 9.2% and 12.2%. A bouquet of the fuel material was exposed to an industrial electrical arc of certain power (P [kVA]) as can be seen in Figure 8. The time (t [s]) elapsed from the beginning of discharge until the evidence of combustion was measured. The energy (E[kJ]) required for ignition was determined using Equation 1.

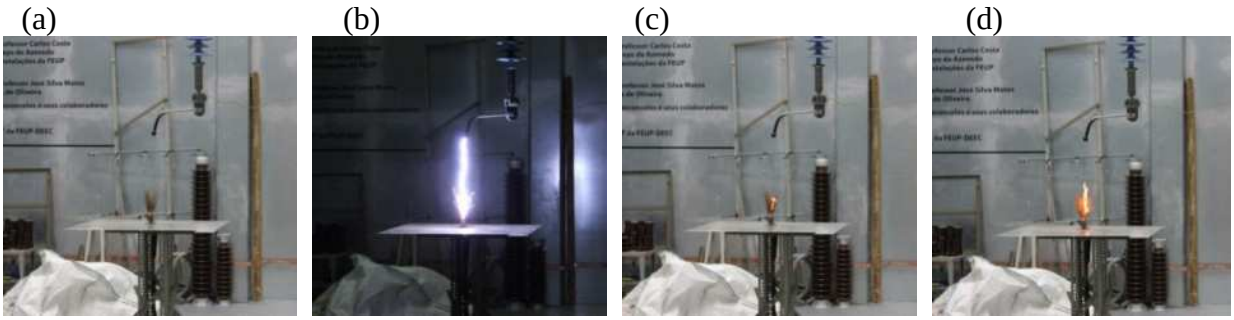

Figure 8. Sequence of images of a laboratorial test to determine the energy required for ignition by industrial electric discharge.

$$E = P \times t \qquad \textbf{[1]}$$

It was found that the probability of ignition was not significantly different for the several tests at different conditions of FMC or different types of fuel (straw or pine needles) and also the fuel load does not seem really relevant for the probability of ignition. This statement should be considered preliminary since not many tests with fuels other than straw and pine needles were carried out and the range of fuel moisture content was not very extensive. It also refers specifically to the situation of a cascading effect scenario, i.e. the possible spot ignition by electric discharge. Findings might be different for other ignition causes where fuel and soil moisture are expected to play a more significant role and are therefore sometimes regionally monitored to identify and address potential susceptible areas (Aubrecht *et al*., 2011).

Using the data collected in the laboratory experiments, we estimated the parameter of different competing probabilistic models in order to find the distribution providing the best description of the laboratory observations. As possible competing models we used the Log-normal, Gamma, Normal, Weibull and Exponential distributions. We estimate the model parameters for each candidate model using a Maximum Likelihood Estimate (MLE) approach, and use the Akaike Information criteria (AIC, Akaike 1974) for the model selection. The AIC is a tool based on the concept of entropy and offers a relative measure of the information lost when a given model is used to describe some data (a trade off between accuracy and complexity of the model).

Table 1 summarizes the functional form of the PDF, estimated (MLE) parameters (and uncertainties), and the AIC for all the probabilistic models considered. Using a Kolmogorov–Smirnov test, we cannot reject the Log-normal, Gamma, and Normal hypotheses (at significance level of 0.05), which means that, from a statistical point of view, all these probability models successfully explain the observed data. However, according with the AIC values, the preferred model (i.e. that with the lowest AIC value) is the Log-normal.

Table 1. Candidate distributions, PDF, estimated (MLE) model parameters and uncertainties, and Akaike Information Criteria (AIC). According to the AIC information, the model that best describes the data is the Lognormal

Model	Probability density	Parameters (MLE)	AIC
Log-normal (μ,σ)	$\boldsymbol{y = f(x\|\mu,\sigma) = \frac{1}{x\sigma\sqrt{2\pi}} e^{-\frac{(\ln x-\mu)^2}{2\sigma^2}}}$	μ=6.334 [6.329,6.339] σ=0.246 [0.243,0.250]	– 62803
Gamma (a,b)	$\boldsymbol{y = f(x\|a,b) = \frac{1}{b^a \Gamma(a)} x^{a-1} e^{-\frac{x}{b}}}$	a=16.68 [16.22,17.14] b=34.84 [33.87,35.83]	– 62845
Normal (μ,σ)	$\boldsymbol{y = f(x\|\mu,\sigma) = \frac{1}{\sigma\sqrt{2\pi}} e^{-\frac{(x-\mu)^2}{2\sigma^2}}}$	μ=581.0 [578.1,583.8] σ=146.3 [144.2,148.3]	– 63319
Weibull (a,b)	$\boldsymbol{y = f(x\|a,b) = \frac{b}{a}\left(\frac{x}{a}\right)^{b-1} e^{-\left(\frac{x}{a}\right)^b}}$	a=637.1 [633.7,640.6] b=3.87 [3.81,3.92]	– 63832
Exponential (μ)	$\boldsymbol{y = f(x\|\mu) = \frac{1}{\mu} e^{-\frac{x}{\mu}}}$	μ=581.0 [569.7,592.6]	– 72815

Figure 9a shows the cumulative probability (CDF) of the candidate distributions and the empirical CDF of the observed data, while the Figure 9b shows the CDF and related uncertainties of the Log-normal model.

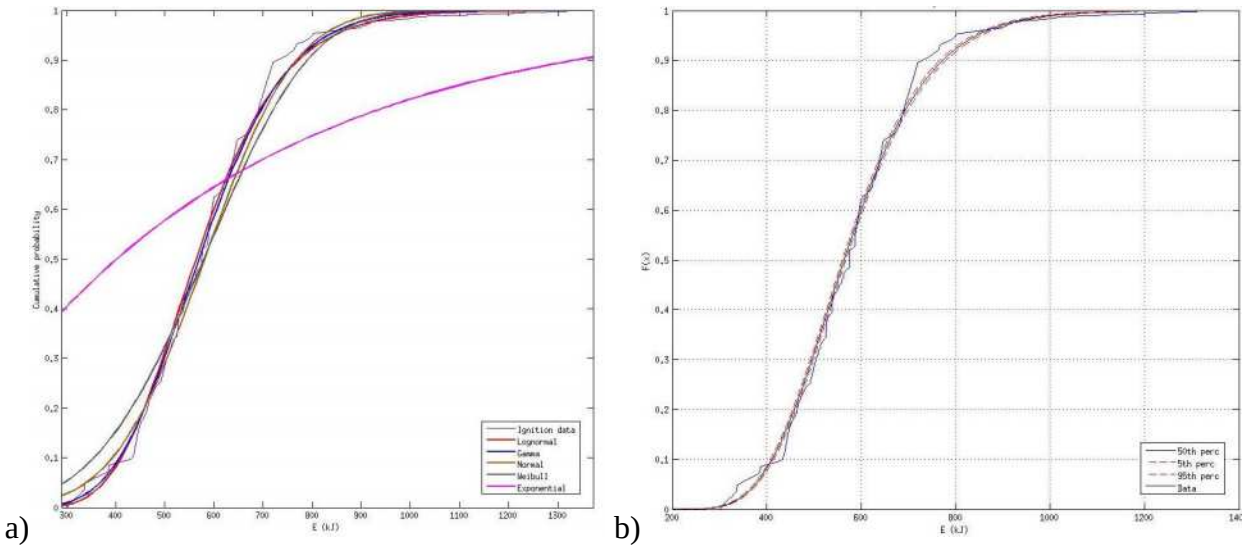

Figure 9. a) Plot of the Cumulative Distribution Function (CDF) of Log-normal, Gamma, Normal, Weibull, and Exponential competing models, and the empirical CDF of the observed data; b) CDF of the Log-normal (with parameters as those presented in Table XX), selected as the best model describing the observations

Therefore, the model selected to describe the energy required to start an ignition is a Log-normal with parameters μ=6.334 [6.329, 6.339] and σ=0.246 [0.243, 0.250], where the values in parenthesis represent uncertainty bounds. The Log-normal model is therefore used for the determination of the probability of fire ignition given the occurrence of an electric discharge. Since for simplicity we consider that an electric cable failure will always generate an electric discharge, this model consequently also represents the probability of a fire ignition given a cable failure.

As previously mentioned, there was no significant difference in the results achieved for pine needles as compared to straw. Therefore, for simplification, we assume that the model can provide the probability of ignition for all fuel classes other than urban areas, where the probability of ignition by electric discharge is assumed to be zero. This assumption seems reasonable as commonly, for prevention reasons, the area below electric cables is cleaned of heavy fuels.

Results

In this section, the maps summarizing the results obtained for event probabilities at different parts of the event chain are presented. Figure 10a shows the map representing the probability of cable failure in the electric network given the occurrence of a Mw5.6 seismic event in the NE part of the study area.

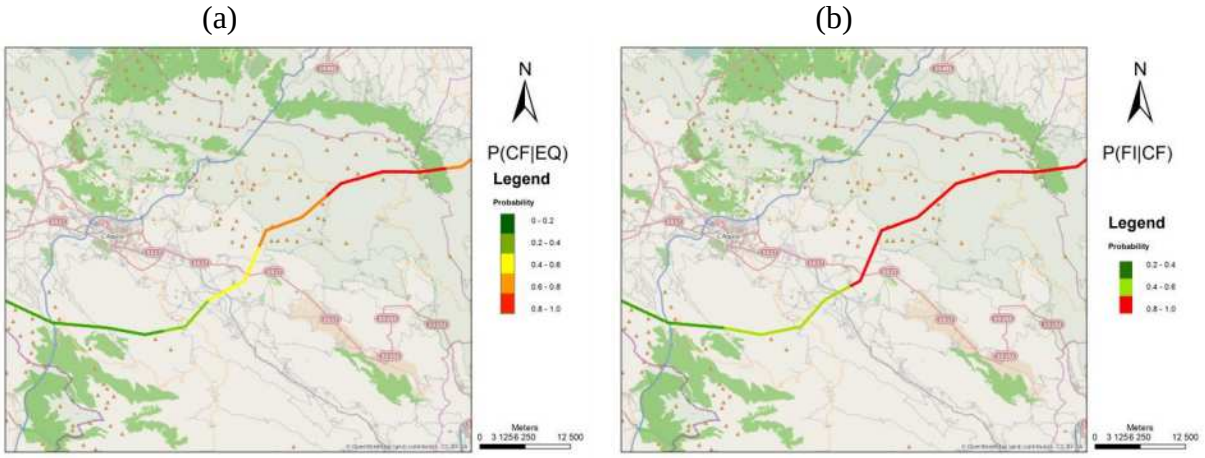

Figure 10. Maps for: a) probability of cable failure, and b) probability of fire ignition due to an electric cable failure

As it was previously explained, cable failures occur close to the electric poles. Therefore, the information on the cable failure probability is presented around the poles. In this case, a single electric poles fragility curve was used (X_{MAX}=1) and therefore the probability of cable failure depends exclusively on the distance between each pole and the seismic epicentre.
Besides the visualization of the map for probability of cable failure due to the triggering EQ event, the assessment of the probabilities of fire ignition due to cable failure also needs to be considered. This information is provided in the form of a distribution map as shown in Figure 10b. The map for distribution of fire ignition by electric cable failure is obtained from the fuel map (Figure 6), the geographic location of the electric network (Figure 1) and the probability function of fire ignition.
It is worth noting that the probability of fire ignition is strongly dependent on the energy released by the electric discharge. The amount of energy released during the discharge was determined by fixing a trigger time (electric interruption) of 0.1s, a power of 8,000kVA (current of 53A and voltage value of 150kV) and consequently 800kJ of energy for the first 20km of electric line (first 67 poles on the right side of Figure 10b). Furthermore, a withdrawal of 100kJ of energy was assumed due to energy consumption and losses for every 20km of electric line, resulting in a decrease of fire ignition probability along the electric network.
Finally, to evaluate the fire ignition probability given the occurrence of the seismic event, the full path of the selected scenario can be assessed. In this case, the probability of fire ignition is the product of the probability of cable failure due an EQ of a certain seismic intensity distribution, the probability of a fire ignition due to a cable failure (Equation 3), and the probability of having the PGA value calculated at the pole site (which in this case is 1 because we neglect uncertainties in ground motion prediction equations). Figure 11 shows the probability map of fire ignition triggered by the occurrence of the seismic event considered in the worked scenario.

$$p(FI) = p(FI|CF) \times p(CF|PGA) \times p(PGA) \quad \textbf{[3]}$$

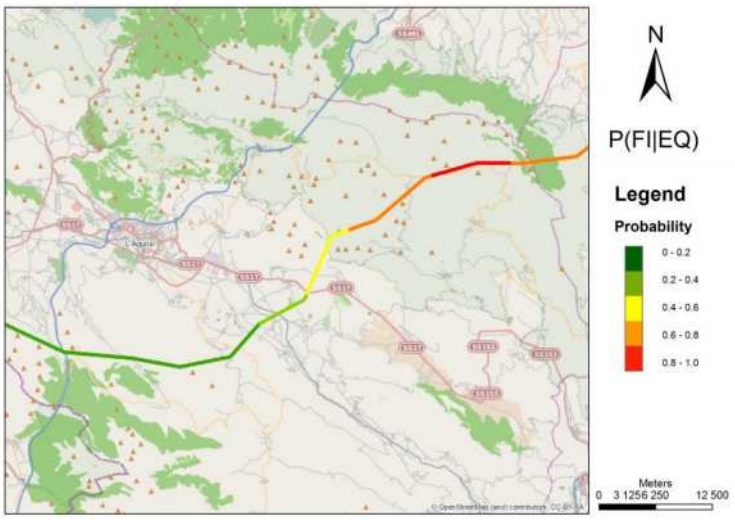

Figure 11. Map for probability of fire ignition due to the Mw5.6 earthquake considered in thestudied scenario

Supported by the information on the probability of a fire ignition around each pole, the simulation of an ignition and the subsequent fire development is commonly the following step. For a given pole with a calculated probability of fire ignition, we perform a fire propagation simulation using the FireStation tool in order to forecast the spread of the fire and other parameters of interest, as shown in Figure 12 The comparison of impacts caused by both EQ and forest fire in a cascade effect event may be an important information to support the decision making process. As outlined by Aubrecht *et al.* (2014), the temporal evolution of the entire cascading effects scenario also provides crucial input for

evacuation planning and societal impact assessment, taking into consideration dynamic population exposure models to cover the respective world state states.

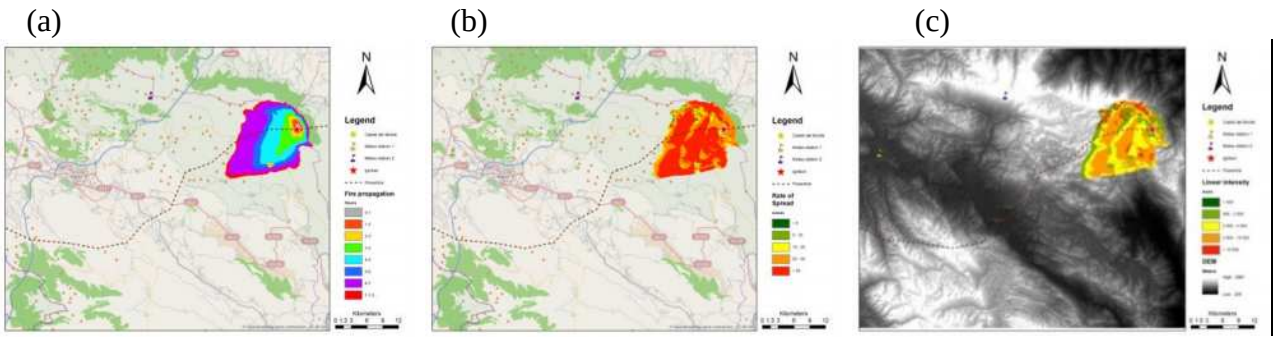

Figure 121 – Map of the evolution of the forest fire (a) after the ignition by the electric discharge from a probable ignition point and other possible outputs from the FireStation software: b) rate of spread, c) linear intensity.

Summary

The occurrence of a surprising cascading event chain may complicate an emergency situation caused by the occurrence of an adverse event since the initial strategy may become useless for the new scenario of multiple hazards occurring in a given chain of events. The probabilistic assessment of cascading effect scenarios is therefore of great relevance for precautionary reasons as this evaluation is useful before the hazard transition occurs. The probabilistic assessment of cascading effects scenarios shall be performed in a short and long term planning phase. Short term planning is related to a scenario where the triggering event has occurred and strategic plans are being designed in order to eliminate or mitigate further impacts. Long term planning is associated to a scenario where the triggering hazard event has not yet occurred but plans are being made in advance for preventive or preparative reasons.
A methodology for the probabilistic assessment of cascading effects was described using a sample scenario of an EQ as triggering event. After collecting the reauired data, it was possible to quantify the probability of fire ignition around the electric poles located in the study area. The anticipated perception of the likelihood of secondary events may support decision-making in order to avoid larger impacts caused by the triggered events (as the wild fires considered here) that would cause additional impacts respect to those directly caused by the triggering EQ event.

Acknowledgements

The presented study was performed in the framework of the CRISMA project (www.crismaproject.eu). CRISMA is funded from the European Community's Seventh Framework Programme FP7/2007-2013 under grant agreement no. 284552. The content of this paper has the contributions of many colleagues of the CRISMA Project Consortium to whom we would like to address our acknowledgment and appreciation.

References

Akaike H (1974). A new look at the statistical model identification. IEEE Trans Automat Contr AC 19:716–723

Alexander D and Magni M (2013). Mortality in the L'Aquila (Central Italy) Earthquake of 6 April 2009. Version 1. PLoS Currents 2013 January 7. Published online 2013 January 7. doi: 10.1371/50585b8e6efd1.

Almeida M, Ribeiro LM, Viegas DX, Garcia-Aristizabal A, Zuccaro G, Polese M, Nardone S, Marcolini M, Grisel M, Coulet C and Pilli-Sihvola K (2014). D42.3 - Database and Model for Dynamic scenario assessment. Deliverable of CRISMA FP7 European Project. http://www.crismaproject.eu/

Aubrecht, C, Elvidge CD, Baugh K, Hahn S (2011). Identification of wildfire precursor conditions: Linking satellite based fire and soil moisture data. In Tavares J.M.R.S., Natal Jorge R.M. (eds.), Computational Vision and Medical Image Processing: VipIMAGE 2011. CRC Press/Balkema (Taylor & Francis), 347-353.

Aubrecht C, Almeida M and Freire S (2014). Evaluating the benefits of spatio-temporal population dynamics data for protective action decision support in wildfire emergency management. 7th International Conference on Forest Fire Research (ICFFR). Proceedings. Coimbra, Portugal, November 17-20, 2014.

Lopes AMG, Cruz MG and Viegas DX (2002). FireStation - An integrated software system for the numerical simulation of wind field and fire spread on complex topography. Environmental Modelling & Software, Vol.17, N.3, pp. 269-285.

Pondrelli S, Salimbeni S, Morelli A, Ekstrom G, Olivier M and Boschi, E.(2010) Seismic moment tensors of the April 2009, L'Aquila (Central Italy), earthquake sequence, Geophys. J. Int., 180(1), 238–242.

Marzocchi W, Mastellone ML, Di Ruocco A. Novelli P, Romeo E and Gasparini P (2009). Principles of multi-risk assessment. Interaction amongst natural and man-induced risks. Project Report, FP6 SSA Project: Contract No. 511264

Marzocchi W, Garcia-Aristizabal A, Gasparini P, Mastellone ML, and Di Ruocco A (2012). Basic principles of multi-risk assessment: a case study in Italy, Nat. Hazards, 62(2), 551-573 DOI: 10.1007/s11069-012-0092-x.

Assessment of risk index for urban vegetation fires of Juiz de Fora, MG, Brazil

Fillipe Tamiozzo Pereira Torres, Guido Assunção Ribeiro, Sebastião Venâncio Martins, Gumercindo Souza Lima

[a]*Universidade Federal de Viçosa, DEF, campus universitário 36570-000, torresftp@yahoo.com.br, gribeiro@ufv.br, venancio@ufv.br, gslima@ufv.br*

Abstract

The impact caused by forest fire, although it is an old subject, but increasingly larger proportions, has stimulated the development of new methods for the prevention and reduction of risks in the environment. The use of a reliable index of risk among the existing preventive measures is fundamental to a more efficient planning of prevention and an effective action of fight. The work involving the forest fire prevention must use all the tools available since it is a complex task and one that shows great variability in the time of occurrence. One such tool is the degree of danger by means of an index that reflects the probability of fire occurrence. Meteorological indices have shown good results in predicting events and contributing to the work of forecasting fire in forests. The aim of this study was to analyze 4 descriptive fire risk indices for the period from 01/01/2006 to 12/31/2012. Each of them was built with 4 hazard classes of risk. The indices used were Formula de Monte Alegre (FMA), Index of Nesterov, Index of Telicyn and P-EVAP According to the results, the rate of P-EVAP performed better in accuracy of forecasts of occurrences within the class of High Risk, while the FMA was the most effective in the forecast of no occurrence in classes of Low Risk and No Risk. The days classified as Medium Risk in Telicyn indices and P - EVAP presented closest to the average of occurrences in the entire series averages. Knowledge of descriptive classes of indices for predicting fire is valuable to communicate with public, help the actions of awareness, prevent and plan accident. The results had shown some similarities with studies of Torres *et al*. (2009). They used the Skill Score (SS) method and concluded that the logarithmic index of Telicyn showed the best results for the study area.

Keywords*: Index of danger, descriptive classes, fires*

Introduction

Forest fires contribute to air pollution, climate change and are among the most damaging to some ecosystems events (Magalhães, Lima & Ribeiro, 2011). In areas of economic development, the pressures that forest areas suffer due to the need for new areas intended for agricultural activities, have greatly increased the number of fires and the extent of burned areas due to bad use of fire as an agricultural tool (Alves & Nóbrega, 2011).

In recent years, debates involving fires have increased significantly because there is a great concern due to the release of CO2 and other gases to atmosphere, which are residues from the vegetation combustion. Brazil, in general, is considered as a great contributor of CO2 emissions resulting from forest fires. Globally fires and emissions cause severe losses of biodiversity, interfere in a water cycle and in carbon cycle in the atmosphere. This cause economic, landscaping and ecological loss, reaching protected areas, farms, roadsides, urban areas and nearby areas of reforestation, besides other places (Souza, Casavecchia & Stangerlin, 2012).

One way to prevent these fires is through knowledge of the degree of the risk, which reflects the possibility of an event to occur. These indices can be supported by environmental variables, usually related to weather conditions and can be estimated by indices constructed with different combinations of variables (Tetto *et al*., 2010).

The risk assessment is based, in general, in an integration of the factors that contribute to the risk of the forest fire model. This method of risk assessment is reflected generally in indexes that can be

materialized in maps which are expressed areas or levels of risk (Antunes, Viegas and Mendes, 2011). Besides to allow the correct planning Borges *et al*. (2011) argue that the use of a risk index reliably fire is critical to the establishment and mapping of risk areas, defining the number and location of fire observation towers and public warning level risk, which is considered an important factor in environmental education programs. The first step is determine the danger of fire occurrence. For this, several methods have been developed and refined over the years and in different countries.
According Carapiá (2006), rates of fire risk are influenced by several factors, usually fuels, topography and weather. The choice of variables and methods used in this combination results in a variety of approaches. Faced with this diversity, several solutions have been proposed for classification. Depending on the input data, two main groups of methods may be identified: 1) weather risk, which is based solely on data of weather conditions (like temperature, relative humidity, rainfall and wind speed) and 2) potential risk, when are considered more advanced approach, and includes as input the state of vegetation, type of fuel and its moisture content.
The aim of this study was to compare the efficiency of 4 weather indices: Formula de Monte Alegre (FMA) (Soares, 1972), Logarithmic Index of Telicyn, Nesterov Index and Cumulative Index P-EVAP. Will be analysed the relationship of hazard classes of each index with the occurrences of forest fires in the urban area of Juiz de Fora, MG, Brazil, whereas the use of a reliable index of danger is a fundamental factor for efficient planning of measures prevention and to adopt quick and effective actions in fighting fires, in order to reduce losses and, consequently, of any financial losses resulting from the occurrence of catastrophic events.

Methods

In this study was analyzed a time series of 01/01/2006 to 31/12/2012. Meteorological data were provided by LabCAA (Laboratory of Climatology and Environmental Analysis) of the Federal University of Juiz de Fora (UFJF). The information on 3,135 occurrences of forest fires in urban area, were provided by the 4th Battalion of Military Firefighters (4th BBM).
An analysis of days according to the hazard class of each index was taken, noting occurrences per day, percentage of days with occurrences and percentage of occurrences of each class in relation to the whole period.
The calculation of each index was performed as follows:

2.1. Fórmula de Monte Alegra - FMA

$$FMA = \sum_{i=1}^{n} (100/Hi)$$

where:
FMA = Monte Alegre index.
H = relative humidity (%).
n = number of days analysed

The index value is subject to restrictions according to the precipitation, as shown in Table 1:

Table 1. Modification in the FMA value in agreement with the precipitation

Rain day (mm)	Modification of the calculation
≤2,4	None
2,5 a 4,9	Shoot down 30% in the FMA calculated before and add (100 / H) of the day
5,0 a 9,9	Shoot down 60% in the FMA calculated before and add (100 / H) of the day
10,0 a 12,9	Shoot down 80% in the FMA calculated before and add (100 / H) of the day
>12,9	Interrupt the calculation (FMA=0), starting over the sum in the next day or when rain to cease.

Source: Torres *et al*. (2009)

Telicyn Logarithmic Index

$$I = \sum_{i=1}^{n} \log (ti - ri)$$

where:
I = Telicyn index
T = air temperature in °C
r = dew point temperature in °C
log = logarithm to the base 10

Restriction Index: whenever a precipitation equal or higher than 2.5 mm occurs, abandon the sum and start calculating the next day or when the rain stopped. In this case the index value is zero.

Nesterov Index

$$G = \sum_{i=1}^{n} di \cdot ti$$

where:
G = Nesterov Index
d = saturation deficit of the air in millibars
T = air temperature in °C
n = number of days analysed

The saturation deficit of the air, in turn, is equal to the difference between the maximum water vapor pressure and the real pressure of water vapor, which can be calculated by the following expression:

$$d = E (1-H/100)$$

where:
d = saturation deficit of the air in millibars
E = maximum pressure of water vapor in millibars
H = relative humidity in%

The sum is limited or changed by the occurrence of precipitation according to Table 2.

Table 2. Modification in the G calculation in agreement with the precipitation

mm Rain day	Modification of the calculation
≤2,0	No
2,1 a 5,0	Shoot down 25% in the G value calculated to the day before and add (dt) of the day
5,1 a 8,0	Shoot down 50% in the G value calculated to the day before and add (dt) of the day
8,1 a 10,0	Abandoning the previous sum and start new calculation, ie, G = (dt) of the day
>10,0	Interrupt the calculation (G=0), starting over the sum in the next day or when rain to cease.

Source: Torres *et al*. (2009)

2.4. P-EVAP

The P-EVAP cumulative index proposed by Sampaio (1991), relates the difference between precipitation (P) and evaporation (EVAP), both daily measured in mm. The restrictions on the calculus are the same of Nesterov index (Table 2).

To normalize the number of classes of indices, the class named as Most High Danger of FMA and Nesterov index was grouped within the class of High Risk. For Index-P EVAP, descriptive classes were determined according to the average of occurrences per day. The descriptive classes of each index are shown in Table 3.

Table 3. Descriptive classes of the indices

Indexes	Hard	Middle	Low	Null
FMA	>8,0	3,1 a 8,0	1,1 a 3,0	≤1,0
Telicyn	> 5,0	3,6 a 5,0	2,1 a 3,5	≤ 2
Nesterov	> 1000	501 a 1000	301 a 500	≤300
P-EVAP	< -44,9	- 17 a - 44,9	- 5 a - 16,9	> -5

Adapted from: Torres *et al*. (2009)

3. Results and Discussion

In the time series, the average was 1.14 events per day. The indices of Nesterov and FMA were those with more days classified as High Risk (Table 4). At Average Risk, FMA and P-EVAP had a greater number of days. Classes of Low and Zero Risk indices with the highest number of days were P-EVAP and Telicyn.

Table 4. Number of days of each index by danger class

Index	Hard	Middle	Low	Null	Total
FMA	1293	495	347	605	2740
Telicyn	990	213	245	1292	2740
Nesterov	1453	295	157	835	2740
P-EVAP	663	487	495	1095	2740

Analyzing the descriptive class of High Risk (Table 5) it is observed that the P-EVAP index showed the highest number of occurrences per day within the period (3.0), and 81% of days classified as High Risk for fires that occurred. On the other side presented the lowest number of occurrences within the period (63%), while Nesterov index record higher percentage of occurrences (88%).

Table 5. Analysis of the descriptive class of High Risk

Index	Events/day	% of days with occurrences	% of occurrences
FMA	2.06	68%	85%
Telicyn	2.42	74%	77%
Nesterov	1.90	64%	88%
P-EVAP	3.00	81%	63%

Regarding the days classified as Medium Risk (Table 6), it was observed that the index of P-EVAP showed the most occurrence per day (1.12), where 54% of days with occurrence and 17% of occurrence on the period. Furthermore, Nesterov and FMA indexes showed less occurrences per day, being classified as Medium Risk (0.56) and percentage of days with events (30% and 31%). However, there was a difference in the percentage of occurrences within the class in relation to the series studied, the FMA had the second highest percentage (9%) while the Nesterov index ranked last (5%).

Table 6. Analysis of the descriptive class of Medium risk

Index	Events/day	% of days with occurrences	% of occurrences
FMA	0.56	31%	9%
Telicyn	0.92	48%	6%
Nesterov	0.56	30%	5%
P-EVAP	1.12	54%	17%

In the days classified as Low Risk (Table 7), the FMA showed the least amount of occurrences per day (0.26), a lower percentage of days with occurrences (14%) and second lowest percentage of occurrences for the period around (3%). The Telicyn index had shown the highest number of occurrences per day (0.82) and percentage of days occurring within the class (42%). The P-EVAP index showed the highest percentage of occurrences in relation to the 2740 days of the series (11%).

Table 7. Analysis of the descriptive class of Low Risk

Index	Events/day	% of days with occurrences	% of occurrences
FMA	0.26	14%	3%
Telicyn	0.82	42%	6%
Nesterov	0.37	25%	2%
P-EVAP	0.68	37%	11%

In the of Null Risk class (Table 8), the FMA and Nesterov index got the best performance in relation to the number of occurrences per day (0.18 and 0.19), percentage of days with no occurrence (92% and 91%) and concentrated the lowest number of occurrences in relation to the whole period (3% and 5%). While the Telicyn index got the highest number of occurrences per day (0.27), a lower

percentage of days without incidents (85%) and the highest concentration of occurrences in relation to the whole period (11%).

Table 8. Analysis of the descriptive class of null risk

Index	Events/day	% of days with occurrences	% of occurrences
FMA	0.18	92%	3%
Telicyn	0.27	85%	11%
Nesterov	0.19	91%	5%
P-EVAP	0.23	88%	8%

The results showed some differences and similarities with the studies by Torres *et al*. (2009) They used the Skill Score (SS) method which is the ratio of the difference between the occurrences in the forecast and the expected number of occurrences; and the difference between the observed number of days and number of days with forecast adjustments. It was concluded that the Telicyn logarithmic index achieve the best results for the characteristics of Juiz de Fora territory. However, in an individual analysis of the occurrences predictions and no occurrences of fires, it is observed that the most effective index was the P-EVAP with 77% of correct predictions, while the FMA was the index that best answered forecasts of not fires occurrences with 90% accuracy.

Conclusion

The data showed a wide variety in the results of each index . However it can be concluded that for days with high fires risks, the rate of P - EVAP performed better in accuracy of forecasts of occurrences also concentrating the highest average successes per day within the period.
Furthermore, the FMA showed the best results for days classified as Low Risk and No Risk , with higher percentage of success in forecasting of non occurrences and lower value of occurrences per day in class.
Analysing the days classified as Medium Risk , P – EVAP and Telicyn indices were closer to the values from the average of daily occurrences on the whole period studied.
The knowledge of descriptive classes of indices for predicting fire can be very valuable in informing the public, helping the actions of awareness and prevention of more serious accidents.

References

Alves, K. M. A. da S.; Nóbrega, R. S. (2011). Uso de dados climáticos para análise espacial de risco de incêndio florestal. Mercator, Fortaleza, v. 10, n. 22, p. 209-219.

Antunes, C. C.; Viegas, D. X.; Mendes, J. M. (2011). Avaliação do Risco de Incêndio Florestal no Concelho de Arganil. Silva Lusitana, Oeiras, v.19, n.2, p.165-179.

Borges, T. S. *et al.* (2011). Desempenho de Alguns Índices de Risco de Incêndios em Plantios de Eucalipto no Norte do Espírito Santo. Floresta e Ambiente, Seropédica, v. 18, n.2, p. 153-159.

Carapiá, V. R. (2006). Predição do índice de risco de incêndios e modelagem computacional do comportamento do avanço da frente do fogo no Parque Nacional da Floresta da Tijuca. Tese (Doutorado em Engenharia Civil) – COPPE, Universidade Federal do Rio de Janeiro, Rio de Janeiro.

Magalhaes, S. R. de; Lima, G. S.; Ribeiro, G. A. (2012). Avaliação dos incêndios florestais ocorridos no Parque Nacional da Serra da Canastra - Minas Gerais. CERNE, Lavras , v. 18, n. 1, p.135-141.

Sampaio, O. B. (1991). Estudo comparativo de índices, para previsão de incêndios florestais, na região de Coronel Fabriciano, Minas Gerais. Dissertação (Mestrado em Ciência Florestal) - Universidade Federal de Viçosa, Viçosa.

Soares, R. V. (1972). Índice de Perigo de Incêndio. Floresta, Curitiba, v.3, n.3, p.19-40.

Souza, A. P.; Casavecchia, B. H.; Stangerlin, D. M. (2012). Avaliação dos riscos de ocorrência de incêndios florestais nas regiões Norte e Noroeste da Amazônia Matogrossense. Scientia Plena, Aracajú, v.8, n.5, p.1-14.

Tetto, A. F. *et al.* (2010). Comportamento e ajuste da fórmula de Monte Alegre na Floresta Nacional de Irati, Estado do Paraná. Scientia Forestalis**, Piracicaba, v. 38, n. 87, p.409-417.**

Torres, F. T. P. *et al.* (2009). Relações entre incêndios em vegetação e elementos meteorológicos na cidade de Juiz de Fora, MG. Revista Brasileira de Meteorologia, São José dos Campos, v. 24, p.379-389.

Characterizing pyroregions in south-eastern France

Thomas Curt, Thibaut Fréjaville, Christophe Bouillon

[a] *IRSTEA-EMAX Mediterranean ecosystems and risks, 13185 Aix en Provence (France),*
thomas.curt@irstea.fr, thibaut.frejaville@irstea.fr, christophe.bouillon@irstea.fr

Abstract
Efficient fire policies may rely on good knowledge of the regional variations of fire activity and of fire drivers. South-eastern France comprises a range of pyroclimates, i.e. regions with contrasted fire activity (from fire-prone Mediterranean areas to mountain areas with few fires) and contrasted climate and fire weather. We tested if these pyroclimates also corresponded to specific hierarchy among environmental and human variables which drive fire activity. We used a 1973-2009 georeferenced fire database, and we computed how the landscape compartmentalization, the fuel coverage, the human density and the fire suppression capacity varied at a 2x2 km scale. The first pyroregion regroups two maritime fire-prone mountains (Corsica and the maritime Alps) in which there are no clear limitation to fire activity because of high human activity (i.e. numerous ignitions), no fuel limitation, and no weather limitation. The area is especially fire-prone because the suppression capacity is low to medium, and because the compartmented landscape hinders the activity of firemen. In the second pyroregion (fire-prone Mediterranean plains and foothills), fire activity is neither weather-limited (especially during dry summers) nor fuel-limited. It is clearly controlled by fire suppression which is especially active. In the third pyroregion (cool peri-Mediterranean mountains), fire activity remains low in spite of low fire suppression capacity and high landscape compartmentalization, because human activity is low and fire weather is unfavorable on average. We discuss to which extent the present fire suppression strategy (i.e. fast, hard-hitting initial attack on all fires) is adapted to these different pyroregions. In the fire-prone maritime mountains, it would be useful to increase the fire suppression forces. In fire-prone plains and foothills, the current plan of action is well suited, but large and destructive fire may persist due to the climate change and the fuel accumulation. In mountainous areas with low fire activity, fire suppression forces will likely have to adapt to the forecasted increase of fire activity.

Keywords*: pyroregion; pyrogeography; k-means clustering; fire hazard; France*

Introduction

Wildfires are major disturbances in many terrestrial ecosystems worldwide. In south-eastern France, fires have major impact on humans, infrastructures, and ecosystems (Curt, Borgniet *et al*. 2013). Basically, wildfire activity and fire regime depend upon three main requirements: sources of ignitions, a fuel to burn (i.e. vegetation and land covers), and a favorable climate and weather acting on fire ignition and propagation (Krawchuk, Moritz *et al*. 2009). The chief drivers of fires are thus: (i) climate which promotes the weather conditions favorable to fire ignition and propagation; (ii) human activities which provide a part of the ignitions, which modify land uses and vegetation, but which also suppress fires; and (ii) vegetation and land uses. The environmental conditions as the topography modify fire propagation. Pyrogeography (*sensu* (Krawchuk, Moritz *et al*. 2009) suggests that interactions among these drivers create specific landscape patterns of fire distribution. Here we call 'pyroregion' an area characterized by a typical spatiotemporal pattern of fires driven by a typical hierarchy among fire drivers (weather, fuels, humans).
Characterizing pyroregions is crucial for fire science and fire policy. Actually, it can help understanding the contribution of each fire driver from past to present. The fire policy and the fire suppression strategy may thus adapt to the regional variations of fire regime.
The south-eastern part of France is a good study case because it comprises a range of regions with different fire activity, and presumably different hierarchy among fire drivers. A simple view of the 1973-2009 fire maps shows that fire size, fire pattern, and fire number varies strongly within study

area (Figure 1). The southernmost part of this area comprises Mediterranean-type ecosystems which are especially fire-prone. The peri-Mediterranean areas have less summer fires but more prescribed burning in winter and spring (Fernandes, Davies *et al*. 2013). The mountain areas (southern French Alps, Eastern Pyrénées and Massif Central) are less fire-prone but some of them have experienced increased fire activity during the last decades. A precedent study (Fréjaville & Curt, this issue) partitioned the south eastern France into pyroclimatic regions based on spatiotemporal patterns of fire and climate. We tested to which extent these pyroclimatic regions also corresponded to specific hierarchy in the environmental and human drivers, including fire suppression.

Methods

In this study we characterized how areas characterized by similar fire regime, climate and similar temporal trend (i.e., pyroclimatic regions) depicted hierarchy in environmental and human drivers throughout southern France, i.e. what are the pyroregions. For this purpose we used a georeferenced fire database (1973-2009), and data on human activities, fuels, weather, and topography.

Study area

The study area was the whole south-eastern France (ca. 80,500 km²), including the 15 departments most frequently subjected to wildfires. This area has varied rates of coverage by flammable fuels such as forests and shrublands (15 to 70%). The main forest types are oaks forests (*Quercus ilex, Q. pubescens*), pine forests (*Pinus halepensis, P. sylvestris, P. nigra, P. pinaster*), and mixed oak-pine forests. At higher elevation, forests comprise *Larix decidua, Fagus sylvatica, Abies alba*, *Picea abies,* and *Pinus cembra*. Flammable shrublands (so-called *garrigues* and *maquis*) are common in the southernmost part of the study area. They are dominated by *Quercus coccifera*, *Ulex parviflorus*, *Cistus* spp., and *Erica arborea*. At high elevation, the dominant shrubs are *Vaccinium myrtillus* and *Arctostaphyllos uva-ursi*. The study area covers a large gradient of elevation from the sea level to the subalpine ecosystems of the French Southern Alps (ca. 2500 m asl).

The southern part of the study area along the Mediterranean sea has typical Mediterranean climate with hot and windy summers which favor fire activity. The peri-Mediterranean area has a supra-Mediterranean climate with hot summer temperature but cold winters, and the mountain climate of the French Alps is typically cold in winter and cool in summer.

Wildfire activity heterogeneously impacted the ecosystems and the landscapes in the study area (Figure 1), with a clear gradient from the highly fire-prone coastal areas located near the Mediterranean sea, to peri-Mediterranean mid-elevation mountains which experience frequent fires, then to subalpine mountains which historically experienced fires but at much lower frequency and intensity (Genries, Mercier *et al*. 2009). Fire is a major driver of vegetation dynamics in the Mediterranean part of the study area: about 6% of the wildland being has burned at least once between 1960 and 2011. In this area, stand-replacing fires are predominant and mostly occur in summer (Curt, Borgniet *et al*. 2013). Fire is also frequent in the peri-Mediterranean area all along the coast. Mountain areas (notably subalpine areas of the Pyrenees and Alps) experienced quite frequent fires along the Holocene but these fires were mostly surface fires. All the study area is under the protection of the fire suppression crews and services, but regional variations in fire suppression means exists (see below 2.6).

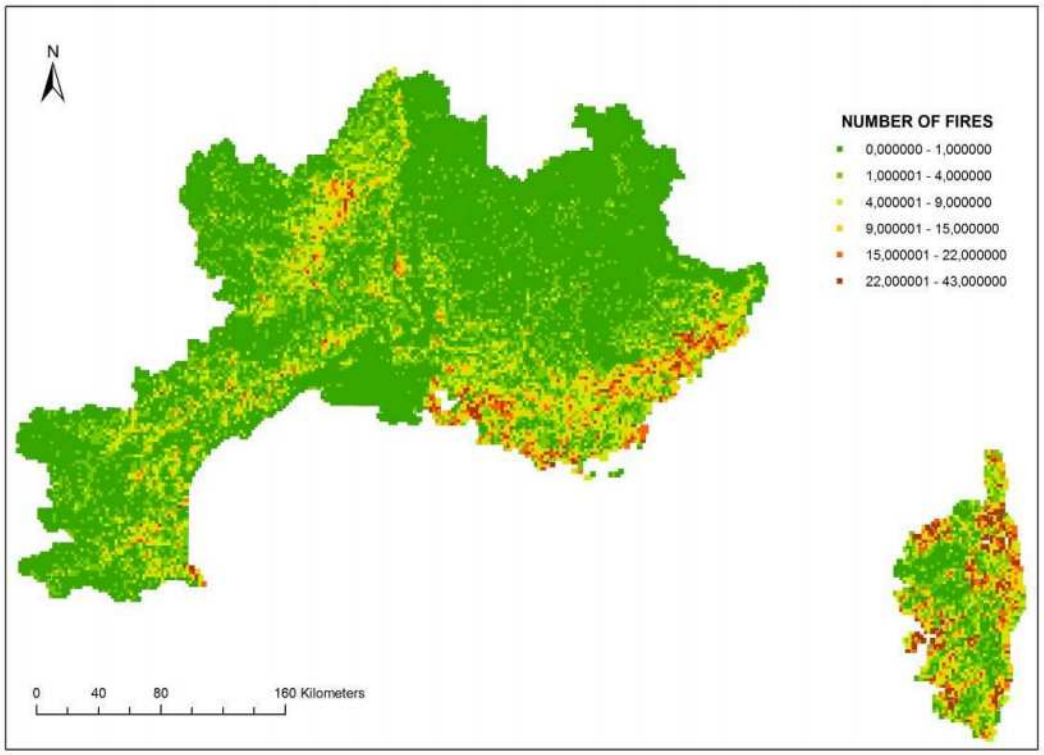

Figure 1. Fire density in south-eastern France (number of fire from 1973 to 2009)

2.2. Fire Data

We used the French Prométhée fire database (Prométhée 2011) which gathers all wildland and forest fires and indicates their date, hour, size, and location on a 2*2 km grid since 1973. We analyzed data for the 1973-2009 period. Fire activity was characterized by three variables: fire density was computed as the number of fires recorded in a 2*2 km pixel, the burned area computed as the total area burned in each pixel (calculated as the sum of all individual fires), and the fire length season which was calculated as the number of days during which fires occurred in a given year in each pixel along the 1973-2009 period.

2.3. Fire Weather

We used the fire weather index (FWI) and its sub-indices (FFMC, DMC, DMC) to assess the mean weather during a fire event, which is crucial for explaining its size and pattern. The FWI is a unitless index that was designed originally to forecast fire risk in Canada on the basis of past and current weather conditions (van Wagner 1987) including air temperature and relative humidity, surface wind speed, and rainfall in the past 24 hours. It provides a uniform, numeric method of rating fire danger throughout an area (Aguado, Chuvieco *et al*. 2003). The FWI aims to predict the probability and ease of ignition and propagation of a fire on the forest floor, taking into account the weather conditions. High FWI values indicate high fire danger.

2.4. Land covers and fuels

The type of land cover may affect the propensity to burn because all land covers do not have the same flammability, and because some land covers are preferentially burned for agricultural purpose or other purposes. The main types of land covers have been assessed using the CORINE 2006 database. We

regrouped the land uses in main categories including forests (pine, oak, and mixings), shrublands, pastures, agricultural lands, urban lands, and other types such as lakes and rivers.
It is of importance to assess the fuel coverage in each pixel of the study area. For this purpose we transformed the CORINE land covers (see above) into flammable fuels (forests, shrublands, and pastures) and non-flammable fuels (i.e. all other types of land cover). Each pixel was assigned a value of fuel coverage computed using a fuel connectivity index for the 8 adjacent pixels. If the central pixel and the 8 adjacent pixels comprised flammable fuels, the fuel coverage was coded as 1, and coded as 0 if fuel was absent from all pixels. Increasing values of fuel coverage suggest higher contagion of flammable vegetation.

2.5. Topography

Topography is acknowledged to affect the likelihood of fire ignition but mostly the behavior of fire (Pyne, Andrews *et al*. 1996). Flat landscapes promote rapid fire rate of spread and large, regular fire shapes while heterogeneous landscapes make fires contours more heterogeneous and generally result in smaller fires. Southern aspects generally favor ignitions and fire propagation since fuels may be drier. Slopes oriented towards dominant summer winds would also favor fire propagation. We assessed three main topographic variables for each pixel: slope, aspect, and a synthetic index of landscape complexity. This index is oriented towards the determination of the extent to which landscape is compartmented and how this may affect fire propagation and size, and the activity of firemen. Actually, a compartmented landscape with steep slopes, deeps valleys, variations of aspect, ridges would both limit fire extension but also hinder the work of firefighters (Pyne, Andrews *et al*. 1996). This index was computed as the cumulated absolute differences in elevation and aspect between each pixel and the eight surrounding pixels. High values of the index of complexity suggest complex fire contours and high difficulty for fire suppression.

2.6. Human activities

Humans have two contradictory incidences on fires. First, they provide most ignitions as lightning fires remain very likely rare in our study area. Secondly, they also prevent and suppress fires. Human activities strongly impact fire activity since fire is both a natural disturbance but also a tool for vegetation management, and sometimes conflicts. Fire causes were not explicitly considered as this information remained fragmentary until the mid-1990s: less than 50% of causes really known (Prométhée 2011). We considered the main variables expressing the pressure exerted by humans on fire activity in each pixel: the density of roads, the density of wildland-urban interfaces, and the population density. Indeed, high density of roads, houses and humans likely increases the number of ignitions.
Data from the French firefighting services were used to assess the regional variations in the fire suppression capacity. We computed a synthetic score using different information. First, we assessed the number of fire suppression forces, specific fire suppression material resources (trucks) and mean annual investment in suppression resource for each of the 15 departments of the study area (corresponding to districts of 3,567 to 6,925 km²). These data were recoded as scores from 1 (very low) to 5 (very high) according to iso-range values. Secondly, in order to get a more detailed view of the location of the fire suppression forces, we used a georeferenced database of all firehouses. Each firehouse was affected a code according to the number of fire crew (1 = low; 2 = medium; 3 = high). Then, we computed an inverse distance weighted function from each firehouse, which represents the capacity or the time needed to suppress a fire from each firehouse. Finally, we combined these two sets data to get a map of the score of fire suppression capacity. It indicates the number and location of human and mechanical means that can suppress a fire in any pixel of the landscape, under the assumption that higher and closer fire suppression resources would suppress more effectively fires, and prevent them from becoming large and destructive.

2.7. **Data Analyses**

A precedent study (Fréjaville & Curt, this issue) partitioned the south eastern France into pyroclimatic regions based on spatiotemporal patterns of fire and climate (Figure 2). We used this pyroclimatic classification as a basis to test if the different pyroclimates corresponded to specific hierarchies in the environmental and human drivers, including fire suppression. In a first step, we used a principal component analysis (PCA) in order to determine the redundant variables, and to select the most influential environmental and human variables. The fire and climate variables were put as supplementary variables because they were prior used to discriminate pyroclimatic regions. In a second step, we plotted the values of these influential variables as a function of the pyroclimatic groups in order to determine which variables discriminated each pyroclimatic group.

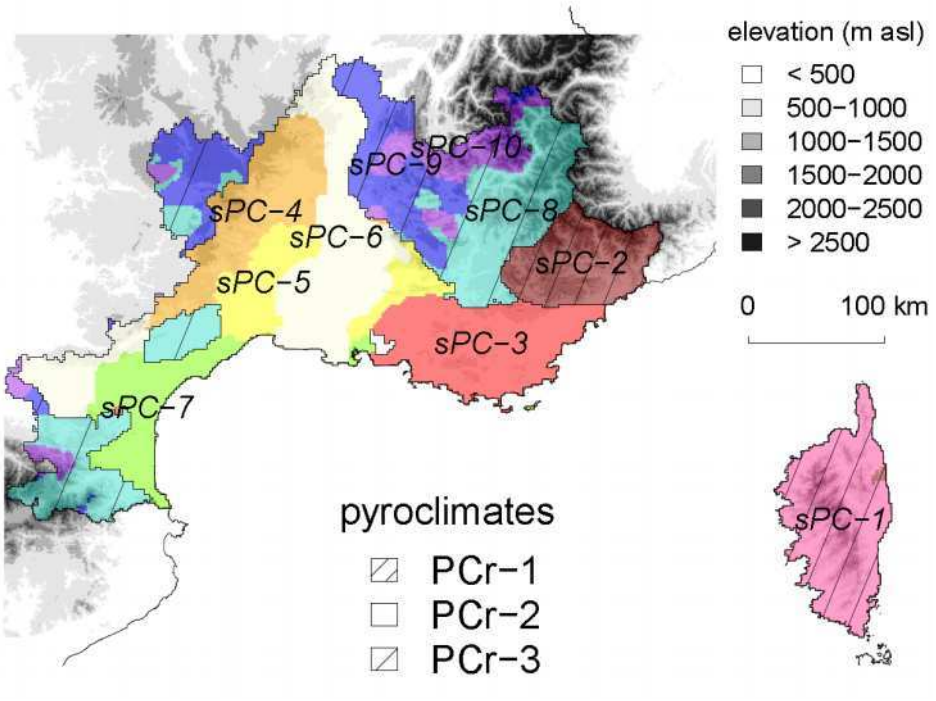

Figure 2. Pyroclimatic regions of south-eastern France. (From Fréjaville & Curt, see this special issue and Table 1)

Table 1. Main characteristics of the pyroclimatic regions of south-eastern France1973-2009 (From Fréjaville & Curt, see this special issue)

	PCr-1	PCr-2	PCr-3
Fire activity	Maximal fire density Medium and large fires Long fire season	High fire density Small to large fires Long fire season	Low fire density Small fires Short fire season
Fire activity trend	Increasing fire density at spring and autumn	Decreasing fire density and size in almost all seasons	Increasing fire density in summer, decreasing fire size in summer and winter
Climate	High summer and winter precipitation	Hot summer temperature, high 95th percentile FFMC and FWI	High spring and summer precipitation
Climate trend	High increase 95th percentile FWI and DMC	Decreasing FWI in spring	Increasing summer temperature, decreasing winter precipitation

Results

The PCA allowed determining the most influential environmental and humans variables, and discarding the redundant variables. Finally, the PCA indicated two main groups of environmental and human variables (Figure 2). The first comprises high fuel coverage, wildland flammable vegetation (predominantly forests and shrublands), and compartmented terrains which are difficult to access. This group corresponded to areas with high mean annual rainfall. At the opposite, the other group corresponded to areas with high human activity (high housing density, high road density), and high capacity of fire suppression. It corresponded to high mean annual temperature and high values of FWI and the associated indices (FFMC, DMC, DC).

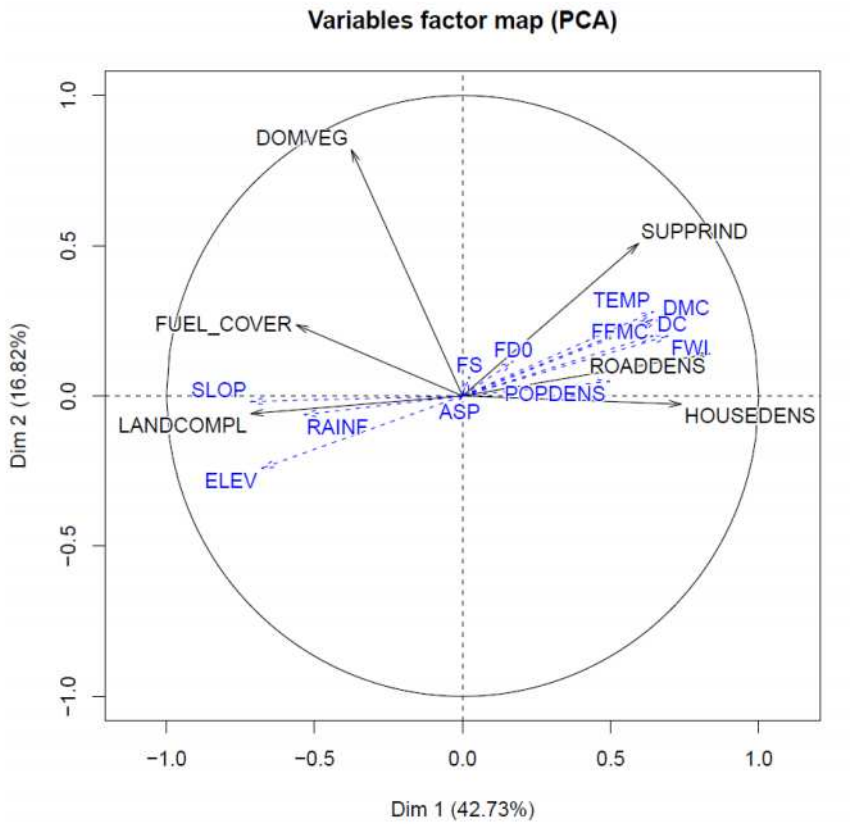

Figure 3. Principal component analysis of the main fire drivers in south-eastern France. Variable in black are active variables (FUEL_COVER: fuel coverage, LAND_COMPL: compartmentalization of the landscape, IND_LUTTE: fire suppression capacity index, Lroute: road density, SUM_Sbati: surface of habitations). Variables in blue are supplementary variables

The comparison of the main environmental and human variables for the three pyroclimatic regions (Figure 4) indicated that the first pyroclimatic region was characterized by a medium to high human activity, a very high fuel coverage and a highly compartmented landscape, but a low to medium fire suppression capacity. The second pyroclimatic region was characterized by high human activity but high fire suppression capacity, a low compartmented landscape, and low fuel coverage. The third pyroclimatic region was characterized by high fuel coverage and highly compartmented landscape but a low human activity and fire suppression capacity.

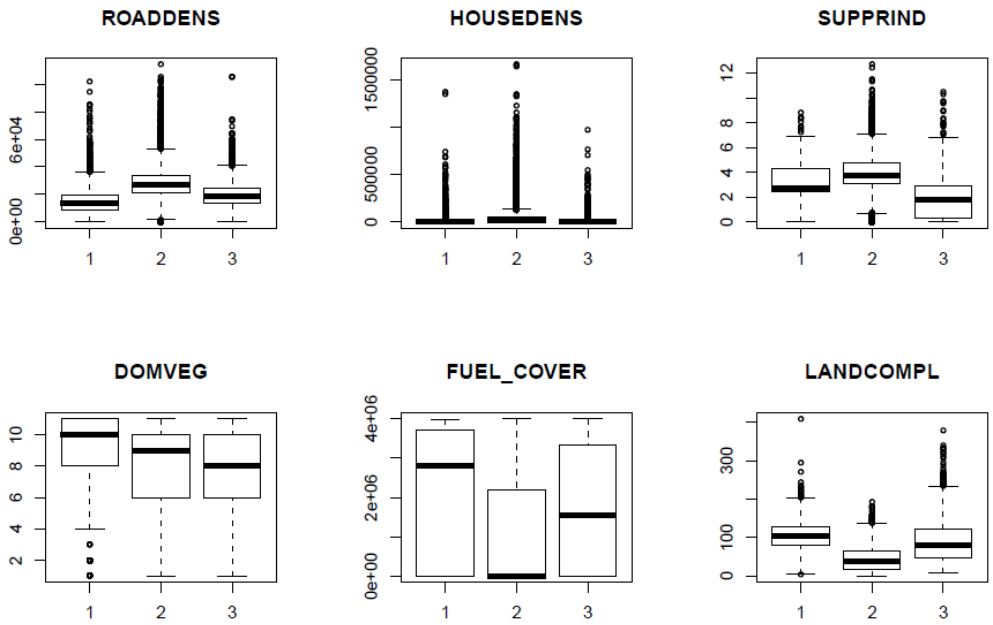

Figure 4. Boxplots of the main fire drivers for the three pyroregions of south-eastern France

Discussion

4.1. Pyroregions

The combination of the pyroclimates regions with human and environmental variables provided a description of three main pyroregions, which all have a specific combination of fire activity, fire weather and climate with specific features of human activity, fuel coverage, land compartmentalization, and fire suppression capacity.

The first pyroregion regroups two maritime fire-prone mountains: Corsica and the maritime Alps. Both areas have high fire density, medium to large fires, and a long fire season. Fire density increased in spring, autumn and winter along the past decades. Climate is favourable to fires and the climate-based fire danger indices increased strongly along the 1973-2009 period (Frejaville *et al*., this issue. Human activity is strong, fuel coverage is high, the landscape is difficult to access, and the fire suppression fire is low to medium. These maritime mountains have thus many factors conducive to fire, and a limited ability to suppress them. In brief, this pyroregion has a high probability of human-caused ignitions, no major fuel limitation, and no major weather limitation. In addition, the forecasted increases of fire weather indices seem favourable to an extension of the fire season.

The second pyroregion regroups the fire-prone Mediterranean plains and foothills. These areas have medium-to-high fire density, fires of all size, predominantly in summer. Fire weather is characterized by hot summer spells and extreme values of FWI during few weeks in summer. Fire size and fire density have strongly decreased along the recent decades while climate-induced fire danger has increased. This pyroregion has very high human activity and very high fire suppression capacity, low fuel coverage (due to landscape fragmentation) and a low-compartmented landscape. In brief, fire activity is neither weather-limited (especially during dry summers) nor fuel-limited. Fire activity is clearly controlled by fire suppression which is especially efficient and favoured by a relatively flat landscape, and a dense road network.

The third pyroregion regroups the cool peri-Mediterranean mountains with low fire activity. However, fire density has locally increased during the two past decades in parallel to an increase of annual FWI means and extremes. In this pyroregion, fuel coverage is non-limiting to fire activity. The high landscape compartmentalization and the low fire suppression capacity may favour fires, which are clearly limited by low ignition (due to low human activity) and low by fire unfavourable fire weather in average. Fire suppression means, even low, are likely to be adapted to the present low fire activity.

4.2. Implications for fire policy

This study demonstrated that fire activity varies in south-eastern France, in parallel to fire weather, human activity, and fuel coverage. Fire activity and fire drivers vary strongly within a rather small geographic area. Indeed, fuel limitation exists in lowlands dominated by agricultural lands and urban areas while weather limitation exists in mountain environments. A major implication of these findings is that all pyroregions do not require exactly the same fire suppression effort. Fire prevention can be efficiently applied anywhere, but the fire suppression strategy could be adapted to local features.

The present suppression strategy in south-eastern France relies on a fast, hard-hitting initial attack on all fires to prevent them becoming large and destructive. In the highly fire-prone areas, fire prevention is especially active with terrestrial fire patrols, lookout towers, and the regulation of public frequentation in wild-land area during the fire peak season (generally July and August). In addition, specific and reinforced means have been established with the pre-positioning of fire suppression crew at strategic places where fires occur preferentially, a dense network of lookout towers, and fire trackers planes flying during all the peak fire season to detect fires as rapidly as possible. This study suggests that enhancing fire suppression means would help controlling fire activity in the maritime mountains (Corsica and Maritime Alps), which have high fuel loads and compartmented landscapes limiting firemen activity. It should be noted that recent progress has been done for controlling pastoral and agricultural fires during the fire danger peaks. This progress has likely contributed to the recent decrease of fire activity, especially in Corsica. In fire-prone Mediterranean plains and lowlands, fire prevention and suppression is especially active. It has likely strongly contributed to the decrease of fire activity. However, this efficient fire policy can paradoxical effects referred to as the ‘fire paradox’ (Sande Silva *et al*. 2011): if fire suppression is effective and reduces the area burned yearly, then wildland fuels accumulate and fuel connectivity increases across the landscape. In turn, this will increase the likelihood of large fires when fire suppression forces cannot control them at the initial stage. In cool peri-Mediterranean mountains, fire activity will likely remain limited but it will likely increase, and fire season will likely expand due to climate change. In the mid-term, it is of importance to increase prevention, surveillance, and the fire suppression capacity in order to prepare to future.

References

Aguado, I., E. Chuvieco, P. Martin and J. Salas (2003). "Assessment of forest fire danger conditions in southern Spain from NOAA images and meteorological indices." International Journal of Remote Sensing 24(8): 1653-1668.

Curt, T., L. Borgniet and C. Bouillon (2013). "Wildfire frequency varies with the size and shape of fuel types in southeastern France: Implications for environmental management." Journal of Environmental Management 117: 150-161.

Fernandes, P. M., G. M. Davies, D. Ascoli, C. Fernandez, F. Moreira, E. Rigolot, C. R. Stoof, J. Antonio Vega and D. Molina (2013). "Prescribed burning in southern Europe: developing fire management in a dynamic landscape." Frontiers in Ecology and the Environment 11: E4-E14.

Genries, A., L. Mercier, M. Lavoie, S. D. Muller, O. Radakovitch and C. Carcaillet (2009). "The effect of fire frequency on local cembra pine populations." Ecology 90(2): 476-486.

Krawchuk, M. A., M. A. Moritz, M.-A. Parisien, J. Van Dorn and K. Hayhoe (2009). "Global Pyrogeography: the Current and Future Distribution of Wildfire." PLoS ONE 4(4): e5102.

Prométhée (2011). "La banque de données sur les incendies de forêts en région Méditerranéenne en France." http://www.promethee.com/.

Pyne, S. J., P. L. Andrews and R. D. Laven (1996). "Introduction to wildland fire." 2nd ed. New York, NY: John Wiley & Sons: 808 pp.

van Wagner, C. (1987). "Development and structure of the Canadian Forest Fire Weather Index System." Forestry Technical Report - Canadian Forestry Service(No. 35): viii + 37 pp.

Daily maps of fire risk over Mediterranean Europe based on information from MSG satellite imagery

Carlos C. DaCamara[a], Teresa J. Calado[a], Sofia L. Ermida[a], Isabel F. Trigo[a,c], Malik Amraouia[b], and Kamil F. Turkman[d]

[a] *University of Lisbon, Instituto Dom Luiz, 1749-016 Lisbon, Portugal*
[b] *University of Trás-os-Montes e Alto Douro, School of Sciences and Technology, 5001-801 Vila Real, Portugal*
[c] *Instituto Português do Mar e da Atmosfera, IPMA, 1749-077 Lisbon, Portugal*
[d] *University of Lisbon, DEIO-CEAUL, 1749-016 Lisbon, Portugal*

Abstract
Here we present a procedure that allows the operational generation of daily maps of fire danger over Mediterranean Europe. These are based on an integrated use of vegetation cover maps, weather data, and fire activity as detected by remote sensing from space. It is demonstrated that statistical models based on two-parameter Generalized Pareto (GP) distributions adequately fit the observed samples of fire duration and that these models are significantly improved when the Fire Weather Index (FWI), that rates fire danger, is integrated as a covariate of scale parameters of GP distributions. Probabilities of fire duration exceeding specified thresholds are then used to calibrate FWI leading to the definition of five classes of fire danger. Fire duration is estimated on the basis of 15-minute data provided by Meteosat Second Generation (MSG) satellites and corresponds to the total number of hours fire activity is detected in a single MSG pixel during one day. Defined classes of fire danger provide useful information for wildfire management and are on the basis of the Fire Risk Mapping (FRM) product that is being disseminated on a daily basis by the EUMETSAT Satellite Application Facility on Land Surface Analysis (LSA SAF).

Keywords*: Fire danger; Weather; Fire management; Generalized Pareto distribution; Remote sensing.*

Introduction

Representing more than 85% of burned area in Europe, the Mediterranean is one of the regions of the world most affected by large wildfires that burn half a million of ha of vegetation cover every year causing extensive economic losses and ecological damage (San-Miguel-Ayanz *et al.* 2013).
Fire in the Mediterranean is a natural phenomenon linking climate, humans and vegetation (Lavorel *et al.* 2007). Fire activity is therefore conditioned by natural and anthropogenic factors. Natural factors include topography, vegetation cover and prevailing weather conditions (San-Miguel-Ayanz *et al.* 2003) which are linked to several atmospheric mechanisms working at different temporal and spatial scales (Trigo *et al.* 2006). At the regional and at the seasonal or inter-annual time scales, rainy and mild winters, followed by warm and dry summers, lead to high levels of vegetation stress that make the region particularly prone to the occurrence of fire events (Pereira *et al.* 2005). At the local and daily scales, extreme weather conditions (e.g. temperature, wind speed, atmospheric stability, fuel moisture and relative humidity) play in turn a key role in the setting and spreading of wildfires (Amraoui *et al.* 2013).
Since 1990 the European Commission has been implementing actions aiming at the organization of a Community forest-fire information system and at the development and implementation of advanced methods for the evaluation of forest fire danger and the estimation of burnt areas at the European scale (San-Miguel-Ayanz *et al.* 2012).

Forecasts of fire danger over Mediterranean Europe up to three days in advance are also currently being disseminated within the framework of the Satellite Application Facility on Land Surface Analysis (LSA SAF, Trigo *et al.* 2011) which is part of the distributed Applications Ground Segment of EUMETSAT (the European Organization for the Exploitation of Meteorological Satellites).
The goal of the present study is to quantify and predict the randomness in the distribution of duration of fire events using statistical modelling, and therefore provide a robust estimation of fire danger instead of a simple characterization using basic FWI statistics.

Background

Fire prevention requires adequate knowledge about time when and location where a fire event is likely to happen as well as on the potential damage that may result on wildland and urban values (Finney 2005). These two aspects, respectively referred to as fire danger and vulnerability, constitute the two main components of fire risk assessment (Chuvieco *et al.* 2010). The first component deals with fire behaviour probabilities and wildfire potential assessment that encompasses potential fire ignition, propagation and difficulty of control. The vulnerability component includes the assessment of the negative effects which mainly relate to socio-economic values, degradation potential of soil and vegetation conditions and landscape value.
The focus of the present study is on wildfire potential assessment that is usually based on fire danger rating systems (Fujioka *et al.* 2009), which provide indices to be used on an operational basis for fire prevention management. Because of the availability of near-real time weather observations and forecasts, most of danger rating systems make use of indices that are based on meteorological parameters (Bovio and Camia 1997).
Here, fire danger is rated based on the Fire Weather Index that is part of the Canadian Forest Fire Weather Index System (CFFWIS, Van Wagner 1974). CFFWIS has shown to be particularly suitable as a fire rating system for Mediterranean Europe. Dimitrakopoulos *et al.* (2011) have shown that CFFWIS components, in particular FWI, are suitable to rate fire danger in the eastern Mediterranean. Since 2007, FWI is the main component of the EFFIS Danger Forecast module (San-Miguel-Ayanz *et al.* 2012).
When applied to ecosystems other than Canadian forests, CFFWIS must be calibrated to the new environmental conditions by means of a reliable database of fire events (Carvalho *et al.* 2008). The process of calibration usually involves establishing a set of break points that result from the analyses of fire weather history and time series of the CCFFWIS components, namely FWI (van Wagner 1987). Established break points are then used to define fire danger classes (Kiil *et al.* 1977). In the present study, breakpoints of FWI are based on estimates of fire danger provided by statistical models of fire activity based on the FD&M product from the LSA SAF. The proposed approach has the advantage of rating fire danger based on statistical models of extreme fire events, which allow quantifying the contribution of meteorological factors in terms of increasing or decreasing the probability that the duration of a fire event exceeds a given threshold.

3. Data and methods

3.1. Study area and period

Encompassing Mediterranean Europe, the study area (Figure 1) is delimited by the latitude circles of 35º and 45ºN and the meridians of 10ºW and 37ºE. In order to be consistent with related LSA SAF products, all data fields are mapped in the so-called Normalized Geostationary Projection (NGP) of MSG (EUMETSAT 1999). The MSG pixel resolution is 3 km at the nominal sub-satellite point (0º lat, 0º lon), progressively deteriorating with increasing distance, reaching values of about 5 km over Mediterranean Europe.

Baseline information about land cover is obtained from the 1 km resolution Global Land Cover 2000 (GLC2000) dataset as derived from SPOT-4 VEGETATION (Bartholomé and Belward 2005). GLC2000 data comprise 22 land-use types which were grouped into three main classes of vegetation cover (Figure 1): forests (GLC2000 classes 1, 2, 4 and 6); shrubs (classes 11, 12 and 14); and cultivated areas (class 16). The three main classes were mapped from the original 1 km resolution to the NGP of MSG by assigning to each (~5 km) MSG pixel the most frequent class falling inside that pixel.

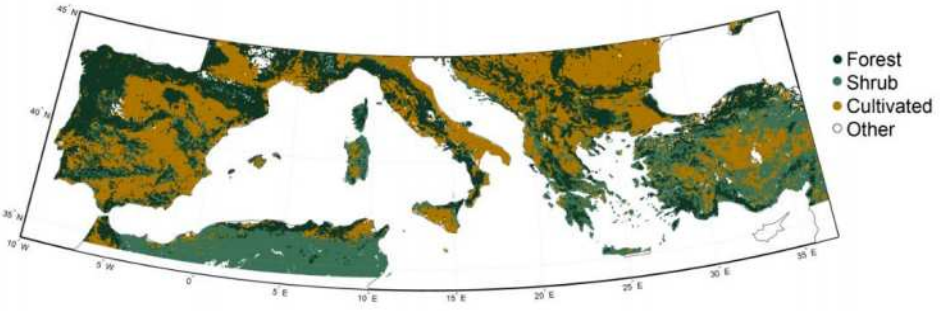

Figure 1. Geographical distribution of the three main vegetation types as derived from GLC2000.

The study covers the months of July and August of 2007, 2008 and 2009. This period may be regarded as representative of fire activity in Mediterranean Europe taking into account the official statistics of burned area provided by the European Commission for Portugal, Spain, France, Italy and Greece.

3.2. Meteorological data

Daily values of FWI over the study area are derived from meteorological fields provided by ECMWF operational model for 12 UTC, covering the period of July and August, from 2007 to 2009. Originally obtained over a 0.25°×0.25° latitude/longitude grid, the meteorological fields were re-projected onto NGP. Data consist of 2-meter air temperature, 2-meter dew point temperature, 10-meter wind speed and 24-hour cumulated precipitation; temperature and dew point were topographically corrected by applying a constant lapse rate of -0.67ºC/100m to the difference between ECMWF (coarser) orography and NGP pixel altitude. Relative humidity of air was computed by combining dew point temperature and temperature according to Magnus' expression (Lawrence 2005). For each pixel and day, anomalies of FWI, hereafter referred to as FWI*, were computed as departures from the 30-year means for the reference period 1980-2009, i.e., the anomaly FWI^*_{pd} for MSG pixel *p* and day *d* is defined as:

$$FWI^*_{pd} = FWI_{pd} - \overline{FWI}_p \quad (1)$$

where FWI_{pd} is the value of FWI for pixel *p* and day *d* and $\overline{FWI}_p$ is the time mean performed for that pixel and day over the 30-year reference period.

3.3. Fire activity and duration

Information on fire activity every 15 min on an MSG pixel basis is available from the above-mentioned FD&M product that is currently generated within the framework of the LSA-SAF (Trigo *et al*. 2011). Duration of fire δ may be estimated by summing the number detected fires in a given pixel *p* and a given day *d* during the study period. For each pixel *p*, at day *d*, there are 96 observations (one every 15 min) made by the SEVIRI instrument on-board MSG. Let $\mathbf{I}_{pd}(i)$ be an indicator function that is equal to one if the i^{th} MSG image has captured fire activity inside pixel *p* during day *d* and is equal to zero otherwise. The fire duration δ_{pd}, for pixel *p* during day *d*, is defined as:

$$\delta_{pd} = 0.25 \times \sum_{i=1}^{96} \mathbf{I}_{pd}(i) \quad (2)$$

Units of δ are hours, the coefficient 0.25 converting into hours the sampling interval of 15 min between consecutive MSG images. Fire duration δ may be viewed as a proxy of fire intensity and burn extent but it should be noted that δ is not to be interpreted as the duration of individual fire events.

3.4. Statistical models of fire duration

The statistical distribution of fire duration δ is modelled using the Peaks Over Threshold (POT) approach (Pickands 1975), which is a commonly used tool to quantify fire danger (de Zea Bermudez *et al.* 2009). The POT approach uses the Generalized Pareto (GP) distribution as a model to assign probabilities to the exceedances of duration δ over a threshold, *i.e.* to values $x=\delta-\delta_{min}$ (with $\delta>\delta_{min}$) where δ_{min} is a prescribed minimum value (de Zea Bermudez and Kotz 2010b).
The GP probability density function g is given by:

$$g(x \mid \alpha,\sigma) = \frac{1}{\sigma}\left(1+\frac{\alpha}{\sigma}x\right)^{-1-\frac{1}{\alpha}} \tag{3}$$

where x is the exceedance, and α and σ are the shape and scale parameters. The corresponding GP cumulative distribution function is:

$$G(x \mid \alpha,\sigma) = 1-\left(1+\frac{\alpha}{\sigma}x\right)^{-\frac{1}{\alpha}} \tag{4}$$

When $\alpha<0$ the distribution is upper bounded, with $0 < x < -\sigma/\alpha$. A complete description of the GP distribution may be found in de Zea Bermudez and Kotz (2010a).
The minimum threshold δ_{min} is estimated using a graphical approach (Coles 2001) where the chosen value is such that the sample mean of the values exceeding successive thresholds larger than δ_{min} becomes a linear function when plotted against the respective thresholds.
Once δ_{min} is determined, the shape (α) and the scale (σ) parameters are estimated using the maximum likelihood method (Grimshaw 1993); 95% confidence intervals for α and σ are asymptotically estimated using normal distributions for α and for log(σ) (Kotz and Nadarajah 2000). Goodness of fit is assessed by means of the A^2 test (Anderson and Darling 1952), a nonparametric test that is especially appropriate to models based on long-tailed distributions.
For each vegetation type, POT is applied to the exceedances x of all fire pixels that were recorded during the study period (July-August 2007-2009). Obtained models, hereafter referred to as static models, may be improved by incorporating daily anomalies, FWI*, as a covariate of scale parameter in the GP distributions, in particular by assuming a linear dependence of σ on FWI*:

$$G(x, FWI^* \mid \alpha,a,b) = 1-\left(1+\frac{\alpha}{a\times FWI^*+b}x\right)^{-\frac{1}{\alpha}} \tag{5}$$

Estimates of shape parameter (α) and of coefficients of the linear relationship $\sigma=a\times FWI^*+b$ are again obtained using the maximum likelihood method. Performance of the new alternative models, hereafter referred to as daily models, is compared against the respective null models (i.e. the original static models) by using the so-called standard likelihood ratio test (Neyman and Pearson 1933). The test is based on statistic Λ defined as:

$$\Lambda = 2(\ln L' - \ln L) \tag{6}$$

where L is the maximum likelihood function of the static model and L' is the maximum likelihood function of the daily model.

3.5. Meteorological danger

Static models allow estimating baseline danger D_{b0} which represents the probability that exceedance x is above a given fixed threshold x_0:

$$D_{b0} = D_b(x_0) = 1 - G_{static}(x_0 \mid \alpha, \sigma) \quad (7)$$

Conversely, the threshold value of exceedance x_0, corresponding to a specified level of baseline danger, D_{b0}, may be estimated, for each vegetation cover, by inverting the previous relationship:

$$x_0 = x(D_{b0}) = G_{static}^{-1}(1 - D_{b0}) \quad (8)$$

In a similar way, daily models allow estimating daily danger D_d which represents the probability that exceedance x is above a given fixed threshold x_0 for a given value of FWI*:

$$D_d(x_0, FWI^*) = 1 - G_{daily}(x_0, FWI^* \mid \alpha, a, b) \quad (9)$$

The role played by meteorological conditions on wildfire potential may then be uncovered by defining meteorological danger D_m, which combines information about static and daily danger for a given day and pixel according to the following procedure:

1. A given threshold of baseline danger, D_{b0}, is fixed over the entire study area;
2. For each vegetation cover, baseline thresholds of exceedances x_0 are computed using the appropriate static models of fire duration (Eq. 8);
3. For each day and pixel location, daily models are then used to estimate daily danger, D_d, based on the corresponding baseline threshold and the observed daily value of FWI* (Eq. 9);
4. Meteorological danger, D_m, is finally defined by the ratio of daily danger D_d to prescribed baseline danger D_{b0}:

$$D_m(x_0, FWI^*) = \frac{D_d(x_0, FWI^*)}{D_{b0}} \quad (10)$$

Meteorological danger provides a coherent basis to set break points in FWI* to be used in the definition of classes of meteorological fire danger. Given a baseline danger D_b, break point BP_L will be defined as the value of FWI* associated to meteorological danger L, i.e.

$$D_m(x_0, BP_L) = \frac{D_d(x_0, BP_L)}{D_{b0}} = \frac{1 - G_{daily}(x_0, BP_L \mid \alpha, a, b)}{D_{b0}} = L \quad (11)$$

Values of BP_L may be estimated by inverting the previous equation e.g. using the bisection method (Faires and Burden 1985).

Results

4.1. General characteristics of fire duration

Duration of fire activity for the three vegetation types (Table 1) is characterized by long tailed distributions, with values of δ <3 h representing about 85, 82 and 94% of the sample in the case of forest, shrub and cultivated areas, respectively . Besides being less frequent in both absolute and relative terms, duration of fire activity in cultivated areas has a shorter tail than duration in forest or shrub. For instance the relative frequencies of very long lasting fire activity (δ>12 h) over forest and shrub are 0.52 and 0.89% respectively, about three times and more than five times the value of 0.17% corresponding to cultivated areas. Long-lasting fire episodes are therefore more expected through shrub land and forests than over agricultural areas, a result in close agreement with findings in previous works either at the scale of the Mediterranean basin (Fernandes, 2013) or at the national levels of Portugal (Barros and Pereira 2014), Spain (Moreno *et al.* 2011) and Italy (Bajocco and Ricotta 2008). Such differences in land cover burning are likely to be driven by different interacting factors which include fuel connectivity, topography, population density, meteorological conditions and fire suppression (Brotons *et al.* 2013). For instance, the proximity of agricultural lands to populated areas and the social and economic value attributed to agricultural activities is expected to steer an increase

of the level of effort in fire suppression and therefore to a decrease in the likelihood of large fire events (Moreira *et al.* 2010).

Table 1. Distribution frequencies of fire activity for the three types of vegetation. The distributions of fire activity refer to the study period of July-August 2007-2009; for each class the absolute frequency is shown together with the relative frequency (% in brackets).

Classes of duration δ (h)	0.25 to 3.00	3.25 to 6.00	6.25 to 9.00	9.25 to 12.00	12.25 to 15.00	15.25 to 18.00	18.25 to 21.00	Total
Forest	3 321	387	128	34	15	4	1	3 890
[%]	*[85.37]*	*[9.95]*	*[3.29]*	*[0.87]*	*[0.39]*	*[0.10]*	*[0.03]*	*[100.00]*
Shrub	2 240	292	114	47	17	7	0	2 717
[%]	*[82.44]*	*[10.75]*	*[4.19]*	*[1.73]*	*[0.63]*	*[0.26]*	*[0.00]*	*[100.00]*
Cultivated	2 205	118	23	4	3	1	0	2 354
[%]	*[93.67]*	*[5.01]*	*[0.98]*	*[0.17]*	*[0.13]*	*[0.04]*	*[0.00]*	*[100.00]*

4.2. Static models

Results from the previous exploratory analysis suggest choosing POT and use GP distributions to model the exceedances of duration δ for each vegetation type. For each vegetation type, a common minimum threshold of 3 h was therefore set for δ_{min}. The largest scale (σ) parameter is the one for shrub, followed by forest and cultivated areas (Table 2). The shape (α) parameters are negative for all vegetation cover types, indicating that exceedances are upper limited. The largest negative value is also the one for shrub, followed by forest and cultivated areas. The predominant effect of the scale (σ) parameter on the fitted GP models becomes apparent when plotting the cdf curves for the three vegetation cover types (Figure 2), the shrub model presenting the longest tail, followed by forest and cultivated areas.

4.3. Daily models

The role played by meteorological factors may be assessed by looking at the impact of FWI on fire activity. The dataset of exceedances x for each vegetation type was subdivided into subgroups associated with different ranges of FWI; 51 groups of fire pixels were defined as respectively associated with values of FWI between percentile 0 and percentile 50, between percentile 1 and percentile 51, and so on up to between percentile 51 and percentile 100. GP distributions were then adjusted to each subset and plots were made of estimated values of scale σ versus the mean value of FWI in the considered range.

For all types of vegetation cover, the scale (σ) parameter tends to linearly increase with increasing FWI. Each type presents a characteristic range of FWI, the largest values being observed for shrub and the lowest for forest. There is a close relationship between vegetation cover and range of FWI. However the spatial distribution of FWI is affected by other factors than vegetation. For instance, the Eastern and Southern borders of the Mediterranean basin present higher values of FWI. The impact of regional effects other than vegetation may be mitigated by replacing daily values of FWI at a given pixel by respective departures (FWI*) from 30-year means for the reference period 1980-2009.

Table 2. Static GP models for each vegetation type. Columns 1-5 indicate the following: vegetation type, sample size and corresponding percentile of original data sample (% in brackets), estimated values and 95% confidence intervals (in brackets) of the shape (α) and scale (σ) parameters, and confidence levels (CL) of the Anderson-Darling tests.

Vegetation type	Sample size [Percentile]	α	Σ	CL
Forest	569 *[85%]*	-0.06 *[-0.13,0.02]*	2.92 *[2.61,3.26]*	98%
Shrub	477 *[82%]*	-0.14 *[-0.22,-0.05]*	3.70 *[3.27,4.18]*	93%
Cultivated	149 *[94%]*	-0.01 *[-0.15, 0.12]*	2.31 *[1.87,2.86]*	91%

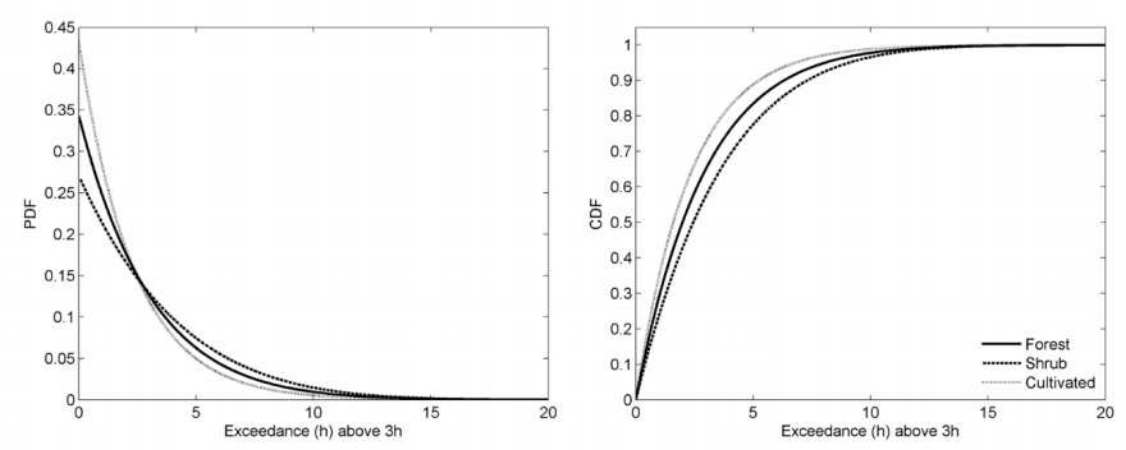

Figure 2. Probability density functions (left panel) and cumulative distribution functions (right panel) of fitted GP models of exceedances x=δ-δmin (with δmin = 3 h) for forests (solid curve), shrubs (dashed curve) and cultivated areas (dotted curve).

Impact of meteorological conditions was therefore modelled by introducing FWI* as a covariate of the scale parameter of the GP models using linear relationships of the type σ=a+b×FWI* (Table 3). In all cases p-values of the maximum likelihood ratio test are lower than 0.5% meaning that the null hypothesis that the daily models have a better fit than the corresponding static ones cannot be rejected at the 0.5% significance level. The sensitivity of scale parameters to changes in FWI* also reflect on the probabilities of exceedance of duration (Figure 3).

Table 3. Daily GP models for each vegetation type. Columns 2-4 indicate the following: shape (α) parameter, dependence of scale (σ) parameter on FWI* and p-values of the maximum likelihood ratio tests.

Vegetation type	α	σ=a+b×FWI*	p-value (%)
Forest	-0.074	σ=2.04 + 0.038×FWI*	1.39×10^{-5}
Shrub	-0.15	σ=2.37 + 0.052×FWI*	1.20×10^{-6}
Cultivated	-0.027	σ=1.33 + 0.042×FWI*	0.46

4.4. Calibration of FWI

For each vegetation type the respective static and daily models were used to compute the dependence of meteorological danger D_m on FWI* (Eq. 10). For a fixed baseline danger D_b = 33%, four break points of FWI* were obtained, respectively associated to levels of meteorological danger of 0.25, 0.50, 0.75 and 1.00. Estimates of break points (Table 4) were obtained by solving Eq. (11) using the bisection method. The three vegetation types present differences that are worth being noted. The largest value of the baseline threshold of fire duration (associated to baseline danger D_b=33%) is the one of shrub (x_0=3.8 h) followed at similar intervals of about 0.6-0.7 h by forest (x_0=3.1 h) and cultivated areas (x_0=2.5 h). The four defined break points allow defining five classes of meteorological fire danger, respectively "low" when $D_m < 0.25$, , "moderate" when $0.25 \leq D_m < 0.5$, "high" when $0.5 \leq D_m < 0.75$, "very high" when $0.75 \leq D_m < 1$ and "extremely high" when $D_m \geq 1$.

Table 4. Break points of FWI* for each vegetation type. Lines 2-6 indicate the following: baseline threshold of fire duration (x0) associated to a fixed baseline danger (D_b=33%) and break points of FWI* ($BP_{0.25}$, $BP_{0.50}$, $BP_{0.75}$ and $BP_{1.00}$) corresponding to different levels (L) of meteorological danger D_m (0.25, 0.50, 0.75 and 1.00, respectively).

	Forest	Shrub	Cultivated
x_0	3.1 h	3.8 h	2.5 h
$BP_{0.25}$	-17.5	-10.4	-6.5
$BP_{0.50}$	-4.7	0.8	-2.9
$BP_{0.75}$	8.7	12.6	12.8
$BP_{1.00}$	24.0	26.2	24.1

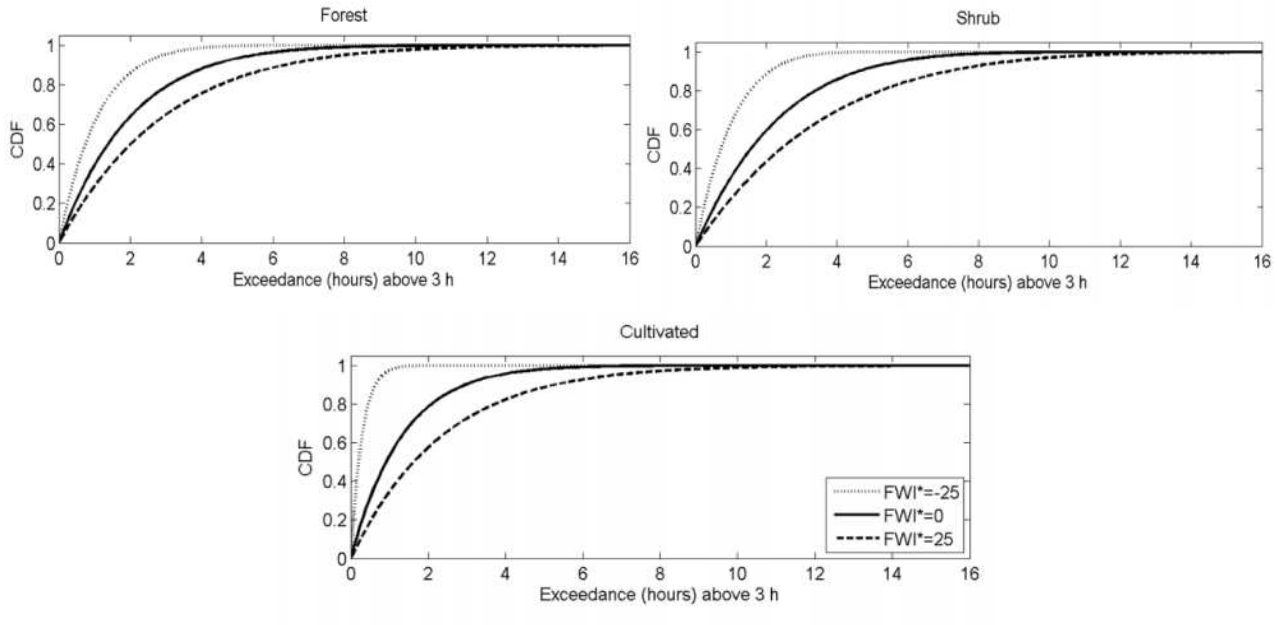

Figure 3. Cdf curves for three fixed values of FWI* (-25, 0 and +25) in the case of the daily GP model for forests (top left panel), shrubs (top right panel) and cultivated areas (bottom panel).

Discussion

The case of August 25th 2007, when Greece and Albania were struck by very severe fire events, provides an interesting example of the obtained product that is worth analysing in detail. Two impressive clusters of fire pixels with duration longer than 6 hours may be observed over Greece

(Figure 4, bottom panel). The larger cluster spreads over western Peloponnese and contains a large number of fires that lasted more than 12 hours, and the other one locates over eastern Attica and Evia. The map of classes of fire danger (Figure 4, top panel) shows that both clusters are part of a large core labelled "extremely high" which covers the entire territory of Greece and extends eastwards into Anatolia and towards the northeast over Bulgaria and Romania up to Crimea. An event lasting more than 12 hours also occurred in Albania, inside a large patch labelled "very high" which covers the territories of Albania, Montenegro and Bosnia and Herzegovina, and extends towards the northeast up to Ukraine. No fire events occurred in regions labelled "low", and "moderate".

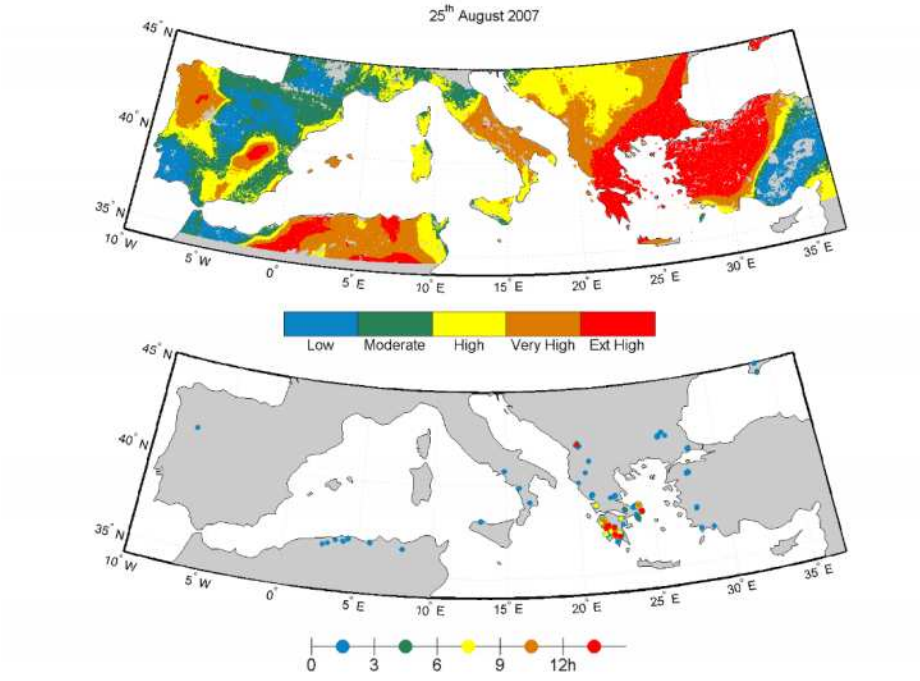

Figure 4. Map of classes of fire danger (top panel) and corresponding spatial distribution of observed fire events and respective duration (bottom panel) for August 25th 2007. Colorbars identify classes of fire danger (upper panel) and fire duration (lower panel).

An assessment of the global consistency (in space and time) of results obtained was performed by analysing, for the entire study area and the entire study period, the number of observed events that belong to a given interval of fire duration and were assigned to a given class of fire danger (Table 5). The percentage of fires within any given duration interval (***bold italics***) steadily decreases with decreasing danger, with the exception of fires of very short duration (less than 1h) where the "high" class is the modal one. Such decrease is especially steep in the cases of the upper intervals of duration. With the exception of fires of very short duration where the fraction is only 1%, there is no fire activity in the case of "low" danger. When considering fixed classes of danger, it may be noted that the percentage of events associated with any given duration interval (*underlined italics*) always decreases with increasing duration, the steepest declines being observed in the lower danger classes.
When looking at maps of classes of fire danger (Figure 4) it may be noted that areas of "high" and "very high" fire danger spread over regions where no fire activity is detected. This is to be expected since both static and daily models allow computing probabilities of exceedance provided there is an event with minimum duration of 3 h.

Conclusions

The calibration approach adopted in this study is based on an integrated use of information about meteorological conditions provided by the European Centre for Medium-Range Weather Forecasts (ECMWF), vegetation land cover from Global Land Cover 2000 (GLC2000) and fire duration as detected by the SEVIRI instrument on-board Meteosat Second Generation (MSG) satellites. The main difference of the proposed methodology to existent others is that it takes full advantage of the temporal resolution of SEVIRI that allows detecting fire events every 15 minutes. This information is used to make daily records of fire duration that are essential to calibrate meteorological danger and establish classes of fire danger. Traditional approaches rely on calibration procedures performed through analyses of fire weather history based on ground observations of amount of burned area or number of fire occurrences. Several factors may affect the reliability of ground observations; recorded values are not only determined by visual inspection which may nevertheless affect their accuracy but they are also determined by the policy of individual countries, which may further change in time (Pereira *et al.* 2011). Approaches based on the use of satellite data have the advantage of being more consistent in space and time. They also benefit from not depending on the availability of ground fire records from each country, which are neither easily obtainable, nor available in the short term.
Finally, it is worth stressing that the Fire Risk Mapping (FRM) product is entirely based on a set of estimated probabilities, in particular meteorological danger. These probabilities are derived from statistical models that may be readily updated and continuously tuned, which represents an advantage from the operational point of view. The fact that the FRM product is currently being disseminated within the framework of the Land Surface Analysis Satellite Application Facility (LSA SAF) will also allow tailoring the product according to specific needs of a broad community of users.

Table 5. Distribution of fire events by classes of fire danger and by fire duration. Each cell contains the number of observed daily fire events (first line), the corresponding fraction (%) of the total number of events with the same fire duration interval (second line, bold italics) and the corresponding fraction (%) of the total number of events in the same class of fire danger (second line, underlined italics).

	Classes of fire danger										
Duration (hours)	Low		Moderate		High		Very high		Extremely high		All Classes
0 – 1	68		634		2111		1853		1327		5983
	1	*99*	***11***	*89*	***35***	*75*	***31***	*66*	***22***	*53*	***100***
1 – 2	1		46		361		379		382		1169
	0	*1*	***4***	*6*	***31***	*13*	***32***	*13*	***33***	*15*	***100***
2 – 3	0		14		132		215		225		586
	0	*0*	***3***	*2*	***22***	*5*	***37***	*8*	***38***	*9*	***100***
3 – 6	0		12		180		267		338		797
	0	*0*	***2***	*2*	***23***	*6*	***33***	*9*	***42***	*14*	***100***
6 – 9	0		7		29		77		150		263
	0	*0*	***3***	*1*	***11***	*1*	***29***	*3*	***57***	*6*	***100***
9 –12	0		0		6		28		51		85
	0	*0*	***0***	*0*	***7***	*0*	***33***	*1*	***60***	*2*	***100***
12 – 15	0		0		2		8		25		35
	0	*0*	***0***	*0*	***6***	*0*	***23***	*0*	***71***	*1*	***100***
15 – 18	0		0		1		3		8		12
	0	*0*	***0***	*0*	***8***	*0*	***25***	*0*	***67***	*0*	***100***
> 18	0		0		0		0		1		1
	0	*0*	***0***	*0*	***0***	*0*	***0***	*0*	***100***	*0*	***100***
All durations	69	*100*	703	*100*	2822	*100*	2830	*100*	2507	*100*	8931 ***100***

7. Acknowledgements

This study was performed within the framework of the EUMETSAT Satellite Application Facility on Land Surface Analysis (LSA SAF). Part of the research was supported by the EU 7th Framework Program through project FUME (contract number 243888). The Portuguese Science Foundation (FCT) has supported the research work by M. Amraoui (grant SFRH/BD/36964/2007), S. L. Ermida (grant in project PTDC/AAC-AMB/104702/2008) and K. F. Turkman (projects PEst-OE/MAT/UI0006/2011 and PTDC/MAT/118335/2010).
This work partly reproduces results already published in the following article:
DaCamara CC, Calado TJ, Ermida SL, Trigo IF, Amraoui M, Turkman KF, (2014). Calibration of the Fire Weather Index over Mediterranean Europe based on fire activity retrieved from MSG satellite imagery. *International Journal of Wildland Fire*, doi: 10.1071/WF13157

8. References

Amraoui M, Liberato MLR, Calado TJ, DaCamara CC, Coelho LP, Trigo RM, Gouveia CM (2013) Fire activity over Mediterranean Europe based on information from Meteosat-8. *Forest Ecology and Management* **294**, 62-75.

Anderson TW, Darling DA (1952) Asymptotic Theory of Certain "Goodness of Fit" Criteria Based on Stochastic Processes. *Annals of Mathematical Statistics* **23,** 193–212.

Bajocco S, Ricotta C (2008) Evidence of selective burning in Sardinia (Italy): which land-cover classes do wildfires prefer? *Landscape Ecology* **23**, 241–248. doi:10.1007/s10980-007-9176-5

Barros AMG, Pereira JMC (2014) Wildfire Selectivity for Land Cover Type: Does Size Matter? *PLoS ONE*, **9**, e84760.

Bartholomé E, Belward AS (2005) GLC2000: a new approach to global land cover mapping from Earth Observation data. *International Journal of Remote Sensing*, **26**, 1959-1977.

Bovio G, Camia A (1997) Meteorological Indices for Large Fires Danger Rating. In 'A review of remote sensing methods for the study of large wildland fires'. Megafires project ENV-CT96-0256 (Ed Chuvieco E) pp. 73-90. (Universidad de Alcalá: Alcalá de Henares, Spain)

Brotons L, Aquilué N, de Cáceres M, Fortin M-J, Fall A (2013) How Fire History, Fire Suppression Practices and Climate Change Affect Wildfire Regimes in Mediterranean Landscapes. *PLoS ONE*, **8**, e62392.

Camia A, Amatulli G (2009) Weather factors and fire danger in the Mediterranean. In 'Earth observation of wildland fires in Mediterranean ecosystems'. (Ed Chuvieco E) pp. 71-82. (Springer-Verlag: Berlin, Germany)

Carvalho A, Flannigan M, Logan K, Miranda A, Borrego C (2008) Fire activity in Portugal and its relationship to weather and the Canadian Fire Weather Index System. *International Journal of Wildland Fire* **17**, 328–338.

Chuvieco E, Aguado I, Yebra M, Nieto H, Salas J, Martín MP, Vilar L, Martínez J, Martín S, Ibarra P, de la Riva J, Baeza J, Rodríguez F, Molina JR, Herrera MA, Zamora R (2010) Development of a framework for fire risk assessment using remote sensing and geographic information system technologies. *Ecological Modelling* **221**, 46–58.

Coles S (2001) An Introduction to Statistical Modeling of Extreme Values, 208 pp. (Springer-Verlag: London).

de Zea Bermudez P, Mendes J, Pereira JMC, Turkman KF, Vasconcelos MJP (2009) Spatial and temporal extremes of wildfire sizes in Portugal (1984–2004). *International Journal of Wildland Fire* **18**, 983-991.

de Zea Bermudez P, Kotz S (2010a) Parameter estimation of the generalized Pareto distribution — Part I. *Journal of Statistical Planning and Inference* **140**, 1353-1373.

de Zea Bermudez P, Kotz S (2010b) Parameter estimation of the generalized Pareto distribution — Part II. *Journal of Statistical Planning and Inference* **140**, 1374-1388.

Dimitrakopoulos AP, Bemmerzouk AM, Mitsopoulos ID (2011) Evaluation of the Canadian fire weather index system in an eastern Mediterranean environment. *Meteorological Applications* **18**, 83–93.

EUMETSAT (1999) Coordination Group for Meteorological Satellites LRIT/HRIT Global Specification, EUMETSAT, 53 pp., http://www.eumetsat.int/groups/cps/documents/document/pdf_cgms_03.pdf

Faires JD, Burden RL (1985) Numerical Analysis. (Prindle, Weber & Schmidt: Boston)

Fernandes PM (2013) Fire-smart management of forest landscapes in the Mediterranean basin under global change. *Landscape and Urban Planning* **110**, 175–182.

Finney MA (2005) The challenge of quantitative risk analysis for wildland fire. *Forest Ecology and Management* **211**, 97–108.

Fujioka FM, Gill AM, Viegas DX, Wotton BM (2009) Fire danger and fire behavior modeling systems in Australia, Europe and North America. In 'Wildland fires and air pollution'. (Eds Bytnerowicz A, Arbaugh M, Riebau A, Andersen C), Developments in Environmental Science, vol 8, pp. 471-498. (Elsevier, Amsterdam, The Netherlands)

Grimshaw SD (1993) Computing Maximum Likelihood Estimates for the Generalized Pareto Distribution. *Technometrics* **35**, 185-191.

Kiil AD, Miyagawa RS, Quintilio D (1977) Calibration and performance of the Canadian fire weather index in Alberta. Information Report NOR-X-173, Northern Forest Research Centre, Canadian Forestry Service. (Edmonton)

Kotz S, Nadarajah S (2000) Extreme Value Distributions: Theory and Applications. (Imperial College Press: London)

Lavorel S, Flannigan MD, Lambin EF, Scholes MC (2007) Vulnerability of land systems to fire: interactions between humans, climate, the atmosphere and ecosystems. *Mitigation and Adaptation Strategies for Global Change* **12**, 33-53.

Lawrence MG (2005) The Relationship between Relative Humidity and the Dewpoint Temperature in Moist Air, A simple Conversion and Applications. *Bulletin of the American Meteorological Society* **86**, 225–233.

Moreira F, Catry FX, Rego F, Bacao F (2010) Size-dependent pattern of wildfire ignitions in Portugal: when do ignitions turn into big fires? *Landscape Ecology* **25**, 1405–1417.

Moreno JM, Viedma O, Zavala G, Luna B (2011) Landscape variables influencing forest fires in central Spain. *International Journal of Wildland Fire* **20**, 678–689.

Neyman J, Pearson ES (1933) On the Problem of the Most Efficient Tests of Statistical Hypotheses. *Philosophical Transactions of the Royal Society of London A* **231**, 289-337.

Pereira MG, Trigo RM, DaCamara, CC, Pereira JMC, Leite SM (2005) Synoptic patterns associated with large summer forest fires in Portugal. *Agricultural and Forest Meteorology* **129**, 11-25.

Pereira MG, Malamud BD, Trigo RM, Alves PI (2011) The history and characteristics of the 1980–2005 Portuguese rural fire database. *Natural Hazards and Earth System Sciences* **11**, 3343–3358.

Pickands J (1975) Statistical inference using extreme order statistics. *The Annals of Statistics* **3**, 119-131.

San-Miguel-Ayanz J, Carlson JD, Alexander M, Tolhurst K, Morgan G, Sneeuwjagt R, Dudley M (2003) Current Methods to Assess Fire Danger Potential. In 'Wildland Fire Danger Estimation and Mapping' (Ed Chuvieco E) pp. 20-61 (World Scientific Publishing: Singapore)

San-Miguel-Ayanz J, Schulte E, Schmuck G, Camia A, Strobl P, Liberta G, Giovando C, Boca R, Sedano F, Kempeneers P, McInerney D, Withmore C, Santos de Oliveira, S, Rodrigues M, Durrant T, Corti P, Oehler F, Vilar L, Amatulli G (2012) Comprehensive Monitoring of Wildfires in Europe: The European Forest Fire Information System (EFFIS). In 'Approaches to Managing Disaster –

Assessing Hazards, Emergencies and Disaster Impacts' (Ed Tiefenbacher J) pp. 87-108 (InTech: Rijeka, Croatia)

San-Miguel-Ayanz J, Moreno JM, Camia A (2013) Analysis of large fires in European Mediterranean landscapes: Lessons learned and perspectives. *Forest Ecology and Management* **294**, 11-22.

Trigo IF, DaCamara CC, Viterbo P, Roujean, J-L, Olesen F, Barroso C, Camacho-de-Coca F, Carrer D, Freitas SC, García-Haro J, Geiger B, Gellens-Meulenberghs F, Ghilain N, Meliá J, Pessanha L, Siljamo N, Arboleda A (2011) The Satellite Application Facility for Land Surface Analysis. *International Journal of Remote Sensing* **32**, 2725-2744.

Trigo RM, Pereira JM, Pereira MG, Mota B, Calado MT, DaCamara CC and Santo FE (2006) Atmospheric conditions associated with the exceptional fire season of 2003 in Portugal. *International Journal of Climatology* **26**, 1741-1757.

Van Wagner CE (1974) Structure of the Canadian Forest Fire Weather Index. Publication No. 1333, Department of the Environment, Canadian Forestry Service. (Ottawa)

Van Wagner CE (1987) Development and structure of the Canadian Forest Fire Weather Index System. Technical Report No. 35, Canadian Forestry Service. (Ottawa)

Evaluation of a system for automatic dead fine fuel moisture measurements

Christian Schunk[a], Michael Leuchner[a,b], Annette Menzel[a,b]

[a] *Technische Universität München, Chair of Ecoclimatology, Hans-Carl-von-Carlowitz-Platz 2, 85354 Freising, Germany, schunk@wzw.tum.de*
[b] *Technische Universität München, Institute for Advanced Study, Lichtenbergstraße 2a, 85748 Garching, Germany*

Abstract
Dead fine fuel moisture content is a key parameter for wildfire ignition and behaviour: the higher the fine fuel moisture content, the more activation energy has to be spent on the evaporation of this moisture before the fuels can ignite and release their energy of combustion. Thus, high fuel moisture leads to a lower probability of ignition and a more moderate fire behavior.
These facts have been recognized for a long time and fine fuel moisture has become an essential part of several fire danger rating systems (e.g. 1- and 10-hour dead fuel moisture in the National Fire Danger Rating System (NFDRS) and Fine Fuel Moisture Code in the Canadian Forest Fire Danger Rating System (CFFDRS)). Additionally, dedicated fine fuel moisture models are available as well.
Nevertheless, direct information on dead fine fuel moisture can be valuable for monitoring, scientific research as well as during exceptional conditions, e.g. extreme fire danger with exceptional temporal or spatial distribution of fire danger, for the management of large wildfires. However, dead fine fuel moisture measurements are hard to obtain since common methods involve manual sampling in the field and potentially oven-drying, adding a time delay before the results become available.
In this study, a thorough evaluation of the Campbell Scientific, Inc. instrumentation for automated 10-hour dead fuel moisture (CS506-L fuel moisture sensor) has been carried out. Ten fuel moisture sensors and associated *Ponderosa pine* dowels were obtained and subjected to tests in a constant climate chamber as well as at two field sites in Central Europe for one fire season. The comparability of the values determined from these ten different dowels as well as a potential influence of weathering were investigated along with correlations to manual-gravimetric fuel moisture.
Results show that dowel-to-dowel comparability is relatively good but may be further increased by additional calibration. In the field, there was an excellent correlation between 10-hour fuel moisture as measured by the CS506-L sensors and fast-drying dead fuels such as needle litter and dead grass (R^2 0.81 and 0.82, respectively). Weathering effects during the study period had no major influence on sensor performance.

Keywords*: fine fuel moisture, 10-hour fuel moisture, automatic measurement*

Introduction

Fine fuel moisture has been recognized as a key parameter for forest fire danger, ignition and behaviour and thus also for fire-fighting (Pyne *et al.* 1996). This is because most fires start and spread, at least initially, in fine fuels located on the forest floor and their water content plays an important role for ignitability and combustibility. Wet fuels tend to ignite less easily and to burn more moderately (if there is sustained combustion at all), since a large amount of energy has to be spent on evaporating the moisture (Pyne *et al.* 1996). This additionally leads to a cooling effect (Britton *et al.* 1973) and to a dilution of combustible gases (Chandler *et al.* 1983). Thus, fine fuel moisture is an important parameter in the field and the basis of several forest fire danger rating systems, such as the National Fire Danger Rating System (NFDRS, USA (Bradshaw *et al.* 1983)) and the Canadian Forest Fire Danger Rating System (CFFDRS (Van Wagner 1987)).
Despite its high significance, there is no straightforward way of measuring fine fuel moisture automatically in the field. Gravimetric measurement following manual sampling is the standard procedure (Britton *et al.* 1973; Norum and Miller 1984; Viegas *et al.* 2006), which however requires

a person to travel to the respective field site(s) and to take fuel samples. These samples need to be transported back to a laboratory, weighed wet, oven dried and weighed again in a dry state. In addition to the multitude of steps required, drying time (24 hours in many studies) leads to an additional delay before the fuel moisture measurements become available, rendering them useless for any immediate prevention or fire management decisions.
Several methods have been developed to overcome these problems. One of them is based on an observation made by early US fire researchers in Scandinavia, where local foresters used wood as a reference material that was easier to observe that the fine fuels (Hardy and Hardy 2007). This method was extended by Gisborne (1933), who set up rules to standardize the so-called fuel moisture sticks and trimmed them to exactly 100 g dry mass (Fischer and Hardy 1976; Hardy and Hardy 2007). Following this standardization, moisture content of the reference sticks could be determined using a simple balance in the field. Later on, the dead fuel moisture components of the NFDRS were based on those measurements and on theoretical considerations for drying and wetting of cylindrical objects (Bradshaw *et al.* 1983; Burgan 1988; Cohen and Deeming 1985). However, an influence of wood decay on the long-term stability of the measurements was detected (Haines and Frost 1978). Finally, several instrument manufacturers (e.g. Campbell Scientific (North Logan, UT, USA), Vaisala (Helsinki, Finland) and Forest Technology Systems (Victoria, BC, Canada)) have found ways to automatically measure the stick's moisture content, e.g. using capacitive sensing. Although some of the manufacturers had to adapt the stick dimensions to their techniques, this widely increases the potential use of fuel moisture measurements. For example, automated fuel moisture sensors are part of many RAWS stations in the US (NWCG 2009). Nevertheless, the precision, reliability and long-term performance of these systems remain somewhat dubious (Gibos 2010) and are examined in this study.

Methods

The measuring system developed by Campbell Scientific consists of a fuel moisture stick (26601 CS506, also called "dowel") connected to a so-called fuel moisture sensor (electronics unit, CS506-L) and associated data logger. In order to evaluate the measuring system, a total of 8 fuel moisture sensors, 10 fuel moisture sticks and three data loggers (CR800) were acquired. The fuel moisture sticks are made of *Ponderosa pine* wood into which two stainless steel electrodes are pressed and secured by cable ties. They have a nominal dimension of 1.3 cm (0.5") diameter and 50.8 cm (20.0") length and are meant to represent the 10-hour fuel moisture class of the NFDRS. The RMS error and maximum usage time reported by the manufacturer are 0.75-2.27% and one season, respectively. The sensors were tested in two forest sites in Bavaria, southern Germany, for one fire season, during which manual gravimetric measurements of fine fuel moisture were made regularly. Before and after the field tests, reference measurements were made in a climate chamber. At the end of the study, the fuel moisture sticks were separated in hygroscopic (wood) and non-hygroscopic (electrodes and cable ties) material and the wood parts were oven-dried.

2.1. Reference measurements in the climate chamber

In the climate chamber, only one fuel moisture sensor (electronics unit) was used, to which the 10 fuel moisture sticks were connected sequentially. This was performed regularly during the two desorption runs before and after the field measurements, which included the following conditions: soaking the fuel moisture sticks for one hour, subjecting them to 23°C and 90, 80, 70, 60, 50, 40, 30, 20% relative humidity until equilibration before the field measurements and to 23°C and 90, 55, 20% relative humidity (shortened desorption run) after the field measurements. Equilibration of the sticks' moisture content was assessed using both the automated measurements and additional manual weighing. The climate chamber was of a walk-in type (3.9 m² floor space) and had a typical accuracy of ±0.2°C and ±5% relative humidity, respectively.

2.2. Field measurements

Following the initial climate chamber tests, the two forest climate stations "Altdorf" (49.4175° N, 11.3125° E, approx. 15 km east of Nuremberg, pure Scots pine (*Pinus sylvestris*) stand) and "Freising" (48.4102° N, 11.6595° E, approx. 30 km north of Munich, mixed European beech (*Fagus sylvatica*) and pedunculate oak (*Quercus robur*) stand) of the Bavarian State Forest Institute (Bayerische Landesanstalt für Wald und Forstwirtschaft, LWF) were equipped with three fuel moisture sensors and sticks each. The measurements were carried out from end of March until end of October 2013, and after each third of the measuring period, one fuel moisture stick was exchanged by a spare that had been stored in a laboratory for this purpose. The fuel moisture sensors were mounted according to the manufacturer's instructions at a height of 30.5 cm (12") above the ground, facing south. The setup at the Altdorf station is shown in Figure 1 as an example. Their values were measured and stored at 15-minute intervals, according to the measurement intervals of the existing forest climate stations.

Figure 1. Arrangement of fuel moisture sticks at the forest climate station Altdorf.

During the measuring period, fuel moisture samples of litter (Altdorf and Freising) and dead grass from the previous season (Altdorf only) were taken regularly. While it was our aim to sample in the early afternoon, at least weekly during wet periods and at least every other day in dry periods, a certain variation occurred due to the availability of sampling personnel. Additionally, dry grass sampling at Altdorf had to be terminated in the end of August as the grass had decayed in a way that it was no longer relevant to fire danger and that sampling became impossible. For each day and fuel, three samples were taken, which were stored in air-tight polypropylene bottles and shipped to the laboratory within a maximum of 7 days. The fuel moisture was calculated gravimetrically (in % of dry mass), following oven-drying at 105°C for 24 hours.

2.3. Data analysis

The data thus gathered were combined, processed and analyzed in a way that the relationship of the automatically measured fuel moisture values to relative humidity and gravimetric stick moisture in the climate chamber before and after the field measurements could be shown. The field measurements themselves are presented as progressions of the measured stick moisture over time and as correlations of stick moisture and gravimetric fine fuel moisture content. Linear regressions are used for showing and modelling relationships between the different measurement variables, where appropriate. All data processing, statistics and plotting were performed in R, version 3.0.3, and its packages xlsx, doBy, and RODBC.

Results and discussion

Reference measurements before the field campaign

Before the field campaign was started, a relatively high resolution desorption run was carried out in a climate chamber in order to compare the fuel moistures of each stick, measured both by the automatic system and gravimetrically. The gravimetric moisture values were obtained by weighing the fuel moisture sticks repeatedly and combining these values with the mass of the non-hygroscopic material and the oven-dry mass of the wood determined at the end of the study. Results for both automatically measured and gravimetric moisture of the sticks are shown in Figure 2.

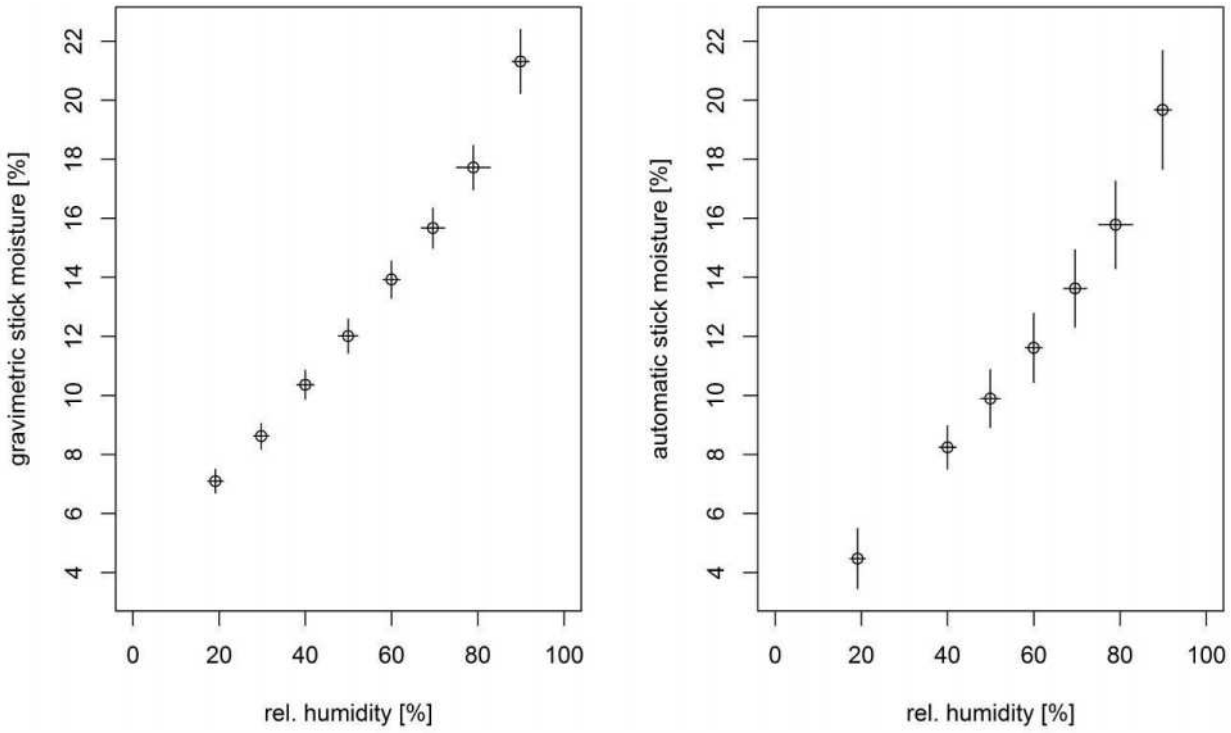

Figure 2. Results of the initial climate chamber desorption run. Left graph: gravimetric fuel moisture, right graph: fuel moisture as measured by the automated system.

The left graph in Figure 2 represents the gravimetric fuel moisture during the desorption run and is thus a classic sorption isotherm. In contrast to isotherms from literature for wood (Kollmann *et al.* 1986*;* Forest Products Laboratory 1999) and fine fuels (Van Wagner 1972; Anderson 1990; Blackmarr 1971; Lopes *et al.* 2010), it lacks the typical sigmoid shape. Apart from this, an increasing standard deviation with increasing relative humidity can be observed. Comparing this to the automated measurements in the right chart of Figure 2, their absolute values are not identical to the gravimetric measurements and the standard deviations are substantially higher. This is not surprising as the gravimetric technique is by far more accurate than the capacitive sensing of the automated measurement. Additionally, the dry mass of the sticks (not shown) had a variation >5%, influencing the automated measurements as they in fact react to the density surrounding the electrodes.

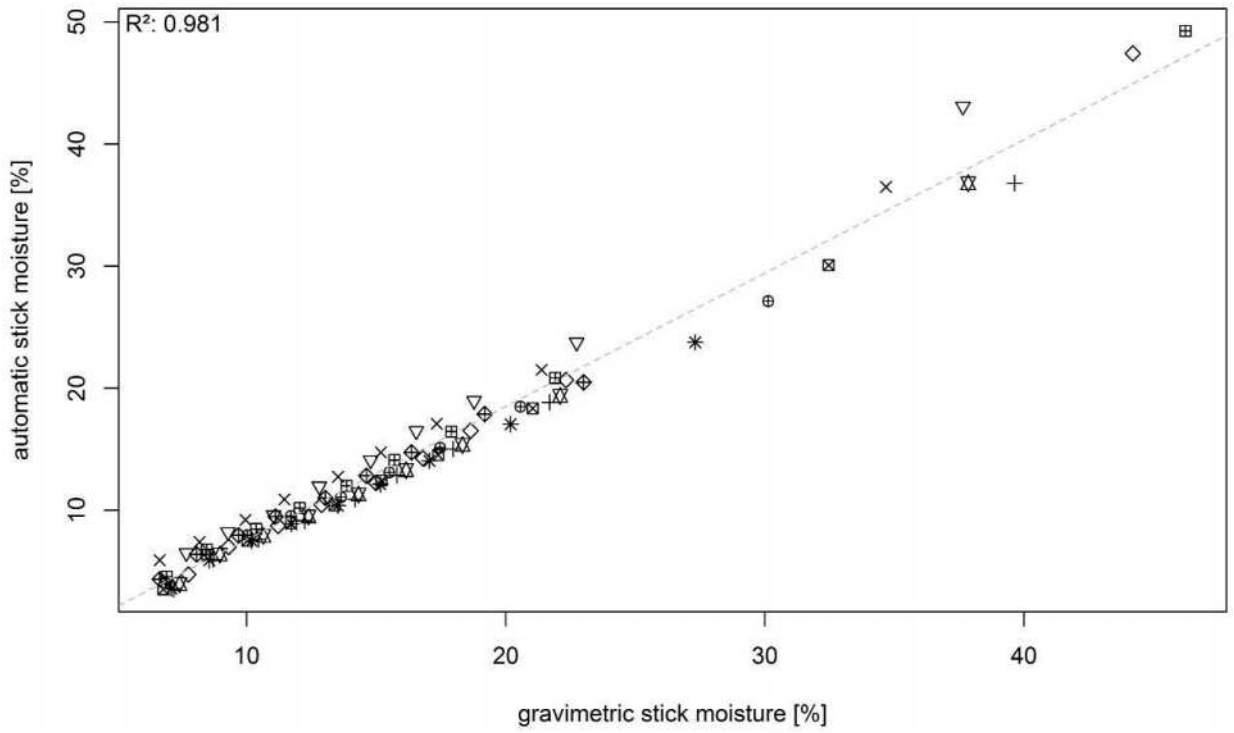

Figure 3. Automated fuel moisture values of the initial desorption run in dependence of the gravimetric fuel moisture. The different symbols correspond to the individual fuel moisture sticks.

When the automated values are shown in dependence of the gravimetric fuel moisture (Figure 3, including the values of the soaked sticks), a distinct and highly significant correlation of these values (R^2 0.981) is obvious. However, not all individual fuel moisture sticks follow a common regression line. Linear calibration for each stick can be used to correct this and to make the absolute automated fuel moisture values identical to the gravimetric moisture content of the sticks (not shown). However, this procedure is very laborious, as a full desorption run and an estimation of the stick's dry mass is necessary.

Field measurements

The progression of the automatically measured fuel moisture during the field campaign is shown in Figure 4. Whenever a new fuel moisture stick was used, all values until the first substantial precipitation event were removed. It can be seen that the accordance of the individual fuel moisture sticks is quite good and that there are no obvious shifts when the sticks were exchanged (lighter shades of gray represent longer ageing and use in the field). However, high moisture contents are usually accompanied by a higher variation from stick to stick than low moistures. During dry conditions, a daily cycle of fuel moisture can be observed that corresponds to textbook examples (cf. Pyne *et al.* 1996).

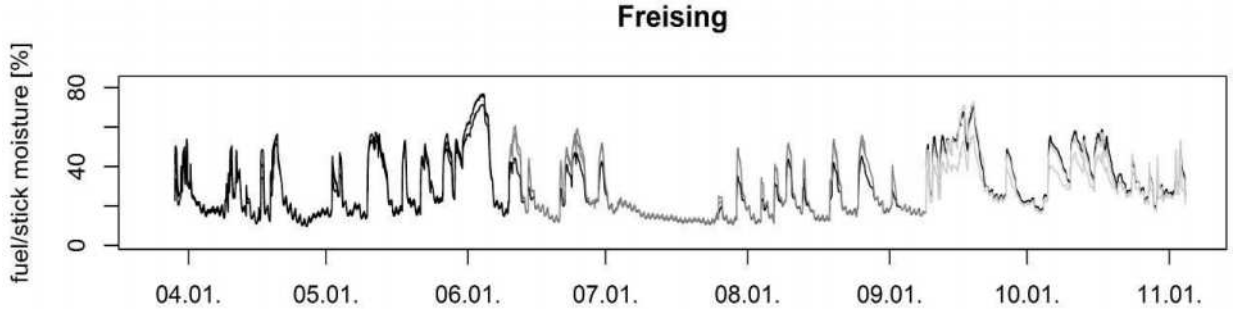

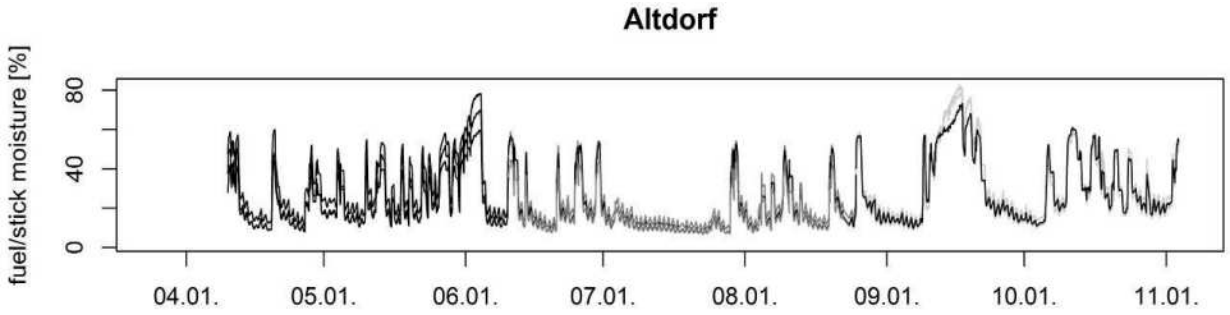

Figure 4. Progression of fuel moisture during the field measurements. Lighter shades of gray represent longer ageing of the sticks and thus longer use in the field, i.e. black-coloured lines represent fuel moistures that have been determined during initial exposure of any fuel moisture stick; dark gray lines an extended exposure of another third of the measuring period and light grey lines an exposure over the whole measuring period.

When the automated fuel moisture measurements are compared to simultaneously sampled gravimetric values of local dead fine fuels (Figure 5), correlations of varying strength and significance can be observed. For the thick, rather slow drying layers of European beech and pedunculate oak leaves at Freising, R^2 of the linear regression is smaller (0.44) than for the values of Scots pine litter and dead grass from the previous season (Altdorf, R^2 0.81 and 0.82, respectively). These are good, despite the fact that the type of material, dimensions, and arrangement are substantially different.

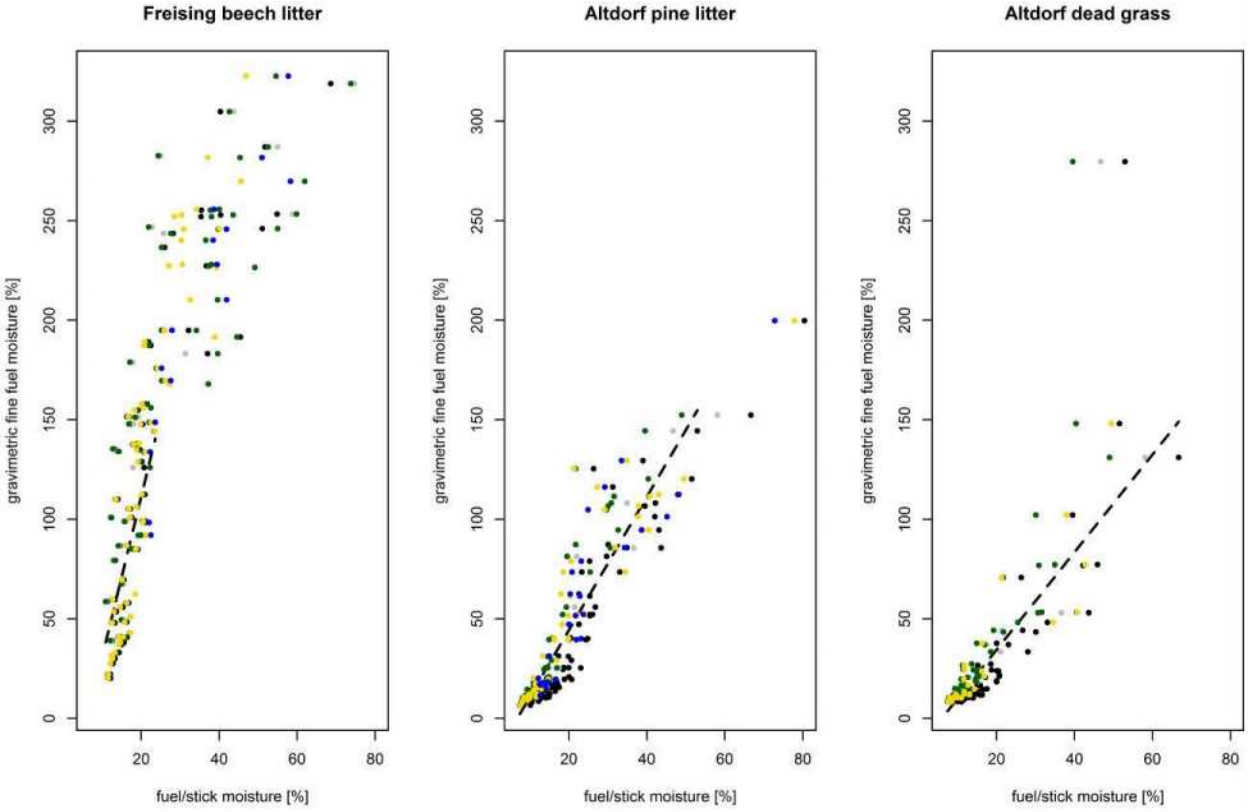

Figure 5. Correlations of (left to right) automatically measured and manually determined fuel moisture for European beech (Freising) and Scots pine (Altdorf) litter, as well as dead grass from the previous year (Altdorf).

3.3. Reference measurements after the field campaign and long-term stability

Besides comparing the continuity of the measuring signal when the fuel moisture sticks were replaced in the field (cf. Figure 4), additional reference measurements were made in the climate chamber after the field exposure of the sticks. These are compared to the initial desorption run in Figure 6, where the initial values are shown in black, the associated confidence intervals as dashed orange lines and the final reference values as red circles.

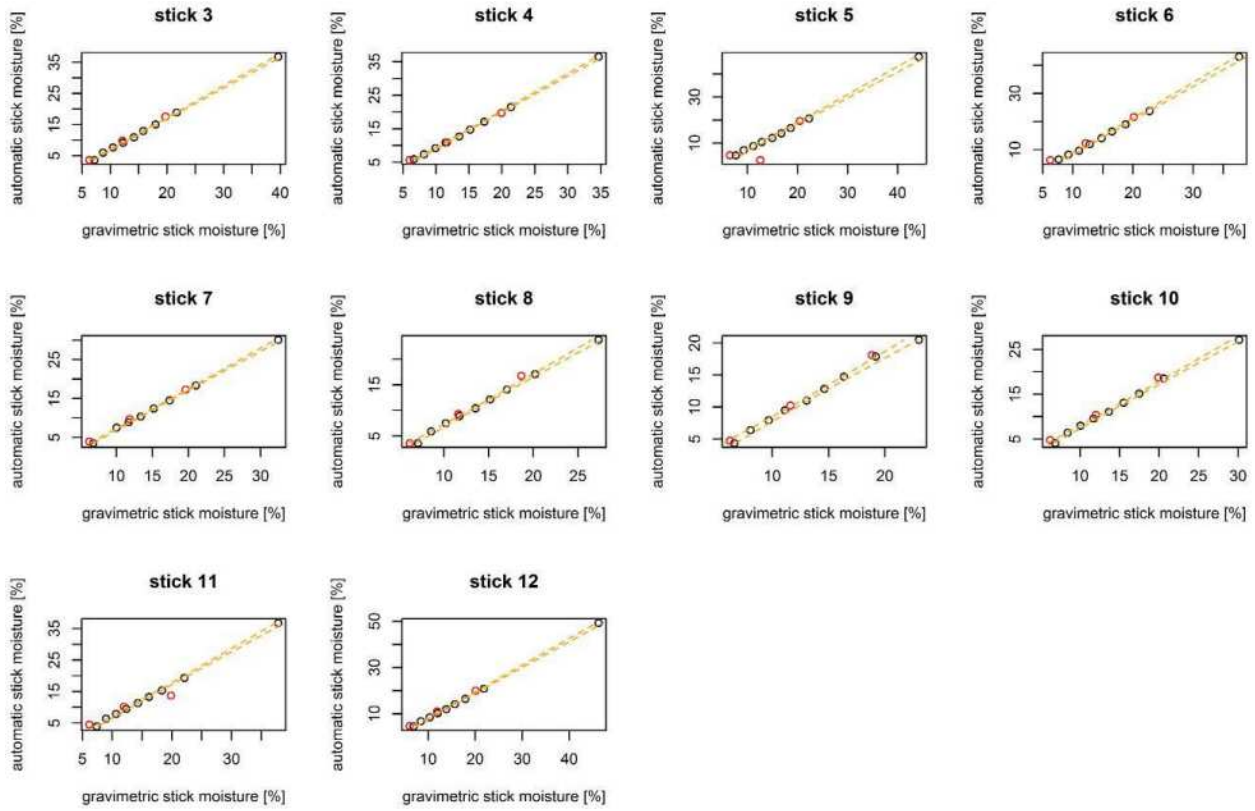

Figure 6. Correlations of automatic and gravimetrically measured fuel moisture of the sticks before (black circles) and after (red circles) the field campaign, determined in steady-state conditions in the climate chamber. The orange dashed lines correspond to the confidence interval of the initial measurements.

Except for very few outliers that were probably caused by measuring errors, no relevant differences in the signal before and after the field exposure can be discovered. Thus, the long-term stability of the fuel moisture sticks can be constituted as sufficient for (at least) one fire season under conditions similar to this central European setting.

Conclusions

This study was carried out to evaluate the performance of the automated Campbell Scientific fuel moisture measurement system (CS506-L). Using measurements in controlled environments, at field sites and a comparison to manual sampling and gravimetric moisture content determination, it could be shown that the stick-to-stick deviation is tolerable, no relevant ageing effects are expected to occur during one fire season and there is a correlation of the automated 10-hour fuel moisture values to common dead fine fuel moisture (ranging from R^2 0.44 to 0.88 depending on the type of fuel). Overall, this system is a satisfactory option when a direct measure of an (analogous) fuel moisture value is required, yielding values that can be deemed at least acceptable for this hard-to-measure parameter. The automated operation as well as the possibility for immediate data transmission and availability is

a great benefit of this system. However, even changing the fuel moisture sticks annually is rather cost-intensive when the original fuel moisture sticks are used. Additional work (not reported here) has shown that replacement sticks could be self-manufactured relatively easily. However, ensuring correct calibration/repeatability is an issue in this case.

Acknowledgements

The authors would like to thank all persons who helped carrying out the project, in particular the local fuel moisture samplers Klaus Oblinger and Helmut Rüger at Altdorf and the colleagues of the Bavarian State Forest Institute (LWF). Financial support is acknowledged from the Bavarian State Ministry for Food, Agriculture and Forestry through project ST288 and from the European Research Council under the European Union's Seventh Framework Programme (FP7/2007-2013)/ERC grant agreement no. 282250. The authors furthermore gratefully acknowledge the support of the Institute of Advanced Study and the Faculty Graduate Center Weihenstephan of TUM Graduate School at Technische Universität München, Germany.

References

Anderson HE (1990) Predicting equilibrium moisture content of some foliar forest litter in the northern Rocky Mountains. USDA Forest Service, Intermountain Research Station Research Paper INT-429. (Ogden, UT)

Blackmarr WH (1971) Equilibrium moisture content of common fine fuels found in southeastern forests. USDA Forest Service, Southeastern Forest Experiment Station Research Paper SE-74. (Asheville, NC)

Bradshaw LS, Deeming JE, Burgan RE, Cohen JD (1983) The 1978 National Fire-Danger Rating System: Technical Documentation. USDA Forest Service, Intermountain Forest and Range Experiment Station General Technical Report GTR INT-169. (Ogden, UT)

Britton CM, Countryman CM, Wright HA, Walvekar AG (1973) The effect of humidity, air temperature, and wind speed on fine fuel moisture content. *Fire Technology* **9,** 46–55. doi:10.1007/BF02624840

Burgan RE (1988) 1988 Revisions to the 1978 National Fire-Danger Rating System. USDA Forest Service, Southeastern Forest Experiment Station Research Paper SE-273. (Asheville, NC)

Chandler C, Cheney P, Thomas P, Trabaud L, Williams D (1983) 'Fire in Forestry - Forest Fire Behaviour and Effects' (Wiley: New York)

Cohen JD, Deeming JE (1985) The National Fire Danger Rating System: basic equations. USDA Forest Service, Pacific Southwest Forest and Range Experiment Station General Technical Report PSW-82. (Berkeley, CA)

Fischer WC, Hardy CE (1976) Fire-weather observer's handbook. US Department of Agriculture, Agriculture Handbook No. 494. (Washington, DC)

Forest Products Laboratory (1999) Wood handbook - wood as an engineering material. USDA Forest Service, Forest Products Laboratory General Technical Report FPL-GTR-113. (Madison, WI)

Gibos KE (2010) Effect of slope and aspect on litter layer moisture content of Lodgepole pine stands in the eastern slopes of the Rocky Mountains of Alberta. University of Toronto, Master thesis. (Toronto, ON)

Gisborne HT (1933) The wood cylinder method of measuring forest inflammability. *Journal of Forestry* **31,** 673–679.

Haines DA, Frost JS (1978) Weathering effects on fuel moisture sticks: corrections and recommendations. USDA Forest Service, North Central Forest Experiment Station Research Paper NC-154. (St. Paul, MN)

Hardy CC, Hardy CE (2007) Fire danger rating in the United States of America: an evolution since 1916. *International Journal of Wildland Fire* **16,** 217–231. doi:10.1071/WF06076

Kollmann F, Côté WA, Jr., Kuenzi EW, Stamm AJ (1968) Sorption and equilibrium moisture. In 'Principles of Wood Science and Technology. Vol. 1: Solid Wood' (Eds. F Kollmann, WA Côté Jr) pp. 189-195. (Springer: New York)

Norum RA, Miller M (1984) Measuring fuel moisture content in Alaska: standard methods and procedures. USDA Forest Service, Pacific Northwest Forest and Range Experiment Station General Technical Report PNW-171. (Fairbanks, Alaska)

NWCG (2009) Interagency wildland fire weather station standards & guidelines. National Wildfire Coordination Group Report PMS-426-3. (Boise, ID)

Pyne SK, Andrews PL, Laven RD (1996) 'Introduction to Wildland Fire' (Wiley: New York)

Van Wagner CE (1972) Equilibrium moisture contents of some fine fuels in eastern Canada. Canadian Forest Service, Petawawa Forest Experiment Station Information Report PS-X-36. (Chalk River, ON)

Van Wagner CE (1987) Development and structure of the Canadian Forest Fire Weather Index System. Canadian Forestry Service, Forestry Technical Report 35. (Ottawa, ON)

Lopes S, Lemos LT, Viegas DX, (2010) Modeling moisture content of dead fine forest fuels common in Central Portugal. In 'Proceedings of the VI International Conference on Forest Fire Research', 15-18 November 2010, Coimbra, Portugal. (Ed. DX Viegas) (CD-ROM) (ADAI: Coimbra, Portugal)

Viegas DX, Lopes SMG, Viegas MT, de Lemos LT (2006) Moisture content of fine forest fuels in the central Portugal (Lousa) for the Period 1996-2004. In 'Proceedings of the V International Conference on Forest Fire Research', 27-30 November 2006, Coimbra, Portugal. (Ed. DX Viegas) (CD-ROM) (Elsevier: Amsterdam)

Expanding the horizons of wildfire risk management

Matthew P Thompson[a], Joe Scott[b], Julie W Gilbertson-Day [a], Jessica R Haas [a], and David E Calkin [a]

[a] *Rocky Mountain Research Station, US Forest Service, Missoula, MT, USA, mpthompson02@fs.fed.us, jgilbertsonday@fs.fed.us, jrhaas@fs.fed.us, decalkin@fs.fed.us*
[b] *Pyrologix, LLC, Missoula, MT, USA, joe.scott@pyrologix.com*

Abstract
Owing to increased computational capacity and other factors, wildfire simulation methodologies are becoming increasingly sophisticated, and are subsequently seeing increasing use for federal fire management within the United States. State-of-the-art simulation systems account for the occurrence, topological spread, and behaviour of wildfire, all within a spatially-explicit, stochastic framework. Leveraging these advancements in burn probability modelling, researchers and managers alike are better able to assess the hazards and risks associated with wildfires and to identify effective and efficient risk mitigation opportunities. In this paper, we review the role of stochastic simulation modelling in wildfire risk assessment, focusing on how simulation results can be used to support risk-informed decision making across planning contexts. Our principal focus will be describing how novel assessment tools can be brought to bear to analyse risks to the wildland urban interface and to municipal water supplies. We will review how assessment results can inform high-level prioritization and allocation decisions, as well as more in-depth, spatial suppression response and fuel treatment planning.

Keywords*: wildfire management, spatial analysis, simulation analysis, econometric analysis*

The views expressed here are the authors', and do not necessarily represent the views of the USDA

Introduction

Wildfire is a global phenomenon with potentially devastating consequences to human life, air quality, water quality, homes, infrastructure, and natural and cultural resources. At the same time, wildfire is an important component of many ecosystems, potentially resulting in substantial ecological benefits. There is a critical need, therefore, to understand where and under what conditions alternative fire management strategies should be employed to balance costs and the impacts of fire, both positive and negative.

Recognizing the inherent uncertainty associated with wildfire processes, federal wildfire management in the United States, the primary focus of this paper, is increasingly adopting risk analysis principles. Principally this entails implementation of a quantitative, integrated wildfire risk assessment framework – the primary components of which are depicted in Figure 1. The likelihood and intensity of wildfire, along with the susceptibility of resources/assets to wildfire, collectively define the three legs of the "wildfire risk triangle." Stochastic wildfire simulation is therefore a foundational component of wildfire risk assessment.

A key aim of this paper is to demonstrate the value of stochastic wildfire simulation to support risk-informed land and fire management decisions. Recent advances in burn probability modelling have enabled the estimation of spatially-resolved fire likelihood and intensity metrics across landscapes, with a growing array of applications. Prominent uncertainties and informational needs vary across planning context, and resultantly a variety of simulation approaches exist, which will be compared and contrasted. In addition to highlighting several real-world planning examples focusing on risks to human life and health, this paper will identify emerging and future applications of stochastic wildfire simulation.

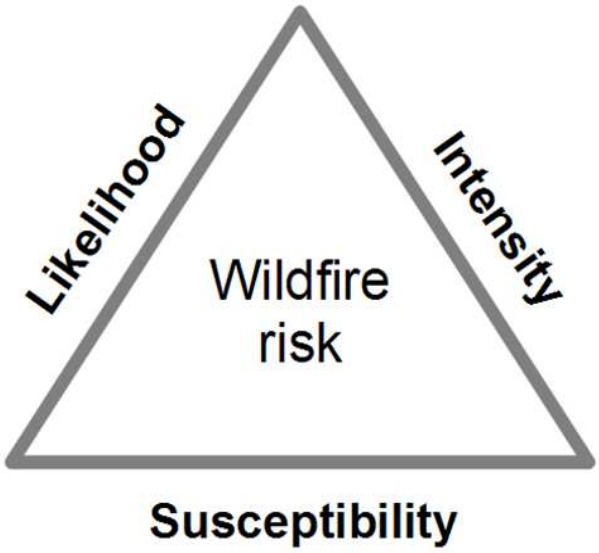

Figure 1. Wildfire likelihood and intensity, along with resource/asset susceptibility comprise the three legs of the "wildfire risk triangle." (Scott et al. 2013)

The Role of Simulation and Risk Analysis to Support Planning

Figure 2 identifies the primary sources of variability and their relation to wildfire risk mitigation and planning contexts. In pre-fire environments, the ignition date and location, as well as fire weather conditions influencing fire behaviour are uncertain. The date of the ignition is important because fires earlier in the season may have a longer temporal horizon over which to grow given the right weather conditions, whereas ignitions late in the fire season may be less of a concern as temperatures and dryness levels decrease. The location of an ignition is important relative to fuels and topographic conditions capable of supporting large fire spread, as well as proximity to fire-susceptible resources and assets. By contrast, after a wildfire incident has been detected, the primary source of uncertainty is fire weather, which is generally less uncertain relative to pre-fire contexts due to availability of short-term weather forecasts..

Figure 2 also identifies three primary types of wildfire management decisions: pre-fire fuel treatment planning, which entails manipulation of vegetation and fuel conditions to modify fire behaviour; pre-fire response planning, which entails the stratification of objectives and strategies according to possible wildfire scenarios as well as the location of firefighting resources (e.g., crews, dozers, helicopters); and wildfire incident response, which entails the implementation of strategies and tactics to achieve objectives, and the ordering and deployment of firefighting resources. Ideally these three planning processes are linked, so that for instance fuel treatments are designed to enable safe and effective firefighting response. Not included in this figure, although potentially important depending upon context, are efforts aimed at preventing human-caused ignitions.

Expanding upon the sources of variability depicted in Figure 2, Figure 3 displays the primary inputs and outputs feeding stochastic wildfire simulation models. As described above, ignition patterns, fire weather patterns, and the conditions of fuels and vegetation all influence the likelihood and intensity of wildfire across the landscape. The fundamental unit of simulation is a wildfire event and/or a wildfire season, the latter of which may entail multiple wildfire events in a given season. Fire spread modelling is built upon pixel-based, or rasterized, geospatial data, where each pixel represents a composite of topographic and vegetation-related variables, and the continuity of fuels across pixels

along with weather patterns drives simulated fire spread. There are two primary sources of outputs: pixel-based outputs that aggregate results across simulated fire events to characterize localized burn probabilities and fire intensity distributions; and event-level or polygon-based outputs that summarize simulation results for individual fires or individual fire seasons.

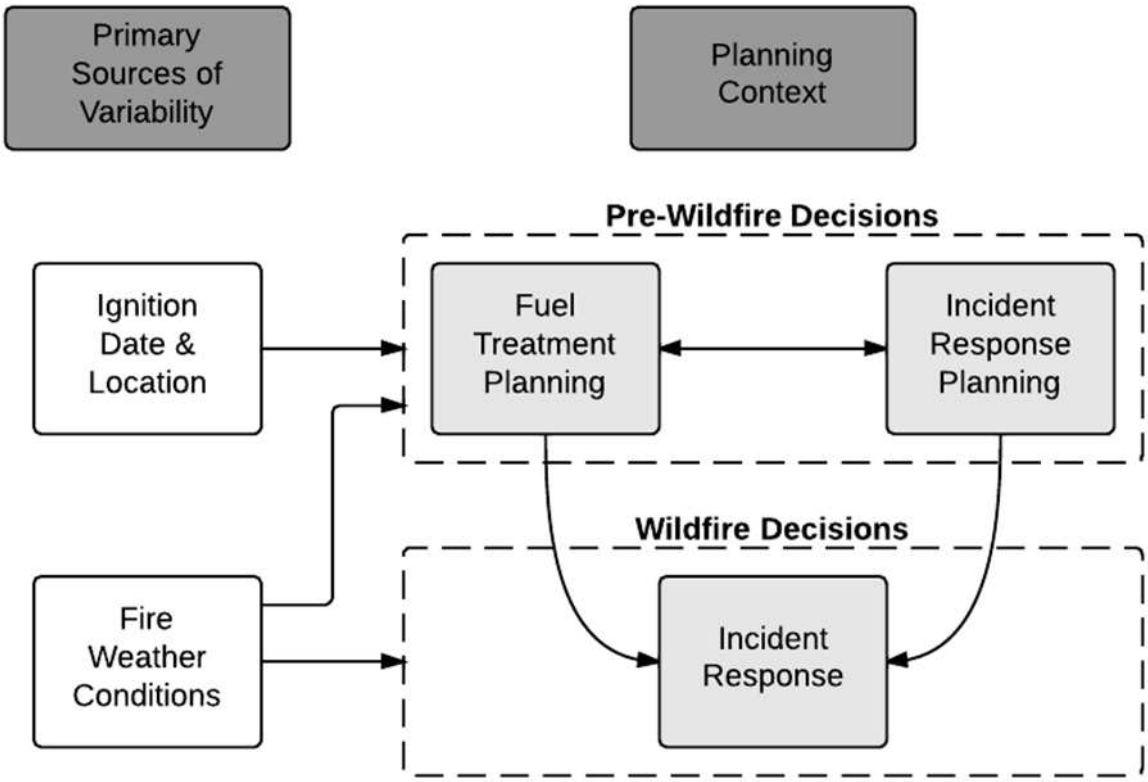

Figure 2. Primary sources of variability concerning wildfire occurrence and behaviour, and their relation to wildfire management planning contexts.

The advent of widespread burn probability modelling for wildfire management in the United States came with the development of the Fire Spread Probability (FSPro) modelling functionality within the Wildland Fire Decision Support System (WFDSS), used for active large wildfire incidents (Calkin *et al*. 2011). Referring to Figure 2, this entails ensemble simulations accounting for thousands of possible realizations of fire weather conditions, given an observed ignition. FSPro simulations depict contours of equal burn probability given fire spread potential over a given time duration, which roughly resemble concentric circles augmented by factors such as topography and forecasted wind direction. Figure 4 displays example FSPro burn probability contours for a large wildfire event in California, USA.

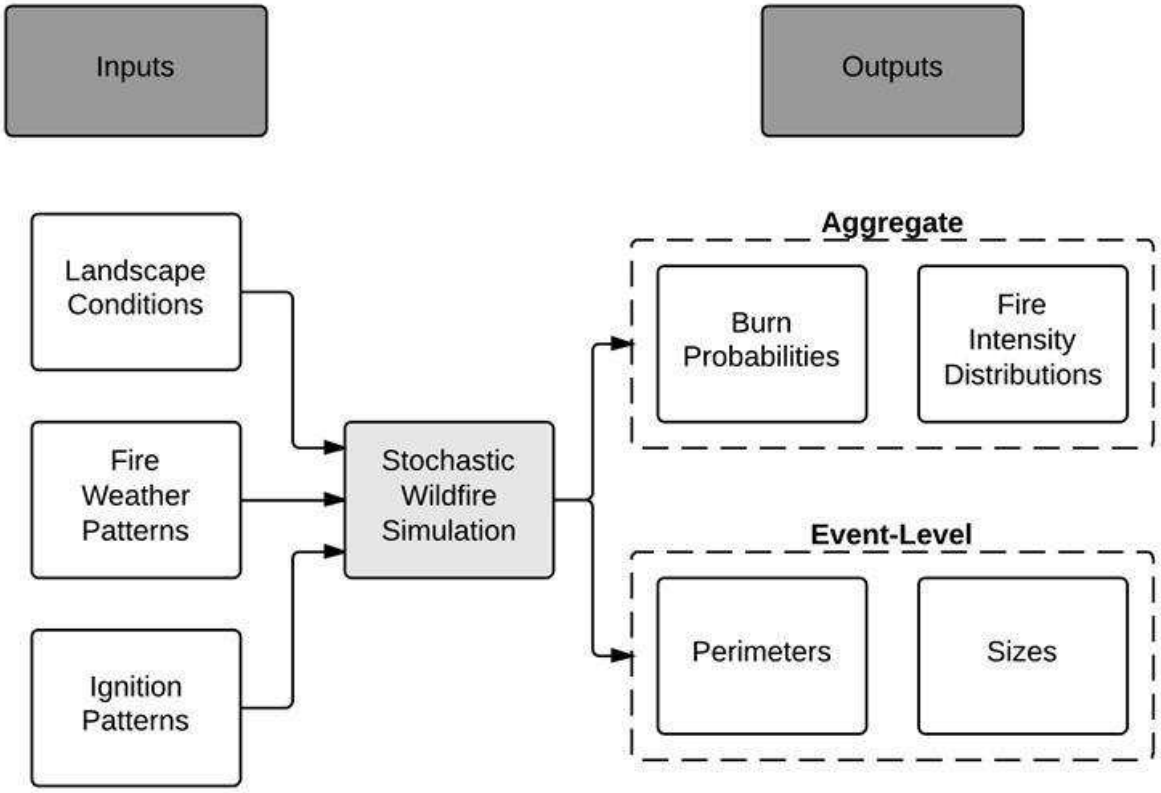

Figure 3. Primary inputs and outputs of stochastic wildfire simulation modelling

As adoption of risk analysis principles has increased, attention has turned to the application of stochastic wildfire simulation to pre-fire planning contexts. Figure 5, for instance, displays spatial burn probability modelling results for a landscape encompassing the Bridger-Teton Nation Forest in Wyoming, USA. Note the stark differences in patterns of probability between Figures 4 and 5, with the results presented in the latter figure capturing multiple ignitions along with variable fire weather conditions. The use of stochastic simulation in pre-fire planning contexts allows for more deliberative, structured decision processes (e.g., Marcot *et al*. 2012), incorporating not just fire modelling results but also information on resource/asset exposure, potential fire effects, and managerial priorities (Thompson *et al*. 2013a). Risk-based assessments built upon pixel-based burn probability results are now being widely used to support land and fire management decisions, in various geographic locations and at various planning scales (Thompson *et al*. 2011; Salis *et al*. 2012). Further, stochastic simulation can be used in comparative analysis frameworks to evaluate the impacts of alternative management strategies and to evaluate how past fuel treatments may have altered fire outcomes (Ager *et al*. 2010; Cochrane *et al*. 2012).

Another major expansion in application of stochastic wildfire simulation has been the transition to utilizing event-level results. That is, instead of focusing on localized burn probabilities and flame length distributions, analyses have focused on aggregating results across simulated events themselves. One prominent example is using simulation outputs to feed economic models predicting suppression costs based upon individual fire sizes, among other variables (Thompson *et al*. 2013b). Use of perimeters is also useful, particularly for capturing the range of variation for possible fire outcomes. For instance, whereas the expected area burned within a given polygon of interest (e.g., municipal watershed) can be captured by summing the product of pixel area and pixel burn probability for all pixels within the area, the use of simulated perimeters can characterize the entire distribution of conditional polygon area burned (Thompson *et al*. 2013c).

One promising application of perimeters is in capturing risk transmission across landscapes and identifying potential fire spread pathways (Ager *et al*. 2012). This type of analysis can estimate the likelihood of ignitions in various locations reaching some resource/asset of interest, for instance isolated patches of wildfire habitat or the wildland-urban interface (Scott *et al*. 2012; Thompson *et al*. 2013c). Spatially identifying the area within which ignitions can reach an area of interest can lead to delineation of a "fireshed" boundary, or the area within with ignitions can transmit risk to the area of interest. As an illustration, Figure 6 displays the location of all simulated ignitions whose perimeters can reach the municipal watershed for Helena, Montana, USA The outer boundary of these ignitions is delineated using a convex hull, with the left panel indicating all ignition locations and right panel further indicating the percentage of watershed burned associated with each ignition.

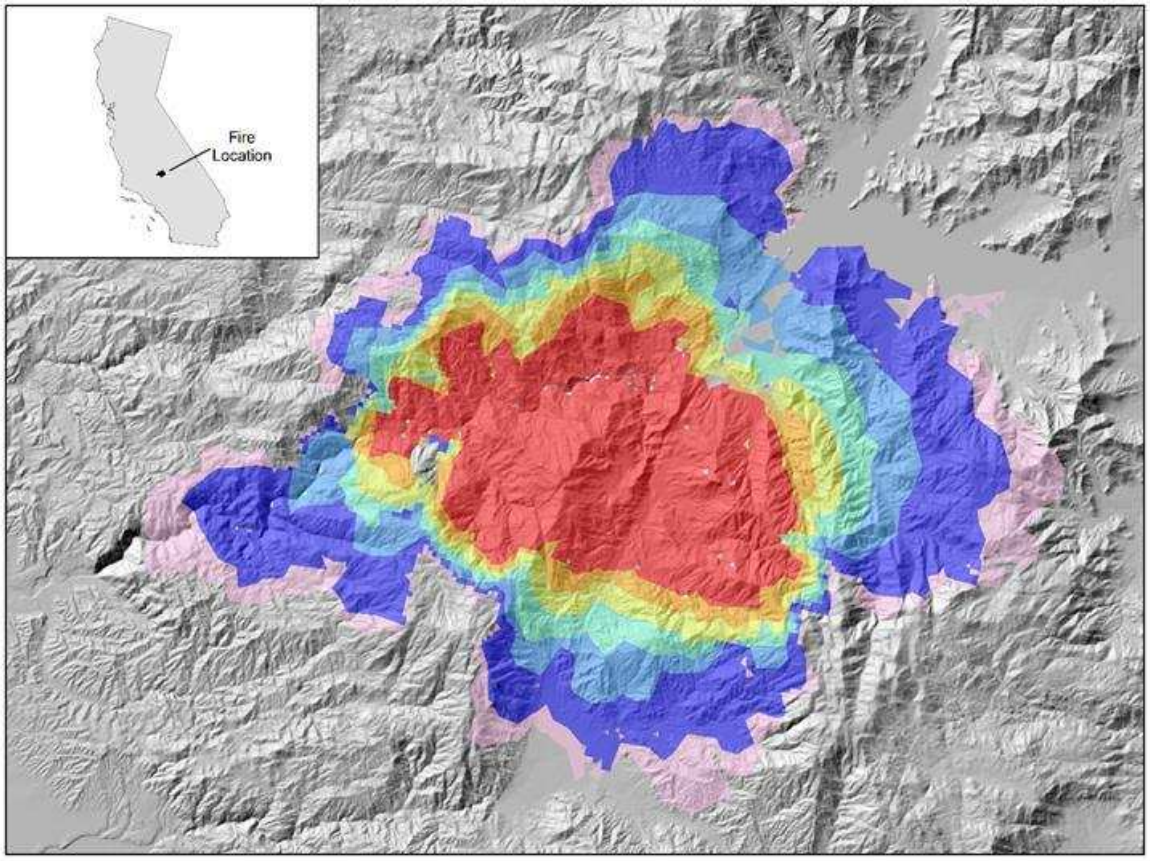

Figure 4. Simulated burn probability contours for a large wildfire event, given an ignition and fire weather forecasts. (Thompson et al. 2012)

The attribution of fire-level impacts to ignition locations has great potential to identify and differentiate areas of high risk transmission, and further to inform pre-fire strategies for mitigating risk. One prominent question in wildfire management, for instance, is which landowners comprise the greatest share of contributed risk and therefore bear the greatest burden for investing in risk mitigation. Figure 7 presents results from an analysis in the Front Range of Colorado, USA, examining the potential amount of human population affected within each simulated perimeter. The figure presents probabilities of exceeding a given amount of population impacted, charts which are commonplace in other arenas such as flood modelling but are only now being integrated into fire modelling. In this case, the impacts of ignitions are partitioned according to whether the fire ignited on federal or non-federal land, with results indicating non-federal ignitions have a greater potential to impact populated areas, due to geographic patterns of land ownership and human development in this region.

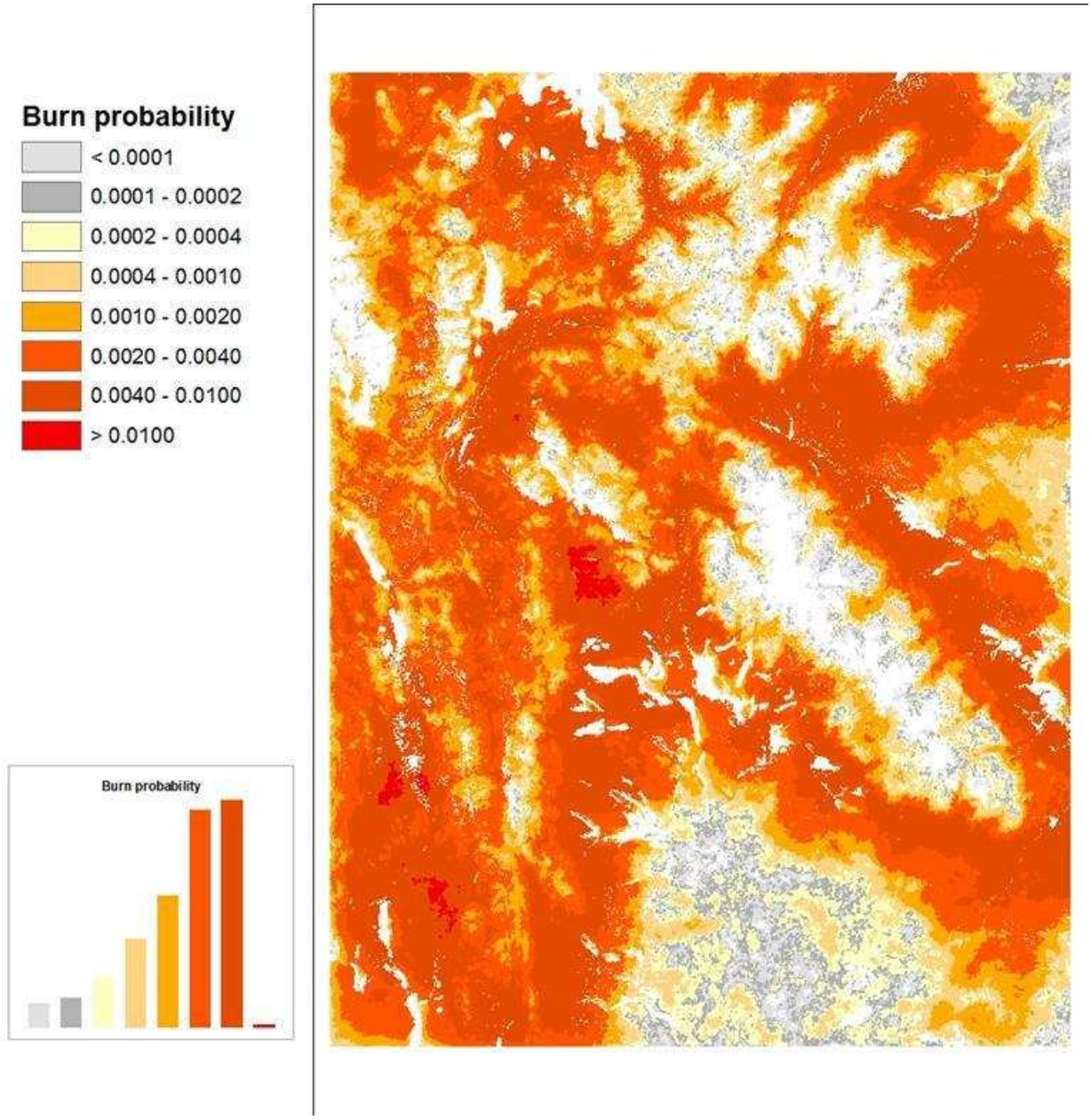

Figure 5. Annual burn probability results for thousands of simulated large wildfire events, with variable ignitions and fire weather conditions. (Scott et al. 2013)

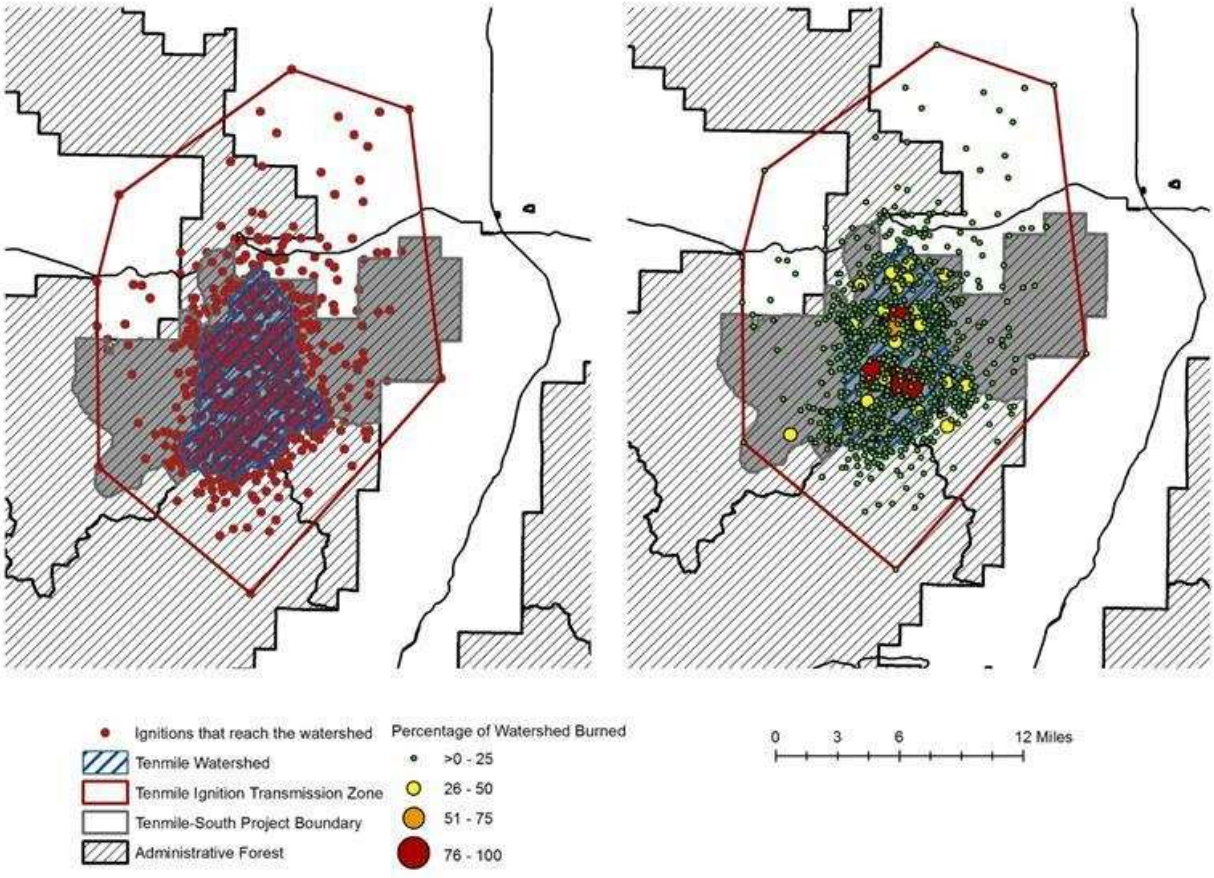

Figure 6. Fireshed (ignition transmission zone) delineation for all ignitions reaching the municipal watershed, along with area burned attributed to ignition.

3. Future Research Directions

Practically speaking, one key future direction of stochastic simulation is expanded application to other geographic regions throughout federally managed lands in the United States and elsewhere. Early adopters have largely reported beneficial outcomes, setting the stage for broader-scale adoption in a variety of contexts and planning scales. Notably, many of the assessments performed to date have occurred within collaborative planning environments, which in the ideal scenario will lead to less conflict and more streamlined implementation of risk mitigation activities. The availability of fire and fuel modellers, geospatial analysts, and process experts may largely determine the application rate of stochastic wildfire simulation and geospatial risk assessment frameworks, an area ripe for science delivery and technology transfer from the research world to land and fire managers.

Three arenas of active research are worth mentioning. First, decision makers would benefit from increased application of stochastic wildfire simulation and associated modelling efforts to better understand the impacts of fire management policies. Such efforts are by necessity interdisciplinary, for instance combining risk analysis, fire ecology, and economics, to better understand the likely costs and benefits of alternative strategies. Second, stochastic wildfire simulation outputs can help better characterize the range of potential post-fire consequences, and in particular can help with probabilistic characterization of nested disturbance processes such as post-fire debris flows. Third, stochastic wildfire simulation, in combination with other modelling efforts, can help better capture spatiotemporal dynamics of ecosystems and wildfire impacts. These questions are far more complex

and uncertain, and require consideration of vegetation succession, disturbance processes, the impacts of current decisions on future conditions, and climate change. There are clear roles for expanded application of sensitivity analysis, scenario analysis, and uncertainty analysis, among other approaches.

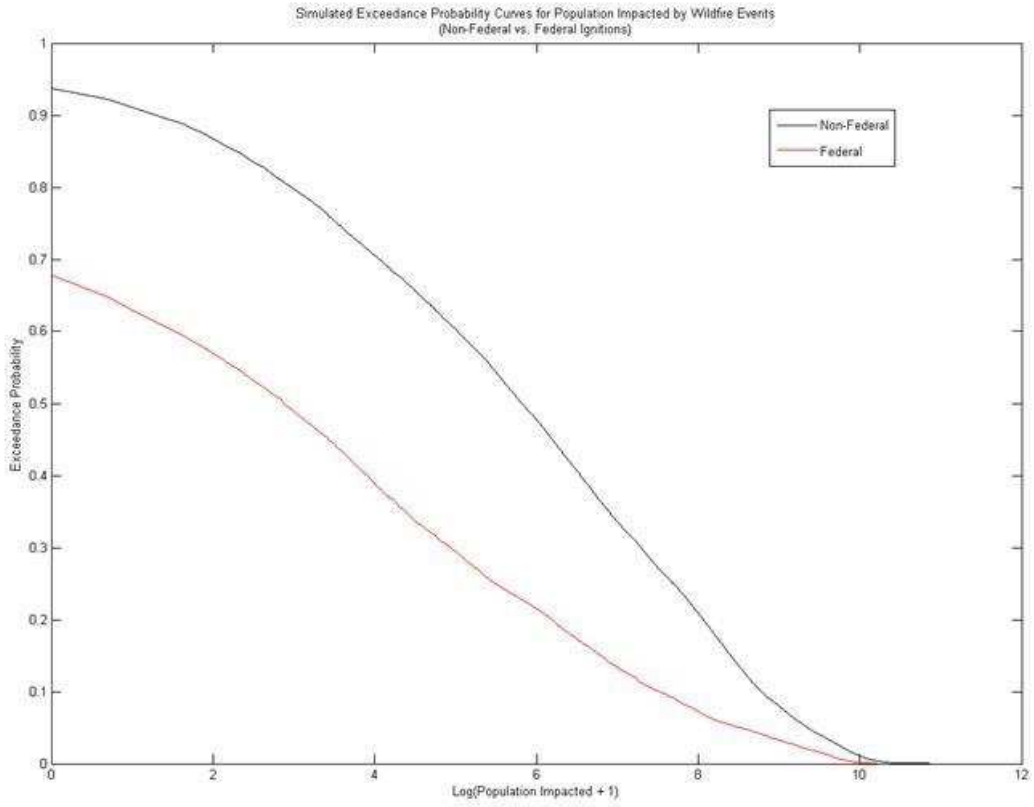

Figure 7. Exceedance probability charts for human population affected per simulated fire event, partitioned according to ownership at ignition location

Acknowledgements

The Rocky Mountain Research Station and the National Fire Decision Support Center supported this effort. Don Helmbrecht and Jon Rieck helped generate figures and/or contributed to the wildfire risk assessments discussed in this paper.

References

Ager, A. A., M. A. Finney, A. McMahan, and J. Cathcart (2010), Measuring the effect of fuel treatments on forest carbon using landscape risk analysis, Natural Hazards and Earth System Sciences 10, 2515-2526.

Calkin, D. E., M. P. Thompson, M. A. Finney, and K. D. Hyde (2011), A real-time risk assessment tool supporting wildland fire decisionmaking, Journal of Forestry, 109(5), 274-280.

Cochrane, M., C. Moran, M. Wimberly, A. Baer, M. Finney, K. Beckendorf, J. Eidenshink, and Z. Zhu (2012), Estimation of wildfire size and risk changes due to fuels treatments, International Journal of Wildland Fire, 21(4), 357-367.

Finney, M. A., C. W. McHugh, I. C. Grenfell, K. L. Riley, and K. C. Short (2011), A simulation of probabilistic wildfire risk components for the continental United States, Stochastic Environmental Research and Risk Assessment, 25(7), 973-1000.

Finney, M., I. C. Grenfell, and C. W. McHugh (2009), Modeling containment of large wildfires using generalized linear mixed-model analysis, Forest Science, 55(3), 249-255.

Holmes, T. P., and D. E. Calkin (2013), Econometric analysis of fire suppression production functions for large wildland fires, International Journal of Wildland Fire, 22(2), 246-255.

Gebert, K. M., D. E. Calkin, and J. Yoder (2007), Estimating suppression expenditures for individual large wildland fires, Western Journal of Applied Forestry, 22(3), 188-196.

Hand, M. S., K. M. Gebert, J. Liang, D. E. Calkin, M. P. Thompson, and M. Zhou (2014), Modeling Fire Expenditures with Spatially Descriptive Data, in Economics of Wildfire Management, edited, pp. 37-48, Springer New York.

Mendes, I. (2010), A theoretical economic model for choosing efficient wildfire suppression strategies, Forest Policy and Economics, 12(5), 323-329.

Moghaddas, J. J., and L. Craggs (2008), A fuel treatment reduces fire severity and increases suppression efficiency in a mixed conifer forest, International Journal of Wildland Fire, 16(6), 673-678.

Parks, S., C. Miller, C. Nelson, and Z. Holden (2014), Previous Fires Moderate Burn Severity of Subsequent Wildland Fires in Two Large Western US Wilderness Areas, Ecosystems, 17(1), 29-42.

Scott, J., D. Helmbrecht, S. Parks, and C. Miller (2012), Quantifying the threat of unsuppressed wildfires reaching the adjacent wildland-urban interface on the Bridger-Teton National Forest, Wyoming, USA, Fire Ecology, 8(2), 125-142.

Short, K. (2013), A spatial database of wildfires in the United States, 1992–2011, Earth System Science Data Discussions, 6(2), 297-366.

Stephens, S. L., J. D. McIver, R. E. Boerner, C. J. Fettig, J. B. Fontaine, B. R. Hartsough, P. L. Kennedy, and D. W. Schwilk (2012), The effects of forest fuel-reduction treatments in the United States, BioScience, 62(6), 549-560.

Thompson, M. P., and D. E. Calkin (2011), Uncertainty and risk in wildland fire management: a review, Journal of Environmental Management, 92(8), 1895-1909.

Thompson, M. P., N. M. Vaillant, J. R. Haas, K. M. Gebert, and K. D. Stockmann (2013), Quantifying the potential impacts of fuel treatments on wildfire suppression costs, Journal of Forestry, 111(1), 49-58.

Wimberly, M. C., M. A. Cochrane, A. D. Baer, and K. Pabst (2009), Assessing fuel treatment effectiveness using satellite imagery and spatial statistics, Ecological Applications, 19(6), 1377-1384.

Zimmerman, T. (2012), Wildland Fire Management Decision Making, Journal of Agricultural Science and Technology, B(2), 169-178.

Fine forest fuels moisture content monitoring in Central Portugal - a long term experiment

Sérgio Lopes[a], Domingos Xavier Viegas[b], Luís de Lemos[a], Maria Teresa Viegas[b]

[a] *Environment Department, Technology and Management School of Viseu, Polytechnic Institute of Viseu, Campus Politécnico de Repeses 3504-510 Viseu, Portugal; slopes@estv.ipv.pt*
[b] *ADAI/Mechanical Engineering Department, University of Coimbra, Polo II, Pinhal de Marrocos, 3030-790 Coimbra, Portugal; xavier.viegas@dem.uc.pt*

Abstract
Forest fuel moisture content is a fundamental parameter in forest fire research and management. Due to the complexity of fuel moisture content modelling, direct field measurement is a necessary step to establish a monitoring program for fire risk applications or to assess the validity of existing models applied to different environmental conditions.
In the present study partial results from a long-term program with direct field measurements performed in Central Portugal were used to improve the knowledge on fine forest fuel moisture content.
The objective of this study is to describe seasonal and spatial patterns of the moisture content and to analyse the relation between the moisture content of the studied species.
In terms of seasonal variation, it was found that dead tree species foliage moisture content behaves in a similar way during the year. and that the average live foliage moisture content of these species is nearly constant during the year. For the shrub species, in the period between August to September, fuel moisture content decreases till its minimum yearly value.
The relation between the studied species moisture content was analysed. The relation between the dead tree species and between the shrub species presented the best correlation performance.

***Keywords**: Fine fuels, moisture content.*

Introduction

Forest fuel moisture content (FMC) is a fundamental parameter in forest fire research and management given its implication in many aspects of fire risk including ignition probability, number and extension of fires, mode of fire spread, fire line intensity, ease of extinction and mop up (e.g. Blackmarr 1972; Rothermel 1972; Van Wagner 1987; Viegas *et al.* 1992; Dimitrakopoulos and Papaioannou 2001; Chuvieco *et al.* 2004). Due to the complexity of FMC modelling, direct field measurement is a necessary step to establish a monitoring program for fire risk applications or to assess the validity of existing models applied to different environmental conditions.
In order to assess fire risk several prediction methods that give satisfactory results, such as the Canadian Forest Fire Weather Index (Van Wagner 1987), can be used. This index mimics the moisture content trends of relevant types of fuels but direct measurements of FMC guarantee more reliable data. Despite its difficulty and cost, direct measurement of FMC does not have some of the limitations of the prediction models (Viegas *et al*. 1992).
In the present study partial results from a long-term program with direct field measurements performed in Central Portugal since 1986 (Viegas *et al*. 1992; Viegas *et al*. 2001) were used to improve the knowledge on fine forest fuel moisture content. The FMC variation range of the studied species, the seasonal FMC variation, the relations between the studied species and the relations between meteorological data and FMC will be analysed for more than 15 years of the monitoring program.

Methods

In the present study, sampling was carried out in Central Portugal, near Lousã for the period between 1996 and 2012, near Silvares and near Olho Marinho for the period between 1996 and 1999. The sampling site of Silvares is distant 5.5 km from the Lousã site, the sampling site of Olho Marinho is distant 7.7 km from Lousã site (*vide* Figure 1 and Table 1).
In the present research program, the moisture content of living and dead tree foliage from *Pinus pinaster* and *Eucalyptus globulus* and living shrub foliage and extremities from *Calluna vulgaris* and *Chamaespartium tridentatum* that are very common in the forests of Central Portugal was measured by field sampling throughout the year from 1986 to present date. In this paper the available values for the period 1996-2012 were systematized and analysed.
Living tree foliage correspond to needles of *Pinus pinaster* and leaves of *Eucalyptus globulus*, as well as small branches and leaves of *Calluna vulgaris* and *Chamaespartium tridentatum*. Dead tree foliage corresponds to needles of *Pinus pinaster* and leaves of *Eucalyptus globulus* from the litter.
Samples were daily collected at Lousã during the summer months (June to September) and once or twice a week during the rest of the year (October to May), between 12:00h and 14:00h LST.

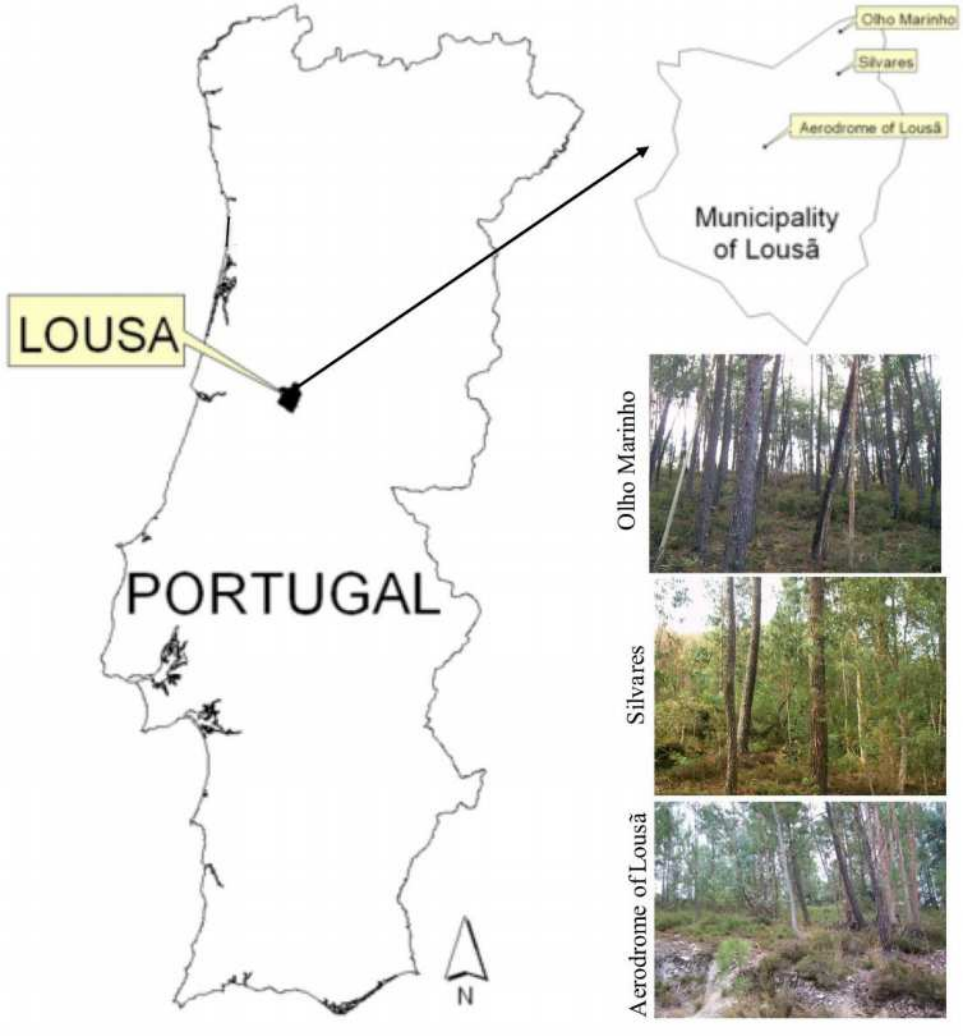

Figure 1. Geographical location of the study sites

Table 1. Main physical, climatic and vegetation characteristics of the study sites

Sampling Site	Coordinates	Altimetry (m)	Aspect	Slope (%)	Lithology	Tree height (m)	Crown closure	Vegetation
Lousã	40º8'30''N 8º14'30''W	200	South	30	Schist	10	Medium	Pinus pinaster Eucalyptus globulus Calluna vulgaris Chamaespartium tridentatum
Silvares	40º10'27''N 8º11'50''W	200	East	20	Schist	10	High	
Olho Marinho	40º11'35''N 8º11'46''W	250	East	30	Schist	10	Medium	

After the collection of approximately 50 grams of each fuel, samples were stored in a thermal bag to avoid moisture loss and immediately transported to the laboratory located in the Aerodrome of Lousã and prepared for tests. The time delay between sample collection and sample preparation was usually less than 30 minutes. If the foliage was wet with dew or rain, sampling did not occur to avoid moisture content errors.

For each fuel type, 4 samples weighing approximately 5 grams each (wet weight) were prepared and oven-dried for 24 hours at 105ºC. After the drying process, samples were weighed again in order to obtain the dry weight. The daily value of moisture content was the average of the 4 samples (*vide* Figure 2).

Figure 2. Sampling and determination procedures on the FMC research program of Lousã

3. Results

3.1. Seasonal moisture variation of the studied species

In Figure 3 the monthly FMC statistical parameters of the studied species for the period 1996–2012 is shown. As can be seen, for dead tree foliage from *Pinus pinaster* and *Eucalyptus globulus* values of moisture content between 2.6% and 182.9% were measured. For live tree foliage values of FMC between 68.8% and 225.3% were measured. The shrub foliage and extremities of *Calluna vulgaris* and *Chamaespartium tridentatum* presented values of FMC between 36.5% and 206.0%.

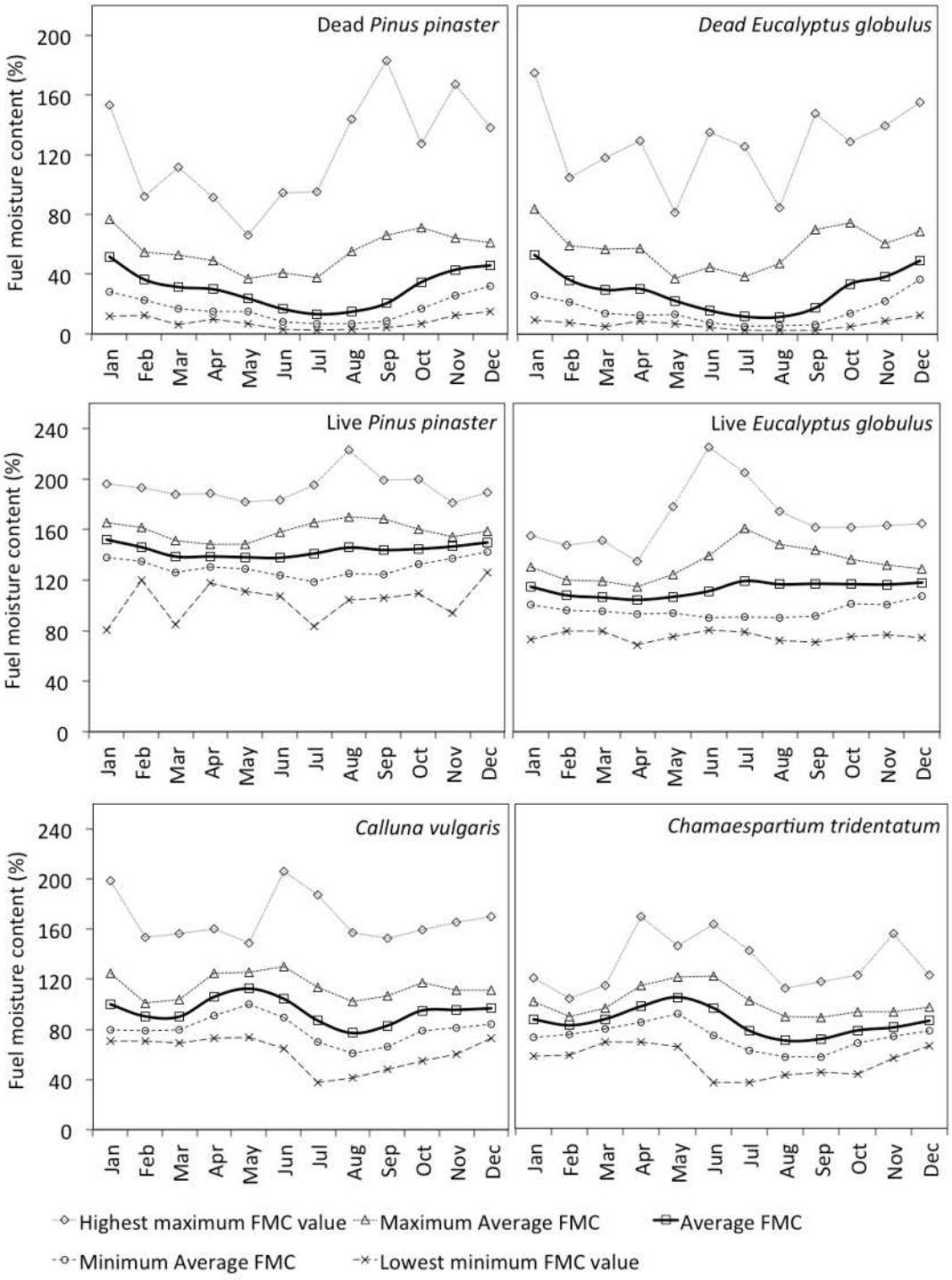

Figure 3. Monthly FMC statistical parameters of the studied species (Pinus pinaster, Eucalyptus globulus, Calluna vulgaris and Chamaespartium tridentatum) for all studied period (1996-2012)

In terms of seasonal average FMC variation, both dead tree species foliage behave in a similar way during the year. FMC is near 50% in the beginning, decreasing till a minimum of 10% in the summer months, coinciding with the forest fire period in Portugal. At the end of the year, the moisture content increases again till 50%. The average FMC of live foliage of *Pinus pinaster* is nearly constant during the year, between 140% and 150%. The same happens with live foliage of *Eucalyptus globulus* with average values of FMC between 105% and 120%. For the shrub species, in the period between August

and September, FMC decreases till 80% for *Calluna vulgaris* and till 70% for *Chamaespartium tridentatum*.

3.2. Relationship between the studied species fuel moisture content

The relationship between the FMC of the studied species are analysed through the Pearson correlation coefficients presented in Table 2. Such relationship allows the estimation of the FMC of species A through the knowledge of the FMC of species B as defined in Eqn 1. In Table 3 the model parameters estimation defined in Eqn 1 are shown. This estimation was performed using linear least squares fitting based on the field measurements. As expected, the relationship between the dead tree species and the relation between the shrub species present the best performance.

Table 2. Pearson correlation coefficients between the FMC of the studied species

Relation	Dead *P. pinaster*	Live *P. pinaster*	Dead *E. globulus*	Live *E. globulus*	*C. vulgaris*	*C. tridentatum*
Dead *Pinus pinaster*	1	0.183$^{(**)}$	0.909$^{(**)}$	0.098$^{(**)}$	0.467$^{(**)}$	0.417$^{(**)}$
Live *Pinus pinaster*	-	1	0.200$^{(**)}$	0.090$^{(**)}$	0.093$^{(**)}$	0.088$^{(**)}$
Dead *E. globulus*	-	-	1	0.107$^{(**)}$	0.486$^{(**)}$	0.443$^{(**)}$
Live *E. globulus*	-	-	-	1	0.095$^{(**)}$	0.051$^{(*)}$
Calluna vulgaris	-	-	-	-	1	0.734$^{(**)}$
C. tridentatum	-	-	-	-	-	1

$^{(**)}$ Significant at 0.01 level; $^{(*)}$ Significant at 0.05 level; (ns) Not significant

$$FMC_{Specie\ A} = aFMC_{Specie\ B} + b \quad (1)$$

Table 3. Model parameters of Eqn 1 and statistical parameters

Specie A	*Specie B*	*a*	*Std. dev.*	*b*	*Std. dev.*	*n*	R^2 *adj.*
Dead *Eucalyptus globulus*	Dead *Pinus pinaster*	1.001 $^{(**)}$	0.011	-2.395 $^{(**)}$	0.337	1692	0.826
Calluna vulgaris	Dead *Pinus pinaster*	0.456 $^{(**)}$	0.021	79.372 $^{(**)}$	0.635	1692	0.218
Chamaespartium tridentatum	Dead *Pinus pinaster*	0.330 $^{(**)}$	0.017	72.554 $^{(**)}$	0.528	1692	0.174
Chamaespartium tridentatum	*Calluna vulgaris*	0.594 $^{(**)}$	0.013	26.695 $^{(**)}$	1.223	1692	0.539

$^{(**)}$ Significant at 0.01 level; $^{(*)}$ Significant at 0.05 level; (ns) Not significant

3.3. Spatial representativity

In Viegas *et al* (1992) it was shown that dead fine FMC measurements in Lousã could be used as an indicator of fire occurrence of Central Portugal. Therefore, it is important to understand how representative the Lousã measurements are spatially in order to use this data as a fire risk indicator of a larger area.

As defined in Van Wagner (1987), the Canadian Forest Fire Weather Index (CFFWI), namely in its the sub-indexes Fine Fuel Moisture Code (FFMC), Duff Moisture Code (DMC) and Drought Code (DC), the moisture content indicators of litter and other cured fine fuels in a forest stand, represent respectively, loosely compacted decomposing organic matter, and deep layer of compact organic matter. In the specific case of DC it is also an indicator of live fine FMC as shown in Viegas (2001).

Thus, for the period between 1999 and 2008, fine FMC measurements of Lousã were correlated with CFFWI moisture content sub-indexes for several weather stations in the Portuguese territory shown in the map ofFigure 4, in order to verify the existence of potential relations between the measured moisture content and CFFWI predicted moisture content and to determine the spatial representativeness of the studied species FMC.

Figure 4. Geographical location of weather stations

For this purpose, Table 4 shows the Spearman non-linear correlation coefficients between the sub-index FFMC and dead needles of Pinus Pinaster moisture content measurements and the sub-index DC and live *Chamaespartium Tridentatum* moisture content measurements.
In general terms, Table 4 and Figure 5 show that dead fine FMC measurements of Lousã can be used as a fire risk indicator with a high representativeness in the central and northeast Portuguese territory and a medium representativeness in the littoral and south regions. In terms of live fine FMC, namely for shrub species, the representativeness is, in general, medium in the central and north part of the territory and low in the rest of the territory.

Table 4. Representativeness of fine FMC measurements of Lousã in terms of the Portuguese territory

Weather Station	Dead *Pinus pinaster* / FFMC		*Chamaespartium tridentatum* / DC	
	Spearman coefficient	Representativeness	Weather Station	Spearman coefficient
Aveiro	-0,609	Medium	-0,581	Medium
Beja	-0,693	Medium	-0,535	Low
Braga	-0,721	High	-0,598	Medium
Bragança	-0,708	High	-0,557	Medium
Castelo Branco	-0,728	High	-0,540	Low
Coimbra	-0,798	High	-0,619	Medium
Évora	-0,701	High	-0,540	Low
Faro	-0,512	Low	-0,430	Low

Weather Station	Dead *Pinus pinaster* / FFMC		*Chamaespartium tridentatum* / DC	
	Spearman coefficient	Representativeness	Weather Station	Spearman coefficient
Leiria	-0,698	Medium	-0,502	Low
Lisboa	-0,710	High	-0,502	Low
Portalegre	-0,740	High	-0,586	Medium
Porto	-0,656	Medium	-0,569	Medium
Santarém	-0,706	High	-0,516	Low
Setúbal	-0,650	Medium	-0,445	Low
Viana do Castelo	-0,668	Medium	-0,580	Medium
Vila Real	-0,762	High	-0,545	Low
Viseu	-0,745	High	-0,595	Medium

High representativeness: Spearman Coefficient >0.70; Medium representativeness: 0,55< Spearman Coefficient <0.70; Low representativeness: Spearman Coefficient <0.55
All correlations are significant at the 0.01 level

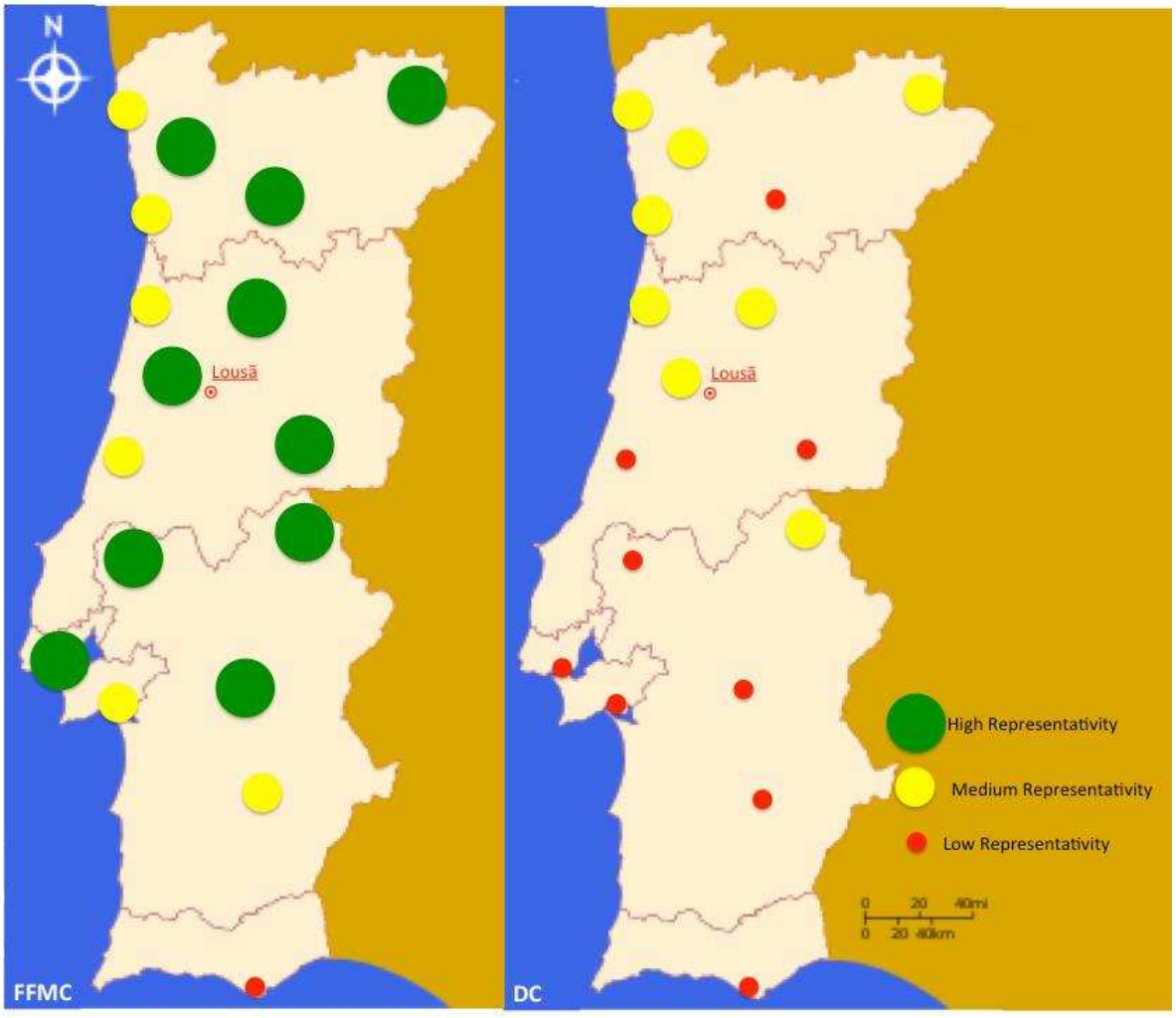

Figure 5. Representativeness of fine FMC measurements of Lousã in terms of the Portuguese territory

In order to quantify the spatial FMC patterns of the studied species (dead and live foliage of tree species, namely *Pinus pinaster* and *Eucalyptus globulus* and live shrub species, namely, *Calluna vulgaris* and *Chamaespartium tridentatum*), the data from the four sampling sites previously presented (Lousã, Silvares, Olho Marinho and Viseu) were compared. Such quantification allows the estimation

of FMC of each species, in a specific location from the knowledge of the FMC of that species in a different location.

In Table 5 the Pearson correlation coefficients between the FMC for the different species measured in Lousã and in the other two sampling sites are shown. The FMC of dead foliage of the tree species (*Pinus pinaster* and *Eucalyptus globulus*) and FMC of live shrub species (*Calluna vulgaris* and *Chamaespartium tridentatum*) show good relation between the sampling site Lousã and other three sampling sites. FMC of living foliage of the tree species shows no relation.

Due to the proximity between sites, the best relations were established between Lousã and Silvares namely for dead foliage with a Pearson correlation coefficient of 0.917 for *Eucalyptus globulus* and 0.884 for *Pinus pinaster*. As expected, the relationship between FMC measured in Lousã and FMC measured in the other three sampling sites decreases as distance increases.

The linear relation between FMC of the studied specie "*A*" at the site "*X*" and the moisture content of the same species at the site "Y" for the species that show a significant Pearson correlation coefficients were calculated using a linear equation:

$$FMC_{Specie\ A\ in\ Site\ X} = a.FMC_{Specie\ A\ in\ Site\ Y} + b \qquad (1)$$

These equations were determined using the least square method. The coefficients ***a*** and ***b*** and the respective standard error, as well as the number of data (***n***) and the adjusted determination coefficient (R^2) of the obtained equations for each species are shown in Table 6.

This analysis shows that in the lack of data, it is possible to estimate the FMC of some species in a specific location from the knowledge of the FMC of that species in a different location, using linear relationships.

Table 5. Pearson correlation coefficients between the FMC values for the different species measured in Lousã and in the other three sampling sites (Silvares and Olho Marinho)

	Dead *Pinus pinaster*	Dead *Eucalyptus globulus*
Lousã and Silvares	$0.884^{(**)}$	$0.917^{(**)}$
Lousã and Olho Marinho	$0.855^{(**)}$	$0.844^{(**)}$
	Live *Pinus pinaster*	Live *Eucalyptus globulus*
Lousã and Silvares	$0.092^{(ns)}$	$0.017^{(ns)}$
Lousã and Olho Marinho	$0.168^{(**)}$	$0.086^{(ns)}$
	Calluna vulgaris	*Chamaespartium tridentatum*
Lousã and Silvares	$0.654^{(**)}$	$0.676^{(**)}$
Lousã and Olho Marinho	$0.569^{(**)}$	$0.606^{(**)}$

(**) Significant correlations at 0.01; (*) Significant correlations at 0,05; (ns) not significant

Table 6. Coefficients, a and b, number of data (n) and adjusted determination coefficient (R^2) of the obtained relation for dead tree and shrub species

Species	***Relation***	***a***	***Std. Error***	***b***	***Std. Error***	***n***	***Adjusted R^2***
Dead Pinus pinaster	Lousã (X) and Silvares (Y)	$0.678^{(**)}$	0.023	$5.295^{(**)}$	0.651	239	0.781
	Lousã (X) and Olho Marinho (Y)	$0.799^{(**)}$	0.031	$3.570^{(**)}$	0.881	239	0.730
Dead eucalyptus globulus	Lousã (X) and Silvares (Y)	$0.943^{(**)}$	0.027	$1.644^{(**)}$	0.631	239	0.841
	Lousã (X) and Olho Marinho (Y)	$0.972^{(**)}$	0.040	$2.628^{(**)}$	0.951	239	0.712
Calluna vulgaris	Lousã (X) and Silvares (Y)	$0.646^{(**)}$	0.041	$27.615^{(**)}$	3.573	329	0.426
	Lousã (X) and Olho Marinho (Y)	$0.649^{(**)}$	0.052	$37.866^{(**)}$	4.490	329	0.321
Chamaespartium tridentatum	Lousã (X) and Silvares (Y)	$0.782^{(**)}$	0.782	$25.716^{(**)}$	3.526	329	0.456
	Lousã (X) and Olho Marinho (Y)	$0.682^{(**)}$	0.050	$31.458^{(**)}$	3.705	329	0.365

(**) Significant correlations at 0.01; (*) Significant correlations at 0,05; (ns) not significant

Conclusion

The moisture content of forest fuels is very important in terms of forest fire research given its implication in many aspects of fire risk, fire spread and fire ecology. The long-term experience with direct field measurement in Lousã enables the study of several aspects related to fine fuel moisture content, being fundamental for fire risk applications or to assess the validity of existing or future FMC models.

In terms of seasonal variation, the litter moisture content of both tree species behaves in a similar way during the year, being close to 50% in the beginning, decreasing till a minimum of 10% during the summer months, coinciding with the forest fire period in Portugal. At the end of the year, the litter moisture content species increases again till 50%. Live *Pinus pinaster* average fuel moisture content is nearly constant during the year, between 140% and 150%. Live *Eucalyptus globulus* average fuel moisture content is also nearly constant during the year, between 105% and 120%. For the shrub species, in the period between August to September, fuel moisture content decreases till 80% for *Calluna vulgaris* and till 70% for *Chamaespartium tridentatum*.

The correlation between the studied species fuel moisture content was analysed. Such correlation allows the estimation of the fuel moisture content of one specie through the knowledge of the fuel moisture content of another specie. As expected, the relation between the dead tree species and the relation between the shrub species present the best performance. This representativeness allowed the establishment of linear relations between the FMC of a studied species at one site based on the FMC of that species in another site. This was performed between three sampling sites.

Dead fine FMC measurements of Lousã can be used as a fire risk indicator with a high representativeness in the central and northeast Portuguese territory and a medium representativeness in the littoral and south regions. In terms of live fine FMC, namely for shrub species, the representativeness is, in general, medium in the central and north part of the territory and low in the rest of the territory

References

Blackmarr WH (1972) Moisture content influences, ignitability of slash pine litter. United States Department of Agriculture. Forest Service. Research Note SE-173

Chuvieco E, Aguado I, Dimitrakopoulos AP (2004) Conversion of fuel moisture values to ignition potential for integrated fire danger assessment. *Canadian Journal of Forest Research* 34, 2284–2293.

Dimitrakopoulos AP, Papaioannou KK (2001) Flammability assessment of Mediterranean forest fuels. Fire Technology 37, 143–150.

Rothermel RC (1972) A mathematical model for predicting fire spread in wildland fuels. United States Department of Agriculture. Forest Service. Research Paper INT-115

Van Wagner CE (1987) Development and Structure of the Canadian Forest Fire Weather Index System. Canadian Forestry Service, Forestry Technical Report 35, Ottawa.

Viegas DX, Viegas MT, Ferreira AD (1992) Moisture content of fine forest fuels and fire occurrence in central Portugal. *Int. J.Wildland Fire* 2: 69–86,

Viegas, D.X., Pinol, J., Viegas, M.T., and Ogaya, R. (2001) Estimating live fine fuels moisture content using meteorologically-based indices. *Int. J. Wildland Fire*, 10(2): 223–240.

Fire and deforestation processes represented in vegetation models for the Brazilian Amazonia

Manoel Cardoso, Gilvan Sampaio, Vinicius Capistrano, Marcos Sanches

Instituto Nacional de Pesquisas Espaciais (INPE), Cachoeira Paulista SP 12630-000 Brasil
manoel.cardoso@inpe.br

Abstract
Dynamic global vegetation models need to be improved to accurately represent fire and land-use change in Amazonia. To this end, we are working on improving existent dynamic vegetation models to account for such strong disturbances, and aim to perform new analyses to quantify how fire, deforestation and climate change may combine to affect the distribution of major biomes and climate in the region. At present, we concentrate the development and implementation of new fire models on the simulation of fire probability and effects on vegetation dynamics, based on methods already tested in global dynamic vegetation models where fire potential is driven by the combination of presence of fuel, flammability, and sources of ignitions. To account for fire disturbance we assumed that the fraction of the vegetation affect by fires is proportional to the fire probability. Deforestation is directly interpreted as a fraction of the affected vegetation, and it is assumed to disturb tropical, temperate and conifer broadleaf, evergreen and deciduous trees. Both disturbances affect biomass, leaf area index, and total ecosystem aboveground net primary productivity, modifying the fractional cover of forest and herbaceous canopies. These implementations represent important steps towards the development and use of vegetation models that can account for major contemporary disturbances in the study region.

Keywords*: Fire, deforestation, model, Amazonia*

Introduction

Dynamic global vegetation models with improved representation of surface process are being developed to access the impacts of fire and land-use change in Amazonia. In addition to represent major features such as vegetation distribution, terrestrial carbon cycle and links between land surface and atmosphere, the models need to be improved to account for major disturbances in the region. Fires and deforestation have substantial impacts on the ecosystems of Amazonia, causing rapid shifts in surface cover, atmospheric emissions of greenhouse gases, and modifications fluxes of moisture and energy from the surface. To this end, we are working on improving existent dynamic vegetation models to account for fires and deforestation in Amazonia.

The current developments for representing fire and deforestation processes in vegetation models for Amazonia were implemented in a revised version of the IBIS model (Integrated Biosphere Simulator), which has the ability to simulate land-surface processes such as vegetation dynamics and terrestrial carbon cycle, based on dominant climate and soil properties (Foley *et al*. 1996, Kucharik *et al*. 2000). The model offered the possibility of performing global and regional simulations from common input datasets, and was tested using several experiment configurations and evaluations of model outputs. One test was the compatibility between model and observed values of evapotranspiration globally (Baumgartner and Reichel, 1975).

Our improvements of IBIS evolved into the Brazilian Integrated Land Surface Processes Model (Inland), first released on November 2012 during a workshop at INPE (http://www.ccst.inpe.br/inland). The development of the model aims global applications with emphasis on improvements and performance for ecosystems in South America and Brazil, and is part of a broad effort in Earth System modelling in Brazil [ref BESM]. From Inland 1.0, we have

implemented a new fire scheme and the ability of the model to account for deforestation disturbances, including the assimilation of deforestation scenarios for Amazonia, as summarized below.

Methods

Fire occurrence and effects

The development of the new fire model implemented in Inland was based on methods already tested in global dynamic vegetation models (Cardoso *et al*. 2013). From the methods considered, we adopt the work of Arora and Boer (2005) (AB2005) where fires are simulated as burning occurrence (probability of fire) and effects (burned area and emissions). At this initial stage, we concentrated the development and implementation of the fire model for Inland on the simulation of fire probability and effects on vegetation dynamics only. For that, we implemented the fire occurrence probability equations of AB2005, where fire potential is driven by the combination of presence of fuel, flammability, and sources of ignitions.

Presence of fuel is represented as in AB2005, which determines that a minimum of 200 gC/m2 of plant biomass is required to sustain a fire. In the Inland implementation, plant biomass was considered the sum of stem and leaf biomass from all vegetation types over land. Flammability, as described in AB2005, increases exponentially as soil moisture at the root zone approaches the wilting point. In Inland, we calculate flammability based on the moisture at the model's first soil layer, where most of roots are located. Our approach to represent ignitions sources from lightning differed from AB2005 as we assumed that lightning activity is simply random. Final fire occurrence probability is calculated by multiplying these three estimates, as in AB2005.

To account for fire disturbance, we propagated the fire occurrence probability estimation into the calculation of vegetation dynamics, following the original IBIS formulation for considering disturbances. That was done by assuming that the fraction of the vegetation affect by fires is proportional to the fire probability. As disturbances (fraction of affected vegetation) were considered in IBIS, Inland considers that fires affect biomass, leaf area index, and total ecosystem aboveground net primary productivity, which in turn modify the fractional cover of forest and herbaceous canopies.

2.2. Deforestation processes

Based on a similar approach used for fire, deforestation processes were considered in Inland also by accounting for this disturb when calculating the dynamics of the vegetation. In this case, no additional assumptions were made, and input deforestation data is assimilated by directly interpreting it as a fraction of affected vegetation. However, we assume that the grid-cell fraction of vegetation affected by deforestation only impacts tropical, temperate and conifer broadleaf, evergreen and deciduous trees. For these classes, deforestation changes plant biomass, leaf area index and net primary productivity.

In Inland, the treatment of the fire and deforestation consequences follows the original IBIS formulation, and the possibility to consider a general natural disturbance rate is also maintained. In order to avoid overly-high (greater than 100%) fractions of affected vegetation, the balance between disturbance rates is evaluated in each grid cell by assuming precedence of natural causes, than fires, and finally deforestation, and by limiting the overall annual disturbance rate for each model grid cell to a maximum of 100%.

Results

The new implementations of fire and deforestation processes in the Inland model were tested in simulations where the model was run for a total of 699 years (1400-2099), to allow for equilibrium of the slow carbon pools and to test the model stability. There was an initial spin-up period of 366 years (from 1400-1765) under constant pre-industrial atmospheric CO2 value (278 ppm). The runs were continued from 1766 to 2005 with increased prescribed atmospheric CO2 concentrations (from 278 to

378 ppm), and from 2005 to 2099 with atmospheric CO2 concentrations following the Coupled Model Intercomparison Project 5 (CMIP5) protocols. From 1400 to 2005, climate data was applied cyclically, and after 2005 from CMIP5 models. Deforestation data is based on the work of Aguiar *et al*. (2012). The results presented here represent only contemporary conditions of the study region.

Figure 1 below shows the effect of considering fires in Inland. Top panels (a, b) show the spatial distribution of evergreen trees (tropical and temperate broadleaf trees, and boreal and temperate conifers) biomass. The bottom panels (c, d) show the spatial distribution of grasses (warm and cool grass) biomass. On the left the maps show simulation results without fires, and on the right considering fires. As shown, the simulation of the transition between forests and grasslands in the Brazilian Amazonia (approximately highlighted by the dotted ellipsis) is affected by the consideration of fire in the formulation of the model. As simulated, there is an expansion of grasses over forest areas noticeable in the border between the two regions dominated by these types of vegetation.

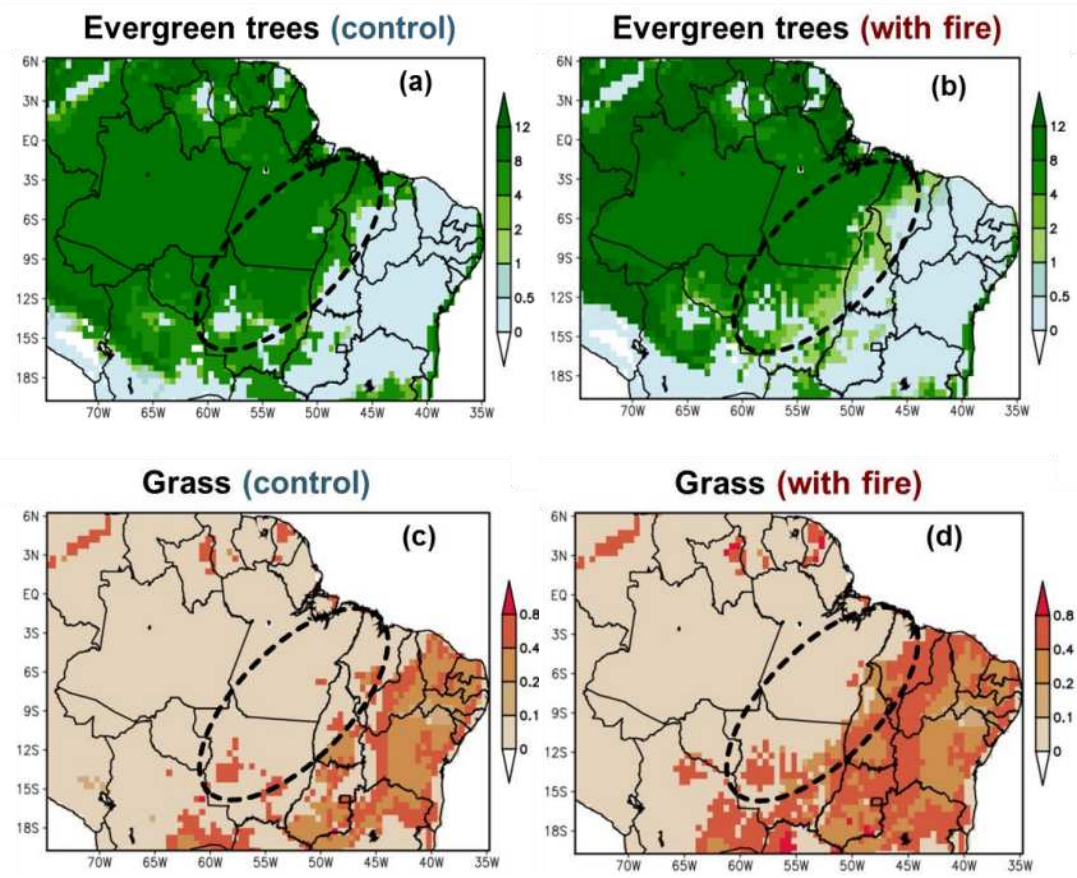

Figure 1. Contemporary distribution of evergreen trees and grasses biomass over the Brazilian Amazonia as simulated by the Inland model. Top panels (a, b) show the spatial distribution of evergreen trees (tropical and temperate broadleaf trees, and boreal and temperate conifers) biomass, and bottom panels (c, d) show the spatial distribution of grasses (warm and cool grass) biomass. On the left the maps show simulation results without fires, and on the right considering fires. The black dotted ellipsis approximately highlights the transition between forests and grasslands in the Brazilian Amazonia.

Figure 2 below shows the effect of considering deforestation on the contemporary distribution of evergreen tropical and temperate broadleaf trees biomass over the Brazilian Amazonia simulated by the Inland model. Panel (a) shows the spatial distribution of biomass without considering deforestation effects. Panel (b) shows the spatial distribution of the simulated biomass considering disturbance from deforestation based on Aguiar *et al*. (2012). As shown, the simulated biomass differs substantially by

considering deforestation. In relation to panel (a), (b) shows patterns of reduced tree biomass that resembles the observed contemporary maps of forests distribution in the study region.

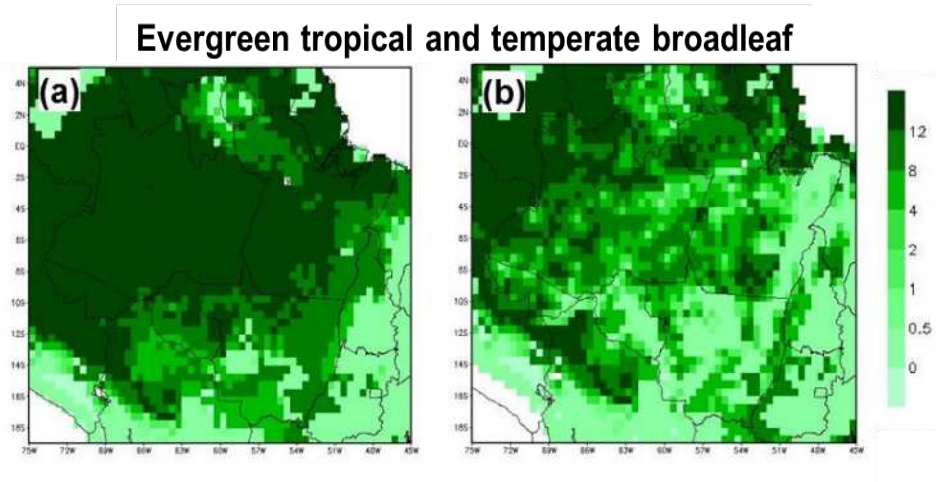

Figure 2. Effect of deforestation on the contemporary distribution of evergreen tropical and temperate broadleaf trees biomass over the Brazilian Amazonia simulated by the Inland model. Panel (a) shows the spatial distribution of the simulated biomass without considering deforestation effects. Panel (b) shows the spatial distribution of the simulated biomass considering disturbance from deforestation based on Aguiar et al. (2012).

Conclusions

At present, our implementations of major contemporary disturbances to ecosystem in Amazonia (fires and deforestation) are very simple, but they represent important steps towards the development and use of vegetation models for the study region. These new features are also important for broader analyses, where connections with prevailing environmental conditions such as climate can be considered. In specific, our preliminary results (not shown here) from offline and coupled vegetation-climate projections under current (5th Assessment Report of the Intergovernmental Panel on Climate Change) protocols of evaluations of future climate, indicate that the impacts of climate change in Amazonia will potentially intensify when combined to fires and deforestation. It is expected, for example, increase in dry season length, and reduction in the upper-canopy biomass related to an increase of the biomass in grasses from replacements of tropical forest by seasonal forest and savanna. These effects can have important implications for the distribution and stability of the vegetation in the region. Our future research activities include further model improvements and runs to understand the potential for changes and the connections between the ecosystems of the region and global environmental conditions and processes, such as carbon cycling and climate dynamics.

Acknowledgments

We thank Thiago Veloso, Luciana Soler, and Celso von Randow for earlier discussions on deforestation data assimilation in Inland. This work was developed within the scope of the research programs lead by the Brazilian National Counsel of Technological and Scientific Development (CNPq) and São Paulo Research Foundation (Fapesp) (CNPq Process 573797/2008-0, Fapesp Process 2008/57719-9), and project IRTG 1740 / TRP 2011/50151-0 funded by the DFG / Fapesp.

References

Aguiar APD, Ometto JP, Nobre CA, Lapola DM, Almeida C, Vieira IC, Soares JV, Alvala R, Saatchi S, Castilla-Rubio JC (2012) Modeling the spatial and temporal heterogeneity of deforestation-driven carbon. Global Change Biology 18, 3346–3366, doi: 10.1111/j.1365-2486.2012.02782.x

Arora VK, Boer GJ (2005) Fire as an interactive component of dynamic vegetation models. Journal of Geophisycal research, vol 110, doi:10.1029/2005JG000042.

Cardoso M, Sampaio G, Shimizu MH, Sanches M, and Nobre CA. (2013) Improvements of land-surface models to account for fire-climate feedbacks in the Amazon region. Natural Hazards (NH) Wildfires on landscapes: theory, models, and management. American Geophysical Union Meeting of Americas, Cancun, Mexico, 14-17 May 2013.

Baumgartner, A., Reichel, E. (1975) The world water balance: mean annual global, continental and maritime precipitation, evaporation and runoff, first ed. Elsevier Science Pub. Co., New York.

Foley, J.A., I.C. Prentice, N. Ramankutty, S. Levis, D. Pollard, S. Sitch, and A. Haxeltine (1996). An integrated biosphere model of land surface processes, terrestrial carbon balance, and vegetation dynamics. Global Biogeochemical Cycles 10(4), 603-628.

Kucharik, C.J., J.A. Foley, C. Delire, V.A. Fisher, M.T. Coe, J. Lenters, C. Young-Molling, N. Ramankutty, J.M. Norman, and S.T. Gower (2000). Testing the performance of a dynamic global ecosystem model: Water balance, carbon balance and vegetation structure. Global Biogeochemical Cycles 14(3), 795-825.

FireDST: a simulation system for short-term ensemble modelling of bushfire spread and exposure

Ian A. French[a b], Thomas J. Duff[c b], Robert (Bob) P. Cechet[d b], Kevin G. Tolhurst[c b], Jeff D. Kepert[e b] and Mick Meyer[f b]

[a] *Geoscience Australia, Canberra, Aust. Capital Territory (A.C.T.), 2609 Australia*
[b] *Bushfire Cooperative Research Centre, Melbourne, Victoria, 3002, Australia*
[c] *The University of Melbourne, Victoria, 3010, Australia*
[d] *University of New South Wales (ADFA), Canberra (A.C.T.), 2610, Australia*
[e] *Australian Bureau of Meteorology, Melbourne, Victoria, 3008, Australia*
[f] *CSIRO Marine and Atmospheric research, Aspendale, Victoria, 3195, Australia*
Contact author: b.cechet@adfa.edu.au

Abstract
The impact of bushfires in Australia can be enormous when considered in terms of loss of life, assets, infrastructure and productivity. The FireDST "proof-of-concept" system links various databases and models, including the Australian Bureau of Meteorology's new "high resolution" ACCESS (Australian Community Climate and Earth-System Simulator) numerical weather prediction system, the PHOENIX RapidFire fire behaviour model, the Commonwealth Scientific and Industrial Research Organisation's (CSIRO) smoke dispersion model as well as infrastructure and demographic databases provided by Geoscience Australia. FireDST runs multiple simulations of a bushfire utilising varying inputs (such as different ignition points, different start times, different fuel characteristics and variations in the weather) based on an understanding of what may occur. FireDST amalgamates all the simulations into a single ensemble visualisation for the fire.
This paper provides an overview of the FireDST system and examines the potential for using ensemble simulations to predict short-term (1-2 days) potential impacts from wildfires. We introduce variability in the numerical weather prediction model for three case-study fires to demonstrate the ensemble modelling system. FireDST can produce both exposure and impact statistics for the ensemble fire spread, however only exposure is covered in this paper. Such information is potentially useful in assisting in the operational management of bushfires, landscape planning (such as locating infrastructure to reduce exposed to fire) and in education and training.

Keywords*: wildfire hazard/impact simulation, ensemble modelling, integrated modelling*

Introduction

Extreme bushfires are complex physical phenomena that occur under extreme weather and environmental conditions. They are often exceedingly difficult to manage and cause sizable impacts on individuals, communities and the economy. For instance, the Victorian Black Saturday fires of February 2009 directly caused 173 deaths, over 800 admissions to emergency hospital care, destroyed 2133 houses and burned over 430,000 ha of land. It was also estimated that the fires caused a negative impact on the Australian economy of more than 4 Billion Australian dollars (VBRC 2010).
At the incident management level there have been many improvements in the ability to manage active bushfires. In particular, the last few decades have seen the development of computerised bushfire simulation models that produce a single deterministic simulation of the fire spread. These models include PHOENIX Rapidfire (Tolhurst *et al.*, 2008) in Australia, FARSITE (Finney, 1998), FlamMap (Finney, 2006) in the USA and PROMETHEUS, the Canadian wildland fire growth simulation model (Tymstra *et al*., 2009). All are able to assimilate information on the terrain, vegetation load and type and weather predictions (some also consider the built environment), to produce a single graphical output of the progress of a fire. The models, which are calibrated against how past fires have typically

progressed, consider vegetation type, terrain and topography, a fire's perimeter, air temperature, wind, and humidity. They then model where a fire will go and when it will arrive at a certain location. Incident management teams then use these predictions to help manage public warnings, evacuations and the placement of fire fighting resources.

Unfortunately there are many uncertainties in the inputs to these models (such as variations in fuel moisture, wind speed and temperature) and uncertainties in the modelling of the physics of the fire environment. These uncertainties can lead to inaccurate predictions being generated by the software. Inaccurate predictions could lead to dangerous decisions in the incident control centre and sizable effort is required to improve these simulation models. Even though accuracy is improving with new developments such as higher resolution vegetation mapping and improved fire modelling, it may never be possible to produce sufficient accuracy in every case. Recently there has been a move to incorporate uncertainty into fire modelling. Systems such as the Wildland Fire Decision Support System- Fire Spread Probability Model (WFDSS-FSPro) (USDA Forest Service, 2012) use a Monte-Carlo method to introduce uncertainty into the weather, producing a synthetic weather stream to generate a long range weather forecast. These models require an advanced understanding of the past weather and the variability in the weather that usually occurs at the time of the fire to generate this weather forecast. FSPro generates thousands of possible long range forecasts (assuming a constant weather and wind for each day) and runs a fire simulation for each. The multiple fire simulation results are then amalgamated to produce a map of fire spread probability. FSPro also places an extra level of complexity on the users of the system in understanding what the output probabilities actually mean in a physical sense. Monte-Carlo methods to generate long range weather forecasts with uncertainty, producing fire shapes which consider uncertainty, have also been used in research by Anderson *et al*. (2007), Cruz (2010) and Finney *et al*. (2011).

In 2011 the Australian Bushfire Cooperative Research Centre initiated the FireDST research project (Fire Impact and Risk Evaluation Decision Support Tool). One of the main aims of the project was to develop a "proof-of-concept" system that would allow users to easily view and assess the short-term (1-2 days) impact of various uncertainties in the information supplied to any fire spread model. The approach taken to address this aim was novel in that the FireDST system would not define the probability of an uncertainty occurring. Instead it would build an ensemble from individual fire spread simulations each with a different variation in the input condition and initially weighting each with the same probability. For example FireDST could produce an ensemble from individual fire simulations where the temperature has been varied up or down by five degrees Celsius in steps of one degree. A number of meteorological variables are varied to produce the ensemble. This paper concentrates on uncertainties in the weather however the research has also been applied to uncertainties in the vegetation and fire ignition location as well as location of synoptic frontal systems.

After producing the individual fire simulations we investigated how they could be amalgamated into a single ensemble view of the fire spread. Ensemble prediction has been applied successfully for the modelling of weather (such as the UK Met office ensemble MOGREPS[1] system) and in modelling of the paths of tropical cyclones (Zhang & Krishnamurti, 1997, Buckingham *et al*. 2010). The fire spread ensemble was then used to calculate the exposure of the ensemble footprint on people and buildings. Finally we addressed whether the smoke and combustion products from the fire could also be modelled using an ensemble.

[1] http://www.metoffice.gov.uk/research/areas/data-assimilation-and-ensembles/ensemble-forecasting/MOGREPS

Methodology

Concept design

We designed the FireDST system to follow the information flow defined in the Bushfire Risk Assessment Framework (Jones *et al. 2012*). The framework defines an information flow for computational analysis of bushfires from the definition of the hazard, through exposure, vulnerability and impact to calculation of the bushfire risk.

The core of the FireDST system is the Ensemble Generator (Figure 1) which controls the generation of the multiple variations for input, simulates each individual variation and creates the ensemble. Initially the supplied weather is perturbed by the Weather Ensemble Generator to provide new weather sets containing the variation in humidity, temperature, wind speed and wind direction. The supplied fuel information is also perturbed to provide variations in fuel load. Finally, the ignition information is perturbed to provide variation in the ignition location and ignition time. Once all the variations in input conditions have been created, the Ensemble Generator simulates each individual fire and amalgamates them all into an ensemble footprint of the fire.

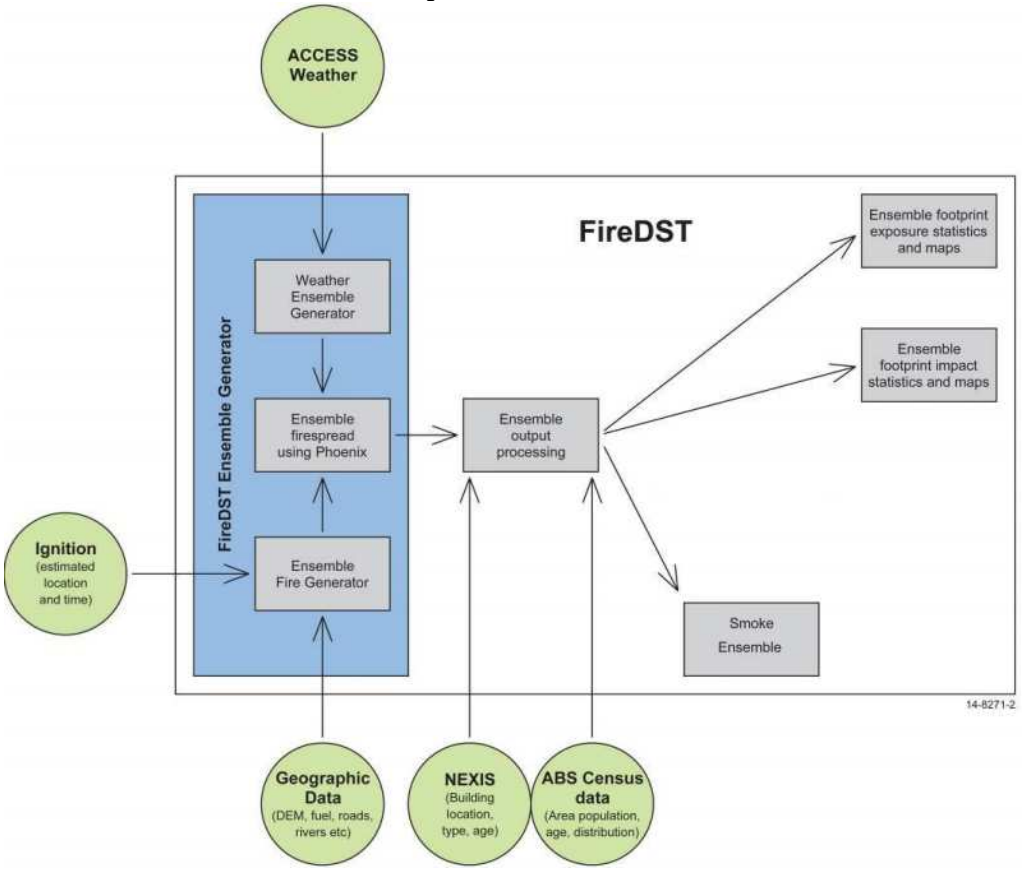

Figure 1. Information flow in FireDST

FireDST Ensemble Generator

The weather is one of the most critical inputs required for simulating bushfires. The Australian Bureau of Meteorology supplied an ACCESS (Australian Community Climate and Earth-System Simulator)(Puri, 2011) research mode numerical weather prediction for 48 hours in 5 minute time steps at horizontal grid spacing of 0.036° latitude/longitude grid spacing, which is approximately 4.0 km in the north-south direction. Each ACCESS simulation included separate grids of temperature, relative humidity, wind speed and wind direction.

The Weather Ensemble Generator allows the user to define a set of rules for creating a weather ensemble every time a new ACCESS weather forecast is produced by the Bureau of Meteorology. The Weather Ensemble Generator modifies the weather grids to produce different combinations of weather that the user considers likely to occur (i.e. takes into account some of the uncertainties in weather conditions). Simple rules were used to modify individual weather scenarios. Examples are changing the wind speed grid to increase all wind speeds by five meters per second, or changing the temperature grid to increase the temperature by two degrees. The rules also allow a more complex weather scenario by creating a profile that includes a combination of changes to humidity, temperature, wind speed or wind direction. These weather variations are stored as a weather ensemble for later use when a fire ignition location is supplied to FireDST. For this research we did not attempt localised weather change in particular areas within each weather file.

FireDST uses PHOENIX RapidFire (Tolhurst *et al*. 2008) to run each single simulation of the fire. To create a fire ensemble, FireDST uses the ignition point rules to generate other fires around the user specified ignition point (e.g. 200 meters to the North, South, East and West). 200m is the minimum distance utilised as the PHOENIX Rapidfire grid cell size is 180m in size and we wanted to ensure that each new ignition started in a new cell. Ignition time was varied from 20 minutes before to 20 minutes after the actual ignition in steps of 5 minutes. The rules can also vary the vegetation conditions (such as variations in fuel load and moisture) and their application for each weather ensemble. The FireDST Ensemble Fire Generator rules also allow the modification of wind speed based on the local terrain/topography using the Wind Ninja system (Forthofer *et al*., 2009). The user also specifies the information that is required by PHOENIX Rapidfire including the fuel type grid, a digital elevation model, road disruptions and fire history database.

The Ensemble Fire Generator then combines all of the individual PHOENIX simulations into a single ensemble view of the fire. This is achieved by taking the simulated fire area of the individual fire and converting the area inside the fire shape to "1" and everything outside to "0". An ensemble fire shape is produced by overlaying each converted fire spread simulation shape and adding the area values. For example where two fires cover the same location the ensemble fire location then contains "2", where there is no overlap the ensemble shape just contains "1". Everywhere else is "0". An example of how this is undertaken is shown in Figure 2. The overlap values are then converted to a percentage overlap in the final shape which can be displayed in discrete intervals. Typically, either half-hourly or hourly time increments are used to understand the progression of the fire.

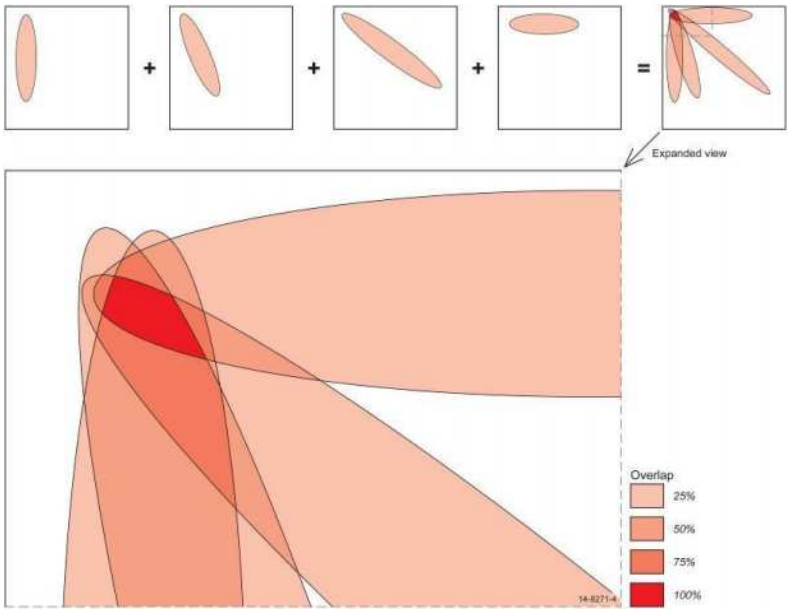

Figure 2. Example of how an ensemble likelihood shape is produced. The fire scars of the four different notional fire simulations are combined to compute the likelihood that a particular location will burn.

2.3. Ensemble Output Processing – Exposure Statistics

FireDST has been setup to display statistics and maps of residents and structures exposed to the ensemble fire spread. Geoscience Australia supplied the building database National EXposure Information System (NEXIS) (Nadimpalli *et al*. 2007; Canterford, 2011). NEXIS identifies the house location and attributes of the house (age, wall construction, roof type). NEXIS also contains quantity surveying information such as estimated building replacement cost and estimated contents value. Population statistics were extracted from the 2006 Australian Bureau of Statistics (ABS) Census at the Collection District reference level and allocated as averages to all the individual houses in that collection district. The 2006 Census information contains 14 vulnerability indicators (fields) that have been included in FireDST (Canterford 2011). The exposure statistics are produced by overlaying the ensemble fire footprint with each building location (which includes the population and vulnerability indicator statistics).

2.4. Ensemble Output Processing – Smoke Dispersion

Finally, all the individual fire simulations included in FireDST's ensemble can be passed to a new atmospheric numerical model (supplied by CSIRO Marine & Atmospheric Research) that simulates the spread of gaseous fire combustion materials such as smoke, ozone, particles smaller than 2.5 microns in size ($PM_{2.5}$), Nitrogen Monoxide (NO) and Carbon Monoxide (CO) from a single fire. Information regarding the supplied atmospheric model and smoke dispersion technique can be found in Cechet *et al.* (2014). FireDST takes the individual fire atmospheric spread results and amalgamates them into two ensemble maps of the concentration and percent overlap of the various products of bushfire combustion. The amalgamation technique is the same as described in Figure 2. These maps can be overlaid with the population statistics and building locations to display the impacted population. These maps can be useful to assist in managing public health warnings and in the movement of people and emergency service teams.

2.5. Case studies

FireDST was tested in Australia on three case studies. The Kilmore fire of 9 February 2009 was selected because the fire progressed through various terrain types and there was a high level of fire reconstruction information available. The Kilmore fire started around 11:45 and burnt 125,383 hectares, resulted in the deaths of 119 people and destroyed 1,242 homes. A comprehensive assessment of the Kilmore East fire can be found in Chapter 5 of the Victorian Bushfires Royal Commission report (VBRC, 2010). A comparison of the ACCESS weather simulation with all the Automated Weather Stations (AWS) in the region indicated a good match for temperature, humidity, wind direction and the timing of the wind change. However the 10 metre wind speed comparison found that the simulation of the wind speed was under-predicted by 5 to 7m s-1. A summary of the comparison is contained in the FireDST final report (Cechet *et al*. 2014). This deficiency in wind speed was able to be corrected by calculating wind speed bias correction factors that were then applied to the ACCESS wind speed file. This technique is fully discussed in the Kilmore Case Study report (French *et al*. 2014a). Smoke dispersion simulations were only conducted for this case study due to the excessive computer time necessary to run these simulations.

The second case study was the South Australian Wangary bushfire of 10 January 2005 which resulted in the burning of 77,964 hectares of mainly farmland, in the deaths of nine people and the destruction of 93 homes on January 11 (SA Coroner 2007). On January 10 the fire appeared to be contained, however the fire broke out at three locations during the morning of the 11th. The fire progressed through very open terrain and mainly crops, providing a contrast to the terrain and vegetation of the Kilmore fire. As with the Kilmore case study, comparison of the ACCESS weather with all the AWS observations in the region indicated a good match for temperature, humidity, wind direction and the timing of the wind change. However the 10 metre wind speed comparison found that the simulation

under predicted the actual wind speed. A summary of the comparison is contained in the FireDST final report (Cechet *et al*. 2014). The Wangary case study report (French *et al*. 2014b) contains details of the wind speed bias correction factors that were calculated and used in this case study.

The third case study was a portion of the Mt Hall fire that occurred on 24 December 2001 in New South Wales. The Mt Hall fire was ignited by lightning on the 24th of December 2001 in a rugged region of the Blue Mountains. The fire was not contained on the 24th due to excessive weather conditions and crossed Lake Burragorang at around 13:00 on the 25th of December 2001. The fire then impacted the townships of Warragamba and Silverdale destroying 30 properties. The case study covered this fire from when it jumped the lake until it impacted the townships, primarily to evaluate whether an ensemble could be used to model part of a bushfire. Comparison of the ACCESS weather with the AWS observations showed that significant aspects of the AWS meteorological observations were missing or otherwise inadequately represented. The relatively poor simulation may be due to the initial conditions, the complex topography or that the synoptic forcing was weaker. A summary of the comparison is contained in the FireDST final report (Cechet *et al*. 2014). Unfortunately due to the distance of this fire from the nearest AWS there was no ability to calculate wind speed bias correction factors.

Simulation Variability

The main uncertainty in calculating fire spread is a combination of changes in the environmental inputs particularly the meteorological parameters. This paper uses variability in the weather to demonstrate FireDST ensemble functionality. The standard perturbations initially used in each case study are outlined in Table 1. These values were chosen based on the Bureau of Meteorology's comparison of the ACCESS simulation and the observations for Kilmore and Wangary. This results in a standard set of 31 simulations including a simulation with the supplied weather.

Table 1. Standard variability initially used in all case studies

	Minimum	Maximum	Increment	Units/Comment
Temperature	-2	+2	1	Degrees Celsius
Humidity	-2	+2	1	Percent
Wind Direction	-2	+2	1	Degrees
Wind Speed	-5	+5	1	Meters/second
Ignition Time	-10	+10	5	Minutes
Ignition point				200m to the N, S, E and W of the original ignition

2.6. Ensemble Validation

Ensemble validation was conducted by comparing the ensemble shape at various time steps in the footprint with a reconstruction of each of the case studies at the same time step. Individual fire simulations were also compared with the reconstruction using the Area Difference Index (ADI) technique defined in Pugnet *et al*. (2013). This technique has the ability to also compare individual simulations that will in time assist to constrain the variability in the input parameters considered for use in the ensemble.

Results

3.1. Weather variability results

A 30 member ensemble for the Kilmore case study is displayed in Figure 3. Displayed on top of the ensemble are the blue isochrones of the reconstruction of the Kilmore fire at the same time. The reconstruction, which fitted in the ensemble footprint, indicates that the choice of ensemble members provided a wider range of variation than actually occurred in the real fire.

The Wangary fire was contained to a swamp area on 10 January 2005, but there were three outbreaks to the south-east in the morning of the 11 January. Figure 4 shows that if an ensemble was constructed on the 11th and initiated with the actual location and time of each of the breakouts, the ensemble would accurately predict the fire impacting the township of North Shields (which was impacted by the fire).

Despite many attempts it proved difficult to get a realistic ensemble using the standard perturbations for the Mt Hall fire. More variability was required in both wind direction and wind speed to achieve a realistic ensemble shape. Figure 5 is an ensemble simulation for the Mt Hall fire to 1930 EDT on 25th of December 2001. The ensemble fire spread has clearly impacted both Warragamba and Silverdale. The ensemble spread also shows the continuing path of the fire to the east. Although this ensemble simulation closely resembles the reconstruction, the choices of individual simulations in the ensemble had the largest variation from the ACCESS model output compared to the other two case studies. For example in this ensemble the minimum wind direction was increased to 25 degrees less than the ACCESS model output and the wind speed was increased to 20 $m.s^{-1}$ higher than the ACCESS model.

Table 2 displays the actual variability used to produce these ensembles. Mt Hall ensemble had the largest variation, probably due to the fact that the ACCESS weather simulation validated poorly for the available weather observations. Despite the extra variations, the ensembles still produced fire shapes that reflected the actual fire shapes.

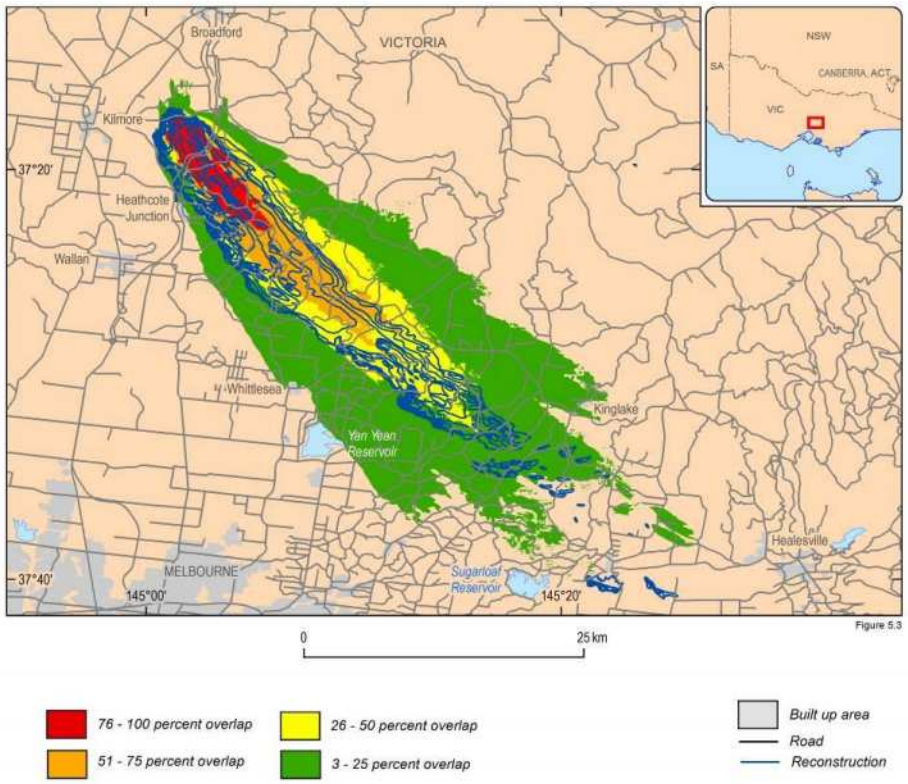

Figure 3. 30 member ensemble simulation for the Kilmore fire with the actual fire reconstruction from Gellie et.al (2012) (blue isochrones).

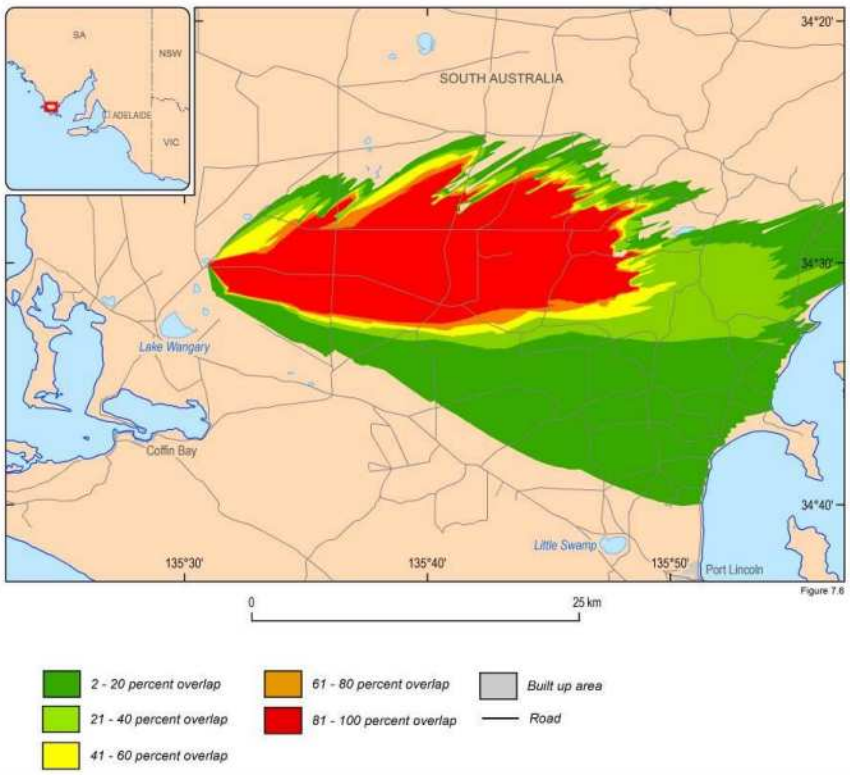

Figure 4. 39 member ensemble shape file output for Wangary to 15:50 CDT using the actual location and time of the fire breakouts on 11/1/2005.

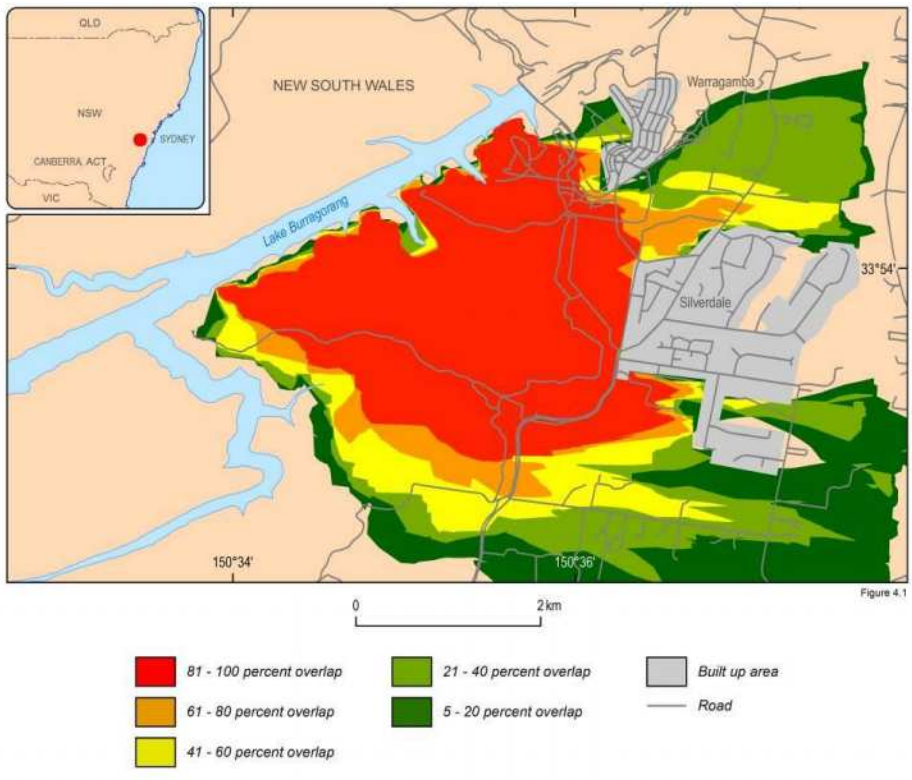

Figure 5. 25 member ensemble simulation for the Mt Hall fire to 19"30 on 25/12/2001

Table 2. Actual variability initially used in the case study examples where the letter "S" stands for the supplied information

	Kilmore		Wangary		Mt Hall		
Members	30		39		25		
	Min	Max	Min	Max	Min	Max	Units/Comment
Temperature	-2	+5	S	+10	S	+10	degrees Celsius
Humidity	-2	+5	-5	S	-5	S	percent
Wind Direction	-10	+10	-5	+25	-5	+25	degrees
Wind Speed	-5	+5	S	+10	-5	+20	meters/second
Ignition Time	S	S	S	S	S	S	minutes
Ignition point	Y		S		S		200 to the north,south,east and west

3.2. Exposure of buildings to the firespread ensembles

Figure 6 shows an example for the Kilmore case study of how the house locations can be displayed overlaid on the ensemble footprint. This overlay provides a direct visual representation of the exposure of the buildings to the ensemble footprint. FireDST can then automatically calculate from the building location the number of buildings and people that are potentially exposed to this fire.

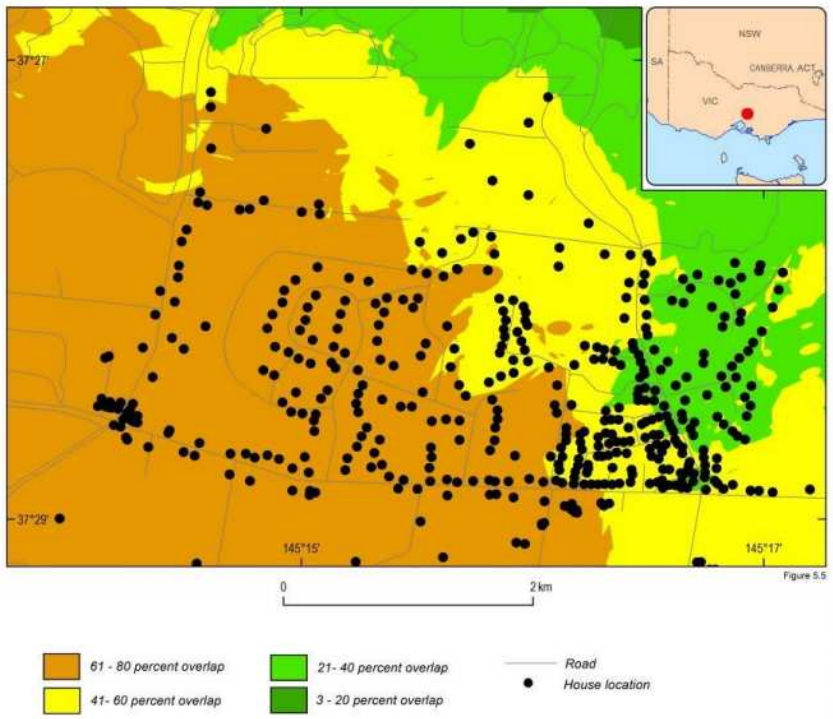

Figure 6. Kilmore fire, ensemble fire spread with house locations displayed.

3.3. Exposure of buildings/people to the bushfire smoke ensembles

FireDST is able to extend the ensemble approach to smoke and combustion element spread from a bushfire. The ensemble smoke spread was only completed for the Kilmore fire due to the computer processing time taken to produce the multiple simulations (Meyer *et.al*. 2013). Figures 7 and 8 show an example for the maximum concentration and percent overlap of Carbon Monoxide (CO) for an ensemble of 4 fire spread simulations that had different ignition points 500m to the North, South, East and West of the Kilmore ignition point. The two images are required to be considered together.

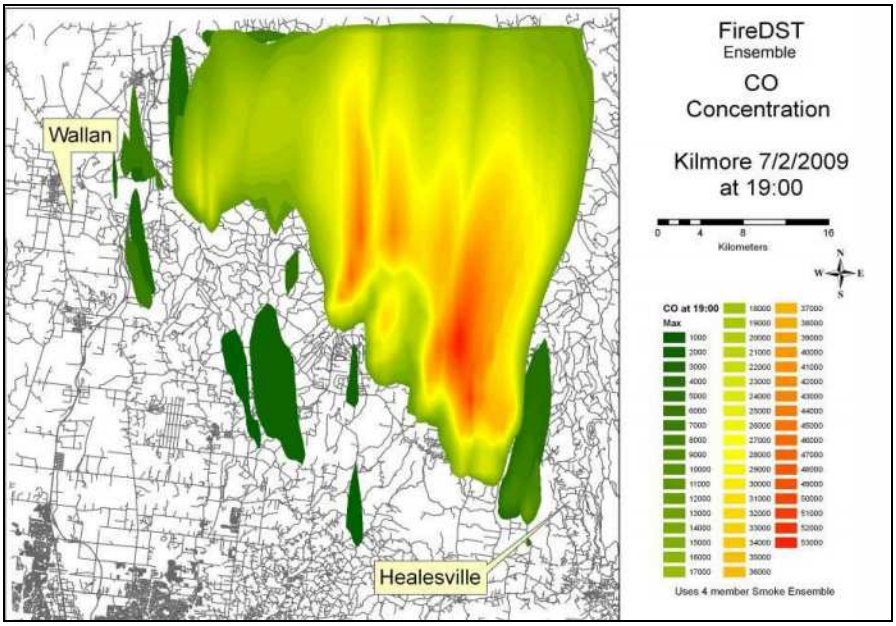

Figure 7. Map of the concentration of CO at 1900 for the 4 simulations of the Kilmore fire. This concentration map must be used in conjunction with the probability map.

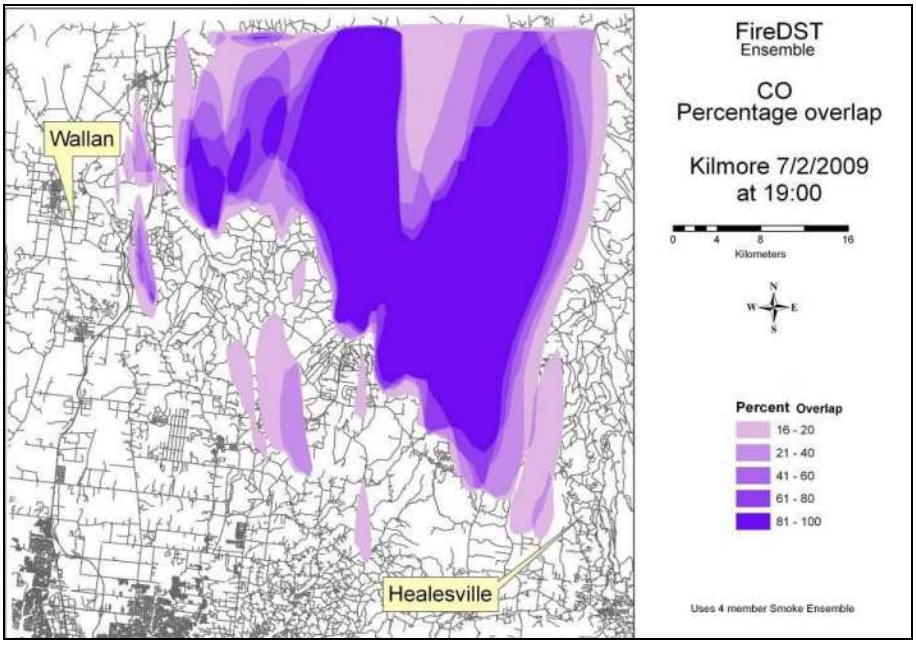

Figure 8. Ensemble map of the percentage overlap of CO at 1900 for the 4 simulations of the Kilmore fire. This probability map must be used in conjunction with the concentration map.

Discussion, Conclusions and Future Work

With the FireDST "proof-of-concept" system we have demonstrated the successful generation of short-term ensemble fire spread as well as modelling associated exposure. FireDST has shown the utility of generating multiple scenarios and generating an ensemble fire spread. FireDST has also demonstrated the ability to derive and display statistical information about people and buildings that are exposed to the ensemble footprint. Graphs and tables can be displayed showing the exposure across the ensemble footprint (e.g. an estimate of those houses and people in the 76-100% probability area for the simulations considered in the ensemble).

This research has shown the development of a simple ensemble overlap of all the individual fire simulations. However it may be possible in the future to include known probabilities for the likelihood of occurrence of each of the individual simulations. The probabilities could be supplied as part of a weather ensemble similar to the weather ensemble produced by the UK Meteorological Office. The probabilities can then be incorporated into the ensemble to produce a probabilistic fire spread which informs users of the likelihood of each ensemble area occurring (i.e. the 3-25% percent overlap area might only have a 10 % likelihood but the 76 to 100% area would have a 100% likelihood.

The next challenge is the operational implementation of this new technology. More work is needed in association with the fire agencies to define a business case for predictive models such as FireDST and a sustainable implementation plan that includes further research, training and field trial validation. A national collaborative effort among Australian fire agencies is clearly required. As a prototype, FireDST has already revolutionised fire simulation modelling. The methodologies developed in the project promise to be an invaluable asset to fire managers working under pressure to make quick decisions that affect lives and infrastructure. Operational fire decision support models could conceivably produce continually updated simulations of severe fire events which address the uncertainty in the input parameters (including the assimilation of fire ground intelligence and real-time performance statistics relating to the fire weather predictions). These simulations, developing products relating to fire spread and impacts, could provide valuable decision support for emergency management. Fire agencies face a steep learning curve in dealing with scenario information which attempts to capture the outcome sensitivity by considering the uncertainty in model inputs. The development of a national approach to fire spread and impacts, as well as standardisation and consistency with the underpinning datasets, would help enable all fire managers to become accustomed to 'what if' scenarios, and to allow transparency in utilisation, validation and learnings across state boundaries.

Acknowledgements

This study was partly supported by the Bushfire Cooperative Research Centre as part of the "*Understanding Risk*" theme.

References

Anderson, K., Reuter, G. & Flannigan, M.D. (2007) Fire-growth modelling using meteorological data with random and systematic perturbations. Int. J. Wildland Fire, 16, 174-182.

Buckingham, C., Marchok T., Ginis I., Rothstein L., Rowe D. (2010) Short- and medium-range prediction of tropical and transitioning cyclone tracks within the NCEP Global Ensemble Forecasting System. Weather and Forecasting, 25, 1736–1754.

Canterford,S. (2011) Locating People Spatially:2006,2010,2100 and 2:36PM on Friday, Aust. J. of Regional Studies, (17) 1,46-59

Cechet R.P., French I.A., Kepert J.D., Fawcett R.J.B., Tory K.J., Thurston W., Tolhurst K.G., Duff T.J., Chong D.M., Meyer M., Keywood M., Cope M., (2014) Fire Impact & Risk Evaluation Decision Support Tool (FireDST) Final Report , Bushfire Cooperative Research Centre

Cruz, M.G. (2010) Monte Carlo-based ensemble method for prediction of grassland fire spread. Int. J. Wildland Fire, 19, 521-530.

Finney, M. A. (1998) FARSITE: Fire Area Simulation – Model development and evaluation. USDA Forest Service, Rocky Mountain Research Station, Research Paper RMRS-4.

Finney, M.A. (2006) An overview of FlamMap modelling capabilities. In: P.L. Andrews, B.W. Butler (comps.). Fuels Management – How to measure success: Conference Proceedings. RMRS-P-41. p 213-219.

Finney, M.A., Grenfell, I., McHugh, C., Seli, R., Trethewey, D., Stratton, R. & Brittain, S. (2011) A method for ensemble wildland fire simulation. Environmental Modelling and Assessment, 16, 153-167.

Forthofer, J., Shannon, K., and Butler, B. (2009) Simulating diurnally driven slope winds with Wind Ninja. Proc. 8th Symposium on Fire and Forest Meteorology, October 13-15; Kalispell, MT

French I. A, Woolf, M., Cechet, B., Yang, T., and Sanabria, A. (2014a) GA 4-1-5A Acknowledging and Understanding Uncertainty in Simulating Bushfires - Part 1 - Evaluation of FireDST against the Kilmore fire of 7 February 2009, Geoscience Australia Record (in press)

French I. A, Woolf, M., Cechet, B., Yang, T. and Sanabria, A. (2014b) GA 4-1-5B Acknowledging and Understanding Uncertainty in Simulating Bushfires - Part 2 - Evaluation of FireDST against the Wangary fire of 10 January 2005, Geoscience Australia Record (in press)

French I. A, Woolf, M.,Cechet, B., Yang, T. and Sanabria, A. (2014c) GA 4-1-5C Acknowledging and Understanding Uncertainty in Simulating Bushfires - Part 3 - Evaluation of FireDST against the Mt Hall fire of 24 December 2001, Geoscience Australia Record (in press)

Gellie, N., Gibos, K., Mattingley, G.,Wells, T., Salkin, O. (2012) Reconstruction of the spread and behaviour of the Black Saturday fires, 7th February 2009, Department of Sustainability and Environment, Government of Victoria, Draft Version 3.3

Jones, T., Woolf, M., Cechet, R.P. and French, I. (2012) Quantitative bushfire risk assessment framework for severe and extreme fires, Australian Meteorological and Oceanographic Journal (62), 171–178

Meyer, C.P., Lee, S. and Cope, M. (2013) Smoke impacts from prescribed burning in Victoria; developing a risk climatology. Proc. 20th International Congress on Modelling and Simulation (MODSIM 2013), Adelaide, December 2-6th

Nadimpalli, K. Edwards, M. and Mullaly, D. (2007) National EXposure Information System (NEXIS) for Australia: Risk Assessment Opportunities. Proc. 17th International Congress on Modelling and Simulation (MODSIM 2007), 1674-1680

Pugnet, L, Chong, DM, Duff, TJ, Tolhurst (2013) 'Wildland-urban interface (WUI) fire modelling using PHOENIX RapidFire: A case study in Cavaillon, France. Proc. 20th International Congress on Modelling and Simulation (MODSIM 2013), Adelaide, December 2-6th

Puri, K. (2011) Overview of ACCESS, http://www.cawcr.gov.au/bmrc/basic/wksp18/papers/Puri.pdf

SA Coroner (2007) Finding of inquest, Inquest into the deaths of Star Ellen Borlase, Jack Morley Borlase,Helen Kald, Castle, Ludith Maud Griffith, Jody Maria Kay, Graham Joseph Russell, Zoe Russell-Kay, Trent Allan Murnane and Neil George Richardson, South Australia Coroner's Office

Tolhurst, K.G., Shields, B.J. and Chong, D.M. (2008) PHOENIX: development and application of a bushfire risk management tool. Australian Journal of Emergency Management, 23(4), 47-54

Tymstra, C.; Bryce, R.W.; Wotton, B.M.; Armitage, O.B. (2009) Development and structure of Prometheus: the Canadian wildland fire growth simulation model. Inf. Rep. NOR-X-417. Nat. Resour. Can., Can. For. Serv., North. For. Cent., Edmonton, AB.

USDA Forest Service, Wildland Fire Decision Support System: Reference Guide, FSPro Overview 1.0, http://wfdss.usgs.gov/wfdss/pdfs/fspro_reference.pdf, accessed June 2012

VBRC (2010). The 2009 Victorian Bushfires Royal Commission final report. Summary and four volume report tabled July 31st; available at http://www.royalcommission.vic.gov.au/Commission-Reports

Zhang, Z., T. N. Krishnamurti, (1997) Ensemble Forecasting of Hurricane Tracks. Bulletin of the American Meteorological Society, 78, 2785–2795

Fuel types identification for forest fire risk assessment in Bulgaria

E. Velizarova[a], T. Stankova[a], M. Glushkova[a], G. Xanthopoulos[b], Vl. Konstantinov[c], D. N. Dimitrov[a]

[a] *Forest Research Institute – Bulgarian Academy of Sciences, 132 Kl. Ohridsky blvd., 1756, Sofia, Bulgaria. velizars@abv.bg; tatianastankova@yahoo.com; m_gluschkova@abv.bg; mitkomit@mail.bg*
[b] *Hellenic Agricultural Organization "Demeter". Institute of Mediterranean Forest Ecosystems and Forest Products Technology. Terma Alkmanos, Ilisia, 11528, Athens, Greece. gxnrtc@fria.gr*
[c] *Ministry of Agriculture and food, Executive Forests Agency | Directorate - Prevention and control of the forests territories. 55 Hr. Botev blvd., 1040 Sofia, Bulgaria. vl_konstantinov@nug.bg*

Abstract
Knowledge of the spatial distribution of fuel types is essential for implementation of the fire models predicting fire behaviour, severity and spread. In the present study, the most commonly used fuel classifications systems currently employed worldwide and the associated methods for generating a fuel type classification has been examined and compared. Based on a critical analysis of the state-of-the-art and on the main advances achieved in different classification systems, a simple quantitative methodology for development of a fuel type model has been developed. The results obtained showed that Austrian stands are characterized by a higher fuel load concerning both – live and dead biomass. The load of the dead material ranged from 13.3 t/ha to 47.0 t/ha and the load of the live fuel material was within the range 1.60 kg/m2 - 2.08 kg/m2. The density of the crown was also higher and equal to 0.354 kg/m2. The moisture content of the live leaves branches and dead material for Austrian pine and beech stands was relatively low in comparison with those for the other tree species.

***Keywords**: forest fuels, fuel type, fire behaviour prediction*

Introduction

Numerous forest fire studies report relationships between fire behaviour, fire suppression and their dependence on the forest fuels (Burgan and Rothermel, 1984; Fryer and Johnson, 1988; Burgan *et al*., 1998; Chuvieco *et al*., 1999; Arroyo *et al*., 2006). The rationale for using vegetation characteristics to classify fuels is that fuels are ultimately derived from vegetation. The increase in density and surface and canopy fuels has enhanced the risk of high-severity fires (Miller *et al*., 2009, 2012; Taylor *et al*., 2014). The fuel type classifications are usually based on the vegetative characteristics of a particular site or location. Fire behaviour fuel models are used as input to the Rothermel´s (Rothermel, 1972) fire spread model, which is used in a variety of fire behaviour modelling systems. Different kinds of fuel models are used in fire science (Rothermel, 1972; Albini, 1976; Anderson 1982). The variation in predicted spread rate among models is attributed to fuel load by size class (0 to 0.64 cm, 0.64 to 2.54 cm, and 2.54 cm to 7.62 cm diameter), fuel-bed depth, and fuel particle size, surface-area-to-volume (SAV) ratio by component. Later, the fuel particle heat content was included as a fuel model parameter for the BEHAVE fire behaviour prediction (Andrews, 1986; Burgan and Rothermel, 1984), FARSITE (Finney, 1998) and BehavePlus (Andrews *et al*., 2003) models. It should be mentioned that Albini's fuel models specified an extinction moisture content value for each fuel model, whereas this parameter was held constant for Rothermel's fuel models. The fuel moisture was considered for distinguishing the two major groups of fuel models: live and dead. The 1-, 10-, 100-, and 1000-h time-lag classes represent the dead fuels (Cohen and Deeming, 1982). The live fuels are further classified into herbaceous and woody shrub.
FARSITE (Fire Area Simulator) model developed by Finney (1998), includes both type of models - for crown fire behaviour as well as surface fuel models and therefore require information of crown fuel

parameters such as percentage canopy cover, canopy height, crown base height and crown bulk density. The next fuel models in the USA paid attention on the fuel beds and their classification according to the capacity to support fire and consume fuels (Sandberg *et al*., 2001; Ottmar *et al*., 2007). The fuel classification system called Prometheus has been adapted for Mediterranean conditions (Arroyo *et al*., 2006). The main criterion of classification in this system is the type and height of the propagation element divided into three major groups: grass, shrubs or ground litter and trees. The main approach of the BEHAVE system was applied for developing the other systems, such as the CARDIN system in Spain (Caballero *et al*., 1994) and for development of general fuel models for some regions in Greece (Dimitrakopoulos *et al*., 1999, Dimitrakopoulos *et al*., 2001) and photo keys (ICONA 1990) for different environments. Knowledge of the spatial distribution of fuel types is also essential for implementation of the fire models predicting fire behaviour, severity and spread.
In this paper, we examine the most commonly used fuel classifications systems currently employed worldwide and the associated methods for generating a fuel type classification. Based on the analysis of state-of-the-art and on the main advances achieved in different classification systems, a simple quantitative methodology for development of a fuel type model is presented.

Methods

Six sampling sites (SS) have been established in the western region of Bulgaria (Government Forestry Enterprises "Nevestino"), which is one of the most frequently affected by forest fires (Figure 1). The main tree species are *Fagus sylvatica L., Pinus sylvestris L., Pinus nigra Arn., Quercus cerris L., Quercus frainetto Ten.*. The main characteristics of the location and the stand's surface biomass parameters have been collected. At field conditions, the following parameters of the stands were measured: the crown cover, crown height, diameter at breast height (D.B.H.), height difference between surface and first tree branches. Information on the distribution of live and dead fuels in the pre-specified four size classes was obtained by separating all live and dead fuels in 1 m^2 plots and weighing them. The fine live biomass - leaves, twigs and branches less than 0.64 cm in diameter and thicker and live shrub biomass (if present at sampling sites) have been also collected. The dead woody fuel loading was measured collecting the material from 50 cm x 50 cm square plots in three replications at each sampling site. The material was divided into classes characterizing the drying rates of the various fuel particles, so called 1-, 10-, 100- and 1000 h time lag fuels. The fuel load values for collected size classes for live biomass and dead material were determined.
The moisture content of the various elements of the fuel complexes (live needles and leaves, woody shrub stems, ground litter, duff, etc.) was also determined by collecting samples from the sampling sites, weighing them, oven-drying them for 48 hours at 1050C, and weighing them again. This information was used to adjust all measured weights in the sample plots to oven-dry fuel loadings.

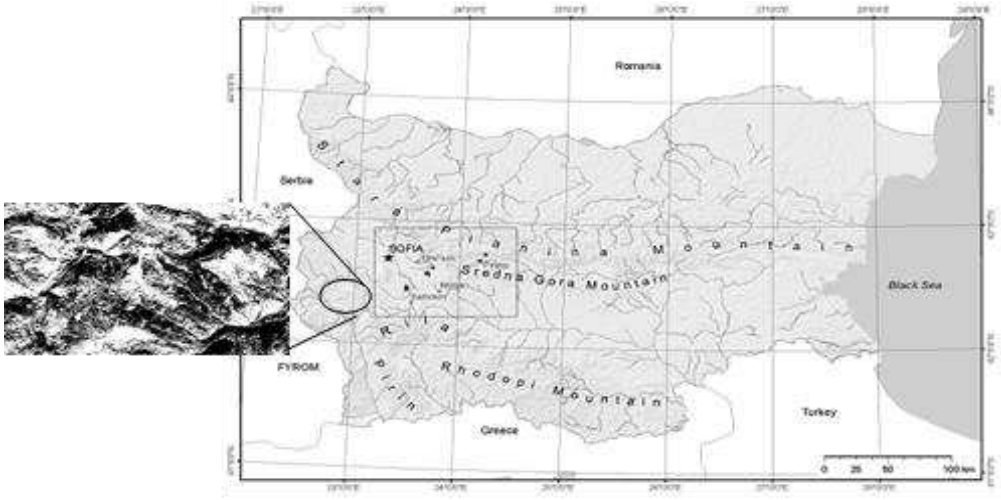

Figure 1. Legend of figure 1

Results

For the current investigation, the live fuel load (LFL) in the tree crown was determined as the weight of the lives/needles for the unit horizontal area (in kg/m2). The calculation was performed using equations 1, 2 and 3. The diameter at breast height (D.B.H.) of all trees from the sampling plot was used.

For Austrian pine: $CrFL = 1.324 - 0.13dbh + 0.025dbh^2$ (1)

for Scots pine: $CrFL = 0.023dbh^{1.802}$ (2)

where *CrFL* [kg] is the weight of crown fuel material of a tree with diameter at breast height (dbh).

$$CFL = \frac{\sum_{i=1}^{n} CrFL}{PP}\left[kg/m^2\right] \quad (3),$$

where *CFL* is the quantity of the fuel material of the continuous canopy (in kg/m^2), represented as the sum of the quantities for all separated trees on the territory of the studied sampling site, divided by its area *PP* (m^2).

The fuel load for live biomass of the deciduous forest was not determined, as its role in crown forest fires is negligible. The quantity of the fuel load of the dead material is important in case of surface fires in coniferous and deciduous forests. The highest fuel load of live biomass was found for Austrian pine stands – from 1.60 kg/m^2 to 2.08 kg/m^2 (Table 1).

Besides the fuel load, the moisture content of the various fuel materials was determined (Figures 2, 3).

Table 1. Crown fuel characteristics

SS	Main tree species	Crown fuel (leaves and twigs) (kg/m^2)	Height of crown (m)	Crown fuel density (kg/m^2)
SS1	Beech			
SS2	Scots pine	1.04	10.54	0.188
SS3	Austrian pine	2.08	12.50	0.354
SS4	Oak			
SS5	Austrian pine	1.17	11.96	0.147
SS6	Austrian pine	1.60	8.02	0.294

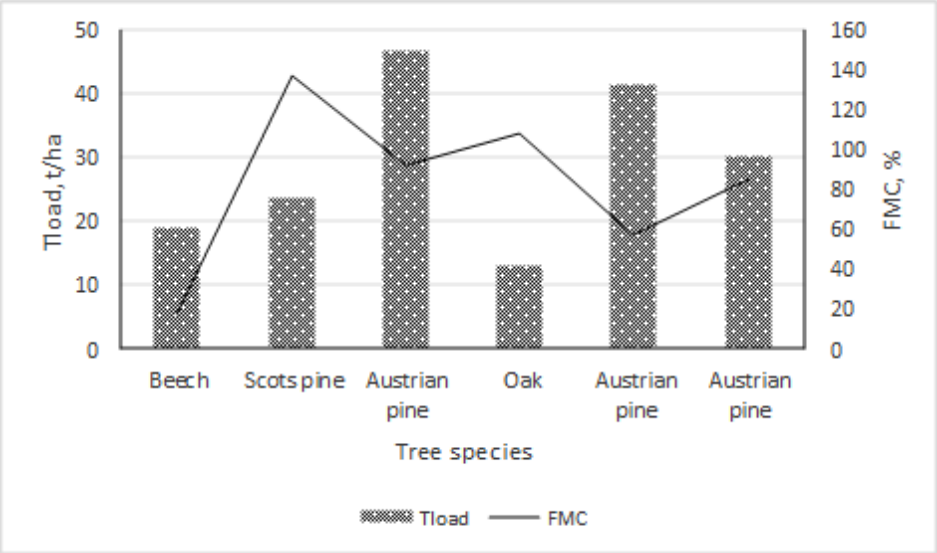

Figure 2. Fuel characteristics of sampling sites (Tload – total load; FMC – Fuel moisture content, %).

The most important variable of interest for the analysis is the total fuel loading (TLOAD), for each location. For our purpose, TLOAD represents the sum of litter load (LL), 1-hr dead woody fuel, 10-hr dead woody fuel, 100-hr dead woody fuel, cones, and bark. Similar to the load of the live biomass, the highest TLOAD was found for Austrian pine stands – from 30.0 t/ha to 47.0 t/ha (Figure 2).
Fuel moisture affects ignition by absorbing energy when being vaporized, and by diluting flammable volatiles, which increases the ignition delay time. Moist fuels reduce to less intense fires in contrast to the dry fuels that burn more fiercely (Van Wagner, 1967; Catchpole and Catchpole, 1991).

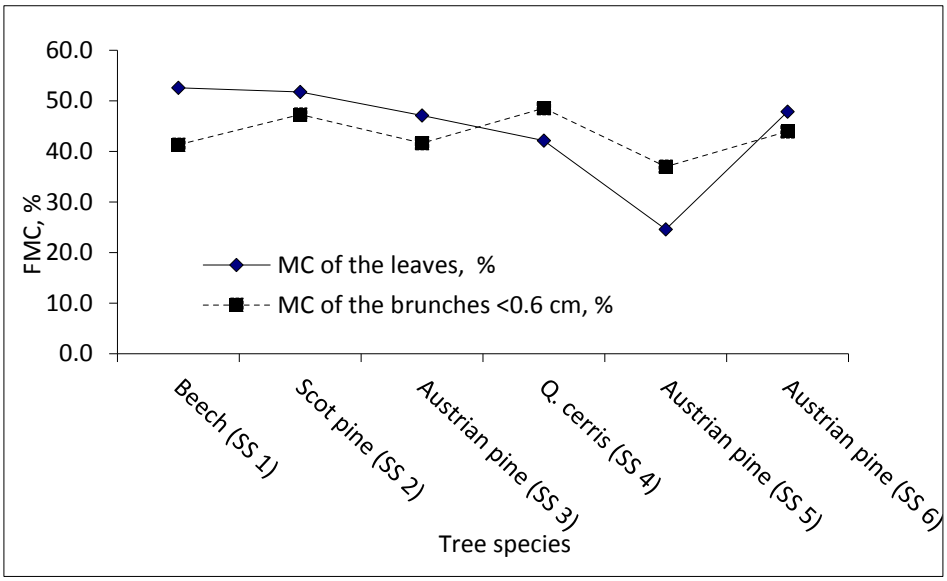

Figure 3. Moisture content (MC) of the live fuel load.

The experimental results show that the FMC of the live leaves/needles and brunches varies from 24. 6% to 52,6 %. Based on the definition of the moisture of extinction (ME) (32% of plant fresh weight), in could be noted that very flammable is the plantation of the Austrian pine from SS 5, as its moisture content was less than 25% (Figure 3). The MC of the brunches changes within narrower limits.

Conclusions

The results obtained clearly show that Black Pine stands are characterised by a higher fuel load concerning both – live and dead biomass. The load of the dead material ranged from 13.3 t/ha to 47.0 t/ha and the load of the live fuel material was in the range 1.60 kg/m2 - 2.08 kg/m2. The density of the crown was also higher and equal to 0.354 kg/m2. The moisture content of the live leaves branches and dead material for Black pine and beech stands was relatively low in comparison with those for the other tree species.

Acknowledgements

We wish to thank the Bulgarian Found for Scientific Investigations, Bulgarian Ministry of education and Science for providing financial support through Project DFNI-I-01/0006 “Simulating the behaviour of forest and field fires”.

References

Albini, F. A. 1976. Estimating wildfire behaviour and effects. Gen. Tech. Rep. INT-30. Ogden, Utah: Department of Agriculture, Forest Service, Intermountain Forest and Range Experiment Station. 92 p.

Anderson, H. E. 1982. Aids to determining fuel models for estimating fire behavior. Gen. Tech. Rep. INT-122. Ogden, UT: U.S. Department of Agriculture, Forest Service, Intermountain Forest and RangeExperiment Station. 22 p.

Andrews, P. L. 1986. BEHAVE: Fire behavior prediction and fuel modeling system — BURN Subsystem, Part 1. Gen. Tech. Rep. INT-194. Ogden, UT: U.S. Department of Agriculture, Forest Service, Intermountain Forest and Range Experiment Station. 130 p.

Andrews, P. L.; Bevins, C. D.; Seli, R. C. 2003. BehavePlus fire modeling system, version 2.0: User's Guide. Gen. Tech. Rep. RMRS-GTR-106WWW. Ogden, UT: Department of Agriculture, Forest Service, Rocky Mountain Research Station. 132 p.

Arroyo, L.A., Healey, S.P., Cohen, W.B., Cocero, D., 2006. Using object-oriented classification and high-resolution imagery tomap fuel types in aMediterranean region. Journal of Geophysical Research 111, G04S04

Arroyo, L.A., S.P. Healey, W.B. Cohen, D. Cocero. 2006. Using object-oriented classification and high-resolution imagery to map fuel types in a Mediterranean region. Journal of Geophysical Research 111, G04S04 doi: 10.1029/2005JG000120.

Burgan, R. E. and R. C. Rothermel. 1984. BEHAVE: Fire behavior prediction and fuel modeling system - FUEL subsystem. USDA For. Serv. Gen. Tech. Rep. INT-167. 126 p.

Burgan, R. E., Rothermel, R. C. 1984. BEHAVE: Fire behavior prediction and fuel modeling system – FUEL subsystem. Gen. Tech. Rep. INT-167. Ogden, UT: U.S. Department of Agriculture, Forest Service,Intermountain Forest and Range Experiment Station. 126 p.

Burgan, R., Klaver, R., Klaver, J., 1998. Fuelmodel and fire potential fromsatellite and surface observations. International Journal of Wildland Fire 8, 159–170

Chuvieco, E., Carvacho, L., Rodrıguez-Silva, F., 1999. Integrated fire risk mapping. In: Chuvieco, E. (Ed.),Remote Sensing of LargeWildfires. Springer, Berlin, pp. 61–84.

Cohen, J.D., Deeming, J.E., 1982. The National Fire Danger Rating System: basic equations. Rep. No. PSW-82. Pacific Southwest Forest and Range Experiment Station, Berkeley, CA.

Dimitrakopoulos, A. P., G. Xanthopoulos, and V. Mateeva. 1999. Statistical classification of Mediterranean fuel types in Greece. pp. 125-131. In Proc. Int. Symposium on "Forest Fires: Needs and Innovations". November 18-19, 1999, Athens, Greece. Published by CINAR S.A., Athens, Greece, under the auspices of the European Commission DG XII. 419 p.

Dimitrakopoulos, A. P., V. Mateeva, and G. Xanthopoulos. 2001. Fuel models for Mediterranean vegetation types in Greece. Geotechnical Scientific Issues (Geotechnical Chamber of Greece): Series VI, vol. 10(3): 192-206 (in Greek).

Finney, M. A. 1998. FARSITE: Fire Area Simulator—model development and evaluation. Res. Pap. RMRS-RP-4. Fort Collins, CO: U.S. Department of Agriculture, Forest Service, Rocky Mountain Research Station. 47 p.

Miller, J.D., Safford, H.D., Crimmins, M. & Thode, A.E. 2009. Quantitative evidence for increasing forest fire severity in the Sierra Nevada and southern CascadeMountains, California and Nevada, U.S.A. Ecosystems 12: 16–32.

Miller, J.D., Skinner, C.N., Safford, H.D., Knapp, E.E. & Ramirez, C.M. 2012. Trends and causes of severity, size, and number of fires in northwestern California, USA. Ecological Applications 22: 184–203.

Ottmar, R.D., Sandberg, D.V., Riccardi, C.L., Prichard, S.J., 2007. An overview of the fuel characteristics classification system—quantifying, classifying, and creating fuelbeds for resource planning. Canadian Journal of Forest Research 37, 2383–2393.

Rothermel, R. C. 1972. A mathematical model for predicting fire spread in wildland fuels. Res. Pap. INT-115. Ogden, UT: U.S. Department of Agriculture, Forest Service, Intermountain Forest and Range Experiment Station. 40 p.

Sandberg, D.V., Ottmar, R.D., Cushon, G.H., 2001. Characterizing fuels in the 21st Century. International Journal of Wildland Fire 10, 381–387.

Taylor A. H., A. M. Vandervlugt, R. S. Maxwell, R. M. Beaty, C. Airey, C.l N. Skinner. 2014. Changes in forest structure, fuels and potential fire behaviour since 1873 in the Lake Tahoe Basin, USA Applied Vegetation Science Volume 17, 1, 17–31, DOI: 10.1111/avsc.12049

Viegas D. X., Viegas M. T., Ferreira A. D. 1992. Moisture content of forest fuels and fire occurrence in central Portugal. International Journal of Wildland Fire 2: 69–86.

Global assessment of fire risk: using a global fuel map and climatological data to estimate fire behavior with FCCS

M. Lucrecia Pettinari[a], Emilio Chuvieco[b]

[a] *Environmental Remote Sensing Research Group, Universidad de Alcalá, Calle Colegios 2, 28801-Alcalá de Henares, Spain. mlucrecia.pettinari@uah.es*
[b] *Environmental Remote Sensing Research Group, Universidad de Alcalá, Calle Colegios 2, 28801-Alcalá de Henares, Spain. emilio.chuvieco@uah.es*

Abstract
The spatial distribution, structure, and environmental conditions of the fuels are key variables in wildland fire behavior and effects. This study developed environmental scenarios, based on global weather information and topography, in order to calculate surface fire behaviour parameters using the Fuel Characteristic Classification System and a global fuel map previously developed.
The results show the geographic variation in monthly mean wind speeds and fuel moisture content for the months of January and July and for the period 1981-2010. Also, the worst monthly conditions were evaluated, corresponding to the maximum monthly wind speeds and minimum fuel moisture content. From these environmental scenarios, the rate of spread for the global fuels was mapped, obtaining more realistic results than in the past.

Keywords*: Fire risk, FCCS, global fuel map, fire behavior, ECMWF*

Introduction

Surface fire behaviour is dependent on the available fuels and also on the environmental conditions when the fire occurs. Specifically, fuel moisture, slope and wind speed affect the speed in which fire spreads, and the energy released by it (Rothermel 1983). The different fire behaviour systems that are currently widely used, such as BehavePlus (Andrews *et al.* 2008), the National Fire Danger Rating System (Cohen and Deeming 1985), the Canadian Fire behaviour prediction (Stocks *et al.* 1989), the Fuel Characteristic Classification System (Ottmar *et al.* 2007), etc., include these environmental conditions in the calculation of the surface fire parameters.

The Fuel Characteristic Classification System (FCCS) (Ottmar *et al.* 2007) was designed to represent the structural and geographic diversity in wildland fuels, and combines the fuel properties into "fuelbeds", which include the physical and chemical variables used to model fire behavior and fuel consumption, and predict emissions (Riccardi *et al.* 2007). FCCS uses fuel characteristics (e.g. percentage cover, loading, depth) to calculate and report nine fire potentials, organised into three categories: surface fire behaviour potential, crown fire potential and available fuel potential (Sandberg *et al.* 2007a). Also, based on input environmental variables, the FCCS also predicts surface fire behaviour parameters using a reformulation of the Rothermel (1972) fire behaviour model (Sandberg *et al.* 2007b).

During previous work developing fuel maps using FCCS (Pettinari *et al.* 2013a; Pettinari *et al.* 2013b), default environmental parameters were used to estimate fire potentials and surface fire behaviour such as rate of spread, flame length, and reaction intensity. The use of a defined set of environmental conditions allowed the comparison of the different fuelbeds based solely on their intrinsic characteristics, but they did not reflect the variations of weather conditions around the world, which influence fire behaviour. In this study we focused on improving the fire behavior results by means of applying more realistic environmental conditions to the different regions of the world.

Methods

To run FCCS, it is necessary to select the fuelbeds that will be included in the calculations, and also the environmental variables that affect fire behaviour. These environmental conditions are: fuel moisture content (FMC) for different fuel classes, wind speed and slope. The required FMCs are: 1-, 10- and 100-h dead fuel moisture, and live-herb, live-shrub and live-crown moistures. The FMCs can be input as individual FMCs, or a Fuel Moisture Scenario (FMS) can be used. The 16 combinations of the Scott and Burgan (2005) dead and live FMSs are already input as selectable FMSs. Terrain slope is input in units of % slope, and wind speed is input in units of miles per hour (mph).
For the purpose of this study, we selected FMSs from the existing ones in FCCS according to their dead 10-h FMC, and we created slope and wind scenarios to reflect the influence of these variables in surface fire behaviour. All the calculations were done using FCCS version 3.0 module inside the Fuel and Fire Tools (http://www.fs.fed.us/pnw/fera/fft/index.shtml, accessed June 2014) version 3.03.203.
The climatic data was extracted from the European Centre for Medium-Range Weather Forecast (ECMWF). We used the ERA-Interim Global Reanalysis (Dee *et al.* 2011) because it includes all the climatic variables required to calculate the environmental variables for the FCCS run, and it is the latest release of the ECMWF reanalyses. The data covers a 30-year period, from 1981 until 2010, and was rescaled from the original 0.75º grid to a 0.50º grid covering the whole globe directly at the ECMWF Data Server. ERA-Interim provides daily forecast information for 8 hours UTC (time steps): 0, 3, 6, 9, 12, 15, 18 and 21 hr. Since the lowest fuel moisture content usually occurs at early afternoon, the globe was divided in 8 strips of 45º longitude, each one including information of local solar time (LST) between 12 hr. (in the western part of the strip) and 15 hr. (in the eastern part of the strip). For example, the data of UTC 15:00 was used for the strip extending between 45º and 90º, and that information represents weather conditions at 12 hr for the longitude 45º, 13 hr. for latitude 60º, 14 hr. for latitude 75º and 15 hr. for latitude 90º. Table 1 summarises the climatic variables used for this study and their characteristics.

Table 1. Climatic variables from the ERA-Interim Reanalysis used for this study

Variable Name	Variable Code	Units	Type of Level	Stream	Other information
10 m Wind Speed	207	m s^{-1}	Surface	Synoptic Monthly Mean	Produced by forecast. Monthly average at time step.
Total Cloud Cover	164	Fraction of cover (0-1)	Surface	Daily	Produced by forecast. Instantaneous at time step.
Snow Depth	141	m of water equivalent	Surface	Daily	Produced by forecast. Instantaneous at time step.
Total Precipitation	228	m of water	Surface	Daily	Produced by forecast. Accumulated from the previous 24 hr.
2 meter Dew Point	168	ºK	Surface	Daily	Produced by forecast. Instantaneous at time step.
2 meter Temperature	167	ºK	Surface	Daily	Produced by forecast. Instantaneous at time step.

2.1. Fuel map

The fuel distribution and their physical and chemical variables related to fire behaviour were extracted from the Global Fuelbed Map developed by Pettinari and Chuvieco (2013a). This map is based on vegetation data provided by the GlobCover V2.2 product (Bicheron *et al.* 2008), and has a spatial resolution of 10 arc seconds (~300 m at the Equator). Its legend was defined using the Land Cover Classification System (Di Gregorio 2005). The land cover information was sub-divided using the biomes described in the Map of Terrestrial Ecoregions (Olson *et al.* 2001), in order to account for differences in vegetation characteristics due to the influence of climate. This map (see Fig 1) has a total of 166 Fuelbeds, some of them subdivided according to their percentage of canopy cover. Each

fuelbed is identified by a number, where the thousands value corresponds to the biome, and the following three values identify the land cover type associated with each pixel. For example, fuelbed 13140 is in the Desert and Xeric Shrublands biome: "13", and associated with grass vegetation: "140".

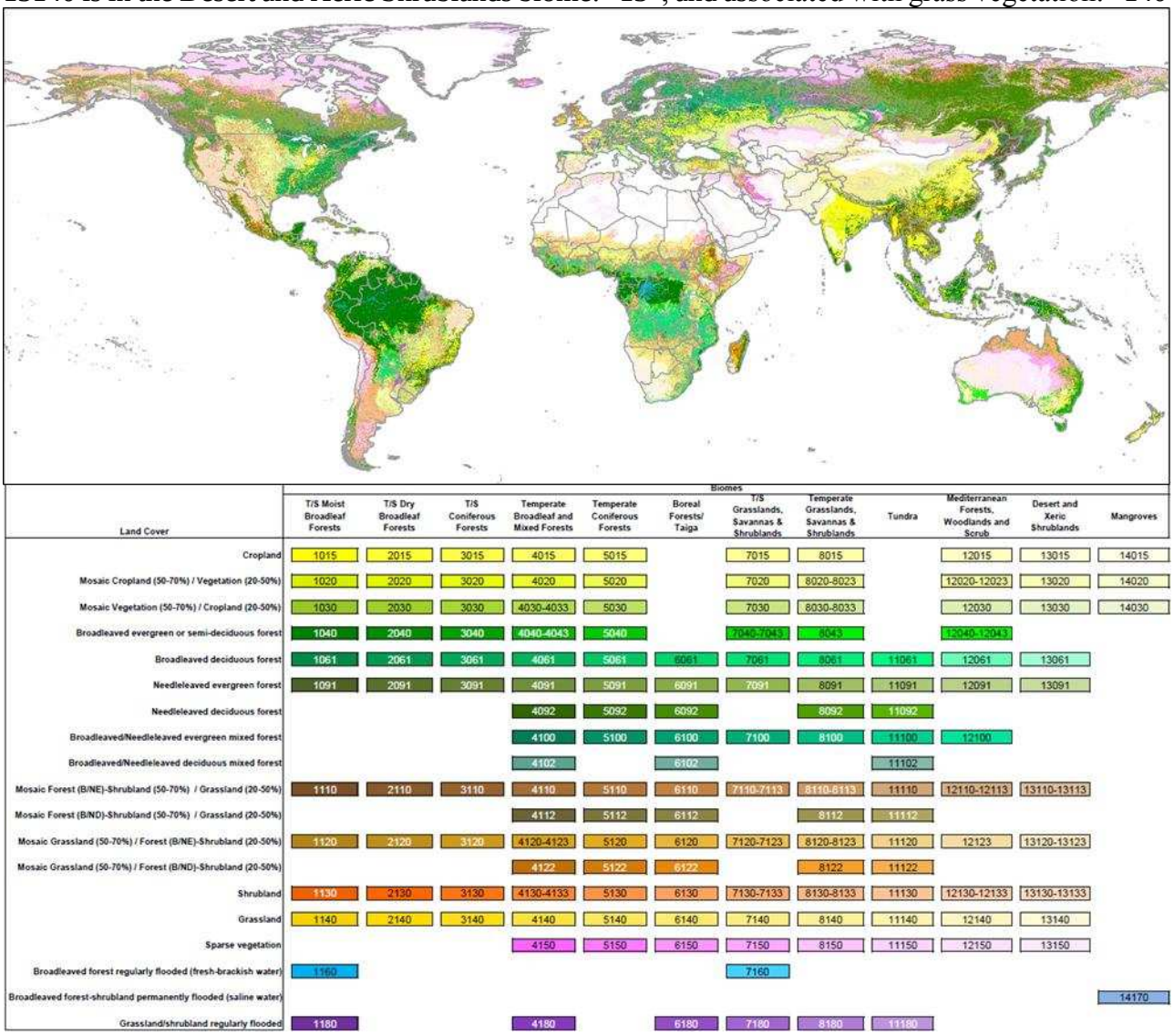

Land Cover	T/S Moist Broadleaf Forests	T/S Dry Broadleaf Forests	T/S Coniferous Forests	Temperate Broadleaf and Mixed Forests	Temperate Coniferous Forests	Boreal Forests/ Taiga	T/S Grasslands, Savannas & Shrublands	Temperate Grasslands, Savannas & Shrublands	Tundra	Mediterranean Forests, Woodlands and Scrub	Desert and Xeric Shrublands	Mangroves
	Biomes											
Cropland	1015	2015	3015	4015	5015		7015	8015		12015	13015	14015
Mosaic Cropland (50-70%) / Vegetation (20-50%)	1020	2020	3020	4020	5020		7020	8020-8023		12020-12023	13020	14020
Mosaic Vegetation (50-70%) / Cropland (20-50%)	1030	2030	3030	4030-4033	5030		7030	8030-8033		12030	13030	14030
Broadleaved evergreen or semi-deciduous forest	1040	2040	3040	4040-4043	5040		7040-7043	8043		12040-12043		
Broadleaved deciduous forest	1061	2061	3061	4061	5061	6061	7061	8061	11061	12061	13061	
Needleleaved evergreen forest	1091	2091	3091	4091	5091	6091	7091	8091	11091	12091	13091	
Needleleaved deciduous forest				4092	5092	6092		8092	11092			
Broadleaved/Needleleaved evergreen mixed forest				4100	5100	6100	7100	8100	11100	12100		
Broadleaved/Needleleaved deciduous mixed forest				4102		6102			11102			
Mosaic Forest (B/NE)-Shrubland (50-70%) / Grassland (20-50%)	1110	2110	3110	4110	5110	6110	7110-7113	8110-8113	11110	12110-12113	13110-13113	
Mosaic Forest (B/ND)-Shrubland (50-70%) / Grassland (20-50%)				4112	5112	6112		8112	11112			
Mosaic Grassland (50-70%) / Forest (B/NE)-Shrubland (20-50%)	1120	2120	3120	4120-4123	5120	6120	7120-7123	8120-8123	11120	12123	13120-13123	
Mosaic Grassland (50-70%) / Forest (B/ND)-Shrubland (20-50%)				4122	5122	6122		8122	11122			
Shrubland	1130	2130	3130	4130-4133	5130	6130	7130-7133	8130-8133	11130	12130-12133	13130-13133	
Grassland	1140	2140	3140	4140	5140	6140	7140	8140	11140	12140	13140	
Sparse vegetation				4150	5150	6150	7150	8150	11150	12150	13150	
Broadleaved forest regularly flooded (fresh-brackish water)	1160						7160					
Broadleaved forest-shrubland permanently flooded (saline water)												14170
Grassland/shrubland regularly flooded	1180			4180		6180	7180	8180	11180			

Figure 1. Global fuel map. The table legend lists the 166 fuelbeds developed. B: Broadleaf, NE: Needleleaf Evergreen, ND: Needleleaf Deciduous.

Each fuelbed has several structural, physical and chemical parameters, necessary to run FCCS. These parameters were extracted from global products based on remote sensing when possible, or from existing databases. The percentage of tree cover was extracted from the MODIS Vegetation Continuous Field, Collection 5, product (Carroll *et al.* 2011), and canopy height was derived from the map developed by Simard *et al*. (2011). For each fuelbed, the mean value of these variables was used. Representative tree, shrub and grass species were assigned based on the description of the ecoregions of the World Wildlife Fund Ecoregions' database (http://worldwildlife.org/science/wildfinder/, accessed June 2014). The remaining variables for each fuelbed (canopy height to live crown (HLC), tree density, diameter at breast height (DBH), the presence or absence of ladder fuels, shrub height, grass height and load, dead woody fuels cover and depth, fuel loads by size class of dead woody fuels, and litter and duff cover and depth) were assigned selecting the most similar fuelbeds from the ones in the FCCS database or from the Natural Fuels Photo Series from Mexico and Brazil (Ottmar *et al.* 2001; Morfín-Ríos *et al.* 2008).

Slope

Percentage slope was calculated using the GTOPO30 product, which is a global digital elevation model with a horizontal grid spacing of 30 arc seconds (approximately 1 kilometre at the Equator), developed by the United States Geological Survey (USGS) - EROS Data Center (https://lta.cr.usgs.gov/GTOPO30, accessed June 2014).

Three slope classes were established with the following criteria (see Figure 2):

- Slope class 1: 0% slope (for slope ranges between 0 - 5%)
- Slope class 2: 30% slope (for slope ranges between 5 - 45%)
- Slope class 3: 70% slope (for slopes higher than 45%)

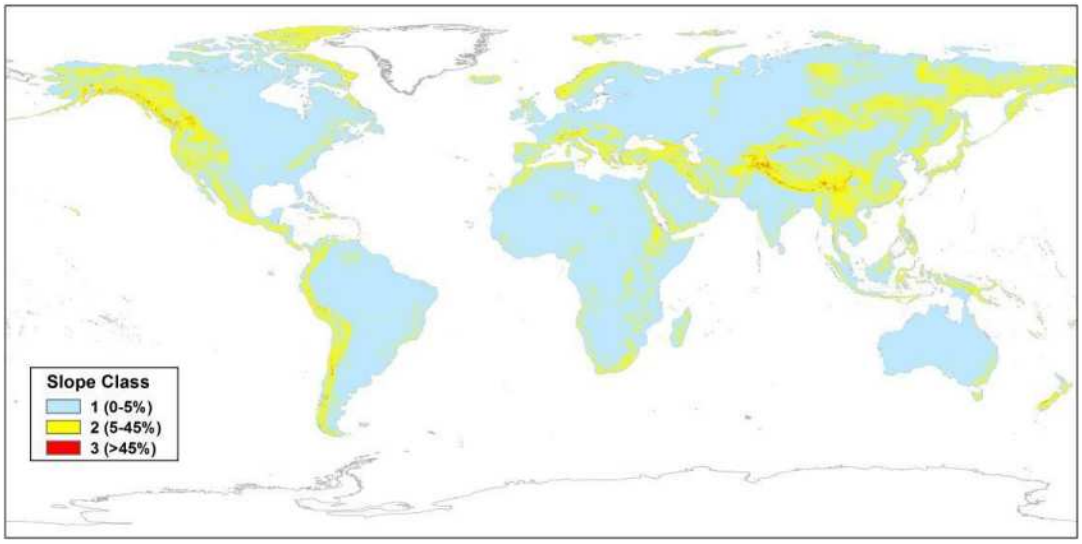

Figure 2. Slope classes derived from GTOPO30.

Wind Speed

The wind speed data was downloaded from the ECMWF Data Server directly as a monthly mean wind speed for each time step. The mean value of wind speed for each month within the 30-year period was calculated, and also the maximum monthly wind speed was identified.

The wind data correspond to 10 m winds, but the FCCS input requires the midflame wind speed, which is the average wind velocity that affects surface fire spread, and is usually referred as to the velocity of the wind taken at the mid-height of the flames. To convert from 10 m to midflame wind speed, a wind adjustment factor (WAF) is used. This WAF is dependent on the sheltering from overstory vegetation above the fire, and take values from 0.6 (for unsheltered fuels) to 0.1 (for sheltered fuels), based on 6.01 m (20-ft) wind speeds (Andrews 2012). For this study, a general intermediate WAF of 0.4 for 20-ft winds was used, which corresponds to 0.348 for 10-m winds (Turner and Lawson 1978).

As with the slope, three wind speed classes were established, to account for the contribution of wind speeds to fire spread:

- Class 1: 0 – 1.0 m/seg (0 – 2.24 mph). Assigned to 1.0 mph in FCCS.
- Class 2: 1.0 – 2.5 m/seg (2.24 – 5.59 mph). Assigned to 4 mph in FCCS.
- Class 3: 2.5 – 5 m/seg (5.59 – 11.18 mph). Assigned to 7 mph in FCCS.

2.4. Fuel Moisture Content

Four FMSs were selected to represent different moisture conditions, based on their 10-hr fuel moisture content. They combine Scott and Burgan's Dead Fuel Moisture Scenario (DFMS) and Live Fuel Moisture Scenario (LFMS). Their FMCs are described in Table 2.

Table 2. FMCs of different fuel classed assigned to each FMS. Extracted from the FMS table inside FFT

FMS Code	FMS description	Herb	Shrub	Crown	1-hr	10-hr	100-hr
D1L1	Very low dead, fully cured herb	30	60	60	3	4	5
D2L2	Low dead, 2/3 cured herb	60	90	60	6	7	8
D3L3	Moderate dead, 1/3 cured herb	90	120	120	9	10	11
D4L4	High dead, fully green herb	120	150	150	12	13	14

The 10-hr FMC was calculated using the equations formulated for the National Fire-Danger Rating System (Cohen and Deeming 1985). Relative humidity was calculated from temperature and dew point using the formulas described in Wanielista *et al*. (1997), because there were not data for relative humidity in ERA-Interim for the 8 time steps. Cloud cover data was converted to the State of Weather code (SoW), which was in turn used to adjust the temperature and humidity values. The 10-hr FMC was calculated daily for each month and for the 30-year period. Wet fuel conditions were assigned for a day when the snow depth was higher than 0 m of water equivalent, or if the total precipitation in the previous 24 hr was higher than 0.01 m. In that case, the 10-hr FMC was assigned to 35%.

From the daily 10-hr FMC, monthly mean values were computed, and from those, the monthly mean value for the 30-year period was obtained, and also the minimum monthly mean value was identified. 10-hr FMC was converted to FMS according to the following classification:

- D1L1: 10-hr FMC < 5.5%.
- D2L2: 5.5% < 10-hr FMC < 8.5%.
- D3L3: 8.5% < 10-hr FMC < 11.5%.
- D4L4: 10-hr FMC > 11.5%.

Results and discussion

Figure 3 shows the wind speed classes for January and July, for both the mean monthly conditions and the worst monthly conditions, corresponding to the maximum monthly wind speeds in the 30-year period. The highest mean monthly wind speed values during July are found in the Horn of Africa, where the maximum value is 4.6 m/seg for the mean monthly values, and 5.6 m/seg for the worst year. During January, the highest mean monthly wind values are found in the coast of southern Argentina and Chile, the Great Lakes, the coasts of the United Kingdom, a region in northern Siberia and the Borkou region in Chad. The maximum mean monthly value is 4.15 m/seg, and during the worst monthly conditions the maximum value is 5.18 m/seg.

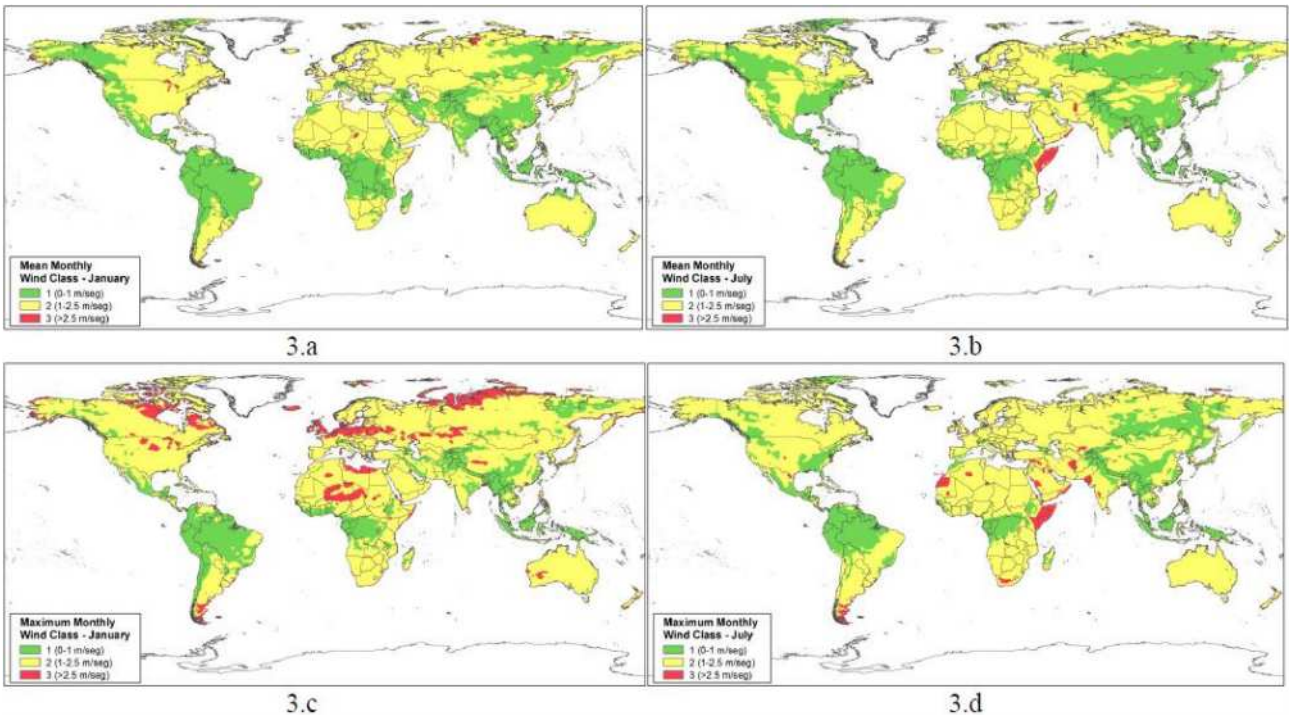

Figure 3. Wind classes calculated for the 1981-2010 period. 3.a: Mean January wind class; 3.b: Mean July wind class; 3.c: Maximum January wind class; 3.d: Maximum July wind class.

Wind speed varies greatly, even at very short time scales (seconds to minutes), and is also influenced by topography, vegetative sheltering, local heating or cooling, and surface friction (Rothermel 1983). The use of different wind classes does not intend to predict wind conditions for a particular moment or point in space, but to identify general regions and time periods where and when faster winds could occur compared with other parts of the world or seasons, and hence more severe surface fire behaviour could be expected.

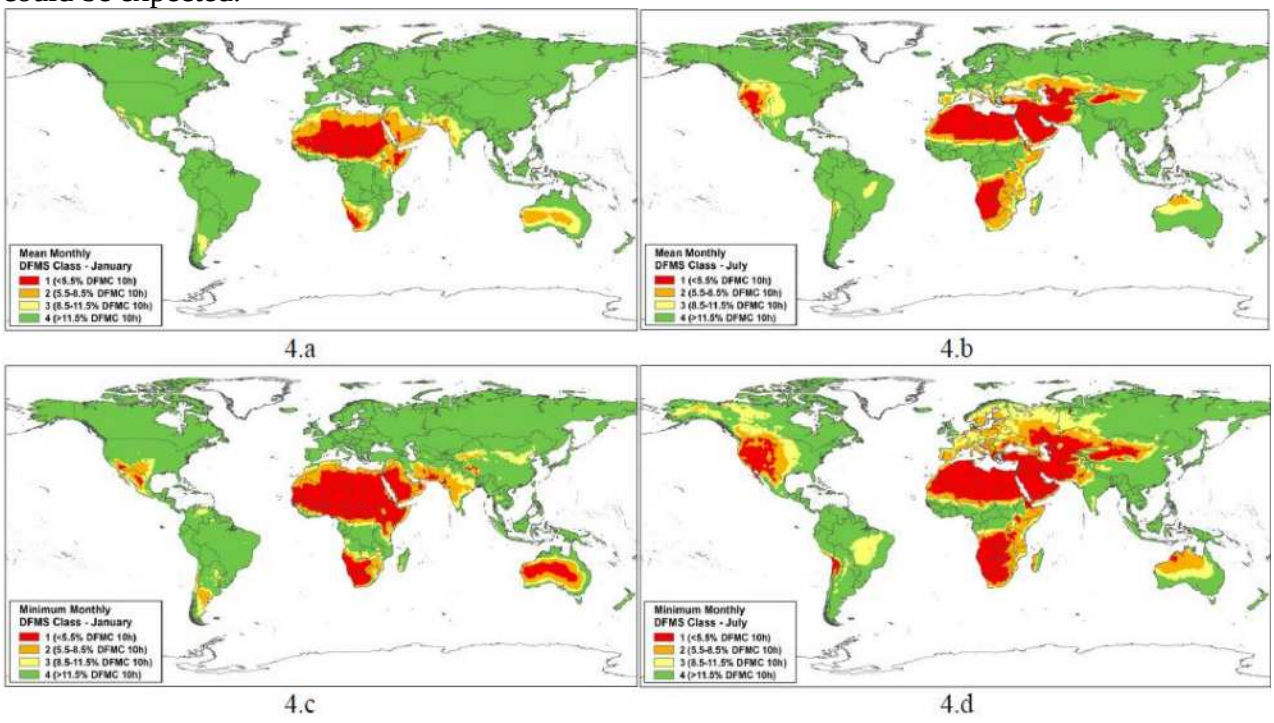

Figure 4. Dead Fuel Moisture Scenario calculated for the 1981-2010 period. 4.a: Mean January DFMS; 4.b: Mean July DFMS; 4.c: Minimum January DFMS; 4.d: Minimum July DFMS.

The result of the calculation of the 10-hr FMC, which determined the assignation of a Dead Fuel Moisture Scenario (DFMS), is shown in Figure 4. This figure includes the DFMS for January and July, for both the mean monthly conditions and the worst monthly conditions, corresponding to the minimum monthly FMC found in the 30-year period. During January, the highest latitudes of the northern hemisphere are covered in snow, and hence are considered to have wet fuels, and a FMS of D4L4. On the other hand, January means summer for the southern hemisphere, and higher temperatures determine lower FMCs in regions such as Australia and Patagonia. During July, the tropical rain belt is located in the northern hemisphere, and the tropics below the Equator have a dry season, which causes the fuel moisture content to be lower compared to January. This process is particularly noticeable in the southern African savannahs and in the Brazilian cerrados. On the contrary, during January the savannahs above the Equator are drier than during July, due to the shift of the tropical rain belt to the southern hemisphere.

The use of longitude strips derived in brusque changes in weather conditions along the borders of the strips, where at the west of the border the weather data corresponds to 15 hr. LST, while at the east it corresponds to 12 hr. LST. Although in most of the borders that situation did not produce differences in the wind or DFMS classes, it did in some cases, most prominently at longitude 0º in Northern Africa. But since that region is mostly desert, and has few vegetation, it did not cause an important effect in the resulting fire behaviour results.

The combination of the 4 possible FMSs, the 3 wind classes, and the 3 slope classes, produced a total of 36 different environmental conditions, which were used to run FCCS with the exiting fuelbeds. The environmental scenarios are classified as D(a)L(a)W(b)S(c), being a the FMS, b the wind class, and c the slope class. As an example, an environmental scenario of D2L2W1S3 would mean a FMS of 2, a wind class of 1 and a slope class of 3.

For the purpose of showing the differences in fire behaviour due to changing environmental conditions, Figure 5 show the rate of spread values obtained for January and July, during the mean and worst monthly conditions.

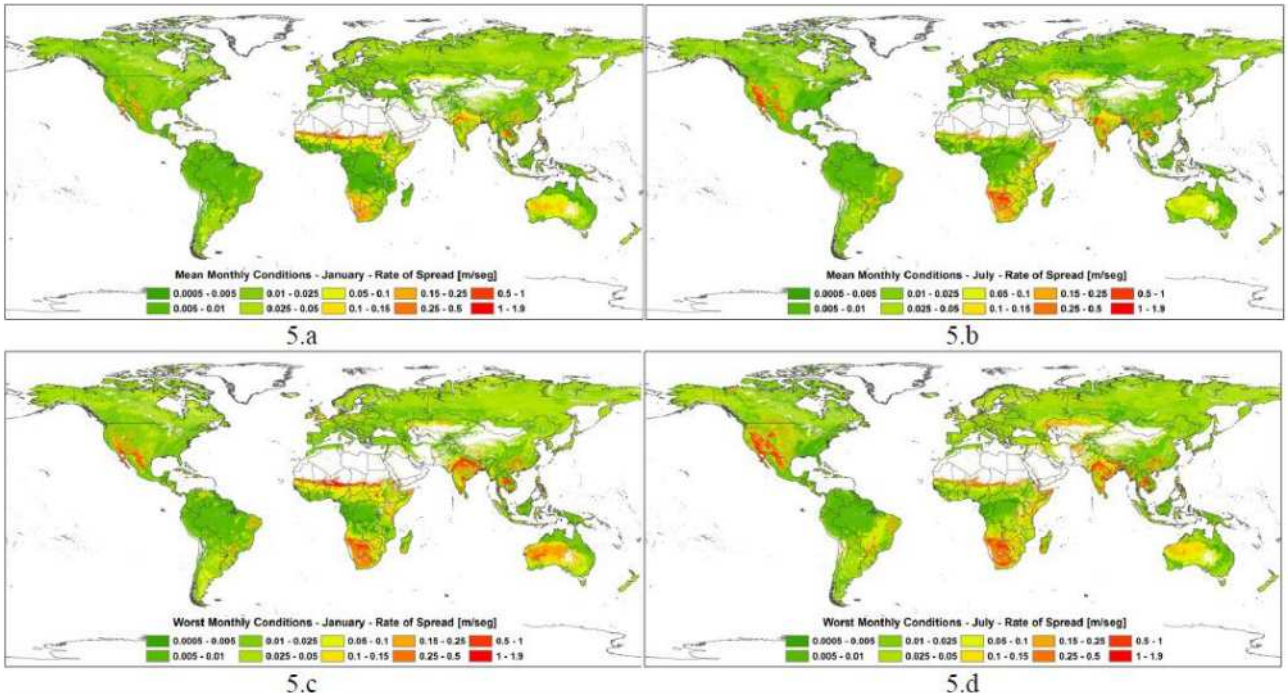

Figure 5. Rate of spread calculated for the global fuelbeds using the environmental conditions detailed in the legend of the maps.

The highest ROS values in Figure 5 (higher than 1 m/seg) belong to fuelbeds associated with grasslands (fuelbed numbers finishing in 140 or 180) and croplands (fuelbeds finishing in 015). The highest ROS correspond to rice croplands in tropical regions (fuelbeds 1015, 2015 and 14015), and vary in their value depending on the environmental conditions. The highest mean value for January is 1.63 m/seg, obtained for an environmental scenario D4L4W3S3. For the mean conditions in July, as well as the worst conditions in January, the highest value is 1.83 m/seg, for an environmental scenario D1L1W2S3. In the worst July conditions, the highest ROS value is 1.88 m/seg, but with an environmental scenario D2L2W3S2. These results indicate the prominent influence of wind on the rate of spread, as specified by the Rothermel's (1972) equations used in FCCS and in other fire behaviour systems such as BehavePlus (Andrews *et al.* 2008) or FARSITE (Finney 2004).
The results of the rate of spread show the variation with the different environmental conditions in different seasons, as exemplified for January and July. This is particularly evident in the North American and Australian deserts, as well as in the African savannahs. The comparisons between the mean and worst monthly conditions also reflect the inter-year variability of the weather conditions, and should be taken into account when evaluating possible fire behaviour results. The existence of extreme weather seasons can significantly increase the surface fire behaviour, as shown in Figs 5.b and 5.d regarding the Brazilian Cerrado, or Figs. 5.a and 5.c in Africa.

Conclusion

This study developed environmental scenarios, based on global weather information and topography, in order to calculate the surface rate of spread using the Fuel Characteristic Classification System and a global fuel map previously developed. The results shown correspond to the months of January and July, in order to illustrate the temporal variability of the environmental conditions in different geographic regions. These results allowed obtaining more realistic results than in the past, where only one set of environmental conditions had been used for the whole globe.
Still, these are preliminary results, and further refinement is needed. Future research will focus on improving the weather data to eliminate brusque changes in weather conditions along some longitudes, incorporating live fuel moisture scenarios to increase the environmental variability, and calculating other fire behaviour parameters.

Acknowledgements

The authors thank Susan Prichard, Anne Andreu and Paige Eagle for their help and support in the use of FCCS, and Roger Ottmar for his suggestions in the definition of the environmental thresholds.

References

Andrews, PL (2012) Modeling wind adjustment factor and midflame wind speed for Rothermel's surface fire spread model. USDA Forest Service, Rocky Mountain Research Station. Gen. Tech. Rep. RMRS-GTR-266, Fort Collins, CO.

Andrews, PL, Bevins, CD, Seli, RC (2008) BehabePlus fire modeling system Version 4.0. User Guide. USDA Forest Service General Technical Report. RMRS-GTR-106WWW.

Bicheron, P, Defourny, P, Brockmann, C, Schouten, L, Vancutsem, C, Huc, M, Bontemps, S, Leroy, M, Achard, F, Herold, M, Ranera, F, Arino, O (2008) GLOBCOVER: Products description and validation report. MEDIAS-France/POSTEL. Available at http://ionia1.esrin.esa.int/ [Accessed July 2012].

Carroll, M, Townshend, J, Hansen, M, DiMiceli, C, Sohlberg, R, Wurster, K (2011) MODIS Vegetative Cover Conversion and Vegetation Continuous Field. In 'Land Remote Sensing and

Global Environmental Change.' (Eds B Ramachandran, CO Justice, MJ Abrams) pp. 725-745. (Springer New York)

Cohen, JD, Deeming, JE (1985) The National Fire-Danger Rating System: basic equations. USDA Forest Service, Pacific Southwest Forest and Range Experiment Station. General Technical Report PSW-82, Berkeley, CA.

Dee, DP, Uppala, SM, Simmons, AJ, Berrisford, P, Poli, P, Kobayashi, S, Andrae, U, Balmaseda, MA, Balsamo, G, Bauer, P, Bechtold, P, Beljaars, ACM, van de Berg, L, Bidlot, J, Bormann, N, Delsol, C, Dragani, R, Fuentes, M, Geer, AJ, Haimberger, L, Healy, SB, Hersbach, H, Hólm, EV, Isaksen, L, Kallberg, P, Köhler, M, Matricardi, M, McNally, AP, Monge-Sanz, BM, Morcrette, J-J, Park, B-K, Peubey, C, de Rosnay, P, Tavolato, C, Thépaut, J-N, Vitart, F (2011) The ERA-Interim reanalysis: configuration and performance of the data assimilation system. Quarterly Journal of the Royal Meteorological Society 137, 553-597.

Di Gregorio, A (2005) 'Land Cover Classification System. Classification concepts and user manual, Software version 2.' (FAO: Rome)

Finney, MA (2004) FARSITE: Fire Area Simulator - Model development and evaluation. USDA Forest Service, Rocky Mountain Research Station.

Morfín-Ríos, JE, Alvarado-Celestino, E, Jardel-Peláez, EJ, Vihnanek, RE, Wright, DK, Michel-Fuentes, JM, Wright, CS, Ottmar, RD, Sandberg, DV, Nájera-Díaz, A (2008) Photo series for quantifying forest fuels in Mexico: montane subtropical forests of the Sierra Madre del Sur and temperate forests and montane shrubland of the northern Sierra Madre Oriental. Pacific Wildland Fire Sciences Laboratory Special Pub. Nº 1; University of Washington, College of Forest Resources. Seattle. Available at http://www.fs.fed.us/pnw/fera/publications/fulltext/PhotoSeriesMexicoUW-FERAPublication.pdf.

Olson, DM, Dinerstein, E, Wikramanayake, ED, Burgess, ND, Powell, GVN, Underwood, EC, D'Amico, JA, Itoua, I, Strand, HE, Morrison, JC, Loucks, CJ, Allnutt, TF, Ricketts, TH, Kura, Y, Lamoreux, JF, Wettengel, WW, Hedao, P, Kassem, KR (2001) Terrestrial Ecoregions of the World: A New Map of Life on Earth. BioScience 51, 933-938.

Ottmar, RD, Sandberg, DV, Riccardi, CL, Prichard, SJ (2007) An overview of the Fuel Characteristic Classification System-Quantifying, classifying, and creating fuelbeds for resource planning. Canadian Journal of Forest Research 37, 2383-2393.

Ottmar, RD, Vihnanek, RE, Miranda, HS, Sato, MN, Andrade, SMA (2001) Stereo Photo series for quantifying cerrado fuels in Central Brazil - Volume I. Pacific Norhtwest Research Station, USDA Forest Service. General Technical Report PNW-GTR-519, Seattle.

Pettinari, ML, Chuvieco, E, Ottmar, RD Uo Leicester (Ed.) (2013a) 'Development of a global fuel map using FCCS: mapping fuel characteristics to obtain fire potentials, 9th EARSeL Forest Fire Special Interest Group Workshop.' University of Leicester, UK. Available at http://earsel-ffsig.web.auth.gr/images/PDF/9th_EARSeL_Forest_Fire_SIG_Workshop_Proceedings.pdf

Pettinari, ML, Ottmar, RD, Prichard, SJ, Andreu, AG, Chuvieco, E (2013b) Development and mapping fo fuel characteristics and associated fire potentials for South America. International Journal of Wildland Fire 12.

Riccardi, CL, Ottmar, RD, Sandberg, DV, Andreu, A, Elman, E, Kopper, K, Long, J (2007) The fuelbed: a key element of the Fuel Characteristic Classification System. Canadian Journal of Forest Research 37, 2394-2412.

Rothermel, RC (1972) A mathematical model for predicting fire spread in wildland fuels. USDA Forest Service, Intermountain Forest and Range Experiment Station. Research Paper INT-115, Odgen, Utah.

Rothermel, RC (1983) How to predict the spread and intensity of forest and range fires. US Department of Agriculture - Forest Service. INT-143.

Sandberg, DV, Riccardi, CL, Schaaf, MD (2007a) Fire potential rating for wildland fuelbeds using the Fuel Characteristic Classification System. Canadian Journal of Forest Research 37, 2456-2463.

Sandberg, DV, Riccardi, CL, Schaaf, MD (2007b) Reformulation of Rothermel's wildland fire behaviour model for heterogeneous fuelbeds. Canadian Journal of Forest Research 37, 2438-2455.

Scott, JH, Burgan, RE (2005) Standard fire behavior fuel models: a comprehensive set for use with Rothermel's Surface Fire Spread Model. USDA Forest Service. RMRS-GTR-153, Fort Collins, CO. Available at http://www.fire.org/downloads/behaveplus/3.0.0/rmrs_gtr153.pdf.

Simard, M, Pinto, N, Fisher, JB, Baccini, A (2011) Mapping forest canopy height globally with spaceborne lidar. Journal of Geophysical Research 116, 12.

Stocks, BJ, Lawson, BD, Alexander, ME, Van Wagner, CE, McAlpine, RS, Lynham, TJ, Dubé, DE (1989) Canadian Forest Fire Danger Rating System: an overview. Forestry Chronicle 65, 258-265.

Turner, JA, Lawson, BD (1978) Weather in the Canadian Forest Fire Danger Rating System: a user's guide to national standards and practices. Canadian Forest Service, Pacific Forest Research Centre. Victoria, British Columbia. Available at http://cfs.nrcan.gc.ca/pubwarehouse/pdfs/1843.pdf.

Wanielista, M, Kersten, R, Eaglin, R (Ed. Wiley (1997) 'Hydrology: Water Quantity and Quality Control, 2nd Edition.' (Wiley)

Haines Index and the forest fires in the Adriatic region of Croatia

Tomislav Kozaric[a], Marija Mokoric[b]

[a] *Meteorological and Hydrological Service, Croatia, Zagreb, Gric 3, tomislav.kozaric@cirus.dhz.hr*
[b] *Meteorological and Hydrological Service, Croatia, Zagreb, Gric 3, marija.mokoric@cirus.dhz.hr*

Abstract
It is known that the weather conditions can greatly affect the frequency of forest fires and their behaviour and thus the size of the burned area. Besides the wind, the instability of the atmosphere also affects the fire behaviour and that kind of fires are called "plume dominated". In the dry and unstable atmospheric environment fires are intensified and may behave abnormally. As a quantitative measure of the instability in the dry atmosphere and potential for large fire growth Haines Index is used. Higher value of Haines Index (or the class) means higher potential for fire growth. In this work performance of Haines Index was tested for the Adriatic area, part of Croatia with Mediterranean climate where forest fires are the most common and severe. The distribution of the low-elevation Haines Index calculated from upper air soundings was analyzed as well as relationship between Haines Index and forest fire number and burned area. Analysis was done particularly for Zadar region in summer fire seasons of 2011, 2012 and 2013. In all seasons the smallest percentage of high class of Haines Index was noticed, proportion which was desirable and expected. Surprise was a large proportion of moderate class, which stands out in comparison to the other classes. This result disagreed to the Haines Index statistics found in the literature. However, results showed an obvious connection between Haines Index and forest fires in Adriatic region, particularly Zadar area. In the majority of days of fire seasons the increase of class of Haines Index was related to the increase of number of fires and larger burned area. On average the largest number of fires and largest burned area were associated with the high class. The impact of high class of Haines Index to fire behaviour was pointed out the most when the three-day moving sums/averages were applied. Conclusion is that Haines Index can be used also in the Adriatic region of Croatia as an additional tool for issuing warnings on severe fire weather related to instability. However, there is some place for improvements and further research.

Keywords*: Adriatic, atmospheric instability, forest fire, Haines Index*

Introduction

It is known that the weather conditions can greatly affect the frequency of forest fires, their behaviour and thus the size of the burned area.
The instability of the atmosphere, besides the wind, also strongly affects the fire behaviour by generating covective plumes (columns). Forest fires are then denoted "plume dominated". In dry and very unstable atmosphere this kind of fires are intense due to development of stong indrafts with more oxygen entraining from the surrounding environment. Also they may behave abnormally showing high rates of spread, extensive spotting, crowning etc. As a quantitative measure of the instability of the dry atmosphere Haines Index is used.
In this work the performance of Haines Index was tested for the Adriatic area, part of Croatia with Mediterranean climate where forest fires are the most common and severe. Haines Index in Croatia has been used operationally since 2011.
The distribution of the Haines Index calculated from upper air soundings data at Zadar station was analyzed as well as its relationship with the forest fires in the surrounding area during the summer fire seasons.

Methods

The summer forest fire season in Croatia typically lasts from the beginning of June to the end of September. Fire seasons in 2011, 2012 and 2013 were considered and during this period all available forest fire data in the Zadar area were collected and analyzed. Also Haines Index data from the Zadar upper air soundings were calculated for the same period.

Haines Index

Haines Index is a simple index that is based on the vertical lapse rate in some layer of air as well as on moisture content in that layer as described by Haines (1988).
Haines Index is calculated from empirical relation:

$$\mathbf{HI=A(}T_p\mathbf{-}T_{p1}\mathbf{)+B(}T_p\mathbf{-}Td_p\mathbf{)},$$

where A is a function of temperature difference (lapse rate) between the levels of the atmospheric pressure *p* and *p1* and B is a function of a dewpoint depression at the level of pressure *p*. Haines Index is, therefore, the simple sum of stability term (A) and moisture term (B).
Because of the difference in altitudes of certain areas, three elevation variants of Haines Index are calculated: low variant (elevations below 500 m.a.s.l.), middle variant (elevations from 500 to 1500 m.a.s.l.) and high variant (elevations above 1500 m.a.s.l.). The layers *p* and *p1* are chosen considering ground elevation and also high enough above the ground to ignore the daily variability of surface temperature and surface temperature inversions. Depending on the upper level atmospheric conditions terms A and B may get values 1, 2, or 3 for each of the variants (Table 1), so Haines Index values between 2 and 6. Lower values are in thermally stable and more humid air and higher values in thermally unstable and drier air.

Table 1. Three elevation variants of Haines Index depending on the terrain elevation and upper level atmospheric conditions, i.e. lapse rate and dewpoint depression.

Lapse rate T_p-T_{p1}			
A	Low 950 - 850 hPa	Middle 850 - 700 hPa	High 700 - 500 hPa
1 2 3	<4 4 to 8 >=8	<6 6 to 11 >=11	<18 17 to 22 >=22
Dewpoint depression T_p-Td_p			
B	Low 850 hPa	Middle 850 hPa	High 700 hPa
1 2 3	<6 6 to 10 >=10	<6 6 to 13 >=13	<15 15 to 21 >=21

The relationship between Haines Index and potential for large forest fires growth or unpredictable behaviour is shown in Table 2.

Table 2. Classes of Haines Index. Values 2 and 3 of Haines Index are combined together in one class (very low).

Haines Index	Class (potential for large fire growth)
2 or 3	very low
4	low
5	moderate
6	high

Generally, Haines Index is designed in the way that low classes are expected most often and accompanied by low potential for large fire growth, while high class is expected rarely but accompanied by high potential for large fire growth. Some additional research on Haines Index can be found in Werth and Ochoa (1993).

In a preliminary analysis conducted in this work the low-elevation variant Haines Index was used because Zadar area has elevation mostly lower than 500 m.a.s.l. (higher mountains occupy smaller part in the north of the region). At this stage possibility of using a middle-elevation variant Haines Index for Zadar area was left for further examination.

Distribution of Haines Index, i.e. percentage of days of the fire season with different Haines Index values, and missing data were calculated for a whole range of soundings and separately for those at 00 and 12 UTC. Analysis is made for all three fire seasons and 122 days per season were taken into account. Also the analysis of stability and moisture terms was performed in the same way to investigate how the values of A and B were distributed and which of them contributed the most.

Forest fires and Haines Index

The available data on forest fires contained information about the location, date, starting time and duration of the fire and the size of burned area. Fire locations were chosen to be less than 100 km away from the station in Zadar. In that case upper air soundings were supposed to be valid for all chosen locations. The proximity condition was satisfied by the total of 930 forest fire cases in 244 days corresponding 21489 hectares of burned area (356 fires in 91days of the fire season 2011 wasted 6369 ha of vegetation, 402 fires in 88 days of fire season 2012 wasted 13206 ha and 172 fires in 65 days of fire season 2013 wasted 1914 ha). In the whole analyzed period there was no significant wind over the area of interest, so all forest fires cases were taken into consideration. It was considered also that a large number of this fires were "plume dominated", i.e. under the strong influence of the atmospheric instability. For fires lasting more than 2 days burned area was reduced by linear interpolation to the size which might burn in the first 36 hours. This time period was chosen arbitrarily but reasonably so that the reduced burned area could be associated with the Haines Index on the day of the occurrence of fire. Also different truncation times were tested but results showed no significant differences. However, it should be noted that there were just 16 long-lasting forest fires but the idea was not to exclude them.

The relationship between the number of fires in one day and the associated Haines Index at 00 and 12 UTC of the same day was analyzed using box plot statistical method, as well as relationship between total area burned in those fires and Haines Index. Days with missing Haines Index data were omitted. Identical procedure was done with moving sums of number and burned area of fires and the associated moving averages of Haines Index. The idea was not just to test the impact of atmospheric instability on forest fires in one day, but also to see how longer periods with unstable dry weather conditions impact forest fires. Different time (day) windows were used, but three-day forward oriented window seemed to be appropriate for moving sums and averages.

Results and conclusions

In all three forest fire seasons the smallest percentage of high class (value 6) of low-elevation Haines Index was noticed. Such a small proportion of high class was desirable and expected. Surprise was a large proportion of moderate class (value 5), which stands out in comparison to the other classes (Figure 1). This was the case for a whole data set and separately for sets at 00 and 12 UTC.

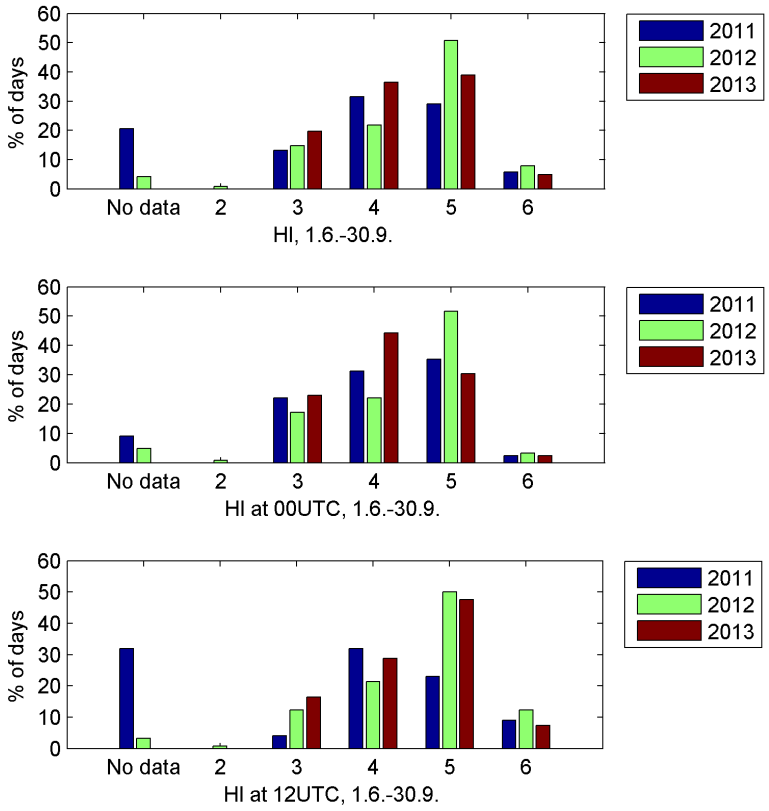

Figure 1. Distribution of Haines Index calculated from upper air soundings at Zadar station for three forest fire seasons. 12 UTC data set is shown in the lower plot, 00 UTC in the middle and a whole data set is in the upper plot. Missing data were also taken into account.

The resulting distribution of Haines Index did not match distributions found in the literature. The possible issue was strange distribution of the stability term A with too large proportion of value 3 (not shown). With a given distribution the performance of low-elevation variant Haines Index as a marker of severe fire weather conditions in the Zadar/Adriatic area may be reduced. But as already mentioned, the further plan is to test the middle-elevation variant in the calculation of Haines Index, in other words taking into account the effects of higher topography. Also a calibration of the original set up of Haines Index to the Mediterranean climate of the Adriatic can be carried out (particularly through tuning the thresholds of the stability term A) but this procedure requests for longer and more detailed data series of forest fires in the Adriatic region.

In any case there was an obvious relationship between Haines Index and forest fires in Adriatic region, particularly Zadar area. Haines Index at 12 UTC showed similar connection to the forest fires behaviour as Haines Index at 00 UTC but with a little bit better correlation, probably because daylight heating of land surface still had some small effect on instability in the upper levels.

In the majority of days of fire seasons the increase of the class of Haines Index was related to the increase of number of fires (Figure 2) and larger burned area (Figure 3).

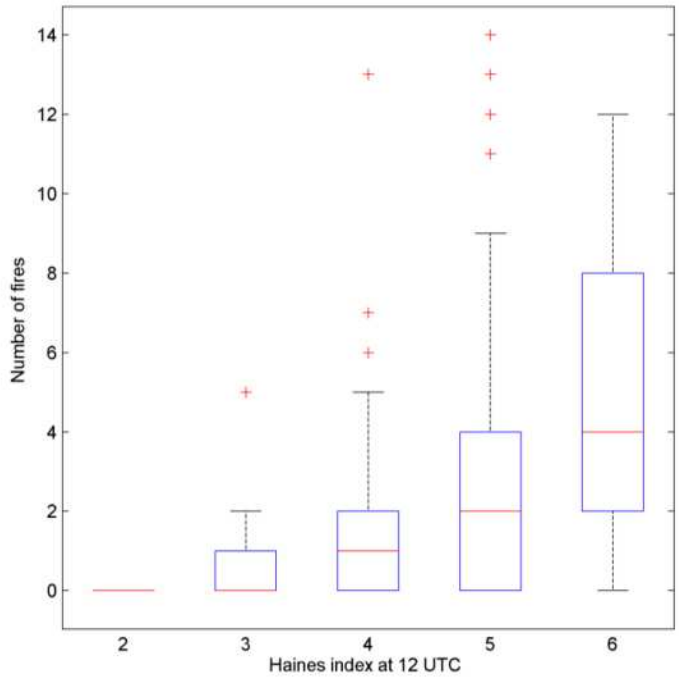

Figure 2. Box and whisker plot of the number of forest fires in one day against Haines Index class at 12 UTC same day. Red lines are medians, blue boxes represent interquartile range, black lines at the top of the whiskers are extremes and red pluses indicate outliers, i.e. cases not belonging to the set.

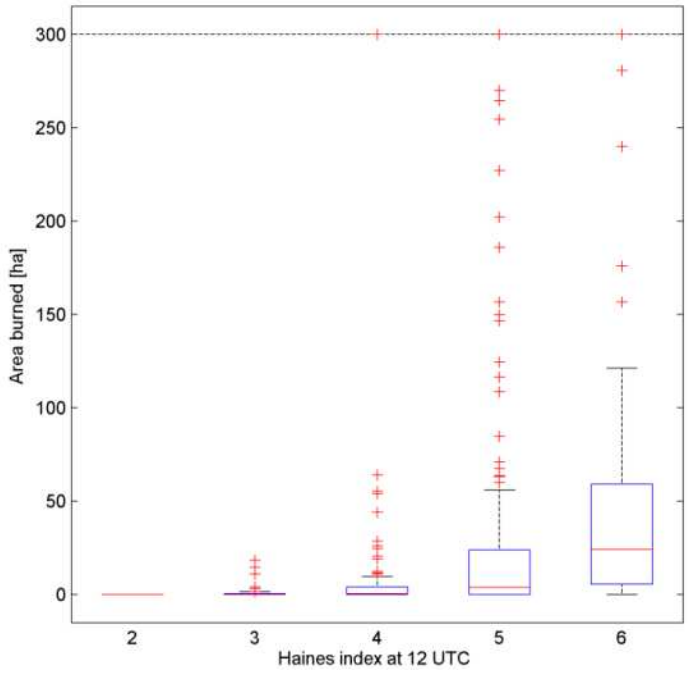

Figure 3. Same as Figure 2, but for an area burned in one day.

According to the results of box plot statistics the largest number of fires and the largest burned area were associated with the high class of Haines Index as seen in higher values of both median and upper quartile in comparison to moderate class and especially low classes. Despite the procedure of reducing size of long-lasting fires, there was still large number of outliers, especially for burned area. This could be explained by the fact the forest fires are not affected just by weather conditions but also by other factors, e.g. fuel availability, topographic characteristics, fire suppression efficiency and others.

The positive correlation of forest fires behaviour with the unstable dry air mass was even stronger when the three-day moving sums/averages were applied to the number of fires, burned area and associated Haines Index. Then the high class of Haines Index was pointed out the most as seen in Figures 4 and 5. Longer periods, in this case three consecutive days with unstable dry weather conditions had obviously strong impact on forest fire behaviour.

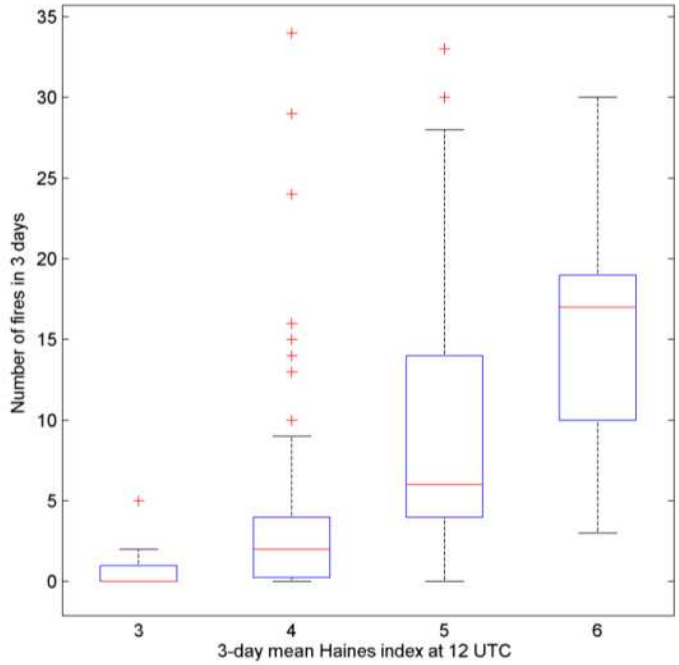

Figure 4. Box and whisker plot of a total number of forest fires in three days against three-day average of Haines Index classes at 12 UTC. Red lines are medians, blue boxes represent interquartile range, black lines at the top of the whiskers are extremes and red pluses indicate outliers, i.e. cases not belonging to the set.

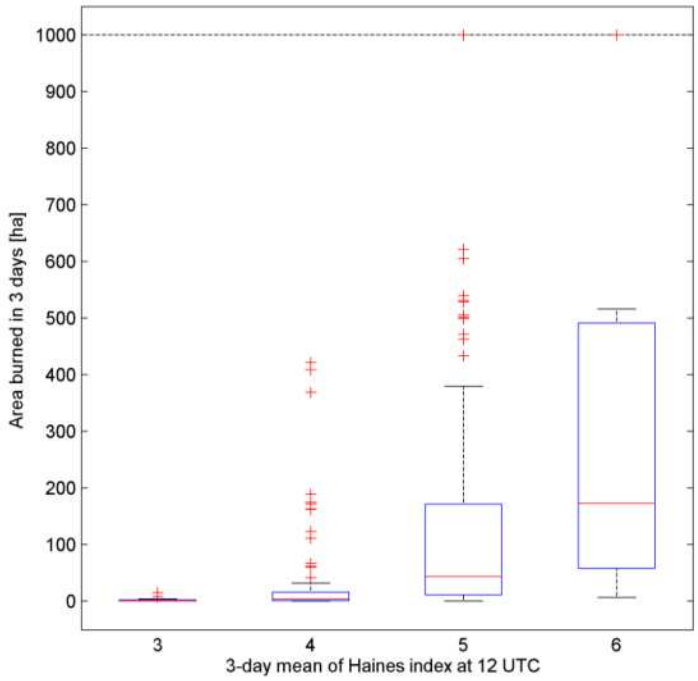

Figure 5. Same as Figure 4, but for a total area burned in three days.

Final conclusion is that the original set up of Haines Index can still be used in the Adriatic region of Croatia as an additional tool for issuing warnings on severe fire weather related to atmospheric instability. At least high class of Haines Index can be used what is currently the case in Croatia. However, as shown in this work, there is place for improvements and further research.

Acknowledgments

Authors thank to Robert Rozic from the National Protection and Rescue Directorate of Croatia (Fire Fighting Sector) on providing the data on forest fires, and to Lovro Kalin from Meteorological and Hydrological Service of Croatia on constructive comments.

References

Haines D.A., 1988: A lower atmosphere severity index for wildland fire, *Natl. Wea. Dig.*, **13**, 23-27.

Werth P. and R. Ochoa, 1993: The evaluation of Idaho Wildfire Growth Using the Haines Index, *Weather and Forecasting*, **8**, 223-234.

Impacts of climate change on forest fire risk in Paraná State-Brazil

Antonio Carlos Batista[a], Alexandre França Tetto[a], Flavio Deppe[b], Leocádio Grodzki[c]

[a] *Federal University of Paraná, Av. Pref. Lothário Messner 900, Curitiba - Brazil, batistaufpr@ufpr.br, tetto@ufpr.br*
[b] *SIMEPAR Institute, Centro Politécnico da UFPR - Curitiba – Brasil, deppe@simepar.br*
[c] *IAPAR, Rua Máximo João Kopp, 274 - Santa Candida, Curitiba - Brasil, grodzki@hotmail.com*

Abstract
Forest fires are a global phenomenon due to the interaction between climate, fuels and human activities. Fires are also a critical component in the dynamics of planet earth and atmosphere. Recent advances in remote sensing products gathered via sensors on board satellites, have demonstrated the possibility of fire identification and monitoring on a global scale. The weather and climate are the major factors directly affecting fire and are being modified due to climate change caused mainly by man. There is an expectation of most researchers that changes in climate over the next 100 years will cause a major impact on forest ecosystems. The aim of this study was to determine, by decade, forest fire risk zoning for the State of Paraná, Brazil, based upon the scenarios predicted by the Intergovernmental Panel on Climate Change (IPCC) in 2007. Vegetation maps, fuel moisture, Monte Alegre Formula (FMA) for forest fire risk, slope, population density and road network, were used. These information, after being classified according to the risk of fire hazard, were weighted in a mathematical model. The determined values were then used to compose the Forest Fires Zoning Risk (ZRIF) per decade for the State of Paraná. Results showed that for the best scenario, which considers an increase of 1.8 ºC in the average temperature of the Earth by year 2100, there will be an increase in class extreme risk of forest fires, rising from 1.80% of the area of the State in 2020 to 8.49% in 2100. The same applies to the class of very high risk, which rises from 10.43% (2020) to 32.38% (2100). For the worst scenario, which considers an increase of 4.0 ºC in the average temperature of the Earth by 2100, the class of extreme risk rises from 2.18% (2020) to 22.72% (2100). The higher risk class rises from 13.93% (2020) to 55.95% (2100). It was concluded that, if the IPCC predictions were confirmed, there will be an increase in the number of occurrences and area affected by forest fires in the State of Paraná, which will require integrated actions to prevent and suppress forest fires to minimize environmental, social and economic damages.

Keywords*: forest fire risk, climate change, forest fire zoning risk, FMA fire risk*

Introduction

The effects of fire on the forests affect not only vegetation but also soil, fauna and atmosphere characteristics, and can be highly destructive when it is a forest fire. A fire occurs in the simultaneous presence of oxygen, fuel and heat source (Marques *et al*., 2011). According to the terminology of wildfires proposed by the Food and Agriculture Organization (FAO), "fire hazard" is defined as the probability of starting a fire due to the presence and activity of active causal agents. Also, "fire hazard" is used to express the degree of involvement of fixed and variables factors that determine the ease of ignition, rate of spread, difficulty of control and impact of fires, usually expressed as an index (FAO, 2007).
The assessment of the risk of forest fires is a critical part in fire prevention, since for pre-suppression planning and fire-fighting tools are needed to monitor when and where a fire can occur or when its effects will be more negative (Chuvieco *et al*., 2010).
Several factors may explain the ignition and spread of forest fires, such as: the characteristics of fuels, weather conditions, sources of ignition and topography. Fuel characteristics depend on the structure

and composition of vegetation, allied to anthropogenic factors (Marques *et al*., 2011). Another important ignition factor is the influence of human activities, which increase the risk of fire in the vicinity of road networks and urban areas (Cardille *et al*., 2001).

The risk of fires has been assessed by means of fixed and variable environment factors (e.g. fuels, weather and topography), that determine the ease of ignition, rate of spread, the difficulty of control, and the impact of forest fires (Vadrevu *et al*., 2010).

The importance of drawing up forest fire risk maps is evident for a long time (Show; Clarke, 1953). A very simple way to achieve a forest fire risk map is through the use of fire reports of previous years and plotting on a map the areas affected by fires. When there are multiple-year records, one can define a pattern for the areas of greatest occurrence and draw boundaries that define areas of risk (Brown; Davis, 1973; Chandler *et al*., 1983).

Several researchers have developed forest fires risk zones, using methods that allow to associate environmental factors with forest fires, allowing in this way to map the potential risk of fires according to the sensitivity of the factors related to fire. The main factors used in these studies, in order to establish different levels of forest fires risk, were: type of vegetation, characteristics of forest fuels, weather variables (temperature, air humidity, speed and direction of winds and precipitation), topography and ignition human activities (roads, demographics and usage type and occupation of land) (Salas; Chuvieco, 1994; Ferraz; Vettorazzi, 1998; Verde, 2008; Chuvieco *et al*., 2010; Marques *et al*., 2011; Oliveira *et al*., 2012).

Climate change can affect the number of fires that occur annually, the duration of the fire season and the area burned by fires. It also can increase the intensity of fire. Changes in these properties result in a direct influence of fire, increasing their frequency and intensity, and therefore, greater potential of fire (IPCC, 2007).

Several studies have demonstrated the impact of climate change on the behaviour of forest fires in various parts of the world, such as the research of Liu *et al*. (2012), on spatial patterns of fire occurrence and its future trend in Northeast China; Liu *et al*. (2010), on global trends of forest fire potential in the light of climate change, and the research conducted by Westerling and Bryant (2008), about climate change and California wildfires.

Flannigan *et al*. (2009a) reviewed the current understanding of what the future can bring with respect to forest fires. Research conducted in China by Tian *et al*. (2011), indicated a general increase in burned areas and in cases of fires, but with a considerable spatial variation, with some areas without alteration or even decrease in burned areas and the number of occurrences of fires.

Recent studies conducted by Flannigan *et al*. (2009b), suggest a doubling of burned areas, and an increase of 50% of the occurrences in several parts of the boreal forests by the end of this century. Fire seasons are expanding in the temperate and boreal regions and this trend should continue in the hottest regions of the world.

The Paraná is a State with a long tradition in the use and management of forest resources, mainly due to the exploration of extensive areas of forest with Araucaria covering almost the entire territory of Paraná in 20 mid-century (Maack, 2012). It is also the State in which occurred one of the biggest forest fires in the world, which in 1963 burned an area of 2 million hectares (20,000 hectares of plantations, 500,000 hectares of primary forests and 1,480,000 hectares of fields, secondary forests and brushlands) (Soares; Batista, 2007). And since that time the State of Parana has been a pioneer in research on control of forest fires in Brazil (Soares *et al*., 2009).

In view of the importance of forest fire risk zones and considering the hypothesis that the frequency and intensity of forest fires will increase in the light of global warming, the objective of this work was to evaluate the risk of forest fires for the State of Paraná, considering the scenarios predicted by the Intergovernmental Panel on climate change (IPCC) in 2007.

Methods

Study Area

The study area comprises the whole territory of the State of Paraná, located between the Parallels 22º 58' 30'' and 26º 43' 00'' South latitude and the Meridians 48º 05' 37''and 54º 37' 08'' West longitude. The territory comprises an area of 199,281 km^2, which corresponds to 2.34% of the total area of Brazil and 34.61% of the area of the southern region. In 2010, the State had 399 municipalities, 10,444,526 inhabitants and a population density of average 52.40 inhab/km^2, and much of this population live in urban area (85.30%). In the State of Paraná the altitudes range from sea level to 1,922 m at Peak of Paraná, located at Serra do Mar, highest elevation in the State and also in the southern region (IBGE, 2000, 2010).

Due to geographical location and topography, Paraná State has two dominant types of climate, having a third covering small land area between the coastline and the Valley of Ribeira (IAPAR, 1994). According to the Köppen classification (Trewartha; Horn, 1980), based on temperature and rainfall, Paraná State has the following climatic types: Cfa, Cfb and Af.

The less rainy months of June, July and August, shows that South and Southeast regions have rainfall between 350 and 450 mm, followed by Central and West regions, between 250 to 350 mm. The North region near the edge of the Paranapanema River, bordered by the State of São Paulo, rainfall is between 150 and 250 mm). The combination of low temperatures with occurrence of frosts and the decrease of precipitation make this quarter (June, July and August), most favourable to dry, making it susceptible to forest fires (Grodzki *et al*., 1996).

Collection and analysis of data

To obtain the necessary information to carry out the research, the following data set was used: historical series of temperature, relative humidity and precipitation of 28 weather stations operated by IAPAR from a period of 40 years (1970 to 2010); slope, aspect and elevation (INPE, 2008); demographic density (IBGE, 2010); map of State of Paraná with states and county boundary in 1:250,000 scale (IBGE, 2007); vegetation types map (Probio, 2005); road network map (DER, 2010). The method consisted in the elaboration of preliminary risk maps for each variable under study: vegetation type, moisture of forest fuel, fire danger index (FMA), slope, elevation, aspect, population density and road network. These maps were integrated by means of a weighted sum of the characteristics of fuels, weather and ignition sources, according to the equation:

RIF=0.33*((MC+UMC)/2)+0.33*((FMA+DE-Hipso+Orient)/4)+0.33*((DD+SV)/2)

Where:
RIF = risk of wildfire computed in each unit of analysis;
MC = forest fuel;
UMC = forest fuel moisture;
FMA = fire danger index;
DE = slope;
Hipso = elevation;
Orient = aspect;
DD = population density;
SV = road network.

The risk map depending upon vegetation type (forest fuel), was prepared based on a map of vegetation type of PROBIO (2005). This variable was considered static for the period under examination. The 55 vegetation types found in this survey were grouped into the following classes: agriculture, pasture/fields, forest cover, forest cultivation and no information.

The forest fuel moisture was estimated by the equation proposed by Simard (1968):

$$E = 21.06 – 0.4944*H + 0.005565*H^2 – 0.000638*H*T \ (H > 50)$$

Where:
E = forest fuel moisture, in percentage;
H = relative humidity, in percentage;
T = air temperature in °C.

Two scenarios were generated according to the IPCC report of 2007: (i) The best scenario, considering 1.8 °C increase in the average temperature of the Earth by 2100, (ii) The worst scenario, considering 4.0 °C increase in the average temperature of the Earth until 2100.
For the estimation of the necessary weather variables, stochastic simulations were carried out with the program PGECLIMA_R (Das Virgens Filho *et al*., 2011), for the period of 2010 to 2100.
The cumulative index of fire danger was calculated for the period of 2010 to 2100 and for both scenarios, using the fire risk index called Monte Alegre Formula (FMA). After generating the indexes, the values were classified into 5 classes through the method of Quantile and interpolated using Kriging method.
The variables slope, aspect and elevation were considered static variables for the analysis, and were generated using TOPODATA data set (INPE, 2008). Ratings were established on the basis of Soares and Batista (2007), Salas and Chuvieco (1994) and Fernandez and Vettorazzi (1998), respectively.
To generate the variable population density (dynamic variable), data were used from Brazilian Institute of Geography and Statistics (IBGE) related to 1991, 2000 and 2010 census for each municipality in the State of Paraná, as well as population estimates from 2000 to 2009. Initially it was necessary to estimate the population every decade for further calculation of the density. For this the method of Von Sperling (2005) was used. Population projections were generated using descending rate of growth. The observed values for the population density by municipality were distributed into five classes adapted from Guillhermo Julio (1992).
Considering that distance from the road system is inversely proportional to the risk of forest fire, buffers were established from the roads and railway network (DER, 2010). This was adapted from Salas and Chuvieco (1994) method. This variable was considered static for the analyzed period.
The final risk map was obtained applying GIS algebra operations between the preliminary risk maps (Salas; Chuvieco, 1994, Souza *et al*., 1996, Ferraz; Vettorazzi, 1998). After that, the risk map was classified into five classes of risk (low, moderate, high, very high, extreme), using the Quantile method. Finally, maps were generated for both, best and worst scenarios.

Results and discussion

The forest fire risk map depending on the vegetation cover featured a 4,263,177 ha (21.53% of the area of the State) in the extreme risk class, while the area for the very high class indicated 6,187,629 ha (31.25%). These areas where concentrated in the East and Northwest of the State.
In the eastern region are the most extensive forest fragments in the State, while the Northwest region is dominated by extensive grazing areas. These higher-risk areas reflect the largest vegetation flammability when compared with other types of vegetation found in the State of Paraná.
Considering the fuel moisture variable, in the best case scenario simulation, classes were not observed with very high and extreme risk in 2020. While in 2100 these classes have covered more than half of the State area (56.08%). The extreme class concentrated in the northern region with 11.97% of the State area. The worst case scenario simulation also failed to provide the most extreme classes (very high and extreme) in 2020, when compared to the best case scenario. However, in 2100 much of the State was ranked in the extreme risk of forest fire, reaching 91.33%. The moisture content is the most

important property that controls the flammability of living and dead fuels (Soares; Batista, 2007). Therefore, it has great influence on the risk of fire (ADAB *et al*., 2013). The moisture of forest fuels is the result of climate and atmospheric conditions. The results showed that as climate becomes drier over the years, according to the IPCC scenarios, there were more extensive areas with drier forest fuels and therefore, more dangerous and more flammable.

Regarding the simulation to the best case scenario of the FMA, it was observed a discrete spatial variation in the behaviour of the index, with little variation in terms of area in the State. In 2020 the high, very high and extreme classes resulted in 62.58% of the State area, keeping this extension in 2100. For the worst case scenario, it was noticed a significant spatial variation in the analysis period, with very high and extreme classes with more than half of the State at the end of the period. In this scenario the high and very high classes resulted in 56.82% in 2020, reaching 96.89% of the area in 2100.

For the slope variable, the State presented largely in low and moderate risk classes. The low risk class totalled 12,802,087 ha (64.41% of the area of the State) and the moderate class 3,845,465 ha (19.35%). The extreme risk concentrated in the Serra do Mar and Ribeira Valley and corresponded to 3.00% of the total area. According to Adab *et al*. (2013), the slope is one of the parameters that influence the rate of spread of fire. The fire runs faster uphill than downhill. In addition, the rate of spread of fire can increase on the steepest slopes, because the flames are tilted closest to the surface of the soil, and the process of heat convection may be increased by the wind.

The risk of fire in terms of elevation showed that much of the State was ranked in high risk and very high, totalling 98.23% of area (altitude less than 1,200 m above sea level). As Hernandez-Leal *et al*. (2006), the altitude is a physiographic variable that is associated with the temperature, moisture and wind. Therefore, it plays an important role in fire propagation. The altitude influences the structure of the vegetation, air moisture and fuel. It was observed that the humidity and temperature have greater influence over fire in areas with higher altitude. It has also been reported that the fire behaviour trends are less severe on higher places due to higher rainfall (Chuvieco; Congalton .1989).

The classes of fire risk due to the aspect of the slopes were low, with 36.59% of the area, followed by a very low, with 25.20% and high, with 12.93 %. The aspect of the slopes is correlated with the amount of solar energy that an area receives (Soares; Batista, 2007). The north-facing slopes receive more sunlight and high temperatures, high winds, low humidity and low fuel moisture in the southern hemisphere. Therefore, the vegetation is typically drier and less dense in the northern slopes (Vadrevu *et al*., 2010; Soares; Batista, 2007). Because of this, the driest fuels are more exposed to ignition (Adab *et al*., 2013).

The simulation of population density and its classification in terms of risk of forest fire showed a continuation of higher risk in the North, East and West of the State. The State had, in 2010, 76.41% of its area in the low risk class, which fell in the period under examination, passing to 69.70% of the area. The extreme risk class increased from 7.83 % to 12.72%, which represented an increase of 62.4%. Humans are the cause of the vast majority of fires and therefore, the population density is a factor which expresses the omnipresent effect of population on the ignition and spread of fire. In this sense, Marques *et al*., 2011, claim that the population density has been singled out as the main source of ignitions of fires in Portugal.

The road network has an area of influence of 831,534 ha (4.38% of the State area). This area is divided into 170,692 ha with low risk, 167,645 ha with moderate risk, 166,028 ha with high risk, 164,268 ha on the degree of risk too high and 162,900 ha in degree of extreme risk. The road network showed no influence on 95.62% of the area of the State. It is necessary to emphasize that human activities are one of the basic factors that affect fire occurrences (Xu Dong *et al*., 2005). Due to more intensive human activities, the fire risk is larger and offers plenty of opportunity for the unexpected fire ignition (Alencar *et al*., 2004). Proximity of roads and road density are potentially important parameters once the roads facilitate access of people in areas of forest and pasture and this can cause fires (Jaiswal *et al*., 2005).

In figures 1 and 2 are presented forest fires risk zones in the years 2020 and 2100, for the best scenario. In the first decade (2020) the risk was concentrated in the moderate and high classes, with 33.04% and 54.64%, respectively. Areas located in the North region of the State and in the surrounding areas of the metropolitan region of Curitiba, concentrated much of the extreme risk of forest fires, which totalled 1.80% of the total area. This value increased in the following decade, passing to 2.51%. The same behaviour is observed for the very high class, ranging from 10.43 % to 13.82 %.
This behaviour has remained throughout the period under examination. In 2100, the area corresponding to the low risk class was 0.01 %, while the moderate class corresponded to 7.66 %, the high class 51.47%, very high class to 32.38% and extreme class to 8.49%.

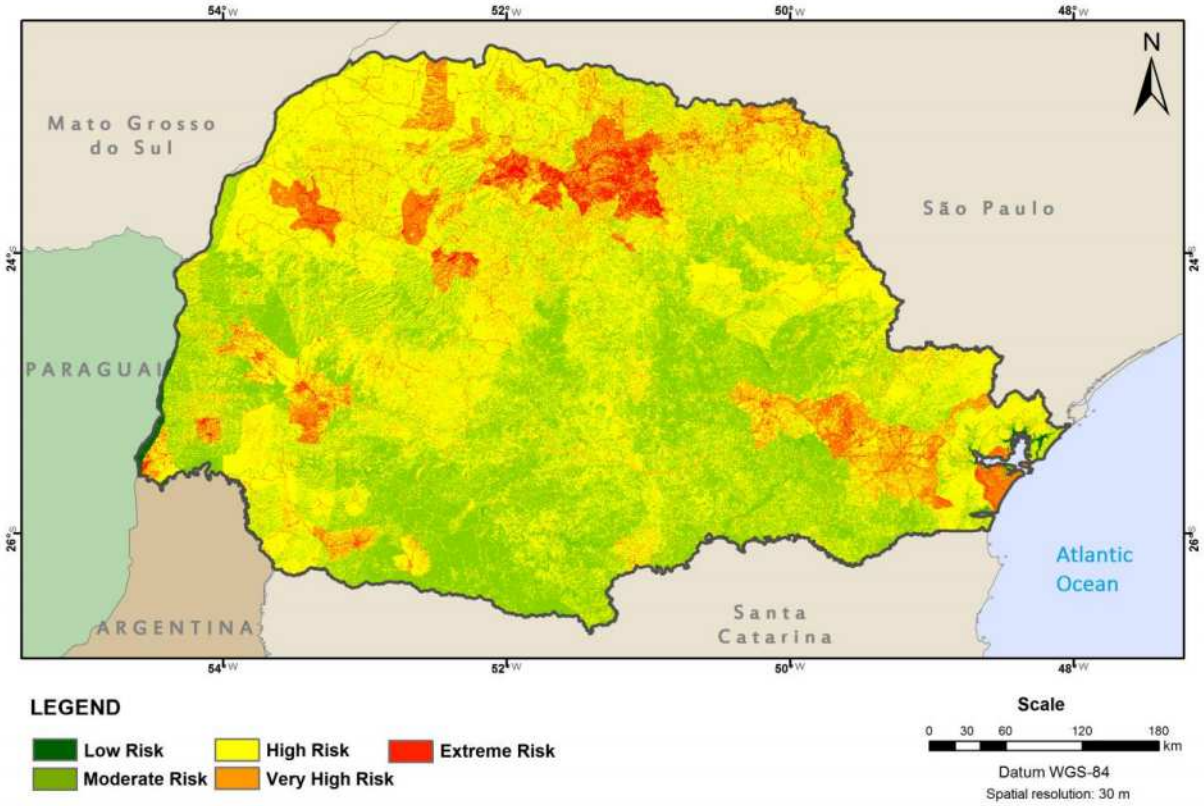

Figure 1. Risk of wildfire in 2020 (best case scenario).

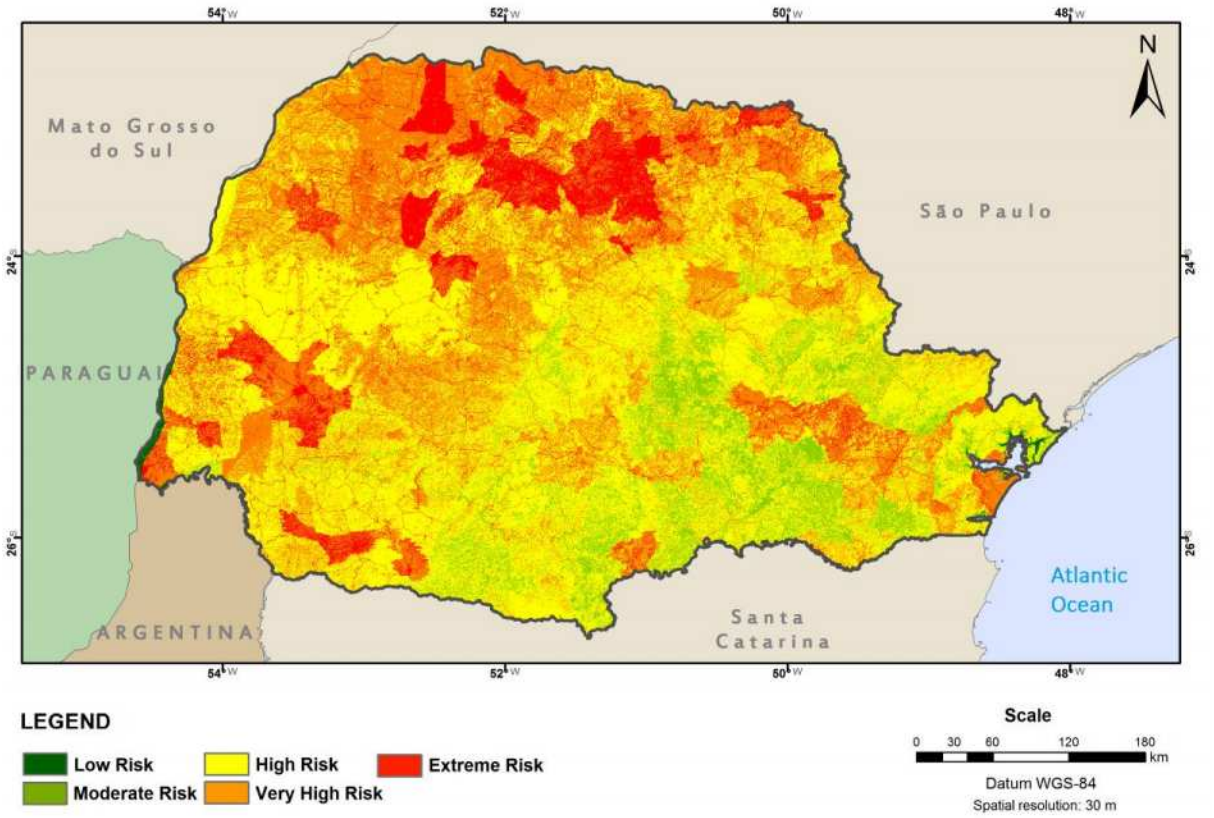

Figure 2. Risk of wildfire in 2100 (best case scenario)

In figures 3 and 4 are presented the forest fires risk zones, in the years 2020 and 2100, for the worst case scenario. In the 2020 decade, much of the State performed at high-hazard class (51.74% of the area), followed by the moderate (32.08%) and very high (13.93%). The class of extreme danger, with 2.18% of the area, passed the decades following the 3.54% and 5.98%, respectively.

At 2100 the State failed to provide more area in the low risk class and the moderate risk class corresponded to 0.07% of the State. The high class, that in 2020 was 51.74%, showed 21.27%. The classes very high and extreme, both with significant increment, represented 55.95% and 22.72% of the total area.

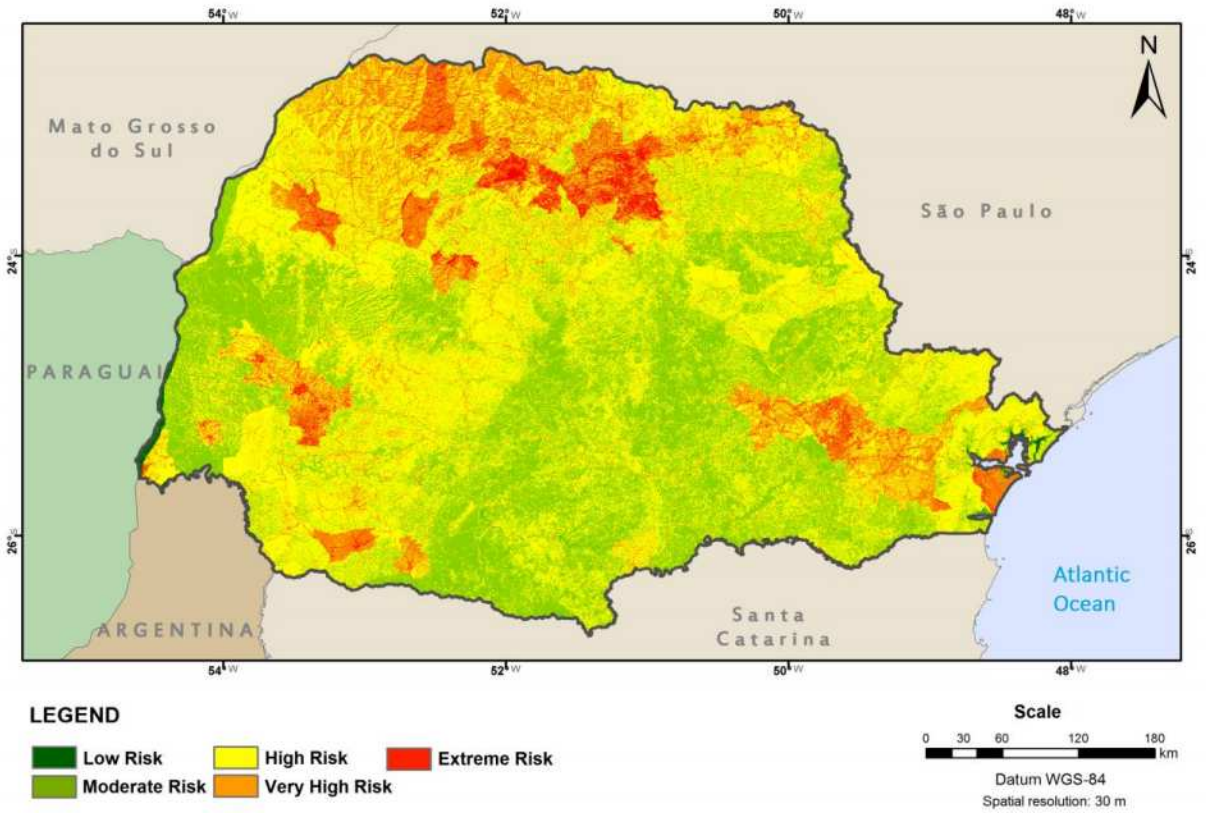

Figure 3. Risk of wildfire in 2020 (worst case scenario)

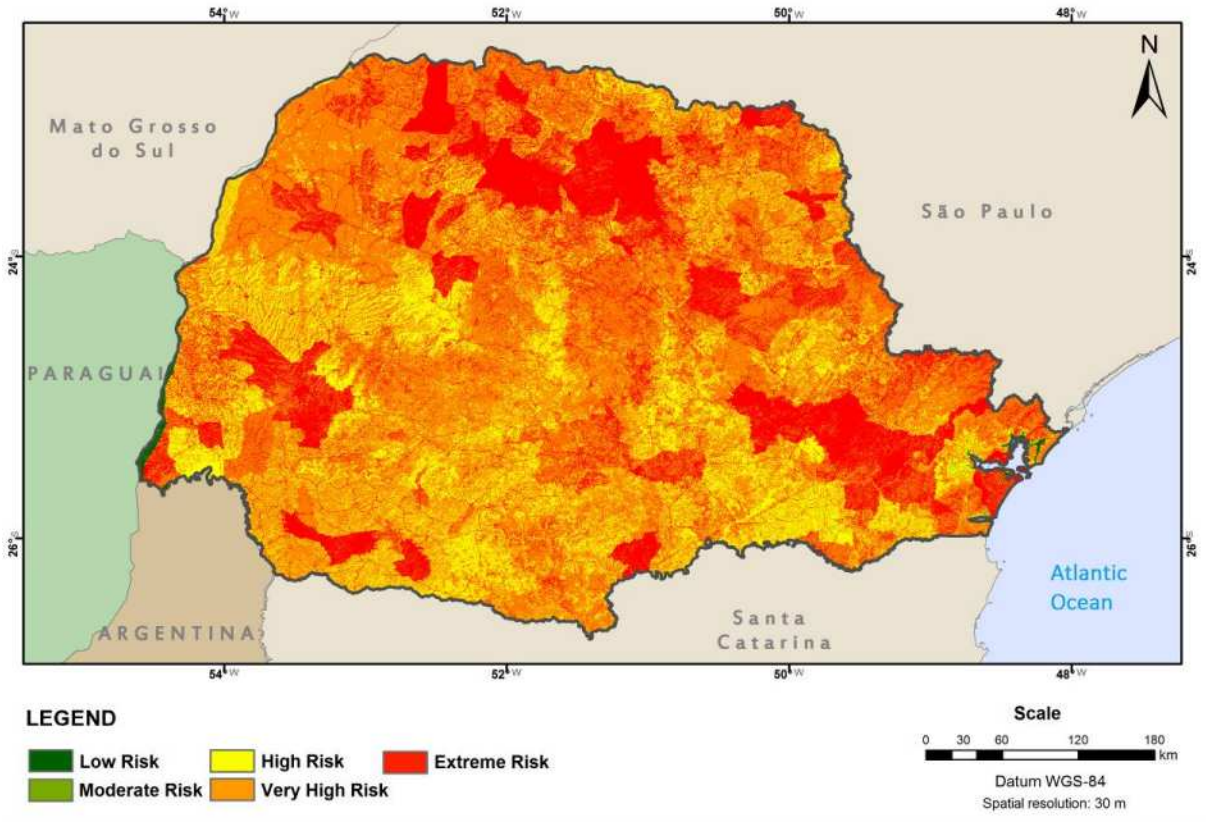

Figure 4. Risk of wildfire in 2100 (worst case scenario)

Conclusions

The dynamic variables (demographic density, fuel moisture, fire danger index (FMA) and forest fire risk zoning), showed an increase in higher classes of danger from fires over time. This behaviour was observed for both the best and the worst scenarios of temperature increase (in accordance with the IPCC).
The data integration model used showed generate consistent results, considering that the mapping of the exposure classes obeyed an evolution according to the decades.
The hypothesis that there will be an increase in the risk of forest fires in the event of an increase in the average temperature of the Earth, was accepted. It is concluded that, if the IPCC predictions are confirmed, there will be an increase in the number of fire events in the State of Paraná, which will require integrated actions for preventing and fighting forest fires to minimize possible environmental, social and economic damages.

Aknowledgments

To FINEP for enabling the accomplishment of this work.
To professionals of IAPAR and SIMEPAR: Paulo Henrique Caramori, Luciane Christina Pinheiro, Roberto Oliveira Santos, Fábio Sato and Livia Maria Pereira for all the support.
To the students of the forest fire Laboratory of the Federal University of Paraná (UFPR), SIMEPAR and IAPAR: Igor K. Takashina, Regiane Kock de Sousa, Luciana Pereira Lauthert, Rafaela de Asunção, Chaiane Cristina Rech Leiva and João Jankowski Saboia.

References

Adab, H.; Kasturi Devi Kanniah, K. D.; Solaimani, K. Modeling forest fire risk in the northeast of Iran using remote sensing and GIS techniques. Nat Hazards, v. 65, p. 1723 – 1743, 2013.

Alencar; A. A. C.; Solorzano, L. A.; Nepstad, D. C. Modeling forest understory fires in an eastern amazonian landscape. Ecological Applications, v. 14, n. 4, p. S139 – S149, 2004 (supplement).

Bergeron, Y.; Cyr, D.; Girardin, M. P.; Carcaillet, C. Will climate change drive 21st century burn rates in Canadian boreal forest outside of its natural variability: collating global climate model experiments with sedimentary charcoal data. International Journal of Wildland Fire, v. 19, p. 1127 – 1139, 2010.

Brown, A. A.; Davis, K. P. Forest fire: control and use. 2 ed. New York: McGraw Hill Book, 1973.

Cardille, J. A.; Ventura, S. J.; Turner, M. G. Environmental and social factors influencing wildfires in the Upper Midwest, USA. Ecological Applications, v. 11, n. 1, p. 111 – 127, 2001.

Chandler, C.; Cheney, P.; Thomas, P.; Trabaud, L.; Williams, D. Fire in forestry: forest fire behavior and effects. New York: J. Wiley, 1983.

Chuvieco, E.; Aguado, I.; Yebra, M.; Nieto, H.; Javier Salas, J.; Martín, M. P.; Vilar, L.; Martínez, J.; Martín, S.; Ibarra, P.; La Riva, J.; Baeza, J.; Rodríguez, F.; Molina, J. R.; Herrera, M. A.; Zamora, M. Development of a framework for fire risk assessment using remote sensing and geographic information system technologies. Ecological Modelling, v. 221, p. 46 – 58, 2010.

Chuvieco, E.; Congalton, R. G. Application of remote sensing and geographic information systems to forest fire hazard mapping. Remote Sens. Environ., v. 29, p. 147 – 159, 1989.

Der - Departamento De Estradas De Rodagem. Mapa político rodoviário do estado do Paraná, 2010. (Escala 1:200.000).

FAO - Food And Agriculture Organization. Fire management: global assessment 2006. Roma, 2007. 159 p. (FAO Forestry Paper 151).

Ferraz, S. F. B.; Vettorazzi, C. A. Mapeamento de risco de incêndios florestais por meio de sistema de informações geográficas (SIG). Scientia Forestalis, Piracicaba, v. 53, p. 39 – 48, jun. 1998.

Flannigan, M. D.; Krawchuk, M. A.; Groot, W. J.; Wotton, B. M.; Gowman, L. M. Implications of changing climate for global wildland fire. International Journal of Wildland Fire, v. 18, p. 483 – 507, 2009a.

Flannigan, M. D.; Stocks, B. J.; Turetsky, M. R.; Wotton, B. M. Impact of climate change on fire activity and fire management in the circumboreal forest. Global Change Biol., v. 15, p. 549 – 560, 2009b.

Grodzki, L.; Caramori, P. H.; Bootsma, A.; Oliveira, D.; Gomes, J. Risco de ocorrência de geada no estado do Paraná. Revista Brasileira de Agrometeorologia, Santa Maria, v. 4, n. 1, p. 93 - 99, 1996.

Guillhermo Julio, A. Método de determinación de prioridades de protección. Santiago: Universidad de Chile, Facultad de Ciencias Agrarias y Forestales, 1992. 27 p. (Manual n. 10).

Hernandez-Leal, P. A.; Arbelo, M.; Gonzalez-Calvo, A. Fire risk assessment using satellite data. Advances in Space Research, v. 37, p. 741 – 746, 2006.

IAPAR - Instituto Agronônico Do Estado Do Paraná. Cartas climáticas do estado do Paraná. Londrina: IAPAR, 1994. 45 p. (Documento 18).

IBGE - Instituto Brasileiro De Geografia E Estatística. Anuário estatístico do Brasil. Rio de Janeiro: IBGE, v. 60, 2000.

Mapa do estado do Paraná. Brasília: IBGE, 2007. Escala 1:250.000.

Censo2010. Disponível em: http://www.censo2010.ibge.gov.br. Access: 11/12/2012.

INPE - Instituto Nacional De Pesquisas Espaciais. TOPODATA: banco de dados geomorfométricos do Brasil 2008. Disponível em: <www.dsr.inpe.br/topodata/>. Access: 11/12/2012.

IPCC - Painel Intergovernamental De Mudanças Climáticas. Relatório do IPCC/ONU: novos cenários climáticos, 2007. 21 p.

Jaiswal, R.K.; Krishnamurthy, J.; Mukherjee, S. Regional study for mapping the natural resourcesprospect & problem zones using remote sensing and GIS. Geocarto Int, v. 20, n. 3, p. 21 – 31, 2005.

Liu, Y.; Stanturf, J.; Goodrick, S. Trends in global wildfire potential in a changing climate. Forest Ecology and Management, v. 259, p. 685 – 697, 2010.

Liu, Z.; Yang, J.; Chan Y.; Weisberg, P. J. Spatial patterns and drivers of fire occurrence and its future trend under climate change in a boreal forest of Northeast China. Global Change Biology, v. 18, p. 2041 – 2056, 2012.

Maack, R. Geografia física do estado do Paraná. 4. ed. Ponta Grossa: Editora UEPG, 2012, 526 p.

Marques, S.; Borges, J. G.; Garcia-Gonzalo, J.; Moreira, F.; Carreiras, J. M. B.; Oliveira, M. M.; Cantarinha, A.; Botequim, B.; PereirA, J. M. C. Characterization of wildfires in Portugal. Eur J Forest Res, v. 130, p. 775 – 784, 2011.

Oliveira, S.; Friderike Oehler, F.; San-Miguel-Ayanz, J.; Camia, A.; Pereira, J. M. C. Forest Ecology and Management, v. 275, p. 117 – 129, 2012.

Probio. Mapa de cobertura vegetal, 2005. Available: <http://homolog-w.mma.gov.br/index.phpido=conteudo.monta&idEstrutura=14>. Acces: 11/12/2012.

Salas, J.; Chuvieco, E. Geographic information systems for wildland fire risk mapping. Wildfire, Washington, v. 3, n. 2, p. 7 – 13, jun. 1994.

Show, S. B.; Clarke, B. Elements of forest fire control. Roma: FAO, 1953.

Simard, A. J. The moisture content of forest fuels – I. Ottawa, Ontario: Forest Fire Research Institute, 1968. 47 p. (Inf. Report FF – X – 14).

Soares, R. V.; Batista, A. C. Incêndios florestais: controle, efeitos e uso do fogo. Curitiba, 2007. 250 p.

Soares, R. V.; Batista, A. C.; Nunes, J. R. S. Incêndios florestais no Brasil – o estado da arte. Curitiba, 2009. 246 p.

Sousa, C.; Pinheiro, D.; Grilo, F.; Guerreiro, J.; Mendonça, M.; Caridade, M. L.; Castro, M.; Mesquita, P.; AlmeidA, R. Relatório do projeto de cartografia de risco de incêndios florestais, 1996. available: <http://valpacos.no.sapo.pt/relatorioflorestal.html>. Access: 07/11/2013.

Tian, X.; Shu, L.; Wang, M.; Zhao, F. Forest fire danger ratings in the 2040s for northeastern China. For. Stud. China, v. 13, n. 2, p. 85 – 96, 2011.

Trewartha, G. T.; Horn L. H. An introduction to climate. New York: McGraw-Hill, 1980. 416 p.

Vadrevu, K.·P.; Eaturu, A.;·Badarinath, K. V. S. Fire risk evaluation using multicriteria analysis: a case study. Environ Monit Assess, n. 166, p. 223 – 229, 2010.

Verde, J. C. Avaliação da perigosidade de incêndio florestal: Liboa – Portugal. 109 p. Dissertação (Mestrado em Geografia) - Universidade de Lisboa, Faculdade de Letras, Departamento de Geografia, Lisboa, Portugal, 2008.

Virgens Filho, J. S.; Félix, R. P.; Oliveira, P. M.; Leite, M. De L. Pgeclima_R - gerador estocástico de cenários climáticos, 2011.

Von Sperling, M. Princípios do tratamento biológico de águas residuárias: introdução à qualidade das águas e ao tratamento de esgotos. 3. ed. Departamento de Engenharia Sanitária e Ambiental: UFMG, 2005. 452 p.

Westerling, A. L.; Bryant, B.P. Climate change and wildfire in California.

Climatic Change, v. 87, p. S231 - S249, 2008. (Supl)

Xu, D.; Dai, L.; Shao, G.; Tang, L.; Wang, H. Forest fire risk zone mapping from satellite images and GIS for Baihe Forestry Bureau, Jilin, China. Journal of Forestry Research, v. 16, n. 3, p. 169 – 174, 2005.

Impacts of climate change on the fire regime in Portugal

Carlos C. DaCamara[a], Mário G. Pereira[b,a], Teresa J. Calado[a], Tomás Calheiros[a]

[a] *Instituto Dom Luiz, , Universidade de Lisboa, Lisboa, Portugal, cdcamara@fc.ul.pt, mtcalado@fc.ul.pt, tlmenezes@fc.ul.pt*
[b] *Centro de Investigação e de Tecnologias Agro-Ambientais e Biológicas CITAB, Universidade de Trás-os-Montes e alto Douro, UTAD, Quinta de Prados, 5000-801 Vila Real, Portugal, gpereira@utad.pt*

Abstract
Wildfires in Portugal are a major problem, with about 18 500 fires and 110 000 ha burnt every year and an increasing trend of the large fires (>100 ha) during the 1980 – 2011 period. In previous studies, climate and weather conditions were identified as the most important drivers of annual total burnt area in the country which inspire assessing potential changes in the statistical distribution of the areas burnt by fires in the expected warmer and drier conditions of future climate. The aim of the study is therefore to project area burnt by vegetation fires in Portugal for different future climate scenarios using an appropriate Burnt Area Model (BAM). The BAM is a multiple regression model that shown to be able to simulate the burnt areas in July and August with just two predictors: the Daily Severe Rating (DSR) in the pre-fire season (May and June) and during the fire season (July and August). Then, the regression model is fed with simulated data by a Global Climate Model (GCM) respecting to present climate and to future IPCC emission scenarios B1 and A1B. It is shown that samples of observed and simulated logarithms of burnt areas follow normal distributions. Changes in measures of location and dispersion (mean and variance), from recent past to future climates, are analysed after statistically removing the effects due to the limitations of the GCM and the BAM. When comparing present climate with future climate scenario B1 (A1B), maximum increases in the averages of the decimal logarithm of July and August burnt area are of 11% (28%) while the standard deviation remaining almost unchanged for scenario B1 and presenting an increase of 25% for A1B. Obtained estimates need to be looked at with due care but the developed approach consistently points towards an increasing risk of fire under future climate conditions, inter-annual variability and likelihood of having much larger fire events.

Keywords*: Forest fire; Climate change; GCM; Fire risk/danger*

Introduction

Assessing the potential impacts of climate change on the fire regime is especially relevant in Portugal, where according to the Portuguese National Forest Authority (*Instituto de Conservação da Natureza e das Florestas*, ICNF) and the European Forest Fire Information System (EFFIS), more 610 000 fires and 3,5 million ha have burnt between 1980 and 2012, almost 1 million ha of which between 2003 and 2005 (Calado and Dacamara 2008). Besides, the number of large fires (with more than 100 ha), amount of burnt area (hereafter, BA) and fire severity have lately increased in Portugal (Pereira *et al.* 2011). Weather and climate are considered the most important drivers of fire activity, even more important than fuel pattern and topography in determining BA in simulated landscapes due to the direct and indirect profound influence they have on wild land fire ignition potential, fire behaviour and severity (Cary and Banks 2000; Benson *et al.* 2008). The climatic conditions determine the existence, type and life cycle of the vegetation which helps explaining the strong resemblance between the spatial patterns of the global pyrogeography (Krawchuk *et al.* 2009) and the updated world map of the Köppen-Geiger climate classification (Peel *et al.* 2007). On the other hand, weather conditions such as lightning promotes fire ignition, while air temperature, wind, atmospheric stability and air relative humidity determine the fuel moisture content and fire spread and, on the contrary, precipitation, even in small amounts, contributes to fire extinction (Pereira *et al.* 2013).

Climate and weather play a particularly important role in the fire regime in Portugal, where long-term climatic pre-conditions (e.g. temperature and precipitation in winter and spring before the summer fire peak season) and short-term synoptic forcing (e.g. extreme synoptic weather patterns and weather types from classifications schemes) are able to explain about two thirds of the variance in the annual, seasonal and monthly total BA (Pereira *et al.* 2005; Pereira *et al.* 2013; Trigo *et al.* 2013). Extreme fire activity as recorded in 2003 and 2005 tends to occur under (also) extreme and consistent weather conditions from the surface to high levels of the atmosphere (Trigo *et al.* 2006) and is related to the evolution of the synoptic- and meso-scale wind, temperature and humidity patterns associated to the appearance of the Iberian thermal low (Hoinka *et al.* 2009).

These factors are continuously changing due to natural climate variability and human-caused climate change (Stocker *et al.* 2013) which may contribute to the high inter-annual variability and increasing trends observed in the last decades (Pereira *et al.* 2005; Pereira *et al.* 2011) and legitimizes the ambition to try to estimate future fire activity.

Many of the most recent studies on the impacts of climate change on some aspect of the fire regime and wildfires has focus on North (Johnstone *et al.* 2010; Wotton *et al.* 2010; Westerling *et al.* 2011; Rocca *et al.* 2014) and South America (Silvestrini *et al.* 2011), Australia (Pitman *et al.* 2007; Murphy and Timbal 2008; Clarke *et al.* 2011) Lynch *et al.*, 2007), in boreal forests of North America and Eurasia (Kilpeläinen *et al.* 2010; Liu *et al.* 2012; De Groot *et al.* 2013), in Europe (Moriondo *et al.* 2006; Batllori *et al.* 2013; Cane *et al.* 2013; Bedia *et al.* 2014; Karali *et al.* 2014) and even at global scale (Moritz *et al.* 2012). However, and despite the magnitude of the problem in Portugal, a very short list of studies have dealt with the impact of climate change on wildfire risk in Portugal (Durão and Corte-Real 2006; Carvalho *et al.* 2008; Carvalho *et al.* 2010; Pereira *et al.* 2013).

The projection of future fire activity requires the development of robust and resistant fire-vegetation-weather/climate relationships to be used in future climate conditions and the availability of sufficiently long and reliable datasets of observed and simulated values of meteorological and fire variables (Pereira *et al.* 2013). Portugal holds one of the largest (in terms of total number of recorded fires) and most comprehensive rural fire databases, not only in European context but also in comparison to many other countries worldwide (Pereira *et al.* 2011).

Currently, a large set of long and reliable meteorological datasets of analysis and reanalysis are available for climate research studies which includes the European Centre for Medium-Range Weather Forecasts (ECMWF) ECMWF 40-year Reanalysis (ERA-40), the ECMWF Interim Reanalysis (ERA-Interim), the Japanese 25-year (JRA-25) and 55-year Reanalysis (JRA-55), the NASA Modern Era Reanalysis for Research and Applications (MERRA) and (MERRA2), the National Centers for Environmental Prediction (NCEP) Climate Forecast System Reanalysis (CFSR) and NCEP/DOE Reanalysis II and the NOAA-CIRES 20th Century Reanalysis V2.

On the other hand, General Circulation Models (GCMs) are nowadays recognized as suitable tools for climate modelling because they are based on well-established physical principles, able to simulate global- and many regional-scale observed features of contemporary climate, past climate changes and there is significant confidence that GCM provide credible quantitative estimates of future climate change (Randall and Fichefet 2007). In this sense, most climate models are able to derive fire danger and thereby characterize a probable fire regime (Lynch *et al.* 2007). In addition, climate change data, which may include climate estimates from observations, socio-economic data and scenarios, global climate model data simulated by different GCM and for different future climate scenarios may be easily obtained from many different data providers such as the Data Distribution Centre (DDC) of the Intergovernmental Panel on Climate Change (IPCC) or the Program for Climate Model Diagnosis and Intercomparison which provides the World Climate Research Programme Coupled Model Intercomparison Project, WCRP CMIP datasets (Meehl *et al.* 2007). Recently, a Burnt Area Model (BAM) was developed for Portugal based on multiple regression analysis of meteorological parameters with the aim to model the BA during the summer months and be used as a BA generator (Pereira *et al.*

2013). Therefore, the aim of this study is to produce and compare projections of future BA in Portugal by means of the BAM for different future climate change scenarios.

Materials and Methods

This study is based on a fire database and on daily meteorological data of both analysed and simulated fields. Indices of fire risk that integrate the Canadian Forest Fire Danger Rating System (CFFDRS) are then computed using the appropriate meteorological data.

Data

The fire database was provided by the Institute for the Conservation of Nature and Forestry (*Instituto da Conservação da Natureza e das Florestas*, ICNF) and consist of detailed information (e.g., fire ignition location, in terms of administrative division of Portugal, fire ignition and extinction date and time, fire area in forest, shrublands and agricultural land cover type) obtained from ground measurements for each fire occurred in Continental Portugal between 1980 and 2011. This dataset is an extension of the Portuguese Rural Fire Database (Pereira *et al.* 2011) and after correcting the additional data for inconsistencies and errors using the same procedures, monthly cumulated values were computed for the considered 32 – year period.

The observed meteorological database consist of analysed fields from the ERA-Interim which is the latest global atmospheric reanalysis produced by the ECMWF to replace the ERA-40 with a new atmospheric reanalysis which will extend back to the early part of the twentieth century and able to provide a better representation the hydrological cycle, improve the quality of the stratospheric circulation and the consistency in time of the reanalysed fields (Dee *et al.* 2011). The ERA-Interim data server surface archive has a mixture of analysis fields, forecast fields and fields available from both the analysis and forecast which is determined by the step variable: 0 for analysis (which are available for 0000, 0600, 1200 and 1800 UTC); 3, 6, 9 or 12 for forecast fields which are produced from forecasts beginning at 0000 and 1200 UTC). The other daily archives have only analysis data.

The selected meteorological fields are: 2 meter air temperature, 2 meter dew point temperature, 10 meter zonal and meridional components of wind speed and 24 hour cumulated precipitation (all at 12 UTC). The air relative humidity was computed with the Magnus formula (using 2 meter air temperature, 2 meter dew point temperature) and corrected according to the altitude. All meteorological fields are defined on a 0.75°×0.75° latitude/longitude grid over Continental Portugal. Spatial means were then computed over the selected grid points and monthly means were finally derived for all meteorological data.

The simulated meteorological database consist of outputs from the Model for Interdisciplinary Research on Climate (MIROC), which is a coupled Atmosphere-Ocean GCM that comprises five components, namely atmosphere, land, river, sea ice and ocean. Developers of MIROC are at the Centre for Climate System Research (CCSR), the University of Tokyo, the National Institute for Environmental Studies (NIES) and the Frontier Research Centre for Global Change (FRCGC). Several different model comparison studies identify MIROC as one of the best models (Lucarini *et al.* 2007; Scherrer 2011; Watanabe *et al.* 2011; Watanabe *et al.* 2011; Mochizuki *et al.* 2012; Chikamoto *et al.* 2013) with especial good performance over the Iberian Peninsula (Nieto and Rodríguez-Puebla 2006; Errasti *et al.* 2011).

For comparison purposes, data for three grid points were selected from MIROC 3.2 medres grid, all approximately at the same longitude but at different latitudes: two of them located over Portugal (one in the south and another in the centre) and one at north of Portugal, in Spanish region of Galicia. Daily grid values of 10 m wind speed, 24h cumulated precipitation, surface air temperature and relative humidity were extracted for 1951 – 2000 period respecting to the recent past conditions (20th century) model simulations (20C3M), and for the 2051 – 2100 respecting to IPCC Special Report on Emissions Scenarios (SRES) B1 and A1B (Nakicenovic and Swart 2000). The B1 scenario corresponds to a high

level of environmental and social consciousness accompanied by rapid changes in economic structures and the introduction of cleaning technologies. On the other hand, the A1B scenario reflects a future world of very fast economic growth, low population growth, with a rapid introduction of new and more efficient technology, and a balanced mix of technologies and supply sources.

The Canadian Forest Fire Weather System

In this study, the indices of the Canadian Forest Fire Weather Index (FWI) were used to account for the effect of weather on fuels and fire behaviour. The FWI System (Figure 1) comprises six components: the first three components, the Fine Fuel Moisture Code (FFMC), the Duff Moisture Code (DMC) and the Drought Code (DC), are fuel moisture codes which aim respectively to rate the moisture content of litter and other fine fuels, the average moisture content of loosely compacted organic layers of moderate depth, and the average moisture content of deep, compact organic layers; the remaining three components, the Initial Spread Index (ISI), the Build Up Index (BUI) and the Fire Weather Index (FWI), are fire behavior indices, which characterize the rate of fire spread, the fuel available for combustion, and the frontal fire intensity (Van Wagner and Pickett 1985; Van Wagner 1987). Finally, the Daily Severity Rating (DSR) is simply a power function of FWI ($DSR = 0.0272 \times FWI^{1.77}$), with the aim to rate the difficulty of controlling fires and specifically designed for averaging either in time or in space in opposition to FWI that is suitable as a single day value. All these indices are computed solely with the values of four meteorological variables and their values increase with the rise of fire danger (Van Wagner and Pickett 1985). The FWI System was developed for Canada but has been successfully used all over the world (Amiro *et al.* 2005; Wotton 2009) and shown to be especially useful in Portugal to assess the fire behaviour potential in maritime pine stands (Palheiro *et al.* 2006) and to rate fire risk in Portugal during the summer season (Rainha *et al.* 2002; Viegas *et al.* 2004; Carvalho *et al.* 2008; Carvalho *et al.* 2010). Since 1998, the System has been operationally used by the Portuguese Weather Service.

Values of the FWI and DSR derived on selected grid points based on daily values of the above-listed meteorological values (analysed and simulated) and then, spatial averages were computed over grid points and monthly means were finally computed.

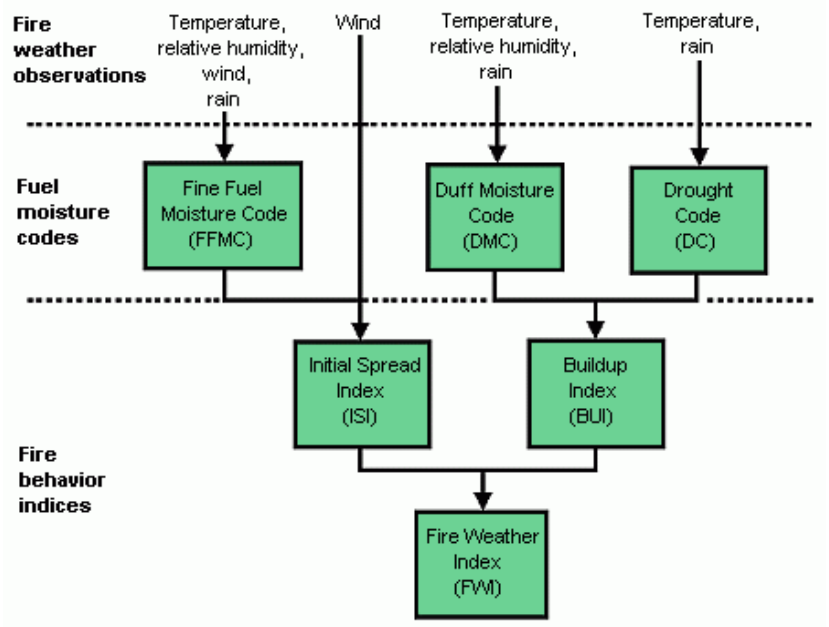

Figure 1. The Structure of the FWI System. The components of the FWI System are computed with consecutive daily observations of air temperature, relative humidity, wind speed, and 24-hour rainfall. The six standard components provide numeric ratings of relative potential for wildland fire. Adapted from Natural Resources Canada (http://cwfis.cfs.nrcan.gc.ca/background/summary/fwi).

Results

The observed summer burnt areas

The annual cycle of monthly BA for Continental Portugal during the considered 32 – year period is shown in Table 1. It is well apparent that the vast majority of area burnt by forest (71% of the total BA) take place during the summer months of July and August. The close agreement between the time series of annual and July plus August BA and the very large inter-annual variability dominated by the outstanding values registered in the years of 2003 and 2005 (Figure 2) suggest that the annual fire regime is dominated by the events that take place in July and August and to restrict the study to those two summer months.

Table 1. Annual cycle of monthly burnt area in Portugal for the period 1980 − 2011. Values of simple and robust and resistant statistics including the maximum, upper quartile (Q3) median, lower quartil (Q1), minimum, interquartile range (IQR), range and total.

Burnt area (ha)

Statistics	Jan	Feb	Mar	Apr	May	Jun	Jul	Aug	Sep	Oct	Nov	Dec
Maximum	1100	3118	14780	11360	3987	18962	99087	261481	66015	27606	9157	3734
Q3	115	513	2161	1447	1074	6197	43856	60237	25123	4548	102	93
Median	34	124	585	352	372	2112	16780	30779	11679	1632	18	17
Q1	10	12	85	109	145	555	7979	18337	6246	479	2	0
Minimum	0	0	3	0	3	27	529	3571	3325	0	0	0
IQR	106	501	2076	1338	929	5643	35877	41900	18877	4069	100	93
Range	1100	3118	14777	11360	3983	18935	98559	257910	62690	27606	9157	3734
Total	4775	14247	67787	36393	21801	140834	845584	1612525	574751	122332	13206	5908
Total (%)	0%	0%	2%	1%	1%	4%	24%	47%	17%	4%	0%	0%

This behaviour is expected in Mediterranean regions since vegetation presents elevated levels of water stress as induced by periods of dry conditions and relatively high temperatures that often characterise the late spring and the beginning of summer (Viegas *et al.* 2001; Pereira *et al.* 2005; Trigo *et al.* 2006). The inter-annual variability (as measured by the inter-quartile range) is also clearly larger during the summer months and it is worth noting that the variability of July and August is about twice the one of September.

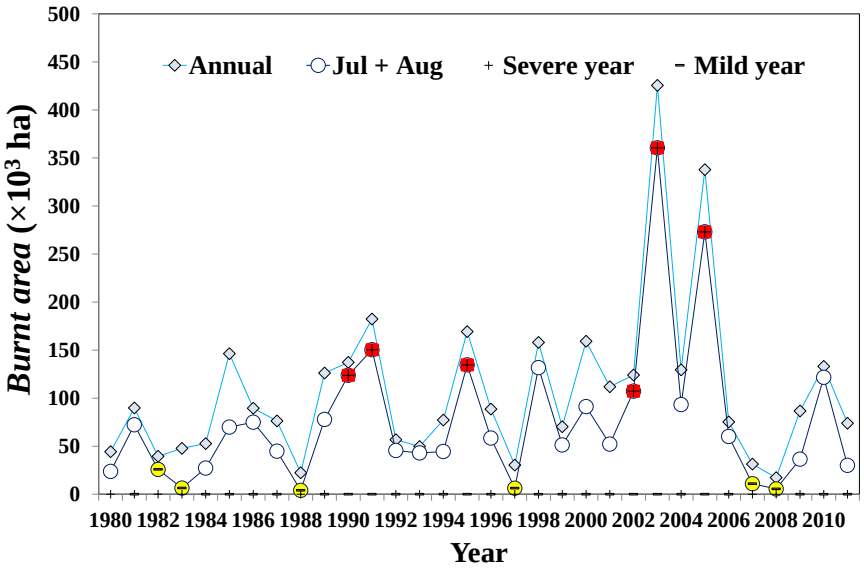

Figure 2. Inter-annual variability of burnt area amounts in Continental Portugal for the whole year (Annual) and just for July + August (Jul + Aug), for the period 1980−2011. Severe (+) and mild (–) years signs inside respective red and yellow circles.

It is also important to underline some of the results of correlation analysis during the period 1980 – 2011, namely: (*i*) the existence of a positive and statistical significant (p-value<0.0001) value of the Pearson Product-Moment correlation coefficient (r = 0.66) between the areas burned in July and in August; (*ii*) the very low (r =0.22) and statistically not significant correlation between the DSR monthly means of July and August; (*iii*) despite the significant (p-value<0.0001) high value of the correlation coefficient between DSR and the decimal logarithm of monthly BA for the months of July and August, (r = 0.76 and r = 0.59, respectively). These results underline the usefulness of the DSR to rate the meteorological fire danger and suggests the existence of a pre-summer season climatological background that would condition the fire regimes of both July and August.

The Burnt Area Model

With the aim of identifying the most promising predictors of BA in July and August and characterizing the climatological background, a composite analysis (Pereira *et al.* 2005; Trigo *et al.* 2006) of all the analysed meteorological fields was performed for two classes of extreme summer fire seasons, respectively severe and mild (Figure 2), defined depending on the monthly BA of July and August are both greater/lesser than the upper/lower tercile of the respective month (i.e. greater than 40,000 ha for July and 46,000 ha for August).

Results reveal that, from the meteorological standpoint, major differences between mild and severe years may be found during the months preceding and during the summer fire season (Figure 3). In the pre fire season, severe years are associated to positive anomalies of precipitation in the early spring (March), which favours the growth of vegetation, followed by significant negative anomalies of precipitation and air relative humidity and positive air temperature anomalies in May and June. This climatic pattern is consistent with the atmospheric circulation from NE, over Portugal during this period and, as expected, the increasing trend of positive DSR anomalies from April to June reflect the above-described cumulative behaviour of temperature, relative humidity, wind and precipitation. During the fire season, major statistically significant differences between severe and mild fire seasons are naturally found in all meteorological variables and, consequently, in DSR. Severe fire seasons are characterised by extreme negative precipitation and humidity anomalies and positive temperature anomalies associated to south-eastern winds leading to utmost DSR anomalies. In the case of mild years, the opposite behaviour is observed.

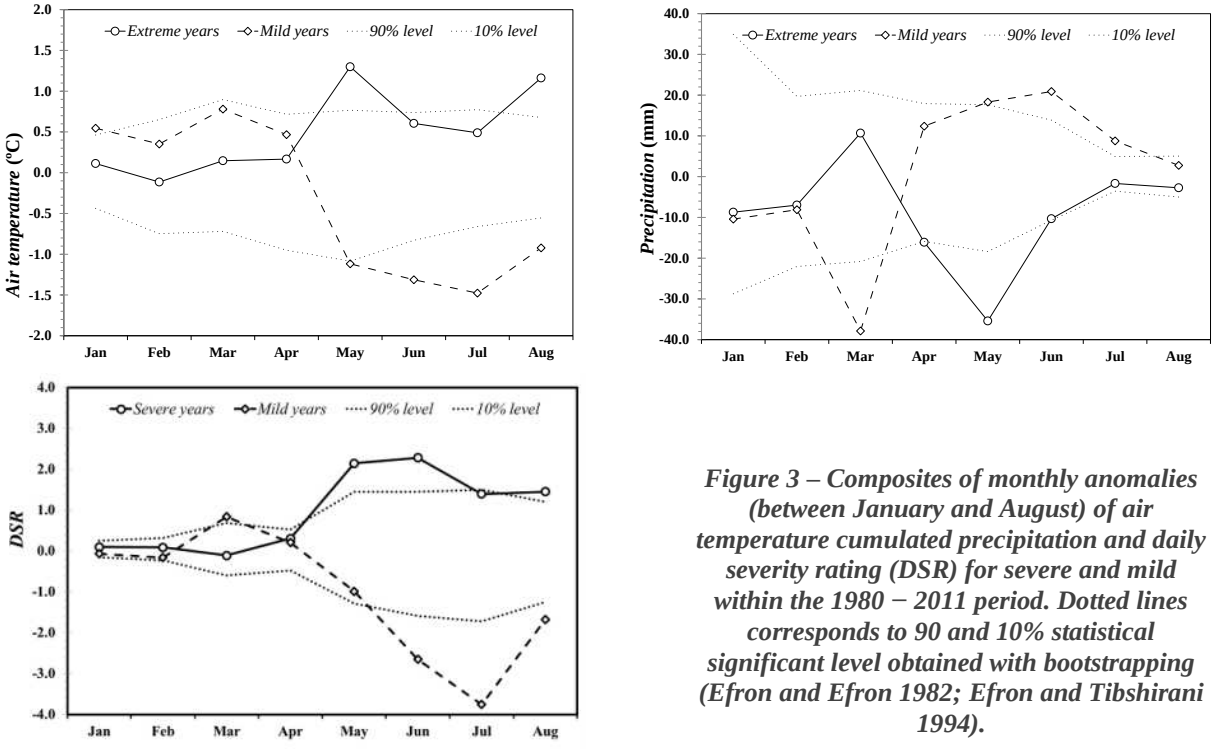

Figure 3 – Composites of monthly anomalies (between January and August) of air temperature cumulated precipitation and daily severity rating (DSR) for severe and mild within the 1980 − 2011 period. Dotted lines corresponds to 90 and 10% statistical significant level obtained with bootstrapping (Efron and Efron 1982; Efron and Tibshirani 1994).

These results suggest the development of a multiple linear regression BAM for decimal logarithm of monthly BA (due to the highly asymmetrical character of monthly BA) in summer months using, as predictors, meteorological variables and/or fire risk indices respecting to the pre-fire and/or fire seasons. In order to mitigate the effects of over fitting, the performance of the experiments was evaluated using a leave-one-out-cross validation scheme (Wilks 2011). Several selection methods (e.g., stepwise, forward, backward and explained variance) using different criteria were tested to select the best and parsimonious BAM for BA time series in July, August and July + August for the 32-year period using the equation presented in Table 2 where the $Log_{10}BA_{J/A}$ is the decimal logarithm of monthly BA in July or in August; DSR_{PF} is the monthly mean of DSR during the pre-fire period (PF), defined as May and June when the predictand is the decimal logarithm of monthly BA in July ($Log_{10}BA_J$) and May, June and July when the predictant is the decimal logarithm of monthly BA in August ($Log_{10}BA_A$); $Log_{10}BA_{J/A}$ is the monthly mean of DSR in July or in August depending if the predictand is the monthly BA in July or August, respectively.

Table 2 – Burnt Area Model regression and ANOVA analysis for July, August, and July + August (1980 − 2011). Statistics includes which includes: regression coefficients (A, B and C) and St. Error, R^2, adjusted R^2 (R^2_{adj}) F-statistic (Regression F) and significance of F (Significance F)

Regression and ANOVA analysis

$$\mathbf{Log_{10}BA_{J/A} = A + B \times DSR_{J/A} + C \times DSR_{PF}}$$

July	**Regression stats**		***Coefficients***	***St. error***	***t Stat***	***P-value***	
	R	0.78	**A**	2.4952	0.2650	9.4163	0.0000
	$\mathbf{R_{adj}}$	0.75	**B**	0.0973	0.0336	2.8921	0.0072
	St. Error	0.36	**C**	0.1009	0.0233	4.3326	0.0002
				ANOVA			
			df	***SS***	***MS***	***Regression F***	***Significance F***
	Regression		2	5.7904	2.8952	21.9352	1.58E-06
	Residual		29	3.8277	0.1320		
	Total		31	9.6181			
August	**Regression stats**		***Coefficients***	***St. error***	***t Stat***	***P-value***	
	R	0.77	**A**	2.4715	0.3104	7.9632	0.0000
	$\mathbf{R_{adj}}$	0.75	**B**	0.1005	0.0295	3.4003	0.0020
	St. Error	0.32	**C**	0.1072	0.0247	4.3353	0.0002
				ANOVA			
			df	***SS***	***MS***	***Regression F***	***Significance F***
	Regression		2	4.4198	2.2099	21.7332	1.71E-06
	Residual		29	2.9488	0.1017		
	Total		31	7.3686			
July + August	**Regression stats**		***Coefficients***	***St. error***	***t Stat***	***P-value***	
	R	0.80	**A**	2.4952	0.2650	9.4163	0.0000
	$\mathbf{R_{adj}}$	0.79	**B**	0.0973	0.0336	2.8921	0.0072
	St. Error	0.34	**C**	0.1009	0.0233	4.3326	0.0002
				ANOVA			
			df	***SS***	***MS***	***Regression F***	***Significance F***
	Regression		2	11.7115	5.8557	52.2081	6.11E-14
	Residual		61	6.8419	0.1122		
	Total		63	18.5533			

Results of the regression analysis and analysis of variance (ANOVA) obtained independently for July and August (Table 2) are very similar for both months not only in what respects to regressions statistics (R^2 = 0.59 – 0.61, R^2_{adj} = 0.56 and standard error of 0.32 (August) – 0.36 (July), respectively), regression coefficients (A, B and C), statistical significance (Student's *t* distribution statistic and significance of *F-statistic*). Results for BA in July and August (jointly) are even slightly better (R^2 = 0.64, R^2_{adj} = 0.62) but regression coefficients are very similar to those obtained independently for July and August.

The two predictors are statistically significant and were selected in the same order they appear in the equation, with increasing R^2 value from 0.44, when $Log_{10}BA_{J/A}$ is the only predictor, to 0.630 when the model has both predictors. Several other aspects are worth being noted namely: the overall good agreement between observed and modelled values of the decimal logarithm of BA; the relatively high value of the coefficient of determination R^2 = 0.64 (p-value<0.001) for July and August BA; which means that the BAM is able to explain, in cross-validation mode, almost 3/5 of the total variance. Finally, the normality of the values of the logarithm of the values of BA observed, modelled and residuals from the use of the BAM was confirmed by the Kolmogorov-Smirnov test. All these features are especially important and will be exploited in the next subsection when the BAM will be used as a generator of monthly BA scenarios in recent past and future climate conditions.

3.3. The simulated summer burnt areas

Simulated time series of BA in July and August were generated by feeding the BAM with DSR values computed for the pre-fire period and for the fire season with GCM outputs respecting to present (20C3M) and to future B1 and A1B climate scenarios. The Kolmogorov-Smirnov (K-S) test was used to check that the simulated BA for all cases are normally distributed at the 5% significant level (Table 3). Values of the mean and standard deviations of $Log_{10}BA_{J/A}$ reveal that, as expected, the use of the multiple linear models with observed DSR leads to a simulated BA samples with the same mean as the one of the observed sample but with smaller variance. However, when feeding the BAM with

Table 3 – Mean, standard deviation (SD) and p-value of the one-sample Kolmogorov-Smirnov test for normality of burnt area time series for July and August observed and simulated by the BAM when fed with ERA-Interim (Modelled) and with GCM outputs (BAM+MIROC) for different periods of scenario B1 and A1B.

Model	Scenario	Period	Mean	SD	p
BAM	Observed	1980 - 2011	4.31	0.54	0.41
	Modelled	1980 - 2011	4.31	0.43	0.85
BAM + MIROC	20C3M	1971 - 2000	5.06	1.06	0.42
	B1	2051 - 2080	5.63	0.72	0.38
		2071 - 2100	6.03	1.07	0.68
	A1B	2051 - 2080	6.72	0.97	0.68
		2071 - 2100	7.48	1.36	0.29

simulated data by a GCM for future climate scenarios there is an increase in both the mean and the variance, even for the recent past conditions (20C3M). The latter case is an expected consequence of the GCM's characteristics, namely the known fact that the simulated meteorological fields by MIROC, or by other climate models, are biased and have too much variability. Accordingly, changes in the mean and in the standard deviation are due to climate change (signal) and to the limitations of BAM and GCM (noise) to properly reproduce the observed reality. With the aim of, at least reduce the model bias, the $Log_{10}BA_{J/A}$ obtained for the recent past conditions (20C3M scenario) were corrected to have mean and standard deviation equal to the observed values. Then, time series of $Log_{10}BA_{J/A}$ for the future scenarios were transformed with exactly the same correction factors.

Comparison between future projections of the normal distributions may be performed on the basis of the descriptive statistics of the decimal logarithm of BA (Table 4). When compared with the present climate scenario (20C3M), there are increases in the means of $Log_{10}BA$ for both future climate scenarios periods, respectively of 7% and 11% (20% and 29%) from the 20C3M to the 2051 – 2080 and 2071 – 2100 periods of the B1 (A1B) scenario. The standard deviation remains almost unchanged from the 20C3M to the last (first) period of B1 (A1B) scenario, but presents a decrease (increase) of about 32% (28%) from the 20C3M to the first 30-year of B1 (A1B) scenario. It is also worth noting that differences in percentiles changes with increasing percentiles, e.g. from 0.39 (0.36) in P5 to 0.48 (0.57) in P50 and to -0.28 (0.38) in P95 when going from present climate to first (last) 30-year period of B1 scenario while the correspondent differences for A1B scenario are even higher (about the double). This is an important aspect, since it reveals that in the B1 scenario conditions, for the 2051 – 2080 period major increases in burnt area are only expected for values below P75 and the larger increases should be expected for P10 (0.58) values of burnt area while for the 2071 – 2100 period the increases are therefore to be expected for all values of burnt area nonetheless larger increases are found between P10 (0.55) and P75 (0.47). A similar changing pattern is expected for A1B scenario during the first period but increasing changes may be expected from P5 (0.85) to P95 (1.47). As expected, differences are even more impressive when analysing changes in BA (and not in the logarithm) from present to future climate scenarios. The median may change from 16,000 ha in 20C3M scenario to 49,000 ha (158,000 ha) and 61,000 ha (294,000 ha), respectively in the first and second 30-year period of B1 (A1B) scenario. On the other hand, the mean remains unchanged from recent past climate scenario to 2051 – 2080 period of B1 but increase to 158,000 ha in the 2071 – 2100 period of future scenario. Values of the mean BA for A1B scenario are even higher (270,000 and 1,500,000 ha).

Table 4 – Descriptive statistics of corrected log-normal distributions of monthly burnt area for present (20C3M) and future (B1 and A1B) climate scenarios. P: percentiles, IQR: inter-quartile range, RD: Relative dispersion.

	20C3M	B1		A1B	
	1971-2000	2051-2080	2071-2100	2051-2080	2071-2100
Mean	4.31	4.60	4.80	5.16	5.54
SD	0.54	0.37	0.54	0.49	0.69
P5	3.60	3.99	3.96	4.35	4.46
P10	3.65	4.23	4.20	4.55	4.65
P25	3.94	4.43	4.44	4.79	5.14
P50	4.21	4.69	4.79	5.20	5.47
P75	4.63	4.85	5.11	5.48	5.89
P90	5.20	5.01	5.48	5.68	6.41
P95	5.36	5.08	5.75	5.94	6.83
IQR	0.69	0.43	0.66	0.69	0.76
RD	0.08	0.05	0.07	0.07	0.07

Conclusions

This study shown that the annual total BA in Continental Portugal is dominated by the fire events taking place in July and August which accounts for almost 3/4 of the total burnt area. The influence of weather conditions on the BA in these summer months was disclosed by the results of composite analysis of relevant meteorological variables performed for severe and mild years, defined as those where both the monthly BA of July and August are higher or lower than the respective upper or lower terciles, respectively. Results indicated that severe years are related to averaged anomalies of precipitation in March followed by positive anomalies of temperature and negative anomalies of precipitation and relative humidity in pre fire season. These climatic patterns are consistent with the atmospheric circulation over Portugal and with the anomalies of DSR becoming increasingly positive and statistically significant from May to June for severe years. Differences were also obtained during the fire season (July and August), where extreme meaningful positive anomalies of temperature and DSR (i.e., above the 90% significant level) were found for severe and negative for mild year composites.

These differences in the meteorological parameters have a profound impact on the life cycle and the thermal and hydric stress of the vegetation. In fact, during severe years a higher averaged precipitation and relative humidity in March increases the likelihood of a healthy growth of vegetation while the lower values of precipitation that follow in May and June, together with the higher values of temperature, increase the stress in a more abundant vegetation contributing to a larger amount of available fuels and burnt area. This process is particularly highlighted if, during the fire season, Portugal is affected by atmospheric circulation patterns that induce extreme hot and dry spells (heat waves) over the territory.

A Burnt Area Model (BAM) was developed to simulate the decimal logarithm of monthly burnt areas in July and August using, as predictors, the DSR during the pre-fire and the fire season. This model is able to explain almost 2/3 of the total observed variance and is almost unaffected by over fitting which increase the confidence in their use in practice with future unknown validation dataset. The BAM was then fed with simulated data by the MIROC climate model respecting to present climate conditions (20C3M) and to future climate IPCC emission scenario B1 and A1B and the bias of the BAM and GCM was corrected before proper comparison between projections of future BA.

When compared with the recent past climate scenario (20C3M) with the two periods (2051 – 2080 and 2071 – 2100) of future climate scenarios B1 and A1B, increases in the means of the logarithm of July and August BA ranges, respectively between 7% and 11% for B1 and between 20% and 29% for A1B whereas the standard deviation remained almost unchanged in the latter case of scenario B1, presented a decrease of about 30% and 9% in the case of the former period of both B1 and A1B and an increase of 28% in the last period of A1B scenario. Differences in percentiles (between present and future climate scenarios) increased with increasing percentiles indicating that the larger increases in burnt area are to be expected for all fire events at the end of the XXI century.

It is very likely that the simulated BA are overestimated due, at least to three orders of reasons: (*i*) the use of global (GCM) or regional (RCM) circulation models (which are just limited representations of the observed reality); (*ii*) the use of a linear BAM (which prevents the existence of feedback mechanisms that might reduce the amounts of burnt area); and, (*iii*) not taking into account other important factors for fire occurrence and size such as those related to changes in fuel structure (Pausas and Paula 2012; Gibson *et al.* 2014); climate-vegetation dynamics and conservation planning (Krawchuk *et al.* 2009); patterns of lightning strikes (Wotton *et al.* 2010; Wendler *et al.* 2011; Liu *et al.* 2012); and anthropogenic activities and drivers of fire, such as control over ignition, fire management, suppression activities, land use/land cover changes (Krawchuk *et al.* 2009; Le Page *et al.* 2010; Aldersley *et al.* 2011; Costa *et al.* 2011; Kloster *et al.* 2012). Nevertheless, obtained results are of the same order of magnitude of other similar studies (Le Goff *et al.* 2009; Carvalho *et al.* 2010; Westerling *et al.* 2011; Nitschke and Innes 2013).

Finally, despite all the identified limitations, the developed approach consistently points towards an increasing of: (*i*) the meteorological fire danger; (*ii*) having much larger fire events; (*iii*) inter-annual variability of the fire regime under future climate, which together with the positive bias will have dramatic consequences at the social, economic and environmental levels. These conclusions could be even more dramatic as an increase of the fire season length is very likely to be expected in boreal and temperate climates (Flannigan *et al.* 2009; Wotton *et al.* 2010; Carvalho *et al.* 2011; Westerling *et al.* 2011; Kloster *et al.* 2012).

Acknowledgements

This work was supported by national funds by FCT - Portuguese Foundation for Science and Technology, under the project PEst-OE/AGR/UI4033/2014 and by the project "SUSTAINSYS: Environmental Sustainable Agro-Forestry Systems" – NORTE-07-0124-FEDER-0000044. The authors are especially thankful to Dr. Manabu Abe, from Lab. Climate Risk Section, CGER, NIES, from Japan, for providing the MIROC data and to Cátia Pinto Teixeira for the spelling and grammar review of the manuscript.

References

Aldersley A, Murray SJ and Cornell SE (2011) Global and regional analysis of climate and human drivers of wildfire. Science of the Total Environment 409,3472-3481

Amiro BD, Logan K, Wotton B, Flannigan M, Todd J, Stocks B and Martell D (2005) Fire weather index system components for large fires in the Canadian boreal forest. International Journal of Wildland Fire 13,391-400

Batllori E, Parisien MA, Krawchuk MA and Moritz MA (2013) Climate change-induced shifts in fire for Mediterranean ecosystems. Global Ecology and Biogeography 22,1118-1129

Bedia J, Herrera S, Camia A, Moreno J and Gutiérrez JM (2014) Forest fire danger projections in the Mediterranean using ENSEMBLES regional climate change scenarios. Climatic Change 122,185-199

Benson RP, Roads JO and Weise DR (2008) Climatic and weather factors affecting fire occurrence and behavior. Developments in Environmental Science 8,37-59

Calado T and DaCamara C (2008) in 'Dating fire events on end of season maps of burnt scars.' (Eds pp. 323-333. (Springer)

Cane D, Wastl C, Barbarino S, Renier L, Schunk C and Menzel A (2013) Projection of fire potential to future climate scenarios in the Alpine area: some methodological considerations. Climatic Change 119,733-746

Carvalho A, Carvalho A, Martins H, Marques C, Rocha A, Borrego C, Viegas D and Miranda A (2011) Fire weather risk assessment under climate change using a dynamical downscaling approach. Environmental Modelling & Software 26,1123-1133

Carvalho A, Flannigan M, Logan K, Miranda AI and Borrego C (2008) Fire activity in Portugal and its relationship to weather and the Canadian Fire Weather Index System. International Journal of Wildland Fire 17,328-338

Carvalho A, Flannigan MD, Logan KA, Gowman LM, Miranda AI and Borrego C (2010) The impact of spatial resolution on area burned and fire occurrence projections in Portugal under climate change. Climatic Change 98,177-197

Cary GJ and Banks JC (2000) in 'Fire regime sensitivity to global climate change: an Australian perspective.' (Eds pp. 233-246. (Springer)

Chikamoto Y, Kimoto M, Ishii M, Mochizuki T, Sakamoto TT, Tatebe H, Komuro Y, Watanabe M, Nozawa T and Shiogama H (2013) An overview of decadal climate predictability in a multi-model ensemble by climate model MIROC. Climate Dynamics 40,1201-1222

Clarke HG, Smith PL and Pitman AJ (2011) Regional signatures of future fire weather over eastern Australia from global climate models. International Journal of Wildland Fire 20,550-562

Costa L, Thonicke K, Poulter B and Badeck F-W (2011) Sensitivity of Portuguese forest fires to climatic, human, and landscape variables: subnational differences between fire drivers in extreme fire years and decadal averages. Regional Environmental Change 11,543-551

de Groot WJ, Flannigan MD and Cantin AS (2013) Climate change impacts on future boreal fire regimes. Forest Ecology and Management 294,35-44

Dee D, Uppala S, Simmons A, Berrisford P, Poli P, Kobayashi S, Andrae U, Balmaseda M, Balsamo G and Bauer P (2011) The ERA-Interim reanalysis: Configuration and performance of the data assimilation system. Quarterly Journal of the Royal Meteorological Society 137,553-597

Durão R and Corte-Real J (2006) Alterações climáticas: futuro dos acontecimentos extremos e do risco de incêndio. Incêndios Florestais em Portugal: Caracterização, Impactes e Prevenção 231-255

Efron B and Efron B (Eds) (1982) 'The jackknife, the bootstrap and other resampling plans.' (SIAM)

Efron B and Tibshirani RJ (Eds) (1994) 'An introduction to the bootstrap.' (CRC press)

Errasti I, Ezcurra A, Sáenz J and Ibarra-Berastegi G (2011) Validation of IPCC AR4 models over the Iberian Peninsula. Theoretical and Applied Climatology 103,61-79

Flannigan MD, Krawchuk MA, de Groot WJ, Wotton BM and Gowman LM (2009) Implications of changing climate for global wildland fire. International Journal of Wildland Fire 18,483-507

Gibson RK, Bradstock RA, Penman TD, Keith DA and Driscoll DA (2014) Changing dominance of key plant species across a Mediterranean climate region: implications for fuel types and future fire regimes. Plant Ecology 215,83-95

Hoinka KP, Carvalho A and Miranda AI (2009) Regional-scale weather patterns and wildland fires in central Portugal. International Journal of Wildland Fire 18,36-49

Johnstone JF, Chapin FS, Hollingsworth TN, Mack MC, Romanovsky V and Turetsky M (2010) Fire, climate change, and forest resilience in interior Alaska This article is one of a selection of papers from The Dynamics of Change in Alaska's Boreal Forests: Resilience and Vulnerability in Response to Climate Warming. Canadian Journal of Forest Research 40,1302-1312

Karali A, Hatzaki M, Giannakopoulos C, Roussos A, Xanthopoulos G and Tenentes V (2014) Sensitivity and evaluation of current fire risk and future projections due to climate change: the case study of Greece. Natural Hazards and Earth System Science 14,143-153

Kilpeläinen A, Kellomäki S, Strandman H and Venäläinen A (2010) Climate change impacts on forest fire potential in boreal conditions in Finland. Climatic Change 103,383-398

Kloster S, Mahowald N, Randerson J and Lawrence P (2012) The impacts of climate, land use, and demography on fires during the 21 st century simulated by CLM-CN. Biogeosciences 9,509-525

Krawchuk MA, Moritz MA, Parisien M-A, Van Dorn J and Hayhoe K (2009) Global pyrogeography: the current and future distribution of wildfire. PLoS One 4,e5102

Le Goff H, Flannigan MD and Bergeron Y (2009) Potential changes in monthly fire risk in the eastern Canadian boreal forest under future climate change. Canadian Journal of Forest Research 39,2369-2380

Le Page Y, Oom D, Silva J, Jönsson P and Pereira J (2010) Seasonality of vegetation fires as modified by human action: observing the deviation from eco-climatic fire regimes. Global Ecology and Biogeography 19,575-588

Liu Z, Yang J, Chang Y, Weisberg PJ and He HS (2012) Spatial patterns and drivers of fire occurrence and its future trend under climate change in a boreal forest of Northeast China. Global Change Biology 18,2041-2056

Lucarini V, Calmanti S, Dell'Aquila A, Ruti PM and Speranza A (2007) Intercomparison of the northern hemisphere winter mid-latitude atmospheric variability of the IPCC models. Climate Dynamics 28,829-848

Lynch AH, Beringer J, Kershaw P, Marshall A, Mooney S, Tapper N, Turney C and Van Der Kaars S (2007) Using the paleorecord to evaluate climate and fire interactions in Australia. Annu. Rev. Earth Planet. Sci. 35,215-239

Meehl GA, Covey C, Taylor KE, Delworth T, Stouffer RJ, Latif M, McAvaney B and Mitchell JF (2007) The WCRP CMIP3 multimodel dataset: A new era in climate change research. Bulletin of the American Meteorological Society 88,1383-1394

Mochizuki T, Chikamoto Y, Kimoto M, Ishii M, Tatebe H, Komuro Y, Sakamoto TT, Watanabe M and Mori M (2012) Decadal prediction using a recent series of MIROC global climate models. 気象集誌. 第 2 輯 90,373-383

Moriondo M, Good P, Durao R, Bindi M, Giannakopoulos C and Corte-Real J (2006) Potential impact of climate change on fire risk in the Mediterranean area. Climate research 31,85-95

Moritz MA, Parisien M-A, Batllori E, Krawchuk MA, Van Dorn J, Ganz DJ and Hayhoe K (2012) Climate change and disruptions to global fire activity. Ecosphere 3,art49

Murphy BF and Timbal B (2008) A review of recent climate variability and climate change in southeastern Australia. International Journal of Climatology 28,859-879

Nakicenovic N and Swart R (2000) Special report on emissions scenarios. Special Report on Emissions Scenarios, Edited by Nebojsa Nakicenovic and Robert Swart, pp. 612. ISBN 0521804930. Cambridge, UK: Cambridge University Press, July 2000. 1,

Nieto S and Rodríguez-Puebla C (2006) Comparison of precipitation from observed data and general circulation models over the Iberian Peninsula. Journal of climate 19,4254-4275

Nitschke CR and Innes JL (2013) Potential effect of climate change on observed fire regimes in the Cordilleran forests of South-Central Interior, British Columbia. Climatic Change 116,579-591

Palheiro PM, Fernandes P and Cruz MG (2006) A fire behaviour-based fire danger classification for maritime pine stands: comparison of two approaches. Forest Ecology and Management 234,S54

Pausas JG and Paula S (2012) Fuel shapes the fire–climate relationship: evidence from Mediterranean ecosystems. Global Ecology and Biogeography 21,1074-1082

Peel MC, Finlayson BL and McMahon TA (2007) Updated world map of the Köppen-Geiger climate classification. Hydrology and earth system sciences discussions 4,439-473

Pereira M, Malamud B, Trigo R and Alves P (2011) The history and characteristics of the 1980–2005 Portuguese rural fire database. Natural Hazards and Earth System Science 11,3343-3358

Pereira MG, Calado TJ, DaCamara CC and Calheiros T (2013) Effects of regional climate change on rural fires in Portugal. Climate research 57,187-200

Pereira MG, Trigo RM, da Camara CC, Pereira J and Leite SM (2005) Synoptic patterns associated with large summer forest fires in Portugal. Agricultural and Forest Meteorology 129,11-25

Pitman A, Narisma G and McAneney J (2007) The impact of climate change on the risk of forest and grassland fires in Australia. Climatic Change 84,383-401

Randall DA and Fichefet T (2007) Climate models and their evaluation.

Rocca ME, Brown PM, MacDonald LH and Carrico CM (2014) Climate change impacts on fire regimes and key ecosystem services in Rocky Mountain forests. Forest Ecology and Management

Scherrer SC (2011) Present-day interannual variability of surface climate in CMIP3 models and its relation to future warming. International Journal of Climatology 31,1518-1529

Silvestrini RA, Soares-Filho BS, Nepstad D, Coe M, Rodrigues H and Assunção R (2011) Simulating fire regimes in the Amazon in response to climate change and deforestation. Ecological Applications 21,1573-1590

Stocker TF, Qin D, Plattner G-K, Tignor M, Allen SK, Boschung J, Nauels A, Xia Y, Bex V and Midgley PM (2013) Climate change 2013: The physical science basis. Intergovernmental Panel on Climate Change, Working Group I Contribution to the IPCC Fifth Assessment Report (AR5)(Cambridge Univ Press, New York)

Trigo RM, Pereira J, Pereira MG, Mota B, Calado TJ, Dacamara CC and Santo FE (2006) Atmospheric conditions associated with the exceptional fire season of 2003 in Portugal. International Journal of Climatology 26,1741-1757

Trigo RM, Sousa PM, Pereira MG, Rasilla D and Gouveia CM (2013) Modelling wildfire activity in Iberia with different atmospheric circulation weather types. International Journal of Climatology

Van Wagner C (Eds) (1987) 'Development and structure of the Canadian forest fire weather index system.')

Van Wagner C and Pickett T (Eds) (1985) 'Equations and FORTRAN program for the Canadian forest fire weather index system.')

Viegas D, Piñol J, Viegas M and Ogaya R (2001) Estimating live fine fuels moisture content using meteorologically-based indices. International Journal of Wildland Fire 10,223-240

Viegas DX, Reis RM, Cruz MG and Viegas MT (2004) Calibração do sistema canadiano de perigo de incêndio para aplicação em Portugal. Silva Lusitana 12,77-93

Watanabe M, Chikira M, Imada Y and Kimoto M (2011) Convective control of ENSO simulated in MIROC. Journal of climate 24,543-562

Watanabe S, Hajima T, Sudo K, Nagashima T, Takemura T, Okajima H, Nozawa T, Kawase H, Abe M and Yokohata T (2011) MIROC-ESM 2010: Model description and basic results of CMIP5-20c3m experiments. Geoscientific Model Development 4,845-872

Wendler G, Conner J, Moore B, Shulski M and Stuefer M (2011) Climatology of Alaskan wildfires with special emphasis on the extreme year of 2004. Theoretical and Applied Climatology 104,459-472

Westerling A, Bryant B, Preisler H, Holmes T, Hidalgo H, Das T and Shrestha S (2011) Climate change and growth scenarios for California wildfire. Climatic Change 109,445-463

Wilks DS (Eds) (2011) 'Statistical methods in the atmospheric sciences.' (Academic press)

Wotton B, Nock C and Flannigan M (2010) Forest fire occurrence and climate change in Canada. International Journal of Wildland Fire 19,253-271

Wotton BM (2009) Interpreting and using outputs from the Canadian Forest Fire Danger Rating System in research applications. Environmental and Ecological Statistics 16,107-131

Investigation of the weather conditions leading to large forest fires in the area around Athens, Greece

G. Xanthopoulos[a], A. Roussos[a], C. Giannakopoulos[b], A. Karali[b], M. Hatzaki[b]

[a] *Hellenic Agricultural Organization "Demeter". Institute of Mediterranean Forest Ecosystems and Forest Products Technology. Terma Alkmanos, Ilisia, 11528, Athens, Greece. gxnrtc@fria.gr*
[b] *Institute for Environmental Research and Sustainable Development,National Observatory of Athens, Athens, Greece. I. Metaxa and V. Pavlou Street, Palaia Pendeli, 15236, Athens, Greece cgiannak@meteo.noa.gr*

Abstract
Large forest fires are of great concern in all fire prone countries. Understanding them and predicting the possibility for their occurrence can be very helpful for forest fire management. They usually occur under very adverse fire weather conditions so any investigation about them is sure to take this into consideration. The Fire Weather Index (FWI) of the Canadian Forest Fire Danger Rating System which enjoys very broad use not only in the vast forests of Canada but also in other parts of the world, is a composite index that represents fire weather conditions quite well. The study presented here is an investigation of the possibility to associate fire weather conditions, as captured by FWI, with the occurrence of large forest fires in the broader area around Athens, the capital of Greece. It is based on forest fire data from the Greek Fire Service for the 2003-2011 period, matched to FWI values for this period, calculated using gridded observation data from the ERA Interim data sets, that were interpolated using the Thin Plate Spline Technique in order to obtain high resolution (1 km) spatial analysis data. Correlations between FWI and burned area per fire proved to be very poor, precluding regression modelling, so an alternative analysis method was used in order to determine, according to the data for the study period, the minimum FWI above which it is possible for fires to exceed certain burned area thresholds.

Keywords*: Fire Weather Index (FWI), large forest fires, Athens, Attica, Greece*

Introduction

In the world of forest fire management the need for understanding and prediction of fire ignition probabilities and difficulty of control is the main reason for collecting fire statistics and for the development and use of fire danger rating systems. A significant number of such systems have been developed around the world, some having more global characteristics and use than others. Among them the Canadian Forest Fire Danger Rating System (CFFDRS) (Stocks *et al*. 1989, Forestry Canada Fire Danger Group, 1992) enjoys very broad use not only in the vast forests of Canada but also in other parts of the world including Europe where the System's Fire Weather Index (FWI) was evaluated favourably, among others, by Viegas *et al*. (1999) in comparison with four other methods of fire danger evaluation, and was adopted since 2007 at the EU level by the European Forest Fire Information System (EFFIS) of the Joint Research Centre of the European Commission (http://forest.jrc.ec.europa.eu/effis). The FWI was also evaluated favourably by Dimitrakopoulos *et al*. (2011) and by Karali *et al*. (2014) in Greece. Both these studies proposed FWI value classes for association with fire danger.
Although the FWI, according to most evaluation studies produces good predictions, its use can become much more meaningful for use in operational fire management if it is further investigated and calibrated to the specific fire conditions in the region where it is to be applied (e.g. Fogarty *et al*. 1998, Rainha and Fernandes 2002). Furthermore, it makes sense to examine if its predictions and utility can be improved by introducing additional information to the one already required for FWI calculation.

The study presented here is an investigation of the fire weather conditions leading to large forest fires in the broader area around Athens, the capital of Greece. It was prompted by the operational need to tie the potential for such fires to FWI, in conjunction with the finding of studies like the one by Dimitrakopoulos *et al*. (2011) that the Fire Weather Index (FWI) while highly correlated to fire occurrence is only moderately correlated to burned area.

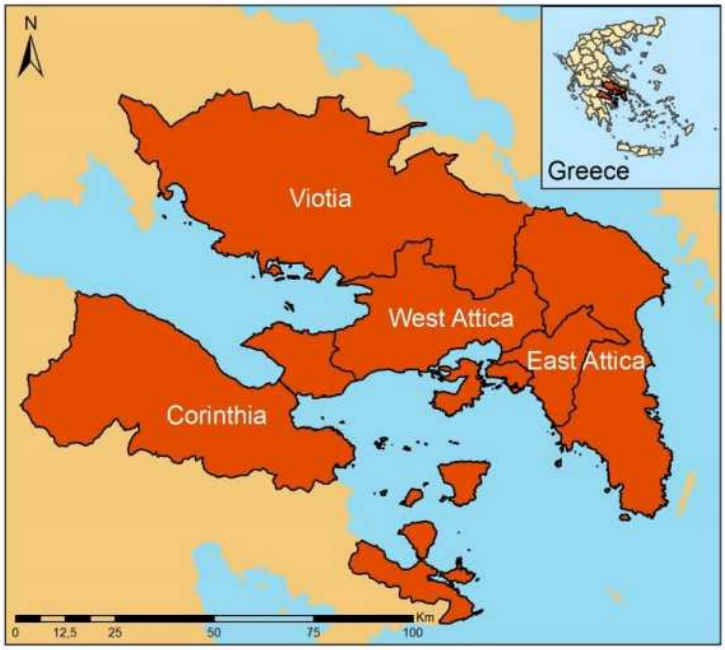

Figure 1. Map of the study area in Greece.

Methods

The study area covered the prefectures of East Attica, West Attica, Corinthia and Viotia (Figure 1). For this area forest fire data (dates, number of fires, burned area) for the 2003-2011 period, were obtained from the Greek Fire Service. Meteorological data were obtained from the ERA Interim data set (Dee *et al*. 2011) at a horizontal resolution of 0.75° (approximately 82km). The gridded meteorological data were firstly interpolated from the 82 km grid to a high spatial resolution 1-km grid using the 3D Thin Plate Spline technique (Hutchinson 1998). Subsequently, the interpolated meteorological data were used to calculate FWI values for a particular representative site on Mount Hymettus near Athens. Forest fire data were then matched to the calculated FWI values. Further to this, each fire was associated with representative predawn water potential (WP) measurements for roughly the same day, collected during the 2003-2011 period on the same site on Mount Hymettus (Xanthopoulos *et al*. 2006). These WP measurements were carried out for three representative Mediterranean species: *Pinus halepensis*, *Quercus coccifera and Cistus creticus.* This trial aimed to examine if the drought experienced by the living forest plants can play an important role in the occurrence of large fires in addition to the influence of the current weather condition captured by the FWI.

Analysis and results

The total number of fires reported in the four prefectures in the period of interest reached 6,860. They had burned a total area of 43,569 ha, roughly 5% of the study area. Some of them were identified as

non forest fires (e.g. agricultural residue burning) and were dropped from the database. The rest of the fires were analyzed putting emphasis on the large fires that occurred in this time period.
The FWI for all days with fire, varied between 0.0001 and 102.92. On the day of the highest FWI (August 22, 2010) six fires were reported. Their burned area ranged between 0.05 and 7 ha. The maximum burned area for one fire was 17,500 ha. This historic fire started on August 21, 2009, under an FWI of 71.845.
Focusing on large fires, a sub-sample of the data set was created with all fires having a burned area equal to or larger than 10 ha. The number of observations was 175. This smaller data set was examined in regard to the correlation of burned area with FWI. The Pearson correlation proved to be very low (0.133) and non-significant. The existence of the large 17,500 ha fire of August 2009 in the dataset was considered as a probable reason for this low correlation. However, even when this data point was removed (N=174), the correlation reached only 0.183 and became significant at the 0.05 level (2-tailed). Obviously, these low correlations preclude any effort for predictive regression modelling. Figure 2 is a plot of the 174 point data set, after omission of the 17,500 ha fire.

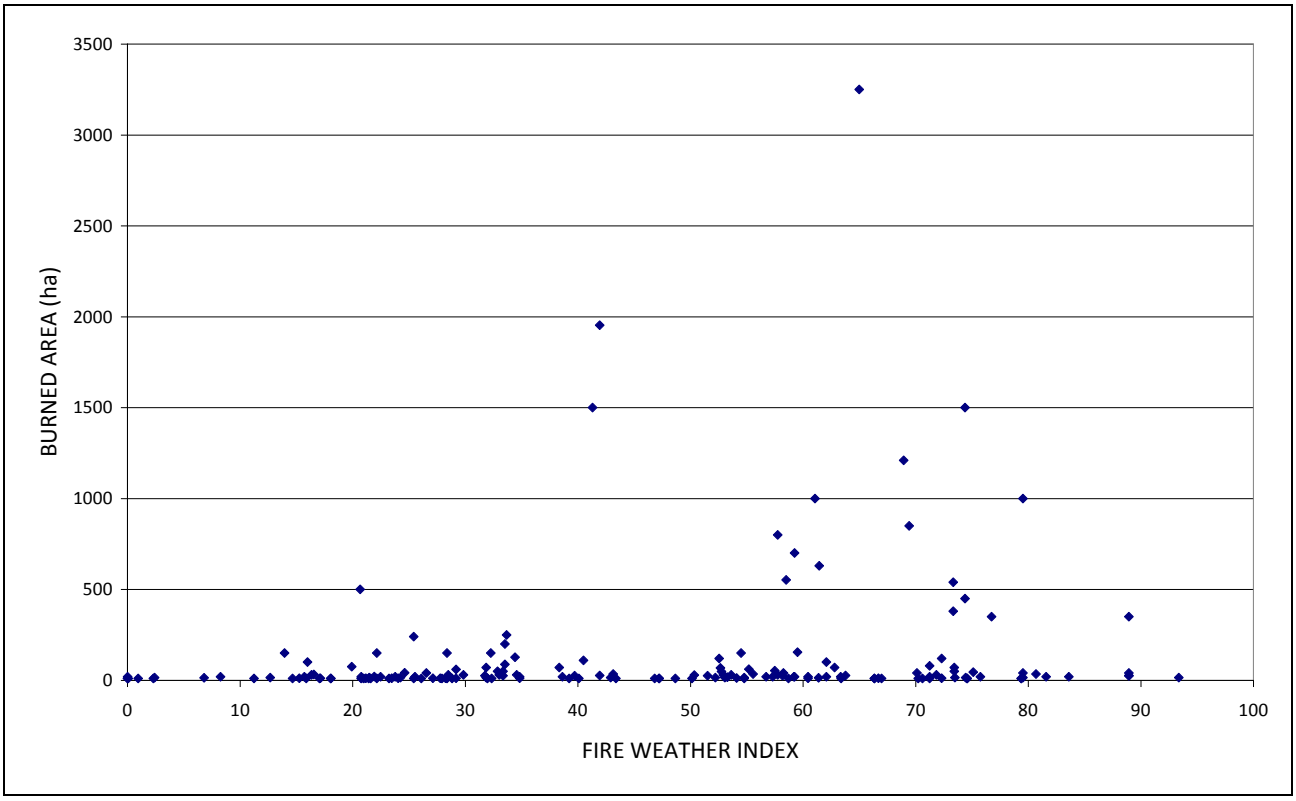

Figure 3. Plot of the Fire Weather Index versus the burned area of the 174 largest fires in the study region in the 2003-2011 period, omitting for scaling purposes the largest fire of 17,500 ha that occurred under a FWI of 71.845

The water potential data for the three species examined also had poor correlation with burned area. The same was true when the product of FWI with water potential was examined for correlation with burned area, so at this stage the WP data were not examined further.
These results illustrated the problem of the potential discrepancies between FWI and burned area and called for a different ad-hoc approach for analysing the data set in regard to large fires. This approach was as follows: selecting sub-samples of the database that included only the fires that burned an area larger than a specific threshold (ha), the minimum FWI and maximum FWI for each sub-sample were entered in a table (Table 1) and were also plotted against that threshold.

Table 1. Number of fires, Minimum FWI, and Maximum FWI for subsets of the complete dataset that each included only the fires above a selected burned area threshold (ha).

Burned Area Threshold (ha)	Number of fires	FWI Min	FWI Max
10	175	0,00705	93,37405
20	100	0,01265	88,93933
30	69	13,95373	88,93933
40	56	13,95373	88,93933
50	48	13,95373	88,93933
60	44	13,95373	88,93933
70	41	13,95373	88,93933
80	36	13,95373	88,93933
90	34	13,95373	88,93933
100	34	13,95373	88,93933
110	32	13,95373	88,93933
120	31	13,95373	88,93933
130	28	13,95373	88,93933
150	28	13,95373	88,93933
170	22	20,67158	88,93933
200	22	20,67158	88,93933
250	20	20,67158	88,93933
300	19	20,67158	88,93933
350	19	20,67158	88,93933
400	16	20,67158	79,54018
500	15	20,67158	79,54018
600	12	41,3183	79,54018
700	11	41,3183	79,54018
800	10	41,3183	79,54018
900	8	41,3183	79,54018
1000	8	41,3183	79,54018
1200	6	41,3183	74,38725
1400	5	41,3183	74,38725
1600	3	41,3183	74,38725
1800	3	41,3183	74,38725
2000	2	64,99238	71,84505
3300	1	71,84505	71,84505

As shown in table 1, 175 fires had each burned an area equal to or exceeding 10 ha (N_{10}=175). The minimum FWI value among these fires was 0.007 and the maximum FWI was 93.374. This means that a fire may reach or exceed 10 ha even at an FWI=0.007.

When setting the threshold at 20 ha the number of fires dropped to N_{20}=100, the minimum FWI was 0.012 and the maximum FWI was 88.894. This means that even at this minimum FWI value a fire may exceed 20 ha. The smaller maximum FWI value in this subset means that a fire that occurred with an FWI of 93.374 and was included in the previous subset because it had burned over 10 ha, did not exceed the 20 ha threshold and was left out of this second subset.

The next subset with the threshold burned area set at 30 ha, had a minimum FWI of 13.95 and N_{30}=69. The same minimum FWI remained for the next subsets until the threshold was set to 170 ha (N_{170}= 22) and the minimum FWI became 20,672.

Following the same logic, the plot of Figure 3 was created. It shows the minimum FWI thresholds that make it possible for fires to exceed initial attack capabilities and, as long as there is available fuel in their path, to become large or very large.

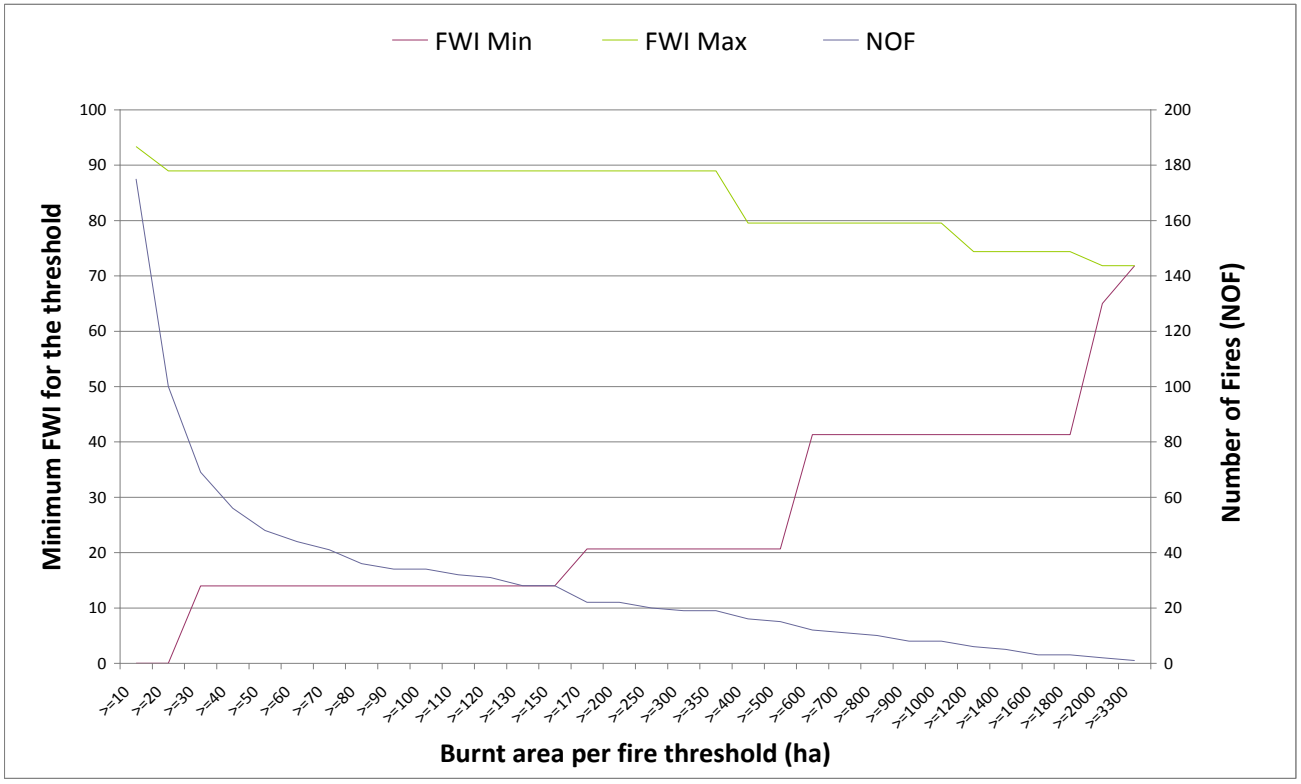

Figure 3. Minimum FWI that may allow forest fires to exceed certain burned area thresholds for the conditions (vegetation, firefighting resources, etc.) in the study area around Athens, in Greece.

Discussion and conclusions

The efforts spent looking for a mathematically expressed relation between FWI and burned area did not produce any results. This is in agreement with the conclusions of Dimitrakopoulos *et al*. (2011). It is clear that whereas fire ignition probabilities correlate reasonably well with the weather conditions as captured by FWI, things are quite different in regard to burned area. The varying capability of firefighting resources, temporally and spatially, is a significant factor affecting the evolution of each fire. The existence of fuel in the path of a fire is also another important factor that acts randomly on every fire depending on where it starts and on the direction of its spread. Further to the above, there are various sources of errors in the data set that may have added "noise" reducing correlations further. These sources of error are:

- Inaccuracy of reported burned area per fire by the Fire Service (it is called an estimate, not a measurement)
- Calculation of FWI over broad areas rather than based on the local conditions of each fire.
- Using one value of water potential per species (average of two measurements) from one location in Attica and from the closest available date to the date of the fire.

On the other hand, the alternative method of analysis used here, as shown in Table 1 and Figure 3, provides some thresholds that can be useful for setting mobilization levels according to predicted

weather conditions and FWI, and also for guiding pre-fire positioning of firefighting resources and for supporting dispatching decisions in case of fire eruption. More specifically, it can be concluded that:

- If the FWI exceeds 0,01 fires exceeding 20 ha are possible.
- If the FWI exceeds 13,95 fires exceeding 30 ha are possible.
- If the FWI exceeds 13,95 fires exceeding 30 ha are possible.
- If the FWI exceeds 20,67 fires exceeding 170 ha are possible.
- If the FWI exceeds 41,32 fires exceeding 600 ha are possible.
- If the FWI exceeds 64,99 fires exceeding 2000 ha are possible.
- If the FWI exceeds 71,84 fires exceeding 3300 ha are possible.

Acknowledgements

The research reported here was carried out in the frame of a research project of the Institute of Mediterranean Forest Ecosystems and Forest Products Technology (IMFE&FPT) titled "Investigation of the relation between the water potential of forest plants and forest fires", and a second project titled "Contribution to Fire Prevention in 2013-2014 using the INCA methodology". This latter project was funded by the Special Secretariat for Forests through the "Green Fund" of the Greek Ministry of Environment, Energy, and Climate Change.

References

Dee DP, Uppala SM, Simmons AJ, Berrisford P, Poli P, Kobayashi S, ... & Vitart, F (2011) The ERA-Interim reanalysis: Configuration and performance of the data assimilation system. Quarterly Journal of the Royal Meteorological Society 137(656), 553-597.

Dimitrakopoulos AP, Bemmerzouk AM, Mitsopoulos ID (2011) Evaluation of the Canadian fire weather index system in an eastern Mediterranean environment. Meteorological Applications 18(1), 83-93.

Fogarty LG, Pearce HG, Catchpole WR, Alexander ME (1998) Adoption vs. adaptation: lessons from applying the Canadian forest fire danger rating system in New Zealand. In Proceedings, 3rd International Conference on Forest Fire Research and 14th Fire and Forest Meteorology Conference, Luso, Coimbra, Portugal. (Ed. DX Viegas)pp. 1011-1028. (ADAI: Coimbra, Portugal).

Forestry Canada Fire Danger Group 1992. Development and structure of the Canadian Forest Fire Behavior Prediction System. Forestry Canada, Ottawa, ON. 63 p. Information Report ST-X-3.

Hutchinson MF (1998) Interpolation of rainfall data with thin plate smoothing splines—part II: analysis of topographic dependence. Journal of Geographic Information and Decision Analysis 2:152–167.

Karali A, Hatzaki M, Giannakopoulos C, Roussos A, Xanthopoulos G, Tenentes V (2014) Sensitivity and evaluation of current fire risk and future projections due to climate change: the case study of Greece, Nat. Hazards Earth Syst. Sci., 14, 143-153.

Stocks BJ, Lynham TJ, Lawson BD, Alexander ME, Wagner CV, McAlpine RS, Dube DE (1989) The Canadian forest fire danger rating system: an overview. The Forestry Chronicle 65(4), 258-265.

Van Wagner CE (1987) Development and structure of the Canadian Forest Fire Weather Index System. Canadian Forestry Service, Forestry Technical Report 35. Ottawa, Ontario, Canada.

Viegas DX, Bovio G, Ferreira A, Nosenzo A, Sol B (1999) Comparative study of various methods of fire danger evaluation in southern Europe. International Journal of Wildland Fire 9, 235–246.

Xanthopoulos G, Maheras G, Gouma V, Gouvas M (2006) Is the Keetch-Byram drought index (KBDI) directly related to plant water stress? In "Forest Ecology and Management", Vol. 234, Supplement 1, (Ed. DX. Viegas), p. 27 (abstract). (Elsevier Publishers, Amsterdam). Full text, in Proceedings of the 5th International Conference on Forest Fire Research. November 27-30, 2006, Figueira da Foz, Portugal (on CD).

Modeling fire behaviour and carbon emissions

William J. de Groot, Alan S. Cantin, Natasha Jurko, Alison Newbery

Canadian Forest Service, 1219 Queen St. E., Sault Ste. Marie, ON Canada P6A 2E5.
bill.degroot@nrcan.gc.ca, alan.cantin@nrcan.gc.ca, natasha.jurko@nrcan.gc.ca, alison.newbery@nrcan.gc.ca

Abstract
Wildland fire is an important component of the earth system and global carbon cycle, burning about 350 M ha of vegetated land and contributing 2.0 Pg C to the atmosphere in direct emissions every year. Wildland fire carbon emissions are directly related to fuel consumption, which is a key component of fire behaviour. Fuel consumption varies greatly by fuel (vegetation type, load, size, spatial distribution, moisture content) and weather (temperature, relative humidity, wind speed, rainfall) parameters. In forested regions where wildfires may burn for extended periods of time, carbon emissions can vary by an order of magnitude between stands within a single fire due to complex fuel structures and distribution patterns, and constantly changing fire weather conditions. Modelling stand-level fire behaviour and carbon emissions and compiling simulation results over large areas is commonly used as a bottom-up approach to summarizing fire regimes and estimating wildland fire emissions at large scales.
This paper presents a summary of studies simulating stand-level fire behaviour and carbon emissions using the Canadian Fire Effects Model (CanFIRE). CanFIRE simulates fire behaviour in standing timber, grass, and slash vegetation types, or combinations of these vegetation types. In standing timber vegetation types, the forest stand is simulated as 3 distinct fuel components: forest floor (herbaceous plant, litter and organic soil layers), surface fuels (dead woody debris), and overstory (tree) fuels. Modelled fire behaviour and carbon emission results from studies in various global regions of different vegetation types and climate zones are presented, including comparisons using different fuels and weather/climate datasets and comparison to other carbon emission estimation methods. Sensitivity of the model outputs to driving input variables is presented. In particular, the influence of stand composition, structure, surface fuel load and distribution, and organic soil characteristics are reviewed. Annual and seasonal trends in fire behaviour and carbon emissions are also presented. Recommendations for basic data standards to provide reliable and consistent modelling results are discussed.

Keywords*: Canadian Fire Effects Model, crowning, fire intensity, forest carbon, fuel consumption, rate of spread, wildland fire emissions, North American forest regions, circumpolar boreal forest*

Introduction

Numerous studies have been conducted over the last decade to estimate wildland fire carbon emissions using various models and methods (e.g., French *et al*. 2011). Global-level estimates have been produced using the Global Fire Emissions Database (GFED3) (Van der Werf 2010). At national and sub-national scales, wildfire carbon emissions are typically estimated using a fire behaviour-based, bottom-up method using models such as the Canadian Fire Effects Model (CanFIRE, de Groot 2006, 2010), the First Order Fire Effects Model (FOFEM, Reinhardt *et al*. 1997), CONSUME (Ottmar *et al*. 2009) and the Wildland Fire Emissions Information System (WFEIS, French *et al*. 2009), which is based on the CONSUME model. These models quantify fuel consumption at the stand level and scale-up by aggregating stand emissions data over landscapes with fire mapping products (e.g., de Groot *et al*. 2007, French *et al*. 2011) Stand-level fuel consumption can be calculated with fuels data from a variety of sources and spatial resolution, and fire weather data with a range of spatial and temporal resolutions. Using different databases with various scales contributes to the variability of wildland fire carbon emission estimates that are produced (c.f., French *et al*. 2011). Adding to this uncertainty is that there are very few verified field data sources to compare with modelled results (Ottmar 2014).

The purpose of this paper is to review applications of the Canadian Fire Effects Models to estimate carbon emissions in the circumpolar boreal forest region, in North American forests (including boreal and western forest regions), and within the Canadian boreal forest region, and to compare results using different fuels and weather data bases at different scales.

The Canadian Fire Effects Model

The Canadian Fire Effects Model (CanFIRE) is an integrated science-management model of the Canadian Forest Fire Danger Rating System (Stocks *et al*. 1989). It was originally developed as the Boreal Fire Effects Model (BORFIRE) to conduct fire, climate change, and vegetation dynamics research in the Canadian boreal forest (de Groot *et al*. 2002, 2003). The model was later expanded to include all Canadian forest regions (renamed CanFIRE) for use as an operational model to calculate annual national wildland fire carbon emissions (de Groot 2006, de Goot *et al*. 2007). The model has since been re-designed for fire and forest management applications and is available as an Excel spreadsheet[1], a cross-platform Windows and Unix application[1], and as a web application[2].

CanFIRE simulates stand-level physical and ecological fire effects. It is a fire behaviour-based model driven by fuels and fire weather data. Fuels are characterized by tree species in the stand (including age, height, dbh, and density data) and fuel loads for stand components of the forest floor (litter and other fine fuels, fermentation, and humus layers), dead and downed woody debris (multiple roundwood diameter size classes), and aboveground tree biomass (live and dead; stem, branch, bark and foliage components). Fire weather data are provided to CanFIRE using the Canadian Forest Fire Weather Index (FWI) System (Van Wagner 1987) components. The model calculates fire behaviour (rate of fire spread, fuel consumption, type of fire, and fire intensity) and resulting physical (depth of burn, crown scorch, carbon emissions) and ecological (tree mortality/survival, regeneration rate, long-term post-fire succession) effects. CanFIRE uses the rate of spread algorithms of the Canadian Forest Fire Behavior Prediction (FBP) System (Forestry Canada Fire Danger Group 1992); type of fire is determined using Van Wagner's (1977) crown fire threshold model; fuel consumption is calculated using fuel load data and new fuel consumption algorithms (de Groot *et al*. 2009); and resulting fire intensity is calculated using Byram's (1959) equation. CanFIRE can be used to simulate fire behaviour and effects of a single fire event, or the accumulated effects of many fires occurring over many years on a defined landscape (i.e., simulating fire regime).

CanFIRE has been modified and used for numerous fire and carbon modelling applications in different regions since the original BORFIRE model. The purpose of this paper is to provide a review of CanFIRE applications to estimate wildland fire carbon emissions using different data sources and simulation methods, and to compare with results from other emission models.

Wildland Fire Carbon Emission Studies with CanFIRE

Circumpolar Boreal Fire Carbon Emissions

A comparison of wildfire carbon emissions in western Canada and central Siberia, Russia during 2001-2007 was conducted with remotely-sensed area burned polygons and fire weather data used to simulate fire behaviour and carbon emissions with CanFIRE (de Groot *et al*. 2013a). Russia-specific fuel models were setup in CanFIRE by assigning an FBP System fuel type, and adjusting tree heights and crown length factors for Russian tree species. The primary effect of this was to adjust the crown fire

[1] Contact Bill de Groot (bill.degroot@nrcan.gc.ca) or Alan Cantin (alan.cantin@nrcan.gc.ca)
[2] http://www.glfc.forestry.ca/canfire/index.cfm

threshold for Russian boreal tree species. Fuels load and type data were obtained from national sources and fires were mapped with different remote sensing products. As a result, input data had different spatial characterization and resolution. However, the data was sufficient to calculate stand-level fire behaviour for all large (>200ha) fires in both study areas for the 7-year period. All fires were burned using fire weather conditions interpolated from station data to all MODIS hot spots within a 1 km buffer around each fire and taking the mean, thus weighting the fire weather to the date of greatest fire activity. Results of the study comparison indicated divergent continental fire regimes in the circumpolar boreal region, which was attributed to differences in tree species morphology and fire ecology traits. In particular, the fire regime of the Canadian study area was characterized by infrequent, very large, high intensity crown fires; whereas, the Russian study area was characterized by moderately frequent, large surface fires of moderate to high intensity (Table 1). Fire seasons were also different with most large fires occurring in Russia in the spring, and during summer in Canada. The carbon emissions rate (t C·ha^{-1} within burned area polygons) in Canada was 50% higher than in Russia mostly because of higher forest floor fuel loadings and fuel consumption but also, to a lesser degree, due to higher crown fuel consumption rates in Canada. However, the total C emissions rate (t C·ha^{-1} per 100 M ha of forest area) was two times greater in Russia because of the much higher annual area burned rate.

CanFIRE was also used to simulate C emissions in the same Canadian and Russian study areas under future climate change scenarios (de Groot *et al*. 2013b). That study examined the impact of changing fire weather on carbon emissions by the end of this century. Three Global Climate Models (Canadian CGCM3.1, HadCM3, and IPSL-CM4) and three climate change scenarios (A1B, A2, and B1) (IPCC 2000) were used to determine nine sets of future fire weather conditions for the CanFIRE simulations. All climate change models and scenarios indicated greater fire weather severity across the circumboreal region, although conditions will be slightly more severe in the western Canada study area. The future fire season will have two extreme fire intensity peaks in western Canada in spring and later summer, and one extreme peak in central Russia in late spring/early summer. Higher carbon emission rates (t C·ha^{-1}) will occur in western Canada due to a higher fuel consumption rate but central Russia will have greater total carbon emission rates (t C·ha^{-1} per 100 M ha forest area) due to higher annual area burned rates.

Table 1. Summary of annual average fire regime characteristics in western Canada and central Russia boreal forest during 2001-2007 (de Groot et al. 2013a)

	Canadian Study Area	Russian Study Area
Number of fires (per 100 M ha forest)	93.7	1441.9
Area burned (M ha/100 M ha forest)	0.56	1.89
Mean fire return interval (yrs)	179.9	52.9
Large fire size (ha)	5930	1312
Crown fire (%)	57.1	6.5
Head fire intensity (kW/m)	6017	4858
Fuel consumption (kg/m^2)	5.68	3.73
C emissions rate (t/ha)	28.4	18.5
Total C emissions rate (Mt/100 M ha forest)	15.8	35.0

North American Wildland Fire Carbon Emissions

In a study of six terrestrial models, French *et al*. (2011) compared wildland fire carbon emissions from five large fires across North America. CanFIRE was applied to the three forest-dominated fires of that study, but not to the two fires in southern California chaparral because CanFIRE does not currently

have a shrub fuel model. Fuels data for the large fires in Oregon and Alaska were provided from the Fuels Characteristic Classification System (FCCS, Ottmar *et al*. 2007) and from fuel load models of Lutes *et al*. (2009). Fuels data in the Saskatchewan large fire were obtained from provincial forest inventory and interpreted as FCCS fuels. All fires burned over many days and were simulated in CanFIRE and WFEIS as multi-day events using daily fire progression (as determined by MODIS hot spots) and daily fire weather data. Additional WFEIS, CONSUME and FOFEM estimates were obtained using single day simulations with standard fuel moisture scenarios. FBP estimates were multiple day simulations using FBP System fuel types interpreted from the FCCS data (Oregon and Alaska) or forest inventory data (Saskatchewan).

Despite using the same original fuels and weather databases, emission estimates showed considerable variation depending on model and fire location. A detailed field-based survey of carbon emissions was available for the Oregon Biscuit fire (Campbell *et al*. 2007), which reported an average carbon emissions rate of 1.9 kg $C \cdot m^{-2}$. The CanFIRE estimate was 3% higher, and FOFEM 5.7 ranged from 17% lower to 4% higher (3 scenarios using revised fuels map); the FBP System was 11% lower, GFED was 14% higher, CONSUME 3.0 was 10-30% lower (3 scenarios using revised fuels map), and WFEIS was 61-63% higher (3 scenarios using revised fuels map). A field-based survey was also available for the Alaska Boundary fire, resulting in an emissions rate of 2.59 kg $C \cdot m^{-2}$. For that fire, the GFED estimate was 14% lower, CONSUME was 10-45% lower, CanFIRE was 40% higher, the FBP System was 48% lower, and FOFEM was 73-136% higher. Field data were not available for the Saskatchewan Montreal Lake fire for comparison, but the estimated emission rates were 0.79 kg $C \cdot m^{-2}$ (FBP), 1.26 kg $C \cdot m^{-2}$ (GFED), 1.6 kg $C \cdot m^{-2}$ (WFEIS), 2.32 kg $C \cdot m^{-2}$ (CanFIRE), 2.23-3.32 kg $C \cdot m^{-2}$ (CONSUME), and 4.76-6.51 kg $C \cdot m^{-2}$ (FOFEM). A previous estimate for the same fire using CanFIRE and national forest inventory data (Power and Gillis 2006) was 1.70 kg $C \cdot m^{-2}$, and using the national fuels database (Nadeau *et al*. 2005) with the FBP System was 1.20 kg $C \cdot m^{-2}$.

Canadian Wildland Fire Carbon Studies

CanFIRE has been used operationally since 2004 to calculate annual national wildland fire carbon emissions as part of the National Forest Carbon Monitoring, Accounting and Reporting System (Kurz and Apps 2006) to meet United Nations Framework Convention on Climate Change and other international reporting obligations (de Groot *et al*. 2007). CanFIRE was modified to utilize a national database of carbon pools provided by the Carbon Budget Model of the Canadian Forest Sector (CBM-CFS3, Kurz *et al*. 2009) as a replacement for fuel type and fuel load data. This is a spatially-explicit procedure using primarily satellite-mapped burned areas, daily hot spots and fire weather data. In brief, every forest stand within each mapped fire perimeter was burned in the model as a single-day event. Fire weather was calculated by interpolating FWI System values to each MODIS and AVHRR hot spot, and averaging all those data annually for the fire season for each ecoregion-provincial unit, and applying those results to all fires contained in each unit. In this way, the FWI system data are weighted by days of highest fire activity within the ecoregion-provincial unit for the year.

More recently, 43 large fires from Ontario, Saskatchewan, Alberta, and British Columbia were used in an ongoing study to compare Canadian wildland fire carbon emissions using different fuels data and simulation methods. The initial phase of the study examined 24 large boreal wildfires from 2006–2008 ranging in size 95–62,670 ha. These fires were selected because they occurred in areas where detailed provincial forest inventory data were available, which allowed stand-level simulations with CanFIRE to calculate direct carbon emissions. In a second analysis, an additional 10 large fires (446–22,116 ha) occurred in Alberta during the same time period and were combined with the original 24 fires plus 9 large fires from 2010 (1,943–28,182 ha) in British Columbia and used for carbon emission calculations using the national fuel type map of Nadeau *et al*. (2005) (resolution of 1 km^2) and standard fuel loads for FBP System fuel types. The fires were simulated as a single-day event (date selected by weighted average of hot spots), and as a multi-day event (daily fire spread using hot spots) for comparison.

Results using the large scale national fuels database (n=43 fires) and standard FBP System fuel types and fuel loads showed very little difference when using single- or multi-day simulations (Figure 1). Emissions were generally higher in Alberta and lower in Ontario. In the comparison of 33 fires with forest inventory available to use as input fuels data (Figure 2), carbon emission estimates increased for the British Columbia fires and decreased for all others, including a very sharp decrease in the Alberta and Saskatchewan fires (although there were only two large fires in Alberta with forest inventory available). These results were consistent for both single- and multi-day simulations. When all provincial data were combined, the forest inventory method produced lower carbon emissions estimates than the FBP method. Overall, there was almost no difference between single- and multi-day estimates (Figure 3).

Discussion

The previous studies using CanFIRE to estimate wildland fire carbon emissions have demonstrated that many different fuel and weather data sets can be used as input variables to CanFIRE (Table 2). The question of which database and/or what data resolution is the most appropriate or accurate to use is still not clear. As Ottmar (2014) pointed out, there are very few datasets available to test model accuracy, and there is also very little information available about the sensitivity of models to data input variability.

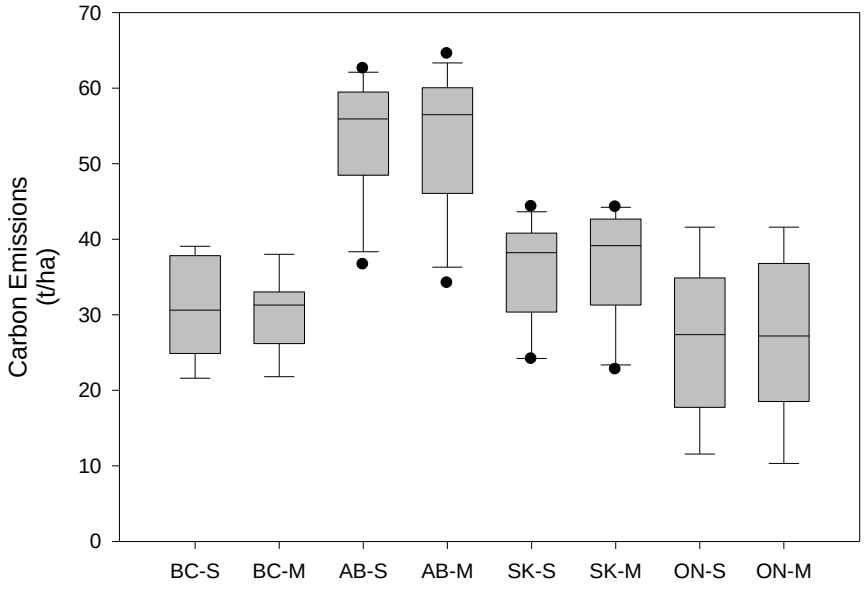

Fig 1. Summary of wildland fire carbon emissions in the provinces of British Columbia (BC) (n=9), Alberta (AB) (n=12), Saskatchewan (SK) (n=13), and Ontario (ON) (n=9) using single-day (S) and multi-day (M) simulation methods with CanFIRE. Fuels data were obtained from the spatial national fuel type map of Nadeau et al. (2005) using standard fuel loads for FBP System fuel types.

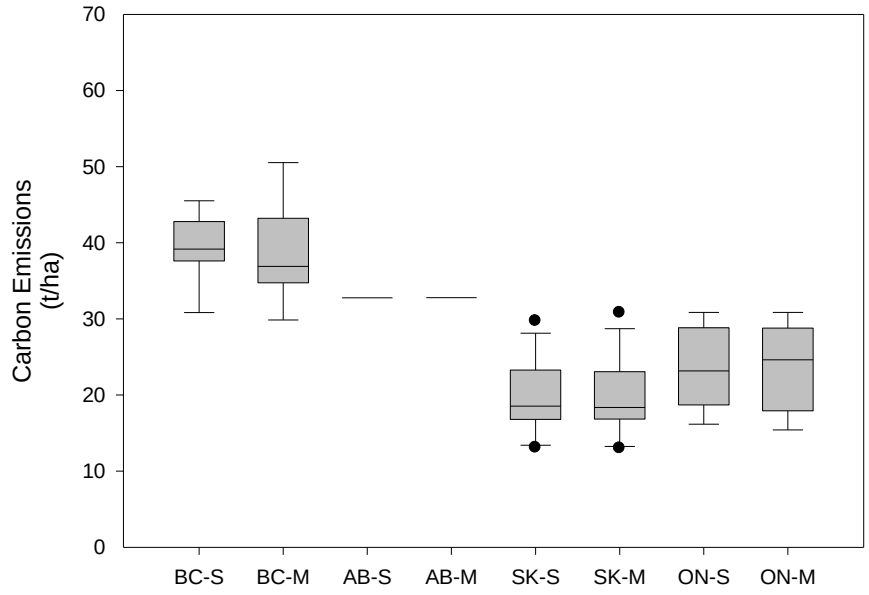

Fig 2. Summary of wildland fire carbon emissions in the provinces of British Columbia (BC) (n=9), Alberta (AB) (n=2), Saskatchewan (SK) (n=13), and Ontario (ON) (n=9) using single-day (S) and multi-day (M) simulation methods with CanFIRE. Spatial provincial forest inventory was used to interpret stand-level species composition and corresponding fuel load was calculated using forest inventory with provincial growth and yield models.

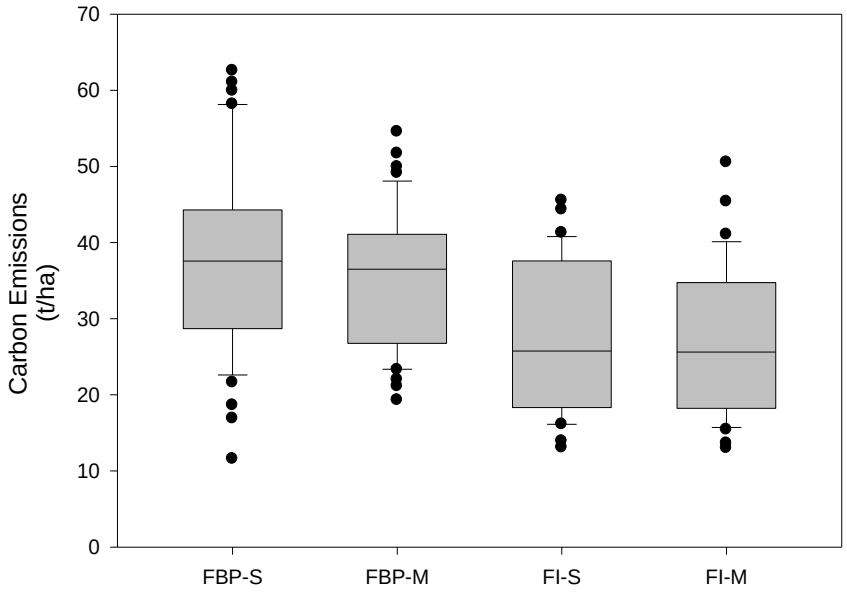

Fig 3. Summary of average wildland fire carbon emissions in the provinces of British Columbia, Alberta, Saskatchewan, and Ontario using the national fuels database (FBP) and provincial forest inventory (FI) for fuels information, and using single-day (S) and multi-day (M) simulation methods with CanFIRE.

One of the most important observations in comparing these wildland fire carbon emissions studies is the influence of fuels input data. The CanFIRE estimate of emissions on the Montreal Lake fire in French *et al*. (2011) was almost twice as high as the previous estimate in de Groot *et al*. (2007), which was entirely the result of different input fuels data. Similarly, emission estimates using CONSUME

and FOFEM on the Biscuit fire were up to three times higher for the same model, depending on the fuels data source (original and revised fuels maps; French *et al*. 2011). The impact of different fuels data on emission estimates was also identified in the circumboreal comparison study (de Groot *et al*. 2013a), which showed substantially higher carbon emissions rates (t/ha) from Canadian fires than Russian fires. That result was attributed to underestimated forest floor fuel loads in the Russian database because fire weather conditions were fairly similar.

French *et al*. (2011) provide a good summary of differences in the six tested models that can lead to different emission estimates. In that study, emission estimates from a few models aligned fairly close on some fires but not on others, and there was no obvious overall trend. This suggests that wildland fire emission models may need to be regionally calibrated. However, one common result was that FBP System estimates were lower than most of the other model estimates. This agrees with previous results from de Groot *et al*. (2007) that indicated FBP System estimates were about 30% lower than CanFIRE estimates in central Canada. Low emission estimates from the FBP System are attributed primarily to an underestimation of forest floor fuel consumption. CanFIRE uses more recent forest floor fuel consumption algorithms (de Groot *et al*. 2009) than currently included in the FBP System, but which will be incorporated in the next generation FBP System.

Table 2. Summary of fire simulation methods, weather and fuels data for wildland fire carbon emission studies using CanFIRE

Study	Fire simulation method	Weather data		Fuels data	
		Source	Resolution	Source	Resolution
Boreal fire emissions in Canadian and Russian study areas (2001-2007) (de Groot *et al*. 2013a, 2013b)	Canadian large fires burned as single day events on most active fire day (by MODIS hot spots)	Canadian national weather station network	Daily	National fuel type map, standard FBP fuel loads	1 km^2
	Russian large fires burned as single day events on most active fire day (by MODIS hot spots)	Russian national weather station networks	Daily	National forest carbon database	Ecoregion and oblast-level summaries (semi-spatial)
North American study (French *et al*. 2011)	3 large fires (Oregon, Alaska, Saskatchewan) burned as single and/or multi-day events	Nearby fire weather stations	Daily	FCCS and FLM[a]	1 km^2
Canadian annual carbon emissions reporting (de Groot *et al*. 2007)	All fires burned as single day event using averaged fire weather from active fire days	National and provincial fire weather station network	Daily, averaged seasonally by hot spot occurrence over ecoregion-provincial units	CBM-CFS3 carbon pools	Stand-level
Canadian large fires	Large fires burned as single- and multi-day events	National and provincial fire weather station networks	Daily	National fuel type map and standard FBP system fuel loads	1 km^2
	Large fires burned as single- and multi-day events	National and provincial fire weather station networks	Daily	Provincial forest inventory	Stand-level

[a] Fuel Characteristic Classification System (Ottmar *et al*. 2007) and Fuel Loading Models (Lutes *et al*. 2009)

The amount of detail (or scale) to use for wildland fire emissions modelling has been a lingering question. Forest inventories have many advantages as a fuels data source: they are small scale (stand-level), have detailed species information for fuel typing, integrate well with forest growth and yield models for dynamic fuel modelling, and integrate well with tree biomass algorithms to properly distribute fuel load in multiple stand components. However, there are many deficiencies: inventories are often old, they are only as reliable as the original photo interpretation and areas are so vast that ground checking is often limited, fuels data for some stand components are usually missing (e.g., forest floor and dead woody debris), inventory methods are usually not consistent across land jurisdictions which makes large scale simulation difficult, and there are many areas without forest inventory. There are numerous other vegetation, fuels, and biomass inventories that can be used for calculating wildland fire emissions, and all will produce different results. The question remains: what are the best criteria to use for selecting a fuels database, understanding that many factors have to be balanced (i.e, accuracy vs. efficiency)? It is still an open question because test datasets to assess accuracy are very few. However, large-scale data consistency is important in terms of modelling efficiency. At this point, the general recommendation is to use stand-level data if it is consistent in content across the simulation area, and if not available, then to use coarser resolution fuels data at a larger scale. To provide the best fire behaviour-based estimate of wildland fire carbon emissions, the selected fuels database should provide fuel type and load data that can be separated into discreet stand components (forest floor, dead woody debris, tree crown, etc.) in order to properly simulate stand-level fire behaviour dynamics.
In terms of temporal scale, the question of detail is much less critical. In the Canadian fire study, CanFIRE emission estimates showed very little difference between single- and multi-day simulations (Figure 1-3) even though some fires burned for over a month. The comparison of single- and multi-day WFEIS simulations (French *et al*. 2011) also showed the same results. This suggests that the procedure used for single-day simulation (i.e., using fire weather and fuel moisture data based on daily-weighted hot spot occurrence) captures the most important weather information driving these fire behaviour-based models.

Conclusions

Fuels data source is a critical factor influencing wildland fire carbon emission estimates for all fire behaviour-based models, including CanFIRE. Consistency in data content across the simulation area is important, and it is preferable to have stand-level detail so that fuel load can be distributed in the different stand components. Multiple-day simulations of fire spread do not appear necessary, as single-day simulations using a hot spot-weighted average of daily fire weather provide very similar emission estimates.

Acknowledgments

We thank David McNeice for preparing the FBP System database; Nathan Sauvé for translating provincial inventory to CanFIRE input data; Edward Fong (Inventory Branch, BC Ministry of Forests) for providing VRI data; and Richard Carr and Peter Englefield (CFS) for providing FWI System data.

References

Byram GM (1959) Combustion of forest fuels. Forest Fire: Control and use. K. P. Davis. New York, McGraw-Hill.

Campbell J, Donato D, Azuma D, Law B (2007) Pyrogenic carbon emission from a large wildfire in Oregon, United States. *Journal of Geophysical Research* **112**, G04014, doi:10.1029/2007JG000451.

de Groot WJ (2006) Modeling Canadian wildland fire carbon emissions. Proceedings of the IV International Conference on Forest Fire Research (Nov. 2006, Coimbra, Portugal). D.X. Viegas, ed. CD-ROM. Elsevier BV: Amsterdam.

de Groot WJ (2010) Modeling fire effects: integrating fire behaviour and fire ecology. In: Viegas, D.X. (Ed.), VI International Conference on Forest Fire Research, ADAI/CEIF Univ. Coimbra, Portugal (CD ROM)

de Groot WJ, Bothwell PM, Carlsson DH, Logan KA (2002) Simulating the impacts of future fire regimes and fire management strategies on vegetation and fuel dynamics in western Canada using a boreal fire effects model (BORFIRE). CD-ROM in Proceedings of the IV International Conference on Forest Fire Research and Wildland Fire Safety Summit (Luso, Portugal). Viegas, D.X. (ed.). Millpress, Rotterdam.

de Groot WJ, Bothwell PM, Carlsson DH, Logan KA (2003) Simulating the effects of future fire regimes on western Canadian boreal forests. *Journal of Vegetation Science* **14**, 355–364.

de Groot WJ, Landry R, Kurz WA, Anderson KR, Englefield P, Fraser RH, Hall RJ, Banfield E, Raymond DA, Decker V, Lynham TJ, Pritchard JM (2007) Estimating direct carbon emissions from Canadian wildland fires. *International Journal of Wildland Fire* **16**, 593–606.

de Groot WJ, Pritchard J, Lynham TJ (2009) Forest floor fuel consumption and carbon emissions in Canadian boreal forest fires. *Canadian Journal of Forest Research* **39**, 367–382.

de Groot WJ, Cantin AS, Flannigan MD, Soja AJ, Gowman LM, Newbery A (2013a) A comparison of Canadian and Russian boreal forest fire regimes. *Forest Ecology and Management* **294**, 23–34.

de Groot WJ, Flannigan MD, Cantin AS (2013b) Climate change impacts on future boreal fire regimes. *Forest Ecology and Management* **294**, 35–44.

French NHF, Erickson TA, McKenzie D, Billmire M, Hatt C (2009) The Wildland Fire Emissions Information System: Providing information for carbon cycle studies with open source GIS tools, paper presented at North American Carbon Program—2nd All-Investigators Meeting, San Diego, Calif.

French NHF, de Groot WJ, Jenkins LK, Rogers BM, Alvarado E, Amiro B, de Jong B, Goetz S, Hoy E, Hyer E, Keane R, Law BE, McKenzie D, McNulty SG, Ottmar R, Pérez-Salicrup DR, Randerson J, Robertson KM, Turetsky M (2011) Model comparisons for estimating carbon emissions from North American wildland fire. *Journal of Geophysical Research* **116**, G00K05.

Forestry Canada Fire Danger Group (1992) Development and structure of the Canadian Forest Fire Behaviour Prediction System. Forestry Canada, Ottawa, ON. Inf. Rep. ST-X-3.

IPCC (2000) Emissions scenarios. Cambridge University Press, Cambridge.

Kurz WA, Apps MJ (2006) Developing Canada's national forest carbon monitoring, accounting and reporting system to meet the reporting requirements of the Kyoto Protocol. *Mitigation and Adaptation Strategies for Global Change* **11**, 33–43. doi:10.1007/S11027-006-1006-6

Kurz WA, Dymond CC, White TM, Stinson G, Shaw CH, Rampley GJ, Smyth C, Simpson BN, Neilson ET, Trofymow JA, Metsaranta J, Apps MJ (2009) CBM-CFS3: a model of carbon-dynamics in forestry and land-use change implementing IPCC standards. *Ecological Modelling* **220**, 480–504.

Lutes DC, Keane RE, Caratti JF (2009) A surface fuels classification for estimating fire effects. *International Journal of Wildland Fire* **18**, 802–814, doi:10.1071/WF08062.

Nadeau LB, McRae DJ, Jin J-Z (2005) Development of a national fuel-type map for Canada using fuzzy logic. Natural Resources Canada, Canadian Forest Service, Inf. Rep NOR-X-406 (Edmonton, Alberta)

Ottmar RD (2014) Wildland fire emissions, carbon, and climate: Modeling fuel consumption. *Forest Ecology and Management* **317**, 41–50.

Ottmar RD, Sandberg DV, Riccardi CL, Prichard SJ (2007) An overview of the Fuel Characteristic Classification System (FCCS)— Quantifying, classifying, and creating fuelbeds for resource planning. *Canadian Journal of Forest Research* **37**, 2383–2393, doi:10.1139/X07-077.

Ottmar RD, Miranda A, Sandberg D (2009) Characterizing sources of emissions from wildland fires, in Wildland Fires and Air Pollution, edited by A. Bytnerowicz *et al*., pp. 61–78, Elsevier, Amsterdam.

Power K, Gillis MD (2006) Canada's forest inventory 2001. Natural Resources Canada, Canadian Forest Service, Inf. Rep. BC-X-408E (Victoria, BC)

Reinhardt ED, Keane RE, Brown JK (1997) First Order Fire Effects Model: FOFEM 4.0, user's guide. USDA For. Serv., Washington, DC. Gen. Tech. Rep. INT-GTR- 344.

Stocks BJ, Lawson BD, Alexander ME, Van Wagner CE, McAlpine RS, Lynham TJ, Dube DE (1989) Canadian Forest Fire Danger Rating System: an overview. *Forestry Chronicle* **65**, 258–265.

van der Werf GR, Randerson JT, Giglio L, Collatz GJ, Mu M, Kasibhatla PS, Morton DC, DeFries RS, Jin Y, van Leeuwen TT (2010) Global fire emissions and the contribution of deforestation, savanna, forest, agricultural, and peat fires (1997–2009). *Atmospheric Chemistry and Physics* **10**, 11707–11735.

Van Wagner CE (1977) Conditions for the start and spread of crown fire. *Canadian Journal of Forest Research* **7**, 23-34.

Van Wagner CE (1987) Development and structure of the Canadian forest fire weather index system. Canadian Forest Service. Ottawa, Canada. For. Tech. Rep. 35.

New method of forecasting forest fire risk in Poland

Mirosław Kwiatkowski, Ryszard Szczygieł, Bartłomiej Kołakowski

Forest Research Institute. Sękocin Stary, 3, Braci Leśnej Street, 05-090 Raszyn, Poland.
r.szczygiel@ibles.waw.pl, m.kwiatkowski@ibles.waw.pl, b.kolakowski@ibles.waw.pl

Abstract
The possibility of reducing losses caused by forest fires, apart from preventative activities, should be sought primarily in limitation of the area burnt as a result of fires. This objective may be achieved through optimisation of extinguishing activities. The basic requirement of such activities is accurate forecasting of forest fire risk depending on meteorological and physical conditions in forests. The purpose of the research was to prepare a new method of forecasting forest fire risk, which would enable a more precise method of evaluation of the risk of an outbreak of fire in relation to existing and forecast meteorological conditions in forests.

Establishing provisional assumptions of the new method accepted:
- possibility of determining actual fire risk,
- possibility of forecasting forest fire risk for the afternoon hours in the morning hours of the given day and the following day,
- possibility of forecasting the moisture content of pine litter (Pinus silvestris L.),
- preparation of a method enabling limitation of fire prevention system operating costs.

To enable drawing up a fire risk forecast (in the morning for the hours of the afternoon and the following day) formulae were drawn up equally enabling calculation of predicted moisture content of pine litter on the basis of its actual current values and forecast meteorological values. The basis for assessment of the proposed method were data relating to the frequency of occurrence of particular degrees of risk, average number of fires in forecast zone depending on the degree of risk and also the average area of fire at the given degree.
The drawn up method is based on moisture measurements of flammable material, which has a significant relationship to its precision. Selection of test material – pine litter is adjusted to the specific conditions occurring in the majority of pine stands (Pinus silvestris L.) in Poland. As a result of the work it was possible to create a prognosis method enabling precise establishment of the fire risk in forests according to the accepted assumptions. The results obtained during testing of this method indicate a high accuracy in forecasting fire risk and a satisfactory precision of formulae for calculating moisture content of litter. On this basis it may be stated that the drawn up method enables a decidedly better means to define the actual fire risk, simultaneously providing its forecast for later hours and it is currently introduced for application in fire protection of Polish forests. Such a solution may bring about a significant limitation of fire protection operating costs in forests and facilitate organisation of the work of the services responsible for it.

***Keywords**: Forecasting fire risk, forest fires, moisture of flammable material*

Introduction

Permanent increase of fire risk, the effect of which is the increasing number of fires and area burnt and also the increasing operating costs of the fire prevention system were the stimuli to undertake research intended to limit fire losses. The possibility of reducing losses, apart from prevention activities, should be sought primarily in limiting the surface area burnt as a result of fires. This objective may be achieved by optimising fire extinguishing activities. The basis for this is accurate forecasting of fire risk of forest based on meteorological and physical conditions prevailing in the forest. This information enables specification of the required state of operational readiness of the services responsible for forest fire prevention.

The objective of the research was the drawing up of a new method of forecasting the risk of forest fire, which enables a more precise means of evaluation of the risk of occurrence of fire in relation to actual and forecast conditions in forests.
The basis for evaluation of conditions of the occurrence of fires in forests was data of the National Forests from the years 2002-2008. This analysis equally included the occurrence of fires in relation to stand conditions, types of fires, temporal analysis of occurrence in particular months and times of day, as also the occurrence of fires in relation to meteorological conditions.

Methods and results

On the basis of this analysis it may be clearly seen, that most of the frequently burning stands are pine of a young age class growing in coniferous habitats. The decided majority of them are fires of the soil covering, which constitutes 85.5% of the general number of fires. The majority of fires occur from March to September, and the most, close to 25% occur in April. Approximately 70% of all fires in total occur between the hours of 11.00 and 19.00. Whereas the greatest intensity - 10.7% occurs at the hour of 15.00. (figure 1)

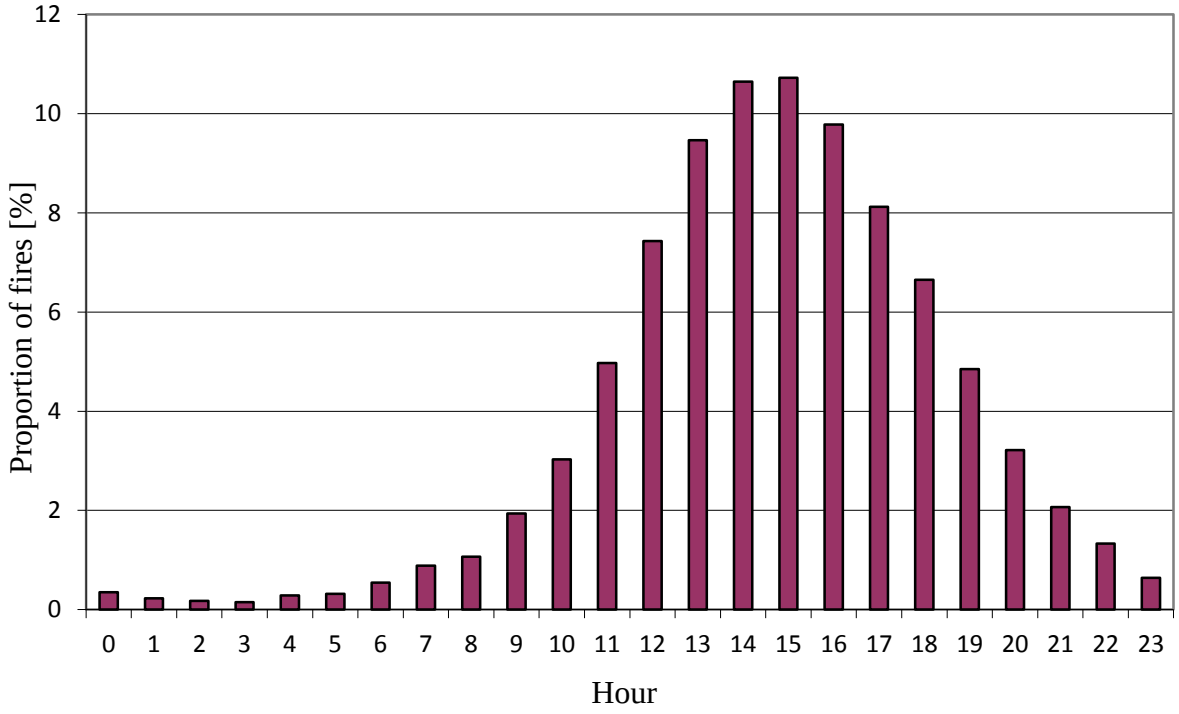

Figure 1. Occurrence of forest fires depending on the time of day

In the analysis of occurrence of fires in relation to meteorological conditions and moisture of litter 25,000 fires were considered. It consisted primarily of evaluation of the number of fires in relation to the values of these parameters. In the analysis of this value from the hour of 9.00 in relation to fires, this occurred between the hours of 9.00 and 13.00. The dependency of the occurrence of fires on the given parameter may be characterised by the frequency of occurrence of fires, being in relation to the number of occurrences of the given value of this parameter. In figure 2 is presented an example schedule of frequency of occurrence of fires depending on moisture of litter as also is presented the expected schedule and the strength of the connection between observed and expected values expressed as a value of the coefficient of determination and R2.

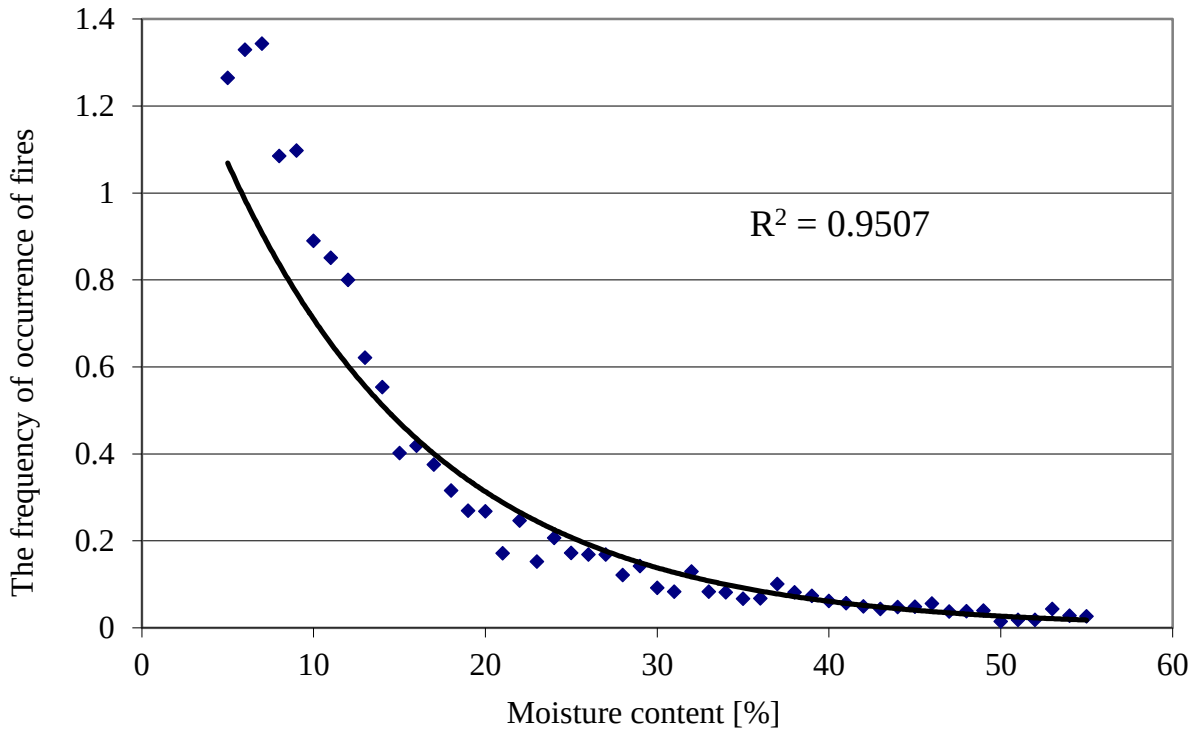

Figure 2. Frequency of occurrence of fires after the hour 13.00 in relation to moisture content of litter at 13.00

Establishing provisional assumptions of the new method included:

- possibility of determining actual risk of fire for given area, being the average for all measurement points located on the terrain equally those in which the moisture content measurement of litter has not been performed.
- possibility of forecasting the risk of forest fire for the afternoon in the morning hours of the given day,
- possibility of forecasting fire risk for the following day,
- forecasting moisture content of litter for the afternoon and of the given day and for the following day,
- drawing up a method enabling limitation of operational costs of fire prevention system.

All analyses of occurrences of fires in relation to the above-mentioned parameters were performed using the reverse step multiple regression method. On this basis polynomials enabling establishment of fire risk for particular points were calculated. In order to standardise the principles of defining the degree of fire risk from the values of polynomials particular formulae were converted in such a manner that the specified degree of fire risk from the value of polynomial of particular formulae were converted in such a way that the specified range of polynomial values always corresponded to the same degree of fire risk. Depending on the values thus calculated for the polynomial, it is possible to establish the degree of fire risk for the given point.

Polynomial risk for forecast point at the hour of 9.00

Polynomial _forecast_09 = f $_{(TP\_09, WP\_09, OP\_09, WS\_09)}$

Polynomial risk of forecast point at 13.00

Polynomial_forecast_13 = f $_{(TP\_09, WP\_09, WS\_09, TP\_13, WP\_13)}$

Polynomial risk for forecast point at 13.00 with regard to moisture content of litter at 13.00
Polynomial_forecast_13P = f (TP_09, WP_09, OP_09, WS_09, TP_13, WP_13, WS_13)

Polynomial risk for auxiliary point at 9.00
Polynomial_measurement_09 = f (WP_09, WS_09P)

Polynomial risk for auxiliary point at 13.00
Polynomial_measurement_13 = f (WP_09, TP_13, WP-13, TP_09P, WP_09P, WS_09P, WP_13P)
where:

TP_09	- air temperature at 9.00,
TP_13	- air temperature at 13.00,
WP_09	- relative air moisture at 9.00,
WP_13	- relative air moisture at 13.00,
OP_09	- 24-hour sum of atmospheric precipitation at 9.00,
WS_09	- moisture content of litter at 9.00,
WS_13	- moisture content of litter at 13.00,
TP_09P	- air temperature at 9.00 at forecast point,
WP_09P	- relative moisture content of air at 9.00 at forecast point,
WP_13P	- relative moisture content of air at 13.00 at forecast point,
WS_09P	- moisture content of litter at the 9.00 at forecast point.

To enable drawing up a fire risk forecast (in the morning for the hours of the afternoon and the following day) formulae were calculated also enabling calculation of forecast moisture content of litter on the basis of its actual value and also current and forecast meteorological conditions. During analyses of the dependency of litter moisture content in the afternoon hours and the following day on its actual value and also on meteorological parameter values not included in the previously referred to data, used in forecasting meteorological parameter values based on a numerical weather model obtained from the Interdisciplinary Mathematical Modelling Centre of the University of Warsaw. The accepted principle was to achieve the highest possible verifiability of prognosis with maximal error tolerance amounting to 20% of actual value, for actual values of litter moisture content less than 40%. Such an assumption guarantees appropriate calculation of litter moisture content for the extent of its moisture, at which the occurrence of fire is possible, so doing taking into consideration the possibility of a certain variation in moisture contents in the area of the whole zone. Similarly to the case of the previously described analysis for evaluation of the dependency between litter moisture in the hours of the afternoon and the following day on its actual value and meteorological parameters values used in multistep regression analysis, but in this instance the dependency was significantly greater (values of coefficient of determination from 0.52 to 0.83). On this basis formulae were drawn up enabling calculation of moisture content of litter both at the hour of 13.00 of the current day has also in the morning of the following day.

Moisture of litter forecast for the hour of 9.00 the following
moisture_1_09 = f (TP_09, OP_09, WS_09, WS_13_1, WS_09_A1, TP0_13, WP0_13, OP0_13, Z0_13, VW0_13, TP1_09, WP1_09, VW1_09)

Moisture content of litter forecast for the hour 9.00 on the following day with regard to measurement data from the hour of 13.00

moisture_1_09_13 = f (TP_09, WP_09, WS_09, TP_13, WP_13, WS_13, WS_09_A1, Z0_13, VW0_13, TP1_09, WP1_09, VW1_09)

Moisture content forecast for 13.00
moisture_0_13 = f (WP_09, OP_09, WS_09, WS_09_1, WS_13_1, TP0_13, WP0_13, OP0_13, Z0_13)
where:

TP_09 - air temperature at 9.00,
WP_09 - relative air moisture at 9.00,
OP_09 - 24-hour sum of atmospheric precipitation at 9.00,
WS_09 - moisture content of litter at 9.00,
WS_09_1 - moisture content of litter at 9.00 the previous day,
WS_13_1 - moisture content of litter at 13.00 the previous day,
TP0_13 - air temperature forecast for 13.00,
WP0_13 - relative air moisture forecast for 13.00,
OP0_13 - sum of forecast precipitation at 13.00,
VW0_13 - wind speed forecast for 13.00,
WP_13 - relative air moisture at 13.00,
WS_09_A1 - average moisture content of litter at 9.00 for 4 successive previous days,
Z0_13 - cloudiness forecast for 13.00,
TP1_09 - air temperature forecast for the 9.00 on the following day,
WP1_09 - relative air moisture forecast for 9.00 the following day,
VW1_09 - wind speed forecast for 9.00 the following day,
TP_13 - air temperature at 13.00,
WS_13 - moisture content of litter at 9.00,

The basis of assessment of the proposed method was data concerning the frequency of occurrence of particular degrees of risk established according to tested methods, average number of fires in the zone in relation to the degree of risk and average surface area of fire at the given degree. These values for afternoon hours are shown in figure 3 and also in table 1.

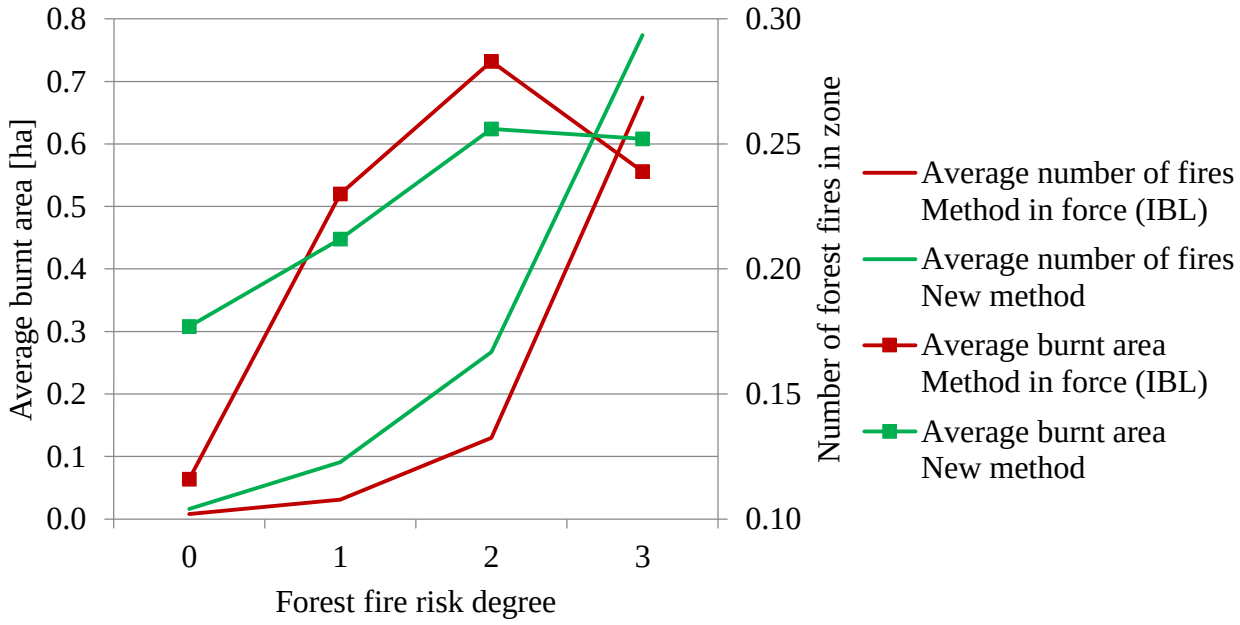

Figure 3. Average number of fires and fire area according to degree of forest fire risk at 13.00

Table 1. Presentation of data relating to forecast of forest fire risk at 13. 00

		unit	Degree of risk			
			0	1	2	3
IBL method	number of days with degree	item	3075	2458	4524	3337
	average number of fires	item	0,008	0,031	0,130	0,674
	average area of fire	ha	0,116	0,230	0,283	0,239
New method	number of days with degree	item	4210	4133	3054	1997
	average number of fires	item	0,016	0,091	0,267	0,774
	average area of fire	ha	0,177	0,212	0,256	0,252

On the basis of the data presented it is clearly seen that with the method in force in Poland a higher fire risk occurs significantly more frequently in comparison to the new method. Concerning occurrence of fires the increase in their numbers together with increased risk is clearer and more balanced for the new method. Significantly greater differences between degrees occur in the case of average fire areas. With the method in force the greatest area of fires, which occurred after 13.00 were at degree 3. Reduction in this case of the area by 3 degrees might be connected with the conduct of extinguishing activity. If it concerns the relationship of surface area of fire to the degree established according to the tested method for afternoon hours, for the new method a clear increase of average area is visible from 0 to 2 degrees whereas the area at degree 3 is almost equal to the area at degree 2. The analysis presented above clearly shows that the newly drawn up method enables significantly better definition of actual fire risk in comparison to the method currently applied.

The condition for appropriate forecasting of fire risk for the following day and the afternoon hours of the given day is precise calculation of envisaged moisture content of litter at those hours. The evaluation of accuracy performed for actual values less than 40% (with tolerance of margin of error amounting to ± 20% of actual value) of drawn up formulae enables obtaining accuracy at a level of 60% for forecasts in the morning for the following day and 70% for the afternoon of the current day.

The schedule of forecast of litter moisture content values in relation to their actual values is shown in figures 4 and 5.

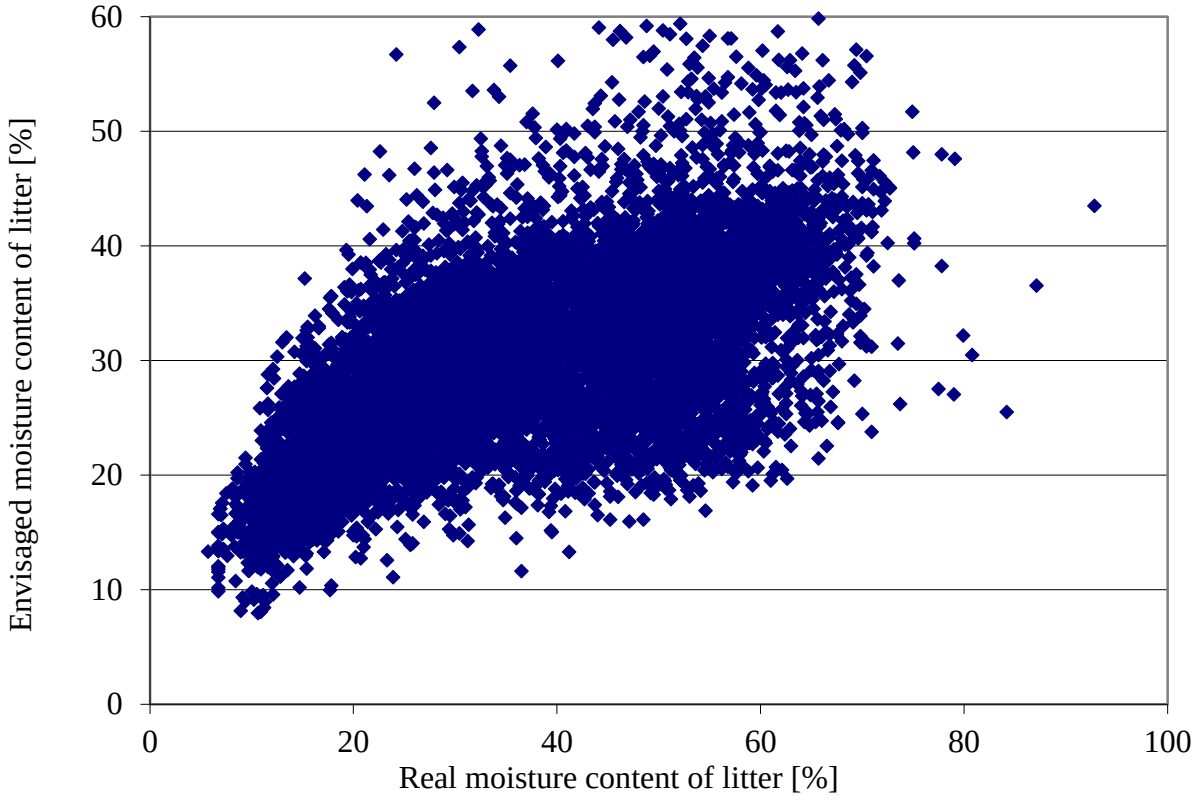

Figure 4. Schedule of litter moisture content forecast for 9.00 the following day

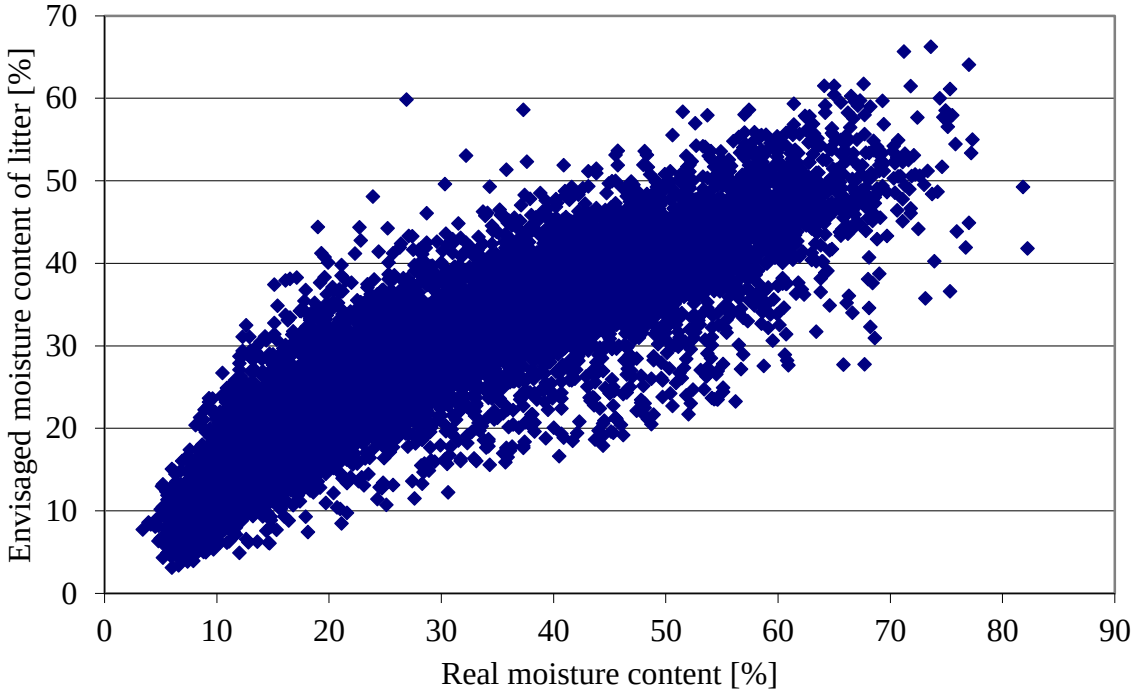

Figure 5. Schedule of litter moisture content forecast for 13.00

In the economic analysis of forest fire protection costs in relation to the applied method of forecasting forest fire risk, only those elements of the system are considered, which are operationally dependent on actual fire risk. This assessment is to a significant degree approximate, because it accepts identical costs for forestry areas counted to a specified category of fire risk. In the conduct of economic analysis

it is accepted that particular activities in the extent of forest fire protection are performed in relation to the degree of risk. On this basis is calculated the cost of the operation of fire prevention protection with regard to affiliation of particular forestry administration areas to the forecast prognosis zones. It shows the possibility of obtaining, as a result of applying the new method, economies in the operation of the forest fire prevention system at a level of 10,000,000 PLN annually or approximately 30% of these costs.

Summary

The drawn up method is based on the measurement of the moisture content of inflammable material, which to a significant extent as an influence on its precision. The choice of test material - pine litter is appropriate to the specific characteristics of forest fires occurring in Poland. As a result of the work a forecasting method was successfully established enabling precise determination of fire risk in forests. The presented results obtained during testing of this method indicate great accuracy in forecasting forest fire risk and satisfactory accuracy of formulae enabling calculation of litter moisture content. On the basis of the entirety of the material presented in this study it may be stated that the drawn up method enables a decidedly better definition of the actual fire risk, simultaneously providing the possibility of its prognosis for later hours and should be introduced for application in forest fire protection. Such a solution may bring about significant limitation of forest fire prevention operating costs and facilitate the organisational work of the services responsible for forest fire protection.

Potential impact of climate change on live fuel moisture dynamic at local scale

Grazia Pellizzaro[a], Martin Dubrovsky[b], Sara Bortolu[a], Bachisio Arca[a], Andrea Ventura[a], Pierpaolo Duce[a]

[a] *Institute of Biometeorology (CNR-IBIMET), Sassari, Italy, g.pellizzaro@ibimet.cnr.it*
[b] Institute of Atmospheric Physics, Praha, Czech Republic

Abstract
According to projections on future climate, an increase in risk of summer droughts is likely to take place in Southern Europe. More prolonged drought seasons induced by climatic changes are likely to influence general flammability characteristics of fuel, affecting species composition and live and dead fuel ratio. Moreover, variations in precipitation and mean temperature could directly affect live fuel water content, and length of critical periods of high ignition danger for Mediterranean ecosystems. The flammability of vegetation is influenced by several factors that include structural properties, chemical properties and moisture content. Several studies have also highlighted the importance of vegetation moisture content in relation to ignition and rate of spread in Mediterranean shrubs.
The main aim of this work was to propose a method for evaluating possible impacts of future climate change on live moisture dynamic and length of fire danger period at local scale by using weather generator techniques. In particular, in this work i) threshold values for drought indices that indicate the end of fire season due to live fuel status in Mediterranean shrubland were identified, and ii) potential impacts at local scale of future climate changes on the duration of fire danger period were simulated. The study was carried out in Sardinia (Italy). Moisture content of live fuel (LFMC) was determined periodically for 8 years on three shrub species. Seasonal patterns of LFMC were compared with the Drought Code (DC) of the Canadian Forest Fire Weather Index and the Keetch–Byram Drought Index. A threshold value of DC useful to determine the end of the potential fire season due to fuel status was identified. A weather generator linked to climate change scenarios derived from 17 available General Circulation Models (GCMs) was used to produce synthetic weather series, representing future climates, and then the expected changes of the fire season length was determined. Results confirmed that the projected climate scenarios over the Mediterranean area will determine an overall increase of the fire season length.

Keywords*: Forest fires, Mediterranean shrubs, Fuel status, Fire danger season*

Introduction

Shrubs are an important component of Mediterranean vegetation: live shrubs are often the main component of the available fuel which catches fire and constitute the surface fuels primarily responsible for the ignition and the spread of wildland fires.
Vegetation flammability is influenced by several factors including structural properties, chemical properties and moisture content. However, it is well known that moisture content of plants is an essential factor influencing the fire ignition and spread. Several authors have found relationships between vegetation water content and ignitability in several Mediterranean species (Hernando *et al.*1994; Dimitrakopoulos and Papaioannou 2001; Pellizzaro *et al.* 2007). Some authors highlighted the importance of vegetation moisture content in relation to crown fire potential, ignition and rate of spread in shrubs (Van Wagner 1977; Chandler *et al*. 1983; Agee *et al*. 2002; Davis *et al*. 2009). Studies carried out in Mediterranean areas have shown that burned areas tend to increase as live fuel moisture decreases (Davis *et al*. 1995; Schoenberg *et al.* 2003; Chuvieco *et al*. 2004; Dennison *et al*. 2008).
The relationship between fire occurrence and drought is well known; forest fires mainly occur during dry summer periods when air temperature is high, air humidity is low and fuel moisture reduced (Piñol

et al. 1998). According to projections on future climate, an increase in risk of summer droughts is likely to take place in Southern Europe (Giorgi *et al*. 2004; Giannakopoulos *et al*. 2009). More prolonged drought seasons induced by climatic changes are likely to influence general flammability characteristics of fuel, affecting species composition and live and dead fuel ratio. Moreover, variations in precipitation and mean temperature could directly affect live fuel water content, and length of critical periods of high ignition danger for Mediterranean ecosystems (Westerling *et al.* 2006; Flannigan *et al.* 2009; Flannigan *et al.* 2013; Liu *et al.* 2013).
Therefore, considering the observed climatic variations and foreseen future scenarios, an evaluation of the impact of these variations on fire danger seems essential.
The climate data provided by the general circulation models (GCMs) are characterized by low resolution and are often not recommended for application at local scale. This constraint could be overcame by using the weather generator approach. Weather generators linked to climate model can transform the raw outputs from the climate models into data with more realistic structure and create synthetic weather series representing present and future climates at local scale.
The main aim of this work was to propose a novel methodology for evaluating the possible impacts of future climate changes on moisture dynamic and length of fire danger period at local scale in the Mediterranean area. Specific objectives were: i) identify threshold values for drought indices that indicate the length of fire season due to fuel status in Mediterranean shrubland, and ii) simulate the potential impacts of future climate changes on the duration of fire danger period.

Methods

The study was carried out in a nature reserve located in North Western Sardinia, Italy (40° 36' N; 8° 09' E, 30 m a.s.l.). The climate is Mediterranean with water deficit conditions occurring from May through September and precipitation mainly concentrated in autumn and winter. The mean annual rainfall is 640 mm and the mean annual air temperature is 16.8 °C. The vegetation cover of the study area consists mainly of Mediterranean maquis and garigue, grown after a fire event occurred in mid '70s.
Moisture content of live fuel (LFMC) was determined periodically for 8 years on three shrub species: *Cistus monspeliensis* L., *Juniperus phoenicaea* L., and *Rosmarinus officinalis* L., which are very common species in the Western Mediterranean Basin. Samples of live fine fuel, consisting of terminal twigs with diameter not greater than 6 mm, were collected from each species.
To determine the live fuel moisture, three samples of each species were weighed, dried and reweighed. Live fine moisture content was expressed as a percentage of dry weight. Meteorological data were also collected from an automated weather station located in the study site.
Drought conditions that occurred during the LFMC sampling period were assessed by calculating the Drought Code (DC) of the Canadian Forest Fire Weather Index System (Van Wagner 1987). DC is widely used worldwide in wildfire danger assessment as an indicator of the moisture content of very slow drying fuels and its values have been shown to be associated with occurrence of drought (Girardin *et al*. 2004; Wotton 2009). DC is similar to other drought models such as the Keetch–Byram Drought Index (Keetch and Byram 1968; Burgan 1988) and the Palmer Drought Index (Palmer 1965) and is calculated from daily rainfall and air temperature. Previous studies showed that DC is well related to LFMC of shrub species (Pyne *et al*. 1996; Viegas *et al*. 2001). In the current FWI System, DC values equal to 0 correspond to saturation moisture content, with increasing values indicating drier conditions without a specific maximum value (Van Wagner 1987). In this work, the DC code was calculated using the equations given by Van Wagner and Pickett (Van Wagner and Pickett 1985)

Analysis of cumulative distribution curves of DC values for only those days characterized by LFMC values over the critical threshold for fire ignition and spread was performed in order to identify the DC values that indicate the end of the fire danger season. Based on available literature, LFMC

values below 95% were used as threshold values for indicating ignition and fire spread danger over Mediterranean shrubs.
The M&Rfi weather generator (Dubrovsky *et al* 2004) linked to climate change scenarios derived from 17 available General Circulation Models (GCMs) (see Table 1 for details) was used to produce synthetic weather series, representing present and future climates, for four selected sites located in North Sardinia, Italy. The projected future climates were then used to determine the expected changes of the fire season length.

Table 1. General Circulation Models (GCMs) used in conjunction with the M&Rfi weather generator to produce synthetic weather series representing present and future climates at four location in North Sardinia, Italy.

BCM2	Bjerknes Centre for Climate Research, Norway
CGMR	Canadian Center for Climate Modelling and Analysis, Canada
CNCM3	Centre National de Recherches Meteorologiques, France
CSMK3	Commonwealth Scientific and Industrial Res. Organisation, Australia
ECHOG	Met. Inst. Univ. Bonn + Met. Res. Inst., Korea + Model and Data Groupe at MPI-M, Germany
GFCM20	Geophysical Fluid Dynamics Laboratory, USA
HADCM3	UK Met. Office, UK
HADGEM	UK Met. Office, UK
INCM3	Institute for Numerical Mathematics, Russia
MIMR	National Institute for Environmental Studies, Japan
MPEH5	Max Planck Institute for Meteorology, Germany
MRCGCM	Meteorological Research institute, Japan
NCCCSM	National Centre for Atmospheric Research, USA
NCPCM	National Centre for Atmospheric Research, USA
GFCM21	Geophysical Fluid Dynamics Laboratory, USA
GIER	Geophysical Fluid Dynamics Laboratory, USA. Model E20/Russel
IPCM4	Institute Pierre Simon Laplace, France

3. Results

In general, LFMC values of all species were correlated with the Drought Code values. The analysis showed significant and negative correlation between LFMC and DC for all species ($P \leq 0.05$). High correlation coefficients were obtained for *Cistus* and *Rosmarinus* throughout the entire study period ($P \leq 0.01$). Similar results were also observed for the KBDI ($P \leq 0.05$).
LFMC and DC patterns were also compared with the purpose of evaluating whether or not DC values could be useful to describe the seasonal changes of LFMC.
DC and KBDI patterns were very close to LFMC during the rising phase of moisture content (from mid-summer to autumn). During the moisture falling phase (from mid-spring to the beginning of summer), although the weather indices are correlated to LFMC values, the response of both codes does not match very well the short-term variations of LFMC due to resprouting and flowering phases of plants (Fig.1). Therefore, it seems more appropriate the use of the codes to identify the end of fire danger season rather than the date of starting.

With the purpose of evaluating the effectiveness of both indices, we performed the analysis of frequency distribution as suggested by Andrews *et al* (2003). Figure 2 shows the distribution of DC and KBDI for all days from July 1 (plots on the top), and only for those days from July 1 with LFMC values higher than 95% (plots on the bottom). For DC the distribution shifts to the right, with most of the DC values below 700, when the analysis is performed using only days with LFMC higher than 95%. This behavior is less pronounced in the case of KBDI, so that Drought Code seems to be a better indicator for predicting the end of fire danger season than KBDI.

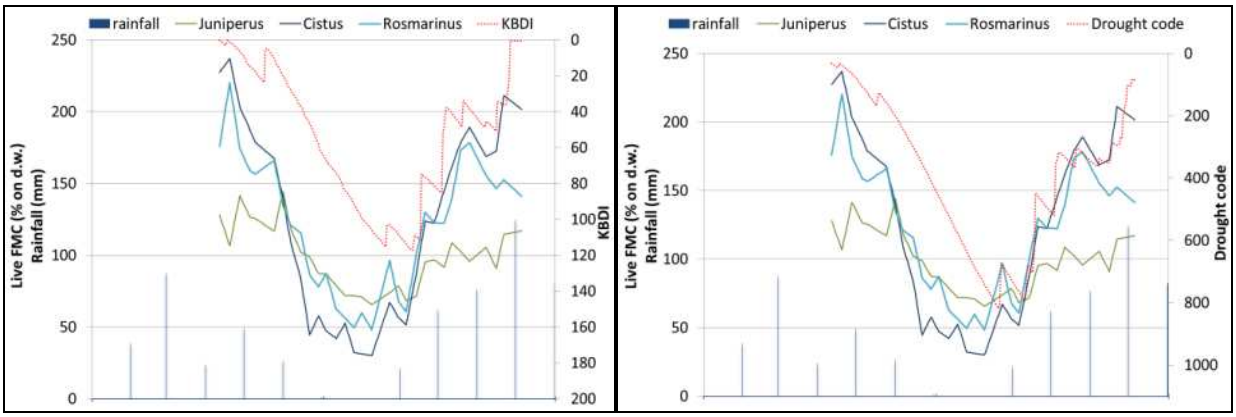

Figure 1. Seasonal trends of Keetch and Byram (KBDI) and Drought Code (DC) and live fuel moisture content (LFMC) values observed for Cistus monspeliensis, Juniperus phoenicaea and Rosmarinus officinalis at the experimental site during April-November 2005.

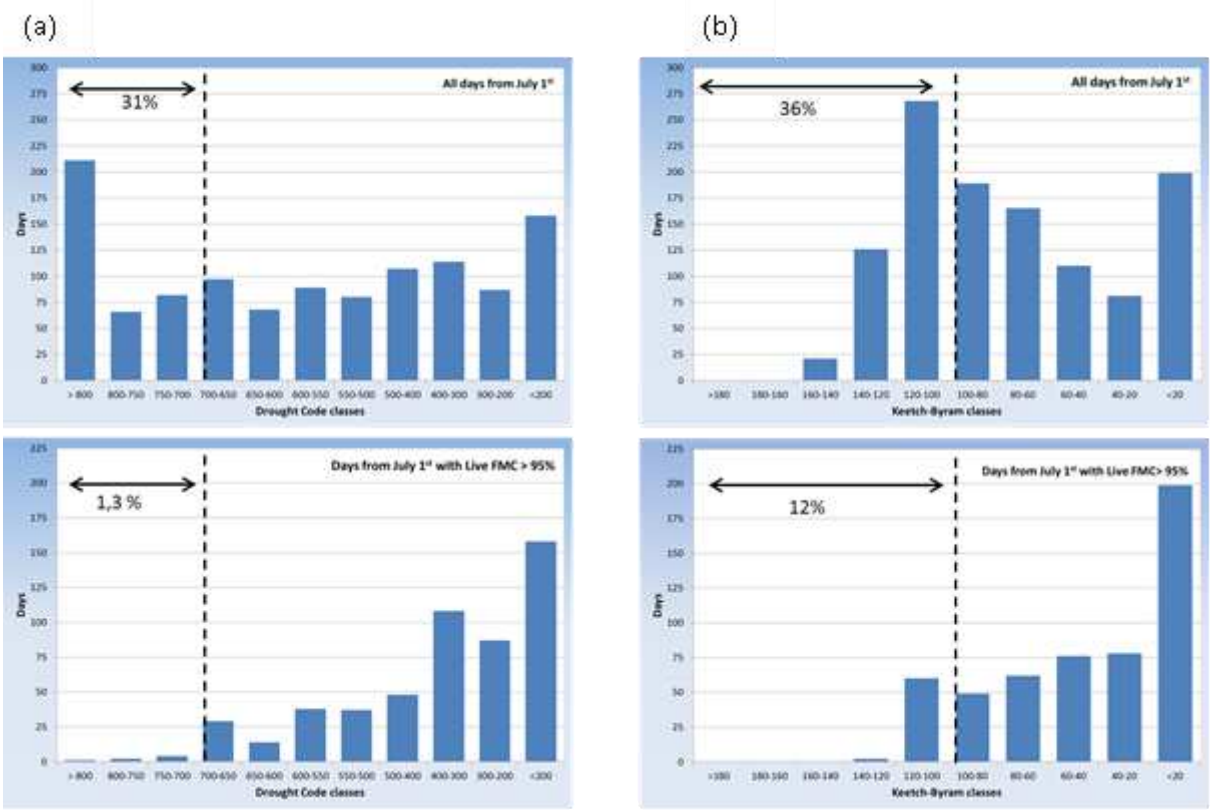

Figure 2. Frequency distribution of Drought Code (a) and Keetch and Byram Drought Index (b) for all days from July 1 (plots at the top) and for all days from July 1 with LFMC values higher than 95%.

The cumulative distribution curves of DC (LFMC rising phase), calculated for all days from July 1 with LFMC values above 95%, shows that most of the DC values are below 700 when LFMC values are above the critical moisture threshold of 95% (Figure 3). Therefore, a DC threshold of 700 was used to estimate the end of fire danger season due to LFMC of Mediterranean shrubs.

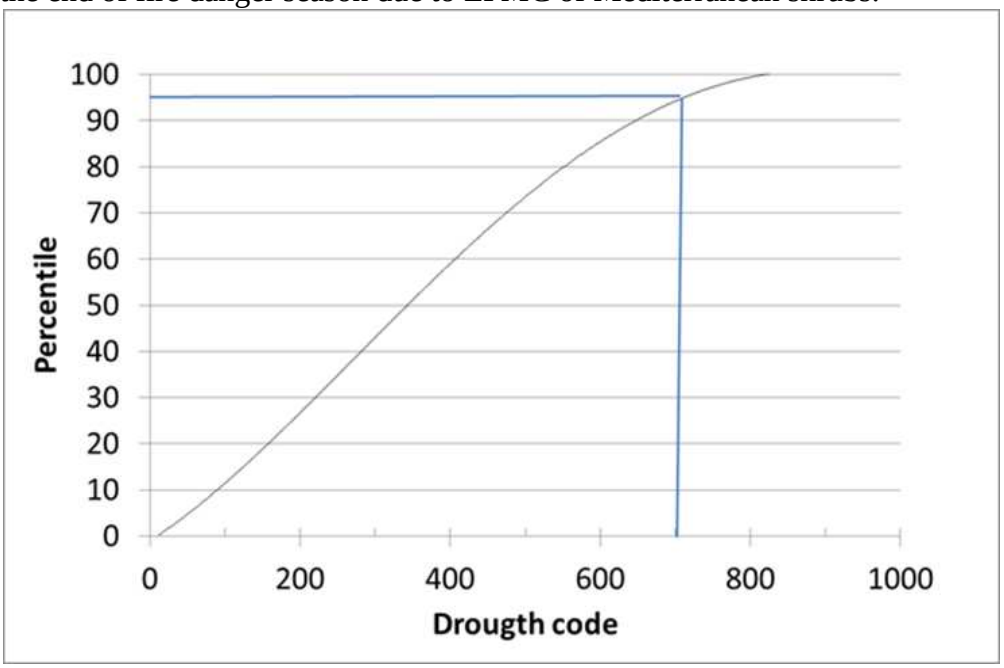

Figure 3. Cumulative distribution of Drought Code values observed during days with LFMC values above 95% (rising phase of LFMC).

Projections of future likely dates of the end of the fire season were obtained using 17 climate change scenarios derived from a subset of available GCMs combined with synthetic weather data from M&Rfi weather generator.

The actual and projected average dates of the end of fire season for the experimental site are shown in Figure 4 and Table 2. The actual ending date of the fire danger season calculated by using the synthetic weather series is October 14 (DOY = 287). The calculation of the DC values derived from 17 climate change scenarios resulted in a general increase of the duration of the fire danger season. Scenario B1 determines little variations compared to scenarios A2 e A1B. Scenario B1 shows an extension of the fire season ranging from 3 days (2050) to 5 days (2100), with a spread of predictions ranging from 1 to 14 days. Results from scenarios A1B e A2 and mid-century (2050) indicate a possible extension of the fire season of more than 1 week with a spread of the predictions ranging from few days to 3 weeks. For both scenarios A1B and A2, the fire season length indicated by 2100 projections is much larger: about 2 (A1B) and 3 (A2) weeks with a maximum spread of predictions around 1 month.

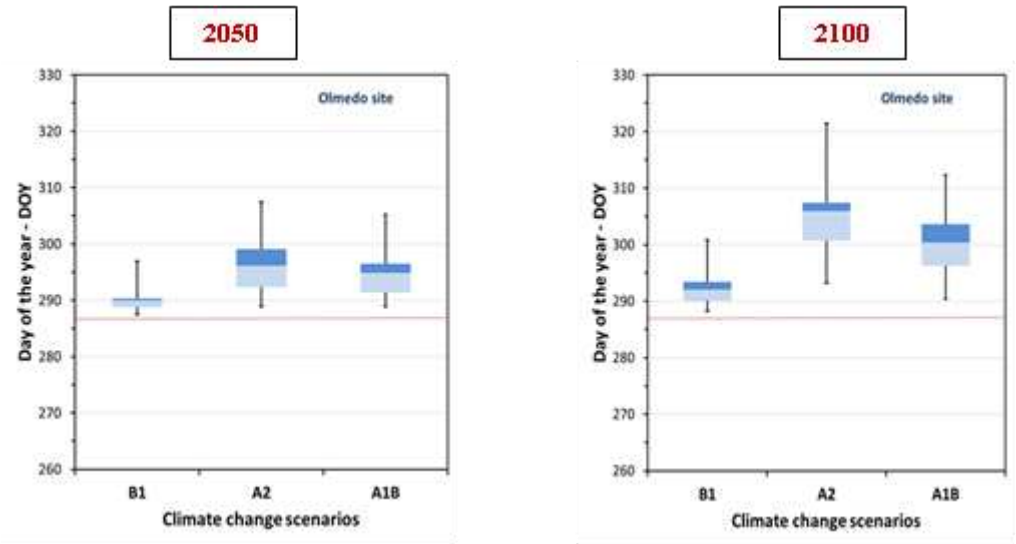

Figure 4. Boxplot of the actual (red) and projected (blue) average fire season ending dates relative to three climate change scenarios (B1, A1B, and A2). The charts show the minimum, maximum and mean values, and the lower and upper quartiles.

Table 2. Projections of future extension of fire season (in days) by climate change scenario and time period. Spread of predictions (in days) are reported in brackets.

Years	B1	A2	A1B
2050	**3 (1 – 10)**	**9 (2 – 20)**	**8 (2 – 18)**
2100	**5 (1 – 14)**	**19 (6 – 35)**	**13 (3 – 25)**

Conclusions

The results reported in this paper are based on local data and information and on the calibration of the commonly used DC code. Our study confirms that projected climate scenarios over the Mediterranean area could affect the duration of the fire danger season causing a delay in the ending dates of high ignition danger periods. Several authors suggested that an earlier spring could lead to an earlier fire season (Westerling *et al* 2006; Flannigan *et al* 2009; Matthews *et al* 2012). In this work, we did not investigate on the impact of climate change on starting date of fire season, since weather indices used as a proxy of vegetation moisture content showed poor performances in following the variations of LFMC in spring. During this period, the moisture content of living plants of Mediterranean species is also affected by phenological phases that depends by both endogenous rhythm of the plant and weather conditions occurred before vegetative growth. In this context, the use of models that also include phenological response to weather of Mediterranean shrubs could provide an appropriate tool for a better description of live fuel moisture seasonal changes in Mediterranean shrublands.

Acknowledgements

This work was partly supported by the EU 7th Framework Program (FUME) contract number 243888. The authors are also grateful to Mr Angelo Arca and Mr Pierpaolo Masia for their valuable support in the field work.

References

Agee JK, Wright CS, Williamson N, Huff MH (2002) Foliar moisture content of Pacific Northwest vegetation and its relation to wildland fire behaviour. Forest Ecology and Management 167, 57-66.

Andrews P, Loftsgaargen DO, Bradahaw S (2003) Evaluation of fire danger rating indexes using logistic regression and percentile analysis. International Journal of Wildland Fire 12, 213-226.

Burgan RE (1988) 1988 revisions to the 1978 national fire-danger rating system. Asheville, N.C., U.S. Dept. of Agriculture, Forest Service, Southeastern Forest Experiment Station, pp. 39.

Chandler P, Cheney P, Thomas L, Trabaud L, Williams D (1983) Fire in forestry. Vol. 1. John Wiley & Sons (New York, USA).

Chuvieco E, Aguado I, Dimitrakopoulos A (2004) Conversion of fuel moisture content values to ignition potential for integrated fire danger assessment. Canadian Journal of Forest Research 34, 2284-2293.

Davis F, Michaelsen J (1995) Sensitivity of fire regime in chaparral ecosystems to climate change. In Global Change and Mediterranean-Type Ecosystems. (Eds JM Moreno, WC Oechel) pp. 435-456. (Springer: NewYork).

Davis FW, Legg CJ, Smith AA, MacDonald AJ (2009) Rate of spread of fires in Calluna vulgaris-dominated moorlands. Journal of Applied Ecology 46, 1054-1063.

Dennison PE, Moritz MA, Taylor RS (2008) Examining predictive models of chamise critical live fuel moisture in the Santa Monica Mountains, California. International Journal of Wildland Fire 17, 18-27.

Dimitrakopoulos AP, Papaioannou KK (2001) Flammability Assessment of Mediterranean Forest Fuels. Fire Technology 37, 143-152.

Dubrovsky M, Buchtele J, Zalud Z (2004) High-Frequency and Low-Frequency Variability in Stochastic Daily Weather Generator and Its Effect on Agricultural and Hydrologic Modelling. Climatic Change 63 (1-2), 145-179.

Flannigan MD, Krawchuk MA, de Groot WJ, Wotton BM, Gowman LM (2009) Implications of changing climate for global wildland fire. International Journal of Wildland Fire 18, 483-507.

Flannigan M, Cantin AS, de Groot WJ, Wotton M., Newbery A, Gowman L (2013) Global wildland fire season severity in the 21st century. Forest Ecology and Management 294, 54-61.

Giannakopoulos C, Le Sager P, Bindi M, Moriondo M, Kostopouloua E, Goodess CM (2009) Climatic changes and associated impacts in the Mediterranean resulting from a 2 °C global warming. Global and Planetary Change. 68, 209-224.

Giorgi F, Bi XQ, Pal J (2004) Mean, interannual variability and trends in a regional climate change experiment over Europe. II: climate change scenarios (2071- 2100). Climate Dynamics 23, 839-858.

Girardin MP, Tardif J, Flannigan MD, Wotton BM, Bergeron Y (2004) Trends and periodicities in the Canadian Drought Code and their relationships with atmospheric circulation for the southern Canadian boreal forest. Canadian Journal Forest Research 34(1), 103-119.

Hernando Lara C, Moro C, Valette JC (1994) Flammability parameters and calorific values of Erica arborea and Arbutus unedo. In Proceedings of the 2nd International Conference on Forest Fire Research, Vol. II, 481-489, Coimbra, Portugal.

Keetch JJ, Byram GM (1968). A drought index for forest fire control. Research Paper SE-38. Asheville, NC, U.S. Department of Agriculture, Forest Service, Southeastern Forest Experiment Station. pp. 32.

Liu Y, Goodrick SL, Stanturf JA, (2013) Future U.S. wildfire potential trends projected using a dynamically downscaled climate change scenario. Forest Ecology and Management 294, 120-135.

Matthews S, Sullivan AL, Watson P, Williams R, (2012) Climate change, fuel and fire behaviour in a eucalypt forest. Global Change Biology, 18 (10), 3212-3223.

Palmer WC (1965) Meteorological drought. Research Paper No. 45. (Washington DC: U.S.) Department of Commerce Weather Bureau.

Pellizzaro G, Duce P, Ventura A, Zara P, (2007) Seasonal variations of live moisture content and ignitability in shrubs of Mediterranenan Basin. International Journal of Wildland Fire 16, 633-641.

Piñol J, Filella I, Ogaya R, Peñuelas J. (1998) Ground-based spectroradiometric estimation of live fine fuel moisture of Mediterranean plants. Agricultural and Forest Meteorology 90, 73-186.

Pyne SJ, Andrews PL, Laven R. (1996) Introduction to Wildland Fire, 2nd ed., 769 pp. John Wiley and Sons, (Toronto, Canada)

Schoenberg FP, Peng R, Huang Z, Rundel P (2003) Detection of nonlinearities in the dependence of burn area on fuel age and climatic variables. International Journal of Wildland Fire 12, 1-6.

Van Wagner CE (1977) Conditions for the start and spread of crown fires. Canadian Journal of Forest Research 7,23-34.

Van Wagner CE, Pickett TL (1985) Equation and FORTRAN program for the Canadian Forest Fire Weather Index System. Canadian Forestry Service, Forestry Technical Report 33.(Ottawa, ON, Canada).

Van Wagner CE (1987) The development and structure of the Canadian Forest FireWeather Index System. Canadian Forest Service, Petawawa National Forestry Institute. Chalk River, Ont. FTR-35.

Viegas DX, Pinol J, Viegas MT, Ogaya R (2001) Estimating live fine fuels moisture content using meteorologically-based indices. International Journal of Wildland Fires 10, 223-240.

Wotton M (2009) Interpreting and using outputs from the Canadian Forest Fire Danger Rating System in research applications. Environmental and Ecological Statistics 16, 107-131.

Westerling AL, Hidalgo HG, Cayan DR, Swetnam TW (2006) Warming and Earlier Spring Increase Western U.S. Forest Wildfire Activity. Science 313, 940-943.

Predicting wildfire ignitions, escapes, and large fire activity using Predictive Service's 7-Day Fire Potential Outlook in the western USA

Karin L. Riley[a], Crystal Stonesifer[b], Haiganoush Preisler[c], and Dave Calkin[d]

[a] *College of Forestry and Conservation, University of Montana, 32 Campus Drive, Missoula, Montana, USA, 59812, karin.riley@umontana.edu*
[b] *Human Dimensions, Rocky Mountain Research Station, 200 East Broadway, Missoula, Montana, USA 59807, csstonesifer@fs.fed.us*
[c] *Pacific Southwest Research Station, 800 Buchanan St., West Annex Building, Albany, California, USA, 94710, hpreisler@fs.fed.us*
[d] *Human Dimensions, Rocky Mountain Research Station, 200 East Broadway, Missoula, Montana, USA 59807, decalkin@fs.fed.us*

Abstract
Can fire potential forecasts assist with pre-positioning of fire suppression resources, which could result in a cost savings to the United States government? Here, we present a preliminary assessment of the 7-Day Fire Potential Outlook forecasts made by the Predictive Services program. We utilized historical fire occurrence data and archived forecasts to assess how well the 7-Day Outlook predicts wildfire ignitions and escaped fires, ultimately to help characterize the effectiveness of this tool for prepositioning national firefighting resources. The historical fire occurrence data track ignitions on all land ownerships; from this dataset, we established number and location of ignitions and final fire size for the years 2009-2011 for Predictive Service Areas (PSAs) within the Northwest and Southwest Geographic Areas. These data were then matched to the corresponding PSA and appropriate forecast for each of the seven days prior to the ignition date. Final fire size was used as a metric to establish whether an ignition escaped initial attack, with fires greater than 121.4 hectares (300 acres) considered escaped. Our results show that 7-Day Outlook values yield better-than-random prediction of large fire activity, although there is wide variation in this relationship among individual PSAs. In addition, the number of escaped fires increased with the number of ignitions, with this relationship showing a distinct regional pattern. Fires were more likely to escape during certain times of the year, with this season being earlier in the Southwest than in the Northwest. Significantly higher numbers of escaped fires per ignition occurred during days considered to be high risk by the meteorologist than on lower-risk days.

Keywords*: forecasting; fire danger; ignitions; escaped fires; large fire activity*

Introduction

Accurate predictions of days and locations with heightened potential for significant wildfire activity would be valuable for a number of planning functions, including giving land managers time to evaluate potential responses in the event of an ignition, such as prepositioning of fire suppression resources. The 7-Day Fire Potential Outlook forecasts issued by the Predictive Service program in the United States (US) might be suitable for such tasks, but they have not yet been assessed at the necessary national scale. In this manuscript, we present preliminary assessment of this product for two regions of the US.

The Predictive Services program was created under the National Wildfire Coordinating Group in 2001 to address the need for long- and short-term decision support information for fire managers and operations personnel. The primary mission of Predictive Services is to integrate fire weather, fire danger, and resource availability in order to enable strategic fire suppression resource allocation and prioritization. The conterminous United States is divided into ten Geographic Coordination Areas (GCAs; Figure 1), which are in turn comprised of individual forecast units called Predictive Service Areas (PSAs; Figure 2). PSAs are delineated within each GCA to represent geographic areas of similar

climate based on statistical correlation of observed weather and fuel moisture data, or based on political or land ownership boundaries. In 2006, Predictive Services began daily production of the 7-Day Significant Fire Potential Outlook for each PSA on weekdays during the core fire season to support efforts at informed regional and national fire suppression resource allocation and prepositioning.

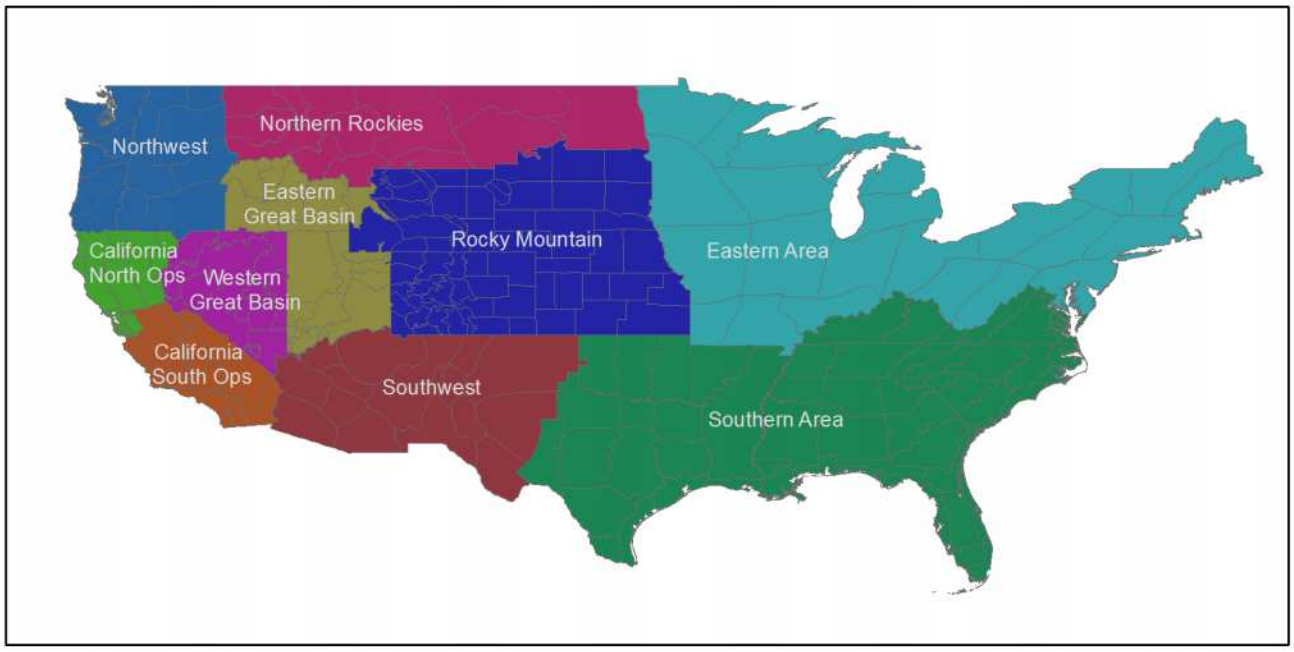

Figure 1. Geographic Coordination Areas (GCAs) of the conterminous US. The boundaries of the Predictive Service Areas (PSAs) for the year 2012 are shown in gray.

The 7-Day Outlook uses forecasted fuel dryness and specific high-risk weather events to predict the location and timing of demand for regionally and nationally shared suppression resources. Thus, it is essentially designed to anticipate significant fire activity. More specifically, Predictive Services defines "Significant Fire Potential" as "the likelihood that a wildland fire event will require mobilization of additional resources from outside the area in which the fire situation occurs" (www.nwccweb.us/content/products/fwx/fdrop/FDROP.pdf, accessed May 9, 2014). "Significant fires" are defined to be those larger than a threshold size, which varies geographically, based on historical fire sizes.

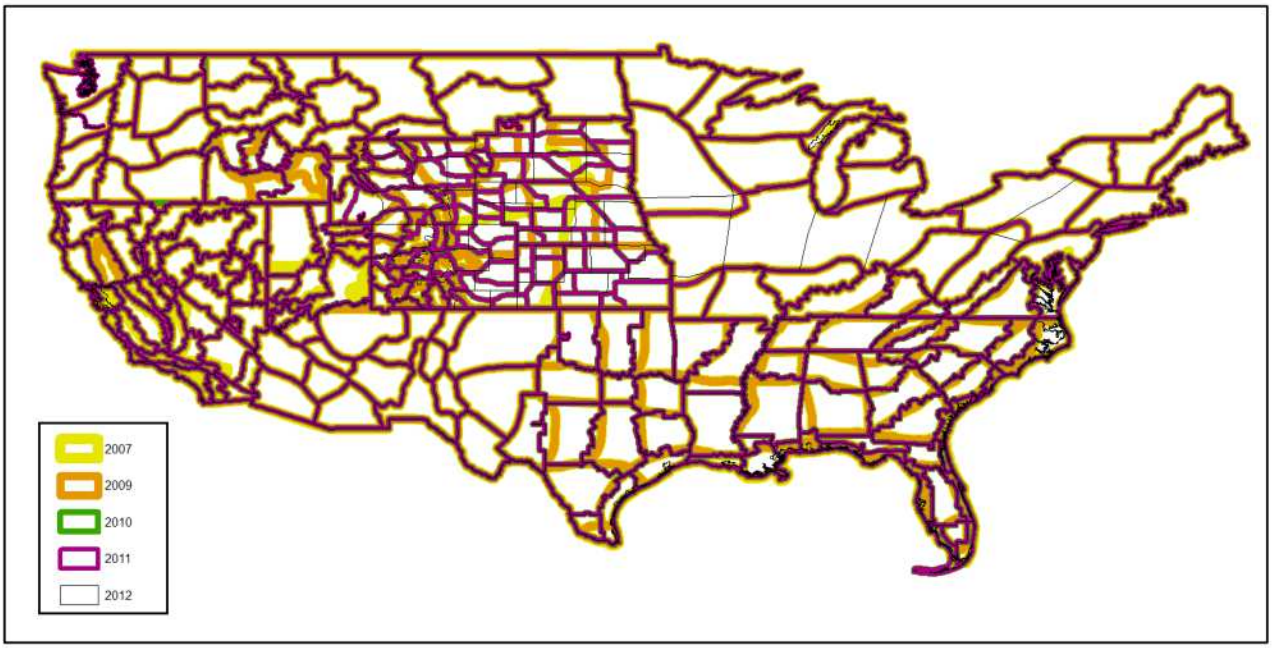

Figure 2. Boundaries of Predictive Service Areas (PSAs) in the conterminous US. Boundaries have changed significantly in some GCAs since their inception in 2006.

The Fire Potential Forecasts are made on a categorical scale of 1 to 9 for the current day and each of the following six days, and combine forecasted fuel dryness level, ignition triggers (from lightning and recreation), critical burn environment conditions (windy, unstable, hot and dry), and resource availability (Table 1). Each day's forecast consists of one and only one of the nine categorical values. Forecasting methodologies vary across GCAs and across PSAs within a GCA, based on the expert opinion of the meteorologist and statistical correlations of weather and fuel dryness variables with large fire activity. Forecast categories 1-3 are based on fuel dryness alone, and indicate increasing fuel dryness. Categories 4-9 indicate "high risk" days on which the meteorologist predicts a greater than 20% chance of significant fire activity. High risk days can be caused by an elevated chance of ignitions, from either lightning (category 4) or recreation (category 8), a forecast value which is issued primarily on the 4th of July when fireworks are commonly set off during celebrations. Weather factors may also cause the meteorologist to issue a high risk forecast, due to wind (category 5), unstable atmosphere and associated possible thunderstorm development (category 6), hot and dry weather (category 7), or dry weather (category 9).

When the forecast takes on a high risk value, regional staff often consults with the meteorologist in order to decide whether to preposition firefighting resources within the GCA. At high national preparedness levels, when firefighting resources are in high demand across the country, staff at the National Interagency Coordination Center in Boise, Idaho, use the 7-Day Fire Potential Outlook as an input into resource allocation decisions, along with existing fire activity and risks, socio-political considerations, and forecasted weather.

In this manuscript, we present preliminary analysis of the 7-Day Fire Potential Outlook, assessing the forecast's ability to predict ignitions and escaped fires in the Northwest and Southwest GCAs during the years 2009-2011.

Table 1. 7-Day Significant Fire Potential Outlook forecast values. Each day's forecast corresponds to one and only one of these values.

	Forecast Value	Forecast Description	Fire Environment
Increasing fuel dryness ↓	1	Moist Fuel Conditions	Little or No Risk of Large Fire
	2	Dry Fuel Conditions	Low Risk of Large Fire
	3	Very Dry Fuel Conditions	Low-Moderate Risk of Large Fire
High risk	4	Lightning	Ignition Trigger
	5	Windy	Critical Burn Environment Factor
	6	Unstable	Critical Burn Environment Factor
	7	Hot & Dry	Critical Burn Environment Factor
	8	High Recreation	Ignition Trigger
	9	Dry	Critical Burn Environment Factor

Methods

To assess the skill of the 7-Day Outlook, we obtained archived daily forecast values for PSAs in the Northwest (NWA) and Southwest (SWA) geographic coordination areas. Preliminary analyses were spatially constrained to these two geographic areas, and temporally constrained to 2009-2011, in order to refine our methods prior to initiating a nationwide analysis. While each day the forecast is issued for the current day and following six days, our initial analysis concentrates on the forecast values issued the for the current day (referred to as the Day 1 forecast) and Day 7 forecast.

To compare historical predicted fire occurrence (via the 7-Day Outlook) with actual historical fire occurrence, we utilized the national all-lands wildfire occurrence database (Short 2013, 2014). Fire ignition locations from the fire occurrence database (FOD) were intersected with annual PSA boundaries in ArcGIS 10.1. We utilized final fire size from the FOD to assess whether a fire escaped initial attack containment efforts; for our initial analysis, an escaped fire was defined as any incident with a final fire size greater than or equal to 121.3 hectares (300 acres).

Boxplots were used to assess the total number of ignitions by forecast level, as well as the total number of escaped fires by forecast level. We calculated 95% thresholds for number of ignitions and number of escaped fires, in order to establish confidence levels. Skill of the forecast was assessed in more detail within the NWA, where we used the log likelihood ratio to test whether the distribution of fire activity given the forecast was different from what would be expected randomly. The R statistical package was used to perform a G-test of independence with William's correction, and p-values were reported as a test of significance.

- Null hypothesis: fire activity occurs randomly with respect to forecast (therefore, the differences observed in the parallel boxplots are not statistically significant)

- Alternative hypothesis: fire activity is significantly different than random with respect to the forecast (the differences observed in the parallel boxplots are statistically significant)

In this work we conclude that a forecast has skill if the null hypothesis is rejected (in other words, fire activity is significantly different than random with respect to the forecast), and the boxplots show a positive pattern in numbers of ignition or escapes with increasing forecast risk level.
In addition, we fitted a generalized additive Poisson regression model with spline functions to describe the potentially non-linear relationships that might exist between expected number of escapes and the three explanatory variables, number of ignitions, the day of the year, and the next-day forecast value (note that the next-day forecast value is used since a fire ignited on one day is not likely to escape containment efforts until the next day). The estimated effects of each of the explanatory variables were then graphed to illustrate the additive increase or decrease from average (with 0 on the y axis corresponding to average) due to the particular explanatory variable.

Results

The most frequently issued forecast value was 1 (moist), followed by 2 (dry), and 3 (very dry). Since increasing fuel dryness is meant to convey a heightened awareness of significant fire potential, it seems appropriate for the very dry fuel category to appear less often than the moist category (Table 2). Similarly, "high risk" forecast values (category 4-9) were issued much less frequently than fuel dryness forecasts (category 1-3), which again seems appropriate since they are meant to convey elevated risk of significant fire activity to resource managers. The NWA currently uses empirical regression equations between the predicted amount of lightning, fuel dryness, and predicted number of fire starts to decide when to issue a forecast of 4 (lightning ignition trigger). They use the other high risk forecast values more rarely, since the required 20% probability of a large fire threshold is seldom attained for any weather condition other than a lightning event. The recreation ignition (category 8) trigger was issued only four times during the period of analysis, and the dry forecast (category 9) was not issued at all during the period of analysis in these two GCAs.

Table 2. Number of times each forecast level was issued for Day 1 (current day) forecasts, between 2009 and 2011, in the Southwest and Northwest Geographic Coordinating Areas (GCAs).

Forecast Level	1	2	3	4	5	6	7	8
NW	3133	1150	202	60	16	58	0	2
SW	5672	3456	2035	79	544	3	75	2
Total	8805	4606	2237	139	560	61	75	4

Patterns demonstrating the skill of the 7-Day Outlook in forecasting ignitions and escaped fires are evident in boxplots appearing in Figures 3 and 4. The number of ignitions per PSA is lower at dryness level 1 (moist) than at dryness levels 2 (dry) and 3 (very dry), which have roughly the same distribution of number of ignitions. Since the distribution of number of ignitions was similar during forecast levels 2 and 3, it seems the forecast does not exhibit skill in discerning the number of ignitions during dry versus very dry conditions. This result is perhaps not surprising, since the dryness levels were calibrated to the probability of large fires, not total ignitions.

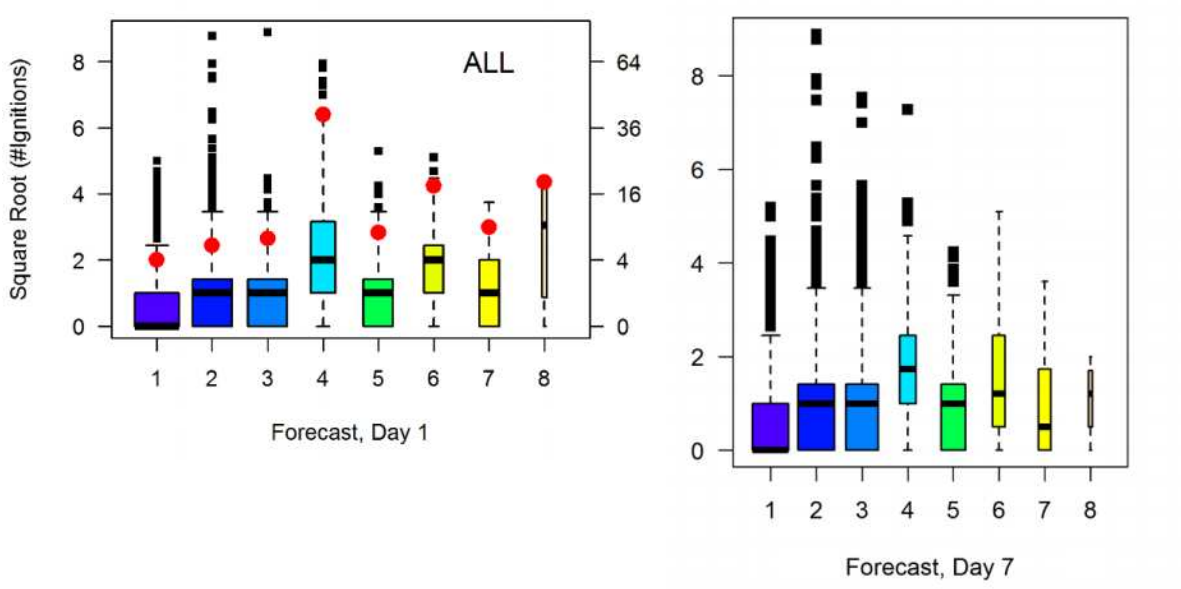

Figure 3. Distributions of number of ignitions (boxplots) in the Northwest and Southwest GCAs by forecast value, for forecast for current day (left panel) and seven days prior (right panel). Note that the y-axis represents the square root of the number of ignitions. The width of each boxplot is proportional to the square root of the number of times that value was forecasted (Table 2). Red dots in left panel indicate the 95th percentile of the distribution.

On average, a higher number of historical ignitions occurred coincident with ignition trigger and critical burn environment forecast values (4 through 8) than for dryness level 1 (moist), indicating some skill in predicting ignitions in these high risk forecast levels as well. In the same-day forecast, on average, the highest numbers of ignitions occurred under forecast level 8 (high recreation), followed by level 6 (unstable), and level 4 (lightning), with the ignition numbers being higher than those for dryness levels 2 and 3 on average. Evidently, days that the meteorologists forecast lightning do indeed experience higher lightning levels, judging by higher ignitions on those days. The level 6 forecast indicates unstable atmospheric conditions, which are often associated with thunderstorm development and lightning, and thus elevated numbers of ignitions. The level 5 forecast (windy day) had a similar distribution of number of ignitions as dryness levels 2 and 3, which is not surprising since wind would be expected to promote fire growth but not ignitions. The patterns in the boxplots are similar for the forecast values seven days ahead, suggesting that the forecast may be used up to a week ahead to indicate days with heightened levels of ignitions.

Boxplots give the 25th, 50th, and 75th percentiles of the distribution in addition to outliers. Ninety-fifth percentiles may also be a useful tool for managers. These were calculated for the number of ignitions and escaped fires by forecast value and added to the boxplots (Figures 3 and 4). For example, historically, fewer than four ignitions per PSA were observed on 95 percent of days forecasted as moist (level 1) conditions (Figure 3). The 95th percentile for ignitions is highest for days with lightning forecasts (level 4), at approximately 40 ignitions.

As noted above, the forecast was designed to predict significant fire activity rather than ignitions, although of course ignitions are a prerequisite to significant fire activity. Thus, we also assessed the performance of the forecast with regard to escaped fires (Figure 4). Because escaped fires are rare, the median (50th percentile) number of escaped fires on any given day per PSA is zero across all forecast values. However, the 95th percentile is one escaped fire during same-day forecasts of 3 (very dry), 4 (lightning), 5 (windy), and 7 (hot and dry), indicating that there is a 5% chance of having at least one escaped fire during days with these forecasts. Conversely, managers may expect no escapes on 95 percent of the days when the forecast is 1 (moist), 2 (dry), 6 (unstable), or 8 (recreation). In other words, there is less than a 5 percent chance of having at least one escape. Specifically, during days

with forecast level 4, the estimated probability of at least one escape was 0.22 for the same-day forecast in the NW, with 95% confidence limit between 0.13 – 0.31, and 0.14 in the SW, with 95% confidence limit between 0.05 – 0.23. Because a forecast level 4 is issued to indicate a 20% or greater risk of a significant fire event, this result indicates good skill of the category 4 forecast in that the 20% probability fell within the confidence interval of the observed proportion of escapes in both GCAs. However, the Day 7 forecasts for level 4 had less skill in predicting the probability of at least one escape, with estimated probability of 7.5% (1.4 -15%), which was significantly different than the expected 20% or greater risk. Thus, the forecast seven days in advance does not have as much skill in predicting escaped fires as the same-day forecast. The number of cases in forecast level 8 is too small to make any conclusions about the skill of the forecast for escapes for this level. The pattern is quite similar in both the Day 1 (same day) and Day 7 forecasts, indicating that the 7-Day Outlook forecast might be useful in indicating PSAs where firefighting resources might be prepositioned up to seven days ahead in order to prevent escaped fires. It should be noted that we used a threshold of 121.4 hectares (300 acres) across all PSAs to indicate an escaped fire, while each PSA has a different threshold for determining the size of a "Significant Fire", varying from 20.2 to 4046.9 hectares (50 to 10,000 acres), so there is some discrepancy in the definitions used to define an escaped versus significant fire.

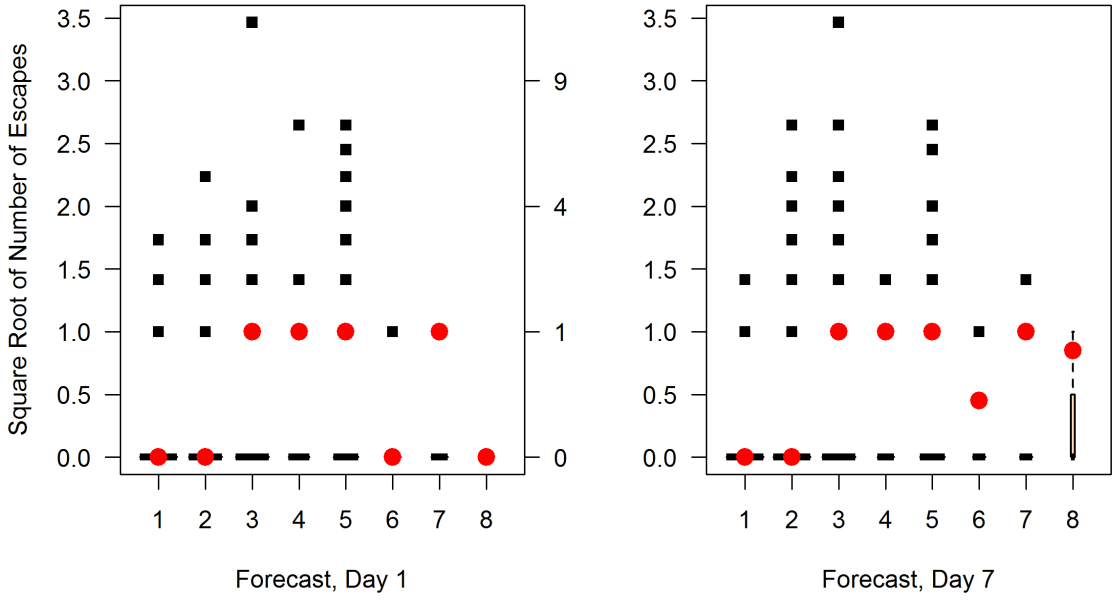

Figure 4. Distributions of number of escaped fires (final fire size >=121.4 hectares (300 acres)) using the same day forecast (left panel) and forecast value from seven days ahead (right panel) in the Northwest and Southwest GCA by forecast value. The red dot signifies the 95th percentile of the distribution. Escaped fires were lagged one day, assuming that a fire ignited on one day will not usually escape initial attack and grow to 121.4 hectares (300 acres) until the next day.

The statistical significance of the differences seen in the boxplots was tested using the log likelihood ratio. In the GCA as a whole (totals for all PSAs), fire activity with respect to the forecast occurred differently from random, indicating the forecast has skill at predicting ignitions and escaped fires at the GCA level (p<=1.06e-14). The log likelihood ratio tests, which were also performed for the Day 1 forecasts in each PSA in the NWA, indicate skill of the 7-Day Outlook in predicting ignitions in 11 of 12 PSAs and escaped fires in only 5 of 12 PSAs. Escaped fires are likely more challenging to predict than ignitions for several reasons, including their rarity. In fact, the log likelihood ratio test may not have had an adequate number of escaped fires in some PSAs, and may have failed to indicate statistical significance due to the low sample size.

Although the skill of the forecasts look good probabilistically, in absolute numbers there may be many days where the forecast missed predicting high fire risk. For example, although the chance of at least one escape was very small (approximately 2 percent) on days with forecast prediction level 1 (moist) or 2 (dry), indicating low risk of significant fires, the actual number of days that had at least one escape in these forecast levels and over the three years of the study was 318. Seven of those 318 days had more than three escapes. Up to 10 escaped fires occurred within a PSA on days when the forecast was not being issued; sometimes these days were during winter months that may not have been considered part of the core fire season, but other times these days occurred during the summer months.

We analysed the number of escaped fires as a function of number of ignitions, day in year, and next day forecast level (grouped into two groups, the "high risk" forecast values of 4-7 and the dryness levels 1-3), using Poisson regression (Figure 5). The number of escapes increased with the number of ignitions in both the NWA and SWA. In the SWA, an increase in the number of escaped fires is seen up to about 10 ignitions, after which there is no further increase. In the NWA, we see a similar pattern up to about 50 ignitions, with perhaps another increase above 60 ignitions, although the standard errors are large. The seasonal patterns in the SWA and NWA are different, with the SWA showing more escapes on average around 100-150 days into the year (mid-April through late May), corresponding with spring dryness before the arrival of monsoon rains, while the NWA shows more escapes around 210-250 days into the year (early August through mid-September), corresponding with dry fuels at the end of the summer season and possibly convective thunderstorm development. In the SWA, the high risk forecast days (categories 4-7) show an estimated 2.35 times more escaped fires per ignition than days with a dryness level forecast (categories 1-3), with a 95% confidence interval of 1.9 – 2.87. In the NWA, a similar pattern is evident, with about four times more escaped fires per ignition on high risk forecast days (95% confidence interval 2.5 – 6.4).

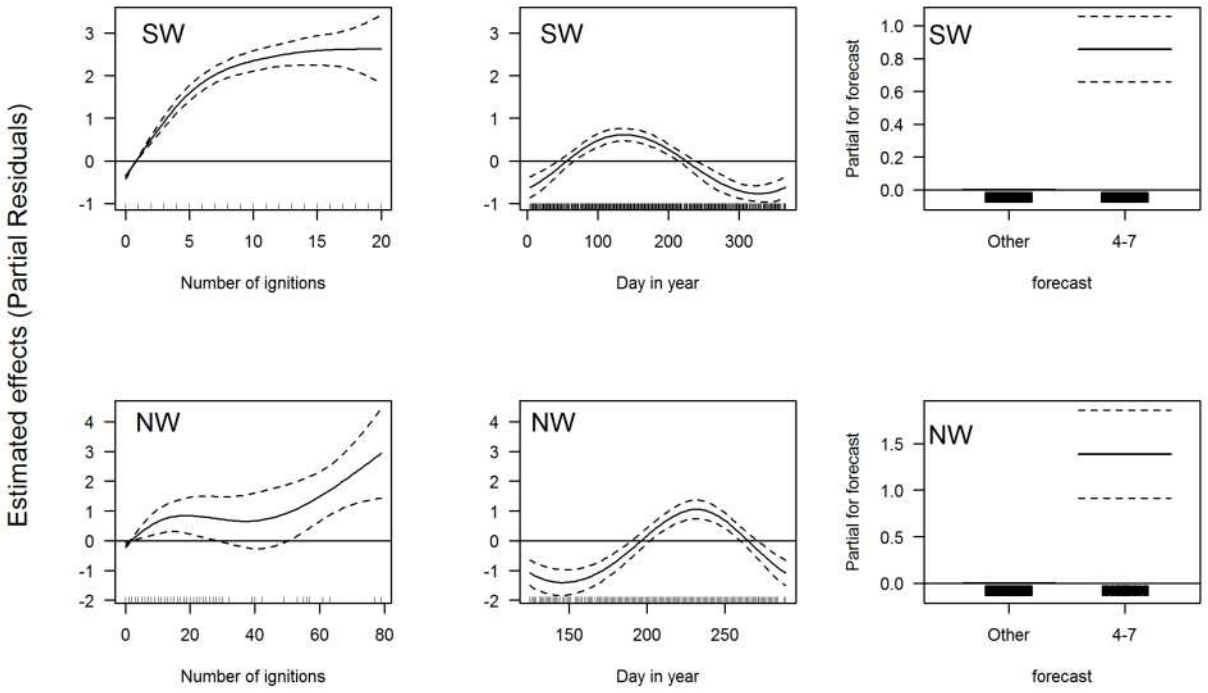

Figure 5. Partial residuals from Poisson regression demonstrating estimated effects of number of ignitions, day in year, and 7-Day Outlook forecast on number of escaped fires in the Northwest (NW) and Southwest (SW) Geographic Coordinating Areas. The partial residual plots show the additive increase or decrease from average (with 0 on the y axis corresponding to average) due to the particular explanatory variable. The y axis is in units of the natural log.

Discussion and Conclusions

Generally speaking, the 7-Day Fire Potential Outlook demonstrated better than random prediction of wildfire activity in the NWA. In the NWA and SWA, numbers of ignitions were lower at dryness level 1 (moist) than at dryness levels 2 (dry) and 3 (very dry) and on days with forecasts indicating lightning, unstable conditions, high recreation, windy conditions, or hot and dry conditions. Escaped fires were more likely under forecast levels 3 (very dry), 4 (lightning), 5 (windy), and 7 (hot and dry) than forecasts 1 (moist) and 2 (dry), with forecasts 6 (unstable) and 8 (high recreation) showing predictive skill seven days ahead but not during the same-day forecasts. In general, the forecasts showed skill in identifying days with elevated numbers of ignitions and potential for escaped fires not only for the current day's forecast, but also for forecasts made a week before, indicating the forecast might be useful in prepositioning of fire suppression resources nationally up to seven days in advance. In spite of this demonstrated skill, the forecasts missed many days with escaped fires.

The relationship between fuel dryness and fire ignitions is well established in the literature (Andrews *et al.* 2003), and thus the increasing number of ignitions across dryness levels 1 to 3 makes sense, but the weather conditions leading to significant fire activity are less well understood, adding to challenges in predicting fire activity and escapes. The rarity of escaped fires alone makes their prediction challenging. Adding to the difficulty in forecasting rare events, gridded weather model output also contains uncertainties and imperfections, which are then passed to the fire models. Wind speeds and directions tend to vary considerably within PSAs, causing spatial variation in the potential for fires to grow large. Additionally, if regional and national decision makers utilize a skilled forecast to effectively preposition suppression resources, which then successfully contain a fire while it is small, the performance of the forecast could appear poor in some cases, since it would appear that significant fires did not occur on days with high risk forecasts, when in fact the forecast itself contributed to containment during initial attack.

We found that the number of escaped fires increased with the number of ignitions in both the SWA and NWA, with the number of escaped fires per ignition being higher in the SWA than in the NWA. Different seasonal trends in escaped fires are present in the SWA and the NWA, with the most common period for escaped fires coming earlier in the year in the SWA (mid-April through late May, corresponding with spring dryness before the arrival of monsoon rains) than in the NWA (early August through mid-September, corresponding with dry fuels at the end of the summer season and possibly convective thunderstorm development). These findings illustrate the different fire regimes and response capabilities of fire suppression resources in these two GCAs. Forecasted high risk days (categories 4-7) had about twice as many escaped fires per ignition in the SWA and about four times more escaped fires per ignition in the NWA. On days with high risk forecasts, prepositioning of fire suppression resources or implementation of fire prevention measures might bring down the number of escaped fires, where desired in order to meet land management objectives.

In this initial work, we focused only on the three years 2009, 2010, and 2011, and on two of the ten geographic areas in the conterminous US. We are currently in the process of expanding the analysis to include a total of six years of reliable historical forecast data (2007 to 2012). Expanding the dataset will help to address the statistical issues with small sample sizes of escaped fires. We will also incorporate analysis of additional GCAs, in order to begin to be able to address national-level resource allocation issues. In addition, we will examine geographical and fuels characteristics as well as longer term fire history data to determine if additional non-weather-related variables (e.g. fuel type, land ownership) may improve the skill of the forecasts, in particular, by decreasing the number of days when escaped fires occurred but were not predicted.

References

Andrews, PL, Loftsgaarden, DO, Bradshaw, LS (2003) Evaluation of fire danger rating indexes using logistic regression and percentile analysis. International Journal of Wildland Fire 12, 213-226.

Short, KC (2013) 'Spatial wildfire occurrence data for the United States, 1992-2011 [FPA_FOD_20130422].' (RMRS USDA Forest Service: Fort Collins, CO). Available at http://dx.doi.org/10.2737/RDS-2013-0009

Short, KC (2014) A spatial database of wildfires in the United States. Earth System Science Data 6, 1-27.

Pyroclimatic classification of Mediterranean and mountain landscapes of south-eastern France

Thibaut Fréjaville, Thomas Curt

IRSTEA, UR EMAX, 3275 route Cézanne, F-13185 Aix en Provence, France.
thibaut.frejaville@gmail.com, thomas.curt@irstea.fr

Abstract
Fire risk is expected to increase in the Mediterranean Basin like in many areas worldwide. Climate is likely the main driver of fire activity by conditioning fuel dryness and fire weather. However fire-climate relationships are conditioned by other environmental dimensions like fuel structure (composition and spatial arrangement of flammable vegetation) and human activities. Therefore assessing how climate controls fire activity in heavily anthropized landscapes like European Mediterranean regions requires to design analyses in appropriate geographic units to encompass the dominant fire drivers. We aimed to assess how spatiotemporal patterns of both fire activity and climate structured south-eastern France into homogeneous geographic unit which we defined as 'pyroclimatic' regions.
We performed a pyroclimatic classification of Mediterranean and mountain areas of south-eastern France at 2 km resolution from the national fire database and daily atmospheric parameters over 1973-2009. This classification was based on multidimensional and clustering analyses. South-eastern France is characterized by three main 'pyroclimatic' regions and ten sub-regions from high fire-prone maritime mountains to moderate fire-prone hot lowlands and low fire-prone inner moist mountains. These geographic units are discriminated from each other by fire activity, fire seasonality, fire weather and their recent evolution.
We demonstrated that fire activity and fire weather of south-eastern France are highly dynamic in space and time. Characterizing pyroclimatic regions offers new regional perspectives of fire management and policy because two areas having similar fire weather, fire regime and recent temporal trends would benefit for specific attention.

Keywords*: pyrogeography, climate change, fire danger, fire activity, fire density, burned area, Mediterranean ecosystems, mountain.*

Introduction

Future changes of fire activity would be highly heterogeneous in space and time (Flannigan *et al.* 2009; Moritz *et al.* 2012). Spatial patterns of fire activity are governed by environmental gradients of climate, vegetation and ignition which drive pyrogeography worldwide (*sensu* Krawchuk *et al.* 2009). In this sense, authors argued that global changes are likely to have different effects on fire regimes respective to the predominant drivers (Bradstock, 2010; Krawchuk & Moritz, 2010). Climate is likely the main driver of fires because it controls both fire weather and fuel moisture (e.g. Flannigan *et al.* 2000) such as fuel amount (Bond and Keeley 2005). Otherwise, human influence on current and past fires has been emphasized as a key process (Bowman *et al.* 2011). In particular, the fire-climate relationship at a regional scale should be offset by temporal changes in land use and or fire management policies (Mouillot and Field 2005; Marlon *et al.* 2008). Therefore, it appears that no description or prediction of climate effects on wildfires makes sense without reference to particular climatic, ecological and human contexts. Human influence on fire activity has already been highlighted in Mediterranean areas through transformation of land cover and ignition potential (Loepfe *et al.* 2012). On the other hand, the northern Mediterranean Basin are facing an increasing fire risk with ongoing climate change (Bedia *et al.* 2013) and because fires are expected to be primarily limited by weather conditions in these areas (Batllori *et al.* 2013). We aimed to assess the diversity of French Mediterranean 'pyroclimates', i.e. regions having similar fire regime, similar climate, and similar recent trends of both. We expect that partitioning south-eastern France into pyroclimates will allow testing the variability in local fire drivers

because fire activity varies strongly across the study area (Figure 1). Moreover characterizing 'pyroclimates' has management implications since two areas having similar fire weather, fire regime and temporal trends would benefit from similar fire management and policy. So we aimed to assess the spatiotemporal patterns of fire weather and fire regime across south-eastern France and test how they are distributed into homogeneous geographic units, i.e. pyroclimatic regions.

Methods

Fire regime and fire weather of south-eastern France were quantified over 1973-2009 at two kilometre resolution from the national fire georeferenced database (Prométhée 2011) and daily atmospheric parameters of Safran reanalysis system (Vidal *et al.* 2010).

Fire regime was quantified from 2*2 km aggregates of i) fire season length (number of days between the first and the last fire of the year), ii) yearly and seasonal fire occurrence (fire density) and iii) yearly and seasonal cumulated size of fires which ignited in a given pixel. As we aim to capture regional variation in fire regime, we applied an inverse distance weighting function to smooth fire statistics over a larger moving window (30 km). A spatial smoothing of fire metrics allowed us to emphasize their deterministic part by reducing the stochasticity inherent to the fire process. Moreover, as fire regime may need more than four decades to be assessed in the less fire-prone regions, we expanded the spatial search range of fire occurrence in a given pixel from two (pixel resolution) to ten kilometres (moving window of 5 km radius). Fire danger was assessed from components of the Canadian Fire Weather Index System which rate the initiation, spread and control of forest fires. Fire weather index (FWI) and its drought components (FFMC, DMC, DC) were computed from the equations of Van Wagner and Pickett (1985) based on daily noon parameters (Van Wagner 1987). The use of instantaneous conditions (12h GMT) instead of daily means was recently pointed out to get reliable estimates of mean and extreme conditions of fire danger (Herrera *et al.* 2013). Climate patterns were assessed from monthly and yearly averages of temperature and precipitation whose computations are based on daily mean temperature and cumulated rainfall respectively. All these indices were downscaled from height to one kilometre resolution by the help of regional statistical modelling following standard procedures (Zimmermann and Kienast 2009; Zimmermann *et al.* 2013). Specifically downscaling procedure was based on vertical gradient modelling *per* homogeneous climatic regions ('symposium', Vidal *et al.*, 2010) and anomaly inference. Fire danger and bioclimatic indices were first computed before downscaling and then aggregated to 2*2 km (fire database resolution). Temporal trends over 1973-2009 were quantified for all fire regime variables and downscaled climatic indices by the statistics of a modified Mann-Kendall trend test (Hamed and Ramachandra Rao 1998).

We carried out the pyroclimatic classification of south-eastern France by ordination and clustering analyses on four subsets: i) fire regime metrics, ii) climate (fire danger and bioclimatic indices) and iii-iv) their past temporal trends. First, we independently synthesized each of the four subsets from Principal Components Analyses (PCA) with backward selection procedure. Backward selection was applied to remove the least contributory variables in order to synthesize the multidimensional variability of fire, climate and temporal trends into a reduced number of gradients (i.e., principal components). We prior standardized seasonal fire and climatic variables by pixel (0-1) to limit autocorrelation with annual means and to study the seasonal distribution of them among pyroclimatic regions. Secondly, we performed a hierarchical agglomerative clustering (HAC) on principal components based on a Euclidean distance matrix and the Ward criterion (Ward 1963). The number of group was given by the Calinski-Harabasz criterion (Caliński and Harabasz 1974) applied on an independent k-means clustering with Monte Carlo simulations (Makarenkov and Legendre 2001). All analyses and calculations were performed on R environment (R Core Team 2013), with the help of the 'fume' package for FWI calculations and trend tests (Santander Meteorology Group 2012).

Results and discussion

Average patterns over 1973-2009 of annual fire density and size show a high variability of fire activity across South-eastern France (Figure 1). We find the most fire prone areas in the eastern Mediterranean coast where from west to east, calcareous and siliceous Provence, the maritime pre-Alps and Corsica have experienced both the highest density of fires and the highest burned area. In the western coast, we find several fire-prone islands around major cities with high burned areas and moderate fire density. A third area with high density and cumulated size of fires was found in north-western inlands (Ardeche plateau). Elevated mountain areas in Eastern Pyrenees, Cevennes and Southern Alps (from west to east) are less fire-prone. These spatial gradients of fire activity are partly related to fire weather ones, depicted by the drought code (DC) and the fire weather index (FWI) of the Canadian Fire Weather Index System (Figure 1). Annual extremes (95th percentile) of DC and FWI are maximal in the western Mediterranean coast and minimal in elevated mountain areas which are relatively characterized by high *versus* low fire activity respectively.

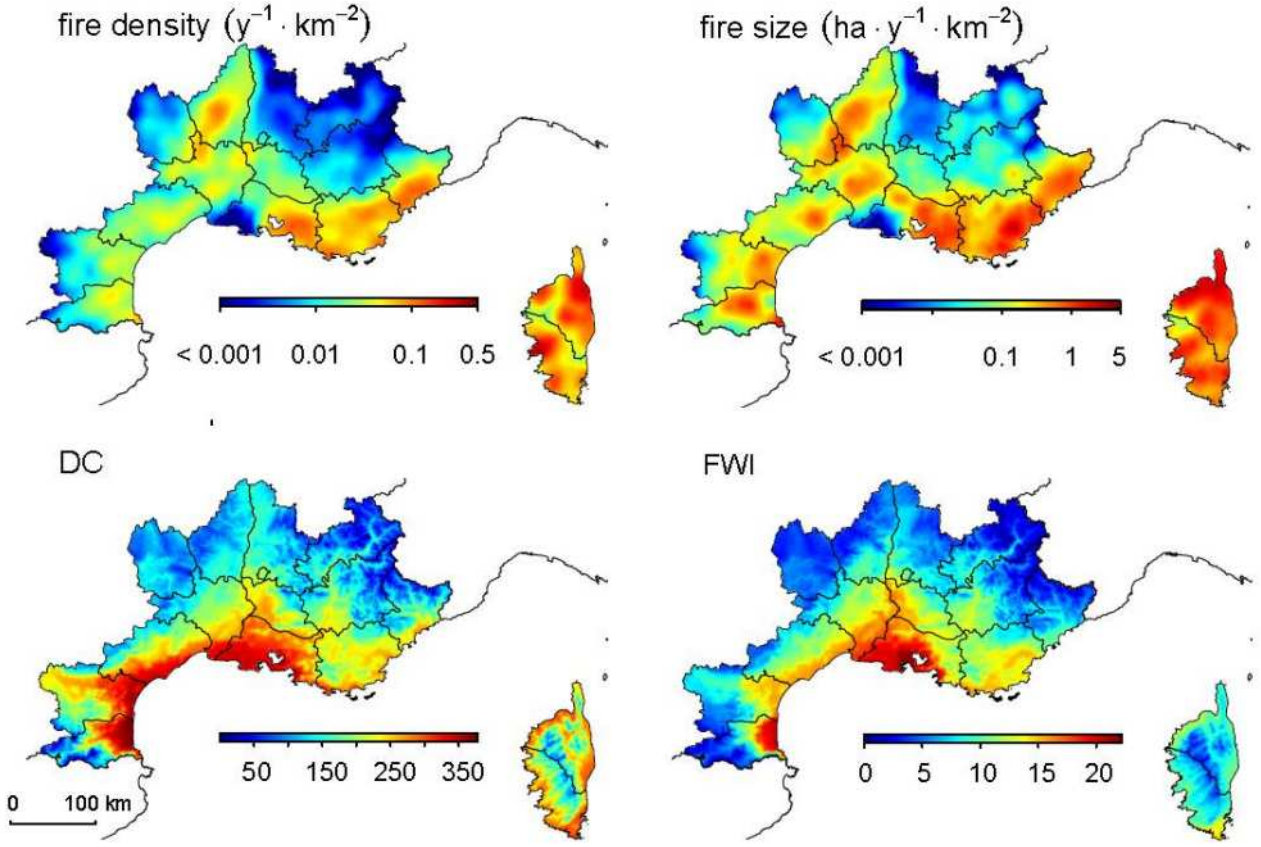

Figure 1. Spatial patterns of annual fire density, fire size, Drought Code and Fire Weather Index in the 15 departments of south-eastern France (1973-2009 averages). Fire metrics were smoothed by an inverse distance weighting function on a 30 km moving window (log-scale). Fire size represents here the cumulative size of fires which ignited in a given square kilometre per year. Maps of fire weather indices have been computed from extreme annual values (95th percentile).

By taking into account fire activity, fire weather and their temporal trends over 1973-2009, clustering analyses indicated that south-eastern France is divided into three pyroclimatic regions and 10 sub-regions (Figure 2). These regions constitute specific combinations of climate and fire regime from the highest fire-prone maritime mountains (Corsica and maritime pre-Alps, PCr-1) to high fire-prone Mediterranean-climate lowlands (Mediterranean coast and Rhone valley, PCr-2) and low fire-prone moist and cold inner mountains (eastern Pyrenees, Cevennes and southern Alps, PCr-3).

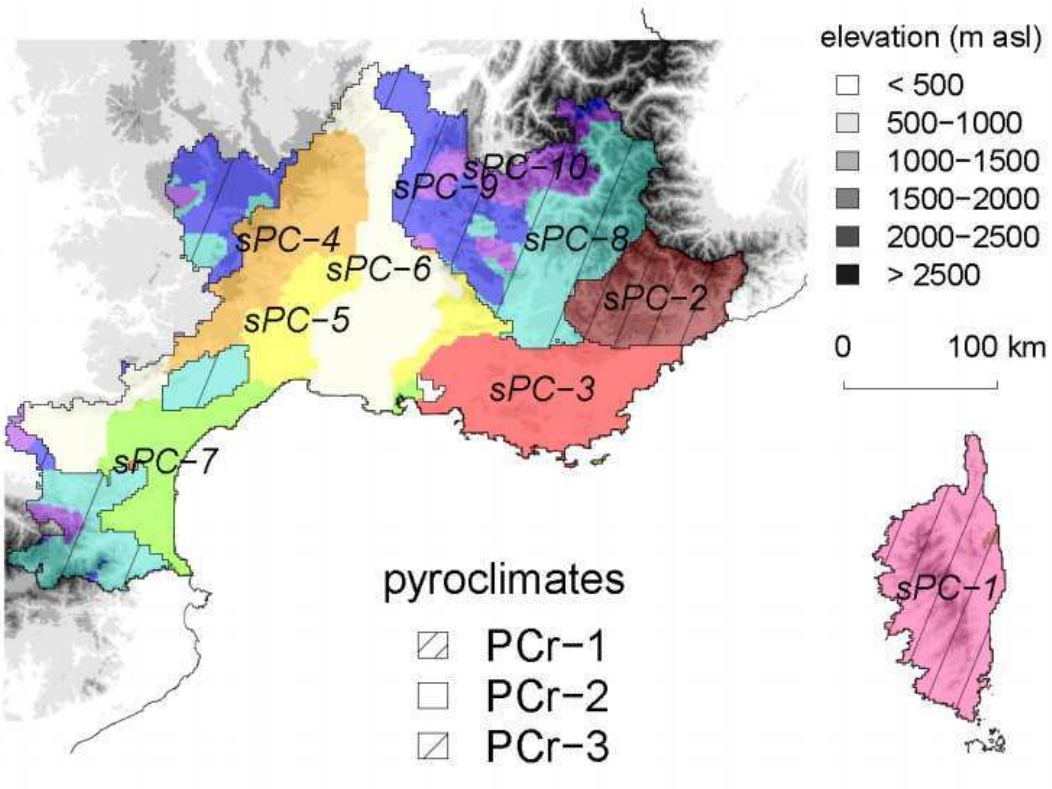

Figure 2. Pyroclimatic regions of south-eastern France. Pyroclimatic regions (PCr) were subdivided into 10 sub-pyroclimates (sPC). Sub-regions sPC-1 and 2 belong to pyroclimate PCr-1; sPC-2 to sPC-7 belong to PCr-2 and sPC-8 to sPC-10 belong to PCr-3. See Method section for details on pyroclimate partitioning.

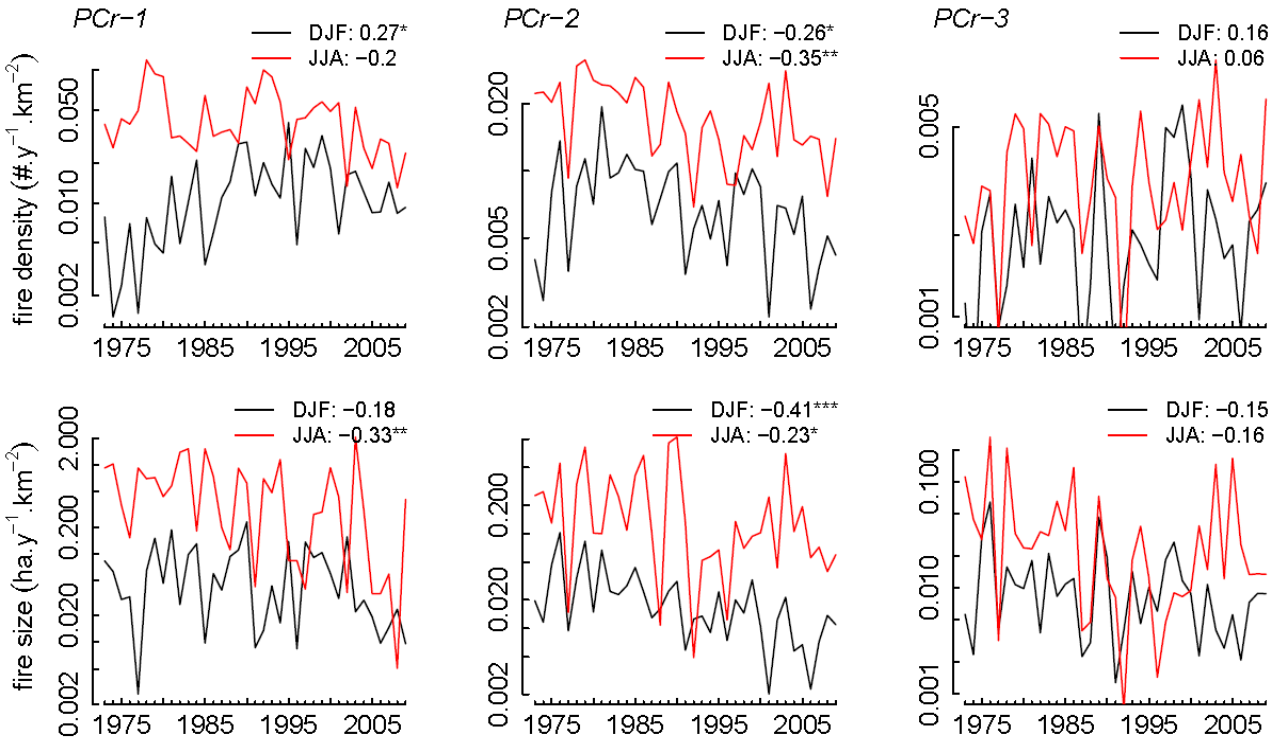

Figure 3. Averaged temporal trends (1973-2009) of winter (DJF) and summer (JJA) fire density and fire size (log-scale) within the three pyroclimatic regions. Correlation coefficient (t) and significance ($p < 0.05$, ** $p < 0.01$, *** $p < 0.001$) are presented for Mann-Kendall modified trend tests. Fire size represents here the cumulative size of fires which ignited in a given square kilometre per year.*

Fire danger is the highest in PCr-2 and the lowest in PCr-3 in respect to annual mean and 95th percentile of FWI and DC (Figure 1). Trend tests over the four past decades indicated that mean fire danger has significantly increased in all three regions, depicted by yearly mean FWI (tau > 0.42, p < 0.01). Fire danger extreme conditions have followed the same increasing trend (95th percentile FWI: tau > 0.39, p < 0.05). These findings corroborate previous study in Mediterranean areas (Carvalho *et al.* 2008; Bedia *et al.* 2013). Otherwise fire activity is largely seasonally restricted with one peak in winter and one in summer. The two most fire-prone regions PCr-1 and PCr-3 are characterized by a predominant fire activity in summer compared to PCr-3 (69, 73 and 45 % of annual burned area, respectively). On the contrary, winter burned area is higher in annual proportion within the less fire-prone elevated-mountain region PCr-3 (30 % against 19 % and 10 % in PCr-1 and PCr-2 respectively). In these more weather-limiting landscapes spring fires contribute to 18 % of annual burned area, whereas autumn fires are poorly contributing with less than 7 % of annual burned area whatever the pyroclimatic region. 1973-2009 trends of seasonal fire activity showed contrasted patterns too (Figure 3). Indeed winter fire density has increased in PCr-1 (p < 0.05), decreased in PCr-2 (p < 0.05) while both fire density and size have not significantly changed in winter and in summer across PCr-3 (p > 0.05). Overall in the two most fire-prone regions, both summer fire density as winter and summer fire size have decreased these past decades (Figure 3) with higher significant trends for the hotter and dryer pyroclimatic region (PCr-2, p < 0.05).

We demonstrated that south-eastern France has contrasted geographic units, i.e. pyroclimatic regions, which revealed differences in both spatial and temporal patterns of fire and climate. This classification would offer new regional perspectives in fire management policy by defining regional affinities in both fire weather and fire regime dynamics. In the heavily anthropized landscapes of south-eastern France, fire activity appear likely more heterogeneous in space and time than in other Mediterranean areas where burned area has increased since the seventies (Pausas 2004; Carvalho *et al.* 2008). Indeed we found that fire density and fire size have increased in some regions and decreased in others with season-specific trends. These findings point out that changes in fire activity may strongly differ between closed regions without *a priori* evident climatic explanation. This may involve a stronger expression of climatic-independent altering dimensions such as fire suppression strategies (Mouillot and Field 2005; Brotons *et al.* 2013) or land cover transformation (Loepfe *et al.* 2012). This study highlights that the predominance of fire drivers among climate, vegetation and human factors may likely differ across small spatial ranges and may counteract the effects of climate change on future regional fire activity.

Acknowledgements

Financial support was provided by the FUME Project under the European Union's Seventh Framework Programme (FP7/2007-2013) and by grants from the National Research Institute of Science and Technology for Environment and Agriculture (IRSTEA) to TF. Authors acknowledge the national meteorological agency Météo-France and Jean-Philippe Vidal for providing climate data. We also acknowledge the public institutions that have fueled the fire national database Prométhée and Christophe Bouillon for help in formatting this database.

References

Batllori E, Parisien M-A, Krawchuk MA, Moritz MA (2013) Climate change-induced shifts in fire for Mediterranean ecosystems. *Global Ecology and Biogeography* **22**(10), 1118–1129. doi:10.1111/geb.12065.

Bedia J, Herrera S, Camia A, Moreno JM, Gutiérrez JM (2013) Forest fire danger projections in the Mediterranean using ENSEMBLES regional climate change scenarios. *Climatic Change* 1–15. doi:10.1007/s10584-013-1005-z.

Bond WJ, Keeley JE (2005) Fire as a global 'herbivore': the ecology and evolution of flammable ecosystems. *Trends in Ecology & Evolution* **20**(7), 387–394.

Bowman DMJS, Balch J, Artaxo P, Bond WJ, Cochrane MA, D'Antonio CM, DeFries R, Johnston FH, Keeley JE, Krawchuk MA, Kull CA, Mack M, Moritz MA, Pyne S, Roos CI, Scott AC, Sodhi NS, Swetnam TW (2011) The human dimension of fire regimes on Earth. *Journal of Biogeography* **38**(12), 2223–2236. doi:10.1111/j.1365-2699.2011.02595.x.

Brotons L, Aquilué N, de Cáceres M, Fortin M-J, Fall A (2013) How Fire History, Fire Suppression Practices and Climate Change Affect Wildfire Regimes in Mediterranean Landscapes. *PLoS ONE* **8**(5), e62392. doi:10.1371/journal.pone.0062392.

Caliński T, Harabasz J (1974) A dendrite method for cluster analysis. *Communications in Statistics* **3**(1), 1–27. doi:10.1080/03610927408827101.

Carvalho A, Flannigan MD, Logan K, Miranda AI, Borrego C (2008) Fire activity in Portugal and its relationship to weather and the Canadian Fire Weather Index System. *International Journal of Wildland Fire* **17**(3), 328–338.

Flannigan MD, Krawchuk MA, de Groot WJ, Wotton BM, Gowman LM (2009) Implications of changing climate for global wildland fire. *International Journal of Wildland Fire* **18**(5), 483–507.

Flannigan MD, Stocks BJ, Wotton BM (2000) Climate change and forest fires. *Science of the total environment* **262**(3), 221–229.

Hamed KH, Ramachandra Rao A (1998) A modified Mann-Kendall trend test for autocorrelated data. *Journal of Hydrology* **204**(1), 182–196.

Herrera S, Bedia J, Gutiérrez JM, Fernández J, Moreno JM (2013) On the projection of future fire danger conditions with various instantaneous/mean-daily data sources. *Climatic Change* **118**(3-4), 827–840. doi:10.1007/s10584-012-0667-2.

Krawchuk MA, Moritz MA, Parisien M-A, Van Dorn J, Hayhoe K (2009) Global Pyrogeography: the Current and Future Distribution of Wildfire. *PLoS ONE* **4**(4), e5102.

Loepfe L, Martinez-Vilalta J, Piñol J (2012) Management alternatives to offset climate change effects on Mediterranean fire regimes in NE Spain. *Climatic Change* **115**(3-4), 693–707. doi:10.1007/s10584-012-0488-3.

Makarenkov V, Legendre P (2001) Optimal Variable Weighting for Ultrametric and Additive Trees and K-means Partitioning: Methods and Software. *Journal of Classification* **18**(2), 245–271. doi:10.1007/s00357-001-0018-x.

Marlon JR, Bartlein PJ, Carcaillet C, Gavin DG, Harrison SP, Higuera PE, Joos F, Power MJ, Prentice IC (2008) Climate and human influences on global biomass burning over the past two millennia. *Nature Geoscience* **1**(10), 697–702.

Moritz MA, Parisien M-A, Batllori E, Krawchuk MA, Van Dorn J, Ganz DJ, Hayhoe K (2012) Climate change and disruptions to global fire activity. *Ecosphere* **3**(6), art49. doi:10.1890/ES11-00345.1.

Mouillot F, Field CB (2005) Fire history and the global carbon budget: a 1°× 1° fire history reconstruction for the 20th century. *Global Change Biology* **11**(3), 398–420. doi:10.1111/j.1365-2486.2005.00920.x.

Pausas JG (2004) Changes in Fire and Climate in the Eastern Iberian Peninsula (Mediterranean Basin). *Climatic Change* **63**(3), 337–350. doi:10.1023/B:CLIM.0000018508.94901.9c.

Prométhée (2011). "La banque de données sur les incendies de forêts en région Méditerranéenne en France." http://www.promethee.com/.

R Core Team (2013) R: A language and environment for statistical computing. R Foundation for Statistical Computing (Vienna, Austria) URL http://www.R-project.org/.

Santander Meteorology Group (2012) fume: FUME package. R package version 1.0. URL http://CRAN.R-project.org/package=fume.

Vidal J, Martin E, Franchistéguy L, Baillon M, Soubeyroux J (2010) A 50-year high-resolution atmospheric reanalysis over France with the Safran system. *International Journal of Climatology* **30**(11), 1627–1644. doi:10.1002/joc.2003.

Van Wagner CE (1987) Development and structure of the Canadian Forest Fire Weather Index System. Canadian Forestry Service, Forestry Technical Report 35. (Ottawa, ON)

Van Wagner CE, Pickett TL (1985) Equations and FORTRAN program for the Canadian Forest Fire Weather Index System. Canadian Forestry Service, Forestry Technical Report 33. (Ottawa, ON)

Zimmermann NE, Gebetsroither E, Zuger J, Schmatz D, Psomas A (2013) Future Climate of the European Alps. 'Management Strategies to Adapt Alpine Space Forests to Climate Change Risks'. (Ed G Cerbu)(InTech)

Zimmermann NE, Kienast F (2009) Predictive mapping of alpine grasslands in Switzerland: species versus community approach. *Journal of Vegetation Science* **10**(4), 469–482.

Rainfall effects on fine forest fuels moisture content

Sérgio Lopes[a], Domingos Xavier Viegas[b], Luís de Lemos[a], Maria Teresa Viegas[b]

[a] *Environment Department, Technology and Management School of Viseu, Polytechnic Institute of Viseu, Campus Politécnico de Repeses 3504-510 Viseu, Portugal;slopes@estv.ipv.pt*
[b] *ADAI/Mechanical Engineering Department, University of Coimbra, Polo II, Pinhal de Marrocos, 3030-790 Coimbra, Portugal; xavier.viegas@dem.uc.pt*

Abstract
The main purpose of the present study was to develop and test different approaches to predict fuel moisture content after rainfall episodes based on field measurements. These approaches were validated also with field measurements that indicate which as the best performance. It was also an objective to establish a low risk or safe period in terms of forest fires occurrence through the analyses of fuel moisture content after rainfall episodes comparatively to the value observed before the episodes.
Although the influence of rainfall on forest fuel moisture content is quite complex we found that the simplified assumptions made in the present study and the simple mathematical models that were proposed exhibit suitable performances in the prediction of fuel moisture content change after rainfall episodes. In the present study good prediction results were obtain for dead foliage of the tree species of *Pinus pinaster* and *Eucalyptus globulus*. It was also verified that a safe time period regarding the occurrence of forest fires depending on the summer rainfall episode intensity could be established.

Keywords*: Fuels, moisture content, rainfall, fire risk.*

Introduction

Rainfall has a significant effect in forest fire danger. Depending on the period of the year, it can contribute to increase fine fuel growth and therefore increase fire danger during the fire season (Viegas and Viegas 1994). On the other hand rainfall episodes during the fire season will increase fuel moisture content (FMC) and therefore reduce fire danger, establishing a low risk period regarding the occurrence of forest fires. In order to predict FMC it is important to estimate the increase of moisture as a result of a given amount of rainfall and also to predict the decrease of moisture and consequently the duration of the low risk period. The influence of rainfall on FMC of dead fine fuels is well known but it is a complex process that cannot be simply a matter of directly equating the changes in moisture content with the amount of rainfall (Viney 1991).
The increase of FMC can decrease with the increase of rainfall amount and initial FMC. Thus as the amount of rainfall increases, a smaller proportion of it could be held by the fuels, also the higher the fuel's initial moisture content, the less rain it could absorb (Van Wagner 1987).
The main purpose of the present study is to develop and test different approaches to predict FMC after rainfall episodes based on field measurements. These approaches will be validated also with field measurements that will indicate which as the best performance. It is also an objective to establish a safe time period regarding the occurrence of forest fires through the analyses of FMC after rainfall episodes comparatively to the value observed before the episodes.

Field measurements

In the present study, FMC of dead foliage from *Pinus pinaster* and *Eucalyptus globulus* tree species and living shrub foliage and extremities from *Calluna vulgaris* and *Chamaespartium tridentatum* (that are very common in the forests of Central Portugal) was measured by field sampling throughout the year from 1996 to 2010. Samples were daily collected at Lousã during the summer months (June to September) and once or twice a week during the rest of the year (October to May), between 12:00h

and 14:00h LST. FMC was determined by oven-drying the fuel samples for 24 hours at 105°C, as presented in Figure 1. The total daily rainfall measured at the Lousã Weather Station obtained by the Portuguese Institute of Meteorology for the same period was used in the present analysis. Similar sampling was performed in Viseu (80km apart from Lousã) for the following species: dead foliage of *Pinus pinaster* and *Eucalyptus globulus* and living *Calluna vulgaris* from 2007 to 2010.
For FMC prediction after rainfall episodes, model evaluation was performed using data from of a series of rainfall episodes at Lousã and model validation was performed comparing predicted values with FMC measured in Viseu for well characterized rainfall episodes. For establishing the low risk period after the rainfall episodes data from Lousã and Viseu were used.

Figure 1. Sampling and determination procedures on the FMC research program of Lousã and Viseu

In Figure 2 some examples of studied rainfall episodes occurred in Lousã and Viseu are presented. As can be seen there are some rainfall episodes with only one day while in other examples there are several consecutive days of precipitation. In some of them rainfall intensity increased and in other cases rainfall intensity decreased.
Analysing all the available episodes occurred in Lousã and Viseu, depending on rainfall intensity and on the initial moisture content of forest fuels, after the rainfall episode we can establish period of time with low risk of fire ignition.
It can be observed that an episode with intensity up to 10 mm/day shows a 1 to 2 days safe period till it returns to the initial value of FMC before the episode. An episode with intensity higher than 10 mm/day can result in at least 3 days of low risk period.

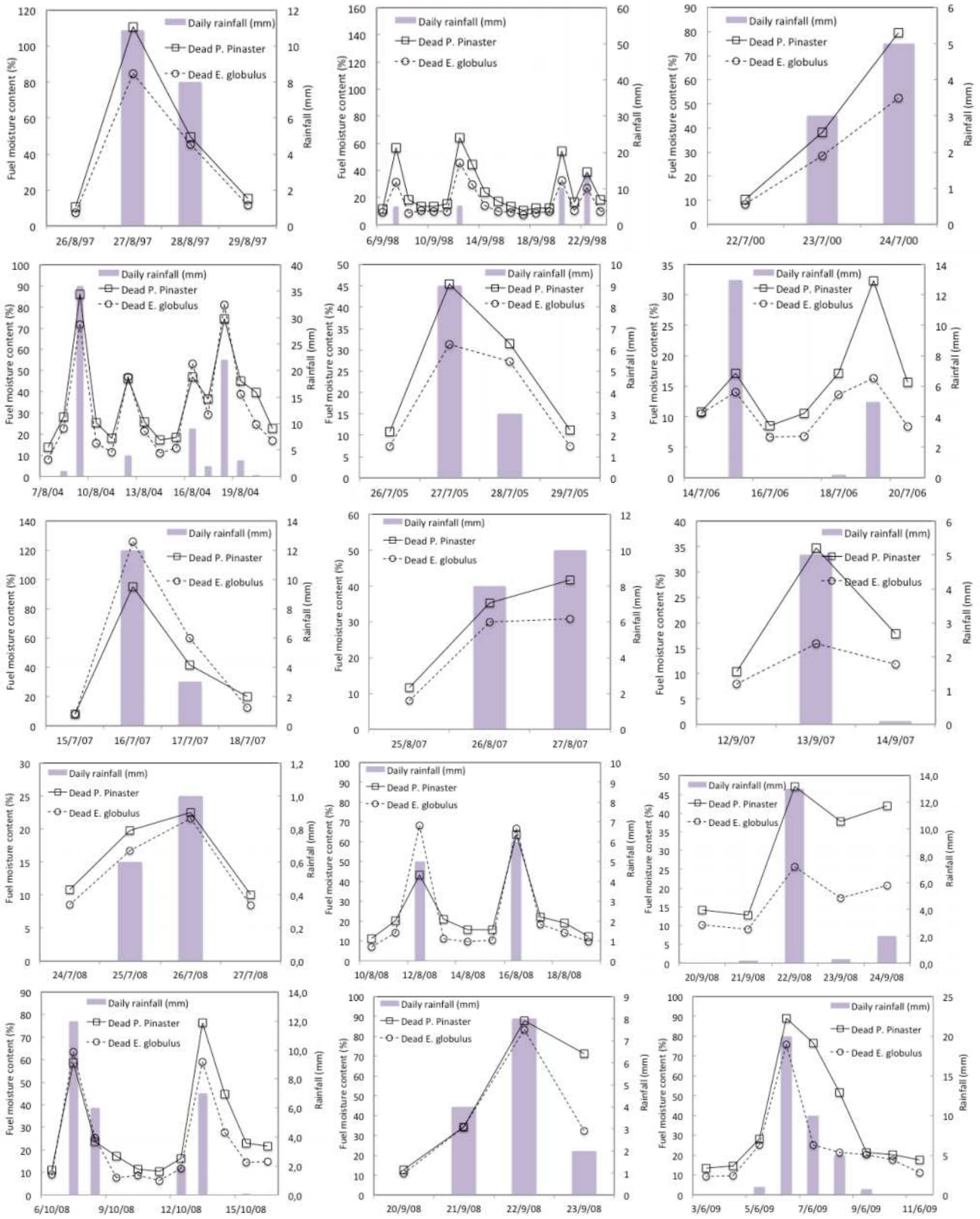

Figure 2. Examples of studied rainfall episodes that occurred in Lousã and Viseu.

FMC Variation Models

As can be seen in Table 1, for a correlation analysis, the Spearman nonlinear correlation coefficients were calculated between the FMC variation, Δm (variation between the FMC of one day and the FMC of the day before**)** and the rainfall intensity**,** I_d (total rainfall of the last 24h), rainfall variation, ΔI (variation between the rainfall intensity of one day and the rainfall intensity of the day before) and the initial FMC, m_0 (FMC of the day before).
The correlation analysis shows that, for dead foliage (*Pinus Pinaster* and *Eucalyptus globulus)*, rainfall intensity I_d and rainfall variation ΔI have a significant positive correlation with FMC variation Δm and a significant negative correlation with FMC variation/rainfall intensity $\Delta m/I_d$. For shrub foliage of *Calluna vulgaris* a medium positive correlation with Δm and also a significant negative correlation with $\Delta m/I_d$ was observed.

***Table 1. Correlation analysis between the FMC variation and rainfall intensity**, rainfall variation and initial FMC*

			FMC variation	FMC variation/ Rainfall intensity
			Δm (%)	Δm /I_d (%.mm^{-1})
Dead Pinus pinaster	Rainfall intensity	I_d (mm)	0.683$^{(**)}$	-0.763$^{(**)}$
	Rainfall variation	ΔI_{d-d-1}(mm)	0.692$^{(**)}$	-0.611$^{(**)}$
	Initial FMC	m_0	0.059$^{(ns)}$	-0.380$^{(**)}$
Dead Eucalyptus globulus	Rainfall intensity	I_d (mm)	0.597$^{(**)}$	-0.750$^{(**)}$
	Rainfall variation	ΔI_{d-d-1}(mm)	0.608$^{(**)}$	-0.656$^{(**)}$
	Initial FMC	m_0	0.122$^{(ns)}$	-0.361$^{(**)}$
Calluna vulgaris	Rainfall intensity	I_d (mm)	0.316$^{(**)}$	-0.755$^{(**)}$
	Rainfall variation	ΔI_{d-d-1}(mm)	0.328$^{(**)}$	-0.651$^{(**)}$
	Initial FMC	m_0	0.291$^{(**)}$	0.025$^{(ns)}$
Chamaespartium tridentatum	Rainfall intensity	I_d (mm)	0.128$^{(ns)}$	-0.815$^{(**)}$
	Rainfall variation	ΔI_{d-d-1}(mm)	0.060$^{(ns)}$	0.000$^{(ns)}$
	Initial FMC	m_0	0.041$^{(ns)}$	-0.086$^{(ns)}$

$^{(**)}$ Significant at 0.01 level; $^{(*)}$ Significant at 0.05 level; (ns) Not significant

Based on the Lousã FMC field measurements and considering the previous correlation analysis, three models were developed and tested, each one with the same purpose of determining the FMC m_d of the day d by adding a FMC increase/decrease value Δm to the FMC observed before the episode m_0 as defined in Eqn 1.

$$m_d = m_0 \pm \Delta m \qquad 1$$

A daily basis time resolution for FMC modelling was adopted, not considering crown interception, fuel immersion in water, changes of intensity and duration of rainfall with less than 24h resolution.
It is observed that for a given fuel with initial FMC value equal to m_o, expressed in [%] in a given day d if there is a rainfall with intensity I_d, expressed in [mm] on the previous 24 hours then there will be a FMC variation Δm.

In Model 1 we assume that for fine dead fuels this Δm is an increase value to m_o depending only on the amount of rainfall of day d as defined in Eqn 2.

$$\Delta m = a_1 . I_d{}^{b_1} \quad (2)$$

It was also found that Δm could depend not only on I_d but also on m_o.

We propose Model 2 to estimate the relationship between the increase in FMC and rainfall intensity expressed by $\Delta m / I_d$ and the initial FMC m_o as defined in Eqn 3.

$$\Delta m / I_d = a_2 . m_0{}^{b_2} \quad (3)$$

Models 1 and 2 do not consider FMC change due to consecutive days with rainfall, which are observed quite often. For this purpose we propose Model 3 to take into account, not only the occurrence of rainfall in one day but also in two consecutive days with values I_d and I_{d-1}, respectively for the last 24 hours and the previous 24 hours. Depending on the sign of rainfall variation $\Delta I = I_d - I_{d-1}$ we will have two situations:

(i) If $\Delta I > 0$ then the FMC variation value Δm is positive and we will have a moisture increase given by Eqn 4:

$$\Delta m = a_3 . \Delta I_{d-d_{-1}}{}^{b_3} \quad (4)$$

(ii) If $\Delta I < 0$ then the FMC variation value Δm is negative and we will have a moisture decrease given by Eqn 5:

$$\Delta m = -a_4 . \left|\Delta I_{d-d_{-1}}\right|^{b_4} \quad (5)$$

Where a_1, a_2, a_3, a_4, b_1, b_2, b_3 and b_4 are empirical model parameters estimated with field measurements.

Results

In Table 2 the FMC prediction model parameters estimation defined in Eqn 2 to 5 are shown. This estimation was performed using linear least squares fitting based on the field measurements. The graphical representation of the studied models is shown in **Erro! A origem da referência não foi encontrada.**.

Table 2. Model parameters of Eqns 2 to 5 and statistical parameters

Model	*Species*	*i*	a_i	*Std. dev.*	b_i	*Std. dev.*	*n*	R^2 *adj.*
Model 1	*Dead Pinus pinaster*	1	15.180$^{(**)}$	1.100	0.445$^{(**)}$	0.037	14	0.917
	Dead Eucalyptus globulus		18.476$^{(**)}$	1.811	0.364$^{(**)}$	0.049	15	0.794
	Calluna vulgaris		22.961$^{(**)}$	1.458	0.211$^{(**)}$	0.029	9	0.794
Model 2	*Dead Pinus pinaster*	2	189.453$^{(*)}$	77.246	-0.981$^{(**)}$	0.137	9	0.863
	Dead Eucalyptus globulus		172.720$^{(**)}$	44.379	-0.960$^{(**)}$	0.091	8	0.940

Model 3 Moisture increase	*Dead Pinus pinaster*	3	14.146 (**)	1.566	0.495(*)	0.070	6	0.906
	Dead Eucalyptus globulus		17.594(**)	1.338	0.384(*)	0.044	5	0.950
Model 3 Moisture decrease	*Dead Pinus pinaster*	4	11.620(*)	1.337	0.398(**)	0.052	11	0.866
	Dead Eucalyptus globulus		7.789(*)	5.254	0.591(ns)	0.290	9	0.282

(**) Significant at 0.01 level; (*) Significant at 0.05 level; (ns) Not significant

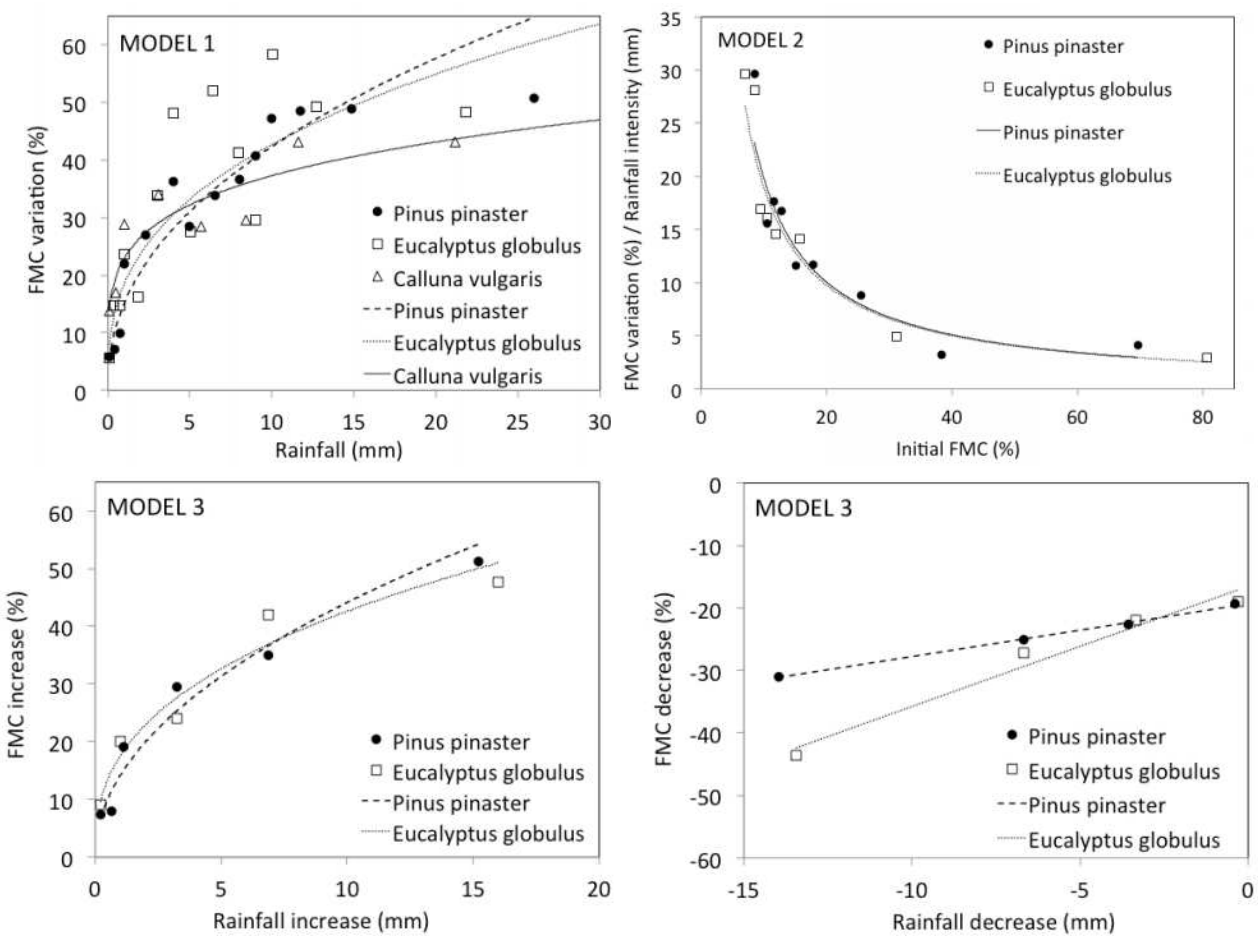

Figure 3. Graphical representation of the studied models

Model validation

In order to validate the previously developed models 1 to 5the predicted FMC values with *Pinus pinaster* dead needles, *Eucalyptus globulus* dead leaves and *Calluna vulgaris* live extremities FMC measured in Viseu between 2007 and 2010 were compared.

In Figure 4, an example comparing predicted FMC values with the ones measured between July and September 2008, taking into account the rainfall effects is presented. Note that the predicted FMC values are calculated only when there is occurrence of rainfall.

Results of the Statistical model validation are presented inTable 3, comparing Viseu field measured values with predicted values, in terms of mean absolute error (MAE), root mean squared error (RMSE) and determination coefficient (R^2), for dead foliage (*Pinus pinaster* and *Eucalyptus globulus*) the best

performance was obtained with Model 3 (MAE: 15.8%, RMSE: 23.6% and R^2: 0.668). Although Model 2 showed a medium R^2 (0.514) the MAE is very high (46.6%), thus indicating that the difference between the model and the measured data is significant.
The results for shrub foliage of *Calluna vulgaris*, considered only in Model 1, that are shown in Table 3 did not exhibit a suitable performance (MAE: 44.5%, RMSE: 64.2% and R^2: 0.287).

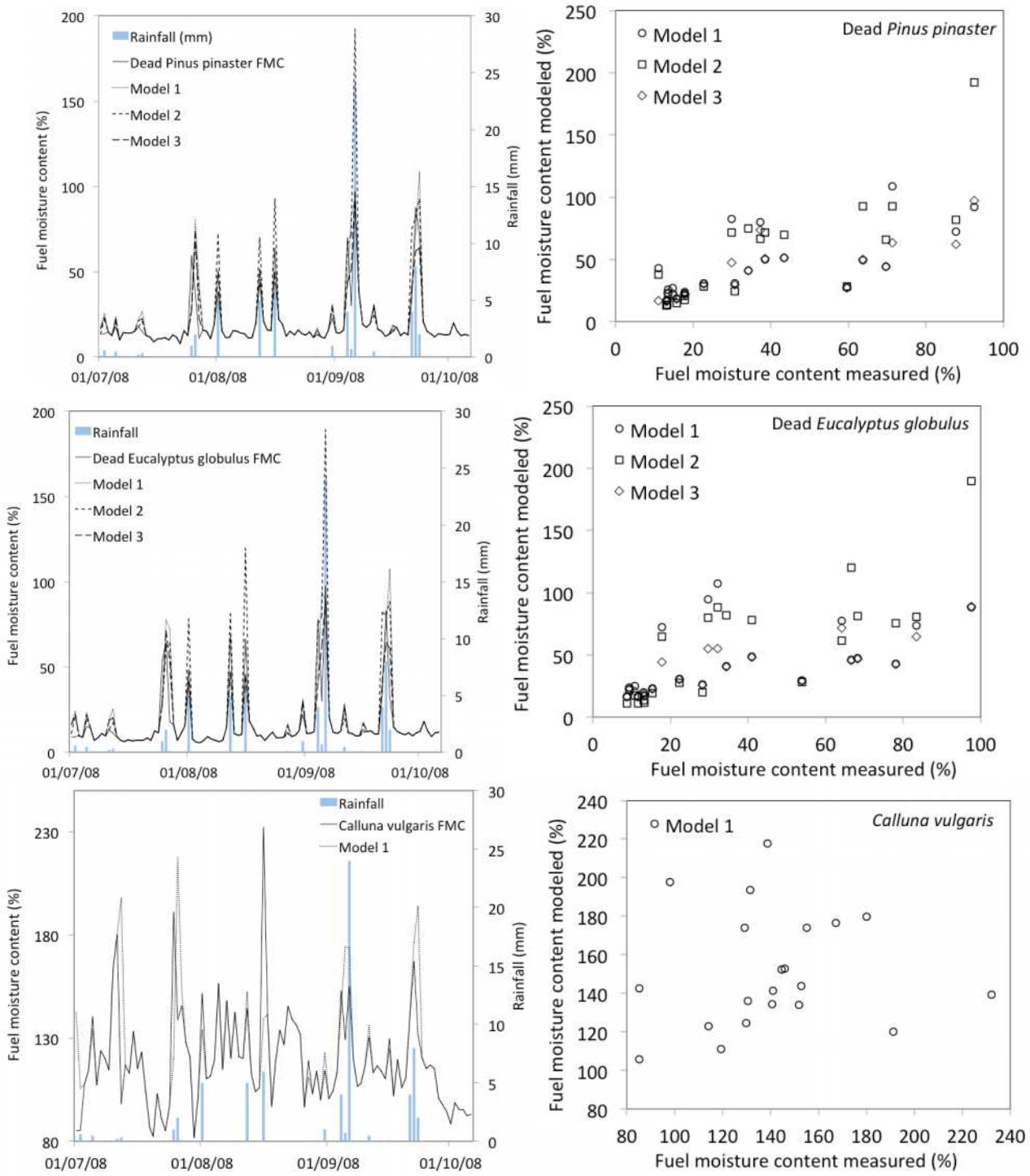

Figure 4. Example comparing predicted FMC values with the measured ones taking into account the rainfall effects.

Table 3. Model validation results

Specie	Statistical parameters	Model 1	Model 2	Model 3
Pinus pinaster	MAE	0.223	0.466	0.158
	RMSE	0.304	0.794	0.236
	R^2	0.596	0.514	0.668
Eucalyptus globulus	MAE	0.242	0.498	0.177
	RMSE	0.323	0.848	0.224
	R^2	0.627	0.529	0.743
Calluna vulgaris	MAE	0.445	-	-
	RMSE	0.642	-	-
	R^2	0.287	-	-

Conclusion

Although the influence of rainfall on forest fuel moisture content is quite complex we found that the simple assumptions that were made in the present study and the mathematical models that were proposed show suitable performances in the prediction of FMC change after rainfall episodes.
In the present study good results for dead foliage of *Pinus pinaster* and *Eucalyptus globulus species* prediction were obtained. In validation tests the best performance was obtained with Model 3, a model that takes into account, not only the occurrence of rainfall in one day but also in two consecutive days. Analysing all the available episodes that occurred in Lousã and Viseu, we found that a low risk period can be established after a rainfall episode. The duration of this period depends on rainfall intensity and on the initial value of moisture content of forest fuels. After an episode up to 10 mm/day a low period of one or two days can be expected while for an episode of more than 10 mm/day this duration can be extended to three days or more.
Further research has to be carried out to check the validity of the proposed models in other conditions and to compare their performance with that of other models.

References

Van Wagner CE (1987) Development and Structure of the Canadian Forest Fire Weather Index System. Canadian Forestry Service, Forestry Technical Report 35, Ottawa

Viegas DX, Viegas MT (1994) A relationship between rainfall and burned area for Portugal. International Journal of Wildland Fire, 4(1), 11-16. doi:10.1071/WF9940011

Viney NR (1991) A review of fine fuel moisture modelling. *International Journal of Wildland Fire* 1, 215–234. doi:10.1071/WF9910215.

Statistical evaluation of site-specific wildfire risk index calculation for Adriatic regions

Marin Bugarić, Darko Stipaničev, Ljiljana Šerić

University of Split Faculty of Electrical Engineering, Mechanical Engineering and Naval Architecture, Department for Modelling and Intelligent Systems Ruđera Boškovića 32, 21000 Split, Croatia. marin.bugaric@fesb.hr

Abstract
Wildfires are great threat to nature and humans. Predicting fire occurrence, early fire detection and intervention can significantly diminish hazardous consequences. Therefore, fire risk index is used to quantify probability of fire occurrence at certain time and place, in order to help fire managers to organize fire protection in a better way. In this paper we have performed statistical analysis of past fires detected by satellites in respect to various parameters. We have taken into account meteorological, topological and anthropological parameters and study their influence on fire occurrence. Based on this study we proposed an improved method for calculating a site-specific fire risk index (SWRI), especially tuned for the Adriatic region.

***Keywords**: wildfires, wildfire risk index, Adriatic region, statistical evaluation*

Introduction

Wildfires are important class of natural hazards especially in areas with mild and hot climate such as Mediterranean region. Fire management deals with predicting, preventing and detecting wildfires, as well as fire suppression after it ignites. For all these activities, fire risk index can be useful indicator. Fire risk index represents a numerical description probability of fire ignition and spread on a certain place and time. Wildfire risk index determination is of great importance for both wildfire prevention and protection. Even before the actual wildfire, identifying the fire danger is of great importance as it can be useful for planning firefighting activities. By using wildfire risk index, it is possible to achieve a more successful surveillance of the surrounding terrain by raising the level of alertness of automatic fire detection system or human observers on areas where current risk index is high. Beside that, wildfire risk index could help improve fire alertness for all the citizens who may be affected by wildfires.
Most countries exposed to wildfires have either developed or use one of the existing methods for wildfire risk index calculation. However, most of these indexes are not adequate for the use in the Adriatic region. Even more, not many existing wildfire risk indexes were site-specific developed with a focus on a micro-location, and therefore they have a rather low spatial resolution.
In this paper we propose a calculation method for **Site-specific Wildfire Risk Index (SWRI)** with quite satisfactory spatial resolution. The proposed wildfire risk index is not based solely on the meteorological parameters, like most existing wildfire risk indexes. It also takes into account other parameters for which we have, after carrying out a detailed statistical analysis, proven that they have a significant influence on the risk of wildfires in the Adriatic region, particularly on the central part of the Adriatic. More specifically, the proposed wildfire risk index is based on the following parameters: climatological and meteorological parameters, vegetation, terrain configuration and anthropogenic parameters. An example of the developed site-specific wildfire risk index for Split and Dalmatia County in Croatia, during a relatively high-risk index is shown in Figure 1.

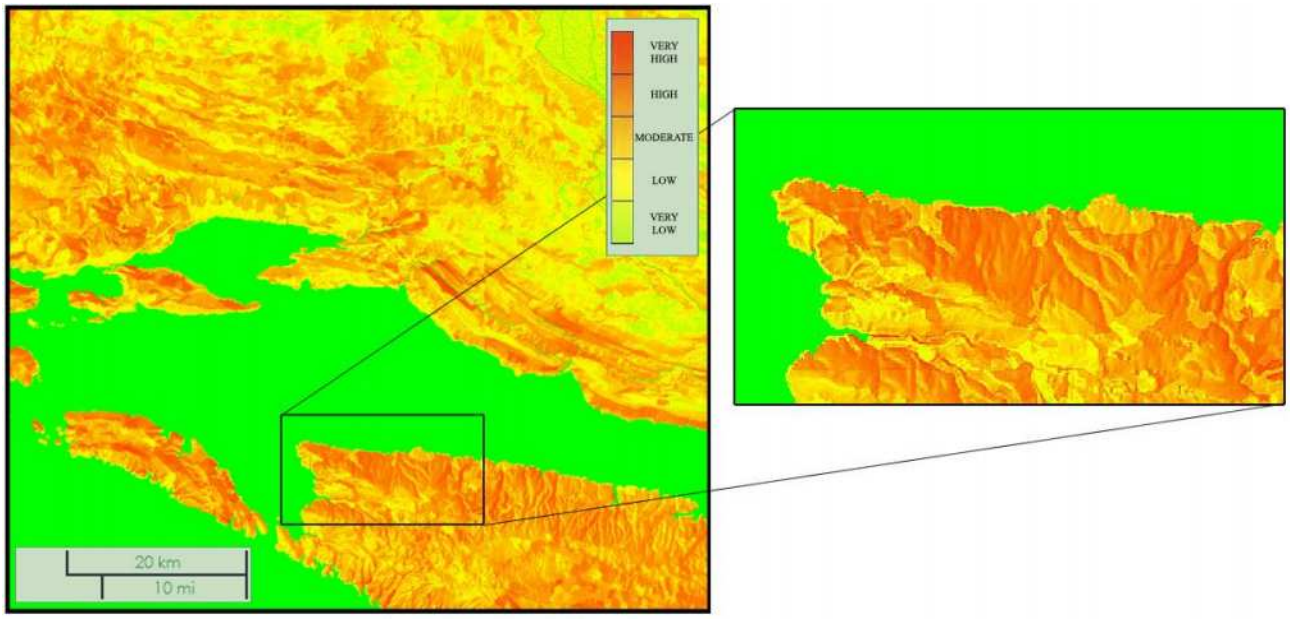

Figure 1. An example showing the proposed micro-location wildfire risk index

Our paper is organized as follows: In Section 2 we give a short overview of the existing wildfire risk indexes. In Section 3 we describe all the data required for a statistical evaluation of the proposed wildfire risk index in the Adriatic region. In Section 4 we studied different parameters in detail and calculated the correlation with wildfire frequency in the past for the Adriatic region. In Section 5 we define what we mean by a site-specific wildfire risk index. Finally, in Section 6 we carried out the evaluation of the proposed index.

Related work

In fire management, operatives usually use some kind of risk predication and assessment. Also, many counties adopted or developed a method for fire risk index calculation. Wildfire risk indexes are often classified into two categories: static and dynamic ((Gould, 2003, (Hernandez-Leal, 2008, (San-Miguel-Ayanz, 2002). Static indicators of wildfires change slowly over time; therefore they can be computed once before each fire season. In contrast, dynamic indicators of wildfires depend upon current conditions and must be calculated at least on a daily basis.
In the United States, National fire danger rating system (NFDRS, 1988) is used for ignition and spread risk assessment. Widely used fire risk index is Canadian Fire Weather Index (FWI), based on Canadian empirical fire model (FWI, 2009). FWI is calculated on the basis of weather conditions (temperature, humidity, wind, rain). Some authors also propose risks estimation based on Normalized Difference Vegetation Index (NDVI, 2014) obtained by remote sensing. In Europe, frequently used wildfire risk index is European Forest Fires Risk Forecasting System (EFFRFS) ((Gould, 2003, (San-Miguel-Ayanz, 2002), where the probability of fire occurrence and likely damage belong to static indicators, and meteorological fire risk and vegetation stress fire risk belong to dynamic indicators.
Geographic information system is used in wildfire risk models described in ((Erten, 2002, (Setiawan, 2004). In ((Zhijun, 2009) elevation, meteorological conditions and vegetation belong to main parameters for wildfire risk index. Other solutions were also proposed like (Silveira, 2008, Preisler, 2004, Vasilakos, 2007, (Netolicki, 2012, (Bugaric *et al*., 2009).
We used a slightly different approach. First we performed a detail statistical analysis of input parameters important for wildfire risk index calculation for Split and Dalmatia County. Based on this analysis a number of parameters were selected and in this first version of our model a linear correlation

of selected parameters was considered. Genetic algorithms were used for calculation of coefficients in the model. The final evaluation has confirmed the reasonable assumptions of our model.

Input data for the statistical analysis

Meteorological data used for the impact assessment of different parameters on a site-specific wildfire risk index were collected for the time period from January 1st 2012. to January 1st 2014. Croatian Meteorological and Hydrological Service (DHMZ) calculates Canadian wildfire index (FWI) for several meteorological station across Adriatic coast several times a day. In collaboration with DHMZ, we have collected for Split-Dalmatia County their FWI as well as other meteorological data concerning wind, rain and humidity, with spatial resolution of 2km.
Vegetation parameters were based on Corine Land Cover (CLC) categorization. Unfortunately, fuel maps that classify vegetation in relation to the characteristics of combustibility were not developed for the Adriatic region. We proposed a simple conversion table to convert from CLC classification to a well-known Fire Behaviour Prediction System (FBPS) models introduced by ((Burgan, 1998, (Anderson, 1982, (Scott & Burgan, 2005).
Terrain configuration data was based on NASA SRTM (Shuttle Radar Topography Mission) ((van Zyl, 2001). These data are currently distributed free of charge, and provide digital elevation model with 3-arc seconds resolution (approximately 90m) for the Adriatic region.
Anthropogenic parameters were extracted from OpenStreetMap ((OpenStreetMap,) that is open data, licensed under the Open Data Commons Open Database License (ODbL). More specifically, we extracted information about roads, railroads, buildings and transmission lines.
The evaluation of the proposed site-specific wildfire risk index was performed using history of wildfires database. This database is based on MODIS ((NASA,) data from Terra and Aqua satellites, which are capable of detecting wildfires with minimal area 1km2. History of wildfires was collected for the period from January 1st 2001 to January 1st 2013 and consists of 1146 records of fire in Split-Dalmatia County.
A site-specific wildfire risk index (SWRI) was completely implemented using GRASS GIS ((NASA, 2014) http*://earthdata.nasa.gov/data/near-real-time-data/data/firms/active-fire-data, Active Fire Data | EOSDIS - Earth Data Website, 06. June 2014.*
(NDVI, 2014) http://earthobservatory.nasa.gov/Features/MeasuringVegetation/
(Neteler & Mitasova, 2008) software and for visualization Mapserver (Mapserver, 2014) as well as Open Source Web GIS technology based on Openlayers (Openlayers, 2014) were used. First the impact assessment of input parameters on the site-specific wildfire risk index in the Adriatic region is given. Please note that all the values were normalized into interval [0-255] where 0 represents low, and 255 high wildfire risk index. For most of the parameters we have calculated Pearson correlation coefficient (Pearson, 1805), later used in model definition.

Impact assessment of input parameters on wildfire risk index

4.1. Climatological and meteorological parameters

While meteorological parameters refer to current weather parameters, climate refers to pattern of meteorological parameters over long periods of time. Climatological parameters can influence wildfire risk index in several ways. Climatological parameters determine the type of vegetation growing at certain territory. Drier climate usually means higher value of insolation and air temperature. Finally, strong winds can also have a great impact on the wildfire rate of spread, and thus on wildfire risk index. The proposed SWRI index is a dynamic index, where dynamics depends mostly on meteorological and climatological parameters. In our solution, wildfire risk index depends on: temperature, relative humidity, rainfall, wind speed, wind direction and cumulative FWI.

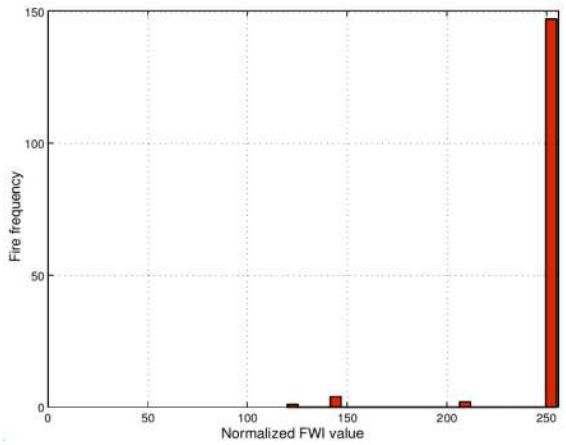

Figure 2. Relation between normalized FWI index R_{FWI} and fire frequency during year 2012.

Figure 2 shows the relation between FWI index and 154 historical wildfires that occurred during the year 2012. As we can see from the figure, most of the wildfires occurred under a very high FWI index; however, this is due to the low spatial resolution of FWI index where most of the terrain during the summer season is labelled as a high-risk territory. Although we believe that there exists territory with lower level of wildfire risk, we decided to take FWI index as a parameter in the calculation of the proposed site-specific wildfire risk index. Let us denote parameter based on Canadian fire feather index as RFWI.

Our study has shown that the slope of the terrain in combination with wind speed (Rst) as well as the aspect of the terrain in combination with wind direction (Rat) have greater influence on wildfire risk than wind speed and wind direction alone. We use the following equations to calculate those two sub-indexes:

$$R_{st} = (wind_{speed} + slope)_{norm\_0-255}, R_{at} = (|\cos(\frac{wind_{dir} - aspect}{2})|)_{norm\_0-255} \quad \textbf{(2)}$$

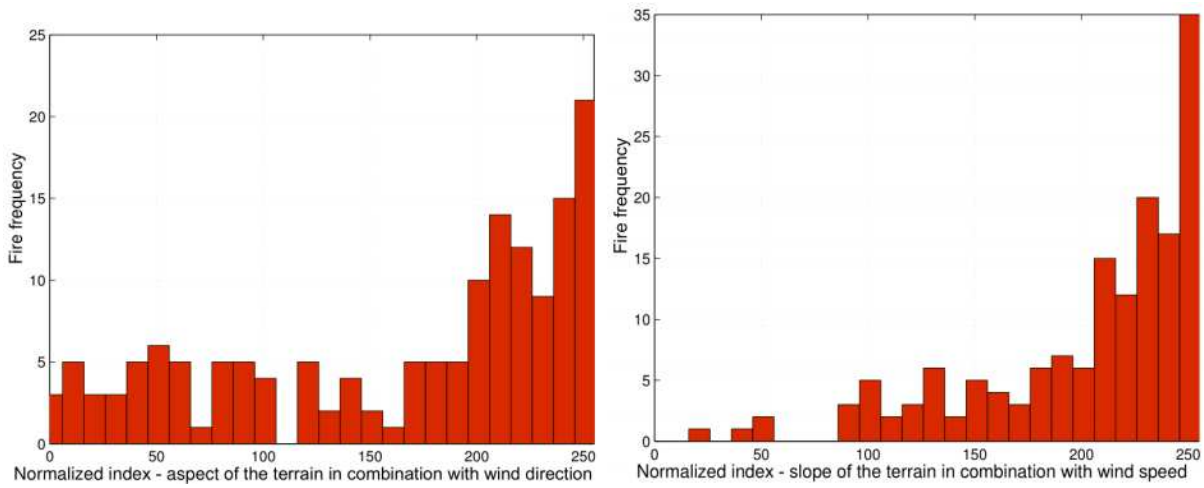

Figure 3. Relation between normalized indexes based on terrain and wind conditions (R_{at},R_{st}) and fire frequency during year 2012.

The graphs showing the normalized indexes are presented in Figure 3. Again, 154 historical wildfires that occurred during the year 2012 were taken into account.

4.2. Vegetation parameters

Fire spreads after ignition by igniting surrounding fuel in presence of oxygen. Amount of fuel depends on type of vegetation and soil. As already mentioned, FBPS fuel model was not developed for the Adriatic region, therefore in this paper we propose a conversion table used to convert from CLC classes to FBPS fuel model (Table 1).
Categories from FBPS fuel model were also normalized into interval [0 255]. Relation between the fuel model sub-index (Rfm) and 1146 historical wildfires that occurred in Split-Dalmatia County from January 1st 2001 to January 1st 2013 is given in Figure 4 (left).

Table 2. Conversion of CLC (Corine Land Cover) classes to FBPS fuel classes

CLC	111	112	121	122	123	124	131	132	133	141	142	211	212	213
FBPS	0	0	0	0	0	0	0	0	0	0	0	11	0	0
CLC	221	222	223	231	241	242	243	311	312	313	321	322	323	324
FBPS	2	10	7	1	12	12	12	9	8	8	1	0	5	2
CLC	331	332	333	334	411	421	422	423	511	512	521	523		
FBPS	0	0	0	0	0	0	0	0	0	0	0	0		

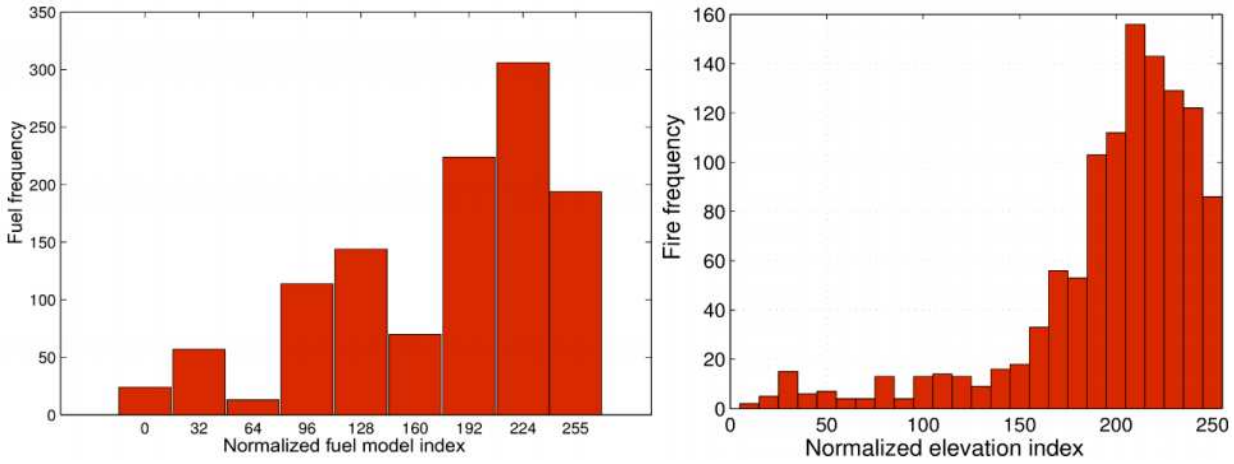

Figure 4. Relation between normalized fuel model index R_{fm} and historical wildfires (left) and relation between normalized elevation index R_{el} and historical wildfires (right)

4.3. Terrain configuration

Terrain configuration has two effects, first it has an influence on wildfire risk, but also it has an inevitable impact on the way the fire spreads after the ignition. In the previous sections we have already shown how terrain configuration in combination with wind speed and wind direction affects the wildfire risk index. In this section we investigate the influence of the terrain elevation.
Higher altitude means lower temperatures, what has a direct impact on the risk of fire ignition. There is also an indirect impact on wildfire risk index through the type of vegetation growing at certain altitudes. Normalized elevation sub-index (R_{el}) was created by normalizing altitudes from 0m to 1000m into interval [0 255] (whereas lower altitude represents higher index). The relation between normalized elevation index and 1146 historical fires is shown in Figure 4 (right).

4.4. Anthropogenic parameters

In most cases of wildfires, humans are often responsible for fire ignition. Human activity is highly correlated with wildfires, no matter if fires were caused deliberately, or started by human negligence or ignorance. Fires caused by arson are often in a close proximity to humans and human infrastructure.

On the other hand, negligence, such as uncontrolled agricultural burning, can also be a significant cause of wildfires. These are just a few examples where the human is the main culprit for wildfire ignition.

A first group of anthropogenic parameters refers to the distance from the human activities. In our study we investigated: the distance from roads and the distance from settlements. In order to determine the influence of the roads, we first formed a corridor close to the roads because we suppose that close to the roads the wildfire risk is higher. The width of the corridor was set to 2000 m, since in our study we observed that most of the historic wildfires occurred within this distance. Similarly, for the influence correlated with the distance from settlements, we formed a zone around the settlements of 15 000 m (again, highest value of the normalized sub-index is in the close vicinity of the settlements). Graphs representing the relation of historical wildfires with normalized sub-indexes representing distance from roads (R_{ro}) and buildings (R_{bu}) are given in Figure 5.

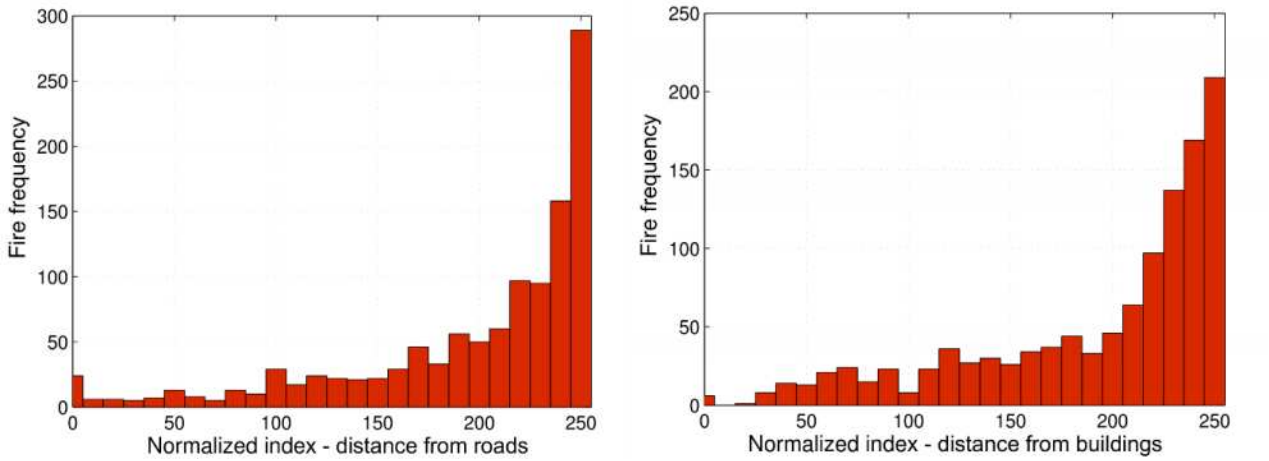

Figure 5. Relation between normalized index based on distance from roads R_{ro} and historical wildfires (left), relation between normalized index based on distance from settlements R_{bu} and historical wildfires (right)

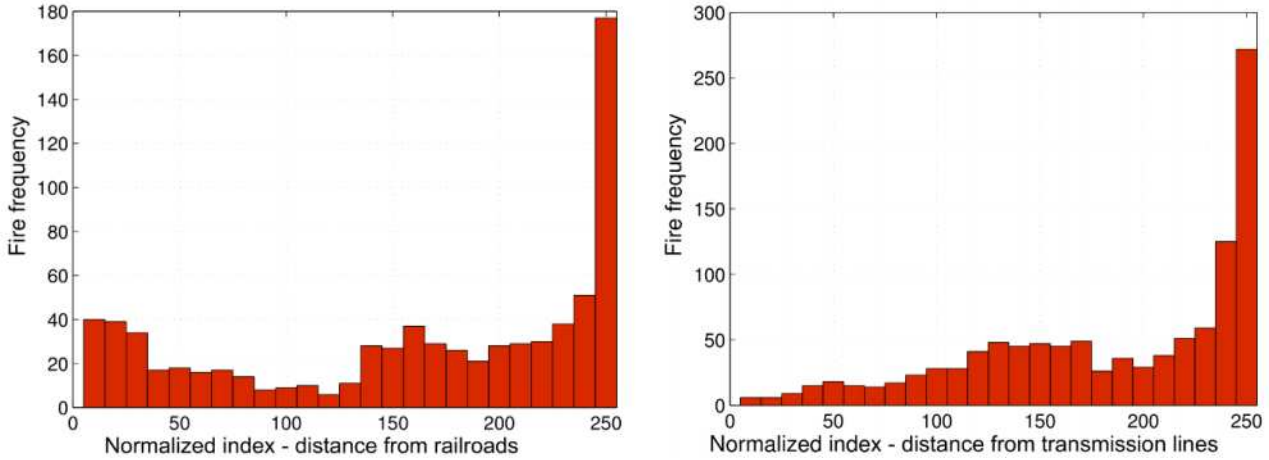

Figure 6. Relation between normalized index based on distance from railroads and historical wildfires (left), relation between normalized index based on distance from transmission lines R_{tl} and historical wildfires (right)

The second group of anthropogenic parameters refers to the distance from human infrastructure, i.e., the distance from railroads and the distance from transmission lines. In the vicinity of the railroads wildfires often start from sparks caused by braking of the trains. However, our study has shown low correlation between historical wildfires and distance from railroads, therefore we decided to omit this sub-index from the final model (Fig 6 (left)). When we studied influence of transmission lines on

wildfire risk index, we formed a corridor with width 2000 m. Normalized index that takes into account the distance from transmission lines (R_{tl}) is shown in Figure 6 (right).
For all the parameters we have calculated Pearson correlation coefficients, as shown in Table 2. Pearson correlation coefficient is a measure of the linear correlation (dependence) between two variables, in this case between a certain sub-index and fire frequency. Maximal correlation is 1.

Table 2. Pearson correlation coefficients for sub-indexes building used for SWRI index calculation

	Sub-index	**Pearson correlation coefficient**
R_{el}	Elevation index	0.8404
R_{fm}	Fuel model index	0.8340
R_{bu}	Index based on distance from buildings	0.7814
R_{st}	Index based on slope of the terrain and wind speed	0.7740
R_{ro}	Index based on distance from roads	0.7044
R_{at}	Index based on aspect of terrain and wind direction	0.6470
R_{tl}	Index based on distance from transmission lines	0.6408

Site-specific wildfire risk index (SWRI) model definition

Site-specific wildfire risk index (SWRI) takes the following sub-indexes as inputs: Canadian fire weather index (R_{FWI}), elevation index (R_{el}), fuel model index (R_{fm}), index based on the distance from buildings (R_{bu}), index based on the slope of terrain and wind speed (R_{st}), index based on the distance from roads (R_{ro}), index based on the aspect of the terrain and wind direction (R_{at}) and index based on the distance from transmission lines (R_{tl}). An overview of all sub-indexes and their dependencies is given in Figure 7.
In order to calculate SWRI index we have used in this phase a simple linear model of superposition of input parameters, as shown in the following linear equation:

$$SWRI = k_1 \cdot R_{FWI} + k_2 \cdot R_{el} + k_3 \cdot R_{fm} + k_4 \cdot R_{bu} + k_5 \cdot R_{st} + k_6 \cdot R_{ro} + k_7 \cdot R_{at} + k_8 \cdot R_{tl} \qquad (3)$$

where $\sum_{n=1}^{8} k_n = 1$. In order to determine the values k_n we have decided to use genetic algorithms (**Goldberg, 1989**). Genetic algorithm is a search heuristic that mimics the process of natural selection. It is used to generate solution to optimization problems using techniques inspired by natural evolution, such as inheritance, mutation, selection and crossover. The most difficult task in genetic algorithm designing is to define a fitness function for measuring the quality of the represented solution.
Our approach was to defined two sets of geographic locations for which we wanted to calculate a site-specific wildfire risk index. The first set consisted of locations of real historical wildfires that occurred during year 2012 in Split-Dalmatia County (we have randomly chosen 100 historical wildfires from that period). The second set consisted of randomly chosen locations in Split-Dalmatia County (we have selected 250 locations).
The following requirements for the data set representing the SWRI index calculated for locations of real historical wildfires were defined: a) the data set should be as close as possible to maximal value 255, b) the data set should be normally distributed - for normality test we used the Spiegelhalter test (Spiegelhalter, 1983), and c) the data set should be maximally skewed to the left, measured using Fisher-Pearson standardized moment coefficient (Doane & Seward, 2011).

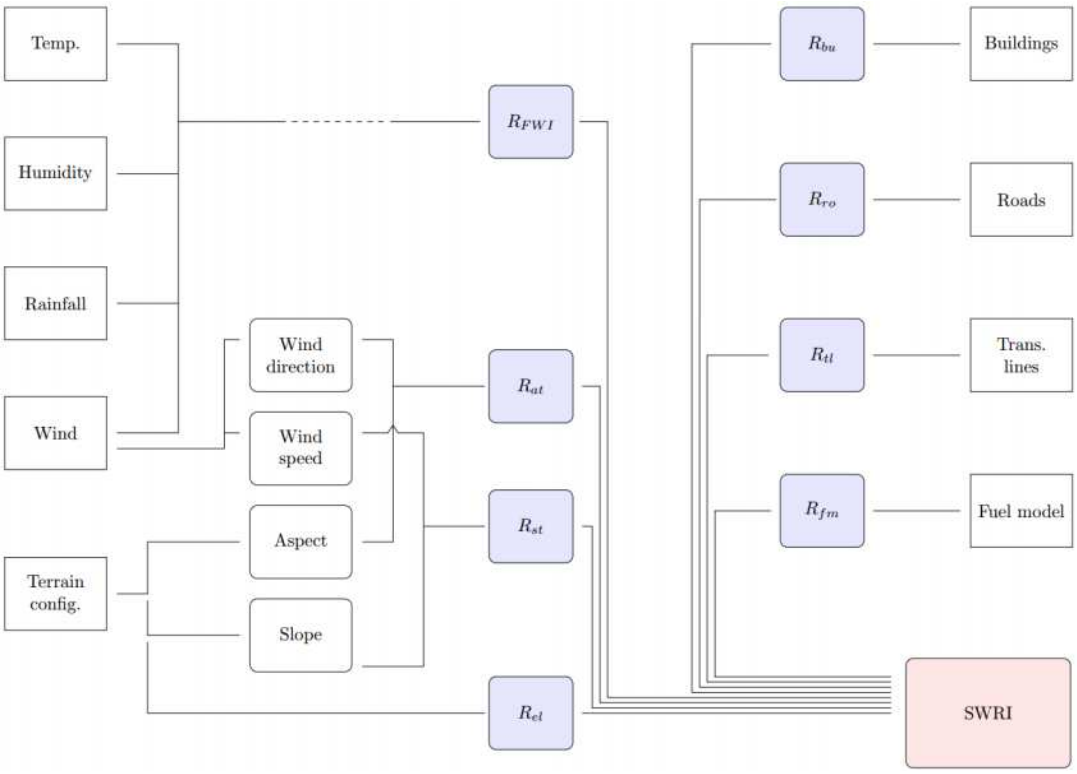

Figure 7. Overview of all inputs and sub-indexes that build up the final site-specific wildfire risk index

The requirements for the data set representing the SWRI index calculated for randomly chosen locations were defined as follows: a) the data set should be normally distributed (also measured using Spiegelhalter test for normality), b) the standard deviation of the data set should be as high as possible. Using the aforementioned requirements we represented the wildfire risk index model definition as an optimization problem. We included Pearson correlation coefficients into the fitness function for the genetic algorithm in a way it defines the mutual ratio of coefficients k_n with the following restriction $\sum_{n=1}^{8} k_n = 1$. The value of the fitness function z was defined by:

$$z = -0.5 \cdot |G_{real} \cdot \overline{Mode_{real}} \cdot p_{real}| - 0.5 \cdot |\overline{\sigma_{random}} \cdot p_{random}| \tag{2}$$

where subscript $(\cdot)_{real}$ represents real historical wildfires, and $(\cdot)_{random}$ represents randomly chosen locations. Parameter G represents Fisher-Pearson standardized moment coefficient where negative values represent skewness to the left, $\overline{Mode}$ is the mode of the dataset normalized into interval [0 1], p the value of Siegelhalter test for normality where value 1 represents normal distribution, and $\overline{\sigma}$ represents a standard deviation normalized into interval [0 1]. Siegelhalter test for normality p is calculated using a set of equations shown in (3):

$$p = 1 - \left|\frac{2}{\sqrt{\pi}} \int_0^{\frac{s}{\sqrt{2}}} e^{-t^2} dt\right|, \quad s = \frac{R - 0.73 \cdot I}{0.8969 \cdot \sqrt{I}}, \quad R = \sum_{i=1}^{I} \left[\left(b_i - \bar{b}\right) \cdot \rho\right]^2 \cdot \ln\left\{\left[\left(b_i - \bar{b}\right) \cdot \rho\right]^2\right\}, \quad \rho = \sqrt{\frac{1}{I} \sum_{i=1}^{I} (b_i - \bar{b})^2} \tag{3}$$

where $\bar{b}$ represents the arithmetic mean of the data set and I represents the number of elements of the same data set. Fisher-Pearson standardized moment coefficient G is defined by

$$G = \frac{I}{(I-1)(I-2)} \cdot \sum_{i=1}^{I} \left(\frac{b_i - \bar{b}}{\sigma} \right)^3 \quad (4)$$

Table 3. Results of the genetic algorithm

Randomly chosen locations representing historical wildfires			**Randomly chosen locations**		
$\overline{Mode_{real}}$	p_{real}	G_{real}	$\overline{\sigma_{random}}$	p_{random}	z
0.8824	0.9216	-0.6951	0.1522	0.0788	-0.2886

Please note that the more negative values of the fitness function z, the better the results. The output of the genetic algorithm (Table 3) provided us with the final linear equation that defines the site-specific wildfire risk calculation:

$$SWRI = 0.399 \cdot R_{FWI} + 0.097 \cdot R_{el} + 0.096 \cdot R_{fm} + 0.09 \cdot R_{bu} + 0.089 \cdot R_{st} + 0.081 \cdot R_{ro} + 0.075 \cdot R_{at} + 0.073 \cdot R_{tl} \quad (5)$$

Equation was implemented into Grass GIS software to calculate SWRI index several times a day. The output of the calculation is a SWRI index in a raster format. Using Mapserver we create a WMS layer that can easily be shown using Openlayers in a web based user interface. As shown in Figure 8, our system automatically communicates with Croatian Meteorological and Hydrological Service (DHMZ) several times a day in order to retrieve the latest data such as current temperature, wind speed, wind direction, rainfall, humidity, as well as the Canadian Forest Fire Weather Index (FWI).

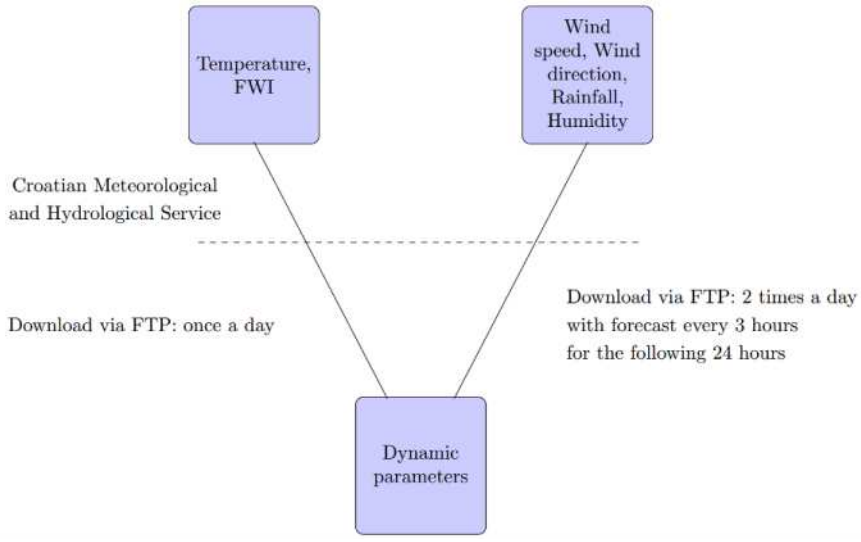

Figure 8. Communicating with Croatian Meteorological and Hydrological Service

SWRI model evaluation

The level of forest fire risk in Croatia is determined by the "Static forest fire risk" defined in the *"Criteria for assessing the risk of forest fires"* (**(MUP, 2003)**, therefore we decided to compare it to

the proposed SWRI index. Parameters taken into account in "Static forest fire risk" are as follows: vegetation cover, anthropogenic parameters, climate, habitat, insolation and forest order. For this index, regions are classified into 4 categories depending on the level of risk: i.e., category IV: low risk, category II: moderate risk, category II: high risk and category I: very high risk. Figure 9 (left) shows the region of Split-Dalmatia County classified into 4 aforementioned categories, while Figure 9 (right) shows the relation between 154 historical wildfires (that happened during year 2012. in the Adriatic region of Croatia) and the *"Static forest fire indexes".* As seen in this figure, most of the wildfires occurred in low risk regions, meaning that the *"Static forest fire risk"* does not predict wildfire risk index with high accuracy.

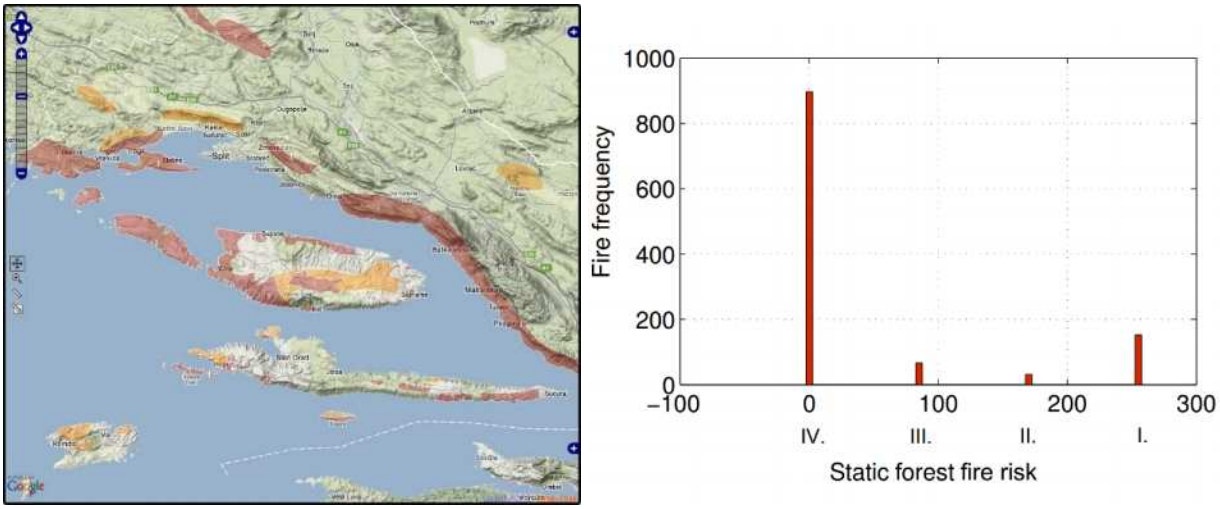

Figure 9. The region of Split-Dalmatia County classified into 4 static risk categories, where dark red colour represents the highest risk (left), and relation between historical wildfires that occurred during year 2012 "with Static forest fire indexes" (right).

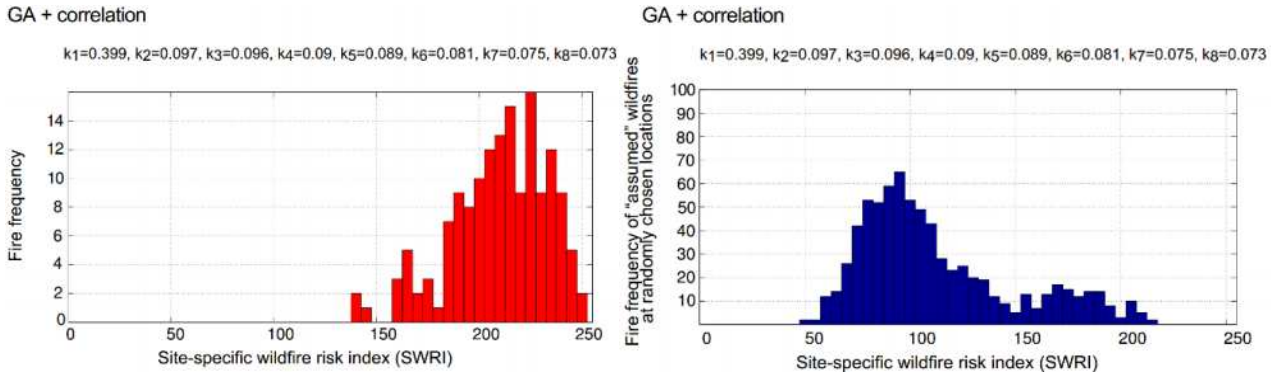

Figure 10. SWRI index for the 154 actual wildfires that occurred during year 2012 (left), and SWRI index for a randomly chosen locations and time moments during the same year

On the other hand, Figure 10 (left) shows the proposed SWRI index for the same 154 historical wildfires that occurred during the year 2012. From this figure it is obvious that most of the wildfires occurred in high risk regions. Nevertheless, in Figure 10 (right) we can see that, for 750 randomly chosen locations and time moments during the same year, the value of SWRI in most cases does not exceed 150, meaning that most of the regions are labelled as low or moderate risky regions. This is expected, as we have modelled SWRI index to be a site-specific index with a focus on a micro-location.

7. Conclusions

In this paper we proposed a novel method for wildfire risk index calculation - the **Site-specific Wildfire Risk Index (SWRI)**. The overall SWRI index is calculated based on 8 sub-indexes: Canadian fire weather index, elevation index, fuel model index, index based on the distance from settlements, index based on the slope of terrain and wind speed, index based on the distance from roads, index based on the aspect of the terrain and wind direction and index based on the distance from transmission lines. All sub-indexes were chosen based on the statistical evaluation, where we have, for all sub-indexes, calculated Pearson correlation coefficients that show their relation to the historical wildfires in the Adriatic region. In other words, for all sub-indexes we have proven their influence on the actual wildfires that occurred in Split-Dalmatia County in the history.

Using genetic algorithms and calculated Pearson correlation coefficients, we have created a final model of SWRI index. We carried out the evaluation of the proposed site-specific wildfire risk index and compared it to the "Static forest fire index", where we have shown that SWRI index provides good correspondence with the actual wildfires that occurred in the Adriatic region in recent years. On the other hand, for randomly chosen locations, the value of SWRI index in most cases indicated a low or a moderate level of risk. This was expected, since SWRI index was modelled with focus on a micro-location and the fact that even in the fire season not all regions should be labelled as regions of high risk.

SWRI index is calculated using geographical information system (GIS), and its main purpose is to display relevant information important for firefighting activities before and during the actual wildfire. The SWRI index should also be optimized for other parts of Adriatic regions besides Split-Dalmatia County using the same methodology for more general results.

8. References

(Anderson, 1982) Anderson, H. E. 1982. *Aids to determining fuel models for estimating fire behavior*. Tech. rept. U.S.D.A. Forest Service, Intermountain Forest and Range Experiment Station, Ogden, Utah.

(Bugaric *et al.*, 2009) Bugarić, M., Jakovčević, T., & Stipaničev, D. 2009 (May). Automatic adjustment of detection parameters in forest fire video monitoring system. *Pages 270–275 of: Proc. of 32. Int. Conference MIPRO*.

(Burgan, 1998) Burgan, R. E., Klaver, R. W., & Klaver, J. M. 1998. Fuel models and fire potential from satellite and surface observations. *International Journal of Wildland Fire*, 8(3), 159–170.

(Doane & Seward, 2011) Doane, David P., & Seward, Lori E. 2011. Measuring Skewness: A Forgotten Statistic: *Journal of Statistics Education*, 19(2), n2.

(Erten, 2002) Erten, E., Kurgun, V., & Musaoglu, N. 2002. Forest Fire Risk Zone Mapping From Satellite Imagery And GIS: A Case Study. *International Journal of Applied Earth Observation and Geoinformation*, 4, 1–10.

(FWI, 2009) "Canadian Forest Fire Weather Index (FWI) System". Background Information. Natural Resources Canada. 2009. Retrieved 2009-09-13.

(Goldberg, 1989) Goldberg, David E. 1989. *Genetic algorithms in search, optimization, and machine learning*. Addison-Wesley Professional.

(Gould, 2003) Gould, Michael, Laurini, Robert, & Coulondre, Stéphane. 2003. *AGILE 2003: 6th AGILE Conference on Geographic Information Science*. PPUR presses polytechniques.

(Hernandez-Leal, 2008) Hernandez-Leal, P.A., Gonzalez-Calvo, A., Arbelo, M., Barreto, A., & Alonso-Benito, A. 2008. Synergy of GIS and Remote Sensing Data in Forest Fire Danger Modeling. *IEEE Journal of Selected Topics in Applied Earth Observations and Remote Sensing*, 1(4), 240 – 247.

(Mapserver, 2014) http://mapserver.org/, Welcome to MapServer - MapServer 6.4.1 documentation, *06. June 2014.*

(MUP, 2003) 2003. *Ministarstvo unutarnjih poslova, Pravilnik o zaštiti šuma od požara*.

(NASA, 2014)http://earthdata.nasa.gov/data/near-real-time-data/data/firms/active-fire-data, Active Fire Data | EOSDIS - Earth Data Website, 06. June 2014.

(NDVI, 2014) http://earthobservatory.nasa.gov/Features/MeasuringVegetation/

(Neteler & Mitasova, 2008) Neteler, Markus, & Mitasova, Helena. 2008. Open Source GIS: A GRASS GIS Approach. The International Series in Engineering and Computer Science. Springer New York Inc.

(Netolicki, 2012) Netolicki, Antonija, Blaževic, Tomislav, & Antolovic, Andrija. 2012. Multicriteria Analysis of Fire Risk in the Split-Dalmatia County. Kartografija i geoinformacije, 11(17), 4, 5–24, 24.

(NFDRS, 1988) Burgan, Robert E. 1988. 1988 revisions to the 1978 National Fire-Danger Rating System. Res. Pap. SE-273. Asheville, NC: U.S. Department of Agriculture, Forest Service, Southeaster Forest Experiment Station. 39 pp

(Openlayers, 2014) http://openlayers.org/, Openlayers: Home, , 06. June 2014.

(OpenStreetMap, 2014) http://www.openstreetmap.org/, OpenStreetMap, 06. June 2014.

(Pearson, 1805) Karl Pearson,1895, Notes on regression and inheritance in the case of two parents, Proceedings of the Royal Society of London, 58 : 240–242.

(Preisler, 2004) Preisler, H. K, Brillinger, D. R, Burgan, R. E, & Benoit, J. W. 2004. Probability based models for estimation of wildfire risk. International Journal of Wildland Fire, 13(2), 133–142.

(San-Miguel-Ayanz, 2002) San-Miguel-Ayanz, J. 2002. Towards a coherent forest fire information system in Europe: the European Forest Fire Information System (EFFIS). Forest fire research & wildland fire safety, 46, 5–16.

(Scott & Burgan, 2005) Scott, J. H., & Burgan, R. E. 2005. Standard fire behavior fuel models: a comprehensive set for use with Rothermel's surface fire spread model. Tech. rept. USDA Forest Service, Rocky Mountain Research Station.

(Setiawan, 2004) Setiawan, I., Mahmud, A. R, Mansor, S., Shariff, A. R.M, & Nuruddin, A. A. 2004. GIS-grid-based and multi-criteria analysis for identifying and mapping peat swamp forest fire hazard in Pahang, Malaysia. Disaster Prevention and Management, 13(5), 379–386.

(Silveira, 2008) Silveira, H. L.F, Vettorazzi, C. A, & Valente, R. O.A. 2008. Multi-criteria evaluation of a GIS environment in a forest fire hazard mapping for the Corumbata River basin, SP, Brazil. Revista Árvore, 32(2), 259–268.

(Spiegelhalter, 1983) Spiegelhalter, D. J. 1983. Diagnostic tests of distributional shape. *Biometrika*, 70(2), 401–409.

(van Zyl, 2001) van Zyl, J. J. 2001. The Shuttle Radar Topography Mission (SRTM): a breakthrough in remote sensing of topography. *Acta Astronautica*, 48(5), 559–565.

(Vasilakos, 2007) Vasilakos, C., Kalabokidis, K., Hatzopoulos, J., Kallos, G., & Matsinos, Y. 2007. Integrating new methods and tools in fire danger rating. *International Journal of Wildland Fire*, 16(3), 306–316.

(Yang & Di, 2011) Yang, Guang, & Di, Xueying. 2011 (June). Adaptation of Canadian Forest Fire Weather Index system and it's application. *Pages 55–58 of: IEEE International Conference on Computer Science and Automation Engineering (CSAE)*, vol. 2.

(Zhijun, 2009) Zhijun, T., Jiquan, Z., & Xingpeng, L. 2009. GIS-based risk assessment of grassland fire disaster in western Jilin province, China. *Stochastic Environmental Research and Risk Assessment*, 23(4), 463–471.

The development of a web-application for improved wildfire risk management in Lebanon

George Mitri[a], Mireille Jazi[a], Edward Antoun[a], David McWethy[b], Rabih Kahaleh[c], Manal Nader[a]

[a] *Institute of the Environment, University of Balamand, Lebanon, george.mitri@balamand.edu.lb*
[b] *Department of Earth Sciences, Montana State University, Montana, USA*
[c] *Department of Information Technology, University of Balamand, Lebanon*

Abstract
Lebanon's National strategy for forest fire management emphasizes the need to enhance the capacity of stakeholders in Lebanon to assess and manage wildfire in light of future climate change and residential expansion into wildland areas. In this context, we developed a web-based decision framework to improve fire risk management. The primary objective of the application (FireLab) was to provide an online user-friendly interface for displaying data that are critical for making informed fire-management decisions. Data include 257 variables related to fire activity, risk, and hazard and are generated at the municipality level for all of Lebanon. FireLab is delivered through a web browser, making it widely accessible to the public in a format that allows users to easily display wildfire conditions and to describe and share modeled wildfire potential scenarios of current and future conditions.

Keywords*: wildfire risk management, climate change, web-application, decision framework*

Introduction

During the past decade, Lebanon has experienced a number of large wildfires that have had dramatic impacts on large areas of forests and the livelihoods of local communities. In addition, projections for continued climate warming are likely to further promote fire risk (Salloum and Mitri, 2014).
While the risks of fires are increasingly becoming a concern, a common database documenting spatial and temporal patterns of fire and their proximity to settlements is lacking. Currently, there is little information with which to anticipate and predict which areas of Lebanon are most vulnerable to future fire risk and hazard data.
Previously, we set out to assess drought conditions in Lebanon based on climatic variability to gain a better understanding of the temporal and spatial changes in wildfire potential (Mitri *et al.*, 2014). Wildfire potential was assessed with the use of spatial climatic data, and the temporal and spatial variability of wildfire potential was investigated accordingly. In addition, an updated wildfire risk map of Lebanon was produced involving the use of extensive biophysical and socio-economic datasets.
Maps and models have long been an integral part of the environmental decision making process (Walker and Chapra, 2014). However, the abilities of resource managers, policy makers, and stakeholders to understand how these maps and models work and what they represent are limited due to the required technical expertise (NRC, 1999).
In this context, it was essential to build a generic and simple data infrastructure for individual communities to access in relation to their needs. The development of this infrastructure was important because land owners, managers, and decision makers have a major role in fire risk reduction for communities with different needs.
According to Goodall *et al*. (2011), the availability of online databases and models as web services allows for their inclusion not only in professional workflows, but also in interactive tools for data querying and simulation aimed at decision-making. The science of visualizing data has a long history (Tufte, 2001; Spiegelhalter *et al*. 2011). Implementing environmental models in a web context is necessary to help bridging the gap between high-level environmental data analysis and access and

usability for and by the general public. This approach promises greater transparency and inclusive participation of citizens in environmental data monitoring, research, and decision-making (Buytaert *et al*., 2012).
Lebanon's National strategy for forest fire management (Decision No. 52/2009) highlighted the need of information to describe the magnitude and urgency of the problem to decision makers and make them prioritize the necessary measures to prevent or minimize fire risk (MOE/AFDC, 2009). In this context, the development and dissemination of detailed information on fire risk assessment and monitoring across Lebanon is critical to improve fire risk management at both local and National levels.
To address these needs, we developed a web-based application to host multiple data types related to fire risk and management. The primary objective of the application (called FireLab) was to provide an online user-friendly interface where relevant fire data can be accessed to make informed fire-management decisions.

Methods

The development of the web-application model comprised 1) the web browser or the user interface, 2) the dynamic content generation technology, and 3) the database server containing all generated data (Figure 1).

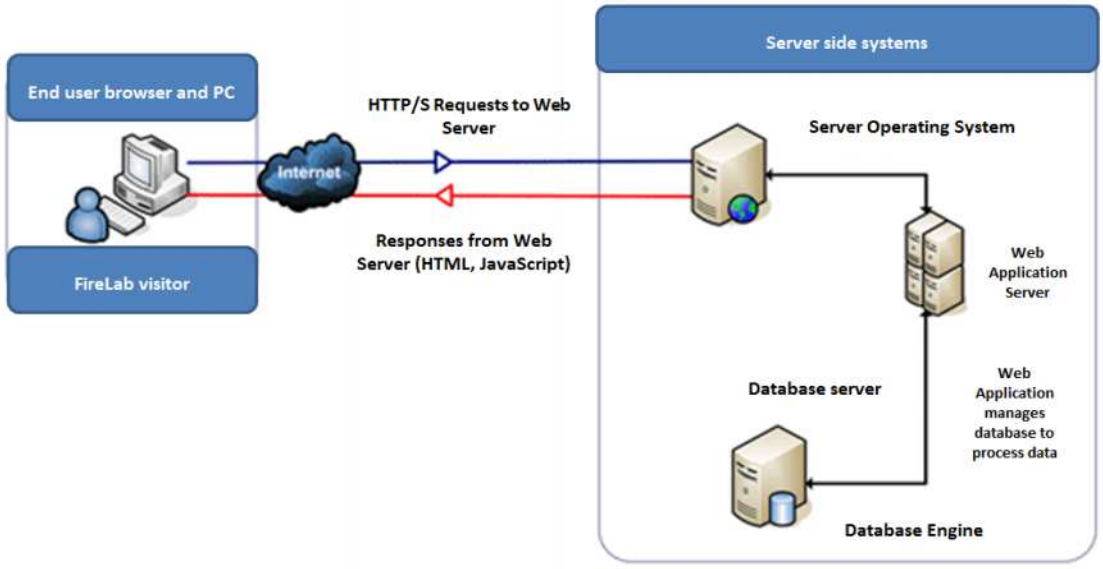

Figure 1. Architecture of the web-application model

The user interface was designed to be self-exploratory and easy to use. Users only need to provide minimal input to achieve the desired outputs. Technically, the web-application queries the content server (a content repository database) and dynamically generates web documents to serve to the user. The documents are generated in a standard format to allow support by all browsers (e.g., HTML).
In addition, the development of the web-application involved the use of Microsoft Visual Studio 2010, C#, asp.net and JQuery. The technology is accessible by all electronic tablets and mobile phones, easily accessed by mobile operators, reliable, secure, and without major technological restrictions.
The database comprised 257 variables generated at the village level and covering the entire country. The variables included information about landcover/landuse, fire hazard, vulnerability, overall fire risk (Figure 2), future fire hazard in association with projected climatic data, and Wildland-Urban Interface (WUI), among others. Most importantly, the application allows data to be constantly updated in the system so that new information can be used to guide management. Finally, a comprehensive glossary

was developed and integrated in the system describing the main terminologies employed in the queries of the application.

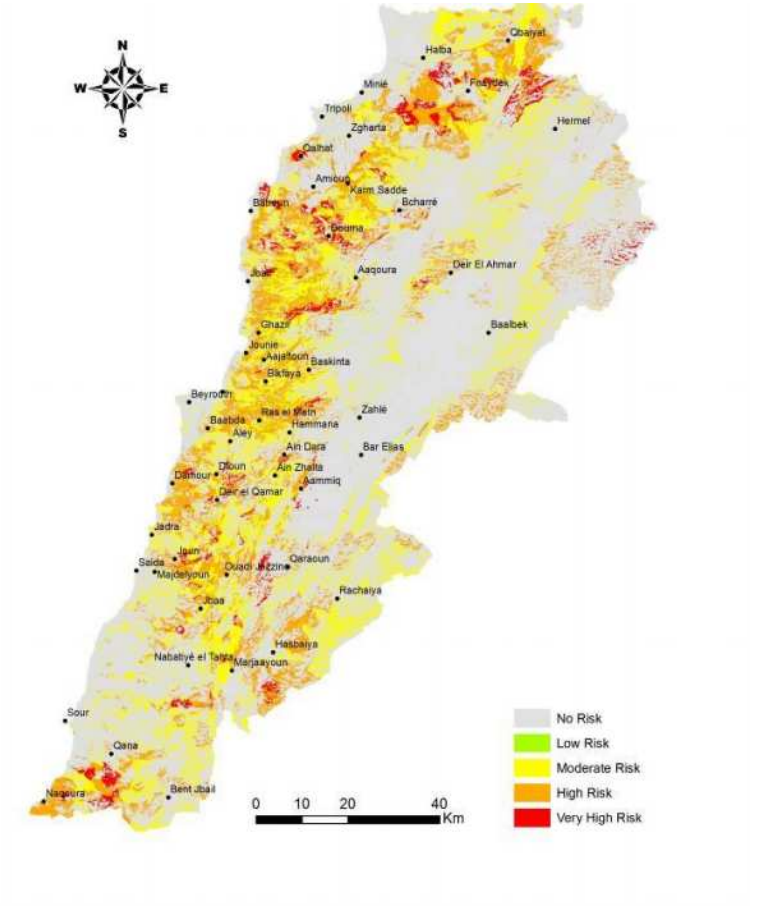

Figure 2. Overall fire risk map of Lebanon

Results and discussion

The main four queries of the web-application interface (Figure 3) included: 1) the selection of the area of interest (e.g., village) and the visualization of a specified type of information for the selected area in form of tables and diagrams, 2) the listing and sorting of summary statistics of required information in a country table view, 3) the listing and sorting of summary statistics of required information for a group of administrative units (e.g., villages) within the same broader administrative unit (called Kadaa), 4) the generation of a detailed wildfire profile including a full graphical report about each category of available data for each individual village, and 5) the generation of an annual country profile of fire statistics (based on field collected data previously entered in the database). In addition, the web-application allows further data entry through private access.

The user interface included an administrative map for each Mohafazat (administrative region) in Lebanon. These comprised Bekaa, Beirut, Nabatieh, North and Akkar, Mount Lebanon and South. The user has the possibility to select the Mohafazat of interest, visualize its coverage map and the name of each village, and select the village of interest. Accordingly, all data for the selected village can be visualized in form of tables and graphs. A full report of each village can be generated in a PDF format.

Overall, the application was not only viewed as a scientific tool, but also it was considered as a management and outreach mechanism. This is reflected in its capability of providing the public with the data needed at different levels, namely at the municipality, regional, and National levels. Also, the fact that the application allows further data entry in the system based on a specific data entry sheet, makes it a dynamic tool that incorporates new information with which to inform management.

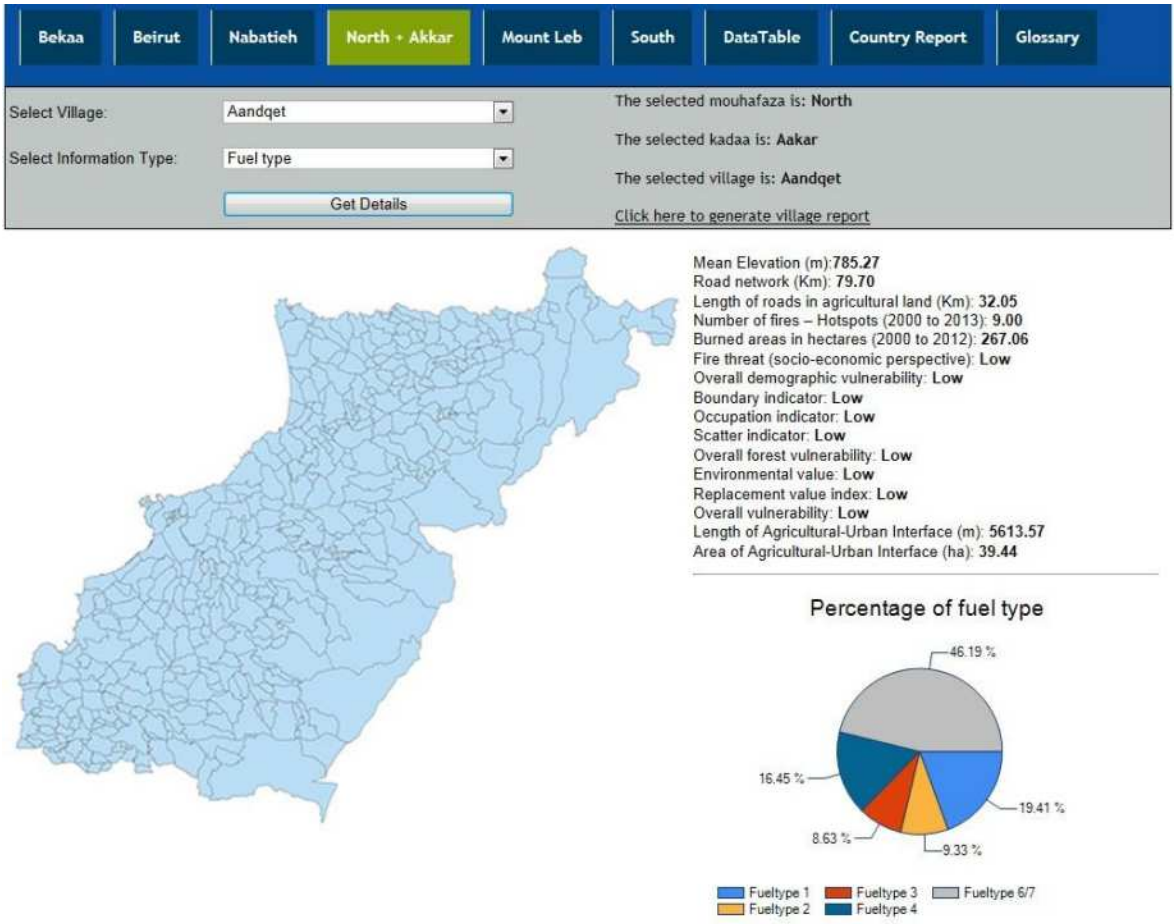

Figure 3. A screen shot of the main interface of the web-application

Conclusions

With projections for increased fire activity in Lebanon there is a critical need to provide spatially explicit wildfire data with which to assess fire risk and hazard at the village level. To address this need, we made fire data publicly available through an online web-application and within a framework where management decisions could easily be made. Additionally, we developed a structure where users can contribute to the development and dissemination of new knowledge, and to a more transparent and effective decision-making and policy assessment. Future work will involve collecting feedback from end-users on the use of such developed tool in order to evaluate its functionality and future improvement.

Acknowledgements

This material was published in association with the project "Towards a better assessment and management of Wildfire Risk in the Wildland-Urban Interface in Lebanon: gaining from the US

experience" supported by the Partnerships for Enhanced Engagement in Research (PEER), sponsored by USAID. The contents do not necessarily reflect the views of USAID or the United States Government.

References

Buytaert W, Baez S, Bustamante M, Dewulf A (2012). Web-Based Environmental Simulation: Bridging the Gap between Scientific Modeling and Decision-Making. *Environmental Science and Technology* **46**, 1971-1976.

Goodall JL, Robinson BF, Castronova AM (2011) Modeling water resource systems using a service-oriented computing paradigm. *Environmental Modelling and Software*, 573– 582.

Mitri G, Jazi M, McWethy D (2014) Investigating temporal and spatial variability of wildfire potential with the use of object-based image analysis of downscaled global climate models. *South-Eastern European Journal of Earth Observation and Geomatics* **3**, 251-254.

MOE/AFDC (2009) Lebanon's National Strategy for Forest Fire Management. Decision No. 52 – 2009 (Mitri, G. Editor). A publication of the Ministry of Environment and the Association for Forests, Development and Conservation – Beirut, Lebanon.

NRC (1999) National Research Council (NRC). New strategies for America's watersheds. National Academies Press, Washington, D.C.

Salloum L, Mitri G (2014) Assessing the temporal pattern of fire activity and weather variability in Lebanon. *International Journal of Wildland Fire*. doi: 10.1071/WF12101.

Spiegelhalter D, Pearson M, Short I (2011) Visualizing uncertainty about the future. *Science* **333**, 1393– 1400. doi: 10.1126/science.1191181.

Tufte E (2001) The Visual Display of Quantitative Information; Graphics Press: Cheshire, CT,

Walker J, Chapra S (2014) A client-side web application for interactive environmental simulation modeling. *Environmental Modelling and Software*, **55**, 49-50.

The weather circulation analysis over Adriatic region of Croatia in warm period 1981-2013

Marija Mokorić, Lovro Kalin

Meteorological and Hydrological Service of Croatia, Gric 3, Zagreb, mokoric@cirus.dhz.hr, kalin@cirus.dhz.hr

Abstract
The most frequent natural hazard in the Adriatic region are the forest fires, which are strongly affected by weather conditions. This is particularly stressed in the last two decades, when large fires occurred. Furthermore, the season has been expanded and large fires appeared also in early summer and early autumn, which was not so common before. In order to explain such a behaviour, an analysis of the atmospheric circulation patterns has been performed. The results reveal that the frequency of weather types conected to dry and warm conditions has been increased, and frequency of weather types with wet weather has been reduced. This is especially pronounced in June and September. Additionally, a change of number of days with precipitation has been observed, with less days with smaller precipitation and more days with larger precipitation. This can lead to additional drying of the fuel. The risk- and fire-managers should be aware of these trends in the future.

***Keywords**: forest fires, atmospheric circulation, weather types, climate change*

Introduction

Most frequent natural hazards on the Adriatic region are forest fires. They strongly depend upon weather conditions such as dry and warm periods, which are connected with weather types and atmospheric circulation.
A large number of forest fires appeared in 2000s. They occurred not only on the coast, but for the first time in the mountain region as well. Furthermore, since 2005 the most dangerous fires appeared at the end of August and first part of September, which was not common before. Recently – particularly in 2012 - fires became more frequent in interior parts also.
In order to find a possible explanation of such behaviour, an analysis of the upper atmosphere circulation was done for warm season for period 1981-2013.
Additionally, the analysis of mean monthly number of days with precipitation has been performed also.

The atmospheric circulation

There are seven main atmospheric circulations patterns in upper atmosphere: upper atmospheric ridge (R), non-gradient field (NG), front side of the ridge (FR), upper through (TR), back side of the upper through or north-west stream (NW), west-stream (W), front side of upper through or south-west stream (SW).
First three types are associated with relatively dry and warm weather, which could be connected with an increased number of forest fires. North-west stream brings cold air with local showers or thunderstorms. West stream is characterized by moderate temperatures and precipitation, while south-west stream and upper through usually cause more precipitation.
The analysis is done for Adriatic coast for years 1981-2013 for period May to October. Charts of mean monthly circulation AT 500 hPa on the Northern hemisphere (Deutscher Wetterdienst and European Centre for Medium-Range Weather Forecast) were used. The weather pattern typing is done manually.

Results

Most frequent situations are north-west and west stream with relative frequency about 25%, the same as non-gradient field and the upper ridge (although the upper ridge is most common in July and August, and very rare - with only one case - in September). Frequency of upper through is about 15%, mostly in September. The southwest stream, which brings more rain, has the frequency 6%, and is most common in September. This distribution of weather circulation pattern is expected.

A further analysis showed that in May and June the non-gradient field and upper ridge mean monthly circulation has appeared more frequently since 2000. In July the distribution of patterns is dispersed. The west and north-west stream were most frequent in August, the west stream particularly in the first decade.

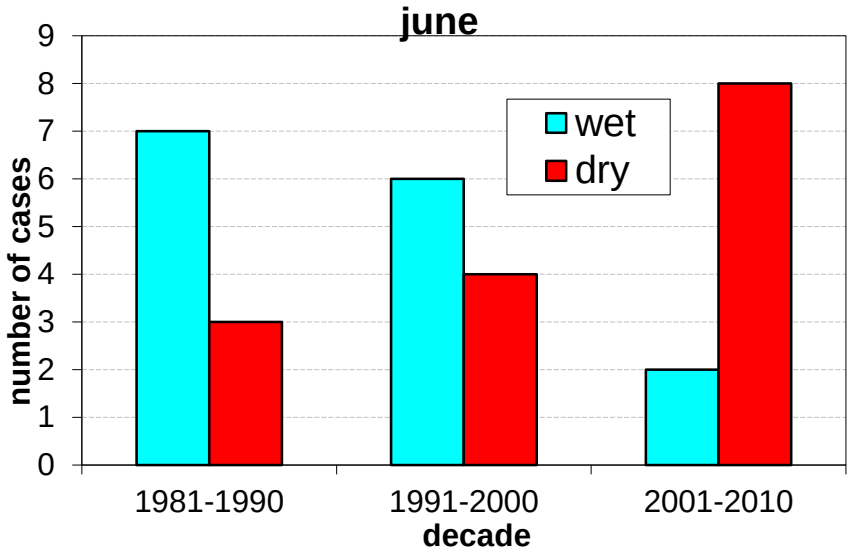

80’s	TR	NW	NW	W	W	SW	SW	W	NW	W
90’s	W	NG	W	R	TR	W	W	R	W	R
00’s	TR	R	FR	NW	NW	NW	W	NG	NW	NG

Figure 1. The frequency of relatively dry (filled red) and wet (filled blue) weather types in June, for period 1981-2010.

Finally, in September and October the most frequent types are north-west stream, upper through and - particularly in October - southwest stream. However, since 2005 non-gradient field appeared more often, characterized by less precipitation.

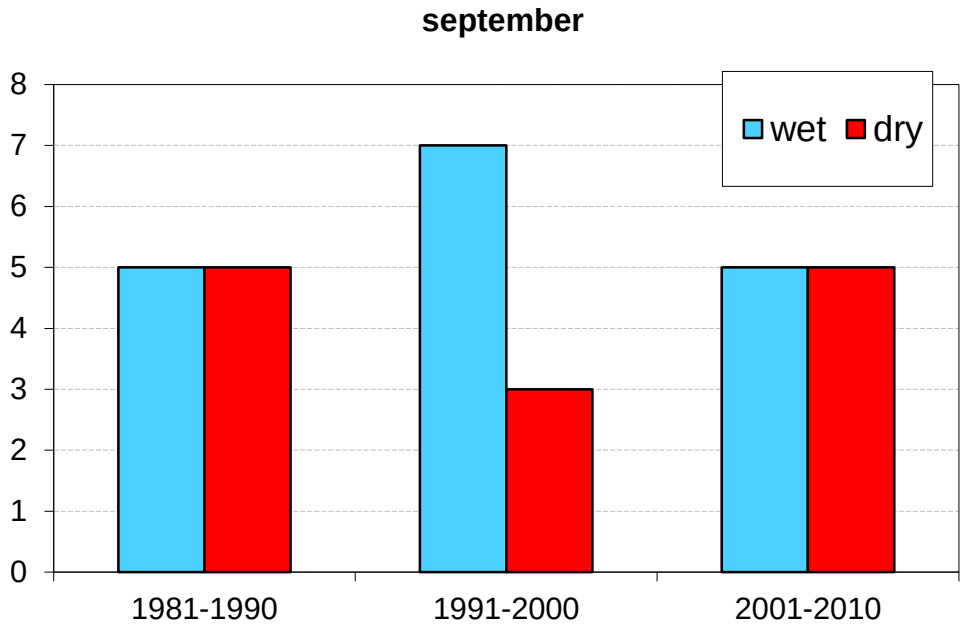

80's	W	NG	NW	SW	R	W	W	TR	NG	NW
90's	NW	W	W	TR	TR	TR	NW	W	NG	W
00's	TR	TR	TR	NW	SW	NG	W	NW	NG	NW

Figure 2. The frequency of relatively dry (filled red) and wet (filled blue) weather types in September, for period 1981-2010.

To estimate the potential influence of such a distribution to the precipitation regime on the Adriatic, an analysis of number of days with precipitation has been conducted also. The goal of such analysis is to provide the information about the distribution of precipitation events, and its possible trends.
A mean number of days with precipitation greater than 1mm, 10 mm, 20 mm and 50 mm is calculated for individual months (May, June, July, August, September and October). Data are based on 63 climatological stations on the Adriatic, for period 1981-2013.
A simple and preliminary analysis reveals that the number of days with smaller precipitation is generally found to be decreasing towards the end of the observed period. Meanwhile, number of days with larger precipitation thresholds is significantly increasing. This feature is observed for both June and September.

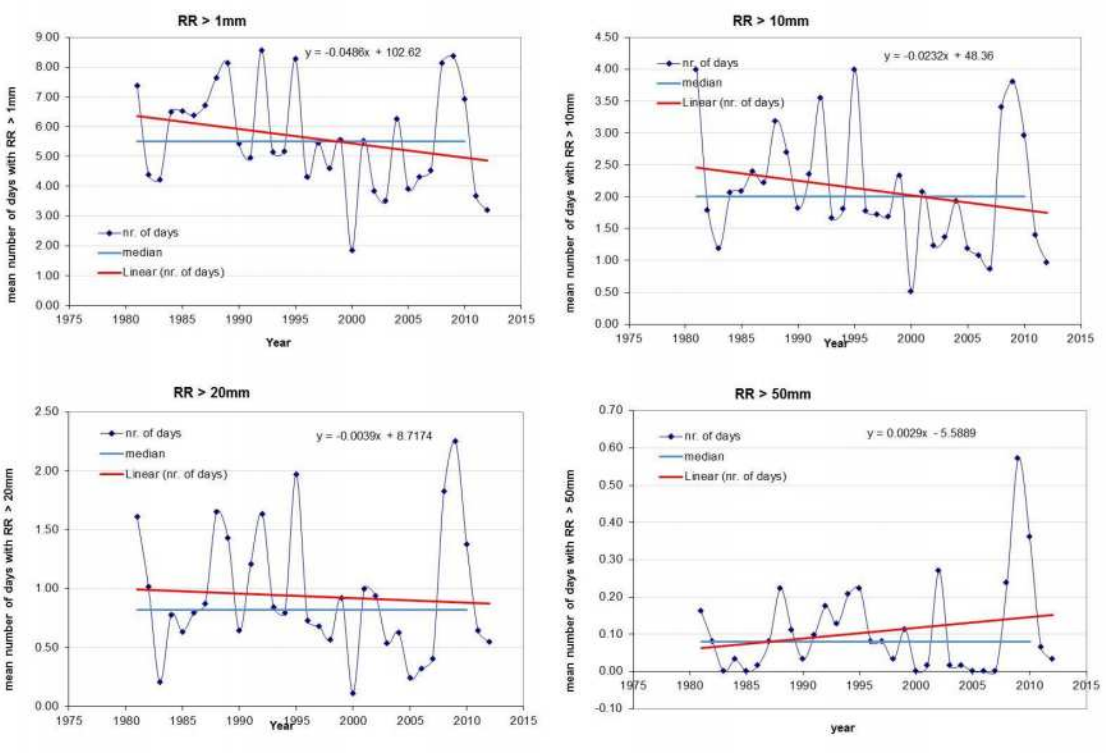

Figure 3.: Mean number of days with precipitation bigger than 1mm, 10 mm, 20 mm and 50 mm, for June (period 1981.-2013.), with corresponding linear trends.

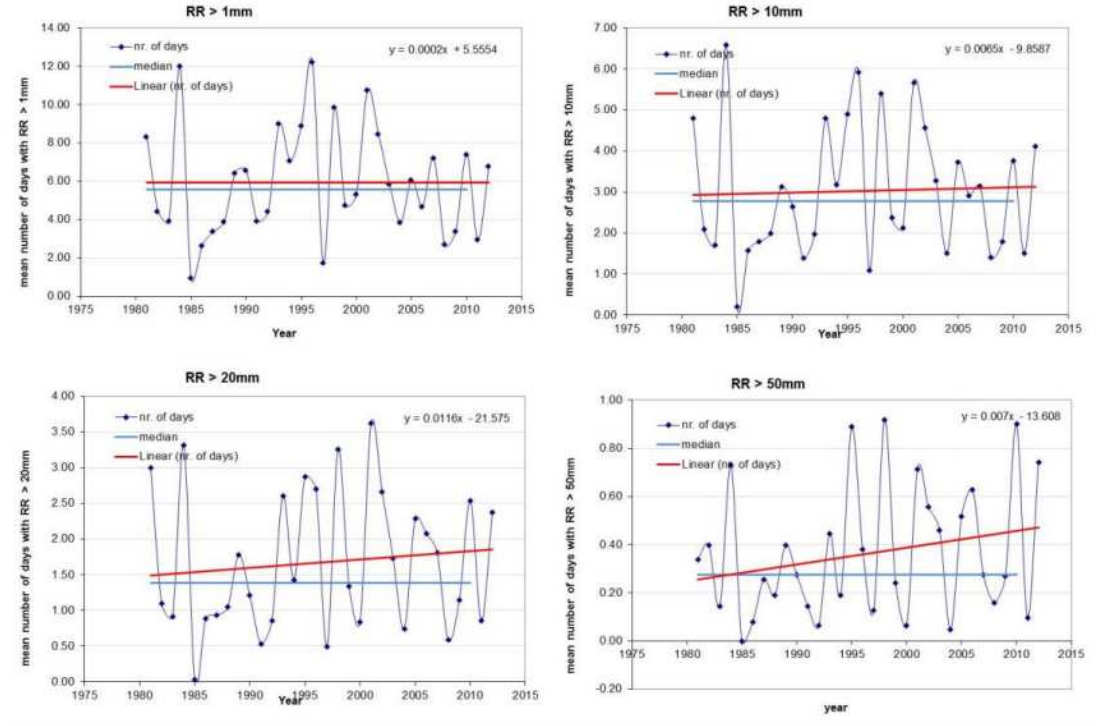

Figure 4.: Mean number of days with precipitation bigger than 1mm, 10 mm, 20 mm and 50 mm, for September (period 1981.-2013.), with corresponding linear trends.

Such trends, caused by changes of weather types, are not desired in hydrological and agrometeorological (silvometeorological) sense. Decrease of frequency of days with smaller precipitation and increase of frequency of days with larger (extreme) precipitation eventually leads to

prolonged dry spells on a wider area, and to the lack of water. This reflects significantly on the fuel condition.

Conclusions

To summarize, these possible changes of atmospheric circulation in the last decade can be connected to more frequent weather conditions associated with high forest fire risk, particularly in May, June and September. So, the risk- and fire-managers should be aware of more probable such weather circulation pattern in the Adriatic region in the future.

Understanding risk: representing fire danger using spatially explicit fire simulation ensembles

Thomas J. Duff[a], Derek M. Chong[a], Brett A. Cirulis[a], Sean F. Walsh[a], Trent D. Penman[b], Kevin G. Tolhust[b]

[a] *University of Melbourne, Burnley, Victoria Australia 3121, tjduff@unimelb.edu.au, derekmoc@unimelb.edu.au, sean.walsh@unimelb.edu.au*
[b] *University of Melbourne, Creswick, Victoria Australia 3363, trent.penman@unimelb.edu.au kgt@unimelb.edu.au*

Abstract
Forest fires are periodic occurrences in many parts of the world. Where they coincide with human populations, they have the potential to have substantial impacts on human values. Consequently, strategies are adopted by land managers to reduce the probability of fire occurrence and, in the event of a fire, reduce subsequent impacts. One such strategy has involved the adoption of fire danger ratings. These are levels of alertness that are applied at a regional level on a daily basis. They are based on preceding and forecast weather and provide an indication of the potential severity of fire behaviour. Danger ratings are generally based on weather derived indices and have limited ability to represent the contribution of landscape attributes to potential impacts, including the properties of vegetation (fuels) and the amount and spatial configuration of vulnerable assets. We propose an alternative method for representing fire danger using fire simulation. An ensemble approach is demonstrated whereby thousands of virtual fires are ignited on a regular grid and simulated on a daily basis using forecast weather with the model PHOENIX RapidFire. Each fire is simulated in succession and burns for a specified period. Fire simulations integrate the contributions of local fuel, topography and weather to fire behaviour. The resultant fires can be aggregated to provide spatially explicit representations of potential spread patterns. These maps can be combined with asset registers to quantify potential impacts and assist with the prioritisation of response and protection measures.

Keywords*: bushfire; PHOENIX RapidFire; Monte-Carlo; risk; simulation; vulnerability; weather; wildfire*

Introduction

Fire danger ratings are used to influence the behaviour of the community at times of high fire risk. They are used to provide warnings, set preparedness levels and invoke regulations that reduce risky behaviour (Taylor and Alexander 2006). They are valuable tools to reduce the probability of fire occurrence and, in the event of a fire, enable the planning of effective responses to reduce subsequent impacts. As a consequence, they have been widely adopted throughout the world (Lin 2000). They provide an indication of the likelihood of a fire starting and for fires that do occur, an indication of the difficulty of suppression and potential damage.

In the context of this article, we define fire danger ratings as the descriptive classes used to communicate fire danger to the public. These danger ratings are typically based on quantitative indices of fire behaviour. Fire danger index systems are used worldwide, including the United States National Fire Danger Rating System (Cohen and Deeming 1985), the McArthur Fire Danger Index (FFDI) used in Australia (Noble *et al.* 1980) and the Canadian Forest Fire Weather Index used in a number of different countries (van Wagner 1974). Fire Danger Indices are calculated using models that are specific to broad landscape types (i.e. forest or grass) and are computed for specific points in space and time using preceding and forecast weather parameters (typically rainfall, temperature, wind speed and humidity (Fujioka *et al.* 2008; Matthews 2009)). To disseminate this information to the public, these indices are summarised on a regional basis using ordinal 'adjective classes' that describe increasing levels of potential fire behaviour (e.g. high, very high and extreme) (Hardy and Hardy

2007). While predominantly derived from fire danger indices, fire danger ratings can also incorporate some expert adjustment to account for additional considerations such as assets at risk, seasonal population movements and public holidays.
For communication purposes fire danger ratings are applied over defined regions, districts or management areas. As a consequence, large geographic areas can be given the same danger rating even though there can be substantial heterogeneity in the expected fire potential resulting from differing combinations of fuel (Duff *et al.* 2012), expected weather, topography (Schunk *et al.* 2013), ignition likelihood (Penman *et al.* 2013) and vulnerable assets (Cheney and Gould 1995; Bones *et al.* 2007). While the zoning of fire rating districts can be optimised to minimise within-district variation (Gouma and Chronopoulou-Sereli 1998), the dynamic nature of fuel and weather means that a single rating is unlikely to be representative of the entire mapped region it denotes (Cheney and Gould 1995). This may contribute to confusion in the community with regards to the intended meaning of danger ratings, or what the most appropriate action should be (Dawson 1988; Reid and Beilin 2013).
As fire danger indices are more quantitative, they can be more easily represented at higher spatial resolutions (e.g. Chowdhury & Hassan (2013)). However, as they were designed for informing land managers about fire spread potential and suppression difficulty, they are not necessarily suitable to provide to the public as information of fire hazard to the community (Cheney and Gould 1995). Current indices are generated from fixed (fuel and topography) and varying (weather) parameters, but are effectively point estimates. They have no way of incorporating landscape context related elements that can greatly contribute to expected fire impacts. These include predominant wind direction, changing patterns of weather throughout the day, the scale and relative position of fuels to assets and variation in the likelihood of human caused ignition. Furthermore, despite the use of the word 'danger' in the term 'fire danger index', there is no explicit evaluation of danger in the context of values at risk. As values in the landscape are unevenly distributed, two fires under similar weather conditions can have substantially different impacts. This can be seen in a recent study by Blanchi *et al* (2010), where high fire danger indices were clearly correlated with maximum house loss potential (extreme days had the potential to result in greater house loss) but only weakly associated with average house loss potential (fires under extreme conditions did not necessarily impact settlements).
We propose an alternative method for representing fire danger at a regional and local level utilising the ability of dynamic fire behaviour models to simulate of fire spread and characterise impacts. Such models have been used to estimate long term fire danger (e.g. Weise *et al* (2010)) however we suggest that ensembles of predictions can be effectively used as indications of daily fire danger potential. To do this, ensembles of fires can be ignited on a regional grid using each day's forecast weather to guide fire progression. Maps of the resulting fires impact characteristics can then be used to differentiate areas of varying fire danger. These maps can be combined with asset registers in order to quantify potential asset impacts and assist with the prioritisation of fire prevention and protection measures. Combined with ignition probability maps, hazard (combining likelihood and consequences) to specific assets can also be quantified. The process was demonstrated using the state of Victoria, Australia, as a test case with fires simulated from gridded weather forecasts using the simulator PHOENIX RapidFire (Tolhurst *et al.* 2008).

2. Methods

Method framework

Dynamic fire behaviour models have developed rapidly in recent years. Advances in computing power mean that fires can be rapidly simulated on a desktop computer. We propose that a parallel processing framework be used to simulate a large (>1000) ensemble of independent fires within the jurisdiction of interest using a regular ignition grid. These can be run on a daily basis using weather forecasts. The results of these simulations can then be combined to produce daily products that represent fire danger to particular assets of interest. The process is outlined in Fig 1.

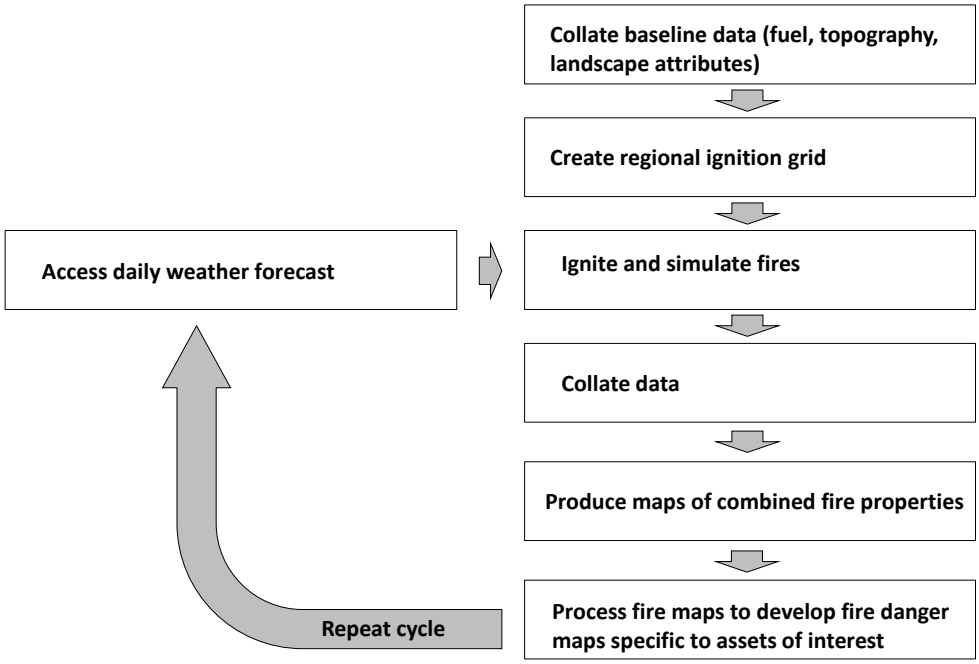

Figure 1. Framework methodology for producing simulation based fire hazard maps

Case study

We used the state of Victoria, Australia, to demonstrate the proposed methodology. Covering an area of 227 000 km^2, Victoria has a Mediterranean type climate and has been subject to a number of severe wildfires, including the Black Saturday fires of 2009.

To capture the spatially and temporally explicit nature of fire spread and resulting fire characteristics, we selected the model *PHOENIX RapidFire* (Tolhurst *et al.* 2008), a dynamic fire model developed explicitly for Australian conditions and used operationally by fire management agencies (Paterson and Chong 2011). The baseline data (fuel hazard, topography, roads, fuel barriers, fire history and wind modifiers) necessary to run simulations was sourced from the Department of Environment and Primary Industries (DEPI), Victoria.

Four days where total fire bans had been declared for the entire state of Victoria were selected from the 2013/2014 fire season. The dates and maximum temperatures at Melbourne Airport (a location of relatively central latitude in the state) are presented in Table 2. These days all had a similar level of alertness communicated to the public.

Table 1. State wide total fire ban days for 2013/2014 fire season showing a reference maximum daily temperature at Melbourne Airport (source Australian Bureau of Meteorology)

Total Fire Ban Date	Daily Max Temperature (ºC)	Total processing time (hrs)
15 January 2014	41.7	0.19
28 January 2014	42.0	0.30
8 February 2014	41.0	0.23
9 February 2014	40.4	0.82

Weather forecasts for the selected days were sourced from the Australian Bureau of Meteorology in the form of state wide NetCDF grids containing the required weather parameters for PHOENIX RapidFire. Inputs of wind speed and direction, temperature, relative humidity and cloud were supplied

at hourly intervals, whilst curing and drought factor were daily values. The NetCDF grids had a longitudinal resolution of 0.03 degrees (approximately 2.6 km) and a latitudinal resolution of 0.02 degrees (approximately 2.2 km). PHOENIX RapidFire continuously interrogates the forecast weather grids at all points along the modelled fire perimeter in order to capture the spatial and temporal variability of the weather across the landscape.

Daily fire potentially was evaluated by modelling ignitions on a regular 5 km grid across the entire state. For each day, ignitions times were calculated using a diurnal fuel moisture content derived FFDI as described by the Matthews fuel moisture model (Matthews 2006) and a nominal threshold FFDI value of 23 to capture the point at which fires become difficult to contain (Mason *et al.* 2011). Where the threshold value is not met, the peak FFDI value between 6am and 6am the following day is used. Ignitions are then modelled until 6am the following day. Grid ignition simulations were run with a nominal 'first attack' suppression allocation to reflect current operational practices. Each daily iteration consisted of a set of 9088 ignitions. The extent of each modelled fire is processed on completion, whereby they are aggregated to provide a state wide spatially explicit indication of the number of impacts affecting each point in the landscape. In addition, an expected house loss map was generated by combining the probability of house loss with the number of houses impacted in each fire (Tolhurst and Chong 2011). House loss results for each fire were represented at the ignition locations. Ignitions were processed in parallel using a 24 core, 2.7 GHz Xeon desktop running Windows 7 Professional with 64 GB of ram. Fires were modelled at 180m resolution which is the recommended resolution for operational use of PHOENIX RapidFire. This is also the reporting resolution for the aggregated results from all ignitions.

To contrast the method, we compare the ensemble generated maps with maps of the daily maximum FFDI sampled at the ignition grid points.

Results

All four days were processed in under an hour respectively, with the maximum ignition grid simulation time of .82 hours and the fastest day processed in 0.23 hours (Table 2).

Despite all four days being classified as total fire bans and the very similar maximum temperatures at Melbourne airport, all four days exhibited substantial spatial variation and range of fire impact values across the state.

The calculated maps showing peak FFDI display a large spatial variation of daily maximums across the state and within defined fire ban districts (Fig 2). Peak values range from the danger classes Low (<12) to Code Red (>100). There were substantial differences between days. In particular, the 9th of February had substantially elevated FFDI in the north and east of the state. The 28th of Janurary had substantially elevated FFDI In the west of the state.

The simulated burn frequency maps were generated for all days (Fig 3). In these, there were some key differences to the FDI maps. In particular, there were a number of parts of the state that had low impacts despite high FDIs (i.e. north-central, south and North West). There were also substantial differences in pattern between days. For example, the 9th of February shows an increased burn frequency in the east of the state.

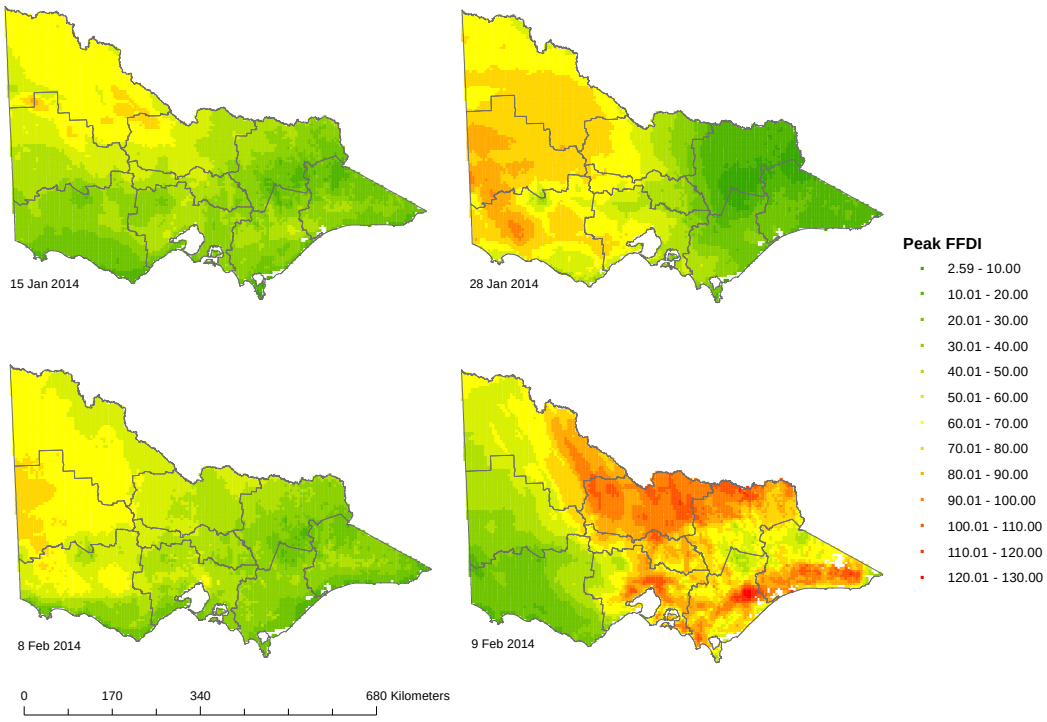

Figure 2. Calculated daily maximum Forest Fire Danger Index values for the state of Victoria, Australia

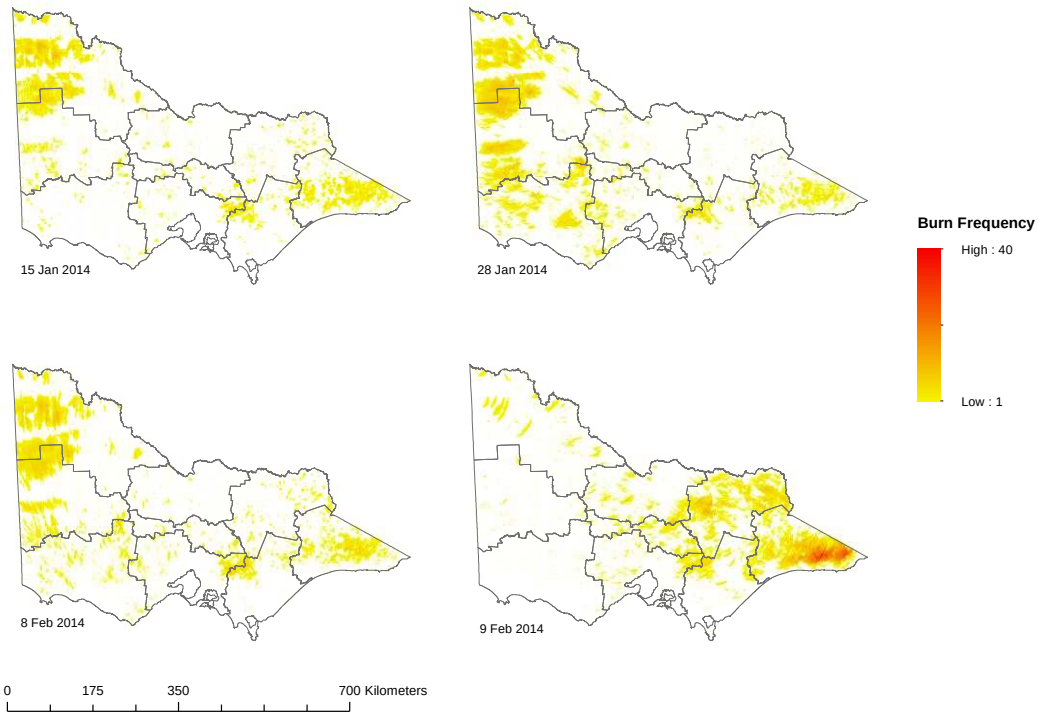

Figure 3– Cumulative burn simulated frequency for fires simulated from gridded ignitions in the state of Victoria, Australia

Resulting house loss values displayed against source ignition points (Fig 4) also show a large spatial variation in impacts across the landscape on each day. In contrast to FDI and burn frequency, there were proportionally higher expected house losses in the centre of the state.

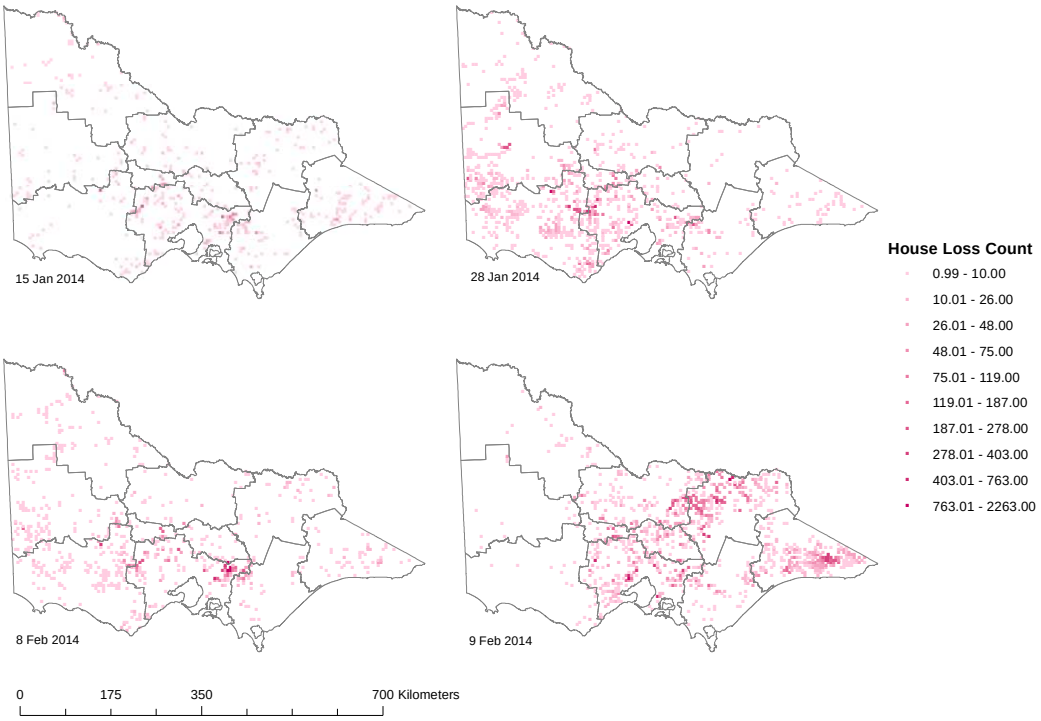

Figure 4– Modelled expected house loss for fires simulated from gridded ignitions in the state of Victoria, Australia

Closer examination of individual fires around the regional centre of Bendigo on the days of the 9th of February and the 28th of January show a clear difference in spread direction and area impacted (Fig 5).

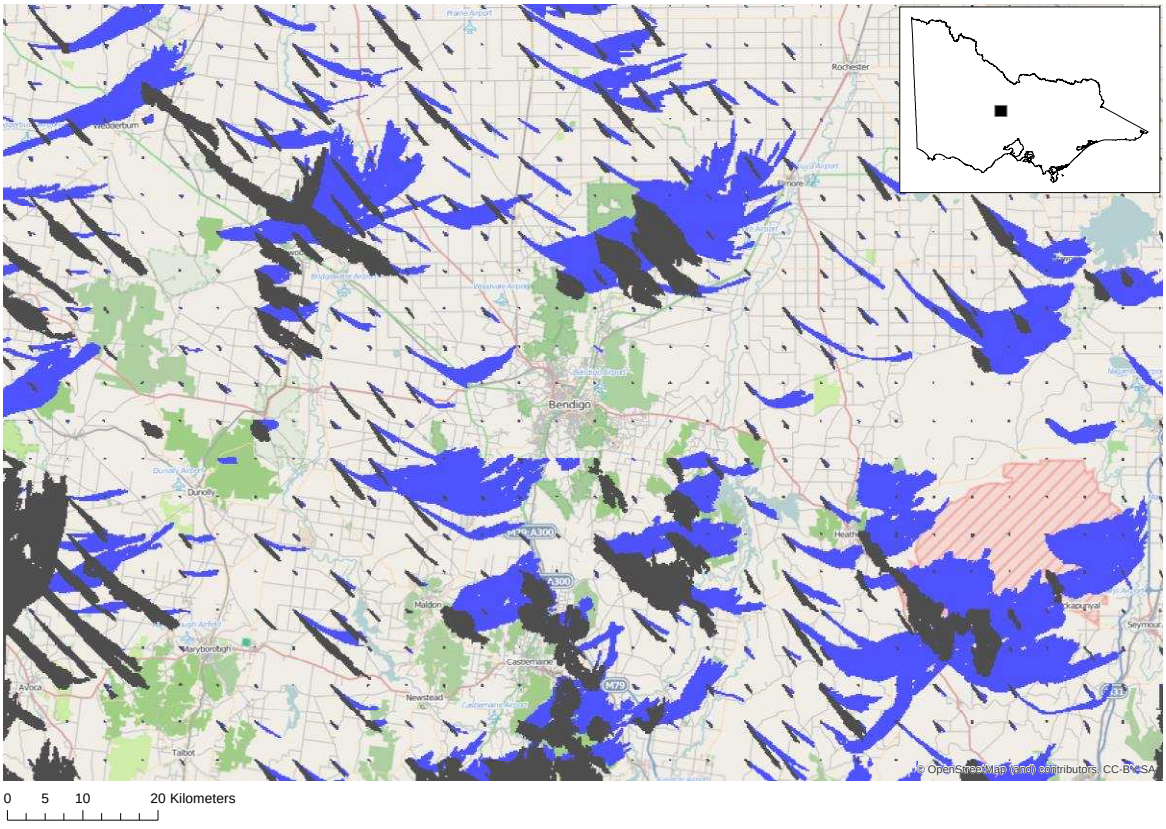

Figure 5- Simulated fire footprints from 9th February (Blue) and 28th January (Dark Grey) surrounding Bendigo, Victoria, Australia

Discussion

The ensemble fire prediction process was demonstrated to have the potential to produce forecasts of fire impacts in operationally useful timeframes. Forecasts of fire potential at operational resolutions for an entire state were all calculated on a desktop computer. As fires were processed in parallel, there is the potential to further decrease processing times with additional hardware.

Such simulation derived products of fire behaviour have substantial advantages over maps of fire danger indices. As they emulate the process of a spreading fire, they have much greater potential to consider temporal dynamics (such as the likely influences of weather fronts or wind changes influencing an area throughout the day) and spatial dynamics (such as the spatial context of varying fuel levels) in relation to values of interest. This means that fire simulations can provide more detail on likely fire behaviour and results will be more locally relevant than what can be produced by pure weather indices.

This is evident in Figure 3, where on all days there was low fire activity in the north-central part of the map due to grassland fuel types. The temporally dynamic nature of fire is evident in the map for the 9th of February, where there was limited fire behaviour in the north and west of the map despite declared total fire ban due to the wind change passing through early in the day bringing cooler conditions. In addition, In Figure 5, the orientations of the fires are markedly different on different days. This is due to the timing of the weather front moving from west to east throughout the day, a common fire weather pattern in South Eastern Australia (Long 2006). Wind changes that occur during fires can greatly effect on the size and overall impacts of a fire (Cheney *et al.* 2001). This means that in addition to the degree of fire threat that a point in the landscape faces, detailed information on the nature of the threat can also be obtained that can be used to guide daily readiness measures. Furthermore, while single day predictions were produced for case study purposes, the method can be validly applied to longer term outlooks. In localities where there is a 7 day weather forecast, there is the potential to produce equivalent fire behaviour forecast maps for each day of weather available. Fire behaviour forecasts could be automatically generated when weather forecasts become available (in Victoria, approximately 5am and 5pm daily).

An additional advantage of the use of ensemble simulations is that a wide variety of products that can be produced. In the example presented, we represent potential fire impacts as the number of fires impacting on a particular point in the landscape. However, other fire properties can also be represented; dynamic fire models can also produce a range of other outputs including fire intensities, cumulative ember loads, rates of spread and flame heights. Empirical data can be used to relate these to impacts on particular values of interest. By overlaying this information with other data sources, a single ensemble prediction can be processed to yield a wide range of information, including potential impacts to water resources, carbon storage, critical infrastructure, biodiversity, houses and human lives. In this study we demonstrated this by assessing the expected impact to houses of each fire (Fig 4). Of note are the higher expected house losses in the centre of the state in all cases. This phenomenon is due to the high concentration of houses in association with wildland fuels in this part of the state. This effect is also evident with the contrast between high FFDI forecasts, high fire impacts and low expected house loss in the north west of the state. While there is high fire potential in the north west, the housing density is very low, so the threat to the community is reduced. As simulation approaches are a way to integrate weather, the landscape, fire behaviour and impacts, they are an ideal way to get a clear idea of potential fire impacts on particular values.

The method presented here can be further extended by incorporating ignition probabilities. The maps presented here represent a regular grid of fires where each fire is given the same weighting. By weighting by ignition probability the likelihood of fires can be represented in the final output. By combining the likelihood of fires and empirically derived consequences (such as house loss in the example above) the method we present can be used to spatially represent fire hazard in a quantitative manner. This means that potential fires can be considered objectively and preparedness measures can

be efficiently designed to be proportional to expected impacts. In contrast, methods based purely on weather derived 'danger' indices cannot truly represent danger as there is no potential to objectively incorporate values at risk.

Ensemble derived maps are able to provide a more nuanced indication of fire risk to the public than regional fire danger ratings. This has the potential to reduce of type I 'false alarm' errors (Taylor and Alexander 2006). However, as sources of public information, weather forecast style fire danger outlooks may not be ideal for all uses. When weather conditions become extreme, members of the public may look for 'threshold' style indicators to spur them to undertake a particular response (Reid and Beilin 2013). Currently total fire bans and 'red alert' warnings used by agencies as unambiguous triggers for action. While the prediction ensemble products may assist in declaring fire bans, bans are likely to remain a valuable tool in fire management. As with fire danger ratings, fire bans are declared over particular regions. While our results have indicated that the regions are not representative of fire behaviour, by aggregating the results of many daily ensembles, there is the potential to use fire simulation to better redraw fire danger declaration regions to create districts with more homogenous expected fire behaviour (Gouma and Chronopoulou-Sereli 1998).

Conclusion

Our results indicate that there is substantial spatial heterogeneity in fire impact within fire danger rating districts. This means that the daily rating applied to a district is unlikely to relevant to all parts of that district. For a particular area, if fire danger ratings are commonly too high, complacency may result. Conversely if ratings are conservative, the residents may not understand the true level of threat. Our methods provide an alternative way to understand and represent fire danger that is more locally relevant. In addition, simulation approaches can give a greater indication of the nature of the fire threat that particular localities may face.

Acknowledgements

The Department of Environment and Primary Industries, Victoria, Australia provided support in the development of this research.

References

Blanchi, R, Lucas, C, Leonard, J, Finkele, K (2010) Meteorological conditions and wildfire-related houseloss in Australia. International Journal of Wildland Fire 19, 914-926.

Bones, H, Pearce, HG, Langer, ER (2007) Communication of fire danger warnings in New Zealand and overseas Ensis Forest Biosecurity and Protection Group, Christchurch, New Zealand.

Cheney, N, P., Gould, J, McCaw, L (2001) The deadman zone: a neglected area of firefighter safety. Australian Forestry 64, 45-50.

Cheney, NP, Gould, JS (1995) Separating fire spread prediction and fire danger rating. CalmScience 4, 3-9.

Chowdhury, E, Hassan, Q (2013) Use of remote sensing-derived variables in developing a forest fire danger forecasting system. Natural Hazards 67, 321-334.

Cohen, JD, Deeming, JE (1985) The national fire danger rating system: basic equations. Forest Service, U.S. Department of Agriculture No. PSW-82, Berkeley, California.

Dawson, MP (1988) Fire bans and public perception of fire danger. In 'Conference on bushifre modelling and fire danger rating systems. Canberra, Australia'. (Eds NP Cheney, AM Gill) (CSIRO

Duff, TJ, Bell, TL, York, A (2012) Predicting continuous variation in forest fuel load using biophysical models: a case study in south-eastern Australia. International Journal of Wildland Fire -.

Fujioka, FM, Gill, AM, Viegas, DX, Wotton, BM (2008) Chapter 21 Fire Danger and Fire Behavior Modeling Systems in Australia, Europe, and North America. In 'Developments in Environmental Science.' (Eds MJAARR Andrzej Bytnerowicz, A Christian.) Vol. Volume 8 pp. 471-497. (Elsevier:

Gouma, V, Chronopoulou-Sereli, A (1998) Wildland fire danger zoning; a methodology. International Journal of Wildland Fire 8, 37-43.

Hardy, CC, Hardy, CE (2007) Fire danger rating in the United States of America: an evolution since 1916. International Journal of Wildland Fire 16, 217-231.

Lin, CC (2000) The Development, Systems, and Evaluation of Forest Fire Danger Rating: A Review Taiwan Journal of Forest Science 15, 507-520.

Long, M (2006) A climatology of extreme fire weather days in Victoria. Australian Meteorological Magazine 55, 3-18.

Mason, C, Sheridan, G, Smith, H, Chong, DM, Tolhurst, KG (2011) Wildfire risk to water supply catchements: a Monte Carlo simulation model. In 'MODSIM2011, 19th International Congress on Modelling and Simulation. Perth, Australia', December 2011. (Eds F Chan, D Marinova, RS Anderssen) pp. 2831-2837. (Modelling and Simulation Society of Australia and New Zealand

Matthews, S (2006) A process-based model of fine fuel moisture. International Journal of Wildland Fire 15, 155-168.

Matthews, S (2009) A comparison of fire danger rating systems for use in forests. Australian Meteorological and Oceanographic Journal 58, 41-48.

Noble, IR, Gill, AM, Bary, GAV (1980) McArthur's fire-danger meters expressed as equations. Austral Ecology 5, 201-203.

Paterson, G, Chong, D (2011) 'Implementing the Phoenix fire spread model for operational use, Proceedings of the Surveying and Spatial Sciences Biennial Conference 2011.' Wellington, New Zealand. (New Zealand Institute of Surveyors and the Surveying and Spatial Sciences Institute:

Penman, TD, Bradstock, RA, Price, O (2013) Modelling the determinants of ignition in the Sydney Basin, Australia: implications for future management. International Journal of Wildland Fire 22, 469-478.

Reid, K, Beilin, R (2013) Where's the Fire? Co-Constructing Bushfire in the Everyday Landscape. Society & Natural Resources 27, 140-154.

Schunk, C, Wastl, C, Leuchner, M, Schuster, C, Menzel, A (2013) Forest fire danger rating in complex topography: results from a case study in the Bavarian Alps in autumn 2011. Natural Hazards and Earth System Sciences 13, 2157-2167.

Taylor, SW, Alexander, ME (2006) Science, technology, and human factors in fire danger rating: the Canadian experience. International Journal of Wildland Fire 15, 121-135.

Tolhurst, KG, Chong, DM (2011) Assessing potential house losses using PHOENIX RapidFire. In 'Proceedings of Bushfire CRC & AFAC 2011 Conference. Sydney, Australia'. (Ed. RP Thornton) pp. 74-86.

Tolhurst, KG, Shields, B, Chong, D (2008) PHOENIX: development and application of a bushfire risk management tool. Australian Journal of Emergency Management 23, 47-54.

van Wagner, CE (1974) Structure of the Candadian forest fire weather index. Canadian Forestry Service, Ottawa, Canada.

Weise, DR, Stephens, SL, Fujioka, FM, Moody, TJ, Benoit, J (2010) Estimation of fire danger in Hawai'i using limited weather data and simulation. Pacific Science 64, 199-220.

Use of weather generators for assessing local scale impact of climate change on dead fuel moisture

Grazia Pellizzaro[a], Martin Dubrovsky[b], Sara Bortolu[a], Bachisio Arca[a], Andrea Ventura[a], Pierpaolo Duce[a]

[a] *National Research Council, Institute of Biometeorology (CNR-IBIMET), Traversa La Crucca 3 Sassari Italy, g.pellizzaro@ibimet.cnr.it*
[b] *Institute of Atmospheric Physics, Praha, Czech Republic, madu1110@gmail.com*

Abstract
The main aims of this work are to identify useful tools to determine potential impacts of expected climate change on dead fuel status in Mediterranean shrubland and, in particular, to estimate the effect of climate changes on the number of days characterized by critical values of dead fuel moisture. Measurements of dead fuel moisture content in Mediterranean shrubland were performed in North Western Sardinia (Italy) for six years by using humidity sensors. Meteorological variables were also recorded. Data were used to determine the accuracy of the Canadian Fine Fuel Moisture Code (FFM code) in modelling moisture dynamics of dead fuel in Mediterranean vegetation. Critical threshold values of FFM code for Mediterranean climate were identified by percentile analysis, and new fuel moisture code classes were also defined.
A stochastic weather generator (M&Rfi), linked to climate change scenarios derived from 17 available General Circulation Models (GCMs), was used to produce synthetic weather series, representing present and future climates, for the selected site located in North Western Sardinia, Italy. The number of days with critical FFM code values for present and future climate were calculated and the potential impact of future climate change was analysed.

***Keywords**: Forest fires, Mediterranean shrubs, Fine fuel moisture code, Downscaling techniques*

Introduction

The moisture content of dead fuel (FMC) is an important variable in fire ignition and fire propagation and is strongly affected by changes in atmospheric conditions. According to projections of future climate in Southern Europe, changes in temperature, precipitation and extreme events are expected (Christensen *et al*. 2007; Giannakopoulos *et al*. 2009; Giorgi *et al*. 2004). More prolonged drought seasons could influence fuel moisture content and, consequently, the number of days characterized by high ignition danger in Mediterranean ecosystems (Flannigan *et al*. 2009; Flannigan *et al*. 2013; Liu *et al*. 2013; Matthews *et al*. 2012; Westerling *et al*. 2006).
The low resolution of the climate data provided by the general circulation models (GCMs) represents a limitation for evaluating climate change impacts at local scale. For this reason, the climate research community has called to develop appropriate downscaling techniques. One of the downscaling approaches, which transforms the raw outputs from the climate models (GCMs or RCMs) into data with more realistic structure, is based on linking a stochastic weather generator with the climate model outputs. Weather generators linked to climate change scenarios can therefore be used to create synthetic weather series (air temperature and relative humidity, wind speed and precipitation) representing present and future climates at local scale.
Moisture exchange in dead materials is controlled by physical processes, and is clearly dependent on rapid atmospheric changes. Therefore, some meteorological danger indices can be used for modelling the moisture dynamics of dead fuel (Van Wagner 1977; Chandler *et al*. 1983; Van Wagner 1985; Wotton, 2009; Matthews, 2014).

The main aims of this work are to identify useful tools to determine potential impacts of expected climate change on dead fuel status in Mediterranean shrubland and, in particular, to estimate the effect of climate changes on the number of days characterized by critical values of dead fuel moisture

Materials and Methods

The study was carried out in in North Western Sardinia, Italy (40° 36' N; 8° 09' E, 30 m a.s.l.). Climate is Mediterranean with water deficit conditions occurring from May through September and precipitation mainly concentrated in autumn and winter. The mean annual rainfall is 640 mm and the mean annual air temperature is 16.8 °C. The experimental area is mainly covered by Mediterranean shrubs.

Figure 1. Experimental site location

The study was carried out in two different phases. In the first one, FMC values (1 hour and 10 hours fractions) were periodically determined during six consecutive years on three Mediterranean shrub species: *Cistus monspeliensis* L., *Pistacia lentiscus* L., and *Juniperus phoenicaea* L. During the same period meteorological variables and temporal patterns of moisture content, measured by using humidity sensors, were recorded. The relationships between direct field measurements and FMC values given by moisture sensor were analysed. Then, the Canadian Fine Fuel Moisture Code (FFM code) was calculated. Finally, FMC values obtained from fuel sensors were used to develop appropriate FFM code danger classes specific for Mediterranean climate.
In the second step the potential climate change impact on fuel status and ignition danger season in Mediterranean area was simulated. The weather generator M&Rfi (Dubrovsky *et al*. 2005, 2007) linked to climate change scenarios derived from 17 available General Circulation Models (GCMs), was used to produce synthetic weather series, representing present and future climate (2100) for the selected site (Table 1). The downscaling of future climate projections was made using three scenarios (A2, B1, and A1B) from the IPCC Special Report on Emission Scenarios (Nakicenovic *et al.* 2000) . The projected future climates were then used to calculate the FFM code of the Canadian Forest Fire Weather Index System (Van Wagner 1987) and to estimate possible impacts of climate change on dead fuel moisture content pattern.

Table 1. General Circulation Models (GCMs) used in conjunction with the M&Rfi weather generator to produce synthetic weather series representing present and future climates at four location in North Sardinia, Italy

BCM2	Bjerknes Centre for Climate Research, Norway
CGMR	Canadian Center for Climate Modelling and Analysis, Canada
CNCM3	Centre National de Recherches Meteorologiques, France
CSMK3	Commonwealth Scientific and Industrial Res. Organisation, Australia
ECHOG	Met. Inst. Univ. Bonn + Met. Res. Inst., Korea + Model and Data Groupe at MPI-M, Germany
GFCM20	Geophysical Fluid Dynamics Laboratory, USA
HADCM3	UK Met. Office, UK
HADGEM	UK Met. Office, UK
INCM3	Institute for Numerical Mathematics, Russia
MIMR	National Institute for Environmental Studies, Japan
MPEH5	Max Planck Institute for Meteorology, Germany
MRCGCM	Meteorological Research institute, Japan
NCCCSM	National Centre for Atmospheric Research, USA
NCPCM	National Centre for Atmospheric Research, USA
GFCM21	Geophysical Fluid Dynamics Laboratory, USA
GIER	Geophysical Fluid Dynamics Laboratory, USA. Model E20/Russel
IPCM4	Institute Pierre Simon Laplace, France

Results

A highly significant relationship (R^2=0.82; p< 0.001) between direct measurements of FMC and values given by fuel moisture sensor was observed. Therefore, we used FMC values by sensor measurements to calibrate FFM code for Mediterranean species.

The range of values of FFM code (from 10 to 95) was divided into 35 classes of equal width (2.5). The frequencies of number of days characterized by values lower than 20% and 15% for each FFM code class were calculated. Figure 2 shows that most of days with moisture content lower than 20% and 15% are included in the FFM classes 87.5 and 90, respectively, and corresponded to 85th and 95th percentile of FFM series, respectively. Therefore, threshold values equal to 85th and 95th percentile of FFM code values calculated by synthetic weather series representing present and future climates were selected to identify days characterized by high (85th percentile) and extreme (95th percentile) fire danger.

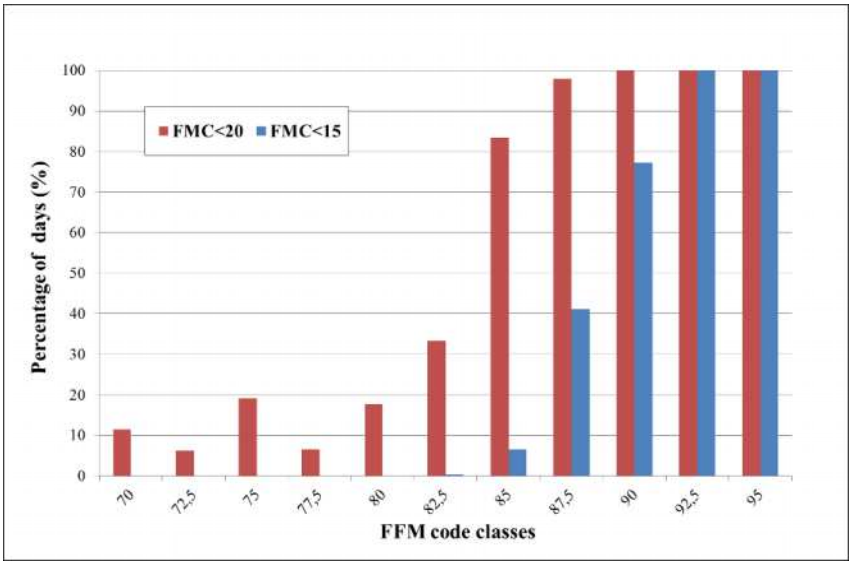

Figure 2. Frequency distribution (percentage) of days when dead fuel moisture content values (FMC) were less than 15% and 20% by FFM code classes (2007-2012)

Figures 3 and 4 show the forecasted total number of days characterized by high and extreme fire danger for each GCM and scenario (actual and 2100 projection) relative to April - October months.

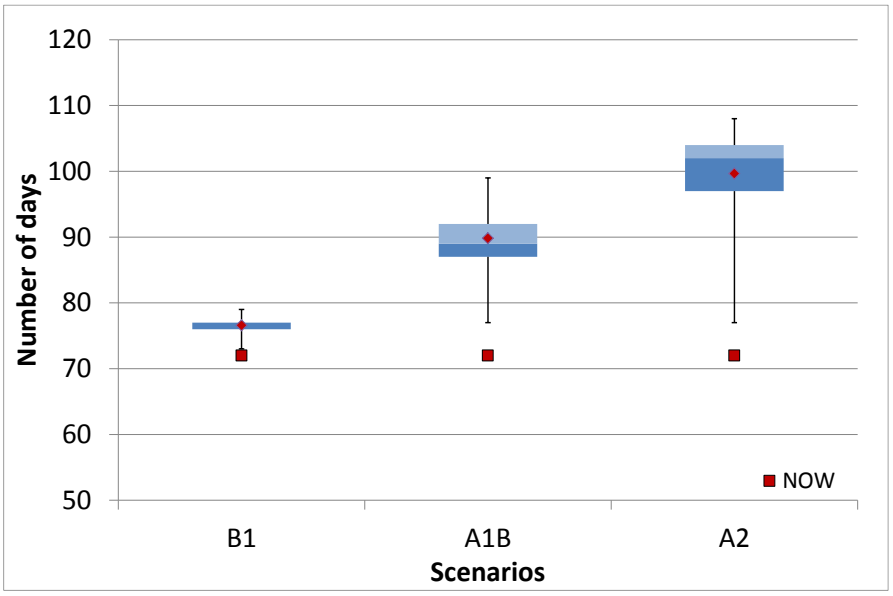

Figure 3. Boxplot of the actual and projected (blue) number of days characterized by high danger (85th percentile) relative to three climate change scenarios (B1, A1B, and A2). The chart shows the mean (red diamond), median, minimum and maximum values, and the lower and upper quartiles. The actual number of days characterized by high danger are indicated by the red squares (April - October period).

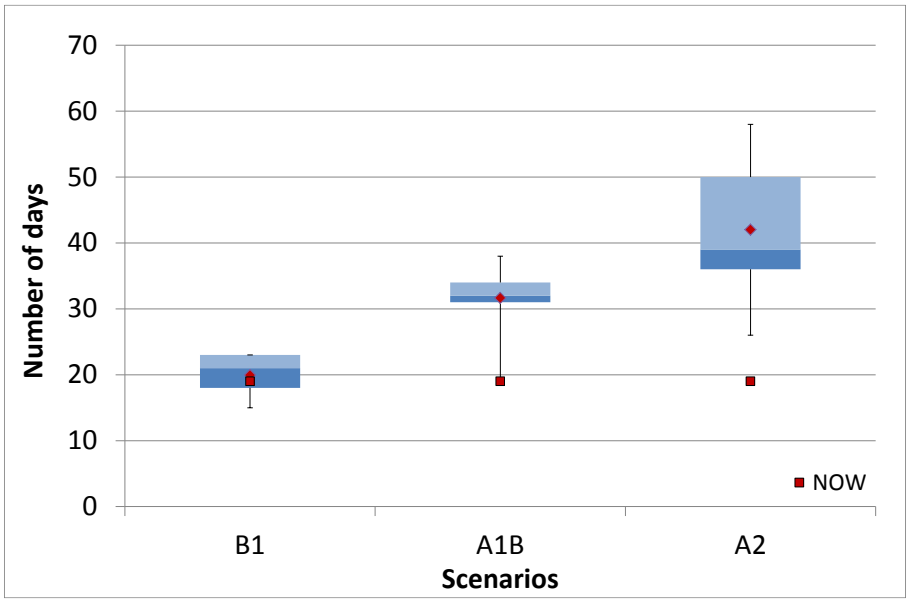

Figure 4. Boxplot of the actual and projected (blue) number of days characterized by extreme danger (95th percentile) relative to three climate change scenarios (B1, A1B, and A2). The chart show the mean (red diamond), median, minimum and maximum values, and the lower and upper quartiles. The actual number of days characterized by extreme danger are indicated by the red squares (April - October period).

No evident differences between baseline period and future were observed for B1 scenario especially regarding days characterized by extreme danger. More evident changes were observed for A1B and A2 scenarios. For A1B scenario the mean total number of high and extreme danger days is expected to increase by 18 and 12 days, respectively, compared to the present climate. The increase of high and extreme danger days reached 27 and 23 days in the case of A2 scenario.

Analysis of distribution of danger days throughout the April - October period shows that in general the increase of days characterized by high danger (85th percentile) is likely to occur during the second half of summer. For all three scenarios, in fact, the number of danger days increased in August and September. In addition, our results suggest that the fire season may end later than today (scenarios A1B and A2), although scenario A2 projections indicate a possible anticipation of the fire season.
With reference to extreme days (95th percentile), a general increase of number of critical days is likely to occur on the basis of A1B and A2 scenarios that are characterized by intermediate (A1B) and high (A2) anthropogenic greenhouse gas emissions.
In conclusion, this study confirms that an increase of number of days critical for fire occurrence and a longer fire season could be expected also in Mediterranean areas as a consequence of climate change projections.

Acknowledgements

This work was partly supported by the EU 7th Framework Program (FUME) contract number 243888. The authors are also grateful to Mr Angelo Arca and Mr Pierpaolo Masia for their valuable support in the field work

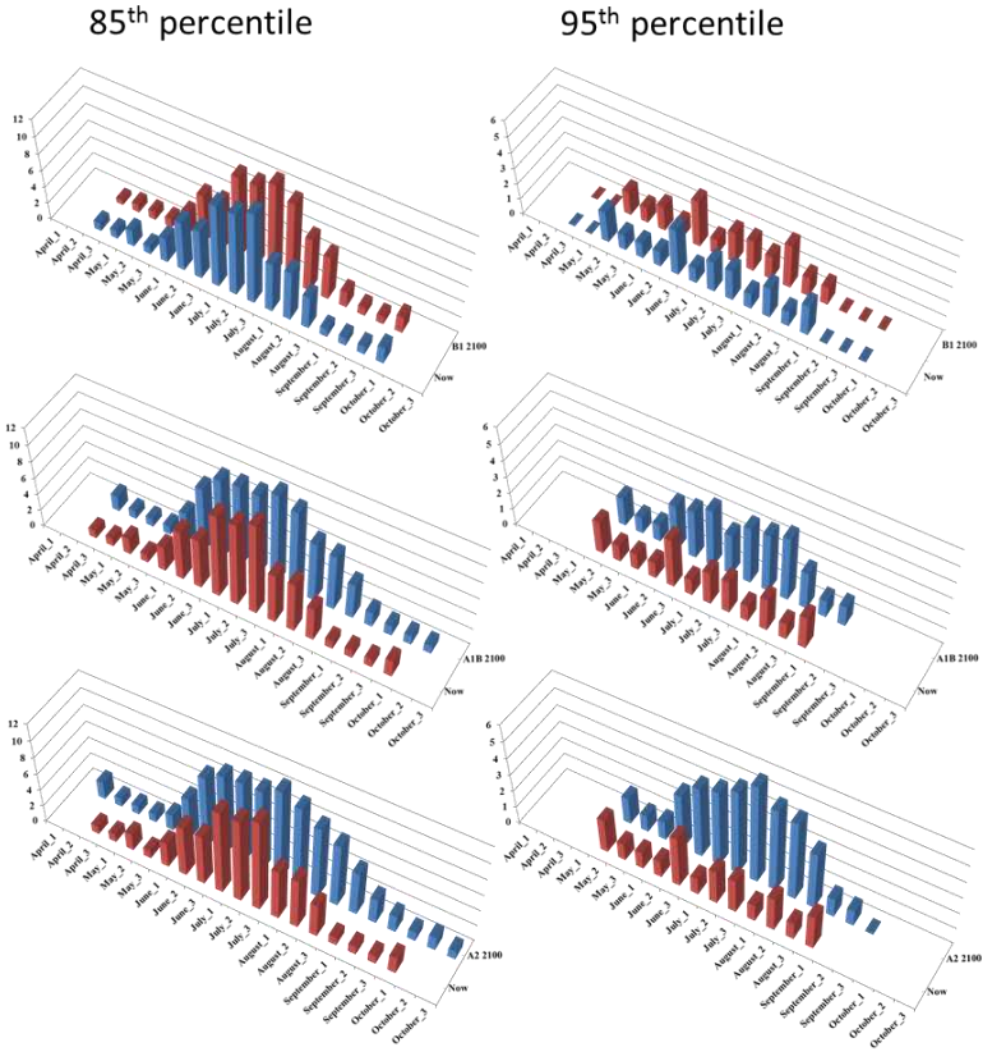

Figure 5. Mean total number of days with high (85th percentile) and extreme danger (95th percentile) at the end of the century during the period April 1st to October 30th. Mean values were calculated per ten-days periods and three climate change scenarios (B1, A1B, and A2) .

References

Chandler P, Cheney P, Thomas L, Trabaud L & Williams D (1983) *Fire in forestry*. Vol. 1. John Wiley & Sons (New York, USA)

Christensen JH, Hewitson B, Busuioc A, Chen A, Gao X, Held I, Jones R, Kolli RK, W.-T. Kwon, Laprise R., Magaña Rueda V., Mearns L., Menéndez C.G., Räisänen J., Rinke A., Sarr A. & Whetton P. (2007), Regional Climate Projections. In: Climate Change 2007: The Physical Science Basis. Contribution of Working Group I to the Fourth Assessment Report of the Intergovernmental Panel on Climate Change [Solomon, S., D. Qin, M. Manning, Z. Chen, M. Marquis, K.B. Averyt, M. Tignor and H.L. Miller (eds.)]. Cambridge University Press, Cambridge, United Kingdom and New York, NY, USA.

Dubrovsky M, Nemesova I, Kalvova J, (2005) Uncertainties in climate change scenarios for the Czech Republic, *Climate Research*, **29,** 139-156

Dubrovsky M, (2007) M&Rfi Weather Generator. http://www.ufa.cas.cz/ dub/ wg/ marfi/ marfi.htm, 34 p

Flannigan MD, Krawchuk MA, de Groot WJ, Wotton BM, Gowman LM (2009) Implications of changing climate for global wildland fire. *International Journal of Wildland Fire* **18**, 483–507.

Flannigan M, Cantin AS, de Groot WJ, Wotton M., Newbery A, Gowman L, (2013) Global wildland fire season severity in the 21st century. *Forest Ecology and Management* **294**, 54-61.

Giannakopoulos C, Le Sager P, Bindi M, Moriondo M, Kostopouloua E, Goodess CM (2009) Climatic changes and associated impacts in the Mediterranean resulting from a 2 °C global warming. *Global and Planetary Change.* **68**, 209-224.

Giorgi F, Bi XQ, Pal J (2004) Mean, interannual variability and trends in a regional climate change experiment over Europe. II: climate change scenarios (2071- 2100). *Climate Dynamics* **23**, 839-858.

Liu Y, Goodrick SL, Stanturf JA, (2013) Future U.S. wildfire potential trends projected using a dynamically downscaled climate change scenario. *Forest Ecology and Management* **294**, 120-135.

Matthews S, Sullivan AL, Watson P, Williams R, (2012) Climate change, fuel and fire behaviour in a eucalypt forest. *Global Change Biology* **18**,3212–3223.

Matthews S (2014) Dead fuel moisture research: 1991–2012 *International Journal of Wildland Fire* **23**, 78–92.

Nakicenovic N. *et al*. (2000) Special Report on Emissions Scenarios. A Special Report of Working Group III of the Intergovernmental Panel on Climate Change. Cambridge University Press: Cambridge. 599 pp.

Van Wagner CE (1977) Conditions for the start and spread of crown fires. *Canadian Journal of Forest Research* **7**,23-34.

Van Wagner CE & Pickett TL (1985) Equation and FORTRAN program for the Canadian Forest Fire Weather Index System. Canadian Forestry Service, Forestry Technical Report 33.(Ottawa, ON, Canada)

VanWagner CE (1987) The development and structure of the Canadian Forest FireWeather Index System. Canadian Forest Service, Petawawa National Forestry Institute. Chalk River, Ont. FTR-35.

Westerling AL, Hidalgo HG, Cayan DR, Swetnam TW (2006) Warming and Earlier Spring Increase Western U.S. Forest Wildfire Activity. *Science* **313**, 940-943

Wotton BM (2009) Interpreting and using outputs from the Canadian Forest Fire Danger Rating System in research applications. *Environmental and Ecological Statistics* **16**, 107–131. doi:10.1007/S10651-007- 0084-2

Chapter 5
Fire Suppression and Safety

A Landsat-TM/OLI algorithm for burned areas in the Brazilian Cerrado – preliminary results

Arturo E. Melchiori, Alberto W. Setzer, Fabiano Morelli, Renata Libonati, Pietro de Almeida Cândido, Silvia C. de Jesús

INPE, R. dos Astronautas 1758, São José dos Campos, SP, Brazil. {emiliano.melchiori; alberto.setzer; fabiano.morelli; renata.libonati; pietro.candido}@cptec.inpe.br, silvia.jesus@inpe.br

Abstract

Accurate burned area information is required and of particular interest for the scientific communities dealing with land use and climate changes. Currently, due to the very broad spatial extent and the limited accessibility of some of the largest regions affected by fire, instruments on-board satellites provide the only available operational systems capable to collect cost-effective burned area data.

This paper presents the initial results of an algorithm for automatic extraction of burned area scars using Landsat TM and OLI imagery in the Cerrado (savannah) biome of Brazil. Development and validation tests were conducted for the "Jalapão" region, which has been intensely affected by fire in the last years; during the 2010 dry season, it accounted for 60% of all active fire pixels detected in the Cerrado.

A series of Landsat TM and /OLI 52 scenes (path/row: 221/067) covering the period of 2000 - 2013 was used. Input images were accepted only with cloud cover up to 10%, and the maximum period of time between consecutive scenes was up to 1 month. Composite images with differences in NDVI (dNDVI) and NBRL (dNBRL) of consecutive scenes were used to identify fire scars. The algorithm computes and filters the rate of change in dNDVI and dNBRL indexes, relative to the pre-fire condition. The value of the dNBRL change is then used in the calculation of the burned area mask.

Results of the automatic extraction were evaluated against maps of burned scar produced by visual photo interpretation of the composite images for the reference period of 2004 - 2010. Omission and commission errors were obtained, and the reliability of the algorithm and the burned area match levels were calculated for the image series. Omission Errors ranged from 4.8% to 21.0%, and Commission Errors from 2.3% to 24.1%. Reliability of the Algorithm and Burned Area Match varied from 75.8 % to 97.2%, and from 79 to 95.2%, respectively. These values are comparable to the best reported in the literature for other regions. Commission errors were associated mainly to clouds and their shadows in the images; agricultural practices were another source of error. Detailed error analysis and results are included in the text.

The algorithm developed is currently being implemented for operational and automatic generation of burned scar maps at a regional scale, particularly for conservation areas.

***Keywords**: fires, burned area, automatic extraction, Landsat, Cerrado*

Introduction

The Brazilian Cerrado extends over 2000000km^2, occupying almost a fourth of the country's territory, and is considered the most bio diverse Savannah of the world. Deforestation already reduced this biome to be at least 50%, and if degradation is also considered, this value increases significantly (Klink and Machado, 2005). Conservation areas account only for 8.2% of the Cerrado, and an additional 4.4% are preserved as indigenous territories (MMA, 2014a; Klink and Machado, 2005). The study area is located in the Jalapão region, at the northeast portion of central Brazil, comprising the largest and more important conservation areas of the Cerrado biome – see Figure 1. Its elevation ranges from 150 m to 950 m, and the climate in the region is hot semi-humid, with a pronounced drought season. Rains are concentrated in the October-to-April so-called summer season, with up to about 600 mm of average precipitation in the rainiest trimester, while winter, from May through September, may accumulate as little as 25 mm. Soils have a large proportion of quartz sands, almost 50%; vegetation types include

the main physiognomies of the Cerrado/Savannah, and the population density is below 2.5 inhabitants/km^2 [INMET, 2014, SEPLAN, 2013; Prado dos Santos *et al*, 2011].
Increasing efforts are being made by federal and state agencies in this region to control deforestation processes and anthropic vegetation fires [MMA, 2012; MMA, 2014b]. During the severe drought period of 2010, 60% of all fires in the Cerrado biome were detected in the Jalapão ecologic corridor. Remote sites and fire brigade's limited operational conditions contribute to an inefficient control of fires. The total fire pixel detections by Projeto Queimadas of INPE, Brazil [INPE, 2014], accounts for 83575 events in the period 2004-2013, with a mean annual value of 8357 [Candido 2014]; this value refers to multiple satellite platforms, when a unique fire event might have simultaneous detections from more than one satellite.
Mapping burned areas requires the development of methods to process massive mid-resolution (e.g. Landsat TM and OLI) image data bases to produce results of practical use; unfortunately, no reliable products are available on an operational basis. Remote sensing techniques are now recognized as the only cost-effective source of information for mapping burned areas from regional/national up to global scale [Stroppiana *et al* 2012]. Burned area mapping using mid-resolution sensors has been classically oriented toward local-scale studies, but the current availability of such images without costs allows their use in larger scales [Bastarrika *et al* 2011]. Our study area is contained in the Landsat TM/OLI scene path/row 221/067. Figure 1 shows the study area within the context of the South American continent.

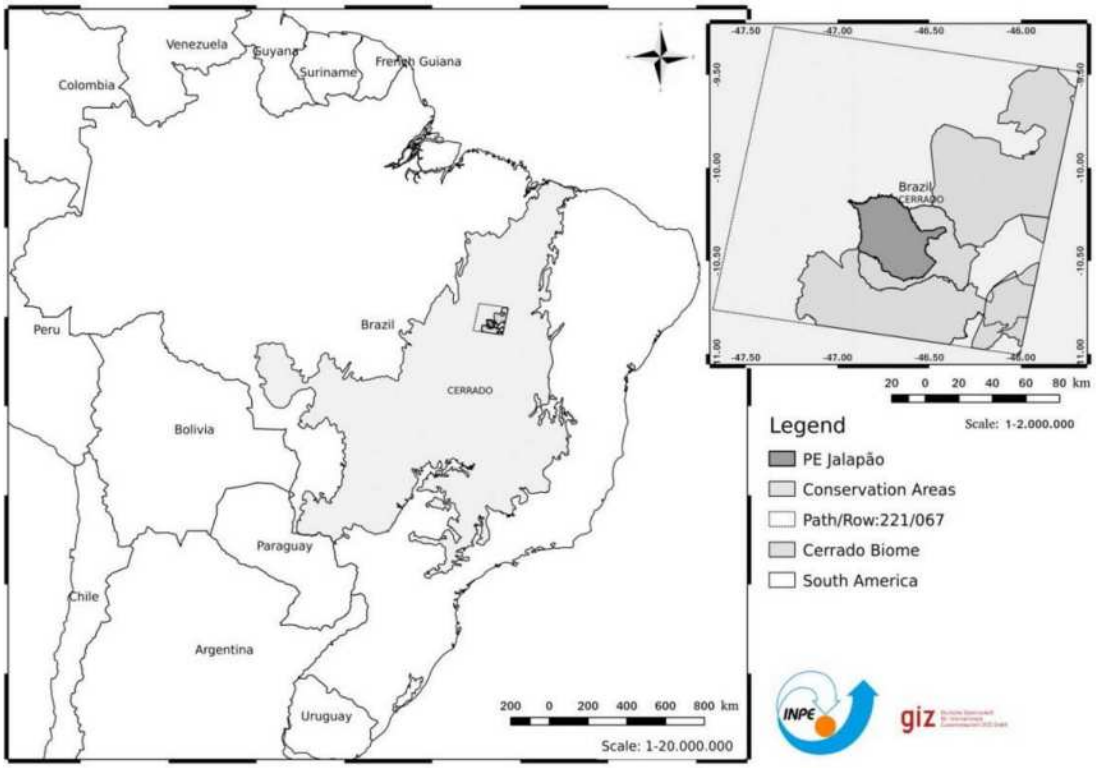

Figure 1. Location of the study area.

Landsat TM sensor images have been widely used for precise mapping due to its 30 meters spatial resolution in both visible and infrared channels [Stroppiana *et al*, 2012]. OLI sensor's images present strong improvements regarding the TM sensor, in both spectral and radiometric resolution. While temporal resolution might be adequate for multi-temporal mapping in ideal atmospheric conditions, the occasional presence of clouds and cloud shadows over the study region impair the regularity of the temporal series, even causing its interruption.

In this present work, the cloud content of any image used in the temporal series was limited up to 10% of total image special coverage. The amount of cloud cover was established by visual inspection. All images were downloaded from the USGS server [USGS, 2014]. The high quality of their geo-processing grants their use in automatic and operational processes.
The entire procedure for image processing was developed in the Python 2.7.4 programming language, using freely available function libraries like gdal, numpy, scipy, scikit, among others. Inter-operation among these libraries greatly simplifies the process work flow. The application developed allows the processing of raw image series, generating derived series as a result. Results from the sub-process stages like statistical information, objects mapped, thresholds used for classification, among other data, are logged in a file for further analysis.

Methods

Several processing routines were defined to process the Landsat TM/OLI images and obtain burned scar maps in a semi-automatic mode, file downloads and decompressing, generation of a layer stack, cropping, processing and comparisons with reference data.
Input data consisted of compressed Landsat TM and OLI imagery in the tar.gz format, downloaded from the USGS server [USGS, 2014]. Output data were the burned scar maps, in raster and vector file formats, reflectance images, and composite RGB files used for burned scar visual photo analysis [Candido, 2014]. The download process involved selecting, within the available images, those with less than 10% cloud cover. An automated routine was developed to handle the compressed data and generate the corresponding layer stacks of radiance images; it avoids compression tools and GIS systems to prepare data for processing, saving many hours per image set for the operators. Each uncompressed radiance stack layer obtained is accompanied by its metadata file for later reflectance conversion.
The next step in the process is the cropping stage, where radiance stack layers are cropped to a polygon vector file of the study area, using another specific automated routine developed for this purpose. The cropped layer stacks, with their corresponding metadata file, are the input for the main procedure.

Main procedure for burned area mapping

The main core of this classification procedure is based on calculations of the NDVI (Normalized Difference Vegetation Index) [Gitelson *et al*, 1996; Stroppiana *et al*, 2012] and the NBRL (Normalized Burn Ratio Long SWIR Variation) [Bastarrika *et al*, 2012; Key & Benson, 2006] indexes calculated from reflectance data. Conversion from sensor radiance to TOA reflectance was done following the work of Chander *et al*, 2009.
The detection and extraction of burned scars in the images is based on the concept that in conservation areas, the behaviour of the vegetation cover does not present sudden changes, and if they occur, they are very likely the result of fires. To evaluate this pattern change caused by fires, the variation in time of NDVI and NBRL, as described in equations 1 and 2, was evaluated in a similar way to the work of Miller and Thode (2007). In that work, they have used the positive square root of the absolute initial value divided by 1000. In this case, we directly used the absolute values. Considering two consecutive images of the same area with a maximum period between images of one month, the change rate for each index is defined by:

$$crndvi = \frac{ndvi(data1) - ndvi(data2)}{abs\big(ndvi(data1)\big)}$$

$$crnbrl = \frac{nbrl(data1) - nbrl(data2)}{abs(nbrl(data1))}$$

Outliers in ratio values may be found when a very low value (near zero) is present in data1. To avoid these extreme cases, a limitation threshold was used in the NBRL difference.

$$dnbrl = nbrl(data1) - nbrl(data2)$$

For each equation, a threshold was used to separate burned from unburned areas, where the complete masking procedure results as follows:

$$Bmask = (crnbrl \geq Tcnbrl) * (crndvi \geq Tcndvi) * (dnbrl > Tdnbrl)$$

Used thresholds were: *Tcrnbrl*= 0.5, *Tcrndvi*= 0.45 and *Tdnbrl*= 0.10, and they were obtained by qualitative comparisons. For OLI images, a different set of thresholds were used, and the NDVI threshold was lowered to 0.35, while *Tdnbrl* was lowered to 0.06.
The final operation is the vectorization, which is optional. To speed up the process, the vector file creation procedure can be cancelled. All these processes are straightforward using functions in the gdal, numpy and other python libraries. The complete work flow of the burned mapping process is presented in Figure 2.

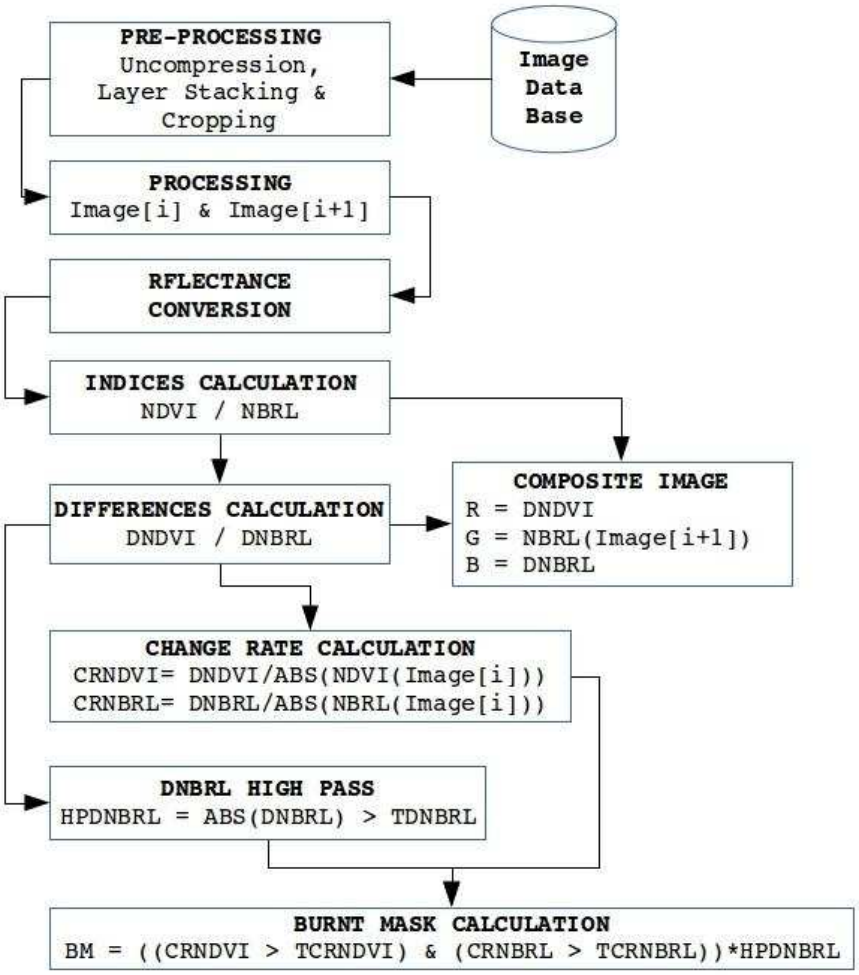

Figure 2. Flux diagram of developed process.

Evaluation of the algorithm's performance was made using burned area manually mapped from visual photo interpretation in the period 2004 – 2010 [Candido, 2014]. As mentioned by Congalton 1991, the accuracy of photointerpretation has been accepted as correct without any confirmation, and digital classifications are often assessed with reference to it leading to sometimes poor and unfair assessments. According to Blaschke *et al* (2008), visual photo interpretation is the ultimate benchmark for any classification and segmentation procedure. Omission and commission errors were obtained from image differencing between the reference data manually digitized and the algorithm's burned area (BA).

$$Omission\ Error = Reference - Algorithm's\ Burned\ Area$$

$$Commission\ Error = Algorithm's\ Burned\ Area - Reference$$

Burned Match (BM) and the Algorithm Reliability (AR) were obtained with the following formulas.

$$Burned\ Match = \frac{Algorithm's\ BA - CommissionError}{Algorithm's\ BA}$$

$$Algorithm\ Reliability = \frac{(Algorithm's\ BA - Commission\ Error)}{Reference}$$

Results

A total of 52 Landsat TM/OLI scenes from path/row 221/067 covering the period of 2000 – 2013 were processed. Over two thirds of the complete set was evaluated against visual photo interpretation of the burn scars, while the remaining 15 images were processed without a visual evaluation because this works was not yet available. For the 37 images in the 2004 – 2010 period, the obtained results are presented in the following tables.

Table 1. Scene date (day/month of the last image), algorithm burned area, reference burned area, commission error, omission error, burned match and reliability in percentages for year 2004.

2004	Alg [ha]	Ref [ha]	Comm %	Omission %	B. Match %	A. Reliability %
02/06	57415	57435	15.8	15.9	84.1	84.1
04/07	96064	98558	11.7	14.3	86.0	88.2
20/07	42975	44628	8.9	12.8	87.6	91.0
05/08	73097	76786	4.5	9.5	90.9	95.5
06/09	207589	213562	7.2	10.1	90.1	92.7
Total	**477140**	**490968**	**9.6**	**12.5**	**87.8**	**90.3**

Table 2. Scene date (day/month of the last image), algorithm burned area, reference burned area, commission error, omission error, burned match and reliability in percentages for year 2005.

2005	Alg [ha]	Ref [ha]	Comm %	Omission %	B. Match %	A. Reliability %
23/07	60536	68046	4,1	16,5	85,3	95.9
08/08	67321	71017	7,9	13,4	87,3	92.1
24/08	78788	85490	2,7	11,2	89,6	97.2
09/09	112800	125704	3,0	14,4	87,0	97.0
Total	**319445**	**350256**	**4.4**	**13.9**	**87.3**	**95.5**

Table 3. Scene date (day/month of the last image), algorithm burned area, reference burned area, commission error, omission error, burned match and reliability in percentages for year 2006.

2006	Alg [ha]	Ref [ha]	Comm %	Omission %	B Match %	A. Reliability %
08/06	36319	35851	13.4	9.3	87.7	86.5
24/06	46208	41725	20.9	11.2	87.6	79.1
26/07	97734	95515	10.4	8.1	91.7	89.6
11/08	73420	75630	7.1	10.1	90.2	92.9
27/08	105949	106607	4.2	4.8	95.2	95.8
Total	**359631**	**355328**	**11.2**	**8.7**	**90.5**	**88.8**

Table 4. Scene date (day/month of the last image), algorithm burned area, reference burned area, commission error, omission error, burned match and reliability in percentages for year 2007.

2007	Alg [ha]	Ref [ha]	Comm %	Omission %	B. Match %	A. Reliability %
27/06	122041	129975	7.1	13.3	87.5	92.9
13/07	106922	111613	4.2	8.6	91.7	95.7
29/07	84500	86719	5.4	8.1	92.1	94.5
14/08	83659	87798	4.4	9.3	91.1	95.6
30/08	153121	155883	4.2	6.0	94.1	95.8
Total	**550602**	**571987**	**5.1**	**9.1**	**91.3**	**94.9**

Table 5. Scene date (day/month of the last image), algorithm burned area, reference burned area, commission error, omission error, burned match and reliability in percentages for year 2008.

2008	Alg [ha]	Ref [ha]	Comm %	Omission %	B. Match %	A. Reliability %
15/07	77942	91987	6.7	24.8	79.0	93.2
31/07	57383	53040	24.1	16.5	82.1	75.8
16/08	51192	59116	5.9	21.4	81.4	94.0
17/09	139085	157851	3.2	16.7	85.2	96.7
Total	**325602**	**361994**	**10**	**19.9**	**81.9**	**90.0**

Table 6. Scene date (day/month of the last image), algorithm burned area, reference burned area, commission error, omission error, burned match and reliability in percentages for year 2009.

2009	Alg [ha]	Ref [ha]	Comm %	Omission %	B. Match %	A. Reliability %
19/08	58495	69751	2.3	21.5	81.9	97.2

Table 7. Scene date (date/month of the last image), algorithm burned area, reference burned area, commission error, omission error, burned match and reliability in percentages for year 2010.

2010	Alg [ha]	Ref [ha]	Comm %	Omission %	B. Match %	A. Reliability %
19/06	73822	65861	18.1	7.4	91.7	81.8
05/07	111983	114114	8.2	10.1	90.1	91.8
06/08	150513	145396	10.7	7.3	92.4	89.3
22/08	152316	154458	6.8	8.2	91.9	93.2
07/09	194168	190690	6.9	5.1	94.8	93.1
23/09	211921	222384	4.4	9.3	91.1	95.6
Total	**894723**	**892904**	**9.2**	**7.9**	**92.0**	**90.8**

Table 8. Algorithm burned area, reference burned area, commission error, omission error, burned match, reliability in percentages and total scenes processed for the period 2004-2010.

Year	Alg. [ha]	Ref. [ha]	Comm %	Omission %	B. Match %	A. Rel.%	T. Scenes
2004	477140	490968	9.6	12.5	87.8	90.3	6
2005	319445	350256	4.4	13.9	87.3	95.5	5
2006	359631	355328	11.2	8.7	90.5	88.8	6
2007	550602	571987	5.1	9.1	91.3	94.9	6
2008	325602	361994	10	19.9	81.9	90.0	5
2009	58495	69751	2.3	21.5	81.9	97.2	2
2010	894723	892904	9.2	7.9	92.0	90.8	7
Mean	**426520**	**441884**	**8.2%**	**11.8%**	**88.6%**	**91.8%**	**Sum=37**

The mean burned Match for the whole 2004 – 2010 series was 88.6%, while the mean algorithm reliability was 91.8%. Mean commission error was 8.2%, while mean omission error was 11.8%. These results are considered excellent when one analyses similar studies found in the literature [Bastarrika, 2011], which normally indicate more limited classification skills; in addition, the study region is particularly difficult for mapping burned areas with mid-resolution imagery due to the low biomass volume and sparse vegetation in many locations. The results of the classification algorithm for the remaining 15 images of the series, without validation of the fire scars, are listed in Table 9, with total burned area for each year and the corresponding number of processed images.

Table 9. Year, algorithm burned area and number of scenes processed.

	2000	2001	2013	Mean	Total
Burned Area [ha]	472817	461377	401922	**445372**	
Scenes	3	5	7		**15**

The means for the Algorithm Reliability and Burned Match obtained for the other subset of 37 images can be also included, thus resulting in a mean annual burned area for the total period of 432175 ha. The figure with the accumulated burned pixels was obtained for the whole period 2000-2013, and as it can be seen on Figure 3, most of the area covered by the image was burned; from the total 30707018 pixels of our study area, 23021994 were burned at some occasion, or almost 75% of the pixels.

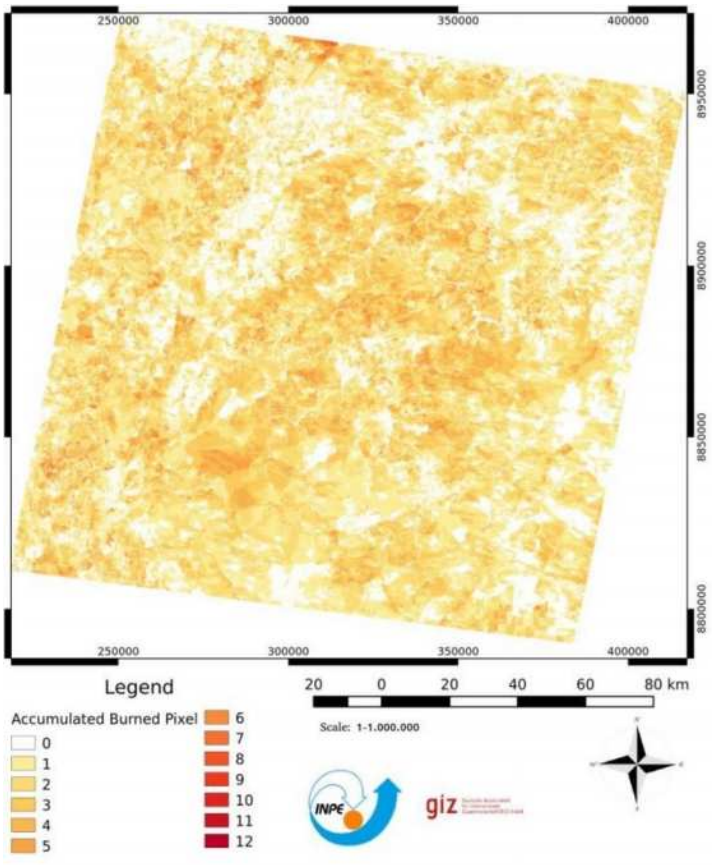

Figure 3. Cumulative burned pixels for the study area in the period of 2000-2013.

Conclusion

A relatively simple and reproducible concept for mapping burned area at the Cerrado-Jalapão region based on NDVI and NBR is presented. The Algorithm Reliability and Match coefficients suggest the usefulness of the tool developed and its application in other biomes. In particular, its use for conservation units could minimize the impact of land cover changes of anthropic origin.

Sudden changes in the spectral reflectance of the vegetation normally indicate perturbing events. The overlap of mapped burned scars with updated land use cover maps can identify the type of vegetation burned, allowing estimates of carbon and pollution emissions.

Agricultural land practices were a source of error in the mapping of fire scars, together with clouds and cloud shadows. Masking these three classes automatically will reduce the uncertainty of the process and improve the Burned Match; further work in this direction is currently in progress.

A reliable spatial reference is fundamental to validate a digital automatic process [Congalton 1991], but this condition is rarely found in the analysis of the results of algorithms to map burned area at regional and continental scales. The systematization of the processing stages herein proposed and their integration with a geographical data base engine could foster an operative system to process large image repositories. The implementation of software applications without proprietary libraries or closed systems grants the portability and free distribution of the developed tools, either in a dedicated system or as part of any processing chain.

Acknowledgments.

The authors acknowledge the support of the GIZ - German Technical Cooperation Agency through the MMA Project "Prevenção, controle e monitoramento de queimadas irregulares e incêndios florestais no Cerrado", as well as the scientific grants CNPq 309199/2008-5 and FAPESP 2010/19712-2.

References

Bastarrika. A.; Chuvieco, E. Martín, M.P. Mapping burned areas from Landsat TM/ETM+ data with a two phase algorithm: Balancing omission and commission errors. Remote Sensing of Environment. 2011. 105:1003-1012

Blaschke, T.; Lang, S.; Hay, G.J. Object-Based Image Analysis. Spatial Concepts for Knowledge-Driven Remote Sensing Applications. Springer. 2008. ISBN 978-3-540-77057-2

Candido, P.A. Monitoramento de Queimadas e Incêndios na Região do Parque Estadual do Jalapão em 2004 e 2013. 2014. Relatório Atividades GIZ, Internal Report.

Chander, G.; Markham, B.L.; Helder, D.L. Summary of current radiometric calibration coefficients for Landsat MSS, TM, ETM+ and EO-1 ALI sensors. Remote Sensing of Environment. 2009. 113:893-903

Congalton, R.G. A Review of Assessing the Accuracy of Classifications of Remotely Sensed Data. Remote Sensing of Environment. 1991. 37:35-46

Gitelson, A.A.; Kaufman, Y.J.; Merzlyak, M.N. Use of a Green Channel in Remote Sensing of Global Vegetation from EOS-MODIS. Remote Sensing of Environment. 1996. 58:289-298.

INMET. Instituto Nacional de Meteorologia, Climatologia da Faixa Normal – dados de 1961-2010. http://www.inmet.gov.br/portal/index.php?r=clima/faixaNormalPrecipitacaoTrimestral. Access on 14/July 2014.

INPE – Instituto Nacional de Pesquisas Espaciais – Projeto Queimadas. 2014. http://www.inpe.br/queimadas Access on 14/July/2014.

Key, C.H. Benson, N.C. Landscape assessment (LA): Sampling and Analysis Methods – Remote Sensing of severity, the Normalized Burn Ratio. USDA Forest Service Gen. Tech. Rep. RMRS-GTR-164-CD. 2006. LA1-LA5.

Klink, C. and Machado, R.B. Conservation of the Brazilian Cerrado. Conservation Biology, 19 (3), 707-713, 2005.

MMA – Ministério do Meio Ambiente. Plano de Ação para Prevenção e Controle do Desmatamento e das Queimadas no Cerrado, Brasília, 2010. http://www.mma.gov.br/estruturas/201/_arquivos/ppcerrado_201.pdf Access on 14/July/2014.

MMA – Ministério do Meio. Ambiente. Contra o fogo no Cerrado. 2012. http://www.mma.gov.br/informma/item/8482-contra-o-fogo-no-cerrado Access on 14/July/2014.

MMA – Ministério do Meio. Ambiente. O Bioma Cerrado. http://www.mma.gov.br/biomas/cerrado Access on 15/July/2014.

MMA – Ministério do Meio Ambiente. Plano de Ação para Prevenção e Controle do Desmatamento e das Queimadas no Cerrado. 2014b. http://www.mma.gov.br/florestas/controle-e-preven%C3%A7%C3%A3o-do-desmatamento/plano-de-a%C3%A7%C3%A3o-para-cerrado-%E2%80%93-ppcerrado . Access on 14/July/2014.

Miller, J.D.; Thode, A.E. Quantifying burn severity in a heterogeneous landscape with a relative version of the delta Normalized Burn Ratio (dNBR). Remote Sensing of Environment. 2007. 109:66-80.

Prado dos Santos, R.; Crema, A.; Szmuchrowski, M.A.; Asado, K. Kawaguchi, M. Atlas do Corredor Ecológico da Região do Jalapão. 2011. Instituto Chico Mendes de Conservação de Biodiversidade. Versão Digital.

SEPLAN – Secretaria de Planejamento e Meio ambiente. Plano de Manejo do Parque Estadual do Jalapão, Palmas, TO, 132 pp. 2003.

Stroppiana, D.; Bordogna, G.; Carrara, P.; Boschetti, M.; Boschetti, L.; Brivio, P.A. A method for extracting burned áreas from Landsat Tm/ETM+ images by soft aggregation of multiple spectral indices and a region growing algorithm. ISPRS Journal of Photogrammetry and Remote Sensing. 2012. 69:88-102.

USGS – United States Geological Survey. 2014. http://www.earthexplorer.usgs.gov

A wearable system for firefighters smoke exposure monitoring

P. Azevedo[a], F. Marques[b], J.M. Fernandes[c], J.H. Amorim[b], J. Valente[b], A.I. Miranda[b], C. Borrego[b], J.P.S. Cunha[a,c]

[a] INESC-TEC/Faculty of Engineering, University of Porto, Portugal. *paulo.r.azevedo@inescporto.pt, jpcunha@fe.up.pt*
[b] *CESAM & Department of Environment and Planning, University of Aveiro, 3810-193 Aveiro, Portugal, fabiomauricio@ua.pt, amorim@ua.pt, joanavalente@ua.pt, miranda@ua.pt, cborrego@ua.pt*
[c] *IEETA/Department of Electronics, Telecommunications and Informatics, University of Aveiro, 3810-193 Aveiro, Portugal, jfernan@ua.pt*

Abstract
Firefighters (FF) have to deal in their routine with dangerous situations, exposing themselves to extreme environmental conditions, which can put their lives at risk. Extreme heat exposure, smoke inhalation and reduced visibility are among the most significant hazards to firefighters involved in the suppression of forest fires. In this sense, some new technologies were built addressing the monitoring of firefighters health in the field, mainly sport-oriented solutions adapted for both scientific studies and commercial solutions. However, none of those aim at the mitigation of the main reason for incidents involving firefighters: the exposure to dangerous concentrations of air pollutants.
Our purpose is the development of an integrated hardware and software solution that allows the online monitoring of vital and environmental parameters, helping the FF to preserve their personal health and safety. The system is composed of a specific hardware device attached to the helmet that measures several parameters of interest (e.g. elevation, air temperature, atmospheric pressure, luminosity, exposure to carbon monoxide and nitrogen dioxide), and a mobile application running in a smartphone, which processes information gathered by the helmet hardware to determine if the firefighter is at an acceptable level of exposure/danger and triggers an alarm, if necessary.
From an operational point of view, this work proposes a cost-effective solution to monitor FF smoke exposure in typical adverse scenarios such as forest fires, allowing the detection and mitigation of hypothetical intoxication incidents. The hardware component is easily integrated in standard firefighter's protection equipment and the mobile application can run in any "off-the-shelf" mobile computing device. Beyond the stand-alone firefighters monitoring perspective, this wearable technological solution opens several opportunities as a data source. In this sense, under development is the integration of the near real-time observations into a Decision Support System (DSS) aiming to provide knowledge-based aid to firefighters at critical decision-making situations, thus helping with the safe and successful management of fire fighting.

Keywords*: fire safety; smoke exposure; wearable sensor.*

Introduction

Firefighters (FF) have to deal, in their quotidian, with dangerous situations, exposing themselves to extreme environmental conditions, which put their lives at high risk. Extreme heat exposure, smoke inhalation and reduced visibility are among the most significant hazards to firefighters involved in the suppression of forest fires.
In this sense, there are some new technologies that enable the monitoring of some FF health parameters (e.g. heart rate, ventilation frequency, r-r interval) for commercial [Zephyr Technology, 2014] and scientific purposes [Heimburg *et al*., 2006]. However, these technologies are only partial solutions and mostly oriented to the offline analysis of physiological data, not taking into consideration the problem

of aiding the FF in the terrain nor the needed environmental data. Even the commercial solutions are actually adaptations of sport-oriented systems, and are not well suited for realistic operational conditions [Teie, 2005], letting important issues as ergonomic, needed monitoring variables or operational concerns out of their scope.

An illustrative example is the synergy between wearable technologies and mobile computing [Coimbra *et al*., 2012], in which FF were monitored by their own smartphone [Colunas *et al*., 2011] and using wearable sensors [Cunha *et al*., 2010, Cunha, 2012] (see Figure 1). In this previous work, physiological variables were nicely adapted to a wearable system that was specifically developed to FF requirements. Nevertheless, the needed environmental variables were not integrated.

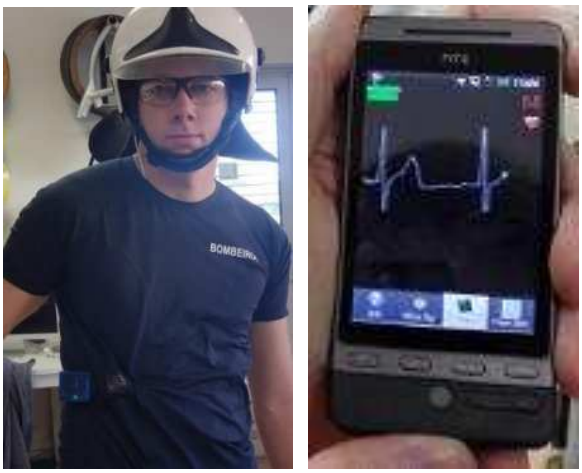

Figure 1. Vital Responder setup: wearable hardware (on the left) and the mobile application (on the right).

Recognising the power of mobile computing devices features (e.g. computational power, wireless networks) using wearable hardware as terrain sensors, our purpose is to contribute for mitigating one of the main reasons for incidents involving firefighters: the exposure to dangerous concentrations of air pollutants [Miranda *et al*., 2012]. The main goal of this research is the development of an integrated hardware and software solution that allows online monitoring of vital and environmental parameters that influence the firefighter's health and safety.

System Description

To achieve the referred goal, two technological paradigms were merged: wearable electronics development and mobile programming, as it is depicted in Figure 2.

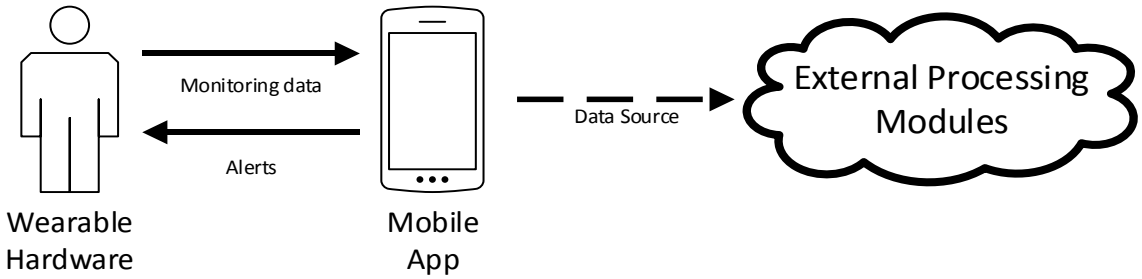

Figure 2. System interaction.

The wearable hardware consists on a sensored helmet unit (Figure 3) to be used by the firefighter. This device allows the measurement of elevation, air temperature, atmospheric pressure, as also the personal exposure to carbon monoxide (CO) and nitrogen dioxide (NO_2). These specific air pollutants are known to cause short term effects (e.g. headache, dizziness, nausea, dyspnea, loss of consciousness) [Treitman *et al*., 1980; Morrow, 1984; Sandstrom *et al*., 1990; Prockop *et al*., 2007] that can put a firefighter's life in immediate danger. In order to allow online processing of these variables, the hardware module transmits the information over a Bluetooth network that can be used by smartphones to receive and process the information.
The mobile application uses the information gathered to determine if the firefighter is at an acceptable level of exposure/danger and triggers an alarm, if necessary. Another potential feature of the mobile App is to add some information (e.g. GPS, fall detectors) to the hardware stream and relay it to some kind of superior monitoring platform over Wi-Fi networks. This information can then be used by the team leader to monitor his crew.

Hardware Modules

The hardware modules were developed in-house. The development process was based on the requirements identified based on the outcomes from two research projects:

- FUMEXP (PTDC/AMB/66707/2006), with special emphasis on sensors choice for a set of air pollutants of interest and corresponding typical ranges;
- VitalResponder (CMU/PT/CPS/0046/2008), due to the usability concerns and the technological possibilities already assessed.

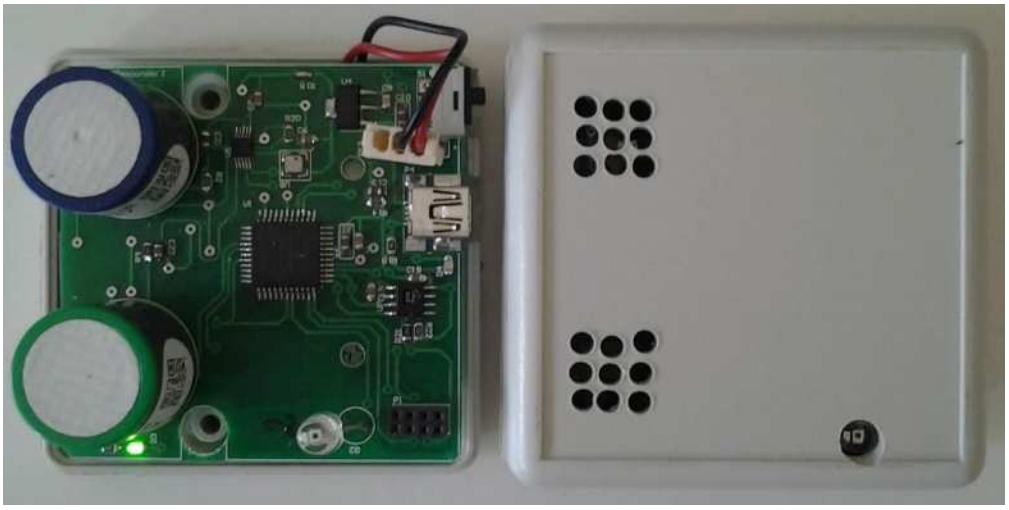

Figure 3. Helmet module prototype: hardware picture (on the left) and its integration on suitable box (on the right).

First of all, a requirement analysis was performed taking into consideration the state of the art on firefighters monitoring systems. It was concluded that the commercial solutions available for the monitoring of human exposure (usually in industrial environments) are not well suited to firefighting operational conditions due to their weight, discomfort and positioning. To mitigate these gaps, and after consulting stakeholders from several fire departments, a hardware device was designed with the objective of being placed on the firefighter's helmet. This approach presents several advantages, but the most representative are:

- ergonomy: with an approximate weight of just 150 g the device becomes imperceptible to the firefighter that is being monitored;
- proximity to the firefighter airways, allowing accurate measurement of the pollutants inhaled;

- usability: once the helmet is a part of the mandatory protection equipment, firefighters do not have to take extra concerns about the monitoring device;
- endurance: due to the environmental factors surrounding a wildfire scenario, it's very difficult to keep an electronic device working properly. For this reason, attaching the monitoring device on the helmet improves the hardware's safety and accuracy.

However, attaching a monitoring device on a firefighter helmet is not a trivial process due to its ratification standards (e.g. EN 443 for helmets hull, EN 16471 for wildland firefighting helmets). In order to surpass these constraints, an embedded helmet socket (Figure 4. left) was used to attach the monitoring hardware module (Figure 4. right). Originally, this socket was designed to support attachments as flash lights and fulfils the applied standards.

Figure 4. Helmet module prototype integration: original firefighter helmet (on the left) and helmet equipped with monitoring hardware (on the right).

Therefore, in order to build an electronic device small enough to be integrated on a firefighter helmet, we tried to achieve a suitable agreement between the technological possibilities and the most representative environmental variables to measure. Finding support on scientific studies [Ferreira *et al*., 2011], our helmet unit has sensors to monitor the data depicted on Table 1.

Table 1- Environmental data acquired by the Helmet module

Variable	Units
NO_2	ppm
CO	ppm
Atmo. Pressure	hPA
Elevation	m
Humidity	%
Temperature	ºC
Luminosity	%

Technologically, we developed a custom printed circuit board to support all the above mentioned sensors and the remaining necessary components:
- electronic front-ends to bridge all sensors with an Analog-to-Digital conversion
- a microcontroller (MCU) unit to gather and process data from all sensors;
- a bluetooth interface, in order to relay data frames processed by the MCU;
- a battery, providing an autonomy of 24 hours, approximately.

CO and NO_2 sensors were calibrated using a calibration gas with a known concentration (100 ppm for CO and 10 ppm for NO_2).

Mobile application

The mobile application is an evolution of the Android based DroidJacket system [Colunas *et al.*, 2011] with support to receive and process data from the helmet unit described on the above section. It can run in an off-the-shelve Android smartphone supporting bluetooth communication, or it can be integrated on a Wi-Fi network and relay data to any connected device.

To extend the DroidJackets physiological monitoring capabilities with the environmental data relayed by the new Helmet Unit we follow the application's original software architecture, replicating the functionalities implemented for VitalJacket®. This approach enables us to maintain all application features (e.g. visualization, persistence, danger alarms, network connection) on an already successful evaluation platform.

More specifically, pairing the smartphone with the Helmet Unit, the smartphone receives, displays (Figure 5), stores and relays all environmental data through a Wi-Fi network, if available.

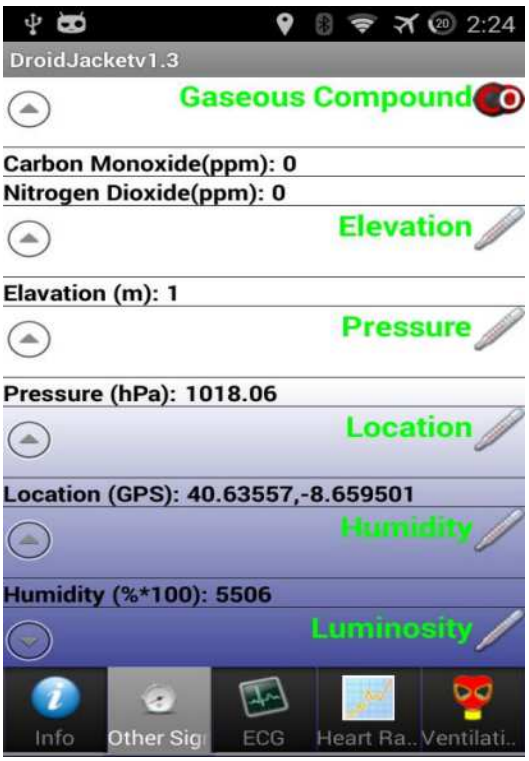

Figure 5 –Improved DroidJacket Version.

Besides the data provided by the Helmet Unit, and other external sensor (e.g. Vital Jacket), the application can use the smartphone's built-in sensors to provide additional information (e.g. GPS, accelerometers, battery).

Integrability and Scalability

The Hardware setup was built with the aim of integrating new sensors on an effortless manner, enhancing integrability and scalability of the overall solution of the Vital Responder project. In this case, we could integrate the previous physiological wearable platform [Coimbra and Cunha, 2012] with the environmental helmet monitoring unit and a GPS. In that sense, the main challenge was related with the sensors size and form-factor

At the software level, DroidJacket application was used and enhanced. It is an example of scalability, once it has been evolved over several iterations of the project with increasing new features [Marques *et al*. 2013]. At this point, the DroidJacket Android App can gather, in one smartphone, physiological data (ECG, heart rate and actigraphy, from VitalJacket®), environmental data (from Helmet Unit presented above) and GPS location. Furthermore, it enables to add more sensing devices up to the limit of the bluetooth connections (7 channels) or the smartphone processing capabilities.
Under development is an ad-hoc data networking technique that will allow the real-time data acquired in the terrain by several of these wearable monitoring equipments and its bridging to a cloud service that will allow numerical forecast that will enable projections of fire progression, smoke levels and critical exposure, aiming to permit safe and efficient positioning of crews.

2.4. System Evaluation

The whole system will be tested, on a stand-alone mode, during the summer of 2014. We will deploy the system on two fire departments, at two different operational zones. There will be firefighters equipped with our system and all monitored data will be stored on the smartphones, without connectivity between each other. Additionally, we will ask firefighters to produce mission reports to selectively tag relevant events (arrival to fire scene, approach a fire front, etc.) so that all collected data can be analysed for the intended evaluation.

Conclusions

Smoke exposure is identified as one of the most important cause of incidents among firefighters. Since the physiological monitoring of firemen has been already addressed, this work signifies one step ahead in this matter, pursuing not only the identification of high risk situations in the terrain, but also contributing to prevent them.
This work proposes a cost-effective solution to monitor firefighters smoke exposure in typical adverse scenarios such as forest fires, allowing the detection and mitigation of hypothetical intoxication incidents. The system is composed of a hardware component easily integrated in standard firefighter protection equipment and a mobile application that can run in any "off-the-shelve" mobile computing device.
Beyond the stand-alone firefighters monitoring perspective, this wearable technological solution opens several opportunities as a data source. In this sense, under development is the integration of the near real-time observations into a Decision Support System (DSS) aiming to provide knowledge-based aid to firefighters at critical decision-making situations, helping with the safe and successful management of fire.

Acknowledgements

The authors would like to thank the contribution of Oscar Pereira to the work here reported. This work was supported by European Funds through COMPETE and by National Funds through the Portuguese Science Foundation (FCT) within projects PEst-C/MAR/LA0017/2013 and VitalResponder2 (PTDC/EEI-ELC/2760/2012), and the Post-Doc grants of J.H. Amorim (SFRH/BPD/48121/2008) and J. Valente (SFRH/BPD/78933/2011).

References

Zephyr Technology, Available: http://zephyranywhere.com/training-systems/first-responders/ , (last accessed July 2014)

von Heimburg E. D., *et al*., Physiological Responses of Firefighters and Performance Predictors During a Simulated Rescue of Hospital Patients, *Ergonomics*, vol. 49, No. 2, 2006, 111-126

Teie W. C., *et al.* , *Firefighter's Handbook on Wildland Firefighting: Strategy, Tactics, and Safety*, 3th edn., U.S.:Deer Valley Press 2005

Coimbra, M., & Cunha, J. P. S., 2012. Vital Responder – Wearable Sensing Challenges in Uncontrolled Critical Environments. In F. Martins, L. Lopes & H. Paulino (Eds.), *Sensor Systems and Software* (Vol. 102, pp. 45-62): Springer Berlin Heidelberg.

Colunas M. M. F., Fernandes J.M.A., Oliveira I.C., Cunha J.P.S., 2011. Droid Jacket: a mobile monitoring system for a team, In Proc. of: *7th International Wireless Communications and Mobile Computing Conference*, IWCMC 2011, 2157-2161.

Cunha J.P.S., Cunha B., Pereira A.S., Xavier W., Ferreira N., Meireles L., 2010. Vital Jacket: A wearable wireless vital signs monitor for patients' mobility in Cardiology and Sports. 4th International ICST Conference on Pervasive Computing Technologies for Healthcare 2010 (ACM, IEEE and IMIA sponsored). Munich, Germany.

Cunha, J.P.S., 2012. *pHealth and Wearable Technologies: a permanent challenge*, in *Studies in Health Technology and Informatics*, B. Blobel, P. Pharow, and F. Sousa, Editors. 2012, IOS Press: Amsterdam. p. 185-195.

Miranda A.I., Martins V., Cascão P., Amorim J.H., Valente J., Borrego C., Ferreira A.J., Cordeiro C.R., Viegas D.X., Ottmar R., 2012. Wildland smoke exposure values and exhaled breath indicators on firefighters. Journal of Toxicology and Environmental Health - Part A: Current Issues 75 (13-15), 831-843.

Treitman RD, Burgess WA, Gold A. Air contaminants encountered by firefighters. Am Ind Hyg Assoc J 1980; 41:796-802.

Morrow PE. Toxicological data on NOx: an overview. J Toxicol Environ Health 1984; 13: 205-227.

Sandstrom T, Andersson MC, Kolmodin-Headman B, Stjernberg N, Angstrom T. Bronchoalveolar mastotytosis and lymphocytosis after nitrogen dioxide exposure in man: a time kinetic study. Eur Respir J 1990; 3:138-143.

Prockop LD, Chichkova RI, 2007. Carbon monoxide intoxication: an updated review. *Journal of the Neurological Sciences*, Vol. 262, 122–130.

Ferreira A.J., Cordeiro R.C., Ferreira P., Miranda A.I., Martins V. Viegas D.X., 2011. Firefighter occupational exposures in forest fire settings – Three years of the FUMEXP project, European Respiratory Journal, Vol. 38, p4169.

Marques F., Azevedo P., Cunha J.P.S., Cunha M.B., Brás S., Fernandes J.M., 2013. FIREMAN: FIRefighter team brEathing Management system using ANdroid. In Proc. Of: 17 *th International Symposium on Wearable Computers*,ISWC 2013, 133-134

Analysis of the effectiveness of fire detection systems in different dimensions

Agoston Restas

National University of Public Service, Budapest, Hungary, Restas.Agoston@uni-nke.hu

Abstract
Introduction: One of the key elements of the cheap but effective fire suppression is early fire detection and quick initial response. There are many ways of fire detection; in many cases taking an overview of the effectiveness is not useless. Methods: Firstly paper shows the basic principles of the economical effectiveness of the fire management. Afterwards, research turns to the different dimensions and basically counts with aerial flight patrol. Looking at the monitored forest as a flat area gives a 2 dimension analysis but as an articulated area gives a 3 dimension analysis. If research counts with the time scale, meaning the way weather condition changes, it gives a 4 dimension analysis. Results and discussion: Research says in the 2 dimension model the aerial flight patrol cannot be effective, a tower based fire detection system is required.
In case of 3 dimensions model the balance between the methods of aerial flight patrol or the tower based fire detection system depends on feature and rate of the area articulation. The 4 dimensions analysis says that the balance between the methods of aerial flight patrol or the tower based fire detection system can correlate to the fire weather index.

Keywords*: aerial patrol, UAS application, tower based fire detection system, dimension analysis*

Introduction

One of the key elements of the cheap but effective fire suppression is early fire detection and quick initial response. There are many ways of solutions for the fire detection, such as satellite in orbital equipped with special sensors, manned or unmanned aerial (UAV) flight patrol at different altitude, many kinds of tower based automatic fire detection systems, or mobile human surveillance. Each of them has operation costs, in many cases not negligible, therefore taking an overview of the effectiveness is not useless.
Satellite can be a very effective tool for fire detection but there are some problems with the application. Satellites at geostationary can monitor huge areas but the distance is too far from the Earth to detect hot spots in small size. Sensors with higher resolution could help to detect smaller size fire but there are other problems, like higher price or more false alarms (Pennypacker, 2013). Satellite with closer orbit than geostationary can be also a nice solution but keeping the distance from the Earth requires higher speed meaning that the same area can be monitored cyclically (Giglio at al., 2008). In this case we can count a *monitored time* and a *blind time*; latest means that area is not monitored continuously (Restas, 2012). This satellite can be a good solution at huge forested areas such as North and South America, Africa or Siberia.
Human surveillance is also a kind of fire detection method, however the effectiveness is many cases accidental. Closing out the human beings measuring the effectiveness of the human surveillance is more or less similar to tower based fire detection systems. Assuming continuous monitoring and taking into account the horizontal position of the "sensor" to the fire human surveillance can mean the one, on satellite installed sensor the other wings as extremes in the range of different fire detection solutions.
All method mentioned above belongs to strategic solutions for hot spot detection however at the beginning of the intervention managers also require tactical solutions. It can mean horizontal observation from the ground or human with special technical equipment like fire truck or UAS.

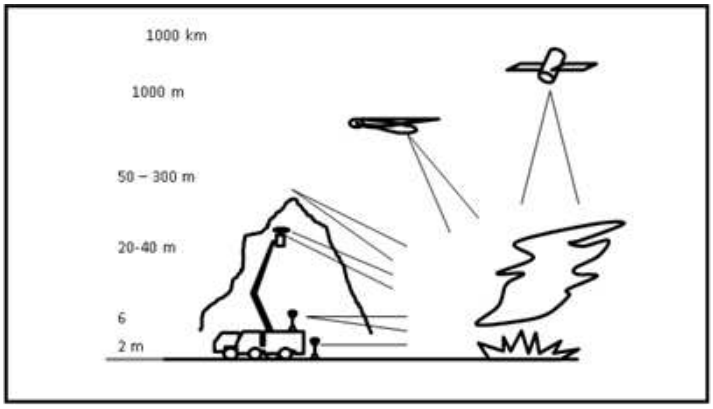

Figure 1. Different solutions for fire detection: from human on ground to on satellite installed sensors

Damage – time function analysis

When anybody assesses efficiency, it is usually the return on investment and the period of time required for such returns to be realized that we take into account. The concept of efficiency is applicable to firefighting as well, but the way it is applied differs from the traditional interpretation mentioned above. In the case of firefighting and other interventions, efficiency is measured either by the quantity of value saved or by the actual damage, which, of course, should be as small as possible.
The value of forest is not homogenous; it depends on variety, age, quality, etc. But forests have not only economical but a social, biological, goodwill, etc. value as well. The goodwill value is much higher than the simply economic value. It applies even more to national parks. Despite this statement this method basically takes into account only the economic value.
The value of saved forest is also not homogenous, neither in time nor in field. Usually it doesn't take into account the total price of the forest. Destruction depends on the age of the forest, the type of the trees, the combustible materials and weather parameters. They are separated not in a discrete value but a complex continuities function.
On the other hand, there are years when the risk is very high, the value of destruction is extreme and in other years much less. Let us look at this curve in the case of a forest fire. The damage-time function gives an exponential curve that diverges to infinity.

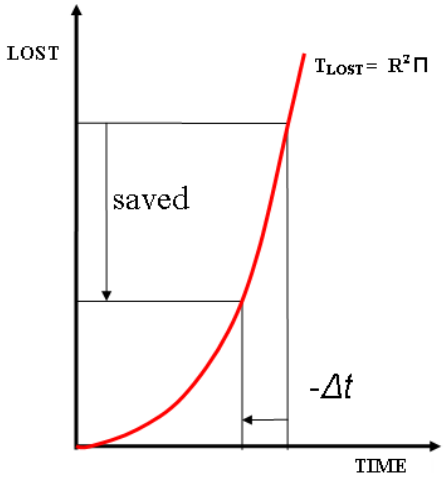

Figure 2. Damage-time function. Basic shape at uncontrolled forest fire

It is easy to recognise if for any period Δt is reduced, the area burnt and thereby the damage caused is reduced exponentially. The smaller the area affected by the fire, the smaller the quantity of resources to extinguish it.

Aerial patrol for hot spot detection – 2 dimensions analysis

Basic elements of the effectiveness

The basic assumption is that by using aerial patrol the fire service can save forest of more value than without it. The economic efficiency will materialize if the saved forest is more than the all expenditure of fire service regarding using aerial surveillance. At the strategical level, author means a bigger scale, let's say at a government level, we have to take into account all the expenditure of aerial surveillance and all the saved forest of the country.
Aerial patrol can detect hot spots very quickly and it is able to give the first fire report to fire brigades; it can reduce the time of first attack.

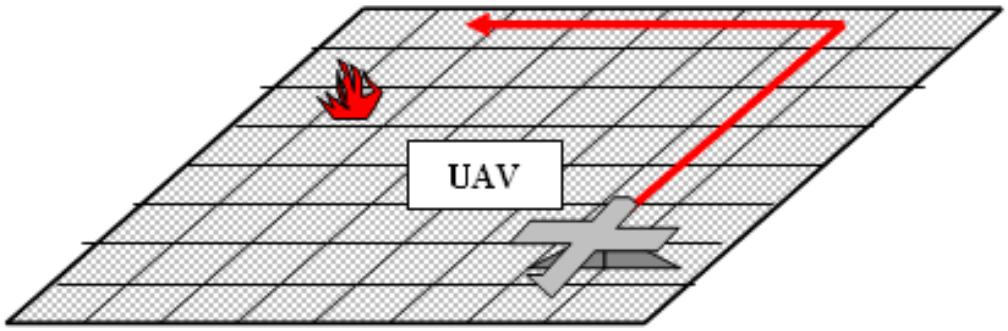

Figure 3. Aerial surveillance e.g. using UAV for hot spot detection

For hot spot detection spotter makes a patrol following the pre-programmed flight path usually as routine task. Obviously, the average delay of the aerial fire report must be less than the average delay of the civil report. This condition is necessary even if not sufficient for satisfying the requirements of economic efficiency of aerial surveillance, in this example UAV flight.
From the ignition (fire starts) till the aerial based fire report takes different time depending on the position of the UAV and the position of the ignited fire crossed by planned flight path. Obviously large number of fire detection (statistical data base) gives for the time of average fire report as a half time of the UAV patrol time. This statement can be accepted also by logical conclusion.

$$\bar{t}_{UAV\_report} = \frac{1}{2} t_{UAV\_patrol} \qquad (1)$$

$$\bar{t}_{UAV\_report} < \bar{t}_{Civil\_report} \qquad (2)$$

- t_{UAV_patrol} - full time of a flight patrol, made by UAV;
- t_{UAV_report} - average time of fire report given by UAV, making fire patrol;
- t_{Civil_report} - average time of fire report, given by civilians.

The other criteria for satisfying the economically efficiency is that based on aerial surveillance (e.g. UAV use) fire service must save forest of more value than the costs of the surveillance (aerial patrol).

A quick fire report results in quick answer; short uncontrolled fire means less damages but more saved value.
If the intervention starts very soon after ignition, the savings will come not just from the saved forest but also from a shorter use of the special equipment required to suppress the fire (figure 4).

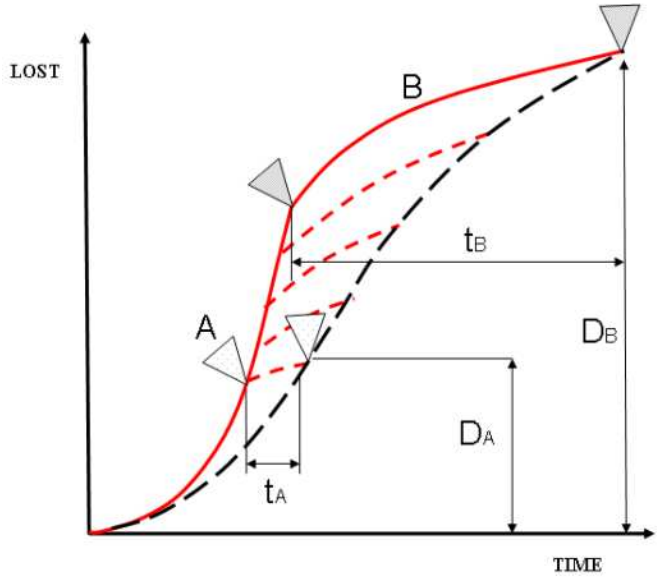

Figure 4. Structure of damage – time functions taking into account the quick fire report

Modelling the extinguishing of the fire by the damage – time functions the beginning of the response will break the fire curve (figure 2 → figure 4). The intensity and the length of the modified fire curve will depend on the time between the ignition and the beginning of the response. In case of A the time is shorter than in case of B therefore in case of A the intensity is lower and the length is shorter of the modified fire curve than in case of B (figure 4). The response in case of A results in lower damage (lost) and shorter time of intervention; this latest one results also in lower costs of the intervention. The shorter the time is between the ignition and the beginning of the response, the lower the intensity and the shorter the modified fire curve is. The above criteria can be expressed also by the next formulas:

$$S \Rightarrow D\left[\bar{t}_{Civil\_report} - \frac{1}{2}t_{UAV\_patrol}\right] > \Sigma C_{UAV\_patrol} \qquad (3)$$

$$\int_{\frac{1}{2}t_{UAV\_patrol}}^{\bar{t}_{Civil\_report}} D \; > \Sigma C_{UAV\_patrol} \qquad (4)$$

- S (D) - damages between the average term of civil report and aerial report;
- A - characteristic of suppression using UAV support;
- B - characteristic of suppression without UAV support.

Till the above formulas are valid the criterion of the economically based efficiency is satisfied at UAV patrol based fire management.

3.2. Moving to higher effectiveness – flight speed analysis

Since the efficiency obviously depends on the difference of the civil based and aerial supplied report's time, the question spontaneously arises, how can we make longer term between these reports? Based on the above formulas the delay of civil report is relatively stable, while the aerial based hot spot detection depends mainly on flight regimes. Therefore, making the aerial based hot spot detection more efficient we must face fly parameters. Logically we can test the flight speed, the altitude and the visual or camera (UAV) focus. During the analysis idealistic circumstances are supposed: there is no wind, it counts just with one hot spot, price of the technical elements, like camera does not change, weather does not limit the visibility, area is flat, etc. This latest one, the flat area means that we monitor 2 dimensions extension.

The purpose of reducing the average detection time requires the flight speed rise. With this process the flight path will not change but the time of aerial patrol will reduce. In case of a 24 km x 24 km area, with about a 180 kmh^{-1} flight speed and about a 3 km x 3 km monitored (camera) pixel in a moment (e.g. UAV) the monitored time for 1 pixel is 1 minute then 63 minutes are blind; the rate of monitored and blind area is 1:63. Raising the speed the cycle will reduce but the rate of the monitored and blind area will not. The problem is that the flight speed rise is objectively limited.

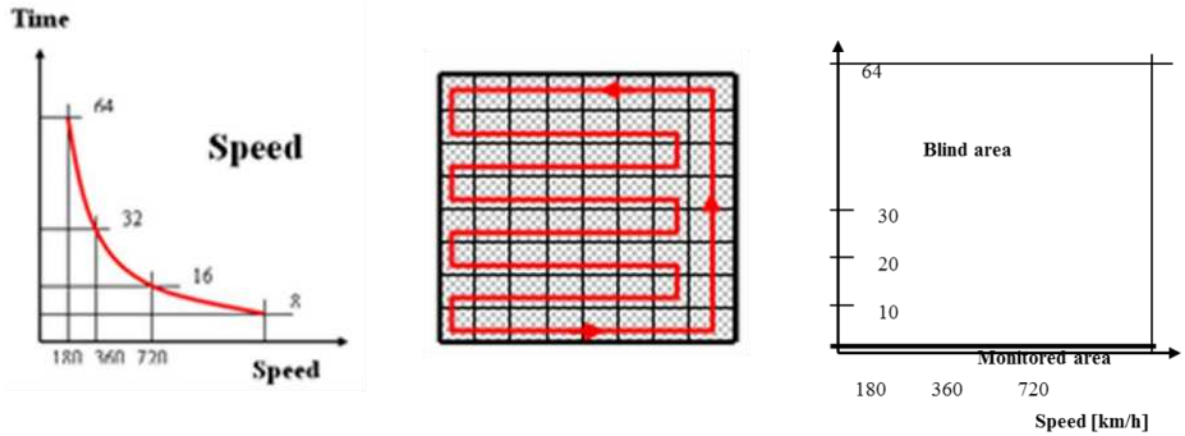

Figure 5– Example for moving towards the higher effectiveness of the fire detection. Raising the flight speed neither the flight path nor the rate of monitored and blind area do not change

3.3. Moving to higher effectiveness – camera focus and altitude analysis

The analyses of camera focus and altitude gives a little bit different results. Rising the altitude the on board installed camera monitors larger area (pixel). If the frame of the supervised area remains but the monitored pixel is larger than earlier, it means that the flight path can change; obviously it will be shorter. The flight path will move to the center of the area. Step by step continuing this process it reaches the end values when the flight path will concentrate at the middle point of the supervised area. It means our aerial means hangs on the central point of the area without flight speed! Logically the end value doesn't require the manned or unmanned flight; in this case a tower based camera system can be an alternative solution with the same effectiveness.

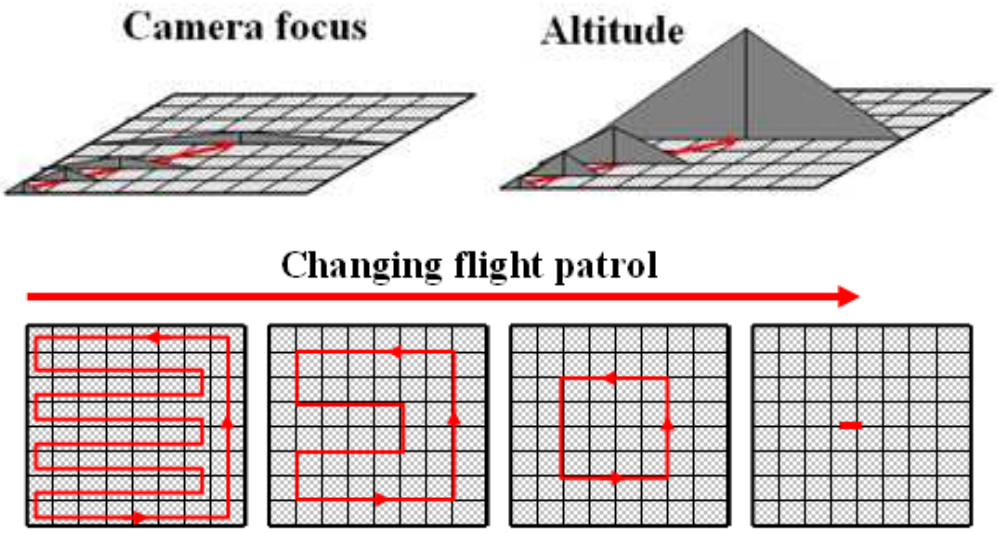

Figure 6– Example for moving towards the higher effectiveness of the fire detection. Raising the angle of camera focus or the altitude the flight path changes; it moves to the centre of the monitored area

Without deeper explanation it can be accepted the analysis of camera focus with similar way as above gives the same results. In this case there is no or insignificant difference between the altitude of aerial "surveillance" –hanging on the center point of the area – and tower based fire detection system.
In both cases the rate of the monitored and blind area also changes; it drastically turns beneficially. At the end of the process the rate is 1:0; which means all area is monitored continuously. Even if the effectiveness of both systems – aerial surveillance and tower based fire detection system – can be similar that is not sure in case of efficiency. If all the costs of using tower based fire detection system and the aerial surveillance are similar the efficiencies are also similar. In the assumptions we took into account same technical parameters – it means camera installed on board or tower too – therefore, the difference of the efficiency generates from the all costs of using the systems. This is true in case of UAV use too, even if it is supposed to be a cheaper solution than manned aircraft. In this case the tipping point – meaning the balanced costs – can be lower.

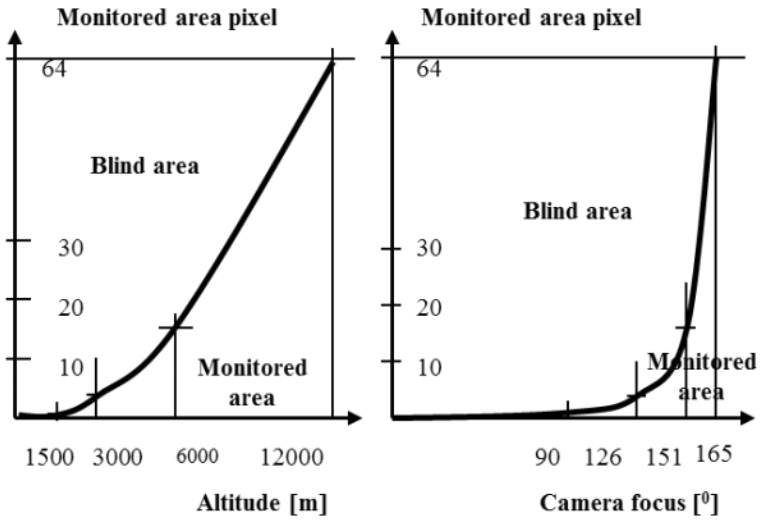

Figure 7– The rate of the monitored and blind area changes drastically positive

Geographically high articulated area – 3 dimensions analysis

Based on the above using tower based fire detection system in case of flat area – 2 dimensions extension – is more effective. The question is that in what or when the higher efficiency can be limited. As a first step, author extended flat – 2 dimensions – area to geographically high articulated – 3 dimensions – area.
In case of flat area tower based fire detection system can detect hot spots by direct way; it means there is no natural or manmade barrier to "see" the hot spots by the camera or sensor. In case of articulated areas the way for fire detection can be different. If the ignition is at the valley or at the bottom of the slope it can be in shadow of the hills, therefore, tower based fire detection system can detect fire in many cases only by indirect way; it means fire is in the shadow of the hill, camera or sensor cannot detect the fire but the smoke column or plum of it.
Naturally the smoke column in indirect way can be detected later than fire in direct way. Depending on different circumstances – wind power and direction, inversion, fire intensity, rate and way of the articulation, etc. – the detection of smoke column can delay significantly. It means that not just the effectiveness of the tower based fire detection system reduces but also the efficiency of it. The rate of reduction naturally depends on the rate and way of articulation; this is a circumstance that does not change in time. In case of high articulation reduction of effectiveness is surely higher; however, the rate of correlation between them requires advanced research. Moreover, the way of articulation is also important.

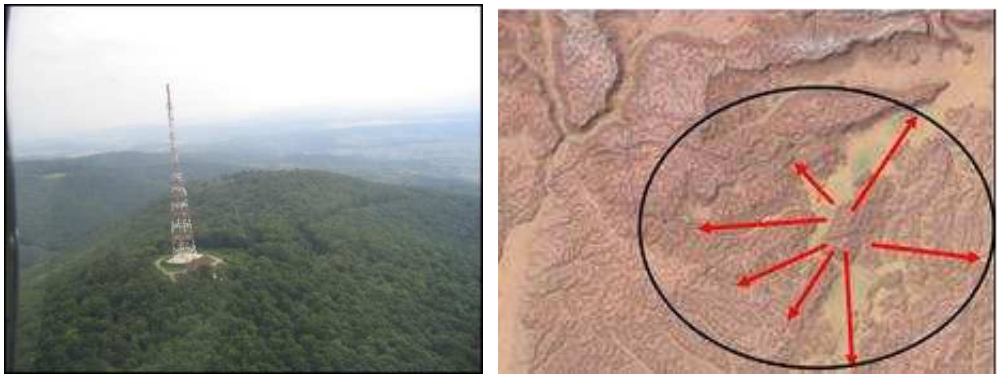

Figure 8– Example for a geographically good positioned tower based fire detection system. Aggtelek National Park - Szendro Fire Department, Hungary, Installation: 2005

There is an example where tower based fire detection system was installed in such an advantageous way that the valley's position looks like radiation spread from it (Restas, 2006). Positioning this kind of system is very important; it basically determines its potential of both effectiveness and efficiency. Good positioning – even if just a limited way, but – can reduce the shadow effect of hills.
When positioning of the system cannot be advantageous but the area is high articulated the rate of direct detection and indirect detection can be also very bad. The smoke emission from the valley stand ignited fire can be detected only with such delay so the advantages of low yearly costs evaporate.
Obviously the mission costs of aerial surveillance do not depend or just to a limited extent on the rate of area articulation. On the other hand, during flight patrol the shadow effect of hills can be relevant only for that pixel where the aircraft flies above. Naturally this effect is much lower in this case than in case of tower based fire detection system. Since the effectiveness and efficiency correlate to each other, the higher costs of aerial surveillance can be balanced by the lower effectiveness of the tower based system. It can be explained by other words too; the rate of catching hot spots in time by aerial surveillance is higher than in case of tower based system. The disadvantageous rate of monitored and

blind area is balanced by higher rate of quick fire report regarding shadow area. The above criterion can be expressed by formula (1) and (5) too.

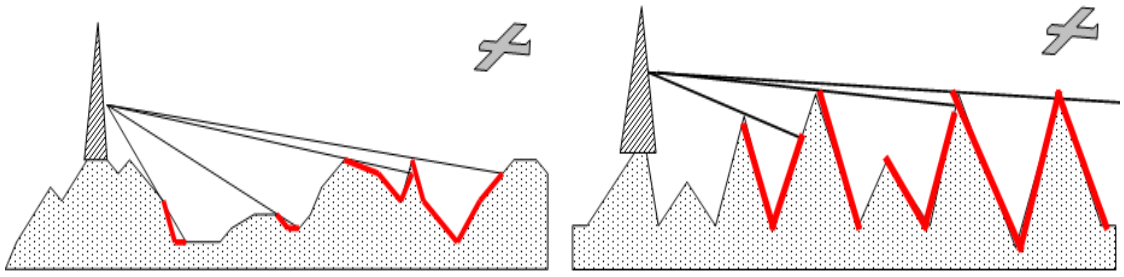

Figure 9– High articulated area: direct detection versus indirect detection (red colored slopes).

Aerial surveillance versus tower based fire detection system

$$\bar{t}_{UAV\_report} = \frac{1}{2} t_{UAV\_patrol} \qquad (1)$$

$$\bar{t}_{UAV\_report} < \bar{t}_{delay\_tower\_report} \qquad (5)$$

- $t_{delay\_tower\_report}$ -average delay of fire report, given by tower based fire detection system.

As the formulas (1) and (3) are logically same at time factor, formula (3) and (6) also have logical similarity in costs factor.

$$S \Rightarrow D\left[\bar{t}_{delay\_tower\_report} - \frac{1}{2} t_{UAV\_patrol}\right] > \Sigma C_{UAV\_patrol} \qquad (6)$$

It means also that it must satisfy other basic criterion too, as quicker average fire report than report of civilians. Till the above formulas are valid the criterion of the economically based efficiency is satisfied at aerial surveillance versus tower based fire detection system.

Extremely High Fire Weather Index – 4 dimensions analysis

Analysis above focused on physical extension of the given area; 2 dimensions counted as flat area, 3 dimensions as articulated area. In any case, there is no difference in time range; it takes into account time range as standard condition, however areas are threatened by fire risk usually cyclically so-called fire seasons. If the fire risk is cyclic, the question arises spontaneously, can it be even cyclic or not monitoring the area? If we take into account the cyclic – fire seasons – as time factor, it can mean as 4 dimensions analysis.
It is known, fire seasons strongly correlate to weather conditions; for measuring it different type of index – fire weather index (FWI) – were created, e.g. Canada: McArthur FWI (Dowdy at al., 2010), Germany: Waldbrandgefahrenindex WBI (König, 2007). That is obvious, area monitoring is the more required the higher the fire risk; in this case probability of matching hot spots is higher, which is shown by FWI. Therefore, it is practical to find correlation between FWI and effectiveness of fire detection.

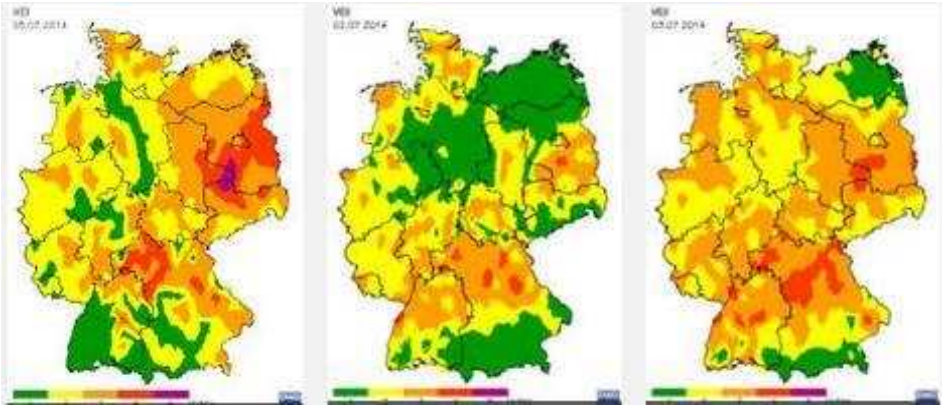

Figure 10. Examples for Waldbrandgefahrenindex, July 2014, Germany

Following the correlation, FWI based planning of applied system for fire detection does not require area monitoring all year round. This condition is not relevant for tower based fire detection system because its installation fix and it is able to work during all year. It means we need count with its all year costs. In case of aerial surveillance we have to count with costs only for that period when it is occasionally demanded.

There are some options for analyzing the efficiency: areas extension can be taken as 2 dimensions or 3 dimensions, however the essence of both results must be similar.

In case of same effectiveness – the average rate of fire detection is equal – the cheaper solution takes the higher efficiency, however this possibility has low chance. The other situation is when there are differences between both the average rates of the fire detection and the costs of using the different systems; obviously the higher costs of the aerial fire detection are suspected. In case of same efficiency the higher costs of aerial fire detection must be balanced by the higher rate of matching hot spots; it is the tipping point. Above this threshold – taking into account fix price for the flight hour – aerial fire detection is more efficient, otherwise not.

Otherwise, if there is difference in match of hot spot detection we have to calculate the rate of the difference between the saved forest and costs. In basic situation the criterion can be expressed by the next formula:

$$\Sigma C_{UAV\_occasionally} < \Sigma C_{Tower\_yearly\_costs} \quad (7)$$

$\sum C_{UAV\_occasionally}$ - occasional costs of UAV, used it at extremely high FWI;
$\sum C_{Tower\_yearly\_costs}$ - yearly costs of the tower based fire detection system.

Till the above formula is valid the criterion of the economically based efficiency is satisfied at extremely high FWI term.

It can be seen, this latest analysis contains the most vulnerable elements. Therefore, this paper just shows some directions for further research, exact definition of the tipping point as well as determines the correlation between the higher rate of matching hot spots and the efficiency requiring more study.

Summarizing

There is no doubt one of the key elements of the cheap but effective fire suppression is the early fire detection and quick initial response. There are many solutions for the fire detection however in many cases taking an overview of the effectiveness is not useless.

This paper firstly described the basic principles of the economical effectiveness of the fire management. Afterwards, research turned to the different dimensions and basically counts with aerial

flight patrol. Looking at the monitored forest as a flat area, it gives 2 dimensions analysis but as an articulated area it gives 3 dimensions analysis. Research counted also with the time scale, meaning that weather conditions can change; it gave the 4 dimensions analysis.
Based on the research in the 2 dimension model the aerial flight patrol cannot be effective, a tower based fire detection system is required. In case of 3 dimensions model the balance between the methods of aerial flight patrol or the tower based fire detection system depends on feature and rate of the area articulation. The 4 dimensions analysis says that the balance between the methods of aerial flight patrol or the tower based fire detection system can correlate to the fire weather index.
Research pointed out that applied analysis contains many vulnerable elements. Therefore, this paper just shows some directions for further research, exact definition of the tipping point as well as determines the correlation between the higher rate of matching hot spots and the efficiency requiring more study.

References

Dowdy, A.D., Graham A. Mills G.A., Finkele1, K., Groot, W.: Index sensitivity analysis applied to the Canadian Forest Fire Weather Index and the McArthur Forest Fire Danger Index; Meteorological Applications, 17 (3), pp. 298–312, September 2010 DOI: 10.1002/met.170

Giglio, L., Csiszar, I., Restas, A., Morisette, J.T., Schroeder, W., Morton, D., Justice, C.O.: Active fire detection and Characterization with the Advanced Spaceborne Thermal Emission and Reflection Radiometer (ASTER) Elsevier Science, Remote Sensing of Environment 112 (2008) 3055-3063

König, H.C.: Waldbrandschutz. Kompendium für Forst und Feuerwehr. Edition GefahrenAbwehr; Supplement (Band 1). Fachverlag Grimm, Berlin 2007, 197 S., ISBN 978-3-940286-01-7 oder ISBN 3-940286-01-X

Pennypacker, C.R., Jakubowski, M.K., Kelly, M., Lampton, M., Schmidt, C., Stephens, S., and Tripp, R.: FUEGO — Fire Urgency Estimator in Geosynchronous Orbit — A Proposed Early-Warning Fire Detection System; Remote Sensing, 2013 5(10) ISSN 2072-4292

Restas, A.: Integrated Vegetation Fire Management at Aggtelek National Park. Wildfire Management Program from Hungary; International 5th ICFFR, Conference on Forest Fire Research; Coimbra, Portugal, 2006

Restas, A.: An Approach for Measuring the Economic Efficiency of UAV Applications at Forest Fires Helping Decision Makers; AUVSI 2012: The First International Conference on Unmanned Systems in Israel. Tel Aviv, Israel, 2012.

Analysis of the thermophysiological response to cooling techniques in firefighters

R. Marcelo Abreu, António M. Raimundo* and Divo A. Quintela

ADAI-LAETA, Department of Mechanical Engineering, University of Coimbra - Pólo II, Rua Luís Reis Santos, 3030-788 Coimbra, Portugal. antonio.raimundo@dem.uc.pt; +351.239790738

Abstract
Firefighting has often been compared to a fight against an enemy capable of both material and lives' loss. It is a physical activity that requires a rare combination of strength, flexibility, endurance and intelligence to survive under extreme conditions. When it comes to firefighting, men fighting fires are potential victims of heat stress because they go through long periods of hard work in hot environments. The present work's target is the analysis of firefighters' thermophysiological reactions to heat stress situations caused by hyperthermia. Using a *software* that simulates the human body's thermophysiological behavior, several aspects, such as the fire intensity's influence on the thermal state of the firefighter, the exposure time and the body cooling technique used to attenuate heat stress, are highlighted. With the goal of embracing the most possible situations, three intensity levels of impinging radiation that come from the fire and affect men fighting fires are analyzed: low; medium; and high. Three alternative body cooling techniques are considered: the traditional one; by immersion of forearms and hands in water at 20ºC; and by immersion of forearms and hands in 10ºC water. Normal ingestion of water during recovering breaks (matching the cooling times) was also in focus in the simulations.

Keywords*: Safety firefighting; Human thermophysiological response; Body cooling techniques*

Introduction

Firefighting has often been compared to a fight against an enemy capable of both material and lives' loss. It is a physical activity that requires a combination of strength, flexibility, endurance and intelligence. Men fighting fires are potential victims of heat stress because they go through long periods of hard work in very hot environments (Barr *et al.*, 2009).
Heat stress is defined as the amount of heat that needs to be dissipated or produced in order to maintain the body in a safety thermal balance (WHO, 1969). When the thermoregulatory system is unable to compensate the overload of heat imposed to the human body, the system gets unbalanced and the individual begins to suffer from hot heat stress. This kind of thermal stress occurs due to internal factors, such as the metabolic heat and individual differences, due to the person activity intensity and the garments that uses, and due to the surrounding thermal environment (Sharkey, 1999; McLellan & Selkirk, 2005). Any job or task that may cause an increase in the body core temperature elevates the risk of hyperthermia (heat stress caused by over accumulated heat in the body). Operations involving high air temperatures, high level of moisture, impinging radiation from heat sources, direct physical contact with hot objects, or very intense physical activities have a high potential risk of hyperthermia. Firefighters on duty are potential victims of numerous pathologies related with excess of heat and the consequent increase in body core temperature. These heat-related illnesses are introversion (violent sweating, misleading, amnesia, etc.), heat-stroke (fainting and eventually stop of sweating, central nervous system alteration, etc.), superficial skin damages (pain and first-degree burns), and permanent injuries (second-degree burns or higher, brain damage or, in more serious cases, death).
In order to satisfy all the demands of the firefighting activity, it might be necessary to use recovery strategies for physical recuperation and for body cooling as a way of thermal stress attenuation (Barr *et al.*, 2009). The purpose of the body cooling process after the firefighting activity is to restore the

thermophysiological balance of the body in the shortest time possible and thus avoid harmful effects to health trying at the same time help the recovery of the individual for any subsequent activity.
Body cooling techniques can be passive or active. Passive cooling methodologies are much simpler to implement then the active ones. Normally, passive cooling is implemented by the moving of the firefighter to a secluded area far from the fire front, if possible shaded, and removing some of his personal protective ensemble. Active body cooling techniques requires the same actions as the passive ones and an additional cooling process, for instance forced air convection, immersion of body segments in water, etc. The drinking of water (preferably moderately cold) is also fundamental, but for body hydration as its effect on body cooling is only marginal.
The body cooling by forced air convection is based on the use of fans in order to impose a strong air speed (Carter *et al.*, 1999). This technique is reasonable effective but somehow unpractical to improve. By other hand, the techniques based on immersion of body parts in cold water have good efficacy if applied to areas with a high concentration of arteriovenous anastomoses, as the case of hands, forearms and legs (Magalhães *et al*., 2001; Barr *et al*., 2009). This technique is simple and easy to implement due to the availability of water supply from wells or rivers, which is usually at temperatures of the order of 15 to 20°C, making this technique often used. Studies have shown that for an individual who is in a state of hyperthermia the water temperature should be not lower than 10ºC in order not compromising vasodilation (Selkirk *et al*. 2004; Carter *et al.*, 2007; Barr *et al*., 2009). In the case of immersing the forearms and the hands in water, the highest cooling rates occur when the water temperature is 10°C (Giesbrecht *et al.*, 2007; Barr *et al*, 2009).
The main objective of this work is the establishment of secure protocols to fight high intensity fires. The emphasis will be given to the identification and analysis of the effectiveness of body cooling techniques capable to mitigate the risk of heat stress by hyperthermia. It also aims to determine the influence of the intensity of the fire on the risk of incidents related with hot heat stress, as well as the maximum exposure times of firefighting to prevent any body thermal conditions that may constitute a hazard.
Three intensity levels of radiation are considered: low, medium and high. As alternative body cooling techniques, applied during regular time-breaks, attention was given to the most traditional passive method (the firefighter goes away from the fire front to rest in a shaded location) and to the immersion of forearms and hands in water at 20ºC and at 10ºC. During these periods the firefighter is dressed with his personal protective ensemble, but without the helmet, the balaclava, the coat, and the gloves. The normal ingestion of water was also taken into account.

2. Calculation Tool

To obtain the results presented in this study, a computer program implemented by the authors (Raimundo and Figueiredo, 2009; Raimundo *et al*. 2008 and 2012) is used for the simulation of heat and mass transfer and thermophysiological response of a male firefighter exposed to extreme environmental conditions, such as those occurring in the proximity of a high intensity fire front. This program is composed by nine modules. However, for present purposes are used only the ones for the calculation of (*i*) person thermophysiological response, (*ii*) heat and water transport through the clothing, (*iii*) heat (by conduction, convection and radiation) and mass exchange between the external surface of clothing (or skin) and the environment and surroundings, (*iv*) start and evolution of skin injuries (pain and burn) and (*v*) detection of specific incidents within the human being.
The simulation of man thermophysiological response is based on the Stolwijk (1971) thermoregulation model, improved with knowledge found in the literature (e.g., Henriques, 1947; Weaver and Stoll, 1969; Konz *et al*., 1977; Wissler, 1985; Huizenga *et al.*, 1999; Fiala *et al*., 1999; Tanabe *et al.*, 2002). This enhanced 89-node model considers the human body divided in 22 segments (face, scalp, neck, chest, abdomen, upper back, lower back, pelvis, left shoulder, right shoulder, left arm, right arm, left forearm, right forearm, left hand, right hand, left thigh, right thigh, left leg, right leg, left foot and right

foot). Each body segment is composed of 4 layers (core, muscle, fat and skin), the 89th node being the central blood compartment. The model was implemented for an average man of 1.72 m tall, weighing 74.43 kg and with 14% of body fat (1.869 m^2 of skin). For other anthropometric data, the appropriated coefficients are proportionally changed in function of the body weight, skin area and body fat. Nevertheless, the model does not take into account the influence of barometric pressure and hydration status of the subject, because there is a lack of information in the literature about the relationship between these physical and physiological parameters and the human thermophysiological response.
The simulation of heat and water transport through the clothing is based on the formulation purposed by Havenith *et al*. (2002). The calculations are made for each specific human body segment. Then, individual values of the local clothing parameters (intrinsic insolation, mass, specific heat, vapour permeability and radiation emissivity) must be specified for each of the 22 human body segments considered. Each section is either completely clothed or nude.
The modeling of skin burn process implemented in the software is based on Henriques' theory (Henriques, 1947; Weaver and Stoll, 1969), which represents the skin thermal damage as chemical rate phenomena. As they don't start at same instant, the prediction of the skin pain threshold is also useful. This is important because, as reported by Stoll and Greene (1959), when the pain is felt, it is often too late to avoid a 2nd degree skin burn or, in some extreme situations, a heat stroke or even death. Empirical correlations have been developed that allow the prediction of the time until pain is felt, some of them reported in Wenger (1988), SFPE guide (2000) and Gagnon (2000). In the present program, the onset of skin pain is marked when epidermis-dermis interface temperature (T_{edi}) reaches 45ºC (Havenith and Heus, 2000) or when Henriques (1947) integral injury parameter (Ω) equals 0.53, depending on what occurs first (generally, T_{edi} = 45ºC).
In order to understand the significance of the calculated body temperatures, it is necessary to identify the values for which there is the probability of occurrence of specific incidents in the human body. Normally, the rectal temperature is used to identify the risk of thermal injuries. Nevertheless, the temperature of blood reaching the hypothalamus is regarded as a major afferent stimulus for the intensity of the effective response of sweating, vasomotor activity and shivering. Then, a better relationship may be expected between hypothalamus temperature (T_{hyp}) and the various physiological and sensory states (Pascoe *et al*., 1994; Kenney *et al*., 2004, Raimundo and Figueiredo, 2009; Raimundo *et al*., 2012). In the module of the program for the detection of specific incidents, the temperature limits are set as function of the hypothalamus temperature (T_{hyp}) following the Pascoe *et al*. (1994) scale: $\leq$ 25ºC → death, $\leq$ 28ºC → ventricular fibrillation, $\leq$ 30ºC → stop shivering and fainting, $\leq$ 34ºC → introversion and violent shivering, 34 < T_{hyp} < 39ºC → normal thermoregulation, $\geq$ 39ºC → introversion and violent sweating, $\geq$ 41ºC → heat stroke (stop sweating and fainting), $\geq$ 42ºC → brain damage (permanent injuries) and $\geq$ 44ºC → death.

Problem Description

It is assumed that the firefighter in question has a physique corresponding to the average of worldwide adult male population. This corresponds to 1.72 m tall, 74.43 kg of weight and 14.5% of body fat (Tanabe *et al*., 2002; Raimundo and Figueiredo, 2009).
The protocol adopted in this study submits the firefighter to several phases. Each firefighting period is followed by a time break where a body cooling technique is applied and a normal ingestion of water is also taken into account.
Three alternative body cooling techniques were analyzed: the most traditional method (the firefighter goes away from the fire front to rest in a shaded location) and the immersion of forearms and hands in water at 20ºC and at 10ºC. With the aim to determine how long it took until the manifested of the various heat stress related pathologies, simulations were also performed without the application of any cooling technique.

In order to verify the usefulness of each body cooling technique, simulations were made taking into account three levels of fire intensity: low, medium and high. The corresponding impinging radiation fluxes are quantified in the Table 1.

Table 1. Characterization of the impinging radiation fluxes for the various fire intensities.

Radiation from / Intensity	Impinging radiation fluxes [W/m^2]		
	Low	Medium	High
North	3 000	6 000	9 000
South	60	120	180
East	1 200	2 400	3 600
West	1 200	2 400	3 600
Top	120	240	360
Ground	60	120	180

The following phase sequence was assumed: neutral (stabilization), pre-firefighting, firefighting, time break with cooling, firefighting, time break with cooling, firefighting, time break with cooling.
The neutral phase is foreseen to ensure that all firefighters submitted to this protocol start equally in a state of thermal neutrality. It should be noted that at this stage it is considered that the firefighter is nude.
During pre-firefighting the firefighter is moving towards the scene of the fire or making preparations for firefighting in this vicinity. At this stage the firefighter is dressed with a shirt, pants of protective clothing and boots.
The firefighting phase is when the firefighter is in front of the fire to fight it. It is assumed that the firefighter is facing the fire and thus exposed to incident radiation from the flame which varies according to the intensity of the fire (see Table 1). At this stage the firefighter is equipped with all parts of his personal protective ensemble.
The cooling phase aims to lower the core temperature of the firefighter in order to prevent the harm caused by heat exposure and to recover him in the shortest time possible. The firefighter is dressed with protective clothing but without: the helmet, the balaclava, the coat, and the gloves.
The simulation process requires a complete characterization of each phase. Namely, it must be defined the firefighter parameters (activity intensity, posture, orientation relatively to the fire, garment and food or water intake), the description of the thermal environment (temperatures, impinging radiation, relative humidity, etc.) and several calculation controlling parameters. A short of the required parameters is summarized in Table 2.

Table 2. Summary of the parameters required for the simulation of each phase.

Parameter	Neutral phase	Pre-firefighting phase	Fire fighting phase			Time break and cooling phase
			Low intensity	Medium intensity	High intensity	
Duration	120 min	30 min	20 min	15 min	10 min	15 min
Activity level	0.8 met	1.5 met	3.0 met	3.0 met	3.0 met	1.0 met
Man posture	Sitting	Standing	Standing	Standing	Standing	Sitting
Man orientation	North	North	North	North	North	North
Mass of food ingested	0	0.66 kg	0	0	0	0.66 kg
Temperature of food	0	15ºC	0	0	0	15ºC

Specific heat of food	0	4 186 J/(kg ºC)	0	0	0	4 186 J/(kg.ºC)
Clothing global intrinsic insolation	0.00 clo	1.53 clo	2.45 clo	2.45 clo	2.45 clo	1.53 clo
Total mass of clothing (including the helmet and the boots)	0.0 kg	2.8 kg	5.3 kg	5.3 kg	5.3 kg	2.8 kg
Clothing specific heat	1 000 J/(kg.ºC)	1 000 J/(kg.ºC)	1 000 J/(kg.ºC)	1 000 J/(kg.ºC)	1 000 J/(kg.ºC)	1 000 J/(kg.ºC)
Clothing global vapour permeability	1.00	0.42	0.22	0.22	0.22	0.42
Clothing global external surface emissivity	0.93	0.91	0.90	0.90	0.90	0.91
Air temperature	29ºC	35ºC	35ºC	35ºC	35ºC	35ºC
Surrounding temperature	29ºC	30ºC	40ºC	40ºC	40ºC	30ºC
Air relative humidity	50%	40%	40%	40%	40%	40%
Air velocity	0.1 m/s	3.0 m/s	5.0 m/s	5.0 m/s	5.0 m/s	3.0 m/s
Impinging radiation	0	0	Values from Table 1			0

Results and Discussion

As far as safety is concerned, the most important indicators seem to be the times delays for the starting of heat stroke (fainting) and of skin pain, mainly the first one. These and other pathologies can occur, but only for continuous firefighting circumstances (without time breaks). This aspect is remarked in Table 3, where the instants for the beginning of skin pain, introversion, heat stroke, brain damage and lethal conditions, are represented as functions of the intensity of the radiation that impinges the firefighter.

Table 3. Time delay (after firefighting start) for the occurrence of undesired pathologies with the man for continuous firefighting circumstances.

Time delay [minutes] for	Impinging radiation intensity		
	Low	Medium	High
Skin pain	130	74	50
Introversion	23	15	12
Heat stroke	45	29	21
Brain damage	64	39	28
Death	128	74	50

As stated in Table 3, undesired pathologies can occur with the man if no time breaks are applied. The threshold for introversion is a good indicator for exposure limits that must not be exceeded. However, even for low incident radiation flux, this pathology and worst can occur for a continuous firefighting. Skin pain situation is reached only after death. Then no pain is felt by the firefighter, which can be a trap. This fact was also reported in the bibliography (e.g. Stoll and Greene, 1959; Raimundo and Figueiredo, 2009). This is perhaps one of the reasons why many experienced firefighters refuse to wear protective clothing in some body parts (ears, hands, neck, etc.). Traditionally the ears were used by firefighters as in indicator of dangerously high temperatures. A good clothing insolation protects against the incoming of external heal but also can allow a firefighter to stay in dangerously hot places, and remain there for unsafe times without any warning.

To avoid the undesired pathologies the firefighter must stay enough away from the fire to be exposed to impinging radiant fluxes lower than the specified in Table 1. If it is not possible, then the firefighting period must be of limited duration and followed by recovering periods. It is recommended the application of a body cooling technique during these time breaks, which is the main subject of this work.

In the analysis of the results for firefighting following the protocol defined in previous section (with recovering body cooling periods), the emphasis is given to the hypothalamus, rectal and skin temperatures and to the maximum variation of the heat stored by the body over time. This is due to the fact that these variables are considered to be the most important to characterize the evolution of the thermal state of the human body. The main conclusions will be drawn about the relationship between these factors and the intensity of impinging radiation on the firefighter and of the recovery technique used.

In Figures 1, 2 and 3 are represented the results obtained with the simulations for the evolution of the thermophysiological state of the firefighter during the protocol adopted, assuming that the firefighter keeps a distance from the fire front from which results a low intensity of incident radiation and for the three cooling techniques considered.

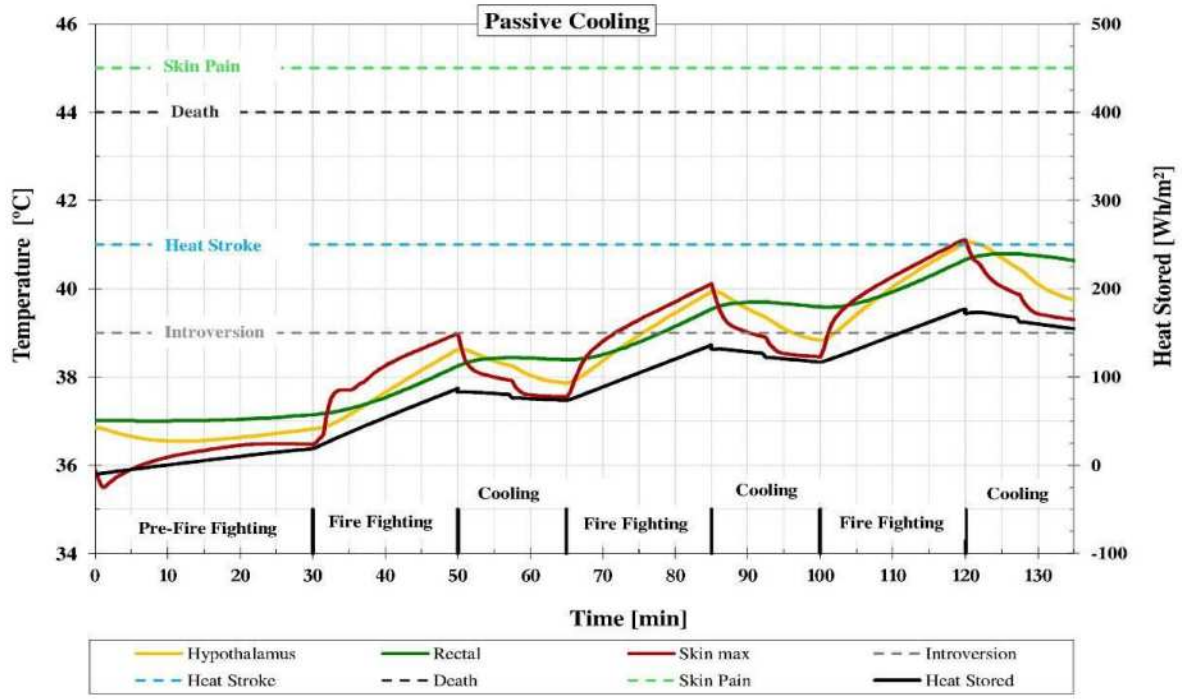

Figure 1. Evolution of firefighter thermophysiological state for low intensity incident radiation and passive cooling recovery.

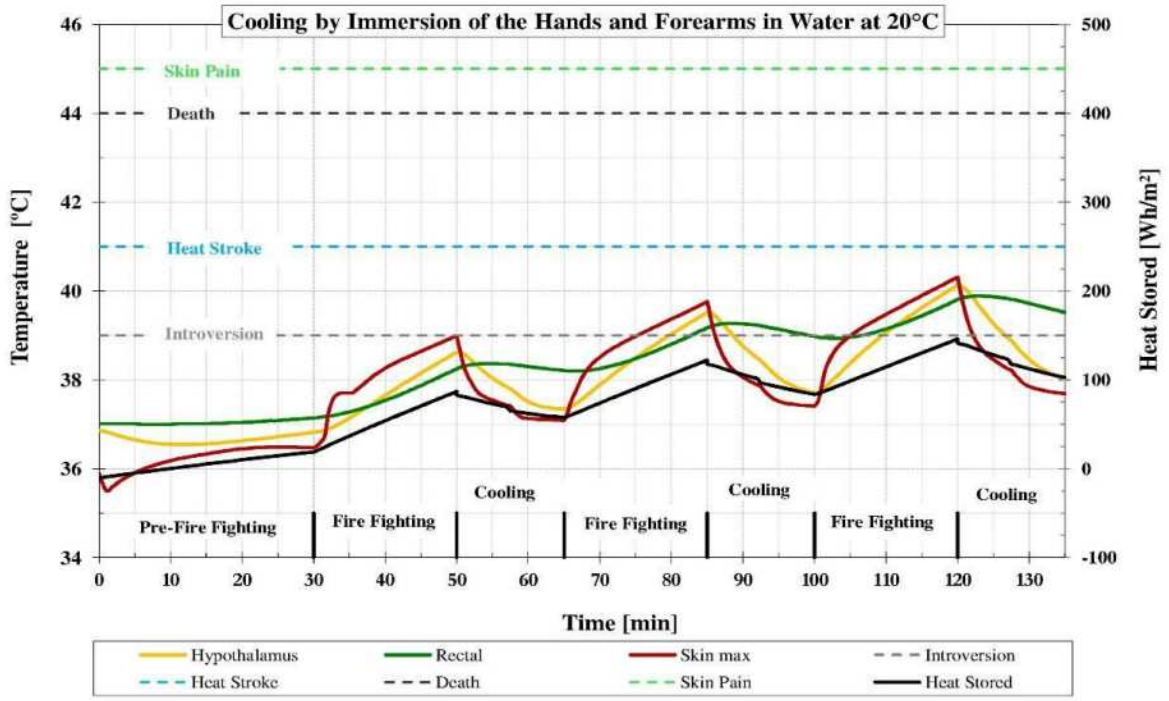

Figure 2. Evolution of firefighter thermophysiological state for low intensity incident radiation and cooling by immersion of the hands and forearms in water at 20°C.

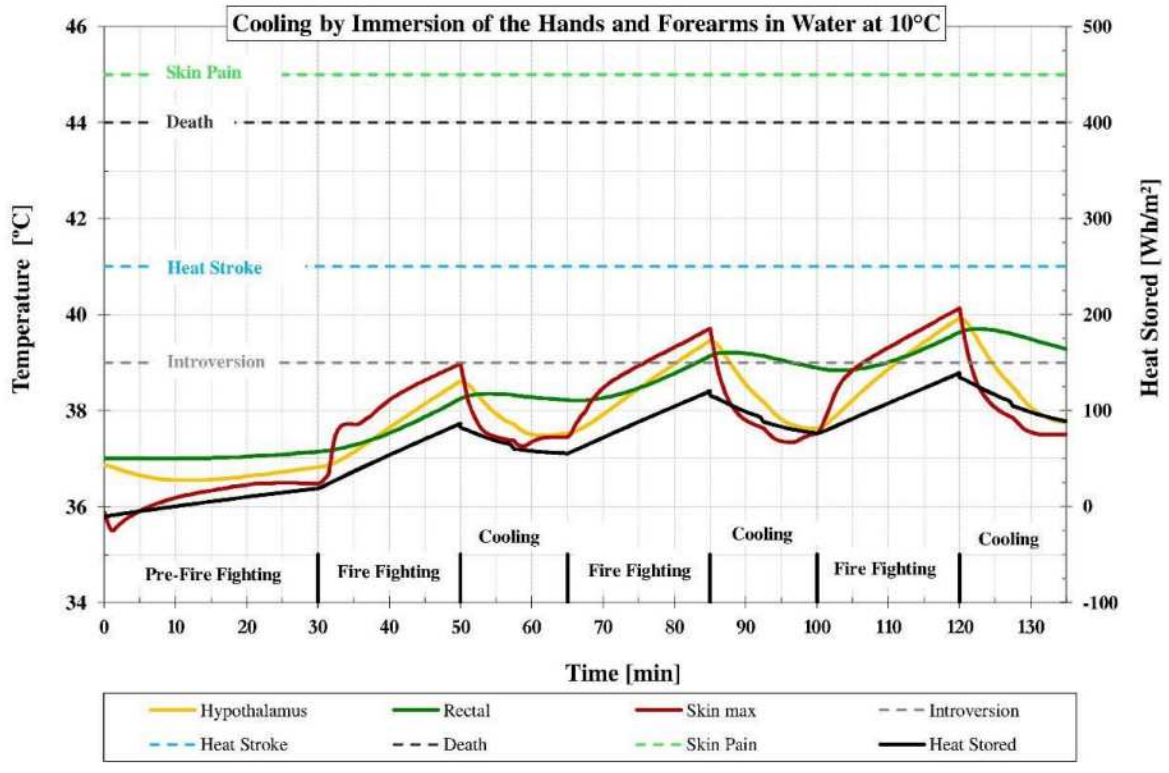

Figure 3. Evolution of firefighter thermophysiological state for low intensity incident radiation and cooling by immersion of the hands and forearms in water at 10°C.

As it can be seen in Figures 1 to 3, passive cooling for the conditions defined in this case proves to be a recovery strategy with a reduced efficacy when compared with the techniques of immersion of the

hands and forearms in cold water. The strategy of passive cooling (Figure 1) attenuates the heat stress felt by the firefighter but is not enough to prevent the rising of the hypothalamus temperature causing a decompensation to the thermoregulatory system, thus increasing the possibility of firefighter to come into introversion and even faint.

The cooling techniques by immersion of the hands and forearms have a greater efficacy and it would be expected that the lower the water temperature the higher the cooling produced, but it didn´t happened in an obvious manner. In some cases the cooling effects are higher when the water is at 20°C (Figure 2) than 10ºC (Figure 3). This is due to the fact that the temperature of the hypothalamus may not be high enough (slight degree of hyperthermia), thus the immersion of hands and forearms in water at 10ºC promotes the appearance of cold signals, then leading to the occurrence of vasoconstriction and shivering. The vasoconstriction reduces the body cooling rate and the shivering increases the internal heat production.

By other hand, the values of the rectal temperature and of the heat stored were lower and the cooling rate (ºC/min) is higher by applying the cooling technique of hands and forearms immersion in water at 10 ºC. So it can be stated that this is the most effective cooling technique for heat stress reduction on fighting fires where low radiation intensity impinges the firefighter.

Similarly to the previous case, Figures 4, 5 and 6 summarize the results previewed by the simulations for the evolution of the thermophysiological state of the firefighter during the protocol adopted, but now assuming he keeps a distance from the fire front resulting in a medium intensity of incident radiation and for the three cooling techniques considered.

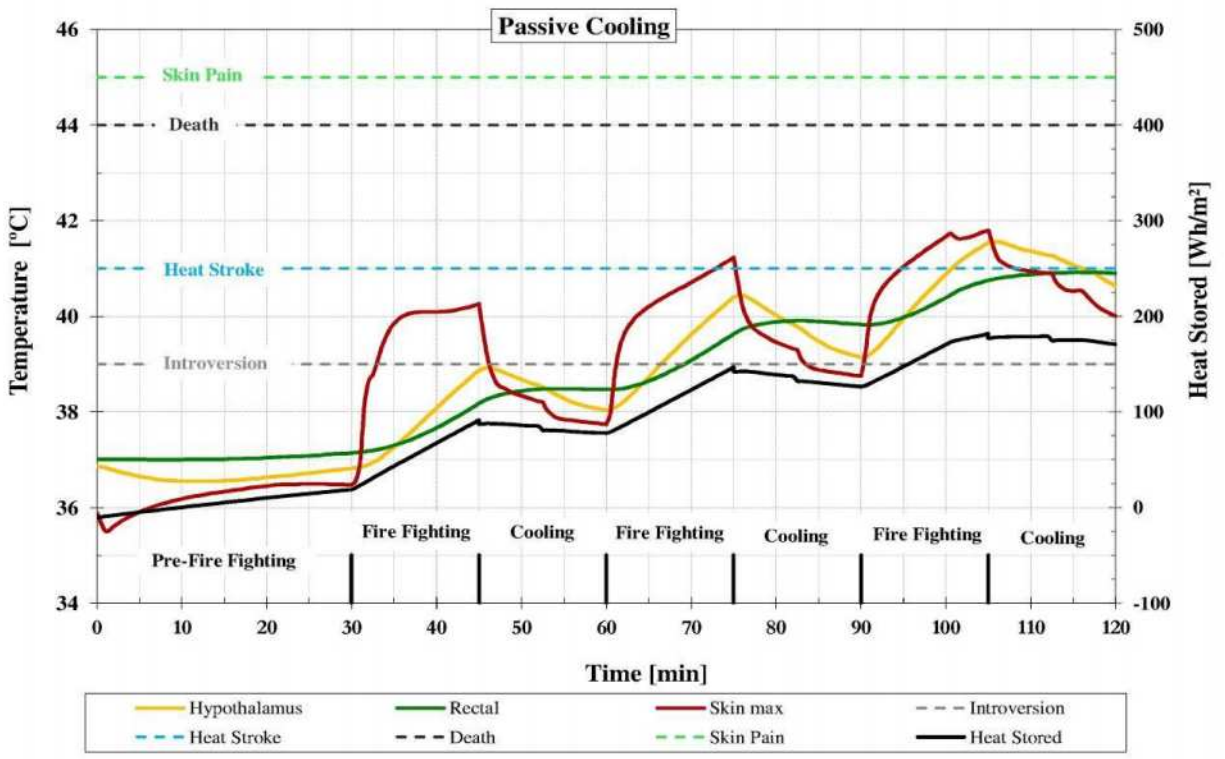

Figure 4. Evolution of firefighter thermophysiological state for medium intensity incident radiation and passive cooling recovery.

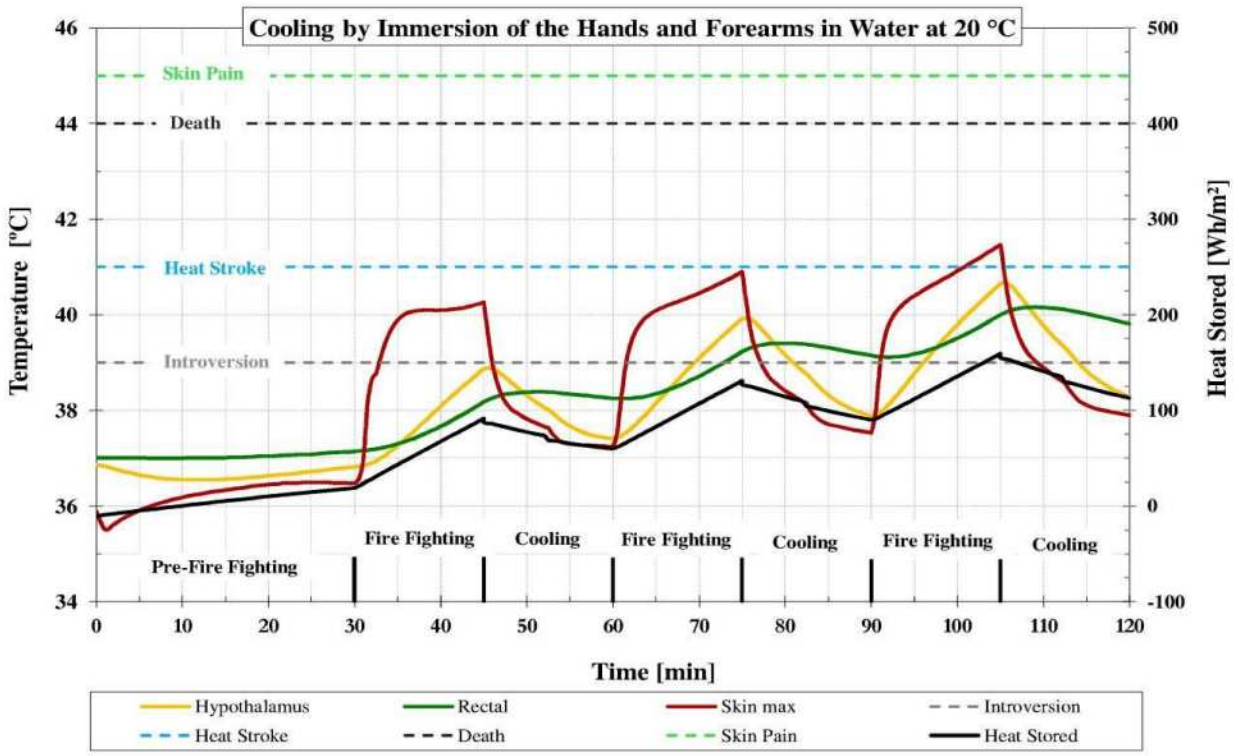

***Figure 5. Evolution of firefighter thermophysiological state for medium intensity incident radiation and cooling by** immersion of the hands and forearms in water at 20°C.*

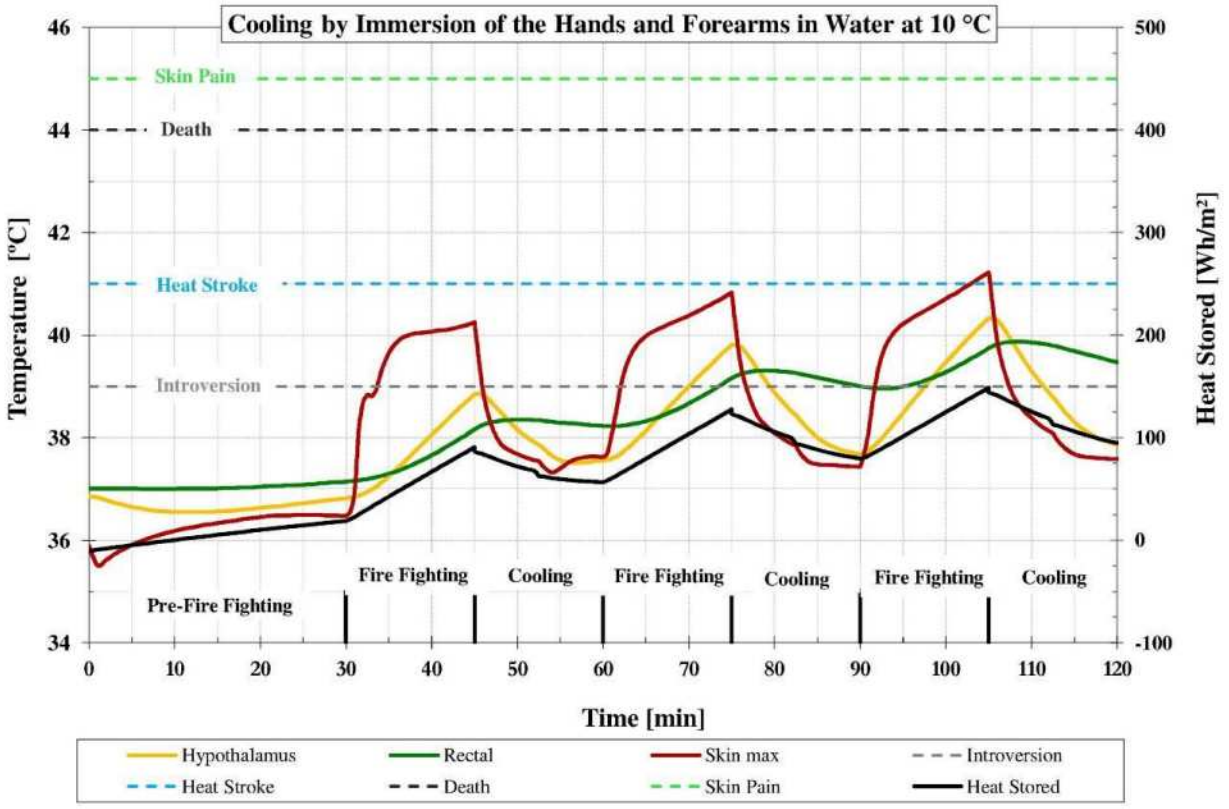

***Figure 6. Evolution of firefighter thermophysiological state for medium intensity incident radiation and cooling by** immersion of the hands and forearms in water at 10°C.*

Just like what happened in the previous case, the passive cooling (Figure 4) does not show results that allow us to state that this is an efficient solution for the attenuation of heat stress. This intensity of fire causes the hypothalamus temperature to rise 2°C for every 15 minutes of firefighting while the passive cooling technique can only lower this temperature 1°C for every 15 minutes of cooling. This generates a decompensation of the thermoregulatory system thus increasing the possibility of the firefighter to be affected by introversion or even by a heat stroke, which, if occurs, prevents the firefighter of getting out of the way of fire by himself.

The cooling techniques by immersion of members in cold water (Figure 5 and Figure 6) proved to be more efficient since they can provide a greater and faster reduction of hypothalamus temperature. After the entry of the firefighter in the state of introversion, they always succeeded to recover and restore the hypothalamus temperature within the range where thermoregulation occurs normally. Following the same trend previously verified the cooling technique with the immersion of hands and forearms in water at 10ºC (Figure 5) is the more efficient, even in spite of the occurrence of vasoconstriction in a first cooling phase. This is the body cooling technique which promotes the lower values for the temperatures (hypothalamus, rectal, skin max, etc.) and for the heat stored and guaranties the higher cooling rates (ºC/min). Then, also for the case of fire with a medium intensity of incident radiation this is the most effective technique in the attenuation of the heat stress.

Figures 7, 8 and 9 shown the results obtained with the simulations for the evolution of the thermophysiological state of the firefighter in the case when he is kept at a distance from the fire front leading to a high intensity of incident radiation.

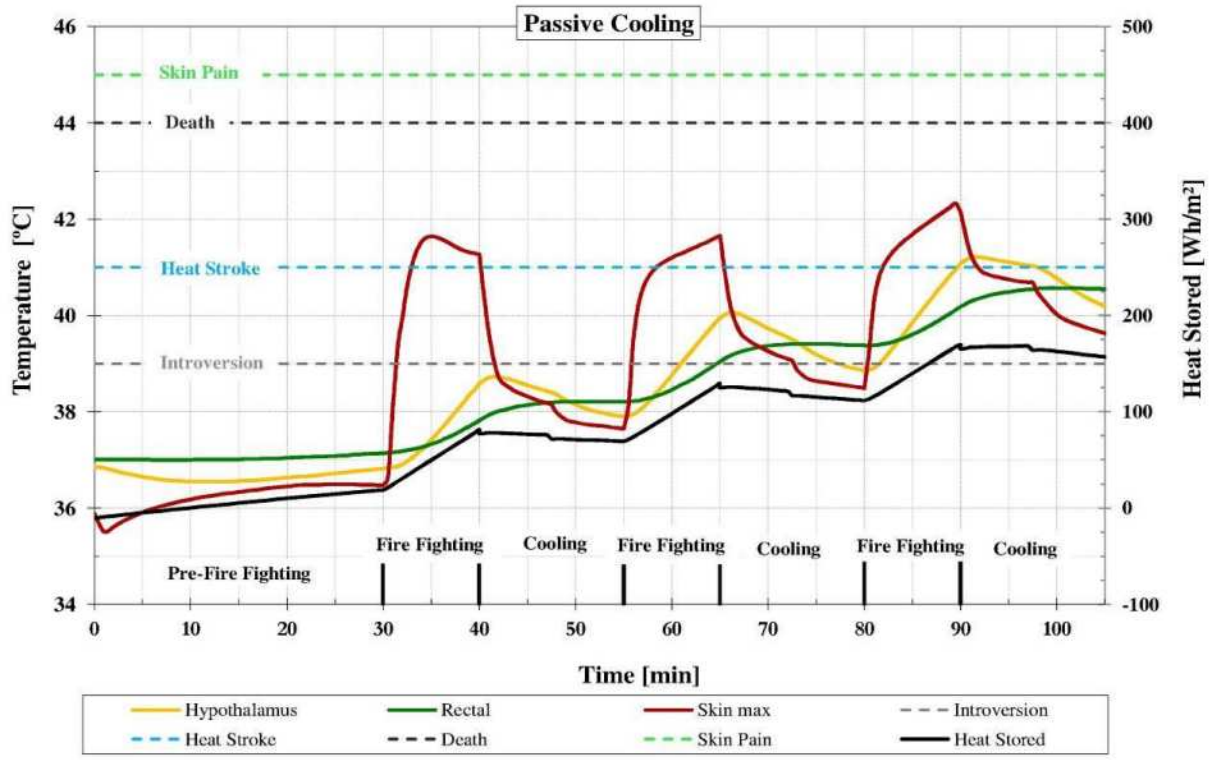

Figure 7. Evolution of firefighter thermophysiological state for high intensity incident radiation and passive cooling recovery.

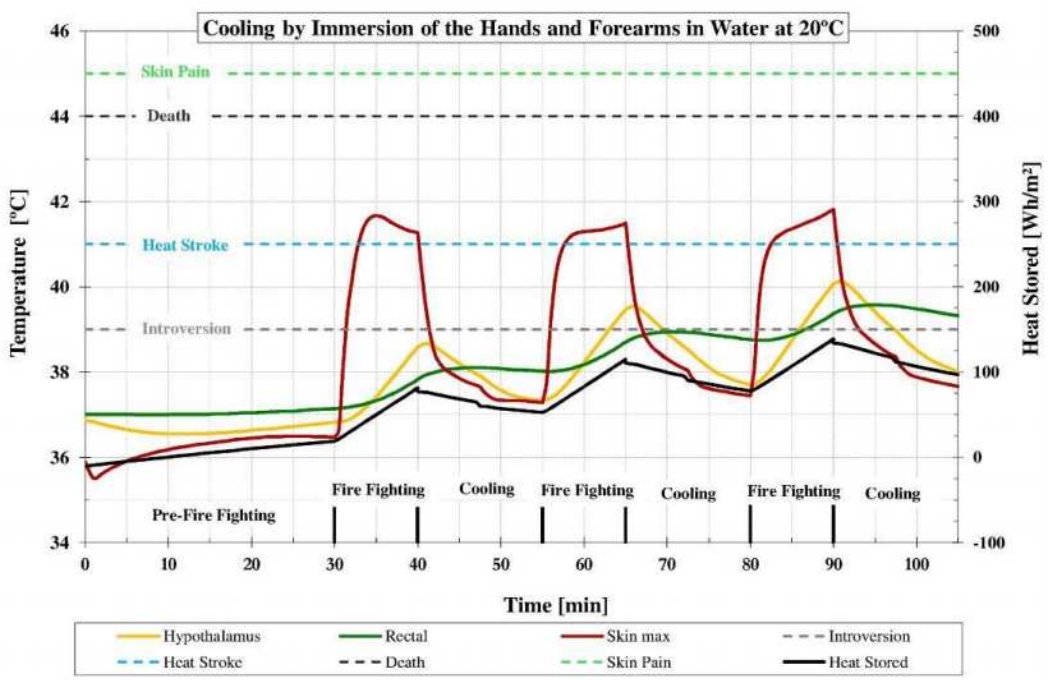

Figure 8. Evolution of firefighter thermophysiological state for high intensity incident radiation and cooling by immersion of the hands and forearms in water at 20°C.

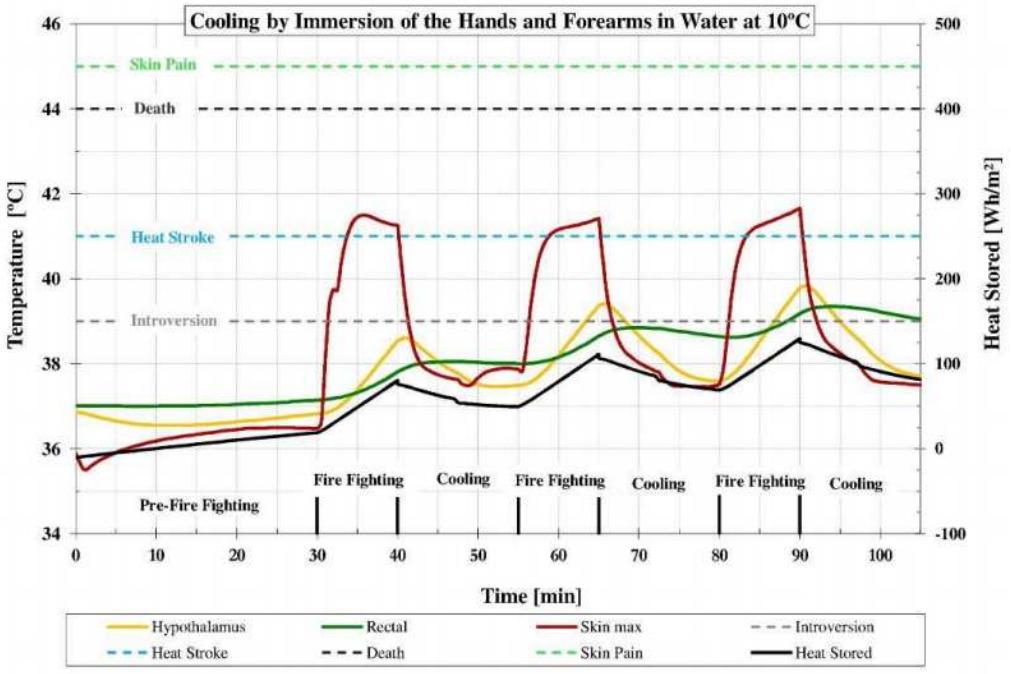

Figure 9. Evolution of firefighter thermophysiological state for high intensity incident radiation and cooling by immersion of the hands and forearms in water at 10°C.

Following the example in the analysis of the results obtained with the two types of fires previously seen, the technique of passive cooling (Figure 7) presents a decrease of hypothalamus temperature lower than those obtained through the cooling techniques by immersion of members in cold water. Otherwise, even if vasoconstriction occurred in the first cooling phase with water at 10 °C, this

technique turned out to be the most effective one in attenuating the heat stress for the same reason mentioned above in the other two cases.
In short, among the tested, the cooling technique of immersion of the hands and of the forearms in cold water at 10ºC proved to be the more efficient, even in spite of the occurrence of vasoconstriction (and in some cases shivering) in the first cooling phase. This is the body cooling technique which promotes the lower values for the temperatures (hypothalamus, rectal, skin max, etc.) and for the heat stored and guaranties the higher cooling rates (ºC/min).

Conclusions

During this work several aspects related to the activity of fighting fires, including the intensity of the impinging radiation on the firefighters, exposure time, pathologies related with heat stress and recovery strategies (active and passive) were explored.
The intensity of the incident radiation on the firefighters during the specific fighting phase, as well as the time of heat exposure are crucial for the occurrence of heat stress.
Among the simulated cases, it can be stated that the exposure time without affecting the physical integrity of the firefighter (hypothalamus temperature lower than 39ºC), decreases with the increasing of the intensity of the incident radiation in the fighting phase.
In relation to the cooling techniques, it was found that the body cooling by immersion of the hands and of the forearms in cold water is much more efficient than the passive air cooling, which is in good agreement with other results available in the literature.
In spite of causing vasoconstriction, and in some cases shivering, when the degree of hyperthermia is high, the strategy of body cooling by immersion of the hands and of the forearms in cold water at 10 ºC provides the best results in the attenuation of heat stress. Among the three body cooling techniques tested this was the one with the highest cooling rate (°C/min) and the lower values for the temperatures and for the heat stored in the human body. Then, this is the one that sustains the firefighter effectiveness during more time.

References

Barr D, Gregson W, Sutton L, Reilly T (2009), "A practical cooling strategy for reducing the physiological strain associated with firefighting activity in the heat", Ergonomics, Vol. 52 (4), pp. 413–420.

Carter JB, Banister EW, Morrison JB (1999), "Effectiveness of rest pauses and cooling in alleviation of heat stress during simulated fire-fighting activity", Ergonomics, Vol. 42 (2), pp. 299-313.

Fiala D, Lomas KJ, Stohrer M (1999), "A computer model of human thermoregulation for a wide range of environmental conditions – the passive system", J. Applied Physiology, Vol. 87, pp. 1957-1972.

Gagnon BD (2000), "Evaluation of new test methods for firefighting clothing", MSc thesis, Worcester Polytechnic Institute.

Giesbrecht GG, Jamieson C, Cahill F (2007), "Cooling hyperthermic firefighters by immersing forearms and hands in 10°C and 20°C water", Aviation Space Environmental Medicine, Vol. 78, pp. 561-567.

Havenith G, Heus R (2000), "Ergonomics of protective clothing", Proc. of Nokobetef 6 and 1st European Conference on protective clothing. Kuklane, K. and Holmér, I., (eds.), Stockholm, Sweden, May 7–10.

Havenith G, Holmér I, Parsons K (2002), "Personal factors in thermal comfort assessment - clothing properties and metabolic heat production", Energy and Buildings, Vol. 34, pp. 581-591.

Henriques F (1947), "Studies of thermal injury V. The predictability and the significance of thermally induced rate processes leading to irreversible epidermal injury", Archives of Pathology, Vol. 43, pp. 489–502.

Huizenga C, Zhang H, Duan T, Arens E (1999), "An improved multinode model of human physiology and thermal comfort", Proceedings of IBPSA Building Simulation 99, Kyoto, Vol. 1, pp 353-359.

Kenney W, DeGroot D, Holowatz L (2004), "Extremes of human heat tolerance - life at the precipice of thermoregulatory failure", J. Thermal Biology, Vol. 29, pp. 479-485.

Konz S, Hwang C, Dhiman B, Duncan J, Masud A (1977), "An experimental validation of mathematical simulation of human thermoregulation", Computers in Biology and Medicine, Vol. 7, pp. 71–82.

Magalhães S, Albuquerque RR, Pinto JC, Moreira AL (2001), "Termorregulação", Faculdade de Medicina da Universidade do Porto, Serviço de Fisiologia.

McLellan TM, Selkirk GA (2005), "The management of the heat stress for the firefighter", DRDC, Toronto, Canada.

Pascoe DD, Bellingar TA, McCluskey BS (1994), "Clothing and exercise. II. Influence of clothing during exercise/work in environmental extremes", Sports and Medicine, Vol. 18, pp. 94-108.

Raimundo AM, Oliveira AVM, Gaspar AR, Quintela DA (2008), "Thermophysiological response of human beings working in cold thermal environments", 7i3m – 7th International Thermal Manikin and Modelling Meeting, 3-5 of September, Coimbra, Portugal, pp 1-11.

Raimundo AM, Figueiredo AR (2009), "Personal protective clothing and safety of firefighters near a high intensity fire front", Fire Safety Journal, Vol. 44, pp. 514-521.

Raimundo AM, Oliveira AVM, Quintela DA, Gaspar AR (2012), "Development and validation of a computer program for simulation of the human body thermophysiological response", 2nd Portuguese Meeting in Bioengineering, Portuguese chapter of IEEE-EMBS, Coimbra, Portugal, 23-25 February, pp. 1-4.

Selkirk G, McLellan TM, Wong J (2004), "Active versus passive cooling during work in warm environments while wearing firefighting protective clothing", Journal of Occupational Environment and Hygiene, Vol. 1, pp. 521-531.

SFPE Task Group on Engineering Practices (2000), "Predicting 1st and 2nd degree skin burns from thermal radiation", Society of Fire Protection Engineers, Bethesda, MD.

Sharkey BJ (1999), "Heat stress", Wildland firefighter health and safety recommendations, April 1999 Conference, Missoula Technologic and Development Center, USDA Forest Service, Montana.

Stoll A, Greene L (1959), "Relationship between pain and tissue damage due to thermal radiation", Journal of Applied Physiology, Vol. 14, pp. 373-382.

Stolwijk JAJ (1971), "A mathematical model of physiological temperature regulation in man", NASA contractor report CR-1855, NASA, Washington DC.

Tanabe S, Kobayashi K, Nakano J, Ozeki Y, Konishi M (2002), "Evaluation of thermal comfort using combined multi-node thermoregulation (65MN) and radiation models and computational fluid dynamics (CFD)", Energy and Buildings, Vol. 34, pp. 637-646.

Weaver J, Stoll A (1969), "Mathematical model of skin exposed to thermal radiation", Aerospace Medicine, Vol. 40, pp. 24-30.

Wenger CB (1988), "Human heat acclimatization", In: Pandolf K, Sawka M, Gonzalez R, eds, Human performance physiology and environmental medicine at terrestrial extremes. Indianapolis Benchmark Press (now: Cooper Publishing Group), pp. 153-197.

WHO (1969), "Health factors involved in working under conditions of heat stress", World Health Organization, Technical Report Series, nº 412, Genève.

Wissler EH (1985), "Mathematical simulation of human thermal behaviour using whole body models", In: Shitzer A, Eberhart RC, eds, Heat transfer in medicine and biology - analysis and applications. Plenum, New York London, pp 325-373.

Consideration of an Empirical Model for Wildland Firefighter Safety Zones

B. Butler

USDA Forest Service, Rocky Mountain Research Station, Fire Sciences Laboratory 5775 W US Highway 10 Missoula MT 59808, USA bwbutler@fs.fed.us t:406 329 4801

Abstract
The term safety zone was first introduced into the official literature in 1957 in the aftermath of the Inaja fire that killed 11 firefighters. Since then identification of safety zones has been a primary duty of all wildland firefighters. Unfortunately, information regarding what constitutes an adequate safety zone is not well defined. Measurements of energy release from wildland fires have been used to develop an empirically based safety zone guideline. The proposed model is compared against past fire entrapments in North America. The comparison indicates that the empirical model does provide an extra margin of safety over most entrapments that are associated with injury or fatalities but it seems to underpredict the separation distance needed to meet the full definition of a safety zone.

***Keywords**: Fire behavior, prescribed fire, firefighter safety*

Introduction

Wildland firefighting by its nature is inherently dangerous. 699 wildland firefighters died in fire related accidents between 1910 and 1996 in the United States, 384 of those were directly related to fire entrapments (National Wildfire Coodinating Group 1997). Wildland firefighters must consider the risks to themselves and others when approaching, suppressing, and managing wildland fire and take action to minimize those risks (National Wildfire Coodinating Group 2004). The identification of suitable safety zones for firefighters during daily fire management operations is perhaps one of the most critical decisions made on wildland fires.
All wildland firefighters in the United States are required to identify safety zones when working on or near fire. Until1998 the regulatory agencies responsible for wildland fire management in North America did not provide any quantitative information about safety zone characteristics other than that proposed by Butler and Cohen (1998) which was subsequently included in the Fireline Handbook (National Wildfire Coodinating Group 2004). The safety zone guidelines are based on the assumption that the fire and safety zone were located on flat terrain. The minimum safe distance for a firefighter to be from a flame was calculated as that corresponding to a radiant incident energy flux level of 7.0 kW-m-2. This was determined to be the level at which exposed human skin will develop a 2nd degree burn in less than 90 seconds. An approximate correlation was derived from this model that indicated a minimum separation between the firefighter and fire should be equal to four times the flame height. For a circular safety zone this would be equal to the safety zone radius. When fires are burning on flat terrain, convective energy transfer is primarily upward in the plume while radiant energy transfer occurs out ahead of the fire front. Current firefighter safety guidelines are based on the assumption that radiant energy transfer is the dominant energy transfer mode. Measurements have verified the accuracy of this assumption but have also indicated that when fires are burning on slopes or under the influence of wind convective energy transfer ahead of the fire front can be significant. Intuition, professional observations, and experimental measurements indicate that when fires are located on slopes or ridges or are burning with a strong wind convective energy transfer may reach distances two to four or more flame lengths ahead of the fire front. This implies that the current safety zone guidelines may be invalid in some situations. It is also clear from site visits to designated safety zones on

numerous wildland fire incidents that considerable ambiguity exists regarding identification or creation of true 'safety zones,' versus 'deployment zones.'
Measurements of energy release from fires have been gathered from a range of ecosystem and vegetation types. The data were used to calculate the distribution of energy in and around those flames (Frankman *et al*. 2012a). Measurements and analysis of fires and safety zones on flat terrain showed that the current safety zone guidelines were adequate with the assumption that both the fire and safety zone were on flat terrain. Additional guidelines were developed that related safety zone size in acres to flame height in feet and to account for changes in safety zone size necessary to accommodate equipment and multiple personnel. When the influence of slope on fire intensity and spread is considered, the current safety zone guidelines that were designed for flat terrain and low wind clearly become inadequate. With this need in mind efforts have focused on measuring energy release from fires burning in natural conditions. While a very small subset of the data collected corresponds to fire on slopes, the data suggest a potential safety zone rule that encompasses all terrain and weather conditions as a function of vegetation type. These measurements are analysed to propose an empirically based firefighter safety zone rule.

Methods – Energy Measurements

Definition of a firefighter safety zone requires determination of the fire energy source strength; calculation of burn injury as a function of heating magnitude and duration; and estimation of safe separation distance (SSD) from the fire to prevent injury.
Energy is transported from wildland fires primarily by two heating modes: 1) radiative energy transport (Albini 1986; Viskanta 2008) and 2) convective energy transport (Yedinak *et al*. 2006; Anderson *et al*. 2010). Some cases exist where radiation dominates fire energy transport, for example a fire spreading through grass in the absence of wind would seem to be driven by radiant heating ahead of the flaming front, or a large crown fire with minimal ambient wind would also be characterized by primarily radiant heating although in both cases it is difficult to separate the radiant heating from the advective influence of lofting and ignition from burning embers that act as ignition pilot sources (Albini 1986). Logically, convective heating should also play a critical role in fire spread, for example a fire burning through grass in the presence of a very strong ambient wind where the wind causes the flames to reach ahead of the burning front preheating vegetation far in advance of the fire through direct contact between the flames and unignited fuels. In this case convective energy transport would dominate energy transport and fire spread. Recent measurements support this (Yedinak *et al*. 2010; Frankman *et al*. 2012a).
Safety zone studies have assumed that radiative heating is the primary heating mode (Butler and Cohen 1998; Zarate *et al*. 2008; Rossi *et al*. 2011). Various methods have been used to measure radiant energy release from wildland flames. Butler (1993) describes a simple radiometer. Packham and Pompe (1971) measured radiative heat flux from a fire in Australian forest lands. Heating reached 100 kW m-2 when the flame was adjacent to the sensor and 57 kW m-2 when the sensor was a distance 7.6 m from the flame (King 1961), no description of flame dimensions were provided. Butler *et al*. (2004) presented temporally resolved irradiance measurements in a boreal forest crown fire burning primarily in jack pine (Pinus banksiana) with an understory of black spruce (Picea mariana). Irradiance values reached 290 kW m-2, flames were 25 m tall, and fire spread rates were nominally 1 m s-1. Morandini *et al*. (2006) measured time-resolved irradiance values from flames burning in 2.5 m tall Mediterranean shrubs (Olea europea, Quercus ilex, arbustus unedo, Cistus Monspeliensis and Cytisus triflorus). Radiative heat fluxes peaked at 1, 2.2 and 7.8 kW m-2for distances to flames of 15, 10 and 5 m respectively. Silvani and Morandini (2009) measured time-resolved radiative and total heat fluxes incident on the sensor in fires burning in pine needles and oak branches. For the burn conducted on a slope of 36% with flame heights of 5.6 m the peak radiative and total heating at the sensor were 51 kW m-2 and 112 kW m-2 respectively, implying that convective heating was nominally of the order

of the radiative heating. Frankman *et al*. (2012a) report measurements from fires burning in a variety of vegetation and terrain. Irradiance from two crown fires burning in lodgepole pine (Pinus contorta) peaked at 200 and 300 kW m-2 respectively with flames reaching 30 m, convective fluxes were 15 to 20% of the peak radiative fluxes. Peak irradiance associated with fires in grasses and leaf and pine needle litter in southern longleaf pine (Pinus palustris) reached 100 kW m-2 with a mean value of 70 kW m-2 for flames nominally 2 m tall, convective heating were equal to or greater than the radiative flux. Fires burning in sagebrush (Artemisia tridentata subsp. Wyomingensis) dominated ecosystems generated peak radiant energy fluxes of 132 kW m-2 with a mean value of 127 kW m-2 for flames less than 3 m tall, peak convective heating was 20 to 70% of the radiative heating magnitudes on slopes of 10 to 30%. Napier and Roopchand (1986) report an average incident radiant flux of 7.5 kW m-2 159 m away from LNG flames 80 m tall and 31 m in diameter. Measurements incidate that flame increases nearly monotonically with approach of the flame front and declines exponentially with its passage. Irradiance beneath crown fires peaks at 300 kW m-2, peak irradiance associated with fires in surface fuels reaches 100 kW m-2 with a mean value of 70 kW m-2; the peak for fires burning in shrub fuels was 132 kW m-2 with a mean value of 127 kW m-2.

Recent measurements of convective energy transport have shown that instantaneous peak convective energy fluxes inside flames may significantly exceed the radiant fluxes although convective heating based on 2 s moving averages are nominally 70% of similarly averaged radiant heating values (Frankman *et al*. 2012b). Measurements of flame geometry ahead of a spreading fire front suggest as slope exceeds nominally 30% flames begin to attach to the surface and high temperature gases are convected along the slope (Viegas 2004). Crown fires in lodgepole pine (Pinus contorta) resulted in 2 second averaged convective fluxes from 15 to 20% of the peak radiative fluxes. However, fires in surface fuels characteristic of a southern longleaf pine (Pinus palustris) ecosystem showed convective heating equal to or greater than the radiative flux. Fires burning in sagebrush (Artemisia tridentata subsp. Wyomingensis) or similar shrub dominated ecosystems produced peak convective heating 20 to 70% of the radiative heating magnitudes.

Results

It is commonly believed that radiant energy decays as the inverse of the square of the distance away from the source. This is based on energy transport theory and ideally holds true. While it is somewhat arbitrary, the data collected as part of this study were grouped according to the vegetation and fire type (i.e. grass, brush, moderate intensity crown and high intensity crown). Measurements of total incident heating are plotted below and compared to the ideal decay model (Figure 1). Clearly the correlation is not entirely accurate. It appears that "real" wildland flames do not necessarily represent ideal flame models. Logically departure from theoretical flame behavior can be attributed to three primary factors: 1) absorption of energy by water vapor and carbon dioxide in the atmosphere, 2) convective energy transport away from the fire, and 3) varying temperature and emissivity of the flame. The implications from these data are that the 1/r2 rule (which theoretically applies to radiative heating) does not seem to apply to total energy transfer from fires suggesting that convective energy transport extends the distance over which heating from the flames occurs. In the context of firefighter safety zones, these results suggest that convective heating can be a significant contributor to energy transfer from fires.

Figure 2 presents energy levels as a function of vegetation type which is intended to be a surrogate for fire intensity. The burn injury threshold of 7 kW m-2 is displayed in both graphs. Based on these groupings, the decay in intensity with distance can be simulated using a model of the form q=m/rn where (q) is incident heating level at distance (r) from the flame, (m) is a constant, and the exponent (n) is 0.75 for these data. The values for (m) scale nominally with the observed peak total heating values measured in each grouping, the exponents (n) were held constant. The largest discrepancy between this model and the data occurs for the moderate intensity crown fire data. These data are based on measurements over a range of topographical and vegetation types. Also the arbitrary nature of the

grouping could alter the results. However, there is some intuitive comfort derived from the correlation between peak total heating values and the constant multiplier values.

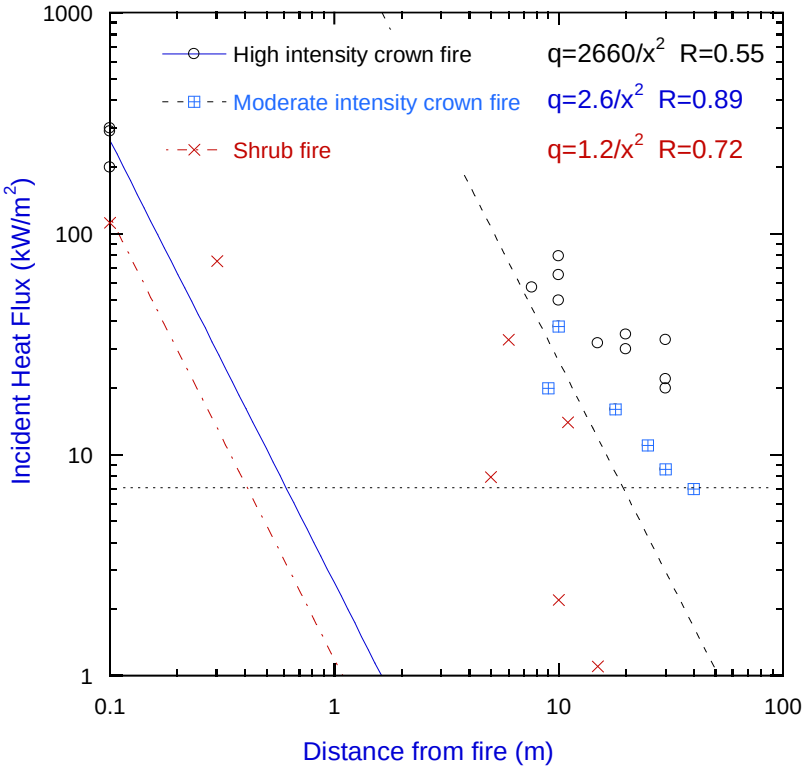

Figure 1—Comparison of measurements to inverse squared law.

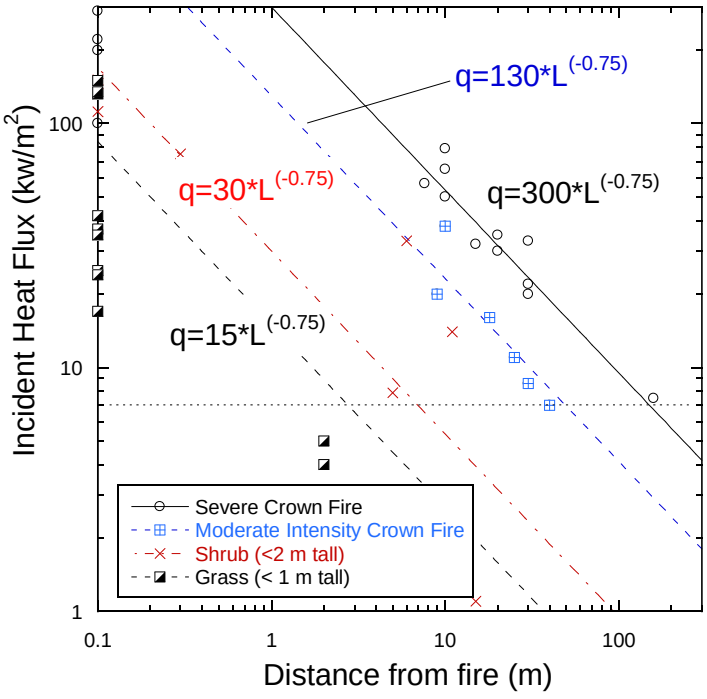

Figure 2-- Exponent based models for energy decay with distance for wildland fires.

Four heating regimes are identified for these data. The lowest being that associated with fire in grass vegetation (nominally less than 1 m tall). The measurements are best fit by a line defined as q=15/L0.75 where L is the distance between the receptor and the fire. The next highest heating level is associated with shrub vegetation similar to sage brush. Nominally 1 to 2 m tall. The best fit for heating level as function of distance from flame is q = 30 / L0.75. For taller shrubs (e.g. gamble oak or other shrubs 2 to 5 m tall) or low intensity crown fires the fit is q = 130 / L0.75. Finally when considering the most intense fires such as those typically associated with forest crowns the best fit is q = 300 / L0.75. The horizontal dashed line represents the level at which second degree burn injury will occur in roughly 30 to 60 seconds. Logically the point at which the best fit for energy distribution crosses the burn injury limit would represent the minimum distance required from a fire in the particular vegetation type to prevent injury. Based on these data a rule for SSD that is dependent only on vegetation type is proposed. The rule is based on extrapolating vertically downward from the intersection of the line corresponding to each fire (or vegetation) type and the burn injury limit of 7 kW m-2 to the horizontal axis. The intersection with the horizontal axis would be the distance from the fire necessary to maintain an exposure below the burn injury limit. Thus for the highest intensity crown fires nominally 105 m is required, for moderate intensity crown fires or fire in 2 to 5 m tall shrubs the minimum distance is 60 m, for fires in 1 to 2 m tall shrubs or tall grass the minimum distance is 8 m and for fires in grass less than 1 m tall the minimum separation distance is 3 m. This approach includes wind and slope implicitly in the data set. There is no direct accounting for steep slopes or strong winds. Additionally only a few data points were collected in steep terrain or windy conditions, thus this empirical model does not have a strong slope or wind component.

Butler (2014) evaluates safety zones for selected firefighter entrapments over the past 70 years in the United States. Figure 3 compares entrapment data presented in that study as well as a few other entrapments in the context of the empirical SSD model for the entrapments. Table 1 summarizes the entrapment incident details. The data indicate that for all but two fire incidents the empirical model suggests a larger SSD is required. In most cases the difference between the actual SSD and the suggested SSD is significant (for example consider the Mann Gulch, Inaja, Dude, Thirtymile, Cramer, and Yarnell Hill fires). The suggested SSD is significantly larger than the actual SSD. All of these are associated with fatal entrapments. However the Blackwater, Butte, South Canyon-II deployment are fires where firefighters deployed fire shelters, or in the case of the Blackwater fire took evasive action and survived, albeit in some cases very uncomfortably. The Butte fire and South Canyon-II entrapments had actual SSD greater than that specified from the empirical model. In the Butte fire incident, firefighters deployed aluminium fire shelters in a prepared safety zone. They had to move from one side of the clearing to the other as the fire burned around the area. In the South Canyon-II entrapment, 8 firefighters deployed on a rocky ridge nominally 160 m from the primary vegetation (Gambel Oak). At no time did they feel threatened in their shelters and some indicated they believe they would have been safe without the shelters. These two incidents suggest that the empirical model seems to underpredict the minimum distance needed.

The empirical model is attractive from the standpoint that it is simple to memorize and apply, it does not require that the firefighter visualize the fire behaviour, and can be applied quickly. But it does not consider slope or wind both of which are considered shortcomings in the present safety zone rule applied in the United States. These shortcomings might be the reason why there are some fires where the proposed SSD was lower than the actual SSD (i.e. Butte, and South Canyon-II).

Table 1—Fire incident details

Incident	Fatalities	Injuries	Vegetation	Vegetation Ht (m)	Flame Ht (m)	Actual SSD (m)	Actual SSD/Flame Ht	Empirical SSD/Flame Ht
Blackwater		36	Timber	25	80	30	0.37	1.3
Mann Gulch	13	1	Timber	20	10	13	1.3	10
Inaja	11		Shrub	8	12	5	0.42	3.3
Loop	10	12	Brush	6	10	15	1.5	5.0
Battlement Mesa	3	1	Brush	5	14	5	0.36	3.6
Butte		73	Timber	30	70	125	1.8	1.4
Dude	6		Timber	15	50	5	0.10	2.0
So Can-I	14		Brush	5	29	2	0.069	1.7
So Can-II		8	Brush	5	29	160	5.5	1.7
30-mile	4	12	Timber	25	50	5	0.10	2.0
Cramer	2		Timber	20	30	3	0.10	3.3
Esperanza	5		Brush	5	20	10	0.50	2.5
Yarnell Hill	19		Brush	5	30	5	0.17	1.7

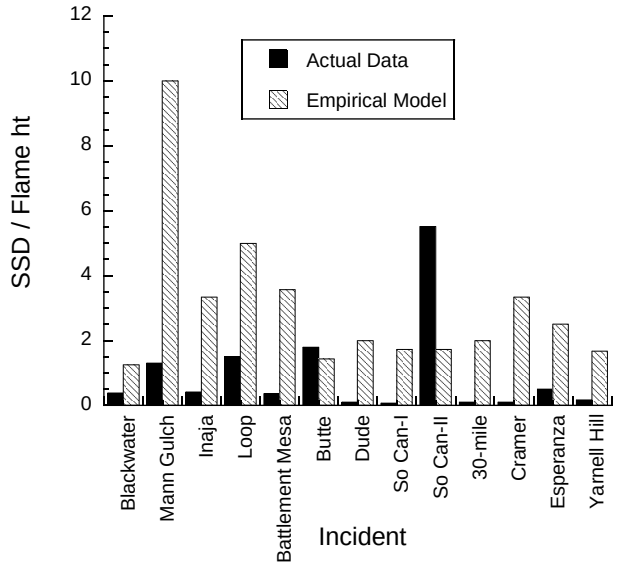

Figure 3—Comparison of actual entrapments and empirical safety zone SSD model.

Conclusions

Many questions remain regarding how energy is generated and released from wildland flames and the implications of energy distribution on safety zone effectiveness. It is only recently that measurements have identified the range of heating magnitudes that can be expected from wildland flames. The prediction of fire behaviour, especially during dynamic fire operations can be very difficult even with access to sophisticated computer models and hardware. Current studies suggest that heating levels of 6 to 7 kW m-2 generally represent burn injury limits, however a more appropriate metric is thermal dosage unit that includes both heating magnitude and exposure time (Butler 2014). Comparison between a selected set of fire entrapments and the empirical model derived from the data presented here suggests that the empirical model suggests SSD on the order of the current guideline based on earlier work (Butler and Cohen 1998). Intuition, professional observations, and the few experimental measurements that have been reported indicate that when fires are located on or adjacent to slopes or

ridges or are exposed to winds convective energy transfer may reach distances equal to 2 to 3 or more flame lengths ahead of the fire front (Frankman *et al*. 2012a). This implies that the empirical model may underestimate SSD in some situations. This conclusion is supported by the comparison to fire entrapments. Recent measurements suggest that in the context of wildland firefighter safety zones on slopes an accurate accounting of energy transport requires consideration of both convective and radiative heating. The inclusion of convective heating implies that slope steepness, ambient wind, and safety zone geometrical location relative to terrain slope are all relevant.

Acknowledgements

This work could not have been accomplished without the financial support provided by the Joint Fire Sciences Program, as well as support from fire managers in the Bureau of Land Management and the National Park Service when we were deploying sensors in and around fires. We also acknowledge the enthusiastic support from many fire crews, as well as forest service district, and forest staff.

References

Albini, FA (1986) Wildland fire spread by radiation-- a model including fuel cooling by natural convection. Combustion Science & Technology 45, 101-113.

Anderson, WR, Catchpole, EA, Butler, BW (2010) Convective heat transfer in fire spread through fine fuel beds. International Journal of Wildland Fire 19, 284-298.

Butler, BW (1993) Experimental measurements of radiant heat fluxes from simulated wildfire flames. In '12th International Conference of Fire and Forest Meteorology, Oct. 26-28, 1993. Jekyll Island, Georgia', Oct. 26-28, 1993. (Eds JM Saveland, J Cohen) Volume 1 pp. 104-111. (Society of American Foresters, Bethesda, MD:

Butler, BW (2014) Wildland firefighter safety zones: a review of past science and summary of future needs. International Journal of Wildland Fire 23, 295-308.

Butler, BW, Cohen, J, Latham, DJ, Schuette, RD, Sopko, P, Shannon, KS, Jimenez, D, Bradshaw, LS (2004) Measurements of radiant emissive power and temperatures in crown fires. Canadian Journal of Forest Research 34, 1577-1587.

Butler, BW, Cohen, JD (1998) Firefighter safety zones: a theoretical model based on radiative heating. International Journal of Wildland Fire 8, 73-77.

Frankman, D, Webb, BW, Butler, BW, Jimenez, D, Forthofer, JM, Sopko, P, Shannon, KS, Hiers, JK, Ottmar, RD (2012a) Measurements of convective and radiative heating in wildland fires. International Journal of Wildland Fire 22, 157-167.

Frankman, D, Webb, BW, Butler, BW, Jimenez, D, Harrington, M (2012b) The impact of sampling rate on interpretation of the temporal characteristics of radiative and convective heating in wildland flames. International Journal of Wildland Fire

King, AR (1961) Compensating radiometer. British Journal of Applied Physics 633.

Morandini, F, Silvani, X, Rossi, L, Santoni, P-A, Simeoni, A, Balbi, J-H, Louis Rossi, J, Marcelli, T (2006) Fire spread experiment across Mediterranean shrub: Influence of wind on flame front properties. Fire Safety Journal 41, 229-235.

Napier, DH, Roopchand, DR (1986) An approach to hazard analysis of LNG spills. Journal of Occupational Accidents 7, 251-272.

National Wildfire Coodinating Group, NIFC, 1997. Historical Wildland Firefighter Fatalities 1910-1996. National Interagency Fire Center, Boise, ID. PMS 822 NFES 1849: 42.

National Wildfire Coodinating Group, NIFC, 2004. NWCG Fireline Handbook. National Wildfire Coordinating Group, Boise, ID. NWCG Handbook 3, PMS 410-1, NFES 0065:

Packham, D, Pompe, A (1971) Radiation temperatures of forest fires. Australian Forest Research 5, 1-8.

Rossi, JL, Simeoni, A, Moretti, B, Leroy-Cancellieri, V (2011) An analytical model based on radiative heating for the determination of safety distances for wildland fires. Fire Safety Journal 46, 520-527.

Silvani, X, Morandini, F (2009) Fire spread experiments in the field: Temperature and heat fluxes measurements. Fire Safety Journal 44, 279-285.

Viegas, DX (2004) On the existence of a steady state regime for slope and wind driven fires. International Journal of Wildland Fire 13, 101-117.

Viskanta, R (2008) Overview of some radiative transfer issues in simulation of unwanted fires. International Journal of Thermal Sciences 47, 1563-1570.

Yedinak, KM, Cohen, JD, Forthofer, JM, Finney, MA (2010) An examination of flame shape related to convection heat transfer in deep-fuel beds. International Journal of Wildland Fire 19, 171-178.

Yedinak, KM, Forthofer, JM, Cohen, JD, Finney, MA (2006) Analysis of the profile of an open flame from a vertical fuel source. Forest Ecology and Management 234, S89-S89.

Zarate, L, Arnaldos, J, Casal, J (2008) Establishing safety distances for wildland fires. Fire Safety Journal 43, 565-575.

Determining a safety condition in the prevention of eruptive fires

Chatelon F.J.[a], Balbi J.H.[a], Rossi J.L.[a], Simeoni A.[b], Viegas D.X.[c], Marcelli T.[a]

[a] *Università di Corsica, Systèmes Physiques pour l'Environnement, UMR CNRS 6134, Campus Grossetti, 20250 Corti, chatelon@univ-corse.fr, balbi@univ-corse.fr, rossi@univ-corse.fr, marcelli@univ-corse.fr*
[b] *Centre for Fire Safety Engineering, Institute for Infrastructure and Environment, University of Edinburgh, A.Simeoni@ed.ac.uk*
[c] *Centre of Studies on Forest Fires, ADAI, University of Coimbra, Portugal, xavier.viegas@dem.uc.pt*

Abstract
Eruptive fires are one of the main causes of human losses in forest fire fighting. This phenomenon is fairly rare, unpredictable and thus extremely dangerous for firefighters (or civilians). Many casualties result from several accidents identified in the last fifty years around the world. Indeed, people involved in fire fighting activities are not prepared for facing such an unpredictable phenomenon. Very few literature is available to support either modelling or occurrence prediction for this phenomenon. Eruptive fire behaviour usually describes an extreme case of dynamic fire behaviour in which a sudden increase of the fire front rate of spread (ROS) in a short lapse of time is observed. So the question of predicting an eruption's occurrence is a crucial point for the fire fighters' safety. In this study, it is assumed that the eruption is due to physical considerations. The mechanism responsible for this erratic behaviour is the pioneering interpretation proposed by Viegas (2005) which consists in a feedback between the ROS and a convective air flow created by the fire itself. A physical modelling for this "induced wind" is given and is coupled with a simplified physical propagation model for surface fires. If the solution of the coupled system usually converges, it may diverge under certain conditions, leading to a fire eruption. It is then possible to obtain a physical condition which gives the impossibility (or not) for a fire to turn into an eruptive fire and the model is able to predict the occurrence of a fire eruption according to the triangle of fire. The model is tested by comparing its numerical results on the one hand to a set of experiments carried out at laboratory scale and on the other hand to an outdoor wildfire (Kornati accident).

Keywords*: Eruptive fire, fire spread, physical model, prevention, eruption's occurrence*

Introduction

The term 'blowup' used in wildland fires by Butler *et al*. (1998) indicates a rapid change from a low intensity surface fire to a high fire burning through the whole vegetation complex, from surface to canopy and demonstrates dramatically larger flame heights, higher energy release rates and rates of spread that are faster than usual fires. As this work focuses on the acceleration of surface fires, the designation of fire eruption proposed by Viegas (2005) is used and describes the sudden change in rate of spread of the head fire and in energy release within a very short lapse of time. Viegas and Simeoni (2011) reviewed the mechanisms (physical or chemical considerations, variation of external conditions, etc…) that are described in literature to explain the onset and development of fire eruptions. The major part of these diagnoses are refuted by examples of real fires occurred in the past. Among all these explanations, the pioneering interpretation proposed by Viegas (2005) must be highlighted. Actually, it is based on the coupling of the own properties of the spreading fire with other conditions (wind, topography) and consists in a feedback effect caused by the convective flow induced by the fire in the presence of wind or/and a positive slope. The fire creates an 'induced wind' which transports oxygen to the reaction zone which intensifies the combustion process and consequently flame length and ROS. So the reaction needs more and more ambient air. This feedback process will increase continuously and the ROS could reach very important values if it is not inhibited by some external mechanisms. This strong air flow movement was proved at the laboratory scale by Viegas and Pita

(2004) and observed at the field scale (Viegas *et al*. 2002). Moreover, the testimony of the one fire fighter who survives the Kornati fire accident (Stipanicev and Viegas, 2009), the meteorological measures of the wind speed during the freixo accident (Viegas 2005) are clear evidences of the importance and the relevance of the induced wind. Viegas (2005) suggested a mathematical model (constituted by a non linear differential equation) that predicts the fast increasing of the ROS. One can also cite the model developed by Dold *et al*. (2011) in which the phenomenon is the result of a flow attachment and the ROS is assumed to vary as a power-law of the fireline intensity. If these empirical models can reproduce the fire behaviour during the eruption, they do not predict the eruption's onset and to our knowledge, such a model does not exist.
This work focuses on the existence of a condition for predicting either extreme or usual fire behaviour. A physical modelling of the induced wind is coupled with the simplified physical propagation model for surface fires developed at the University of Corsica (Balbi *et al*. 2007, 2009, 2010). In some cases, this coupling can diverge, leading to a fire eruption's onset.

Equations of the simplified physical propagation model

As some authors (*e.g*. Albini 1985, Telisin 1974, Van Wagner 1967) assumed that radiation was the dominant process in the contribution of heat to unburnt fuel, the propagation model developed at the University of Corsica (Balbi *et al.* 2007) was only based on radiation. It was elaborated to be as complete as possible with regard to the equations that govern fires, whilst also being computationally cheap. To this end, the use of partial differential equations was avoided because of their associated long calculation times and also because of the difficulty of making a sensitive study of the fire behaviour with respect to the different parameters involved (e.g. environmental, topographic, or fuel bed properties). This model was later improved and successfully confronted to sets of experiments at the laboratory scale with aligned slope and wind and at the field scale (Balbi *et al.* 2009) or confronted to the set of experiments conducted by Viegas (2004a) where slope and wind are not aligned. The improvements brought by Chatelon *et al.* (2010) or Marcelli *et al.* (2011) have changed the propagation model into a complete fire behaviour model in which rate of spread (ROS), flame tilt angle, flame temperature, flame length, radiant fraction and vertical velocity due to buoyancy are given.
The two main algebraic equations of the model are the following:

$$\tan\gamma = \tan\alpha + \frac{U}{u_0} \quad (1)$$

$$R = R_b + R_f \quad (2)$$

Equation (1) gives the flame tilt angle γ depending on the slope angle α, the normal component of the wind velocity U and the upward gas velocity u_0. Equation (2) provides the ROS R as a function of the two radiative contributions from the flame (R_f) and from the burning fuel bed (R_b). These contributions are obtained by considering the flame and the base of the flame as grey radiant panels:

$$R_b = \frac{e}{\sigma}\,\frac{B\,{T_b}^4}{C_p\Delta T + m\Delta h} \quad (3)$$

$$R_f = A\,R\,\frac{1+\sin\gamma-\cos\gamma}{1+\frac{R\cos\gamma}{r_0}} \quad (4)$$

where C_p denotes the specific heat of the vegetative fuel, B the Stefan-Boltzmann constant, m the fuel moisture content, Δh the heat of latent evaporation, σ the fuel load, e the fuel bed depth, T_b the fuel burning particles temperature and $\Delta T = T_i - T_a$ the difference between ignition temperature and ambient

air temperature. The coefficient r_0 is a ROS factor that can be expressed as a function of the surface area to volume ratio of the fuel elements (Chatelon *et al.* 2010).
The coefficient *A* in equation (4) involves flame radiation. It represents the magnitude of the flame radiation related to the ignition energy. Its expression given in equation (5) depends on the heat of combustion of the pyrolysis gases ΔH, a radiant factor χ_0, the absorption coefficient ν and a corrective term *Y* to the view factor introduced by Koo *et al.* (2005) in order to improve Pagni and Peterson's model (Pagni and Peterson 1973). This term *Y* depends on dynamic fire parameters (ratio between fire front width *W* and flame length *l*).

$$A = \nu \frac{\chi_0 \, \Delta H}{4\left(C_p \Delta T + m \Delta h\right)} \, Y \qquad (5)$$

This model was successfully used to model several laboratory experiments (e.g. Guijarro *et al.* 1997, Mendes-Lopes *et al.* 2003, Viegas 2004b) and applied to some field-scale fires (e.g. McArthur 1969, Cheney and Gould 1995, Fernandes 2001). As this model is a steady-state model, it cannot reproduce a fire eruption which is an unsteady phenomenon (Viegas 2005, Dold and Zinoviev 2009). Thus a sub-model which describes the effect of the induced wind defined by Viegas (2005) has to be added.

Induced wind modelling

Under slope and weak wind conditions, the fire creates an induced airflow U_i in order to compensate the draught caused by the hot gases moving upwards. Considering a positive slope, the airflow comes from both sides of the fire front but only the airflow coming from the burned zone enters the flame. Indeed, the flame geometry causes an important deviation of the trajectory of the fresh air stream coming from the unburnt zone. So, the induced wind velocity under the flame is assumed to be practically zero. Consequently, there is no indraft at the fire front. On the other hand, the airflow coming from the burned zone is only slightly deviated, particularly near the ground, as it gets into the flame and supplies the reaction zone with oxygen.
Viegas and Pita (2004) clearly showed the presence of induced wind at the laboratory scale. Their experiments consisted in measuring the fire spread in canyons, using a combustion table with two inclined faces in order to create a canyon geometry. A first set of experiments in opened canyons showed a very fast spreading fire, which can be considered as eruptive. When the induced-wind was inhibited by a plate placed across the base of the canyon, the spread was much slower and the fire never showed an eruptive nature.
At the field scale, the Freixo de Espada-a-Cinta accident reported by Viegas (2004c) is a good example of the presence of an induced wind. Indeed, when the fire reached the base of a canyon, it was given as practically extinguished and the wind was blowing from the northwest in a downslope direction with a velocity on the order of 15 km/h. Suddenly, the wind turned to south-southwest, which is approximately the upslope direction and rose to 65 km/h 30 minutes later, with gusts up to 96 km/h. These data were retrieved by a meteorological station located on top of the ridge that was located in the spreading direction of the fire front. They clearly showed the impact of the induced wind because no other atmospheric phenomenon can explain this eruption.
The induced wind formulation is derived from a simplified mass balance based on the geometrical flame characteristics between the top of the vegetal stratum and the mid-height flame. The equality between inflow and outflow can be written as:

$$\rho_a \, \frac{H}{2} \, U_i = \rho \, \frac{L}{2} \, u \, \cos\alpha \qquad (6)$$

where U_i is the self induced wind, ρ is the combustion gases density, ρ_a is the ambient air density, *L* is the flame depth, *H* is the flame height and *u is* the upward gases velocity with slope (see Figure 1).

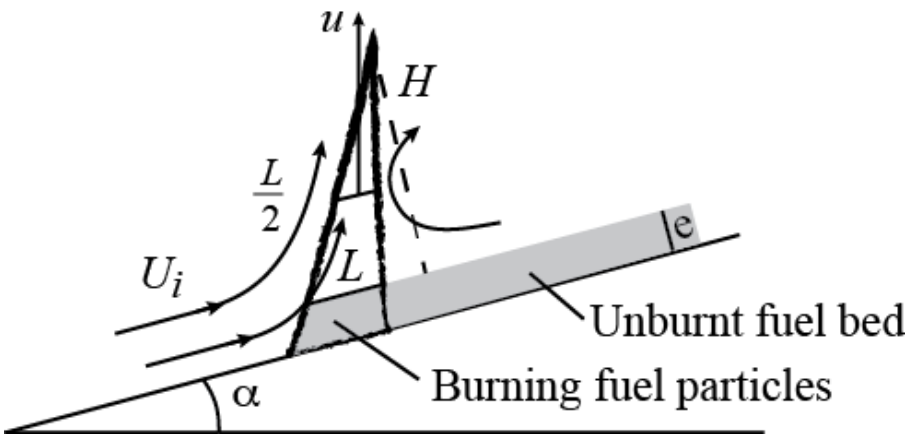

Figure 1. Qualitative description of the flame geometry.

Using the relationship $u = \frac{u_0}{\cos\alpha}$ (Balbi *et al.* 2009), the ratio between induced wind (U_i) and upward gases velocity at mid-height flame (u_0) is

$$\frac{U_i}{u_0} = \frac{\rho}{\rho_a}\frac{L}{H} = \frac{\rho}{\rho_a}\frac{R\,\tau}{H} = \frac{R}{p} \tag{7}$$

where τ is the flame residence time and

$$p = \frac{T}{T_a}\frac{H}{\tau} = 2\,\frac{\chi_0\,\Delta H\,\rho_v\,v\,r_0}{B\,T_a\,T^3\,\tau_0} \tag{8}$$

with the flame height given by Marcelli *et al.* (2011)

$$H = \frac{2\chi_0\Delta H\,\rho_v v r_{00}}{BT^4} \tag{9}$$

The flame residence time τ in equation (8) is expressed by using the relationship provided by Anderson (1969): $\tau = \tau_0 / s$ with τ_0 = 75591 m^{-1}·s. This time is inversely proportional to the fuel surface area to volume ratio *s*. Notice that this relationship is currently used in BEHAVE (Andrews 1986) in operational conditions. Using equation (7), the relationship (1) is changed in

$$\tan\gamma = \tan\alpha + \frac{R}{p} \tag{10}$$

Finally the fire spread behaviour taking into account the self-induced wind, is obtained by solving the following system:

$$R = p(\tan\gamma - \tan\alpha) \tag{11}$$

$$R = R_b + A\,R\,\frac{1+\sin\gamma-\cos\gamma}{1+\frac{R\cos\gamma}{r_0}} \tag{12}$$

The safety condition

In the coordinate system (tan γ, *R*), the steady solutions of the model are defined as the intersection of the growing function given by equation (12) and the straight line given by equation (11). Chatelon *et*

al. (2010) have showed that equation (12) exhibits two different behaviours for the ROS depending on the value of the coefficient *A*. Indeed the ROS *R* given by equation (12) is always a growing function which presents an horizontal asymptote when *A* is smaller than ½ and an affine asymptote (whose slope denoted by p_∞ is equal to $r_0(2A\text{-}1)$) otherwise (see figure 2).

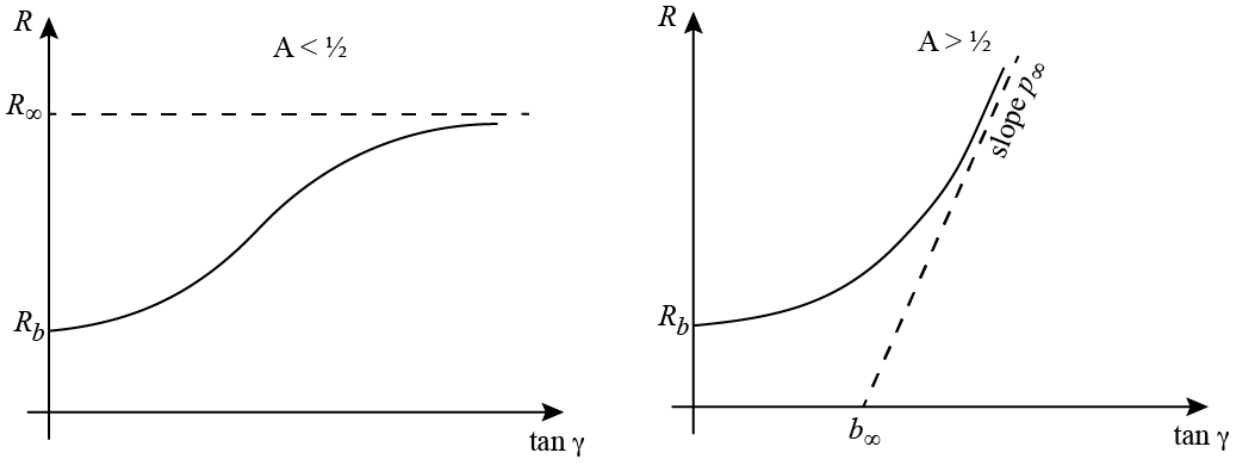

Figure 2. Qualitative illustration of the different rate of spread behaviours as a function of the flame tilt angle according to the value of the coefficient A.

A qualitative graphic analysis leads to several different cases, according to the values of the slope angle and the coefficients *A* and *p*:

- When $A < ½$, at least one solution of the system (11-12) always exists and is finite due to the horizontal asymptote exhibited by the ROS given by equation (12). So a fire eruption is impossible because the ROS cannot go to infinity. (see left side of figure 3)
- When $A > ½$, if *p* is greater than p_∞, the intersection of the ROS given respectively by equations (11) and (12) always exists. Its value may be great (when the slope is steep) but is always finite. So the fire never erupts (right side of figure 3).
- When $A > ½$, if *p* is smaller than p_∞, a fire eruption is possible but not sure. It depends on the value of the terrain slope angle. When α is greater enough, fire inevitably erupts.

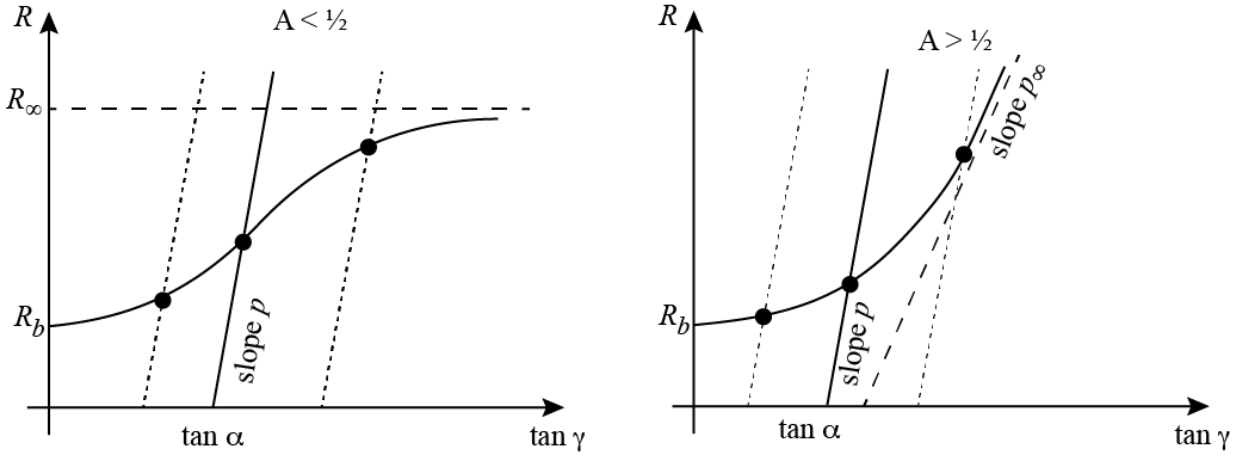

Figure 3. Qualitative illustration of the intersection of equations (11-12) when coefficient A is smaller than ½ (left side) and when A is greater than ½ (right side).

Consequently, two safety conditions with regard to fire eruptions can be expressed. The first one, i.e. $A < ½$ is usually obtained when the fuel bed arrangement is well ordered (e.g. with vertically-oriented fuel particles at the laboratory scale) or when the number of gaps in the vegetal stratum is very important (at the field scale). This condition is rarely satisfied when facing an eruptive fire.
Using equations (5), (7) and the expression of p_∞ previously given, the second condition i.e. $A > ½$, $p > p_\infty$ leads to the following ratio

$$\left(\frac{p}{p_\infty} = \frac{\rho_v}{\tau_0\, B\, T_a\, T^3\left[\frac{Y}{4(C_p\,\Delta T + m\Delta h)} - \frac{1}{2\,\nu\,\chi_0\,\Delta H}\right]}\right) > 1 \qquad (13)$$

where T_a is the ambient temperature, T the flame temperature, τ_0, B and χ_0 are constant values.
When the inequality (13) is satisfied, a fire eruption cannot occur. As soon as the ratio p/ p_∞ is smaller than 1, a fire eruption becomes possible but not sure. In fact the lower the value of the ratio p/ p_∞ the more the fire eruption risk grows.
Several factors contribute to reduce the value of the ratio p/ p_∞:

- Fuel bed properties
  - A low density vegetation with small specific heat, where its density ρ_v and the specific heat of vegetative fuel C_p are small.
  - A vegetative fuel with a light ligneous component. Indeed, the heat of combustion of the pyrolysis gases can be written as $\Delta H = (1\text{-}c)\ \Delta H_T - c\ \Delta H_c$, where ΔH_T is the heat of combustion of fuel ($\Delta H_T \approx 1.8\times10^7$ J·kg^{-1}), c the percentage of char and ΔH_c the heat of combustion of the char (Leroy *et al.* 2009). So, low char contents induce high values for ΔH, and then the ratio given by equation (13) decreases. Furthermore, the cubic flame temperature T^3 strongly increases with ΔH.
  - A sufficient fuel load. Coefficient ν must be as great as possible (ν=1 is the perfect situation for an eruption). As $\nu = \min(1, S/4)$, the leaf area S must be greater than 4. Moreover, as $S = \frac{s\,\sigma}{\rho_v}$, a low buoyancy (low density) and thin (important surface area to volume ratio) fuel satisfies this condition with a minimal fuel load of $\frac{4\,\rho_v}{s}$.
  - A dry vegetal stratum. Indeed, the moisture content m is lower than the moisture content of a living vegetal stratum and the greater m, the smaller the ratio p/p_∞.
- Environmental factors
  - A high ambient temperature. T_a plays a direct part in equation (13) but also through $\Delta T = T_i - T_a$ and through the flame temperature T (Balbi *et al.* 2009). Note that a specific work (Chetehouna *et al.* 2009) shows that if summer temperatures are extreme (≈ 40°C), some volatile organic compounds are probably emitted in a sufficient quantity to burn at a temperature lower than the usual temperature given for T_i (around 550 K). This issue deserves to be deepened and it would be useful to have a law for ΔT as a function of T_a.
  - Assuming a homogeneous fuel bed (or a dead fuel bed), a low relative air humidity induces a low fuel moisture content (Ascoli and Bovio 2010).
- Factors related to fire dynamics
  - A strong coefficient Y (close to 1). This coefficient depends on the fire front width/flame length ratio. When the fire front width is large compared to the flame length, the coefficient Y is close to 1 (*e.g.* in field scale configurations).

To summarize, the required conditions to increase the fire eruption risk are:

- A low buoyancy vegetation, weakly ligneous, with a sufficient fuel load,
- Bad meteorological conditions (high ambient temperature, low relative humidity),
- A large fire front.

Dold and Zinoviev (2009) emphasized the impossibility to describe an eruption phenomenon with a steady-state model for the ROS. In our case, the steady state propagation model is only used to obtain the safety condition (13) because the danger condition represents its limit case. The expression of the ROS and consequently the fire behaviour during the eruption is obviously obtained using the unsteady version of the propagation model but this aspect is not studied in this work which only focuses on the eruption's occurring.
When the condition (13) is no longer satisfied, a fire eruption is probable but does not inevitably occur. The eruption's onset depends on the value of the slope angle. One can note that the safety condition (13) does not depend on the slope angle. If the slope angle is greater than a threshold value α_c, fire will erupt. It is not possible to obtain an analytic expression of this threshold but only a numerical value which is found at any precision by solving the coupled model (11-12) with a fixed-point method.
One can also note that the model (11-12) can be used when a fire spreads downslope (*i.e.* for negative slope angle values) or on flat ground (as the eruptive fire occurred without wind and slope in the Saint-Génis Des Fontaines' local site in the south of France in 2005). But in these cases, the value of the ratio p/p_∞ has to be very small in order to obtain an eruption.

Confrontation with laboratory experiments and a real accident

Sets of data describing an eruptive behaviour are very rare in literature. So, testing the proposed approach is a difficult task. Two sets of laboratory scale experiments and a wildland fire that occurred on Kornati Island in 2007 were selected.
The first set of experiments was carried out by Viegas (2004b). Notice that the main goal of that set of experiments was only to observe fire propagations on slope.
The experimental bench (DV2 inclination table) had a useful 3m x 3m area that could be inclined at any desired angle α between 0° and 40°. The fuel bed used was made with dead pine needles (Pinus pinaster). The average fuel load was 0.8 kg m^{-2}. The average moisture content was about 10-11%.
No eruptions were observed, even with the steepest slopes (30° to 40°). This is due to the intrinsic properties of the pinus pinaster needles and to a pointed head of the fire front, leading to a fast decrease of the fire front width, especially with steep slopes and then to a weak ratio fire front width/flame length W/l. The flame length is approximately 1 m. The greatest width of the fire front (3 m wide) leads to a value of the coefficient Y equal to 0.75. In this "worst" case, the value of coefficient A is greater than ½ ($A = 0.91$) and the value of the ratio p/p_∞ is much greater than 1 ($p/p_\infty = 1.73$). So the model does not predict any eruption even for a 40° slope angle.
The second set of laboratory experiments was conducted by the CEIF (Centro de Estudos sobre Incêndios Florestais) laboratory of ADAI (Association for the Development of Industrial Aerodynamics) for Dold (2010) in which eruptions are observed for slope angles greater or equal than 30°.
The experiments consist in five trench fire experiments at 15°, 20°, 25°, 30° and 35° slope angles. For the three lower slopes, the fire spreads in a usual way, but a very fast spread is observed for the two higher slopes. So eruption happens between 25° and 30°.
The characteristics of the fuel bed (straw) that were used lead a lot more easily to a fire eruption than pinus pinaster's ones. Indeed, the great surface area to volume ratio ($s = 10000$ m^{-1}) or the small density of the vegetal particles ($\rho_v = 450$ kg.m^{-3}) involve a smaller value of the ratio $\boldsymbol{p/p_\infty}$ than the one obtained for pinus pinaster needles.

Moreover, vertical walls are located on the sides of the inclination table. According to Catchpole *et al.* (1998), the role of these walls is to mimic a wider fire front by preventing indraft into the combustion zone and by reflecting some of the radiation.
The model provides a value of 1.21 for coefficient *A* and a ratio p/p_∞ smaller than 1 ($p/p_\infty = 0.76$). Then a fire eruption is possible. The value of the threshold slope angle is obtained in solving the equations (11-12). A 26° slope angle is found which means that the fire eruption will occur only if the slope angle is greater than 26°. This threshold value is in accordance with the observed results.
The model was also confronted to a real fire that happened on the Kornati Islands, Croatia in 2007. This fire led to a dramatic fire-fighting accident causing the death of 12 fire fighters and severe burns for another one. The full description of this accident is detailed in Viegas *et al.* (2008) and Stipanicev *et al.* (2008).
The accident took place in the island of Kornat (the largest of 365 islands in Croatia's Kornati National Park). The fire started 6.6 km from the accident, which occurred in a small canyon (500 m long). The fuel load was low and made of sparse vegetation, mostly grass of approximately 30 cm with a few small isolated trees and bushes. The fuel load ranged from 0.561 $kg \cdot m^{-2}$ to 0.837 $kg \cdot m^{-2}$ and the average vegetation low heating value was estimated to be 1.8×10^7 $J \cdot kg^{-1}$. The moisture content of the fine fuel mass was equal to 10-12%. The canyon's main axis was directed to the north with a 15% (about 9°) average slope. A camera was found at the location of the accident. A large fire front (of about 50 m) was clearly seen on a photo from this camera (Stipanicev and Viegas 2009), with small flame lengths (below 1 m). So the parameter Y is close to 1 in this case ($Y = 0.98$).
On the Kornat Island, the fire was pushed by a S-E wind (about 40 km/h at 10 m height). According to the only fire-fighter who survived the accident of Kornati, the important fact was the very strong wind. In the canyon, the wind changed its direction to become parallel to the main canyon axis and the fire front was spreading at very high speed, maybe 6 or 7 $m \cdot s^{-1}$. His words are confirmed by the melted particles of a fire-fighter belt buckle found on a stone behind the place where his body was laying, which prove that the wind generated by the fire was very strong and coming from the south. The fire-induced wind, which grew to be stronger than the S-E wind and changed its direction, had clearly a key role in the occurrence of the eruption. Note that the few trees here have not been burnt. That means that flames were very slanted (in agreement with the flame attachment assumption).
The simulation results with Y = 0.98 and an average fuel load (0.7 kg·m-2) give the initiation of eruption for a slope angle $\alpha = 8°$, which is in accordance with the average slope of the canyon. Indeed, the value of coefficient *A* is equal to 1.24 and the ratio $\boldsymbol{p}/\boldsymbol{p}_\infty$ is smaller than 1 ($\boldsymbol{p}/\boldsymbol{p}_\infty = 0.86$).

Conclusion

If a few works about modeling of a fire ROS during an eruption can be found in the literature (e.g. Viegas 2005, Dold *et al*. 2011), to our knowledge none of them are able to predict the eruption's onset. This work focuses on a physical safety condition which means that a fire cannot erupt if this condition is satisfied. Otherwise, an eruption is either possible or certain. The physical model proposed in this work consists mainly of one propagation equation and one equation providing the induced wind created by the fire.
The explanation of the eruption phenomenon is the following: if the slope angle is sufficient enough, the combustion of the pyrolysis gases creates an indraft proportional to the flow of these gases that is related to the fire front depth and then to the ROS. So, there is a coupling between ROS and induced wind that created a feedback effect leading to unsteady growing propagation. Note that this interpretation was given by Viegas (2005).
Usually this unsteady phase converges to a steady phase, but under some conditions, this unsteady phase grows exponentially and a fire eruption occurs.
The specific conditions leading to certain eruption ($p < p\infty$ and $\alpha > \alpha c$) are obtained with:

- Dry summer conditions (weak humidity, great ambient temperature),

- Low density vegetation, slightly ligneous (e.g. grass),
- View factor of the fire front close to 1,
- Slope angle important enough.

The two last conditions are usually contradictory: it is well known that if the slope is steep, the fire front presents a 'pointed' effect with a narrow fire head. Then, the coefficient *Y* is small and the condition $p < p_\infty$ is satisfied with difficulty. This pointed effect is due to the induced wind, which reduces the view factor on the edges of the fire front. The ROS at the edges of the fire front is then close to the backward ROS.

The right situation for a fire eruption is obtained when this induced wind downslope does not exist. This can happen when:

- The inclined plane is lined with 'walls', i.e. a trench effect or corridor topography. The nature of this topographic concavity may be geological (rocks) or constituted by a vegetation stratum (e.g. hillside lined with forests). So, in order to obtain a Y coefficient close to 1, the fire front width must be much greater than the flame length. The eruption can only develop in long corridors that let the positive feedback happen before the fire reaches any topographic limits. The trench effect defined by Sharples *et al*. (2010), especially the King Cross underground disaster, is part of this first case.
- Vegetation made of two different layers – a lower stratum and a higher stratum, such as shrubs and trees – is covering a hill. If the lower layer is burning and the induced wind is strong enough, the flames will not reach the canopy and the fire will remain a surface fire. The induced wind coming upslope can enter the flame front from the burned area but vegetation slows down the induced wind coming downslope and the pointed head effect will not appear. So, the fire front width may be much greater than the flame length and then, $Y \propto 1$. For example, the Canberra fire in 2003, or the black Saturday fires in 2009, may be part of this second case.

In these two cases (corridor and bi-strata), the Y coefficient is close to 1. If the moisture content is of the order of 10%, a fuel bed with averaged properties (surface area to volume ratio, density, specific heat, height, fuel load) will give the following results: $p_\infty = 2p$, $\alpha_c = 15°$, $R = 6.4\ m \cdot s^{-1}$ after 60 s and L = 128 m. This example corresponds to the blow up phenomenon described by the fire-fighters.

Apart from these two cases, the decrease in coefficient Y will not provide a fire eruption faced to topographies as inclined plateau or hill with convex shape.

References

F.A. Albini (1985) A model for fire spread in wildland fuels by radiation, Combustion Science and Technology, 42, 229-258.

H.E. Anderson (1969) Heat transfer and fire spread, United States Department of Agriculture Forest Service, Research Paper INT-69.

P.L. Andrews (1986) BEHAVE: fire behavior prediction and fuel modelling system – BURN Subsystem, part 1, General Technical Report INT-194. Ogden, UT: U.S. Department of Agriculture, Forest Service, Intermountain Research Station, 130p.

D. Ascoli, G. Bovio (2010) Appraising fuel and fire behaviour for prescribed burning application in heathlands of Northwest Italy, D.X. Viegas (Ed.) VI International Conference on Forest Fire Research proceedings, Coimbra.

J.H. Balbi, J.L. Rossi, T. Marcelli, P.A. Santoni (2007), A 3D physical real-time model of surface fires across fuel beds, Combustion Science and Technology, **179:12**, pp. 2511-2537.

J.H. Balbi, F. Morandini, X. Silvani, J.B. Filippi, F. Rinieri (2009), A physical model for wildland fires, Combustion and Flame, **156**, 2217-2230.

J.H. Balbi, J.L. Rossi, T. Marcelli, F.J. Chatelon (2010), Physical modeling of surface fire under nonparallel wind and slope conditions, Combustion Science and Technology, **182**, pp. 922-939.

B.W. Butler, R.A. Bartlette, L.S. Bradshaw, J.D. Cohen, P.L.Andrews, T. Putnam, R.J. Mangan (1998), *Fire behavior associated with the 1994 South Canyon Fire on Storm King Mountain, Colorado*, USDA, Forest Service, RMRS-RP-9, Ogden, UT, 82 p.

W.R. Catchpole, E.A. Catchpole, B.W. Butler, R.C. Rothermel, G.A. Morris, D.J. Latham (1998) *Rate of spread of free-burning fires in woody fuels in a wind tunnel*, Combustion Science and Technology, **131**, 1-37.

F.J. Chatelon, J.H. Balbi, B. Moretti, T. Marcelli, J.L. Rossi (2010), Fast and slow regimes of fire propagation, D.X. Viegas (Ed.) VIe ICFFR proceedings, Coimbra, 2010.

N.P. Cheney, J.S. Gould (1995) *Fire Growth in Grassland Fuels*, International Journal of Wildland Fire, 5(4), 237-247.

K. Chetehouna, T. Barboni, I. Zarguili, E. Leoni, A. Simeoni, A.C. Fernandez-Pello (2009) *Investigation on the emission of Volatile Organic Compounds from heated vegetation and their potential to cause an eruptive forest fire*, Combustion Science and Technology, 181:10 (2009), pp. 1273-1288.

J.W. Dold, A. Zinoviev (2009), *Fire eruption through intensity and spread rate interaction mediated by flow attachment*, Combustion Theory and Modelling, **13**, pp. 763-793.

J.W. Dold (2010), *Flow attachment in eruptive fire growth*, D.X. Viegas (Ed.) *VI International Conference on Forest Fire Research proceedings*, Coimbra, 2010.

J.W. Dold, A. Zinoviev, E. Leslie, (2011) *Intensity accumulation in unsteady firelines: A simple model for vegetation engagement*, Fire Safety Journal, **46**, pp. 63-69.

P.A. Fernandes (2001) *Fire spread prediction in shrub fuels in Portugal*, Forest Ecology Management, 144, 67–74.

M. Guijarro, C. Hernando, J.A. De Los Santos, C. Diez (1997) Forest Fire behaviour on the wind tunnel, Hefaistos Project Report, ENV4-CT96-0299.

E. Koo, P. Pagni, J. Woycheese, S. Stephens, D. Weise, J. Huff (2005) A Simple Physical Model for Forest Fire Spread Rate, In 'Fire Safety Science-Proceedings of the eighth international symposium', 851-862.

V. Leroy, D. Cancellieri, E. Leoni, (2009) *Relation between forest fuels composition and energy emitted during their thermal degradation*, Journal of thermal analysis and calorimetry, **96(1)**, pp. 293-300.

A.G. McArthur (1969), The behavior of mass fires in felled eucalypt forest originating from a simultaneous grid or line ignition system, in Mass Fire Symposium, Defense Standards Laboratory, Canberra, Australia, Paper A1.

T. Marcelli, J.H. Balbi, B. Moretti, J.L. Rossi, F.J. Chatelon (2011) Flame height model of a spreading surface fire, In 'Proceedings of the seventh Mediterranean Combustion Symposium (The Combustion Institute)', Chia Laguna, Cagliari, Italy, september 11-15, pp 12.

J.M.C. Mendes-Lopes, J.M.P. Ventura, J.M.P. Amaral (2003) *Flame characteristics, temperature-time curves, and rate of spread in fires propagating in a bed of Pinus pinaster needles*, International Journal of Wildland Fire, 12, 67-84.

P.J. Pagni, G. Peterson (1973) Flame spread through porous fuels, In 'proceedings of 14th Symposium (International) on Combustion', 1099-1107. (The Combustion Institute)

J.J. Sharples, A.M. Gill, J.W. Dold (2010) The trench effect and eruptive wildfires: lessons from the King's Cross underground disaster, Proceedings AFAC 2010.

D. Stipanicev, Z. Spanjol, M. Vucetic, V. Vucetic, R. Rosavec, Lj.Bodrozic (2008) The Kornati fire accident facts and figures – configuration, vegetation and meteorology, Witpress (Ed.) Modelling, Monitoring and Management of forest fires, Vol. I, pp 387-396.

D. Stipanicev, D.X. Viegas (2009), *The accident of Kornati (Croatia) 2007*, Recent Forest Fire Related Accidents in Europe, JRC Scientific and Technical Reports, 75 pp., 26-53, doi:10.2788/50781.

H.P. Telisin (1974) Flame radiation as a mechanism of fire spread in forests, In 'Heat Transfer in Flames', Afgan N.H. and Beer J.M. (Eds), John Wiley and Sons, New York, p. 441.

C.E. Van Wagner (1967) Calculations on forest fire spread by flame radiation. Special paper for the sixth World Forestry Conference, 1-14.

D.X. Viegas, M.G. Cruz, L.M. Ribeiro, A.J. Silva, A. Ollero, B. Arrue, R. Dios, F. Gomez-Rodriguez, L. Merino, A.I. Miranda, P. Santos (2002) Gestosa fire spread experiments. In 'Proceedings of the IV ICFFR, Luso, Portugal, 18-23 November 2002', (Ed. DX Viegas)(Millpress Science Publishers: Rotterdam, The Netherlands).

D.X. Viegas (2004a), *Slope and wind effects on fire propagation*, International Journal of Wildland Fire**, 13**, pp. 143-156.

D.X. Viegas (2004b), *On the existence of a steady state regime for slope and wind driven fires*, International Journal of Wildland Fire, **13**, pp. 101-117.

D.X. Viegas (2004c), Cercados pelo Fogo (in Portuguese), Minerva Editora (Eds), 274 pp.

D.X. Viegas (2005), *A mathematical model for forest fires blowup*, Combustion Science and Technology**, 177:1**, pp. 27-51.

D.X. Viegas, L.P. Pita (2004), *Fire spread in canyons*, International Journal of Wildland Fire, **13**, pp. 253-274.

D.X. Viegas, D. Stipanicev, L. Ribeiro, L.P. Pita, C. Rossa (2008) The Kornati fire accident – eruptive fire in relatively low fuel load herbaceous fuel conditions, Witpress (Ed.) Modelling, Monitoring and Management of forest fires, Vol. I, pp. 365-375.

D.X. Viegas, A. Simeoni (2011) *Eruptive behaviour of forest fires*, Fire Technology, **47(2)**, pp. 303-320, doi: 10.1007/s10694-010-0193-6.

Development and application of wildfire suppression expenditure models for decision support and landscape planning

Michael S. Hand[a], Matthew P. Thompson[a], David E. Calkin[a]

[a] *US Forest Service Rocky Mountain Research Station, Missoula, Montana, USA, mshand@fs.fed.us, decalkin@fs.fed.us, and mpthompson02@fs.fed.us*

The opinions expressed in this paper are the authors' and do not necessarily reflect the views of the U.S. Department of Agriculture

Keywords: suppression expenditures; spatial models; decision support; fuel treatments

Extended abstract

A major consequence of large wildfires is the budgetary impact on public agencies tasked with wildfire management and suppression efforts. In wildfire seasons with a high incidence of large and expensive fires, agency budgets for non-fire activities can be threatened when the immediate needs of wildfire management are prioritized. In the United States, wildfire management already accounts for a large and increasing share of the U.S. Forest Service's (USFS) budget, which strains other land management needs. Between 1992 and 2011, the annual budget dedicated to fire management grew from 13 to over 40 percent of total agency appropriations.

This extended abstract describes the development of expenditure models that are capable of providing spatially and temporally explicit information about costs, and provides examples of how such models can complement sophisticated fire simulation models used to support incident management decisions and landscape-scale fire planning. To date, expenditure modelling efforts have yielded insights into the geographic, landscape, socio-political, and management characteristics associated with wildfire suppression expenditures. These insights are based on models that relate characteristics associated with the location and date of ignition of wildfires to expenditure records (e.g., Gebert *et al*. 2007; Gude *et al*. 2013; Donovan *et al*. 2011; Yoder and Gebert 2012). However, decision support tools and wildfire modelling efforts increasingly use detailed spatial and temporal descriptions of geographic, landscape, and weather conditions. Accounting for heterogeneity of such conditions in management expenditure models may improve link between fire modelling outputs and expenditure models for fire management planning and decision support.

Incorporating spatial characteristics in expenditure models has limited precedent in the literature. Priesler *et al*. (2011) create spatially explicit forecasts of expenditures, but the underlying expenditure model is based on ignition-point data. Liang *et al*. (2008) incorporated spatial characteristics of the area within fire perimeters to account for observed spatial autocorrelation of expenditures for limited set of fires in the Northern Rockies region of the United States. Hand *et al*. (2014, ch.4) extend the approach in Liang *et al*. (2008) to include fires in the entire Western United States, but did not evaluate the role of heterogeneity or assess model performance relative to ignition-point models. The data and methods in Hand *et al*. (2014) form the basis of the empirical models in this paper.

To develop spatially and temporally descriptive expenditure models, final fire perimeters were gathered for a sample of large fires (greater than 121 hectares) from the western United States. In total, 406 fires from fiscal years 2006 to 2011 are used in the final estimation sample. The fire perimeters were used in conjunction with several geo-spatial data layers to describe the extent and variation of geographic and landscape characteristics that are thought to be associated with expenditures. The time period between the discovery date of the fire and the date of control or containment was used to examine landscape and geographic characteristics within the fire perimeter that may vary over time.

The spatially and temporally descriptive characteristics are used as independent variables in a regression model to predict total incident expenditures by Federal management agencies.[1] Table 1 describes the variables used in the regression model and the corresponding variables in ignition-point expenditure models that the spatially and temporally descriptive variables replace.

Table 1. Variables used in spatially descriptive regression with corresponding ignition-point variables; obs. = 406

Variable	Description	Source (see table footnote)	Corresponding ignition-point variables
lnexp	Natural log of total federal suppression expenditures in constant 2012 $ (Dep. Var.)	FFIS	--
lnacres	Natural log of area within final fire perimeter	NIFC FTP	--
erc_max	Maximum relative ERC percentile observed during the fire within the final perimeter	GIS calculation of data from Abatzoglou (2011)	ERC at ignition point and time
erc_std	Standard deviation of relative ERC observed during the fire within the final perimeter	GIS calculation of data from Abatzoglou (2011)	ERC at ignition point and time
lnavelev	Natural log of the average elevation within the final perimeter	LANDFIRE	Elevation at ignition point
wild_burn	Burned within Wilderness area (binary)	WFDSS	Ignition within Wilderness area (binary)
wild_sh	Share of final burned area within a Wilderness area	WFDSS	Distance of ignition point from Wilderness boundary
ira_burn	Burned within an Inventoried Roadless Area (binary)	WFDSS	Ignition within Inventoried Roadless Area (binary)
ira_sh	Share of final burned area within an IRA	WFDSS	Distance of ignition point from IRA boundary
other_burn	Burned within other specially designated area (binary)	WFDSS	Ignition within other specially designated area (binary)
other_sh	Share of final burned area within a SDA	WFDSS	Distance of ignition point from SDA boundary
slope1	Share of final burned area with slope less than 20% (omitted reference category)	LANDFIRE	Percent slope at ignition point
slope2	Share of final burned area with slope between 20% and 40%	LANDFIRE	
slope3	Share of final burned area with slope between 40% and 60%	LANDFIRE	
slope4	Share of final burned area with slope between 60% and 80%	LANDFIRE	
slope5	Share of final burned area with slope greater than 80%	LANDFIRE	
usfs_sh	Share of final burned area in USFS ownership	WFDSS	USFS ownership at ignition point (binary)
doi_sh	Share of final burned area in Dept. of Interior ownership	WFDSS	DOI ownership at ignition point (binary)
grass_sh	Share of final burned area with grass fuels	LANDFIRE	Grass fuels at ignition point (binary)
brush_sh	Share of final burned area with brush fuels	LANDFIRE	Brush fuels at ignition point (binary)

[1] The sample of fires includes only fires managed primarily by the U.S. Forest Service. However, other Federal agencies may incur a minority of expenses for the management of these fires. The dependent variable represents total Federal expenditures.

timber_sh	Share of final burned area with timber fuels	LANDFIRE	Timber fuels at ignition point (binary)
slash_sh	Share of final burned area with slash fuels	LANDFIRE	Slash fuels at ignition point (binary)
lnhousein	Natural log of housing value within the final perimeter in constant 2012 $	U.S. Census	n/a
lnhouse5_perim	Natural log of housing value within 5 miles of final perimeter in constant 2012 $	U.S. Census	Housing value within 5 mi. of ignition point
lnhouse10_perim	Natural log of housing value between 5 and 10 miles from perimeter in constant 2012 $	U.S. Census	Housing value within 10 mi. of ignition point
lnhouse20_perim	Natural log of housing value between 10 and 20 miles from perimeter in constant 2012 $	U.S. Census	Housing value within 20 mi. of ignition point
asp_123	Share of final burned area with North, Northeast, or East aspect	LANDFIRE	Sine and cosine of aspect (in radians) at ignition point
asp_456	Share of final burned area with Southeast, South, or Southwest aspect	LANDFIRE	
asp_78	Share of final burned area in West or Northwest aspect (omitted reference category)	LANDFIRE	
duration	Fire duration in days, top-coded at 90 days	NIFMID	--
dur2	Square of *duration*	NIFMID	--
dur3	Cubic of	NIFMID	--
reg_1	Northern region identifier (binary, omitted reference category)	NIFMID	--
reg_2	Rocky Mountain region indicator (binary)	NIFMID	--
reg_3	Southwest region indicator (binary)	NIFMID	--
reg_4	Great Basin region indicator (binary)	NIFMID	--
reg_5	California region indicator (binary)	NIFMID	--
reg_6	Northwest region indicator (binary)	NIFMID	--
fy06	Fiscal year 2006 indicator (binary, omitted reference category)	NIFMID	--
fy07	Fiscal year 2007 indicator (binary)	NIFMID	--
fy08	Fiscal year 2008 indicator (binary)	NIFMID	--
fy09	Fisal year 2009 indicator (binary)	NIFMID	--
fy10	Fiscal year 2010 indicator (binary)	NIFMID	--
fy11	Fiscal year 2011 indicator (binary)	NIFMID	--

-- indicates no change in the variable between ignition point and spatially descriptive model.
n/a indicates that the variable was not used in the ignition point model.
Data sources: FFIS – Foundation Financial Information System, which is being replaced by the Financial Management Modernization Initiative (FMMI), available at http://info.fmmi.usda.gov/, accessed 9/3/2013. NIFMID – National Interagency Fire Management Integrated Database, maintained at the USDA National Information Technology Center in Kansas City, MO; NIFMID variables are self-reported by managers for each wildfire. NIFC FTP – available at ftp://ftp.nifc.gov/Incident_Specific_Data/, accessed 7/24/2013; WFDSS – Wildland Fire Decision Support System databases available at http://wfdss.usgs.gov/wfdss/WFDSS_Data_Downloads.shtml, accessed 7/24/2013; LANDFIRE – version 1.2.0 available at http://www.landfire.gov/lf_120.php, accessed 7/24/2013.

Preliminary results suggest that spatial heterogeneity of geographic and landscape characteristics affect suppression expenditures. In particular, the spatial pattern of surface fuels, protection designation (e.g., Wilderness Areas), land ownership, and housing values are significant predictors of expenditures. Further, the temporal pattern of fire weather and fuel moisture conditions is an important predictor of expenditures. The spatially descriptive model also improves prediction accuracy and

model fit as compared with analogous models based on ignition-point characteristics. Table 2 compares the size of the standardized residuals (in standard deviation, or s.d., units) in the spatial/temporal model to those in the comparable ignition-point model.

Table 2. Comparison of standardized prediction errors between spatial/temporal model and ignition-point model

Size of standardized residual	Spatial model frequency	Ignition-point model frequency
<= 1 s.d.	104	94
1 - 2 s.d.	101	77
2 - 3 s.d.	87	69
>4 s.d	114	166
All obs.	406	406

An immediate use of the spatially and temporally descriptive expenditure model is to improve the accuracy of expenditure predictions when the final burned area is known. For example, after-season reviews of fire-specific expenditures can be compared to predicted expenditures using the final fire perimeter and the spatial/temporal expenditure model. The results indicate that the modest improvements in prediction accuracy can lead to more reliable comparisons in the future.

The model can also be used to improve the functionality of decision support tools that include predictions of total incident expenditures. In the Wildland Fire Decision Support System (WFDSS), the ignition-point expenditure model is currently used to provide information about expected expenditures for an incident under given conditions (Noonan-Wright *et al*. 2011). The spatially and temporally explicit model may yield more nuanced information about expenditures because it can, in theory, be paired with fire models in WFDSS that result in predicted fire perimeters. For example, the expenditure model can be paired with fire spread models to generate spatially explicit expected expenditure maps. Such an application would leverage variations in fire behaviour generated by the fire spread model (which determines the size and areal extent of the fire), as well as spatial and temporal variations in characteristics that are related to expenditures. As risk management becomes a greater focus of wildfire management, risk-based expenditure information may assist managers in making strategic decisions during a fire incident.

Incorporating spatially descriptive data can provide richer information about how expenditures are affected by alternative land management scenarios. Planning and prioritizing the treatment of hazardous fuels to affect future fire behaviour may incorporate impacts on expected suppression expenditures (Fitch *et al*. 2013; Thompson *et al*. 2013). The spatial/temporal expenditure model could provide greater detail about how changes in fire behaviour relate to expenditures. For example, hazardous fuel treatments may not necessarily affect the expected number of ignitions or number of large fires in a given season, but could affect the spatial pattern of where fires are likely to burn. Ignition-point models of expenditures currently in use (e.g., in Thompson *et al*. 2013) only account for changes in fire size. But fuel treatments are an inherently spatial endeavour, and the location and pattern of treatments may have impacts on wildfire management that extend beyond changes in final fire size. Understanding the magnitude of any potential suppression cost trade-offs can assist managers in determining whether such investments are worth the cost.

In summary, spatially and temporally descriptive models of wildfire management expenditures show promise for improving predictions of expenditures and providing nuanced information for decision support and land management planning. Accounting for heterogeneity of characteristics in space and over time improves the fit and predictive power of wildfire expenditure models, and are readily adaptable to spatially explicit fire modelling tools. The models investigated in this paper are limited

by the fact that they use relatively coarse geospatial data, and do not explicitly model how the progression of fire relates to expenditures. Future research using time-series panel data and finer scale geographic data may help alleviate these limitations.

References

Abatzoglou, J.T., 2013. Development of gridded surface meteorological data for ecological applications and modelling. *International Journal of Climatology* 33,121-131.

Fitch, R.A.,, Kim, Y-S., Waltz, A.E.M., 2013. Forest restoration treatments: their effect on wildland fire suppression costs. Northern Arizona University, Ecological Restoration Institute – Issues in Forest Restoration. Available at: http://library.eri.nau.edu/gsdl/collect/erilibra/index/assoc/D2013009.dir/doc.pdf, accessed April 15, 2014.

Gebert, K.M., Calkin, D.E., Yoder, J., 2007. Estimating suppression expenditures for individual large wildland fires. *Western Journal of Applied Forestry* 22, 188-196.

Gude, P.H., Jones, K., Rasker, R., Greenwood, M.C., 2013. Evidence for the effect of homes on wildfire suppression costs. *International Journal of Wildland Fire* 22, 537-548.

Hand, M.S., Gebert, K.M., Liang, J., Calkin, D.E., Thompson, M.P., Zhou, M., 2014. *Economics of wildfire management: the development and application of suppression expenditure models*. Springer Briefs in Fire, Springer, New York.

Liang, J., Calkin, D.E., Gebert, K.M., Venn, T.J., Silverstein, R.P., 2008. Factors influencing large wildland fire suppression expenditures. *International Journal of Wildland Fire* 17, 650-659.

Noonan-Wright, E., Opperman, T.S., Finney, M.A., Zimmerman, T., Seli, R.C., Elenze, L.M., Calkin, D.E., Fiedler, J.R., 2011. Developing the U.S. wildland fire decision support system. *Journal of Combustion* 2011 (Article ID 168473), 14pp.

Preisler, H.K., Westerling, A.L., Gebert, K.M., Munoz-Arriola, F., Holmes, T.P., 2011. Spatially explicit forecasts of large wildland fire probability and suppression costs for California. *International Journal of Wildland Fire* 20, 508-517.

Thompson, M.P., Vaillant, N.M., Haas, J.R., Gebert, K.M., Stockmann, K.D., 2013c. Quantifying the potential impacts of fuel treatments on wildfire suppression costs. *Journal of Forestry* 111, 49-58.

Yoder, J., Gebert, K.M., 2012. An econometric model for ex ante prediction of wildfire suppression costs. *Journal of Forest Economics* 18, 76-89.

Evaluating wildfire simulators using historical fire data

George J Milne, Joel K Kelso, Drew Mellor and Mary E Murphy

University of Western Australia. Perth, Australia. george.milne@uwa.edu.au

Abstract
High-performance wildfire simulators allow the future location of a wildfire to be rapidly predicted. The accuracy of such simulators needs to be evaluated; this can be achieved by comparing simulated and observed spread for documented historical fires. A key issue relates to the accuracy of data obtained from historical fires, such as the time-varying fire location, fire-ground weather and accuracy of fuel type, load and structure data. A methodology used to evaluate the accuracy of wildfire simulators using historical fire data is presented and applied to the AUSTRALIS wildfire simulator using the four distinct phases of a large-scale wildfire occurring in Western Australian sand-plain heathlands and a fire reconstruction report on this fire produced by a wildfire expert. Challenges encountered in performing this validation exercise are highlighted.

***Keywords**: wildfire simulation, GIS, fire behaviour models, simulator testing*

Introduction

A methodology used to evaluate the accuracy of wildfire simulators using historical fire data is presented. Application of the methodology was examined using the four phases of a large-scale wildfire occurring in Western Australian sand-plain heathlands and a fire reconstruction report on this fire produced by a wildfire expert. The spatio-temporal dynamics estimated from the reconstruction report was compared with simulated fire behaviour, as produced by the AUSTRALIS wildfire simulator. The availability of rapid automated fire prediction permits the many variables which influence fire spread to be quickly examined by changing simulator input parameters, such as forecast wind speed and direction, to determine how such changes may impact on the spread characteristics of the fire. While simulators such as the AUSTRALIS wildfire simulator allow the future location of a wildfire to be rapidly predicted, and geographical information systems (GIS) maps with forecast fire-lines overlayed on them to be quickly made available to fire managers, the accuracy of such simulators needs to be examined by application to high-quality datasets from prior fires. A key issue relates to the accuracy of data obtained from historical fires, such as time-varying fire location, fire-ground weather and accuracy of fuel type, load and structure data, which are necessary if meaningful comparisons are to be made.

2. Methods

Simulating the spread of wildfire across a real landscape may, like simulation of other complex natural phenomena, be impacted by multiple sources of inaccuracy. First, the input data used for simulation will be subject to inaccuracy. For example, spatial boundaries in vegetation maps have limited precision and may have changed since the map was generated; initial fire perimeters are generally approximate; the closest meteorological observations may have been taken tens of kilometres from the fire-site. Second, predictive models relevant to fire behaviour, such as fire behaviour models for predicting rate of spread, slope correction, two-dimensional fire shape models, and fuel accumulation models, are all idealised models that approximate real phenomena. Third, the simulation methodology itself can introduce inaccuracy. For example, the discrete event simulation approach of AUSTRALIS (Johnston *et al.* 2008) relies on spatial discretisation, where the landscape is partitioned into cells that are assumed to have homogeneous attributes, such as vegetation, slope and aspect. When the spatial

resolution of the cell grid is coarse relative to the features being modelled, then the assumption of homogeneity is likely to be inaccurate for many cells. Given the need for accurate wildfire spread prediction these issues need to be overcome, and this provides the rationale for the reported study.

The general validation technique used in this paper is as follows:

- Obtain topographic, meteorological and fuel data for a historical fire event. Also obtain reconstructed fire spread perimeters and initial ignition/fire front locations
- Simulate the fire using the obtained data and generate a progression of fire spread perimeters
- Compare the level of agreement between the simulated and reconstructed fire progression perimeters
- Assess the impact of uncertainty in the input data, fire behaviour models, and simulation algorithm on simulation accuracy by extensive sensitivity analyses.

In this paper, a case study of the above methodology is presented in which the AUSTRALIS wildfire simulator (Johnston *et al.* 2008) is applied to a large-scale historical fire that occurred in the vicinity of the Boorabbin National Park, Western Australia (WA) in December 2007 and January 2008.

This fire burned a total area of approximately 18,000 hectares over the 4 phases that were simulated. The topography consisted of gently undulating sand-plains and broad, shallow valleys. Two types of vegetation were present: Eucalypt woodland characterised by a very sparse understorey layer and a lack of fuel continuity, and semi-arid sand-plain heath (see Figure 1). Two government reports into the Boorabbin fire were produced as part of a coronial inquest following deaths which occurred on the fourth phase of the fire. These reports provided (i) a comprehensive assessment of the fuel and meteorological conditions occurring during the course of the fire (Bureau of Meteorology 2008; de Mar 2008), and (ii) a reconstruction of the fire perimeters over several phases of the fire at time steps ranging from 15 minutes to 3.5 hours (de Mar 2008). The existence of this detailed fire reconstruction data facilitated use of the following method.

Comparison between the simulator-generated, time-varying progression of the fire-line and an independently produced fire behaviour reconstruction produced as part of a coronial inquiry into deaths resulting from one of the four constituent fire phases was made. The accuracy of the simulated fire against the fire reconstruction contained in the report was determined using a number of measures, such as agreement of the headfire rate-of-spread (RoS) and the fit of the time-varying fire perimeters. The reconstruction report made use of high-resolution (less than 20m) satellite imagery to establish the final fire perimeter; however very limited data (i.e. firefighter recollection and limited aerial and ground photography) was available for the estimation of intermediate perimeters. Four distinct component fire phases were simulated, with the maximum Fire Danger Index ranging from 28 (high) to 104 (very extreme) across the four fire phases.


Figure - 1 Predominant vegetation present at the fireground. Left: sandplain heath-scrub. A short scrub assemblage typical of that occurring in the higher parts of the landscape. Note the low, patchy nature of the vegetation. The taller, isolated shrubs in the background are mature Callitris, and indicate that this area has not been burnt for 25 years. Right: unburnt Tamma scrub. An expanse of Tamma scrub similar to the vegetation that burnt during the run of the fire to the highway where the fatalities occurred. Note the short, relatively dense vegetation structure. Tamma scrub is one of the denser heath-scrub assemblages (high level of fuel continuity) likely to support faster moving fires than occur in patchier heath scrub vegetation types. Photographs and annotations taken from (de Mar 2008).

Simulated fire progression perimeters were generated using the AUSTRALIS simulator, using fuel type and coverage data from the reports, a national vegetation mapping data set (Australian Government Department of the Environment 2014), meteorological data from the nearest Bureau of Meteorology Automatic Weather Station (AWS) at Southern Cross, and a fire behaviour (rate-of-spread) model developed for arid heathland (Cruz *et al.* 2010). Simulator accuracy was assessed via a statistical comparison of the spatial extent of the simulated perimeters against the estimated perimeters taken from the reconstruction report, at corresponding time-steps.

AUSTRALIS employs a discrete event simulation technique (Zeigler *et al.* 2000) that is based on partitioning the landscape into a collection of two dimensional cells and calculating the propagation delay between an 'ignited' cell and each of its 'unburnt' neighbours. Each cell contains state information ('unburnt' and 'ignited') and a number of attributes relevant for calculating propagation delay, including location, elevation, and fuel characteristics such as vegetation type and fuel load. In contrast to other cell-based approaches to wildfire simulation, the cell locations are distributed randomly, rather than regularly, across the landscape. This is done to avoid a form of fire shape distortion that results from using a regular partition, such as with a rectangular or square grid. For all simulations in this study, the average distance between cell centroids was 50 m. Other fire spread simulation systems that use a discrete cellular representation of the landscape include FSPro, part of the U.S. Forest Service WFDSS system (Finney 2002; Finney *et al.* 2011), PYROCART (Perry *et al.* 1999), and FireStation (Lopes *et al.* 2002).

The validation technique presented in this paper may be used to validate any fire spread simulation system that predicts fire-front time of arrival across the landscape. Systems that do not use an underlying cellular landscape structure, such as FARSITE (Finney and Ryan 1995), Prometheus (Tymstra *et al.* 2010), and SIROFire/Phoenix (Coleman and Sullivan 1996; Tolhurst *et al.* 2008), may be accommodated by first running fire spread simulations and then rasterising both the estimated and simulated fire arrival time maps to generate cells for the purpose of accuracy assessment (see below). We note that in order to conduct extensive sensitivity analyses of the type presented in this paper, the ability to run many (hundreds) of fire spread simulations rapidly is beneficial, and it may not be practical to apply this kind of sensitivity analysis to computationally intensive, physics-based simulation systems such as FIRETEC (Linn *et al.* 2002).

The accuracy of the AUSTRALIS simulator at predicting the fire spread progression of the Boorabbin fire was measured as follows. At the conclusion of a simulation, AUSTRALIS output the fire arrival time for each cell that ignited. The accuracy of the simulated fire spread was assessed by comparison to a

detailed reconstruction of the estimated fire progression which had mapped intermediate fire perimeters throughout the course of the fire at time step intervals of at most 3.5 hours over the four phases of interest. Accuracy was determined using Cohen's kappa coefficient (*K*), a statistical measure of agreement between two geo-spatial datasets, which has been used previously for assessing the accuracy of fire spread simulation (Arca *et al.* 2007). Cohen's kappa is given by:

$$K = \frac{N\sum_{i=1}^{k} x_{ii} - \sum_{i=1}^{k}(x_{i+} - x_{+i})}{N^2 - \sum_{i=1}^{k}(x_{i+} - x_{+i})}$$

where x is the error matrix, i.e. xij is the number of simulation cells where the simulated and reconstructed fires arrive in time period i and j respectively; , $xi+$ and $x+i$ are the marginal totals of row i and column i respectively, and N is the total number of samples. Kappa typically varies over [0,1], where $K = 0$ indicates that agreement is due to chance alone, and $K = 1$ indicates perfect agreement.

Results

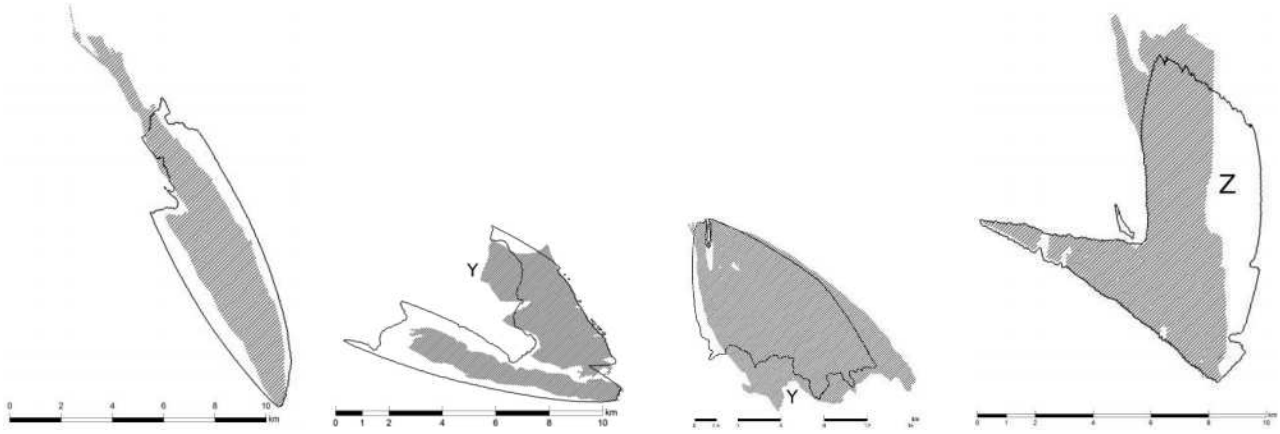

Phase 1: 2359 kappa = 0.62 | Phase 2 : 1900 kappa = 0.49 | Phase 3a: 1900 kappa = 0.33 | Phase 3b : 2359 kappa = 0.42

Figure 2. Final fire perimeters estimated by the reconstruction report (shaded) and simulated by AUSTRALIS (black line) at the end of each phase. The agreement statistic kappa is given for each phase, which takes into account agreement between intermediate estimated and simulated fire perimeters (not shown). Spread under-predictions in Phase 2 and 3a marked Y are due to vegetation mapping inaccuracies; spread over-prediction in Phase 3b (marked Z) is due to weather data inaccuracy.

Using the available data AUSTRALIS were able to approximately reproduce the observed fire behaviour in each of the four phases, as shown in Figure 2.

Following the initial simulations of the four phases, an extensive series of sensitivity analysis experiments were conducted in order to determine the factors which limited the accuracy of the simulation system. The simulation input parameters that were varied and the range of values used are given in Table 1. In the case of the weather time series, adjustments were made by adding or subtracting a fixed amount from the value of the variable at each time step. For vegetation cover, all landscape cells containing heath vegetation were set to an alternative percent cover score (PCS) value. For fire behaviour models, each sensitivity analysis simulation used an alternative fire behaviour model to calculate rate of spread occurring in heath vegetation.

Table 1. Simulation parameters varied in sensitivity analysis simulations and the series of parameter values examined for each. Abbreviations are as follows. AWS – automatic weather station; U10 – 10 m wind speed recorded at the Southern Cross AWS; WD – wind direction (degrees clockwise from North); WS – wind speed (kilometres per hour); T – temperature (degrees Celsius); RH – relative humidity (percentage); PCS – percentage cover score; HE – semi-arid heath model (Cruz et al. 2010); MH1 – mallee heath (McCaw 1997); MH2, MH3 – semi-arid mallee heath (Cruz et al. 2010); SH – shrubland (Catchpole et al. 1998); HG - (Burrows et al. 2009).

Simulation parameters and models	Baseline value/model	Sensitivity analysis range
Cell grid		
Cell size (m)	50	50, 100, 250, 500, 750 5 randomly generated grids at each size.
Meteorological variables		
Wind speed measured at 10 m (km/h)	Southern Cross AWS (U10)	U10 ± 5, U10 ± 10, U10 ± 15, U10 ± 20
Wind direction (°)	As above (WD)	WD ± 5, WD ± 10, WD ± 15
Temperature (°C)	As above (T)	T ± 5, T ± 10, T ± 15
Relative Humidity (%)	As above (RH)	RH ± 5, RH ± 10, RH ± 15
Fuel variables		
PCS of elevated fuel layer (0–4)	1.5	1, 1.5, 2, 2.5, 3, 3.5, 4
Fire behaviour models		
Fire behaviour model for heath vegetation	HE	HE, MH1, MH2, MH3, SH, HG

In the following subsections we summarise the results of these sensitivity analyses. We describe the outcome of the analyses in two parts: the effect of simulation algorithm cell size, and results showing a dichotomy between the first two phases of the fire and the second two phases, which occurred under extreme fire weather conditions.

Impact of the cell grid on simulation accuracy

As described previously, the AUSTRALIS simulator discretises the landscape into a set of randomly placed cells. This technique potentially introduces two sources of inaccuracy into the simulation results. Firstly, as with any simulation algorithm based on a cellular landscape discretisation, if cells are too large, it will not be possible for any set of simulation-generated cells to represent realistic fire shapes without either under- or over-fitting. Secondly, since the cell locations used by AUSTRALIS are randomly generated, simulation outputs can vary from one simulation run to another, even with identical simulation inputs. Both of these potential sources of inaccuracy decrease with decreasing cell size, as illustrated in Figure 3. In Figure 3A it can be seen that with a large cell size, the simulation of an ideal elliptical fire spread shape is considerably distorted, whereas in Figure 3B the elliptical fire shape is closely approximated. Comparing Figure 3B with 3C, it can be seen that simulations using two different randomly chosen grids with the same small cell size give rise to very similar fire shapes.

A **B** **C**

Figure 3. Three AUSTRALIS simulation outputs for an idealised case with uniform fuel and a northerly wind. A (left) cell spacing 750m, B (middle) cell spacing 150m, C (right) cell spacing 150m, but with different randomly generated grid.

In order to quantify these effects of cell size in the context the Boorabbin simulation study, each of the four phases of the fire were simulated using cell grids generated with cell spacing ranging between 50–750 m, with five random cell grids being generated for each cell size. Two important results were apparent. Firstly, accuracy (i.e. agreement between estimated and simulated fire spread) increased as cell size decreased from 750 to 250 m, and remained constant below 250 m, indicating that below this cell size inaccuracy in simulation output was not due to discretisation error but was due to other sources (as discussed below). Secondly, the variance in simulation outputs due to the random nature of the cell grid diminished with cell size. For the 50m cell size used in the rest of the study, the results indicated that random grid variance artefacts do not significantly influence our results (95% confidence intervals for Kappa values were +/- 0.016 or smaller).

Impact of extreme fire weather on simulation accuracy

In this section we describe a clear distinction in the simulation accuracy sensitivity analysis results between the first two phases of the fire, during which the fire danger index (McArthur 1966) ranged from 20 – 28 (High), and the third and fourth phases, during which the fire danger index ranged from 47 to 104 (Extreme). For each of 4 key simulation parameters, Table 2 shows which parameter value resulted in the most accurate simulation i.e. the highest kappa value *k*. If this value was not the baseline parameter value (baseline values are given in Table 1), the variation from the baseline is given along with the improvement in kappa over the baseline.

Table 2. Summarised results of sensitivity analysis simulations, showing the best accuracy value kappa (k) achieved by varying each simulation parameter. Where the best k value is greater than that of the baseline simulation, the baseline k value is given in parenthesis for comparison. The simulation parameter value that gave the best accuracy is also shown: where the notation "baseline" is used, this value was the baseline value shown in Table 1; otherwise, the deviation from the baseline value is given.

	Phase 1		Phase 2		Phase 3A		Phase 3B	
Variable	best *k*	value for best *k*	best *k*	value for best k	best *k*	value for best *k*	best *k*	value for best *k*
wind speed	0.63 (0.62)	– 5kph	0.49	*baseline*	0.44 (0.33)	+ 20km/h	0.58 (0.42)	+ 20km/h
wind direction	0.62	*baseline*	0.49	*baseline*	0.47 (0.33)	– 15°	0.42	*baseline*
PCS	0.62	*baseline*	0.49	*baseline*	0.54 (0.33)	+ 3.5	0.58 (0.42)	+ 1.5
FBM	0.62	*baseline*	0.49	*baseline*	0.49 (0.33)	MH1	0.56 (0.42)	MH1

The sensitivity analysis simulations revealed that for Phases 1 and 2, the most accurate simulation results were given by the baseline parameter settings. In other words, the weather time series from the Southern Cross AWS, the estimate of vegetation cover (PCS) as having a value of 1.5, and the selection of the heathland fire behaviour model yielded the most accurate simulation results. In the case of the wind speed during Phase 1, a very slight improvement in simulation accuracy was given by reducing the Southern Cross AWS wind speed by 5 km/h Note that this is not a claim that the baseline parameter values were "correct" – rather, these results show that simulation inaccuracies are not simply explained by errors in the weather data, vegetation coverage estimate, or selection of an inappropriate fire behaviour model. For example, one apparent source of inaccuracy was due to the resolution of the vegetation map. Inspection of the Landsat imagery of the area showed that some areas of the map marked as Eucalypt woodland were interspersed with heath and carried fire; simulation in these areas under-predicted the extent of fire-spread (see areas marked Y in Figure 2).

The situation for Phases 3A and 3B is quite different. In terms of wind direction, in Phase 3A the simulation with the greatest accuracy occurred for a wind direction series in which all wind readings were rotated 15° counter-clockwise from the (northerly) winds recorded at the Southern Cross AWS. This result is consistent with de Mar's (2008) analysis that transient westerly winds occurred during this phase at the fire-site and impacted the shape of the perimeters. In Phase 3B, the wind direction was clearly inaccurate at the beginning of the period (see Figure 4, up to 2100), resulting in over-prediction of westerly spread in the area marked 'Z' in Figures 2 and 4. Unlike Phase 3A, no simple uniform alteration of wind direction improved accuracy.

Table 2 shows that simulation accuracy is improved if the wind speed during the Phases 3A and 3B were 20km/h *faster* than the value recorded at Southern Cross AWS. Simulation accuracy was *also* improved if it was assumed that the vegetation cover of the heath vegetation burned during Phases 3A and 3B was higher than estimated, *or* if a Mallee Heath (MH1) fire behaviour model was used for heath vegetation. These three sensitivity analysis results are actually manifestations of a single factor: that the baseline simulation systematically under-predicted the *rate of spread* during Phase 3B. This is illustrated in Figure 4, which shows both estimated and simulated fire perimeters at 2030, 2045, 2100 and 2359. In each case the simulated fire front lags the fire front position estimated from the fire reconstruction report. The under-prediction of the rate of spread may thus be due to:

1. The actual wind speed being higher than the value recorded at Southern Cross. Given that the Southern Cross AWS was located 75km from the fire ground, and the clear discrepancies in wind direction noted above, discrepancies in wind speed are plausible. The HE fire behaviour model would then predict a faster rate of spread, more closely matching the estimated fire behaviour. Or,
2. The heath vegetation burned during Phase 3B having a higher vegetation cover than in the previous phases. Although the available vegetation input map data did not distinguish between heath scrub types, according to (de Mar 2008) the fire site contained both 'heath-scrub' and 'Tamma scrub'. Of these two types of heath vegetation Tamma scrub, which was present in some areas burnt during Phase 3B, had characteristically higher levels of cover. With a higher vegetation cover, the HE fire behaviour model predicts a faster rate of spread. Or,
3. The HE fire behaviour model under-predicting the rate of spread in extreme fire weather conditions. This is plausible, given that the heathland experimental fires on which the HE model was based were conducted under less severe weather conditions: the maximum experimental fire danger rating was Very High compared to the Extreme conditions during Phase 3B, and maximum experimental wind speeds were approximately 18 km/h, compared to the average Phase 3B wind speed of 37 km/h. Or,
4. Some combination of the above.

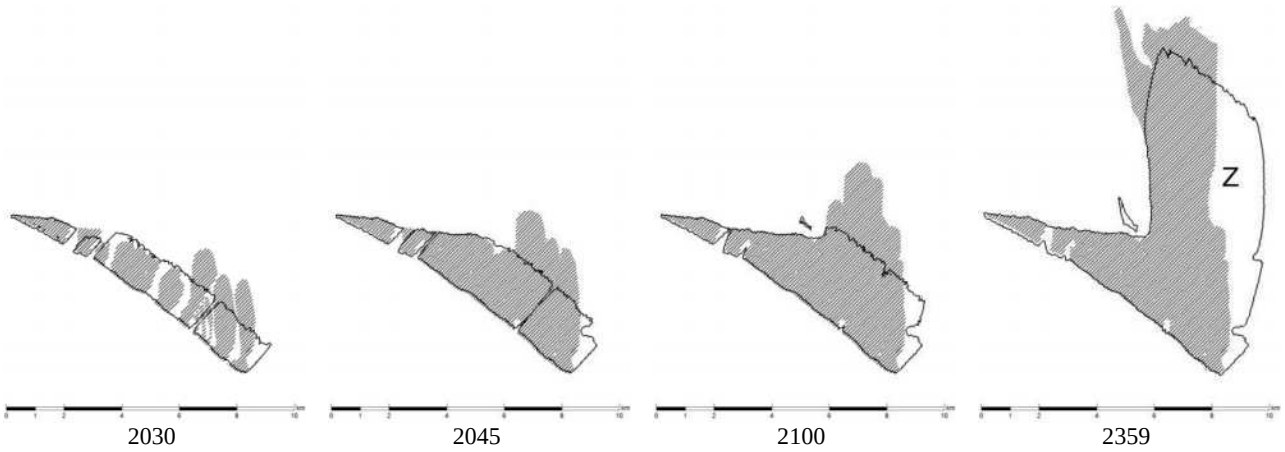

Figure - 4 The progression of the fire during Phase 3B. Simulated (black line) and estimated (shaded) fire perimeters are shown for times 2030, 2045, 2100 and 2359. The annotation "Z" is discussed in the text.

Using the data available for our validation analysis, we were not able to distinguish between the possibilities 1-3 above.

Discussion

Several previous studies have sought to validate fire spread simulation systems by comparing simulated fire spread against historical fire data, for example the studies of Finney (Finney 2000), Fujioka (Fujioka 2002), Arca *et al* (Arca *et al.* 2007), and Fillipi *et al* (Filippi *et al.* 2014). In common with previous validation exercises, this study found that that the ability to perform validation was limited by the reliability of available data, with fireground weather presenting the largest obstacle. While this study identified that the AUSTRALIS simulation system under-predicted the of rate of spread in arid heathland vegetation under extreme fire conditions, it was not possible to further diagnose either wind data, fuel mapping data, or fire behaviour models as the cause of the under-prediction.
The very features which this study highlighted as presenting difficulties in conducting a validation of the accuracy of computer simulation of wildfire spread (using high quality data) are exactly those which impact on the use of such simulation technology "in the field". As well as conducting simulation model validation using historical fire data, there is a pressing need to collect accurate fire data during active wildfires, rather than conducting analysis after the event. Such data-gathering efforts include regular fire line mapping at hourly intervals and the recording of fire ground weather conditions. Together, accumulated GIS data on fuel types, fuel load, and the development of fire behaviour rate-of-spread models which are experimentally calibrated for extreme fires, these data will facilitate: (1) higher fidelity simulator validation studies and, (2) more accurate prediction of "live" wildfires, which currently may be compromised by source data quality. Fire agencies and fire personnel organisations are to be encouraged to address these data issues.

Acknowledgements

The authors acknowledge funding for the study from the Australian Research Council, Fire and Emergency Services WA, and Landgate WA.

References

Arca B, Duce P, Laconi M, Pellizzaro G, Salis M, Spano D (2007) Evaluation of FARSITE simulator in Mediterranean maquis. International Journal of Wildland Fire 16, 563-572.

Australian Government Department of the Environment (2014) 'National Vegetation Identification System.' Available at
http://www.environment.gov.au/topics/science-and-research/databases-and-maps/national-vegetation-information-system
Bureau of Meteorology (2008) Meteorological Aspects of the Boorabbin Fire (28 December 2007 - 8 January 2008). Western Australian Regional Office, Bureau of Meteorology, Perth, WA Available at http://www.bom.gov.au/wa/sevwx/fire/20071228/boorabbin_fire_rpt.pdf
[Accessed May 2012].
Burrows ND, Ward B, Robinson A (2009) Fuel Dynamics and Fire Spread in Spinifex Grasslands of the Western Desert. In 'Proceedings of the Royal Society of Queensland'. Volume 115 pp. 69-76. Available at
http://search.informit.com.au/documentSummary;dn=590969984229226;res=IELHSS [Accessed 8th July 2014].
Catchpole W, Bradstock R, Choate J, Fogarty L, Gellie N, McCarthy G, McCaw L, Marsden-Smedley J, Pearce G (1998) Cooperative Development of Prediction Equations for Heathland Fire Behaviour. In 'Proceedings of the 3rd International Conference on Forest Fire Research and 14th Conference on Fire and Forest Meteorology'. pp. 631-645.
Coleman JR, Sullivan AL (1996) A real-time computer application for the prediction of fire spread across the Australian landscape. Simulation 67, 230-240.
Cruz MG, Matthews S, Gould J, Ellis P, Henderson M, Knight I, Watters J (2010) Fire Dynamcis in Mallee-Heath: Fuel, Weather and Fire Behaviour Prediction in South Australian Semi-Arid Shrublands. Bushfire CRC Available at
http://www.bushfirecrc.com/resources/research-report/report-fire-dynamics-mallee-heath [Accessed 8th July 2014].
de Mar P (2008) Goldfields Fire 13 (Boorabbin Fire) - Fire Development Chronology. GHD Pty Ltd, Sydney, NSW Available at
http://www.dec.wa.gov.au/pdf/boorabbin/goldfields_fire_13_chronology.pdf
[Accessed 8th July 2014].
Filippi J-B, Mallet V, Nader B (2014) Representation and evaluation of wildfire propagation simulations. International Journal of Wildland Fire 23, 46-57.
Finney MA (2000) Efforts at comparing simulated and observed rire growth patterns. Systems for Environmental Management, Missoula MT, USA. Available at
http://www.firemodels.org/downloads/farsite/publications/Finney_2000_FarsiteValidation_FinalReport.pdf [Accessed 8th July 2014].
Finney MA (2002) Fire growth using minimum travel time methods. Canadian Journal of Forest Research 32, 1420-1424.
Finney MA, Grenfell IC, McHugh CW, Seli RC, Trethewey D, Stratton RD, Brittain S (2011) A method for ensemble wildland fire simulation. Environmental Modeling & Assessment 16, 153-167.
Finney MA, Ryan KC (1995) Use of the FARSITE fire growth model for fire prediction in U.S. national parks. In 'The International Emergency Management and Engineering Conference'. Nice, France. (Eds JD Sullivan, JL Wybo, L Buisson) pp. 183-189.
Fujioka FM (2002) A new method for the analysis of fire spread modeling errors. International Journal of Wildland Fire 11, 193-203.
Johnston P, Kelso J, Milne GJ (2008) Efficient simulation of wildfire spread on an irregular grid. International Journal of Wildland Fire 17, 614-627.
Linn R, Reisner J, Colman JJ, Winterkamp J (2002) Studying wildfire behavior using FIRETEC. International Journal of Wildland Fire 11, 233-246.

Lopes AMG, Cruz MG, Viegas DX (2002) FireStation — an integrated software system for the numerical simulation of fire spread on complex topography. Environmental Modelling & Software 17, 269-285.

McArthur AG (1966) 'Weather and grassland fire behaviour.' (Forest Research Institute, Forestry and Timber Bureau of Australia: Canberra)

McCaw L (1997) Predicting fire spread in Western Australia mallee-heath shrubland. University of New South Wales.

Perry GL, Sparrow AD, Owens IF (1999) A GIS-supported model for the simulation of the spatial structure of wildland fire, Cass Basin, New Zealand. Journal of Applied Ecology 36, 502-518.

Tolhurst K, Shields B, Chong D (2008) Phoenix: development and application of a bushfire risk management tool. The Australian Journal of Emergency Management 23, 47-54.

Tymstra C, Bryce RW, Wotton BM, Taylor SW, Armitage OB (2010) Development and structure of Prometheus: the Canadian wildland fire growth simulation model. Canadian Forest Service, Edmonton, Canada. Available at http://cfs.nrcan.gc.ca/bookstore_pdfs/31775.pdf

[Accessed 8th July 2014].

Zeigler BP, Praehofer H, Ki TG (2000) 'Theory of modelling and simulation: Integrating discrete event and continuous complex dynamic systems.' (Academic Press: San Diego, California)

Fire detection with a frame-less vision sensor working in the NIR band

Juan A. Leñero-Bardallo[a], Jorge Fernández-Berni[a] , Ricardo Carmona-Galán[a], Philipp Häfliger[b], Ángel Rodríguez-Vázquez[a]

[a] *Institute of Microelectronics of Seville (CSIC – Universidad de Sevilla), Avda. Américo Vespucio s/n Seville (Spain), juanle@imse-cnm.csic.es*
[b] *Department of Informatics, University of Oslo, Oslo, Norway, PO Box 1080, Blindern, Contact. hafliger@ifi.uio.no*

Abstract
This paper draws the attention of the community about the capabilities of an emerging generation of bio-inspired vision sensors to be used in fire detection systems. Their principle of operation will be described. Moreover experimental results showing the performance of an event-based vision sensor will be provided. The sensor was intended to monitor flames activity without using optic filters. In this article, we will also extend this preliminary work and explore how its outputs can be processed to detect fire in the environment.

Keywords*: Flame monitoring, event-based vision sensors, fire detection, NIR, image processing.*

Introduction

Infrared cameras can easily detect fire and hot spots. Unfortunately, they are expensive, difficult to handle, and fragile (Briz *et al*. 2003). For this reason, CMOS cameras are still preferred for some applications where it is not strictly necessary operating in the whole infrared band, (Cheon *et al*. 2009, Naoult *et al*. 2007, Bendiscio *et al*. 1998, Fernandez-Berni *et al*. 2012). Silicon can detect Near Infrared Radiation (NIR) within the band [700 1,100] *nm*. This property can be exploited to monitor flame and fire activity.
Flames have a very characteristic oscillatory behavior. They flicker with certain frequency components that depend on their nature. The study of these frequency components is interesting for industrial processes and applications. Traditionally CMOS cameras with NIR filters have been employed (Yan *et al*. 2006). As an alternative to this traditional approach, recently we proposed a bio-inspired event-based system to monitor flame activity without using optic filters (Leñero-Bardallo *et al*. 2013). The idea behind this method was to compare the photocurrents of stacked photodiodes at different depths. The top one was more sensitive to shorter wavelengths and the bottom one was more sensitive to longer wavelengths, having a very good sensitivity within the NIR band. Just comparing the difference between their photocurrents, we were able to determine if the incident radiation was within the NIR band without optic filters. Moreover, we could process with a real-time algorithm the temporal variations of the NIR levels in the visual scene provoked by flames and compute their frequency components values.
This paper studies how the prior work to monitor flame activity could be extended to detect fire in the environment and emit an alarm in case. We will show that the previously implemented algorithm outputs can be processed to detect fire with a low computational load. Up to date, all the forest fire detection systems with cameras use frame-based vision sensors. With this contribution, we also want to draw the attention of the community about this new generation of bio-inspired vision sensors.
This document is organized as follows: In Section 3, we explain briefly the fundamentals of bio-inspired vision sensors and we discuss their feasibility for fire detection; Section 4 explains what kind of radiation can be sensed with CMOS sensors; Section 5 describes our sensor and algorithm to process its outputs and detect radiation within the NIR band; Section 6 provides experimental results when our system is employed to monitor flame activity; Section 7 explores how the NIR separation algorithm

can be modified to emit an alarm if there is fire in the environment; finally, Section 8 draws some conclusions.

Bio-inspired Event-based Vision Sensors

Conventional vision sensors are frame-based systems (also known as smart imagers). A frame is a 2D-dimensional matrix that contains information about the visual scene (typically light intensity or color). Such sensors always provide a continuous output data flow (frames are transmitted with a continuous periodicity) that can be very redundant if the visual scene does not change. If we compare their performance with the human retina, we can state that they perform worse in the majority of uncontrolled situations and environments: their dynamic range is much lower, their sensitivity to light is also lower, and their power consumption is much higher.
For these reasons, some authors considered the idea of developing bio-inspired vision sensors (also called retinas, (Mahowald 1994, Leñero-Bardallo *et al*. 2010, Leñero-Bardallo *et al*. 2011). These sensors try to mimic the interactions of the cells of the human retina. The retina operates in a very different way to conventional vision sensors. Its cells process the visual information before transmitting it to the brain. Thus, redundant information is not sent through the optical nerve. Retinal cells can compute the spatio-temporal contrast that contains almost all the relevant information about the visual scene. This information is transmitted continuously. There is a massive parallel architecture and cells can send anytime spikes to the brain. Therefore biological systems are inherently faster than classic imagers which bandwidth is limited by the frame rate.
The main drawback of artificial event-based sensors is their low pixel fill factor. Their pixels have more transistors than commercial frame-based pixels with three or four transistors. Extra circuitry per pixel is required to process the visual information and to implement and asynchronous pixel communication (Häfliger 2000). However, such sensors are good candidates for applications like fire detection or surveillance, where high image quality is not mandatory, and speed and low power consumption are preferred. They have a great potential to be nodes of wireless sensor networks. In such networks it is mandatory to minimize the amount of data transmitted from the sensors to a central node which processes the information.

Fire Detection in the NIR Band

A CMOS camera without filters detects radiation beyond the visual spectrum, i.e. Ultra Violet ([250, 390] nm), visible ([390, 750] nm), and NIR ([750, 1100] nm). Hot spots, fire or flames can be detected with a CMOS sensor with a NIR filter (Naoult *et al*. 2007), (Li *et al*. 2010) (hot spots need to be above 350Cº). Smoke detection is possible too when employing NIR sources (e.g. NIR LEDs).
In our particular case, we developed a system (Leñero-Bardallo *et al*. 2013) with an event-based sensor to monitor the temporal variations of the visual scene provoked by flames. Flames have frequency components within the interval [0, 250] Hz and their flickering can easily be tracked with an asynchronous sensor.
As a continuation of this preliminary work, we propose to develop new real-time algorithms, (Leñero-Bardallo *et al*. 2013), to detect fire in indoors and outdoors environments. According to our experimental results, flames provoke very fast and periodic variations of NIR levels in the visual scene that can be identified from other NIR sources like sunlight. Such periodic variations of the NIR levels are easy to detect when they appear, just computing the standard deviation of previously recorded NIR levels and normalizing it.

Methodology

We employ an event-based vision sensor to detect the NIR variations of the visual scene (Leñero-Bardallo *et al*. 2013). The sensors pixels are made up of three stacked photodiodes at different depths. Each one is connected to a circuitry that sends pulses out the chip, with a frequency proportional to its local photocurrent (see Figure 1). The top one is more sensitive to shorter wavelengths. The bottom one is more sensitive to longer wavelengths and to the radiation within the NIR band. This property is based on the light penetration depth. Shorter wavelengths photons have more energy and on average, they travel less time before they generate electron-hole pairs. Longer wavelengths have less energy and they travel more time across the silicon before generating electron-hole pairs.

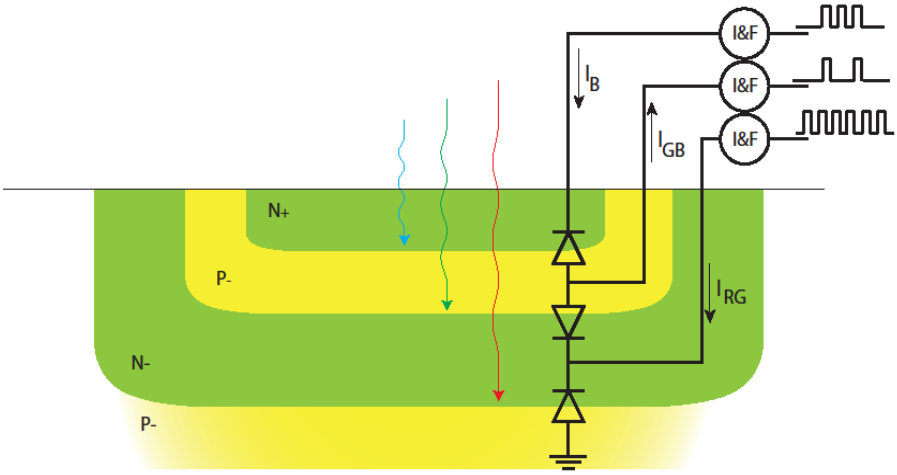

Figure 1. Experimental setup: vision sensor and data logger. Photodiodes cross-section. Each one is connected to circuitry (channel) that generates pulses with a frequency proportional to its inputs photocurrents.

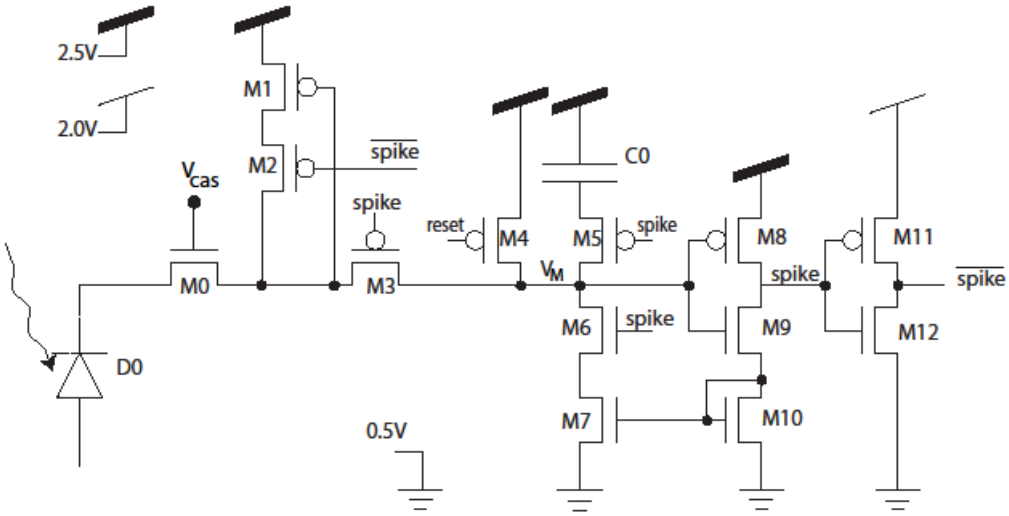

Figure 2. Integrate-and-fire neuron. This circuitry is replicated three times within each pixel. Depending on the input is connected to the photodiode cathode/anode, we use this circuit or a complementary version of it, with p-MOS transistors instead n-MOS transistors and vice versa.

Note that the photocurrents at the inputs of the integrate-and-fire neurons do not correspond with each photodiode current. For this reason it is necessary to process the events outputs to estimate the photocurrent of each photodiode. Unfortunately, we do not know the photodiodes quantum efficiencies, their doping profiles, and the PN junction depths (such information was not disclosed by the foundry). For this reason, it is impossible to know the exact photocurrent values. We denote the photocurrent estimations after processing the integrate-and-fire outputs as $I'_{\{B,GB,RG\}}$. However, to represent the color information of each pixel, we only need to know the relative values of each photocurrent. For this reason, it is possible to represent RGB images after processing the channels outputs. Every time that a pixel integrate-and-fire neuron spikes, its frequency f_* is updated. Periodically, the estimation of the photocurrents is computed according to the following equations:

$$I'_B = \frac{f_B C_B \Delta V_{th\_B}}{e_B} \quad (1)$$

$$I'_G = \frac{f_{GB} C_{GB} \Delta V_{th\_GB} - I'_B e_B}{e_G} \quad (2)$$

$$I'_R = \frac{f_{RG} C_{RG} \Delta V_{th\_GB} - I'_G e_B}{e_G} \quad (3)$$

Where $C_{\{B,GB,RG\}}$ are the photodiodes capacitances, $\Delta V_{th\_\{B,GB,RG\}}$ are the voltage increments at the integrate-and-fire neurons capacitances to elicit one spike, and $e_{\{B,GB.RG\}}$ are parameters that represent the photodiodes quantum efficiencies.

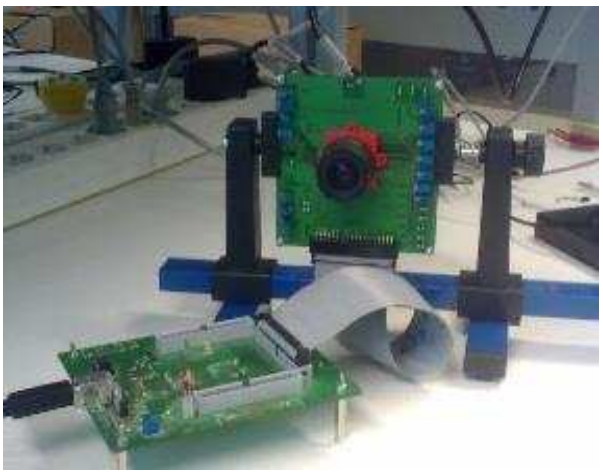

Figure 3–Experimental setup: vision sensor and data logger.

Experimental Results

Figure 3 shows the experimental setup. We designed a custom board for the vision sensor. That board is connected to a data logger that sends the output data to a PC. We programmed a dedicated Java interface (jAER open source) to compute the values of $I'_{\{B,GB,RG\}}$ and show real-time color images. Main system specifications are summarized on Table I.

Table 1 –System Specifications

Array Size	22x22
Technology	STM 90nm
Power Supply	2.5V
Chip Size	1mm x 1mm
Pixel Size	31μm x 31μm
Fill Factor	28%
Power Consumption	0.03mA @ 10Keps
Dynamic Range	>60dB

5.1. Detection of NIR levels

A real-time NIR extraction algorithm was proposed, (Leñero-Bardallo *et al*. 2013). It operates with photocurrents estimations I'_G and I'_R. The NIR levels are proportional to the photocurrents ratio after a certain number of events are received:

$$NIR = \frac{I'_R}{I'_G} I'_R \tag{4}$$

Its performance is depicted in Figure 4. Within the NIR band, the value of I'_R is larger than I'_G. To take into account the light intensity, we multiply $\frac{I'_R}{I'_G}$ by I'_R. Once we have estimated the NIR levels of each pixel, we can use this information to either create intensity images proportional to the NIR levels that each pixel detects or to estimate global NIR levels variations of the visual scene. This can be done computing the FFT of the global NIR levels within a time interval. The pixel updating frequency is in the order of *KHz* and the main NIR frequency components of a flame are below *100Hz*. Hence, the system is fast enough to track flames flickering.

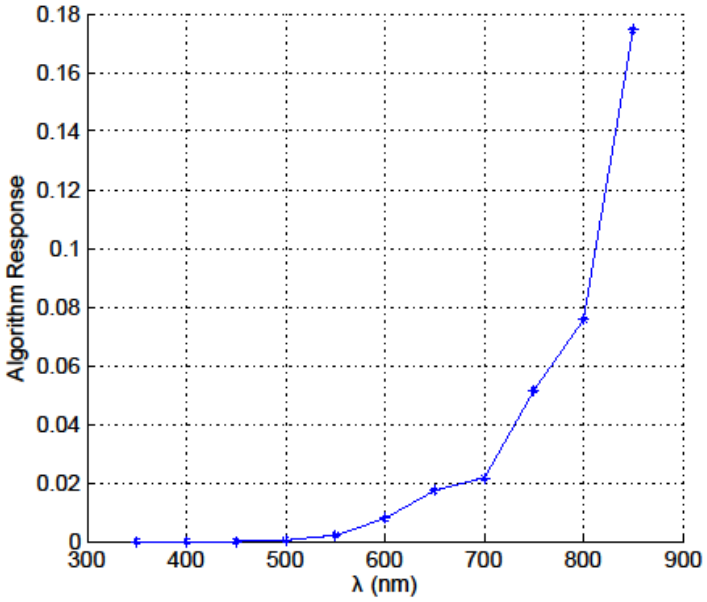

Figure 4. Algorithm response on infrared detection mode. The sensor was stimulated with a monochromator emitting light at different wavelengths.

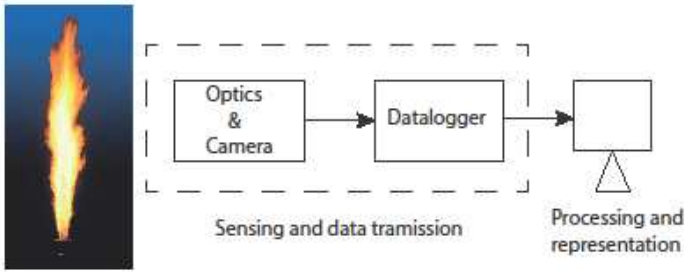

Figure 5. System Diagram for fire detection.

Figure 5 shows a diagram of the experimental setup operating with flames. A gas lighter emitting flames was placed in front of the sensor at a distance of *0.5m*. Figure 6 displays the temporal variations of the NIR levels of the visual scene with and without flames. With flames the NIR levels change with a very characteristic periodicity due to the flames flickering. Without flames, the NIR levels are much more stable. Figure 7 shows the spectra of temporal NIR variations with flames in indoors and outdoors environments. Results are quite similar to the ones reported by other authors with other methods based on optic filters (Yan *et al*. 2006). Sunlight provokes an increase of the average NIR level of the scene and makes more challenging the frequency analysis.

A custom Java interface (jAER open source) was programmed to show real-time NIR images as it is depicted in Figure 8. The interface can display images and implements the NIR algorithm previously explained. Figure 9 shows a snapshot of the NIR levels emitted by a flame. The different regions of the flame can be distinguished. The root and the central region of the flame have less energy than the periphery where the flame emits more energy in the NIR band.

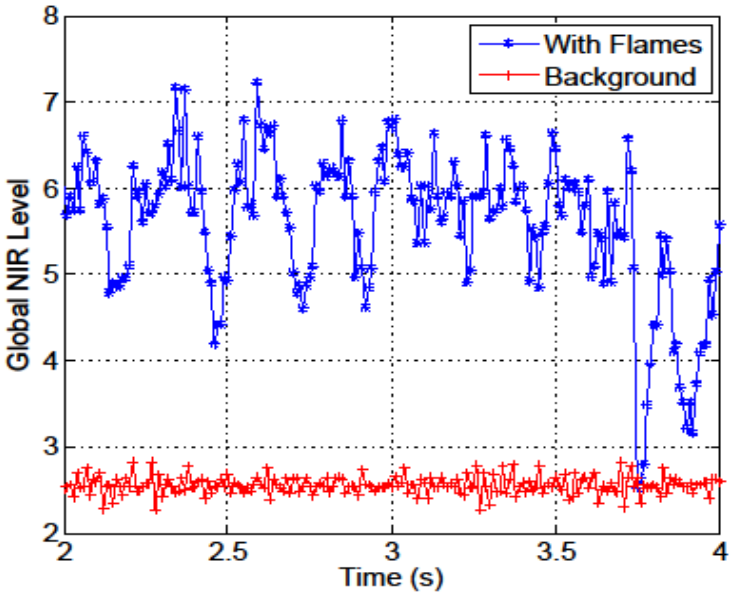

Figure 6. Real-time temporal variations of the NIR levels of the visual scene in different environments with and without flames.

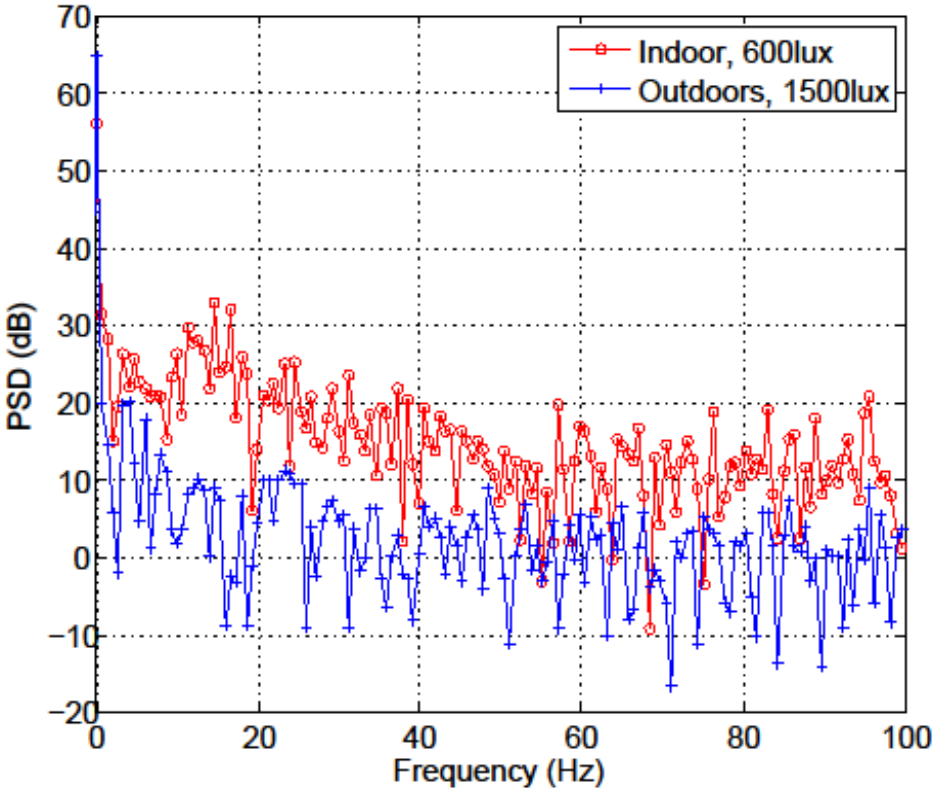

Figure 7. Frequency components emitted by a flame in indoors and outdoors environments. Outdoors the average NIR level is higher due to sunlight.

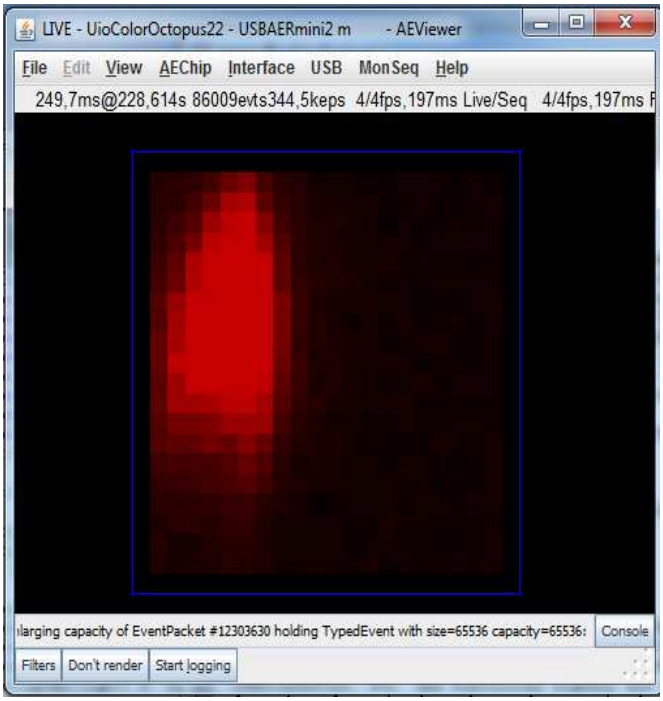

Figure 8. Computer interface showing real-time NIR levels emitted by one flame.

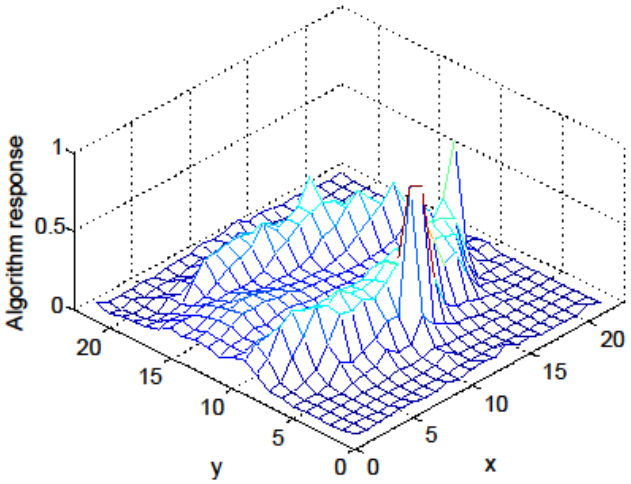

Figure 9. Snapshot showing NIR levels when the sensor was exposed to a flame. It is possible to distinguish the different regions of the flame according to (Yan et al. 2006).

New approach to detect fire

So far an algorithm has been successfully employed to monitor NIR variations of the visual scene and to compute the flame frequency components: see 0 and 0. Once we have computed the global NIR levels in the scene, we can compute periodically the standard deviation of the previously recorded NIR levels and normalize it.

$$A[n] = \frac{\sigma_{NIR} \cdot N}{\sum_{k=0}^{N-1} NIR[n-k]} \tag{5}$$

The parameter $A[n]$ represents the variations of the NIR levels within the visual scene. It does not depend on illumination. If its value exceeds a certain limit, we can assume that there are flames in the scene. Depending on how many previously recorded samples are considered to compute the average NIR levels (see 0), the value of $A[n]$ with and without flames will be different. Thus there is a trade-off between algorithm execution speed, the algorithm robustness to false alarms, and the number of events that have to be received to detect fire. 0 illustrates the values of the normalized standard deviation computing the average NIR levels of the scene with different number of global NIR levels previously computed. Without flames, $A[n]$ values are always lower than 5%. With flames, such value is higher two or three times higher. To prevent generate fire alarms, a value of $A[n] \geq 10\%$ seems to be practical according to our measurements.

The algorithm only requires to store N previously estimated NIR levels and to update the value of $A[n]$ periodically. To reduce the computational cost detecting fire $A[n]$ could be updated every second, for instance.

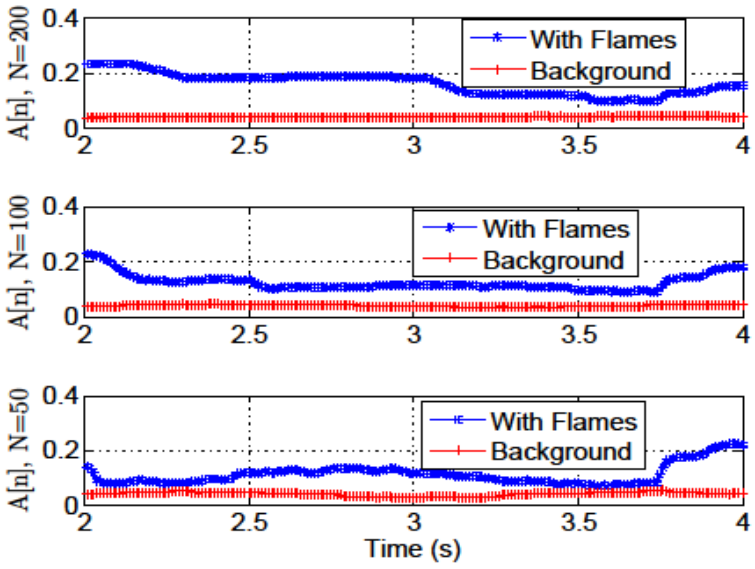

Figure 10. Normalized standard deviation computation. With flames, the value is always higher than without flames. The normalized value does not depend on illumination conditions.

7. Conclusions

In this paper we have presented event-based sensors as an alternative to classic frame-based vision sensors for fire detection and surveillance systems. One particular example of a system with a bio-inspired camera that can be used to monitor flame activity is shown. The sensor outputs can be processed real-time to obtain NIR levels from the visual scene. Furthermore, we have extended this prior work define a real-time algorithm that detects fire in the environment analysing the transient variations of the NIR levels of the scene. Our goal is to create a portable system that emits an alarm if fire is detected in the visual scene. Experimental results with flames are provided. 0 summarizes the main system features.

8. Acknowledgements

This research work was partially funded through projects TEC2012-38921-C02-02 MINECO (European Region Development Fund, ERDF/FEDER), IPT-2011-1625-430000 MINECO, IPC-20111009 CDTI (ERDF/FEDER), ONR grant no. N000141410355 (Office of Naval Research (USA)), and TIC 2012-2338 (Junta de Andalucía, Consejería de Economía, Innovación, Ciencia y Empleo (CEICE)). Chips and system fabrication were funded by the Department of Informatics of the University of Oslo (Norway).

9. References

Briz S, Castro A de, Aranda J, Melendez J, and Lopez F (2003). Reduction of false alarm rate in automatic forest fire infrared surveillance systems. *Remote Sensing of Environment*, 19–29.

Bendiscio P, Francesconi F, Malcovat P, Malobert F, Polett M, and Valacca R (1998). A CMOS integrated infrared radiation detector for flame monitoring. *IEEE International Symposium on Circuits and Systems*, ISCAS, **6**, 625–628.

Cheon J, Lee J, Lee I, Chae Y, Yoo Y, and Han G (2009). A single-chip CMOS smoke and temperature sensor for an intelligent fire detector. *IEEE Sensors Journal*, **9**, 625–628.

Fernandez-Berni J, Carmona-Galan R, Martinez-Carmona JF, and Rodriguez-Vazquez A (2012). Early forest fire detection by vision-enabled wireless sensor networks. *International Journal of Wildland Fire*, **21**, 938–949.

Gang L, Yong Y, Colechin M, and Hill R (2006). Monitoring of oscillatory characteristics of pulverized coal flames through image processing and spectral analysis. *IEEE Transactions on Instrumentation and Measurement*, **55**, pp. 226–231.

Häfliger P (2000). A spike based learning rule and its implementation in analog hardware. *Ph.D. dissertation, ETH Zürich, Switzerland*. http://www.ifi.uio.no/ ~hafliger.

jAER open source project. http://sourceforge.net/projects/jaer/.

Leñero-Bardallo JA, Serrano-Gotarredona T, and Linares-Barranco B (2010). A 5-decade dynamic range ambient-light-independent calibrated signed-spatial-contrast AER retina with 0.1ms latency and optional time-to-first-spike mode. *Transactions on Circuits and Systems*, Part-I, **57**(10), 2632-2643.

Leñero-Bardallo JA, Serrano-Gotarredona T, and Linares-Barranco B (2011). A 3.6μs latency asynchronous frame-free event-driven dynamic-vision sensor. *IEEE Journal of Solid-State Circuits*, **46**(6), 1443–1455.

Leñero-Bardallo JA, Bryn DH, and Häfliger P (2013). Flame monitoring with an AER color vision sensor. *IEEE International Symposium on Circuits and Systems, ISCAS 2013.*

Leñero-Bardallo JA, Bryn DH, and Häfliger P (2013). Bio-inspired asynchronous pixel event tri-color vision sensor. *IEEE Transactions on Biomedical Circuit and Systems*, 1-13, DOI: 10.1109/TBCAS.2013.2271382.

Li Q, Hao Q, and Zhang K (2010). Smart wireless video sensor network for fire alarm. *6th International Conference on Wireless Communications Networking and Mobile Computing (WiCOM)*, 1–4.

Mahowald M (1994). An Analog VLSI System for Stereoscopic Vision. *Kluwer*, 1994.

Naoult Y L, Sentenac T, Orteu J, and Arcens J P (2007). A new approach based on a low cost CCD camera in the near infrared. *Fire Detection*, 193–206.

Fire safety management based on integrated monitoring and forecast of smoke exposure

J.H. Amorim[a], A.I. Miranda[a], J. Valente[a], F. Marques[a], C. Borrego[a], J.M. Fernandes[b], R. Ottmar[c], S.J. Prichard[d], A. Andreu[d], P.M. Fernandes[e], J.P.S. Cunha[f]

[a] *CESAM & Department of Environment and Planning, University of Aveiro, 3810-193 Aveiro, Portugal, amorim@ua.pt, miranda@ua.pt, joanavalente@ua.pt, fabiomauricio@ua.pt, cborrego@ua.pt*
[b] *IEETA/DETI, University of Aveiro, 3810-193 Aveiro, Portugal, jfernan@ua.pt*
[c] *Pacific Wildland Fire Sciences Laboratory, US Forest Service Pacific Northwest Research Station, Seattle, Washington 98103, USA, rottmar@fs.fed.us*
[d] *University of Washington, Seattle, Washington, USA, sprich@u.washington.edu, agandreu@u.washington.edu*
[e] *Centro de Investigação e de Tecnologias Agro-Ambientais e Biológicas (CITAB), University of Trás-os-Montes and Alto Douro, 5001-801 Vila Real, Portugal, pfern@utad.pt*
[f] *INESC-TEC/Faculty of Engineering, University of Porto and IEETA, Portugal, jpcunha@fe.up.pt*

Abstract
Decisions made by firefighters during suppression operations are highly dependent on personal judgement, experience, and senses. However, recent scientific and technological advances offer a vast number of possibilities towards advanced emergency preparedness during firefighting operations, if integrated in a single on-line platform. In this context, this paper addresses the following question: can models be successfully merged with personal sensors aiming to build an advanced Decision Support System (DSS) focused on the preservation of firefighter's safety, while pursuing an enhanced response to wildfires?
The goal of this research is to develop an emergency response support system for firefighting ground-based operations during forest fire events. The target of the under-development computational tool is to provide knowledge-based aid to firefighters at critical decision-making situations, helping with the safe and successful management of fire. This DSS will support the following features:
- capture of 'live' sensor data from a set of wearable monitoring equipment that will be based on a previously developed certified medical wearable technology named "VitalJacket®";
- capture of meteorological observations from a mast placed in one of the vehicles;
- enable projections of fire progression, smoke levels and critical exposure in a predefined time-step (up to 30 minutes);
- interpretation of results in an easy and intuitive form to be used by fire managers or firefighters involved in operations.
To achieve this goal hardware technology (e.g. wearable, mobile, communications) was combined with processing/simulation software algorithms that run under a user interactive interface. A data assimilation technique will allow near real-time observations from wearable monitoring equipment to be integrated into the exposure forecast modelling system, increasing the accuracy of the estimates.
A first prototype of the DSS, running in off-line mode, will be tested in the terrain during the fire season of 2014. An improved online version of the prototype will be tested in the following autumn in a series of prescribed burns.
In conclusion, this work proposes the development and testing (under real conditions) of a DSS intended to provide optimized firefighting efficiency, enhanced hazard awareness, and knowledge-based response to forest fire events. Advances in the computational modelling of fire and smoke behaviour, in conjunction with personal monitoring data, provide near real-time simulation of local fire conditions and short-term smoke exposure forecasts, with the needed advance in time to permit the safe and efficient positioning of crews in the terrain.

***Keywords**: fire safety; smoke exposure; emergency response support system.*

Introduction

At the operational level, firefighters face extremely severe conditions including steep terrain, falling debris, obstructions to movement, heavy equipment, high temperatures, reduced visibility and toxic atmosphere. Smoke is, in this context, a magnifier of the destructive potential of fire. In fact, a significant number of the casualties occurring in forest fires is caused by smoke inhalation and consequent faint or disorientation due to heavily impaired visibility conditions [e.g., Miranda *et al*., 2005, 2012a]. Firefighters, in particular, are affected by short to long-term health disorders, as shown by several studies [Reinhardt and Ottmar, 2004; Reisen and Brown, 2009; De Vos *et al*., 2009; Reisen *et al*., 2011; Miranda *et al*., 2005, 2010, 2012a]. Miranda *et al*. [2010, 2012a] have shown that forest firefighting can expose firefighters to very high concentrations of carbon monoxide (CO), and also to high concentrations of nitrogen dioxide (NO_2), volatile organic compounds and particulate matter, with potential harmful effects on health, even in wildfires with small burnt areas. A particular concern is the peak and short-term exposure to CO because of the strong increase of the exhaled CO and carboxyhemoglobin (COHb) observed in firefighters after the exposure to smoke, meaning that the oxygen delivery to the body's organs and tissues is strongly diminished after smoke exposure.
Despite the advances on the numerical simulation of fire progression and smoke dispersion, operational models for assisting with decision are still limited in accuracy, resolution, and performance. Meteorological and air quality forecasts can provide some additional help but they are limited to coarse spatial and temporal resolutions.
However, recent developments on new sensor technologies, connectivity solutions and numerical models open unprecedented opportunities for anticipating or mitigating the risks associated to the inhalation of toxic gases. In this context, this paper addresses the following question: can models be successfully merged with personal sensors aiming to build an advanced Decision Support System (DSS) focused on the preservation of firefighter's safety, while pursuing an enhanced response to wildfires?

DSS development and testing

The goal of this research is to develop an emergency response support system for firefighting ground-based operations during forest fire events. The target of the under-development computational tool is to provide knowledge-based aid to firefighters at critical decision-making situations, helping with the safe and successful management of fire. This DSS will support the following features:
- capture of 'live' sensor data from a set of wearable monitoring equipment [Teles *et al*., 2011] that will be based on a previously developed certified medical wearable technology named "VitalJacket®" [Cunha *et al*., 2010; Cunha, 2012] [http://www.biodevices.pt];
- capture of meteorological observations from a mast placed in one of the vehicles;
- enable projections of fire progression, smoke levels and critical exposure in a predefined time-step (up to 30 minutes);
- interpretation of results in an easy and intuitive form to be used by fire managers or firefighters involved in operations.
To achieve this goal hardware technology (e.g. wearable, mobile, communications) was combined with processing/simulation software algorithms and user interactive interfaces. In that sense, and as a result of the requirement analysis, a conceptual architecture of the system was designed, as schematically represented in Figure 1, which relates the different modules and actors intervening in the process.

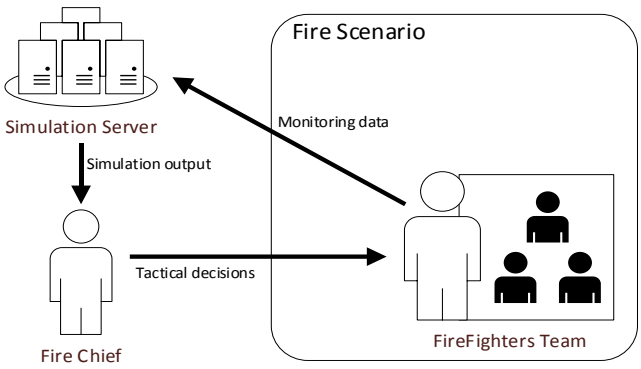

Figure 1. Schematic representation of system deployment.

General framework

As can be depicted in Figure 1 the dataflow relies on a modelling system capable of providing the needed information on fire and smoke behaviour. A simplified scheme of this integrated modelling tool is shown in Figure 2.

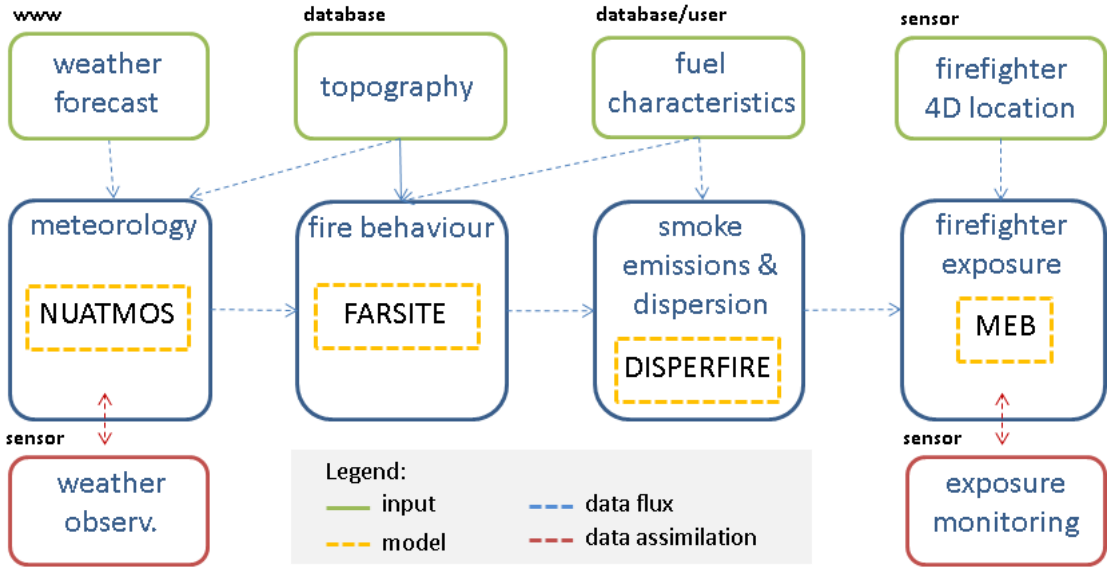

Figure 2. Schematic representation of the DSS core structure.

Graphical user interface

In order to provide a friendly way to interact with the end users, a JAVA Server Faces web interface called “VRTeam” was developed. This web developing platform was chosen because of its flexibility, for instance, the user can access the interface through any computing device (e.g., laptop, tablet, smartphone) with a standard browser and internet connection.

In terms of implementation, the interface works as a client application of two web services:

- "VRData", a JAVA Rest web service (jax-rs standard) that receives, processes and provides the monitoring data acquired in the terrain;
- "VRSimulationEngine", a JAVA WSDL web service designed to operationalize the numerical simulation models and return the results.

Concerning the interface graphical aspect, a hybrid approach between visual attraction and operability aspects was followed, as it is presented in Figure 3.

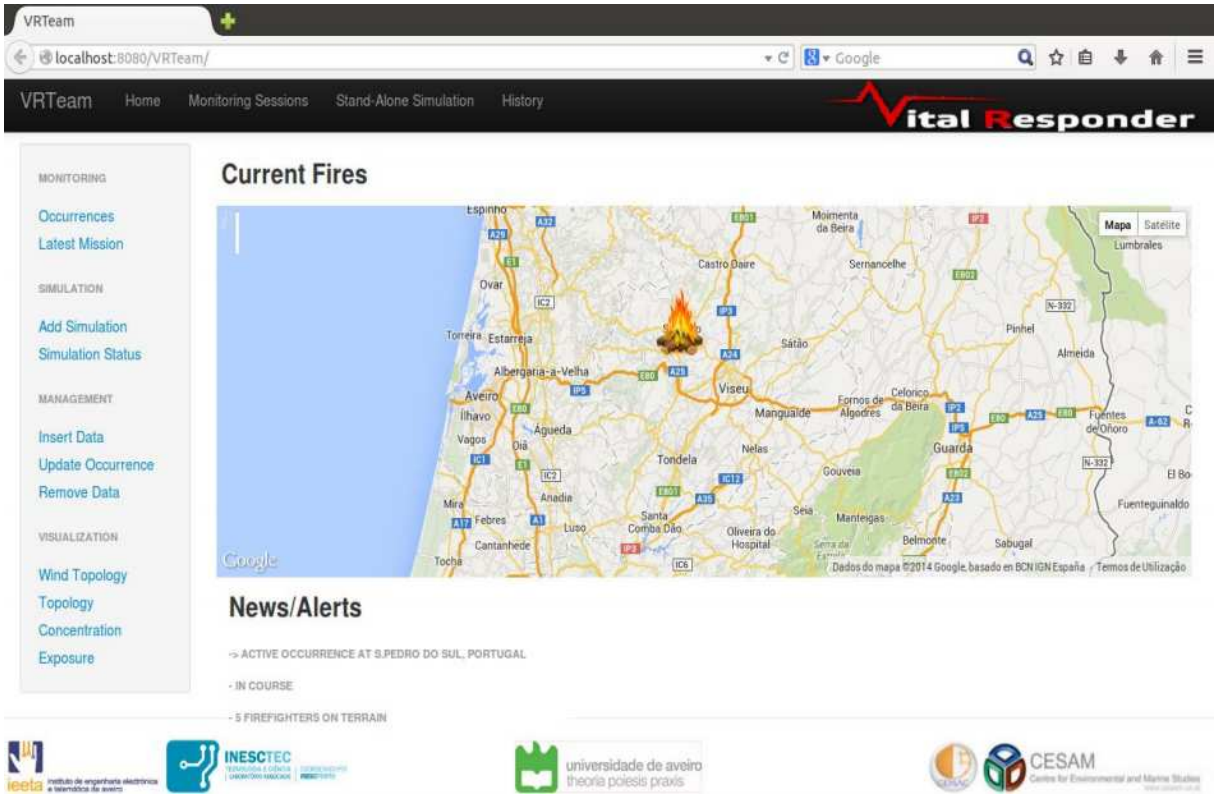

Figure 3. Main menu of the graphical user interface (GUI).

As can be seen in the above figure, the home page consists of a dashboard allowing users to view all active fire occurrences in course. Option buttons (in the left and top of the screen) are available that enable the access to all features provided by the system, namely:
- visualize monitoring data from active fire occurrences;
- simulate fire/smoke behaviour for an active occurrence;
- perform a stand-alone simulation for a random area.

Under development are other capabilities, such as the enriched visualization of occurrences history and monitored/simulated data, visual warnings of hazardous conditions for firefighters and advanced data analysis features for research purposes.

2.3. **Modelling system**

As shown in Figure 2 the numerical modelling architecture is composed of 4 independent models, which compose the main cores of the numerical system. These models are responsible for the simulation of local meteorological fields, fire progression, fuel consumption, smoke production and atmospheric dispersion, and human exposure. The numerical codes implemented have been previously tested [e.g. Valente *et al*., 2007] although not as an integrated system.

The different modules have been linked using a web service developed in JAVA (WSDL standard). This web application implements the workflow depicted in Figure 2 in a way that each numerical model corresponds to one execution stage. Any client application can make execution requests on the web service that are performed by the GUI application. Once an execution request is made, a simulation session for that user is created, and the forecast workflow begins. All related data is kept in cache so every user can have feedback about his simulation job status (see Figure 4).

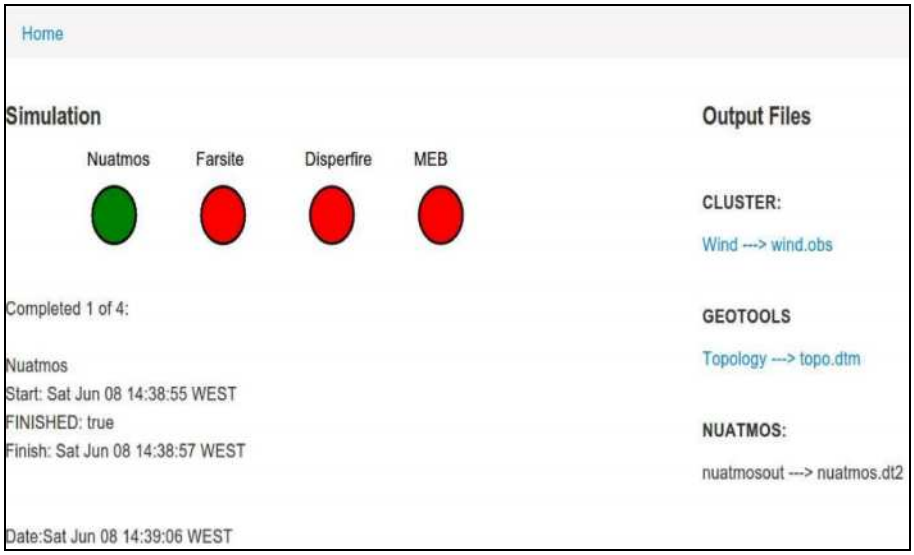

Figure 4. Example of GUI's feedback about the simulation status.

At the end of each execution, the results are stored in the cloud file system (e.g. Dropbox), and the outputs can be viewed using the GUI (section 2.5).
The main features of the numerical modules are hereafter briefly described.

Fuel

An adequate representation of the structural complexity and diversity of fuels, encompassing all the components that have the potential to burn (as trees, shrubs, grasses, woody material, litter, and duff) is needed for an accurate simulation of fire progression and smoke emission. Under development the incorporation into the system of a fuel classification tool based in the Fuel Characteristic Classification System (FCCS) [Ottmar *et al*., 2007] that will allow capturing the structural complexity, geographic diversity and potential flammability of typical Portuguese fuels. This tool is based in the concept of fuelbeds, which provides an easy identification of fuel characteristics in the terrain, and an accurate estimation of fire hazard and smoke emissions. Typical Portuguese fuelbeds were identified and built using the National Forest Inventory, other fuels datasets, published scientific literature, and fuel photo series. The mapping of the defined fuelbeds using vegetation classification and quantitative vegetation data is under development, as also the possibility of the user define the fuel model by selecting, through a touch-screen button, the corresponding image in the interface.

Meteorology

The diagnostic wind model NUATMOS [Ross *et al*., 1988], which has already been tested in this scope with good results [Valente *et al*., 2007; Borrego *et al*., 1999], produces a 3D mass consistent wind field through the interpolation of meteorological values distributed throughout the domain of interest. Instead of relying on meteorological observations, the system is connected to the meteorological forecast modelling system running at the University of Aveiro, thus providing also forecasts for the area.

Fire behaviour

The fire growth simulation model FARSITE [Finney, 2004] incorporates existing models of surface fire, crown fire, point-source fire acceleration, spotting, and fuel moisture. The model produces vector fire perimeters (polygons) at specified time intervals, which makes it adequate for the integration in the DSS.

Smoke behaviour

The estimation of forest fire emissions and the simulation of the atmospheric dispersion of the emitted pollutants are carried out by DISPERFIRE [Miranda *et al*., 1994; Valente *et al*., 2007]. Emission factors specific for southern European conditions, and particularly for the Portuguese forest and shrubland [Miranda, 2004], are implemented. The injection height of the smoke plume is estimated following the Sestak and Riebau [1988] methodology, while the subsequent transport and dispersion mechanisms are tracked using a 3D Lagrangian approach.

Firefighter's exposure to air pollution

It is important to distinguish between concentration and exposure. While the first is a physical characteristic of the environment at a given place and time, the latter quantifies the interaction between the polluted atmosphere and the person [Ott, 1982]. The exposure of each individual in the crew is estimated with MEB model [Miranda *et al*., 2012b], which follows the microenvironment approach from Hertel *et al*. [2001]. Basically, the time evolution of the exposure is simulated by tracking, in each time-step, the georeferenced firefighter's position and the corresponding concentration on that location and time.

2.4. Data assimilation

Under development is a data assimilation technique that will allow near real-time observations from wearable monitoring equipment to be integrated into the exposure forecast modelling system, increasing the accuracy of the estimates.

2.5. Outputs

As described, the system handles two types of data: monitoring data acquired by sensors on terrain and numerical forecasting outputs. Hereafter, the data provided by the system, and corresponding graphical output on VRTeam interface, are briefly described.

Monitored data

The system was designed to support a vast number of monitoring variables due to the scalability properties needed at this level (namely, the possibility of adding more sensors to the grid). At the present version the tool is capable of receiving, processing and displaying the following physiological and environmental variables:

Table 1- Monitored data.

Variable	Units
Terrain elevation	m
Atmospheric pressure	hPA
Air humidity	%
Air temperature	ºC
Luminosity	%
CO concentration	ppm
NO_2 concentration	ppm
Firefighter's location	UTM
Firefighter's heart rate	beats/min
Firefighter's R-R interval	s

The monitoring data is handled by *VRData* module. This module performs the caching of the last data received from the sensors in the terrain during half an hour periods (maximum caching time window). *VRTeam* interface consumes the online cache of *VRData* to present all information to end users, as line charts or custom grid tables (see Figure 5).

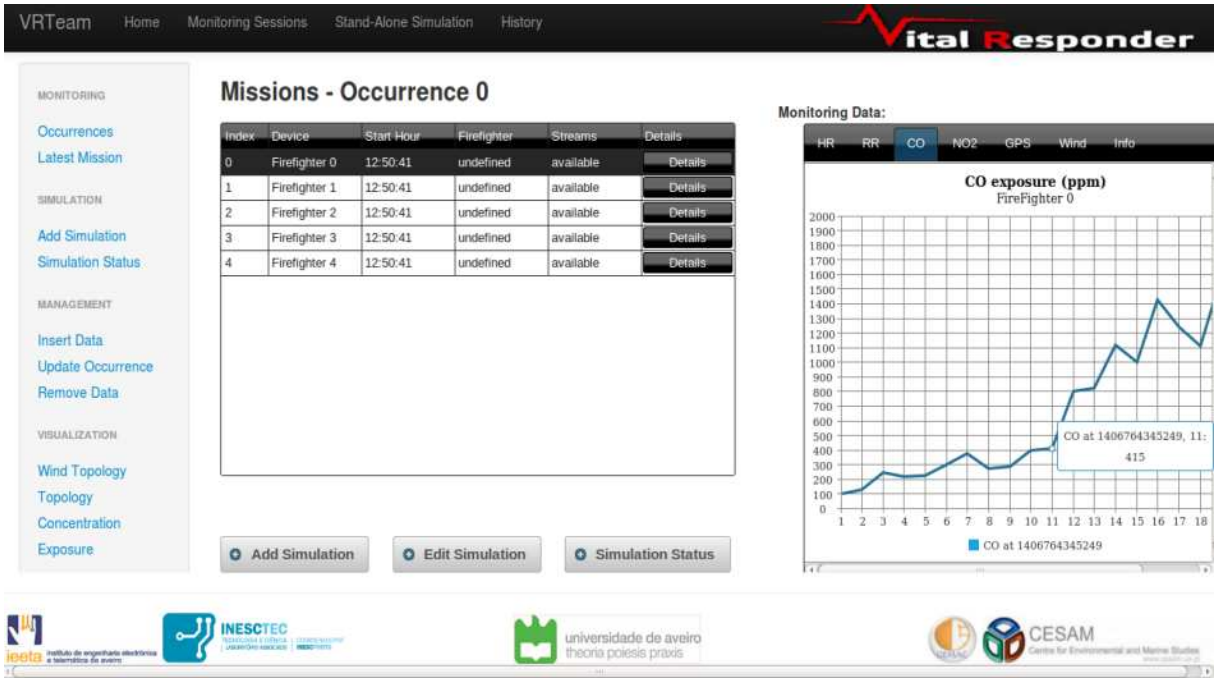

Figure 5. Example of monitored data shown in the GUI.

Simulated data

The results of the simulation's workflow are produced by the *VRSimulationEngine*, which runs the different numerical modules. Figure 6 shows an example of the information available to the *VRTeam* users after a complete simulation session. Enriched visualization of simulation results is shown using multi-dimensional representation of the outputs.

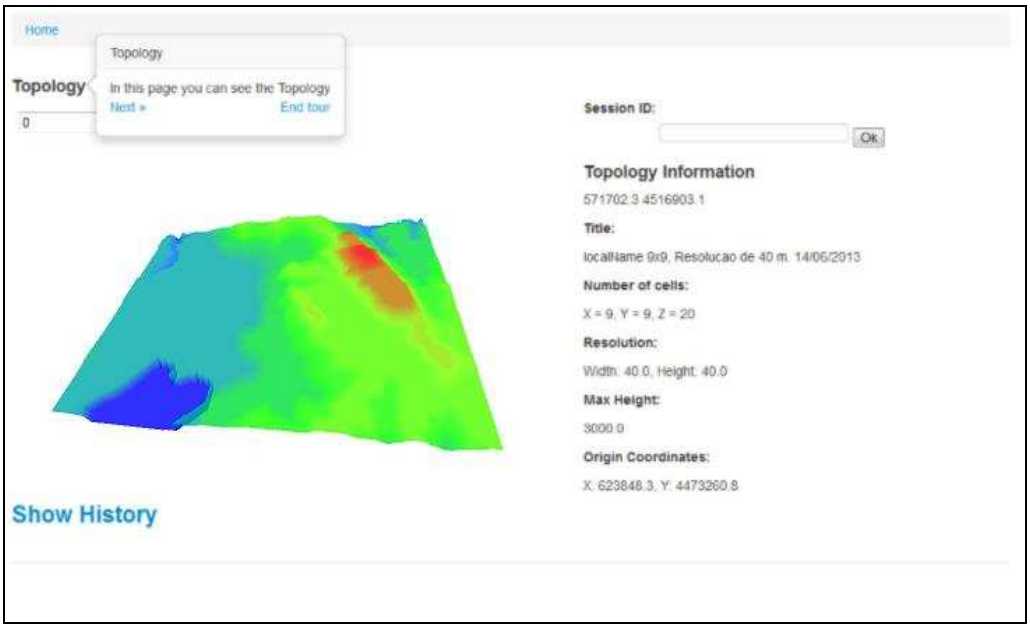

Figure 6. Example of simulation data shown in the GUI.

2.6. Operational testing

A first prototype of the DSS, running in off-line mode, will be tested in the terrain during the fire season of 2014. An improved version of the prototype will be tested in prescribed burning occurring in the autumn of 2014.

Conclusions

Decisions made by firefighters during suppression operations are highly dependent on personal judgement, experience, and senses. However, recent scientific and technological advances offer a vast number of possibilities towards advanced emergency preparedness during firefighting operations, if integrated in a single on-line platform.

This work proposes the development and testing (under real conditions) of a DSS that will provide optimized firefighting efficiency, enhanced hazard awareness, and knowledge-based response during wildland fire. Advances in the computational modelling of fire and smoke behaviour, in conjunction with personal monitoring data, will provide near real-time simulation of local fire conditions and short-term smoke exposure forecasts, with the needed advance in time to permit the safe and efficient positioning of crews in the terrain.

Acknowledgements

This work was supported by European Funds through COMPETE and by National Funds through the Portuguese Science Foundation (FCT) within projects PEst-C/MAR/LA0017/2013 and VitalResponder2 (PTDC/EEI-ELC/2760/2012), and the Post-Doc grants of J.H. Amorim (SFRH/BPD/48121/2008) and J. Valente (SFRH/BPD/78933/2011).

References

Borrego C., Carvalho A.C. & Miranda A.I., 1999. Numerical simulation of wind field over complex terrain. In 'Measuring and modelling investigation of environmental processes'. R. San Jose (Ed.). WIT Press. Southampton, UK. 271-298.

Cunha J.P.S., Cunha B., Pereira A.S., Xavier W., Ferreira N. & Meireles L.A., 2010. *Vital Jacket: A wearable wireless vital signs monitor for patients' mobility in Cardiology and Sports*. 4th International ICST Conference on Pervasive Computing Technologies for Healthcare 2010 (ACM, IEEE and IMIA sponsored). Munich, Germany.

Cunha J.P.S., 2012. *pHealth and Wearable Technologies: a permanent challenge*. In *Studies in Health Technology and Informatics*, B. Blobel, P. Pharow, and F. Sousa (Eds). IOS Press: Amsterdam. 185-195.

De Vos A.J., Reisen F., Cook A., Devine B. & Weinstein P., 2009. Respiratory irritants in Australian bushfire smoke: air toxics sampling in a smoke chamber and during prescribed burns. Archives of Environmental Contamination and Toxicology 56, 380-388.

Finney M.A., 2004. FARSITE: Fire Area Simulator–model development and evaluation. Research Paper RMRS-RP-4 Revised. Department of Agriculture, Forest Service. Ogden, USA.

Hertel O., Leeuw F.D., Raaschou-Nielsen O., Jensen S.S., Gee D., Herbarth O., Pryor S., Palmgren F. & Olsen E., 2001. Human exposure to outdoor air pollution - IUPAC Technical Report. Pure and Applied Chemistry 73(6), 933-958.

Miranda A.I., Borrego C. & Viegas D.X., 1994. Forest fire effects on the air quality. In 'Air pollution II, computer simulation'. J.M. Baldasano, C.A. Brebbia, H. Power, P. Zannetti (Eds). Computational Mechanics Publications. Southampton, UK. 191-199.

Miranda A.I., Ferreira J., Valente J., Santos P., Amorim J.H. & Borrego C., 2005. Smoke measurements during Gestosa 2002 experimental field fires. International Journal of Wildland Fire (IJWF) 14(1), 107-116.

Miranda A.I., Martins V., Cascão P., Amorim J.H., Valente J., Tavares R., Borrego C., Tchepel O., Ferreira A.J., Cordeiro C.R., Viegas D.X., Ribeiro L.M. & Pita L.P., 2010. Monitoring of firefighters exposure to smoke during fire experiments in Portugal. Environment International 36, 736-745.

Miranda A.I., Martins V., Cascão P., Amorim J.H., Valente J., Borrego C., Ferreira A.J., Cordeiro C.R., Viegas D.X. & Ottmar R., 2012a. Wildland smoke exposure values and exhaled breath indicators on firefighters. Journal of Toxicology and Environmental Health - Part A: Current Issues 75(13-15), 831-843.

Miranda A.I., Amorim J.H., Martins V., Cascão P., Valente J., Ottmar R., Ribeiro L.M., Viegas D.X. & Borrego C., 2012b. Modelling the exposure of firefighters to smoke based on measured data. 3rd International Conference on Modelling, Monitoring and Management of Forest Fires (Forest Fires 2012). 22-24 May, 2012. New Forest, UK.

Ott W.R, 1982. Concepts of human exposure to air pollution. Environment International 7, 179-196.

Ottmar R.D., Sandberg D.V., Riccardi C.L. & Prichard S.J., 2007. An overview of the Fuel Characteristic Classification System (FCCS) - quantifying, classifying, and creating fuelbeds for resource planning. Canadian Journal of Forest Research 37, 1-11.

Reinhardt T.E. & Ottmar R.D., 2004. Baseline measurements of smoke exposure among wildland firefighters. Journal of Occupational and Environmental Hygiene 1, 593-606.

Reisen F., Hansen D. & Meyer C.P., 2011. Exposure to bushfire smoke during prescribed burns and wildfires: firefighters' exposure risks and options. Environment International 37, 314-321.

Reisen F. & Brown S.K., 2009. Australian firefighters' exposure to air toxics during bushfire burns of autumn 2005 and 2006. Environment International 35, 342-52.

Ross D., Smith I., Manins P. & Fox D., 1988. Diagnostic wind field modelling for complex terrain: model development and testing. Journal of Applied Meteorology 27, 785-796.

Sestak M.L. & Riebau A.R., 1988. SASEM – Simple Approach Smoke Estimation Model. US Department of the Interior, Bureau of Land Management Technical Note 382. Denver, USA.

Teles D.C., Colunas M., Fernandes J.M., Oliveira I.C. & Cunha J.P.S., 2011. iVital: A Real Time Monitoring System for First Response Teams. In: Pentikousis Kea, editor. MONAMI 2011, LNICST 97. 396-404.

Valente J., Miranda A.I., Lopes A.G., Borrego C., Viegas D.X. & Lopes M., 2007. Local-scale modelling system to simulate smoke dispersion. International Journal of Wildland Fire 16(2), 196-203.

Forest fire detection wireless sensor node

George E. Sakr[a], Rafik Ajour[a], Areej Khaddaj[a], Bahaa Saab[a], Alaa Salman[a], Ola Helal[a], Imad H. Elhajj[a], George Mitri[b]

[a] *Electrical and Computer Engineering Department, American University of Beirut, Beirut, Lebanon, ges07@aub.edu.lb, rafikajour@gmail.com, areej.khaddaj@gmail.com, bahaa.saab@gmail.com, alaasalman@gmail.com, olahelal@hotmail.com, ie05@aub.edu.lb*
[b] *Institute of Environment, University of Balamand, Tripoli, Lebanon, george.mitri@balamand.edu.lb*

Abstract
Wireless sensor networks have attracted a great deal of research due to the wide range of applications that are enabled by such networks. Sensor networks are used for ecological monitoring, military surveillance and biomedical detection. This paper describes a design of a wireless sensor node to be used for early forest fire detection; it utilizes the WSN principle where each node is a sensing device with various sensors attached, powered by solar recharging and supports wireless data transmission. Each one of these nodes sends its collected data through the network to reach a sink node. The latter has a direct link with a base station (weather station, civil defence operation room, or scientific research center). The base station analyses the received data and takes the decision accordingly to raise a fire alarm or not. The main parameters involved in the decision making are smoke, CO, temperature, humidity and methane gas. This paper details the design as well as the experimental activities which demonstrated that this device is capable of early forest fire detection.

Keywords*: Forest Fire, Detection, Wireless Sensor Network, Energy Efficient.*

Introduction

Forest fires pose a menacing danger to the socio-economical, ecological, and environmental aspects of a community. Moreover, forest fires cause severe “ecological imbalances" through endangering the natural habitats of animals, disrupting the food chain in a vast area that exceeds the burned zone, reducing ground water levels, polluting rivers, and preventing vegetation from growing in burned zone. More specifically increasing fire frequency and severity, threatening forest ecosystems and economic development [Mitri, 2009]. All this gives rise to the urgent need to detect forest fires as fast as possible, so as to limit these effects.
Systems used for forest fire detection can be divided into three groups based on where the sensors are deployed: aerial, terrestrial, or combination. It is worth noting that in many cases similar sensors are used in aerial and terrestrial systems. However, depending on the location of deployment there might be different advantages and disadvantages.

1.1. Aerial Forest Fire Detection

The areal detection is subdivided into two main categories: Satellite Systems and Autonomous Aerial Vehicles. There are two types of satellites that appear in the context of forest fire detection. These are the geostationary satellites and the polar orbiting satellites. The geostationary satellites maintain a higher temporal resolution compared to the orbiting ones. This is the reason why geostationary satellites have an advantage over the polar orbiting satellites in near-real time active forest fire detection. In most cases the satellites are used with a base station that collects the data sent by the satellite(s) and runs the analysis [Manyangadze, 2009, Zhou, 2004, Kelh, 2000, Abuelgasim, 2002]. Satellite imaging is used by several agencies for detecting and tracking fires; such as the Canadian Wildland Fire Information System of the Canadian Fire Service. Three well known satellite systems used for fire detection are the (AVHRR) launched by the National Oceanic and Atmospheric

Administration (NOAA) in 1998, the Moderate Resolution Imaging Spectroradiometer (MODIS) launched by NASA in 1999 on board of the Aqua satellite and the National Aeronautics and the Space Administration's Moderate Resolution Imaging Spectroradiometer (MODIS). The use of satellites for forest fire detection and monitoring remains a dominant option. Yet, this system suffers from a set of disadvantages:

- There is a minimum detectable fire size, usually 0.1 ha. This means that there is some delay to detect the fire, which is at least equal to the time it takes for the fire to go beyond 0.1 ha.
- The accuracy of the system is within 1 km of the actual location of the fire.
- Satellites typically provide images of the monitored area every 1 to 2 days, which is a limitation as fires could go undetected for a long time.
- Clouds greatly affect the Top of Atmosphere temperature as they may lower the temperature measured by the satellite. The interpretation being that clouds usually have cold tops and hence low brightness temperature; thus, fires under these clouds are missed.
- Selection of the processing algorithm varies for different sensors with each having its specific limitations.

Autonomous Aerial Vehicles use a helicopter with infrared and visual cameras [Dios, 2005, Casbeer, 2005]. These helicopters are called “Autonomous Aerial Vehicles" or “Unmanned Aerial Vehicles" (UAVs). A base station is needed as well where the collected data is analyzed. Fire detection is initiated in missions where a UAV fleet embarks on patrolling the forest in question. In order to decrease the probability of false alarms, this system relies on the combined results obtained from the analysis of infrared and visual images. Navigation sensors are installed on the UAV to compute the position and the orientation of the cameras. These calculated positions are then collected in order to locate the actual fire. This system suffers from some disadvantages such as:

- Covering large forests requires the use of a larger number of UAVs or a longer flight time per vehicle, which means more consumption of fuel yielding a higher overall operational cost.
- Monitoring a forest is very difficult when unfavourable or extreme weather conditions are present. In addition, limited visibility when smoke is present.
- Assessing fires will vary significantly depending on the topology of the forest in question.
- Scheduling of the flights poses another concern in this mechanism since issuing UAV flights throughout the day will result in a waste of resources and in an increase in cost.
- Radio communication can be hindered in mountainous areas
- Cost of UAV's starts at around 7000$ and they require specialized personnel to operate and maintain them.

1.2. Terrestrial Forest Fire Detection

Several terrestrial systems have been investigated which include: video surveillance, radio acoustic sounding, fiber optic sensor network, wireless sensor network and a combination of the above.
Video surveillance systems are the most widely used for forest fire detection [Kovcs, 2004, Losso, 2006, Stipanicev, 2006, Bodrozic, 2006, Dios, 1999, Arrue, 2000, Bosch, 2007]. In this system, camera sensors are mounted on communication towers that are placed on a location overlooking a large part of the forest. It is not uncommon for cameras to be mounted on towers of elevation often surpassing 30m, making maintenance and even initial deployment a non-trivial affair. In order to provide a full view of the forest, or a specific portion of it, a rotational mechanism is installed to enable the camera

to rotate. The images obtained by the sensors are processed to detect smoke. This is made possible by the use of algorithms that takes into consideration atmospheric conditions.
Radio Acoustic Sounding System (RASS) refers to the use of wave radiation in order to obtain the atmospheric structure. This system utilizes two main devices which are the radio with fire watch towers and the acoustic source [Sahin, 2009]. The approach is to form thermal maps of forest areas for the detection of potential fires. This relies on the fact that radio acoustic sounding techniques have much higher sensitivity to temperature changes and can remotely provide more accurate air temperature measurements. The process of temperature measurement using acoustic sound waves is made available by a Sonar, or acoustic radar, that operates by transmitting acoustic pulses into the atmosphere and detecting echoes backscattered from atmospheric thermal inhomogeneites. This technique is very effective and reliable and it is believed that, in terms of accuracy, it surpasses any other fire detection technique. Yet, it still has several disadvantages and technical difficulties that are:

- The deployment strategy of this system is critical to the performance. This is due to the fact that echoes in collected data are caused by ground clutter.
- It is reported that the scanning area is to be limited to a certain height that is just above the trees.
- The performance is sensitive to the frequency matching and the power of the signal. The optimal results are only obtained once the frequency and the power of the acoustic signals are determined, taking into consideration several issues such as the forest surface density and the distance between the radar and acoustic sources.

Fiber Optic Sensor Network uses a network of fiber optic sensors based on “Fiber Bragg Grating" (FBG) devices, distributed sensors and gas analyzers, and optoelectronic piloting unit for the grid of fiber optic sensors [Corsi, 2006]. This system is composed of FGB temperature sensors, an FBG acquisition assembly to collect data from FBG sensors, distributed fiber optical sensors to collect distributed temperature variation over the fiber, roads upon which to lay the cable through the forest, and gas sensors and their acquisition unit. The number of sensors and the length of the fiber optic cable depend on the nature of the forest. The FBG temperature sensors measure the temperature values in the presence of fire. The gas sensors collect samples of air, measure the content for CH4, and report the results to their respective acquisition unit. The advantage of this system is that the effect of temperature variation on the wavelength of fiber optics can be exploited to generate ultra-stable temperature sensors. This system has two main drawbacks:

- The fiber optic cables need to be installed throughout the forest on a special type of road or path.
- Crown fires take longer time to be detected, if ever, depending on the height of the trees. This is the case since the cables are laid on ground level.

Recently, a promising technology has emerged based on Wireless Sensor Networks [Hefeeda, 2007]. Sensible Solutions Sweden AB developed robust and environmentally friendly sensors, which can be placed in trees. When high temperatures are detected for a few seconds these sensors transmit a radio signal alerting of the possibility of a fire. The disadvantage of such a system is that it does not provide any environmental measurements which can be used to assess the risk of a fire starting. In addition, they are based on detecting high temperatures, which might take a long time to reach a sensor and which implies sensors only detect fires that do reach them. Temperature, relative humidity and barometric pressure where used in a wireless sensor network to demonstrated experimentally that variations in these parameters could be used to detect fires [Doolin, 2005]. The Forest Fire Surveillance System was designed and deployed in South Korea [Son, 2006]. The nodes used measure temperature, humidity and light. Neither of these approaches used smoke detection to improve the performance of the network. In addition, neither of the references discussed the practical requirements of packaging needed to deploy the sensor network. Several papers had mentioned wireless sensor networks as a tool

for forest fire detection [Yu, 2005, Chaczko, 2005]. However, these papers focused on theoretical issues related to sensor networks in general such as in-network processing and data collection. The work in both papers was theoretical with no actual nodes or network being designed and deployed. Also, they had minimal contribution to the task of early forest fire detection. Combination Forest Fire Detection systems integrate the use of a network of optical cameras linking to a multi-layer GIS database operated by Control Operating Center [Tsiourlis, 2009]. This is referred to as the ``SITHON'' system. The SITHON system consists of a wireless network of optical cameras and an airborne fire detection system based on a fully digital thermal imaging sensor. In turn, the network of optical sensors consists of monitoring towers, transmitters, and wireless transmission links up to an integrated GIS environment. This system shares the drawbacks of all of its components.
In addition to the above mentioned systems, is the none traditional Mobile Biological Sensors [Sahin, 2007]. Animals living in a forest are used to assist in the early detection of the fire. These animals are technically referred to as ``Mobile Biological Sensors'' (MBSs). This system is composed of the MBSs, thermal and radiation GPS equipped sensors, access points for wireless communication, and a central computer system. Data is checked for sudden movement of group of animals, which is believed to be a result of panic among those animals. There are some technical limitations involved in this method:

- Animals and sensors should be chosen in accordance with the characteristic of the forest in question and the forest fire type to be detected. For example, crown fires, surface fires, and ground fires cannot all be detected by installing sensors on reptiles.
- Sensor selection depends on the animal species that is chosen.
- Powering these sensors is another concern as they are expected to operate for a long time.

In this paper we present the design and evaluation of a wireless sensor node for the early detection of forest fires. The rest of the paper is organized as follows. Section 2, describes the proposed design, the operation and the packaging of the device. Section 3 reports the experimental results.

Methods

In order to achieve fire detection within a reasonable time, a number of detection devices (including all its subcomponents) should be deployed in different strategic spots in the forest. This implies that there should be a wireless network linking all these devices together. All the data and signals collected, shared, and transmitted between these devices ought to be sent to a remote base station, located somewhere inside or even outside the forest itself. This base station may be a civil defense office, weather station, office for statistics and analyses, or any concerned authority. Therefore, in order to link this sub-network in the forest to that base station, at least one of the devices in the forest has to serve as a gateway or a “sink" of all the signals and data emanating from the forest devices (sources) to their final destination. Note that these sinks are detection devices as well. The only two differences are that they can communicate with the base station and they have their own schedule of operation. The number of these gateways depends on the topography of the terrain, area of the forest, number of regular devices inside it, and the amount and frequency of data to be sent. The general structure of the network is shown in Figure 1. The figure shows a typical architecture of a deployed network where a number of nodes are mounted on trees or poles. These nodes report to a base station with Internet access to send remote alerts of the occurrence of a forest fire.

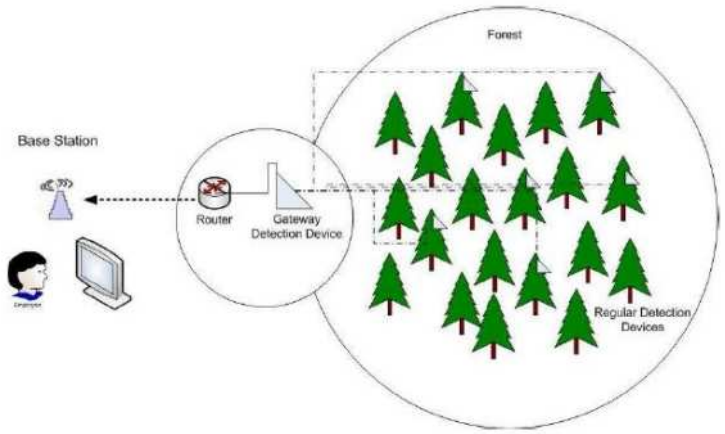

Figure 1. Network Structure

This paper discusses the design and implementation of the nodes used for fire detection. The deployment strategy is beyond the scope of this paper. The device makes use of the components shown in Figure 2.

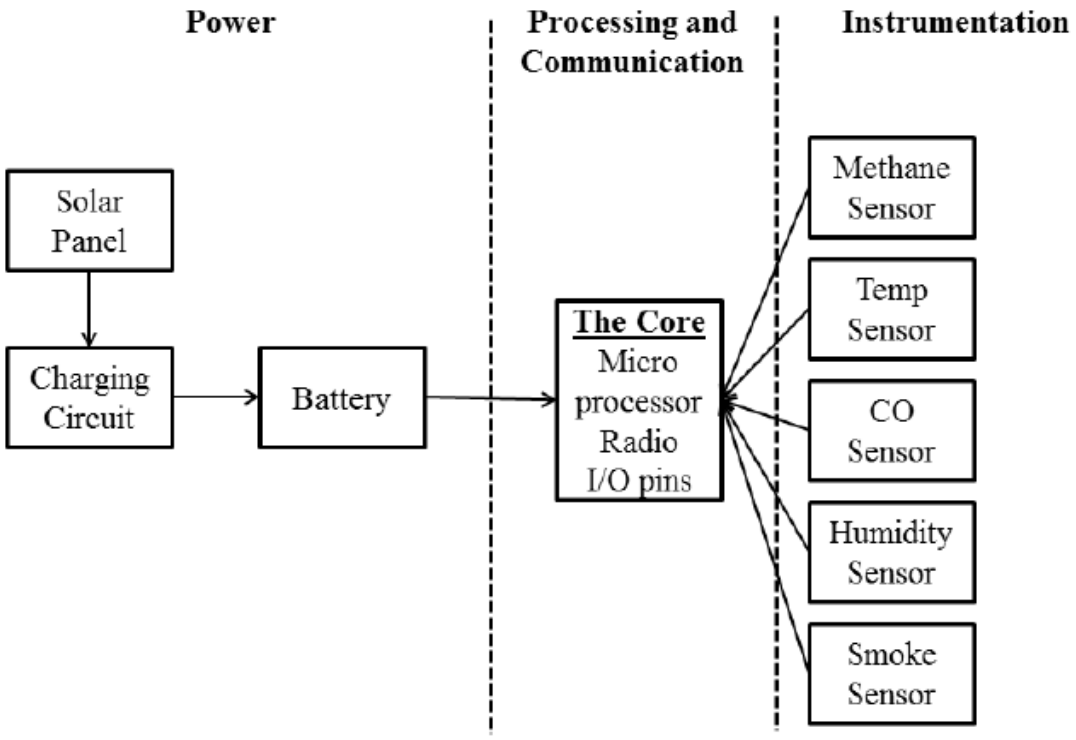

Figure 2. Device's Components

Smoke sensor can provide great help when detecting fires since smoke is the most common and spontaneous product of fire. The smoke sensor chosen is a light Scattering Photoelectric Detector. This smoke sensor produces an output of 1.5 V with a response time which varies between 10 and 20 seconds depending on the concentration of smoke.

Temperature sensor: When a forest fire occurs, huge masses of timber, shrubs, and various plants are burnt, releasing vast amounts of energy in the form of heat. This heat is dissipated in the surrounding atmosphere, causing an increase in temperature. Although this increase in temperature might be a couple of degrees, this can still be a valid indicator especially when combined with other factors. The temperature sensor used is the one built-in the Berkeley Mote (Tmote)
Humidity Sensor: Built-in the Tmote, the humidity has a significant impact on the reliability of the system design since high levels of relative humidity may deceive the smoke sensor, resulting in false alarms. So this sensor can be used to reduce false alarms.
CO Sensor: Carbon Monoxide (CO) is an evident gas released from a forest fire. The S+4CO by Sensor Direct has been used, this sensor is linear, it has a response less than 30 sec, with a resolution of 1 ppm, and a range of 0-500 ppm. However, its sensitivity is considerably low (70 nA/ppm). This implies that a very low output voltage is produced, even for the maximum input value. For instance, if the CO concentration was 500ppm, then the output of the sensor would be 35µA, which is an undetectable value by the Mote. To solve this issue, a special Potentiostatic circuit, recommended by National Semiconductor has been used. This circuit is shown in Figure \ref{circuit} and includes the LMP7721 amplifier which input bias current is only 3fA. The final output voltage of the circuit is the current value multiplied by 10000, which end up being 350mV, an easily detected value by the Mote.
Methane Sensor: Forest fires release huge quantities of combustible gases such as, Methane with average emission rate of 4.96g/kg of dry weight of trees burned. Other combustible gases have lower rates: CH3COOH (3.96), HCOOH (2.61), CH3OH (2.06), C2H4 (0.94), and C2H6 (0.58). Therefore, among the combustible gases, it is most valuable to measure methane levels, in order to help in detecting forest fires. The Methane sensor chosen is the KGS 701 by Korea New Ceramics Co., Ltd. which has an input range of (0-100\% LEL),with a sensitivity 27±5mV / % methane and with a response rate less than 10sec. This sensor also can detect a wide range of combustible gases, mainly propane, iso-butane and pentane.
Battery: a rechargeable Li-ion battery has been chosen. This battery is characterized by a high energy density, a long life cycle (around 300 to 500 cycles), a high drain capability and a fast charge capability. We have chosen a battery with an energy capacity close to 1800mAh and a voltage of 3.7V, since the mote operates on a voltage range of 2.1V to 3.6V.
The Li-ion battery needs a special recharging circuit that guarantees its power functioning and protects it from being damaged. Several requirements are to be considered:

- Set a minimum threshold of input charging voltage.
- Maintain a constant charging voltage independent from the variation of the solar panel's output voltage.
- Stop charging when the battery if full
- Prevent the battery from discharging into the panels when the voltage is low
- Prevent an over-current to enter into the battery, which may damage it.
- To achieve the special charging, the most appropriate IC found was the LTC 1734 by LTC 1734 by Linear Technology, described as “A Lithium-ion Linear Battery Charger". Some of the characteristics of the LTC 1734 are:
- Programmable charge current: 50mA to 180mA
- 1% accurate pre-set voltage: 4.2V
- Charge current monitor output for charge termination
- Automatic sleep mode with input supply removal
- Negligible battery drain current in shutdown
- Under-voltage lockout
- Self protection for over-current/over-temperature

Linear Technology recommends a special circuit to include the LTC 1734 within. Figure 4 shows the LTC 1734 designed to deliver a current of 80mA.
The resistor connecting pin 4 to ground is the control element, which determines the delivered current, based on the following equation:

$$I_{Bat} = \frac{375}{R_{Prog}}$$

Solar Panel: Solar energy is selected due to its higher energy density, simple implementation, reliability, and cost effectiveness. Six solar panels are used to deliver the appropriate energy needed; each rated at 3.7V and 85mAh. This bank of panels is connected as shown in figure 3.

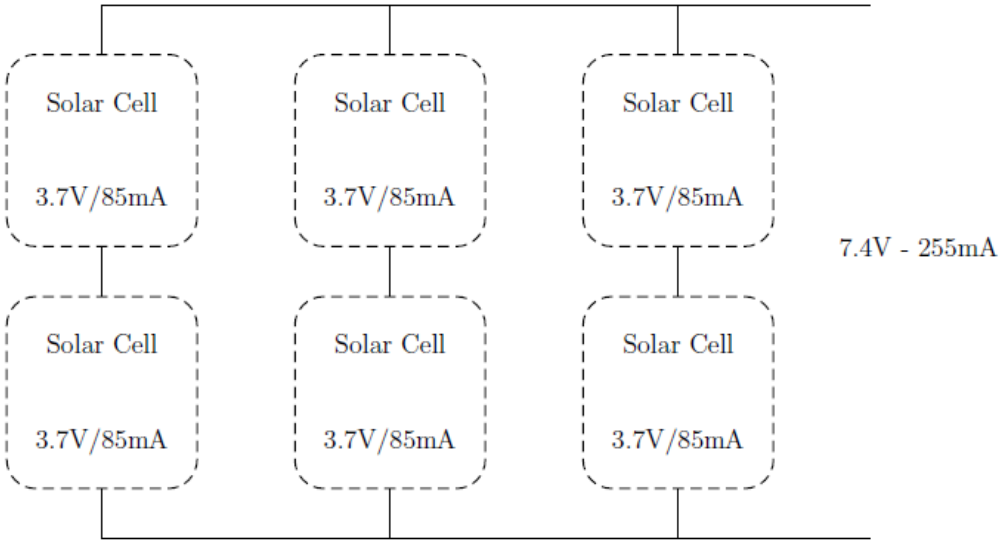

Figure 3. Solar Panel Connections

This configuration produces a nominal rated voltage of 7.4V that is sufficiently higher than the required charging voltage of the battery.
Tmote Sky (Mote-developed by Berkeley University): The core of the node is the processing needed for the sensor outputs, communicating the data to the sink, and checking if there is a fire. The core includes a microcontroller to collect the data coming from the sensors and communicate them. This core is the mote named Tmote Sky that is ultra-low power device and was intended to be used in wireless sensor networks. The mote can be connected to the USB ports of the computer where it can be programmed. Besides, it includes Chipcon CC2420 radio for wireless communication that supports IEEE 802.15.4. It operates at 2.4GHz frequency, and it may communicate with other motes that use the same standard. Hence, the different motes can establish a network automatically upon booting up within their communication vicinity.
The Mote uses MSP430F1611 microcontroller that includes the MSP430 microprocessor produced by Texas Instruments. The 16-bit RISC processor features extremely low active and sleep current which reduces its power consumption. This permits the mote to run for years on a pair of AA batteries. Moreover, it can function on high level operating systems like the TinyOs. This eases the programming of the mote using the NesC language supported by TinyOs.
The module of the mote was designed to fit two AA batteries; however its operating voltage ranges between 2.1V to 3.6V DC. Whenever attached through the USB port, the mote takes its power from the computer. Its power consumption depends on its operation. Consequently, different types of sleep modes can be applied by stopping the components that consume power.

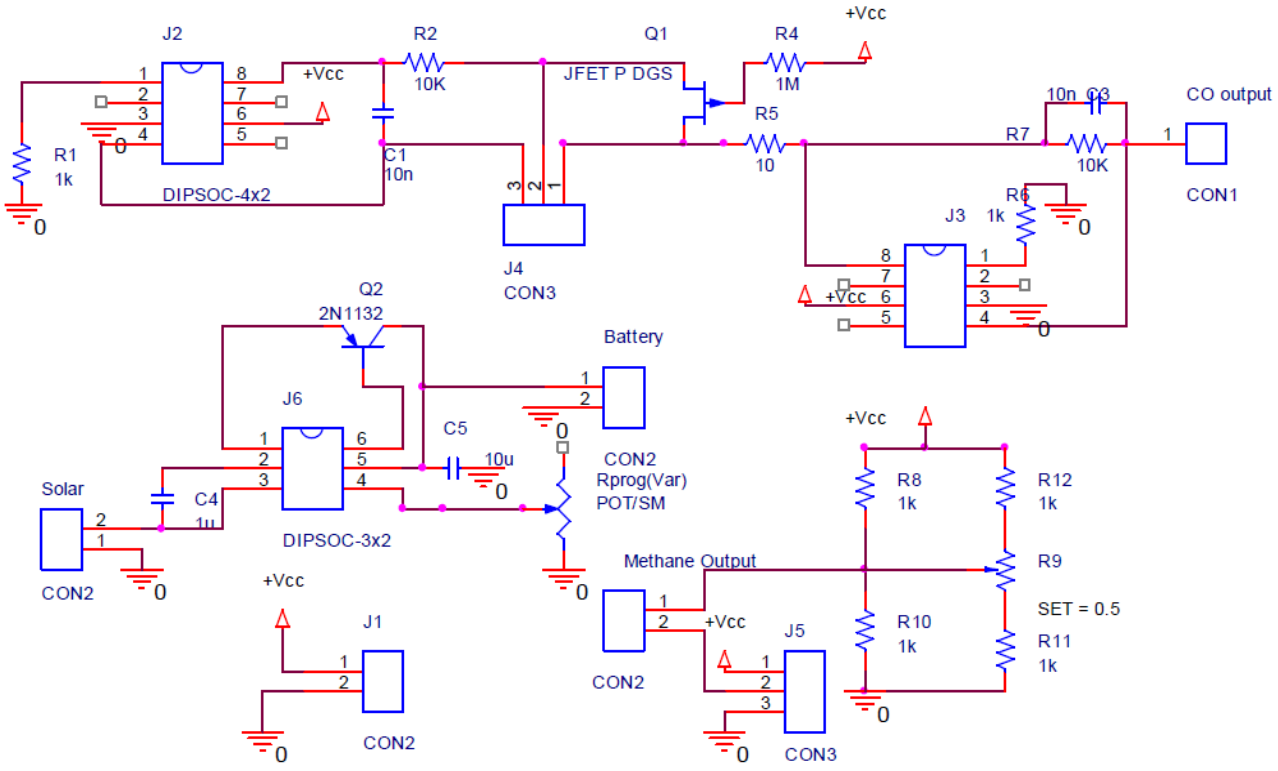

Figure 4. Circuit Design

Design Operation

The main implementation aspect of the mote is its software. The software consists of two main parts: the program on the nodes in the forest and the program on the sink (base station node). Each node shall sense the different parameters (methane, smoke, CO, humidity and temperature) and send them in a single packet to the base station that reads and processes them. The IEEE802.15.4 wireless communication protocol permits automatic setup of the network between the motes that are within communication range. Thus any packet will be routed to its destination by the network itself. The routing supported by the motes was used without modification.

The program proceeds as follows: the sampling timer is initialized by the value set by the base station, whenever it is fired; it turns the output voltage on; this will power the CO and the methane sensor circuits. Then it will initialize a 1min stabilizing timer that will wait for the sensors outputs to stabilize. After the stabilizing timer is fired the program acquires the output of the built-in sensors on the mote, the value of the operating voltage on the mote, and the output voltage of the methane, smoke and CO sensors. Finally all the read values are added to the packet and sent to the base station. The sampling timer can be configured by the base station. The inputs and outputs of the sensor are connected to the expansion pins of the mote where they can take power and send their outputs. The Mote will be in sleep mode when the sampling timer is running. See Figure 5 for the flowchart of the code.

For design reliability, the smoke sensor will remain always on as an existence of smoke will surely mean that there is fire and its output will be used as an interrupt that will awake the mote and send the alarm packets whenever there is smoke. For the methane, its output is the difference between high and low outputs. The two outputs are connected to the mote and their values are subtracted through the software. Both the Smoke and the CO sensors outputs are acquired directly.

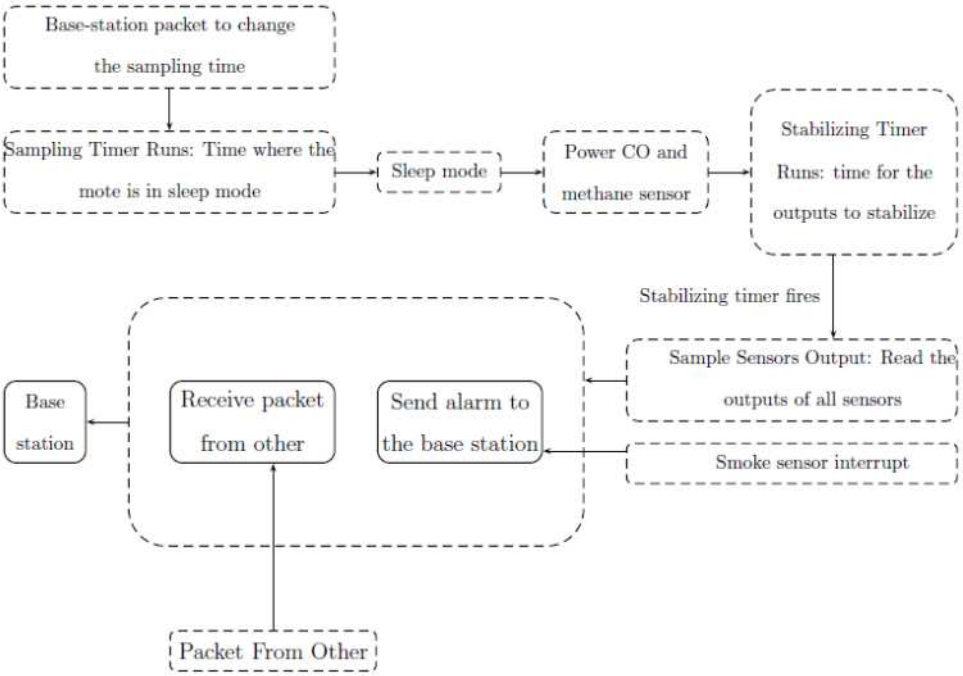

Figure 5. Script Flowchart

Device Packaging

The general shape of the package is right triangular prism where the sensors emerge from the bottom facing downwards. The top cover holds the solar panels and makes an angle of 34^o with the base of the package to increase the solar radiation. The device can be mounted on a pole or tree form the vertical side and its base will be parallel to the horizontal plane. One of the sides can be easily removed in case any component needs to be replaced, modified, or introduced. Figure 6 shows the finalized package.

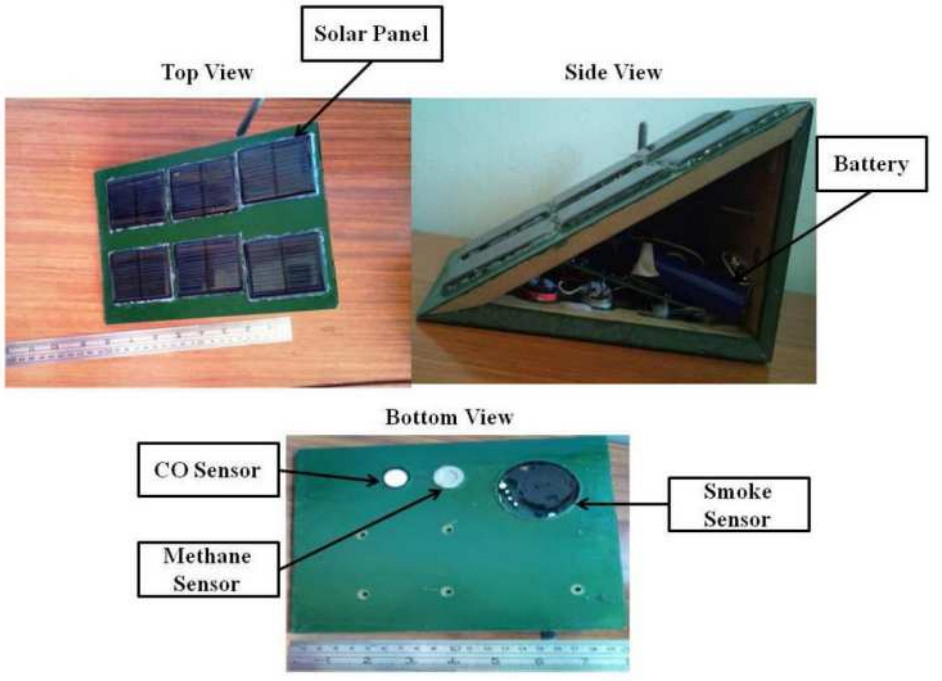

Figure 6. Fire Sensor Module Different Views

Results

Tests were conducted for each sensor and fires were burnt in controlled conditions at different heights. Ash and paper were burnt at the vicinity of the smoke sensor to test its performance. Ten experiments were conducted and the resulting outputs are shown in Table 1.

Table 1. Smoke Sensor Performance T: time, H: height, 1: fire detected, 0: fire missed

T / H	t	t+1	t+2	t+3	t+4	t+5	t+6	t+7	t+8	t+9	Average
0.5 m	0	1	1	1	0	1	1	1	1	1	80%
1 m	1	0	1	1	1	0	0	1	1	1	70%
1.5 m	0	1	0	0	1	1	1	0	1	0	50%

Table2 - CO Sensor Concentration in ppm T: time, H: height

T / H	t	t+1	t+2	t+3	t+4	t+5	t+6	t+7	t+8	t+9	Average
0.5 m	129.2	141.2	114.5	149.5	156.4	147.4	150.4	153.1	145.4	142.1	142.9
1 m	111.7	86.8	115.2	121.4	130.4	117.7	103.0	98.0	105.7	100.5	109.0
1.5 m	84.2	50.8	46.0	86.4	63.4	43.71	74.8	56.8	47.1	49.8	60.3

Table 3- Methane Sensor - % of air composition by volume T: time, H: height

T / H	t	t+1	t+2	t+3	t+4	t+5	t+6	t+7	t+8	t+9	Average
0.5 m	3.463	5.130	5.104	4.230	4.815	3.593	4.111	5.026	4.800	5.107	4.538
1 m	4.085	2.833	3.289	2.863	2.956	3.900	4.063	3.363	4.537	2.841	3.473
1.5 m	2.293	2.185	2.896	2.952	1.826	2.385	2.304	2.678	2.793	2.878	2.519

The results recorded in Table 1 show that the smoke sensor succeeded in detection 80%, 70% and 50% of the time at 0.5m, 1m and 1.5m respectively. The average amplitude of the output voltage generated by the smoke sensor varied from one experiment to another with an average value of 1.5V, which is easily digitized by the mote. It is also important to note that the detection is performed quickly and in close range which is necessary to detect small fires that satellites cannot detect.

Ten experiments of incomplete combustion were done to test the CO sensor with its circuit. A big piece of paper was slightly burnt and then inserted in a bottle. The bottle was closed and got filled with CO. The bottle is then opened and exposed to the sensor. The output CO concentration is shown in Table 2.

The values obtained in Table 2 vary between 46ppm and 156ppm, with an average of 120ppm, which is the typical concentration of CO in such a fire. Moreover the concentration decreases as the distance between the sensor and complete combustion increases. The output voltage ranged between 100 and

130mV, with an average value of 120mV. Taking into consideration the 20mV offset, the output increase is 100mV, which is a significant value, compared to the amount of released CO.
The methane sensor was tested using an unregulated methane source in 10 experiments. We exposed the output of the source to the membrane of the sensor with separation of about 10cm, and released the gas. The average response time was two seconds. The output voltage ranged between 80mV and 160mV, with an average of 110mV. These values signified that the sensor and circuit were working correctly. The percentage decreases as the distance between the sensor and the source increases.
It is worth noting that for all sensors the accuracy of measurement is not critical as the sensitivity. The detection works on processing change in normal operation to detect an increase of a gas. So the absolute value is not as important as the change in the sensor output.

Conclusion

This paper described a sensor node to be used for forest fire detection. The sensing device is characterized by various sensors attached to a mote, solar recharging mechanism, and wireless data transmission capability. The main parameters involved in the decision making are smoke, CO, temperature, humidity and methane gas. The results show high accuracy (80%) of fire detection for close range and slightly lower but acceptable accuracy for higher ranges (60%). As for future work, this device can be used for forest fire prediction in addition to detection. Moreover, the deployment plan and strategy has to be developed to optimize the operation of the overall network.

Acknowledgment

This research was funded by the Association for Forests, Development and Conservation (AFDC), American University of Beirut University Research Board, Dar Al-Handassah (Shair \& Partners) Research Fund and the Rathman (Kadifa) Fund.

References

Abuelgasim, 2002 Abuelgasim, A., Fraser, R., 2002. Day and night-time active fire detection over north america using noaa-16 avhrr data, in: Geoscience and Remote Sensing Symposium, 2002. IGARSS'02. 2002 IEEE International, IEEE. pp. 1489–1491.

Losso, 2006 Andrea Losso, Lorenzo Corgnati, G.P., 2006. Early forest fires detection: smoke identification through innovative image processing using commercial sensors. Technical Report. Environment Including global Change, Palermo, Italy.

Arrue, 2000 Arrue, B., Ollero, A., Matinez de Dios, J., 2000. An intelligent system for false alarm reduction in infrared forest-fire detection. Intelligent Systems and their Applications, IEEE 15, 64–73.

Bodrozic, 2006 Bodrozic, L., Stipanicev, D., Stula, M., 2006. Agent based data collecting in a forest fire monitoring system, in: Software in Telecommunications and Computer Networks, 2006. SoftCOM 2006. International Conference on, IEEE. pp. 326–330.

Bosch, 2007 Bosch, I., Gomez, S., Vergara, L., Moragues, J., 2007. Infrared image processing and its application to forest fire surveillance, in: Advanced Video and Signal Based Surveillance, 2007. AVSS 2007. IEEE Conference on, IEEE. pp. 283–288.

Casbeer, 2005 Casbeer, D., Beard, R., McLain, T., Li, S., Mehra, R., 2005. Forest fire monitoring with multiple small uavs, in: American Control Conference, 2005. Proceedings of the 2005, IEEE. pp. 3530–3535.

Chaczko, 2005 Chaczko, Z., Ahmad, F., 2005. Wireless sensor network based system for fire endangered areas, in: Information Technology and Applications, 2005. ICITA 2005. Third International Conference on, IEEE. pp. 203–207.

Corsi, 2006 Corsi, N., Gemelli, A., 2006. An innovative approach to forest-fire detection and monitoring: The eu-fire project.

Dios, 1999 Martinez-de Dios, J., Arrue, B., Ollero, A., 1999. Distributed intelligent automatic forest fire detection system. Proceedings of INNOCAP 99.

Dios, 2005 Mart´ınez-de Dios, J., Merino, L., Ollero, A., 2005. Fire detection using autonomous aerial vehicles with infrared and visual cameras, in: Proceedings of the 16th IFAC World Congress.

Doolin, 2005 Doolin, D., Sitar, N., 2005. Wireless sensors for wildfire monitoring, in: Proceedings of SPIE, p. 477.

Hefeeda, 2007 Hefeeda, M., 2007-2008. Forest Fire Modeling and Early Detection using Wireless Sensor Networks. Technical Report. School of Computing Science, Simon Fraser University.

Manyangadze, 2009 Manyangadze, T., 2009. Forest fire detection for near real-time monitoring using geostationary satellites. Technical Report. International Institute for Geo-information Science and Earth Observation, Enschede, Netherlands.

Mitri, 2009 Mitri, G., 2009. Lebanon's National Strategy for Forest Fire Management. Technical Report. Ministry of Environment and AFDC, Beirut.

Kovcs, 2004 Rka Kovcs, Blint Kiss, k.N.G.V., 2004. Early Detection System for vegetation Fire in the Aggtelek National Park. Technical Report. Budapest University of Technology and Economics.

Sahin, 2007 Sahin, Y., 2007. Animals as mobile biological sensors for forest fire detection. Sensors 7, 3084–3099.

Sahin, 2009 Sahin, Y., Ince, T., 2009. Early forest fire detection using radio-acoustic sounding system. Sensors 9, 1485–1498.

Son, 2006 Son, B., Her, Y., Kim, J., 2006. A design and implementation of forest-fires surveillance system based on wireless sensor networks for south korea mountains. IJCSNS 6, 124.

Stipanicev, 2006 Stipanicev, D., Vuko, T., Krstinic, D., Stula, M., Bodrozic, L., 2006. Forest fire protection by advanced video detection system-croatian experiences, in: Third TIEMS Workshop-Improvement of Disaster Management System, Trogir.

Tsiourlis, 2009 Tsiourlis, G., Andreadakis, S., Konstantinidis, P., 2009. Sithon: A wireless network of in situ optical cameras applied to the early detection-notification-monitoring of forest fires. Sensors 9, 4465–4482.

Kelh, 2000 Vin Kelh, Yrj Rauste, A.B., 2000. Forest Fire Detection by Satellites for Fire Control. Technical Report. European Space Agency, Finland.

Yu, 2005 Yu, L., Wang, N., Meng, X., 2005. Real-time forest fire detection with wireless sensor networks, in: Wireless Communications, Networking and Mobile Computing, 2005. Proceedings. 2005 International Conference on, Ieee. pp. 1214–1217.

Zhou, 2004 Zhou, Y., Chen, S., Zhou, W., Wang, L., 2004. Early warning and monitoring system for forest and grassland fires by remote sensing data, in: Geoscience and Remote Sensing Symposium, 2004. IGARSS'04. Proceedings. 2004 IEEE International, IEEE. pp. 4799–4802.

Generation of simulated ignitions for the continental United States

Isaac C. Grenfell[a], Mark A. Finney[b], Dianne Trethewey[c]

[a] *RTL Networks, 5775 US Highway 10 W, Missoula, Montana, USA, 59808, igrenfell@gmail.com*
[b] *Missoula Fire Sciences Laboratory, Rocky Mountain Research Station, U.S. Forest Service,5775 US Highway 10 W, Missoula, Montana, USA, 59808, mfinney@fs.fed.us*
[c] *Missoula Fire Sciences Laboratory, Rocky Mountain Research Station, U.S. Forest Service,5775 US Highway 10 W, Missoula, Montana, USA, 59808, dtrethewey@fs.fed.us*

Abstract
Fire suppression continues to be a costly endeavour in the United States and elsewhere. In order to develop a systematic approach to allocating resources to fight wildland fire, it is necessary to understand the underlying process by which ignitions occur on a continental scale with respect to fire weather. We therefore developed a technique that simulated a gridded fire weather index from historical observations and then simulated ignitions at a local scale. The procedure required two steps. First, a model for fire-days (at least one fire occurring on each 30km pixel) used the localized percentile of the ERC (energy release component) as a predictor. A logistic regression model using ERC percentile at that pixel predicted a binary response (fire-day/no-fire-day). Then, for those pixels where at least one ignition occurs, a VGAM (vector generalized additive model) with a Pareto response also used ERC percentile as the predictor. This yielded a dataset of simulated ERC percentiles and the associated number of ignitions for each pixel and each day. The related metadata for each ignition (cause, time of detection, etc.) are sampled from the historical distributions conditional on location. What results is a simulated equivalent of the Fire Occurrence Database which is ready for use in applications for strategic planning.

Keywords*: Spatial temporal simulation, ignition generation, energy release component, Pareto distribution*

Introduction

In order to develop a system to test various fire suppression resource allocation strategies, it is necessary to have a mechanism to simulate the distribution of ignitions across very large land areas. The main problems facing resource allocation are 1) local scarcity of resources created by ignition episodes (large number in short time frame), and 2) broad-scale scarcity of resources created by spatial synchronicity of fire ignition episodes. Firefighting resources dispatched and coordinated at a national scale, meaning that fire occurrence patterns must reflect spatial and temporal patterns at that scale.
There are several attributes that are necessary to constitute a good practical simulation method. First, the distribution of the simulated ignitions must follow approximately that of the historical distribution at the local scale. This means that the overall shape of the distribution, the rough total number of ignitions, as well as extreme behavior must be similar to a great extent. Second, the overall number and seasonal distribution over the entire country must be similar. Third, the method must make use of the historical relationship between the number of ignitions and fire weather. Regarding the first two points, there is no statistical method that systematically provides all of these desired attributes simultaneously. Thus, we must make use of expertise and intuition in order to evaluate what constitutes an acceptable or unacceptable method.

Methods

The method consists of statistically simulating the spatial and temporal patterns of fire occurrence based on gridded daily fire danger rating index. In (Grenfell 2010), a method was described to simulate fire weather at a continental scale that has the same seasonal variability, spatial, and temporal

autocorrelation. The fire danger rating index Energy Release Component (ERC) from this modeling was used to generate ignitions. The key result from the simulation method developed there was to have simulated fire weather with similar temporal and spatial autocorrelation as the historical data. We rely on the relationship between ignition occurrence and this spatially/temporally correlated weather to provide generate the pattern of coincidence (both spatially and temporally) of ignitions. The technique relies upon a fire occurrence database (FOD) (Short 2013) which contains fire records from 1992-2011 coincident with the years generated by the weather simulation model. To choose the appropriate model, data exploration were conducted.

From the FOD, we see that the distribution of the number of ignitions at a particular pixel generally appears to follow a Pareto distribution. In Figure 1, data for a Fire Planning Unit (FPU Colorado-05) are plotted as a histogram of the observed number of ignitions, a histogram where zero ignition-days were excluded, a histogram of 1000 simulated Poisson values from the estimated mean of the historical data, and 1000 simulated Pareto values with the same shape parameter as that of the historical data.

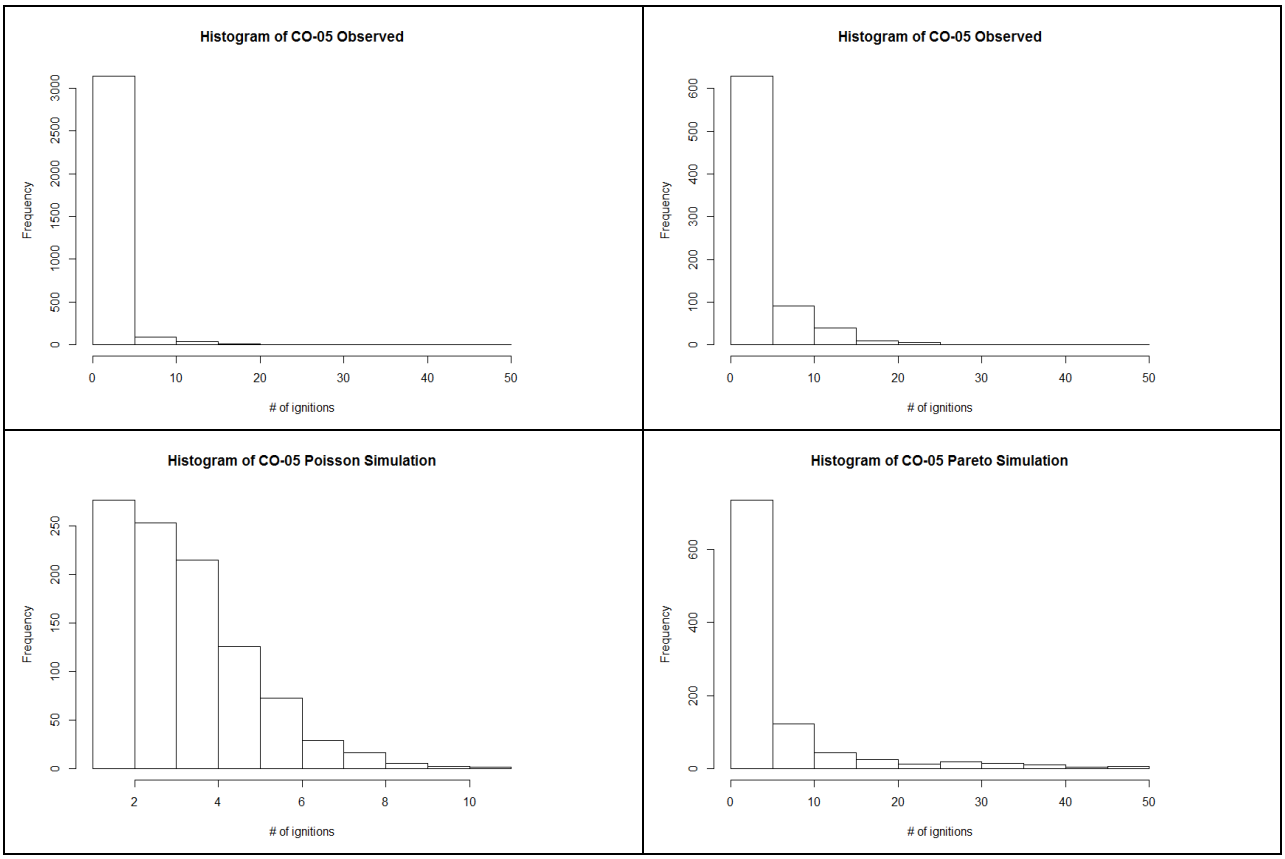

Figure 1- Above left (a), histogram of number of ignitions in FPU CO-05. Above right (b) histogram of number of ignitions on days with at least one ignition. Below left(c) histogram of 1000 simulated days using the average number of ignitions from (b). Below right (d) Histogram of 1000 simulated days using the shape parameter estimated from (b).

Notice that there are more zero-values in the historical histogram than in the simulated dataset. This is a commonly observed phenomenon known as overdispersion. In order to resolve this, we built a two stage model. For the first model, we perform a logistic regression with ERC percentile from the NARR grids being the predictor and the response being whether there are zero ignitions (0) or greater than zero (1). We use percentiles rather than just the ERC values because there are different local relationships with ERC and ignitions (a location where an ERC value of 60 would be in the 90th percentile would be indicative of high fire danger in some places, whereas a location where an ERC value of 60 would be in the 50th percentile in another location would be indicative of far more moderate fire danger).

Once we have developed the logistic models to determine whether ignitions (at least one ignition) have occurred or not, we then use the VGAM package in R in order to perform a Vector Generalized Additive Model regression. This regression method allows for a much broader set of response variables, in this case a response with a Pareto distribution. It is here that the virtues of the Pareto distribution become a hindrance, as left unsupervised the erratic nature of distribution in the right tail can come to dominate the overall phenomenon. To avoid this, we truncate the maximum number of ignitions that can occur at one pixel in one day at fifty percent above the value of the 4th from last order statistic. This allows for the simulation method to produce results greater than what was observed in the historical record (which is the reason for not simply using the historical distribution in a bootstrap-like approach), while not having values so extreme that the overall behavior of the simulated results becomes unrecognizable.

With the two sets of models in hand, we can now begin the process of simulation. It is essentially just the estimation process but in reverse. First, we derive the ERC percentiles from the simulated ERC grids. We then use the percentiles at each location on each day to determine from the logistic model whether or not there will be ignitions. If there are, we use that ERC percentile in the VGAM model to determine how many ignitions will be simulated on that day. In figure 2, we se a selected day from a simulated season (Julian day 180), with a grid of the ERC values (not percentiles). In addition, we can pass on simulated metadata values taken from the FOD, such as cause and time of day. For our purposes, we simply built tables for each location and drew a sample from that.

3. Results

In order to assess the overall quality of the simulation method, we evaluate the simulated tables of ignitions and consider several qualities- the overall number of ignitions, the behavior of the extreme values of the distribution, and patterns of seasonality. To get a sense of the scale and variability in the historical and simulated data, we examine a table of the mean, median, standard deviation, median absolute deviation, and maximum for both the 19 historical years and the 41 simulated years.

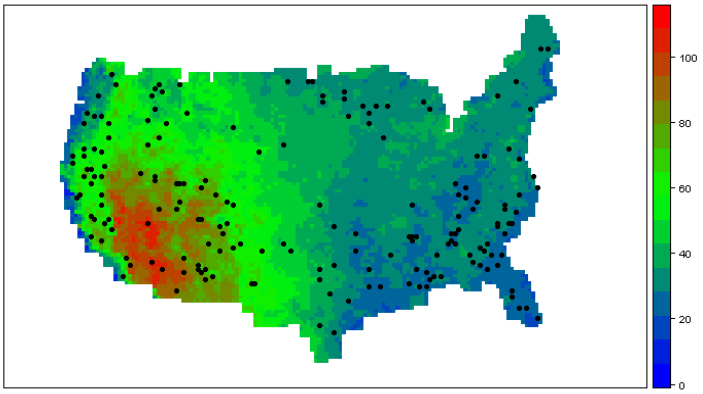

Figure 2. An example of a day's worth of simulated ERC values across the continental United States and the associated simulated ignitions for that day.

	Historical (19 yrs)	*Simulated (41 yrs)*
Mean	65,309	71,780
Median	61,225	71,556
SD	14,369	17,554
MAD	15,280	21,822
Maximum	103,120	109,930

Both the mean and median are within one standard deviation or MAD (respectively) for both the historical and simulated sets of ignitions, providing good evidence that the simulation method is doing a good job of matching the overall behaviour of the historical data.

References

Grenfell, I.C. , Finney, M. A, Jolly, M. Simulating spatial and temporally related fire weather. Proceedings of the VI International Conference on Forest Fire Research; 15-18 November 2010; Coimbra, Portugal. Coimbra, Portugal: University of Coimbra.

Short, K. C. A spatial database of wildfires in the United States, 1992-2011 Fort Collins, CO: USDA Forest Service, Rocky Mountain Research Station. http://dx.doi.org/10.2737/RDS-2013-0009

Hose laying rates for forest firefighting in Greece

Gavriil Xanthopoulos[a], Ioannis Kousaridas[b]

[a] *Hellenic Agricultural Organization "Demeter". Institute of Mediterranean Forest Ecosystems and Forest Products Technology. Terma Alkmanos, Ilisia, 11528, Athens, Greece. gxnrtc@fria.gr*
[b] *Ministry of Public Order and Citizen Protection. Fire Service Headquarters. 4 Mourouzi street, Kolonaki, 10674, Athens, Greece. kousjo@gmail.com*

Abstract
Knowledge and models of firefighting are of great importance for decisions on presuppression planning, dispatching of firefighting forces and operational planning of fire suppression. Significant research effort has been devoted to built such knowledge so far. However, all such information has to be interpreted carefully because it can be affected by various local factors. One example of missing information in regard to firefighting performance is the rate of hose laying by ground forces trying to reach and follow the head or flanks of a fire. Such knowledge is necessary for modelling fire suppression in countries such as Greece where direct attack on the flames using water provided by fire trucks is the main ground firefighting method. The study presented here is an experimental effort to identify some of the key factors affecting the hose laying rate and to establish some initial values for commonly encountered situations in Greece.
Data were collected by building hose lays in Aleppo pine (*Pinus halepensis*) forests with shrub understory on mount Hymettus near Athens, Greece. The hose lays were built by professional firefighters on forest roads or trails that did not hinder their movement. The parameters that were varied were a) Number of firefighters (FF); there were 2 or 3 firefighters laying hose in addition to the driver, as is usually the case with firetrucks in Greece b) Site slope (%) (SLOPE); it varied between -28 and 27%, and c) Length of hose lay (LENGTH); three lengths were selected: 100, 200, and 300 m. The trials were timed with a chronometer and a hose laying rate (HLR) was calculated. Multiple linear regression analysis of the data resulted in the following equation:

HLR = 1.028 - 0.003 * LENGTH + 0.477 * FF -0.024 * ABS_SLOPE

Where (ABS_SLOPE) is the absolute value of SLOPE and FF is the number of firefighters. The value of the equation, its limitations and its potential uses are discussed in relation to the approaches taken in other studies on fireline production rates.

Keywords*: forest firefighting, hose laying rate, Greece*

Introduction

In forest fire management, decisions on presuppression planning, dispatching of firefighting forces and operational planning of fire suppression require knowledge of the productivity, the effectiveness and the limitations of the aerial and ground resources (Xanthopoulos 2002). Numerous studies have examined and tried to model the firefighting process (Fried and Fried 1996, Fried *et al*. 2006), building on other studies that examined, for example, fireline production rates with bulldozers and hand crews (Broyles 2011), length of fire front extinguished by water and retardant drops from various types of aerial resources, etc. All such information has to be interpreted carefully because it can be affected by various local factors (Fried and Gilless 1989, Hirsch and Martell 1996). The same is true for the development and use of firefighting models.
One example of limited reliable information in regard to firefighting performance has to do with use of water under pressure and the related production rates. The studies focusing on this subject, either based on in-field measurements or on expert opinion, are relatively few and the results are very variable (Parker *et al*. 2007). This variability is the result of the multitude of influencing factors such terrain, wind speed, flame height and fuel type. It might be possible to reduce this variability if the effect of

various factors is first measured separately and then the effects are combined. For example, in regard to water based ground firefighting, it might be possible to examine the rate of hose laying by ground forces trying to reach and follow the head or flanks of a fire, before considering the difficulty of extinguishment posed by the variation in flame length.
The study presented here is an experimental effort to identify some of the key factors affecting the hose laying rate (HLR) and to establish some initial values for commonly encountered situations in Greece. This subject has received relatively limited attention globally and there is no specific knowledge for Greek conditions. Such knowledge is necessary for modelling fire suppression in countries such as Greece where direct attack on the flames using water provided by fire trucks is the main ground firefighting method.

Methods

Data were collected by building hose lays in Aleppo pine (*Pinus halepensis*) forests with shrub understory on mount Hymettus near Athens, Greece. The hose lays were built by professional firefighters on forest roads or trails without vegetation that would hinder their movement. The hose used for all tests was of the type most commonly used for forest firefighting by the Fire Service in Greece: 2.5 cm (1 inch) in diameter adhering to the standard PR EN 1924-1, in lengths of 25 meters with Storz type couplings. The parameters that were varied were:

- Number of firefighters (FF). There were 2 or 3 firefighters laying hose in addition to the driver, as is usually the case with firetruck crews in Greece.
- Slope (SLOPE). It varied between -28 and +27%.
- Length of hose lay (LENGTH). Three lengths were selected: 100, 200 and 300 m.

The experiments took place between June and November 2012. Weather conditions, namely air temperature, relative humidity, wind speed, sunshine or cloudy conditions, were recorded for each trial. The aim was to check for probable influence of these factors in the performance of the firefighters. The trials were timed with a chronometer and a hose laying rate (HLR) was calculated by dividing the length by the time (m/s). A total of 24 trials were performed (Figure 1).

Figure 1. A photo of one of the hose laying trials

Analysis and results

The data were analyzed using the SPSS statistical software. The descriptive statistics of the data set are shown in Table 1. HLR varied between 0.7 and 2.44 m/s (2.052 to 8.784 km/h). The highest HLR was achieved by 3 firefighters creating a 100 m long hose lay downslope, on a 14% slope.

Table 1. Descriptive statistics of the 24 record data set.

Parameter	N	Minimum	Maximum	Mean	Std. Deviation
Temperature (ºC)	24	15.0	32.0	22.79	5.2670
Relative humidity (%)	24	24.0	75.0	59.79	18.2350
Wind speed (km/h)	24	1.9	27.8	10.500	5.7424
Number of firefighters (FF)	24	2.0	3.0	2.50	0.5110
SLOPE (%)	24	-28.0	27.0	1.125	17.7462
LENGTH (m)	24	100.0	300.0	175.00	84.6990
HLR (m/s)	24	0.57	2.44	1.3041	0.52909

Multiple linear regression analysis using the stepwise procedure excluded the weather parameters from the list of selected independent variables. As steep slope may impede efforts both upslope and downslope a derived variable ABS_SLOPE, equal to the absolute value of SLOPE, was calculated and tried. The model developed is:

$$HLR = 1.028 - 0.003 * LENGTH + 0.477 * FF - 0.024 * ABS\_SLOPE \quad (1)$$

The multiple regression equation has a p-value<0.001 and an adjusted R^2= 0.641. The constant of the equation has a p-value = 0.013. All the coefficients of the variables are statistically significant at the 0.005 level.

The effect of slope was investigated further by plotting SLOPE against HLR for the laying of 100 m of hose by two firefighters (six measurements) and by three firefighters (six more measurements). The data points and the polynomial lines capturing the trends are shown in figure 2. As seen, HLR increases for downslope hose laying on gentle slope, up to approximately 10%, but then drops as a steeper slope makes downslope firefighter movement more difficult.

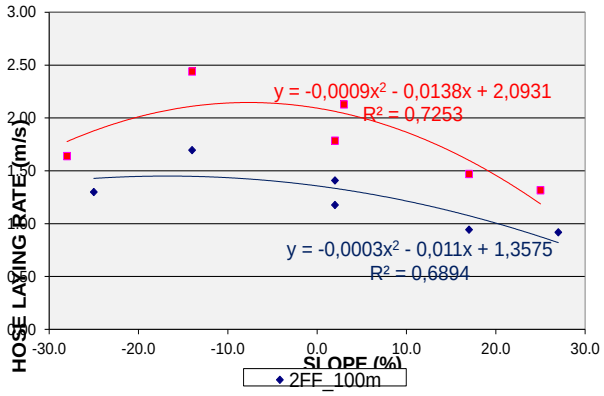

Figure 2. The effect of SLOPE on HLR for hose laying tests of 100 m LENGTH by two or three firefighters.

Discussion and conclusions

The equation developed identified three of the important variables affecting HLR and can be useful in ground fire fighting modelling in Greece, namely number of firefighters, length of hose lay and slope. The lack of influence of weather conditions can be explained by the lack of extreme conditions at the time of the tests and the short duration of each trial which does not allow fatigue to build-up. These conditions may be important if firefighting continues for hours.

The equation can be used for quick calculations either in the form of a table or of a graph (figure 3). It is recognized that it has limitations due to the small sample size, the limited range of values of the variables and the omission of certain other influencing factors such as building hose lay in thick vegetation that impedes movement of the firefighters. The most important weakness is that it does not account for the increase in HLR when hose is laid downslope on slopes less than about 15%. A larger data set would be needed in order to establish with confidence the exact slope threshold beyond which negative slope reduces HLR. If using the equation for estimating HLR for laying hose on negative slopes (downslope) in the range 5-15%, for example in a computer based model for fire suppression, it is suggested to use the HLR estimated for 0% slope increased by 10% in order to reduce error.

The HLR values calculated by equation (1) should be considered as optimum. Such performance can be expected realistically by non-fatigued initial attack firefighter crews arriving to a fire. Future work on the subject is expected to provide additional data and to even allow examination of a non-linear influence of the independent variables on HLR outside the range of values tested so far.

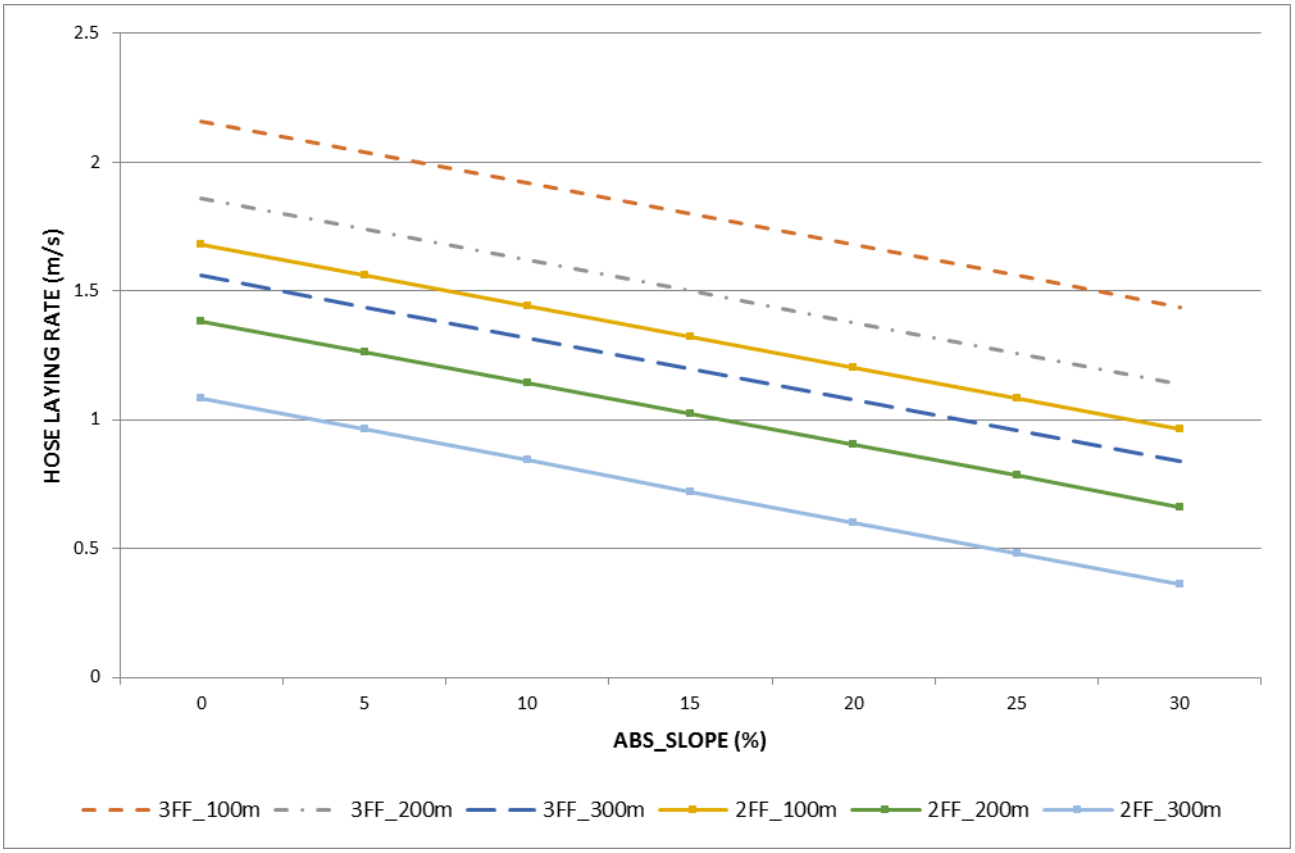

Figure 3. HLR vs ABS_SLOPE according to equation (1), for teams of 2 and 3 firefighters and hose lay lengths of 100, 200 and 300 m.

As a final note, it should be mentioned that the HLR values reported here are not comparable with the values reported in studies such as those of Fried and Gilless (1989) or reviewed by Parker *et al*. (2007) because they do not include fire extinguishment of any short as is the case in those studies. Thus, they can be used, for example, when trying to estimate the time required for reaching a fire front or flanking with hose. Then, the fireline production rates with engine hose lay depending on the type of vegetation (as for example reported in Table 1 of Fried and Gilless (1989)) can be used.

Acknowledgements

The research reported here is part of the work of the second author for a M.Sc. degree at the National and Kapodistrian University of Athens. The first author participated in the frame of a project of the Institute of Mediterranean Forest Ecosystems and Forest Products Technology (IMFE&FPT) titled "Contribution to Fire Prevention in 2013-2014 using the INCA methodology". The project was funded by the Special Secretariat for Forests through the "Green Fund" of the Greek Ministry of Environment, Energy, and Climate Change.

References

Broyles G (2011) Fireline production rates. San Dimas, CA: US Department of Agriculture, Forest Service, San Dimas Technology and Development Center. 5100—Fire Management 1151 1805P.

Parker R, Ashby L, Pearce G, Riley D (2007) Review of methods and data on rural fire suppression resource productivity and effectiveness. Ensis Forest Biosecurity and Protection, Scion, Rotorua, New Zealand.

Fried JS, Gilless JK (1989) Expert Opinion Estimation of Fireline Production Rates. Forest Science 35(3), 870-877.

Fried JS, Fried BD (1996) Simulating wildfire containment with realistic tactics. Forest Science 42(3), 267-281.

Fried JS, Gilless JK, Spero J (2006) Analysing initial attack on wildland fires using stochastic simulation. International Journal of Wildland Fire 15(1), 137-146.

Hirsch KG, Martell DL (1996) A review of initial attack fire crew productivity and effectiveness. International Journal of Wildland Fire 6, 199–215.

Xanthopoulos G (2002) The DISPATCH program for the dispatching of Canadair CL-215 and fire trucks in Greece. In proceedings of the International Workshop on "Improving Dispatching for Forest Fire Control". December 6-8, 2001. Chania, Crete, Greece. Ed. G Xanthopoulos) pp. 133-141. (Mediterranean Agronomic Institute of Chania, Chania, Crete, Greece)

Instant foam technology to improve aerial firefighting effectiveness

Agoston Restas

National University of Public Service, Budapest, Hungary, Restas.Agoston@uni-nke.hu

Abstract
Introduction: This paper describes a new technology, making the process of aerial firefighting more effective. Instant foam technology based on adopted patent, called Foam Fatal, used by petrol industry. Methodology: Before starting the project prepared a study which is focused the economic efficiency of aerial firefighting. This study says that the effectiveness of aerial firefighting using just pure water is very limited but there are possibilities for extending this effectiveness. Instant foam technology can use any traditional foam solution in a special tank installed on board and this liquid emitted in the required place by pressure. Whit this process the quality of the created foam become very homogeneous and some feature also can be modified during the process. Results and discussion: No doubt, in the market there are already some special water tanks, even with pressured systems, however the results comparing the extended efficiency of the instant foam technology to the others is notable. Moreover, instant foam technology is even cost effective, making the process of aerial firefighting real effective.

Keywords*: instant foam, homogenous foam structure, effective fire suppression, aerial firefighting*

Introduction

One effect of global climate change is the increased risk of forest and vegetation fire and the higher intensity of these fires, thus the resulting damage is more severe. The application of aircraft and helicopters in large-scale forest fires is a globally widespread practice. They can transport great amount of extinguishers, mainly water to places which road vehicles cannot reach. However, even this amount is often not enough. The author aims to present a potential new method of increasing the effectiveness of extinguishers.
The new technology is based on a Hungarian patent[1], whose goal is to effectively extinguish extensive fires of containers used in petroleum industry with instant foam. The adaptation of this technology in forest fire fighting has raised interest. Thus, the author wishes to introduce and develop this technology as an innovation in the market of forest and aerial fire fighting with the consent of the owner of the patent. The article describes the author's related research, result and the adaptation of the technology.

Possibilities and barriers of water extinguishing

Theoretical backgrounds of water extinguishing

The most common extinguishing material used in fighting against forest fire is water. Unfortunately its maximum volume is objectively limited on surface (Csontos *et al*., 2007). Twigs of an average age (40 – 80 years) pine forest is able to hold about 4 – 5 litres water per square meter. These amounts of water makes the surface wet but using more amounts will drop to ground and be out of the burning zone without any effect. All resources we used for carrying this water can be evaluated as a waste and useless expenditure.

[1] Foam Fatal technology; http://foamfatale.com/

Based on specific heat capacity of 1 litre of 20 C^0 water [1] (4.2 kJ/kgC^0 x 80 C^0 = 336 kJ/kg) and counts with its evaporation heat[2] (2684 kJ/kg) the cooling capacity is 3020 kJ/kg. Based on the 5 l/m^2 maximum weight of water on the surface its cooling capability without waste is 15100 kJ.
The volume of the biomass per square meter at a mature forest obviously can move at a wide scale. Based on the author's experience its volume which can catch fire during burn is about 6 – 10 kg/m^2. Based on Nagy (2007) its heat of combustion (≈18500 kJ/kg) is about 111000 – 185000 kJ.
Water content of the biomass is taken as 70 % (Nagy, 2007) during an extreme weather condition perhaps less. Based on the above the rate of water of a 6 – 10 kg bulk is about 4.2 – 7 kg that has to be evaporated by its own combustion heat. Cooling capacity of the above amount of water is between 12684 – 21140 kJ.
The heat combustion of the part of pine bulk, can be count during burn is (111000-185000 kJ) much higher than the common cooling capacity of water content of the bulk (12684-21140 kJ) and the maximum water amount on its surface (15100 kJ). It means with water the suppression of a developed fire is objectively not possible. The difference between the combustion heat and the cooling capacity is at the lower threshold 4 times, at the upper level 5 times higher for the combustion heat! Based on the above the practice can be demonstrated, above that fire intensity where 5 kg/m^2 water is not enough for suppression, the active, fighting tactics is avoided with pure water even in case of aerial firefighting (Georges, 1975; Hardy, 1985).

Losses of aerial firefighting

Losses during transportation

In case of helicopters there are significant water losses during transportation. Bucket has no cap therefore there is a friction between the water surface and moving air. This effect, like the Bernoulli principle, takes lots of water out from the bucket and it looks like an evaporation cloud above-after the bucket. This loss depends mainly on the speed of transportation and the carrying distance. The other type of losses is caused by mechanical effect, mainly immediately after the upload but also during the whole transportation route. Water swing in the bucket and clashing to the wall lots of water will splash out from the bucket. Based on some observers above losses can be over 30 %, in extreme conditions even 50 % (Jambrik, 2007, Imreh at al., 2009).

Figure 1. Losses of aerial firefighting

[1] Specific heat capacity (c) of water is: 4.2 kJ/kgC^0; Formula is: E_c = c m dT = 1680 kJ
[2] Evaporation heat (p) is: 2684 kJ/kg; Formula is: E_p = p m

Losses during water dropping

After opening the valve water decomposes to drops creating water cloud. Usually it is generated by the strong airflow spontaneously; however there can be generated also some technical means. Raising the speed of the fly the rate of spray will also rise. Unfortunately, the very small water drops can leave the requested area without significant help in the suppression or the rate at the surface is below the effectiveness threshold. Some observations say this loss can be about 5 – 10 % (Delforge, 2001).

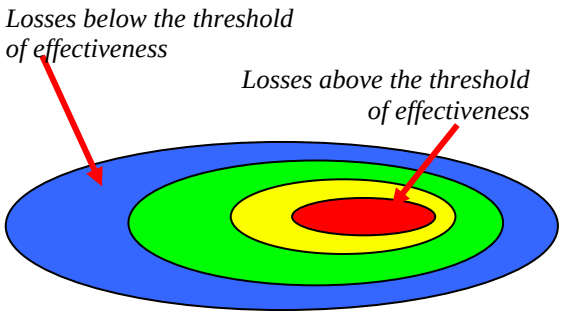

Figure 2. Losses above and below the threshold of effectiveness

Losses above and below the thresholds of effectiveness

For the effective suppression we must ensure there is enough water quantity per square meter. If this water quantity is below a threshold there is no suppression effect of water; it means this volume is lost. All resources we spent for this volume to be carried to the fire front is a useless expenditure. Since the footprint of water dropping is never homogenous, from the middle to the edge less and less, unfortunately this loss can't be avoided. Even if experts keep this minimum threshold volume different[1] it is between 0.2 – 0.8 l/m^2.

In the middle of the footprint of dropping water the water quantity can be higher than it is required. Bulk can hold no more than 5 l/m^2 water on leaves. Above this quantity water drip to the ground and there is no effect for crown fire; it means this volume is loss. All resources we spent on this volume to be carried to the fire front is also a useless expenditure. The rate of losses above and below the thresholds of effectiveness is about 10 – 20 %.

Loss of evaporation

If water dropping is not directly to fire front but some meter before it making a wetting zone a significant evaporation loss can be noticed. It is caused by the huge surface (wetting leaves), small water drops and high temperature. It takes time the fire front moving ahead and reach the wetting zone. Depending on the distance and the speed of fire propagation the time interval – fire front reaches the wetting zone – can be significant and during this time loss of evaporation can be remarkable; it means evaporated volume is loss which can be more than 25 % (Delforge, 2001).

Other losses

There are other losses, like targeting, navigation or coordination losses, however these are almost the same technologies, therefore different analysis is not necessary.

Based on the above, author counts with the average rate of losses 25 % in case of on-board installed tanks and 50 % in case of buckets.

[1] It depends on literatures, those are differences, e.g. 0.5 l/m^2 (Szabo, 1994); 0.8 l/m^2 (Delforge, 2001)

2.3. Possibilities enhancing water capabilities

Regarding the above problems experts search different ways to enhance water capabilities. It means different applications, like using retardant, gel, foam agent, specially developed explosion extinguishers[1] or even developing new kind of extinguisher materials[2].

Technical solutions

Based on the above analysis, it can be seen one part of losses are not avoidable, other part – mainly in case of helicopter – it relates to using bucket. This latest one – because of the Venturi effect – can cause even more than 30 % losses of transport capacity. This loss can eliminate in case of using tank, therefore different types of its appeared like on-board[3] or to belly installed tank[4].

Knock out effect

In many cases practice uses the kinetic energy of dropped water to suppress fire, so called „knock out" effect. In this case aircraft pilot drops water directly to the fire front and besides the cooling effect the kinetic energy of water mass also helps to suppress the fire; it breaks the chain reaction of burning process tearing down the flames. This method gladly used by aerial firefighting. An aircraft with flight speed of 180 km/h and altitude of 20 m generates kinetic[5] and potential[6] energy of 1 kg water about sum 1.45 kJ. The problem is that even if this method many times effective way to suppress – "knock out" – a short section of the fire front but the used kinetic energy of 1 kg water is much less than either the specific heat capacity or the evaporation heat capacity of water. Economically author evaluates this method waste because the extinguishing potential of the carried water is much higher than just the kinetic energy. (Naturally during knock out effect besides kinetic energy the cooling effect has also an important role. Its rate requires more analysis.)

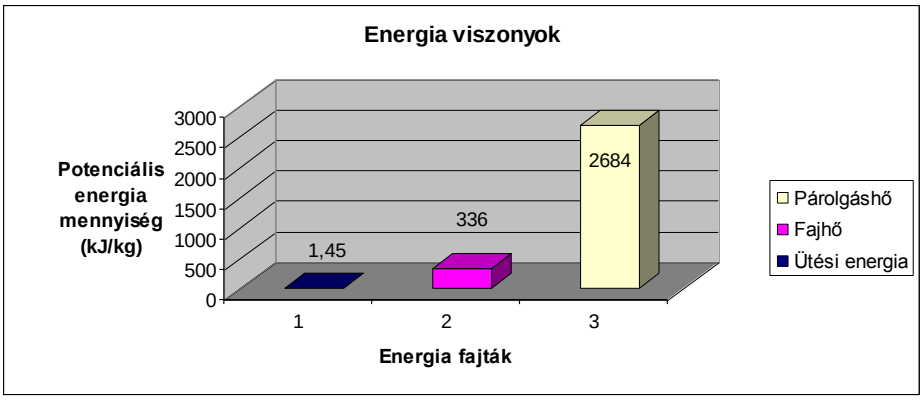

Figure 3. Kinetic energy (1 / blue), heat capacity (2 / purple) and evaporation heat (3 / yellow) of dropped unit water. Source: R-Fire Ltd. I4F technology Manuscript

[1] e.g. Beaextin S.L., http://www.lucka.be/brandbeveiliging/extras/efp-fire-suffication.pdf

[2] Special salt mix; 2 years research project, BASF presentation, Aerial Fire Fighting Conference, 2008, Athens, Greece

[3] e.g. Coulson C-130 Next Gen Airtanker: http://fireaviation.com/2013/07/12/removing-coulsons-c-130-tank/

[4] e.g. Simplex: http://www.simplex.aero/fire-attack/

[5] $E_{kinetic} = ½ m v^2$; in the above example 1250 J

[6] $E_{potential} = mgh$; in the above example 200 J

Retardants

There are also other solutions to enhance water capability which are based on different agent additions. One of these is using retardant that makes water drops more homogeneous causing less waste and there are not just cooling but also chemical based effects. Author focused on energy balance and potential suppression capability of extinguishing materials therefore the water equivalent of chemical based effects of retardant is missing however the value of its obviously can be very interesting and also planned to be one of author's next research topic.

Foam

Besides the retardant there is another method to enhance water suppression capability that is using agents to generate foams from its solution. In case of foam beside the cooling effect there can be also extra extinguishing effects. One of them is that agent reduces water's surface tension therefore the pine bulk can be covered by more homogenous foam drained solution. Other kind of the effect is that the structure of foam creates an isolation effect that can protect leaves from heat radiation. Based on this extra extinguishing effect fire propagation can reduce significantly and there is no enough radiation heat to keep chain reaction of flames alive. Based on authors study there is a way to optimize the isolation effect of foam and expand its capability to that dimension where pure water objectively can't be effective.

Figure 4. Aerial firefighting with using foam traditionally

Opposite to generate a foam structure there can be another aim to use foam agent. As mentioned above minimal rate of foam agent mixed to water can reduce the surface tension. In this case the rate of agent can remain below 1 % however this amount is enough to enhance the water effectiveness. Before fire it means water can cover pine bulk homogenous, after fire water can wet the glowed or sooty surface more effectively.

In case of foam using the evaporation loss is also less. Other side depending mainly on the type of foam agent the water draining from foam structure is natural phenomenon. Unfortunately this phenomenon reduces the foam effectiveness however with a good firefighting tactic – optimizing the distance between the fire front and foamed strip – it can minimize, that means a minimum „waiting time" fire front reaches the foamed zone.

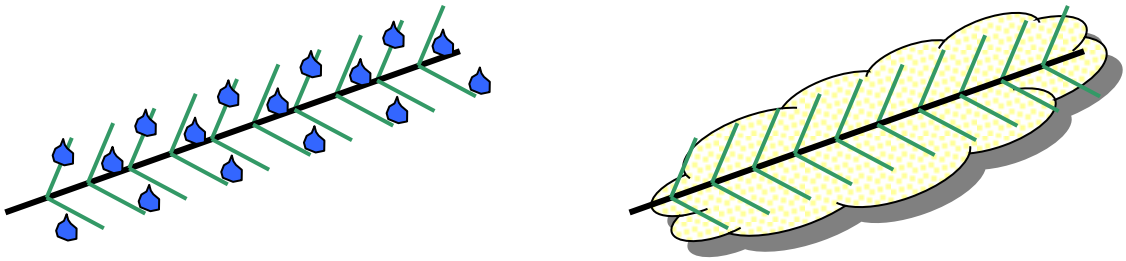

Figure 5. Water drops and foam blanket on pine bulk. Structural graphic

Based on the above, next part uses practical and theoretical investigations focusing on the possibilities of raising foam effectiveness.

Problems extinguishing with foam

In common cases using modern foam are believed to be very effective. Firstly, as addition of agent it is able to reduce the surface tension resulting better wetting effect, the other one is that with different equipment we are able to generate a foam structure. This structure depends on many conditions however in most cases it generates mechanically by the collision of solution and equipment dropping solution to air.
In case of aerial firefighting we can also face to use foam however there are some barriers of effective use. Dropping solution from the tank it strikes a grid or net to mix with air and generate foam but in most cases solution collide with air spontaneously (Figure 4), resulted foam. In case of bucket a special „foam sack" attached to water sack and its net mix air and solution generating inhomogeneous foam structure.
The effectiveness of foam depends on many conditions, like the mixing rate, expanditure rate, speed of solution dropping (flight speed), altitude and also the homogeneity.

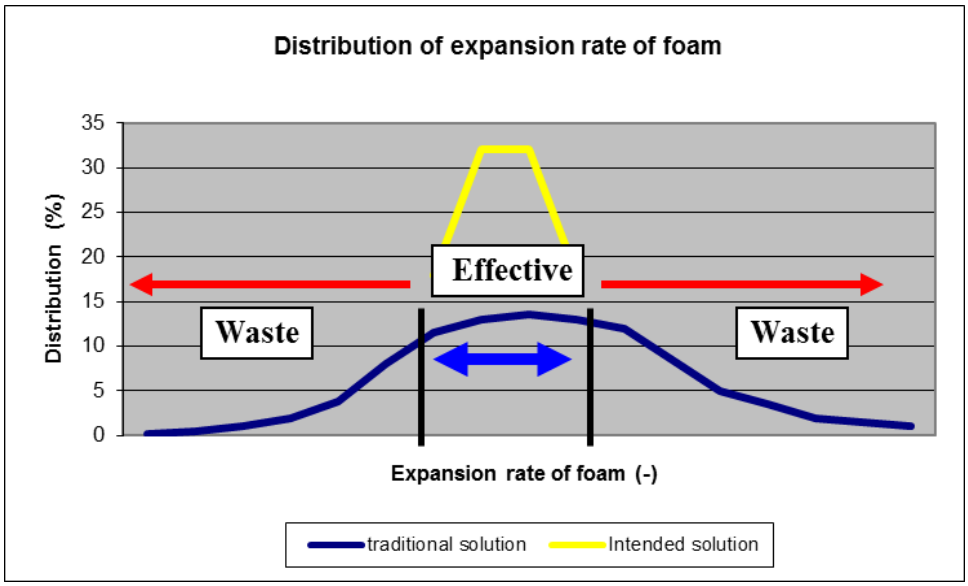

Figure 6. Foam bulb's distribution of traditional and new technologies depending on expansion rate

Foams with different structure and feature have different behaviour. Foams with large expanditure rate can be driven from the required place by the rotor wind of helicopter or by the fire caused convection

and there is no effect to suppress fire. Foams habitant on crown depends on its dense; light dense foam remains on the top of the crown, heavy dense foam – like a Newtonian fluid – flown down to ground. The effective suppression requires that the foam need to be – more or less – homogenous at all cross-section of the crown. Naturally the crown structure is not ideal thus the foam homogenate can't also be ideal. Probably there is no technology to create an ideal foam homogenate at all cross-section of the crown however the technology to improve it will result higher foam effectiveness.

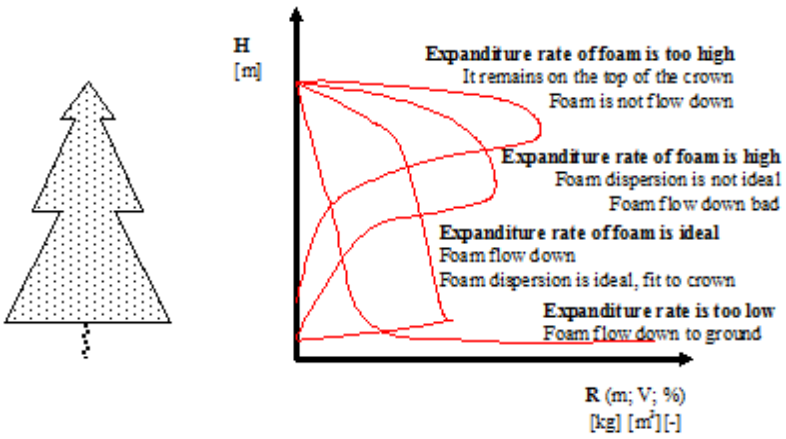

Figure 7. Foams blanket depending on expanditure rate

Basic requirements of foam for effective suppression:

1. Expanditure rate of foam must be such quality it ensures both the cross flown the canopy and its remaining on twig surface to cover it.
2. The foam weight on the unit surface must be such quantity it ensures to stop fire propagation.
3. The foam structure must be such quality it ensures the minimum water drain and long term stability.

Summarizing the problems regarding using foam:

1. The foam we need is of homogenous quality. Its density is suitable to maintain its insulation effect yet it can flow down from the crown and provide protection for the required time.
2. The foams designed specially for fighting forest fire meet the condition of remaining on the surface for the required time based on author's assumptions and the information provided by the manufacturers.
3. The current transport methods and means can only partially meet the condition of homogenous quality. It reduces the extinguishing capability of foams.
4. The favourable features of foams are present even at lower foam expenditure for a certain period.
5. In the case of low foam expenditure, the foam maintains it fluidity, typical of Newtonian fluids.

Instant foam for fighting forest fire – I4F technology – is able to ensure that the quality of foam structure is enough homogeneous therefore the losses caused by the different expanditure rates can be reduced and minimized.

Summarizing – concept of adaptation Foam Fatal technology

Based on the R-20F method foam has an extra extinguishing effect caused by the isolation effect; total suppression effect of foam is – averagely – twice higher than just the quantity of water that foam

contains (Restas, 2012). Other side, based on the R-10A method the foam remains on canopy 3 times more weight than just pure water (Restas, 2014). Above extra effects can give 6 times more effectiveness than just pure water per unit surface. It means new technology is able to protect the unit surface of vegetation against 6 times higher heat radiation of fire.

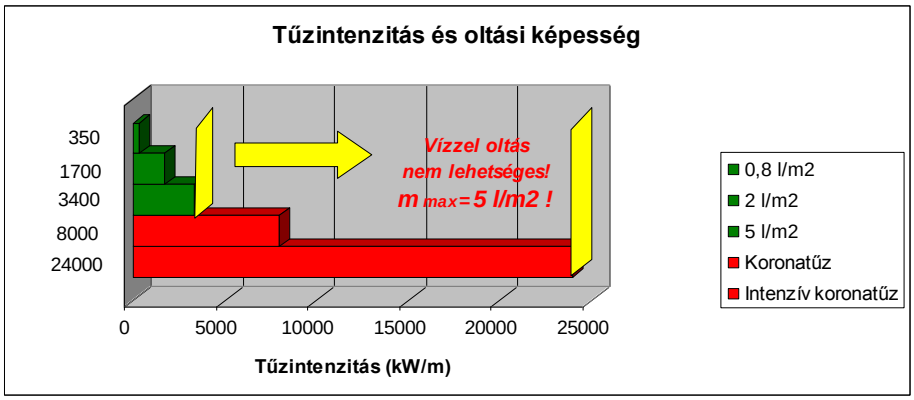

Figure 8. Capability of water and fire intensity. Above 3400 kW/m fire intensity water is not effective (red tubs)

The maximum amount of water remains on canopy surface is about 5 l/m^2; it is enough to suppress fires no more than with about 3400 kW/m intensity; it means both the effectiveness (capability) and also the barriers of pure water. However in case of canopy fire we can face about 8000 kW/m, in extra situation to about 24 000 kW/m fire intensity. Logically follows that using water traditionally is objectively can't be effective in case of canopy fire. Based on the above it also follows that using new technology the extinguishing capability of foam theoretically can extend even to 6 times higher fire intensity – it can be above 20 000 kW/m – similar to water capability. It means using new technology canopy fires can be supressed that was unable by traditional solution. The above clearly shows the benefits of new technology, which can be supplemented with the comparison of losses.

Table 1—Losses depending on technology

Losses	On-board tank	New technology
Loss caused by inhomogeneity	30 %	0%
Loss caused by technology	0%	15%

The basic difference between the two technologies can be found in the quality of the foam, which can be demonstrated by inhomogeneity. With the application of new technology the losses are reduced by half.

Extinguishment with instant foam is not new. It is present in hand portable extinguishers, and in petroleum industry at storage tanks as a Hungarian patent. It should be noted that author does not differentiate between instant foam and compressed air foam system (CAFS) regarding the extinguishing capability.

Tank must to be filled about of 4/5 part with water, then add the required amount of foam-forming agent (0.1 – 6 %). After that, with the help of a special pump we add gas to the solution until the pressure reaches the suitable value. Practically, the instant foam is ready. The extinguishment starts with the wide opening of the valve of the container. Within an instant, the solution is able to leave the container through the pipeline. As a result, the pressure suddenly and drastically drops which causes

the solution to become foam. The continual release of gas results in the slow decrease in pressure within the container, which enables the continual and quick release of the liquid and the instant foam. The special hose at the end of the pipeline the homogenous instant foam can reach long distances similarly to water jet.

Figure 9. Foam Fatal tank made of composite and install on helicopter board

In order to install the system on board making composite tank instead of meatal one is required. It maximizes the useful part of the loading capacity and makes aerial firefighting more cost effective solution. Author plans to finish tests in 2015.

References

Csontos P.: Feketefenyveseink kutatása (Research for pine forests in Hungary), MTA-ELTE Elméleti Biológiai és Ökológiai Kutatócsoport, Budapest, 2007

Delforge, P.: Guide d'emploi des moyens aeriens en feux de forets (Handbook for aerial firefighting) Minister de L'Interieur, Paris, France, 2001

Georges, W. C.: Fire retardant ground distribution Patterns from CL-215 air Tanker, USDA Forest service – Research note, INT-165. United States, 1975

Hardy, C.: Chemicals for Forest Fire Fighting, Study, NFPA, National Fire Protection Association, Boston, United States, 1985

Imreh, L., Blaskovits, Zs., Restas, A.: Új módszerek a légi tűzoltásban (New systems in aerial firefighting), Repüléstudományi közlemények, 2009 (2) pp. 1-5, Szolnok, Hungary, HU ISSN 1789-770X

Jambrik, R.: Légi támogatás nélkül nehéz lett volna (It is difficult without aerial support), Vedelem, XIV. (6), pp. 51 – 53, Budapest, Hungary, 2007, ISSN: 1218-2958

Nagy D.: A közvetlen taktika korlátainak fizikai/égéselméleti háttere (Physics backgrounds of fire hindering direct firefighting tactics); Vedelem, XIV 2007 (6), Budapest, Hungary, ISSN: 1218–2958

Restas, A.: R-20F Method: An approach for measuring the isolation effect of foams used fighting forest fires, Academic and Applied Research in Military Science 11: (2) pp. 233-247. 2012

Restas, A.: I4F technology, Manuscript, R-Fire Ltd, Szendro, Hungary, 2013

Restas, A.: Suppression capability of foams used fighting against forest fires with the test of weight rate remained on the crown surface R-10A Method - weight effectiveness experiment; Manuscript, under publishing, 7th ICFFR, Coimbra, Portugal, 2014

Szabo, G.: Erdőtűz (Forest fire), Study, 1994. http://speed.eik.bme.hu/~gergo/html, downloaded: 2011.05.10.

Mobile application based on a physical model to calculate Acceptable Safety Distance

Paul-Antoine Bisgambiglia, Romain Franceschini, François-Joseph Chatelon, Jean-Louis Rossi, Paul Antoine Bisgambiglia

[a] *University of Corsica - UMR SPE CNRS 6134, Campus Grimaldi bat PPDB 20250 Corti FRANCE. bisgambiglia@univ-corse.fr, r.franceschini@univ-corse.fr, chatelon@univ-corse.fr, rossi@univ-corse.fr, bisgambi@univ-corse.fr*

Abstract
The purpose of this paper is to present a multidisciplinary work in order to propose a simple tool that forecasts fuelbreak safety zone sizes at the field scale. The main question associated with safety zones is determining the Acceptable Safety Distance (ASD) between the fire and firefighters required to prevent injury. This distance is usually set thanks to a general rule-of-thumb: it should be at least 4 times the maximum flame length. A common assumption consists in using an empirical relationship between fireline intensity and flame length. To quantify the fireline intensity, a closed physical model is applied. So, this Web Service uses a simulation framework based on Discrete EVent system Specification formalism (DEVS), a theoretical fire spreading model developed at the University of Corsica and a mobile application based on a Google SDK to display the results.

***Keywords**: Decision-Making Tool, Fire Model, Acceptable Safety Distance, ASD, Calculation Tool, DEVS, Mobile Application*

Introduction

In the last few years the increasing influence of global warming on the environment has produced periods of drought which in turn have led to wildfires with devastating consequences. There is a growing need for firefighters to have decision-making tools. However, wildfires are so unpredictable that reducing their impact is still a complex task.
For several years, our *fire team* works on a models set. These different models are used to fire studies at different detail level, from fire laboratory to real forest fire. Recently, we developed some models to calculate the radiation rate and thereby compute the safety distances. In this work, we propose its integration into an online calculator: a Web Service. This web service will be interrogated by a mobile application to provide, as shown in Figure 1, an acceptable safety distance defined from a geographical area (GIS: Geographical Information System). These first results were introduced in Bisgambiglia *et al.*, (2013).
Our tool has been designed with and for fire-fighters, to meet their needs. A mobile application is of great interest because it is portable and allows you to go on the ground.
In the first and second part, we present the physical model and the formalism used to implement it. Fire model is an analytical model based on University of Corsica's forest-fire propagation model. The model is called ASD for *Acceptable Safety Distance*. It is used to place the fire-fighters on the ground and assess the radiation rate to which they are exposed. The role of this system is twofold: (1) it calculates a safe distance for the prevention of forest fires. This distance is used to realize a fuel break by vegetation clearing; (2) it can also calculate a safety distance during the struggle. This distance informs the fire-fighters on the degree of heat in the vicinity of the fire front. This is an analytical model based on radiative heating, and a whole set of parameters, such as vegetation, meteorology, topography, etc. The flame model adopted is based on the radiant surface approach; it is generalized to take into account the effect of the fire front width. So far this model prediction has been compared against measured flame length of several experimental fires conducted at the field scale through a

variety of natural vegetation in Corsican mountain region. The used formalism is called DEVS for *Discrete EVent system Specification;* it can be defined as multi-formalism and seen as a computational tool. DEVS is flexible, fast and open. In the field of Discrete Event Systems, many efforts have been devoted to develop appropriate tools to study, and model in a formal way the dynamics and the mechanisms of interaction of the natural systems. For several years the community is changing the DEVS formalism so that it can become a powerful tool for modelling complex systems. DEVS allows the reusing models through library already developed and also interconnecting of these models to compose heterogeneous models based on different formalisms.
In the third part, we will detail our software architecture. Including how the physical model has been modelled in our framework and what are the input data used. Then, we present how our DEVS models were migrated into a Web Service. Finally, we will detail the mobile application and its GUI (graphical user interface). Fire models have been implemented in a DEVS framework and coupled with a computational model of acceptable safety distance (ASD). The simulator is hosted on a Server to be queried remotely. At the start of the process, the user sends to the server a message with several positions. The server queries the Web Services to determine local parameters (slope, wind, etc.), and for each position compute the ASD. Finally, results are returned to the client for visualization in GIS.
In the fourth part, we describe our results. In collaboration with fire-fighters, we defined five vegetation types. These types have been incorporated in the software. With the GUI, the user can choose a vegetation type. We propose a comparison of results based on different vegetation.

Figure 1. An overview of the application

Physical Models

The fire behaviour at the field scale is difficult to forecast. It is a tricky task because the physical processes of combustion and heat transfer and how they are influenced by meteorological conditions and the arrangement and type of fuel are complex. It belongs to the framework of strongly coupled non linear transport phenomena. The aim of this section is to propose a model of fire behaviour that is

simple in concept and transparent to parameterize too. The main objective of this approach is to facilitate the use of existing vegetation models. A simplified surface fire spread model has been developed since 2007 at the University of Corsica in France. It has been tested on experiments carried out across fuel beds under slope and wind conditions at different field scales (Balbi *et al.*, 2007; 2009; 2010). The two main equations of this physical 3D model are the following:

$$\left.\begin{aligned} \tan\gamma &= \tan\alpha + \frac{U_n}{u_o} \\ R &= R_o + AR\,\frac{1+\sin\gamma-\cos\gamma}{1+\dfrac{R\cos\gamma}{r_o}} \end{aligned}\right\} \quad (1)$$

where R is the fire spread rate across an equivalent homogeneous combustible medium and under slope and wind conditions. It is obtained by using a thermal balance assessment in the combustible zone downstream to the fire front. This relationship is the sum of two terms. The first one, R_o, evaluates the rate of spread under no wind and no slope (it represents the contribution of the radiation from the fuel burning particles area). The second one determines the radiant heat flux, which comes from the flame body. γ represents the flame tilt angle. This angle is calculated using the local slope (α), the normal wind speed to the fire front (U_n) and the upward gas velocity (u_o). For an in-depth look at the determination of the rate of spread on the basis of this physical model, readers are encouraged to consult scales (Balbi *et al.*, 2007; 2009; 2010).

A flame height submodel (Marcelli *et al.*, 2011) is added to the simplified physical rate of spread model described by equation (1). As $h_f = l_f \cos\gamma$, where l_f and h_f denote the flame length and the flame height respectively, the flame length is expressed as

$$l_f = \frac{2\chi_0 r_{00}\Delta H \rho_v \nu}{BT^4\cos\gamma} \quad (2)$$

where χ_0 is a radiant factor (usually close to 0.3), r_{00} is a universal rate of spread (ROS) factor (equal to 2.5×10^{-5}), ΔH is the heat of combustion of the pyrolysis gases, ρ_v is the fuel density, ν is the fuel absorption coefficient, B is the Stefan-Boltzmann constant and T_f is the mean flame temperature.

The main question associated with safety zones is determining the safety distance between the fire and firefighters required to prevent injury. This distance is usually set thanks to a general rule-of-thumb: it should be at least 4 times the maximum flame length (Butler and Cohen, 1998).

Fuelbreaks divide expanses of natural fuels into smaller units. Native vegetation on these strategically located wide strips of lands is modified so that fire burning into them can be more readily and safely controlled. Fuelbreak generally has a low-growing ground in order to protect the soil against erosion. But, fuelbreaks with safety zones providing safety for firefighting personnel and equipment under critical conditions should be wider than other parts of a fuel break. In selecting the widths of fuelbreaks safety zone, the forest manager must estimate the distance from the flame front necessary to prevent serious burns from radiated heat and direct ignition from radiation too. Green and Schimke (1971) estimated that the distances from the flame front necessary to prevent ignition from radiation are half of the distances considered necessary to prevent disabling burns. Hence, ignition from radiation across a wide fuelbreak should not be a problem. Assuming that the safety distance is in the center of the break, the total width of a fuelbreak safety zone must be equal to 2 times this distance.

DEVS formalism

Simulation is used to study fire evolution model. For example, the DEVS formalism has been used to model physical equations describing fire evolution; we can quote (Harzallah *et al.*, 2008; Muzy *et al.* 2002; Bisgambiglia *et al.*, 2006; Nader *et al.*, 2011). This work focuses on the spreading aspect; our application aims to provide a safety distance.

Since the 1970s, formal tasks have been performed to develop the theoretical foundations of modelling and simulating of discrete event systems. Discrete Event System Specification is an extension of the Moore machine formalisms which is used for modelling and analyzing general systems. Our interest focuses on the *Discrete EVent system Specification* formalism (Ziegler *et al.*, 2000). DEVS provides a way of expressing discrete event models and a basis for an open distributed simulation environment. DEVS is universal for discrete event dynamic systems and is capable of representing a wide class of other dynamic systems. Universality for discrete event systems is defined as the ability to represent the behaviour of any discrete event model where represent and behaviour are appropriately defined. Concerning other dynamic system classes, DEVS can too simulate discrete time systems such as cellular automata and approximate, as closely as desired, differential equation systems. It also supports hierarchical modular construction and composition methodology. This bottom-up methodology keeps incremental complexity bounded and permits stage-wise verification since each coupled model build can be independently tested (Ziegler, 2005).

Major efforts have been made to adapt this formalism to various domains and situations as to study forest fire spreading (Harzallah *et al.*, 2008; Innocenti *et al.*, 2009; Muzy *et al.*, 2005; Ntaimo *et al.*, 2004; 2008; Nader *et al.*, 2011). DEVS permits the modelling of causal and deterministic systems with two types of components. A DEVS model is either an Atomic (AM) or a Coupled (CM) model. An AM is a structure: $<X, Y, S, \delta ext, \delta int, \lambda, ta>$ with

- X the set of external events,
- Y the set of output events,
- S the set of sequential states,
- $\delta ext: Q \times X \longrightarrow S$ the external state transition function,
- where
- $Q = \{(s,e) \mid s \text{ in } S, 0 \leq e \leq ta(s)$ and
- e is the elapsed time since the last state transition;
- $\delta int\ S \longrightarrow S$ the internal state transition function;
- $\lambda: S \longrightarrow Y$ the output function and
- $ta: S \longrightarrow R+0 \longrightarrow \infty$ the time advance function.

The AM describes the behaviour of the system. A atomic model is based on continuous time, inputs, outputs, states and functions (output, transition and lifetime of states). More complex models are constructed by connecting several atomic models in a hierarchical way. The interactions are created via the models' input and output ports, which favours modularity. A CM describes the composition of several DEVS sub-models, i.e AM or CM, it is described by the following formula: CM: $< X_M; Y_M; C_M;$ EIC; EOC; IC; L >.

Where,

- X_M: is the set of input ports;
- Y_M: is the set of output ports;
- C_M: is the list of models that composed the coupled model CM;
- EIC: is the set of the input couplings, which links the coupled model to its components;
- EOC: is the set of the output couplings, which links the components to the coupled model;
- IC: is the set of the internal couplings, which links the components to one another; and,
- L: is a list of priorities among components.

Many works have been proposed with the aim of mapping DEVS models in Web Services (Harzallah *et al.*, 2008; Al-Zoubi and Wainer, 2009; Kim and Kang, 2005; Mittal *et al.*, 2007; Wainer *et al.*, 2008). Generally the aim of this works is twofold: (1) provide a service based on a DEVS model, and (2) extend the interoperability of DEVS formalism. We do not propose evolution at these levels, but simply the use of these concepts applied to another application field: the ASD calculation. Our approach is general because we want to use DEVS as a calculation tool. We also propose a comparison

with a calculation program scientist and to equivalent results our environment is much more efficient. In addition, we can use DEVS to transform our calculation tool in online tool, and propose complete software architecture; efficient and adapted to the problem we were asked. That is to say: developing a tool for fuelbreak dimensioning.

Application and software architecture

In Bisgambiglia *et al.*, (2013) the software architecture of our application was introduced. To summarize, our tool is fairly standard, it looks like in this work (Harzallah *et al*., 2008), and is based on DEVS-Ruby framework (Franceschini *et al.*, 2014). We constructed a computational service as Web Service. Our Web Service is based on the DEVS formalism. It allows sending a safety distance, used to planning aid (fuelbreak) and prevention against forest fires. For our calculations, we need a certain number of data, and these data are either acquired locally, such as geolocation, or retrieved through other Web Services, such as ground slope. A main Web Service hosting a DEVS simulator to calculate the ASD. It can connect to another Web Services. The client sends data and displays the results. The Figure 2 describes this architecture. A main Web Service hosting a DEVS-Ruby simulator to calculate the ASD. It can connect to another Web Services. The client sends data and displays the results.

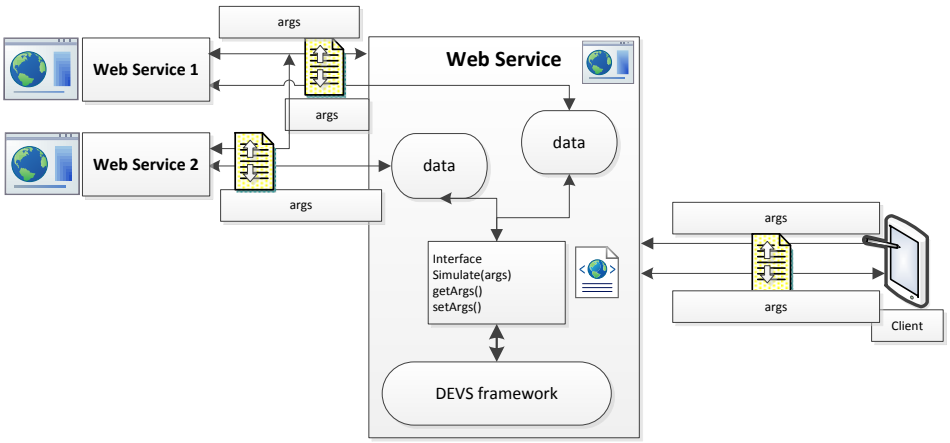

Figure 2. An overview of the overall approach.

The first step was to map the physical models to a DEVS models, then identify the major input parameters and finally transform the DEVS models to a DEVS Web Service. The computer architecture and the underlying technologies are described in Bisgambiglia *et al.* (2013).
Modelling the vegetation, denoted hereafter by fuel, is essential for the purpose of predicting the behaviour of a fire, either for fire danger rating system or fire spread model as well as to assess the impact of fire. Characterization of fuel particles is therefore required as an input to semi-empirical and physical fire behaviour models. The physical, chemical and thermal properties of fuel particles are assessed at the level of the individual particle or element
The different fuels characterization which are used in the mobile application in order to compare the values of the acceptable safety distances are presented in table 1.

Table 1. Examples of fuel description in the Mediterranean

Fuel type	Corsican tall shrub	Corsican shrub	Sardinian shrub (type 1)	Sardinian shrub (type 2)	grassland
Fuel Height (m)	4	2	0.48	1.8	0.3
Fuel load (kg m-2)	0.89	0.39	0.39	1.2	0.166
Fuel Moisture Content	0.08	0.08	0.08	0.08	0.08
Surface area-to volume ratio	5544	10200	2000	2400	11400
Heat of Combustion (kJ kg-1)	19640	18620	18620	18620	18620
Fuel density (kg m-3)	720	750	478	734	288
Specific Heat (J kg-1 K-1	1912	1900	1740	1820	1440

Results

5.1. Confrontation of the proposed physical model with field scale experiments

This section deals with the comparison of thirteen experimental literature field shrubland fires with model results.

Experiments were located in mountain areas in the southern Cape Province of South Africa. Fires were conducted at two sites. The first site is situated in the Kogelberg State Forest (110 m above the sea level). Detailed experiments description can be found in Van Wilgen *et al.* (1985).

Table 2. Observed and predicted flame lengths during the Kogelberg State Forest experiments.

	Flame length (m)						*NMSE (%)*	*FB (-)*
Wind speed ($m \cdot s^{-1}$)	3.56	1.5	2.67	2.67	3.11	3.11		
Rate of spread ($cm \cdot s^{-1}$)	44	36	21	30	37	47		
Observed	3.2	2.4	2	4.3	3	4		
Physical model	4.15	2.11	3.47	3.48	4.23	3.99	7.9	0.13
Burrows (1994)	15.39	12.12	10.10	15.9	20.52	17.97	326.3	1.31
Butler *et al.* (2004)	7.33	5.96	5.09	7.55	9.41	8.39	80.1	0.80
Byram (1959)	4.99	4.32	3.88	5.09	5.93	5.47	23.3	0.46
Catchpole *et al.* (1998)	5.15	4.33	3.80	5.28	6.35	5.77	27.1	0.49
Clark (1983)	5.65	4.15	3.29	5.90	8.19	6.90	45.3	0.55
Fernandes *et al.* (2009)	6.15	5.20	4.57	6.30	7.54	6.87	48.6	0.65
Fernandes *et al.* (2000)	3.11	2.70	2.43	3.17	3.69	3.41	4.06	0.006
Nelson (1980)	4.09	3.50	3.11	4.18	4.94	4.53	9.57	0.27
Nelson and Adkins (1986)	4.12	3.53	3.14	4.20	4.95	4.55	9.84	0.28
Van Wilgen (1986)	4.80	4.09	3.62	4.90	5.81	5.32	20.1	0.42
Vega *et al.* (1998)	7.54	6.47	5.76	7.70	9.07	8.33	82.6	0.82

Table 3. Observed and predicted flame lengths during the Cederberg State Forest experiments.

Wind speed ($m \cdot s^{-1}$)	1.92	2.83	3.56	2.5	1.03	1.89	3.11	2.67		
Rate of spread ($cm \cdot s^{-1}$)	32	80	89	52	4	52	78	55		
	Flame length (m)								*NMSE (%)*	*FB (-)*
Observed	4	6	7	5	1.4	6.5	5	5		
PM	4.52	5.27	6.65	4.84	3.94	3.99	6.27	5.63	7.66	0.09
Burrows (1994)	17.55	59.03	45.32	19.23	3.78	26.40	40.38	33.34	582.9	1.33
Butler *et al.* (2004)	8.22	23.52	18.70	8.90	2.17	11.71	16.92	14.33	140.9	0.80
Byram (1959)	5.4	11.15	9.52	5.70	2.15	6.89	8.88	7.92	20.7	0.35
Catchpole *et al.* (1998)	5.67	13.69	11.30	6.06	1.86	7.63	10.39	9.04	39.26	0.43
Clark (1983)	6.69	31.90	22.70	7.53	0.92	11.32	19.57	15.29	220.1	0.70
Fernandes *et al.* (2009)	6.75	15.91	13.20	7.20	2.28	9.01	12.17	10.63	62.2	0.59
Fernandes *et al.* (2000)	3.36	6.87	5.88	3.55	1.36	4.28	5.59	4.91	5.48	-0.11
Nelson (1980)	4.46	9.81	8.26	4.73	1.64	5.82	7.67	6.77	11.12	0.18
Nelson and Adkins (1986)	4.48	9.74	8.23	4.75	1.67	5.82	7.64	6.76	10.81	0.18
Van Wilgen (1986)	5.23	11.76	9.86	5.57	1.88	6.87	9.13	8.03	24.03	0.34
Vega *et al.* (1998)	8.20	17.84	15.06	8.70	3.07	10.66	13.99	12.38	87.4	0.74

With regard to flame length models, four models are quite adequate to predict flame length in the Kogelberg (Table 2) and the Cederberg experiments (Table 3). These data are accurately fitted with the empirical relationships proposed by Fernandes', Nelson's, Nelson and Adkins's laws and by the physical model too.

Empirical laws are useful to quantify flame length but should not be used to compare fires in fuel types, which are structurally very different (Morvan *et al.*, 2002). Besides, really hazardous fires, such as those burning under conditions of strong wind at the field scale, cannot be properly quantified because of the contribution of heat convection to the heat transport ahead of the flame front. Moreover, empirical laws are not predicted. It is a strong argument for a physical approach. So, a physical simplified approach is applied to obtain an analytical expression of the flame length.

5.2. Comparison of the results given by the mobile application on various vegetation types

This section deals with the computation of Acceptable Safety Distances in which a fire spreads across five different fuels in the Mediterranean area (the intrinsic characteristics of each fuel are detailed in table 1). Two wind speed values are randomly chosen (3 and 5 $m.s^{-1}$). Table 4 presents the ASD obtained with the rule-of-thumb stated by Butler and Cohen (1998) and the physical model presented in section two.

Table 4. Comparison of the ASD values (m) obtained with a rule-of-thumb, applied to five different fuels in the Mediterranean.

Wind (m.s-1)	Corsican tall shrub	Corsican shrub	Sardinian shrub (type 1)	Sardinian shrub (type 2)	grassland
3	10.14	11.16	11.05	10.48	8.86
5	14.87	16.06	20.46	15.32	14.37

If the values of ASD are similar for a 3 $m.s^{-1}$ wind speed whatever the fuel bed, they are quite different when the wind speed increases. As the physical model (especially the flame length sub-model) gives a good precision (see the errors given in tables 2 and 3), it is necessary to have either accurate characteristics of the vegetal stratum or a good modelling for an equivalent fuel.

5.3. Graphical user interface

ASD results provided by our Web Service are useful for firefighters on field when evaluating distances for fuelbreak, the client side must then provide a clear GUI to visualize the terrain and our results, an unobtrusive way to feed input data and a way to retry computations in case of a network failure. In order to fit such requirements, the client has been implemented as a mobile application on both iOS and Android platforms and designed to run primarily on tablets. The results presented are from iOS client. The application is in French. The user interface will be essentially composed of:
(1) a sliding panel on the left side providing a section containing a list of previous cached computations and the ability to create a new one. Another section is there for configuration purposes. This menu is shown in Figure 3.a, it also allows you to select a fuel types (Corsican tall shrub, Corsican shrub, Sardinian shrub (type 1), Sardinian shrub (type 2), grassland), or configure a local wind;
(2) a map fitting the whole screen and representing the current selected computation. The map contains the user location if available; the path for which we want the results and when these are available, the ASD zone is drawn as a polygon. The user can touch the zone to display detailed information about results (Figure 3.b);

(a) left menu (b) drawing the path (c) result

Figure 3. Display example.

(3) the map has three distinct modes: the normal mode, the user-tracking mode and the drawing mode. Each of these are detailed respectively below : (3.1) the normal mode displays all available data for the current selected computation and allows user interaction to show detailed information; (3.2) since our Web Service input is essentially a set of coordinates, these GPS enabled devices allow us to provide

a handy user-tracking mode. Thereby, as the user location is updated we can spawn requests to our Web Service and draw a polygon that will represent the ASD; (3.3) finally, the drawing mode allows the user to place a set of locations directly on the terrain and adjust each of them. The final result is shown in Figure 3. We can see the contours of the safety zone.

Conclusions

This paper presents a multidisciplinary work and argues a software tool to compute Acceptable Safety Distance (ASD). This distance was usually set thanks to a general rule-of-thumb: it should be at least 4 times the maximum flame length. This distance is very important because it is used to design fuel breaks. In our approach, to quantify the fireline intensity, a closed physical model is used. The model is hosted as a web service, and used a simulation framework based on Discrete EVent system Specification formalism (DEVS). In this new work, we present various results based on the vegetation characterization.

One goal of this study is to provide an accurate quantification of a safety zone at the field scale. To quantify this area different flame models (one simplified physical model and twelve empirical correlations) are tested using several experiments. Model predictions are compared against measured flame length of spreading fires through shrub vegetation. This work shows that the simplified physical approach presents a main advantage: its capability to be used for all types of fires under a wide range of conditions if fuel models, describing structural types of vegetation, are available. So, this model can be seen as an alternative operational length flame model, which can be applied to calculate more accurately safety distances.

Now, as expected fire-fighters, we will now turn our application on desktop.

References

Al-Zoubi K., Wainer G. (2009) Using REST Web-Services Architecture for Distributed Simulation, Principles of Advanced and Distributed Simulation, PADS'09. ACM/IEEE/SCS 23rd Workshop, June 22-25, pp 114-121, doi:10.1109/PADS.2009.16

Balbi J.H., Rossi J.L., Marcelli T., Santoni P.A. (2007) A 3D physical real-time model of surface fires across fuel beds, Combustion Science and Technology, 179:12, 2511-2537.

Balbi J.H., Morandini F., Silvani X., Filippi J.B., Rinieri F. (2009) A physical model for wildland fires, Combustion and Flame, 156, 2217-2230.

Balbi J.H., Rossi J.L., Marcelli T., Chatelon F.J. (2010) Physical modeling of surface fire under nonparallel wind and slope conditions, Combustion Science and Technology, 182, 922-939.

Bisgambiglia P.-A., Filippi J.B., De Gentili E. (2006) A fuzzy approach of modelling evolutionary interfaces systems, In 'Proceedings of the ISEIM 2006 (IEEE eds)', Corte, France, 98-103.

Bisgambiglia P.-A., Franceschini R., Chatelon F.J., Rossi J.L., Bisgambiglia P. (2013) Discrete Event Formalism To Calculate Acceptable Safety Distance, In "proceedings of the 2013 Winter Simulation Conference (Pasupathy R., Kim S.-H., Tolk A., Hill R. and Kuhl M.E. Eds), Washington DC, USA, pp 217-228.

Burrows, J.K. (1994) Experimental development of a fire management model for jarrah (Eucalyptus marginata Donn ex Sm) forest. PhD thesis, Australian National University, Canberra.

Butler, B.W, Cohen, J.D.; 1998. Firefighter Safety Zones: A Theoretical Model Based on Radiative Heating. International Journal of Wildland Fire. 8(2), 73-77.

Butler, B.W., Finney, M.A., Andrews, P.L., Albini, F.A., (2004) A radiation-driven model of crown fire spread. Canadian Journal of Forest Research, 34, 1588-1599.

Byram, G.M., (1959) Combustion of forest fuels, in: Davis, K. P. (Eds.), Forest Fire: Control and Use, McGraw_Hill, New-York, pp. 61-80.

Catchpole, W.R., Bradstock, R.A., Choate, J., Fogarty, L.G., Gellie, N., McCarthy, G., McCaw, W.L., Marsden-Smedley, J.B., Pearce, G., (1998). Cooperative development of equations for healthland fire behavior, in Viegas, D.X. (Eds.), in Proceedings 3rd International Conference on Forest Fire Research and 14th Conference on Fire and Forest Meteorology, Coimbra, pp. 631-645.

Clark, R.G., (1983) Threshold requirements for fire spread in grassland fuels. PhD thesis, Texas Tech. University, Lubbock.

Fernandes, P.M., Catchpole, W.R., Rego, F.C., (2000) Shrubland fire behavior modeling with microplat data. Canadian Journal of Forest Research, 30, 889-899.

Fernandes, P.M., Botelho, H.S., Rego, F.C., Loureiro C., (2009) Empirical modeling of surface fire behavior in maritime pine stands. International Journal of Wildland Fire. 18, 698-710.

Franceschini R., Bisgambiglia P.-A., Bisgambiglia P.A., Hill D.R.C. (2014) DEVS-Ruby: a Domain Specific Language for DEVS Modeling and Simulation (WIP), In 'proceedings of the symposium on Theory of Modeling & Simulation', DEVS Integrative M&S Symposium, Tampa, Florida, USA.

Green L.R., Schimke H.E. (1971) Guides for fuel-breaks in the Sierra Nevada mixed-conifer type, Berkeley, California, USDA Forest Service, Pacific SW, Forest and Range Experimental Station.

Harzallah Y., Michel V., Liu Q., Wainer G. (2008) Distributed Simulation and Web Map Mash-Up for Forest Fire Spread, Services – Part I, IEEE Congress on, pp 176-183, doi:10.1109/SERVICES-1.2008.74.

Innocenti E., Silvani X., Muzy A., Hill D.R.C. (2009) A software framework for fine grain parallelization of cellular models with OpenMP: Application to fire spread, Environmental Modeling and Sofware, 24(7), 819-831.

Kim K.-H., Kang W.-S. (2005) A web services-based distributed simulation architecture for hierarchical DEVS models, In 'Proceedings of the 13th international conference on AI, Simulation and Planning in High Autonomy Systems', Berlin, Heidelberg, pp 370-379.

Marcelli T., Balbi J.H., Moretti B., Rossi J.L. Chatelon F.J. (2011) Flame height model of a spreading surface fire, In "proceedings of the seventh Mediterranean Combustion Symposium", September 11-15, Chia Laguna, Cagliari, Italy, 2011.

Mittal S., Risco J.L., Ziegler B.P. (2007) DEVS-Based simulation web services for net-centril T&E, In 'proceedings of the 2007 Summer Computer Simulation Conference', San Diego, California, USA, pp 357-366.

Morvan D., Tauleigne V., Dupuy J.L. (2002) Flame geometry and surface to crown fire transition during the propagation of a line fire through a Mediterranean shrub, In 'Proceedings of the fourth International Conference on Forest Fire Research and Wildland Fire Safety (Ed. D.X. Viegas)', Luso-Coimbra, Portugal, November 16-20, CD-ROM, ADAI, Millpress:Rotterdam.

Muzy A., Innocenti E., Aïello A., Santucci J.F., Santoni P.A., Hill D.R.C. (2005) Modelling and simulation of ecological propagation processes: application to fire spread, Environmental Modelling and Sofware, 20(7), 827-842.

Nader B., Filippi J.-B., Bisgambiglia P.-A. (2011) An experimental frame for the simulation of forest fire spread, In "proceedings of the 2011 Winter Simulation Conference", pp 1010-1022.

Nelson, R.M. Jr., (1980) Flame characteristics for fires in southern fuels. U.S.D.A. Forest Service, General Research Paper SE-205. Southeast. Forest Experimental Station, Asheville, NC, USA.

Nelson, R.M. Jr. and Adkins, C.A., (1986) Flame characteristics of wind-driven surface fires. Canadian Journal of Forest Research. 16, 1293-1300.

Ntaimo L., Hu X., Sun Y. (2008) DEVS-FIRE: Towards an Integrated Simulation Environment for Surface Wildfire Spread and Containment, Simulation, 84(4), 137-155.

Ntaimo L., Ziegler B.P., Vasconcelos J., Khargharia B. (2004) Forest Fire Spread and Suppression in DEVS, Simulation, 80(10), 479-500.

Van Wilgen B., Le Maitre D.C., Kruger F.J. (1985) Fire behaviour in South African fynbos (Macchia) vegetation and predictions from Rothermel's fire model, Journal of Applied Ecology,22(1), 207-216.

Vega, J.A., Cuinas, P., Fonturbel, T., Perez-Gorostiaga, P., Fernandez, C., (1998) Predicting fire behavior in Galician (NW Spain) shrubland fuel complexes, in Proceedings 3rd International Conference on Forest Fire Research and 14th Conference on Fire and Forest Meteorology, Coimbra, pp. 713-728.

Wainer G.A., Madhoun R., Al-Zoubi K. (2008) Distributed simulation of DEVS and Cell-DEVS models in CD++ using Web-Services, Simulation Modeling Practice and Theory, 16(9), 1266-1292.

Ziegler B.P., Praehofer H., Kim T.G. (2000) Theory of Modeling and Simulation, Second Edition.

Ziegler B.P. (2005) Discrete Event Abstraction: An emerging paradigm for modelling complex adaptative systems, In 'Perspectives on Adaptation in Natural and Artificial Systems Chapter 6 (Booker L., Forrest S., Mitchell M., Riolo R. eds)', Oxford, England, New York: Oxford University Press.

Monitoring forest fires and burnings with weather radar

Ernandes A. Saraiva[a, d], Ronaldo Viana Soares[b], Antônio Carlos Batista[b], Horácio Tertuliano[b], Ana Maria Gomes[c]

[a] *CAPES/Federal University of Parana State, Curitiba, Brazil, ernandessaraiva@gmail.com*
[b] *Federal University of Parana State, Curitiba, Brazil, rvsoares@ufpr.br*
[c] *Meteorological Research Institute - IPMet/UNESP, Bauru, Brazil, ana@ipmet.unesp.br*
[d] *Federal University of Parana State – UFPR / CAPES – Depto de Ciências Florestais*
Av. Pref. Lothário Meissner, 900 – Jardim Botânico – 80210-170 – Curitiba – PR – Brasil

Abstract
The efficiency on forest fire control is directly related to the quickness on detection and localization, which significantly can minimize the potential of damages. The current technology used in the manufacture of weather radars has opened new opportunities for research, making it possible to detect small signals, not necessarily used in the daily rain observations. The objective of this research is to use the capacity of weather radar, configured to execute tasks of high sensitivity, to monitor and detect "non meteorological targets", i.e., the smoke produced by sugar cane burnings and, by similarity, forest fires. An experimental model was developed and applied to the S-band weather radar operated by the Meteorological Research Institute – IPMet/UNESP, located in the central region of the State of São Paulo, Brazil. In the first experiment, all the monitored sugar cane burnings were efficiently detected by the radar with a delay of 2 to 9 minutes, with an average of 4.67 minutes, a significant reduction in the response time of 15 minutes, considered optimal for conventional detection systems. In the second experiment, the weather radar monitored forest area when the fire danger rating index was medium or high and the same events observed by the observation towers were detected by the weather radar. The methodology used in this study can add significant value to the information in the forest fire suppression decision-making. The results showed the efficiency of weather radar to detect smoke. Therefore, weather radars systems could be used, in the absence of rain echoes, for monitoring agriculture burnings and detecting forest fires.

***Keywords**: Fire detection, Weather radar, Forest fire*

Introduction

The efficiency on forest fire control is directly related to the rapidness on the occurrences detection and localization, what significantly minimizes the potential of damages. There are several difficulties and limitations in the most widely method used for monitoring and detection of forest fires, the observation towers. The high cost of installation and operation is one of the handicaps of the system. When the number of towers is not sufficient, some fires are detected when the intensity is already high and the suppression more difficult.

Trying to improve monitoring and detection of forest fires, this research used the remote sensing technology to detect events related to fire. The biomass combustion process produces large amounts of smoke, an excellent target which can be detected by deploying various electromagnetic wavelengths. The particles and water vapor that constitute the smoke is an excellent electromagnetic spreader.

Due to the absence of rain, during the dry season, the degree of fire hazard increases. Therefore an experimental model of fire detection was developed, and initially tested on the frequent and programmed sugar cane harvesting burnings in the central region of São Paulo State, which is monitored by a weather radar equipment "S-band Doppler", operated by the Meteorological Research Institute, UNESP, located in Bauru. County. In the same region covered by the radar system, there are

large plantations of pine and eucalyptus owned by Duratex, that in the second phase of the experiment were monitored during high fire danger indices

Methods

Weather Radar

The Radar (***Ra**dio **D**etection **A**nd **R**anging)* is considered an active element, considering that it illuminates the target with a microwave beam and identifies this target through the detection of the energy portion reflected back. The choice of the operation wavelength (λ) is primarily defined according to the type and size distribution of the targets to be investigated or detected. (Doviak 1992; Lhermitte 2002).

Detection Capability

Operacional and research weather radars have already been deployed in the past to observe "non-meteorological targets" such as: wind speed profiles, gust fronts, particles in suspension, flocks of birds, clusters of insects as well as smoke plumes (Banta and Olivier 1992; Calheiros and Gomes 1999; Erkelens and Venema 2000; Gary *et al*. 1998; Held *et al*. 2011). This became even more feasible with the continuous technological advances of data acquisition and signal processing, sensitivity and improved detection capability as well as mitigating the associated measurements errors.

2.3. Fire Detection

The detection of a fire occurs indirectly, since it is detects not the fire flame or the heat, but the smoke produced by the biomass burning. Initially, a high sensitivity parameter task is programmed (low PRF, pulse length of 2 microseconds). Unlike its conventional Unlike its conventional operation mode, while the radar monitors rain from up to the soil surface, in the forest fire detection the monitoring occurs from the soil surface to up in the sky.

When forest fuel or biomass burns, the released smoke rises and crosses the microwave beam of the radar, backscattering incident energy, resulting in the event detection (figure 1). An important detail is the effect of the curvature of the earth in determining the height of the center beam, because the height relative to the ground increases with distance from the radar site. The purpose of this study was the detection of smoke originated from biomass burning as close to the ground as possible.

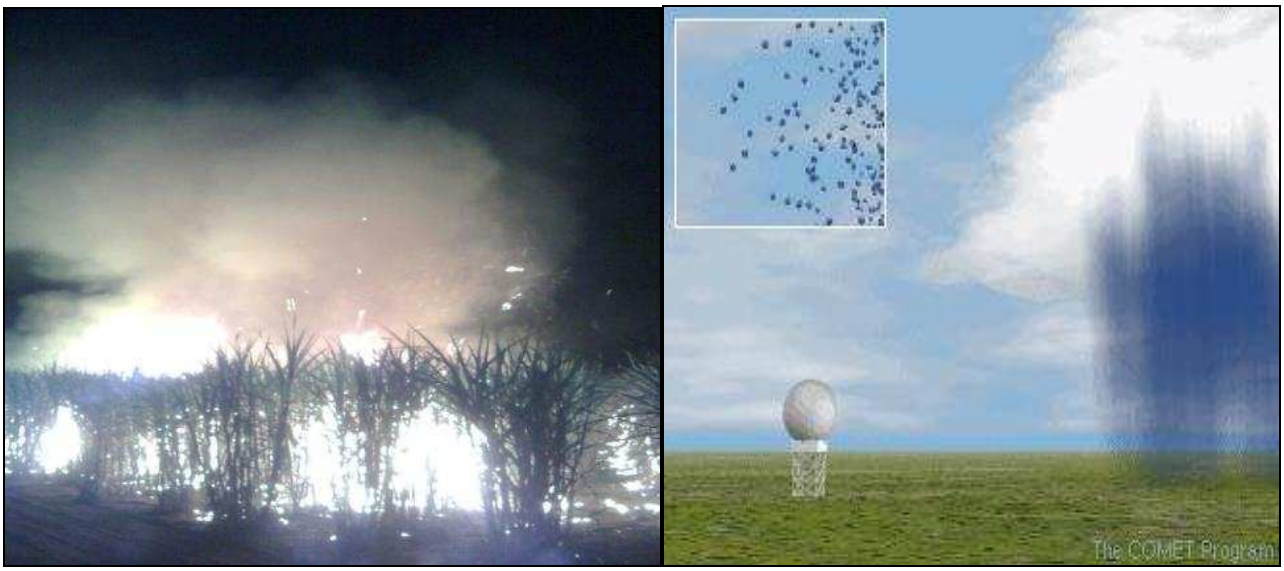

Figure 1. Vegetation fires release smoke and intercept the radar beam.

As the fire starts in the soil surface and the quicker it is detected easier is its control. Idealy the radar beam should be as low as possible on height above the monitoring area, but not too low as reflect ground echoes and contaminate the image with noises**.**
The study area should not be too close to the radar in order to avoid the effects of side lobes of antenna radiation that impair detection efficiency. With the distance of around 50 km from the radar, and antenna elevation between 0.3 and 2 degrees, the beam intercept smoke up to 2000 meters above ground level.

Results

Data from the burned plots, including time of ignition and detection, duration of fire, and response time between ignition and detection are showed in Table 1.

Table 1. Summary of monitored and detected events

Sample	Area (ha)	Schedule of Burnings (GMT)			Radar Detection	Response Time (min)
		Start (hh:mm)	End hh:mm)	Duration (min)	Start (hh:mm)	
1	6,42	22:28	22:48	20	22:30	2
2	15,11	22:17	22:31	14	22:20	4
3	10,29	22:56	23:20	24	23:00	4
4	4,86	22:20	22:36	16	22:29	9
5	8,73	22:07	22:19	12	22:13	6
6	8,35	22:07	22:24	17	22:11	4
7	8,68	21:48	22:13	25	21:52	4
8	5,56	21:02	21:18	16	21:07	5
9	**8,23**	**22:02**	**22:32**	**30**	**22:07**	**5**
10	5,81	22:25	23:02	37	22:30	5
11	10,85	21:18	21:32	14	21:22	4
12	3,99	21:26	21:42	16	21:31	5

Running task with high sensitivity and temporal sampling of 7.5 minutes, the S-band Doppler weather radar monitored the 12 burning events in the sugar cane plots. All the burnings were accompanied *in situ*, and with the time synchronized to the radar time system; the exact ignition time and the events duration were recorded.
The radar data have been treated with the TITAN software, developed at NCAR (National Center for Atmospheric Research), for applications in nowcasting the displacement of storms based on the methodology of centroids (Dixon and Wiener 1993). The images used are Cartesian products called CAPPIs (Constant Altitude Plan Position Indicator) with the viewing plane at constant average height of 1.5 km amsl (above mean sea level). Figure 2 shows the area of study and distance of radar site.
The response time ranged from 2 to 9 minutes with an average of 4.67 minutes (table 1), reducing in 68.9% the response time considered ideal in the conventional detection systems (Soares and Batista 2007).
Figure 3 shows the sample n° 9 (table 1), before ignition of burning and without radar echoes (22:00 GMT), while figure 4 (22:07 GMT) depicts it 5 5 minutes after ignition (22:02 GMT) and with the first radar echoes. The figures 5 and 6, show the area of sample n° 9 with the radar echoes during burning (22:15 and 22:22 GMT).

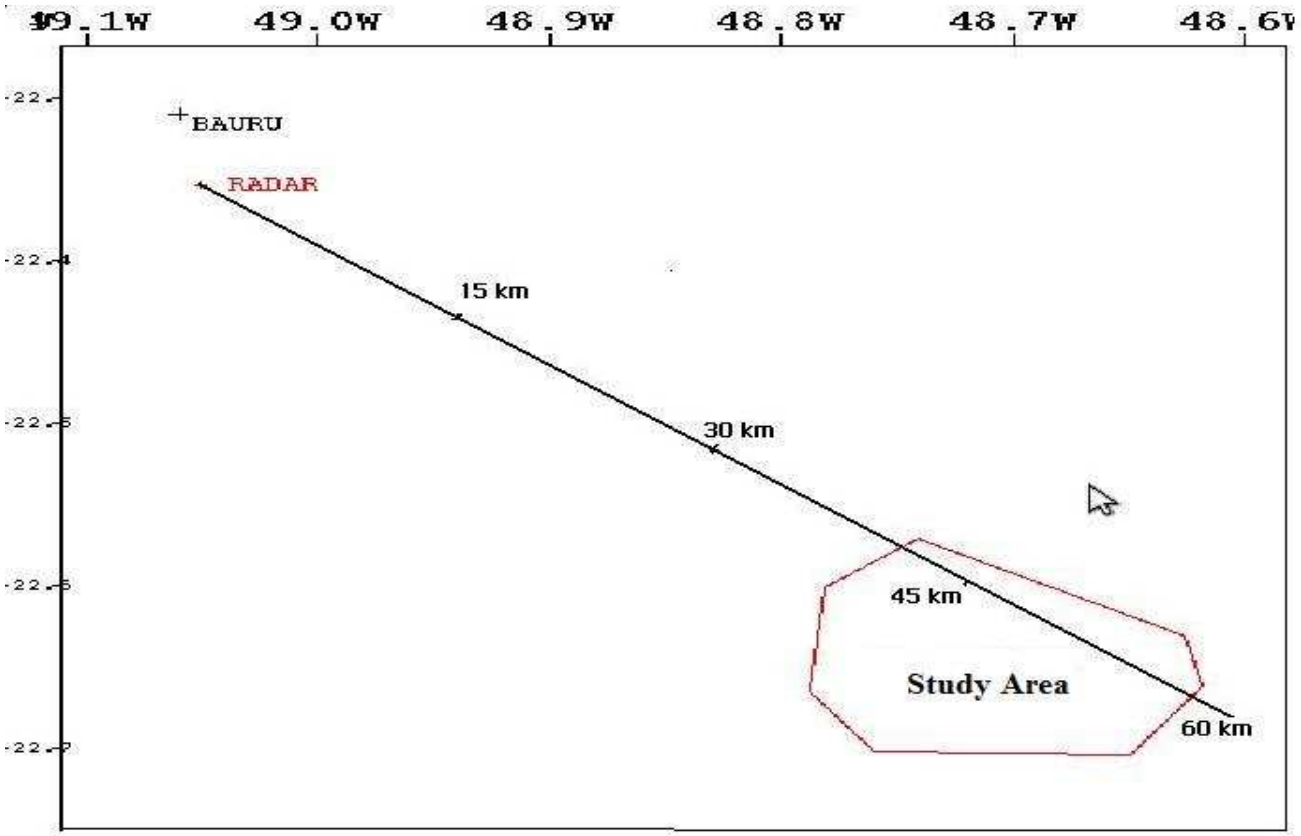

Figure 2. Study area (red polygon) and distance of radar site

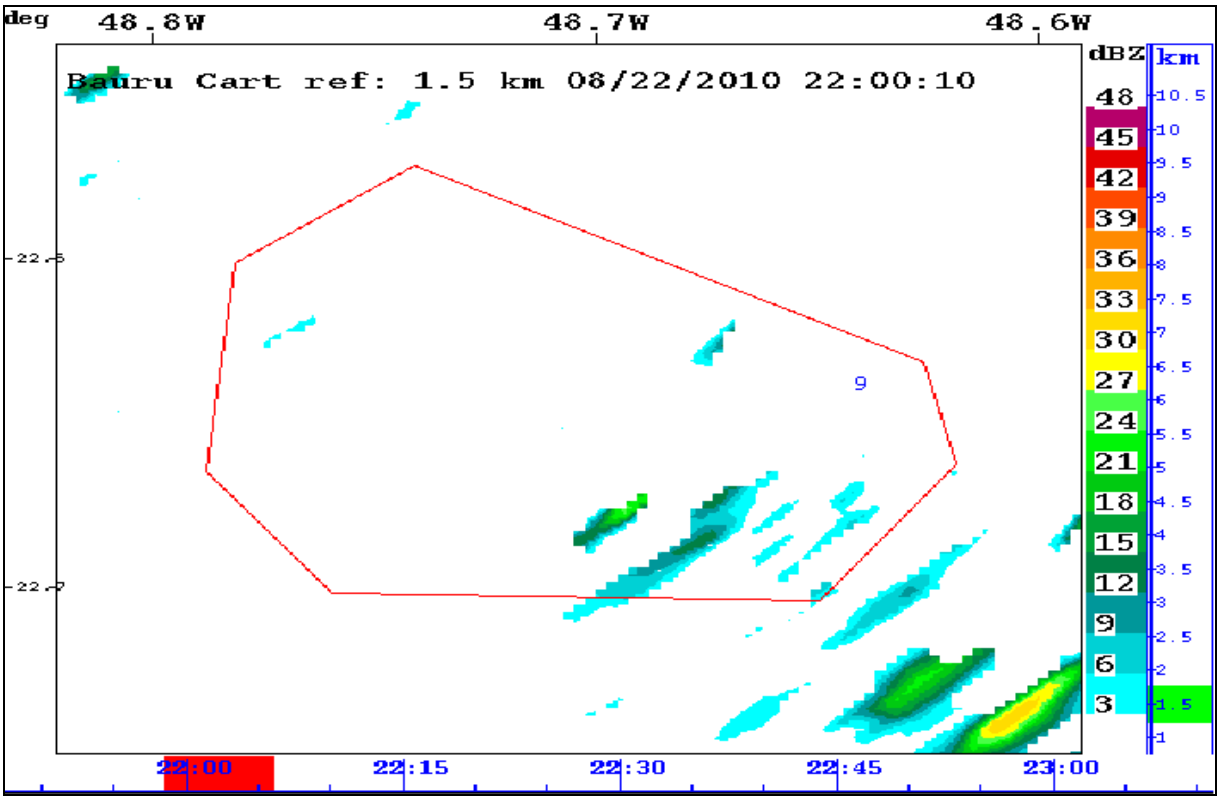

Figure 3. Image of the location of sample n° 9 (indicated by the number 9)

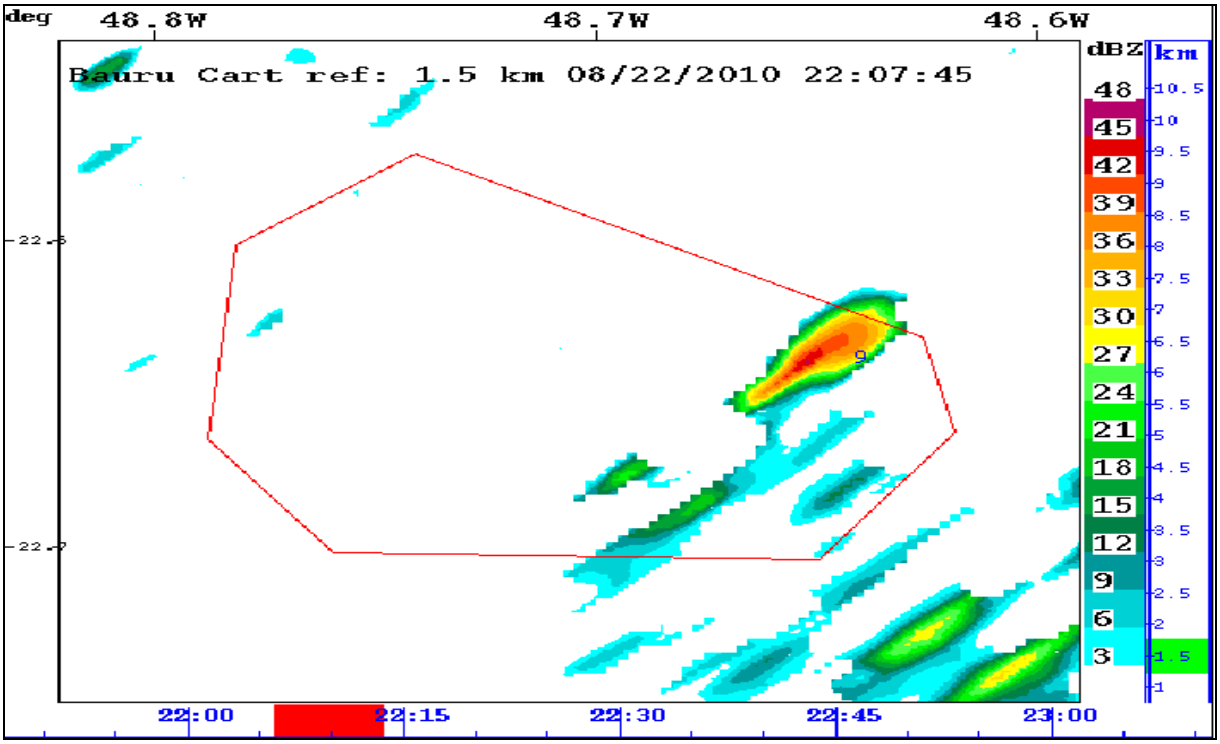

Figure 4. Location of sample n° 9 with the first radar echo after ignition

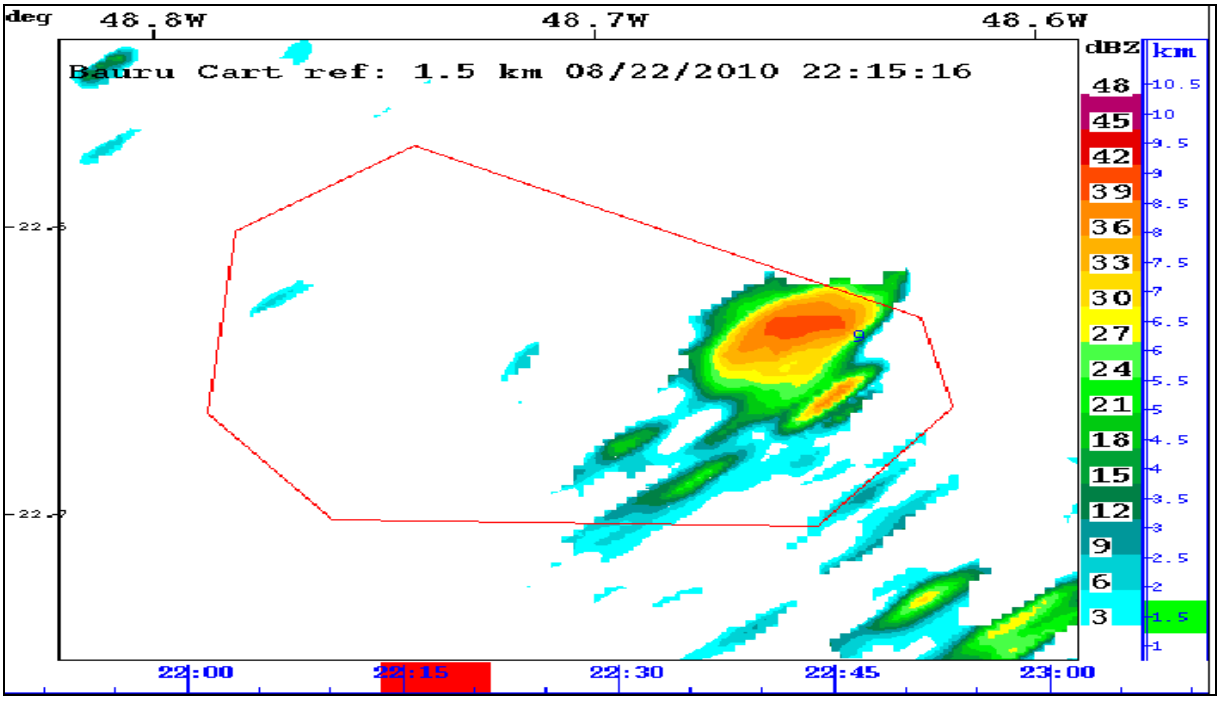

Figure 5. Location of sample n° 9 with radar echoes during the fire (22:15)

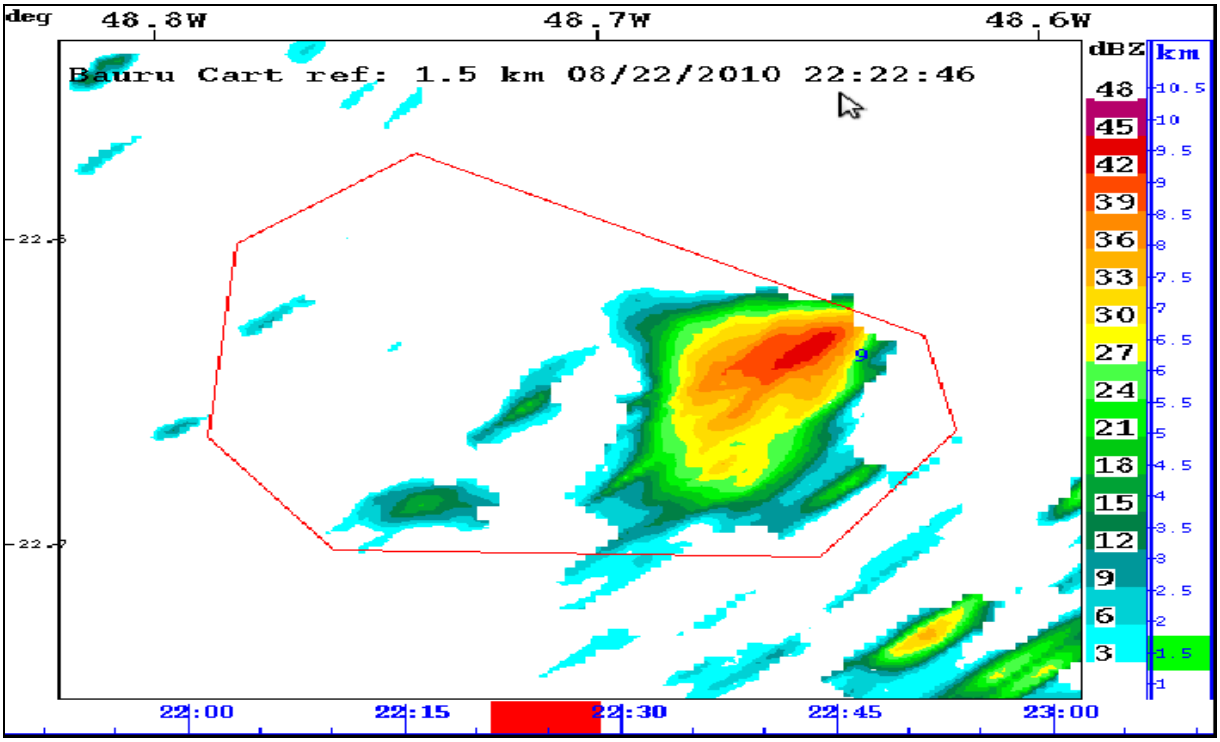

Figure 6. Location of sample n° 9 with radar echoes during the fire (22:22)

The figures 7 and 8 shows the sample n° 9 at 22:37 and 22:45 GMT, 5 and 13 minutes, respectively, after the end of burning and already without radar echoes within the monitoring area.

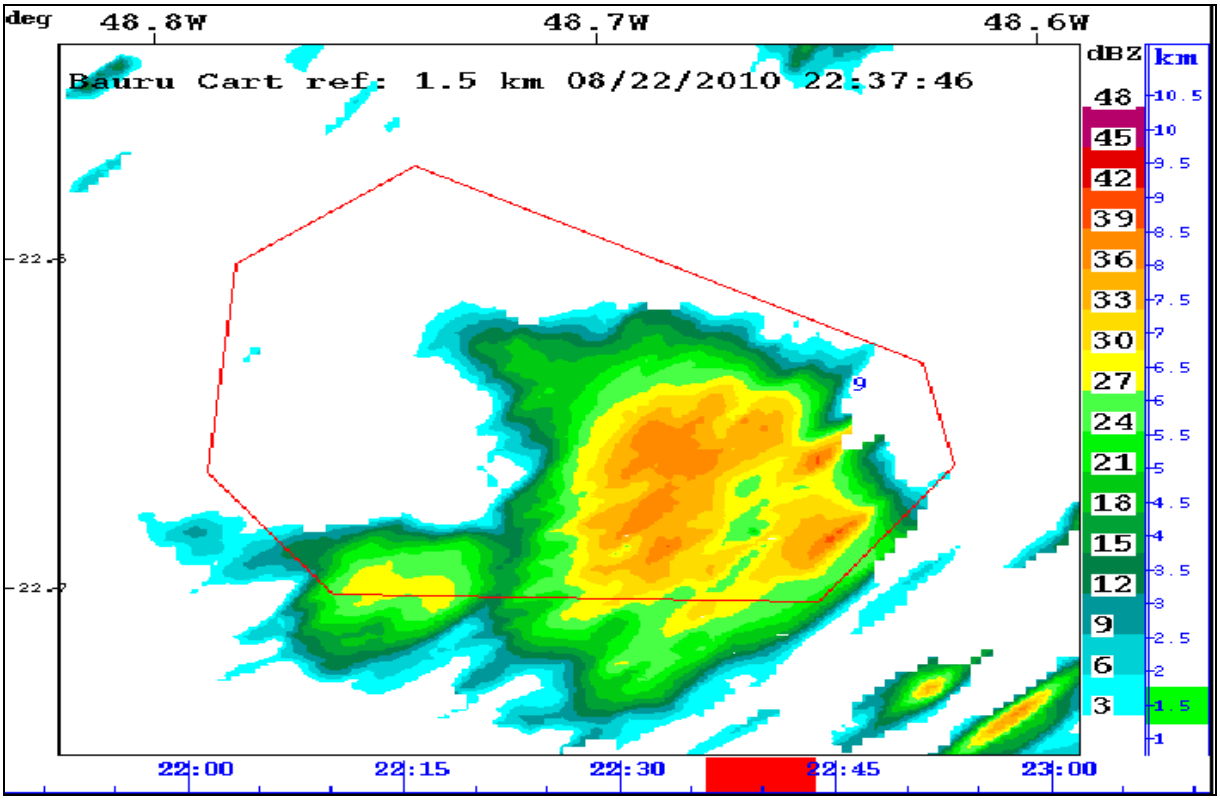

Figure 7. Sample n°9 after burning and without radar echoes (22:37)

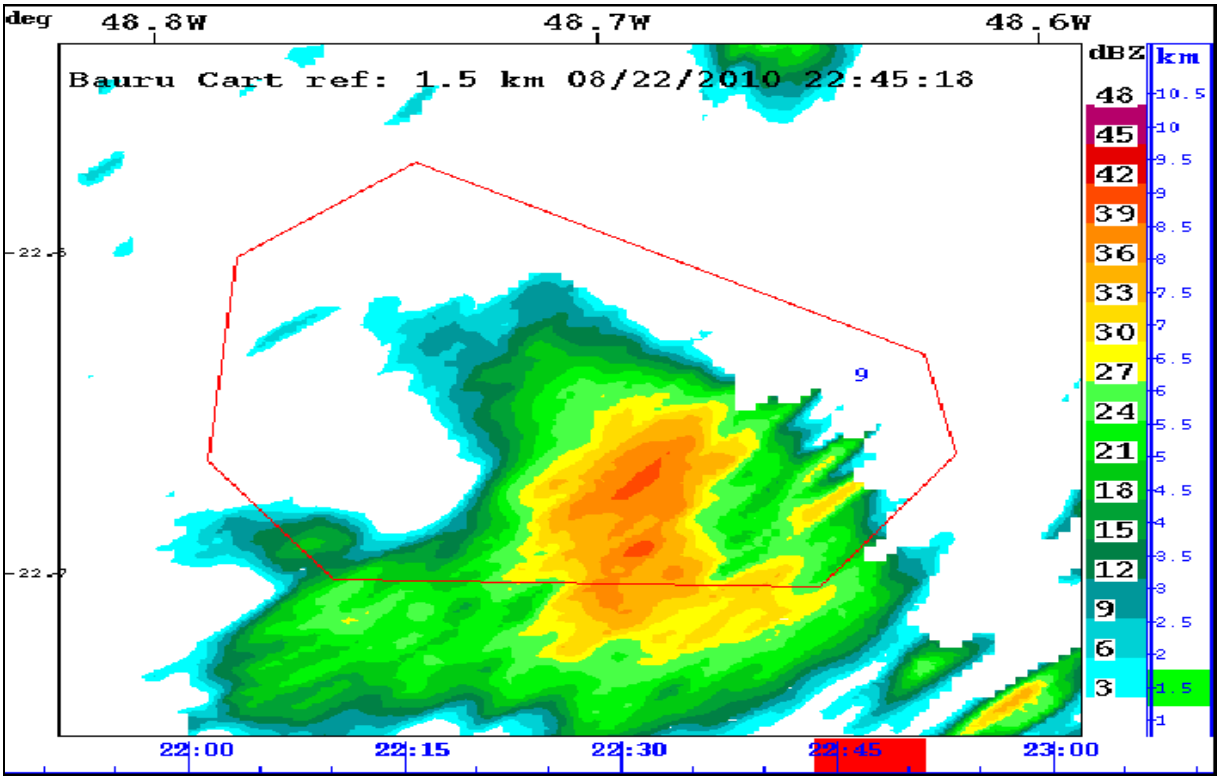

Figure 8. Sample n°9 after burning and without radar echoes (22:45)

Durant August 2013, which was a period of high index of fire danger in the region, the radar was operated again with high sensitivity and the temporal resolution shortened to 5 minutes, monitoring the reforestation areas owned by Duratex Company. The only two small fire spots detected by the company's observation towers were also detected by the radar system. Synchronizing the time from the radar and the observation tower, the radar detected the fires 6 an 8 minutes in advance, respectively.

Conclusions

The Bauru S-band Doppler weather radar had successfully detected of burning of 12 plots of sugar cane. The two events identified by the observation towers in the reforestation area during the second experiment were also monitored and detected by the radar.

Based on the results, weather radar can be considerate an important auxiliary tool for detecting unauthorized burning and forest fires, adding significant value to the information for decision-making in monitoring, detecting and suppressing wildfires.

The X-band radar, for example, with its own technical characteristics combined with increased temporal resolution, would be more suitable for smaller targets and smoke, could be an even better alternative to fire detection, and shorter response time.

References

Banta, R. M., Olivier, L. D. Smoke-Column Observations from Two Forest Fire Using Doppler Lidar and Doppler Radar. In: Journal of Applied Meteorology, vol 31, p.p. 1328-1349, 1992.

Calheiros, R. V., Gomes, A. M., Wind Profiling in Clear Air: a radar-radiosonde comparation. Locarno, Proceedings of the International Seminar on Advanced Weather Radar Systems, p. 678-687, 1999.

Dixon, M. and Wiener, G. (1993), TITAN: Thunderstorn Identification, Tracking, Analysis and Nowcasting – a radar-based methodology, J. Atmos, Oceanic Technol., 10, p. 785-797.

Doviak, R. J.,(1992). Doppler Radar and Weather Observations. Dusan S. Zrnic. -2nd ed. 562pp.

Erkelens, J. S., Venema, V. K. C. Coherent Scattering of Microwaves by Particles: Evidence from Clouds and Smoke**.** In: American Meteorologcal Society, p. 1091, 2000

Gary, L., Hufford, H., Lee, K e Willians, S. Use of Real-Time Multisatellite and Radar Data to Support Forest Fire Management. In: Weather and Forecasting, vol 13, p. 592, 1998.

G. Held, F.J.S. Lopes, J.M. Bassan, J.T. Nery, A.A. Cardoso, A.M. Gomes, T. Ramires, B.R.O, Lima, A.G. Allen, L.C. Silva, M.L. Souza, K.F. Souza, L.R.F. Carvalho, R.C. Urban, E. Landulfo, A.M. Decco, M.L.A.A. Campos, M.E.Q. Nassur, R.F.P. Nogueira. Raman Lidar monitors emissions from sugar cane fires in the State of São Paulo: A Pilot-Project integrating Radar, Sodar, Aerosol and Gas observations, Revista Boliviana de Física, V.20, 24-26, 2011.

Lhermitte, R. Centimeter & Millimeter Wavelength Radars in Meteorology. Miami, University Publications, 2002

Soares, R. V.; Batista, A. C. Incêndios florestais – controle, efeitos e uso do fogo. Curitiba. 250 p. 2007.

Monitoring the amount of carbon released into the atmosphere in Portugal due to forest fires, in the summer of 2013

Lourdes Bugalho[a], Luís Pessanha[a], L. M. Ribeiro[b], M. Almeida[b], Ricardo Oliveira[b] D. X. Viegas[b,c]

[a] *Instituto Português do Mar e da Atmosfera, Portugal.* Lourdes.Bugalho@ipma.pt
[b] *CEIF/ADAI/LAETA – University of Coimbra, Portugal*
[c] *Department of Mechanical Engineering of the University of Coimbra, Portugal*

Abstract
Forest fires are one of the most devastating natural disasters occurring in Portugal mainland over the summer season, with a strong impact on the economy, environment and climate. In last four decades the increase of wildfires problems in Portugal linked to Industrialization, urbanization, rural exodus (in recent past), and emigration (nowadays), with tendency to be worst in the future, lead to a mutation in Portuguese society. Severity of wildfires its worst year to year, besides the effort of the State, increasing human, operational, technical and economic resources to solve the problem. The fire combat continue very difficult and the number of occurrences of fires getting out of control, becoming larger and larger with a heady impact the increase of destruction.
Present work aim to contribute to a development of a support decision tool to be used in combat operations, monitoring fire spots and fire evolution using LSA SAF (*Land Surface Analysis Satellite Application Facilities*) products. The FRP (*Fire Radiative Power*) a product of LSA SAF are available and free distributed, in NRT (*Near Real Time*) and off-line, every 15 minutes for all pixels with a delay of about 20 minutes. These data can, subsequently, be used to obtain the carbon (or the equivalent CO_2), estimated for each pixel and integrated for a given area and period of time or, simply, to map and monitor forest fires.
This work is showing the possibility of monitoring forest fires, using FRP product with about 4 km of spatial resolution, taking advantage of the very interesting temporal resolution (15 minutes). As test, two major wildfires of 2013 had been used: Alfândega da Fé (Picões), from 8 to 11 July, and another one, in the region of Caramulo, from 21 to 30 August. Burnt area was, respectively, 14000 ha and 9416 ha, according data provide *by ICNF*.

Keywords: carbon release; monitoring forest fires; meteorological satellites; LSA; SAF; EUMETSAT

Introduction

The spectral characteristics, temporal resolution and coverage of meteorological satellites, allow, in addition to weather monitoring, surveillance and forecast, the use of data in other areas of activity, such as climate monitoring, agriculture and forestry support, namely, on forest fires monitoring.
The operation of the European System of Geostationary Satellites (METEOSAT SECOND GENERATION – MSG) is under the responsibility of EUMETSAT (https://www.eumetsat.int/). EUMETSAT ground segment includes, not just a central unity, *Central Application Facility* (CAF), but also, several different centres for satellite applications, *Satellite Application Facilities* (SAF).
The Portuguese Sea and Atmosphere Institute (IPMA) is responsible for the *Land Surface Analysis Satellite Application Facilities* (LSA SAF), ensuring the development of algorithms for obtaining various biophysical parameters on the ground, such as descendant radiative fluxes on small and long wavelength (DSSF and DSLF), the surface temperature of the earth (LST), various vegetation parameters (LAI, FVC, fAPAR) and also the radiative power of forest fires (FRP) (Trigo *et al*, 2011). From these basic parameters it is possible to compute the radiative balance which plays a crucial role in the control of soil moisture and evapotranspiration processes, in turn, depending on the type, level and condition of vegetation and photosynthetic activity. Table 1, shows four LSA SAF products linked with forest fires together with a summary of some of the features of the products.

Table 1. LSA SAF products linked with forest fires

	Processing frequency	Product Name	Status	Observation
FD&M	15 Minute	*Fire Detection and Monitoring*	Operational	Identification of pixels with fires in Europe and Africa
RFM	Daily	*Risk of Fire Map*	Operational	Index associated with the forest fire risk in Europe
FRPPixel	15 Minute	*Fire Radiative Power*	Operational	Fire Power in each pixel - MSG resolution
FRP-GRID	Hourly	*Fire Radiative Power – Gridded*	Operational	Fire Power in a 5º resolution grid

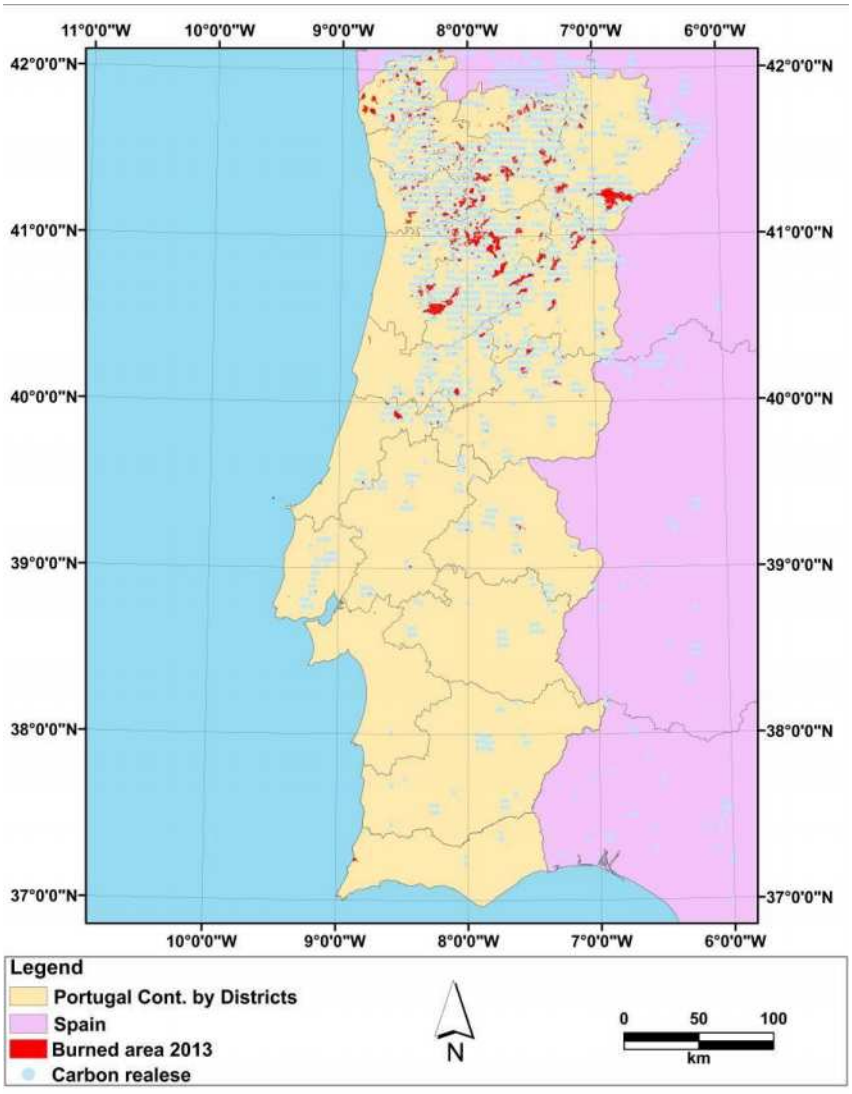

***Figure 1** - Forest fires map to 2013, based on FRP-Pixel LSA SAF product*

SEVIRI (*Spinning Enhanced Visible and Infrared Imager*), is the radiometer on board of MSG satellite systems, with 12 spectral channels each with 3 km spatial resolution (1 km for the high-resolution visible channel) at nadir (Latitude and Longitude are ear 0º, 0º) corresponding, in our latitudes, to a spatial resolution of about 4 km. Temporal revisiting time is of 15 minutes.

Navigation of pixels is possible (associating a Latitude and Longitude to the centre of each *pixels*) and can be used to navigate fire occurrences mapping Carbon or CO_2 over Portugal. Figure 1 shows a fire map for Portugal (January to October 2013): burnt area and CO_2 estimated thorough FRPPixel.

The map was done extracting Portugal mainland from the Europe window of the LSA SAF FRP product distribution. All these products are available for other windows, namely, Europe, Africa (two windows Northern and Southern regions) and South America where this methodology can also be used.

This paper is showing the possibility of monitoring forest fires using FRP product over a region, such as districts, municipalities or other areas of interest, taking advantage of the temporal resolution (15 minutes) of the system. Monitoring specific areas during consecutive days to get information about the evolution of large fires can also be done.

This capability will be illustrated using two large fires: Alfândega da Fé, Picões, (from 8 to 13 July) with 14000 ha of burned area and, in the region of Caramulo (from 21 to 30 August), with 9416 ha according data provide by ICNF (*Instituto de Conservação da Natureza e Florestas*). These 2 large fires where studied in detail by the CEIF (*Centro de Estudos de Incêndios Florestais*) team (Viegas *et al*, 2013).

Data and Methodology

Using the *Fire Radiative Power* (FRP), it is possible to estimate the amount of carbon emitted into the atmosphere, due to forest fires. These parameters can be used in various fields of applications, such as mapping fire carbon emissions over the country, allowing strategic decisions to minimize the effects as, for example, reducing health impact.
The FRP estimate the power of wildfires. It is calculated in megawatts (MW) representing the radiant energy, released per unit time, during the forest fire (Wooster *et al*., 2005). The time integration of the FRP during the wildfire lets allows to estimate the total energy released FRE (*Fire Radiative Energy*). The energy released is directly related to combustion and to the rate of fuel consumed process, through a thermal efficiency rate, where carbon is oxidized releasing CO_2. One fraction is emitted as electromagnetic radiation, which can be detected using remote observation (in the case the SEVIRI sensor, installed in the MSG system). The rate of consumption of biomass (TCB), measured in kg/s, is given by the following expression:

$$TCB\ (kg / s) = 0.368\ (\pm 0.015) \bullet FRP\ (MW)$$

Consumption of biomass (CB) estimated in kg, can be calculated from the following expression:

$$CB\ (kg) = 0.368\ (\pm 0.015) \bullet FRE\ (MJ)$$

From the biomass, it is possible to estimate the amount of carbon (C) released into the atmosphere, using a linear statistical approach to estimate the value (in g) for each kg of fuel burned.

$$C\ (g) = 0.47 \bullet CB\ (kg)$$

The statistical value usually used is 0.47. The equivalent amount of CO_2 released into the atmosphere, is approximately four times higher the amount of carbon.
Either, the equivalent amount of CO_2 or the Carbon released into the atmosphere due to forest fires, presents a good fit with the burnt area provided by the Institute of Nature Conservation and Forestry (ICNF) (Bugalho, L. and Pessanha, L., 2011).
IPMA forest fire reports are including, since 2011, a comparison of the full amount (per day) of carbon/CO_2eq released into the atmosphere, and burnt areas (ha), provided by ICNF. Figure 2 represents the CO_2 equivalent released into atmosphere and the burnt area, in 2013 (May to October), for full Portugal mainland.

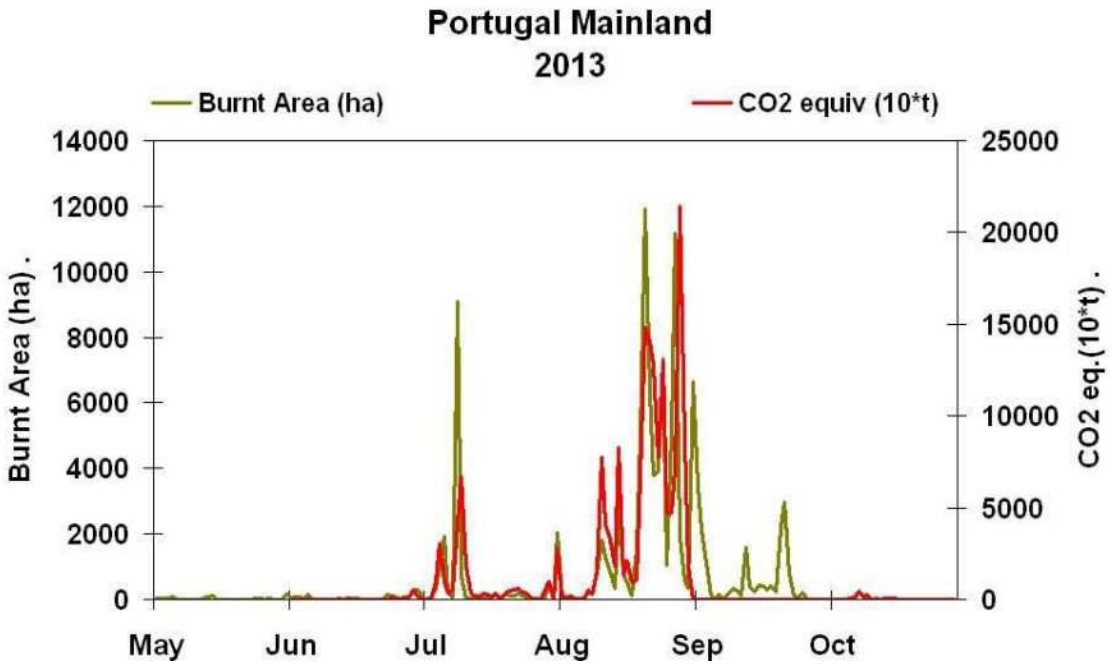

Figure 2. Daily evolution of the equivalent amount of CO2 released into the atmosphere by forest fires across the country (red, 10*tons), based on FRP and burnt area provided by ICNF updated on November 12/2013 (green, ha)

LSA SAF FRP is produced and distributed, in NRT (Near Real Time) and off-line, every 15 minutes for all pixels. These data can, subsequently, be used to obtain the Carbon (or equivalent CO_2), estimated for each pixel and integrated for a given area and period of time. Can also to be used to map and monitor forest fires.

This work is showing the possibility of monitoring forest fires, using Carbon computed based on FRP with 4 km of spatial resolution, taking advantage of the temporal resolution (15 minutes) of the system. As test, two major wildfires of 2013 had been used: Alfândega da Fé (Picões), from 8 to 11 July, and another one, in the region of Caramulo, from 21 to 30 August. Burnt area was, respectively, 14000 ha and 9416 ha, according data provide by ICNF.

On July 8th of 2013, at 14:44 h the biggest wildfire register in Portugal in 2013, ignited in the inhabited village of Cilhade, parish of Felgar, municipality of Torre de Moncorvo, district of Bragança, northeast region of Portugal. Few minutes (less than 10 min) after the initial alarm, all the human and material resources available in the region were fighting this wildfire. The combat to fire was difficult by the extreme slope, characterised in this region. On the July 8^{th,} after a few hours of fighting, the fire was dominated and the progression stopped near to Picões in the municipality of Alfândega da Fé (Figure 3), with a burned area relatively small of 180 ha. Despite all the efforts and vigilance strategies of the firelighters of Alfândega da Fé, on July 9th at 14:00 h the fire rekindle and outbreak the perimeter and started a new event with capacity to evolve to a large fire. This wildfire became known as Picões fire, due the location of the rekindle.

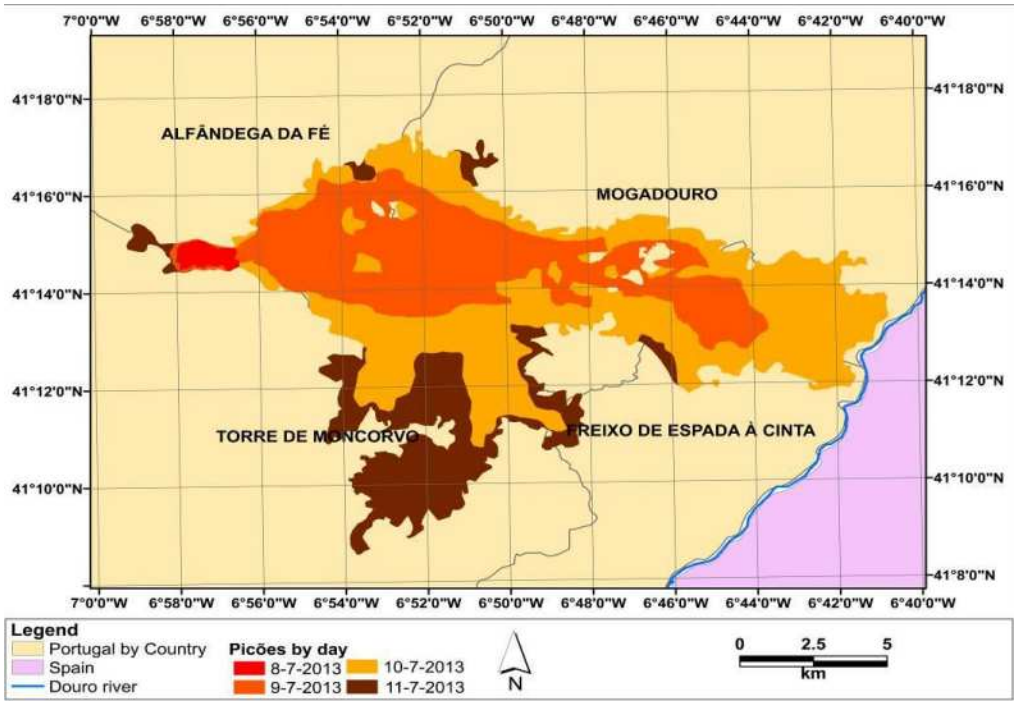

Figure 3. Daily evolution of the burnt area for Alfandega da Fé forest fires

To a better understand of the fire behavior, it is necessary to characterize the region, land use and vegetation, as well as, climate and meteorological aspects.

The geographic characterization of the region from the physical aspect, is continuous mountains with steep slopes and several waterlines running belonging to the basin of the Sabor river.

Land use was mainly occupied for subsistence agriculture, connected to an aged population, olive oil and almond production. *Pinus pinaster* and *Eucalyptus globulus* stands for production of pulp paper.

Meteorologically, the year of 2013 started with large amounts of rainfall. The values of accumulated amounts of precipitation between October 1 of 2012 and June 30 of 2013 were, in general, higher than the normal (average), and ranged from 100% to 150%. The meteorological condition in Portugal mainland, for the initial 10 days of July 2013, according to Novo *et al*, was characterized by an anticyclone system located near to Golf of Biscay, after the 3 of July and again between July 6 and July 10, leading to a very dry and warm air mass, transported from the centre of Spain, resulting in heat wave around the country which last to July 13.

On the July 9th the air temperature record (IPMA meteorological station of Torre de Moncorvo), on the Northeast region of Portugal at 14:00 h (rekindle of the Picões wildfire) attained values over 38ºC, the relative humidity was lower than 13% and the maximum wind velocity was close to 45 km/h. Due the extreme weather conditions the moisture content of fine forest fuels are close to 7%. These conditions were favorable to the development of large fires (slopes, high temperatures, low moisture content of fine forest fuels, strong wind aligned with the drainage basin of the Sabor river).

The wildfire of Caramulo occurred from August 21 to August 30, Figure 4. Most than 20 occurrences were register in these period of time, grouped in three major wildfires, Alcofa (1522 ha of burned area), Silvares (1346 ha of burned area) and Guardão (6548 ha of burned area). These wildfires are the most deadly recording in 2013, reaping the life of four fire-fighters and injuries in several crew members in two human accidents register. Each fire are aggravated by the difficult of the terrain (slope), stands, fuels that provoked embers and burning particles starting often new fire focus and, also, the human limitation to fighting in such conditions.

On August 20th at 23:54 h the Centre of Operations of Tondela firehouse, received an alarm of a wildfire near to the small village of Alcofra. The main cause of this fire was, according to the Portuguese authority, arson.

Reconstruction of these fires was made by the CEIF team, using testimonies of the main interlocutors such as fire-fighters, hotshots, crew members, authority's, civil protection members and local habitants.

The geographic characterization of the region from the physical aspect is continuous mountains with steep slopes. Land use was mainly occupied for subsistence agriculture, connected to an aged population, shrubs, *Pinus pinaster, Eucalyptus globulus* stands, and a Forestry Park under the jurisdiction of the National Forestry Service (ICNF).

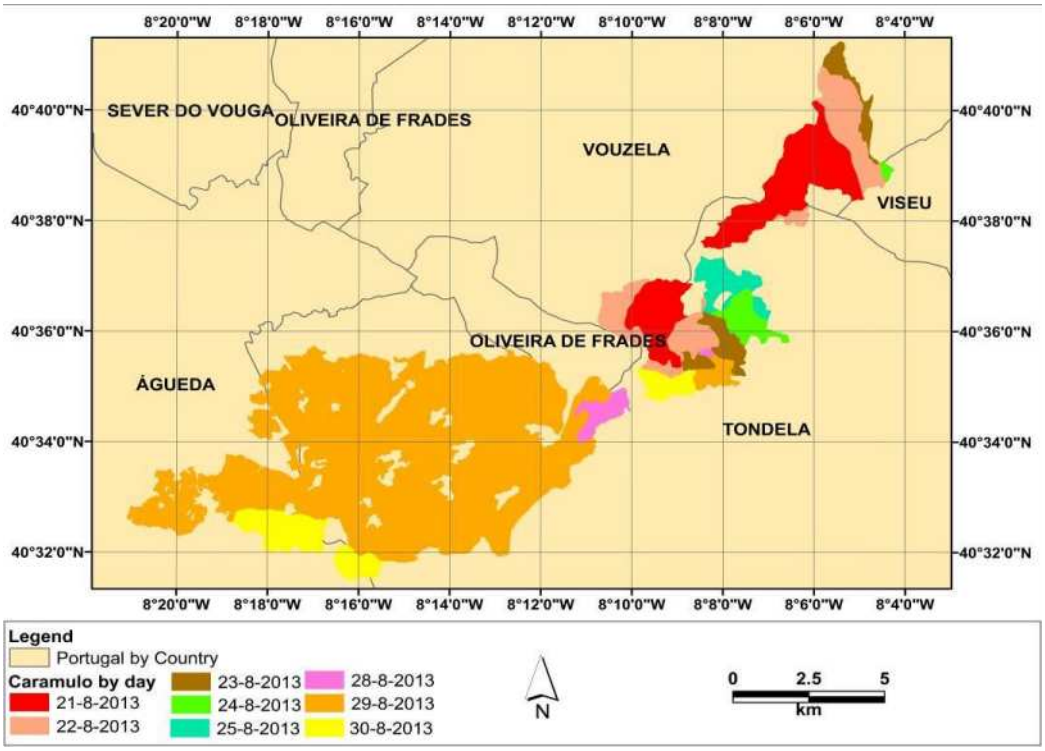

Figure 4. Daily evolution of the burnt area for Caramulo forest fires

The meteorological records shows, from August 21 to August 30, in the station of Viseu, 30ºC of temperature, relative humidity near to 20% and 27 km wind velocity without defined direction, in the first hours of the Alcofa wildfire. The next two days presented same conditions without changes on meteorological conditions. After the August 24, the temperature registered in Viseu oscillated in the range of 10 to 20ºC during the night to around the 30ºC during the day. The wind velocity increased to 50km/h with maximum speed of 60km/h.

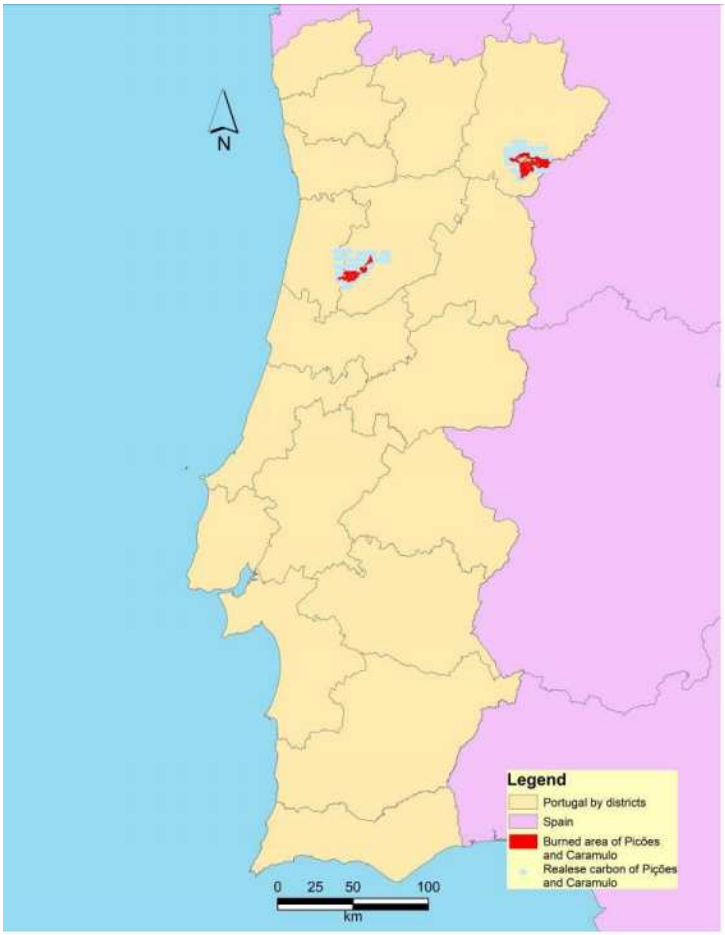

Figure 5 - Localization of two forest fires (Alfandega da Fé and Caramulo). The burnt area measure in red and the FRP product for the same days in blue

Latitude and Longitude of centre of pixels of LSA SAF products are available (geolocation), making possible to map products. For each of the selected wildfire periods already indicated, (8 to 11 July 2013 for Alfandega da Fé and 21 to 31 August 2013 for Caramulo) Carbon data was used to map fires in the correspondent area.

It is possible to observe (Figure) the very good fit of the areas: burnt area prepared by ICNF (*Instituto de Conservação da Natureza e Florestas*) and LSA SAF Carbone map estimated after the integration of the FRP product for the correspondent period of the fires and areas, using all 15 minutes LSA SAF FRP.

Limits for the selection were established:

- Alfândega da Fé: Latitude from 41º 8'N to 41º 18'N, longitude from -6º 59'W to -6º 40'W (Figure 3).
- Caramulo: Latitude from 40º 32'N to 40º 42'N, Longitude from -8º 20'W to -8º 0' W (Figure 4).

3. Results and Discussion

Figure 6 (A and B) shows the evolution of the amount of Carbon released into the atmosphere corresponding to the integrated value (15 minutes), for the each of the two study areas, Alfandega da Fé and Caramulo, for July and August respectively. Analyzing the figures it can be observed a large amount of carbon released into the atmosphere by forest fires from 8 to July 11 in the area of Alfandega da Fé and, on days 21 to 31 August (mainly in 29 and 30), in the Caramulo region.

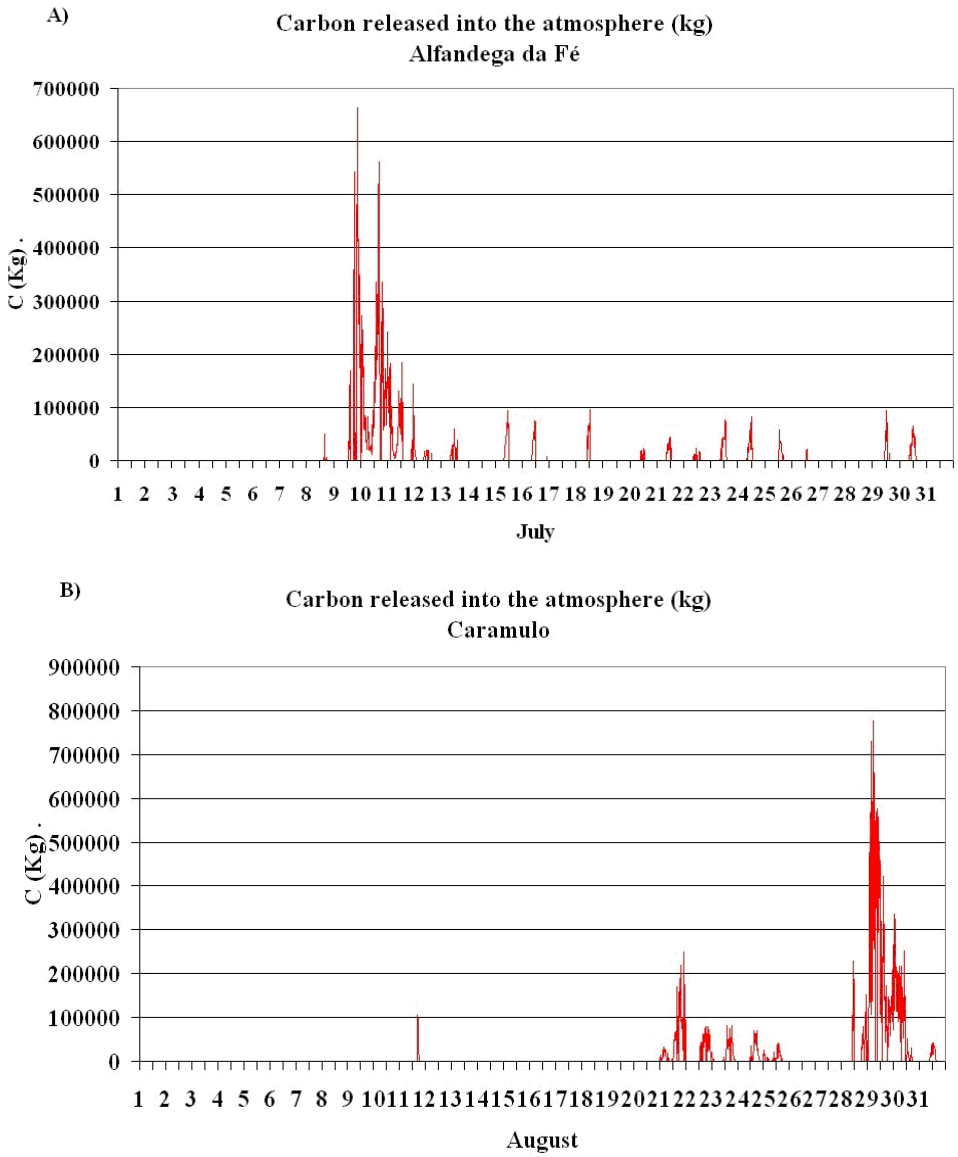

Figure 6 - Daily evolution of the equivalent amount of CO2 released into the atmosphere by forest fires across the Alfandega da Fé area before defined (A) and Caramulo area before defined (B) (red, tons)

Figure 7 (A and B) shows also the evolution of Carbon released into atmosphere around the periods of maximum emission: Alfandega da Fé (8 to 11 July 2013) and Caramulo (21 to 31 August 2013). A moving average of one hour (in blue) was also included. It is possible to verify that Carbon emission was very high, with a maximum of more than 664 tons of Carbon in 15 minutes, released at 21:00 of 9 July 2013 in Alfandega da Fé and a maximum of more than 777 tons released in 15 minutes on 29 August 2013 at 05:00.

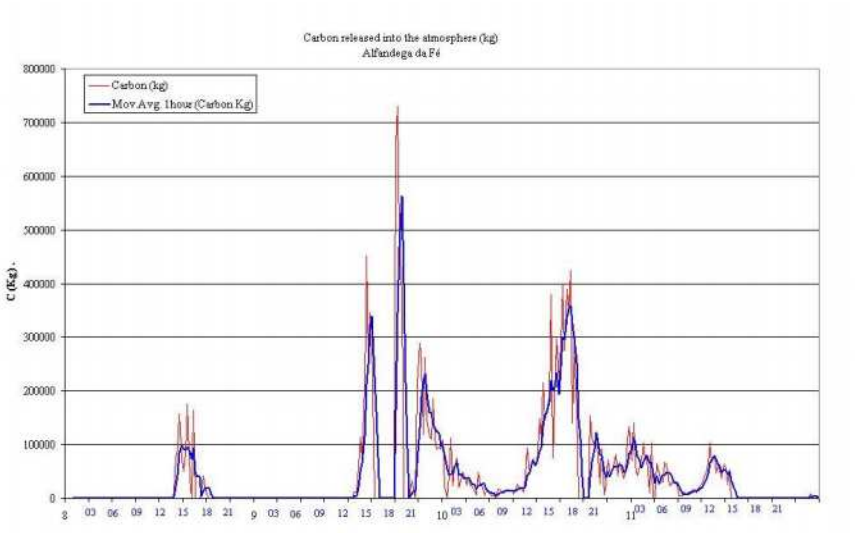

A

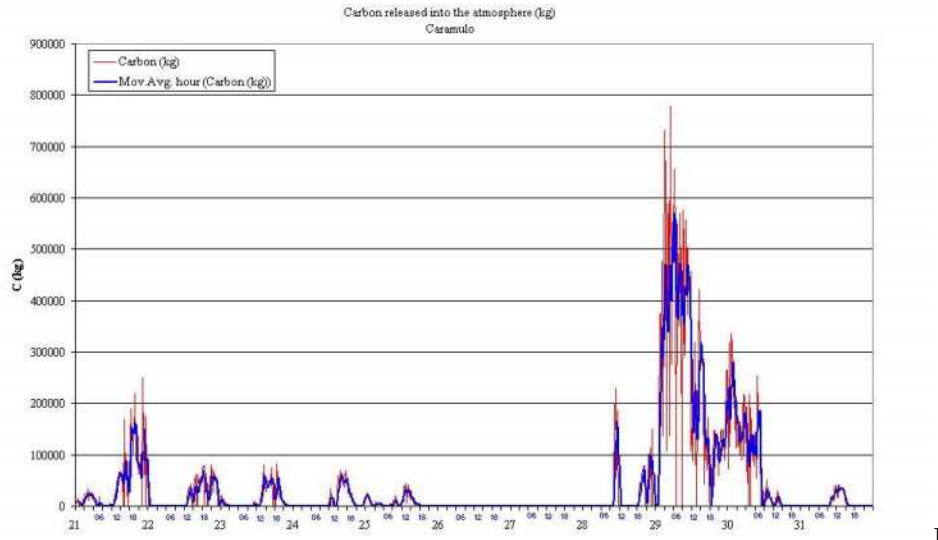

B

Figure 7 - The same of Figure 5 during the periods 8 to 11 July and 21 to 31 August, 2013 (red) and moving average of one hour (blue)

The daily evolution of burned areas can be associated to pixels where there are values of Carbone, ie, where it is possible using remote observation, detection of forest fires associated with biomass burning. Figure 8A and B shows the overlay of information about daily evolution of the area burned by forest fires, and pixels. The colour is giving the information about the day of occurrence.

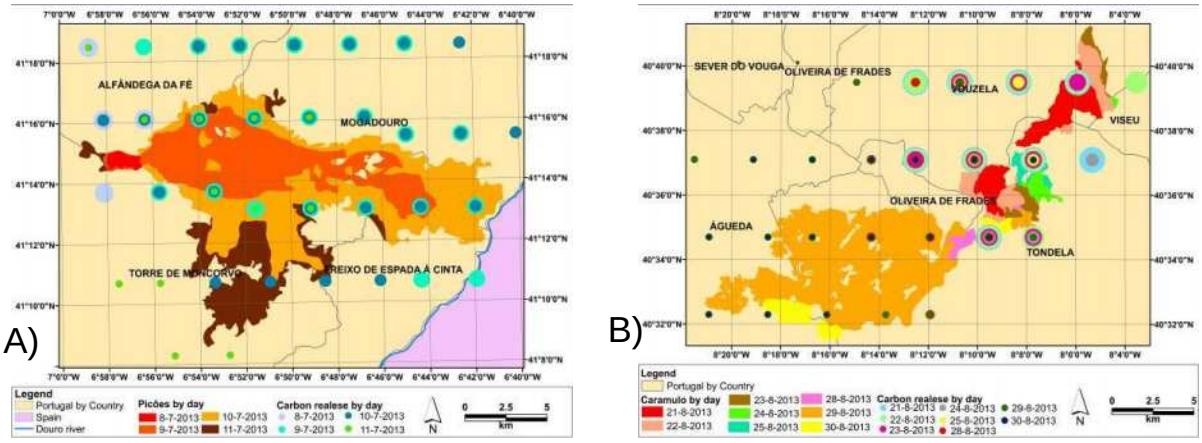

Figure 8- The daily evolution of burnt area for Alfandega da Fé (Picões), (A) and Caramulo (B) and the pixels with FRP values for each day

Note that the location is placed on the centre of the pixel but the fire can be in any place inside of the pixel (or even out the limits of the pixel). Also, geometric correction of the input MSG image can have some impact (geometric corrections done by EUMETSAT) when trying to use in applications near the pixel size. Nevertheless, analyzing Figure 8A and 7B, it is possible to verify that the evolution of spot fires follow the wildfire. For example, in Picões (Alfandega da Fé), Figure 8A, the fire started in further west, on the 8th of July, and it is possible to observe pixels with values of Carbone in light blue in the Figure 8A. On following days (9 and 10), the forest fire migrate to the river eastward. This behaviour is also accompanied by the evolution of Carbone released. On day 11, the wildfire occurs further south, being also accompanied by the Carbone released. Due to the error associated with the pixel size and the geolocation error, associated to remote sensing technique, the pixels with values of Carbone are not always over wildfire.

Conclusion

It is possible to conclude that:

- Results obtained so far shows a good correlation between burnt areas and Carbone (or CO_2) released in the atmosphere;
- In the case of the two large fire events in 2013 this is especially true.
- The monitoring Carbon (or CO_2) release in the atmosphere during forest fires, seems good and shall be used as an environmental tool.
- It seems possible to used the estimation of Carbon (or CO_2) released into the atmosphere as an economic way of estimating burned area, with enough quality to be used in NRT (*Near Real Time*).
-

References

Bugalho, L., Pessanha, L. (2011) – Prevenção dos Fogos Florestais: Contribuição da Observação Remota ("*Prevention of Forest Fires: The Contribution of Remote Sensing")* – Proceeding of 7º Simpósio de Meteorologia e Geofísica da APMG, 28 a 30 Março, 2011

Govaerts, Y; Wooster, M.; Lattanzio, A. (2009) Roberts, G. Algorithm Theoretical Basis document for MSG SEVIRI fire radiative power (FRP) characterisation. Project documentation (https://landsaf.ipma.pt/).

Novo, I.; Rio, J.; Silva, P; Ramos, R. e Moreira, N. (2013). Incêndios Florestais no Verão de 2013: Análise Meteorológica e Comportamento do Vento. Novembro de 2013. Divisão de Previsão Meteorológica, Vigilância e Serviços Espaciais. Instituto Português do Mar e da Atmosfera.

Trigo, I. F.; Dacamara, C. C.; Viterbo, P.; Roujean, Jean-Louis; Olesen, F.; Barroso, C.; Camacho-de-Coca, F.; Carrer, D.; Freitas, S. C.; García-Haro, J.; Geiger, B.; Gellens-Meulenberghs, F.; Ghilain, N.; Meliá, J.; Pessanha, L.; Siljamo, N. and Arboleda, A. (2011). The Satellite Application Facility for Land Surface Analysis. International Journal of Remote Sensing, 32:2725-2744

Product User Manual (PUM FRP) FIRE RADIATIVE POWER (2009) - Issue/Revision Index: Issue 1.1. Project documentation (https://landsaf.ipma.pt/).

Wooster, M. J., G. Roberts, G. L. W. Perry, and Y. J. Kaufman (2005) Retrieval of biomass combustion rates and totals from fire radiative power observations: FRP derivation and calibration relationships between biomass consumption and fire radiative energy release, J. Geophys. Res., 110, D24311, doi:10.1029/2005JD006318.

Viegas D.X, Ribeiro L.M, Almeida M.A., Oliveira R., Viegas M.T., Raposo J.R., Reva V., Figueiredo A.R., Lopes S. (2013) Grandes Incêndios Florestais e os Acidentes Mortais Ocorridos em 2013 – Parte 1 – ADAI

New generation of automatic ground based wildfire surveillance systems

Darko Stipaničev, Marin Bugarić, Damir Krstinić, Ljiljana Šerić, Toni Jakovčević, Maja Braović, Maja Štula

University of Split Faculty of Electrical Engineering, Mechanical Engineering and Naval Architecture, Department for Modelling and Intelligent Systems Ruđera Boškovića 32, 21000 Split, Croatia. darko.stipanicev@fesb.hr

Abstract

The paper presents a state of the art in the research area of ground based wildfire surveillance systems with special emphasis on their latest generations proposed and developed in the last couple of years. We have focused primarily on novel, more efficient algorithms for wildfire detection, but other topics like fusion of video based systems with other wildfire detection systems and their integration with Geographic Information Systems (GIS) systems has also been analyzed. Our particular focus was on research carried out in our Department. Last but not least, we give our opinions and assumptions about future development of such systems.

Keywords*: wildfires, forest fires, smoke and fire detection, wildfire monitoring, wildfire surveillance, augmented reality, GIS, wildfire monitoring network, fusion of video data.*

Introduction

Wildfires are still a constant threat to ecological systems, as well as human safety, causing rapid reduction of forest stand. Many efforts in fire prevention and protection are aimed to reduce not only the number of fires, but also the fire damage. It is well known that early fire detection and quick and appropriate intervention are the most important measures for wildfire damage minimization. Once a wildfire has expanded, it is very difficult to control and extinguish. Therefore in countries that have a great wildfire threat, there are a lot of efforts to organize appropriate and efficient wildfire surveillance. Wildfire surveillance1 is still mostly based on a traditional human wildfire observers, specially trained people located on selected spots with a good visual coverage of protected area, usually equipped only with binoculars, maps and communication units. Their task is to detect wildfire in the incipient stage, try to locate it on the map and to alert the appropriate fire department. In fire season human observers are engaged 24 hours a day and they are exposed to isolation, extreme weather conditions, especially high temperatures and a need for continuous concentration.

Therefore, since 1932 when the inventor called Osborne designed a swing-lens panoramic camera used by USDA Forest Service for wildfire detection (Kresek, 2007), until today a lot of research was done with the aim of photo and video based systems in wildfire detection to make the observers' job less

[1] *Concerning wildfire observation two terms could be encountered – wildfire surveillance and wildfire monitoring. They are often thought as synonymous, but there is a certain difference in their meaning and a lot of discussions about these differences. More or less in all discussions people agree that they are identical in the fact that they collect routinely information on phenomena, but surveillance is more than monitoring. Under surveillance the information collected are analyzed, interpreted and action taken while in monitoring the action might not necessarilly be there, depending on the purpose of this monitoring. The other difference is that term surveillance is mostly used when information is collected primarily by vision sensors, and in monitoring it is not necessary to have a vision sensor at all and instead any other kind of sensors could be used. As our focus is primarily on vision based systems in this paper we will use the term wildfire surveillance.*

strenuous and easier. These research efforts were particularly intensive after 80s, thanks to development of video technology. At the beginning, that was only dislocation of the observer to the observation center and installment of pan, tilt, zoom controlled video cameras on monitoring spots, but quite soon more advanced systems have been proposed with the ability of automatic wildfire detection (Cappellini *et al*., 1989). Human observer no longer needs to constantly look at the monitor. His/her job is now to check and verify whether the raised alarm is real or false. Such automatic systems could be used not only for early fire detection, but also for distant video presence, a task very important for preventive inspection of the protected area as well as for fire-fighting coordination when the fire starts, so they are usually called automatic wildfire surveillance systems and to emphasize that they are located on the ground automatic ground based wildfire surveillance systems.
Since the end of the 80s, a few generations of such systems have been developed, designed and deployed, not only as experimental, but also as real working systems (Kührt, 2001) (Dedeoglu *et al*., 2005) (De Dios *et al*., 2008) (Stipaničev *et al*., 2010). Improvements have occurred on different parts and functions, both on hardware and software level. This paper focuses on the last generation of such systems that have been proposed in the last couple of years. Our attention is particularly focused on:

a) Algorithms for wildfire smoke and fire detection, resulting in significant improvement of detection features,

b) Fusion of video detection in various electromagnetic ranges, as well as fusion of video detections with other sensor types,

c) Close integration of wildfire surveillance and monitoring and systems with Geographic Information Systems (GIS), resulting in new features in both fire detection and distant video presence modes,

d) Synergy effect of wildfire observer network consisting of mutually connected individual wildfire observers working together in cooperation.

The paper presents a state of the art in this research area with emphasis on the research carried out in our Department in the last couple of years (Stipaničev *et al*., 2010) (Šerić *et al*., 2011) (Jakovčević *et al*., 2013) (Bugarić *et al*., 2014). We have worked and we are working on almost all of the topics listed above, both on the experimental, laboratory level but also on practical implementation.

Improvements in algorithms for wildfire smoke and fire detection, resulting in significant improvement of detection features

Vision based wildfire detection systems are mainly focused on smoke detection during the day and fire detection during the night. Since 80s, a lot of different algorithms have been proposed based on different smoke and fire visual characteristics. In this review we have been focused on recent works since 2011. Review of the previous works in this field could be found in (Jakovčević *et al*., 2011).
Most of the methods for smoke detection are based on the moving region detection as the first step of the detection process. Ashish at al. proposes an algorithm (Ashish *et al*., 2013) based on the background subtraction method introduced by Collins at al. (Collins *et al*., 1999). In detected regions, color is used as discriminatory characteristic where smokes colored pixels are expected to have small aberration in red, green and blue channels from the average value of all three channels. Another distinctive characteristic of smoke is perimeter to area ratio that is expected to be above the predefined threshold. Finally, suspicious regions that satisfy above given conditions are checked against dynamic property of the smoke that it continuously moves in upward direction. Brovko *et al*. (Brovko *et al*., 2013) proposed an algorithm based on motion and contrast, with wavelet transform applied as a preprocessing step to reduce the image size and to remove high frequencies details. Slowly moving areas are detected by frame differencing of 3 consecutive frames. Model for blending semitransparent objects with background is introduced with:

$$I_{t+1}(x,y) = b \times F_{t+1}(x,y) + (1 - b) \times B_t(x,y) \quad (1)$$

where $I_{t+1}(x,y)$ is the current frame, β is the blending parameter and $B_t(x,y)$ is the background from the previous step. As soon as frame $I_{t+1}(x,y)$ is obtained, foreground can be estimated from equation (1). Smoke propagation direction based on optical flow calculation is used as a final test for suspicious regions.

Complex wildfire smoke detection technique is proposed by Labati *et al*. (Labati *et al*., 2013) based on the previous work by Genovese *et al*. (Genovese *et al*., 2011) using computational intelligence methods to dynamically adapt to the environment. Proposed algorithm can be summarized in the following steps: moving region detection, smoke-color analysis, sharp edge detection, growing region detection, rising region detection, perimeter disorder analysis and feature set computation. Moving region detection is based on the work of Collins *et al*. (Collins *et al*., 1999). Two different background images are estimated. The first one is updated at every frame and the second is updated with a period of 1 second. Two background images are used to extract slow moving regions. A matrix D_M representing the motion of every pixel is computed according to:

$$D_M(x,y,t) = \begin{cases} 0, & if \left| B_f(x,y,t) - B_s(x,y,t) \right| \le T_l \\ \left(\left| B_f(x,y,t) - B_s(x,y,t) \right| - T_l \right) / (T_h - T_l), & if\ T_l \le \left| B_f(x,y,t) - B_s(x,y,t) \right| \le T_h \\ 1, & if\ T_h \le \left| B_f(x,y,t) - B_s(x,y,t) \right| \end{cases} \quad (2)$$

where $0 < T_l < T_h$ are fixed threshold values. In the next step color feature matrix is computed based on the work of (Toreyin *et al*., 2009) and pixels not satisfying predefined conditions are discarded. Sharp edge detection step aims to search high differences in the luma channel of adjacent frames, usually not present in the regions containing smoke. Growing region matrix is computed as the difference between the moving regions at the time instants *t* and *t-1* and only positive values of growth are considered to avoid excessive data fluctuations. Finally, rising value of the moving pixel and the perimeter disorder is computed. Two different algorithms use the computed features set. In *Algorithm A* the features are extracted for every pixel of each frame of the frame sequence and in *Algorithm B* the features are extracted globally for each frame. Feature selection algorithm based on kNN is applied separately for different scenarios. Obtained features are used as inputs for computational intelligence and statistical classifiers.

Park *et al*. (Park *et al*., 2013) proposed an algorithm for wildfire smoke detection using spatial-temporal bag-of-features (BOF) technique. Slow moving regions are extracted by key-frame detection, followed by rejection of non-smoke colored blocks based on probability density function of smoke color model learned from the training data. For the remaining suspicious blocks, combining the candidate blocks with 100 corresponding blocks in previous frames creates a spatial-temporal 3D volume. Histogram of optical flow (HOF) is extracted as a temporal feature and histogram of gradients (HOG) extracted from the current block is used as a spatial feature. Random forest classifier trained from the training data is used as a final confirmation of smoke.

Vipin (Vipin, 2012) proposed a rule-based system for forest fire detection. Fire-colored regions are detected by processing input images in RGB and YCbCr color spaces. Avgerinakis *et al*. (Avgerinakis, 2012) proposed an algorithm based on temporal HOGHOF descriptors and color energy. Separation of moving from static pixels is based on the assumption that real motion introduces deviation from the Gaussian distribution of motion vector induced by noise. Moving blocks are constructed in regions

where at least 50% of pixels are detected as moving. HOG descriptors are calculated for moving blocks and HOF is constructed from previous set of frames. Extracted HOG and HOF descriptors from the training set are used to train SVM classifier. When a frame with smoke is detected, second stage of the algorithm takes place, where statistics based on the color energy of the candidate blocks are analyzed to determine whether they contain smoke or not.

Algorithm proposed by Lee *et al*. (Lee *et al*., 2012) is based on hybrid motion segmentation using frame differencing and Gaussian mixture model. For the regions with detected motion spatial and temporal features are extracted. Spatial wavelet analysis detects loss of energy in high frequencies is followed by temporal energy analysis differencing sudden loss of energy corresponding to rigid objects from the gradual loss of energy which may represent smoke. Color information is used as the third characteristics for identifying smoke in a video. Based on the empirical analysis, authors assume that smoke affects every component in the RGB color space. However, it does not drastically change the configuration of the normalized rgb color system. Described features extracted from the training data set are combined and used to train SVM classifier. Final verification of the smoke is based on temporal consistency. The alarm is raised if smoke is detected for over 50% of a predefined time interval. In the study presented by Ko *et al*. (Ko *et al*., 2012) moving regions are detected using key-frame differencing. Features extracted from the training data are used to train two random forest (RF) classifiers. One is trained using temporal features, namely: average hue, saturation, intensity and skewness of the hue, average wavelet energy and skewness of the wavelet energy and spatial motion orientation from the preceding 100 frames. Histogram of gradients (HOG) from the current block is used to train the other classifier. A candidate block is declared as smoke block if the average probability of two RF classifiers in a smoke class is maximum.

Surit and Chatwiriya (Surit, 2011) proposed a technique based on frame differencing. Moving blocks are examined and confirmed as smoke based on color. Habiboglu *et al*. (Habiboglu *et al*., 2011) proposed an algorithm based on two background models, where one is optimized to detect fast moving objects used to differentiate ordinary objects from smoke-like moving regions. Set of thresholds in YUV color space is used to further filter non-smoke from smoke colored pixels. Slow moving region detection was based on GMM background models. Background model optimized to detect fast moving objects is used to differentiate ordinary objects from smoke-like moving regions. Set of thresholds in YUV color space is used to further filter non-smoke from smoke colored pixels. For each pixel satisfying the color condition a set of covariance descriptors is extracted, including luminance, chrominance, intensity and its temporal derivatives. The video is divided into blocks that do not overlap in spatial domain but there is 50% overlap in time domain. SVM classifier is trained for classification. Similar technique based on the covariance descriptors and SVM classification was also proposed for flame detection (Habiboglu *et al*., 2012).

Last but not least let us mention the work of our Department concerning improved algorithms for wildfire smoke detection. Interesting and promising research work was integration of context information in wildfire detection, together with motion, chromatic, texture and shape analysis (Jakovčević *et al*., 2011). Visual context analysis was performed by region merging segmentation, classification and applying context rules based on shape analysis. The phase of classification into classes smoke, low clouds and fog, sun and light effects, water surface and sky, distance landscape and vegetation, was not used for detection itself, but as a validation process for false alarms reduction. Fig 1 shows an example of input and classified image.

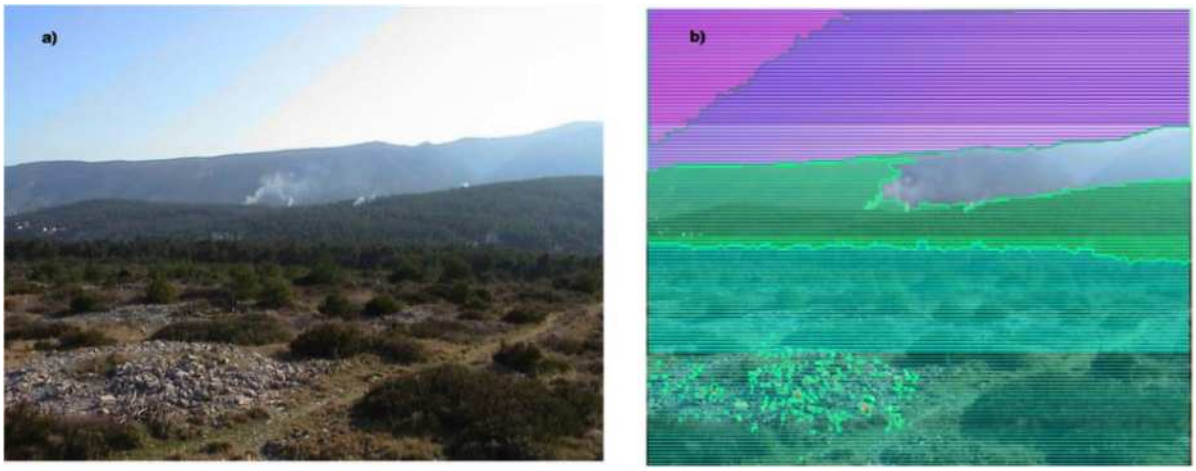

Figure 1. a) Input image and b) classified image used in visual context analysis

Fusion of video detection in various electromagnetic ranges and fusion of video detections with other sensor types

Sensory data fusion is today one of the top themes in artificial perception inspired by human perception. Humans usually use the fusion of data from more than one sensor in order to understand their surroundings. Usually the fusion processes are divided in low level or data fusion, intermediate level or feature fusion and high level or decision fusion (FireSense, 2010). Low level fusion or data fusion combines various raw data to produce new raw data having additional information in comparison with input data. Intermediate fusion or feature fusion is a fusion of features primarily extracted from row data. High level fusion or decision fusion is performed on the decision making level when various sources are used only for final decision making. In wildfire surveillance all three fusion types could be used and realized as fusion of video data captured in various electromagnetic ranges, usually visible and IR spectra and fusion of video data with other sensors data, particularly meteorological sensors data. Fig 2 shows an example of smoke visibility during typical hot summer day in visible and far IR spectra.

The research presented in (Verstockt *et al*., 2012) describes a multi-sensor approach to smoke detection using visible and thermal imaging. The information from both sensors is analyzed in order to extract moving objects that could potentially represent smoke. The silhouette of the moving objects is examined in order to determine the appearance of smoke in the scene. In order to implement this type of multi-sensor detection process, images for two different sources have to be registered. The registration is performed using a contour-mapping algorithm where the rotation, scale and translation of moving objects are discovered.

Figure 2. Smoke visibility during typical hot summer day in visible spectra (left) and far IR spectra (right)

Another approach, presented in (Torabnezhad *et al*., 2013), describes a new method of smoke detection based on fusion of information from IR and visible sensors, since each source alone cannot provide the full information about the potential event. The method is designed for smoke detection on short distances. The smoke is not visible in the IR images, so this feature is used to distinguish between smoke and objects/phenomena visually similar to smoke. The method consists of two phases. In the first phase the input from both sources is used to generate a potential-smoke mask. The mask from the visual source is obtained using background subtraction and a smoke color model, while the mask from the IR source is obtained using hot object segmentation where due to invisibility of smoke in the IR image the smoke pixels are not segmented as hot objects. The potential smoke mask is built using these two masks as input. The second step is based on disorder measurements and energy calculation in order to reduce false alarms. The authors characterize the method as very effective and accurate.
Work presented in (Verstockt *et al*., 2010) describes a new multi-sensor fire detection system operating on ordinary video and long wave infrared (LWIR) thermal images. The detection process consists of several phases. When dealing with thermal images, the detector extracts hot objects using dynamic background subtraction and histogram based segmentation. Similarly, when dealing with ordinary video, moving objects are extracted using dynamic background subtraction. Both types of objects, hot and moving, are further analyzed using flame features based on specific geometric, temporal and spatial disorder characteristics of flame regions. By combining probabilities of visual and thermal features, according to authors it is possible to detect fire at an early stage.
Salah *et al*. (Salah *et al*., 2011) describes an FP7 project dealing with protection of cultural heritage sites from the risk of fire and extreme weather conditions. The fire protection is provided using a fusion of information obtained from IR and visible images. The main problem with this type of approach is the image registration between two different sources. The objective is to discover the correspondences between images. When the correspondences have been found the images can be transformed into the same reference so it is possible to achieve information fusion. The process of registration is challenging because the wavelengths of the IR and visible spectrum are different, so the general approaches such as SIFT and RANSAC do not work properly in this case. Authors have discussed several different registration approaches and proposed explicit alignment of lines derived from edge pixels. The individual extracted points could not always match correctly, so a Hough transform is used to generate lines. Using four of the generated lines it is possible to obtain perspective transformation matrix used for registration. The paper does not present explicit results for the fire detection process.
Although detection of wildfires using fusion of video data is most common, there are some drawbacks to this approach, primarily fusion of video based systems and other sensor types. Various types of sensors are used in wildfire detection, primarily meteorological sensors like temperature, pressure, humidity, wind and sun radiation sensors, but chemical sensors sensing carbon monoxide, carbon

dioxide and nitrogen dioxide are also used. The main problem in video - sensors data fusion is the correct fusion application for heterogeneous sensor types. Interesting example of smoke video detection and meteorological information fusion were presented by Štula *et al*. (Štula *et al*., 2011) where fuzzy cognitive maps with 4 concepts: current wind, conclusion on alarm (true/false), false alarms generated in the last 24 hours and current humidity was used for false alarms reduction in image post-processing phase.
Fire detection on Wild-land Urban Interface (WUI) using wireless sensor network was studied in SCIER project (Sekkas *et al*., 2010). The system architecture consists of three layers: Sensors, Local Area Control Unit (LACU) and Computing Subsystem. Sensors that are measuring temperature, humidity and vision sensors are organized into local clusters. LACU is responsible for administration of local sensor network. First level of fusion is performed on local cluster by calculating cumulative sum (CUSUM test) of local sensors and assigning basic probability of fire to each of them. Computing subsystem perform second level of fusion. Data from all LACU units are fused using Dumpster-Shafer evidential theory.
In (Šerić *et al*., 2011) authors proposed framework for multi sensor data fusion based on vision sensor and environmental sensors with goal of forest fire detection and false alarm reduction. The framework utilizes formal theory of perception and describes data fusion aiming to detect sensors and network failure (syntactic and semantic data validation) and occurrence of wildfire phenomenon. The system is also interesting, because it is entirely based on software agent's architecture. Software agents and intelligent software agents are responsible for everything from image and data collection to final wildfire recognition.

Integration of wildfire surveillance and monitoring systems with GIS

GIS can be of great benefit for wildfire surveillance, regardless of whether it is used in the phase before, during or after the wildfire (pre-fire, fire and post-fire). Geographic position of wildfire, as well as the time of ignition, is of vital importance in many aspects of human and material safety.
In the 'pre-fire phase' GIS could be used to calculate the probability of fire occurrence. Wildfire risk index is a numerical indicator that defines the level of fire risk and as such is associated with a certain geographic area. For this reason, GIS is the right tool that could be used to develop advanced wildfire risk models. We have developed a site-specific wildfire risk index (SWRI) that is focused on the micro-location and based on climatological and meteorological parameters, vegetation, terrain configuration and anthropogenic parameters (Bugarić *et al*., 2014).
SWRI could be quite useful in wildfire surveillance systems, particularly in its automatic mode for more successful wildfire detection. An example is recent work of Bugarić *et al*. (Bugarić *et al*., 2014) where it was shown how any existing smoke detection methods could be improved by the automatic adaptation of smoke detection parameters based on SWRI. Almost every existing smoke detection method depends on various detection parameters that could be manually edited and change to adapt the algorithm and particularly its sensitivity, on the current weather situation. Normally this is a job of system operators, but in practice we could encounter that operators are not very keen to interact with detection procedure and change parameters. One of the possible solutions is automatic adaptation of smoke detection parameters. In our approach it was based on GIS and Augmented Reality (AR). GIS was used for calculation of SWRI and augmented reality scene calibration. The idea was to find link between real world scene and digital elevation model based on GIS. Then the calculated SWRI map in GIS could be transformed to word scene as Fig 3 shows and applied for adaptation of detection parameters. On all those image parts where fire risk index is high the detection algorithm sensitivity will be also higher and vice versa where there is small fire risk index, for example on river parts the algorithm sensitivity could be lowered to zero.

Figure 3. Original image of detection area and synthetic AR image of the same view with superimposed site-specific wildfire risk index

Augmented Reality based mixing of real images and GIS produced data could be used not only for automatic adjustment of motion detection sensitivity, but also to selective blurring of input images based on point distance from the camera, definition of the minimal candidate region size and dynamics analysis based on detected region growth.

Augmented reality in combination with GIS could be useful in manual mode of wildfire surveillance and monitoring systems as well. The important fact is that these systems are geo-referenced, so for every pixel in the image the corresponding geo-coordinate is known and vice versa. Therefore, in manual mode, relevant GIS information such as toponyms, compass, geographic coordinates or altitudes could be presented on a real-time video stream. Another important capability of GIS, useful in the phase before the wildfire, is interpreting and visualizing the current weather conditions, such as wind speed and direction, temperature or humidity. These data could be of great importance in the case of organizing fire-fighting activities. Figure 4a shows an example of dynamic presentation of meteorological data where weather information is automatically and dynamically retrieved from a Croatian Meteorological and Hydrological weather server several times a day. Important is to note that this feature is of equal importance also in the fire phase when it is important to predict the future fire behavior.

Visibility of any point manually chosen on the map could be easily verified using simple trigonometry and Digital Elevation Models. Note that visibility maps and elevation profiles could also be generated using GIS, as this feature is suitable for better understanding of what is visible in the camera image. Another important feature that GIS systems provide is the determination of azimuth, elevation and field of view of the actual video camera viewing as Fig 4b shows.

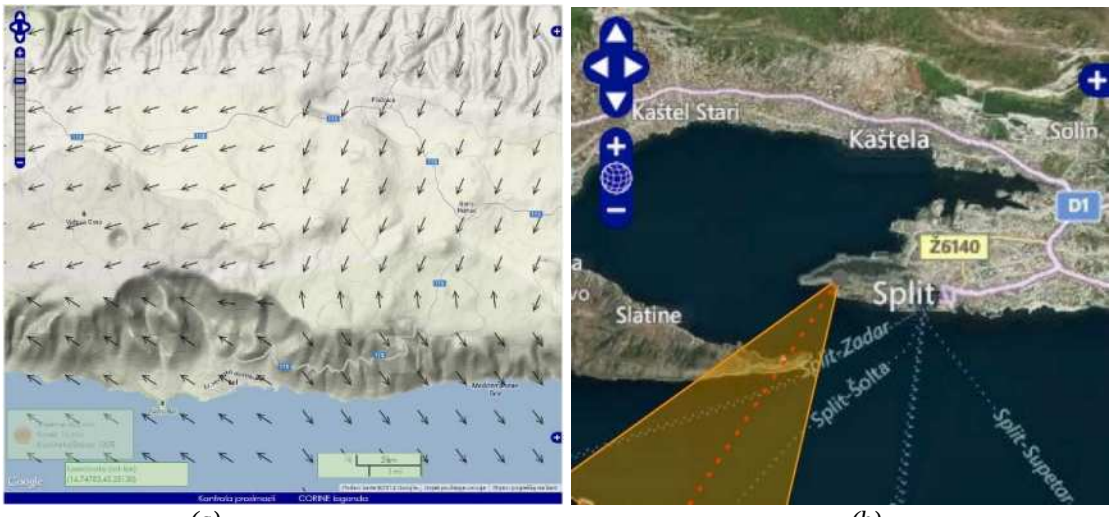

(a) *(b)*

Figure 4. a) Superposition of dynamic meteorological data on GIS maps and b) presentation of cameras azimuth and field of view on GIS map

When wildfire is spotted the 'fire phase' start. For wildfire damage minimization it is important to have a rapid and well-organized response. Apart from the information concerning the current weather conditions, knowledge about the wildfire features is equally important as it may affect the final outcome. These features include the time and geographic coordinates of the ignition, the way in which the wildfire spreads, real-time tracking of the fire front and the current location of fire-fighting units in the field.

After a successful detection of the wildfire, determining the ignition point and displaying it on the map could be done using 'alidade'-like devices such as Osborne Fire Finder or DragonPlot (Guth et.al., 2005). However, more advanced methods using vision based wildfire surveillance and GIS could be used. Almost all wildfire surveillance systems on the market have this ability, either as cameras azimuth ray intersection with digital elevation model, triangulation if few cameras could see the fire location or based as afore mentioned AR systems that we have developed (Bugarić *et al*., 2014). It has the ability to extract geographic coordinates by simply clicking on any pixel on real life image using AR based pre-calculated image templates where for every image pixel its corresponding lat-long-height coordinate is determined.

(a) *(b)*

Figure 5. a) Simulated wildfire spread shown on GIS map and b) superimposed in real time on real camera view using Augmented Reality methods

Wildfire propagation modeling and simulation is another feature for wildfire surveillance, useful in pre-fire and fire phase. Based on vegetation characteristics, landscape and meteorological conditions the future fire spread could be simulated in appropriate time steps. Fig 5a shows result on one such simulation for SE winds. In pre-fire phase it could be used for training and in fire phase for proper intervention planning and management. Augmented Reality could be used for superposition of fire spread simulation results on real life image as Fig 5b shows.

Synergy in wildfire observance networks

Aristotle coined that "The whole is more than the sum of its parts." This sentence was later used to describe the synergy, the effect that exists between parts of a system working together in a cooperative effort. Therefore, having a wildfire observance network of mutually connected individual wildfire observers working together in cooperation, could give the overall effect greater than the sum of their individual effects. Cooperation of individual wildfire observers could be used to improve automatic wildfire detection as well as to enhance manual camera PTZ control.

Let us suppose that we have a region covered by a network of wildfire observers and that certain part could be seen from three different observation points. The biggest problem in visual wildfire detection is still rather high false alarms rate, so any effort in order to minimize false alarm rate is welcomed. A

network of wildfire observers could be used for that, because it is unlikely to have a false alarm on the same location on all three observers units. If observers exchange information about alarms and their estimated locations a simple procedure could be used for additional false alarms reduction.
Also using the wildfire observer network the manual PTZ cameras control could be improved and simplified. An example is 'one click multiple cameras control' principle (Stipaničev et.al., 2009), (Stipaničev *et al*., 2011). One click means that all cameras covering the same region could be controlled by simple click on the map. The system automatically calculate the target point visibility from various observation points and appropriate cameras pan and tilt movements for all those cameras that could see the selected location.

Conclusion

In the future we could expect more and more wildfires, therefore in countries where wildfire risk is high, a lot of time and money is spent to minimize the wildfire effects. Maybe it is difficult to drastically reduce the number of fire ignitions, but the damage could be minimized by early wildfire detection and quick and appropriate intervention. Early wildfire detection is usually organized as a wildfire surveillance service and today this service is more and more based on application of modern ICT technologies, particularly new sensors, processing units, algorithms and calculation procedures. In this paper our focus was on automatic wildfire surveillance systems. They have evolved a lot in the last few years. More and more sophisticated algorithms for wildfire smoke and fire detection were developed, fusion of video detection in various electromagnetic ranges and fusion of video detections with other sensor types are today used, as well as close integration of wildfire surveillance and monitoring and systems with GIS, resulting in new features in both fire detection and distant video presence modes. Last but not least we have discussed a synergy effect of wildfire observer network consisting of mutually connected individual wildfire observers working together in cooperation. Although a lot of new wildfire surveillance systems has been developed and applied in various regions our opinion is that in the future we should expect even greater achievements in automatic wildfire surveillance systems development and implementation. Today human wildfire observers are still dominant (Matthews *et al*., 2010), but we are sure that high definition cameras, more advanced algorithms and powerful processing engines will improve automatic wildfire detection and reduce the difference between human and machine wildfire detection.

References

Ashi *et al*., 2013 Ashish A., Narwade, V., Chakkarwar, A. "Smoke Detection in Video for Early Warning Using Static and Dynamic Features." *Int. Journal of Research in Eng and Tech.* 02, no. 11: 610-614. 2013

Avgerinakis *et al*., 2012 Avgerinakis, K., Briassouli, A., Kompatsiaris, I. "Smoke Detection Using Temporal HOGHOF Descriptors and Energy Colour Statisrics from Video." *Proc. of the Int.l Workshop on Multi-Sensor Systems and Networks for Fire Detection and Management.* Antalya, Turkey, 2012

Brovko *et al*., 2013 Brovko, N., Bogush, R., Ablameyko, S. "moke detection algorithm for intelligent video surveillance system." *Computer Science Journal of Moldova* 21, no. 161) 2013): 142-156.

Bugarić *et al*., 2014 Bugarić, M., Jakovčević, T., D. Stipaničev, D. "Adaptive estimation of visual smoke detection parameters based on spatial data and fire risk index ." *Computer Vision and Image Understanding* 118 (2014): 184–196.

Bugarić *et al*., 2009 Bugarić, M., Jakovčević, T., D. Stipaničev, D. "Automatic Adjustment of Detection parameters in Forest Fire Video Monitoring System," *32nd Int. Conf. MIPRO 2009.* Opatija, 270-275.

Bugarić *et al*., 2013 Bugarić, M., Braović, M., Stipaničev, D. "Augmented reality based segmentation of outdoor landscape images," , Sept 2013, pp. 43–48." *8th International Symposium on in Image and Signal Processing and Analysis (ISPA).* 2013. 43-48.

Bugarić *et al*., 2014 Bugarić, M., Stipaničev, D., Šeric, Lj. "Statistical evaluation of micro-location wildfire risk index calculation for Adriatic regions." *VII Int. Conference on Forest Fire Research.* Coimbra, 2014.

Cappelini *et al*., 1989 Cappellini, V., Mattii, L., Mecocci, A. "An intelligent system for automatic fire detection in forests." *Third Int. Conference on Image Processing and its Applications.* 1989. 563-570.

Collins Bugarić *et al*., 1999 Collins, R. T., Lipton, A. J., Kanade, T. "A System for Video Surveillance and Monitoring." *8th Int. Topical Meeting on Robotics and Remote Systems.* Pisttsburgh, 1999.

De Dios *et al*., 2008 De Dios, J.R.M., Arrue, B.C., Ollero, A., Merino, L., Gómez- Rodríguez, F. "Computer vision techniques for forest fire perception." 26, no. 4 2008: 550–562.

Dedeoglu *et al*., 2005 Dedeoglu, Y., Töreyin, B., Güdükbay, U., Çetin, A.E. "Real-time fire and flame detection in video." *Proc. of IEEE Int. Conf. on Acoustics, Speech, and Signal Processing.* Phil, 669-672.

FireSense, 2010 Del.No.D4 – "Preliminary Report on User Requirements Identification and Analysis", FireSense Project, 2010, http://www.firesense.eu/ .

Genovese *et al*., 2011 Genovese, A., Labati, R.D. Piuri, V., Scotti, F. "Wildfire Smoke Detection Using Computational Intelligence Techniques." *IEEE International Conference on Computational Intelligence for Measurement Systems and Applications (CIMSA 2011),.* Ottawa, Canada, 2011. 1-6.

Guth *et al*., 2005 Guth, P.L., Vraven, T., Chester, T., O'Leary, Z., Shotwell, J. "Fire location from a single Osborne Firefinder and DEM." *ASPRS 2005 Annual Conference Geospatial Goes Global: From Your Neighborhood to the Whole Planet.* Baltimore, 2005.

Habiboglu *et al*., 2012 Habiboglu, Y. H., Gunay, O., Cetin, A. E. "Covariance matrix-based fire and flame detection method in video." *Machine Vision and Applications* 23, no. 6 (2012.): 1103-1113.

Habiboglu *et al*., 2011 Habiboglu, Y. H., Gunay, O., Cetin, A. E. "Real-Time Wildfire Detection Using Correlation Descriptors." *European Signal Processing Conference.* Barcelona, Spain, 2011.

Jakovčević *et al*., 2011 Jakovčević, T., Braović, M., Stipaničev, D., Krstinić, D. "Review of Wildfire Smoke Detection Techniques based on Visible Spectrum Video Analysis." *Proc. of International Symposium on Image and Signal Processing and Analysis.* Dubrovnik, Croatia, 2011. 480-484.

Jakovčević *et al*., 2011 Jakovčević, T., Stipaničev, D., Krstinić, D. "Visual context-based forest-fire smoke sensor." *Machine Vision and Applications* 24, no. 4 2013: 707-719.

Kührt *et al*., 2001 Kührt, E., Knollenberg, J., Mertens, V. "An automatic early warning system for forest fires." *Ann. Burns Fire Disasters* 14, no. 3 2001: 151-154.

Ko *et al*., 2001 Ko, B., Kwak, J., Nam, J. "Wildfire smoke detection using temporspatial features and random forest classifiers." *Optical Engineering* 51, no. 1 2012.

Kresek, 2007 Kresek, Ray. "History of the Osborne Firefinder ." 2007. http://www.nysforestrangers.com/archives/osborne%20firefinder%20by%20kresek.pdf .

Labati *et al*., 2013 Labati, R.D., Genovese, A., Piuri, V., Scotti, F. "Wildfire Smoke Detection using Computational Intelligence Techniques Enhanced with Syntetic Smoke plume Generation." *IEEE Trans. on Systems, Man, and Cybernetics* 43, no. 4 2013: 1003-1012.

Lee *et al*., 2012 Lee, C., Lin, C., Hong, C., Su, M. "Smoke Detection Using Spatial and Temporal Analyses." *int. Journal of Inovative Computing, Information and Control* 8, no. 7 2012.

Matthews *et al*., 2010 Matthews, S., Sullivan, A., Gould, J., Hurlay, R., Ellis, P., Larmour, J. "Evaluation of three fire detection systems." Bushfire Cooperative Research Center, Canberra, 2010, 82.

Park *et al*., 2013 Park, J., Ko, B., Nam, J. "Wildfire Smoke Detection Using Spatio Temporal Bag-of-Features of Smoke." *IEEE Workshop on Appl. of Computer Vision (WACV 2013).* Clearwater Beach, FL, USA, 2013.

Salah *et al*., 2011 Salah A. A., Han J., Pauwels E., de Zeeuw P. "Multimodal Monitoring of Cultural Heritage Sites and the FIRESENSE Project." *Proceedings of the 4th International Symposium on Applied Sciences in Biomedical and Communication Technologies.* 2011. 152:1-152-5.

Sekkas *et al*., 2010 Sekkas, O., Hadjiefthymiades, S., Zervas, E. "A Multi-level Data Fusion Approach for Early Fire Detection." *Proceedings of the 2010 International Conference on Intelligent Networking and Collaborative Systems INCOS '10.* Washington, 2010. 479-483.

Stipaničev *et al*., 2009 Stipaničev, D., Bugarić, M., Bodrožić, Lj. "Integration of Forest Fire Video Monitoring System and Geographic Information System ." *Proc. of 51st Int. Symp. ELMAR 2009.* Zadar, 2009. 49-52.

Stipaničev *et al*., 2010 Stipaničev, D., Štula, M., Krstinić, D., Šerić, Lj. jakovčević, T. M.Bugarić,. "Advanced automatic wildfire surveillance and monitoring network." *VI International Conference on Forest Fire Research.* Coimbra, 2010.

Stipaničev *et al*., 2011 Stipaničev, D., Bugarić, M., Šeric, Lj., Jakovčević, T. "Web GIS Technologies in Advanced Cloud Computing Based Wildfire Monitoring System." *5th International Wildland Fire Conference WILDFIRE 2011.* Sun City, 2011.

Surit *et al*., 2011 Surit, S., Chatwiriya, W. "Forest Fire Smoke Detection in Video Based on Digital Image Processing Approach with Static and Dynamic Characteristics Analysis." *First ACIS/JNU International Conference on Computers, Networks, Systems and Industrial Engineering CNSI*, 2011.

Šerić *et al*., 2011 Šerić, Lj., Stipaničev, D., Štula, M. "Observer network and forest fire detection." *Information Fusion* 12, no. 3 2011: 160-175.

Štula *et al*., 2011 Štula, M., Stipaničev, D., Šerić, Lj., Krstinić, D. "Fuzzy Cognitive Map for decision support in image post-processing." *Proc. of IWSSIP 2011.* Sarajevo, 2011. 311-314.

Torabnezhad *et al*., 2013 Torabnezhad M., Aghagolzadeh A., HadiSeyedarabi H. "Visible and IR image fusion algorithm for short range smoke detection." *First RSI/ISM International Conference on Robotics and Mechatronics ICRoM.* 2013. 38-42.

Toreyin, 2013 Toreyin, B. U. "Fire detection algorithms using multimodal signal and image analysis." 2009.

Verstock *et al*., 2012 Verstockt S., Poppe C., Van Hoecke S., Hollemeersch C., Merci B., Sette B., Lambert P., Van de Walle R. "Silhouette-based multi-sensor smoke detection." *Machine Vision and Applications* 23, no. 6 2012: 1243-1262.

Verstock *et al*., 2010 Verstockt S., Vanoosthuyse A., Van Hoecke S., Lambert P., Van De Walle R. "Multi-sensor Fire Detection by Fusing Visual and Non-visual Flame Features." *Proceedings of the 4th International Conference on Image and Signal Processing.* 2010. 333-341.

Vipin, 2012 Vipin, V. "Image Processing Based Forest Fire Detection." *Int. Journal of Emerging Technology and Advanced Engineering* 2, no. 2 2012.

NITROFIREX: Existing technologies and nighttime aerial firefighting solutions.

Luis M. Bordallo, Alexander Burwitz

NITROFIREX S.L. C/ Islas Baleares 4 Santiago De La Ribera (30720) Murcia Spain.
luisbordallo@nitrofirex.com / alexander.burwitz@nitrofirex.com

Abstract
The maturity of the technologies for the guidance and control of UASs allows proposing innovative operational options such as the ability to spray (a liquid) or spread (a powder) a significant amount of an agent of any sort at a pre-established point in the atmosphere.
This is the case of NITROFIREX, an innovative Spanish project that integrates available technologies from the defense industry to achieve this operational capability

Keywords*: nighttime aerial fire fighting, new technologies, UAS, launcher aircraft, autonomous gliders containers, risky operation, operative and economical efficiency*

Introduction

It may be the controversial climate change or perhaps human pressure on the natural environment but the fact is that, year after year, alarming reports of devastating forest fires monopolize the media. The past summer of 2012 saw how catastrophic fires razed through the U.S.A., Portugal, Canada and especially Spain and in previous summers how Russia, Bolivia, Israel, California, Australia or Greece stood by helplessly before the devastation of their natural heritage. In the coming years, and this is unfortunately more than likely, we shall have to continue suffering from this modern plague that is ravaging our forests.
In facing this bitter reality it is necessary to ask whether political, economic and technical levels are contributing in finding solutions, or at least methods to efficiently avoid and relieve these disasters. Unfortunately the answer is a very clear and definite negative.
According to estimates from the IPCC (Intergovernmental Panel on Climate Change) forest fires create at least 20 % of all CO2 projected into the atmosphere annually. On the other hand, all the activity of commercial aviation worldwide causes only 2 % of all the emission.
For example, the European project CLEANSKY has a budget estimated at 1.600 millions of Euros in order to obtain a higher efficiency of engines, the employment of biofuels, intelligent wings and the reduction of weight, etc. Paradoxically, very little technological effort is being put into research regarding the elimination or the reduction of the 14-20% emission of CO2 that results from wild fires and, above all, the lack of research into aerial fire extinction - the most versatile and effective method to fight fires.
In the face of the social alarm, political upheaval and vast economic losses engendered by these wildfires, why is it that so few technical resources are available to fight these fires with the greatest efficiency possible? Why, for example, having at our finger tips technology that literally allows us to place a guided bomb carrying 200 or 300 kilos of explosives and fired from a warplane some dozens of miles away through a window (see photo below)… why can't we use the same technology to drop, throughout the night, loads of 2,000 to 3,000 litres of water continuously over a burning forest?

Figure 1

Why is it that an aeronautical sector, which internationally moves thousands of millions of $/€, is still confined to using methods, techniques and procedures developed some 60 years ago in extreme high risk operations for their crews? Why not integrate available technology and develop the capacity to drop more fire extinguishing agents in less time, but above all, to be able to do so at night. Have we forgotten that the inability to fly at night is the greatest operative lack in present day fire fighting?

State of the art

The fixed-wing aircraft employed to combat wildfires at present are principally slow-moving turboprops and the majority are planes used exclusively for the job. In isolation and in numerous high-risk operations for crews they visually discharge their loads only between sunrise and sunset.
Apart from the fact that the power plants have changed from piston to turbo, few other technical advances have been applied to the fire fighting fleets since the Second World War. And yet, as we have seen in other fields of aeronautics, the progress has been spectacular.
There is a great concern at the business and academic level to provide answers to the challenge of extinguishing forest fires. In the last decade several solutions have appeared. A good example is the use of huge transport aircraft such as the B-747 Jumbo or DC-10 aircraft, employed by the American Company Evergreen (http://www.evergreen.com), because of their capacity to drop far greater loads of extinguishing agents.
Obviously these aircraft are able to discharge vast amounts of extinguishing agent, but because of their lack of manoeuvrability at low altitudes, their scope of action is greatly reduced. Their excessive length of reaction time and high operational costs render them non-effective in 'first line attack' on the fire. They only become effective once the fire has reached huge dimensions.
But, above all, the use of these big aircraft offers no solutions to nocturnal fire fighting due to their inability to operate visually at night and at low altitude.
Another project also aimed at changing methods and techniques of aerial wildfire fighting is the Precision Container Air Delivery System (PCADS). Supported by Boeing and Weyerhaeuser their method consists of launching, by means of parachutes with no guides of any type, via the rear ramp of heavy-duty transport aircraft a series of biodegradable cubic containers with a capacity of 250 gallons (some 950 litres) each of extinguishing agent from about 500 feet AGL. Once in the air and at about 200 feet AGL these containers open and scatter their cargo over the fire. (web: http://www.flexiblealternatives.com/products/pcads). A similar system is the Israeli Caylym Guardian Deployment System (http://www.caylym.com/the-guardian/). In this case the containers are launched at some 1.500 feet AGL.

The precision of the drop point achieved by a parachute without any form of guidance in an adverse atmospheric environment caused by wind, turbulence and the thermal currents produced by the on-going wildfire, does not appear to be sufficient enough to produce a coordinated and efficient action of extinction. At the same time this concept entails that all the solid components, although biodegradable, will be spread all over the fire zone. It doesn't either permit night-time operation due to the low altitude demanded by the operation.
Another method proposed by Boing is that of using 'water bombs' (bomblets), a type of biodegradable dodecahedra shaped container filled with 50lbs of water (23litres). Using path-calculating systems, 2800 of these 'bomblets' would be launched via the rear ramp of a C-17 from between 1.000 to 2000 feet above the fire to drop freely, with no form of guidance whatsoever. (web:http://www.boeing.com/news/frontiers/archive/2003/august/i_ids4.html).
Assuming that the path calculating systems allow sufficient precision to allow the drop to occur within the designated zone, this would still imply that the impact of the bomblets, dropping at great speed in free fall onto the ground would in the first place result in a high risk factor for ground crews, people and possessions in the fire area. Secondly, the water would on impact extinguish some of the fire but the effect would not be optimal since the always desired atomisation of the water never occurs, therefore the amount of energy absorbed is highly reduced, implying a big reduction in the extinguishing effect.
This concept, as with the two previous ones, is also not applicable to night-time operations because of low altitude flying. Should the altitude be raised to a 'safe altitude' the precision of the drops would decrease and the risk factor increases because of the higher speed at impact of the 'water bombs'.

The NITROFIREX concept

The developing technologies in the control and guiding of UAV's allow for the development of innovative operational options such as the possibility of 'spraying' (a liquid) or 'scattering' (a powdered solid) an important amount of extinguishing agent from a programmed point in the atmosphere.
This is the case of NITROFIREX, an innovative project that integrates the industrial technologies of the Defence Force in order to attain an operative capability that could be applied in the battle against wildfires, to combat against an atomic, chemical or biological emergency, to operate with meteorological phenomena (inducing rain, avoiding hail, dissipating fogs), to fight against plagues or to sow in remote or inaccessible regions and also the fumigation of drug plantations at night.
Discarding all these possible applications, and due to the ecological harm caused, the social alarm generated as well as the human and economic losses that they bring forth, the project that NITROFIREX is developing with maximum priority is the one to combat wildfires. For that very reason NITROFIREX is concentrating on its night-time operations as an indispensible and necessary complement to aerial means already in use during daytime.
Heavy transport planes will be responsible for moving great quantities of useful cargo (extinguishing agents in the case of wildfires) to the operative zone. These planes are designed to transport at great speed big quantities of cargo at a cost per unit far lower to that of a smaller plane.
This is the NITROFIREX proposal: Launcher Aircraft, LAs (the heavy transport aircraft equipped with a rear ramp) will be employed to transport the NITROFIREX Airborne Glider Containers, AGCs (already containing ±2.500 litres of payload) to the programmed drop zone. See figure number 1.
The LA will then launch the AGCs from the rear ramp in a programmed sequence and immediately return to the operation base. Once released, the AGCs will automatically home in onto their programmed target area within the drop zone and, with great accuracy, drop their load in the core of the fire. Once the drop of the fire-extinguishing agent on the fire has taken place, these containers return to base performing an "escape" manoeuvre from the danger zone by taking advantage of the great and sudden loss of weight as well as the extra speed.

Figure 2

Then the empty NITROFIREX AGC begins its autonomous return to the operations base of the launcher aircraft where it can be swiftly reused and loaded into the LA thus beginning a constant turnaround operation until sunrise.

The NITROFIREX Project

Although, as we have seen in the previous paragraph, the concept has a wide application, NITROFIREX is, first and foremost, a completely innovative project focused on night-time aerial wildfire fighting.
As we have seen, the main element used is the NITROFIREX AGC, launched at medium altitude (six to ten thousand feet), from the rear ramp of the cargo bay of a heavy transport aircraft, such as the C-130 Hercules, AN-12, KC-390, A400M, IL-76, C-17 or even aircraft with greater cargo capacity, which perform as the LA (launcher aircraft). These containers, loaded with a fire-extinguishing agent, are capable of gliding in their initial phase and are equipped with a guidance system (satellite, inertial and infrared). They fly automatically into the fire zone and drop their load, in sequence and with great accuracy, on the targeted area.

Figure 3

For safety, but also economic reasons, the NITROFIREX AGC's (Glider Containers) are recoverable. Once the drop of fire-extinguishing agent on the fire takes place, the NITROFIREX AGC performs an escape manoeuvre from the danger zone. Taking advantage of the great and sudden loss of weight as well as the surplus speed, the empty glider container is transformed, thanks to the activation of the small engine that propels it, into an UAV and returns autonomously to the operation base of the launcher aircraft where it can be swiftly reused.
In its guided bomb role the glider container flies no more than 90 seconds from the launcher aircraft to its target over the fire. When compared to a guided bomb, it carries a bigger payload and has more wing surface and but with an equal gliding and guide capacity. After concluding its 'escape' from the

target area and until it lands at the launcher aircraft's operation base, it navigates at night as a UAV at 1,000 feet above ground level and attains speeds of up to 70Kts.

Figure 4

By no means does NITROFIREX want to substitute current aerial means whose efficiency in daytime operations has been demonstrated over decades. The truth is that NITROFIREX aims to be their night-time counterpart in order to achieve H-24 aerial combat against wildfires (24 hour non-stop fighting) and to make use of, as the toiling ground crews well know, the better weather conditions that the night usually has to offer. In the following graphics one can analyse these advantages from:

1. The operative point of view (litres launched per hour of the operation),
2. The economic point of view (litres launched per hour and flight plus the cost of each litre launched)
3. The development of the NITROFIREX concept according to the type of AL used.

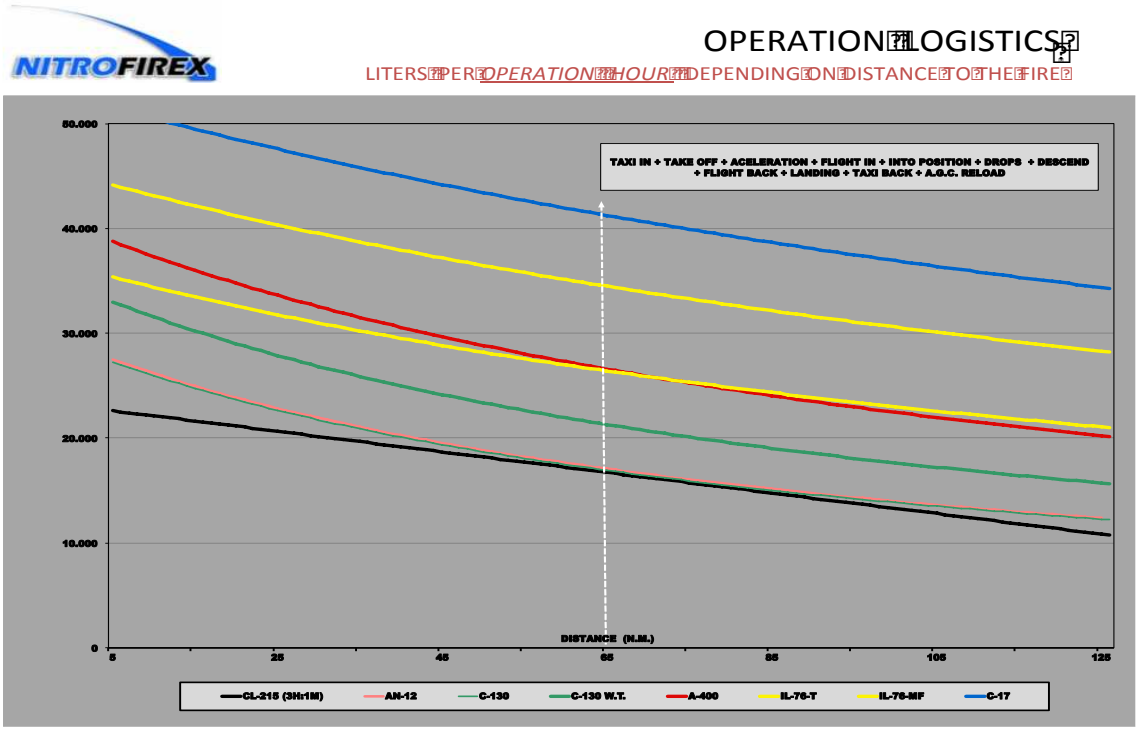

Figure 5

NITROFIREX

OPERATION LOGISTICS

DROPPED LITERS PER FLIGHT HOUR DEPENDING ON DISTANCE TO THE FIRE

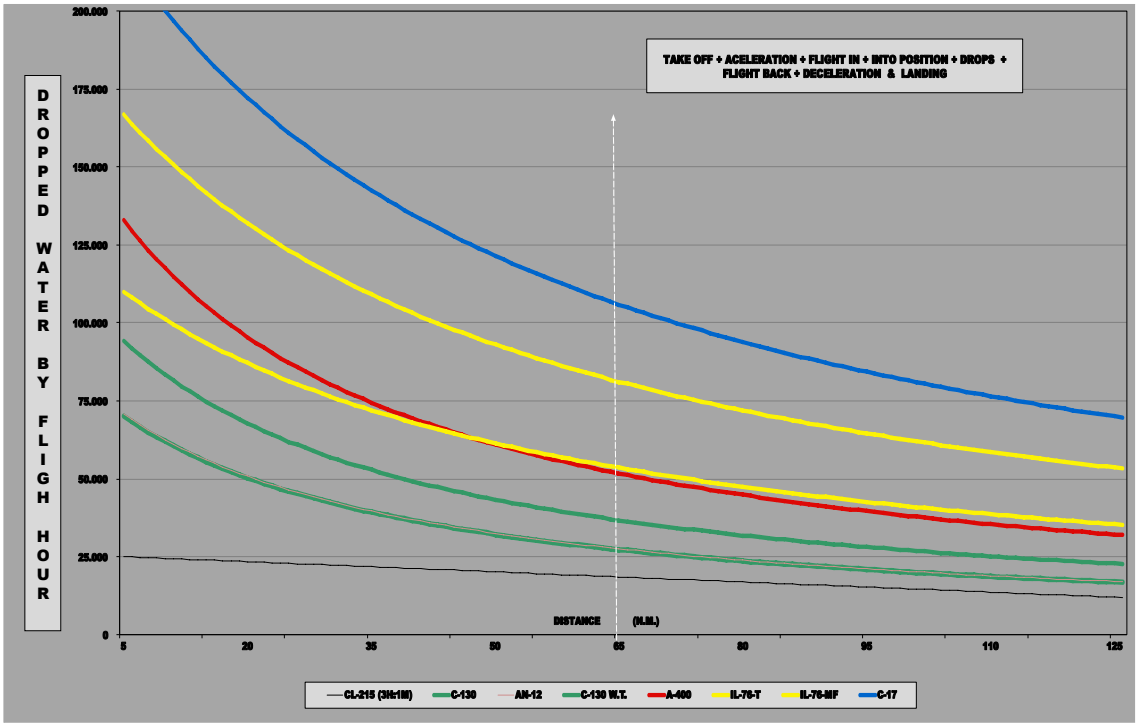

Figure 6

NITROFIREX

OPERATION LOGISTICS

DROPPED LITERS COST DEPENDING ON DISTANCE TO THE FIRE

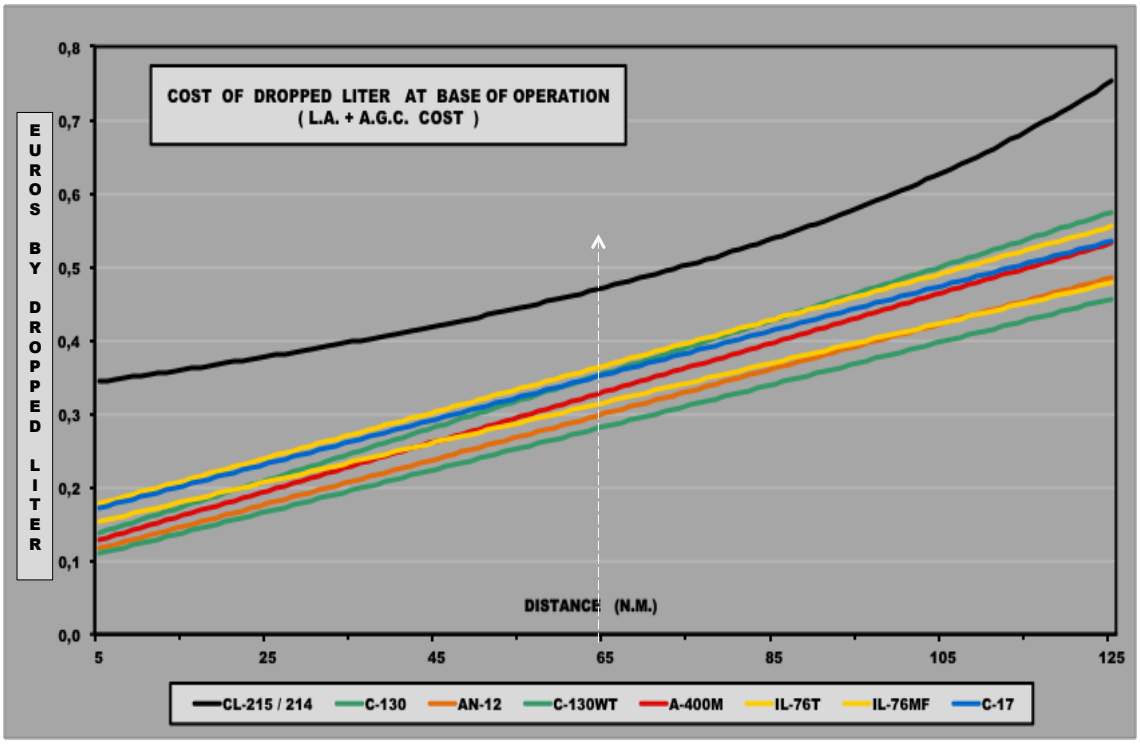

Figure 7

Operational model

Because of the great cargo capability and the increased deployment speed that the NITROFIREX LAs offer, a new operational model will have to be put into use. This will include a regional operational base that could be situated in a strategic site in accordance to the operations area.
Should a supranational operation come to be, the ideal base that would cover, for example, the Mediterranean Basin, would be Marseille in France or Olbia in Sardinia. Since the NITROFIREX operation is nocturnal, we can assure that under normal conditions, at least half a day would be needed to detach the LA to any airport in any country within the Basin.

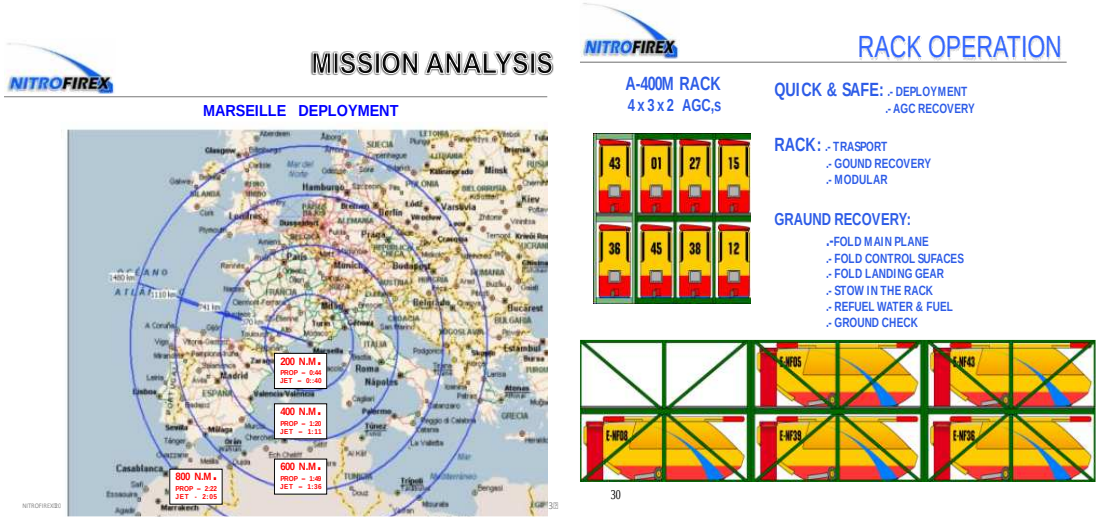

Figure 8

The NITROFIREX AGCs are transported from the regional operational base to the mission base (airport, air base or aerodrome closest to the fire). Two sets of empty NITROFIREX AGCs are stacked on two levels in a 'rack' or specifically designed shelving in the cargo hold of the LA. Later, during the mission this 'rack' will be used for the fast turn-around (pre-flight check, fuelling, loading of extinguishing agent and re-stacking) of the AGCs returning from the fire zone.
Once a wildfire alarm has been activated, the LA fly from their regional base to the detachment base, the airport closest to the fire, where the operation begins by downloading the rack of empty NITROFIREX AGCs and the rest of the necessary equipment so as to proceed with the final preparation. The first set of NITROFIREX AGCs (on the lower level of the 'rack') are filled with the extinguishing agent and are once again stacked in the LA leaving them ready for take off at dusk.
As night falls they fly to the fire zone and, coordinated by the ground teams who provide direct support, the LA begins launching the NITROFIREX AGCs in groups with a 90º 'angle off' to the fire front – the goal being that at the moment of leaving the LA the DPA's make a 90º turn, so that when the 4 or 6 NITROFIREX AGCs leave the LA they can form up in a trail formation and attack the fire. The extinguishing agent is dropped over the area preselected by the fire management officer. In order to maximize the extinguishing effect the drops are overlapped.
Once the first set of NITROFIREX AGCs have left the LA, it returns to base to load the second set of NITROFIREX AGCs so it can then return to the fire area in order to continue the attack on same fire or to attack more than one fire simultaneously. The NITROFIREX AGCs autonomously return to mission-base after each drop.

For example, one could consider an operation of an A-400 with a cargo capacity of 12 full DPA's. Flying to the mission-base with a 'rack' holding 24 empty containers, it starts operating at dusk and launches in each flight 12 containers filled with the extinguishing agent and rapidly returns to load the next 12. In the case of the A-400 the cargo load of each DPA would be 2,583 litres, which

means that a single flight of an A-400 would be approximately equivalent to 6 drops of the Canadair CL-215/415. At a distance of 120km (65 N.M.) between the mission base and the fire zone an A-400 can perform 9 flights in one night dropping 12 DPA's with each flight.
According to operative analyses done by NITROFIREX, and assuming the loading and stowage coefficients for the NITROFIREX AGCs, one can establish that having one LA and its two sets of NITROFIREX AGCs detached to a mission base within 120 km, the operation over the fire zone would be non-stop. The LA turn-around at mission base for loading the NITROFIREX AGCs would ensure a relentless dropping of water over the intended targets. See graphics number 4 and number 5.

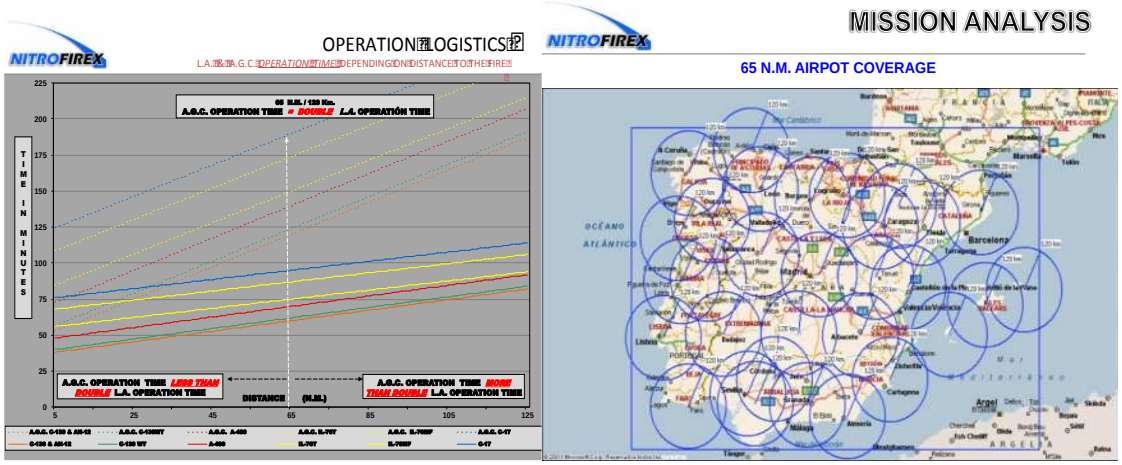

Figure 9

Drop optimization

Present day aerial resources used in fighting wildfires manually execute the drops of extinguishing agent directly over the fire, to either extinguish or to cool down the zone. So the effectiveness and efficiency of a drop depends on the pilot's, as well as the fire management officer's experience and ability.
If the drop is performed at an excessive height, the water is atomized by the fall and because of thermal convection it does not manage to reach the core of the fire thus greatly diminishing the effectiveness of the release. Conversely, if the release is excessively low the water reaches surface still compacted, without atomizing sufficiently. Here it evidently achieves some success but does not reach its full potential.
But if the drop is done at the ideal height most of the atomized water reaches the core of the fire. The maximum transfer of energy is obtained between the fire and the water. The resulting dowsing action of the water mass on the fire can be considered to be ideal.
Therefore we face the problem of drop optimization, which to date has not yet been studied. One has to find the exact point where, during the drop, water atomization allows water droplets of the smallest possible diameter to reach the fire surface, therefore favouring the heat exchange between the agent and the fire.
The fundamental factors for optimizing the release are the height above the ground and the speed of the aircraft/glider container at the point of water release. Relying on these two essential parameters, it is possible to optimize the minimal size of the drops landing on the ground depending on the desired launch strategy.
There are other parameters to be taken into consideration at the moment of optimizing the release. These are the diving angle at the moment of the release and the use of a thickener to change the surface tension of the water at the planned high-speed release from the glider containers so as to control the

minimum size of the droplets at the moment of the impact and thus obtaining a higher capability of penetrating the core of the fire.
In the NITROFIREX project the release from the NITROFIREX AGC will be completely automatic. The research on release parameters (height, speed, diving angle and surface tension) must be undertaken in order to obtain the maximum efficiency from the release.
The release of a considerable mass of water (thousands of litres) from an air vehicle (plane, helicopter or glider container) at a relatively high speed can be studied initially from a theoretical point of view as a problem of fluid dynamics in order to establish a mathematical model that will assist in establishing the ideal parameters of the release.
The idea consists of establishing a simplified model in order to optimize the operation. It is necessary to bear in mind that it is a question of a two-phase flow (air - water), turbulence and having different parameters within the same plume of water. These, the main parameters that determine the nature of the problem, are the dimensionless numbers of Reynolds (turbulence) and Weber (effects of the surface tension), which can be considered infinite to practical effects in the exit area or water door of the glider container.
The subject of the release can be split into several areas ranging from the NITROFIREX AGC to the ground. The first area can be considered of potential flow, just at the exit of the glider container. It is followed by an area where a primary atomization takes place, where droplets of the smallest diameter are obtained. An area starts then to configure where a Rayleigh-Taylor instability prevails after which an area comes forth where a secondary atomization takes place, where you can find droplets increasing in size due to the decrease in the speed of the water plume. Knowing parameters such as speed, height and dive angle, it is possible to estimate an average or statistical distribution of the size of the drops, therefore allowing to adjust this distribution so as to perform each release in the most effective way, under any given conditions.
The study for the optimization of the release is a process requiring both basic research in fluid mechanics and applied research that could also be of great help in improving conventional means of operation.

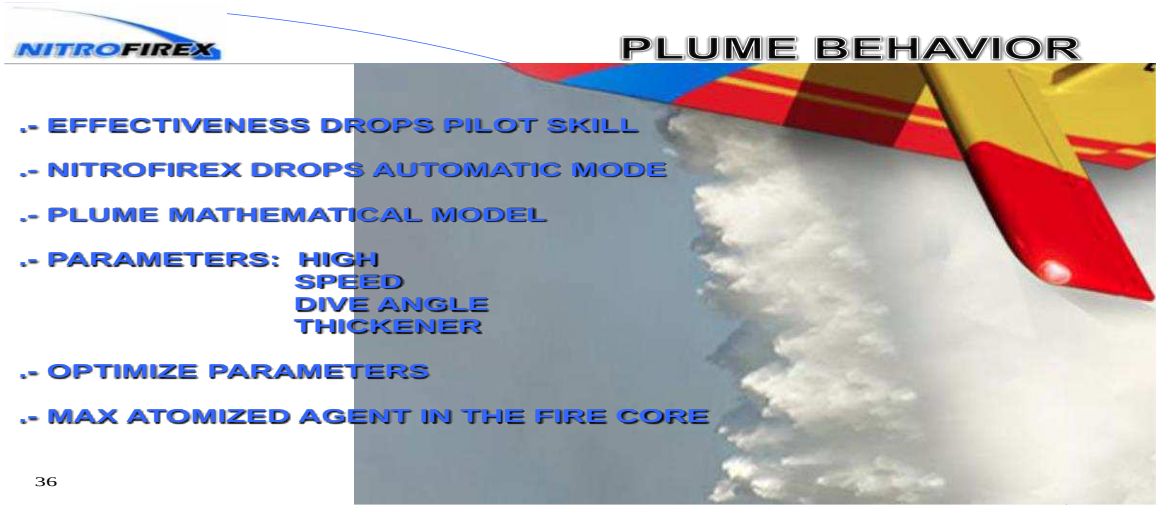

Figure 10

Coordination and safety

Those dedicated to aerial fire fighting know the importance of ground/air coordination to ensure an efficient and safe operation. With this objective in mind NITROFIREX proposes the implementation of new operative protocols and rules of communication with ground crews that are needed to adapt to the requirements of this project.

It should be the fire management officer who maintains radio contact with the LAs and the mission-base to coordinate the whole operation, principally the waiting points of the LAs as well as the approach routes and drop points of the NITROFIREX AGCs.
At night it becomes very important that the ground crews can see the approach and the drop from the NITROFIREX AGCs. For that reason, apart from the standard lights of all aerial vehicles (navigation, beacon, strobe and logo lights), the NITROFIREX AGCs are equipped with lights illuminating the fuselage as well as powerful headlamps. These headlamps are aimed forwards so that ground crews will be able to see them in the far distance and calculate the speed of approach to the drop point. So, ground crews will be able to very clearly see the approach, the actual drop and its effect on the fire as well as the NITROFIREX AGCs departure from the drop point.
In any type of aerial operation safety is of primordial importance at the time of planning, something NITROFIREX is not indifferent to. Consequently the NITROFIREX AGCs in their approach to the drop as well as in the recovery phase to mission base will have their flight parameters programmed and will accomplish them automatically and autonomously. But the safety concept of 'a man in a loop', in the case of having to abort the drop or reprogram the recuperation route, has been considered fundamental for the safety of the operation.
Therefore, during the approach phase, the NITROFIREX AGCs will be capable of manually or automatically aborting their approach to the drop point, releasing their cargo at the abort point and then proceeding automatically into the escape and recovery phase. Should the flight trajectory deviate from the one established or an unexpected event occurs during the approach to the drop point and it becomes advisable not to continue, the abort can be manual, carried out by the NITROFIREX AGCs operators at mission-base or from the LA and decided by anyone of them or by the fire management officer. The NITROFIREX AGC can automatically abort if its flight path does not match with what had been programmed or if it approaches the ground and/or a non-desired location.
In any case, the NITROFIREX AGC never reaches the ground filled with extinguishing agents, because if any thing deviates from what was programmed the cargo is immediately released and it then moves into the recovery phase.
On the other hand, the return route of the NITROFIREX AGCs to mission base will be programmed for the night (they have all day to do it in), at 500ft or less and over uninhabited areas. Should, by chance, the NITROFIREX AGCs engine have a flameout or any other malfunction during the return it is equipped with a parachute and an airbag, which opens up automatically and that allows for a 'soft landing', minimizing any possible damage.

8. Technical regulations for the operation of UAV's

Today the great stumbling block in operating UAVs in purely civilian aerial operations is the lack of rules and regulations controlling the airspace where both manned and unmanned aircraft could operate. For promoting the development of such rules and regulations at an international level two basic kinds of operations have been established: VLOS and BVLOS.
VLOS are those UAVs that operate in 'Visual Line of Sight' conditions, that is to say that at all moments there is visual contact between the vehicle and the operator. The operator's responsibility is to avoid any situation that could endanger any other aerial vehicle (manned or unmanned) or persons or properties on the ground. International regulation of UAVs operating within VLOS is meant to be available by 2015 since no technical or regulatory drawbacks exist, the operator being solely responsible for the safety of the vehicle.
BVLOS are those UAVs that operate under conditions 'Beyond Visual Line Of Sight', that is to say that in given distances and altitudes required for its employment the operator loses sight of the vehicle whilst electronic control is still maintained. These UAVs tend to have a great range and normally require the same airspace and altitudes of operation of manned aircraft.

Therefore regulating BVLOS UAVs is more complex, entailing greater technical requirements that will be needed because of the new players involved. These players range from the UAV operator to the air traffic controllers as well as the pilots of the manned aircraft.
Logically NITROFIREX stands in the second group of UAVs that operate under conditions of 'Beyond Visual Line Of Sight'. But the airspace required by the NITROFIREX project is in fact minimal: A segregated airspace over of the fire would be used for an LA flying at an altitude no more of 6.000 feet and a distance of no more of 6NM in respect to the intended drop zone. The LA will launch the NITROFIREX AGCs that would need no more than 90 seconds with their filled tanks, and finally no more than an hour of navigation at an altitude of 500 feet between the fire and the mission base (the LA operating base).
What manned aircraft could be flying in the proposed zone? That is to say a zone at an altitude of 500 feet or less between a fire and the LA's mission base? It is for this very reason that a night-time operation is proposed, so that the regulations established could serve as a stepping stone for future operational regulations for UAVs in a civilian environment that need more flight time and airspace for manoeuvres.
Understanding the flight envelope proposed, and in context with the BVLOS regulatory authority, the profile of the NITROFIREX AGCs recovery as proposed by NITROFIREX should be the first to be regulated because the operational hours and the airspace required cannot affect manned traffic. This would serve the use of UAVs in a safe and secure manner within the civilian environment of the BVLOSs. At the same time, it may take advantage of using it as a 'launching pad' for future regular BVLOS operations in the upper layers of airspace where safety requirement and coordination are far superior owing to the altitudes and flight times needed for UAV operations.
In one word, if in a BVLOS operation the low altitude profile, as proposed by NITROFIREX, is not regulated and it will be extremely difficult to regulate profiles requiring higher altitudes and longer time spans.

9. The aeronautical industry and UAV's

In the emerging and promising world of UAV's, aeronautical businesses as well as different governments and organizations are vying for good places in this race for the civil & military market of the future that unmanned air vehicles can provide.
The aeronautical industry and her official organizations will participate in this race with different products and business initiatives. But, owing to the on going economic crisis and the lack of rules and regulations, the short and medium future of the UAV's in our country is a singular challenge.
In addition to the profound economic crisis in which we are at present immersed, the defence and social security budgets are the first to be cut and readjusted. So, at the present moment, the UAV industry has to resort to ecological projects and appeal for social and political support to be able to support its participation in the development of the emergent world of unmanned aerial vehicles. The expensive and more complex projects must wait for better times.
Regarding past circumstances and now facing actual circumstances, the approach should be to find low cost projects operating in 'marginal airspace' with the purpose of keeping the regulatory bodies to a minimum.
The NITROFIREX Project entails all the previously mentioned connotations. As an air vehicle, it must obviously fly –both in the glider phase as well as in the UAV phase. Of course the NITROFIREX AGC must be able to navigate and release its cargo as programmed. One could propose an aircraft or a high performance aerodynamic vehicle or high performance aeronautic vehicle that would be evaluated, developed and whose final cost would never reach that of other projects with more demanding technical and operative objectives.
In addition to, and taking into account present circumstances, it should be the responsibility of the organizations and businesses involved in the development of the UAV's to refer to the economic

losses, the political concern and the social fear that wild-fires generate, in order to obtain economic aid and above all political aid that a project of this nature needs for its development.
Given its relatively simple technique and minimum requirements when compared to the other UAV projects, the NITROFIREX project can and should be dealt with solely aeronautical industry, instead of having to resort to complex and problematical international alliances. In these difficult times this would allow companies to find a niche in the complex and competitive world of unmanned aerial vehicles, serving at the same time as a launching pad for the aeronautical industry to find a good position within the UAV world by the time the civil employment of these vehicles becomes standard.
NITROFIREX has been presented in Madrid at the Spanish summit of unmanned vehicles, UNVEX-12 and at the Defence and Security Fair HOMSEC13. In both cases, great interest was shown amongst the official organizations (Spanish and European) as well as private businesses in this sector, especially regarding the exclusive and original approach on the operative and technical levels of the project.
During these two fairs it was obvious that the greater majority of UAV's are conceived for military or paramilitary employment. Consequently they are designed to transport technology composed of sensors and/or cameras with the object of obtaining and/or transmitting information. In order not to be detected or seen they are un-illuminated and are painted in discreet colours.
On the contrary the NITROFIREX AGCs are designed primarily for civil employment and conceived to spray/dust large quantities of non-technological substances at a programmed point of the atmosphere. In order to be seen by all involved in the operation they are illuminated (night flight) and painted in striking colours or marked by smoke generators (day flight).
Likewise, NITROFIREX's presentation at the International Aerial Fire Fighting Meeting in Aix en Provence (Marseille-France) April 2013 and in Sacramento March 2014 awoke enormous interest amongst the international aeronautic community for wildfire fighting. Our presence in the regulatory aspect brought us to give another speech in Eurocontrol in Brussels.
The importance and the concern of night-time fighting was obvious. The need to confront wildfires with security and efficiency is the great operational lack in of aerial means, a shortcoming and a total disregard for its importance!
The NITROFIREX Company has developed the conceptual phase of the project at its technical level as well as the operative and economic levels. It is now in the phase of consolidating the agreements between industrial/technological associates so as to confront the first phase of the construction of a concept demonstrator and subsequently the development of the Project.
The NITROFIREX concept is patented in those countries which have an economic and aeronautic capacity to face this type of project and who also have serious wildfire problems such as the USA, Canada, Australia, the Russian Federation and Europe (Spain, France, Italy, Germany England, Switzerland and Sweden). In addition, NITROFIREX is a member of the European organization EUROCAE and leads the work-group GW93. This group is responsible for editing the rules pertaining to the first phase, a phase that regulates UAS flights in non-segregated airspace in Europe.

10. **Conclusions**

It doesn't make sense that, well into the XXI century, at a time when ecology in all its aspects (climate change, CO2 emissions, deforestation, etc.) becomes a red hot topic on the political, social and economic levels, we've not bothered to integrate these demands in order to combat forest fires by night.
The use of an autonomously guided glider container, such as the one proposed in the NITROFIREX Project, allows for nocturnal aerial fire fighting operations, eliminates risks for crews and increases the accuracy and concentration of the releases. Besides all this, the amount of water dropped both per operating hour and per flight hour is increased with respect to the aerial methods currently used.
In addition, the launcher aircraft to be used are large military transport airlifters that are not single-role and they will continue performing cargo operations for the rest of the year once the summer forest fire

season is over. This will help bring down to a great extent the final flight-hour cost (considering acquisition amortization in addition to maintenance, personnel, etc.) for the part of operations performed on fire fighting, and ultimately the cost of each dispatched litre.
The new technologies have already been developed, matured and made available. It is only necessary to integrate them towards the objective that concerns and worries us. It is therefore up to the politicians and technicians in charge of the operation to accept the seriousness of the problem and to raise a new strategy against the ecological damage, the economic loss and the social alarm that forest fires produce. It is high time for the managerial and academic worlds to take on the challenge that an R&D project of this nature and relevance imposes.
The challenge consists in daring to develop this technological integration here and now with political decision, managerial initiative and technological drive.

Radiative properties of firefighters' protective clothing worn during forest fire operations

Alexis Marchand [a], Anthony Collin [a], Pascal Boulet [a], Zoubir Acem [a], Françis Magnolini [b], Hervé Charette [b], Marc Lepelletier [c], Yann Van Waelfelghem [c]

[a] *LEMTA, Université de Lorraine – 2 Avenue de la forêt de Haye – 54504 – Vandœuvre lès Nancy – France. alexis.marchand@univ-lorraine.fr*
[b] *SDIS 54 – 75, rue Lavoisier – 54710 – Ludres – France*
[c] *SDIS 85 – Les Oudairies – 85017 – La Roche sur Yon – France*

Abstract
The present work addresses the spectral radiative characterization of firefighters' jackets, which are the main component of their Personal Protective Equipments (PPE). During their tasks firefighters have to wear their PPE that must ensure simultaneously comfort, mobility and first and foremost thermal protection. Over time the nature and constituents of the firefighter's coats have strongly evolved. They were made up with leather for a long time, and are mainly designed in multiple-layer fabrics today. Given that, we can find many garments which overcome with one or several specifications in terms of comfort, thermal protection, heat dissipation, moisture barrier, mobility, weight … Numerous studies are found in the literature dedicated to one of these properties. None of the works related to their thermal performance considers the spectral radiative properties, however. Obviously, thermal protection is of primary importance and since firemen may be exposed to various heat threats, which present different spectral characteristics, it becomes also of prime interest to investigate the spectral radiative properties of these new products. To our best knowledge, the last study which referred to the spectral properties dates back to 1974 with the work by Quintiere [1] who provided the spectral radiative properties of several fabrics, within a relatively wide spectral range from 0.3 to 22 μm. The present study aims at investigating the spectral radiative properties of currently available fabrics used by French firefighters in the range from 0.25 to 16 μm covering both IR-Visible range.

Keywords*: Fire protective clothing, radiative properties, absorptivity*

Introduction

A standard fire intervention jacket (fig 1 (a)) is made of four layers (fig 1 (b)): a fire resistant outer layer in aramid (fig 2 (a)), a moisture barrier layer (fig 2 (b)) and a double inner layer for thermal barrier and comfort (fig 2 (c) and (d)). Our study is focused on the measurements of radiative properties of five fire intervention jackets provided by the Rescue Service Department of Meurthe et Moselle and of Vendée, France. Jacket #1 and #2 are blue, #3 is orange and #4 is gold. The fifth fire jacket is made of leather and is no more used in fire intervention in France since 2002.

Figure 1. Standard fire protective jacket (a). Samples of the different layers involved (b)

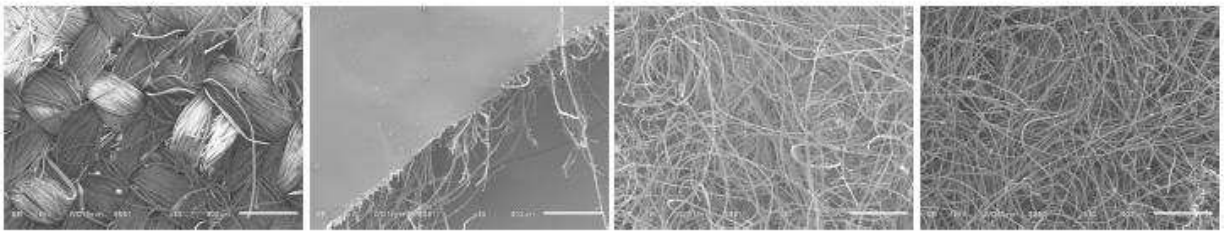

(a) *(b)* *(c)* *(d)*

Figure 2. The different layers of the jacket zoomed 50x (a) Outermost layer (b) Moisture barrier (c) Innermost layer #1 (d) Innermost layer #2

The experimental set-up used for the radiative property measurement was described in a previous study [2]. The radiative properties measured are the directional-hemispherical transmissivity τ_ν and directional-hemispherical reflectivity ρ_ν. These properties depend on the wavelength. Then, the spectral absorptivity α_ν is deduced from the radiative balance,

$$\rho_\upsilon + \tau_\upsilon + \alpha_\upsilon = 1$$

Directional-hemispherical transmissivity and reflectivity measurements were carried out in the visible-infrared range from 450 cm^{-1} to 25000 cm^{-1}. An FTIR spectrometer (Vertex 80 Bruker), an IR integrating sphere by Labsphere and an MCT detector by InfraRed Associates were used for the radiative properties in the IR range. In the visible range, a sphere from Labsphere and a spectrophotometer Cary 500 of Varian were used.
In the present study the homogeneity of the radiative properties was tested first. Then, a specific evaluation was conducted on the individual radiative properties of each layer of the fire intervention jacket #1. Finally, the effect of the fabric color and of the dyeing mode was evaluated, comparing the results for the different fire jackets.

Results

Repeatability test

Radiative properties may depend on the localization of the sample on the fire jacket. Three samples were selected from the jacket: on the front face, on the back face and on the jacket arm. The directional-hemispherical transmissivity, the directional-hemispherical reflectivity and the absorptivity for one fire jacket are presented in Figure 3, allowing to check for the homogeneity of the radiative properties on the jacket.

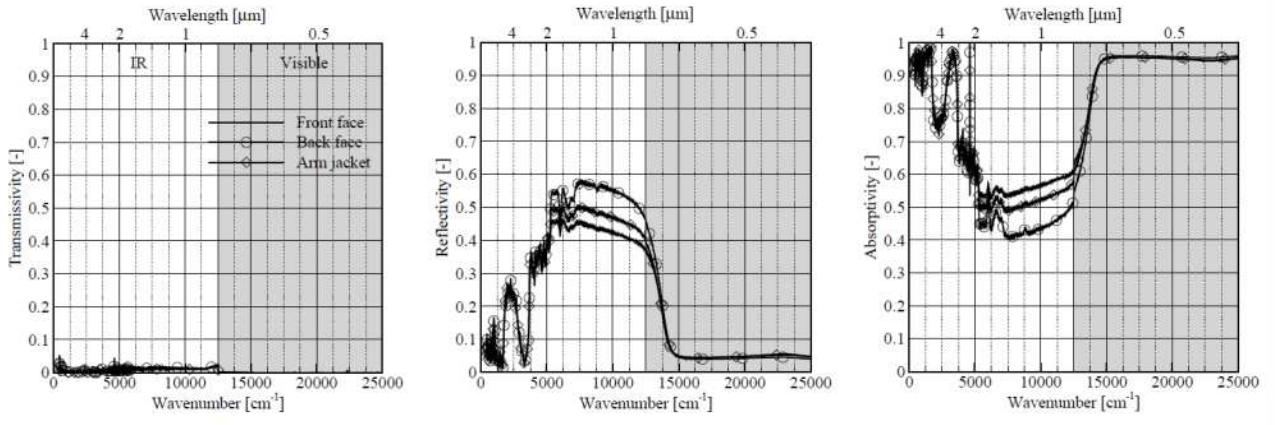

(a) Transmissivity *(b) Reflectivity* *(c) Absorptivity*

Figure 3. Radiative properties of three samples selected on the same fire jacket #1

Results reveal that the properties are quite similar for the three samples and that the radiative properties of the fire jacket are near homogeneous. It can be observed that the spectral transmissivity is quasi-null, whereas the spectral reflectivity can reach up to 55%. The average absorptivities over the whole spectral range are estimated to 80%. Consequently, no direct radiative transfer will occur through the jacket considering the zero transmission, but the high absorptivity will result in heat absorption which will be partly transferred from layer to layer through the jacket.

Radiative properties of the different layers

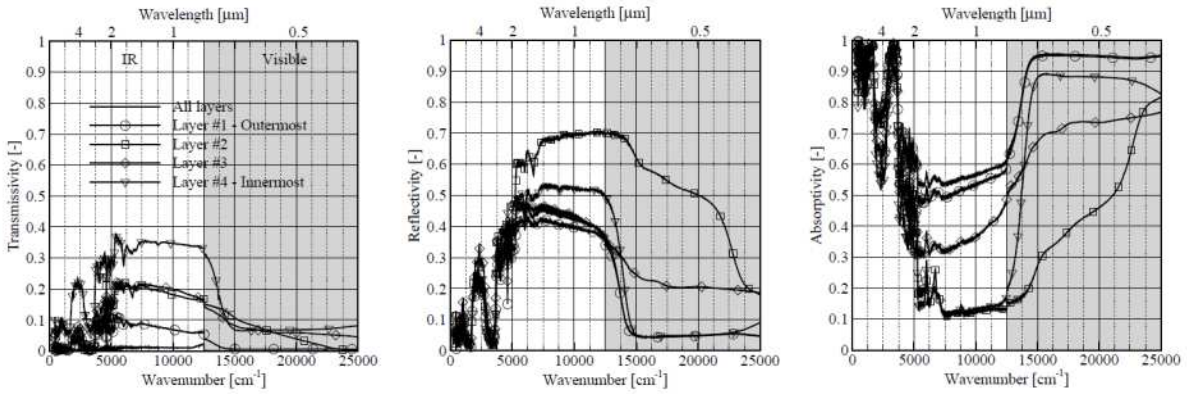

(a) Transmissivity *(b) Reflectivity* *(c) Absorptivity*

Figure 4. Radiative properties of different layers of the fire intervention jacket #1

The jacket #1 is made up with the 4 layers presented previously. Their respective radiative properties are presented in Figure 4 and compared with the complete jacket properties. The first observation is that each layer has a non zero transmissivity, but their product involved in the complete jacket finally results in a transmissivity equal to zero (fig 4 (a)). Note that the transmissivity of the outermost layer is too weak to allow significant multiple reflections inside the jacket. The reflectivity of the fire jacket is mainly due to the outermost layer (the curves of the reflectivity for this layer and the one of the complete jacket are superimposed in figure 4(b)). Strong variations of the absorptivity are observed as a function of the wavenumber (fig 4 (c)). The absorptivity is significantly lower for the inner layers, which results in a global behavior mainly influenced by the outermost layer, in particular in the infrared range. Globally, the radiative heat transfer through the fire intervention jacket is mainly controlled by the outermost layer.

Effect of the fabric color

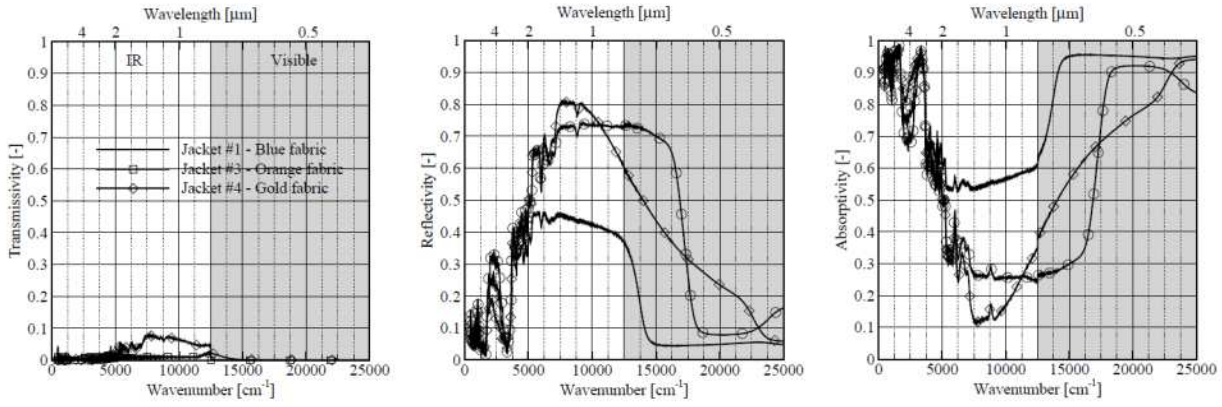

(a) Transmissivity *(b) Reflectivity* *(c) Absorptivity*

Figure 5. Comparison of radiative properties of different sample for a same fire jacket

Three different jackets (jacket #1, jacket #3 and jacket #4) with different colors (blue, orange and gold, respectively) have been tested in order to evaluate the impact of the fabric color.
Transmissivity values are still very low (fig 5 (a)) close to zero, except for jacket #4 for which values up to 9 % are obtained. The effect may due to the weaving mode which produces some little gaps between the polymer fibers, making the surface porous. The reflectivity is larger for the orange and gold jackets than for the blue one (fig 5(b)). Consequently, the spectral absorptivities of the orange and gold jackets are weaker than the one of Jacket #1(fig 5(c)). However, these discrepancies are mainly observed in the near IR and in the visible domain. They are very weak in the middle IR range, which results in close average values for all the jackets, since presented average values correspond to Planck's averaging performed for radiative sources with temperature in the range between 800 and 1400 K. A maximum absorptivity of 80% is finally found for the gold jacket, while a minimum value of 75% is obtained for the orange one. As a summary, the fabric color only slightly modifies the radiative properties in the spectral range concerned by radiative heat transfer and thermal protection.

2.4. Effect of dyeing

The dyeing is the process of adding color to the textile products. There are two dyeing modes involved in the fire intervention jacket manufacturing. The first consists in applying pigments during the polymer fiber production and then in weaving them to form the jacket. The second approach adds pigments after the jacket weaving.
Two different blue jackets (#1 and #2) with the two dyeing modes were compared (jacket #1 is a jacket dyed as a whole and jacket #2 is made of dyed fibers). Figure 6 presents the radiative properties for these jackets. The behavior of jacket #2 is close to be grey with an average absorptivity close to 90% (figure 6 (c)) while jacket #1 shows a weaker absorptivity, close to 80% in average.
Hence, the dyeing mode has a more important impact than the color itself, on the radiative properties of the jacket.

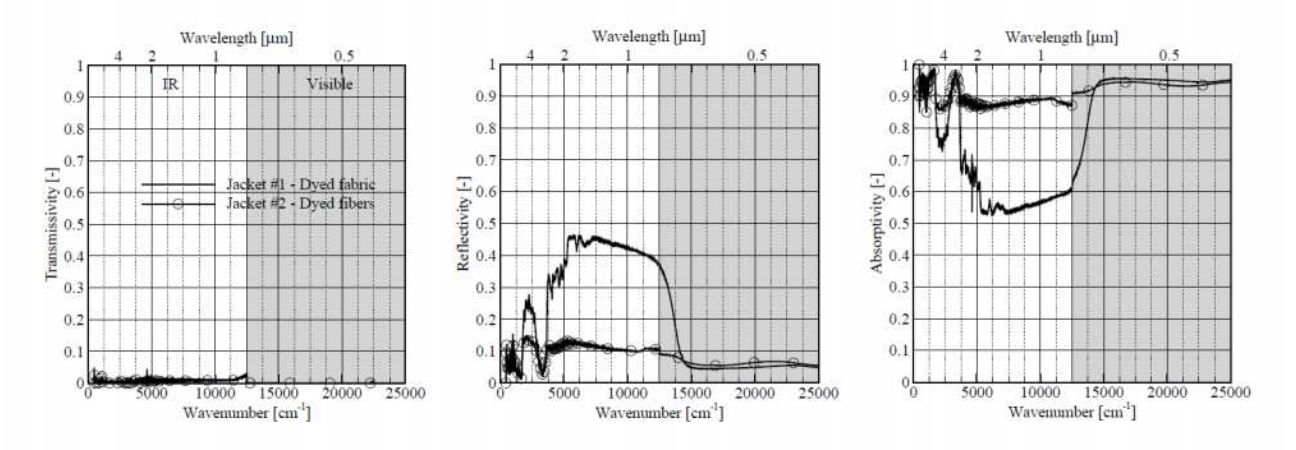

(a) Transmissivity *(b) Reflectivity* *(c) Absorptivity*

Figure 6. Radiative properties of different two jackets with different dyeing mode

3. Conclusions

Radiative properties were measured over the visible-IR range for different Personal Protection Equipments used by firefighters. Results show that fire protective clothings have a high spectral absorptivity in the IR range (between 80 and 90%). This is an important observation since the heat absorbed will be transferred through the jacket by conduction. The thermal protection improvement would require a decrease of the absorptivity, using layers with higher reflectivity. The effect of the

fabric color on the radiative properties is not significant. However dyeing mode of the jacket may have a more important effect: a weakest absorptivity is observed for a dyed fiber jacket.
Future work will be focused on the heat transfer between personal protection equipment and the skin of a firefighter.

References

[1] J. Quintiere, Radiative Characteristics of Fire Fighters' Coat Fabrics, Fire Technology, Vol. 10 (2), pp. 153-161, 1974.

[2] A. Collin, A. Marchand, A. Kadi, Z. Acem, P. Boulet, J. Pageaux, S. Pinson, M. Lepelletier, Y. Van Waelfelghem, F. Magnolini and H. Charette. Study on visible-IR radiative properties of personal protective clothings worn during firefighting operations. Fire Safety Journal. Submitted. 2014.

Results of the R-20F Method for Measuring the Water Equivalence of the Isolation Effect of Foams Used in Fighting Forest Fires

Agoston Restas

National University of Public Service, Budapest, Hungary, Restas.Agoston@uni-nke.hu

Abstract
Introduction: Aerial firefighting is a very expensive solution; however bombing just pure water is not always enough to suppress the fires. In many cases retardants or special agents are added to water to increase efficiency, wetting it or creating foam. Methods: This research used dried pine wood pieces as samples. Samples were divided into different groups: not treated samples for giving the reference data or treated samples to ensure data for calculating the isolation effect of foam. During the experiment with a randomly chosen foam agent product a 3% foam solution was mixed. From this solution 6 – 9 – 12 expansion rate foams were generated. Samples were also provided with a metal ring to ensure the exact depth of water or foam blanket. Each sample was put in a special heat oven which ensured the permanent 35 kWm^{-2} heat fluxes and measured the different ignition time. Results and discussion: Experiment demonstrated that the ignition times in case of foams are longer than in case of same equivalent pure water. The longer ignition time of foams can be expressed by the pure water amount. Results say that the maximum rate of isolation effect in value of water equivalent is more than 2.3 but always significantly more than just pure water.

Keywords*: isolation effect, foam, water equivalence of isolation effect*

Introduction

Based on author's experience there is no objective method known for measuring the complex effect of the efficiency of foams while suppressing fires. The suppression potential of foams such as Class A foams specially used for structure or forest fires is measured by a special way; bonfires classified by international standards are extinguished by the foams and the potential is evaluated by the size of the bonfires. This method, measuring the active impact of foams is appropriate and accepted as international standards for structure fires.
The standard methods are not measuring the isolation effect of foams, however there were more initiatives regarding this topic (Boyd and Merzo, 1996; STP 2007 Standard Test Procedures). But each manufacturer characterizes their agent with the "*good*" isolation effect. The isolation effect is not an active action against the flame but passive influence of the ignition caused by the blanket covering the surface (Igishev and Portola, 1993; Salgado and Paz-Andrade, 2009).
Since there is no accepted method for measuring the isolation effect of foams, and each producer characterizes its own foam as having "*good*" isolation effect, it is required to develop a process which is objective, practical and ready to demonstrate the different isolation effects of the different type of foams.
To start with, the reference base to which the effect is evaluated and expressed in equivalent must be declared. Pure water is the most frequently used material for fire suppression that is why it was taken as base and the scale of equivalent.
As usual foam is characterised as having passive isolation effect but not as having the active extinguishing potential; this feature also can be very important during intervention, especially in case of forest fires using aerials. The added value of using foam for the fire suppression is not only isolation of the combustible material against heat radiation but it also plays an active role in suppression. If the quality or quantity of foam blanket is not suited for stopping the spread of fire it means that the consumed resources were ineffective, spending on aerials used was wasteful.

Methods

The method was developed in order to measure the extinguishing potential of foam blanket. This procedure following the below assumptions got a fantasy name and was called R-20F method. As usual foam is characterised as having passive isolation effect but not as having the active extinguish potential; however this feature also can be very important during intervention.

Prepare the process

Below is declared the main important things for preparing the test, and some basic process for being ready to measure the ignition time of samples.
Means required for the process:

1. Radiant heater: KAL VK1[1] - with 35 kWm^{-2} heating flux[2];
2. Samples with metal rings – 0,06m x 0,06m x 0,01m dried pine wood samples;
3. Pure water, temperature 293 K;
4. Foams , made from type EVAM[3] agent, 3% mixed rate solution, expenditure rate in series 6 – 9 – 12.

Special metal ring stacked to each sample in order to ensure the same thickness of foam blanket covering the samples. Ring is made of steel, with 0.06m diameter and 0.008m sheet thickness, in series of 2 – 3 – 4 – 5 mm ring height. Rings are fixed by heat resistant stove glue, purchased from the market.

Ignition time

During the experience three different ignition times were measured: A) It is necessary to measure the natural sample for getting the net ignition time; B) The measurement of the sample treated with water gives the reference base; C) The sample treated with foam is measured for the purposes of the test method.
Ignition time of natural sample: Natural sample with metal ring but without any surface treatment is needed to put in to the radiant heater and measured the ignition time. As usual, the space between the foam blanket and the heater is fix and have to ensure that the radiant heat fluxes is 35 kWm^{-2} continuously. At least 3 or more samples are needed for measuring the ignition times.
Ignition time of water treated sample: The effect of water's ignition delay relates to the ability of heat abstraction; it is used as a base, similar to the effect of foam's ignition delay. Ring on sample is needed to fill with 293 K temperature pure water by the volume of rings depending on the series. Sample is needed to put in to the radiant heater and measured the ignition time. As usual, the space between the rim of ring and the heater is fix and have to ensure that the radiant heat fluxes is 35 kWm^{-2} continuously. At least 3 or more samples are needed for measuring the ignition times, in series with 2 – 3 – 4 – 5 mm deep water column.
Ignition time of foam covered sample: From pure water and foam agent have to prepare a solution with 3% mix rate. From the solution different expansion rated foam is prepared in series 6 – 9 – 12. Ring on sample is needed to fill with foam by the volume of rings depending on the series. Sample is needed to put in to the radiant heater and measured the ignition time. The space between the rim of ring and the heater is fix and have to ensure that the radiant heat fluxes is 35 kWm^{-2} continuously. At least 3 or more samples are needed for measuring the ignition times, in series with 2 – 3 – 4 – 5 mm thick foam blanket.

[1] KAL VK1 radiant heater: produced by KALÓRIA Hőtechnikai Kft., H-1071 Budapest, Bethlen út 43 Hungary
[2] Certificated by Szent Istvan University, Ybl Miklos Department, Budapest
[3] Foam agent for universal applications in Hungary and neighbor countries, used also for fighting against forest fire; it is made by EVM Rt., H-1172 Budapest, Cinkotai út 26. Hungary.

The effect of foam is obviously influenced both by the structure made by air bulbs and the solution itself the foam contains (water and agent). Since the R-20F method focuses to measuring typically the isolation effect of foam, influence of the solution is needed to exclude. The effect of solution is taken away from the complex effect; it depends on the different quantity in series of the solution the foam contains. Since the extract rate is very low (3%) the effect of pure water and solution is taken equal.
Based on the measured data, it is required to calculate different parameters. For calculations and evaluating the measured value, notations and different mathematical formulas were used. Because of their complexity, formulas (F.x) can be found in the Appendix separated. These formulas marked in brackets signed in many places (text and tables) make the process of following easier.

Study for ignition time

This study contains only the extracted data meaning usually the average value of measured ignition time but in explanation deviations also mentioned. The whole study located in the author's archive.

Measured ignition times of different treated samples

The first test result used for this study for further calculation. The *Table 1* contains the average value of measured ignition time.

Table 1—Measured data of ignition time.

R-20F		No treatment	Blanket sample covered [mm]			
			2	3	4	5
		Ignition time [sec]				
Nature		19				
Water			108	-	-	-
Foam	Rexp6		45	51	58	60
	Rexp9		42	47	50	53
	Rexp12		36	44	46	44

Legend: Nature: samples without treatment
R_{exp}6/9/12: Expansion rate of foam used for series

Based on the measured data and mathematical formulas different calculations were made. The series of this calculation can be followed in Table 2, Table 3 and Table 4.

Net time of ignition delay

To evaluate the results different calculations were made. Firstly, the ignition delays of differently treated sample were measured; in case of no treatment (nature) *F.13*, water *F.14* and foam *F.16* figures meaning. These results can be evaluated as "net effect" of ignition delay of extinguishing material covering the samples. For the calculations *F.15* (water) and *F.17* (foam) formulas were used (*Table 2*).

Table 2—Net time of ignition delay

No	Height of the ring (F.1) h [mm]	Expansion rate of the foam (F.9) y [-]	Ignition time gross (F.14) (F.16) t [sec]	Ignition time nature (F.13) t [sec]	Ignition time net (F.15) (F.17) t [sec]
1.	2	0 (water)	108	19	89
2.		6	45	19	26
3.		9	42	19	23
4.		12	36	19	17
5.	3	0 (water)	153	19	134
6.		6	51	19	32
7.		9	47	19	28
8.		12	44	19	25
9.	4	0 (water)	197	19	178
10.		6	58	19	39
11.		9	50	19	31
12.		12	46	19	27
13.	5	0 (water)	242	19	223
14.		6	60	19	41
15.		9	53	19	34
16.		12	44	19	25

3.3. Foam's efficiency and expression by water equivalent

Secondly, the water content of the foam, expressed by water column happens (F.19). Logically samples covered with water also belong to this series (F.18). Thereafter the ignition delay of water, foam contains is calculated (F.21). Samples covered with water belong again to this series (F.20). Based on the *F.17* and *F.21* a coefficient created (F.23) expressed the relation between the ignition delay in case of same water quantity but different features (water-foam). As before, samples covered with water also belong to this series (F.15 and F.20) meaning the base to this calculation (F.22) and logically ratio always results *1* (*Table 3*).

Table 3—Coefficient of ignition delay

No	Height of the ring (F.1) h [mm]	Expansion rate of the foam (F.9) y [-]	Ignition time net (F.15) (F.17) t [sec]	Water content in water column height (F.18) (F.19) h [mm]	Ignition time of water quantity (F.20) (F.21) t [sec]	Coefficient of ignition delay (F.22) (F.23) Y [-]
1.	2	0 (water)	89	2	89	1
2.		6	26	0,333	14,8	1,76
3.		9	23	0,222	9,9	2,32
4.		12	17	0,167	7,4	2,3
5.	3	0 (water)	134	3	134	1
6.		6	32	0,5	22,3	1,43
7.		9	28	0,333	14,8	1,89
8.		12	25	0,25	11,2	2,23
9.	4	0 (water)	178	4	178	1
10.		6	39	0,667	29,7	1,3
11.		9	31	0,444	19,8	1,57
12.		12	27	0,333	14,8	1,82
13.	5	0 (water)	223	5	223	1
14.		6	41	0,833	37,2	1,1
15.		9	34	0,555	24,8	1,37
16.		12	25	0,417	18,6	1,34

Table 4—Foam's extra ignition delay and its expression by water equivalent

No	Height of ring (F.1) h[mm]	Expansion rate of the foam (F.9) y [-]	Coefficient of ignition delay (F.22) (F.23) Y [-]	Water content in water column height (F.18) (F.19) h [mm]	Water equivalent of ignition delay (F.24) (F.25) Z [mm]
1.	2	0 (water)	1	2	2
2.		6	1,76	0,333	0,586
3.		9	2,32	0,222	0,515
4.		12	2,3	0,167	0,384
5.	3	0 (water)	1	3	3
6.		6	1,43	0,5	0,715
7.		9	1,89	0,333	0,629
8.		12	2,23	0,25	0,558
9.	4	0 (water)	1	4	4
10.		6	1,3	0,667	0,867
11.		9	1,57	0,444	0,697
12.		12	1,82	0,333	0,606
13.	5	0 (water)	1	5	5
14.		6	1,1	0,833	0,916
15.		9	1,37	0,555	0,76
16.		12	1,34	0,417	0,559

Based on the coefficient (F.23) and water content (F.19) of the foam the ignition delay can be calculated expressed by the equivalent of water column (F.25). This equivalent means that water has *extra ignition delay effect* in case of foam formulas (*Table 4*).

Evaluation

As a first step, the ignition time of samples without treatment (nature) was measured. For the correct base nature samples were measured also during series. Precision of measuring ignition time was below *1* second. Based on 6 samples the average ignition time is 19 seconds with minimal deviation (+3/-2 seconds).
In the series, the samples covered with water were measured firstly. To make measurement more precise, the 2 mm high ring samples were filled with water using hypodermic syringe, to make the volume precise.

$$V = hA = h\frac{d^2\Pi}{4} = 2x10^{-3}m\frac{\left(60x10^{-3}m\right)^2 x3{,}14}{4} = 5{,}652x10^{-6}m^3 = 5{,}65cm^3$$

Based on five measures the average ignition time was 108 seconds, with +15/-18 seconds maximal deviation; the rate of deviation is not bigger than with natural samples.
The speciality of water series was that no more measures with precision could be carried out with higher ring on samples. Unfortunately the rings separated from the sample surface (3 mm) and causing some water leakage during tests spoiled the genuine process. The problem was identified as a minimal deformation of samples' surface caused by water and cement was not enough flexible to compensate the minimal gap. Therefore in case of 3-4-5 mm high ring there was no measured value only calculated in scale based on linear interpolation.
Due to the above, some results can be taken into account with due critical considerations; and additional test series are also required. But results were evaluated as a tendency rather than principle of each measured data.

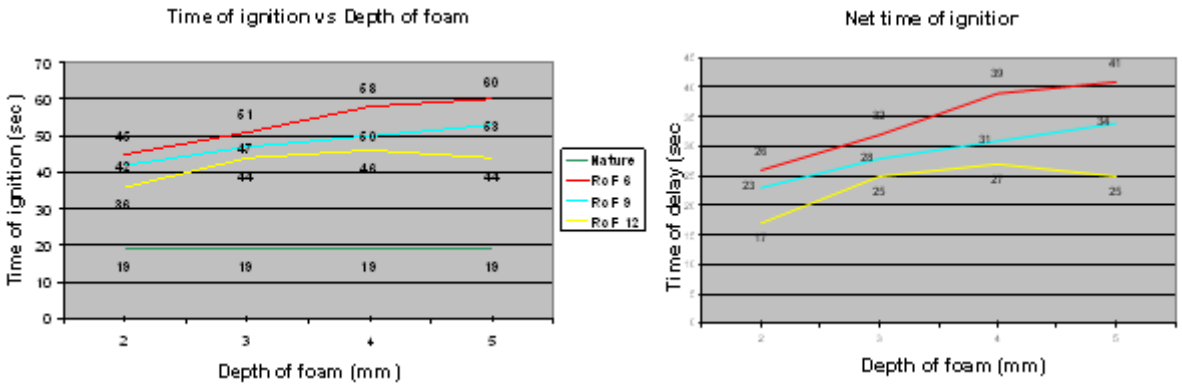

Figure 1. Time and Net time of Ignition versus Depth of foam

In the next series the different expansion rated foams were tested with different depth of blanket covering the samples. The same quantities of foam in each sample were assured by rings. The measured values are in the *Table 1* and *Figure 1* also shows values in the graphics. The graphics show not just the time of ignition but the tendency of the change hanging on the depth of foam covering samples.

The study focused on the inspection of how the ignition delay changed and what is the tendency of it hanging on the own quality of the foams. That is why the ignition time of not treated sample (nature) required subtracting from the ignition time of treated samples (water and foam). In this case the data shows the "net ignition time" of substances hanging on their own features (Figure 1). Based on measured data and graphics next conclusion were stated:

1. Rising the depth of foam covering samples the time of ignition delay also rise. Tendency yes, but exact data for rising characteristic was not established; more test needed.
2. Rising the depth of foam a special symptom, co-called "foam boiling" was observed. This symptom was more intensive during raising the depth of foam, especially in case of 5 mm foam blanket with high expansion rated foam (exp. rate = 12). It modified the result, obviously reduced the delay of ignition time.
3. Taking into account the symptom of foam boiling (see above) and the curve tendency of foams (expansion rate is 6 - 9, and depth of foam is 2-5 mm) the tendency more or less can be also linear.
4. Since the technical difficulties and the assumed rate for higher mistake this study didn't measure the 1 mm high ring samples, however the *Figure 2* generated the data by linear interpolation.

The effect of foam's ignition delay is aggregated by two different factors as below; the first counts with the quantity, the other with the quality:

Factor of quantity: Mechanical foam is made of special solution and air bulbs; solution consists of pure water and special foam agent. The mixture rate hangs on conditions intervention having; ratio is required usually between 0.1 – 6 %. During the study of R-20 method 3 % solution was used. Since the rate was relatively low and the heat capacity of the agent doesn't differ drastically from the water, the value of solution was taken equal to water. Obviously during the test radiation heat evaporated the solution meaning that its heat capacity influenced the ignition time, delayed it similarly to water.

Factor of quality: Foam has a special effect not just having water quantity. Isolation, the additional feature of foam is an extra effect. Fire fighters often use this isolation effect even if the practice does not know exactly what is it or with more precisions what the background of this effect is. Obviously the isolation effect often means defence against radiation heat but also separation between flammable liquid and oxygen. R-20F method focuses on the study of the extra effect caused by the special feature

of foam. The interest focuses not on the feature of foam but finding a common scale expressing this extra effect and measures these with water equivalent, understood by any fire fighter.
If the foam produces longer ignition delay than ignition delay belongs to its own water quantity, it means that this extra effect is caused by the special features the foam has.
In order to reduce the possibility of mistake during test, series started from 2 mm high covering. Value before it was rated logically. *Figure 2* left from the broken line shows the estimated value, right the measured except in case of water. Problem of water was mentioned above.
Based on the own water quantity of foam (F.7) the ignition delay belonged to it was determined by linear interpolation (F.9). Dividing the time of measured ignition delay to its own water quantity results a rate. If the value of this rate is more than *1* means that foam has extra delay effect (F.11).
Based on the R-20F study the analysis of measured data resulted that this rate is significantly always more than *1*. It means that foam has extra isolation effect than just the effect of its own water quantity.

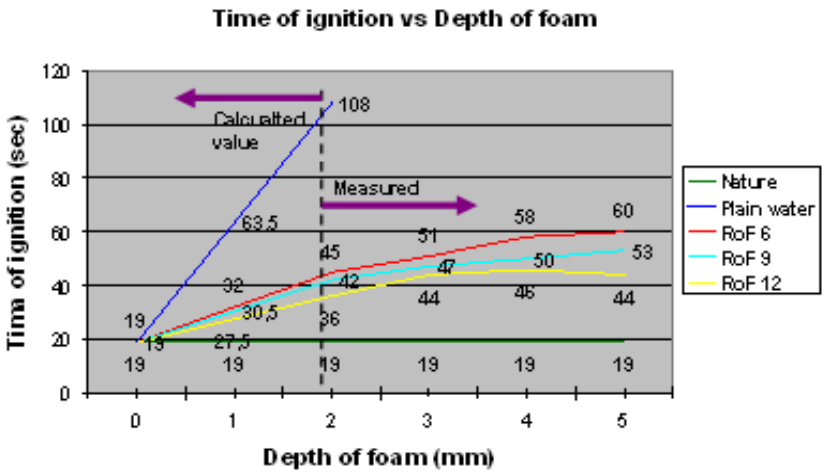

Figure 2. Measured and interpolated value of ignition time

The efficiency of foams with different features is represented in different functions as can be seen below:

1. Expansion rate on "x" axis and hanging on depth of foam efficiency shown in *Figure 3a*;
2. Depth of foam on "x" axis and hanging on expansion rate efficiency shown *Figure 3b*;
3. For better demonstration both diagram were made in 3 dimensional versions using belt diagrams *Figure 4a* and *Figure 4b*.

Based on experience during the test, calculations and graphics there are statements as can be seen below:

1. The efficiency of foam rises with raising the expenditure rate. The characteristic of this raise can't be surely stated; taking into account the deviations from the average, the near linear curve can't be excluded.
2. The efficiency of foam reduces with raising the thickness. The characteristic of this reduce can't be surely stated; taking into account the deviations from the average, the near linear curve here also can't be excluded (but logically in ideal circumstances it must be).
3. Relatively thin foam blanket but high expansion rate results in high efficiency.

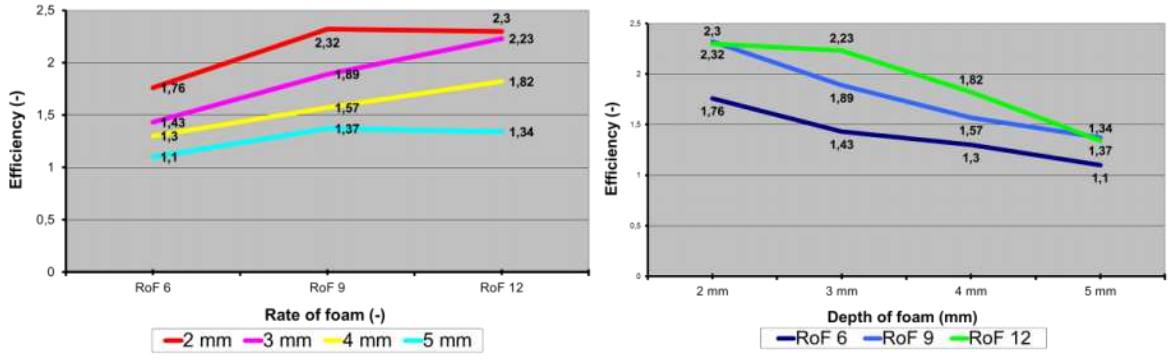

Figure 3. Efficiency versus rate of foam (a) and depth of foam (b)

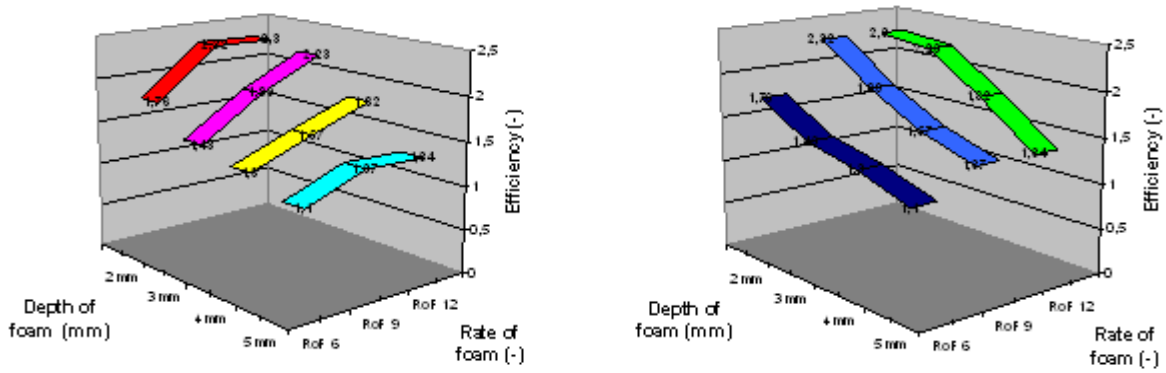

Figure 4. Efficiency versus rate of foam (a) and depth of foam (b); belt diagrams

After determining the efficiency of foams, R-20F method focuses on the expression of this extra effect by practical method; to be able to explain this extra effect also to fire fighters. Water equality as an easiest way can give the solution (F.25). The water equality of foam with its own water quantity can be also demonstrated in a function shown by *Figure 5*. The difference between values in vertical shows also the extra ignition delay effect of foam.

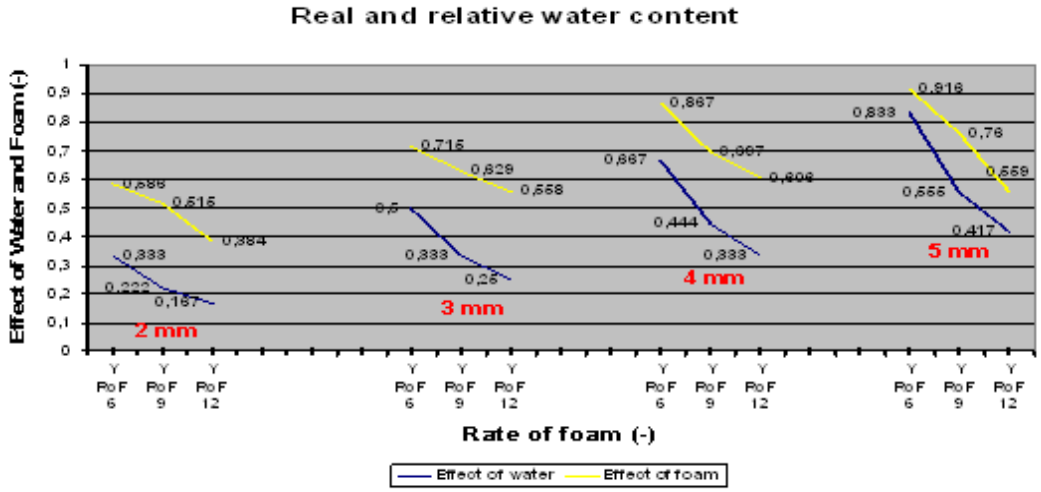

Figure 5. Real and relative water content

The graphic also demonstrates that raising the thickness of foam (2 mm ⇒ 5 mm) moves the curves close to each other; consequently the delay effect reduces. This statement harmonises to *Figure 6*. With fine analysis it can be observed that the angle with "x" axis rises in both case (real and equivalent water quantity of foam's curve) if thickness of foam blank*et al*so rises.

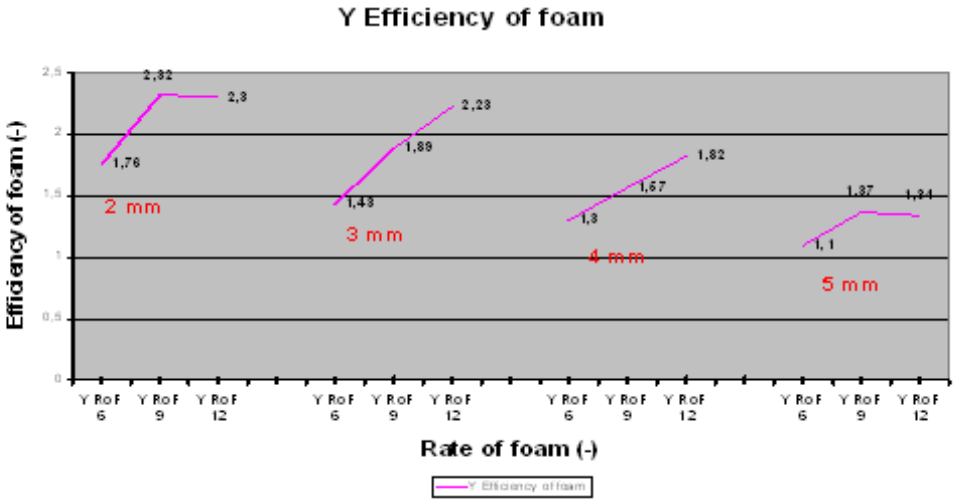

Figure 6. Efficiency of foam

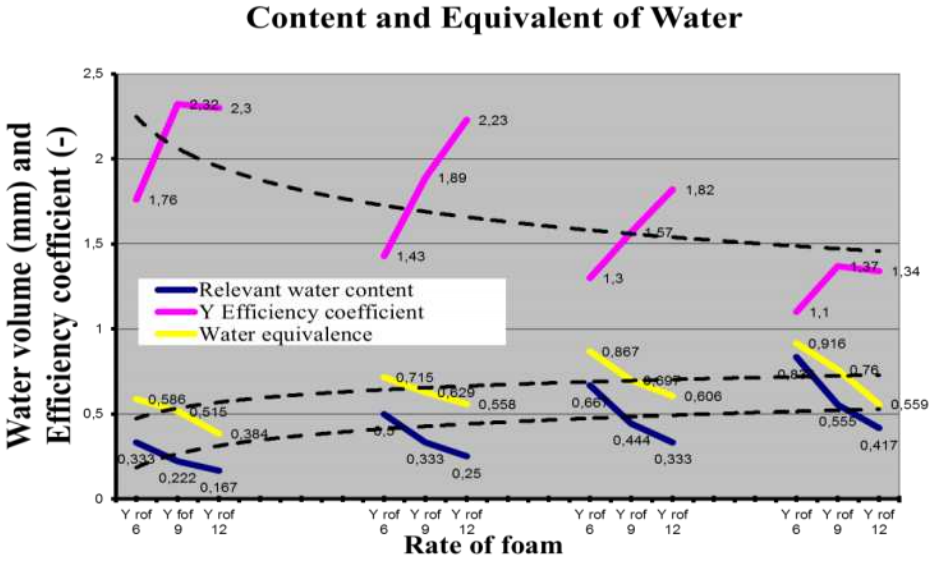

Figure 7. Content and equivalent of water

The coefficient reduces while raising the thickness of foam blanket, parallel to the angle between curves and "x" axis (Figure 7). Harmony is also demonstrated in the function where foams with different features, the real and equivalent water contain of foams and coefficient is represented.

Summarizing

Based on the R-20F method commonly used firefighting foam was tested. There are many experiences after making test series. Main statements:

1. R-20F is appropriate method to determine the extra effect of foam which is caused by the special feature of the structure and resulted longer ignition delay than should by own water contain.

2. R-20F is appropriate method drawing conclusion regarding most effective intervention, determine the quality and quantity of foam used especially in case of forest fire.
3. Results given by R-20F method declare that the most effective structure of foam is a relatively thin foam blanket (≤ 5 mm) but higher expenditure rate than 6.

For better and more precise results additional test are required using different foam concentrate especially used for fighting forest fires even by aerials. Based on the results some traditional tactic can change and cause more effective fighting against forest fires.

Appendix – Mathematical formulas used for calculations

1. h — Height of the metal ring [mm]; (F.1)
2. t — Ignition time [sec]; (F.2)
3. "h" — Upper index, height of water column or thick of foam blanket (height of the metal ring) [mm]; (F.3)
4. "nature" — Lower index, untreated sample; (F.4)
5. "B" — Lower index, gross ignition time [sec]; (F.5)
6. "N" — Lower index, net ignition time (measured ignition time reduced by the ignition time of the untreated sample) [sec]; (F.6)
7. "W" — Lower index, ignition time of water treated sample [sec]; (F.7)
8. "F" — Lower index, ignition time of foam treated sample [sec]; (F.8)
9. "y" — Lower index, expansion rate of the foam [-]; (F..9)
10. W — Water content of the foam/water expressed by water column height [mm]; (F.10)
11. Y — Effect of ignition delay regarding water content [-]; (F.11)
12. Z — Effect of ignition delay expressed by water equivalent [-]; (F.12)
13. t_{nature} — Ignition time, nature sample [sec]; (F.13)
14. t_{BW}^{h} — Gross ignition time, sample covered with "h" mm height water column [sec]; (F.14)
15. t_{NW}^{h} — Net ignition time, gross ignition time reduced by t_{nature}, sample covered with "h" mm height water column [sec]; $t_{NW}^{h} = t_{BW}^{h} - t_{nature}$ (F.15)
16. t_{BFy}^{h} — Gross ignition time, sample covered by „h" mm thick and "y" expansion rated foam [sec]; (F.16)
17. t_{NFy}^{h} — Net ignition time, gross ignition time reduced by t_{nature}, sample covered with "h" mm thick and "y" expansion rated foam [sec]; $t_{NFy}^{h} = t_{BFy}^{h} - t_{nature}$ (F.17)
18. W_{W}^{h} — Water content of "h" mm height water column [mm]; (F.18)
19. W_{Fy}^{h} — Water content of „h" mm thick and „y" expansion rated foam, expressed by water column height [mm]; $W_{Fy}^{h} = \frac{h}{y}$ (F.19)

20. $t^h_{W/W}$ Ignition time measured (2 mm) or linear calculated (3-4-5 mm), sample covered with "h" mm height water column [sec]; $t^h_{W/W} = t^h_{NW}$ (F.20)

21. $t^h_{W/Fy}$ Ignition time calculated with water quantity of foam contains, sample covered by „h" mm thick and „y" expansion rated foam [sec]; $t^h_{W/Fy} = \frac{t^h_{W/W} W^h_{Fy}}{W^h_W}$ (F.21)

22. Y^h_W Coefficient, meaning the effect of water's ignition delay, sample covered with "h" mm water column, evaluated by water equivalent. Rate = 1 [-]; $Y^h_W = 1$ (F.22)

23. Y^h_{Fy} Coefficient, meaning the extra effect of foam's ignition delay correlate to its own water content, sample covered with "h" mm thick and "y" expansion rated foam [-]; $Y^h_{Fy} = \frac{t^h_{NFy}}{t^h_{W/Fy}}$ (F.23)

24. Z^h_{EquW} Water equivalent of water's ignition delay, expressed by „h" mm high water column. [mm]; $Z^h_{EquW} = W^h_W$ (F.24)

25. Z^h_{EquFy} Water equivalent of foam's ignition delay, evaluated by "h" mm height water column equivalent, foam blanket „x" mm thick and „y" expansion rated foam[mm]; $Z^h_{EquFy} = Y^h_{Fy} W^h_{Fy}$ (F.25)

References

Boyd, C.F., Merzo, M. 1996 Fire Protection Foam Behavior in a Radiative Environment; Final Report, Mechanical Engineering Department, University of Maryland, US

Igishev, V.G., Portola V.A. 1993 Evaluation of foam parameters in extinction of self-ignition sources; Mine Aerodynamics, Institute of Mining, Russian Academy of Sciences, Prokopyevsk, Fiziko-Tekhnicheskie Problemy Razrabotki Poleznykh Iskopaemykh, No. 4, Russia

Salgado, J., Paz-Andrade, M.I. 2009 The effect of Firesorb as a fire retardant on the thermal properties of a heated soil; Journal of Thermal Analysis and Calorimetry, Vol. 95 (2009) 3, Akadémiai Kiadó, Budapest, Hungary

STP 2007 Standard Test Procedures, Evaluation of Wildland Fire Chemicals, Lateral Ignition and Flame Spread (LIFT), STP 2.2, Revised 5/30/07, Department of Agricultural, Forest Service, US Source: http://www.fs.fed.us/rm/fire/wfcs/tests/documents/stp_02_2.pdf Internet, Downloaded: 2012.08.28.

Safety at the WUI: a firefighters view

Clara Quesada-Fernández[a], Daniel Quesada-Fernández[b]

[a] *Universidad de Córdoba, Spain.* claraquesada@gmail.com, danielquesadafernandez@gmail.com

Abstract
Firefighting is a risky task. Every year during an even longer fire season we attend to many injuries and fatalities of civilians and firefighters in the frame of forest fires activities, especially in wildland urban interface fires situations. Every fatality and injury are investigated, in most of cases they are object of scientific research in order to learn from mistakes. Extracting the learned lessons helps to try not to repeat the situation. In case of recurrent risks personnel can be prepared to deal with them safely. Research in materials, procedures, protocols and many others, most of them are measurable aspects. State and regional agencies invest resources in education and training of its personnel in fire situations. However, in some cases it is not assessed enough those involved (firefighters) on their own identification and perception of risks.

Keywords*: communities, fire emergency, emergency evacuation, emergency preparedness, firefighting, fire prone areas, fire risk, forest fires, hazard, how to prevent, human behavior, personnel safety, prevention, risk, safety, wildland urban interface fire hazards.*

Introduction

Firefighting is a risky task. Every year during an even longer fire season we attend to many injuries and fatalities of civilians and firefighters in the frame of forest fires activities, especially in wildland urban interface fires situations. Every fatality and injury are investigated, in most of cases they are object of scientific research in order to learn from mistakes. Extracting the learned lessons helps to try not to repeat the situation. In case of recurrent risks personnel can be prepared to deal with them safely. Research in materials, procedures, protocols and many others, most of them are measurable aspects. State and regional agencies invest resources in education and training of its personnel in fire situations. However, in some cases it is not assessed enough those involved (firefighters) on their own identification and perception of risks.
Sometimes an excess of confidence or a lack of it due to a misperception of risk involve the occurrence of an accident. They are very little analyzed the so-called almost accidents. This situation is particularly relevant in wildland/rural urban interface areas.

Methods

The current situation about safety risks in the firefighting tasks shows identified risks and other unknown or not identified as risks. It is discussed the risk perception/vision of firefighters fronting fires in wildland urban interface areas.
The study examines the case of several working groups. In particular we study cases in Spain, located in different areas of the territory (peninsular, islands) with different working protocols to fighting fires in the WUI areas as common work situation to all of them. We show the analysis of different Fire Services situations all of them in fire prone areas throught the view of their firefighters.
Collected data were obtained from a 151 firefighters sample in Spain from base to higher levels in the firefighting scale. They collaborated in a extended survey during six months. In some of the cases firefighters had a specialized work in forest fires, following a Forest Model. In others cases existed a structural fire-based Service fronting forest fires.
The process consisted of a survey containing 50 questions about risk perception in firefigting tasks at the WUI. Each thematic block in which was divided the survey was presented with some introductory comments that summarized the contents. The first section of topics was dedicated to recognising the

main activity of firefighters at their Service structure, experience in fighting fires, personal data (sex, age). The second part followed knowledge on the topic of forest fires from the perspective of fire management, fire fighting, wildland urban interface and the state of the art in their territories and others places. We asked about the perception of risk levels and existence of aditional types and risks levels working at forest areas and wui areas. The third part analyzed the perception of human relations between professionals and citizens. The last section was dedicated to a miscelanea of questions about the perception of firefighting future at the WUI.

Results and discussions

The first section dedicated to recognising the main activity of firefighters showed 151 firefighters (141 men, 10 women) working on preventing and fighting forest fires (97% of them, 3% only prevention tasks) with more of ten years of activity. They described their activity as interesting (35%), usefull (33%) and risky (28%) and by calling as firefighting (70%). A minimun of 4% considered the activities as no risky tasks.

The second part followed knowledge on the topic of forest fires from the perspective of fire management, firefighting, wildland urban interface and the state of the art in their territories and others places. It was carried out using a four-level grid consisting of progressive steps of assessment from level 1 (no fires) to level 6 (catastrophic). The Do not know (Dk) answer was also avalaible. As shown in *Figure 1* the most popular argument tended to be referred to levels 3 (medium) to 6 (catastrophic) in the own country (Spain, 94% of data collected), the region (82%), working areas supossed to be well known (77%) and other places in the world (32% of referred data "Do not know" and 62% referred to levels 3 to 6).

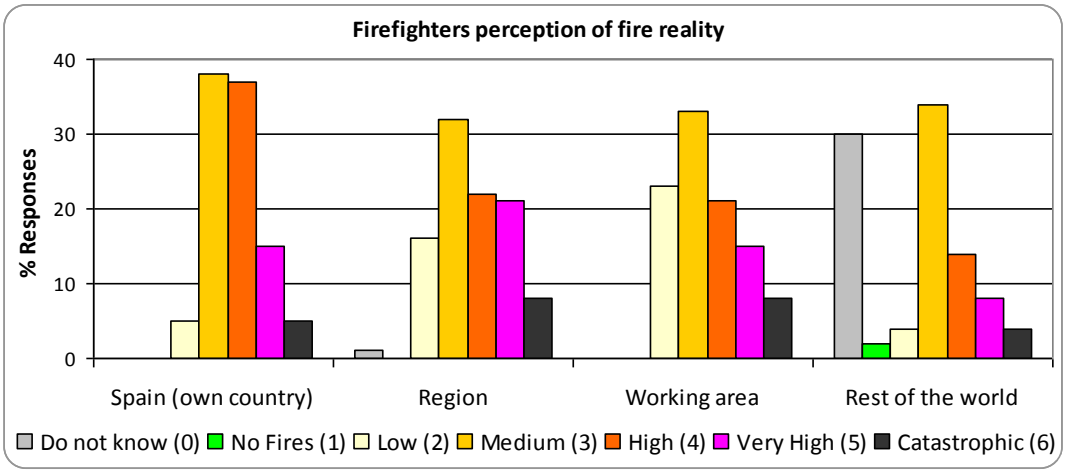

Figure 1. Perception of fire reality. Source: Quesada, C. & Quesada, D., 2014.

We asked about the perception of risk levels and existence of aditional types and risks levels working on fires in forest areas and WUI areas in Spain. To the question "Special risk at wui firefighting tasks" a number of 18% answered that the risks at the WUI were exactly the same as those on fighting forest fires. It is pretty clear to them the number of aditional risks as seen in *Figure 2*.

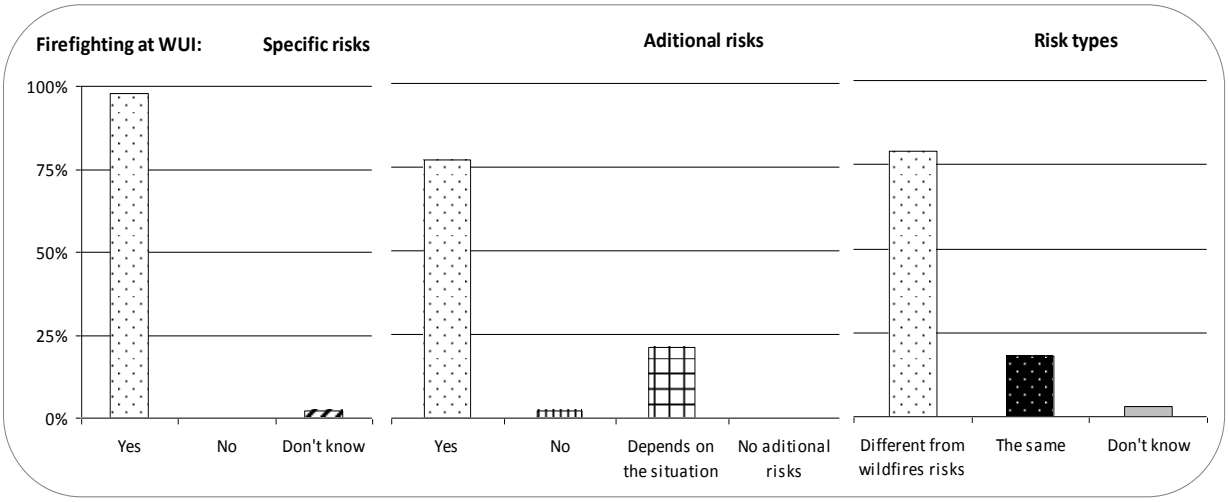

Figure 2. Perception of firefighting risks at WUI. Source: Quesada, C. & Quesada, D., 2014.

The third part analyzed the perception of human relations between professionals and citizens. A number of 28% admited that they ignored if civilians (residents, owners, tourists) had been previously informed about prevention and fighting policies and activities at WUI areas. More than 30% of professionals perceived that civilians didn't know about firefighting tasks neither who were the professionals responsible for that. If they did (firefighters fight forest fires and WUI fires) they didn't recognize their work as relevant or even consider that as an important task. This fact was specially relevant at WUI and rural areas.

Asking about WUI areas a number of 11% didn't know what WUI meant. This data corresponded to those professionals working in forest areas with an inexistent participation in fires in those areas. However, most of firefighters have expressed their lack of knowledge and how to proceed in a WUI fire. Referring to firefighing strategies and tactics at WUI areas a high number answered about an inappropiate situation in terms of not specific tools with their actual PPE (37%), hand tools (26%), trucks, engines or vehicles on the road (25%) and a general lack of eficiency (41%).

The last section was dedicated to a miscelanea of questions about the perception of firefighting future at the WUI. More than 69% of professionals answered they didn't feel recognised in their work by superiors into the organizational structure.

Conclussions

It would be reasonable to think that a 4% of participants considering the firefighting activities as no risky tasks is a difficult situation even with a low porcentage. The special risk at wui firefighting tasks, with a number of 18% answering exactly the same risks as those on fighting forest fires, it is understandable from the point of view of personal safety and related risks of this type of activity.

The situation in nearest places (provinces, regions, own country) is perceived as worse than in the rest of the territories (other countries, other regions, rest of the world). This perception is not necessary related to real situation is some cases. Some example cases as australian (Victoria State) and north and south american fire seasons (USA, Canada, Chile) are not seen as specially relevant situation from the point of view of fires and related events by an important part on the participants in this study.

It should be necessary to facilitate more oportunities to see greater exchange and more numerous examples of collaborative activities between professional and citizens (civilians, owners, residents, tourists) including knowledge and information sharing, research and training in WUI areas assessing wildland fire safety programs and firefighters and public safety in the WUI.

At the same time those professionals working in forested areas need to know that the emergency response services are more and more directed to a global situation (forest areas, civilians, buildings, engines) and not only the forest one that they are used to. These experiences can also contribute to prevent safety lapses, to create a new crew cohesion and wildland firefighter safety. Firefighters can increase feelings as recognised professionals in their work by superiors into the organizational structure.

Future works

We are now extending the study to other areas of the Mediterranean (France, Greece and Portugal), other Mediterranean climate areas in other latitudes (United States and Australia) and places with similar problems in fighting fires at the WUI (Chile). One interesting fact will study two cases analyzing the situation of a Fire Service confronting the challenges of all fire emergencies (Portugal, France) not only forest fire Services neither those Services mostly specialized in urban and structural fires.

References

Quesada, C., Pous, E. 2008. *The Helitransport Brigade Technician: Toward Professionalization of the Sector* in Proceedings of the Third International Symposium on Fire Economics, Planning, and Policy: Common Problems and Approaches. April 29 to May 2, 2008, Carolina, Puerto Rico. Pp 210-225. United States Department of Agriculture Forest Service. Pacific Southwest Research Station, General Technical Report PSW-GTR-227 (English). November 2009.

Quesada, C., Pous, E. 2009. *¿Hay futuro para el Técnico de Brigada Helitransportada?* in Revista Incendios Forestales, nº 20, april, 2009. Ed. Aifema, Granada.

Quesada, C.; Quesada, D. 2013. *Firefighters risk perception on firefighting tasks at the WUI* in Proceedings of the International Conference on Forest Fire Risk Modelling and Mapping. "Vulnerability to forest fire at wildland-urban interfaces". Aix en Provence, France, 30 September-2 October 2013.

TEIE, W. 2005. *Firefighter's Handbook on Wildland Firefighting: Strategy, Tactics and Safety*. 3rd edition. Deer Valley Press. California, USA.

Troup, B. 2013. *The Basics of Firefighter Safety in the Wildland Urban Interface* in Firerescue Magazine, march 2013.

Safety zones and convective heat: numerical simulation of potential burn injury from heat sources influenced by slopes and winds

Russell A. Parsons[a], Bret. W. Butler[b], William "Ruddy" Mell[c]

[a] *USDA Forest Service RMRS Fire Sciences Laboratory, 5775 Highway 10 W. Missoula, MT 59808, rparsons@fs.fed.us*
[b] *USDA Forest Service RMRS Fire Sciences Laboratory, 5775 Highway 10 W. Missoula, MT 59808, bwbutler@fs.fed.us*
[c] *USDA Forest Service PNW Pacific Wildland Fire Sciences Laboratory, 400 N. 34th St. Suite 201 Seattle, WA 98103 wemell@fs.fed.us*

Abstract
Although slope and winds are common factors in most wildland fires, current guidelines for safety zone dimensions used in the United States assume flat ground and do not consider wind speed as a factor. Similarly, while convective heat transfer is an essential part of fire behavior and is often highly significant to firefighter safety, it has not been considered in past work establishing safety zone criteria. In recent years, 3D, dynamic, physics-based dynamic fire models have been developed which can help us to understand fire behavior and firefighter safety. Here, we used a 3D dynamic fire model, WFDS, to explore different factors influencing potential burn injuries that could arise from both radiative and convective heat transfer over a range of heat sources, slopes and wind speeds. In the present study, we considered a fixed (non-moving) heat source on an inclined plane. Above this heat source, at regular intervals along the slope, synthetic "sensors" tracked wind velocities, temperature, radiative and total heat fluxes, facilitating analysis of potential burn injury as a function of distance from the heat source, analogous to the radius of a safety zone. Our primary finding was that convective heat could result in burn injuries at distances several times what would result from radiation alone. We also found that, while all factors were important, the nature of the heat source (heat release rate per unit area, flaming zone depth and residence time) had more pronounced effects on potential burn injury than slope or wind speed. Both of these findings have significant implications for how we think about firefighter safety, both in terms of how big safety zones might need to be to protect firefighters from convective heat, and in terms of characterizing the fuel as a heat source. This is a new arena of research investigation, and our work is just an early step; more work is needed to fully understand the implications of convective heat for firefighter safety and decision support.

***Keywords**: Firefighter safety zones, fire behaviour, fire safety, fire modeling*

Introduction

The United States Forest Service defines safety zones as "a preplanned area of sufficient size and suitable location that is expected to protect fire personnel from known hazards without using fire shelters" (National Wildfire Coodinating Group 2004). Subsequent definitions in 2012 added detail and broadened this concept to include safety zones more typically encountered operationally, "an area cleared of flammable materials used for escape in the event the line is outflanked or in case a spot fire causes fuels outside the control line to render the line unsafe. In firing operations, crews progress so as to maintain a safety zone close at hand allowing the fuels inside the control line to be consumed before going ahead. Safety zones may also be constructed as integral parts of fuelbreaks; they are greatly enlarged areas which can be used with relative safety by firefighters and their equipment in the event of blowup in the vicinity." (National Wildfire Coodinating Group 2012).
Although institutional culture and policy, firefighter safety training and tactical approaches have significantly improved over the years, often in response to firefighter fatality incidents (e.g. McArdle 1957), recent tragedies such as the June 2013 Yarnell Hill fire in Arizona underscore the ongoing need

for continued improvement in consideration of the potential risk exposure of firefighting personnel in wildland fire incidents and how such risks can be mitigated.

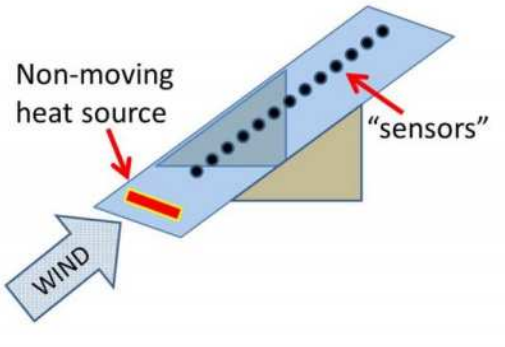

Figure 1. Schematic diagram of general experiment, consisting of a heat source at the lower end of an inclined plane. Above the heat source, sensors record key quantities used to evaluate incident heat flux. Slope was modeled through modification of the gravity vector rather than as shown here.

Most of the firefighter fatality or near-fatality events that have occurred in the United States and elsewhere over the last several decades have taken place in conditions in which slope and winds significantly influenced observed fire behaviour. Well documented examples include, among many others, the August 1949 Mann Gulch (Rothermel 1993), the 1994 South Canyon (Butler *et al* 1998), and the July 2001 Thirtymile fires (USDA Forest Service 2001) in the US; the 2003 Freixo de Espada-a-Cinta fire in Portugal (Viegas *et al* 2005), the 1998 Kareas fire in Greece (Xanthroupolous 2007), as well as the 1983 Grays Point, 1998 Johnstones Creek and 1998 Linton fires in Australia (Cheney *et al* 2001).

While slope and wind have been recognized as critical factors in fire behaviour for some time (Rothermel 1972), most research work examining safe separation distance characterizing safety zone dimensions to date has focused on radiation as the primary mechanism of heat transfer (Albini 1986, Rossi *et al* 2011, Zarate 2008); convection has often been considered as a less significant influence, with a common assumption that the buoyancy of heated gases would result in vertical transport, reducing the effect on persons or objects located some distance laterally from the flames (e.g. Gettle and Rice 2002). Consequently, current guidelines for safety zone dimensions used in the United States assume flat ground and do not consider wind speed as a factor (Butler and Cohen 1998a, 1998b). Recent work, however, suggests that convective heat transfer is more important to fire behaviour than had been thought in the past (Frankman *et al* 2010, Frankman *et al* 2012), with potentially significant implications for firefighter safety. A recent review of safety zones and entrapment incidents suggests that safety zone specifications can be improved through inclusion of convection (Butler 2014).

In recent years, dynamic fire behavior models have emerged which model the dominant physical processes driving fire behavior; unlike simpler semi-empirical models (e.g. Rothermel 1972), different mechanisms of heat transfer are modeled, facilitating detailed analysis of the roles and impacts of radiation and convection in fire behavior. Two such models are HIGRAD/FIRETEC (Linn *et al* 2002; Linn and Cunningham 2005; Linn *et al* 2007) and WFDS (Mell *et al* 2007; Mell *et al* 2009). Due to their dynamic nature, these models offer potentially valuable insights in examining interactions between fire, the atmosphere, vegetation, and topography to help improve our understanding of fire behavior and firefighter safety.

Our objective in this study was to use a physics-based fire model, WFDS, to explore the relative impact of different factors influencing potential burn injuries over a range of heat sources, slopes and wind speeds. A secondary objective was to assess the relative contribution of radiative vs convective heat in potential burn injury over a range of conditions. Using thermal dosage, an integrative measure based on magnitude and duration of exposure (Eisenberg *et al* 1975) which has been correlated to different burn injuries (Hymes *et al* 1996), we examined potential burn injuries resulting from either radiative

or convective heat alone, or both mechanisms of heat transfer in combination, over a range of distances from the heat source.

Methods

Using WFDS, we carried out 288 simulations with a rectangular domain measuring 252m in length, 40 m wide in width and 35m in height, with a constant resolution of 1 m in x, y and z dimensions. These experiments spanned a range of levels for several key factors, two representing key aspects of the fire environment (slope and wind) and three representing key aspects of the heat source, presented in Table 1, below. Our simulations spanned environmental conditions ranging from no-wind, no-slope up to substantial winds (10 m/s) on 50% slope.

Table 1. Factors used in numerical experiments examining safe separation distance from a non-moving heat source. For each factor, the number of different levels is presented in parentheses before the values.

Factor Group	Factor and units	Levels
Environment	Slope (%)	(6) 0,10,20,30,40,50
Environment	Wind speed, m/s	(4) 0,2.5,5,10
Heat Source	HRRPUA[1] (kW/m^2)	(3) 550,1500,2500
Heat Source	Heat Area Depth (m)	(2) 5,10
Heat Source	Duration (s)	(2) 30,60

[1]Heat Release Rate Per Unit Area

We used mirror boundary conditions on lateral boundaries to emulate a fireline of infinite width; the ceiling boundary was open. Within this domain, an inclined plane was simulated by altering the gravity vector. Winds were represented with an atmospheric profile with simple laminar flow. A fixed (non-moving) heat source, perpendicular to the wind flow, was located at ground level several meters from the inflow boundary along the inclined plane. Each heat source case was characterized with three variables: heat release rate per unit area (kW/m2), depth (width in meters) and duration in seconds. A ramp function was used to both initiate and terminate the heat source in time. Beyond the heat source, at regular 3m intervals along the slope, synthetic "sensors" tracked wind velocities, temperature, radiative and total heat fluxes. We calculated convective heat fluxes through standard heat transfer coefficient calculations based on cylinder geometry with a characteristic diameter of 0.1m and a length of 0.65m, intended to represent a person's arm.

To assess the relative contribution to potential burn injury from different heat transfer mechanisms, for each sensor over time, we calculated the thermal dosage from radiation only, from convection only, and from the two mechanisms of heat transfer combined. Thermal Dosage, V, is calculated as $V=tI^{4/3}$ where t is time, I is total incident heat flux, and V is the thermal dosage, measured with Thermal Dosage Units (TDU); one TDU = 1 $(kW/m^2)^{4/3}$.s (Eisenberg *et al* 1975, Tsao and Perry 1979, Torvi *et al* 2000). We used three thresholds of Thermal Dosage which have been identified to correlate with burn injuries (to exposed bare skin) as follows: 550 TDU indicates onset of 1st degree burns, a value of 1050 represents onset of 2nd degree burns, and a value of 2300 corresponds to full depth 3rd degree burn, as well as 50% lethality TDU for a typical subject (Hymes *et al*. 1996).

Summarizing the Thermal Dosage at each sensor over the time interval extending from the start of heat release from the heat source until thirty seconds after heat release terminated, we assessed the farthest sensor from the heat source experiencing each of the three thresholds. This provided us with a means of assessing potential burn injury as a function of distance from the heat source as well as the other factors in the experiment.

Results

Figure 2 shows a series of graphs for an individual simulation. The top three panels show convective, radiative and total incident fluxes with different coloured lines for each sensor over time. The bottom panel shows thermal dosage (for total incident heat flux) as a function of distance from the heat source for the slope and wind conditions of that simulation; different symbols correspond to different thresholds of potential injury as quantified with Thermal Dosage.

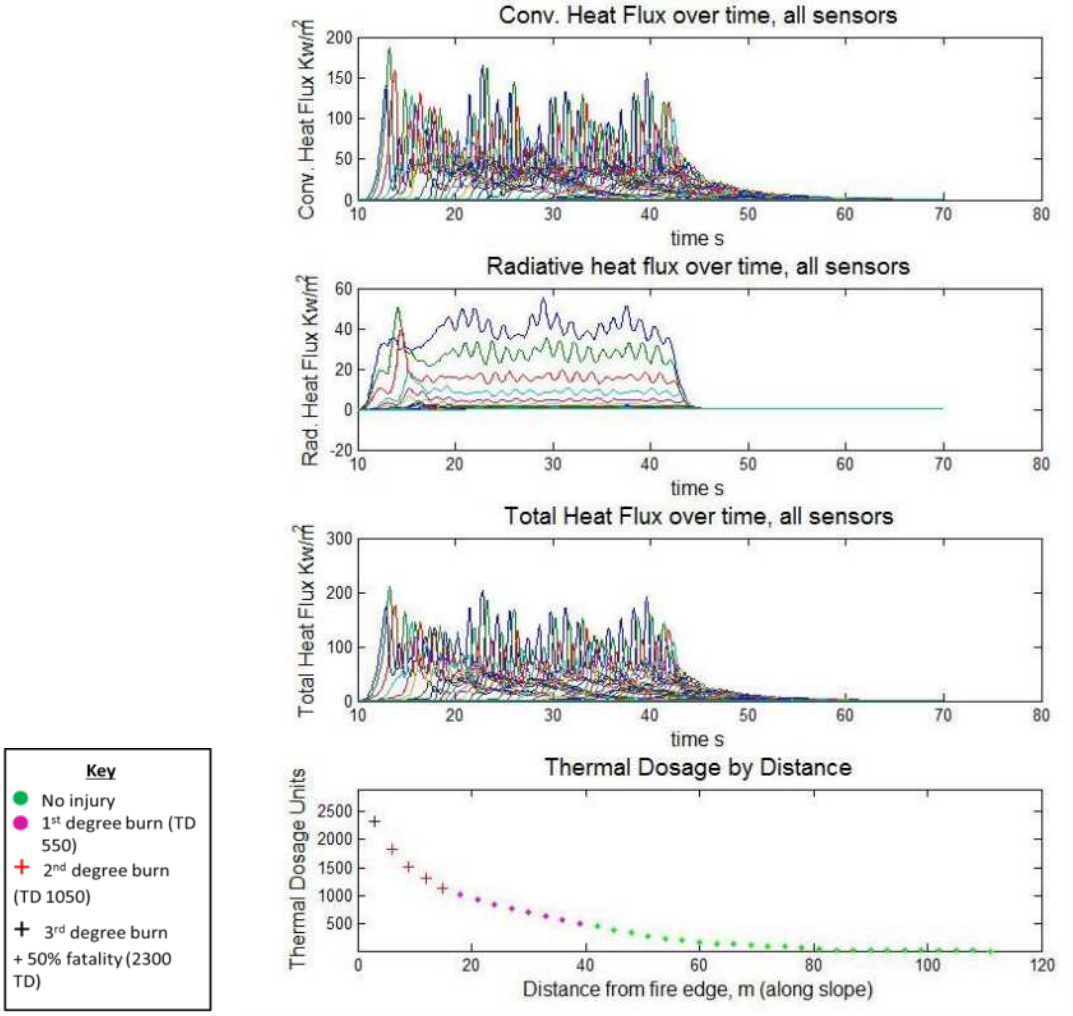

Figure 2. Simulation output for a given simulation. Top three panels show plots of convective heat flux, radiative heat flux and total heat flux over time at points spaced along the slope a fixed height above the ground. Bottom panel shows thermal dosage for each point over distance from heat source. Thermal dosages are very high close to the heat source but diminish with distance; markers in bottom panel correspond to injury key, shown above

In this example, at distances 40m or greater from the heat source, no injury is predicted to occur; injuries increase as sensors approach the heat source, with 1st degree burns predicted for 18 to 39 m, 2nd degree burns predicted from 6 to 15 m from the heat source, and full depth 3rd degree burns and 50% mortality predicted at distances below 6 m.

The range of conditions examined resulted in a wide range of outcomes, with very little predicted injury under more mild heat source cases, light winds and low slopes, ranging to very extreme effects at great distances from the heat source under high winds, high slopes and more severe heat source cases. The relative contribution of radiative vs convective heat transfer to Thermal dosage varied as well with the conditions. In the case shown in Figure 2, convective heat flux was typically around twice the radiative heat flux.

Heat fluxes from the numerical experiments were similar to values reported in measurements. For example, radiative heat flux for Figure 2 is in a similar range to values reported for measurements taken in burning pine needles and oak branches in southern France (Silvani and Morandini 2009).

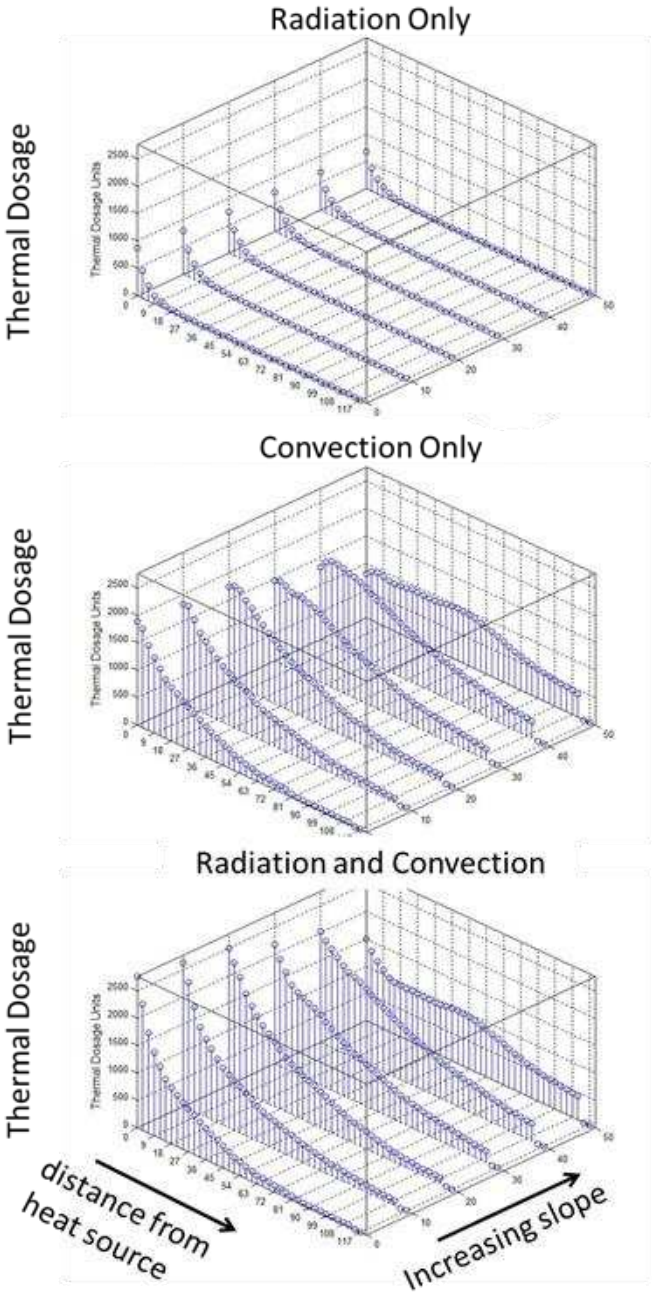

Figure 3. Simulated thermal dosage, a measure of potential burn injury, at different distances from a heat source, and on different slopes for a particular wind speed and set of heat source parameters. Top panel shows radiation, middle shows convection, and bottom shows combined effects.

All three characteristics used to describe the heat source (heat release rate per unit area, depth and duration) significantly impacted the safe separation distance; all three factors interacted with slope and wind as well. In general, Thermal Dosage increased as all three of these factors increased.

Our primary finding, however, was that inclusion of convective heat associated with wind and slope effects could result in burn injuries at distances often several multiples of what would result from radiation alone. Prior rules of thumb used for field personnel in the US, based on radiation alone, for flat ground, with no wind, would characterize safe separation distance as a multiple of four times the

flame length (Butler and Cohen 1998a and b). In contrast, in the most extreme cases we tested, safe separation distance could potentially be nearly an order of magnitude greater, or forty times the flame length.

Discussion

We conducted a series of numerical experiments examining potential thermal exposure at a range of distances from a fixed heat source under a range of wind, slope conditions and with different heat source parameters. We found that safe separation distances may need to be much larger to ensure firefighter safety in wind and slope conditions. This has potentially significant implications for firefighting tactics, design and planning of safety zones, as well as in consideration of escape routes and the safety margins in time needed to ensure safe evacuation (Beighley 1995, Baxter *et al* 2004).

An additional finding of potential consequence was that the characteristics of the heat source were all highly significant to predicting safe separation distance. The intense energy release rates from crown fires are certainly well known but dynamic aspects of convection arising in these intense situations could pose dangers to firefighters. For example, intense jets of superheated air have been observed in crown fire situations (Coen *et al* 2004). Research is needed to better characterize the frequency and magnitude of such events and their potential for firefighter injury. While most interest in fire behaviour emphasizes the active flaming front, our results suggest that heavy fuels and duff, which often burn for long duration and cover large areas, may potentially contribute sufficient energy to affect safe separation distance. We expect that, under some topographic configurations and atmospheric conditions, long burning fuels such as these, contributing energy over often large areas, could potentially result in longer safe separation distances. More research is needed to examine whether this is truly a possibility or not.

It is important to recognize that this work represents a simple early step in investigations along these lines. We expect that future work will provide greater refinement of the concepts we present here. This is a natural and expected course of how scientific knowledge unfolds. Our numerical experiments have a very simple configuration; our use of a non-moving heat source is convenient and tractable for a first approach but is not very representative of a real wildfire; more work must be carried out with moving heat sources. Additional work must be carried out as well to ensure that results such as those presented here are not highly influenced by domain width, domain size, resolution or other potential numerical artifacts. Investigation should examine how vegetation might reduce (or increase) the safe separation distance effects we observed here.

Particularly important, however, is to examine how more complex terrain configurations could influence outcomes. We expect that under many circumstances in real fires these slope/wind multipliers may be less than we observed here, as convective cooling could play a significant role. However there may be cases of particular topographic configurations that could lead to greater distance effects; this could be disastrous. Recent work suggests that particular wind/terrain alignment scenarios can have very significant effects, resulting in rapid changes in fire behavior (Sharples *et al* 2010, Sharples *et al* 2012). More research is needed to link potential burn injury to firefighters, dynamic fire behavior, and atmospheric / topographic interactions such as these.

Using a dynamic, physics-based fire model, we assessed Thermal Dosage arising from radiation alone, convection alone, and both combined. In general, measurement of convective processes can pose significant challenges in the field, typically requiring a great deal of instrumentation and often only permitting a relatively small sample of observations (Kaimal *et al* 1976); inferences made from point observations may result in uncertainties when applied over larger areas (Linn *et al*. 2012). A significant advantage of using a physics-based model, as we did here, is that these quantities, and the dynamic interactions between different influential factors, can be examined in detail, facilitating improved understanding. Such models provide a unique value in that they can provide an experience analogous to laboratory experiments; modeling efforts are uniquely complementary to physical experiments in

laboratories and in larger field campaigns. Fire science benefits from all of these approaches to learning.

Finally, our finding that safe separation distances may need to be much larger to ensure firefighter safety in wind and slope conditions suggests a possible paradigm shift. This shift may already be underway. When we first encountered these results we were somewhat discouraged, as it seemed likely that managers might interpret these results as extremely restrictive, unreasonable, and, in many cases, unattainable, particularly in areas of complex terrain as are common throughout areas within the US and elsewhere where fires often occur. However, in presentations with several groups of managers in the United States, their response has often been quite different; some managers were encouraged that these results could provide them with justification for not sending firefighters into areas from which escape in the event of a blow-up could be very tenuous. We hope that this research, and subsequent work which follows it, may promote the use of more indirect attack tactics and other approaches which limit firefighter risk exposure.

References

Albini, FA (1986) Wildland fire spread by radiation-- a model including fuel cooling by natural convection. Combustion Science & Technology 45, 101-113.

Beighley, M. 1995. Beyond the safety zone: creating a margin of safety. Fire Management Notes 55(4):21–24

Baxter G, Alexander M, Dakin G (2004) Travel rates of Alberta wildland firefighters using escape routes on a moderately steep slope. Forest Engineering Research Institute of Canada Advantage Report. Vol. 5 No. 25. Pointe Claire, QC and Vancouver, BC. 15 pp.

Butler, Bret W.; Bartlette, Roberta A.; Bradshaw, Larry S.; Cohen, Jack D.; Andrews, PatriciaL.; Putnam, Ted; Mangan, Richard J. 1998. Fire behavior associated with the 1994 South Canyon Fire on Storm King Mountain, Colorado. Res. Pap. RMRS-RP-9. Ogden, UT: U.S. Department of Agriculture, Forest Service, Rocky Mountain Research Station. 82 p

Butler, BW, Cohen, JD (1998a) Firefighter safety zones: how big is big enough? Fire Management Notes Vol. 58, 13-16.

Butler, BW, Cohen, JD (1998b) Firefighter safety zones: a theoretical model based on radiative heating. International Journal of Wildland Fire 8, 73-77.

Butler, BW, Cohen, J, Latham, DJ, Schuette, RD, Sopko, P, Shannon, KS, Jimenez, D, Bradshaw, LS 2004. Measurements of radiant emissive power and temperatures in crown fires. Canadian Journal of Forest Research 34, 1577- 1587.

Butler B. W. (2014) Wildland firefighter safety zones: a review of past science and summary of future needs. International Journal of Wildland Fire 23, 295–308.

Cheney, Phil, Jim Gould, and Lachie McCaw. "The dead-man zone—a neglected area of firefighter safety." Australian Forestry 64, no. 1 (2001): 45-50.

Coen, Janice, Shankar Mahalingam, and John Daily. "Infrared imagery of crown-fire dynamics during FROSTFIRE." Journal of Applied Meteorology 43, no. 9 (2004): 1241-1259.

Frankman, D, Webb, BW, Butler, BW (2010) Time-resolved radiation and convection heat transfer in combusting discontinuous fuel beds. Combustion Science & Technology 182, 1-22.

Frankman, David, Brent W. Webb, Bret W. Butler, Daniel Jimenez, Jason M. Forthofer, Paul Sopko, Kyle S. Shannon, J. Kevin Hiers, and Roger D. Ottmar. "Measurements of convective and radiative heating in wildland fires."International Journal of Wildland Fire 22, no. 2 (2013): 157-167.

Furnish, Jim; Chockie, Alan; Anderson, Leslie; Connaughton, Kent; Dash, Dave; Duran, Joe; Graham, Brenda; Jackson, George; Kern, Tony; Lasko, Rich; Prange, Jim; Pincha-Tulley, Jeanne; Whitlock, Chuck. 2001. Thirtymile Fire. Accident Investigation Factual Report. U.S. Department of Agriculture, Forest Service. 95p Available at http://www. fs. fed. us/r6/wenatchee/fire/thirtymile-reports. html

Gettle, G, Rice, CL (2002) Criteria for determining the safe separation between structures and wildlands. In 'IV International Conference on Forest Fire Research & Wildland Fire Safety Summit. Luso, Coimbra, Portugal', 18-23 November, 2002. (Ed. DX Viegas) pp. 9. (Millpress: Rotterdam)

Hymes, I, Boydell, W, Prescott, B (1996) 'Thermal Radiation: Physiological and pathological effects.' (Insititution of Chemical Engineers: Rugby, Warwickshire, UK)

Kaimal, J. C., J. C. Wyngaard, D. A. Haugen, O. R. Coté, Y. Izumi, S. J. Caughey, C. J. Readings, 1976: Turbulence Structure in the Convective Boundary Layer. J. Atmos. Sci., 33, 2152–2169.

Linn R., Winterkamp J., Colman J., Edminster C. and Bailey J. 2005. Modeling interactions between fire and atmosphere in discrete element fuel beds. International Journal of Wildland Fire 14: 37-48.

Linn R., Wintercamp C., Edminster C., Colman J. and Smith W. 2007. Coupled influences of topography and wind on wildland fire behavior. International Journal of Wildland Fire 16: 183-195.

Linn R.R., Reisner J., Colman J.J. and Winterkamp J. 2002. Studying wildfire behavior using FIRETEC. International Journal of Wildland Fire 11: 233-246.

Linn, Rodman, Kerry Anderson, Judith Winterkamp, Alyssa Brooks, Michael Wotton, Jean-Luc Dupuy, François Pimont, and Carleton Edminster. "Incorporating field wind data into FIRETEC simulations of the International Crown Fire Modeling Experiment (ICFME): preliminary lessons learned."Canadian Journal of Forest Research 42, no. 5 (2012): 879-898.

Mell W., Jenkins M.A., Gould J. and Cheney P. 2007. A physics-based approach to modelling grassland fires. International Journal of Wildland Fire 16: 1-22.

Mell W., Maranghides A., McDermott R. and Manzello S.L. 2009. Numerical simulation and experiments of burning douglas fir trees. Combustion and Flame 156: 2023-2041.

National Wildfire Coordinating Group [NWCG]. [N.d.].Glossary of wildland fire terminology. http://www.nwcg.gov/pms/pubs/glossary/index.htm. (June 1, 2011).

McArdle, RE (1957) Standard fire fighting orders. Fire Control Notes 18, 151-152.

Rothermel R.C. 1972. A mathematical model for predicting fire spread in wildland fuelsResearch Paper INT-115. United States Department of Agriculture, Forest Service, Intermountain Forest and Range Experiment Station,, Ogden, Utah. p. 40.

Rossi, JL, Simeoni, A, Moretti, B, Leroy-Cancellieri, V (2011) An analytical model based on radiative heating for the determination of safety distances for wildland fires. Fire Safety Journal 46, 520-527.

Sharples, J. J., R. H. D. McRae, and R. O. Weber. "Wind characteristics over complex terrain with implications for bushfire risk management." Environmental Modelling & Software 25, no. 10 (2010): 1099-1120.

Sharples, Jason J., Richard HD McRae, and Stephen R. Wilkes. "Wind–terrain effects on the propagation of wildfires in rugged terrain: fire channelling."International Journal of Wildland Fire 21, no. 3 (2012): 282-296.

Silvani, X, Morandini, F (2009) Fire spread experiments in the field: Temperature and heat fluxes measurements. Fire Safety Journal 44, 279-285.

Torvi, DA, Hadjisophocleous, GV, Hum, J (2000) A new method for estimating the effects of thermal radiation from fires on building occupants. In 'Proceedings of the ASME Heat Transfer Division. pp. 65-72. (National Research Council Canada. Available at www.nrc.ca/irc/ircpubs

Tsao, C.K. and Perry, W.W., 1979, "Modifications to the Vulnerability Model: A Simulation System for Assessing Damage Resulting from Marine Spills (VM4)," ADA 075 231, US Coast Guard NTIS Report No. CG-D-38-79.

Viegas, D. X., L. P. Pita, L. Ribeiro, and P. Palheiro. "Eruptive fire behaviour in past fatal accidents." Proceedings, Eighth International Wildland Fire Safety Summit (2005): 26-28.

Xanthopoulos, G. 2007. Forest fire related deaths in Greece: confirming what we already know. In: Proceedings of "Wildfire 2007", Sevilla, Spain, pp. 1-12.

Zarate, L, Arnaldos, J, Casal, J (2008) Establishing safety distances for wildland fires. Fire Safety Journal 43, 565-575.

Sensor grid for fine particles monitoring during a fire: implications to firefighter's safety

J.H. Amorim[a], A.I. Miranda[a], J. Valente[a], P. Cascão[b], V. Martins[a], L.M. Ribeiro[c], and D.X. Viegas[c]

[a] *CESAM & Department of Environment and Planning, University of Aveiro, 3810-193 Aveiro, Portugal, amorim@ua.pt, miranda@ua.pt, joanavalente@ua.pt, veram@ua.pt*
[b] *Ecotech Pty Ltd, Knoxfield, Vic. 3180 Australia, pedro.cascao@ecotech.com*
[c] *Association for the Development of Industrial Aerodynamics, University of Coimbra, 3031-601 Coimbra, Portugal, luis.mario@adai.pt, xavier.viegas@dem.uc.pt*

Abstract
Forest fires are a massive source of air pollutants to the atmosphere causing several environmental and human impacts. It is generally accepted that firefighters are potentially exposed to critical levels of air pollution during fire suppression activities (both in direct combat and mop-up), but the concentrations attained in these areas are still scarcely quantified because of the difficulty inherent to the monitoring of air quality close to the fireline. The goal of this work is to provide a better understanding of the spatiotemporal dynamics of the smoke plume, and resulting levels of fine particles, in the proximity of a fire, and how this translates into human safety issues. The experimental study area is located in the mountain range of Lousã, Central Portugal. Ten in-continuum monitoring sensors were positioned at a distance of 5 m (8 sensors) and 10 m (2 sensors) from the top boundary of the burn plot, and at 1.7 m above ground. The concentration of particulate matter with an equivalent aerodynamic diameter smaller than 2.5 µm (PM2.5) was measured during a total period of 50 minutes, capturing the effect of both flaming and smouldering emissions.
The results presented in this work highlight the fact that the concentration of fine particles in the atmosphere close to the fireline is extremely dynamic, with differences between sensors that go up to 540% in terms of average concentrations and 170% in peak values. This is particularly relevant taking into account that these values correspond to sensors at a distance of 10 m. This conclusion suggests that in a single fire crew considerable differences in the exposure of its members can occur depending on their task/position relating the fireline.
For this particular burning plot the time evolution of the observations reveals a dip in PM2.5 concentration that is not explained by the analysis of smoke plume dynamics in video recordings, suggesting that under certain circumstances the visual estimate of fire safety conditions can be misleading due to e.g. reduced visibility. In wildfire suppression operations the safety of the involved personnel should rely also in the use of personal exposure monitoring equipment for the prevention of potentially critical exposure.

Keywords*: real scale fire experiments; smoke emissions; fire safety; smoke exposure.*

Introduction

Forest fires are a massive source of air pollutants to the atmosphere causing several environmental and human impacts. At the operational level, firefighters are confronted with extremely severe environmental conditions, including reduced visibility and toxic atmosphere. In this context, particulate matter, which is abundantly produced during forest fires, has significant effects over the safety and health of personnel in the terrain (e.g., Reinhardt and Ottmar [2004] and Miranda *et al*. [2010, 2012]). In fact, the International Agency for Research on Cancer (IARC) stated that the occupational exposure of a firefighter is possibly carcinogenic [IARC, 2010a]. There are a number of factors that affect the impacts of smoke on firefighter's health, including the concentration of specific air pollutants within the breathing zone, the exposure duration, the exertion levels, and the individual susceptibility (e.g., pre-existing lung or heart diseases) [Reisen and Brown, 2009]. In what relates specifically to smoke particles, the associated health effects not only depend on the chemical and toxic

characteristics but also on their morphological properties, such as size, shape and density [Dost, 1991; Schwela, 2001; Naeher *et al*., 2007].
Despite the research studies carried out in the United States of America [Reinhardt *et al*., 2000; Reinhardt and Ottmar, 2000 and 2004], Australia [McMahon and Bush, 1992; Materna *et al*., 1993; Reisen and Brown, 2009; Reisen *et al*., 2011] and Portugal [Miranda *et al*., 2010 and 2012], the current state of knowledge in this field is still scarce. The difficulty inherent to the monitoring of air quality and personal exposure levels during a fire has largely contributed to this scientific gap.
The complex mixture of smoke constituents induces adverse health effects such as acute and instantaneous eye and respiratory irritation and shortness of breath, that can potentially develop into headache, dizziness and nausea lasting for hours, and mild impairment of lung function for hours to days [Reinhardt *et al*., 2000], while long-term effects are characterized by impaired respiratory function, increased risk of cancer, and cardiovascular disease [Rothman *et al*., 1991]. Special concern is raised by the exposure to respirable particles and potentially toxic compounds adsorbed to them, such as polycyclic aromatic hydrocarbons (PAHs) and semivolatile organic compounds, some of which may be carcinogenic [Le Masters *et al*. 2006; Youakim, 2006; IARC, 2010b].
Aiming to establish cause/effect relationships between exposure to smoke and firefighter's health effects it is fundamental to improve the current understanding about the spatial and temporal dynamics of air pollution levels close to the fireline. It is widely known that the composition of smoke depends on several factors, namely the type of vegetation consumed, the efficiency of combustion, the fuel moisture content, the fire temperature, and the weather conditions [Reisen and Brown, 2009]. However, the extent of the impact of smoke plume dynamics on individual exposure is scarcely documented by field observations. The main goal of this work is to evaluate the spatial and temporal variation of fine particles concentration during a bushfire, and how this potentially translates into human safety issues during firefighting operations.

Fire experiments description

The experimental study area is located in the mountain range of Lousã, Central Portugal (40° 15'N, 8° 10'W), at an elevation of approximately 1,000 m. The fire experiments described in this paper were carried out in May 6, 2010. The characteristics of the burn plot are described in Table 1.

Table 1. Physical characteristics of the burn plot. Fuel moisture was sampled 40 min before the fire ignition.

Area (m^2)	Avg. slope (°)	Fuel cover (%)	Avg. fuel height (m)	Avg. fuel load ($ton.ha^{-1}$)	Avg. fuel moisture (%)	Fuel species
853	16	67	0.31	32.50	Live: 46.6 Dead: 9.0	*Erica umbellata, Erica australis, Ulex minor, Chamaespartium tridentatum*

Average meteorological data acquired during the burn are shown in Table 2.

Table 2. Average meteorological data observed from 10:00 to 10:50.

Wind velocity ($m.s^{-1}$)	Wind direction (-)	Air temperature (ºC)	Air humidity (%)
3.1	East (uphill)	12.8	45.6

As shown in Figure 1, no significant variation of wind velocity and direction was reported in this period.

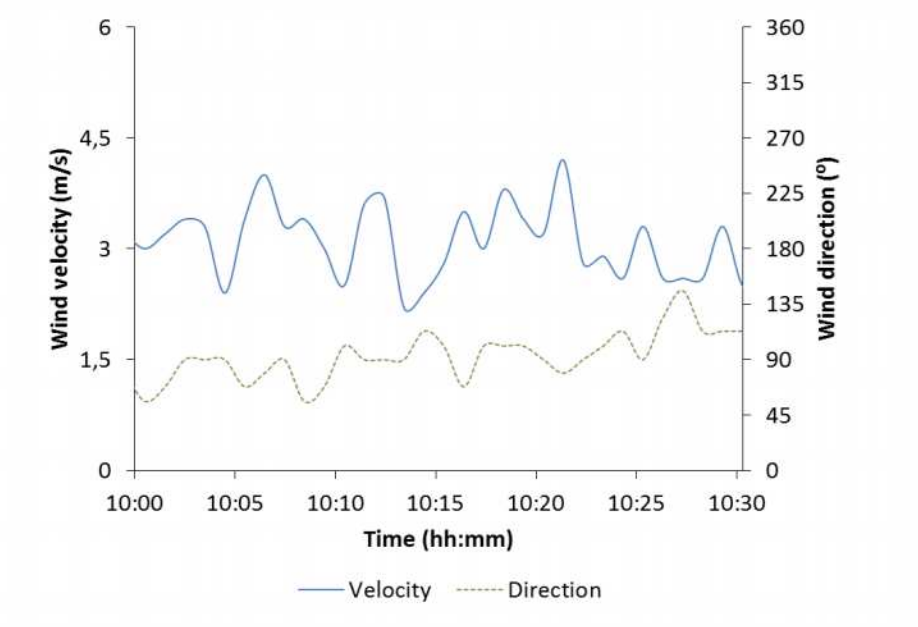

Figure 1. Meteorological data measured during the experiment.

The procedure for the fire ignition is presented in Table 3.

Table 3. Fire ignition (Δt indicates time after ignition).

Fire ignition (hh:mm)	End of flaming stage (hh:mm)	End of smouldering stage (hh:mm)	Fire ignition description
10:00 (Δt=0min)	10:30 (Δt=30min)	10:50 (Δt=50min)	Δt=0min: Linear ignition along the top (West) boundary of the plot starting at the right (North) side; Δt=7min: Linear ignition parallel to the initial one and starting at the left (South) side; Δt=13min: Downhill linear ignition along the right (North) boundary of the plot; Δt=16min: Downhill linear ignition along the left (South) boundary of the plot; Δt=19min: Linear ignition along the bottom (East) boundary of the plot starting at the right (North) side and covering the first 1/3 of the total width; Δt=27min: Linear ignition along the bottom (East) boundary of the plot, covering the remaining 2/3 of the total width.

A snapshot of the plot burning is shown in Figure 2. The effect of the uphill wind is evident in the behaviour of the smoke plume. Also, the effect of the decreased heat release in the smouldering stage is evident in the diminishing of the plume rise in image (d).

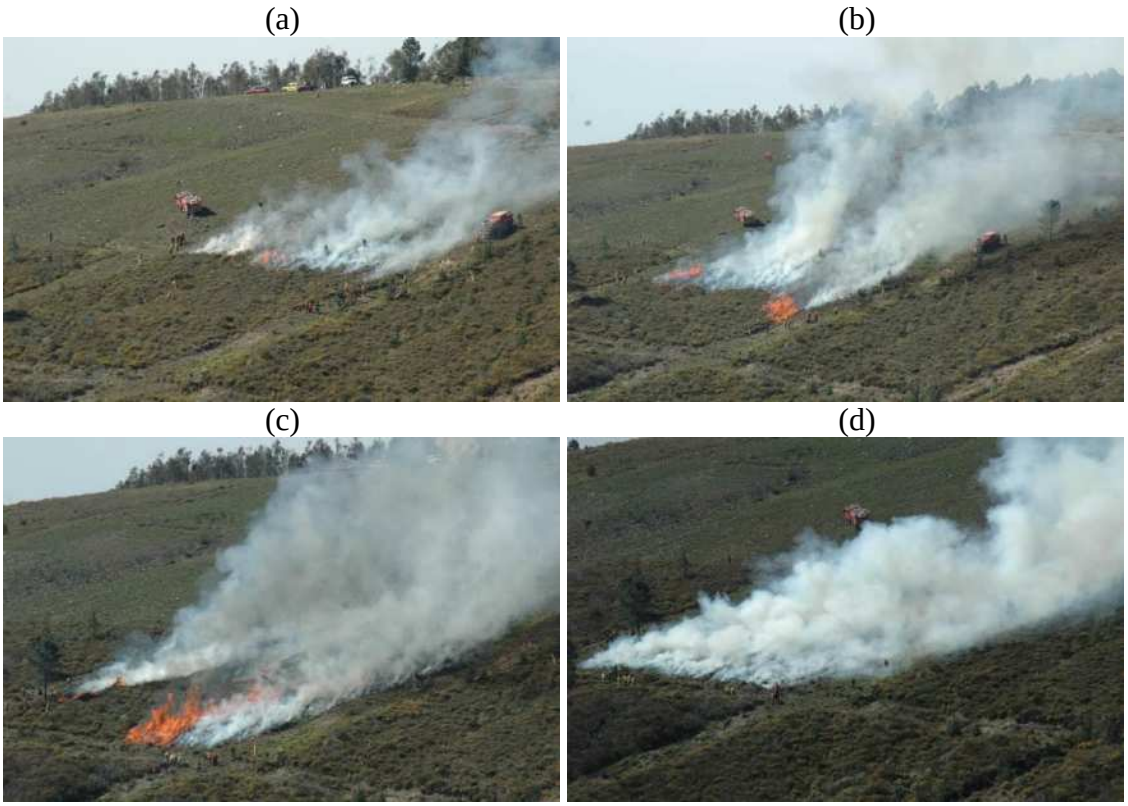

Figure 2. Sequence of photos showing the plot burning at: (a) 10:05 (Δt=5 min), (b) 10:14 (Δt=14 min), (c) 10:22 (Δt=22 min), and (d) 10:32 (Δt=32 min, corresponding to the start of the smouldering stage).

The layout of the sensor grid is schematically shown in Figure 3. Ten in-continuum air quality monitoring sensors were distributed at intervals of 5 m along the top boundary of the plot. The two lines of sensors are, respectively, at 5 m (8 sensors) and 10 m (2 sensors) from the top (West) boundary of the plot. This grid was defined according to the prevailing winds during the burns, with the objective of capturing the smoke plume.

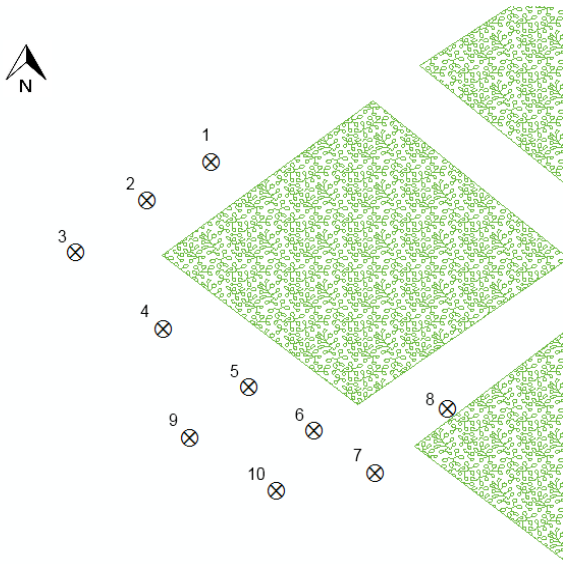

Figure 3. Sensors grid layout.

The equipment used for the measurement of the concentration of particles with an equivalent aerodynamic diameter smaller than 2.5 µm (PM2.5) was a SidePack AM510 (TSI^{TM}) (for more details on the sensors see Miranda *et al*. [2010]). Each sensor was fixed to a mast at a height of approximately 1.7 m above ground, as can be seen in Figure 4.

Figure 4. PM2.5 monitoring sensors indicated by the circles.

3. Experimental data analysis

Figure 5 shows the PM2.5 concentration acquired in each sensor normalized by the global average for all sensors.

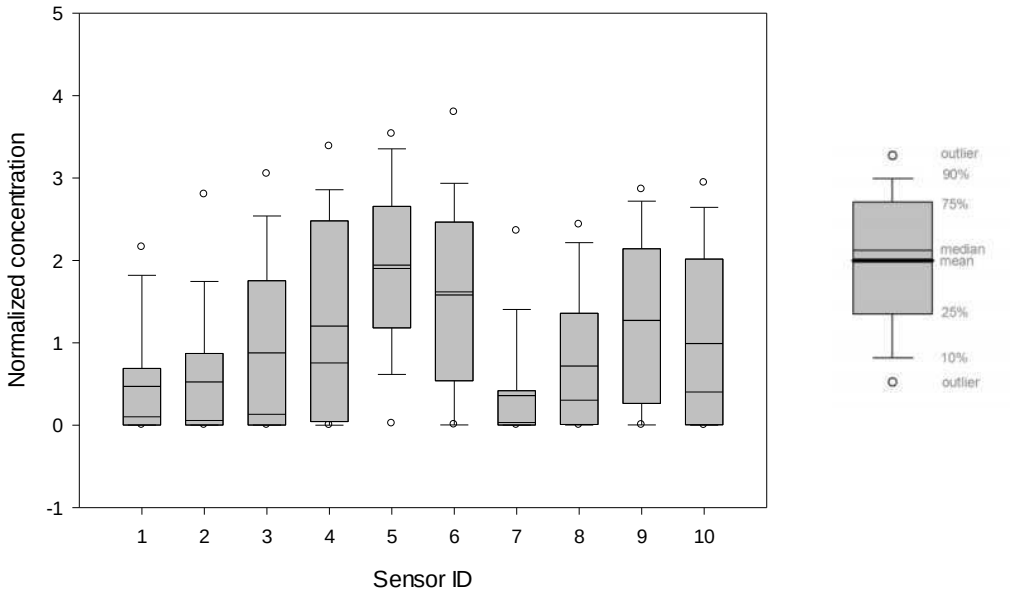

Figure 5. Box plots of normalized 1 min averaged PM2.5 concentration per sensor.

Figure 5 shows a clear discrepancy on the magnitude of the concentrations attained, with sensor 5 hitting an average concentration 5.4 times higher than sensor 7, and 1.7 times higher in the case of peak values, despite the short distance (10 m) between these sensors. Standard deviation is also dependent on sensor location, ranging from 0.6 (sensor 7) to 1.2 (sensor 4). These conclusions are in agreement with previous measurements carried out by the authors [Miranda *et al*., 2010] in similar plots but in which the measuring equipment was used by firefighters (consequently, not representing a specific spot but a given job in the crew).

For an additional understanding of the time evolution of PM2.5 levels, 1 minute averaged normalized values are shown in Figure 6.

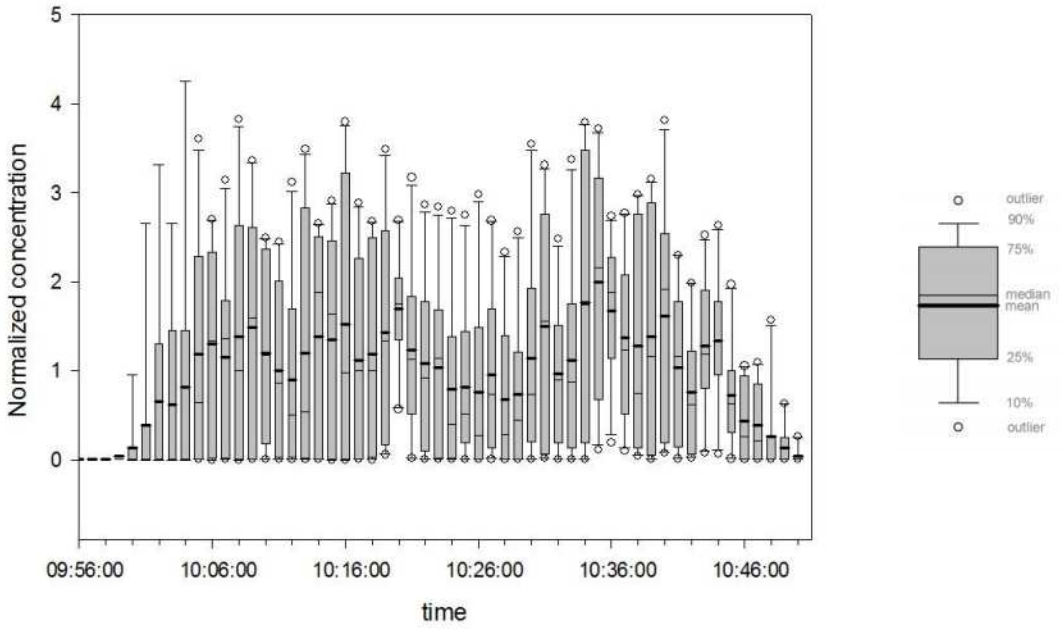

Figure 6. Box plots of normalized 1 min averaged PM2.5 concentration per sensor (a) and per minute (b).

The decrease of concentration around 10:26 shown in Figure 6 corresponds to the end of the flaming stage (at 10:30), thus revealing two distinct fire stages. It is possible to conclude that the PM2.5 levels captured during the first 30 minutes are resulting from a combination of both flaming and smouldering emissions, while the second peak in concentration (around 10:36) is exclusively caused by smouldering emissions, showing the significant contribution of the smouldering phase to the emission of fine particles, again in the agreement with the previous campaign by Miranda *et al*. [2010]. In fact, the (1 minute) average concentration values are higher in this second stage, which is also a consequence of the weakened plume rise (as already observed in the analysis of Figure 2).
Additionally, it is worth to observe in Figure 6 that in the flaming stage a dip in PM2.5 concentration was observed for approximately 6 minutes, starting at 10:10. This effect is not explained by the analysis of smoke plume dynamics in video recordings (at least from the observation point), in which a significant (horizontal or vertical) deviation of the plume was not observed, neither a decrease on fire intensity.

Conclusions

It is generally accepted that firefighters are potentially exposed to critical levels of air pollution during fire suppression activities (both in direct combat and mop-up), but the concentrations attained during these operations are still scarcely quantified. The goal of this work is to give a better understanding of the spatiotemporal dynamics of the smoke plume, and resulting PM2.5 levels, in the close proximity of a fire.
The results presented in this work highlight the fact that the concentration of fine particles in the atmosphere close to the fireline is extremely dynamic, with differences between sensors that go up to 540% in terms of average concentrations and 170% in peak values. This is particularly relevant taking into account that these differences were registered in sensors at a distance of 10 m. This conclusion suggests that in a single fire crew considerable differences in the exposure of its members can occur depending on their task/position in relation to the fire front.
Data analysis suggests also that the visual estimate of fire safety conditions can be misleading, as concluded from the comparison between monitored PM2.5 levels and video footage, as a consequence of e.g. reduced visibility. In wildfire suppression operations the safety of the involved personnel should rely also on the use of personal exposure monitoring equipment for the prevention of potentially critical exposure.
In agreement with previous field measurements [Miranda *et al*., 2010] the smouldering stage can be critical to the security of firefighters in the terrain, because of the higher emission of fine particles (when compared to the flaming phase) and the ‘immersion’ of firefighters in smoke when carrying out mopping operations (due to the decreased fire intensity).

Acknowledgements

This work was supported by European Funds through COMPETE and by National Funds through the Portuguese Science Foundation (FCT) within projects PEst-C/MAR/LA0017/2013, FUMEXP (PTDC/AMB/66707/2006) and VitalResponder2 (PTDC/EEI-ELC/2760/2012), and the Post-Doc grants of J.H. Amorim (SFRH/BPD/48121/2008) and J. Valente (SFRH/BPD/78933/2011).

References

Dost FN, 1991. Acute toxicology of components of vegetation smoke. Rev Environ Contam Toxicol 119, 1-46.

IARC, 2010a. International Agency for Research on Cancer. IARC Monographs on the Evaluation of Carcinogenic Risks to Humans. Volume 98 - Painting, Firefighting, and Shiftwork. Lyon, France. 804 p.

IARC, 2010b. International Agency for Research on Cancer. IARC Monographs on the Evaluation of Carcinogenic Risks to Humans. Volume 92 - Some Non-Heterocyclic Polycyclic Aromatic Hydrocarbons and Some Related Exposures. Lyon, France. 868 p.

LeMasters GK, Genaidy AM, Succop P, Deddens J, Sobeih T, Barriera-Viruet H, Dunning K & Lockey J, 2006. Cancer risk among firefighters: a review and meta-analysis of 32 studies. J Occup Environ Med 48(11), 1189-1202.

Materna BL, Koshland CP & Harrison RJ, 1993. Carbon monoxide exposure in wildland firefighting: a comparison of monitoring methods. Appl Occup Environ Hyg 8(5), 479-87.

McMahon CK & Bush PB, 1992. Forest worker exposure to airborne herbicide residues in smoke from prescribed fires in the southern United-States. Am Ind Hyg Assoc J 53(4), 265-72.

Miranda A.I., Martins V., Cascão P., Amorim J.H., Valente J., Borrego C., Ferreira A.J., Cordeiro C.R., Viegas D.X. & Ottmar R., 2012. Wildland smoke exposure values and exhaled breath indicators on firefighters. J Toxicol Env Heal A 75(13-15), 831-843.

Miranda A.I., Martins V., Cascão P., Amorim J.H., Valente J., Tavares R., Borrego C., Tchepel O., Ferreira A.J., Cordeiro C.R., Viegas D.X., Ribeiro L.M. & Pita L.P., 2010. Monitoring of firefighters exposure to smoke during fire experiments in Portugal. Environ Int 36, 736-745.

Naeher LP, Brauer M, Lipsett M, Zelikoff JT, Simpson CD, Koenig JQ & Smith KR, 2007. Woodsmoke health effects: a review. Inhalat Toxicol 19, 67-106.

Reinhardt T.E. & Ottmar R.D., 2004. Baseline measurements of smoke exposure among wildland firefighters. J Occup Environ Hyg. 1, 593-606.

Reinhardt TE & Ottmar RD, 2000. Smoke exposure at western wildfires. USDA Forest Service Pacific Northwest Research Station Research Paper; 525 p.

Reinhardt TE, Ottmar RD & Hanneman A, 2000. Smoke exposure among firefighters at prescribed burns in the Pacific Northwest. USDA Forest Service Pacific Northwest Research Station Research Paper 526, 1-45.

Reisen F. & Brown S.K., 2009. Australian firefighters' exposure to air toxics during bushfire burns of autumn 2005 and 2006. Environ Int 35, 342-52.

Reisen F., Hansen D. & Meyer C.P., 2011. Exposure to bushfire smoke during prescribed burns and wildfires: firefighters' exposure risks and options. Environ Int 37, 314-321.

Rothman N, Ford D.P., Baser M.E., Hansen J.A., O'Toole T., Tockman M.S. & Strickland PT, 1991. Pulmonary function and respiratory symptoms in wildland firefighters. J Occup Med 33(11), 1163-1169.

Schwela D, 2001. Fire disasters: the WHO-UNEP-WMO health guidelines for vegetation fire events. Ann Burns Fire Disasters 13, 178-179.

Youakim S, 2006. Risk of cancer among firefighters: a quantitative review of selected malignancies. Arch Environ Occup Health 61(5), 223-231.

Sources and implications of bias and uncertainty in a century of us wildfire activity data

Karen C. Short

USDA Forest Service, Missoula Fire Sciences Laboratory, 5775 US Hwy 10 W, Missoula, Montana, 59808, USA, kcshort@fs.fed.us

Abstract
Analyses to identify and relate trends in wildfire activity to factors such as climate, population, land use/land cover, and wildland fire policy are increasingly popular in the United States (US). There is a wealth of US wildfire activity data available for such analyses, but users must be aware of inherent reporting biases, inconsistencies, and uncertainty in the data in order to maximize the integrity and utility of their work. Data for analysis are generally acquired from archival summary reports of the federal or interagency fire organizations; incident-level wildfire reporting systems of the federal, state, and local fire services; and, increasingly, remote-sensing programs. This paper provides an overview of each of these sources and the major reporting biases, inconsistencies, and uncertainty within them. Use of the national fire reporting systems of state and local fire organizations has been rising in recent decades, providing an improved set of incident-level data for all-lands analyses of wildfire activity. A recent effort to acquire, standardize, error-check, compile, scrub, and evaluate the completeness of US federal, state, and local wildfire records from 1992-2012 has been completed for the national Fire Program Analysis (FPA) application. The resulting FPA Fire-Occurrence Database (FPA FOD) currently includes nearly 1.7 million records from the 21-year period, 1992-2012, with values for at least the following core data elements: location (fire origin) at least as precise as a Public Land Survey System section (2.6 km^2 grid), discovery date, and final fire size. The FPA FOD is publicly available from the US Forest Service Research Data Archive (http://dx.doi.org/10.2737/RDS-2013-0009.2). While necessarily incomplete in some aspects, the database is intended to facilitate fairly high-resolution geospatial analysis of US wildfire activity over recent decades.

Keywords*: wildfire occurrence, reporting, data, statistics, bias, uncertainty, USA*

Introduction

The statistical analysis of wildfire activity is a critical component of national wildfire planning, operations, and research in the United States (US). Wildfire activity data have been collected in the US for over a century. Yet, to this day, no single, unified system of wildfire record-keeping exists. Data for analysis are generally harvested from archival summary reports of the federal or interagency fire organizations; incident-level wildfire reporting systems of the federal, state, and local fire services; and, increasingly, remote-sensing programs. It is typical for research into wildfire activity patterns for all or part of the last century to require data from several of these sources and perhaps others. That work is complicated by the disunity of the various datasets and potentially compromised by inherent reporting biases, inconsistencies, and errors or uncertainty in the data, as described here.

2. Data sources

Data for analyses of variables like wildfire numbers and area burned in the US are available in various forms from the early 20th century to the present. Figure 1 shows the general temporal coverage of key data sources, grouped into three categories: (1) archival summary reports, (2) documentary fire records, and (3) remotely sensed data.

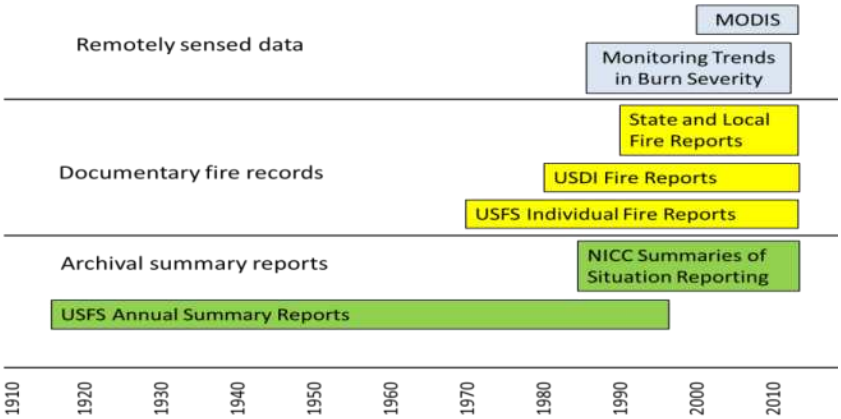

Figure 1. Timeline showing the general temporal spans of the sources of US wildfire activity data discussed in this paper.

The longest time period is covered by the archival summary reports, circa 1916 to 1997, from the US Forest Service (USFS). These reports include annual estimates of wildfire activity on all US lands (forest and non-forest) that qualified for organized wildfire protection in any given year, as per the statutory requirements of the 1911 Weeks Law and subsequent legislation. Figures were reported for each US state and included estimates of wildfire numbers and area burned by land ownership, fire cause, and fire size class. The National Interagency Coordination Center (NICC) began issuing an independently sourced set of similar reports in 1983. The basic fire occurrence information in those annual summaries comes from the NICC's Situation Reporting module, which gets daily activity reports from wildland fire dispatch offices during fire season and weekly reports otherwise. Together, the USFS and NICC archival summary reports provide over a century of wildfire-activity data (Figure 1), and are commonly used to characterize trends in variables like wildfire area burned over lengthy periods at the national level or by interstate region (e.g., Houghton *et al*. 2000, Mouillot and Field 2005, Collins *et al*. 2006, Littel *et al*. 2009).

Documentary fire records, which are created using standard forms issued by the various federal, state, and local fire organizations, are warehoused and readily available in electronic format for several recent decades (Figure 1). These fire reports are intended to capture the basic facts about each individual wildfire occurrence – including point of origin, date, cause, and final fire size – as well as additional information about responses and impacts associated with the incident. The USFS, bureaus of the US Department of Interior (USDI), state fire authorities, and local fire departments use different forms and reporting systems to capture these incident-level data, and their electronic archives span different time periods (approximated by Figure 1). Some states, like California and Alaska have digital archives (including locally mapped perimeters of large fires) that extend over longer historical periods than Figure 1 indicates; but their extensive electronic archives are exceptional cases. The fire-climate analyses of Westerling *et al*. (2003, 2006) are examples of work based on documentary wildfire records.

For recent decades, remotely sensed fire data are also available, including satellite-derived perimeters, or burn scars, of large (i.e., >405 ha) fires dating back to 1984, from the Landsat-based Monitoring Trends in Burn Severity (MTBS) project (Eidenshink *et al*. 2007). The MTBS data have increasingly been used to identify trends in and drivers of large-fire activity in the US (e.g., Riley *et al*. 2013, Dennison *et al*. 2014, Lannom *et al*. 2014). The remote sensing group (Figure 1) also includes satellite fire detection data like the active fire (hotspot) and burned area products that date back to circa 2000 from use of the Moderate Resolution Imaging Spectroradiometer (MODIS) on board the Aqua and Terra satellites (Giglio *et al*. 2003). While other satellite sensors have advanced fire detection capabilities, including the Geostationary Operational Environmental Satellite (GOES) system and the

Visible Infrared Imaging Radiometer Suite (VIIRS), this paper focuses on just the MODIS products due to their widespread use in fire activity analyses in the US and elsewhere over the past decade (Mouillot *et al*. 2014, Schroeder *et al*. 2014; e.g., Urbanski *et al*. 2011, Hawbaker *et al*. 2013, Parks 2014).

Bias and uncertainty

The following sections are intended to provide an overview of the major reporting biases, inconsistencies, and sources of errors and uncertainty in the different types of US wildfire activity datasets (Figure 1). It is beyond the scope of this paper to daylight and detail every issue that may concern a keen analyst. When topics have been covered in more depth elsewhere, readers will be referred to other published work for further information.

Archival summary reports

The USFS annual summary reports cover the longest time period, but are neither complete nor consistent over the ~80 years that they are available, because wildfire activity was tallied from an increasing land area over time. This changing baseline must be taken into account when analyzing and interpreting the data. The reporting area more than triples in size from 1926 to 1983 (Figure 2), which is the time period for which area-reporting figures are included in the USFS annual summaries. The reporting area rises as the land base qualifying for the federal fire protection program that required the reports grows from just the forested and other critical watersheds mandated by law in the earliest years to nearly the total burnable US land area by the early 1980s (Fig 2). (The estimate of total burnable wildland in the US used here is based on data generated by the national LANDFIRE program using circa 2000 satellite imagery [Reeves *et al*. 2006]). Even then, not all of the reporting area was formally protected from wildfire under the program requiring the statistics. Therefore the USFS wildfire activity data are classified as from "protected" and "unprotected" areas, with unprotected areas having no organized fire protection despite their need for it as per the national directive at the time (explained further by Houghton *et al*. [2000]). The total area of protected land estimated in the USFS reports does not reach total US burnable area until the last year it is included in the reports, which is 1990 (Fig 2).

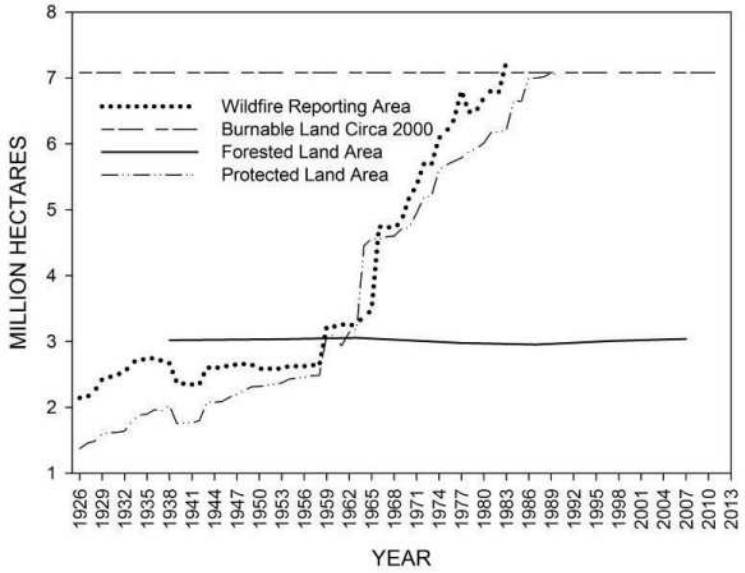

Figure 2. US wildfire reporting area (dotted line), 1926-1983, and protected land area (dot-and-dash), 1926-1990, from the USFS archival summary reports. The upper dashed reference line represents the ~700 million ha of US land, including Alaska, mapped as burnable from circa 2000 satellite imagery by the national LANDFIRE program. The lower horizontal reference line represents approximately 750 million acres of US forested land estimated at various points in time during this period by the national Forest Inventory and Analysis program.

Because the USFS summary reports are broken down by US state, the reporting biases can be examined further at that resolution. Figure 3 shows the percent burnable area reporting, by contiguous US state, as an average within the three decades from 1950 to 1979, which correspond to a collective period of marked increase in land area accounted for in the USFS reports (see Figure 2). By the 1970s, the reporting area begins to reach what could be considered an "all-lands" coverage, but not in all states. Some states, like Alaska and Kansas, are completely unaccounted for in the USFS wildfire activity statistics prior to the 1940s and 1950s; others, like Texas and North Dakota, remain poorly accounted for well into the 1970s.

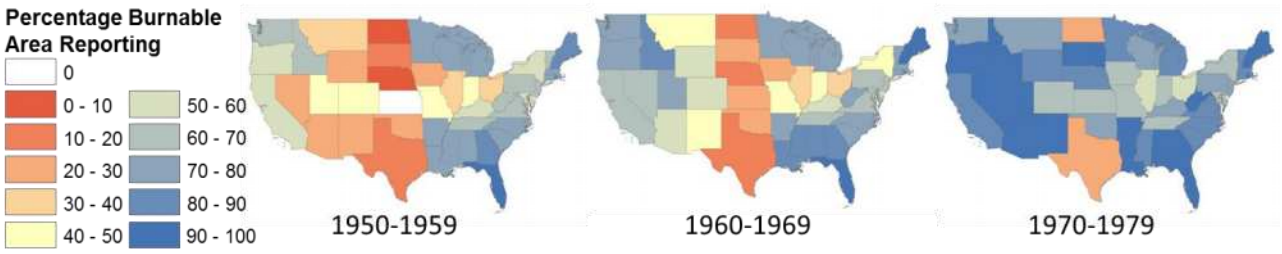

Figure 3. Percent burnable land area accounted for in the USFS annual wildfire summary reports, as an average for each contiguous US state during the three decades from 1950-1979.

One reason for the large increase in land area accounted for in the USFS wildfire summary reports during the 1960s is the inclusion of an additional ~70 million hectares (ha) of western US rangelands administered by the USDI Bureau of Land Management (BLM) (Figure 4). This addition occurred after wildfires burned several hundred thousand acres of BLM lands near Elko, Nevada, in 1964 and brought the BLM fully into the cooperative fire control program for which the USFS reports were generated (Pyne 1982). Estimates of wildfire activity levels on BLM lands in the contiguous US (CONUS) were first included in the 1966 USFS summary reports. Prior to 1966, the USFS statistics accounted for wildfire activity on only about half of the contemporary federal land base in the 11 westernmost states in the CONUS (Figure 4). Littel *et al*. (2009) recognized the reporting bias and, as part of their analyses of fire-climate relationships in the western US, multiplied the USFS-reported wildfire-area-burned (WFAB) estimates "by the ratio of the total area protected in 2003 to the area protected in a given year." Such adjustment assumes that wildfire activity levels are largely equivalent on a per-acre basis between the reporting and non-reporting areas. However, the areas unaccounted for in the early USFS wildfire statistics (e.g., pre-1960s) for the US West should comprise a much greater proportion of non-forested land than the areas reporting, potentially invalidating any assumption of comparable fire-activity levels and possibly contributing to the underperformance of fire-climate models based on WFAB estimates that included the early USFS figures (e.g., pre-1977) versus those that did not (Littel *et al*. 2009).

In addition to the area-reporting bias in the USFS summary reports, analysts should be aware of other inconsistency and uncertainty in the wildfire activity estimates that are included, especially for unprotected areas. Intentional, or controlled burning, was used extensively for vegetation management on nonfederal lands, especially in the southeastern US during the early 20th century. While now used to a lesser extent (but on both federal and nonfederal lands) in the US, intentional burning is not classified in the current reporting systems as "wildfire" unless the controlled burn escapes and requires a suppression response. However, the early USFS wildfire activity summaries do include millions of acres of intentional burning on "unprotected" lands, which, until about the mid-20th century was viewed by the USFS as akin to wildfire, as something that should be prevented and ultimately eradicated (Pyne 1982). Controlled burning became accepted as an acceptable land management practice over time and persists to this day (Melvin 2012); however, statistics regarding its use have not been included in summaries of "wildfire" activity for several decades. Furthermore, the USFS includes with its unprotected area estimates the

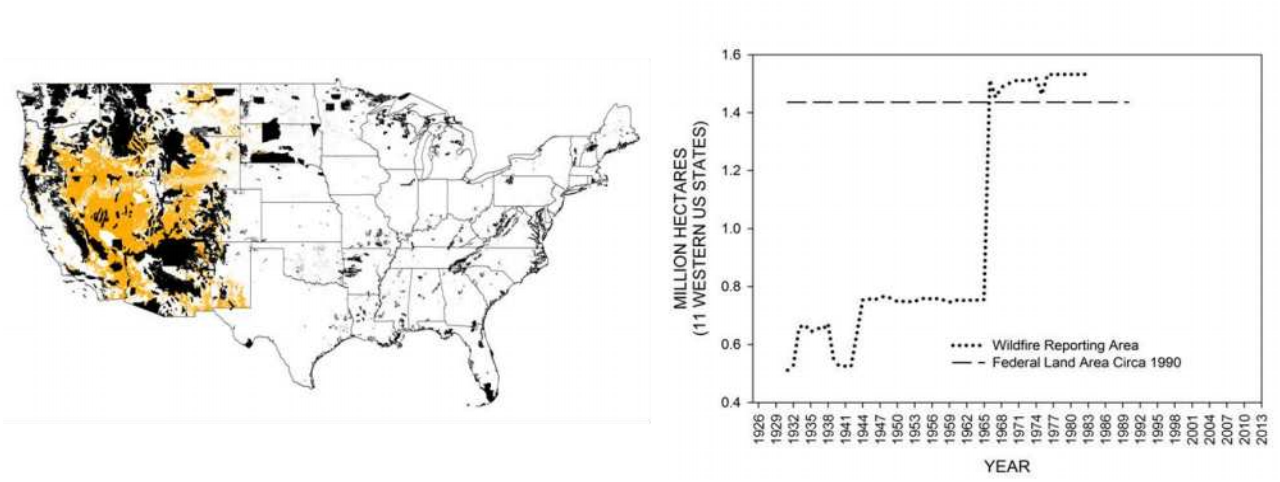

Figure 4. Map of the CONUS showing lands administered by the USDI Bureau of Land Management (BLM) in orange and other federal lands in black. Wildfires on these BLM lands, which include ~70 million ha of largely non-forested area in the western US, are not accounted for in the USFS wildfire summary reports until 1966, after the BLM joined the cooperative fire control program for which the USFS reports were generated. The graph at right shows the spike in reporting area. The dashed reference line represents the ~140 million ha of total federal land in the 11 westernmost states of the CONUS as of the year 1990.

following caveat: "since no field organizations are established in unprotected areas to report fires, the statistics on such unprotected areas are merely the best estimates by local agencies." Although the degree of error in the reported figures cannot be known, egregious errors apparently exist at least in some of the WFAB estimates from unprotected and protected areas. For example, the USFS annual summary reports for 1976-1983 indicated that ~800,000 ha were burned by wildfires in Texas during each of four years within that eight-year period. Those are levels comparable to those witnessed in the state during what have been considered unprecedented fire seasons of 2006 and 2011 – seasons that prompted disaster declarations by the Federal Emergency Management Agency. There are multiple independent sources, including remotely sensed data, that corroborate the 2006 and 2011 estimates; but no records, including media reports, have been found to corroborate the similarly high USFS estimates from 1976-1983. Several authorities within the Texas state fire service have asserted that the USFS estimates must be in error, because the fire service has no recollection of large fires burning in 1976-1983 on par with those in 2006 and 2011; and those recent "outbreak" years were so significant that records of similar years, had they occurred just a few decades prior, would abound, especially in media archives (C. Stripling, T. Spencer, B. Smith: personal communication). If millions of acres did not burn in Texas during each of several years 1976-1983, then any regional or national WFAB estimates based on the USFS summary reports are inflated as well. The total US WFAB reported by the USFS for each of the affected years is 1.6-2 million ha, with 35-50% based on the apparently inflated Texas unprotected-area estimates.

Potential errors in the wildfire activity statistics in the USFS annual summary reports are not limited to Texas, nor are they limited to figures from unprotected areas. Another potentially significant example is found in the USFS report for 1977. In that year, the USFS WFAB figure for protected lands in Alaska is 40,000 ha. However, WFAB estimates for that state in 1977 (~900,000 ha) published by Gabriel and Tande (1983) and several media outlets indicate that the USFS figure is an extreme underestimate.

While the reporting biases and potential errors in the wildfire activity statistics in the USFS annual summary reports should be recognized and addressed in analyses for which they are used, a portion of the data have been made readily available online with no formal citation or any reference to their source. At the time of this writing, the excerpt includes estimates of total wildfire numbers and area burned for the US from 1960-1982, and exists in tabular form on the website of the External Affairs

section of the National Interagency Fire Center (NIFC), which is where the NICC is located. The NIFC webpage with figures for a total span of 1960-2013, http://www.nifc.gov/fireInfo/fireInfo_stats_totalFires.html, is among the first returned in an Internet search for "wildfire statistics" or a similar term. While the estimates are identified as "total wildland fires and acres," at the time of this writing, the figures represent wildfires only, and exclude intentional, or controlled burning, which is a type of wildland fire by definition of the National Wildfire Coordinating Group (NWCG 2014). The figures for 1983-2013 are attributed to the Situation Reporting system that generates the estimates of wildfire numbers and area burned in the NICC annual reports described in Sect. 2 (see also Figure 1). However, the same footnote explains that "prior to 1983, sources of these figures are not known, or cannot be confirmed, and were not derived from the current situation reporting process. As a result the figures prior to 1983 shouldn't be compared to later data." Yet, when the NIFC figures are plotted with the USFS annual summary reports (Figure 5), whether as wildfire numbers or area burned, it is clear that NIFC External Affairs is using USFS estimates for 1960-1982.

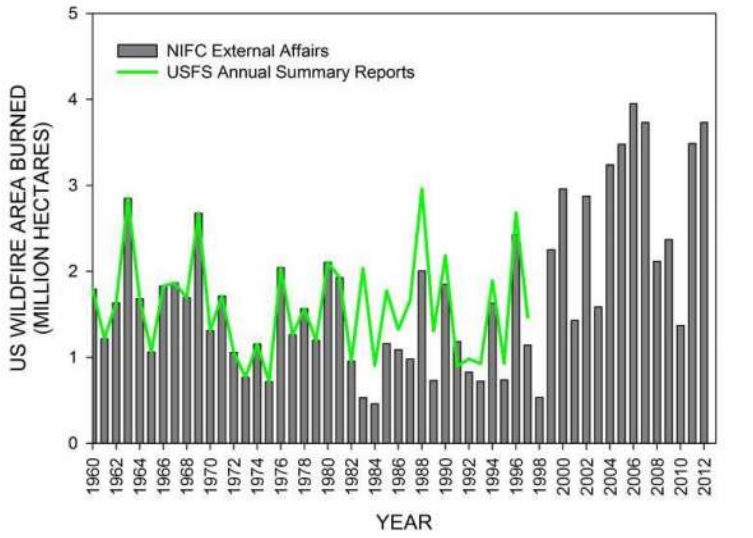

Figure 5. Comparison of US wildfire area burned estimates distributed by NIFC External Affairs for 1960-2012 (bars) compared with estimates for 1960-1997included in the USFS archival summary reports (line). The figures, whether wildfire numbers or wildfire area burned are identical between the sources for 1960-1982, indicating that the USFS summary reports are the source of the NIFC figures. The figures for 1983-2012 differ between the sources, because, as NIFC explains, those estimates are from the NICC summaries of the Situation Reporting data.

When the estimates from the USFS publications and the NIFC estimates sourced from the NICC Situation (SIT) Reporting summaries overlap in 1983-1997, the USFS figures tend to meet or exceed the values in the NICC summaries. As noted above, the USFS estimate for US WFAB for 1983 may be inflated by as much as 800,000 ha. While additional errors may exist in the USFS statistics, the NICC numbers may be biased downward during at least a portion of the period of overlap. Use of the SIT Reporting application, on which the NICC summary reports are based, is required only by agency and local dispatch offices associated with federal lands; it is effectively optional for nonfederal units with wildfire protection responsibility only for nonfederal lands. Voluntary SIT Reporting by nonfederal units may result in considerable underestimation of elements like wildfire numbers and area burned in the NICC annual reports. The magnitude of the discrepancies between the USFS reports and the NICC numbers appears largest in the earliest years of SIT Reporting (circa 1983; Figure 5), when the network of participating units was likely at its smallest

3.2. Documentary fire records

In general, documentary fire records of the federal, state, and local fire organizations are warehoused and available in electronic format only for a relatively recent period of several decades (Figure 1). The numerous US fire organizations have separate wildfire reporting requirements, standards, protocols, and archival systems, and compilation of data from multiple systems is difficult and time consuming (Short 2014). It is therefore typical for wildfire activity analyses based on the documentary fire records to be limited to a single agency, like the USFS, or to federal lands only (e.g., Westerling *et al*. 2003, 2006).

Yet, even within a single fire organization's system of record, the available electronic archive does not necessarily provide a complete or consistent accounting of actual wildfire activity. The USFS digital fire-reporting archive, for example, extends back to 1970. However, records from 1970-1992 were stored on computer tape before they were migrated, in 1992, to the current database archive (Bunton 2000). Bunton (2000) explains that, once the data from that early period were written to tape, no corrections could be made. Moreover, "some fire reports were never added to the tape files, and . . . most of the missing fires were very large fires that were still active (not declared out) until well after the annual report for the year was completed" (Bunton 2000). Once they were migrated from tape to database, records from prior to 1986 remained un-correctable, although Bunton (2000) indicates that some records of missing large fires were added after the current archival system was initiated in 1992. Analysts commonly consider the USDI fire records complete only back to 1980, because the digital archive is erratically populated prior to that year. However, formal and comprehensive fire reporting was not consistently mandated by the USDI bureaus until the mid-1980s, and the USDI archive suffers from many of the data quality and completeness issues as does that of the USFS prior to circa 1992 (S. Larrabee, personal communication).

Each of the fifty US states experiences wildfires that occur outside of the protection responsibility areas of federal government, and each maintains records of those events in non-federal reporting systems. While the period of record in the digital archives differs among the various non-federal fire organizations, the degree and quality of formal fire reporting has generally risen over time (Thomas and Butry 2012, Short 2014). For analyses of wildfire activity that include figures from states like Texas, for which wildfire protection and reporting is almost entirely the responsibility of the state or local service (see Artley 2009), it will be crucial to recognize and account for any nonfederal reporting idiosyncrasies within the domain of interest; they can be substantial (Short 2014).

The content, quality, and completeness of the available data can vary considerably among organizations and over time. For example, in the federal systems, the spatial resolution, or precision, of a fire's reported point of origin has generally improved over time from a legal description – township, range, and section – to actual point coordinates in latitude and longitude. However, most local fire department records can be spatially resolved to county or zip code at best – often referencing the zip code of a responding fire station. Location information from the state reporting systems can span the whole spectrum from a latitude-longitude point of origin to a nominal state designation only. Fire cause and final fire size are other basic occurrence-related elements that tend to range in both specificity and accuracy, if reported at all (Prestemon *et al*. 2013). Estimates of fire size from locally (e.g., manually) mapped and satellite-derived fire perimeters (polygons) may differ from that included in the incident reports; and all may overestimate area burned by including unburned islands within the fire perimeter (Kolden and Weisberg 2007).

3.3. Remotely sensed data

The use of satellite-derived fire detection and mapping products in wildland fire science has been expanding in the US and across the globe in recent decades (Mouillot *et al*. 2014). These remotely sensed datasets have proven particularly valuable where ground data are lacking or otherwise incomplete (Mouillot *et al*. 2014). In the US, areas of limited ground-based documentary wildfire data

may include lands for which fire protection is the responsibility of a local fire service that does not submit fire activity information to the (voluntary) national fire department reporting system. Millions of burnable hectares, including large fire-prone areas within several states in the south-central US (e.g., Kansas, Oklahoma, and Texas) may fall into this category in any given year (Short 2014). However, the MODIS active fire and burned area products have a relatively short history among the US wildfire activity datasets, dating back only to circa 2000 (Figure 1). To benefit from the enhanced fire detection capability of dual sensors (Hawbaker *et al*. 2008), analyses of MODIS products must be restricted to post-2003, which is the first full year that instruments were in use on both the Aqua and Terra satellites. The current MTBS large-fire perimeter (and burn severity) dataset nominally spans a lengthier period, 1984-2012, although it does not account for the majority of large fires in Alaska prior to 1999.

At present, the 30 m resolution MTBS burn scar dataset affords a consistently generated geospatial archive of large fire occurrence for nearly 30 years across most of the US. Fires are mapped regardless of land ownership or agency affiliation, and therefore the MTBS dataset can be used for all-lands analyses of spatially explicit large fire activity in recent decades. Yet, although it is intended to represent all fires greater than 404 ha in the western US and those greater than 202 ha in the eastern US, the MTBS dataset does miss some fires. Landsat scene selection in the MTBS mapping process is directed by reports of large fires in a compilation of documentary fire records from federal and state wildland fire reporting systems (Eidenshink *et al*. 2007). Fires missing from the MTBS compilation of documentary records – and fires with records lacking adequate temporal or spatial information to point to a specific Landsat scene – are unlikely to be included in the MTBS perimeter dataset, unless the burn scars are discovered by chance in the process of mapping other fires. Fires may likewise be missed or incompletely mapped due to poor scene quality (e.g., clouds, smoke, shadows), obstructive tree canopy over surface fire scars, patchy burning within pixels, mismatches in pre- and post-fire imagery related to sun angle and phenology, or rapid (<1 year) post-fire vegetation recovery (e.g., in some grassland and sprouting-shrub systems) (Kolden and Weisberg 2007, Kolden *et al*. 2012).

While the MTBS data suite includes pixel-level severity estimates for mapped fires, the identified unburned areas are not excised by rote from fire perimeters included in the polygon-based MTBS product. The unburned portions within the MTBS (and other) mapped perimeters can be substantial. Kolden *et al*. (2012) reported a total of 14-35% unburned area within fire perimeters from three national parks in the western US, 1984-2009, mapped using the MTBS protocol. Kasischke and Hoy (2012) found a similar average of 20% unburned within fire perimeters from Alaska forest fires in 2004 and 2006-2008. However, the unburned fraction can vary greatly among fires, and has been found to be inversely related to factors like fire size and severity (Kolden *et al*. 2012). If the size and severity of wildfires, for example, increase over time, the unburned portions within fire polygons may decrease. Kolden and Weisberg (2007) describe in further detail the challenges and associated sources of error in the mapping and measuring of wildfire area burned, both locally and remotely via the MTBS protocol, and readers are referred to that publication for more on these topics.

The MTBS dataset identifies prescribed (or controlled) burns separately from wildfires. This "fire type" attribute is useful for screening out the intentional, controlled burns for an analysis of wildfire activity. However, prior to the 2014 release, fires mapped by MTBS defaulted to a fire-type label of "wildfire," and that default label was updated to another type (e.g., prescribed fire) only when the associated fire report specified accordingly. For this reason, all fires mapped without the aid of documentary records (e.g., fires discovered in the process of mapping others) were all identified as wildfires. In the 2014 release, this issue was remedied to some degree by relabeling any fires of uncertain fire type to "unknown." Of the ~23,000 fire polygons in the 2014 MTBS product release, 4,500 (20%) are now labeled as unknown fire type. Analysts must determine the appropriate use of these uncertain types. Many of the fires of unknown type map within the Flint Hills region of Kansas and northern Oklahoma, where ~700,000 ha are intentionally burned each spring for rangeland improvement (KDHE 2010, Melvin 2012). Fires of unknown type in that region are prime candidates for exclusion from MTBS-based analyses of wildfire activity.

Improvements in spaceborne sensors over the past couple of decades have expanded the available set of data products characterizing fire activity and associated burned area (Mouillot *et al*. 2014). Products derived from MODIS sensors are increasingly used for analyses of wildland fire activity, as the instruments employ what are considered to be the most useful channels (spectral bands) for fire monitoring and mapping – at spatial resolutions of 500 m (burned area) to 1 km (active fire). The MODIS active fire product (Giglio *et al*. 2003) is based on detection of thermal anomalies; and while strictly a fire detection product, it has been used to estimate burned area in the US (e.g., Wiedinmyer *et al*. 2011, Hawbaker *et al*. 2013). Temporal sampling by the MODIS sensors (on two Earth Observation Satellites) is relatively limited: a total of four satellite overpasses comprise a midday pair and a nighttime pair. Thus the sensors will not always overpass as burning occurs, and clouds (or smoke) may preclude active fire detection during the limited overpasses (Giglio *et al*. 2006, Hawbaker *et al*. 2008, Urbanski *et al*. 2009). In general, the MODIS active fire product is subject to high omission errors with regard to fires of small size, short duration, or low-intensity and may underestimate area burned by large, rapidly moving fires that travel across multiple MODIS pixels between overpasses (Hawbaker *et al*. 2008). The MODIS sensors are generally considered to have a lower fire-size detection threshold of ~100 m^2 under the most favorable conditions (Giglio *et al*. 2003). But above that size threshold, omission errors can be quite high and tend to be much greater in grasslands and open shrublands than in forested areas (Hawbaker *et al*. 2008, Urbanski *et al*. 2009, Mouillot *et al*. 2014). According to Urbanski *et al*. (2009), "even large rangeland fires (>2000 ha) may completely evade MODIS detection." Within a given vegetation type, however, active-fire omission errors tend to decrease with increasing fire size (Hawbaker *et al*. 2008, Urbanski *et al*. 2009).

Errors of commission in the MODIS active fire product may result from confusion of highly reflective non-fire surfaces with true fires, or, due to its contextual algorithm, from sharp radiometric contrasts between adjacent non-fire elements, like certain vegetation and soils (Hawbaker *et al*. 2008). More importantly and despite omission errors, burned areas derived from MODIS active detection products tend to overestimate the true burned area because the sensor's detection threshold of ~100 m^2 is much lower than the product's 1 km pixel resolution (Giglio *et al*. 2006). Thus, while MODIS active fire product may capture the majority of certain types of large fire events (e.g., forest fires), the corresponding burned area estimates are highly error prone. Adjustments to initial burned area estimates, including scaling by fraction of vegetation cover or a combination of vegetation cover and fire-pixel clustering, may improve burned area estimates derived from the active-fire product (Giglio *et al*. 2006, Wiedinmyer *et al*. 2011).

Aside from the thermal-based active-fire product, several 500-m resolution MODIS burned area products based on surface reflectance (burn scars) have been generated (Mouillot *et al*. 2014). Roy *et al*. (2005) and Giglio *et al*. (2009) identify burn scars based on changes in surface reflectance, while Urbanski *et al*. (2009) developed an algorithm to produce near-real-time burn scar data using a single observation of surface reflectance. The burn scar algorithm of Roy *et al*. (2005) is employed in the standard, monthly MODIS burned area product distributed by the US National Aeronautics and Space Administration. Both Giglio *et al*. (2009) and Urbanski *et al*. (2009) leverage the active fire detections in their algorithms to confirm burn scars and reduce uncertainty in burned area estimates; using a version of this method (and MTBS burned pixels rather than NICC burned area estimates as "ground-truth" data) Urbanski *et al*. (2011) were able to reduce the apparent upward bias in MODIS burned area estimates for the western US, 2003-2008, to 7% and estimated uncertainty in their annual estimates of area burned by wildland fire to $\leq$5%.

From a *wildfire* activity standpoint, another important source of uncertainty in the MODIS-based products is the conflation of wildfire and intentional, controlled (or prescribed) burning in both wildland and agricultural areas. All of the controlled burning must be screened from remote sensing fire products for any analyses of wildfire activity, *per se*. According to estimates from the NICC, an average 800,000 ha of wildlands have been intentionally burned (with prescribed fire) in the US annually since the NICC began keeping records in 1998. However, that figure is a conservative

estimate, because much controlled burning on private lands, including commercial timberlands, is not reported to the NICC. An independent survey of controlled burning levels for the year 2011 by the National Association of State Foresters and the Coalition of Prescribed Fire Councils, suggests that the total area deliberately burned in the US during that year was 8 million ha, or *ten times* the NICC estimate (Melvin 2012). Of that total, 39% (3.1 million ha) was reported as controlled burning on forested lands, predominantly in the southeastern US; while the remainder was considered agricultural burning, largely in western and central plains states (Melvin 2012). Assuming the 2011 controlled burning figures are typical, which Melvin (2012) suggests, and given that the average annual area burned by wildfire over the past 20 years is estimated (from several sources) as ~2.3 million ha (Short 2014), then the vast majority of area burned annually in the US is not from wildfire, but from intentional burning for agricultural or other land management purposes. Moreover, the contemporary annual area burned by wildfire in the US appears likely to be less than that burned deliberately for forestry objectives. Therefore, even if MODIS detection rates from agricultural areas are expected to be relatively low (Hawbaker *et al*. 2008) and even if remotely sensed landcover maps can be used to exclude detections in pixels mapped as developed or agriculture/cropland (McCarty *et al*. 2007, Urbanski *et al*. 2011, Hawbaker *et al*. 2013), additional efforts must be made to exclude controlled burning in forested areas. Otherwise, "wildfire" activity levels would likely be greatly overestimated from MODIS products, especially if the southeastern US is included in the analysis.

Mouillot *et al*. (2014) expand on many of the points made here with regard to potential limitations of the MODIS (and other satellite-based) products and discuss them specifically in light of potential uses of the data, including for hazard assessment, mobilization of firefighting resources, and emissions modeling; readers seeking more information on these topics are encouraged to consult that publication. With growing interest in MODIS-based active fire count and burned area datasets there is increasing pressure to improve the accuracy, resolution, and temporal specificity of the products (Mouillot *et al*. 2014, Schroeder *et al*. 2014). Any changes in detection capabilities or processing algorithms that result in such improvements must be taken into account in any multiannual analysis to potentially mitigate influences of temporal instability in the datasets.

Summary and Conclusion

There is a wealth of US wildfire activity data available for analyses today, but analysts must be aware of inherent reporting biases, inconsistencies, and uncertainty in the data in order to maximize the integrity and utility of their work. Users of data from archival summary reports should recognize that the estimates come from an increasing land area over time, and even the most recent annual wildfire summary reports from the NICC do not account for all wildfire activity (especially fire numbers) in the US, due in part to limited wildfire reporting by local fire departments (Thomas and Butry 2012). Moreover, all estimates are just that, and area-burned estimates are inherently uncertain. Burned area estimates based on fire perimeters, which often include significant unburned portions, are typically biased high (~15-30%). Analysts attempting to assess MODIS burned area products have, for example, adjusted the NICC reference figures of area burned by a factor of 0.72 to account for a perceived overestimation of 28% (Urbanski *et al*. 2009). Unadjusted, area burned figures based solely on the MODIS active fire product tend to be overestimates, due to the ability of the sensors to detect fires smaller than the products' pixel sizes. Algorithms that use the active fire detections to confirm burn scars can generate MODIS burned area products that align well with those estimated from MTBS burn scars (with unburned islands excluded).

All remotely sensed datasets intended for analyses of wildfire activity, per se, must be carefully screened to remove areas burned intentionally for in both agricultural areas and wildlands, which may account for 80% of the total area burned in the US in any given year. Millions of ha of intentional burning in the southeastern US are included as part of the annual estimates of wildfire activity on unprotected lands for several early decades of the USFS annual summary reports. It is inappropriate

to compare, for example, the early total area burned estimates, which factor in "prescribed fire," to the statistics in later USFS reports, which omit it, or to compare them to figures post-1998 in the NICC reports, which greatly underestimate levels of intentional burning in the US.

Documentary fire records from the digital archives of federal wildfire reporting may not fully represent total wildfire activity levels in years prior to 1992, but it is unclear how much data is missing. Use of the national fire reporting systems of state and local fire organizations has been rising in recent decades, providing an improved set of incident-level data for all-lands analyses of wildfire activity. Short (2014) expanded on earlier efforts of Schmidt *et al* (2003) to compile federal and nonfederal wildfire data from the various reporting systems for the national Fire Program Analysis system. The resulting FPA Fire-Occurrence Database (FPA FOD) currently includes nearly 1.7 million records from the 21-year period, 1992-2012, with values for at least the following core data elements: location (fire origin) at least as precise as a Public Land Survey System section (2.6 km^2 grid), discovery date, and final fire size. The FPA FOD is publicly available from the USFS Research Data Archive (http://dx.doi.org/10.2737/RDS-2013-0009.2). While necessarily incomplete in some aspects (Short 2014), the database is intended to facilitate fairly high-resolution geospatial analysis of US wildfire activity over recent decades. Additional elements added to the original fire records, including the unique MTBS perimeter identifiers, effectively provide a "bridge" between the ground- and satellite-based datasets, and the MTBS perimeters can be used in conjunction with the FPA FOD to expand upon geospatial analyses possible with point-of-origin information in the original fire reports (Short 2014).

References

Artley DK (2009) Wildland fire protection and response in the United States: the responsibilities, authorities, and roles of federal, state, local, and tribal government. Report for the International Association of Fire Chiefs.

Bunton DR (2000) Wildland fire and weather information data warehouse. In 'Proceedings of the Seventh Symposium on Systems Analysis on Forest Resources', 28-31 May 1997, Traverse City, MI, USA. USDA Forest Service, North Central Forest Experiment Station, General Technical Report GTR-NC-205, pp. 297-302 (St. Paul, MN).

Collins BM, Omi PN, Chapman PL (2006) Regional relationships between climate and wildfire-burned area in the Interior West, USA. *Canadian Journal of Forest Research* **36**, 699-709.

Dennison PE, Brewer SC, Arnold JD, Mortiz MA (2014) Large wildfire trends in the western United States, 1984-2011. *Geophysical Research Letters* **41**, 2928-2933.

Eidenshink J, Schwind B, Brewer K, Zhu Z, Quayle B, Howard S (2007) A project for monitoring trends in burn severity. *Fire Ecology* **3**, 3-21.

Gabriel HW, Tande GF (1983) A regional approach to fire history in Alaska. USDI Bureau of Land Management, BLM-Alaska Technical Report No. 9 (Anchorage, AK).

Giglio L, Descloitres J, Justice CO, Kaufman YJ (2003) An enhanced contextual fire detection algorithm for MODIS. *Remote Sensing of Environment* **87**, 273-282.

Giglio L, van der Werf GR, Randerson JT, Collatz GJ, Kasibhatla P (2006) Global estimation of burned area using MODIS active fire observations. *Atmospheric Chemistry and Physics* **6**, 957-974.

Giglio L, Loboda T, Roy DP, Quayle B, Justice CO (2009) An active-fire based burned area mapping algorithm for the MODIS sensor. *Remote Sensing of Environment* **113**, 408-420.

Hao WM, Larkin NK (2014) Wildland fire emissions, carbon, and climate: Wildland fire detection and burned area in the United States. *Forest Ecology and Management* **317**, 20-25.

Hawbaker TJ, Radeloff VC, Syphard AD, Zhu Z, Stewart SI (2008) Detection rates of the MODIS active fire product in the United States. *Remote Sensing of Environment* **112**, 2656-2664.

Hawbaker TJ, Radeloff VC, Stewart SI, Hammer RB, Keuler NS, Clayton MK (2013)

Human and biophysical influences on fire occurrence in the United States. *Ecological Applications* **23**, 565-582.

Houghton RA, Hackler JL, Lawrence KT (2000) Changes in terrestrial carbon storage in the United States. *Global Ecology & Biogeography* **9**, 145-170.

Kasischke ES, Hoy EE (2012) Controls on carbon consumption during Alaskan wildfires. *Global Change Biology* **18**, 685-699.

[KDHE] Kansas Department of Health and Environment (2010) Flint Hills smoke management plan. A report of the State of Kansas.

Kolden CA, Weisberg PJ (2007) Assessing accuracy of manually mapped wildfire perimeters in topographically dissected areas. *Fire Ecology Special Issue* **3**, 22-31.

Kolden CA, Lutz JA, Key CH, Kane JT, van Wagtendonk JW (2012) Mapped versus actual burned area within wildfire perimeters: characterizing the unburned. *Forest Ecology and Management* **286**, 38-47.

Lannom KO, Tinkham WT, Smith AMS, Abatzoglu J, Newingham BA, Hall TE, Morgan P,

Strand EK, Paveglio TB, Anderson JW, Sparks AM (2014) Defining extreme wildland fires using geospatial and ancillary metrics. *International Journal of Wildland Fire* **23**, 322-337.

Littel JS, McKenzie D, Peterson DL, Westerling AL (2009) Climate and wildfire area burned in western US ecoprovinces, 1916-2003. *Ecological Applications* **19**, 1003-1021.

McCarty JL, Justice CO, Korontzi S (2007) Agricultural burning in the Southeastern United States detected by MODIS. *Remote Sensing of Environment* **108**, 151-162.

Melvin M (2012) National prescribed fire use survey report. Coalition of Prescribed Fire Councils, Inc., Technical Report 01-12.

Mouillot F, Schultz MG, Yue C, Cadule P, Tansey K, Ciais P, Chuvieco E (2014) Ten years of global burned area products from spaceborne sensing – A review: Analysis of user needs and recommendations for future developments. *International Journal of Applied Earth Observation and Geoinformation* **26**, 64-79.

Mouillot F, Field CB (2005) Fire history and the global carbon budget: a 1^{o} x 1^{o} fire history reconstruction for the 20^{th} century. *Global Change Biology* **11**, 398-420.

[NWCG] National Wildfire Coordinating Group (2012) Glossary of wildland fire terminology. NWCG Publication PMS-205 (Boise, ID).

Parks SA (2014) Mapping day-of-burning with coarse resolution satellite fire-detection data. *International Journal of Wildland Fire* **23**, 215-223.

Prestemon, JP, Hawbaker TJ, Bowden M, Carpenter J, Brooks MT, Abt KL, Sutphen R, Scranton S (2013) Wildfire ignitions: a review of the science and recommendations for empirical modeling. USDA Forest Service, Southern Research Station, General Technical Report SRS-171 (Asheville, NC).

Pyne SJ (1982) 'Fire in America: a Cultural History of Wildland and Rural Fire' (University of Washington Press: Seattle).

Reeves MC, Kost JR, Ryan KC (2006) Fuels products of the LANDFIRE project. In 'Fuels Management – How to Measure Success: Conference Proceedings', 28-30 March 2006, Portland, OR, USA. (Eds Andrews PL, Butler BW) pp. 239-252. USDA Forest Service, Rocky Mountain Research Station, Proceedings RMRS-P-41 (Fort Collins, CO).

Riley KL, Abatzoglou JT, Grenfell IC, Klene AE, Heinsch FA (2013) The relationship of large fire occurrence with drought and fire danger indices in the western USA, 1984-2008: the role of temporal scale. *International Journal of Wildland Fire* **22**, 894-909.

Roy *et al*. (2005) Prototyping a global algorithm for systematic fire affected area mapping using MODIS time series data, *Remote Sensing of Environment* **97**, 137-162.

Schmidt KM, Menakis JP, Hardy CC, Hann WJ, and Bunnel DL (2002) Development of coarse-scale spatial data for wildland fire and fuel management. USDA Forest Service, Rocky Mountain Research Station, General Technical Report RMRS-87 (Fort Collins, CO).

Schroeder W, Oliva P, Giglio L, Csiszar IA (2014) The new VIIRS 375 m active fire detection product: algorithm description and initial assessment. *Remote Sensing of Environment* **143**, 85-96.

Short KC (2014) A spatial database of wildfires in the United States, 1992-2011. *Earth Systems Science Data* **6**, 1-27.

Thomas DS, Butry DT (2012) Wildland fires within municipal jurisdictions. *Journal of Forestry* **110**, 34-41.

Urbanski SP, Salmon JM, Nordgren BL, Hao WM (2009) A MODIS direct broadcast algorithm for mapping wildfire burned area in the western United States. *Remote Sensing of Environment* **113**, 2511-2526.

Urbanski SP, Hao WM, Nordgren B (2011) The wildland fire emission inventory: western United States emission estimates and an evaluation of uncertainty. *Atmospheric Chemistry and Physics* **11**, 12973-13000.

Wiedinmyer C, Akagi SK, Yokelson RJ, Emmons LK, Al-Saadi JA, Orlando JJ, Soja AJ (2011) The fire INventory from NCAR (FINN): a high resolution global model to estimate the emissions from open burning. Geoscientific Model Development 4, 625-641.

Westerling AL, Gershunov A, Brown TJ, Cayan DR, Dettinger MD (2003) Climate and wildfire in the western United States. *Bulletin of the American Meteorological Society* **84**, 595-604.

Westerling AL, Hidalgo HG, Cayan DR, Swetnam TW (2006) Warming and earlier spring increase western US forest wildfire activity. *Science*, **313**, 940-943.

Suppression capability of foams used fighting against forest fires with the test of weight rate remained on the crown surface R-10A Method - weight effectiveness experiment

Agoston Restas

National University of Public Service, Budapest, Hungary, Restas.Agoston@uni-nke.hu

Abstract
Introduction: The effectiveness of the foams used in fighting against forest fire depends on common effect of some coefficients. Cooling and isolation effects as main extinguishing effects as well as side extinguishing effects, like evaporation, blanket and separation effects are also included. Under the same conditions, the more extinguisher remains on the surface, the more extinguishing effect it has. Methods: A product for the test was randomly chosen out of the ones on the market. Spruce was chosen for the test due to its high flammability. The goal was to determine the amount of extinguisher at the end of the branches in the foliage. Groups of the same size were created in the selected foliage. To start with, the weight of the untreated foliage was measured, followed by the groups of foliage dipped in water and foaming agents. Results and discussion: According to the findings of research, the amount of foam remaining on the foliage is remarkably higher than that of water. Its rate is 3.36-3.76 compared to water. The research also revealed that this rate does not significantly depend on expansion rate. As a result, the fire intensity which can be extinguished by using foams expands as well.

Keywords: suppression capability, foam, weight effectiveness experiment, R-10A method

Introduction

The effectiveness of the foams used in fighting against forest fire depends on common effect of some coefficients. Cooling and isolation effects as main extinguishing effects as well as side extinguishing effects, like evaporation, blanket and separation effects are also included (Kuncz, 1972). The efficiency of isolation effect certainly depends on the amount of extinguishing agent measured in unit area of surface, which in the case of not horizontal surfaces is in correlation with the adhesion of the extinguisher that is the rate of remaining on the surface. Under the same conditions, the more extinguisher remains on the surface, the more extinguishing effect it has.
Since the quantity of the extinguisher has a great impact on the firefighting techniques applied as well as the effectiveness of the techniques applied (Bleszity, 1990), it is recommended to review the various factors not only because of their importance but also because of the safety of the intervention crew (Pantya, 2011). Several studies are dealing with the effectiveness of extinguishers and separate measurement methods were created (Batista, 2011; Morris, 2011). However, researches aimed at the extinguisher remaining on the foliage may be scarce, according to the author. The paper wishes to present a unique approach to this topic, comparing water and foam as extinguishers with different structures and their ability to remain on the surface. This procedure following the below assumptions got a fantasy name and was called R-10A method.

Methods

The method was developed in order to measure the rate of foam remained on the vegetation surface (spruce) to determine the extinguishing potential of foam blanket. This problem can have not just one aspect. In case of using very “light” foam – meaning that the expansion rate of foam is large, with other words the density is low – it will remain on the top of the crown, therefore it is unable to protect

the bulk from the radiation heat or it can be blown over by the wind. In other case, when using very "heavy" foam – meaning that the expansion rate is low or the density is high – it takes the features as Newtonian fluid and will drip to ground resulting that the larger part of foam will not remain in the area of the burning cell. Both case causes useless waste. Even if the ideal expanditure rate of foam can be different depending on the situation or the type of vegetation but author's experience say it must be higher than 6 but below 13. As a series in this research author used foams expanditure rate of 6 – 9 – 12.

The other aspect is that, what is the difference between the weights of the extinguisher materials remaining on the surface (crown).

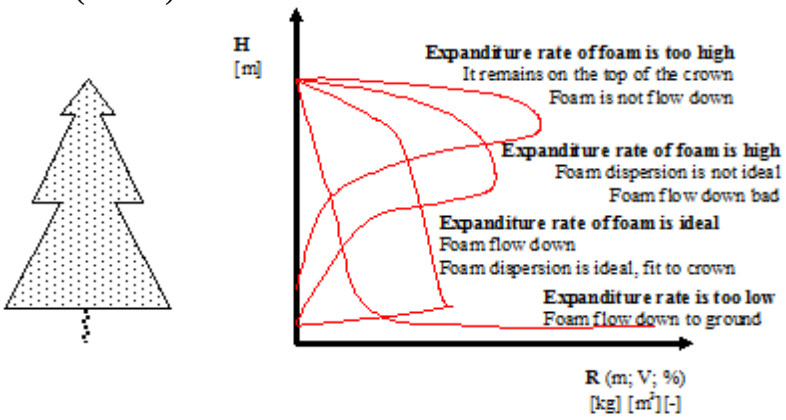

Figure 1. Structure of foam remaining on the crown depending on the rate of expanditure

Prepare the process

During the research the goal has been formulated to develop a simple, easily reproducible method used for both illustration and teaching which proves the differences in the extinguishers' adhesion and presents its consequences. The author opted for analysing the mass/volume of extinguisher left on the surface. A product was randomly chosen out of the ones on the Hungarian market. It is named Light Water, what is used in Hungary as common foam concentrate, even in case of serious forest fire, however this type of foam not typical at the international practice (or at forest fire). Using this foam is acceptable, because the aim of the test is not to determine the efficiency of the extinguisher, but to demonstrate its application.

Spruce was chosen for the test due to its high flammability. The goal was to determine the amount of extinguisher at the end of the branches in the foliage. Groups of the same size were created in the selected foliage. To start with, the weight of the untreated foliage was measured, followed by the groups of foliage dipped in water and foaming agents. In the case of the latter groups, the weight of the foliage itself was subtracted from the total weight, giving us the maximum amount of the extinguisher remaining on the foliage. During the experiment 6 – 9 – 12 expansion rated foams were applied.

Below is declared the main important things for preparing the test, and some basic process for being ready to measure the mass/volume foam left on the surface. Means required for the process:

1. Choosing samples: The highly flammable spruce was chosen as a sample. Twigs of 100-150 mm were cut down (4x10pcs= 40pcs). Thus, that part of the spruce was examined which has the greatest role both in fire spread and keeping the extinguisher.
2. Preparing the samples: the twigs are dried in sun for 4 hours in 30°C. Thus, the surface becomes totally dry similarly to the typical conditions of intense fire periods.
3. Preparing the matrix holding the samples: a matrix was created according to the set of measurements. It included the boxes (altogether 4x10 pcs) to keep water and the foams of 6 – 9 – 12 expanditure (Hk = 6 – 9 – 12).

4. Preparing the extinguishers to be examined: normal tap water and foam-forming substance was used in the experiment. The foam-forming substance was Light Water, which is generally used in Hungary.
5. The preparation of the extinguishers: Water was 20°C, normal temperature, 15 ^{0}dH (water hardness in German degrees). Preparing a foam solution in measuring bottles: the foam-forming substance is Light Water, out of which foams of different expanditure were created, using a mixture of 3%. These were in three different bottles: Hk = 6; Hk = 9; Hk = 12.

Figure 2. Preparing the spruce twigs for measurement

2.2. Measured data of different treated samples1

The measurements clearly show that water and foam remain on the surface of the foliage in completely different shapes (Figure 3). Water is not evenly distributed, but it sticks to the surface in drops, separately, while the foam surrounds the twig in a homogenous mass. In spite of the conspicuous difference, we do not know if the difference in structure causes any significant difference in the extinguishers' ability to remain on the surface. If so, then the extinguisher which has more quantity on surface possesses more heat capacity proportionately.

Figure 3. Different treated samples – foam and water

1 Author made this measurement in 8th May, 2013, Szendro, Hungary

The findings of the measurements carried out and the values obtained from the data can be found in Table 1.

Table 1—Measured data

R-10A	**Measured weight** (gram)			
Weight of untreated samples (n=10) (avarage:34,17)	33,48	34,26	35,33	33,60
1. Sample group				
Weight of samples treated by water (net)	50,52	-	-	-
Weight of water	17,04	-	-	-
Rate of extinguisher (water) to max. water on surface	1	-	-	-
2. Sample group				
Weight of samples treated by foam, Hk=6 (net)	-	98,33	-	-
Weight of foam, Hk=6	-	64,07	-	-
Rate of ext. (foam, Hk=6) to max. water on surface	-	3,76	-	-
3. Sample group				
Weight of samples treated by foam, Hk=9 (net)	-	-	94,84	-
Weight of foam, Hk=9	-	-	59,51	-
Rate of ext. (foam, Hk=9) to max. water on surface	-	-	3,49	-
4. Sample group				
Weight of samples treated by foam, Hk=12 (net)	-	-	-	90,81
Weight of foam, Hk=12	-	-	-	57,21
Rate of ext. (foam, Hk=12) to max. water on surface	-	-	-	3,36

2.3. Calculations

The following calculations were made to assess the findings. To start with, the author specified the average weight of the samples from each sample group, and then calculated the weight of the individual sample by averaging.

Secondly, by dipping the samples into water, the author specified the maximum value of water saturation. Thus the water retention capacity of the samples can be determined, by considering the differences in weight.

Thirdly, foams of different expanditure and their ability to remain on the surface were examined. The samples were dipped into foam (it results also the maximum weight on surface), weighed and then the relevant data were calculated by averaging.

The ability of the extinguisher to remain on the surface was determined by subtracting the weight of the untreated samples from the values measured. Then we get the values of the foam by comparing these data to the data of the samples treated with water. The calculations produce the following results:

1. Average weight of the individual samples of the 4 sample groups

$$\overline{m}_{P\_Nature} = \frac{\sum_{i=1}^{n} m_{P\_Nature\_n}}{n} = \frac{33{,}48g}{10} = 3{,}348g$$

$$\overline{m}_{P\_Nature} = \frac{\sum_{i=1}^{n} m_{P\_Nature\_n}}{n} = \frac{34{,}26g}{10} = 3{,}426g$$

$$\overline{m}_{P\_Nature} = \frac{\sum_{i=1}^{n} m_{P\_Nature\_n}}{n} = \frac{35{,}33g}{10} = 3{,}533g$$

$$\overline{m}_{P\_Nature} = \frac{\sum_{i=1}^{n} m_{P\_Nature\_n}}{n} = \frac{33{,}60g}{10} = 3{,}360g$$

2. Average of the average samples of the sample groups

$$\overline{m}_{P\_Nature} = \frac{\sum_{i=1}^{4} m_{P\_Nature\_n}}{n} = \frac{3{,}348g + 3{,}426g + 3{,}533g + 3{,}360g}{4} = 3{,}417g$$

3. The average weight of the spruce sample dipped into water

$$\overline{m}_{P\_H_2O} = \frac{\sum_{i=1}^{n} m_{P\_H_2O\_n}}{n} = \frac{50{,}52g}{10} = 5{,}052g$$

4. The average weight of the spruce sample treated with foam of expanditure Hk

$$\overline{m}_{P\_Foam\_H_K=6} = \frac{\sum_{i=1}^{n} m_{P\_FoamH_K\_n}}{n} = \frac{98{,}33g}{10} = 9{,}833g$$

$$\overline{m}_{P\_Foam\_H_K=9} = \frac{\sum_{i=1}^{n} m_{P\_FoamH_K\_n}}{n} = \frac{94{,}84g}{10} = 9{,}484g$$

$$\overline{m}_{P\_Foam\_H_K=12} = \frac{\sum_{i=1}^{n} m_{P\_FoamH_K\_n}}{n} = \frac{90{,}81g}{10} = 9{,}081g$$

5. The average weight of the water on the spruce sample

$$\overline{m}_{H_2O} = \overline{m}_{P\_H_2O} - \overline{m}_{P\_Nature} = 5{,}052g - 3{,}348g = 1{,}704g$$

6. The average weight of the foam of expanditure H_K on the spruce sample

$$\overline{m}_{Foam\_H_K=6} = \overline{m}_{P\_Foam\_H_K} - \overline{m}_{P\_Nature} = 9{,}833g - 3{,}426g = 6{,}407$$

$$\overline{m}_{Foam\_H_K=9} = \overline{m}_{P\_Foam\_H_K} - \overline{m}_{P\_Nature} = 9{,}484g - 3{,}533g = 5{,}951$$

$$\overline{m}_{Foam\_H_K=12} = \overline{m}_{P\_Foam\_H_K} - \overline{m}_{P\_Nature} = 9{,}081g - 3{,}360g = 5{,}721$$

7. The rate of foam of expanditure H_K and water on the spruce samples

$$R_\gamma = \frac{\overline{m}_{Foam\_H_K=6}}{\overline{m}_{H_2O}} = \frac{6{,}407g}{1{,}704g} = 3{,}76$$

$$R_\gamma = \frac{\overline{m}_{Foam\_H_K=9}}{\overline{m}_{H_2O}} = \frac{5{,}951g}{1{,}704g} = 3{,}49$$

$$R_\gamma = \frac{\overline{m}_{Foam\_H_K=12}}{\overline{m}_{H_2O}} = \frac{5{,}721g}{1{,}704g} = 3{,}36$$

Results

According to the findings of research, the amount of foam remaining on the foliage is remarkably higher than that of water. Its rate is 3.36-3.76 compared to water. The research also revealed that this rate does not significantly depend on expansion rate. The surface of the foliage in a full-grown forest is able to hold 4-5 kgm^{-1} water, which is enough to control a fire of about 3400 kWm^{-1} fire intensity. We can come to the conclusion that if fire intensity is so high that the cooling capability of water is not enough to extinguish the fire, applying foam can extend the range of extinguishing possibilities to dimension where extinguishing with water is not possible for objective reasons. Its reason is that by applying foam, the mass remaining on the surface, thus the cooling capability of the extinguisher, can be tripled. As a result, the fire intensity which can be extinguished expands as well.
We have to add that in addition to the foam's weight effectiveness increase, insulation effects can be noticed, too, resulting in additional extinguishing effects. Weight effectiveness and insulation effects do not add up but multiply, which is yet another proof of the advantages of foams.
The above results show that the factor of weight effectiveness of the foams is significant, which offers the opportunity of increasing the amount of extinguisher on one unit of surface. The unsatisfactory extinguisher effect of water can be improved and extinguisher solutions have become available which have been impossible so far.

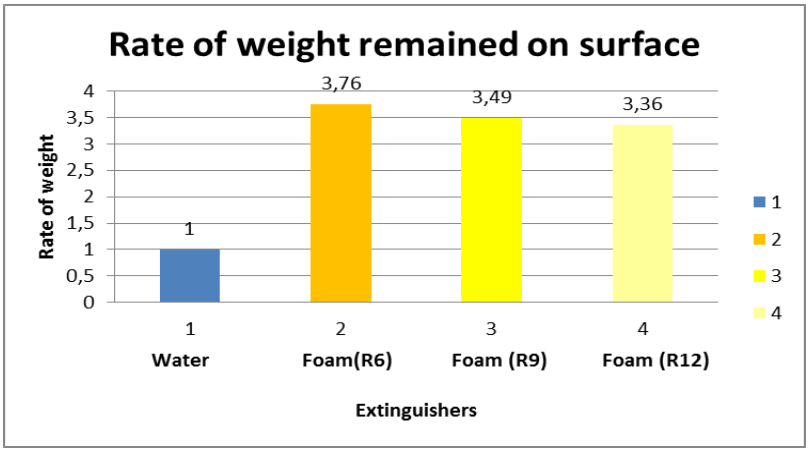

Figure 4. Rate of weight remained on surface depending on the expanditure rate of foams

Appendix A – Notation

1. m_{P_Nature} = the weight of the individual twig (sample), untreated;

2. $\overline{m}_{P\_Nature}$ = the average weight of the untreated samples;
3. $m_{P\_H_2O}$ = the weight of the individual samples treated with water;
4. $\overline{m}_{P\_H_2O}$ = the average weight of the samples treated with water;
5. $m_{P\_Foam\_K_k}$ = the weight of the individual samples treated with foam of H_K expanditure;
6. $\overline{m}_{P\_Foam\_K_k}$ = the average weight of the samples treated with foam of H_K expanditure;
7. $\overline{m}_{H_2O}$ = the average weight of the water remaining on the samples;
8. $\overline{m}_{Foam\_H_K}$ = the average weight of the foam of H_K expanditure remaining on the samples;
9. R_γ = the weight of the foam of H_K expanditure and water remaining on the samples;
10. $m_{\max H_2O\_m^2}$ = the weight of the water remaining on one unit of surface (constant) = 5kg;
11. $m_{\max FoamH_K\_m^2}$ = the weight of the foam of H_K expanditure remaining on one unit of surface.

Appendix B – Mathematical formulas used for calculations

1. The average weight of the untreated spruce sample

$$\overline{m}_{P\_Nature} = \frac{\sum_{i=1}^{n} m_{P\_Nature\_n}}{n}$$

2. The average weight of the spruce sample dipped into water

$$\overline{m}_{P\_H_2O} = \frac{\sum_{i=1}^{n} m_{P\_H_2O\_n}}{n}$$

3. The average weight of the spruce sample dipped into foam of H_K expanditure

$$\overline{m}_{P\_Foam\_H_K} = \frac{\sum_{i=1}^{n} m_{P\_FoamH_K\_n}}{n}$$

4. The average weight of the water remaining on the spruce sample

$$\overline{m}_{H_2O} = \overline{m}_{P\_H_2O} - \overline{m}_{P\_Nature}$$

5. The average weight of the foam of H_K expanditure remaining on the spruce sample

$$\overline{m}_{Foam\_H_K} = \overline{m}_{P\_Foam\_H_K} - \overline{m}_{P\_Nature}$$

6. The rate of the average foam of H_K expanditure and water remaining on the samples

$$R_\gamma = \frac{\overline{m}_{Foam\_H_K}}{\overline{m}_{H_2O}}$$

7. The amount of water effectively remaining on one unit of surface

$$m_{\max H_2O\_m^2} = const = 5kg$$

8. The amount of foam of H_K expanditure remaining on one unit of surface

$$m_{\max FoamH_K\_m^2} = m_{\max H_2O\_m^2} R_\gamma$$

References

Batista, A.C.: Combustion characteristics tests of Magnolia grandiflora and Michelia champaca for potential use in fuelbreaks in south region of Brazil, Wildfire 2011 Conference, Sun City, South Africa, 2011.05.9-13.

Bleszity, J., Zelenák, M.: Tűzvédelmi ismeretek (Firefighting basic knowledge), Budapest: Szövetkezeti Szervezési Iroda, 272 p. 1990

Kuncz, I.: A tuz es oltoanyagai (Physics of fire and extinguishers), BM Kiado, Budapest, Hungary, p 240. 1972

Morris C.J.: A simulation study of fuel treatment effects in dry forests of the western United States: testing the principles of a fire-safe forest, Wildfire 2011 Conference, Sun City, South Africa, 2011.05.9-13.

Pantya, P.: A tűzoltói beavatkozás biztonságának növelése zárttéri tüzeknél (Safety of firefighters during interventions in different areas), HADMÉRNÖK 6: (1) pp. 165-171.

SWeFS: Sensor Web Fire Shield for forest fire detection and monitoring

George Bismpikis, Vassilis Papataxiarhis, Nikos Bogdos, Elias S. Manolakos and Stathes Hadjiefthymiades

Department of Informatics and Telecommunications, Pervasive Computing Research Group. National and Kapodistrian University of Athens, 15784, Greece. gbismpikis@di.uoa.gr, vpap@di.uoa.gr, bogdos@di.uoa.gr, eliasm@di.uoa.gr, shadj@di.uoa.gr

Abstract

Fires are a common, disastrous phenomenon (hazard) that constitutes a serious threat for many years. Due to their speed of propagation and intensity they often lead to property damages, personal injuries and loss of human lives. The probability of forest fire eruption in the Wildland-Urban Interface (WUI) is steadily increasing due to the climate change and human activities. WUI refers to all types of areas where forests, water bodies, and rural lands interface with homes, other buildings and infrastructures, including first and secondary home areas, industrial areas and tourist developments.

The Sensor Web Fire Shield (SWeFS) research project designs, develops and demonstrates an integrated system of sensors, networking and computing infrastructure aimed to detecting, monitoring, predicting and assisting in natural hazards such as forest fires at the WUI zones. Its goal is to deliver: (i) a methodology for developing a novel Sensor Web platform for dynamic data-driven assimilation (DDDAS) for securing the WUI zones against environmental risks, and, (ii) a prototype DDDAS system specifically optimized/tuned for addressing the serious threat of forest fires in Greece. SWeFS pushes the state-of-the-art by combining and using technologies derived from multidisciplinary research in the areas of sensor networks, distributed vision systems, remote sensing, geographical information systems (GIS), data stream fusion, space-time predictive modeling and control systems.

Keywords*: fire detection and monitoring, active sensing, wireless sensor networks, dynamic data driven assimilation, data fusion, space-time predictive modelling, closed-loop architecture*

Introduction

Countries in the Mediterranean basin suffer from 50.000 fires annually with damaged land that covers 600.000 hectares. The cost of fire prevention and fire fighting in the Southern European countries scales up to 1 billion USD. The cost of the destructive fires of 2007 in Greece has been estimated to 1 billion euros. The land impacted by fires annually in the same region is equivalent to the surface of Crete or Corsica while the fires in Spain, Portugal, France, Italy and Greece have quadrupled since the 1960's. The rapid development of WUI areas is the outcome of pollution and overpopulation of city centers that grew in the ‘70s. Settlements were built without efficient road networks while homes and other buildings were developed in or near areas that form the flood plain of water catchments.

To minimize the aforementioned damages, early detection of environmental hazards like forest fires is critical. It is also very important to have early and accurate information about the exact origin(s) of the fire and its course as it spreads. Great technological effort has been invested on the design of systems for fire detection and monitoring. From an engineering perspective, machineries can be designed and used to help with detection or prediction of the disastrous events. One technology that enables (near) real-time detection of such events is the so-called Wireless Sensor Networks (WSNs). WSNs typically consist of a large number of small, low-cost sensor nodes distributed over a large area. The sensor nodes are integrated with sensing, processing and wireless communication capabilities. A simple WSN could be based only on a network of multi-sensor field devices that are able to detect increases in the temperature and/or decreases in the humidity percentage. However, the most promising approach for the early forest fire detection in WUI zones is the combination of various

heterogeneous sensors. Typical temperature and humidity sensors can be combined with video-capable wireless sensors, optimally placed in an area of interest, to better observe the outbreaks of various hazardous phenomena. The prediction accuracy of such an approach could be enhanced through the exploitation of remote sensing products such as satellite monitoring (another source of information interfaced to the systems). Of course, one of the requirements that have to be addressed is the optimal placement of the available sensor infrastructure in order to maximize the coverage of the monitored area. WSN systems can reach, at a reasonable cost, the density of physical parameter measurements needed for an accurate and timely fire detection, localization and progress monitoring.

During the past years, a lot of research has been conducted in the area of forest fire detection. The study from Elmas et. al. (2011) discusses a Forest Fire Decision Support System (FOFDESS) model, which is a multi-agent Decision Support System for Forest Fire. Depending on the existing meteorological state and environmental observations, FOFDESS does the fire danger rating by predicting the forest fire and it can also approximate fire spread speed and quickly detect a started fire. The considered model adopts data fusion algorithms such as Artificial Neural Network (ANN), Naive Bayes Classifier (NBC), Fuzzy Switching (FS) and image processing. The SFEDONA project (co-funded by ESA) deals with a complete end-to-end fire detection and alerting application which makes use of state-of-the-art fire detection technologies based on terrestrial optical cameras and sensors, data fusion, satellite and wireless communications as well as modern IT technologies. The SFEDONA project adopts a terrestrial wireless network for the interconnection of various components installed on-field such as optical and panoramic PTZ cameras, weather monitoring stations and wireless environmental sensors, as well as of a SatCom (satellite) network for the interconnection of the end user's premises with local field. The SatCom connection is used for delivering alarms on fire events to the core control center. The model presented by Li et. al. (2005) discusses a hybrid contextual fire detection algorithm for airborne and satellite thermal images. This model essentially treats fire pixels as anomalies in images and can be considered a special case of the more general clutter or background suppression problem. The system from Lloret et. al. (2009) deploys wireless IP multi-sensors able to sense fire by infrared radiation and smoke. The system sends an alarm to the control system if the combination of physical sensors reports a fire event. When a fire is detected, the sensor alarm is sent through the wireless network to the control center. The center selects the closest wireless IP cameras to the sensor and sends them a signal in order to receive real-time images from the affected zone. Regarding the cases where the fire detection algorithms use satellite remote sensing capabilities, most of them are based on a single sensor approach and are using basic signal processing techniques. Specifically for MSG/SEVIRI data, the different approaches rely on variations of EUMETSAT's (the international organization managing the Meteosat series of geostationary meteorological satellites) proposed classification methodology. Sifakis et. al. (2011) from ISARS/NOA and Carvalheiro et. al. (2010), among others, have adopted a similar approach for identifying hotspots. It should be noted that the method presented by Calle et. al. (2006) was applied in the framework of SAFER (EC/GMES) project with noticeable omission errors for Greece, mainly attributed to insufficient customization for the geographic area's special characteristics in terms of vegetation species and underlying land cover. Finally, in the context of the EU project SCIER (Sensor and Computing Infrastructure for Environmental Risks management) as described from Sekkas et. al. (2010), a scalable system architecture that integrates private and public sensor and camera networks in a hierarchy has been developed and tested. The system was designed to protect WUI areas by adopting a scalable and modular approach for early detection and effective fire management. In addition to the sensory system (WSNs), SCIER provided the capability of performing parallel simulation (using Grid computing) of multiple fire scenarios corresponding to different environmental conditions (e.g. wind direction and speed). This unique capability was an innovation offered for the first time by SCIER. However, SCIER and the rest of the aforementioned approaches did not attempt to integrate WSN sensing and predictive modeling with remote sensing and GIS into a *closed-loop active sensing system* and implement a DDDAS scheme for fire detection and management. This unique innovative approach is pursued in

SWeFS. Moreover, SWeFS deals with multiple parameters and trade-offs, hence, considers and aims both for energy-efficiency and early-detection. The Sensor Web Fire Shield (SWeFS) research project aims at delivering: (i) a methodology for developing a novel Sensor Web platform as a Dynamic Data-Driven Assimilation System (DDDAS) for securing the WUI zones against environmental risks, and, (ii) a prototype DDDAS specifically optimized/tuned for addressing the serious threat of forest fires at national and international level.

SWeFS High Level Architecture

SWeFS adopts a combination of heterogeneous sensors including remote sensing and predictive risk propagation models in a *single closed loop active sensing system*. The first step towards the completion of SWeFS architecture (Figure 1) is the *efficient collection and processing of data streams* that is provided from the various subsystems of the Input Block (IB) (i.e., network of sensors, cameras, remote sensing and unmanned air vehicles).

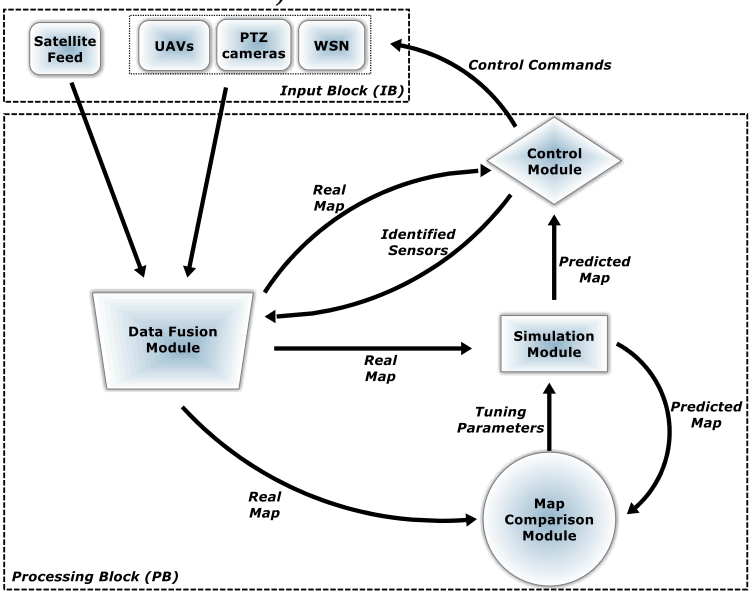

Figure 1- Interconnection of SWeFS components

The remote sensing methodologies employed in SWeFS greatly facilitate the early detection and monitoring of wildfires while the active sensing techniques give an identification mechanism for the type and combination of sensors that provide the most useful measurements from the field. In addition, the ability provided by SWeFS to simulate multiple scenarios in parallel is important from a management point of view since it enables "what if" type queries and worst case scenario identification in real-time. Of course, the prediction mechanism is equally important for the encapsulation of the DDDAS scheme in SWeFS. The processing of the streaming data derived from the IB is operated by the components of the Processing Block (PB), in a closed loop approach, in order to provide accurate information regarding the exact origin(s) of the fire and its course as it spreads. The outcome is the visualization of hazard maps for the monitored phenomenon on a map based graphical user interface (GUI). To the best of our knowledge, SWeFS is pioneer to its domain with respect to the adoption of a closed loop approach in order to detect and monitor the evolution of a hazardous phenomenon such as forest fires at the WUI zones.

Another important element of innovation in SWeFS is the simultaneous implementation of both asynchronous and synchronous communication, which is defined according to the type of functionalities and the information handled: in the former case (asynchronous), new information or information updates are either published from the components of the IB or consumed from the components of the PB as soon as they become available, while in the latter one (synchronous), access

to the needed data (i.e., spatial data for available sensors, fuel data, etc.) and functionalities (i.e., control of the sensory infrastructure) happen "on request". This architecture is achieved through the utilization of a Message Oriented Middleware (MOM) to act as the communication infrastructure for the interconnection of the SWeFS structural components. Publisher and Subscriber entities are present in the various modules belonging either in the IB or the PB to respectively publish and consume information of interest through the MOM.

Input Block

The Input Block (IB) of SWeFS consists of a heterogeneous infrastructure of sensors that provides the means for the optimal collection of measurements related to a fire incident in the monitored area. Currently, the following categories of sensors are integrated:

- In-field sensors able to measure temperature, humidity and gas concentrations,
- Weather stations that provide additional information about rain rate, wind speed and wind direction
- Out-of-field sensors like:
    - Pan-Tilt-Zoom (PTZ) and Fixed Cameras
    - Unmanned Air Vehicles (UAVs) equipped with cameras
- Remote sensing and processing facilities

Figure 2-SWeFS Sensory Infrastructure

Raw data stemming from in-field sensors provide on-the-run information about the actual progress of the phenomenon to experts. On the other hand, the data coming from the satellite feed and the available camera network constitute pre-processed streams that provide an estimation (i.e., probability values) regarding the occurrence of a fire incident in the area that falls in their supervision. The processing stage of such feeds is based on widely accepted image processing techniques from the research community. These operations are either performed locally on the nodes, through the exploitation of Field-Programmable Gate Arrays (FPGAs) (i.e., camera feed processing) or centrally on the back-end infrastructure of the system (i.e., process satellite feed).

Due to the heterogeneity of the sensor sources, the description of the sensed information must be homogenized. Since the main idea in SWeFS is to take advantage and reuse open standards that secure the inbound interoperability, we have adopted the Open Geospatial Consortium (OGC) Sensor Observation Service (SOS) in order to provide access to sensor descriptions and observations. The SOS specification leverages the Observations and Measurements (O&M) specification to encode observations and the Sensor Model Language (SensorML) specification to encode sensor descriptions. Both of these formats are based on the Extensible Markup Language (XML). The SOS standard defines a Web-based interface (Web service) that allows querying observations, sensor metadata or representations of observed features. Further, this standard provides means to register new sensors or remove existing ones. It also defines operations to insert new sensor observations. The SOS operations follow the general pattern of other OGC Web Services and inherit or re-use, when needed, elements defined previously. For every available sensor category we developed the corresponding proxies that ensure the robust communication of the sensory infrastructure with the rest architecture. The role of

each proxy is twofold since the sensors supporting SWeFS, apart from providing their sensing capabilities, can be also externally controlled in order to optimize the capabilities of the system. This broader meaning assigned to the sensing devices is illustrated in Figure 3.

Figure 3. Sensor Entity of SWeFS

A proxy that lies upon a sensing element, on the one hand transforms/encapsulates the sensed values in SOS compliant messages which are subsequently forwarded to the MOM. On the other hand, these proxies act as controllers that translate and forward the consumed control commands and inform the rest system for the result. However, a fundamental issue is the way to process and combine the collected data streams and subsequently control the identified sensors of interest in order to reach to a meaningful decision related to the fire phenomenon. In SWeFS, the components of the PB undertake this task.

Processing Block

The building components of the PB are interconnected in a way to achieve the smart closed loop integration approach. The designed workflow is triggered by information derived from the elements of the IB. The processing task of the collected sensor data streams is assigned to the Data Fusion Module (DFM) while the Control Module (CM), the Map Comparison Module (MCM) and the Simulation Module (SM) enhance the active sensing capabilities and the DDDAS nature of SWeFS. As depicted inFigure Figure 1, an inner/smaller closed loop is shaped between these components. The DFM is the entry point for the sensor measurements in this circle while the CM is the component that broadcasts the result of the processing chain to the sensory infrastructure in the form of control commands. A description regarding each one of these modules follows.

Data Fusion Module (DFM): The DFM facilitates the integration and interpretation of different types of sensor data. In addition to the statistical advantage gained by combining same-source data (e.g., obtaining an improved estimate of a physical phenomenon via redundant observations), the use of multiple types of sensors increases the accuracy with which a quantity can be observed, interpreted and used for an event recognition in the context of SWeFS. The most fundamental mechanism of the DFM involves (i) the detection of pre-defined events, (ii) the decision or inference regarding the characteristics of an observed entity and (iii) an interpretation of the observed entity in the context of a surrounding environment and relationships to other entities.

The SWeFS sensor infrastructure provides an indication of the spatiotemporal evolution of the fire front. Such input can be highly localized (e.g., an alarm originating at a certain ground sensor) or of broader spatial scope (e.g., a sizeable ground segment of the observed terrain). The DFM processes data streams received from the available infrastructure in order to detect possible changes in their typical (no-event) distribution. Both types of input (coarse- and fine-grained) are taken into account for establishing the actual fire front (i.e., a time-invariant polygon that is approximated by the real feed; ground sensors, visual and satellite observations).

DFM architecture is partially based on the contextor's theory presented by Coutaz et. al. (2002) and leverages the SOS standard for the interoperable integration of sensor data. A typical contextor is a software abstraction that models a relation between variables of an Observed System Context which is the composition of situations as observed by the system. A contextor does not exist as an isolated entity but rather as a part of a connected directional graph, produced by connecting Data-In channels with compliant Data-Out. The core principle of the DFM design is that each contextor encapsulates the functionality provided by a specific algorithm (e.g. Bayesian Network, Cumulative Sum, Linear

Opinion Pool, etc.) or operator (e.g., minimum, maximum, average, threshold, etc.). The DFM provides the necessary middleware services which will allow contextors to acquire data, execute the encapsulated algorithms, exchange information with each other, and finally produce the desired output. From an operational perspective, the DFM can be characterized as an event based system, which can run specific fusion applications. A fusion application comprises from a directional acyclic graph (DAG) of contextors with defined external inputs and defined outputs. Each input is a data flow coming from the network (i.e., sensory infrastructure), while each output is another data flow dispatched in specific format using a specific protocol adapter. What accounts as an event is a new value produced by an input data flow, both in macroscopic and microscopic level. So, in macroscopic level, this means that a new value coming from the network (e.g., a sensor) will trigger the engine by forcing the specific contextor which receives the corresponding data flow in its Data-In channel to execute. But, also, microscopically seen, inside the DFM, each output produced by a specific contextor, flows through its Data-out channel, to its connected contextor's Data-In channel, producing a corresponding event. This sequence of events results to the output of the DFM application which can be delivered in various formats using a variety of transport protocols such as http, email, etc. Both formatters and protocol adapters are pluggable modules which means that new implementations of both can be added at any time to the engine. DFM applications are modeled using a specific xml-based language, the Application Description Language (ADL). An XML parsing subcomponent inside the DMF is responsible to simply transform the static information of a script to Fusion Engine directives, used to build the application context inside the DFM.

The definition of the detected events depends upon the specific application under consideration. In a very simple scenario, the event detection mechanism in DFM could be based on certain pre-defined thresholds for evaluating the occurrence of an event. However, the combination of multiple sensor data sources and the implementation of advanced detection and fusion algorithms could achieve satisfactory detection levels in a variety of operating conditions. The output of the DFM can be an improved estimate on an event occurrence. The aforementioned capitalize on the dual nature of the DFM in the SWeFS context. On the one hand, through the exploitation of a simple fusion application script based on thresholding operators over the available sensor streams, the DFM can operate in a *detection mode*. In this case, the localization of the incident in the monitored area is pursued. On the other hand, by taking advantage of the detection mode's outcomes and the active sensing approach adopted in SWeFS, the DFM can also operate in a *monitoring mode*. The results of this mode are continuously improved through the periodic deployment of more sophisticated and near-to-real application scripts with respect to the selected data sources that participate in the process. These scripts are created dynamically in compliance with the outcomes of the active sensing process. Through the DDDAS approach and the active sensing scheme, the information of the sensor sources that should participate in each round is constantly refined and consequently, the fusion scripts are refined as well. This results in more accurate estimations regarding the current state of the monitored fire front. The output of the DFM in SWeFS is provided in the form of ASCII Raster files that describe the estimated probability maps (probabilistic and binary) for the monitored area.

Simulation Module (SM): Due to the dynamic nature of the wind, which is the most influential fire simulation parameter, the SM was developed around the notion of *Multiple Simulation Scenarios* (MSS). Multiple wind direction and speed scenarios are generated as perturbations around an expected average scenario and executed in parallel. When combined, the MSS simulation results give rise to a map of burn probabilities that can be visualized as a fire hazard map. The capability to simulate multiple scenarios in parallel is also important from a management stand point since it allows the Tactical Commanders to pose "what if" type queries in the field and identify worst case scenarios faster than real-time. Furthermore, it greatly facilitates dynamic sensor selection (active sensing) and accurate fire course predictive modeling.

The SM is based on *fireLib* by Bevins (1996), and it stems from a previous work on the Fire Logic Animator (*FLogA)* interactive wildfire simulator by Bogdos et. al. (2013). However, instead of using

fireLib's default fire propagation algorithm (which exploits only 8 possible fire propagation directions) the SM utilizes a more flexible 16-neighbors scheme. Consequently, the fire front's propagation is less biased and the resulting propagation distortion is not noticeable under spatially heterogeneous conditions. Furthermore, the SM is designed to take advantage of CPUs with multiple processor cores in order to take advantage of parallelism and reduce execution time, i.e. the different simulation scenarios are executed in parallel by adopting a Master-Workers processing pattern.
As suggested by the interaction of the various SWeFS modules depicted in Figure , the SM is triggered each time the DFM produces estimations for the current state of an ongoing fire. Just before generating and executing the MSS, the SM consumes the up-to-date weather data from the MOM and uses the current wind parameter values to define the mean of the sampling ranges to be used for the MSS generation. Moreover, the relative air moisture value is used to calculate the 10hr dead fuel moisture content value reduction (10-H timelag) as in Vasilakos *et al*. (2007).

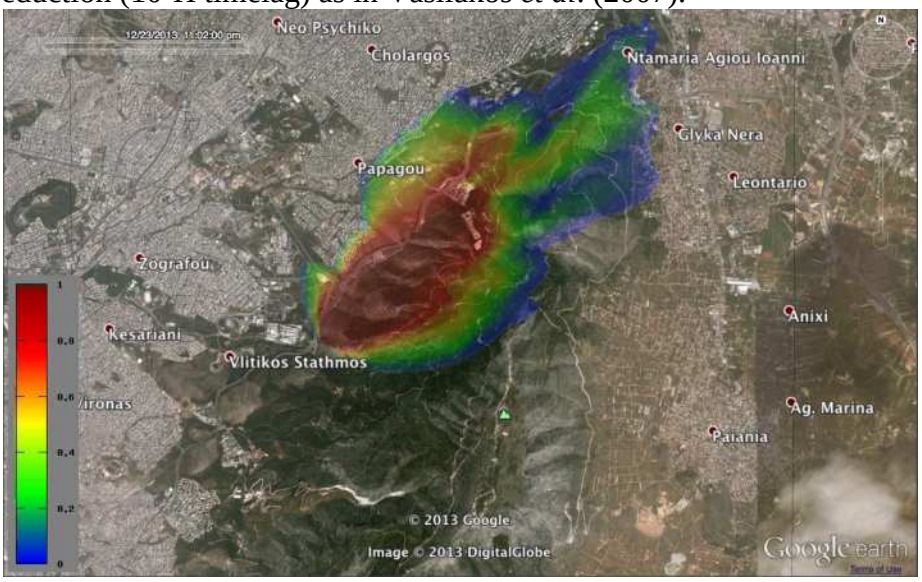

Figure 4: Visualization of a fire hazard map considering an MSS with 64 scenarios and equidistant (deterministic) parameters sampling around the expected wind direction and speed values.

The SM generates an MSS by performing deterministic or random sampling in a configurable wind speed and direction parameters range. Subsequently, the SM simulates the generated multiple scenarios as a combinatorial experiment, which means that it executes a wildfire simulation for each possible parameter values combination. The results are combined to produce KML visualization files using ground overlay images produced automatically by Gnuplot (2014) for the flame length of each scenario as well as the combined hazard map of the whole MSS. Figure 4 provides an example of a fire hazard map visualization based on a 8x8=64 scenarios MSS ignited at the northern end of the NKUA campus, in Athens. The prediction window was 2 hours while the ranges of the wind speed and direction parameters were 5m/s - 7m/s and 200º - 250º respectively (remaining constant throughout the simulation time). Moreover, equidistant (deterministic) parameters sampling was used.

Map Comparison Module (MCM): The DFM and the SM provide an estimation for the real map that describes the current state of the monitored fire front and a prediction for the phenomenon's possible evolution respectively. One of the objectives of the DDDAS approach is the continuous recalibration of the various components of a system in order to produce results as close as possible to the real situation. Hence, the actual fire front can be compared against the estimated (predicted) one derived through simulations in order to establish model accuracy metrics by taking into account the uncertainty in parts of the forest where data is not confirmatory of the real fire status. Such metrics (e.g., percent overlap between the estimated and the observed fire front) can be used for deciding on the recalibration

of the model (simulator). A refined simulation outcome will result in a refined product from the CM's procedures as well, thus, the overall quality of the produced results is improved. This important task for the realization of the DDDAS approach in SWeFS is undertaken by the MCM.
The MCM receives at each *processing round* of the closed-loop the estimated real map from the DFM along with the prediction of the SM for the phenomenon's evolution. The input from the SM is multidimensional since parallel processing is performed and several simulation scenarios are produced in every simulation step from the engine. The MCM, by taking into account the spatial characteristics of the affected area, compares every received estimated map with the real one from the DFM. To eliminate possible map alignment issues the same coordinate system is utilized for the produced probability maps from DFM and SM. The metrics provided for the calculation of the overlap percent among the maps are the Jensen-Shannon Divergence, the Pearson Correlation Coefficient, the Kullback-Leibler Divergence and the Similarity Score. From these metrics, although the simplest one, the Similarity Score seems to outperform the other ones for map comparisons with respect to calculation accuracy and processing time in SWeFS.
Through the processing circle of the MCM an evaluation of the simulation results is performed by ranking the multiple simulation results (that refer to the same time horizon) based on the achieved score. This ranking is subsequently forwarded to the SM which in turn evaluates it and recalibrates, if need be, the appropriate internal tuning parameters. Should the MCM outcomes indicate that the simulation presents large deviation from the actual evolution of the phenomenon (i.e., quite low scores in terms of coverage percent), the SM restarts the simulation procedure by considering as ignition area the currently estimated real map from the DFM.

Control Module (CM): Through the existence of the CM, the active sensing aspect is implemented. Active sensing techniques are capable of identifying the type and combination of sensors that provide the most useful measurements (e.g., because they are placed close to the observed phenomenon). The CM receives the products of the DFM and SM, i.e., actual and predicted probability maps respectively, correlates them with the deployed sensor infrastructure and the spatial characteristics of the monitored region (e.g., elevation, slope, etc.) and identifies the sensor nodes that should be controlled. The algorithm that is used as the core of this internal procedure is based on the so called Cognitive-based Adaptive Optimization (CAO) approach presented by Kosmatopoulos et. al. (2009). CAO transforms the energy efficiency and the coverage problem into an optimization one where in every processing round the goal is to optimize the sensing capabilities of the available sensor resources so to meet the objective of the monitored area's optimal coverage with respect to energy efficiency. For instance, the CM can alter the sampling frequency and/or the strength of the transmitted signal for the in-field sensors, steer the available PTZ cameras by providing a new triplet of pan, tilt and zoom control directives and transmit a new waypoint for the available UAVs. This dynamic management of the infrastructure has a positive impact on the optimal monitoring of the affected area and the energy consumption of the nodes.
The CM outcomes are equally important for the recalibration of the results derived from the fusion processing. Since forest fires is a rapidly growing phenomenon as time evolves and the output of the DFM is highly correlated with the quality of the accounted data streams, is of paramount importance to know, at each iteration of SWeFS closed-loop processing, the combination of sensor sources that can monitor the phenomenon's evolution optimally. The CM is able to identify with accuracy these sensors. This information is forwarded via the MOM to the DFM in order to recalibrate its operation by dynamically configuring and deploying timely and accurate fusion application scripts. Through this procedure is assured that the produced result of the DFM is aligned with the evolution of the fire front and one aspect of the DDDAS nature of SWeFS is materialized.

DDDAS Approach

Unsurprisingly, a lot of praise has been given to the Dynamic Data-Driven Assimilation Systems (DDDAS) concept following its introduction from Darema (2004). In the classic simulation approach the applications are using a static input dataset. An inherent disadvantage of such applications is that they are not able to adjust the model parameters in case of significant simulation drift. Conversely, the DDDAS paradigm entails the ability to receive and respond to online data and measurements, thus recalibrating the simulation and allowing for more accurate predictions. The benefits of adopting a sound DDDAS strategy are indisputable for numerous environmental applications. For example Douglas (2005) mentions that before DDDAS it was more probable for meteorologists to fail in predicting the path and the scale of storms while the Forest Services were more likely to ignite controlled burns that would eventually become proper wildfires.

SWeFS aims to not only assimilate online measurements but also utilize them to improve the quality of the monitoring process (active sensing). To do this effectively, the SM needs to provide an accurate fire evolution prediction, so as to offer valuable data for the CM to steer the sensory infrastructure effectively based on the near future fire evolution predictions. This is why it is crucial for the SM to also conform to the DDDAS principles in order to provide as accurate predictions to the CM as possible.

One important point in taking a decision to calibrate the SM is to be able to discover how much the simulation has drifted from reality, by effectively comparing the simulation predictions and the field measurements. We approached the problem of comparing the predicted and real fire maps by borrowing some ideas from the image-processing field. Specifically, we observed that a fire hazard map in the form of a burn probability distribution shares many properties with a saliency map. We experimented extensively with various map comparison metrics reported in the literature and found that the simplistic Similarity Score by Judd et. al. (2012) is the most advantageous. Specifically, when comparing two burn probability maps (in the MCM) generated by two different MSSs, this comparison metric has the following desirable attributes:

1. The returned similarity scores reflect consistently the difference in the weather parameter values between the two MSS
2. The similarity scores remain unaffected by the size of the fire fronts
3. The calculation performance for the metric meets our real time constraints

Each time the SM is triggered by the DFM, it utilizes the comparison results from the MCM to obtain the Total Similarity Value (TSV) for the simulated MSS against the estimation of the real fire map (DFM outcome) and the Scenario Similarity Value (SSV), which is an indication for the accuracy of each scenario. Our DDDAS approach for the next step is to use two predefined threshold values thresh1 and thresh2, with thresh1 > thresh2, as follows:

1. If the *TSV > thresh1* then the simulation drift is considered *insignificant* and the SM continues with the same/previous settings.
2. If thresh2 < TSV < thresh1 then the simulation drift is considered *moderate* and the SM uses the SSV of each scenario to modify its weight coefficient used to compute the burn probability distribution of the MSS. More specifically, the weight of each scenario is modified as: $w_i = \frac{SSV_i}{\sum_1^n SSV_i}$, where n is the number of simulation scenarios in the MSS. In this case the results of the individual scenarios do not change, as the MSS parameters remain unaltered. What changes is how these individual results are combined to produce the burn probability distribution of the MSS.
3. If TSV < thresh2 the simulation drift is considered *significant* and the SM adopts the wind speed and direction values of the best scenario (highest SSV) as the posterior mean wind speed and wind direction values to be used for the MSS redefinition at the next time step.

The CM consumes the updated prediction of the burn probability distribution raster file instantly and the latest fire hazard maps are updated automatically in the provided GUI.

Conclusions

In this paper we have discussed the SWeFS approach that delivers an integrated solution able to detect, monitor, predict and assist in the management of natural hazards at WUI areas. SWeFS enables several desired features of monitoring and surveillance systems, such as fusion of sensor data streams, remote sensing, forest fire simulation and closed-loop integration. The paper presents the overall system architecture describing the design approaches followed during the development phase as well as certain implementation details.
Through the flow of information within the SWeFS architecture, data assimilation is also accomplished to better observe a detected phenomenon. Consequently, SWeFS can be characterized as a DDDAS which constitutes a unique innovative approach in forest fire monitoring.
The presented sensor web based closed loop fire shielding system provides:

1. *Real-time data stream processing* for the estimation of parameters that affect the fire spreading models.
2. *Fast simulation of multiple fire scenarios* for predicting fire evolution and provisioning of dynamic (time varying) probabilistic hazard maps for a given area.
3. *Intelligent closed-loop control mechanism* acting on the basis of available measurements and estimating the most important sensors for optimized active sensing.

Future work includes the improvement of the existing sensor data fusion mechanism by implementing and integrating new data aggregation algorithms. Finally, we are planning to develop optical detection algorithms that can be deployed in the cameras located in the available UAVs targeting at the localization of a forest fire front. The latter will take into consideration data related to the current position, height and angle of the UAV.

Acknowledgments

This work has been co-financed by the European Union (European Social Fund – ESF) and Greek national funds through the Operational Program "Education and Lifelong Learning" of the National Strategic Reference Framework (NSRF) in the scope of the Research Funding Program: THALES-UOA-Sensor Web Fire Shield (SWeFS).

References

Bevins, C. D., (1996). fireLib User Manual and Technical Reference, (October 1996). http://www.fire.org/downloads/fireLib/1.0.4/doc.html (accessed 24 June 2014)

Bogdos, N., Manolakos, E.S. (2013), A tool for simulation and geo-animation of wildfires with fuel editing and hotspot monitoring capabilities, Environmental Modelling & Software, http://dx.doi.org/10.1016/j.envsoft.2013.03.009

Calle, A., Casanova, J., Romo, A., "Fire detection and monitoring using MSG Spinning Enhanced Visible and Infrared Imager (SEVIRI) data", Journal of Geophysical Research, 111, 2006

Carvalheiro, L.C., Bernardo, S.O., Orgaz, M.D.M., Yamazaki, Y., "Short communication: Forest fires mapping and monitoring of current and past forest fire activity from meteosat second generation data", Environ. Model. Softw., 25, 1909-1914, 2010

Cetin Elmas and Yusuf Sonmez. 2011. A data fusion framework with novel hybrid algorithm for multi-agent Decision Support System for Forest Fire. Expert Syst. Appl. 38, 8 (August 2011), 9225-9236

Coutaz, J. & Rey, G. (2002), Foundations for a Theory of Contextors, in CADUI 2002, May 15-17, Valenciennes, France

EUMETSAT, “Active Fire Monitoring with MSG Algorithm - Theoretical Basis Document”, Eumetsat: Darmstad, Germany, 2007

Gnuplot, http://www.gnuplot.info/, (accessed 24 June 2014)

Jaime Lloret, Miguel Garcia, Diana Bri, Sandra Sendra, A Wireless Sensor Network Deployment for Rural and Forest Fire Detection and Verification, Sensors 2009, 9(11), 8722-8747; doi:10.3390/s9110872

Judd, T., Durand F., and Torralba, A. (2012). A Benchmark of Computational Models of Saliency to Predict Human Fixations, MIT: Computer Science and Artificial Intelligence Laboratory Technical Report, 1–24

Kosmatopoulos E.B., Kouvelas A.. Large-scale nonlinear control system fine-tuning through learning. IEEE Transactions Neural Networks, 20(6):1009–1023, 2009

O. Sekkas, D.M. Manatakis, E.S. Manolakos and S. Hadjieythimiades, “Sensor and Computing Infrastructure for Environmental Risks – The SCIER system”, Chapter in the book “Advanced ICTs for Disaster Management and Threat Detection: Collaborative and Distributed Frameworks”, E. Asimakopoulou and N. Bessis Editors, IGI Global Publ, 2010

Sensor Observation Service (SOS), http://www.opengeospatial.org/standards/sos, (accessed 26 June 2014)

SFEDONA - Satellite-based FirE DetectiON Automated system (ESA ARTES), http://telecom.esa.int/telecom/www/object/index.cfm?fobjectid=29777, (accessed 26 June 2014)

Sifakis, N., Iossifidis, C., Kontoes, C. and Keramitsoglou, I., “Wildfire Detection and Tracking over Greece Using MSG-SEVIRI Satellite Data”, Journal of Remote Sensing, Vol.3, pp 524-538, 2011

Vasilakos, C., Kalabokidis, K., Hatzopoulos, J., Kallos, G., & Matsinos, Y. (2007). Integrating new methods and tools in fire danger rating. International Journal of Wildland Fire16(3), 306-316. doi:10.1071/WF05091

Ying Li, Anthony Vodacek, Robert Kremens, Ambrose Ononye, Chunqiang Tang, A Hybrid Contextual Approach to Wildland Fire Detection Using Multispectral Imagery, IEEE T. Geoscience and Remote Sensing, 43(9), 2005, 2115—2126

The effectiveness of suppression resources in large fire management in the US; A Review

David Calkin[a], Hari Katuwahl[b], Michael Hand[a], and Tom Holmes[c]

[a] *US Forest Service Rocky Mountain Research Station, Missoula, Montana, USA, decalkin@fs.fed.us and mshand@fs.fed.us*
[b] *University of Montana, Missoula, Montana, hkatuwahl@fs.fed.us*
[c] *US Forest Service Southern Research Station, Research Triangle Park, NC, USA, tholmes@fs.fed.us*

Abstract
Wildfire management currently represents nearly 50 percent of the US Forest Service's total budget. In both 2012 and 2013 large fire suppression exceeded the Agency's budget allocations by over $400 million (US$). Despite the scale of this investment relatively little is understood about how suppression actions influence large wildfire spread and those conditions that ultimately lead to containment. There is considerable uncertainty in managing large wildfires including the quality of weather forecasts, complex environmental conditions, variation in the type and quality of suppression resources, and whether or not requested suppression resources will be assigned.
In this presentation we review several recent studies that attempt to understand how suppression actions influence fire progression of large wildland fires in the US. Finney et al. (2009) who established the critical importance of quiescent fire growth periods in achieving final fire containment. Holmes and Calkin (2013) used econometric analyses including Cobb-Douglas production functions and production possibility frontiers to examine the effect of different suppression resources and fire characteristics on daily reported fire containment. We extend the Holmes and Calkin (2013) analysis by focusing on geospatially delineated fire progression maps to identify how suppression resources and fire characteristics influenced the amount of fire perimeter that held on a given day. Additionally we review a small sample of large fires where field based data collection allows us to better understand the types of mission and relative efficiency and effectiveness of field based crews.
Despite these recent efforts, there remains limited understanding of suppression effectiveness. These results suggest that modelling large fire containment as a production process of fireline construction similar to traditional initial attack models is inappropriate. Improved understanding of large fire management effectiveness and efficiency will require spatially tracking individual resource assignments, activities, and tactics within the broader suite of fire management objectives and strategies.

Keywords*: wildfire management, suppression effectiveness*

Introduction

Wildfire management currently represents nearly 50 percent of the US Forest Service's (USFS) total budget. Suppression of large wildland fires represents the single largest outlay within wildfire management; currently the USFS consistently exceeds $1 billion (US) annually in large fire suppression costs alone. In both 2012 and 2013 the Agency exceeded its large fire suppression budg*et al*location by over $400 million. A majority of wildfire ignitions (96-98 percent) are captured during initial attack, or the first burning period with only a small percentage exceeding initial attack capability. Although these escaped fires constitute a small portion of the total number of fires, they account for the majority of the suppression expenditures of all wildfire management activities (Calkin *et al*. 2005). Despite the scale of the investment in large wildfire suppression, relatively little is understood about how suppression actions influence large wildfire spread and those conditions that ultimately lead to containment (Finney *et al*., 2009). Wildfire containment under initial attack (IA) has typically been

modelled by evaluating the elliptical rate of spread of an ignition under identified fuel and weather conditions compared with the productive capacity and arrival time of IA resources (see for example Fried and Fried, 1996). However, the large fire environment presents additional complexity and it has not been demonstrated if the IA containment approach is relevant to large wildfire suppression.

There is considerable uncertainty in managing large wildfires including the quality of weather forecasts, complex environmental conditions, variation in the type and quality of suppression resources, and whether or not requested suppression resources will be assigned (Thompson and Calkin, 2011). Additionally, many resources are engaged in non-line building activities such as point protection, contingency line development and mop-up. Further, given that the wildfire escaped IA it is likely that the characteristics of wildfire growth are such that line building efforts may not be feasible or effective.

Data necessary to understand suppression effectiveness within the US can be difficult to obtain. Some recent studies have relied on primary reporting systems such as the ICS-209 Situation report. However, these data do not provide spatial characteristics of the fire environment and rely on self-reporting by the incident team responsible for managing the events. In particular some of the most relevant data for suppression modelling contained within the ICS 209; specifically percentage of the wildfire contained, growth potential, and reported values at risk are subjective and may not be accurately reported (Holmes and Calkin, 2013). Despite these challenges several authors have examined the 209 data to model suppression effectiveness

Finney *et al* (2009) modelled the probability that on a given day a large fire would be declared fully contained by examining wildfire suppression resource assignment, daily fire growth, fuel model and other reported data within the 209 reports. The most significant finding to achieving wildfire containment was the critical importance of quiescent periods during the fire. That is, the most important factors in determining if a wildfire was fully contained were the number of low growth fire days and the number of previous intervals of low growth. Containment probability was negatively related to the presence of timber fuel types. No significant relationship was found between likelihood of containment and fire size or number of personnel assigned.

Holmes and Calkin (2013) utilized similar data from the ICS 209 to examine the relative efficiency of suppression resources by comparing published resource line building production rates published by Broyles (2011) with daily line built estimated from reported fire size and percentage containment. The results indicated that the actual production rates of suppression resources on a set of large wildland fires in 2009 were between 14 to 93% of the reported standard production rates. Further, the econometric models indicated that the marginal productivity of all inputs increased as total resources assigned increased. This result may indicate economies of scale in fire suppression or, alternatively, that fire managers learn how resources may be deployed more productively over the course of a fire.

In this paper we evaluate recent efforts to better understand the effectiveness of suppression resources in containing large fires. Given results from recent and current studies we identify potential opportunities for future research efforts that will allow us to better understand the implications of the existing research and improve the effectiveness of future large wildfire management.

2. Methods

We examine fireline productivity and suppression effectiveness for large wildland fire suppression activities as fire progresses using geospatial perimeter data. We estimate suppression effectiveness using stochastic frontier analysis. We modelled wildfire containment as a production process where crews are resources are assigned to build fireline until the amount of built fireline along the final fire perimeter equals the current fire perimeter. Production of controlled fireline on a particular fire day is the final output of the daily production operation. A mixture of resources are engaged in a large wildland fire suppression operation, and the production of controlled fireline depends on combination

of these major inputs (e.g. crews, dozer, engines, helicopter and air tanker). The ability of a production unit to transform inputs into corresponding outputs is affected not only by the combination of major inputs but also by exogenous environmental factors. We include these weather and landscape related variables on the right hand side of the frontier production function as the inefficiency effects component of our model to capture effect of these characteristics on productivity and suppression effectiveness.

Results

The coefficient of all suppression resource input variables are significant and as of the expected direction of a priori assumptions with the exception of a negative and significant coefficient for ground crew resources. That is the presence of additional ground crews results in a reduction in held fireline for that day. Estimates from the inefficiency effect model provide the direction of the influence of the corresponding variables to efficiency. However, these coefficients do not provide magnitude of the effect and cannot be interpreted reasonably.
Results from the marginal effects of inefficiency model indicate that efficiency increases if firelines are built along the natural break see table 1. However, marginal effects are fairly small. Previous fires seem to play a significant role in increasing efficiency of controllable fireline production. Again, marginal effects are fairly small. Relative day seems to be one of the strongest factors that influence efficiency. Every one day increase fire days increases the efficiency by about 7 percentage points suggesting that contained fireline increases over time possibly due to learning how best to engage the fire with improved suppression strategies and tactics. Efficiency gain is highest on those fires where full suppression is identified as the preferred strategy.

Table 1. Marginal Effect of specified variables on daily fireline produced.

Variable	Marginal Effect
max_gust_	0.04556
max_rh_lag	-0.05212
timber	1.021
rivers	0.1074
roads	0.01456
full_suppress	2.646
previous _fire	0.07543
relative_days	7.151

Most interesting, our results indicated that the number of assigned crews is not significantly related to the amount of permanently controlled fireline. This is most likely related to our definition of the objective of suppression efforts. Our definition of the suppression objective is to produce controlled fireline on a given day that ultimately is along the final fire perimeter. It should be noted that it does not include any fireline that may have been produced, but ultimately burned over, nor any built fireline such as contingency lines that never engage the fire. Further, on many fires strategies may include significant effort on burn out operations. In these circumstance significant resource effort is assigned to construct indirect line over several days that is ultimately burned out. This results in all of the effects of the effort being recognized on a single operational day when the burnout was conducted. Additionally, on many fires significant suppression effort is assigned to assure that controlled fireline along already burned areas does not reignite by “mopping up” any burning material within the fire’s interior.

In a related effort we collected field based data for a small set of individual large fires that provide the ability to link the specific assignment of all ground suppression crews assigned to the fire. Results from this small sample of large fires demonstrate that only 22 percent of all ground crew assignments were related to direct line building missions whereas approximately 60 percent of all assignments were related to indirect line building, holding, or mopping up a fire.

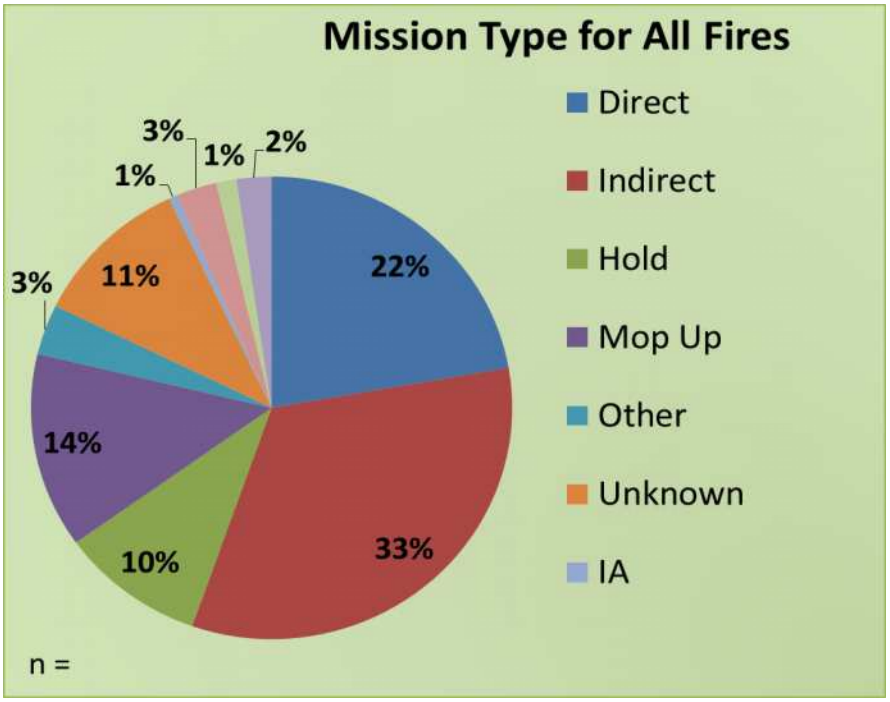

Figure 1. Ground crew mission type for 5 large US Forest Service Fires

The fire environment is the most important factor that can determine the success or failure of suppression effort. Obviously, fire managers have no control over topographic or weather elements. There could be several other variables that influence fire behaviour and efficiency of fireline production but are not included in our analysis. With these caveats in mind, our results suggest that production of controllable fire line is more efficient if they are built along the natural lines such as rivers and roads. However, these effects are only marginally significant and fairly small. Similarly, if there are areas that were burnt by previous fires, it is more efficient to construct the controllable fireline. Thus, efficiency analysis provides useful information in that it identifies the circumstances under which the suppression effort (as defined in this analysis) is more efficient

Discussion

These results collectively call for a re-evaluation of how we model the effectiveness of wildfire suppression actions and the productivity of individual resource categories assigned to large wildland fires. Uncertainty around fire progression, weather, and individual resource effectiveness make developing wildfire suppression strategies extremely challenging. Improving our understanding of how resources contribute to reducing wildfire related losses is critical to improving the safety, effectiveness, and efficiency of large wildfire management.

References

Broyles, G., 2011. Fireline production rate. USDA Forest Service, National Technology & Development Program, Fire Management Report 1151-1805, San Dimas, CA.

Calkin, D.E., K.M. Gebert, J.G. Jones, and R.P. Neilson. 2005. Forest Service Large Fire Area Burned and Suppression Expenditure Trends, 1970-2002. Journal of Forestry. 103(4): 179-183.

Finney, M., Grenfell, I.C., McHugh, C.W., 2009. Modeling containment of large wildfires using generalized linear mixed-model analysis. Forest Science 55, 249–255.

Fried, J.S. and B.D. Fried. 1996. Simulating wildfire containment with realistic tactics. Forest Science. 42: 267-281.

Holmes, T.P., Calkin, D.E., 2013. Econometric analysis of fire suppression production functions for large wildland fires. International journal of wildland fire 22, 246–255.

Thompson, M.P. and D.E. Calkin. 2011. Uncertainty and risk in wildland fire management: A review. Journal of Environmental Management. 92: 1895-1909.

The ODS3F project: evaluating and comparing the performances of the ground optical and thermal fire monitoring systems.

G. Laneve[a], Roberto De Bonis[a], Pablo Marzialetti[a], Yiannis Bakouros[b], Paraskevi Giourka[b], Riccardo Castellini[c], Remi Savazzi[d], Maria Rosa Grisolia[e]

[a] *University of Rome 'La Sapienza', Dipartimento di Ingegneria Astronautica, Elettrica e Energetica, Roma, Italy; laneve@psm.uniroma1.it; robertodebonis@yahoo.it*
[b] *University of Western Macedonia, Kozani, Greece; ylb@uowm.gr; g_vivi@hotmail.com*
[c] *CESEFOR, Soria, Spain; riccardo.castellini@cesefor.com*
[d] *Office National des Forets, Aix-en-Provence, France; remi.savazzi@onf.fr*
[e] *Provincia di Roma, Roma, Italy; mr.grisolia@provincia.roma.it*

Abstract
The ODS3F project (funded in the framework of the EC Civil Protection Financial Instrument) is devoted to the development of a common understanding of the capabilities of vision (optical or thermal) and detection systems on which a fire remote detection network can be based.
This paper illustrates the project results.

Keywords*: camera, fire, performances, comparison*

Introduction

The ODS3F project (funded in the framework of the EC Civil Protection Financial Instrument) is devoted to the development of a common understanding of the capabilities of vision (optical or thermal) and detection systems on which a fire remote detection network can be based. The main objective of such project is the technical assessment and operational comparison between remote visual systems devoted to monitor wooded areas or areas of particular environmental, touristic and/or cultural interest. In particular, apart from the definition of an optimal way to obtain the information needed to detect a fire at the early stage, the project aims at evaluating the possibility of exploiting such information for simulating the fire propagation behavior. Furthermore, the project has the objective to promote the cooperation in spreading and sharing objectively recognized successful practices in reducing the incidence of forest fires or improving the reaction time allowing an enhanced distribution of the human and means resources on the ground
The project originates from the evidence that several surveillance systems devoted to monitor vegetated areas are available in Europe. In particular, the activity of the project relies on the availability of a system based on visible cameras operated in Italy, France and Greece and a system based on thermal cameras operated in Spain. Therefore, this project aims at: - evaluating, through an agreed evaluation scheme, the performances of the already available monitoring systems based on visible or thermal camera already available in the project partners countries; - comparing the results taking into account the different characteristics of the monitored area and the observation system; - assessing the possibility of complementing the monitoring network with a system capable to simulate the fire behaviour providing the most probable, time dependent, propagation conditions by taking into account the meteorological conditions, the orography and fuel (vegetation) type and status; - defining agreed criteria capable to guide the decision about the adoption of situation reports devices based upon remote observation system, in terms of convenience and/or basic characteristics (visible or thermal camera).
The paper is devoted to illustrate the project results.

Methods

The ODS3F project contemplates two levels of analysis:
- one devoted to evaluate the performances of the camera based surveillance systems in terms of omission and/or commission errors by comparing the events detected by such system with the events reported by other sources (watchtowers, satellite sensors, fire brigade or forest corps reports);
- the second one devoted to define the basic elements to be taken into account for a correct comparative evaluation of the different systems performances.

The first level of analysis (system performances) has been addressed by comparing the alarms (omission errors) provided by the system with the events detected by satellite systems (MODIS, SEVIRI) or reported by Forest Corps or Fire Brigades. Also the number of false alarms (commission errors) is taken into account.
The comparison among systems has been carried out taking into account:
- the land characteristics (as topography, vegetation type),
- main weather conditions in which each system operates,
- the landscape characteristics that could affect the contrast approach.

We assume that an analysis aimed at characterizing the ground/weather/contrast of each area of interest could be carried out, with more or less success depending mainly on the availability of accurate weather data.

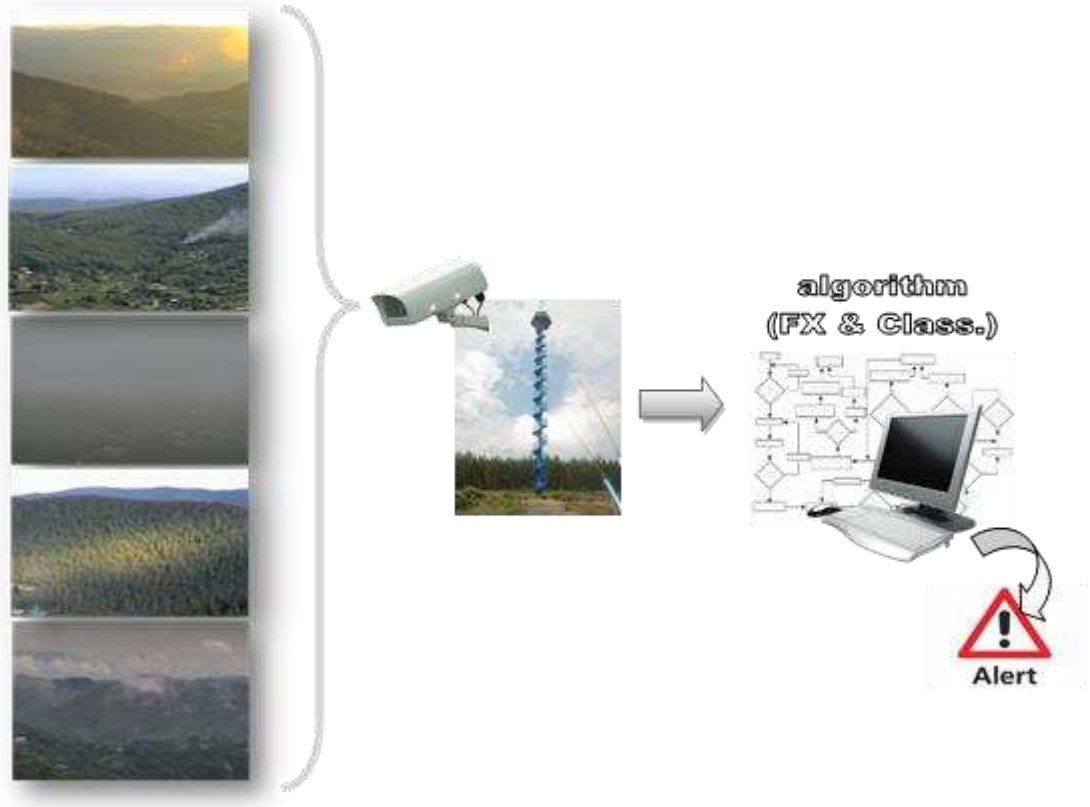

Figure 1. Fire monitoring/detection system.

Furthermore, we proceed by introducing an analysis of the algorithms on which the fire detection is based. Considering an outline of a monitoring/detection system architecture (Fig.1), beyond the above mentioned inherent complexity related to a landscape characterization due to its high dynamism, and leaving out a technical characterization of the cameras installed within the consortium, we intend to address the problem of how each system analyzes the information acquired by the cameras.

Smoke detection and feature extraction processing is a topic developed in many studies, focusing on different approaches (as wavelet decompositions, histogram-based smoke segmentations, colour space transformations, multi-temporal differences, area growth variable and smoke growth rate, spatial characteristics of smoke column, fractal self-similarity properties, RGB space thresholds, texture analysis with gray level co-occurrence matrix, irregular boundaries and background subtraction, neural network and support vector machine classifications).
Then we intend to give as an input in each system an imagery dataset including a number of different context situations (illumination, sunrises and sunsets, foggy and other extreme weather conditions, etc.) in order to evaluate the performance of each classification algorithm in several contrast circumstances.

Results

This paragraph is devoted to describe more in detail the results of the camera systems performances analysis (Figure 2 and Figure 3) and the strategy adopted for comparing the different systems in a way that will take into account the different conditions in which such systems are operating.

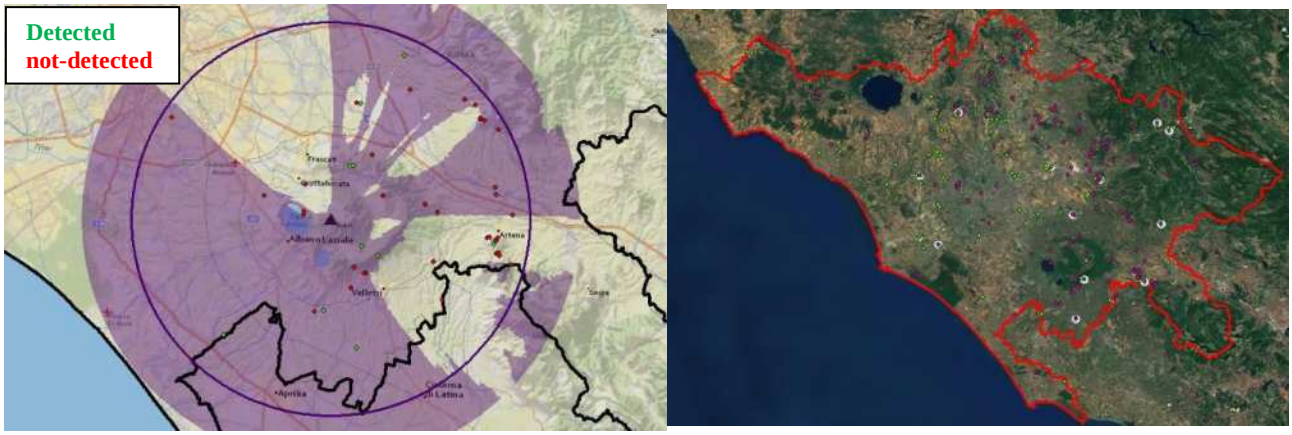

Figure 2. (left) CICLOPE system (Province of Rome) performances analysis. Comparison between camera system reported events (a single camera has been considered) and those provided by Italian Forest Corps, the camera visibility is shown in violet, the fires not detected by CICLOPE are given in red whereas those detected are shown in green. (right) Comparison between Forest Corps events (violet) and MODIS sensor based hot spot (green), the coincident events are highlighted with a cyan circle for the whole Province of Rome.

Figure 2 refers to the system available in the Lazio region (Italy) based on visible camera. Regarding the system based on thermal cameras operating in the Castilla y Leon region (Spain), some results of the analysis of the performances of the detection system are shown in Figure 3. The system is operational since 2006, even if, the number of cameras has increased with time. Figure 3 shows the increasing trend of the effectiveness of the system, reaching an average efficiency of 32%, from the date (2006) of commissioning to 2013.
Table 1 shows, more in details the results concerning the years 2012 and 2013. The year 2012 had a number of fires over the average of the decade. But, only 24 of them exceeded one hectare of burned area. However, to evaluate the full performance of the detection systems in 2012, all the occurred fires were considered, even in farmland.
2013 was one of the best years of the last decade in terms of the number of fires and burned surface in Soria province. 40% fewer fires than the average of the decade. This low incidence of fire in 2013 not facilitates to test the efficiency of the cameras and be able to provide data representative of actual performance. So we also considered all the occurred fires.

These data indicate an effectiveness in **viewed area** of **26,9%** and an effectiveness in all detection range (8km buffer) of 16,3% .

Table 1. Comparison of the surveillance system performances for years 2012 and 2013

	2012	2013
Nº Total fires in the year throughout the province	**207**	**76**
Forest fires	**156**	**47**
Fires between June and October	**110**	**67**
Fires in detection buffer (all the year)	**46**	**20**
Fires in detection buffer and in period of detection	**27**	**16**
Fires in viewed area	**28**	**10**
Fires in viewed area and in period of detection	**17**	**9**
Fires Detected	**4**	**3**
Monitored Fires	**35**	**10**

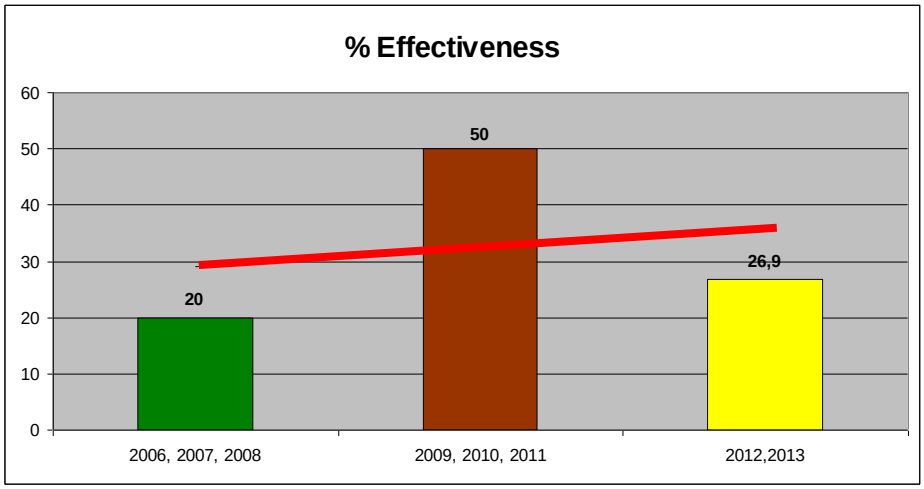

Figure 3. Trend of the effectiveness of the thermal system in Castilla y Leon.

The main causes of this, still low efficiency are:

- A high number of systems failures.
- Short operating time during the year.
- Low rotation speed of some systems.
- Bad calibration for fire detection under adult trees.
- High occurrence of small fire and fast extinction.
- Low visual coverage.
- Absence of qualified personnel throughout all the operation time.

From such analysis we come out with the idea that, besides trying to correct the technical failures and extend the system operating time during the year, it will be necessary to make changes in the operations protocol and mostly important to proceed with a new **calibration of the cameras.**

With reference to the definition of the parameters characterizing the operational 'environment' of the cameras we have identified:

- **terrain characteristics**. The topography of the area monitored by cameras can be characterized by introducing the:

- TPI (topographic Position Index) that gives an estimate of the landform type (Figure 4);

- Aspect, that identifies the downslope direction of the maximum rate of change in value from each cell to its neighbors (Figure 5 left);
- Illumination, which put into evidence different hillshades depending on different hours of the day, providing relative measures of solar illumination (Figure 5 right), which potentially define contrast values with previous Aspect direction;
- Binary Viewshed analysis, which gives the possibility to quantify the amount of covered area seen at surface level, especially useful for thermal cameras (Figure 6 left) and Minimum Smoke Height maps (Figure 6 right), which evidence the Minimum Smoke Height that a smoke column need to reach in order to be seen by the camera.

- **weather conditions** capable to produce fog that can impact the detection capabilities of the system.
  - The frequency of fog conditions can be evaluated introducing the FSI (Fog. Stability Index) based on the knowledge of meteorological data (Figure 7 left);
  - The impact on visibility can be approximated from FSI values by a comprehensive statistical analysis (Figure 7 right).

- **land cover/fuel type**. The vegetation type and status (dryness), potentially, define the amount and 'color' of the smoke, that should be taken into account for detection.

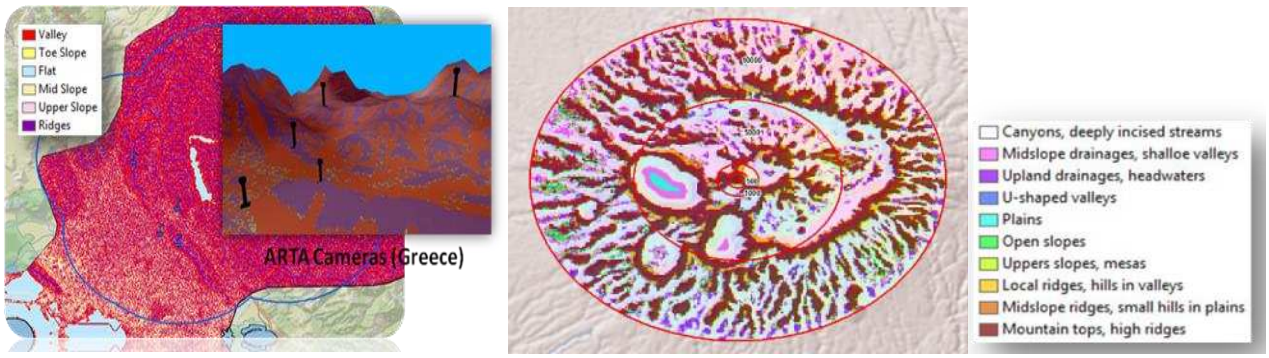

Figure 4. Topographic analysis of the Greek's system in Arta region (right), Provence Region (right)

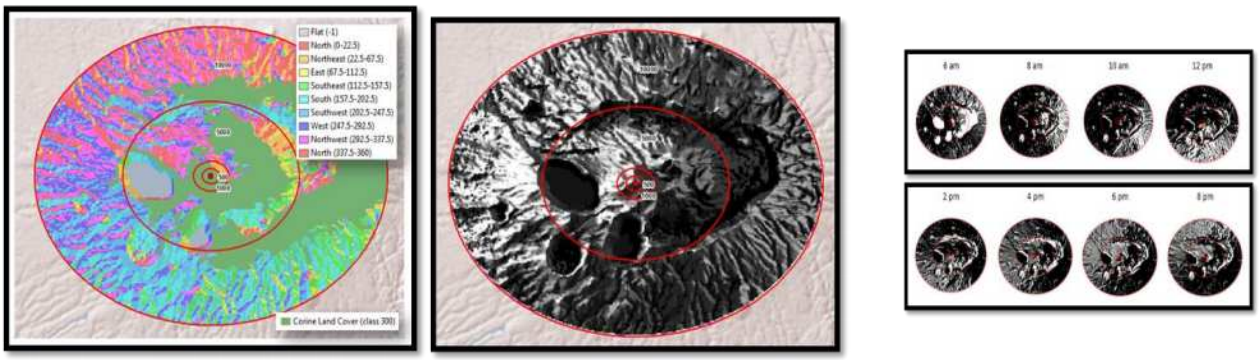

Figure 5. Aspect (left) & Illuminations products (right)

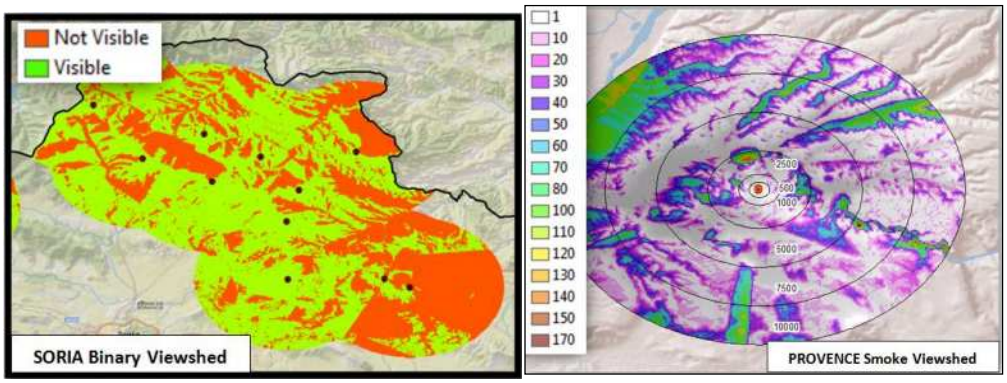

Figure 6. Example of Binary Viewshed analysis of Soria (left), and Minimum Smoke Heights maps of Provence (right).

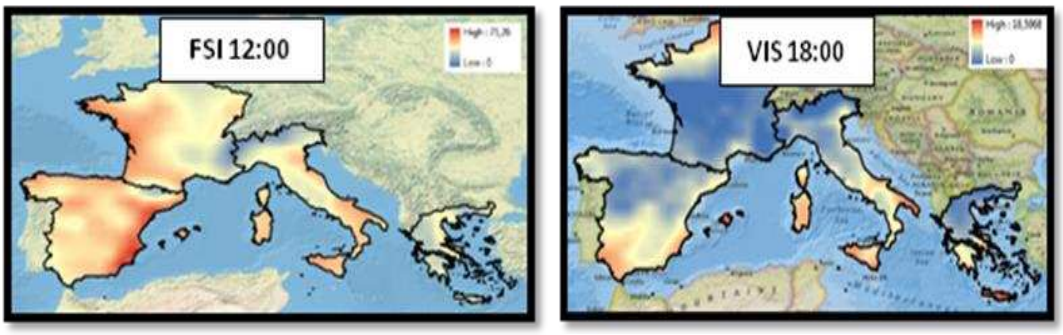

Figure 7. Examples of assessment of the FSI (left) and the visibility (right) for ODS3F countries.

From the different parameters and classes extracted and described above the potential weight that each parameter has can be measured to better understand principal omission and commission errors, and in a further work the potential influences of the territory on each fire monitoring system (Figure 8).

If from a side, as explained above, we are trying to define the 'environmental' parameters which can affect the effectiveness of the camera based surveillance system, on the other side, for comparing the different systems, it is also necessary to set certain common criteria related to the events analyzed.
In fact, during the summer 2014 a campaign covering the summer season will be carried. During such campaign, for each alarm provided by the fire detection systems under study, a template containing a minimum set of variables that could vary according to the detection type systems (heat or smoke) opportunely identified, will be filled:

- Type of detection: thermal or smoke, Kind of sensor and algorithm used.
- Detection range: maximum distance that can detect a fire. (radius).
- Nº Forest Fires in detection range: Official data of the fires that have occurred in the detection range of each system along the period of study.
- Fire forest in detection range and in operational time: Official data of the fires that have occurred in the detection range of each system and in its working time.
- Fire forest in detection range, operational time and in viewed area: Official data from fires that should have been detected by the system
- Fire Forest detected: Number of automatic real detections of fire
- Fire forest Monitoring: Number of fires not detected by the system but monitored
- % Effectiveness of detection: fires detected divided between those who should have detected

Other variables taken into account are:

Operability:

- Work time day / year: how many days the systems work during the year.
- Work time hour / day: how many hours the systems works during the day.

False Alarms:

- Type 1 (Technical): generated by the system when there is some kind of technical failure.
- Type 2 (Natural): are originated by natural causes, such as sunrise and sunset, reflections, clouds, etc.
- Type 3 (Realistic): any other cause giving rise to a hot spot or a column of smoke but no actual case of a wildfire. Such equipment, barbecue, fireplaces, agricultural practices.

Other:

- Installation cost: The cost of systems, excluding tower infrastructure.
- Maintenance cost: cost of commissioning, calibration and annual maintenance (€ / year / system).
- Lifetime of each system: estimated duration that each system can have with correct operation.

Product	Class 1	Class 2	Class 3	Class 4	Class 5	Class 6
Illumination	08:00 – 12:00	12:00 – 16:00	16:00 – 20:00			
Aspect	0	315º-45º	45º-135º	135º-225º	225º-315º	
Binary Viewshed	Visible	Not visible				
Minimum Smoke Height	0	< 10 mts.	< 20 mts.	< 50 mts.	< 100 mts.	> 100 mts.
Visibility	0	< 500	< 1000	< 2500	< 5000	> 5000
Fog Stability Index	low	medium	hight			
Slope Position Classification	Valley	Plain	Ridge			
Distance	500 mts.	1000 mts.	2500 mts.	5000 mts.	7500 mts.	10000 mts.
Corine Land Cover	Forest	Agricultural	other			

characteristic	event #1	event #2	event #3	...	event # n
Illumination	C1	C2	C2	...	C2
Aspect	C2	C5	C4	...	C1
Binary Viewshed	C1	C1	C2	...	C2
Minimum Smoke Height	C3	C5	C2	...	C2
Visibility	C4	C4	C1	...	C3
Fog Stability Index	C3	C2	C2	...	C2
Slope Position Classification	C3	C3	C2	...	C3
Distance	C2	C4	C6	...	C4
Corine Land Cover	C3	C2	C1	...	C1
event detected	X	√	√		√
false alarm	X	X	√		X

Omission errors (event Not Detected that is a not a False Alarm) >> **Need to be reduced**

Note: Event = feature detected by the system, not necessarily a fire/smoke event

Commission errors (event Detected that is a False Alarm) >>**Need to be reduced**

Figure 8. Classes extracted from parameters

Conclusions

The ODS3F project objectives originate from the circumstance that even if the systems based on (visible and thermal) cameras devoted to monitor/detect fires are spreading all over Europe a comprehensive study, of such systems and their limits compared with the environment where they operate is not available yet.
Through the comparisons of different systems ODS3F aims at defining an optimized system, a standardized set of information, a common method of using the situational reports for enhancing the correct, effective and efficient utilization of the available data in facing emergencies (as wildfires are) and in reducing their consequences. Finally, a guidelines document describing the elements to be taken into account for selecting the most suitable surveillance system for monitoring, protecting a given area of interest and for optimizing the exploitation of the produced information will be issued.

Thematic division and tactical analysis of the UAS application supporting forest fire management

Agoston Restas

National University of Public Service, Budapest, Hungary, Restas.Agoston@uni-nke.hu

Abstract
Introduction: This paper describes many initiatives and shows also practical examples which have happened using Unmanned Aerial Systems to support fire managers in different ways. Since the operation of manned aircraft at forest fires is usually expensive, in many cases managers miss the aerial activity even for reconnaissance however that would be required for the effective intervention. Today more and more experts say Unmanned Aerial Systems can give real alternatives for aerial reconnaissance even if this application is far from manager's mentality yet. Methods: Author used thematic division of Unmanned Aerial Systems applications; it is based on two key elements, one of them is the time flow of fighting forest fires, the other is its tactical requirements. Research used mainly author's own experiences in this field, accompanied by function analysis, practical experiments, economic analysis and also expert estimation. Results and discussion: Logically Unmanned Aerial Systems can be used before fire for hot spot detection, before starting the intervention for fire reconnaissance, during the intervention for intervention monitoring and after suppression for post fire monitoring. The method of prescribed fire can also be in the focus of Unmanned Aerial Systems use as a special application for fire prevention.

***Keywords**: Unmanned Aerial Systems (UAS), tactical analysis, forest fire management, fire detection, fire monitoring, prescribed fire*

Introduction

The operation of manned aircraft at forest fires is usually expensive, therefore in many cases managers miss the aerial activity even for reconnaissance or supporting decision making, even if that would be required for the effective intervention. Today's experiences say Unmanned Aerial Systems[1] (UAS) can give real alternatives of manned aircraft's operation not just for aerial reconnaissance but even other activities. This paper describes many initiatives and shows also practical examples which have happened using UAS to support fire managers in different ways.
UAS activities regarding forest fire is not new. We can reel off activities using UAS to fight against forest fire in the United States (Ambrosia and Hinkley, 2009), in Croatia (Hucaljuk, 2004; Restas, 2013), in Spain (Ollero, 2004; Pastor, 2008). In Hungary the Szendro Fire Department carried out many activities helping fire management using UAS (Restas, 2004).
This paper gives an approach for thematic division of using UAS at forest fires; it is based on the tactical differences. Logically UAS can be used *before fire* for hot spot detection, *during the intervention* helping fire management and *after suppression* for post fire monitoring. The method of prescribed fire can be also in the focus of UAS use as a *special application* for fire prevention. (Restas, 2011)
The paper uses the chronological flow of fighting forest fire for thematic divisions, although the last part of this paper, the *UAS generated prescribed fire* can be disputed; it could have been also the first part. As a latest development of this application author found it as the latest place for the best.

[1] There are other abreviations like UAV (Unmanned Aerial Vehicle) or RPAS (Remotely Piloted Aircraft Systems) meaning the similar technology as UAS. „Drone" is also used for this technology.

Aerial patrol for hot spot detection

Aerial patrol with manned aircraft is a commonly used procedure for detecting hot spot. Many countries such as Australia, Canada, France, Russia, Spain, and United States regularly use this procedure while others such as Germany and Poland used to apply it but today not.

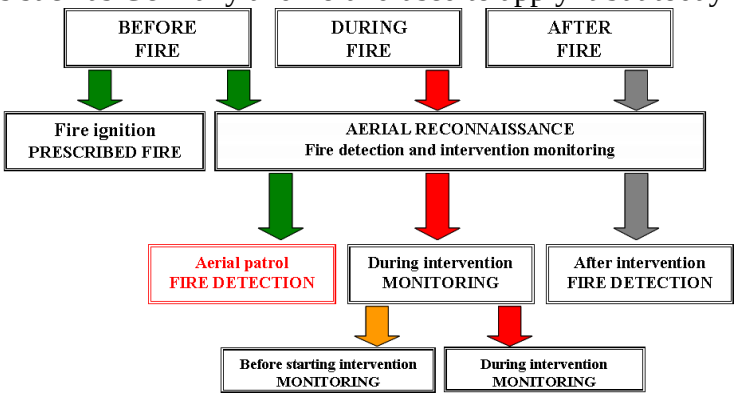

Figure 1. Aerial patrol for hot spot detection in the structure of thematic division of UAS use

Detecting hot spots by aerials earlier than reporting it by civilians obviously helps fire managers limit the damages fires cause. Unfortunately, the main reason why this method is not always used is the huge costs of aerials. If the procedure made by UAS is cheaper than the traditional one (manned aircraft), it means that the option of UAS use is the better solution. Naturally this case assumes the similar professional efficiency of different methods.

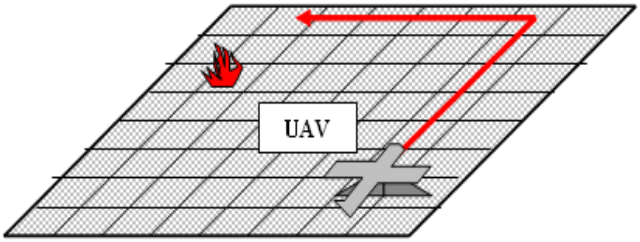

Figure 2. Planning UAS mission for hot spot detection

During this task UAS makes a patrol following the pre-programmed flight path and based on the real time video supply the staff in the control station can detect and check any hot spots. In case of real danger staff reports it to the fire service.

Figure 3. UAS mission in the United States. Ikhana strategic UAS

Figure 4. UAS based hot spot detections: in Croatia (2011) and the first one in Hungary (2004)

No doubt, aerial patrol by UAS can detect hot spots very quickly and it is able to give the first fire report to fire brigades. It can reduce the time of first attack but study says that based on economic calculations, this application can be effective just under special conditions such as at extremely high Fire Weather Index and at geographically high articulated area. Detailed criteria must be developed in the future for optimizing the effectiveness of UAS applications.
For effective hot spot detection different type of UAS can be used. Depending on the area staff responsible for both strategic and operational UAS can be effective tool for the early hot spot detection. In the United States the high altitude long endurance (HALE) Ikhana was used for both early detection and intervention monitoring. In Croatia and Hungary tactical UAS were also used for hot spot detection.

Aerial reconnaissance before starting intervention

When starting intervention the main problem is the lack of objective information regarding the affected area, fire intensity, etc. (Bleszity, 1989). Operational used UAS could help in this case; below just a few minutes it can be ready for launch and 2-3 minutes later it transmits the real time pictures about the fire and their circumstances.

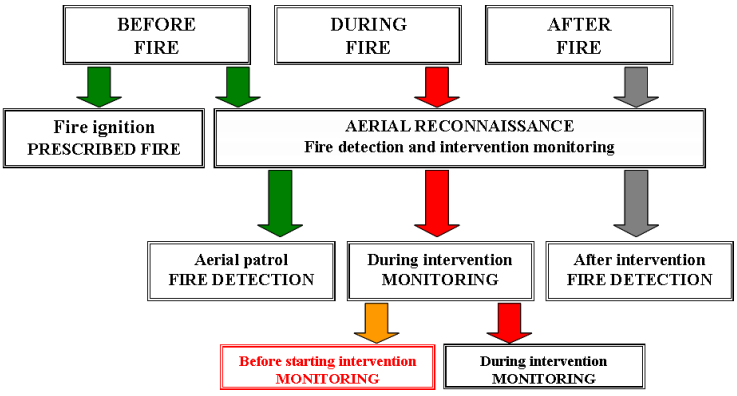

Figure 5. Aerial reconnaissance before starting intervention in the structure of thematic division of UAS use

For aerial patrol aimed at hot spot detection the reasonable type of UAS belongs to the category of high altitude, long endurance or medium altitude long endurance (HALE, MALE) band. In this case a special UAS service can also be used effectively. In case of aerial reconnaissance before starting

intervention the situation is totally different. Fire managers require some basic information about fires immediately and for this task a highly qualified UAS service is not applicable.
In case of aerial reconnaissance the quick access to the information is much more important than the quality (e.g. resolution of the video, photos) of that. Therefore the simple but *immediately ready for start* UAS is required for this type of task. Capability of this type of UAS is limited. Fire manager needs objective information about the fire characteristic, fire intensity, speed of spreading fire, smoke emission, wind direction, etc. but very quickly. For this task a hand launch, by electric engine powered UAS is considered the best solution.

Figure 6. Launch of fix wing UAS (Fenix) for fire reconnaissance before starting intervention. Rotary wings UAS (Bee) hovering at forest fire. Source: 6DOF (Croatia) and R-Fire Ltd. (Hungary)

The simple criterion for economic effectiveness is that all costs of UAS use must remain below the value of the forest saved by this process.

Figure 7. Differences between fire fronts can be seen face to face or from the air after arriving. UAS supported intervention in Hungary (DRAVIS II, 2011)

Aerial reconnaissance during intervention

During intervention, where aerial reconnaissance is required but manned aircraft is above price, UAS could give also a cost effective solution. If the commander of fire-fighting operations is at the scene, he is too close to the fire to be able to manage it along with its environment. Quite literally, he cannot see the forest for the trees! As the extinction of forest fires is a protracted process in time, and since during that time the fire will continue to spread, the ability to manage a fire together with its environment is an indispensable precondition for the efficient extinguishing of a fire.
Manned aircraft is used on several occasions to assist with the reconnaissance of forest fires. However, these fires cover very large areas and putting them out takes several days, and the fire-fighting action

is managed at higher levels of the organisation, usually at executive staff level. These experiences indicate that air reconnaissance is effective.

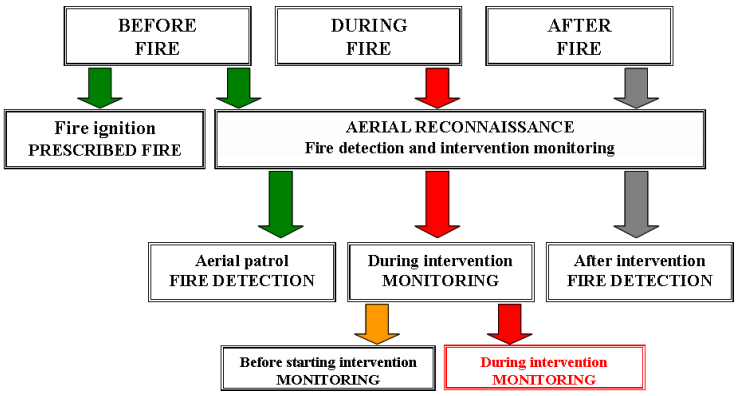

Figure 8. Aerial monitoring during intervention in the structure of thematic division of UAS use

During intervention the UAS use can be very effective because obtaining an overview of several hundred or even thousand hectares of forest allows intervention measures to be co-ordinated. Without air reconnaissance, co-ordination of measures can only be based on the information circulating between the commanders of individual units at various locations. But the assessment of the scope of their individual situations by commanders located at various sites may be completely subjective and not made in relation to the other sites. Air reconnaissance helps to eliminate subjectivity in such judgements and to rank the individual sites in relation to the others.

Figure 9. Typical fire forms: spot fire and linear fire spread. Photos made by UAS in Croatia (2011)

At huge fires using manned aircraft for bombing water or just to support the reconnaissance with information is a normal procedure. On the other hand, small fires don't require aerial support; these are managed by traditional equipment. Between these extremes, logically, there is a sector, where fire size is larger than management could suppress successfully just with traditional equipment, but not large enough to ask manned aircraft for help. In this case the manned aircraft is economically, obviously, not effective, but a solution such as UAS - which is cheaper than the use of manned aircraft – can already be.

If the UAS based aerial reconnaissance satisfies the minimum criteria of the professional requirements of the effective reconnaissance, it means that this solution can be even economically effective.

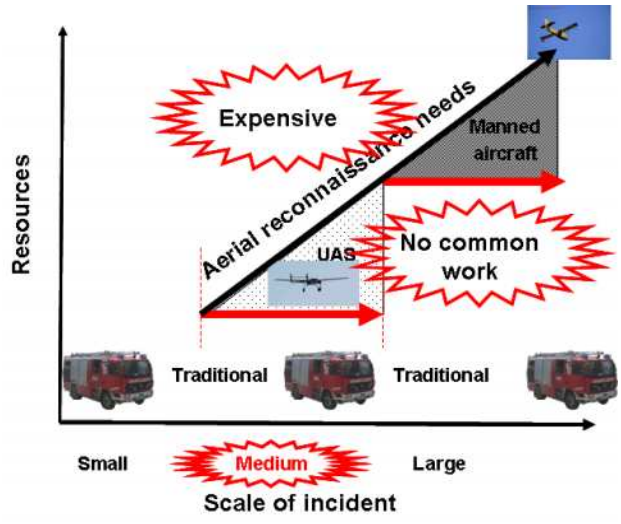

Figure 10. Efficiency of UAS application depends on fire size

We can demonstrate the effectiveness of UAS based aerial reconnaissance also by the *damage – time function.* This kind of applications is not just reducing the damages caused by the fire but even reducing the time of the intervention. Shorter intervention is reducing also the risk posed to citizens caused by the lack of fire fighters who are ready for alarm in case of accident, house fire, etc. Unfortunately this kind of risk is usually assessed much lower than the reality requires.

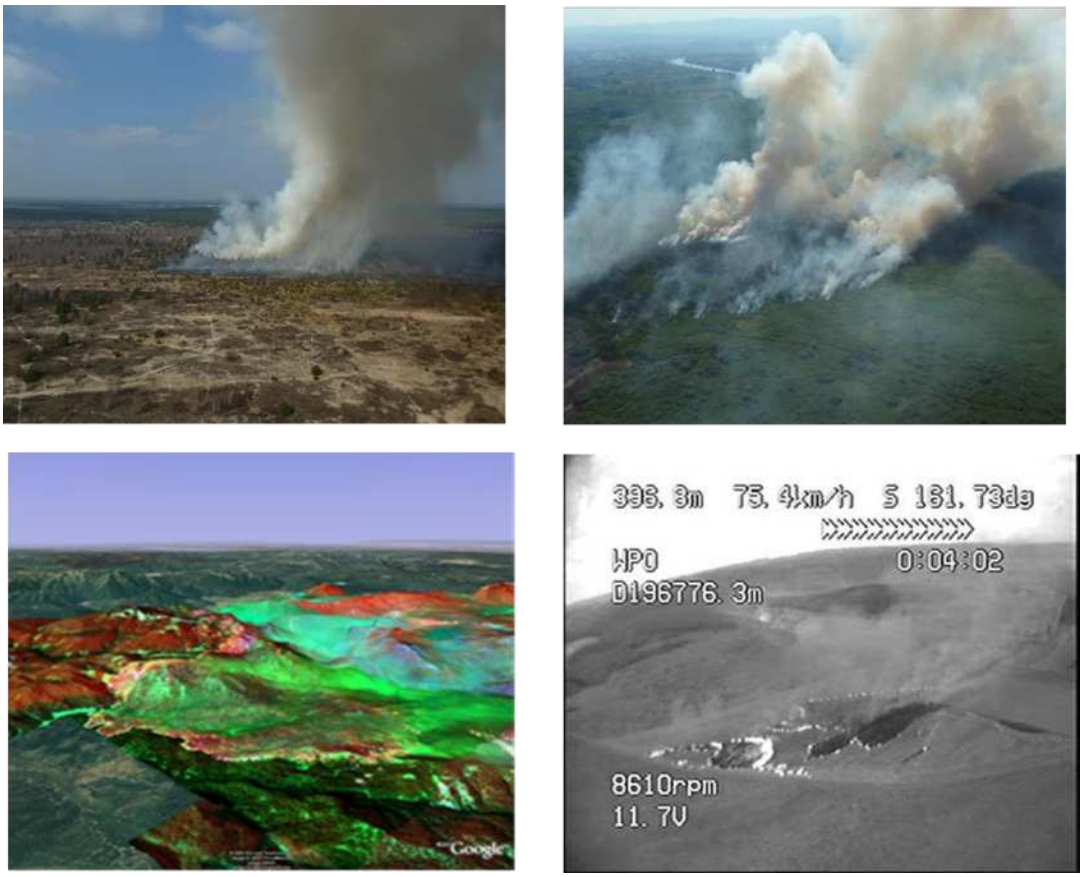

Figure 11. Intervention supported by UAS: forest fires in coloured (Bee, Germany, 2010, and Phoenix, Croatia, 2011), artificial coloured (Ikhana, US, 2007) and black and white photos (Hungary, 2004)

Post-fire monitoring

After suppressions, many times, area surveillance is required to prevent starting fire again by remained cinder. UAS equipped with IR camera can detect the critical points easily and with a small team can manage hot spots while let fire fighters leave the area.

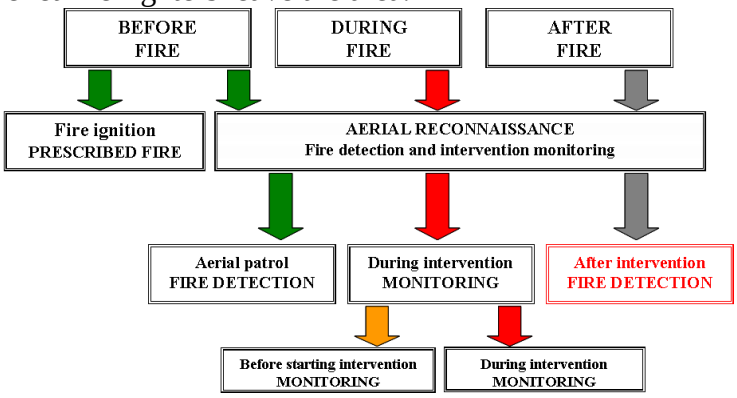

Figure 12. Post-fire monitoring in the structure of thematic division of UAS use

Burnt area monitoring besides the tactically advantages gives also other options. Since many cases UAS use is optimal when it is in the hand of fire service, the post fire monitoring is ideal for training recruit. After the intervention, there is no stress regarding success, no pressure from media or residents. But post fire monitoring is a real task while its environment means a reality. It means hot spots, remained cinder what also requires responsible management.

Figure 13. Thermo cam is installed on UAS board and able to detect the remained cinder

Planning the post-fire monitoring UAS must fly around the extinguished fire front instead of monitoring the whole area (hot spot detection). For this task a simple but with IR equipped UAS is required.

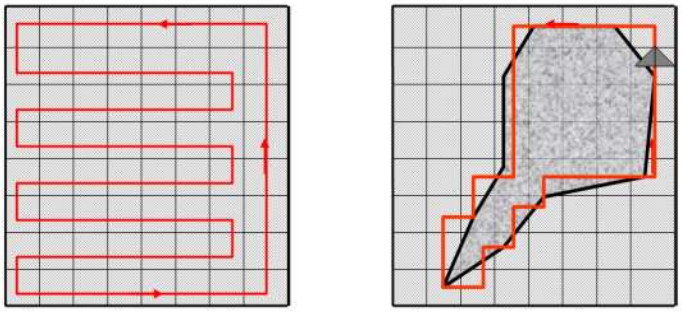

Figure 14. Differences between planning UAS mission for early fire detection and remained cinder detection

Prescribed fire – made by UAS

There are other initiatives such as making prescribed fires with using medium size UAS. The special equipment filled with fire eggs or pastilles weighs less than the payload capacity of UAS. It means UAS can provide also this task, giving more possibilities for managers using prescribed fires method with limited costs.

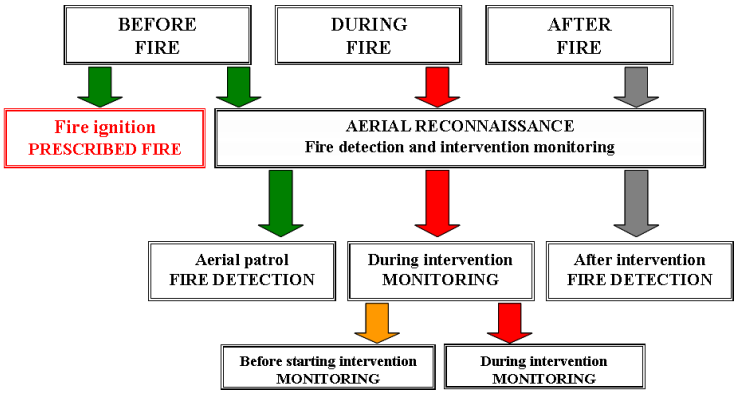

Figure 15. UAS generated prescribed fire in the structure of thematic division of UAS use

No doubt, prescribed fire is a very effective management tool for avoiding the serious fires in critical seasons. In this process fire managers burn areas with controlled fire reducing the fuel load of the territories. Less fuel load means less fire intensity and damage. There are different ways from hand tools (drip torch) till aerial means making this process.
For the sake of better efficiency today managers can use special equipment for this task such as fire eggs and pastilles. These equipment weighs about 20 kg. This method means that a light helicopter carries these 20 kg weight machines for dropping the eggs or pastilles. Since both fix wing and rotary wings UAS are able to carry this machine, we can supply this task also with UAS.
Professionally there is no difference in effectiveness between manned aircraft or UAS. There are other tactical advantages of using UAS for generating controlled fire. UAS can fly not just in day mission but also at night widening the term when control fire can be made. It means the possibilities of UAS generated fire is more than just giving an alternative solution.

Figure 16. Example for the special equipment generating prescribed fire and a real application

As usual we can demonstrate the effectiveness of UAS generated control fire also by the damage – time function. Since the prescribed fire reduced the fuel load in case of not intended fire the fire intensity will remain at low level. Low level fire intensity means reduced fire spread, more time for intervention and limited severity.

Figure 17. Method of UAS generated prescribed fire and an example of UAS ready for doing it

7. Results

Based on the above examples UAS can be a very effective tool in the hand of fire managers. After launch the UAS can supply real time data continuously, therefore within in the first few minutes it can provide effective support for the decisions of the commander. One such element of decision support is that even before the UAS returns, it will be possible to establish the extent of the burning area and to request the assistance of further units. This will save a significant amount of time.
Another example of decision support: if commanders are able to manage the entire area in a complex way, it may be the case that protecting the area where the fire is currently most intense is the most important task. It is possible that our forces need to be concentrated in a location other than that furnished by the initial assessment.
While firefighting is in progress, the fire continues to spread in the areas where no countermeasures are taken, and indeed it may meet natural obstacles or barriers. A river, a wider road or glade may stop the fire as a natural barrier, so beginning fire-fighting measures at a distance of 100 or 200 metres from such a natural barrier can only be considered efficient if we have plenty of resources.
On the other hand, it is also possible that in a direction which currently has low parameters for spread and is thus assessed as lower priority, there lies a much more valuable area, such as a highly protected plant community, a habitat of protected animals, or perhaps an area of vegetation with higher parameters for spread.
The above examples show that the most efficient intervention is not necessarily the same as intervention at the point where the fire is the most intense. In order to make the best decision, the area of the fire must be managed in a complex manner, together with its environment.
The tactical UAS, which has proven effective, can be made available to even the smallest fire brigades. Traditional reconnaissance no longer provides information of a quality and quantity sufficient for today's applications. Increasing the efficiency of reconnaissance will result in increasingly efficient interventional measures. This will increase the area of forests saved while reducing the areas destroyed. The workload of fire-fighters may be reduced; in many instances there may be no need to mount a response at all. The elimination of unnecessary responses will reduce the level of risk to citizens, resulting in a higher level of fire safety.

8. References

Ambrosia, V. and Hinkley, E.: UAS Applications: Science, Applied Science, and Civil Applications "UAS For Earth Remote Sensing Workshop" International Symposium on Remote Sensing of Environment (ISRSE), Stresa, Italy, 3 May 2009

Bleszity J. and Zelenak, M.: A tuzoltas taktikaja (Tactics of firefighting) Ed.: BM Konyvkiado, Budapest, 1989

Hucaljuk M. 2004. "Remote Sensing of Wild Fires by an Ultra-light Unmanned Aerial Vehicle", 24th EARSeL Symposium New Strategies for European Remote Sensing, Dubrovnik, Croatia, 25-27 May 2004

Ollero A., Hommel G., Gancet J., Gutierrez L.G., Viegas X.D., Forssén P.E., González M.A.: "COMETS: A multiple heterogeneous UAV system". IEEE International Workshop on Safety, Security and Rescue Robotics SSRR 2004, Bonn, Germany, May 24-26, 2004.

Pastor, E. (*et al*.): Project SKY-EYE, Applying UAVs to Forest Fire Fighter, Support and Monitoring; Department of Computer Architecture; Technical University of Catalonia, Spain, 2008

Restas, A.: Robot Reconnaissance Aircraft. UAVnet 9th Meeting, Amszterdam, Netherlands, 2004

Restas, A.: UAV Applications From Aerial Patrol to Prescribed Fires; Wildfire2011 The 5th International Wildland Fire Conference, Sun City, South Africa, 9-13 May 2011

Restas, A.: Cost Effective Solution of Aerial Means for Supporting Large Scale Firefighter's Incidents, Advances Fire and Safety Engineering, Zilina, Slovakia, 2013

Towards an ultra-low-power low-cost wireless visual sensor node for fine-grain detection of forest fires

J. Fernández-Berni[a], R. Carmona-Galán[a], Juan A. Leñero-Bardallo[a], R. Kleihorst[b], Á. Rodríguez-Vázquez[a]

[a] *Institute of Microelectronics of Seville (CSIC – Universidad de Sevilla), Avda. Américo Vespucio s/n Seville (Spain), berni@imse-cnm.csic.es*
[b] *Ghent University/iMinds/TELIN-IPI. St-Pietersnieuwstraat 41 Ghent (Belgium), rkleihor@telin.ugent.be*

Abstract
Advances in electronics, sensor technologies, embedded hardware and software are boosting the application scenarios of wireless sensor networks. Specifically, the incorporation of visual capabilities into the nodes means a milestone, and a challenge, in terms of the amount of information sensed and processed by these networks. The scarcity of resources – power, processing and memory – imposes strong restrictions on the vision hardware and algorithms suitable for implementation at the nodes. Both, hardware and algorithms must be adapted to the particular characteristics of the targeted application. This permits to achieve the required performance at lower energy and computational cost. We have followed this approach when addressing the detection of forest fires by means of wireless visual sensor networks. From the development of a smoke detection algorithm down to the design of a low-power smart imager, every step along the way has been influenced by the objective of reducing power consumption and computational resources as much as possible. Of course, reliability and robustness against false alarms have also been crucial requirements demanded by this specific application. All in all, we summarize in this paper our experience in this topic. In addition to a prototype vision system based on a full-custom smart imager, we also report results from a vision system based on ultra-low-power low-cost commercial imagers with a resolution of 30×30 pixels. Even for this small number of pixels, we have been able to detect smoke at around 100 meters away without false alarms. For such tiny images, smoke is simply a moving grey stain within a blurry scene, but it features a particular spatio-temporal dynamics. As described in the manuscript, the key point to succeed with so low resolution thus falls on the adequate encoding of that dynamics at algorithm level.

Keywords*: forest fires, surveillance systems, wireless sensor networks, automatic early detection, artificial vision, low-power sensors, vision algorithms.*

Introduction

Wireless Sensor Networks (WSNs) (Akyildiz *et al*. 2002) constitute an enabling technology for the paradigm of *pervasive computing* (Weiser 1991). One of the most representative application frameworks of this paradigm is *environmental monitoring*. Typical scenarios are precision agriculture (McCulloch *et al*. 2008), forest canopy analysis (Tolle *et al*. 2005), volcanic studies (Werner-Allen *et al*. 2006), meteorological station networks (Barrenetxea *et al*. 2008) etc. In all these cases, the network nodes incorporate particular sensing capabilities according to the requirements of the application considered. These capabilities share a common feature: they provide scalar measurements, e.g. temperature, humidity or wind speed. Moreover, the data sampling rate is usually low or moderate at most, leading to a reduced amount of information to be handled locally by the nodes. These conditions significantly change when it comes to the in-node implementation of multimedia sensing (Akyildiz *et al*. 2007). Specifically, the implementation of vision hardware at WSN nodes is not a trivial issue at all since the visual stimulus implies to deal with a massive flow of multidimensional information. Taking into account the very strict power budgets allocated to the nodes, the mere capture and digitization of an image sequence could represent a significant percentage of their energy consumption.

But the critical point arises just afterwards. On the one hand, the sequence could simply be transmitted for remote processing, affecting dramatically the scalability and bandwidth of the network. On the other hand, the node itself could deal with the image sequence by taking advantage of its processing capabilities. In this case, the nature of such processing is greatly influenced by the energy constraints, demanding new strategies which permit to reach the targeted result with the minimum possible power cost.

Most WSN applications take a new dimension when imaging is added to the catalogue of in-node sensing capabilities. A clear example is wildfire monitoring. Image processing permits not only to monitor a certain area from the perspective of environmental conditions (Hefeeda 2007, Aslan *et al.* 2012), but also to carry out visual inspection in order to perform early detection of smoke or flames (Fernández-Berni *et al.* 2012, Jakovcevic *et al.* 2013). At the moment, two fundamental intertwined challenges are hindering the commercial exploitation of vision-enabled WSNs performing fine-grain detection of forest fires: node cost and battery life. A scalable deployment of sensors across typical regions of interest for fine-grain detection, e.g. Wild-land Urban Interfaces (WUIs), demands a competitive cost per node, what in turn demands the use of standard technologies and reduced form factors. Maintenance also plays a key role in terms of system cost when hundreds of vision-enabled nodes are to be deployed. Frequent change of batteries directly impacts the commercial viability of the network. Rechargeable batteries making use of solar panels or other energy-scavenging devices could be a solution, but they significantly increase the node form factor and the cost. They also strongly influence the locations of the sensors, which must be adequate for the particular physical process collecting energy. These considerations again point to ultra-low power consumption as the primary requirement of vision-enabled WSNs, a fact that is emphasized for the specific application of forest fire detection.

All in all, we summarize in this paper our contribution to the power-efficient implementation of vision hardware on wireless sensor network nodes targeting early detection of forest fires. This contribution is the result of long-term research. The tasks carried out range from devising a robust vision algorithm for smoke detection to the design and physical implementation of a power-efficient smart imager tailored to the characteristics of such an algorithm. By integrating this smart imager with a commercial wireless platform, we endowed the resulting system with vision capabilities and radio communication. Numerous tests were arranged in different natural scenarios in order to progressively tune all the parameters involved in the autonomous operation of this prototype node. We have also studied the performance of another platform based on commercial components, the so-called *Silicam IGO* (Silicam 2014). This smart camera includes two low-cost image sensors with a resolution of only 30×30 pixels. Reliable smoke detection is still possible in real scenarios even for such a small amount of visual information. Indeed, the low resolution itself can be a helpful mechanism to filter out spurious data. Experimental results are presented for both systems.

Methodology

The methodology followed to address early forest fire detection by vision-enabled WSNs comprises: i) the development of a reliable vision algorithm for smoke detection suitable for embedded systems, that is, featuring low computational load and undemanding memory requirements; ii) the recording of meaningful footage for algorithm parameter tuning and off-line tests; iii) the implementation of the algorithm on a commercial system for preliminary field tests; iv) the design and implementation of a vision-enabled WSN node based on a full-custom smart imager; v) field tests in real scenarios; and vi) exploration of a new low-cost platform aiming at increasing power efficiency while preserving system reliability and robustness against false alarms.

Vision algorithm for smoke detection

The general conditions in which the visual inspection of a vegetation area will take place for the targeted system must be specified before addressing the design of a vision algorithm for smoke detection. The requirements for camera systems surveying extensive areas from very tall towers – the most usual scenario for automatic detection of forest fires – are very different to those of vision-enabled nodes in a WSN. In our case, we are pursuing an arrangement of watching devices like the one depicted in Figure 1. This arrangement presents several advantages when compared to current automatic ground systems (Fernández-Berni *et al.* 2008). Basically, the objective is to exploit the low-cost and low-power features of the nodes in order to increase the surveillance grain, what in principle should lead to a faster, more reliable and more robust detection. We therefore devised a vision algorithm assuming that each vision sensor surveys a small vegetation area located around it within a limited range (typically 1km).

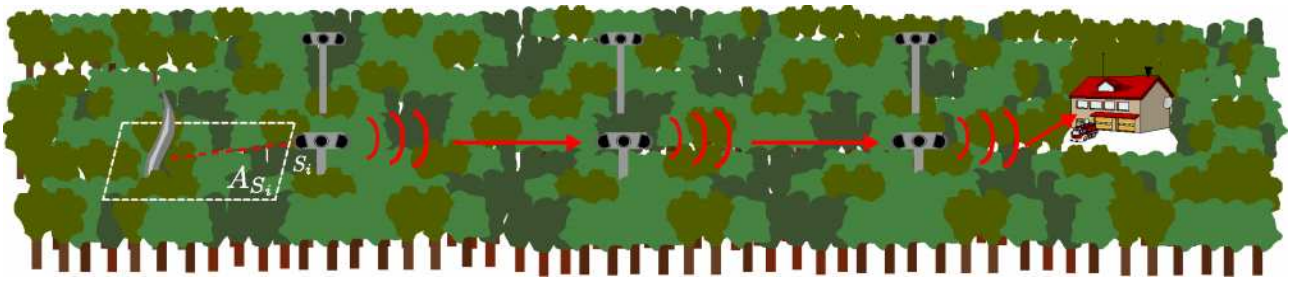

Figure 1. Proposed arrangement for visual detection of smoke.

Most of the details of the algorithm were described in (Fernández-Berni *et al.* 2012). However, we have introduced some minor modifications that were applied for the tests realized after that publication. They have resulted in higher robustness against false alarms. The modifications consisted in: i) setting a longer time interval for the maximum detection period and for the confirmation phase, now encoded by $T_{D_{MAX}} = 60\text{s}$ and $T_C = 12\text{s}$; ii) making the transition between the detection phase and the confirmation phase more flexible by not updating the background model as soon as the number of candidate bins goes below the corresponding threshold, as was the case for the previous version. The new flowchart of the algorithm is represented in Figure 2. These modifications are really interrelated since it is the larger values of $T_{D_{MAX}}$ and T_C what allows for accommodating a wider spectrum of smoke dynamics without triggering false alarms.

Parameter tuning and off-line tests

The discriminative power of the proposed algorithm is fundamentally supported by an adequate setting of the thresholds associated to its parameters. Such setting was performed by a thorough analysis of different sequences recorded in a natural environment, using commercial pyrotechnic material as smoke generator. We also recorded additional footage useful as a testbench and took a number of photographs in the variety of real scenarios we visited during all the field tests arranged the last few years. Most of this material is available for download at http://www.imse-cnm.csic.es/vmote (accessed 21 May 2014).

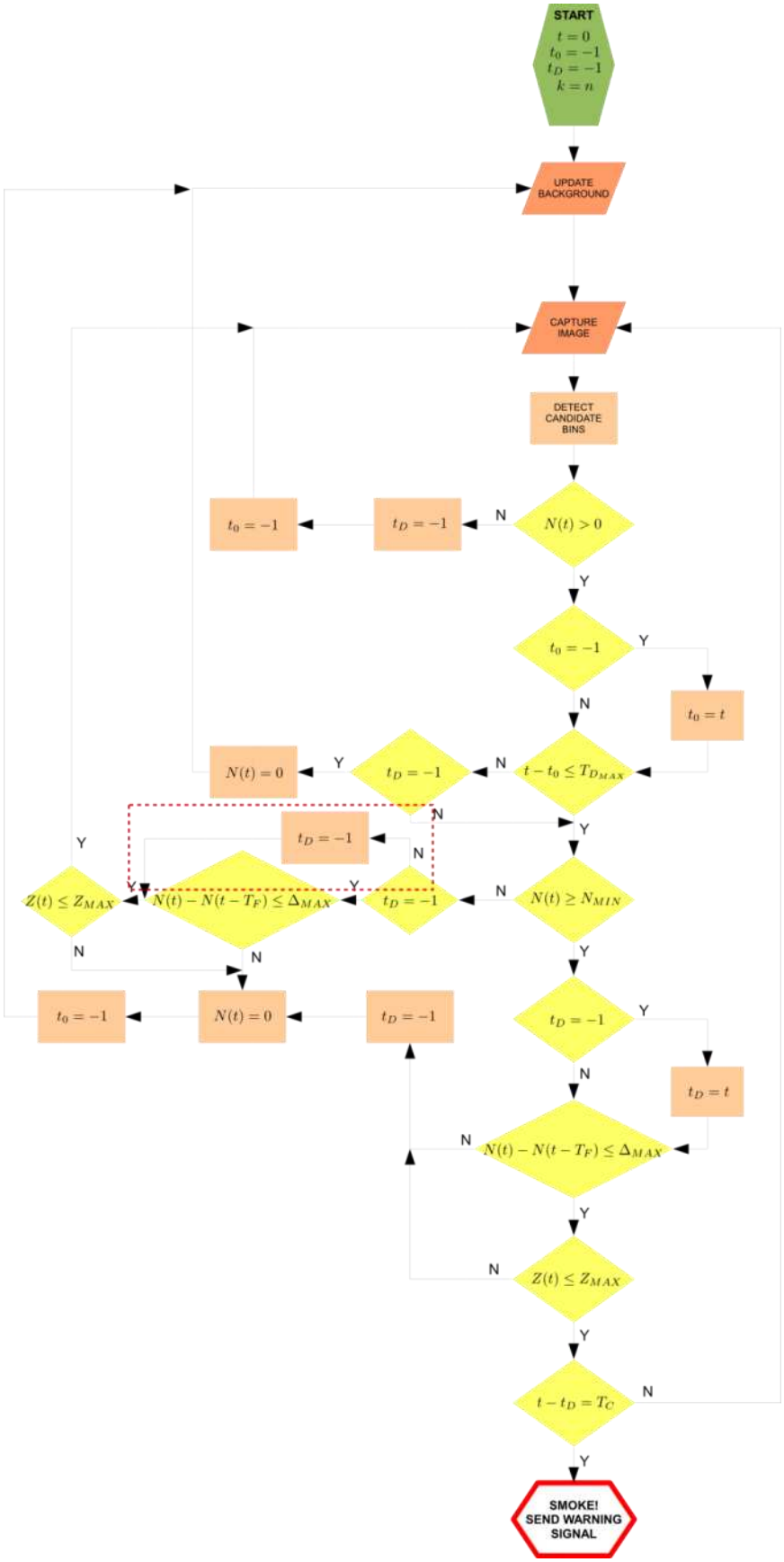

Figure 2. Flowchart of the algorithm. The modification related to the transition between the detection phase and the confirmation phase is highlighted by a red dashed rectangle.

2.3. Field tests with a commercial system

Once the algorithm was tuned for smoke detection, we programmed it into the *EyeRIS v1.2*, a commercial autonomous vision system built by AnaFocus Ltd (Seville, Spain, http://www.anafocus.com, accessed 22 May 2014). After a setup stage in the laboratory, two controlled burns of forest debris were surveyed by this system in order to test the algorithm in a real scenario. This test was also useful to learn and cope with typical operational problems of field experiments, permitting a better arrangement in following trials. All the details about these burns can be found in (Fernández-Berni *et al.* 2012). As a summary, smoke was detected without false alarms in both cases. In the first, the alarm was triggered at 2min 50s from ignition, whereas in the second, the alarm was delivered after 57 s. The most remarkable aspect about the results was the algorithm´s ability to filter motion other than smoke.

2.4. Design and implementation of a vision-enabled WSN node

The successful tests with the *EyeRIS* system demonstrated the viability of reliable forest fire smoke detection with low-power low-resolution autonomous vision systems in a scenario like that of Figure 1. But we wanted to go further concerning power efficiency and also to incorporate wireless communication to the sensor node. Based on our expertise on microelectronics, and specifically on vision sensor chips, we addressed the design and implementation of an ultra-low-power smart imager embedding different processing capabilities (Fernández-Berni *et al.* 2011-1). This chip met several academic purposes, one of which was to play a key role in the prototype vision-enabled WSN node we built, the so-called *Wi-FLIP* system (Fernández-Berni *et al.* 2011-2), shown in Figure 3. This system resulted from the integration of our smart imager and Imote2, a commercial WSN platform from MEMSIC Corporation (Andover, MA, www.memsic.com, accessed 22 May 2014). This platform is built around a microprocessor that can operate in a low-voltage low-frequency mode, hence allowing low-power operation. A ZigBee-compliant radio is also integrated into the Imote2 system.

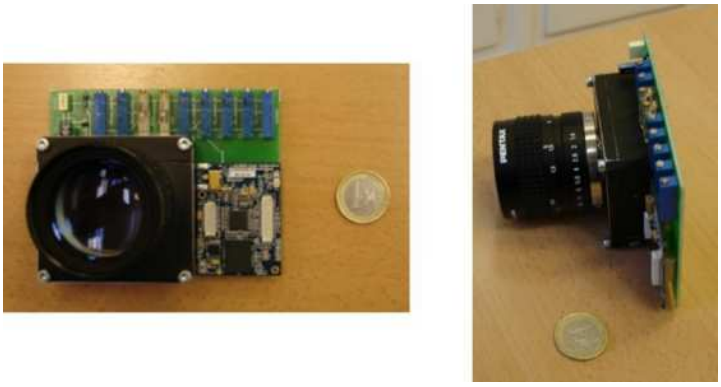

Figure 3. Wi-FLIP, a vision-enabled WSN node based on a focal-plane low-power image processor.

2.5. Field tests in real scenarios

As for the *EyeRIS* system, we also arranged for some preliminary tests with the *Wi-FLIP* system after the corresponding setup in the laboratory. Such tests took place in the same public park where we recorded the smoke sequences enabling the algorithm parameter setting. Once the whole system was tuned during these preliminary trials, additional tests involving controlled burns of vegetation areas were carried out in collaboration with the Andalusian Forest Fire Suppression and Prevention Service (INFOCA). These tests, whose results will be described in the next section, generated alarm signals as an outcome. The alarms were wirelessly sent to a base station located within a range of 30m. Also images were sparsely broadcast from *Wi-FLIP* since an alarm signal was triggered. This would permit

further visual checking from personnel supervising the network. Some of the scenarios where the field tests took place are depicted in Figure 4.

Figure 4. Some of the scenarios where our field tests took place.

2.6. Exploration of a new ultra-low-power low-cost vision platform

As stated in Section 1, node cost and battery life are currently hindering the commercial exploitation of vision-enabled WSNs for fine-grain detection of forest fires. The performance of the *Wi-FLIP* system has been remarkable as a first prototype, providing autonomous operation for ~10h powered by small commercial batteries. However, further steps must be given to reach much better performance figures at lower cost. In this context, we have had the possibility of running the algorithm on the images provided by the platform *Silicam IGO* (Silicam 2014). This is the first version of a commercial embedded vision system including, among other components, two grayscale 30×30-px image sensors and a radio module with 64 channels whose cost does not go beyond a few dollars. Indeed, the imagers are high-performance optical mouse sensors. A really competitive network node in economic terms can be built up from these extremely cheap modules. But the first step is to evaluate how the algorithm performs when being fed by so coarse images. This is what we have done during the realization of new field tests by making use of the *Silicam IGO* platform. A couple of snapshots of this system are shown in Figure 5.

Figure 5. Silicam IGO platform capturing images for on-site smoke detection.

Results

This section reports the experimental results achieved from both the *Wi-FLIP* and the *Silicam* systems. Concerning *Wi-FLIP*, some results were already described in (Fernández-Berni *et al.* 2012) but we are gathering here those results together with the new ones obtained after that publication. A complete perspective of the *Wi-FLIP* performance is thus provided.

Wi-FLIP

As mentioned in Section 2.5, the operation of *Wi-FLIP* was first tuned in the same public park where the video sequences for the algorithm settings were recorded. The setting up of these tests was complicated due to strong gusts of wind. Nevertheless, no false alarm was triggered during eight sequences of smoke generation and detection was successful in five of them. Smoke was not successfully detected in the others because, owing to the wind, the pyrotechnic material burnt out before it had entered the field of view of *Wi-FLIP* sufficiently to be registered.

The next test consisted in surveying the prescribed burning of a 95×20-m^2 area of vegetation in a public forest in collaboration with INFOCA. This area was mechanically divided into three zones of similar sizes according to the density of vegetation. *Wi-FLIP* was placed ~80m away and monitored all the activity occurring in it for over 2h. The first zone presented very sparse vegetation, generating very thin smoke that was not detected by *Wi-FLIP*. However, successful detection took place for the second and third zones. A first alarm was triggered 5min 28s after ignition for the second zone whereas it took 3min 29s to trigger an alarm for the third zone. No false positives were triggered either before or after the prescribed burn, despite the fact that many people and vehicles were moving around.

Finally, a new test similar to the just described was arranged in a different location of the same public forest. In this case, the operation conditions were harder. To start with, the wireless vision system was placed ~200m away from the prescribed burning. Fast cloud motion was constantly changing the illumination conditions. The motion of people and vehicles was even more intense than for the previous test. The surveillance period was ~2h. Two false alarms were triggered during this interval. The first one was caused by clouds that entered the field of view of *Wi-FLIP* rapidly. The second one was generated by a sudden change of illumination. Despite these false alarms, the algorithm was capable of filtering out most of the constant activity taking place in the scene other than smoke. Detection was successful for the three zones of the prescribed area progressively burnt. The detection time from ignition was always below 8min: 3min 40s for the first zone, 5min 4s for the second one and 7min 26s for the last zone. The background model just before starting to survey the third controlled burn along with the foreground segmentation of smoke at the detection instant and the first image sent via radio are depicted in Figure 6. It can be seen that some false candidate bins were segmented at the

detection instant. However, it did not prevent the fire from being detected. We have summarized the experimental results achieved with *Wi-FLIP* in Table I.

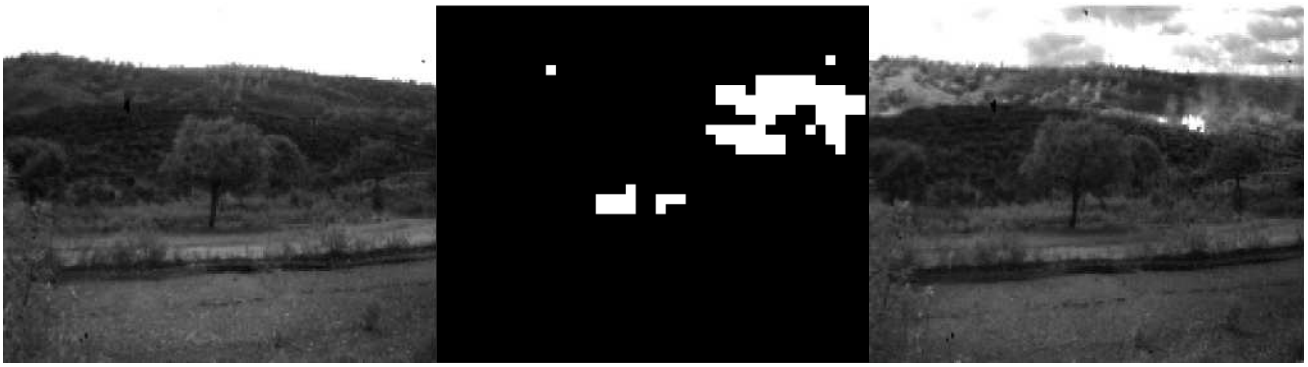

Figure 6. Initial background (left), foreground segmentation (center) and image sent via radio by Wi-FLIP (right) during one of the field tests carried out.

Table I – Summary of the experimental results achieved with Wi-FLIP.

Test#-Location	Smoke source	Surveillance period	True positives	False positives	False negatives	Detection time (distance)
#1-Public park	Pyrotechnic	~20m	5	0	3	43s max (~100m)
#2-Public forest	Controlled burns	~2h 30m	2	0	1	5m 28s max (~80m)
#3-Public forest	Controlled burns	~2h	3	2	0	7m 26s max (~200m)

3.2. Silicam

We also arranged for a first set of field trials with *Silicam* in a public park. Pyrotechnic material was again used as smoke source. It was burnt out within distances between ~50m and ~100m with respect to the vision system. Only one of the imagers of *Silicam* was used. No false alarm was triggered during the seven smoke sequences analysed at four different locations. There was only one false negative due to lack of contrast of the generated smoke against the background. Successful detection was achieved for the other six sequences. The background model at the detection instant along with the captured image and foreground segmentation at that same moment for one of these sequences are depicted in Figure 7.

A controlled burn in a public forest could be surveyed with *Silicam* too. However, the arrangements for this test were far from ideal. First of all, the vegetation to be burnt was sparse and relatively damp, generating thin smoke. The characteristics of the surroundings were not suitable either for adequate surveillance: tall trees prevent the thin smoke arising from the burn from being detected from higher locations. The trees also caused high illumination contrast in the visual scene, making the detection more challenging. We had to place *Silicam* very close to the ignition points, what at least permitted to confirm once again the robustness of the algorithm against false alarms: there was only one throughout the over 2h of visual inspection. Detection was successful in three of the sequences analysed. Concerning false negatives, we consider that the smoke was thick enough to have being detected in other three sequences. One of the successful detections is shown in Figure 8. A couple of photographs taken during the realization of this test are included in Figure 9. The results achieved with *Silicam* are summarized in Table II.

Figure 7. Background model (left), captured image (center) and foreground segmentation (right) just at the detection instant of smoke from pyrotechnic material with Silicam.

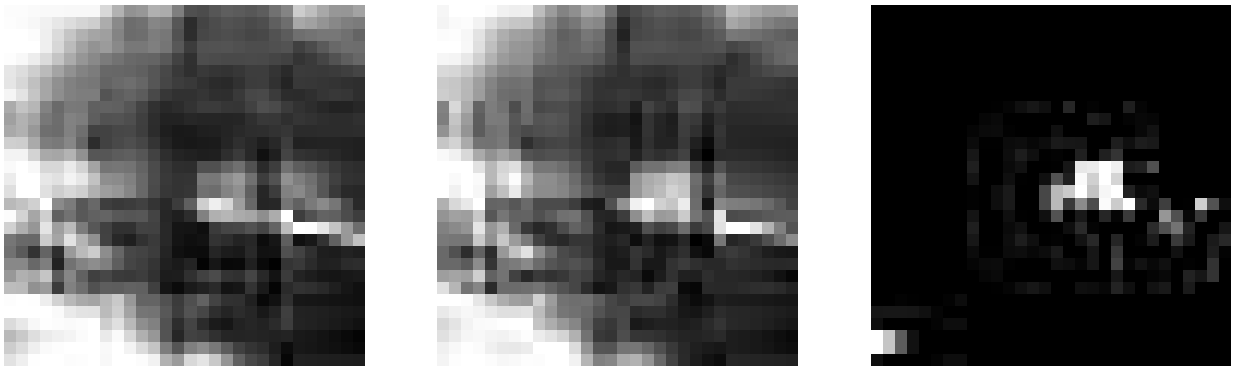

Figure 8. Background model (left), captured image (center) and foreground segmentation (right) just at the detection instant of smoke from controlled burn with Silicam.

Figure 9. Snapshots taken during the controlled burn surveyed by Silicam.

Table II – Summary of the experimental results achieved with Silicam.

Test#-Location	Smoke source	Surveillance period	True positives	False positives	False negatives	Detection time (distance)
#1-Public park	Pyrotechnic	~45m	6	0	1	51s max (~100m)
#2-Public forest	Controlled burns	~2h 15m	3	1	3	4m 7s max (~30m)

Conclusions

Fine-grain detection of forest fires is technologically possible nowadays. State-of-the-art vision-enabled WSN nodes can be deployed throughout a region of interest to locally survey small vegetation areas and wirelessly send alarm messages by multi-hopping. However, operational costs still seem to be very high for a dense deployment. Node cost and battery life demand new strategies that permit to reduce the former while increasing the latter. In this paper, we have described our contribution to achieve such objective. Tight integration of the different system components arises as a major requirement. Among these components, the vision algorithm for detection stands out as the primary demander of computational power and hence of power consumption. The algorithm proposed in this manuscript features low computational load and can also cope with very low resolution images. The results from the numerous field tests presented suggest pushing in this direction by further algorithm tuning. To this end, the feedback provided by real deployments in different locations and circumstances is mandatory, according to our experience. Ultra-low power consumption and miniaturization should ultimately lead to the seamless integration of vision within the catalogue of sensing capabilities available for WSNs.

Acknowledgments

The authors express their deep gratitude to Mr Salvador Benítez Moscoso, Mr Manuel Larios de la Carrera and Mr Francisco Senra Rivero of INFOCA for arranging the burns. This work has been funded by the Spanish Government through projects TEC2012-38921-C02 MINECO (European Region Development Fund, ERDF/FEDER), IPT-2011-1625-430000 MINECO and IPC-20111009 CDTI (ERDF/FEDER), by Junta de Andalucía through project TIC 2338-2013 CEICE, by the Office of Naval Research (USA) through grant N000141410355 and by Ghent University through its BOF program for visiting foreign researchers.

References

Akyildiz IF, Su W, Sankarasubramaniam Y, Cayirci E (2002) A survey on sensor networks. *IEEE Communications Magazine* **40**(8), 102–114.

Akyildiz IF, Melodia T, Chowdhury KR (2007) A survey on wireless multimedia sensor networks. *Computer Networks* **51**(4), 921–960.

Aslan YE, Korpeoglu I, Ulusoy O (2012) A framework for use of wireless sensor networks in forest fire detection and monitoring. *Computers, Environment and Urban Systems* **36**(6), 614-625.

Barrenetxea G, Ingelrest F, Schaefer G, Vetterli M (2008). The hitchhiker's guide to successful wireless sensor network deployments. In 'Proc. of 6th Int. Conf. on Embedded Network Sensor Systems (SenSys)', 43-56.

Fernández-Berni J, Carmona-Galán R, Carranza-González L, (2008) A vision-based monitoring system for very early automatic detection of forest fires. In 'Proc. of I Int. Conf. on Modelling, Monitoring and Management of Forest Fires', 161-170.

Fernández-Berni J, Carmona-Galán R, Carranza-González L, (2011-1) FLIP-Q: A QCIF resolution focal-plane array for low-power image processing. *IEEE Journal of Solid-State Circuits* **46**(3), 669-680.

Fernández-Berni J, Carmona-Galán R, Liñán-Cembrano G, Zarándy Á, Rodríguez-Vázquez Á, (2011-2) Wi-FLIP: A wireless smart camera based on a focal-plane low-power image processor. In 'Proc. of IEEE/ACM Int. Conf. on Distributed Smart Cameras (ICDSC)'.

Fernández-Berni J, Carmona-Galán R, Martínez-Carmona JF, Rodríguez-Vázquez A, (2012) Early forest fire detection by vision-enabled wireless sensor networks. *International Journal of Wildland Fire* **21**, 938–949.

Hefeeda M, (2007). Forest fire modeling and early detection using wireless sensor networks. Tech. rept. School of Computing Science, Simon Fraser University.

Jakovcevic T, Stipanicev D, Krstinic D, (2013) Visual spatial-context based wildfire smoke sensor. *Machine Vision and Applications* **24**(4), 707-719.

McCulloch J, McCarthy P, Guru SM, Peng W, Hugo D, Terhorst A, (2008) Wireless sensor network deployment for water use efficiency in irrigation. In 'Proc. of Workshop on Real-World Wireless Sensor Networks (REALWSN)', 46-50.

Silicam (2014). http://silicam.org/welcome/ [Online; accessed 04-May-2014].

Tolle G, Polastre J, Szewczyk R, Culler D, Turner N, Tu K, Burgess S, Dawson T, Buonadonna P, Gay D, Hong W, (2005). A macroscope in the redwoods. In 'Proc. of 3rd Int. Conf. on Embedded Networked Sensor Systems (SenSys)', 51-63.

Weiser M, (1991) The Computer for the 21th Century. *Scientific American* **265**(3), 94-104.

Werner-Allen G, Lorincz K, Ruiz M, Marcillo O, Johnson J, Lees J, Welsh M (2006). Deploying a wireless sensor network on an active volcano. *IEEE Internet Computing* **10**(2), 18-25.

Tropical forest degradation in the Brazilian Amazon – relation to fire and land-use change

Ana Cano-Crespo[a,b], Paulo J. C. Oliveira[a], Manoel Cardoso[c], Kirsten Thonicke[a]

[a]*Potsdam Institute for Climate Impact Research (PIK). Telegraphenberg A62, 14473 Potsdam, Germany. a.cano@pik-potsdam.de*
[b]*Geography Department, Humboldt University of Berlin. Alfred-Rühl-Haus, Rudower Chaussee 16, 12489 Berlin (Adlershof), Germany.*
[c]*Instituto Nacional de Pesquisas Espaciais, Centro de Ciência do Sistema Terrestre (INPE/CCST), 12630-000 Cachoeira Paulista, São Paulo, Brazil.*

Abstract
While deforestation represents an obvious ecosystem change, forest degradation is often more difficult to discern or quantify, but it impacts a number of ecosystem functions which are vital for biodiversity and climate feedbacks. In the Brazilian Amazon, land-use changes increase fire occurrence, especially in fragmented forests close to managed land. We used remote sensing imagery to estimate the extent and impact of forest fires in degraded tropical rain-forest in the Brazilian Legal Amazon between 2007 and 2010 and examined land-use establishing in degraded areas. The trends in degraded area vs. burned area were different. Even though degradation increased one year after a high fire year, there was no spatial overlap, which points to other causes for degradation. Up to 11% of the degraded area was burned in the same year, playing escaping fires from managed and deforested lands a significant role in degradation by fire. Eighty-four percent of 2007s degraded area remained forest one year later, whereas the rest was identified as deforestation, secondary vegetation or pasture. Three years after degradation, 80% remained forest, the proportion of deforested area decreased and areas in regeneration after being deforested increased. Monitoring of forest degradation across tropical forests is critical for developing land management policies and for carbon stocks/emissions estimation.

Keywords*: forest degradation, logging, forest fires, land-use, Brazilian Amazon.*

Introduction

In Brazilian Amazonia, the extent of canopy and subcanopy disturbance has been underestimated and often exceeds the total area deforested (Peres *et al.*, 2006; Souza Jr. *et al.*, 2013). Deforestation in the region is superimposed upon synergistic processes of anthropogenic forest degradation (events when, unlike in deforestation processes, the forest canopy cover is only partially or temporarily removed), which implies the reduction in the overall capacity of a forest to supply goods and services (Simula, 2009). Several aspects of the forest may be affected by degradation including productive capacity, protective capacity, biodiversity and health and carbon storage (Parrotta *et al.*, 2012). The proximate drivers of forest degradation include unsustainable and illegal logging, human-induced fires, over-harvest of fuelwood and non-timber forest products, overgrazing and poor management of shifting cultivation (Chazdon, 2008; Kissinger *et al.*, 2012). In addition to these adverse impacts of land-use change and human-induced forest degradation, climate change poses an increasing threat to tropical forest ecosystems increasing the frequency of severe droughts (Malhi, 2012).
In the Brazilian Amazon humans have substantially altered forest fire regimes and fires have increased in extent and frequency as a result of forest fragmentation, the expansion of managed lands and logging (Asner *et al.*, 2005; Morton *et al.*, 2008; Armenteras *et al.*, 2012), thus contributing to forest degradation and reducing forest resilience (Barlow and Peres, 2008; Nepstad *et al.*, 2008). Moreover, forest fire can increase susceptibility to further burning in a positive feedback by killing trees, opening the canopy and

increasing solar penetration to the forest floor (Cochrane and Laurance, 2008; Alencar *et al.*, 2011). Anthropogenic forest disturbance from fires produces long lasting changes in forest structure and biomass but the changes are sometimes hard to detect in satellite imagery and are quickly obscured by the regenerating forest canopy (Matricardi *et al.*, 2010), which makes it difficult to properly assess forest degradation by fire.

In 2007, at its 13th Conference of the Parties, the UN Framework Convention on Climate Change recognized forest degradation as an important contributor to global carbon emissions by incorporating it into the Reducing Emissions from Deforestation and Forest Degradation (REDD+) mechanism (UNFCCC, 2008). According to van der Werf *et al.* (2010), the global sum of deforestation, degradation, and peat fire emissions accounted for about a quarter of total carbon emissions. Another study by Asner *et al.* (2005) estimated that emissions caused only by selective logging were equivalent to between 60 and 123% of previously reported deforestation emissions in five states of the Brazilian Amazon, which accounted for 90% of all deforestation in the region, while Pearson *et al.* (2014) found that Brazil's emissions from logging were small and equivalent to 10% of those from deforestation. Nevertheless, the release of carbon by degradation still remains largely overlooked, and limited information is available to achieve a full carbon accounting for REDD+ (Morton *et al.*, 2011a). The scientific, conservation, and climate policy importance attracted previous studies to analyse forest degradation processes in the Brazilian Amazon through field research (Xaud *et al.*, 2013; Berenguer *et al.*, 2014) and remote sensing observations (Matricardi *et al.*, 2010; Souza Jr. *et al.*, 2013). Further progress, however, is yet to be made in quantifying the extent and intensity of less-visible forms of nonstructural habitat disturbance underneath the forest canopy. In this line, our study pursues the quantification of the degraded area affected by fires in the Brazilian Amazon and also their temporal changes using 30x30 m land-cover information (INPE and EMBRAPA, 2013). Specifically, we answer three main questions. 1) What is the relation between forest degradation and fire? 2) To what extent do fires escaping from managed land contribute to forest degradation? 3) What are the temporal dynamics of degraded areas and their conversion to other land-use types?

Methods

Study area

The Brazilian Amazon contains about 3.2 million square kilometers of the Amazon forest (INPE and EMBRAPA, 2013) and stores the majority of the 126 Pg of carbon reported for the entire Amazonia (Malhi *et al.*, 2006). About 80% of the forest remains intact (FAO-ITTO, 2011), although substantial areas have been deforested (INPE, 2013a), selectively logged (Asner *et al.*, 2005; Matricardi *et al.*, 2010) or affected by fires in recent decades (Morton, 2013; Xaud *et al.*, 2013). As a consequence of that rapid land-cover change, the forest has been fragmented by logging gaps and mosaics of cattle ranching and agricultural settlements, mainly along the arc of deforestation in southern and eastern Brazilian Amazon (Houghton *et al.*, 1991; Lambin *et al.*, 2003; Lepers *et al.*, 2005). In this paper we use the Brazilian Legal Amazon definition, the largest Brazilian socio-geographic division (Figure 1), which, in 2010, was covered by primary or secondary forest (76%), savanna-type vegetation (18%), concentrated mainly in the southeast, and 6% was detected as cleared areas (Figure 1a).

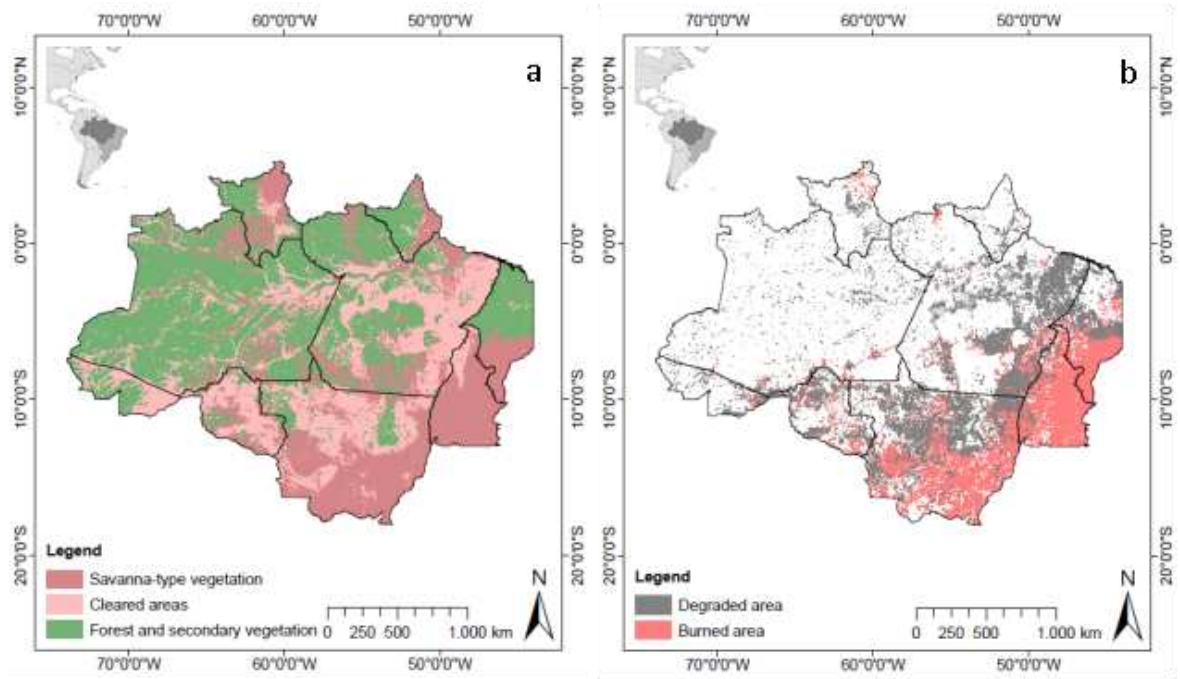

Figure 1. a) Map showing the extension and land-cover of the Brazilian Legal Amazon according to TerraClass 2010. Savanna-type vegetation includes cerrado, campinas and campinaranas. Cleared areas includes agricultural fields, pasture lands and deforested areas. b) Map of degraded and burned area detected from 2007 to 2010.

Datasets

We used degradation maps provided by the DEGRAD project (http://www.obt.inpe.br/degrad/dados/) which monitors the degradation of the Brazilian Amazon forest caused by wood extraction or by recurrent fires (INPE, 2013b). Forest areas likely to become deforested where the canopy has not been totally removed are considered by DEGRAD as degraded areas. It is based on the Landsat Thematic Mapper and CBERS satellites to detect clearings of at least 6.25 ha size annually from 2007 to 2010 at 60 m spatial resolution.

Annual deforestation maps for the same period were obtained from the PRODES project which has been monitoring Brazilian Amazon deforestation since 1988 (INPE, 2013a, http://www.dpi.inpe.br/prodesdigital/prodes.php). PRODES combines satellite data from the Thematic Mapper (LANDSAT), DMC (Disaster Monitoring Constellation) and CCD (CBERS) sensors, and their successors for recent years, and detects clearings of at least 6.25 ha where deforestation by clear cutting has occurred at 60 m spatial resolution and one map each year.

The Moderate Resolution Imaging Spectroradiometer (MODIS) on board the polar orbiting Terra and Aqua satellites maps fire affected areas since 2000 (Roy *et al*., 2008). We used the re-projected monthly Geotiff version of MODIS collection 5 Burned Area Product (MCD45, National Aeronautics and Space Administration, University of Maryland FTP server: ftp://ba1.geog.umd.edu) from 2007 to 2010 (500-m resolution, windows 5 and 6).

Land-cover maps of the Legal Amazon were produced by the TerraClass project (http://www.inpe.br/cra/projetos_pesquisas/terraclass2008.php) showing a very detailed land-use classification in 15 categories at 30-m resolution with data generated from the interpretation of images Landsat/TM5 for the years 2008 and 2010 (Almeida *et al*., 2009; INPE and EMBRAPA, 2013).

2.3. Data analysis

We worked with the geographical information system (GIS) package ArcGIS 10.1 (Esri) to conduct all digital spatial and temporal analysis. While TerraClass and DEGRAD files were provided in Esri

shapefile format, burned area files needed a preliminary transformation into polygon shapefiles. Burned and degraded area maps were overlaid for computing the temporal and spatial relation between them for each year of the study period (2007-2010), after aggregating degradation data to 500 m to fit its resolution to the fire data. The same overlay operation was applied to the degraded area layers and land-use maps (in 2008 and 2010) to track their evolution over time. Potential escaping fires from pasture fields, agricultural lands and deforested areas into the forest contributing to degradation were evaluated by creating buffer zones of different size (from 0.5 to 3 km, every 0.5 km) around the burned areas occurring in managed lands to examine the proportion of forest patches that were burned, and therefore classified as degraded areas (hereafter referred to as fire-related degraded area) within each buffer. The coordinate system of the files was converted to the geographic South American Datum 1969, when working with Amazonia, or to the state corresponding projected coordinate system according to the Universal Transverse Mercator scheme. This way a proper fit between the different information layers was achieved and accurate area calculations of the polygons were performed.

3. Results

In the period from 2007 to 2010, 395549 km² of burned area were detected in the Brazilian Legal Amazonia (8% of the territory) and 64308 km² of forest were registered as degraded (2% of the forested area within the study region in 2010). Both variables showed an uneven spatial distribution. Burned area was concentrated in southern Mato Grosso, Tocantins and southern Maranhão, which corresponds to the extension of the savannah-type vegetation, while degraded area was mainly located along the arc of deforestation (Rondônia, northern Mato Grosso, eastern Pará and northern Maranhão) (Figure 1b). The highest amount of burned area was found in 2010 (177615 km²), while the maximum amount of degraded area was detected in 2008 (27478 km²) (Figure 2a) with all nine states in the region presenting the same trend (Figure 2b). Most burned area was observed in the state of Mato Grosso contributing 44% of the total, followed by Tocantins (30%), Maranhão (13%) and Pará (12%). The states contributing the greatest amounts of degradation were Mato Grosso (51%), Pará (27%) and Maranhão (14%) (Figure 2b). In 2007 and 2010, the two high fire years of the period, 11% of the degraded area was detected as burned in the same year, while figures were lower than 1% in 2008 and 2009 (Figure 3a).

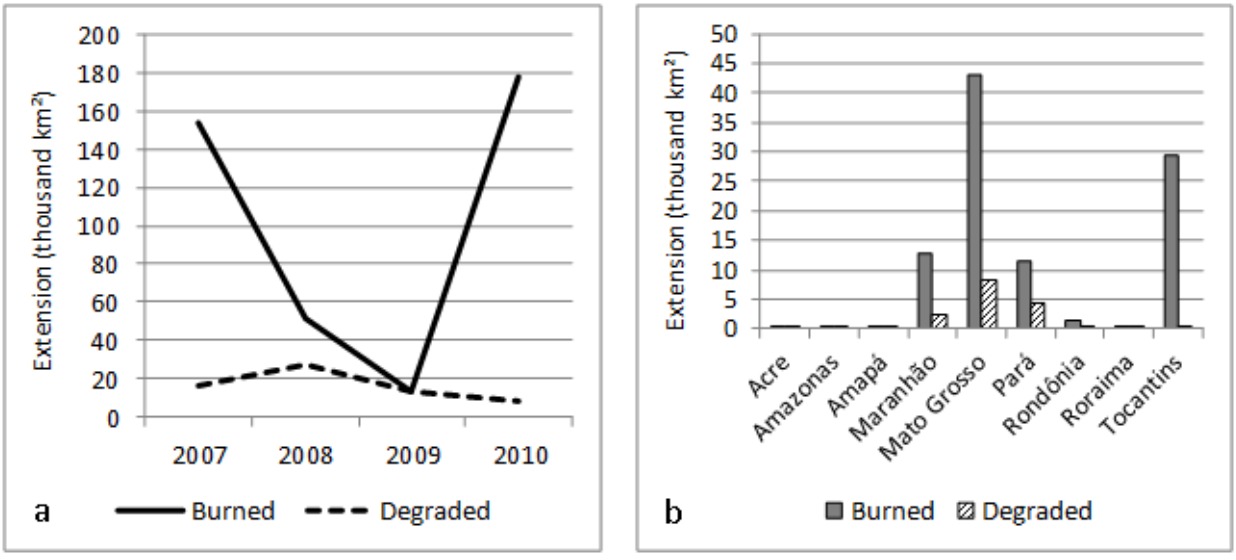

Figure 2. a) Annual burned (solid line) and degraded (dashed line) area for2007-2010 in the Brazilian Legal Amazon (in thousand km²). b) Amount of burned and degraded area in the different states (in thousand km², averaged over the period 2007-2010).

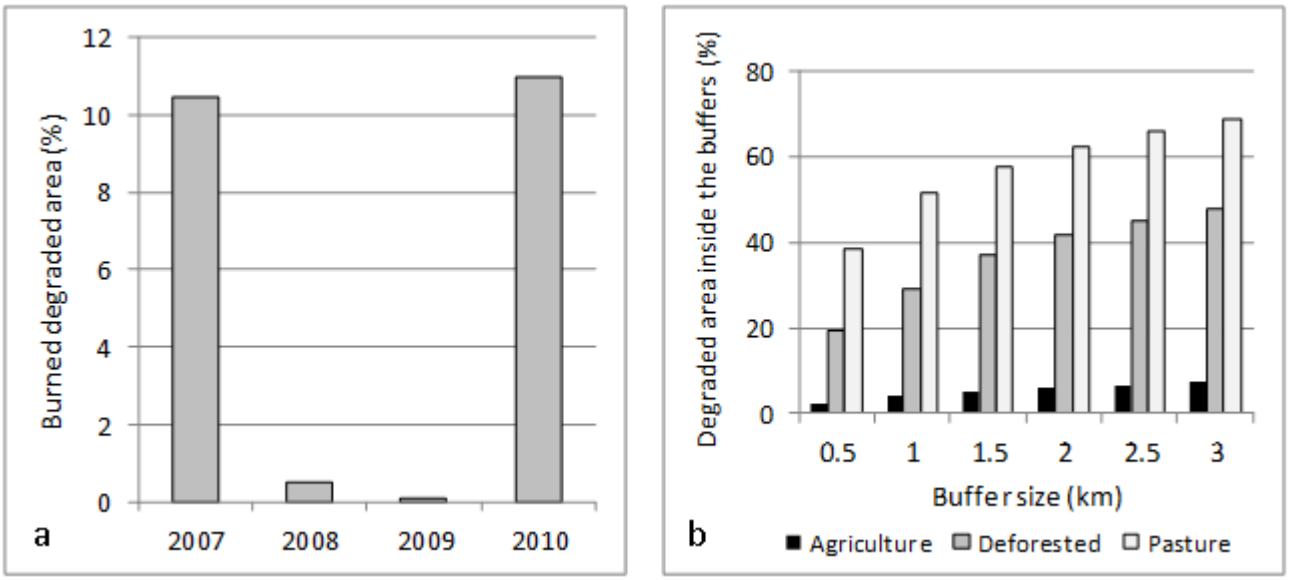

Figure 3. a) Percentage of degraded area that was also detected as burned area by MODIS in the same year. b) Percentage of fire-related degraded area that was connected to burnings in managed lands and deforested areas averaged over 2008 and 2010 in the Brazilian Legal Amazonia.

Fires escaping from agricultural fields in the vicinity of forest may cause between 2 (0.5-km buffer) and 7% (3-km buffer) of forest degradation, which means that between 6 and 31 km² of the fire-related degraded area were within the 0.5-km buffer and 3-km buffer zone, respectively, established around the burned area polygons in agricultural lands, averaged over 2008 and 2010 (Figure 3b). The proportion of the fire-related degraded area that overlapped the buffers delimited around pasture burned area polygons was higher for all the buffer sizes compared to agricultural buffers, between 39 and 69% of the fire-related degraded area (between 107 and 300 km²), averaged over 2008 and 2010 (Figure 3b). Fires occurring in deforested areas may be responsible for 19 to 48% of the forest degradation caused by fire (between 73 and 191 km²), averaged over 2008 and 2010 (Figure 3b). Concurrent with the greatest annual burned area figures in the period, the year 2010 presented higher overlap values between the buffers and the fire-related degraded area than 2008 for all the three land-uses: agricultural, pasture and deforested lands.

Of the degraded area detected in 2007, 23% was still considered as such one year later, 7% two years later and 3% three years later (data not shown). According to Terraclass, 84% of the forest classified as degraded in 2007 remained forest one year later. The remaining degraded area was registered in 2008 as deforestation (11%), secondary vegetation (2%), pasture (1%) and degraded pasture (1%) (Figure 4a). Three years after degradation, 80% of 2007's degraded area was detected as forest, the proportion of deforested area decreased (3%) while the area covered by areas in regeneration after being deforested and used for agriculture or pasture (7%), pasture (4%) and degraded pasture (3%) increased, and a similar extension of secondary vegetation was found (2%), compared to the figures observed in 2008 (Figure 4b).

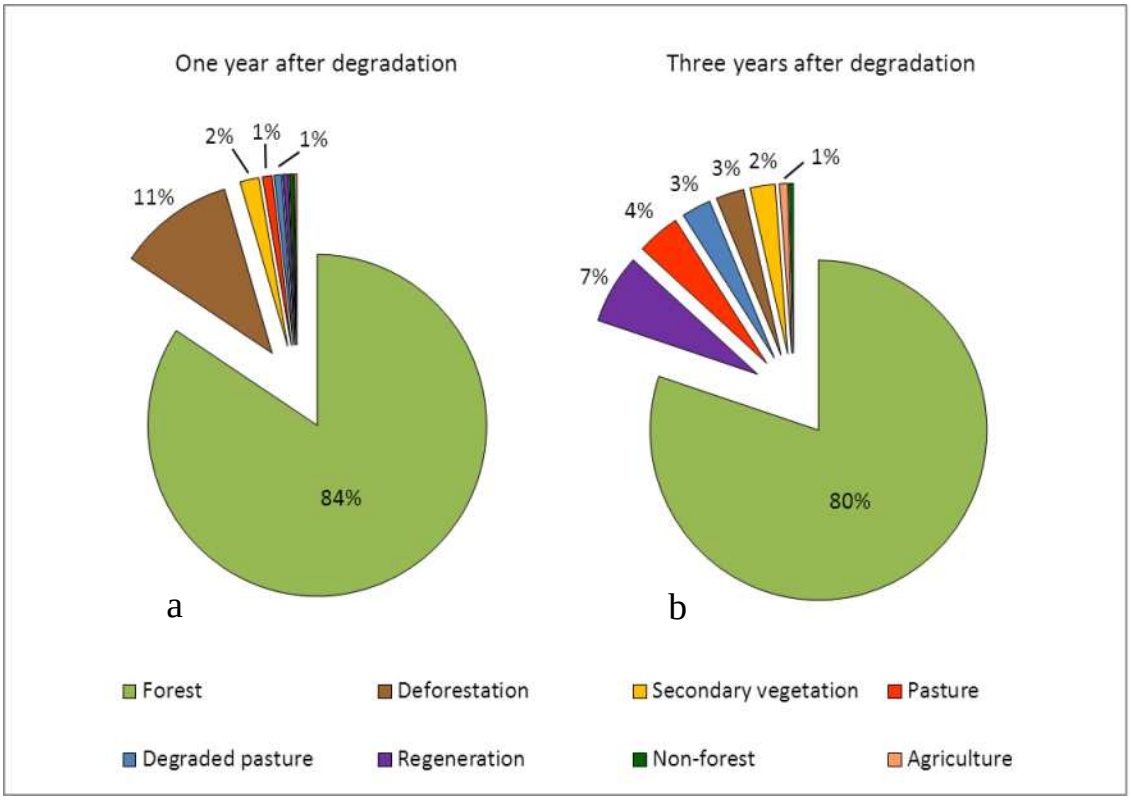

Figure 4. a) Land-use of the degraded area assigned by TerraClass one year after degradation, in 2008, and b) three years after degradation, in 2010 (averaged over the Brazilian Legal Amazonia).

Discussion

The above results underscore the relatively low proportion of degraded area solely related to forest fires, being 11% the maximum percentage of annual degraded area that was connected to burning events in the detection year (Figure 3a). However, it is important to consider the difficulty in obtaining accurate burned area mapping within tropical closed-canopy forest by MODIS (Giglio *et al.*, 2006), which can lead to underestimation of burning occurrence in the forest, e.g., small surface fires can be overlooked (Morton *et al.*, 2013). The analysis detected evidence of the link between degradation fires and land-use change processes. Even when considering the conservative 0.5-km buffer, 2, 19 and 39% of the fire-related degraded area may be the result of escaping fires from the adjacent agricultural lands, deforested areas and pasture fields, respectively, and the figures increase as the buffer size grows (Figure 3b). These findings support the idea of burning events becoming much more frequent and widespread across the Amazon forests as a consequence of deliberate fire use for land clearing and field maintenance (Cochrane, 2003; Cardoso *et al.*, 2009; Davidson *et al.*, 2012).

Since the forest degradation drivers contemplated by the DEGRAD system are selective logging and fire (INPE, 2008), the results of the fire vs. degraded area analysis indicated a stronger influence of selective logging in degradation. Unfortunately, we do not have logging data for the study period to confirm this premise, but different studies have identified logging as the process responsible for the largest proportion of forest degradation (Matricardi *et al.*, 2010). Kissinger *et al.*, (2012) in their report for REDD+ policymakers stated that unsustainable logging accounted for more than 70% of forest degradation in Latin America. Moreover, once disturbed by selective logging activities, the amount of dead slash or dried biomass increases and forest becomes more susceptible to fire (Uhl and Kauffman, 1990; Holdsworth and Uhl, 1997).

Around 80% of the degraded forest was still classified as forest one and three years later (Figure 4). After 12 years, Matricardi *et al.* (2010) found that 70% of the total forest area disturbed in their study area in the state of Mato Grosso had sufficiently recovered to become undetectable using satellite data. Degraded forests can often remain in a degraded state for long periods of time if degradation drivers remain, or if ecological thresholds have been passed, and yet remain officially defined as forests for classification purposes (Murdiyarso *et al.*, 2008; Sasaki and Putz, 2009), thus, regrowing vegetation can lead to misclassification in the absence of accompanying field data. The climax of forest regeneration seems to be 3 to 5 years following logging activities and 3 to 10 years after a forest fire event (Matricardi *et al.*, 2010), which explains why Stone and Lefevre (1998) observed in their study in the state of Pará that within 3 to 5 years degradation signal by selective logging was obscured by the regenerating forest canopy. Even though most of the degraded forest regenerated, 11% was deforested one year later, which is comparable with previous estimates of 16% due to logging alone by Asner *et al.* (2006) for the early 2000s, when deforestation rates were higher.

Recent research has contributed to substantial improvements in remote sensing based techniques to evaluate extent and impacts caused by selective logging and forest fires (Matricardi *et al.*, 2010; Morton *et al.*, 2011b; Andersen *et al.*, 2013). However, a large-scale and long-term evaluation of processes causing forest degradation is still lacking, but is required to understand ecological and climate-related consequences of tropical forest impoverishment through logging and fire.

Conclusions

Based on these research results we can conclude that forest degradation is not mainly controlled by fire, which suggests that the major driver in the Brazilian Amazonia is selective logging. The occurrence of fire in the forest, in most of the cases, is the result of land-use change processes, and escaping fires from pasture management play a crucial role. Only a small percentage of degraded forest becomes deforested or develops to other land-uses one and three years after degradation, while the majority of it recovers and is still detected as forest. Continuous monitoring of forest degradation across tropical forests is critical for developing land management policies, as well as for an accurate estimation of carbon stocks/emissions. At the same time, global Earth system models must incorporate dynamic models of land-use change driving deforestation, forest degradation and vegetation fires for a better carbon balance simulation.

Acknowledgements

This paper was developed within the scope of the IRTG 1740/TRP 2011/50151-0, funded by the DFG/FAPESP. ArcGIS software license was provided by the German Research Centre for Geosciences (GFZ, Potsdam).

References

Alencar, A., Asner, G. P., Knapp, D. and Zarin, D. (2011). Temporal variability of forest fires in eastern Amazonia. *Ecological Applications 21*, 2397-2412.

Almeida, C., Pinheiro, T., Barbosa, A., Abreu, M., Lobo, F., Silva, M., Gomes, A., Sadeck, L., Medeiros, L., Neves, M., Silva, L. and Tamasauskas, P. (2009). *Metodologia para mapeamento de vegetação secundária na Amazônia Legal.* Technical Report. Brazil's National Institute for Space Research, São José dos Campos, Brazil.

Andersen, H. E., Reutebuch, S. E., McGaughey, R. J., d'Oliveira, M. V. N. and Keller, M. (2013). Monitoring selective logging in western Amazonia with repeat lidar flights. *Remote Sensing of Environment*, doi:10.1016/j.rse.2013.08.049.

Armenteras, D., González, T. M. and Retana, J. (2012). Forest fragmentation and edge influence on fire occurrence and intensity under different management types in Amazon forests. *Biological Conservation 159,* 73-79.

Asner, G. P., Knapp, D. E., Broadbent, E. N., Oliveira, P. J. C., Keller, M. and Silva, J. N. (2005). Selective logging in the Brazilian Amazon. *Science 310,* 480-482.

Asner, G. P., Broadbent, E. N., Oliveira, P. J. C., Keller, M., Knapp, D. E. and Silva, J. N. (2006). Condition and fate of logged forests in the Brazilian Amazon. *Proceedings of the National Academy of Sciences 103,* 12947-12950.

Barlow, J. and Peres, C. A. (2008). Fire-mediated dieback and compositional cascade in an Amazonian forest. *Philosophical Transactions of the Royal Society B-Biological Sciences 363,* 1787-1794.

Berenguer, E., Ferreira, J., Gardner, T. A., Aragão, L. E. O. C., de Camargo, P. B., Cerri, C. E., Durigan, M., de Oliveira, R. C., Vieira, I. C. G. and Barlow, J. (2014). A large-scale field assessment of carbon stocks in human-modified tropical forests. *Global Change Biology*, doi: 10.1111/gcb.12627.

Cardoso, M., Nobre, C., Sampaio, G., Hirota, M., Valeriano, D. and Camara, G. (2009). Long term potential for tropical-forest degradation due to deforestation and fires in the Brazilian Amazon. *Biologia 64,* 433-437.

Chazdon, R. L. (2008). Beyond deforestation: restoring forests and ecosystem services on degraded lands. *Science 320,* 1458-1460.

Cochrane, M. A. (2003). Fire science for rainforests. *Nature 421,* 913-919.

Cochrane, M. A. and Laurance, W. F. (2008). Synergisms among fire, land use, and climate change in the Amazon. *Ambio* 37, 522-527.

Davidson, E. A., de Araújo, A. C., Artaxo, P., Balch, J. K., Brown, I. F., Bustamante, M. M. C., Coe, M. T., DeFries, R. S., Keller, M., Longo, M., Munger, J. W., Schroeder, W., Soares-Filho, B. S., Souza Jr., C. M. and Wofsy, S. C. (2012). The Amazon basin in transition. *Nature 481,* 321-328.

FAO-ITTO (2011). *The State of Forests in the Amazon Basin, Congo Basin and Southeast Asia*. Food and Agriculture Organization, Rome. **http://www.fao.org/docrep/014/i2247e/** i2247e00.pdf

Giglio, L., van der Werf, G. R., Randerson, J. T., Collatz, G. J. and Kasibhatla, P. (2006). Global estimation of burned area using MODIS active fire observations. *Atmospheric Chemistry and Physics 6,* 957-974.

Holdsworth, A. R. and Uhl, C. (1997). Fire in Amazonian selectively logged rainforest and the potential for fire reduction. *Ecological Applications 7,* 713-725.

Houghton, R. A., Lefkowitz, D. S. and Skole, D. L. (1991). Changes in the landscape of Latin America between 1850 and 1985. I. Progressive loss of forests. *Forest Ecology and Management 38,* 143-172.

INPE (2008). *Monitoramento da cobertura florestal da Amazônia por satellite: sistemas PRODES, DETER, DEGRAD e queimadas.* Brazilian Institute for Space Research, São José dos Campos, Brazil.

INPE (2013a). *Projeto PRODES. Monitoramento da floresta Amazônica brasileira por satélite.* Brazilian Institute for Space Research, São José dos Campos, Brazil. http://www.obt.INPE.br/prodes/

INPE (2013b). *Projeto DEGRAD. Mapeamento da degradação florestal na Amazônia Brasileira.* Brazilian Institute for Space Research, São José dos Campos, Brazil. http://www.obt.inpe.br/degrad/

INPE and EMBRAPA (2013). *Projeto TerraClass*. Brazilian Institute for Space Research-Amazon Regional Center, Belém, and the Brazilian Enterprise for Agricultural Research, Brasília, Brazil. http://www.inpe.br/cra/projetos_pesquisas/ terraclass2008.php

Kissinger, G., Herold, M. and De Sy, V. (2012). *Drivers of Deforestation and Forest Degradation: A Synthesis Report for REDD+ Policymakers*. Lexeme Consulting, Vancouver.

Lambin, E. F., Geist, H. J. and Lepers, E. (2003). Dynamics of land-use and land-cover change in tropical regions. *Annual Review of Environment and Resources 28*, 205-241.

Lepers, E., Lambin, E. F., Janetos, A. C., DeFries, R., Achard, F., Ramankutty, N. and Scholes, R. J. (2005). A synthesis of information on rapid land-cover change for the period 1981-2000. *BioScience 55*, 115-124.

Malhi, Y., Wood, D., Baker, T. R., Wright, J., Phillips, O. L., Cochrane, T., Meir, P., Chave, J., Almeida, S., Arroyo, L., Higuchi, N., Killeen, T. J., Laurance, S. G., Laurance, W. F., Lewis, S. L., Monteagudo, A., Neill, D. A., Núñez Vargas, P., Pitman, N. C. A., Quesada, C. A., Salomão, R., Silva, J. N. M., Torres Lezama, A., Terborgh, J., Vásquez Martínez, R. and Vinceti, B. (2006). The regional variation of aboveground live biomass in old-growth Amazonian forests. *Global Change Biology 12*, 1107-1138.

Malhi, Y. (2012). The productivity, metabolism and carbon cycle of tropical forest vegetation. *Journal of Ecology 100*, 65-75.

Matricardi, E. A. T., Skole, D. L., Pedlowski, M. A., Chomentowski, W. and Fernandes, L. C. (2010). Assessment of tropical forest degradation by selective logging and fire using Landsat imagery. *Remote Sensing of Environment 114*, 1117-1129.

Morton, D. C., Defries, R. S., Randerson, J. T., Giglio, L., Schroeder, W. and van der Werf, G. R. (2008). Agricultural intensification increases deforestation fire activity in Amazonia. *Global Change Biology 14*, 2262-2275.

Morton, D. C., Sales, M. H., Souza Jr., C. M. and Griscom, B. (2011a). Historic emissions from deforestation and forest degradation in Mato Grosso, Brazil: 1) source data uncertainties. *Carbon Balance and Management 6*, doi:10.1186/1750-0680-6-18.

Morton, D. C., DeFries, R. S., Nagol, J., Souza Jr., C. M., Kasischke, E. S., Hurtt, G. C. and Dubayah, R. (2011b). Mapping canopy damage from understory fires in Amazon forests using annual time series of Landsat and MODIS data. *Remote Sensing of Environment 115*, 1706-1720.

Morton, D. C., Le Page, Y., DeFries, R., Collatz, G. J. and Hurtt, G. C. (2013). Understorey fire frequency and the fate of burned forests in southern Amazonia. *Philosophical Transactions of the Royal Society B-Biological Sciences 368*, http://dx.doi.org/10.1098/rstb.2012.0163.

Murdiyarso, D., Skutsch, M., Guariguata, M., Kanninen, M., Luttrell, C., Verweij, P. and Stella, O. (2008). *Measuring and monitoring forest degradation for REDD: Implications of country circumstances*. Center for International Forestry Research (CIFOR) info briefs 16.

Nepstad, D. C., Stickler, C. M., Soares-Filho, B. and Merry, F. (2008). Interactions among Amazon land use, forests and climate: prospects for a near-term forest tipping point. *Philosophical Transactions of the Royal Society B-Biological Sciences 363*, 1737-1746.

Parrotta, J. A., Wildburger, C. and Mansourian, S. (Eds.). (2012). *Understanding relationships between biodiversity, carbon, forests and people: The key to achieving REDD+ objectives*. IUFRO World Series Vol. 31.

Pearson, T. R. H., Brown, S. and Casarim, F. M. (2014). Carbon emissions from tropical forest degradation caused by logging. *Environmental Research Letters 9*, doi:10.1088/1748-9326/9/3/034017.

Peres, C. A., Barlow, J. and Laurance, W. F. (2006). Detecting anthropogenic disturbance in tropical forests. *Trends in Ecology & Evolution 21*, 227-229.

Roy, D. P, Boschetti, L., Justice, C. O. and Ju, J. (2008). The collection 5 MODIS burned area product-Global evaluation by comparison with the MODIS active fire product. *Remote Sensing of Environment 112*, 3690-3707.

Sasaki, N. and Putz, F. E. (2009). Critical need for new definitions of forest and forest degradation in global climate change agreements. *Conservation Letters 2*, 226-232.

Simula, M. (2009). *Towards defining forest degradation: Comparative analysis of existing definitions*. FAO Forest Resources Assessment (Working Paper 154), Rome.

Souza Jr., C. M., Siqueira, J. V., Sales, M. H., Fonseca, A. V., Ribeiro, J. G., Numata, I., Cochrane, M. A., Barber, C. P., Roberts, D. A. and Barlow, J. (2013). Ten-year Landsat classification of deforestation and forest degradation in the Brazilian Amazon. *Remote sensing 5*, 5493-5513.

Stone, T. and Lefebvre, P. (1998). Using multi-temporal satellite data to evaluate selective logging in Pará, Brazil. *International Journal of Remote Sensing 19*, 2517-2526.

Uhl, C. and Kauffman, J. B. (1990). Deforestation, fire susceptibility, and potential tree responses to fire in the eastern Amazon. *Ecology 7*, 437-449.

Van der Werf, G. R., Randerson, J. T., Giglio, L., Collatz, G. J., Mu, M., Kasibhatla, P. S., Morton, D. C., DeFries, R. S., Jin, Y. and van Leeuwen, T. T. (2010). Global fire emissions and the contribution of deforestation, savannah, forest, agricultural, and peat fires (1997-2009). *Atmospheric Chemistry and Physics 10*, 11707-11735.

UNFCCC (2008). *United Nations Framework Convention on Climate Change Report of the Conference of the Parties on its thirteenth session*, Bali. FCCC/CP/2007/6/Add.1.

Xaud, H. A. M, Martins, F. da S. R. V. and dos Santos, J. R. (2013). Tropical forest degradation by mega-fires in the northern Brazilian Amazon. *Forest Ecology and Management 294*, 97-106.

Wettability and extinguishing power of different wetting composition for wildland fire fighting

Joanna Rakowska[a], Bożenna Porycka[a], Katarzyna Radwan[a], Ryszard Szczygieł[b], Mirosław Kwiatkowski[b]

[a] *Science and Research Centre for Fire Protection – National Research Institute, Nadwiślańska 213, 05-420 Józefów, jrakowska@cnbop.pl*
[b] *Forest Research Institute, Sekocin Stary, Braci Lesnej 3, 05-090 Raszyn, R.Szczygiel@ibles.waw.pl*

Abstract
Extinguishing fires of forests is a serious problem for fire services since vast areas can be involved in a relatively short time. For extinguishing fire of forests and peat-bogs is indispensable employment of wetting agents, which by its specificity multiplies speed of penetration burning material. Water is the most frequently used extinguishing agent, but when it is used to extinguish the fires of forests, shrubs, peat-bogs or wildland its efficiency is poor because of its weak capacity to wet and penetrate the cracks of the hydrophobic forest floor. The extinguishing efficiency can be enhanced by adding extinguishing concentrates which reduce the water surface tension. The optimum solution is to use wetting extinguishing agents which hamper the development of a fire by reducing the rate of the fire spread and the combustion intensity.
Wetting agent are mixtures of many components inclusive of surfactants, which are well soluble in water and which lower surface tension value of aqueous solutions and boost ability of solution to wetting of surface hydrophobic material. When added to water, those compounds improve its fire extinguishing properties, and thus improve efficiency of rescue actions. Wetting agents are assigned for extinguishing fire of wood (forest) and peat-bogs, cotton, coal and other smoldering and glowing fires.
This study presents the results of laboratory tests of wetting compositions. The purpose of this study was to determine the wetting power, adsorbing power and extinguishing tests for the wetting agents intended to fight forest fires.

Keywords*: wetting agent, wildland fire-fighting, forest fire*

Introduction

Extinguishing fires of forests is a serious problem for fire brigades since vast areas can be involved in a relatively short time. For extinguishing fire of forests and peat-bogs is indispensable employment of wetting agents, which by its specificity multiplies speed of penetration burning material. Wetting agent are mixtures of many components inclusive of surfactants, which are well soluble in water and which lower surface tension value of aqueous solutions and boost ability of solution to wetting of surface hydrophobic material. Wetting agents are used to extinguish both the flaming and glowing phases of combustion by application on the burning fuel. Their effectiveness relies also on their ability to retain moisture and absorb heat by cooling. They remain effective until all water has been removed from the fuel by evaporation [1].
When added to water, those compounds improve its fire extinguishing properties, and thus improve efficiency of rescue actions. Wetting agents are assigned for extinguishing fire of wood (forest) and peat-bogs, cotton, coal and other smoldering and glowing fires. Surfactants in this type of compounds are selected under their abilities to reduce surface tension value in water solutions and increase wetting. The purpose of tests and search for new agents is certainly development and implementation of the best and most effective arrangements. Efficiency of wetting agent is a function of the concentrations and types of the active ingredients that are delivered into the solution. The foam generation, more or less important depending on additive quality and concentration, gives a better insulation of the fire by

flame covering. Additionally, the water coming from drainage helps to cool down the fire and so enhances the extinction.
The wettability is an advantage for forest fire-fighting as it makes better the penetration and spreading of the liquid over a thick vegetal cover.
The foam achieved from solutions of commercial wetting agent and in a concentration 1.0% (v/v), prepared by using municipal water were also compared.

Materials and Methods

Materials

In our studies five commercial extinguishing and wetting agents were used. Characteristic of tested compositions is showed in Table 1.

Table 1. Commercial fire-fighting agents

Commercial fire-fighting agent	Field of application	Recommended concentration [%]	Basic surfactants
Biofor C	forest fires and urban fires plastics, tyres, cotton hydrocarbon fuel	0,1-1,0	salts of fatty alcohol ether sulfates C_{12}-C_{14} - anionic surfactant
Prosintex A	structures and buildings hydrocarbon fuel rubber, plastic, tyres paper, wood, forest fires	0,1-1,0	salts of fatty alcohol ether sulfates C_{10}-C_{14} - anionic surfactant
Forexpan S	forestry and wildland fire structural fires tyres and rubber fires hydrocarbon spill fires	0,1-1,0	salts of fatty alcohol ether sulfates C_{10}-C_{16} - anionic surfactant
Sthamex cl. A	cotton, peat, pulverised coal fires forest and bush fires	0,1 – 1,0	polyoxyethylene glycol dodecyl ether- nonionic
Amber One	forest fires, bush fires and peat bog fires, cotton, wood, paper, pulverised coal fires	0,1 – 1,0	fatty alcohol C12-C15 ethoxy sodium sulphates

Surface tension

Equilibrium surface tension was measured using the du Noüy ring technique with a Krüss K9 ET tensiometer (Germany) with platinum ring [2]. The surface of each solution was cleaned immediately prior to measurement.
Aqueous solutions were prepared in a wide range of concentrations immediately prior to measurements. All measurements were carried out at 294 K. The average standard deviation of these determinations was equal to 0.2 $mN \cdot m^{-1}$. In all the systems, re-distilled water with conductivity equal to 3 μS was used as the aqueous phase.

Foaming power

The foam was generated according to standard EN 1568-3 [3] from an aqueous solution of the wetting agent at a concentration of 1.0 %. This method consists of measuring the foam volume in a 1 L cylinder.

The expansion ratio (E), given in Eq. (1), is the proportion of the volume of foam (V_{foam}) to the volume of solution ($V_{solution}$) from which it was made.

$$E = \frac{V_{foam}}{V_{solution}} \quad (1)$$

All measurements were carried out at 294±2 K. The average standard deviation of expansion ratio determinations was equal to 1.5 %.

2.4. Wettability

100 g of wetted material (peat or wood bark) was dried in order to achieve moisture content of approximately 8–10 % . Next the wetted material was placed in steel mesh baskets, weighed, and spayed by studied solutions of wetting mixtures. Then, the bottom of the basket was dried with absorbent paper and the basket with wetted material was weighed. For estimating wettability W (%) the following equation was used:

$$W = \frac{m_1 + m_0}{m_0} \cdot 100\% \quad (2)$$

where m_1 is the mass of wetted material after spaying by tested solution and m_0 is the mass of dry peat or wood bark which is equal to 100 g.

Measurements were conducted at 294±2 K. The average standard deviation of these determinations was equal to 3 %.

2.5. Extinguishing test

Tests of the effectiveness of extinguishing fires of solid materials were performed in accordance to method described in standard EN 3-7 [4] using portable fire extinguishers of 2 L volume filled with 1% solutions of the wetting mixtures analysed. After extinction no burnback was observed for any studied compositions.

Measurements were carried out at 294±5 K. The average standard deviation of extinction time determinations was up to 2s.

2.6. Retardancy

The peat was soaked by 1% solutions of wetting compositions and dried to obtain moisture below 13%. Next the 100 g of peat was put in basket and ignited by propan (propan-butan) pilot burner. Measurements were conducted from the start of ignition of pilot burner till the smoldering of fuel was observed.

Measurements were carried out at 294±5 K. The average standard deviation of extinction time determinations was up to 2s.

Results

3.1. Surface tension

In the Figure 1 values of surface tension of studied agents were showed. The surface tension of the analysed wetting compositions varies between 26 mN/m (for Sthamex A) to almost 30 mN/m (for Amber One). Typical values of surface tension for solutions of extinguishing agents is below 35 $mN \cdot m^{-1}$.

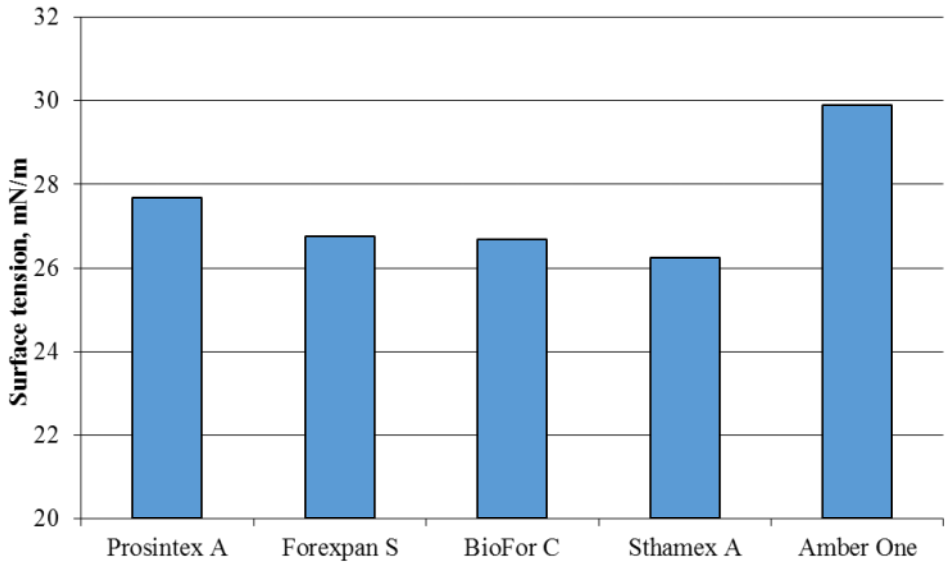

Figure 1. Surface tension of the analysed wetting compositions

Foaming power

The results of foaming properties were presented in the Figure 2. The foaming power of analysed wetting compositions varies between 5 (for Prosintex A) to 8 (for Sthamex). For good properties of wetting and extinguishing fire of natural hydrophobic material a low foamability (between 4-6) is required.

In the Fig 3 time to drainage of 25% and 50% of foam volume were showed. Short time of draining is demanded for quick speeding of wetting agent on the flammable surface.

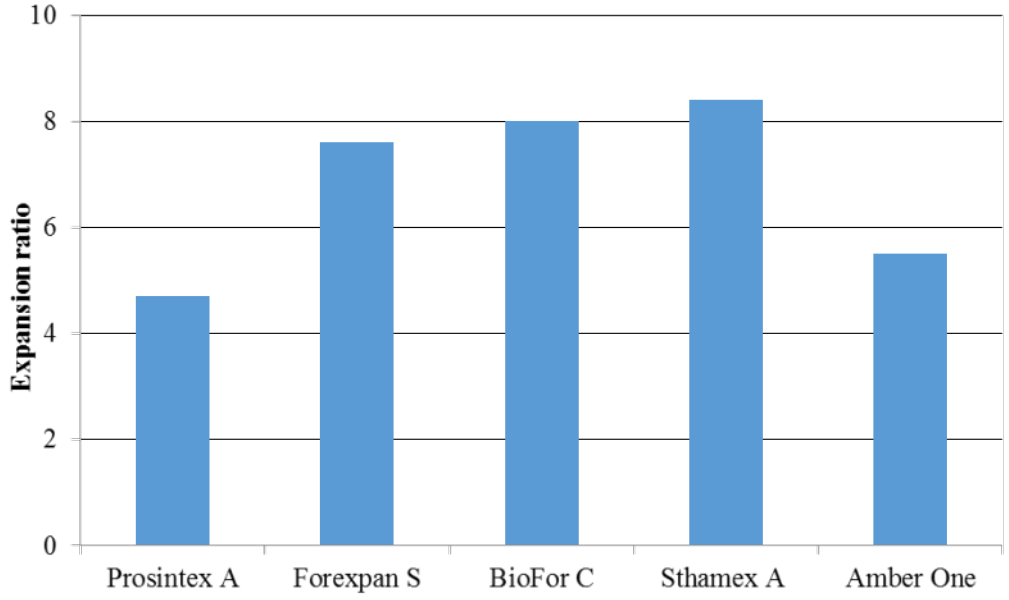

Figure 2. Foaming power of analysed wetting compositions

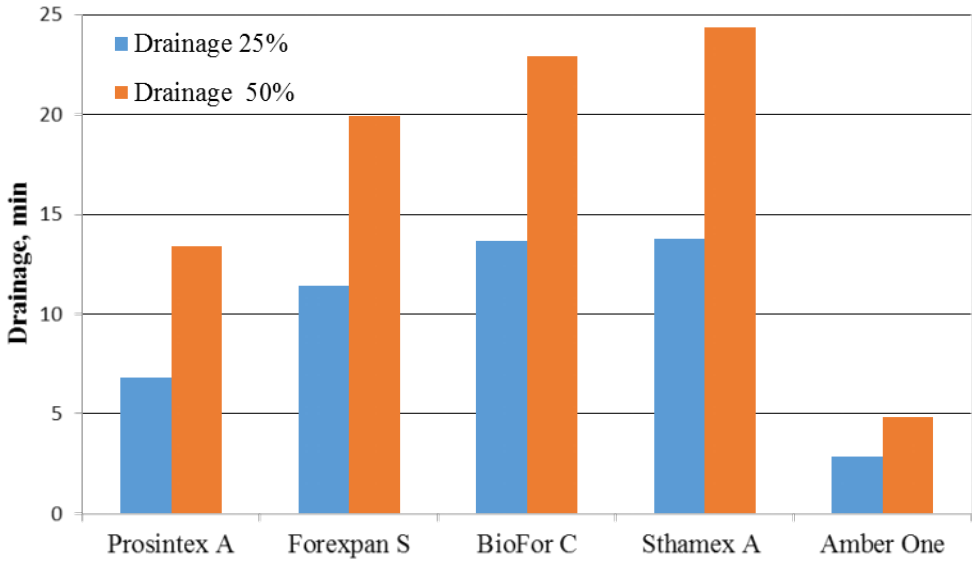

Figure 3. Drainage time of the produced foam for analysed wetting compositions

3.3. Wettability

In the Fig 4 and Figure 5 the wetting power of studied wetting agents were showed. At the concentration of 0,10% all of the analysed wetting compositions have comparable wettability of peat. The highest wettability was recorded for Amber One and Forexpan S. Wettability for this two wetting compositions was comparable at concentration 0,5% and 1,0%.

The highest wettability of bark was recorded at the concentration of 1,0%. In this respect the best was BioFor C and next Sthamex A, Forexpan S and Amber One.

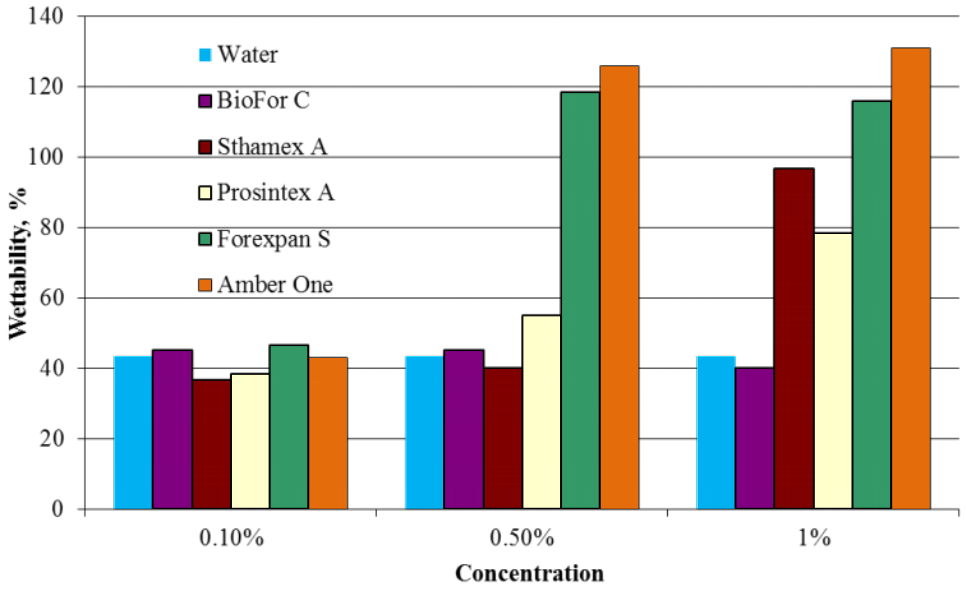

Figure 4. Wettability of peat with the analysed wetting compositions versus to concentration

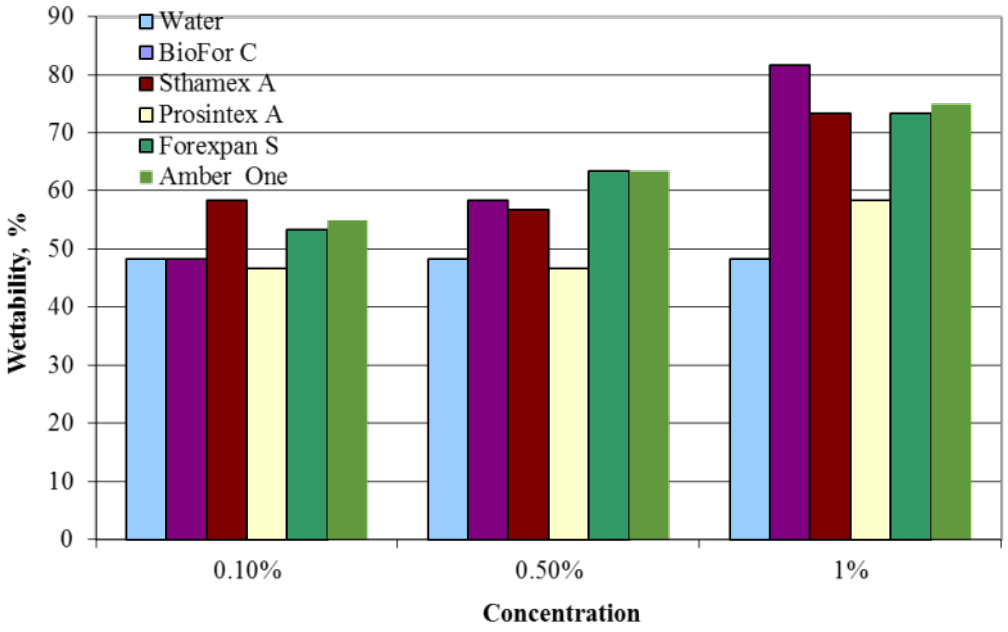

Figure 5. Wettability of bark with dispersed stream of the analysed wetting compositions.

3.4. Extinguishing test

The results of extinguishing tests were presented in the Figure 6. The times required for the wetting agents used to extinguish fires proved to be up to two times shorter than the time required for synthetic extinguishing agents typically applied in fighting fires of solid porous materials. Once the flames were extinguished by applying each of the solutions investigated, no return of fire was observed.

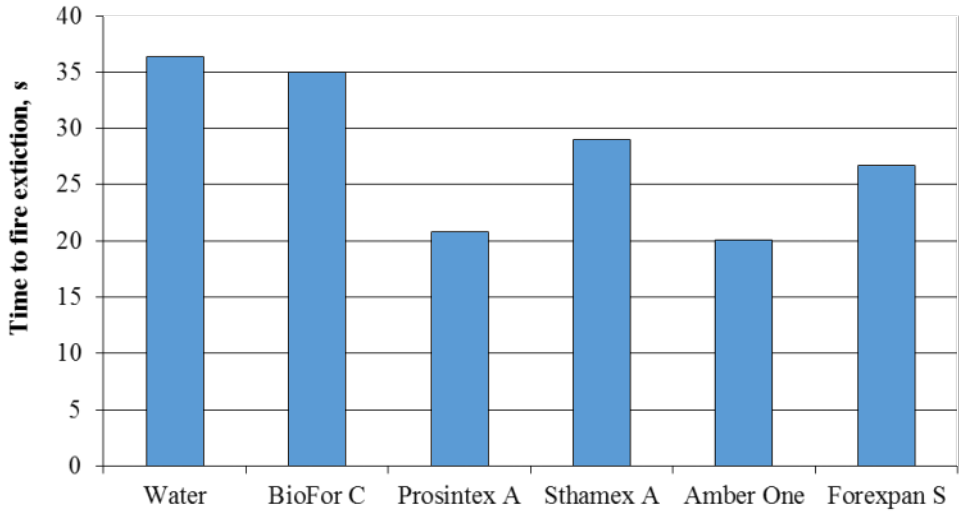

Figure 6. Extinguishing time of test fire 5A [5]

3.5. Retardancy

In the Figure 7 a comparison of delaying time to inflammation of dry peat was presented. Unprotected peat sample has an inflammation time of 25s. After wetting composition treatment inflammation time was extended by 5s (for Biofor C) up to 15s (Forexpan S).

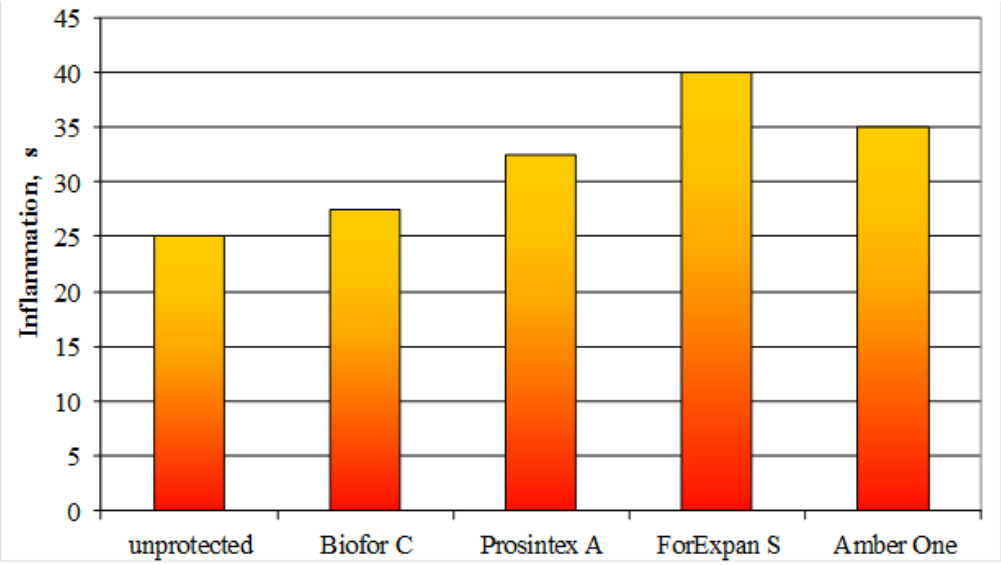

Figure 7. Inflammation time of peat sample

Conclusions

- Wetting agents added to water for lowering surface tension and improving wettability. The foaming of extinguishing agent for suppression wildland fire should not be so high like to agent used to extinction for liquid fuel.
- The use of wetting agents reduces the time to extinguish the fire and delaying burnback.
- Wetting agents can be used as a short-term retardants.
- Application of the wetting agent helps to reduce the size of burnt areas of forest and decreases the number of fatalities, as well as material and ecological losses.

Aknowledgement

This work was financially supported by MNiSW as project R00-O0046/03 in years 2007-2010 and 016/BC/CNBOP-PIB/2011-2016.

References

[1] S. Liodakis, V. Tsapara, I.P. Agiovlasitis, D. Vorisis, Thermal analysis of Pinus sylvestris L. wood samples treated with a new gel–mineral mixture of short- and long-term fire retardants, Thermochimica Acta (2013) 568, 156–160. DOI: 10.1016/j.tca.2013.06.011

[2] Lunkenheimer, K., & Wantke, K. D. (1981). Determination of the surface tension of surfactant solutions applying the method of Lecomte du Noüy (ring tensiometer). *Colloid and Polymer Science*, *259*, 354–366. DOI: 10.1007/bf01524716.

[3] EN 1568-3:2008 Fire extinguishing media — Foam concentrates - Part 3: Specification for low expansion foam concentrates for surface application to water-immiscible liquids

[4] EN 3-7: 2007 Portable fire extinguishers - Part 7: Characteristics, performance requirements and test methods

[5] J. Rakowska, K. Prochaska, B. Twardochleb, M. Rojewska, B. Porycka, A. Jaszkiewicz, Selection of surfactants as main components of ecological wetting agent for effective extinguishing of forest and peat-bog fires, *Chemical Papers* 68 (6) 823–833. DOI: 10.2478/s11696-013-0511-9

Chapter 6
Forest Management

A fire effects index for overall assessment of wildfire events in Greece

Kostas Kalabokidis, Palaiologos Palaiologou, Nikolaos Athanasis

Department of Geography, University of the Aegean, GR-81100 Mytilene, GREECE.
kalabokidis@aegean.gr

Abstract
Greece is faced with increased wildfire activity on an annual basis. Large-scale wildfires along with limited economic resources do not allow application of rehabilitation measures for the vast majority of burned areas, and when restoration takes place it is not based on sound scientific evidence. A scientific approach is missing based on wildfire classification and overall assessment of fire effects. Severity of a wildfire is perceived by the authorities only from the total area burned. These facts prompted our research thoughts about the need for introducing a new ranking method that will be based on expert judgment, with scientific evaluation of what has happened and what it is expected to occur based on several fire related aspects and parameters. The backbone of our proposed Fire Ranking and Effects Index (FIRE Index) is the Analytical Hierarchical Process (AHP) that is used to combine the scores of seven categories and 56 criteria that comprise them. These categories form two groups of effects: Environmental Fire Effects with three categories (Landscape and Vegetation; General Environment Impacts; Regeneration Potential/Vegetation Recovery); and Socioeconomic Fire Effects with four categories (Casualties and Fatalities; Destructions/Damages on Infrastructure; Economic Losses; Firefighting/Wildfire Confrontation). Each of the 56 criteria, along with four different general multipliers, describes a different anticipated fire effect. The magnitude of the effects is estimated by one or more persons/ assessors in a multi-level evaluation procedure. Then, AHP pair-wise comparisons are applied in two levels, i.e. within the criteria of each category and among the seven categories. Weighted scores of criteria are summed and normalized in a 0-100 scale; and the same procedure is applied on categories to calculate the final FIRE Index value. End-users are thus able to estimate the FIRE Index in a user-friendly, web-based platform that provides all the necessary feedback and literature justification, while conducting all the necessary calculations in the background.

Keywords*: Wildfire Effects Evaluation; Analytical Hierarchical Process; Fire Index; Greece*

Introduction

Increased frequency and intensity of wildfire events for the past two decades in the Mediterranean Basin resulted in millions hectares of burned land, causing hundreds of fatalities and extensive losses on socioeconomic and natural resources (Moreira *et al.* 2011). There are several explanations for this large wildfire breakout, ranging from climate change (Trigo *et al.* 2006; Founda and Giannakopoulos 2009) to socioeconomic reasons, but it is generally agreed that human activities is the main cause for their geometrical increase (Pausas 2004). Either from arsons, negligence or need, the human-ignited fires are constantly destroying forest lands, accelerating phenomena such as erosion, desertification, land use changes, species extinction and degradation of the natural environment (Shakesby and Doerr 2006; Pausas *et al.* 2008; Moreira *et al.* 2011). Furthermore, the cost of rehabilitating the landscape, repairs on infrastructures and properties and economic compensations burden the national budgets (Butry *et al.* 2001; Steelman and Burke 2007). Societies are forced to spend vast amounts of economic and human resources to confront these events and to mitigate their catastrophic effects. Inability of evaluating each wildfire event from the importance of the causing effects usually leads to overestimate or underestimate of the real situation that emerged after the event, resulting in enforcing either a wrong recipe for post-fire management or do nothing.
Our proposed Fire Ranking and Effects Index (FIRE Index) in this study adds to the current fire effects evaluation procedures a comprehensive methodology that allows the classification of wildfires based

on an evaluation of multiple fire effects categories and criteria. Its primary evaluation principle considers the social perspective of wildfires, by incorporating into the evaluation procedure a logic derived from how people understand fire effects during their lifetimes. The social perspective of wildfires dominates most of the criteria but co-exists with the ecological perspective of others. In the case of a conflict between those two approaches, the social always prevails. The above indicate that the assessor must rate the criteria based on what is important for human beings and societies, as well as, how they understand and experience ecology and environment.

Materials and Methods

The main tools used for the conceptual design and implementation of the proposed FIRE Index are based on approaches and applications used to estimate and assess burn severity and first order fire effects on the field (Composite Burn Index - CBI) from Key and Benson (2006); in conjunction with ranking the academic performance of world universities (The World University Rankings - Thomson Reuters[1]). The backbone of the ranking method among the different fire effects is the Analytical Hierarchical Process (AHP) (Saaty 1977). The FIRE Index has been designed for fire events that occur in Greece, but, given the necessary modifications and inputs can be expanded to other countries and regions.

The first level of wildfire evaluation is the *Fire Effect Category* (FEC: seven in total). Each category is composed of *Criteria* (56 in total). Each criterion has its own set of *Choices*, defining the magnitude of fire effects it describes on a scale of 0 (No effect) to 100 (High effect) (Table 1). The choices for each criterion were derived by the detailed study of the relevant local and international literature (wildfire and ecology studies) for several wildfire incidents as well as from the knowledge and experiences gained from several case studies across Greece. These choices portray the significance of the effects and outcomes caused by the wildfire. The assessor has the ability to provide any value through the predefined scale, with the exception of those values for certain choices that have been excluded or are not available by the initial criterion design. For example, if a criterion has two available choices that can both describe a certain fire effect with values 100 and 60, then the assessor can choose either the middle values of the two choices (80) or, a value that is closer to one choice depending on his judgment for the current situation (70 or 90).

Table 1. Fire effects evaluation scale from 0 (none) to 100 (high)

No Effect		Low		Moderate		High
0	10	20	40	60	80	100

Two criteria were assigned with *Additive Terms* (AT) that can aid in a more detailed description of the fire effects. The criterion score is modified by the AT value, but, eventually the final score will fall in the range of 0 to 100, due to an average estimation of the scores. For example, a forest under protection status will receive the highest value if it is an old-growth forest that comprises more than 50% of the burned area. Another concept in the evaluation procedure is the *Criterion Descriptor* that allows the attribution of a percentage value to each choice to achieve a better description of what has happened on a landscape level. For example, the assessor can describe the percentage of area occupied by pine trees or other vegetation types, achieving a more detailed allocation of the criterion value. The sum of all the values of criterion descriptor should not exceed 100%.

Some of the FEC's (five out of seven) were assigned with a *General Multiplier* (GM) that is evaluated on a scale of 0.5 to 3 having a 0.5 interval. These GM's were derived from evaluation of important

[1] http://www.timeshighereducation.co.uk/world-university-rankings/2013-14/world-ranking/methodology

wildfire attributes and characteristics, such as fire size, ecological condition and protection status, and post-fire vegetation condition. They provide the ability to decrease (by selecting a value from 0.5 to 0.9), keep it the same (values equal to 1) or increase (values greater than 1) the overall FEC score based on the assessor's answer. AT's were also assigned to two GM's and their value is defined by the average of all answers. The majority of criteria and multipliers can be evaluated by simply selecting one from the available choices or provide a user defined score; but there are some that have a particular logic behind them that it is noted in their description.

Prioritization of Categories and Criteria

For each category and criterion, weights were derived to achieve a prioritization among them based on their relative importance at the category and final index levels, by using the AHP method developed by Saaty (1977). Initially, a pair-wise comparison matrix is designed (Equation 1), where the relative importance between two criteria is measured according to a numerical scale from 1 to 9, where 1 denotes equal importance and 9 denotes that the first is absolutely more important than the second criterion.

$$A = \begin{bmatrix} 1 & a_{12} & \cdots & a_{1n} \\ a_{21} & 1 & & a_{2n} \\ \vdots & & \ddots & \vdots \\ a_{n1} & a_{n2} & \cdots & 1 \end{bmatrix} \qquad (1)$$

where, $\alpha_{jk} = 1/ a_{kj}$ and k,j = 1, …., *n*.

Once the matrix is built, it is possible to derive a normalized pair-wise comparison matrix (i.e. A_{norm}) by making equal to 1 the sum of the entries on each column. Each entry $\bar{a}_{jk}$ is computed by Equation 2:

$$\overline{a}_{jk} = \frac{a_{jk}}{\sum_{l=1}^{m} a_{lk}} \qquad (2)$$

Then, the criteria weight vector w (that is an m-dimensional column vector) is built by averaging the entries on each row of the A_{norm} matrix with Equation 3 (results were checked to ensure that they are consistent):

$$w_j = \frac{\sum_{l=1}^{m} \bar{a}_{jl}}{m} \qquad (3)$$

To conduct all the necessary calculations for the final FIRE Index estimation, the calculation of all criteria and multipliers scores is required. Each criterion is weighted and then summed with the others from the same category. If a GM exists, it is applied on the weighted sum. Then, a normalization of the outcome is performed on a scale of 0 to 100 by using the higher and lower value that each category can achieve with the Equation 4:

$$x_i = \frac{(R_i - R_{min})}{(R_{max} - R_{min})} * SR \qquad (4)$$

where, R_i is the outcome weighted value of the category i, R_{min} and R_{max} are the lower and higher values respectively the category can achieve, and SR is the standardized range.

Finally, the value from each of the seven categories is also weighted and then summed with the others to derive the final FIRE Index value on a scale of 1-100.

Results

Categories and Criteria of Fire Effects

By studying several wildfire case studies that occurred during the past 40 years in Greece, seven general wildfire effects categories were derived, forming two groups: the Environmental Fire Effects (Figure 1) and the Socioeconomic Fire Effects (Figure 2). The first fire effects category is the "Effects on Landscape and Vegetation" and examines the wildfire consequences on the landscape in terms of air quality and soil condition. It also examines the vegetation type, rarity, protection status based on a social perspective of the prioritization of forest resources. It is composed by five criteria and one GM. Initially, the assessor must define the landscape type in which the wildfire took place, by choosing among flat terrain/agricultural land, highlands, wildland-urban interface and mountainous areas. Then, in the criterion "Dominant Land Use/Land Cover types" (LULC), the vegetation composition inside the burned area is defined by providing the percentage estimation of its cover. The available choices are: bare soil; grass or short shrub; shrubland; agricultural land or orchard; mixed or broadleaf forest; and conifer forest. Then, the percentage fraction provided for each choice is multiplied by its relevant score. If the choices involve either "Mixed/Broadleaf forest" or "Conifer forest", then the two AT are activated, defining the vegetation types that exist inside the fire perimeter. For the case of mixed/broadleaf forest types, the available choices are: *Quercus* spp. or *Olea sylvestris*; *Fagus* spp. or *Juglans regia* or *Castanea* spp. or Cold Climate Broadleaf Evergreens; and mixed conifer/broadleaf forest. For the case of conifer forest types the available choices are: *Pinus brutia* or *Pinus halepensis*; *Juniperus* spp. or *Cupressus* spp.; *Pinus nigra* or *Pinus pinea*; and *Abies* spp. or mixed Fir/Pine forest or *Pinus sylvestris* or *Pinus heldreichii*. The assessor must provide the type of each forest and, depending on what is chosen, the AT score is multiplied by the fraction of cover for this particular LULC, summed with the initial LULC score and then averaged. The final criterion value is derived by summing the scores of each LULC type, including the average values derived by the possible usage of AT.

The next criterion defines if the burned area is under Greek or international conservation and protection status of forested areas and on what percentage it is inside the fire perimeter. The choices are: lake or seashore forests; recreational forests; national parks; and old-growth forest. If the assessor chooses a value different from "None" (which means a zero value for the criterion), he must then define the percentage that this protected area type is occupying inside the burned area. The two scores are then summed and averaged to derive the final criterion value. The effects on air quality are defined by providing information that describes the size and type of the affected populated areas and to what extent (Sastry 2002; Vedal and Dutton 2006). The available choices are: away from settlements; small-scale visibility reduction and smoke impacts near small villages; visibility reduction inside medium/large sized populated areas; and severe smoke impacts inside medium/large sized populated areas. Finally, the last criterion describes the probabilities to occur land degradation, erosion and soil losses phenomena (none; low; moderate; high) (Robichaud 2000; Parsons *et al.* 2010). The assessor must also define the percentage of area that is expected to have those probabilities. The percent fraction is then multiplied with the score of each choice and summed to derive the final criterion score. Upon the completion of the above criteria, the size of burned area must be defined to act as the category's GM. Based on a detailed study of the frequency, size and number of fire events on Greece, the available choices are: fire size <10 ha; 10 to <100 ha; 100 to <500 ha; 500 to < 2,000 ha; 2,000 to <7,000; and >7,000 ha.

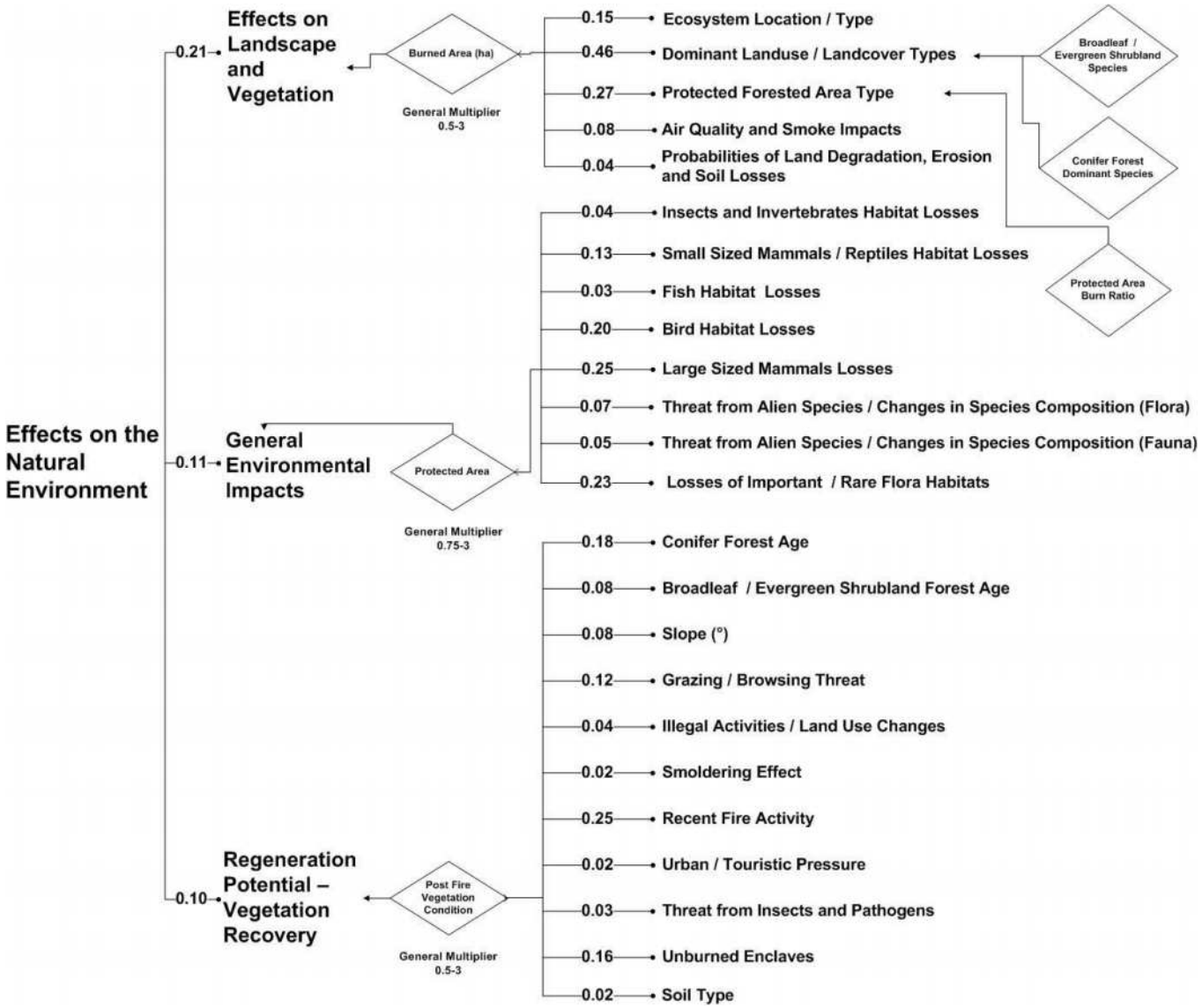

Figure 1. Structure of criteria and categories with their attributed weights for natural environment fire effects evaluation

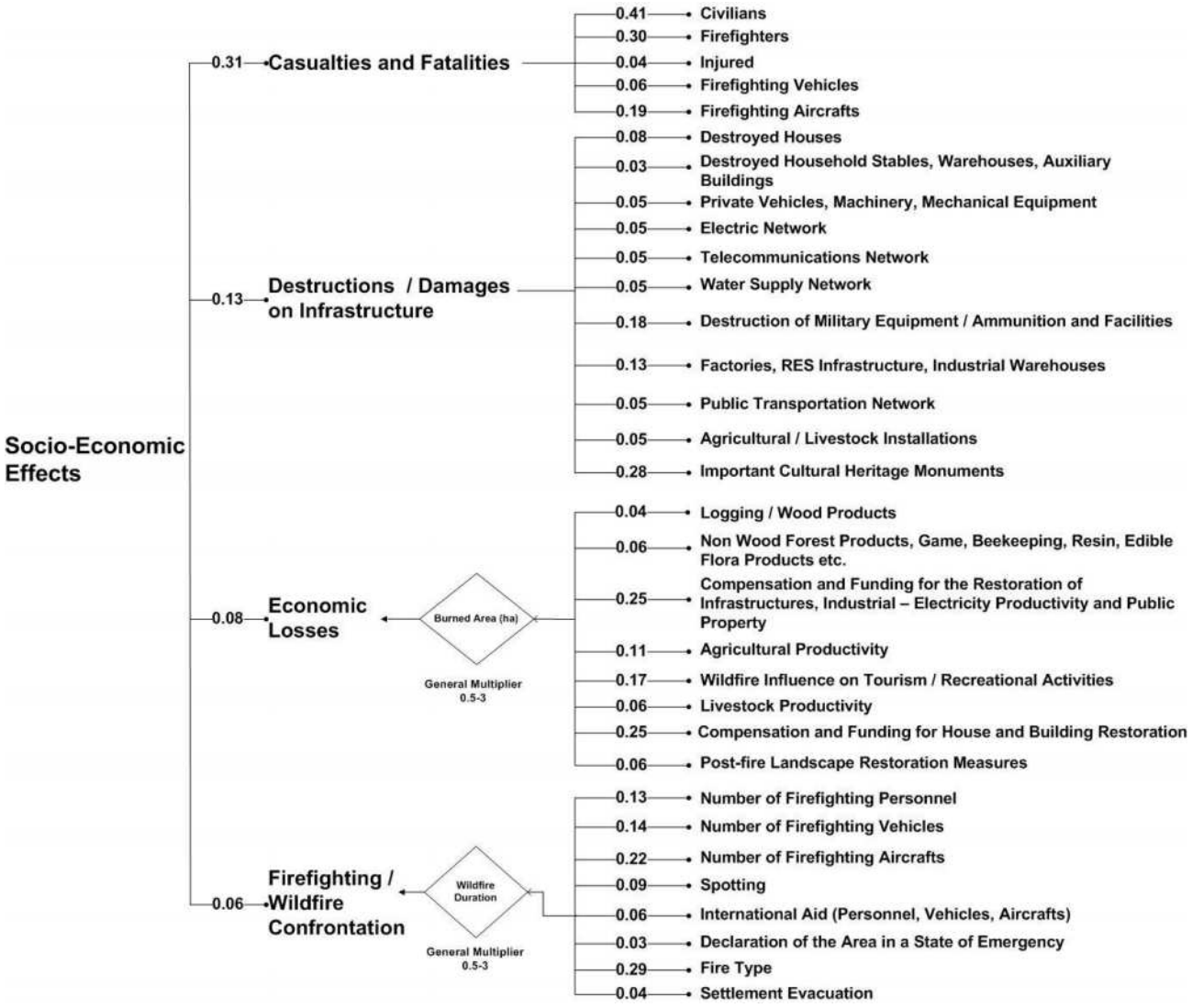

Figure 2. Structure of criteria and categories with their attributed weights for socioeconomic fire effects evaluation

The second category is the "General Environmental Impacts" that evaluates the wildfire effects on the fauna and flora of the affected area, as well as on the environmental quality and biodiversity. It is composed of eight criteria and one GM. Initially, the assessor must define the losses (if any) on important fauna habitats for five criteria (insects and invertebrates; small mammals/reptiles; fish; birds; and large-size mammals) (Smith 2000). The available choices are: none; few; several; and extended. The assessor must, prior to any judgment, acquire knowledge about the species composition of the area, their vulnerability to wildfires, their projected population response, their rarity and the extent of their habitat on the broader area. The sixth criterion evaluates the losses and possible endangering of important/rare flora species (Phitos *et al*. 1995; Brown and Smith 2000; Georghiou and Delipetrou 2010). The available choices for the assessor include: zero losses due to the lack of important/rare species; few losses with regeneration potential; extended losses with alteration on habitat conditions and strong population stresses; and intense, with possible species extinction or disappearance from the area. The next two criteria estimate the threat for exotic species invasion or the modification of the current abundance of local fauna and flora species. The available choices for both criteria are: none; local; extended; and intense. The assessor must gain knowledge about possible exotic species/invaders that reside inside or adjacent to the affected area that can encroach into it and to estimate if there will be any changes in species abundance and composition (Vitousek 1990; D 'Antonio and Vitousek 1992; Daehler and Strong 1994; Wilcove *et al.* 1998; Pimente 2002). Finally, one GM with an AT will define if the affected area is under any protection status and to what extent (Dimopoulos 2005; Mazaris *et al.* 2008). The available choices for the assessor are: none; wildlife habitats/NATURA 2000 areas; protected natural areas; areas of complete and strict protection; and biogenetic/biosphere reserves. If the choice is different than "None" (score = 1), the percentage of burned area that belongs to the selected type should be defined on the AT. The two scores are summed and averaged to derive the final GM score.

The third category is the «Regeneration Potential/Vegetation Recovery» and examines the fire behavior, pre-fire landscape and vegetation conditions, fire history and human pressures on the affected area. It is composed of 11 criteria and one GM. Initially, the assessor must define the age of conifer species that existed in the area prior to the fire (if present). The available choices are: not applicable; >100 years; 60-100 years; 20-60 years; 15-20 years; and <15 years. It is assumed that the younger the conifer forest is the more difficult it is to regenerate (Thanos and Daskalakou 2000; Tapias *et al*. 2001; Ne'eman *et al.* 2004; Climent *et al.* 2008). In the second criterion, the age of broadleaf species/evergreen shrublands must be defined (if present). The available choices are: not applicable; 10-15 years; 15-20 years; 20-60 years; 60-80 years; and >80 years or <10 years old. It is assumed that the older (or very younger) the broadleaf forest/evergreen shrublands is the more difficult it is to regenerate (Johnson and Godman 1983; Stroempl 1983). For these two criteria, it is important to define the age of the dominant vegetation types across the landscape instead of a detailed approximation at a stand level. The next criterion describes the topography of the area in terms of slope, and the assessor must calculate and provide information about the portions of the landscape that have a certain slope choice. The available choices are: 0-5°; 5-10°; 10-15°; 15-20°; 20-30°; 30-45°; and >45°.

The imminent threat from grazing must be evaluated by understanding the amount of livestock that resides inside or on the periphery of the burned area. It is assumed that as the grazing is increased in frequency and range, the conditions for potential successful vegetation regeneration are dramatically reduced (Perevolotsky and Haimov 1992; Campbell and Donlan 2005). The available choices are: none; partial; extended; and intense. The recent fire activity is an important parameter that has a substantial effect on regeneration. It is assumed that there are more chances for a successful regeneration if the fire return interval is large (Agee 1990). The available choices are: >100 years; >50 years; >30 years; and <30 years. It is frequent that post-fire vegetation recovery is depended on unburned forest patches and individual trees, providing a seed bank to colonize and repopulate the burned area, and it is assumed that the more dispersed and abundant these unburned patches are, the better is for regeneration (Lentile *et al.* 2005; Arianoutsou *et al.* 2010). The available choices are:

many (dispersed); many (gathered); few (dispersed); few (gathered); none. Illegal activities that may cause land use changes or interference into formerly vegetated areas can have a substantial negative effect, so the assessor must identify if there is any evidence that such activities have happened in the past (e.g. illegal logging, construction of buildings, roads and houses, conversion of forests into agricultural lands, etc.) (Tacconi *et al.* 2003). The available choices are: none; partial; extended; and intense. Another important criterion is the influence humans can have into the burned area by applying urban or touristic pressures. This can usually take the form of frequent tourist trips into the burned forests and people visits for recreational activities (Kuvan 2005). These pressures are usually performed into the wildland urban interface environment (Atmiş *et al.* 2007). The available choices are: none; partial; extended; and intense.

Fire smoldering effect can cause serious implications in vegetation recovery, mainly by modifying significant soil properties that prevent seeds from growing or resprouting (Ryan and Noste 1985). The assessor must have evidence if smoldering has happened and to what extent. The available choices are: none; partial; extended; and intense. Another important threat is the outbreak of diseases or harmful insect's population expansion that can cause negative effects on areas that survived the fire (de Dios 2007; Hansen 2008). Often, seeds and genetic material is transferred from these areas to other nearby burned parts, colonizing the landscape and reestablishing vegetation. If those surviving areas or individuals are affected, then the process of forest regeneration can be halted or lead to vegetation alterations (Winder and Shamoun 2006). The available choices are: none; partial; extended; and intense. Finally, the soil type plays an important role on resprouting and seed germination ability. This criterion assumes that deep soils with small amount of rocks are more preferable compared to shallow skeletal soils (steep slopes or exposed parent material) (López-Soria and Castell 1992; Minotta and Pinzauti 1996; Spanos *et al.* 2001). The available choices are: deep soils with small amount of rocks; deep soils with moderate amount of rocks; moderate depth soils with small amount of rocks; moderate depth soils with moderate amount of rocks; shallow soils with moderate amount of rocks; and shallow exposed soils with large amount of rocks. The GM is composed of three parts that must be evaluated and averaged. In particular, the assessor must define the percentage of burned, scorched and unburned vegetation (black, brown and green), in a similar way to CBI estimation for the overstory vegetation condition (Key and Benson 2006). The sum of the percentage choices from the three answers should not exceed 100%.

The main operational priority for most firefighting agencies across the world is focused on the protection of civilian and personnel lives, followed by the protection of firefighting infrastructure, properties and the natural environment. Societies often evaluate the importance of a wildfire from the number of fatalities it has caused and the total burned area (Haynes *et al.* 2010). Thus, a category with criteria able to estimate what has happened in terms of casualties is extremely important. The category «Casualties and Fatalities» determines the human death toll caused by the fire, along with the number of injured individuals and the number of destroyed firefighting vehicles and aircrafts. This category is composed of five criteria; three of them describe the fire effects on human lives and two on firefighting infrastructure. The last two criteria were selected for that they are caused due to the operational activities of firefighting forces and can be seen as causalities (Mangan 2007).

To include the proper choices on each criterion, a detailed study on the number of fatalities caused during the past 40 years from fire events across Greece was conducted. The available choices for the civilian fatalities criterion are: 0; 1; <5; 5 to 10; and >10. The available choices for firefighting personnel deaths criterion are: 0; 1; 2 to 3; 4 to 5; and >5. Usually, the firefighting personnel losses are less compared to civilians from a single fire event. The available choices for injured people criterion are: 0; 1; <5; <10; 10 to 20; 20 to 30; and >30. It is more common to have destroyed firefighting vehicles compared to aircrafts, thus, the available choices for firefighting vehicles losses criterion are: 0; 1; 2; 3; 4 to 5; and >5. Finally, the available choices for firefighting aircraft losses criterion are: 0; 1; 2; and >2.

The fire effects Category «Destructions/Damages on Infrastructure» is composed of 11 criteria and estimates the magnitude of destructions and damages caused by the fire event on property, public infrastructures, monuments and capital. Initially, the assessor must provide data regarding the destroyed houses due to the fire activity, providing their absolute number by selecting among these choices: 0; 1; 3; 5; <10 and >10. Based on the same logic, the number of destroyed household stables, warehouses or auxiliary buildings must be provided by selecting among these choices: 0; 1; 3; 5; <10; <20; and >20. The following eight criteria are evaluated based on their repair or acquisition cost. The assessor must provide estimation of the cost required to replace or restore this infrastructure to its pre-fire working condition. The third criterion estimates the fire damage cost caused on mobile property such as cars, machinery and other equipment. For the next four criteria, the fire damage cost on transportation, electric, water supply and telecommunication networks is estimated. The available choices for the above criteria are: no damages; minor costs <15,000€; small cost <30,000€; medium cost <100,000€; and important high cost damages >200,000€. The next three criteria examine the cost of damages on military facilities, ammunition and equipment; on factories, renewable energy sources (RES) installations and industrial warehouses; and on Agricultural/Livestock installations. The available choices for the above criteria are: no damages; minor costs <50,000€; small cost <100,000€; medium cost <200,000€; and important high cost damages >300,000€. Finally, it is very important to assess if there were any damages or destruction of important cultural heritage monuments, and if so, the assessor must select a monument category that is based on time. The following choices are available: no damages; recent monuments aged <200 years; historic monuments aged >200 years; and world heritage sites and monuments.

The category «Economic Losses» accounts for the changes that are expected to occur on the local or regional economic structure, emphasizing on the market price drop of some valued items/products, the inability to produce or collect them and the amount of money that will be spent for productivity restoration or compensations (Donovan and Rideout 2003; Calkin *et al.* 2007). It also estimates the relative cost of post-fire landscape treatment measures that are going to be applied on the affected area. The main difference with the previous category is that it does not just account the costs of damages and destructions the fire has caused, but the cost of anticipated rehabilitation measures and future economic losses. It is composed by eight criteria and one GM.

Initially, the assessor must provide information about the timber production and wood harvesting practices of the affected area. If the area was under a management status with frequent or upcoming timber harvesting then it is very probable that some kind of economic losses might occur. Several individuals or industries exploit the non-timber forest/nature products, such as game, honey production, resin extraction, pharmaceutics and medicine products, wild food, etc. These lead to the development of a small scale local or regional economy around these activities. The assessor must evaluate which were the fire effects on them and if economic losses have already happened or is expected to occur in the future. In Greece, it is very often for a wildfire to cause negative effects on agricultural and livestock production (Henderson *et al.* 2005; Moreira *et al.* 2011). This is usually done by destroying the means to produce income from these activities (animal deaths, burning of crops or orchards, destruction of infrastructure such as greenhouses, etc.). The cost includes possible compensations and future revenue losses from the inability to produce (e.g. in case of destroyed orchards). The assessor must assess those costs for these criteria. The available choices for the four criteria are: non productive area; minor; small; moderate; high economic losses; and total destruction. To restore the industrial and electric production, or to repair infrastructures and public property, compensations or funding must be paid from the state or insurance companies, otherwise negative effects can arise for the whole society. The same applies for houses and buildings. The available choices for these two criteria are: no cost; minor; small; moderate; and very high costs. The next criterion assesses the fire effect on tourism by evaluating the aesthetic, recreational and tourist infrastructure potential of the area (Kuvan 2005). The assessor must understand how large the touristic value of the area is and what kind of activities take place in the broader affected landscape. A link

must also be established between the values of the burned area and how important is for selecting it for tourist purposes, along with the predicted economic losses it might be caused. The available choices are: non touristic area; seashore related tourism area, scenery landscape close to intensely developed touristic areas; and forested area used for recreational/touristic purposes. The last criterion estimates the cost of landscape rehabilitation measures that are expected to be applied on the affected area. Usually, the type and range of their application depends on the available money the state is willing to spend. It is assumed that as the type changes and range of application increases, so does the cost (Napper 2006). The available choices are: no measures; small; medium; or high scale reforestations/counter-erosion/counter-flooding measures. Finally, one GM will define the size of burned area, assuming that as the fire size increase so does the overall economic losses.

The last category is the «Firefighting/Wildfire Confrontation» and evaluates the wildfire effects caused during firefighting activities and the wildfire confrontation strategy implemented. The category is composed of eight criteria and one GM, defining the general firefighting context and its operational costs. Furthermore, it considers the equipment and machinery wear, as well as the personnel fatigue. In the first criterion, the assessor must describe the fire behavior type that occurred in the majority of the burned area. This information can be derived either from observations or from the firefighting personnel. The available choices are: surface fire; torching/ passive crown fire; and active crown fire. Next, it must be defined if any spotting of fire re-bursts occurred. The available choices are: none; few; constant. The next three criteria count the number of people and vehicles that participated during the firefighting operations, to figure out confrontation difficulty. The available choices for the number of people/ firefighting personnel are: <10; 10-24; 25-39; 40-54; 55-70; and >70. The available choices for the number of ground vehicles are: 1-4; 5-9; 10-14; 15-19; 20-25; and >25. The available choices for the number of firefighting aircrafts are: 0; ≤2; 3-5; 4-5; and >5. All the above choices were derived by the study of several past wildfire events of Greece and are in proportion with their severity and confrontation costs. The international aid and reinforcements on personnel, vehicles and aircrafts add substantially to the firefighting operations, but is an indicative fact of the wildfire suppression difficulty, as well as of the costs associated with them. The available choices are: none; personnel; vehicles; and aircrafts. The declaration of the area in a state of emergency has two options (either no or yes), and is another indicative criterion of the wildfire difficulty. The evacuation of settlements adds a very complex parameter in the whole operation, increasing the costs and difficulty of operation. The available choices are: none; <2; 2 to 5; and >5 settlements. Finally, the category has one GM which accounts for the fire duration, providing the following choices: 0-2; 3-15; <24; <48; <72; and >72 hours.

3.2. Web-Based Software Architecture

To easily calculate and account for the complex interactions between and among criteria and categories, it was necessary to design a web-based software/ platform that will enable the assessor to provide inputs in a user-friendly Graphical User Interface (GUI), thus automating the calculation procedures and return the intermediate and final FIRE Index values (Figure 3). Furthermore, users can instantly test several different choices and options and understand their influence on the final index value (Figure 4). A detailed help section exists inside the GUI covering all the aspects of the methodology, providing explanation and documentation about what is being evaluated and the logic behind the available provided choices.

Figure 3. Initial evaluation screen and selection among categories

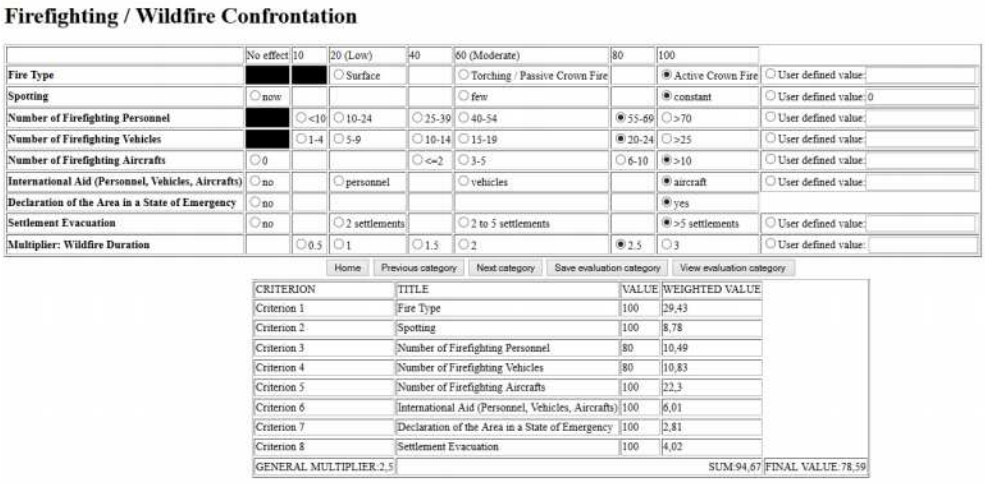

Figure 4. Web-based fire effects evaluation for the firefighting/wildfire confrontation category

Discussion and Conclusions

This version of FIRE Index is the first and has the primary goal of defining an evaluation context by creating a hierarchy among the categories, criteria and choices and by setting the rules that determine the combination of scores. Given its limitations and assumptions, the FIRE Index attempts to reveal an aspect of reality that allows people to evaluate possible scenarios that might happen in the future or to better understand what is been happening during the present time or to discover what has happened in the past. The FIRE Index does not portray or explains with full detail all the complexity, interrelationships and multivariate range that appear after a wildfire but, rather, it can quantify and

record systematically what has happened for a large number of fire effects, while for some others can estimate what is going to happen.
There is a large number of criteria, AT's and GM's (approximately 1/3 of the total number) that can be evaluated by providing spatial data together with their descriptive information. The usage of Geographic Information Systems (GIS) in a next version of the FIRE Index can perform the necessary spatial queries and interactions that are required to provide answers for several criteria. For example, the size of burned area and their boundaries can be provided in a very short time after the wildfire event by EFFIS[1]. These data can be used to derive information from other spatial layers such as the LULC types or the location of protected areas. Spatial data from satellite products or other study methods (such as burn severity, erosion and soil type maps) can also be included in the process if they are provided. The assessor then just has just to accept, reject or apply corrections on the derived choices.
There are several limitations and assumptions in the FIRE Index evaluation context. The main assumption is that each fire effect can be evaluated by a single criterion that has predefined choices on a scale from 0 to 100, thus providing a numerical value for its significance. This is not a problem for criteria like "Burned Area", but for example applying scores on fatalities may cause misinterpretations, disagreement and confuse. However, choices were derived from detailed studies of hundreds of fire events. The way those choices have been placed on the scale is more a descriptive/ qualitative approach rather than a numerical one. The current approach scales the choices from lower to higher impacts, and thus, the assessor should rate them with this logic. The numerical values are used primarily for the calculations, but their meaning lies on the way the assessor chooses them on the predefined scale. Another assumption that has been made for the "Destructions/Damages of Infrastructure" category, where there are several criteria on which a market value has been applied. The main limitation on this approach is that the total damage cost can greatly exceed the predefined choices and the assessor is limited on the higher ranked choice, without the ability of inserting this extra amount on the procedure. The evaluation context of the FIRE Index is designed to catch the variability between and among the different wildfires and not to actually portray everything that has happened and with absolute detail. The last assumption, that is simultaneously a limitation, is the usage of AHP method to derive criteria and categories weights. The AHP method requires user inputs to set a hierarchy among criteria and categories, thus, it is vulnerable to subjective judgment. Different people can consider differently their importance and this will lead to alterations in weights. The AHP was evaluated by the authors of this study by considering the social perspective of fire effects as the most important issue that determines the FIRE Index value, followed by environmental and economic perspectives.
By combining the scores of criteria for each category and by producing a total score for the wildfire event, public authorities and societies will be able to understand if during this event more or less serious effects have happened to one or more environmental and socioeconomic attributes; an approach that is beyond a simple measure of the burned area. This will allow a shift to occur in the current perspective of wildfires in Greece (and maybe elsewhere) and will enable the introduction of a scientific approach in the evaluation of each wildfire. It is anticipated that fire effects will be seen as an overall sum of negative and positive consequences that should be dealt either combined or individually to mitigate their impacts on nature and humans. It will also enhance the public awareness and will provide a comprehensive information source regarding several aspects of wildfires. The FIRE Index will not substitute a thorough study for the wildfire event with well established methods and techniques for the estimation of first and second order fire effects, but, in contrary, it will be enhanced by those studies that can provide the necessary inputs, with scientific evidence, and increased detail and accuracy.

[1] http://forest.jrc.ec.europa.eu/effis/applications/current-situation/

Acknowledgments

This work has been funded by the research project “AEGIS: Wildfire Prevention and Management Information System” {Code Number 1862}, which is implemented within the framework of the Action ARISTEIA of the Operational Program "Education and Lifelong Learning" (Action’s Beneficiary: General Secretariat for Research and Technology), and is co-financed by the European Social Fund (ESF) and the Greek State.

References

Agee, J.K., 1990. The historical role of fire in Pacific Northwest forests. In: Natural and prescribed fire in Pacific Northwest forests. (eds. Walstad, J.D., Radosevich, S.R., Sandberg, D.V.), pp. 25-38. (Corvallis: Oregon State University Press).

Arianoutsou, M., Christopoulou, A., Kazanis, D., Tountas Th, G. E., Bazos, I., and Kokkoris, Y., 2010. Effects of fire on high altitude coniferous forests of Greece. In: 6th international conference on forest fire research, 15-18 November 2010, Coimbra, Portugal.

Atmiş, E., Özden, S. and Lise, W., 2007. Urbanization pressures on the natural forests in Turkey: an overview. *Urban Forestry and Urban Greening*, **6(2)**, 83-92.

Brown, J.K. and Smith, J.K., (Eds.) 2000. Wildland fire in ecosystems: effects of fire on flora. USDA Forest Service, Rocky Mountain Research Station, General Technical Report RMRS-GTR-42-vol. 2. (Ogden, UT).

Butry, D.T., Mercer, E.D., Prestemon, J.P., Pye, J.M. and Holmes, T.P., 2001. What is the price of catastrophic wildfire? *Journal of Forestry*, **99(11)**, 9-17.

Calkin, D.E., Hyde, K.D., Robichaud, P.R., Jones, J.G., Ashmun, L.E. and Loeffler D., 2007. Assessing post-fire values-at-risk with a new calculation tool. USDA Forest Service, Rocky Mountain Research Station, General Technical Report RMRS-GTR-205. (Fort Collins, CO).

Campbell, K.J and Donlan, C.J., 2005. A review of feral goat eradication on islands. *Conservation Biology*, **19(5)**, 1362-1374.

Climent, J., Prada, M. A., Calama, R., *et al*., 2008. To grow or to seed: ecotypic variation in reproductive allocation and cone production by young female Aleppo pine (Pinus halepensis, Pinaceae). *American Journal of Botany*, **95(7)**, 833-842.

Daehler, C.C., and Strong, D.R., 1994. Native plant biodiversity vs. the introduced invaders: status of the conflict and future management options. In: Biological Diversity: Problems and Challenges. (Eds. Majumdar, S.K., Brenner, F.J., Lovich, J.E., Schalles, J.F. and Miller, E.W.), pp. 92- 113. (Easton, PA: Pennsylvania Academy of Science).

D'Antonio, C.M. and Vitousek, P.M., 1992. Biological invasions by exotic grasses the grass/fire cycle, and global change. *Annual Review Of Ecology And Systematics*, **23**, 63-87.

de Dios, V.R., Fischer, C., and Colinas, C., 2007. Climate change effects on Mediterranean forests and preventive measures. *New forests*, **33(1)**, 29-40.

Dimopoulos, P., Bergmeier, E., Theodoropoulos, K., Fisher, P. and Tsiafouli, M., 2005. Monitoring Guide for Habitat Types and Plant Species in the Natura2000 Sites of Greece with Management Institutions. University of Ioannina and Hellenic Ministry for Environment, Physical Planning and Public Works.

Donovan, G.H. and Rideout, D.B. 2003. A reformulation of the cost plus net value change (C+ NVC) model of wildfire economics. *Forest Science*, **49(2)**, 318-323.

Founda, D. and Giannakopoulos, C., 2009. The exceptionally hot summer of 2007 in Athens, Greece – a typical summer in the future climate? *Global and Planetary Change*, **67**, 227-236.

Georghiou, K. and Delipetrou, P., 2010. Patterns and traits of the endemic plants of Greece. *Botanical Journal of the Linnean Society*, **162**, 130-422.

Hansen, E.M, 2008. Alien forest pathogens: Phytophthora species are changing world forests. *Boreal Environmental Research*, **13**, 33-41.

Haynes, K., Handmer, J., McAneney, J., Tibbits, A. and Coates, L., 2010. Australian bushfire fatalities 1900–2008: exploring trends in relation to the 'Prepare, stay and defend or leave early'policy. *Environmental Science & Policy*, **13(3)**, 185-194.

Henderson, M., K. Kalabokidis, E. Marmaras, P. Konstantinidis, and M. Marangudakis. 2005. Fire and society: a comparative analysis of wildfire in Greece and the United States. Human Ecology Review, **12(2)**,169-182.

Johnson, P.S. and Godman, R.M., 1983. Precommercial thinning of oak, basswood, and red maple sprout clumps. In: Silviculture of established stands in north. Stier, Jeffrey C. (Ed.). SAF Region V Technical Conference, Duluth, Minnesota. Society of American Foresters, pp. 124-142. (Washington, DC: USA).

Key, C.H. and Benson, N.C., 2006. Landscape assessment: Sampling and analysis methods. In: FIREMON: Fire effects monitoring and inventory system. USDA Forest Service, Rocky Mountain Research Station, General Technical Report RMRS-GTR-164-CD. (Fort Collins, CO).

Kuvan, Y., 2005. The use of forests for the purpose of tourism: the case of Belek Tourism Center in Turkey. *Journal of environmental management*, **75(3)**, 263-274.

Lentile, L.B., Frederick, W.S. and Wayne, D.S., 2005. Patch structure, fire-scar formation, and tree regeneration in a large mixed-severity fire in the South Dakota Black Hills, USA. *Canadian Journal of Forest Research*, **35(12)**, 2875-2885.

López-Soria, L., and Castell, C., 1992. Comparative genet survival after fire in woody Mediterranean species. *Oecologia*, **91(4)**, 493-499.

Mangan, R., 2007. Wildland firefighter fatalities in the United States: 1990–2006. National Wildfire Coordinating Group. *Safety and Health Working Team, National Interagency Fire Center*, NWCG PMS, **841**.

Mazaris, A.D., Kallimanis, A.S., Sgardelis, S.P. and Pantis, J.D., 2008. Does higher taxon diversity reflect richness of conservation interest species?: the case for birds, mammals, amphibians, and reptiles in Greek protected areas. *Ecological indicators*, **8(5)**, 664-671.

Minotta, G. and Pinzauti, S., 1996. Effects of light and soil fertility on growth, leaf chlorophyll content and nutrient use efficiency of beech (Fagus sylvatica L.) seedlings. *Forest Ecology and Management*, **86**, 61-71.

Moreira, F., Viedma, O., Arianoutsou, M., *et al.*, 2011. Landscape–wildfire interactions in southern Europe: implications for landscape management. *Journal of Environmental Management*, **92(10)**, 2389-2402.

Napper, C., 2006. Burned area emergency response treatments catalog. USDA Forest Service, National Technology and Development Program, Watershed, Soil, Air Management, 0625 1801—SDTDC. (San Dimas: CA).

Ne'eman, G., Goubitz, S. and Nathan, R., 2004 . Reproductive traits of Pinus halepensis in the light of fire — a critical review. *Plant Ecology*, **171**, 69-79.

Parson, A., Robichaud, P.R., Lewis, S.A., Napper, C. and Clark, J.T., 2010. Field guide for mapping post-fire soil burn severity. USDA Forest Service, Rocky Mountain Research Station, General Technical Report RMRS-GTR-243. (Fort Collins, CO).

Pausas, J.G., 2004. Changes in fire and climate in the eastern Iberian Peninsula (Mediterranean basin). *Climatic change*, **63(3)**, 337-350.

Pausas, J.G., Llovet, J., Rodrigo, A. and Vallejo, R., 2008. Are wildfires a disaster in the Mediterranean basin? – A review. *International Journal of Wildland Fire* **17**, 713-723.

Perevolotsky, A. and Haimov, Y., 1992. The effect of thinning and goat browsing on the structure and development of Mediterranean woodland in Israel. *Forest ecology and management*, **49(1)**, 61-74.

Phitos, D., Strid, A., Snogerup, S. and Greuter, W., 1995. The red data book of rare and threatened plants of Greece. World Wide Fund for Nature (WWF).

Pimentel, D., 2002. Biological Invasions: Economic and Environmental Costs of Alien Plant, Animal, and Microbe Species. (CRC Press: Boca Raton, Florida).

Robichaud, P.R., 2000. Fire effects on infiltration rates after prescribed fire in Northern Rocky Mountain forests, USA. *Journal of Hydrology*, **231-232**, 220-229.

Ryan, K. and Noste, N., 1985. Evaluating prescribed fires. In: Symposium and Workshop on Wilderness Fire. USDA Forest Service Intermountain Forest and Range Experiment Station, General Technical Report INT-182, pp. 230-238. (Lotan, J.E., *et al*. (tech. coord.).

Saaty, T., 1977. A scaling method for priorities in hierarchical structures. *Journal of Mathematical Psychology*, **15 (3)**, 234-281.

Sastry, N., 2002. Forest fires, air pollution, and mortality in Southeast Asia. *Demography*, **39(1)**, 1-23.

Shakesby, R.A. and Doerr, S.H., 2006. Wildfire as a hydrological and geomorphological agent. *Earth-Science Reviews*, **74**, 269-307.

Smith, J.K., (Ed.) 2000. Wildland fire in ecosystems: effects of fire on fauna. USDA Forest Service, Rocky Mountain Research Station, General Technical Report RMRS-GTR-42-vol. 1. (Ogden, UT).

Spanos, I.A., Radoglou, K.M. and Raftoyannis, Y., 2001. Site quality effects on post-fire regeneration of Pinus brutia forest on a Greek island. Applied vegetation science, 4(2), 229-236.

Steelman, T.A. and Burke, C.A., 2007. Is wildfire policy in the United States sustainable? *Journal of Forestry*, **105(2)**, 67-72.

Stroempl, G., 1983. Thinning clumps of northern hardwood stump sprouts to produce high quality timber. In: Forest Research Information Paper, Canadian Ministry of Natural Resources (Maple: Ontario).

Tacconi, L., Boscolo, M. and Brack, D., 2003. National and international policies to control illegal forest activities. *Report for the Ministry of Foreign Affairs, Government of Japan. CIFOR, Bogor, Indonesia*.

Tapias, R., Gil, L., Fuentes-Utrilla, P. and Pardos, J.A., 2001. Canopy seed banks in Mediterranean pines of southeastern Spain: A comparison between *Pinus halepensis* Mill, *P. pinaster* Ait, *P. nigra* Arn. and *P. pinea* L. *Journal of Ecology*, **89**, 629-638.

Thanos, C.A. and Daskalakou, E.N., 2000. Reproduction in Pinus halepensis and P. brutia. In: G. Ne'eman and L. Trabaud [eds.], Ecology, biogeography and management of Pinus halepensis and P. brutia forest ecosystems in the Mediterranean Basin, 79 – 90. Backhuys Publishers, Leiden, Netherlands.

Trigo, R.M., Pereira, J., Pereira, M.G., Mota, B., Calado, T.J., Dacamara, C.C. and Santo, F.E., 2006. Atmospheric conditions associated with the exceptional fire season of 2003 in Portugal. *International Journal of Climatology* **26**, 1741-1757.

Vedal, S. and Dutton, S.J., 2006. Wildfire air pollution and daily mortality in a large urban area. *Environmental research*, **102(1)**, 29-35.

Vitousek, P.M., 1990. Biological invasions and ecosystem processes: towards an integration of population biology and ecosystem studies. Oikos, **57**, 7-13.

Wilcove, D.S., Rothstein, D., Dubow, J., Phillips, A. and Losos, E., 1998. Quantifying threats to imperiled species in the United States. *BioScience*, **48**, 607-615.

Winder, R.S. and Shamoun, S.F., 2006. Forest pathogens: friend or foe to biodiversity. *Canadian Journal of Plant Pathology*, **28**, 1-7.

Accuracy assessment of a mediterranean fuel-type map for wildland fire management at national scale: the cases of greece and portugal

Ioannis D. Mitsopoulos[a] , Luis .M. Ribeiro[b], G. Eftychidis[a], D.X. Viegas[b]

[a] *Algosystems SA, Athens, Greece, ioanmits@gmail.com*
[b] *ADAI, Coimbra, Portugal, luis.mario@adai.pt*

Abstract
Classification and mapping of wildland fuel is one of the most important factors that should be taken into consideration for wildland fire prevention and planning. In this paper we demonstrate the accuracy assessment of "ArcFUEL" project which has delivered a complete, up-to-date, methodology for Fuel Classification Mapping (FCM on a Web-Geodatabase) based on "readily available" data, harmonized, accessible & interoperable according to INSPIRE principles, for the Mediterranean Region. The fuel layer has been evaluated in terms of spatial and thematic thematic accuracy by employing an extensive field campaign in Portugal and Greece and standard photointerpretation procedures. For Greece, the overall accuracy was found to be 80.59 % , while the Kappa value was 0.74. For Portugal the overall accuracy was found to be 67% and the Kappa value was 0.63.The spatial fuel maps is an end-product essential for computing spatial fuel hazard, fire risk and simulation, fire growth and intensity and post fire effects across a landscape at national and regional scale.

Keywords*: Fuel Mapping, Fuel Management, Accuracy Assessment, Greece, Portugal, Fire Management*

Introduction

Increased wildland fire activity over the last 30 years has had profound effects on budgets and operational priorities of the Forest Service, Civil Protection agencies, Fire Service and local entities with wildland fire responsibilities in Mediterranean Basin. Both the number and the average size of large fires have shown an increasing trend over the last several decades causing extensive financial and ecological losses and often human casualties (Dimitrakopoulos and Mitsopoulos 2006). Mediterranean region is also considered a ''hot spot'' for fire studies, not only because of its high sensitivity to changes in recent decades such as processes of rural depopulation, land abandonment and reduction of traditional forest use but also for the reason that according to the majority of climate models the most likely evolution of this region is towards a hotter and drier climate, with a significantly higher risk of intense heat wave episodes as well as an increase in fire hazard and occurrence (Giannakopoulos *et al*. 2009; Dimitrakopoulos *et al*. 2011; Koutsias at al. 2013).
Fuel maps are an essential tool in fire management since they characterize, in a landscape level, the only factor that fire and land managers can control over many scales – fuel parameters. Coarse resolution fuel maps are useful in global and national fire and fuel hazards assessments because they help fire managers effectively plan, allocate, and mobilize suppression resources (Burgan *et al*. 1998). Regional fuel maps are useful as inputs for simulating fire behavior, fuel consumption, carbon release, smoke dispersion scenarios, as well as for describing fire hazards to support fire suppression and resources deployment (Leenhouts 1998; Leinhan *et al*. 1998). Medium and fine-resolution fuel maps are important for proposing and evaluating tactical fuel treatments, assessing fire hazard and risk, helping in environmental assessments and computing fire danger (Gonzalez *et al*. 2007). However, landscape-level fuel maps have been proved the most appropriate in fire management because they provide the required inputs for the spatially explicit fire behavior and growth models used to simulate fire propagation (Keane *et al*. 2006).
Many different approaches have been used in order to map wildland fuels (Keane at al. 2001; Arroyo *et al*. 2008). Most efforts have tried to map important fuel characteristics such as the fuel model as a

function of vegetation type (Menakis *et al*. 2000) and topography (Rollins *et al*. 2004) to create spatial layers in a Geographical Information System (GIS). Some researchers have qualitatively or quantitatively related fuel information to various forms of remote sensing data at multiple scales, including digital photographs (Oswald *et al*. 1999), LANDSAT images (Wilson *et al*. 1994), ASTER images (Falkowski *et al*. 2005), AVHRR images (Burgan *et al*. 2005), Quickbird and EO-1 Hyperion (Mallinis *et al*. 2014), microwave-radar images (Arroyo *et al*. 2008), and LIDAR data (Mutlu *et al*. 2008). Other efforts have mapped fuels using statistical modeling techniques coupled with detailed field data and knowledge-based systems (De Vasconcelos *et al*. 1994). Recently, the "ArcFUEL" project delivered a complete, up-to-date, methodology for Fuel Classification Mapping (FCM on a Web-Geodatabase) based on "readily available" data, harmonized, accessible & interoperable according to INSPIRE principles, for the Mediterranean region (Bonazountas *et al*. 2012). ArcFuel utilized many and various ancillary data and delivered a consistent and systematic ex novo methodology and workflow for large scale classification and mapping of forest fuels and production of Fuel Classification Maps.

For many reasons it is difficult to map wildland fuels. The most notable factor that prevent accurate mapping is the high temporal and spatial variability of fuel parameters (Keane 2008). Fuel properties are also highly variable and vary across multiple scales; fuel strata consists of many fuel components, including litter, duff, dead twigs, shrubs, herbs and the properties of each component, such as its heat content, moisture content, and size, can be highly variable even within a single type of fuel. The variability of fuel loads within a stand, for example, can be as high as the variability across a landscape, and this variability can be different for each fuel component and property. The main objective of the current study was to assess and validate the accuracy of the Fuel Types maps developed at national scale in Greece and Portugal using the ArcFuel production chain.

Methods

Plots selection

In order to select the validation dataset in both countries the next steps were followed:

- Selection of LUCAS plots matching to the ArcFUEL classification: Based on SQL queries the LUCAS dataset was separated into two subsets of data, one with the LUCAS points of which the description coincided with ArcFUEL characterization and another with the LUCAS points of which it differed (FPP sample). The first subset was used as part of the ArcFUEL validation data set.
- Selection of plots visited in the field, based on the LUCAS dataset: Based on the first step, a stratified random sampling design (considering minimum representation) was applied in representative regions of the two countries and an additional subset created including a number of plots defined for field visit. This subset included conflicting with ArcFuel, LUCAS points and plots located above 1000m of altitude, which aren't considered in the LUCAS data set. Additional plots were added ad hoc during the field survey based on the fuel types occurring in each region according to the estimation of the surveyors. Field surveys have been carried out by trained personnel through the entire country in Greece and Portugal.

Field work

Field work organized for validating ArcFuel map created for the participating countries. It should be stated that ArcFuel map covering the entire country created only for Greece and Portugal. A proper field data collection protocol was defined and field campaings organized in order to create the appropriate data sets for validating the accuracy of the maps for Greece and Portugal. Although a common protocol was used the field survey implemented based on the use of different data collection

technologies. A extended field campaign for collecting information necessary to validate the accuracy of the ArcFuel map was planned covering all the geographic regions of Greece. A suitable field survey daily plan was elaborated, using GPS routing optimization, for reducing travel distances, minimizing total time required for the data collection and comply with vegetation growth status in the regions visited. A commercial GPS application (Navigon) allows reaching nearby the plot, providing its coordinates. In the plot, a properly developed mobile android application installed in a tablet was used for collecting and storing in-situ the information required for the validation purpose. The information collected is based on observations referred to the description of the vegetation composition and the fuel bed horizontal and vertical structure. The ArcFuel android application provides access to a previously uploaded list of survey plots and their relevant data according to the ArcFuel map. These data are presented in a digital form, in which field data are also recorded, supporting thus a direct comparison between mapped and observed data. The field recorded data are uploaded through the web to a proper server on a daily base. Sample screens of the mobile application are shown in Figure 1. The application is available in the Google play store of android applications.

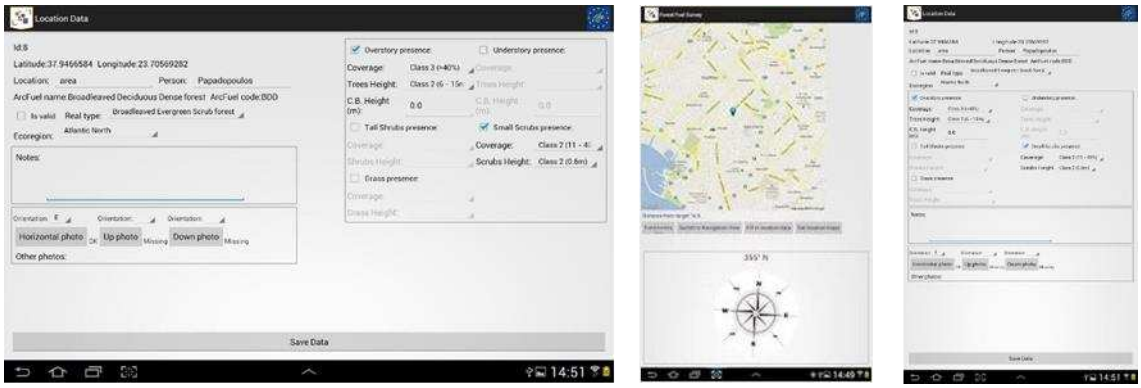

Figure 1. Fuel data collection mobile application of ArcFuel

The field data stored in the server were organized in an on-line data base (http://webservices.g-fmis.com:48080/WebArcfuel/login.jsp) with web interface. Screens of the web interface of the on-line ArcFuel data base of fuel sample plots are shown in Figure 2.

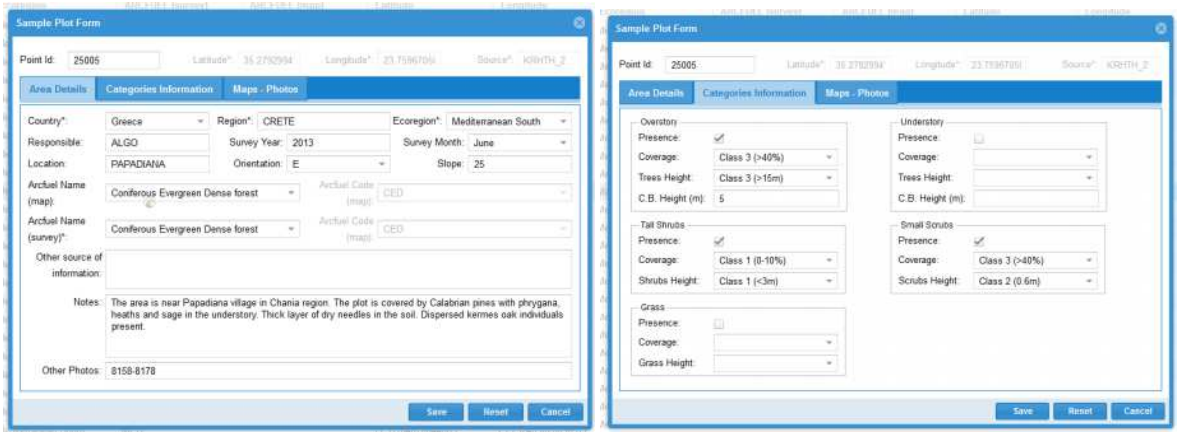

Figure 2. On-line data base of ArcFuel field plots

The data base can be extended with additional data collected in context of relevant forest fuel management campaigns. Thus map validation can be continuous and the ArcFuel mapping accuracy can be improved significantly.

2.3. Accuracy assessment

All the data from the above subsets were aggregated in order to derive the final ArcFUEL validation data set consisting of 1288 points in Greece and 275 in Portugal. In addition, information obtained through photointerpretation of large scale orthophotographs of the KTIMATOLOGIO SA for Greece (http://gis.ktimanet.gr/wms/ktbasemap/default.aspx) which are publicly available through a WMS server and VHR satellite imagery available through Google Earth, was considered along the validation process. During the photointerpretation process, an area equal to 0.25 ha corresponding to the ArcFUEL pixel size, around each point was inspected. To estimate the accuracy of the ArcFUEL map an error matrix was derived. The Kappa coefficient of agreement was also calculated (Fleiss *et al*. 2003). A slightly different methodology was applied in Portugal, deriving the accuracy matrices independently for LUCAS and the remaining field points. Furthermore, three classes that identified "deciduous conifers" during the methodology application were removed from the final analysis as they were considered erroneous a priori. There are no deciduous conifers in Portugal, at least not at a scale that would allow its identification using ArcFUEL methodology.

Results and discussion

For Greece, the overall accuracy was found to be 80.59 % (Figure 3), while the Kappa value was 0.74. For Portugal the overall accuracy was found to be 67% (Figure 4), the Kappa value was 0.63.

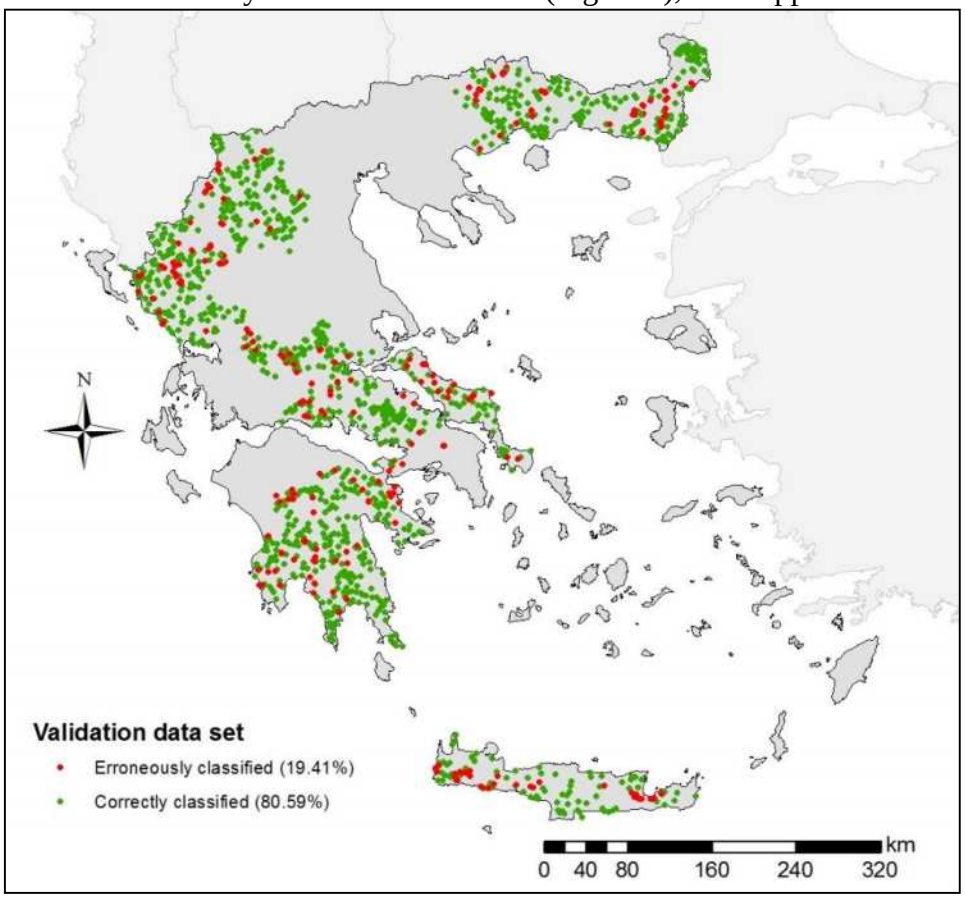

Figure 3. Validation findings based the 1288 point dataset in Greece

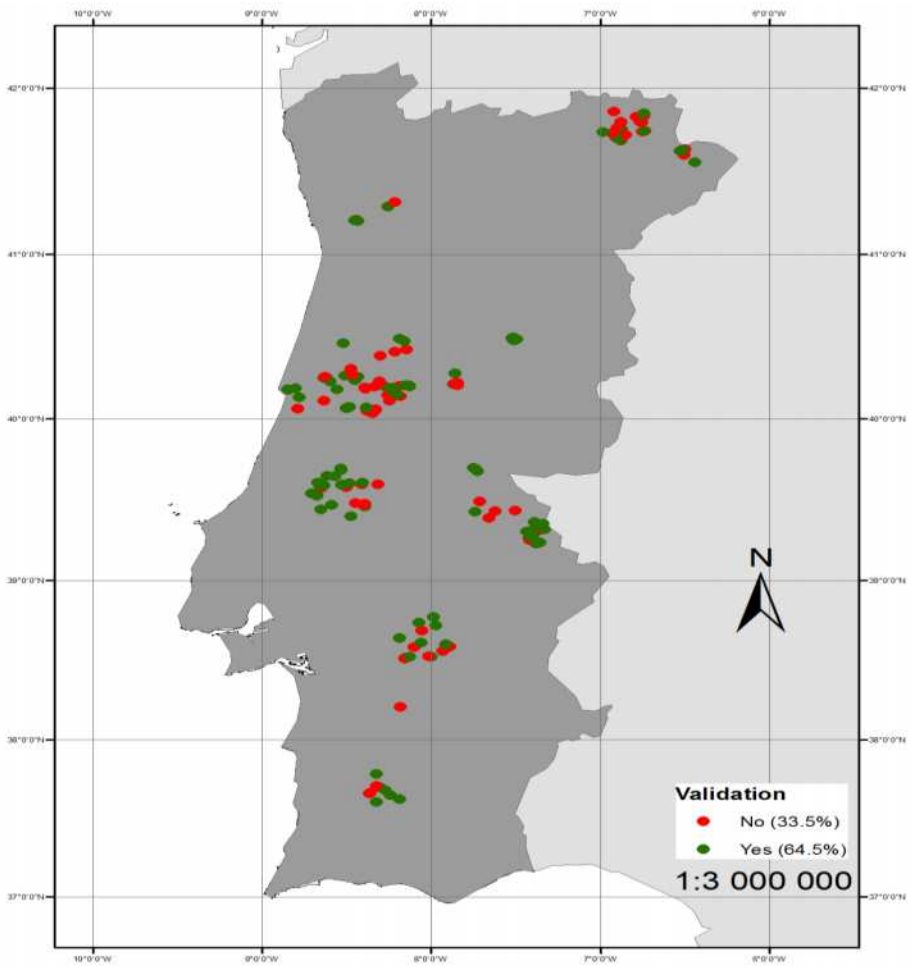

Figure 4. Validation findings based the 1288 point dataset in Greece

Two main efforts have been conducted in Europe for generating fuel maps at large scale. The European Fuel Map developed by Joint Research Center (JRC) (Sebastián López *et al*. 2002), where 44 fuel types were classified by using two databases: the CORINE Land Cover (CLC) and the Map of Natural Vegetation of Europe (MNVE). The CLC classes were stratified into sub-regions according to phyto-sociological criteria, which accounted for the floristic composition and other factors governing the distribution of the vegetation. These sub-regions were then linked to the National Fire-Danger Rating System (NFDRS) Fuel Model map in order to assign a fuel type to each of the sub-regions. The NFDRS fuel load corresponding to each of the fuel model classes was then assigned to each of the fuel models. However, the fairly poor spatial resolution of the datasets prevents the use of the data set for fine scale fire behavior and effects modeling. In 1999, the Prometheus project a new fuel type classification system was developed to better represent the fuel characteristic of the European Mediterranean ecosystems (Lasaponara and Lanorte 2006). However, this classification is principally based on the height and density of fuel, which directly influences the intensity of a wildfire and does not take into consideration the fuel physical and chemical properties which are required for simulating fire behavior and growth. In the USA, the recent LANDFIRE project feature 30-m raster grids of fuel models at national scale by integrating many geospatial technologies including biophysical gradient analyses, remote sensing, vegetation modeling, ecological simulation, landscape disturbance and successional modeling (Rollins 2009).

In United States the most commonly used fuel classifications are the 13 models of Anderson (1982) and the 40 models of Scott and Burgan (2005), all of which are used as inputs in the BEHAVE, FARSITE and FLAMMAP fire prediction systems, and the 26 fire danger models of Deeming *et al*.

(1977) that are used in the US National Fire Danger Rating System. Several surface fuel models are currently used by fire and forest management agencies in the United States, Europe, Canada and Australia, and most of these systems have the same categories, components and description variables (Sandberg 2001). In Mediterranean Basin, Mallinis *et al*. (2008) created a set of custom fuel models that were mapped across a large landscape using Quickbird imagery for input to the FARSITE model. In Italy, Santoni *et al*. (2011) developed two fuel models in order to simulate fire behaviour for various shrubland ecosystems and Bacciu *et al*. (2009) used field loading data to create fuel models for Mediterranean vegetation types for FARSITE simulations. To evaluate fire hazard in Portugal, Fernandes (2009) created a set of 19 fuel models based on the dominant vegetation types in Portuguese forests. Despite of fire behavior studies, fuel classification systems have been used as primary inputs for estimating fuel consumption and smoke emissions models (Reinhardt *et al* 2001), fire danger models (Deeming *et al*. 1977) and fire risk studies (Thompson *et al*. 2011).

Quantitative accuracy assessments are essential for evaluating map quality and fire simulation outputs. Fire growth predictions should, for example, identify those fuel types that generate high fire intensities but are mapped with poor accuracy. Furthermore, accuracy assessments should indicate if additional fuel sampling is needed for the fuel models mapped with a low level of reliability. Accuracy assessments are critical in fuel mapping because most fuel classifications efforts use indirect techniques where the vegetation types are the main mapped entity and not the fuel beds. For that reason, accuracy assessments should be explicitly built into any standardized fuel mapping approach. Moreover, low accuracies could also be a result of inherent sampling and analysis errors such as scale differences in field data and mapped elements, improper use of vegetation as fuels classifications and differences fuel spatial variation.

Conclusions

This study performed an extensive accuracy assessment of the ArcFUEL fuel types based on a field campaign and standard photointerpretation procedures The resulted fuel type maps accompanied by accurate measurements of fuel physical and chemical properties (fuel load, bulk density, surface area to volume ratio, moisture of extinction, heat content) would provide high resolution raster files of fuels which are the required inputs in most fire simulation systems, such as FARSITE and FlamMap. Further validation of the data set by sampling a larger number of field plots would substantially improve the ArcFUEL spatial data set.

Maps depicting fuel types are essential to fire and land management at many scales because they can be used to compute fire hazard, risk, behavior, and effects for planning and real time wildfire applications. Future efforts for classifying and mapping fuels need to incorporate measurements of canopy fuels (e.g., Mediterranean conifer forests), as well as, the quantification of fuel spatial variability in order to play an important role in revising and refining the resulted fuels maps. Since no other spatial fuel data sets exist with capabilities in wildfire behavior and effects, the proposed fuel classification scheme could be applied for supporting fire management activities on interim basis.

Acknowledgements

The research was partially supported by the European Community‘s Environment LIFE+ Program Project ArcFUEL: Forest Fuel Mapping Service (EC-LIFE10 ENV/GR/617).

References

Anderson H (1982) Aids to determining fuel models for estimating fire behavior. USDA, Forest Service Intermountain Research Station, General Technical Report INT-122 (Odgen, UT)

Arroyo L, Pascual C, Manzanera J (2008) Fire models and methods to map fuel types: the role of remote sensing. Forest Ecology and Management 256, 1239–1252.

Bacciu V, Arca B, Pellizzaro G, Salis M, Ventura A, Spano D, Duce P (2009) Mediterranean maquis fuel model development and mapping to support fire modeling. Geophysical Research Abstracts EGU2009- 13148-1.

Bonazountas M, Kallidromitou D, Astyakopoulos A (2012) ArcFIRE™/ArcFUEL™: Forest fire management geoplatform and fuel maps. In: 'Modeling, Monitoring and Management of Forest Fires III' (Eds Brebbia C, Perona G) pp. 1790-1802. (Wit Press)

Burgan R, Klaver R, Klaver J (1998) Fuel models and fire potential form satellite and surface observations. International Journal of Wildland Fire 8, 159-170.

Burgan R, Klaver R, Klaver J (1998) Fuel models and fire potential from satellite and surface observations. International Journal of Wildland Fire 8, 159–170.

Conganlton R (1991) Accuracy assessment and validation of remotely sensed and other spatial information. International Journal of Wildland Fire 10, 321–328.

De Vasconcelos M, Paúl J, Silva S, Pereira J, Caetano M, Catry F. Oliveira T (1994) Regional fuel mapping using a knowledge based system approach. In: '3rd International Conference on Forest Fire Research and 14th Conference on Fire and Forest Meteorology' (Ed Viegas D), pp. 2111–2123. (University of Coimbra)

Deeming J, Burgan R, Cohen J (1977) The National Fire-Danger Rating System - 1978. USDA Forest Service Intermountain Research Station, General Technical Report INT-39 (Odgen, UT)

Dimitrakopoulos A, Vlahou M, Anagnostopoulou Ch, Mitsopoulos I (2011) Impact of drought on wildland fires in Greece; Implications of climatic change? Climate Change 109, 331-347.

Dimitrakopoulos A, Mitsopoulos I (2006) 'Thematic report on forest fires in the Mediterranean Region'. In: A.P. Vuorinen (Ed.), Global Forest Resources Assessment, 2005, Forest Fire Management Working Paper 8, FAO. 43 p.

Falkowski M, Gessler P, Morgan P, Hudak A, Smith A (2005) Characterizing and mapping forest fire fuels using ASTER imagery and remote sensing. Forest Ecology and Management 217, 129–146.

Fernandes P (2009) Combining forest structure data and fuel modelling to classify fire hazard in Portugal. Annals of Forest Science 66, 415- 423.

Fleiss J, Levin B, Paik M (2003) Statistical methods for rates and proportions. 3rd ed. (John Wiley & Sons, Hoboken)

Giannakopoulos C, Le Sager P, Bindi M, Moriondo M, Kostopoulou E, Goodess C (2009) Climatic changes and associated impacts in the Mediterranean resulting from a 2°C global warming. Global Planetary Change 68, 209–224.

Gonzalez J, Kolehmainen O, Pukkala T (2007) Using expert knowledge to model forest stand vulnerability to fire. Computers and Electronics in Agriculture 55, 107–114.

Keane R (2008) Biophysical controls on surface fuel litterfall and decomposition in the northern Rocky Mountains, USA. Canadian Journal of Forest Research 38, 1431-1445.

Keane R, Burgan R, Wagtendonk J (2001) Mapping wildland fuels for fire management across multiple scales: integrating remote sensing, GIS, and biophysical modeling. International Journal of Wildland Fire 10, 301–319.

Keane R, Frescino T, Reeves M, Long J (2006) Mapping wildland fuels across large regions for the LANDFIRE prototype project. In: 'The LANDFIRE prototype project: nationally consistent and locally relevant geospatial data for wildland fire management.' (Eds Rollins M, Frame C) USDA, Forest Service, Rocky Mountain Research Station, RMRS-GTR-175 (Ogden, UT)

Koutsias N, Xanthopoulos G, Founda D, Xystrakis F, Nioti F, Pleniou M, Mallinis G, Arianoutsou M (2013) On the relationships between forest fires and weather conditions in Greece from long-term national observations (1894-2010). International Journal of Wildland Fire 22, 493-507.

Lasaponara R, Lanorte A (2006) Multispectral fuel type characterization based on remote sensing data and Prometheus model. Forest Ecology and Management 234, S226

Leenhouts B (1998) Assessment of biomass burning in the conterminous United States. Conservation Ecology 2, 1–23.

Lenihan J, Daly C, Bachelet D, Neilson R (1998) Simulating broad scale fire severity in a dynamic global vegetation model. Northwest Science 72, 91–103.

Mallinis G, Galidaki G, Gitas I (2014) A comparative analysis of EO-1 Hyperion, Quickbird and Landsat TM imagery for fuel type mapping of a typical Mediterranean landscape. Remote Sensing 6, 1684-1704.

Mallinis G, Mitsopoulos I, Dimitrakopoulos A, Gitas I, Karteris M (2008) Local-scale fuel-type mapping and fire behavior prediction by employing high-resolution satellite imagery. IEEE Journal of Selected Topics in Applied Earth Observations and Remote Sensing 1, 230–239.

Menakis J, Keane R, Long D (2000) Mapping ecological attributes using an integrated vegetation classification system approach. Journal of Sustainable Forestry 11, 245–265.

Mutlu M, Popescu S, Zhao K (2008) Sensitivity analysis of fire behavior modeling with LIDAR-derived surface fuel maps. Forest Ecology and Management 256, 289–294.

Oswald B, Fancher J, Kulhavy D, Reeves H (1999) Classifying fuels with aerial photography in East Texas. International Journal of Wildland Fire 9, 109–113.

Reinhardt E, Keane R, Brown J (2001) Modeling fire effects. International Journal of Wildland Fire 10, 373–380.

Rollins M (2009) LANDFIRE: a nationally consistent vegetation, wildland fire, and fuel assessment. International Journal of Wildland Fire 18, 235–249.

Rollins M, Keane R, Parsons R (2004) Mapping fuels and fire regimes using remote sensing, ecosystem simulation and gradient modeling. Ecological Applications 14, 75-95.

Sandberg D, Ottmar R, Cushon G (2001) Characterizing fuels in the 21st century. International Journal of Wildland Fire 10, 381–387.

Santoni P, Filippi J, Balbi J, Bosseur F (2011) Wildland fire behaviour case studies and fuel models for landscape-scale fire modeling. Journal of Combustion 1, 1–12.

Scott J, Burgan R (2005) A new set of standard fire behavior fuel models for use with Rothermel's surface fire spread model. USDA, Forest Service Rocky Mountain Research Station, General Technical Report RMRS-GTR-153 (Fort Collins)

Sebastián López A, San-Miguel-Ayanz J, Burgan R (2002) Integration of satellite sensor data, fuel type maps and meteorological observations for evaluation of forest fire risk at the pan- European scale. International Journal of Remote Sensing 23, 2713-2719.

Thompson M, Calkin D, Gilbertson-Day J, Ager A (2011) Advancing effects analysis for integrated, large-scale wildfire risk assessment. Environmental Monitoring and Assessment 179, 217-239.

Wilson B, Ow C, Heathcott M, Milne D, McCaffrey T, Ghitter G, Franklin S (1994) Landsat MSS classification of fire fuel types in Wood Buffalo National Park, Northern Canada. Global Ecology and Biogeography Letters 4, 33–39.

Addressing trade-offs among fuel management scenarios through a dynamic and spatial integrated approach for enhanced decision-making in eucalyptus forest

Brigite Botequim [a*], Alan Ager [b], Abílio P. Pacheco[c], Tiago Oliveira [d], Joao Claro [c], Paulo M. Fernandes [e], José G. Borges[a]

[a] *Departamento de Recursos Naturais, Ambiente e Território, Instituto Superior de Agronomia (ISA),Universidade de Lisboa, Tapada da Ajuda, 1349-017 Lisboa, Portugal. *bbotequim@isa.ulisboa.pt, joseborges@isa.ulisboa.pt*
[b] *USDA Forest Service, Pacific Northwest Research Station, Western Wildland Environmental Threat Assessment Center, 3160 NE 3rd Street, Prineville, OR 97754, USA. aager@fs.fed.us*
[c] *INESC TEC (INESC Porto) and Faculdade de Engenharia, Universidade do porto, Campus da FEUP, Rua Dr. Roberto Frias, 378, 4200-465 Porto, Portugal.abilio.p.pacheco@inescporto.pt, jclaro@fe.up.pt*
[d] *Forest Protection, grupo Portucel Soporcel(gPS), Edifício Mitrena, Apartado 55, 2091-861 Setúbal, Portugal.tiago.oliveira@portucelsoporcel.com*
[e] *Centre for the Research and Technology of Agro-Environmental and Biological Sciences (CITAB), University of Trás-os-Montes e Alto Douro, Quinta de Prados, 5001-801 Vila Real, Portugal. pfern@utad.pt*

Abstract
Addressing sustainability concerns in Mediterranean forest ecosystems management with the growing incidence of fires impacting the forest areas over the past decades is a complex task. The current framework was driven taking into account several decision support tools of the United States Wildfire Modeling System for wildfire risk management, which focuses on a three-tiered approach strategy calibrated and applied in Portugal. In addition, contains spatial and temporal dimensions to integrate landscape-scale properties required to meet fire management goals, without encroaching budget constraints, while meeting demands for timber values. Explicitly : i) Developing and applying a Forest System Dynamic Model for identifying temporal stand-scale and understory fuel dynamics, including a site and regional percentage of burnt probability; ii) Building for each landscapes fuel population distribution the expected fire behaviour curve trends, i.e. the corresponding spread rate and flame length using EXRATE tool and FlamMap simulator, respectively, thereby allowing the calculation of changes in the annual expected wood loss; iii) Spatially optimize in the Landscape Treatment Designer tool (LTD) the location of fuel treatments distribution. For testing and demonstration purposes, the research considered an application encompassing three properties of pulp mill's from the Grupo Portucel Soporcel (gPS) in the North, Central and South of Portugal, where eucalypt (E. globulus) is predominant (extent ≈ 3665 ha). A sensitivity analysis was performed by measuring trade-offs among specific treatment scenarios: "treated" vs "untreated" or "treated considering neighbors". The effect of each scenario was changed by a set percentage of optimal parameters and a series of LTD runs was recorded as a project. The protection of the eucalyptus trees from potential wildfires loss was assumed as a key primary goal, following by a set of quantitative target stand structures, budgets and policies constraints in proportion of area treated, and fire behaviour thresholds for each farm. Parameters decisions were assessed to address the identification of thresholds for radical change in fire behavior, and further insight to support hazard-reduction fuel practices. The accuracy of the results demonstrates the usefulness and relevance of the pursued to calculate the potential effect of treatments strategies on improving fire resiliency. Further, the approach provided an overview of management guidelines for fuel modifications to make the gPS eucalyptus farms in Portuguese conditions more resistant to fire, selecting priority intervention areas and designing effective strategies.

***Keywords**: Forest System dynamic Model; Fire behavior; Spread rate; budget constraints; Landscape Treatment Designer; Fuel management strategies.*

Introduction

About 35.4% of the area of Portugal is covered by forest. Nonetheless in the Mediterranean and in Portugal the forest composition is strongly determined by wildfires. Indeed, is the smallest country in southern Europe but has the highest fire incidence in the region. The management of such ecosystems sustaining the forest ecological base, in a changing physical, socio-economic, cultural, demographic and political context is a challenge. Thus, fires should be taken into account when developing forest management plans. We have little or no control over most factors in the fire behavior triangles. However, one element we can control is the common denominator - fuel. Indeed, fire risk and wildfire damage can be reduced by removing or reducing fuels in strategic locations. Fuel structure and flammability are primary conditions for fire spread (Pausas and Paula 2012) and fuel treatments have been found to decrease wildfire size (e.g. Baeza and Vallejo 2008; Rideout *et al.* 2008; Boer *et al.* 2009). Fuel treatment positively affects suppression efforts by reducing fire spread and fire intensity (Rideout *et al.* 2008). Thus, the emphasis today in forest management is on forest restoration and fuels reduction. Nevertheless, there is an urgent need for decision support tools to enable effective fire management.

Where to treat? How much? Shape and size? In this sense, for handling with the complexity of such forest management problems that wildfire risk implies for forest owners and policy-makers, the present research try to answer the above-mentioned questions focusing on techniques for address the problem of spatially optimize treatments to prioritize fuel management activities, aimed at disrupt fire spread and protect eucalyptus areas from burning without have loss of important ecological and commercial timber values. For that purpose, a Forest System Dynamic Model have been developed and coupled with spatial optimization software (Landscape Treatment Designer - LTD, Ager *et al.* 2012) to design efficient landscape fuel treatment plans.

The current framework includes a three-tiered approach strategy such as i) developing a Forest System Dynamic Model; ii) Characterizing the expected fire behaviour characteristics (e.g. spread rate and flame length); iii) Explore the optimal levels of fuel landscape treatment configurations in the LTD tool. The pursued are tested and results are discussed for a large-scale application encompassing over 3365 ha of eucalyptus in North, Centre and Southern Portugal.

Methods

The framework presented here was based on an extensive literature review (e.g. Finney 2003; Alan *et al.* 2013), field work to assign fuel model distribution, and analysis of a database within three Eucalyptus farms located in the North (1471, 48 ha), Centre (173, 34 ha) and South region (2020, 34 ha) from the Grupo Portucel Soporcel (gPS), a European company dedicated to produce and market high quality paper for office and offset uses (Figure 1). Inventory data represent conditions of the year 2013 in the study area.

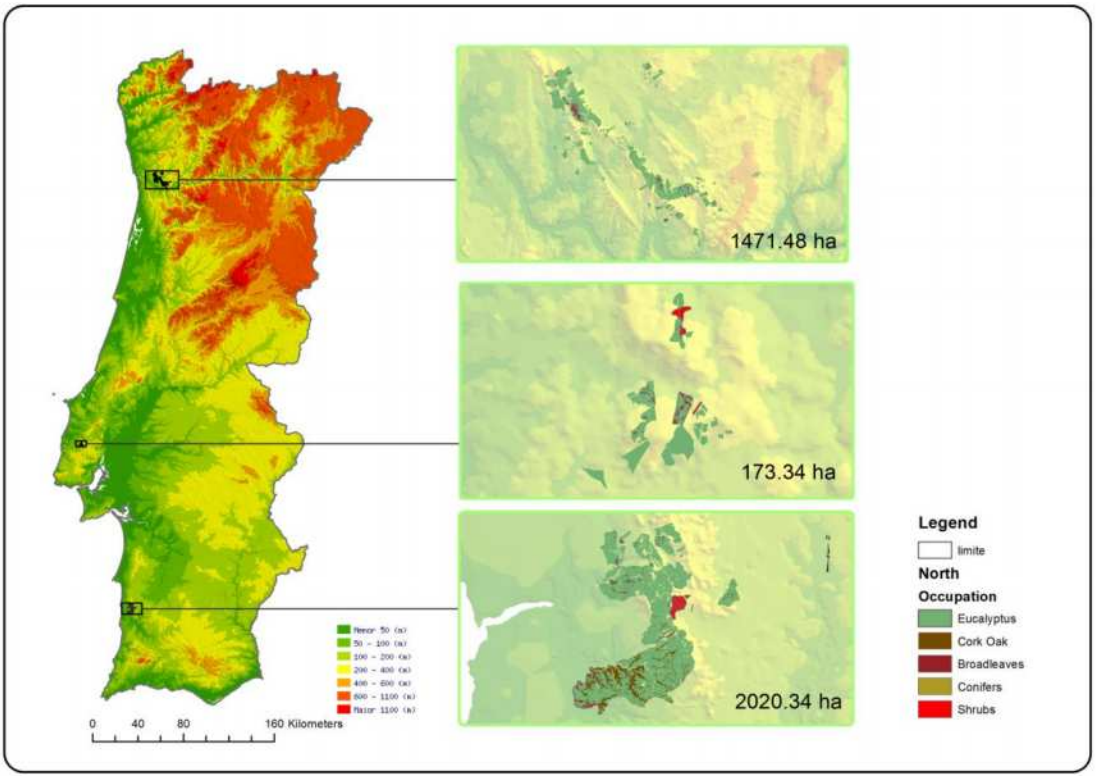

Figure 1. Portugal: location and cover types of the three farms from the Grupo Portucel Soporcel

Developing a Forest System Dynamic Model

In order to identify temporal trends for guiding LTD, a Forest System Dynamic Model (FSDM) was developed to examine stand-scale and fuel dynamics. The model incorporates both well-defined, quantitative field data and qualitative expert gPS opinion. Note that all the spatial fuel types under eucalyptus cover were collected "in loco" and assessed by the field guide-fuel from Project Vesta (Cheney *et al.* 1998; Gould *et al.* 2007). Further, enumerated using a set of customized fuel models developed for eucalyptus stands in Portugal (Fernandes *et al.* 2009). Such dynamic model was used to classify fuel over time due to planting operations, harvesting, and vegetation regrowth.

In addition, an estimate of total burnt probabilities (TBP, %) on each eucalyptus farm was also integrated in the model as a "burnt factor" based on landscape and site scale wildfire modelling information available in Portugal. In the former, each stand burns considering an adjusted burnt probability based on the regional fire frequency analysis (Oliveira *et al.* 2012) and the fire regimes at the municipality-level obtained by multiple correspondence analysis and spatial clustering (Pereira *et al*. submitted). For the site-scale the probability of wildfire occurrence in Eucalyptus stands was calculated by Botequim *et al.* (2013). Furthermore, wildfire impacts and resulting damage over time at stand and tree level across the eucalyptus farms was include using Marques *et al.* (2012) post- fire mortality equations. Thus, landscape data were generated for random mixtures of several fuel types in various proportions over time and replicated because of expected variation in weather scenarios (increase the number of additional fuel configurations).

2.2. Characterizing the expected fire behaviour characteristics

Current fire behavior characteristics for each stand, i.e. spread rate (SR, m/min) and flame length (FL, m) for randomness of the fuel arrangements was calculated on the program EX-RATE (Finney 2003) and FlamMap simulator (Finney 2006), respectively. Each fuel configuration has a well-defined maximum spread rate (minimum travel time algorithm, Finney 2003). Different spread rate ratios show a sigmoid trend over the range of proportions of fuel populations. These outputs can be used to estimate

the change in the annual expected timber loss (TL), as well to demonstrate reductions in the ΔSR and ΔFL from the effect of fuel treatments, to further aid in spatial allocation of fuel strategies across the eucalypt farms.

2.3. Explore the optimal levels of fuel landscape treatments

Spatial data for each farm indicating: (i) potential fire behavior as represented by SR and FL, (ii) expected TL in the stand for both treat and untreated conditions (iii) stand area (ha), (iv) biometric patterns such as crown base height (CBH), crown bulk density (CBD), type of fuel model (shrub or litter) for predicting fire activity (Botequim *et al.* in preparation); and (v) annual budget capacity for gPS fire management, was created to explore in LTD tool (Ager *et al.* 2012) the optimal levels of fuel landscape treatment configurations.

The protection of the eucalyptus trees from potential wildfires loss was assumed as primary goal, i.e. minimize the total predicted expected TL and maximize delta SR. Activity constraints on policy and annual budget restrictions to represent the total treatment allowance (area, ha) for fire management were considered. Thresholds were measured by potential FL, and a set of biometric patterns for each eucalypt stands.

In addition, to better understand how expected loss was affected by the above treatment parameters a sensitivity analysis using several LTD simulations was performed across all the stands in response to different investment levels, treatment intensity. The trade-offs associated with these divergent management strategies including percentage of treated and untreated areas to calculate potential mortality to eucalyptus trees were quantified to examine change in risk on improving fire resiliency.

Results

The current work expands the application in fuel spatial optimization for eucalyptus stands, and demonstrates a decision support approach computationally feasible to address the most fire-prone areas in each region and prioritize fuel management efforts based on respective management goals. The model seeks to locate project areas to most efficiently reduce potential wildfire loss of fire resilient eucalyptus trees while creating contiguous areas within which managed fire can be effectively used to maintain low-hazard conditions. Indeed, the approach identifies the aggregate of polygons that minimize the expected timber loss E(TL), and maximize the delta Spread rate (ΔSR) objectives, and the polygons that require treatment, i.e. the percentage of stand - treatment densities optimal in terms of the overall reduction in the potential wildfire mortality. Furthermore, the sensitivity analyses based on a series of test landscapes allows the identification of investment trade-offs with easily interpretable results. Finally, this research have real implications for spatial strategies of fuel treatments on gPS farms, and can contribute to enhance the coordination of seasonal budget for fire prevention, directing their actions to the most susceptible areas in case of extreme, and uncontrollable, weather events.

Acknowledgment

This work was financed by the European Regional Development Fund (ERDF) through the COMPETE Programme (Operational Programme for Competitiveness), by National Funds through the Fundação para a Ciência e a Tecnologia (FCT, Portuguese Foundation for Science and Technology) within projects «FCOMP - 01-0124-FEDER-022701» and «FIRE-ENGINE - Flexible Design of Forest Fire Management Systems/MIT/FSE/0064/2009», in the scope of the MIT Portugal Program, and by grupo Portucel Soporcel. FCT has also supported the research performed by Brigite Roxo Botequim (Grant SFRH/BD/44830/2008) and by Abílio P. Pacheco (Grant SFRH/BD/92602/2013).

References

Ager AA, N. Vaillant DE, Owens S, Brittain JH (2012) Overview and example application of the Landscape Treatment Designer. PNWGTR- 859. USDA Forest Service, Pacific Northwest Research Station, Portland, Oregon, USA.

Ager AA, Vaillant, NM, McMahan A (2013) Restoration of fire in managed forests: a model to prioritize landscapes and analyze tradeoffs. *Ecosphere* **4**:art29.

Baeza MJ, Vallejo VR (2008) Vegetation recovery after fuel management in Mediterranean shrublands. *Appied Vegetation Science* **11**:151–158.

Boer MM, Sadler RJ, Wittkuhn RS, McCaw L, Grierson PF (2009) Long-term impacts of prescribed burning on regional extent and incidence of wildfires e evidence from 50 years of active fire management in SW Australian forests. *Forest Ecology and Management* **259**, 132-142

Botequim B, Garcia-Gonzalo J, Marques S, Ricardo A, Borges JG, Oliveira MM, Tomé J, Tomé M (2013). Developing wildfire risk probability models for Eucalyptus globulus stands in Portugal. *iForest* **6**:217-227. doi: 10.3832/ifor0821-006.

Botequim B, Fernandes PM, Garcia-Gonzalo J, Silva A, Borges J. Modeling fire behavior and risk in Portuguese´s forest: guidelines for sustainable landscape management (unpublished data).

Cheney NP, Gould JS, McCaw L (1998) Project Vesta: research initiative into the

effects of fuel structure and fuel load on behaviour of wildfires in dry eucalypt forest. In: Proceedings 13th International Conference of Forest Fire and Meteorology. International Association of Wildland Fire, pp. 375–378.

Cheney NP, Gould JS, McCaw L, Anderson WR (2012) Predicting fire behaviour in dry eucalypt forest in Southern Australia. *Forest Ecology and Management* **280**,120-131.

Fernandes P, Gonçalves H, Loureiro C, Fernandes M, Costa T, Cruz M, Botelho 2009. Modelos de combustível florestal para Portugal. Proceedings Congresso Florestal Nacional, Açores.

Finney M (2003) Calculation of fire spread across random landscapes. *International Journal of Wildland Fire* **12**, 167-174.

Finney M (2006) An overview of FlamMap fire modeling capabilities. In: Andrews PL, Butler BW (eds) Fuels management-how to measure success:conference proceedings.RMRS-P-41. USDA Forest Service, Rocky Mountain Research Station,Portland, pp 213–220.

Gould JS, McCaw WL, Cheney NP, Ellis PE, Knight IK, Sullivan AL (2007) Project Vesta. Fire in Dry Eucalypt Forest: Fuel Structure, Fuel Dynamics, and Fire Behaviour. Ensis-CSIRO, Canberra, ACT and Department of Environment and Conservation, Perth, WA, Australia.

Marques S, Garcia-Gonzalo J, Borges JG, Botequim B, Oliveira MM, Tomé J, Tomé M (2011) Developing post-fire Eucalyptus globulus Labill stand damage and tree mortality models for enhanced forest planning in Portugal. *Silva Fennica* **45** (1): 69-83. ISSN 0037-5330.

Oliveira S, Pereira JMC, Carreiras JMB (2012). Fire frequency analysis in Portugal (1975-2005), using Landsat-based burnt area maps. *International Journal of Wildland Fire* **21**,48-60.

Rideout DB, Ziesler P, Kling R, John B, Loomis R, Botti SJ (2008). Estimating rates of substitution for protecting values at risk for initial attack planning and budgeting. *Forest Policy and Economics* **10**, 205-219.

Analysis of burnt areas and number of forest fires in the Iberian Peninsula

Marta M. Mato[c], José Luis Legido [c], Eva Miguez[c], Vicente Caselles[d], Eulogio Jiménez[e], Tarsy Carballas[b], Maria I. Paz Andrade[a]

[a] *Departamento de Física Aplicada, Microcalorimetría, Facultad de Física, Universidade de Santiago de Compostela, Campus Universitario Sur, E-15782 Santiago de Compostela, Spain, inmaculada.paz.andrade@usc.es*
[b] *Instituto de Investigaciones Agrobiológicas de Galicia (IIAG-CSIC), Campus Universitario Sur, Apartado 122, E-15780 Santiago de Compostela, Spain, tcf@iiag.csic.es*
[c] *Departamento de Física Aplicada, Universidade de Vigo, Vigo, Spain, xllegido@uvigo.es*
[d] *Departamento de Física de la Tierra y Termodinámica, Universidad de Valencia, Valencia, Spain, vicente.caselles@uv.es*
[e] *Departamento de Física, Universidade de A Coruña, A Coruña, Spain, ejimenez@udc.es*

Abstract
The Iberian peninsula has suffered for many years from large scale forest fires, which in the past decades have been devastating for all components of the environment: destruction of biological systems, loss of organic matter from soils and alteration of atmospheric and climatic processes.
In this study we analyse the variation in number and burnt areas in the Iberian Peninsula (Portugal and Spain), using mathematical functions. The results obtained are compared with other European Mediterranean countries such as France, Italy and Greece. More than 1.5 million fires were recorded in the Mediterranean countries between 1980 and 2011, involving a burnt area of approximately 15 million hectares, where 67% of the fires and 60% of the burnt area lay in the Iberian Peninsula. Upon using the adjustment functions, the evolution of the number of fires in the Iberian Peninsula shows a growth rate between 1980 and 2000, while a decline in fires was observed after 2001. There is a continuous decrease in burnt area throughout these years.
The evolution of the number of fires in Spain and Portugal presents a behaviour that is quite similar to that in the Mediterranean countries. However, this is not true for the burnt areas, where an increase in Spain from 1980 to1985 was observed, and this decreased after 1986. Portugal on the other hand presents an increase in burnt areas from 1985 to 2003.

***Keywords**: Iberian peninsula, burnt areas, number of forest fire, mathematical function*

Introduction

Spain like Portugal and other Mediterranean countries are suffering the dramatic consequences of the forest fires, which in the last years have produced a big deforestation that provokes degradation of the environment and important socio-economical losses. Their direct destructive effects are manifested in all components of the environment: the vast forest area burnt (forest and scrub); the destruction of the fauna; the loss of soil organic matter, with the consequent variation of all its properties and the loss of soil quality; and altering atmospheric and climatic processes due to particles and smoke released by the fire, which also contains hydrocarbons, greenhouse gases and toxic substances for humans and animals In addition, there are indirect effects caused by the destruction of the vegetation cover, which leaves the soil unprotected against the impact of the rain, and subsequent post-fire erosion, producing the drag of the finest components of topsoil (seeds, organic and inorganic substances) necessary for normal development of the vegetation, and in extreme conditions, the irreversible loss of soil and even the rock outcrop. The drag of water and sediments caused by the erosion and deposition away from the fire epicenter will alter aquatic and marine ecosystems and habitat for fish, shellfish, etc. This has

negative social and economic impacts. Consequently, it is of paramount importance to develop efficient tools for the integral forest fire fighting.

Most of the total burned area and the largest numbers of fires in Europe are found in southern European countries, namely in Portugal, Spain, France, Italy and Greece. The characteristics that define the fire events have been characterised using qualitative or quantitative methods, from local to regional or global scales. For example, San-Miguel-Ayanz *et al*. (2013) published an analysis of trends in the number of forest fires and burnt areas in the Mediterranean region (Galicia-Spain, Portugal and Greece). Pereira *et al.* (2011) studied the number of fires per year and burnt area per year for five Mediterranean countries (Portugal, Spain, France, Italy and Greece). Sarris and Koutsias (2014) investigated correlations between climate, vegetation and fire statistics in four Mediterranean countries (Spain, France, Italy and Greece). Oliveira *et al*. (2012) identified the main structural factors that explain the likelihood of fire occurrence at Europan scale (Portugal, Spain, France, Italy, Greece). The factors influencing fire occurrence, fire risk, or fire statistics in Mediterranean countries, have been investigated at local or regional level by several authors who have focused on Portugal (Viegas *et al*. 1992; Moreira *et al*. 2001), Spain (Chuvieco *et al.* 2009; Fuentes-Santos *et al*. 2013; Moreno and Chuvieco 2013; Martínez-Fernández *et al*. 2013; Turco *et al.* 2013; Martin-Martin *et al*. 2013), France (Ganteaume and Jappiot 2013; Sarris and Koutsias 2014), Italy (Salis *et al.* 2014), Croatia (Jurjevic *et al.* 2009) and Greece (Koutsias *et al*. 2012; Koutsias *et al*. 2013; Sarris and Koutsias 2014; Polychronaki and Gitas 2012).

The principal aim of this paper is to analyse the variation in number of fires and burnt areas in the Iberian Peninsula (Portugal and Spain), using mathematical functions.

Methods

Study area and fire databases

The study area for this investigation is the entire Iberian Peninsula (figure 1). This region is located in south-western Europe (western Mediterranean Basin), and includes two countries: Portugal and Spain. The results obtained are compared with other European Mediterranean countries such as France, Italy and Greece.

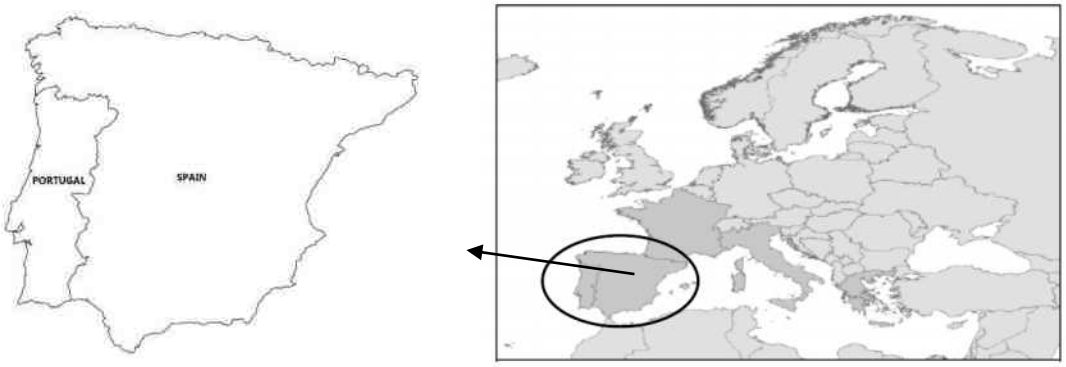

Figure 1. Study area.

In order to compile the required information for the temporal analysis on the variation in number of fires and burnt area in the Iberian Peninsula, a fire database for the Iberian Peninsula was developed from the information contained in both national official databases. The Spanish Forest Fire Prevention Service compiles a fire database based on the forest fire reports by the autonomous regions and provinces, since 1968. Data of fire occurrence and burned area in Portugal and Southern most affected European Countries (Spain, Portugal, France, Italy and Greece) were obtained from the Autoridade

Florestal Nacional (AFN) and from Join Research Center (JRC Tecnical Reports, Forest Fires in Europe Middle East and North Africa 2011), respectively. The data series from 1980 to 2011 was used in the present study.
More than 1.5 million fires were recorded in the Mediterranean countries between 1980 and 2011, involving a burnt area of approximately 15 million hectares, where 67% of the fires and 60% of the burnt area lay in the Iberian Peninsula and 31% of the fires and 36% of the burnt area corresponding to Spain.

Equations

In this study, data of the number of forest fires and burnt area in the Spain, Portugal, Iberian Peninsula and European Mediterranean countries (Portugal, Spain, France, Italy and Greece) from 1980 to 2011 were fitted to variable-degree polynomials such as:

$$f(x) = \sum_{i=1}^{n} A_i \cdot x^{i-1} \qquad (1)$$

where $x = x' - x_o$, x' is the year of study, $x_o = 1979$ is the year zero, f(x) is the number of fires or the burn area in the study interval. The fitting parameters A_i were computed from the unweighed least-squares method using a non-linear optimization algorithm.

In addition, the burned area and the number of fires have been considered to assess the evolution of forest fires in the different temporal periods. Then, mean number of fires and mean area burned are studied in periods of two years, three years, four years, and so on.

Results

Trends in number of fires and burnt areas in the Iberian Peninsula, Spain and Portugal was analysed. The results obtained in this study were compared with the trends followed by the set of several Mediterranean countries. Figure 2 shows the annual series of burned area and number of fires in the Iberian Peninsula, in España and Portugal, and in the set of Mediterranean countries (España, Portugal, France, Italy and Greece).

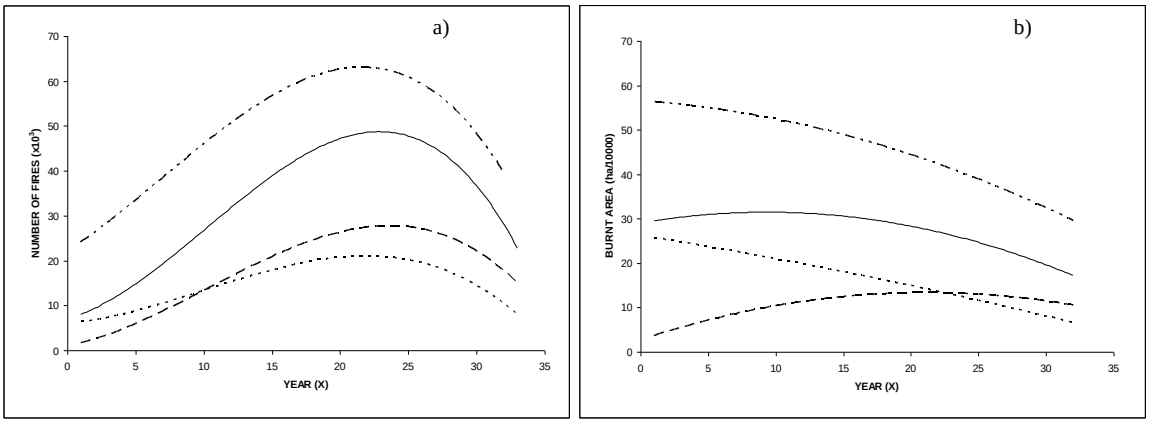

Figure 2. a) Evolution of the forest fire number registered between 1980 and 2011, b) Evolution of the burned area between 1980 and 2011. — · · — Set of the mediterranean countries, ——Iberian peninsula, – – – – Portugal, ·····Spain

It can be seen that the evolution of the number of fires in the Iberian Peninsula shows a growth rate between 1980 and 2000, while a decrease of fires is observed after 2001. The number of fires in Spain and Portugal has a very similar trend. Moreover, there is a continuing decline in the area burned along these years in Spain, Iberia Peninsula and in the set of Mediterranean countries studied. However, it is noted that in Portugal the area burned increases smoothly along these years.
The functions obtained for annual data shown in Figure 2 are compared with the obtained functions for the mean data in several time intervals, of between 2 and 5 years, presented in Figure 3. The best correlations were obtained with polynomials of degree three for the number of fires and polynomials of degree two for area burned. The coefficients of correlation obtained from the fitting curves of degree three for the mean number of fires are shown in Table 1.

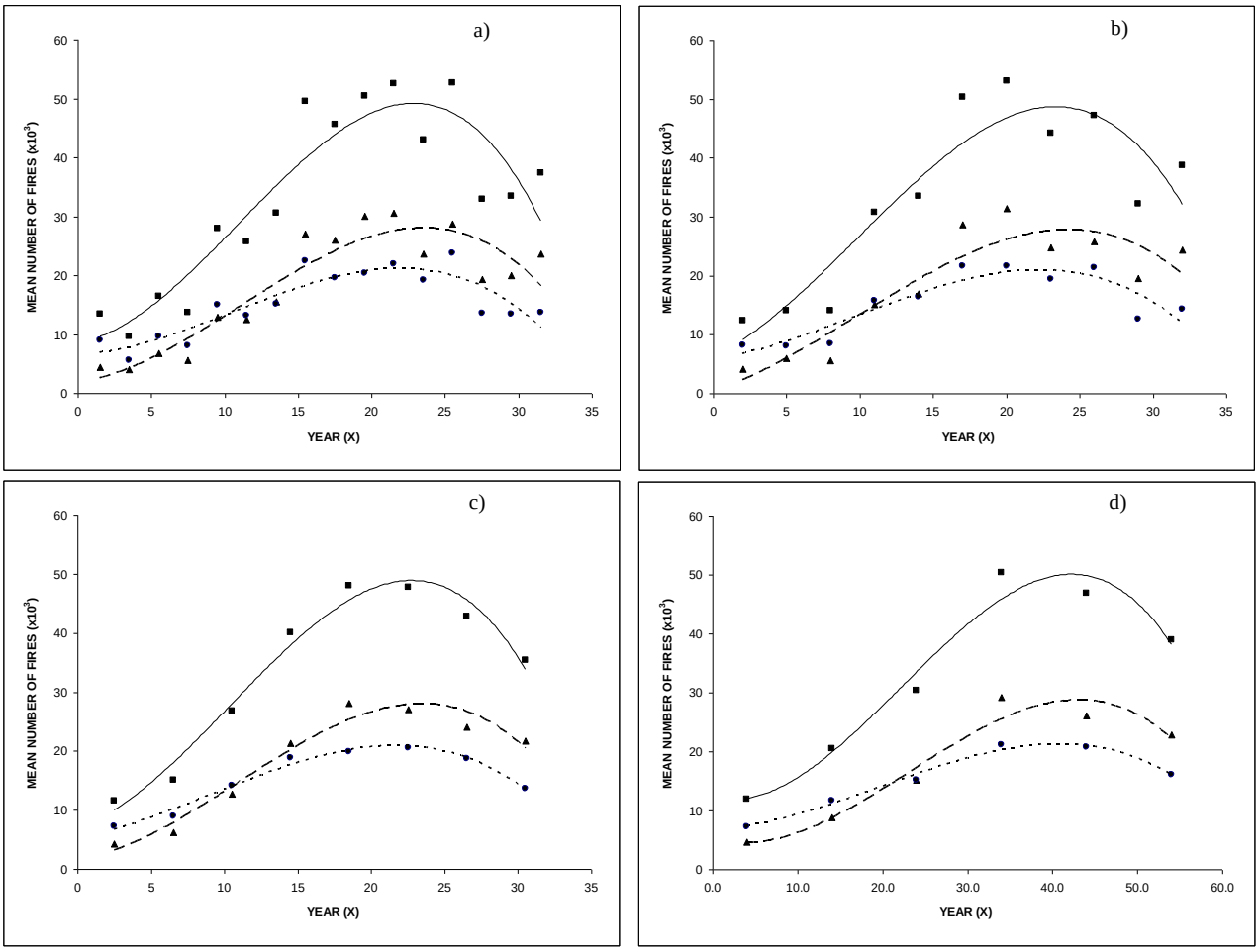

Figure 3- Evolution in several time intervals of the forest fire number registered between 1980 and 2011. a) 2 years, b) 3 years, c) 4 years, d) 5 years. Fitting curves: —— Iberian peninsula, – – – – Portugal, ·····Spain. Mean number of fires: ■ Iberian Peninsula, ▲ Portugal, ● Spain.

Table 1. The correlation coefficients, R^2, of the fitting curves of degree three for the number of fires.

	1 year	2 years	3 years	4 years	5 years
Iberian Peninsula	0.7163	0.8453	0.8433	0.9752	0.9647
Portugal	0.7709	0.8568	0.8411	0.9606	0.9466
Spain	0.6591	0.7967	0.8302	0.9815	0.9849

A similar study to that presented in Table 1 for the number of fires was performed to analize the area burned. The best results were obtained with a time interval of 4 years, for both the number of fires as for the burned area.
From the fitting curves, the maximum value for the mean number of fires in the Iberian Peninsula is about 47 000 fires in 2002, around 28 000 fires in Portugal for 2002, and 22 000 fires in Spain for 2001. In accordance with real data.

References

Chuvieco E, González I, Verdú F, Aguado I, Yebra M (2009) Prediction of fire occurrence from live fuel moisture content measurements in a Mediterranean ecosystem *International Journal of Wildland Fire* **18**, 430–441.

Fuentes-Santos I, Marey-Pérez MF, González-Manteiga W (2013) Forest fire spatial pattern analysis in Galicia (NW Spain) *Journal of Environmental Management* **128**, 30-42.

Ganteaume A, Jappiot M (2013) What causes large fires in Southern France *Forest Ecology and Management* **294**, 76–85.

García Lázaro JR, Moreno Ruiz JA, Arbeló M (2013) Effect of spatial resolution on the accuracy of satellite-based fire scar detection in the northwest of the Iberian Peninsula *International Journal of Remote Sensing* **34**, 4736–4753.

Jurjevic P, Vuletic D, Gracan J, Seletkovic G (2009) Forest fires in the Republic of Croatia (1992-2007) *Sumarski List* **133**, 63-72.

Koutsias N, Arianoutsou M, Kallimanis AS, Mallinis G, Halley JM, Dimopoulos P (2012) Where did the fires burn in Peloponnisos, Greece the summer of 2007? Evidence for a synergy of fuel and weather *Agricultural and Forest Meteorology* **156**, 41– 53.

Koutsias N, Xanthopoulos G, Founda D, Xystrakis F, Nioti F, Pleniou M, Mallinis G, Arianoutsou M (2013) On the relationships between forest fires and weather conditions in Greece from long-term national observations (1894–2010) *International Journal of Wildland Fire* **22**, 493–507.

Martinez-Fernandez J, Chuvieco E, Koutsias N (2013) Modelling long-term fire occurrence factors in Spain by accounting for local variations with geographically weighted regression *Nat. Hazards Earth Syst. Sci.* **13**, 311–327.

Martín-Martín C, Bunce RGH, Saura S, Elena-Rosselló R (2013) Changes and interactions between forest landscape connectivity and burnt area in Spain *Ecological Indicators* **33**, 129– 138.

Moreira F, Rego FC, Ferreira PG (2001) Temporal (1958–1995) pattern of change in a cultural landscape of northwestern Portugal: implications for fire occurrence *Landscape Ecology* **16**, 557–567.

Moreno MV, Chuvieco E (2013) Characterising fire regimes in Spain from fire statistics *International Journal of Wildland Fire* **22**, 296–305.

Oliveira S, Oehler F, San-Miguel-Ayanz J, Camia A, Pereira JMC (2012) Modeling spatial patterns of fire occurrence in Mediterranean Europe using Multiple Regression and Random Forest *Forest Ecology and Management* **275**, 117–129.

Pereira MG, Malamud BD, Trigo RM, Alves PI (2011) The history and characteristics of the 1980–2005 Portuguese rural fire database *Nat. Hazards Earth Syst. Sci.* **11**, 3343–3358.

Polychronaki A, Gitas IZ (2012) Burned area mapping in Greece using SPOT-4 HRVIR images and object-based image analysis *Remote Sens.* **4**, 424-438.

Rego F, Catry FX, Montiel C, Karlsson O (2013) Influence of territorial variables on the performance of wildfire detection systems in the Iberian Peninsula *Forest Policy and Economics* **29**, 26–35.

Román MV, Azqueta D, Rodrígues M (2013) Methodological approach to assess the socio-economic vulnerability to wildfires in Spain *Forest Ecology and Management* **294**, 158–165.

Salis M, Ager AA, Finney MA, Arca B, Spano D (2014) Analyzing spatiotemporal changes in wildfire regime and exposure across a Mediterranean fire-prone area *Natural Hazards* **71**, 1389-1418.

San-Miguel-Ayanz J, Manuel Moreno J, Camia A (2013) Analysis of large fires in European Mediterranean landscapes: Lessons learned and perspectives *Forest Ecology and Management* **294**, 11-22.

Sarris D, Koutsias N (2014) Ecological adaptations of plants to drought influencing the recent fireregime in the Mediterranean *Agricultural and Forest Meteorology* **184**, 158– 169.

Turco M, Llasat MC, Tudela A, Castro X, Provenzale A (2013) Decreasing fires in a Mediterranean region (1970–2010, NE Spain) *Nat. Hazards Earth Syst. Sci.* **13**, 649–652.

Viegas DX, Viegas TP, Ferreira AD (1992) Moisture content of fine forest fuels and fire occurrence in central Portugal *International Journal of Wildland Fire* **2**, 69–85.

Anticipating the severity of the fire season in Northern Portugal using statistical models based on meteorological indices of fire danger

Sílvia A. Nunes[a], Carlos C. DaCamara[a], Kamil F. Turkman[b], Sofia L. Ermida[a], and Teresa J. Calado[a]

[a] *Instituto Dom Luiz, Faculdade de Ciências, Universidade de Lisboa, 1749-016 Lisboa, Portugal, sanunes@fc.ul.pt, cdcamara@fc.ul.pt , snermida@fc.ul.pt , mtcalado@fc.ul.pt*
[b] *DEIO-CEAUL, Universidade de Lisboa, 1749-016 Lisboa, Portugal, kfturkman@fc.ul.pt*

Abstract
Climate and weather are major drivers of fire activity in Portugal. The aim of the present study is to assess the role of meteorological factors on the inter-annual variability of burned area, for the period 1980-2011, over a region of Central Portugal. Although occupying only 18% of the territory of Portugal, the chosen area is responsible for 43% of all the burned area in August during the study period.
A normal distribution model is fitted to the decimal logarithms of monthly burned area during August over the study area. This model is then improved by introducing as covariates two different measures of prevailing meteorological conditions as derived from Daily Severity Rate (DSR), namely a top-down factor which consists of daily cumulated values of DSR from April up to July and a bottom-up factor defined as the square root of the mean of the squared daily positive deviations of DSR in August from the daily climatology. The two models are used to derive a model of fire severity that allows quantifying the probability of having a severe or weak fire season.

Keywords*: fire activity, burned area, indices of fire danger, meteorological conditions, statistical models*

Introduction

The number and extension of fires and the large amounts of burned area that are observed in Mediterranean Europe have strong adverse impacts at the social, economic, ecological and environmental levels that include the destruction and change of the landscape and the emission of greenhouse gases (Pausas and Vallejo, 1999). The increase in temperature that is to be expected according to future climate scenarios may also turn more frequent fire episodes of large magnitude (Flannigan *et al*., 2013; Liu *et al*., 2010; Mori and Johnson, 2013; Yongqiang *et al*., 2010). It is therefore crucial to improve our knowledge about fire behaviour (especially about extreme fire events), that will help taking adequate measures to mitigate the adverse effects.
The Mediterranean region is responsible for 85% of burned area in Europe, causing extensive economic losses and ecological damages (San-Miguel-Ayanaz *et al*., 2013). In particular, Portugal presents the highest score of fire occurrences in the Mediterranean Basin (Pereira *et al*., 2005). According to official records of *Instituto de Conservação da Natureza e das Florestas* (ICNF), the Portuguese authority for forests, 3,468,986 hectares have burned in Continental Portugal during the period 1980-2011, the equivalent to three fifths of the total forested area of the country; in the last few years, a significant increase has also been observed in the amount of total burned area, number of large fires and fire severity (Pereira *et al*., 2011).
Fire activity in Mediterranean Europe, is a natural phenomenon linking climate, humans and vegetation (Lavorel *et al*., 2007). Fire activity is therefore conditioned by natural and anthropogenic factors (San-Miguel-Ayanz *et al*., 2003). According to Costa *et al*. (2011) and Ganteaume *et al*. (2013) the most important factors for fire occurrence in Mediterranean Europe are anthropogenic and environmental. The first one is the main cause of ignition, reaching 95% of all cases (San-Miguel-Ayanz *et al*., 2013) whereas the most significant environmental factors are weather, fuel availability and topography. Even though most of fire events are human caused, several studies show that climate

and associated weather conditions are major drivers for fires with extensive burned area. For instance, rainy and mild winters followed by warm and dry summers lead to high levels of vegetation stress making the region particularly prone to the occurrence of fire events (Pereira *et al*., 2005); while precipitation and temperature in the pre-fire season have a determinant role in fuel availability and vegetation stress, temperature, wind and precipitation in the fire season are crucial for the development and extinction stages (Aldersley *et al*., 2011; Dale *et al*., 2001; Pereira *et al*., 2013; Trigo *et al*., 2013). The aim of the present study is to contribute to a better understanding of the meteorological factors that affect the inter-annual variability of burned area in August over a region in Central Portugal. Meteorological information is used to derive the so-called Daily Severity Rate (DSR), an index of fire danger that is part of the Canadian Forest Fire Weather Index System (CFFWIS). This index is then used to characterize the pre-fire season in terms of levels of heat and stress of vegetation, as well as an indicator of extreme meteorological conditions taking place in summer. A normal distribution model is fitted to the decimal logarithms of monthly burned area during August over the study area. This model is then improved by introducing as covariates two different measures of prevailing meteorological conditions as derived from the Daily Severity Rate (DSR); a top-down factor, DSR_{td}, which consists of daily cumulated values of DSR from April up to July and a bottom-up factor, DSR_{bu}, defined as the square root of the mean of the squared daily positive deviations of DSR in August from the daily climatology. A model of fire severity is finally derived that allows quantifying the probability of having a severe or weak fire season.

Data and methods

Study area and period

The study area is located in Central Portugal (Figure 1) and encompasses 53 counties (*concelhos*). The study area covers 1,805,226 ha, 30% of which are covered by forest. The two main species in the forested area are *Pinus Pinaster* (58%) and *Eucalyptus* (22%). The high percentage values of maritime pine and eucalyptus, that are extremely flammable in summer (Núñez-Regueira *et al*., 1996), can explain the fact that although the study area occupies only 18% of all the territory of Portugal it is responsible for 43% of the total burned area in August during the study period (Figure 2).

Figure 1. Location of the study area (left panel), RGB zoom image of the area from ArcGlobe 10 (middle panel) and GLC2000 map (right panel) identifying forest (green), cultivated and managed areas (cyan), shrubland (orange) and bare soils and sparse vegetation (red).

The study covers the 32-year period 1980-2011, and focuses on yearly amounts of cumulated burned area (*BA*) in August over the study area. As shown in Figure 2, the time series of *BA* presents a very large inter-annual variability and is highly correlated (r = 0.93) with the time series of Continental Portugal.

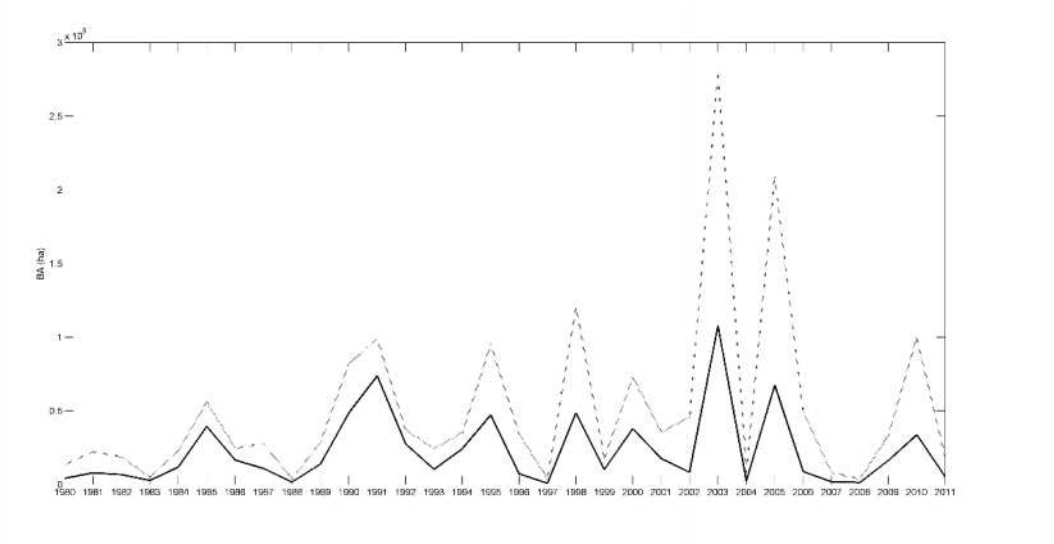

Figure 2. Time series of cumulated burned area in August over the study area (black curve) and over Continental Portugal (dotted curve)

2.2. Fire database

Values of burned area in Portugal are derived from the official Portuguese Rural Fire Database (PRFD) provided by ICNF. The database covers a 32-year period (1980-2011) and includes more than half a million records of fire events over forest, shrubland, grassland and agricultural land. It includes the data and time of ignition and extinction, total burned area, cause of fire, land cover type and location of ignition in terms of administrative division of Portugal.

The database was screened for inconsistencies, such as records with null values of burned area, with the same date, time and spatial location, negative durations, missing and/or suspicious information about area and duration. Pereira *et al*. (2011) provide a full description of these inconsistencies and a detailed description of the corrected PRFD.

2.3. Fire danger rating

Fire danger is based on the so-called Daily Severity Rating (DSR) that is part of the the Canadian Forest Fire Weather Index System (CFFWIS). This system has been in operational use in Portugal since 1998 by the national weather service (*Instituto Português do Mar e da Atmosfera*, IPMA) (Pereira *et al*., 2013). CFFWIS involves six different components based on fuel moisture and wind; three fuel based mechanisms and three fire behaviour indices that are based on daily fields of temperature, relative humidity, wind speed and 24-hour cumulated precipitation at 12 UTC (Van Wagner, 1987). DSR is derived from the Fire Weather Index (FWI), the last component of CFFWIS by means of a simple power function and may be viewed as a numeric rate of the difficulty of controlling fires. DSR was specifically designed for averaging or accumulation in time or space and is currently used in the official annual reports of fire activity in Portugal.

2.4. Statistic model of burned area

Pereira *et al*. (2013) have shown that the decimal logarithm of *BA* recorded in July and August over Portugal in the 32-year period 1980-2011 follows a normal distribution. Normal models were accordingly fitted to the recorded sample of $x=\log_{10}(BA)$. Estimates of the mean (μ) and standard deviation (σ) were obtained by maximum likelihood (Wilks, 2006).

Following DaCamara *et al*. (2014) the fitted model, hereafter referred to as null model of fire danger, may be used to estimate baseline danger D_{bo} which is defined as the probability that a prescribed threshold x_0 of $\log_{10}(BA)$ is exceeded:

$$D_{bo} = D_b(x_0) = 1 - N_x(x_0|\mu, \sigma) \quad (1)$$

Conversely, the excess threshold associated to a prescribed level of baseline danger D_{bo} may be estimated by inverting the previous equation:

$$x_0 = x(D_{b0}) = N^{-1}(1 - D_{b0}) \quad (2)$$

Normal models for $\log_{10}(BA)$ may be improved by incorporating meteorological covariates that numerically rates fire danger at different temporal and spatial scales. Let ψ and χ be two such meteorological covariates and let us assume a linear dependence of the mean (μ) of the normal distribution on the covariates:

$$\mu = a \times \psi + b \times \chi + c \quad (3)$$

Estimates of coefficients *a*, *b*, *c* and of σ are again obtained by maximum likelihood. Performance of the new alternate model, hereafter referred to as the meteorological model of fire danger, is compared against the null model (i.e. the normal without covariates) by using the standard likelihood ratio test.

The meteorological model allows estimating the "climate + weather" danger D_{c+w} which is defined as the probability that a certain threshold, x_0, of $\log_{10}(BA)$ is exceeded given two values of ψ and χ:

$$D_{c+w}(x_0, \psi, \chi \mid a, b, c, \sigma) = 1 - \mathrm{N}(x_0 \mid a \times \psi + b \times \chi + c, \sigma) \quad (4)$$

Results

Null model

A normal model was fitted to the 32-year sample (1980-2011) of cumulated BA in August (Figure 3). Obtained maximum likelihood estimates of mean and standard deviation are μ = 4.07 and σ = 0.55 and the probability associated to the Anderson-Darling statistics is 0.66, meaning that the null hypothesis that the sample is normally distributed cannot be rejected at the level of 5%.

Two different thresholds were chosen, one to discriminate between severe and non-severe years and the other one to discriminate between moderate and weak years. The first threshold, x_{20}, is associated to a baseline danger of 20%, whereas the second one, x_{80}, is associated to a baseline danger of 80%. Values were estimating using Eq. (2), leading to x_{20}=4.6 and x_{80}=3.6 that correspond to values of BA of 34,295 ha and 4,025 ha, respectively. These thresholds were then used to classify each year into one of three categories, namely severe, moderate and weak; as shown in Figure 3, severe (weak) years are those such that $x > x_{20}$ ($x < x_{80}$), the remaining ones being classified as moderate.

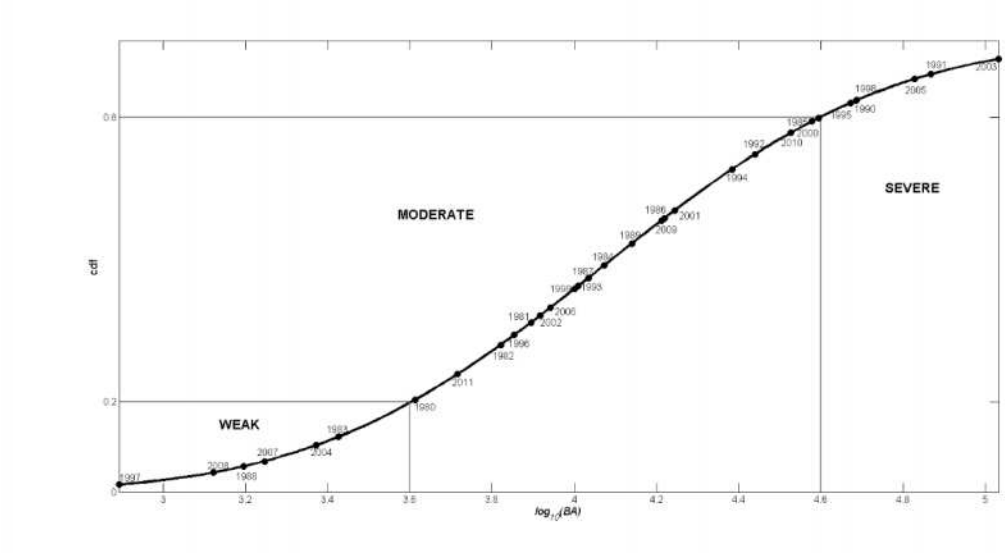

Figure 3. Cumulative distribution function of the baseline model. Dashed lines indicate thresholds x_{20} and x_{80} associated to baseline risks of 20% and 80%, which are used to stratify the 36-year sample into classes of weak, moderate and severe years represented by black squares, open triangles and black circles, respectively.

Meteorological factors

Pereira *et al*. (2005) have shown that the inter-annual variability of burned area in Portugal during the fire season is conditioned by two main meteorological factors that work at different temporal and spatial scales; i) a top-down factor (referred to as the "climate anomaly"), linked to long dry periods with absence of precipitation in late spring and early summer, which induce heat and water stress in the vegetation and ii) a bottom-up factor (referred to as the "weather anomaly"), related to the occurrence of very intense dry spells in days of extreme synoptic situations.

Top-down factor

Pereira *et al* (2013) have recently shown that the "climate anomaly" may be quantified using cumulated values of DSR in the pre-fire season (May and June). As shown in Figure 4 (left panel) severe (weak) years tend to present larger (smaller) values of cumulated DSR than the overall median. As discussed in Pereira *et al* (2013) the larger values of cumulated DSR in the case of severe years is associated to systematic increases in temperature and decreases in precipitation that take place in the pre-fire season and drive biomass to high levels of heat and water stress, making them prone to trigger large wildfires in case of favourable meteorological conditions in the fire season, which are very likely to occur in hot and dry summers. The opposite situation is observed in the case of weak years, where the tendency towards lower values of DSR than the overall median is associated to decreases in temperature and to increases in precipitation that make vegetation much less prone to trigger large wildfires, even in case of favourable meteorological conditions.

The role played by the "climatological background" associated to the prevailing meteorological conditions during the pre-fire season was therefore characterized by means of cumulated values of DSR since April 1 till June 15 / June 30 / July 15 / July 31, depending on the model to be developed. Values of cumulated DSR will be hereafter referred to as the top-down factor and denoted DSR_{td},. Choice of the term top-down is because DSR_{td} has a time scale longer than the monthly scale of BA.

Bottom-up factor

Trigo *et al*. (2006) and Amraoui *et al*. (2013) pointed out the crucial role played by heatwaves associated to extreme synoptic situations in the onset and spreading of extreme fire events. In the case of Portugal such extreme synoptic situations favour the advection of very hot and dry air throughout central Iberia (Pereira, *et al*., 2005) and are usually associated to sequences of days, within the month, characterized by large positive departures of DSR from the respective daily climatology, i.e. days with values of anomaly A_d defined as:

$$A_d = DSR_d - \overline{DSR_d} \tag{5}$$

where DSR_d and $\overline{DSR_d}$ denote the daily value of DSR for August on day d of a given year and the respective daily climatological mean performed over the 32-year period. The role played by "daily weather " associated to extreme synoptic conditions that favour or prevent fire onset and spreading within a given month was characterized by hereafter referred to bottom-up factor, DSR_{bu}, defined by the square root of the mean of squared anomalies performed over the days where $DSR > \overline{DSR_d}$, hereafter referred to as:

$$DSR_{bu} = \sqrt{\frac{\sum_{d=1}^{31} H[A_d]\,(A_d)^2}{\sum_{d=1}^{31} H[A_d]}} \tag{6}$$

where H[x] is the Heaviside step function whose value is zero for negative argument and one for positive argument. As opposed to DSR_{td}, the bottom-up factor DSR_{bu} reflects the effects associated to daily time scales that are smaller than the monthly scale of BA. As shown in Figure 4 (right panel), severe (weak) years tend to present larger (smaller) values of DSR_{bu} than the overall median.

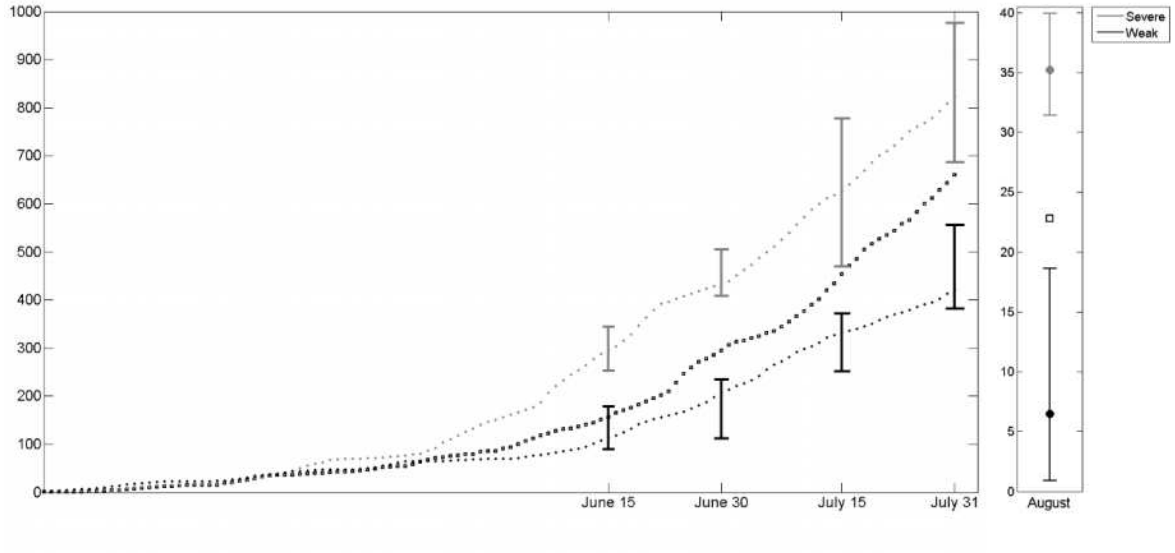

Figure 4. Left panel: daily values from April 1 to July 31 of median values of DSR_{td} for the entire period (1980-2011) (large black circle) and for the subsample of severe years (small light grey circles) and of weak years (small dark grey circles); whiskers in the two subsamples delimit the first and third quartiles of DSR_{td}. Right panel: as in the left panel but for the distribution of DSR_{bu} in August.

Meteorological model

Values of DSR_{td} and DSR_{bu} were used as covariates of the normal model of x, assuming a linear dependence in μ as in Equation (3) with $\psi = DSR_{td}$ and $\chi = DSR_{bu}$.. Obtained maximum likelihood estimates are a=0.09, b=0.02, c=3.07 and σ = 0.55 and the p-value of the likelihood ratio test is 0.0001, indicaing that adding the two covariates results in an improvement in the model that is statistically significant at the 0.01% level.

3.3. Model of fire severity

Model in diagnostic mode

Following DaCamara *et al*. (2014), the impact of the top-down and bottom up factor on burned area was statistically characterized by defining meteorological fire danger *MFD*, according to the following procedure:

1. A given threshold of baseline danger, D_{b0}, is fixed over the entire study area and the corresponding threshold x_0 is computed using Eq. (2);
2. For each year, the meteorological model is used to estimate the "climate + weather" danger, D_{c+w}, using Eq. (4) with threshold x_0 as defined in the previous step and the values of DSR_{td} and DSR_{bu};
3. Meteorological fire danger, *MFD*, is finally defined as the ratio between "climate + weather" danger, D_{c+w} and prescribed baseline danger D_{b0}:

$$MFD = \frac{D_{c+w}}{D_{b0}} \qquad (7)$$

The usefulness of meteorological fire danger may be assessed by making a model of fire severity that assigns levels of severity (low, medium, high) to a given year based on values of D_{md} associated to values of baseline danger D_{b0} of 20% and 80%. The procedure is shown in Figure 5, where values, MFD_{20} (MFD_{80}) of meteorological fire danger associated to a baseline danger D_{b0} of 20% (80%) are shown in the upper (lower) panel, using values of top-down factor DSR_{td} accumulated until July 31. The severity level of a given year is classified as high (not-high) if $MFD_{20} \geq 1.5$ ($MFD_{20} < 1.5$); a not-high year is then classified as a low (medium) level year if $MFD_{80} \leq 0.76$ ($MFD_{80} > 0.76$).
Results obtained are shown in Tables 1 and 2. There is a very good agreement between categories based on observed values of BA (weak, moderate and severe) and modelled levels of fire severity (low, medium, high); 25 (78%) were correctly classified out of 32 cases; all the remaining years were nevertheless attributed the immediate level and 2007 is the only misclassified extreme year (i.e. a weak year classified as one of medium level).

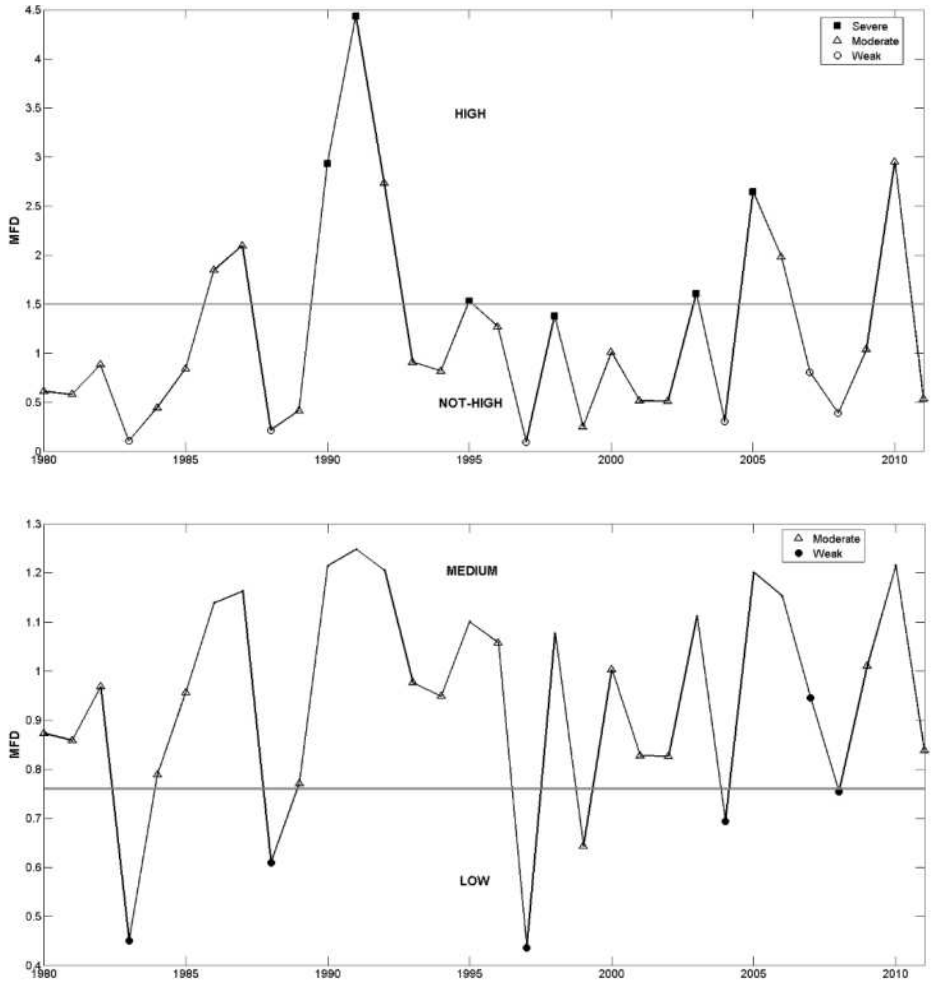

Figure 5. Time series of Meteorological Fire Danger (MFD) associated to values of baseline danger D_{b0} of 20% (upper panel) and 80% (lower panel). The horizontal dotted lines define the thresholds of 1.50 (upper panel) and of 0.76 (lower pane) that are used to classify a given year as high/not high (upper panel) and as low/medium level (lower panel). Squares, triangles and circles indicate years according to the categories of severe, moderate and weak according to the observed value of BA (Figure 3).

Table 1. Quality assessment of the fire danger model; years correctly classified by the model are printed in bold.

Modelled		**Years**
High		1986 1987 **1990 1991** 1992 **1995 1998 2003 2005** 2006 2010
Not high	*Medium*	**1980 1981 1982 1984 1985 1989 1993 1994 1996 2000 2001 2002** 2007 **2009 2011**
	Low	**1983 1988 1997** 1999 **2004 2008**

Table 2. Contingency tables of observed categories of burned severity (Figure 3) versus modelled levels of severity.

		Modelled levels of Severity		
		High	*Medium*	*Low*
Observed Categorie	*Severe*	**6**	0	0
	Moderate	5	**14**	1
	Weak	0	1	**5**

Model in prediction mode

The developed model of fire severity may be used in prediction mode at different stages of the year, namely. June 15, June 30, July 15 and July 31 when only the corresponding value of top-down danger D_{td} is known. The procedure is as follows:

1. Maximum likelihood estimates of parameters a, b and c of meteorological models are estimated that use as covariates D_{bu} in August and D_{td} accumulated until each stage (Table 3):
2. Value of D_{c+w}=0.3 for the high severity threshold is obtained by inverting Eq. (7) using MFD_{20}=1.50 and D_{b0}=20%. In a similar way value of D_{c+w}=0.6 for low severity is obtained using MFD_{80}=0.76 and D_{b0}=80%.
3. Value of μ^{+}=4.25 is obtained by inverting Eq. (4) using D_{c+w}=0.3, x_{20}=4.6 and σ=0.55. Value of μ^{-}=3.76 is similarly obtained using D_{c+w}=0.6, x_{80}=3.6 and σ=0.55.
4. Values of DSR_{bu}^{+} and DSR_{bu}^{-} are obtained by inverting Eq. (3) and using observed value of DSR_{td}: and appropriate coefficients a, b and c (Table 3):

$$DSR_{bu}^{+} = \frac{\mu^{+} - a \times DSR_{td} - c}{b} \quad (8)$$

$$DSR_{bu}^{-} = \frac{\mu^{-} - a \times DSR_{td} - c}{b} \quad (9)$$

5. The severity of the year is classified as "not high" if Prob$\{DSR_{bu} > DSR_{bu}^{+}\}$<20%; in a similar way the severity is classified as "not low" if Prob$\{DSR_{bu} < DSR_{bu}^{-}\}$<20%. When none of the two conditions is satisfied the level of severity is considered unknown. Probabilities are empirically estimated by fitting a normal distribution to the 32-year sample of observed values of DSR_{bu} (1980-2011).

Table 3. Maximum likelihood estimates of parameters a, b and c for meteorological models of fire danger using values of* DSR_{td} *observed at four different stages of the year.

	June 15	**June 30**	**July 15**	**July 31**
a	0.05	0.09	0.08	0.09
b	0.02	0.02	0.02	0.02
c	3.39	3.25	3.19	3.07

Obtained results are shown in Table 4 and it may be noted that models for June 15, June 30, July 15 and July 30 correctly anticipate years with levels of severity of "not low" in 17 out of 19 classifiable cases, in 18 out of 19, in 18 out of 19 and in 20 out of 21 years, respectively; the models are also able to correctly anticipate years with levels of severity of "not high" in 1 out of 2 classifiable cases, in 9 out of 10, in 8 out of 9 and in 10 out of 11 years, respectively. It is apparent that years with levels of "not low" may be correctly anticipated at an earlier stage of the year than those with levels of "not high"; this is especially true when comparing severe years that are never classified as "unknown" by the model with the case of weak years where the same only occurs for the model of July 31. Finally it is worth noting that all model (since June 15) are able to correctly classify as "not low" all but one of the severe years, the only exception (1998) being erroneously classified as "not severe" by models at all stages of the year. A possible explanation is an anomalous accumulation of biomass, given the fact that 1997 was by far the year with lowest burned area. Predictions seem less robust for weak years, all but one year (2004) being correctly classified as "not high" at the last stage (July 31); again the exception is incorrectly classified at all stages but it is worth noting that large fires occurred in the first days of September (which if included would turn 2004 into a moderate year).

Table 4. Results from model of fire severity used in prognostic mode at four different stages of the year. Symbols ✓, ✗ and ? identify correctly classified, incorrectly classified and unknown years.

			June 15		***June 30***		***July 15***		***July 31***	
Classification	**rank**	**year**	**Not-high**	**Not-low**	**Not-high**	**Not-low**	**Not-high**	**Not-low**	**Not-high**	**Not-low**
Severe	1	2003		✓		✓		✓		✓
	2	1991		✓		✓		✓		✓
	3	2005		✓		✓		✓		✓
	4	1998	✗		✗		✗		✗	
	5	1990		✓		✓		✓		✓
	6	1995		✓		✓		✓		✓
Moderate	7	1985	?	?	✓		✓		✓	
	8	2000	?	?		✓		✓		✓
	9	2010		✓	✓		?	?		✓
	10	1992		✓		✓		✓		✓
	11	1994		✓		✓		✓		✓
	12	2001		✓		✓		✓		✓
	13	1986		✓		✓		✓		✓
	14	2009		✓		✓		✓		✓
	15	1989	?	?	✓		✓		✓	
	16	1984	✓		✓		✓		✓	
	17	1987		✓		✓	?	?	✓	
	18	1993	?	?	✓		✓		✓	
	19	1999		✓		✓		✓		✓
	20	2006		✓		✓		✓		✓
	21	2002		✓		✓		✓		✓
	22	1981	?	?		✓		✓		✓
	23	1996		✓		✓		✓		✓
	24	1982		✓		✓		✓		✓
	25	2011	?	?	?	?		✓		✓
	26	1980	?	?	✓		?	?		✓
Weak	27	1983	?	?	?	?	✓		✓	
	28	2004		✗		✗		✗		✗
	29	2007	?	?	✓		✓		✓	
	30	1988	?	?	✓		✓		✓	
	31	2008	?	?	✓		?	?	✓	
	32	1997		✗	?	?	✓		✓	

Conclusions

A study was performed aiming to assess the role of meteorological factors on the inter-annual variability of burned area over a region of Central Portugal. The study covers a 32-year period that extends from 1980 to 2011. The study region is dominated by forest, the predominant species being maritime pine and eucalyptus. The large fractions of the forested area and the high percentages of tree species that are extremely flammable in summer explain the fact that, although occupying only 18% of the territory of Portugal, the chosen study area is responsible for 43% of the burned area in August during the study period.

A normal distribution model was fitted to the 32-year sample of decimal logarithms of monthly burned area. This model was then improved by introducing as covariates two different measures of prevailing meteorological conditions as derived from Daily Severity Rate (DSR), an indicator of meteorological fire danger; a top-down factor, DSR_{td}, which consists of cumulated values of monthly means of DSR from April 1 to July 31 and a bottom up factor, DSR_{bu}, defined as the square root of the mean of the squared daily deviations of DSR in August from daily climatology, the average being performed only over days of positive deviation.

The two models, the one without and the one with meteorological covariates, allow estimating baseline and climate+weather fire danger, both defined as the probability that the monthly burned area exceeds a given threshold. These two quantities allow defining meteorological fire danger, based on which a probabilistic model of fire severity is built that assigns levels of severity to a given year. This model may be used in either diagnostic or prognostic modes. When used in diagnostic mode, 25 (78%) out of 32 cases were correctly classified. When used in prognostic mode, at four different stages of the year (June 15, June 30, July 15 and July 31), the very large majority of years with levels of severity classified as "not low" (17 out of 19 classifiable cases, 18 out of 19, 18 out of 19 and 20 out of 21 years, respectively) were correctly anticipated. Good results were also obtained for years with levels of severity classified as "not high" (1 out of 2 classifiable cases, 9 out of 10, 8 out of 9 and in 10 out of 11 years, respectively).

Results from the present study put into perspective the key roles played by meteorological factors associated to different spatial and temporal scales on the occurrence of fire seasons characterized by very high or very low fire activity. This information may be of use to forest managers when organizing fire preventing measures and firefighting capacity and when allocating resources for both. It may be also useful when developing an on-line alarm system to predict the event of extreme fires since such a system depends on constructing a sound model that links the fire size process to the multivariate exploratory variables.

Acknowledgements

This study was performed within the framework of the EUMETSAT LSA SAF project. The LSA SAF has also supported research grants of Sílvia A. Nunes, Sofia L. Ermida and Teresa J. Calado. The Portuguese Science Foundation (FCT) has supported the research work by K. F. Turkman (projects PEst-OE/MAT/UI0006/2011and PTDC/MAT/118335/2010).

References

Aldersley A, Murray SJ, Cornell SE (2011). Global and regional analysis of climate and human drivers of wildfire. *Science of The Total Environment* **409**, 18, 3472-3481. doi: 10.1016/j.scitotenv.2011.05.032

Amraoui M, Liberato MLR., Calado TJ, DaCamara CC, Coelho LP, Trigo RM, Gouveia CM (2013). Fire activity over Mediterranean Europe based on information from Meteosat-8. *Forest Ecology and Management* **294**, 62-75. doi: 10.1016/j.foreco.2012.08.032

Costa L, Thonicke K, Poulter B, Badeck F (2011). Sensitivity of Portuguese Forest Fires to Climatic, Human, and Landscape Variables: Subnational Differences between Fire Drivers in Extreme Fire Years and Decadal Averages. *Regional Environmental Change* 11, 543–51. doi: 10.1007/s10113-010-0169-6

DaCamara CC, Calado TJ, Ermida SL, Trigo IF, Amraoui M, Turkman KF, (2014). Calibration of the Fire Weather Index over Mediterranean Europe based on fire activity retrieved from MSG satellite imagery. *International Journal of Wildland Fire*, doi: 10.1071/WF13157

Dale VH, Joyce LA, McNulty S, Neilson RP, Ayres MP, Flannigan MD, Hanson PJ, Irland LC, Lugo AE, Peterson CJ, Simberloff D, Swanson FJ, Stocks BJ, Wotton BM (2001). Climate change and

forest disturbances. *BioScience* **51**, 723-734. doi: 10.1641/0006-3568(2001)051[0723:CCAFD]2.0.CO;2

Flannigan M, Cantin AS, de Groot WJ, Wotton M, Newbery A, Gowman LM (2013). Global wildland fire season severity in the 21st century. *Forest Ecology and Management* **294**, 54-61. doi: 10.1016/j.foreco.2012.10.022

Ganteaume A, Camia A, Jappiot M, San-Miguel-Ayanz J, Long-Fournel M, Lampin C (2012). A review of the main driving factors of forest fire ignition over Europe. *Environmental Management* **51**, 651-662. doi: 10.1007/s00267-012-9961-z

Lavorel S, Flannigan MD, Lambin EF, Scholes MC (2007). Vulnerability of land systems to fire: Interactions among human, climate, the atmosphere, and ecosystems. *Mitigation and Adaptation Strategies for Global Change* **12**, 33-53. doi: 10.1007/s11027-006-9046-5

Liu Y, Stanturf J, Goodrick S (2010). Trends in global wildfire potential in a changing climate. *Forest Ecology and Management* **259**, 658-697. doi: 10.1016/j.foreco.2009.09.002

Mori AS, Johnson EA (2013). Assessing possible shifts in wildfire regimes under a changing climate in mountains landscapes. *Forest Ecology and Management* **310**, 875-886. doi: 10.1016/j.foreco.2013.09.036

Núñes-Regueira L., Añón J. A. R., Castiñeiras J. P. (1996). Calorific values and flammability of forest species in Galicia. Coastal and hillside zones. *Bioresource Technology* **57**, 283-289. doi: 10.1016/S0960-8524(96)00083-1

Pausas JG, Vallejo V R (1999). The role of fire in European Mediterranean ecosystems. In "Remote sensing of large wildfires in the European Mediterranean basin". (Chuvieco, E.) pp. 3-16. (Springer, Berlin). doi: 10.1007/978-3-642-60164-4_2

Pereira MG, Trigo RM, DaCamara CC, Pereira JMC, Leire SM (2005). Synoptic patterns associated with large summer forest fires in Portugal. *Agricultural and Forest Meteorology* **129**, 11-25. doi: 10.1016/j.agrformet.2004.12.007

Pereira MG, Malamud BD, Trigo RM, Alves PI (2011). The history and characteristics of the 1980-2005 Portuguese rural fire database. *Natural Hazards and Earth System Sciences* **11**, 3343-3358. doi: 10.5194/nhess-11-3343-2011

Pereira MG, Calado TJ, DaCamara CC, Calheiros T (2013). Effects of regional climate change on rural fires in Portugal. *Climate Research* **57**, 187-200. doi: 10.3354/cr01176

San-Miguel-Ayanz J, Carlson JD, Alexander M, Tolhurst K, Morgan G, Sneeuwjagt R, Dudley M (2003). Current Methods to Assess Fire Danger Potential. In "Wildland Fire Danger Estimation and Mapping". (Chuvieco, E.) pp. 20-61. (World Scientific Publishing, Singapore)

San-Miguel-Ayanz J, Moreno JM, Camia A (2013). Analysis of large fires in Mediterranean landscapes: Lessons learned and perspectives. *Forest Ecology and Management* **294**, 11-22. doi: 10.1016/j.foreco.2012.10.050

Trigo RM, Pereira JMC, Pereira MG, Mota B, Calado TJ, DaCamara CC, Santo FE (2006). Atmospheric conditions associated with the exceptional fire season of 2003 in Portugal. *International Journal of Climatology* **26**, 13, 1741-1757. doi: 10.1002/joc.1333

Trigo RM, Sousa PM, Pereira MG, Rasilla D, Gouveia CM (2013). Modelling wildfire activity in Iberia with different atmospheric circulation weather types. *International Journal of Climatology* **294**, 54-61. doi: 10.1016/j.foreco.2012.10.022

Van Wagner CE, 1987. Development and structure of the Canadian Forest Fire Weather Index System. *Canadian Forestry Service*, Forestry Technical Report **33** (Ottawa)

Wilks DS (2006). Parametric Probability Distributions. In "Statistical methods in the atmospheric sciences". (Academic Press) 2nd edition, vol. 91, pp. 111-116

Yongqiang L, Stanturf J, Goodrick S (2010). Trends in global wildfire potential in a changing climate. *Forest Ecology and Management* **259**, 685-697. doi: 10.1016/j.foreco.2009.09.002

Application of simulation modeling for wildfire risk assessment and management

Michele Salis[a,b], Alan A. Ager[c], Mark A. Finney[d], Fermin Alcasena Urdiroz[b], Bachisio Arca[e], Olga Muñoz Lozano[a], Paul Santoni[f], Donatella Spano[a,b]

[a] *University of Sassari, Department of Science for Nature and Environmental Resources (DIPNET), Via Enrico De Nicola 9, I-07100, Sassari, Italy, miksalis@uniss.it*
[b] *Euro-Mediterranean Center on Climate Change (CMCC), IAFENT Division, Via De Nicola 9, I-07100, Sassari, Italy*
[c] *USDA Forest Service, Pacific Northwest Research Station, Western Wildland Environmental Threat Assessment Center, 3160 NE 3rd Street, Prineville, OR 97754, USA*
[d] *USDA Forest Service, Rocky Mountain Research Station, Fire Sciences Laboratory, 5775 Highway 10 West, Missoula, MT 59808, USA*
[e] *National Research Council (CNR), Institute of Biometeorology (IBIMET), Traversa La Crucca 3, I-07100 Sassari, Italy*
[f] *Université de Corte, Forest Fire Research Team, Campus Grimaldi, BP 52, 20250 Corte, France*

Keywords*: simulation modeling; fire risk assessment and management; mitigation strategies; burn probability; case studies*

Abstract

The growing incidence of large wildfires impacting urban interfaces and values of interest over the past decades has led to extensive research on decision support tools for fire risk assessment and management. The inherent complexity of risk management and fuel treatment planning has led to a rapid increase in the application of fire spread and behavior modeling software for both research and operational applications. Simulation models are now routinely used to analyze potential fire behavior and to develop risk assessments and mitigation strategies, over a range of scales, from forest stands (a few hectares) to large landscapes. Fire behavior models mainly used for fuels planning in the US and elsewhere include NEXUS, FVS-FFE, FARSITE, FlamMap, RANDIG, and FSIM. The geospatial interface to these models, ArcFuels, is used to streamline preparation of input files and post-process simulation outputs. The majority of these landscape fire simulation models use the minimum travel time algorithm, a compact fire simulation algorithm that makes it computationally feasible to simulate thousands of fires and generate burn probability and intensity maps over large areas. The outputs can be used to study wildfire topology on complex landscapes, and analyze uncertainty associated with wildfire events in terms of timing, location, intensity, and duration. Wildfire simulation models have also been coupled with spatial optimization software to design efficient landscape fuel treatment plans. From a risk assessment standpoint, the key benefit of newer wildfire simulation approaches, compared to previous work on spatial patterns in ignition patterns, is that the former accounts for risk factors that influence landscape wildfire spread, while the latter does not. Overall, properly calibrated and validated, wildfire simulation methods offer a dramatic increase in information content for conservation, restoration, and fire protection planning on fire-prone landscapes. Risk assessments using simulation methods have now been completed for a range of issues including carbon offsets, endangered wildlife species, habitat conservation, watersheds and WUI protection, and protection of biodiversity. In this talk, we will discuss the application of wildfire simulation models and geospatial tools for wildfire risk assessment and management for several study areas including the western US and the Mediterranean Basin.

Introduction

To reduce the growing financial and ecological losses from large wildfires, risk assessment and cost-effective mitigation activities have become a challenge for planners, policy makers, fuel managers and

Forest Services (Ager *et al.* 2011; Calkin *et al.* 2011). The relevant importance of wildfire risk assessment and fuel management will play a key role with urban expansion into the wildlands, land use variations and climate-change effects on fire occurrence frequency, burn probability, fire intensity and the related consequences (Brown *et al.* 2004; Westerling *et al.* 2006; Moreira *et al.* 2011; Arca *et al.* 2012; Kloster *et al.* 2012; Brotons *et al.* 2013; Ager *et al.* 2014). Since weather and topography are beyond human control (Finney 2007), wildfire mitigation activities encompass a wide range of operational methods including thinning, mechanical treatments for limiting fuel load and continuity, prescribed burning, and creation of infrastructures and fuelbreaks (Agee and Skinner 2005; Montiel and Kraus 2010). These activities have the aim of reducing both surface and canopy fuel load and continuity, to ultimately bring down the occurrence of uncharacteristic wildfires (Agee *et al.* 2000; Cochrane *et al.* 2012). Fire mitigation projects vary widely depending on ecosystems and ecological conditions, a strong role being played by historical fire regimes, weather, topography, and the spatial pattern of values at risk. For instance, some treatments are designed as localized fuelbreaks to minimize fire occurrence within highly valued social and ecological values as well as susceptibility, while others are designed to impede or slow down the spread of fire over large landscapes (Ager *et al.* 2011).
In this paper, we define fire risk as the expected loss or benefit after the fire, and fire exposure as the analysis of the probability of a fire at given intensities (Figure 1; Fairbrother and Turnley 2005; Finney 2005; Salis *et al.* 2013). We define risk factors as the individual contributing components to risk (likelihood, intensity and susceptibility). Quantitative assessment of wildfire risk requires (a) the probability of a fire at a specific location; (b) the conditional fire intensity, measured by flame length; (c) the resulting net value change in financial or ecological value (Finney 2005; Miller and Ager 2013). Wildfire exposure is a necessary step in risk assessment and does not include the quantification of expected wildfire impacts.

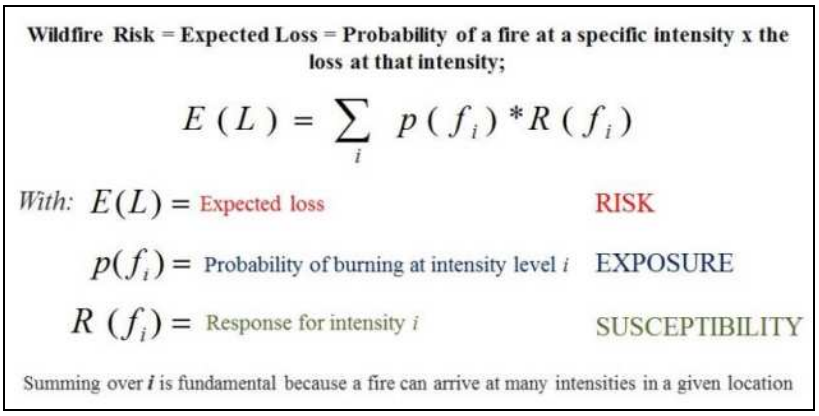

Figure 1. Overview of the definition used for fire risk, exposure, and susceptibility in this paper

From a risk standpoint, it is important to note that in all ecosystems a very small proportion of wildfires globally accounts for most of the burned area, as well as the resulting damages and human casualties: thus, accounting for the risk posed by large destructive wildfires requires consideration of their behavior and spread over large areas (Viegas 2004; Finney *et al.* 2005; Viegas *et al.* 2006; Ager *et al.* 2010*a*, 2013; Salis *et al.* 2013). The complexity of fire risk assessment and management and the abovementioned points have led to a rapid increase in the application of fire behavior modeling software in both research and operational contexts. Simulation models are now routinely used to analyze potential fire behavior and to develop risk assessments and mitigation strategies, over a range of scales, from forest stands (a few hectares) to landscapes ($< 10^5$ ha), regional ($< 10^7$ ha) or national scales (Calkin *et al.* 2011). Fire behavior models used for fuels planning include NEXUS (Scott 1999), BehavePlus (Andrews 2007), FVS-FFE (Rebain 2010), FARSITE (Finney 1998), FlamMap (Finney 2006), RANDIG (Finney 2002), and FSIM (Finney *et al.* 2011). The geospatial interface to these

models, ArcFuels, is used to streamline preparation of input files and post-process simulation outputs (Vaillant *et al.* 2013). To analyze uncertainty associated with wildfire events in terms of timing, location, rate of spread, intensity, and duration, simulation of thousands fires at landscape scales are commonly performed. A number of supporting models and software can be used, in conjunction with historical databases, to estimate appropriate wind, weather, dead and live fuel moisture, and other input variables required to run a fire behavior model (Nelson 2000; Butler *et al.* 2006; Stratton 2006; Forthofer 2007). While the application of non-spatial fire behavior models for a single fuel type and constant weather conditions is relatively straightforward, the design and evaluation of large-scale risk assessment and management activities requires more complex landscape fire modeling to fully characterize fire exposure and potential effects of events burning with diverse conditions in an area. The abovementioned issues have created a strong demand for an integrated modeling system to assess current wildfire exposure and risk, and to analyze the potential benefits of proposed fuel management and other mitigation activities (Miller and Ager 2013). The majority of these landscape fire simulation models use the minimum travel time algorithm (MTT, Finney 2002), a compact fire simulation algorithm that makes it computationally feasible to simulate thousands of fires and generate burn probability and intensity maps over large areas (Ager *et al.* 2012). The MTT algorithm searches for the fastest path of fire spread along straight-line transects connected by the cell corners (nodes) (Figure 2; Finney 2002, 2006): MTT pathways are then interpolated to reveal the fire perimeter positions at specific instants in time.

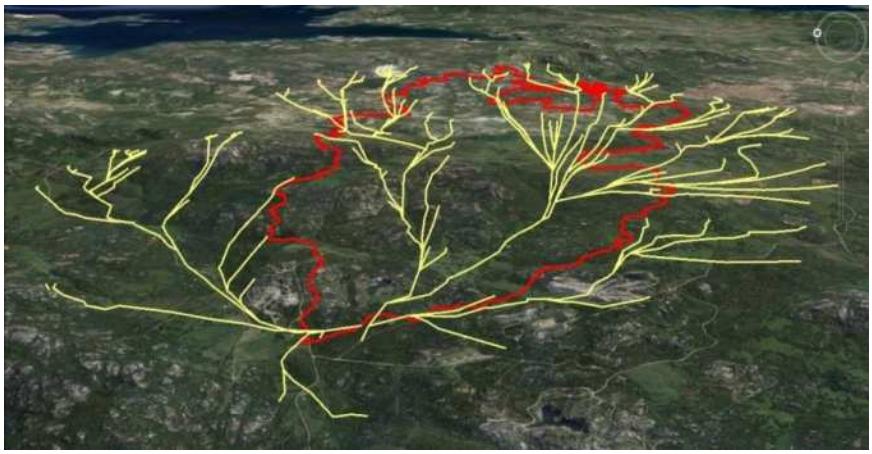

Figure 2. Major fire flow paths (yellow) and observed wildfire perimeter (red) over an aerial photograph. The flow paths, obtained by the MTT spread algorithm, searches for the fastest path of fire spread along straight-line transects connected by nodes. The example refers to a wildfire occurred in North-East Sardinia, Italy (Lu Lioni, Arzachena, August 2004).

The outputs can be used to study wildfire topology on complex landscapes, and analyze uncertainty associated with wildfire events in terms of timing, location, intensity, and duration. Wildfire simulation models have also been coupled with spatial optimization software to design efficient landscape fuel treatment plans (Finney 2006; Seli *et al.* 2008). From a risk assessment standpoint, the key benefit of newer wildfire simulation approaches, compared to previous works on spatial patterns in ignition occurrence patterns, is that the former accounts for risk factors that influence landscape wildfire spread, while the latter does not (Ager *et al.* 2011, 2014). Overall, properly calibrated and validated, wildfire simulation methods offer a dramatic increase in information content for conservation, restoration, and fire protection planning on fire-prone landscapes (Arca *et al.* 2007; Ager *et al.* 2007, 2010*a*; Salis *et al.* 2013). Risk assessments using simulation methods have now been completed for a range of issues including carbon offsets, wildlife habitat conservation, WUI protection, and protection of biodiversity. In this paper, we will discuss the application of wildfire simulation models and

geospatial tools for wildfire risk assessment and management for several study areas including the western US and the Mediterranean Basin.

Methods

The majority of fire behavior models are derived from systems that model one-dimensional fire behavior as part of a spreading line fire. Most models linked or integrated Rothermel's models for predicting surface and crown fire rates of spread with VanWagner's or Scott's crown fire transition and propagation models, and provided outputs of diverse fire behavior characteristics (rate of spread, fireline intensity, flame length, crown fire activity, etc.) (Rothermel 1972; Anderson 1983, Van Wagner 1993; Scott and Reinhardt 2001). In depth discussions of these models and their limitations, as well as programs and tools to determine appropriate weather inputs, to select fuel management scenarios, or to streamline preparation of input files and post-process simulation outputs, can be found in several recent papers, as presented in the Introduction.
The minimum travel time (MTT) fire spread algorithm of Finney (2002) is one of the most used to analyze fire exposure and characterize fire behavior. The MTT algorithm has been extensively described elsewhere and is routinely applied to fire management problems in the US and elsewhere; initial calibration (Figure 2) and validation of the Rothermel's fire spread model as implemented in FARSITE and the MTT were performed and described by several research papers (Ager *et al.* 2007, 2012; Arca *et al.* 2007; Duguy *et al.* 2007; Andrews 2009; Salis 2008; Salis *et al.* 2013, 2014).
FlamMap MTT utilizes the same set of gridded spatial inputs as the FARSITE simulation system. The spatial inputs include eight grid themes that describe fuel canopy characteristics, surface fuel model, and topography, which are combined into a binary landscape (LCP) file (Figure 3; Finney 1998). Surface fuels are described by fuel models that characterize dead and live fuel load (by size class), surface-area-to-volume ratio for live and dead fuels, fuelbed depth, moisture of extinction, and heat content. Fuel models are derived by field measurements, selected using photo guides, or obtained from other data sources (Anderson 1982; Scott and Burgan 2005; Arca *et al.* 2009). Canopy fuels are described by percentage of cover, crown bulk density, crown base height, and average height.

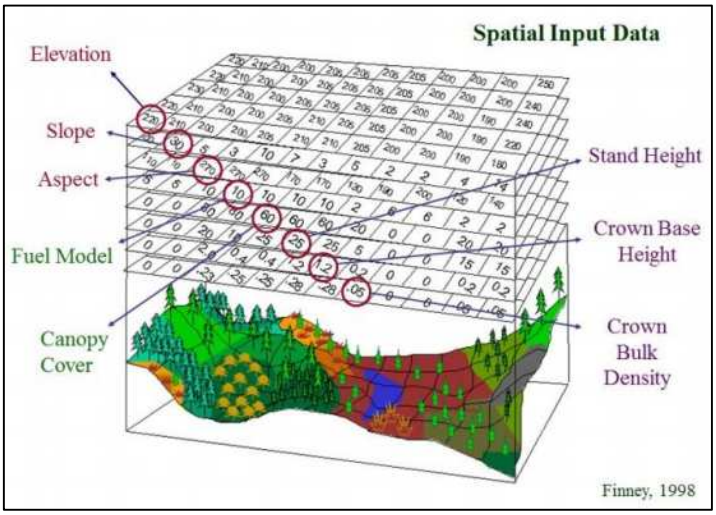

Figure 3. Topography, surface and crown fuels grid data used for wildfire simulations by FlamMap, FARSITE, Randig, and FSIM. The data are easily converted with ArcFuels scripts to the binary format (landscape file) required by the abovementioned fire models.

With the MTT approach, multiple fires are simulated to generate burn probabilities and fire behavior outputs (Figure 4). A user-defined number of random or historic based ignitions (from 1 to more than 100,000) for fixed or variable burn periods are simulated. The MTT reports a conditional burn

probability at each pixel for twenty 0.5-m intervals (0–10m). The conditional burn probability is the chance that a pixel will burn at a given flame length interval, considering one ignition in the whole study area under the assumed conditions. Fireline intensity outputs are converted to flame length based on Byram's (1959) equation: the modeled intensity depends on the direction in which the fire encounters a pixel relative to the major direction of spread (i.e. heading, flanking or backing fire), as well as slope and aspect (Finney 2002). Fire size and ignition coordinates for each simulated fire are also generated as output.

Overall, three widely recognized issues with the application of the fire behavior models are the choice of the most appropriate fuel model, the quantification of canopy fuels, and the limitation of Rothermel's model in complex terrains. About the first point, several fire behavior models require a surface fuel model, which is typically chosen from standard or custom models. Fuel models are difficult to calibrate and are rarely validated with observed fire behavior (Arca *et al.* 2007; Salis 2008; Ager *et al.* 2011). Also, known limitations exist with estimates of canopy fuel characteristics, critical to model crown fire behavior (Cruz and Alexander 2010). Canopy base height and foliar moisture content are both used to calculate the critical fireline intensity, and canopy bulk density is used to determine active crown fire rate of spread. Because destructive measuring on canopy fuels is not feasible and expensive, indirect methods using tree inventory data are necessary (Reinhardt *et al.* 2006). Vegetation modeling systems such as FVS-FFE are used to process inventory data to determine the effective canopy base height and canopy bulk density using a running mean. Furthermore, fire behavior models rely on the Rothermel's surface fire equations, and fire behavior is only represented for frontal combustion. This is a limitation for wildfires spreading in complex terrains, where specific physical phenomena associated to wildfires (e.g.: fire channeling) are not properly captured by the Rothermel's spread model (Viegas and Pita 2004; Viegas 2006; Sharples *et al.* 2012).

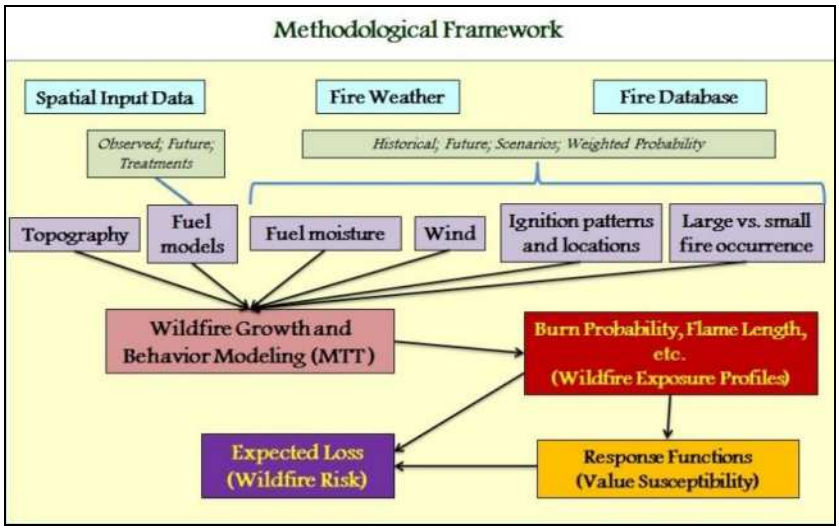

Figure 4. Methodological framework for wildfire growth and behavior modeling and wildfire risk evaluation

Results

The MTT algorithm was applied to complete several case studies in the Mediterranean Basin and in the US, as for instance 1) to quantify landscape wildfire exposure and risk, 2) to determine fire exposure profiles for values at risk, 3) to assess temporal variation in fire exposure, 4) to compare fuel treatment alternatives, and 5) to examine expected carbon offsets from fuel treatments.

In the first application, wildfire risk was calculated for northern spotted owl (*Strix occidentalis caurina*) habitat, old growth forests, and carbon in several studies in Oregon (Figure 5; Ager *et al.*

2007, 2010*a*, 2010*b*). In the first case study, the probabilistic risk analysis system was used for quantifying wildfire threats to spotted owl habitat. 10,000 wildfire simulations with randomly located ignitions were run to calculate spatially explicit probabilities of habitat loss for fuel treatment scenarios on a 70,245 ha study area. A flame length threshold for each spotted owl habitat stand was determined using FVS-FFE and used to predict the proportion of fires that resulted in habitat loss.

In later work, simulation modeling was used to analyze spatial variation in wildfire exposure on the island of Sardinia (24,000 km^2), Italy (Salis *et al.* 2013). Weather conditions associated with large escaped fires were used as input to simulate 100,000 fire events within the study area, randomly drawing from the frequency distribution of burn periods and wind directions. Historical data and wildfire simulations were used to estimate burn probabilities, flame length and fire size. Spatial patterns in modeled outputs were strongly related to fuel loadings and weather conditions, although topographic and other influences were apparent. Both studies allowed to quantify exposure profiles (burn probability, flame length, fire size) and to identify landscapes able to support large and severe fires.

In a subsequent application, the analyses were scaled up to analyze wildfire exposure factors (burn probability, fire intensity) to social and ecological values on Oregon and Washington States, and Sardinia (Italy) (Ager *et al.* 2012; Salis *et al.* 2013). Example plots of fire exposure factors can be used to identify highly valued resources at risk, and to prioritize fuel management activities.

Another application to quantify fire risk based on fire modeling was presented by Thompson *et al.* (2011), which described a quantitative, geospatial fire risk assessment tool based on burn probability modeling, identification of values at risk, and production of response functions.

In another paper, the spatiotemporal changes in wildfire exposure in Sardinia (Italy) from 1980 to 2009 in relation to historical changes in fire ignition patterns, weather, suppression activities, and land uses were analyzed (Figure 6; Salis *et al.* 2014). 100,000 fire events were simulated for two time frames, reflecting the 1980-1994 and 1995-2009 conditions, drawing from the frequency distribution of the specific burn periods and wind directions associated with large wildfires observed in the island. In that research paper, along with a net reduction in area burned and ignitions, an advance of 15 days for the fire season peak, and an increase in spring temperatures, the wildfire modeling highlighted strong spatial variations in burn probability and increments in fire exposure for WUI areas. Considering that little change was observed for land use types and associated fuels for the analyzed timeframes, a combination of social factors and suppression capabilities may be responsible of the above mentioned results.

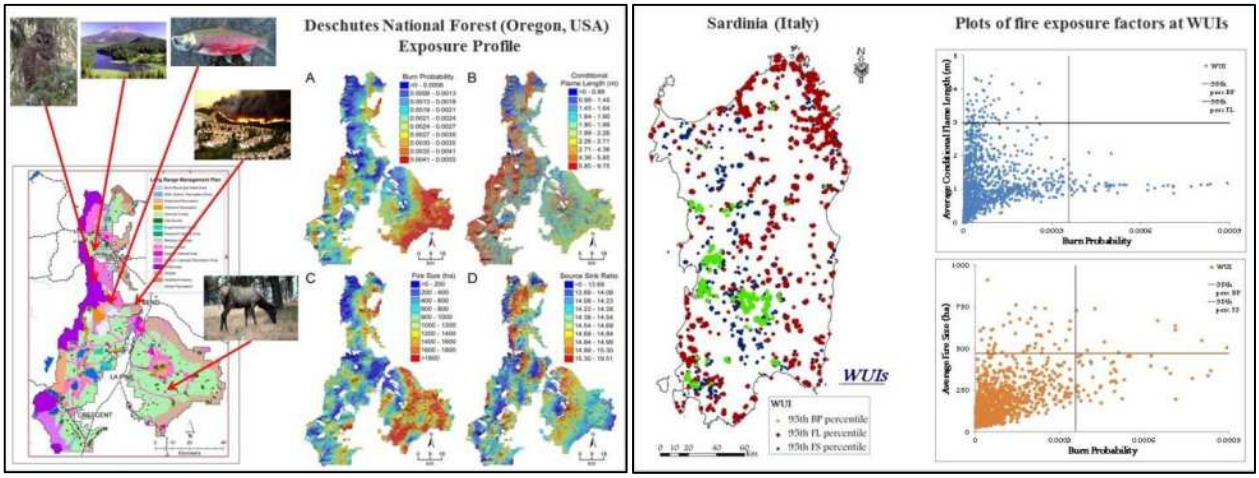

Figure 5. On the left, maps of burn probability (BP, a), conditional flame length (CFL, b), fire size (FS, c), and source sink ratio (SSR, d) for the for northern spotted owl habitat in central Oregon, US. On the right, scatterplots of fire exposure factors (BP vs CFL and BP vs FS) for wildland urban interfaces in Sardinia, Italy. The map shows the WUIs with BP, FL and FS values higher than the 95th percentile

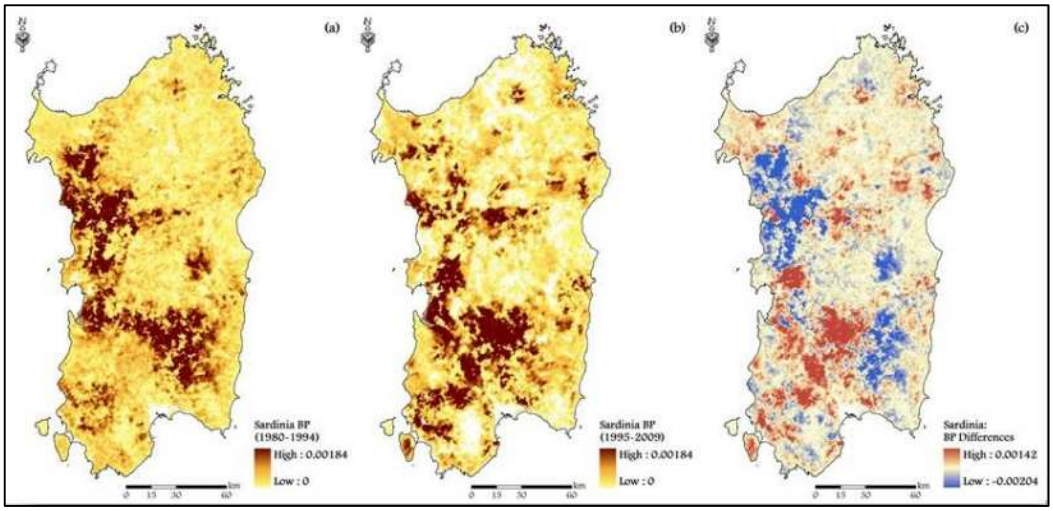

Figure 6. Variation in BP between 1995-2009 and 1980-1994 study periods in Sardinia, Italy. BP is the chance that a pixel will burn, considering one ignition in the whole study area under the assumed conditions

In another study, a risk framework was used to analyze tradeoffs between ecological management objectives (large fire resilient trees) versus the protection of residential structures in the wildland urban interface (WUI) (Figure 7; Ager *et al.* 2010*a*). The former was quantified using the expected mortality of large trees and the latter with burn probability in the location of residential structures. This study was conducted in a 16,000 ha study area in Oregon, US, to examine tradeoffs between placing fuel treatments near residential structures within an urban interface, versus treating stands in the adjacent wildlands to meet forest health and ecological restoration goals. The treatment strategies were evaluated by simulating 10,000 wildfires with random ignition locations, and replicating severe fire events based on 97th percentile historic weather conditions.

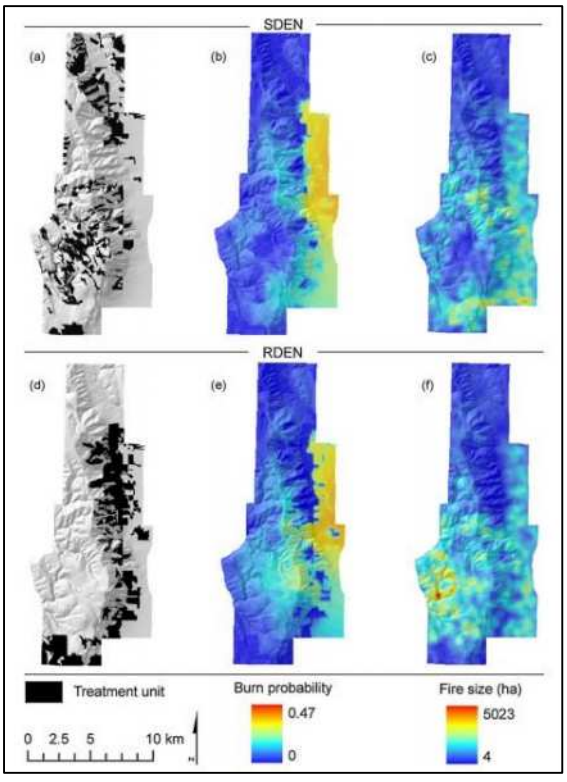

Figure 7. Maps of treatment units (a and d), burn probabilities (b and e), and kernel smoothed fire size (c and f) for the 20% treatment area for the stand density (SDEN) and the residential density (RDEN) treatment priorities, for the study area close to La Grande, OR (USA)

The main findings were that treatments strategically located on a relatively minor percentage of the landscape (10%) resulted in a roughly 70% reduction in the expected wildfire loss of large trees for the restoration scenario; treating stands near residential structures resulted in a higher expected loss of large trees, but relatively lower burn probability and flame length within structure buffers.
About mitigation activities and landscape fuel management, both positive and negative carbon impacts have been reported (Finkral and Evans 2008; Mitchell *et al.* 2009; Reinhardt and Holsinger 2010). A 70,000 ha watershed on the Fremont-Winema National Forest in southern Oregon, US, was used as case study to assess the expected carbon change from fuel treatments, combining carbon loss functions with the flame length probability outputs (Figure 8; Ager *et al.* 2010*b*). As result, a probabilistic estimate of carbon impacts that accounted for the uncertainty about future wildfire events was yielded. In this work, 30,000 wildfires were simulated with random ignition locations under both treated and untreated landscapes. The results suggested that the carbon loss from implementing fuel reduction treatments exceeded the expected carbon benefits associated with lowered burn probabilities and reduced fire severity on the treated landscape.

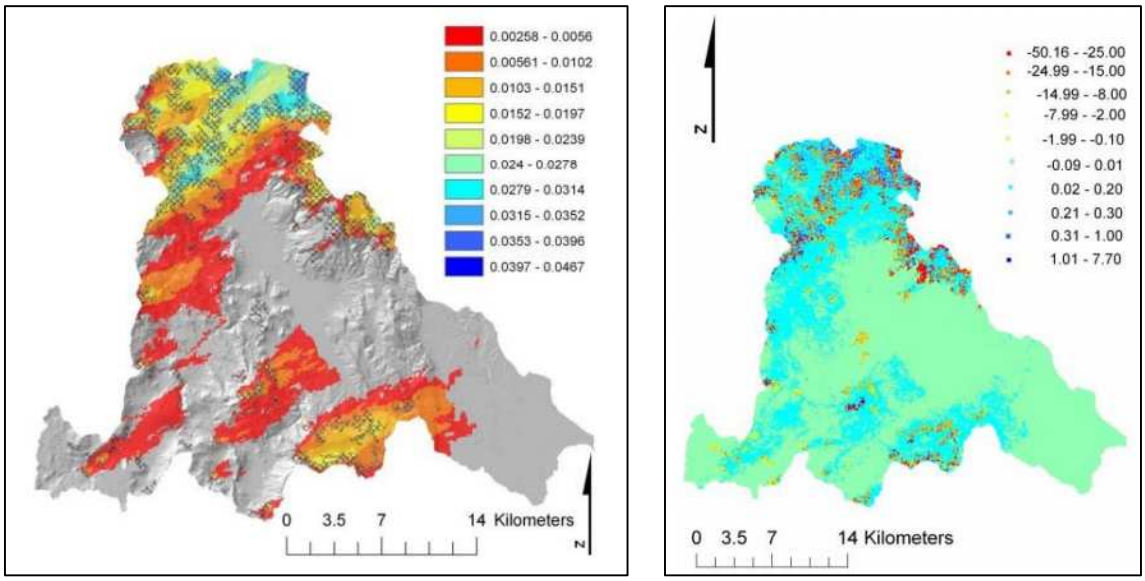

Figure 8. On the left, difference in BP between the non-treatment and treatment scenario for the Drews Creek watershed, Fremont - Winema National Forest (Oregon, USA). Stands selected for fuel treatments are hatched. Areas not shaded had differences less than 0.00258. On the right, expected carbon differences (tonnes ha^{-1}) between non-treatment and treatment scenarios

Discussion and Conclusions

Although our example applications are related to case studies from US national forests and Sardinia (Italy), the proposed methods for quantifying fire exposure and risk and for supporting fuel management planning can be applied elsewhere. When the MTT fire spread algorithm for FlamMap was parallelized for multithreaded processing, it became computationally feasible to simulate thousands of fires to generate spatially explicit fine scale burn probability and intensity maps over large areas (Ager *et al.* 2012). Extensive testing has shown that this algorithm can replicate fire size distributions in the North American ecosystems and the Mediterranean areas (Ager *et al.* 2007, 2010a, 2012; Parisien *et al.* 2007; Bar Massada *et al.* 2009; Salis *et al.* 2013, 2014). In addition, the incorporation of the MTT algorithm into fire behavior models make it feasible to rapidly generate fire exposure and risk maps for different fuel management, weather, fuel conditions, or ignition scenarios (Ager *et al.* 2011).

Newer models that use the MTT algorithm include spatiotemporal probabilities for ignition, escape, and burn conditions, and yield estimates of annual burn probabilities; the identification of the areas characterized by the highest exposure and risk, as well as the zones to be prioritized for mitigation strategies, can be easily determined with the abovementioned approach. A strong effort in the integration of tools, scientific findings and data for an operational application of the fire behavior models was addressed, with the aim of supporting wildfire risk assessment and management (Forthofer 2007; Vaillant *et al.* 2013). An important end-product is providing an efficient working environment that allows users to interact with fire behavior models in a geospatial context, and thus gain a better understanding of their limitations and biases. Application of fire behavior modeling continues to grow among planners and researchers alike, especially as land management agencies and policy makers require integrated landscape analyses (Ager *et al.* 2013). The analysis framework proposed contributes to a consistent analytical process for assessing the level of exposure and risk that communities and highly valued resources face from wildland fires. Risk provides a comprehensive index of likelihood, intensity, and potential effects. Burn probability modeling and exposure analyses play an important role in research to address a number of management problems, including analyzing carbon offsets, understanding temporal and spatial tradeoffs of fuel treatments, climate changes impacts, post fire recovery, soil erosion, and wildfire impacts to ecological conservation reserves.

Acknowledgments

This work was partially funded by the GEMINA Project (MIUR/MATTM n. 232/2011), by the EXTREME Project (Legge Regione Sardegna 7/2007, CRP-25405), and by the Project ‘‘Modeling approach to evaluate fire risk and mitigation planning actions’’ (P.O.R. Regione Sardegna F.S.E. 2007-2013, Asse IV Capitale Umano, Linea di Attività l.3.1).

References

Agee JK, Bahro B, Finney MA, Omi PN, Sapsis DB, Skinner CN, van Wagtendonk JW, Weatherspoon CP (2000) The use of shaded fuelbreaks in landscape fire management. *Forest Ecology and Management* 127, 55–66.

Agee JK, Skinner CN (2005) Basic principles of forest fuel reduction treatments. *Forest Ecology and Management* 211, 83–96.

Ager AA, Buonopane M, Reger A, Finney MA (2013) Wildfire Exposure Analysis on the National Forests in the Pacific Northwest, USA. *Risk Analysis* 33, 1000–1020.

Ager AA, Finney MA, Kerns BK, Maffei H (2007) Modeling wildfire risk to northern spotted owl (Strix occidentalis caurina) habitat in Central Oregon, USA. *Forest Ecology and Management* 246, 45–56.

Ager AA, Finney MA, Mcmahan A, Cathcart J (2010b) Measuring the effect of fuel treatments on forest carbon using landscape risk analysis. *Natural Hazards and Earth System Science* 10, 2515–2526.

Ager AA, Preisler HP, Arca B, Spano D, Salis M (2014) Wildfire risk estimation in the Mediterranean area. *Environmetrics*. DOI: 10.1002/env.2269.

Ager AA, Vaillant N, Finney MA (2011) Application of fire behavior models and geographic information systems for wildfire risk assessment and fuel management planning. *Journal of Combustion*, http://dx.doi.org/10.1155/2011/572452.

Ager AA, Vaillant NM, Finney MA (2010a) A comparison of landscape fuel treatment strategies to mitigate wildland fire risk in the urban interface and preserve old forest structure. *Forest Ecology and Management* 259, 1556–1570.

Ager AA, Vaillant NM, Finney MA, Preisler HK (2012) Analyzing wildfire exposure and source-sink relationships on a fire prone forest landscape. *Forest Ecology and Management* 267, 271-283.

Anderson HE (1982) Aids to determining fuel models for estimating fire behaviour. USDA Forest Service, Intermountain Forest and Range Experiment Station, General Technical Report INT-GTR-122. (Ogden, UT).

Anderson HE (1983) Predicting wind-driven wildland fire size and shape. Tech. Rep. INT-305, USDA Forest Service, Intermountain Forest and Range Experiment Station, Ogden, Utah, USA.

Andrews PL (2007) BehavePlus fire modeling system: past, present, and future. In: Proceedings of 7th Symposium on Fire and Forest Meteorological Society, pp. 1–13, Bar Harbor, Maine, October 2007.

Andrews PL (2009) BehavePlus fire modeling system, version 5.0: Variables. USDA Forest Service, Rocky Mountain Research Station, General Technical Report RMRS-GTR-213WWW Revised. (Fort Collins, CO).

Arca B, Bacciu V, Pellizzaro G, Salis M, Ventura A, Duce P, Spano D, Brundu G (2009) Fuel model mapping by IKONOS imagery to support spatially explicit fire simulators. In '7th International Workshop on Advances in Remote Sensing and GIS Applications in Forest Fire Management towards an Operational Use of Remote Sensing in Forest Fire Management', 2–5 September 2009, Matera, Italy. (Eds E Chuvieco, R Lasaponara) pp. 75–78.

Arca B, Duce P, Laconi M, Pellizzaro G, Salis M, Spano D (2007) Evaluation of FARSITE simulator in Mediterranean maquis. *International Journal of Wildland Fire* 16, 563–572.

Arca B, Pellizzaro G, Duce P, Salis M, Bacciu V, Spano D, Ager AA, Finney MA, Scoccimarro E (2012) Potential changes in fire probability and severity under climate change scenarios in Mediterranean areas. In Spano D, Bacciu V, Salis M, Sirca C (eds.), 2012. Modelling Fire Behaviour and Risk, pag. 92-98. ISBN: 978-88-904409-7-7.

Bar Massada A, Syphard AD, Hawbakr TJ, Stewart SI, Radeloff VC (2011) Effects of ignition location models on the burn patterns of simulated wildfires. *Environmental Modelling & Software* 26, 583–592.

Brotons L, Aquilué N, de Caceres M, Fortin M-J, Fall A (2013) How fire history, fire suppression practices and climate change affect wildfire regimes in Mediterranean landscapes. *PLoS One* 8(5), e62392. doi:10.1371/journal.pone.0062392.

Brown TJ, Hall BL, Westerling AL (2004) The impact of twenty-first century climate change on wildland fire danger in the western United States: an applications perspective. *Climate Change* 62, 365–388.

Butler BW, Finney MA, Bradshaw L, Forthofer JM, McHugh CW, Stratton RD, Jimenez D (2006) WindWizard: A New Tool for Fire Management Decision Support. In: Proceedings of the Fuels Management-How to Measure Success, pp. 787-796, Portland, Oregon, USA, March 2006

Byram GM (1959) Combustion of forest fuels. In 'Forest Fire: Control and Use'. (Ed. KP Davis) pp. 61–89. (McGraw-Hill: New York).

Calkin DE, Ager AA, Thompson MP (2011) A comparative risk assessment framework for wildland fire management: the 2010 cohesive strategy science report. Gen. Tech. Rep. RMRS-GTR-262. Fort Collins, CO: U.S. Department of Agriculture, Forest Service, Rocky Mountain Research Station. 63 p.

Cochrane MA, Moran CJ, Wimberly MC, Baer AD, Finney MA, Beckendorf KL, Eidenshink J, Zhu Z (2012) Estimation of wildfire size and risk changes due to fuels treatments. *International Journal of Wildland Fire* 21, 357–367.

Cruz MG, Alexander ME (2010) Assessing crown fire potential in coniferous forests of western North America: a critique of current approaches and recent simulation studies. *International Journal of Wildland Fire* 19, 377–398.

Duguy B, Alloza JA, Roder A, Vallejo R, Pastor F (2007) Modeling the effects of landscape fuel treatments on fire growth and behaviour in a Mediterranean landscape (eastern Spain). *International Journal of Wildland Fire* 16, 619–632.

Fairbrother A, Turnley JG (2005) Predicting risks of uncharacteristic wildfires: application of the risk assessment process. *Forest Ecology and Management* 211, 28–35.

Finkral AJ, Evans AM (2008) The effects of a thinning treatment on carbon stocks in a northern Arizona ponderosa pine forest. *Forest Ecology and Management* 255, 2743–2750.

Finney MA (1998) FARSITE: fire area simulator—model development and evaluation. Tech. Rep. RMRS-RP-4, USDA Forest Service, Rocky Mountain Forest and Range Experiment Station, Ogden, Utah, USA.

Finney MA (2002) Fire growth using minimum travel time methods. *Canadian Journal of Forest Research* 32(8), 1420–1424.

Finney MA (2005) The challenge of quantitative risk analysis for wildland fire. *Forest Ecology and Management* 211, 97–108.

Finney MA (2006) An overview of FlamMap fire modeling capabilities. In: Proceedings of the Fuels Management-How to Measure Success, pp. 213–220, Portland, Ore, USA, March 2006.

Finney MA, Grenfell IC, McHugh CW, Seli RC, Trethewey D, Stratton RD, Brittain S (2011). A method for ensemble wildland fire simulation. *Environmental Modeling and Assessment* 16: 153-167.

Finney MA (2007) A computational method for optimising fuel treatment locations. *International Journal of Wildland Fire* 16, 702–711.

Forthofer JM (2007) Modeling wind in complex terrain for use in fire spread prediction. PhD thesis. Colorado State University.

Kloster S, Mahowald NM, Randerson JT, Lawrence PJ (2012) The impacts of climate, land use, and demography on fires during the 21st century simulated by CLM-CN. *Biogeosciences* 9, 509-525.

Miller C, Ager AA (2013) A review of recent advances in risk analysis for wildfire management. *International Journal of Wildland Fire* 22, 1–14.

Mitchell SR, Harmon ME, O'Connell KEB (2009) Forest fuel reduction alters fire severity and long-term carbon storage in three Pacific Northwest ecosystems. *Ecological Applications* 19, 643–655.

Montiel C, Kraus D (2010) Best Practices of Fire Use – Prescribed Burning and Suppression Fire Programmes in Selected Case-Study Regions in Europe. European Forest Institute Research Report 24. Joensuu, FI.

Moreira F, Viedma O, Arianoutsou M, Curt T, Koutsias N, Rigolot E, Barbati A, Corona P, Vaz P, Xanthopoulos G, Mouillot F, Bilgili E (2011) Landscape - wildfire interactions in southern Europe: Implications for landscape management. *Journal of Environmental Management* 92(10), 2389-2402.

Nelson RM (2000) Prediction of diurnal change in 10-h fuel stick moisture content. *Canadian Journal of Forest Research* 30, 1071-1087.

Parisien MA, Junor DR, Kafka VG (2007) Comparing landscape-based decision rules for placement of fuel treatments in the boreal mixed wood of western Canada. *International Journal of Wildland Fire* 16, 664–672.

Rebain SA (2010) The fire and fuels extension to the forest vegetation simulator: updated model documentation. Tech. Rep., USDA Forest Service, Forest Management Service Center, Fort Collins, USA.

Reinhardt E, Holsinger L (2010) Effects of fuel treatments on carbon-disturbance relationships in forests of the northern Rocky Mountains. *Forest Ecology and Management* 259, 1427–1435.

Reinhardt E, Scott J, Gray K, Keane R (2006) Estimating canopy fuel characteristics in five conifer stands in the western United States using tree and stand measurements. Canadian Journal of Forest Research 36, 2803–2814.

Rothermel RC (1972) A mathematical model for predicting fire spread in wildland fuels. USDA Forest Service, Intermountain Forest and Range Experiment Station, Research Paper, INT-115. (Ogden, UT).

Salis M (2008) Fire behaviour simulation in Mediterranean maquis using FARSITE (Fire Area Simulator). Tesi di dottorato. Università degli Studi di Sassari. Available at http://eprints.uniss.it/23/.

Salis M, Ager AA, Arca B, Finney MA, Bacciu V, Duce P, Spano D (2013) Assessing exposure of human and ecological values to wildfire in Sardinia, Italy. *International Journal of Wildland Fire* 22, 549–565.

Salis M, Ager AA, Finney MA, Arca B, Spano D (2014) Analyzing spatiotemporal changes in wildfire regimes and exposure across a Mediterranean fire-prone area. *Natural Hazards* 71(3), 1389-1418.

Scott JH (1999) NEXUS: a system for assessing crown fire hazard. *Fire Management Notes* 59, 21–24.

Scott JH, Burgan R (2005) Standard fire behavior fuel models: a comprehensive set for use with Rothermel's Surface Fire Spread Model. USDA Forest Service, Rocky Mountain Research Station, General Technical Report RMRS-GTR-153. (Fort Collins, CO)

Scott JH, Reinhardt E (2001) Assessing crown fire potential by linking models of surface and crown fire behavior. RMRS-RP-29, USDA Forest Service, Rocky Mountain Research Station, Fort Collins, USA.

Seli RC, Ager AA, Crookston NL, Finney MA, Bahro B, Agee JK, McHugh CW (2008) Incorporating landscape fuel treatment modeling into the Forest Vegetation Simulator. In: Havis RN, Crookston NL (2008) Third Forest Vegetation Simulator Conference; 2007 February 13–15; Fort Collins, CO. Proceedings RMRS-P-54. Fort Collins, CO: U.S. Department of Agriculture, Forest Service, Rocky Mountain Research Station. p. 27-39.

Sharples JJ, McRae RHD, Wilkes SR (2012) Wind–terrain effects on the propagation of wildfires in rugged terrain: fire channelling. *International Journal of Wildland Fire* 21, 282–296.

Stratton RD (2006) Guidance on spatial wildland fire analysis: models, tools, and techniques. Tech. Rep. RMRS-GTR-183, USDA Forest Service, Rocky Mountain Research Station, Fort Collins, USA.

Vaillant NM, Ager AA, Anderson J (2013) ArcFuels10 system overview. Gen. Tech. Rep. PNW-GTR-875. Portland, OR: U.S. Department of Agriculture, Forest Service, Pacific Northwest Research Station. 65 p.

Van Wagner CE (1993) Prediction of crown fire behavior in two stands of jack pine *Canadian Journal of Forest Research* 23, 442–449.

Viegas DX (2006) Parametric study of an eruptive fire behaviour model. *International Journal of Wildland Fire* 15, 169-177.

Viegas DX, Abrantes T, Palheiro P, Santo FE, Viegas MT, Silva J, Pessanha L (2006) Fire weather during the 2003, 2004 and 2005 fire seasons in Portugal. In 'V International Conference on Forest Fire Research', 27–30 November 2006, Figueira da Foz, Portugal. (Ed. DX Viegas).

Viegas DX, Pita LP (2004) Fire spread in canyons. *International Journal of Wildland Fire* 13, 253–274.

Westerling AL, Hidalgo HG, Cayan DR, Swetnam TW (2006) Warming and earlier spring increase Western U.S. forest wildfire activity. *Science* 313, pp. 940–943.

Ash deposition during wildfire and its threat to water quality

Cristina Santín [a], Stefan H. Doerr[a], Chris J. Chafer[b]

[a] *Department of Geography , College of Science, Swansea University , Singleton Park, Swansea SA2 8PP - United Kingdom; c.s.nuno@swansea.ac.uk; s.doerr@swansea.ac.uk*
[b] *Sydney Catchment Authority, PO Box 323 Penrith, NSW, 2750 Australia; chris.chafer@sca.nsw.gov.au*

Abstract
The highly erodible ash material that covers the ground after fire is increasingly gaining attention as a potential major contributor to water contamination in fire-affected landscapes.
The recent and severe forest fires near Sydney (October 2013) provided an ideal opportunity to identity and quantify the potential main threats to water quality from pollutants present in the ash. These fires affected forests in the greater Sydney catchment, raising serious concerns about the risk of drinking water contamination from post-fire erosion.
An extensive sampling campaign (sampling points = 120) was carried out in Jan. 2014 along a ridge with homogeneous vegetation and soils, but affected by a range of burn severities. Burn severity was classified based on the differenced Normalised Burn Ratio obtained from satellite imagery, validated by field observations and linked to estimates of fire intensity.
Three burn severities were sampled: extreme (>70,000 kW m-1); moderate (7000-500 kW m 1); and low (<500 kW m-1). At each sampling point, the entire ash layer was collected from a square are of a specified size. The ash layer comprised the loose, charred and wettable material (<1 cm size) lying on top of uncharred water-repellent mineral soil.
Total loads of ash increased substantially with burn severity with averages of 35 16 and 6 t/ha for extreme, moderate and low severity sites, respectively. Notable differences exist in ash composition between fire severities, from comprising mainly charcoal and fine charred particles (derived largely from combustion of litter and vegetation) at low severity sites to a more mineral enriched composition (with substantial contribution from charred mineral soil) at extreme severity sites.
Results in bulk chemical composition of ash and main pollutants availability will be presented and discussed with special focus on potential implications for water quality impacts based on a series of post-fire rainfall and erosion scenarios.

Keywords*: Australia, bushfire, fire severity, eucalypt forest, drinking water, pollutants.*

Introduction

Wildfire enhances the risk of soil erosion and sediment transfer through the removal of vegetation and litter, and changes to soil wettability with associated contamination risks for surface water bodies. Most previous studies on post-fire erosion have focused on soil erosion and associated sediment transfer. The highly erodible ash material that covers the ground after fire and which can be rapidly mobilised and transferred into water bodies by water and wind erosion, however, has been largely overlooked to date. This ash, generated from combustion of vegetation, litter and surface soil, is increasingly gaining attention as a potential major contributor to post-fire water contamination (Bodi *et al*. 2014).
An extensive wildfire near Sydney (October 2013) provided us with an ideal opportunity to determine the quantities of ash produced during wildfire in relation to burn severity and to identity and quantify the main threats to water quality from contaminants contained in the ash. The fire affected parts of the Nepean catchment, which contributes to the greater Sydney water supply system, raising serious concerns about the risk of water contamination from post-fire erosion.

Methods

In October 2013, severe wildfires burnt 10,000 ha of dry sclerophyl eucalypt forest near Sydney (NSW, Australia). Sampling was carried along at a ridge in the Nepean catchment with homogeneous vegetation species composition, fuel load and soil characteristics, but with a range of burn severities, resulting from wind-driven differences in fire behaviour. Burn severity was determined using the differenced normalised burn ratio (dNBR) obtained from satellite images immediately before (1 day) and after (1 week) the fire, supported by on site determination of fuel consumption completeness and linked to estimates of fire intensity. Between the fire and the sampling campaign (early January 2014), rainfall was very limited so that there had been no significant redistribution of material by water erosion.

Three burn severities were sampled: *i) extreme* (>70,000 kW m^{-1}), *ii) moderate* (7000-500 kW m^{-1}), and *iii) low* (<500 kW m^{-1}). For each burn severity, three replicate sites were sampled with 30 sampling points each. At each sampling point, a square of known size was sampled by careful brushing together and collecting the entire ash layer. The ash layer comprised the loose, charred and wettable material (<1cm size) material lying on top of uncharred water-repellent mineral soil. It included residues from the burning of aboveground vegetation and litter, as well as the completely-charred and structureless surface mineral soil. Litter and soil was also samplied at a long-unburned control site on the same ridge.

All samples being analysed for basic parameters (pH, CEC, and total carbon, phosphorous and nitrogen concentrations) as well as total concentrations of trace elements at the time of writing. In addition, leaching tests (Hageman *et al*. 2008) will be also performed on selected representative samples to assess biochemical availability of toxic elements (metals and metalloids) and eutrophication agents (nutrients).

3. Results

Irrespective of burn severity the ash layer was consistently wettable and dark in colour whereas the underlying uncharred soil was highly water repellent and lighter in colour. However, notable differences exist in ash composition between the different fire severities, from comprising mainly charcoal and fine charred particles (derived largely from combustion of litter and understory vegetation) at low severity sites to a more mineral enriched composition (probably with substantial contribution from charred mineral soil) at extreme severity sites.

Total loads of ash increased substantially with burn severity with averages of 35 (±2.0 Standard Error of Mean), 16 (±0.9 SEM) and 6 t/ha (±0.7 SEM) for extreme, moderate and low severity sites, respectively. Ash bulk density also increased with burn severity with values of 58.9 (STDEV 6.4) , 53.7 (STDEV 14.9) and 34.5 g cm^3 (STDEV 16.4) for extreme, moderate and low severity sites, respectively, which supports the increasing contribution from charred mineral soil with burn severity. Results regarding bulk chemical composition of ash and the availability of main pollutants will be presented and discussed with special focus on potential implications for water quality impacts based on a series of post-fire rainfall and erosion scenarios.

Figure 1. Extreme severity (left) and Low Severity (right) sampling sites 3 months after fire.

References

Bodí M.B., Martin D., Balfour V.N., Santín C., Doerr S.H., Pereira P., Mataix-Solera J., Cerdà A. 2014. Wildland fire ash: production, composition and eco-hydro-geomorphic effects. Earth-Science Reviews 130:103–127.

Hageman, P.L., Plumlee, G.S., Martin, D.A., Hoefen, T.M., Adams, M., Lamothe, P.J., Todorov, T., Anthony, M.W., Leachate Geochemical Results for Ash Samples from the June 2007 Angora Wildfire near Lake Tahoe in Northern California, 2008: U.S. Geological Survey Open-File Report 2008-1170. http://pubs.usgs.gov/of/2008/1170/

Assigning dates to burned areas in Portugal based on NIR and the reflected component of MIR as derived from MODIS

Jéssica Panisset[a], Renata Libonati[b], Carlos C. DaCamara[c], Ana Barros[c]

[a] *Universidade Federal do Rio de Janeiro, Departamento de Meteorologia, Rio de Janeiro - RJ, Brazil - jessicapanisset@gmail.com, leonardo.peres@igeo.ufrj.br*
[b] *Instituto Nacional de Pesquisas Espaciais, Cachoeira Paulista - SP, Brazil - renata.libonati@cptec.inpe.br*
[c] *Instituto Dom Luiz / Universidade de Lisboa, Lisboa, Portugal - cdcamara@fc.ul.pt*

Abstract
Accurate information about location and extent of burnt area is required and of particular interest for the scientific communities dealing with meteorological and climate models in what respects to reliable estimations of biomass burned. An automated procedure is here presented that allows identifying and assigning dates of occurrence to burned areas in Portugal using daily reflectance from NIR (near-infrared) and MIR (middle infrared) bands, obtained from the MODIS instrument on-board Aqua and Terra satellites. The algorithm detects persistent changes in the so-called (V, W) Burned Index time series, and the day of maximum change is then identified as the burning day. The procedure was applied to the extreme summer of 2005 and results were validated against a reference map derived from Landsat imagery. Comparison between the burned map as obtained using the developed procedure and the reference map resulted in a Proportion Correct of 96%. Probability of Detection was 63%, meaning that the algorithm was able to identify almost two thirds of the scars occurred in 2005. An assessment of the temporal accuracy of the dating procedure was also conducted. Results show that 75% of burnt pixels were correctly dated by the algorithm with differences to the hotspots dates less than five days.

***Keywords**: Burned areas, NIR and MIR bands.*

Introduction

Portugal is the European country most prone (per unit area) to fire occurrences, which are responsible for many damages, like the emission of greenhouse gases and pollutants, the loss of vegetation and lives, the soil erosion, the proneness to floods in the period following the fire events and the economic impact, among others.
Instituto de Conservação da Natureza e das Florestas (ICNF), the Portuguese authority for forests, has been producing yearly maps of fire perimeters. The fire atlas uses end of fire season Landsat TM/ETM imagery to map all fire perimeters with areas larger than 5 ha. Because it relies on end-of-season imagery, the atlas provides a spatial snapshot of the yearly area burned, and dates of burning for individual events cannot be estimated. However, such information is required to fully understand the fire regime and fire seasonality and to disentangle the complex interactions among fire, land cover and meteorology.
The aim of this work is to apply the so-called (V,W) Burned Index in order to identify and assign dates of occurrence to burned areas in Portugal using daily reflectances from NIR (near-infrared) and MIR (middle infrared) bands, obtained from the Moderate Resolution Imaging Spectrometer (MODIS) instrument on-board Aqua and Terra satellites.

Methods

2.1. Data

Data consist of top of the atmosphere values of MIR radiance, NIR reflectance and thermal infrared (TIR) brightness temperature, acquired by the MODIS instrument on-board Aqua and Terra satellites during July, August and September 2005, together with the respective solar zenith angles. Data were obtained from the Aqua and Terra / MODIS Level 1B 1 km V5 product, MOD021 and MYD021, (MCST, 2006) and respect to channels 2 (centred at 0.858μm), 20 (centred at 3.785μm), and 31 (centred at 11.017μm). Surface values of MIR reflectance are then retrieved by applying the methodology developed by Kaufman and Remer (1994), paying special attention to the possible drawbacks previously pointed out by Libonati *et al*. (2010). Data from Aqua and Terra / MODIS Geolocation Fields Level 1A V5 are also used (MOD03 an MYD03).
Validation of results from the analysis performed on MODIS images is mainly carried out based on the annual atlas provided by the ICNF, based on end of fire season Landsat TM/ETM imagery. Validation of the dates assigned is based on the comparison of estimated dates by the developed procedure and dates of hot spots as identified by Modis.

2.2. The "V,W" Burned Index

Following the procedure described in Libonati *et al*. (2011), the "V,W" burned index is computed for each image based on differences (ξ index) between the reflected component of MIR (middle-infrared, centred at 3.785 μm) and NIR (near-infrared, centred at 0.858 μm) together with the distance (η index) to a convergence point in MIR/NIR space, representative of a totally burned surface. Information of hot spots extracted from the MODIS Fire and Thermal Anomalies Product (MOD14A1/ MYD14A1) is also used.
Coordinate V has a very small scatter for pixels associated with vegetated surfaces and coordinate W covers a much wider range of values, allowing the identification of water content of vegetative surfaces.

2.3. Identification of Burned Areas

Monthly minimum value composites of W are computed and seed points of potentially burned areas are selected based on pre-specified thresholds of W and on temporal differences of W between composites; seed points also have to be located inside a buffer around MODIS hot spots.
Burned areas are identified by expanding the search around selected seed points. Pixels considered as burned are identified based on relative thresholds whose values are contextually derived from the pixels in the neighbourhood. A spatial filter is finally applied to remove outliers.

2.4. Assigning dates to burned areas

The algorithm detects persistent changes in the (V, W) burned index time series, and the day of maximum change is then identified by means of discrimination index S (Giglio *et al*., 2009), which estimates the time separability between two groups of W observations a given day D (the first group consists in the 6 days before D and the second one in the 6 days following D). A large and abrupt decrease in the W values therefore implies positive values of S that is defined as:

$$S(x,y) = \frac{\Delta W(x,y)}{\left[\sigma_{pre}(x,y) - \sigma_{pos}(x,y)\right]/2} \quad (1)$$

$$\Delta W(x,y) = \bar{W}_{pre}(x,y) - \bar{W}_{pos}(x,y) \quad (2)$$

Results

Erro! A origem da referência não foi encontrada. shows the values of W_t and $\Delta W_{t(t-1)}/W_t$ for July, August and September 2005, as obtained by the algorithm. Burned areas are concentrated in pixels with low values of W and/or with negative values of $\Delta W_{t(t-1)}/W_t$ (normalized difference between the value of W in the current and the previous month), namely pixels whose value of W has decreased from one month to another.

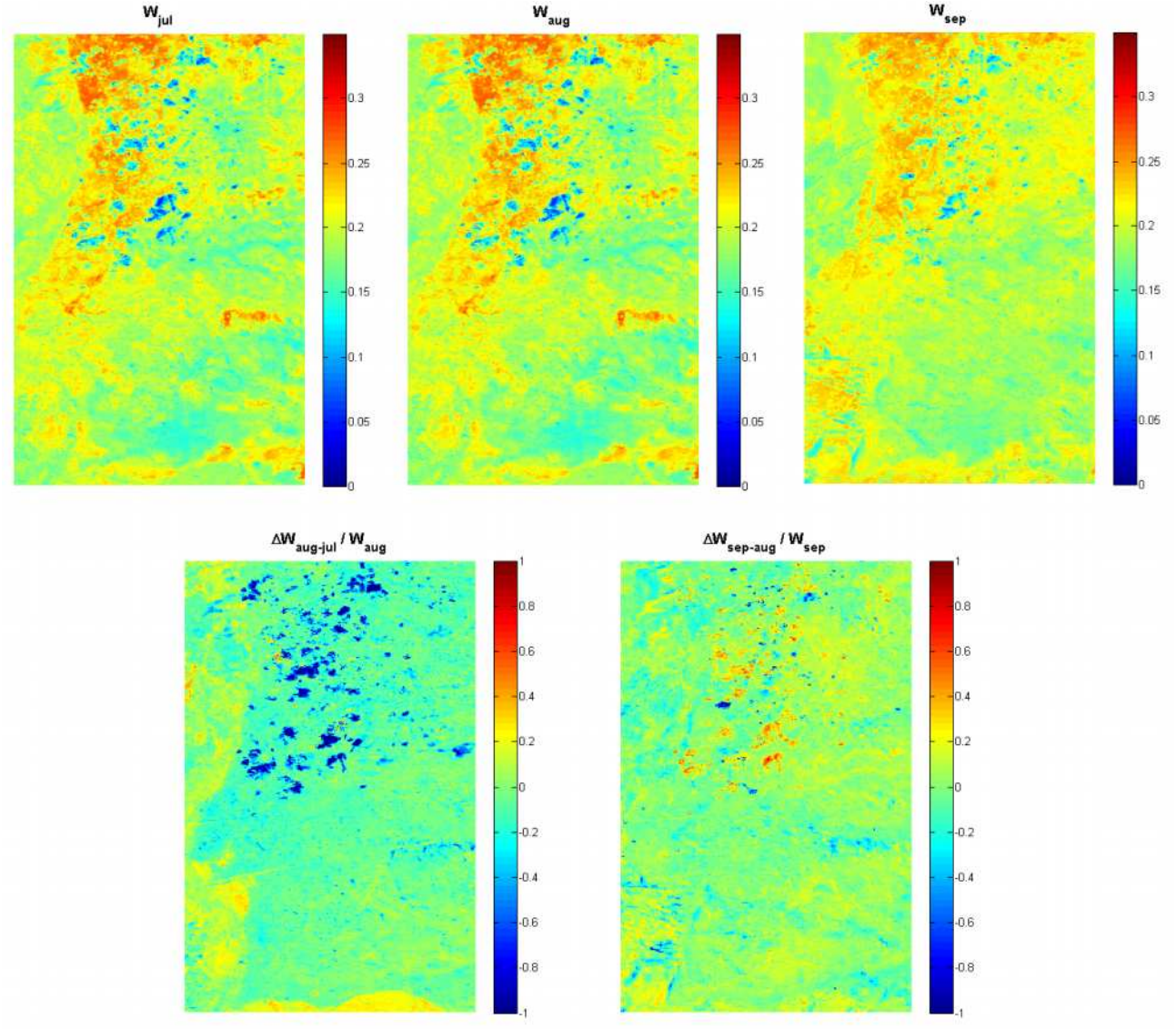

Figure 1. Minimum value composites of W Index for July (upper left panel), August (upper central panel) and September 2005 (upper right panel). Normalized differences between the composites for August and July (lower left panel) and between the composites for September and August (lower right panel).

As mentioned before, fixed thresholds and contextual algorithms are applied to the temporal composites of W_t and $\Delta W_{t(t-1)}/W_t$. This methodology is applied to both August and September 2005, resulting in two scar maps that are on the basis of the burned area map of August and September 2005 (Figure 2).

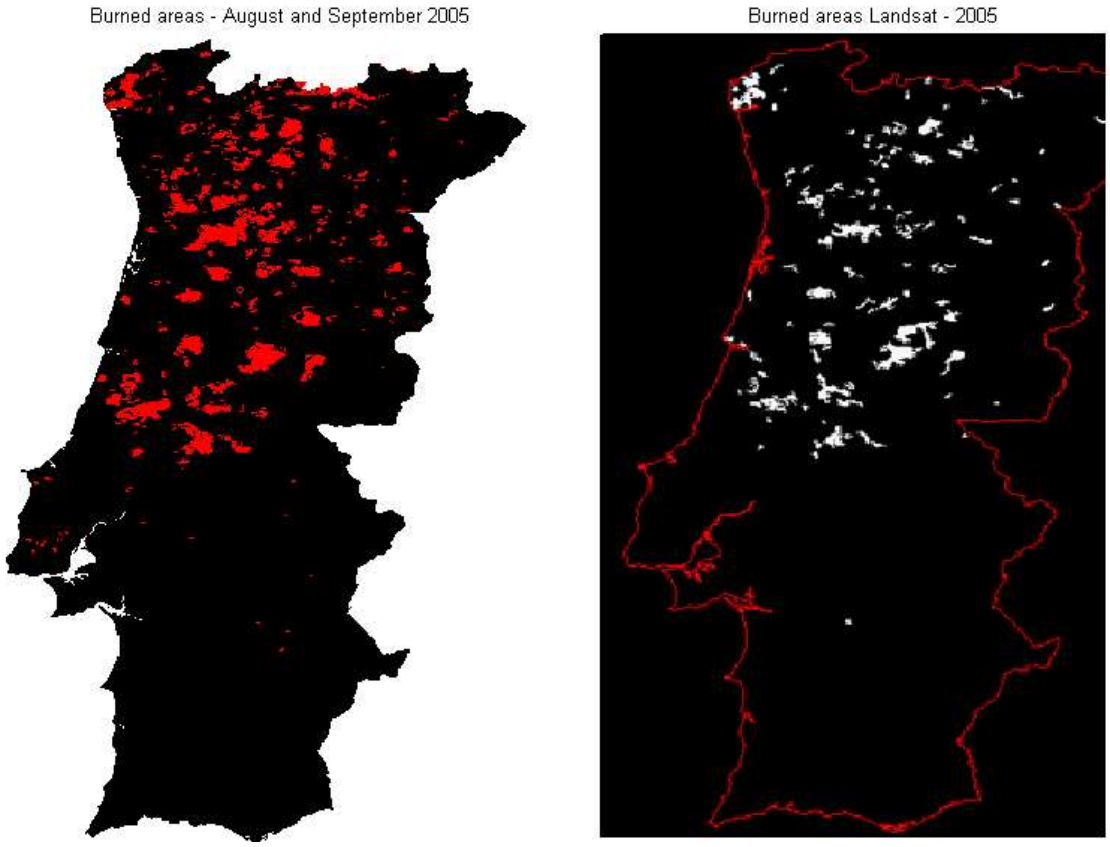

Figure 2. Burned area map for August and September 2005, as obtained by the algorithm based on MODIS imagery (a - left panel) and the reference map for the whole year of 2005, based on Landsat imagery (b - right panel).

Validation of burned area is based on the comparison of the map obtained by the developed algorithm (Figure 2a) with the one derived from scar vectors independently obtained from an end of season Landsat image by ICNF (Figure 2b). For this purpose, the reference map of scar vectors was rasterized to 1 km resolution, the same of MODIS imagery. In this process, however, some pixels, mainly the ones located in the borders of the scars, do not represent totally burned areas. Because of this, each pixel of the reference map have associated to it a value which represents the percentage of burned area (Figure 3).

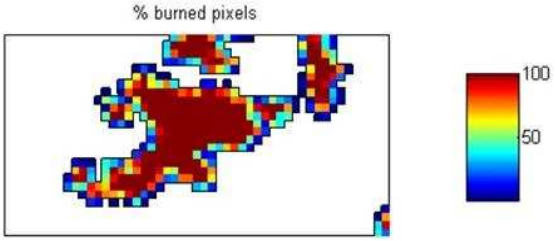

Figure 3. Proportion of burned area in pixels of the reference map, based on Landsat imagery.

Comparison between both maps is performed based on a contingency table (also known as confusion matrix), where all pixels correctly classified are located in the main diagonal, and the incorrect ones, in the remaining cells. The contingency table allows computing a set of accuracy measures, namely Proportion Correct (PC), Commission Error (CE), Omission Error (OE) and Probability of Detection (POD). These measures were computed according to the studies carried out by Binaghi *et al*. (1999), where agreement or disagreement between reference data (with high resolution) and classified data

(low resolution) are calculated taking into account the proportion of burned/unburned area of the reference data inside each pixel of classified data. Tables 1 and 2 present the confusion matrix and the accuracy measures, respectively.

Table 1. Contingency table calculated according to studies carried out by Binaghi et al. (1999). Classification was made based on MODIS instrument data, while reference data were based on Landsat imagery.

		LANDSAT		
MODIS		BURNED	UNBURNED	**Total**
	BURNED	1596.7	3165.0	**4761.7**
	UNBURNED	943.7	87765.6	**88709.4**
	Total	**2540.4**	**90930.6**	**93471.0**

Table 2. Accuracy measures calculated from the contingency table: Proportion Correct (PC), Commission Error (CE), Omission Error (OE) and Probability of Detection (POD).

Accuracy Measures	
PC	96%
CE	66%
OE	37%
POD	63%

The spatial distribution of omission errors, commission errors and hits is presented in Figure 5. Green, red and magenta pixels indicate correctly identified burned areas; commission errors and omission errors, respectively.

According to Table 2, 63% of burned pixels identified by ICNF (based on the end of fire season Landsat imagery) were correctly classified by the algorithm (based on MODIS imagery). This is a very good result, since the algorithm only detects scars corresponding to August and September, while the reference map refers to the whole year of 2005. In other words, using only images of July, August and September, the algorithm was able to detect more than a half of burned area in the year of 2005.

Cases of omission error represent 37% of burned pixels of the reference map. Taking into account hotspots dates, it is found that 23% of all omission errors refer to wildfires occurred in months that are neither August nor September. Therefore, 23% of all omission errors refer to wildfires that occurred outside the period of imagery used, not being detectable by the algorithm. Most of these cases are related to hotspots detected in July (15), namely the largest scar not detected by the algorithm, highlighted in the right panel of Figure 4. On the other hand, almost 30% of omissions have an associated hotspot detected in August or September, and should have been identified by the algorithm (Figure 5). Almost half of omission cases occurred in pixels without the presence of hotspots. This may be due to the following three causes:

a) Hotspots used were restricted to those with confidence over 50%;
b) The MODIS algorithm of detection of hotspots failed;
c) The scar map of ICNF may be incorrect in some cases, presenting scars that do not correspond to wildfires (e.g., deforestation).

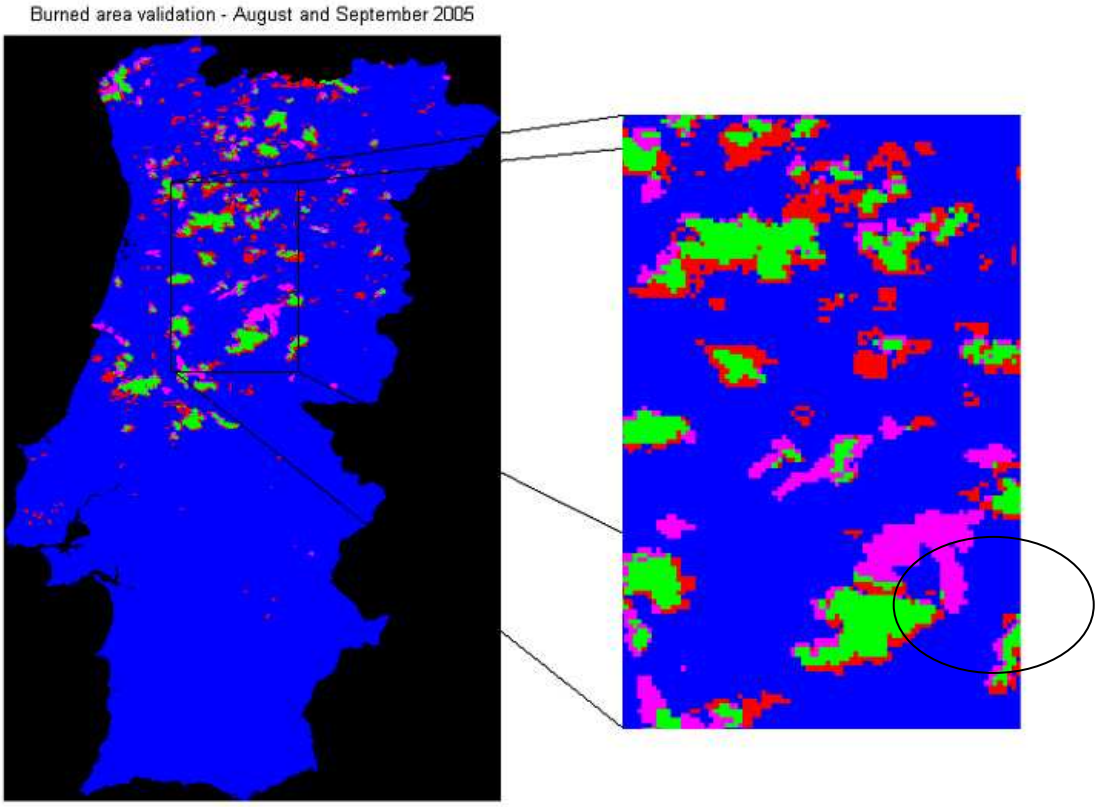

Figure 4. Validation of detection of burned areas. Green pixels indicate agreement between Modis and Landsat; magenta pixels indicate omission errors; red pixels indicate commission errors.

Another important question relates to the proportion of burned pixels area. More than a half (55.4%) of all omission errors refers to MODIS pixels in which only 1-50% of the area is burned (Figure 6). These pixels are, therefore, more difficult to be detected by the algorithm that uses low resolution (1 km) data.

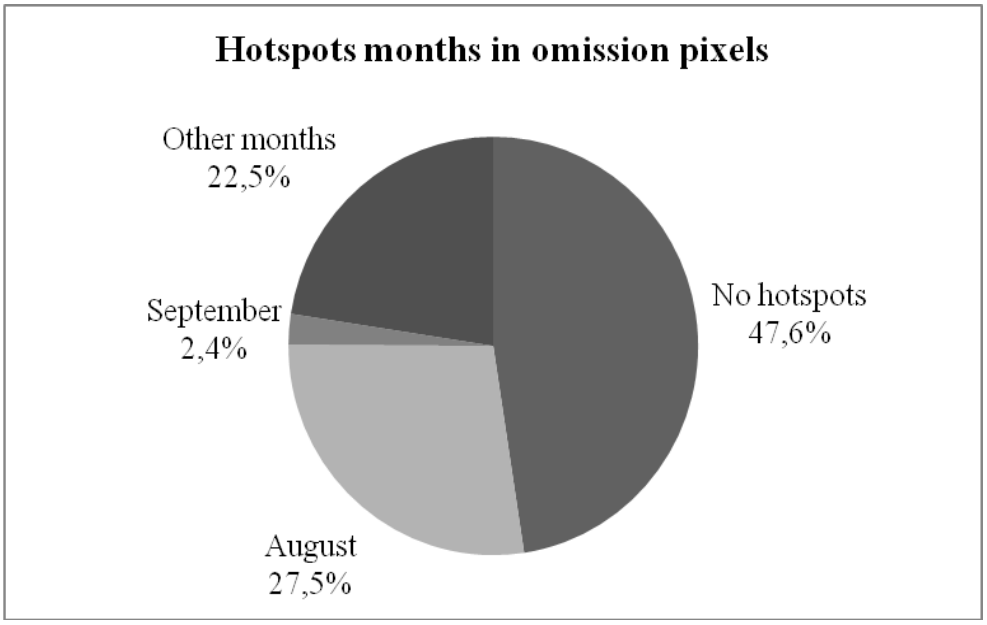

Figure 5. Relative frequency of monthly distribution of hotspots in pixels characterized as omission errors; 62.2% however, do not have associated hotspots.

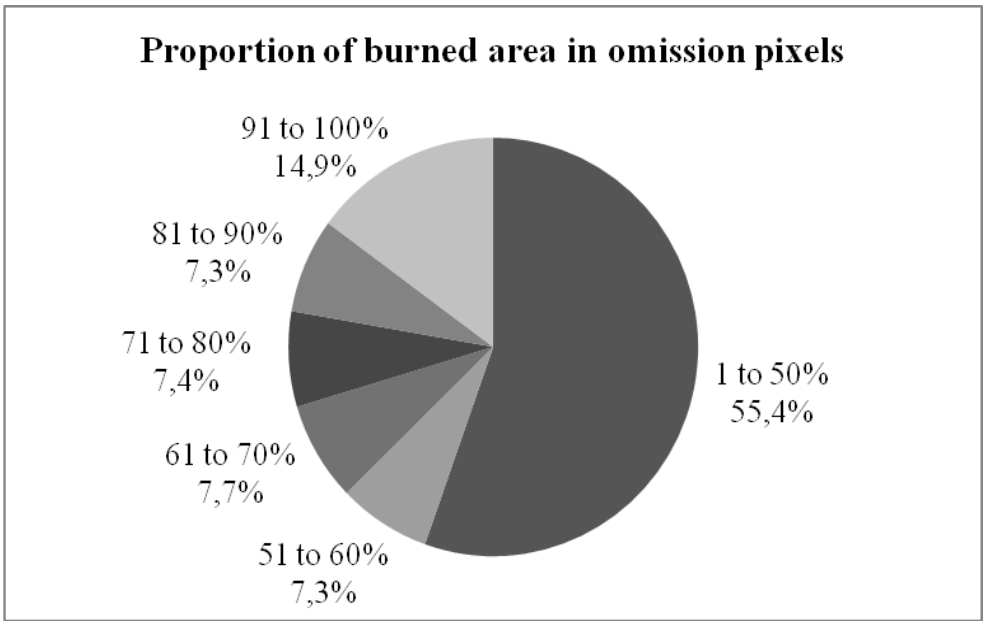

Figure 6. Proportion of burned area of pixels characterized as commission errors. Only 18.4% correspond to pixels in which 90 to 100% of the area is burned.

Two thirds (66.5%) of the pixels detected as burnt by the algorithm were commission errors. However, 14.8% of them have associated hotspots in August and September (Figure 7). Being classified as burned by the algorithm, these pixels are associated to W low values, and since at least one hotspot has been detected it is quite likely that they have burned in fact; the discrepancies may therefore be due to inaccuracies in the reference map, which, despite having a higher spatial resolution and having been prepared with due care, is also subject to errors, mainly because of its lower temporal resolution.

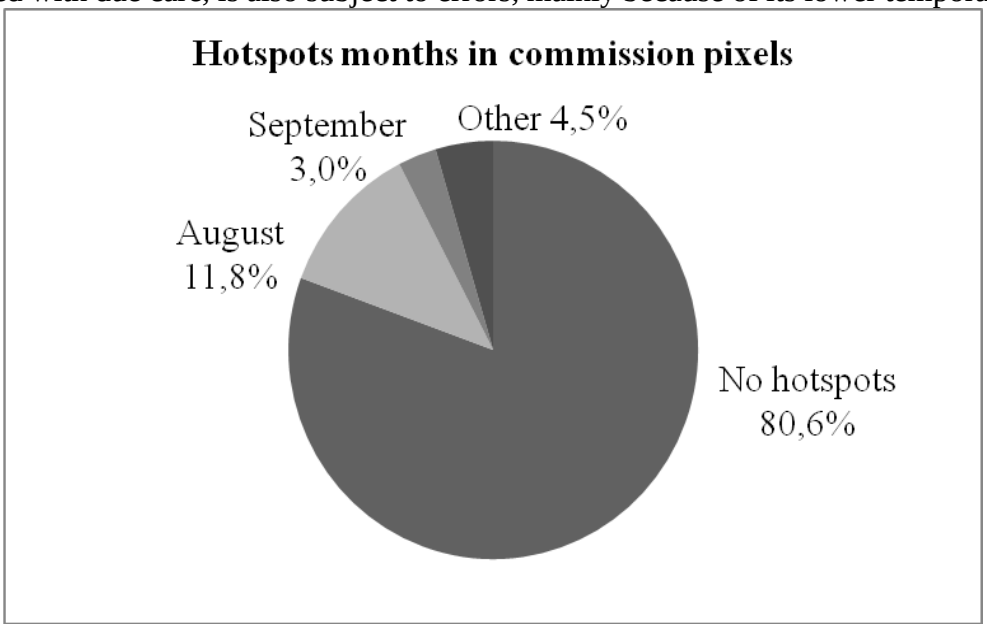

Figure 7. Relative frequency of monthly distribution of hotspots in pixel with commission errors. 20.7% of commission errors have hotspots in August and September, a possible indication of hit of the algorithm and omission of the reference map.

Dates assigned by the algorithm are presented in Figure 8. Attribution of dates was only made for pixels correctly identified as burned (left panel); hotspots dates are also presented for the same pixels, when available (right panel). Validation was performed by comparing these dates (between August 1 and September 30). It may be noted that we opted to restrict to hotspots with confidence higher than 50%, so they are supposed to represent wildfires in fact.

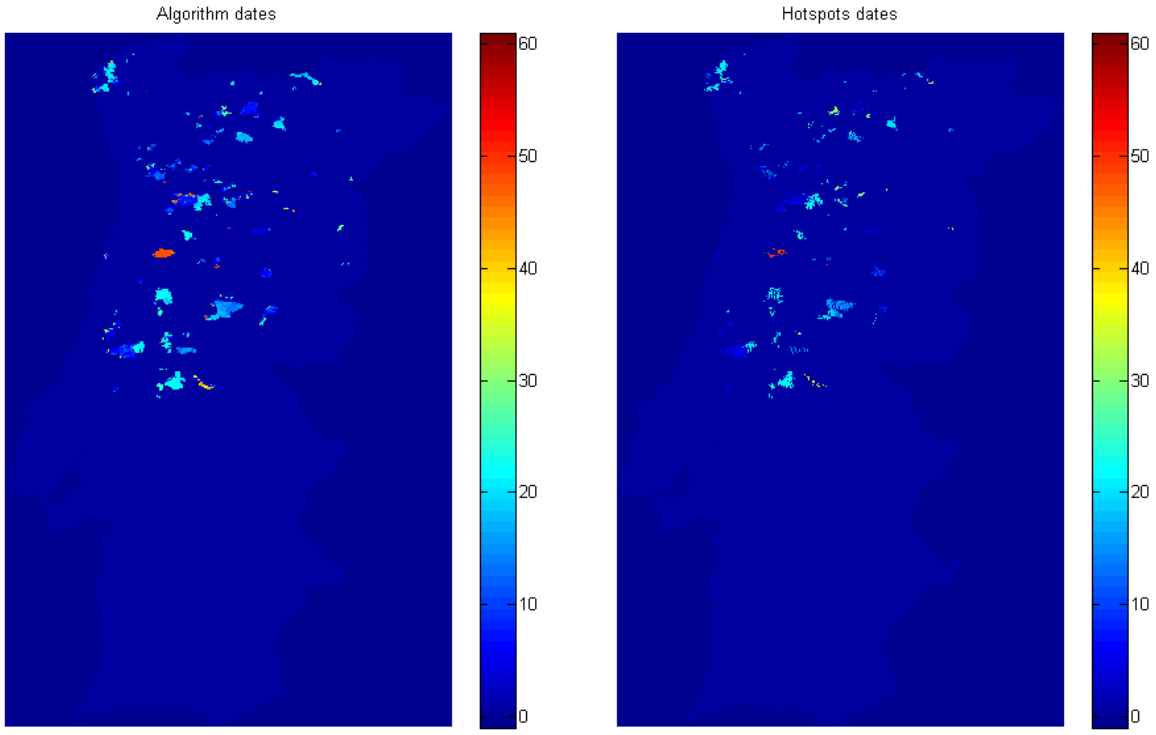

Figure 8. Days of wildfires occurrence. Day 1 refers to August 1, and day 61, to September 30, 2005. Darker blues refer to unburned pixels (zero value) and pixels outside Portugal (negative values) (left panel). On the right panel, are presented days of occurrence of hotspots in the same pixels, when available.

Comparison of estimated dates by our procedure and dates of hotspots as identified by MODIS showed that more than 3/5 of cases (63.5%) have differences between -2 and +2 days and that 3/4 of cases (75.0%) have differences between -5 and +5 days (Figure 9).

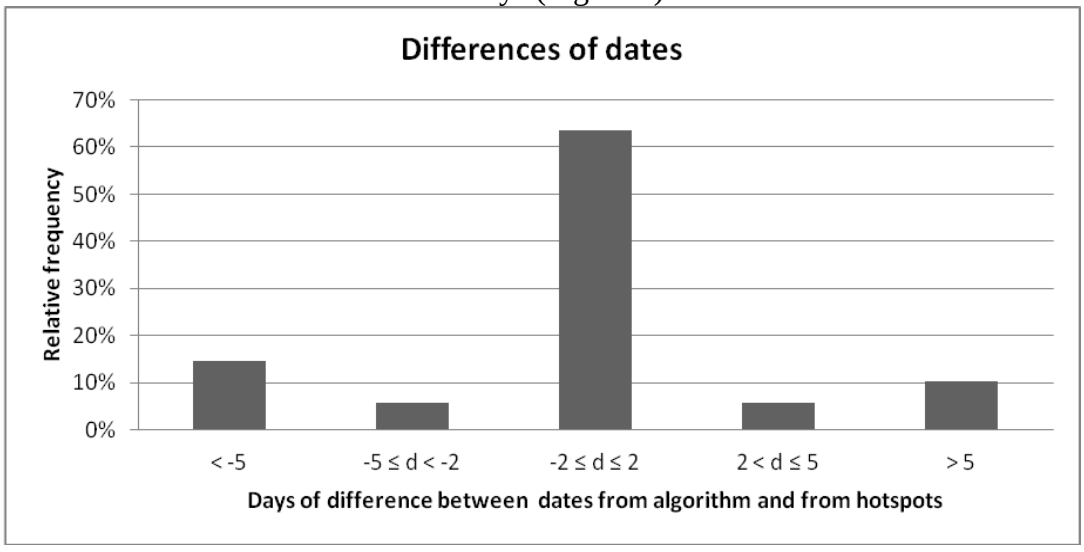

Figure 9. Differences between dates assigned by the algorithm and dates of hotspots occurrence. 75% of dates were correctly attributed.

Discussion

A new automated method of detection and of date assignment to burned areas was applied to Portugal, based on daily reflectances from NIR (near-infrared) and MIR (middle infrared). A total of 170 images from MODIS instrument on-board Aqua and Terra satellites were used during July, August and September 2005, the second worst year in terms of burned area in Portugal.

The algorithm uses MIR and NIR information to calculate the (V, W) Burned Index. Burned pixels are identified by means of fixed and contextual thresholds on monthly composites, and burned area maps are generated. Comparison between generated and reference maps, the latter based on end of fire season Landsat imagery resulted in an agreement of 95.6%, and a Probability of Detection of 62.9%, which means that with only low resolution images for July, August and September, the automated procedure was able to detect almost two thirds of all scars occurred in 2005.

Omission and commission errors were observed mainly on the scars borders, where the proportion of burned area is not so large and the spectral signal on the W Index is not so pronounced. Commission errors were also observed in isolated scars, generally small ones and associated to hotspots. It is possible that these cases are actually omission errors of the reference map and hits by the algorithm. This would be possible given the fact that the reference map is based on end of fire season imagery, when the radiometric signal of some small scars could have been already extinguished. Besides, the lower temporal resolution of Landsat when compared to MODIS, naturally leads to a smaller number of available images.

Omission errors were also observed in isolated scars, generally large ones. Analyzing dates of hotspots in these pixels, when available, it was noted that these undetected scars correspond to wildfires that have not occurred in August and September. Notably the greatest scar, located in the central of the country, in which hotspots indicate wildfires occurred in July. Therefore it was not supposed to be detected by the algorithm.

The attribution of dates to the scars was made based on analysis of W Index values, being the day with the greatest variation (greatest temporal separability) considered the day of burn. Validation shown that 63.5% of the pixels were correctly dated, with differences of the hotspots occurrence between -2 and +2 days. Allowing differences of up to 5 days, the matching score increases to 75.0%.

Results from this work open very promising perspectives towards the operational identification and the assignment of dates to burned areas, therefore contributing to a better understanding of fire regimes.

References

Barbosa, P. M., Grégoire, J. M., & Pereira, J. M. C. (1999). An algorithm for extracting burned areas from time series of AVHRR GAC data applied at a continental scale. *Remote Sensing of Environment*, *69*(3), 253-263.

Binaghi, E., Brivio, P. A., Ghezzi, P., & Rampini, A. (1999). A fuzzy set-based accuracy assessment of soft classification. *Pattern recognition letters*,*20*(9), 935-948.

Boyd, D. S., & Duane, W. J. (2001). Exploring spatial and temporal variation in middle infrared reflectance (at 3.75@ m) measured from the tropical forests of west Africa. *International Journal of Remote Sensing*, *22*(10), 1861-1878 apud Libonati, 2010.

Direcção Geral Dos Recursos Florestais. *Incêndios Florestais – Relatório de 2005.* Lisboa, 2006. 27p. Available at: <http://www.icnf.pt/portal/florestas/dfci/Resource/doc/rel/if-rel2005.pdf>. Last visited: 2014, 26 January.

Earth Observing System Data and Information System. *Near Real-Time Data - FAQ.* Available at: <https://earthdata.nasa.gov/data/near-real-time-data/faq/firms>. Last visited: 2014, 05 March.

Fraser, R. S., & Kaufman, Y. J. (1985). The relative importance of aerosol scattering and absorption in remote sensing. *Geoscience and Remote Sensing, IEEE Transactions on*, (5), 625-633.

Giglio, L., Loboda, T., Roy, D. P., Quayle, B., & Justice, C. O. (2009). An active-fire based burned area mapping algorithm for the MODIS sensor. *Remote Sensing of Environment*, *113*(2), 408-420.

Holben, B. N. (1986). Characteristics of maximum-value composite images from temporal AVHRR data. *International Journal of Remote Sensing*, *7*(11), 1417-1434.

Kaufman, Y. J., & Remer, L. A. (1994). Detection of forests using mid-IR reflectance: an application for aerosol studies. *Geoscience and Remote Sensing, IEEE Transactions on*, *32*(3), 672-683.

Libonati, R., DaCamara, C. C., Pereira, J. M., Setzer, A., & Morelli, F. (2007). A New Optimal Index for Burnt Area Discrimination in Satellite Imagery. In*2007 EUMETSAT Meteorological Satellite Conference and the 15th Satellite Meteorology & Oceanography Conference of the American Meteorological Society*.

Libonati, R., DaCamara, C. C., Pereira, J. M. C., & Peres, L. F. (2011). On a new coordinate system for improved discrimination of vegetation and burned areas using MIR/NIR information. *Remote Sensing of Environment*, *115*(6), 1464-1477.

Libonati, R., DaCamara, C. C., Pereira, J. M. C., & Peres, L. F. (2010). Retrieving middle-infrared reflectance for burned area mapping in tropical environments using MODIS. *Remote Sensing of Environment*, *114*(4), 831-843.

Libonati, R., DaCamara, C. C., Pereira, J. M. C., & Peres, L. F. (2012). Retrieving middle-infrared reflectance using physical and empirical approaches: implications for burned area monitoring. *Geoscience and Remote Sensing, IEEE Transactions on*, *50*(1), 281-294.

Libonati, R. *Using middle-infrared reflectance for burned area detection*. 2010. 182 p. Tese (Doutorado em Ciências Geofísicas e da Geoinformação - Meteorologia) – Faculdade de Ciências, Universidade de Lisboa, Lisboa, 2010.

Libonati, R. (2010). *Using middle-infrared reflectance for burned area detection*.Ph.D. dissertation, University of Lisbon, Lisbon, Portugal.

Libonati, R.; Setzer, A. W.; Morelli, F. Algoritmo automático de detecção de áreas queimadas em imagens MODIS – aplicação na região de Jalapão, TO. *In: Proceedings of XVI Simpósio Brasileiro de Sensoriamento Remoto*. Foz do Iguaçu, 2013.

Mieville, A., Granier, C., Liousse, C., Guillaume, B., Mouillot, F., Lamarque, J. F., ... & Pétron, G. (2010). Emissions of gases and particles from biomass burning during the 20th century using satellite data and an historical reconstruction. *Atmospheric Environment*, *44*(11), 1469-1477.

National Aeronautics and Space Administration. *About Modis*. Available at: < http://modis.gsfc.nasa.gov/about/>. Last visited: 2014, 24 February.

Pereira, J. M. (1999). A comparative evaluation of NOAA/AVHRR vegetation indexes for burned surface detection and mapping. *Geoscience and Remote Sensing, IEEE Transactions on*, *37*(1), 217-226.

Pereira, M. G., Calado, T. J., DaCamara, C. C., & Calheiros, T. (2013). Effects of regional climate change on rural fires in Portugal. *Climate research*,*57*(3), 187-200.

Pereira, M. G., Trigo, R. M., da Camara, C. C., Pereira, J., & Leite, S. M. (2005). Synoptic patterns associated with large summer forest fires in Portugal. *Agricultural and Forest Meteorology*, *129*(1), 11-25.

Pereira, M. G., Malamud, B. D., Trigo, R. M., & Alves, P. I. (2011). The history and characteristics of the 1980–2005 Portuguese rural fire database.*Natural Hazards and Earth System Science*, *11*(12), 3343-3358.

Roy, P. S. (2003). Forest fire and degradation assessment using satellite remote sensing and geographic information system. *Satellite Remote sensing and GIS applications in agricultural meteorology*, 361.

Roy, D. P. (1999). Multi-temporal active-fire based burn scar detection algorithm. *International Journal of Remote Sensing*, *20*(5), 1031-1038.

Verstraete, M. M., & Pinty, B. (1996). Designing optimal spectral indexes for remote sensing applications. *Geoscience and Remote Sensing, IEEE Transactions on*, *34*(5), 1254-1265.

Characterizing the secondary peak of Iberian fires in March

Carlos C. DaCamara, Ricardo M. Trigo, Manuel L. Nascimento

Instituto Dom Luiz, Faculdade de Ciências, Universidade de Lisboa, 1749-016 Lisboa, Portugal, cdcamara@fc.ul.pt, rmtrigo@fc.ul.pt, mlnascimento@fc.ul.pt

Abstract
Mediterranean Europe is strongly affected by wildfires that burn half a million of hectares of vegetation cover every year causing extensive economic losses and ecological damage. Most studies about fire activity over the Iberian Peninsula (IP) are focused on the summer months, from June to September, as these correspond to the vast majority of BA, but it is important to note the occurrence of a secondary peak during late winter and early spring. This peak is particularly prominent during the month of March, although its relevance changes considerably for different Iberian regions. While the causes of fire activity in March in IP are mainly anthropogenic, either because of negligence or arson, meteorological factors also play an important role in the ignition and spread of wildfires.
The main aims of the present study are threefold: 1) to identify the areas of the IP where fires in March play an important role and have a coherent inter-annual variability; 2) to relate burned areas in March to meteorological danger and 3) to characterize the synoptic conditions that constitute the meteorological background in extreme events (i.e. large burned areas in March).

Keywords*: burned area, meteorological factors, extreme events*

Introduction

Mediterranean Europe is strongly affected by wildfires that burn half a million of hectares of vegetation cover every year causing extensive economic losses and ecological damage (San-Miguel-Ayanz *et al*. 2012). According to reports of the European Commission (European Commission, 2011), during the period 1980-2010 the Iberian Peninsula (IP) has contributed to 60% of the total burned area of 14,620,968 ha that was recorded in five Southern Member States (Portugal, Spain, France, Italy and Greece). As discussed in previous works, e.g. in Trigo *et al*. (2013), this may be attributed to a number of factors that include both natural and anthropogenic factors. Natural factors include geographical location, topography, vegetation cover as well as climate background and extreme meteorological conditions (Pausas, 2004; Pereira *et al*., 2005; Trigo *et al*., 2006). Anthropogenic factors range from land management practices and fire prevention, management and suppression efforts, up to socio-economic and demographic trends (Cueva *et al*., 2006; Costa *et al*., 2010).
Most studies about fire activity over IP are focused in the summer months, from June to September, as these correspond to the vast majority of BA. However, it is important to note the occurrence of a secondary peak during late winter and early spring. This peak is especially conspicuous in the month of March, although its relevance changes considerably for different Iberian regions (Trigo *et al*. 2013). The existence of a secondary peak was known for some northern sectors of IP, but the absence of a pan-Iberian dataset undermined a more thorough analysis on the exact nature and extension of this secondary peak. This caveat was solved to a large extent in Trigo *et al*. (2013) that have used a consistent dataset for the entire Iberian region and applied a k-means cluster analysis to identify large areas characterized by similar fire regimes. The most compelling results were obtained for four clusters (Northwestern, Northern, Southwestern and Eastern) whose spatial patterns and seasonal fire regimes are shown to be related with constraining factors such as topography, vegetation cover and climate conditions. Interestingly, two of the identified clusters present two maxima, with the Northwestern cluster revealing a much larger peak in August and a smaller one in March. The northern most areas of Iberia are concentrated in the Northern cluster that presents two peaks, both comparable in

magnitude (although relatively small), in early spring (March) and late summer (September). Finally, the two remaining clusters (Southwestern and Eastern) are characterized by a single summer maximum in either July or August. Therefore, considering the fact that these March fires affect not only ecosystems but also local populations, they should not be neglected, and deserve to be further investigated. While the causes of fire activity in March in IP are mainly anthropogenic, either because of negligence or arson, meteorological factors also play an important role in the ignition and spread of wildfires. The main aims of the present study are threefold: 1) to identify the areas of the IP where fires in March play an important role and have a coherent inter-annual variability; 2) to relate burned areas in March to meteorological danger and 3) to characterize the synoptic conditions that constitute the meteorological background in extreme events (i.e. large burned areas in March).
For that purpose, monthly amounts of BA are analyzed for each administrative region of Portugal and Spain, covering the period 1980-2005. The study area is first identified based on a ranking of relative BA in each region (i.e. in terms of percentage of the total area of the region) and two regions with distinct inter-annual variability are defined based on cluster analysis performed on time series of BA. The impact of meteorological danger is then assessed by means of the so-called Daily Severity Rating (DSR), an indicator of fire danger which is part of the Canadian Forest Fire Weather Index System (CFFWIS). Finally, meteorological charts of sea-level pressure, 500 hPa height, 2m-temperature and zonal and meridional components of the wind are analyzed for extreme years of BA during the period of study.

Data and methods

Burnt area data

Fire data were supplied by the Autoridade Florestal Nacional (AFN, 2011) and by the Dirección General de Biodiversidad, the national authorities for Portugal and Spain, respectively. The datasets cover the period from 1980 to 2005. Following Trigo *et al*. (2013), data for both countries were merged into a single dataset of monthly amounts of BA, spatially organized into administrative regions, respectively *distritos* for Portugal and *provincias* for Spain. Therefore, the database spatial domain is constituted by a total of 66 regions, 18 for Portugal and 48 for Spain.

Meteorological data

Following Pereira *et al*. (2013) meteorological danger of fire was evaluated based on DSR which integrates the Canadian Forest Fire Danger Rating System (CFFDRS). This system is composed of a set of quantitative indices of fire potential, which are used as guides in a wide variety of fire management activities. For instance, DSR is considered to be a good indicator about the expected efforts required for fire suppression and was specifically designed for averaging either in time or in space (Van Wagner 1987).
Daily values of all components of CFFWIS, in particular DSR, were computed based on ERA-interim reanalysis data at 12 UTC for the period 1979-2012. DSR fields are defined in a 0.05º by 0.05º grid covering the region delimited by latitude circles 35° and 45° N, and by meridians 10° W and 5° E which encompasses IP as well as a part of France and North Africa.

Synoptic conditions

Information about synoptic conditions associated with extreme events was obtained using the Koninklijk Nederlands Meteorologisch Instituut (KNMI) Climate Explorer tool. Synoptic information consists of maps of monthly anomalies defined as departures from climatological normal of 1981-2010 of sea-level pressure (SLP), 500 hPa geopotential fields (Z500), 2m-temperature (T2). Besides the aforementioned anomalies, monthly means of zonal and meridional wind magnitudes at 10 meters (U10 and V10, respectively) were also used. Maps of SLP and Z500 are defined on a large window, centred over IP and covering Europe and North Africa, delimited by latitude circles of 30° and 70° N

and by meridians of 45° W and 45° E, whereas maps of T2, U10 and V10 are defined on a smaller window covering the North of IP, defined between 40° and 45°N and between 10°W and the Greenwich meridian.

Results

Spatial analysis of BA in March

The total amount of BA in March, for each region, was sorted in descending order. However, because the considered regions have quite different surface areas, the analysis was performed on relative values of BA for each region, which were obtained by dividing the total amount of BA of each region by the total area of the region. All but one region that rank in the first 24 are spatially contiguous, spreading over the North and Northwest of IP. The exception is the region of Castellon (located over the East of IP) that ranks 19. This suggests considering the 23 contiguous regions as the study area for March BA over IP.

Inter-annual variability of BA in March

In order to identify regions of consistent inter-annual variability within the study area, a k-means clustering analysis was performed on time series of March BA for each region.

The k-means clustering analysis was applied to the 23 regions that constitute the study area, each one viewed as a point in a 26 dimensional space, each axis being the value of BA (normalized in time) for a specific year during the 26-year period 1980-2005. The k-means clustering analysis is performed by pre-specifying a given number *k* clusters (*k* was set to 2) and by successively assigning each point to the nearest centroid of the clustering, computing the centroids of obtained new clusters, and repeating the process until the assignment of members does not change. As shown in Fig 1, the two clusters obtained, hereafter referred to as East cluster and West cluster, present spatial continuity and are separated from each other by the Cantabrian mountain ranges.

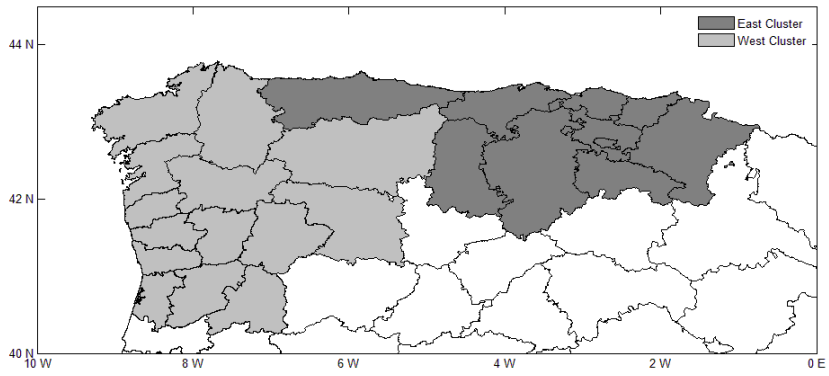

Figure 1. The k-means determined clusters of Northern Iberia

As shown in Figure 2, the time series for the two clusters of normalized burnt area present distinct behaviour, especially in terms of years of extreme BA. The years of 1981 and 1989 correspond to high values of burnt area for the East cluster, whereas the years of 1997 and 2000 are the ones of higher values of burnt area for the West cluster. The year of 1997 is especially conspicuous since both regions present high values of burnt area.

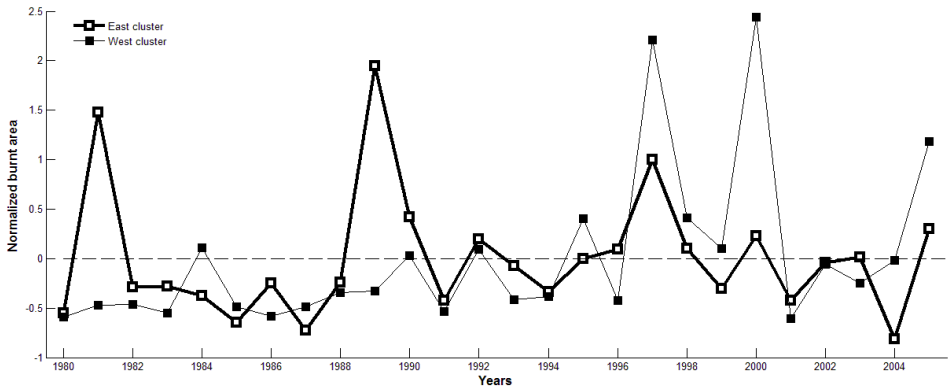

Figure 2. Time series of normalized BA for East and West clusters

Using polygon shapefiles for the administrative regions, a spatial mask for each cluster was defined and spatial means of daily values of DSR in March were accordingly computed. Then, for each year and for each cluster, the average of these DSR daily values above the monthly median was assigned to each year. This value, hereafter referred to as DSR+, is expected to reflect (at the monthly level) the presence of the usually small number of days that have high values of DSR and are associated to large fire activity that virtually explain the monthly amounts of BA. This is illustrated in Figure 3, where high values of DSR, for the West cluster in 2005, concentrate in a period of 5 days, from March 16th to 20th.

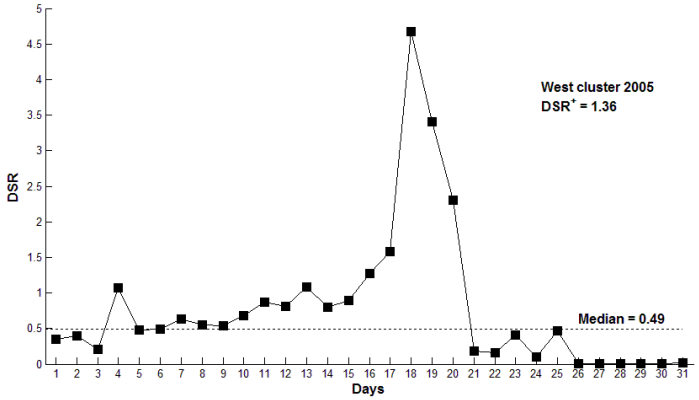

Figure 3. Time series of daily values of DSR for March 2005, for the West cluster

The time series of DSR$^+$ for both clusters are shown in Figure 4. As expected, because of the magnitude of the spatial scale associated to synoptic conditions, the two time series present a coherent temporal behaviour which reflects on the value of the correlation between the two (r = 0.88). The peak in both series occurring in 1997 is worth being noted since it corresponds to a year of high values of NBA in both East and West clusters. The same happens in 2005 which is associated to high values of NBA in both clusters and to high values of DSR$^+$ in both time series. The year of 2000, associated to a high value of NBA in the West cluster is also associated to a high value of DSR$^+$. However, the years of 1981 and 1989, where peaks of NBA may be identified in the East cluster, are associated to relatively low values of DSR$^+$.

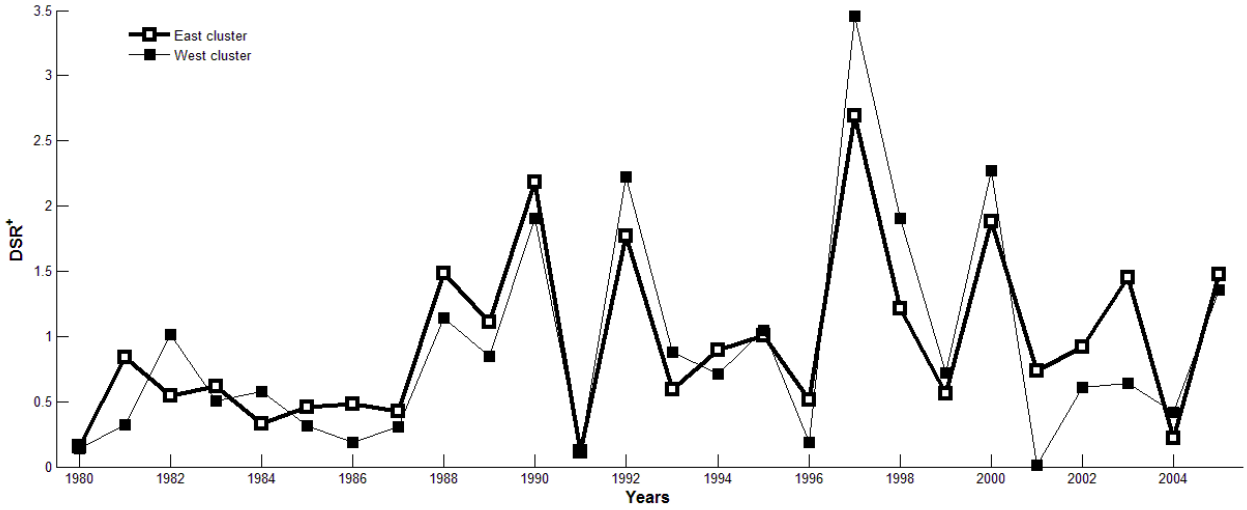

Figure 4. As in Figure 2 but for time series of DSR+.

3.3. The role of meteorological danger

Results from the previous sections suggest that the relationship between DSR+ and NBA in each cluster should be further investigated. Figure 5 presents scatter plots of DSR+ versus NBA for the West cluster (left panel) and the East cluster (right panel). In the case of the West cluster, results provide evidence of a linear relationship between the two analyzed time series. A linear model was fitted by least square regression which explains almost two thirds (65%) of the total variance.

In the case of the East cluster the above-mentioned year of 1981 and 1989 appear as outliers from a distribution that again suggests a linear relationship between DSR+ and NBA. These two outliers were disregarded and a linear regression model was fitted to the data, with good results, explaining three quarters (75%) of the total variance.

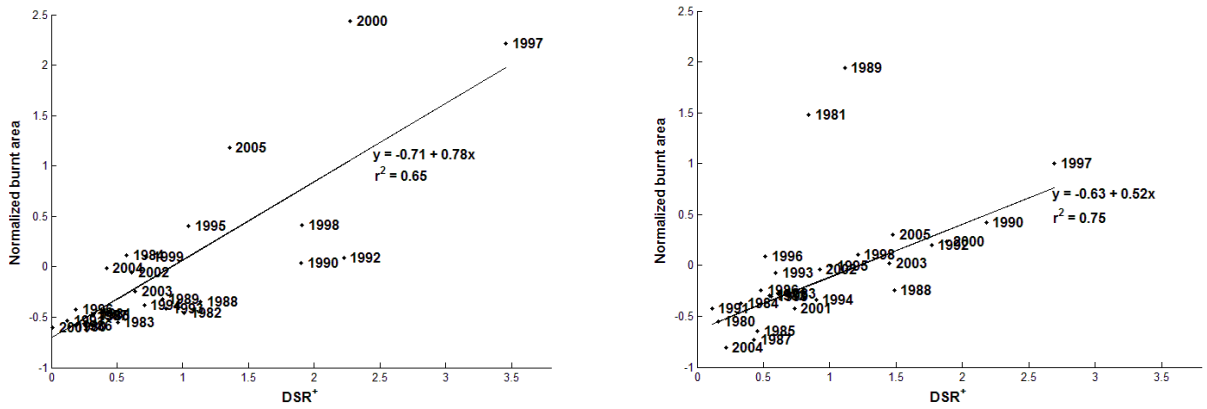

Figure 5. Scatter plots of NBA vs. DSR+ for the West (left panel) and East (right panel) clusters. Straight lines were obtained by linear regression that was applied to all years in the case of the West cluster and to all years but 1981 and 1989 in the case of the East cluster.

Results suggest that inter-annual variability of March NBA in the two clusters is linked to meteorological conditions that induce meteorological danger of fire ignition and fire spread. Nevertheless, the two highest years of BA in the East cluster present a different behaviour that deserves

to be further investigated. However, and as to be expected, even for all remaining cases in both clusters there is still a substantial amount of inter-annual variability that is not explained by such a simple model (about one third and one fourth of total variability for West and East clusters, respectively).

3.4. Atmospheric patterns associated to extreme years of burnt area

The linkage between DSR^{+} and NBA was further investigated by analyzing the synoptic circulation patterns that prevailed for years characterized by very large amounts of March NBA for each or both clusters. Figure 6 presents the values of NBA in descending order for the West cluster (left panel) and the East cluster (right panel). The four (six) highest years for the West (East) cluster are labelled.

First a detailed analysis will be presented for the year of 2000, associated to the highest value of NBA in the West cluster. Then a similar analysis is provided for the year 1989, associated to the highest value of NBA in the East cluster and finally for the year 1997 associated to high values of NBA in both clusters (ranking 2nd and 3rd in the West and East clusters, respectively).

As shown in Figure 7 (top panel), the extreme event of 2000 covers the majority of the area of the West cluster, with all regions ranging from the top to the 5th position, half of the 14 regions occupying the 1st rank in BA.

In the case of the extreme event of 1989 (Figure 7, central panel), the large majority of regions that form the East cluster occupy the first three positions, the exception being the provinces of Asturias and Cantabria, located in the northwest coast of the East cluster.

In the case of 1997 (Figure 7, bottom panel), 19 regions out of the 23 regions that form the East and West clusters occupy the first five positions, 12 of them ranking 1st and 2nd. The exceptions are the easternmost regions of Guipúzcoa, Vizcaya, Navarra and La Rioja that rank in positions 12, 13, 15 and 19.

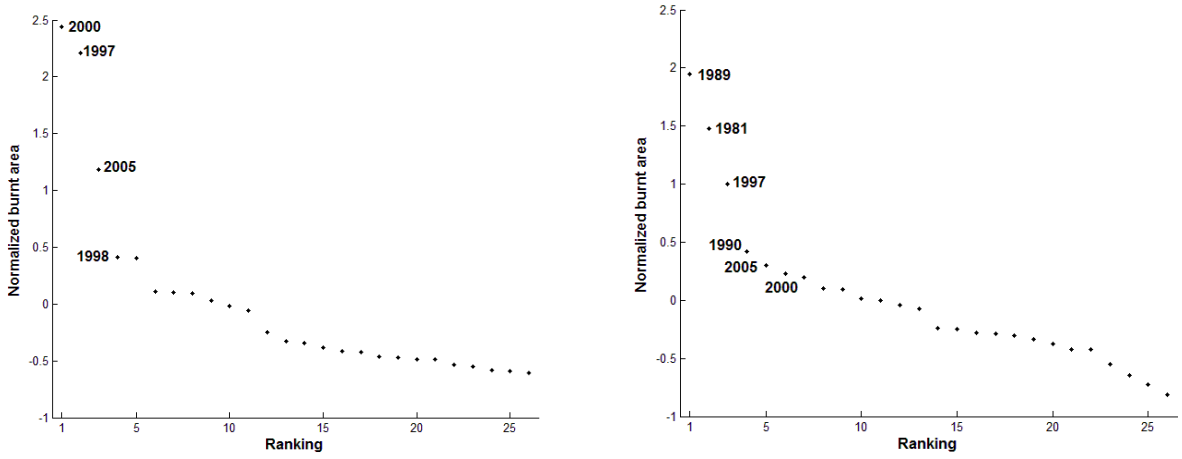

Figure 6. Values of NBA sorted in descending order for the West (left panel) and East (right panel) clusters.

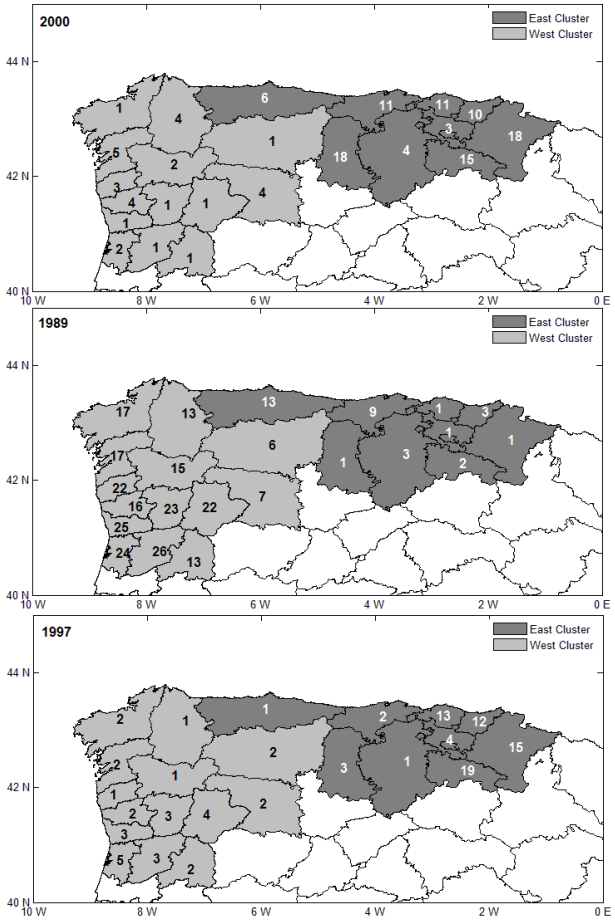

Figure 7. Ranking of administrative regions in the study area according to the amount of BA for the extreme events of March 2000 (top panel), March 1989 (middle panel) and March 1997 (bottom panel).

3.5. The extreme cases in the West cluster (March 2000), the East cluster (March 1989) and both clusters (March 1997)

The atmospheric circulation relative to March 2000 is characterized by the presence of an intense anticyclonic pattern centred just west of the British Islands (Fig 8, top panel). This structure is characterized by positive anomalies of SLP (Figure 8, top left panel) and geopotential height at the 500hPa level, which are characteristic of a hot quasi-barotropic anomaly. The location of such patterns, farther North than usual, corresponds to a typical Winter-Spring blocking pattern (Trigo *et al.*, 2004) that disrupts the usual path of low pressure systems from the Atlantic towards Europe. The negative values of zonal and meridional winds for the West cluster point to a North-eastern continental air flow which results in negative temperature anomalies along the northern coast of Spain as a consequence of the advection of cold air from northern Europe (Trigo *et al.*, 2004). Positive temperature anomalies may however be observed for Northern Portugal and Galicia (Figure 8, top right panel), as a result from an intense Föhn effect over the Cantabrian mountains with warmer and drier air descending the southern flank. The warm temperatures and downwind are associated to meteorological conditions favouring the onset and spreading of fires, which translates into an increase of meteorological danger of fire. This is clearly shown in the daily time series of DSR for March 2000 where a steady increase may be observed since the 7th until the 20thof March (Figure 9, top left panel).

When compared with March 2000, the atmospheric circulation of March 1989 presents an almost inverted pattern, with an intense low pressure system crossing the Atlantic with its centre placed just south of Iceland (Figure 8, central panel). The presence at high latitudes of highly negative anomalies of SLP (Figure 8, central left panel) and geopotential height at the 500 hPa level associated with

positive anomalies in the lower latitudes induce stronger than usual westerly winds, with the advection of warm and moist being responsible for the positive anomalies that are observed over the study area. Warming of air is further enhanced by the Föhn effect when the flow crosses the Cantabrian mountain ranges, resulting in hot (and dry) anomalies close to the Basque country and Pyrenees that could induce fire activity (Figure 8, central right panel). This is supported by the behaviour of time series of DSR that presents a sequence of three small peaks of increasing amplitude in the first 17 days of March, the third one centred on March 16th, followed by a very large peek centred on March 27th (Figure 9, top right panel). The fact that extreme values of DSR are concentrated on this last very short period of time makes it very difficult to perform an analysis of the events at the monthly scale and explains the apparently anomalous behaviour of March 1989 when looking at scatter plots of DSR^{+} versus NBA (Figure 5, right panel).

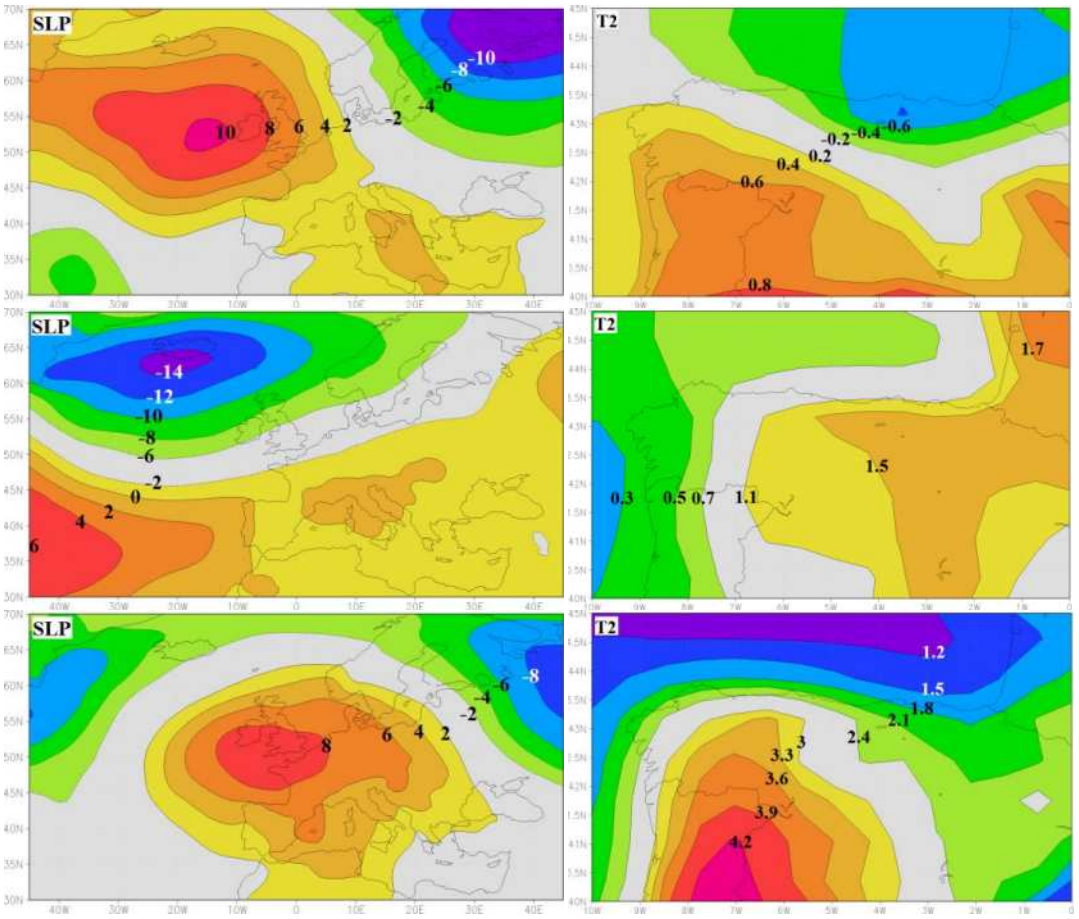

Fig 8 –Monthly anomaly charts for the West cluster of March 2000 (top panel), the East cluster of March 1989 (central panel) and for both clusters of March 1997 for two atmospheric fields. Contour lines delineate anomaly fields of SLP (hPa), and T2 (°C)

The atmospheric circulation of March 1997 is very similar to the one of March 2000, being dominated by a strong anticyclonic pattern centred above the English Channel (Figure 8, bottom panel). Two intense positive anomalies of both SLP (Figure 8, bottom left panel) and Z500 may be again identified, suggesting a hot barotropic anomaly, typical of a blocking pattern. The resulting Northeastern winds induce a small positive anomaly over the easternmost regions of the East cluster and the air is further warmed by the Föhn effect when crossing the Cantabrian Mountains into Galicia and Northern Portugal. This effect is clearly illustrated by the daily time series of DSR over the West and East clusters (Figure 9, bottom panel), where two large peaks may be identified in the last ten days of March, the peaks in the time series of the West cluster being substantially higher than the

corresponding ones in the East cluster. The two time series present a coherent variability during the month, especially during the last 10 days, a feature that explains the high values of burned area that were registered in both clusters.

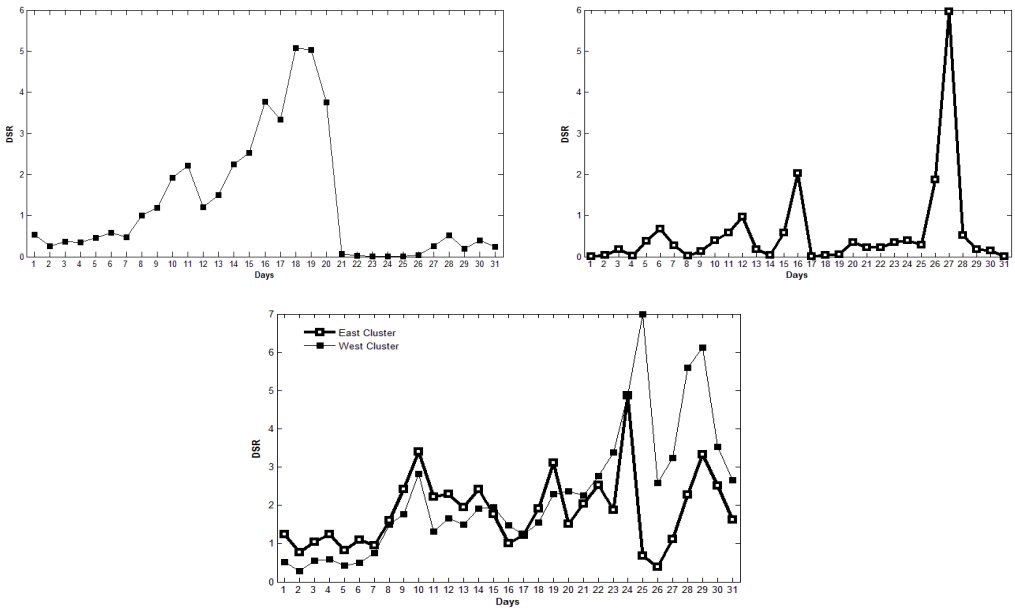

Fig 9 – Daily values of mean DSR for the West cluster of March 2000 (top left panel), for the East cluster of March 1989 (top right panel) and both clusters of March 1997 (bottom panel)

3.6. The role of large-scale atmospheric patterns

The role played by large scale atmospheric patterns in the establishment of meteorological conditions favouring the occurrence of fire events may be put into evidence by analyzing the atmospheric patterns of 1989, 1997 and 2000, associated to these three extreme events. As shown in Figure 8, in all three events the study area is crossed either by Northeastern flow (cases of March 2000 and of March 1997) or by Southwestern flow (case of March 1989); in all cases the flow crosses the Cantabrian mountains and the associated Föhn effect induces warm and dry conditions downstream where fire activity is observed.

Such large scale flow is induced by well-defined anomalies west of the British Isles, with a barotropic structure which are either positive anomalies (of blocking-type) or negative. These barotropic anomalies tend to be stationary for several days and together with the Föhn effect are on the origin of the observed peaks of daily DSR (Figure 9), i.e. of meteorological danger.

This simple conceptual model was applied to the seven cases where amounts of BA ranked in the top four positions in the case of the West cluster and in the top six positions in the case of the East cluster (i.e. the two outliers of 1981 and 1989 and the following four years of higher BA). The chosen years are identified in Figure 6 and in Table 1, the latter showing the ranks and the type of anomaly located in the Atlantic Ocean near the British Isles.

It may be observed that the two extreme cases in the East cluster (March 1981 and 1989) are associated to an intense negative anomaly that steers Southwestern flow and that all remaining 5 cases are associated to a blocking-type positive anomalies that induces Northeastern flow. It may be further noted that 3 out of these 5 cases (i.e. March 1997, March 2000 and March 2005) correspond to high values of BA in both clusters.

Table 1. Extreme years, West and East ranking and occurrence of blocking event.

Year	Large-scale pattern	West cluster rank	East cluster rank
1981	Negative anomaly	19	**2**
1989	Negative anomaly	13	**1**
1990	Positive anomaly	9	**4**
1997	Positive anomaly	**2**	**3**
1998	Positive anomaly	**4**	8
2000	Positive anomaly	**1**	**6**
2005	Positive anomaly	**3**	**5**

Conclusions

A study was performed on BA in the IP associated to fire activity in March. The study relies on monthly values of BA for a set of 66 regions covering the period 1980-2005 (Trigo *et al*., 2013). The annual cycle of BA for the entire IP was determined, showing two peaks of BA, a first large peak centred in August and spreading over summer and a secondary one centred in March and spreading over late winter-early spring.

The 66 regions were sorted by decreasing order of relative BA, which was obtained by dividing the total amount of BA for each region by the corresponding total area, therefore ensuring equal weights from the regions. The ranking procedure allowed defining a spatially contiguous study area formed by 23 regions that ranked in the first 24 places; the region of Castellon, that ranked 19th was discarded because of the spatial location, out of the area covered by the remaining ones.

Time series of BA for each of the 23 regions were normalized by subtracting the respective time mean and dividing by the standard deviation and a cluster analysis was performed on time series of NBA leading to the identification of two clusters, each one presenting a characteristic inter-annual variability. The two clusters, the so-called West cluster and East cluster, are formed by contiguous regions and are separated by the Cantabrian Mountains. Extreme events were identified in each or both clusters, namely March 1997 for both clusters, March 2000 and March 2005 for the West cluster, and March 1981 and March 1989 for the East cluster.

For each cluster, the associated meteorological conditions were analyzed by inspecting time series of DSR, an index of meteorological danger, i.e. of meteorological conditions that might induce fire onset and fire spread. Because fire events tend to be associated to a small number of days with higher meteorological danger, the monthly values of meteorological danger were assigned in terms of DSR^{+}, i.e. on time means performed on days with DSR above the monthly median. Time series of DSR^{+} for each cluster show peaks in March 1997 for both clusters, as well as in 2000 and 2005 for the West cluster. These results indicate that high levels of meteorological fire danger are associated to large values of NBA; however, the years of 1981 and 1989, associated to the highest values of NBA in the East cluster, present rather low values of DSR^{+} in that cluster.

In order to further investigate the relationship between fire danger and monthly burned area, linear regression models were developed relating DSR^{+} and NBA in each cluster. The models were able to provide good results in both the West and the East clusters, but in the case of the latter cluster the extreme years of 1981 and 1989 had to be disregarded. Results suggest that inter-annual variability of March NBA in the two clusters may be partly understood in terms of the prevalence of meteorological conditions that induce meteorological danger of fire ignition and fire spread.

The role of meteorological conditions was further investigated by analysing the synoptic atmospheric circulation that prevailed during March of the extreme events in the West cluster (March 2000), in the East cluster (March 1989) and in both clusters (March 1997). Results indicate that in all cases, there is an intense prevailing atmospheric flow over the Cantabrian Mountains, either from the Northeast

(March 2000 and March 1997) or from the Southwest (March 1989), which are driven by the presence of barotropic anomalies located near the British Isles. These steady anomalies are negative in the case of northwestern flow over the study region and positive in case of northeastern flow, being in this associated to blocking-type patterns. The prevailing NE-SW or SW-NE directions are essential since they allow the establishment of a Föhn effect when the air flow crosses the Cantabrian Mountains originating warm and dry air downstream that favours the onset and spreading of fire events.
This simple conceptual model was finally successfully applied to seven cases where amounts of BA ranked in the top four positions in the case of the West cluster and in the top six positions in the case of the East cluster. Results obtained provide a conceptual framework that may assist in developing warning systems of fire danger in March over IP.

References

Costa L, Thonicke K, Poulter B, Badek F (2010) Sensitivity of Portuguese forest fires to climatic, human, and landscape variables: subnational differences between fire drivers in extreme fire years and decadal averages. Regional Environmental Change 11, 543-551, DOI: 10.1007/s10113-010-0169-6

Cueva AV, Barrio JMG, Quero MO, Palomares OS (2006) Recent fire regime in peninsular Spain in relation to forest potential productivity and population density. International Journal of Wildland Fire 15, 397-405, DOI: 10.1071/WF05071

European Commission (2011) Forest Fires in Europe 2010, EUR 24910 EN, Publication Office of the European Union (Luxembourg)

Pausas JG (2004) Changes in fire and climate in the Eastern Iberian Peninsula (Mediterranean Basin). Climatic Change 63, 337-350. DOI: 10.1023/B:CLIM.0000018508.94901.9c

Pereira MG, Trigo RM, DaCamara CC, Pereira JMC, Solange ML (2005) Synoptic patterns associated with large summer forest fires in Portugal. Agricultural and Forest Meteorology 129, 11-25, DOI: 10.1016/j.agrformet.2004.12.007

Pereira MG, Malamud BD, Trigo RM, and Alves PI (2011) The history and characteristics of the 1980–2005 Portuguese rural fire database, Natural Hazards and Earth System Sciences 11, 3343-3358, DOI: 10.5194/nhess-11-3343-2011

Pereira MG, Calado TJ, DaCamara CC, Calheiros T (2013) Potential effects of regional climate change on rural fires in Portugal. Climate Change (in press)

San-Miguel-Ayanz J, Schulte E, Schmuck G, Camia A, Strobl P, Liberta G, Giovando C, Boca R, Sedano F, Kempeneers P, McInerney D, Withmore C, Santos de Oliveira, S, Rodrigues M, Durrant T, Corti P, Oehler F, Vilar L, Amatulli G (2012) Comprehensive Monitoring of Wildfires in Europe: The European Forest Fire Information System (EFFIS). In 'Approaches to Managing Disaster – Assessing Hazards, Emergencies and Disaster Impacts' (Ed Tiefenbacher J), 87-108 (InTech: Rijeka, Croatia), DOI: 10.5772/28441

Trigo RM, Trigo IF, DaCamara CC, Osborn TJ (2004) Climate impact of the European winter blocking episodes from the NCEP/NCAR Reanalyses. Climate Dynamics 23, 17-28, DOI: 10.1007/s00382-004-0410-4

Trigo RM, Pereira JMC, Pereira MG, Mota B, Calado MT, DaCamara CC, Santo FE (2006) Atmospheric conditions associated with the exceptional fire season of summer 2003 in Portugal. International Journal of Climatology 26, 1741-1757, DOI: 10.1002/joc.1333

Trigo RM, Sousa P, Pereira M, Rasilla D, Gouveia CM (2013) Modeling wildfire activity in Iberia with different atmospheric circulation weather types, International Journal of Climatology, DOI: 10.1002/joc.3749 (in press)

Van Wagner CE (1987) Development and structure of the Canadian Forest Fire Weather Index System. Technical Report No. 35, Canadian Forestry Service (Ottawa).

Anderberg M.R (1973) Cluster Analysis for Applications, Academic Press, New York San Francisco London, pp. 162-163.

AFN (Autoridade Florestal Nacional). 2011. Statistics: Wildfire Data [Online] Available at: http://www.afn.min-agricultura.pt/portal/dudf/estatisticas/estatistica-2013-dados-sobre-incendios-florestais [Accessed 1 March 2011].

KNMI Climate Explorer (http://climexp.knmi.nl)

Spanish shapefiles: http://geocommons.com/overlays/168393 [Accessed May 28th 2013]

Portuguese shapefiles: http://geocommons.com/overlays/226435 [Accessed May 28th 2013]

Climate. *Forest Ecology and Management* **259**, 685-697. doi: 10.1016/j.foreco.2009.09.002

Experimental research of penetration hearth of burning in the peat layer.

M. Grishin, V.P. Zima, D. P. Kasymov

National Research Tomsk State University, 634050, Russia, Tomsk, 36, Lenin Avenue
denkasymov@gmail.com

Abstract
The present paper considers, on the basis of the available data and experimental studies, a variant of deepening of the combustion site with account for the botanical composition. After analyzing the thermocouple data, the experiment have shown that there is a steady transition of combustion from a ground forest fire to the deep layer of peat at a low humidity content and sufficient stock of forest fuel.
The presence of combustion conductors and their chaotic arrangement promote combustion propagation in both the horizontal and the vertical planes.

Keywords*: combustion process, peat, botanical composition, combustion conductors.*

Introduction

According to different estimates, the world′s deposit of peat varies from 250 to 500 billion tons (counting moisture content). Peat is widely used in various branches of national economy, in agriculture, medicine, biology, power engineering, etc. Peat is valuable due to the fact that its deposits can regenerate. So, in the world up to 3 billion square meters of peat deposits are formed yearly, which is about 120 times more than used. Peat is characterized by a high natural moisture content of up to 96%, and its porosity amounts to 96% with an average diameter of water-conducting pores of the order of 8.2 μm (Grishin *et al.* 2013).
It should be noted that in determining the kind of peat the most important index is also the degree of decomposition (Nikitin *et al.* 1986). Since peat is an organic compound, under certain conditions its combustion takes place. Peat combustion under natural conditions depends on a complex connected with climatic, meteorological, and topographical factors. This dependence shows up most clearly in a prolonged droughty period when it is necessary to take into account the solar radiation intensity, the air temperature, the time of the day, the ground water level, and many other factors (Belozerov 2010). Peat ignition sources may be different: the sparks from the wires, electrical sparks produced during short-circuit current-carrying wires and cables to the units, careless use of fire, the heat of the sun. Ignition of peat may be due to one of many different causes: sparks from wires, electric sparks produced by short circuit of current-carrying wires and cables to assemblies, careless use of fi re, and the heat of sunbeams. Most often peat beds catch fire from ground forest fires. Three stages of development of a peat fire are distinguished. The first stage has a small area of the site and a low temperature in the combustion zone. It has been established that in the first 1.5–2 hours a peat layer of thickness $(2-4)\cdot 10^{-2}$ m burns up. The second stage is characterized by an increase in the burning velocity and an increase in the zone temperature. The area of the fire increases to several thousands of square meters, and the combustion becomes stable. Acrid fume propagates for a long distance. The third stage is characterized by a large combustion area, a high temperature in the combustion zone, a high smoke content, and a high fi re propagation velocity (Grishin *et al.* 2013).The fire area is calculated by the formula:

$$F_n = \frac{\Pi \cdot V_n^2 \cdot t_p^2 \alpha}{360} = 0{,}00873 V_n^2 \cdot t_p^2 \alpha$$

The approximate change with time in fire areas at various wind velocities is presented in paper (Grishin *et al.* 2013).
It should be noted that the burning of peat in natural conditions is carried out with an excess moisture content and lack of oxidant decay mode (Grishin 1986). Combustion has a diffusive character as limited intake of oxidant environment.
It should be noted that all the well-known works do not consider a botanical composition of peat to be a factor for penetration of the combustion front in the mass of peat. The influence of the botanical composition on ignition of peat is given in the work (Grishin *et al.* 2006) that provides the results of experiments for determination of the minimum ignition energy, and in the work (Loboda 2012) that provides the results of experimental studies to determine the depth of the combustion front in the peat layer. The samples represented four types of peat with different characteristics (botanical composition, density, humidity content and degree of decomposition). We have found that the depth of the combustion front in peat is varied in the range of 10-28 mm, depends on the type of peat, the degree of decomposition, the density and is weakly dependent on the changes of humidity content in the range from 2.6 to 17.3% and does not depend on the size of the sample in the range from $0.3 \times 0.3 \times 0.3$ to $0.35 \times 0.15 \times 0.15$ m.
In this work we suggest an explanation of self-penetration of the combustion front, taking into account the botanical composition of peat. Peat is characterized by the bimodal particle size distribution connected, on the one hand, with the presence of coarse particles of plants and, on the other hand, with a finely-dispersed fraction consisting of the decomposition products. Coarsely dispersed residues, forming a carcass grid or representing a «filler», have an average particle size from 0.1 to 4.5 mm (Churaev 1961).

Technique of the experiment

We assume that peat fire occurs due to the ground forest fire initiated by needle and leaf litter. In the work, the mechanism for penetration of combustion is investigated and evaluated in the peat layer of a different botanical composition.
When the ignition takes place on the surface, combustion (smouldering) will be propagated in the mass of peat. In order to check this assumption, in the laboratory we conducted a series of experiments for modeling the ignition of peat from ground forest fire (Figure 1) using a test complex (Grishin *et al.* 2009).

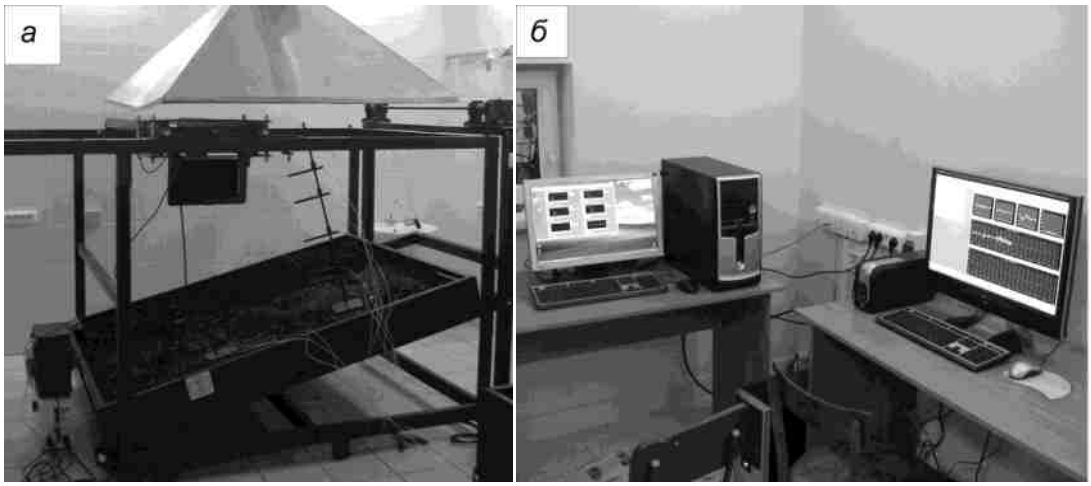

Figure 1. Facility for physical modeling of ground and steppe fires (a); system of data input and registration (б) (Grishin et al. 2009).

There are a complex of measuring equipment and an automated data acquisition and recording system based on a computer and three five-channel ADCs with chromel-alumel thermocouples. The input data recording program was developed on the basis of the Labview program complex. The humidity content of peat is determined using a humidity analyzer A&D HX-50 with an accuracy up to 0.01%. The weight of the samples was determined using an electronic balance A&D HL-400 with an accuracy of 0.1g. Forest fuels (FF) was ignited using a linear source of ignition in the form of a spiral. Combustion temperature was measured by a thermocouple method using chromel-alumel thermocouples.
The scheme of the experiment is presented in Figure 2. A peat sample (2) with sizes $(0.08 \times 0.065 \times 0.05) \cdot m^3$ is placed on the bottom of the metal box (1). Four thermocouples were set in the peat sample: one in the near-surface layer closer to the FF (3), one on the axis inside the peat layer at a distance of $1 \cdot 10^{-2}\ m$ (4), one on the axis at a distance of $2 \cdot 10^{-2}\ m$ (5), and thermocouple (6) was set below thermocouple (3) at a distance of $1 \cdot 10^{-2}\ m$ from it and at a distance of $2 \cdot 10^{-2}\ m$ from the peat surface adjoining the FF. Ignition was realized by means of a point source.

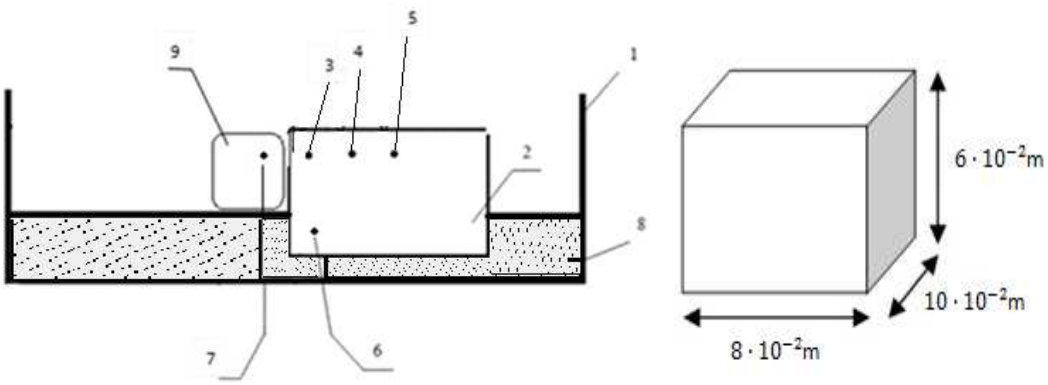

Figure 2. The scheme of the experiment (side view) and dimensions of peat samples (right one). 1 - metal box-testing area; 2 - peat sample; 3,4,5,6 - thermocouple in the peat sample, 7 – thermocouple in the FF layer; 8 - ground substrate; 9 - FF layer.

Since the underlying surface is over peat in the nature, we modeled two variants for the development of underground fire (Figure 3):

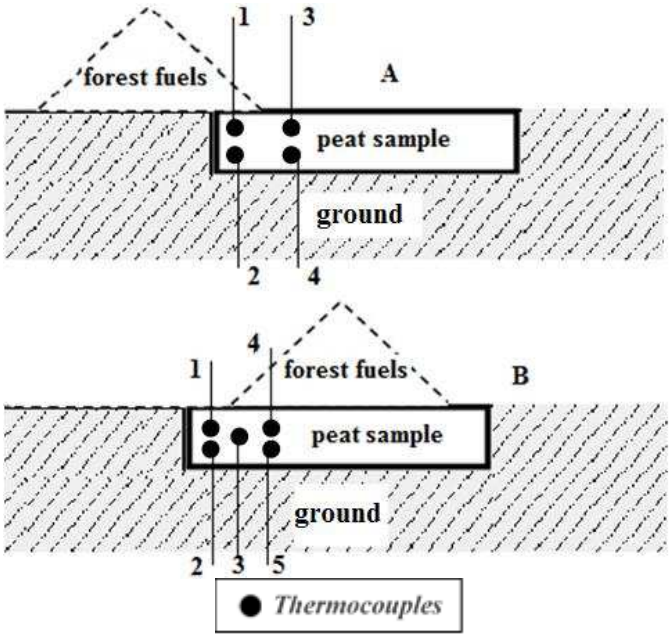

Figure 3. The scheme of experiment: A – Ground forest fire front coming to peat layer, buried in the ground; B - Initiation of ground forest fire occurs directly above the peat, buried in the ground;

The main parameters:
$M_{peat} = 27{,}3$ г, $M_{FF} = 20$ г, $W_{peat} = 4{,}7$ %, $W_{FF} = 5{,}7$ %, $T_{initial} = 17^0 C$.

We studied the samples with a different botanical composition of peat (Grishin *et al.* 2013).

Analysis of the structure of peat samples

To analyze the structure of the peat layer, peat samples with a different humidity content were photographed using the microscope. Figure 4 shows the photographs with a vertical section of peat samples (deposit in the settlement of Plotnikovo, Tomsk region) with a magnification of 200 times. Plant residues ***A*** and water-conducting pores ***B*** are clearly observed.

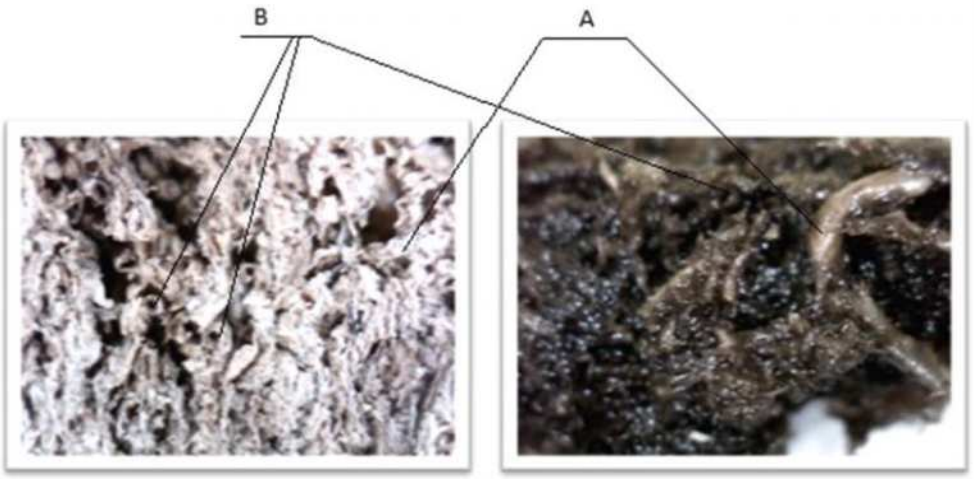

Figure. 4. Vertical slice of peat sample: $W = 4{,}7$ % (left one) u $W = 57{,}7$ % (right one).

Taking into account the properties and the role of initiation and propagation of fires, the components of the ground layer forming peat are unequal and divided into three classes: conductors of combustion, materials supporting combustion and retarding combustion propagation (Grishin *et al.* 2013).

The conductors include the materials that quickly become wet and then quickly become dry. Therefore, they are the materials that ignite very fast and provide a continuous propagation of flame over the ground cover.

Materials supporting combustion include live plants regulating evaporation, with a constant high humidity (more than 70%) and a small volume weight of the layer. This fact does not allow combustion to propagate spontaneously. They can burn only together with the conductors of combustion, increasing the total intensity of the fire line.

Materials retarding propagation of combustion are the materials which can not burn naturally due to the high humidity. They significantly reduce the total intensity of combustion, since the ignition and combustion requires a large amount of heat.

Analysis of experimental data

Figure 5A shows time dependence of the temperature change for the humidity content of the peat $W =$ 4.7% according to the first scheme of the experiment (Figure 2).

Figure 5B shows time dependences of the temperature change for the humidity content of the peat $W = 57.7\%$ according to the same scheme of the experiment.

.

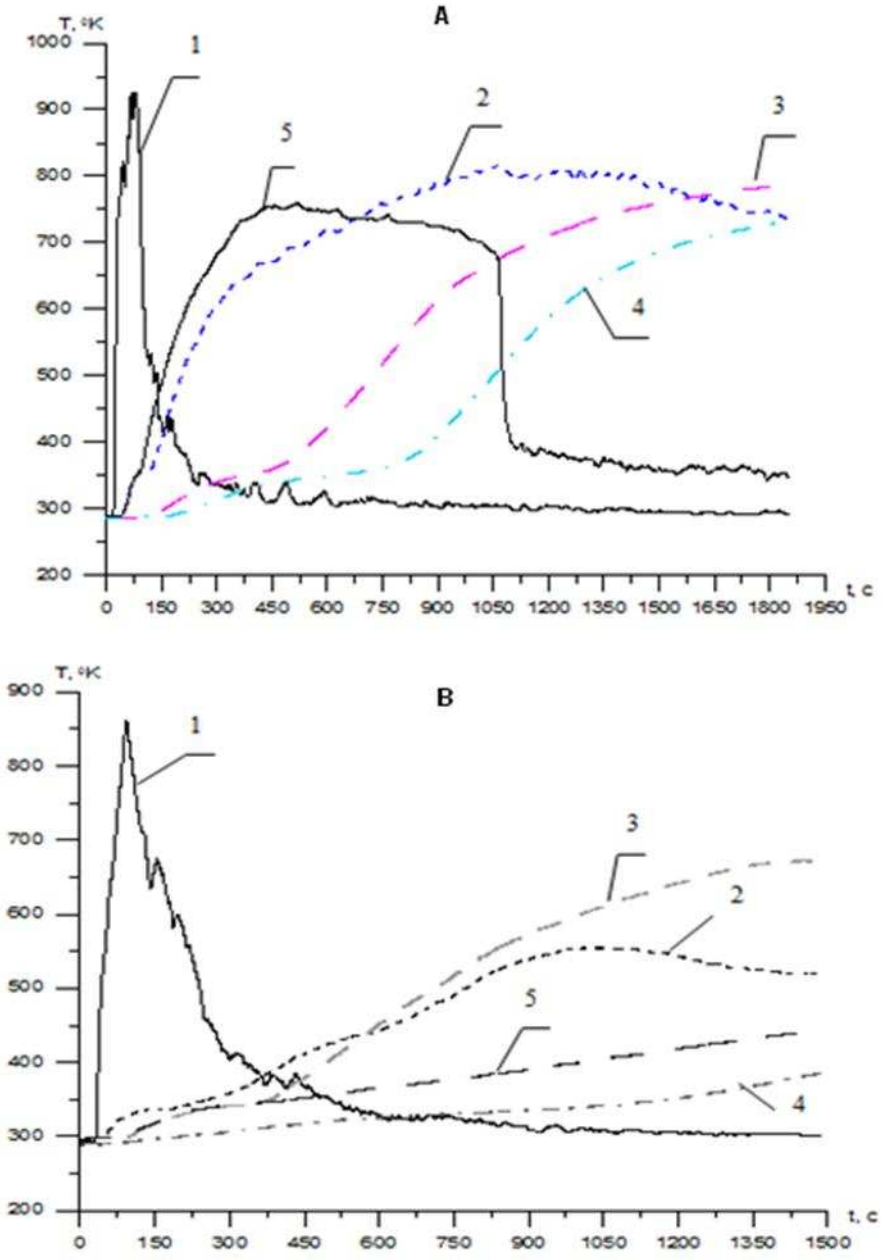

Figure. 5. Time dependences of the temperature change (A-moisture of peat samples $W = 4.7\%$, B-moisture of peat samples $W = 57.7\%$): 1- temperature in the FF layer, 2- temperature change at the boundary between the layer of peat and FF, 3- temperature change on the axis in the layer of peat at the distance of $1 \cdot 10^{-2}$ m from the thermocouple 3 (Figure 3), 4- temperature change on the axis in peat at a distance of $2 \cdot 10^{-2}$m, 5-temperature change in the lower part of peat layer.

Thus, combustion (smouldering) propagates in the mass of the peat sample (2) faster than in the horizontal direction. The rate of the fire front is approximately 0.19 mm/s at a distance of $1 \cdot 10^{-2}$ m between the thermocouples.

Analyzing the plots, it is seen that the transition of combustion from FF to peat is slower for the more wetted sample of torus. In general, combustion has a focal character, which is consistent with the different works (Reardon 2007; Ohlemiller 2002). Thus, combustion (smouldering) propagates in the mass of the peat sample (2) faster than in the horizontal direction. The rate of the fire front is approximately 0.19 mm/s at a distance of $1 \cdot 10^{-2}$ m between the thermocouples (Grishin *et al*. 2013).

Time dependences of the temperature change in accordance with second scheme of experiments (Figure 3A) are shown on Figure 6.
Figure 7 shown the time dependences of the temperature change for the case where the seat of the fire was initiated immediately above peat layer (Figure 3B).

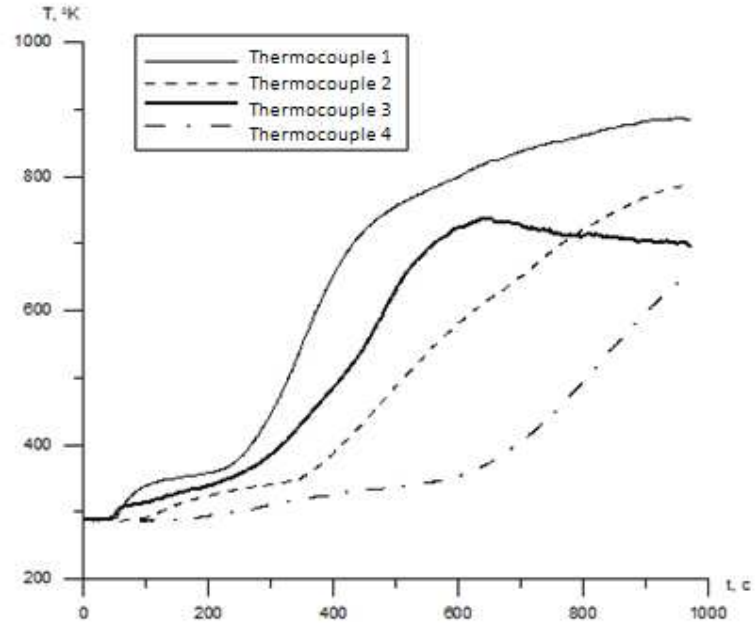

Figure 6. Time dependences of the temperature change. The numbering of the curves corresponds to the numbering of thermocouples in Figure 3A.

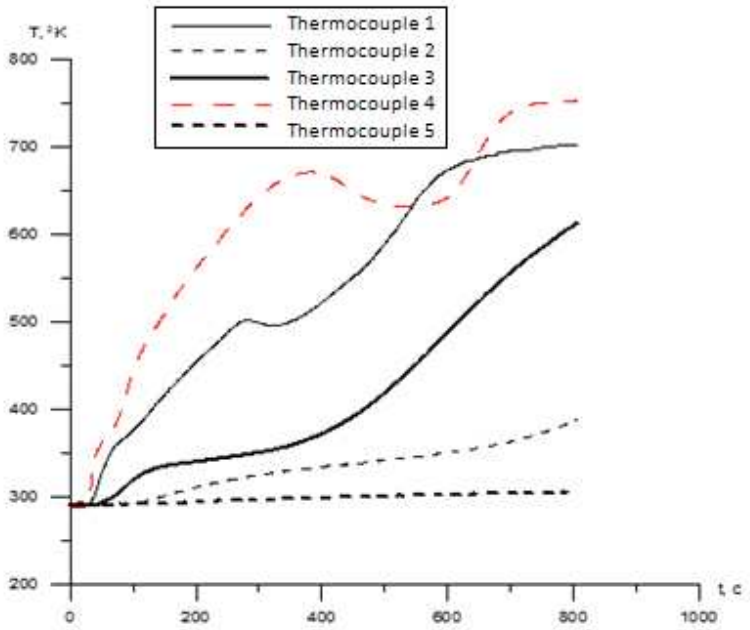

Figure 7. Time dependences of the temperature change. The numbering of the curves corresponds to the numbering of thermocouples in Figure 3B.

After analyzing the thermocouple data, the experiment have shown that there is a steady transition of combustion from a ground forest fire to the deep layer of peat at a low humidity content and sufficient

stock of forest fuel. The mechanism of penetration is mainly dependent on the botanical composition of peat. The presence of combustion conductors and their chaotic arrangement promote combustion propagation in both the horizontal and the vertical planes.
Complete understanding of the mechanism of penetration of combustion in peat layer requires additional investigations involving IR-methods, as well as mathematical modeling and comparison with the existing data.

Results

1. The experiments to study the deep of combustion in the peat layer from the front of a ground forest fire have been prepared and conducted.
2. The rate of peat burning has a value of about 0.19 mm/s.
3. The combustion has a site character, which agrees with the data of (Reardon 2007; Ohlemiller 2002).
4. Analysis of the structure of peat samples has been conducted. It has been noted that the characteristic of peat structure is the presence of burning conductors and water conveyance pores. The penetration of combustion may occurs on them.

Acknowledgements

This work was supported by the Tomsk State University Competitiveness Improvement Program, the Government Task in the Field of Scientific Activity (number 1624) and the Russian Foundation for Basic Research (project number 12-01-00142-a and 14-01-00211-a).

References

Belozerov VV, Nesterov AA, Plakhotnikov YuG, and Prus YuV, A method and automated complex for detecting, preventing, and quenching extinguishing peat fires, *Intern.-Zh. "Tekhn. Tekhnosfer. Bezop."* (http://ipb.mos.ru/ttb/), No. **5** (33) (2010).

Churaev NV, *Water Properties, Structure, and Moisture Transfer Processes in Peat*, Doctoral Dissertation (in Engineering), Moscow (1961).

Grishin AM, *Physics of Forest Fires* [in Russian], Izd. Tomsk. Gos. Univ., Tomsk (1986).

Grishin AM, Golovanov AN, and Sukov YaV, Experimental determination of the thermophysical, thermokinetic, and filtration characteristics of peat, *Inzh.-Fiz. Zh.*, **79**, No. 3, 131–136 (2006).

Grishin AM, Zima VP, Kuznetsov VT, and Fil′kov AI, *A Test Complex for Modeling Forest, Steppe, and Peat Fires*, RF Patent No. 237/220, No. 2008/17660 of 0.4.05.2008. Published 27.10.2009, Byull. No. 30.

Grishin AM, Zima VP, Kasymov DP, On the depending mechanism of the site of peat combustion, *Inzh.-Fiz. Zh*., **86**, No. 5, 996-1001 (2013).

Loboda EL, Experimental study of the depth of peat combustion front with IR methods // Atmospheric and Ocean Optics, Izd. IOA SB RAS, No. **25** (5), Pp. 451-455 (2012).

Nikitin YuA, Rubtsov VF Prediction and extinguishing of fires in forests and peatlands. M.: Rosselizdat, 1986, 95 pp.

Ohlemiller TJ "Smoldering Combustion", *in SFPE Handbook of Fire Protection Engineering*, 3rd ed., Massachusetts, 2002, Pp. 2.200 – 2.210.

Reardon J, Hungerford R, Ryan K Factors affecting sustained smouldering in organic soils from pocosin and pond pine woodland wetlands // *International Journal of Wildland Fire*, 2007, No.**16**, Pp. 107 – 118.

Forest fire risk related to the railway transport and evaluation of the effectiveness of firebreaks

Ryszard Szczygieł, Mirosław Kwiatkowski, Bartłomiej Kołakowski, Józef Piwnicki

Forest Research Institute. Sękocin Stary, 3, Braci Leśnej Street, 05-090 Raszyn, Poland.
r.szczygiel@ibles.waw.pl, m.kwiatkowski@ibles.waw.pl, b.kolakowski@ibles.waw.pl, j.piwnicki@ibles.waw.pl

Abstract
The study contains an evaluation of the occurrence of forest fires caused by rail transport and the effectiveness of the firebreaks beside railway lines. Analysis was conducted on the basis of information given in a questionnaire completed by forest administration units, inspection of the actual condition of equipment and maintenance of firebreaks and data are obtained from Polish State Railways and the State Fire Service. Analysis showed that approximately 65% of firebreaks are located in forests most subject to forest fires, 90% of firebreaks are made in pine stands, mainly of over 30 years of age (81.8%). Most forest fires occur in coniferous forest habitats (58.3%). Over 60% of all fires occurred in pine stands. Most frequently stands aged from 30 to 60 years (28%). From analysis of the effectiveness of the application of firebreaks beside railway lines it is shown that the first furrow of the firebreak was crossed by 27.3% of all fires. The conduct of extinguishing operations in the case of forest fires adjacent to railway lines is significantly hindered primarily by the late discovery of the fire, difficult access and initiation of burning along a significant length. The conducted investigations indicated the necessity of making and maintaining firebreaks in order to reduce the risk of fire to adjacent forest areas, which appropriately maintained are capable of reducing the risk of fire. The accuracy of this statement is also confirmed by the fact that such a method of protection is applied in many European countries. On the basis of the analysis conducted, a modification proposal has been drawn up for the existing firebreaks also with guidelines, concerning forest fire prevention in forest areas.

***Keywords**: Firebreaks, forest fire risk, railway transport*

Introduction

Rail transport, despite technical progress, still constitutes a significant fire risk to forest areas. It is true that over the last 30 years[1] a trend of reduction of the number of fires beside railway lines has been observed (in the years 1981–1990 rail transport was the cause of 5.92% fires, in the years 1991–2000 – 2.1%, and in the years 2001–2010 – 0.81% of all fires recorded), the greatest forest fire disasters occurred beside railway lines (Forest District: Rudy Raciborskie – 9060 ha and Potrzebowice – 5130 ha). Among the established causes of fires, those, which occurred because of rail transport, are seventh out of nine in statistical classification. The frequently compared cause - road transport - in the years 2001-2010 constituted the cause of 0.34% of forest fires, which is under half of the number of fires caused by rail transport.
According to the analysis of the Railway Scientific-Technical Centre[2] over 90% of forest fires were caused by sparks from brake blocks, or as a result of their friction. In such a situation, where fire embers are caused, the role of passive fire protection is filled by the firebreak, executed alongside the railway line, the role of which is to prevent or limit the possibility of the spread of fire to the adjacent

[1] Statistical data of the Forest Research Institute
[2] Prevention of fires beside rail routes. Rail Scientific-Technical Centre, Warsaw 1994

forest area protection. This method of fire prevention protection of forests against the risk caused by rail transport has been known since the mid-19th century and with certain modifications is currently applied also in countries other than Poland. Appropriately prepared and maintained, a belt of land is capable of preventing the spread of fire and limiting its speed and area.
Refraining from the making of firebreaks beside railway lines was the reason for undertaking the study, which was intended to assess the risk of forest fire from rail transport and the effectiveness of fire prevention protection in the form of firebreaks executed beside railway lines. The study was also required because of the lack of a complete insight concerning the cause of forest fires as a result of rail transport, concerning not only the number of fires caused and their surface area, but also fire risk development tendencies, spatial occurrence of fires in relation to firebreaks, evaluation of their effectiveness in the instance of occurrence of fire, the costs of execution and maintenance of firebreaks and also occurrence of fires in relation to habitat factors.
Obtaining reliable and complete data would provide the basis for assessment of activities, concerning protection of forests against fires and its adequacy with regard to the existing risk from rail transport and possible proposals for changes.

Methods

In the research information was used concerning the occurrence of fires beside railway lines and equipment and the maintenance of firebreaks from the State Forests, State Fire Service, Polish State Railways (PKP) and the Forest Research Institute.
The sources of this information are:

1) questionnaire information about the principles of fire prevention protection beside railway lines in Europe and analysis of the legal situation in Poland,
2) questionnaire information from 314 forest district offices from the years 2000–2010,
3) information from the incident registration system of the State Fire Service (EWID), from the years 2006–2010,
4) information from Polish State Railways Polish Railway Lines (PKP PLK) from the years 2002–2011,
5) information from terrain inspections conducted in selected forest districts.

Analysis of the fire risk from rail transport and the effectiveness of firebreaks consisting of the following stages. The first analysis stage was assessment of the conditions of performance of firebreaks. It was composed of analysis of the results of questionnaires and assessment of the execution of firebreaks on site. The basis for assessment of location of firebreaks maintained beside railway lines was information obtained through research questionnaires from forestry districts in the year 2010, containing information about all firebreaks maintained beside railway lines in the territory of Poland. In this stage, inspections were made of existing methods of creating firebreaks in other European countries and in Poland. In the second stage the hypothesis was verified, that forests lying beside railway lines are subject to a greater degree of fire risk, in comparison to other forests. Verification was based on the density of occurrence of fires and the average size of single fire. For this purpose was calculated the density of occurrence of fires and the average area per single fire beside railway lines in the years 2000–2009, on the basis of data are obtained from research questionnaires. The data was compared with data concerning the remaining forests. The third stage was detailed analysis of the occurrence of fires beside railway lines conducted according to the number of fires, area burnt, causes, place of occurrence and type of fire. Because only data for fires occurring as a result of two causes (faults of means of transport – code 26, incorrect use of means of transport - code 27) is available from the information system of the State Fire Service (EWID), the analysis was performed on the basis of information from the State Forests from the years 2007–2010, which is available in the National Forest Fires Information System. The fourth stage of the analysis was the assessment of the effectiveness of

firebreaks in the limitation of the spread of forest fires. It included the number of fires occurring in front of the first furrow of the firebreak, which crossed that furrow, the number of fires occurring between furrows, which crossed the second furrow and the number of fires that crossed both furrows. These analyses were conducted with regard to the type of forest, age of stand and prevalent species of trees.

Results

Legal status of fire prevention protection of forests beside railway lines in Poland

3.1.1. *Current situation in Poland*

According to statutes currently valid in Poland railway managements and hauliers and also users of rail sidings are obliged to fulfil technical and organisational conditions assuring fire prevention protection and environmental protection (art.17. point 1.3 of the Rail Transport Statute of the 28th of March 2003 – Journal of Laws no. 16 entry 94). The principles for the execution of firebreaks beside railway lines are regulated by the *Ordinance of the Minister for Internal Affairs and Administration of the 17th June 2010 concerning the fire protection of buildings, other building structures and land areas (Journal of Laws no. 109 entry 719) and the Ordinance of the Minister of Infrastructure of the 7th of August 2008 concerning the requirements in the extent of distance and permissible conditions of situation of trees and bushes, acoustic elements and the performance of earthworks adjacent to railway lines and also the manner of execution and maintenance of snow protection shields and firebreaks (Journal of Laws 2008 no. 153 entry 955).*

According to these regulations, beside railway lines on which traffic is conducted a firebreak shall be executed in the form of two furrows of a width of at least 2 metres, at a distance from each other from 10 to 15 m and connected with each other every 25 to 50 m by transverse furrows of the same width.

3.1.2. *Protection of forests in Europe*

Analysis concerning execution of firebreaks beside railway lines in particular European countries conducted on the basis of questionnaires, which were sent to services and institutions concerned with fire prevention protection. Countries/regions, which did not declare the execution of firebreaks beside railway lines running through forested areas are: Austria, Bulgaria, the Czech Republic, Germany (landers (provinces): Baden-Wurttemberg, Bavaria, Hesse, Rhine-Westphalia), Norway, Great Britain and Sweden. Respondents justified the lack of firebreaks by the slight risk of fire in those territories. From the questionnaire it is plainly shown that in a decided majority of states the responsibility for protecting forested areas against the risk of fire caused by rail traffic is borne by the managements of railway lines. This responsibility is regulated legally or constitutes a type of agreement between railway line management and the manager of afforested land (e.g. Turkey). The costs of these measures are borne by the railway line management or are divided between the rail management and the forest management (Slovakia).

The majority of the replies obtained from representatives of German landers indicated Deutsche Bahn Ag.DB, as the entity responsible for fire prevention protection. Only in one case (Mecklenburg-Pomerania) were the entire costs of fire prevention protection of forests borne by the private owners or managers of forests. The determining factor of the location of firebreaks is mainly the intensity of rail traffic and the susceptibility of afforested areas to the spread of fire. In the case of Switzerland and France the location of the so-called spark barriers was emphasised in places, in which trains frequently brake (downward gradients, curves), where obviously there is an increased risk of sparking from brake blocks. In Greece, Romania Portugal and in Lithuania firebreaks are executed along the entire length of rail routes running through afforested areas.

As a result of the information collected concerning methods and frequency of renewal of firebreaks, in the majority of cases they are renewed at least annually before the beginning of the fire season (April-September). Some questionnaire respondents also declared repetition of this activity in the

autumn. The main methods of renewal of firebreaks include clearing vegetation from the specified area measured from the external edge of the tracks by mowing or application of chemicals (herbicides). Use of chemical substances in order to prepare firebreaks was emphasised in information obtained from Greece and Spain. In the countries where questionnaires were sent the assessment of the effectiveness of firebreaks was mainly specified as good and very good.

3.1.3. *Assessment of execution of firebreaks beside railway lines*

Assessment of preparation and maintenance of firebreaks based on information from 1879 enquiries. The enquiries indicated that the combined length of firebreaks in Poland amounted to 5926.6 km, and that the decided majority of them (90.4%) were maintained by PKP PLK. The State Forests maintained 248.1 km of firebreaks, and other entities maintained 322.3 km. The majority of the land (66%), on which the firebreaks were situated was maintained by the State Forests, 29% were the property of PKP, and the remainder (5%) were managed by other entities. The annual cost of maintenance of firebreaks in the State Forests amounted to approximately 60,000 PLN. Whereas the Company PKP Polskie Linie Kolejowe [Polish Railway Lines] spent on average annually approximately 2,000,000 PLN, with the exclusion of the year 2011 when execution and renewal of firebreaks was limited. The results of analyses are presented in tables or directly in the text.

The results of analysis of the establishment of firebreaks along railway lines depending on the habitat type of forest are shown in table 1. Close to 65% of firebreaks are located in forest habitats, being the most subject of fires, 90% of the firebreaks executed are in pine stands, of over 30 years old (81.8%). Site terrain inspections, for the purpose of assessing the means and conformity with regulations for creating and maintaining firebreaks along railway lines were conducted at 67 selected locations. Among them, 46 were places where fires had occurred in the area of the railway track in 2010. The remaining 21 inspections were made in average places for the whole length of firebreaks in forestry districts, in which a significant number of fires have occurred beside railway lines. Evaluating the distance of the first furrow from the railway embankment it is confirmed that only in 48% of cases was the distance according to the regulations. In 19% instances the distance was less, and in 33% greater. Conformity of distance between the furrows was confirmed in 44% of cases, in 14% the distance was less, in 42% the distance was greater. The width of furrows was confirmed in the case of the first in 84% of instances, and in the case of a second in 93% of instances. At 7 inspection locations it was confirmed that firebreaks had not been renewed for a year or maybe two years.

Table 1. Firebreaks length according to the forest habitat types

Forest habitat type	Lenght [km]	Share [%]
BMśw	2093,4	35,6
Bs	20,3	0,3
Bśw	1509,3	25,6
Bw, BMw, Bb, BMb	297,3	5,0
Ł, Ol, OlJ, Lw	88,9	1,5
LMśw	1146,3	19,4
LMw, LMb	202,8	3,4
Lśw	267,4	4,5
other	228,9	3,9
mountain	2,7	0,0
upland	47,8	0,8

3.2. Occurrence of forest fires beside railway lines

In the years 2000–2009 in State Forests on the belt of ground 50 m wide beside railway lines there were 599 fires that burnt a combined area of 350.9 ha w. In the incident registration system (EWID) the State Fire Service registered 757 fires in forests, including all forms of ownership, which occurred

by railway lines in the years 2006-2010. Whereas according to the information of PKP Polskie Linie Kolejowe S.A. in the years 2002–2011 28 fires were noted involving an area of 84.19 ha. The information obtained from PKP PLK is grossly disproportionate to the information provided by the State Forests and the State Fire Service. The discrepancy probably results from internal instructions of PKP, that only incidents of fires that constitute a significant threat and the existence of which might be a liability to PKP PLK are recorded. With regard to the completeness of information, further analysis was conducted on the basis of information obtained from the State Forests. In order to verify the hypothesis stating that forests lying beside railway lines are at a greater risk of fire than the remaining afforested areas, the density of occurrence of fires was calculated and also their average surface area with regard to the category of forest fire threat (kzpl). The results shown in table 2 indicate that the density of occurrence of fires beside railway tracks (2.0 fires /1000 ha) was almost threefold greater in comparison to forests classified as I and II kzpl (0.7 fires/1000 ha).

Table 2. Density of forest fires occurrence and average burnt area in the relation to localization of the forest fire

Place of the fire occurrence	Forest fire risk category	Average annual density of the fire occurrence [fires/1000 ha]	Average burnt area [ha]
I and II forest fire risk category (kzpl)	I	1,1	0,28
	II	0,3	0,32
	I i II	0,7	0,31
Forests area along the railway	I	2,5	0,65
	II	1,3	0,41
	I i II	2,0	0,59

Comparing individual density in particular categories of fire risk it is shown that in afforested areas I kzpl is over twice as great in comparison to the remaining areas included in this category. Whereas in areas II kzpl this difference is over four times as great. The density of occurrence of fires beside railway lines in areas classified as I kzpl was almost twice as great as that of areas classified as II kzpl. Evaluating the average area of single fire and for forests lying beside railway lines in comparison to the remaining forests classified as I and II kzpl it may be seen, that beside railway lines it is almost twofold greater.

3.3. The occurrence of forest fires beside railway lines in relation to stand conditions and the size of the burnt area.

Analysis of the occurrence of fires beside railway lines in relation to forest habitat type is shown in table 3.

Table 3. Number of forest fires along the railway in the relation to the forest habitat type

Forest habitat type	Total forest fire		Ground cover forest fire		Together	
	number	share[%]	number	share[%]	number	share[%]
BMśw	38	50,0	139	26,9	177	29,8
Bs			3	0,6	3	0,5
Bśw	12	15,8	122	23,6	134	22,6
Bw,BMw,Bb,BMb	6	7,9	26	5,0	32	5,4
Ł, Ol, OIJ, Lw	2	2,6	10	2,0	12	2,0
LMśw	10	13,1	76	14,7	86	14,5
LMw, LMb	4	5,3	8	1,5	12	2,0
Lśw	3	4,0	14	2,7	17	2,9
undefined			116	22,7	116	19,6
upland	1	1,3	3	0,6	4	0,7

Most forest fires occurred in forest habitats (58.3%), including fresh mixed coniferous forest (BMśw) 29.5% and fresh coniferous forest (Bśw) 22.6%. 21.4% of fires occurred in forest habitats, including fresh mixed broadleaved forest (LMśw) 14.5%. There is a lack of clear difference of combined number of forest fires between stand age categories. Most fires (28%) occurred in stands aged from 30 to 60 years. Over 60% of all fires occurred in pine stands, and next (at a similar level) in stands, in which the principal species were birch and oak. Information presented in the above tables enables one to state that the flammability of forests beside railway lines is typified with a certain variability in comparison to the remaining forests. Apart from "particularly flammable" (Bs, Bśw, BMśw) attention is drawn to the significant flammability of stands growing in moist and boggy habitats (Bw, BMw, Bb, BMb, Ł, Ol, OlJ, Lw), which may arise from the presence on track side shoulders of a strongly developed grass cover, which during times of drought and in spring-autumn periods constitutes a high fire risk.

Size of burnt area

Analysis conducted on 553 fires since the remaining 46 fires did not spread to the forests, including within its reach exclusively the tracks and therefore omitted. Most fires were germinal, the area of which did not exceed 0.05 ha, and then small (from 0.06 do 1 ha). With regard to percentage share by size of fires occurring in all forests the results were similar. This however does not apply to large fires (from 10.1 to 100 ha), 1.6% of which occurred beside railway lines, and only 0.1% in remaining forests. This indicates that the probability of occurrence of a large fire beside a railway track is significantly greater.

The most frequent cause of forest fires according to information from the National Forest Fires Information System was rail transport, which caused 39.9% of all fires. Next in order were: arson (7.3%), carelessness of adults (5.2%), spread of fire from non-forested areas (1.6%) and electric power line malfunction and carelessness of children accounting for 0.5%. It was not possible to establish the cause in the case of 44.6% of all fires. Quite different information is given by PKP PLK, according to which arson is the dominant cause (39.3%), and followed by: blocked brake blocks (21.4%), sparks from locomotive funnel, electrical equipment faults and starting fire from train at 3.6%. Fires for which no cause was established constituted 28.5%.

3.4. Assessment of the effectiveness of firebreaks in limiting the spread of fires in forest

Analysis of the effectiveness of firebreaks along railway tracks in the limitation of the spread of fires was conducted on the basis of questionnaire concerning 417 forest fires in.

In the assessment were considered:

- the number of fires occurring in front of the first furrow, which crossed that furrow,
- the number of fires which crossed both furrows,
- the number of fires occurring between furrows, which crossed the second furrow.

Results with regard to stand conditions are shown in tables 4–6.

Table 4. Number of forest fires occurred before the first firebreak furrow and which crossed the first firebreak furrow according to the forest habitat type

Forest habitat type	Number of fires which crossed the first firebreak furrow	Total number of fires	Share[%]
BMśw	33	112	29,5
Bs	2	2	100,0
Bśw	30	96	31,3
Bw, BMw, Bb, BMb	15	20	75,0
Ll, Ol, OlJ, Lw	5	10	50,0
LMśw	14	55	25,5
LMw, LMb	3	9	33,3
Lśw	4	9	44,4
undefined	5	95	5,3
mixed	2	7	28,6
upland	1	2	50,0
together	114	417	27,3

Presented in table 4 information confirming significantly greater threat to forests by fires, in more fertile and moist habitats. They are places, in which on nonforested areas an abundant grass cover growth may occur and certainly for that reason a greater number of fires crossed the first furrow. Analysing the effectiveness of limiting the spread of fire by the first furrow in relation to the age of the stand it may be stated that its effectiveness increases together with the age of the stand. However similarly to the assessment conducted with regard to habitat type of forest is the situation in the case of prevailing species. From the data analysed it is shown that the first furrow was crossed by 27.3% of all fires.

The next aspect of information analysis was the assessment of effectiveness of the first furrow depending on the place of occurrence of fire (table 5).

Table 5. Number of forest fires occurred before the first firebreak furrow and which crossed the first firebreak furrow according to the place of the fire outbreak

Place of the fire outbreak	Number of fires which crossed the first firebreak furrow	Total number of fires	Share[%]
Between railway and the edge of embankment or ditch	68	227	30,0
Between the edge of embankment or ditch and first firebreak furrow	46	190	24,2

Approximately 6% more was the number of fires, which crossed the first furrow in the case of fires, which occurred within the vicinity of a railway line (to the edge of embankment or ditch) in comparison to the fires, which occurred from the edge of embankment or ditch to the first furrow. This probably results from the time of free spread of these first fires until the moment of reaching the first furrow was longer, and because of that attained a greater intensity, which facilitated overcoming obstacles.
In the case of fires, which crossed both furrows, the analysis included fires occurring in front of the first furrow, which crossed this furrow and analysis of what proportion of them cross the second furrow – table 6. Of the fires, which crossed the first furrow 22.8% also spread beyond the second furrow. The spread of fires, which occurred in more fertile, though moist habitats in deciduous stands, was

significantly more effectively stopped by the second furrow than by the first furrow. This is probably connected with the significantly weaker spread of herbaceous soil cover inside the stand in comparison to the sunlit part in front of the first furrow. Investigating the age of the main stand the least fires crossed the second furrow in stands with an age of 30–60 years.

Table 6. Number of forest fires occurred before the first firebreak furrow and which crossed the second firebreak furrow according to forest habitat type

Forest habitat type	Number of fires which crossed the second firebreak furrow	Total number of fires	Share[%]
BMśw	6	33	18,2
Bs		2	
Bśw	10	30	33,3
Bw, BMw, Bb, BMb	5	15	33,3
Ł, Ol, OlJ, Lw		5	
LMśw	1	14	7,1
LMw, LMb	1	3	33,3
Lśw	2	4	50,0
undefined		5	
mixed	1	2	50,0
upland		1	
together	26	114	22,8

According to questionnaire data only 98 fires occurred between furrows, and only 1 fire, which occurred in a pine stand aged >60 growing in a BMśw (fresh mixed coniferous forest habitat) crossed the second furrow, which constituted 3.8% of all analysed occurrences. Attention should be drawn to the fact that the conduct of fire extinguishing operations in the case of forest fires by railway lines is significantly hindered primarily by late discovery of fire, impeded access and initiation of burning along significant distance. From reports in the EWID State Fire Service system it is shown that burning on a section from 100 to 500 m occurred in 5.4% of all occurrences, on a section from 500 to 1000 m in 2.1%, and 7.3% of incidents were noted when the section was longer than 1000 m.

Summary

The conducted research showed the necessity of creating firebreaks beside railway lines, which appropriately maintained are capable of reducing the fire risk to adjacent areas of forest areas. The correctness of this statement is equally confirmed by the fact of the application of such a means of protection in many European countries. Also in those, in which the rail rolling stock used is significantly more modern than in Poland and creates less fire risk. In the majority of states in which firebreaks are executed beside railway lines, they have a mineralised form, or vegetation free belts of a width from 2 to 20 m. The factor, which is considered in making the decision of location of firebreak, is primarily the density of rail traffic, the level of risk and the susceptibility of afforested terrain to fire. Firebreaks are renewed at least once a year prior to the forest flammability season, by removal of vegetation by mowing or by application of chemical substances.
Considering the research results, from which it is shown that approximately 54% of forest fires beside railway lines occurred in front of the first firebreak furrow and of these fires almost 27% crossed this belt, drawing up a modification of the means of executing firebreaks one is guided primarily by the need to halt or limit the spread of fire of relatively low burning intensity. This may be achieved, if the

barrier belt shall be situated as close as possible to the railway line, thereby limiting the time of unimpeded fire development of fire, fire loading shall be reduced and a mineralised belt shall be wider. For these reasons the proposed firebreaks beside railway lines should have the form of one mineralised belt of a width of a least 4 m placed as close as possible to the line (Fig.1). Additionally it is recommended that the belt section be extended to public or fire access road executed in such a way that it might simultaneously fulfil such a role. Firebreaks should be situated in forests, through which railway lines pass and that are classified as having I and II category fire risk.

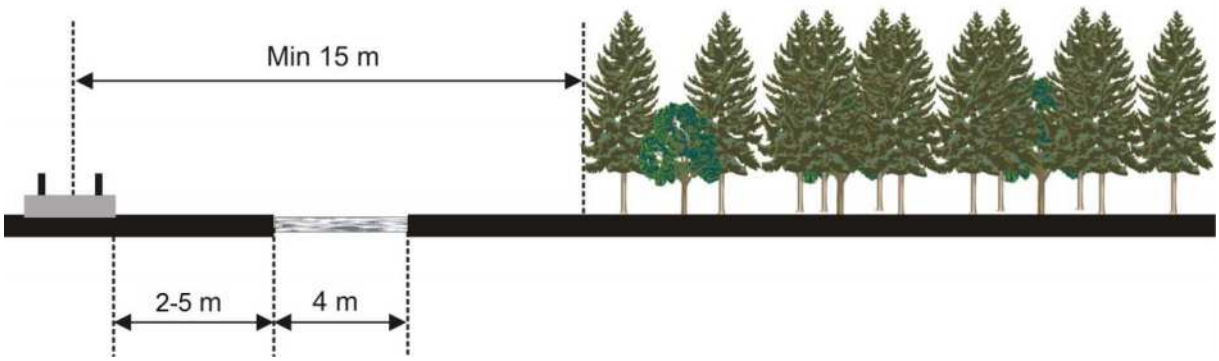

Figure 1. Scheme of the modified firebreak beside the railway

Figure 2. Modified firebreak beside the railway

In the case of modernisation of existing firebreaks it is recommended to use the existing first furrow, executing widening of this furrow to the required width from the side of the tracks, as the ground conditions permit. In connection with the above it has become essential to change the regulations currently in force through agreement of the ministers responsible for supervision of rail traffic, forests and fire prevention protection.

The amendment of the regulation became legally valid through the *Ordinance of the Minister of Transport, Building and Marine Economy of 15 March 2013.*

Abbreviation:

BMśw – *fresh mixed coniferous forest*
Bs – *dry coniferous forest*
Bśw – *fresh coniferous forest*
Bw – *moist coniferous forest*
BMw – *moist mixed coniferous forest*
Bb – *bog coniferous forest*
BMb – *bog mixed coniferous forest*
Lł – *riparian forest*
Ol – *alder forest*
OlJ – *alder-ash forest*
Lw – *moist broadleaved forest*
LMśw – *fresh mixed broadleaved forest*
LMw – *moist mixed broadleaved forest*
LMb – *bog mixed broadleaved forest*
Lśw – *fresh broadleaved forest*

References

Prevention of fires beside railway routes. Railway Scientific-Technical Centre, Warsaw 1994

Forest fire severity in NW Spain: a case of study

Fernández-Alonso, J.M., Vega Hidalgo, J.A., Jiménez Carmona, E.

Centro de Investigación Forestal de Lourizán. PO Box 127. 36080, Pontevedra. Spain.
txema182@gmail.com

Abstract
Wildfires have become a main forestry concern for pine stands in Galicia (NW Spain). Burned forested areas have patterns of varying burn severity as a consequence of various topographic, vegetation and meteorological factors. Determining the relative importance of these factors is necessary to predict fire severity in the canopy, and therefore, base decisions on fuel management. A spatial study of fire severity for a large wildfire (Oia, Pontevedra) is presented here. Pine stands within the fire were classified according to the fire severity. The effect of meteorological (simulated wind speed and direction), topographic (aspect, slope and combined variables) and canopy fuel structure (LIDAR data) variables was described and then modeled. The presence of high fire severity patches was significantly linked to areas of higher simulated wind speed, to lower height stands and to sunny slopes. Simulated wind speed was the most important variable determining the high intensity areas in the rank order of importance analysis, meanwhile slope and aspect were the second and third most important variables. Canopy structure presented low variability in the studied area, which leads to a low importance in classifying fire severity. Variables evaluating alignment of forces, slope and wind direction, have not been found to be important predictors.

Keywords*: Random forests model, Pinus pinaster Ait., fire severity, landscape-base*

Introduction

Fire severity reflects the impact of heat pulses aboveground and belowground and it can be assessed as the degree of organic matter consumed (Ryan and Noste 1985, Keeley 2009). Crown fire is considered as extreme fire behavior (Alexander and Cruz in Werth *et al* 2011) and it is generally considered as one of the highest degrees of fire severity, where tree canopies are killed and needles are consumed (Key and Benson 2006; Lentile *et al* 2006; Keeley 2009; Holden *et al* 2009; Lecina *et al* 2014). That type of stand replacement fires means a challenge for fire managers: they pose an important risk to population and firefighting crews due to difficulty to suppress them. They also are a threat to forest production by removing much or the entire tree canopy in a particular area, and resulting in considerable C emissions (Jimenez *et al* 2013). They reset the successional and growth processes of stands and forests (Graham *et al*, 2004) and can change post-fire dominant vegetation type (Holden, 2009). Moreover that type of fire by consuming all canopy needles leave soil unprotected and prone to post-fire degradation and erosion (Robichaud *et al* 2000, Alexander *et al* 2006, Jain and Graham 2004).
Predicting high severity fire is essential to define areas to apply fuel treatments for severity mitigation or forest restoration works (Lentile *et al* 2006, Holden *et al* 2009, Amato *et al* 2013), nevertheless spatial patterns of burn severity over time remain poorly understood to date (Alexander *et al* 2006; Fernandes *et al* 2010; Sikkink and Keane 2012). Topography, vegetation and weather vary over space and time and they interact in complex ways to influence fire extent and fire occurrence (Turner and Romme, 1994, Odion *et al* 2004; Holden *et al*, 2009). Understanding the relative importance with which these factors contribute to fire severity is critical information for land managers of fire-prone landscapes (Graham *et al* 2004; Holden *et al* 2009 Sikkink and Keane 2012) since they may permit to prioritize investments in fuel treatments or to plan suppression tactics.
Despite the relevance of this topic, most of the studies published to date on fire severity are focused in the USA (Turner *et al* 1994, Lentile *et al* 2006, Alexander *et al* 2006, Collins *et al* 2007, Holden *et al*

2009, Dillon *et al* 2011, Amato *et al* 2013). Fire severity studies in Europe were carried out mainly in Mediterranean forests (NE Spain) (Broncano and Retana 2004, García-Martín *et al* 2008, Oliveras *et al* 2009, Roman-Cuesta *et al* 2009, Alvarez *et al* 2013, Lecina-Diaz *et al* 2014). Most of the studies assess fire severity using medium resolution satellite imagery data (Turner *et al* 1994, Lentile *et al* 2006, Collins *et al* 2007, Holden *et al* 2009, Dillon *et al* 2011, Bradstock *et al* 2010, García-Martín *et al* 2008, Oliveras *et al* 2009, Roman-Cuesta *et al* 2009, Lecina-Diaz *et al* 2014), whereas less studies used a field sampling-based approach (Broncano-Retana 2004, Holden 2009, Fernandes *et al* 2010, Alvarez *et al* 2013). Information from satellite imagery allows assessing fire severity patterns across a large scale and over time. This is useful to reflect the complexity of the interaction among topography, vegetation cover and weather (Amato *et al* 2013). However field data –based studies supply with more detailed information on that interaction and at finer scale.
In Galicia (northwestern Spain), a territory of about 30,000 km2, more than 10,000 fires occur annually (D.X. Montes 2010). That represents about than half of fires in Spain (MARM 2010). In that area, suitable conditions for biomass growth, summer drought and abundant ignition sources coincide (Vazquez 2006; Moreno and Chuvieco 2013), favoring high severity fires. Most of these fires occur in very continuous and productive conifer stands frequently resulting in stand replacement crown fires. These fires cause important economical losses and severe ecological impacts. Given the dominance of rainy climate and the steep terrain in the area, the main undesirable post-fire consequence is the soil erosion. This problem is more dramatic in crown fire-affected areas where soil losses measured following this type of fire in Galicia are considered the highest rates after wildfire in the Southern Europe, requiring costly rehabilitation treatments (Fernandez *et al* 2011; Vega *et al* 2014).
Despite of the tremendous impact of the high severity fires in Northwestern Iberian Peninsula, not a single study has been carried out on this topic in that area. Therefore, we considered essential to gain knowledge in how fine scale variables, used as inputs from empirical fire behavior models (Rothermel 1972, Rothermel 1991, Van Wagner 1977, Cruz *et al* 2004) and their spatial and temporal variability during the occurrence of a wildfire, can affect the severity patterns in a landscape scale. In the present paper we used fire related variables (topography, weather and fuel structure parameters) to evaluate their importance on high severity fire patterns in Oia fire in Galicia. More specifically we addressed: (i) assessing the differences of these variables between high-severity crown fire areas and low severity areas (ii) fitting statistical models to determine their capability to predict high-severity fire occurrence and the relative importance of each predictor variable.

Methods

Study area

Our research focused on the Oia wildfire (area > 500 ha) occurred during the summer of 2013 in the coastal area of Galicia (Northwestern Spain) (Fig 1). This wildfire affected mainly *Pinus pinaster* Ait. (maritime pine) pole-size stands.

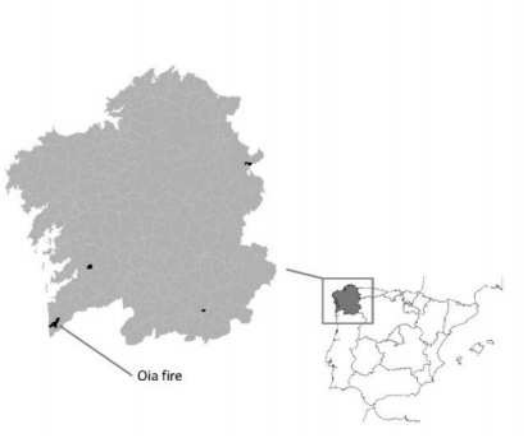

Figure 1. Location of the study area, in Galicia (NW Spain)

The Oia fire occurred in the municipalities of Oia and O Rosal (Pontevedra province). The elevation of the study area ranged from 30 to 515 m. The aspect was generally southeast, with slopes between 0 and 65%. Maritime pine and *Eucalyptus globulus* Labill. (blue gum) were the dominant tree species and the main shrub species were *Ulex europaeus* L., *Pteridium aquilinum* (L.) Kuhn, and *Pterospartum tridentatum* (L.) Wilk. The fire was human-caused and started in 26th August 2013. It was brought under control two days after the ignition. It burned 1810 ha. According to Spain Lithological Map 1/50.000 (http://www.igme.es/internet/cartografia/cartografia/magna50.asp, accessed on 21st June 2014), the soils in this area are developed from schist, slates and granite.
Meteorological conditions during the wildfire are presented in Table 1.

Table1 - Meteorological conditions during the wildfire. Variables from Canadian Forest Fire Weather Index (Van Wagner 1987): FFMC: Fine Fuel Moisture Code; DMC: Duff Moisture Code; DC: Drought Code; ISI: Initial Spread Index; BUI: Buildup Index; FWI: Fire Weather Index. Data from meteorological station located at 4 km from the burned area (Meteogalicia, Xunta de Galicia)

Variable	26th August	28th August
Temperature (ºC)	18.8(13.4-26.1)	20.6(15.3-26.7)
Relative humidity (%)	63.3(44-85)	61.6(45-79)
Wind speed (km h-1)	20.4(5.4-33.3)	17.7(6.1-33.8)
Wind gusts (km.h-1)	36.2(15.1-53.6)	33.3(11.7-56.7)
Wind direction (º)	50	76
FFMC	88	88
DMC	87	87
DC	512	512
ISI	5	5
BUI	122	122
FWI	21	23

Field sampling and spatial data

Wind speed and direction, fuelbed load and structure, slope, fuel moisture content, distance from the surface fuelbed to the lower limit of the canopy stratum and crown bulk density are the input variables determining crown fire occurrence (Van Wagner 1977, Cruz *et al* 2004).
Fieldwork was carried out in the following weeks after the fire. Areas affected by crown fire were visually identified as the patches where the crown fine fuel consumption was complete. The perimeters were tracked using a Trimble Juno 5B GNSS to delimit these areas from where tree crown were totally or partially scorched in the same stand. The areas of interest for the present study were delimited in a Geographic Information System (GIS) as continuous stands where the high-severity fire (crown fire) occurred and surface or low severity fire was observed in the surrounding area. In this way, two contrasted fire severity levels were considered: high and low.
A grid of 100 m was overlaid on a map of the areas of interest. The starting sample point was randomly chosen and 41 sample points were selected. Circular plots of 10 m radius were established on each point. In each plot, all trees with diameter at breast height (Dbh) >5 cm were tagged. Diameter at breast height, total height and post-fire crown base height were measured for each tagged tree. Descriptive characteristics of the plots are presented in table 2. Fire direction was determined observing the char patterns on the tree trunks and the stuck pine needles.

Table2. Mean characteristics and range of monitored plots. Dbh: diameter at breast height; Ht: total height; CBH: crown base height, G: basal area. Minimum and maximum observed values of means per plot between brackets

Type of fire	Density (trees.ha^{-1})	Dbh (cm)	Ht(m)	CBH(m)	G(m^2.ha^{-1})
High-severity	1364(265-2487)	16.4(11.2-22.9)	12.4(8.8-15.8)	6(1.9-9.7)	29.4(9.9-56.7)
Low-severity	881(368-1741)	21.5(14.9-36.6)	15.3(9.4-29.6)	8.4(2.5-23.1)	32.4(7.9-53.8)

Given the landscape-scale and spatial characteristics of a large wildfire, we used the methodology proposed by Stratton *et al* (2006) for wildland fire spatial analysis of the fire environment (weather, fuel, topography) variables.

Grid-based digital elevation model (DEM) at horizontal resolution of 25 m was obtained for the study area from the Spanish Geographic National Institute (http://www.ign.es/ign/layoutIn/modeloDigitalTerreno.do, accessed on 21st June 2014). The DEM was used to calculate the slope and aspect (topography variables) within each fire digital perimeter in ArcGIS v. 9.3 (ESRI 2008).

The same DEM was utilized to simulate the wind fields within the fire perimeters with WindNinja (Forthofer, 2007). WindNinja is a mass-consistent fluid flow dynamics models that estimates the modifying effects of topography on synoptic winds. Although presumably local wind field could be significantly affected by the fire itself, obtaining direct information on wind field within fire perimeter was not an operational option. Wind and temperature data were obtained from Meteogalicia weather stations network (http://www2.meteogalicia.es/galego/observacion/estacions/estacions.asp, accessed on June 21, 2014). The two closest weather stations were selected to supply with the information necessary for the corresponding wind simulations. Characteristics of weather stations are shown in table 3. Wind simulations were made for the wildfire at ignition time and at different moments of the fire run by dividing burned area in function of the approximated position of the fire front, by using the information provided by the suppression crews. Vector files (point geometry) containing wind speed and wind direction were generated and clipped for the study area.

Table3 - Characteristics of weather stations used in the wind simulation (Meteogalicia, Xunta de Galicia)

Station name	Elevation (m)	Distance to study area (km)
Castro Vicaludo	440	4
Aloia	480	15

A database was created including topography (aspect and slope) and simulated wind variables (wind speed and direction) for each pixel within the fire perimeter. With the aim of evaluating if the concurrent effects of the simulated wind and slope is determinant for the occurrence of high-severity crown fire in the same way it is for fire behavior (Weise and Biging, 1997) two combined variables were calculated and included:

a) Terrain slope in the wind direction (fig 2), ranging from positive value of maximun slope (wind vector aligned with upslope vector) to negative value of maximum slope (wind aligned downslope) and

b) the difference between upslope direction and wind direction (fig 3) vectoring as described in Rothermel (1983), where 0º is complete alignment of slope and wind blowing upslope, and 180º means alignment of slope and wind blowing downslope.

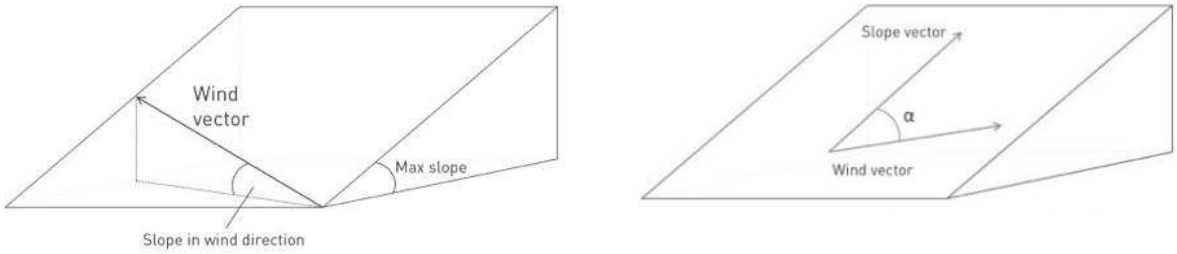

Figure 2 and 3. Sketches of: slope in wind direction calculation, referenced to maximum slope (left) and degree of alignment between slope and wind vector (α), referenced to the slope vector (maximum slope) (right)

National Aerial Ortophoto Program (PNOA) LIDAR data (http://www.ign.es/PNOA/presentacion.html) was used to account for the effect of vegetation structure on fire severity. Light Detection and Ranging (LIDAR) technology has proven its capability to measure canopy and surface fuel structure and to generate landscape-scale maps of these variables (Riaño *et al* 2004, Andersen *et al* 2005, Skowronski *et al* 2011, Mutlu *et al* 2008,van Aardt *et al* 2011, Jakubowski *et al* 2013; Gonzalez-Olabarría *et al* 2012). In fact, these studies have shown that LIDAR data allow to fit models to estimate variables directly linked with crown fire behavior, such as canopy bulk density (CBD), crown fuel load (CFL), canopy base height (CBH), and also understory stratum. In this area of study the LIDAR flights were carried out in the year 2009. Values of the laser height distribution (mean, minimum, maximum, mode and percentiles) and canopy cover above 2 m were added to the statistical analysis as a potential predictor for fire severity on canopy, given the above relationship between these variables and the vegetation variables that drive crown fire initiation (CBH, surface fuel structure) and spread (CFL, CBD).

2.3. Statistical analysis

Two statistical tests were applied to the variables distribution to assess significant differences between the two severity categories considered. The Kruskal-Wallis one-way analysis of variance was used to examine significant differences for each potential continuous variable. Fisher's Exact Test was applied to the contingency table to examine the significance of the association between fire severity and aspect class.

Random Forests (RF) (Breiman, 2001) is a variant of Classification and Regression Trees (CART). This technique is an ensemble method that fits many classification trees to a data set and then combines the predictions from all the trees. Approximately 66% of the data are used in a classification tree with the remaining data used as a validation data set (called out-of-bag observations). An estimate of the error rate is obtained based in this out-of-bag, or OOB, data. RF has shown its power in the analysis of ecological data in a landscape base in the Cutler *et al* (2007) study, in which RF showed higher classification accuracy than four other commonly statistical classifiers. Holden *et al* (2009) used Random Forest to assess the ability of landscape variables to predict severe fire occurrence and Pierce *et al* (2012) also used RF for modeling and mapping four canopy fuel variables at a landscape level.

We used this statistical approach to assess the ability of topography, fuel and wind variables to predict fire severity on forest canopy layer. We used the Random Forest Package developed for R (R Core Team, 2013) by Liaw and Weiner (2002). A first RF model was adjusted containing weather and topographic variables (6 variables) and all the LIDAR variables (67 variables) into the dataset to compare the goodness-of-fit of each model and to select the most relevant variables. For a suitable evaluation of the variable importance, multicollinearity between variables was analyzed using the Pearson's correlation coefficient: the threshold of 0.75 was applied as criteria for removal any of the correlated variables. The final RF models were adjusted with the dataset containing the remaining variables (6 or 7 variables). Sampsize option was used to account for the lack of balance in the datasets.

High-severity observations were less than the low-severity ones, so sampsize was set up in order to RF select the same number of observations for each type of fire severity by randomly decreasing the sampling size of scorched fire observations.
Model error stabilized after 2000 bootstrap replicates. The m parameter (number of predictors randomly selected at each tree node as potential variables to base the split on) was optimized with 3 of the 6 explanatory variables. Variance plots were used to identify the relative strength of each predictor variable.

Results

Variables related to fire severity

Mean value of terrain slope was higher in low severity-affected stands than in high severity patches (table 4), but the difference was less than 4%. Mean wind speed was higher for high-severity patches than for low-severity ones, with a difference of 2.2 km.h-1 between them. Minimum wind speed values were also higher for high-severity patches. Mean values for simulated wind direction were very close between fire severity levels: 66 and 67 degrees for high and low severity respectively. Mean values for slope in wind direction were very close, with a difference of 2.4% between fire severity levels and very similar ranges for both. Angle between maximum slope and wind direction showed a higher mean value for high severity patches, 109 degrees, and the difference with low severity patches was 9 degrees.
Kruskal-Wallis one-way analysis of variance test determined that only the distribution of terrain slope, wind speed, and angle between maximum slope direction and wind direction values were significantly different ($p<0.05$) between fire-severity levels.

Table 4- Mean and range for topography and weather variables values in the studied area. SD = standard deviation. Obs = number of observations

Fire type	Statistics	Slope (%)	Wind Speed (km/h)	Wind direction (º)	Slope in wind direction (%)	Max.slope-wind direction (º)	Obs
High severity	Min.	4.0	12.6	55	-44.7	1	3335
	Max.	60.6	27.6	81	58.7	180	
	Mean	26.4	20.3	66	-3.4	109	
	SD	12.5	2.5	4	18.1	45	
Low severity	Min.	0.3	8.7	53	-48.7	0	7781
	Max.	65.8	27.6	109	65.5	179	
	Mean	30.2	18.1	67	-1.0	100	
	SD	14.7	3.1	8	23.6	48	

Table 5 shows the observed percentage distribution, in aspect class, for each severity level. High severity fire was significantly more frequent in S, SE and SW aspect classes (sunny slopes) (Fisher's Exact Test; p-value < 0.01). Conversely, E, N, NE and NW aspect classes showed more low-severity points.

Table 5- Percentage of pixels by aspect class in the studied area. Obs = number of observations

Fire type	Flat	N	NE	NW	E	S	SE	SW	W	Obs
High-severity	0.0%	1.8%	2.7%	7.2%	7.5%	20.9%	26.9%	16.1%	17.0%	335
Low-severity	0.0%	5.0%	7.0%	14.3%	9.5%	15.9%	19.1%	9.6%	19.6%	781

RF model

Table 6 shows the statistics for the only relevant LIDAR variable in classifying high severity fire after fitting the RF model. According the RF classification, maximum elevation (Elev max) of LIDAR pulse appeared to be the only important variable, and it was significantly different (Kruskal-Wallis test, $p<0.05$) between high and low severity areas. Mean value of LIDAR maximum elevation was higher for low severity patches than for high severity ones.

Variable	Type of fire	Mean	SD	Minimum	Maximum
Elev max	High-severity	8.00	3.27	0.61	18.93
	Low-severity	9.27	4.54	0.46	33.59

Table 6. LIDAR variable used for determining severity crown fire occurrence. Elev max = maximum elevation of LIDAR pulse.

Table 7 shows the out-of-bag (OOB) estimate of error rate for the classification of fire severity. Total OOB estimate was 18.46%. For high severity estimations the number of misclassified observations was 23.72%.

Table 7. Confusion matrix for the Random Forests model predicting severity crown fire occurrence in each severity level. Obs = observed fire, Pred = predicted fire, OOB= out-of-bag estimation of error.

	Pred.		
Obs.	Low-severity	High-severity	
Low-severity	700	137	16.37%
High-severity	79	254	23.72%
		OOB estimate:	**18.46%**

Figure 4 shows rank orders of variable importance for the RF model. The most important variables classifying fire severity are at the top of the y-axis. A weather variable, wind speed, was the most important one for this fire. Slope and aspect class, both topography variables, were the second and the third most important variables. Maximum elevation of LIDAR pulse, a fuel variable, was the less important variable in classifying fire severity.

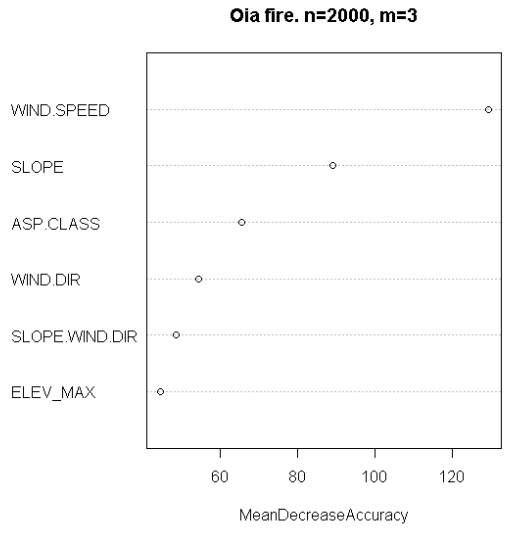

Figure 4. RF variable importance rank plot for the studied area. The most important variables predicting crown fire severity are at the top of the y-axis. n= number of trees in the RF model and m = number of predictors randomly selected at each tree node as potential variables to base the split on.

Discussion and conclusions

4.1. Variables related to fire severity

The effect of slope on severity is dissimilar in literature. Some authors have found positive correlations between fire severity and slope (Jimerson and Jones 2003, Alexander *et al* 2006, Holden *et al*, 2009). Contrarily, Bradstock *et al* (2010) found a negative correlation between fire severity and slope, which is explained by the authors as a possible effect of rocks outcrops, common in slopes, lowering the fire intensity. Although the slope was significantly different between severity levels in our study, difference in mean values was less than 4%, which we consider not having a large effect on fire behavior.

Few studies have taken into account the effect of wind speed on fire severity and all of them have followed different approaches to the one we used in this study. Dillon *et al* (2011) used mean and maximum values of wind speed for a 10-days period starting on the detection date of each fire and number of days with wind speed above 20 miles/hour. These wind variables were positively related to fire severity in only one of the six studied regions. Collins *et al* (2007) used mean wind speed values for each burning period in two fires and they observed contrasting associations between wind speed and fire severity. Bradstock *et al* (2010) found a positive association between high severity and extreme weather, variable that includes the effect of wind speed. Our approach, in which wind speed was simulated taking into account the effect of topography, seems hardly comparable. However, the positive association we found between high severity fire and wind speed seems consistent with the results in the above studies.

Alignment of wind and slope did not seem essential for high severity occurrence. Statistical difference was found for the variable angle between slope and wind direction between fire severity levels. Despite of these results, difference for mean values between fire levels was only 9 degrees. This scarce difference between fire severity levels may point out that was not determinant for high severity occurrence in the studied area.

Studies in fire severity have found dissimilar results regarding the effect of aspect on fire severity. Weatherspoon and Skinner (1995) and Alexander *et al* (2006) have found that patterns of severity were associated to the aspect, underlining that south-facing slopes or flat terrains tended to burn with higher severity than other aspects. Holden *et al* (2009) found that at lower elevations, north-facing slopes were proner to have high intensity fire likely because a higher vegetation growth than in south-facing slopes, whereas at higher elevations solar insolation would increase drying of surface fuels in south-face slopes, which are associated to higher burn severity. Dillon *et al* (2011) also found north-facing slopes to focus high severity fires for five of six ecoregions studied. Nevertheless, in the Pacific ecoregion the probability of high severity fire was highest in the warmest aspects, which may be explained because aspect is not a limiting factor for productivity in these areas with high precipitation. In our study, given that the elevations were relatively low and the annual rainfall is high, we consider that the fuel availability is not limited by the aspect. Summer drought is common during the fire season in Galicia, which could act drying the sunny slopes and leading to an increased probability of severe fire in those aspects.

ELEV_MAX variable was positively correlated to canopy height (Andersen *et al*, 2005), so looking at table 4 one can say that, under the same under conditions, high severity fire tended to occur more frequently in lower (i.e younger) stands. Studies in maritime pine stands for the same area (Jimenez *et al* 2013, Fernandez-Alonso *et al* 2013, Gomez-Vazquez *et al* 2013) have shown that there is a positive correlation between mean stand height or dominant height and canopy base height (CBH). Thus, higher stands may have also higher CBH values and therefore, lower possibilities of crown fire occurrence.

4.2. RF model

Despite of the correction for the unbalanced dataset, since the number of high severity observations was lower than low severity observations, results showed that RF had more difficulties to correctly

classify high severity observations. A possible explanation for such phenomenon is that less information on high severity occurrence was available for RF, which complicated its correct classification. Anyway, RF model was a useful tool to determine which variables were related with high severity occurrence and which was the relative importance of each of them.

This case of study was a good example of wind-driven fire. Meteorological station data (not shown) presented a constant wind conditions during the fire and the fire shape (Anderson, 1983) was narrow and elongated, with an approximated length to width ratio of 4:1. Information provided by fire fighting services described the fire as driven by strong winds, with high spotting activity and the most of the fire runs occurring during the first night. Our results seem compatible with these observations. High wind gusts were observed for the closest weather station and mean wind speed was considerably high during the fire. Under these conditions it seems reasonable that wind speed played a determinant role in the fire behavior in this area and, hence, controlling fire severity, as it was shown by the RF model. Fuel variables were the last in the importance ranking determining high severity occurrence for this fire. A possible explanation is the homogeneity of canopy fuel structure within this area: mean values for LIDAR maximum elevation of canopy layer were very close between fire severity levels. This fact supports that studied stands were considerably similar for this fire and canopy structure did not play an important role in high severity occurrence.

Regardless of the favorable results, some limitations of our approach are evident. We used driver variables of fire behavior to estimate fire severity, but we acknowledge that fire behavior models do not necessarily provide good predictions of fire severity (Alexander *et al* 2006). Nevertheless, studied variables here are well-known for affecting fire intensity, and in the case of a tree stand, a higher intensity can lead to crown activity and to a higher canopy fuels consumption (Alexander, 1982).

The effect of wind speed explaining high severity occurrence must be taken with caution. Windninja simulation only accounts for the effects of topography, but obviously there was an interaction between fire and the atmosphere surrounding fire that affects the crown fire activity (Coen *et al* 2004). In cases with moderate wind conditions, these interactions may become more important for fire behavior than local winds as convective plume created by the fire modifies notably its surrounding atmosphere (Potter, 2012) and fire -induced turbulence can be critical to understand apparently inexplicable fire behavior (Seto *et al*. 2013).

Results regarding the variable importance should be taken in the context of the studied area. In our study most of the stands had similar ages and all of them were pure and even-aged, which means that canopy fuel structure was quite similar within each stand. Moreover, fuel treatments aimed at reducing fire severity on canopy were not identified in the studied area. Under those conditions is understandable that weather variables were the most important predictors of high severity in two of the fires because their higher variability within the perimeter.

However our results seem reasonable and consistent with the current knowledge on fire severity phenomenon. In despite of the limitations of the wind simulation approach used, wind speed emerged as the most important variable predicting high severity occurrence. That agrees with the central role the current models give to wind in fire intensity and rate of spread, and accordingly, to fire severity. Our results also suggest that slope and aspect class, the latter likely as a surrogate of fuel moisture, seemed to play an important role in determining crowning occurrence and fire severity on canopy. Having into account the rate of accuracy of the RF model, this methodology may be helpful for fire managers to delimitate and plan fuel treatment works for severity mitigation, in areas where fire events recur under a fixed synoptic wind condition and post hoc case study

Acknowledgments

The research was funded by the agreement between the Spanish Ministry of Agriculture and INIA, Project RTA2009-0153- C03-01.

References

Alexander JD, Seavy NE, Ralph CJ, Hogoboom B (2006) Vegetation and topographical correlates of fire severity from two fires in the Klamath-Siskiyou region of Oregon and California. Int J Wildland Fire 15: 237–245

Alexander ME (1982) Calculating and interpreting forest fire intensities. Canadian Journal of Botany 60, 349–357.

Alvarez A, Gracia M, Castellnou M, Retana J (2013) Variables That Influence Changes in Fire Severity and Their Relationship with Changes Between Surface and Crown Fires in a Wind-Driven Wildfire. For Sci 59: 139–150.

Amato, V.J.W.; Lightfoot, D.; Stropki, C.; Pease, M. 2013. Relationships between tree stand density and burn severity as measured by the Composite Burn Index following a ponderosa pine forest wildfire in the American Southwest. Forest Ecology and Management 302: 71-84.

Andersen, H. E., McGaughey, R. J., & Reutebuch, S. E. (2005). Estimating forest canopy fuel parameters using LiDAR data. Remote Sensing of Environment, 94, 441−449.

Anderson, H.E. 1983. Predicting wind-driven wildland fire size and shape. USDA For. Serv. Res. Pap. INT-305.

Bradstock RA, Hammill KA, Collins L, Price O (2010) Effects of weather, fuel and terrain on fire severity in topographically diverse landscapes of south-eastern Australia. Landsc Ecol 25: 607–619.

Breiman, L. "Random forests, 2001" Machine Learning, vol. 45, no. 1, pp. 5–32

Broncano MJ, Retana J (2004) Topography and forest composition affecting the variability in fire severity and post-fire regeneration occuring after a large fire in the Mediterranean basin. Int J Wildland Fire 13: 209–216

Coen, J., S. Mahalingam, and J. Daily (2004), Infrared imagery of crown-fire dynamics during FROSTFIRE, J. Appl. Meteorol., 43,1241–1259.

Collins BM, Kelly M, van Wagtendonk JW, Stephens SL. 2007. Spatial patterns of large natural fires in Sierra Nevada. Landsc Ecol 22:545–57

Cruz MG, Alexander ME, Wakimoto RH (2004) Modeling the likelihood of crown fire occurrence in conifer forest stands. Forest Science 50, 640–658.

Cutler, D.R., Edwards Jr., T.C., Beard, K.H., Cutler, A., Hess, K.T., Gibson, J., Lawler, J.J., 2007. Random forests for classification in ecology. Ecology 88 (11), 2783–2792

Dillon, G.K., Holden, Z.A., Morgan, P., Crimmins, M.A., Heyerdahl, E.K., Luce, C.H., 2011. Both topography and climate affected forest and woodland burn severity in two regions of the western US, 1984–2006. Ecosphere 2 (12).

D.X. Montes 2010. Memoria do Plan de Prevención e Defensa contra Incendios Forestais de Galicia. Consellería de Medio Rural. Xunta de Galicia. Santiago de Compostela

Fernandes, P.M., Luz, A., Loureiro, C., 2010. Changes in wildfire severity from maritime pine woodland to contiguous forest types in the mountains of northwestern Portugal. Forest Ecology and Management 260, 883-892.

Fernández, C.; Vega J.A.; Jiménez, E. ; Fonturbel, M.T, (2011), Effectiveness of three post-fire treatments at reducing soil erosion in Galicia (NW Spain). International Journal of Wildland Fire . (20) p. 104-114.

Fernández-Alonso, J.M.; Alberdi, I.; Alvarez-González, J.G.; Vega, J.A.; Cañellas, I.; Ruiz-González, A.D., (2013), Canopy fuel characteristics in relation to crown fire potential in pine stands: analysis, modelling and classification. European Journal of Forest Research. (132) p. 363-377.

Forthofer J.M., 2007. Modeling wind in complex terrain for use in fire spread prediction. Masters thesis. Colorado State University, USA. 123 pp.

García-Martín, A., Pérez-Cabello, F., de la Riva, J.R., Montorio, R., 2008. Estimation of crown biomass of Pinus spp. from Landsat TM and its effect on burn severity in a Spanish fire scar. IEEE Journal of Selected Topics in Applied Earth Observations and Remote Sensing 1, 254–265.

Gómez-Vázquez I, Crecente-Campo F, Diéguez-Aranda U, Castedo- Dorado F (2013) Modelling canopy fuel variables for Pinus pinaster Ait. and Pinus radiata D. Don in northwestern Spain. Ann Sci 70: 161–172

Gonzalez-Olabarria, J.R.; Rodrigez, F.M.; Fernandez-Landa, A.; Mola-Yudego, B. (2012): Mapping fire risk in the Model Forest of Urbión based on airborne LiDAR measurements. Forest Ecology and Management. 282: 149-156

Graham, Russell T.; McCaffrey, Sarah; Jain, Theresa B. (tech. eds.) 2004. Science basis for changing forest structure to modify wildfire behavior and severity. Gen. Tech. Rep. RMRS-20 GTR-120. Fort Collins, CO: U.S. Department of Agriculture, Forest Service, Rocky Mountain Research Station. 43 p

Holden, Z.A., P. Morgan, and J.S. Evans. 2009. A predictive model of burn severity based on 20-year satellite-inferred burn severity data in a large southwestern U.S. wilderness area. Forest Ecology and Management. 258 (11), 2399-2406.

Jakubowski, M.K.; Guo, Q.; Kelly, M. Tradeoffs between lidar pulse density and forest measurement accuracy. Remote Sens. Environ. 2013, 130, 245–253, doi:10.1016/j.rse.2012.11.024.

Jiménez, E.; Vega, J.A.; Ruiz-González, A. D., Guijarro, M.; Alvarez-González, J. G.; Madrigal, J.; Cuiñas, P.; Hernando, C.; Fernández-Alonso, J.M., (2013), Carbon emissions and vertical pattern of canopy fuel consumption in three Pinus pinaster Ait. active crown fires in Galicia (NW Spain).. Ecological Engineering . (54) p. 202-209.

Jimenez, E., J. A. Vega, J. M. Fernandez-Alonso, D. Vega-Nieva, J. G. Alvarez-Gonzalez, and A. D. Ruiz-Gonzalez. 2013. Allometric equations for estimating canopy fuel load and distribution of pole-size maritime pine trees in five Iberian provenances. Canadian Journal of Forest Research, v. 43, no. 2, p. 149-158. 10.1139/cjfr-2012-0374

Jimerson, T.M., Jones, D.W. (2003). Megram: Blowdown, Wildlife, and the Effects of Fuel Treatment. T. T. R. Station. Miscellaneous Report No. 13, 55–59.

Keeley, J.E., 2009. Fire intensity, fire severity and burn severity: a brief review and suggested usage. International Journal of Wildland Fire 18, 116–126.

Key CH, Benson NC (2006) Landscape assessment (LA): sampling and analysis methods. In FIREMON: Fire Effects Monitoring and Inventory System. General Technical Report RMRS-GTR-164-CD. USDA Forest Service, Rocky Mountain Research Station, Fort Collins, Co.

Lecina-Diaz J, Alvarez A, Retana J (2014) Extreme Fire Severity Patterns in Topographic, Convective and Wind-Driven Historical Wildfires of Mediterranean Pine Forests. PLoS ONE 9(1): e85127. doi:10.1371/journal.pone.0085127

Lentile LB, Holden ZA, Smith AMS, Falkowski MJ, Hudak AT, *et al*. (2006) Remote sensing techniques to assess active fire characteristics and post-fire effects. Int J Wildland Fire 15: 319–345.

Liaw, A., Weiner, M., 2002. Classification and regression by Random Forests. R News 2, 18–22.

MARM (2010) Anuario de estadı´stica. Ministerio de Medio Ambiente y Medio Rural y Marino, Madrid

Moreno M. Vanesa, Chuvieco Emilio (2013) Characterising fire regimes in Spain from fire statistics. *International Journal of Wildland Fire* 22, 296–305.

Mutlu, M., Popescu, S. C., Stripling, C., & Spencer, T. (2008). Assessing surface fuel models using lidar and multispectral data fusion.Remote Sensing of Environment,112, 274−285.

Oliveras I, Gracia M, More´ G, Retana J (2009) Factors influencing the pattern of fire severities in a large wildfire under extreme meteorological conditions in the Mediterranean basin. Int J Wildland Fire 18: 755–764.

Pierce, A. D., C. A. Farris, and A. H. Taylor. 2012. Use of random forests for modeling and mapping forest canopy fuels for fire behavior analysis in Lassen Volcanic National Park, California, USA. Forest Ecology and Management, v. 279, p. 77-89. 10.

Potter, B.E., 2012a. Atmospheric interactions with wildland fire behaviour – I. Basic surface interactions, vertical profiles and synoptic structures. Int. J. Wildand Fire 21, 779–801.

Robichaud, P.R. 2000. Fire effects on infiltration rates after prescribed fire in northern Rocky Mountain forests, USA. Journal of Hydrology 231-232: 220-229.

Róman-Cuesta, R.M., Gracia, M., Retana, J., 2009. Factors influencing the formation of unburned forest islands within the perimeter of a large fire. Forest Ecology and Management 258, 71–80.

Rothermel RC (1972) A mathematical model for predicting fire spread in wildland fuels. USDA Forest Service, Intermountain Forest and Range Experiment Station, Research Paper INT-115. (Ogden, UT)

Rothermel RC (1983) How to predict the spread and intensity of forest and range fires. USDA Forest Service, Intermountain Forest and Range Experiment Station, General Technical Report INT-143. (Ogden, UT)

Rothermel RC (1991) Predicting behavior and size of crown fires in the Northern Rocky Mountains. USDA Forest Service, Intermountain Research Station, Research Paper INT-438. (Ogden, UT)

Ryan, K.C., Noste, N.V., 1985. Evaluating prescribed fires. In: Lotan, J.E., Kilgore, B., Fischer, W., Mutch, R. (Tech. Coords.), Proceedings—Symposium and Workshop on Wilderness Fire. USDA Forest Service, General Technical Report INT-182, Intermountain Forest and Range Experimental Station, Ogden, UT, pp. 230–238.

Seto, D., Clements, C.B., Heilman, W.E., 2013. Turbulence spectra measured during fire front passage. Agric. Forest Meteorol. 169, 195–210Riaño, D., Chuvieco, E., Condes, S., Gonzalez-Matesanz, J., & Ustin, S. L. (2004). Generation of crown bulk density for Pinus sylvestris L. from lidar. Remote Sensing of Environment, 92, 345−352.

Sikkink, Pamela G.; Keane, Robert E. 2012. Predicting fire severity using surface fuels and moisture. Res. Pap. RMRS-RP-96. Fort Collins, CO: U.S. Department of Agriculture, Forest Service, Rocky Mountain Research Station. 37 p

Skowronski NS, Clark KL, Duveneck M, Hom J, (2011) Three-dimensional canopy fuel loading predicted using upward and downward sensing LiDAR systems, Remote Sensing of Environment, Volume 115, Issue 2, 15 February 2011, Pages 703-714, ISSN 0034-4257

Stratton, Richard D. 2006. Guidance on spatial wildland fire analysis: models, tools, and techniques. Gen. Tech. Rep. RMRS-GTR-183. Fort Collins, CO: U.S. Department of Agriculture, Forest Service, Rocky Mountain Research Station. 15 p

Turner MG, Romme WH (1994) Landscape dynamics in crown fire ecosystems. Landsc Ecol 9: 59–77. Odion, D.C., Frost, E.J., Strittholt, J.R., Jiang, H., Dellasala, D.A., Moritz, M.A., 2004. Patterns of fire severity and forest conditions in the western Klamath Mountains, California. Conservation Biology 18, 927–936.

Turner, M.G., Hargrove, W.W., Gardner, R.H., Romme, W.H., 1994. Effects of fire on landscape heterogeneity in Yellowstone National Park, Wyoming. J. Veg. Sci. 5, 731–742.

van Aardt, J. A. N., Wynne, R. H., & Oderwald, R. G. (2006). Forest volume and biomass estimation using small-footprint Lidar-distributional parameters on a per-segment basis. Forest Science, 52(6), 636−649

Van Wagner CE (1977) Conditions for the start and spread of crown fire. Canadian Journal of Forest Research 7, 23–34. doi:10.1139/ X77-004

Vázquez de la Cueva, A., J. M. Garc´ıa del Barrio, M. O. Quero, and O. S. Palomares. 2006. Recent fire regime in peninsular Spain in relation to forest potential productivity and population density. International Journal of Wildland Fire 15:397–405

Vega J.A.; Fernández, C.; Fonturbel, T.; González-Prieto, S.; Jiménez, E., (2014), Testing the effects of straw mulching and herb seeding on soil erosion after fire in a gorse shrubland. Geoderma 223-225: 79-87.

Weise, D.R., Biging, G.S., 1997. A qualitative comparison of fire spread models incorporating wind and slope effects. For. Sci. 43 (2), 170–180.

Weatherspoon, C. P., and C. N. Skinner. 1995. An assessment of factors associated with damage to tree crowns from the 1987 wildfires in northern California. Forest Science 41:430– 451

Werth, Paul A.; Potter, Brian E.; Clements, Craig B.; Finney, Mark A.; Goodrick, Scott L.; Alexander, Martin E.; Cruz, Miguel G.; Forthofer, Jason A.; McAllister, Sara S. 2011. Synthesis of knowledge of extreme fire behavior: volume I for fire managers. Gen. Tech. Rep. PNW-GTR-854. Portland, OR: U.S. Department of Agriculture, Forest Service, Pacific Northwest Research Station. 144 p.

Implementation of different techniques for controlling post-fire erosion in the N.W. of the Iberian Peninsula

M. Díaz-Raviña[a], A. Martín[a], A. Barreiro[a], A. Lombao[a], J.A. Vega[b], M.T. Fontúrbel[b], C. Fernández[b], T. Carballas[a]*

[a] *Departamento de Bioquímica del Suelo, Instituto de Investigaciones Agrobiológicas de Galicia (IIAG-CSIC), P.O. Box 122, 15780 Santiago de Compostela, Spain, *tcf@iiag.csic.es*
[b] *Centro de Investigación Forestal-Lourizán, Consellería de Medio Rural e do Mar, P.O Box 127, 36080 Pontevedra, Spain, maria.teresa.fonturbel.lliteras@xunta.es*

Abstract
The effect of two post-fire stabilization treatments (seeding and mulching) on some selected physical, chemical, biochemical and microbiological properties as well as the efficacy of these treatments on post-fire erosion control was investigated. The study was performed in two scrubland areas of Galicia (N.W. Spain), susceptible to suffer post-fire erosion (slope 30-50%) after an experimental fire and a wildfire, respectively. Soil samples were taken from the A horizon at different sampling times over one year after the fire event as well as from the corresponding unburnt soil located in an adjacent plot used as control; the sediments from the burnt soils, with and without different post-fire stabilisation treatments, were periodically collected after precipitation events. The results showed that initially the wildfire induced important changes in most properties measured and that these effects persisted 12 months after the fire; in contrast, the experimental fire provoked slight changes in the physic-chemical and chemical properties but moderate changes in the biochemical properties. They also indicated that both stabilisation treatments had no effects on the soil properties analysed and then on soil quality, but reduced significantly the sediments yield compared to the control burnt soil. The mean efficiency of the seeding and mulching treatments in preventing soil erosion was 21-31% and 85-88%, respectively, showing that, in the short- and medium-term (12 months), the straw mulching was the most effective treatment for reducing the post-fire erosion in both burnt areas.

Keywords*: experimental fire, wildfire, soil quality, post-fire soil erosion, post-fire rehabilitation.*

Introduction

High severity forest wildfires are common in the N.W. of Spain and the risk of post-fire erosion is very high due to the presence of forest ecosystems located in pronounced relief terrains, in combination with abundant precipitations (Carballas 2014; Carballas *et al.* 2009; Vega *et al.* 2013). It is well known that post-fire stabilisation treatments such as seeding, mulching and erosion barriers can reduce surface runoff and keep post-wildfire soil in place and thereby prevent sediment deposition in unwanted areas, being regarded as a defensive first line against post-fire erosion and sediments movement (Robichaud *et al.* 2005). Therefore, the implementation of post-fire stabilisation techniques in burnt forest ecosystems could reduce post-fire erosion; however, studies on this topic are scarce and have been mainly performed in USA. Since post-fire stabilisation treatments are expensive they should only be applied where and when they are required; therefore, studies on monitoring the efficacy of these techniques are necessary to compare their effectiveness and determine if they should be implemented in burned areas of the N.W. of the Iberian Peninsula. The aim of this investigation was to evaluate the effectiveness of two stabilisation techniques, seeding and mulching, in reducing soil erosion as well as their effects on the soil quality.

Methods

The study was performed on two scrubland hill slopes areas located in Galicia (N.W. of Spain), one affected by an experimental fire of low severity (Monte Cabalar, Pontevedra; E soil), and the other affected by a high severity wildfire (Laza, Ourense; W soil) and highly susceptible to suffer post-fire erosion (slope 30-50%). In both areas, experimental plots (E soil, 30 m long x 10 m wide; W soil, 20 m long x 5 m wide) were installed by triplicate (W soil) or quadruplicate (E soil) and four treatments were established: unburnt control soil (U); burnt control soil (B); burnt soil with seeding (B+S; a mixture of seeds at a rate of 45 g m^{-2} in the E soil; and rye seeds at a rate of 10 g m^{-2} in the W soil); and burnt soil with straw mulch (B+M; straw at a rate of 250 g m^{-2}) (Figs. 1. 2, 3). For the different soil treatments, the sediments production (Figure 4) as well as the analysis of different physical, chemical and microbiological properties of the soil samples collected from the A horizon (0-5 cm) was performed over an one year period. A detailed description of the experimental set up as well as the methods used for the sediments and soil characterization are given in Fontúrbel *et al.* (2012) and Díaz-Raviña *et al.* (2012). Soil characterization included a wide range of physical (texture, water retention, water repellence, aggregate stability), physic-chemical (pH, electric conductivity), chemical (total C, soluble C, soil carbohydrates, total N, ^{13}C, ^{15}N, inorganic N, macro- and micro-nutrients) and biochemical and microbiological (microbial biomass, soil enzymes of C, N and P, bacterial activity, soil respiration, microbial biomarkers such as phospholipids fatty acids –PLFA pattern) properties, as well as sediment characterization, performed at different sampling times over one year period. However, to facilitate the interpretation of data, only 11 soil properties measured 1 day and 365 days after the application of the treatments were here used for evaluating the soil quality status in the two experimental burned areas.

In order to evaluate the effect of the fire and the post-fire stabilisation treatments, the values of three-four plots with the same treatment were averaged (mean ± SE). The data were analyzed by a standard analysis of variance (ANOVA1) and, in the cases of significant F statistics, the Turkey's minimum significant difference test was used to separate the means. In addition, a principal component analysis (PCA) was carried out on the physical, chemical and biochemical data for the evaluation of the soil status. All statistical analyses were made using SPSS 15.0 statistical package.

Figure 1. Partial view of the macro-plots in the area affected by an experimental fire (Monte Cabalar, A Estrada, Pontevedra; E soil).

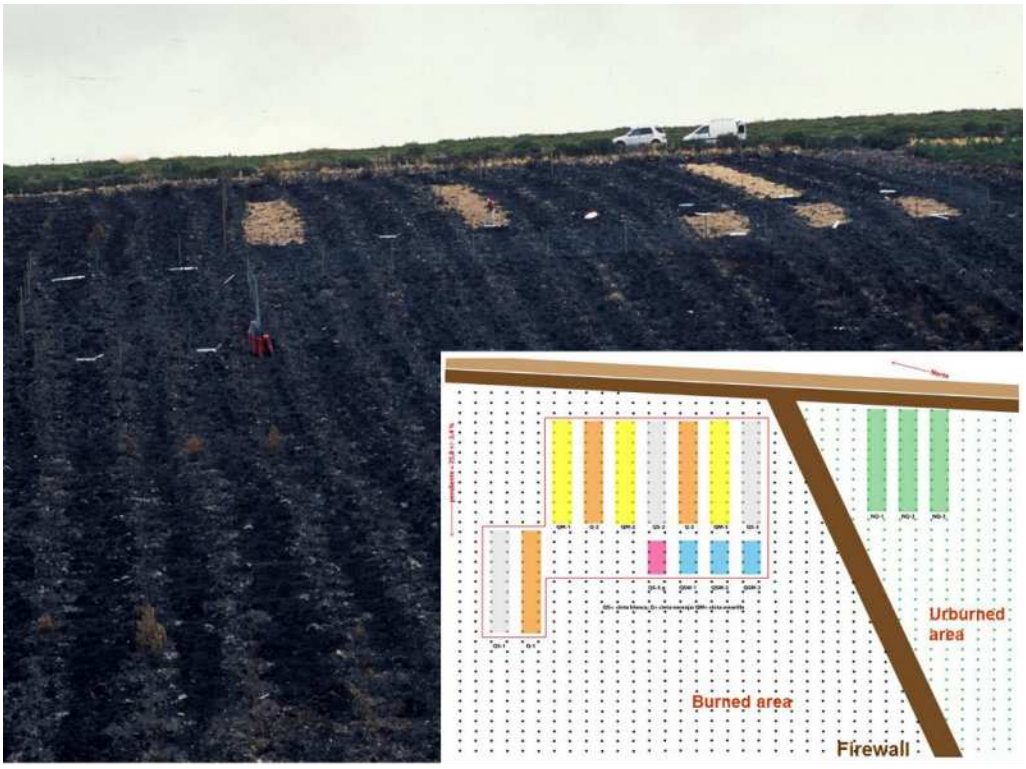

Figure 2. Partial view of the experimental area affected by a wildfire (Laza, Ourense; W soil).

Figure 3. Burnt soil protection against post-fire erosion with straw mulching.

Figure 4. View of the macro-plots delimited by geotextile fabrics to measure post-fire erosion.

Results and discussion

The main topsoil characteristics of the unburnt and burnt soil samples 1 day and 365 days after the wildfire are showed in Figures 5 and 6. The soils studied had an acid pH, elevated content of organic matter and microbial biomass C and low nutrient availability and microbial activity values, these results being representative of forest soils under shrub land vegetation in the Atlantic humid temperate zone of the N.W. of the Iberian Peninsula. Compared to the corresponding unburnt soil samples (U), significant positive or negative effects in most physic-chemical, chemical and biochemical properties were observed immediately after the wildfire (W soil) and less marked or even no significant changes in the soil affected by the experimental fire (E soil). These results can be explained by the temperatures reached during the fire event; the prescribed fire was of low severity, reaching temperatures of 153ºC in the mineral soil surface and 34ºC at 2 cm soil depth (Fontúrbel *et al.* 2012) whereas the uncontrolled fire was of moderate to high severity as it was indicated by the presence of black and white ashes and the total consumption of the ground plant communities (Vega *et al.* 2013). The microbial biomass and the activity values were lower in the burnt soils than in the corresponding unburnt soils, indicating that the fire had negative effects on the microbial population (death of microorganisms by soil sterilization). It should be noticed that for both soils, the fire induced more marked changes in the biochemical properties (microbial C, glucosidase activity, urease activity) than those observed in the physic-chemical and chemical properties. This is consistent with earlier studies performed with soils from the same region showing the usefulness of the more labile and active fraction of the soil organic matter, the microbial component, to detect the impact of prescribed fires (Barreiro *et al.* 2010; Basanta *et al.* 2004) or wildfires of medium and high intensity (Prieto *et al.* 1998; Villar *et al.* 2004).
One year after the wildfire, except for the electric conductivity, the burnt soils showed values for the physic-chemical, chemical and biochemical parameters different from those reported for the corresponding unburnt soil, indicating that the adverse fire impact persisted over time. This behaviour can be explained by the high temperatures reached during the fire as well as the low recovery of the vegetation.

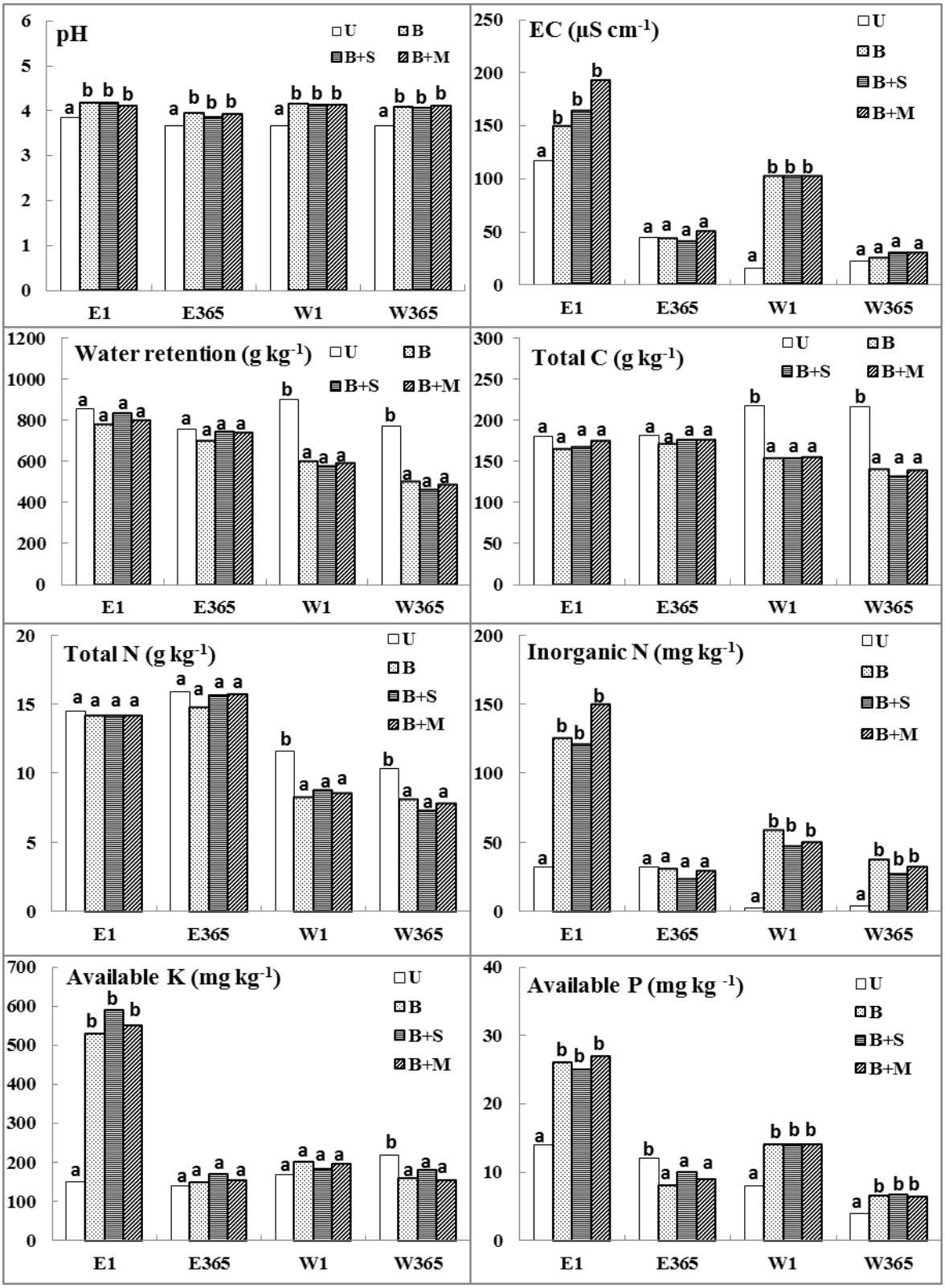

Figure 5. Soil physical and chemical properties for the different soil treatments 1 day and 365 days after the experimental fire (E) or the wildfire (W) (mean values of 3-4 replicates). Treatments: U, unburnt soil; B, burnt soil; B+S, burnt soil plus seeding; B+M, burnt soil plus straw addition. For the same soil and sampling time different letters denote significant differences ($p<0.05$) among treatments. Available nutrients were taken from Gómez-Rey et al. (2013) and Gómez-Rey and González-Prieto (2014).

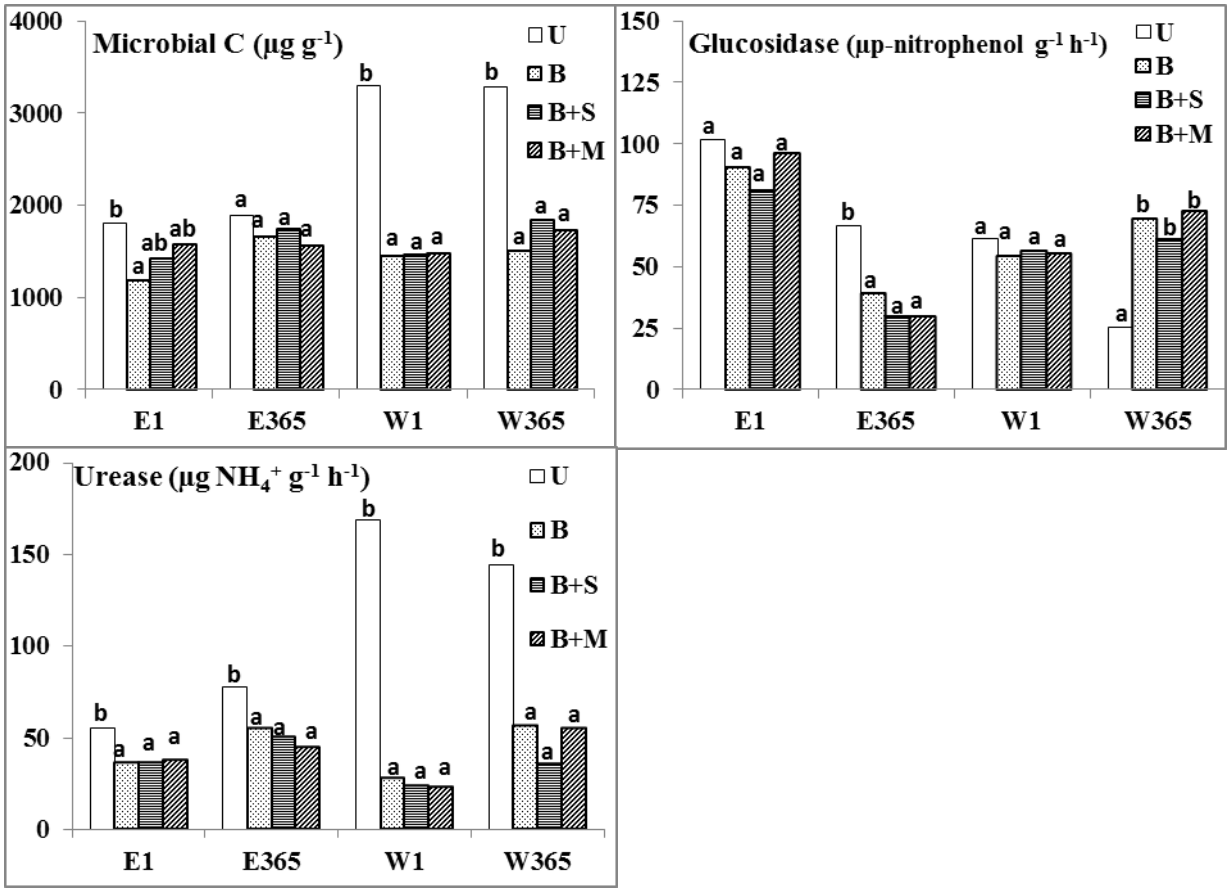

Figure 6. Soil biochemical properties in the different soil treatments 1 day and 365 days after the experimental fire (E) or the wildfire (W) (mean values of 3-4 replicates). Treatments: U, unburnt soil; B, burnt soil; B+S, burnt soil plus seeding; B+M, burnt soil plus straw addition. For the same soil and sampling time different letters denote significant differences ($p<0.05$) among treatments.

With regard to the experimental fire, a positive fire influence on pH and a negative effect on the glucosidase and the urease activities were still maintained after 365 days.

The comparison of the values obtained for the selected soil properties analyzed in the burnt plots under seeding and mulching treatments (B+S, B+M) 365 days after the fire with those of the corresponding untreated burnt soil (B) allowed us to determine the effect of these two post-fire stabilisation treatments on the soil quality. Likewise, the analysis of the sediments corresponding to the above treatments allowed us to determine their effectiveness on the control of soil erosion. The results clearly indicated that, independently of the fire event, there were no significant differences between the B+S and B+M treatments and the corresponding burnt control (B) for any of the soil properties studied, which showed that at least after one year these two stabilisation treatments did not modify the burnt soil quality (Figures 5 and 6).

In order to compare the soil quality in the unburnt and the burned samples collected in the two experimental areas, all physic-chemical, chemical and biochemical properties should be used together. Consequently, a Principal Component Analysis (PCA) was used to analyse the 11 soil properties of the whole data set of the samples analyzed (n = 16 samples) (Figure 7). The main two factors identified accounted for 68% of the variance. The factor 1, which accounted for 42% of the variance, is defined at its positive extreme by the pH, the electric conductivity, the inorganic N and the available P; and at its negative extreme by the microbial biomass C and the urease activity. The

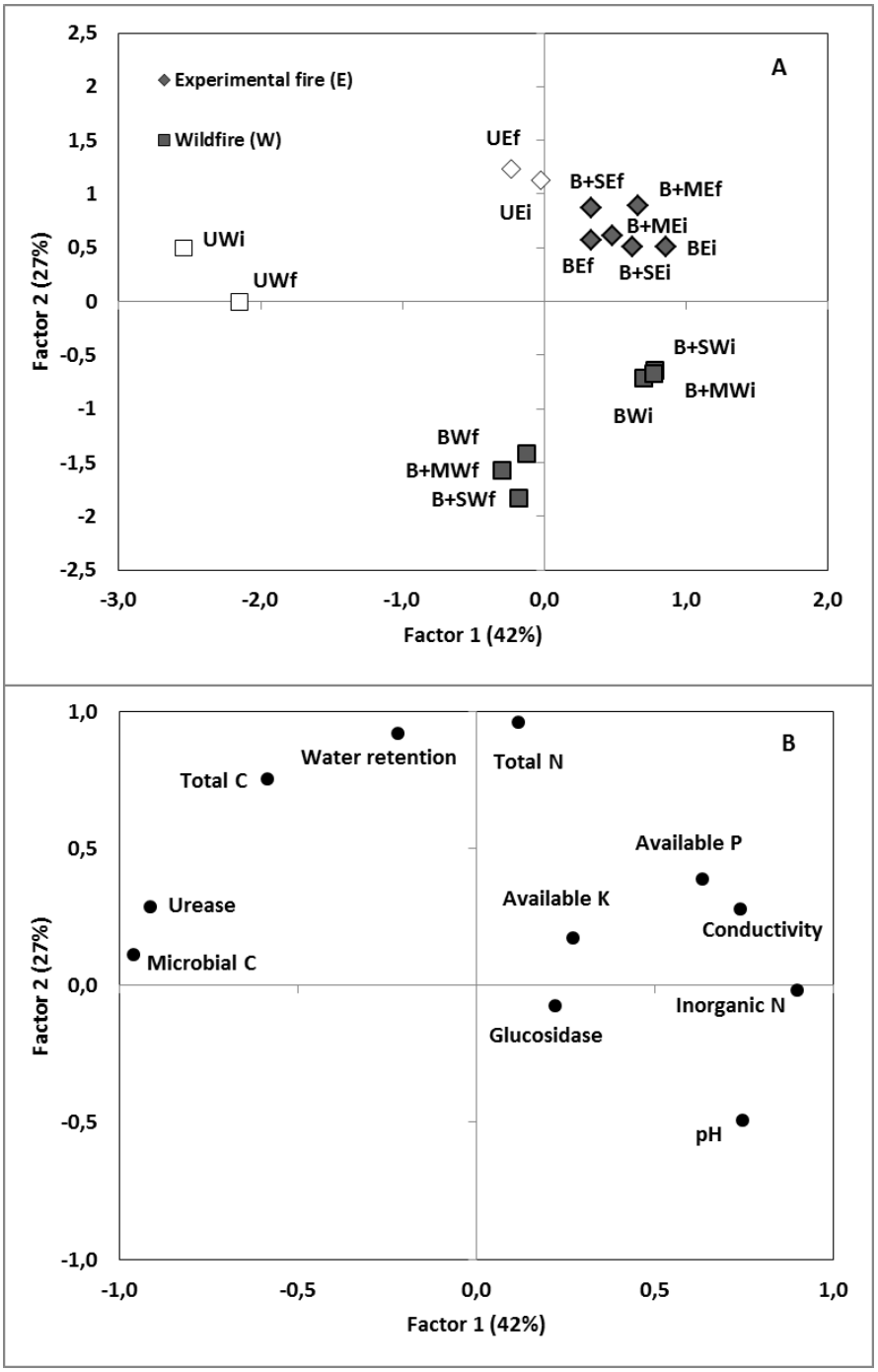

Figure 7. Score (A) and loading plots (B) from principal component analysis performed on the physical, chemical and biochemical properties of the studied soil treatments 1day (i) and 365 days (f) after the experimental fire (E) or the wildfire (W). Treatments: U, unburnt soil; B, burnt soil; B+S, burnt soil plus seeding; B+M, burnt soil plus straw addition.

factor 2, which accounted for 21% of the variance, is defined at its positive arm by variables related to the organic matter (total N, total C and water retention). The distribution of the samples in the plane defined by the Factors 1 and 2, make it possible to separate clearly the unburned samples of the soil affected by the wildfire from the corresponding burnt samples and even the burnt soil sample from the two treatments collected at different soil sampling time (1 day and 365 days); and, in a lesser extent, the burnt samples of the soil affected by the experimental fire from the corresponding unburnt control soil, suggesting that the factors 1 and 2 are related to the fire impact. The results showed that the fire

provoked a decrease in the microbial C, the urease activity and the organic matter content; and an increase in the available nutrients, electric conductivity and soil pH. These findings are consistent with the results obtained in previous studies performed in the same region (Carballas *et al.* 2009; Martín *et al.* 2012). Likewise the data indicated that the effect of the wildfire on the soil quality was much more accentuated than that observed for the experimental fire (the unburned samples of the E soil were grouped closer to the corresponding samples from the burnt treatments, whereas the unburned samples of the W soil were clearly separate from the samples corresponding to the burnt treatments).

With regard to the soil stabilisation treatments effects, it should be noticed that, independently of the experimental area considered, the burned treatments of the same soil (B, B+S, B+M) are grouped together, indicating that the post-fire stabilisation treatments did not change at medium-term (1 year) the quality of the burnt control soil.

The total loss of soil in the soil affected by the experimental fire and the wildfire within 12 months, without and with two different post-fire stabilisation treatments, is showed in Figure 8. The values were 3,628 kg ha^{-1} in the burnt E soil and 1,206 kg ha^{-1} in the burnt W soil, with 60-80% of sediments production in the 2-5 months following the treatments application. The soil loss values obtained lied in the reported range given for burnt soils of the temperate humid zone (Vega *et al.* 2013); however, it should be noticed that the area affected by the wildfire (W soil) exhibited lower values than those observed in the area subjected to the experimental fire (E soil). This behaviour can be explained according to the rainfall amount and intensity that differed notably between the two experimental areas, the rain events and the erosive power being higher in the E soil than in the W soil. The results clearly indicated that important post-fire erosion processes can occur following a low severity fire and that the climate rather than the fire intensity can be more determinant for the production of sediments under specific environmental conditions such as those in the present study (N.W. of the Iberian Peninsula).

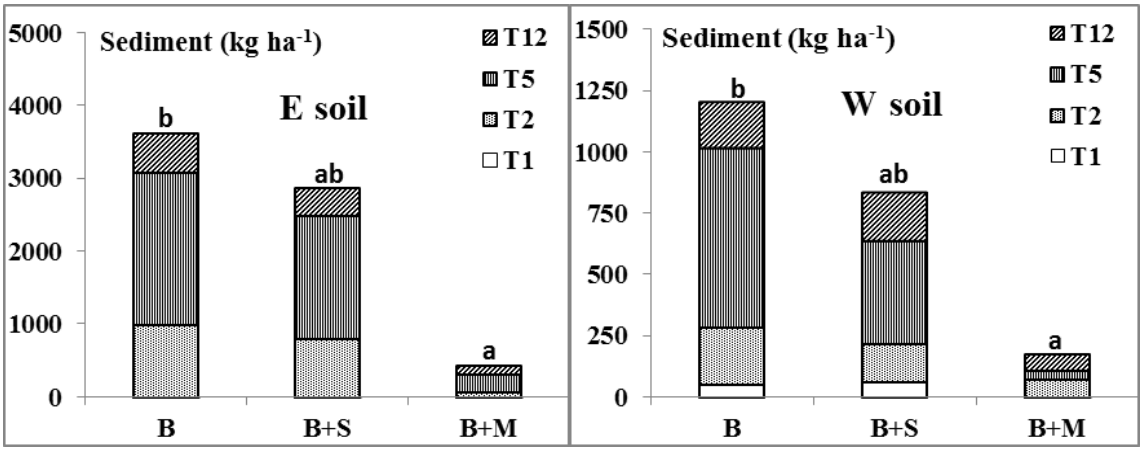

Figure 8. Accumulated sediment yield during the first 1, 2, 5 and 12 months following the experimental fire (E) or the wildfire (W) (11 variables, n = 16 samples). Treatments: U, unburnt soil; B, burnt soil; B+S, burnt soil plus seeding; B+M, burnt soil plus straw addition.

The soil losses accumulated during the study period from the plots with post-fire stabilisation treatments were much lower than those registered for the burnt control. The sediment yield data indicated that the mulching treatment was the most effective to control the post-fire erosion since compared to the control the soil losses were reduced by 75-95% in the four evaluation dates, whereas the seeding reduced the soil losses by 20-42%. At the end of the experiment the efficiency of the seeding was 21% in the E soil and 31% in the W soil, whereas the mulching reduced the erosion by 88% in the E soil and 85% in the W soil; therefore the mean efficiency of the treatments were similar independently of the fire severity. The efficiency values of these soil stabilisation treatments differed

notably from the values obtained in the NE of Spain (Badía and Martí 2000) but are in accordance with those observed in recent studies performed in the NW of the Iberian Peninsula (Prats *et al.* 2013; Vega *et al.* 2013).

Conclusions

The results showed that initially the wildfire induced important changes in most properties analyzed and that these effects persisted 12 months after the fire; in contrast, the experimental fire provoked slight changes in the physic-chemical and chemical properties but moderate changes in the biochemical and microbiological properties. They also indicated that both stabilisation treatments had no effects on the soil properties analyzed and then on the soil quality, but reduced significantly the sediments yield compared to the control burnt soil. The mean efficiency of the seeding and mulching treatments in preventing soil erosion was 30-40% and 70-90%, respectively, showing that, in the short- and medium-term (12 months), the straw mulching was the most effective treatment for reducing post-fire erosion in both burnt areas. Therefore, taking into account their effects on soil quality as well as their effectiveness, treatments such as seeding and mulching are recommended to control the post-fire erosion in this temperate humid region. However, since post-fire stabilisation techniques are expensive, the straw mulching rather than seeding should be implemented due to its lower cost/benefits ratio.

Acknowledgements

This study was supported by the Consellería de Medio Rural de la Xunta de Galicia (08MRU002400PR) and by the Ministerio de Ciencia e Innovación (AGL2008-02823) of Spain.

References

Badía D, Martí C (2000). Seeding and mulching treatments as conservation measures of two burned soils in the central Ebro valley, NE Spain. *Arid Soil Research Rehabilitation* **13**, 219-232.

Barreiro A, Martín T, Carballas T, Díaz-Raviña M (2010). Response of soil microbial communities to fire and fire-fighting chemicals. *Science of the Total Environment* **408**, 6172-6176.

Basanta MR, Díaz-Raviña M, Cuiñas P, Carballas T (2004). Field data of microbial response to a fire retardant. *Agrochimica* **48**, 51-60.

Carballas T (2014). 'El suelo y los incendios forestales en Galicia' (Ed Academia de Farmacia de Galicia), 82 pp. ISBN: 978-84-941537-8-5. (NINO, Santiago de Compostela, Spain)

Carballas T, Martín A, Díaz-Raviña M (2009). Efecto de los incendios forestales sobre los suelos de Galicia. In 'Efectos de los incendios forestales sobre los suelos en España. El estado de la cuestión visto por los científicos españoles'. (Eds A Cerdà, J Mataix-Solera), pp. 269-301. (Cátedra Divulgación de la Ciencia. Universitat de Valencia, Valencia, Spain).

Díaz-Raviña M, Martín A, Barreiro A, Lombao A, Iglesias L, Díaz-Fierros F, Carballas T (2012). Mulching and seeding treatments for post-fire soil stabilisation in NW Spain: short-term effects and effectiveness. *Geoderma* **191**, 31-39.

Fontúrbel MT, Barreiro A, Vega JA, Lombao A, Martín A, Jiménez E, Carballas T, Fernández C (2012). Effects of an experimental fire and post-fire stabilization treatments on soil microbial communities. *Geoderma* **191**, 51-60.

Gómez-Rey MX, Couto-Vázquez A, García-Marco S, González-Prieto SJ (2013). Impact of fire and post-fire management techniques on soil chemical properties. *Geoderma* **195-196**,155-164.

Gómez-Rey MX, González-Prieto SJ (2014). Short and medium-term effects of a wildfire and two emergency stabilization treatments on the availability of macronutrients and trace elements in topsoil. *Science of the Total Environment* **493**, 251-261.

Martín A, Díaz-Raviña M, Carballas T (2012). Short- and medium-term evolution of soil properties in Atlantic forest ecosystems affected by wildfires. *Land Degradation and Development* **12**, 427-439.

Prats SA, Malvar MC, Vieira DCS, MacDonald L, Keizer JJ (2013). Effectiveness of hydromulching to reduce runoff and erosion in a recently burnt Pine plantation in Central Portugal. *Land Degradation and Development*. In press, http://dx.doi.org/10.1002/ldr.2236.

Prieto-Fernández A, Acea MJ, Carballas T (1998). Soil microbial and extractable C and N after wildfire. *Biology and Fertility of Soils* **27**, 132-142.

Robichaud PR, Beyers JL, Neary DG (2005). Watershed rehabilitation. In 'Wildland fire in ecosystems: effects on soils and water'. (Eds DG Neary, KC Ryan, LF Debano), pp 179-197. (General Technical Report RMRS-GTR-42-Vol.4. U.S. Department of Agriculture, Forest Service, Rocky Mountain Research Station).

Vega JA, Fontúrbel T, Fernández C, Arellano A, Díaz-Raviña M, Carballas MT, Martín A, González-Prieto S, Merino A, Benito E (2013) (Eds). 'Acciones urgentes contra la erosión en áreas forestales quemadas. Guía para su planificación en Galicia'. (Tórculo Artes Gráficas, Santiago de Compostela, Spain).

Villar MC, Petrikova V, Díaz-Raviña M, Carballas T (2004). Changes in soil microbial biomass and aggregate stability following burning and soil rehabilitation. *Geoderma* **122**, 73-82.

LIFE ArcFUEL: Mediterranean fuel-type maps geodatabase for wildland & forest fire safety

M. Bonazountas[a], A. Astyakopoulos[a],G. Martirano[b], A. Sebastian[c], D. De la Fuente[c], L.M. Ribeiro[d], D.X. Viegas[d], G. Eftychidis[e], I. Gitas[f], P. Toukiloglou[f]

[a] *Epsilon International SA, Monemvasias 27 Marousi-Greece, bonazountas@epsilon.gr*
[b] *Epsilon Italia srl, Via Pasquali 79 Mendicino-Italy, g.martirano@epsilon-italia.it*
[c] *GMV Aerospace & Defence SA, Juan de Herrera Boecillo Valladolid-Spain, asebastian@gmv.com*
[d] *ADAI, Coimbra, Rua Pedro Hispano 289 Coimbra-Portugal. luis.mario@adai.pt, xavier.viegas@dem.uc.pt*
[e] *Algosystems SA, Syggrou 206 Athens-Greece, geftihid@algosystems.gr*
[f] *AUTH, Aristotle University of Thessaloniki P.O. Box 248-Thessaloniki Greece, igitas@for.auth.gr*

Abstract
ArcFUEL [1] is a LIFE+ Project that involves six European Partners with the objective of producing updated fuel maps to be used in forest fire management operations and geoplatforms. The ArcFUEL project delivers a complete, up-to-date, methodology for Fuel Classification Mapping (FCM on a Web-Geodatabase) based on "readily available" data, harmonized, accessible and interoperable according to INSPIRE principles, for the Mediterranean Region. This paper outlines the: (i) history of the Fuel Classification Maps (FCMs), (ii) the problem targeted in fuel mapping, (iv) the significance of FCMs for Forest Fire (FF) Management, (v) the ex-novo ArcFUEL methodology developed within the project, (vi) two case studies applied in Spain and Portugal, (vii) the field validation process and (viii) the final results derived from the project.

Keywords*: wildland, forest fire management, fuel maps, fuel types, LIFE, ArcFUEL, ESRI ArcGIS, QRASS GIS*

History

Fuel Classification Maps (FCMs) production started in the 90's when experts used the reclassification vegetation type's method to produce Fuel Maps from Forest & National Maps based on assumptions [2]. In the last decade established forest fuel catalogues (NFFL, Scott & Burgan, and PROMETHEUS) were used in several FCM projects in combination with Remote Sensing Techniques [3] [4] [5] [6] [7] [8]. A number of projects on fuel mapping for operational purposes have been accomplished in several European countries [9]. However, with some exception [10], these efforts concentrated at local or regional scale, and no maps at national scale are produced. Fuel type mapping was also approached at a pan-European within the FUELMAP Project [11]. This project derived a novel fuel classification adapted to European environments that enables a high level harmonization of the different fuel mapping initiatives. Yet, the JRC's fuel map was not meant for local scale applications.

ArcFUEL compiles information from past FCM efforts, utilizes ancillary data, and delivers a new era of FCMs, an ex-novo methodology and workflow.

The problem targeted

Effective Forest Fire (FF) Management requires knowledge of Fuel Classification Maps (FCMs) that are poorly available in Mediterranean countries since they are produced only at local or regional scale, without any regular updates and/or using standardized methodologies. Therefore available FCMs cannot support the systematic use of FF modelling at operational levels (prevention, suppression planning) of FF management.

Why FCMs for FF Management?

Forest vegetation is considered as a "fuel" and its structure and status govern the dynamics of a fire. This is the reason why Fuel Models and their spatial patterns (i.e. FCMs) are significant for FF Management Actions during all four phases of the FF lifecycle: 1 (Awareness phase - prior to the fire), 2 (Emergency phase - during the fire), 3 (Impacts phase - after the fire), 4 (Dissemination phase - lesson learnt). Moreover, fuel models are dynamic; either due to natural or anthropic causes (mostly because of the latter), the composition and loading of forest fuel changes and hence the need for up-to-date forest fuel information.

The ArcFUEL methodology

The ArcFUEL methodology consists of cascaded steps based on the use of multi-temporal LANDSAT [12] Thematic Mapper (TM) images for the distinction of fuel classes with different seasonal characteristics and further refinement based on ancillary data, such us burned areas, and canopy cover density data [13] derived from satellite observations. In more details, the ArcFUEL methodology is accomplished in 2 major blocks: (i) pre-processing of Landsat satellite imagery and (ii) forest fuel classes mapping.

The pre-processing of Landsat scenes involved:

1. Searching, selecting, ordering / downloading Landsat scenes (5TM or 7 ETM+ SLC-) of interest via the official sources (USGS' Landsat archive, GloVis and EarthExplorer web-services). The selection criteria are strict in the sense to get as much as possible cloud free acquisitions which, in addition, were timely as close as possible. All Landsat scenes in a geospatial database
2. Trimming scene border fringes
3. Converting Digital Numbers (DNs) to Top-of-Atmosphere Reflectances (ToAR) by normalizing either a statistical approach for most cloud-free scenes, or the 6S algorithm for scenes that were significantly cloud-contaminated (as per the cloud cover percentage estimation given in the metadata, as well as after visual control).
4. Detecting clouds and cloud shadows
5. Topographically correcting Imagery by using the Minnaert method (insert reference?) based on the ASTER GDEM2 dataset.
6. Relatively normalizing images (separate handling for each spectral band and season) to balance up seasonal radiometric variations based on the Histogram Matching technique.
7. Creating a large surface reflectance mosaic (for each band) for the whole study area.

The forest fuel classes map production comprised the following steps:

1. Extracting major vegetation classes from existing land data bases, i.e. (i) forested areas (Broadleaved, Coniferous and Mixed) from JRC's Forest Type Map (2006), (ii) surface fuels from JRC's Forest Fuel Type Map (2006), (iii) ground and azonic fuels (and non-fuels) as the remaining areas from the Corine Land Cover 2000/6.
2. Separating deciduous and evergreen vegetation (and, similarly, grasses and shrubs) is done via a bi-temporal classification approach, i.e. clustering and classifying the seasonal vegetation index difference inside the two main vegetation categories (forest and surface fuels) [14] [15]. Clustering is performed by implementing a modification of the K-Means algorithm.
3. Sub-classifying the above vegetation classes based on forest density criteria [16]. This is done by using JRC's up-to-date Tree Cover Map.
4. Filtering spatially and temporally relevant burned areas extracted from JRC's [17] Burnt Area Perimeters data base [18].

5. Additionally, sub-classifying the fuel type classes can be achieved by incorporating JRC's Environmental Zones [19] (Eco-Regions) classification.

Figure 1 below presents the whole ArcFUEL methodology.

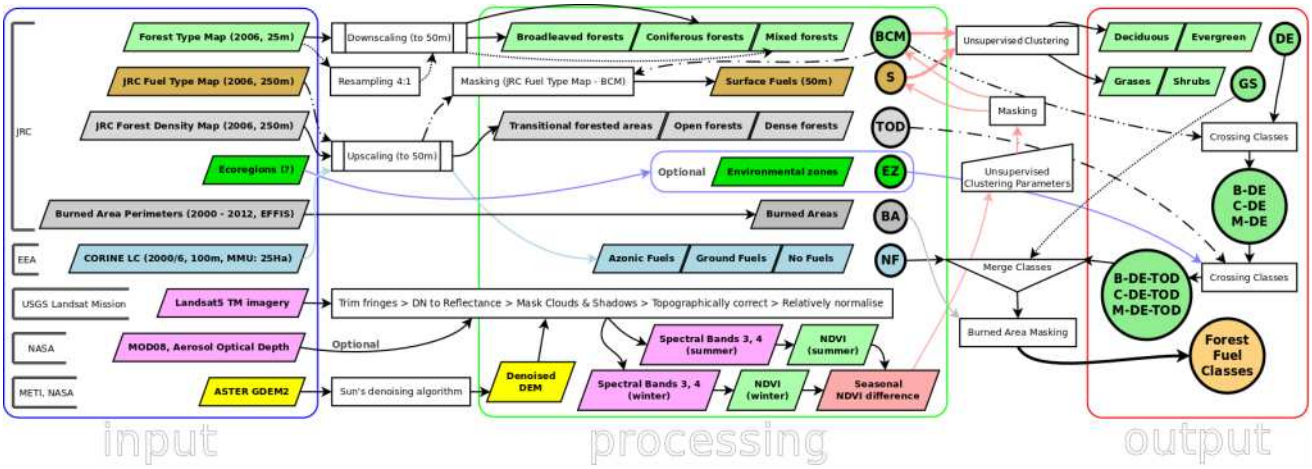

Figure 1. ArcFUEL methodology

Case Study

Two case studies are presented, one in Portugal and the second in Spain. In both cases the study consisted on two phases, a prior testing of the methodology in a smaller pilot area, and the implementation of the refined methodology over a larger area of interest.

Phase I: The pilot area chosen was located in Central Portugal in the area of the Lousã Mountains, part of the NATURA 2000 Network (Figure 2). The most representative species of forest stands and shrublands for Portugal occur in this region. It is an area of 10000 ha delimited by the coordinates 40º7'N – 40º13'N and 8º15'W – 8º7'W, and with altitudes ranging 80-700m. The region, falls inside the "Lusitanian" Ecorregion.

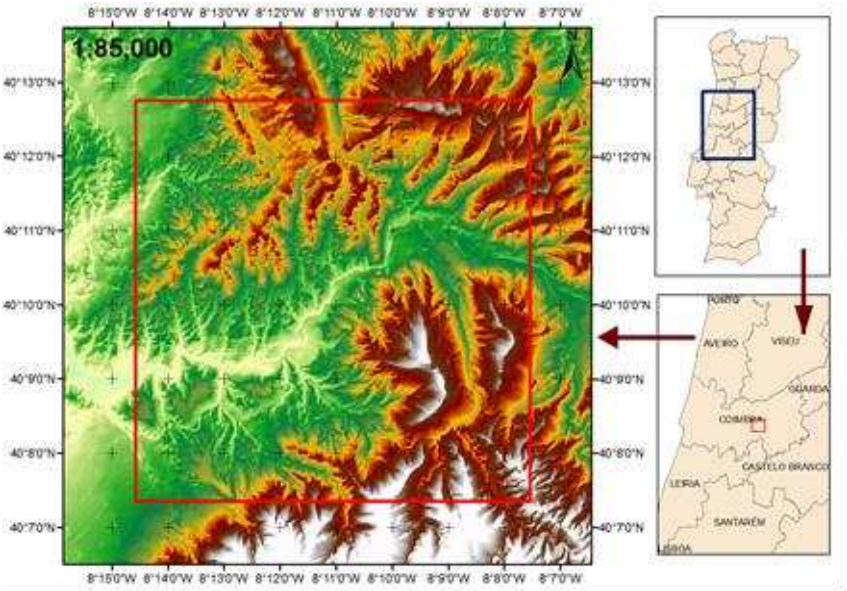

Figure 2. Portuguese pilot area (red box) (Phase I)

The application of the methodology in this first phase produced the map shown inFigure 3. It was proven to be an easy to use procedure although some fine tunings had to be done, particularly regarding the definition of the density parameter. A couple of methodologies were tested and it was finally decided to use the density cover map produced by JRC [20] and freely available.

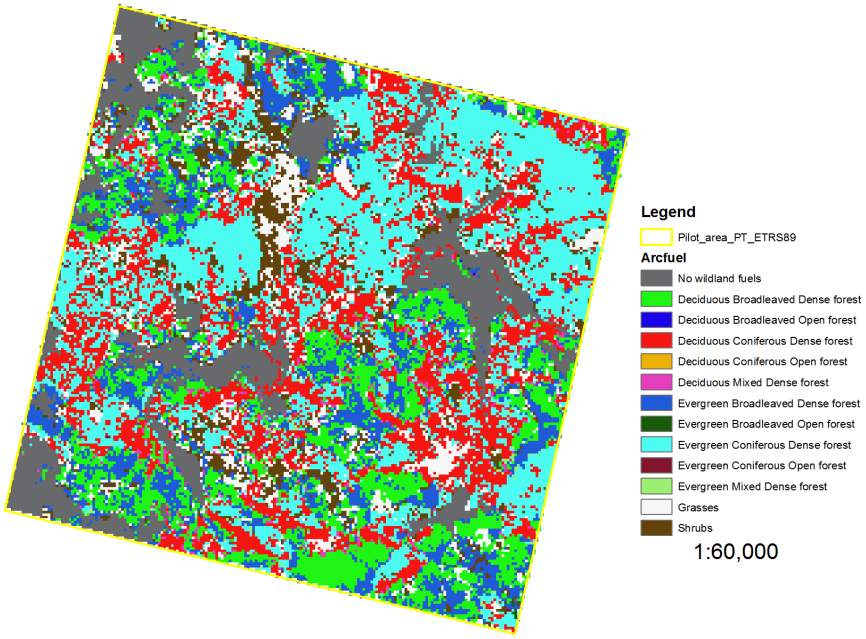

Figure 3. Phase I PT Pilot Area fuel map (reprojected to ETRS 89))

Phase II: After tuning the methodology the ArcFUEL fuelmap was produced for the entire Portuguese (islands excluded). The work was performed with the GIS tools ArcMap 10.1 [21] and Grass GIS 7.0 [22]. The workflow consisted of the following general steps of the production chain:

- Mapping of the main ArcFUEL vegetation classes
- Multi-temporal analysis
- Refinement of the produced fuel classes based on density cover
- Merge of all the produced map layers in a single one
- Combination of the fuel classes with Ecoregions data

A crucial part of the methodology application was the selection of good clear Landsat images. For Portugal we had to go back to 2007 and use Landsat 5 images as they were the only acceptable ones covering the entire country. The new Landsat 8 should provide new up to date images that will allow us to update the maps. All areas burned in 2007 were masked from the final map (Figure 4).

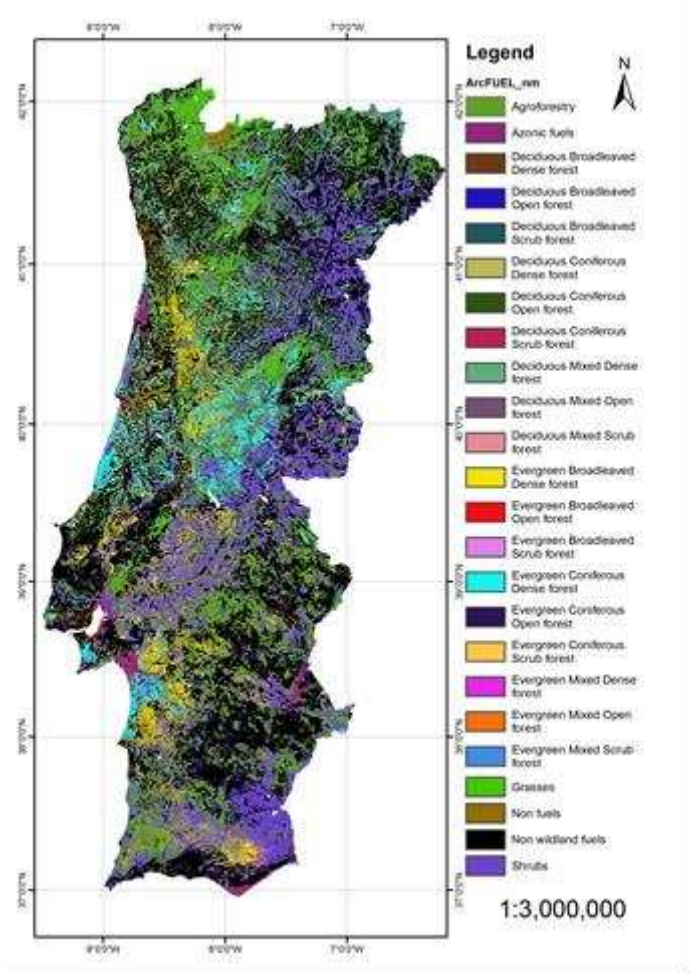

Figure 4. Final ArcFUEL map for Portugal mainland

The accuracy assessment of the produced map is currently being performed. A predefined number of control points is being directly checked in the field in order to check for the map consistency and reliability. At the moment, and after slightly more than 2/3 of the field campaign finished, the matching between the produced map and the reality can be considered visually satisfactory. Further statistical analysis will allow us to define a more reliable accuracy percentage.

5.1. Case study in Spain

The pilot area chose for Phase I was the Sierra de Las Nieves Natural Park, located west of Málaga province (Andalucía region), inside a Biosphere Reserve of the same name, showing very high terrestrial biodiversity. The area covers 20.163 ha and shows a high elevation gradient, raging in few km, from near the sea level to circa 2000 m (highest elevation peak at 1.919 m).

The area of interest (AOI) selected for Phase II in Spain was made up by the provinces of Málaga and Córdoba (north of Málaga), both in Andalucía region.

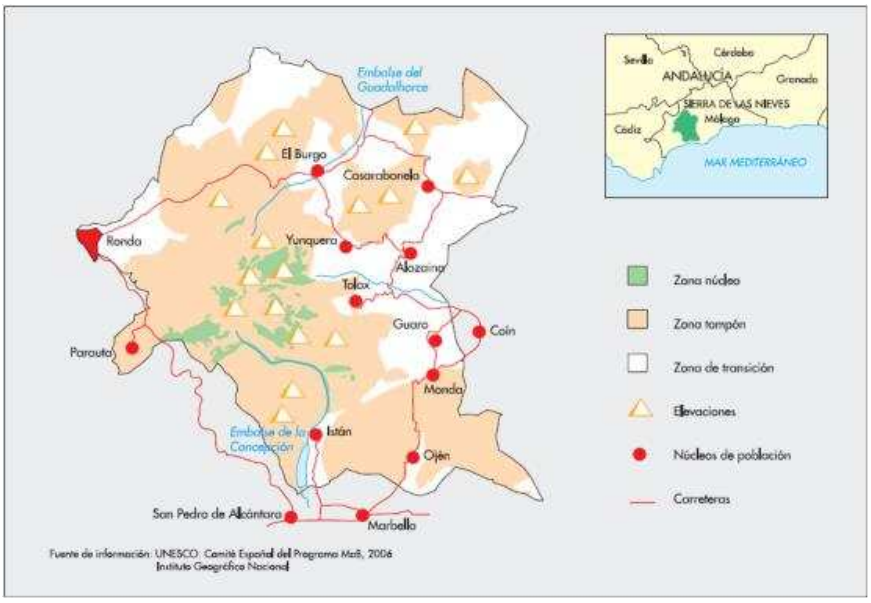

Figure 5. Biosphere Reserve of Sierra de las Nieves (Phase I)

Six Landsat 5TM images were used to cover the entire area in spring-summer, and another six to cover it in winter. Images date from year 2009, 2010 and 2011.

Erro! A origem da referência não foi encontrada. below shows the ArcFUEL fuel types derived over the entire area of study in Spain. The map shows a clear predominance of a few classes: Broadleaved Evergreen Scrub (18%), Broadleaved Evergreen Dense (32%), Coniferous Evergreen Dense (21%) and above all, Shrubs (42%). The non-wildland fuels represent a 17% of the study area. To assess these results a two-step validation was performed:

Validation step 1 (over pilot area)**:** focused on the discrimination between deciduous and evergreen species. This was done using the National Forest Inventory (NFI3) field plots, distributed in a regular 1-km grid.

Crossing the ground- truth with the classification values at each of the 163 IFN3 plots falling within the "Deciduous"/ "Evergreen" classes of the pilot area yielded very satisfactory results (95,6% overall accuracy), particularely in what concerns Evergreen forests. Conversely the discrimination of Decidous trees in the classification was not always correct (33% commission error). The impact of this is not relevant since the percentage of the area covered by Deciduos vegetation was less than1,6%. A similar procedure was followed to assess the discrimination of Shrubs and Grasses, and comparable results were obtained: (86,7% overall accuracy).

Validation step 2 (over Málaga and Córdoba): focused on the discrimination of vegetation assemblages, a concept closer to the term "fuel type" (e.g.: dense pine plantation with high shrubs, or abandoned olive trees plantation with grasses and dispersed shrubs).

For this purpose two ancillary sources having information on vegetation assemblages were used as ground truth:

I. The LUCAS (Land Use / Cover Area Frame Statistical Survey) multipurpose (agriculture, environment) field survey, with more than 250.000 sample points throughout the EU. LUCAS 2009 campaign was downloaded from EUROSTAT Web site [23] (free access).

II. The Integrated product "SIOSE" [24] plus "Vegetation map of Andalucía" (scale 1:10.000), property of the Andalusian Government (free access).

By crossing the classification values with the validation sources (LUCAS and SIOSE) at the 171 valid LUCAS plots falling within the AOI, we deduced that 136 of them were correctly classified (80%) while 35 were not (20% error).
The analysis per fuel type class showed again particularly good results for the Shrubs (90%) and Coniferous Evergreen classes (96%). Whereas the plots falling in the Broadleaves Evergreen Dense, and specifically those in deciduous classes (incorrectly classified) were not enough in number to draw any conclusion.

It must be noted that several inconsistencies were observed between LUCAS and the Andalusian Land Use/Vegetation Map, on the one hand, and the EU layers defining the first levels of ArcFUEL classification on the other (CLC [25], the Forest Types Map). Nonetheless results yielded (80% of correctly classified plots) evidence a satisfactory performance.

Overall this work has been a rather intense exercise of assessment, as the classification was crossed with field data and local scale maps with information on vegetation assemblages in a significant number of points. Moreover, this exercise was difficult since the intervening ancillary datasets have different reference date (2005 and 2009), level of detail and legends. It is concluded that the difference in dates (Landsat scenes leading to the classification map dated 2009-2011) might be behind the poor results shown by the most dynamic classes: Grasses, on the one hand, and Deciduous species, on the other.

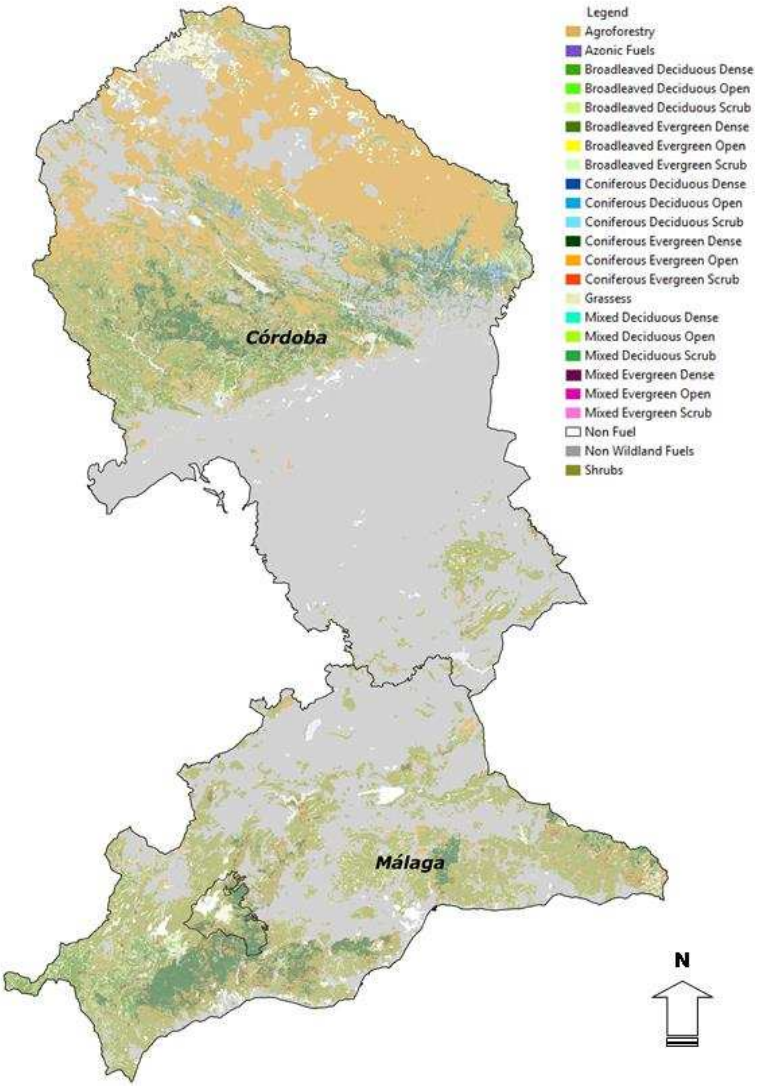

Figure 6. ArcFUEL fuel types over the study area in Spain (21.077 km2) and Pilot area (202 km2).

Field Validation

Purpose of the field validation is to create a dataset of point values for validating the ArcFUEL map. This comprises of the following steps:

1. We overlay LUCAS points to the ArcFUEL map and we separate LUCAS in two subsets of data, one with the LUCAS points which description coincide with ArcFUEL characterization and another with the LUCAS points which description differs from ArcFUEL. We keep the first subset as part of the ArcFUEL validation data set.
2. We use the second subset of point 1 and apply the following methodology per region:
    a. We select in each region randomly LUCAS points from the second subset and create the second part of ArcFUEL data set.
    b. We define a number of sampling points per region depending on its extent.
    c. We take care including all ArcFUEL types (AFT) in the data set derived.
    d. Sample points are located in a distance <300m from road and in slope <40%.
3. We randomly select 5% of the number of points defined in 2.b in elevation >1000m (LUCAS points are up to 1000m) taking into account the coverage of the ArcFUEL types.
4. During the field work:
    a. We fill the form with the data that we have defined (we have developed an android application for collecting these data).
    b. We allow taking as sample point a point close to the LUCAS point but representing better the forest fuel type in the specific location.
    c. We take additional sample points of representative fuel types along the way moving from one point to another.

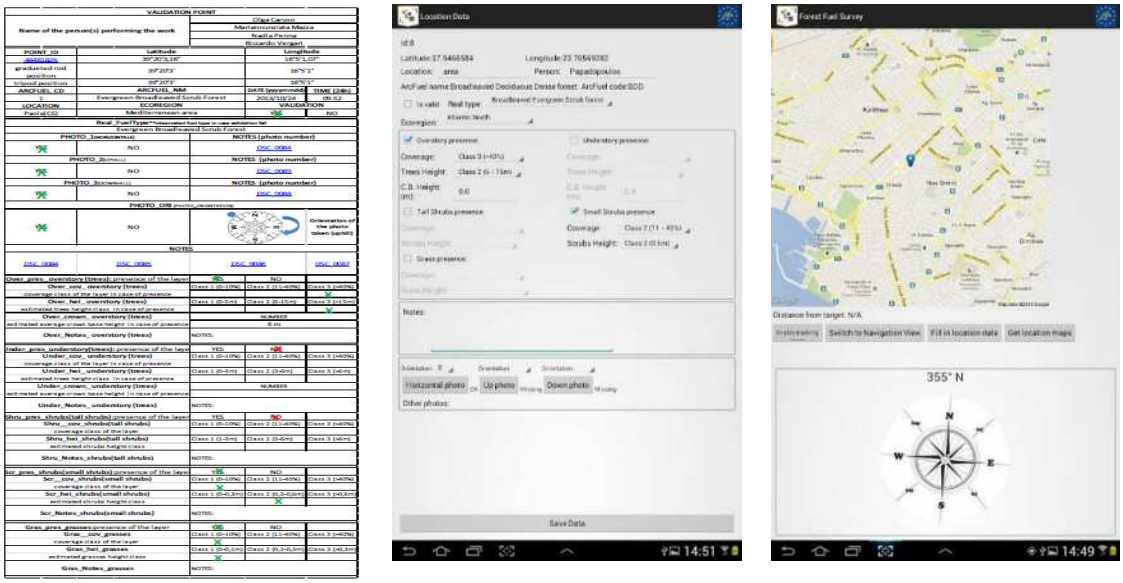

Figure 7. Field validation application, location data

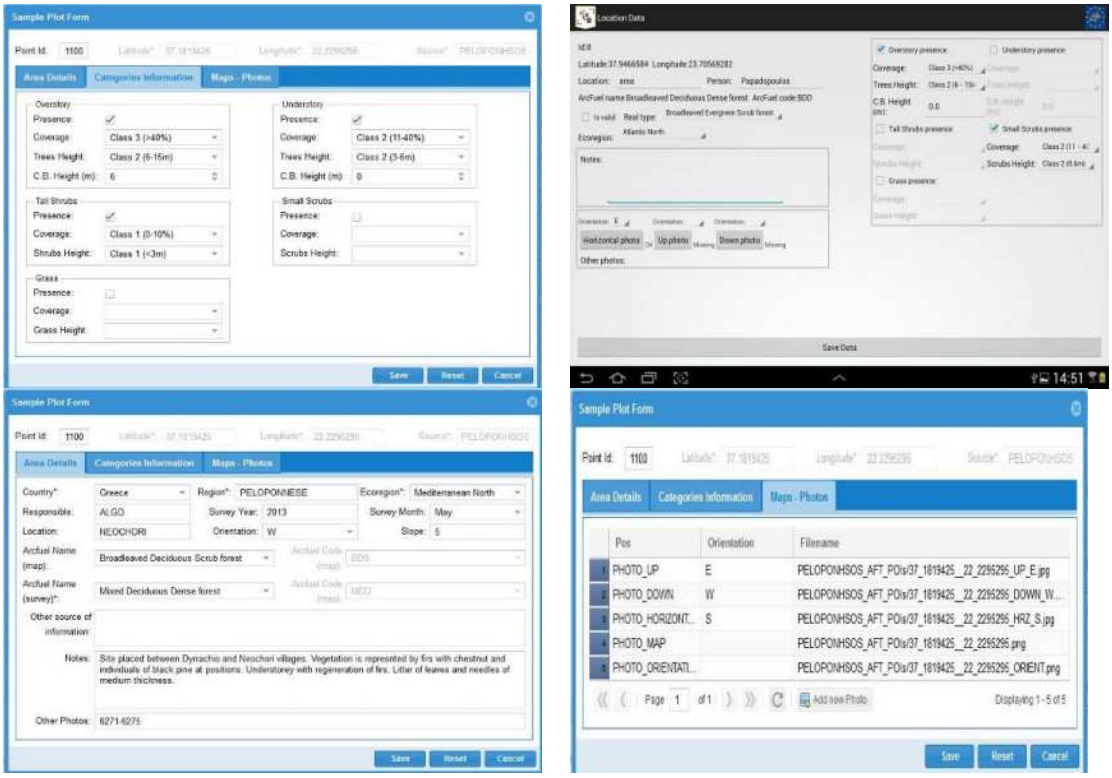

Figure 8. Field validation application, sample plots

5. We aggregate all data from the subsets mentioned above in point 2 (LUCAS=AFT), 3 (LUCAS≠AFT), 4 (>1000m) and 5 (additional AFT based points) for deriving the ArcFUEL validation data set.
6. In defining the above methodology we consider:
    a. We wanted to create a data set of point information for validating the accuracy and quality of the ArcFUEL map. Thus the main purpose was to create such a data set with distributed points, covering the area of interest and including all the fuel types present in each of the areas.
    b. We used LUCAS points in order to have information for a number of these points without new ArcFUEL survey but based on the new LUCAS survey data.
    c. We had to check deviation from LUCAS characterization in the field to see if and what the problem is.
    d. We had to enrich the ArcFUEL data set with additional points e.g. points at elevation greater than 1000m or points of representative fuel types.
    e. We considered 250 sample points to be distributed all over Greece and Portugal for the ArcFUEL map validation data set after the end of the field survey.

Fuel maps.

The LUCAS point dataset description was checked again to the ArcFUEL classification map to isolate points correctly classified. In addition to this overlay approach visual inspection using large scale orthophotographs of KTIMATOLOGIO SA [26] and Google Maps [27] was performed in order to identify any inconsistencies. A selective sample of these points is presented especially for randomly selected NATURA sites around project's areas.

Figure 9. Visual inspection to identify inconsistencies

8. Conclusions

The ArcFUEL methodology was tested and demonstrated producing forest fuel maps for Greece and Portugal at national scale and Italy and Spain at regional scale. The quality of the mapping was validated against field data.

During the field survey the ArcFUEL Consortium visited a total of 670 points in 4 countries, namely Greece, Portugal, Italy and Spain. The accuracy of the ArcFUEL methodology proved quite good, as it reached 73,2%. In detail, number of points visited during the field survey and accuracy of the ArcFUEL methodology in each country was:

- Greece: 298 points (81%)
- Portugal: 275 points (67%)
- Italy: 41 points (76%)
- Spain: 56 points (60%)

ArcFUEL delivered forest fuel maps with spatial resolution of 50x50m for Greece and Portugal at the country level and fuel maps of selected regions in Italy (Calabria and Sardinia) and Spain (Malaga, Cordoba).

ArcFUEL methodology proved to be a comprehensive method for rapid classification of forest vegetation into fuel types, delivering relevant input layers for fire modeling at an appropriate spatial resolution, using freely available data. Any future update of the input maps used in the ArcFUEL project will strongly improve the accuracy of the forest fuel maps. Synchronizing further the time reference of the input layers in the FCM production shall greatly improve the quality and accuracy of the ArcFUEL products.

The final fuel maps for Greece, Portugal, Italy and Spain are presented below:

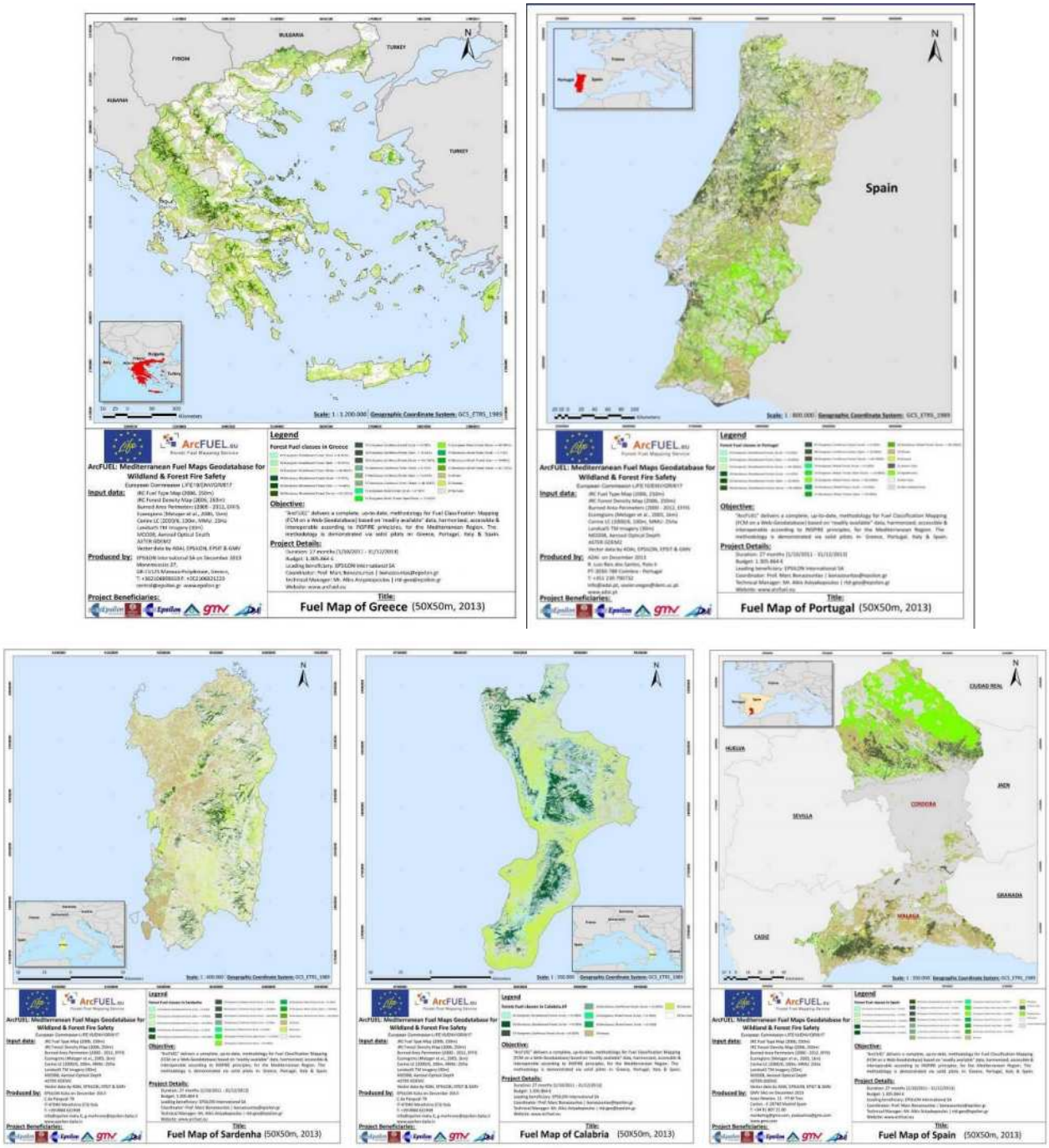

Figure 10. ArcFUEL final fuel maps

9. References

[1] ArcFUEL Official Website. Available online from: http://www.arcfuel.eu/index.php/en/

[2] RUIZ DE LA TORRE J., 1990. Distribucion y caracteristicas de las masas forestales espanolas. Ecologia Fuera de Serie 1, 11-30

[3] Bachmann, A. and Allgower, B. (1998). Framework for wildfire risk análisis. III International Conference on Forest Fire Research – 14th Conference on Fire and Forest Meteorology. ADAI, Coimbra, pp.2177-2190

[4] David Riaño, Emilio Chuvieco, Javier Salas, Alicia Palacios-Orueta, Aitor Bastarrika, Generation of fuel type maps from Landsat TM images and ancillary data in Mediterranean ecosystems- Canadian Journal of Forest Research, 2002, vol 32, issue 8, pp 1301-1315
[5] Gitas I.Z. and Devereux B.J. (2006). The role of topographic correction in mapping recently burned Mediterranean forest areas from LANDSAT TM images. International Journal of Remote Sensing. Vol.27, No.1, 41-54
[6] Gitas, I. Z., Polychronaki, A., Katagis, T., and Malinis, G.: Contribution of remote sensing to disaster management activities: A case study of the large fires in the Peloponnese, Greece, Int. J. Remote Sens., 29(6), 1847-1853, 2008
[7] Lasaponara, R. and Lanorte, A.:Remotely sensed characterisation of forest fuel types by using satellite ASTER data, Int. J. Appl. Earth Obs., 9, 225-234, 2007
[8] Dimitrakopoulos, A.P. 2002. Mediterranean fuel models and potential fire behaviour in Greece. International Journal of Wildland Fire, v. 11, no. 2, p. 127-130
[9] The 1990 Forest Fire Season in Spain, available online from: http://www.fire.uni-freiburg.de/iffn/country/es/es_1.htm
[10] The 1990 Forest Fire Season in Spain, available online from: http://www.fire.uni-freiburg.de/iffn/country/es/es_1.htm
[11] FUELMAP project 2011. Final Classification and Mapping of EU Fuel Complexes. Deliverable 2. JRC-ITT/RFQ Reference 2008/S 116-153998. June 2011
[12] Bolstad, P.V. &Lillesand, T.M., 1992. Improved classification of forest vegetation in northern Wisconsin through a rule-basedcombination of soils, terrain, and Landsat Thematic Mapper data.Forest Sci. 38 (1): 5–20
[13] Rikimaru, A., 1996. Landsat TM data processing guide for forest canopy density mapping and monitoring model. In: International Tropical Timber Organization (ITTO) workshop on utilization of remote sensing in site assessment and planning for rehabilitation of logged-over forest, Bangkok, Thailand, pp. 1–8.
[14] Wolter, P. T., Mladenoff, D. J., Host, G. E. & Crow, T. R., 1995. Improved forest classification in the northern Lake States using multitemporal Landsat imagery. Photogr. Eng. Remote Sensing61 (9): 1129–1143.
[15] Van Wagtendonk, J., W. and Root, R. R., 2003. The use of multitemporal Landsat Normalized Difference vegetation Index (NDVI) data for mapping fuel models in Yosemite national Park, USA. International Journal of Remote Sensing, 24, 1639-1651.
[16] Rikimaru A. Roy P.s., Miyatake S., 2002. Tropical forest cover density mapping. Tropical ecology 43, 39-47
[17] Barbosa, P., Amatulli, G. Camia, A. Kucera, J., San-Miguel-Ayanz, J., Strobl, P. 2007. "European Forest Fire Information System (EFFIS), rapid management assessment: appraisal of burnt area maps in southern Europe using MODIS data (2003 to 2006), In: Proc. Wildfire2007 IV International Wildland Fire Conference. Seville, Spain 13-17 May
[18] Mitri G.H. and Gitas I.Z., 2004. A semi-automated object-oriented model for burned area mapping in the Mediterranean region using Landsat-TM imagery. International Journal of Wildland Fire, Volume 13, Number 3, 367-376.
[19] Mücher, C.A., Bunce, R.G.H., Jongman, R.H.G., Klijn, J.A., Koomen, A.J.M., Metzger, M.J., Wascher, D.M., 2003. Identification and Characterisation of Environments and Landscapes in Europe. Alterra-rapport 832. Alterra, Wageningen.
[20] Joint Research Centre (JRC) EFFIS (European Forest Fire Information System) . Available online from: http://forest.jrc.ec.europa.eu/effis/
[21] ESRI ArcGIS Desktop. Available online from: http://www.esri.com/software/arcgis
[22] GRASS GIS. Available online from: http://grass.osgeo.org/
[23] Statistical Atlas – LUCAS (Land Use and Cover Area Frame Survey). Available online from: http://ec.europa.eu/eurostat/statistical-atlas/gis/viewer/?myConfig=LUCAS-2012.xml

[24] SIOSE Geoportal. Available online from: http://www.siose.es/siose/
[25] European Environmental Agency 2007. CLC2006 technical guidelines. Technical report No 17/2007. Luxembourg: Office for Official Publications of the European Communities, 2007, ISSN 1725–2237
[26] National Cadastre and Mapping Agency S.A. Available online from: http://gis.ktimanet.gr/wms/ktbasemap/default.aspx
[27] Google Maps. Available online from: https://www.google.gr/maps

Monitoring erosion risk with ERMIT model: a case study in North Sardinia, Italy

Romina Secci[a], Annalisa Canu[b], Andrea Motroni[c], Andrea Ventura[b], Gabriele Uras[a]

[a] *University of Cagliari, DICAAR, romysecci@gmail.com*
[b] *CNR - IBIMET Sassari, canu@ibimet.cnr.it*
[c] *ARPAS - Meteo-Climatic Department, amotroni@arpa.sardegna.it*

Abstract
Wildfires are one of the most widespread factors of ecosystem degradation around the world. The present note reports the first experimental results of a wider-scale research project, whose aim is to develop methods for the analysis and the collection of field data, by means of a multidisciplinary approach, to evaluate land erosion hazard.
The experimental area is located in Mediterranean basin, on a steep slope in a hilly area of north-western Sardinia (Municipality of Ittiri, Italy), where a human caused fire occurred in August 2013. The area is mainly covered by the typical Mediterranean vegetation. The forest fire spread through the study area in August 2013 and the burn severity has been moderate, according to USDA burn severity classification system. After the fire, sediment fences were installed to trap sediments eroded by natural rainfall. Precipitations were recorded using tipping bucket rain gauge installed at the site.
Soil erosion rates from experimental plots were measured and estimated with silt fences technique taking into account different slopes and vegetation distribution. The study aims to compare the results obtained by ERMIT (Erosion Risk Management Tool) model application and post-fire sediment yields measured in the study area.
The application of the model shows that the area experienced most of erosion after the first rain events after fire occurring. Comparing experimental and model estimated data, there is evidence of ERMiT model overestimating in respect of sampled data for the first year. Future experimental data are needed to confirm this assumption and to contribute to calibrate ERMiT in a Mediterranean typical vegetation and climate environment.

Keywords*: erosion risk, ERMIT, burned area, forest fire effects*

Introduction

Several authors suggest that in the early months following the passage of a fire, the soil erosion increases dramatically (DeBano *et al*., 1998; Campo *et al*., 2006), even if gaps and further investigation in this field can be easily outlined and recommended (Shakesby, 2011). High soil temperatures can increase the erodibility of the soil surface, giving an indication of the susceptibility of the soil to the impact of raindrops, to runoff, and other erosive processes (Moody and Martin 2009, Scott *et al*., 2009). In extreme situations, burned areas of unstructured soils may be interested by processes of waterproofing and soils becoming hydrophobic (Imeson *et al*., 1992). Available sediment can be eroded from slopes and channels, transported and deposited downward in the valley driven by erosion energetic inputs: precipitation, runoff, wind, and gravity. The loss of vegetation and forestry sediments increase surface runoff in sloppy areas because longer flow paths are formed without interruption, without surface roughness, and because the wind speed increase. These changes increase the amount of energy available for erosion and sediment transport (Moody and Martin 2009a). The effects of fire on hydrology can be mitigated by the presence of ash: forest fires can leave a dry, porous layer of ash that covers the mineral soil (Cerdà and Robichaud, 2009).
The increase of landslide phenomena in slope areas crossed by forest fires, is well documented in the scientific literature (Curran *et al*. 2006; DeBano *et al*. 1998; Lane *et al*. 2006; Moody *et al*. 2009;

Neary *et al*. 2005). In general, the hydrological response at the catchment scale is inversely correlated to the effectiveness of the after fires treatment (Robichaud *et al*. 2008).
ERMiT is a web-based application developed by USDA (Robichaud, 2007a) that uses Water Erosion Prediction Project (WEPP) technology to estimate soil erosion, in probabilistic terms, on burned lands with and without the application of erosion mitigation treatments. Data inputs are: climate parameters, vegetation type, soil type, topography, and soil burn severity class. The above parameters were applied to the ERMIT model and it was possible to predict the probably erosion risk for the next 5 years.
The objective of this work is to show preliminary results of erosion sediments yield in a hilly burned area of north-western Sardinia (Italy) and the correspondent output data from the application of ERMiT model.

Methods

Study site and data collection

The experimental area is located in a hilly area of north-western Sardinia, (around urban area of Sassari, Italy, 40° 33'N; 8° 31'E), where a human caused fire occurred in August 2013 and burned an area of 28 hectares (Figure 1). The area is mainly covered by typical Mediterranean chaparral vegetation.
The climate is typically Mediterranean with water deficit conditions occurring from May through September and precipitations mainly concentrated in autumn and winter.
The mean annual rainfall is 730 mm and annual mean air temperature is 16.8 °C. Most fires occur during the summer season, from June to September.

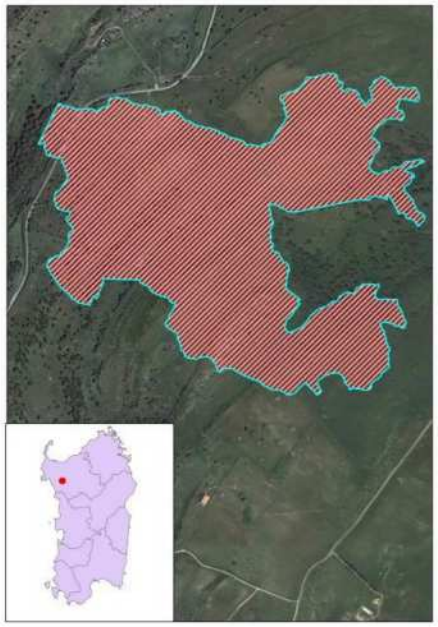

Figure 1. Study area and perimeter of burned area

In August 2014, sediment fences were installed in 10 plots in an area with a slope of 20% to capture sediment produced by natural rainfall (Robichaud and Brown, 2002).

ERMIT model

ERMiT (Erosion Risk Management Tool) is a web-based application that uses Water Erosion Prediction Project (WEPP) technology to estimate erosion in probabilistic terms, on burned and recovering forest, range, and chaparral lands with and without the application of erosion mitigation treatments. User inputs are processed by ERMiT to combine rain event variability with spatial and

temporal variabilities of soil burn severity and soil properties, which are then used as WEPP input parameters. ERMiT produces a distribution of rain event sediment delivery rates with a probability of occurrence for each of five post-fire years. In addition, event sediment delivery rate distributions are generated for post-fire hillslopes that have been treated with seeding, straw mulch, and erosion barriers such as contour-felled logs or straw wattles. In this work for every simulation has been considered only the results of the untreated hillslope.
User inputs for ERMiT are climate, soil texture, soil rock content, vegetation type (forest, range, chaparral), hillslope gradient and horizontal length, soil burn severity class for range and chaparral, and pre-fire plant community description (relative distribution of shrub, grass, and soil cover in percentages). User inputs are entered on a single interactive browser screen. ERMiT's "event sediment delivery exceedance probability" output can help managers to decide where, when, and how to apply treatments to mitigate the impacts of post-wildfire runoff and erosion on life, property, and natural resources. With ERMiT, managers can establish a maximum acceptable event sediment yield and use ERMiT to determine the probability of "higher than acceptable" sediment yields occurring (Robichaud, 2007b).
Simulations were carried out for the burned area taking into consideration the same input parameters for all the runs. The only change was made for the vegetation values immediately and 6 months after fire occurring. Successive validation of ERMiT was completed with field data.
Hill slope burned area was divided in 10 plots (10 m x 3 m) limited in the downhill edge by silt fences in order to contain eroded soil and debris of each specific plot. Silt fences used in this study are easy to be installed and costless (Robichaud and Brown, 2002), being made of wooden posts and geotextile fabric (figure 2). Eroded material is collected, weighted and analysed possibly soon after the major rain events.

Figure 2. Example of sample plot and sediment trapped in the silt fence

2.2.1. *Climate parameters*

Climatic data for ERMiT simulations referred to the closest weather station of Hydrological Department of Sardinia. Temperature and precipitation data series for the period 1988-2002 were considered. In ERMiT simulation runs, the monthly means of rainfall and the number of rainy days for each month of the year are considered. Mean, maximum and minimum temperature values were also input data for modeling.

2.2.2. *Vegetation*

Prevailing surrounding vegetation is Mediterranean chaparral in garrigue association, while as the areas where fire occurred is dominated by oak tree (*Quercus suber* spp.) forest. Ground cover ocular estimation (percentage of herbaceous, bare soil and stoniness surface) were made using a 1 m^2 point frame with wire intersections at 10 cm intervals (figure 3) with 3 repetitions per plot.

Vegetation cover measurements were made both soon after fire occurring in late August 2013 and in early days of May 2014, so after about 8 months. In this way different recovering attitudes and characteristics of the plots inside the area were considered.

Figure 3. Vegetation cover measurement

2.2.3. *Type of soil*

Several soil samples were collected at 0-10 cm depth, in burned plots. Analysis were performed in collaboration with the Geotechnical laboratory of Cagliari Province. Two trials of texture repetitions were conducted considering both sieving (for 0.075÷100 mm grains) and sedimentation (0.0055÷0.1117 mm grains). Results are shown in table 1. Soil is therefore constituted mostly by sand and clay.

Table 1. Basic statistics for each soil property

	pH	N g Kg^{-1}	% OC	P_2O_5 ppm	Silt %	Clay %	Sand %	2 mm %	1 mm %	0,5 mm %	0,2 mm %
mean	6,36	3,68	3,70	12,86	26,13	26,61	47,26	31,76	2,21	1,41	3,30
st. dev.	0,11	1,23	0,21	1,87	4,61	7,18	3,40	9,78	0,79	0,56	0,88

2.2.4. *Slope*

Slope was measured in the field using a digital level instrument (Stabila 86 Electronics). Several measures were made for each plot and the average slope was considered (20% in this case).

2.2.5. *Soil burn severity*

Burn severity was estimated applying USDA methodology as reported in the "Field guide for mapping soil burn severity" (Parsons *et al.*, 2010). Ocular estimation of fire severity and damages caused by burning and the comparison with clear pictures of similar situations allows to have a fast, reasonably precise classification of burn severity. The severity of the fire was considered "moderate" based on post fire analysis and vegetation recovering capacity, together with vegetation damages and limited infiltration rates of topsoil.

3. Results

Figure 4 shows the daily cumulative, maximum intensity 30 minute rainfall (I_{30} max) and the sample dates. The total precipitation recorded in the period September 2013 - April 2014 (653 mm) is about 90% of the mean annual rainfall. Four periods of sediment accumulation were carried out during the

experimentation, and sediments were removed from the silt fence on 10 September 2013, 29 January, 19 March, and 10 April 2014. These dates are reported in the figure 4 in black (sample).

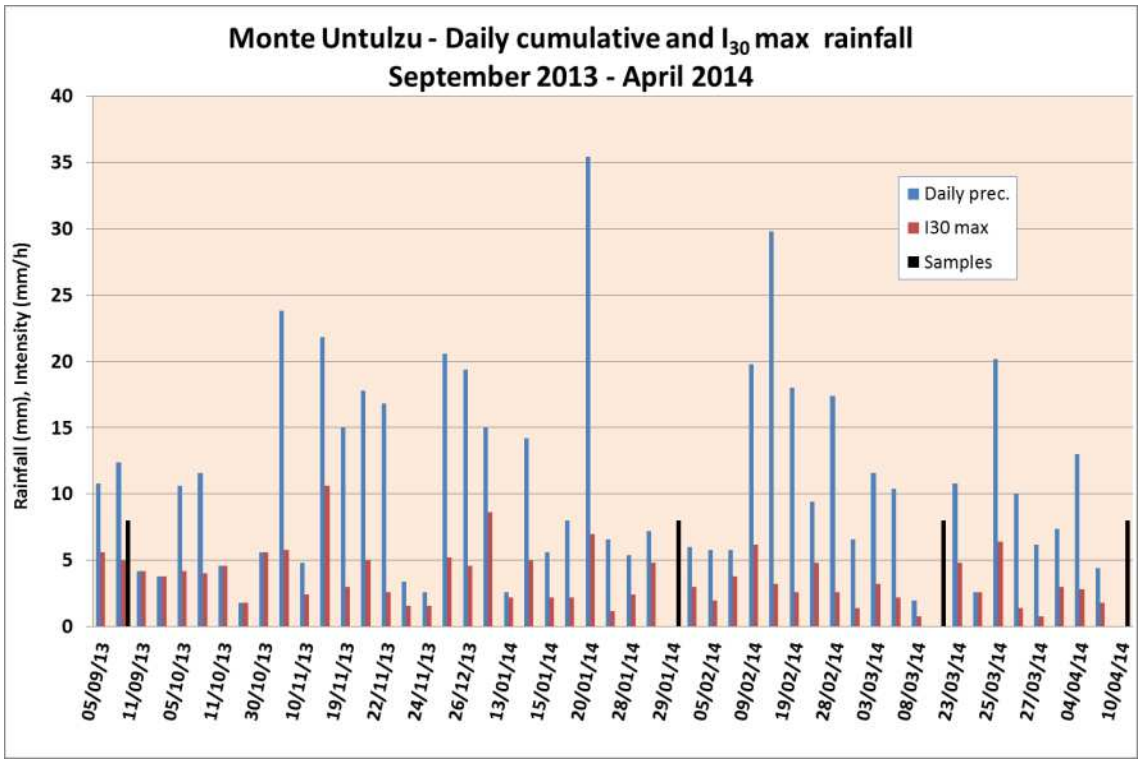

Figure 4. Daily cumulative rainfall and $I_{30\ max}$

Mean values of measured soil loss for each sample of plots with slope of 20% are reported in figure 5. The highest erosion was observed in the first sample (1.6 t ha^{-1}), whereas, in the last sample, event erosion rate was very low, only 0.02 t ha^{-1}.

Total soil erosion loss recorded during this study was 2.8 t ha^{-1}. Vacca *et al*. (2000) had much lower results in erosion plots under burned chaparral in southern Sardinia (0.51 – 0.26 t ha^{-1}); even lower sediment values (0.014 t ha^{-1}) were recorded in Bonassai, northwestern of Sardinia, on burned pasture (Rivoira *et al*., 1989) this low values are probably due to the low severity of fire.

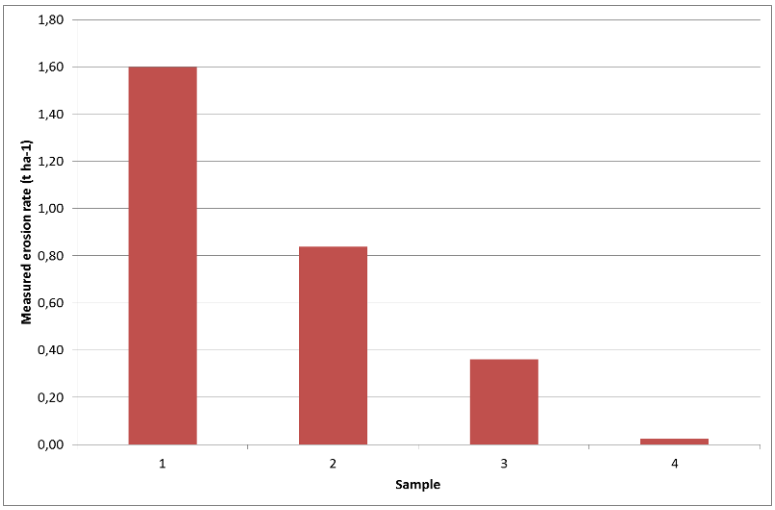

Figure 5. Mean values of measured soil loss (t ha^{-1})

The results of ERMiT simulations are shown in figures 6 and 7. Only untreated estimates were considered with different probability that sediment yield will exceed a certain threshold. Soil losses estimated by ERMiT for the first year are 3.23 and 3.13 t ha^{-1}, soon after fire and six months after fire, respectively.
Model results compared with the field measurements show how ERMIT model tends to overestimate erosion rates in typical Mediterranean vegetation and soil conditions. These preliminary results need to be confirmed by further investigation in coming years and also in different sites with similar vegetation, slope and soil conditions, given a defined fire severity and precipitation patterns.

Sediment Delivery					
Probability that sediment yield will be exceeded 20 % go	Event sediment delivery (t ha^{-1})				
	Year following fire				
	1st year	2nd year	3rd year	4th year	5th year
Untreated	3.23	1.66	0.7	0.6	0.5
Seeding	3.23	0.9	0.6	0.5	0.5
Mulch (1 t ha^{-1})	0.7	0.7	0.7	0.6	0.5
Mulch (2 t ha^{-1})	0.6	0.6	0.7	0.6	0.5
Mulch (3.5 t ha^{-1})	0.58	0.6	0.7	0.6	0.5
Mulch (4.5 t ha^{-1})	0.56	0.6	0.7	0.6	0.5
Erosion Barriers: Diameter 0 m Spacing 50 m go ?					
Logs & Wattles	3.23	1.66	0.7	0.6	0.5

Figure 6. Example of ERMiT output of sediment delivery 20% exceedance probability

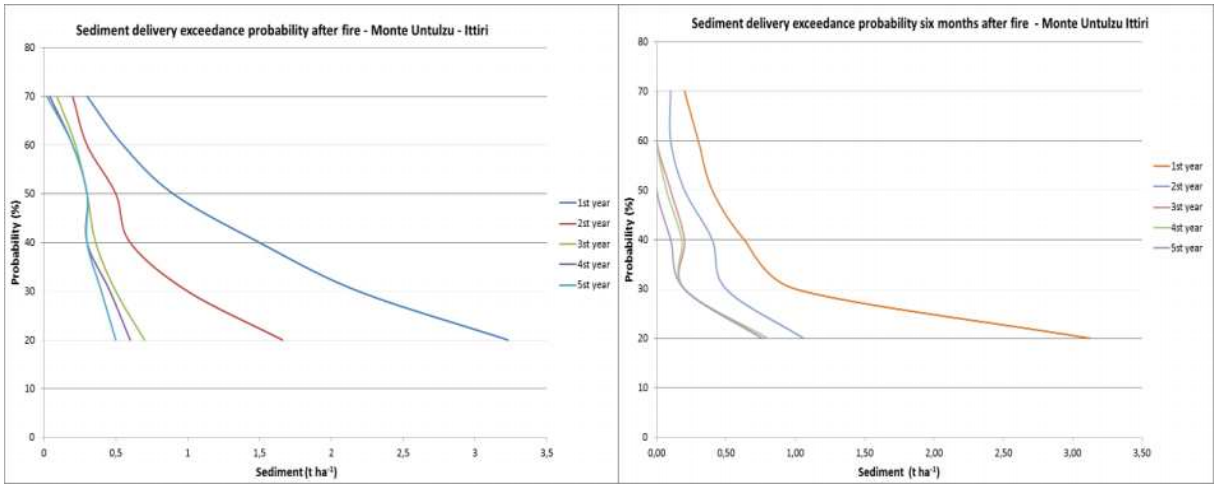

Figure 7. Exceedance probability vs event sediment delivery for five years after the fire(left) and after six months in the study area (right)

References

Campo, J.; Andreu, V.; Gimeno-García, E.; González, O.; Rubio, J.L.; 2006. The occurrence of soil erosion after repeated experimental fires in a Mediterranean environment, Geomorphology vol 82, n. 3-4, 376- 387.

Cerdà, A.; Robichaud, P.R., eds. Fire effects on soils and restoration strategies., 2009, Enfield, NH, USA, Science Publishers. pp. 589.

Curran, M.; Chapman, B.; Hope, G.; Scott, D. 2006. Large-scale erosion and flooding after wildfires: understanding the soil conditions. B.C. Tech. Rep. 030. Victoria, B.C. Canada: B.C. Ministry of Forests and Range, Research Branch. 18 p.

DeBano, L.; Neary, D.; Folliott, P. 1998. Fire's effects on ecosystems. New York, NY: John Wiley & Sons. 333 p.

Imeson, A.C. ; Verstraten, J.M.; van Mulligen, E.J.; Sevink, J.; 1992, The effects of fire and water repellency on infiltration and runoff under Mediterranean type forest, Catena, 19: 345-361.

Lane, P.N.J.; Sheridan, G.J.; Noske, P.J. 2006. Changes in sediment loads and discharge from small mountain catchments following wildfire in south eastern Australia. Journal of Hydrology. 331: 495-510.

Moody, J. A.; Martin, D. A.; 2009. Synthesis of sediment yields after wildland fire in different rainfall regimes in the western United States, International Journal of Wildland Fire 18(1) 96–115 http://dx.doi.org/10.1071/WF07162.

Neary, Daniel G.; Ryan, Kevin C.; DeBano, L. F.; eds. 2005. (revised 2008). Wildland fire in ecosystems: effects of fire on soils and water. Gen. Tech. Rep. RMRS-GTR-42-vol. 4. Odgen, UT: U.S. Department of Agriculture, Forest Service, Rocky Mountain Research Station. 250 p.

Parsons, A., Robichaud, P.R., Lewis, S.A., Napper, C., Clark, J.T. 2010. Field guide for mapping post-fire soil burn severity. Gen. Tech. Rep. RMRS-GTR-243. Fort Collins, CO: U.S. Department of Agriculture, Forest Service, Rocky Mountain Research Station. 49 p.

Rivoira, G.; Roggero, PP.; Bullitta, S.; 1989. Improvement techniques and erosion of hillside pasturelands, Rivista di agronomia, 23/4, 372-377 (in Italian).

Robichaud, P.R.; Brown, R.E.; 2002, Silt Fences: An economical technique for measuring hillslope soil erosion,.USDA Forest Service Gen. Tech, Rep., RMRS – GTR – 94.

Robichaud, P.R.; Elliot, W.J.; Pierson, F.B.; Hall, D.E.; Moffet, C.A.; 2007a. Predicting postfire erosion and mitigation effectiveness with a web-based probabilistic erosion model. Catena 71: 229–241

Robichaud, P.R.; Elliot, W.J.; Pierson, F.B.; Hall, D.E.; Moffet, C.A.; Ashmun, L.E.; 2007b. Erosion Risk Management tool (ERMIT) Manual (version 2006.01.18),USDA, RMRS, General Technical Report RMRS-GTR-188,31 p.

Robichaud, P.R.; Wagenbrenner, J.W.; Brown, R.E.; Wohlgemuth, P.M.; Beyers, J.L.; 2008. Evaluating the effectiveness of contour-felled log erosion barriers as a post-fire runoff and erosion mitigation treatment in the western United States. International Journal of Wildland Fire. 17: 255-273.

Scott, D.F.; Curran, M.P.; Robichaud, P.R.; Wagenbrenner, J.W. 2009. Soil erosion after forest fire. In: Cerdà, A.; Robichaud, P.R., eds. Fire effects on soils and restoration strategies. Enfield, NH: Science Publishers: 178-195.

Shakesby, R.A. Post-wildfire soil erosion in the Mediterranean: Review and future research directions, 2011. Earth-Science Reviews 105: 71–100.

Shakesby, R.A.; Coelho, C.O.A.; Ferreira, A.D.; Terry, J.P.; Walsh, R.P.D.; 1993. Wildfires impacts on soil erosion and hydrology in wet Mediterranean forest, Portugal. Int. J. Wildland Fire 3-2., 95–110.

Vacca, A.; Loddo, S.; Ollesch, G.; Puddu, R.; Serra, G.; Tomasi, D.; Aru, A. 2000. Measurement of runoff and soil erosion in three areas under different land use in Sardinia, Italy. Catena 40: 69–92.

Multitemporal analysis of burned areas of the Selva El Ocote Biosphere Reserve, Mexico, using satellite data

Lilia Manzo-Delgado[a], Aide Franco-Martínez[b], Gloria León-Rojas[c]

[a, c] *Instituto de Geografía, Universidad Nacional Autónoma de México. Av. Universidad 3000, Ciudad Universitaria, 04510 Coyoacán, México, D.F. Apartado Postal 20-394, llmanzo@igg.unam.mx , glorisa.leon@gmail.com*
[b] *Facultad de Ciencias, Universidad Nacional Autónoma de México. Av. Universidad 3000, Ciudad Universitaria, 04510 Coyoacán, México, D.F., aideframa@ciencias.unam.mx*

Abstract
The aim of this study was to map the burned areas of the Selva El Ocote Biosphere Reserve for the period 1998–2012, using Landsat TM/ETM+ images. The method was based on a visual comparison of false color images and the pre/post-fire spectral indices Normalized Burn Ratio (NBR) and Normalized Difference Vegetation Index (NDVI); it used official records of wildfires from the National Commission for Natural Protected Areas and National Forestry Commission, and hotspots identified by the National Commission for Knowledge and Use of Biodiversity and the Fire Information for Resource Management System. Landsat images were downloaded during the fire season, January–June, for each year. According to the results, 54,756 ha were affected by 1095 fires during 1998–2012. We estimated that 352 of them involved tropical forest and 743 pasture, savannah and secondary tropical forest. The catastrophic years were associated with El Niño events 1998 (42,240 ha), 2003 (1,643 ha) and 2005 (1,248 ha), suggesting that the meteorological conditions contributed to the vulnerability of vegetation to fire. These results illustrate a method for analysing the pattern of spatial and temporal distribution of burned areas and for identifying zones that merit priority attention with regard to agricultural burning and wildfires.

Keywords*: burned area, Landsat, NBR, NDVI*

Introduction

Each year, Natural Protected Areas in Mexico are affected by wildfires of varying frequency, intensity and extent (Ressl *et al*., 2009). The factors influencing the occurrence of forest fires are physical (topography and climate), biological (community structure and functioning) and anthropogenic (often caused by the cultural use of fire, tourism and transport). In recent decades, the combination of climatic anomalies such as hurricanes, followed by long dry periods associated with the El Niño Southern Oscillation (ENSO) phenomenon (particularly during 1998, 2003 and 2005) has produced much organic combustible material and large forest fires. In southeastern Mexico all these factors converge to favour extensive burned areas in tropical rainforest (Román-Cuesta *et al*., 2003). To counter this, a global integrated fire management programme was developed for protected areas. The Selva El Ocote Biosphere Reserve in Chiapas State was the first to adopt and adapt this programme, including prevention, suppression, fire use and registration of all annual records of wildfires (CONANP & TNC, 2009). However, this programme does not have maps of burned areas.
For more than two decades, remote sensing techniques and satellite imagery have been used in various regions of the word to identify burned areas, using principles based on the spectral response of the deposits of ash and charcoal left after combustion of plant material. The spectral behaviour of burned areas is characterised by an increase in the reflectance of wavelengths in the visible region (0.4–0.7 µm), a decrease in the near-infrared region (0.78–0.90 µm), and an increase again in the mid-infrared region (1.3–8.0 µm) and thermal region (8.0–14.0 µm). These changes are related to the interruption of photosynthetic activity, changes in the internal structure of leaves and loss of water (Pereira *et al*.,

1999). Although scars may persist, burned areas may be remove by wind and rain a few weeks or months after the fire. Burn scars are more evident when trees or shrubs have been eliminated: whereas the effect remains for two to three weeks in pasture it can persist for several years in temperate forest (Robinson, 1991; Pereira *et al.*, 1999).

The discrimination of burned areas is based on the use of vegetation indices such as NDVI (Normalized Difference Vegetation Index), false color images, supervised classification and principal components (Roy *et al.*, 2005a; Chuvieco *et al.*, 2005); however, Normalized Burn Ratio (NBR) and Burned Area Index (BAI) are a better alternative because they use near infrared and short-wave infrared bands, which are more sensitive to the presence of charcoal and ash on the soil (Pereira *et al.*, 1999; Cocke *et al.*, 2005). This process includes a visual analysis of multitemporal images or automated detection using algorithms; both need to consider the wide diversity caused by severity of the fire and the time elapsed since the fire was extinguished, and vegetation type (Bastarrika *et al.*, 2011).

Several products based primarily on data with coarse spatial resolution can be used to survey burned areas at the global level. For example, the project Global Burnt Area (GBA) 2000, with 1 km spatial resolution, was developed during 2000 with SPOT-VEGETATION data, later named L3JRC, and generated results until 2007 (Tansey *et al.*, 2007). Also, the official product for burned areas MCD45, from Moderate Resolution Imaging Spectroradiometer (MODIS) images, with 500 m spatial resolution, has provided monthly reports from 2000 to the present (Roy *et al.*, 2005b). Similarly, some regional studies have been developed, such as in Latin America (Chuvieco *et al.*, 2006). All information has been limited to large fires (> 250 ha). Nevertheless, local-level studies require high spatial resolution images such as Landsat Thematic Mapper (TM), Enhanced Thematic Mapper (ETM+) or SPOT (Bastarrika *et al.*, 2011; Polychronaki & Gitas, 2012).

The Landsat near-infrared and middle-infrared bands provide stronger burned area discrimination than the visible bands and are less sensitive to smoke aerosol. The burned areas have low reflectance in all these bands, and so appear dark. The spatial and spectral appearances of the burned area vary within and between the two dates (Roy *et al.*, 2005a).

The aim of this study was to map burned areas in the Selva El Ocote Biosphere Reserve, Chiapas, for the period 1998–2012, using visual analysis of multitemporal Landsat TM/ETM+ images, in order to contribute to the spatial and temporal analyses of these events and identify priority areas regarding fire risk.

Methods

2.1. Study area

The study area is in southeastern Mexico, in western Chiapas State, south of the Nezahualcoyotl dam (16° 45’42” to 17° 09’00” N, and 93° 54’19” to 93° 21’20” W). At the end of 2000, the Selva El Ocote Biosphere Reserve, was established; it consists of 101,288 ha divided into two core zones with a total area of 40,432 ha and a buffer zone of 60,856 ha (Diario Oficial de la Federación, 2000) and its elevation ranges from 180 to 1500 m asl. It is a mountainous karstic region, with shafts, sinkholes and caverns. Warm and humid climates dominate, favouring the development of tropical rainforest, dry tropical forest and savannah, as well as pasture and agriculture lands.

Fire data and satellite images

The official fire records were provided by the National Commission for Natural Protected Areas (CONANP) and the National Forestry Commission in Chiapas State (CONAFOR). Also, hotspots (active fire) identified by the National Commission for Knowledge and Use of Biodiversity **(**CONABIO) and the Fire Information for Resource Management System (FIRMS) were downloaded (https://conabio.gob.mx; https://earthdata.nasa.gov/data/near-real-time-data/firms). The different data were visualised in layers and organised monthly with ArcMap software.

Fifty-nine Landsat TM/ETM+ images (Path/Row 22/48) for the period January – June from 1998 to 2012 were downloaded from the USGS Global Visualization Viewer (http://glovis.usgs.gov), Geotiff format, Level-1G, <43% cloud cover and georeferenced (Universal Transverse Mercator projection), with a ground spatial resolution of 30 m. Eight images were acquired out of the fire season to ensure cloud-free data for multitemporal comparisons.

The Land Cover maps produced by the National Institute of Statistics, Geography and Information Technology (INEGI) at scale 1:250000 were also available for the study area. This information was used to identify land cover classes affected by fire.

2.3. Discrimination of burned areas

Discrimination was based on a visual analysis of consecutive false color images Landsat images: bands 5(15.5–17.5 µm), 4(7.50–9.00 µm), 3(6.30–6.90 µm) and 7(20.90–23.50µm), 4(7.50–9.00 µm) 3(6.30–6.90 µm) displayed as red (R), green (G), and blue (B) respectively (Roy *et al.*, 2005a). Dark-red or purple areas (Figure 1) were considered to be potential burned areas that could be associated with charcoal and ash deposited after the combustion of plants (Pereira *et al.*, 1999). At the same time, the official fire records and hotspots were overlayed.

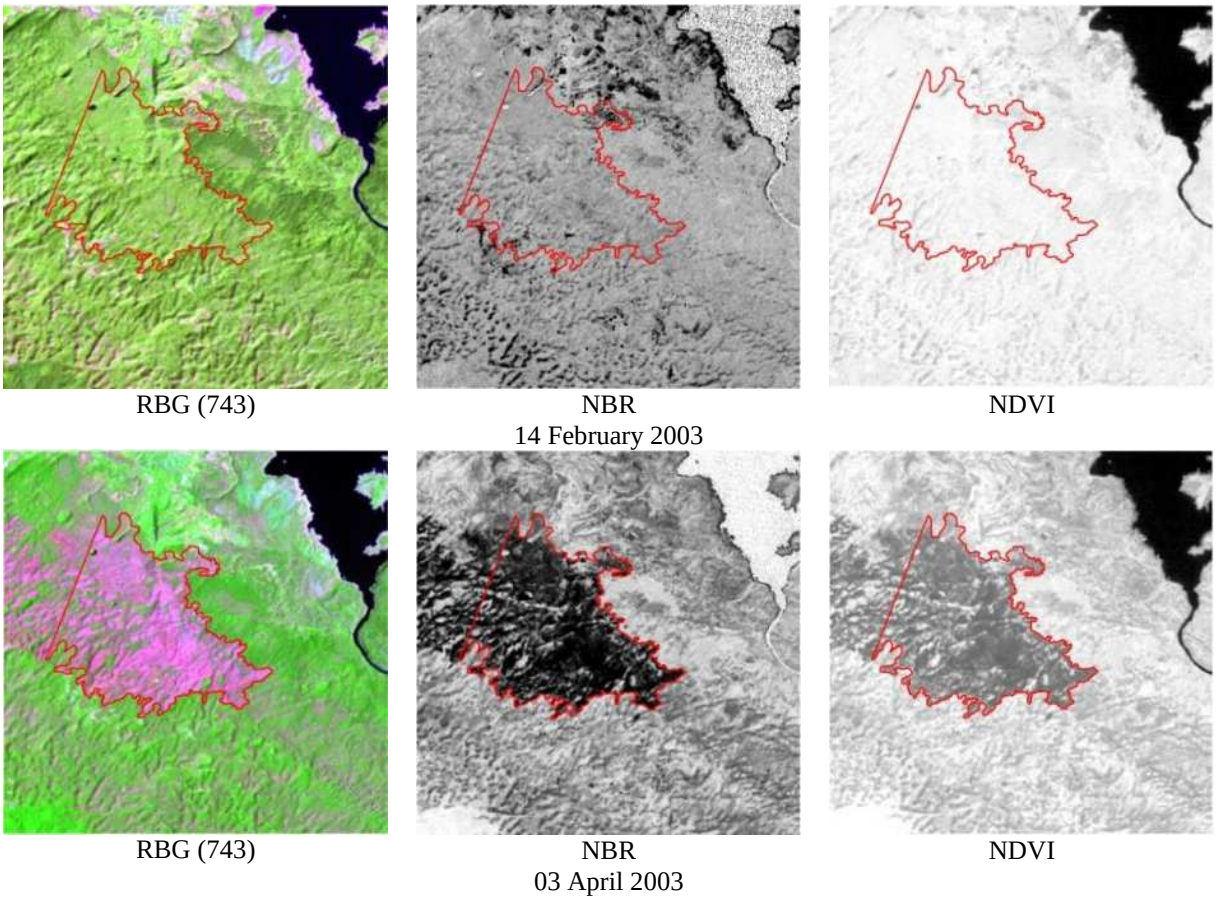

Figure 1. Visual comparison between pre/post-fire (top/bottom) Landsat ETM+ images. The fire perimeter in the Reserve is the red outline. At the top is part of the Nezahualcoyotl Dam.

To confirm the areas thus identified, a visual comparison between pre/post-fire spectral indices NBR (Normalized Burn Ratio: B4 - B7/B4 +B7) was used. A diminished NBR confirms the presence of a burned area (Cocke *et al.*, 2005). During this phase, the vegetation index NDVI (B4 - B3/B4 +B3) was also used to identify significant changes in the areas affected by fire (Figure 1). Fire perimeters were

digitised and labelled with the dates of images, the official record and the hotspot, as well as vegetation type. The different processes were supported by ArcMap and ENVI.

Results

According to the visual comparison in 1998, 229 fire perimeters were delimited, with surface variation from 0.3 to 2600 ha, and 42,240 ha affected; this was less than half of the total area. During 1999–2012, 866 fire perimeters were delimited, with surface variation from 0.3 to 600 ha, and 12,517 ha affected. We estimated that 352 involved tropical forest (wildfires) and 743 pasture, savannah and secondary tropical forest (agricultural burning). With the exception of 1998, burned areas smaller than 20 ha were more frequent (90%) at the buffer zone and near to villages and roads, confirming the relation with traditional fire use. Nowadays, in the core zone, many areas affected during 1998 have recovered their forest density; however, the portion west of the core zone sometimes experiences severe fires (Figure 2).

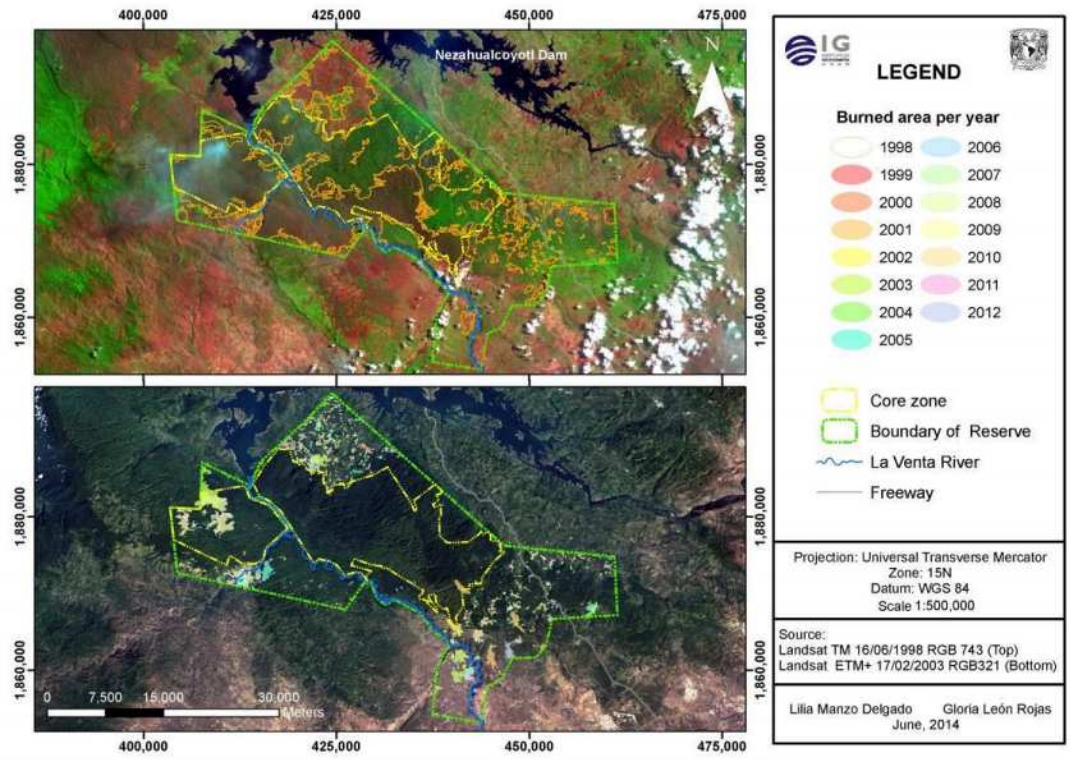

Figure 2. Burned areas of the Selva El Ocote Biosphere Reserve, Mexico, 1998 (top), 1999-2012 (bottom), from Landsat TM/ETM+

The catastrophic years were associated with El Niño events 1998 (42,240 ha), 2003 (1,643 ha) and 2005 (1,248 ha), suggesting that the meteorological conditions contributed to increased vulnerability of vegetation to fire. Comparative analysis between total fires and affected areas from Landsat images and official records of fires within the Reserve showed important differences each year (Table 1).

Table 1. Annual burned area derived from Landsat TM/ETM+ and official records of wildfires

Year	Landsat TM/ETM+				Official records	
	Agricultural burning (Number)	Surface (ha)	Wildfires (Number)	Surface (ha)	Wildfires (Number)	Surface (ha)
1998	111	10243	118	31997	7	22000
1999	3	13	2	12	2	1
2000	21	116	21	66	0	0
2001	9	195	31	893	6	211
2002	34	155	29	123	1	8
2003	12	342	17	1301	28	9275
2004	20	179	10	186	1	4
2005	35	571	29	677	10	553
2006	13	85	7	115	1	20
2007	13	130	13	76	8	82
2008	169	1063	14	78	3	5
2009	67	809	6	1537	6	2743
2010	57	732	25	547	3	24
2011	124	1676	29	104	0	0
2012	55	729	1	8	4	8

The month of May saw more agricultural burnings because it is a better time to prepare cropland, just before the start of the rainy season. At the same time, fires are common in the buffer zone; sometimes a few grow out of control and become forest fires in the core zone. The fire team of the Reserve are always alert; they have a range of measures for monitoring fire, such as CONABIO hotspots and fire reports, fire brigades and involvement of inhabitants of the communities in fire fighting. However, agricultural fires are a threat to the conservation of the Reserve.

High clouds from May to October are very common in the study area. This hindered identification of burnt areas for some years, particularly for 2003 during which there were many forest fires.

Hotspots were important for the discrimination of burned areas. A hotspot represented small agricultural burning (<1 ha) into contiguous land; multiple hotspots in the same area were associated with large wildfires (> 10 ha) that remained active for more than two days.

Official fire reports for the Reserve include underground fires; however, neither hotspot nor Landsat images could confirm these events. This issue is very important and it will be convenient necessary to use other methods to study these fires.

Conclusions

Visual analysis of multitemporal Landsat TM/ETM+ images was a good method for obtaining the first local burned areas map of the Selva El Ocote Biosphere Reserve, Chiapas, for 1998 and the period 1999–2012. These results illustrate an alternative means for analysing the pattern of spatial and temporal distribution of burned areas and for identifying zones that merit priority attention with regard to wildfires.

References

Bastarrika A, Chuvieco E, Martín MP (2011) Mapping burned area from Landsat TM/ETM+ data with a two-phase algorithm: Balancing omission and commission errors. *Remote Sensing of Environment* **115**, 1003–1012.

Chuvieco E, Ventura G, Martín MP, Gómez I (2005) Assessment of multitemporal compositing techniques of MODIS and AVHRR images for burned land mapping. *Remote Sensing of Environment* **94**, 450-462.

Cocke AE, Fule PZ, Crouse JE (2005) Comparison of burn severity assessments using Differenced Normalized Burn Ratio and ground data. *International Journal of Wildland Fire*. **14**, 189-198.

CONABIO (National Commission for Knowledge and Use of Biodiversity). Program for heat points detection using remote sensing techniques: http://conabio.gob.mx

CONANP, TNC (2009) Programa de manejo integral del fuego, Reserva de la Biosfera Selva El Ocote, Chiapas, México 2009-2012. 43 pp.

Diario Oficial de la Federación (2000) Decreto de la Reserva de la Biosfera Selva El Ocote, México D.F. 97 pp.

FIRMS (Fire Information for Resource Management System) https://earthdata.nasa.gov/data/near-real-time-data/firms

GLOVIS (The USGS Global Visualization Viewer) http://glovis.usgs.gov/

INEGI (National Institute of Statistics, Geography and Information Technology) 2001, 2006, 2011, 2012. Cartas de uso del suelo y vegetación E15-8, E15-11, escala 1:250000.

Pereira JMC, Sá ACL, Sousa AMO, Silva JMN, Santos TN, Carreiras JMB (1999) Spectral characterization and discrimination of burnt areas. In 'Remote sensing of large wildfires in the European Mediterranean basin' (Ed E Chuvieco) pp. 123–138. (Springer: Madrid).

Polychronaki A, Gitas IZ (2012) Burned area mapping in Greece using SPOT-4 hrvir images and object-based image analysis. Remote Sensing **4**, 424-428.

Ressl R, López G, Cruz I, Colditz RR, Schmidt M, Ressl S, Jiménez R (2009) Operational active fire mapping and burnt area identification applicable to Mexican Nature Protection Areas using Modis and NOAA-AVHRR direct readout data. *Remote Sensing of Environment* **113**, 1113 - 1122.

Román-Cuesta RM, García M, Retana J (2003) Environmental and Human Factors influencing fire trends in ENSO and Non-ENSO years in tropical México. *Ecological Applications* **13**, 1177-1192.

Robinson JM (1991) Fire from space: global fire evaluation using infrared remote sensing. *International Journal of Remote Sensing* **12**, 3-24.

Roy DP, Frost PGH, Justice CO, Landmann T, Le Roux JL, Gumbo K, Makungwa S, Dunham K, Du Toit R, Mhwandagaraii K, Zacarias A, Tacheba B, Dube OP, Pereira JMC, Mushove P, Morisette JT, Santhana Vannan SK, Davies D (2005a) The Southern Africa Fire Network (SAFNet) regional burned-area product-validation protocol. *International Journal of Remote Sensing* **26**, 4265 - 4292.

Roy D, Jin Y, Lewis P, Justice C (2005b) Prototyping a global algorithm for systematic fire-affected area mapping using Modis time series data. *Remote Sensing of Environment* **97**, 137-162.

Tansey K. Gregoire, JM, Pereira, JMC, Defourny P, Leigh R, Pekel, JF, Barros A, Silva J, Van Bogaert E, Bartholomé E, Bontemps S (2007) L3JRC - A global, multi-year (2000-2007) burnt area product (1 km resolution and daily time steps). *Remote Sensing and Photogrametry Society Annual Conference 2007*, Newcastle upon Tyne, UK.

Post fire erosion control mulch effects on soil organic matter turnover

Erin Berryman[a], Deborah Page-Dumroese[b], Martin Jurgensen[c], Peter Robichaud[d]

[a] *Research Ecologist. USGS Geosciences and Environmental Change Science Center. Lakewood, Colorado. USA. eberryman@usgs.gov*
[b]*US Forest Service Rocky Mountain Research Station, Moscow, Idaho, USA, ddumroese@fs.fed.us*
[c]*Michigan Technological University, School of Forest Resources and Environmental Sciences, Houghton, Michigan, USA, mfjurgen@mtu.edu*
[d]*US Forest Service Rocky Mountain Research Station, Moscow, Idaho, USA, probichaud@fs.fed.us*

Keywords*: wheat straw, wood strands, decomposition, aerial mulching, rehabilitation*

Extended Abstract

Introduction

An increasingly common post fire rehabilitation practice is the aerial application of mulch or hydromulch to the soil surface, with the goal of reducing post fire erosion. Mulch has the potential to alter soil organic matter cycling compared to areas that are allowed to naturally recover following high-severity wildfire. Following wildfire, soil surfaces are exposed to higher amounts of solar radiation and have low albedo; surface mulch can increase surface albedo and may decrease soil temperature in the summertime. In addition, mulch may alter soil moisture patterns by providing to a barrier to both surface water inputs and surface moisture evaporation. These alterations in temperature and moisture may have important impacts for soil microbial activity responsible for processing soil organic matter left behind following a wildfire. In addition, mulch provides a carbon substrate for soil microorganisms with little nitrogen to support its metabolism. As a result, mulch may induce net N immobilization with potential feedbacks to soil organic matter processing. These changes to the soil physical and chemical environment can alter soil organic matter turnover rates with important implications for soil productivity during post fire recovery.

Methods

We monitored changes in soil organic matter turnover resulting from aerial mulching practices on two large fires in the western United States: the 2002 Hayman Fire in the Rocky Mountains of Colorado and the 2005 School Fire in the Blue Mountains of eastern Washington and Oregon. Plots were established within hillsides treated with agricultural straw, hydromulch, wood strands, contour felling (Hayman Fire only), and unmulched areas in both burned and unburned areas. To supplement this monitoring, a controlled experiment was established on the 2012 High Park Fire in the Rocky Mountains of Colorado to determine effects of different mulch application rates on soil organic matter turnover. Plots contained two application rates each of agricultural straw and wood strands.

Soil organic matter turnover and soil environment

In two subplots per treatment, soil organic matter turnover was measured by monitoring changes in mass loss of buried wooden stakes over time. Control over organic matter quality was achieved by using the same organic material among sites and treatments, which assures comparison of decomposition as a function of treatment-induced abiotic and biotic soil conditions. Wood is a major component for surface and mineral forest soil, and has a slow decomposition rate that integrates changes in soil conditions over a long period of time. Wood is also an important factor after burning since wood is often left within the soil profile or on the surface. Aspen (*Populus tremuloides*) and pine

(*Pinus taeda*) stakes (dim: 2.5 x 2.5 x 30 cm) were buried vertically to a depth of 30 cm in the mineral soil, buried between the mulch and soil interface, and secured on top of the mulch surface. Each year, five replicate stakes from each fire, treatment and position were retrieved, dried, weighed for mass loss determination, and measured for loss in tensile strength. Soil temperature was monitored at all three sites. At the High Park Fire controlled experiment, soil moisture at two depths (5 cm and 20 cm) was also continuously monitored.

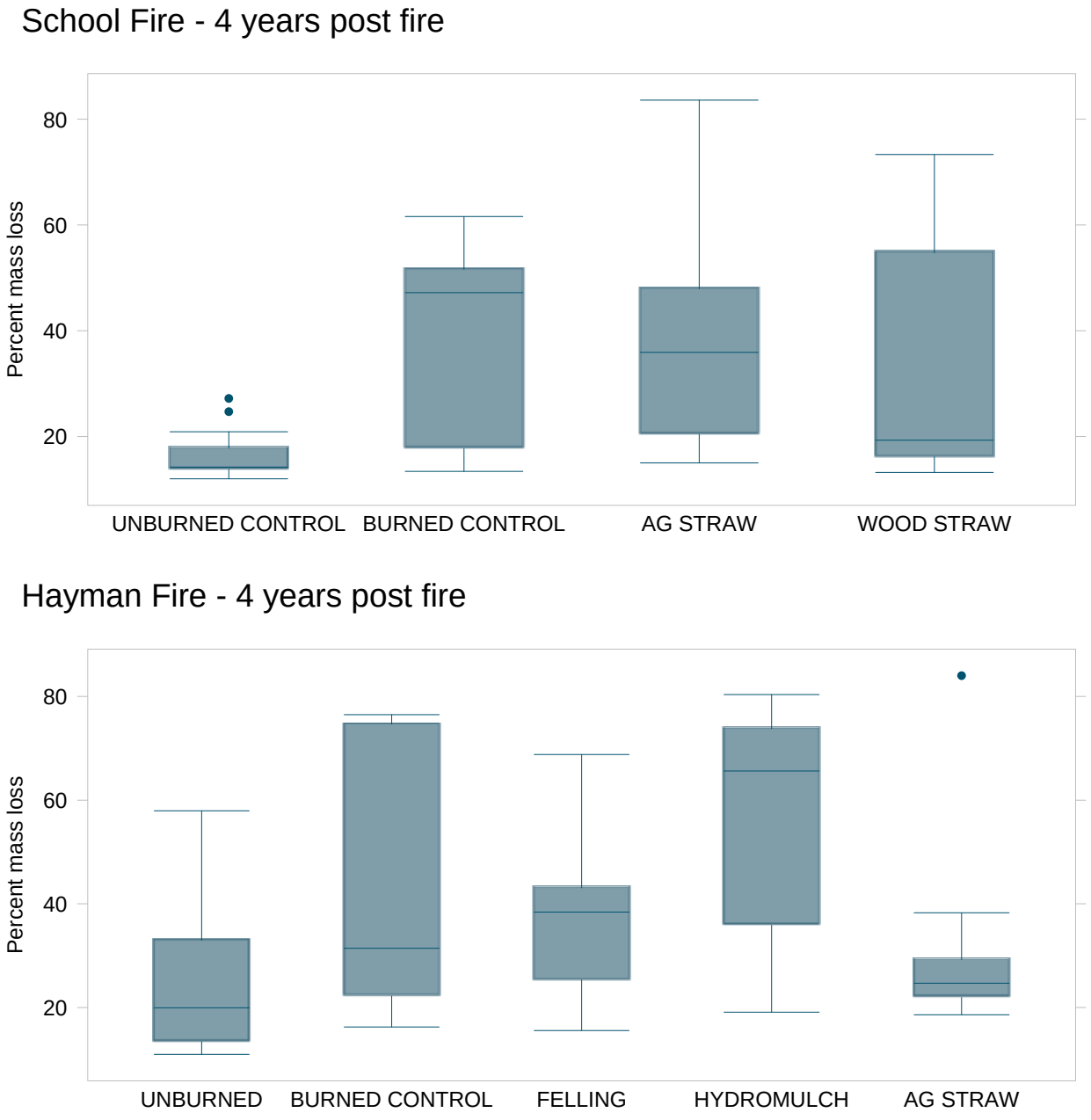

Figure 1. Mass loss from wood stakes four years following fire and mulch application at the School Fire (top) and Hayman Fire (bottom).

Results

Four years following fire, stake decomposition was increased in burned soil compared to unburned soil at both the Hayman and the School Fire (Figure 1). Following wildfire, char on the soil surface

decreases albedo and increases solar radiation absorption, which leads to temperature increases. Temperature is a key control over biological and chemical reactions involved in soil organic matter processing. In addition, wildfire often leads to an increase in soluble nitrogen to the soil; such nitrogen may allow for increased metabolism of carbon in the decomposition stakes by soil microorganisms.

Four years following application, mulch had little effect on stake decomposition at both the School Fire and the Hayman Fire (Figure 1). Initial differences in treatment, such as increased stake decomposition underneath hydromulch in the first year, disappeared later in the trajectory, leading to no differences among treatment seven years after mulch applications.

On the School Fire, wheat straw led to increased stake decomposition compared to the Hayman Fire. This may have been due to differences in climate, vegetation or soil texture between the two sites. The controlled experiment at the High Park Fire provided insight to mulch effects on soil organic matter turnover. Mulch increased summer time soil moisture, with the greatest effects seen at the 20 cm depth.

Conclusions

These findings support the idea that fire enhances soil organic matter turnover, at least in the first several years post burn. In addition, we have demonstrated that mulch applications may alter the initial stages of soil organic matter turnover, but with little long-term effects beyond the first few years. The Hayman Fire and the School Fire data have important limitations, however, due to the unreplicated nature of the hillside-scale mulch applications. The controlled experiments at the High Park Fire allowed a more robust test of mulch application on soil processes, suggesting that these initial effects on stake decomposition are derived from an altered soil environment. It remains unknown whether these intitial mulch effects on soil organic matter turnover establish a unique plant response trajectory compared to unmulched areas. More replicated mulching studies are needed, covering a range of soil textures and climates, that explicitly monitor soil processes important for organic matter turnover and soil productivity and tie these to plant responses.

Spatio-temporal monitoring of burned area to evaluate post-fire damage: application on Fontanès wildfire (France)

Marlène Long-Fournel, Gabrielle Mattei, Denis Morge, Johan Blanpied, Roland Esteve, Fabien Guerra, Christian Ripert, Marielle Jappiot

Irstea, 3275 route de Cézanne – CS 40061, 13182 Aix en Provence Cedex 5, marlene.long@irstea.fr, denis.morge@irstea.fr, roland.esteve@irstea.fr, fabien.guerra@irstea.fr, christian.ripert@irstea.fr, marielle.jappio@irstea.fr

***Keywords**: Wildfire, post-fire damage, spatio-temporal monitoring, remote sensing data*

Extended Abstract

Introduction

Even if the contribution of temporal series of remotely sensed data is well-admited, the use of temporal series of high spatial resolution images is limited because of the lack of data allowing developing these applications. The French project TOSCA is related to the analysis and the applications of multi-temporal remote sensing Landsat images. The aim of this project is showing the interest of multi-temporal series of data to obtain accurate information on large territories. For this project, multi-temporal Landsat images were tested for the spatio-temporal monitoring of burned area to evaluate post-fire damage.

The application of temporal Landsat images was realized on the Fontanès wildfire which occurred in Herault French department on the 30th August 2010 and which burned 2,590 hectares area.

Figure 1. Localisation of the study area according to Google Earth data (left side) and Fontanes wildfire on post fire Landsat 5 image (right side).

Two Landsat 5 images with 30 metres spatial resolution were considered: one acquired before the wildfire on the 12th September 2009, one acquired immediately after the wildfire on the 15th September 2010.

Methods to evaluate post-wildfire damages

Damages evaluation on the field

The monitoring of burned area consisted to relate post-fire damage levels evaluated on the field after the wildfire with vegetation there before the fire. 90 field surveys were spread uniformly on the study site to evaluate post-fire damage on homogenous vegetation types. For each field survey, damages were observed on four height strata of the vegetation (0-1 metres, 1-4 metres, 4-10 metres and more than 10 metres) and on each structural element of the vegetation (trunk, branch, leaf, fruit). Then, a level of damage was affected to each field survey:

- 0: no damage observed,
- 1: partially burned,
- 2: completely burned,
- 3: deep damages.

The weight given to the highest strata is more important than the other strata in order to take into account to the perception of the satellite sensor which considers the highest strata of the vegetation.

Damages evaluation according remote sensing techniques

Atmospheric corrections to detect clouds and aerosol and corrections to reduce environmental effects (fuzziness due to the atmosphere, lightning variation due to topography, etc.) were made by the CESBIO. Then, according to the field survey, supervised classifications were performed on the principal component analysis of the images: before the fire to identify fuel types, after the fire to characterize damage levels.

Results

3.1. Damages evaluation on the field in relation with the strata height

High and very high levels of damages concern lowest strata (0-1 m and 1-4 m strata) whereas moderate or low damages concern strata more than 4 metres. So damages decrease at the same time the height of the strata increases.

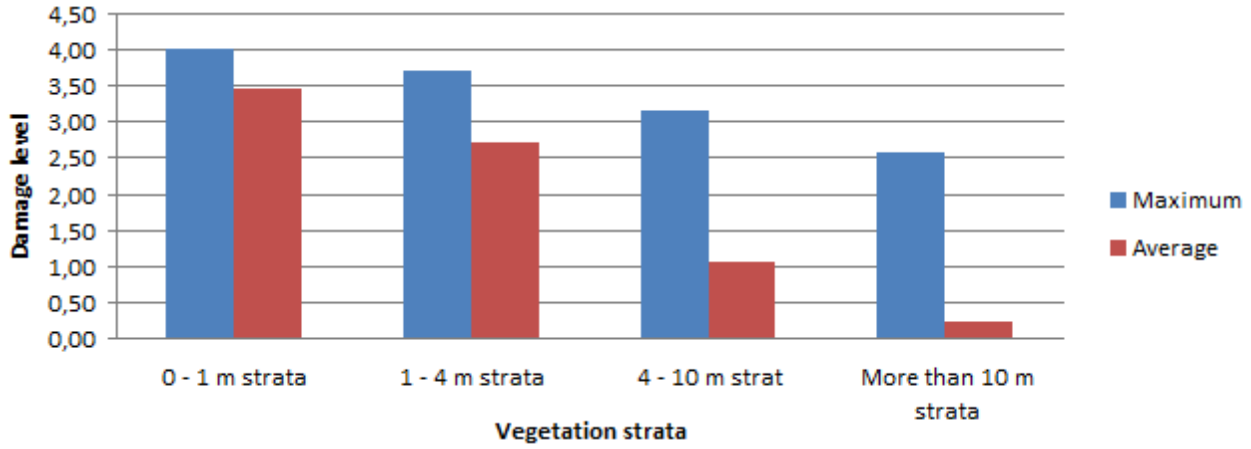

Figure 2. Damage observed on field data on the different vegetation strata

Damages evaluation by remote sensing techniques in relation with fuel type

The image before the wildfire allowed distinguishing 6 land cover classes, 5 of them characterizing fuel types: mature pine stand, young pine stand, hardwood, high and low shrublands, bare-ground. The image after the wildfire allowed distinguishing 6 levels of damage: no damage, moderate damage, high and very high damage on shrublands (high S, very high S), high and very high damage on tree stands. The comparison between observed damage and fuel types showed the most important damage on young pine stand and high shrublands. Damages are less important in mature pine stand characterized on your study site by vertical and horizontal continuity of the vegetation.

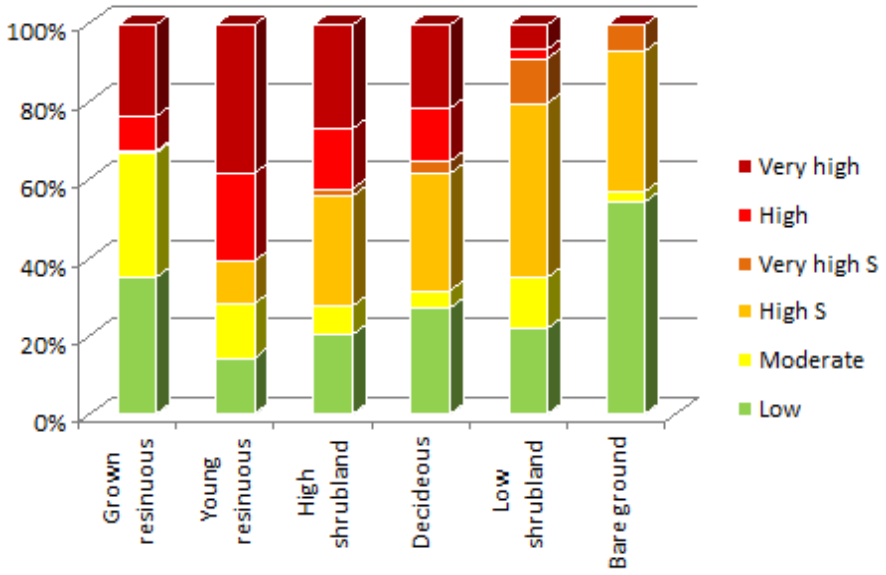

Figure 3. Damage observed according the post-wildfire image on the different fuel types

Conclusion

The spatio-temporal monitoring of burned area with remote sensing data allows the identification of the most sensitive fuel types against wildfire which is an important help to wildfire managers in the post-crises analysis but also in the wildfire prevention.

The Greek National Observatory of forest fires

Ioannis Gitas[a], George Zalidis[b], George Eftychidis[b]

[a] *Aristotelian University of Thessaloniki -AUTH, Thessaloniki, Greece (igitas@for.auth.gr)*
[b] *Interbalkan Environment Center; Loutron 18, 57200 Thessaloniki, Greece (zalidis@balcenv.gr; g.eftychidis@gmail.com)*

Abstract
The Greek Forest Service has recently established the National Observatory of Forest Fires (NOFF) in collaboration with the Laboratory of Forest Management and Remote Sensing, Aristotle University of Thessaloniki (AUTH) and the Interbalkan Environment Center (i-BEC). The purpose of the i-BEC is to support the systematic monitoring of the quality of the environment in Greece, the assessment of potential risk related to natural hazards and the development of relevant technology and sound knowledge, applicable in the Balkan region. A series of indicators and decision support applications is used for the monitoring of selected environmental parameters in real time in order to support operational early warning and documented risk assessment.

Keywords*: National Observatory, wildfire, forest fire, risk assessment, Balkans, fire management*

The problem targeted

The adverse effects of forest fires can be prevented, or at least minimised, by implementing successful prevention, suppression and mitigation measures. The design and consequent success of such measures is highly dependent on the availability and reliability of up-to-date fire-related data, such as burned area or fire risk maps. Such data are often collected locally and inconsistently in order to be used in context of independent projects; hence, they can rarely be found in a consistent format and content over extensive areas. The lack of such data inhibits the capacity of designing successful measures at regional or national scales. This is also the case in Greece, despite the capacity brought by new technologies and the progress made during the last decades in the topics of fire risk assessment, fire modelling and spatial data management. The quality, completeness and reliability of the fire data in Greece is still questioned due to lack of operational and procedural standardization and data interoperability.
NOFF aims to collect various environmental data related to forest and fire management and to develop a series of modern products and services that will support the design of efficient forest fire prevention policies in Greece and the Balkan region, as well as the assessment of the fire impact. The observatory aims to become the focal point in Greece and a major Center in the Balkan region in handling forest fire related information.

Products and services

A number of different activities are planned for the following years including the development of a number of spatial products, information tools and fire management support services aiming to support all Balkan countries, the creation of the Greek forest fire web-portal, an early warning service, as well as dissemination and capacity building actions.
Currently, the development of the following products and services is in progress:

- A consistent methodology for mapping the forest fuel types occurring in the Balkan region.
- A fire risk index adapted to the soil, climate and vegetation peculiarities of the region.

- A methodology for the accurate mapping of burned areas using high resolution satellite imagery, which will be delivered within a service that can provide burned area maps on a yearly base or on demand.
- An interactive Fire Forest portal and associated mobile applications which will make the products and services of NOFF available to stakeholders, policy makers, and local and regional authorities.

The aforementioned products will be designed for operational use and they will be tested in cooperation with relevant public services. The developed tools are planned to have graphical and multilingual user interface that could be easily employed by experts in all Balkan countries. The rest of this section details the aforementioned products.

2.1. Forest fuel type mapping

Forest fuel maps are primarily used by fire behaviour simulation models, in order to accurately perceive and assess the risk, severity, propagation and environmental impact of forest fires. The developed methodology would have to be able to regularly map forest fuels over extensive areas at a low cost so that its operational use will be feasible. Towards this end, it will benefit from the experience already gained by previous forest fuel mapping projects (e.g. ArcFuel and FUELMAP) and minimise the need for costly field data collection, by primarily relying on the processing of readily available ancillary data—consistently available across the Balkan countries—and remotely sensed images.
The combined use of ancillary data, such as the CORINE land-cover map and the Joined Research Centre (JRC) forest type map, will allow the mapping of certain forest fuel types. The remaining forest fuel types will be mapped by processing remotely sensed images using object-based image analysis (OBIA) and advanced image classification algorithms (fuzzy rules, decision trees, support vector machines). These images will be collected during the summer and winter seasons by a Disaster Monitoring Constellation (DMC) sensor at a 22 m spatial resolution. Images from both seasons will be used to facilitate the distinction between forest fuels which display different seasonal behaviour, such as evergreen and deciduous tree species.
The methodology will initially be applied over the prefecture of Chalkidiki, which is located in northern Greece and extents over an area of about 2900 km2 covered by a representative range of forest fuel types found across Greece. The resulting forest fuel map will be validated with a series of field visits.

2.2. Fire risk index

An efficient index for mapping forest fire risk is currently being developed. The fire risk index will be computed based on soil, climate and vegetation peculiarities of the region. The production of the fire risk index takes advantage of the use of Landsat 8 images that are freely and regularly distributed over the internet, being thus capable to provide seasonal assessment of fire risk based on deviation from normal vegetation, topographic and meteorological conditions. The calculation of the fire danger index will be adjustable to local data, thus being easily applicable to the different countries of the region.
The operational fire risk index will be linked online via SMS and e-mail with the Greek Special Secretariat of Forests and the local forest services. For the creation of this index an algorithm will be developed that also takes into account historical weather data and the fire regime of each area. The final value will be weighted by a set of selected parameters and the development and the accuracy assessment of the fire danger index will be applied at the Region of Central Macedonia.

2.3. Burned area mapping

An in-house method for the accurate mapping of burned areas is currently being developed, using high resolution satellite imagery. The method can be used operationally at several scales (local, regional and national). The employed methodology will be implemented in two stages:

- Initially, the satellite image will be segmented through the application of an object-based image analysis (OBIA) technique. A number of higher order features will be extracted from the original image (on an object level basis) and a set of prototype reference objects will be selected by the user.
- Subsequently, a small subset of highly informative features will be determined through the application of an advanced feature selection methodoly, based on the principles of the so-called Fuzzy Complementary Criterion (FuzCoC). The burned area map will be produced by employing a Support Vector Machine (SVM) classifier on the selected feature subset, which presently constitutes one of the most accurate classification techniques based on supervised learning.

The first stage will be employed using a well-known commercial image processing software. For the second stage, a custom user interface is being developed, which will be used to apply the feature selection method and subsequent classification with minimum user interaction.
The employed method, which is sensor independent, is normally applied for mapping older fires, but it can also be used operationally to map new fires as well as for the reconstruction and mapping of historical events and the assessment of the fire regime. Initially, the methodology will be employed and validated in two areas of Greece recently affected by fires (Parnitha and Rhodes), using two IKONOS very high resolution satellite images. Ultimately, the whole methodology will be delivered within a service which will provide burned area maps on a yearly base or on demand.

2.4. Web portal and applications

A Forest Fire web portal will be created with the purpose of disseminating the NOFF's products and services to stakeholders, policy makers, and local and regional authorities. It will be accessible through a web browser and allow interested parties to visualise and interact with the maps and tools provided by NOFF through a friendly user interface. Thus, users will be able to benefit from what NOFF has to offer without the need to install and operate specialised and expensive software or a deep understanding of forest fire science. The portal will also host a depository for fire related data that will accommodate the data exchange within the scientific community and promote research.
In addition to the above, the Forest Fire web portal is planned to include a Public Participation GIS (PPGIS) that will bring the academic practices of GIS and mapping to the local level in order to support transfer of knowledge and promote the development of new knowledge. The idea behind PPGIS is to use and produce digital maps, satellite imagery, sketch maps, and many other spatial and visual products and tools in order to promote geographic involvement and awareness on a local level. Apart from the PPGIS, the Forest Fire portal will include the frequently updated map of fire risk and the most updated map of forest fuel types.
A number of mobile applications (SMS alerts, smart phone application) are anticipated for the ubiquitous access to the data resources as well as for distributing information and relevant early warning messages related to the level of fire risk to pertinent fire management groups including the Forest Service and Fire Service personnel.

Main results

Apart from the networking and capacity building objectives, the results expected from the establishment of NOFF are related to the integration of scientific knowledge and technological tools in the operational practice of fire prevention and forest protection. A series of mapping products and a suite of EO data processing services will be available through the NOFF to all Balkan countries, thus providing several opportunities for scientific cooperation among the neighbouring countries. The forest fuel map, the Fire Danger Index and the Burned area mapping service are the key results that

NOFF delivers. Furthermore a web repository of fire management data and information related to this region of Europe will be also developed.

Conclusions

The objective of the NOFF is to develop and promote the aforementioned fire management information products and services to interested parties and forest fire stakeholders both at national and a regional (Balkan region) level. This will be accomplished through the organisation of workshops, seminars and short courses that will ensure the optimization of use and performance of the products and services described above. The aim of NOFF is to become a regional center of fire management technology and information, providing the background for organizing relevant inter-Balkan activities with the participation of fire experts and potential end-users from different Balkan countries.

Trends and changes of fire danger in Italy and its relationships with fire activity (1985-2008)

Valentina Bacciu[a,b], Francesco Masala[b], Donatella Spano[b,a], Costantino Sirca[b,a]

[a] *CMCC, Euro-Mediterranean Center on Climate Change, IAFENT Division, via E. de Nicola 9 (Sassari), valentina.bacciu@cmcc.it*
[b] *DipNeT, Dipartimento di Scienze della Natura e del Territorio, University of Sassari, via E. de Nicola 9 (Sassari), cosirca@uniss.it*

Abstract
The comprehensive understanding of trends in fire activity and associated drivers is crucial to anticipate future trends and regulate fire potential impacts, by means of efficient fire and fuel management strategies. A valuable tool to examine past changes on fire potential and danger across fire regions is represented by fire weather indexes. In this study, spanning from 1985 to 2008, recent trends and patterns of fire danger and the relationships between the Canadian Fire Weather Index (FWI) System components and fire activity were investigated across Italy. Although time series trend analysis revealed a statistically significant increase in temperature, no clear pattern of fire danger increase was unveiled, while the number of days with high fire danger level increased significantly, especially in central and southern Italy. Monthly fire activity was modeled using as explanatory variables FWI components and significant coefficient of determination were obtained. The applied statistical approach (multiple linear regression) explained a consistent part of the fire occurrence variance all year long ($p<0.001$), although relevant differences across Italy were found.

Keywords*: fire danger indexes, percentile analysis, trend analysis*

Introduction

According to the last Intergovernmental Panel on Climate Change (IPCC, 2014), observed climate trends showed a variation in temperature and rainfall over Europe. There are different degrees of confidence that future climate will show an increase in high temperature extremes (*high confidence*) and meteorological drought (*medium confidence*), but small or no changes in wind speed extremes (*low confidence*), with diverse patterns varying considerably within and between regions.
It is well known that extreme weather events, such as extended drought and heat waves, facilitate and promote forest fire activity in Southern Europe. For example, during the dry spells in 2005, 2007 and 2009 a high number of large wildfires were recorded in South European countries (Pereira *et al*., 2005; EEA, 2010c; Koutsias *et al*., 2013; Salis *et al*., 2013). Future fire risk is projected to increase in Southern Europe (Carvalho *et al*., 2011; Dury *et al*., 2011; Vilén and Fernandes, 2011; Lung *et al*., 2013), along with the occurrence of high fire danger days (Arca *et al*., 2012) and fire season length (Pellizzaro *et al*., 2010). In this framework, the analysis of past conditions and the factors that shaped fire pattern plays a crucial role for the comprehensive understanding of trends in fire activity, so as to anticipate future fire potential and changes (e.g., Carvalho *et al*., 2010; Zumbrunnen *et al*., 2011; Amatulli *et al*., 2013), and to assess the ecological effects of forest fires, thus reaping the benefits (Moreno and Chuvieco, 2012).
During the last decades, fire weather indexes were often used to examine past changes on fire potential and danger across fire regions (e.g. Camia *et al*., 2008; Carvalho *et al*., 2008; Mäkelä *et al*., 2012; Wastl *et al*., 2012). These systems, combining relevant weather variables into suitable indexes, are usually valuable tools to estimate potentially dangerous conditions, as fire intensity or large size fires, and to help forest fires services in effective prevention and response to forecasted danger. A clear comprehension of the relationships between these indexes and fire occurrence features, as well as their

efficiency, is of paramount importance in the implementation of fire policies and management (Carvalho *et al*., 2008; Bedia *et al*., 2012). Furthermore, the identification of areas with high fire danger and risk under severe and extreme environmental conditions is of utmost importance to cope and regulate their potential impacts through fire and fuel management (e.g. Fernandes, 2009; Arca *et al*., 2009; Salis *et al*., 2012b). Moreover, fire danger measurements are very valuable for all fire-fighting services, as they enable minimizing the level of uncertainty by combining scientific knowledge and operational experience (Valese 2008; Taylor and Alexander 2006).

One of the most commonly used fire danger rating systems across the world is the Canadian Fire Weather Index System (FWI), developed by Van Wagner and Pickett (1987). FWI has been very effective not only in Canada, where it was developed, but also in the Mediterranean area, as demonstrated in literature (e.g., Viegas *et al*., 1999; 2001). An important comparative study assessing the performance of different danger indexes in Southern Europe has revealed that FWI is the fire danger index best correlated with fire occurrence in Spain, France, Italy and Southern Portugal (Viegas *et al*., 1999). Therefore, FWI is a reliable fire danger system also in dry Mediterranean vegetation and climate conditions, which are very different from Canadian conditions where FWI was designed. However, despite its successful application in recent studies in Mediterranean regions (Moriondo *et al*. 2006; Valese 2008; Carvalho *et al*. 2008), it is noticeable that the performance of FWI and its relationship with fire occurrence show different response patterns according to the area considered (Carvalho 2008).

In relation to this, few works are available in Italy. With the intention to fill this knowledge gap and thus contribute to the understanding of past fire danger conditions, the main goals of this study are to (i) investigate and characterize recent trends and patterns of weather and fire danger in Italy, and then to (ii) unravel the relationships among the Canadian Fire Weather Index (FWI) System components and both fire number and burned area.

Methods

Study area and data collection

The area under investigation is Italy, which covers an area of about 301,000 km^2 comprising the boot-shaped Italian Peninsula and a number of islands including the two largest of the Mediterranean sea, Sicily and Sardinia. The climate of Italy, according to Köppen-Geiger (1954) climate classification, can be distinguished into 7 broad climatic regions, from the Mediterranean climate (characteristic of all coastal areas excluding the North-East) with mild and wet winter and hot and dry summers, to the Tundra climate with mean temperature below 10°C all year long. According to the Corine Land Cover classification (CLC 2006; EEA, 2007), agriculture is the main land use in Italy, covering 51.8% of the territory, closely followed by forested areas (40.2%). Artificial surfaces occupy about 5% of the territory.

National fire data were obtained for the period 1985-2008 from two sources of data, the European Fire Database (EFD) from the Joint Research Center (JRC) and the Sardinian Forestry Corp (CFVA, Corpo Forestale e di Vigilanza Ambientale della Regione Sardegna) database. The EFD is the largest repository of information on individual fire events in Europe (Camia *et al*., 2010). The database summarizes, on a monthly basis, the number of fire events and the total burned area of a given NUTS (Nomenclature of Territorial Units for Statistics) 3 unit (administrative level of province). A preliminary analysis of the EFD database revealed a data gap for Sardinia Region from 1985 up to 1997, so the CFVA fire daily database was used instead for the whole study period.

The weather data were obtained from the interpolated (25x25 km) daily meteorological database developed in the framework of "Monitoring of Agriculture with Remote Sensing" (MARS) project. The database was created using different weather data sources such as direct observations from meteorological stations, and from remote sensing platforms. The dataset, comprising the time period 1985-2008, consists of daily value of air temperature, precipitation, wind speed, and vapour pressure.

Since relative humidity data were not available in the MARS database, we estimated it from the air temperature, vapour pressure, and the dew point temperature (Snyder and Show, 1984).
Finally, fire and weather datasets were aggregated in a database at 25 km resolution grid and on a monthly basis using ArcGIS 9.3 ©-ESRI.

Fire danger indexes and statistical analyses

Fire danger was calculated through the Canadian forest Fire Weather Index System (FWI), which provides a rating of fire danger through fuel moisture and fire behaviour potential (Van Wagner, 1987). The FWI is composed by 6 sub-codes, the first 3 rating fuel moisture content of the forest floor layers and the other 3 the potential fire behaviour. The Fine Fuel Moisture Code (FFMC) rates the moisture of litter and other dead fine fuels at the top of the surface fuel layer; Duff Moisture Code (DMC) embodies the moisture content of loosely compacted, decomposing organic matter weighing about 5 kg m^{-2}, when dried (this is an indicator of fuel consumption in moderate duff layers and medium-sized woody material (Carvalho 2010)); and the Drought Code (DC) represents the moisture content of the deep layer of compact organic matter.
As outlined above, the other 3 sub-codes estimate the potential fire behaviour, combining the previous fuel moisture codes and weather. The Initial Spread Index (ISI), obtained by the combination of wind and the FFMC component, assesses the rate of fire spread without the influence of variable quantities of fuel; the Build Up Index (BUI) combines DMC and DC components to represent the total fuel available for combustion; and the final Fire Weather Index (FWI) is the combination of ISI and BUI components and represents the intensity of fire spreading as a rate of energy output per unit of fire front length. As highlighted by Alexander (2008), each individual component of the FWI system is actually a fire danger index, revealing different aspects of fire danger that are difficult to synthesize into one single number.
Usually, the FWI system is computed by daily meteorological variables recorded at noon. In this study, FWI was computed using daily meteorological values from MARS database as proxy of instantaneous values at 12:00. After the FWI system calculation, the dataset comprised daily values for all the 565 cells derived from the MARS dataset and for the whole 24-year period.
To handle this amount of data, a preliminary hierarchical cluster analysis, based on the fire/weather dataset, was performed to identify homogeneous areas in terms of fire occurrence and climate (pyro-climatic areas) (Bacciu *et al*., 2014) (**Erro! A origem da referência não foi encontrada.**). The Mann-Kendall non-parametric statistical test was thus applied to evaluate the existence of trends on fire danger components and weather data series. As commented by Wastl *et al*. (2012), a shift in fire danger might be induced by an increase of either absolute index values or number of days with elevated index values. We thus calculated the number of days, for each year and pyro-climatic area, exceeding the threshold of the FWI 95th percentile of the whole time period. Then we proceeded with the Mann-Kendall non-parametric statistical test over the past 24 years to investigate on the eventual increase of fire extreme days. Mann-Kendall test was performed using an Excel macro named MAKESENS created by Salmi *et al*. (2002).
Finally, historical fire activity was analysed in relation to monthly averages of FWI system components to understand the relationships among variables and to develop statistical models to be used to project fire activity in the near future. Separate analyses were carried out at cluster level and a classical stepwise Multiple Linear Regression analysis was applied for the period 1985-1999 (training dataset). The Multiple Linear Regression is one of the most common methods applied to analyse relationships between fire activity and fire danger/weather parameters (e.g. Carvalho *et al*., 2008; Camia and Amatulli, 2009; Bacciu *et al*., 2014). The stepwise approach combines entry and removal of regression terms, which were accepted or discharged as long as they meet significance criteria. The natural logarithm was used to normalise burned area and fire number for the normality requirement, as it is a common procedure followed in other modelling works (Carvalho *et al*., 2008; Amatulli *et al*., 2013). The 9-year period 2000-2008 was then used as external validation dataset. The performances

of the model equations were evaluated using the R^2 coefficient of determination between estimated and measured values.

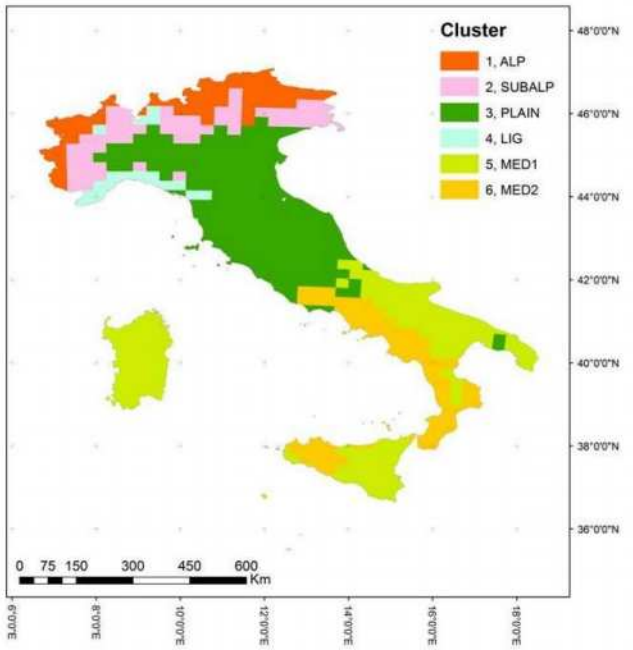

Figure 1. Map of pyro-climatic regions in Italy (from Bacciu et al., 2014)

Results

The descriptive statistic of the fire-regime metrics at cluster level is shown in Table 1. The most fire-prone zones are located in the Southern clusters (MED1 and MED2) although a marked fire activity also occurred in LIG (19% burned area over total, 2 fires km^{-2}). From 1985 to 2008, about 2.5 million of hectares were burned (~10% over the Italian total area), about 230,000 fire ignitions occurred, and the annual average burned area was ~100,000 ha. The maximum recorded area burned was in 1993 and 2007 (9.2% and 9.1% over the total, respectively). High level of inter-annual variability of burned area (computed through the coefficient of variation, cv) was found in Northern clusters (ALP and SUBALP) with low fire activity (0.2-0.4 fires km^{-2}), suggesting a stronger influence by weather and climate. As expected, clusters with marked Mediterranean climate and significant fire activity (i.e. Sardinia, Calabria, and Sicily, which had the highest area burned values and number of occurrences in Italy) showed a low inter-annual variability in both fire number and burned area, probably due to persistent human activities.

Five-year averages of maximum and minimum temperatures as well as precipitation and relative humidity are displayed in **Erro! A origem da referência não foi encontrada.** for each pyro-climatic area. The Mann-Kendall trend test highlighted a generalized significant positive pattern for air temperature variables in all clusters (overall almost 0.5°C and 0.7°C per decade for maximum and minimum temperature, respectively). On the other hand, annual precipitation trends were not significant and the signs of the slopes were different across areas, while on the contrary relative humidity showed overall a significant negative pattern.

Table 1. Number of fire (FN) and burned area (BA) statistics at cluster scales, for the period 1985-2008. CV is the coefficient of variation

CLUSTER	CODE	FN (*1000)	BA (ha*1000)	% BURNED OVER TOTAL	FIRE DENSITY (FN km^{-2})	AVG FIRE SIZE (ha)	CV FN	CV BA	FIRE SEASON (Month)
Cluster 1	ALP	6,2	62,0	1,99	0,20	9,97	0,49	1,22	12,1,2,3
Cluster 2	SUBALP	13,8	147,5	4,27	0,40	10,66	0,46	1,20	12,1,2,3
Cluster 3	PLAIN	37,2	279,1	2,62	0,35	7,50	0,47	0,77	7,8,9
Cluster 4	LIG	21,4	193,9	19,00	2,10	9,06	0,52	0,76	12,1,2,3,8
Cluster 5	MED1	89,8	1109,9	13,90	1,12	12,36	0,38	0,60	6,7,8,9
Cluster 6	MED2	64,4	669,4	16,90	1,63	10,40	0,41	0,66	6,7,8,9

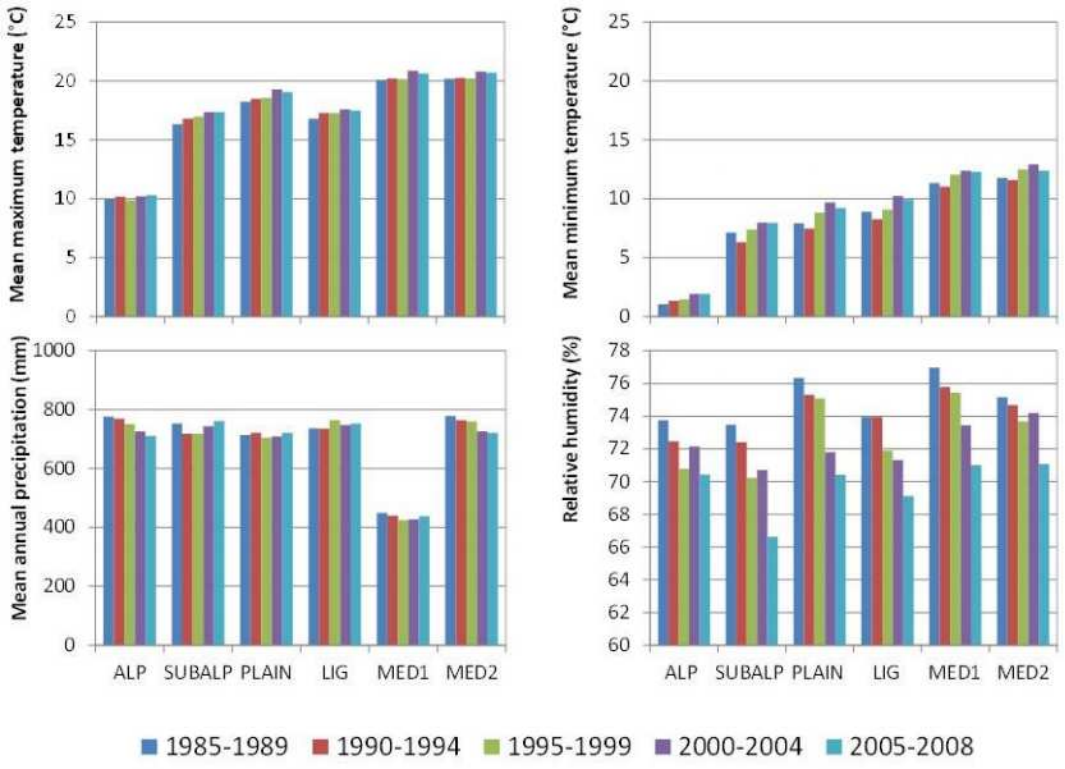

Figure 1. Evolution of mean maximum and minimum temperature, annual precipitation and relative humidity on a five-year basis (1985-1989, 1990-1994, 1995-1999, 2000-2004-2005-2008) in pyro-climatic areas

Overall, the statistical analysis of the mean forest fire danger index values (**Erro! A origem da referência não foi encontrada.**) revealed few significant changes during the 24 year of analysis. According to the Mann-Kendall trend test, there was a significant downward trend ($p<0.01$) in DC for ALP cluster, and a significant upward trend in four out to six cluster in ISI index. The number of days with exceptionally high meteorological fire danger was assessed calculating the annual number of days above the 95th percentile threshold. The analysis showed overall a statistically significant increase during the analyzed period, ranging from 1 to 8 days per decade. Overall, the mean number of extreme fire danger days ranged from 4 in cluster ALP to 30 in cluster MED1. The most important increase in number of extreme fire danger days were recorded in PLAIN and MED1 clusters. Ranging from an average of 22 days in 1985-1996 to 39 days in the period 1997-2008, MED1 exhibited a significant

increase of 43%. A stronger increase (65%) was recorded in SUBALP area, which went through an average of 7 days during the first period to 19 days in the period 1997-2008.

Table 2. Mann-Kendall trend test (Z score) results for mean FWI System components for each pyro-climatic area and mean annual number of days exceeding the FWI 95th percentile of the whole 24-year period.

** p= 0.05; ** p= 0.01; ***p= 0.001*

	Mann-Kendall trend Test Z						Estreme fire danger days	
CLUSTER	FFMC	DC	DMC	ISI	BUI	FWI	1985-1996	1997-2008
ALP	-0,06	-4,69**	-0,21	0,00	-0,39	-0,03	2	4
SUBALP	0,07	-3,29	0,07	0,04**	-0,08	0,02	7	19
PLAIN	0,10	0,02	0,45	0,04**	0,49	0,03	14	32
LIG	0,07	2,24	0,26	0,02*	0,43	0,03	9	24
MED1	0,03	-3,83	0,32	0,04**	0,00	0,02	19	29
MED2	0,08	-0,85	-0,06	0,01	-0,11	0,02	22	39

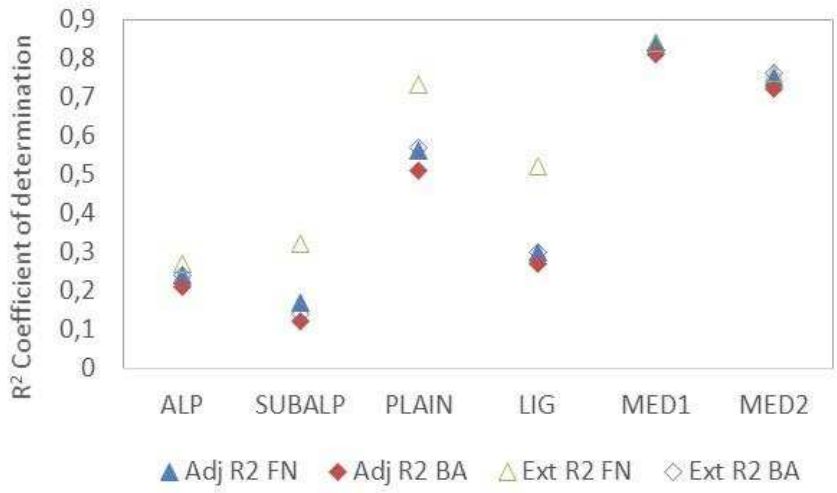

Figure 3. Monthly fire number and burned area explained variance (Adj R^2) and external validation values (Ext R^2)

Coefficients of determination (R^2) resulting from the Multiple Linear Regression analysis of monthly area burned and monthly number of fires considering the whole year for the six clusters across Italy are given in Figure 3. All coefficient were highly significant with $p<0.001$. We also checked for collinearity through the variance inflation factor (VIF). In those cases where predictors entered the final stepwise model and their VIF was higher than the value of 10, thus creating multicollinearity problems (Myers, 1990), we decided to exclude those variables from the regression in order to avoid any further inconsistencies. Finally, an informal analysis of the data using histograms and scatterplots was performed to reveal threats to the assumption of linearity of residuals of the dependent variable (data not shown).

The explained variance ranged from 17 to 84% for fire number and from 12 to 71% for burned area. Clusters in northern and central regions showed the lowest variances, accounting from 17% up to 56% for fire number and from 12% to 51% for burned area in cluster SUBALP and in cluster PLAIN, respectively. On the other hand, pyro-climatic areas in southern regions exhibited variances above 70%, for both fire number and burned area. The external validation R^2 values (period 2000-2008) are slightly bigger than the internal validation.

Discussion and conclusion

In this study, we investigated recent trends in both climate and fire danger parameters and we highlighted the relationships between the FWI System components and fire activity in the 6 pyro-climatic areas identified by Bacciu *et al*. (2014).
As a first analysis, we applied the non parametric Mann-Kendall test to assess the statistical significance of weather and fire danger trends. The results of our study indicated the overall increase of temperatures, highlighting that the warming did not have homogeneous impacts all over the country, corroborating other findings over the past decades in Italy and in other areas of the Mediterranean Basin (e.g., Brunet *et al*., 2007; del Rio *et al*., 2012; Koutsias *et al*., 2012). Furthermore, annual precipitation records presented an unclear trend, except in the Alpine area. This data is consistent with the findings of Wastl *et al*. (2012), which reported for this area a slight increase of about 8% in annual precipitation. Moreover, our results highlighted a dichotomy in signs that seems to be in agreement with the results of other researchers.
Generally, the slope of the mean annual fire danger was positive at nearly every cluster, statistically significant in MED1. The situation in ALP cluster, as revealed by the weather variables, was the opposite with a statistically significant downward trend in mean values, probably influenced by the increase in total precipitation. The first results are in agreement with Moriondo *et al*. (2006), who found an increase in mean fire danger in the Mediterranean Basin. On the other hand, the clear decrease of the danger in ALP pyro-climatic area is in contrast with findings reported by Wastl *et al*. (2012) that showed a general increase of fire danger despite this trend was highly variable in consideration of the spatial and the time scale. The wide-ranging positive trend in fire danger corresponded also to a general increase in the frequency of extreme fire danger events. The analysis of the annual number of days above the 95^{th} percentile threshold showed that although southern clusters were characterized by a high number of extreme fire danger days, considerable increment occurred also in northern and central clusters.
Finally, by modelling both fire number and burned area on the basis of monthly FWI components in the different clusters, this study contributes to the understanding of the relationships between fire activity and fire danger indices. Although the study area presented a generalized decrease in both fire number and burned area for the period 1985-2005 (Spano *et al*., 2014; Bacciu *et al*., 2014), the multiple regression analysis showed that FWI system components (especially FFMC and ISI) are good predictors, especially for the clusters with summer fires. Similarly, Amatulli *et al*. (2013) highlighted the drought code (DC) and the initial spread index (ISI) as predictors consistently selected in the equations using the Multiple Linear Regression approach. Results achieved by Carvalho *et al*. (2008) in Portugal revealed that FWI mean and maximum values contributed to explain a great part of the variance in burned area.
Although fire activity in Italy is influenced by a number of factors not related, as fire danger, to weather conditions, the simple statistical models developed in this work can reproduce an important part of the inter-annual fire variability. Thus, the identified relationships could be incorporated in predictive models of fire risk and short- and long-term fire planning strategies that, in turn, could be boosted by the enhancement and a wider use of long-range climate outlooks (such as the seasonal and decadal predictions, e.g. Borrelli *et al*. (2012); Bellucci *et al*. (2014)). Furthermore, the developed models could be used as inputs for the construction of future fire scenarios (e.g., Amatulli *et al*., 2013) to understand the future magnitude of the issue and thus to develop new fire risk mitigation strategies.

Acknowledgements

The Authors would like to thank the JRC and Forest Service of Sardinia (CFVA) for providing fire occurrence data for this study. The researchers leading this work received funding from the Italian Ministry of Education, University and Research and the Italian Ministry of Environment, Land and

Sea under the GEMINA project, from the OFIDIA Project "Operational FIre Danger preventIon plAtform" (European Territorial Cooperation Programme Greece-Italy 2007-2013), and from the PRIN CARBOTREES Project- "Climate change mitigation strategies in tree crops and forestry in Italy" (Prot. 201049EXTW).

References

Alexander ME (2008) Proposed revision of fire danger class criteria for forest and rural areas in New Zealand. Christchurch: National Rural Fire Authority, Wellington, in association with the Scion Rural Fire Research Group.

Amatulli G, Camia A, San-Miguel-Ayanz J (2013) Estimating future burned areas under changing climate in the EU-Mediterranean countries. Sci Total Environ 450-451:209-222

Arca B, Bacciu V, Pellizzaro G, Salis M, Ventura A, Duce P, Spano D, Brundu G (2009) Fuel Model Mapping by IKONOS Imagery to Support Spatially Explicit Fire Simulators. Proceedings of the 7th International Workshop on Advances in Remote Sensing and GIS Applications in Forest Fire Management towards an Operational Use of Remote Sensing in Forest Fire Management. Matera, Italy, 2-5 September 2009. ISBN: 978-88-904367-0-3.

Arca B, Salis M, Pellizzaro G, Bacciu V, Spano D, Duce P, Ager Aa, Finney MA (2010) Climate change impact on fire probability and severity in Mediterranean areas. In: Viegas D.X. (Ed.), VI International Forest Fire Research Conference, Coimbra, Portugal, electronic edition.

Bacciu V, Masala F, Salis M, Sirca C, SpanO D (2014) Analysis of weather conditions influencing fire regime in Italy. Geophysical Research Abstracts, vol. 16, ISSN: 1607-7962.

Bedia J, Herrera S, Gutierrez Jm, Zavala G. Urbieta Ir, Moreno Jm (2012) Sensitivity of fire weather index to different reanalysis products in the Iberian Peninsula, Nat. Hazards Earth Syst. Sci., 12, 699-708, doi:10.5194/nhess-12-699-2012.

Bellucci A, Haarsma R, Gualdi S, Athanasiadis Pj, Caian M, Cassou C, Fernandez E, Germe A, Jungclaus J, Kröger J, Matei D, Müller W, Pohlmann H, Salas Y Melia D, Sanchez E, Smith D, Terray L, Wyser K, Yang S (2014) An assessment of a multi-model ensemble of decadal climate predictions, Climate Dynamics, DOI 10.1007/s00382-014-2164-y

Borrelli A, Materia S, Bellucci A, Alessandri A, Gualdi S (2012) Seasonal Prediction System at CMCC. Research Papers Issue RP0147

Brunet M, Jones Pd, Sigro J, Saladie O, Aguilar E, Moberg A, Della-Marta Pm, Lister D, Walther A, Lopez D (2007) Temporal and spatial temperature variability and change over Spain during 1850–2005, J. Geophys. Res., 112, D12117, doi:10.1029/2006JD008249

Camia A, Durrant Houston T, San-Miguel J (2010) The European Fire Database: Development, Structure and Implementation In: Viegas D.X. (Ed.), Proc. VI International Conference on Forest Fire Research. Coimbra

Camia A, Amatulli G (2009) Weather Factors and Fire Danger in the Mediterranean. In: Chuvieco E, editor. Earth Observation of Wildland Fires in Mediterranean Ecosystems. Berlin: Springer-Verlag; 2009. p. 71-82. JRC55075

Camia A, Amatulli G, San-Miguel-Ayanz J (2008) Past and future trends in forest fire danger in Europe, JRC Scientific and Technical Reports, EUR 23427 EN, 7 pp., Ispra, Italy.

Carvalho A, Flannigan M, Logan K, Gowman L, Miranda Ai, Borrego C (2010) The impact of spatial resolution on area burned and fire occurrence projections in Portugal under climate change. Climatic Change 98, 177–197 DOI: 10.1007/s10584-009-9667-2

Carvalho A, Flannigan Md, Logan K, Miranda Ai, Borrego C (2008) Fire activity in Portugal and its relationship to weather and the Canadian Fire Weather Index System, Int. J. Wildland Fire, 17, 328–338.

Carvalho Ac, Carvalho A, Martins H, Marques C, Rocha A, Borrego C, Viegas Dx, Miranda AI (2011) Fire weather risk assessment under climate change using a dynamical downscaling approach. Environmental Modelling & Software, 26, 1123–1133.

Dury M, Hambuckers A, Warnant P, Henrot A, Favre E, Ouberdous M, François L (2011) Responses of European forest ecosystems to 21st century climate: assessing changes in interannual variability and fire intensity. iForest 4: 82-99

EEA (2007). European Environment Agency: CLC2006 Technical Guidelines. Copenhagen

EEA (2010c) The European environment — state and outlook 2010: assessment of global megatrends, European Environment Agency.

Del Rio S, Cano-Ortiz A, Herrero L, Penas A (2012) Recent trends in mean maximum and minimum air temperatures over Spain (1961–2006). Theor Appl Climatol 109:605–626. doi:10.1007/s00704-012-0593-2

Fernandes PM (2009) Combining forest structure data and fuel modelling to classify fire hazard in Portugal. Annals of Forest Science 66 (4), 415-415

IPCC (2014) Climate Change 2014: Impacts, Adaptation, and Vulnerability. Part B: Regional Aspects. Contribution of Working Group II to the Fifth Assessment Report of the Intergovernmental Panel on Climate Change [Barros, V.R., C.B. Field, D.J. Dokken, M.D. Mastrandrea, K.J. Mach, T.E. Bilir, M. Chatterjee, K.L. Ebi, Y.O. Estrada, R.C. Genova, B. Girma, E.S. Kissel, A.N. Levy, S. MacCracken, P.R. Mastrandrea, and L.L. White (eds.)]. Cambridge University Press, Cambridge, United Kingdom and New York, NY, USA, XXX pp.

Köppen W, Geiger R (1954) Klima der Erde (Climate of the Earth). Wall Map 1:16 Mill. Klett-Perthes, Gotha.

Koutsias N, Xanthopoulos G, Founda D, Xystrakis F, Nioti F, Pleniou M, Mallinis G (2013) On the relationships between forest fires and weather conditions in Greece from long-term national observations (1894-2010). International Journal of Wildland Fire 22(4) 493-507 http://dx.doi.org/10.1071/WF12003

Lung T, Lavalle C, Hiederer R, Dosio A, Bouwer LM (2013) A multi-hazard regional level impact assessment for Europe combining indicators of climatic and non-climatic change. Global Environ Change 23:522–536

Mäkelä Hm, Laapas M, Venäläinen A (2012) Long-term temporal changes in the occurrence of a high forest fire danger in Finland, Nat. Hazards Earth Syst. Sci., 12, 2591–2601, doi:10.5194/nhess-12-2591-2012

Moreno Mv, Chuvieco E (2013) Characterising fire regimes in Spain from fire statistics. International Journal of Wildland Fire 22, 296–305. http://dx.doi.org/10.1071/WF12061

Moriondo M, Good P, Durão R, Bindi M, Giannakopoulos C, Corte-Real J (2006) Potential impact of climate change on fire risk in the Mediterranean area. Climate Research 31, 85-95. doi: 10.3354/cr031085

Pellizzaro G, Ventura A, Arca B, Arca A, Duce P, Bacciu V, Spano D (2010) Estimating effects of future climate on duration of fire danger season in Sardinia. In: Viegas D.X. (Ed.), VI International Forest Fire Research Conference, Coimbra, Portugal, electronic edition.

Pereira Mg, Trigo Rm, Dacamara Cc, Pereira Jmc, Leite SM (2005) Synoptic patterns associated with large summer forest fires in Portugal. Agricultural and Forest Meteorology 129:11–25.

Salmi T, Määttä A, Anttila P, Ruoho-Airola T, Amnell T (2002) Detecting trends of annual values of atmospheric pollutants by the Mann–Kendall test and Sen's slope estimates – the Excel template application MAKESENS. (Finnish Meteorological Institute: Helsinki, Finland)

Salis M, Ager Aa, Arca B, Finney Ma, Bacciu V, Duce P, Spano D (2013) Assessing exposure of human and ecological values to wildfire in Sardinia, Italy. International Journal of Wildland Fire 22(4):549-565. http://dx.doi.org/10.1071/WF11060

Salis M, Diana G, Casula F, Farris G, Farris O, Licheri F, Musina G, Orotelli S, Peluffo L, Pirisi Am, Bacciu V, Fois C, Sirca C, Spano D (2012b) Potential effects of prescribed burning and tactical

fires on fire risk mitigation. In: D. Spano, V. Bacciu, M. Salis, C. Sirca (ed) Modelling Fire Behaviour and Risk. Nuova Stampa Color: pp 174-180. ISBN: 978-88-904409-7-7

Snyder R, Show (1984) Converting Humidity Expressions with Computers and Calculators. Volume 21372, University of California Division of Agricultural Sciences Leaflet (University of California (System). Division of Agriculture and Natural Resources)

Spano D, Camia A, Bacciu V, Masala F, Duguy B, Trigo R, Sousa P, Venäläinen A, Mouillot F, Curt T, Moreno Jm, Zavala G, Urbieta Ir, Koutsias N, Xystrakis F (2014) Recent trends in forest fires in Mediterranean areas and associated changes in fire regimes. In: Josè M. Moreno (ED), Forest fires under climate, social and economic changes in Europe, the Mediterranean and other fire-affected areas of the world. p. 6-7, ISBN: 9788469597590.

Taylor Sw, Alexander Me (2006) Science, technology, and human factors in fire danger rating: the Canadian experience. Int. J. Wildland Fire 15, 121–135

Valese E, Anfodillo T, Rossi S, Carraro V, Deslauriers A, Carrer M, Monai M, Lemessi A, Ramon E (2008) Realizzazione di un sistema di calcolo e di spazializzazione dell'indice canadese di pericolo d'incendio boschivo FWI (Fire Weather Index) per la Regione Veneto. Forest@ 5: 176-186 [online: 2008-06-20] URL: http://www.sisef.it/forest@/.

Van Wagner Ce, Pickett TL (1987) Equations and Fortran program for the Canadian Forest Fire Weather Index System. Canadian Forestry Service, Forestry Technical Report 33, Ottawa.

Van Wagner CE (1987) Development and Structure of the Canadian Forest Fire Weather Index System. Ottawa, ON, Can. For. Serv., Tech. Rep. 35

Viegas Dx, Bovio G, Ferreira A, Nosenzo A, Sol B (1999) Comparative study of various methods of fire danger evaluation in southern Europe. Int. J. Wildland Fire 9, 235–246

Viegas Dx, Piñol J, Viegas Mt, Ogaya R (2001) Estimating live fine fuels moisture content using meteorologically-based indices. International Journal of Wildland Fire 10, 223-240

Vilen T, Fernandes P (2011) Forest Fires in Mediterranean Countries: CO_2 emissions and mitigation possibilities through prescribed burning. Environmental Management, 48(3), 558-567

Wastl C, Schunk C, Leuchner M, Pezzatti G, Menzel A (2012) Recent climate change: long-term trends in meteorological forest fire danger in the Alps. Agr. Forest Meteorol., 162–163, 1–13

Zumbrunnen T, Pezzatti GB, Menendez P, Bugmann H, Burgi M, Conedera M (2011) Weather and human impacts on forest fires: 100 years of fire history in two climatic regions of Switzerland. Forest Ecology and Management 261 (12):2188-2199. - doi:10.1016/j.foreco.2010.10.009

Validation of burn scar mapping: Pilot case in Peloponnesus, Greece

G.Eftychidis[a], G.Leventakis[a], B.Hirn[b], F.Ferrucci[c] and G.Laneve[d]

[a] *Center for Security Studies -KEMEA, Athens, Greece (g.eftychidis@kemea-research.gr; gleventakis@kemea.gr)*
[b] *IESConsulting, Roma, Italy; b.hirn@iesconsulting.net*
[c] *University of Calabria, Rende, Italy; f.ferrucci@gmail.com*
[d] *University of Rome 'La Sapienza', Dipartimento di Ingegneria Astronautica, Elettrica e Energetica, Roma, Italy; laneve@psm.uniroma1.it*

Abstract
The PREFER FP7 project aims delivering a series of map products based on Earth Observation data, which can support and improve fire and forest management in EU. Among these products are maps of Burn Scars from forest fires which are created using complex remote sensing techniques and image processing algorithms. In this paper is presented the validation methodology and the results relative to the evaluation of the burn scar product of PREFER in Greece.

Keywords*: PREFER, burn scar, burned area mapping, validation, Greece, fire management, forest management*

Introduction

Every year Southern Europe is affected by numerous uncontrolled forest fires having large impact on the natural environment and the regional economies. PREFER project of the FP7 Space Theme aims to support forest fire preparedness and prevention as well as post-fire management for vegetation recovery. The project has the objective to develop an on line service for delivering a series of map products, that are based on the use of Earth Observation data from space-borne sensors, which may support the improvement of fire management in EU. Among the products are maps of scars caused by forest fires that are produced using complex remote sensing techniques and image processing algorithms.
PREFER is designed to improve systematically the current capacity of mapping burnt areas both in terms of area threshold (EFFIS' current thresholds are 40 ha in Rapid Fire and ca.10 ha in Fire Damage assessment modes) as well as in terms of spatial resolution (currently 250m in Rapid Fire and 30-50m in Fire Damage assessment modes, respectively). The need of systematic mapping at much higher resolution combined with the task of managing large number of fires in real time require improved process automation and robust solutions for operational burn scar mapping at national or regional level. The high accuracy of mapping burn scars allows assessment of fire affected areas to become operational.

The problem targeted

In recent decades, a higher frequency of wildfire in mid- and high latitudes has been observed, partly as a result of climate warming. Burn scar refers to areas that are destroyed by forest fire, grass fire and controlled burning and have not yet recovered (Liu *et al*, 2014). To assess and estimate the impact of the fire on forest ecosystems, the area of the burn scars, as the most significant parameter for running post-fire models, has to be acquired (Vafeidis and Drake 2005). At this stage, the task of burn scar identification and mapping is undertaken mainly through analysis of remotely sensed data. Multi-temporal satellite data provide several interpretative advantages over single date data for mapping

burned areas (Pereira *et al*. 1997, 1999, Eva and Lambin 1998). These include a reduction in the likelihood of spectral confusion with spectrally similar static land cover types, the option to use relative rather than absolute changes in spectral values to account for spectral differences between pixels and dates, and the opportunity to define the date of burning more precisely.
The underlying problem for most of the burn scar mapping methods is that each of them can only capture limited aspects of burned vegetation, but very few of the methods can comprehensively examine as many aspects as possible, through which a more reliable result should be achieved. Another problem with existing burn scar mapping methods is the difficulty in choosing an optimal threshold. However, it has been noted that fixed threshold methods performed poorly for varying atmospheric effects and different land covers (Barbosa *et al*., 1999).
The Burn Scar mapping capacity is particularly challenging in areas with limited visibility because of persistent cloud cover, haze and/or smoke (G.Laneve and G.Cadau, 2006). Such cases require the development of robust mapping techniques based on X-band (Cosmo-SkyMED, TerraSAR-X) very high spatial resolution data and C-band (Radarsat-2 and the forthcoming ESA Sentinel-1) Synthetic Aperture Radar data. Three different products namely Burn Scar Map HR Optical at scale 1:25,000-1:50,000, Burn Scar Map HR SAR at scale 1:10,000-1:50,000 and Burn Scar Map VHR at scale 1:2,000-1:5,000 are produced using the multi-patented (B.Hirn and F.Ferrucci 2003 and 2006) procedure called MYME2 (B.Hirn and F.Ferrucci, 2005), based on Pseudo Invariant Targets (PCT/IT04/000376,WO2005/005926A1,EP/1642087).
The accuracy and quality of the burn scar layers, which are produced following the above mentioned automatic procedures, have to be tested and validated in order to verify the performance of the algorithms and the accuracy of the approach adopted for the development of the relative products.

Methodology

The objective of the validation is to identify any systematic deviation between burn scar mapping and real data based on observations as well as to identify eventual false detected fire spots in order to investigate the source of the errors and potentially improve or document the performance of the PREFER algorithms and the data processing techniques.

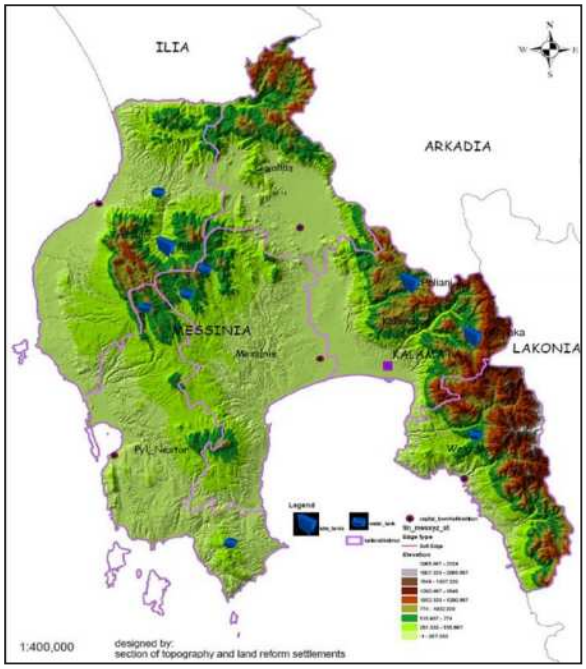

Figure 1. Pilot area of PREFER project in Greece (Messinia Region)

The validation of the burn scar product includes comparison of the data layers produced by the automated PREFER techniques and the MYME2 procedures against field observed or ancillary and archived fire data in the pilot areas of PREFER established in all the Mediterranean EU countries. The Greek pilot area (Figure 1) for the PREFER project, where the PREFER burn scar mapping products are validated, is the region of Messinia in Peloponnesus (Greece). Furthermore PREFER results are compared with data delivered by other automated burned area mapping services.
Mountainous areas cover the northern and eastern part of the Greek pilot area although low forest vegetation is spread in the entire region. Forest fire problem is quite significant in the region, which suffered severe damages during the mega-fires of 2007 in Peloponnesus.
For the map validation, fire data and burned scar maps provided by IESC were considered. The assessment was done during ground survey conducted the autumn of 2013. The survey referred to the burned areas of the year 2013 while for the previous years (2009-2012), fire data from the files of the Forest Service, the Hellenic Fire Corps and the Messinia Regional Administration services were used.

Figure 2. Missed fire (left), false fire (center) and properly detected fire (right) in the Greek pilot area of PREFER

The validation methodology of the burn scar mapping includes both qualitative and quantitative aspects. Missed fires (not detected) and false fires (detected without being verified in the field or the fire records) define the qualitative aspects of the validation methodology (Fig.2). Assessment of the accuracy of the burned area and calculation of the fire perimeter are considered as quantitative aspects of the metthodology (Fig.3). Burn scar mapping data can be compared with GPS measurements on the

ground and field collected data in case of recent fire (before the rain period start) as well as with fire records in case of past fires, in which case fire trace are lost.

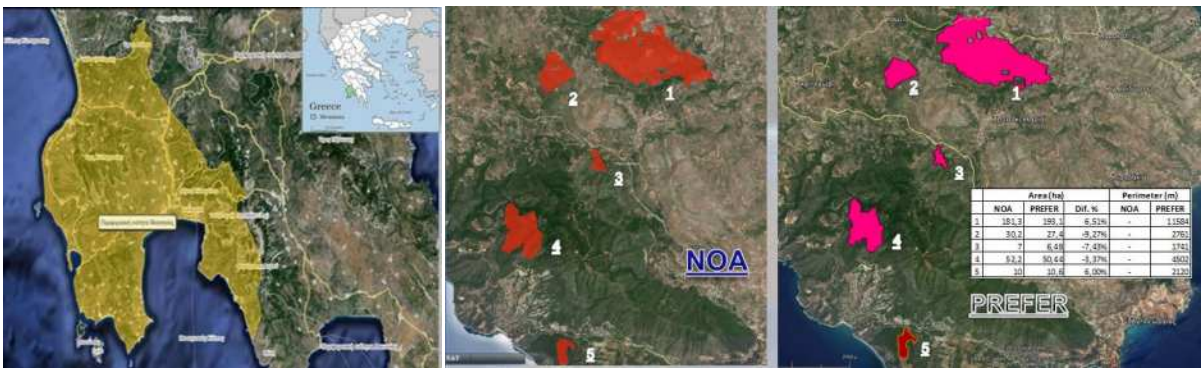

Figure 3. Greek pilot area of PREFER (left) and comparison of PREFER Burn Scar Map (right) and Diachronic BSM of NOA (center)

Vector data of the burned areas within the reference period (2009-2013) were collected from the Forest Service and compared with the produced burn scar maps of PREFER.

Interviews with potential stakeholders of the specific PREFER product are organized in order to ensure the user acceptance concerning the accuracy of the product as well as for collecting feedback concerning the final design of the burn scar maps that will be delivered by the on-line service of PREFER.

Main results

Although the validation task shall continue for the next years, preliminary results show that the PREFER algorithms perform quite well and the results of qualitative validation against the 2013 fires are very accurate. Some minor issues that identified concerning past fires need to be checked further since they may be influenced by the reliability of the fire records kept by the public services.

The length of time that the spectral signature of the burned area is detectable after the fire depends on the physical evolution of the post burn surface (vegetation regrowth, dissipation of ash and charcoal by wind and rain). Thus the dates of the satellite images can be important in particular towards the beginning and the end of the fire season. Similarly distinction among scars due to vegetation loss caused by forest fires and vegetation loss caused by other factors (eg forest area clearing) shall be further investigated.

A first quantitative comparison of the results against records of the forest service show that the accuracy of areal extent ranges between 73% and 92%. In any case the estimation of the relevant PREFER service is more accurate than other automated products tested in the same region in the past. Furthermore the burn scar mapping product of PREFER need to be designed properly in order to fulfill the operational requirements of the potential end users (Forest Service, Fire Service, Environmental organizations, Local and Regional Authorities) distinguishing among wildfires and prescribed fires in agricultural areas. Finally product availability, continuity and cost issues shall be considered in context of the PREFER service exploitation plan.

Conclusions

The results of the validation of the burn scar mapping products of the PREFER portfolio of EO-based maps are quite encouraging. The product specifications and its accuracy are suitable for addressing the operational fire management needs. Further validation and redesign of the product format in context of the PREFER service will be required. Relevant inputs from the respective stakeholders' groups are

currently collected in order to document thoroughly the required performance of the relative technique and procedures as well as for shaping properly the product in order to be acceptable by competent end users.

Acknowledgements

The work described in this paper has been co-funded by the European Union's Seventh Framework Programme under Grant Agreement no. 312931 (Project PREFER Space-based Information Support for Prevention and REcovery of Forest Fires Emergency in the MediteRranean Area). The content of this publication is the sole responsibility of the authors and does not necessarily reflect the views of the European Commission.

References

Barbosa P.M., Gregoire J.M. and Pereira J.M.C., 1999. An algorithm for extracting burned areas from time series of AVHRR GAC data applied at a continental scale.Remote Sensing of Environment, 69, pp. 253–263.

Eva H. and Lambin E.F., 1998. Remote sensing of biomass burning in tropical regions: Sampling issues and multisensor approach. Remote Sensing of Environment, 64, pp.292–315.

Hirn B. and Ferrucci F. "Automatic method for detectingand mapping burnt areas without vegetation", Patent 1642087, 2006

Hirn B. and Ferrucci F. "Metodo Automatico Di Rilevazionee Mappatura, in Particolare Di Aree Bruciate E Prive Di Vegetazione, e RelativoApparato", PatentRM2003A000336, 2003

Hirn B. and Ferrucci F. 2005. MYME2: A multi-payload integratedprocedure for the automated, high-resolution remote sensing of burn scars, *Proc. IEEE IGARSS*, 2005

Laneve G. and Cadau E. G. 2006. Assessment of the fire detectionlimit using SEVIRI/MSG sensor, *Proc. IEEE Geoscienceand Remote Sensing Symp., IGARSS06*, pp.4157 -4160 2006

Liu Y, Dai Q, Liu J, Liu S, Yang J, 2014. Study of Burn Scar Extraction Automatically Based on Level Set Method using Remote Sensing Data. PLoS ONE 9(2): e87480. doi:10.1371/journal.pone.0087480

Vafeidis A.T. and Drake N.A., 2005. A two-step method for estimating the extent of burnt areas with the use of coarse-resolution data. International Journal of Remote Sensing,26, pp. 2441–2459.

Validation of the burned area "(V,W)" Modis algorithm in Brazil

Renata Libonati[a], Carlos C. DaCamara[b], Alberto W. Setzer[a], Fabiano Morelli[a], Silvia C. de Jesus[a], Pietro A. Candido[a], Arturo E. Melchiori[a]

[a] *Instituto Nacional de Pesquisas Espaciais, Cachoeira Paulista - SP, Brazil - renata.libonati@cptec.inpe.br; alberto.setzer@cptec.inpe.br; fabiano.morelli@cptec.inpe.br; silvia.jesus@cptec.inpe.br; pietrocandido@cptec.inpe.br, emelchiori@gmail.com@cptec.inpe.br*
[b] *Instituto Dom Luiz / Universidade de Lisboa, Lisboa, Portugal - cdcamara@fc.ul.pt*

Abstract
This work presents an automated regional algorithm that allows detecting burned areas in Brazil based on information from TERRA/AQUA MODIS data. The procedure relies on the so-called W burning index, that requires daily reflectance from the 1km MODIS Level 1B calibrated radiance from bands 2 (near infrared) and 20 (middle infrared). Burned pixels are first identified as those located in the neighbourhood of active fires and associated to values of W and temporal changes in W larger than a fixed threshold. Pixels in the neighbourhood of the previously identified ones are then tested as burned ones based on contextual tests performed on associated values of W and temporal changes in W. Validation of results was performed over Cerrado region using high resolution burned area maps derived from Landsat imagery, paying special attention to the omission and commission errors. For comparison, validation of NASA/MODIS burned area products MCD45A1 and MCD64A1 is also carried out over the same area. Results from the new algorithm present considerably lower omission error when compared to NASA/MODIS products. The two NASA products present very low commission errors (ranging from 2 to 10%) but they are affected by very high occurrence of omission errors (greater than 60% in almost all cases analysed). The new product has larger commission errors (ranging from 20 to 40%) but a large fraction of those (more than 40%) occur at the borders of the scars and may therefore not be strictly viewed as false alarms; there is also a clear reduction of the omission cases (below 40% in all cases).

Keywords*: Burned areas, MODIS, remote sensing.*

Introduction

In Brazil, the conversion of vegetation into pasture and agricultural land using fire practices is a key source of greenhouse gases and trace gases to the atmosphere. Besides, lower moisture conditions enable the use of fire as a tool for land management during the dry season. Furthermore, fire used for burning crops and pastures frequently goes beyond control affecting neighbouring vegetation and becoming a major concern due to the potentially vast area of vegetation affected.
Despite the explicit vulnerability for fire of Brazilian ecosystems, together with the unequivocal need for reliable fire information, to the best of our knowledge hardly any products were developed to operationally monitor burned area in the Brazilian ecosystems. This issue is of particular interest since the accuracy of burned area (BA) maps is closely related to the specific characteristics of a given region (e.g., pre-fire land-cover type and conditions, background soil, fire severity, post fire processes and atmospheric conditions).
The aim of the present work is to develop an automated regional algorithm that allows detecting burned areas in Brazil based on information from TERRA/AQUA MODIS data. The procedure relies on the so-called W burning index (Libonati *et al*., 2011), that uses daily reflectance as obtained from the 1km MODIS Level 1B calibrated radiance from band 2 (near infrared - NIR) and band 20 (middle infrared - MIR). Burned area pixels in the images are first searched in the neighbourhood of active fires, selecting the pixels where specific thresholds of W and of temporal W changes are exceeded. Pixels in the neighbourhood of the previously identified ones are then considered as burned pixels based on contextual tests performed on associated values of W and respective temporal changes. Validation of

results is performed over Cerrado region using high resolution BA maps as derived from Landsat imagery, paying special attention to the omission and commission errors. For purposes of comparison, a similar validation of NASA/MODIS BA products MCD45A1 and MCD64A1 is also carried out over the same area.

Data

Calibration data consist of top of the atmosphere (TOA) values of MIR radiance, NIR reflectance and thermal-infrared (TIR) brightness temperature, as acquired by the MODIS instrument on-board TERRA and AQUA satellites. Data were extracted from the TERRA/AQUA MODIS Level 1B 1 km V5 product, MOD021/MYD021 (MCST, 2006) and correspond to channels 2 (NIR, centered at 0.858 μm), 20 (MIR, centered at 3.785 μm) and 31 (TIR, centered at 11.017 μm). Geolocation data as well as land/sea mask and solar and view angle information for each MODIS 1-km sample were obtained from the MODIS Geolocation product (MOD03 and MYOD03). Both MODIS Level 1B 1 km V5 and MODIS Geolocation products were obtained from the Image Generation Division (DGI) of the Brazilian National Institute for Space Research (INPE). DGI/INPE is responsible for, among other satellites and sensors, the reception, processing and distribution of MODIS images acquired by TERRA and AQUA satellites and the products are made available in Hierarchical Data Format (HDF) format. It may be noted that all MODIS products mentioned above are also free available via the MODIS website.

Information about active fires was based on data provided by GOES, NOAA, MSG-2, TRMM, ATSR, AQUA and TERRA satellites. Data were acquired from INPE active fire database.

Results obtained in the present work were compared with reference BA data as derived from Landsat TM imagery over Jalapão, a region located in the state of Tocantins (Figure 2). The BA scars dataset was derived using a semi-automatic algorithm developed at INPE and the results were verified by independent analysts. The methodology is based on multi-temporal compositing of Landsat imagery and priority is given to select cloud free images less than 32 days apart. The periods covered by the BA dataset July-August 2005, June-September 2006 and June-September 2010. The study region covers about 187 x 187 km^2 and lies within Landsat TM paw/row 221/67. The region belongs to the Cerrado biome and has been increasingly affected by fire in the last years. For instance, during the 2010 dry season, Jalapão has accounted for 60% of all fire events detected in the Cerrado biome.

Results were further compared with those from the two MODIS BA official products namely the MCD45A1 Burned Area Product (Roy *et al*., 2005) and MCD64A1 Direct Broadcast Monthly Burned Area Product (Giglio *et al*., 2006). MCD45A1 and MCD64A1 BA products were freely downloaded from the University of Maryland ftp sites. Tiles for the two BA products over Brazil between 2005 and 2010 were then mosaicked and remapped using the Modis Reprojection Tool.

MCD45A1 is a monthly Level 3 gridded 500 m product containing per-pixel burning and quality information, and tile-level metadata. Quality information is given using five confidence levels of detection from 1 (most confident) down to 4 (least confident). Confidence level 5 denotes detections over agricultural areas, as identified by the MCD12 land cover mask. As stated in MODIS Collection 5.1 - Burned Area Product - MCD45 User's Guide, level 5 detections should not be used in any quantitative analysis because of the low accuracy of BA detection when fire is due to agricultural practices. The MCD45A1 Science Data Sets used in our analysis include all quality assurance flags from 1 to 4.

MCD64A1 is globally available on a monthly basis back to August 2000 at 500m resolution. The MCD64A1 Direct Broadcast Monthly Burned Area Product is currently used in the framework of the Global Fire Emissions Database (GFED) initiative and will replace MCD45A1 in the upcoming MODIS Collection 6. Among the five data layers from MCD64A1, only the Burn Date was used in our study, as this product does not have flags containing confidence levels.

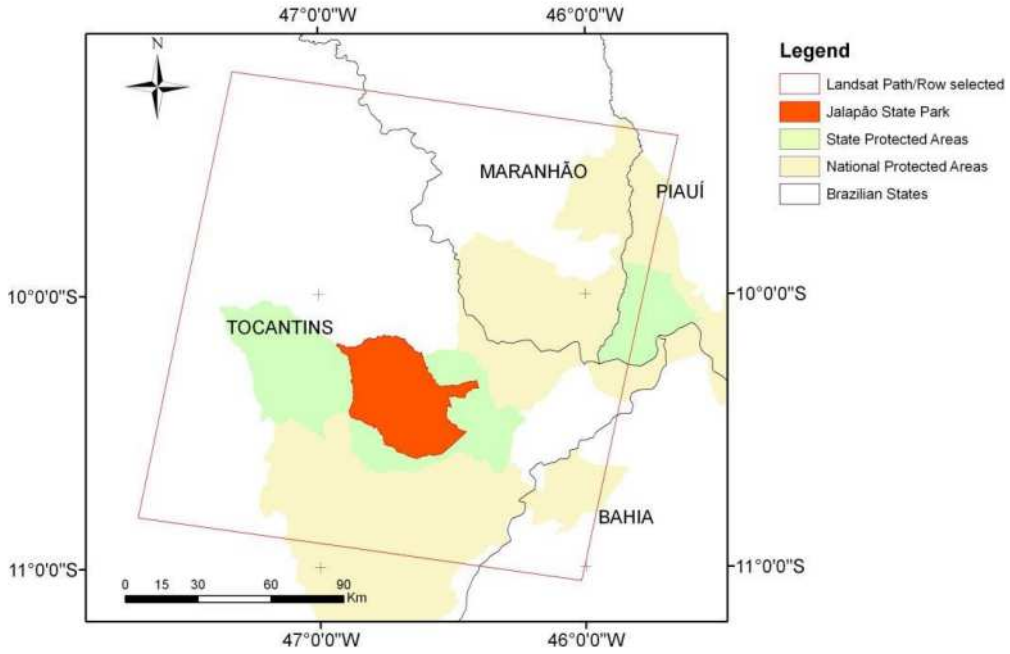

Figure 1. Location of the validation site of Jalapão in the state of Tocantins.

Methods

3.1. Pre-processing

Values of MIR reflectance were retrieved from MODIS channel 20 (MIR) radiances by applying to daytime imagery the methodology developed by Kaufman and Remer (1994) and using TIR (MODIS channel 31) brightness temperature as a surrogate for land surface temperature. Following Libonati *et al*. (2011), special attention was paid to the presence of high solar zenith angles (SZA), all images acquired at solar zenith angles greater than 55° having been rejected. When TERRA and AQUA images were both available for the same day, the image selected was the one with the lowest SZA. Images with view zenith angles (VZA) greater than 45° were also rejected in order to prevent large distortions in pixel size. Pixels associated to water bodies were also masked using the land/sea mask from the MODIS Geolocation product (MOD03, MYD03).

As discussed in Libonati *et al*. (2011), burned surfaces tend to have values of W very close to zero, especially shortly after the fire event, whereas green vegetation tends to be characterized by higher values of W (about 0.3). Intermediate values of W generally correspond to vegetation of small density and/or to the emergence of the soil background. Clouds and cloud shadows are often associated to high values of W (greater than 0.4). We have accordingly rejected pixels associated to W values greater than 0.4, which were flagged as contaminated by clouds/shadows.

3.2. Temporal composites

Multi-temporal image compositing is an operational means of mitigating the gap of information about the land surface due to the presence of cloudy pixels which is especially high in the tropics (Sousa *et al*. 2003). Compositing also contributes to reducing the daily reflectance variability and residual atmospheric effects (Holben *et al*., 1986). Compositing techniques have been therefore widely used for BA detection (Barbosa *et al*., 1998; Stroppiana *et al*., 2002; Sousa *et al*., 2003; Stroppiana *et al*., 2003; Chuvieco *et al*., 2008).

Following these approaches, monthly minimum composites of W were computed, the chosen span of one month representing a compromise between the need to retain the burned signal and the requirement of having a reasonable number of pixels to generate a meaningful minimum value of W.

3.3. Selection of burned pixels (stage I)

Identification of burned pixels is performed in two stages. First (stage I), the analysis is restricted to pixels belonging to 3x3 pixel buffer zones centred in pixels where active fires were identified during the compositing period. Information on active fires is extracted from the INPE database (see http://www.dpi.inpe.br/proarco/bdqueimadas/) as obtained from data provided by GOES, NOAA, MSG-2, TRMM, ATSR, AQUA and TERRA satellites. The defined buffer may be viewed as an area of influence/coverage of the identified active fires, taking into account that we are using data with different spatial resolutions (e.g. 3 km for MSG/SEVIRI, 1 km for TERRA/MODIS).

As pointed out by Giglio *et al*. (2006), algorithms aiming at BA detection based on active fire detection (Roy *et al*. (1999), Fraser *et al*. (2000), Pu *et al*. (2004), George *et al*. (2006), Loboda *et al*. (2007)) may fail to uncover burned areas due to active fire omissions either because of the time of satellite overpass or due to obscuration by clouds, smoke and vegetation. Schroeder *et al*. (2008) have quantified the impact of cloud obscuration on GOES active fires in the Brazilian Amazonia. They showed that in some regions 15% of GOES active fires were omitted due to cloud cover. When assessing fire continuity over time and space, Schroeder *et al*. (2005) suggest the integration of multiple datasets in order to reduce the uncertainties in fire counts when derived using a single system. Giglio *et al*. (2009) also pointed out that BA detection may benefit from the fusion of multi-sensor active fire observations. We therefore believe that the problems associated to active fire omissions are considerably mitigated by relying on information on hot spots from a collection of sensors on board different satellites.

Pixels in the 3x3 buffer zone are then classified as burned ones when there is a change in W between monthly composites that is likely to have been induced by a fire event. It is worth mentioning that in stage I, such changes in W have to be large enough so that possible contaminations by active fire commission errors (false alarms) is substantially reduced.

Let W1 and W2 be the values of W for a given pixel in two successive monthly composites. This pixel is considered as burned if the following conditions are all fulfilled:

I. the pixel belongs to a 3x3 pixel buffer;

II. $W2 \leq 0.16$;

III. $\Delta W = W2 - W1 \leq 0.0$.

Estimates of thresholds of W2 and ΔW were obtained by applying classification trees using observed values of W2 and ΔW for burned and unburned pixels in a sample of around 25,000 MODIS pixels covering Amazonia and Cerrado. Figure 2 shows maps of W for September 2005 composite (left) and of ΔW for differences of W composites between September and August over the study region. It may be noted that areas affected by fire present values of W well above the prescribed threshold of 0.16 together with negatives values of ΔW.

3.4. Selection of burned pixels (stage II)

Stage II of the selection procedure aims at identifying pixels that although presenting less intense signals in either W or ΔW are likely to be burned ones because of their vicinity to pixels already classified as burned. The weaker radiometric signal may be due to partial burning or to low fire severity. The procedure consists in the following steps:

I. L*et al*l pixels classified as burnt pixels in stage I be considered as seed points;

II. For each seed point, let N be the total number of seed points inside a grid of 5x5 pixels centred at the considered seed point; in case N>=3, let $\hat{W}$ and δW be the mean and the mean absolute deviation of seed points within the grid. Let W* be the value of W for a pixel inside the grid that is not a seed point; this pixel is then classified as a burned pixel and considered as a new seed point if the two following conditions are fulfilled:

   a. $\Delta W^* = W^*2 - W^*1 \leq 0.0$

   b. $W^* \leq \hat{W} + (\delta W)$

III. Step II is recursively performed until no new seed points are generated.

IV. The burned area is obtained by summing up all identified burned pixels.

Figure 3 presents an example of the procedure. It may be noted that most burned pixels are identified in stage I, using the most restrictive criteria; then, during stage II, the number of added burned pixels steeply decreases with the number of iterations.

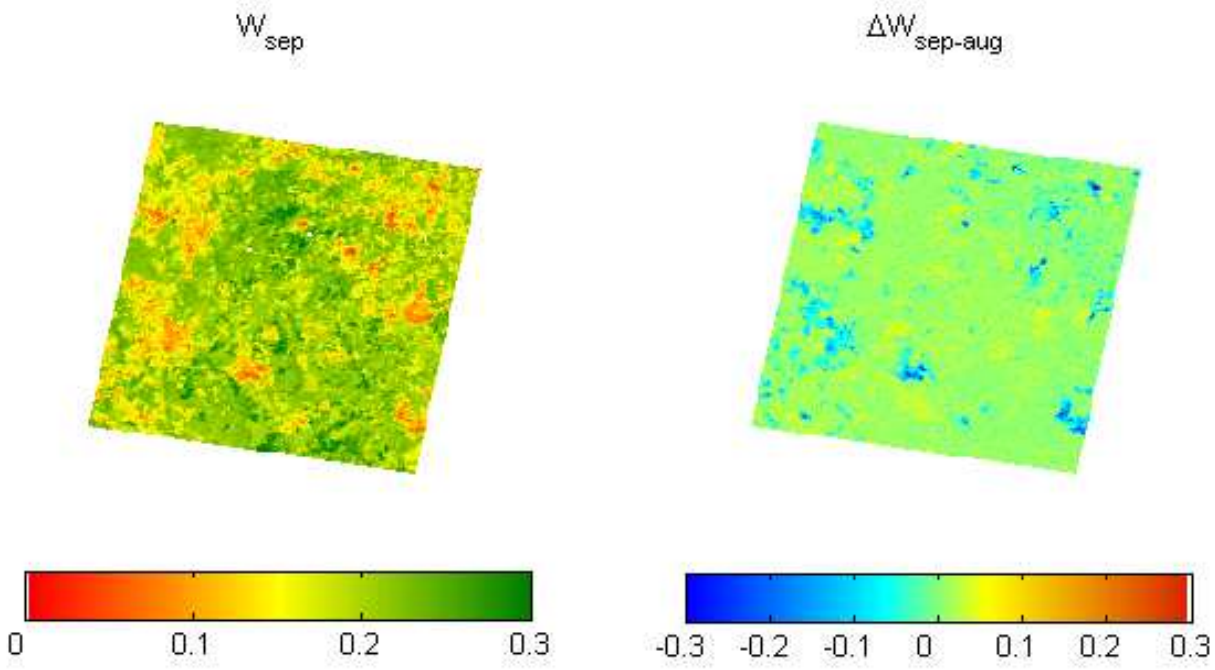

Figure 2. Maps of W for September 2010 composite (left) and of ΔW between September and August composites over the study region shown in Figure 1.

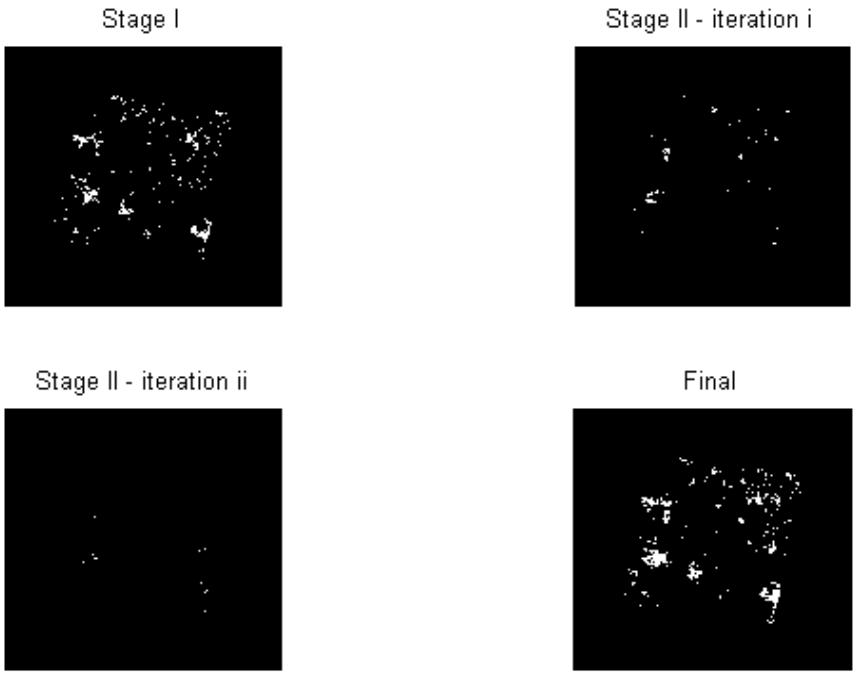

Figure 3. An example of results obtained during stages I and II of the algorithm.

Validation

The quality of a given thematic map derived from remote sensing is usually assessed based on a systematic comparison with other maps (reference maps) also derived from remote sensing. The evaluation is often made based on contingency tables, also known as confusion or error matrices (Story and Congalton, 1986; Smits *et al*., 1999; Foody, 2002). Contingency tables (Table 1) provide a very effective means to analyse the number of correctly and incorrectly classified pixels over a study region. The quality assessment will rely on the following four verification measures that may be derived from contingency tables:

1. The overall accuracy (OA), defined as the fraction of correctly classified pixels, either as burned or unburned:
   $OA=(a+d)/(a+b+c+d)$ (1)

2. The omission error (OE), defined as the fraction of burned pixels in the reference map that were not classified as such in the BA product:
   $OE=c/(a+c)$ (2)

3. The commission error (COE), defined as the fraction of pixels classified as burned in the BA product that are unburned pixels in the reference map:
   $COE=b/(a+b)$ (3)

4. The bias (B), defined as the ratio of the number of pixels classified as burned in the BA product to the number of burned pixels in the reference map:
   $B=(a+b)/(a+c)$ (4)

Whereas OA reflects the agreement between the BA product and the reference map, OE and CE provide information about the reliability and discrimination power of the developed classifier. An unbiased classification exhibits in turn a value of bias equal to one, whereas a bias greater (less) than one indicates the events were over (under) classified.

Table 1. Contingency table for the dichotomous case of pixels classified as burned vs. unburned over a given study region. The total number n of pixels number of pixels is split into four categories with number of occurrences given by a, b, c and d.

		REFERENCE MAP		
		Burned	Unburned	
BA PRODUCT	Burned	a	b	a+b
	Unburned	c	d	c+d
		a+c	b+d	n=a+b+c+d

The traditional contingency table assumes that each pixel belongs to a single class; however, several studies (Foody, 1996, 2002; Gong and Howarth, 1990; Karaska *et al*., 1995) have shown that use of pure pixel approaches is a common source of error in the accuracy assessment of remote sensing products, since reference maps generally have higher resolution than the map being tested. As shown by Binaghi *et al*. (1999), the problems posed by mixed pixels may be circumvented by using fuzzy theory, which allows each pixel to belong to multiple classes with different degrees of membership.
In the present work, the agreement/disagreement between the Landsat TM reference data (30 m resolution) and either our product (1 km resolution) and MODIS MCD64A1 and MCD45A1 products (500 m resolution) are computed taking into account the proportion of BA from reference data within the product pixel. This approach is based on the work by Boschetti *et al*. (2004) who pointed out the need of taking into account the percentage of BA in each pixel of the coarse product when comparing coarse and high resolution BA maps. For instance, if a pixel is classified as burned by the BA product and has 60% of BA from reference data, so this pixel will have a proportion of 0.6 as true burned and 0.4 as commission error (as opposed to a weight of 1 as true burned and 0 as commission error that would be assigned following the traditional approach). In the same way, if a pixel is classified as unburned by the BA product and has 20% of BA from reference data, so this pixel will have a proportion of 0.8 as true unburned and 0.2 as omission error of the non-occurrence. This kind of approach seems to be fairer to the computation of the measures accuracy than the traditional one, since it takes into account the real proportion of reference burned pixel within the product pixel. Recently, Padilla *et al*. (2014) and Tsela *et al*. (2014) have conducted similar approaches when validating algorithms for global BA.

Results

The very own characteristics of the BA product based on the above-described algorithm, hereafter referred to as AQM (from "área queimada", meaning burned area in Portuguese) may be brought into evidence by comparing its performance with the ones of MODIS MCD64A1 and MCD45A1 products. As described in section 3.3, performance of the three products was validated against a reference map of burned scars derived from Landsat TM using verification measures derived from confusion matrices where a mixed-pixel approach is followed that takes into account the proportion of the BA from reference data within the pixel. The same procedure was applied to AQM and the two MODIS global

products. As described in section 3.1, the study was conducted over Jalapão, for a period of 3 years (2005, 2006 and 2010).

In general, the overall accuracy (OA) for MCD64A1 and MCD45A1 BA products is slightly higher than for AQM (Figure 4); it may be however noted that OA satisfies the principle of equivalence of the events (Wilks, 2006), giving equal credits for burned and unburned classes. This property is not always desirable, particularly in the case of BA detection studies where the burned event is more relevant than the non-occurrence event (unburned event). Both MCD64A1 and MCD45A1 products present very low values of CE but they are affected by quite high values of OE; the two NASA BA products appear therefore as conservative in the sense that a low level of false alarms is attained at the cost of quite high occurrence of omission cases. The AQM product presents in turn a rather low value of CE together with a clear reduction of OE that reflects a higher probability of detection of burned pixels. Finally, the AQM product presents an unbiased behaviour (B~1), whereas the NASA BA products tend to underestimate the number of pixels classified as burned in the reference map (B<1).

A better insight into the different characteristics presented by AQM and the two NASA BA products is obtained by looking at the characteristics of pixels correctly classified as burned areas (hits) or contributing to omission and commission errors (Table 2), as obtained when comparing AQM and MODIS MCD64A1 and MCD45A1 versus reference map of burned scars derived from Landsat TM over Jalapão in 2005, 2006 and 2010. Corresponding fractions of pixels located inside (I), on the external border (B) and outside (O) the reference scars were also computed and, for hits and omissions, evaluations were also made of the fractions of low burned pixels (L), i.e. those covered less than 50% by burned areas in Landsat reference map and of high burned pixels (H), i.e. those covered more than 50% by burned areas.

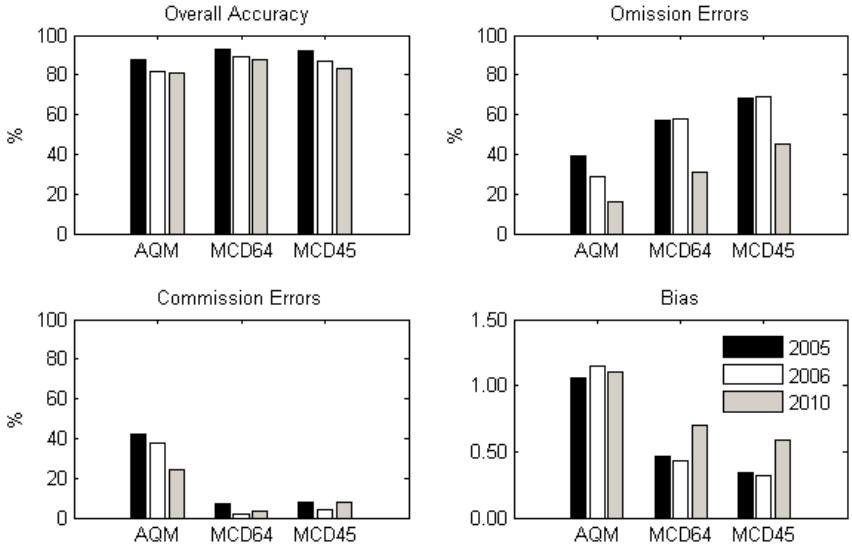

Figure 4. Verification measures as obtained from confusion matrices of AQM and MODIS MCD64A1 and MCD45A1 versus reference map of burned scars derived from Landsat TM over Jalapão in 2005, 2006 and 2010.

As shown in Table 2, for all three products the large majority of hits is associated to pixels located inside burned scars, but the AQM is able to correctly identify a substantially larger number of burned pixels, 30% of them located in the external borders of the scars (an amount quite larger than those by the NASA products that are below 20%).On the other hand, the AQM product is able to correctly identify as burned 43% of pixels with low fraction of burned area (less than 50%), an amount that is more than the double of that by MCD64A1 (21%) and almost the double than that by MCD45A1 (23%). The AQM product presents a substantially lower number of omission errors than the NASA

products, but for all three products the larger fractions are associated to pixels located in the borders of scars and to pixels with low fraction of burned area (less than 50%). The very large number of commission errors by AQM also presents a large contrast with the very low number by the two NASA products; however, more than two fifths of commission errors in AQM are associated to occurrences in pixels located in the borders of the scars suggesting that they are not to be viewed as 'false alarms' in the strict sense, but as an overestimation of the size of the real scars. This problem is likely to be associated to errors in geo-referencing of a small number of MODIS images that propagate into the multi-image composites. Obtained results may be visually confirmed in Figure 5 that shows pixels where true burned areas were detected (green), together with omission (blue) and commission (red) errors from AQM (left) and MCD64A1 (right) in Jalapão during 2010. The AQM product shows higher probability of detection of burned pixels, i.e. lower OE than MCD64A1 that presents a higher value of OE and a very low value of CE. A large fraction of pixels with commission errors in AQM are located in the external borders of the scars (delimited by the black lines).

Table 2. Number of hits, omission errors and commission errors when comparing AQM and MODIS MCD64A1 and MCD45A1 versus reference map of burned scars derived from Landsat TM over Jalapão in 2005, 2006 and 2010 together with corresponding fractions of pixels located inside (I), in the external border (B) and outside (O) the scars in reference maps and, for hits and omissions, the fractions of low burned pixels (L), i.e. covered less than 50% by burned areas in Landsat reference map and of high burned pixels (H), i.e. covered more than 50% by burned areas.

	Hits	Omissions	Commissions
AQM	15961 I=70%; B=30% L=43%; H=57%	12649 I=42%; B=58% L=64%; H=36%	7466 O=59%; B=41%
MCD64A1	9492 I=82%; B=18% L=21%; H=79%	19118 I=46%; B=54% L=67%; H=33%	325 O=51%; B=49%
MCD45A1	7132 I=81%; B=19% L=23%; H=77%	21478 I=50%; B=50% L=62%; H=38%	545 O=43%; B=57%

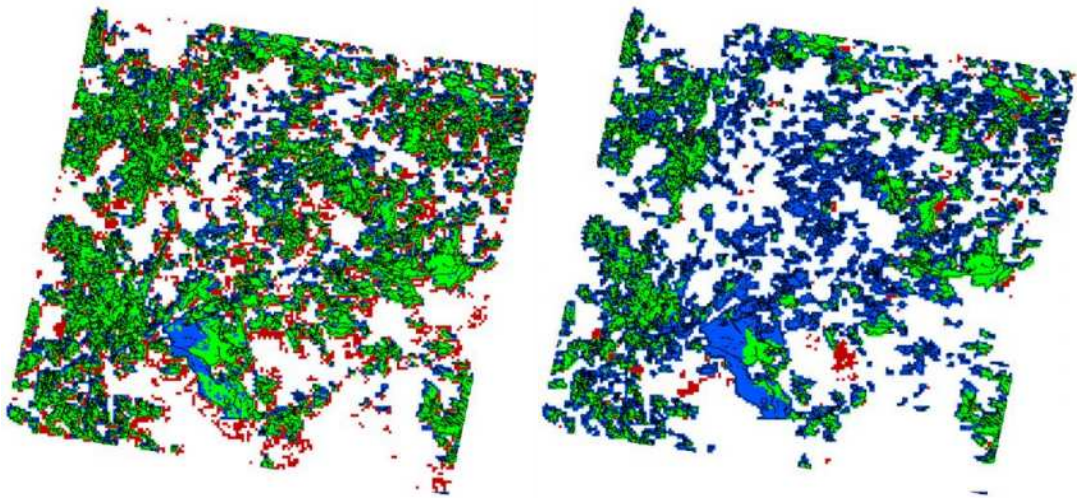

Figure 5. Maps showing pixels where true burned areas were detected (green), together with omission (blue) and commission (red) errors. TM reference scars (black lines) are superimposed. Results shown are those obtained from AQM (left panel) and MCD64A1 (right panel) over Jalapão in 2010.

As shown in Table 3, during the three years analysed the area of study was characterized by high frequency (87-90%) of small scars (<100ha) that accounts for a small percentage (8-19%) of the total BA. Large scars (> 1000ha) are rare (1-2%) but they account for a large amount (42-64%) of the total BA. As opposed to regions where large scars are predominant, low resolution instruments will tend to underestimate BA in regions where burned scars are small and fragmented. A large number of omission errors in therefore to be expected It is therefore to be expected in all three analysed products (Table 2) but, as already pointed out, the AQM is able to identify a larger fraction of low burned pixels than the NASA products. The AQM product appears therefore as more sensitive to sub-pixel burned areas, even when working at a lower spatial resolution (1km) than the NASA products (500m); this is probably due to the use of MIR reflectance by the algorithm.

Table 3. Fractions of total number of scars and of total burned area for three classes of scars as derived from Landsat TM data over Jalapão in 2005, 2006 and 2007.

	Classes	Fraction of total number of scars	Fraction of total burned area
2005	<100ha	90%	16%
	100-1000ha	9%	38%
	>1000ha	1%	46%
2006	<100ha	89%	19%
	100-1000ha	10%	39%
	>1000ha	1%	42%
2010	<100ha	87%	8%
	100-1000ha	11%	27%
	>1000ha	2%	64%

Conclusions

An automated regional algorithm able to detect burned areas in Brazilian biomes was developed using information from MODIS imagery at 1km resolution. The algorithm relies on the so-called W burning index that is defined in a transformed NIR-MIR space. Pixels are classified as burned ones when there is a change in W between 30-day composites that are likely to have been induced by a fire event. Identification of burned pixels is performed in two stages. First, the algorithm is restricted to pixels belonging to buffer zones centred in pixels where active fires were identified from a variety of sensors on-board geostationary satellites and polar orbiters. Then the algorithm is successively applied to pixels in the vicinity of pixels that were classified as burned.

The resulting AQM product was validated against reference maps of scars derived from Landsat TM images over a study region located in the Cerrado biome. For purposes of performance assessment, two operational NASA products, MCD64A1 and MCD45A1, were also validated against the same reference maps. Because the products to be validated have different spatial resolutions than that of reference maps (e.g. AQM with 1km and Landsat scars with 30 m), the error matrix was estimated following a new approach based on the assumption of mixed pixels, where the agreement/disagreement between product and reference data are computed taking into account the proportion of BA from reference data within the product pixel.

The two NASA products present very low commission errors (ranging from 2 to 10%) but also very high occurrence of omission errors (greater than 60% in almost all cases analysed). The AQM product has larger commission errors (ranging from 20 to 40%) but a large fraction of those (more than 40%)

occur at the borders of the scars and may therefore not be strictly viewed as false alarms; there is also a clear reduction of the omission cases (below 40% in all cases).
Performance of the AQM product may be attributed to two main factors. On the first hand, the usage by the algorithm of the W index, that was specifically designed to identify burned areas and takes advantage of the ability of MIR reflectances to discriminate burned areas. On the second hand, the usage of multiple sensor active fire observations that considerably contribute to mitigating the problem of failing to uncover BA due to active fire omissions either because of the time of satellite overpass or due to obscuration by clouds, smoke and vegetation. It is worth mentioning that active fire information from NPP/VIIRS (which is being disseminated by INPE since 25/09/2013) is also planned to be introduced operationally in the algorithm, contributing to increase the spatial and temporal coverage of fire observations.
The AQM approach is currently in pre-operational phase at INPE and additional tuning experiments are currently being carried on. More validation sites are also being developed at INPE using Landsat TM imagery that will allow performing accuracy assessments of the algorithm for different biomes.

7. Acknowledgments

Research was supported by the scientific grants FAPESP 2010/19712-2 and CNPq 309199/2008-5, and the GIZ - German Technical Cooperation Agency through the MMA Project "Prevenção, controle e monitoramento de queimadas irregulares e incêndios florestais no Cerrado". Research was also supported by the EU 7th Framework Program (FUME) contract number 243888.

8. References

Barbosa, P. M., Pereira, J. M. C., and Gregoire, J.-M. (1998). Compositing criteria for burned area assessment using multitemporal low resolution satellite data. Remote Sens. Environ., 65, 38– 49.

Binaghi, E., Brivio, P. A., Ghezzi, P., and Rampini, A. (1999). A fuzzy set-based accuracy assessment of soft classification.Pattern Recognition Letters, 20, 935–948.

Boschetti, L., Flasse, S.P., and Brivio, P.A. (2004). Analysis of the conflict between omission and commission in low spatial resolution dichotomic thematic products: The Pareto Boundary. Remote Sens. Environ., 91, 280–292.

Chuvieco, E., Englefield, P., Trischenko, A., and Lio, Y. (2008). Generation of long time series of burn area maps of the boreal forest from NOAA-AVHRR composite data. International Journal of Remote Sensing, 23, 5103–5110.

Fraser, R. H., Li, Z., and Cihlar, J. (2000). Hotspot and NDVI differencing synergy (HANDS): A new technique for burned area mapping over boreal forest. Remote Sens. Environ., 74, 362−376.

Foody, G.M. (1996). Approaches for the production and evaluation of fuzzy land cover classications from remotely-sensed data .Internat. J. Remote Sensing, 17(7), 1317-1340.

Foody, G.M. (2002). Status of land cover classification accuracy assessment. Remote Sens. Environ., 80,185–201.

George, C., Rowland, C., Gerard, F., and Balzter, H. (2006). Retrospective mapping of burnt areas in Central Siberia using a modification of the normalized difference water index. Remote Sens. Environ., 104, 346−359.

Giglio, L., Loboda, T., Roy, D. P., Quayle, B., and Justice, C. O. (2009). An active-fire based burned area mapping algorithm for the MODIS sensor, Remote Sens. Environ., 113, 408–420.

Giglio, L., van der Werf, G. R., Randerson, J. T., Collatz, G. J., and Kasibhatla, P. S. (2006). Global estimation of burned area using MODIS active fire observations. Atmospheric Chemistry and Physics, 6, 957−974.

Gong, P., and Howarth, P. J. (1990). The use of structural information for improving land-cover classification accuracies at the rural –urban fringe.Photogrammetric Engineering and Remote Sensing, 56, 67–73.

Karaska, M. A., Huguenin, R. L., Van Blaricom, D., and Savitsky, B. (1995). Subpixel classification of cypress and tupelo trees in TM imagery. Proceedings of the 1995 ACSM/ASPRS Annual Convention and Expo-sition, 3, 856–865.

Kaufman, Y. J., and Remer, L. (1994). Detection of forests using mid-IR reflectance: An application for aerosol studies. IEEE Trans. Geosci. Remote Sens., 32(3), 672−683.

Libonati, R., DaCamara, C. C., Pereira, J. M. C., and Peres, L. F. (2011). On a new coordinate system for improved discrimination of vegetation and burned areas using MIR/NIR information. Remote Sens. Environ., 114, 831−843.

Loboda, T., O'Neal, K. J., and Csiszar, I. (2007). Regionally adaptable dNBR-based algorithm for burned area mapping from MODIS data. Remote Sensing of Environment, 109, 429−442.

Padilla, M., Stehman, S.V., Litago, J., Chuvieco, E. (2014). Assessing the temporal stability of the accuracy of a time series of burned area products. Remote Sens., 6, 2050.2068.

Pereira, J. M. C. (1999). A comparative evaluation of NOAA/AVHRR vegetation indexes for burned surface detection and mapping. IEEE Trans. Geosci. Remote Sens., 37(1), 217−226.

Pu, R., Gong, P., Li, Z., and Scarborough, J. (2004). A dynamic algorithm for wildfire mapping with NOAA/AVHRR data. International Journal of Wildland Fire, 13, 275−285.

Roy, D. P., Giglio, L., Kendall, J. D., and Justice, C. O. (1999). Multi-temporal active-fire based burn scar detection algorithm. International Journal of Remote Sensing, 20, 1031−1038.

Roy, D.P., Jin, Y., Lewis, P.E., e Justice, C.O. (2005). Prototyping a global algorithm for systematic fire-affected area mapping using MODIS time series data. Remote Sens. Environ., 97(2), 137–162.

Schroeder, W., Csiszar, I., and Morisette, J. (2008). Quantifying the impact of cloud obscuration on remote sensing of active fires in the Brazilian Amazon. Remote Sens. Environ., 112, 456-470.

Schroeder, W., Morisette, J., Csiszar, I., Giglio, L., Morton, D., Justice, C.O., (2005) Characterizing Vegetation Fire Dynamics in Brazil through Multisatellite Data: Common Trends and Practical Issues. Earth Interact., 9, 1–26.

Smits, P.C., Dellepiane, S.G., and Schowengerdt, R.A. (1999). Quality assessment of image classification algorithms for land-cover map-ping: A review and a proposal for a cost-based approach. International Journal of Remote Sensing, 20:1461–1486.

Sousa, A. M. O., Pereira, J. M. C.. and Silva, J. M. N., (2003). Evaluating the performance of multitemporal image compositing algorithms for burned area analysis. International Journal of Remote Sensing 24(6): 1219-1236.

Story, M., and Congalton, R.G. (1986). Accuracy assessment: A user's perspective, Photogrammetric Engineering and Remote Sensing, 52:397–399.

Stroppiana, D., Pinnock, S., Pereira, J.M.C, and Gregoire, J-M. (2002). Radiometric analysis of SPOT-VEGETATION images for burnt area detection in Northern Australia. Remote Sens. Environ., 82, 21-37.

Stroppiana, D., Tansey, K., Gregoire, J-M. and Pereira, J.M.C, (2003). An algorithm for mapping burnt areas in Australia using SPOT-VEGETATION data, IEEE Trans. Geosci. Remote Sens., 41, 4,.907 -909.

Tsela, P., Wessels, K., Botai, J., Archibald, S., Swanepoel, D., Steenkanp, K., Frost, P. (2014). Validation of the tow standard MODIS satellite burned area products and an Empirically-derived merged product in South Africa. Remote Sens, 6, 1275-1293.

Wilks, D. (2006). Statistical methods in the atmospheric sciences. Second Edition. Academic Press, pp 627.

Chapter 7
Social and Economic Issues

ANN multivariate analysis of factors that influence human-caused multiple fire starts

Sergi Costafreda-Aumedes[a], Cristina Vega-Garcia[b]

[a] *Agriculture and Forest Engineering Department, University of Lleida, Alcalde Rovira Roure 191, 25198, Lleida, Spain, E-mail: scaumedes@gmail.com*
[b] *Agriculture and Forest Engineering Department, University of Lleida, Alcalde Rovira Roure 191, 25198, Lleida, Spain, E-mail: cvega@eagrof.udl.es*

Abstract
Delays in the initial attack of new fire starts can happen locally when two or more fires burn simultaneously. The occurrence of multiple-fire-day situations may pose a real problem if suppression resources are limited, which almost always are. We analyzed multiple-fire-days in Galicia (Spain) from 2002 to 2005 with the goal of predicting these multiple fire situations by using Artificial Neural Networks. We carried out two types of analysis with our seasonally-structured data: to identify the relevant variables in the multiple versus single daily outcome (classification problem) and to predict the number of fires within the multiple-fire-days observations (prediction problem). The accuracy for the best Spring model was around 59-60% which located multiple occurrences in higher altitudes and public forest properties, near roads and recreation areas, with lower temperatures, lower quantity of pastureland and higher FFMC. Best classifications for the Summer period were around 60-61% and associated multiple fires to lower elevation areas, higher proportion of public and communal forests, near roads and higher drought indices. Predictions of actual number of fire occurrences in the Spring period reached 62% accuracy with a similar variables selection as the Spring classification model. Predictions for the Summer period lacked accuracy (44-50%) suggesting more complex patterns, probably due to mixed causes.

Keywords*: Artificial Neural Network, Daily Fire Prediction, Human-caused fires, Simultaneous fires*

Introduction

Short-term forest fire suppression performance depends on number and behavior of active fires (Haight and Fried 2007). Fire behavior is set by conditions in the fire environment that are difficult or impossible to control (fuels, weather, and topography), but numbers of ignitions in many countries, and particularly in the Mediterranean, are linked to human risk. Delays in the start of initial attack of new fires can happen locally when two or more forest fires are burning simultaneously, and the time required to extinguish a forest fire grows exponentially with detection and response time. For fire suppression resources sufficient to manage one fire, the simultaneous occurrence of two, three or more fires do create a challenge (Rachaniotis and Pappis 2006, IAFC and NFPA 2010). Forest fire managers must make crucial decisions every day on the amount and the type of fire suppression resources required and their allocation. Budgetary constraints under rising fire extinction costs (Liang *et al.* 2008, Calkin *et al.* 2014) often prevent maintaining enough suppression resources to potentially manage all possible active fires in all subdivisions of a region (i.e. Galicia, Alonso-Betanzos *et al.* 2003). When worse-case scenarios occur, and unlikely high-risk peaks couple with favorable conditions for burning in the fire environment, available fire suppression resources stretch beyond planned levels and are overloaded.
The prediction of these rare days with multiple fire starts, or multiple-fire-days (MFD), would be useful to fire managers (De Haan 2006). There are many studies which have focused on deployment of suppression resources (from Simard and Young 1978 to Calkin *et al.* 2014), but only Kirsch and Rideout (2005) and Haight and Fried (2007) tried to incorporate the effects of a number of possible simultaneous fires, but without estimating a probability or modeling this process. Previous studies

which attempted to predict MFD occurrence relied only on daily weather data or danger indices by using a Poisson distribution (Martell *et al.* 1987), binary logistic models (Andrews and Bradshaw 1997) or non-linear models (Garcia Diez *et al.* 1994, 1996, 1999). Garcia Diez *et al.* (1994, 1996, 1999) analyzed data between 1986 and 1993 in Galicia, concluding that fires (all causes) were primarily related to unfavorable weather conditions (past- and present-day weather). Their best MFD prediction had an accuracy varying between 52 and 72% over their study period.

Although MFD may be associated in some countries (Canada, USA) with dry lightning storms (Rorig *et al.* 2007), in most countries they are associated mainly to human activity (Omi 2005, Tanskanen and Venäläinen 2008, IAFC and NFPA 2010). Arsonists often set several ignition points to increase damage before firefighters arrive (Omi 2005, De Haan 2006), as do farmers in agrarian traditional rural activities (i.e. pastoral use of fire to regenerate rangelands in the Mediterranean, Ruiz-Mirazo *et al.* 2012). Martell *et al.* (1987), Garcia Diez *et al.* (1994, 1996, 1999) and Andrews and Bradshaw (1997) only considered weather variables related to the biophysical fire environment in their MFD occurrence analysis and did not include human risk factors.

There are already an important number of research papers on the general topic of fire occurrence prediction and the analysis of human risk in the fire literature (from Crosby 1954 to Rodrigues *et al.* 2014) and in Spain (i.e. Lozano *et al.* 2007, Chuvieco *et al.* 2009, Vasilakos *et al.* 2009, Vilar *et al.* 2010, Padilla and Vega-Garcia 2011, Vilar del Hoyo *et al.* 2011, Rodrigues *et al.* 2014). Fire occurrence studies have dealt with socioeconomic (i.e. Martínez *et al.* 2009) or geographic factors and biophysical variables (Lozano *et al.* 2007), but the occurrence of multiple-fire-day situations has been rarely approached.

Our aim was to explore these relationships between human risk factors, biophysical variables and multiple fires caused by people on a daily basis, with a view to aid fire management to anticipate and locate potential fire suppression overload events.

Methods

Study area

The study area is the Autonomous Community of Galicia, the Northwestern region of Spain (Figure 1). Galicia encompasses around 3 million ha (6 % of the Spanish territory) near the Atlantic Ocean (North and East boundaries). The humid Atlantic climate provides an average annual rainfall over 1,200 mm that favors the rapid growth of vegetation, which would be grasses and broadleaved tree species in natural conditions. The Galician vegetation has been highly modified through time. Population is distributed over 3,000 towns with a higher concentration on the coast and forests, mainly located in rural areas in the interior, that have long been highly fragmented by this human impact. Forest ownership is private (33 % of forests) either individually (64 % private forest area) or communally (36%). About 40% of forests have artificial origin, as many properties were reforested after the 1950's with *Pinus pinaster* and *Eucalyptus globulus* for their high economic interests for the pulp and plywood markets. Historical evidence attests the use of pastures by livestock for at least 6000 years (Kaal *et al.* 2011) and livestock production is currently the most important economic activity in the region.

Galicia is the Spanish administrative region with the highest number of human-caused forest fires (HCFF) (MAGRAMA 2013). Between 2001 and 2010, 86,036 HCFF have occurred in Galicia, a 44.1 % of all human-caused forest fires accounted for in the country in the same period, and the trend appears to be growing in this Atlantic region of the Iberian Peninsula (Carvalho *et al.* 2010). Fires take place basically into two well-defined time periods, end of winter and summer (Marey-Pérez *et al.* 2010), and are linked to socio-economic activities and the traditional pastoral use of fire (Marey-Pérez *et al.* 2010, Torre-Antón 2010). The high mean annual number of fires, and the spatiotemporal clustering of part of these fires in MFD in Galicia, led to its selection as study area.

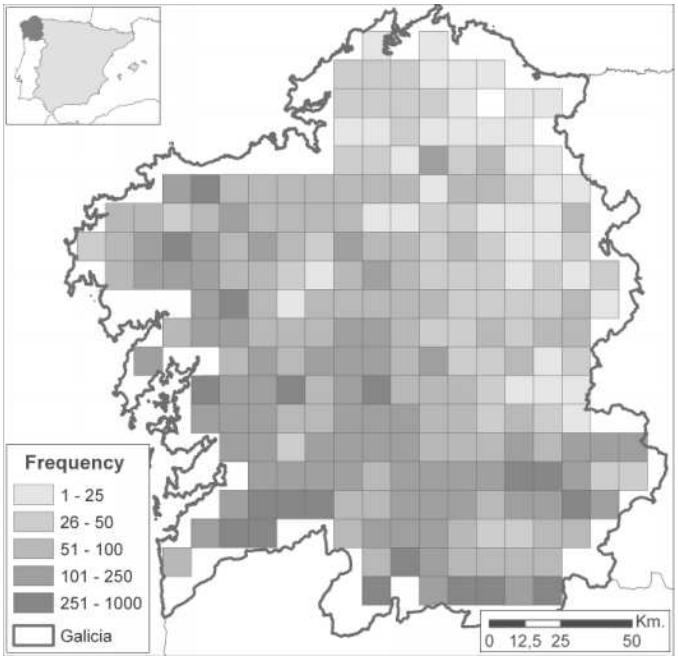

Figure 1. Galicia's location. This figure shows the human-caused forest fire frequency occurred during the period 2002 to 2005 in each of the 239 10x10 sq km UTM quadrates.

2.2. Study period

The data consisted on historical records of daily HCFF occurrences, daily weather data and geographic characteristics for Galicia in a 10x10 sq km UTM grid, for the period from 2002 to 2005. This period was restricted to four years due to data acquisition limitations (the spatially interpolated daily weather data available (Padilla and Vega-Garcia 2011)), but 4-5 years is the usual planning period for fire prevention in Spain.

2.3. Fire data

The Spanish fire history database (EGIF, 1983 – 2011) was provided by the Spanish Forest Service of the Ministry of Agriculture, Food and Environment (MAGRAMA). We extracted 28,442 HCFF records between 2002 and 2005 (both included) and summarized daily number of fires in a 10x10 sq km UTM grid for Galicia (19,612 observations). The grid consisted of 239 quadrates, after some irregular units in the coastal line were excluded in order to obtain a regular grid of equal-area (100 ± 1 km^2) quadrates. There was only one quadrate in which there was no fire in the study period. Though one fire occurrence per quadrate and day is quite common in Galicia (14,340 cases), MFD occurrences are rarer events (5,272 cases). In our study period, number of fires per day and quadrate ranged from 2 (3,354 observations) to 15 fires (just 1 observation).

The database was divided according to the seasonality of fires in Galicia (Marey-Pérez *et al*. 2010, Xunta de Galicia 2014). "Seasons" were defined by considering the daily frequency of the HCFF data, summarized by quadrate, and separating periods by minimum peaks of occurrence. Accordingly, the first period comprised from January 19th to May 11th (5,472 cases, 8,699 Spring fires), the second from May 12th to October 21st (13,735 cases, 19,248 Summer fires) and the third from October 22nd to January 18th (407 cases, 475 Winter fires). The third period had a very low number of records, so it was discarded for modeling.

We carried out two types of analysis with our data. Our first goal was the identification of variables that were relevant in the multiple (MFD) versus single (SFD) daily outcome. This classification analysis required coded data: SFD observations were coded as Y = (1, 0) (just one fire occurred in the day and quadrate) and MFD observations were coded Y = (0, 1) (more than one fire occurred in the

quadrate and day). In order to have a balanced database for analysis (Vega-Garcia *et al.* 1996) we randomly selected the same number of cases for SFD and MFD records. This database contained 3,532 records in Spring and 6,900 in the Summer seasonal period (10,544 observations in total, annual data). The second goal was to predict quantitatively the number of HCFF within the MFD observations. We randomly selected the same number of observations for each class in order to have a balanced database for analysis. We limited the minimum number of observations per class to 100 because an increase of the daily fire frequency diminishes the number of cases and the modeling errors could increase. The maximum number of classes to predict was 6 (X = 1, 2, 3, 4, 5 and more than 5 HCFF per quadrate and day) when working with all the data (annual data) and five (X = 1, 2, 3, 4 and more than 4 HCFF per quadrate and day) when working with the data for each seasonal period. The seasonal MFD databases contained 820 and 1,055 observations for the Spring and Summer periods, respectively.

2.4. Explanatory variables

Our explanatory variables (Table 1) were the same as in the study of daily HCFF occurrence in Spain by Padilla and Vega-Garcia (2011). The cartographic information on these factors came from the Biodiversity database of the Spanish Ministry of Environment. Weather was provided by the Department of Geography of the University of Alcalá with permission of Meteológica SA (Madrid, Spain). The geographic factors included forest land ownership and infrastructures; physiography was described by elevation, slope and aspect variability; vegetation was represented by the percentage occupied by each Rothermel's fuel model (1972) in the quadrate. The weather data included daily records of rainfall, temperature, relative humidity, maximum dew point temperature, wind speed at 12 hours UTC, solar radiation, presence of snow and cloudiness. The Meteorological Fire Danger Index Processor (MFDIP) described in Camia *et al.* (1998) was used to compute several fire danger rating indices widely used.

2.5. Methodological approach. Cascade correlation ANN

Artificial Neural Networks (ANN) models are a reliable alternative to traditional statistical methods, especially when dealing with large databases, non-linear systems (Scrinzi *et al.* 2007), not normally distributed variables (Hilbert and Ostendorf 2001) or highly correlated variables (Vega-Garcia and Chuvieco 2006). For a given database representing a set of historical events these algorithms are capable of identifying and fitting very complex non-linear patterns by iterative adjustment (Kuplich 2006). These models have been applied before to the study of forest fires (e.g. Vega-Garcia *et al.* 1996, Vasconcelos *et al.* 2001, Alonso-Betanzos *et al.* 2003, Vega-Garcia and Chuvieco 2006, Vasilakos *et al*. 2009) reaching good accuracies and good generalization capability, so ANN models were selected for this work in an attempt to gauge their potential in modeling MFD events.

As losing generalization capacity by overtraining a net is a common problem, it is customary to apply an *early stopping* procedure, based on the separation of the database in two subsets: one for training or "learning", and part (test set) used to control the evolution of error committed in this independent set, and stop training if the error starts to increase (Hasenauer *et al*. 2001, Jutras *et al*. 2009). Accordingly, before construction of the models the database was randomly split in two subsets: 70 % of the cases were used for the training process, and the remaining 30 % were used to test the progression of the iterative learning processes and to prevent overtraining of the models that might limit their generalization capacity. No independent validation dataset was segregated (100% cases were used for validation), as the models were designed to be explicative and not to predict future occurrences.

Table 1. Acronyms and abbreviations of each independent variable

Acronyms and Abbreviations	Variable	Acronyms and Abbreviations	Variable
Geographical variables		Geographical variables	
Human Risk Factors		Physiography	
Forest Land Tenure		DEM_MN	Elevation mean
FOREST_PV	Private	DEM_SD	Standard deviation of the elevation
FOREST_PB	Public	SLOPE_MN	Slope mean
FOREST_VC	Communal	SLOPE_SD	Standard deviation of the slope
FOREST_PR	Protected	ASPECT_VAR	Number of aspect classes
Infrastructure		Meteorological variables	
TOWN_DI	Distance to towns		
RECRE_DI	Distance to recreational areas	Raw weather variables	
RESER_DI	Distance to reservoirs	P24	Daily rainfall
ROAD_DI	Distance to roads	T_MAX	Maximum temperature
DENS_PO	Density of population	RH_MIN	Minimum relative humidity
		DewTmpMax	Maximum dew point temperature
Vegetation		WIND	Wind speed at 1200 hours UTC
Area occupied by each	Rothermel's fuel type (%)	SOLAR_R	Solar radiation
FUEL_01	Fuel type 1	CLOUD	Cloudiness
FUEL_02	Fuel type 2		
FUEL_03	Fuel type 3	Fire danger rating indices	
FUEL_04	Fuel type 4	FWI	Canadian Fire Weather Index
FUEL_05	Fuel type 5	FFMC	Canadian Fine Fuel Moisture Code
FUEL_06	Fuel type 6	DMC	Canadian Duff Moisture Code
FUEL_07	Fuel type 7	DC	Canadian Drought Code
FUEL_08	Fuel type 8	PROB	Portuguese Drought Index
FUEL_09	Fuel type 9	ISI	Initial Spread Index
FUEL_00	No vegetation		
FUEL_TY	Number of different fuel types		

The backpropagation algorithm (Rumelhart *et al*. 1986) associated to the multilayer perceptron (Hecht-Nielsen 2005), with one hidden layer and a sigmoid activation function, has been the algorithm most often used for predicting fire occurrence (Vega-Garcia *et al*. 1996, Vasilakos *et al*. 2009), but other techniques such as genetic algorithms (Vasconcelos *et al*. 2001), Levenberg-Marquardt models (Alonso-Betanzos *et al*. 2003), perceptron neural networks (Bisquert *et al*. 2012) or cascade-correlation networks (Vega-Garcia and Chuvieco 2006) have also been used for modeling forest fire occurrence.

The cascade-correlation model created by Fahlman and Lebiere (1990) was used in this work, following the procedure described in Alcázar *et al*. (2008) and Vega-Garcia and Chuvieco (2006). Initial architecture was set to two layers (input/output), and no hidden units. The number of hidden nodes was optimized during the training phase, as candidate hidden units were tested and added (or not), creating an optimal multi-layer structure (Fahlman and Lebiere 1990) at the end of the learning phase. We controlled final size to make sure number of weights was within the order of magnitude that our data would allow, and favored simple architectures. Training was based on an adaptative gradient learning rule (Bridle 1990, Fahlman and Lebiere 1990), a fast variant of the general algorithm of back-propagation (Werbos 1994) that featured a weight decay factor to reduce complexity of the

models (NeuralWare 2009). Several models were built and tested starting training with different random weights, and with different random distributions of individual observations among the three datasets (training, test and validation).
Classification performance for the two cases (SFD and MFD) in the three datasets (training, test and validation) was evaluated by using the total percentage correctly classified, or Accuracy, and the confusion matrix provided by Predict® 3.24 software (NeuralWare 2009). The predictive capacity of the number of daily forest fires (X = 1, 2, 3, 4, 5, 6) was evaluated by using the linear correlation (r) between the observed and the estimated fire occurrences in three data subsets (training, testing and validation). In the selection of the best models, other diagnostics were analyzed, such as relative entropy of the network (the lower, the better the model was), internal correlation (the higher, the better) (NeuralWare 2009), and architecture complexity (we favored models with low number of input variables, processing elements and layers as stated before).
We sought balanced accuracies for the three datasets. For the best model, a sensitivity analysis was applied to identify relevant variables by computing a matrix of partial derivatives of the output variables with respect to each of the input variables (NeuralWare 2009). High values of this sensitivity measure indicated that slight variations of an input variable produced considerable changes in the classification of SFD or MFD, and vice versa. A positive sign in the sensitivity analysis would generally indicate a direct relationship between dependent and independent variable; a negative sign would indicate an inverse relationship. This is a standard diagnostic procedure commonly used to gain insight into a multilayer neural network solution (Alonso-Betanzos *et al.* 2003, Alcázar *et al.* 2008).

Results

Cascade-correlation binary classification accuracies were around 60% with a 7-8-2 ANN structure, for the annual data. This model suggested that MFDs occurred in areas with lower elevation (DEM_MN, average MDF value: -0.200) and lower temperatures (T_MAX, -0.107), higher FFMC (1.321) and higher DC (0.125).

Table 2. Accuracy and sensitivity analysis of the Spring cascade-correlation binary classification model (CL_SP). Network structure: 6-2-2

	Accuracy	Relative Entropy		FOREST_PB	ROAD_DI	RECRE_DI	FUEL_02	DEM_MN	FFMC
SFD	0.653	0.639	Av. SFD	-0.411	0.441	0.268	0.413	-0.392	-1.469
MFD	0.576	0.676	Av. MFD	0.411	-0.441	-0.268	-0.413	0.392	1.469
Train	0.615	0.657							
SFD	0.625	0.649	Av. Sq.	0.204	2133	0.219	0.237	0.201	3.938
MFD	0.582	0.698	Variance	0.036	1939	0.148	0.066	0.047	1.779
Test	0.603	0.674							
SFD	0.645	0.642							
MFD	0.578	0.683							
Validation	0.611	0.662							

SFD, Single-Fire-Days; MFD, Multiple-Fire-Days; Av. SFD, Average SFD value per variable; Av. MFD, Average MFD value per variable; Av. sq. Average square of each variable

Accuracy for the best Spring model (CL_SP) was also around 59-60% (Table 2), but DEM_MN had a positive response (contrariwise to the annual binary classification model). T_MAX was included in some models evaluated, with negative sign. MFD occurred more frequently in higher altitudes, with higher percentages of public forests (FOREST_PB), where temperatures are lower and near roads

(ROAD_DI) and recreation areas (RECRE_DI), with lower quantity of pasture FUEL_02 and higher FFMC.

Best classifications for the second seasonal period (Summer, CL_SU) were located again around 60-61%, similar to the first period. T_MAX was included only in few models, but in those cases, the sign of T_MAX was positive. MFD (Table 3) were associated to lower elevation areas with higher proportion of public and communal forests (FOREST_PB and FOREST_VC), near roads, and higher drought indices (DMC and DC).

Table 3. Accuracy and sensitivity analysis of the Summer cascade-correlation binary classification model (CL_SU). Network structure: 7-4-2

	Accuracy	Relative Entropy		FOREST_PB	FOREST_VC	ROAD_DI	DEM_MN	DMC	DC
SFD	0.595	0.663	Av. SFD	-0.056	-0.118	0.672	0.220	-0.226	-0.182
MFD	0.607	0.662	Av. MFD	0.056	0.118	-0.672	-0.220	0.226	0.182
Train	0.601	0.663							
SFD	0.609	0.659	Av. Sq.	0.004	0.097	0.575	0.425	0.067	0.227
MFD	0.614	0.669	Variance	0.001	0.083	0.124	0.377	0.016	0.194
Test	0.611	0.664							
SFD	0.599	0.662							
MFD	0.609	0.664							
Validation	0.604	0.663							

SFD, Single-Fire-Days; MFD, Multiple-Fire-Days; Av. SFD, Average SFD value per variable; Av. MFD, Average MFD value per variable; Av. sq. Average square of each variable

Numerical models

No model could be accepted to adequately discriminate the exact number of human-caused forest fires per day and quadrate for the annual data, so we focused our efforts on the seasonal models.

Table 4. Accuracy and sensitivity analysis of the Spring cascade-correlation predictive model (PR_SP). Network structure: 11-14-1

PREDICT	R	Av. Abs.	Max. Abs.	RMS	Accuracy (20%)	Conf. Interval (95%)
Train	0.609	0.927	2.950	1.109	0.471	2.161
Test	0.597	0.958	2.957	1.162	0.462	2.273
Validation	0.606	0.936	2.957	1.125	0.468	2.191

	FOREST_PB	FOREST_PV	DENS_POB	FUEL_06	SLOPE_MN	SLOPE_SD	PROB	DMC
Average	-0.273	0.324	-0.988	1.531	0.187	-0.198	0.276	0.720
Average Square	0.123	0.232	3.857	43.264	1.332	0.142	0.151	0.844
Variance	0.049	0.127	2.884	40.969	1.299	0.103	0.075	0.326

SFD, Single-Fire-Days; MFD, Multiple-Fire-Days; Av. Abs., Average Absolute Error; Max. Abs., Maximum Absolute Error

Predictions of fire occurrences (1 to 5 values) in the Spring seasonal period (PR_SP) reached 61% accuracy (Table 4). The structure of the net was relatively complex (high number of variables in the hidden layer, structure 11-14-1). The average error was approximately 1 fire, with an absolute error of 3. In this case, higher HCFF occurred in quadrates with higher percentage of private forest (FOREST_PV), but lower public forest (FOREST_PB), lower population density, higher shrub fuel (FUEL_06) percentage located in high slopes, and higher PROB and DMC (drought indices).

Results in the Summer period (PR_SU) were somewhat worse (44-50% in the best model, Table 5). Drought indices (DC, DMC, etc.) were the most often selected variables. In the best model, the quantity of input variables was high, but the net had only 3 nodes in the hidden layer (24-3-1). A large quantity of anthropogenic-related variables was included in this net model, locating fires mainly near roads and recreational areas, but far from towns and reservoirs. This model indicated that HCFF were more numerous in locations near roads and recreational areas, higher proportion of public and protected forests, lesser percentage of private and communal forests, lesser altitude and slope variation, and higher danger and drought indices.

Table 5. Accuracy and confusion matrix of the Summer cascade-correlation predictive model (PR_SU). Network structure: 24-3-1

PREDICT	R	Av. Abs.	Max. Abs.	RMS	Accuracy (20%)	Conf. Interval (95%)	Records
Train	0.437	1.102	3.214	1.288	0.358	2.510	738
Test	0.499	0.986	2.910	1.187	0.423	2.317	317
Validation	0.456	1.067	3.214	1.259	0.377	2.450	1055

Av. Abs., Average Absolute Error; Max. Abs., Maximum Absolute Error

Discussion

Multiple fire days in quadrates in Galicia could be correctly separated from the more usual occurrence of single fire days in seasonal time spans using Cascade-Correlation models. Variables and trends were similar in most of the models evaluated, which suggested robustness in the model building processes and relevance of these variables in the final solution. Binary classification seasonal models (X = 1 or more than 1 human-caused forest fire per day and quadrate) have higher accuracy than predictive models (X = 1, 2, 3, 4 or more than 4 HCFF per day and quadrate) especially for the Spring "season". This better accuracy suggests that Spring fires caused by humans are probably more homogeneous and related to a smaller number of causes mainly linked to vegetation management, like agricultural residues burning or shrubs removal (Chas-Amil *et al.* 2010a). On the contrary, the lower accuracy and the higher number of variables of the Summer models seem to reveal that human-caused forest fires in summer are more heterogeneous in cause (i.e. agricultural burning, shrubs removal, arsonists, negligence, machinery), making especially difficult trying to predict the number of fires per quadrate and day (Morillo 2013, personal communication).

Our models show that the probability of MFD was influenced by structural or geographic variables -population, forest ownership, vegetation and topography- and by temporally changing daily variables -weather variables and fire danger assessment indices- during the study period. While accuracy was similar in all the models (around 60%), some variables were different or exhibited opposite trends in them. These findings are in agreement with known causes of fires and their temporal distribution, as described previously (Chas-Amil *et al.* 2010a). Our results indicate that fire activity can vary considerably between different locations in a given day in Galicia in agree to Marey-Perez *et al.* (2010), as in other work elsewhere by i.e. Boychuck and Martell (1988) in Canada or Vasilakos *et al.* (2009) in Lesbos Island (Greece).

Regarding weather variables, the maximum temperature factor influence varied with season, but fire danger indices were positively related to higher fire incidence in all seasons. Spring and Summer MFD were more likely on windy days with lower relative humidity, which may be translated as days with higher danger indices (FFMC, DMC, DC or PROB) in agreement with Garcia Diez *et al.* (1994, 1996, 1999) and Vasilakos *et al.* (2009). The Galician weather is humid and rainy most of the year except in Summer, but there are inland areas where a geographic gradation towards the Mediterranean climate creates drier weather conditions (and higher danger indices) than in the Atlantic region. In Galicia, danger indices may be high when dry weather conditions prevail, such as in summertime with the

higher maximum temperatures and fuel moisture deficit, but also with low daily relative humidity and atmospheric stability in winter (colder days) (Garcia Diez *et al.* 1999) which explains the opposite seasonal temperature pattern found in different models. Spells of low relative humidity (RH) in late winter – early spring produce vegetation water stress during these periods and facilitates fuel ignition, which is why shrublands burning takes place mainly in late winter - early spring, but it is also carried out during the summer, when is masked by other agricultural burning activities and other arson or negligence fires (Chas-Amil *et al.* 2010b, Morillo 2013, personal communication).

The selection of the structural/geographic variables is consistent with the descriptions of the fire problem in Galicia by Chas-Amil *et al.* (2010a, 2010b) and also helps to understand this pronounced seasonality. Altitude is the main distinctive geographic factor. Spring MDFs are more usual in higher altitudes (generally inland); meanwhile Summer MDFs mainly occur in lower altitudes (generally coastal).

According to the Spanish forest fire database, about 75 % of human-caused forest fires in Galicia are related to the rural use of fire for vegetation management (Torre-Antón 2010). Fire use is common in Southern rural areas inland, with higher altitudes and slopes, where most wildfires take place (Chas-Amil *et al.* 2010a, 2010b). Rural population concentrates in valley areas with high livestock productivity, mainly cattle, which feed on grasses. Livestock management requires grasses and the cheapest and traditional way to eliminate shrubs, mainly gorse and heather (Díaz-Vizcaino 2005), is the use of fire (Kaal *et al.* 2011). The second most common fire cause in Galicia is agricultural residues burning. Agriculture is also an important economic activity in Galician rural areas and stubble burning is quite common (MAGRAMA 2013).

Lower altitudes are located in Western and Northern Galicia (Fig 1., at the boundary with the Atlantic Ocean). According to Chas-Amil *et al.* (2010b), in Western Galicia, human-caused forest fires have more diverse motivations. The Southwest is dominated by arsonists; meanwhile the Northwest is dominated by unspecified motivations as revenge, timber prices, land use changes or resentments. Other near township's fires are related to agricultural and livestock activities. As in Vasilakos *et al.* (2009), our models related summer MDFs to lower altitudes in which human settlements (towns, recreational areas, etc.) are more usually placed and recreation and agriculture are the most important economic activities (Chas-Amil 2007). These activities are related to forest fires especially in the boundary of human activities-forest interfaces (Martinez *et al.* 2010). In these Galician regions forest are not valued by the population (Marey-Pérez *et al.* 2010, Torre-Antón 2010), which increases the risk of fires. Public forests and Communal forests were selected in our best Summer binary and predictive models, also in agreement to the conclusions of Marey-Perez *et al.* (2010).

Useful as these explanatory models may be, we are driven to consider that complex spatiotemporal patterns exist. In order to better to explore these relationships between human risk factors, biophysical variables and multiple fires caused by people on a daily basis, with a view to aid fire management to anticipate and locate potential fire suppression overload events, causality will have to be specifically incorporated in future models. However, cause records are currently incomplete, as full investigations are precluded by the high daily fire loads.

Acknowledgements

he authors gratefully acknowledge the fire occurrence historical data from the National Forest Fire Statistics database (EGIF), Ministry of Environment and Rural and Marine Affairs (MAGRAMA) and weather data from the Department of Geography of the University of Alcalá and Meteológica SA (Madrid, Spain). Arsenio Morillo (Xunta de Galicia) provided helpful advice and on-site expertise.

References

Alcázar J, Palau A, Vega-García C (2008) A neural net model for environmental flow estimation at the Ebro River Basin, Spain. *Journal of Hydrology* **349**, 44-55.

Alonso-Betanzos A, Fontenla-Romero O, Guijarro-Berdiñas B, Hernández-Pereira E, Paz Andrade MI, Andrade P, Jiménez E, Legido Soto JL, Carballas T (2003). An intelligent system for forest fire risk prediction and fire fighting management in Galicia. *Expert Systems with Applications* **25**, 545-554.

Andrews PL, Bradshaw LS (1997) The FIRES computer program. General Technical Report - US Department of Agriculture, Forest Service, Issue INT-GTR-365

Boychuk D, Martell DL (1988) A Markov Chain Model for Evaluating Seasonal Forest Fire Fighter Requirements. *Forest Science* **34**, 647-661.

Bridle JS (1990) Alpha-nets: A recurrent 'neural' network architecture with a hidden Markov model interpretation. *Speech Communication* **9**, 83-92.

Camia A, Bovio G, Gottero F (1998) Algorithms to compute the Meteorological Danger Indices included in MFDIP. Megafires Project, Final Report.

Carvalho A, Flannigan MD, Logan KA, Gowman LM, Miranda AI, Borrego C (2010) The impact of spatial resolution on area burned and fire occurrence projections in Portugal under climate change. *Climatic Change* **98**, 177-197.

Chas-Amil ML (2007) Forest fires in Galicia (Spain): Threats and challenges for the future. *Journal of Forest Economics* **13**, 1-5.

Chas-Amil ML, Touza J, Prestemon JP (2010a) Spatial distribution of human-caused forest fires in Galicia (NW Spain). *Ecology and the Environment* **137**, 247-258.

Chas-Amil ML, Touza J, Prestemon JP, McClean Colin J (2010b) Sociorvonomic analysis of forest fires causes and motivations: A case study of Galicia. VI International Conference on Forest Fire Research. In: Viegas DX (Ed), Coimbra, Portugal.

Chuvieco E, González I, Verdú F, Aguado I, Yebra M (2009) Prediction of fire occurrence from live fuel moisture content measurements in a Mediterranean ecosystem. *International Journal of Wildland Fire* **18**, 430-441.

Crosby JS (1954) Probability of fire occurrence can be predicted. *USDA, Forest Service, Central States Forest Experiment Station, Technical Paper* **143**, 14-14.

De Haan JD (2006) Kirk's Fire Investigation. Prentice Hall, ISBN 9780131719224

Donovan GH, Rideout DB (2003) A reformulation of the cost plus net value change (C+NV) model of wildfire economics. *Forest Science* **49**, 318-323.

Falham SE, Lebiere C (1990) The Cascade-Correlation Learning Architecture. Advances in Neural Information Processing Systems 2. Morgan Kaufmann, San Francisco, CA, USA. 13 pp

Garcia Diez EL, Rivas Soriano L, de Pablo F, Garcia Diez A (1994) An objective model for the daily outbreak of forest fires based on meteorological considerations. *Journal of Applied Meteorology* **33**, 519-526.

Garcia Diez EL, Rivas Soriano L, Garcia Diez A (1996) Medium-range forecasting for the number of daily forest fires. *Journal of Applied Meteorology* **35**, 725-732.

Garcia Diez EL, Rivas Soriano L, de Pablo F, Garcia Diez A (1999) Prediction of the daily number of forest fires. *International Journal of Wildland Fire* **9**, 207-211.

Haight RG, Fried JS (2007) Deploying Wildland Fire Suppression Resources with a Scenario Based Standard Response Model. *INFOR* **45**, 31-39.

Hassenauer H, Merkl D, Weingartner M (2001) Estimating tree mortality of Norway spruce stands with neural networks. *Advances in Environmental Research* **5**, 405-414.

Hilbert DW, Ostendorf B (2001). The utility of artificial neural networks for modelling the distribution of vegetation in past, present and future climates. *Ecological Modelling* **146**, 311–327.

IAFC, NFPA (Eds) (2010) Fire Officer: Principles and Practice. Jones and Bartlett Publishers, Sudbury, MA, USA

Islam KMS, Martell DL (1998) Performance of initial attack airtanker systems with interacting bases and variable initial attack ranges. *Canadian Journal of Forest Research* **28**, 1448-1455.

Jutras P, Prasher SO, Mehuys GR (2009) Prediction of street tree morphological parameters using artificial neural networks, Computers and Electronics in Agriculture 67, 9-17.

Kaal J, Carrión Marco Y, Asouti E, Martín Seijo M, Martínez Cortijas A, Costas-Casáis M, Criado Boado F (2011) Long-term deforestation in NW Spain: linking the Holocene fire history to vegetation chance and human activities. *Quaternary Science Reviews* **30**, 161-175.

Kirsch AG, Rideout DB (2005) Optimizing initial attack effectiveness by using performance measures. System Analysis in Forest Resources: Proceedings of the 2003 Symposium In: (Eds M Bevers, TM Barrett). pp. 183-187 (Portland, OR)

Kuplich TM (2006) Classifying regenerating forest stages in Amazonia using remotely sensed images and a neural network. *Forest Ecology and Management* **234**, 1-9.

Liang J, Calkin DE, Gebert KM, Venn TJ, Silverstein RP (2008) Factors influencing large wildland fire suppression expenditures. *International Journal of Wildland Fire* **17**, 650-659.

Lozano FJ, Suárez-Seoane S, de Luis E (2007) Assessment of several spectral indices derived from multi-temporal Landsat data for fire occurrence probability modelling. *Remote Sensing of Environment* **107**, 533-544

Marey-Pérez MF, Gómez-Vázquez I, Díaz-Varela E (2010) Different approaches to the social vision of communal land Management: the case of Galicia. *Spanish Journal of Forest Research* **8**, 848-863.

Martell DL, Otukol S, Stocks BJ (1987) A logistic model for predicting daily people-caused forest fire occurrence in Ontario. *Canadian Journal of Forest Research* **17**, 394-401.

Martínez J, Vega-Garcia C, Chuvieco E (2009) Human-caused wildfire risk rating for prevention planning in Spain. *Journal of Environmental Management* **90**, 1241-1252.

MAGRAMA (2013) Forest Fires in Spain 2012, Area of Defense Against Forest Fires. Madrid.

Morillo A (2013) Coordinator of Prevention and Forest Valoration Area of Consellería do Medio Rurale do Mar, Xunta de Galicia, Spain.

NeuralWare (2009) NeuralWorks Predict®. The complete solution for neural data modeling. NeuralWare, Pittsburg, PA, USA

Omi PH (2005) Forest fires: a reference handbook. Contemporary world issues. Santa Barbara, California, USA

Padilla M, Vega-Garcia C (2011) On the comparative importance of fire danger rating indices and their integration with spatial and temporal variables for predicting daily human-caused fire occurrences in Spain. *International Journal of Wildland Fire* **20**, 46-58.

Rachaniotis NP, Pappis CP (2006) Scheduling fire-fighting tasks using the concept of "deteriorating jobs". *Canadian Journal of Forest Research* **36**, 652-658.

Rorig ML, McKay SJ, Ferguson SA, Werth P (2007) Model-Generated Predictions of Dry Thunderstorm Potential. *Journal of Applied Meteorology and Climatology* **46**, 605-614.

Rothermel RC (1972) A mathematical model for predicting fire spread in wildland fuels, Res. Pap. INT-115. Ogden, UT: U.S. Department of Agriculture, Intermountain Forest and Range Experiment Station

Rumelhart DE, Hinton HE, Williams RJ (1986) Learning integral representations by error propagation. In: Parallel distributed processing: explorations in the microstructure of cognition. Foundations (Eds DE Rumelhart, JL McClelland). MIT Press Vol. 1. pp. 318-362.

Scrinzi G, Marzullo L, Galvagni D (2007) Development of a neural network model to update forest distribution data for managed alpine stands. *Ecological Modelling* **206**, 331-346.

Simard AJ, Young A (1978) AIRPRO - an air tanker productivity computer simulation model - application. Ontario Information Report FF-X-69. (Forest Fire Research Institute, Canadian Forest Service: Ottawa)

Tanskanen H, Venäläinen A (2008) The relationship between fire activity and fire weather indices at different stages of the growing season in Finland. *Boreal Environment Research* **13**, 285-302.

Torre-Antón M (2010) La situación actual de los incendios forestales en España. Conferencias y Ponencias del 5º Congreso Forestal Español, *Cuadernos de la Sociedad Española de Ciencias Forestales* **31**, 179-195.

Vasconcelos MJP, Silva S, Tome M., Alvim M, Pereira JMC (2001) Spatial prediction of fire ignition probabilities: Comparing logistic regression and neural networks. *Photogrammetric Engineering and Remote Sensing* **67**, 73-81.

Vasilakos C, Kalabokidis K, Hatzopoulos J, Matsinnos I (2009) Identifying wildland fire ignition factors through sensitivity analysis of a neural network. *Natural Hazards* **50**, 125-143.

Vega-Garcia C, Chuvieco E (2006) Applying local measures of spatial heterogeneity to Landsat-TM images for predicting wildfire occurrence in Mediterranean landscapes. *Landscape Ecology* **21**, 595-605.

Vega-Garcia C, Lee BS, Woodard PM, Titus SJ (1996) Applying neural network technology to human-caused wildfire occurrence prediction. AI Applications **10**, 9–18.

Vilar L, Woolford DG, Martell DL, Martín MP (2010) A model for predicting human-caused wildfire occurrence in the region of Madrid, Spain. *International Journal of Wildland Fire* **19**, 1-13.

Vilar del Hoyo L, Martín MP, Martínez-Vega FJ (2011) Logistic regression models for human-caused wildfire risk estimation: Analysing the effect of the spatial accuracy in fire occurrence data. *European Journal of Forest Research* **130**, 983-996.

Werbos, PJ (1994) The roots of backpropagation: from ordered derivatives to neural networks and political forecasting, John Wiley & Sons, Inc, New York, USA, 319 pp.

Xunta de Galicia (2014) Plan prevención e defensa contra os incendios forestais de Galicia (PLADIGA) Memoria 2014. Consellería do medio rural, Dirección Xeral de Montes.

Common analysis of the costs and effectiveness of extinguishing materials and aerial firefighting

Agoston Restas

National University of Public Service, Budapest, Hungary, Restas.Agoston@uni-nke.hu

Abstract
Introduction: Aerial firefighting is known to be a very costly firefighting technique, which encourages professionals to investigate its effectiveness and to be aware of the influential factors as well as to strive to find a way to reduce costs and increase efficiency prior to making a decision. Method: examination is basically based on mathematical calculations, comparative analyses and proportioning. Simple charts, matrixes and graphs help to evaluate the findings and to explain and illustrate the relationship between them. Among the research methods, logical deductions and the application of practical experience can be found. Results: the research introduces a new method of examining the effectiveness of aerial firefighting, which helps to conduct analyses and comparisons based on real data. This method contributes to a better understanding of key factors affecting effectiveness, gives guidance on the possible ways to increase effectiveness, their potentials and limitations.

Keywords*: aerial firefighting, professional effectiveness, economic efficiency, absolute index, standard index, comparative index, vertical and horizontal divisions, matrix analysis*

Introduction

Although aerial firefighting is known to be a very costly firefighting technique, we must admit that in several cases it is the only possibility to extinguish large-scale forest fires. The high expenses of firefighting must urge professionals to investigate effectiveness of aerial firefighting and to be aware of the influential factors as well as to strive to find a way to reduce costs and increase efficiency prior to making a decision.
The success and effectiveness of aerial firefighting is influenced by many factors. It would be a complex and complicated task, if not impossible, to evaluate all of them. Despite this, the author picked a few basic factors which have considerable impact on the economic efficiency of aerial firefighting. One of them is the extinguisher itself together with its extinguisher ability. It certainly varies from extinguisher to extinguisher. The promotion materials of different companies selling extinguishers clearly demonstrate these differences, by highlighting the unique, beneficial feature of the given extinguisher.
The other basic factor is the cost of the transportation of the extinguishers to the scene or with other words, its efficiency. If we accept that there are differences in the extinguisher ability, we must conclude that the more effective extinguishers are worth being used despite the higher transportation costs. The extent of the efficiency of the latter factor is influenced by not only the transportation costs but the costs of the extinguisher itself. The author studies the correlation between the above factors.

2. The effectiveness of the extinguishers and related expenses

We know several methods of examining the effectiveness of extinguishers. Some of them are generally accepted and standardised in certain countries, e.g. LIFT[1], TM2[2] methods, while others are merely

[1] LIFT – Lateral Ignition and Flame Spread
[2] TM2 – Test Method 2 Combustion Retarding Effectiveness Test

used for the purposes of researches (Batista, 2011; Fiorucci, 2011a; Fiorucci, 2011b; Morris, 2011). The effectiveness of the extinguisher is shown by the way it puts out a fire, that is, how it is able to reduce the speed of fire spread (v_0) or even stop it (v_x; $v_x<v_0$, or $v_x=0$). Obviously, the latter is the final solution, but with most methods, their ability to reduce the speed of spread is considered a sign of their effectiveness (e.g. LIFT). The author accepts the previous method to analyse this topic, that is, an extinguisher is considered effective not only if it extinguishes the fire completely but also if it reduces the speed of fire spread. In the end, the steady reductions of the speed results in stopping the fire spread or, in other words, complete extinguishment. As a result, the effectiveness of extinguishers reducing the speed of fire spread to varying extents is different, too. Obviously, the more it reduces the speed of fire spread, the more effective it is.

The varying abilities to extinguish a fire must be accompanied by further differences, so the expenses are most likely to be dissimilar. Provided that we accept the previous statement, that is, not only the total extinguishment of the fire is effective, but also the reduction of the speed of fire spread, then professional effectiveness depends on the extent of speed reduction. Professional effectiveness considers significant only the goal, which is in this case the higher extent the extinguisher reduces the speed of fire spread. The resources used and the expenses are, however, ignored (Restas, 2011). Extinguishers reducing the speed of fire spread by the same extent are assessed as having the same professional effectiveness, irrespective of the expenses they incur.

Nevertheless, efficiency in terms of economics is about much more than the above; in addition to the speed of spread, the costs entailed also need to be taken into account. If we bear the costs in mind as well, the extinguisher of the same effectiveness but with lower prices is clearly more efficient economically.

The most general extinguisher is water. Its cost is so insignificant compared to other extinguishers that it is often overlooked. Water is not only used by itself but to produce other extinguishers like retardants or foams. If we disregard the cost of water, the cost per unit of extinguishers depends on two factors: mixing rate of the agent (R_{foam}) and the price of one unit of the agent (p_{foam}).

$$c_{foam} = R_{foam} p_{foam} \qquad (1)$$

In the case of advanced foams, the prescribed mixing rate is 0.5-3%, which means that 5-30 litres of concentrate is needed to make 1 m^3 solution. This solution produces 6-12 m^3 foam, which stops or reduces fire spread by covering the vegetation. The extinguisher ability of foams is naturally a combination of several factors, e.g. separation, isolation, cooling effects.

Identical extinguisher abilities may be characterised by expanditure rate as well, in the case of foams; in the example above this value is 6-12 ($R_{exp\ foam} = 6 \div 12$). Certainly, other features are also important, but expanditure rate is generally regarded as a feature indicating the initial extinguishing ability of the foams. Foam of low expanditure (high foam density) will stream down to the ground – like Newtonian fluid – instead of staying on the vegetation, thus it will not take part in effective extinguishment. Conversely, foam of high expenditure (low foam density) can be blown away by airflows.

If both the cost per unit and the extent to which it is able to reduce the speed of fire spread are dissimilar, then – assuming linear change – the ratio between them and its scale determine which extinguisher is more efficient economically. In this study, the author presumes that the effect resulting from the changing prices of the extinguishers and the related effect on the speed of fire spread (affecting effectiveness) is a linear variable.

The analysis of the extinguishers' effectiveness

Evidently, we need to take into account the different types of extinguishers and we had better start with the simplest one. The most general extinguisher is water, it is often used by itself, but it can also

be mixed with retardants or foam-forming substances. The additives, obviously, are aimed at increasing the effectiveness of extinguishing with water, so they are more effective. As a result, it is logical to start with water and use it as a reference point. This is the simplest solution, which often succeeds in reducing the speed of fire spread ($v_w<v_0$) by itself. In terms of professional effectiveness, it represents one of the extreme values (the starting value) in the above range.

If we use retardants or foam-forming substances, we have to compare their ability to reduce the speed of fire spread to that of the water and to each other's (e.g. v_A, v_B). When comparing them to water – whether we look at the retardant or the foam –, professional effectiveness must be higher, since in the opposite case it would not make sense to waste resources on them.

The goal of extinguishers is to put out the fire or to reduce the speed of its spread. The extent of the reduction ($v_0 \rightarrow v_x$) is obviously correlated to the initial speed of fire spread (v_0). When comparing the different values of professional effectiveness, it reasonable to use the most simple extinguisher's, the water's effect as a starting point, that is, to what extent it is able to reduce the speed of fire spread; then compared to this value, the effects of the other extinguishers can be ranked. The author examined two different extinguishers (foam) in the experiment without naming them so that it does not harm the producers' interests (foam "A" and foam "B").

Different extinguishers are very likely to reduce the speed of fire spread by different extents. The difference between the speeds of fire spread measured at places treated (v_x) and not treated (v_0) with extinguishers can be determined simply by deducting one from the other, so the results can be ranked.

$$v_W = v_0 - v_1 \quad (2)$$

$$v_A = v_0 - v_2 \quad (3)$$

$$v_B = v_0 - v_3 \quad (4)$$

$$v_0 > v_1 > v_2 > v_3 \quad (5)$$

Based on the above the following are regarded as base values (with sample values):

- The speed of fire spread: v_0 (=10 mmin^{-1})
- The speed of fire spread when using water: v_1 (= 6 mmin^{-1})
- The speed of fire spread when using foam "A": v_2 (= 5 mmin^{-1})
- The speed of fire spread when using foam "B": v_3 (= 4 mmin^{-1})

Based on the values in the previous example we can calculate the effects of reducing speed:

- The effect of water to reduce speed: v_W =4 mmin^{-1}
- The effect of foam "A" to reduce speed: v_A =5 mmin^{-1}
- The effect of foam "B" to reduce speed : v_B =6 mmin^{-1}

Ranking the above figures:

$$v_W < v_A < v_B \quad (6)$$

In addition to the speed of fire spread, we can certainly examine other parameters, too. Presumably, we can put out the fire completely using the extinguishers, but the length (e.g. l_x) of the segment extinguished varies from one extinguisher to the next. Basically, this method can be applied in this case as well, the results do not change.

$$l_W < l_A < l_B \quad (7)$$

We can conclude from the above that they do help to determine the ranking of professional effectiveness, but actually they cannot provide guidance in comparing neither their relative effectiveness nor their economic efficiency.

Indexes describing the extinguishers' effectiveness

In order to determine effectiveness more precisely, we can make calculations using different factors, whose results can be used as indexes.

4.1. Absolute index

We get absolute index (Y_x) if we correlate the extinguishers' effect to reduce the speed of fire spread to the initial speed of the fire.

$$Y_W = \frac{v_0 - v_W}{v_0} = 1 - \frac{v_W}{v_0} \quad (8)$$

Based on the above the absolute indexes of the three extinguishers (water, foam "A", foam "B") are the following:

$$Y_W = 1 - \frac{v_W}{v_0} \quad (9) \qquad Y_A = 1 - \frac{v_A}{v_0} \quad (10) \qquad Y_B = 1 - \frac{v_B}{v_0} \quad (11)$$

The absolute indexes provide guidance on the extent by which the different extinguishers are able to reduce the speed of fire spread. Its value may be 1 or lower than 1; in the first case, the extinguisher not only slowed down fire spread but extinguished it completely. The closer the result is to 1, the slower the fire spread became, and in other words, the more effective the given extinguisher is. As a matter of logic, the other extreme value is possible as well. Thus, when $Y_x=0$, the extinguisher failed to reduce the speed of fire spread.

Table 1—Absolute indexes of extinguishers (with example values)

	Y_W	Y_A	Y_B
Water	$1 - \frac{v_W}{v_0}$ (0.4)		
Foam A		$1 - \frac{v_A}{v_0}$ (0.5)	
Foam B			$1 - \frac{v_B}{v_0}$ (0.6)

4.2. Standard index

The professional effectiveness of extinguishers can be expressed in other ways, too. The reduction of the speed of fire spread can be correlated not only to the initial speed of fire spread but also to the effect of the reference extinguisher. The author calls it standard index (Z_x). By correlating them to water, the simplest extinguisher, it becomes apparent how the professional effectiveness of the other extinguishers vary – affected by the additional costs, the expenditure. In terms of professional effectiveness, it is a more accurate guidance, as it does not compare the extinguisher directly to the fire but to the reference point, to water (having the lowest cost).

$$Z_A = \frac{Y_A}{Y_W} \text{ (12), and} \qquad Z_B = \frac{Y_B}{Y_W} \text{ (13)}$$

Table 2—Standard indexes of extinguishers (with example values)

	Z_A	Z_B
Foam A	$\frac{Y_A}{Y_W}$ (1.25)	
Foam B		$\frac{Y_B}{Y_W}$ (1.5)

Obviously, values higher than 1 are acceptable in the above case. If the value is 1, it shows that using additives in water does not result in increased effectiveness, so the resources spent on them were wasted. The higher the value is or the farther it is from 1, the more effective the extinguisher is.

4.3. Comparative index

Following the idea above, we can get the relative difference between the effectiveness of the two different extinguishers by using relation. This is the comparative index (G), the ratio of the standard indexes of the two different extinguishers to be compared.

$$G = \frac{Z_B}{Z_A} \text{ (14)}$$

The result shows the relation between the professional effectiveness of the two extinguishers. The farther its value is from 1, the bigger the difference is between the effectiveness of the two extinguishers. If the value is 1, there is no difference the professional effectiveness of the two extinguishers.

It does not affect our calculations which data (feature) we use as divisor or dividend. Naturally, we get a higher quotient by dividing the higher value, so that extinguisher is more effective professionally. On the basis of the values of the example, foam "B" performed better in the test (G=1.5/1.25=1,2), its effectiveness is 1.2 times higher or 20% higher than that of foam "A".

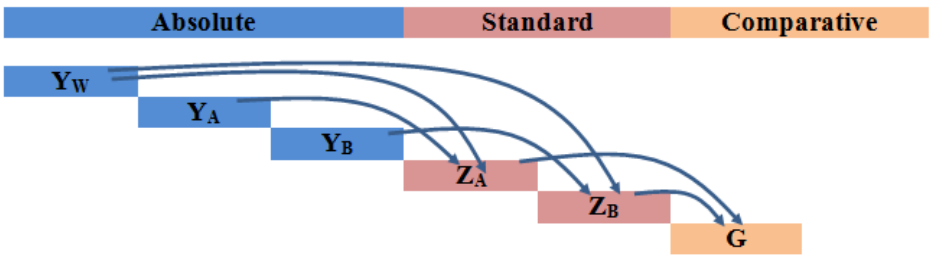

Figure 1. Logic of the indexes of the professional effectiveness of the extinguishers

Based on the above, we determined the professional effectiveness of particular extinguishers, but we do not know how much a unit of them costs. We need to answer it later on. The relationship between the indexes of the professional effectiveness of the extinguishers is depicted in Figure 1.

Effectiveness of the logistic – costs of aerial firefighting

After the examination of the professional effectiveness of the extinguishers, the following questions arise: How is the given extinguisher transported to the frontline? How much does it cost? Its logistics is conducted by air transportation (aerial firefighting), which is known to be very costly. The cost analysis of this logistics task raises the issue of economic efficiency, which, by itself, still shows only professional effectiveness, as we will see.
The cost of aerial firefighting consists of several parts: the operation of the aircraft as well as the price of the extinguisher used. According to the author, it is a common mistake that the two are often dealt with separately, which might lead to false conclusions. It will be demonstrated later on. When assessing the economic efficiency of the extinguishment, it is imperative to treat both of them together. Provided the costs of the aircraft are constant and we calculate with a definite amount, then the efficiency of aerial firefighting depends on the price of the extinguisher and its extinguishing effectiveness.
The operation cost per unit (c_{aff}) is decisive in the cost per unit of the aircraft (c_{AFF}), that is, the efficiency. Besides this, we also have to take into account the transport capacity of the aircraft (Q_{aff}) and in a given unit of time how many turns or deliveries it can carry out (n_{aff}), that is, what is the cost of transporting a unit of extinguisher to the fire front.
Following the above idea, we need the following information to calculate effectiveness (with sample:

- The cost of the aircraft in an hour: (=1000 €h^{-1})
- The transport capacity of the aircraft: (=1000 kg)
- The number of turns (deliveries): (= 10 h^{-1})

The transport cost of one unit of extinguisher can be calculated in the following way using the data above:

$$c_{AFF} = \frac{c_{aff}}{Q_{aff} n_{aff}} = (0.1 €kg^{-1}) \quad (15)$$

Similarly to the principles applied in the assessment of the professional effectiveness of the extinguishers, the transportation costs (aerial firefighting) need to be ranked as well. Water is applied in many cases, but its cost is rarely taken into account or not at all (e.g. from lakes, the sea), so in fact, only the costs of the aircraft are looked at, they dominate. The above suggests that this case ought to be viewed as the starting point or reference point. Regarding the costs, it represents one of the extreme values of the above range.
If we use retardants or various foam-forming substances, beside their effect of reducing the speed of fire spread, we also have to consider their related costs. In this case, the operation cost of the aircraft (15) and the cost of the extinguisher (1) together make up the total cost.
In the simplest case, we need to consider only the costs related to water. Based on the above, its reason is that the cost of water as an extinguisher is not regarded at all or only as a minimal amount ($C_w \approx 0$). Thus, we only have to calculate with the operation cost of the aircraft. In order to make the comparison simpler, it is reasonable to discuss the cost of one unit of the extinguisher (c_{AFF}).
It follows from the above that in the case of two aircrafts with identical operation costs – and other conditions also being identical, – that one is more efficient which is able to deliver more extinguisher to the scene within a given time. If the amounts are the same, the aircraft with lower cost can be viewed

as more efficient. To determine the latter, the costs of the given extinguisher have to be specified; the data required to do so:

- The required mixing rate of foam "A": 3 %
- The price of foam-forming substance "A": 6 €kg^{-1}
- The required mixing rate of foam "B": 3 %
- The price of foam-forming substance "B": 12 €kg^{-1}

Calculating the costs of the two extinguishers with the help of the form (1):

$c_A = R_A p_A = 0.018\,€\text{kg}^{-1}$ (16), and $c_B = R_B p_B = 0.036\,€\text{kg}^{-1}$ (17)

Indexes describing the aerial firefighting's effectiveness

Similarly to the indexes of the professional effectiveness of the extinguisher, those of the aerial firefighting can be specified, too. In the following section, these calculations will be presented, illustrated with examples.

6.1. Absolute index

Based on the above water can be regarded as the reference point. Now mostly, the operation costs of the aircrafts are taken into account, while with the other extinguishers we need to add the costs of the extinguishers as well. This is the absolute index (C_x):

$$C_W = \frac{c_{AFF}}{c_{AFF} + c_W} \cong 1 \quad (18)$$

Based on the above, the formulas to determine the costs of the extinguishers can be constructed:

$$C_W = \frac{c_{AFF}}{c_{AFF} + c_W} \quad (19) \qquad C_A = \frac{c_{AFF}}{c_{AFF} + c_A} \quad (20) \qquad C_B = \frac{c_{AFF}}{c_{AFF} + c_B} \quad (21)$$

The cost of the water is not ignored. The author determined its value arbitrarily to be 5% of the operation cost of the aircraft.

Table 3—Absolute indexes of aerial firefighting (with example values)

	C_W	**C_A**	**C_B**
Water	$\frac{c_{AFF}}{c_{AFF} + c_W}$ (0.95)		
Foam A		$\frac{c_{AFF}}{c_{AFF} + c_A}$ (0.33)	
Foam B			$\frac{c_{AFF}}{c_{AFF} + c_B}$ (0.43)

The absolute index correlates the total cost of the extinguisher used to the cost per unit of the aircraft. Then, according to the values we get, the logistics methods can be simply ranked, which is about professional effectiveness strictly in terms of the expenses. Without the effectiveness of the extinguisher, this is not a relevant economic analysis either.

Its value can be 1 or less than 1; in the former case we do not look at the cost of the extinguisher (water), while in the latter one we do. The closer the value is to 1, the lower the cost of the extinguisher itself relative to the cost per unit of the aircraft.

6.2. **Standard index**

Similarly to the professional effectiveness of the extinguishers, the standard indexes of the logistic (U_x) can be created, too. In this case we correlate the cost per unit of the different extinguishers to that of the water. Then we get the quotient of the cost of the extinguisher and that of the water, as a reference cost.

$$U_A = \frac{R_A p_A Q_{aff} n_{aff}}{c_{aff}} = \frac{C_A}{C_W} \quad (22)$$

The formula for the two extinguishers:

$$U_A = \frac{C_A}{C_W} \quad (23), \text{ and} \quad U_B = \frac{C_B}{C_W} \quad (24)$$

The above offer us a more accurate guidance in the effectiveness of logistic, because they do not correlate directly to the cost per unit of the aircraft, but to the cost related to a reference point, that is, the water. It is also correct if the cost of the water is minimal, then the index value of its effectiveness will obviously be higher. If we ignore the cost of water and its index value is 1, the absolute and standard index values of the other extinguishers will be identical.

Table 4—Standard indexes of aerial firefighting (with example values)

	U_A	**U_B**
Foam A	$\frac{C_A}{C_W}$ (0.35)	
Foam B		$\frac{C_B}{C_W}$ (0.45)

6.3. **Comparative index**

Following the above idea, the relative difference between the effectiveness of the delivery of the two extinguishers can be calculated with relation. This is the comparative index (W), which is the quotient of the standard index values of the two different extinguishers.

$$W = \frac{U_B}{U_A} \quad (25)$$

The result shows the difference between the effectiveness of the delivery of the two extinguishers. The farther its value is from 1, the bigger the difference is between the effectiveness. If the result is 1, there is no difference between the effectiveness of the delivery of the two extinguishers. It does not affect our calculations which data we use as the divisor or the dividend. Naturally, we get a higher quotient by dividing the higher value, so that extinguisher is more effective professionally.

On the basis of the values of the example, foam “B” performed better in the test (W=0.45/035=1.29), its effectiveness is 1.29 times higher or the effectiveness of aerial firefighting (delivery) is 29% higher than that of foam “A”. The relationship between the indexes of the delivery is depicted in Figure 2.

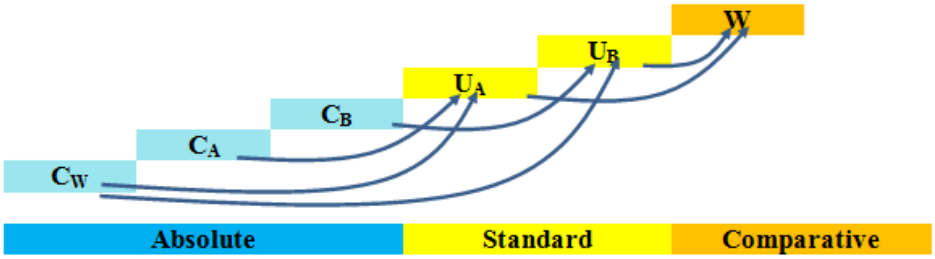

Figure 2. Logic of the indexes of the professional effectiveness of the delivery

Qualifier indexes describing the aerial firefighting's efficiency

In the previous sections the professional effectiveness of both the extinguishers and the application of aircrafts were outlined. The comprehensive evaluation of the effectiveness of the firefighting can be conducted by consulting the so-called qualifier indexes created by the author.

7.1. Absolute index

The absolute index of qualifier (M_x) is the product of multiplying the absolute indexes of the extinguishers and the delivery, which show their professional effectiveness. They can be determined in the following way:

$$M_W = C_W Y_W \quad (26) \qquad M_A = C_A Y_A \quad (27) \qquad M_B = C_B Y_B \quad (28)$$

The above details are summarized in Table 5. The table contains the values of the calculations with the data of the example as well.

Table 5—Absolute indexes of qualifying the aerial firefighting efficiency

	M_W	M_A	M_B
Water	$C_W Y_W$ (0.38)		
Foam A		$C_A Y_A$ (0.175)	
Foam B			$C_B Y_B$ (0.27)

The relationship between the indexes is shown in Figure 3, which clearly shows that we can get the qualifier indexes by combining the professional indexes of the extinguishers and their logistics needs, that is, aerial firefighting. These indexes move towards economic efficiency.

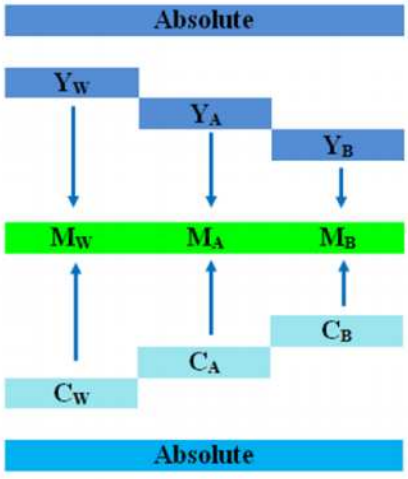

Figure 3. Logic of the absolute indexes of qualifying the efficiency of the aerial firefighting

Numerous calculations can be made with the data above, whose results are inequations that show the threshold values of efficiency. They are summarised in Tables 6-8 to aid understanding. Theoretically, the following deductions can be made from the data of Table 6 regarding water and foam "A":

- Water has an economic advantage as long as $C_W > 0.184$ or $Y_W > 0.438$ remains constant under other conditions.
- Application of foam "A" may gain an economic advantage if $C_A > 1.15$ or $Y_A > 0.76$.

The above has a theoretical approach, for example the value of C_A cannot exceed 1, since it would mean putting out the fire. It shows that the goal of the above is not specifying the extreme values, but rather finding a reasonable and beneficial way to increase the effectiveness of the extinguisher – by increasing its extinguishing ability or improving its delivery method. In practice, it is probable that the joint, though minor improvement of both factors is more feasible than a major improvement of a single factor, even if the mathematical results are the same.

Table 6— Conditions of the efficiency of the "A" foam

$C_W > \frac{C_A Y_A}{Y_W}$	$C_W > 0.184$	$C_A > 1.15$	$C_A > \frac{C_W Y_W}{Y_A}$
	$C_W = 0.4$	$C_A = 0.5$	
$C_W Y_W > C_A Y_A$	$M_W = 0.38$	$>$ $M_A = 0.175$	$C_W Y_W > C_A Y_A$
	$Y_W = 0.95$	$Y_A = 0.33$	
$Y_W > \frac{C_A Y_A}{C_W}$	$Y_W > 0.438$	$Y_A > 0.76$	$Y_A > \frac{C_W Y_W}{C_A}$

The above can be applied with the other extinguisher, too. Thus, theoretically, the following deductions can be made from the data of Table 7 regarding water and foam "B".

- Water has an economic advantage as long as $C_W > 0.284$ or $Y_W > 0.675$ remains constant under other conditions.
- Application of foam "A" may gain an economic advantage if $C_B > 0.884$, or $Y_B > 0.63$.

The statements made earlier also apply to this case. Increasing the effectiveness of the foam from two directions could be simpler or more beneficial than improving a single factor significantly.

Table 7— Conditions of the efficiency of the "B" foam

$C_W > \frac{C_B Y_B}{Y_W}$	$C_W > 0.284$	$C_B > 0.884$	$C_B > \frac{C_W Y_W}{Y_B}$
	$C_W = 0.4$	$C_B = 0.6$	
$C_W Y_W > C_B Y_B$	$M_W = 0.38$	$>$ $M_B = 0.27$	$C_W Y_W > C_B Y_B$
	$Y_W = 0.95$	$Y_B = 0.43$	

$Y_W > \frac{C_B Y_B}{C_W}$	Y_W >0.675	Y_B >0.63	$Y_B > \frac{C_W Y_W}{C_B}$

The above implies the foams could also be compared to each other instead of the water. It produces the values in Table 8. Theoretically, the following deductions can be made from the data above regarding foam "A" and foam "B".

- Foam "B" has an economic advantage as long as $C_B > 0.41$ or $Y_B > 0.29$ remains constant under other conditions.
- Application of foam "A" may gain an economic advantage if $C_A > 0.82$ or $Y_B > 0.54$.

Table 8— Conditions of the efficiency of the foam "A" and "B" to each other

$C_B > \frac{C_A Y_A}{Y_B}$	C_B >0.41	C_A >0.82	$C_A > \frac{C_B Y_B}{Y_A}$
	C_B =0.6	C_A =0.5	
$C_B Y_B > C_A Y_A$	M_B =0.27 >	M_A =0.175	$C_B Y_B > C_A Y_A$
	Y_B =0.43	Y_A =0.33	
$Y_B > \frac{C_A Y_A}{C_B}$	Y_B >0.29	Y_A >0.54	$Y_A > \frac{C_B Y_B}{C_A}$

It is logical that the statements made earlier are also valid in this case, that is, enhancing the unfavourable features from two directions could be simpler or more beneficial than improving a single factor significantly.

7.2. **Standard index**

Similarly to the previous ones, the standard qualifier indexes (H_x) are the products of multiplying the professional effectiveness of the extinguisher by that of aerial firefighting. The data above are summarised in Table 9. The table contains the values of the calculations with the data of the example as well.

$$H_A = Z_A U_A \quad (28) \text{ and } H_B = Z_B U_B \quad (29)$$

Table 9—Standard indexes of qualifying the aerial firefighting efficiency

	H_A	H_B
Foam A	$Z_A U_A$ (0.438)	
Foam B		$Z_B U_B$ (0.675)

Numerous calculations can be made with the data above, whose results are the threshold values of effectiveness. They are summarised in Tables 10-11.

$$Z_A U_A = Z_B U_B \quad (30) \quad H_A = Z_A U_A \quad (31)$$

$$H_B = Z_B U_B \quad (32) \qquad Z_A U_A < Z_B U_B \quad ..(33)$$

The relationship between the qualifier standard indexes is shown in Figure 4, which clearly shows that we can get the qualifier indexes by combining the professional indexes of the extinguishers and their logistics needs, that is, aerial firefighting.

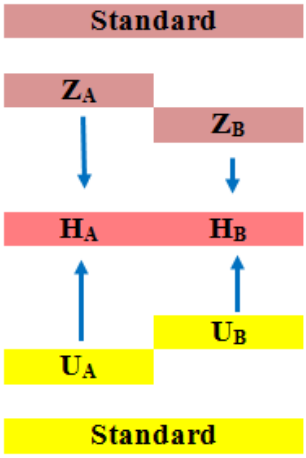

Figure 4. Logic of the standard indexes of qualifying the efficiency of the aerial firefighting

Theoretically, the following deductions can be made from the data regarding the relationship between foam "A" and foam "B".

- Foam "B" has an economic advantage as long as $Z_B > 0.97$ or $U_B > 0.29$ remains constant under other conditions.
- Application of foam "A" may gain an economic advantage if $Z_A > 1.93$ or $U_A > 0.54$ remains constant under other conditions.

Table 10— Conditions of the efficiency of the foam "A" and "B" to each other

$Z_A < \frac{Z_B U_B}{U_A}$	Z_A<1.93	Z_B>0.97	$Z_B > \frac{Z_A U_A}{U_B}$
	Z_A=1.25	Z_B=1.5	
$H_A = Z_A U_A$	H_A=0.438	< H_B=0.675	$H_B = Z_B U_B$
	U_A=0.35	U_B=0.45	
$U_A < \frac{Z_B U_B}{Z_A}$	U_A<0.54	U_B>0.29	$U_B > \frac{Z_A U_A}{Z_B}$

Based on the previous reasoning it is still valid in this case, that enhancing the unfavourable features from two directions could be simpler or more beneficial than improving a single factor significantly.

7.3. **Comparative index**

We can get the qualifier comparative index (B) in two ways. Either by multiplying the comparative indexes of the professional effectiveness of the extinguisher by that of the logistics (34) or as the quotient of the standard qualifier indexes of the two extinguishers (35). Both build on the previous reasoning.

$$B = GW \quad (34), \text{ and } B = \frac{H_A}{H_B} \quad (35)$$

The two mathematical processes must yield the same results. The result reveals the difference between the economic efficiency of the two extinguishers, which can be higher or lower than 1, depending on which extinguisher is the divisor and the dividend in the relation. Obviously, it has no significance in multiplication. The farther the value is from 1, the bigger the difference is between the economic efficiency of the two extinguishers. If the result is 1, there is no difference between the extinguisher and the related aerial firefighting in terms of economics despite the dissimilar partial results.
It does not affect our calculations with the qualifier indexes which data (the extinguisher and the related aerial firefighting) we use as the divisor or the dividend (35). Naturally, we get a higher quotient by dividing the higher value, so that extinguisher is more effective professionally. On the basis of the values of the example, foam "B" performed better in the test (B=0.68/0.44=1.54), its effectiveness is 1.54 times or 54% higher than that of foam "A". We get the same product in multiplication, too (B=1.2x1.29=1.54). Figure 11 presents the comparative indexes of qualifying the aerial firefighting efficiency.

Table 11— Comparative indexes of qualifying the aerial firefighting efficiency

	B	
From standard qualifier indexes	$\frac{H_A}{H_B}$ (1.54)	
From comparative indexes		GW (1.54)

The two types of relationship between the comparative qualifier indexes are presented in Figure 5. On the one hand, the indexes of economic efficiency are quotients of the professional indexes of the extinguishers and the related logistics needs. On the other hand, they are the products of multiplying the standard qualifier indexes of the two extinguishers.

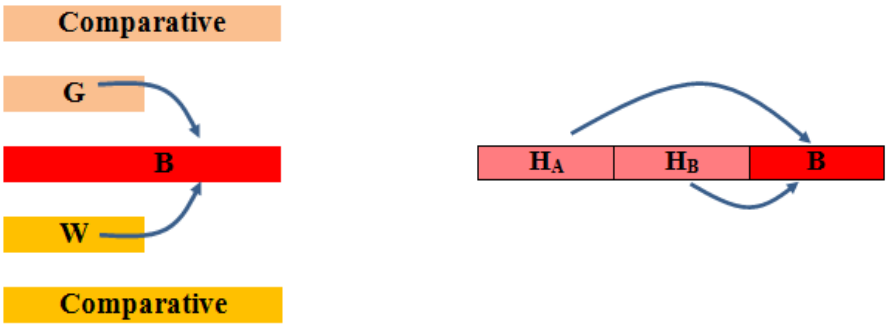

Figure 5. Logic of the comparative index of qualifying the efficiency of the aerial firefighting by two different ways

8. Summarizing

The creation of indexes and the calculations can be looked upon as a kind of mathematical game. It can be clearly seen how one consequence generates another one and also that, by keeping the basis of correlation, the new relations do not necessarily yield new results but rather a new approach to the results. The relationship between the indexes are summarised in Figure 6.

Despite the above, the creation of the indexes was not for their own sake. The paper has drawn attention to the fact that the extinguisher ability of extinguishers and the cost of their delivery can be examined together and that the separate analyses of their effectiveness do not necessarily lead to the correct conclusions. According to author's approach, it is possible - however difficult it is - to analyse and evaluate the effectiveness of aerial firefighting beyond the producers, distributors of the extinguishers and the marketing tricks of service providers of aerial firefighting even if the paper does not discuss each and every factor in detail.

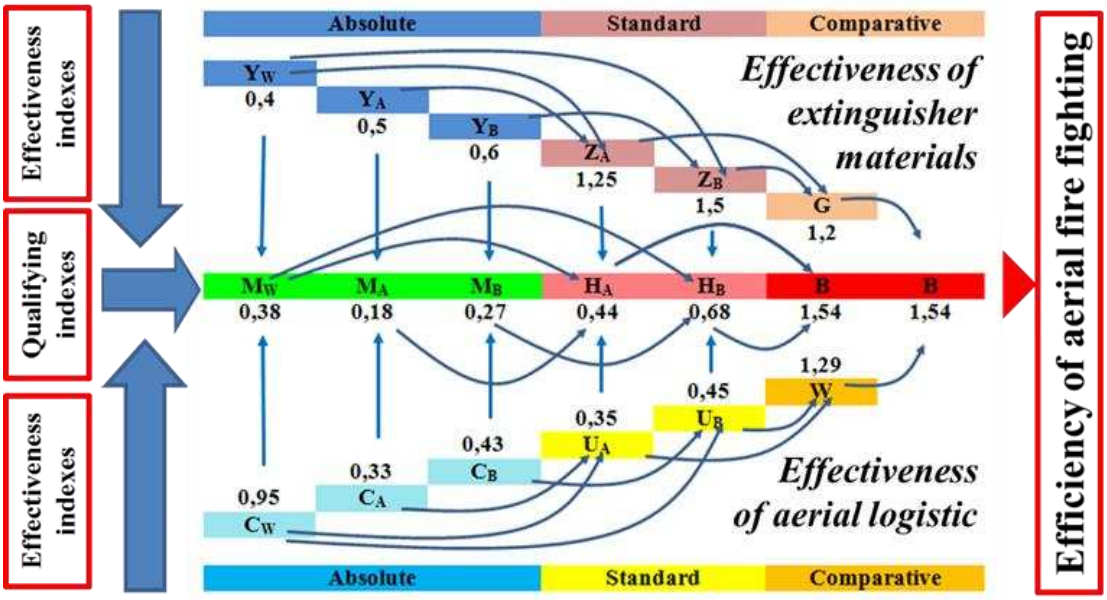

Figure 6. Complex logic of the indexes

The reasoning in the paper obviously changes with the modification of the influencing factors. We might assign different delivery means to the various extinguishers or even increase the number of extinguishers to be compared. We can get the results by expanding the formulas above or by interpolating the already existing results.

9. References

American Society for Testing and Materials. Standard Test Method for Determining Material Ignition and Flame Spread properties; E1321-1997(02).

Batista, A.C.: Combustion characteristics tests of Magnolia grandiflora and Michelia champaca for potential use in fuelbreaks in south region of Brazil, Wildfire 2011 Conference, Sun City, South Africa, 2011

Fiorucci, P. a): PROPAGATOR: A Rapid and Effective Tool for Active Fire Risk Assessment, Wildfire 2011 Conference, Sun City, South Africa, 2011

Fiorucci, P. b): RISICO: A Decision Support System (DSS) for Dynamic Wildfire Risk Evaluation in Italy, Wildfire 2011 Conference, Sun City, South Africa, 2011

Morris C.J.: A simulation study of fuel treatment effects in dry forests of the western United States: testing the principles of a fire-safe forest, Wildfire 2011 Conference, Sun City, South Africa, 2011

Restas, A.: Az erdotuzoltas hatekonysaganak kozgazdasagi megkozelitese (Economical approach of the effectiveness of suppressing forest fire) Vedelem, 18:(5) pp. 47-50. (2011) ISSN 1218-2958

Underwriters Laboratories Inc. Project Reports to USDA Forest Service; 98NK32277, 99NK35219, 01NK12843, 03NK13445, 04NK16188, and 06CA42655.

Crossing the crossroad: challenges for the implementation of a collaborative wildfire management program in Portugal.

António Patrão

Institute for Interdisciplinary Research, University of Coimbra (IIIUC),
uc1997105312@student.uc.pt

Abstract
Wildfires represent the main natural risk in Portugal. Since 2003 the territory has been affected by extreme wildfires which have consumed more than 1.2 million ha. Following those events, several modifications were introduced in wildfire policies to preserve forest and increase the resilience of communities facing wildfires. These modifications suggest that the wildfire management strategies in Portugal are changing from a response based paradigm (wildfire combat capability) to a paradigm based on prevention and community collaboration. The goal of this paper is to identify this set of transformations, analysing the main features of the wildfire management program between 2003-2013 and the challenges for the implementation of a collaborative wildfire management framework. Wildfire policies and legislation created since 2003 were collected and submitted to content analyses to identify the main resolutions and strategies for wildfire management and to explore the extent of community involvement and participation. Results suggest that since 2003 many changes were implemented in the system, setting a positive context for wildfire prevention. But these measures still reveal a low potential for community participation and empowerment towards wildfire risk. New models of risk communication and information sharing with communities that increase their involvement in the decision process are needed.

Keywords*: wildfire management, collaborative framework, wildfire policies, community.*

Introduction

Wildfires represent the main natural risk in Portugal. Since 2003 the territory has been affected by extreme wildfires which have consumed more than 1.2 million ha and destroyed and many tangible and intangible resources, including human lives. These great wildfires, with catastrophic features, highlight the need for reviewing the policies of wildfire management and to develop systematic actions to preserve forest, guarantee the security and increase resilience of communities (adaptative capacity) when facing wildfires. Therefore, following a tendency common to other countries such as the United States of America or Australia, where catastrophic wildfires are common, wildfire management strategies in Portugal are changing from a response based paradigm to a more collaborative/resilience oriented framework based on prevention and community participation (Pearce, 2003). After 2003 several changes were introduced in the national system for the defence of forest against wildfires, focusing in creating more resilient and safe territories. However, recent studies indicate that wildfire risk is still very high and that there is an urgent need to work on prevention issues and with communities: individual risk behaviours continue high and the collaboration of people/communities has been identified as one of the major factors to the success of the wildfire national policies (Viegas *et al*, 2012; Tedim & Paton, 2012). This paper analyses the main legislative and policy context of wildfire management framework in order to understand the changes that emerged following the 2003 wildfires and analyse at what extent these measures are favourable to the new paradigm based on prevention and community participation.

Objectives

The goal of this paper is to identify and analyse the main modifications in wildfire policies following the catastrophic wildfires of 2003. Specifically it characterizes the framework of wildfires management, from 2003-2013, identifying the main resolutions and strategies for wildfire management, and exploring the degree of community involvement and participation involved on it. Results highlight the legislative framework, its main principles and orientations, suggesting the challenges facing professionals and other stakeholders in the implementation of a more collaborative orientation within the wildfires management cycle.

Methods

In order to understand the main orientations of the policies following the 2003 wildfire catastrophic events legislative instruments (policies and legislation) focusing on wildfire management, between 2003 and 2013 were selected using wildfire as key-words and submitted to content analysis (Miles & Huberman, 1994). The data base of the national forestry services-ICNF (http://www.icnf.pt/portal/icnf/legisl/lex-flor/flor-incen-agric#dfci) which contains the majority of legislative documents connected to the Portuguese forestry sector, since 1901, was used. Legislative instruments (law, decree-law, resolution of the council of ministers and parliamentary resolution and ordinance, decree, order and legislative order) were selected on the basis of their aims and field.

Data analysis

The selected documents were integrally read and then submitted to content analysis (Miles & Huberman 1994) within the emergency management cycle framework (NFPA 1600) (Figure 1).

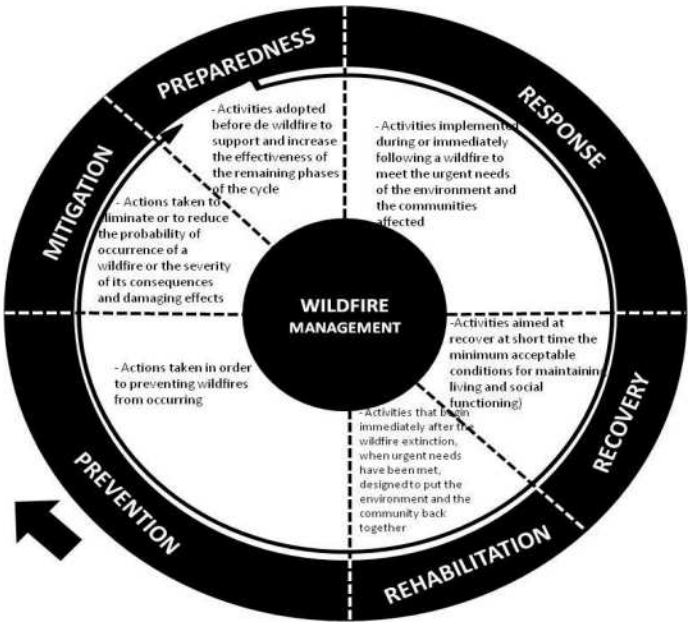

Figure 1. Wildfire Management cycle

The analysis aimed to describe and characterize the main features of the wildfire management framework: core themes, strategies used within the emergency cycle, amount of attention devoted to each of the cycle phases. Categorisation system was gradually refined by two independent judges. Each judge read the legislative documents and drew up a list of categories and subcategories based on the phases of the wildfire management cycle (Figure 1). The inter-judgment agreement score (number

of agreements / total number of agreements plus disagreements) was 80%; this reliability may be considered high (Miles & Huberman, 1994). A list of categories and sub-categories, which included definitions was produced (Table 2). Then the legislative documents were classified to the (sub)categories (judges were in full agreement) (table 3).

Results

4.1. Main topics/themes within the wildfire management cycle

Prevention /Mitigation is the most frequent topic within the Portuguese wildfire management cycle (Table 3). Forest management strategies (plans for sustainable management of wildfire hazardous areas at regional, local and operational level) are the most significant topics within this matter. Funding and support and the reinforcement of agents, organizations and human resources to work on prevention and mitigation actions were also underlined by the legislative instruments. Public education (focused on education to the correct use of fire and wildfire risk awareness) and prescribed burning are also present but are a lot less expressive.

Rehabilitation is the second most recurrent category (Table 3). Most common issues are support programs and funding to face the effects of wildfires, which emerged from a Disaster Declaration in August, 2003. Rehabilitation issues also emphasize operational/technical procedures (e.g. reforestation programs; harvest burned timber; control erosion; preserve water resources) to recover the burned areas, specially following the wildfires occurred in 2003-2006. The regulation of burned timber trade market was included but is less expressive.

Table 2. Themes and contents of wildfire policies and legislation: categories and subcategories within the emergency cycle

Category/	***subcategory***	***Definition***
Prevention/Mitigation: Reducing the chance of occurrence and the damaging effects of wildfires.	1.1. Forest management and planning strategies	Plans for sustainable management of wildfire hazardous areas (regional, local and operational level).
	1.2. Fuel management tools	Fuel reduction techniques (e.g. prescribed burning).
	1.3. Funding and support	Financial support (from European Community and fuel taxes) for prevention and education campaigns and plantation programs
	1.4 Reinforcement of agents, organizations and human resources. (prevention specialists)	Specialized entities and committees; specialized forest brigades; and volunteers programs.
	1.5. Public education/communication	Warning systems, definition of critical risk periods, reinforcement of the legal framework.
Response/Immediate Recovery: meeting the urgent needs of the environment/communities affected;	2.1. Reinforcement of human resources(combat specialists)	Special fire fighters; coordination between fire-fighters and civil protections agent in combat.
	2.2.Communication systems/technology	Communication systems to improve combat and the interaction/connection between entities involved.
	2.3. Special combat/response equipment	Special funding conditions to rent forest fire combat aeroplanes.
Rehabilitation: putting the environment and the community back together	3.1. Support programs (financial, social and operational)	Criteria for the attribution of financial support to repair the damages; special credit lines (preservation of pine and eucalyptus timber; *Quercus suber* plantations and cork extraction).

	3.2. Reinforcement of agents, organizations and human resources (Rehabilitation specialists)	Agents and procedures and to cope with wildfire consequences and recovery of burned areas (reforestation programs; harvest burned timber; control erosion; preserve water resources).
	3.3 Regulation of burned timber trade market	Creation and establishment of burned timber points.
System for forest defence against wildfires: setting the frame	4.1. General framework	Interventions related to the prevention and defence of forest against wildfires accomplished by the public entities and private agents (public education and awareness, conservancy and land use planning, forestry, surveillance, detection, combat and aftermath of wildfires).

Response/Immediate recovery is the third category (Table 3). Most frequent issue within this topic is the reinforcement of organizational and human resources involved in combat. It centres on the coordination between national forestry services, the national civil protection services and the law forces in combat scenarios and in the specialization of professionals to work on the field (fire-fighters, law forces, forest workers and fire specialists). The allocation of special services, like combat aeroplanes and the acquisition of communication systems are also contemplated.
System for forest defense (general framework) is the fourth general category (Table 3). It contains documents related to the definition, implementation and adjustment of a National Wildfires Defense System, which were publicized in the immediate sequence of the great wildfires (years 2004, 2005, 2006).

Table 3. Classification of the fire policies and legislation on the themes (categories and subcategories) between 2003 - 2013.

Categories/subcategories	**%**
1.Prevention/ Mitigation	66,2
1.1. Forest management and planning strategies	22,1
1.2. Fuel management tools	2,6
1.3. Funding and support	15,6
1.4 Reinforcement of agents, organizations and human resources. (prevention specialized)	15,6
1.5. Public education/communication	10,4
2. Response/Immediate recovery	9,1
2.1. Reinforcement of human resources(combat specialists)	5,2
2.2. Communication systems/technology	1,3
2.3. Special combat/response equipment	2,6
3.Rehabilitation	19,5
3.1 Support programs (financial, social and operational)	11,7
3.2. Reinforcement of agents, organizations and human resources (Rehabilitation specialists)	5,2
3.3 Regulation of burned timber trade market	2,6
4. System for forest defence against wildfires (general framework)	5,2
Total	100

Discussion

5.1. General framework of the wildfire management (context)

The results of this study suggest the embracing of two major topics for wildfire management in Portugal: prevention /mitigation and rehabilitation. Together both areas integrate nearly 85% of all legislative publication, mostly issued between 2003 and 2009. This seems to point out to a turning point on the wildfire management framework, towards a more preventive/resilience orientation. However recent data evidence that funding and financial support continue to reinforce response and combat over prevention. Decision makers centre the discussion on prevention vs. response, dismissing other phases of the emergency management cycle, namely preparedness (Figure 2). Moreover, nonetheless the results suggest that public policies put an emphasis on rehabilitation the guidelines of the legislative instruments are not being successfully imported and transferred to those who implement recovery actions on the field.

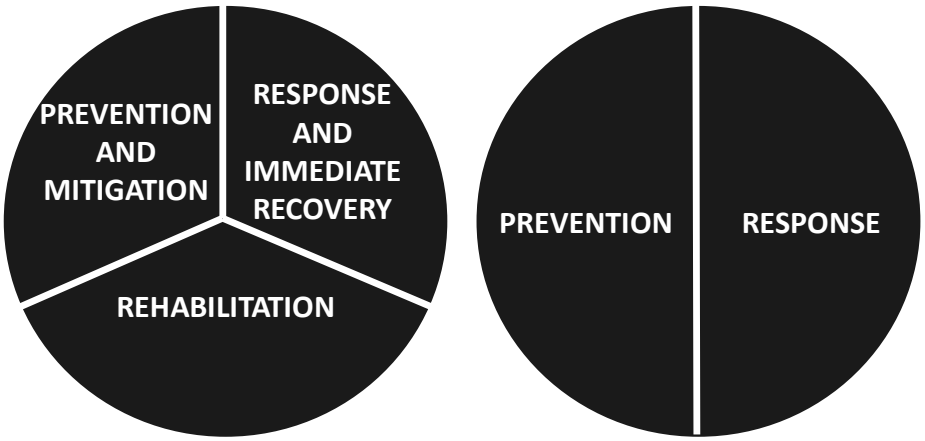

a) legislative frame *b) perspective of decision makers (action on the field)*

Figure 2. Features of the wildfire management framework:

Therefore, recent studies and reports continue to point out to a deficit on prevention, structural problems connected to individual property and land use (large areas of abandoned or unattended lands with unmanaged or inadequately managed flammable vegetation), individual risk behaviours (high number of human-caused ignitions) and to the need to persist on community involvement and participation (Tedim & Paton 2012; Viegas *et al* 2012).

5.2. Community involvement and collaboration (challenges)

Content analysis suggests that the degree of community involvement and collaboration provided by Portuguese policies for wildfire management is still low. The contents analysed referred mainly to education and risk communication based on the diffusion of general information (e.g. pamphlets, media advertisements) and to the increase of the legal framework as an instrument of regulation (define what to do and how to do in a top-down orientation).

These measures represent passive forms of communication that fail to address the diversity of needs and expectations within a community and also fails to engage people in ways that facilitate their ability to make decisions (Prior & Paton, 2008). They share the assumption that providing the public with information on wildfires and the protective measures to prevent it will automatically translate into preventive behaviours, which is a wrong assumption (Paton 2003). Behaviour change in wildfire risk situations demands for the active engagement of community members within the risk communication process and the use of interactive risk communication procedures. Professionals and agencies connected to wildfire management should act as facilitators or consultants to communities rather than directing the change process in a top down manner. One possible approach would involve invite

representatives of community groups and stakeholders to review wildfire scenarios in regard to the potential challenges, opportunities and threats they could pose for each group.
Another important dimension of participation is related to the sharing and construction of knowledge between people and specialists (Callon, Lascoumes & Barthe 2001). Results suggest that the framework gives a great emphasis to the specialization of human resources (creating specialists) but less to the acknowledgment and integration of local knowledge. Within these circumstances people tend to rely on the action of the specialists, placing the responsibility of change on their shoulders and disconnecting from the field (Patrão 2010). This is important because such an orientation has the potential to increase the sense of conflict, rivalry and distrust that historically has been characterizing the relationship between the sate and the communities within the forest management (Soares e Oliveira 2006; Mendes & Tavares 2009). Community participation requires the use of strategies to promote the articulation between the scientific community, the political actors, professionals and the citizens (Mendes & Tavares 2009). Socially Fire Regimes framework (Goldstein & Hull, 2008) represent an innovative intervention on this subject.

Conclusions

Since 2003, Portugal has implemented many (and mainly positive) changes in its wildfire management program. However the framework for action includes only three (3) of the six (6) steps of the emergency management cycle, developing in a triadic structure around mitigation/prevention-response-rehabilitation, mainly in a mandatory and directive orientation (top-down). Moreover giving their structural features, many of these changes are still maturing and may take several years to bear fruit. This is special relevant in the process of community collaboration.
The framework is in a period of transformation and transition between paradigms: the system aims at a more collaborative stance but remains trapped in a top-down orientation. It demands new forms of communication, networking and deliberation to foster learning, transform values and cultivate new identities among the communities, the fire professionals and specialists (Goldstein & Butler 2012). It is necessary to develop a culture that embraces the value of empowering communities.
This exploratory study highlighted the legislative framework of the wildfire management in Portugal, its main principles and orientations, summarising some of the obstacles professionals and other stakeholders are facing in the implementation of a more collaborative wildfire management framework.. Future studies are needed to study people (communities) and fire professionals´ attitudes towards different risk communication techniques and to deepen the knowledge about collaborative processes in wildfire management, namely through action research methodology.

References

Callon, M, Lascoumes, P & Barthe Y 2001, Agir dans un monde incertain. Essai sur la democratie technique, Seuil, Paris.

Goldstein, B., Butler, W 2012, "Collaborating for tansformative resilience" In Collaborative resilence: moving through crisis to opportunity, eds B Goldstein & W Butler, The MIT Press, Cambridge, Massachussetts, pp 339-358.

Goldstein, B., Hull, R. 2008, "Socially Explicit Fire Regimes." Society &Natural Resources, 21:6, pp 469-482.

Mendes J & Tavares A 2009, "Building resilience o natural hazards." In Safety, reliability and risk analysis, eds Martorell *et al*, Taylor & Francis Group, London.

Miles, M & Huberman, M 1994, Qualitative data analysis: An expanded sourcebook, Sage, Thousand Oaks, CA.

NFPA, 2013, NFPA 1600 Standard on Disaster/Emergency Management and Business Continuity Programs, NFPA Edition, Quincy, MA

Paton D 2003, “Disaster Preparedness: A social-cognitive perspective”, Disaster Prevention and Management, 12, pp. 210-16.

Patrão, A, 2010, "Social paths towards wildfire risk mitigation" In Proceedings from the 6th International Conference o Forest Fire Research, eds D. X. Viegas, Coimbra, pp 313.

Pearce, L 2003, "Disaster management and community planning, and public participation.", Natural Hazards, vol 28, pp 211-228.

Prior, T & Paton, D 2008, “Understanding the context: the value of community engagement in bushfire risk communication and education”, The Australasian Journal of Disaster And Trauma Studies, 2.

Soares, J & Oliveira, T 2006, "Políticas públicas recentes para a protecção da floresta" In Incêndios Florestais em Portugal, eds J. S. Pereira *et al*, ISA Press, Lisboa..

Taylor, P 2011, “Shifting boundaries: From management to engagement in complexities of ecosystems and social contexts," in Ecosystem Based Management for Marine Fisheries., eds A. Belgrano & C. Fowler, .Cambridge University Press, Cambridge, pp. 248-263.

Tedim, F & Paton, D (eds.) 2012. A dimensão social dos incêndios florestais, Estratégias Criativas, Lisboa.

Viegas, X *et al* 2012, Relatório do incêndio florestal de Tavira / São Brás de Alportel - 18 a 22 de Julho de 2012. Universidade de Coimbra, Centro de Estudos sobre incêndios florestais, ADAI/LAETA.

Determining the economic damage and losses of wildfires using MODIS remote sensing images

Juan Ramón Molina Martínez[1], Miguel Castillo Soto[2], Francisco Rodríguez y Silva[1]

[1] *Forest Fire Laboratory. Forest Engineering Department. University of Cordoba Leonardo da Vinci Building. Campus de Rabanales. 14071 Córdoba (Spain), jrmolina@uco.es; ir1rosif@uco.es*
[2] *Fire Management Laboratory. Faculty of Forest Sciences and Nature Conservation. University of Chile. Santiago, Chile. migcasti@uchile.cl*

Abstract
The economic evaluation of damage and losses of the areas affected by forest fires requires comprehensive studies covering a wide range of natural resources. The assessment of fire impacts requires the individualized study of each resource, such as timber resources, fruit production and hunting activity, and the analysis of their net value change based on fire intensity and ecosystem resilience. As a consequence, this concept of net value change extends the study beyond an economic valuation, integrating two concepts, the value of the resource and fire behavior. However, field sampling on large fires becomes complex because of the costs involved in field tasks and the time that will elapse before the assessment is available.
The incorporation of satellite imagery to the economic valuation of fire impacts provides a new tool of undoubted interest. This paper details the methodology and the results obtained in the economic assessment of two medium (between 200-500ha) and two large fires (more than 500 ha) in the south of Spain. MODIS data were suitable for mapping medium and large fires (more than 200 ha). The advantage of using MODIS satellite images in relation to other remote sensors lies in the free download (zero cost) and temporal resolution. As other studies have shown, the normalized vegetation index was not presented as the best identifier of the burned area. However, RdNBR index allowed us to obtain reliable relationships between its value and the depreciation ratio for each resource due to the differences among resources based on fire intensity.
Economic resources valuation and MODIS images (pre and post-fire) can be integrated into Geographic Information System (GIS), in order to obtain, in a geo-referenced way, the economic value per hectare resulting from fire impact. This tool should provide a procedure to help improving fire management and take more appropriate decisions about budg*et al*location and rehabilitation of areas affected by fires. Given current economic constraints, the use of a geo-referenced tool with free download and regular update (MODIS) allows us to the inclusion of changes, improvements and temporal or spatial adaptations according to the needs of forest managers. The methodological approach for assessing the economic impact of forest fires provided allows the application of this simple and flexible technique to any territory by previous economic valuation of natural resources presented in the interesting area.

Keywords*: Economic losses; net value change, vegetation indices, remote sensing, fire management*

Introduction

Forest fires are a major factor of environmental transformation in a wide variety of ecosystems (FAO, 2007). Although fire has been used since ancient times in crop rotation, agricultural plowing and pasture creation for the purpose of livestock use, socio-economic changes have led to an abandonment of traditional uses. This neglect results in a greater accumulation of scrub (Perez, 1990; Rodriguez y Silva and Molina, 2010), which, along with the accentuation of climate conditions (Piñol *et al*., 1998), are transforming fire into a threat to the biodiversity and conservation of Mediterranean ecosystems (Brook *et al*., 2003).
Remote sensing is commonly used for monitoring wildfires using various space-borne sensors, such as Landsat and MODIS (Chuvieco *et al*. 2005; Devineau *et al*., 2010). MODIS (Moderate Resolution

Imaging Spectroradiometer) data were suitable for mapping medium and large (50-500 ha) burn scars that accounted for the majority of all fire-damaged forests (Morton *et al*., 2011). MODIS makes up to four daily observations from each of the Terra and Aqua satellites providing consistent data on fire development with high temporal frequency. The use of MODIS satellite images enabled us to map wildfires at a national scale due to the high temporal resolution of the sensor (Levin and Heimowitz, 2012). In other works, MODIS has been used to the classification of fires into headfire and backfire types in assessing pollutant emissions to the atmosphere (Smith and Wooster, 2005). The incorporation of satellite imagery to the economic evaluation provides, in a novel way, a tool of undoubted interest to accurately identify the natural resources affected by fire (Rodríguez y Silva *et al*., 2009, 2012a). The advantage of using MODIS satellite imagery lies in the availability of real-time information at zero cost.

The economic evaluation of damage and losses of the areas affected by forest fires requires comprehensive studies covering a wide range of natural resources. The valuations of natural resources tend to underestimate the real value of the forest (Constanza *et al.*, 1997). Unlike traditional economic activity, the forest environment is characterized by the extraordinary relevance of externalities that involve harm or benefits of considerable magnitude to others (Riera, 2000). From forest management standpoint, it is necessary to express all the natural resources in monetary terms. The economic valuation requires the identification of the "net change value" of the resources affected by fire. As a consequence, this concept of "net value change" extends the study beyond an economic valuation, integrating two concepts, the value of the resource and fire behavior (Rodríguez y Silva and González-Cabán, 2010).

Wildfires are the most important disturbance in the Mediterranean area causing damages to tangible assets, environmental services and landscape goods. The spatial assessment of fire impacts is indisputable in the identification of effective rehabilitation actions. However, this evaluation becomes complex when the size of the affected area makes gathering the information unfeasible, mainly because of the costs involved in obtaining the information and the time that will elapse before the final assessment is available. The aim of this paper is to assess the economic fire impacts of medium and large fires based on satellite images and fire intensity level. One of the most difficult concepts to value the economic impact of fire on natural resources is determining the net value change or economic value loss. MODIS images identify value change based on the differences in spectral information based on fire behavior. The socioeconomic vulnerability model was incorporated into a Geographic Information System (GIS) that facilities the development of spatiotemporal tracking cartography, at both the individual resource level and the integrated ecosystem vulnerability level. The impacts valuation using satellite images and GIS achieves in a versatile geo-referenced tool understanding of the forest system vulnerability to wildfires, at virtually real time.

Methods

The economic evaluation of fire impacts by MODIS images has been carried out for four large fires in Andalusia, in the south of Spain. These four fires provide a wide range of Mediterranean ecosystems and topographical characteristics: burned area from 275 to 7,300 ha, range of altitudes between 423 and 1,200 m meters above sea level and different stand areas (*Quercus ilex*, *Castanea sativa*, *Alnus glutinosa*, *Pinus pinea* and *Pinus pinaster*) and treeless (chaparral, *Cistus* genus, *Pistacia lentiscus*, *Rosmarinus officinalis* and *Juniperus oxycedrus*).

The economic impact assessment of a large forest fire requires the following phases of analysis and development:

a) Economic valuation of natural resources
b) Spatial identification of different damage levels
c) Identification of the net value change in the resources
d) Economic valuation of fire impacts

Economic valuation of natural resources

Although economic valuation of natural resources must incorporate three types of resources: tangible assets, environmental services and landscape goods, this paper only includes tangible assets covering timber and non-timber resources. The methodology for the evaluation of timber resources consists of an algorithm integrating the method in the National Fire Management Analysis System (NFMAS) developed by the USDA Forest Service and the method used by the Spanish Forest Service (Rodríguez y Silva *et al*., 2012b). NFMAS is based on the concept of natural restoration while Spanish system considers artificial restoration based on stand development stage and rotation age of the species.

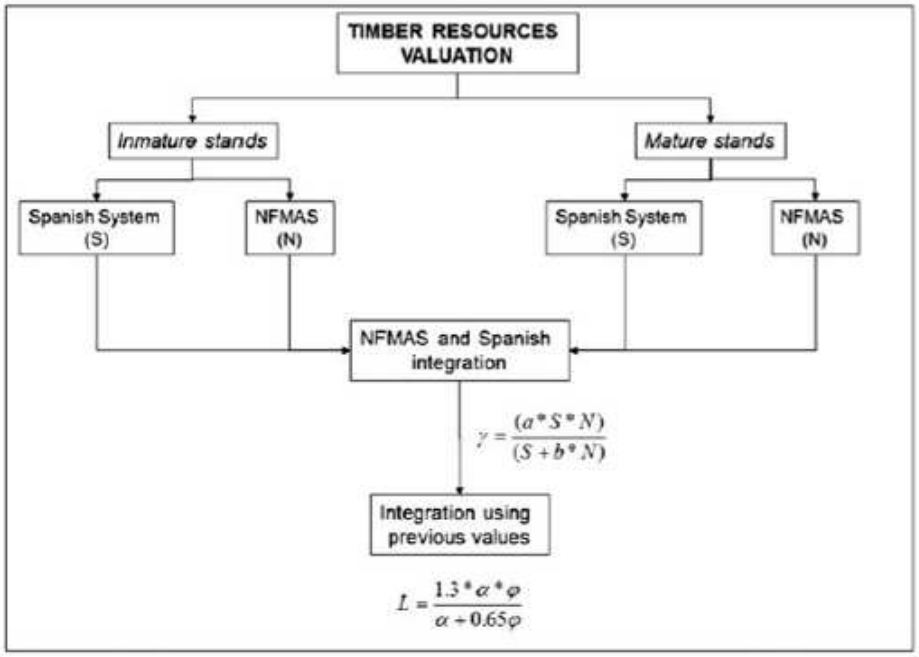

Figure 1. Methodological scheme for the valuation of timber losses (Rodríguez y Silva et al., 2012b)

Non-timber losses should be calculated depending on the generated annual income from resources production, such as pasture, acorn and pine nut production (Table 1). A problem exists because of the number of years without resource production or vegetation resilience (Molina *et al*., 2011; Roman *et al*., 2013). Valuation of grassland impact requires information on the available production, nutritional value of the grass and the carrying capacity of the area. On the other hand, fruit production per hectare is given by the tree production and the canopy closure adjusted for site index and phytosanitary condition. Finally, the hunting resource is based on the acquisition of a hunting assessment by updating the annual profit plus the stock or replacement value of the reproductive wildlife (Zamora *et al*., 2010).

Table 1. Mathematical formulations used for economic valuation

Resource	Formula	Potential status	Source
Timber	$\gamma = (a*S*N)/(S+b*N)$	Immature and mature stands	Rodríguez y Silva *et al*. 2012
	$S = C_0*t\,[r^e + i(r^e - 1)] + F*(r^e - 1)$	Immature stands	
	$N = [(P*V*1.025^y)/1.04^y]*\,[1-(1.025/1.04)^e] * [1 + M*c*t]$	Immature stands	
	$S = [P*V - P_1*V_1] + P*V\,[(r^{(R-e)} - 1)/(r^{(R-e)})]$	Mature stands	
	$N = V*c*t[C*P + (1 - C)*P_1]$	Mature stands	
Firewood; fruit production	$L = A_p*P_r*[((1+r)^y - 1)/(r*(1+r)^y]$	Mature stands	Martínez, 2000; Molina *et al*., 2011
Pasture production	$L = V*[((1+0.06)^n - 1)/(0.06*(1+0.06)^n]$	Livestock and/or game area	Martínez, 2000; Molina *et al*., 2011
Hunting activity	$L = V*[((1+0.06)^n - 1)/(0.06*(1+0.06)^n] + S$	Game area	Zamora *et al*., 2010

where " γ " is the timber valuation (€/ha), "S" is the valuation according the Spanish system (€/ha), "N" is the valuation adapted from NFMAS (€/ha), "a" takes the value of 1.7 or 2.6 according to protection or recreational function, or timber forest respectively, "b" takes the value of 0.85 or 0.25 base on the same reasons, "C_0" is the reforestation cost per hectare (€/ha), "t" is the percentage burned stand based on fire behavior, "r" is the compound annual interest rate and depends on species growth rate: fast growth (1.06), medium growth (1.04), slow growth (1.025) and very slow growth (1.015); "e" is the estimated stand age, "i" is the annual silvicultural cost factor and depends on species growth rate: fast growth (1.27), medium growth (1.1) slow growth (1.1) and very slow growth (0.93), "P" is the price of the timber (€/m^3), "V" is the timber volume (m^3/ha), "y" is the time or years remaining in the harvesting rotation or senescence age, "M" is the tree mortality coefficient depending on fire intensity, "c" is the percentage of immature or mature timber in stand, "P_1" is the price of affected timber with commercial use (€/m^3), "V_1" is the volume of burned timber (m^3/ha), "R" is the rotation age, "C" is the percent of non-commercial timber, "L" is the resource loss (€/ha), "A_p" is the annual production (kg/ha), "P_r" is the estimated resource price (€/kg), "V" is the annual income given the carrying capacity of the site (€/ha), "n" is the estimated number of years until recovery (vegetation resilience), "S" is the reproductive stock (€/ha)

Spatial identification of different damages levels

The spatial and spectral information from satellite images before and after fire let us to identify fire severity (Chuvieco *et al*., 2008). MODIS images were assessed in order to characterize fire impacts and to relate them with land cover. The spatial identification of the different damage levels was performed using MODIS images (Terra and Aqua) for a previous date as well as for a post-fire date. The MODIS products (both pre and post-fire) were downloaded from the United States Geological Service's LP DAAC Server (https://lpdaac.usgs.gov/get_data/data_pool). These images were already geometrically corrected. The original reference and coordinate system was transformed to the ETRS89 30N system making the overlapping of the images with the fire perimeter in vector format. The identification of damage levels was obtained based on the spectral and spatial differences between pre and post-fire images. Figure 2 shows a framework for the methodology proposed in this paper.

The surface reflectance, both for the Terra and Aqua platforms, was identified in the electromagnetic spectrum of 620-670nm (Red-NIR) for band 1, and 841-876nm (NIR) for band 2. In the case of images with a spatial resolution of 500 meters, the band 7 used ranged from 210-215nm. Geo-referencing and adjusting of the final fire perimeter was performed with ArcGIS© software, keeping a 150-meter tolerance buffer in order to include the effect of the proximity to the burned area. In order to harmonize MODIS bands (1, 2 and 7) and land use cartography for the calculation of the fire impacts, all inputs were resampled from original spatial resolution to 25 m (cell size = 0.625 ha).

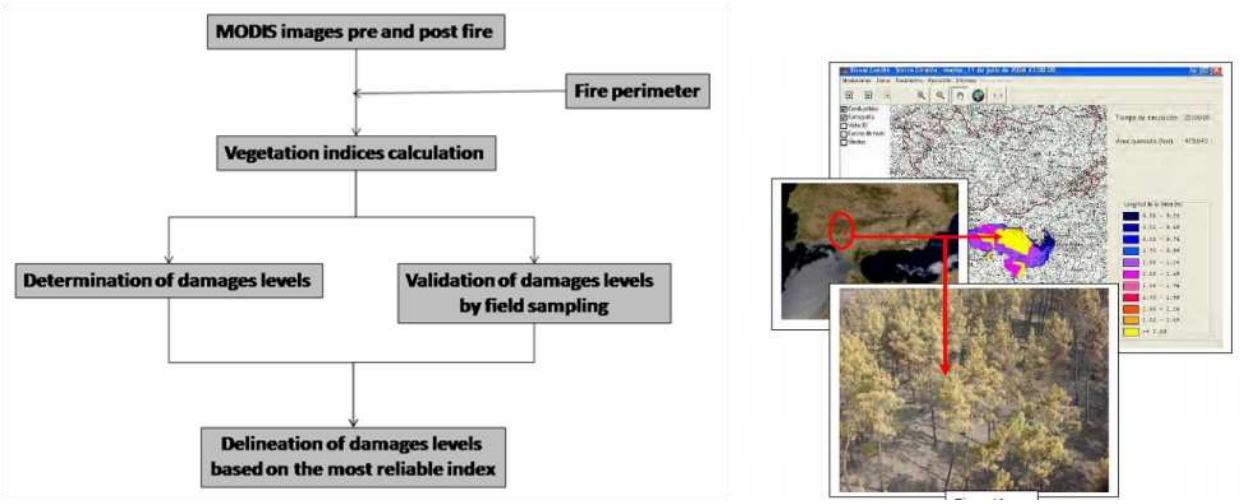

Figure 2. Framework of the methodological proposed in this paper

Three vegetation indices were considered: Normalized Difference Vegetation Index (NDVI), Normalized Burn Ratio (NBR) and a relative differenced Normalized Burn Ratio (RdNBR).The calculation of these indices requires mid-infrared (MODIS band 7) and near infrared (MODIS band 7) information. MODIS band 7 was very important due to its intrinsic ability to identify fuel moisture.

At the Red-NIR spectral space, NDVI (Chuvieco *et al*., 2002) was computed as follow:

$NDVI = (\rho_{NIR} - \rho_R) / (\rho_{NIR} + \rho_R)$
where ρ_{NIR} is the reflectance in the NIR (MODIS band 2) and ρ_R is the reflectance in the RED (MODIS band 1).

In the NIR-SWIR spectral space, NBR (Key and Benson, 1999) was calculated as follow:

$NBR = (\rho_{NIR} - \rho_{LSWIR}) / (\rho_{NIR} + \rho_{LSWIR})$
where ρ_{NIR} is the reflectance in the NIR and ρ_{LSWIR} is the reflectance in the SWIR (MODIS band 7).

In both vegetation indices the value range oscillates between -1 and 1. While values close to zero generally correspond to bare soil areas, positive values represent shrublands or grasslands (lower positive values) and forest lands (values close to one). The identification of the damage level of each "cell" (0.625 ha) was estimated by the differences in the values of vegetation indices, pre and post fire:

dNDVI = PreFire NDVI – PostFireNDVI
dNBR = PreFire NBR – PostFire NBR

Since chlorophyll contents vary due to vegetation type and density, each absolute differenced image should ideally be stratified by pre-fire vegetation type and independently calibrated. Therefore proposed the creation of a relative differenced NBR (RdNBR) to remove the biasing of the pre-fire vegetation by dividing dNBR by the square-root of the pre-fire NBR as follows (Miller and Thode, 2007):

RdNBR = dNBR / [Square Root (ABS (PreFire NBR/1000)]

We scale NBR by 1,000 to transform the data to integer format (Key and Benson, 2005); therefore the pre-fire NBR must be divided by 1,000 in the RdNBR formula. Positive RdNBR values remain

representing a decrease in vegetation cover, while negative values represent an increase in vegetation cover.

2.3. Identification of the net value change in the resources

The economic assessment of fire impacts on natural resources requires knowledge of the fire severity. The net value change in the resources is computed as a function of fire severity, which is determined by Fire Intensity Level (FIL) (Molina *et al*., 2011; Rodriguez y Silva *et al*., 2012b). To estimate the rates of depreciation for each resources based on fire behavior we used the following 13 large fires (year of fire in parenthesis) in Andalusia: Huétor (1993), Aznalcollar (1995), Los Barrios (1997), Estepona (1999), Cazorla, Segura and Las Villas Natural Park (2001, 2005), Ojen (2001), Aldeaquemada (2004), Minas de Río Tinto (2004), Alajar (2006), Obejo (2007), Cerro Catena (2009) and Cerro Vértice (2011). For the valuation of hunting activity, information from Monfragüe National Park, Aldeaquemada and Minas de Río Tinto were used to test the annual hunting profit and number of years until recovery (vegetation resilience) (Zamora *et al*., 2010).
Different sampling plots (10 and 15 m square plot) were established according to forest characteristics and average flame length in each fire event. We used flame length as a simple parameter "in situ" for fire severity. The creation of a direct relationship between fire severity and flame length increases the flexibility and simplicity of this methodological approach. In addition, a photographic overview was taken as a virtual key to identify vegetation resilience.

2.4. Economic valuation of fire impacts

We used Geographic Information Systems (GIS) to assess the socio-economic impacts on natural resources. The use of GIS allows us the option to link the economic value of natural resources and damage levels obtained by MODIS images. An extrapolation of sampling depreciation rates for each damage level could be extrapolated to large burned area with the help of remote sensing. The depreciation rate is estimated individually for each resource based on damage level depending on fire intensity. The integration of both economic value and real fire impacts provides the economic vulnerability of each resource. Final economic vulnerability is the sum of the vulnerabilities of the resources present in each burned area. Economic vulnerability cartography was developed showing fire impacts by hectare.

Results

3.1. Economic valuation of natural resources

It was necessary to characterize vegetation (combination between stand cover and understory association) to identify the natural resources presented in each area. In stand areas, immature and mature condition could be determined from the rate of growth and rotation length, as well as approximate stand age that is necessary for some resources valuations. Once the vegetation structure was characterized, a spreadsheet was used to identify the economic vulnerability of each area based on the mathematical formulations (Table 1). This characterization was related to dominant species, as a consequence, to the ecosystem resilience, that can be defined as the time needed by a species to recuperate to its original condition as a result of fire. Resilience was assigned based on restoration planning (large fires in Andalusia) and the experiences in the maintenance of the preventive infrastructure in wildfire risk areas (Zamora *et al*., 2010).
As an example of the application of this methodological approach, we incorporated the economic valuation of natural resources from "Catena fire" (Table 2). Economical results indicated that timber is the most important resource (€ 194,093.17), given the natural condition of the *Pinus pinaster* and their longevity (over 100 years in some stands). Tangible assets valuation reaches to € 263,568.69, showing a value per unit area of 1,261.1 €/ha.

Table 2. Tangible assets valuation for one example fire

Resource	Valuation (€)	Valuation per unit area (€/ha)	Representativeness (%)
Timber	194,093.17	928.68	29.35
Non-timber resources	60,771.17	290.77	9.19
Hunting activity	8,704.35	41.65	1.32

Spatial identification of different damages levels

MODIS images were assessed in order to characterize fire damages levels based on field sampling plots. In order to the size of the fire, we can identify four or six fire intensity levels according to the flame length (directly related to the fire line intensity) and spatial resolution. In this sense, four fire intensity levels were differentiated by medium fires (between 200 and 500 ha):

- Damage level I: this level corresponded to a flame length lower than 3 meters
- Damage level II: this level corresponded to a flame length between 3 and 6 meters
- Damage level III: this level corresponded to a flame length between 6 and 10 meters
- Damage level IV: this level corresponded to a flame length exceeding 10 meters

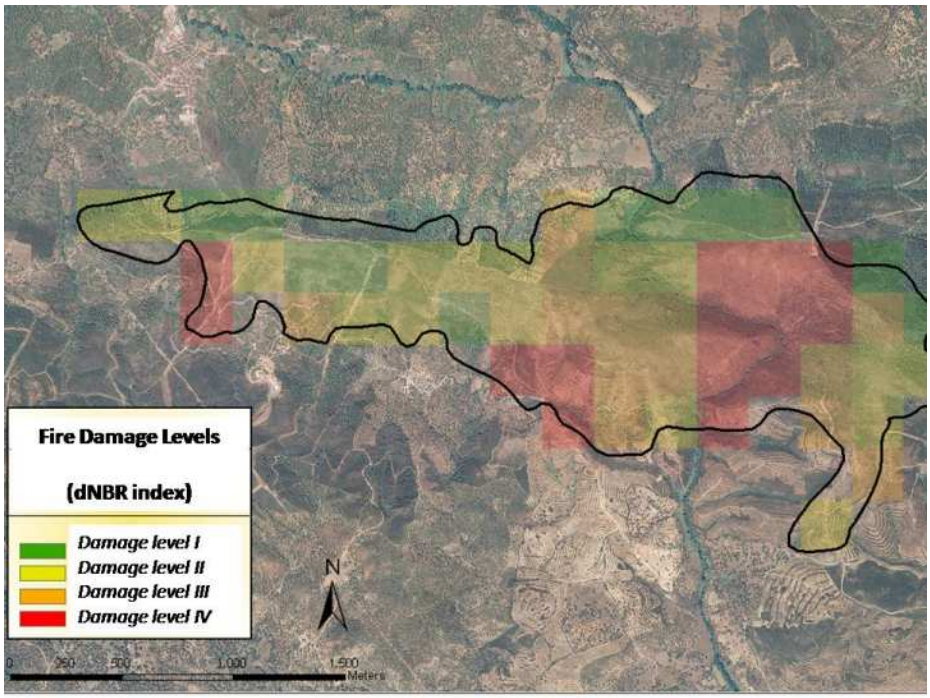

Figure 3. Fire damage levels from medium fire (275 ha)

In the case of large fires (more than 500 ha), the damage scale was extended to six categories due to the large sampling area and the most different fire behavior:

- Damage level I: this level corresponded to a flame length lower than 2 meters
- Damage level II: this level corresponded to a flame length between 2 and 3 meters
- Damage level III: this level corresponded to a flame length between 3 and 6 meters
- Damage level IV: this level corresponded to a flame length between 6 and 9 meters
- Damage level V: this level corresponded to a flame length between 9 and 12 meters
- Damage level VI: this level corresponded to a flame length exceeding 12 meters

The selected index should have adequate differences among damage levels, to avoid potential omission error in the automatic remote sensing process. The observed behavior of the different indices, regarding the identification of different damage levels, was heterogeneous. In general, better results were obtained with NBR index in relation to NDVI indices, since it allowed better discrimination and contrast of the fire impacts (Figure 4). Pre-fire and post-fire values (dNDVI) showed a difference (0.128) higher than dNBR (Terra bands 2 and 7) due to the post-fire photosynthetic activity. The indicator RdNBR allowed eliminating existent correlation between the result of the ratio and the pre-fire NBR value showing the most reliable relation between reflectance fire response and damage levels.

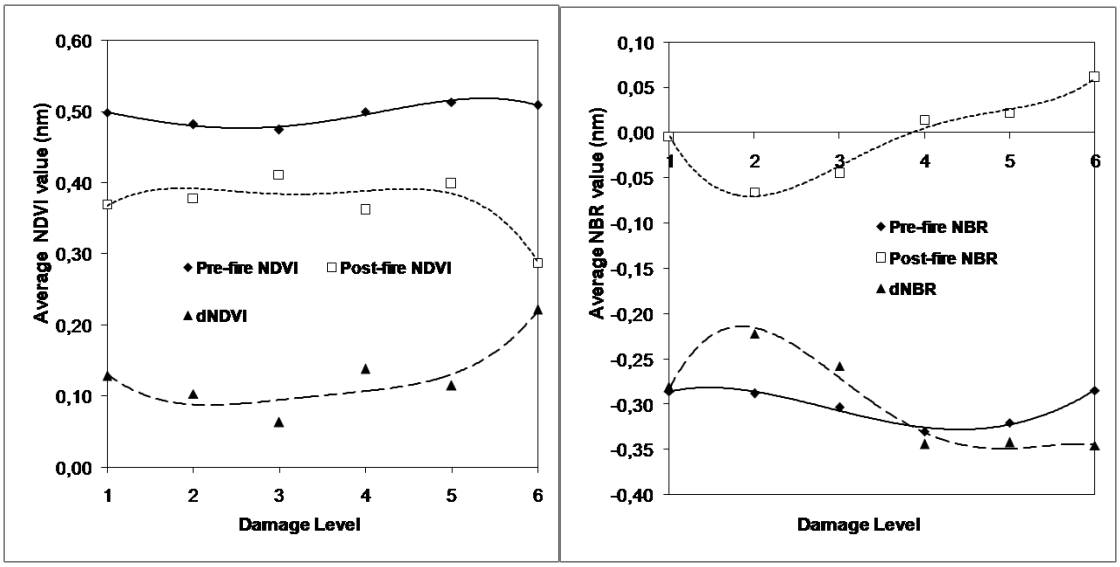

Figure 3. Comparison between dNDVI and dNBR for the same large fire

3.3. Identification of the net value change in the resources

The economic impact was determined by the fire intensity level. Therefore, a relationship had to be established between fire intensity level (directly related to flame length) and resource depreciation caused by the fire. The net value change expressed as different percentage intervals were from the result of some research projects and direct experiences from large fires in the region of Andalusia (Figure 4 and Table 4).

Figure 4. Sampling plots inventory on burned stand to determinate the net value change

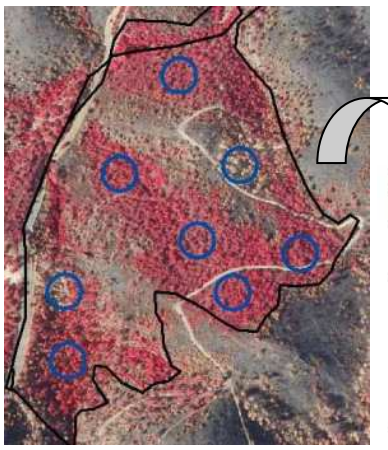

Table 1
Timber resource deterioration by fire intensity level.

Average flame length (m)	Fire intensity levels (FIL)	Timber resources deterioration (%)	Tree mortality coefficient (x)
< 2	I	8.33 (±6.58)	0
2–3	II	16.65 (±5.89)	0
3–6	III	38.58 (±6.27)	0.5
6–9	IV	57.85 (±13.74)	0.5
9–12	V	82.79 (±1.81)	1
>12	VI	89.41 (±2.82)	1

Table 4. Depreciation matrix (net value change for each resource based on fire intensity level)

Resource	Fire Intensity Level			
	I	II	III	IV
Timber	16.65 (±5.89)	38.58 (±6.27)	57.85 (±13.74)	89.41 (±2.82)
Firewood/fruit production	6 (±3.53)	14.2 (±5.03)	44.1 (±26.62)	73.40 (±5.65)
Hunting activity	40 (±17.67)	65 (±19)	84 (±15.27)	99 (±3.53)

*Depreciation matrix was more-detailed by other scientific papers: Rodríguez y Silva *et al*., 2012 (timber resource); Molina *et al*., 2011 (non-timber assets) and Zamora el al., 2010 (hunting activity)

Each resource change o depreciation value was adjusted with RdNBR index (the best index for the identification of the four damage levels) showing greatest correlation. We chose the logarithmic approach since it provides a reliable and easy way for the valuation of fire impact. In this sense, it is possible to provide the deterioration ratio (depreciation caused by fire and the residual economic benefits of vegetation unaffected) for each resource based on the spatial identification of the RdNBR index by MODIS images.

$y = a \ln(x) - b$
where " γ " is the net value change or depreciation ratio (%) and "x" is the value of RdNBR index

3.4. Economic valuation of fire impacts

MODIS data were suitable for mapping medium and large fires (more than 50 ha) similar to other studies (Morton *et al*., 2011). The spatial identification of damage levels with satellite imagery supported by a field inventory facilitates the extrapolation of the field information to the burned area (Devineau *et al*., 2008). The final step in the process, once the losses were determined and damage levels map was complete, was the preparation of a GIS-based data layer portraying the economic impacts to each studied fire (on a 25 x 25 m spatial resolution).

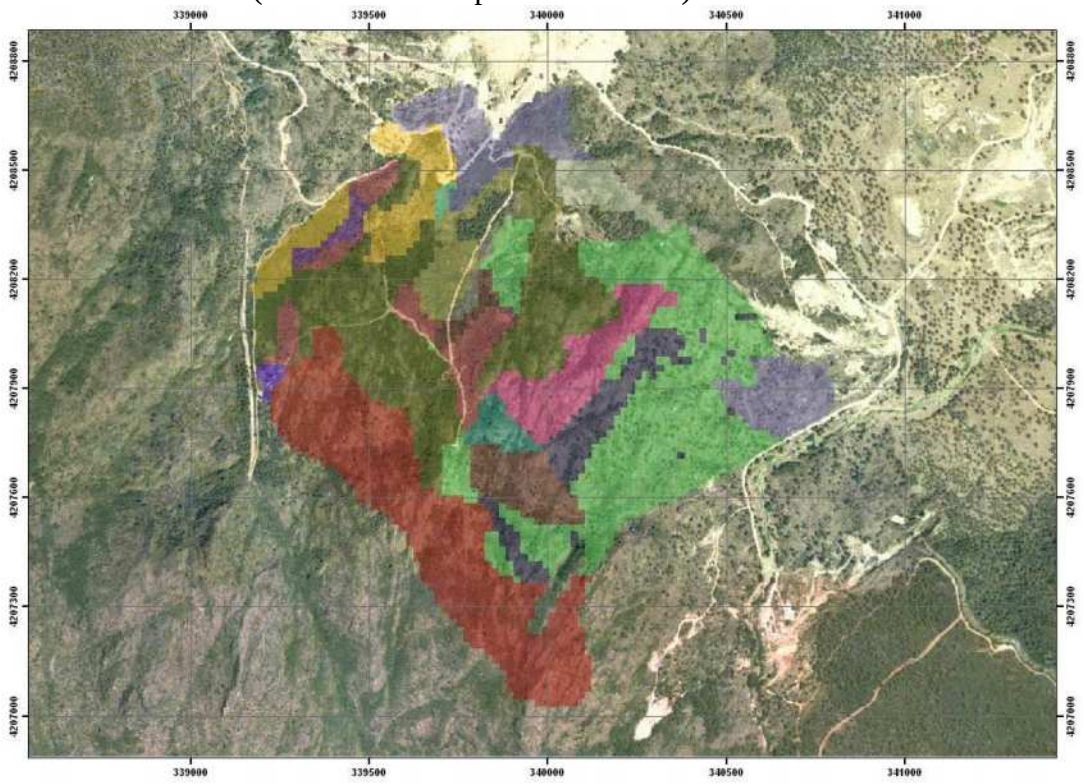

Figure 5. Economic valuation of burned area based on the socio-economic value of each ecosystem and the fire behavior

Conclusions

The integral valuation of forest ecosystems is essential for spatiotemporal planning conducted by forest managers. It is necessary to express non-timber resources in monetary terms. The incorporation of satellite imagery to the economic valuation of fire impacts provides a new tool of undoubted interest. The model should provide a sound procedure to help improving pre-fire management and take more appropriate decisions about rehabilitation of areas affected by fires.
The increasing demand for thematic mapping by government agencies with management responsibilities implies the need to develop tools and products based on Geographic Information Systems (GIS) and remote sensing. The use of GIS and remote sensing in spatial economic valuation provides flexibility when doing spatial ordination of the territory and increases the dynamisms of planning and systems protection tools. Given current economic constraints, the use of a geo-referenced tool with free regular updates (MODIS) allows us to the inclusion of changes, improvements and temporal or spatial adaptations according to the needs of forest managers.

Acknowledgements

The authors of this article express special gratitude to the INFOCOPAS project of the Ministry of Science and Innovation (RTA2009-00153-C03-03).

References

Brook B.W., Sodhi N.S., Ng P.K.L., 2003. Catastrophic extinctions follow deforestation in Singapore. Nature 424, 420–423.

Chuvieco E., Ventura M., Martín P., Gómez I., 2005. Assessment of multitemporal compositing techniques of MODIS and AVHRR images for Burneo land mapping. Remote Sensing of Environment 94, 450-462.

Constanza R., D'Arge R., de Groot R., Farber S., Grasso M., Hannon B., Limburg K., Naeem S., O'Neill R.V., Paruelo J., Raskin G.R., Sutton P., Van der Belt M., 1997. The value of the world's ecosystem services and natural capital. Nature 387, 253-260.

Devineau J.L., Fournier A., Nignan S., 2010. Savanna fire regimes assessment with MODIS fire data: their relationship to land cover and plant species distribution in western Burkina Faso (West Africa). Journal of Arid Environments 74, 1092-1101.

FAO, 2007. Fire Management-Global Assessment 2006. A Thematic Study Prepared in the Framework of the Global Forest Resources Assessment 2005. FAO, Rome.

Key C.H., Benson N.C., 1999. The Normalized Burn Ratio (NBR): A Landsat TM radiometric measure of burn severity. U.S. Dept. interior, Northern Rocky Mountain Sci. Center. Bozeman, MT.

Levin N., Heimowitz A., 2012. Mapping spatial and temporal patterns of Mediterranean wildfires from MODIS. Remote Sensing of Environment 126, 12-26.

Miller J.D., Thode A., 2007. Quantifying burn severity in a heterogeneous landscape with a relative version of the delta Normalized Burn Ratio (dNBR). Remote Sensing of Environment 109(1), 66.80.

Molina J.R., Herrera M.A., Zamora R., Rodríguez y Silva F., González-Cabán A., 2011. Economic losses to Iberian Swine production from forest fires. Forest Policy and Economics 13, 614-621.

Morton D., DeFries R., Nagol J., Souza C., Kasischke E., Hurtt G., Dubayah R., 2011. Mapping canopy damage from understory fires in Amazon forests using annual time series of Landsat and MODIS data. Remote Sensing of Environment 115, 1706-1720.

Pérez M.R.,1990. Development of Mediterranean agriculture: an ecological approach. Landscape Urban Planning 18, 211–220.

Piñol J., Terradas J., Lloret F., 1998. Climate Warming, Wildfire Hazard, and Wildfire Occurrence in Coastal Eastern Spain. Climatic Change 38(3), 1480-1573.

Riera A., 2000. Mass tourism and the demand for protected natural areas: A travel cost approach. Journal of Environmental Economics and Management 39, 97-116.

Rodríguez y Silva F., Molina J.R., Herrera M.A., Zamora R., 2009. The impact of fire and the socioeconomic vulnerability of forest ecosystems: A methodological approach using remote sensing and Geographical Information Systems. General Technical Report PSW-GTR-227. Pacific Southwest Research Station. Forest Service, U.S. Department of Agriculture; 151 - 168.

Rodríguez y Silva F., González-Cabán A., 2010. "SINAMI": a tool for the economic evaluation of forest fire management programs in Mediterranean ecosystems. International Journal of Wildland Fire 19, 927-936.

Rodríguez y Silva F., Molina J.R., 2010. Manual Técnico para la Modelización de la Combustibilidad asociada a los Ecosistemas forestales Mediterráneos. Departamento de Ingeniería Forestal. Universidad de Córdoba. Córdoba. España.

Rodríguez y Silva F., Molina J.R., Castillo M., 2012a. A methodological approach for assessing the economic impact of forest fires using MODIS remote sensing images. Papers of the Fourth International Symposium on Fire Economics, Planning and Policy: Climate Change and Wildfires. Mexico City, Mexico.

Rodríguez y Silva F., Molina J.R., González-Cabán A., Herrera M.A., 2012b. Economic vulnerability of timber resources to forest fires. Journal of Environmental Management 100, 16-21.

Román M.V., Azqueta D., Rodríguez M., 2013. Methodological approach to assess the socio-economic vulnerability to wildfires in Spain. Forest Ecology and Management 294, 158–165.

Smith A., Wooster M., 2005. Remote classification of head and backfire types from MODIS fire radioactive power and smoke plume observations. International Journal of Wildland Fire 14(3), 249-254.

Zamora R., Molina J.R., Herrera M.A., Rodríguez y Silva F., 2010. A model for wildfire prevention planning in game resources. Ecological Modeling 221, 19-26.

Fire extremes and the triangle of climate, fuels and people

Timothy J. Brown[a] and Tamara U. Wall[b]

[a] *Desert Research Institute, Reno Nevada USA, tim.brown@dri.edu, tamara.wall@dri.edu*

Abstract
Over the past decade or so, statements by fire personnel claiming unusual fire behaviour beyond training or experience levels seem to be increasing. This is occurring globally. Concurrently, climate and weather extreme events have been increasing, fuel loads have notably increased due to both natural occurrence and management practices, and the people have been expanding into the wildland and rural interfaces. All of these factors appear to be intersecting causing an increase in "extreme" fire events based on another fire triangle of climate, fuels and people. Megafires (for those comfortable with the term and lack of official definition) could be considered the extreme of the extremes, but many large fires can be categorized as extreme events. But for these extreme events to occur, not all three factors on the triangle need necessarily be extreme simultaneously. For example, strong winds need not be out of the ordinary (e.g., Santa Ana in southern California), but combined with continuous and heavy fuel in a highly populated area can lead to "never seen before" occurrences. Sometimes fire personnel are surprised at how large a fire becomes. In some cases, the extreme event is truly a surprise; in other cases, while seemingly a surprise at the time, upon further reflection perhaps it should not have been. In either event, personnel safety can easily be at higher risk during extreme events, as these situations tax critical thinking given they are outside the common fire experience.
This presentation discusses a project that draws upon quantitative assessment of physical observations (e.g., climate, weather, fuels) along with qualitative assessment of firefighter claims to 1) determine if indeed there is a common trend and intersection of these factors; 2) determine if situational awareness factors can be identified to lessen the surprise of these events; and 3) provide recommendations that incorporate knowledge of extreme events into fire management training.

Keywords*: Fire extremes, large fires, human factors, climate, fuels, fire behaviour*

Introduction

This project is driven by the phrase “I’ve never seen fire do that before” and the concern that fire fighters in the US are being surprised by wildfire behaviour, which then raises concerns about fire fighter safety and if levels of training and situational awareness are sufficient to address current patterns of fire behaviour. Fire is inherently a complex environment, and by extension, almost all questions related to the intersection of fire and people will be equally complex. Added to this is a convergence of climate (hotter and drier), fuels loading (high in many areas), and expanded residential areas in fire-prone areas. In summary, by any measure, addressing the question of fire extremes, both in terms of a quantitative assessment of climate, weather, and fuels and a qualitative assessment of fire fighter perceptions of extreme wildfire behaviour, requires a method that can absorb the variability in this complex problem.

2. Methods & Timeline

Our methodological approach in this project uses a software developed by Cognitive Edge, SenseMaker®, which uses narrative story prompts to ask for “microstories” about an event or experience in someone’s life (Figure 1). Once a person has either dictated or typed a brief narrative into the collection device (using either a app or website using a smartphone, tablet, or computer), they then answer a series of questions about the event or experience, applying context and meaning to their story. The questions employ a level of ambiguity to 1) deter “satisfying” or giving the “right answer”

to a question and 2) to provide the storyteller the ability to respond with complex answers—if you ask specific questions, you will get specific answers. While that may be advantageous for some questions, it does not provide the complexity needed in this situation. Survey's, for example, tend to provide averages of responses to a question. In this problem, an average is exactly the wrong metric to use—what we need are a diversity of stories that provide an array events across geographies, timescales, and situations in response to surprising, unexpected, or extreme wildfire behaviour. This diversity and quantity of stories/context questions will provide us with an authentic reflection of reality that can then be analysed for weak signals and patterns to identify factors involved with fire fighters responses to these situations. The primary data in this methodology is not the stories themselves, but rather the responses to the questions that apply the context and meaning of the story to create a quantitative dataset that can then be analysed statistically.

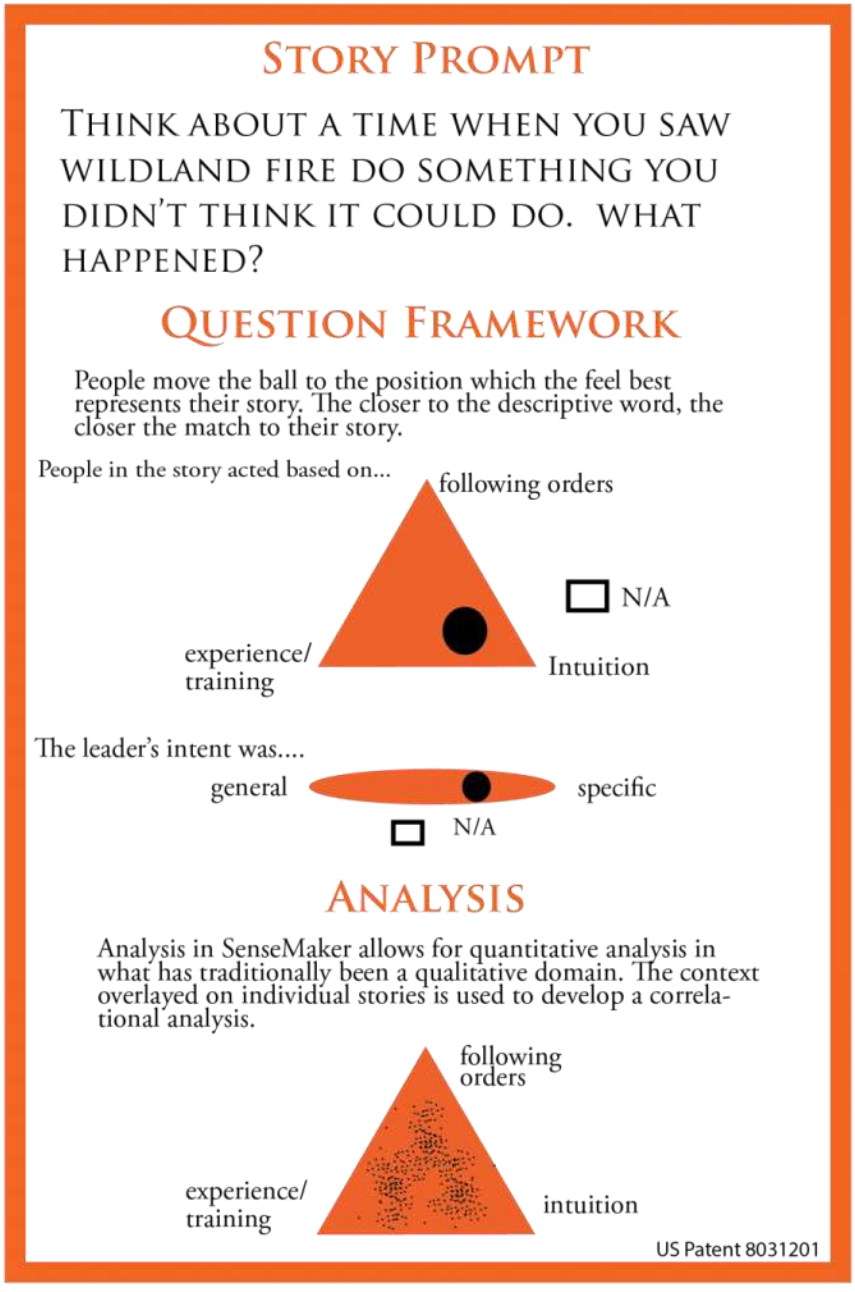

Figure 1. SenseMaker framework.

For this project, we worked iteratively with several groups of expert fire fighters and supervisors, as well a consultant experienced in SenseMaker® to develop the initial question framework. SenseMaker® uses a series of questions that are framed as triads and dyads (Figure 1). Once a preliminary framework was developed, we tested pen/paper versions with several different fire crews to finalize the framework. At this point the framework was coded, and uploaded to a demo server where it was tested again on the website, as well as both iOS and Android operating systems, and the mobile apps.

Quantitative analysis of the physical side of fire - fuels, weather and climate - will be done in association with the stories and other analyzed case studies. This quantitative analysis will assess the extent that fuels, weather and climate are associated with firefighters view of extreme fire. The data for this project component includes weather observations, climate background (e.g., extent of drought), fuels conditions (e.g., moisture, fire danger), and atmospheric synoptic characteristics that might be associated with the fire.

Summary

At the time of this writing, we are about to launch the data collection system and are developing and deploying an extensive outreach strategy to reach both current and past wildland fire fighters in the United States. We hope to gather approximately 1000 stories through December of this year. Analysis of the data will occur simultaneously with the data collection. We will also develop a workshop and/or series of webinars to explore the data themes and results with the fire community early in 2015. Following the U.S. analysis, we would to begin collecting stories in Australia, Canada and Europe.

Flexible design of a cost-effective network of fire stations, considering uncertainty in the geographic distribution and intensity of escaped fires

Abílio Pereira Pacheco[a], Richard de Neufville[b], João Claro[a], Hèctor Fornés[b]

[a] *INESC TEC (formerly INESC Porto) and Faculdade de Engenharia, Universidade do Porto, Campus da FEUP, Rua Dr. Roberto Frias, 378, 4200-465 Porto, Portugal, apacheco@mit.edu*
[b] *Engineering Systems Division, Massachusetts Institute of Technology, 77 Massachusetts Avenue, Building E40-261, Cambridge, MA 02139-4307, USA*

Abstract
This paper proposes an improved strategy for allocating fire-fighting vehicles to Local Dispatch Centers (LDCs) over a region. By considering the uncertainties in fire location and intensity, and a flexible design, it develops a plan more cost-effective than that from a traditional deterministic approach, reducing the number and cost of required vehicles.
While small fires occur regularly and call for 'first response' equipment to be available close to susceptible fire-prone areas, large fires occur rarely and take time to develop. Thus the 'extended attack' equipment needed for larger fires can be held in reserve over a larger area, serving in effect as insurance against rare events. A layered strategy removes specialized equipment from the front lines and locates it in strategic reserves located in some of the pre-existing fire stations. The proposed solution thus reduces specialized equipment.
Innovatively, the analysis applies simulation to the management of fire-fighting resources, in order to deal with uncertainty in the number of deployments and location of fires over time. The approach first uses location algorithms to calculate optimal sets of fire stations. It then uses simulation to determine the probability distributions of outcomes of several performance measures (e.g., distance run by vehicles, vehicle utilization, or fire access time). The simulation implements flexibility by considering decision rules to open and close LDCs, according to recent observations of leading parameters. The outcomes of the simulation allow decision-makers to evaluate the performance of the flexible design in four different scenarios: as-is, intensification through wildland urban interface expansion or climate change, and attenuation (i.e., surveillance investment and law enforcement).
Finally, we use data available from ANPC and AFN/ICNF to compare the current design with the proposed flexible design, in a case study of the district of Porto, in Portugal. The results show that this design (a partially centralized strategy) leads to a cost-effective allocation of equipment and could reduce investment costs up to about 68 percent.

Keywords*: forest fire suppression, flexibility, network design, capacity planning, operations strategy*

Introduction

Portugal has an old and hardly used fleet of fire-fighting vehicles. These vehicles have more than 34 years on average and their underutilization is reflected by the mere 80 km they travel every year on average. The main goal of this research is to define a flexible design for the location of this fleet, to improve vehicle utilization efficiency without compromising its effectiveness.
We propose the centralization in Local Dispatch Centers (LDC), located in pre-existing fire stations (*Corporações de Bombeiros*), of some of the vehicles used in extended attack, deployed well after the initial emergency call, when containment by initial attack fails. These vehicles do not need to be immediately close to potential fires to ensure current levels of protection.
The model carries out a simulation to compare the current design with a proposed flexible allocation of equipment to LDCs, which can adjust to the changing location and nature of the forest fires. To deal with the uncertainty in the number and location of fires, a flexible approach opens and closes LDCs, according to recent observations of leading parameters - some of the current fixed locations as the

LDCs are selected to be open each year, according to the severity of the past three seasons and the number of LDCs open in the previous year.
Using the district of Porto, one of the eighteen districts of Portugal, as a case study, four envisioned trends are also analysed in independent scenarios: business as usual, evolution of the Wildland-Urban Interface, increased forest surveillance and law enforcement.

Methodology

Our model combines optimization and simulation to assess the flexible design in each of the four scenarios, over a 20-year period, considering one-year time-steps.
First, for each possible number of LDCs in a given range, and using historical data, we determine the set of LDC locations that minimizes the total distance run by vehicles (Cooper 1963; Kotian *et al.* 2009; Aravind *et al.* 2010). The potential locations are the currently existing firehouses, to decrease the costs of implementing the new design.
Second, in the simulation component, the model uses the locations of LDCs and the uncertain XY coordinates of fires to calculate the distance run by vehicles. The main driver of uncertainty is the total number of deployments per year, which depends on fire weather, modeled as an independent mean reverting process (Chow and Regan 2011). Empirical data is used to obtain this parameter and generate grid-based spatial distributions of vehicle deployments for each scenario, i.e., specific 2D distributions for each time-step, accounting for the uncertainty in the location and intensity of fires (Figure 1).

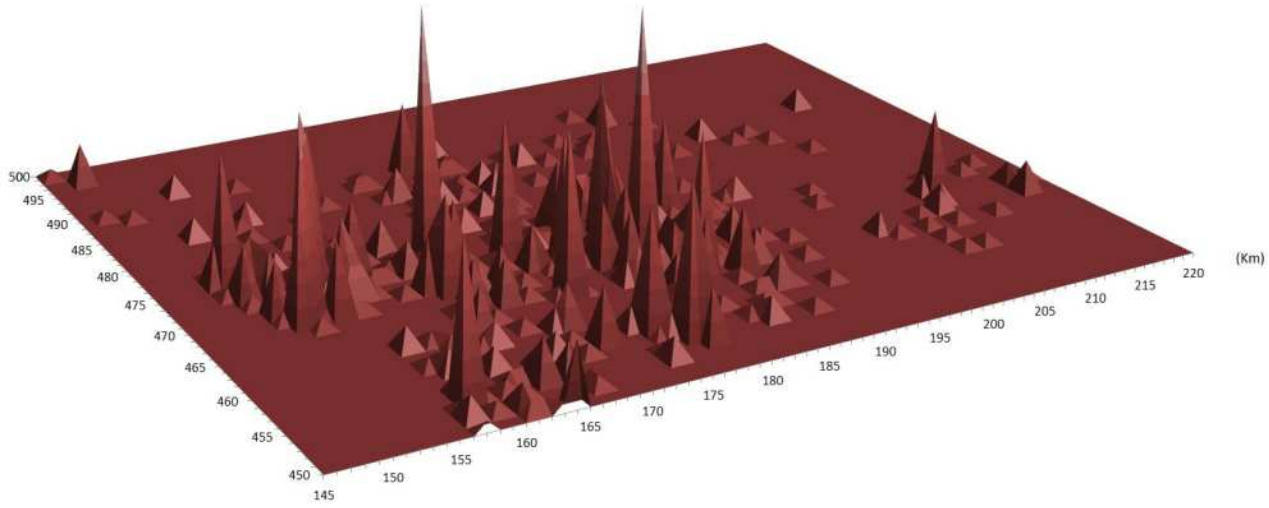

Figure 1. Graphical representation of a 2D distribution of escaped wildfires in the district of Porto, generated from a grid of one square kilometre

The model includes flexibility by applying, at each time-step, two decision rules to determine whether LDCs should be opened and/or closed given the new fire scenario conditions. Once the LDCs are fixed, the model calculates trip distance, time required to access fires, and thus extra time spent. The same procedure is repeated for the current network of firehouses, to compare the current and the proposed flexible design.

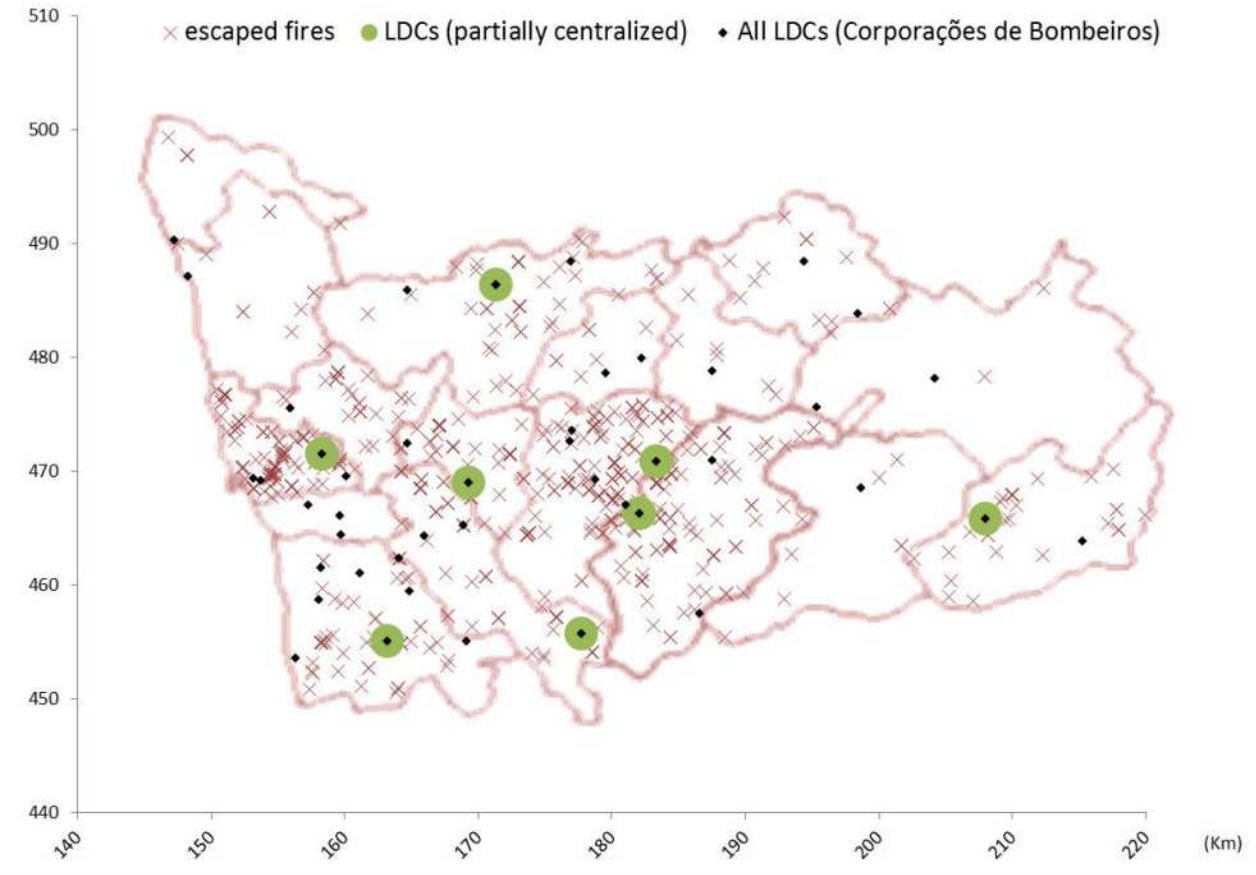

Figure 2. The best 8 (out of the current 45) LDC locations and randomly generated escaped fires, preserving the spatial pattern of historical forest fire data

For all the parameterizations, we use the Portuguese official fire databases, from ANPC and AFN/ICNF, the latter being the largest such database in Europe in terms of total number of recorded fires in the 1980–2005 period (Pereira *et al.* 2011).

Findings

Using one of the eighteen districts of Portugal as a case study (Porto, Figure 2), in the flexible design, the current fixed 45 locations were reduced to no more than 16 in the four scenarios. This design leads to a cost-effective allocation of equipment. Indeed, just in the case of the Porto district, it could reduce the investment in vehicles by about 6.5 M€, for a potential fleet reduction of up to 68%.
Additionally, the protection levels remain constant by keeping 90% of the potential fire-events within 10 km of the closest LDC and an average extra access time of sixteen minutes: these two indicators are reasonable given that they concern vehicles that are deployed after the fire escapes the first containment.

Contribution

This research tackles the issue of how to manage fire-fighting resources more cost-effectively. Analysis of empirical data of 2003 through 2005 provided by ANPC and AFN/ICNF, shows that Portugal has a very old and hardly used fleet of fire-fighting vehicles.
Our results show that a partial centralization by applying the proposed flexible design improves vehicle utilization efficiency while maintaining its effectiveness. The increased utilization reduces the number of vehicles needed and thus the cost of renewing the fleet (by about 100 M€). Policy makers might

consider using this new design as a strategy to address the lack of a management plan to procure equipment, since it eases the modernization of the current fleet.

Acknowledgements

This work was financed by the European Regional Development Fund (ERDF) through the COMPETE Programme (Operational Programme for Competitiveness), by National Funds through the Fundação para a Ciência e a Tecnologia (FCT, Portuguese Foundation for Science and Technology) within projects «FCOMP - 01-0124-FEDER-022701» and «FIRE-ENGINE - Flexible Design of Forest Fire Management Systems/MIT/FSE/0064/2009», in the scope of the MIT Portugal Program, and by grupo Portucel Soporcel. FCT has also supported the research performed by Abílio P. Pacheco (Grant SFRH/BD/92602/2013).
We are grateful to Rui Almeida on the Instituto da Conservação da Natureza e das Florestas (ICNF, Portuguese Institute for Nature Conservation and Forestry), who compiled the forest fire suppression historical data used in this research.

References

Aravind, H, Rajgopal, C, Soman, K (2010) A Simple Approach to Clustering in Excel. International Journal of Computer Applications 11, 19-25.

Chow, JYJ, Regan, AC (2011) Resource Location and Relocation Models with Rolling Horizon Forecasting for Wildland Fire Planning. INFOR 49, 31-43.

Cooper, L (1963) Location-allocation problems. Operations Research 11, 331-343.

Kotian, SR, Bonilla, C, Hale, TS (2009) The Planar k-Centra Location Problem. Open Industrial & Manufacturing Engineering Journal 2, 42-49.

Pereira, MG, Malamud, BD, Trigo, RM, Alves, PI (2011) The history and characteristics of the 1980–2005 Portuguese rural fire database. Nat. Hazards Earth Syst. Sci. 11, 3343-3358.

Flexible planning of the investment mix in a forest fire management system: spatially-explicit intra-annual optimization, considering prevention, pre-suppression, suppression, and escape costs

Abílio Pereira Pacheco[a], João Claro[b]

[a] *INESC TEC (formerly INESC Porto) and Faculdade de Engenharia, Universidade do Porto, Campus da FEUP, Rua Dr. Roberto Frias, 378, 4200-465 Porto, Portugal, app@fe.up.pt*
[b] *INESC TEC (formerly INESC Porto) and Faculdade de Engenharia, Universidade do Porto, Campus da FEUP, Rua Dr. Roberto Frias, 378, 4200-465 Porto, Portugal, jclaro@fe.up.pt*

Abstract
We model intra-annual management as a multistage capacity investment problem, considering a portfolio of resources enabling fuel treatment and fire suppression, and having fires as the demand.
The solutions are spatially explicit and our Mixed Integer Programming model considers two types of flexibility: capacity commitment postponement (prevention, pre-suppression, and suppression) and spatial flexibility (ground crews and aerial resources).
The results confirm that higher volatilities in weather conditions lead to commitment postponement, and we have found that the prevention/suppression balance changes qualitatively according to the burnt hectare value. The changes in the investment mix correspond to real world behaviors and challenge several myths. We have also found that above a certain threshold for the burnt hectare value, fuel treatments are always needed.

Keywords*: forest fire management, risk management, multi-resource investment, stochastic optimization*

Introduction

There are few natural phenomena with the scope and complexity of wildland fires (Van Wagner 1985). Highly unpredictable factors, such as weather, suppression performance, or fire behaviour, spread, and effects, have to be addressed in most Forest Fire Management (FFM) decisions. With limited financial funds, equipment, and human resources, policy makers must decide their most efficient and effective distribution among alternative FFM options, such as community prevention, fuel treatment, pre-suppression, suppression, and restoration (Mavsar *et al.* 2010).
In Portugal, forest fires are a severe problem, accounting for more than half the fires in the EU Mediterranean region (San-Miguel-Ayanz *et al.* 2013). In recent years, the consequences of forest fires have been particularly severe, with multiple catastrophic fire seasons (2003, 2005, 2013), and every year, on average, close to 2.5% of forestland burned, total direct losses near 250 M€, and more than 120 M€ spent in fire prevention and suppression.
To help tackle some of the challenges raised by the complexity and the large uncertainties in FFM systems, we use optimization to study the relationship between different types of operational flexibility, when used to mitigate exposure to uncertainty.

Methods

Using data and insights from our previous studies and fieldwork, we propose a Stochastic Mixed Integer Programming (MIP) model focusing on fuel treatment planning, but taking into account escape and suppression costs. We model intra-annual FFM as a multistage capacity investment problem, considering a portfolio of resources (Chod *et al.* 2010) enabling fuel treatment and fire suppression, and having fires as the demand.

Demand uncertainty has two origins: inter-annual weather variability (oscillations in fire season severity); and uncertainty in micro-scale factors (ignition, time, place, escape probability, and specific fire severity). We focus our analysis on mismatch risk (the cost of supply differing from demand): over-investment in FFM capacity will lead to unused capacity costs, whereas under-investment will lead to forest value loss. We model inter-annual weather variability with a scenario tree (considering conditions for winter, and spring) and micro-uncertainty with a spatial grid, each cell characterized by maximum ignition probability.

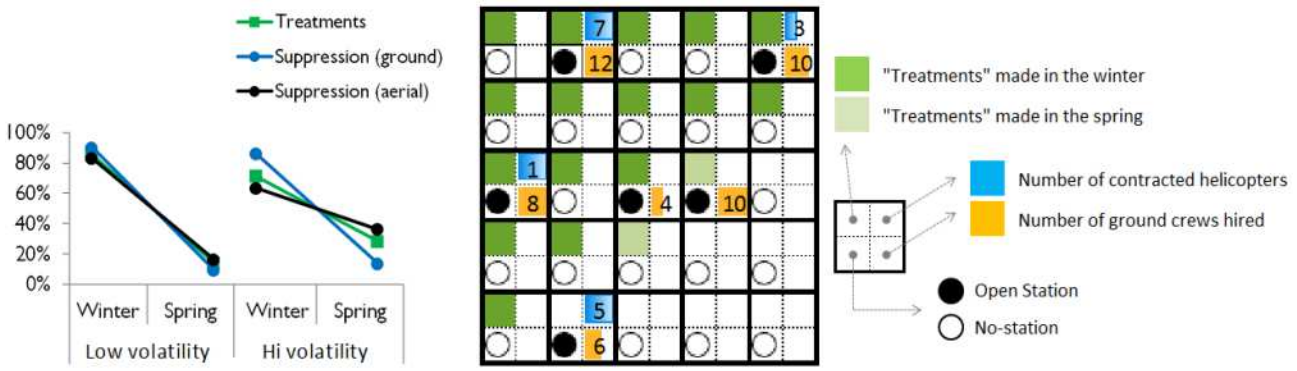

Figure 1. Low/high volatility vs. investment postponement % (left); spatial solution example (right).

We consider two types of flexibility (the ability to adapt to change): postponement of the commitment to each type of capacity (prevention and suppression), fine-tuning the capacity mix as the year evolves (and the weather conditional probabilities change); and spatial flexibility in a trade-off with the costs of the different suppression resource types (e.g., helicopters and ground crews).

3. Findings

Preliminary results point in three promising directions. First, the evolution of the investments along the year confirms that higher volatilities in weather conditions lead to their postponement (figure 1, left), and the results provide an estimate of the value for this source of flexibility. In addition, the solutions are spatially explicit (figure 1, right).
Second, we found that the balance between prevention and suppression changes qualitatively in the system (figure 2), according to the expanded cost attributed to each escaped fire (i.e., ignitions for which the initial attack fails, and come to be big or catastrophic fires), resulting in three system states.
Finally, fuel treatments are always of value above a certain cost per hectare. Indeed, independently of how the escape cost rises above that threshold, the optimal absolute value of the budget for fuel treatments remains almost constant (figure 2, solid green line).

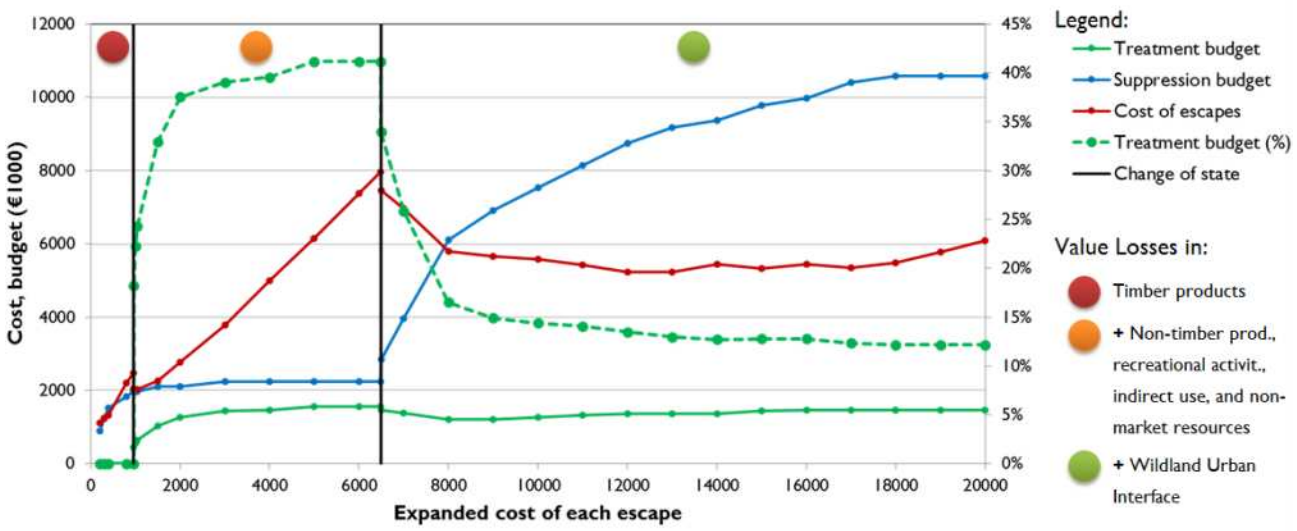

Figure 2. Global system behaviour and change of state (no prevention, prevention focused, and suppression dominance) according to the cost of each escaped forest fire.

Contribution

Studies addressing fuel treatment and fire suppression within the same model are scarce (Rideout *et al.* 2008), even more with the use of MIP, as in Minas *et al.* (2013), or Mercer *et al.* (2008). The latter inspired our model, which in turn modifies the standard-response model of Haight and Fried (2007) to include the effects of fuel treatment; in addition, we use insights from some of our previous studies (Collins *et al.* 2013; Pacheco *et al.* 2014).
Our results show that an integrated intra-annual FFM leads to a cost-effective allocation of the budget reducing the losses with catastrophic fires. In addition, the investment mix in each system state corresponds to different real world behaviours, challenging several FFM myths (e.g., prevention is always good; the prevention budget proportion should be at least one third; the utilization of helicopters is always a waste). Moreover, after a certain threshold the investments in fuel treatments are stable and always needed.

Acknowledgements

This work was financed by the European Regional Development Fund (ERDF) through the COMPETE Programme (Operational Programme for Competitiveness), by National Funds through the Fundação para a Ciência e a Tecnologia (FCT, Portuguese Foundation for Science and Technology) within projects «FCOMP - 01-0124-FEDER-022701» and «FIRE-ENGINE - Flexible Design of Forest Fire Management Systems/MIT/FSE/0064/2009», in the scope of the MIT Portugal Program, and by grupo Portucel Soporcel. FCT has also supported the research performed by Abílio P. Pacheco (Grant SFRH/BD/92602/2013).
We are grateful to Rui Almeida on the Instituto da Conservação da Natureza e das Florestas (ICNF, Portuguese Institute for Nature Conservation and Forestry), who compiled the forest fire suppression historical data used in this research.

References

Chod, J, Rudi, N, Van Mieghem, JA (2010) Operational flexibility and financial hedging: Complements or substitutes? Management Science 56, 1030-1045.

Collins, RD, de Neufville, R, Claro, J, Oliveira, T, Pacheco, AP (2013) Forest fire management to avoid unintended consequences: A case study of Portugal using system dynamics. Journal of Environmental Management 130, 1-9.

Mavsar, R, Cabán, AG, Farreras, V (2010) The Importance of Economics in Fire Management Programmes Analysis. In 'Towards Integrated Fire Management – Outcomes of the European Project Fire Paradox.' (Eds JS Silva, F Rego, P Fernandes, E Rigolot.) Vol. 23 pp. 230. (European Forest Institute: Torikatu 34, 80100 Joensuu, Finland)

Mercer, DE, Haight, RG, Prestemon, JP (2008) Analyzing trade-offs between fuels management, suppression, and damages from wildfire. In 'The Economics of Forest Disturbances.' pp. 247-272.

Minas, J, Hearne, J, Martell, D (2013) An integrated optimization model for fuel management and fire suppression preparedness planning. Annals of Operations Research 1-15.

Pacheco, AP, Claro, J, Oliveira, T (2014) Simulation analysis of the impact of ignitions, rekindles, and false alarms on forest fire suppression. Canadian Journal of Forest Research 44, 45-55.

Rideout, DB, Wei, Y, Kirsch, AG, Botti, SJ (2008) Toward a Unified Economic Theory of Fire Program Analysis with Strategies for Empirical Modeling. In 'The Economics of Forest Disturbances: Wildfires, Storms and Invasive Species.' (Eds TP Holmes, JP Prestemon, KL Abt.) pp. 361-380. (Springer Verlag:

San-Miguel-Ayanz, J, Moreno, JM, Camia, A (2013) Analysis of large fires in European Mediterranean landscapes: Lessons learned and perspectives. Forest Ecology and Management 294, 11-22.

Van Wagner, CE (1985) 'Fire behavior modelling - How to blend art and science, Eight Conference on Fire and Forest Meteorology.' Detroit, Michigan, USA, April 29-May 2. Available at http://cfs.nrcan.gc.ca/publications?id=23547

Forest fires hotspots in EU Southern Member States and North Africa: a review of causes and motives

Tedim F.[a], Meddour-Sahar O.[b], Lovreglio R.[c], LeoneV.[d]

[a] *University of Porto, Faculty of Arts, Via Panorâmica s/nº 4150-564 Porto, Portugal, ftedim@letras.up.pt*
[b] *University Mouloud Mammeri, Faculty of Biological Sciences and Agronomy, BP 17 RP, Tizi Ouzou, 15000, Algeria, o.sahar@yahoo.fr*
[c] *University of Sassari, Department of Agriculture, v. Cristoforo Colombo 1, I-08100 Nuoro, Italy, rlovreglio@uniss.it*
[d] *University of Basilicata (retired), Department of Crop Systems, Forestry and Environmental Sciences, I-85100 Potenza, Italy, vittorio.leone@tiscali.it*

Abstract
Despite enhanced fire suppression efforts the number of fires has increased in Europe and in North Africa, above all in Portugal, and the extinction oriented model of fire control is no more suitable to change the trend. Hence, the need of shifting from a reactive model grounded on a fast and strong reaction, to more pro-active procedures supported by prevention, aimed not only to fuel reduction but also to gradually intervene on the causes of fires. In this perspective, a fair knowledge of man-caused fire outbreak motives is a crucial point. This paper intended to compare and interpret those motives in Portugal, Italy and Algeria obtained through the perception of experts (forest experts and other practitioners). In this research new data was collected in the North Region of Portugal and data already available for Algeria and Italy was commented.
The results of the research highlighted great similarities of the main fire causes and motives identified by the experts from the case-studies in the three countries. Fire outbreak motives are not related with deliberate fire setting but, mainly, with the use of fire in rural activities. Fire is a manageable tool that is still needed in many agro-forestry systems. One of the findings of this study pointed out the need to design and develop specific prevention programs able to reduce fire incidence and promote practices more respectful of the tradition and needs of rural communities, often criminalized for their habitudes of using fire as a multipurpose tool. Deliberate fire can represent isolated and sporadic actions however, some of them result from organized and even criminal interests. Finally, this paper argues that improved fire prevention to address the roots of fire problems cannot be achieved without a deep knowledge of the complexity and diversity of the fire outbreak motives.

Keywords*: CBFiM, concertation, Delphi technique, EU, fire outbreaks motives, forest fire cause, integrated fire management, North Africa, occupational fire, prevention*

Introduction

Each year burned area continues to be substantial in Europe and in other Mediterranean countries (Table 1). Enhanced fire suppression efforts and investments in human and technical resources (e.g. important aerial fleets; updated methods and technology to fight fires; emergency response organization, coordination and support) limited the damages but did not solve the fire problem which is far from being controlled. The incapacity of reducing the number of ignitions, the apparition of events that grow to previously unheard sizes, and more frequent and complex fires in the wildland urban interface, are alerting signals of the need to improve and change forest fires policies. A mainly extinction oriented model of fire control seems not well adapted to cope with new forest fire scenarios (Molina *et al.* 2010; Montiel and Herrero 2010; Sebastián López *et al.* 2011).

Table1 - Forest fires in Southern European and North Africa countries

Country	Average yearly burnt area (ha)*	Average yearly number of fires (no.)*	Maximum annual burnt area (ha)	Average forest fire density no. fires/ km²	AAR**
Spain (*1980-2012)*	171,593	15,263	484,476[1]	3.0	0.84
Portugal (*1980-2012)*	108,334	18, 613	425,726[2]	20.3	3.31
Italy (*1980-2012)*	113,496	9,736	227,729[3]	3.2	1.14
Greece (*1980-2012)*	47,141	1,554	225,734[3]	1.2	0.57
Algeria (*1986- 2010)*	35,025	1,637	271,598[4]	0.07	0.85
France (*1980-2012)*	26,383	4,880	75,566[5]	0.9	0.53
Morocco (*1960-2009)*	2,987	260	11,174[6]	0.06	<0.01
Tunisia (*2005-2010)*	1,554	750	3,551[7]	0.5	<0.01

[1]In 1985; [2]In 2003; [3]In 2007; [4]In 1994; [5]In 1989; [6]In 2012; [7]In 2010

Source: *European Commission, 2013; **Annual Average Risk (AAR) i.e. the percentage of the wooded area burnt each year (FAO, 1999)

Even though forest fires have not usually been considered as a natural hazard by the scientific community (McCaffrey 2004), since the last decades of 20th century they have been recognized as natural hazards (e.g. floods, earthquakes) by the state agencies and institutions, such as NASA or European Union (EU) (Leone and Lovreglio 2003) and, consequently, as a problem to be covered by Civil Protection (or Civil Defence in some countries). Forest fires are a civil protection/defence problem in the moment of suppression, but they are the result of complex interrelationships between society-environment-economy, thus requiring a rather different approach shifting from the reactive model, typical of Civil Protection, to more pro-active procedures supported by a prevention strategy (EFIMED 2012; Xanthopoulos 2012; Marino *et al.* 2014; Raftoyannis *et al.* 2014).

A symptomatic solution dealing with problems, as they arise, but failing to address the underlying causes, can increase the chance that the same problem will crop up in the future. In the case of forest fires, this means to allocate resources to short-term fixing of symptoms, increasing emphasis on fire suppression, instead of dealing with the causes of problems (Collins *et al.* 2013), so neglecting fire prevention. The "*firefighting trap*" metaphor as used in business domain (Collins 2012; Collins *et al.* 2013) well depicts such a short sighted cycle of problem-solving.

Policy makers and fire managers should pursue a balanced approach to suppression and prevention activities (Collins *et al.* 2013) aimed not only at fuel management but also to intervene on the causes of forest fires which are predominantly the result of anthropic activities (FAO 2012).Thus, actions must effort to change individual, social and institutional behaviours, but they meet a weak point in the general lack of in-depth knowledge of causes and forest fire outbreaks motives which according to FAO (1999) is a "*precondition for the implementation of prevention adapted solutions*" (p. 41). It is actually biased by the relevant incidence of unknown causes [e.g. 95% in Morocco (European Commission 2013), 80% in Algeria (Meddour-Sahar *et al.* 2013), 60% in Tunisia (Ben Jamaa and Belhaj 2011), 16% in Italy (CFS 2012), 49% in Portugal (ICNF 2012)]. This is due to the current system of producing forest fires statistics through an a-critical processing of individual forest fires reports, compiled soon after control activity is over. The task is difficult without appropriate surveys, which are impossible in the presence of a great number of events, most of them of less than 5 ha, and without the identification of each ignition point.

This study intended to interpret the motives (i.e. "the intentional state which prompts or moves one to act"; Wrathall 2005: p. 118) of forest fires outbreaks in Portugal through the perception of forest experts, and compared the results with previous studies realized in Italy and Algeria, by a method which consistently reduces the incidence of unknown motives. This paper argues that improved fire

prevention to address the roots of fire problems requires a deep knowledge on the complexity and diversity of man-induced fire causes and motives and should be sensitive to their spatial variation.

Methods

In the absence of sufficient data and/or complete knowledge in regard to forest fires motives the Delphi technique, grounded on a structured process to collect opinions from a group of experts, can be used. This collective judgment, although made up of subjective opinions, is considered to be more reliable than individual statements and is thus more objective in its outcomes.

In Portugal, a research of forest fires causes using Delphi method was conducted in the North Region (NUT 2), with about 3.6 millions of inhabitants (INE 2012) and a surface of 21,278 km^2. It is among the most fire prone regions of the country where, between 1980 and 2011, a total number of 351,550 fires was recorded which burned 1,219,609 ha. The North Region encompasses 86 municipalities, but the urban municipalities of Porto and S. João da Madeira were excluded from the analysis. To the 84 selected municipalities a questionnaire was sent by email to be answered by the Forest Fire Technical Division of each municipality which is responsible for the Municipal Plan for the Defence of the Forest Against Fire, as established by the Decree-law 17/2009. The questionnaire contained the Portuguese official list of the three level structure of fire causes reporting 68 motives (http://www.icnf.pt/portal/florestas/dfci/Resource/doc/estatist/dgrf-codificacao-causas.pdf; Camia *et al.* 2013), divided into seven main categories (i.e. *negligent usage of fire, accidental, structural causes, incendiary, natural, unknown, and rekindle*) with their identification codes. Experts should identify the fire outbreaks motives in their territories, classifying them by a Likert scale from 1 to 5 (ranging from *not important* to *extremely important*); successively, they were asked to rank the six most important motives in decreasing order of importance from 1 (the *most important*) to 6 (the *least important*). Sixty nine valid answers were received (i.e. a return rate of 82% of the contacted sample). The information from the questionnaire was analysed and a fire motive rank-ordering was established as the mode of rank-scores. The early results of this procedure are presented and discussed in this paper. The following step will be the organization of meetings in different municipalities of the North Region to circulate, validate and discuss the results from the questionnaire.

The procedure used in Portugal was slightly different from the one used in Algeria and Italy concerning the two rounds interspersed with a feedback and the number of ranked motives, only six in Portugal instead of the eight in Algeria and Italy. These differences did not have implications in the comparative study. Detailed information on the methodology used in Algeria and Italy can be found in Meddour-Sahar *et al.* (2013) and Lovreglio *et al.* (2006), respectively.

In Algeria, the Delphi method was used to identify forest fires causes and motives in the three most affected *wilayas* (equivalent of NUTS 3, Departments) i.e. Bouira, Boumerdes, and Tizi Ouzou (Meddour-Sahar *et al.* 2013; Meddour-Sahar 2014).

In Italy, the same method was used in the 29 most affected provinces in the Centre and South of the country, in two National Parks (NP) in the South of the Country (NP of Gargano, NP of Cilento and Vallo di Diano) and in some minor administrative units such as Mountain Communities (MC) (Lovreglio *et al.* 2006; De las Heras *et al.* 2007; Lovreglio *et al.* 2008; Leone and Lovreglio 2009; Lovreglio *et al.* 2010a,b; Marciano *et al.* 2010; Regione Puglia 2012).

Although it was interesting to consider Spain in this study, the data obtained also using Delphi method (APAS and IDEM 2003, 2004; Dolz Reus and Franco Irastorza 2005; Franco Irastorza and Dolz Reus 2007) were not comparable for methodological differences.

3. Results

The frequency analysis of forest fires outbreak motives reported as extremely important by the panel's members in North Region of Portugal showed a large variety of motives, where just five of 68 possible reasons were not identified as extremely important by the experts. The most mentioned were rekindle

(considered by 54% of the municipalities) and management of forestry or agricultural vegetation (e.g. renewing pastures, 48% of the municipalities' responses; clearing of forest areas, 45%; clearing of agricultural areas, 41%). Other motives were related with conflicts in the use of resources (e.g. hunting conflicts, 30%), influence on economic/market activities (e.g. pressure on wood market, 20%), social and interpersonal tensions (e.g. conflicts between neighbours, 26%; revenges and retaliatory actions, 24%), and antisocial behaviours (e.g. pyromania, 38%; vandalism, 32%).

The rank obtained from the modal values of the extremely important motives classified from 1 to 6 by the panel's members highlighted the same reasons although presenting them in slightly different order (Table 2). Thus, the most important fire ignition motive in the North Region of Portugal was renewing pastures which was identified as the first one in 16 municipalities and the second one in another nine municipalities. Still related with management of forestry or agricultural vegetation cleaning the agricultural lands and cleaning forest lands appeared in rank 2 and 3, respectively. Pyromania appeared in rank 4, being the main motivation in eight municipalities. In rank 5, appeared vandalism as well as rekindle. Conflicts between neighbours were classified in rank 6.

The results of the rank ordering in North Region of Portugal were not very different from the ones found in Algeria and Italy. Furthermore, in these countries fire, as a manageable tool needed in many agro-forestry systems, appeared as the main reason for fires outbreaks. In Algeria (Table 3), the use of fire in agricultural works was the main motive in the three wilayas together with vegetation management activities (i.e. creation or renewal of pastures, forest works, and wild honey hunting). Illegal garbage dumping and burning, mentioned in the three wilayas although in different rank position, is an "inevitable ´problem solving´ solution by inhabitants, who have no other more sustainable alternative for waste disposal" (Meddour-Sahar *et al*. 2013: p. 251). Other negligent reason was cigarettes remains. Deliberate fires (i.e. intentionally caused by human, according to the harmonized classification scheme of fire causes in EU, Camia *et al*. 2013) were mainly related with interests in land use changes. Rekindle appeared important in Algeria too, where it is caused by fire crews who do not always ensure the mopping up of controlled fires but as well as by the so called "security fires" (Meddour-Sahar *et al*. 2013).

In Italy (Table 4), with the exception of the Province of Bari, the negligent motives are also more important than deliberate use of fire. Multiple motives in the same rank order reflect the

Table2 -Experts panel perception on forest fire ignitions motivations, in Portugal (answers N=69; orange colour for deliberate causes, green for negligent causes, and grey for rekindle)

Frequency	Rank	Motives	Modal values for its position category					
			1st	2nd	3rd	4th	5th	6th
33	1	Renewing pastures	16	9	1	0	1	1
28	2	Cleaning of agricultural areas	1	10	3	3	4	0
31	3	Cleaning of forest areas	3	3	9	5	2	3
26	4	Pyromania	8	3	3	7	1	2
22	5	Vandalism	8	2	1	2	3	0
37	2	Rekindle	8	6	6	2	3	2
18	6	Conflicts between neighbours	1	4	4	0	2	4

Table 3. ***Perception of experts' panels on forest fire ignitions motivations in Algeria (orange colour for deliberate causes, green for negligent causes, and rekindle in grey)***

Wilaya	1	2	3	4	5	6	Source
Bouira	Agricultural works (stubble burning)	Cigarette remains	Illegal garbage dumping and burning	Creation or renewal of pastures	Interests in land use changes	Wild honey hunting	Meddour-Sahar *et al.* 2013
Boumerdes	Agricultural works (stubble burning)	Rekindle	Forest works (burning of cut bush)	Illegal garbage dumping and burning	Cigarette remains	Interests in land use changes	Meddour-Sahar 2014
Tizi-Ouzou	Agricultural works (stubble burning)	Illegal garbage dumping and burning	Interests in land use changes	Cigarette remains	Rekindle	Forest works (burning of cut bush)	

Table4 -Perception of experts' panels on forest fire ignitions motivations in Italy (N.A.-Not available; orange colour for deliberate causes, green for negligent causes, and rekindle in grey)

NUTS	1	2	3	4	5	6	Source
NUTS2 Basilicata Region	Agricultural works (stubble burning)	Creation or renewal of pastures	Agricultural works (stubble burning)	Creation or renewal of pastures	Ownership controversies	Retaliation against public administration	Lovreglio *et al.* 2006
NUTS3 Province of Taranto	Burning of fallow land	Agricultural works (stubble burning)	Agricultural works (stubble burning)	Creation or renewal of pastures	Creation or renewal of pastures	Illegal garbage dumping and burning	Lovreglio *et al.* 2008
MC of Vallo di Diano	Agricultural uses	Agricultural works (stubble burning)	Hunting products in areas scorched by fire passage (e.g. mushrooms, wild asparagus)	Cigarettes remains	Hunting products in areas scorched by fire passage (e.g. mushrooms, wild asparagus)	Fire-crackers and bottle-rockets	Lovreglio *et al.* 2010a
	Burning of rests		Agricultural works (stubble burning)	Agricultural uses	Burning of rests		
			Ownership controversies		Ownership controversies		
NP of Gargano	Agricultural works (stubble burning)	Creation or renewal of pastures	Protest of seasonal fire-fighters	Agricultural works (stubble burning)	Creation or renewal of pastures	Protest of seasonal fire-fighters	Lovreglio *et al.* 2010a
			Retaliation against public administration				
		Protest of seasonal fire-fighters	Fire caused with the intent of being included in fire-fighting crews	Fire caused with the intent of being included in fire-fighting crews			

NUTS3 Province of Bari	Fire caused with the intent of being included in fire-fighting crews	Agricultural works (stubble burning)	Agricultural works (stubble burning)	Creation or renewal of pastures	Building speculation	Hot vehicle exhaust pipes	Lovreglio *et al.* 2010a
		Protest of seasonal fire-fighters	Cleaning of road/railroad	Fire caused with the intent of being included in fire-fighting crews	Protest of seasonal fire-fighters	Building speculation	
	Agricultural works (stubble burning)	Ownership controversies	Protest of seasonal fire-fighters			Ownership controversies	
NP of Cilento and Vallo di Diano	Creation or renewal of pastures	Hunting products in areas scorched by fire passage (e.g. mushrooms, wild asparagus)	Hunting products in areas scorched by fire passage (e.g. mushrooms, wild asparagus)	Ownership Controversies	Plantation cleaning after harvest	Hunting products in areas scorched by fire passage (e.g. mushrooms, wild asparagus)	Lovreglio *et al.* 2010b
				Agricultural land cleaning after harvesting	Burning of rests		
				Burning of rests		Ownership Controversies	
NP of Gargano	Creation or renewal of pastures	Agricultural works (stubble burning)	Vegetation burning to earn agricultural land	Burning of fallow land	Burning of rests	Agricultural works (stubble burning)	Leone and Lovreglio 2009
						Fire lit to depreciate tourist areas	
						Fire lit for game or divertissement	
29 NUTS3 Central South	Creation or renewal of pastures	Agricultural works (stubble burning)	Agricultural land cleaning after harvesting	Agricultural land cleaning after harvesting	Hunting conflicts and poaching	Mental troubles and pyromania	Marciano *et al.* 2010
NUTS 2 Region of Apulia	Burning of fallow land	Agricultural works (stubble burning)	Burning of fallow land	Burning of rests	Creation or renewal of pastures	Mental troubles and pyromania	Regione Puglia 2012
				Agricultural works (stubble burning)			
				Cleaning of road/railroad			
NUTS2 Region of Sardinia	Agricultural and forest activities (burning of stubble and agricultural wastes)	Rekindle	Careless use of machinery	Non-compliance with Regional regulations	N.A	N.A	Lovreglio *et al.* 2014

difference of experts' perspective. The main negligent reasons (classified in rank 1) in all the study-areas were agricultural burnings (e.g. *stubble burning, creation or renewal of pastures, burning of fallow, burning of rests, agricultural land cleaning after harvesting*). Also considered in the rank of the six most important fire outbreak motives appear: *fire-crackers and bottle-rockets, careless use of*

machinery, *cleaning of road/railroad*, *hot vehicle exhaust pipes*, *cigarettes remains,* and *illegal garbage dumping and burning*. *Garbage dumping and burning* is a negligent action in the current EU causes classification (Camia *et al.* 2013), where it is considered a form of waste management. Anyhow, mainly in the South of Italy, it is related to illegal dumping and successive burning by organized criminality, for which illegal waste and garbage traffic and disposal represent an important eco-business; for this it must be classified as voluntary, related to illegal profits.
Deliberate fires motives in the Italian case-studies appeared very diverse and with different profiles. The most important motives are profit activities to obtain goods, job or even money (e.g. *hunting products in areas scorched by fire passage as mushrooms and wild asparagus; building speculation; vegetation burning to earn agricultural land; fire lit to depreciate tourist area; fire caused with the intent of being included in fire-fighting crews*). Social and interpersonal tensions (e.g. *hunting conflicts and poaching*, *ownership controversies*) can also explain some fire setting. Some forest fires events could be attributed to negligent behaviours (e.g. *fire-crackers and bottle-rockets*; *careless use of machinery*; *hot vehicle exhaust pipes*). The experts also identified fire outbreaks as a mean of protest and contestation against public or installed powers (e.g. *retaliation against public administration* and *protest of seasonal fire-fighters)* as well as *noncompliance with regional regulations*. Antisocial behaviours (e.g. *pyromania, vandalism*) did not appear as relevant as happened in Portugal. *Rekindle* was not considered significant in Italy, and was just mentioned in Sardinia Region.
Forest fires outbreaks motives hotspots in all the case-studies were related with the fire use in agriculture burnings and vegetation management. The representativeness and the profile of deliberate fire motives are distinctive between the case-studies.

Discussion

Forest fire outbreaks motives are not a fixed and immutable concept being used through the centuries. "*Fire's definition has changed with its cultural circumstances. It takes its character from its contex*t" (Pyne 2006: p.1). Main motives behind fire outbreaks found in the study-areas can be categorized in three main groups: traditional fire use (TFU) which refers to communities using fire for land and resources management purposes, based on traditional know-how (Lázaro 2010); deliberate fires; and rekindle, each of them putting different challenges in developing measures to reduce their incidence.
TFU explains most of the fires in Portugal, Italy and Algeria as it is a deeply-rooted tool for land and resources management purposes, namely *agricultural or forest residues burning* and for *creating or renovating pastures*. TFU has been facing a very restrictive legal framework (Lovreglio and Leone 2010) resulting from the incapacity to understand that "*fire for humanity is more than a problem or a process. It is a relationship*" (Pyne 2006: p.6). The illegal use of fire is often carried out as a *hit-and-run* practice (e.g. by shepherds setting fires during the night and escaping to avoid prosecution) many times taking place even in days of high fire danger which can provoke the occurrence of large and severe fires. TFU still represents an efficacious way of "problems-solving" by aged rural societies, whose members persist with practices now considered with disdain by the dominant urban society; the latter sometimes adopts a top-down approach deciding plans and programs in the rural context without concertation nor listening the rural communities. For decades state agencies ignored this reality and the criminalization of TFU in land management activities and the lack or absence of alternatives just aggravated the problem. Problems solving through the use of fire fits with the relevant concept of "*man responsible, but not guilty*" as theorized by Dumas *et al.*(2013) and well indicates a possible direction for prevention measures based on the scientific knowledge, respect and wise re-utilization of T.E.K. (Traditional Ecologic Knowledge: Ribet 2002) in rural areas. The criminalization of TFU and the public strategies to deal with high impact fire events, mainly through subsidies to overlap property damages, can inhibit the TFU and transform it in deliberate fire. Considering the high representativeness of the negligent use of fire in agricultural and forestry works in the investigated fires with known causes (46% in 2012 in Portugal, according to ICNF 2012), an improved action on

TFU could have a significant contribution for a sustained reduction of fire occurrence. The concept of integrated fire management offers the framework to enhance TFU (FAO 2006; Silva *et al.* 2010) which implies making communities part of the solution requiring a community-based fire management (CBFiM) approach i.e. "*an approach to fire management in which local communities are actively engaged in the development, and in some instances the implementation, of fire management strategies designed to prevent, control or utilize fires in ways that will improve their livelihood, health and security*" (FAO 2011: p.4).

Deliberate fires in all study areas represented only a part of the arson motive classification as proposed by NCAVC (National Centre for the Analysis of Violent Crime) of FBI Academy (Icove and Estepp 1987; Douglas *et al.* 1992), namely: *vandalism*, *excitement*, *revenge*, *crime concealment*, *profit*, and *extremist*. These classes were also proposed by the new classification scheme of fire causes in EU (Camia *et al.* 2013). In the study-areas the classes retrieved were mainly *vandalism*, *revenge*, and *profit* (including some cases of deliberate fires by organized crime, e.g. *fire lit to depreciate tourist area* as was mentioned in Italy).

"Logics" behind deliberate fires can be a consequence of processes acting: (i) at different spatial scales (e.g. some fires are related with local conflicts that originate revenges; others can be associated with the constraints of a top-down approach by state agencies, interest of non-local groups or even criminal organizations); (ii) with different frequency (i.e. some fires are isolated events; others can have a high frequency reflecting the repetition of the same fire outbreak motive). The representativeness and the profile of deliberate fire outbreak motives resulted distinctive between the case-studies. Most of the motives identified in the case-studies appeared as a consequence of local dynamics reinforcing the importance of adopting CBFiM approach with adapted strategies of intervention. A small part of deliberate fires can be interpreted as a reaction from the peasantry to the exclusion from their environment imposed by the urban society (Zarraga Moreno 1988) and the top down approach used by the state supporting policies that affect the forms of local life (e.g. forestation of commons, too restrictive nature conservation policies, precluding hunting). Others can be related with taking profit of sectorial policies (e.g. hunting law, nature conservation law) or spatial planning (e.g. urban sprawl planning). Others can result from the management of resources imposed without assessing the impacts on the economic dynamic, environment quality and social relationships in each territory. In some cases they can represent a reaction against benefits established by law which can create conditions favourable to the exploitation of local resources by people from outside the communities, for instance changes of land use. Antisocial behaviours in Algeria and Italy (e.g. *pyromania, vandalism*) did not appear as important as happened in Portugal where *pyromania* can be related with the misuse of the term. There are different solutions to deal with deliberate fires. Law enforcement is important not only to penalize behaviours but mainly to control business opportunities related with fires. However it is not the only solution mainly because "a one fits all" strategy more than solving a problem can develop it.

The importance of *rekindle* is different among the case-studies considered in this paper. The frequency of fire restart is higher in Portugal and the situation has aggravated over the years (Pacheco *et al.* 2012). "*The high number of rekindles results from the pressure on the suppression system which works at constantly very high levels of capacity utilization, and is constantly requested to immediately combat all the new fires*" (Pacheco *et al.* op. cit.: p.10). *Rekindle* is important in Algeria too and can be explained by the pressure on the suppression apparatus, adding to the specific lack of security in some forested areas due to problems of terrorism, which make dangerous working in forests (Meddour-Sahar *et al.* 2013). In Italy, *rekindle* is not present in the official list of motives, with the exception of the autonomous Region of Sardinia where it appeared in the second rank. Reducing the incidence of *rekindle* could be achieved directly by enhancing suppression effectiveness (e.g. better training in mop-up operations), active surveillance, increased crew capacity and by adjusting dispatch rules (Pacheco *et al.* 2014). Indirectly, it could result from the reduction of the number of fire outbreaks which implies a decrease of the pressure on suppression apparatus. Pacheco *et al.* (2013) presented

quantitative evidences of the advantages of investing in prevention to reduce *rekindle* as well as "*to invert the vicious circle of more fire, more teams*" (p.53).

Conclusion

It is a common place to say that addressing current forest fire problems requires more balanced suppression and prevention policies. The "*firefighting trap*" pointed out for the need to increase fire prevention clearly identifying the pitfalls of a single suppression approach. However, it is not possible to enhance prevention without a deep knowledge on the complexity of fire causes and outbreaks motives. This study showed the importance of adopting a cause-based approach focusing on the underlying reasons that induce specific negligent or deliberate behaviours.

Fire occurrence cannot be understood if disconnected from the social environment in which is produced (Zarraga Moreno 1988).The theoretical knowledge of the cultural and social construction of fire outbreak motives based on empirical studies is one of the requirements of paramount importance to enhance prevention. Without this scientific knowledge and its integration with local knowledge and the interests of the communities, the development of prevention programs can be misleading and contribute to discrediting the indisputable role of prevention. However, the immediate consequence should not be the design of a general model indistinctly applied in all contexts even with similar characteristics. From an operational point of view the theoretical framework should support prevention plans using a place-based approach, taking into account that more superficial is the knowledge of forest fire outbreak motives more inefficient and dangerous can be the transfer of findings from one context to another even with the same profile. An improved knowledge on fire ignitions motives can enhance forest fire prevention as implies a collaborative effort and communication between state agencies and local communities, thus necessarily adopting a CBFiM approach. However, it does not mean "a "*one size fits all" approach, but rather it must be tailored to meet specific needs and circumstances to be an effective and sustainable approach to fire management*" (FAO 2011: p.1-2).

Fire prevention oriented to the reduction of fire outbreaks is a complex issue comprising three processes: (i) knowledge of man-caused ignition motives; (ii) the development of specific targeted awareness campaigns promoting communities' engagement to change attitudes and behaviours; (iii) and concertation between communities and public organizations. The latter is a very complex and ambitious goal. It needs to accommodate several interests and solve conflicts between several actors (e.g. forest services, shepherds, farmers) through proper communication, finding concerted and socially acceptable solutions, defining new relations between public policies, administration, and communities.

Acknowledgment

The first author would like to thank the experts from the North Portugal municipalities for their collaboration in this research and CEGOT – Centre for Geography Studies and Spatial Planning, a research unit funded by FCT- Portuguese Foundation for Science and Technology, (PEST-OE/SADG/UI4084/2014) for funding the participation in the VII International Conference in Forest Fire Research.

References

APAS, IDEM (2003) ´Estudio Sociológico sobre la Percepción de la población española hacia los incendios forestales.´ Asociación para la Promoción de Actividades Socioculturales: (MMA: Madrid). Available at http://www. idem21.com/descargas/pdfs/ IncediosForestales.pdf

APAS, IDEM (2004) ´Estado del conocimiento sobre las causas de los incendios forestales en España.´ (MMA: Madrid)

Ben Jamaa ML, Belhaj S (2011) Forest Fire in Tunisia: importance and prevention. CypFire 23-2 Cypress and forest fires: a practical manual. Reports of the Training School. (Florence, IT). Available at http://cupressus.ipp.cnr.it/cypfire/files/Brochure%20Summer%20School-5.pdf

CFS (2013)´Incendi boschivi. Dati di sintesi 2012.´ (Corpo Forestale dello Stato: Roma*)*

Camia A, Durrant T, San-Miguel-Ayanz J (2013) ´Harmonized classification scheme of fire causes in the EU adopted for the European Fire Database of EFFIS Executive report.´(JRC, European Commission: Ispra)

Collins RD (2012) ´Forest Fire Management in Portugal: Developing System Insights through Models of Social and Physical Dynamics´ (SM thesis). (Massachusetts Institute of Technology: Massachusetts)

Collins RD, de Neufville R, Claro J, Oliveira T, Pacheco AB (2013) Forest fire management to avoid unintended consequences: A case study of Portugal using system dynamics. *Journal of Environmental Management* **130**, 1-9.

De Las Heras J, Salvatore R, Rodrigues MJ, Lovreglio R, Leone V, Giaquinto P, Notarnicola A (2007) Wildfire motivation survey through the Delphi method. Actas de la IV Conferencia Internacional sobre Incendios Forestales. (Sevilla: SP). Available at http://www.fire.unifreiburg.de/sevill2007/contributions/doc/SESIONES_TEMATICAS/ST4/Heras_et-AL_SPAIN_ITALY.pdf

Dolz Reus ML, Franco Irastorza I (2005) State of the art of forest fire causes in Spain. In ´Proceedings of II International Conference on Prevention Strategies of Fires in Southern Europe´ (Ed Centre Tecnologic Forestal de Cataluña) pp.325-331. (Centre Tecnologic Forestal de Cataluña: Solsona)

Douglas E, Burgess AW, Burgess AG, Ressler RK (1992) ´Crime Classification Manual: A Standard System for Investigating and Classifying Violent Crimes.´ (Lexington Books: New York)

Dumas P, Toussaint M, Herrenschmidt J-B, Conte A, Mangeas M (2013) Le risque de feux de brousse sur la Grande Terre de Nouvelle-Calédonie: l'Homme responsable, mais pas Coupable. *Revue Géographique de l'Est* [En ligne] **53**/ 1-2 |. Available at http://rge.revues.org/4598

EFIMED (2012) The fight against forest fires: an inconvenient truth? EFIMED network newsaugust-2012, 1. Available at http://news.efi.int/newsletter/view/efimed-newsletter-august-2012/1044

European Commission (2013) ´Forest Fires in Europe, Middle East and North Africa.2012.´ (Publications Office of the European Union: Luxembourg)

FAO (1999) ´FAO Meeting on Public Policies Affecting Forest Fires.´ (FAO: Rome)

FAO (2006) ´Fire Management Voluntary Guidelines. Fire Management.´ (FAO: Rome)

FAO (2011) ´Community-based fire management: A review.´ (FAO: Rome)

FAO (2012) ´State of Mediterranean Forests (SoMF) Concept Paper.´ (FAO: Rome)

Franco Irastorza I, Dolz Reus ML (2007) Análisis de la percepción de la sociedad ante el problema de los incendios forestales: metodología y resultados. In ´Actas de la IV Conferencia Internacional sobre Incendios Forestales´. (Sevilla: SP). Available at http://www.fire.uni-freiburg.de/sevilla-2007/contributions/doc/cd/SESIONES_TEMATICAS/ST1/Franco_Dolz_ SPAIN.pdf

ICNF (2012) ´Relatório anual de áreas ardidas e incêndios florestais em Portugal Continental´. (ICNF, ANPC: Lisboa)

INE (2012) ´CENSOS 2011. RESULTADOS DEFINITIVOS, Norte.´ (INE: Lisboa). Available at http://www.ine.pt/xportal/xmain?xpid=INE&xpgid=ine_main

Icove DJ, Estepp MH (1987) Motive-Based Offender Profiles of Arson and Fire Related Crimes. *FBI Law Enforcement Bulletin* **56**, 17-23.

Lázaro A (2010) Development of prescribed burning and suppression fire in Europe. In ´Best practices of fire use - Prescribed burning and suppression in selected case-study regions in Europe´. (Eds C Montiel, D Kraus) pp. 17–31. (European Forest Institute: Joensuu)

Leone V, Lovreglio R (2009) Parco Nazionale del Gargano Piano di Previsione, Prevenzione e lotta attiva contro gli incendi boschivi Primo Aggiornamento 2009-2011. Available at http://www.minambiente.it/pagina/parco-nazionale-del-gargano-0#sthash.waDv9yTY.dpuf

Leone V, Lovreglio R (2003) Human fire causes: a challenge for modelling. In ´Innovative Concepts and Methods in Fire Danger Estimation´. (Eds E Chuvieco, P Martín, C. Justice) pp.89-98. (Ghent University – EARSeL: Ghent)

Leone V, Lovreglio R, Pilar Martín M, Martínez J, Vilar L (2009) Human Factors of Fire Occurrence in the Mediterranean. In ´Earth Observation of Wildland Fires in Mediterranean Ecosystems´. (Ed E. Chuvieco) pp.149-170. (Springer-Verlag: Berlin, Heidelberg)

Lovreglio R, Leone V, Giaquinto P, Notarnicola A (2006) New tools for the analysis of fire causes and their motivations: the Delphi technique. *Forest Ecology and Management* **234**, 18-33.

Lovreglio R, Rodrigues MJ, Silletti G, Leone V (2008) Applicazione del metodo Delphi per l'analisi delle motivazioni degli incendi: il caso Taranto. *L'Italia Forestale e Montana* **5**, 427-447.

Lovreglio R, Leone V, Giaquinto P, Notarnicola A (2010a) Wildfire cause analysis: four case-studies in southern Italy. iForest **3**, 8-15.

Lovreglio R, Rodrigues MJ, Notarnicola A, Leone V (2010b) From fire motives survey to prevention: the case of Cilento and Vallo di Diano National Park (Italy). In ´Proceedings of the VI International Conference on Forest Fire Research´. (Ed DX Viegas) pp.1-6 (Paper 18) (ADAI/CEIF, University of Coimbra: Coimbra)

Lovreglio R, Mou G, Leone V (2014) Forest fire motives in Sardinia through the perception of experts. In ´Advances in Forest Fire Research´ (Ed DX Viegas). (Coimbra University Press: Coimbra) (in press)

Marciano A, Lovreglio R, Patrone A, Notarnicola A, Leone V (2010) Tecniche di analisi delle motivazioni degli incendi. Applicazione nel territorio del Parco Nazionale del Cilento e Vallo di Diano. *Sherwood* **162**, 13-18.

Marino E, Hernando C, Planelles R, Madrigal J, Guijarro M, Sebastian A (2014) Forest fuel management for wildfire prevention in Spain: a quantitative SWOT analysis. *International Journal of Wildland Fire* **23**, 373-384.

McCaffrey S (2004) Thinking of Wildfire as a Natural Hazard. *Society and Natural Resources* **17**, 509-516.

Meddour-Sahar O, Meddour R, Leone V, Lovreglio R, Derridj A (2013) Analysis of forest fires causes and their motivations in North Algeria: the Delphi technique. *iForest-Biogeosciences and Forestry* **6**, 247-254.

Meddour-Sahar O (2014) ´Les feux de forêt en Algérie: Analyse du risque, étude des causes, évaluation du dispositif de défense et des politiques de gestion.´ (Université Mouloud Mammeri: Tizi Ouzou)

Molina D, Castellnou M, García-Marco D, Salgueiro A (2010) Improving fire management success through fire behaviour specialists. In ´Towards Integrated Fire Management-Outcomes of the European Project Fire Paradox´. (Eds JS Silva, F Rego, P Fernandes, E Rigolot) pp. 105-119. (European Forest Institute: Joensuu)

Montiel C, Herrero G (2010) An overview of policies and practices related to fire ignitions at the European Union level. In ´Towards Integrated Fire Management-Outcomes of the European Project Fire Paradox´. (Eds JS Silva, F Rego, P Fernandes, E Rigolot) pp. 35-46. (European Forest Institute: Joensuu)

Pacheco AP, Claro J, Oliveira T (2012) Rekindle dynamics: validating the pressure on wildland fire suppression resources and implications for fire management in Portugal. In ´Modeling, monitoring and management of forest fires III´. (Ed Wessex Institute of Technology). (WIT-Press: Ashurst, Southampton)

Pacheco AP, Claro J, Oliveira T (2014) Simulation analysis of the impacts of ignitions, rekindles, and false alarms on forest fires suppression. *Canadian Journal of Forest Research* **44**, 45-55.

Pyne S (2006) Fire Ecology: Issues, Management, Policy, and Opinions. A forum for the association for fire Ecology. *Fire Ecology* **2**, 1-6.

Raftoyannis Y, Nocentini S, Marchi E, Calama Sainz R, Garcia Guemes C, Pilas I, Peric S, Paulo JA, Moreira-Marcelino AC, Costa-Ferreira M, Kakouris E, Lindner M (2014) Perceptions of forest

experts on climate change and fire management in European Mediterranean forests. *iForest-Biogeosciences and Forestry* **7**, 33-41.

Regione Puglia (2012) Piano di prevenzione, prevenzione e lotta attività contro gli incendi boschivi 2012-2014. Legge 353/2000. Bollettino Ufficiale Regione Puglia, **59**, 12455-13042.Available at http://www.protezionecivile.puglia.it/public/news.php?extend.630.10

Ribet N (2002) La maîtrise du feu un travail "en creux" pour façonner les paysages. In ´Travail et paysages´. (Ed D. Woronoff) pp.167-198. (Éditions du CTHS: Paris). Available at http://www.ecoanthropologie.cnrs.fr/pdf/Ribet_Trav-Paysa.pdf

Silva JS, Rego F, Fernandes P, Rigolot E (Eds) (2010) ´Towards Integrated Fire Management Outcomes of the European Project Fire Paradox.´ (European Forest Institute: Joensu)

Sebastián-López A, Carmen Hernando L, Planelles R, Buffoni A, Boström C, Alves R, Jappiot M, San Miguel Ayanz J (2011) EU-FIRESMART: Forest and land management options to prevent unwanted forest fires. ´5th International Wildland Fire Conference´, 9-13 May. (South Africa)

Wrathall MA (2005) Motives, Reasons, and Causes. In ´ The Cambridge Companion to Merleau-Ponty´. (Eds T Carman, MBN Hansen) pp. 111-128. (Cambridge University Press: Cambridge)

Xanthopoulos G (2012) Evolution of the forest fire problems in Greece and mitigation measures for the future. In ´Proceedings of the 1st International Conference in Safety and Crisis Management in the Construction Tourism and SME Sectors´ (Eds G Boustras, N Boukas) pp. 736-747 (Brown Walker Press: Boca Raton)

Zarraga Moreno JL (1988) Los incendios forestales y las actitudes de la población de las comarcas afectadas. (Servicio de Estudios e Informes del I.A.R.A. I.A.R.A.: Sevilla)

Forest fire motives in Sardinia through the perception of experts

Lovreglio R.[a], Mou G.[a], Leone V.[b]

[a] *Department of Agriculture, University of Sassari, Cristoforo Colombo 1, 08100 Nuoro, Italy, rlovreglio@uniss.it, gmou@uniss.it*
[b] *University of Basilicata (retired), Department of Crop Systems, Forestry and Environmental Sciences, I-85100 Potenza, Italy, vittorio.leone@tiscali.it*

Abstract

Wildfires statistics for Sardinia (Italy) exhibit a very high number of unknown causes: all merged, they account for about 78%. In order to reduce their number, which really hinders any preventive approach, we tested Delphi method, the structured communication technique which relies on a panel of experts.. Results, obtained in collaboration with the Regional Forestry Service (CFVA), put in evidence the concordance among the highest frequency of motifs in regional statistics, as from CFVA databases and those resulting from Delphi survey. Our study reveals a modest prevalence of intentional causes (53 % of total number), also on a provincial basis, v. unintentional ones (46%). All of them can be classified as negligent use of fire in agriculture, namely stubble (or other agricultural wastes) burning, inappropriate or uncontrolled mop-up , negligent use of motors, open flames, electric or mechanical devices, non compliance with regional reglements concerning fire prevention and control. Voluntary fires are also related with agriculture and a traditional rural society, in which fire is a well rooted tool.

Keywords*: Delphi method, fire causes, fire smart, forest fire protection plans, individual fire report, integrated fire management, negligent behaviour, panel of experts, traditional ecological knowledge.*

Introduction

In this paper, we deal with the implementation of a Delphi survey in the eight provinces of the island of Sardinia (Italy), aimed to produce statistics on wildfires causes mainly avoiding unknown causes which represent about 78% (1998-2011) of the total.
Sardinia is a real hotspot for wild fires, which are a recurrent presence.The second largest island in the Mediterranean Basin after Sicily, with a surface of about 2,408,989 hectares, Sardinia is prevalently hilly; 13.6% of the island is mountainous, 18.5% is flat and 67.9% is rugged and hilly.
Forests cover a total of 1,213,250 hectares of which forest cover respectively 583.472 hectares, i.e 24,22%,; other woodland cover 629.778 hectares i.e. 26,14%; thus Sardinia has a forestry index of 50,36 % (Salis *et al*., 2013).

1.1. Climate and territory of Sardinia

The climate is inner Mediterranean (Chessa & Delitala, 2012; Vacca *et al*., 2002), or dry summer subtropical (*Subtropical Csa* type after Köppen, 1936) with an exceedingly long summer and a short humid winter interspersed with three short rainy seasons.
Maximum temperatures of 35-40 °C are repeatedly recorded and peak temperatures climb occasionally well above 45°C as in 2003 and 2009. An absolute maximum of 48,0 °C was recorded in 1965 in Macomer (Chessa & Delitala, 2012).
Wind speed can largely exceed 13,5 m/s (Chessa & Delitala, 2012) with a maximum registered speeds of 64 knots for NW winds in Cagliari and 59 for W winds in Alghero (respectively 118 and 109 km h^{-1}; Osservatorio Industriale della Sardegna, 2000).

1.2. Fires: number and surfaces

About 600,000 ha of woodland were burned in Sardinia in the last 120 years (D'Angelo & Enne, 2000). In the period 1970-2010 fire occurrence is documented (Regione Autonoma della Sardegna, 2011) by the following data (mean ± S.D. and CV, coefficient of variation) :

Number of fires *3,341 ± 1,113 (0.34)*
Burned surface (ha) *38,336 ± 27,619 (0.70)*
Burned forested surface (ha) 7,701 ± 6,847 (0.87)

Sardinia exhibits the highest incidence of wildfires among Italian Regions.

1.3. Fire suppression effort

To counter such a recurrent calamity, since the '80s the autonomous Region of Sardinia has improved its fire suppression apparatus. Despite relevant investments in human and technological resources, results are apparently acceptable. If burned surfaces diminished, due also to improved suppression procedures which insure initial attack within 14' as an average, thus containing 97% of fires under 10 hectares, the number of events (a yearly average of 2,800-3,000) remains accordingly unchanged along time (Boni, 2004).

1.4. Fire causes

There are a variety of motivations for wildfires in Sardinia and their recognition is the key to finding a solution for a more efficacious control (Jollands *et al*., 2011).
It is actually accepted (Birot, 2009; Montiel & Herrero, 2010) that facing the increasing wildfire threats demands a shift from suppression-oriented policies to preventive and integrative policies aimed at removing the structural causes of wildfires. But this pro-active approach requires a good knowledge of the causes contributing to wildfires.
Forest fire statistics, yearly compiled by CGVA (The Sardinian Forestry Rangers Corps) on the basis of individual fire reports, confirm that agropastoralism still plays a major role among the causes of fires, with a positive correlation between sheep number and burned surfaces.
In Tab. 1 motifs, as assessed by CFVA for 1998-2011 and stored in its databases, are reported with their statistical code, where C stays for involuntary, D for voluntary or deliberate. Only motifs with a frequency > 2.00% are considered.

Tab.1 - Motives in order of importance for provinces (1998-2011) through the official statistics by CFVA

Statistical code	Description	Frequency	Frequency in %	Province where frequency is maximum
C09	Fires caused by agricultural and forest activities (burning of stubble and agricultural wastes)	47	12.40	Oristano
C05	Fires caused by inappropriate or uncontrolled mop-up	28	8.70	Oristano
C11	Fires caused by the careless use of machinery	33	7.80	Sassari-Olbiatempio
C08	Non compliance with the the Regional Ordinance relating to the Prevention and Control of Fires	25	7.60	Oristano
C01	Fires caused by cigarette stubs or matches	27	6.80	Sassari-Olbiatempio
D12	Fires caused by behavioural disturbance (pyromania)	28	6.70	Ca-Carbonia Iglesias

C15	Fires caused by poor power line maintenance	27	6.30	Sassari-Olbiatempio
D02	Fires caused by agricultural and forestry activities for the clearing of uncultivated land	21	6.10	Oristano
D03	Fires caused by conflicts or revenge among private owners (for pasture)	32	6.00	Ca-Carbonia Iglesias
D17	Fires caused with the intent of creating an alert situation in firefighting structure	26	5.90	Nuoro-Ogliastra
D13	Fires caused by revenge or retaliation referable to poaching	15	4.20	Oristano
D04	Fires caused by conflicts or revenge among private owners or shepherds and public agencies (for pasture)	15	2.70	Nuoro-Ogliastra
D18	Fires caused by arson (not otherwise defined)	11	2.60	Nuoro-Ogliastra

Such statistic are based on less than 23% of the 8,428 fires occurred in the period 1998-2011.In many cases motifs are classified as unknown voluntary or unknown involuntary, without a specific motive. All merged, unknown causes account for 77.65% and therefore do not give the sufficient information deemed necessary for a more preventive approach.
In order to reduce the number of unknown events, in collaboration with CFVA we tested the Delphi method.

Materials and methods

The Delphi method

The Delphi method (Dalkey & Helmer 1963, Linstone & Turoff 2002) is an iterative process based on the principle that *"a group of experts usually performs better than any one expert because the group possesses at least as much knowledge as its most knowledgeable member"* (Henderson, 2008).

The panel of experts and the questionnaire

For our Delphi survey, carried out in 2012, experts were the non commissioned officers working for CFVA. As from their statement, their knowledge of wildfires is very good for 54% of them, excellent for 14%. They were convened in four successive sessions from one or several neighboring provinces. Number of experts per session varied from 14 for the merged provinces of Nuoro-Ogliastra to 30 units in the provinces of Cagliari-Carbonia/Iglesias, for a total number of 98. Number of experts was balanced among areas and, in addition, well above the minimum (at least 10, Delbecq *et al*., 1975). Structured questioning was achieved through the use of *ad hoc* questionnaires, reporting the motives of forest fires for Sardinia as used by GFVA in official statistics (Saba, 2004). Experts were asked to recognize the four most relevant fire motives in their area of duty and were then invited to rank such motives in order of decreasing importance, giving a score ranging from 1 (maximum) to 4 (minimum). In previous works we used a range of 1 to 8 (Lovreglio *et al*., 2006, 2008, 2010, 2012 ; Meddour-Sahar et a.l 2013). Reducing rank score range to 1 to 4 obliges respondents to make a more severe selection in their responses. Controlled feedback was achieved by discussing responses, and then asking the panel members whether they wanted to change their judgements.

Results

Rank-ordering is the mode of rank-scores. Causes, from our survey, result involuntary for 46%, voluntary for 53 %, natural for 1 %; values are coherent with the general opinion that voluntary fires are often overestimated or overemphasized (Vélez, 2000).

A comparison between the voluntary/involuntary motifs as detected by CFVA in the period 1998-2011 and the motifs identified by the panel of experts was carried out.
In some provinces voluntary fires are clearly prevailing in CFVA official statistics, with the exception of Cagliari-Carbonia Iglesias, where Delphi assesses a majority of voluntary fires.
Motifs issued from Delphi survey and arranged following the mode of rank-scores are presented in Fig.1. Identification codes in the bar chart reflect the official list of causes as proposed by CFVA (Saba, 2004).

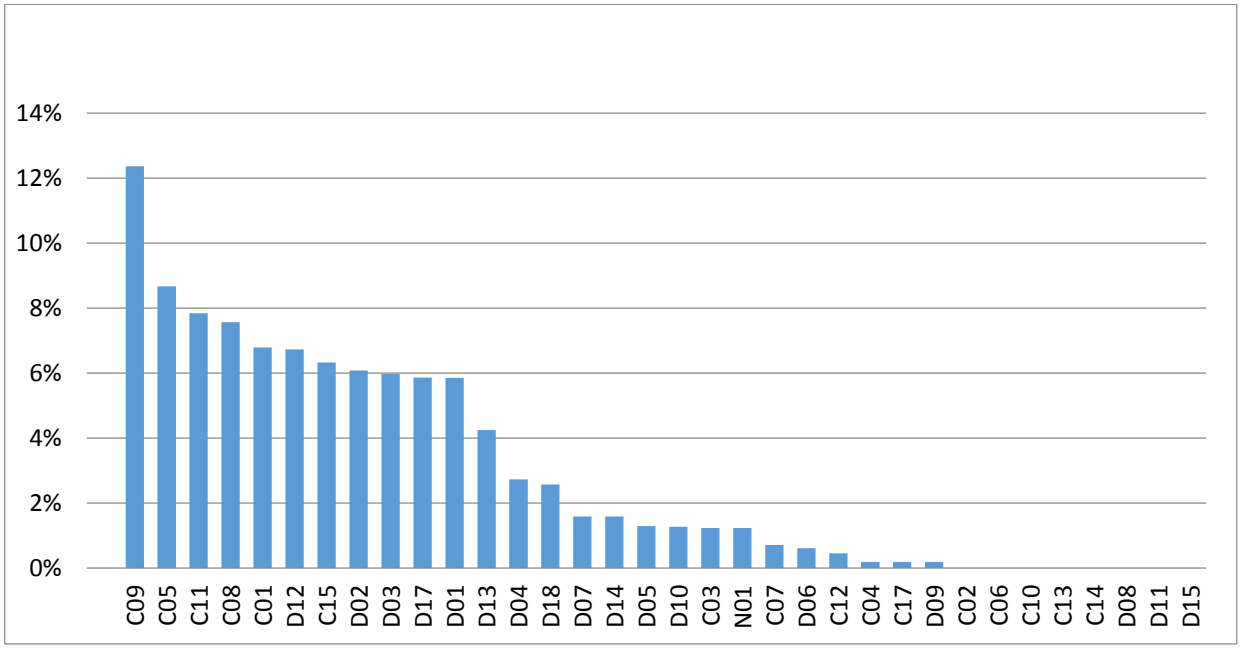

Figure 1 Frequency (%) of the motifs on a regional scale as a result of Delphi method

In Tab. 2 we present the motifs as assessed in the regional wildfires databases and results of our Delphi survey, in terms respectively of frequency and rank order.

Tab.2 - Motives at regional level: comparison between data from regional databases and data from Delphi survey

Motives frequency Data from regional databases		Motives frequency Data from Delphi survey		Motives rank order (1 to 4) Data from Delphi survey	
C09	Fires caused by agricultural and forest activities (burning of stubble and agricultural wastes)	C09	Fires caused by agricultural and forest activities (burning of stubble and agricultural wastes)	1	C09 Fires caused by agricultural and forest activities (burning of stubble and agricultural wastes)
C05	Fires caused by inappropriate or uncontrolled mop-up of fires	C05	Fires caused by inappropriate or uncontrolled mop-up of fires	2	C05 Fires caused by inappropriate or uncontrolled mop-up of fires
C11	Fires caused by the careless use of machinery	C11	Fires caused by the careless use of machinery	3	C11 Fires caused by the careless use of machinery

C08	Non compliance with Regional Ordinance relating to the Prevention and Control of Fires	C08	Non compliance with Regional Ordinance relating to the Prevention and Control of Fires	4	C08 Non compliance with Regional Ordinance relating to the Prevention and Control of Fires

Results put in evidence the full concordance among the highest frequency in regional statistics, as from CFVA databases and the motifs as perceived by the experts in Delphi survey:
In the following Tab. 3 we present the top motives, i.e. those ranked 1 to 4, through the Delphi method, on a provincial scale.

Tab. 3 - Rank order of motifs by Province

Rank	Oristano	Sassari-Olbiatempio	Ca-Carbonia Iglesias	Nuoro-Ogliastra
1	C.05 Fires caused by inappropriate or uncontrolled mop-up	C.11 Fires caused by the use of machinery (motor, flame, electric or mechanical devices)	C.09 Fires caused by agricultural and forest activities (burning of stubble and agricultural wastes)	C.09 Fires caused by agricultural and forest activities (burning of stubble and agricultural wastes
2	C.09 Fires caused by agricultural and forest activities (burning of stubble and agricultural wastes	C.15 Fires caused by poor power line maintenance	D.03 Fires caused by conflicts or revenge among private owners (for pasture)	D.02 Fires caused by agricultural and forestry activities (clearing of uncultivated land)
3	C.08 Non compliance with the Regional Ordinance relating to the Prevention and Controll of Fires and Abusive stubble burning	C.03 Fires caused by cigarette stubs or matches	D.12 Fires caused by behavioural disturbance (pyromania)	C.11 Fires caused by the use of machinery (motor, flame, electric or mechanical devices)
4	D.02 Fires caused by agricultural and forestry activities (clearing of uncultivated land)	C.08 Non compliance with the Regional Ordinance relating to the Prevention and Control of Fires and Abusive stubble burning	D.17 Fires caused with the intent of creating an alert situation in firefighting structure	D.17 Fires caused with the intent of creating an alert situation in firefighting structure

Discussion of results

The results represent only the collective informed opinion and judgement of the experts participating in the panel about fire motives but, at our opinion, there is no alternative way to produce better results,

with the exception of information issued from sentences beyond recall for identified culprits (Leone *et al*., 2009).
Our research was based on the opinions of professionals with an interest, knowledge and field experience in wildfires, assuming that replies are frank and well meditated.Their responses should however be taken to be truth-as-observed by experts not exact science (Jollands *et al*., 2011).
By the Delphi method, unclassified causes of wildfires in Sardinia are eliminated, thus allowing to express more clear information on the possible roots of the phenomenon.
Our results reveal the relevant importance of unintentional causes, which are prevailing also on a provincial basis. All of them can be mainly classified as negligent use of fire in agriculture (burning of residues, stubble burning, negligent use of agricultural machinery, non compliance with regional regulations concerning use of fire..).
A closer analysis of motifs reveals only two cases of voluntary reasons: creating an alert situation in fire fighting structure, though ranked at 4th position, and pasture conflicts; the latter recalls the importance of traditional pastoral activities in the island. If we exclude from analysis pyromania, all others motifs are directly or indirectly connected with agricultural activities and a rural society. In many cases the threshold between voluntary and involuntary is rather fuzzy, such as the case of stubble burning behind official date fixed by regional regulations. Voluntary fires, on the contrary, are more limited but they also partly refer to the use of fire in agriculture.
In the province of Oristano inappropriate mop-up is referred to extinction operations not carefully carried out. Limited to Sassari and Olbia-Tempio province, we notice fire caused by lack of maintenance of power lines. Both situations give a clear info about possible solutions, respectively improving suppression procedures and ensuring power lines efficiency through maintenance.
Results reflect a society accustomed to using forest and rural spaces, with scarce respect and care and without concern for its preservation (Thirgood, 1981; Dimitrakopoulos and Mitsopoulos, 2006).
Causes and their motives, as issued from our research (involuntary for 46%, voluntary for 53 %, and natural for 1 %, as percentages of respondents' judgments), are well consistent with the general trend reported in current literature (Catry *et al*. 2010).
In Sardinia, traditional abilities and know-how of fire use represent a deeply rooted tool for agricultural activities (Silva *et al*., 2010b), a true *TEK, traditional ecological knowledge* (Ribet, 2002) well used by a still fire-relying community (Lazaro & Montiel, 2010).

Conclusions and final remarks

Delphi method for the identification of the major causes and reasons of forest fires exploits the good level of panellists' expertise and their knowledge of the territory and of local socio-economic scenarios behind the phenomenon of wildfire, in a rather quick and easy way (Lovreglio *et al*., 2006, 2008, 2010, 2012; Meddour-Sahar *et al*. 2013).
As in the case of Sardinia, where official info about wildfires is rather poor, Delphi method is intended for use in stuations where statistic method are not possible due to the lack of appropriate data.
Understanding the most frequent causes and reasons in different social contexts can definitely help the prevention measures and the efforts in modifying the behavior of individuals in complex social contexts.In our study area recognizing the presence of a fire-relying community, as from Delphi results, could suggest an approach locally based on a different and fire-smart application of the traditional use of fire, rather than the conventional and regulatory, restrictive measures of prevention. This could represent a fair example of integrated fire management, sensu Fire Paradox.

Acknowledgements

The authors wish to thank dr. C. Masnata, regional head of CFVA and dr. G. Delogu, head of Cagliari provincial CFVA bureau, whose help and collaboration permitted this research. A special thank is also due to all the foresters who accepted to participate in the different Delphi sessions.

References

Birot (2009) Living with wildfires: what science can tell us. European Forest Institute Discussion Paper 15, 82 p.

Boni C (2004) Il fenomeno degli incendi in Sardegna. In: Regione Sardegna Atti del Convegno Incendi boschivi e rurali in Sardegna. Dall'analisi delle cause alle proposte di intervento. Cagliari 14/15 maggio 2004, 9-17.

Catry FX, Rego FC, Silva JS, Moreira F, Camia A, Ricotta C, Conedera M (2010) Fire starts and human activities. In: J.S. Silva, F.C. Rego, P. Fernandes, E. Rigolot (Eds) Towards Integrated Fire Management. Outcomes of the European Project Fire Paradox. European Forest Institute Research Report23, 9-22.

Chessa PA and Delitala A (2012) Il clima della Sardegna.Arpa Sardegna Dipartimento IMC
http://www.sar.sardegna.it/pubblicazioni/notetecniche/nota2/pag001.asp accessed 01.15.2013

Dalkey NC and Helmer O (1963) An experimental application of the Delphi Method to the use of experts. Management Science, 9(3): 458 - 468.

D'Angelo M and Enne G (2000) Monitoring fires in areas characterized by grazing pressure. In: Mediterranean desertification: research results and policy implications Proceedings of the International conference, 29 October - 1 Novembre 1996, Crete, Greece. Luxembourg, Office for Official Publications of the European Communities, 559-568.

Delbecq AL, Van de Ven AH, Gustafson DH (1975) Group techniques for program planning. A guide to nominal group and Delphi processes. Scott, Foresman, and Company, Glenview, IL, USA, pp. 174.

Dimitrakopoulos AP and Mitsopoulos ID (2006) Global forest resources assessment (2005). Report on fires in the Mediterranean Region. Working paper FM/8/E, Forestry Department, FAO. Rome, 43 p.

Köppen W(1936) Das geographische system der klimate, in: Köppen and Geiger (Eds.), Handbuch der Klimatologie, Vol I, Part C, , Gebrüder Borntraeger, Berlin, 44. P.

Jollands M, Morris J and Moffat AJ (2011) Wildfires in Wales. Report to Forestry Commission Wales. Forest Research, Farnham, 107 p.
http://www.forestry.gov.uk/fr/wildfiresinwales#finalreport accessed 09.10.2013

Lazaro A and Montiel C (2010) Overview of prescribed burning policies and practices in Europe and other countries. In: J.S. Silva, F.C. Rego, P. Fernandes, E. Rigolot (Eds) Towards Integrated Fire Management. Outcomes of the European Project Fire Paradox. European Forest Institute Research Report 23, 137-150.

Leone V, Lovreglio L, Martín PM, Martínez J, Vilar L (2009) Chapter 11 Human factors of fire occurrence in the Mediterranean. In: E. Chuvieco (Ed.) Earth observation of wildland fires in Mediterranean ecosystems. Berlin, Heidelberg: Springer-Verlag,149-170.

Linstone HA and Turoff M (2002)The Delphi method methods and applications (digital version). [online] URL: http://is.njit.edu/pubs/delphibook/618 p.

Lovreglio R, Leone V, Giaquinto P, Notarnicola A (2006) Wildfire cause analysis through Delphi Method: Four Case-Studies in Southern Italy . iForest, Biogeosciences and Forestry vol. 3: 8-15 http://www.sisef.it/iforest/contents/?id=ifor0521-003.

Lovreglio R, Rodrigues MJ, Silletti G, Leone V (2008) Applicazione del metodo Delphi per l'analisi delle motivazioni degli incendi: il caso Taranto. L'Italia Forestale e Montana 5: 427- 447.

Lovreglio R, Rodrigues M, Notarnicola A, LeoneV (2010) From fire motives survey to prevention: the case of Cilento and Vallo di Diano National Park (Italy). In: D.X. Viegas (Ed.) Proceedings VI Intern. Conf. Forest Fire Research, Coimbra Nov. 2010, 354 p.

Lovreglio R, Marciano A, Patrone A, Leone V (2012) Le motivazioni degli incendi boschivi in Italia: risultati preliminari di un'indagine pilota nelle Province a maggiore incidenza di incendi Forest@ 9: 137-147.

Meddour-Sahar O, Meddour R, Leone V, Lovreglio R, Derridj A (2013) Analysis of forest fires causes and their motivations in northern Algeria: the Delphi method. iForest-Biogeosciences and Forestry, Vol. 6: 247-254.

http://www.sisef.it/iforest/contents/?id=ifor0098-006 accessed 10.01.2013

Montiel-Molina C (2013) Comparative assessment of wildland fire legislation and policies in the European Union: Towards a Fire Framework Directive. Forest Policy and Economics,Volume 29, Special issue: The FIRE PARADOX project: Setting the basis for a shift in the forest fire policies in Europe: 1‑6.

Montiel C and Herrero G (2010) An Overview of Policies and Practices Related to Fire Ignitions at the European Union Level.In: J. Sande Silva, F. Rego, P.Fernandes, and E.Rigolot (Eds) Towards Integrated Fire Management. Outcomes of the European Project Fire Paradox. European Forest Institute Research Report 23, 35-46.

http://www.efi.int/files/attachments/publications/efi_rr23.pdf accessed 07.01.2013

Osservatorio Industriale della Sardegna (2000) Annuario Statistico della Sardegna 2000 - Dati regionali e provinciali, 497 p.

Regione Autonoma della Sardegna (2011) Piano regionale di previsione, prevenzione e lotta attiva contro gli incendi boschivi 2011-2013, 97 p.

http://www.sardegnaambiente.it/documenti/20_350_20130615120715.pdf accessed 06.10.2013

Ribet N (2002) La maîtrise du feu un travail "en creux" pour façonner les paysages. In: D. Woronoff (dir.), Travail et paysages, Paris, Éditions du CTHS, Actes du 127e Congrès du CTHS Le travail et les hommes, Nancy 15-20 avril 2002 : 167-198.

http://www.ecoanthropologie.cnrs.fr/pdf/Ribet_Trav-Paysa.pdf

Saba F (2004) Le cause degli incendi boschivi e rurali in Sardegna: dalle ipotesi alle analisi dei dati. In: Regione Sardegna Atti del Convegno "Incendi boschivi e rurali in Sardegna. Dall'analisi delle cause alle proposte di intervento. Cagliari 14/15 maggio 2004

Salis M, Ager A, Arca B, Finney M, Bacciu V, Duce P, Spano D (2013) Assessing exposure of human and ecological values to wildfire in Sardinia, Italy. International Journal of Wildland Fire, 22(4): 549-565.

Silva JS, Rego FC, Fernandes P, Rigolot E (2010a) 1.Introducing the Fire Paradox. In: J.S. Silva, F.C. Rego, P. Fernandes, E. Rigolot (Eds) Towards Integrated Fire Management. Outcomes of the European Project Fire Paradox. European Forest Institute Research Report 23, 2-6 and 229.

SilvaJS, Rego FC, Fernandes P, Rigolot E (2010b) 6. Solving the Fire Paradox. Regulating the wildfire problems by the wise use of fire. In: J.S. Silva, F.C. Rego, P. Fernandes, E. Rigolot (Eds) Towards Integrated Fire Management. Outcomes of the European Project Fire Paradox'. European Forest Institute Research Report 23, 219-228.

Thirgood J (1981) Man and the Mediterranean Forest: A History of Resource Depletion. New York, Academic Press, 194 p.

Vacca A , Loddo S, Serra G and Aru A (2002) Soil degradation in Sardinia (Italy): main factors and processes. Options Méditerranéennes, série A n.50 : 413-423.

Vélez R (2000) La defensa contra incendios forestales. Fundamentos y experiencias. McGraw- Hill / Interamericana de España S.A.U., Madrid, Spain, 1360 p.

Human dimension of fire: ten years of Minas de Riotinto fire

Clara Quesada-Fernández[a], Daniel Quesada-Fernández[b]

[a] *Universidad de Córdoba, claraquesada@gmail.com , z32qufec@uco.es*
[b] *danielquesadafernandez@gmail.com*

Abstract
In 2004 one of the most devastating forest fire started since we have official records and statistics of fire occurrence in Spain. On a fire prone context on July 27, 2004, in Minas de Ríotinto (Huelva, Spain) the largest forest fire of the last century and the third largest in the statistical history of Spain initiated. It was extinguished more than three weeks later. The combination of exceptional meteorological, topographic and vegetation conditions resulted a four hours free fire behaviour that burned 4.000 hectares in a 27.000 hectares final perimeter. The economy of the affected settlements and towns was severely damaged not only by the loss of the production of cork, but by the loss of much of its agricultural and livestock production as well as other silvicultural activities, logging and hunting. It was one of the first fires with problems in wildland urban interfaces at large scale because of more than 1000 people evacuated from their homes. Inside this fire prone area, one of the most affected places was the small town of Berrocal which saw how more than 90% of the territory in the municipality was seriously affected by fire. Also, one of the most active firefighting crews working in the fire belonged to this town.

Keywords*: communities assessment, educational aspects, fire culture, fire emergency, environmental education, emergency evacuation, emergency preparedness, firefighting, fire policy, fire prone areas, fire risk, forest fires, hazard, how to prevent, human behavior, prevention, risk, safety, wildland urban interface, wildland urban interface fire hazards.*

Introduction

In 2004 one of the most devastating forest fires started since we have official records and statistics of fire occurrence in Spain. On a fire prone context on July 27, 2004, in Minas de Ríotinto (Huelva, Spain) the largest forest fire of the last century and the third largest in the statistical history of Spain initiated. It was extinguished more than three weeks later. The combination of exceptional meteorological, topographic and vegetation conditions resulted a four hours free fire behaviour that burned 4.000 hectares in a 27.000 hectares final perimeter. More than 1.000 people were evacuated from the towns of Berrocal, Escacena del Campo, Minas de Riotinto, Nerva, Paterna del Campo y Zalamea la Real (Huelva province) and from Aznlacóllar, El Castillo de las Guardas, El Garrobo, Gerena y El Madroño (Seville province). The economy of the affected settlements and towns was severely damaged not only by the loss of the production of cork, but by the loss of much of its agricultural and livestock production as well as other silvicultural activities, logging and hunting.
The catastrophic fire among other material and human damage caused the death of two citizens disoriented by the smoke in the interior of his car. They tried to run out but they were achieved by fire. Some horus later the pilot of one of the extinction helicopters was seriously injuried during the approximation maneuvers to take water.
The Minas de Riotinto Fire was one of the first wildland fires with serious problems in wildland urban interfaces at large scale because of more than 1000 people evacuated from their homes. Inside this fire prone area one of the most affected places was the small town of Berrocal. This area saw how more than 90% of the territory in the municipality was seriously affected by fire. Also, one of the most active firefighting crews working in the fire belonged to Berrocal.

Methods

The present paper researches through personal interviews and analyzes the situation of these people, firefighters (brigade members) and citizens, in 2014, ten years after the fire.
The study work was intended to extract information in order to try to understand one of the most overlooked realities within the human dimension of fire as it is the condition of people who have suffered these losses. A series of interviews was conducted in Berrocal (Huelva, Spain), a 300 habitants towns, with key actors related to the process. It took place at the beginning of 2013.
During the interviews to 25 people (1 wildland firefighting technician, 5 firefighters, 1 mayor and 13 civilians), the goal was to known to the persons affected directly by 2004 fire or not directly affected by suffering the effects ten years later. Among other things, the interviews touched on the so-called message of natural resources but also childhood at Berrocal, memories and future plans. Interviewed were treated sensitively in the interviews, taking into account their serious suffering from the event and even trauma (some cases).
Most of older people in Berrocal were older than 70 years old in 2004 (80 years old in 2014). At this study time there was a part of the population aged below 40 years and other part below 13-15 years.

Results and discussions

Many of citizens of Berrocal feel completely abandoned by regional instituions. The view shared by the majority of participants was indifference from the point of view of refussing to discuss the fire topic (again).
Some of the interviewed belonging to the elder group have not preserved a clear memory of this past situation.
Because they were too young in 2004 the members of the 13-18 years old didn't have memories of those unforgettable days from almost the rest of the population.

Conclusions

This fire events permited an effective learning from past wildland fire incidents and important safety lessons. Also permited a large number of lesson learned from wildland fire incidents from the point of view of managers. However, the human part not belonging to firefighting services felt abandoned a few years after the fire.
The media have contributed in some cases to create a growing excess of pressure in the popolation during the first years focusing on the past not their present even their future.
It seem not to be clear for civilians the human factors in wildland fire safety, including impact of legal and institutional responses on wildland fire.

References

Absher, J.; Kyle, G. 2007. An overview of risk and trust as precursors to defensible space actions by wildland-urban interface residents.

Allen, J.B.; Ferrand, J. 1999. Environmental locus of control, sympathy, and proenvironmental behaviour: a test of Geller's actively caring hypothesis. Environment and Behavior, 31(3): 338–353.

Caballero, D.; Quesada-Fernández, C. 2011. Caracterización del riesgo por incendio forestal en la interfaz urbano-forestal en la Comunidad Autónoma de Andalucía - Zona costera de Málaga y Granada. Junta de Andalucía, Consejería de Medio Ambiente. Spain.

Caballero D., Quesada C. 2011. Evacuation, shelter in place, forced confinement or run-away? The reality of fire situations in the WUI in Europe in Proceedings of the ICFBR 2011 International Conference on Fire Behaviour and Risk. Alghero, Italy - October 4-6, 2011. pp 49.

Cvetkovich, G.T.; Winter, P.L. 2008. The experience of community residents in a fire-prone ecosystem: a case study of the San Bernardino National Forest. Res. Pap. PSW-RP-257. Albany, CA: Pacific Southwest Research Station, Forest Service, U.S. Department of Agriculture.

Kollmuss, A.; Agyeman, J. 2002. Mind the Gap: why do people act environmentally and what are the barriers to pro-environmental behavior? Environmental Education Research, 8 (3).

Molina-García, Y. 2006. La participación comunitaria en la prevención y combate de incendios forestales: estrategias que la promueven. Revista For. Lat 40:107-123.

Mueller, J.M.; Loomis, J.B.; González-Cabán, A. 2008. Do repeated wildfires change homebuyers' demand for homes in high- risk areas? A hedonic analysis of the short and long-term effects of repeated wildfires on house prices in southern California.

Rodríguez-Trejo, D. A.; Rodríguez-Aguilar, M.; Fernández-Sánchez, F. 2001. Educación e incendios forestales. Mundi Prensa. Madrid.

Quesada-Fernández, C. 2007. Simuladores de incendios forestales como respuesta al incendio de Minas Riotinto (Huelva, España) el 27 de julio de 2004 in Proceedings of the IV International Wildland Fire Conference, Sevilla, Spain. 2007.

Quesada-Fernández, C.; Quesada-Fernández, D. 2011. Improving educational aspects as a way to prevent fire risk in fire prone communities in Spain. In Duce, P.; Spano, D. Proceedings of the ICFBR 2011, International Conference on Fire Behaviour and Risk. Alghero. Italy. EDES Sassari. Italy.

Quesada-Fernández, C.; Quesada-Fernández, D. 2012. Improving educational aspects as a way to prevent fire risk in fire prone communities. Cases of study in Spain. In: Spano, D.; Bacciu, V.; Salis, M.; Sirca, C. Modelling fire behaviour and risk. Sassari. 218-223.

Quesada-Fernández, C.; Quesada-Fernández, D. 2013. Fire risk perception in small fire prone communities. Study cases in Proceedings of the International Conference on Forest Fire Risk Modelling and Mapping. "Vulnerability to forest fire at wildland-urban interfaces". Aix en Provence, France, 30 September-2 October 2013.

Vélez, R. 2000. Actuación sobre las causas de origen humano. Persuasión, conciliación y sanción. Legislación preventiva. In: Vélez, R. (coord.). La defensa contra incendios forestales. Fundamentos y experiencias. McGraw-Hill, Madrid. 13.1-13.6 y 13.18– 13.28.

Vélez, R. 2002. Forest fire prevention with a target: The rural people. In: Viegas, D, editor. Proceedings of the IV International Conference on Forest Fire Research. Luso, Portugal.

Vélez, R. 2007. Experiences in Spain of community based fire management. In: Proceedings of the IV International Wildland Fire Conference, Sevilla, 2007.

Vélez, R. 2008. Forest Fires in the Mediterranean Basin. In: González-Cabán, A, coordinator. Proceedings of the III Symposium on Fire Economics. Carolina, Puerto Rico, 2008.

Villalba Ondurria, D.; Martín Pinto, P. 2004. La educación como herramienta fundamental en la prevención de incendios forestales. Tabanque, 18. 189-206.

Identifying risk preferences among wildfire managers and the consequences for incident management outcomes

Michael S. Hand[a], David E. Calkin[a], Matthew P. Thompson[a]

[a] *US Forest Service Rocky Mountain Research Station, Missoula, Montana, USA, mshand@fs.fed.us, decalkin@fs.fed.us, and mpthompson02@fs.fed.us*

The opinions expressed in this paper are the authors' and do not necessarily reflect the views of the U.S. Department of Agriculture

Abstract

Management of wildfire incidents involves trade-offs over risks to firefighting personnel, private property and infrastructure, ecological values, public exposure to harm, and the costs of management. Trade-offs, non-linear probability weighting, and risk preferences among wildfire managers are investigated using a multi-attribute lottery choice experiment. The survey-based experiment asks managers to make strategic choices with varying levels of risk to aviation personnel, property damage, and suppression costs. A latent-class model is estimated to identify two classes of respondents with varying degrees of non-linear probability weighting. Differences between the two classes, explained by differences in educational attainment, suggest that expected outcomes of wildfire can vary depending on risk preferences and individual characteristics of managers.

Keywords*: risk management, decision biases, wildfire outcomes, lottery experiment*

Introduction

Wildfire incidents present a complex risk management environment. Wildfire managers must often make decisions that balance multiple potential outcomes, long-term and short-term risks, and social and political pressures. However, relatively little attention has been paid to how differences in risk preferences among managers affect management decisions and wildfire outcomes. Risk-related decision biases – including risk aversion, probability weighting, and status quo bias, among others – have been demonstrated in a wide variety of decision environments, including wildfire management (Maguire and Albright 2005; Wilson *et al*. 2011; Wibbenmeyer *et al*. 2013). This paper builds on previous work by investigating the role of heterogeneity of risk preferences in determining outcomes on individual incidents and the fire management program.

Of primary interest in this paper is the degree to which risk preferences vary within the population of fire managers. Previous research has established that probability weighting, risk aversion, and information framing drive choices of fire managers that depart significantly from an expected loss-minimization baseline. However, the degree to which managers exhibit risk biases may vary in the population. Differences in risk preferences within the target population can have implications for the expected outcomes of strategic choices made by managers and the extent that choices depart from expected loss-minimizing choices.

Risk preferences are examined using insights from a survey-based experiment administered to Federal wildfire managers in the United States in 2012. The experiment presented managers with a series of strategy choices to respond to a hypothetical wildfire scenario. A random utility model of risky strategic choices is adapted to allow for non-linear probability weighting and risk preferences (e.g., risk aversion). We estimate a latent class model of risk preferences to distinguish between different types (or classes) of respondents in the sample. Latent class models are a way to describe heterogeneity in the sample by identifying different response patterns (usually by estimating some unique parameters for each class) and the factors that are associated with respondents being members of each class

(Greene and Hensher 2013). In this application reported educational attainment is used to identify groups of managers that exhibit varying degrees of risk biases.

A survey-based lottery choice experiment

The primary method used to estimate risk aversion and probability weighting parameters is a multiple-attribute lottery choice experiment. Single-attribute lottery choice (also called multiple price list) experiments have been used to identify risk preferences in a variety of settings, e.g., Holt and Laury (2002) and Taylor (2013). In this study, managers are presented with a series of multi-attribute lotteries; respondents are asked to select strategies that reflect potential responses to a hypothetical wildfire scenario.

Each choice set (i.e., lottery) offered a relatively ``safe'' strategy and a relatively ``risky'' strategy. Both strategies are defined by potential good and bad outcomes that occur with probabilities that vary in the experimental design. The safe strategy represents a situation with moderate use of suppression resources to contain the hypothetical wildfire. The risky strategy involves monitoring the fire with minimal commitment of suppression resources; such strategies are used when potential values at risk are low or favorable conditions are expected to continue for the foreseeable future. As in lottery experiments with financial outcomes, the risky strategy yields good outcomes that are better than the good outcomes in the safe strategy, but bad outcomes that are worse than the bad outcomes in the safe strategy.

The lottery choices require respondents to make tradeoffs over three outcome attributes that are hypothesized to enter the fire manager utility function: Exposure of aviation personnel to the risk of a fatality, damage to private property, and total suppression expenditures for the incident. Potential outcomes for each of the attributes under both the safe and risky strategies are given in table 1. Attribute levels for the good and bad outcomes under the safe strategy and good outcomes under the risky strategy were held constant across all of the choice sets seen by each respondent. The attribute levels in the risky strategy--bad outcome were varied using an experimental design to test risk preferences of respondents across a range of utility values.

Table 1. Attribute levels used in the experimental design

	Safe strategy		Risky strategy[a]		
Attribute	Good outcome	Bad outcome	Good outcome	Bad outcome – low	Bad outcome – high
Aviation exposure	50 hours	75 hours	10 hours	300 hours	1,200 hours
Private property damage	$600,000	$1.25 mil.	$700,000	$3 mil.	$14 mil.
Suppression cost	$300,000	$500,000	$25,000	$2 mil.	$12.5 mil.

[a] Each attribute has two potential bad outcomes under the risky strategy. The Risky-Bad outcomes were varied systematically among the choice sets using a full-factorial design.

To identify how managers respond to lotteries over a range of probabilities, the probability (p) that the good outcome obtains is varied in the experimental design, taking six different values: 0.7, 0.85, 0.9, 0.95, 0.98, and 0.995. Respondents saw probability information displayed as both a percentage (e.g., a 70% chance the good outcome results) and as a frequency (e.g., 700 out of 1,000 fires where the good outcome results).

The risky strategy--bad outcome attributes (two for each of the three attributes) and the outcome probabilities are combined to form choice sets using a 2x2x2x6 full-factorial design, resulting in 48 unique choice sets. A framing experiment was also incorporated into the experimental design. Half of

the sample saw the aviation exposure attribute expressed in expected fatalities per 1,000 incidents (the treatment group) rather than hours of aviation use (the control group). Based on historical accident and fatality rates for the U.S. Forest Service, the aviation exposure attribute was converted to a fatality rate using an average of 4.801 fatalities for every 100,000 flight hours (USDA Forest Service 2010). The econometric models used to analyse the data are estimated separately on the control group sample and the treatment group sample.

The choice sets were blocked into six blocks of eight choice sets, with potential respondents randomly assigned to one of the six blocks. Details of the survey administration can be found in Wibbenmeyer *et al*. (2012). Figure 1 displays sample choice sets for the control and treatment groups.

Strategy A			Strategy B		
90.0% 900 of 1000 wildfires	Aviation Exposure	50 hours	90.0% 900 of 1000 wildfires	Aviation Exposure	10 hours
	Private property damage	$600,000		Private property damage	$700,000
	Suppression cost	$300,000		Suppression cost	$25,000
10.0% 100 of 1000 wildfires	Aviation Exposure	75 hours	10.0% 100 of 1000 wildfires	Aviation Exposure	1200 hours
	Private property damage	$1.25 million		Private property damage	$14 million
	Suppression cost	$500,000		Suppression cost	$12.5 million

A: Control frame

Strategy A			Strategy B		
90.0% 900 of 1000 wildfires	Aviation Exposure	2.4 deaths in 1000 fires	90.0% 900 of 1000 wildfires	Aviation Exposure	0.5 deaths in 1000 fires
	Private property damage	$600,000		Private property damage	$700,000
	Suppression cost	$300,000		Suppression cost	$25,000
10.0% 100 of 1000 wildfires	Aviation Exposure	3.6 deaths in 1000 fires	10.0% 100 of 1000 wildfires	Aviation Exposure	58 deaths in 1000 fires
	Private property damage	$1.25 million		Private property damage	$14 million
	Suppression cost	$500,000		Suppression cost	$12.5 million

B: Treatment frame

Figure 1. Sample choice sets for the control (A) and treatment (B) frames

Econometric specifications

Analysis of the observed lottery choices is conducted using a modified version of a random utility conditional logit model. In this case, assuming that the random component of choices has a type I extreme value distribution (Train 2009, ch.3), the conditional logit model expresses the probability of selecting the "safe" strategy over the "risky" strategy as:

$$(1) \qquad Pr(Safe) = \frac{e^{V_S}}{e^{V_S} + e^{V_R}}$$

where V_S and V_R represent the deterministic component of utility associated with the "safe" and "risky" strategies, respectively. The utility functions are specified using a linear-in-attributes form, modified to accommodate probability weighting and risk preferences. Similar recent examples of this approach include Hensher *et al*. (2011), van Houtvan *et al*. (2011), Sun *et al*. (2012) and Wibbenmeyer *et al*. (2013). Probability weighting is specified using a single-parameter non-linear weighting function of *p* drawn from Prelec (1998): $\pi(p) = exp - (-\ln p)^{\gamma}$. Risk preferences are specified using a constant relative risk aversion form as in Hensher *et al*. (2011). Incorporating probability weighting and risk preferences results in the following utility function for strategy *m*, which is defined by the good (*G*) and bad (*B*) potential outcomes, attribute preference parameters (β_k), the probability weighting parameter (γ), and the risk preferences parameter (α):

$$(2) \qquad V_m = \pi(p_G)\left(\frac{1}{1-\alpha}\right)(\beta_{AE} AE_{mG}^{1-\alpha} + \beta_D D_{mG}^{1-\alpha} + \beta_C C_{mG}^{1-\alpha}) + \big(1 - \pi(p_G)\big)\left(\frac{1}{1-\alpha}\right)(\beta_{AE} AE_{mB}^{1-\alpha} + \beta_D D_{mB}^{1-\alpha} + \beta_C C_{mB}^{1-\alpha})$$

where *AE* is the aviation exposure attribute, *D* is the property damage attribute, and *C* is the suppression cost attribute.

To examine heterogeneity among managers, a latent class model is developed following the approach described in Sun *et al*. (2012) and Greene and Hensher (2003). The latent class model assumes that two distinct classes of strategy choosers exist in the population of managers. The likelihood of belonging to one or the other class is determined by reported educational attainment.[1] The probability that individual *i* is a member of class *q* is specified as a conditional logit:

$$(3)\ H_{iq} = \frac{e^{Z'_i \Theta_q}}{e^{Z'_i \Theta_1} + e^{Z'_i \Theta_2}}, \Theta_1 = 0$$

where *Z* is a vector of educational attainment indicator variables, and Θ is a vector of parameters that describe the relationship between *Z* and the likelihood of membership in class *q*. Θ_1 (corresponding to class 1) is normalized to zero to identify the parameter vector.

Separate choice probabilities (equation 1) are specified for each class. In this application, the choice probability specifications include common attribute preference parameters (βs) and risk preferences parameter (α), but the probability weighting parameter is allowed to vary between the two classes (γ_1 and γ_2 for class 1 and 2, respectively). Although it is possible that other parameters besides those in the probability weighting function vary between classes, holding the other parameters constant

[1] A variety of variables and question responses was used to test class membership probabilities. Educational attainment provided the best fit of candidate regressions.

allows us to isolate differences among managers in responses to probabilities and limits the complexity of the maximum likelihood estimation.[1]

Results

Results from the latent class model suggest that there are at least two classes of respondents in the sample, and that the classes respond to probability differences in distinct ways. Two sets of results are presented in table 2, one each for the control group and the treatment group.

4.1. Latent class model estimates

For both the control group (who saw the aviation exposure attribute expressed as hours of aviation use) and the treatment group (who saw the aviation exposure attribute expressed as expected fatalities), one class exhibited severe probability weighting ($\gamma_1 < 0.2$) and the other class exhibited significant but more moderate probability weighting ($\gamma_2 \sim 0.7$). This suggests that some differences in strategic choices observed in the respondent sample can be attributed to variations in the sample in how managers weight different outcome probabilities.

Table 2. Latent class model parameter estimates by treatment frame

Attribute/parameter	Control frame	Treatment frame
Aviation exposure (flight hours or fatality rate)	-.878***	-2.22***
Private property damage ($)	-1.01***	-.875***
Suppression costs ($)	-.590***	-.192*
Θ_2 (class 2 membership)	-1.08**	-2.06**
Some college education	.906	2.26**
Bachelor's degree	1.76***	2.68***
Graduate degree	1.65***	2.72***
γ_1 (prob. weighting for class 1)	.165***	.137***
γ_2 (prob. weighting for class 2)	.703***	.672***
α (risk preference)	1.02***	.951***
Choice obs (N)	4,097	4,059
Number of respondents	516	511
ln(L)	-2,241	-2,179
AIC	4,501	4,307

*, **, and *** indicate significance at the 90%, 95%, and 99% level respectively.

The observed pattern of probability weighting indicates that managers over-weight low probabilities and under-weight high probabilities. In the case of the extreme probability weighting class (class 1), estimates imply that some managers perceive outcome probabilities to be in the 0.3 to 0.5 range over a large portion of the probability spectrum. Over-weighting low probabilities has the consequence of encouraging managers to avoid strategies with low-likelihood bad outcomes more than they would if they chose according to expected loss minimization, i.e., they appear to avoid taking "good bets" on

[1] The models that allowed additional parameters to vary between the classes, and models with more than two classes, exhibited significant difficulty with maximum likelihood convergence.

low-likelihood bad outcomes. Conversely, under-weighting high probabilities encourages managers to avoid good bets with high-likelihood good outcomes.

Model estimates also show that educational attainment helps explain the likelihood of a respondent belonging to either class. Compared to respondents with a high school diploma or less education, those with a bachelor's or graduate degree are more likely to be members of class 2 (the moderate probability weighting class). For the treatment group, having any amount of college education or more is associated with class 2 membership. This suggests that greater educational attainment is associated with strategy decisions that are more closely aligned with expected loss minimization (at least in terms of probability weighting). However, we cannot assess from the results whether this represents a causal mechanism (i.e., obtaining more education results in less severe probability weighting in decision making), or whether educational attainment is associated with other unobserved characteristics that may drive differences in probability weighting.

4.2. Expected attribute outcomes by educational attainment

The lottery choice experiment was designed such that the (hypothetical) outcomes for each attribute that result from a choice are determined probabilistically. Further, the experimental design and attribute levels were calibrated to ensure that for some lotteries the "safe" option will result in lower expected attribute outcomes, whereas for other lotteries the "risky" option will result in lower expected attribute outcomes. To examine the potential consequences of probability weighting and risk preferences on expected attribute outcomes, we calculated the expected outcomes under an expected loss minimization (ELM) choice pattern (with linear probability weighting and risk neutrality). These were then compared to expected outcomes calculated based on likely strategy choices for the estimated latent class model.

Table 3 displays expected attribute outcomes under ELM choices and under estimated latent class model choices for the control and treatment groups. Under modelled choices, expected outcomes are calculated for each educational attainment category, with choice probabilities for each class weighted by each respondent's likelihood of class 2 membership (note that under ELM there is no difference between classes because all individuals are assumed to exhibit no probability weighting). Attribute preferences (which in part determine choice probabilities) are assumed to be the same for ELM choices and latent class model choices.

Table 3. Average expected attribute outcomes under ELM and modelled choices, by educational attainment.

	Control frame	Treatment frame
Expected loss minimization choices		
Aviation exposure (fatalities per 1,000 fires)	2.6	2.7
Property damage (mil. $)	.785	.815
Suppression costs (mil. $)	.339	.388
Modelled choices		
HS diploma or less		
Aviation exposure (fatalities per 1,000 fires)	4.1	3.3
Property damage (mil. $)	1.25	1.02
Suppression costs (mil. $)	.659	.514
Some college education		
Aviation exposure (fatalities per 1,000 fires)	3.9	3.3
Property damage (mil. $)	1.16	1.06
Suppression costs (mil. $)	.640	.535
Bachelor's degree		

Aviation exposure (fatalities per 1,000 fires)	3.8	3.2
Property damage (mil. $)	1.10	1.05
Suppression costs (mil. $)	.585	.518
Graduate degree		
Aviation exposure (fatalities per 1,000 fires)	3.6	3.1
Property damage (mil. $)	1.12	1.06
Suppression costs (mil. $)	.639	.545

For both the control and treatment groups, modelled choices result in an increase in the number of expected fatalities of between 40 and 60 percent (which represents approximately an additional fatality per 1,000 fires) compared with ELM choices. The amount of expected property damage is also higher under modelled choices by a similar factor, and expected suppression expenditures are higher by between 50 and 100 percent.

The differences in probability weighting between the two classes have implications for expected attribute outcomes. For those respondents with the greatest likelihood of membership in the moderate probability weighting class (class 2), the differences in expected outcomes between ELM and modelled choices are smaller. In the control frame, greater educational attainment in the sample is associated with attribute outcomes that are closer to expected loss minimization, i.e., fewer expected fatalities, less property damage, and less suppression expenditures. In the treatment frame, where the negative consequences of aviation use were highlighted, educational attainment is only associated with reduced expected aviation fatalities. This may be due to respondents in the treatment group exhibiting a greater preference for reducing aviation fatalities than property damage or suppression costs relative to the control group.

Conclusion

Responding to wildfire incidents requires careful consideration of risks and potential outcomes associated with available strategies. This paper has examined how Federal wildfire managers respond to risk by observing hypothetical choices over strategies that involve risk to fire outcomes. An econometric analysis of a survey-based lottery choice experiment indicates that respondents tend to be risk averse and exhibit non-linear weighting of outcome probabilities. Specifically, respondents on average over-weighted low probabilities and under-weighted high probabilities relative to linear probability weights.

Using a latent class model of strategy choices, we discovered that at least two classes of respondents exist in the sample. One class is characterized by extreme non-linear probability weighting, and the other class exhibits non-linear but more moderate probability weighting. The likelihood of class membership is significantly associated with educational attainment; respondents with more education are more likely to be members of the moderate probability weighting class.

Probability weighting, risk aversion, and latent classes have implications for the expected outcomes of the hypothetical wildfires respondents were asked to manage. Compared to an expected loss minimization strategy baseline (i.e., linear probability weighting and risk neutrality), respondents made decisions that on average resulted in greater expected aviation fatalities, property damage, and suppression costs. That is, risk and decision biases tend to result in increased losses to outcome attributes thought to be important to fire managers when they make strategic decisions. However, a portion of the respondent sample exhibited less-severe biases, which tends to mitigate these losses.

It is important to note that the results were obtained using a hypothetical choice scenario, and it is unclear how the quantitative results would apply to real-world fire management scenarios. However, the results suggest that how managers respond to risk can be an important determinant of fire outcomes. Also, a better understanding of heterogeneity of risk preferences among managers could assist training and after-action review efforts to improve risk management skills. Although there is not currently a

reliable way to generate empirical probabilities of strategy outcomes, future research would benefit from a focus on more realistic management scenarios, particularly those that incorporate a temporal dimension of strategic decision making.

References

Greene, W.H., and D.A. Hensher (2003) "A latent class model for discrete choice analysis: contrasts with mixed logit." *Transportation Research Part B: Methodological*, v.37, 681-698.

Greene, W.H., and D.A. Hensher (2013) "Revealing additional dimensions of preference heterogeneity in a latent class mixed multinomial logit model." *Applied Economics*, v.45, 1897-1902.

Hensher, D.A., W.H. Greene, Z. Li (2011) "Embedding risk attitude and decision weights in non-linear logit to accommodate time variability in the value of expected travel time savings." *Transportation Research Part B: Methodological*, v.45, 954-972.

Holt, C.A., S.K. Laury (2002) "Risk aversion and incentive effects." *American Economic Review*, v.92, 322-325.

Maguire, L.A., E.A. Albright (2005) "Can behavioral decision theory explain risk-averse fire management decisions?" *Forest Ecology and Management*, v.211, 47-58.

Prelec, D. (1998) "The probability weighting function." *Econometrica*, v.66, 497-527.

Sun, Z., T. Arentze, H. Timmermans (2012) "A heterogeneous latent class model of activity reschedule, route choice and information acquisition decisions under multiple uncertain events." *Transportation Research Part C: Emerging Technologies*, v.25, 46-60.

Taylor, M.P. (2013) "Bias and brains: Risk aversion and cognitive ability across real and hypothetical settings." *Journal of Risk and Uncertainty*, v.46, 299-320.

Train, K. (2009) *Discrete Choice Methods with Simulation*. New York: Cambridge University Press.

USDA Forest Service (2010). *FY2010 Aviation Safety Summary*. Available at: http://www.fs.fed.us/foresthealth/aviation/safety/safety-statistics.shtml, accessed Feb. 2, 2014.

van Houtvan, G., F.R. Johnson, V. Kilambi, A.B. Hauber (2011) "Eliciting benefit-risk preferences and probability-weighted utility using choice-format conjoint analysis." *Medical Decision Making*, v.31, 469-480.

Wilson, R.S., P.L. Winter, L.A. Maguire, T. Ascher (2011) "Managing wildfire events: risk-based decision making among a group of federal fire managers." Risk Analysis, v.31, 805-818.

Wibbenmeyer, M., M. Hand, D. Calkin (2012) *Preliminary Results From a Survey of U.S. Forest Service Wildfire Managers' Attitudes Toward Aviation Personnel Exposure and Risk*. Research Note RMRS-RN-50WWW. Fort Collins, CO: U.S. Department of Agriculture, Forest Service, Rocky Mountain Research Station.

Wibbenmeyer, M.J., M.S. Hand, D.E. Calkin, T.J. Venn, M.P. Thompson (2013) "Risk preferences in strategic wildfire decision making: a choice experiment with U.S. wildfire managers." *Risk Analysis*, v.33, 1021-1037.

Modelling socio-economic drivers of forest fires in the Mediterranean Europe

Lara Vilar[a], Andrea Camia[b], Jesús San-Miguel-Ayanz[b]

[a] *Centre for Human and Social Sciences, Spanish National Research Council (CSIC), C/Albasanz 26-28, 28037 Madrid, Spain, lara.vilar@cchs.csic.es*
[b] *Joint Research Centre of the European Commission, 21027 Ispra (VA), Italy, andrea.camia@jrc.ec.europa.eu, jesus.san-miguel@jrc.ec.europa.eu*

Abstract
Forest fires in the Mediterranean Europe are mostly related to human activities. More than 90% of fires are originated from either deliberate or involuntary causes. Socio-economic changes occurring in Europe in the last decades (e.g., abandonment of agricultural lands, depopulation of rural areas, changes in agriculture and forestry policies, etc.) have driven landscape transformations affecting fire risk levels through processes like e.g., increase of unmanaged lands, dead and live biomass accumulation, new uses of the forest and natural lands. In this work we analysed and attempted modelling the influence of socio-economic factors and their change over time on forest fire occurrence in the Mediterranean Europe (EU-Med).
Three 6-year time periods were considered (1988-1993, 1998-2003, 2004-2009). Fire data was extracted from the European Fire database of the European Forest Fire Information System (EFFIS). Our analysis was performed in the most fire-affected area of Europe, the European Mediterranean region covered by Portugal, Spain, France, Italy and Greece. Fire data were analysed according to their main fire cause (accident-negligence and deliberate). Both, fires and socio-economic variables, which represent anthropogenic factors related to fire activity, were mapped on a 10 km x10 km grid. Models of forest fire density were derived separately for each period and per cause category using ordinal regression statistical methods. The best predictors by period and fire cause category were assessed and differences between time periods analysed. Our result show that the variable wildland-urban interface (WUI) is related to higher ratings of fire density. This result was consistent for all periods and for the two type of fire cause analysed in our study. The overall fit of the models was 40-50%.for accident-negligence and 50% deliberated caused fires. Despite the relatively homogeneous socio-economic characteristics of the Mediterranean Europe, differences are found at regional level and by fire cause category. The anthropogenic drivers of forest fires are a challenging yet fundamental factor to understand and model the European Mediterranean fire environment.

Keywords*: fire density, fire causes, socio-economic drivers, Europe, EFFIS*

Introduction

Mediterranean ecosystems cannot be fully understood without the role of fires. Natural fires have been essential to maintain biodiversity. Fire has also been a widely used tool to manage territory. In Mediterranean Europe fire regimes have been set directly and indirectly by humans for thousands of years (Pyne, 2009). However, in the last decades, natural fire regimes have experienced significant alterations (fire frequency, intensity and severity), which have aggravated their negative ecological, social and economic consequences (Westerling *et al*., 2006; FAO, 2007). In Mediterranean Europe nowadays, fire does not form a significant part of traditional systems of life; however it continues to be strongly tied to human activity (Leone *et al*., 2009). Socio-economic changes which are occurring in Europe (abandonment of agricultural land, depopulation of rural areas, priority shifts in forestry policy, etc.) result in an increase of unmanaged shrubs and biomass, which increases fire risk (Vélez Muñoz, 2007). Fire risk is also aggravated by the climate conditions in these Mediterranean areas (e.g. hot and dry summers) (Leone *et al*., 2009). Furthermore, research on climate change has indicated that increased fire hazard is likely to arise from global warming (Westerling *et al*., 2006).

Forest fires in the Mediterranean Europe are mostly related to human activities. More than 90% of fires of known cause are originated from either deliberate or involuntary causes (Ganteaume *et al*., 2013).
Fire data were extracted from the European Fire database of the European Forest Fire Information System (EFFIS). EFFIS is the European Commission (EC) focal point for information on forest fires in Europe (San-Miguel-Ayanz *et al*., 2012). It was established by the Joint Research Centre (JRC) and the Directorate General for Environment (DG ENV) of the European Commission to support the services in charge of the protection of forests against fires in the EU and neighbour countries, and also to provide the EC services and the European Parliament with information on forest fires in Europe (San-Miguel-Ayanz *et al*. 2013). Following the recommendations of the European Parliament to further develop the European Forest Information System (EFFIS), a common classification scheme of fire causes was established. This harmonized classification scheme was accepted in 2012 and is currently being adopted by the countries as a common means to record fire causes when reporting national data to EFFIS (Camia *et al*., 2013). This classification was used in our analysis. .
We analysed and attempted modelling the influence of socio-economic factors and their change over time on forest fire occurrence in the Mediterranean Europe (EU-Med). Data from the European Fire database in the European Forest Fire Information System (EFFIS) related to three 6-year time periods were considered: 1988-1993, 1998-2003 and 2004-2009. These three periods will be referred to in the text as 1990s, 2000s and 2006s. Fires were mapped on a 10 km x 10 km grid starting from their location at NUTS3 (Nomenclature of territorial units for statistics, level 3 - province) level resolution using GIS tools. NUTS regions are used by the countries to report national information to the European Commission. Fire density was separated into two cause categories, accident-negligence and deliberate. Socio-economic variables representing anthropogenic factors related to fire activity were also mapped using the same 10 km x 10 km grid.

Methods and materials

Study area

The Mediterranean Europe (EU-Med) area considered for the analysis includes the EU countries Portugal, Spain, Italy, Greece and the Southern provinces of France, with a total area of more than 1 million km^2. Figure 1 shows the area analysed by NUTS3 administrative level (province) and by fire regions agreed by expert knowledge (Camia A, personal communication). Landscape differences between the Mediterranean Basin and the rest of Europe are mainly related to climate, the long and intense human impact and the role of fire (Pausas and Vallejo, 1999). Reflecting the prevailing climate, Mediterranean forests are frequently characterized by fire climax species, i.e. those dependent on the presence of fire in the reproductive cycle (FAO, 2007). Forests, including shrub formations and other semi-natural categories (e.g. transitional woodlands, sclerophyllus vegetation) occupy about 50% of the area. The area is populated by about 137 million people (Eurostat, 2011).

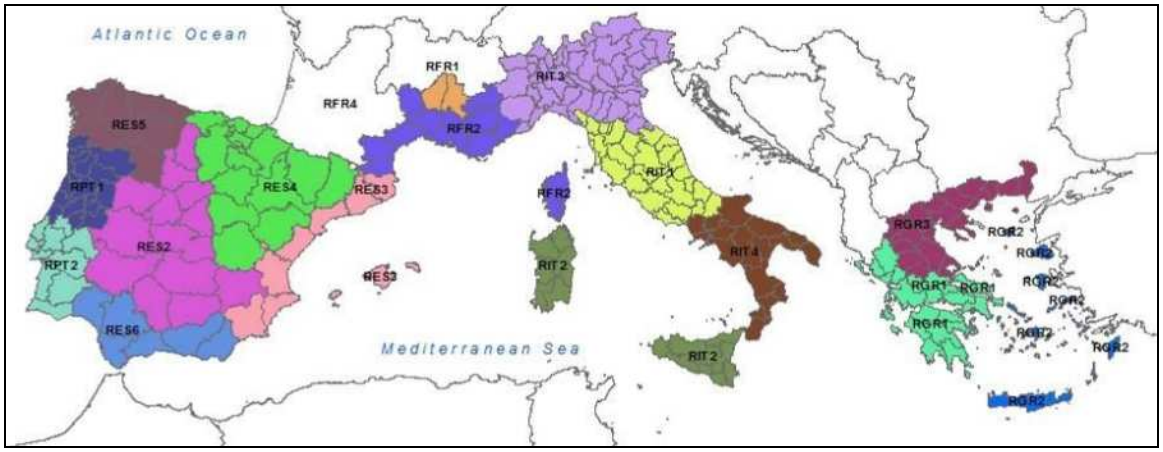

Figure 1- Extent of the analyzed area, separated by NUTS3 administrative level boundaries and fire regions

Data

2.2.1. *Fire occurrence data*

Fire occurrence data was obtained from the European Forest Fire Information System (EFFIS). Three 6-year periods of time were extracted: 1988-1993 (1990s), 1998-2003 (2000s) and 2004-2009 (2006s). The fire records were at NUTS3 (province) level, and included fire occurrence data for months March to November. Fire data was analysed by main fire cause category (accident-negligence and deliberate). Fires of unknown cause were assigned to a known cause on the basis of the proportion of known caused fires in each NUTS3. Also, the number of fires was referred to the wild-land area in the NUTS3. After the pre-processing and selection, the fire data were mapped on a 10 km x 10 km grid (LAEA projection reference grid) following the INSPIRE specifications (EC and EP, 2007). This resulted in fire density values by cause (accident-negligence and deliberate) by grid cell and by period (1990s, 2000s and 2006s). These variables were used as response variables in our modelling. Figure 2 shows as an example the fire density (fires/km^2) by 10 km x10 km grid of deliberated fires in 2000s.

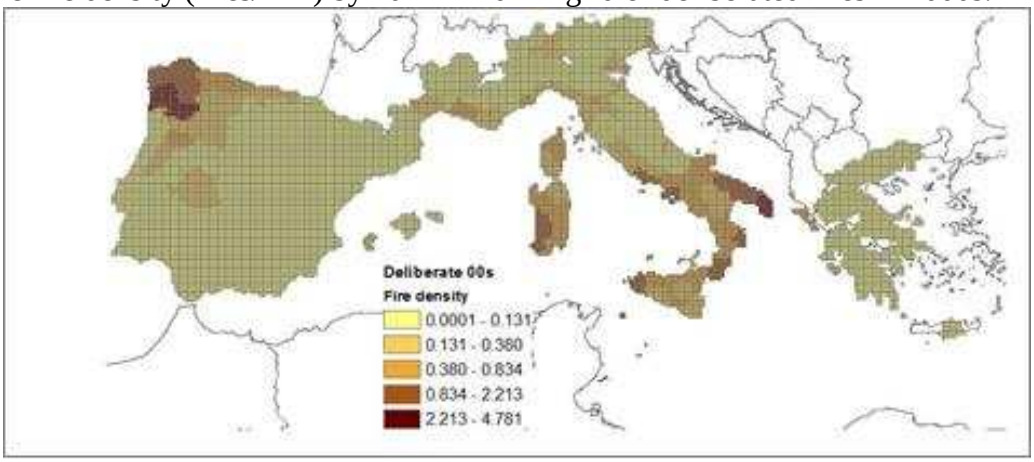

Figure 2- Fire density (fires/km^2) by 10 km x10 km grid. Deliberated fires in 2000s

2.2.2. *Socio-economic factors*

Fire density is influenced by socio-economic factors. These include socio-economic changes in rural and urban areas, traditional activities in rural areas, accidents or negligence, fire prevention activities and other factors that can lead to social unrest (e.g. land use disputes or high unemployment rates) (Martinez *et al*., 2009; Vilar del Hoyo *et al*., 2008; Leone *et al*., 2003). To analyze the impact of these factors on fire density in the EU-Med region, available spatially explicit socio-economic variables

related to the different factors were obtained from different cartographic and statistical sources for the three selected periods of time (1990s, 2000s and 2006s).. All the variables were spatially referred and mapped on the 10 km x 10 km grid. Different spatial analyses were carried out using Geographic Information System (GIS) tools (ArcMap 10, ESRI 2011), including format conversion, re-projection, re-clasification, overlay, calculation of areas, buffer zones and other distance operations such as quantification of different land use interfaces. The variables considered in the analysis are shown in Table 1.

Table 1. Socio-economic variables tested as predictors in the models

Variables [abbreviation]	Unit
Population density [pop_den]	[number/km^2]
Density of labour force in economic sectors *(agriculture, industry, services)* [agri, indus, serv]	[number/km^2]
Agrarian holders older than 55 [holders55]	[number/km^2]
Road network *(road, motorway*) [road, motow]	[total lines/ km^2]
Wildland-Urban interface [WUI]	[km^2]
Number of heads of livestock [bovine, goat, sheep]	[number/km^2]
Full farm time workers (WT) [farmw]	[number/km^2]
Total AA (Agricultural area) Owner Farmed [ofarmed]	[km^2]
Grassland-forest interface [FGI]	[km^2]
Agricultural-forest interface [FAI]	[km^2]
Railway network [railway]	[total lines/ km^2]
Protected areas [NATURA00]	[km^2]
Landscape fragmentation [RPC_A] [RPC_W]	[-]

2.3. Modelling the role of socioeconomic drivers of forest fires

Scientific approaches which include human factors in fire risk assessment were commonly based on statistical models that attempt to explain historical, human-caused fires from a set of independent variables (Vilar del Hoyo *et al*., 2011). Logistic regression analysis was frequently used both to predict and also to explain human-caused fires (Martell *et al*., 1987; Vega-García *et al*., 1995; Chuvieco *et al*., 1999; Lin, 1999; Pew and Larsen, 2001; Vasconcelos *et al*., 2001; Martínez *et al*., 2004; Prasad *et al*., 2008; Martínez *et al*., 2009). Other statistical methods such as linear regression, classification regression trees, neural networks or Bayesian probability were also used in fire risk mapping to generate local risk models (Chao-Chin, 2002; Koutsias *et al*., 2004; Robin *et al*., 2006; Amatulli *et al*., 2006, 2007; Amatulli and Camia, 2007; Syphard *et al*., 2007; Vega-García, 2007; Yang *et al*., 2007; Romero-Calcerrada *et al*., 2008). The response variable in those models always refered to fire occurrence, commonly obtained from information available in forest fire databases.

In order to identify the role of different socio-economic factors on the spatial variation of fire density, the relationships between this response variable and the spatialized socio-economic variables previously described were analized by using regression models for ordinal data, by means of cumulative link models (package ordinal, Christensen, 2012, for R, R Development Core Team, 2011). Fire density was divided into three equiprobable classes (low, medium, high). Models of forest fire density were derived separately for each period and per cause category. A 75% random sample of the input dataset was used to calibrate the models. In particular, the models were initially fitted by a constant and then the relevant socio-economic explanatory predictors were identified by performing a forward stepwise selection procedure, using the Akaike Information Criterion (AIC) as the criterion for variable inclusion. Finally the calibrated model was used to predict the expected fire density class on the 25% of the sample dataset excluded from calibration. The performance of the models was

evaluated by comparing the observed and predicted fire density classes. In particular, a crosstabulation analysis was conducted. This allowed calculating the accuracy by fire density class (user's and producer's accuracy) as well as the overall fit.
The best predictors selected by period and by fire cause category as well as the differences between time periods were analysed.

Results and discussion

Our results in EU-Med study area showed that, for the three periods of time analysed and for accident-negligence and deliberate caused fires, wildland-urban interface (*WUI*) was the variable invariantly selected with positive sign in all periods. For the two types of fire cause analysed the model predicts that the probability of belonging to a higher fire density class increases when *WUI* increases. Tables 2 and 3 show a summary of the results, indicating the significant variables of each model and their signs by period, and by fire cause (accident-negligence vs. deliberated), respectively.

Table 2. Summary of results of ordinal regression models for accident-negligence caused fires in EU-Med: period, variables in the model ordered by AIC step forward, sign and overall fit. In red colour, variables present in all periods with negative sign; in green colour, variables present in all periods with positive sign; in orange colour, variables present in all periods with changing sign

Accident-negligence					
1990s		**2000s**		**2006s**	
Variables (AIC Step forward order)	**Sign**	**Variables (AIC Step forward order)**	**Sign**	**Variables (AIC Step forward order)**	**Sign**
holders55	+	road	+	**bovine**	-
bovine	-	goat	-	**WUI**	+
pop_den	+	**bovine**	-	road	-
sheep	-	pop_den	+	**FGI**	-
FGI	-	agri	+	NATURA00	+
goat	+	RPC_W	-	FAI	+
WUI	+	**WUI**	+		
RPC_W	-	NATURA00	+		
RPC_A	-	RPC_A	+		
		FAI	+		
		FGI	+		
Overall fit	49%	Overall fit	47%	Overall fit	39%

Regarding fires caused by accident-negligence, the variable agriculture-forest interface (*FAI*) enters in the models with positive sign in 2000s and 2006s. This variable is related to vegetation management or agricultural burnings. It must however be noticed that other theoretically important variables show changing signs in the different periods (e.g. *FGI*), and also that high livestock presence (*bovine*) seems to lead to a reduction of expected fire density.

Table 3. Summary of results of ordinal regression models for deliberate caused fires in EU-Med: period, variables in the model ordered by AIC step forward, sign and overall fit. In red colour, variables present in all periods with negative sign; in green colour, variables present in all periods with positive sign; in orange colour, variables present in all periods with changing sign

Deliberate					
1990s		2000s		2006s	
Variables (AIC Step forward order)	**Sign**	**Variables (AIC Step forward order)**	**Sign**	**Variables (AIC Step forward order)**	**Sign**
holders55	+	**goat**	-	**holders55**	+
goat	-	**holders55**	+	**WUI**	+
sheep	-	agri	+	**sheep**	+
WUI	+	**sheep**	+	**FAI**	-
road	+	**WUI**	+	**goat**	-
bovine	-	**FAI**	-	NATURA2000	-
FAI	-	**road**	+	**road**	-
RPC_W90	+	RPC_A	-		
agri	+	FGI	-		
		NATURA2000	-		
		pop_den	-		
Overall fit	56%	Overall fit	53%	Overall fit	50%

Regarding deliberately caused fires, *goat* and *FAI* are the variables that in all periods enter the models with a negative sign, meaning that these variables are less likely to be linked to higher ratings of fire density. *Goat* enters in the models in 1990s and 2000s in the second and first position respectively, while in 2006s in the 5th position. This fact may be related to the loss of the role goats played in the past helping to prevent fire thanks to grazing. *WUI* and *holders55* enter with a positive sign in all periods, meaning they are more likely to be linked to higher ratings of fire density. The overall fit of models was between 40% and 50% for accident-negligence models and above 50% for deliberate fire models. Results were improved when modelling was attempted by sub-country regions, reaching 74% for the best fitting of deliberate fires.

Conclusions

Models show temporal trends in time in the case of the variables *WUI* for both type of fire cause and *goats/FAI* in the deliberated caused fires. For the rest of predictors the models did not highlighted clear trends. This suggests the need to analyse data with larger time span, to include more important socio-economic and territorial changes. The depopulation of rural areas in Europe started after the II World War, being more intense from the 50s and 60s in southern Europe. Changes in regional development have happened since the 60s and 70s. To analyze this issue, homogeneous data would be required for the study area for these periods. The negative sign of some of the variables is non-intuitive. This issue might have a reason related to limitations of the data, lack of explanatory variables or the statistical analysis itself. Further investigation will be needed in these cases. The variables representing the socio-economic issues are an indirect way of measuring the role of socio-economic influence on forest fires. Human behaviour is very difficult to predict and to represent, in particular regarding deliberate actions. Consistent, complete and trustworthy data (both fire data and socioeconomic drivers) is essential to obtain reasonable models.

Generally speaking, the fit is slightly better in the case of the deliberately caused fires. It might be indicative of the influence of fire causality and the scale of the analysis.

Despite the relatively homogeneous socio-economic characteristics of Mediterranean Europe, differences are found at regional level and by fire cause category. The anthropogenic drivers of forest

fires remain a challenging yet fundamental factor to understand and model the European Mediterranean fire environment.

References

Amatulli G, Camia A (2007) Exploring the relationships of fire occurrence variables by means of CART and MARS models. In 'IV International Wildfire Conference', 13-17 May 2007, Seville, Spain

Amatulli G, Pérez-Cabello F., de la Riva J (2007) Mapping lightning/human-caused wildfires occurrence under ignition point location uncertainty. *Ecological modelling* **200**, 321-333

Amatulli G, Rodrigues MJ, Trombetti M, Lovreglio R (2006) Assessing long-term fire risk at local scale by means of decision tree technique. *Journal of Geophysical Research* **111**, G04S05, doi:10.1029/2005JG000133

Camia A, Durrant T, San-Miguel Ayanz J (2013) Harmonized classification scheme of fire causes in the EU adopted for the European Fire Database of EFFIS. Executive report. JRC Scientific and Policy Reports. Report EUR 25923 EN. Available at http://forest.jrc.ec.europa.eu/media/cms_page_media/82/LB-NA-25-923-EN-N.pdf [Verified 14 July 2014]

Chao-Chin L (2002) A Preliminary Test of A Human caused Fire Danger Prediction Model. *Taiwan Journal Forest Science* **17** (4), 525-529

Chuvieco E, Salas FJ, Carvacho L, Rodríguez Silva F (1999) Integrated fire risk mapping. In 'Remote Sensing of Large Wildfires in the European Mediterranean Basin'. (Ed. E Chuvieco) pp. 61-84. (Springer-Verlag: Berlin)

Christensen RHB (2013) Package 'Ordinal' for R. Available at http://cran.r-project.org/web/packages/ordinal/ordinal.pdf [Verified 14 July 2014]

Directive 2007/2/EC of the European Parliament and of the Council of 14 March 2007 establishing an Infrastructure for Spatial Information in the European Community (INSPIRE). OJ L 108, 25.4.2007, p. 1–14 (BG, ES, CS, DA, DE, ET, EL, EN, FR, IT, LV, LT, HU, MT, NL, PL, PT, RO, SK, SL, FI, SV). Special edition in Croatian Chapter 13 Volume 030 P. 270 – 283

EEA reference INSPIRE grid-version 15 (5/2011) Available at http://epp.eurostat.ec.europa.eu/portal/page/portal/eurostat/home/ [Verified 14 July 2014]

ESRI (2011) ArcGIS Desktop: Release 10. Redlands, CA: Environmental Systems Research Institute

EUROSTAT. Basic Figures on the EU. First quarter 2011. Total population at 1/01/2009 Available at http://epp.eurostat.ec.europa.eu/portal/page/portal/eurostat/home/ [Verified 14 July 2014]

FAO (2007) Fire management global assessment. A thematic study prepared in the framework of the Global Forest Resources Assessment 2005. FAO Forestry Paper 151. Food and Agriculture Organization for the United Nations: Rome Available at http://www.fao.org/forestry/fra2005/en [Verified 14 July 2014]

Ganteaume A, Camia A, Jappiot M, San-Miguel-Ayanz J, Long-Fournel M, Lampin C (2013) A Review of the Main Driving Factors of Forest Fire Ignition Over Europe. *Environmental Management*, **51**(3), 651-662

Koutsias N, Kalabokidis KD, Allgöwer B (2004) Fire occurrence patterns at landscape level: beyond positional accuracy of ignition points with kernel density estimation methods. *Natural Resource Modeling* **17** (4), 359-375

Leone V, Koutsias N, Martinez J, Vega-Garcia C, Allgower B, Lovreglio R (2003) The human factor in fire danger assessment. In 'Wildland Fire Danger Estimation and Mapping. The Role of Remote Sensing Data'. (Ed. E Chuvieco) pp. 143–196. (World Scientific Publishing: Singapore)

Lin C (1999) Modelling probability of ignition in Taiwan Red Pine Forests. *Taiwan Journal Forest Science* **14** (3), 339-344

Martell DL, Otukol S, Stocks BJ (1987) A logistic model for predicting daily people caused forest fire occurrence in Ontario. *Caumar*

Martínez J, Martínez J, Martín P (2004) El factor humano en los incendios forestales: Análisis de factores socio-económicos relacionados con la incidencia de incendios forestales en España. In 'Nuevas tecnologías para la estimación del riesgo de incendios forestales'. (Eds. Chuvieco E, Martín P.) pp. 101-142 (CSIC, Instituto de Economía y Geografía: Madrid, Spain)

Martinez J, Vega-Garcia C, Chuvieco E (2009. Human-caused wildfire risk rating for prevention planning in Spain. *Journal Environmental Management* **90**, 1241–1252

Pausas JG, Vallejo VR (1999) The role of fire in European Mediterranean ecosystems. In 'Remote sensing of large wildfires in the European Mediterranean basin'. (Ed. E Chuvieco) pp. 3-16. (Springer: Berlin)

Pew KL, Larsen CPS (2001) GIS analysis of spatial and temporal patterns of human-caused wildfires in the temperate rain forest of Vancouver Island, Canada. *Forest Ecology and Management* **140**, 1-18

Prasad VK, Badarinath KVS, Eaturu A (2008) Biophysical and anthropogenic controls of forest fires in the Deccan Plateau, India. *Journal of Environmental Management* **86** (1), 1-13

Pyne SJ (2009) Eternal Flame: An Introduction to the Fire History. Chuvieco, E. (Ed.) In 'Earth Observation of Wildland Fires in Mediterranean Ecosystems'. (Ed. E Chuvieco) pp 11-27 (Springer-Verlag: Berlin Heidelberg)

R Development Core Team (2011) R: A language and environment for statistical computing. R Foundation for Statistical Computing, Vienna, Austria. Available at http://www.R-project.org/ [Verified 14 July 2014]

Robin JG, Carrega P, Fox D (2006) Modelling fire ignition in the Alpes-Maritimes Department, France. A comparison. In 'V International Conference on Forest Fire Research', 27-30 November 2006, Figueira da Foz, Portugal

Romero-Calcerrada R, Millington JD, Gomez-Jimenez I. (2008) GIS analysis of spatial patterns of human-caused wildfire ignition risk in the SW of Madrid (Central Spain). *Landscape Ecology* **23**, 341-354

San-Miguel-Ayanz J, Schulte E, Schmuck G, Camia A, Strobl P, Libertà G, Giovando C, Boca R, Sedano F, Kempeneers P, McInerney D, Withmore C, Santos de Oliveira S, Rodrigues M, Durrant T, Corti P, Oehler F, Vilar L, Amatulli G (2012) Comprehensive monitoring of wildfires in Europe: the European Forest Fire Information System (EFFIS). In 'Approaches to Managing Disaster - Assessing Hazards, Emergencies and Disaster Impacts' (Ed. J Tiefenbacher) pp. 87-105. (InTech, ISBN 978-953-51-0294-6)

San-Miguel-Ayanz J, Schulte E, Schmuck G, Camia A (2013) The European Forest Fire Information System in the context of environmental policies of the European Union. *Forest Policy and Economics*, **29**, 19-25

Syphard AD, Radeloff VC, Keeley JE, Hawbaker TJ, Clayton MK, Stewart SI, Hammer RB (2007) Human influence on California Fire Regimes. *Ecological Applications* **17** (5), 1388-1402

Vasconcelos MPP, Silva S, Tomé M, Alvim M, Pereira JMC (2001) Spatial Prediction of Fire Ignition Probabilities: Comparing Logistic Regression and Neural Networks. *Photogrammetric Engineering and Remote Sensing* **67** (1), 73-81

Vega-García C, Woodard PM, Titus SJ, Adamowicz WL, Lee BS (1995) A Logit Model for predicting the Daily Occurrence of Human Caused Forest Fires. *International Journal Wildland Fire* **5** (2), 101-111

Vega-García C (2007) Propuesta metodológica para la predicción diaria de incendios forestales. In 'IV International Wildfire Conference', 13-17 May 2007, Seville, Spain

Vélez Muñoz R (2007) Experiences in Spain of Community Based Fire Management. 'IV International Wildfire Conference', 13-17 May 2007, Seville, Spain

Vilar del Hoyo L, Martin Isabel MP, Martinez Vega FJ (2011) Logistic regression models for human-caused wildfire risk estimation: analysing the effect of the spatial accuracy in fire occurrence data. *European Journal of Forest Research*. **130** (6), 983-996

Vilar del Hoyo L, Martin Isabel MP, Martínez Vega FJ (2008) Empleo de técnicas de regresión logística para la obtención de modelos de riesgo humano de incendio forestal a escala regional. *Boletín de la Asociación de Geógrafos Españoles* **47**, 5–29

Westerling AL, Hidalgo HG, Cayan DR, Swetnam TW (2006) Warming and earlier spring increase western US forest wildfire activity. *Science* **313**, 940-943

Yang J, He HS, Shifley SR, Gustafson EJ (2007) Spatial Patterns of Modern Period Human-Caused Fire Occurrence in the Missouri Ozark Highlands. *Forest Science* **53** (15)

The efficiency analysis of the fire control operations using the VISUAL-SEVEIF tool.

Francisco Rodríguez y Silva[a], Juan Ramón Molina[a], Jesus Rodriguez Leal[b]

[a] *Forest Fire Laboratory. Forest Engineering Department. University of Cordoba*
Leonardo da Vinci Building. Campus de Rabanales. 14071 Córdoba (Spain, ir1rosif@uco.es
[b] *Architecture of Computer Department. Computer Engineering School. University of Seville*

Abstract
The suppression costs represent a significant proportion of the total budget available for forest fire protection programs. The need to make efficient use of available budgets requires directing funding towards areas with the lowest costs and maximum benefits. Accordingly, incorporating econometric tools enables establishing criteria to optimize budg*et al*location. Modelling the fire suppression process and budg*et al*location requires knowing how suppression is managed, how resources are dispatched and how costs are incurred.
The methodological approach presented here allows forecasting fire suppression operations productivity, based on suppression difficulty and cost, as well as records from documented fire suppression operation plans from prior fires. On the other side, the value of natural forest resources and the damage and losses from forest fires assessing, help to determining the change net value to estimate the economics fire impacts. For the efficiency analysis of the fire program, is possible using the VISUAL-SEVEIF (Spanish acronym for System for the Economic Evaluation of Wildfires) software tool, to obtain the knowledge of fire behavior and its direct effect on the depreciation of natural resources value, providing the total costs of the losses in the area affected by the wildfire, and the value of the losses for each of the resources identified within the fire perimeter.
This tool work showing both in real time, simulating the spatial development of ground and canopy fires, and the economic losses. The spatial resolution of work will be conditioned by quality and accuracy of fuel model mapping, as well as the characteristics of the digital terrain model, so that in high-precision models the results of the fire behavior dynamic can be up to a square meter. The information layers required by the tool includes one that incorporates the characterization of the natural resources that exist in the area being analyzed and allows determining the economic value of these resources. The import and export possibilities of geo-referenced perimeters, in both vector and raster formats, allows easy transfer of the information generated to geographic information systems (GIS). VISUAL-SEVEIF enables carrying out diagnostic studies of an area that are aimed at the prevention and strategic management of wildfire defense. This paper showing how using this methodology, is possible obtained the efficiency rate of fire suppression activities.

Keywords*: Strategic management, fire prevention, natural resources, GIS, environmental, fire economics, econometrics, fire management, fire program planning, operational plans, fire budgets*

Introduction

Forest fires are one of the biggest environmental problems facing the world today, generating significant consequences with regard to both damage and deterioration of forest landscape and its depreciation and economic and social valuation. The abandonment of forest settings, as areas inhabited and affected by humans in terms of actions related to subsistence and energy use, has generated an increase in the accumulation of high-energy biomass over the past few decades (Rodríguez y Silva and Molina 2010, Vélez 2009). This circumstance, coupled with worsening climatic conditions (Piñol *et al*. 1998), has caused a rise in the potential energy released by fire and consequently the virulence of forest fires, resulting in an increase in fire damage to natural resources and the surrounding environment.
The need for strategic information, in relation to the dynamic, energy and expansive potential of fire runs, led to the development of both analytical and graphical simulators. Increased knowledge in fire

science has allowed addressing prediction and simulation studies, thus facilitating their application in wildfire defense activities.

Today's technology provides appropriate prediction and simulation tools that allow effectively developing attack plans in which the priority focus is on safety; it can thus be concluded that prediction and simulation are an ongoing need in protecting forest areas from fire. Moreover, the prediction and simulation exercise allows reducing the time required to achieve control, while facilitating cost savings by providing critical information for the efficient distribution of firefighting resources.

While there has been significant progress in the quality and accuracy of fire behavior forecasts over recent years, important uncertainties remain to be resolved in relation to the simulation of complex phenomena such as energy feedback, the effect of turbulence on acceleration, and the transition and spread of ground fire to the forest canopy. Regardless of future advances in our understanding of fire's dynamic behavior, there is another important need in forest fire management, which is quantifying it in monetary and therefore budgetary terms. Indeed, it is indisputable that any application of a wildfire defense management model is inextricably linked to budget availability and therefore the establishment of priority-based criteria to determine investment levels to implement the management model.

This discussion highlights the importance of studies, research and developments that enable applying econometric criteria to decision-making. Currently, new tools are available, such as the SINAMI econometric model, which allow analyzing in the context of the area and as a matter of strategic planning the most efficient budg*et al*location, by taking into account: the historical background in the frequency and distribution of fires, fire behavior conditions, the economic value of natural resources and the operational capabilities of the firefighting resources (Rodríguez y Silva *et al*. 2010). As discussed by Thompson and Calkin (2011) uncertainty is a major component to consider in developing decision support methodologies "… to facilitate cost-effective, risk-based wildfire planning efforts (p. 1895)." However, the availability of this model and of its ECONOSINAMI software (Rodríguez y Silva 2009, Rodríguez y Silva and González-Cabán 2010) does not resolve in an integrated manner the expansive simulation of fire behavior and the economic evaluation of damages that the simulated fire can potentially generate. This paper presents the structure and operational flow line of the first simulation tool that incorporates the assessment of economic losses caused by fire based on the linear intensity level that the fire develops (kW/m) by each pixel of spatial resolution with which the simulation is performed.

The VISUAL-SEVEIF model (Rodríguez y Silva *et al*. 2013) has been determined by performing the integration in the VISUAL-CARDIN program (Rodríguez y Silva 1999, Rodríguez y Silva *et al*. 2010) of the set of algorithms for the SEVEIF model (Molina *et al*. 2008, Rodríguez y Silva and others 2007, 2010), which were developed for determining and assessing the impact of fire on natural resources in terms of intensity levels released by fire spread. This model offers real-time economic evaluation of losses from post-fire depreciation of natural resources affected.

Valuations of natural resources tend to underestimate the real value of a forest (Constanza *et al*. 1997). Unlike traditional economic activity, the forest environment is characterized by the extraordinary importance of externalities that entail damages or benefits to others of considerable magnitude. From the socio- economic standpoint, all the natural resources must be expressed in monetary terms. The valuation of damages caused by forest fires requires individualized study of each of the resources (tangible and intangible) and their change in net value in relation to fire severity and ecosystem resilience (Molina *et al*. 2009).

The recognition and valuation of natural resources is essential for spatiotemporal planning of preventive work and post-fire rehabilitation (Molina, 2008). Incorporating the concept of vulnerability extends the study beyond the sphere of traditional economic valuation work, integrating two concepts, on the one hand the value of the resource and on the other fire behavior. The integration of the two concepts is performed using a matrix of depreciation rates based on flame length, called a "depreciation matrix" (Molina *et al*. 2011, Rodríguez y Silva *et al*. 2012).

The socio-economic vulnerability model was made through the configuration of a mathematical algorithm associated with a geographic information system (GIS), facilitating the development of spatiotemporal tracking cartography, both at the individual resource level and at the ecosystem's integral vulnerability level. The automation of the calculation and management through GIS is being conducted under the INFOCOPAS project (RTA2009-00153-C03-03) funded by the National Institute for Agricultural Research (INIA), in order to attain versatile geo-referenced knowledge in almost real-time of forest system vulnerability to forest fires.

Architecture of simulator

The process followed in the definition and development of the operational architecture of the VISUAL-SEVEIF program consisted of the following phases:

- Review of the VISUAL-CARDIN simulator's software structure in order to locate the assembly position of the economic evaluation module in the program's flow line.
- Selection of natural resources for which losses are to be evaluated based on energy intensity levels that simulated fires can develop.
- Programming of economic evaluation algorithms through C++ computer language.
- Development of interactive windows between the VISUAL-SEVEIF program and the user.
- Determination of input variables, which must be entered in order to perform the calculations.
- Implementation of economic evaluation options included in the VISUAL- SEVEIF program:
  1. Calculation of the monetary value of natural resources located within an area or region (area included inside a polygon, both rectilinear and curvilinear). This option allows determining the economic value of the stocks.
- Calculation of the economic losses and depreciation in the economic value of resources as a result of fire spread. In this phase the procedure followed in the SEVEIF model (Rodríguez y Silva *et al*. 2010) is applied by using the "matrix of economic depreciation factors."
- Assignment of the table of values for the different parameters included in the economic evaluation algorithms, in relation to the types of fuel models.
- Design and final construction of the windows for entering data, performing calculations and showing results. Validation of results with valuations available in the database of recorded fires.

VISUAL-CARDIN component

Technological developments in the field of computer science have enabled the development of simulation software of great versatility and usability, offering many tool options that are of great help in decision-making. In this regard, forest fire protection requires specialized programs that provide information on forecasts of dynamic fire behavior associated with fires that evolve in different forest systems. In this sense, the VISUAL-CARDIN program is structured as a deterministic program that works subject to the following conditions:

Simulation model through cellular automaton using the more nearest neighbor

Considerations:

1. Terrain topography.
2. Fuel model in each pixel (cell).
3. Tree height, crown base height, and crown density.
4. Fuel moisture and degree of protection.
5. Wind direction and intensity.
6. Ambient temperature and humidity.

The speed (V) and direction of maximum spread at each point is calculated from the following expression:

$V=(V_0 + V_i \cdot \cos W)\cdot t$ (1)

Where Vo is the rate of spread with zero wind and slope, Vi is the increase in speed in the direction of maximum spread due to the combined effects of wind and slope, φ is the spread radius from the origin of the fire, W represents the angle formed with the maximum spread direction Vi>Vo,
The geometric figure adopted to model the surface expansion of the fire's figure is a cardioid. The excess width on the elliptical reference figure is corrected by a factor (perpendicular to maximum spread). This factor is the ratio between the maximum width provided by the simulation performed by Behave (Andrews 1986) and the maximum width of the theoretical figure produced by the geometry of the cardioid. The maximum width value is determined by the expression (Martínez- Millán 1990, Martínez-Millán *et al*. 1991, Caballero *et al*.1994):

$F= (3V_0 + (V_0^2 + 8Vi^2)^{0,5}) (4V_i^2 - 2V_0^2 - V_0 (V_0^2 + 8V_i^2) / 16V_i^2$ (2)

The input parameters required by the program for the simulation are entered via the module parameters, which allows including data associated with local characteristics through a set of commands. Through the winds command, the characteristics of wind speed and direction measured at six meters above the ground can be entered. The moisture command offers the ability to assign the moisture of both living and dead fuels, with the latter classified according to their geometric characteristics. Alternatively, dead fine fuel moisture can be obtained from a set of calculations based on data such as the date, effects of weather, terrain and vegetative state. The protection command allows assigning the fuel's degree of protection of against wind, whereas the residence command option establishes the flame and ember residence times, allowing assignations to each of the different fuel models. Adjustment of input data using this command allows simulation of the phenomenon of revival from increases in wind speeds. In the simulation, there are some scenarios in which the conditions of transition from a ground to tree-stand crown fire produce a shift in combustion towards the canopy and therefore the fire spreads through the treetops. That is, the model recognizes the possibilities and if conditions allow it, ground, mixed and crown spread are produced. This feature certainly offers great versatility and accuracy in determining the economic impact of fire, by being able to capture the strong energy increases associated with forest canopy spread and thus be able to relate it to damages and losses generated.
Conducting post-fire analysis, in order to reconstruct the behavior of the fire and corroborate the results obtained by the different attack plans applied to extinguish it, is another feature offered by the simulator. This option allows qualifying the final fire reports while at the same time evaluating the performance of the various resources deployed. In this same option, the possible application of educational and technical training courses in fire suppression and behavior can be incorporated.
From the simulation outcomes, a database can be built that interrelates the affected area simulated in freely-evolving, spread dynamics, i.e. without the inclusion of firefighting actions, and the actual final area obtained after extinguishing the fire. The ratio between the two areas determines the spread rate control. This parameter facilitates the development of information bases on the experiences recorded in attack plans developed and implemented. This allows having a query file on those fires that may occur in the future and evolve under similar environmental conditions.
From this historical knowledge, firefighting simulations can be initiated on the set of resources that must be activated to control and extinguish the forest fire. To the extent that the integration of economic evaluation algorithms in the VISUAL- CARDIN software architecture has enabled the calculation of economic losses, the VISUAL-SEVEIF model opens a window to the possibility of making calculations and relationships that link firefighting operations and their costs with the value of the natural resources and the economic losses resulting from fire spread. Efficiency studies on the

results of firefighting operations will help in defining budget options and the best results in wildfire defense planning.
The current version responds to programming in C++ under the Windows operating system, but it will also soon be available for the Linux operating system, and includes significant improvements in pixel-by-pixel information processing, providing more precise information with regard to spread characteristics (rate of spread, linear intensity of the advancing front and flame length).
The graphical environment has also been taken into account in order to facilitate greater mapping options, as the simulation can be performed on raster coverages of the topographic map at different scales. It allows export of the perimeters in raster and vector format, as well as import of fire or area perimeters, measured with GPS and also in vector format. Shown below is the results window, which includes the area covered by the fire in yellow (Figure 1).

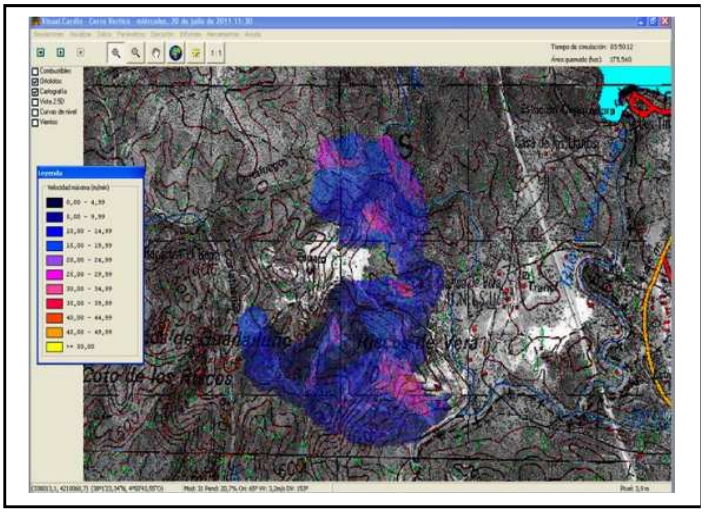

Figure 1—Simulation and analysis of fire behavior using VISUAL-CARDIN software for the Vertice Hill wildfire, 03h:50m after ignition (2011. Cordoba, Spain).

Economic valuation of natural resources: SEVEIF Model

In the first version of the VISUAL-SEVEIF simulator, we have incorporated the most important algorithms corresponding to the natural resources that have high representativeness in forest scenarios and that with the development of the SEVEIF model (Rodríguez y Silva *et al*., 2010) were identified as such.
The natural resources considered for economic valuation are the following: tangible resources, environmental services and landscape assets. The valuation of tangible resources including timber and non-timber products. The methodological approach for valuation of the impact on the timber resource is based on an algorithm that integrates the valuation tools, which include trees of both natural and artificial origin (Rodríguez y Silva *et al*. 2012). The valuation of non-timber resources is based on expressions used in the Manual for the Valuation of Losses and Estimation of Environmental Impact by Wildfires (Martínez Ruíz 2000). The evaluation of the impact on the hunting resource is carried out through the adjustment proposed in Zamora and others 2010.
The valuation of environmental services includes three resources: carbon fixation, erosion control and faunal biodiversity. The valuation of carbon fixation includes both the amount fixed at the time of the fire's occurrence and the amount unfixed from that time on, with prior knowledge of bark, aerial biomass and annual increment volumes being necessary (Table 1). The amount of carbon corresponding to the dry biomass is estimated at 50%. Erosion control will be expressed in economic income loss based on the potential amount of soil lost per unit area. The expression used for the

valuation (Table 1) incorporates a sum in relation to losses incurred during the first rains (bare soil) and a second sum that includes progressive soil losses until recovery of vegetation with similar burn protection (Molina and others 2009). Valuation of faunal biodiversity or unique species is performed using the cost of species recovery programs, or if no specific program is available through the contingent valuation method (Molina 2008).

Resource	Algorithms	Source
Timber	$V_{tim} = (1,7*E*B)/(E+0,85*B)$ $E = C_0*p\ [i^e + g(i^e -1)] + A*(i^e - 1)$ $E = (C_{0/z}*t\ [i^e + g(i^e -1)] + (C_0/z)*0,5*(i^e - 1)$ $E = [P*V - P*V\ ] + P*V\ [(i^{(T-e)} - 1)/(i^{(T-e)})]$ $B = [(V*P*1,025\ )/1,04\ ]*[1- (1,025/1,04)^e]*[1 + X*h*p]$ $B = V*h*t[R*P + (1 - R)*P_1]$	Rodríguez y Silva *et al*. 2012
Firewood us	$V_{firewood} = P_x*R_x*[((1+i)^n - 1)/(i*(1+i)^n]$	Molina *et al*. 2011
Hunting	$V_{hun} = P_x*R_x*[(1+i)^n - 1)/(i*(1+i)^n] + S$	Zamora at al. 2010
Carbon fixation	$V_{carb} = CF*PM + IF*PM*RC*[((1+i)^{T-e} - 1)/(i*(1+i)^{T-e}]$	Molina. 2008
Erosion control	$V_{eros} = R_1*P_1 + R_2*P_2\ [((1+i)^n - 1)/(i(1+i)^n)]$	Molina *et al*. 2009
biodiversity; Landscape; recreation; Unused	$V= Rx*[((1+i)^n - 1)/(i*(1+i)^n]$	Molina. 2008

Table 1. List of the algorithms included in the VISUAL-SEVEIF software, for each different resources considered

where E is the timber valuation based on the traditional Spanish approach (€/ha), B is the timber valuation adapted from the American Model (€/ha), Co is the cost of replanting one hectare of land (€/ha), p is the percentage of the stand affected by fire, i is the annual interest rate, g is annuity dependent on the rotation of the species, A is the value of a hectare of land without trees (€/ha), e is the estimated age of the stand at the time of the fire, V is the timber volume expressed in m^3/ha, P is the m^3 price of felled wood (€), n is the number of years remaining until the hypothetical harvesting rotation, X is the mortality rate dependent on the severity of the flames, h is the percentage of the species in the canopy, z is the reduction in replanting cost due to the self-regenerative phenomenon based on the rotation, P1 is the price of damaged wood with commercial use (€/m^3), V1 is the volume of damaged wood with use (m^3/ha), Px is the price per unit of measurement of the resource (€), Rx is the annual income per unit area, S is the reproductive stock per unit area (€), CF is the amount of CO_2 retained at the time of the fire (t/ha), PM is the price per fixed ton (€/t) , IF is the annual increase in CO_2 retained (t/ha), RC is the income generated by fixing a ton of carbon in a year (€), R_1 is the average amount of soil lost the first year (t/ha), P1 is the estimated price per ton (€), R_2 is the average amount of soil lost until recovery of the original cover (t/ha).

Spatial identification of different damage levels and net change in the value of resources

Determining losses in natural resources, both tangible and intangible, requires knowing the remaining value of the resources, i.e., the "net change in the value of the resources." This concept requires the incorporation of resource depreciation based on fire intensity level. Assigning the depreciation of each

resource based on fire intensity level is made on the basis of depreciation rates or percentage levels, given their greater simplicity and practical applicability.
In the case of the timber and firewood use resources, and under the framework of the FIREMAP, SINAMI and INFOCOPAS research projects, circular plots with a 10-m radius were taken for different plant typologies and degrees of damage in the following fires: Huetor (1993), Aznacollar (1995), Estepona (1995), Los Barrios (1997), Cazorla (2001, 2005), Aldeaquemada (2004), Minas de Ríotinto (2004), Alajar (2006), Gaucin (2006), Obejo (2007), Orcera (2009) and Vértice Hill (2011). For the valuation of losses incurred by the hunting resource, information from Montfrague National Park and the Aldeaquemada and Minas de Ríotinto fires (Zamora *et al*. 2010) was used in order to have not only spatial but also temporal analysis of the natural recovery of reproductive stock and, consequently, of the annual income generated by the hunting resource.
Depreciation levels of the carbon fixation and erosion control resources were estimated based on tree mortality and the consumption level of aerial biomass, from measurements of burned and unburned trees with similar dendrometric characteristics (fires of: Monte Catena, 2009, Obejo 2007, Cazorla 2001, 2005). Economic valuation of erosion damage, or conversion of lost biomass into monetary units, was determined based on the Obejo fire (2007) study, which analyzed the costs associated with the loss of different soil amounts (tons per hectare). In the case of biodiversity, damage valuation is based on the "surrogate value" applied by the Administration (recovery and/or conservation programs) or the value given by the population (contingent valuation methodology). The values obtained for this resource include adjustments based on post-fire costs incurred by the pertinent authorities to prevent the escape and migration of species through the application of food supplementation, predator elimination and competition reduction measures (Molina 2008).
The depreciation rates of landscape assets are very difficult to validate. The aforementioned research projects estimate the depreciation rates for these assets by the technique of social preferences or valuation through indirect landscape perception techniques by pre-fire and post-fire comparison of a territory. Landscape use is affected to a greater extent than leisure and recreational activities. Large wildfires that occurred in Sierras de Cazorla, Segura y Las Villas Natural Park (place where the Catena Hill fires occurred in 2001, 2005 and 2009) provided a good database for quantitative estimates on the impact on landscape assets. It can thus be stated that the 2005 fire resulted in a 40% decrease in the number of tourists and paralyzed numerous business projects for remodeling and expanding recreational facilities. Use of Geographic Information Systems (GIS) allows identification of plant typology and its economic valuation, as well as the availability of information about fire behavior. Based on this, the depreciation rate for each resource is estimated individually. The integration of the two concepts provides the economic vulnerability of each resource present in the burned area. The economic valuation of damages is the sum of the vulnerabilities of the resources present in the burned area.

Classification of fire intensity level from average flame length

Determining the effects of potential fire behavior on the economic valuation of stocks has bee done by identifying the average flame length for each pixel (directly related to the linear intensity of the advancing front). That information is obtained directly from the results provided by the VISUAL-CARDIN program in each of the pixels covered by fire spread. Four fire intensity levels were identified:

Degree of damage I. It corresponds to Fire Intensity Level (FIL) VI or flame length greater than 12 m. Area severely affected. Continuous crown fire is the most representative for this degree.

Degree of damage II. It corresponds to Fire Intensity Level (FIL) V and IV or flame length between 9-12 m and 6-9 m. Moderate affect. Passive crown fire with some crown runs. The ground is left unprotected by clumps due to the intensity. There is almost total surface fuel consumption.

Degree of damage III. It corresponds to Fire Intensity Level (FIL) III or flame length between 3-6 m. Area moderately affected. Ground fire with consumption of surface material. The fire advances with the slope but not the wind. There are isolated scorched trees.

Degree of damage IV. It corresponds to Fire Intensity Level (FIL) II or flame length between 2-3 m. Area slightly affected. Ground fire with consumption of surface material. The fire moves backwards, without slope or wind in its favor.

Identification of net change in the value of the resources and the VISUAL-SEVEIF software flow line

From the experience gained in the large wildfires that occurred in Andalusia during the period 1993-2011 and the scientific results of the FIREMAP, SINAMI and INFOCOPAS research projects, the depreciation matrix was made (Rodríguez y Silva *et al*. 2009), (Figure 2). This matrix is made up of the set of percentage factors based on the fire intensity levels (kW/m) and the corresponding degree of damage, as indicated in the previous section, so that when applied to the initial socio-economic value, it provides both the losses caused by the wildfire and the residual economic value of vegetation unaffected by the fire.

NIF	Vtr	Vfwr	Vhr	Vcar	Verr	Vbir	Vlar	Vler	Vnonr
I	8,33%	5%	20%	10%	10%	20%	5%	2%	4%
II	16,65%	10%	45%	25%	25%	40%	25%	20%	19%
III	38,58%	20%	65%	45%	45%	60%	60%	55%	46%
IV	57,85%	45%	85%	65%	65%	80%	80%	65%	54%
V	82,79%	65%	95%	85%	85%	100%	90%	85%	69%
VI	89,41%	75%	100%	100%	100%	100%	100%	85%	69%

Figure 2—Depreciation matrix ("Vtr", timber resource depreciation (Rodríguez y Silva and others 2012); "Vfwr", firewood use depreciation; "Vhr", hunting resource depreciation; "Vcar"; carbon resource depreciation; "Verr", depreciation of erosion control; "Vbir", depreciation of faunal biodiversity; "Vlar", depreciation of landscape resource; "Vler", depreciation of leisure and recreation resource; "Vnonr", depreciation of non-use resource).

In the VISUAL-SEVEIF software architecture, the depreciation matrix has been integrated in order to provide automatically, and for each pixel concerned, the percentage reduction in the initial economic value as a result of the fire behavior developed in it. The VISUAL-SEVEIF software flow line has been defined by the following sequence of calculation processes (Figure 3):

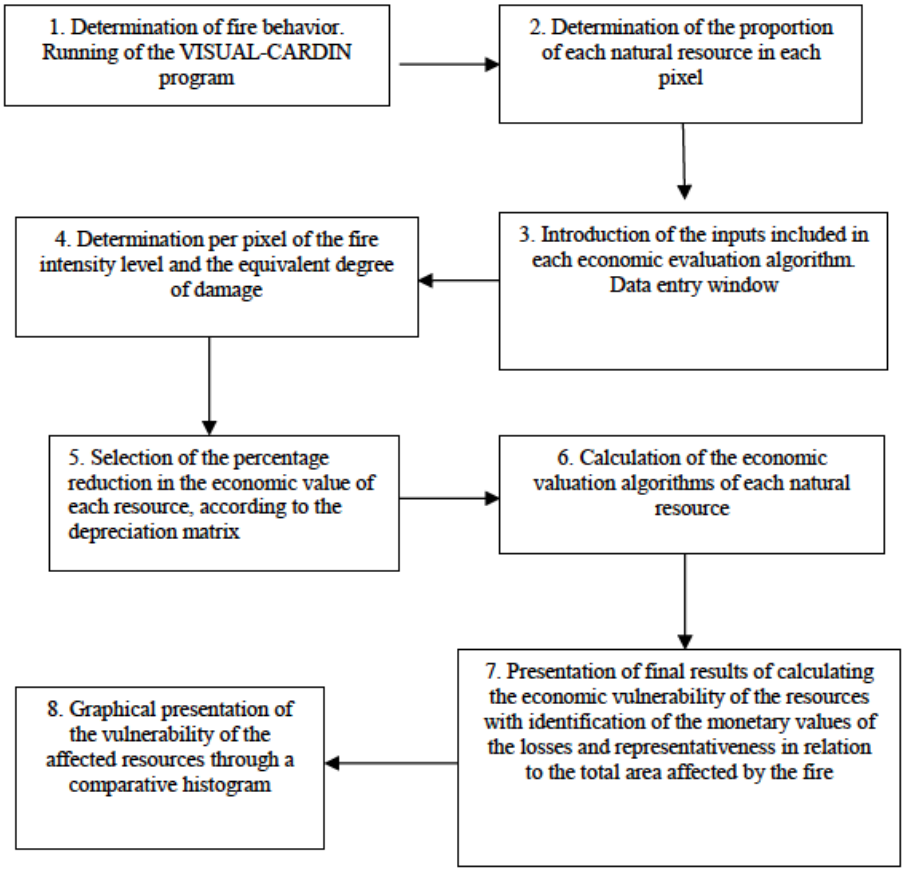

Figure 3—Flow line of the operational process corresponding to the VISUALSEVEIF computer program.

The final windows of the VISUAL-SEVEIF software shown the both report, fire behaviour shape and economic losses affected by different resources (Figure 4).

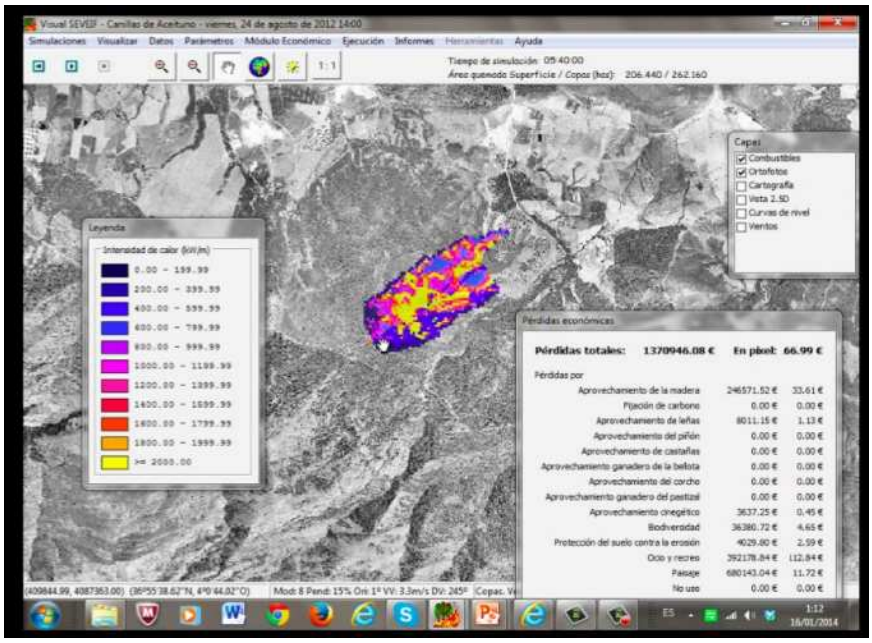

Figure 4. Window of VISUAL-SEVEIF software, showing the fire shape with fire intensity (kw/m) and the economic losses by the resources affected for the fire propagation

7. Estimation of the efficiency of suppression methods using economic losses in natural resources and suppression cost relationship.

Determining the efficiency of production systems, can be understood as an econometric technique through which the existing relationship between the resources employed or assigned and the results obtained, or the target previously set as a goal to be reached, is addressed. That is, it can be understood as the relationship between revenues and expenditures or inputs and outputs generated in a given production system. Conceptually and when evaluating suppression operations, efficiency can be associated with estimating a ratio that allows getting information from the results obtained from using a particular set of suppression resources and their incurred costs on a specific incident or fire (Mendes, 2010).

The efficiency isoquant curve is estimated using data from the fire occurrence database in the forest region or district in which the efficiency analysis is performed. Once the econometric components of the efficiency and its conceptual identification have been achieved the analysis and study of the results of forest fire control and suppression operations can proceed. Using the analysis method for determining efficiency based on econometric model applied to forest fire suppression operations, if necessary to identify for each fire the relationships between the input and the output (Rodríguez y Silva and Gonzalez-Caban. 2013). Inputs refer to the economic value of the area that has been successfully protected based on suppression activities defined when planning the suppression operations. The inputs represents (total economic value saved from the impact of the fire within the fire perimeter), Vr is the economic value of each of the resources in the area where the wildfire has evolved (area bounded by the final fire perimeter), expressed in monetary units (€, $), and Fd is the depreciation factor of the economic value due to the effect or impact of the fire (Molina *et al*. 2009, Rodríguez y Silva and González Cabán 2010, Rodríguez y Silva *et al* 2012). The inputs is obtained using the VISUAL-SEVEIF software.

The outputs or suppression costs are the sum of the individual costs of all suppression resources dispatched to the fire (Ce_j). In terms of efficiency analysis, outputs are the resulting solutions from the combination of suppression resources with a production rate level allocated to the economic value of the resources at risk saved from the impact of the fire. This is the output or suppression costs of the operational suppression system. Accordingly, the efficiency expression can be written as follows, where ET is the efficiency estimator, and all other variables as previously defined (Rodríguez y Silva and Gonzalez-Caban. 2013):

$$ET = 1 - \left[\sum_{j-1}^{j-m} Ce_j / \sum_{i-1}^{i=n} Vr_i\,(1 - Fd_i)\right]$$

From last equation ET values result from the ratio between revenues (outputs) and expenditures (inputs); therefore, it can generalize that:

If 0<ET<1, then the efficiency is low to very high
If ET=1, then the efficiency is in balance

To establish measurement consistency, adjustments are necessary to the ET equation. To do this, weights are introduced that normalize the measurement heterogeneity among the variables in the equation. The weights help put all variables in terms of the ratio of its value to the total overall value for that variable. Thus, for the case of the different suppression resources used (outputs), the weights (β_j) represent the time each resource was used in relation to the total elapsed time from the start of suppression actions until the fire is under control. For the inputs or economic value of each natural resource, the weights (α_i) represents the economic value of each resource relative to the total economic value of all natural resources in the area affected by the fire. By applying the weighting criteria to ET,

we obtain the following equation:

$$ET = 1 - \sum_{j=1}^{j=m} \beta_j (Ce_j) / \sum_{i=1}^{i=n} \alpha_i Vr_i (1 - Fd_i)$$

For simplicity, we suggest a somewhat arbitrary qualitative classification of the results to establish an efficiency ranking (Table 1) by associating the ET estimates to four categorical levels: Low, Moderate, High, and Very High.

Efficiency value interval (ET)	Qualitative classification
0<ET<0.26	LOW
0.26≤ET<0.6	MODERATE
0.6≤ET<0.7	HIGH
0.7≤ET<1	VERY HIGH

8. Conclusions.

The recognition or valuation of forest ecosystems is essential for the spatiotemporal planning work of forest fire managers. The importance of having an evaluation model of socio-economic impacts encompasses a wide range of possibilities, facilitating prevention, valuation and post-fire restoration work. Finally, the methodological approach presented here provides options for the combined study of suppression costs and residual economic valuation of natural resources after the impact of a forest fire. For example, the information produced permit managers not only to analyze and classify the results of agreed upon and applied fire suppression options, but also to make adjustments in the combination of suppression resources assigned if necessary. The VISUAL-SEVEIF software is an objective tool for use in fire economic planning and decision making.

9. References

Andrews, P. 1986. Behave: Fire Behavior Prediction and Fuel Modeling System. Burn Subsystem, part 1. USDA Forest Service. Intermountain Research Station Odgen, UT 84401. General Technical reports INT-194.

Borchert, M., Johnson, M., Schreiner, D., Vander Wall, S. 2003. Early postfire seed dispersal, seedling establishment and seedling mortality of *Pins coulteri* (D.Don) in central coastal California, USA. Plant Ecology 168(2), 207-220.

Caballero, D. Martínez-Millán, J., Martos, J., Vignote, S. 1994. Cardin 3.0. A model for forest fire spread and fire fighting simulation. II International Conference on Forest Fire Research. Proceedings. November 1994. Coimbra. Portugal.

Constanza R., D'Arge, R., de Groot, R., Farber, S., Grasso, M., Hannon, B., Limburg, K., Naeem, S., O'Neill, R.V., Paruelo, J., Raskin, G.R., Sutton, P., Van der Belt, M. 1997. The value of the world's ecosystem services and natural capital. Nature 387: 253- 260.

Martínez Millán, J. 1990. Fire behaviour modelling research and practice. International Conference on Forest Fire Research. Proceedings. November 1990. Coimbra. Portugal.

Martínez Millán, J., Vignote, S., Martos, J., Caballero, D. 1991. Cardín, un sistema para la simulación de la propagación de incendios forestales. Ministerio de Agricultura, pesca y Alimentación. Instituto Nacional de Investigación y Tecnología Agraria y Alimentaria. Investigación Agraria. Sistemas y Recursos Forestales, vol.0-1991- separata no:10. Madrid.

Martínez Ruiz, E. 2000. Manual de Valoración de Montes y Aprovechamientos Forestales. Ediciones Mundi-Prensa, Madrid.

Mendes I. 2010. A theoretical economic model for choosing efficient wildfire suppression strategies. Forest Policy and Economics 12: 323-329.

Molina, J.R. 2008. Integración de herramientas para la modelización preventiva y socioeconómica del paisaje forestal frente a los incendios en relación con el cambio climático. Tesis Doctoral.

Molina, J.R., Rodríguez y Silva, F., Herrera M.A., Zamora, R. 2009. A simulation tool for socio-economic planning on forest fire suppression management. Libro Forest Fires: Detection, Suppression and Prevention. Nova Science Publishers. USA.

Molina, J.R., Herrera, M.A., Zamora, R., Rodríguez y Silva, F., González-Cabán, A. 2011. Economic losses to Iberian Swine production from forest fires. Forest Policy and Economics 13: 614-621.

Piñol, J., Terradas, J., Lloret, F. 1998**.** Climate Warming, Wildfire Hazard, and Wildfire Occurrence in Coastal Eastern Spain. Climatic Change 38(3): 1480-1573.

Rodriguez y Silva, F. 1999. A forest fire simulation tool for economic planning in fire suppression management models: an application of the Arcar-Cardin. Proceedings of the Symposium on Fire Economics, Planning and Policy: Bottom lines, USDA Forest Service. Pacific Southwest Research Station. General Technical Report PSW-GTR- 173. San Diego California**.**

Rodríguez y Silva, F., Molina, J.R., Herrera, M., Zamora, R. 2007. Vulnerabilidad socioeconómica de los espacios forestales frente al impacto de los incendios, aproximación metodológica mediante sistemas de información geográficos (proyecto Firemap). IV International Wildland Fire Conference. Proceedings. Sevilla. (www.wildfire07.es).

Rodríguez y Silva, F., Molina, J.R., Herrera, M.A., Zamora, R. 2009. The impact of fire and the socioeconomic vulnerability of forest ecosystems: A methodological approach using remote sensing and geographical information systems. General Technical Report PSW-GTR-227. Pacific Southwest Research Station. Forest Service, U.S. Department of Agriculture; 151 - 168.

Rodríguez y Silva, F., González-Cabán, A. 2010. "SINAMI": a tool for the economic evaluation of forest fire management programs in Mediterranean ecosystems. International Journal of Wildland Fire 19: 927-936.

Rodríguez y Silva, F., Molina, J.R. 2010. Manual Técnico para la Modelización de la Combustibilidad asociada a los Ecosistemas forestales Mediterráneos. Departamento de Ingeniería Forestal. Universidad de Córdoba. Córdoba. España.

Rodríguez y Silva, F., Molina, J.R., González-Cabán, A.; Herrera, M.A. 2012. Economic vulnerability of timber resources to forest fires. Journal of Environmental Management 100: 16-21.

Rodríguez y Silva, F., Gonzalez-Caban, A. 2013. Forecasting Productivity in Forest Fire Suppression Operations: A Methodological Approach Based on Suppression Difficulty Analysis and Documented Experience. General Technical Report PSW-GTR-245. Pacific Southwest Research Station. Forest Service, U.S. Department of Agriculture; 50 - 65.

Rodríguez y Silva, F., Molina Martínez J. Herrera Machuca M., Rodríguez Leal J. 2013.VISUAL-SEVEIF, a Tool for Integrating Fire Behavior Simulation and Economic Evaluation of the Impact of Wildfires. General Technical Report PSW-GTR-245. Pacific Southwest Research Station. Forest Service, U.S. Department of Agriculture; 163 - 178.

Thompson M, Calkin D**.** 2011. Uncertainty and risk in wildland fire management: A review. Journal of Environmental Management 92: 1895-1909.

Vélez, R. 2009. La Defensa contra incendios forestales. Fundamentos y Experiencias. McGraw-Hill, Madrid.

Zamora, R., Molina, J.R., Herrera, M.A., Rodríguez y Silva, F. 2010. A model for wildfire prevention planning in game resources. Ecological Modeling 221: 19-26.

The impacts of treated landscapes on suppression cost effectiveness

Matthew P Thompson[a], Michael S Hand[a], Jon Rieck [a], Jessica R Haas [a], and David E Calkin [a]

[a]*Rocky Mountain Research Station, US Forest Service, Missoula, MT, USA,*
mpthompson02@fs.fed.us, mshand@fs.fed.us, jrieck@fs.fed.us, jrhaas@fs.fed.us, decalkin@fs.fed.us

Abstract
In this paper we will focus on the role of treated landscapes on suppression costs and suppression effectiveness. We will begin with a framework outlining the pathways through which treatments could influence wildfire management decisions and fire outcomes, rooted in treatment impacts on fire behaviour. We will then synthesize several emerging research threads seeking to characterize treatment impacts on suppression costs and effectiveness: (1) a simulation-based approach combining stochastic fire modelling with statistical cost modelling; (2) an econometric approach analysing historical suppression costs; and (3) a case study approach using spatial fire perimeter and fire line construction data to quantify fire line effectiveness. To conclude we will outline how these threads can be woven with improvements in fire and fuels modelling to better characterize spatiotemporal trends and trade-offs related to fuel treatment and suppression.

Keywords*: wildfire management, spatial analysis, simulation analysis, econometric analysis*

The views expressed here are the authors', and do not necessarily represent the views of the USDA

Introduction

High-quality wildfire suppression decisions require information on the conditions under which alternative strategies and tactics would be safe and cost-effective. Incident management decisions are premised on the acquisition, analysis, and application of timely and accurate fire information (Zimmerman 2012), and recur within a dynamic, uncertain environment (Thompson 2013). Important pieces of information that fire managers must consider include weather forecasts, fire behaviour and fire growth potential, firefighting resource availability and productivity, and the exposure and susceptibility of values-at-risk (Calkin *et al*. 2011). Accurate spatial data on current landscape conditions are essential to predict fire behaviour and identify management opportunities.

A critical component of landscape condition is the location of areas previously treated by wildland fire (i.e., wildfire and prescribed fire) and/or with mechanical methods. Post-fire analyses and simulation modelling demonstrate the potential for treated areas to alter fire behaviour, size distributions, and spatial patterns of burn probability, and to mitigate fire effects (Ager *et al*. 2010; Stephens *et al*. 2012; Parks *et al*. 2014). Less well understood are whether or how these fire-specific changes can meaningfully or measurably lead to changes in incident decisions, expenditures, or effectiveness.

A conceptual model for treatment impacts on suppression cost-effectiveness is presented in Figure 1. The impacts of treated areas have two main pathways. First, altered fuel composition and continuity can directly influence fire behaviour, which can also indirectly influence incident response. Second, the presence of treated areas on the landscape can directly inform the design of incident strategies and tactics, although this is premised on sufficient knowledge regarding the location, age, and type of treatment. In a post-fire environment, the degree and magnitude of treatment impacts may be discerned through interviews with incident management personnel, statistical analyses, and/or retrospective modelling (Moghaddas and Craggs 2008; Wimberley *et al*. 2009; Cochrane *et al*. 2012). In a pre-fire environment, however, treatment impacts are more uncertain and modelling is necessary. Importantly, recognizing the relative rarity of wildfire occurrence and the commensurate low likelihood of treated areas interacting with fire, evaluation of treatment impacts needs to occur within a probabilistic

framework (Thompson and Calkin 2011). Pre-fire risk assessment results can then be shared with fire managers to help inform incident response planning (Scott *et al*. 2012).

Building from this conceptual model, we synthesize several emerging research threads on the effects of treated landscapes on suppression costs and suppression effectiveness: (1) a simulation-based approach combining stochastic fire modelling with statistical cost modelling; (2) an econometric approach analysing historical suppression costs; and (3) a case study approach using spatial fire perimeter and fire line construction data to quantify fire line effectiveness. In concert with improvements in fire and fuels modelling, we believe these research efforts will enable significant advancements in spatiotemporal evaluation of trends and trade-offs related to fuel treatment and suppression.

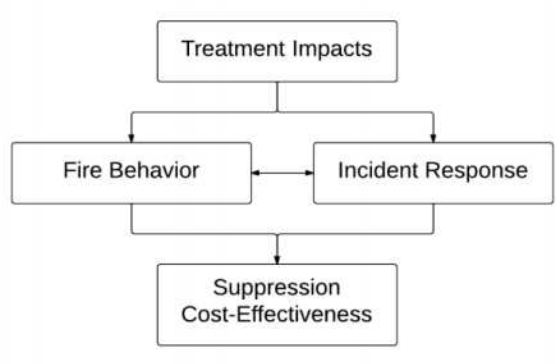

Figure 1. Conceptual model linking treatment impacts to suppression cost-effectiveness

Emerging Research on Suppression Cost-Effectiveness

Interest in whether treated landscapes can measurably influence suppression costs has been around for more than a decade, although only recently have researchers begun to rigorously quantify these potential impacts with geospatial analysis and fire behaviour modelling. Some of these modelling advancements came with the advent of the Collaborative Forest Landscape Restoration Program (CFLRP) in the United States, intended in part to facilitate the reduction of wildfire management costs. In a pilot study, Thompson *et al*. (2013) demonstrated the pairing of stochastic wildfire simulation with suppression cost modelling on landscape in the Deschutes National Forest, using models developed and used by the U.S. Forest Service (Gebert *et al*. 2007; Finney *et al*. 2011). Results indicated the possibility for significant savings given wildfire-treatment interactions, although after considering the likelihood of wildfire occurrence annual savings of any kind only occurred in 1 out of every 4 years.

Simulation of wildfire occurrence and behaviour across the landscape under existing and post-treatment conditions allows for the isolation of fuel treatment impacts on fire metrics and subsequent changes to cost distributions. The spatially-explicit modelling approach captures heterogeneity in fire likelihood and behaviour across the landscape, the size and location of treatments with respect to fire spread direction, and the location of ignitions with respect to factors influencing cost such as land designation and proximity to human development. These techniques are now being systematically applied to evaluate the cost impacts of landscape fuel treatment strategies funded under CFLRP throughout the U.S.

Concurrently with advancements in the coupling of fire and cost models and risk-based evaluation of treatment impacts, researchers have made advancements in the spatiotemporal resolution and predictive power of suppression cost models (Hand *et al*. 2014). One key improvement is the use of spatially descriptive data within the entire perimeter of the fire rather than information based off the ignition location alone, which is made possible by the compilation of a large dataset of spatial fire perimeters from recent fire seasons. The use of perimeters enables, for instance, a more accurate

characterization of the diversity of vegetative and topographic conditions. Additionally, the model can better capture variation in fire weather throughout the course of the incident. With these improvements, cost models will be able to better capture potential treatment impacts by considering not just changes to fire size distributions but also changes in the location and orientation of their footprints with respect to factors known to influence costs.

These improvements further open the door for novel retrospective analysis of historical wildfire-treatment interactions. By leveraging comprehensive, geospatial fire history databases (Short 2013), and possibly agency fuel treatment databases, we will be able to identify the degree to which our dataset of fire perimeters overlaps with previous treatments. Geospatial analyses will allow us to characterize the extent and severity of re-burned areas, and econometric analyses we will allow us to quantify the impact, if any, on observed suppression costs. Figure 2 compares and contrasts these two approaches, both of which should add to the knowledge base of potential treatment impacts on suppression costs.

Better understanding the cost component however does not by itself yield insights into treatment impacts on suppression cost-effectiveness. A third thread of research therefore relates directly to the characterization and quantification of suppression effectiveness. Though theoretical frameworks exist for efficient suppression (Mendes 2010), in practice significant data limitations and knowledge gaps present challenges for identifying factors influencing successful suppression and for characterizing conditions under which alternative strategies and tactics would be safe and effective (Finney *et al*. 2009; Holmes and Calkin 2013). One key challenge is the acquisition and alignment of incident management data from disparate sources such as firefighting resource ordering systems, incident status reporting systems, and operational fire management decision support systems, in addition to data generated and managed at the incident-level. As a result, on-site data collection during an actual wildfire incident is often the best option, despite being time and resource intensive. Specifically, we have been able to collect data on daily assignments by mission type, fire line construction productivity, and daily spatial fire perimeter growth.

With these data, case study analyses can yield new insights into the role of previously treated areas on suppression effectiveness. One initial approach is to query incident decision documentation to qualitatively ascertain the degree to which knowledge of treated areas influenced strategies and tactics. An extra layer of analysis can quantify fire line effectiveness in terms of percent of line held, and can statistically analyse fireline effectiveness within and outside of previously treated areas. The goal of these analyses is to improve our understanding of how suppression resources are used on wildfires and which factors contribute to effectiveness.

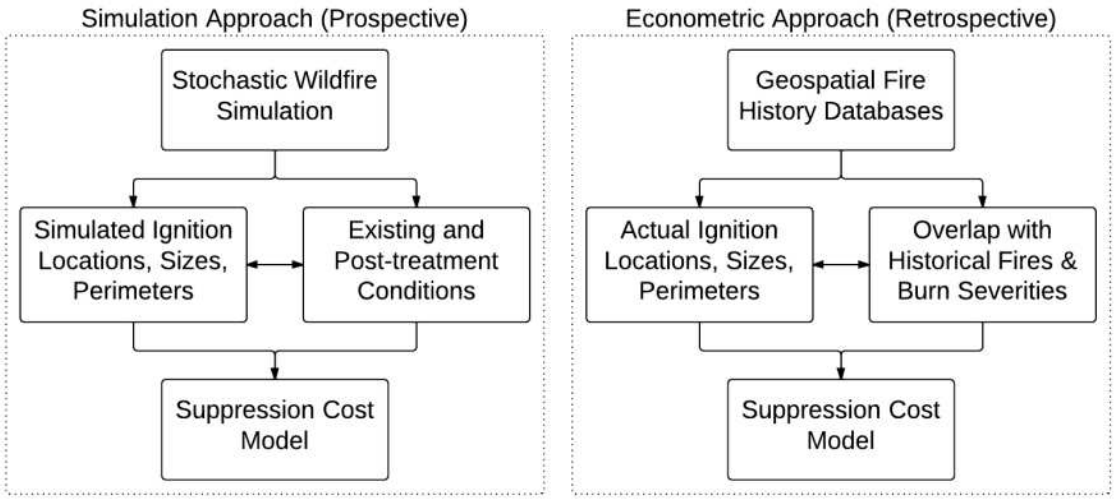

Figure 2. Prospective and retrospective approaches for characterizing potential influences of treated areas on suppression costs

Future Research Directions

The emerging research threads presented in the previous section will set the stage for a wide spectrum of integrated research opportunities. First and foremost we aim to leverage our research with advances in fire and fuels modelling as well as advances in decision support for fuel planning and incident response. Landscape-scale simulation of the spatiotemporal dynamics of wildland fire occurrence, spread, and resulting fuel and vegetation changes will set the stage for life cycle economic analysis of fuel treatment strategies, as well as the costs and benefits of different fire suppression policies. The analytical process can be designed to specifically target salient questions regarding how the spatial and temporal scales of fuel treatment (and retreatment) influence treatment costs and subsequent cost effectiveness. Ultimately the aim of this research is to support evaluation and prioritization of fuel treatment investments at programmatic and landscape scales, and to support risk-informed, forward-looking suppression strategy development.

Acknowledgements

The Rocky Mountain Research Station, the National Fire Decision Support Center, and the Joint Fire Science Program supported this effort.

References

Ager, A. A., M. A. Finney, A. McMahan, and J. Cathcart (2010), Measuring the effect of fuel treatments on forest carbon using landscape risk analysis, Natural Hazards and Earth System Sciences 10, 2515-2526.

Calkin, D. E., M. P. Thompson, M. A. Finney, and K. D. Hyde (2011), A real-time risk assessment tool supporting wildland fire decisionmaking, Journal of Forestry, 109(5), 274-280.

Cochrane, M., C. Moran, M. Wimberly, A. Baer, M. Finney, K. Beckendorf, J. Eidenshink, and Z. Zhu (2012), Estimation of wildfire size and risk changes due to fuels treatments, International Journal of Wildland Fire, 21(4), 357-367.

Finney, M. A., C. W. McHugh, I. C. Grenfell, K. L. Riley, and K. C. Short (2011), A simulation of probabilistic wildfire risk components for the continental United States, Stochastic Environmental Research and Risk Assessment, 25(7), 973-1000.

Finney, M., I. C. Grenfell, and C. W. McHugh (2009), Modeling containment of large wildfires using generalized linear mixed-model analysis, Forest Science, 55(3), 249-255.

Holmes, T. P., and D. E. Calkin (2013), Econometric analysis of fire suppression production functions for large wildland fires, International Journal of Wildland Fire, 22(2), 246-255.

Gebert, K. M., D. E. Calkin, and J. Yoder (2007), Estimating suppression expenditures for individual large wildland fires, Western Journal of Applied Forestry, 22(3), 188-196.

Hand, M. S., K. M. Gebert, J. Liang, D. E. Calkin, M. P. Thompson, and M. Zhou (2014), Modeling Fire Expenditures with Spatially Descriptive Data, in Economics of Wildfire Management, edited, pp. 37-48, Springer New York.

Mendes, I. (2010), A theoretical economic model for choosing efficient wildfire suppression strategies, Forest Policy and Economics, 12(5), 323-329.

Moghaddas, J. J., and L. Craggs (2008), A fuel treatment reduces fire severity and increases suppression efficiency in a mixed conifer forest, International Journal of Wildland Fire, 16(6), 673-678.

Parks, S., C. Miller, C. Nelson, and Z. Holden (2014), Previous Fires Moderate Burn Severity of Subsequent Wildland Fires in Two Large Western US Wilderness Areas, Ecosystems, 17(1), 29-42.

Scott, J., D. Helmbrecht, S. Parks, and C. Miller (2012), Quantifying the threat of unsuppressed wildfires reaching the adjacent wildland-urban interface on the Bridger-Teton National Forest, Wyoming, USA, Fire Ecology, 8(2), 125-142.

Short, K. (2013), A spatial database of wildfires in the United States, 1992–2011, Earth System Science Data Discussions, 6(2), 297-366.

Stephens, S. L., J. D. McIver, R. E. Boerner, C. J. Fettig, J. B. Fontaine, B. R. Hartsough, P. L. Kennedy, and D. W. Schwilk (2012), The effects of forest fuel-reduction treatments in the United States, BioScience, 62(6), 549-560.

Thompson, M. P., and D. E. Calkin (2011), Uncertainty and risk in wildland fire management: a review, Journal of Environmental Management, 92(8), 1895-1909.

Thompson, M. P., N. M. Vaillant, J. R. Haas, K. M. Gebert, and K. D. Stockmann (2013), Quantifying the potential impacts of fuel treatments on wildfire suppression costs, Journal of Forestry, 111(1), 49-58.

Wimberly, M. C., M. A. Cochrane, A. D. Baer, and K. Pabst (2009), Assessing fuel treatment effectiveness using satellite imagery and spatial statistics, Ecological Applications, 19(6), 1377-1384.

Zimmerman, T. (2012), Wildland Fire Management Decision Making, Journal of Agricultural Science and Technology, B(2), 169-178.

Theoretical approaches for evaluating the economic efficiency of the aerial firefighting helping strategic planning

Agoston Restas

National University of Public Service, Budapest, Hungary, Restas.Agoston@uni-nke.hu

Abstract
Introduction: Aerial firefighting is very expensive solution; therefore it isn't useless to study it by the criteria of efficiency. But the meaning of efficiency for fire managers can be different from the meaning of efficiency for economists. Economic efficiency is stricter than technical efficiency. Method: this research created and used rectangular and concentric circles models, than made transport analysis and rate calculation. Results and discussion: The rectangular model shows the criteria of economic efficiency of aerial firefighting. The results from rectangular model can be transferred also to the concentric circles model. Based on the concentric circle model we can define both the economic efficiency of aerial firefighting and minimal criteria of successful suppression expressed by the elementary information we have regarding the actual fire. This paper points also at some principle mistakes often made by marketing to overrate the advantages of some aerial products, agents or procedures. Even if it is very difficult to take into consideration all circumstances and assumptions which are found during firefighting process but there are some theories that can help us to assess the economical effectiveness of aerial product, agent or procedure more precisely than rated nowadays by the marketing.

Keywords*: aerial firefighting, economic efficiency, rectangular model, concentric circle model, transport analysis*

Introduction

In this article author makes a difference between the professional and economical effectiveness that is efficiency. Efficiency is obviously stronger phenomena, in this case not just the professional effectiveness but the criteria of the efficiency must be satisfied. No doubt in the sphere of state protection (police, medical service, disaster management, fire service) it is very difficult to speak about efficiency, much easier about the political or social effectiveness. However author is sure there are ways to find the balance between useful actions and costs. Aerial firefighting is a very expensive extinguishing method; therefore it is not useless to look through some of its economic aspects.
Firstly, author makes two models, which are rectangular and concentric circle model, to make it easier to understand some features of the economic aspects of firefighting. Naturally, the assumptions in both models are idealistic, meaning that they require more development. After models, author focuses on extinguisher materials such as pure water, foam and retardant and gives some different aspects of their effectiveness than usual.

Rectangular model

First model examine a forested area limited by rectangular without concrete geometric data. Assumptions are idealistic, like homogenous forest, flat area; there is no wind, etc. In this model the fire front spreads linearly (Figure 1.). Author demonstrates this theory by more rectangular, placing them next to each other, which shows the fire development by geometric. Some part of this model is similar to the model used by Australian experts however not the same (Gould at al., 2009).
After starting the suppression (B) the controlled line takes „α" with the frame of this example edge (C). During the suppression this controlled line will continue till the opposite edge of the frame, meaning that the fire front is extinguished (D). Based on Pythagoras theory it is easy to understand

that the value of „α" depends on the speed of fire spread (v_{fire}) and the speed of suppression ($v_{suppression}$). The higher the speed of suppression related to speed of fire spread (R), the higher the angle „α" is and vice versa.

$$R\left\langle \frac{v_{fire}}{v_{\sup pression}} \right\rangle \uparrow\downarrow \Rightarrow \alpha \uparrow\downarrow \qquad (2.1)$$

Before the fire front forested area can be saved (M_{forest}), beyond it can be count as damages (K_{forest}). The main purpose of the suppression is that the value of saved forest be as high as possible or the damages be as low as possible. Author means, we search the end values of the positive options.

$$M_{forest} \Rightarrow \max \text{ ; illetve } K_{forest} \Rightarrow \min \qquad (2.2)$$

Above statement can be accepted by the view of professional but since it doesn't count with the cost of extinguishing the result can't be the standard for the view of national economy.

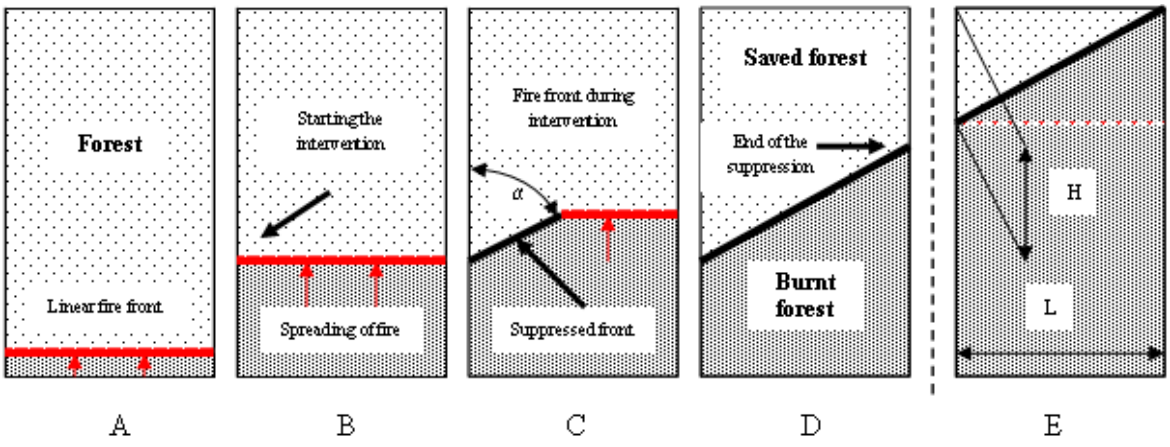

Figure 1. Rectangular model

To maximize the end value of the professional effectiveness' function can't be justify in all cases at the view of national economy. At the latest one all costs of resources must be counted, such as technical and human resources but even the in-material value of the forest and the higher risk of citizens caused by absence of firefighters from urban area.
If the cost of suppression is higher than the saved forest the action is uneconomical in view of national economy. Looking at the rectangular model the efficiency of national economy is valid till the saved forest is higher than the cost of suppression.

$$M_{forest} \geq \Sigma C_{AFF} \Rightarrow \gamma_{NE} \geq 1 \qquad (2.3)$$

M_{forest} – value of the saved forest [€]
C_{AFF} – cost of aerial suppression [€]
γ_{NE} – efficiency of the national economy [-]

Using the notation of the rectangular model the first part of formula (2.3) can be expressed also in another way.

$$\frac{1}{2} LHP_{forest} \geq \Sigma C_{AFF} \qquad (2.4)$$

L – width of the forest area [m]
H – fire spread from the beginning of the suppression till the end of it [m]
P_{forest} – unit value of the forest [€m^{-2}]

This model doesn't count with the burnt area at the beginning of the suppression, not during the action or at the end of it. In this case the efficiency of the suppression in view of national economy doesn't depend directly on the burnt area.
Triangles with „L" width fire front, „α" angles and „H" length in this model are same in any time of beginning the suppression and also same the costs belonged to these triangles.
Based on the rectangular model we get the threshold limit in that case, if the cost of aerial firefighting is equal to the value of the saved forest. In cases of later beginning of the suppression, the cost of aerial firefighting remains the same however the value of the saved forest is reducing continuously till that where remains only the „L-α-H" featured triangle (E). It means the threshold limit of the efficiency geometrically.

$$\lim_{M_{forest} \to \Sigma C_{AFF}} f(M_{forest}) = \Sigma C_{AFF} \qquad (2.5)$$

In this case, if both the above threshold limit is realized and the efficiency of the aerial firefighting is valid, in any earlier beginning time of the suppression will satisfy the requirements of the efficiency too. The earlier is the beginning of the suppression, the higher the value of the saved forest is. The limit value gives just the minimum threshold of satisfying the criteria of the efficiency.
The angle „α" of the suppressed fire front depends on the rate of fire spread and the speed of aerial firefighting. Higher fire spread causes lower angle „α" and longer time of suppression and vice versa. In view of higher efficiency the higher angle „α" is required.

Concentric circles model

The rectangular model counts with linear fire front however in the reality almost each fire starts from small ignition points. In case of ideal and positive spread conditions the fire front will spread radially.

Necessary but not yet sufficient condition for the efficient suppression
Model counts with small ignition point, „v_{fire}" speed of fire spread, „t_{freely}" time of freely fire spread, but other conditions are ignored. In this case the burnt area „A_{fire}" (Figure 2: $A_{t1} – A_{t3}$) can be given with the next formula:

$$A_{fire} = \left(v_{fire} t_{freely}\right)^2 \Pi \qquad (3.1)$$

Following time units (sec, min, hour) burnt areas form concentric circles. This model got its name of these circles. Distance between the circles depends on the rate of fire spread. The „K_{front}" fire front can be given by the formula (3.2) and the changing of it is by the formula (3.3).

$$K_{front} = 2\Pi v_{fire} t_{freely} \qquad (3.2) \qquad\qquad \Delta K_{front} = 2\Delta t v_{fire} \Pi \qquad (3.3)$$

In the formula (3.3) the extent of the „ΔR" radiation change can be given by the formula (3.4).

$$\Delta R = v_{fire} \Delta t \qquad (3.4)$$

The effectiveness of the suppression can be demonstrated by the length of the suppressed fire section per the time units, that is, the speed of fire front suppression.

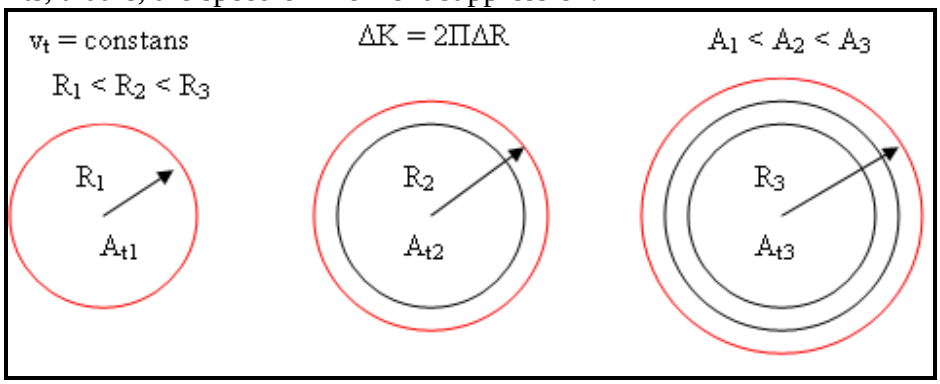

Figure 2. Concentric circles model

Based on the above for demonstrating the capability of the aerial means suppressing fire front author introduce the term of *speed of aerial firefighting* („v_{AFF}"). It means the length of the fire front suppressed by aircrafts.

$$v_{AFF} = \frac{L_{suppression}}{t_{suppression}} \qquad (3.5)$$

- v_{AFF} – speed of aerial firefighting [ms^{-1}; practically it can be $mmin^{-1}$ or $mhour^{-1}$];
- $L_{suppression}$ – length of the suppressed fire front [m];
- $t_{suppression}$ – time for suppression [s; practically min, or hour].

To extinguish the fire successfully, the condition must be met that the interveners suppress fire spread. The firefighters have to extinguish the fire front, whose growth per unit of time is equal to the change in perimeter based on the concentric circles model. Thus, the success and effectiveness of the firefighters' work should not be related directly to the speed of fire spread but rather to the change in perimeter! At the beginning of extinguishment, the speed of the extinguishment of fire front, in this case the speed of aerial firefighting must reach and later exceed the speed of the change of the fire front, that is, the change of the fire front within a given unit of time.

$$L_{suppression} > \Delta K_{front} \qquad (3.6)$$

Using the formula (3.6) to extinguish successfully, the next criteria must be satisfied:

$$v_{AFF} > \frac{\Delta K_{front}}{t_{suppression}} \text{ , or in other form: } v_{AFF} t_{suppression} > \Delta K_{front} \qquad (3.7)$$

By ordering the above, it becomes clear that in practice the initial condition can be calculated in a simplified way, where we need to take the speed of fire spread multiplied by 2Π.

$$v_{AFF} > 2\Pi v_{fire} \qquad (3.8)$$

Above in-equality is necessary but not yet sufficient condition for the efficiency of the national economy. Based on mathematical formulas and the logical deductions regarding the concentric circles model author made the following statements:

1. If the speed of extinguishing the fire front – in this case the speed of the aerial firefighting - is below the speed of changing the fire front, the aerials are unable to extinguish the fire (initial attack).
2. If the speeds above are identical, the length of fire front will remain but the burnt area will extend (beginning situation; later the balance follow 2Πrad).
3. If the speed of extinguishing made by aerials is higher than the increase of the fire front, fire can be suppressed.

Based on the above logical flow we can define both the economic efficiency of aerial firefighting and minimal criteria of successful suppression expressed by the elementary information we have regarding the actual fire. Naturally, the above statements are valid only at the time of beginning the suppression. Later, it modifies as changing the angle of suppressed fire front by the rules of 2Πrad.

Sufficient condition for the efficient suppression

In the examination of the rectangular model, the conditions of efficient extinguishment in terms of the national economy have already been recorded. Based on them, the extinguishment can be regarded efficient if the amount of the saved value reaches the total costs of the extinguishment. Then, the condition of efficiency is met satisfactorily (2.3). It applies to both the rectangular and the concentric circles model.

One feature of extinguishing forest fires is that regardless of the size of the forest burning, we tend to concentrate on the extinguishment of the fire front, which can be regarded as straight fire line suppression. It can be done or it can be accepted because in case of long-lasting uncontrolled fire spread, the curve of the fire front is hardly perceptible, in practice it can be ignored, so it's linear. If we concentrate on a very small section of fire front, the conclusions of the rectangular model can be applied here, too!

Provided we accept the above statements – the adaptation of the limit values of efficiency set in the rectangular model (2.4) to the very small section of the concentric circles model (3.7) – the formula can be created in the following way:

$$\frac{1}{2} LHp_{forest} \geq \Sigma C_{AFF} \Rightarrow \frac{1}{2} \Delta K v_{fire} t_{\sup pression} p_{forest} \geq \Sigma C_{AFF} \qquad (3.10)$$

Moreover, the limit value of the efficiency criterion of aerial firefighting out of formula (3.8):

$$2\Pi v_{fire} = v_{AFF} \qquad (3.9)$$

By reversing the equation and substituting the form pertaining to the actual time of formula (3.3):

$$C_{AFF}^{fly} t_{\sup pression} \leq \frac{1}{2} 2\Pi v_{fire} t_{\sup pression} v_{fire} t_{\sup pression} p_{forest} \qquad (3.10)$$

C_{AFF}^{fly} – unit costs of aerial firefighting [€h^{-1}; €min^{-1}]

$$C_{AFF}^{fly} t_{\sup pression} \leq \frac{1}{2} 2\Pi \left(\frac{v_{AFF}}{2\Pi} \right)^2 t_{\sup pression}^2 p_{forest} \qquad (3.11)$$

Ordering the above formulas and interpret it to a unit time, that is $t_{suppression}$ = 1 min, we can get for the speed of the aerial firefighting the distance of suppression per a minute, that is $v_{AFF} = l_{AFF}$ 1min^{-1}.

$$l_{AFF} \geq \sqrt{\frac{4\Pi C_{AFF}^{fly}}{p_{forest}}} \qquad (3.12)$$

Based on the above formula we can see that some data are enough for the statement of efficient suppression in view of national economy: as the length of suppressed fire front per unit (l_{AFF}), the unit cost of aerial firefighting (C_{AFF}^{fly}) and the unit costs of forest (p_{forest}). Remake the formula and apply it to speed of fire spread:

$$C_{AFF}^{fly} \leq \Pi p_{forest} v_{fire}^2 \qquad (3.13)$$

It has to take into account that the above values are limit values; satisfying them aerial firefighting will satisfy the criteria of efficiency in view of national economy too.

Investigating extinguisher materials

4.1. Extinguishing material is water – using external bucket for bombing

The most common and simplest extinguisher material is water. Using water we count actually only the cost of logistics that is aerial means. In this case the cost of unit water is a quotient of the aircraft cost and water capacity. It can be expressed by the next formula:

$$C_W = \frac{C_A}{V_W} \qquad (4.1)$$

- C_W = cost of water capacity [€kg^{-1}];
- C_A = cost of aircraft per hour [€h^{-1}];
- V_W= volume of water capacity per hour [kgh^{-1}];
- For example, in this article C_W = 0.3 €kg^{-1}

Water, as the most common and simplest extinguisher material, can be taken to the others as a reference regarding extinguishing effects. Therefore author introduce the term of water equivalent per unit of any extinguishing material regarding extinguishing effects ($C_{x=W}$). Naturally, water has its own water equivalent that is cooling effect caused by the specific heat capacity. Moreover not just the extinguishing effects of water but also the cost of water equivalent can be taken as a reference (C_W=$C_{W=W}$). Since the water has its own water equivalent, in the above case it is not important to discuss it. However, later, it gets an important role and as a starting point of a series it belongs logically to water.

Buckets can have significant losses of carried volume during the action, some observer estimate it more than 50 % (Jambrik, 2007; Imreh at al., 2009). Since the losses usually taken with high rate, in this examples author can't ignore it, on average he counts with 25 %. Because of the high rate of losses, we have to take into account not the bucket capacity but the part of it which is dropped to fire front. Consequently, in view of efficiency we have to share the cost of transportation (aerial firefighting) with a reduced volume of the bucket capacity (effective part), resulting higher cost per effective unit water. It can be expressed by the next formula:

$$C_{W\_eff} = \frac{C_W}{\gamma_B} \qquad (4.2)$$

- C_{W_eff} = cost of unit water dropped to fire front [€kg^{-1}];
- γ_B = coefficient of the bucket effectivity [];
- For example, in this article, in case of γ_B = 0.75, C_{W_eff} = 0.4 €kg^{-1}

Based on the above the effectiveness can be expressed by the next statement: the extinguishing capacity of 1 kg „water" at the beginning of the transportation (taking off) expressed by water

equivalent is equal to its own volume, it costs 0.3 €kg^{-1}, regarding the effective part of the capacity at the end of the transportation (dropping to fire front) is 0.4 €kg^{-1}.

4.2. Extinguishing material is foam – using internal tank

In this case the cost of foam concentrate multiplied with the mixing rate has to be added to the quotient of the aircraft cost and water capacity. It can be expressed by the next formula:

$$C_F = \frac{C_A}{V_W} + C_C R_{mix} \qquad (4.3)$$

- C_F = cost of foam solution capacity [€kg^{-1}];
- C_C = cost of foam concentrate [€kg^{-1}];
- R_{mix}= rate of mix [%];
- For example, in this article, in case of $C_C R_{mix}$ = 0.1 €kg^{-1}, C_F = 0.4 €kg^{-1}

Author's experiment shows that beside the cooling effect of foam, caused by the specific heat capacity of the water content, it also has an extra extinguishing effect caused by the structure of the foam that is isolation effect (Restas, 2012). This extra effect delays the ignition of the surface over time than reasonable just by the water content of the foam. This delay, as an extra extinguishing effect, can be expressed by water equivalent. It means, how much water quantity could equal the same delay that is caused by the structure of the foam.
In case of foam author found that it is twice more effective than water (Restas, 2012) however other experts state it 3 times more (Theo, 2009); it generates a coefficient of foam equivalent to water effect. Author insists on his own data; it means 1 kg foam has as much extinguishing effect as 2 kg water (cooling effect) has. In case of cost of extinguishing effect of foam the coefficient also has to be taken into account. It can be expressed by the next formula:

$$C_{F=W} = \frac{C_F}{Y_{exp}} \qquad (4.4)$$

- $C_{F=W}$ = cost of foam solution capacity equivalent to water effect [€kg^{-1}];
- Y_{exp} = coefficient of foam solution equivalent to water effect [];
- For example, in this article, in case of Y_{exp} = 2, $C_{F=W}$ = 0.2 €kg^{-1}

Obviously the on-board installed tank has less transport losses than buckets, many times it is ignored. Author takes into account the losses of on-board tank about 10 %; it means the coefficient of the effectiveness is 0.9. The cost of the effective part of the foam solution dropped from the tank expressed by water equivalent can be given by the next formula:

$$C_{F=W\_eff} = \frac{C_{F=W}}{\gamma_T} \qquad (4.5)$$

- $C_{F=W\_eff}$ = cost of useful part of foam solution capacity equivalent to water effect [€kg^{-1}];
- γ_T = coefficient of on-board tank effectivity [];
- For example, in this article, in case of γ_T = 0.9 , $C_{F=W\_eff}$ = 0.22 €kg^{-1}

Based on the above the effectiveness can be expressed by the next statement: the extinguishing capacity of 1 kg „foam solution" at the beginning of the transportation (taking off) expressed by water equivalent is equal to 2 kg, it costs 0.4 €kg^{-1}, regarding the effective part of the capacity at the end of the transportation (foam on surface) is 0.22 €kg^{-1}.

4.3. Results and discussion regarding foam applications

Based on the results of the practical example, we can deduct that failing to use foams is a professional mistake – if we presume the effectiveness of one unit is twice as much. Yet there is no practical evidence of frequent application of foams. Obviously, it might have numerous reasons. One of them must be the additional cost. It is a mistake to compare the extra cost of foam as an extinguisher to that of water. As water costs practically nothing, regardless of how cheap the foam concentrate is, it would be still significant compared to water. The mistake lies in comparing the costs of the extinguishers or those of the technical equipment (amortisation) instead of comparing the total costs of different extinguishing methods, including the operation cost of the aircraft. The latter one cannot be separated, since it represents a considerable amount within the total cost.

In the above example the difference between the cost of 1 kg water and 1 kg foam solution is very drastic (0 €kg^{-1} => 0.1 €kg^{-1}), but taking into account the cost of transportation (aircrafts) the difference is moderate (0.3 €kg^{-1} => 0.4 €kg^{-1}), it means only 33%! If the effectiveness of the unit foam solution in water equivalent rise also just with 33%, it means, economic point of view there is no difference between the extinguishers. However, the coefficient of the effectiveness of the foam solution in water equivalent is 2, which means the effectiveness rose 100 %!

We have to look for another excuse for failing to use it. In the author's opinion three basic things can hinder the application of foam concentrates.

1. Logistics: The application of foam concentrates requires logistics support. Water is freely available and the loading of aircrafts can be carried out without any external help, so this is the simplest method.
2. Tactics: In aerial firefighting the fire front is directly attacked with water, while in the case of foams the protection strip is targeted primarily.
3. Psychology: The additional related costs the need for logistics support and the difficulties in the application of foams may generate negative prejudices without any professionally valid researches.

Based on the above, in the example, the cost doesn't rise by 33% but in water equivalent reduces by 45% (0.4 €kg^{-1} = > 0.22 €kg^{-1}) !

4.4. Extinguishing material is retardant – using internal tank

In case of retardant the method is similar to the foam concentrate. The cost of retardant multiplied with the mixing rate has to be added to the quotient of the aircraft cost and water capacity. It can be expressed by the next formula:

$$C_R = \frac{C_A}{V_W} + C_{ret} R_{mix} \quad (4.6)$$

- C_R = cost of retardant capacity [€kg^{-1}];
- C_{ret} = cost of retardant [€kg^{-1}];
- R_{mix} = rate of mix [%].

Retardant also has an extra extinguishing effect, therefore the effectiveness in water equivalent – similar to foam solution – have to be counted with coefficient too. It can be expressed by the next formula:

$$C_{R=W} = \frac{C_R}{Y_R} \quad (4.7)$$

- $C_{R=W}$ = cost of retardant capacity equivalent to water effect [€kg^{-1}];
- Y_R = coefficient of retardant equivalent to water effect [].

The cost of the effective part of the retardant dropped from the tank expressed by water equivalent can be given by the next formula:

$$C_{R=W\_eff} = \frac{C_{R=W}}{\gamma_T} \quad (4.8)$$

- $C_{R=W\_eff}$ = cost of useful part of retardant capacity equivalent to water effect [€kg^{-1}];
- γ_T = coefficient of on-board tank effectivity [].

The extinguishing effect of the foam based on water equivalent was determined by tests R-20F (Restas, 2012) and R-10A (Restas, 2014). However, tests targeting the effectiveness of retardants have not been conducted yet so the author has not found any acceptable values to be compared in the specialist literature. Thus, to make practical calculations, I applied logical deductions, expert estimations and hypothesis analysis.

4.5. Results and discussion regarding retardant applications

n the test, the basic conditions are the same as the previous ones. The effectiveness of the retardants is definitely higher than that of water. To determine it, the author makes the following logical deduction:

1. The author accepts that retardants are able to provide protection against crown fire, that is, against fire intensity of 8.000 kWm^{-1};
2. Nobody implies – and there is no practical evidence – that retardants are able to withstand any fire intensity. Its extinguishing effect is obviously lower than the one which is able to suppress extreme fire of 18.000 kWm^{-1} intensity;
3. Based on the author's logical reasoning, the extinguishing effect of retardants is higher than the effect able to suppress fire of 8.000 kWm^{-1} intensity, typical of crown fire, but lower than fire intensity of 18.000 kWm^{-1}, which can be observed in extreme fires.
4. Aerial firefighting can be effective up to 3.400 kWm^{-1} (Silva, 2002). In the comparison of effectiveness its value is 1.
5. If the value of the effectiveness of water is 1 at 3.400 kWm^{-1}, the value of required effectiveness has to be 2.35 at 8.000 kWm^{-1}, and 5.3 at fire intensity of 18.000 kWm^{-1}.

Following from the above, the effectiveness factor of retardants can be considered „4÷5" expressed in water equivalent, based on expert estimation. It implies that it can suppress a quite fierce fire of intensity 13.600 kWm^{-1} - 17.000 kWm^{-1}, which is rather rare. This value takes into account the practical experience that retardants are not always able to provide effective protection against crown fires, though usually they are. For further calculations, the author has rounded the value of professional estimation up to 5, and it will be used for calculations.

In the assessments of the effectiveness of extinguishers, the author has met the opinion several times that foams are 3 times, retardants are 9 times more effective than water (Theo, 2009; George, 2013). The series (water=1, foam=3, retardant=9) obviously reflects rather a logical relationship than actual

effectiveness. The author seeks to determine the effectiveness of retardants with his own hypothesis analysis – because of differing values in his own tests with foams.
Based on the above, the author's hypothesis is that the effectiveness factor of retardants given by the distributor or producer companies reaches the value of 9. It can be examined in several ways, aimed at the following: A) the amount of the extinguisher; B) the intensity of the fire; C) cost-effectiveness. Obviously, there would be a fourth method as well, when all the above are examined together, but it is justifies only in the case, when the hypothesis is affirmed in one of them at least.
A) The producer suggests that the amount of extinguisher needed in one unit of surface is the maximum amount remaining on the foliage in the case of retardants, too. So, we do not meet increased effectiveness in terms of quantity. The hypothesis cannot be justified in terms of quantity.

B) In terms of fire intensity, the effectiveness factor of 9 means that the same amount can suppress fire of intensity which is 9 times higher. It implies that retardants have to be able to suppress forest fires of 30.600 kWm^{-1} intensity. However, practice does not consider such extreme fire intensity. In addition, as it was mentioned before, there is no guarantee that it can suppress fire of 18.000 kWm^{-1} intensity, which happens quite frequently. The hypothesis cannot be justified in this case either.

C) The third way to examine the hypothesis requires a concrete efficiency analysis, which will be detailed below. The price of the retardants has to be at least twice of the price of the foam concentrate; it is not possible to find a product cheaper than 8 $€kg^{-1}$. The mixing rate of retardants suggested by the producers and distributors is at least 25 %, so this percentage was considered in the calculations.
The value of the effectiveness coefficient is counted with 5, given this value by expert estimation, that is $Y_R = 5$. It means, the effectiveness of the retardant is 2.5 higher than the effectiveness of foam. Using on-board installed tank in both cases, the losses are also the same. Example for the above:

- $C_{ret} = 8\ €kg^{-1}$
- $R_{mix} = 25\ \%$
- $C_R = 0.3\ €kg^{-1} + 2\ €kg^{-1} = 2.3\ €kg^{-1}$
- $Y_R = 5$
- $C_{R=W} = 2.3\ €kg^{-1} / 5 = 0.46\ €kg^{-1}$
- $\gamma_T = 0{,}9$
- $C_{R=W\_eff} = 0.46\ €kg^{-1} / 0{,}9 = 0.51\ €kg^{-1}$

Based on the above, the conclusion should be that the efficiency of the retardant expressed by water equivalent is less than that of the water itself. This result obviously can't be logical if the practice uses retardants regularly as an effective extinguishing material. The solution is that the pure water itself is unable to suppress the fire above limited fire intensity (3400 kWm^{-1}), however the retardant is. Therefore, even if water is a cheaper solution in case of higher fire intensity its value is basically nothing. Although retardant seems to be irrationally expensive expressed by water equivalent but the capability extent to such a dimension, where water objectively can't be itself.

References

Fibla D.V.M. and Urbina, J.C.G.: Restardantes en la lucha contra incendios forestales; I. Symposium Internacional, La Gestión de los Medios Aéreos en la Defensa Contra los Incendios Forestales, Córdoba, Spain, 28-30 October, 2002

George, C.: ICL Biogema Sponsor presentation, Aerial Fire Fighting Conference, Aix-en-Provence, France 10-11, April, 2013

Gould, J., Plucinski, M., McCarthy, G., Hollis, J., Handmer, J. and Ganewatta, G.: Effectiveness and efficiency of aerial fire fighting in Australia; Fire Note; Issue 50, 2009 November, Fire Note is

published jointly by the Bushfire Cooperative Research Centre (Bushfire CRC) and the Australasian Fire and Emergency Service Authorities Council (AFAC)

Imreh, L., Blaskovics, Zs. and Restas, A.: Új módszerek a légi tűzoltásban; Repüléstudományi Közlemények 2013. (2) HU ISSN 1789-770X, download: http://www.repulestudomany.hu/kulonszamok/2009_cikkek/Imreh_L-Blaskovits_Zs-Restas_A.pdf

Jambrik, R.: Légitámogatás nélkül nehéz, nagyon nehéz lett volna, Vedelem, ISSN: 1218-2958, 14 (6), pp. 51-52, 2007, download: http://www.vedelem.hu/letoltes/tanulmany/tan126.pdf

Restas, A.: R-20F Method: An approach for measuring the isolation effect of foams used fighting forest fires, ACADEMIC AND APPLIED RESEARCH IN MILITARY SCIENCE 11: (2) pp. 233-247. 2012

Restas, A.: Suppression capability of foams used fighting against forest fires with the test of weight rate remained on the crown surface R-10A Method - weight effectiveness experiment; Manuscript, under publishing, 7th ICFFR, Coimbra, Portugal, 2014

Silva, F. R.: Investigación y Capitalización de la Experiencia en el Empleo de Medios Aéros en la Defensa Contra los Incendios Forestales, La gestión de los Medios Aéros en la defensa conzta los incendios forestales, I. Simposium Internacional, Córdoba, Spain, 2002

Theo, M.T.: Initial Attack Air Tanker - Marsh S-2AT Turbo Tracker; Presentation, Aerial Fire Fighting Conference, Rome, Italy, 3-4 November, 2009

Theoretical solution for a logistic problem: how to raise the effectiveness of aerial water transport

Agoston Restas

National University of Public Service, Budapest, Hungary, Restas.Agoston@uni-nke.hu

Abstract
Introduction: As well-known, aerial firefighting is an effective solution suppressing forest fire, however there is no doubt, this tool in many cases can be the only one effective solution, even if it is very expensive. Following the above idea, any new method that is able to reduce the cost of aerial means supporting forest fire management, is worth examining as a new aerial solution. Methods: This article used practical experiments of the aerial firefighting, created a graphics model to understand the logistic problem, made assumptions to concentrate on the key problems and with mathematical backgrounds some logistic functions meaning distance and capacity axes. Results and discussion: The effectiveness of air tankers depends on the distance between the fire zone and water resource. The shorter the distance is between them, the higher the effectiveness is using aerials. This relation can be shown even at a function; however the change is not linear. The rate of the curve depends on the distance, larger distance means smaller change and vice versa, shorter distance means bigger scale of change. This result gives the tipping point where the higher costs of suggested solution – aerial water supply system - will be balanced by the higher amount of bombed water.

Keywords*: aerial firefighting, water transport, logistic problem, raising effectiveness*

Introduction

Each year thousands of hectares of forests burn causing a lot of damages in life, property and environment. As well-known forest fires cause also the 20% of the CO_2 emission generating greenhouse effects (Spessa, A. at al., 2013). Since the resources of managing forest fires are always limited, any new method, equipment or idea which can help managers is valuable to examine as a new solution.
As well-known, aerial firefighting is an effective solution suppressing forest fire, however there is no doubt, this tool can be the only one solution in many cases, even if it is very expensive (Ganewatta, G. and Handwer, J., 2009). Following the above idea, any new method or equipment, that is able to reduce the cost of aerial means supporting forest fire management, is valuable to examine as a new aerial solution. Higher effectiveness of aerial firefighting means that management can save more life, property and environment or can reduce the cost of intervention.

Problems and theoretical solution

Since the practice using aerial means for bombing water is accepted by the experts as a very effective tool fighting against forest fires, - but its high cost is commonly known also, - the question arises: how could the costs of this application be reduced or how could the effectiveness of this method be raised? Without deeper analysis, it is accepted, the effectiveness of the aerial firefighting strongly depends on the distance between the fire front and water resources. If the distance between them is relatively short, air tankers can take more cycles, it means high effectiveness; however long distance means obviously fewer cycles and lower effectiveness.
Since the distance between the natural water resources and fire front is independent from each other, forest services in many cases create fix, semi-fix or mobile water supply in the most threatened zones in the forest, for example for supporting helicopter attack. This water supply require resources, like

money, time to installation, humans to control, energy for upload, etc. however more and more installation means that, from the point of forest service view these tools are useful and its application is effective.
If fire occurs in the forest where these water supplies had been installed it means that this solution is or can be effective. If fire doesn't occur during the fire season in the forest where water supply had been installed before, all resources that forest service invested in these systems mean wasted money. The experience shows that, even if it has risks in necessity, a lot of efforts are made to install more and more water supply systems.

Figure 1. Mobile water supply system for supporting helicopter attack

The question is, if mobile water supply system is accepted as an effective tool for supporting the (aerial) fight against forest fire, – but it is obviously impossible to install and manage theme in each forest, even if it would be required by experts, – instead of these system an aerial version, like a huge air tanker as an logistic support can be used or not.
Scenario is as follows (Figure 3): a huge capacity air tanker carries the water between the water resource (airport/airfield) and fire zone. At the fire zone, this aircraft flies circles as an aerial water supply system and upload the water to the other, limited capacity air tanker(s). Smaller aircrafts are more mobile, they can bomb water in the most appropriate places, with more precision. In many cases, fire managers require just some water but in the right place to suppress fire, and huge air tankers carry many times more water than it is required for a precisions attack. The water bombed or used ineffectively means that, all the costs invested into carrying it from water resources (airport/field) to fire zone is lost money.

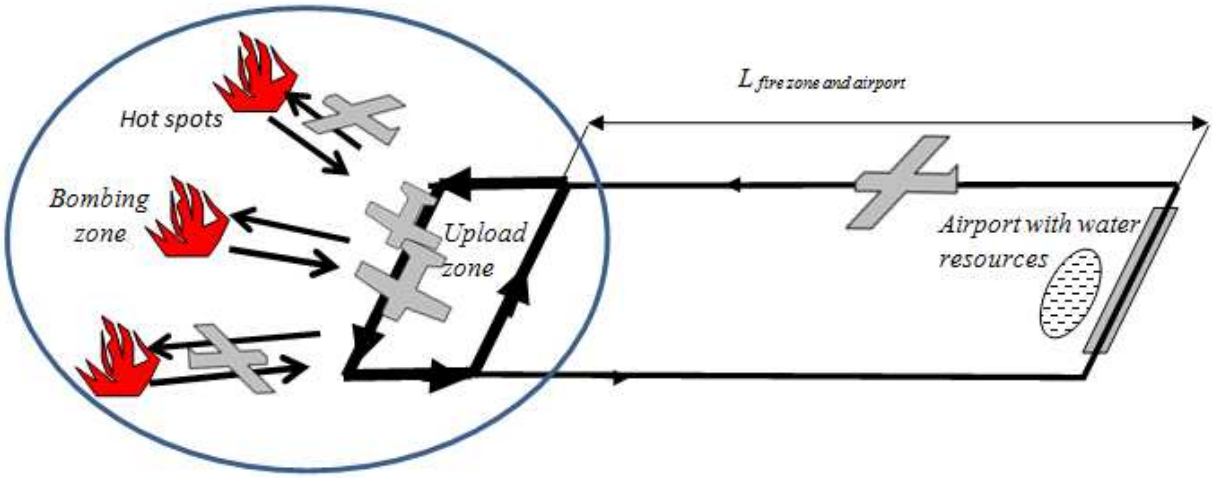

Figure 2. The structure of Aerial Water Supply System (AW2S)

The above scenario seems to be theoretical but not impossible. Many times, the aerial fuel tank is a normal procedure during military operations; therefore, it can be possible to solve the problem of aerial water upload. The question is less technical than economical: the scenario above can be economical effective or not; if the answer is yes, what conditions satisfy the minimum criteria of the required effectiveness?

This study focuses on the possibility of creating a new solution. Because of the limited time, resources and the frame of the study, author determined some assumptions. They make the theory easier to understand and find the essence of the advantages. Assumptions help readers not to get lost in the details but understand the essence.

Even if assumptions make this study simple, it is not allowed to generate false results at the end; counted assumptions are as follows:

- The scale of forest fire is large, aerial firefighting is required;
- Fire intensity is constant, forest area is homogenous, area is flat, there is no wind;
- Extinguishing material is water, aerial firefighting (bombing water) is effective;
- Study focuses on aerials' effectiveness from the logistics point of view but not from firefighting tactics;
- Study uses 2D logistic model;
- There is no problem with water upload from large tanker to small tanker(s).

Features of aerial activity

The effectiveness of air tankers depends on the distance between the fire zone and water resource. The shorter the distance is between them, the higher the effectiveness is using aerials. This relation can be shown even at a function; however the change is not linear. The rate of the curve depends on the distance, larger distance means smaller change and vice versa, shorter distance means bigger scale of change. This curve shows an exponentially decreasing function, where the index depends on the type of aerial tanks. Naturally, the curve never passes the axis; the close has an objective limit.

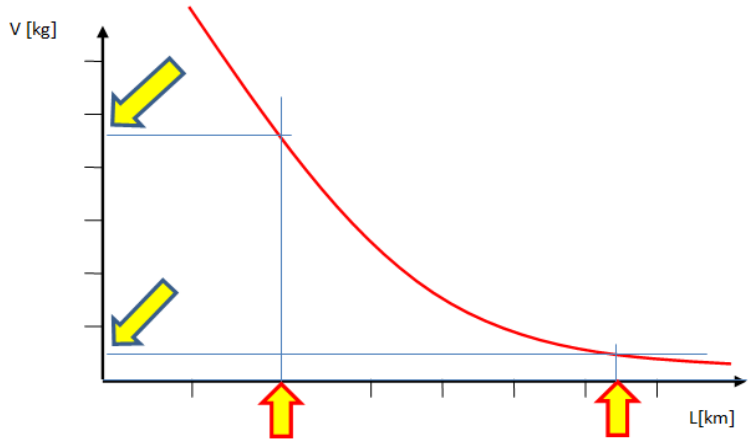

Figure 3- Effectiveness (bombed water) of aerial firefighting depending on the distance between the fire front and the water resource

Again, the shorter the distance is between the fire front and water resource, the more water is carried (bombed) water to fire front, in other words, higher the effectiveness of the aerial firefighting.

Essence of the aerial fire fighting's effectiveness

Experts rarely or never talk about the costs of disaster management. If human life, property or environment is suddenly threatened or hit by a disaster, like large scale forest fires, money doesn't count for politicians, even if the prevention or the higher readiness for response would cost much less. Ethically, human life is invaluable, thus in case of disaster speaking about the money or costs of the intervention is impoliteness.
Despite the above, it is easy to accept that, the essence of the effectiveness depends on the cost of intervention. Based on the given assumptions, the effectiveness takes into account with the amount of water - dropped to fire front, - carried by tankers, and the costs of operation hours paid for tankers' service. The rate of theme gives the costs of dropped extinguish (water) item (1 kg) at fire front (1).

$$\frac{\sum costs\ of\ aerials_{\$}}{\sum carried\ water_{kg}} = x\ \frac{\$}{kg} \qquad (1)$$

Basically, higher effectiveness means that we should carry more water with the same costs, or reduce the costs of the carried amount of water. This study approaches the above question with a special solution. This study examines the opportunity how the effectiveness changes if a large tanker as an aerial water supply is used. For this analysis, it considers two simple cases; they can be developed further based on the results this study determines, or giving up step by step the given assumptions.
In the first case, - let's say case of "A", - all water is carried to the fire front and dropped as usual by 1 small air tanker (2); its feature means:

$$A) \quad 1\ small\ air\ tanker\ (A) \rightarrow \sum water_A \rightarrow \sum costs_A \qquad (2)$$

In the other case, - let's say case of "B", - the water to fire zone is carried by a big air tanker (B) and there it is uploaded by airborne to the smaller air tanker (A). During this process the big tanker serves as a water supply system for the small tanker (A), meaning also that, small tanker can take shorter circles from water resource than without big tanker and resulting also higher amount of water, bombed to fire front (3); its feature means:

$$B) \quad 1\ small\ tanker\ (A) + 1\ big\ tanker\ (B) \rightarrow \sum water_B \rightarrow \sum costs_B \quad (3)$$

In case of "B", there is the same small tanker, as in case of "A", and also a big tanker as an aerial water supply system, meaning that, the total costs in case of "B" are naturally higher than in case of "A" (4):

$$\sum costs_A < \sum costs_B \quad (4)$$

The effectiveness can be expressed not just by the amount of water carried to the fire front, but also by the expenses, the water carried costs. If the costs or the amount of bombed water is equal, the effectiveness can be determined by ranking the other parameter. Since the costs in case of "B" are logically always higher than in case of "A", it is easy to sense that, this study focuses on the *tipping point*, where the higher costs is balanced by the higher amount of water bombed (carried).
Tipping point means that, - with the assumptions given above, - the costs of 1 kg bombed water are equal in both cases; in other words, in both cases the economical effectiveness is the same or equal. In this case, the rate of costs (5) is the same or equal to the rate of water carried (6).

$$R_{costs} = \frac{\sum costs_A}{\sum costs_B} \quad (5)$$

$$R_{water} = \frac{\sum water_A}{\sum water_B} \quad (6)$$

$$\frac{\sum costs_A}{\sum costs_B} = \frac{\sum water_A}{\sum water_B} \quad (7)$$

$$R_{costs} = R_{water} \quad (8)$$

Moreover, the same effectiveness means that, the rate of the costs and the water bombed is equal in both cases (9) (10) (11).

$$R_A = \frac{\sum costs_A}{\sum water_A} \quad (9)$$

$$R_B = \frac{\sum costs_B}{\sum water_B} \quad (10)$$

$$R_A = R_B \quad (11)$$

Since the expenditures of the planes' operation and also the water carried in case of "A" are known, the tipping point ($\Sigma water_B$) can be determined by ordering the above equals (12):

$$\sum water_B = \frac{\sum water_A \sum costs_B}{\sum costs_A} \quad (12)$$

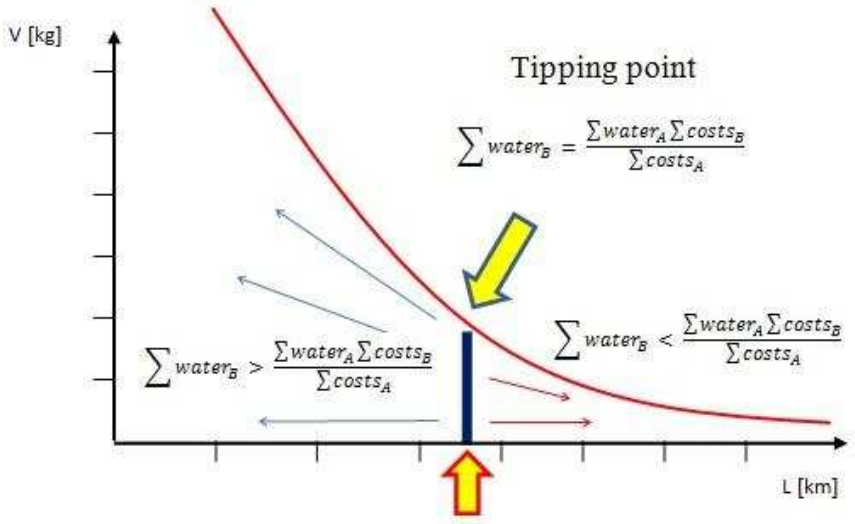

Figure 4. The structure of tipping point

This result gives the tipping point; in any case where the amount of water carried in case of "B" is bigger, the effectiveness is sure. The larger the difference is between the parts of the equal, the higher the effectiveness in the case of "B". Since the costs of case "B" is logically always higher than the costs of case "A", for the equal effectiveness the higher costs of case "B" must be balanced by the higher amount of bombed water.

Required data for finding the tipping point

Following the above, to determine the tipping point the distance between the water resource (airport) and the fire front, the costs of operation hour of used planes and the characteristic of the aircraft's effectiveness function are required to know; based on these data a rate is resulted. Required data for determining the tipping point:

- Characteristic of the aircraft's effectiveness function,
- Operation costs of air tankers (AW2S),
- Distance between the water resource (airport) and the fire front.

From the point of economical view there is no difference between the case of "A" and "B"; higher costs are balanced by more water. This equality doesn't count with the fact that, in the case of "B" the carried (bombed) water is obviously more than in the case of "A"; this fact is an extra advantage (effectiveness) of the case of "B". Considering this advantage or the evaluation of its real value requires another study but the recognition of this fact shows squarely the viability of the aerial water supply system.

Finding examples for the test

Look at an example; if the operation costs of a large tanker is 3 times higher than the small tanker's one, the total costs of the case of "B" are 4 times more than case of "A". Rate of costs is 4, meaning that the required water supply for equal effectiveness by the new system (AW2S) for bombing at the same situation is 4 times more too. Based on table 1, costs are not too far from each other; therefore, there is a chance for finding applicable solution for the aerial water supply system (AW2S).

Table 1—Examples for flying costs[1]

	Type	Costs of flying hour [€h^{-1}]	Costs of flying minute [€min^{-1}]	Source
1.	S-2T	1800	30	Conf. pres.
2.	G-IIIAT	3240	54	Conf. pres.
3-	C-130	6000	100	Internet
4.	C-27 Spartan	7000	117	Internet
5.	CL-415	8640	144	Conf. pres.
6.	BE-200	11500	192	Company
7.	ShinMeiwa	16200	270	Company
8.	B-747 Super tanker	5500[2]	92	Company

To test the new system, author suggests the S-2T as the small aircraft and an often used military plane, example C-130, C-27 or An-26 as the cheapest version of "large" capacity air tanker. Each of them is robust, has relatively low operation costs and easy to test. C-130 can carry much more payload (water) than the difference between the flying costs of S-2T and C-130.

7. Some remarks regarding the results

There are three remarks, first is: naturally other platforms generate other results of the above rate. Even if it seems to be easy to choose or find a version of AW2S which is effective, but the effectiveness is not for itself; it must satisfy the criteria at as low costs level as possible. Results without the latest criteria can satisfy the requirements of the effectiveness of the aerial water supply system but they might not meet the requirements of the effectiveness of aerial firefighting.
Second remark focuses on the tipping point. From the point of economical view they are totally the same, the higher amount of water is carried by a complex system (case of "B" – AW2S) or by the rate times more single solution (in the above example: 4 x case of "A"). Naturally the above statement is valid only at the tipping point.
The difference between the rate of the tipping point and the rate of the payload (water) capacity (6) is very important. The higher the difference is between them, the higher the effectiveness of the aerial water supply system; it results also in a higher effectiveness of aerial firefighting.

8. Analysis of the function's characteristic

Depending on the characteristic of the air tankers' function, the distance between the fire front and water resource (airport) and the rate of costs "A" and "B" gives the orientation of the tipping point on the curve. Even if the above seems difficult, it is not so. If the aerial water supply system can serve more water than the rate is, the system is effective. Not just the payload capacity but also the operation costs of aerial tankers are known by the users, moreover, the distance between the fire front and the water resource (airport) is also known immediately after the fire alarm; thus, using the given equals above the fire management can calculate the tipping point relatively easily helping the quick and right *yes* or *no* decision.

[1] Presentations and expert estimation; Theo, M.T., Aerial Fire Fighting Conference, Rome, Italy, 2009
[2] Special costs, given by the Evergreen service; it seems, must be critics.

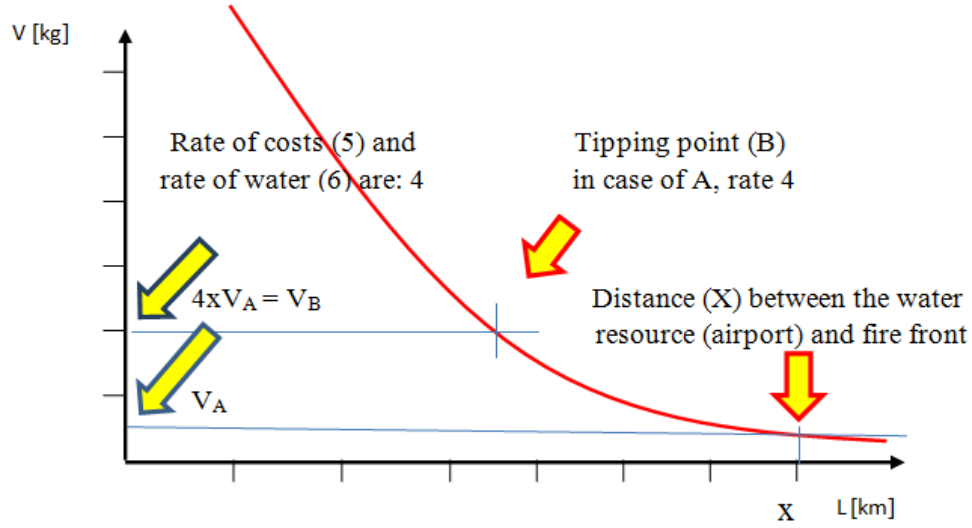

Figure 4. Analysis of the air tanker's effectiveness function

Moreover, to help the effective application even special software can be created for example by GIS based program. On the known parameters the program can classify different zones at the responsible area and indicate it on the intervention map, where the classification can quantify from the point of economical view the effectiveness of the AW2S application.

Based on the characteristic of the function, it is easy to sense that in case of large distance between water resource and fire front it is much easier to reach the tipping point, it is realized at lower level and vice versa, if the distance is shorter, to reach it is more complicated (higher level). Following this process there is a point where the case of "B" practically can't be better solution than the case of "A" because the system objectively can't carry as much water as the balance (tipping point) requires. It is necessary to count with the fact that, the rate of function is not linear, exponential curve has a negative index.

Since the idea generated in this study focuses on the problem of long distance between water resource and fire front, the above extremity is not relevant.

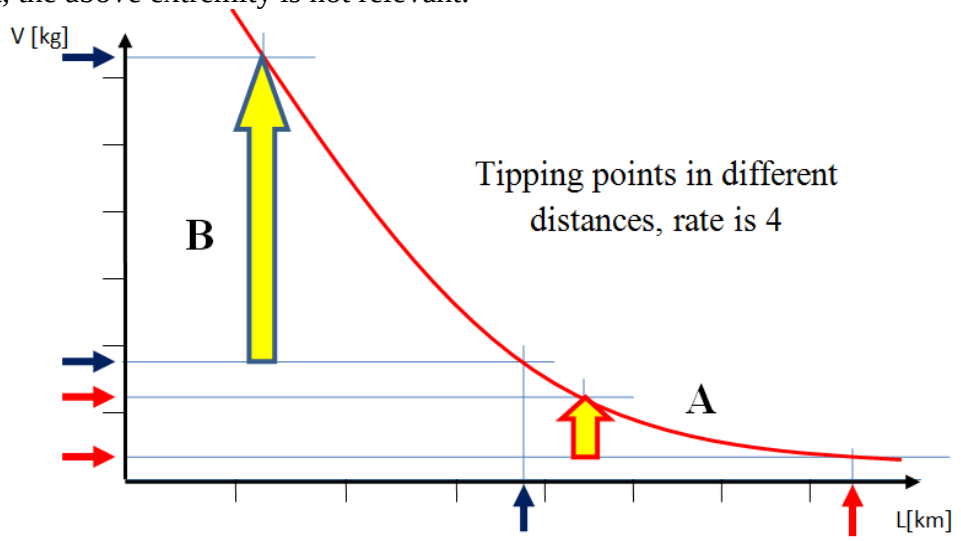

Figure 5. The difference of the requirements depending on the distance between the water resource and the fire front

9. Short summarizing

Based on this study, the aerial water supply system (AW2S) is a good idea and can be an effective solution. Even if the study made assumptions, the end results of the evaluation shows that the AW2S is a viable method not just from the point of professional but also economical effectiveness view. The realization is rather a technical than economical question. There is no doubt, in certain conditions AW2S can be a better and more effective solution than the aerial firefighting pattern used today.

10. References

Ganewatta, G. and Handmer, J.: The Cost Effectiveness of Aerial Fire-fighting in Australia; Centre for Risk and Community Safety, RMIT University, Bushfire CRC, ISBN: 978-0-9804594-3-2, April 2009

Spessa, Allan; van der Werf, Guido; Thonicke, Kirsten; Gomez Dans, Jose; Lehsten, Veiko; Fisher, Rose and Forrest, Matthew . Modeling vegetation fires and fire emissions. In: Goldammer, Johann Georg ed. Vegetation Fires and Global Change – Challenges for Concerted International Action. A White Paper directed to the United Nations and International Organizations. Kessel, 2013. pp. 181–207.

Theo, M.T.: Initial Attack Air Tanker - Marsh S-2AT Turbo Tracker; Presentation, Aerial Fire Fighting Conference, Rome, Italy, 2009

Imprensa da Universidade de Coimbra
Coimbra University Press
Portugal – 2014

· U C ·

IMPRENSA DA UNIVERSIDADE DE COIMBRA
COIMBRA UNIVERSITY PRESS